1001

Heterozygous Disruption of Gsα in Osteocytes Decreases Peripheral Fat without Affecting Bone Mass. Keertik Fulzele*[1], Kevin Barry[2], Sutada Lotinun[3], Roland Baron[4], Lynda Bonewald[5], Jian Feng[6], Min Chen[7], Lee Weinstein[8], Rajaram Manoharan[9], Mary Bouxsein[9], Paola Divieti Pajevic[10]. [1]Massachusetts General Hospital; Harvard Medical School, USA, [2]Endocrine Unit, Massachusetts General Hospital & Harvard Medical School, USA, [3]Harvard School of Dental Medicine, USA, [4]Harvard School of Medicine & of Dental Medicine, USA, [5]University of Missouri - Kansas City, USA, [6]Texas A&M Health Science Center, USA, [7]Metabolic Disease Branch, National Institute of Diabetes & Digestive & Kidney Diseases, National Institute of Health, USA, [8]National Institute of Diabetes & Digestive & Kidney Diseases, USA, [9]Beth Israel Deaconess Medical Center, USA, [10]Massachusetts General Hospital, USA

The stimulatory α-subunit, Gsα, of a heterotrimeric G-protein is a ubiquitously expressed protein that mediates signals from various hormone and neurotransmitter receptors to the generation of cAMP. Gsα is a product of the *Gnas* gene, a complex imprinted gene with multiple products. Heterozygous loss-of-function mutations of Gsα lead to Albright hereditary osteodystrophy (AHO) characterized by skeletal defects and, in case of maternal mutation, results in obesity. To define Gsα actions in bone and specifically in osteocytes *in-vivo*, mice carrying floxed exon-1 alleles of *Gnas* were mated with mice expressing Cre-recombinase driven by 10kb dentin-matrix protein 1 (DMP-1) promoter to generate homozygous (DMP1-GsαKO) or heterozygous (DMP1-GsαHet) deletion of Gsα in osteocytes. Littermates lacking DMP1-Cre expression were used as controls. DXA analysis of 21-week old DMP1-GsαKO mice showed significantly decreased total body BMD (19%) and BMC (21%) ($p<0.01$, $n\geqslant6$). MicroCT analysis of the distal femur showed an 86% decrease in trabecular bone volume in DMP1-GsαKO mice compared to controls ($p<0.01$, $n=5$). Histomorphometry analysis of femurs from 7-week old DMP1-GsαKO mice showed a significant decrease in the number of osteoblasts, BFR, MAR, and the number of osteoclasts indicating a state of low turnover ($p<0.05$, $n\geqslant3$). Despite severe osteopenia in the DMP1-GsαKO mice, the osteocyte density was doubled as compared to controls ($p<0.01$, $n=4$), but resulted in dramatically disorganized canaliculi network as assessed by SEM. Immunohistochemical staining showed a 3-fold increase in sclerostin expression in tibia of DMP1-GsαKO mice indicating possible inhibition of Wnt signaling in osteoblasts. Additionally, DMP1-GsαKO, but not DMP1-GsαHet, mice showed hematopoietic abnormalities. Neither micro-CT nor DXA bone parameters differed between control and DMP1-GsαHet. Interestingly, both DMP1-GsαKO and DMP1-GsαHet mice showed a significant decrease (>40%) in peripheral fat at 21-weeks of age as analyzed by DXA ($p<0.01$, $n\geqslant6$). Preliminary analysis showed no change in fasting insulin and glucose in both DMP1-GsαKO and DMP1-GsαHet mice compared to controls. However, white adipose tissue histology from the mutant mice showed decreased adipocytes size and abnormal morphology suggesting a possible defect in lipid metabolism. These results suggest a possible direct role of Gsα signaling in osteocytes in regulating not only bone metabolism, but also peripheral adiposity.

***Disclosures: Keertik Fulzele**, None.*

1002

Deletion of the Redox Amplifier p66^{shc} Decreases ROS Production in Murine Bone and Increases Osteoblast Resistance to Oxidative Stress in a Cell Autonomous Fashion: Causal Link with the Pro-survival Effects of Sex Steroid. Maria Jose Almeida*, Li Han, Elena Ambrogini, Shoshana Bartell, Aaron Warren, Randal Shelton, Stavros Manolagas. University of Arkansas for Medical Sciences, USA

The age- or gonadectomy-dependant decrease in osteoblast/osteocyte survival is associated with oxidative stress, as illustrated by increased levels of reactive oxygen species (ROS) and phosphorylation of p66^{shc} — an adapter protein that amplifies mitochondrial ROS generation and influences apoptosis and lifespan in mice. We have sought mechanistic evidence causally linking p66^{shc} to the adverse effects of oxidative stress and sex steroid deficiency on osteoblast survival. We report that p66^{shc} deletion in mice (a model provided to us by Dr. T. Prolla, Univ. Wisconsin) caused a decreased in ROS and an increase in the level of glutathione in the bone marrow. Moreover, calvaria-derived osteoblasts from these mice were resistant to H_2O_2-induced apoptosis. Consistent with these findings, silencing of p66^{shc} in established osteoblastic cell models (OB-6 or UAMS-32) abrogated the H_2O_2-, but not etoposide-, induced apoptosis. Silencing of p66^{shc} also reduced NF-kB activation in response to H_2O_2, as determined by the phosphorylation of IkB and the activity of an NF-kB reporter construct. Further, p66^{shc} silencing attenuated the H_2O_2-induced increase in the expression of the NF-kB-target genes IL-6 and TNFα. The H_2O_2-induced apoptosis and NF-kB activation were also attenuated by the specific PKCβ inhibitors hispidin or LY333531. On the other hand, the PKC inducer PMA had similar effects to H_2O_2 on both apoptosis and NF-kB activation. These effects of PMA were abrogated in the absence of p66^{shc} or in the presence of the PKCβ inhibitors, as was the case with H_2O_2, indicating that the effects of H_2O_2 or PMA are indeed dependent on PKCβ. 17β-estradiol (E2), a polymeric form of E2 that is not capable of stimulating the nuclear-initiated actions of ERα (EDC), or the non-aromatizable androgen DHT, prevented H_2O_2- or PMA-induced p66^{shc} phosphorylation, apoptosis, and NF-kB activation. Lastly, each of the three steroids prevented H_2O_2-induced PKCβ phosphorylation. These results demonstrate that p66^{shc} is an essential mediator of the effects of oxidative stress on apoptosis, NF-kB activation, and cytokine production by osteoblastic cells. Estrogens or androgens attenuate these effects by suppressing PKCβ-induced p66^{shc} phosphorylation via a mechanism that does not require the nuclear-initiated actions of the ERα. Thus, p66^{shc} is causally linked to the adverse effects of both aging and sex steroid deficiency on osteoblast survival.

***Disclosures: Maria Jose Almeida**, None.*

1003

Insulin Signaling in Osteoblasts Favors Whole Body Glucose Homeostasis by Activating Osteocalcin. Tatsuya Yoshizawa, Jianwen Wei*, Mathieu Ferron, Patricia Ducy, Gerard Karsenty. Columbia University, USA

Undercarboxylated osteocalcin has been shown recently to act as a hormone favoring b-cell proliferation in the pancreas, insulin secretion by b-cells, insulin sensitivity in peripheral tissues and energy expenditure. An implication of this array of functions is that insulin may, in a feedback loop, regulate osteocalcin expression, secretion and/or its carboxylation. To address these questions we generated, on the one hand, mice lacking the insulin receptor (InsR) only in differentiated osteoblasts and, on the other hand, a dual ELISA enabling us to measure selectively undercarboxylated osteocalcin in mouse serum. We show here that *InsR osb-/-* mice develop a glucose intolerance phenotype similar in severity to the one seen in mice lacking this receptor in liver and identical to the one reported in the literature in the *Osteocalcin -/-* mice. As such, this result underscores the importance of bone in the regulation of glucose metabolism. Three concurrent evidences indicate that insulin signaling in osteoblasts is in fact a major determinant of osteocalcin carboxylation status. First, the level of undercarboxylated osteocalcin was significantly decreased in the serum of *InsR osb-/-* mice compared to wildtype littermates while *Osteocalcin* expression was not affected. Second, continuous delivery of osteocalcin in the *InsR osb-/-* mice significantly improved glucose metabolism; third, compound heterozygous mice lacking one allele of the *InsR* in osteoblasts only and one allele of *Osteocalcin* develop a metabolic phenotype identical to the one reported in the *Osteocalcin-/-* mice and had lower levels of undercarboxylated osteocalcin. Taken collectively, these results demonstrate that insulin signaling in bone is a determinant of whole-body glucose homeostasis to the same extent as insulin signaling in liver is. They also demonstrate for the first time that insulin signaling in osteoblasts is a direct determinant of osteocalcin carboxylation. The unraveling of this feedback loop adds further support to the notion that bone, via osteocalcin, regulates glucose metabolism.

***Disclosures: Jianwen Wei**, None.*

1004

Osteoblast Ablation Compromises Glucose Homeostasis in Mice. Yoshihiro Yoshikawa[1], Lili Xu[2], Mathieu Ferron[2], Jayesh Shah[1], Charles Duncan[1], Aris Economides[3], Marie-Therese Rached[1], Stavroula Kousteni*[4]. [1]Department of Medicine, Division of Endocrinology, College of Physicians & Surgeons, Columbia University, USA, [2]Columbia University, USA, [3]Bone & Cartilage Biology Group, Genome Engineering Technologies Group Regeneron Pharmaceuticals, Inc, USA, [4]Columbia University Medical Center, USA

It has been proposed recently that the skeleton is a regulator of glucose metabolism. Osteoblasts would act through osteocalcin to favor β-cell proliferation, insulin secretion, insulin sensitivity and energy expenditure. This observation suggested that a decrease in osteoblast numbers would be sufficient to compromise glucose metabolism through decreased osteocalcin availability. We tested this hypothesis by inducibly ablating osteoblasts. We used compound mutant mice carrying an inactive form of the diphtheria toxin A chain (DTA) introduced into the ROSA26 locus (Gt(ROSA)26Sor) and a tamoxifen-regulated Cre under the control of the human osteocalcin promoter (DTA;CreERt2). DTA expression is prevented by a DNA sequence which terminates transcription flanked by two loxP sites while administration of tamoxifen activates Cre and allows DTA expression. Adult DTA;CreERt2 mice were injected intraperitoneally with vehicle or 0.07mg/g of tamoxifen daily for 10 days. At this time, mice were either left untreated or were treated intraperitoneally with 30 ng/g per day of recombinant osteocalcin for 4 weeks. We found that 50% of osteoblasts were ablated by DTA expression, as determined by bone histomorphometry in the lumbar vertebrae and by an equivalent 50% reduction in serum osteocalcin levels. Tamoxifen-treated DTA;CreERt2 mice had higher blood glucose and lower insulin levels in the fed state. Consistent with suppressed insulin production, islet numbers and β-cell area were all decreased in tamoxifen-treated DTA;CreERt2 animals. Glucose tolerance and insulin sensitivity were decreased in tamoxifen-treated DTA;CreERt2 mice. There was also a significant decrease in energy expenditure in the tamoxifen-treated mice as measured by heat production, oxygen and CO2 consumption and respiratory rate. In line with the decrease in insulin sensitivity, expression of resistin, an adipokine mediating insulin resistance, was increased by 2-fold in white adipose tissue of mice with osteoblast ablation. Expression and serum levels of adiponectin and leptin, two insulin sensitizing hormones, were not affected by the decrease in osteoblast numbers. Administration of osteocalcin reversed all the metabolic abnormalities resulting from osteoblast ablation and restored glucose metabolism. These observations demonstrate through genetic

means that osteoblasts are necessary for glucose homeostasis and this function occurs, at least in part, through osteocalcin.

***Disclosures: Stavroula Kousteni**, None.*

1005

FoxO1 Interacts with ATF4 in Osteoblasts to Affect Bone Remodeling and Glucose Homeostasis. Maria Theresa Rached*[1], Aruna Kode[1], Charles Duncan[2], Jayesh Shah[2], Stavroula Kousteni[3]. [1]Columbia University, USA, [2]Department of Medicine, Division of Endocrinology, College of Physicians & Surgeons, Columbia University, USA, [3]Columbia University Medical Center, USA

The Forkhead transcription factor, FoxO1 promotes osteoblast proliferation by maintaining redox balance. At the same time, osteoblastic FoxO1 inhibits β-cell proliferation, insulin secretion and sensitivity by suppressing the expression and activity of Osteocalcin. In searching for mechanisms mediating the bone and metabolic actions of FoxO1 we noticed that whereas type I collagen expression was not altered, its production was decreased in the bone of mice with osteoblast-specific deletion of FoxO1 (FoxO1ob-/-). This observation suggested the existence of a defect in amino acid import and protein synthesis in FoxO1-deficient osteoblasts. Supporting this notion, collagen content and osteoid surface was decreased in the bones of the FoxO1ob-/- mice. ATF4 is an osteoblast-enriched transcription factor that, among other functions, controls amino acid import in osteoblasts. Thus, we asked whether FoxO1 interacts with ATF4 to regulate protein synthesis in osteoblasts. We found that FoxO1 co-localizes with ATF4 in the osteoblast nucleus, and physically interacts with and promotes the transcriptional activity of ATF4 in osteoblasts. Consistent with the notion that FoxO1 is required for protein synthesis in osteoblasts and interacts with ATF4, high-protein diet rescued the low osteoblast number/low bone formation phenotype and the increase in oxidative stress in osteoblasts in FoxO1ob-/- mice. More importantly, compound mice lacking one allele of FoxO1 and ATF4 (FoxO1ob+/-;Atf4+/-) recapitulated the low bone formation phenotype of FoxO1ob-/- mice. Next, and because both factors affect glucose metabolism through their expression in osteoblasts we asked whether FoxO1-mediated regulation of glucose homeostasis also occurs through its interaction with ATF4. We found that insulin sensitivity and glucose tolerance were improved in FoxO1ob+/-;Atf4+/- mice. Specifically, FoxO1ob+/-;Atf4+/- mice showed increased β-cell area in the pancreas. Taken together these molecular, histological, metabolic and genetic experiments demonstrate that FoxO1 and ATF4 interact in vivo in osteoblasts to regulate bone remodeling and glucose homeostasis.

***Disclosures: Maria Theresa Rached**, None.*

1006

Decrease Bone Resorption in Mice Deprived of Peripheral Serotonin (Tph1-/-). Corinne Collet[1], Yasmine Chabbi Achengli*[2], Jacques Callebert[1], Francine Côté[3], Marie-Christine De Vernejoul[4]. [1]Laboratoire Biochimie Hopital Lariboisière, France, [2]INSERM U606, France, [3]Hopital Necker UMR 8147, France, [4]Fédération De Rhumatologie Et INSERM U606, France

Serotonin (5-HT or 5-Hydroxytryptamine) was previously shown to be involved in bone metabolism. As tryptophan hydroxylase 1 (Tph1) is the rate-limiting enzyme for peripheral 5-HT synthesis, we investigated the in vivo bone phenotype in Tph1 knock out (Tph1-/-) mice. The Tph1-/- male mice displayed increased bone density (whole body, femur, vertebrae) at the age of 6 and 10 weeks. Bone resorption markers (urinary deoxypyridinoline DPYR, plasma TRAP5b) were also decreased at 6 and 10 weeks (DPYR 6 weeks WT 23.6 $\pm$ 3.7 vs Tph1-/- 9.6 $\pm$ 0.8 $p<0.01$ and 10 weeks WT 22.6 $\pm$ 1.3 vs Tph1 -/- 13.1 $\pm$ 2.0 $p<0.01$) Histomorphometric analysis, carried out in 6 weeks old mice, indicated an increase of trabecular bone volume (+67%) associated with reduced trabecular number and trabecular separation in Tph1-/- mice. Bone formation rate was unchanged whereas osteoclast number and osteoclastic trabecular surfaces were markedly reduced (Oc.S/BS WT 21.4 $\pm$ 3.3 vs Tph1-/- 11.9 $\pm$ 3.2 $p<0.01$). To further study the osteoclast phenotype in Tph1-/- mice, we focused on ex-vivo spleen cells cultured with RANKL and MCSF. Spleen cells from Tph1-/- mice gave rise to both reduced numbers of osteoclasts (WT 3.5 $\pm$ 0.2 vs Tph1-/- 1.4 $\pm$ 0.004, $p<0.0001$) and decreased resorption pits on dentin slices in comparison with WT cells. The Tph1-/- osteoclast precursors displayed a reduced mRNA expression level of TRAP, cathepsin K and TRAF6. Moreover, osteoclastogenesis in Tph1-/- cell cultures was rescued following the addition of 5-HT (10-7 and 10-8M). Spleen cells of WT mice cultured with RANKL and MCSF synthetized 300 $\pm$ 21 ng of 5-HT/mg proteins that was undetectable in Tph1-/- cells. To define how 5-HT regulates osteoclast differentiation, we next focused on serotonergic components, namely the 5-HT transporter (SERT) and 5-HT receptors (5-HTRs). Using paroxetine, a SERT inhibitor, we observed a decrease in osteoclast number in WT but not in Tph1-/- cell cultures, as well as marked reduction in SERT mRNA expression level in Tph1-/- cell cultures. Finally, we observed a strong decrease in osteoclastogenesis in WT cells following the use of ketanserin, which is both a 5HT2AR antagonist and a vesicular monoamine transporter antagonist. In conclusion, murine osteoclasts synthetize minute amounts of 5-HT that appear to enhance osteoclastic differentiation. Our findings favour an autocrine/paracrine way of action for 5-HT and a role for SERT to support osteclastogenesis in presence of Tph1.

***Disclosures: Yasmine Chabbi Achengli**, None.*

1007

A Transcription Factor p63 Controls Extensive Steps of Endochondral Ossification through Distinct Functions of the Isoforms. Yuki Taniguchi*[1], Taku Saito[2], Toshiyuki Ikeda[3], Ung-Il Chung[4], Kozo Nakamura[5], Hiroshi Kawaguchi[6]. [1]University of Tokyo, Japan, [2]University of Tokyo, Graduate School of Medicine, Japan, [3]Information Technology Services, Inc., Japan, [4]University of Tokyo Graduate Schools of Engineering & Medicine, Japan, [5]The University of Tokyo, Japan, [6]University of Tokyo, Faculty of Medicine, Japan

Skeletal development and growth are achieved by the endochondral ossification process which starts with chondrogenic differentiation of mesenchymal cells by the signaling related to SOX9, SOX5 and SOX6. To examine the molecular network, we initially identified a novel core enhancer of the *SOX6* promoter (CES6) which was highly conserved among species. A screening of transcription factors using the CES6 as bait for cartilage-derived libraries identified p63, a p53 family member, as the most potent transactivator. p63 was extensively expressed in chondrocytes of various differentiation stages in mouse embryonic limb cartilage, as well as in cultured mouse chondrogenic ATDC5 cells and limb buds. The knockout ($p63-/-$) mouse embryos exhibited notably short limbs with decreased expressions of not only SOX6, but also SOX9, type II collagen (COL2A1), and COL10A1. Knockdown of p63 by siRNA in ATDC5 cells caused decreases in their expressions. Luciferase assay, electrophoresis mobility shift assay and chromatin immunoprecipitation assay identified respective core responsive elements of p63 in the promoters of *SOX9, COL2A1* and *COL10A1*, as well as the CES6 region in the *SOX6* promoter. Examination of expression profiles of six isoforms of p63 (TAp63α, β, γ, and ΔNp63α, β, γ) using isoform-specific primers and antibodies in the *in vivo* and *in vitro* systems above revealed that TAp63α and TAp63γ were the principal isoforms in chondrocytes, and TAp63α was predominantly expressed in the early differentiation stage while TAp63γ was in the late differentiation stage of chondrocytes. Overexpression of TAp63α in ATDC5 cells caused increases in the early markers like SOX9, SOX6, and COL2A1, while that of TAp63γ increased the late markers like COL10A1. Finally, we generated chondrocyte-specific *TAp63α* and *TAp63γ* transgenic mice driven by the *Col2a1* promoter (*Col2a1-TAp63α* TG and *Col2a1-TAp63γ* TG). Both proliferative and hypertrophic zones were elongated in the limb cartilage of *Col2a1-TAp63α* TG, while only hypertrophic zone was elongated in that of *Col2a1-TAp63γ* TG. We hereby conclude that p63 transcriptionally controls extensive steps of endochondral ossification through functions of TAp63α and TAp63γ in distinct differentiation stages of chondrocytes. Further understanding of the molecular network related to the p63 isoforms will unravel the molecular network underlying the endochondral ossification.

***Disclosures: Yuki Taniguchi**, None.*

1008

Chondrocyte-derived ß-catenin Expression Regulates Secondary Ossification Center and Growth Plate Development. Debbie Dao*[1], Matthew Hilton[2], Di Chen[3], Regis O'Keefe[4]. [1]University of Rochester School of Medicine & Dentistry, USA, [2]University of Rochester School of Medicine, USA, [3]University of Rochester Medical Center, USA, [4]University of Rochester, USA

This study addresses the central question of what role the chondrocyte-derived ß-catenin signal plays in regulating endochondral bone formation. The importance of Wnt/ß-catenin signaling during endochondral bone formation has been previously appreciated; however, the specific cellular contributors of this signal had not been identified prior to this work. Specifically, it was unknown what role the chondrocyte, the predominant cell type in early developing skeletal elements, played. This is partly due to the lack of targeting specificity and to the peri-natal lethality of previous genetic models used to address the question presented above. To overcome these limitations, this study employed the use of Tamoxifen-inducible genetic mouse models in which Cre-recombinase is conjugated to a mutant estrogen receptor and its expression is driven by the *Col2a1* promoter. This promoter is expressed specifically in chondrocytes after embryonic day 12.5 in mice. By injecting Tamoxifen into pregnant female mice after this time point, embryos expressing this enzyme and either *ß-catenin$^{fx(exon3)/wt}$* or *ß-catenin$^{fx/fx}$* alleles experience chondrocyte-specific *ß-catenin* gain- or loss-of-function, respectively.

In these models, *in situ* hybridization and immunohistochemistry studies revealed that ß-catenin in chondrocytes promotes chondrocyte maturation both in the growth plate and the secondary ossification center (SOC). In long bones, secondary ossification centers were present at E18.5 in gain-of-function animals; these centers normally do not appear until post-natal day five in mice. SOC development was delayed in loss-of-function animals. Chondrocyte-derived ß-catenin appeared to have non-cell-autonomous effects in that gain-of-function in chondrocytes promoted bone collar formation. Cartilage canals in developing epiphyses were observed prematurely in gain-of-function embryos, indicating an effect of chondrocyte-derived ß-catenin on vascularization processes. Both *in vivo* and *in vitro* studies revealed enhanced BMP, IHH, and MMP signaling with ß-catenin gain-of-function. These findings indicate that during development, ß-catenin in chondrocytes acts in conjunction with other positive regulators of bone formation to drive both cell-autonomous and non-cell-autonomous maturation. The overall effect of these interactions is accelerated endochondral bone formation as a result of the chondrocyte-derived ß-catenin signal.

***Disclosures: Debbie Dao**, None.*

1009

Wntless is Required for the Secretion of Wnt5a to Promote Distal Limb Growth and Differentiation in Limb Development. Xuming Zhu*[1], Jingjing Cao[2], Lin He[1], Xizhi Guo[3]. [1]Bio-X Center, Shanghai Jiao Tong University, China, [2]Bio-X Center, Shanghai Jiao Tong University, Shanghai, China, [3]Shanghai Jiao Tong University, Peoples republic of china

Wntless is a conserved trans-membrane protein required for Wnt ligands secretion. Although the biochemical nature of Wntless-mediated intracellular transfer and secretion of Wnts has been intensively investigated in fly, its role during mammalian development is still poorly understood, owing to the early lethal effect of Wntless ablation. Here, we generated a conditional knockout mouse for Wntless carrying an exon3 floxed allele. Wntless in limb mesoderm was specifically removed by using *Prx1-Cre* mice. The *Prx1-Cre; Wls$^{c/c}$* mutant mice displayed digits-truncated limb with downsizing elements in stylopod, zeugopod and autopod. Embryonic limb in *Prx1-Cre; Wls$^{c/c}$* mutant exhibited downregulated proliferation and delayed differentiation of mesenchymal progenitor cells around PZ region underneath AER revealed by absence of Sox9 and Ihh expression in the tips of digit, as well as delayed ossification in long bones. However, normal expression of early PZ markers including Fgf10, Msx2 and Bmp4 in early limb patterning indicated that blocking Wnts secretion affected distal limb mesenchymal differentiation at later stage instead of early patterning. All these phenotypes mimicked that observed in *Wnt5a$^{-/-}$* mutants. Actually, immunohistological analysis revealed that Wnt5a protein was accumulated in their producing cells and its secretion was blocked in *Prx1-Cre; Wls$^{c/c}$* mutant. Taken together, our study demonstrated that Wntless was required for the secretion of non-canonical Wnt5a to exert its role in promoting distal limb growth and differentiation in mouse limb development.

***Disclosures: Xuming Zhu**, None.*

1010

Role of CCN2 in Matrix Secretion and Cellular Stress During Cartilage Development. Faith Hall-Glenn*[1], Andrea DeYoung[2], Karen Lyons[1]. [1]University of California, Los Angeles, USA, [2]Baxter, USA

Connective tissue Growth Factor (CCN2) has been described as a matricellular protein, functioning mainly on the cell surface to transduce signals between the extracellular and intracellular environment to regulate cell proliferation, migration and survival. Upon closer inspection of CCN2 knockout mice, defects in extracellular matrix (ECM) deposition were observed and it was hypothesized that CCN2 may play a direct role in chondrocyte ECM assembly and/or secretion. Using electron microscopy for ultrastructural analysis of Ccn2 mutant growth plates, enlarged Endoplasmic Reticulum (ER) and defects in matrix assembly in proliferating chondrocytes were observed (Fig. 1). Components of the Unfolded protein Response (UPR), GRP78 (BiP) and CHOP, visualized via immunoflorescence, were increased in CCN2 mutant growth plates (Fig. 2 A-C). Moreover, the loss of CCN2 leads to increased susceptibility to Thapsigargin (THG) induced ER stress in alginate chondron cultures. Conversely, inducible overexpression of CCN2 in cartilage reduced BiP levels in the growth plate, suggesting attenuation of UPR activation and subsequent ER stress (Fig. 2D,E). All previous examples of ER stress in the growth plate are caused by structural mutations in ECM proteins that lead to misfolding, or mutations in the ER secretory machinery. This is the first time that the absence of a matricellular protein has resulted in ER stress and highlights a novel protective role for CCN2 during ER stress, matrix assembly/secretion and chondrocyte differentiation. The ability of CCN2 to protect against ER stress may be a general feature of the CCN class of matricellular proteins, as mice lacking both CCN1 and CCN2 in cartilage exhibit a far more severe chondrodysplasia than do mice lacking either CCN1 or CCN2 alone.

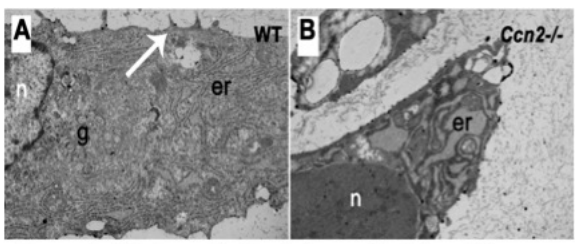

Figure 1. ER stress in *Ccn2-/-* growth plates. Ultrastructural images of chondrocytes in embryonic day (E)17.5 growth plates. Upper epiphyseal chondrocytes from WT and *Ccn2-/-* littermates. The endoplasmic reticulum (er) is grossly distended. The Golgi apparatus (g) in the mutant is vestigial. Arrows in A highlight lamellopodia-like extensions. These are absent in mutant chondrocytes.

Figure 1

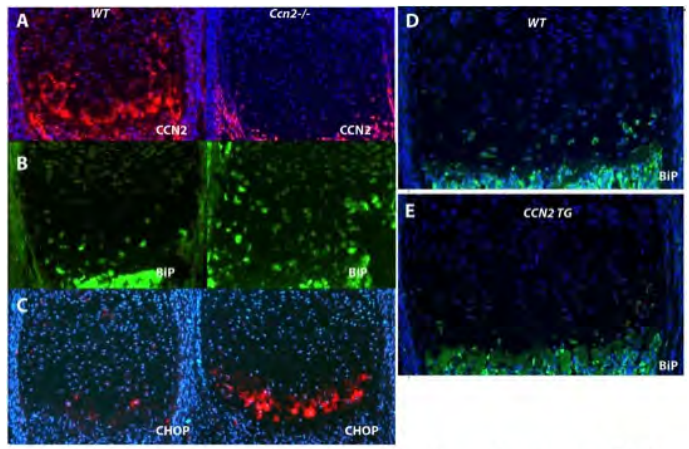

Figure 2: CCN2 mediates ER stress *in vivo*. Immunflorescence of ER stress pathway protein expression in hypertrophic chondrocytes (HC) of E16.5 growth plates. Loss of CCN2 (A) results in increased ER stress markers BiP (B) and CHOP (C) as compared to wildtype growth plates. Overexpression of CCN2 results in an attenuation of BiP (E) compared to wild type samples (D) in Postnatal day 0 growth plates. DAPI-nuclear stain.

Figure 2

***Disclosures: Faith Hall-Glenn**, None.*

1011

The Function of Primary Cilia in Chondrocytes. Ching-Fang Chang*[1], Rosa Serra[2]. [1]University of Alabama at Birmingham, USA, [2]University of Alabama at Birmingham, USA

Primary cilia are microtubule-based non-motile cellular structures, which extend from the surface of almost all cells in our body. The assembly and maintenance of cilia are accomplished by intraflagella transport (IFT). Ift88/Tg737/Polaris is one of the subunits of the anterograde IFT complex. In our previous studies, we used conditional knockout mice Col2aCre;Ift88fl/fl, which had primary cilia specifically deleted in chondrocytes, to study the role of primary cilia in skeletal development. Primary cilia were deleted in mutant mice around e15.5 day. The mutant mice were viable but developed postnatal dwarfism. In histological analysis, the growth plate of mutant mice started to change around postnatal 7 days: the total length of epiphysis was reduced, the columnar organization and orientation of proliferating chondrocytes were altered, and growth plate chondrocytes exhibited reduced proliferation and accelerated hypertrophic differentiation. In order to find out the mechanism of columnar organization in the growth plate, we compared differences in gene expression in proliferating chondrocytes from postnatal 7 day wild type and Col2aCre;Ift88fl/fl mice by microarray analysis. The expression of Ptch1 and Gli-1 (downstream targets of hedgehog signaling), anti-apoptotic protein Bcl2, and several ion channels with ciliary localization, were down-regulated in mutant growth plate. Also, two Wnt signaling antagonists, Secreted frizzled-related protein 5 (Sfrp5) and Sfrp2 were down-regulated and up-regulated, respectively, in mutants. It is well known that primary cilia are required for hedgehog signaling. Based on recent studies implicating the Wnt/PCP pathway in growth plate columnar organization as well as studies suggesting Wnt/ß-catenin signaling can be suppressed by hedgehog through Sfrp-1, we hypothesized that alterations in Wnt signaling downstream of hedgehog could regulate growth plate organization. Our preliminary data showed that Sfrp5, but not Sfrp2 was altered by hedgehog treatment in cultured chondrocytes. Future studies will be focused on rescuing the growth plate phenotype in primary cilia mutants by supplying active Gli-1 or Sfrp5 viruses to metatarsal bones in culture.

***Disclosures: Ching-Fang Chang**, None.*

1012

Chondrocyte-Specific Inactivation of Forkhead Box O (FoxO) Transcription Factors Causes Severe Growth Plate Abnormalities and Increased Bone Volume. Guy Eelen*[1], Christa Maes[2], Conny Gysemans[3], Lieve Verlinden[3], Ji-Hye Paik[4], Ronald DePinho[4], Roger Bouillon[5], Geert Carmeliet[1], Annemieke Verstuyf[3]. [1]Katholieke Universiteit Leuven, Belgium, [2]Laboratory of Experimental Medicine & Endocrinology, K.U.Leuven, Belgium, [3]Laboratory for Experimental Medicine & Endocrinology, Katholieke Universiteit Leuven, Belgium, [4]Belfer Institute for Applied Cancer Science, Department of Medical Oncology, Medicine & Genetics, DFCI, Harvard Medical School, USA, [5]Laboratory for Experimental Medicine & Endocrinology, Belgium

The highly similar and functionally redundant Forkhead Box O (FoxO) transcription factors (TFs) FoxO1, FoxO3a and FoxO4 are ubiquitously expressed and drive diverse key cellular processes such as proliferation, apoptosis and control of intracellular levels of reactive oxygen species (ROS). During endochondral ossification, these processes are tightly controlled in growth plate chondrocytes to ensure adequate bone development and growth. The aim of this study was to determine the role of FoxOs in growth plate chondrocytes and endochondral ossification.

We generated mice lacking FoxO1, 3a and 4 in growth plate chondrocytes (chondrocyte specific triple knock-out; CTKO) by crossing $FoxO1^{L/L}FoxO3a^{L/L}FoxO4^{L/L}$ mice with mice expressing the Cre recombinase driven by the Col2a1 promoter. CTKO mice are viable and are born under normal Mendelian distribution. Histological analyses of the long bones of CTKO neonates (p2 to p10) revealed a significant increase in the length of the hypertrophic zone within the growth plate and this was most obvious in the distal growth plates of tibia and radius/ulna. Quantitative RT-PCR analyses of cultured neonatal growth plate chondrocytes showed a 2-fold decrease in the expression of the pro-apoptotic FoxO target gene bcl-2 interacting mediator of cell death (BIM), suggesting that decreased apoptosis could explain the increased length of the hypertrophic zone. At the age of 8 weeks, CTKO mice showed an increased kyphosis of the spine, increased body and tail length and larger ears. μCT-analyses of tibia at the same age revealed that CTKO mice had a 2-fold increased bone volume and trabecular number in comparison with control littermates. Both serum osteocalcin and serum TRAP5b levels were significantly increased in 8 week old CTKO mice *versus* control mice (osteocalcin: 86.4 ± 7.1 *vs* 53.4 ± 3.1 ng/ml; TRAP5b: 4.0 ± 0.3 *vs* 1.7 ± 0.1 U/L). Histological analyses confirmed the increase in trabecular bone in CTKO mice and in addition revealed a highly disorganized growth plate with complete loss of the columnar appearance of chondrocytes. Safranine O staining showed occasional remnants of chondrocytes within the cortex and trabeculae.

In conclusion, these data show that the expression of FoxO TFs in chondrocytes is indispensable for normal growth plate organization and control of skeletal growth and bone structure.

***Disclosures: Guy Eelen**, None.*

1013

Circulating Osteogenic Cells in Periarticular Non-hereditary Heterotopic Ossification. Kevin Egan, Robert Pignolo*. University of Pennsylvania, USA

In the mature adult skeleton, new bone formation is normally restricted to regeneration of osseous tissue at sites of fracture. However, heterotopic ossification, or the formation of bone outside the normal skeleton, can occur within muscular, adipose, or non-muscle fibrous connective tissue. Periarticular non-hereditary heterotopic ossification (NHHO) may occur after musculoskeletal trauma, following CNS injury, with certain arthropathies, or following injury or surgery that is often sustained in the context of age-related pathology. Recently we identified a novel population of circulating osteogenic precursor (COP) cells which are derived from bone marrow and have the capability to form bone (Suda et al., Stem Cells 27:2209-2219, 2009). These cells are identified by the co-expression of the osteogenic marker type 1 collagen and the hematopoietic marker CD45. COP cells are strongly associated with HO in patients with fibrodyplasia ossificans progressiva, a genetic form of HO, and they can be found in early lesion formation in these individuals. We tested the hypothesis that COP cells may contribute to periarticular NHHO and examined their presence in surgically removed bony lesions after cerebrovascular accident, spinal cord injury, traumatic brain injury, non-neurologic trauma and post-arthroplasty. Using immunohistochemistry, we identified COP cells by co-expression of CD45 and type 1 collagen. There was a statistically significant association between the presence of COP cells and early fibroproliferative lesions of HO. COP cells were negligible or absent in regions of unaffected tissue (no HO). This study provides the first evidence that osteogenic cells in the blood home to distant sites where they are associated with formation of HO caused by diverse traumatic conditions.

***Disclosures: Robert Pignolo**, None.*

1014

The ACVR1 R206H Mutation Recapitulates the Clinical Phenotype of FOP in a Knock-in Mouse Model. Salin Chakkalakal*[1], Deyu Zhang[1], Andria Culbert[1], Alexander C. Wright[1], Andrew D. A. Maidment[1], Frederick Kaplan[2], Eileen Shore[1]. [1]University of Pennsylvania, USA, [2]University of Pennsylvania Hospital, USA

Fibrodysplasia ossificans progressiva is a debilitating genetic disorder characterized by progressive endochondral heterotopic ossification within the soft connective tissues. Patients with classic clinical features of FOP have the identical heterozygous single nucleotide substitution (c.617G>A; R206H) in the gene encoding ACVR1/ALK2, a type I BMP receptor. A genetic knock-in recombineering strategy was used to replace ACVR1 codon 206 (CGC>CAC) in murine Acvr1 exon 5 to develop a mouse model for FOP. Chimeras obtained from knock-in ES cells blastocyst transfers were examined by microCT and X-ray analyses to reveal phenotypes consistent with the clinical features of malformed great toes and post-natal bone formation that characterize FOP. Histological analysis of the HO lesions in R206H chimera mouse displayed all stages of HO formation and paralleled the events in FOP lesion formation. Detailed analysis revealed stages of connective tissue degeneration through apoptosis and an immune response followed by fibroproliferation, chondrogenesis, and ultimately bone with marrow elements. Consistent with data from other models of heterotopic ossification, endothelial Tie-2+ abundantly contribute to heterotopic endochondral ossification in this knock-in mouse model. Further, heterotopic chondrocytes consist of both wild-type and mutant cells, suggesting that cells containing the mutation recruit both normal and mutant progenitor cells. The ACVR1 R206H knock-in mouse provides the first direct *in vivo* evidence that the FOP c.617G>A; R206H ACVR1 mutation induces the characteristic clinical phenotype of FOP and is responsible for the pathophysiology of FOP.

***Disclosures: Salin Chakkalakal**, None.*

1015

Hexa-D-Arginine Reversal of Osteoblast 7B2 Dysregulation in H*yp*-mice Normalizes the *HYP* Biochemical Phenotype. Baozhi Yuan*[1], Jennifer Meudt[2], Robert Blank[2], Jian Feng[3], Marc Drezner[2]. [1]University of Wisconsin, Madison, USA, [2]University of Wisconsin, USA, [3]Texas A&M Health Science Center, USA

Previously we have reported that decreased Phex-dependent osteoblast 7B2 production and diminished 7B2•SPC2 (subtilisin-like protein convertase 2) enzyme activity underlies the biochemical phenotype in hyp-mice. We showed that decreased 7B2•SPC2 function enhanced serum FGF-23 directly by inhibiting degradation of the protein in osteoblasts and indirectly by down-stream effects that stimulate FGF-23 mRNA transcription. As a result, we hypothesized successful therapy of the hypophosphatemic disorder in hyp-mice may depend upon increasing 7B2•SPC2 activity and normalizing FGF-23 degradation and production. Thus, in the present study, we treated normal and hyp-mice for 5 weeks with vehicle or Hexa-D-arginine (D6R [1.5 μmole/kg/day, ip]), a stimulant of 7B2•SPC2 activity and examined the effects on the characteristic biochemical abnormalities. D6R treatment of hyp-mice increased serum P to levels (3.2±0.2 vs 6.3±0.1mg/dl; $p<0.001$) no different than in vehicle or D6R treated normal mice (6.6±0.4 vs 6.8±0.6 mg/dl). Normalization occurred due to an increase of renal tubule Npt2 mRNA (0.7±0.1 vs 1.1±0.1 [relative expression]; $p<0.001$), to levels maintained in vehicle or D6R treated normal mice (1.1±0.1 vs 1.2±0.2). Moreover, in response to D6R treatment, increased renal 25(OH)D-1?-hydroxylase mRNA expression in hyp-mice decreased significantly (2.3±0.1 vs 1.3±0.3 [relative expression]; $p<0.001$) to a similar level as in vehicle and D6R treated normal mice (1.2±0.2 vs 1.3±0.2). These changes were due to resetting osteoblast FGF-23 production and degradation to normal levels. Accordingly, D6R treatment of hyp-mice normalized 7B2•SPC2 dependent intermediate steps in FGF-23 production, including osteoblast production of BMP1 and proteolytic degradation of DMP1 to its 57 kDa C-terminal product. Consequently, FGF-23 mRNA expression (1.2±0.2 vs 0.6±0.1; $p<0.05$) decreased to levels no different than in normal mice (0.5±0.1). Additionally, reduction of the intact FGF-23 to C-terminal fragment ratio in osteoblasts and the circulation indicated D6R treatment also normalized FGF-23 degradation. Thus, treated hyp-mice realized a significant reduction in serum FGF-23 levels (2126±281 vs 1682±191 pg/ml, $p<0.0001$). These observations not only indicate decreased 7B2•SPC2 activity abnormally regulates FGF-23 and P homeostasis, but provide seminal evidence that drug-induced enhancement of enzyme function may serve as a successful treatment for X-linked hypophosphatemia.

***Disclosures: Baozhi Yuan**, None.*

1016

Hypophosphatasia: Enzyme Replacement Therapy for Children Using Bone-Targeted, Tissue-Nonspecific Alkaline Phosphatase. Michael Whyte*[1], Cheryl R. Greenberg[2], Deborah Wenkert[1], William H. McAlister[3], Katherine L. Madson[4], Amy L. Reeves[4], Karen E. Mack[4], Lise Bourrier[5], Alison M. Skrinar[6], Hal Landy[6]. [1]Shriners Hospital for Children, USA, [2]Univ of Manitoba, Canada, [3]Mallinckrodt Inst Radiology, USA, [4]Shriners Hospt for Children, USA, [5]Clinical Research Unit, Manitoba Institute of Child Health, Canada, [6]Enobia Pharma, Canada

Hypophosphatasia (HPP), the inborn-error-of-metabolism characterized by low serum alkaline phosphatase (ALP) activity, is caused by deactivating mutation(s) within the gene encoding the tissue nonspecific isoenzyme of ALP (TNSALP). Natural substrates for TNSALP accumulate extracellularly including inorganic pyrophosphate (PPi), an inhibitor of mineralization, and pyridoxal 5'-phosphate (PLP), the principal form of vitamin B6. Rickets and osteomalacia occur as PPi blocks hydroxyapatite crystal growth within the skeletal matrix. Deranged PLP metabolism reveals TNSALP to be an ectoenzyme. HPP severity spans stillbirth from profound skeletal hypomineralization to osteomalacia presenting late in adult life. There is no established medical treatment. ENB-0040 is a bone-targeted, human recombinant, TNSALP fusion protein that preserved skeletal mineralization and survival in a TNSALP knockout mouse model of severe HPP.[1]

Patient trials began in '08. In a 6-mo, open-label study initially of 6 pts (<3 yrs) with life-threatening HPP, substantial skeletal remineralization, weaning from respiratory support, and improved motor development occurred with ENB-0040 (IV infusion of 2 mg/kg, followed by 1-3 mg/kg SC 3x/wk).[2] Now, 11 patients have been recruited, with 9 (6 girls, 3 boys) having entered an extension study.

Here, we report a phase II, open-label, North American assessment of ENB-0040 in 13 HPP children, ages 5-12 yr (2 girls, 11 boys) randomized to receive either 2 or 3 mg/kg SC 3x/wk for 6 mo. To date, 11 pts have completed Wk 12, one of whom completed Wk 24. The completed study will be reported. Transient injection site erythema was common, but there were no drug-related SAEs. PLP diminished in all 12 patients reaching Wk 6, and was normal for the 9 patients with Wk 12 data. Increases in circulating PTH from enhanced skeletal mineralization occurred, but without hypocalcemia from 'hungry bones'. Skeletal radiographic improvement was observed in all pts by Wk 6 and persisted. All reported increased strength, endurance, and mobility within a few weeks of ENB-0040 treatment. The 9 pts assessed at baseline and at Wk 12 walked 29-121 meters further in a 6-minute walk test (+ 21% on average).

Bone-targeted, tissue-non-specific alkaline phosphatase is a promising enzyme replacement therapy for children with hypophosphatasia.

References:

1) Millan J.L. et al., Enzyme replacement therapy for murine hypophosphatasia. J. Bone. Miner. Res. 23:777-87, 2008

2) In manuscript

Enzyme Knees

***Disclosures: Michael Whyte**, Enobia Pharma, 2; Enobia Pharma, 5*
This study received funding from: Enobia Pharma, Montreal, Canada

1017

Non-redundant Functions of Alkaline Phosphatase and PHOSPHO1 During Endochondral Ossification. Manisha Yadav*[1], Ana Maria Sper Simao[1], Sonoko Narisawa[2], Carmen Huesa[3], Marc McKee[4], Colin Farquharson[3], Jose Luis Millan[1]. [1]Sanford Children's Health Research Center, Sanford-Burnham Medical Research Institute, USA, [2]Sanford-Burnham Medical Research Institute, USA, [3]Roslin Institute, University of Edinburgh, United Kingdom, [4]McGill University, Canada

Endochondral ossification is a carefully orchestrated process mediated by promoters and inhibitors of mineralization. Phosphatases are implicated in mineralization, but their identities and functions remain unclear. Alkaline phosphatase (TNAP) plays a crucial role promoting mineralization of the extracellular matrix by restricting the concentration of the inhibitor inorganic pyrophosphate (PPi). Mutations in the TNAP gene cause hypophosphatasia, a heritable form of rickets and osteomalacia. Here we show that PHOSPHO1, a phosphatase with specificity for phosphoethanolamine and phosphocholine, plays a functional role in the initiation of mineralization and that ablation of both PHOSPHO1 and TNAP prevents skeletal mineralization. Phospho1-/- mice are smaller that WT and heterozygote controls with evidence of spontaneous fractures, bowed long bones, osteomalacia and scoliosis in early life. The difference in weight gain is attributable to reduced food and water consumption by Phospho1-/- mice. Fracture callus and scoliosis are observed from 10 days of age onwards in Phospho1-/- mice and histological analysis revealed deformed growth plates, reduced secondary ossification centers, accumulation of osteoid in the long bones, reduced ash mineral content and bone mineral density of cortical bone in Phospho1-/- mice. qPCR of primary cultures of Phospho1-/- tibial growth plate chondrocytes show decreased Akp2 and increased Enpp1 and Ank expression explaining the increased output of PPi by these cells. A decrease in Col2a1, Mmp13, Aggrecan and Col10a1 gene expression was also observed in day 14 chondrocyte cultures pointing towards a growth plate defect. Chondrocyte cultures and chondrocytes-derived matrix vesicles (MVs) from Phospho1-/-mice also show reduced mineralizing ability. Plasma samples of Phospho1-/- mice have reduced levels of TNAP activity, increased NPP1 activity and elevated plasma PPi concentrations. Normalization of the plasma PPi levels by the transgenic overexpression of TNAP does not correct the bone phenotype in Phospho1-/- mice even at 7 months of age. In turn, deletion of a single TNAP allele (Akp2) onto the Phospho1-null background severely aggravated the phenotypic abnormalities of Phospho1-/- mice and no double homozygote knockout mouse survived past birth. Timed pregnancies revealed the presence of decreased mineralization of the vertebral bones and long bones of E16.5 Phospho1-/-embryos and the total absence of skeletal mineralization in [Phospho1-/-; Akp2-/-] double knockout embryos. We conclude that PHOSPHO1 has a functional role during endochondral ossification and, based on these data and a review of the current literature, we propose an inclusive model of skeletal mineralization that involves intravesicular PHOSPHO1 function and Pi-influx into MVs in the initiation of mineralization, with functions for TNAP, NPP1 and collagen in the extravesicular progression of mineralization in the extracellular matrix.

***Disclosures: Manisha Yadav**, None.*

1018

Teriparatide (Parathyroid Hormone 1-34) Promotes Osseous Regeneration in the Oral Cavity. Jill Bashutski*[1], Robert Eber[1], Janet Kinney[1], Erika Benavides[1], Samopriyo Maitra[1], Thomas Braun[1], William Giannobile[1], Laurie McCauley[2]. [1]University of Michigan, USA, [2]University of Michigan, School of Dentistry, USA

Teriparatide is an established and effective therapy for the treatment of osteoporosis and is currently under investigation for its systemic application to benefit localized osseous defect and fracture healing. The purpose of this study was to evaluate effects of teriparatide in conjunction with periodontal surgery on craniofacial osseous regeneration in patients with advanced periodontal disease. Methods: A double-masked, placebo-controlled study enrolled forty adult subjects with severe periodontal disease including a vertical infrabony defect. Patients received a traditional periodontal surgical procedure along with daily self-administered injections of teriparatide (20 μg) or placebo control, 1000 mg calcium and 800 IU of Vitamin D for 6 weeks. Clinical parameters (probing depth (PD), clinical attachment level (CAL), and bleeding on probing (BOP)), digital standardized radiographs, serum samples, gingival crevicular fluid (GCF) samples, and dual energy x-ray absorptiometry (DXA) scans were evaluated over 12 months. Patients with metabolic bone disease or co-morbid conditions were excluded. Statistical significance of post-treatment differences was determined via two-sample t-test, Wilcoxon, and chi-squared tests. Results: Periodontal surgery significantly improved surgical site clinical parameters in both groups. Teriparatide administration resulted in significantly greater clinical findings of PD reduction (2.42 mm vs. 1.32 mm; $p=0.02$) and CAL gain (1.58 mm vs. 0.42 mm; $p=0.02$) at 12 months. Radiographic alveolar bone defect resolution was significantly greater in the teriparatide group than in controls beginning at 6 months, with a 1.86 mm (29%) versus 0.16 mm (3%) linear defect resolution at 1 year ($p<0.0001$). Serum alkaline phosphatase was increased relative to baseline in teriparatide patients at 6 weeks, an indication of drug compliance ($p=0.003$). No significant differences were noted for other parameters. Conclusions: This is the first report of a prospective study using teriparatide

administration for an application of regenerating craniofacial bone and one of very few studies using teriparatide in a non-osteoporotic population. Teriparatide use for 6 weeks combined with a local surgical therapy resulted in improved clinical outcomes and better alveolar bone defect resolution. The use of a systemic anabolic agent like teriparatide provides an exciting new avenue of therapeutic potential for periodontitis patients.

***Disclosures: Jill Bashutski**, None.*
This study received funding from: Eli Lilly

1019

Low Vitamin D is Related to Increased Risk of Death in Elderly Men. MrOS Sweden. Helena Johansson*[1], Anders Odén[2], John Kanis[3], Eugene McCloskey[4], Mattias Lorentzon[5], Osten Ljunggren[6], Magnus Karlsson[7], Åsa Tivesten[1], Elizabeth Barrett-Connor[8], Claes Ohlsson[9], Dan Mellström[1]. [1]Center for Bone & Arthritis Research at the Sahlgrenska Academy, Institute of Medicine & Geriatrics, University of Gothenburg, Sweden, [2]WHO Collaborating Centre for Metabolic Bone Disease, University of Sheffield, United Kingdom, [3]University of Sheffield, Belgium, [4]University of Sheffield, United Kingdom, [5]Center for Bone Research at the Sahlgrenska Academy, Sweden, [6]Uppsala University Hospital, Sweden, [7]Skåne University Hospital Malmö, Lund University, Sweden, [8]University of California, San Diego, USA, [9]Centre for Bone & Arthritis Research, Sweden

Conflicting results have been presented regarding the association between serum vitamin D and risk of death. We therefore examined the association between serum 25-OH vitamin D (25-OHD) and the risk of death among elderly community dwelling men recruited to the MrOS Sweden study.

The study comprised a random, population-based sample of 3014 men aged 70-80 years. Baseline data included general health and life style questionnaires, femoral neck BMD and 25-OHD. Serum 25-OHD was measured by a competitive RIA (Diasorin, Stillwater, MN). Poisson regression model was used to investigate the association between 25-OHD and the hazard function of death, adjusting for age and time since baseline. A similar approach was used to examine other predictors of mortality and a final multivariate model was constructed to determine independent predictors.

The mean value of 25-OHD in the cohort was 69.7 nmol/l and 2% had 25-OHD <30 nmol/l. The average follow-up was 4.5 years, during which, 382 men died. Low 25-OHD was associated with increased mortality; the gradient of risk (GR) was 1.28 (95% CI, 1.15-1.43) for a 1 SD decrease in 25-OHD. For cardiovascular death the GR was 1.25 (95% CI, 1.04-1.50) and for cancer death the GR was 1.33 (95% CI, 1.11-1.59). Other significant predictors, in univariate analyses, included current smoking, self-estimated health, multiple medications, BMD and known comorbidities (cancer, stroke, myocardial infarction and angina). In multivariate analysis, low 25-OHD remained significantly associated with increased mortality (GR 1.20, 95%CI 1.07-1.34) and was independent of adjustments for a history of cancer, angina, diabetes, BMD, systolic blood pressure and self-estimated health. The Figure shows the relationship between 25-OHD and mortality derived from the multivariate model. Although the nonlinearity of the model was not significant, there appears to be a threshold value for 25-OHD above which survival is not further improved (77 nmol/l). If a causal relationship is assumed, raising 25-OHD levels to 77 nmol/l would decrease the overall mortality by 19% and provide on average 120 days of extended life in a 10 year perspective.

This study shows that low 25-OHD is associated with excess risk of death also when adjusted for comorbidities. These findings indicate that improved vitamin D nutrition has the potential to improve survival and should be examined in prospective trials.

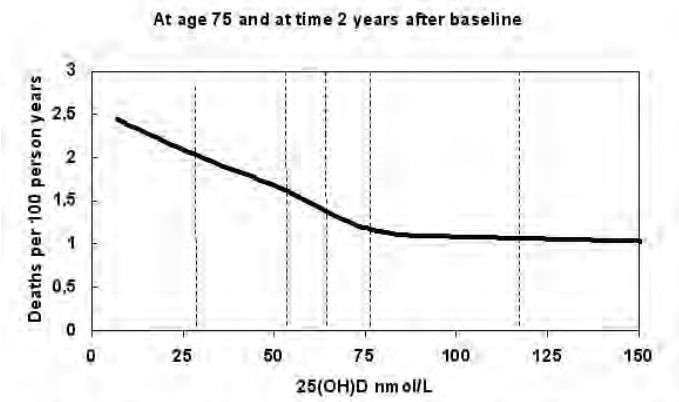

Figure The hazard function of death (momentary risk) according to 25-OHD for men aged 75 (2 years from baseline), with no history of cancer, angina or diabetes. The vertical dashed lines in the figure represent the 1st, 25th, 50th, 75th and the 99th percentiles of 25-OHD.

Figure

***Disclosures: Helena Johansson**, None.*

1020

The Association of Concurrent Vitamin D and Sex Hormone Deficiency with Bone Loss and Fracture Risk in Older Men. Elizabeth Barrett-Connor*[1], Hong Li[2], Gail A Laughlin[3], Tien Dam[4], Jane Cauley[5], Kristine Ensrud[6], Marcia Stefanick[7], Edith Lau[8], Andrew R Hoffman[7], Eric Orwoll[2]. [1]University of California, San Diego, USA, [2]Oregon Health & Science University, USA, [3]University of California San Diego, USA, [4]Columbia University, USA, [5]University of Pittsburgh Graduate School of Public Health, USA, [6]University of Minnesota, USA, [7]Stanford University, USA, [8]Hong Kong Orthopaedic & Osteoporosis Center for Treatment & Research, Hong kong

Background: Low vitamin D (VitD), low sex hormones (SH), and high sex hormone binding globulin (SHBG) levels are common in older men. Using data from the Osteoporotic Fractures in Men study (MrOS), we tested the hypothesis that combinations of low VitD, low SH and high SHBG would have a synergistic effect on BMD, BMD loss and fracture risk in older men.

Methods: For the BMD analysis, 1468 men (mean age 74 yrs) were randomly selected from the MrOS cohort for baseline biochemical measures. Another 278 MrOS men with incident fractures were added for a case-cohort fracture analysis. Total hip BMD was measured by DXA at baseline and follow-up (median 4.6 years). VitD [25(OH)D], testosterone and estradiol were measured by mass spectrometry and SHBG by radioimmunoassay. Abnormal was defined as the lowest quartile for VitD (<20 ng/ml), bioavailable testosterone (BioT), and bioavailable estradiol (BioE), and as the highest quartile for SHBG. Associations with baseline BMD, annualized rate of change in BMD and time to fracture were examined using ANOVA and weighted proportional hazards regressions.

Results: Overall, 10% of participants had only VitD deficiency, 40% had only SH or SHBG abnormalities, and 15% had both. Table 1 presents results of multivariate analyses comparing men with specific combinations of VitD and/or SH/SHBG abnormalities to men with normal levels of all; groups are mutually exclusive. Men with low BioE only or high SHBG only tended to have lower baseline BMD, but did not differ by BMD loss. When combined with low VitD, low BioE (p=.01) and high SHBG (p=.09) were associated with 2-fold greater BMD loss than either low BioE or high SHBG alone. Bone loss was also greater in men with more than one SH/SHBG abnormality and concurrent VitD deficiency. The multivariate-adjusted hazard ratio (95% CI) for non-spine fracture was 1.2 (0.8-1.8) for low VitD alone (n=183); 1.3 (0.9-1.9) for low BioE and/or high SHBG alone (n=356) and 1.6 (1.1-2.5) for low BioE/high SHBG plus low VitD (n=293). Isolated VitD deficiency, and low BioT with or without low VitD, were not significantly related to any bone outcome.

Conclusions: The adverse effects of vitamin D deficiency on bone loss and non-spine fracture in older men were apparent only in the presence of low estradiol or high SHBG. Previous impressions of the effects of VitD or sex steroid abnormalities on bone health in the elderly should be re-examined in light of these findings.

Table 1. Association of Vitamin D and Sex Hormone Groups with Hip BMD & BMD Loss

VitD and SH Group	Baseline			%change/year	
	N	LSMEAN	P value	LSMEAN	P Value
Normal VitD and SH	518	0.97	Ref	-0.31	Ref
Low VitD only	152	0.96	0.40	-0.35	0.65
Low BioT only	121	0.97	0.68	-0.30	0.95
Low BioT + low VitD	52	0.94	0.12	-0.32	0.95
Low BioE only	112	0.95	0.09	-0.33	0.78
Low BioE + low VitD	29	0.92	0.03	-0.79	0.004
High SHBG only	169	0.95	0.02	-0.38	0.37
High SHBG + low VitD	62	0.91	0.0002	-0.63	0.02
>1 SH abnormal only	181	0.94	0.01	-0.41	0.24
>1 SH abnormal + Low VitD	72	0.93	0.005	-0.61	0.048

Adjusted for age, race, BMI, study site and other confounders; SH=sex hormone

Table1

***Disclosures: Elizabeth Barrett-Connor**, None.*

1021

Bone-Muscle Indices as Risk Factors of Incident Fractures in Men. Andy Kin On Wong*[1], Kathy Wilt[2], Peggy Cawthon[3], Yahtyng Sheu[4], Joseph Zmuda[4], Christopher Gordon[1], Kristine Ensrud[5], Lynn Marshall[6], Moira Petit[7], Dennis Black[8], Steven Cummings[9], Jane Cauley[4]. [1]McMaster University, Canada, [2]San Francisco Coordinating Centre, USA, [3]California Pacific Medical Center Research Institute, USA, [4]University of Pittsburgh Graduate School of Public Health, USA, [5]Minneapolis VA Medical Center / University of Minnesota, USA, [6]Oregon Health & Science University, USA, [7]University of Minnesota, USA, [8]University of California, San Francisco, USA, [9]San Francisco Coordinating Center, USA

Background: Bone-muscle (BM) indices describe the interrelationship between bone and muscle strength, and were previously reported to vary with sex, aging and hormones. Objectives: The focus of this study was to examine whether BM indices can assess risk of incident fractures in men.

Methods: Participants in the Osteoporotic Fractures in Men (MrOS) Study completed a peripheral quantitative computed tomography (pQCT) scan of their 66% tibia (Pittsburgh, PA; Minneapolis, MN) in 2005-2006. Bone macrostructure, muscle cross-sectional area and volumetric (v) bone mineral density (BMD) were computed. Total hip and lumbar spine areal (a) BMD was obtained from dual-energy X-ray absorptiometry (DXA). Grip strength and walking speed tests were performed at study visit. Participants were followed prospectively for up to four years to obtain incident fracture data. All adjudicated fractures at any site were included. BM indices were expressed as the ratio of bone-to-muscle strength, mass and area (Table I). We examined the discriminative power of BM indices and aBMD on fractures, reported as a C statistic. Hazard ratios (HR) and 95% confidence intervals relating BM indices to incident fractures were obtained with Cox proportional hazards regression analyses.

Results: Of 1163 men (age: 77.2 $\pm$ 5.2 years, BMI: 28.0 $\pm$ 4.0 kg/m^2) who completed pQCT scans, 79 (6.75%) incident fractures were identified in follow-up. Fractured participants had weaker grip strength ($p<0.01$), and lower aBMD at both the total hip and lumbar spine ($p<0.01$). BM indices were smaller in fractured versus non-fractured groups except for density-weighted BM strength index ($BMSI_D$) and BM areal index (BMAI). One standard deviation decrease in BM indices was associated with increased fracture risk after accounting for age and body mass index. (Table II). After adjustment for functional capacity and lumbar spine aBMD, only BM bending indices ($BMBI_D$, $BMBI_U$) and BM mass index (BMMI) remained significant in identifying increased fracture risk. Discriminative power of BM indices on incident fractures did not improve when combined with aBMD.

Conclusions: Smaller BM indices were associated with increased risk of fractures but did not provide additional value to assessing fracture risk over aBMD. BMMI and BMBI were potential risk factors of fractures but more information is needed to assess whether they provide better sensitivity and specificity for detecting fractures over aBMD.

Table I. Definitions for bone-muscle (BM) indices. SSI = stress-strain index of the bone, MBM = muscle bending moment[a], MSS = muscle-specific strength[b], BMC = total body bone mineral content, LTM = total body lean tissue mass, BSI = bone bending strength index[c], MCSA = muscle cross-sectional area, CoA = cortical area. Subscript D = weighted by bone density, U = not adjusted for bone density.

Bone-Muscle indices	Equation	Units
$BMBI_D$ (density-weighted BM bending index)[a]	SSI/MBM	mm^2/N
$BMSI_D$ (density-weighted BM strength index)[a]	SSI/MSS	mm^5/N
$BMBI_U$ (unadjusted BM bending index)[a,c]	BSI/MBM	mm/N
$BMSI_U$ (unadjusted BM strength index)[c]	BSI/MSS	N^{-1}
BMMI (BM mass index)[d]	BMC/LTM	Index
BMAI (BM areal index)[c]	CoA/MCSA	Index

[a] adapted from Rittweger et al 2000 Bone **27**:319-326
[b] grip strength representing total muscle strength / 66% calf MCSA
[c] adapted from MacDonald et al 2005 Bone **36**:1003-1011
[d] adapted from Cure-Cure et al 2005 Osteoporosis Int **16**:2095-2106

Table I.

Table II. *Risk factors of fractures by bone-muscle (BM) indices.* SD = standard deviation, CI = confidence interval. Hazard ratios (HR) represent values that were age & BMI-adjusted. HRs did not increase significantly when combined with areal bone mineral density (aBMD).

Parameter	HR (95% CI) *per SD decrease*	p-value	C Statistic
$BMBI_U$[a,b]	1.42 (1.09, 1.84)	0.009	0.605
$BMSI_U$	1.28 (0.99, 1.67)	0.064	0.564
$BMBI_D$[a]	1.37 (1.07, 1.75)	0.012	0.611
$BMSI_D$	1.23 (0.95, 1.59)	0.123	0.554
BMMI[a]	1.74 (1.36, 2.24)	<0.0001	0.646
BMAI	1.30 (1.004, 1.69)	0.046	0.581
aBMD hip	2.09 (1.62, 2.69)	<0.0001	0.678
aBMD spine	1.51 (1.15, 1.99)	0.003	0.626

[a] remained significant after additional adjustment for lumbar spine areal bone mineral density and functional capacity measures (walking speed, grip strength)
[b] remained significant after additional adjustment for total hip areal bone mineral density and functional capacity measures (walking speed, grip strength)

Table II.

***Disclosures: Andy Kin On Wong**, None.*

1022

Clinical Vertebral Fracture Risk in Older Men Using Finite Element Analysis of CT Scans. Tony Keaveny*[1], Xiang Wang[2], Arnav Sanyal[2], Lynn Marshall[3], Peggy Cawthon[4], Lisa Palermo[5], Kristine Ensrud[6], Eric Orwoll[3], Dennis Black[5]. [1]University of California, Berkeley, USA, [2]Department of Mechanical Engineering, University of California, USA, [3]Oregon Health & Science University, USA, [4]San Francisco Coordinating Center, California Pacific Medical Center, USA, [5]University of California, San Francisco, USA, [6]Minneapolis VA Medical Center / University of Minnesota, USA

Finite element analysis of quantitative computed tomography (CT) scans is a promising technique for vertebral fracture risk assessment. While it may overcome some of the limitations associated with DXA, it has not yet been prospectively assessed. We used a case-cohort design to assess the ability of finite element analysis of CT scans to predict incident clinical vertebral fractures and to compare it to DXA-measured areal bone mineral density (BMD) at the femoral neck and total lumbar spine. From the MrOS study of 5995 men >65 years, 63 men who experienced incident clinical vertebral fracture (painful fractures presenting clinically and confirmed radiographically) and 242 no-fracture controls (confirmed radiographically) were identified from the approximately 3,500 subjects who had both quantitative computed tomography and DXA scans at baseline. Average follow-up time ($\pm$SD) was 6.5$\pm$2.2 years. Non-linear 3D finite element analysis of L1 (or L2 if L1 was not available for analysis) was performed to derive measures of vertebral strength (N) and volumetric BMD (g/cm^3), and hip and anterior-posterior spine DXA (Hologic 4500) was performed for areal BMD (g/cm^2). All analyses were performed blinded to fracture status. We found that (see Table) the hazard ratio per SD decrease in vertebral strength was 7.6 (95% CI: 4.9–11.9), over two-fold greater than for total spine areal BMD by DXA (3.5; 2.5–4.9). The hazard ratio for volumetric BMD of the whole vertebral body as measured by quantitative CT was comparable with that for strength. The strength-to-(volumetric)-density ratio was an independent predictor of fracture, indicating a significant risk associated with strength beyond that associated with volumetric BMD. The load-to-strength ratio (PHI) was also predictive of fracture. All finite element outcomes, as well as volumetric BMD, remained highly predictive even when LS areal BMD was included in the model and after accounting for the geographic study site. ROC analysis indicated that AUC values for vertebral strength (AUC=0.83) and volumetric BMD (AUC=0.82) were higher ($p=0.017$ and $p=0.038$, respectively) than for LS areal BMD (AUC=0.76). We conclude that, compared to areal BMD, vertebral volumetric BMD and finite element-based vertebral strength each improve prediction of clinical vertebral fracture in elderly men. Future studies should be conducted to confirm these findings in diverse cohorts of men and women.

Table 1: Relative Hazard per unit decrease† in SD (with 95% confidence intervals in parentheses) for each of the main predictor variables of new clinical vertebral fractures, with and without additional predictor variables in the model. N=63 clinical vertebral fractures; N=242 no-fracture controls.

Main Variable	Additional Variables in the Model: None	Age Race BMI	Age Race BMI Site	Age Race BMI Site LS aBMD
DXA:				
LS aBMD (g/cm^2)	3.5 (2.5–4.9)	3.4 (2.4–4.7)	3.4 (2.4–4.9)	
FN aBMD (g/cm^2)	2.1 (1.5–2.8)	2.1 (1.5–3.0)	2.0 (1.4–2.8)	0.9 (0.6–1.4)
QCT:				
Integral vBMD (g/cm^3)	6.1 (4.2–9.0)	5.8 (3.9–8.7)	9.9 (6.0–16.4)	9.4 (5.1–17.4)
FEA:				
Strength (N)	7.6 (4.9–11.9)	7.3 (4.6–11.4)	9.6 (5.7–16.2)	6.5 (4.5–16.2)
PHI (90° flexion with 10 kg)	3.1 (2.6–3.8)	3.0 (2.5–3.7)	3.5 (2.7–4.4)	2.9 (2.2–4.0)
Strength/vBMD (Ncm^3/g)	3.4 (2.5–4.6)	3.3 (2.5–4.5)	3.3 (2.4–4.6)	2.2 (1.6–3.2)

LS — Total lumbar spine; FN — femoral neck; BMI—Body Mass Index; Site — imaging center; integral vBMD is volumetric BMD for the entire vertebral body (without posterior elements but including cortical and trabecular bone); PHI — load-to-strength ratio (ratio of estimated *in vivo* force to vertebral strength; higher values indicate greater risk); † Hazard ratio is per unit *increase* in SD for PHI

Table 1

***Disclosures: Tony Keaveny**, O.N. Diagnostics, 4*

1023

Diagnosis of Vertebral Fracture in Men: What is the Best Agreement Between the Different Approaches? Jacques Fechtenbaum*, Karine Briot, Simon Paternotte, Sami Kolta, Christian Roux. Paris Descartes University, Rheumatology Department, Cochin Hospital, France

Introduction: Reduction in vertebral heights is common in men, because of traumatisms and degenerative spinal diseases. Methods used for vertebral fracture (VF) diagnosis may give different results in a population with high prevalence of vertebral deformities. The aim of the study was to compare the prevalence of VF in men according to 4 methods: 1- Algorithm-Based Qualitative (ABQ)[1], 2- Semi Quantitative with a threshold of 20% (SQ)[2], 3- Semi Quantitative with visual inspection and adjudication by an expert[2,3], 4- Semi Quantitative without grade 1 deformities at the thoracic level[4].

Material and methods: We analysed the X-rays of 261 osteoporotic (Tscore between -2.5 and -4 SD) caucasian men of at least 65 years old, performed with a standardized acquisition. All the methods were used by experienced rheumatologists; method 3 was performed by the same expert as method 2 but 6 months later. Agreement between methods was determined by K statistics and prevalence-adjusted bias-adjusted kappa (PABAK).

Results The prevalence of fractured patients (at least one vertebral fracture from T4 to L4) was 27.2%, 45.2%, 26.4% and 30.7% for the 4 methods. The best agreement for the classification: fractured yes/no, at the patient level was obtained for the methods 1 and 3 with 86.49 % and a PABAK score of 0.73. At the vertebral level, the percentage of agreement between these two approaches was 87.40% to 98.01% with the worse agreements for T8 and T12.

Conclusions. There is a good agreement in vertebral diagnosis in osteoporotic men between ABQ and SQ approach with expert judgement. Methods using only vertebral height reductions give completely different results.

Reference:
1) Ferrar L.and al: J Bone Miner Res 2008; 23: 417-424.
2) Genant HK and al: J Bone Miner Res 1993; 8: 1137-1148.
3) Roux C et al: Osteoporosis Int 2007
4) Szulc P and al: Osteoporos Int 2001:12:302-310.

***Disclosures: Jacques Fechtenbaum**, None.*

1024

Type I Collagen Isomerization (Alpha/Beta CTX Ratio) and Risk of Clinical Vertebral Fracture in Men: A Prospective Study. Douglas Bauer*[1], Patrick Garnero[2], Stephanie Litwack Harrison[3], Jane Cauley[4], Kristine Ensrud[5], Richard Eastell[6], Eric Orwoll[7]. [1]University of California, San Francisco, USA, [2]Molecular Diagnostics, Synarc, France, [3]Research Institute, California Pacific Medical Center, USA, [4]University of Pittsburgh Graduate School of Public Health, USA, [5]Minneapolis VA Medical Center / University of Minnesota, USA, [6]University of Sheffield, United Kingdom, [7]Oregon Health & Science University, USA

We have previously reported that the ratio of urinary alpha (native) to beta (isomerized) type I collagen C-telopeptide fragments (alpha/beta CTX ratio) may reflect bone matrix collagen maturation and is independently associated with hip fracture risk in older men, even after adjustment for hip BMD. The relationship between CTX isomers and vertebral fracture is unknown. We conducted a prospective nested case-cohort analysis in the Osteoporotic Fractures in Men Study (MrOS) to test the hypothesis that higher alpha/beta CTX ratio is associated with an increased risk of symptomatic (clinical) vertebral fracture. Among the 5,995 men enrolled at baseline (mean age: 73.7 $\pm$ 5.9), during a mean follow-up of 7.2 yr. 97 men had new symptomatic vertebral fractures documented on paired spine radiographs. Using fasting urine collected at baseline and stored at –80℃, alpha and beta CTX isomers and urine creatinine (Cr) were obtained on 93 fracture cases and 933 men without known vertebral fracture. Fracture outcomes were examined in logistic models adjusted for age, clinic and total hip BMD (Hologic QDR4500). Compared to men without vertebral fracture, those with incident symptomatic vertebral fracture during follow-up were older (76.5 yr. vs. 73.7) and had lower total hip BMD (0.87 gm/cm^2 vs. 0.96), but had similar BMI (26.9 kg/m^2 vs. 27.4). Higher levels of urine alpha CTX isomer/Cr were associated with a higher risk of clinical vertebral fractures (p trend=0.001), while higher levels of urine beta CTX isomer/Cr were associated with a lower risk (p trend=0.003). Greater alpha/beta CTX isomer ratio was associated with a substantially increased risk of incident clinical vertebral fracture (Figure), particularly in the highest quartile (OR= 9.5, 95% CI: 4.2, 21.6, compared to the lowest quartile). We conclude that the alpha/beta CTX isomer ratio is independently associated with clinical spine fracture risk in older men. These findings support the hypothesis that the alpha/beta CTX isomer ratio reflects some element of bone quality, such as collagen maturation, and may be useful to predict new symptomatic vertebral fractures in older men.

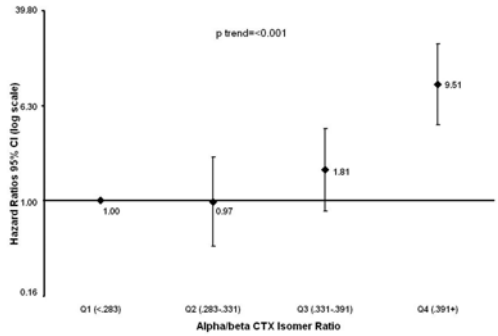

Figure. Quartile of Alpha/Beta CTX Isomer Ratio and Incident Clinical Vertebral Fracture in Men

***Disclosures: Douglas Bauer**, Merck, 2; Novartis, 2; Amgen, 2; Amgen, 5; Merck, 5*

1025

Four Years of Denosumab Exposure in Women With Postmenopausal Osteoporosis: Results from the First Year Extension of the FREEDOM Trial. Socrates Papapoulos*[1], Henry G. Bone[2], Maria Luisa Brandi[3], Jacques Brown[4], Roland Chapurlat[5], Edward Czerwinski[6], Nadia Daizadeh[7], Andreas Grauer[7], Christine Haller[7], Marc-Antoine Krieg[8], Cesar Libanati[7], Zulema Man[9], Dan Mellstrom[10], Sebastião C. Radominski[11], Jean-Yves Reginster[12], Heinrich Resch[13], José A Román Ivorra[14], Christian Roux[15], Steven Cummings[16]. [1]Leiden University Medical Center, The netherlands, [2]Michigan Bone & Mineral Clinic, USA, [3]University of Florence, Italy, [4]Laval University, Canada, [5]E. Herriot Hospital, France, [6]Krakowskie Centrum Medyczne, Poland, [7]Amgen Inc, USA, [8]University Hospital, Switzerland, [9]Centro Médico TIEMPO, Argentina, [10]Sahlgrenska University Hospital, Sweden, [11]Universidade Federal do Paraná, Brazil, [12]CHU Centre Ville, Belgium, [13]Medical University Vienna, Austria, [14]Hospital Dr Peset, Spain, [15]Hospital Cochin, France, [16]San Francisco Coordinating Center, USA

The FREEDOM study established the efficacy and safety of denosumab for 3 years for the treatment of postmenopausal women with osteoporosis. The open-label extension of FREEDOM is evaluating the long-term (up to 10 years) efficacy and safety of denosumab. We report data from the 1st year of follow-up, representing up to 48 months of denosumab exposure.

All subjects who completed FREEDOM were eligible after providing consent to receive a sc injection of denosumab (60 mg) every 6 months during the extension study. For those assigned to the denosumab arm in FREEDOM (long-term group) the data reported here reflects a total of up to 8 injections of denosumab. For those previously assigned to placebo (de novo group) the data are from exposure of up to 2 doses of denosumab for 12 months. All subjects continued to take calcium (1 g) and vitamin D ($\geq$400 IU) supplements daily. Changes in BMD and bone turnover markers (BTM) over 48 months are reported for subjects enrolled in the extension. No formal statistical testing was planned for this interim report. *P*-values are descriptive.

Overall, 4550 (70.2%) eligible subjects from FREEDOM enrolled in the extension study: 2343 in the long-term and 2207 in the de novo group. During the 1st year of the extension study, lumbar spine BMD in the long-term group increased a further 2.0% to a total of 12.1% over FREEDOM baseline at 48 months, and total hip BMD increased an additional 0.8% from extension study baseline to 6.5% at 48 months ($P<0.0001$ for BMD gains during year 4; Figure 1). In the de novo group lumbar spine and total hip BMD increased by 6.0% and 1.7%, respectively (both $P<0.0001$). The magnitude of the rapid reduction in serum C-telopeptide (CTX) after denosumab initiation was similar for the long-term and de novo groups (Figure 2). Reductions in BTM continue to attenuate at the end of the dosing interval as previously reported. Adverse events (AEs) were reported by 70.4% of subjects in the long-term group and 67.9% of subjects in the de novo group. Serious AEs were reported by 9.8% of subjects in the long-term group and 11.2% of subjects in the de novo group. During the 4th year, 31 and 51 osteoporotic nonvertebral fractures were reported in the long-term and de-novo groups, respectively.

These results suggest that 48 months of denosumab continues to significantly increase BMD. Long-term treatment decreases BTM with a similar pattern and to a similar degree as observed with the 1st year of treatment.

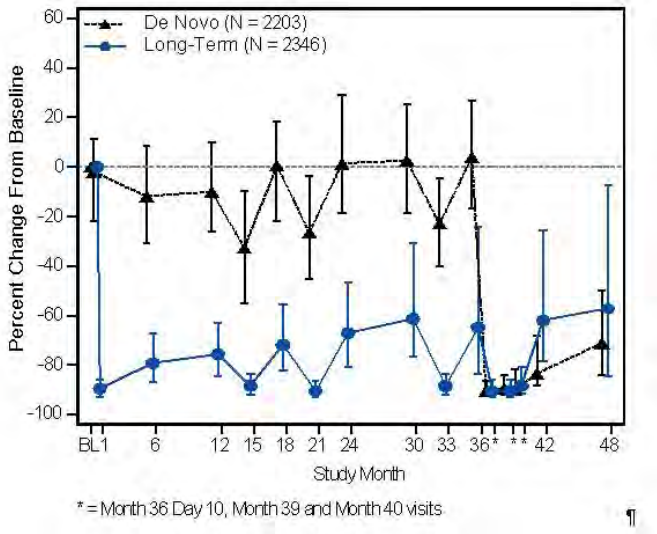

Figure 2: Percentage Change in sCTX Over Time

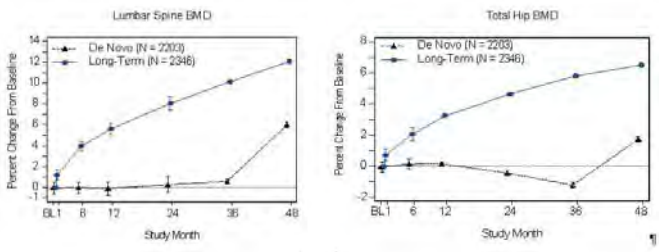

Figure 1: Percentage Change in BMD With Denosumab for 4 Years (Long-term) or 1 Year (De Novo)

Disclosures: Socrates Papapoulos*, Amgen, Merck, Novartis, Lilly, Procter & Gamble, GSK, 5*
This study received funding from: Amgen Inc.

1026

The Value of Monitoring Hip BMD During Treatment with Denosumab: One Year Changes in BMD and Reductions in Fracture Risk. Steven Cummings*[1], Li-Yung Lui[2], Eric Vittinghoff[3], Richard Eastell[4], Matt Austin[5], Steven Boonen[6], Ian Reid[7], Andreas Grauer[8], Cesar Libanati[9], Douglas Bauer[3]. [1]San Francisco Coordinating Center, USA, [2]California Pacific Medical Center Research Institute, USA, [3]University of California, San Francisco, USA, [4]University of Sheffield, United Kingdom, [5]Amgen, Inc., USA, [6]Center for Metabolic Bone Disease, Belgium, [7]University of Auckland, New zealand, [8]Amgen Health Center, USA, [9]Amgen Inc, USA

Some patients lose BMD despite treatment with effective drugs; others gain more than expected. There are few data about whether BMD changes during treatment indicate lesser or greater reduction in risk of fracture, so the value of monitoring BMD is uncertain. If BMD change predicts reduction in risk, then monitoring may be useful. Methods: We studied the association between changes in total hip BMD at one year and reductions in risk of fractures during 3 years of denosumab. We included 5,969 women with osteoporosis who received all 6 planned doses of denosumab 60 mg or placebo subcutaneously every 6 months. We compared fracture rates in the 10% of women who lost hip BMD (≤ 0% change) during the 1st year of denosumab with the 10% who lost the most during the 1st year of placebo. We also compared fracture rates in the 10% of women who gained the most hip BMD (≥ 6.5% increase) on denosumab with the 10% who gained the most on placebo. We also compared fracture rates for the 80% of women whose BMD changes were in between. Logistic models adjusted for differences in baseline BMI and hip BMD; statistical significance was based on tests for interactions.

Results: Overall, denosumab reduced the risk of vertebral fracture by 76% (odds ratio=0.24, 95%CI 0.17-0.34). The decreased risk of vertebral fracture was greater for those who gained hip BMD during the 1st year - 81% (OR=0.19)-than for those who lost BMD (≤0% change): 48% (OR=0.52; interaction P=0.03). Overall, denosumab reduced the risk of nonvertebral fractures by 22% (OR=0.78, 0.64-0.96). The decreased risk appeared to be greater in those who gained the most hip BMD (≥6.5%) during the 1st year-47% (OR=0.53)-than for those who gained less or lost BMD: 18% (OR=0.82). The interaction between increasing BMD on denosumab and decreasing risk of nonvertebral fracture was not statistically significant (P=0.11).

Conclusion: For patients who fully comply with denosumab therapy, those who gain hip BMD during the first year have an 81% reduction in risk of vertebral fracture that is greater than the reduction for patients who lost BMD. Relatively large gains in BMD might indicate a greater reduction in risk of nonvertebral fracture, however additional study of the relationship between change in BMD during treatment with denosumab and risk of nonvertebral fracture is warranted. Our results suggest that monitoring BMD after 1 year of denosumab may give an indication of its antifracture efficacy.

Disclosures: Steven Cummings*, Amgen, Inc., 2; Amgen, Inc., 5*
This study received funding from: Amgen, Inc.

1027

Effect of Whole-Body Vibration on Bone Density and Structure in Postmenopausal Women with Osteopenia: A Randomized Controlled Trial. Lubomira Slatkovska*[1], Shabbir Alibhai[2], Joseph Beyene[3], Angela Cheung[2]. [1]University of Toronto, Canada, [2]University Health Network, Canada, [3]McMaster University, Canada

Purpose: Recent data suggest that whole-body vibration (WBV) may be beneficial to bone health. We conducted a 12-month randomized controlled trial (RCT) to examine WBV effects on bone mineral density (BMD) and bone structure.

Methods: Postmenopausal women with primary osteopenia not on bone medications were randomly assigned to one of three groups: 90 Hz WBV at 0.3*g* (90Hz), 30 Hz WBV at 0.3*g* (30Hz) and control (CON). Women in the 90Hz and 30Hz groups were asked to stand on their WBV platforms for 20mins a day at home. CON group did not receive WBV. Adequate calcium and vitamin D intakes were ensured through diet and supplementation. Bone outcomes were assessed at baseline and 12 months by DXA (dual-energy x-ray absorptiometry; Hologic Discovery A^{TM}, Hologic, Massachusetts) at the lumbar spine, total hip and femoral neck, and by HR-pQCT (high-resolution peripheral quantitative computed tomography; Xtreme CT$^{®}$, Scanco, Switzerland) at the distal tibia and distal radius. Our primary outcome was trabecular volumetric BMD (vBMD) in the distal tibia and secondary outcomes included all other DXA and HR-pQCT parameters. Adherence was recorded by each WBV platform. Between-group differences in absolute pre-post change in bone outcomes were examined using ANOVA. Contrast analyses, specified a priori, were used to study all single pair-wise comparisons and the combined effect of 90Hz and 30Hz versus CON. A priori subgroups were also examined.

Results: 202 women participated in the trial (90Hz: n=67, 30Hz: n=68, CON: n=67): 78% Caucasian, 16% Southeast Asian and 6% other. Mean age was 60 (44-79) years and mean mass was 63 (43-88) kg. Mean daily calcium and vitamin D intakes were 1448 mg and 872 IU. Mean percent adherence was 64% in 90Hz (median=79%) and 66% in 30Hz (median=77%). Using intention-to-treat approach, mean pre-post change in trabecular vBMD of the distal tibia was +0.4, -0.1, -0.2 mg·cm^{-3} in 90Hz, 30Hz, and CON, respectively (between-group differences: p=0.5) (Table 1). There were no statistically significant between-group differences in absolute pre-post change in any primary or secondary bone outcomes using ANOVA and contrast analyses. Subgroup analyses also did not show any effect in women ⩾80% adherent, <65 kg in mass, ≤60 years-old or ≤10 years since menopause.

Conclusions: WBV at 0.3*g* and 30 Hz or 90 Hz 20mins daily for a year did not alter BMD or bone structure in postmenopausal womens with osteopenia.

Bone outcome, mean (SD)	90Hz (n=67)	30Hz (n=68)	CON (n=67)
DXA BMD femoral neck (g·cm^{-2})	-0.005 (0.018)	-0.005 (0.022)	-0.001 (0.020)
DXA BMD total hip (g·cm^{-2})	-0.004 (0.014)	-0.002 (0.016)	-0.002 (0.016)
DXA BMD spine L1-L4 (g·cm^{-2})	-0.006 (0.028)	-0.008 (0.020)	-0.007 (0.020)
HR-pQCT tibia vBMD trabecular (mg·cm^{-3})	0.4 (3.7)	-0.1 (3.3)	-0.2 (3.1)
HR-pQCT tibia vBMD cortical (mg·cm^{-3})	-10.9 (12.7)	-10.4 (14.0)	-9.2 (11.6)
HR-pQCT tibia vBMD total (mg·cm^{-3})	-1.4 (5.4)	-2.3 (5.3)	-1.7 (4.3)
HR-pQCT tibia cortical thickness (mm)	0.000 (0.026)	-0.006 (0.036)	0.001 (0.026)
HR-pQCT tibia trabecular thickness (mm)	-0.003 (0.006)	-0.004 (0.007)	-0.002 (0.006)
HR-pQCT tibia trabecular number (mm^{-1})	0.070 (0.142)	0.078 (0.154)	0.056 (0.128)
HR-pQCT tibia trabecular separation (mm)	-0.022 (0.044)	-0.023 (0.046)	-0.018 (0.048)
HR-pQCT tibia bone volume/trabecular volume (%)	0.000 (0.003)	-0.000 (0.003)	-0.000 (0.003)
HR-pQCT radius vBMD trabecular (mg·cm^{-3})	-2.2 (9.6)	-1.6 (5.0)	-1.0 (4.4)
HR-pQCT radius vBMD cortical (mg·cm^{-3})	-14.8 (17.1)	-10.4 (18.0)	-13.0 (17.1)
HR-pQCT radius vBMD total (mg·cm^{-3})	-5.2 (12.1)	-3.8 (7.5)	-5.2 (9.3)
HR-pQCT radius cortical thickness (mm)	-0.007 (0.032)	-0.006 (0.024)	-0.014 (0.037)
HR-pQCT radius trabecular thickness (mm)	-0.002 (0.006)	-0.002 (0.006)	-0.001 (0.007)
HR-pQCT radius Trabecular number (mm^{-1})	0.031 (0.196)	0.036 (0.137)	0.024 (0.167)
HR-pQCT radius trabecular separation (mm)	-0.002 (0.096)	-0.010 (0.038)	-0.008 (0.052)
HR-pQCT radius bone volume/trabecular volume (%)	-0.002 (0.008)	-0.001 (0.004)	-0.001 (0.004)

Table 1. Mean absolute pre-post change in bone outcomes using intention-to-treat approach

Disclosures: Lubomira Slatkovska*, None.*

1028

Reduction in the Risk of Clinical Fractures after a Single Dose of Zoledronic Acid 5 mg. Dennis Black*[1], Ian Reid[2], Kenneth Lyles[3], Christina Bucci-Rechtweg[4], Guoqin Su[5], Trisha Hue[1], Richard Eastell[6]. [1]University of California, San Francisco, USA, [2]University of Auckland, New zealand, [3]Duke University Medical Center, USA, [4]Novartis Pharmaceuticals Corporation, USA, [5]Novartis pharmaceuticals, USA, [6]University of Sheffield, United Kingdom

Purpose: Studies have shown that compared with placebo, annual infusions of zoledronic acid 5 mg (ZOL) significantly reduce fracture risk over 3 years. However, studies of ZOL, as well as other bisphosphonates, have shown residual effects on BMD and bone turnover over periods ranging from 1 to 5 years after treatment discontinuation. We therefore conducted this post-hoc analysis to investigate the impact of a single infusion of ZOL on fracture risk over a period up to 3 years. This analysis includes women and men from two randomized, double-blind, placebo-controlled trials of ZOL: the HORIZON Pivotal Fracture Trial (PFT) and Recurrent Fracture Trial (RFT). In PFT, 7736 women with osteoporosis were followed for 3 years, whereas, RFT was an event-driven trial in 2127 women and men with recent hip fracture who were followed for as many as 3 years.

Methods: We analyzed the impact of ZOL on fracture risk in a subset of subjects (n=1367) who received only a single, baseline infusion and who completed the respective study. They were followed for a mean of 1.5 years. For comparison, we also analyzed the impact of ZOL in the subset of subjects who received at least 3 infusions (n=6904). These subjects were followed for a mean of 3 years. In both subsets, the incidence rates of fracture were compared in ZOL vs placebo over 36 months using Kaplan–Meier estimates for three categories of fractures: all clinical, non-vertebral and clinical vertebral.

Results: At Month 36, in patients who only received a single ZOL infusion, there was a statistically significant 32% reduction in clinical fracture compared with placebo (p=0.039) and there was a trend toward reductions in clinical vertebral and non-vertebral fractures (p=NS). The magnitude of the risk reduction for the three fracture types in the group who received a single ZOL infusion are similar to those observed with three annual ZOL infusions (34%). Since the subgroup of single infusion patients is based on a post-randomization categorization, the ZOL and PBO groups are not necessarily comparable. However, even after adjustment for confounding variables including age and/or baseline FN BMD T-score (PFT *vs.* RFT), the results remained substantially the same (HR=0.67 [0.47, 0.97] adjusted for age *vs.* HR=0.70 [0.49, 1.01] adjusted for age and FN BMD).

Conclusion: This preliminary analysis demonstrates that a single dose of ZOL in patients with osteoporosis, can reduce the risk of clinical fractures at 3 years.

	Event rate *n* (%)				
	ZOL *N*=746	Placebo *N*=621	HR	(95% CI)	*p*-value
Patients who only received ONE infusion					
All clinical fracture*	53 (11.8)	63 (17.7)	0.68	(0.47, 0.98)	0.039
Clinical vertebral fracture^	5 (0.80)	11 (2.5)	0.44	(0.15, 1.27)	0.12
Clinical non-vertebral fracture	50 (11.4)	53 (15.4)	0.76	(0.51, 1.12)	0.16
Patients who received THREE infusions					
	N=3410	*N*=3494			
All clinical fracture*	279 (8.2)	424 (12.6)	0.66	(0.57, 0.77)	<0.0001
Clinical vertebral fracture^	27 (0.7)	79 (2.5)	0.34	(0.22, 0.53)	<0.0001
Clinical non-vertebral fracture	259 (7.6)	360 (10.5)	0.73	(0.62, 0.85)	<0.0001

*excluding finger, toe, and facial bone fractures; ^ include thoracic spine fracture and lumbar spine fracture

Table: Incidence of clinical fractures after 3 years with ZOL 5 mg

***Disclosures: Dennis Black**, Novartis, 2*
This study received funding from: Novartis

1029

Divergent Trends between Typical and Atypical Hip Fractures and Prevalence of Bisphosphonate Use in the US Elderly, 1996-2007. John Wang*[1], Timothy Bhattacharyya[2]. [1]Intramural Research Program, NIAMS/NIH, USA, [2]Intramural Research Program, NIAMSNIH, USA

Context Though overall hip fracture incidences are declining, increasing numbers of atypical hip fractures have been reported, particularly among elderly patients with long-term use of bisphosphonates. Objective To compare trends between atypical and typical hip fractures and medication use between men and women 65 years or older. Design, Setting, and Patients Cross-sectional studies from 1996 to 2007 on 371 347 respondents to the annual Medical Expenditure Panel Survey and 619 044 hospitalizations in the Nationwide Inpatient Sample with a primary surgical procedure and a primary diagnosis of either a typical closed hip fracture in femoral neck and intertrochanteric regions or an atypical closed fracture in the subtrochanteric region. Main Outcome Measures National estimates and sex-specific, age-adjusted rates of hip fractures. Results Between 1996 and 2007, the annual national estimate for typical hip fractures decreased 12.8% from 263 623 to 229 942. Among women, age-adjusted rates of typical hip fractures decreased by 31.6% (from 1020.5 to 697.4 fractures per 100 000) and among men, by 20.5% (from 424.9 to 337.6 fractures per 100 000). In contrast, national estimates for atypical hip fractures increased 31.2 % from 8 273 to 10 853. Joinpoint regression analysis indicated that trends in age-adjusted rates for atypical hip fractures remained unchanged among men (p=0.34), but increased 20.4% among women from 28.4 (95% Confidence Interval [CI], 27.7-29.1) in 1999 to 34.2 (96% CI, 33.4-34.9) fractures per 100 000 in 2007. The annual percentage increase was 2.1% (95% CI, 1.3-2.8, p<0.001). Meanwhile, prevalence of bisphosphonate use increased more among women (from 3.5% in 1996 to 16.6% in 2007) than in men (2.3% in 2007). Conclusion Typical hip fractures are declining in the US elderly. Hospitalizations for atypical hip fractures, albeit rare, have increased annually since 1999 and were detected mostly among postmenopausal women, a group with prevalent use of bisphosphonates.

***Disclosures: John Wang**, None.*

1030

Atypical Subtrochanteric and Shaft of Femur Fractures - Are they related to Bisphosphonate Therapy? : Blinded radiological review. Christopher Warren[1], Nigel Gilchrist*[2], Mark Coates[3], Joy Helmore[4], John McKie[5], Gary Hooper[5]. [1]Department of Geriatrics, Princess Margaret Hospital, New zealand, [2]CGM Research Trust, New zealand, [3]Department of Radiology, Christchurch Hospital, New zealand, [4]CGM Research Trust, Christchurch, New zealand, [5]Department of Orthopaedic Medicine & Surgery, Christchurch Hospital, New zealand

Purpose: Recent reports have raised the possibility of a relationship between a subset of subtrochanteric and diaphyseal femoral fractures (atypical fractures) and bisphosphonate therapy. A recent review by Black did not show a statistically significant relationship. We undertook a retrospective study of male and female patients admitted with fractures to Christchurch Hospital between 2004 and 2008 to evaluate the relationship between bisphosphonates, this subset of fractures and typical subtrochanteric and diaphyseal femoral fractures.

Methods: The total number of fracture admissions during this period was 18,345. International Statistical Classification of Diseases and Related Health Problems 10th Revision discharge codes (S72.2 subtrochanteric and S72.3 fracture of shaft of femur) were used to identify cases. There were 538 cases identified. Exclusions were a history of motor vehicle accident; age less than 20, misclassification of fracture on x-ray report (intra trochanteric or neck of femur) and tumours identified on x-ray report. There were 336 cases excluded at this stage.

The remaining 202 cases were submitted for independent, blinded single radiologist review. Cases were excluded if they were periprosthetic, or neither subtrochanteric nor diaphyseal femoral fractures. Included fractures were sub classified into typical or atypical (transverse fractures with cortical thickening and beaking of the cortex) fractures. Also excluded were all of those with a history of Paget's disease, malignancy and significant trauma (a fall from greater than standing height). An additional 134 cases were excluded.

Results: There were 61 typical fractures with 9 on alendronate and 5 on etidronate. There were 12 atypical fractures with 4 on alendronate and 0 on etidronate. There was a trend towards alendronate being associated with atypical fractures (relative risk [RR] 2.3) but this did not reach statistical significance (p value 0.12 using chi-squared test). There was less suggestion that any bisphosphonate exposure was associated with atypical fractures, RR 1.7 (p value 0.45).

Conclusions: Atypical femoral fractures are uncommon (<0.1% of total fracture admissions during this study period). Independent radiological review of x-rays is important. This study does not show a statistically significant relationship between alendronate use and atypical subtrochanteric and femoral diaphyseal fractures compared with typical fractures.

***Disclosures: Nigel Gilchrist**, None.*

1031

Genome Wide Association Study Identifies Four Loci that Account for 76% of the Population Attributable Risk of Paget's Disease. Omar Albagha*[1], Micaela Visconti[1], Nerea Alonzo[1], Anne Langston[1], Tim Cundy[2], Rosmary Dargie[3], William Fraser[4], Michael Hooper[5], Giancarlo Isaia[6], Geoffrey Nicholson[7], Javier del Pino[8], Rogelio Gonzalez-Sarmiento[8], Marc di Stefano[6], John Walsh[9], Stuart Ralston[1]. [1]University of Edinburgh, United Kingdom, [2]Faculty of Medical & Health Sciences University of Auckland, New zealand, [3]Glasgow Royal infirmary, United Kingdom, [4]Royal Liverpool University Hospital, United Kingdom, [5]Sydney University & Sydney South West Area Health Service, Australia, [6]University of Torino, Italy, [7]University of Melbourne, Australia, [8]University of Salamanca, Spain, [9]Sir Charles Gairdner Hospital, Australia

Paget's disease of bone (PDB) is a common disorder with strong genetic component that affects up to 2% of Caucasians aged 55 years and above. Genetic factors are known to be important in PDB but so far *SQSTM1* is the only gene that has been confirmed to cause classical PDB. Whilst mutations of *SQSTM1* are found in about 10% of patients with PDB, the remaining genes that contribute to the disease are unclear. Here we report the results of an extended genome-wide association study involving a discovery sample of 750 PDB patients without *SQSTM1* mutations and 2699 controls from the Wellcome trust case control consortium and a replication

sample of 500 PDB cases and 535 controls. Following data cleaning and quality control measures, association testing was performed using the stratified Cochran-Mantel-Haenszel test and stepwise logistic regression. This resulted in the identification of four loci with genome wide significant evidence of association with PDB. These were close to *CSF1* (encoding M-CSF) on chromosome 1p13 ($p=2.1 \times 10^{-26}$; odds ratio (OR)=1.7), within *TM7SF4* (encoding DC-STAMP) on chromosome 8q22 ($p=9.2 \times 10^{-12}$; OR=1.4); within the *OPTN* gene on chromosome 10p13 ($p=1.5 \times 10^{-21}$; OR= 1.6) and close to *TNFRSF11A* (encoding RANK) on chromosome 18q21 ($p=2.4 \times 10^{-13}$; OR=1.4). The M-CSF, DC-STAMP and RANK, genes are strong candidates for PDB since they play key roles in osteoclast differentiation but the function of *OPTN* in bone is as yet unknown. Stepwise regression analysis showed that all four loci were independently associated with PDB and we therefore combined information from all variants to generate a risk allele score and estimate the population attributable risk for PDB. We found that remarkably, the associated SNPs accounted for 76% of the population attributable risk of PDB in the study population with a 16-fold variation in risk between carriers of protective and susceptibility alleles. This study has identified four novel genetic loci that contribute substantially to disease susceptibility. Further work is now required to define the molecular mechanisms responsible for these associations and to determine if predictive genetic testing for these susceptibility alleles might be of clinical value in identifying patients at risk of the disease or complications.

***Disclosures: Omar Albagha**, None.*

1032

Measles Virus Nucleocapsid Gene Expression and the SQSTM1 Mutation Both Contribute to the Increased Osteoclast Activity in Paget's Disease. Noriyoshi Kurihara*[1], Hua Zhou[2], David Dempster[3], Jolene Windle[4], Jacques Brown[5], G. David Roodman[6]. [1]Center for Bone Biology, University of Pittsburgh, USA, [2]Helen Hayes Hospital, USA, [3]Columbia University, USA, [4]Virginia Commonwealth University, USA, [5]Laval University, Canada, [6]VA Pittsburgh Healthcare System (646), USA

The primary cellular abnormality in Paget's disease (PD) resides in the osteoclast (OCL). OCLs in PD are hyper-multinucleated and hyper-responsive to RANKL and 1,25-$(OH)_2D_3$, express increased levels of TAF-12, and secrete high levels of IL-6. Both measles virus and genetic causes have been proposed for the etiology for PD. However, their respective role in PD is unclear. To define the contributions of measles virus and the $p62^{P392L}$ mutation linked to PD to the abnormal OCL activity in PD, OCL precursors from involved and uninvolved bones of 12 PD patients harboring the $p62^{P392L}$ mutation and 6 normals were characterized by qPCR assays for measles virus nucleocapsid protein (MVNP) mRNA expression, OCL formation, and the effects of antisense-MVNP (AS-MVNP) on PCL formation/morphology, bone resorption capacity and 1,25-$(OH)_2D_3$ and RANK ligand (RANKL) responsivity were determined. OCL precursors from involved and uninvolved bones of 1/3 of PD patients expressed MVNP($MVNP^+$) and formed OCLs characteristic of PD in vitro. OCL formation by $MVNP^+$ cells was blocked by AS-MVNP. In contrast, 2/3 of PD patients and all normals which lacked MVNP formed normal OCLs, which were not affected by AS-MVNP. To further characterize the effects of $p62^{P392L}$ and MVNP on OCL activity in vitro and in vivo, we generated $p62^{P394L}$-knock-in ($p62^{P394L}$-KI) mice and crossed them with transgenic mice with targeted MVNP expression to the OCL lineage (T-MVNP mice). OCL precursors from $p62^{P394L}$ KI mice were hyper-responsive to RANKL but not to 1,25-$(OH)_2D_3$, did not form hyper-multinucleated OCLs and the mice developed progress osteopenia rather than PD bone lesions. In contrast, OCLs precursors from T-MVNP mice were hyper-responsive to RANKL and 1,25-$(OH)_2D_3$, expressed increased levels of TAF-12 and formed hyper-multinucleated OCLs in vitro. OCL precursors from $p62^{P394L}$-KI/MVNP were more hyper-responsive to both RANKL and 1,25-$(OH)_2D_3$, showed increased NF-κB, MAPK and PI3K signaling, increased TAF-12 expression, and formed hyper-multinucleated OCLs. These results suggest that both $p62^{P392L}$ and MVNP in vivo contribute to the abnormal OCL activity in PD with $p62^{P392L}$ enhancing the effects of MVNP in pagetic OCL compared to T-MVNP mice.

***Disclosures: Noriyoshi Kurihara**, None.*

1033

***TNFRSF11A* Gene Allelic Variants are Associated with Paget's Disease of Bone and Interact with *SQSTM1* Mutations to Cause the Severity of the Disorder.** Daniela Merlotti*[1], Fernando Gianfrancesco[2], Luigi Gennari[1], Domenico Rendina[3], Marco Di Stefano[4], Giuseppe Mossetti[3], Salvatore Gallone[5], Teresa Esposito[2], Sara Magliocca[2], Daniela Formicola[2], Alessandra Mingione[2], Pierpaola Fenoglio[5], Antonio Criasia[4], Riccardo Muscariello[3], Pasquale Strazzullo[3], Giancarlo Isaia[6], Ranuccio Nuti[1]. [1]Department of Internal Medicine, Endocrine-Metabolic Sciences & Biochemistry, University of Siena, Italy, [2]Institute of Genetics & Biophysics, CNR, Naples, Italy, [3]Department of Clinical & Experimental Medicine, Federico II University of Naples, Italy, [4]Department of Internal Medicine, University of Turin, Italy, [5]Department of Neuroscience, University of Turin, Italy, [6]University of Torino, Italy

Paget's disease of bone (PDB) is a chronic bone disease with a consistent genetic component. Despite mutations in *SQSTM1* gene have been detected in up to 50% of familial cases, phenocopy or incomplete penetrance were described and their prevalence is low in sporadic PDB, likely due to the presence of additional predisposition genes. Although the *TNFRSF11A* gene (encoding RANK, a key protein in osteoclastogenesis) has been associated with different PDB-like syndromes, no *TNFRSF11A* mutations have been reported in PDB patients. In this study we evaluated whether 2 non-synonymous *TNFRSF11A* single nucleotide polymorphisms (SNPs), rs35211496 (H141Y) and rs1805034 (A192V), are associated with PDB and the severity of phenotype in a large population of 580 unrelated consecutive patients that were previously screened for *SQSTM1* gene mutations. 496 age and sex-matched controls were also genotyped for comparison. Both SNPs were associated with PDB in the overall cohort as well as after the exclusion of patients with *SQSTM1* gene mutations (n=79). The largest effect was found for rs1805034, yielding an odds ratio of 1.3 (p=0.006), with the C allele as the risk allele. Moreover, an even more significant p-value (p=0.0009) was observed in the subgroup of patients with *SQSTM1* mutation, with an odds ratio of 1.6, again indicating the C allele to be the risk allele. Interestingly patients with the C allele also showed an increased prevalence of polyostotic disease (68%, 53%, and 51% in patients with CC, CT, and TT genotypes, respectively, p=0.01) as well as an increased number of affected skeletal sites (2.9, 2.5, and 2.0 in patients with CC, CT, and TT genotypes, respectively, p=0.008). These differences increased in magnitude when analyses were restricted to cases with *SQSTM1* mutation, both for the prevalence of polyostotic disease (91%, 77%, and 73% in patients with CC, CT, and TT genotypes, respectively, p=0.03) and the number of affected sites (4.4, 3.3, and 2.8 in patients with CC, CT, and TT genotypes, respectively, p=0.03). No significant differences in relation to *TNFRSF11A* genotypes were observed concerning age of diagnosis and the estimated age of onset of PDB. Haplotype analysis combining the 2 SNPs evidenced an odds ratio of 2.12 in subjects with C-C haplotype (p=0.02). In conclusion, this study provides evidence that *TNFRSF11A* SNPs are associated with the susceptibility to develop PDB and may interact with *SQSTM1* mutations to cause the severity of the disorder.

***Disclosures: Daniela Merlotti**, None.*

1034

Both Hypersensitivity to 1,25-$(OH)_2D_3$ and High IL-6 Levels Are Required to Induce Pagetic Osteoclasts. Noriyoshi Kurihara*[1], Jolene Windle[2], G. David Roodman[3]. [1]Center for Bone Biology, University of Pittsburgh, USA, [2]Virginia Commonwealth University, USA, [3]VA Pittsburgh Healthcare System (646), USA

Our previous studies showed that measles virus nucleocapsid protein (MVNP) can induce development of Paget's disease (PD) osteoclasts (OCL) and pagetic lesions in vivo. MVNP induced hyper-responsivity of OCL precursors to 1,25-$(OH)_2D_3$ through increased expression of a novel VDR co-activator, TAF-12, as well as high levels of IL-6 in the local bone microenvironment. Further, knockdown of TAF-12 blocked formation of pagetic OCL in vitro, but overexpression of TAF-12 in normal OCL precursors did not induce pagetic OCL formation. These results suggest that high levels of IL-6 and hyper-responsivity to 1,25-$(OH)_2D_3$ are both required for development of PD-OCL. To test this hypothesis, TRAP-MVNP mice, which have MVNP targeted to the OCL lineage, using the TRAP promoter and develop pagetic-like bone lesions, were mated with $IL\text{-}6^{-/-}$ mice to generate TRAP-MVNP/$IL\text{-}6^{-/-}$ mice. Bone marrow cells from TRAP-MVNP and TRAP-MVNP/$IL\text{-}6^{-/-}$ mice were then tested for their capacity to form OCL that express a pagetic phenotype in vitro. OCL precursors from TRAP-MVNP but not TRAP-MVNP/$IL\text{-}6^{-/-}$ mice were hyper-responsive to 1,25-$(OH)_2D_3$ and expressed high levels of TAF-12. As expected, OCL precursors in marrow cultures from TRAP-MNVP were hyper-responsive to RANKL. In contrast, OCL precursors from $IL\text{-}6^{-/-}$, MVNP/$IL\text{-}6^{-/-}$ and WT mice were not hyper-responsive to RANKL. OCL from TRAP-MVNP/$IL\text{-}6^{-/-}$, $IL\text{-}6^{-/-}$ and WT were not hyper-responsive to 1,25-$(OH)_2D_3$, did not have increased nuclei per OCL and did not form PD-OCL. Further, in contrast to TRAP-MVNP mice, the bone resorption capacity of OCL formed from TRAP-MVNP/$IL\text{-}6^{-/-}$ was similar to WT. Loss of IL-6 in TRAP-MVNP mice (TRAP-MVNP/$IL\text{-}6^{-/-}$ mice) blunted the enhanced p38 and ERK signaling seen in TRAP-MVNP OCL precursors treated with 1,25-$(OH)_2D_3$. It had no affect on NF-κB and AKT signaling. Further, loss of $IL6^{-/-}$ decreased the enhanced NFATc-1 expression in OCL precursors from TRAP-MVNP

mice. Histomorphometric studies showed that loss of IL-6 significantly decreased osteoblast perimeter and bone formation rate compared to that in TRAP-MVNP mice. These results show that IL-6 is required for hypersensitivity of OCL precursors to 1,25-$(OH)_2D_3$ and that high levels of IL-6 combined with increased TAF-12 expression are necessary to induce PD-OCL and pagetic bone lesions in vivo.

***Disclosures: Noriyoshi Kurihara**, None.*

1035

Effects of Estrogen on Bone Marrow Cytokines/Bone-Regulatory Factors and Osteoprogenitor Cells In Vivo in Elderly Women. Ulrike Moedder*[1], Louise McCready[2], Kelley Hoey[2], Matthew Roforth[2], James Peterson[2], Sundeep Khosla[3]. [1]Mayo Clinic College of Medicine, USA, [2]Mayo Clinic, USA, [3]College of Medicine, Mayo Clinic, USA

Decreases in estrogen (E) levels contribute not only to early postmenopausal bone loss but also to ongoing bone loss with aging in women. E is known to regulate bone turnover; however it is unclear whether E treatment alters peripheral blood (PB) or bone marrow (BM) plasma levels of inflammatory cytokines, sclerostin, or other candidate bone-regulatory factors. In addition, possible effects of E on proliferation or differentiation of human BM osteprogenitor (hematopoietic lineage [lin]-/Stro1+) cells in vivo have not been elucidated. Thus, we treated elderly postmenopausal women (mean age, 71 ± 1 yrs) either with transdermal E2 (0.05 mg/d) or placebo (Control, n=16 per group) for 4 months. PB serum and BM plasma was collected to determine levels of bone formation and resorption markers (P1NP, CTX, TRAP5b) as well as candidate cytokine and other bone-regulatory factors (TNFα, IL-1β, IL-6, RANKL, OPG, adiponectin, DKK1, oxytoxin, serotonin, and sclerostin). Lin-/Stro1+ cells were isolated from BM samples by magnetic activated cell sorting (MACS) for gene expression analysis. As expected, bone turnover markers (P1NP, CTX, TRAP5b) were significantly decreased following E treatment. None of the PB serum or BM plasma marker levels that were determined differed significantly between the two groups, with the notable exception of sclerostin levels, which were significantly lower in the E-treated compared to Control women both in PB (Control, 332 ± 6; E-treated, 207 ± 19 pg/ml, P=0.011) and in BM plasma (Control, 378 ± 41; E-treated, 249 ± 25 pg/ml, P=0.022). There was also a significant correlation between BM plasma and PB serum sclerostin levels (R=0.74, P<0.0001). Gene expression analysis of BM lin-/Stro1+ cells demonstrated a significant decrease in the expression of several proliferation markers (cyclin B1, cyclin E1, E2F1), the BMP target, lysyl oxidase, as well as the master-regulator of osteoblast differentiation, runx-2. In summary, of all the candidate cytokines and other proteins assessed, sclerostin was the only bone-regulatory factor clearly reduced in BM plasma and PB of postmenopausal women following E treatment. Moreover, consistent with the known anti-remodeling effects of E, we demonstrate for the first time in vivo that E suppresses proliferation and expression of runx-2 by early osteoprogenitor cells. Further studies are needed to define whether these effects of E are direct or indirect and whether they differ in early vs late osteoblastic cells.

***Disclosures: Ulrike Moedder**, None.*

1036

Postmenopausal BMD Variation is Strongly Associated with Subsets of MicroRNAs and Other Non-coding RNAs (ncRNAs) Expression Levels. Sjur Reppe*[1], Marit Holden[2], Vigdis T. Gautvik[1], Harish Datta[3], Kaare M. Gautvik[4]. [1]Oslo University Hospital, Ullevaal, Norway, [2]Norwegian Computing Center, Norway, [3]Newcastle University, United Kingdom, [4]Oslo University Hospital, Ullevaal; University of Oslo; Lovisenberg Deacon Hospital, Oslo, Norway

Heritage determines 60-80% of the maximal obtainable bone mineral density (BMD) level in women, and BMD is closely associated with skeletal fractures occurring in about 40% of postmenopausal women in the western world. MicroRNAs are short (19-24) polynucleotides that bind to messenger RNAs of protein coding genes and confer genetic regulation at the post-transcriptional level, affecting a wide range of biological processes. We have identified novel determinants of bone remodeling through global profiling of mature microRNAs and other non-coding RNAs (ncRNAs) in bone biopsies from postmenopausal Caucasian females and calculated their associations to BMD variations. The unrelated women (n=84, 50-86 yr), had diverse BMDs (healthy, osteopenic or osteoporotic) with or without low energy fractures. Out of 667 tested, a set of 24 ncRNAs correlated strongly with total hip BMD adjusted for age and BMI (5% false discovery rate (FDR)). Lasso analysis was used as an alternative statistical method employing cross validations and identified a subset of 10 ncRNAs that explained 32% of the BMD variation in total hip BMD after adjustment for differences in age and BMI. The top ranked 9 Lasso ncRNAs were included among the 24 at 5% FDR level, thus adding strength to the results. High significant correlation between the Lasso ncRNAs and mRNAs previously shown to be highly associated with BMD (Reppe et al., Bone. 2010 46:604-12) suggested reciprocal or similar regulation between several of the RNAs in the two groups, emerging as a closely interconnected net. Target prediction software identified the Adherens Junction, TGFβ and Wnt signaling pathways to be the most implicated. While the TGFβ and Wnt pathways are well known to be important in bone remodeling, the Adherens junction comprising regulation of cell to cell contact via E-Cadherin is a less appreciated complementary system. The results provide novel insight in the functional association between distinct microRNAs / ncRNAs in bone cell metabolism and their possible roles in the pathogenesis of osteoporosis as the ultimate consequence of low BMD.

***Disclosures: Sjur Reppe**, None.*

1037

Inhibiting Cx43 Gap Junction Function in Osteocytes, but not Cx43 Hemichannel Function Results in Defects in Skeletal Structure and Bone Mass. Jean Jiang*[1], Sirisha Burra[2], Stephen Harris[1], Hong Zhao[3], Mark Johnson[4], Lynda Bonewald[5]. [1]University of Texas Health Science Center at San Antonio, USA, [2]University of Texas, USA, [3]School of Dentistry, University of Missouri, USA, [4]University of Missouri, Kansas City Dental School, USA, [5]University of Missouri - Kansas City, USA

Connexin (Cx) 43 plays an important role in maintaining normal bone function and development. Targeted deletion of Cx43 in osteoblasts using either 2.3Col or OC-Cre mice crossed with floxed Cx43 mice results in increased osteocyte apoptosis and osteoclast recruitment leading to reduced bone mass and strength. Cx43 forms both gap junctions and hemichannels. Whereas gap junctions play a role in cell signaling, hemichannels are thought to play a role in both signaling and cell viability. In order to begin to separate the role of gap junctions from hemichannels in osteocyte function, we generated a Cx43 (R76W) mutant construct predicted to block gap junction but not hemichannel function. This construct was expressed in Hela and osteocytic MLO-Y4 cells and tested for Cx43 function. Dye transfer experiments showed that Hela cells expressing Cx43 (R76W) failed to form functional gap junction channels. When co-expressed with wild-type Cx43, this mutant acted as dominant negative for gap junctions. This mutant also inhibited gap junctions formed by endogenous Cx43 when expressed in MLO-Y4 cells. Dye uptake analysis suggested that unlike gap junctions, hemichannel function was not affected by Cx43 (R76W) in both Hela and MLO-Y4 cells.

Next, in vivo studies were performed to determine relative contributions of Cx43 gap junctions to hemichannels in osteocytes by generating mice in which osteocyte specific expression of Cx43 (R76W) was driven by a 10 kb-DMP-1 promoter. At 1 day of age, no differences were observed between controls (C) and heterozygotes (Het) with regards to size, weight, BMD and BMC using x-ray and bone densitometry. To date, no homozygotes have been obtained suggesting lethality. By 4 weeks of age, the heterozygote mice showed a decrease in body weight (15.8/11.7 gm: C/Het) and a decrease in BMD (0.0491/0.0444 g/cm^2: C/Het), but a dramatic decrease in BMC (0.427/0.282; C/Het). By micro-CT analysis, significant increased porosity was observed especially in distal femora and vertebrae (Figure 1). These results suggest that gap junction channels formed by Cx43 in osteocytes are critical for maintaining normal bone density and architecture and potentially postnatal development. Gap junctions, by not hemichannels may be responsible for osteocyte signaling to initiate remodeling. Alternatively, excessive Cx43 hemichannel activity due to the over-expression could also attribute to impaired bone phenotypes exhibited by this transgenic model.

Fig. 1

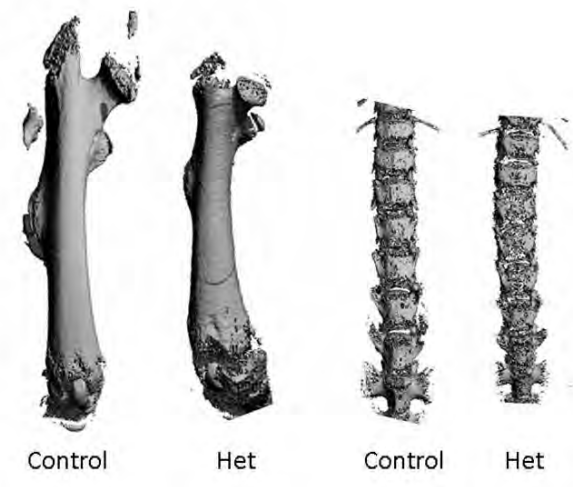

Figure 1

***Disclosures: Jean Jiang**, None.*

1038

Resorption is an Essential Component of Bone Anabolism Induced by Active PTH Receptor Signaling in Osteocytes. Yumie Rhee*[1], Matthew Allen[2], Lilian Plotkin[2], Nicoletta Bivi[3], Racheal Lee[4], Jeffery Benson[4], Virginia Lezcano[5], Ana Ronda[5], Teresita Bellido[2]. [1]IUMS, Yonsei University, College of Medicine, South korea, [2]Indiana University School of Medicine, USA, [3]Indiana University, USA, [4]Department of Anatomy & Cell Biology, Indiana University School of Medicine, USA, [5]Department of Biochemistry, Biology, & Pharmacy, Universidad Nacional de Sur, Argentina

The contribution of remodeling-based bone formation (BF) coupled to osteoclast activity and modeling-based BF that occurs independently of resorption, to the anabolic effect of PTH remains unclear. Earlier work demonstrated that transgenic (TG) mice with constitutive activation of PTH receptor signaling in osteocytes (DMP1-caPTHR1 mice) display increased endosteal remodeling and enhanced periosteal BF. We dissected herein the contribution of resorption to formation induced by PTHR signaling in osteocytes by administering alendronate (ALN, 5.25 mg/kg/week) or vehicle for 2 weeks to 1-month-old DMP1-caPTHR1, DMP1-Sost, double TG, or wild type (WT) littermates. ALN reduced circulating CTX and OCN in all groups, except for OCN in double TG mice that was already low. The increased periosteal BF displayed by DMP1-caPTHR1 mice was reversed by Sost overexpression but still elevated in DMP1-caPTHR1 mice treated with ALN, demonstrating its dependence on the Wnt pathway but not on resorption. In contrast, the increased endocortical MAR of the DMP1-caPTHR1 mice was abolished by ALN indicating that osteoblast activity in this surface is driven by resorption. Moreover, MAR was further increased by Sost overexpression consistent with the higher resorption and low OPG expression exhibited by these double TG mice. However, the increased endocortical MS/BS displayed by DMP1-caPTHR1 mice was not affected by ALN but it was reduced by Sost overexpression, suggesting that the presence of osteoblasts on mineralizing surfaces induced by PTHR signaling is not driven by resorption but depends on the Wnt pathway. Because of the respective lower values of MAR and MS/BS, double TG mice treated with ALN exhibited endocortical BFR even lower than WT mice, demonstrating cooperation between resorption and Wnt activity on remodeling-based BF driven by PTHR signaling in osteocytes. Moreover, whereas Sost overexpression exacerbated the elevated intracortical porosity exhibited by DMP1-caPTHR1 mice, ALN reduced porosity in both DMP1-caPTHR1 and double TG mice. As a result of these combined effects on periosteal and endosteal (endo- and intra-cortical) surfaces, double TG mice treated with ALN exhibited similar bone area in the femoral mid-diaphysis (micro-CT) and femoral BMD (DXA) to WT mice. These findings demonstrate that, although dispensable for periosteal BF, resorption is essential for increasing BF in the endosteal surfaces driven by PTH receptor signaling in osteocytes.

***Disclosures: Yumie Rhee**, None.*

1039

Sclerostin Antibody Protects the Skeleton from Disuse-induced Bone Loss. Alexander Robling*[1], Stuart Warden[1], Chris Paszty[2], Charles Turner[3]. [1]Indiana University, USA, [2]Amgen, Inc., USA, [3]Indiana University, Purdue University Indianapolis, USA

The Wnt signaling pathway is a key modulator of bone metabolism, including responses to the mechanical environment. Soluble inhibitors of Wnt signaling are modulated by mechanical loading and unloading (disuse), and consequently, represent potential targets to alter the naturally occurring responses to those stimuli. We sought to determine whether inhibition of sclerostin, an osteocytic protein that inhibits Wnt signaling through the Lrp5/6 receptors, would protect bone from the bone-wasting effects of mechanical disuse. Adult female mice were subjected to one of two disuse models: tail suspension, or unilateral botox-induced muscle paralysis (Botox; 20 U/kg) of the right lower limb. The left lower limb was injected identically with saline (internal control). The mice underwent disuse for 3 wks in the presence or absence of twice-weekly dosing with a sclerostin neutralizing antibody (Scl-AbIII; 25 mg/kg) injection. In the ground control mice, femoral aBMD did not change significantly over the three week treatment period (+1.7%, p=0.41), but tail suspended mice exhibited a 7% reduction ($p<0.001$). Tail suspended mice treated with Scl-AbIII exhibited a 6.2% increase ($p<0.001$) in femoral aBMD after 3 wks. This increase was significantly greater than that noted for the ground control mice ($p<0.01$), suggesting that Scl-AbIII not only protected these suspended mice from bone loss, but actually increased bone mass over ground control mice, despite the weightless environment. The Botox studies produced similar results to those described for the tail suspension studies. Saline injection into the left lower limb musculature resulted in a slight but significant decrease in femoral aBMD (-2.6%, $p<0.01$) over the 3-wk treatment period, whereas Botox injection into the right limb musculature of these same animals resulted in an 8.4% decrease ($p<0.001$) in femoral aBMD. Mice given Scl-AbIII during the 3 wk period following Botox injection exhibited an 8.0% increase in femoral aBMD in the paralyzed limb. This increase was significantly different from the changes occurring in the saline-injected limbs of mice not receiving antibody ($p<0.001$), suggesting that Scl-AbIII not only protected these paralyzed limbs from bone loss, but actually increased bone mass over non-paralyzed, saline-injected limbs. In summary, these data suggest that sclerostin inhibition is a useful approach for overcoming the bone loss that normally occurs with disuse.

***Disclosures: Alexander Robling**, None.*

1040

A Membrane-Targeted GFP Selectively Expressed in Osteocytes Reveals Cell and Membrane Dynamics in Living Osteocytes. Patricia Veno[1], Yongbo Lu[2], Suzan Kamel[1], Jian Feng[3], Lynda F. Bonewald[4], Sarah Dallas*[4]. [1]University of Missouri, Kansas City, USA, [2]Texas A&M University System Health Science Center, USA, [3]Texas A&M Health Science Center, USA, [4]University of Missouri - Kansas City, USA

Osteocytes, once viewed as quiescent cells, are now known to be capable of modifying their microenvironment, play a key role in phosphate homeostasis and may act to integrate mechanical and hormonal signals to regulate bone mass. We have previously shown in neonatal mouse calvaria that osteocytes within their lacunae may be highly dynamic and show motions of their cell body and dendrites. To further understand the dynamic properties of these cells, we have used live imaging approaches in conjunction with a new transgenic mouse line that selectively expresses a membrane targeted GFP construct in osteocytes.

Transgenic mice were generated expressing a membrane targeted AcGFP variant driven by a 10kb fragment of the Dmp1 promoter. This GFP variant contains the N-terminal 20 amino acids of neuromodulin (GAP-43), which targets the GFP to plasma and intracellular membranes. Living calvarial explants from 5-7 day old mice expressing the transgene were imaged by time lapse fluorescent microscopy. The transgene was expressed in partially and fully embedded osteocytes as well as a sub population of motile cells on the bone surface that we have previously proposed may represent an osteocyte precursor cell. Time lapse fluorescence imaging confirmed motions of the osteocyte cell body and dendrites and also suggested extensive ruffling of the osteocyte cell membrane within its lacuna. Live cell imaging was also performed on primary calvarial osteoblasts isolated from Dmp1-memGFP transgenic mice that were cultured under mineralizing conditions. Mineral deposition occurred exclusively in areas containing clusters of Dmp1-mem-GFP positive cells and was associated with extensive ruffling of the cell membrane of the GFP-positive cells, and apparent shedding of membrane bound vesicles. Confocal microscopy of neonatal Dmp1-memGFP calvaria and immunostaining for the membrane associated osteocyte marker protein, E11/gp38, showed vesicles in the ECM that are apparently shed from the osteocyte dendrites and cell body.

These data underscore the dynamic properties of osteocytes and further reveal their extensive membrane ruffling activity within their lacunae. The shedding of membrane bound vesicles by osteocytes may represent a mechanism for reduction of cytoplasmic volume, may be involved in regulation of mineral deposition and/or may be a mechanism for intercellular communication in the bone microenvironment.

***Disclosures: Sarah Dallas**, None.*

1041

Ablation of Mef2C in Osteocytes Increases Bone Formation and Bone Mass Through Transcriptional Repression of Sclerostin (SOST). Nicole Collette*[1], Aris Economides[2], Liqin Xie[3], Damian Genetos[4], Richard Harland[5], Gabriela Loots[6]. [1]Lawrence Livermore National Laboratory/ University of California, Berkeley, USA, [2]Regeneron Pharmaceuticals, Inc., USA, [3]Regeneron Pharmaceutical company, USA, [4]University of California, Davis, USA, [5]University of California, Berkeley, USA, [6]LLNLUC Merced, USA

Myocyte Enhancer Factors (Mefs) are a family of transcriptional regulators originally described for their key roles in cardiovascular development. In vertebrates there are four closely related Mef2 genes (A, B, C, D) -with overlapping expression patterns in muscle and vasculature. Since Mef2C null mice are embryonically lethal because of their failure to develop hearts, the role of Mef2C in bone metabolism has not yet been described. Recently, MEF2C has been shown to play a role in skeletal development by activating the gene program for chondrocyte hypertrophy. Concomitantly, we found Mef2C and D to be robustly expressed in mineralized bone, suggesting that Mef2 transcription factors may govern similar transcriptional regulatory networks in bone and muscle. Through functional characterization of a distal regulatory element (ECR5) that controls SOST expression specifically in osteocytes, we have previously reported the discovery of a MEF2 response element that is critical for the enhancer activity of this element, in vitro. Since loss of Sclerostin or SOST is responsible for two rare, autosomal recessive disorders characterized by generalized severe hyperostoses of the skeleton [sclerosteosis and Van Buchem Disease (VB)], we aimed to address whether deleting the SOST osteocyte enhancer, ECR5, or the putative upstream regulatory protein, Mef2C, would produce similar phenotypes, in vivo. We examined Mef2C conditional knockout mice in the context of Col1- and Dmp1-Cre in combination with ECR5-LacZ reporter transgenes or Sost-LacZ knock-in alleles. Whereas ECR5-LacZ and Sost-LacZ mice express β-galactosidase in osteocytes in a similar fashion to endogenous mouse Sost, when these reporters were examined in the Mef2C; Dmp1-Cre or Col1-Cre background, the osteocyte-specific ablation of Mef2C in these mice resulted in ECR5-dependent loss of Sost transcription (confirmed histologically and by qRT-PCR). In addition, the osteocyte-specific ablation of Mef2C also causes high bone mass, in these mice. Mef2C; Dmp1-Cre mice showed significant increase in trabecular microarchitecture in both distal femur and lumbar vertebrae relative to WT controls, and strikingly, this phenotype mimicked the bone overgrowth phenotype caused by the loss of ECR5, in vivo. Our results demonstrate that Mef2C is required for the transcriptional activation of Sost in osteocytes and loss of either ECR5 distal enhancer or Mef2C in osteocytes results in a bone phenotype similar to VB.

***Disclosures: Nicole Collette**, None.*

1042

Bone Mass Increases in Osteocyte-specific Mef2c Knock-out Mice are Due to Decreased Bone Resorption. Stefan Baertschi*[1], Ina Kramer[2], Olivier Leupin[1], Hansjoerg Keller[1], Michaela Kneissel[1]. [1]Novartis Institutes for BioMedical Research, Switzerland, [2]Novartis Institutes for BioMedical Research, Che

We discovered previously that myocyte enhancer factor 2 (Mef2) a, c and d transcription factors are expressed in osteocytes and required for expression of the negative bone formation regulator Sost, implicating Mef2s in bone homeostasis. In order to analyze the role of Mef2c, which we found to be most highly expressed amongst the Mef2s in mineralized bone, we generated osteocyte-specific Mef2c deficient mice (Mef2cloxP/loxP;Dmp1-Cre). Previously presented results revealed cancellous and cortical bone mass increases in the axial and appendicular skeleton of male and female Mef2cloxP/loxP;Dmp1-Cre mice during growth and ageing (J Bone Miner Res 23, Suppl.). To gain further mechanistic insights into the observed phenotype we performed qPCR expression profiling utilizing osteocyte-enriched RNA from the femur diaphysis of 3-month-old mice and subjected the cancellous bone in the distal femur metaphysis to histomorphometric analysis.

Mef2c was decreased by 61% in male Mef2cloxP/loxP;Dmp1-Cre mice, consistent with an at least partial deletion of osteocytic Mef2c. Sost expression levels were reduced by 40%. In female mice Mef2c levels decreased by 50 %, while Sost expression decreases of 32 % did not reach significance. Mef2a and Mef2d expression levels were unaffected in both sexes. Despite partial decreases in Sost expression, fluorochrome label based bone formation rates and osteoblast number were largely unchanged in male and female Mef2cloxP/lox;Dmp1-Cre mice. In contrast, we found osteoclast surface to be reduced in male mice by 39 % compared to wildtype controls. Female knock-out animals presented with a decrease of osteoclast surface by 34%. Serum levels of the bone resorption biomarker Trap5b were decreased by 38 % in male mice, while they were not significantly altered in female mice. Expression analysis of bone marker and Wnt/beta catenin target genes revealed increases in expression of soluble RANKL decoy receptor osteoprotegerin (Opg) (70%) in male Mef2c deficient mice, while RANKL was unchanged. Female mice did not show a significant change in Opg expression compared to controls.

In summary, reduction of osteocytic Mef2c results in decreased bone resorption and increased bone mass. Reduced bone resorption is at least in male mice associated with increased Opg levels. Future studies will need to elucidate whether the modulation of Opg levels is dependent on repression of the presumed Wnt/beta-catenin signaling antagonist Sost or is independent of it.

***Disclosures: Stefan Baertschi**, Novartis, 3*

1043

Autophagy Related Proteins Mediate Osteoclast Function in vitro and in vivo. Carl DeSelm*[1], Brian Miller[1], Wei Zou[2], Herbert Virgin[1], Steven Teitelbaum[2]. [1]Washington University School of Medicine, USA, [2]Washington University in St. Louis School of Medicine, USA

Osteoclasts (OCs) degrade skeletal tissue by generating a polarized resorptive microenvironment, between themselves and the bone surface, isolated from the general extracellular space by a sealing zone. Ultimately bone degradation depends upon the cell's capacity to secrete protons, which mobilize mineral, and cathepsin K, which degrades organic matrix, into this sealed compartment. Transport of these molecules, in turn, is mediated by the OC's resorptive organelle, the ruffled border, which is encompassed within the actin ring. The ruffled border is the product of exocytosis of lysosmal vesicles containing the bone-degrading molecules. Thus, the mechanism by which lysosomal vesicles traffic to, and fuse with, the polarized plasma membrane is central to OC function. Autophagy is the process whereby cells degrade intracellular material within the lysosome. Because recent human GWAS data indicates a link between the autophagy pathway and bone density and as autophagy regulates survival and function of some secretory cells, we tested its importance in the OC. Activation of the autophagy pathway results in lipidation of the protein, LC3, which localizes to autophagosomes to promote their development and fusion with lysosomes. LC3 appears in punctate cytoplasmic structures in bone-residing OCs, but also localizes to the ruffled border. Furthermore, inhibition of the autophagy protein Atg4, which mediates lipidation of LC3, prevents LC3 transport to the ruffled border. Confirming this observation, LC3-G120A mutant, which cannot be lipidated, also fails to target to the resorptive organelle. We next turned to Atg5, an essential autophagy protein whose gene we conditionally deleted in OCs. We find Atg5 is also necessary for LC3 localization to the ruffled border and for efficient cathepsin K accumulation within the resporptive micoenvironement. These defects of Atg5-/- OCs are rescued by the WT gene but not its inactive K130R mutant. Establishing physiological relevance, Atg5 deficiency is attended by a ten fold reduction in ruffled border formation and failure to degrade bone slices in vitro, similarly rescued by the WT but not mutant gene. Lack of Atg5 also attenuates resorption in vivo resulting in diminished bone loss following ovariectomy. Thus, autophagy proteins target lysosomal vesicles to the bone-apposed plasma membrane to generate the ruffled border, thus facilitating bone resorption, providing insight into their genetic association with osteoporosis.

***Disclosures: Carl DeSelm**, None.*

1044

MHC Class II Transactivator: A Novel Estrogen-modulated In Vivo Regulator of Osteoclastogenesis and Bone Homeostasis Co-opted from Adaptive Immunity. Elisa Benasciutti*[1], Elisabetta Mariani[2], Egon Perilli[3], Emmanuele Barras[4], Roberta Faccio[5], Nick Fazzalari[6], Walter Reith[4], Simone Cenci[2]. [1]Division of Genetics & Cell Biology, San Raffaele Scentific Institute, Italy, [2]Division of Genetics & Cell Biology, San Raffaele Scientific Institute, Italy, [3]Department of Surgical Pathology, Institute of Medical & Veterinary Science, Australia, [4]Department of Pathology & Immunology, University of Geneva Medical School, Centre Médical Universitaire (CMU), Switzerland, [5]Washington University in St Louis School of Medicine, USA, [6]Institute of Medical & Veterinary Science, Australia

The integrated study of bone and immunity, two co-evolved systems, is greatly expanding our understanding of skeletal biology, with implications for the pathogenesis of bone-wasting diseases. Recent work in mouse models of postmenopausal osteoporosis unveiled an increased expression of the master switch of MHC Class II expression and antigen presentation, CIITA (MHC Class II Transactivator), in osteoclast (OC) precursors. We thus tested the role of CIITA in regulating OC differentiation and activity.

To this aim, we adopted three genetic mouse models, two overexpressing CIITA, either conditionally (CIITA promoter IV-/-) or systemically (CIITA transgenics, Tg) and one lacking CIITA (CIITA-/-). We observed that CIITA potently regulates OC differentiation and bone architecture. 3D microCT analyses on tibial epiphyses show a dramatically reduced trabecular structure in CIITA overexpressing models. Altered architecture is confirmed by histomorphometrical analyses on contralateral bones, that also show increased OC numbers and activity. In parallel, ex vivo OCgenesis from bone marrow monocytes (BMMs) is enhanced in CIITA pIV-/- and CIITA Tg mice, while CIITA-/- monocytes show reduced OC differentiation. Silencing CIITA in BMMs by RNA interference decreases OCgenesis, suggesting that endogenous CIITA levels control OC differentiation in a cell-autonomous fashion. A global increased activation of the signaling pathways downstream of RANK underlies the hyperOCgenic phenotype, indicating the common upstream adapter TRAF6 as a potential target of CIITA.

We also asked if CIITA is regulated by estrogen (E), the main osteotropic hormone whose deficiency represents the main causative factor of involutional osteoporosis. In vivo experiments on OC precursors from ovariectomized mice reveal profound suppressive effects of E on chromatin remodeling at the CIITA locus, reverted by inhibition of histone deacetylases, controlling the inducibility of CIITA target genes. In vitro experiments reveal that E directly regulates CIITA expression in monocytes.

Our study provides compelling genetic evidence that the master immune regulator CIITA controls OC differentiation and bone homeostasis, and is controlled by E in vivo. This work further links bone and adaptive immunity and promises to identify novel therapeutic targets against bone-wasting conditions, in primis osteoporosis.

***Disclosures: Elisa Benasciutti**, None.*

1045

Jmjd5, JmjC-domain-containing Protein, is an Osteoclastogenic Repressor. Min-Young Youn*[1], Ken-ichi Minehata[2], Ichiro Takada[1], Yuuki Imai[3], Takashi Nakamura[1], Takeshi Suzuki[2], Shigeaki Kato[4]. [1]IMCB, University of Tokyo, Japan, [2]Cancer Research Institute, Kanazawa University, Japan, [3]The University of Tokyo, Japan, [4]University of Tokyo, Japan

Osteoclastogenesis is highly regulated by various transcriptional factors, which play pivotal roles by reorganizing gene networks. Recently, epigenetic regulations, such as histone modifications and chromatin remodeling, have been thought to be essential for the regulation of gene expression by transcription factors. Especially, reversibly regulated histone methylation is regarded as the most important storage of epigenetic information that defines cell fate and identity. However, it remains still unknown epigenetic regulations including histone demethylation during osteoclastogenesis. To clarify the roles of epigenetic regulations during osteoclastogenesis, we focused on Jumonji C (JmjC)-domain-containing proteins which are known as histone demethylase family, because their physiological roles in bone are totally unknown. Firstly, we confirmed their significant expressions during RANKL induced osteoclastogenesis using Raw264 cells. Among detected ten kinds of JmjC-domain-containing proteins, we observed that the expression levels of JmjC-domain-containing protein 5 (Jmjd5) was reduced through osteoclastogenesis. To verify its functions in the osteoclast differentiation, a stable cell line constitutively expressing shRNAs against Jmjd5 was established, and then osteoclast formation was assayed by TRAP staining. Notably, down-regulation of Jmjd5 expression resulted in promotion of osteoclast formation with up-regulated expression of osteoclast-specific genes such as DC-STAMP and Cathepsin K (CtsK). These results indicated that Jmjd5 is a negative regulator for osteoclast differentiation. To define the physiological function of Jmjd5 in bone metabolism in vivo, we generated the osteoclast-specific Jmjd5 knockout (Jmjd5?Oc/?Oc) mice by crossing Jmjd5-flox mice with CtsK-Cre mice. Consistent with in vitro function, we could detect the reduced bone mineral density (BMD) of the femurs of 16-week-old Jmjd5?Oc/?Oc mice, when compared with BMD of wild type mice. Taken together, epigenetic regulations, at least methylation and/or demethylation of histone tale, might have an important role in osteoclastogenesis and bone metabolism.

***Disclosures: Min-Young Youn**, None.*

1046

Claudin 18 (Cldn-18), a Novel Bone Resorption (BR) Regulator, Interacts with Zona-occluden-2 (ZO-2) to Modulate RANKL Signaling in Osteoclasts. Gabriel Linares*[1], Robert Brommage[2], David Powell[3], Weirong Xing[4], Catrina Alarcon[1], Anil Kapoor[1], Shin-Tai Chen[1], Kin-Hing William Lau[5], Jon Wergedal[1], Subburaman Mohan[1]. [1]Jerry L. Pettis Memorial VA Medical Center, USA, [2]Lexicon Pharmaceuticals, USA, [3]Lexicon Pharmaceuticals Inc., USA, [4]Musculoskeletal Disease Center, Jerry L. Pettis Memorial Veteran's Admin., USA, [5]Jerry L Pettis Memorial VA Medical Center, USA

Cldn-18 is a member of a large family of transmembrane proteins that have been identified as important components of tight junction (TJ) strands. Targeted disruption of Cldn-18 function in mice decreased total body BMD by 18% ($P<0.01$) at 14 wks of age. μCT measurements at mid-diaphysis of femur revealed no significant change in size but a 20% reduction in cortical thickness ($P<0.01$) in knockout (KO) mice. Trabecular (Tb) bone volume at L5 vertebra was 50% less in KO mice ($P<0.001$) due to significant decreases in Tb number (50%) and thickness (20%) and increased Tb separation (50%). Histomorphometric analyses revealed that resorbing surface (87%) and osteoclast (OC) number (60%) were increased significantly in the KO mice without changes in bone formation parameters. Accordingly serum levels of TRAP5b and expression levels of TRAP and cathepsin K (Ctsk) were increased (60%-80%, $P<0.05$) in the femurs of KO mice. In vitro studies with bone marrow macrophages (BMM) revealed that Cldn-18 disruption significantly increased RANKL-induced OC differentiation (80%, $P<0.01$) but not MCSF-induced BMM proliferation. Consistent with a direct role for Cldn-18 in the regulation of OC differentiation are the findings that OCs express Cldn-18 and overexpression of Cldn-18 in RAW264.7 cells significantly inhibited RANKL-induced OC differentiation. We next tested whether Cldn-18 effects on RANKL signaling are mediated in part via interaction of C-terminal PDZ domain of Cldn-18 with PDZ domain containing protein, ZO-2, since certain Cldns interact with ZO proteins and since ZO-2 was highly expressed and regulated by RANKL in OCs. Accordingly, Cldn-18 interacted with ZO-2 by immunoprecipitation and knockdown of ZO-2 using lentiviral shRNA decreased RANKL induced OC differentiation by 50% ($P<0.001$) and expression of TRAP and Ctsk (43% and 58%, $P<0.05$) in RAW264.7 cells. Nuclear translocation of ZO-2 has been linked to increased gene expression. Accordingly, Cldn-18 overexpression decreased RANKL-induced nuclear levels of ZO-2 by 60% in RAW264.7 cells. Furthermore, knockdown of ZO-2 significantly reduced RANKL induced activation of p-NF-kB-Luc and p-NFATc1-Luc reporters. In conclusion, we demonstrate for the first time that Cldn-18 is a novel regulator of BR that acts by a previously undescribed mechanism involving sequestration of ZO-2 in the cytoplasm to prevent its translocation to the nucleus where it modulates the transcription of RANKL target genes.

***Disclosures: Gabriel Linares**, None.*

1047

The Rac1 Exchange Factor Dock5 Is Essential for Bone Resorption by Osteoclasts. Virginie Vives[1], Mélanie Laurin[2], Gaelle Cres[3], Pauline Larrousse[3], Zakia Morichaud[4], Daniele Noel[5], Jean-François Coté[2], Anne Blangy*[6]. [1]CNRS UMR 5535, France, [2]Clinical Research Institute of Montreal, Canada, [3]CNRS UMR 5237, France, [4]CNRS UMR 5236, France, [5]Inserm U844, France, [6]CNRS UMR 5237 CRBM, France

During bone resorption, actin cytoskeleton in osteoclasts undergoes extensive reorganization while these cells polarize and assemble the sealing zone, the actin based adhesion organelle essential for resorption, typical of osteoclasts. RhoGTPase signaling pathways, as major regulators of actin organization and then of cell adhesion and morphology, have essential functions in osteoclast biology. It is of particular importance when podosomes rearrange into the sealing zone, the osteoclast characteristic adhesion structure necessary for bone resorption.

We previously identified Dock5 as an activator of Rac1 whose expression is strongly induced during osteoclastogenesis (Brazier et al., JBMR, 2006). We found that RAW264.7-derived osteoclasts in which Dock5 expression had been suppressed by shRNAs exhibited an important drop in Rac1 activity accompanied by a low mineral matrix resorption activity.

We used transgenic mice with disrupted Dock5 gene (Dock5-/-) to further examine its function in osteoclasts and the incidence on bone in vivo. In line with our previous observations, bone marrow cells from Dock5-/- mice differentiate into osteoclasts that have highly reduced levels of Rac1 activity and are unable to assemble sealing zones. Dock5-/- osteoclasts result defective for bone resorption, shown by absence of pit formation on bone and reduced release of collagen degradation products into the medium. Osteoclasts lacking Dock5 have adhesion and spreading defects, linked to reduced Rac1 and p130Cas activities. Quantitative RT-PCR showed that osteoclast characteristic genes are expressed normally in Dock5-/- osteoclasts, suggesting the differentiation process is mostly unaltered. Furthermore, M-CSF signaling is normal in the absence of Dock5. Dock5-/- mice are osteopetrotic with normal osteoclast numbers, confirming in vivo that Dock5 is essential for bone resorption but not for osteoclast differentiation. We identified a chemical inhibitor of Rac1 activation by Dock5 and showed that it hinders osteoclast resorbing activity. We found that Dock5 expression is mainly restricted to osteoclasts. In particular, it is asbent in bone forming osteoblasts.

Our findings characterize Dock5 as a novel essential actor in bone degradation, predominantly expressed in osteoclasts. Osteoclast resorbing activity is reduced in the presence of chemical inhibitors of Dock5. Taken together, our observations characterize Dock5 as a novel target to develop antiosteoporotic treatments.

***Disclosures: Anne Blangy**, None.*

1048

Gain of FoxO Function in Osteoclast Precursors and their Progeny Decreases Osteoclastogenesis and Increases BMD in Mice. Elena Ambrogini*, Shoshana Bartell, Li Han, Haibo Zhao, Aaron Warren, Randal Shelton, Xiaohua Qiu, Joseph Goellner, Charles O'Brien, Maria Jose Almeida, Stavros Manolagas. University of Arkansas for Medical Sciences, USA

Skeletal aging is characterized by a decrease in the number of both osteoblasts and osteoclasts and is associated with increased oxidative stress (OS) in mice. Work during the last few years has revealed that FoxO transcription factors are an important defense mechanism against OS and gain or loss of FoxO function in bone has been shown to dramatically alter skeletal homeostasis. Based on evidence that reactive oxygen species (ROS) are required for osteoclast generation and that global combined deletion of FoxO1, FoxO3 and FoxO4 in mice leads to an increase in ROS and osteoclast progenitor number, we investigated here whether FoxO activation in osteoclast progenitors is responsible for the age-related decrease in osteoclast number. To this end, we generated transgenic mice overexpressing FoxO3 in cells of the monocyte/macrophage lineage by crossing FoxO3-flox stop mice with LysM-Cre mice (FoxO3-FS;LysM-Cre). Expression of the FoxO3 transgene was demonstrated in whole vertebrae and bone marrow-derived mature osteoclasts from the FoxO3-FS;LysM-Cre mice; and it was absent in the liver or brain. Strikingly, these mice exhibited a significant increase in BMD, as well as an increase in cancellous bone volume at 3 month of age as determined by micro-CT, in both vertebrae and femora. FoxO3-FS;LysM-Cre mice also exhibited increased trabecular number and decreased trabecular separation. Consistent with the changes in bone, the serum levels of the resorption marker CTx decreased as compared to the controls. Moreover, the mRNA levels of the osteoclast markers TRAP and cathepsin K were decreased in vertebral bone while the osteoblast marker osteocalcin was unaffected. In line with these changes, bone marrow cultures established in the presence of RANKL and M-CSF from FoxO3-FS;LysM-Cre mice exhibited a 30% decrease in osteoclast progenitors and mature osteoclast formation, increased osteoclast apoptosis, but normal macrophage proliferation. Taken together with the results from several other models of genetic manipulation of ROS and FoxOs in cells of the osteoblast lineage, the demonstration of a suppressive effect of FoxOs on osteoclast generation and survival suggests that FoxO activation in response to OS plays a major role in the adverse effects of aging on both osteoblast and osteoclast number. Whether, FoxO3 overexpression interferes with the requirement of ROS for osteoclast generation, function, and survival or has ROS-independent effects requires future work.

***Disclosures: Elena Ambrogini**, None.*

1049

Silencing of PTH Receptor 1 in T Cells Blocks the Bone Catabolic Activity of Continuous PTH Treatment Through a TNF and CD40 Dependent Mechanism. Hesham Tawfeek*[1], Brahmchetna Bedi[2], Jau-Yi Li[2], Jonathan Adams[1], Tatsuya Kobayashi[3], M. Neale Weitzmann[1], Henry Kronenberg[3], Roberto Pacifici[1]. [1]Emory University School of Medicine, USA, [2]Emory University, USA, [3]Massachusetts General Hospital, USA

Hyperparathyroidism in humans and continuous PTH treatment (cPTH) in mice cause bone loss by regulating RANKL/OPG production by stromal cells (SCs) and osteoblasts. Recently, it has been reported that T cells are required for cPTH to induce bone loss as the binding of CD40L T cell costimulatory molecule to CD40 in SCs augments the sensitivity of SCs to PTH. However it is unknown whether direct PTH stimulation of T cells is required for cPTH to induce bone loss. Therefore, PTHR1 (PPR) expression in T cells was conditionally silenced by crossing PPR floxed ($PPR^{fl/fl}$) mice with LCK-Cre mice, a strain that expresses Cre recombinase in the early stages (DN2-DN3) of T cell development. Our data revealed that cPTH infusion (80 μg/kg/day for 2 weeks) caused trabecular and cortical bone loss (as measured by μCT), increased biochemical (serum CTX) and histomorphometric indices of bone resorption, and increased in vitro OC formation in control mice ($PPR^{fl/fl}$ and $PPR^{fl/+}$/Lck-Cre mice). By contrast, in $PPR^{fl/fl}$/Lck-Cre mice cPTH induced a significant increase in trabecular bone volume, did not cause cortical bone loss, and induced a smaller increase in bone resorption and in vitro OC formation. The $PPR^{fl/fl}$/Lck-Cre mice, but not the control mice, were protected against the bone catabolic effect of in vivo cPTH treatment due to impaired production of RANKL to OPG by SCs as a result of blunted expression of CD40. Further studies demonstrated that TNF treatment of SC induces CD40 expression and that T cells produce TNF in a PPR activation dependent manner. Moreover, cPTH treatment was neither able to induce bone loss, nor to regulate SC CD40 expression and RANKL/OPG production in $TNF^{-/-}$ mice. These findings indicate that TNF is a downstream mediator of PPR action in T cells. In support of this hypothesis we found that specific silencing of T cell TNF production by adoptively transferring $TNF^{-/-}$ T cell into T cell deficient nude mice blocked the capacity of cPTH treatment to induce bone loss, stimulate bone resorption, and augment CD40 expression and the RANKL/OPG ratio in SCs.

Indeed, mice lacking T cell TNF production had the same altered response to cPTH as mice lacking functional PPR in T cells. Altogether, these findings demonstrate that PPR signaling in T cells plays an essential role in cPTH induced bone loss by promoting SC osteoclastogenic activity through TNF and CD40 signaling.

***Disclosures: Hesham Tawfeek**, None.*

1050

Deletion of *PTH* Prevents the Premature Aging Phenotype of the *Klotho*-Null Mice. Xiuying Bai*[1], Dinghong Qiu[2], David Goltzman[3], Andrew Karaplis[4]. [1]Lady Davis Institute, Canada, [2]LDI, Canada, [3]McGill University Health Centre, Canada, [4]McGill University, Canada

Mice homozygous for the hypomorphic *Klotho* allele have a short lifespan and show biochemical and morphological features consistent with premature aging. In this study, we have used a mouse genetic approach to investigate *in vivo* the role of PTH in the metabolic and skeletal derangements arising from the absence of *Klotho*. To this end, we crossed mice heterozygous for the hypomorphic *Klotho* allele ($Kl^{+/-}$) to mice heterozygous for the null *Pth* allele and obtained mice homozygous for both the *Kl*-hypomorphic and the *Pth*-null ($Pth^{-/-}/Kl^{-/-}$). Mice were sacrificed and serum and tissues were procured for analysis and comparison to *WT*, $Pth^{-/-}$ and $Kl^{-/-}$ controls.

From 4 weeks onward, $Pth^{-/-}/Kl^{-/-}$ mice were clearly distinguishable from *Klotho*-null mice and exhibited a striking phenotypic resemblance to the $Pth^{-/-}$ controls. The life span of the double mutants increased from 10 weeks to 6 months (as long as they have been observed) as did their body weight, in parallel to the wild type and $Pth^{-/-}$ mice. Serum analysis for calcium, phosphorus, ALP activity, $1.25(OH)_2D_3$, and creatinine confirmed the biochemical similarity between the $Pth^{-/-}/Kl^{-/-}$ and $Pth^{-/-}$ mice and their distinctness from the $Kl^{-/-}$ controls. Interestingly, the extremely high serum FGF23 levels observed in the *Klotho*-null mice were supressed in the double knock-out mice, similar to the serum levels in the wild type mice.The characteristic skeletal changes associated with the absence of *Klotho* were also dramatically converted by the concurrent deletion of *Pth*. Moreover, widespread soft tissue calcification characteristic of the $Kl^{-/-}$ mice was absent in the double mutants.

In summary, our findings substantiate *in vivo* the essential role of PTH in the *Klotho*-null phenotype as its ablation fully reverts the complete spectrum of biochemical and skeletal alternations arising from lack of *Klotho*.

***Disclosures: Xiuying Bai**, None.*

1051

Role of the Transcriptional Co-Activator CITED1 in Bone and its Effect on Anabolic Actions of PTH. Hila Bahar*[1], Jun Guo[2], Dehong Yang[3], Rajaram Manoharan[4], Toshi Shioda[5], Mary Bouxsein[6], F. Richard Bringhurst[2]. [1]MGH & HMS, USA, [2]Massachusetts General Hospital, USA, [3]Endocrine Unit, Massachusetts General Hospital, USA, [4]Orthopedic Biomechanics Laboratory, Beth Israel Deaconess Medical Center, USA, [5]Molecular Profiling Laboratory (T.S.), Massachusetts General Hospital Cancer Center, USA, [6]Beth Israel Deaconess Medical Center, USA

CITED1 is a transcriptional co-activator that interacts directly with CBP/p300 and is capable of enhancing TGF-beta and estrogen-dependent transcription and inhibiting beta-catenin-dependent transcription. CITED1 mRNA expression is rapidly and transiently upregulated by PTH in cultured osteoblasts (Obs) in a manner dependent on cAMP-signaling. Also, the cAMP-mediated Ob-differentiating effect of PTH is selectively suppressed by CITED1 in vitro. Histological observations supported by DEXA measurements indicated that 8-week old CITED1 global knockout C57BL/6 mice (KO) exhibit mild osteopenia, mainly in the primary spongoisa. MicroCT analysis showed a significant reduction in trabecular (Tb) bone volume in KO vertebra, a similar tendency in the Tb bone of the femur and no difference in cortical bone compared to wild type mice (WT). Our is to study the role of CITED1 in PTH's anabolic action on bone. Eight week-old CITED1 KO and WT mice were injected daily with vehicle (VEH), 80 ug/kg of hPTH(1-34) (PTH) or 1600 ug/kg of cAMP-selective PTH analog [G1,R19]PTH(1–28) (GR) for 4 weeks before analysis of blood and bone. MicroCT analysis showed no differences between KO vs. WT VEH-treated controls. PTH significantly augmented both Tb bone at the distal femur (BV/TV, Tb.Th) and cortical thickness at the mid-femur in KO and WT mice, but the overall effect was reduced in KO mice. There was no effect of GR in either WT or KO. BMD of the total body and femur (measured by pDXA) were similar in vehicle-treated KO vs. WT mice. PTH significantly increased BMD in both KO (8%-total body, 10%-femur) and WT (9%, 20%) the increase was significantly less in KO than in WT. GR treatment had no effect on BMD in either WT or KO except for the distal femur that was significantly higher in WT mice (11%). Histological observations were consistent with microCT and pDXA results. Serum P1NP was significantly increased in PTH-treated mice and, to lesser extent, in GR-treated mice in both KO and WT vs. VEH. Serum level of CTX was increased similarly in PTH- and GR-treated WT mice and was not significantly altered in the PTH- and GR-treated KO mice. We conclude that the anabolic effect of PTH and particularly that of the cAMP-selective analog GR, seen in trabecular bone of WT mice is diminished in mice lacking CITED1. CITED1 may be required for a full anabolic response of trabecular bone to PTH.

***Disclosures: Hila Bahar**, None.*

1052

Anabolic Effects of Intermittent PTH Are Impaired in MAP Kinase Phosphatase-1 Knockout Mice. Manshan Xu*, Li Ma, Shilpa Choudhary, Olga Voznesensky, Douglas Adams, Lawrence Raisz, Carol Pilbeam. University of Connecticut Health Center, USA

Mitogen activated protein (MAP) kinase phosphatase-1 (MKP-1) can dephosphorylate and inactivate MAP kinases, including ERK, p38, and JNK. *Mkp-1* is an immediate early gene, expressed in osteoblasts, and upregulated by many factors, including PTH. The aim of this study was to investigate the effect of *mkp-1* deletion on the anabolic responses to intermittent PTH. We used 4-mo old male mice in a C57BL/6 background with global knockout (KO) of MKP-1 developed by Lexicon Genetics. Mice (n=8-11) were injected subcutaneously with vehicle or PTH (80 µg/kg, 1-34 hPTH) daily for 22 days. Percent change in femoral bone mineral density (BMD) was measured by DXA *in vivo*. Mice were euthanized 3 h after the last injection. Trabecular morphometry within the metaphyseal region of the distal femur and cortex in the femoral shaft were measured by µCT. Blood was obtained by heart puncture at time of euthanasia. Tibiae were extracted for RNA. PTH significantly increased femoral BMD 11% in WT mice and 5% in KO mice, but the difference between WT and KO mice was not statistically significant. By µCT, PTH significantly increased trabecular bone volume per total volume (BV/TV) and trabecular thickness (TbTh) 59% and 33%, respectively, in WT mice compared to vehicle-treated controls. Trabecular spacing (TbSp) and trabecular number (TbN) were similar in vehicle- and PTH-treated WT mice. In MKP-1 KO mice, PTH did not increase BV/TV or TbTh relative to vehicle-treated controls. In addition, there was a trend for TbSp to be increased 10% and TbN to be decreased 10% in PTH-treated KO mice relative to vehicle-treated controls. Following PTH treatment, BV/TV, TbTh, and TbN were all significantly lower in KO compared to WT mice, whereas TbSp was significantly higher. Analysis by µCT also showed that PTH stimulated significant increases (20%) in femoral cortical bone thickness and area in WT but not KO mice. PTH increased serum markers of formation (P1NP) and resorption (TRAP 5b and CTX) and gene expression for alkaline phosphatase and RANKL / OPG similarly in WT and KO mice. These data indicate that the anabolic effects of intermittent PTH are impaired by the deletion of *mkp-1* and suggest an important role for MAP kinases in the anabolic effects of intermittent PTH.

***Disclosures: Manshan Xu**, None.*

1053

Signaling Mechanisms Underlying Prolonged Calcemic Actions of Long-Acting PTH Analogs. Akira Maeda*[1], Makoto Okazaki[2], Jun Guo[1], Henry Kronenberg[1], John Potts[1], Thomas Gardella[1]. [1]Massachusetts General Hospital, USA, [2]Chugai Pharmaceutical. Co., Ltd., Japan

We recently reported that high-affinity, N-terminally modified PTH peptide analogs, e.g. and M-PTH(1-34) (M=Ala1,Aib3,Gln10,Har11,Ala12,Trp14,Arg19), produce prolonged calcemic responses in mice following single injection, as compared to PTH(1-34) (Okazaki et al. P.N.A.S. 2008). The unique feature appears to be a prolonged response at constant amplitude, rather than a brisk initial response that subsides over time. The analogs could thus be useful as treatments for hypoparathyroidism. The prolonged responses are not simply explainable by pharmacokinetics, but the underlying molecular and cellular mechanisms, and how they might differ from those mediating the calcemic actions of native PTH, are not well understood. To address these questions, we first compared the blood Ca++ responses induced in normal mice by M-PTH(1-34) at a dose of 10 nmole/kg to those induced by hPTH(1-34) at the higher dose of 100 nmole/kg. We found that the high dose of hPTH(1-34) produced a brisk calcium rise that peaked at two-hours post-injection, and declined to basal by six hours. The M-PTH(1-34) response showed a slightly lower maximum at two-hours, but the elevated levels were maintained for at least four hours, and did not return to basal until 24 hours post injection. To next address the signaling pathways involved, we compared the calcemic actions of M-PTH(1-28), which signals through both the cAMP/PKA and IP3/PKC pathways, to those of Trp1-M-PTH(1-28), which signals efficiently through the former, but not the latter pathway. To compensate for the three-fold lower binding affinity of the Trp1 analog versus that of M-PTH(1-28), the peptides were injected at doses of 20 nmole/kg and 60 nmole/kg, respectively. The resulting blood Ca++ response profiles were largely overlapping, and each was sustained, as compared to that of hPTH(1-34). We further utilized mice having the endogenous PTHR allele homozygously replaced by one encoding a PTHR mutant (DSEL) that is deficient for PLC signaling. These mice produced Ca++ responses to M-PTH(1-28) that were sustained, equivalently to those observed in wild-type mice. Overall, the results suggest that 1) the new long-acting PTH ligands induce increases in blood Ca++ by mechanisms which differ from those utilized by PTH(1-34); and 2) the sustained responses are achieved mainly via the cAMP/PKA signaling pathway. We hypothesize that the mechanisms differ at the level of receptor-interaction and signaling in target cells. In support of this, we found that cAMP levels in homogenates of kidneys obtained from wild-type mice at times after injection with M-PTH(1-34) were elevated for longer times, as compared to with PTH(1-34). Defining more precisely the PTHR signaling and trafficking pathways used by these long-acting PTH analogs in target tissues should further our capacity to treat PTH-related diseases.

***Disclosures: Akira Maeda**, Chugai Pharmaceutical Co. Japan, 2*

1054

Intact Neuropeptide Y Circuit Required for Full Anabolic Response to Parathyroid Hormone in Mice. Natalie Sims[1], Ingrid Poulton[2], Susanna Rossotti[3], Leah Worton[4], Rena Hirani[5], Herbert Herzog[6], Edith Gardiner*[4]. [1]St. Vincent's Institute of Medical Research, Australia, [2]St Vincent's Medical Research Institute, Australia, [3]UQ Diamantina Institute, Australia, [4]University of Washington, USA, [5]Australian Institute for Bioengineering & Nanotechnology, Australia, [6]Garvan Institute of Medical Research, Australia

Neuropeptide Y (NPY) suppresses bone formation via a neural circuit involving both hypothalamic Y2 receptors and osteoblastic Y1 receptors. Germline Y1 or Y2 gene deletion results in enhanced bone formation, and osteoblastic Y1 expression is absent in both Y1 and Y2 knockout (KO) mice. Parathyroid hormone (PTH), a potent anabolic agent for bone, can induce Y1 expression in cultured murine osteoblastic cells, indicating cross-talk between NPY and PTH receptors in bone-forming cells. The present study investigated the interaction between these two anabolic regulatory pathways in the Y2KO mouse model. Male 12 week-old mice were treated with hPTH(1-34) (0.05 mg/kg body weight, 5 days/week for 3 weeks, n=10/group) by subcutaneous injection, with intraperitoneal calcein (10 mg/kg) at days 10 and 19 for histomorphometric analysis of trabecular bone in proximal tibia. As anticipated, PTH exposure significantly increased trabecular bone volume and trabecular thickness in wild type (WT-PTH) mice compared to vehicle (WT-veh) controls; unexpectedly however, neither parameter was significantly affected by PTH treatment in Y2KO-PTH mice. Osteoblast, osteoid and osteoclast surfaces were significantly and similarly elevated in PTH-treated mice of both genotypes (3.1-, 2.9- and 1.8-fold, respectively). PTH treatment also increased single calcein-labeled surface 1.3- to 1.5-fold in WT and Y2KO mice. In contrast,double calcein-labeled surface was significantly reduced (by 53%) in Y2KO-PTH but was not significantly modified in WT-PTH mice. Furthermore, while mineral apposition rate and bone formation rate were significantly increased (1.5- and 1.4-fold) in WT-PTH, there was no change in this parameter in Y2KO-PTH. Y2KO-PTH mice also demonstrated a significant increase (1.7-fold) in osteoid thickness; a change that was not observed in WT-PTH mice. Consistent with these results, although mineralization lag time was significantly increased in both PTH-treated groups, the effect was significantly greater in the Y2KO mice (2.9-fold increase in Y2KO vs 1.8-fold in WT). In summary, genetic ablation of Y2 receptor impaired the response of bone to anabolic intermittent administration of hPTH(1-34), leading to an accumulation of osteoid and longer mineralization lag time in the Y2-deficient animals. The results suggest that in addition to modulating mesenchymal progenitor cell populations, disruption of NPY signaling may also inhibit PTH-stimulated mineralization by mature osteoblasts.

***Disclosures: Edith Gardiner**, None.*

1055

Greater Baseline Lean Mass is Associated With Increased Hip Fracture Risk in Elderly Women: The Framingham Study. Alyssa Dufour*[1], Marian Hannan[2], Kerry Broe[3], Xiaochun Zhang[1], Douglas Kiel[1], Robert McLean[4]. [1]Hebrew SeniorLife, USA, [2]HSL Institute for Aging Researchand Harvard Medical School, USA, [3]Hebrew Senior Life, USA, [4]Hebrew SeniorLife, Harvard Medical School, USA

Reduced muscle mass (sarcopenia) is associated with weakness and poor functioning in elders, yet few data exist on its relation with hip fracture. We previously showed that greater leg lean mass was unexpectedly associated with increased hip fracture risk among older women in the Framingham Original Cohort. Leg lean mass, however, does not account for other muscles that may influence fracture risk or account for body size, and thus may not reflect whether an individual has adequate muscle mass to prevent falls that lead to fracture. As no accepted criteria exist for sarcopenia, we examined whether several measures of sarcopenia predicted hip fracture in women of the Framingham Original Cohort. We hypothesized that higher muscle mass would be associated with lower hip fracture risk even after adjusting for confounders. 419 women with baseline (1992-93) whole body DXA scans (Lunar DPX-L) were followed for incident hip fractures through 12/31/2007. Continuous measures of sarcopenia (lower value=less mass) calculated from DXA scans included: total body lean mass (LM; kg), appendicular lean mass (aLM; arm + leg lean mass, kg); relative lean mass accounting for height (rLM; aLM/ht^2; kg/m^2) as well as the categorical low rLM (poor mass) as rLM£5.67 kg/m^2. Cox proportional hazards regression was used to calculate hazard ratios (HR) and 95% confidence intervals (CI) estimating the risk of hip fracture for each unit increase in LM, aLM and rLM, as well as the risk for those with low rLM vs. those without. Initial analyses adjusted for baseline age (y), weight (lbs), height (in), and physical activity, followed by adjustment for femoral neck bone mineral density (BMD, g/cm^2). Mean age at baseline was 78 y (range 70-92 y) and 59 hip fractures occurred over median follow-up of 10.4 y. Each kg increase in LM and aLM was associated with a 26 and 29% increased hip fracture risk, respectively (Table). The relation was a bit stronger for rLM, with a 1 unit increase associated with an 84% higher fracture risk, however low rLM was not associated with hip fracture risk. The CIs included the null after BMD adjustment, yet HRs were only slightly attenuated. These results confirm our previous unexpected findings of a direct association between lean mass and risk for hip fracture. Future studies should use more precise assessments of physical activity and consider the potential role of sarcopenic obesity in the relation between muscle mass and hip fracture.

Multivariable-adjusted HRs and 95% CIs for risk of hip fracture for different sarcopenia definitions in women from the Framingham Original Cohort

Sarcopenia measure	Mean (SD) or %	HR (95% CI)	
		Model 1*	Model 1 + BMD
LM (kg)	16.31 (2.28)	1.26 (1.02, 1.54)	1.20 (0.97, 1.48)
aLM (kg)	14.96 (2.01)	1.29 (1.03, 1.63)	1.23 (0.97, 1.56)
rLM (kg/m^2)	6.72 (0.77)	1.84 (1.11, 3.03)	1.62 (0.97, 2.72)
Low rLM (yes vs. no)	7.16%	0.99 (0.33, 3.0)	1.05 (0.35, 3.17)

*Adjusted for baseline age, weight, height and physical activity

Table

***Disclosures: Alyssa Dufour**, None.*

1056

Higher Total Protein Intake Associated With Greater Lean Mass and More Favorable Ratio of Low Lean-to-Fat Mass Ratio in Middle-Aged Men and Women: The Framingham Osteoporosis Study. Shivani Sahni*[1], Robert McLean[2], Douglas Kiel[3], Kerry Broe[4], Katherine Tucker[5], L Adrienne Cupples[6], Marian Hannan[7]. [1]Hebrew SeniorLife, Institute for Aging Research, Harvard Medical School, USA, [2]Hebrew SeniorLife, Harvard Medical School, USA, [3]Hebrew SeniorLife, USA, [4]Hebrew Senior Life, USA, [5]Northeastern University, USA, [6]Boston University School of Public Health, USA, [7]HSL Institute for Aging Researchand Harvard Medical School, USA

Protein intake influences muscle mass in younger persons and athletes. Aging is associated with body composition changes, including increases in fat mass (FM) and decreases in lean mass (LM). In one study, protein at RDA level appeared to preserve LM across 3-y in older adults (ages 70-79y). In another study protein was associated with reduced FM among obese subjects. It is unclear what the associations between protein intake and LM (as well as FM) may be in a population of middle-aged men and women. Therefore, we evaluated associations of total protein intake with measures of LM in the Framingham Offspring Cohort. 2,272 participants had a food frequency questionnaire (from either 1995-98 or 1998-2001) and a whole body DXA scan using a Lunar DPX-L (1996-2001). Quartiles of total protein intake (g/day) were created, adjusting for total energy intake (residual method). DXA scans were used to derive leg LM (both legs in kg) and total LM (kg). Participants were also classified (y/n) as having a low lean-to-fat mass ratio (low lean: fat; the lowest sex-specific quintile of total LM to FM ratio). Analysis of covariance was used to compare the least squares-mean leg LM and total LM among quartiles of protein intake and test for a linear trend. Logistic regression was performed to calculate the odds ratio (OR) and 95% confidence intervals (CI) for low lean:fat in each of the upper 3 protein quartiles compared to the lowest quartile (Q1). All models were adjusted for sex, age, height, and total energy intake. Models for leg LM and total LM were additionally adjusted for leg % fat and total % fat, respectively.

Mean age was 55 y (SD=9.6 y, range: 26-86y). Leg LM averaged 14.04 $\pm$ 3.4 kg and total LM averaged 43.28 $\pm$ 10.2 kg. Higher protein intake was associated with greater leg LM (P trend$<$0.001) and total LM (P trend= 0.03, table 1). Those in protein intake quartiles 3 and 4 had 30% (95%CI 0.51-0.96) and 46% (95%CI 0.40-0.73) lower odds of low lean:fat compared to those in Q1, and the trend across quartiles was statistically significant (P$<$0.01).

Our results suggest that higher protein intake is associated with greater leg and total LM in middle-aged men and women. Further, higher protein intake was associated with lower risk of having a low lean-to-fat mass ratio. Future studies should examine the effect of different types of protein intake on age-related loss of LM. As in the elderly participants of the Health ABC cohort, perhaps improving protein intake, even in middle-aged men and women, may help in preserving LM, across the adult age spectrum.

Table 1. Least squares-adjusted leg and total LM, and ORs (95% CIs) for low lean:fat[1], for quartiles of protein intake in middle-aged men and women of the Framingham Offspring Study.

	n	Protein Intake Quartile				*P* trend
		Q1 (low)	Q2	Q 3	Q 4 (high)	
Median protein intake (g/d)		60	66	75	96	
Lean Mass, Mean ± SE[2]						
Leg Lean Mass (Kg)	2791	14.07 ± 0.06[a]	14.31 ± 0.06[b]	14.30 ± 0.06[b]	14.40 ± 0.06[b]	0.0003
Total Lean Mass (Kg)	2266	44.51 ± 0.17	44.68 ± 0.17	44.79 ± 0.17	45.01 ± 0.17	0.03
Low Lean:Fat[1] (%)		15.9	17.6	21.2	25.1	
Low Lean:Fat, OR (95%CI)	1813	1.0	0.90 (0.66-1.23)	0.70 (0.51-0.96)	0.54 (0.40-0.73)	0.007

[1]Lowest sex-specific quintile of the ratio of total lean: fat mass
[2]Means with different superscript are significantly different (*P*≤0.05)

Table 1

***Disclosures: Shivani Sahni**, None.*

1057

Association between Diabetes and QCT Measures of Bone Strength and Prevalent Vertebral Fracture: The Framingham Study. Elizabeth Samelson*[1], Mary Bouxsein[2], Serkalem Demissie[3], Blaine Christiansen[4], Kerry Broe[5], Xioachun Zhang[6], R. Manoharan[7], J. D'Agostino[8], Thomas Lang[9], L. Adrienne Cupples[3], Douglas Kiel[6]. [1]Hebrew SeniorLife, Harvard Medical School, USA, [2]Beth Israel Deaconess Medical Center, USA, [3]Boston University School of Public Health, USA, [4]University of California - Davis Medical Center, USA, [5]Hebrew Senior Life, USA, [6]Hebrew SeniorLife, USA, [7]Beth Israel Deaconness Medical Center, USA, [8]Center for Advanced Orthopedic Studies, Beth Israel Deaconess Medical Center, USA, [9]University of California, San Francisco, USA

Older adults with type 2 diabetes mellitus (DM) have greater BMD yet increased risk of fracture, particularly at peripheral sites, compared to those without DM. At the spine, DM has been shown to increase, decrease or have no association with BMD and fracture. It is difficult to use DXA areal BMD (aBMD) to compare fragility at the spine in persons with and without DM as DXA overestimates aBMD in individuals with larger bones, degenerative conditions and aortic calcification. Moreover, DXA cannot distinguish trabecular bone, the compartment most affected by DM, from cortical bone, and does not allow measures of bone geometry that may be compromised in DM. Some previous studies relied on self-reported DM, clinically diagnosed VF, or were limited to highly selective populations. We compared volumetric QCT measures of the spine and vertebral fracture (VF) prevalence in community-dwelling adults by DM status.

Participants included all 209 individuals with DM (cases) and 418 individuals without DM (controls), selected by stratified random sampling by 5-yr age and sex groups, from 3,479 participants of the Framingham Study who had QCTs in 2002-06. DM was defined by fasting plasma glucose level >126 mg/dl or use of insulin or oral hypoglycemic agents. Custom software (T. Lang, UCSF) was used to measure trabecular, cortical, and integral vBMD, and average cross-sectional area (CSA) of L3. Compressive strength was estimated from CSA and integral vBMD. VF was defined as semi-quantitative grade >1 (mild) assessed from CT lateral scanograms. Regression models were used to compare mean bone measures and prevalence and severity of VF according to DM status, adjusted for age and weight.

Mean age was 64 years, range 40-87. Integral vBMD was 6% higher in women with DM, but trabecular and cortical vBMD, CSA, and compressive strength were similar in cases and controls (TABLE). In men, no differences in bone measures were seen by DM status. Prevalence, number, and severity of VF did not differ by DM status in women or men, however, frequency of persons with >2 VF (7%) or > grade 2 (moderate-severe) VF (3%) was low.

We did not find increased fracture at the spine in persons with DM, and QCT measures of bone strength were similar (or somewhat better) for those with DM. Increased fracture at peripheral sites previously reported for those with DM, but not at the spine in our study, suggests that DM may exert site-specific effects on skeletal fragility.

TABLE. Mean QCT measures of vBMD, cross-sectional area, and compressive strength and fracture prevalence at the spine, adjusted for age and weight, according to diabetes status in women and men in the Framingham Study

	Women			Men		
	Diabetes N=100	No Diabetes N=198	P	Diabetes N= 109	No Diabetes N=220	P
Cross-sectional area (cm^2)	10.181	10.371	0.31	12.389	12.625	0.13
Trabecular vBMD (g/cm^3)	0.140	0.130	0.11	0.137	0.137	0.96
Integral vBMD (g/cm^3)	0.186	0.174	0.04	0.184	0.182	0.71
Cortical vBMD (g/cm^3)	0.230	0.225	0.17	0.247	0.241	0.24
Compressive strength (Newtons)	3889	3705	0.20	4675	4722	0.78
Vertebral fracture (%)	13	18	0.21	22	29	0.52

Table

***Disclosures: Elizabeth Samelson**, None.*

1058

Multi-Phenotype Genome-Wide Association Analysis (GWAS) on both BMD and Glycemic Traits Identified Novel Pleiotropic Genes that Affected Bone Metabolism and Glucose Homeostasis in Caucasian Populations. Yi-Hsiang Hsu*[1], Xing Chen[2], James Meigs[3], L. Adrienne Cupples[4], David Karasik[5], Douglas Kiel[5]. [1]Hebrew SeniorLife & Harvard Medical School, USA, [2]Harvard School of Public Health, USA, [3]Massachusetts General Hospital & Harvard Medical School, USA, [4]Boston University School of Public health, USA, [5]Hebrew SeniorLife, USA

Epidemiological studies suggest that T2DM patients are at increased risk of osteoporotic fractures. A recent rodent study showed that osteocalcin was involved in endocrine regulation of glucose homeostasis, which provided directly evidence linking the skeleton to the pathogenesis of diabetic complications. However, the underlying mechanisms of how the skeleton interacts with glucose homeostasis remain largely unclear. Significantly genetic correlations for BMD with fasting glucose and insulin in the Framingham Study indicates that shared genetic determinants may regulate both bone and energy metabolism. To identify pleiotropic genes associated with both BMD and glycemic traits, we performed a multiple-phenotypes genome-wide association analysis in the Framingham Study by modeling both BMD and glycemic phenotypes simultaneously using our newly developed approach, empirical-weighted linear-combined test statistics (eLC). eLC is a method to directly combine correlated test statistics with a weighted sum of univariate test statistics to maximize the heritability of the overall association tests. From simulation, our eLC approach has outperformed the simple look-up on the overlaps among uni-variate GWAS and traditional methods (such as GEE and PCA). BMD at the lumbar spine (LS) and femoral neck (FN) was measured by DXA. Fasting plasma insulin, proinsulin (radioimmunoassays) and glucose levels (hexokinase) were measured. Affymetrix 550K Gene chips were genotyped and 2.5 millions SNPs were imputed based on HapMap CEU phase II panel. A total of 3,569 Framingham participants (Caucasian with mean age of 61 years old; 1,531 Men and 2,038 women) were analyzed. We first performed univariate GWAS on these 5 phenotypes using linear mixed effects models with adjustment for age, sex, height, weight, ancestral genetic background and pedigree structure. We then applied the eLC method to combine test statistics from univariate analyses. P-values of the multi-phenotype association tests were estimated by permutation. Several associations achieved GWS level ($p < 5x10^{-8}$), i.e. SNPs in or near *TMEM16D, PGAP1, IQCJ* genes. Several suggestive GWS ($p < 5x10^{-6}$) loci were also found, i.e. *KLF14, CHIN, TNFRSF11B, TGFBI, ITGA1, and NPSR1*. Pathway analyses suggested significant clustering of genes involved in cell-cell connection and endocrine metabolism for T1DM. These top associated SNPs are being further evaluated in GEFOS (n=32,000) and MAGIC (n=36,610) consortia. In conclusion, our results reveal novel pleiotropic genes to further elucidate the link between the skeleton and energy metabolisms.

***Disclosures: Yi-Hsiang Hsu**, None.*

1059

Genome-wide Association In the Rotterdam Study Implicates the 16p21 Locus As Determinant of Osteoporotic Vertebral Fractures. Ling Oei*[1], Karol Estrada[2], Martha C. Castano-Betancourt[3], Marjolein van der Klift[4], Hannneke Kerkhof[3], Albert Hofman[3], Huibert Pols[2], Lisette Stolk[3], Joyce B. van Meurs[3], M. Carola Zillikens[3], Andre Uitterlinden[5], Fernando Rivadeneira[2]. [1]Erasmus Medical Center, Nld, [2]Erasmus University Medical Center, The netherlands, [3]Erasmus MC, Netherlands, [4]Erasmus, Netherlands, [5]Rm Ee 575, Genetic Laboratory, The netherlands

Risk for vertebral fractures (VFx), the most common osteoporotic fractures, is a heritable complex trait. No genome-wide association studies (GWAS) searching for genetic susceptibility factors for VFx have been reported to date. The aim of this study was to perform a GWAS for VFx in a large population-based study of Dutch individuals (age >55 years). Radiographs of the thoracolumbar spine were scored for presence of osteoporotic VFx using the McCloskey/Kanis method. Genetic data was available in 329 VFx cases and 2666 controls. We tested 2,543,887 imputed (HapMap CEU release 22, build 36) SNPs for association with risk for VFx using a logistic regression model (MACH2DAT) adjusted for age, sex, and admixture principal components. At a genome-wide significant α-level (GWS) of $5x10^{-8}$, the design has 0.80 power to detect risk effect sizes (OR) of 1.7 to 2.4 for minor allele frequencies (MAF) of 0.20 to 0.05, respectively. A SNP on chromosome 16p21 (MAF=0.10) was associated at GWS level ($P=2x10^{-8}$) with an increased risk for VFx. Heterozygous carriers of the minor allele have 1.7-fold (95%CI: 1.3-2.2) and homozygous carriers 5.8-fold (95%CI: 2.6-12.6) increased risk compared to non-carriers. The VFx-associated SNP maps in a region previously found associated with lumbar spine BMD (LS-BMD) in a meta-analysis of 19,125 individuals, yet represents an independent signal from the reported BMD SNP (LD $r^2=0.002$). The VFx-associated SNP was not associated with LS-BMD. *FOXC2* is a strong candidate gene in the region mapping ~200 Kb upstream from the associated SNP. *FOXC2* is a transcription factor shown to be essential for axial skeletogenesis in mice, highly expressed in human bone tissue and involved in osteoblast differentiation through activation of canonical Wnt-β-catenin signals. Inactivating mutations affecting the FOX gene cluster cause severe vertebral malformations in humans. In conclusion, our findings implicate the 16p21 locus as a strong determinant for osteoporotic VFx. Pleiotropic effects of *FOXC2* are potentially driving these associations with LS-BMD and VFx. Replication within the GEFOS/GENOMOS consortia is currently underway to confirm this finding.

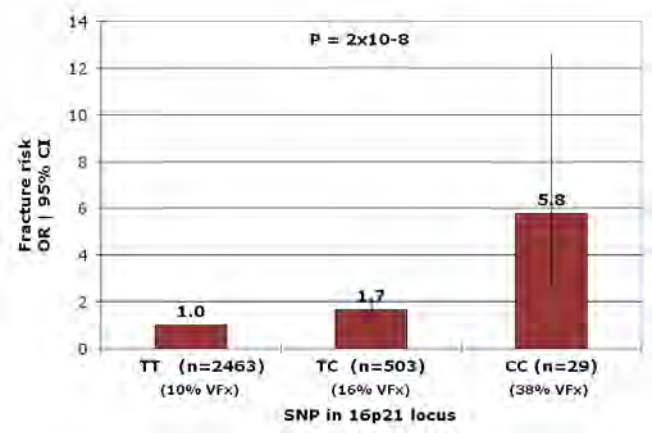

Vertebral fracture risk by 16p21 SNP genotype groups

***Disclosures: Ling Oei**, None.*

1060

Meta-analysis of Genome-Wide Association Study (GWAS) Identifies Several Genes for Hip Bone Geometry in Caucasians: The Genetic Factors for Osteoporosis (GEFOS) Consortium. Yi-Hsiang Hsu[1], Thomas Beck[2], Suzanne J Brown[3], Jane Cauley[4], Serkalem Demissie[5], Karol Estrada[6], Nicole Glazer[7], Stephen Kaptoge[8], Douglas Kiel[9], Brent Richards[10], Fernando Rivadeneira[6], John Robbins[11], Nicole Soranzo[12], Tim Spector[12], Elizabeth Streeten[13], Andre Uitterlinden[14], Scott Wilson[15], Laura Yerges-Armstrong[16], Carola Zillikens[17], David Karasik*[9]. [1]Hebrew SeniorLife & Harvard Medical School, USA, [2]Johns Hopkins Outpatient Center, USA, [3]Sir Charles Gairdner Hospital, Australia, [4]University of Pittsburgh Graduate School of Public Health, USA, [5]Boston Univ. SPH, USA, [6]Erasmus University Medical Center, The netherlands, [7]University of Washington, USA, [8]University of Cambridge Bone Research Group, United Kingdom, [9]Hebrew SeniorLife, USA, [10]King's College London & McGill University, United Kingdom, [11]University of California, Davis Medical Center, USA, [12]King's College London, United Kingdom, [13]University of Maryland School of Medicine, USA, [14]Rm Ee 575, Genetic Laboratory, The netherlands, [15]Sir Charles Gardner Hospital, Australia, [16]University of Maryland, USA, [17]Erasmus MC, Netherlands

Hip geometry has been shown to be an important predictor of fracture. We performed meta-analysis in several large GWAS studies to identify genes associated with proximal femoral geometry phenotypes. We analyzed femoral neck length (FNL), neck-shaft angle (NSA), and narrow neck section modulus (NNZ) estimated by hip structure analysis (HSA) algorithms from DXA scans. GWAS results from the Rotterdam Study (RS, n=4102), Framingham Osteoporosis Study (FOS, n=3414), TwinsUK Study (TUK, n=3815 women), Amish Family Osteoporosis Study (n=806), Erasmus Rucphen Family Study (ERF, n=758), and Cardiovascular Health Study (n=337), were meta-analyzed, with a total of 9132 women and 4100 men (age range 16-93 years).

In each cohort, ~2.5 mil autosomal SNPs were imputed from the International HapMap Project CEU reference panel II, and sex-specific and sex-combined association analyses were performed under an additive model adjusted for age, age^2, height, and BMI. A weighted Z statistic-based fixed-effect meta-analysis implemented in METAL was performed. Since the genomic inflation factor λ_{GC} ranged from 0.996 to 1.049 across different traits, we applied a conservative double-genomic control correction. The genome-wide significance threshold was set at $p<5x10\text{-}8$.

Most significant associations - with FNL in both sexes - were observed over a long region on chromosome 10q24, where cytochrome P450 family member *CYP17A1* is mapped. As follows from the Table, suggestive associations were found between transmembrane proteins *TPRA1*/*GPR175* and NSA and *TMEM38B* and FNL. Also, several sex-specific associations were found, such as an association between forkhead box Q1 (*FOXQ1*) with NSA, and OR4K14 with NNZ, both in women.

In conclusion, we found associations between hip geometry measures and genes belonging to several pathways, most prominently *CYP17A1*, which is located in a previously reported QTL linked to femoral neck cross-sectional geometry. This enzyme catalyzes key steps in human adrenal steroid biosynthesis, therefore participates in sexual development earlier in life. Further replication in additional independent samples is underway to maximize power as well as to determine the relation with hip fractures.

Chr	SNP	Closest Gene	Phenotype	P_value (female)	P_sex	P_value (sexes combined)
3	rs10934815	GPR175	NSA	5.98E-06	0.8294	3.18E-07
6	rs845896	FOXQ1	NSA	1.85E-07	0.04137	2.0E-06
9	rs1516893	TMEM38B	FNL	3.26E-06	0.5708	4.03E-07
10	rs264857	C10orf26/CYP17A1	FNL	1.10E-06	0.7673	**2.07E-08**
14	rs1953999	OR4K14	NNZ	6.78E-07	7.6E-05	n.s.

P_sex = significance of heterogeneity between sexes; n.s.: P > 10-5

Table

***Disclosures: David Karasik**, None.*

1061

Osteocyte-Independent Mechanotransduction of Interstitial Fluid Flow. Ronald Kwon*, Diana Meays, Alexander Meilan, Natalie Kardos, John Frangos. La Jolla Bioengineering Institute, USA

Skeletal adaptation to mechanical loading has long been hypothesized to involve the stimulation of osteocytes by interstitial fluid flow (IFF). Recently, Tatsumi et al. generated mice possessing a diphtheria toxin (DT) receptor transgene driven by the DMP1 promotor (DMP1-DTR), allowing for inducible osteocyte ablation by administration of DT [1]. While these authors found that osteocyte ablation conferred resistance to bone loss upon hindlimb suspension (HLS), mechanotransduction upon reloading was normal, giving rise to the intriguing possibility that loading-induced IFF may be sensed by cells other than osteocytes. We recently developed a microfluidic system for modulating femoral intramedullary pressure (ImP) in alert mice, and showed that the generation of dynamic ImP significantly increased IFF within lacunae and protected against bone loss in mice subjected to HLS [2]. Using this system, we investigated the effects of osteocyte ablation on IFF-induced adaptation. 16wk F wildtype (WT) and transgenic (Tg) DMP1-DTR mice were subjected to HLS for 14d. One limb was exposed to dynamic ImP/IFF (3min/d, 5Hz, peak flow rate: 5uL/s); the other limb served as a sham control. Mice were administered DT (10 or 50ug/kg) 1d prior to HLS and a booster 7d later. BMD and structural indices were quantified at the lesser trochanter using pQCT and uCT [2]. Osteocyte ablation was confirmed by observing empty lacunae (~30%) in H&E-stained sections from Tg mice. In both WT and Tg mice, we observed significant gains in BMD, trabecular volume fraction (BV/TV), cortical thickness (Ct.Th), and cortical area (Ct.Ar) in limbs exposed to flow compared to sham controls (Table 1). In addition, a significant increase in trabecular thickness (Tb.Th) was observed in Tg mice. Interestingly, relative gains (i.e., flow-no flow) in all parameters were greater in Tg mice, indicating that osteocyte ablation did not affect, or even enhanced skeletal adaptation to flow. In particular, rBMD and rTb.Th were significantly different between WT and Tg mice administered 10 or 50ug/kg DT (Table 1). Taken together, osteocyte ablation does not abrogate skeletal adaptation to dynamic ImP/IFF, suggesting that this response occurs independently of flow-induced stimulation of osteocytes. In addition, osteocyte ablation may enhance the response to dynamic ImP/IFF, perhaps by altering the function and/or number of other types of cells within bone.

[1] Tatsumi et al., Cell Metab 2007; [2] Kwon et al., JBMR 2010

Parameter (flow – no flow)		WT (n=15)	Tg+10ug/kg DT (n=11)	Tg+50ug/kg DT (n=5)	One-way ANOVA
	rBMD (mg/ccm)	15.7±4.0**	18.9±6.9*	48.2±17.0*	p<0.05
	rBV/TV (%)	5.8±1.0***	7.0±1.5***	7.0±1.3***	NS
	rTb.Th (um)	0.3±3.1	13.0±3.0**	19.2±1.6***	p<0.01
	rCt.Th (um)	10.9±3.7*	16.2±3.7**	17.3±6.5	NS
	rCt.Ar (mm^2)	0.07±0.02**	0.09±0.02**	0.09±0.03	NS

Table 1. Osteocyte ablation does not affect or enhances skeletal adaptation to dynamic IFF. Values (presented as mean±SE) are relative differences between limbs exposed to dynamic IFF vs. contralateral controls (i.e., flow – no flow) for WT and Tg mice administered 10 or 50ug/kg DT. For WT mice, no differences in relative values were observed for mice administered 10 or 50ug/kg DT, thus for statistical analysis these groups were combined. *,**, or *** indicate $p<0.05$, $p<0.01$, or $p<0.001$ obtained using a one-sample t-test with an assumed zero mean. One-way ANOVA revealed a statistically significant difference between groups (i.e., WT, Tg+10ug/kg DT, and Tg+50ug/kg DT) for rBMD and rTb.Th.

Table 1

***Disclosures: Ronald Kwon**, None.*

1062

Beta-1 Adrenergic Administration Mitigates Negative Changes in Cancellous Bone Microarchitecture and Inhibits Osteocyte Apoptosis During Disuse. Joshua Swift*[1], Sibyl Swift[2], Matthew Allen[3], Florence Lima[2], Susan Bloomfield[2]. [1]United States Navy, USA, [2]Texas A&M University, USA, [3]Indiana University School of Medicine, USA

The sympathetic nervous system (SNS) plays a vital role in mediating bone remodeling. However, the exact role that beta-1 adrenergic (Adrb1) receptors have in this process has not been elucidated. We have previously demonstrated the ability of dobutamine (DOB), primarily an Adrb1 receptor agonist, to mitigate disuse-induced reductions of cancellous bone formation and bone mass at mixed bone sites. The purpose of this study was to characterize the independent and combined effects of DOB and hindlimb unloading (HU) on cancellous bone microarchitecture (by micro-CT), osteocyte apoptosis, and expression of pro- and anti-apoptotic proteins. Male Sprague-Dawley rats, aged 6-mos, were assigned to either normal cage activity (CC) or HU (n=18/group). Animals were given one daily bolus dose (4 mg/kg BW/d) of DOB (n=9) or an equal volume of saline (VEH; n=9). Unloading resulted in significantly lower distal femur BV/TV (-33%), Tb.Th (-11%), and Tb.N (-25%) compared to ambulatory controls (CC-VEH). DOB treatment during HU attenuated these changes, resulting in greater BV/TV (+29%), Tb.Th (+7%), and Tb.N (+21%) vs. HU-VEH. Distal femur cancellous vBMD (+11%) and total BMC (+8%) were significantly greater in DOB- vs. VEH-treated HU rats. Administration of DOB during HU resulted in significantly greater OS/BS (+158%) and Ob.S/BS (+110%) vs. HU-VEH group. Furthermore, Oc.S/BS was significantly greater in HU-DOB (+110%) vs. CC-VEH group. DOB treatment during unloading fully restored bone formation similar to cage control values, resulting in significantly greater BFR (+3-

fold) than in HU-VEH rats. HU resulted in increased prevalence of apoptotic cancellous osteocytes (+85%) vs. CC-VEH, and this increase was prevented with DOB treatment. Osteocyte apoptosis in HU-VEH was associated with greater Bax/Bcl-2 mRNA levels (resulting from increased Bax), and this ratio was not changed in HU-DOB group. Altogether, these data indicate that Adrb1 treatment during disuse mitigates negative changes in cancellous bone microarchitecture and bone mass by inhibiting increases in osteocyte apoptosis and maintaining bone formation. Our findings also suggest that, contrary to findings with Adrb2 receptor agonist treatment, there were no deleterious effects of Adrb1 agonist administration on cancellous bone in weightbearing controls.

Funded by NSBRI through NASA Cooperative Agreement NCC 9-58 and the Sydney and JL Huffines Institute for Sports Medicine and Human Performance.

***Disclosures: Joshua Swift**, None.*

1063

Baseline Bone Turnover Declines with Age but Does Not Limit the Anabolic Response to Mechanical Loading in Mice. Michael Brodt[1], Michelle Lynch[1], Daniel Wood[1], Roberto Civitelli[2], Matthew Silva*[2]. [1]Washington University, USA, [2]Washington University in St. Louis School of Medicine, USA

With aging, the skeleton may become less responsive to mechanical stimuli. Yet we recently reported that aged (22-month old) mice do not have a diminished response to tibial compression compared to young-adult (7-month) mice. In the current study, we extended the age range to include younger, growing mice and asked if the anabolic response to loading depended on the baseline level of bone turnover. After approval from our Animal Studies Committee, female BALB/c mice were studied at 2, 4, 7 and 12 months of age. First, to establish baseline levels of systemic and local bone turnover, mice were euthanized without loading (n=8/age). Serum markers of bone turnover (osteocalcin, CTX) decreased significantly with age. Moreover, qPCR revealed age-related declines in bone turnover in the tibia. Expression of genes associated with bone formation (Alp, Osx, Bmp2) and resorption (Ctsk) were highest at 2 mo and lowest at 7-12 mo. These data confirmed that bone turnover is highest in young mice and declines with age. Next, we subjected the hindlimbs to axial tibial compression in vivo. Peak force values were chosen to produce an estimated peak endocortical strain of -1300 με at the mid-diaphysis. Under anesthesia, right legs were loaded 60 cycles/day, 3 days/wk; left legs were not loaded (control). Changes in bone structure due to loading were evaluated in a 6-week study (n=9/age). Tibias were scanned by in vivo microCT at 0, 3 and 6 weeks. Cortical bone size increased with tibial compression, independent of age (Fig. 1). Cortical bone volume (BV) increased from 0 to 6 weeks in loaded tibias from each age group ($p<0.05$), but did not change in control tibias ($p>0.05$). Cortical bone volume was greater in loaded tibias than controls at 6 wks. Changes in gene expression due to loading were evaluated in a 1-week study (n=4/age). Loading caused a significant upregulation of some genes related to bone turnover, but only in older animals. In particular, expression of Alp and Osx was not stimulated above control levels in the younger animals, yet was significantly increased in loaded limbs of 12 mo animals ($p< 0.05$). In summary, despite the decline in baseline bone formation with age, we found no evidence of an age-related loss of cortical mechanoresponsiveness. Taken together, our data indicate that loading overcomes the age-related decline in bone formation perhaps by increasing the number of committed osteoblasts to levels seen in growing animals.

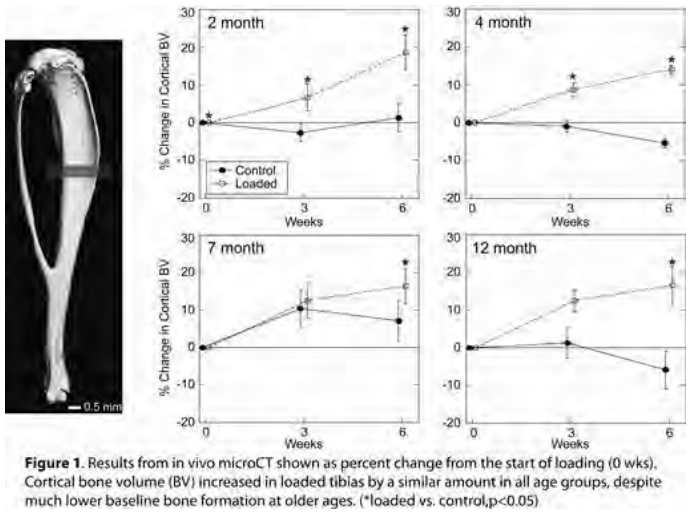

Figure 1. Results from in vivo microCT shown as percent change from the start of loading (0 wks). Cortical bone volume (BV) increased in loaded tibias by a similar amount in all age groups, despite much lower baseline bone formation at older ages. (*loaded vs. control,p<0.05)

Figure 1

***Disclosures: Matthew Silva**, None.*

1064

HIF-1 Antagonizes Load-induced Bone Formation. Ryan Riddle*[1], Ted Gross[2], Thomas Clemens[3]. [1]Johns Hopkins University School of Medicine, USA, [2]University of Washington, USA, [3]Johns Hopkins University, USA

Mechanical loads induce profound anabolic effects in the skeleton but the molecular mechanisms that transduce such signals are still poorly understood. In many non-osseous tissues, mechanical signals induce the expression of hypoxia-inducible factor-1 (HIF-1), a transcription factor originally identified as a regulator of the cellular response to hypoxia. In this study we investigated the role of HIF-1 in skeletal mechanotransduction. Exposure of MLO-Y4 osteocyte-like cells and primary osteoblasts to either fluid shear stress or substrate strain induced the expression of HIF-1α, but not HIF-2α. In MLO-Y4 cells, HIF-1α expression was induced by PGE_2 treatment and prostanoid signaling was required for fluid shear to increase HIF-1α protein levels. Additionally, both PGE_2 and fluid shear activated the Akt/mTOR pathway and treatment with rapamycin abolished the expression of HIF-1α after either stimulus. To determine the role of HIF-1 in load-induced bone formation *in vivo,* we generated mice lacking HIF-1α in osteoblasts and osteocytes (OC-Cre; $HIF1\alpha^{flox/flox}$, ΔHIF1a) and exposed them to 3 weeks of mechanical loading via cantilever bending of the tibia. Compared to control littermates, ΔHIF1α mice were more responsive to mechanical loading. Despite receiving equivalent peak periosteal strain, bone formation rate after loading in ΔHIF1α mice was 2-fold higher than that observed in controls. Similarly, the load-induced increase in mineralizing surface per bone surface in ΔHIF1α mice was 86% higher than controls, which indicates that a greater number of osteoblasts were activated by loading in these mice. Since the Wnt/β-catenin pathway is believed to be critical for load-induced bone formation, and HIF-1 antagonizes this pathway, we investigated the interaction of these transcription factors. Co-immunoprecipitation studies showed that HIF-1α and β-catenin interacted six hours after exposure of MLO-Y4 cells to fluid shear stress. Moreover, osteoblasts over-expressing HIF-1α had reduced levels of the β-catenin target genes *Ccnd1* and *Axin2*. Taken together, these studies identify the hypoxia-inducible factor pathway as a novel regulator of skeletal mechanotransduction, and suggest that HIF-1 acts to suppress load-induced bone formation by altering the sensitivity of bone cells to mechanical signals.

***Disclosures: Ryan Riddle**, None.*

1065

IGF-1 Receptor in Mature Osteoblasts and Osteocytes is Involved in Skeletal Unloading Induced Bone Loss but not in Reloading Induced Bone Acquisition. Takuo Kubota*[1], Hashem Elalieh[1], Yongmei Wang[2], Daniel Bikle[2]. [1]University of California San Francisco/VA Medical Center, USA, [2]Endocrine Research Unit, Division of Endocrinology UCSF, USA

Mechanical loading has a profound influence on bone remodeling. Insulin-like growth factor 1 (IGF-1) signaling also plays a vital role in bone remodeling. IGF-1 production is increased in osteocytes and osteoblasts after mechanical load. Furthermore, skeletal unloading causes a decrease in bone mass with reduced bone formation and increased bone resorption associated with resistance to the anabolic effect of IGF-1. Therefore, we postulated that IGF-1 signaling mediates the skeletal response to unloading and reloading. In the present study, to determine whether the IGF-1 receptor in mature osteoblasts and osteocytes has a role in the skeletal response to unloading and reloading, we evaluated mice in which the IGF-1 receptor was deleted with osteocalcin-driven cre recombinase. These mice were subjected to skeletal unloading using tail suspension and reloading either after unloading or with cyclic axial loading of the right tibia during tail suspension. The micro CT analysis showed that BV/TV was decreased by 19% in the knockout mice compared with control mice at baseline and decreased to 56% below the control mice after two weeks of skeletal unloading. On the other hand, two weeks of reloading after the two-week unloading increased BV/TV in the distal femur by 148% in the knockout mice compared to that in the four-week unloaded knockout mice, a response comparable to the control mice (102% increase). In addition, cyclic loading increased BV/TV in the proximal right tibia of the unloaded knockout mice by 78% compared to the unloaded left tibia, again comparable to that in the control mice (72% increase). These results indicate that the IGF-1 receptor in mature osteoblasts and osteocytes plays a role in preventing bone loss induced by skeletal unloading but not in mediating bone acquisition induced by reloading. Moreover, these results are consistent with recent observations (Tatsumi S, et al. Cell Metab 2007;5:464.) that depletion of osteocytes does not prevent bone gain in response to reloading, and suggest that the IGF-1 receptor in mature osteoblasts and osteocytes helps maintain bone mass during skeletal unloading.

***Disclosures: Takuo Kubota**, None.*

1066

Mesenchymal Loss of BMP2 Primarily Impairs Cortical Bone Structure Causing Only a Modest Decrease in Tissue-Level Modulus. Jeffry Nyman*[1], Giuseppe Intini[2], Matthew R. Murry[1], Daniel Perrien[1], Erik G. Herbert[3], George M. Pharr[3], Gregory R. Mundy[4], Vicki Rosen[2]. [1]Vanderbilt University Medical Center, USA, [2]Harvard School of Dental Medicine, USA, [3]University of Tennessee at Knoxville, USA, [4]Vanderbilt Center for Bone Biology, USA

Mice lacking BMP2 in the cells of the mesenchymal lineage (BMP2fl/fl;Prx1-cre mice) experience spontaneous fractures in both the fore and hind limb by 10 weeks of age. This does not occur in control littermates, and rarely do spontaneous fractures occur in other genetic mouse models, suggesting that loss of BMP2 contributes to fracture risk. We hypothesized that fractures in the BMP2fl/fl;Prx1-cre mice are due to a structural deficit and reduced tissue-level properties. To examine this idea, the left femur was harvested from BMP2fl/fl;Prx1-cre mice and gender- and age-matched control littermates at 10 weeks and 15 weeks of age (n=9/genotype and n=8/genotype, respectively). Then, μCT scans were performed to quantify the structural properties of the diaphysis, trabecular bone architecture of the metaphysis, and mineralization density (mBMD) of both compartments. Next, femurs were embedded in plastic; a cross-section of the diaphysis was polished; and multiple sites throughout the cortex were analyzed by nanoindentation to characterize tissue-level properties. The effect of age and genotype on each bone property was tested for significance using a two-way ANOVA. While no differences were found in trabecular bone volume and architecture between the genotypes, cortical bone structure was vastly different in the absence of BMP2. BMP2fl/fl;Prx1-cre mice had slightly shorter femurs that were greatly reduced in cross-sectional area and moment of inertia when compared to control littermates. Effectively, the mutant diaphysis was more slender than the wild-type diaphysis (Fig. 1), creating a bone in which the mean ratio of body weight to bone slenderness was 4.5x less for mutant than for control mice. To a lesser degree, BMP2 activity appeared to influence tissue properties, with its deletion causing a modest reduction in nanoindentation modulus, and moreover, affecting the direct relationship between tissue modulus and mBMD, suggesting that BMP2 influences the micro-structural organization of the matrix, not just mBMD. Given that structural differences between the genotypes were vastly greater than the tissue-level differences, spontaneous fractures of BMP2fl/fl;Prx1-cre mice likely occur because the lack of BMP2 is preventing proper periosteal expansion of the diaphysis relative to longitudinal growth. Thus, BMP2 expression by cells of the mesenchymal lineage may be important to periosteal apposition and/or the functional adaptation of bone to mechanical loads.

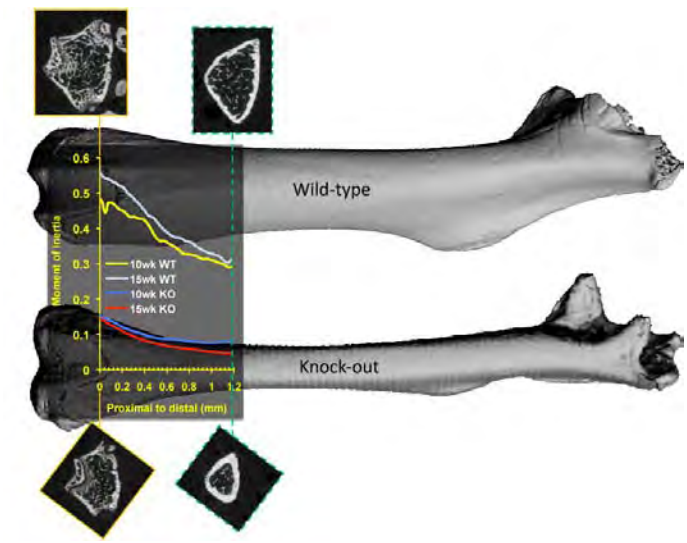

Fig. 1: Structural difference between wild-type and BMP2fl/fl;Prx1-cre femur

***Disclosures: Jeffry Nyman**, None.*

1067

Effect of the Cathepsin K Inhibitor, ONO-5334, on Biochemical Markers of Bone Turnover in the Treatment of Postmenopausal Osteopenia or Osteoporosis. Richard Eastell*[1], Shinichi Nagase[2], Maria Small[2], Michiyo Ohyama[3], Tomohiro Kuwayama[2], Junichiro Manako[3], Steve Deacon[2]. [1]University of Sheffield, United Kingdom, [2]ONO PHARMA UK LTD, United Kingdom, [3]Ono Pharmaceutical Co., Ltd., Japan

The effect of the Cathepsin K inhibitor, ONO-5334 (50mg bd, 100 or 300mg qd), on biochemical markers of bone turnover (BTM) was investigated in the randomised, placebo (PBO)-controlled, double-blind, parallel-group 1 year study enrolling 285 postmenopausal women. Alendronate (ALN, 70mg qw) was used as an active reference. Patients were equally randomised to 5 treatment arms. Calcium and vitamin D were given to all patients. Subjects were 55-75 years old and had osteoporosis (with no fragility fractures) or osteopenia (with a fragility vertebral fracture). We measured CTX, bone ALP, PINP, Osteocalcin, ICTP and TRACP5b in serum(s) and CTX, NTX, DPD in urine(u) throughout the study. Lumbar spine and hip BMD were also assessed.

ONO-5334 appeared to suppress bone resorption markers as potently as ALN (Table). However, the effect on bone formation markers bone ALP, PINP and OC appeared consistently less than ALN. 300mg qd ONO-5334 suppressed these formation markers by approximately 20% with no changes seen with either 50mg bd or 100mg qd ONO-5334. ONO-5334 increased ICTP and there were only small changes in TRACP5b.

All doses of ONO-5334 resulted in significant and dose-dependent increases in spine and total hip BMD vs. placebo (PBO). Mean +/- SE shown. At month 12, 300 mg ONO-5334 increased lumbar spine (LS) BMD by 5.1% (+/- 0.5) ($p<0.001$ vs. PBO 0.6% +/-0.5) and total hip BMD by 3.0% (+/-0.4) ($p<0.001$ vs. PBO 0.9%+/-0.4). ALN BMD results for LS and hip were 5.2% +/- 0.5 and 3.6% +/- 0.4, respectively ($p<0.001$ vs. PBO).

The effect of ONO-5334 on the BTM profile suggests a new mechanism of action vs. standard anti-resorptive agents such as ALN, with less suppression on bone formation markers and TRACP5b. Whether this might indicate a different long-term pattern of BMD change needs to be investigated with long term studies.

	ONO-5334 50mg bd	ONO-5334 100mg qd	ONO-5334 300mg qd	ALN 70mg qw
uCTX	-75 (-82, -64)***	-72 (-80, -60)***	-87 (-91, -81)***	-75 (-82, -65)***
uNTX	-49 (-61, -35)***	-46 (-58, -31)***	-60 (-69, -49)***	-65 (-72, -54)***
PINP	5 (-12, 26)	11 (-7, 33)	-27 (-39, -13)***	-64 (-70, -57)***
bone ALP	2 (-8, 13)	7 (-4, 19)	-15 (-23, -5)**	-34 (-41, -27)***
OC	0 (-14, 17)	1 (-14, 18)	-21 (-32, -7)**	-34 (-43, -23)***
TRACP5b	5 (-3, 14)	12 (4, 22)**	-5 (-13, 3)	-17 (-23, -10)***

Last observation carried forward analysis/Full analysis set were used (** p<0.01, ***p<0.001 vs. PBO as ratio of geometric mean)

Table: Percentage change (95% CI) from baseline as a difference from PBO in BTMs

***Disclosures: Richard Eastell**, Ono Pharmaceutical Co., Ltd., 5*
This study received funding from: Ono Pharmaceutical Co,. Ltd.

1068

The Effects of Denosumab on Bone Mineral Density (BMD) and Fracture by Level of Renal Function. Sophie Jamal*[1], Osten Ljunggren[2], Catherine Stehman-Breen[3], Steven Cummings[4], Michael McClung[5], Stefan Goemaere[6], Peter Ebeling[7], Edward Franek[8], Yu-Ching Yang[3], Steven Boonen[9], Ogo Egbuna[10], Paul Miller[11]. [1]University of Toronto, Canada, [2]Uppsala University Hospital, Sweden, [3]Amgen, Inc., USA, [4]San Francisco Coordinating Center, USA, [5]Oregon Osteoporosis Center, USA, [6]University Hospital, Belgium, [7]University of Melbourne, Australia, [8]Central Clinical Hospital, Poland, [9]Center for Metabolic Bone Disease, Belgium, [10]Amgen, Incorporated, USA, [11]Colorado Center for Bone Research, USA

Purpose

The incidence of osteoporosis and chronic kidney disease (CKD) both increase with age yet there is a paucity of data on treatments for osteoporosis in the setting of impaired renal function. We examined the efficacy and safety of DMAb among subjects with varying level of renal function participating in the FREEDOM study; a 3 year, randomized phase 3 trial of 7808 postmenopausal women with osteoporosis.

Methods

We estimated creatinine clearance (eGFR) using the Cockcroft-Gault equation and defined stage of CKD using the National Kidney Foundation guidelines. We examined incident fracture rates, changes in BMD, serum calcium, creatinine and the incidence of adverse events after 36 months of follow up in subjects receiving DMAb and placebo, stratified by level of renal function using linear regression models adjusted for fracture since aged 45, prevalent vertebral fractures, self reported health status, baseline calcium intake, current smoking, femoral neck BMD T score and years since menopause. We used a subgroup interaction term to determine if there were differences in treatment effect by eGFR.

Results

Most (97%) women were Caucasian, the mean age was 72.3 $\pm$5.2 years, the mean weight was 63.8 $\pm$ 10.41 kg, mean serum creatinine was 70.8 $\pm$ 15.3 mmol/L and mean serum calcium was 2.44 $\pm$0.11mmol/L. 73 women had an eGFR between 15 to 29 ml/min (CKD stage 4); 2817 between 30 to 59 ml/min (CKD stage 3); 4069 between 60 to 89 ml/min (CKD stage 2) and 842 had an eGFR of $\geq$ 90ml/min (CKD stage 1/ normal).

Effects of DMAb, compared with placebo on incident vertebral and nonvertebral fractures and BMD over 36 months, by stage of renal function, are described in Table 1 and illustrated in Figure 1. The test for treatment by subgroup interaction was not statistically significant indicating that fracture risk reduction, as well as the difference in the mean % changes in BMD in subjects treated with DMAb compared to placebo did not differ by level of renal function. Changes in creatinine, calcium and the

incidence of adverse, serious adverse and fatal events were similar between the placebo and treatment groups and did not differ by level of renal function.

Conclusion

DMAb is effective at reducing fracture risk and increasing BMD in women with CKD participating in the FREEDOM trial. Further, the lack of differences in renal and non renal adverse events in the DMAb group compared with placebo suggests that, in this group, no dose adjustments need to be made.

Table 1. Effect of Denosumab, compared with placebo on incident vertebral and nonvertebral fractures and BMD over 36 months, by stage of renal function.

Outcome	Stage 4 CKD eGFR:15-29ml/min (N= 73)	Stage 3 CKD eGFR30-59ml/min (N= 2817)	Stage 2 CKD eGFR:60-89ml/min (N=4069)	Stage 1 CKD/Normal eGFR ? 90ml/min (N=842)
Vertebral Fractures; Odds Ratio (95%CI)	0.31 (0.02 to 5.08)	0.38 (0.26 to 0.57)	0.23 (0.15 to 0.34)	0.33 (0.16 to 0.66)
Nonvertebral Fractures; Odds Ratio (95%CI)	0.51 (0.04 to 7.26)	0.88 (0.66 to 1.16)	0.69 (0.54 to 0.89)	0.89 (0.51 to 1.52)
Lumbar Spine BMD; %change	5.0 (-0.8 to 10.8)	8.9 (8.4 to 9.3)	9.0 (8.6 to 9.4)	8.1 (7.2 to 8.9)
Femoral Neck BMD; %change	5.9 (3.3 to 8.5)	5.1 (4.7 to 5.5)	5.2 (4.9 to 5.5)	5.6 (4.9 to 6.3)
Total Hip BMD; % change	5.9 (3.0 to 8.7)	6.4 (6.1 to 6.7)	6.4 (6.2 to 6.7)	5.8 (5.2 to 6.3)

Note: Odds ratio < 1 in fracture risk or difference in BMD % change >0 in favor of denosumab.

Table 1

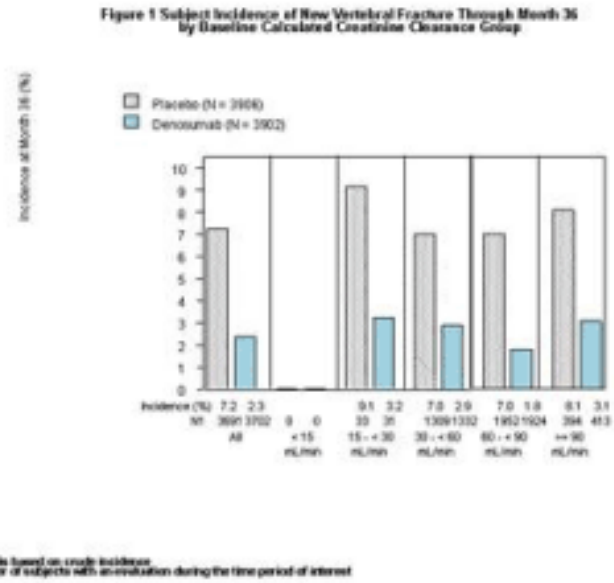

Figure 1

***Disclosures: Sophie Jamal**, Amgen, 8; Amgen, 5*
This study received funding from: Amgen, Inc.

1069

Remodeling Status in Postmenopausal Women Who Discontinued Denosumab Treatment. Jacques Brown*[1], David Dempster[2], Beiying Ding[3], Ricardo Dent[4], Javier San Martin[5], Rachel B. Wagman[6], Jose Ruben Zanchetta[7]. [1]Laval University, Canada, [2]Columbia University, USA, [3]Amgen Inc, USA, [4]Amgen, USA, [5]Amgen, Inc., USA, [6]Amgen Inc. & Stanford University Scool of Medicine, USA, [7]Instituto de Investigaciones Metabolicas (IDIM), Argentina

Denosumab, a fully human monoclonal antibody to RANKL, reduces bone resorption, increases bone mineral density (BMD), and decreases risk for vertebral, nonvertebral, and hip fractures in postmenopausal women with osteoporosis.[1] Transiliac crest bone biopsies from subjects treated with denosumab for 1 to 3 years demonstrate low bone remodeling.[2] The effects of denosumab on biochemical markers of bone turnover (BTM) and BMD are reversible upon treatment discontinuation.[3,4] However, the effects of denosumab discontinuation on bone histology and histomorphometry are not known. Here we report interim results from a cross-sectional transiliac crest bone biopsy study designed to evaluate the effect of denosumab discontinuation on bone remodeling. Eligible subjects completed all denosumab doses in a phase 3 trial after which they received not more than 1 month of osteoporosis treatment. Transiliac crest bone biopsies were obtained for histology and histomorphometry evaluation ≥ 12 and < 36 months after subjects completed the original trial. Fasting serum samples were collected to assess BTM levels at the time of tetracycline (TC) labeling. This study is ongoing with an expected enrollment of approximately 15 subjects. Data from 5 subjects are currently available. Subjects' mean (SD) age at enrollment in the biopsy study was 59.6 (4.3) years. The 1st set of TC labeling occurred after a mean (SD) of 23.4 (2.7) months from denosumab discontinuation. All biopsies showed normal histology without evidence of pathology. Double TC labels were present in all biopsies, suggesting active remodeling. Static and dynamic histomorphometric variables for the 5 subjects are shown (Table). Most histomorphometric parameters of bone remodeling were within the reference values with the exception of an increase in osteoclast number. Both resorption (CTX) and formation (P1NP) markers were similar to the subjects' pretreatment baseline BTM levels. These data demonstrate that bone remodeling returned to pre-treatment levels upon denosumab discontinuation, confirming the reversibility effect of denosumab treatment on suppression of bone turnover.

1. Cummings, et al. *NEJM*. 2009;361:756.
2. Reid, et al. *JBMR*. 2009;24(Suppl 1):S9.
3. Miller, et al. *Bone*. 2008;43:222.
4. Bone, et al. *JBMR*. 2009;24(Suppl 1):S74.

	Reference Range, Mean (SD)*	Subject 1	Subject 2	Subject 3	Subject 4	Subject 5
Eroded surface, %	2.87 ± 1.87	0.82	0.57	1.11	2.20	0.83
Osteoclast number – surface based, per 100 mm	3.97 ± 3.53	21.0	13.0	21.0	52.0	17.00
Osteoid surface, %	8.48 ± 5.23	6.55	7.12	3.27	11.34	2.24
Osteoid width, µm	14.3 ± 7.5	7.18	14.65	9.44	7.77	8.68
Osteoblast–osteoid interface, %	34.01 ± 13.04	15.95	27.68	46.27	32.65	34.73
Single-label surface, %	4.08 ± 2.84	5.38	2.56	3.61	5.82	3.55
Double-label surface, %	8.41 ± 3.89	2.17	8.05	4.07	9.56	1.18
Mineralizing surface, %	n/a	4.91	7.33	5.88	12.49	2.39
Mineral apposition rate, µm/day	0.89 ± 0.18	0.78	0.72	0.69	0.63	0.89
Bone formation rate, %/yr	26.2 ±16.4	30.9	27.3	13.8	34.5	20.3
Activation frequency, year-1	n/a	0.44	0.34	0.20	0.54	0.25

*For women provided by Mayo Clinic Histomorphometry Laboratory, Rochester, MN, USA. n/a = not available

Table. Histomorphometric Parameters for 5 Subjects

***Disclosures: Jacques Brown**, li Lilly, Amgen, Novartis, Merck, Warner Chilcott, 8; Abbott, Amgen, Eli Lilly, Novartis, Merck, Warner Chilcott,5; Abbott, Amgen, Bristol-Myers-Squibb, Eli Lilly, Pfizer, Roche, 2*
This study received funding from: Amgen Inc.

1070

The Effect of 3 Versus 6 Years of Zoledronic Acid Treatment in Osteoporosis: a Randomized Extension to the HORIZON-Pivotal Fracture Trial (PFT). Dennis Black*[1], Ian Reid[2], Jane Cauley[3], Steven Boonen[4], Felicia Cosman[5], P.C. Leung[6], Peter Lakatos[7], Zulema Man[8], Steven Cummings[9], Trisha Hue[1], MaryEllen Ruzycky[10], R Martinez[10], Guoqin Su[11], Christina Bucci-Rechtweg[10], Richard Eastell[12]. [1]University of California, San Francisco, USA, [2]University of Auckland, New zealand, [3]University of Pittsburgh Graduate School of Public Health, USA, [4]Center for Metabolic Bone Disease, Belgium, [5]Helen Hayes Hospital, USA, [6]Chinese University of Hongkong, China, [7]Semmelweis University Medical School, Hungary, [8]Centro Médico TIEMPO, Argentina, [9]San Francisco Coordinating Center, USA, [10]Novartis Pharmaceuticals Corporation, USA, [11]Novartis pharmaceuticals, USA, [12]University of Sheffield, United Kingdom

Purpose: Zoledronic acid 5 mg (ZOL) used annually for 3 years has been shown to be effective in increasing BMD and decreasing fractures. However, it is unknown if increasing the duration of therapy beyond 3 years will maintain BMD and provide additional fracture protection. To address this question, we performed a 3-year extension of the HORIZON-PFT to 6 years.

Methods: A total of 1233 women who had received active ZOL for 3 years in the core study were randomly allocated to 3 additional years of ZOL (Z6, n=616) or 3 years of blinded placebo (Z3P3, n=617). The primary endpoint was percentage change in femoral neck (FN) BMD at Year 6 relative to Year 3 with secondary endpoints including other BMD sites, biochemical markers of bone turnover, fractures and safety. Additionally, a group who received placebo in the core was given 3 years of ZOL (n=1223) in order to retain the core study blind, but results will not be reported here.

Results: FN BMD results are shown in the figure below. In years 3-6, in the Z6 group, FN BMD remained constant while in the Z3P3 group, it dropped slightly (between treatment difference at year 6=1.04%, [95%CI: 0.4,1.7; p=0.0009]) but still remained well above pretreatment levels. Results for other sites of BMD were similar (total hip: 1.2%, $p<0.0001$, lumbar spine: 2.03, p=0.0018). Biochemical markers remained constant in the Z6 group but rose slightly in the Z3P3 group. However, 3 years after discontinuation of therapy in the Z3P3 group, P1NP remained about 47% below pretreatment values. New morphometric vertebral fractures were significantly lower in the Z6 vs. Z3P3 group (RR=0.48, p=0.04) while other categories of fractures including non-vertebral, hip and clinical vertebral were not different across study groups. The overall incidence of adverse events was comparable between groups. A numerical increase in atrial fibrillation SAEs (2.0% in Z6 vs. 1.1% in Z3P3) was not statistically significant (p=0.26). No long-term effect on renal function or difference in adjudicated ONJ events was observed between the two groups.

Conclusions: 6 years of ZOL maintained BMD while discontinuation after 3 years resulted in significant, although small, BMD losses. ZOL showed a comparable safety profile. The BMD results, together with the fracture results, suggest that patients at high risk of fracture, particularly vertebral fracture, should continue on annual ZOL therapy.

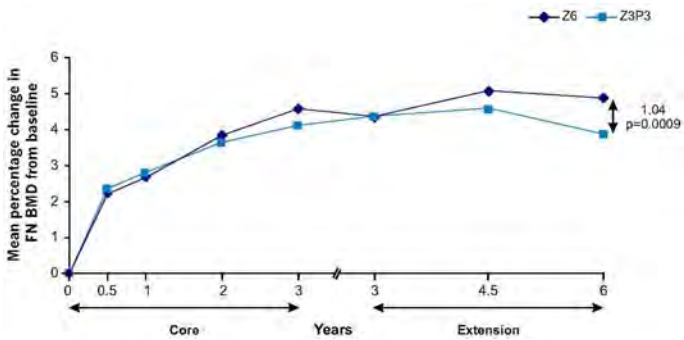

Figure: Femoral neck BMD percentage change over time

***Disclosures: Dennis Black**, Novartis, 2*
This study received funding from: Novartis

1071

Atypical Femoral Fractures Are Associated With Bisphosphonate Use. Christian Girgis[1], Doron Sher[2], Markus Seibel*[3]. [1]Dept of Endocrinology & Metabolism, Concord Repatriation General Hospital, Australia, [2]Dept of Orthopaedic Surgery, Concord Repatriation General Hospital, Australia, [3]Bone Research Program, ANZAC Research Institute, The University of Sydney, Australia

The association between the use of bisphosphonates and the occurrence of subtrochanteric (''atypical'') femur fractures remains controversial.

We reviewed 152 non-hip femoral fractures sustained by 152 patients (mean age 78 ± 5 years; 132 females) admitted to a large tertiary center between June 2003 and May 2008. A senior orthopedic surgeon reviewed the fracture radiographs of every patient in random sequence (Cohen's κ= 0.8) identifying fractures that displayed all criteria for an atypical fracture3,4 (i.e. a lateral transverse or <30 deg oblique fracture line in an area of cortical thickening with a medial unicortical beak).

Twenty of the 152 fractures were atypical. Following unblinding of the database, 17 patients in this group were found to be on current oral bisphosphonate treatment (15 on alendronate; 2 on risedronate; mean treatment duration 5.1 and 3yrs respectively). Of the 132 patients whose radiographs did not fulfill the atypical criteria, 2 were on alendronate (1.5%) and 1 was on risedronate (0.76%), with a mean treatment duration of 3.5yrs and 1yr, resp. Hence, the risk of an atypical vs. typical fracture in non-bisphosphonate-users (3/132, 2.3%) was increased 37.4 fold (95% CI 12.9-119, P<0.001) in bisphosphonate users (17/20, 85%). The atypical fracture pattern was 96.7% specific to bisphosphonate users.

Risk factors for atypical fractures included a history of low energy fractures (OR 3.2, 95%CI 2.1–17.1, P<0.001), glucocorticoid therapy for > 6 months (OR 5.2, 95%CI 1.3–31, P=0.01), active rheumatoid arthritis (OR 16.5, 95% 1.4–142.3, P<0.001) and 25-OH-vitamin D level <16ng/mL [40nmol/L] (OR 3.5, 95%CI 1.7–18.7, P<0.001).

Based on the center's catchment population (~174,448), the mean annual incidence of atypical femur fractures was calculated as 0.23/10,000 of the general population and 1.66/10,000 in people 65 years or older. According to dispensing data and using wide to narrow indices for the catchment locality, the mean annual incidence of atypical fractures was estimated to range from 11 to 33/10,000 amongst alendronate users, and from 2.5 to 7.4/10,000 amongst risedronate users.

We conclude that there is an apparent association between atypical subtrochanteric femur fractures and oral bisphosphonate use. However, the absolute frequency of these fractures is very low and on balance, the anti-fracture effects of bisphosphonates far outweigh their potential risks in patients with established osteoporosis.

***Disclosures: Markus Seibel**, None.*

1072

Risk of Femoral Shaft and Subtrochanteric Fractures In Users of Bisphosphonates, Raloxifene and Strontium Ranelate. Peter Vestergaard*. Aarhus University Hospital, Denmark

Aim: To study the association between use of alendronate and other drugs against osteoporosis and the risk of femoral shaft and subtrochanteric fractures.

Methods: Nationwide cohort study from Denmark. All users of bisphosphonates and other drugs against osteoporosis between 1996 and 2006 (n=103,562) as exposed group and three age- and gender matched controls from the general population (n=310,683). Adjustments were made for prior fracture, use of systemic hormone therapy and use of systemic corticosteroids.

Results: An increased risk of subtrochanteric fractures were seen for alendronate (HR=2.41, 95% CI 1.78-3.27), etidronate (HR=1.96, 95% CI 1.62-2.36), and clodronate (HR=20.0, 95% CI 1.94-205) but not for etidronate (HR=1.06, 95% CI 0.34-3.32). However, an increased risk of subtrochanteric fractures was also present before start of alendronate (OR=2.36, 95% CI 2.05-2.72), etidronate (OR=3.05, 95% CI 2.59-3.58), clodronate (OR=10.8, 95% CI 1.14-103), raloxifene (OR=1.90, 95% CI 1.07-3.40), strontium ranelate (OR=2.97, 95% CI 1.07-8.27). Similar trends were seen for femoral shaft and overall fracture risk. Too few events were present to study subtrochanteric fracture risk after start of strontium ranelate and a number of other drugs against osteoporosis. After start of etidronate no dose-response relationship was present (p for trend 0.54). For alendronate a decreasing risk was present wit increasing dose (p for trend <0.01).

Conclusions: Although an increased risk of femoral shaft and subtrochanteric fractures are seen with use of several types of bisphosphonates, the increased risk before start of the drugs may point at an effect of the underlying disease being treated. The increased risk may thus perhaps be due to confounding by indication.

***Disclosures: Peter Vestergaard**, None.*
This study received funding from: Servier

1073

Deletion of the FoxO1, 3, and 4 Genes from Committed Osteoblast Progenitors Expressing Osterix Increases Wnt Signaling and Bone Mass. Elena Ambrogini*, Li Han, Shoshana Bartell, Aaron Warren, Randal Shelton, Kanan Vyas, Annick Deloose, Robert Weinstein, Charles O'Brien, Stavros Manolagas, Maria Jose Almeida. University of Arkansas for Medical Sciences, USA

Global deletion of FoxOs in 3 month old mice increases reactive oxygen species (ROS) and reproduces the effects of aging on bone; conversely, FoxO3 overexpression in mature osteoblasts decreases OS and increases bone mass. Nonetheless, diversion of the limited pool of β-catenin from Wnt/TCF- to FoxO-mediated transcription in the setting of increased oxidative stress suppresses osteoblastogenesis in vitro and is associated with the old age-dependant decrease in osteoblast number and bone formation in the murine skeleton. To elucidate the significance of the antagonism of Wnt signalling by FoxOs in skeletal homeostasis we deleted FoxO1, 3, and 4 from committed osteoblast progenitors by crossing mice with conditional alleles of FoxO1, 3, and 4 (FoxO1,3,4-flox) with mice expressing the Cre recombinase under the control of the murine osterix promoter (Osx-Cre). Female or male FoxO1,3,4-flox;Osx-Cre mice exhibited an increase in vertebral and femoral BMD (20%) by DEXA at 3, 5 and 8 month of age, as well as increased volumetric BMD, cancellous bone volume, trabecular number, connectivity, and BFR; but not osteoclast gene expression or resorption markers. These mice also exhibited a striking increase in femoral cortical thickness associated with an increase in the external, but not internal, diameter indicating augmented periosteal expansion. Consistent with the contention that FoxOs antagonize Wnt/TCF signaling, the expression of the β-catenin/TCF target genes axin2 and cyclin D1 was elevated, as was the expression of the osteoblast specific gene osteocalcin. In difference to the global deletion of FoxOs that caused a decrease in the number of colony forming unit osteoblasts (CFU-OB), deletion of FoxOs in Osx1 cells, did not affect CFU-OBs. These findings support the working hypothesis that an increase in ROS with advancing age decreases the number of osteoblasts by exhausting adult self-renewing mesenchymal progenitors; restraining the proliferation/differentiation of Osx1 expressing committed osteoblast precursors, at least in part by the diversion of β-catenin from Wnt/Tcf- to FoxO-mediated transcription; and by promoting the apoptosis of post-mitotic osteoblasts/osteocytes. Selective inactivation of FoxOs in Osx positive cells unleashes the restraining effects of FoxOs on Wnt signaling thereby increasing the number of osteoblasts to an extent that overcompensates for the adverse effects of ROS on mature osteoblast survival and causes bone anabolism.

***Disclosures: Elena Ambrogini**, None.*

1074

Homozygous Deletion of Dickkopf1 Results in a High Bone Mass Phenotype. Michelle McDonald*[1], Alyson Morse[2], Paul Baldock[3], Lauren Peacock[2], Poh-Lynn Khoo[4], Patrick Tam[4], David Little[5]. [1]The Childrens Hospital Westmead, Australia, [2]Orthopaedic Research & Biotechnology Dept. The Kids Research Institute, The Children's Hospital Westmead, Australia, [3]Garvan Institute of Medical Research, Australia, [4]Developmental Embryology Dept. The Children's Medical Research Institute, Australia, [5]Orthopaedic Research & Biotechnology Dept, The Kids Research Institute, The Children's Hospital Westmead, Australia

Dickkopf-1 (DKK1), which antagonizes Wnt/β-catenin signaling activity via interaction with the Lrp5/6 co-receptor, is a negative regulator of osteoblast differentiation and bone formation. Complete deletion of *Dkk1* leads to early embryonic lethality and thereby precludes a proper investigation of its role in post natal bone. Recently, adult mice with complete absence of *Dkk1* function have been generated by genetically reducing the activity of Wnt3 during embryonic development. Over 50% of mice of the *Dkk1*-/-; *Wnt3*+/- genotype (HOM/HET) are found viable. We examined the bone phenotype associated with complete loss of *Dkk1* in comparison to *Dkk1*+/+;*Wnt3*+/+ (WT/WT), *Dkk1*+/-;*Wnt3*+/+ (HET/WT) and the *Dkk1*+/+;*Wnt3*+/- (WT/HET) mice.

Analysis of calvarial RNA showed no postnatal expression of Wnt3 in any genotype, as such this tissue in HOM/HET mice is functionally null only for *Dkk1*. Both male and female HOM/HET mice showed no change in body mass compared to WT/WT. Whole body BMC was increased 12% in male and 16% in female HOM/HET mice ($p<0.05$) and BMD was increased 14% in male HOM/HET mice ($p<0.01$) compared to WT/WT. QCT scans of metaphyseal bone revealed increases in trabecular BMC of 67% in female ($p<0.01$ vs WT/WT) and 64% in male HOM/HET mice ($p=0.053$ vs WT/WT). Diaphyseal cortical bone volume was increased by 31% and 27% in female and male HOM/HET mice respectively ($p<0.01$ vs WT/WT). Concurrently, cortical thickness was increased 22% in female ($p<0.01$ vs WT/WT) and 20% ($p<0.05$ vs WT/WT) in male HOM/HET mice. MicroCT scans of metaphyseal bone revealed a 3-fold increase in female and a 2-fold increase in male HOM/HET mice compared to WT/WT for 3D Bone volume/total volume (BV/TV) ($p<0.01$), which is associated with over 2-fold increases in trabecular number in both male and female HOM/HET mice ($p<0.05$). Furthermore, trabecular BMD was increased 83% in female and 104% in male HOM/HET mice compared to WT/WT ($p<0.05$).

Preliminary histological analysis showed a 48% increase in trabecular MAR in female HOM/HET mice compared to WT/WT ($p=0.06$, N=4) but no alterations in osteoclast parameters between genotypes.

In conclusion, our findings have revealed that absence of the WNT antagonist, DKK1, results in a robust phenotype of high bone mass with over 3-fold increase in metaphyseal bone volume. Histological analysis suggests these extensive increases in bone mass are a result of enhanced bone formation without any changes in bone resorption.

***Disclosures: Michelle McDonald**, None.*

1075

Postnatal Inactivation of Beta-catenin in the Cells of the Osteoblast Lineage Causes Progressive Bone Loss, Ectopic Cartilage Formation and Mesenchymal Cell Accumulation. Jun Guo*[1], Minlin Liu[1], Andrew P. McMahon[2], F. Richard Bringhurst[1], Henry Kronenberg[1]. [1]Massachusetts General Hospital, USA, [2]Harvard University, USA

Canonical wnt signaling plays an essential role in skeletogenesis and bone homeostasis. Previous reports have shown that inactivation of β-catenin, a key molecule of the canonical wnt signaling pathway, in mature osteoblasts leads to increased bone resorption through decreased expression of osteoprotegerin in osteoblasts, whereas constitutive deletion of β-catenin in skeletal progenitors or osteoblast precursors blocks osteoblast differentiation. To better understand the role of canonical wnt signaling in osteoblastic cells in postnatal bone homeostasis, we examined mice with postnatal inactivation of β-catenin in the cells of the osteoblast lineage by mating β-catenin floxed ($Ctnnb1^{f/f}$) mice with transgenic mice expressing osterix cre (osx-cre) that is suppressible by doxycycline (Dox) Upon stopping Dox administration, the osx-cre; $Ctnnb1^{f/f}$ mice showed a progressive bone loss, ectopic cartilage formation and "mesenchymal cell" accumulation in the metaphyseal trabecular regions of the tibia. In such accumulated mesenchymal tissue, some cells strongly express mRNAs encoding collagen types II and X and osteopontin, while many other cells express mRNAs encoding α1(I) collagen and Runx2 and to a lesser extent alkaline phosphatase and PTH/PTHrP receptors. However, no mesenchymal cells express osteocalcin. These observations suggest that postnatal inactivation of β-catenin in osteoblast progenitors blocks osteoblast differentiation but promotes chondrocyte differentiation. A dramatic increase in osteoclasts was also observed in both neonatal osx-cre; $Ctnnb1^{f/f}$ mice treated with a low dose of Dox (0.1 mg/ml) and postnatal osx-cre; $Ctnnb1^{f/f}$ mice after withdrawal of a high dose of Dox (1.5 mg/ml). Histologic analysis shows decreased cortical thickness and reduced endosteal osteoblasts in postnatal osx-cre; $Ctnnb1^{f/f}$ mice and the mutant mice showed a striking decrease in bone formation, assessed by double calcein labeling. Consistent with low bone mass and increased osteoclast activity, 12-wk old osx-cre; $Ctnnb1^{f/f}$ mice treated with Dox (1.5 mg/ml) until 7-wk old exhibited significantly decreased serum P1NP, a marker for bone formation and increased serum CTX, a marker of bone resorption. Serum total calcium and inorganic phosphorus were normal in the 12-wk old mutant mice. Taken together, these data indicate that canonical wnt signaling in the cells of the osteoblast lineage is essential for postnatal osteoblast differentiation, bone formation, and regulation of osteoclast-mediated bone resorption.

***Disclosures: Jun Guo**, None.*

1076

sFRP4 Regulates Bone Remodeling by Attenuating Both Wnt and BMP Signaling with Differential Effects on Trabecular- and Cortical Bone in Mice. Hiroaki Saito*[1], Key Yamana[2], Eric Hesse[3], Riku Kiviranta[4], Lynn Neff[1], Marta Hristova[5], Henry Kronenberg[6], Beate Lanske[1], Roland Baron[7]. [1]Harvard School of Dental Medicine, USA, [2]Teijin Institute for BioMedical Research, Teijin Pharma Limited, Japan, [3]Harvard Schools of Medicine & Dental Medicine, USA, [4]University of Turku, Finland, [5]Harvard School of Dental Medicine, Beth Israel Deacones Medical Center, USA, [6]Massachusetts General Hospital, USA, [7]Harvard School of Medicine & of Dental Medicine, USA

Wnt and BMP signaling regulate bone remodeling. Secreted Frizzled Related Protein 4 (sFRP4) is a member of a family of Wnt inhibitors that function as decoy Wnt receptors, thereby depleting Wnt ligands. Unlike Dickkopf 1 (Dkk1) and Sclerostin, sFRP4 suppresses activation of both canonical and non-canonical Wnt pathways. We previously showed that $Sfrp4^{+/-}$ and $Sfrp4^{-/-}$ mice have increased trabecular bone volume (BV) with a more than 2-fold increase in bone formation rate (BFR),due to increased osteoblast (OB) differentiation and activity as demonstrated by increases in OB surface, OB number, mineralizing surface, and mineral apposition rate (MAR), but no change in bone resorption. In contrast, cortical bone in $Sfrp4^{-/-}$ mice was significantly thinner with a decrease in periosteal and endosteal MAR. Thus, deletion of *Sfrp4* favored trabecular BFR and BV but had negative effects on cortical bone in adult mice. This contrasts with the effect of activation of canonical Wnt signaling due to allelic loss of Dkk1 or a lack of Sclerostin expression, but resembles the targeted transgenic *Bmp4* phenotype. We therefore determined whether the trabecular and cortical effects of *Sfrp4* deletion were due to Wnt or BMP signaling. Osteogenic differentiation of $Sfrp4^{-/-}$ calvarial cells was accelerated and analysis of BMP signaling showed increased pSmad protein and upregulation of the BMP target genes Id1, -2 and -3, suggesting that sFRP4 also inhibits endogenous BMP signaling.

To test whether canonical Wnt signaling also contributed to the cortical phenotype, we crossed $Sfrp4^{+/-}$ mice with mice that overexpress *Dkk1* driven by the collagen I-2.3Kb promoter (*Dkk1*-TG). In these mice, canonical Wnt signaling is antagonized whereas the non-canonical pathway is not expected to be affected. *Dkk1*-TG expression in $Sfrp4^{+/-}$ mice normalized the increased trabecular BFR, thereby correcting the high BV. However, the thin cortical bone in $Sfrp4^{+/-}$ mice was not worsened by high levels of Dkk1. These results suggest that activation of non-canonical Wnt and/or BMP signaling pathways when sFRP4 is absent may inhibit cortical bone formation. In conclusion, our results suggest that 1/ sFRP4 deletion activates not only Wnt signaling but also BMP signaling and 2/ while increased canonical Wnt signaling when sFRP4 is deleted has positive effects on trabecular bone formation, activation of non-canonical Wnt and/or BMP signaling may inhibit cortical bone formation.

***Disclosures: Hiroaki Saito**, None.*

1077

Targeted Deletion of Gsα in Early Osteoblasts Leads to Decreased Wnt Signaling and Favors Adipogenic Differentiation of Mesenchymal Progenitors. Partha Sinha*[1], Piia Aarnisalo[2], Min Chen[3], Lee Weinstein[3], Henry Kronenberg[1], Joy Wu[1]. [1]Massachusetts General Hospital, USA, [2]University of Helsinki, Finland, [3]National Institute of Diabetes & Digestive & Kidney Diseases, USA

Progenitors of adipocytes and osteoblasts both arise from mesenchymal stem cells, and animal models and clinical observations suggest an inverse relationship between bone density and bone marrow adiposity. Gsα, a heterotrimeric G protein subunit, mediates cyclic AMP-dependent signaling of G protein-coupled receptors including the parathyroid hormone (PTH)/PTH-related peptide (PTHrP) receptor (PPR). Targeted deletion of Gsα early in the osteoblast lineage (Osterix-Cre:Gsα(fl/fl) mice) leads to osteoporosis and multiple fractures at birth. Histological analysis of bone marrow from mutant mice revealed increased adiposity as compared to wild-type bone marrow. To assess the differentiation potential of bone marrow stromal cells (BMSCs) from these mice and the mechanisms regulating this potential, we isolated BMSCs from Gsα conditional knockout mice and evaluated their differentiation in vitro. Such cells grown to confluence in vitro showed increased adipogenic differentiation as quantitated by oil red O staining. We found that BMSCs isolated from conditional knockout mice formed fewer Colony Forming Unit-Fibroblasts (CFU-F) compared to wild-type BMSCs. Furthermore, knockout BMSCs contained fewer CFU-alkaline phosphatase (CFU-ALP) osteoprogenitors, while the proportion of adipocyte progenitors (CFU-Adip) was increased as compared to wild-type. Loss of Gsα in early osteoblasts may favor adipocyte differentiation because of alterations in canonical Wnt signaling, which regulates the commitment of mesenchymal progenitors into the osteoblast versus adipocyte lineages. We have previously reported that osterix-Cre:Gsα(fl/fl) mice have increased expression of sclerostin, an inhibitor of canonical Wnt signaling secreted by osteocytes. Correspondingly, primary calvarial osteoblasts harvested from knockout mice had decreased mRNA levels of the Wnt targets Tcf1, Lef1, Axin2, and CycD1 as compared to wild-type calvarial osteoblasts. Taken together, these studies point to a key role for Gsα signaling in cells of the early osteoblast lineage in governing the balance of osteoblast and adipocyte progenitors, and suggest this may be mediated by alterations in Wnt signaling.

***Disclosures: Partha Sinha**, None.*

1078

Lrp6 and Lrp5 Exert Distinct Roles in Regulating Bone Acquisition in the Mature Osteoblast. Cassandra R. Zylstra[1], Ryan Riddle*[2], Chao Wan[3], Daniel Robinson[1], Charlotta Lindvall[1], Thomas Clemens[4], Bart Williams[1]. [1]Van Andel Research Institute, USA, [2]Johns Hopkins University School of Medicine, USA, [3]University of Alabama, Birmingham, USA, [4]Johns Hopkins University, USA

Despite the well-accepted role of the canonical Wnt signaling pathway on skeletal development, the specific biological roles of the Wnt co-receptors Lrp5 and Lrp6 in bone have remained controversial. To define the individual contributions of Lrp5 and Lrp6 in skeletal development, we used Cre-LoxP recombination to create mice lacking each co-receptor selectively in osteoblasts. Mice lacking Lrp5 (ΔLrp5) or Lrp6 (ΔLrp6) in mature osteoblasts were generated by crossing Lrp6flox and Lrp6flox mice

with mice expressing cre-recombinase under the control of the human osteocalcin promoter (OC-CreTG) and were born at the expected Mendelian frequence and were viable. DEXA indicated reduced BMD at 3 months in both the ΔLrp6 and ΔLrp5 mice. Assessment of femoral bone morphology by microCT revealed significantly lower bone volume with decreased trabecular numbers in ΔLrp6 mice when compared to controls. Trabecular bone volume was not different from controls in ΔLrp5 mice. By contrast, cortical bone morphology was altered in Lrp5 mutants, which exhibited marked increases in cortical cross-sectional area. Mice deficient for both LRP5 and LRP6 had severely reduced cortical and trabecular bone volume similar in magnitude to that observed previously in mice lacking β-catenin (Holmen, et al, J Biol Chem 2005 280; 21162-8). Quantitative histomorphometric analysis disclosed a dramatically decreased number of osteoblasts in the ΔLrp5;ΔLRP6 mice. In vitro deletion of Lrp6 impaired the differentiation of primary osteoblasts as the expression of alkaline phosphatase, Runx2, and Osteocalcin were significantly reduced. These phenotypic markers were unaffected in Lrp5-deficient osteoblasts differentiated in vitro. Simultaneous disruption of both co-receptors in vitro altered fate-specification of calvarial cells which showed abundant alcian blue staining and increased expression of Sox9, Collagen II and Collagen X mRNA. These results suggest that Lrp5 and Lrp6 can serve overlapping functions in skeletal development, but that Lrp6 is required for normal trabecular bone acquisition, while Lrp5 appear to regulate cortical bone structure.

***Disclosures: Ryan Riddle**, None.*

1079

DAG Coordinates Polarized Secretion in Resorptive Osteoclasts through Activation of the PKCδ- MARCKS Pathway in Vitro and in Vivo. Viviana Cremasco*[1], Roberta Faccio[2]. [1]Washington University School of Medicine, USA, [2]Washington University in St Louis School of Medicine, USA

Both osteoclast (OC) development and bone resorption require the catalytic activity of the lipase PLCγ2, which generates the two second messengers IP3 and DAG. Despite the recognized importance of IP3 in calcium oscillations during OC development, little is known about the role of DAG in these cells. Novel PKC proteins are exclusively activated by DAG and, within this PKC family, we found that PKCδ is highly expressed in OCs. Moreover, consistent with the role of PLCγ2 in generating DAG, adhesion-dependent activation of PKCδ is dampened in PLCγ2-/- OCs. To study the role of DAG-mediated pathways in OCs, we examined the bone phenotype of mice congenitally lacking PKCδ. 6-week old, unmanipulated PKCδ-deficient animals exhibit increased bone mass as determined by histomorphometric analysis (26.9+/-3.2% increase in BV/TV vs WT mice). While OC differentiation is unperturbed, PKCδ-/- OCs are characterized by a flattened morphology in vitro and in vivo, indicative of defective polarization on bone. Despite presence of intact actin rings, genetic disruption of PKCδ significantly impairs OC bone resorption, as determined by collagen type I secretion in the media (CTX 32.7nm in WT and 6.3nm in KO, p=0.04). Strikingly, we observed that PKCδ is required for localization of cathepsin K within actin rings and for its polarized secretion in the resorptive lacunae. Mechanistically, we found that the actin bundling protein MARCKS becomes phosphorylated in a PKCδ-dependent manner upon OC adhesion. Furthermore, MARCKS localizes within the actin ring, implicating this protein in orchestrating polarized secretion during bone resorption. In support of this hypothesis, gene silencing of MARCKS, similarly to PKCδ-deficiency, reduces OC bone resorption (resorbed area/total area 23.5% in WT vs 10.6% in MARCKS knock-down, p=0.03) without affecting cell differentiation. Our results demonstrate a previously unknown role for DAG-PKCδ-MARCKS pathway as a critical regulator of OC polarized secretion during bone resorption, thus positioning this pathway as a possible anti-resorptive target.

***Disclosures: Viviana Cremasco**, None.*

1080

TNF-α Induced Osteoclastogenesis and Inflammatory Bone Resorption are Negatively Regulated by the Notch-RBP-J Pathway. Baohong Zhao*, Xiaoyu Hu, Lionel Ivashkiv. Hospital for Special Surgery, USA

Notch receptors Notch1, 2 and 3 have been implicated in regulation of RANKL-induced osteoclastogenesis in vitro, but the effects are relatively modest, results obtained by different groups were not consistent, and mechanisms of regulation are not clear. The role of Notch signaling in pathologic inflammatory bone resorption is not known. In this study, we investigated the role of Notch signaling in osteoclastogenesis and bone resorption under inflammatory conditions. TNF-α did not detectably induce osteoclastogenesis in wild type (WT) bone marrow macrophages (BMMs). Deletion of RBP-J, the master transcription factor in Notch signaling, resulted in dramatic induction of osteoclastogenesis by TNF-α in the absence of exogenous RANKL, comparable to that induced by RANKL in WT cells. TNF-α-induced mouse osteoclasts derived from RBP-J deficient cells formed actin rings and resorbed dentin slices in vitro. Similar results were obtained using TNF-α-treated human osteoclast precursors in which RBP-J expression was knocked down using RNA interference. RBP-J deficiency had a much more modest augmenting effect on RANKL-induced osteoclastogenesis. TNF-α induced dramatically increased levels of the osteoclast master regulator NFATc1 and osteoclast marker genes including TRAP, cathepsin K, and integrin β3 in RBP-J deficient relative to WT cells. RBP-J deficiency resulted in increased TNF-α-induced NFATc1 transcription and RNA Pol II occupancy at the NFATc1 gene locus. These results show that RBP-J negatively regulates TNF-α-induced osteoclastogenesis by suppressing induction of NFATc1. Mechanisms by which RBP-J suppressed NFATc1 induction included decreasing NF-κB recruitment to the NFATc1 promoter while increasing expression of IRF8, a transcriptional repressor that suppresses osteoclastogenesis. Mice with a myeloid-specific deletion of RBP-J (RBP-J$^{f/f}$ LysM-Cre) did not exhibit a bone phenotype under physiological conditions. However, RBP-J$^{f/f}$ LysM-Cre mice showed dramatically increased osteoclast formation, severe bone destruction and increased serum TRAP levels relative to littermate controls in a TNF-α-induced model of pathological inflammatory bone resorption. These findings identify a key role for Notch component RBP-J in restraining inflammatory TNF-α-induced osteoclastogenesis and provide mechanisms by which RBP-J suppresses NFATc1 induction. Notch/RBP-J signaling plays a more prominent role in inhibiting osteoclastogenesis in inflammatory settings than under physiological conditions.

***Disclosures: Baohong Zhao**, None.*

1081

Itch, an E3 Ligase, Negatively Regulates Osteoclastogenesis by Promoting Deubiquitination of TRAF6 Through Interaction With the Deubiquitinating Enzyme, Cylindromatosis. Hengwei Zhang*[1], Chengyu Wu[2], Lydia Matesic[3], Brendan Boyce[4], Lianping Xing[2]. [1]Univeristy of Rochester, USA, [2]University of Rochester, USA, [3]University of South Carolina, USA, [4]University of Rochester Medical Center, USA

Osteoclastogenesis requires RANKL-induced signaling in osteoclast precursors (OCPs). RANKL binds to RANK leading to TRAF6 ubiquitin-mediated processing. TRAF6 ubiquitination then triggers downstream signaling, leading to osteoclast (OC) differentiation, but the mechanisms whereby this process is controlled have not been well investigated. Here, we report that the E3 ligase, itch, functions as a negative regulator of OC formation by promoting deubiquitination of TRAF6 and thereby limiting RANKL-induced OC formation. Itch is a HECT family E3 ligase, which affects cell function through the regulation of ubiquitination of target proteins, but its role in bone cell function is unknown. First, we demonstrated that Itch-/- cells formed more OCs than WT cells (#OCs/well: 360+24 vs 220+12) in response to RANKL, associated with a 3-4 fold increased expression of c-Fos and NFATc1. We then generated a retroviral expression vector for itch, infected WT and itch-/- OCPs with itch retrovirus, and cultured them with RANKL to form OCs. Itch over-expression significantly reduced RANKL-induced WT OC formation (#OCs/well: 120+12 vs 264+22 in GFP controls) but prevented increased OC formation of itch-/- cells (#OCs/well: 240+18 vs 400+32 in GFP-infected cells). We next used an ubiquitination assay to investigate the mechanism by which itch inhibits RANKL-induced OC formation. Two days of RANKL treatment induced TRAF6 ubiquitination in WT OCPs, the degree of RANKL-induced TRAF6 ubiquitination being similar in itch-/- and WT cells. However, ubiquitinated-(Ub-) TRAF6 disappeared after RANKL withdrawal in WT cells, while Ub-TRAF6 persisted in itch-/- cells, suggesting mis-regulation of TRAF6 ubiquitination in the absence of itch. A recent study reported that the deubiquitinating enzyme, cylindromatosis (CYLD), controls de-ubiquitination of TRAF6, thereby negatively regulating OC formation. We found that flag-tagged itch directly bound to HA-tagged CYLD in 293T cells. In OCPs, endogenous itch interacted with CYLD and TRAF6, but an itch mutant lacking ligase activity did not interact with CYLD. Finally, we found that RANKL increased itch mRNA expression starting at 4 hrs and peaking at 24 hr. RANKL-induced increased itch expression was confirmed by Western blot. Our findings suggest that itch is a new RANKL target gene, which is induced during osteoclastogenesis and functions as a deubiquitinating adaptor molecule to limit RANKL-induced OC formation.

***Disclosures: Hengwei Zhang**, None.*

1082

PTHR1 in Osteocytes Plays a Major role in Perilacunar Remodeling through the Activation of "Osteoclastic" Genes in Osteocytes. Hai Qing*[1], Paola Divieti Pajevic[2], Kevin Barry[3], Vladimir Dusevich[4], John Wysolmerski[5], Lynda Bonewald[6]. [1]UMKC Dental School, USA, [2]Massachusetts General Hospital, USA, [3]Endocrine Unit, Massachusetts General Hospital, USA, [4]University of Missouri-Kansas city, USA, [5]Yale University School of Medicine, USA, [6]University of Missouri - Kansas City, USA

We have previously shown that during lactation, osteocytes directly remodel their perilacunar and pericanalicular matrix, thereby mobilizing calcium and contributing to maternal bone loss. It is known that osteocytes express the type 1 parathyroid-hormone (PTH)/ PTH related peptide (PTHrP) receptor (PTHR1) and that circulating levels of PTHrP are elevated during lactation. To determine if the PTHR1 is involved in perilacunar remodeling, mice lacking the PTHR1 in osteocytes (PTHR1-cKO) were generated by crossing DMP1-Cre mice with PTHR1 fl/fl mice. 12-wk old mice were allowed to become pregnant, deliver and lactate for 12 days before sacrifice. MicroCT analysis showed significant overall bone loss in wild-type lactating compared to wild-type virgin mice that was attenuated in lactating animals with PTHR1 deleted in osteocytes. Unlike control mice, no increase was observed in osteocyte lacunar size in PTHR1-cKO mice during lactation, either in cortical or trabecular bone, and there was no increase of osteocyte-specific TRAP activity. To identify genes potentially

responsible for perilacunar remodeling, microarray analysis was performed on tibiae from CD-1 virgin and lactating mice and mice sacrificed on day 7 post weaning. Periosteum and bone marrow were removed from the tibiae and the bone fragments underwent sequential collagenase/trypsin digestion and were examined histologically to ensure removal of all surface cells and confirm osteocyte enrichment prior to RNA extraction. Microarray data (Affy M430 arrays, n=3 per group) showed that PTHR1 was increased in lactating compared to virgin and post-lactation animals in addition to TRAP, Cathepsin K, ATP6V0D2, NFATc1 and other 'osteoclastic' genes (table). However, there was no significant change in expression of Rank and NF-kB, which are involved in osteoclast formation. These data were validated by qPCR showing a 5.7 ± 3.4 fold ($p<0.05$) increase of TRAP mRNA in lactating mice compared to virgin. A similar increase in TRAP and cathepsin K was also observed by immunostaining. Together these data suggest that osteocytes utilize some but not all of the molecular mechanisms used by osteoclasts to remove perilacunar bone matrix and that PTHR1 expression in osteocytes plays an essential role. These observations support the osteocyte as an important target for PTH/PTHrP actions in bone and suggest that the osteocyte may play a role in directly mobilizing calcium from bone ECM when there is a high calcium demand.

Table

Gene symbol	Gene name	Fold change Lac/virgin	Fold change Post/lac/lac
ATP6V0d2	ATPase, H+ transporting, lysosomal V0 subunit D2	3.6**	−2.9**
Car1	carbonic anhydrase 1	2.2*	−9.8**
Car2	carbonic anhydrase 2	1.8*	−12.7**
CTSK	Cathepsin K	3.6**	−2.5**
NFATc1	nuclear factor of activated T-cells, cytoplasmic, calcineurin-dependent 1	3.8*	−1.5
Nhede2	Na+/H+ exchanger domain containing 2	3.4**	−3.0**
ACP5	acid phosphatase 5, tartrate resistant	3.3**	−3.4*
PTHR1	parathyroid hormone receptor 1	1.5	−0.65

Values shown as fold changes; * P<0.05, ** P<0.01, Lac:lactation, P:p/lac: post lactation

Differentially expressed genes in osteocytes during lactation

***Disclosures: Hai Qing**, None.*

1083

Osteocyte Apoptosis Promotes Angiogenesis and Osteoclast Precursor Adhesion *In Vitro*. Wing-Yee Cheung*[1], Craig Simmons[1], Lidan You[2]. [1]University of Toronto, Canada, [2]Mechanical & Industrial Engineering, University of Toronto, Canada

In vivo studies have shown that osteocyte apoptosis precedes osteoclast resorption at the local remodelling site. Osteoclast precursors are transported from the bone marrow to the remodelling site via the circulation. However, the specific mechanisms by which osteoclast precursors are transported from the capillary in the Haversian canal to the adjacent bone lining surface are not clearly elucidated. We hypothesize that osteocyte apoptosis promotes angiogenic sprouting from the Haversian capillary to aid in osteoclast precursor recruitment, and activates the endothelium to allow for osteoclast precursor adhesion. We found that conditioned media from TNF-α induced apoptotic osteocytes induced a 90% increase in endothelial cell proliferation ($P<0.05$), a 70% increase in endothelial cell migration ($P < 0.05$), and more complex tubule network formation with longer ($P<0.01$) and more ($P < 0.001$) branches compared to treatment with non-apoptotic osteocyte conditioned media. Apoptotic osteocyte conditioned media contained 20% more VEGF than non-apoptotic osteocyte conditioned media ($P=0.01$). The VEGF concentration found in apoptotic osteocyte conditioned media formed endothelial tubule networks with longer ($p<0.05$) and more ($p<0.02$) branches than the VEGF concentration in non-apoptotic osteocyte conditioned media. Blocking VEGF in apoptotic osteocyte conditioned media abolished tubule formation effects ($p<0.001$). Endothelial cells treated with apoptotic osteocyte conditioned media had 130% greater osteoclast precursor adhesion than endothelial cells treated with non-apoptotic osteocyte conditioned media ($p<0.03$). Our results suggest that osteocyte apoptosis assists in osteoclast precursor recruitment by promoting angiogenesis (endothelial cell proliferation, migration and tubule formation) and enhancing osteoclast precursor adhesion to the endothelium.

***Disclosures: Wing-Yee Cheung**, None.*

1084

Talin is Critical for Osteoclast Function by Mediating Inside-Out Integrin Activation. Wei Zou*[1], Brian Petrich[2], Susan J. Monkley[3], David R. Critchley[4], Mark H. Ginsberg[2], Steven Teitelbaum[1]. [1]Washington University in St. Louis School of Medicine, USA, [2]Department of Medicine, University of California, USA, [3]Department of Biochemistry, University of Leicester, United Kingdom, [4]University of Leicester, United Kingdom

Bone degradation by osteoclasts (OCs) depends upon their capacity to organize cytoskeleton, which is mediated by a signaling complex stimulated by the $\alpha v\beta 3$ integrin or the M-CSF receptor. Whether the two receptors activate this complex independently or collaboratively is unknown. We find M-CSF treatment of OCs transits $\alpha v\beta 3$ from a low affinity to a high affinity conformation suggesting M-CSF stimulates the cytoskeleletal signaling complex, indirectly via the integrin (inside-out activation). Talin (TLN) is a large cytosolic protein which by interacting with β cytoplasmic domains is a final step to integrin activation. We asked if TLN mediates M-CSF/$\alpha v\beta 3$-stimulated bone resorption. We find TLN constitutively expressed throughout osteoclastogenesis and M-CSF treatment promotes its association with the $\beta 3$. TLN activates $\alpha v\beta 3$ by associating with specific residues in the $\beta 3$ cytoplasmic domain, including Y747. OCs bearing the β3Y747A (YA) mutation fail to spread or normally resorb bone, in vitro. Affirming that the resorptive defect represents OC dysfunction and not arrested maturation, YA mutants normally express OCs differentiation markers. Furthermore, TLN fail to localize to the plasma membrane in YA OCs, underscoring the biological necessity of $\beta 3$/TLN recognition. Confirming this posture in vivo, YA mice have significantly more bone following OVX than do WT. Having established that mutating the TLN binding site in $\beta 3$ results in impaired OCs function, we asked whether the same obtains in TLN-/- mice. As the TLN-/- mouse is early embryonic lethal, we mated $TLN^{f/f}$ with cathepsin K-cre mice to delete TLN only in mature OCs ($TLN^{\Delta OC/\Delta OC}$) or Lys M-Cre mice to delete TLN in all OC lineage cells. Absence of TLN does not affect macrophage proliferation and apoptosis, it impairs their spreading and diminishes integrin induced cytoskeleton-organizing signals. Mn^{2+}, which directly activates integrins absent inside-out signals, partially rescues this defect. In keeping with inhibited resorption, bone mass is increased 3 fold ($p<0.01$) in $TLN^{\Delta OC/\Delta OC}$ mice as measured by μCT and DEXA. The presence of abundant OCs confirms the enhanced bone mass of $TLN^{\Delta OC/\Delta OC}$ mice reflects resorptive dysfunction and not diminished number. Indicating clinical relevance, $TLN^{\Delta OC/\Delta OC}$ mice are protected from OVX-induced bone loss and the periarticular osteolysis attending inflammatory athritis. Thus, TLN is critical for OC function and mediates M-CSF-induced $\alpha v\beta 3$ integrin activation in OC.

***Disclosures: Wei Zou**, None.*

1085

Increasing Adiponectin Via an Apolipoprotein Peptide Mimetic, L-4F, Reduces Tumor Burden and Increases Survival in a Murine Model of Myeloma. Jessica Fowler*, Seint Lwin, Gregory Mundy, Claire Edwards. Vanderbilt University, USA

Multiple myeloma (MM) remains a fatal malignancy associated with a destructive osteolytic bone disease, and it is essential to evaluate new therapeutic approaches. We have previously identified adiponectin (ADPN) as decreased in mice that are permissive for MM, suggesting a role for this adipokine in MM pathogenesis. *In vitro* studies revealed that ADPN had direct effects on MM cells to increase apoptosis. The aim of the current study was to determine the effect of increasing ADPN on MM development *in vivo*. Treatment of C57Bl/KaLwRij mice for 4 weeks with the apolipoprotein peptide mimetic L-4F (200ug/100g/day) resulted in increased serum ADPN ($p<0.01$, compared to vehicle-treated). Mice were treated with L-4F for 4 weeks prior to i.v. inoculation of 5TGM1 MM cells. Treatment was continued throughout the experiment to maintain the change in ADPN. Measurement of MM-specific IgG2b concentrations demonstrated that mice treated with L-4F had a significant decrease in the rate of MM development ($p<0.01$, compared to vehicle), evident as early as 7 days after tumor inoculation. FACS analysis of GFP-positive MM cells confirmed a significant reduction in tumor burden within the bone marrow (BM) of mice treated with L-4F ($p<0.01$). Immunohistochemical analysis of BM of MM-bearing mice treated with L-4F demonstrated a significant increase in TUNEL positive MM cells ($p<0.05$), indicative of apoptosis. There was also a significant decrease in Ki67 staining in the BM of L-4F-treated mice ($p<0.05$), compared to vehicle. In separate studies, MM-bearing mice treated with L-4F showed an overall increase in survival in comparison to vehicle ($p<0.0001$). In addition, L-4F-treated-mice had a significant increase in bone formation rates compared to vehicle-treated mice ($p<0.001$). *In vitro* studies demonstrated that L-4F had no direct effect on MM cell growth, but directly induced ADPN expression in BM stromal cells (BMSCs). Treatment of MM cells with conditioned media (CM) from L-4F-treated BMSCs increased MM cell apoptosis ($p<0.05$, compared to vehicle CM), suggesting L-4F may increase ADPN expression via the BM microenvironment and so induce MM cell apoptosis. Taken together, our results suggest that increasing ADPN with L-4F may reduce tumor burden via an effect on cells in the host microenvironment, so preventing MM bone disease and increasing survival. These studies identify both ADPN and L-4F as potential therapeutic approaches for the treatment of MM.

***Disclosures: Jessica Fowler**, None.*

1086

Host-derived MMP-7 Decreases Myeloma Progression *In Vivo*: An Unexpected Role for MMP-7 in Myeloma Pathogenesis. Seint Lwin*, Conor Lynch, Jessica Fowler, Gregory Mundy, Claire Edwards. Vanderbilt University, USA

Defining interactions within the bone marrow microenvironment that promote the development of multiple myeloma (MM) is essential to identify new therapeutic approaches. Matrix metalloproteinases (MMPs) are key regulators of tumor:host interactions due to their ability to alter activity of multiple substrates. Increasing evidence supports a critical role for host-derived MMPs in cancer progression and MMP7 has recently been implicated in breast and prostate cancer-mediated osteolysis. We hypothesized that host-derived MMP7 may play a role in MM bone disease *in vivo*. We have previously shown that inoculation of 5TGM1 MM cells into C57Bl/$RAG2^{-/-}$ mice resulted in MM development with osteolytic bone disease identical to that in the syngeneic C57Bl/KaLwRij strain. Our aim was to use Rag2/MMP7 null

($MMP7^{-/-}$) mice to investigate the role of host-derived MMP7 in MM *in vivo*. Inoculation of 5TGM1-GFP MM cells into $MMP7^{-/-}$ mice unexpectedly resulted in a significant increase in the rate of tumor growth, as measured by serum IgG2bk concentrations, when compared to MM-bearing $Rag2^{-/-}$ wild-type mice (WT). This surprising finding suggested that host MMP7 plays a protective rather than a contributory role in MM. FACS analysis of GFP-positive MM cells confirmed a 72% increase in tumor burden within bone in MM-bearing $MMP7^{-/-}$mice, as compared to MM-bearing WT mice ($p<0.01$). MicroCT analysis demonstrated a 47% decrease in BV/TV and 67% increase in osteolytic lesions in MM-bearing $MMP7^{-/-}$mice as compared with MM-bearing WT mice ($p<0.01$). No significant difference in osteoclast or osteoblast number was found. In support of an effect of host-derived MMP7 on tumor growth and/or survival, a 51% decrease in MM cell apoptosis was observed in MM-bearing $MMP7^{-/-}$ mice ($p<0.05$). Furthermore, in vitro studies found no MMP7 expression in MM cells, and no direct effect of MMP7 on MM cell proliferation or apoptosis. Using a candidate list of MMP7 substrates, we identified that $MMP7^{-/-}$mice had increased serum osteopontin (OPN), compared to WT (233 ± 5.7 ng/ml vs. 167 ± 12.3 ng/ml, $p<0.001$). OPN is a MM cell survival factor and we propose that processing of OPN by MMP7 may abrogate the survival effect of full-length OPN. Our studies suggest that host-derived MMP7 inhibits MM growth in vivo, demonstrating that MMPs can play differential roles in specific disease contexts and supporting the rationale for the design of selective MMP inhibitors for the treatment of MM bone disease.

***Disclosures: Seint Lwin**, None.*

1087

Myeloid Derived Suppressor Cells (MDSC) are Responsible for Enhanced Bone Tumor Growth in Osteopetrotic *PLCγ2-/-* mice and are a Direct Target of Zoledronic Acid. Seokho Kim*[1], Deborah Novack[2], Roberta Faccio[3]. [1]Department of Orthopedics, Washington University, St. Louis MO, USA, [2]Washington University in St. Louis School of Medicine, USA, [3]Washington University in St Louis School of Medicine, USA

Despite the well established requirement of active osteoclasts (OC) to sustain tumor growth in bone, we found that PLCγ2-/- mice, with deficiency in OC formation, displayed a 3 fold increase in bone tumor burden compared to WT following intra-tibial (i.t.) and intra-cardiac inoculation of B16 melanoma cells. However, consistent with their OC defect, PLCγ2-/- mice had no tumor-associated bone loss. Even more intriguing, treatment with Zoledronic acid (ZOL), potent inhibitor of bone resorption, significantly suppressed tumor growth in PLCγ2-/- mice, suggesting that another bone-derived cell, targeted by ZOL, modulates tumor growth in these animals. MDSC, a heterogeneous cell population derived from bone marrow, are highly enriched in patients with cancer and potently suppress T-cell mediated anti-tumor responses. Based on the importance of PLCγ2 in myeloid cells, we hypothesized that PLCγ2 may negatively regulates MDSC expansion in tumor bearing mice. In support of this hypothesis, we found that PLCγ2-/- mice i.t. inoculated with B16 or LLC lung tumor cells had enhanced accumulation of MDSC (B16: $8.2 \pm 1.4\%$ in WT, $19 \pm 1.3\%$ in KO; LLC: $14 \pm 1.4\%$ in WT, $31 \pm 1.5\%$ in KO). Importantly, ZOL treatment (100μg/Kg) was sufficient to reverse the increase in MDSC number in vivo and promote apoptosis of MDSC in vitro at 10 and 25 μM, doses too low to directly kill cancer cells. Thus, ZOL may exert an anti-tumor effect in PLCγ2-/- mice by targeting MDSC, independent of its action on the OCs or cancer cells.

Further confirming the relevance of MDSC in tumor growth, WT mice subcutaneously co-injected with tumor cells and MDSC isolated from tumor bearing PLCγ2-/- animals displayed increased tumor burden compared to WT mice receiving tumor alone. Moreover, C57Bl/6 PLCγ2-/- mice, but not WT, allowed growth of the allogenic 4T1 tumor cells derived from BalB/C mice, and this was associated with increased MDSC ($20 \pm 2.7\%$ in WT, $51.6 \pm 3.3\%$ in KO). Taken together, these results indicate that expansion of MDSC is responsible for enhanced tumor burden in bone of osteopetrotic PLCγ2-/- mice. A better understanding of the mechanism leading to MDSC expansion and their targeting by ZOL will be useful for anti-tumor therapy in patients with bone metastases.

***Disclosures: Seokho Kim**, None.*

1088

Multiple Myeloma Cell Induction of GFI-1 in Stromal Cells Suppresses Osteoblast Differentiation in Patients with Myeloma. Sonia D'Souza*[1], Shunqian Jin[1], Benedicte Sammut[1], Chinavenmeni S. Velu[2], Shibing Yu[3], Guozhi Xiao[4], H. Leighton Grimes[2], G. David Roodman[5], Deborah Galson[4]. [1]Center for Bone Biology, University of Pittsburgh, USA, [2]Cincinnati Children's Hospital Medical Center, USA, [3]School of Medicine/Hem-Onc,University of Pittsburgh, USA, [4]University of Pittsburgh School of Medicine, USA, [5]VA Pittsburgh Healthcare System (646), USA

Multiple Myeloma (MM) is a plasma cell malignancy characterized by formation of lytic bone lesions in approximately 90% of the patients which do not heal even after prolonged complete remission. The basis for this selective and protracted suppression of osteoblast (OBL) differentiation from immature bone marrow stromal cells (MSC) is unknown. However, we and others have reported the suppression of RUNX2, a critical transcription factor required for OBL differentiation in MM-altered MSC. The continued inability of MSC to differentiate into OBL even in the absence of MM cells in vivo and in vitro, suggests that the MM cells induced epigenetic changes in the MSC that result in RUNX2 suppression. We have developed a murine model of MM-induced OBL suppression using a murine myeloma cell line engineered to express GFP and thymidine kinase (5TGM1-GFP-TK MM cells). Injection of these 5TGM1-GFP-TK MM cells into SCID mice resulted in persistent and selective inhibition of OBL differentiation even when the MM cells were totally depleted by ganciclovir treatment in vitro. These MM-altered MSC demonstrated RUNX2 suppression and elevated levels of the transcriptional repressor, GFI-1, which can mediate chromatin remodeling. Further, addition of either MM cells in a transwell or TNF-α and IL-7 to MC4, a murine OBL precursor cell line, and to primary murine MSC resulted in inhibition of RUNX2 expression and increased GFI-1 expression. Additionally, neutralizing antibodies to TNF-α and IL-7 blocked MM-induced RUNX2 suppression and GFI-1 expression. Deletion analysis of the RUNX2 P1 promoter revealed that a 1103-bp region (992/+111) containing 29 putative GFI-1 binding sites was responsible for repression of RUNX2 expression by MM cells, TNF-α or by co-transfection with a GFI-1 expression plasmid. A histone deacetylase inhibitor (trichostatin A) abrogated GFI-1 inhibition of the Runx2 promoter reporter. Importantly, MSC from $GFI\text{-}1^{-/-}$ mice are partially resistant to MM-induced RUNX2 expression. In support of these results, we found decreased RUNX2 expression and elevated GFI-1 mRNA and protein levels in MSC from MM patients compared to normals. Significantly, siRNA knockdown of GFI-1 expression partially restored RUNX2, OCN, BSP and OSX expression in both MM exposed MC4 cells and in MSC from MM patients. These results support an important role for GFI-1 in repressing RUNX2 expression in MSC exposed to MM cells, thereby inhibiting osteoblastogenesis in MM.

***Disclosures: Sonia D'Souza**, None.*

1089

Heparanase Promotes Osteoclastogenesis in Multiple Myeloma by Upregulating RANKL Expression. Yang Yang*[1], Yongsheng Ren[2], Li Nan[2], Vishnu C Ramani[2], Larry Suva[3], Ralph D Sanderson[4]. [1]The University of Alabama At Birmingham, USA, [2]Department of Pathology, University of Alabama at Birmingham, USA, [3]University of Arkansas for Medical Sciences, USA, [4]Department of Pathology, Comprehensive Cancer Center & the Center for Metabolic Bone Disease, University of Alabama at Birmingham, USA

Excessive bone destruction is a major cause of morbidity in myeloma patients. However, the biologic mechanisms involved in the pathogenesis of myeloma-induced bone disease are poorly understood. Heparanase, an enzyme that cleaves the heparan sulfate chains of proteoglycans, is upregulated in a variety of human cancers, including myeloma. Using SCID-hu and SCID-tibia animal models with the injection of CAG myeloma cells engineered to express either high or low levels of heparanase, we have demonstrated that heparanase expression promotes both local and systemic osteolysis. To investigate the underlying mechanism in heparanase induced bone destruction, the levels of human RANKL (a primary mediator of osteoclastogenesis) and OPG (a RANKL inhibitor) in these tumors were evaluated by immunohistolochemical staining and western blotting. A significant elevation of RANKL was observed in heparanase-high tumors compared to heparanase-low tumors, while the level of OPG was not affected. In vitro, RANKL levels were significantly elevated in both cell extracts and conditioned medium of CAG myeloma cells when heparanase expression was enhanced. In addition, the elevation of RANKL expression and secretion was also found in other myeloma cell lines (MM.1S and U266) when the cells were cultured in the presence of recombinant human heparanase for 48 hours. To examine the potential clinical significance of heparanase in myeloma bone disease, we investigated whether heparanase expression correlated with RANKL expression in myeloma patients. Heparanase, RANKL and OPG immunohistochemical staining was performed in 20 bone marrow core biopsy specimens of myeloma patients. The results showed a positive, highly significant correlation between the levels of expression of heparanase and RANKL in both myeloma cells and stromal cells in these patients ($p<0.0001$). The expression of OPG was detected in bone marrow cells but not in myeloma cells. However there was no significant correlation between the expression of heparanase and OPG within the bone marrow ($p=0.22$). In addition, increased heparanase expression in clinical samples was associated with an increased number of TRAP positive osteoclasts. These discoveries identify a novel role for heparanase in myeloma, provide new insights into the mechanisms of myeloma-induced bone disease and further validate the use of heparanase inhibitors in the treatment of myeloma bone disease.

***Disclosures: Yang Yang**, None.*
This study received funding from: NIH grant CA135075 and CA138340

1090

A Novel Anti-resorptive Agent, Reveromycin A, Ameliorates Bone Destruction and Tumor Growth in Myeloma. Keiichiro Watanabe*[1], Masahiro Abe[2], Qu Cui[3], Makoto Kawatani[4], Masahiro Hiasa[5], Ayako Nakano[6], Tadashi Jinno[3], Takeshi Harada[3], Shiro Fujii[3], Shingen Nakamura[3], Hirokazu Miki[3], Kumiko Kagawa[3], Kyoko Takeuchi[3], Shuji Ozaki[7], Eiji Tanaka[8], Hiroyuki Osada[4], Toshio Matsumoto[9]. [1]The University of Tokushima Graduate School of Oral Science, Japan, [2]University of Tokushima, Japan, [3]Department of Medicine & Bioregulatory Sciences,The University of Tokushima Graduate School, Japan, [4]Chemical Biology Core Facility, RIKEN Advanced Science Institute, Japan, [5]University of Tokushima Graduate School, Japan, [6]University of Tokushima Graduate School of Medicine, Japan, [7]Division of Transfusion Medicine, Tokushima University Hospital, Japan, [8]Depertmentt of Orthodontics & Dentofacial Orthopedics, The University of Tokushima Graduate School of Oral Sciences, Japan, [9]University of Tokushima Graduate School of Medical Sciences, Japan

Multiple myeloma (MM) develops and expands in the bone marrow, and causes devastating bone destruction by enhancing osteoclastic bone resorption in their close vicinity. In MM bone lesions, thus induced osteoclasts (OCs) in turn enhance MM cell growth and survival, thereby forming a vicious cycle between the progression bone destruction and MM tumor expansion. Reveromycin A (RM-A), a small microbial metabolite, preferentially induces apoptosis in acid-producing OCs, and draws considerable attention as a novel anti-resorptive agent. In the present study, we explored the effects of RM-A on bone resorption and tumor expansion in MM. INA6 and RPMI8226 MM cells potently enhanced osteoclastogenesis and osteoclastic pit formation when cocultured with rabbit bone marrow cells on bone slices. Notably, large multinucleated OCs were almost completely disappeared and pit formation on bone slices was abolished upon the treatment with RM-A at concentrations as low as 100nM. The cocultures with rabbit bone marrow cells stimulated INA6 MM cell growth; RM-A at 1μM was however able to substantially decrease the MM cell viability in the cocultures, although RM-A at this concentration did not affect MM cell growth when MM cells were cultured alone. The suppression of INA6 MM cell viability by RM-A was obviously more potent than that under bisphosphonate treatment in which mature OCs and pits on bone slices similarly decreased in number, suggesting that the anti-MM effects of RM-A is not merely due to depletion of mature OCs. Blockade of acid release from OCs by the proton pump inhibitor concanamycin A abolished such RM-A effects. Given that the acidic microenvironment increases cell permeability of RM-A to cause apoptosis, it is plausible that highly acidic milieu around OCs allows RM-A to act on nearby MM cells as well as OCs. In vivo RM-A effects were next studied using INA6 MM cell-bearing SCID-rab mice. We injected RM-A sc at 4mg/kg twice daily for 18 days to the mice after confirming MM cell growth at 4 weeks after the MM cell inoculation. The RM-A treatment substantially decreased osteolytic lesions in X-ray and μCT images and MM tumor area in bone sections along with a reduction of INA6 cell-derived human soluble IL-6 receptor levels in mouse sera as a marker of MM tumor burden. These results collectively suggest that RM-A may become a novel therapeutic agent against MM with extensive bone resorption.

***Disclosures: Keiichiro Watanabe**, None.*
This study received funding from: Advisory board/Consultant fee: Lilly, Chugai, Teijin, Astellas, Daiichi-Sankyo, JT, Asahi Chemical, Grant support: Ono

1091

Relation of Age, Gender, and Bone Mass to Circulating Sclerostin Levels in Women and Men. Ulrike Moedder*[1], Kelley Hoey[2], Shreyasee Amin[2], Louise McCready[2], L. Joseph Melton[2], Byron Riggs[3], Elizabeth Atkinson[2], Sundeep Khosla[4]. [1]Mayo Clinic College of Medicine, USA, [2]Mayo Clinic, USA, [3]Mayo Clinic College of Medicine,Rochester, MN, USA, [4]College of Medicine, Mayo Clinic, USA

Sclerostin is a potent inhibitor of Wnt signaling and bone formation. However, there is currently no information on the relation of circulating sclerostin levels to age, gender, or bone mass in humans. Thus, we used a recently developed ELISA (Biomedica) to measure serum sclerostin levels in a population-based sample of 365 women (123 premenopausal, 152 postmenopausal not on estrogen treatment [ET], and 87 postmenopausal on ET) and 318 men, age 21 to 97 yrs. In pre- and untreated postmenopausal women combined (n=275), serum sclerostin levels were positively associated with age (R=0.52, $P < 0.0001$); an even stronger association was present in men (R=0.64, $P < 0.0001$). Over life, serum sclerostin levels increased by 2.4- and 4.6-fold in the women and men, respectively. Sclerostin levels were significantly higher in men (mean $\pm$ SEM) (757 $\pm$ 22 pg/ml) versus women (538 $\pm$ 14 pg/ml, $P < 0.001$). In addition, sclerostin levels were significantly lower in postmenopausal women on ET (515 $\pm$ 28 pg/ml) versus untreated women (630 $\pm$ 19 pg/ml, $P < 0.001$). Because sclerostin is produced almost exclusively by osteocytes, we next examined the relation between serum sclerostin levels and total body (TB) bone mass, assessed as TB bone mineral content (TBBMC) by DXA. To reduce confounding by age, we separated the subjects into 3 groups: young (age 20-39 yrs), middle-aged (40-59 yrs), and elderly (60+ yrs). In young women (Figure, Panel A), there was no association between TBBMC and serum sclerostin levels; a modest association was present in middle-aged women (Panel B); the strongest, positive correlations were noted in elderly women (Panel C). As also evident, for a given level of bone mass (TBBMC), sclerostin levels were higher in elderly compared to young women (point 2 vs. 1 in the Figure). Identical findings were noted in men (not shown). In summary, our data demonstrate that (1) serum sclerostin levels increase markedly with age; (2) men have higher serum sclerostin levels compared to women; (3) ET reduces serum sclerostin levels; and (4) compared to young subjects, elderly individuals have higher serum sclerostin levels for a given amount of bone mass. These findings suggest that with aging, individual osteocytes may have increased sclerostin production. Further studies are needed to test this hypothesis as well as the potential role of increases in sclerostin production in mediating the age-related impairment in bone formation.

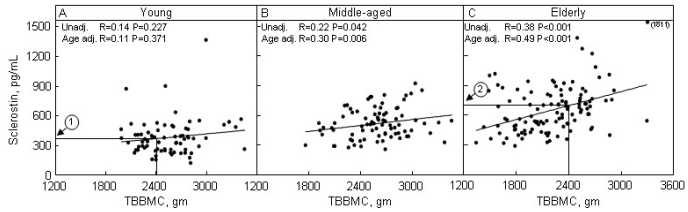

Sclerostin Epid

***Disclosures: Ulrike Moedder**, None.*

1092

Mild Hyponatremia as a Risk Factor for Fractures: The Rotterdam Study. M Zillikens*[1], Ewout Hoorn[2], Joyce Van Meurs[3], Albert Hofman[2], Fernando Rivadeneira[4], Robert Zietse[2], Huibert Pols[4], Andre Uitterlinden[5]. [1]Erasmus MC Rotterdam, The netherlands, [2]Erasmus MC, Netherlands, [3]Erasmus Medical Center, The netherlands, [4]Erasmus University Medical Center, The netherlands, [5]Rm Ee 575, Genetic Laboratory, The netherlands

M. Carola Zillikens MD, PhD1, Ewout J.Hoorn MD, PhD1, Joyce B.J. van Meurs PhD1, Albert Hofman MD, PhD2, Fernando Rivadeneira MD PhD1,2, Robert Zietse MD, PhD1, Huibert A.P. Pols MD, PhD1,2, André G. Uitterlinden PhD1,2

1Department of Internal Medicine, 2Department of Epidemiology, Erasmus Medical Center, Rotterdam, the Netherlands.

Recent studies suggest that mild hyponatremia may be associated with fractures due to increased risk of falling or a decreased bone mineral density (BMD). We investigated in the prospective, population-based, Rotterdam study whether mild hyponatremia at baseline is associated with fractures and studied a relation with recent falls and BMD. We examined 5208 individuals aged 55 years and over who had measurement of serum sodium levels at baseline. Incident non-vertebral fractures (n=926) were recorded during a mean follow-up period of 7.7 years and analyzed in Cox regression models. Vertebral fractures were assessed by X-rays at baseline (n=194) and during a mean follow-up period of 6.4 years (n=139) and analyzed in logistic regression models. Hyponatremia (serum sodium <136 mmol/l,) was detected in 399 subjects (7.7%), with the lowest values of 124 mmol/l. Subjects with hyponatremia were significantly older (73.5 $\pm$ 10.3 vs. 70.0 $\pm$ 9.0 years $P<0.001$), had more recent falls (23.8% vs. 16.4%, $P<0.01$) higher type 2 diabetes prevalence (22.2 vs. 10.3%, $P<0.001$), and used diuretics more often (36.9% vs. 21.3%, $P<0.001$). Hyponatremia was not related to femoral neck or lumbar spine BMD but was associated with increased risk of incident non-vertebral fractures (HR=1.39, 95% CI; 1.11-1.73, P=0.004) after adjustment for age, sex and BMI. Further adjustments for disability index, use of diuretics and psycholeptics, recent falls and prevalent diabetes did not modify the results. Subjects with hyponatremia also had an increased risk of vertebral fractures (combined prevalent and incident) after adjustment for all covariates (OR=1.61, 95% CI; 1.00-2.59, P=0.049). We conclude that mild hyponatremia in elderly subjects is associated with increased risk of recent falls, vertebral fractures and incident non-vertebral fractures but not with BMD. Since increased fracture risk was independent of recent falls and not associated with BMD, a relation with other determinants of bone quality should be studied. When our findings are replicated in an independent population, screening for hyponatremia should be advised for elderly patients with fractures.

***Disclosures: M Zillikens**, None.*

1093

Bone Resorption and Fracture across the Menopausal Transition: The Study of Women's Health Across the Nation (SWAN). Jane Cauley*[1], Michelle Danielson[2], Gail Greendale[3], Joel Finkelstein[4], Yue-Fang Chang[2], Joan Lo[5], Carolyn Crandall[3], Jennifer Lee[6], Robert Neer[4], Mary Fran Sowers[7]. [1]University of Pittsburgh Graduate School of Public Health, USA, [2]University of Pittsburgh, USA, [3]University of California, Los Angeles, USA, [4]Massachusetts General Hospital, USA, [5]Kaiser Permanente, USA, [6]University of California, Davis, USA, [7]University of Michigan, USA

Bone turnover makers have been linked to fracture, independent of bone mineral density (BMD) but the majority of these studies have been carried out in older postmenopausal women. To test the hypothesis that bone turnover markers measured before the final menstrual period predict fracture risk across the menopausal transition and whether changes in bone resorption over the menopausal transition are associated with fractures, we studied 2090 multiethnic women enrolled in SWAN. Women attended up to 8 clinic visits an average of 7.6 ± 1.6 years. Women were pre- or early peri-menopausal at baseline. Self-reported fractures were assessed at each clinic visit. Osteocalcin and urinary cross-linked N-telopeptide of type 1 collagen (NTx) were measured at baseline; NTx was measured at each follow-up. Cox proportional hazards models were used to test whether baseline bone turnover markers predicted fracture; hazards ratios (HR) and 95% confidence intervals were calculated. Repeated measures analyses (generalized estimating equations) were used to test whether changes in NTx from baseline predicted fractures and are expressed as odds ratio (95% CI). Women who fractured (n=181) were more likely to be Caucasian, to report a previous fracture and had lower lumbar spine BMD but not total hip BMD at baseline than women who did not fracture. Baseline NTx was higher in women who fractured compared to women who did not fracture (37.6 vs 34.3 mm BCE/mm Cr, p=0.002) but there was no difference in osteocalcin. Baseline NTx was associated with a higher fracture risk (Table). Women with a baseline NTx greater than the median had a 44% higher risk of fracture over the follow-up period. Women who experienced an increase in NTx greater than the median had a 52% higher risk of fracture. In conclusion, bone resorption markers measured before or during the menopausal transition are associated with fracture risk.

Table: Bone resorption and fracture risk			
	Unit	**HR**	**95% CI**
Baseline NTx and Fracture*			
NTx (log transformed)	1	1.43	(0.99, 2.31)
NTx	>median, 31.9	1.44	(1.04, 2.22)
*Adjusted for fracture history, spine BMD, height, weight, age, race/ethnicity, clinic site, education, smoking, early peri-menopausal status, diabetes.			
	Unit	**HR**	**95% CI**
Changes in NTx from Baseline and Fracture **			
Change in NTx	1 SD	1.15	(1.01, 1.32)
Change in NTx	>median	1.52	(1.08, 2.15)
**Adjusted for baseline NTx, fracture history, spine BMD, changes in spine BMD, height, weight, age, race/ethnicity, clinic site, education, smoking, menopausal status and diabetes.			

Table

***Disclosures: Jane Cauley**, None.*

1094

Association of Menopausal Vasomotor Symptoms with Increased Bone Turnover During the Menopausal Transition. Carolyn Crandall*[1], Chi-Hong Tseng[2], Sybil Crawford[3], Rebecca Thurston[4], Ellen Gold[5], Janet Johnston[6], Gail Greendale[1]. [1]University of California, Los Angeles, USA, [2]UCLA, USA, [3]University of Massachusetts Medical School, USA, [4]University of Pittsburgh School of Medicine, USA, [5]Division of Epidemiology, University of California, Davis, USA, [6]University of Alaska Anchorage Department of Health Sciences, USA

Purpose. To determine the longitudinal association between menopausal vasomotor symptoms (VMS) and urinary N-telopeptide level (Ntx) according to menopausal stage.

Methods. We analyzed data from 2283 participants of the Study of Women's Health Across the Nation, a longitudinal community-based cohort study of women aged 42 to 52 years at baseline. At baseline and annually through follow-up visit 8, participants provided questionnaire data, urine samples, serum samples, and anthropometric measurements. We used repeated measures mixed models to examine associations between annually-assessed VMS frequency and annual Ntx measurements.

Results. After controlling for age, smoking, race/ethnicity, physical activity, alcohol intake, vitamin D intake, calcium intake, body mass index, and study site, mean Ntx was 1.94 nM BCE/mM creatinine higher among early perimenopausal women with any VMS than among early perimenopausal women with no VMS (p< 0.0001). Mean Ntx was 2.44 nM BCE/mM creatinine higher among late perimenopausal women with any VMS than among late perimenopausal women with no VMS (p=0.03). When we compared women with frequent VMS (≥ 6 days in past 2 weeks) and women without frequent VMS, associations between VMS and Ntx additionally reached statistical significance among postmenopausal women. Among premenopausal women, VMS frequency was not significantly associated with Ntx level. Adjustment for serum follicle-stimulating hormone level greatly reduced the magnitudes of associations between VMS and Ntx level.

Conclusion. Among early perimenopausal and late perimenopausal women, those with VMS had higher bone turnover than those without VMS. Prior to the final menstrual period, VMS may be a marker for risk of adverse bone health. The Study of Women's Health Across the Nation (SWAN) and the SWAN Repository (AG017719) have grant support from the National Institutes of Health (NIH), DHHS, through the National Institute on Aging (NIA), the National Institute of Nursing Research (NINR) and the NIH Office of Research on Women's Health (ORWH) (Grants NR004061; AG012505, AG012535, AG012531, AG012539, AG012546, AG012553, AG012554, AG012495). The content of this presentation is solely the responsibility of the authors and does not necessarily represent the official views of the NIA, NINR, ORWH or the NIH.

Associations between VMS and urinary N-telopeptide (Ntx) level in multivariable-adjusted models[1]						
	VMS any vs none: basic model			VMS frequent vs. not frequent[2]: basic model		
Menopausal stage	**β coefficient[3]**	**Standard deviation**	**P value**	**β coefficient[4]**	**Standard deviation**	**P value**
Premenopausal	1.017	0.809	0.17	0.741	1.436	0.61
Early perimenopausal	1.944	0.486	<0.0001	3.077	0.675	<0.0001
Late perimenopausal	2.437	1.011	0.03	3.625	1.069	<0.001
Postmenopausal	1.259	0.769	0.10	1.909	0.799	0.02
	VMS any vs none: model with FSH[4]			VMS frequent vs. not frequent: model with FSH		
Menopausal stage	**β coefficient**	**Standard deviation**	**P value**	**β coefficient**	**Standard deviation**	**P value**
Premenopausal	0.802	0.805	0.32	0.391	1.430	0.78
Early perimenopausal	1.347	0.486	0.006	2.024	0.676	0.003
Late perimenopausal	1.071	1.107	0.33	2.519	1.073	0.02
Postmenopausal	0.546	0.769	0.48	0.919	0.801	0.25
	VMS any vs none: model with estradiol[4]			VMS frequent vs. not frequent: model with estradiol		
Menopausal stage	**β coefficient**	**Standard deviation**	**P value**	**β coefficient**	**Standard deviation**	**P value**
Premenopausal	0.969	0.812	0.23	0.701	1.442	0.63
Early perimenopausal	1.784	0.489	<0.001	2.827	0.679	<0.0001
Late perimenopausal	2.022	1.113	0.07	3.294	1.079	0.002
Postmenopausal	1.307	0.774	0.09	1.748	0.805	0.06
	VMS any vs none: model with FSH and estradiol[5]			VMS frequent vs. not frequent: model with FSH and estradiol		
Menopausal stage	**β coefficient**	**Standard deviation**	**P value**	**β coefficient**	**Standard deviation**	**P value**
Premenopausal	0.787	0.805	0.33	0.443	1.430	0.76
Early perimenopausal	1.336	0.486	0.006	1.022	0.676	0.003
Late perimenopausal	1.042	1.107	0.35	2.492	1.073	0.02
Postmenopausal	0.557	0.769	0.47	0.930	0.801	0.25

[1] Repeated measures models adjusted for age, smoking, body mass index, race/ethnicity, calcium and vitamin D supplement intake, physical activity score (log-transformed), alcohol intake (kcal/d, log-transformed), and study site.
[2] "Frequent VMS" indicates VMS frequency ≥ 5 days in the past 2 weeks. "Not frequent VMS" indicates VMS frequency <5 days in the past 2 weeks.
[3] β coefficient represents the increment in urinary Ntx (nM BCE/mM creatinine) associated with reporting any VMS versus no VMS.
[4] β coefficient represents the increment in urinary Ntx (nM BCE/mM creatinine) comparing frequent VMS compared to not frequent VMS.
[5] Includes variables of basic model, follicle-stimulating hormone level (FSH, IU/l), and menstrual cycle phase (follicular vs. not follicular or unknown phase).
[6] Repeated measures models adjusted for variables of the basic model, serum estradiol concentration (pg/ml), and menstrual cycle phase.
[7] Repeated measures models adjusted for variables of the basic model, serum FSH level, serum estradiol concentration, and menstrual cycle phase.

jpg

***Disclosures: Carolyn Crandall**, None.*

1095

Abdominal Body Composition and Risk of Non-spine Fracture among Elderly Men. Yahtyng Sheu*[1], Lynn Marshall[2], Kathleen Holton[3], Robert Boudreau[1], Peggy Cawthon[4], Jane Cauley[1]. [1]University of Pittsburgh Graduate School of Public Health, USA, [2]Oregon Health & Science University, USA, [3]Oregon Health & Sciences University, USA, [4]California Pacific Medical Center Research Institute, USA

The association of abdominal body composition with incident fracture is unclear. To examine the relationships between incident fracture and abdominal adipose tissue (AT), intermuscular AT (IMAT) and muscle, we performed a case-cohort study of 294 men with incident non-spine fractures confirmed from medical records and a random subcohort of 616 men from the Osteoporotic Fractures in Men study (MrOS). We measured volumes (cm^3) of abdominal subcutaneous AT, visceral AT, total muscle, total muscle IMAT, as well as total abdominal muscle density (HU) and percent total abdominal muscle IMAT, obtained from a single-slice (5-mm) quantitative computed tomography scan at the L4-L5 intervertebral space. Cox proportional hazards regression with a robust variance estimator was used to estimate the hazard ratio (HR) and 95% confidence intervals (CI) of non-spine fracture per standard deviation (SD) increase in the abdominal body composition measure of interest. Standard multivariable models included age, study site, BMI, and dual energy X-ray absorptiometry measure of femoral neck bone mineral density (BMD). The mean age among men in the random cohort was 74.2 ± 6.1 years and the average follow-up time was 5.2 years. Among the case-cohort study, men with incident fractures were older and more likely to have fracture after age 50, and had lower weight, body mass index (BMI), grip strength, and body lean and fat mass than men without fracture. Abdominal subcutaneous and visceral AT, and total abdominal muscle volume were not associated with incident fracture (Table 1). HRs for every SD increase in abdominal muscle density and percent abdominal muscle IMAT were 0.82 and 1.23 with borderline significance, respectively. However, total abdominal muscle IMAT volume was significantly associated with 29% greater fracture risk when the above multivariate model was further adjusted for total abdominal muscle volume. The findings suggest that adipose infiltration may decrease muscle quality and consequently lead to higher fracture risk in older men independent of BMD.

Abdominal measure	Mean±SD	HR per SD increase (95% CI)	p-value
Subcutaneous AT (cm^3)	92.8±32.5	0.99 (0.77, 1.26)	0.92
Visceral AT (cm^3)	67.8±28.4	0.90 (0.72, 1.12)	0.33
Total muscle (cm^3)	63.6±8.4	1.10 (0.88, 1.37)	0.41
Total muscle density (HU)	14.7±16.5	0.82 (0.65, 1.04)	0.10
Total muscle IMAT (cm^3)*	16.2±6.5	**1.29 (1.01, 1.65)**	**0.04**
Percent total muscle IMAT (%)	26.0±10.8	1.23 (0.97, 1.56)	0.09

*Standard multivariable model + abdominal total muscle volume

QCT abdominal body comp & Fx

***Disclosures: Yahtyng Sheu**, None.*

1096

Birth Weight Influences Peak Bone Mass In 25-Year Old Swedish Women. Kristina Akesson[1], Mattias Callréus*[2]. [1]Malmo University Hospital, Sweden, [2]Skåne University Hospital, Sweden

It has been postulated that accrual of bone mass in childhood and adolescence is related to birth weight, however it is not clear to what extent this effect persists to contribute to peak bone mass. The purpose of this study was to evaluate the potential influence of birth weight on peak bone mass, fat mass and lean mass.

Subjects and Methods

1061 young adult women, all 25 yrs old, participated in this population-based study, PEAK-25. DXA was used to assess bone mass and body composition. Bone mineral density (BMD) was determined for spine (LS) and femoral neck (FN). Total body (TB) measurement was used for bone mineral content (BMC), fat mass and lean mass. Information on lifestyle and other health factors were obtained through questionnaire. Birth data was available for 1047 women and obtained from the National Board of Health and Welfare. Pearson Correlation was used to identify correlations between birth weight and assessed parameters. ANCOVA analysis adjusted for current adult body weight, with Bonferroni correction, was applied after dividing subjects into tertiles of birth weight. *Results*

At baseline the women were 25.5 $\pm$ 0.2 yrs, height 167 $\pm$ 6 cm, body weight 65 $\pm$ 11 kg. Mean birth weight was 3 392 $\pm$ 537 gram, and length 50 $\pm$ 2.3 cm. Crude positive correlations with birth weight were identified for TB BMC (r=0.24; p<0.001), FN BMD (r=0.11; p<0.001), fat mass (r=0.10; p=0.001), and lean mass (r=0.29; p<0.001). There was no significant correlation for LS BMD. After adjustment, positive correlations remained for TB BMC (r=0.16; p<0.001), and lean mass (r=0.22; p<0.001). Correlation to fat mass became strongly negatively correlated (r=-0.21; p<0.001). Lean mass demonstrated the highest correlation, even after adjustment. ANCOVA confirmed these findings. Birth weight effects were most pronounced between the low-high birth weight tertiles (p<0.001), and between low-middle birth weight (BMC p=0.002; fat mass p=0.003; lean mass p=0.002). Fat mass changed direction between middle-high birth weight (p=0.013).

Conclusion

This study indicates that birth weight is predictive of peak bone mineral content in women and has a strong influence on future fat and lean mass. In general, the influence appeared more pronounced for women with lower birth weights.

***Disclosures: Mattias Callréus**, None.*

1097

Does the Benefit of Medication Adherence Relate More to a Drug Effect or the Behavior Itself? Quantifying the Effect of Adherence Behavior Using Data From the Placebo Arms of the WHI. Jeffrey Curtis*[1], Joseph Larson[2], Elizabeth Delzell[1], M. Alan Brookhart[3], Suzanne Cadarette[4], Rowan Chlebowski[5], Suzanne Judd[1], Monika Safford[1], Daniel Solomon[6], Andrea Lacroix[2]. [1]University of Alabama at Birmingham, USA, [2]Fred Hutchinson Cancer REsearch Center, USA, [3]UNC-Chapel Hill, USA, [4]Leslie Dan Faculty of Pharmacy, University of Toronto, Canada, [5]UCLA Medical Center, USA, [6]Harvard Medical School, USA

Purpose: The relationship between medication adherence and various outcomes including fracture is of substantial interest, particularly in the osteoporosis community. The extent to which adherence to medications as a behavior is a proxy for other healthy behaviors that affect outcomes is unclear. To better understand the magnitude of the effect of adherence as a behavior, we examined the relationship between adherence to placebo in the hormone therapy (HT) arm of the Women's Health Initiative (WHI) on the risk of fracture, cardiovascular events, malignancy and death.

Method: We used data from those randomized to placebo in the HT arm of the WHI. Adherence was represented as timevarying based upon pill counts and quantified as a medication possession ratio (MPR). Outcome events were identified and validated using medical records as per the original WHI protocol. Confounders were selected a-priori and based upon the ability to adjust the main exposure-outcome relationship by > 10%. Cox proportional hazards models were used to evaluate the relationship between adherence ($\leq$ 50%, 50-80%, $\geqslant$ 80%) and each of the various outcomes, with low adherence as referent. Analyses were censored at the first event specific to each outcome.

Results: A total of 13485 women were randomized to placebo in the HT arm of the WHI and were under observation for 86091 person-years (without respect to censoring). The median (IQR) cumulative adherence to placebo at the end of the trial was 91.3% (81.4, 96.0%). There was a consistent relationship between adherence to placebo and a protective effect of all outcomes that was strongest for death and hip fracture, although not all results were statistically significant (see table). Results were not substantially affected by multivariable adjusted for various confounders.

Conclusion: Medication adherence appears to be a proxy for other unmeasured behaviors and health habits that have important effects on numerous outcomes. The magnitude of this effect was greatest for hip fracture and death. Results of future studies evaluating outcomes related to adherence to specific medications should be interpreted cautiously in light of these results.

Relationship Between Adherence to Placebo and Various Events, High Compared to Low Adherence, WHI Clinical Trial Placebo Arm (N=13,444 Women)

Outcome	Adherence Category	Events	Ann %	Unadjusted Hazard Ratio (95% CI)	Fully Adjusted* Hazard Ratio (95% CI)
Death (all cause)	<80%	109	0.99	1.00	1.00
	≥80%	355	0.59	0.65 (0.52, 0.80)	0.64 (0.51, 0.80)
Hip Fracture	<80%	28	0.25	1.00	1.00
	≥80%	99	0.16	0.68 (0.44, 1.03)	0.50 (0.33, 0.78)
Distal forearm/wrist fracture	<80%	78	0.53	1.00	1.00
	≥80%	475	0.63	1.18 (0.93, 1.50)	1.08 (0.85, 1.38)
Clinical MI	<80%	50	0.46	1.00	1.00
	≥80%	191	0.32	0.73 (0.53, 0.99)	0.69 (0.50, 0.95)
Any Cancer	<80%	138	1.32	1.00	1.00
	≥80%	726	1.24	0.94 (0.79, 1.13)	0.91 (0.76, 1.10)
Invasive breast cancer	<80%	50	0.46	1.00	1.00
	≥80%	215	0.36	0.76 (0.56, 1.04)	0.73 (0.53, 1.00)
Cancer death	<80%	52	0.47	1.00	1.00
	≥80%	163	0.27	0.62 (0.45, 0.85)	0.60 (0.43, 0.82)

CHD = coronary heath disease; MI = myocardial infarction; Ann % = Annualized %

**Adjusted for age, ethnicity, education, smoking, alcohol, fruit/vegetables intake, red meat intake, bmi, physical activity, physical function, any insurance, mammogram, visit to usual care provider in the past year, colonoscopy ever, family history of fracture, family history of breast cancer, self-reported health, history of diabetes, bilateral oophorectomy, age at first birth, age at menarche, depression, aspirin, corticosteroids, fracture medication, beta blockers, thiazides, loop diuretics, PPIs, NSAIDs, lifetime hormone therapy duration, number of medications taken*

Table

***Disclosures: Jeffrey Curtis**, Procter & Gamble, 2; Eli Lilly, 2; Merck, 5; Merck, 2; Eli Lilly, 8; Novartis, 8; Procter & Gamble, 5; Novartis, 2*
This study received funding from: Amgen

1098

Utility of Serial BMD for Fracture Prediction After Discontinuation of Prolonged Alendronate Therapy: The FLEX Trial. Douglas Bauer*[1], Ann Schwartz[1], Lisa Palermo[1], Jane Cauley[2], Kristine Ensrud[3], Marc Hochberg[4], Arthur Santora[5], Dennis Black[1]. [1]University of California, San Francisco, USA, [2]University of Pittsburgh Graduate School of Public Health, USA, [3]Minneapolis VA Medical Center / University of Minnesota, USA, [4]University of Maryland School of Medicine, USA, [5]Merck Research Laboratories, USA

Some clinicians recommend a drug holiday after 5 or more years of bisphosphonate treatment. The utility of serial monitoring with DXA following discontinuation of bisphosphonates is unknown.

The FLEX trial randomized 1099 postmenopausal women previously treated with alendronate (ALN) for approximately 5 years to either continued ALN or placebo for an additional 5 years. Hip DXA (Hologic QDR2000) was obtained at baseline and at each annual visit. Self-reported clinical fractures (non-spine and vertebral) were centrally adjudicated. This analysis is limited to women randomized to placebo in FLEX (N=437). The relationship between FLEX baseline total hip BMD (BMD-BL) or 1-year or 2-year percent change in BMD (ΔBMD) and the risk of clinical fracture were analyzed using age-adjusted Cox models; BMD-BL and ΔBMD were analyzed as continuous variables and tertiles. Among the cohort of 437 women, 109 non-spine and 28 clinical vertebral fractures occurred in 94 women during nearly 5 years of follow-up. Fractures occurring after FLEX baseline but before the follow-up BMD measurement (22 fractures in 19 women during the first year) were excluded.

Compared to women without fracture during follow-up, those with clinical fracture were older (75.2 vs.73.0 yr., p<0.001) and had lower total hip BMD-BL (0.69 vs. 0.73 gm/cm^2, p<0.001), but 1-year ΔBMD was similar (-1.5 vs. -1.3% p=0.59). When analyzed as a continuous variable, or by tertiles (Figure), there were no significant associations between ΔBMD and clinical fracture risk during follow-up, even among the 21% of placebo-treated women in FLEX with >3% bone loss after 1 year (27.5 vs. 19.5%; RH 1.5, 95% CI: 0.9, 2.4, p=0.12). Conversely, BMD-BL was strongly related to the risk of fracture during follow-up (Figure). Results using 2-year ΔBMD gave similar results.

We conclude that among women stopping ALN after 5 years of therapy, hip BMD at the time of discontinuation strongly predicts the risk of clinical fracture over the next 5 years, but 1-year and 2-year changes in BMD after discontinuation of ALN are not associated with subsequent fracture risk. These data suggest repeat BMD

measurements 1-2 years after discontinuation of prolonged ALN therapy may not be useful.

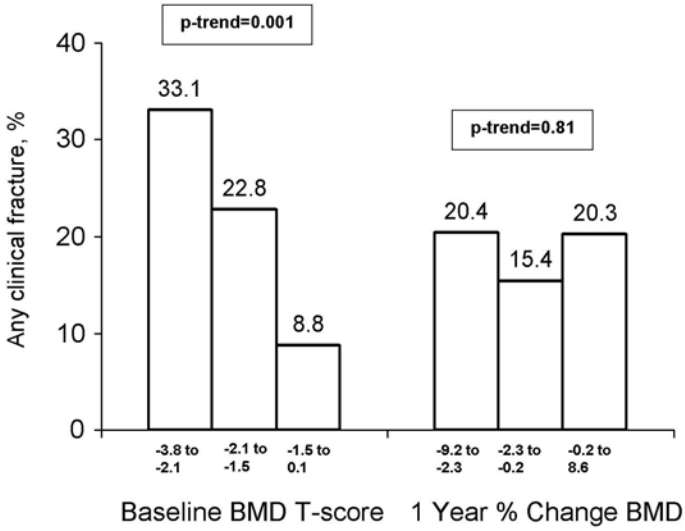

Figure. Clinical Fracture by Tertile of FLEX Baseline BMD and Tertile of 1 Year % Change in Hip BMD

***Disclosures: Douglas Bauer**, Amgen, 5; Novartis, 2; Merck, 5; Merck, 2; Amgen, 2*
This study received funding from: Merck

1099

Denosumab Improves Both Femoral and Vertebral Strength in Women With Osteoporosis: Results From the FREEDOM Trial. Tony Keaveny*[1], Michael McClung[2], Harry Genant[3], Jose Ruben Zanchetta[4], David L. Kendler[5], Jacques Brown[6], Stefan Goemaere[7], Christopher Recknor[8], Maria Luisa Brandi[9], Richard Eastell[10], Klaus Engelke[11], Thomas Fuerst[12], Hoi-Shen Radcliffe[13], Cesar Libanati[14]. [1]UC Berkeley, USA, [2]Oregon Osteoporosis Center, USA, [3]UCSF/Synarc, USA, [4]Instituto de Investigaciones Metabolicas (IDIM), Argentina, [5]University of British Columbia, Canada, [6]Laval University, Canada, [7]Ghent University Hospital, Belgium, [8]United Osteoporosis Center, USA, [9]University of Florence, Italy, [10]University of Sheffield, United Kingdom, [11]Synarc, Germany, [12]Synarc, Inc., USA, [13]Amgen Inc, United Kingdom, [14]Amgen Inc, USA

Denosumab (DMAb), a human monoclonal antibody to RANKL, increased bone mineral density (BMD), decreased bone resorption, and significantly reduced the risk of new vertebral, nonvertebral, and hip fractures in the FREEDOM trial (Cummings et al, NEJM, 2009:361:756). FREEDOM was a phase 3 trial in women 60-90 years old with postmenopausal osteoporosis randomized to 60mg DMAb or placebo (Pbo) every 6 months plus daily calcium and vitamin D supplementation. Patient-specific femoral strength for a simulated sideways fall and L2 vertebral strength for a simulated compression overload were estimated, blinded-to-treatment status, using non-linear 3D finite element analysis of the quantitative computed tomography scans obtained at baseline, 12, 24, and 36 months in a subset of participants (51 DMAb; 48 Pbo). All analyses were exploratory and posthoc. For women treated with DMAb, femoral strength increased significantly compared with baseline by 5.4% ($p<0.0001$) at 12 months, and this strength was augmented over time reaching 8.4% ($p<0.0001$) at 36 months (Table). In contrast, for women treated with Pbo, femoral strength did not change at 12 months and decreased at 36 months compared with baseline (–5.4%, $p<0.0001$). The same temporal trends were seen at the spine but the changes were much larger than at the hip: at 36 months, vertebral strength increased by 18.1% ($p<0.0001$) for the DMAb group and decreased by –4.1% ($p=0.004$) for the Pbo group. For both the hip and spine, DMAb subjects displayed mostly uniform increases in cortical strength, derived from the outer 3mm of bone at the hip and the outer 2mm at the spine, as well as in trabecular strength. Pbo subjects exhibited a preferential loss of trabecular strength. We also found that DMAb-related improvements in strength at the hip and spine were significantly correlated (r=0.38, $p=0.02$, Figure). At 36 months, all DMAb subjects had increased vertebral strength, and all but 2 had increased femoral strength; strength decreases were observed for the majority of Pbo subjects. These improvements in whole-bone strength support the vertebral and nonvertebral fracture efficacy observed with DMAb. We conclude from these findings that DMAb treatment significantly increases both hip and vertebral strength after 12 months compared with both baseline and Pbo, and positively influences both the trabecular and cortical compartments, and that these strength changes improve over 36 months of treatment.

Table.

		FEMUR			SPINE		
		Month 12	Month 24	Month 36	Month 12	Month 24	Month 36
Integral Strength	Pbo	0.7 (-0.9, 2.4)	-1.7 (-3.8, 0.4)	-5.4 (-7.8, -3.0)	-1.0 (-2.6, 0.6)	-1.5 (-3.8, 0.7)	-4.1 (-6.8, -1.4)
	DMAb	5.4 (4.2, 6.6)	6.1 (4.6, 7.7)	8.4 (6.5, 10.4)	11.5 (9.7, 13.2)	15.8 (13.5, 18.1)	18.1 (15.6, 20.5)
Trabecular Strength	Pbo	1.0 (-0.5, 2.4)	-1.0 (-2.6, 0.6)	-2.9 (-4.2, -1.6)	-2.0 (-4.6, 0.5)	-3.4 (-7.0, 0.2)	-8.0 (-12.1, -3.8)
	DMAb	3.5 (2.7, 4.4)	3.3 (2.1, 4.6)	4.3 (2.9, 5.6)	13.3 (10.2, 16.3)	18.2 (14.6, 21.7)	20.2 (16.5, 23.9)
Cortical Strength	Pbo	0.1 (-0.8, 1.0)	-0.4 (-1.3, 0.6)	-0.8 (-2.6, 1.0)	-0.2 (-1.5, 1.1)	-0.3 (-2.3, 1.6)	-1.5 (-4.0, 0.9)
	DMAb	1.8 (1.1, 2.4)	2.3 (1.5, 3.1)	2.8 (1.7, 3.8)	10.5 (9.2, 11.9)	14.5 (12.6, 16.3)	16.9 (14.9, 18.9)

Pbo = placebo; DMAb = denosumab. Values are mean (95% confidence intervals).

Table

Figure. Femoral and Vertebral Strength Change Relationship in Subjects With Evaluable QCT Scans at Baseline and Month 36

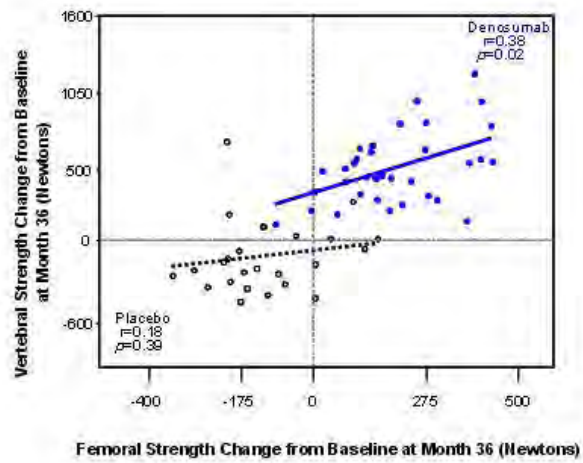

Figure

***Disclosures: Tony Keaveny**, O.N. Diagnostics, 4; Novartis, Merck, 5; Amgen, Merck, Lilly, Novartis, 2*
This study received funding from: Amgen Inc.

1100

Regulators of Bone Formation in Postmenopausal Osteoporosis: Effect of Bisphosphonate Treatment. Richard Eastell, Rosemary Hannon, Fatma Gossiel*. University of Sheffield, United Kingdom

The Wnt signalling pathway is essential for the regulation of bone formation. Serum based immunoassays have recently been developed to measure two key regulators of Wnt signalling, namely Dickkopf-1(Dkk-1) and sclerostin. Postmenopausal osteoporosis is associated with an increase in bone resorption and bone formation. Treatment with oral bisphosphonates results in a decrease in bone formation markers. It is not known whether levels of Dkk-1 and scelrostin are increased in postmenopausal osteoporosis and decrease with bisphosphonate treatment.

The aims were to determine whether 1) Dkk-1 and sclerostin are decreased in postmenopausal osteoporosis and 2) bisphosphonate treatment of postmenopausal osteoporosis results in an increase in these regulators of bone formation.

We recruited 50 postmenopausal women (mean age 68: range 55 to 85 years), with a BMD T-score of <2.5 or <1 and a fracture. They were randomised in to 3 treatment groups: ibandronate (n=15), alendronate (n=19) and risedronate (n=16). 50 healthy premenopausal women (mean age 38: range 35 to 40 years) were also recruited. We measured DKK-1 and sclerostin (Biomedica Gruppe, Austria), Total PINP, osteocalcin and CTX (Roche Diagnostics, Pensberg, Germany) and Intact PINP (IDS, Boldon, UK) in fasting serum samples at baseline and after 48 weeks of treatment in the post menopausal women and once in the premepausal control.

The median levels of total and intact PINP, osteocalcin and sCTX, and sclerostin were significantly higher in osteoporotic postmenenopausal women at baseline compared to the controls, P<0.001. There was no significant difference in median levels of Dkk-1. After 48 weeks of bisphosphonate treatment total and intact PINP, osteocalcin and sCTX decreased by 67%, 68%, 52% and 78% respectively, and no difference in the median levels of Dkk-1 and sclerostin.

We conclude that like bone turnover markers, sclerostin levels are higher in postmenopausal osteoporotic women compared to premenopausal women. This may reflect the impairment of bone formation relative to bone resorption in osteoporosis. Treatment of postmenopausal osteoporosis with oral bisphosphonates results in a decrease in bone turnover as expected. However, there was no increase in Dkk-1 and sclerostin.

The median and 95% confidence intervals for each bone marker and regulators of bone formation in the healthy premenopausal control group and the osteoporotic postmenopausal group at baseline and 48 weeks after bisphosphonates treatment

	Control group (N=50)	Mean B/line (N=50)	Week 48 (N=50)
Total PINP ng/ml	34.1 (30.6-38.4)	54.4 (47.7-62.3)	18.1 (14.3-22.7)
Intact PINP ng/ml	27.5 (25.7-31.9)	44.2 (38.8-53.8)	14.0 (11.7-18.3)
Osteocalcin ng/ml	15.2 (14.35-17.0)	28.8 (22.6-30.2)	13.6 (11.2-13.8)
sCTX ng/ml	0.22 (19.00-0.27)	0.47 (0.39-0.54)	0.10 (0.08-0.12)
Dkk-1 pmol/l	475.3 (436.0-512.8)	452.9 (418.6-487.3)	438.4 (388.4-492.9)
Sclerostin pmol/l	14.9 (11.4-16.6)	20.7 (16.2-24.1)	20.1 (14.7-22.7)

Table

***Disclosures: Fatma Gossiel**, Proctor and Gamble, IDS and Biomedica: Research support, 9*

1101

Risedronate Reduces Deterioration of Cortical Bone Microarchitecture Accompanying Menopause. Ego Seeman*[1], Babul Borah[2], Roland Chapurlat[3], Dieter Felsenberg[4], Lynn Darbie[5], Rene Rizzoli[6]. [1]Austin Health, University of Melbourne, Australia, [2]Procter & Gamble Pharmaceuticals, USA, [3]E. Herriot Hospital, France, [4]Charité - Campus Benjamin Franklin, Germany, [5]Warner Chilcott Pharmaceuticals, USA, [6]University Hospital, Switzerland

Increased remodeling with its negative bone balance contributes to structural deterioration of the skeleton after menopause. While accelerated trabecular bone loss contributes to bone fragility and has been the focus of attention, cortical bone, which constitutes 80% of the skeleton, is a critical but neglected determinant of bone strength because it is believed to remodel slowly. Moreover, most fractures are non-vertebral and arise in women with osteopenia. Risedronate (RIS) reduces the risk for non-vertebral and hip fracture and reduces intracortical porosity as assessed in iliac crest biopsies[1]. To better understand the structural basis of the anti-fracture efficacy of risedronate, particularly in women with osteopenia, we conducted a 12 month double-blind pilot study involving 159 osteopenic women aged 45-55 years within 36 months of menopause. Participants were assigned to oral RIS 35mg/week or placebo (PLB) in a 2:1 randomization. Using high resolution pQCT (XtremeCT, Scanco, 100 µm resolution) ,microstructural parameters were measured at baseline and 12 months at distal tibia (DT) and distal radius (DR). In PLB, DT total and cortical but not trabecular vBMD and cortical thickness decreased. RIS prevented the decline in cortical vBMD in DT (p=0.03); similar observations (not significant) were made for DT cortical thickness and DR cortical vBMD and thickness. No treatment differences were detected in trabecular vBMD, BV/TV or other trabecular bone indices in DT or DR. RIS decreased P1NP (-44.1%) and CTX (-39.4%) and increased aBMD in the lumbar spine (1.4%) and proximal femur (0.5%). The seeming lack of response in trabecular bone may be the result of trabecularization of cortex. Treatment with RIS reduces the deterioration of cortical microstructure, probably due to the reduction of intra-cortical porosity and may therefore protect against developing bone fragility.

[1]Borah et.al., JBMR 2009

Mean % Change (95% CI) of Cortical Parameters at Month 12

	PLB (n=49)	RIS (n=110)	Difference	P-value
DT vBMD	-0.78 (-1.34, -0.23)*	-0.10 (-0.48, 0.27)	0.68 (0.05, 1.30)	0.03
DT Cort Thickness	-1.30 (-2.40, -0.20)*	-0.32 (-1.07, 0.43)	0.98 (-0.26, 2.23)	0.12
DR vBMD	-0.77 (-1.34, -0.21)*	-0.31 (-0.68, 0.07)	0.47 (-0.17, 1.11)	0.15
DR Cort Thickness	-3.47 (-4.93, -2.01)*	-2.40 (-3.42, -1.45)*	1.03 (-0.61, 2.67)	0.21

*significant change from baseline

Table

***Disclosures: Ego Seeman**, sanofi-aventis, 8; sanofi-aventis, 5*
This study received funding from: The Alliance for Better Bone Health, an alliance between Warner Chilcott Company, LLC and sanofi-aventis, U.S.

1102

Fracture Risk Reduction with Zoledronic Acid by Predicted Fracture Risk Score. Jane Cauley*[1], Steven Cummings[2], Lisa Palermo[3], Felicia Cosman[4], Richard Eastell[5], Steven Boonen[6], Trisha Hue[3], Christina Bucci-Rechtweg[7], Dennis Black[3]. [1]University of Pittsburgh Graduate School of Public Health, USA, [2]San Francisco Coordinating Center, USA, [3]University of California, San Francisco, USA, [4]Helen Hayes Hospital, USA, [5]University of Sheffield, United Kingdom, [6]Center for Metabolic Bone Disease, Belgium, [7]Novartis Pharmaceuticals Corporation, USA

Purpose: New NOF treatment guidelines for osteoporosis are based on analyses that assume the same level of drug efficacy regardless of the underlying absolute risk of fracture. In the Health Outcomes and Reduced incidence with Zoledronic Acid Once-Yearly Pivotal Fracture Trial (HORIZON_PFT), zoledronic acid (ZOL) 5mg significantly reduced the risk of vertebral, hip and other fractures by 70%, 41%, and 33%, respectively.

Methods: To test the hypothesis that the effect of ZOL on fracture reduction differs by predicted risk of fracture, we carried out a preplanned analysis in 7,736 women with postmenopausal osteoporosis who were randomized to receive a single annual infusion of ZOL 5mg or PBO over 3 years. Each participant was categorized for 5 year hip fracture risk by adapting a risk facture score developed by Black et al [1]. The assessment tool is comprised of a set of 7 variables: age, BMD T-score, fracture risk after age 50, maternal history of hip fracture, weight <125 lbs, smoking status and using arms to stand. The risk score ranged from 1 to 11. In continuous models, a one unit increase in the fracture score was associated with 1.29 (1.16, 1.44), and 1.11 (1.06, 1.17) increased odds (95% Confidence Intervals, CI) of hip fracture and any clinical fracture, respectively. For analyses, we divided the score into tertiles and calculated the relative risk (95% CI) of hip, all non-vertebral and all clinical fractures in ZOL versus PBO using Cox proportional hazards models and for incident morphometric vertebral fractures using logistic models. Interaction between treatment effect and absolute fracture risk was tested using continuous risk models.

Results: The effect of ZOL on reduction of vertebral, non-vertebral and all clinical fractures was similar regardless of the estimated risk of fracture (Table). However, for hip fractures, there was a trend toward greater reduction in women at the lowest risk, (p=0.056).

Conclusions: We conclude that the effect of ZOL on fracture reduction was consistent for vertebral, all non-vertebral and all clinical fractures across tertiles of absolute fracture risk. The observation that ZOL may have a greater effect on hip fracture among those at lower absolute risk of fracture is consistent with subgroup analyses showing greater benefit among younger women[2].

References: 1. Black DM, et al., Osteoporos Int 2001;12(7):519-28. 2. Eastell R, et al., J Clin Endocrinol Metab 2009;94(9):3215-25.

	Vertebral fx OR (95% CI)	Hip fx RR (95% CI)	Non-vertebral fx RR (95% CI)	All clinical fx RR (95% CI)
Absolute fx risk tertile (hip fx rate per 1000py)				
1 (3.9)	0.20 (0.12, 0.31)	0.29 (0.13, 0.64)	0.70 (0.55, 0.90)	0.65 (0.51, 0.83)
2 (5.7)	0.31 (0.20, 0.47)	0.59 (0.29, 1.22)	0.74 (0.54, 1.01)	0.62(0.46, 0.83)
3 (11.0)	0.32 (0.22, 0.47)	0.78 (0.49, 1.24)	0.79 (0.62, 1.01)	0.70 (0.56, 0.88)
P-value	0.26	0.056	0.72	0.96

Table: Relative risk (odds ratio) of fracture (fx) in women randomized to ZOL versus placebo strati

***Disclosures: Jane Cauley**, Novartis, 5*
This study received funding from: Novartis

1103

A Five Years Exercise Intervention Programme in 7-9 Year Old Children Improve Bone Mass and Bone Structure without Increasing the Fracture Incidence. Magnus Karlsson[1], Jan-Åke Nilsson[2], Fredrik Detter*[3]. [1]Skåne University Hospital Malmö, Lund University, Sweden, [2]Clinical & Molecular Osteoporosis Research Unit, Sweden, [3]Clinical & Molecular Osteoporosis Research UnitLund University, Sweden, Sweden

Purpose: Published pediatric exercise intervention studies that evaluate if exercise may be fracture preventive span at maximum 24 months and uses bone traits as surrogate endpoints for fractures. Furthermore, reports infer physical activity to be associated with more trauma and fractures. Therefore we designed a 5-years population based controlled exercise intervention study with also fracture as endpoint.

Method: The intervention group achieved 40 minutes/day of school physical education and the controls 60 minutes/week. Included were 2395 children aged 7-9 years, 362 girls and 446 boys in the intervention (3152 person-years) and 780 girls and 807 boys in the control group (6761person-years). Fractures were prospectively registered. In 54 girls and 83 boys in the intervention and 53 girls and 58 boys in the control group, skeletal development was followed annually by dual energy X-ray absorptiometry. Slopes and annual changes were calculated for bone mineral density (BMD; g/cm^2) in spine and femoral neck and bone width (mm) in femur. Peripheral computed tomography was applied in forearm and tibia at last measurement. Group

comparisons are reported as mean group difference with 95% CI within brackets and with p-value adjusted for Tanner stage at follow-up.

Results: There were 20.0 fractures/1000 person-years in the intervention and 18.5 fractures/1000 person-years in the control group, leading to a Rate Ratio (RR) of 1.08 (0.79, 1.47) (mean (95% CI)). The mean annual gain in spine BMD was larger in both intervention girls (0.01 g/cm^2 (0.007, 0.02) and intervention boys (0.006 g/cm^2 (0.003, 0.01) and in femoral neck BMD larger in intervention girls (0.007 g/cm^2 (0.00, 0.02) than in the control groups. The gain in femur width was larger in intervention girls (0.3 mm (0.0, 0.6)) and intervention boys (0.1 mm (0.0, 0.4) than in the control groups. The intervention girls had at study end larger mid radial area (11 mm^2 (0.6, 21); p=0.006), more tibia cortical bone mineral content (0.2 g (0.0, 0.4); p=0.01)), larger mid tibial area (17 mm^2 (-3, 36); p=0.03) and larger mid tibial cortical area (17 mm^2 (2, 31); p=0.009) than the control girls The intervention boys had larger mid radial area (7 mm^2 (-3, 18); p=0.04) than the control boys.

Conclusions: Increased duration of school physical education for 5 years in 7-9 year old children could population based be used to improve bone mass and bone structure without increasing the fracture risk.

***Disclosures: Fredrik Detter**, None.*

1104

Habitual Vigorous Physical Activity Increase Cortical Bone Mass In Adolescents, Unlike Light Or Moderate Activity Which Are Without Effect. Jon Tobias, Adrian Sayers*. University of Bristol, United Kingdom

Introduction

How intense habitual physical activity (PA) needs to be affect skeletal development in childhood is currently unclear. To examine this question, we compared the contributions of light, moderate and vigorous day-to-day PA as measured by Actigraph accelerometers, to pQCT-derived cortical bone mineral content (BMCC) of the mid-tibia, in 1748 16-year-old boys and girls from the Avon Longitudinal Study of Parents and Children (ALSPAC).

Methods

Multi-variable analyses were performed to identify independent influences of light, moderate and vigorous physical activity on BMCC. Light, moderate and vigorous physical activity was defined by 2, 4 or 6 METS (kcal.kg^{-1}.h^{-1}) which are associated slow walking, brisk walking and jogging respectively. Further analyses were performed to identify the influences of PA on BMC that were independent of concurrent changes in fat mass (FM) and lean mass (LM). Path analyses were also carried out to identify the relative effects of an increase in periosteal circumference (PC), endosteal circumference adjusted for PC (ECPC) and cortical BMD (BMDC) to associations between PA and BMCC which were present.

Results

In multivariable analyses, vigorous activity had a strong positive influence on BMCC [β 0.082 (95% CI: 0.037, 0.128), p=0.0004], whereas there was no evidence of an effect of light or moderate PA (both P > 0.7) (b represents SD change per doubling of vigorous activity). The effect of vigorous PA on BMCC was largely independent of associated changes in body composition [β 0.070 (95% CI: 0.026, 0.115), p=0. 002, adjusted for FM and LM]. The vigorous PA effect on BMCC was mediated by an increase in PC [β 0.049 (95% CI: 0.018, 0.080), p=0. 002], and a reduction in ECPC [β 0.018 (95% CI 0.010, 0.027), p<0.0001]. There was also evidence of a small negative effect on BMDC [β -0.010 (95% CI: -0.017, -0.003)]. There was no evidence of a differing effect between boys and girls, p=0.47.

Conclusion

The amount of vigorous day-to-day PA exerts important effects on cortical bone development, whereas less intense PA has little discernible effect. Changing the amount of physical activity in childhood is unlikely to benefit skeletal development unless more intense high impact activities such as jogging or running are also increased.

***Disclosures: Adrian Sayers**, None.*

1105

Positive Impact of Both Physical Activity and Protein Intake before Puberty on Biomechanical Strength at Weight Bearing Skeletal Sites 7.8 yrs Later in Healthy Boys. Thierry Chevalley*[1], Jean-Philippe Bonjour[2], Bert Rietbergen[3], Serge Ferrari[4], Rene Rizzoli[5]. [1]University Hospitals of Geneva Division of Bone Diseases, Switzerland, [2]University Hospital of Geneva, Switzerland, [3]Eindhoven University of Technology, The netherlands, [4]Geneva University Hospital & Faculty of Medicine, Switzerland, [5]University Hospital, Switzerland

The influence of environmental factors on adult bone mass and strength appears to be stronger before than after the onset of pubertal maturation. In keeping with this notion we reported in a prospective study in a cohort of 176 healthy boys that the positive impact of relatively high protein intake (superior to median=HProt) and high physical activity (superior to median=HPA) vs. both moderate protein intake (inferior to median=MProt) and physical activity (inferior to median=MPA) evaluated at 7.4±0.4 yrs (±SD) old on areal bone mineral density (aBMD), content (BMC) and width of the femoral neck (FN) measured by DXA before pubertal maturation was observed unabated at the age of 15.2±0.5 yrs. At this age the difference in FN BMD, BMC and width in the HProt-HPA vs MProt-MPA was combined with significant differences (P<0.001) in structural components of distal tibia including cross-sectional area (CSA, mm^2), trabecular number (Tb.N, mm-1), and trabecular space (Tb.Sp, µm) as assessed by high resolution peripheral computerized tomography (HR-pQCT). We now report the influence of HProt-HPA vs MProt-MPA on biomechanical properties of the distal tibia as assessed by micro-finite element analysis (µFEA) based on HR-pQCT measurements. µFEA derived variables reported here include the estimated failure load [N] and the stiffness (kN/mm) as well as the distinct contribution of trabecular and cortical compartments. An increase in PA from 168±40 to 303±54 (±SD) kcal/day under MProt (38.0±6.9 g/day) was associated with increased stiffness and failure load of +0.16 and +0.14 Z-score, respectively. In contrast an increase in PA of similar magnitude from 167±33 to 324±80 kcal/day under HProt (56.2±9.5 g/day) was associated with a larger increase in stiffness and failure load of +0.42 and +0.48 Z-score, respectively (Figure). No difference was observed among these 4 sub-groups in the percentage of load carried by cortical and trabecular bone of the distal tibia. In conclusion, the positive influence of relatively high protein intake on the impact of physical activity observed before puberty and 7.8 yrs later on femoral neck aBMD, BMC and width is also associated with enhanced mechanical resistance at weight bearing site. These results underscore the importance of nutrition and exercise in the early prevention of adult osteoporosis.

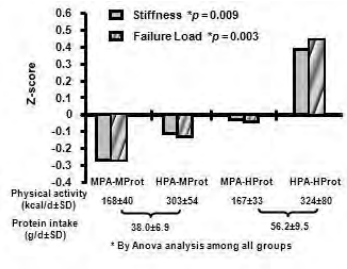

Figure

***Disclosures: Thierry Chevalley**, None.*

1106

Loaded Physical Activity Predicts 12-month Change in Bone Strength and Bone Microstructure at the Distal Tibia in Adolescents. Melonie Burrows*, Danmei Liu, Deetria Egeli, Heather McKay. University of British Columbia, Canada

Randomized controlled intervention trials and long-term prospective studies using dual energy x-ray absorptiometry and peripheral quantitative computed tomography (pQCT) highlight the key role that physical activity (PA) plays to enhance bone mineral content and bone geometry in adolescents across growth. However, there are no high resolution (HR) pQCT studies that assess the effect of PA on bone strength and bone microstructure over time. We conducted a 12-month prospective study to address the following two objectives; 1) To describe 12-month changes in bone strength and bone microstructure in male and female participants, and, 2) To investigate the contribution of loaded physical activity to bone changes. We assessed PA (loaded, hours per week) using the PA Questionnaire for High School Students (1). Using HR-pQCT (Scanco Medical) we assessed the distal tibia (8% site) in 110 male and 80 female participants at baseline (T1) and 12-months (T2). We report the following bone parameters; total area (ToA, mm), total density (ToD, mg/cm^3), cortical density (CoD, mg/cm^3), cortical thickness (Cort.Th, µm), trabecular density (TrD, mg/cm^3) and trabecular number (TbN, 1/mm). Our primary outcome was bone strength index (BSI, mg^2/mm^4 = ToA x ToD^2) (2). We addressed our first objective using ANOVA (P<0.05) and our second objective using regression (adjusting for baseline values, changes in height (cm), weight (kg) and tibial length (cm); STATA, version 10.1). We found significant changes in BSI (12%; 4%), Cort.Th (14%; 2%), TbN (2%; 2%) and ToD (7%; 1%) for male and female participants, respectively. Change in CoD (1%) and TrD (2%) was significant for males only, and change in ToA (2%) was significant for females only (Table 1). A one hour per week increase in PA predicted significant increases in BSI (1%), CoD (1%) and Cort.Th (0.5%) in males only (P<0.05). This could be due to significant increases in PA across the 12-month period in male participants (2%) whereas female's PA decreased (-8%). Our results suggest that PA contributes significantly to bone strength and bone microstructure in adolescent males. It seems important to extend our prospective trial to track whether these relationships persist/change for young adult men and women.

1. Crocker RA et al.(1997) Measuring general levels of physical activity. Med Sci Sports Exerc 29:1344-1349.

2. Martin RB (1991) Determinants of the mechanical properties of bones. J Biomech 24 Suppl 1:79-88.

Table 1. Baseline and 12-month descriptive characteristics and bone outcomes for males and females

	Males (n=110)		Females (n = 80)	
	Baseline	12-months	Baseline	12-months
Age (years)	16.2 (1.7)	17.3 (1.6)†	16.9 (1.8)	17.9 (1.8)†
Height (cm)	174.0 (7.5)	176.0 (7.2)†	163.0 (6.5)	164.0 (7.0)†
Weight (kg)	66.3 (14.3)	69.4 (14.9)†	59.7 (10.2)	61.0 (11.0)†
Tibial length (cm)	41.9 (2.7)	42.4 (26.8)†	38.2 (4.1)	38.7 (2.5)
Physical activity (hrs/wk)	6.6 (6.3)	5.7 (7.9)†	3.7 (4.1)	3.4 (3.6)†
Bone strength index (mg^2/mm^4)	74 (25)	89 (25)†	67 (17)	70 (17)†
Total area (mm^2)	790 (124)	784 (120)	638 (96)	649 (106)†
Total density (mg/cm^3)	304 (52)	324 (47)†	325 (47)	328 (44)†
Cortical density (mg/cm^3)	790 (71)	800 (55)†	874 (33)	866 (34)
Cortical thickness (µm)	1150 (354)	1312 (295)†	1200 (220)	1221 (217)†
Trabecular density (mg/cm^3)	202 (29)	207 (30)†	196 (31)	197 (32)
Trabecular number (1/mm)	1.68 (0.27)	1.91 (0.30)†	1.77 (0.25)	1.80 (0.24)†

Mean (SD). †Significantly different from T1 ($P<0.05$, within sex)

Table 1

***Disclosures: Melonie Burrows**, None.*

1107

Increased Physical Activity Is Associated with Augmented Cortical Bone Size in Young Men: a Five Year Longitudinal Study. Martin Nilsson*[1], Claes Ohlsson[2], Dan Mellstrom[3], Mattias Lorentzon[1]. [1]Center for Bone Research At the Sahlgrenska Academy, Sweden, [2]Centre for Bone & Arthritis Research, Sweden, [3]Sahlgrenska University Hospital, Sweden

Physical activity is believed to have positive effects on the development of cortical bone during growth, but the effects in young adult men has been insufficiently studied. The aim of this five year longitudinal study of young adult men was to determine whether an altered level of physical activity between 19 and 24 years of age was associated with changes in bone mass in general and in cortical geometry in particular. Men from the original Gothenburg Osteoporosis and Obesity (GOOD) Study (n=1068) were contacted by letter and telephone and invited to participate in this five year follow-up study, and a total of 833 men (78%), 24.1 ± 0.6 years of age (mean ± SD), were included. The mean follow-up time was 62.2 ± 2.3 months. A standardized self administered questionnaire was used to collect information about patterns of physical activity at both the baseline and five year follow-up visits. Men were categorized according to physical activity level (Low <4 hrs/wk and High ≥4 hrs/wk) at baseline and at follow up. Areal bone mineral density (aBMD) was measured using dual energy X-ray absorptiometry, whereas volumetric bone mineral density (vBMD) and bone geometry were measured by peripheral quantitative computed tomography. Men who increased their level of physical activity (Low to High), had a more favorable development of total hip aBMD (a yearly increase of 0.3% ± 0.15 (mean ± SEM)) than men who maintained a low level of physical activity (a yearly decrease of 0.4% ± 0.05) during the five year period ($p<0.0001$).

The yearly increase in cortical cross sectional area (CSA) at the tibial diaphysis was greater in men who increased their physical activity level (from Low to High) than the corresponding increase in men with consistently low physical activity level (Fig.1). Men who reduced their physical activity level (High to Low) did not have lesser yearly gains in cortical CSA than men who continued with a high level of physical activity (Fig. 1).

In conclusion, we found that an increased level of physical activity between 19 and 24 years of age was associated with greater increments in cortical bone size and with continued gains in total hip aBMD, indicating that increased physical activity can optimize bone development due to a favourable effect on cortical bone geometry in young adulthood.

Figure 1

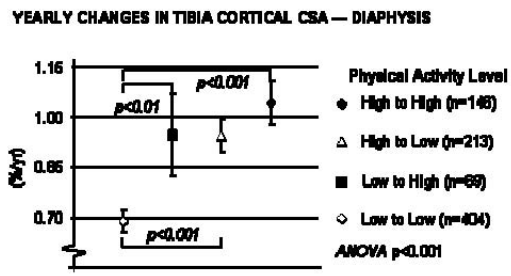

Figure 1

***Disclosures: Martin Nilsson**, None.*

1108

Physical Activity Predicts Bone Mass throughout Childhood: Iowa Bone Development Study Eight-Year Longitudinal Results. Kathleen Janz*[1], Trudy Burns[1], James Torner[1], Julie Eichenberger Gilmore[1], Marcia Willing[2], Steven Levy[1]. [1]University of Iowa, USA, [2]Washington University, USA

Purpose: One strategy to decrease the risk of developing osteoporosis during old age is to ensure optimal bone mass accrual during the growing years. Weight-bearing physical activity (PA) during childhood is associated with bone mass accrual; although most studies examining these relationships have focused on older children (just prior to puberty). Using a longitudinal observational design spanning 8 years of growth, we examined associations between PA and bone mineral content (BMC) in a cohort of healthy young children (n=398, 5 yr at baseline).

Methods: PA and BMC were analyzed in 188 boys and 210 girls participating in the Iowa Bone Development Study at 5, 8, 11, and 13 yr. BMC (hip, spine, whole body) was measured using DXA. PA was measured by the Actigaph monitor and categorized into moderate and vigorous intensity PA (min/d) and total PA (counts/min/d). TV viewing and video gaming, markers of sedentary behaviors, were estimated from parent and child reports. Maturity was estimated using predictive equations by Mirwald. Data were analyzed using multilevel (random- and fixed-effects) regression models which included adjustment for centered age (yr), centered age-squared (yr), height (cm), maturity (0,1), TV viewing (1-5 scale), and video gaming (1-5 scale). Quadratic age was included to allow for non-linear growth. The first-level of the models described the child-specific developmental change of region-specific BMC or whole body BMC over the course of the study (random effect). Adjustment variables and PA variables were added in a stepwise fashion as fixed effects to the second-level of the models. Likelihood ratio statistics were used to determine whether the effects of PA were significant contributors to the models. All models were gender-specific and used a criterion of $p < 0.05$.

Results: Throughout childhood, boys and girls who were the most active had the greatest amount of BMC ($p< 0.05$ all models; all PA measures). Higher intensity PA was more strongly associated with BMC than other PA measures. The association was strongest between higher intensity PA and hip BMC for both boys and girls. In boys, video gaming was inversely associated with BMC in all models ($p < 0.05$).

Conclusions: These results provide evidence that greater amounts and higher intensities of PA are associated with bone mass accrual throughout childhood and during puberty. In boys, decreasing time spent playing video games may contribute to optimal bone development.

***Disclosures: Kathleen Janz**, None.*

1109

Rescue of Active Intestinal Calcium Absorption Reverses the Impaired Osteoblast Function in VDR Null Mice. Ritsuko Masuyama*[1], Liesbet Lieben[2], Ingrid Stockmans[2], Riet Van Looveren[2], Nico Smets[2], Roger Bouillon[2], Geert Carmeliet[2]. [1]Nagasaki University Graduate School of Biomedical Sciences, Japan, [2]Laboratory Experimental Medicine & Endocrinology, Katholieke Universiteit Leuven, Belgium

Systemic vitamin D receptor (VDR) inactivation is characterized by severe hypocalcemia associated with impaired bone mineralization. The normalization of calcium homeostasis by dietary treatment corrects these bone pathologies and strongly suggests that the major target of vitamin D (VD) genomic action is the active intestinal calcium absorption.

To verify this hypothesis, we generated mice expressing VDR exclusively in the intestine (VDR^{res}) by breeding VDR null mice ($VDR^{-/-}$) with transgenic mice expressing VDR under the control of the Calbindin-D9k promoter. After appropriate breeding, VDR^{res}, $VDR^{-/-}$ and wild-type (WT) littermates were phenotypically analyzed.

VDR was expressed in the duodenum of 8-week-old VDR^{res} mice. Although VDR mRNA levels were only 10% of WT levels, serum calcium levels were largely normalized (VDR^{res} 9.0 ± 0.2mg/dL) likely due to increased expression of *Trpv6* by reintroducing VDR expression in the intestine, and resulted in an increased bone volume. Despite the severe hyperparathyroidism in VDR^{res} mice, osteoclast surface was not increased in VDR^{res} compared to WT mice. A possible explanation is that efficient induction of osteoclastogenesis by PTH requires VDR signaling. To substantiate this hypothesis, *RANKL* expression in osteoblasts, derived from bone marrow, was analyzed after PTH and 1,25VD treatment. PTH treatment increased *RANKL* expression in all genotypes, though the induction was much larger in WT osteoblasts. Combinations of PTH with 1,25VD caused synergistic effects in WT cultures whereas these effects were not observed in the cells lacking VDR. These results suggest that VDR-mediate VD signaling is involved in the regulation of *RANKL* expression by PTH. Furthermore, the expanded osteoid surface, a typical finding in $VDR^{-/-}$ mice, returned to normal by correcting serum calcium in VDR^{res}, as did osteoblast differentiation shown by similar *Runx2*, *osteopontin* and *osteocalcin* expression in femur of VDR^{res} compared to WT. To assess whether serum calcium levels directly modulate osteoblast differentiation, mRNA levels of differentiation markers were quantified in WT osteoblasts cultured with different calcium concentrations. Although *Runx2* and *osteopontin* expression was not affected, *osteocalcin* expression dose-dependently increased by calcium concentration.

In conclusion, intestinal VD genomic action promotes active calcium absorption that is required for normocalcemia which on its turn supports local bone turnover directly.

***Disclosures:** **Ritsuko Masuyama**, None.*

1110

Disruption of Pdia3, a Mediator of Rapid Membrane Responses to 1α,25-Dihydroxyvitamin D_3 Results in Embryonic Lethality in Homozygotes and Bone Abnormality in Heterozygotes. Yun Wang*[1], Alex Nizkorodov[2], Kelsie Riemenschneider[2], Chris Lee[2], David Martin[3], Sharon Hyzy[2], Zvi Schwartz[1], Barbara Boyan[1]. [1]Georgia Institute of Technology, USA, [2]Department of Biomedical Engineering & Institute of Bioengineering & Bioscience, Georgia Institute of Technology, USA, [3]Department of Medicine, Emory University School of Medicine, USA

1,25-dihydroxy vitamin D_3 [1α,25$(OH)_2D_3$] is a critical regulator of bone and cartilage development. Protein disulfide isomerase A3 (Pdia3) (also know as 1,25-MARRS, ERp60, ERp57 and Grp58), is a multifunctional protein and expressed in various adult tissues as well as in embryonic stem cells. Previous studies showed that it associates with caveolin-1 and mediates 1α,25$(OH)_2D_3$ initiated-rapid membrane signaling in several cell types. To understand the role of the Pdia3 in regulating skeletal development, we generated Pdia3-deficient mice and examined the physiologic consequence of Pdia3 disruption in embryos and Pdia3 heterozygotes at different ages using stereo confocal microscopy, high-resolution μCT imaging and histomorphometric measurements. No homozygous mice for the Pdia3 deletion were observed at birth nor were embryos after E12.5. Only two homozygous embryos with open neural tube defects and hemorrhage were identified at E10.5, indicating that the targeted disruption of the Pdia3 gene resulted in early embryonic lethality (Fig.1). Heterozygotes aged from 5-weeks-old to 30-weeks-old had 30-50% reduction in Pdia3 expression as shown by real-time PCR and Western blots; no difference in nVDR expression level was observed. Pdia3 heterozygotes of all ages displayed decreased body length (nose to rump) but increased leg length/body length and heart weight/body weight. Pdia3 deficiency also resulted in skeletal manifestations as revealed by μCT analysis. The heterozygous mice had decreased cortical bone area, lower BV/TV and trabecular number compared to wild type mice. In all cases, an increase in tibia growth plate thickness and a reduction in tether volume were observed in heterozygous mice (Fig.2A-D). Histomorphometry showed decreased cell numbers in the resting zone and proliferating zone of the heterozygote growth plate but increased cell numbers in hypertrophic zone compared to wild type mice (Fig.2E,F). Collectively, our findings provide for the first time the in vivo evidence that Pdia3 is essential for normal embryogenesis and play a crucial role in skeletal development. The fact that the Pdia3 heterozygous mice share a similar bone and growth plate phenotype to nVDR knockout mice, suggests that Pdia3 mediated-rapid membrane signaling might be an alternative signal pathway responsible for 1α,25$(OH)_2D_3$'s actions in regulating skeletal development.

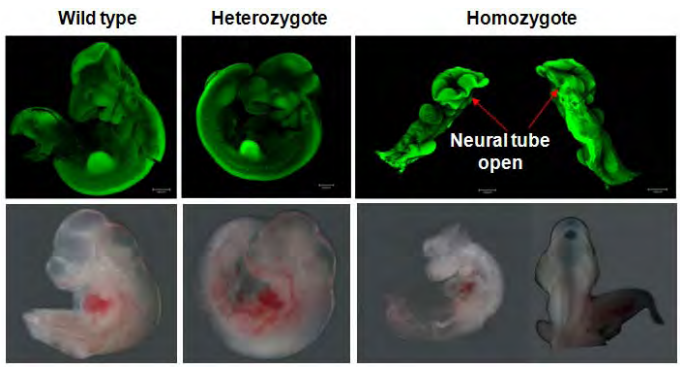

Fig. 1 Stereo confocal microscopy analysis of E10.5 embryos stained with acridine orange.

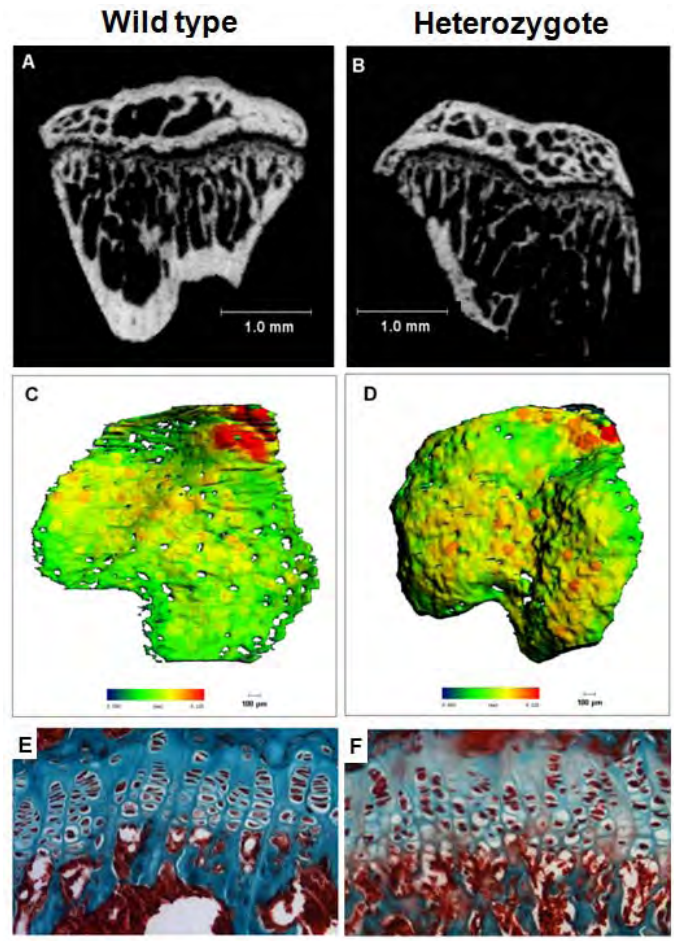

Fig. 2 çCT and histology analysis of 10-week-old wild type and heterozygote growth plate. 2D cross-s

***Disclosures:** **Yun Wang**, None.*

1111

Increased Trabecular Volume in a Novel Mouse Model Expressing a Bone-Specific CYP27B1 Transgene. Andrew Turner*[1], Juliette Tyson[1], Rebecca Sawyer[1], Peter O'Loughlin[1], Gerald Atkins[2], Masakazu Kogawa[2], David Findlay[2], Howard Morris[1], Paul Anderson[1]. [1]SA Pathology, Australia, [2]University of Adelaide, Australia

The endocrine hormone, 1a,25-dihydroxyvitamin D3 (1,25D) is a regulator of calcium homeostasis and bone health. We have shown that a major source of 1,25D within the skeleton are osteoblasts [1], osteocytes and osteoclasts [2] by virtue of their expression of the 25-hydroxyvitamin D 1alpha-hydroxylase (CYP27B1). While locally produced 1,25D in bone may mediate anabolic and/or catabolic activities within the skeleton, in osteoblasts, it is our hypothesis that the synthesis of 1,25D in bone performs autocrine functions that support bone remodelling. In in vitro experiments, we have silenced CYP27B1 mRNA expression in human osteosarcoma (HOS) cells by RNAi technology. In the presence of 100-400nM 25D, inhibition of CYP27B1 expression was accompanied by a marked decrease in the production of 1,25D and abolishment of osteocalcin mRNA levels, which was overcome by the addition of exogenous 1,25D. In in vivo studies, we have constructed a plasmid, in which transcription of the human CYP27B1 sequence is driven by the human osteocalcin promoter (hOcn-CYP27B1). Transient transfection of the hOcn-CYP27B1 construct into HOS cells treated with 25D (50nM), results in higher 1,25D production (63.5±14.8 pM) than control vector transfected HOS cells (7.6±2.1 pM), or transfected kidney 293T cells (3.5±0.7 pM). This construct was recently used to generate transgenic mice, of which two lines (OSC1 and OSC3) are undergoing detailed characterisation. Expression of human CYP27B1 mRNA in both mouse lines, as measured by qRT-PCR, is restricted to bone tissue where it is expressed at high levels (>50-fold higher than any other tissue). OSC mice maintain normal calcium and 1,25D levels in the circulation. Seven week old male OSC1 mice demonstrate a 12.4% increase in BV/TV of the distal femoral metaphysis (n=6/gp, $p<0.05$). This was associated with a 10.8% increase in trabecular number ($p<0.05$) with trabecular thickness unchanged. Dynamic histomorphometry and osteocyte measurements will further clarify the mechanism of increased trabecular bone volume in OSC mice. Our data further support the concept of the skeleton as an intracrine organ for vitamin D, with locally synthesized 1,25D exerting important actions for

bone remodeling and challenging the long-held notion that 1,25D is solely an endocrine hormone.

1. Atkins, G.J., et al., Bone, 2007. 40: 1517-28.
2. Kogawa, M., et al., Journal of Steroid Biochemistry and Molecular Biology, 2010. 118: accepted 13th Mar 2010.

***Disclosures: Andrew Turner**, None.*

1112

Mechanisms Underlying Anabolic Androgen Action in the Periosteum I*n Vivo* and I*n Vitro:* Disparate Response Mediated by Distinct Stem Cell Lineages. Kristine Wiren*[1], Anthony Semirale[2], Xiao-Wei Zhang[3]. [1]Veterans Affairs Medical Center, Oregon Health & Science University Research Ser, USA, [2]Oregon Health Sciences University, USA, [3]VA Medical Center & OHSU, USA

Although androgen is considered anabolic, the consequences of androgen receptor (AR) overexpression in skeletally-targeted AR-transgenic lines highlight the detrimental effect of enhanced androgen sensitivity on cortical bone quality. A compartment-specific anabolic response is observed only in male AR3.6-transgenic (tg) mice, with increased periosteal bone formation and calvarial thickening. Notably, anabolic thickening in vivo is not uniform across the calvaria, occurring only in frontal but not parietal bones. Calvaria provide a unique resource for isolation of multipotent stem cells derived from distinct embryological origins, with frontal bones originating from ectodermal neural crest cells while parietal bones originate from mesoderm mesenchymal cells. Stem-like cells from both sources are multipotent and can differentiate into osteoblasts or adipocytes. To define mechanisms that mediate bone anabolic responses, the consequences of enhanced androgen sensitivity in these distinct stem cell lineages were determined and compared to qPCR array analysis of periosteal vs cortical bone. Fraction 1 frontal bone neural crest stem cell (fNCSC) vs parietal bone mesenchymal cell (pMSC) cultures were isolated after collagenase digestion from AR3.6-tg or wildtype (WT) calvaria. Transgene expression was similar between fNCSC and pMSC cultures. Adipogenesis was significantly reduced in fNCSC cultures from AR3.6-tg compared to WT ($p < 0.05$ at d7; $p < 0.01$ at d10). In contrast, there was no significant difference in WT vs AR3.6-tg pMSC cultures. Notably, osteoblastogenesis was significantly increased in fNCSC cultures from AR3.6-tg compared to WT, with elevated alkaline phosphatase (AP) activity and induction of mineralization and nodule formation by alizarin red and von Kossa staining. Osteocalcin and AP mRNA levels were increased ($p < 0.05$ at d18) in fNCSC cultures from AR3.6-tg vs WT, with no significant difference between the genotypes in pMSC cultures. Expression profiles from AR3.6-tg vs WT long-bone periosteal tissue analyzed by array were recapitulated in fNCSC samples, while pMSCs reflected cortical expression. These observations confirm enhanced osteoblast lineage commitment by androgen in cells derived from neural crest. Combined, these results change our understanding of androgen action and reveal that androgen signaling results in osteogenic responses only in neural crest but not mesodermal lineages, and that the periosteum may have a neural crest origin.

***Disclosures: Kristine Wiren**, None.*

1113

ERα Deletion in Mesenchymal Progenitors or Mature Osteoblasts Decreases Cortical Bone Thickness and Increases Apoptosis, Respectively. Maria Jose Almeida*[1], Elena Ambrogini[1], Marta Martin Millan[2], Shoshana Bartell[1], Aaron Warron[1], Randal Shelton[1], Tony Chambers[1], Jinhu Xiong[1], Robert Weinstein[1], Robert Jilka[1], Charles O'Brien[1], Stavros Manolagas[1]. [1]University of Arkansas for Medical Sciences, USA, [2]University of Arkansas, Center for Osteoporosis & Metabolic Bone Diseases, USA

Estrogens attenuate osteoclast generation and life span via cell autonomous effects; and osteoclast ERα deletion causes loss of cancellous, but not cortical, bone indicating that osteoblasts, osteocytes, and perhaps other cell types are responsible for their protective effects on the cortical compartment. We sought genetic evidence for cell autonomous effects of estrogens at different stages of the osteoblast lineage progression by deleting a conditional ERα allele in early precursors of the mesenchymal lineage of the appendicular skeleton (ERα-flox;Prx1-Cre mice); or in osteoblasts expressing collagen type I (ERα-flox;2.3kbCol1a1-Cre mice). The efficiency of the deletion in these models was determined by measuring ERα mRNA in osteoblasts, generated by culturing adherent bone marrow cells with ascorbic acid, and other non-bone tissues by quantitative RT-PCR. ERα mRNA in osteoblasts from the ERα-flox;Prx1-Cre or ERα-flox;2.3kbCol1a1-Cre mice was decreased by about 60% as compared to the respective controls. Strikingly, cortical thickness in the femurs of 2 month old female ERα-flox;Prx1-Cre was decreased while cancellous bone volume was unaffected, as determined by micro-CT. Moreover, 6 month old ERα-flox;2.3kbCol1a1-Cre mice exhibited a 2-fold increase in osteoblast apoptosis, as determined by ISEL staining in vertebral cancellous bone sections but no changes in cancellous or cortical bone mass under basal conditions. Nonetheless, the number of CFU-OB in ex vivo bone marrow cultures from the ERα-flox;Prx1-Cre mice was 2-fold higher than those from control mice; but indistinguishable from the littermate controls in bone marrow cultures from the ERα-flox;2.3kbCol1a1-Cre mice. These results establish that estrogens acting though the ERα exert cell autonomous effects on osteoblasts; and that these actions are responsible for the protective effects of estrogens on the cortical compartment, as well as the survival of mature osteoblasts in cancellous bone. These findings also suggest that stimulation of differentiation or an increase in osteoblast progenitor survival, or both, may be more important for the effects of estrogens on bone mass than either suppression of progenitor self-renewal or prevention of apoptosis of mature cells. Nonetheless, it remains possible that prevention of osteocytes apoptosis by ERα-mediated effects of estrogens might contribute to strength independently of bone mass.

***Disclosures: Maria Jose Almeida**, None.*

1114

Estrogen Receptor-related Receptor Gamma (ERRg) is a Regulator of Skeletogenesis. Jane Aubin[1], Ralph Zirngibl[2], Marco Cardelli*[2], Ruolin Guo[3], Jonathan Boetto[4]. [1]University of Toronto Faculty of Medicine, Canada, [2]University of Toronto, Canada, [3]University of Rochester, USA, [4]University of Toronto - Molecular Genetics, Canada

Sex steroids, such as estrogen, play a role in the onset and severity of symptoms in arthritis and osteoporosis. Estrogen exerts its activity via its receptors, estrogen receptor alpha and beta, which are members of the nuclear receptor family. There are also members of the family for which ligands have not been identified, the so-called orphan receptors. Amongst these are the estrogen receptor-related receptors (ERRs), ERRα, ERRβ, and ERRγ. Previously, we showed that ERRγ is highly expressed in bone and cartilage and that it plays a functional role in osteogenesis and chondrogenesis *in vitro* (Bonnelye *et al*., 2001; Bonnelye *et al*., 2007). We have also found that ERRγ is expressed in skeletal cells and tissues, albeit at levels significantly lower than ERRα. Consistent with recent evidence from in vitro and ectopic bone formation experiments, suggesting that ERRγ is a negative regulator of osteogenesis, impinging on the BMP-Runx2 pathway (Jeong *et al*., 2009), we also found that knockdown of ERRγ in calvarial cell cultures increases osteoblast differentiation and bone nodule formation (unpublished data). To extend our *in vitro* findings to the whole animal level, we have utilized an ERRγ knockout line (Deltagen). Whole mount skeletal preparations of late embryonic/early postnatal stages revealed an increase in intramembranous bone formation, but no significant difference in long bone length. Preliminary μCT data from 14 week heterozygous mice reveal an increase in trabecular BMD and trabecular bone volume fraction, but no significant difference in cortical bone parameters. Further, *ERRγ* +/- calvaria bones were thicker than their WT counterparts but in a site-specific manner. To investigate the underlying cellular mechanisms, cells were isolated from neonatal knockout and heterozygous calvaria and cultured under osteoblast differentiation conditions. ALP and von Kossa positive staining (number and area) was increased in *ERRγ* +/- and *ERRγ* -/- cultures compared to WT. *In silico* analysis for ERRE consensus sequences identified *Msx2*, *Twist1* and *Alp* as putative ERRγ target genes. Collectively, our data indicate that ERRγ is a negative regulator of osteogenesis and further investigation into its putative target genes and interacting partners will shed light on its mechanism of action.

***Disclosures: Marco Cardelli**, None.*

1115

IGF-I Released during Osteoclastic Bone Resorption Induces Osteoblast Differentiation of BMSCs in the Coupling Process. Lijuan Pang*[1], Xiangwei Wu[2], Weiqi Lei[1], Tao Qiu[2], Feng Li[3], Mei Wan[2], Xu Cao[4]. [1]The Johns Hopkins University School of Medicine, USA, [2]Johns Hopkins University School of Medicine, USA, [3]Department of Pathology, Shihezi University School of Medicine, China, [4]Johns Hopkins University, USA

TGFβ1 has been shown to recruit bone marrow stromal cells (BMSCs) to the bone resorptive sites in response to osteoclastic bone resorption for coupled bone formation. It is, however, still unknown what factor(s) is responsible for the differentiation of BMSCs into osteoblasts during their recruitment. IGF-I is also one of the most abundant factors deposited in the bone matrix. We found that the conditioned medium (CM) from osteoclasts with bone slices induces osteoblast differentiation of BMSCs, and addition of an antibody against IGF-I inhibited the differentiation. Bone resorption CM contains high level of IGF-I, but the control CMs do not have detectable IGF-I, indicating release of IGF-I during osteoclastic bone resorption. To examine the effect of IGF-I on differentiation of BMSCs in the coupling process, we developed osteoprogenitor-specific IGF-IR deficiency mice (IGF-IR-/-) by using osterix promoter-Cre mice. The two-month-old female IGF-IR-/- mice exhibited smaller size with low trabecular bone volume and larger trabecular bone space as measured by μCT. Osteoblast number and area were significantly reduced in IGF-IR-/- mice relative to their WT littermates while osteoclast number and area did not change. Trabecular and endosteal mineral apposition rates were reduced in IGF-IR-/- mice measured by calcein double labeling. Suspensions of BMSCs isolated from the IGF-IR-/- mice and their WT littermates for CFU-F assay. The CFU-Fs were further induced in osteogenic media (CFU-Ob). The number of CFUs of IGF-IR-/- mice was equivalent to their WT littermates, but the number of CFU-Ob significantly decreased, indicating the osteogenic potential of the BMSCs is reduced in IGF-IR-/- mice.

To demonstrate that the role of IGF-I in vivo, GFP-labeled BMSCs isolated from IGF-IR-/- mice were injected into the femur cavity of the immuno-deficient Rag2-/- mice. At two weeks after injection, the GFP-labeled IGF-IR-/- and IGF-IR+/+

BMSCs were largely found at the trabecular bone surface. Importantly, some of the IGF-IR+/+ BMSCs, but no IGF-IR-/- BMSCs were embedded in the trabecular bone at four weeks after injection. Taken together, IGF-I released during bone resorption stimulates osteoblast differentiation of the BMSCs at bone resorptive sites recruited by TGFβ1. Thus, TGFβ1 induces migration of BMSCs to the bone surface in response to bone resorption and IGF-I further stimulates osteoblast differentiation of the recruited BMSCs.

***Disclosures: Lijuan Pang**, None.*

1116

Role of CCL-12 (a.k.a. MCP-5) in Joint Development and Need of TGF-β Signaling in Controlling its Expression. Lara Longobardi*, Tieshi Li, Timothy J. Myers, Froilan Granero-Molto, Yun Yan, Anna Spagnoli. University of North Carolina at Chapel Hill, USA

The Tgfbr2PRX-1KO mouse generated in our laboratory, which lacks the Tgfbr2 in developing limbs, fails joint interzone development. Combining laser-capture microscopy with gene expression microarrays, we found that the interzone is characterized by a down-regulation of the cytokine CCL-12 (a.k.a. MCP-5, homologous of the human MCP-1) compared to the adjacent growth plate, and such regulation is impaired in Tbr2PRX-1KO. Aberrant expressions of MCP-1/CCL12 and its unique receptor CCR2 are involved in OA and RA pathogenesis. Clinical studies aimed at blocking the system in patients with RA are on the way. Our ex-vivo and in vivo studies are aimed at determining whether: #1) an aberrant release of CCL-12 into developing digits disrupts the interzone; #2) the blockage of the CCR2 signaling rescues the Tbr2PRX-1KO phenotype. For purpose #1, using a micro-injector unit and glycol-chitosan-β-cholanic nanoparticles for sustained protein release, either CCL-12 protein or MC-21 antibody (against CCR2) were injected within the developing joints of dissected E13.5 WT or Tbr2PRX-1KO limbs respectively, that were cultured for 2 days. For purpose #2, pregnant females potentially generating Tbr2PRX-1KO, were treated PO with RS504393, a CCR2 inhibitor, starting at E11.5 (4mg/Kg/day). At E18.5 mice were sacrificed and dissected limbs from Tbr2PRX-1KO and control embryos subjected to histological and in-situ hybridization analyses (ISH). Using an immunomagnetic system, TGFβRII+ cells were isolated from E13.5 limb mesenchyme; and treated with increasing doses of CCL-12 The sustained release of CCL-12 into developing WT joints, blocked the interzone development, abolished specific joint marker (i.e. Gdf5) expressions and halted the growth plate segmentation, leading to a continuous pattern of Col2 expressing cells throughout the digit. In-vitro, CCL-12 treatment of TGFβRII+ cells, decreased joint marker (Gdf-5, Wnt9a and Sulf1) and increased Col2 expression. Blockage of the CCR2 signaling in Tbr2PRX-1KO either ex-vivo or in-vivo, led to a rescue of the Tbr2PRX-1KO phenotype restoring interzone and joint formation. In Tbr2PRX-1KO growth plate, CCR2 signaling blockage determined also a more organized pattern in Ihh, Sox9 and Col10 expressions. Our findings provide evidence for new roles for CCL-12 and TGFβRII signaling in joint development, opening novel prospective for their function in adult joint homeostasis and for the prevention and treatment of different forms of arthritis.

***Disclosures: Lara Longobardi**, None.*

1117

Peripheral Actions of the NPY System Regulate Bone Formation via Modulation of PYY. Iris Wong*, Ronaldo F. Enriquez, Amanda Sainsbury, Herbert Herzog, John Eisman, Paul Baldock. Garvan Institute of Medical Research, Australia

The neuropeptide Y (NPY) system regulates bone anabolism through hypothalamic Y2 and osteoblastic Y1 receptors. Hypothalamic NPY expression has a strong, negative relationship to bone anabolism. However, in addition to the central actions of NPY, the NPY system also contains peripheral components which may influence bone homeostasis. Another NPY receptor ligand, peptide YY (PYY) released from the gastrointestinal system, has recently been shown to have an inverse correlation with BMD. Given the critical role of diet in mineral homeostasis, and recent findings regarding serotonin action in bone, we hypothesize that PYY may be a link from gut to skeletal system.

To investigate, we examined bone cell activity and structure of 16 week female mice from two different mouse models – a PYY knockout ($PYY^{-/-}$) model and a model with tamoxifen-inducible PYY over-expression (PYYtg) in the periphery where the ubiquitous gene *ROSA26* is expressed.

Whole body BMD was greater in $PYY^{-/-}$ compared to wildtype (51.8 ±0.8 vs 47.9 ±0.9 mg/cm^2, $p<0.05$). $PYY^{-/-}$ exhibited greater cancellous bone volume (12.9 ±0.7 vs 9.6 ±0.5 %, $p<0.005$) and trabecular number (4.20 ±0.16 vs 3.21 ±0.15 /mm, $p<0.001$) in the distal femur, accompanied by greater mineral apposition rate (MAR) (1.96 ±0.02 vs 1.62 ±0.07 μm/d, $p<0.005$) with no change in osteoclast surface. Endocortical MAR of PYY-/- was also greater (1.70 ±0.20 vs 1.14 ±0.13 μm/d, $p<0.05$).

Importantly, bone cells activities of PYYtg were the opposite of those observed in $PYY^{-/-}$. PYYtg had reduced MAR (1.69 ±0.07 vs 2.01 ±0.05 μm/d, $p<0.005$) and increased osteoclast number (6.01 ±0.21 vs 4.71 ±0.18 /mm, $p<0.001$) and surface (11.43 ±0.42 vs 9.01 ±0.37 %, $p<0.005$) with lower trabecular number (2.98 ±0.18 vs 3.48 ±0.11 /mm, $p<0.05$) and a trend towards reduced cancellous bone volume ($p=0.07$). Endocortical MAR was also reduced in PYYtg (1.57 ±0.06 vs 1.79 ±0.06 μm/d, $p<0.05$).

The contrasting effect of the knockout and transgenic mouse models indicates that peripherally produced PYY regulates bone mass through suppression of osteoblast activity in cancellous and cortical bone. Greater understanding of the role of PYY signalling in bone may reveal novel links between the gut and bone homeostasis.

***Disclosures: Iris Wong**, None.*

1118

Oncostatin M Receptor Signaling Inhibits the Pro-osteoclastic Action of PTH in vivo and in vitro. Emma C Walker[1], Ingrid Poulton[1], Narelle McGregor[1], Elizabeth Allan[1], T John Martin[1], Natalie Sims*[2]. [1]St. Vincent's Institute, Australia, [2]St. Vincent's Institute of Medical Research, Australia

Parathyroid hormone (PTH) acts via osteoblasts to stimulate both osteoclast formation and bone formation. Studies using genetic manipulation and neutralizing antibodies identified that the influence of PTH on osteoclast formation is partially dependent on cytokines that act by binding to the gp130 signal transduction unit (e.g. IL-6, IL-11, oncostatin M (OSM)). Since these cytokines stimulate osteoclast and osteoblast differentiation they may also mediate anabolic effects of PTH.

Microarrays of murine stromal cells identified regulation of gp130-binding molecules by PTH including a 4 fold increase in OSM receptor (OSMR) expression. This was confirmed in primary calvarial osteoblasts, where OSMR expression was increased 12 fold in response to PTH.

To determine whether OSMR signaling is required for PTH anabolic action, 6 week old male OSMR knockout (KO) mice and wild type (WT) littermates were treated with 30μg/kg/day hPTH(1-34) for 3 weeks. In WT mice, PTH increased trabecular bone volume (BV/TV) by 40% ($p<0.05$ vs saline), and increased trabecular thickness by 17% ($p=0.001$). In contrast, the same treatment of OSMR KO mice reduced BV/TV by 22% ($p<0.05$ vs saline) and reduced trabecular number by 27% ($p=0.002$). This difference in response to PTH was not explained by a different bone formation response; osteoblast surface, osteoid surface and mineral apposition rate were increased to the same extent by PTH treatment in WT and OSMR KO mice. In contrast, PTH treatment doubled osteoclast surface in OSMR KO mice ($p=0.003$ vs. saline), an effect that was not observed in WT. This was surprising since OSM stimulates RANKL expression and osteoclast formation via OSMR.

When bone marrow macrophage osteoclast precursors were cultured in the presence of OSMR KO osteoblasts, >3 fold more osteoclasts were formed in response to PTH than when the same precursor population was cultured with WT osteoblasts. Furthermore, even though the cAMP response of OSMR KO osteoblasts to PTH was identical to that of WT osteoblasts, PTH-induced RANKL expression was 5-fold greater in OSMR KO osteoblasts compared to WT, and this high level of RANKL expression was retained at least until 24 hours after PTH exposure.

These data indicate that despite the known pro-osteoclastic and pro-RANKL influence of OSM, OSMR signaling suppresses the action of PTH that enhances RANKL expression in osteoblasts and stimulates osteoclast formation, indicating significant crosstalk between these pathways.

***Disclosures: Natalie Sims**, None.*

1119

The In Vivo Effect of EGFR on Bone. Xianrong Zhang*[1], Ji Zhu[1], Haiyan Chen[2], Xiaoyan Tian[2], Barbara Kream[3], Nicola Partridge[4], Ling Qin[5]. [1]University of Pennsylvania, School of Medicine, USA, [2]University of Utah, USA, [3]University of Connecticut Health Center, USA, [4]New York University College of Dentistry, USA, [5]University of Pennsylvania, USA

The epidermal growth factor receptor (EGFR) has vital roles in developmental and pathological processes. However, its function in the skeletal system has not been well studied. Our previous research demonstrated that its ligands are potent mitogens for osteoprogenitors but strongly suppress osteoblast differentiation in vitro. To address the in vivo role of EGFR in bone, we constructed transgenic and pharmacological mouse models and used microCT and histomorphometry to analyze their bone phenotype. To eliminate the pre/osteoblastic EGFR activity, we generated 3.6 kb collagen1a1-Cre $Egfr^{Wa5flox}$ (Col-Cre $Egfr^{Wa5lf}$) mice harboring an EGFR dominant negative allele, Wa5. At 3-, 5- and 7-months old, these mice exhibited a remarkable 20-40% decrease in tibial trabecular bone volume (BV/TV) with a reduction in trabecular number (17-32%) and trabecular thickness (10%) in both genders. Histological analyses of 7-month old female mice revealed that bone formation and mineralization activities were reduced and bone resorption was elevated. These mice exhibited decreases in osteoblast surface (35%), osteoid surface (34%), mineral apposition rate (MAR, 15%), bone formation rate (BFR, 24%), and an increase in osteoclast surface (78%). Similarly, administration of an EGFR inhibitor into wild type mice caused a 25% reduction in trabecular BV/TV. Histomorphometric analyses suggested similar changes in bone formation and resorption parameters as Col-Cre $Egfr^{Wa5lf}$ mice. In contrast, 3-month old $Egfr^{Dsk5l/+}$ mice with an EGFR constitutively active allele displayed increases in trabecular BV/TV (36-43%) accompanied by an increase in trabecular number (28-35%) and a decrease in trabecular separation (9-17%) in both genders. These structural changes were due to increases in osteoblast surface (37%), osteoid surface (35%), MAR (18%) and BFR (34%) and a decrease in osteoclast surface (27%). Interestingly, we found that EGFR

inhibitor dramatically reduced the number of CFU-F (52%) derived from bone marrow, suggesting that EGFR functions in maintaining the osteoprogenitor pool. In conclusion, our data demonstrate that the EGFR signaling pathway affects both bone formation and bone resorption in vivo and therefore it acts as a novel anabolic regulator for bone metabolism.

***Disclosures: Xianrong Zhang**, None.*

1120

Hypertrophic Chondrocytes and Osteocytes are Essential Sources of RANKL for Bone Growth and for Bone Remodeling, Respectively. Jinhu Xiong*, Melda Onal, Priscilla Cazer, Xinrong Chen, Robert Weinstein, Robert Jilka, Stavros Manolagas, Charles O'Brien. University of Arkansas for Medical Sciences, USA

RANKL is required for osteoclastogenesis and thought to be supplied by cells of the osteoblast lineage. However, ablation of matrix-synthesizing osteoblasts and their immediate replicating precursors does not alter RANKL expression or osteoclast number. Therefore, the identity of osteoclast support cells remains unclear. To address this issue, we created mice with a RANKL conditional allele (RF) and crossed them with mice expressing Cre recombinase under the control of osterix (Osx1-Cre), osteocalcin (OCN-Cre), or dentin matrix protein 1 (DMP1-Cre) gene regulatory elements. Deletion of RANKL using Osx1-Cre or OCN-Cre caused severe osteopetrosis associated with retention of mineralized cartilage in the long bones and spine of 5 wk old mice. Consistent with this, immunohistochemical analysis revealed that both Osx1-Cre and OCN-Cre deleted RANKL from hypertrophic chondrocytes. Osx1-Cre and OCN-Cre activity in hypertrophic chondrocytes was confirmed using the R26R Cre reporter strain. Deletion of RANKL with DMP1-Cre increased bone mass at 5 wk of age, compared to littermate controls, but this was not associated with retention of calcified cartilage. Bone mass continued to increase in DMP1-Cre;RF mice, relative to DMP1-Cre littermates, so that by 6 mo of age, there was a 30% difference in BMD in the spine, suggesting that osteocytes are an essential source of RANKL during bone remodeling. Consistent with this, RANKL mRNA levels were significantly lower in bones from DMP1-Cre;RF mice. However, analysis of DMP1-Cre expression with R26R mice revealed that, in addition to osteocytes, Cre activity was also present in cells on cancellous bone that may be osteoblasts. To confirm that the decrease in RANKL expression caused by DMP1-Cre occurred in osteocytes and not osteoblasts, adult RF mice were treated with OPG for 2 wk to suppress bone turnover, thereby reducing osteoblast number, and were then injected with vehicle or PTH, followed by quantification of RANKL expression. OPG treatment did not change basal or PTH-stimulated RANKL mRNA levels but did potently reduce osteocalcin mRNA. Both basal and PTH-stimulated RANKL were significantly reduced in DMP1-Cre;RF mice. These results, taken together with previous osteoblast ablation studies, demonstrate that hypertrophic chondrocytes are an essential source of RANKL during endochondral bone growth and that osteocytes, but not osteoblasts, are an essential source of RANKL for bone turnover during adulthood.

***Disclosures: Jinhu Xiong**, None.*

1121

Gli2 is Essential for Postnatal Intervertebral Disc Growth and Maintenance. Fanjie Zeng*, Ming Xue, Xinping Zhang. University of Rochester Medical Center, USA

Deterioration of the intervertebral disc (IVD) is common in the elderly and has been shown to be the major cause for back pain. While studies have shown that age-related disc degeneration is associated with enhanced apoptosis and loss of normal extracellular matrix composition in IVD, mechanisms underlying the degeneration of the disc remain poorly understood. Hedgehog (Hh) pathway is critically involved in the vertebral column formation and skeletogenesis. However, due to embryonic lethality, its roles in postnatal IVD growth, maintenance and aging remain unknown. In this current study, we examined the expression of Hh-related genes in young and aged lumbar disc in mice. We found a progressive loss of both Shh and Ihh in aged IVD, associated with significant downregulation of the key transcriptional activator Gli2. Comparing to IVD harvested from the young, aged IVD exhibited loss of proteoglycan, rupture of annulus fibrosus as well as marked induction of apoptosis in endplate. To determine the role of Gli2 in postnatal IVD growth and maintenance, we generated a Gli2f/f;Col2CreER;RosaR mouse model, which permits deletion of Gli2 postnatally in annulus fibrosus, endplate and growth plate following treatment of Tamoxifen (TM). Deletion of Gli2 via Col2CreER led to rapid destruction of cartilaginous tissue in IVD just 3 days following TM injection at postnatal day 18. TUNEL assay showed a near 5-fold increase of apoptosis in endplate and a massive induction of apoptosis in hypertrophic chondrocytes in Gli2f/f;Col2CreER mice, coincided with the severe loss of Col2a1, ColX and MMP13 gene expression as determined by in situ hybridization. In addition to enhanced apoptosis, Brdu labeling showed a near 3 fold reduction of proliferation in growth plate chondrocytes. Deletion of Gli2 further led to disorganization of annulus fibrosus, as evidenced by the loss of Col2a1 expression in the inner layer of annulus but aberrant induction of Col 2a1 expression in the outer layer of the annulus, a phenomenon that was described in the mechanical injury-induced early disc degeneration. By 2 month of age, Gli2-mutant IVD displayed a nearly complete loss of cartilaginous tissue, disruption of endplate, rupture of annulus fibrosus, shrinkage and severe loss of nucleus pulpopus, and fusion of vertebral bodies. Taken together, we conclude that Gli2 plays a critical role in postnatal growth and maintenance of IVD and Hh deficiency could contribute to age-related disc degeneration.

***Disclosures: Fanjie Zeng**, None.*

1122

Conditional Ablation of the Heparan Sulfate-synthesizing Enzyme Ext1 Leads to Dysregulation of BMP Signaling and Severe Skeletal Defects. Yukihide Iwamoto[1], Fumitoshi Irie[2], Yu Yamaguchi[2], Kazu Matsumoto[2], Yoshihiro Matsumoto*[3]. [1]Department of Orthopaedic Surgery kyushu Universtiy School of Medicine, Japan, [2]Sanford-Burnham Medical, Research Institute, USA, [3]Department of Orthopaedic Surgery Kyushu University School of Medicine, Japan

Increasing evidence indicates that heparan sulfate (HS) is an integral component of many morphogen signaling pathways. However, its mechanisms of action appear to be diverse, depending on the type of morphogen and the developmental contexts.

To define the functionof HS in skeletal development, we conditionally ablated Ext1, which encodes an essential glycosyltransferase for HS synthesis, in limb bud mesenchyme using the Prx1-Cre transgene. These conditional Ext1 mutant mice display severe limb skeletal defects, including shortened and malformed limb bones, oligodactily, and fusion of joints. In developing limb buds of mutant mice, chondrogenic differentiation of mesenchymal condensations is delayed and impaired, whereas the area of differentiation is diffusely expanded. Correspondingly, the distribution of both BMP signaling domains and BMP2 immunoreactivity in the mutant limb mesenchyme is broadened and diffuse. In micromass cultures, chondrogenic differentiation of mutant chondrocytes is delayed and the responsiveness to exogenous BMPs is attenuated. Moreover, the segregation of the pSmad1/5/8-expressing chondrocytes and fibronectin-expressing perichondrium-like cells surrounding chondrocyte nodules is totally disrupted in mutant micromass cultures. Together, our results show that HS is essential for patterning of limb skeletal elements, and that BMP signaling is one of the major targets for the regulatory role of HS in this developmental context.

***Disclosures: Yoshihiro Matsumoto**, None.*

1123

Smad7 Mediates Stress Pathways in the Growth Plate. Kristine Estrada*, Fuad Elkhoury, Kelsey N. Retting, Karen Lyons. University of California, Los Angeles, USA

The bone morphogenetic protein (BMP) and transforming growth factor beta (TGF-beta) pathways are important regulators of endochondral bone formation. However, the in vivo regulation of these pathways by inhibitory Smad proteins, Smad6 and Smad7, is unclear. Gain and loss of function studies have revealed potential roles for I-Smads in chondrocytes in vitro, while in vivo studies are limited to demonstrations of prominent roles of Smad6 in the cardiovascular system and of Smad7 in immune responses. Therefore, we characterized the skeletal phenotypes of mice lacking either Smad6 or Smad7 to test the roles of these intracellular inhibitors in the growth plate in vivo. Mice deficient in Smad6 exhibit elevated BMP signaling in the growth plate, while mice deficient in Smad7 exhibit a unique growth plate phenotype. In particular, histological analysis of Smad7 mutant growth plates reveal a delay in chondrocyte hypertrophy. By late gestation, the core of the growth plate is hypocellular, which may be due, at least in part, to increased apoptosis as demonstrated by TUNEL staining. Moreover, Safranin-O staining reveals defective extracellular matrix deposition in this region, partly owing to impaired type II collagen secretion. Given the documented inhibitory effect of Smad7 on canonical BMP and TGF-beta signaling, we expected that effectors of these pathways would be increased in Smad7-/- growth plates. However, reduced levels of both pSmad1/5/8 (BMP signaling) and pSmad2 (TGF-beta signaling) were seen in the core of the neonatal growth plate; levels were unaffected in the hypertrophic zone. Interestingly, pSmad2/3 localization overlaps with that of the most hypoxic regions of the growth plate and with the location of the necrotic core in Smad7 mutants, suggesting a functional connection between TGF-beta signaling and the hypoxic response. This hypothesis is substantiated by the finding that treatment of either ATDC5 or rat chondrosarcoma cells with TGF-beta1 increased *HIF-1alpha* expression. In accordance, knockdown of Smad7 in ATDC5 cells via siRNA led to increased *HIF-1alpha* and *VEGF* expression. Moreover, Smad7-/- mutants exhibited elevated levels of HIF-1alpha throughout the growth plate, with the exception of the necrotic core. These results indicate that Smad7 mediates its effects on hypoxic signaling via increased TGF-beta signaling. More importantly, our results present a novel role for Smad7 in mediating hypoxic stress responses in the growth plate.

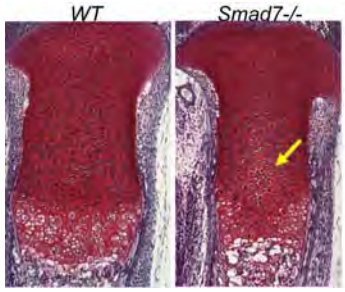

Figure 1. Altered chondrocyte differentiation in Smad7-/- tibial growth plates. Safranin-O staining reveals a paucity of ECM deposition in the medial growth plate (arrow) of Smad7-/- mutants at E17.5.

Figure 1. Altered chondrocyte differentiation in Smad7-/- tibial growth plates.

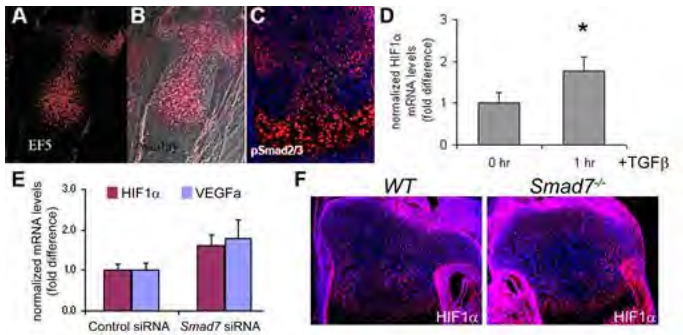

Figure 2. Loss of Smad7 leads to TGFbeta-mediated HIF-1alpha upregulation. ***A,B:*** EF-5 staining (from Schipani, et. al., 2001, Genes Dev.) highlights hypoxic areas. ***C:*** pSmad2/3 localization. ***D:*** Real-time PCR analysis of HIF-1alpha and VEGF mRNA levels in ATDC5 cells treated with control (non-targeting) and Smad7 siRNA. ***E:*** Real-time PCR analysis of HIF-1alpha mRNA levels in ATDC5 cells treated with 5 ng/ml TGF-beta1; *P<0.05. ***F:*** Immunostaining for HIF-1alpha shows increased levels throughout the Smad7-/- medial growth plate at P2.

Figure 2. Loss of Smad7 leads to TGFbeta-mediated HIF-1alpha upregulation.

Disclosures: Kristine Estrada*, None.*

1124

The Oxygen-sensor PHD2 in Chondrocytes Modifies Bone Mass by Regulating Cartilage Collagen Processing. Kjell Laperre*[1], Peter Fraisl[2], Maarten Depypere[3], Stefan Vinckier[2], Nico Smets[1], Roger Bouillon[4], Frederik Maes[3], Peter Carmeliet[2], Geert Carmeliet[5]. [1]Laboratory of Experimental Medicine & Endocrinology, K.U.Leuven, Belgium, [2]VIB Vesalius Research Center, K.U.Leuven, Belgium, [3]Medical image computing (ESAT/PSI), K.U.Leuven, Belgium, [4]Laboratory for Experimental Medicine & Endocrinology, Belgium, [5]Katholieke Universiteit Leuven, Belgium

A balanced supply of oxygen and nutrients is mandatory for bone metabolism. More precisely, an adequate response to hypoxia is critical for the expanding growth plate as lack of the hypoxia inducible factor α (HIFα) in the developing avascular and hypoxic growth plate leads to massive apoptosis. Oxygen sensing is considered to rely on three prolyl-hydroxylase-domain containing (PHD) proteins of which PHD2 seems to be the most important one. To assess the role of PHD2 in bone development, we genetically inactivated *Phd2* in chondrocytes by crossing *Phd2^{fl}* with collagen 2-Cre mice (*Phd2^{chon-}*). The efficient and cell-specific inactivation of *Phd2* resulted in highly increased HIF1α protein levels in growth plate chondrocytes.

Phenotypically, *Phd2^{chon-}* mice were growth retarded and unexpectedly, trabecular bone volume was almost doubled. Yet, *in vivo* and *in vitro* analyses did not reveal major differences in bone formation, resorption or vascularisation. Cartilage remnants were however present in the trabeculae and cortices of *Phd2^{chon-}* mice, suggesting that the cartilage matrix was modified and hence hampered remodeling by osteoclasts.

Mechanistically, *Phd2* null chondrocytes adjusted their energy metabolism in response to the increased HIF1α levels without jeopardizing cell viability: energy production as well as energy expenditure was reduced. Indeed, *Phd2* null chondrocytes displayed a shift towards anaerobic metabolism characterized by increased glycolysis and lactate production associated with decreased glucose oxidation. This adaptation resulted in decreased oxygen consumption and reduced ATP levels. To withstand this challenge, *Phd2* null chondrocytes reduced their energy expenditure by decreasing proliferation and activating the unfolded protein response. The synthesis of proteins and collagen in particular was reduced, but posttranslational processing of collagen was promoted, evidenced by increased mRNA levels of protein disulfide isomerase and lysyl oxidase and the presence of abundant collagen crosslinks. These changes resulted in a denser collagen network in *Phd2* null growth plates and likely rendered the collagen matrix less susceptible to degradation, ultimately leading to cartilage remnants.

In conclusion, deletion of PHD2 in growth plate chondrocytes lowers cellular energy metabolism and activates the unfolded protein response. Hence crosslinked collagens accumulate in the cartilage matrix, precluding remodeling and resulting in increased bone mass.

Disclosures: Kjell Laperre*, None.*

1125

Role of Fibroblast Growth Factor Receptor 3 in bone formation. Emilie Mugniery*[1], Romain Dacquin[2], Caroline Marty[3], Catherine Benoist-Lasselin[1], Arnold Munnich[1], Marie-Christine De Vernejoul[4], Pierre Jurdic[5], Valerie Geoffroy[6], Laurence Legeai-Mallet[1]. [1]INSERM U781, France, [2]Institut de génomique fonctionnelle de Lyon - ENS Lyon, France, [3]INSERM U606, France, [4]Fédération De Rhumatologie Et INSERM U606, France, [5]Ecole Normale Superieure de Lyon, France, [6]INSERM Unit 606, France

Fibroblast Growth Factor receptor 3 (FGFR3) is involved in a family of chondrodysplasias. FGFR3 missense mutations, is associated with achondroplasia, the most frequent form of dwarfism, thanatophoric dysplasia, the lethal form and hypochondroplasia mild form. These mutations induce a constitutive activation of the receptor. To study the role of FGFR3 during bone formation, we first generated a Fgfr3 mouse model which ubiquitously expressed an activating mutation (Y367C). These mice (Fgfr3Y367C/+) exhibit a severe dwarfism, with macrocephaly, short limb and narrow trunk that mimics the human pathology. As in chondrodysplasias, growth plate was severely disorganized and long bones were broad and shortened. Micro-scanner, densitometric and histomorphometry studies revealed a severe primary ossification defect and a significant decrease of bone volume (94%, $p<0,01$), trabecular thickness (16%, $p<0,05$) and trabecular number (66%, $p<0,01$) in the secondary spongiosa in Fgfr3Y367C/+ 3-weeks-old mice. The proliferation and mineralization were decreased in primary cultures of osteoblasts isolated from Fgfr3Y367C/+ mouse calvaria. To highlight involvement of FGFR3 in bone formation, we have established a mouse model (ColI-Fgfr3Y367C/+) that expresses the mutation specifically in osteoblasts. At three weeks of age, these mice (ColI-Fgfr3Y367C/+) do not exhibit any obvious evidence of bone defect. Conversely, at 3 months of age, the mutant mice showed a bone phenotype characterized by a significant increase in bone area at the vertebrae and at the femora (16% and 10% respectively, $p<0.01$). Histomorphometric analysis of secondary spongiosa confirmed an increase in bone diameter (11%, $p<0.002$) and revealed an increase in trabecular thickness (12%, $p<0.003$). In addition, osteoblast number and bone formation rate were both increased in mutant mice. These results indicate that FGFR3 activated mutation disturbs endochondral ossification process. The disorganization of the growth plate induces a severe primary ossification defect. In contrast, when expression of activated FGFR3 was restricted to osteoblasts, the primary ossification process is unmodified. Surprisingly, we observed a significant positive effect on bone formation of activated FGFR3 in this mouse model at adult stage. In FGFR3-related chondrodysplasias, the abnormal bone formation could be due to independent effects of the activated receptor on chondrocytes and osteoblasts.

Disclosures: Emilie Mugniery*, None.*

1126

Cartilage-specific Notch Signaling Regulates Chondrocyte Maturation and Coordinates Osteoblast Differentiation. Anat Kohn*[1], Yufeng Dong[2], Alana Jesse[2], Tasuku Honjo[3], Regis O'Keefe[2], Matthew Hilton[1]. [1]University of Rochester School of Medicine, USA, [2]University of Rochester, USA, [3]Kyoto University Graduate School of Medicine, Japan

Recently, the Notch signaling pathway has been implicated in regulating cartilage maturation during skeletal development. While a strong argument for Notch regulation of these processes has been provided, it still remains unclear whether these processes are regulated via (1) RBPjκ-depended or –independent Notch pathways, and (2) specific Notch signaling in chondrocytes or within multiple mesenchymal cell lineages (chondrocytes, osteoblasts and surrounding connective tissues). Furthermore, it remains to be determined whether Notch signaling in one skeletal lineage can indirectly control the development of another lineage (i.e. – chondrocyte control of osteoblastic differentiation). To identify whether chondrocyte maturation is regulated via RBPjκ-depended or -independent Notch signaling, we first analyzed RBPjk loss-of-function (LOF) (*Prx1Cre;Rbpjκ$^{f/f}$*) and RBPjκ-independent Notch gain-of-function (*Prx1Cre;Rosa-NICD^{fl+};Rbpjκ$^{f/f}$*) mutant embryos at E14.5 and E18.5. Analysis of these embryos, using histology and *in situ* hybridization, revealed that delays in chondrocyte maturation seen in Notch LOF mutants is mediated solely by RBPjκ-dependent pathways. This finding was corroborated *in vitro* using primary chondrocyte cultures from RBPjκ-floxed mice. Finally, analysis of BrdU incorporation in vivo revealed an increase in the rate of chondrocyte proliferation in RBPjκ LOF mutants. Since the Prx1Cre transgene targets multiple cell lineages, we performed similar *in vivo* experiments using the tamoxifen inducible Col2Cre^{ERT2} transgene to ascertain whether the observed effects were due to Notch perturbations in cartilage versus surrounding mesenchymal tissues (*Col2-Cre^{ERT2};Rbpjκ$^{f/f}$, Col2Cre^{ERT2};Rosa-NICD^{fl+}, Col2Cre^{ERT2};Rosa-NICD^{fl+};Rbpjκ$^{f/f}$*). Tamoxifen induction in pregnant mice after E12.5 allows for cartilage-specific Notch

deletion and/or activation. Our results from analyzing these mutant embryos at E14.5 and E18.5 demonstrate conclusively that chondrocyte maturation is regulated via RBPjκ-dependent Notch signaling specifically within chondrocytes. Interestingly, our findings also suggest that Notch signaling specifically within chondrocytes regulates osteoblast differentiation in a cell non-autonomous manner. Continued analyses using both our *in vivo* and *in vitro* approaches will allow us to determine the underlying molecular mechanisms by which Notch signaling regulates chondrocyte proliferation and maturation, while coordinating osteoblast differentiation.

***Disclosures: Anat Kohn**, None.*

1127

Reduced Bone Strength in Young Adult Women with Clinical Fractures During Childhood or Adolescence. Serge Ferrari*[1], Thierry Chevalley[2], Bert Van Rietbergen[3], Jean-Philippe Bonjour[4], Rene Rizzoli[5]. [1]Geneva University Hospital & Faculty of Medicine, Switzerland, [2]University Hospitals of Geneva Division of Bone Diseases, Switzerland, [3]Eindhoven University of Technology, Netherlands, [4]University Hospital of Geneva, Switzerland, [5]University Hospital, Switzerland

We previously reported that young adult women with clinical fractures during childhood/adolescence have decreased peak bone mass (aBMD) at radius and to a lesser extent at femur; lower volumetric bone density, and lower trabecular and/or cortical thickness at distal radius and tibia. These observations raised the possibility that fractures during growth, although most commonly associated with high-impact trauma, could actually be a hallmark of lifelong bone fragility. Whether young adults who experienced a fracture during childhood or adolescence have decreased bone strength, remains to be directly investigated.

We assessed 3D cortical and trabecular bone structure at distal radius and tibia by high-resolution peripheral QCT (HR-pQCT, XtremeCT, Scanco) in 125 women (mean age ±SD, 20.4 ±0.6 yrs) whose clinical fractures had been prospectively recorded since the age of 8 years. The volume of interest (VOI) spans over 1 cm, proximally to a point located at 1 cm and 2.2 cm from the endplate of the radius and tibia, respectively. Using the HR-pQCT measurements, finite element analysis (FEA) was conducted in 95 subjects (34 with fractures, 61 without), simulating an axial compression test to predict bone strength and stiffness, and also separating the contribution of trabecular and cortical compartments.

Adult weight and height were similar in the fracture (Fx) and no fracture (NoFx) groups. Within the VOI, the percentage of load carried by cortical bone decreased from 80-85% proximally to less than 50% more distally, at both radius and tibia. Although no significant differences in the distribution of load between the cortical and trabecular compartments were noted between fracture groups, the percentage of load carried by cortical bone in the distal VOI tended to be lower (-5 to -7%) in Fx compared to NoFx subjects. Bone estimated failure load, stiffness, and apparent modulus of the distal radius were 9-12% significantly lower in Fx than NoFx, both before and after adjustment for age, height, weight, pubertal stage, calcium and protein intakes, and physical activity. At distal tibia, the parameters of bone strength were also 5-9% significantly lower after adjustment for these confounding variables.

In conclusions, young adult women with clinical fractures during growth have decreased bone strength at distal radius and, to a lower extent, distal tibia. These observations further support the possibility that childhood fractures might be a hallmark of persistent bone fragility in adults. Whether these women will sustain more frequent wrist and/or other fractures later in life remains to be determined.

***Disclosures: Serge Ferrari**, None.*

1128

Central QCT Reveals Cortical and Trabecular Structural Deficits in Premenopausal Women With Idiopathic Osteoporosis Whether Diagnosis is Based on Fragility Fracture or Low Areal Bone Mineral Density. Adi Cohen*[1], Thomas Lang[2], Halley Rogers[1], Emily Stein[3], X Guo[4], Xiaowei Liu[4], David Dempster[4], Donald McMahon[3], Joan Lappe[5], Chiyuan Zhang[4], Robert Recker[5], Elizabeth Shane[3]. [1]Columbia University Medical Center, USA, [2]University of California, San Francisco, USA, [3]Columbia University College of Physicians & Surgeons, USA, [4]Columbia University, USA, [5]Creighton University Osteoporosis Research Center, USA

In idiopathic osteoporosis (IOP) in premenopausal women (PreM), young, otherwise healthy women with normal gonadal function present with fragility fractures (Fx). IOP may also be diagnosed on the basis of low areal bone mineral density (aBMD) by DXA in PreM without Fxs, but the clinical significance of isolated low aBMD in young women is controversial. By high-resolution peripheral quantitative tomography (HR-pQCT) of the distal radius and tibia and analysis of transilac bone biopsies, we reported that PreM with IOP (Fx; Low aBMD but no Fx) have low volumetric BMD (vBMD), thin cortices, fewer trabecular (Tb) plates, fewer, longer Tb rods, decreased Tb connectivity and stiffness compared to controls. To assess the central skeleton in PreM IOP, we measured vBMD and stiffness of the spine and hip by quantitative computed tomography (QCT) and finite element analysis (FEA) in 34 Controls (37+9 yrs) and 44 IOP (38+8 yrs; 32 Fx, 12 LowBMD). L1-L2 measures included vBMD of an integral (Int) compartment containing vertebral body and posterior elements (Int vBMD) and of the centrum containing only Tb bone (Tb vBMD). Hip measures included Int, Tb and cortical (Ct) vBMD of femoral neck (FN) and total hip (TH), FN cross-sectional area (FNCS), a measure of bone size, and a ratio of tissue volume in Ct regions of interest to total tissue volume within the periosteal boundaries (C/I), a measure of Ct thickness that correlates with hip Fx At spine and hip, IOPs had comparably lower aBMD by DXA (18-21%), Int vBMD by QCT (17-20%) and stiffness by FEA (19-21%). Tb vBMD was 26% lower at L1-L2 and 37-45% lower at FN and TH ($p<0.0001$). FNCS was 11% and 15% lower in IOP Fx and LowBMD respectively than Controls ($p<0.0001$). Ct vBMD of the hip regions did not differ between Controls and IOP, but C/I was 11-14% lower in IOPs ($p<0.0001$). This suggests that while intrinsic density of Ct bone is retained in IOP, Ct losses occur through thinning, consistent with lower Ct thickness seen on HR-pQCT and transiliac biopsy in these subjects. All differences were significant after controlling for age, height, BMI and FNCS. Moreover, IOP Fx and Low BMD subjects differed comparably from Controls and did not differ from each other. We conclude that in PreM with IOP, low aBMD by DXA is also associated with low vBMD of the central skeleton and is not explained by smaller bone size. We therefore conclude that a history of fragility Fx should not be required for the diagnosis of PreM IOP.

***Disclosures: Adi Cohen**, None.*

1129

Is Screening BMD Testing in Older Women Effective for Fracture Prevention in Routine Clinical Practice? A Matched Case-Control Study. William Leslie*[1], Mahmoud Azimaee[1], Suzanne Morin[2], Colleen Metge[1], Patricia Caetano[1], Lisa Lix[3]. [1]University of Manitoba, Canada, [2]McGill University Health Centre, Canada, [3]University of Saskatchewan, Canada

BMD screening in healthy women after age 65 years, or younger post-menopausal women with additional risk factors, is widely used to identify those that may benefit from anti-osteoporotic therapy. Direct evidence of the effectiveness of this strategy for the prevention of subsequent fractures is limited. OBJECTIVE: To compare fracture rates in relatively healthy women undergoing screening BMD testing with a matched cohort of women that were not screened. METHODS: A database containing all clinical BMD tests for the Province of Manitoba, Canada, was accessed to identify women age 50 and older at the time of baseline (first ever) screening BMD testing (cases) performed during 1998-2007. We excluded women with: any anti-osteoporosis treatment in the prior 12 months; prolonged oral corticosteroid use in the prior 12 months; prior major fractures (hip, wrist, spine, humerus); loss to follow up from migration; use of homecare services or personal care home in the prior 12 months; any hospitalization in the prior 12 months. The index date for the screened cases was the date of BMD testing. Three women who were not screened (controls) were matched to each screened woman using the same exclusion criteria (matching variables age, area of residence, number of comorbid diagnoses). The index date assigned to each control was the date of BMD testing for the matched case. 17,912 screened cases were successfully matched with 53,736 non-screened controls. The outcomes of interest were major osteoporotic fractures (hip, wrist, spine, humerus) and hip fractures alone after the index date. Fractures at fixed intervals (1, 2, 3, 4, 5 years) and at final follow up date (March 31 2008) were established through linkage within a population-based provincial health data repository. RESULTS: No significant reduction in major osteoporotic fractures was seen in the screened women, but hip fractures rates were significantly lower in screened women at all time points after year 1. At final follow up, hip fractures had been diagnosed in 165 (0.9%) of the screened and 621 (1.2%) of the non-screened women ($p=.0091$). The number needed to screen to prevent one hip fracture was 426 (95% CI 249 to 1,472). CONCLUSION: A significantly lower hip fracture rate was seen among screened women. Inability to demonstrate a reduction for other major osteoporotic fractures may indicate residual confounding (referral bias) or greater tendency to diagnose fractures among screened women (ascertainment bias).

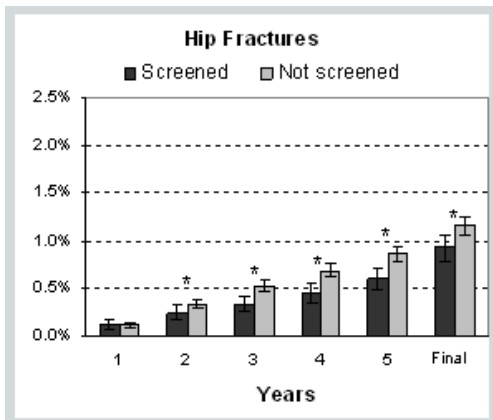

Figure: Percent of screened and non-screened women with hip fractures during follow up (*=p<.05).

***Disclosures: William Leslie**, Amgen, 2*
This study received funding from: Amgen

1130

Determination of an Osteoporosis Screening Interval for Women Aged 67 Years and Older. Margaret Gourlay*[1], John S. Preisser[2], Ryan C. May[2], Li-Yung Lui[3], Kristine Ensrud[4]. [1]University of North Carolina at Chapel Hill, USA, [2]University of North Carolina, USA, [3]California Pacific Medical Center Research Institute, USA, [4]Minneapolis VA Medical Center / University of Minnesota, USA

The US Preventive Services Task Force estimated that a 2-year osteoporosis screening interval for older postmenopausal women might be reasonable considering the precision error of bone densitometry. A bone density screening interval for postmenopausal women has not been determined based on US longitudinal data. We conducted time-to-event analyses of 5035 women aged 67 years and older from the Study of Osteoporotic Fractures to determine an optimal bone mineral density (BMD) testing interval according to baseline T-score category over a total of 15 years of prospective follow-up. We defined an optimal dual energy x-ray absorptiometry (DXA) testing interval as the estimated time during which 10% of women with normal BMD or osteopenia became osteoporotic. All participants underwent DXA and had BMD values at 2 to 5 visits during the study period. Osteoporosis, osteopenia and normal BMD were defined by WHO diagnostic criteria at the femoral neck or total hip. Parametric survival curves for the time to osteoporosis for baseline T-score subgroups were estimated from log logistic survival regression models for interval censored data adjusting for age, BMI, estrogen use, any fracture after age 50 years, current smoking, oral glucocorticoid use and alcohol use. Transitions from osteopenia (n=4278 women) and normal BMD (n=1275 women) were analyzed separately; 518 women who transitioned from normal to osteopenia prior to their last DXA contributed to both analyses. Participants were censored for incident hip fracture or use of bisphosphonate or calcitonin. Adjusting for the covariates, the estimated times for 10% of women to transition to osteoporosis were calculated for the following T-score subgroups: T-score >-2.5 and <=-2, 1.26 years; T-score >-2 and <=-1.5, 5.06 years; T-score >-1.5 and <-1.0, 16.1 years; T-score >=-1, 16.1 years (time conservatively estimated for the lowest BMD in the normal range). The unadjusted estimated times were similar to the adjusted times for the corresponding T-score subgroups (see table). These results suggest that baseline BMD is the most important determinant of a screening interval, and that an interval of 1 year should be considered for older postmenopausal women with a T-score <=-2. An interval of up to 5 years may be reasonable for osteopenia with T-score above -2. For women with normal BMD, repeat DXA before 10 years is unlikely to be informative.

Baseline T-score range	Time interval between DXA exams for 10% of participants to transition to osteoporosis	
	Unadjusted years (95% CI)	Adjusted* years (95% CI)
>-2.5 and <=-2	1.05 (0.93,1.20)	1.26 (1.09,1.44)
>-2 and <=-1.5	4.48 (4.07,4.92)	5.06 (4.54,5.65)
>-1.5 and <-1.0	14.9 (12.5,17.7)	16.1 (13.4,19.4)
>=-1	16.6 (11.3, 24.6)	16.1 (11.3, 23.1)

*adjusted for age, BMI, estrogen use, any fracture after age 50 years, current smoking, oral glucocorticoid use and alcohol use; model for T>=-1 includes continuous BMD and adjusts only for age as only 10 women transitioned from normal BMD to osteoporosis

ASBMR2010Gourlaytable041410

***Disclosures: Margaret Gourlay**, None.*

1131

Predictive value of FRAX® for the prediction of major osteoporotic fractures: The OPUS study. Karine Briot*[1], Simon Paternotte[2], Sami Kolta[3], Richard Eastell[4], Dieter Felsenberg[5], David M Reid[6], Claus C Gluër[7], Christian Roux[2]. [1]Cochin Hospital, France, [2]Paris Descartes University, Rheumatology Department, Cochin hospital, France, [3]Paris-Descartes University, Rheumatology Department, Cochin Hospital, Paris, France, France, [4]Department of Human Metabolism, University of Sheffield, United Kingdom, [5]Charité - Campus Benjamin Franklin, Germany, [6]Division of Applied Medicine, University of Aberdeen, United Kingdom, [7]Medizinische Physik, Klinik für Diagnostische Radiologie, Universitätsklinikum Schleswig-Holstein, Campus Kiel, Germany

Background and objectives: The validity of the WHO 10-yr probability of major osteoporotic fracture model (FRAX®) for prediction of fracture has been tested in few studies. We analyzed how well FRAX® predicted the risk of major osteoporotic fracture over 6 years in the prospective OPUS (Osteoporosis and Ultrasound) cohort.

Patients and methods: The OPUS study consisted of 2409 ambulatory European women aged above 55 years, recruited in 5 European centers from random population samples and followed over 6 years. For this study, we excluded women who didn't have follow-up for fracture assessment (n=670) and women who received an antiosteoporotic treatment (n=268). The population for analysis consisted of 1504 women (mean age of 65.7 years) with information on incident fractures. 607 (40.9%) of them had a prevalent low-trauma fracture (radiographic vertebral fracture included). We analyzed data of FRAX® with ORs and areas under receiver operating characteristics curves (AUC).

Results: 60 (4%) patients with incident major fractures and 9 (0.6%) with incident hip fractures were recorded. FRAX® predicted incident major osteoporotic fracture with an AUC of 0.58. History of low trauma fracture alone (AUC=0.63) predicted incident major osteoporotic as well as a combination of age + femoral neck (FN) BMD (AUC=0.60) and FRAX (AUC = 0.59). In this study, FRAX® did not predict incident hip fracture. In women without any prevalent fracture (n=897), FN BMD and FRAX® predicted incident major osteoporotic with an AUC of 0.63 and 0.55, respectively.

Conclusion: this study suggests that FRAX® predicts major osteoporotic fracture. However, once history of prevalent fracture, FN BMD and age are known, the additional risk factors in FRAX® do not significantly improve the prediction of incident fracture. A combination of history of fracture, age and FN BMD is the strongest predictor of major osteoporotic fractures.

***Disclosures: Karine Briot**, None.*

1132

Force Directions for Optimal Proximal Femoral Strength and Hip Fracture Risk Assessment in Men and Women: The AGES-Reykjavik Study. Joyce Keyak*[1], Agusta Sigmarsdottir[2], Gyda Karlsdottir[2], Sigurdur Sigurdsson[2], Kristin Siggeirsdottir[2], Gudny Eiriksdottir[2], Shoujun Zhao[1], Tamara Harris[3], Gunnar Sigurdsson[4], Vilmundur Gudnason[2], Thomas Lang[5]. [1]University of California, USA, [2]Icelandic Heart Association Research Institute, Iceland, [3]Intramural Research Program, National Institute on Aging, USA, [4]Landspitali, Iceland, [5]University of California, San Francisco, USA

Hip fracture risk is a composite of fall risk and bone strength, which is a function of bone density distribution and geometry, as well as force direction. Finite element (FE) modeling explicitly accounts for all of these factors. The goal of this study was to identify the force directions for which proximal femoral (hip) strength most strongly predicts hip fracture in elderly men and women.

5500 subjects from the AGES-Reykjavik study aged 65-90 years had quantitative computed tomography (QCT) scans of the hip (Siemens Somatom 4, 120 kVp, 150 mAs, 1 mm slice thickness increased to 3 mm). During 3 to 7 years follow-up, 51 men and 76 women sustained hip fractures. For each fracture subject, about 2 sex- and age-matched control subjects (97 men, 152 women) were randomly selected. FE models of the left hip were generated from the QCT scans of each subject, and hip strength was computed for single-limb stance loading (Stance) and fall loading onto the lateral (Lfall), posterior (Pfall), and posterolateral (PLfall) greater trochanter. Proximal femur areal bone mineral density (BMD) was also computed from the CT scans. Logistic regression was used to identify fracture predictors separately in men and women, and odds ratios (OR) per standard deviation were computed with adjustment for age, height and weight. Backward stepwise regression with all FE variables, BMD, age, height, and weight was used to identify the parameters that independently predict hip fracture.

All FE variables and BMD were associated with hip fracture ($p<0.001$; Table), but tended to be more strongly associated with fracture in men than in women. Stance and Pfall were the strongest predictors of fracture in men, and Pfall was the strongest in women. After backwards stepwise regression for men, Stance alone remained (OR=4.3, 95%CI:2.2–8.5), and for women, Pfall (OR=3.3, 95%CI:1.7–6.2) and height (OR=1.6, 95%CI:1.0–2.4) remained, indicating that Lfall, PLfall and BMD did not contribute additional information about fracture risk.

Stance in men and Pfall in women, followed by Pfall in men and Stance in women, most strongly predicted hip fracture, indicating that directly lateral loading may not be optimal for assessing fracture risk. Although a posterior fall is unlikely to impact the greater trochanter, a fall onto the greater trochanter can include a large posterior component. Therefore, hip strength under posterior loading should be considered an important factor for assessing hip fracture risk.

Table. Adjusted Odds Ratios per Standard Deviation from Univariate Analysis

Predictor	Men - OR (95% CI)	Women - OR (95% CI)
Stance	5.3 (2.6 – 10.9)	2.6 (1.5 – 4.3)
Lateral fall	4.0 (2.0 – 8.0)	2.1 (1.2 – 3.7)
Posterior fall	4.5 (2.2 – 9.3)	3.1 (1.8 – 5.4)
Posterolateral fall	2.7 (1.5 – 4.6)	2.2 (1.4 – 3.4)
BMD	3.3 (2.0 – 5.6)	2.5 (1.6 – 3.9)

Univariate Logistic Regression Results

***Disclosures: Joyce Keyak**, None.*

1133

Suppression of FSH Secretion in Postmenopausal Women has No Effect on Bone Resorption Markers. Matthew Drake*[1], Louise McCready[2], Kelley Hoey[1], Elizabeth Atkinson[1], Sundeep Khosla[3]. [1]Mayo Clinic College of Medicine, USA, [2]Mayo Clinic, USA, [3]College of Medicine, Mayo Clinic, USA

It has recently been suggested that the increase in bone resorption following the menopause may not be due principally to estrogen (E) deficiency, but rather to the concomitant increase in circulating follicle stimulating hormone (FSH) levels. This hypothesis is based on in vitro studies demonstrating that FSH increases osteoclastogenesis and the observation that, despite having E deficiency, FSH-

receptor null mice may have normal bone mass, although different laboratories have obtained conflicting data on bone mass in these mice. Furthermore, serum FSH levels have been shown to correlate directly with rates of bone loss in postmenopausal women. However, effects of FSH on bone resorption may differ between rodents and humans, and correlation does not prove causality. Thus, to directly test for possible regulation of bone resorption by FSH in humans, we randomized healthy postmenopausal women to undergo suppression of endogenous FSH secretion using the gonadotropin releasing hormone (GnRH) agonist, leuprolide, 7.5 mg intramuscularly every 28 days (n = 22), or no FSH suppression (placebo injections [Control, n = 20]), for 4 months. To eliminate possible variations in residual E levels as a confounder, both groups were concomitantly treated with the aromatase inhibitor (AI), letrozole, 2.5 mg/d. Fasting (8 AM) serum samples were obtained at baseline (Bsl) and monthly thereafter. As shown in the Figure, Panel A, whereas Control women had a slight, transient increase in serum FSH levels (likely due to the AI-induced suppression of E production), the GnRH group had a marked (~90%) suppression of FSH levels, into the premenopausal range for this assay. Compared to Bsl, 4 month (endpoint, EP) levels of bone resorption markers (serum CTX and TRAP5b) increased slightly in the Control women (Panel B), again likely due to the AI-induced reduction in endogenous E levels. In the GnRH group (Panel C), suppression of FSH secretion did not reduce either CTX or TRAP5b levels; on the contrary, both bone resorption markers increased to a similar extent in the GnRH group as in the Control group. This direct interventional study thus demonstrates that FSH does not regulate bone resorption in postmenopausal women. As such, development of pharmacological antagonists of FSH secretion and/or action is unlikely to be a viable approach for limiting postmenopausal bone loss.

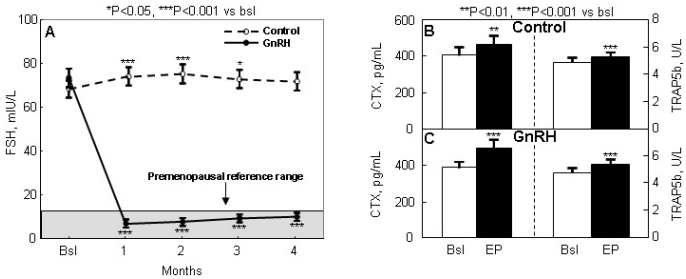

FSH and Resorption Figure

***Disclosures: Matthew Drake**, None.*

1134

Estrogen, but not Testosterone, Suppresses Circulating Sclerostin Levels in Humans. Ulrike Moedder*[1], Jackie Clowes[1], Kelley Hoey[2], James Peterson[2], Louise McCready[2], Merry Jo Oursler[2], Byron Riggs[3], Sundeep Khosla[4]. [1]Mayo Clinic College of Medicine, USA, [2]Mayo Clinic, USA, [3]Mayo Clinic College of Medicine,Rochester, MN, USA, [4]College of Medicine, Mayo Clinic, USA

Sex hormones are important regulators of bone turnover, but the mechanisms of their effects remain unclear. Sclerostin is a major inhibitor of Wnt signaling, but whether sex steroids regulate sclerostin production and whether changes in sclerostin levels are associated with changes in bone formation and/or resorption markers is unknown. Thus, we examined effects of short term sex steroid treatment on serum sclerostin levels (measured by ELISA [Biomedica]) in E-treated postmenopausal women (Study A, n=34, mean age 54yrs) and in elderly men (Study B, n=59, 66yrs) made sex steroid deficient (using a GnRH agonist and an aromatase inhibitor) and on no replacement (-T,-E), E alone (-T,+E), T alone (+T,-E), or on both (+T,+E). E treatment of postmenopausal women for 4 weeks led to a significant decrease in serum sclerostin levels (-27%) compared to controls (+1%, P<0.001, Figure A). In addition, bone formation markers increased in E-treated women (+42% versus +12% in controls for PINP, P=0.012, and +7% versus -2% for osteocalcin, P=0.034) and bone resorption markers decreased (-37% versus -8% for CTX, P<0.001, and -25% versus -3% for TRAP5b, P<0.001). In Study B (men), using a 2-factor ANOVA model comparing the +E to the -E and +T to the -T groups, E, but not T, prevented increases in circulating sclerostin levels following induction of sex steroid deficiency (Figure B). Serum P1NP levels decreased (-13%) and bone resorption markers increased (+56% for CTX and +17% for TRAP5b, respectively, P < 0.05 for all) in the -T,-E group, and these increases were prevented by E (+14% for CTX and +6% for TRAP5b, respectively), but not T (+53% for CTX and +17% for TRAP5b, respectively) treatment. In both sexes, changes in sclerostin levels correlated with changes in bone resorption, but not formation, markers (R = 0.62, P < 0.001 and R = 0.33, P = 0.009 for correlations with changes in serum CTX in the women and men, respectively). Our studies thus establish that in humans, circulating sclerostin levels are reduced by E, but not T. Moreover, while the E-induced reduction in sclerostin production may play a role in the effects of E in maintaining bone formation, the associations we observed between changes in sclerostin levels and in bone resorption markers suggest that, consistent with recent data indicating important effects of Wnts on osteoclastic cells, at least part of the anti-resorptive effects of E may be mediated by changes in sclerostin production.

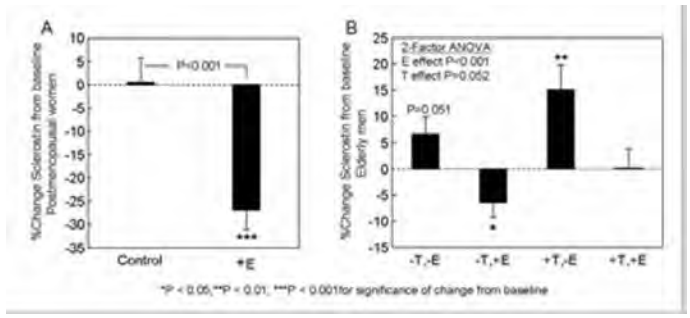

Sclerostin E and T

***Disclosures: Ulrike Moedder**, None.*

1135

Altered Bone Microarchitecture and Decreased Local Runx2, RANKL and SOST Gene Expression in Men with Primary Idiopathic Osteoporosis. Janina Patsch*[1], Paul Roschger[2], Andrea Berzlanovich[1], Christian Muschitz[3], Thomas Woegerbauer[4], Thomas Kohler[5], Heinrich Resch[6], Peter Pietschmann[1]. [1]Medical University of Vienna, Austria, [2]L. Boltzmann Institute of Osteology, Austria, [3]St. Vincent's Hospital, Austria, [4]St. Vincent Hospital Vienna, Austria, [5]b-cube AG, Switzerland, [6]Medical University Vienna, Austria

While postmenopausal osteoporosis is considered to be a high bone turnover disease in the first years after menopause, idiopathic osteoporosis in both premenopausal women and men might be associated with a functional osteoblast defect and/or impaired osteoblast-osteoclast coupling. The aim of this study was to assess the expression of a predefined set of osteoblastic or osteoblast-influencing genes in transiliac bone biopsies of patients with primary male osteoporosis and to relate molecular-biological to micro-structural alterations at the tissue level. 11 men with untreated, primary male osteoporosis underwent a double transiliac bone biopsy. Age-matched control samples (n = 11) were obtained from forensic autopsies following sudden death. One biopsy per patient was used for gene expression analysis the second biopsy was-embedded in PMMA and used for structural characterization. Gene expression levels were analyzed by quantitative real time PCR to assess RANKL, OPG, osterix, runx2, SOST and wnt10b, normalized to GAPDH expression. For structural analysis embedded biopsies were measured by micro-computed tomography (micro-CT) and common morphometric indices were determined for the trabecular bone compartment using a direct 3D approach.The patients' mean age was 52 ±16 years. Their mean T-scores were -2,06 at the lumbar spine (L1-L4) and -2,18 at the (total) hip. Peripheral or vertebral fractures were prevalent in about 90%. 45% of patients had a positive family history for fractures. After normalization to GAPDH, the gene expression of runx2, RANKL and, somewhat surprisingly, SOST expression was significantly lower in osteoporotic patients than in non-osteoporotic controls. Trabecular separation (Tb.Sp) was significantly increased (p=0,012) whereas trabecular number (Tb.N) was (p=0,01) reduced in the patient group. A significant difference in the structure model index (SMI; p=0,014) further indicates a more rod-like appearance of trabeculae in men with primary osteoporosis. The decreased runx2 expression stresses the potential role of a functional osteoblast defect in the pathogenesis of male idiopathic osteoporosis. We speculate that the decreased RANKL and SOST expression reflect an osteoblast-osteoclast coupling effect as well as an indirect sign of osteoblast-osteocyte cross-talk, respectively.

***Disclosures: Janina Patsch**, None.*

1136

Rosiglitazone Decreases Bone Mass and Bone Marrow Fat: A Randomized, Placebo-controlled Trial. Torben Harsloef*[1], Louise Wamberg[2], Louise Møller[3], Steffen Ringgaard[4], Hans Stødkilde-Jørgensen[4], Steen Bønløkke Pedersen[2], Bente Langdahl[5]. [1]Aarhus Amtssygehus, Aarhus University Hospital, Denmark, [2]Department of Endocrinology & Internal Medicine, THG, Aarhus University Hospital, Denmark, [3]Department of Endocrinology & Internal Medicine, NBG, Aarhus University Hospital, Denmark, [4]MR Research Centre, Aarhus University Hospital, Skejby, Denmark, [5]Aarhus Sygehus, Aarhus University Hospital, Denmark

Activation of peroxisome proliferator-activated receptor gamma (PPARγ) is believed to force mesenchymal stem cells of the bone marrow in an adipocyte direction at the expense of osteoblast leading to decreased BMD and increased marrow fat. Some studies, however, suggest that the two cell types can develop independently of

each other and might originate from different clones of stem cells. Rosiglitazone is a PPARγ agonist.

We examined the effect of rosiglitazone (8mg/day) for 14 weeks on BMD assessed by DXA and spine bone marrow fat assessed by magnetic resonance imaging proton spectroscopy (1H-MRS) in 53 healthy, postmenopausal women in a prospective, randomized placebo-controlled trial. Both types of scans were made before and after treatment but 1H-MRS only in a subgroup of 20 randomized participants. 1H-MRS provides a measure of fat content relative to water, the lipid to water ratio (LWR).

At the femoral neck, BMD decreased by 1.34 ± 0.60% (mean ± SEM) in the rosiglitazone group whereas BMD increased by 0.28 ± 0.56% in the placebo group (p=0.055). Changes in BMC were similar although not statistically significant (p=0.16).

At the lumbar spine, BMD decreased by 1.03 ± 0.34% in the rosiglitazone group and by 0.42 ± 0.35% in the placebo group (p=0.22). BMC decreased by 1.38 ± 0.42% in the rosiglitazone group and by 0.24 ± 0.41% in the placebo group (p=0.058).

Bone resorption marker CTx increased 20.4 ± 7.7% (mean ± SEM) in the rosiglitazone group and decreased by 7.1 ± 4.7% in the placebo group (p=0.003). Changes in the bone formation markers PINP, BAP, and osteocalcin were not significantly different between the groups.

In the rosiglitazone treated women spine LWR decreased by 13.5 ± 5.5% (mean ± SEM) whereas in the placebo group an increment of 6.8 ± 7.4% was found (p=0.056).

Our study is the first to examine the effect of rosiglitazone treatment on marrow fat in humans. Contrary to what was expected, spine LWR decreased during rosiglitazone treatment. Furthermore, rosiglitazone treatment results in uncoupling of bone resorption and formation leading to bone loss. Our data confirm that the bone marrow osteoblast/adipocyte relationship is more complex than originally assumed and that the two cell types can be independently affected.

***Disclosures: Torben Harsloef**, None.*

1137

The *Misty* mouse which has minimal brown adipose tissue (BAT) has markedly reduced bone mass and altered microarchitecture. Masanobu Kawai*[1], Sheila Bornstein[1], Sudatha Lotinen[2], Maureen Devlin[3], Mary Bouxsein[3], Mark Horowitz[4], Roland Baron[5], Clifford Rosen[1]. [1]Maine Medical Center, USA, [2]Harvard School of Dental Medicine, USA, [3]Beth Israel Deaconess Medical Center, USA, [4]Yale University School of Medicine, USA, [5]Harvard School of Medicine & of Dental Medicine, USA

Brown adipose tissue (BAT) is critical for non-shivering thermogenesis in young mammals. Recent studies suggest that BAT is also found in adults, particularly in young and thin individuals. Little is known about the relationship between BAT and skeletal remodeling, although expression studies have demonstrated that uncoupling protein-1(UCP-1), a marker of BAT, is highly expressed in some forms of marrow adiposity. To test the hypothesis that alterations in BAT affect bone metabolism, we phenotyped the Misty mouse that has been reported to have minimal BAT and impaired BAT function. Misty has a gray coat color on the B6 background and was previously used as a marker for prediction of the Lepr (db) genotype because the db locus is tightly linked to the Misty mutation. Loss of function of Dock7, a Rho family guanidine exchange factor (GEF) belonging to the DOCK180 protein family has been reported in Misty mice. Initially we performed developmental analyses of body composition in Misty and age and gender-matched B6 control mice. Misty females exhibited decreased body temperature at 16-wks, with altered BAT morphology, and reduced body weight compared to B6 controls across several time points (4-16 wk old). Surprisingly, percent body fat was not different between Misty and B6 at 16-wk of age although Misty had reduced whole body bone mineral content and bone mineral density vs B6 at all ages. MicroCT analysis confirmed that at 16 wks Misty had markedly reduced mid-femoral cortical thickness and decreased trabecular BV/TV and number in both the distal femur and spine ($p<0.01$ for all). Histomorphometric analysis revealed a 3 fold increase in osteoclast number ($p<0.001$) associated with a doubling in eroded surfaces in Misty vs B6, whereas osteoblast number and bone formation were identical to B6. Bone marrow stromal cell cultures revealed that CFU-Fs and CFU-OBs were comparable between Misty and B6, suggesting that the low bone mass phenotype of Misty is not cell autonomous for osteoblasts, despite relatively high expression of Dock7 in those cells. In sum, Misty mice have low bone mass and deteriorated architecture that is likely due to increased bone resorption. While we can not exclude the possibility that the lack of Dock7 directly affects osteoclast function, our data suggest that alterations in BAT have a profound systemic effect on bone acquisition and maintenance.

***Disclosures: Masanobu Kawai**, None.*

1138

PPARβ/δ-deficiency Impairs Muscle and Bone Mass and Worsens its Response to Estrogen-deprivation. Nicolas Bonnet*[1], Beatrice Desvergne[2], Serge Ferrari[3]. [1]Geneva University Hospital, Switzerland, [2]Center for integrative Genomics, Genopodes, Switzerland, [3]Geneva University Hospital & Faculty of Medicine, Switzerland

Ppar beta/delta (ß/δ) is ubiquitously expressed and its prime role is to promote fatty acids oxidation in skeletal muscle and adipose tissue. Pparß/δ-deficient mice have reduced muscle strength and capacity to perform physical activity, but their skeletal phenotype is unknown. We investigated the influence of Pparß/δ on the skeleton and its response to aging and ovariectomy (OVX).

Female Pparß/$\delta^{-/-}$ and Pparß/$\delta^{+/+}$ mice were monitored from 3 to 12 months of age. Another group was OVX or SHAM operated at 6 months and followed 8 wks.

Compared to Pparß/$\delta^{+/+}$, 3-month-old Pparß/$\delta^{-/-}$ mice had lower total body (TB) lean mass (17.9±0.4 vs 19.9±0.3 g, $p<0.001$), TB BMD (0.052±0.001 vs 0.054±0.001 g/cm^2, $p<0.05$), spine BMD (0.073±0.001 vs 0.080±0.002 g/cm^2, $p<0.01$), caudal vertebral BV/TV (8.6±0.3 vs 10.6±0.8 %, $p<0.05$) and tibial cortical (Ct) bone volume (BV, 0.34±0.01 vs 0.38±0.02 mm^3, $p<0.05$). Serum levels of TRAc5b were 20% higher in Pparß/$\delta^{-/-}$ vs PPARß/$\delta^{+/+}$ mice ($p<0.05$). At that age, no significant differences in TB fat mass, femoral BMD, tibial BV/TV or osteocalcin were observed. Between 3 and 12 months, Pparß/$\delta^{-/-}$ had significantly lesser % gain in femur BMD (+4.9% vs +13% in Pparß/$\delta^{+/+}$, $p<0.01$), tibial Ct BV (+9.8% vs +18.2% in Pparß/$\delta^{+/+}$, $p<0.05$), and Ct thickness (+6.0% vs +14.6% in Pparß/$\delta^{+/+}$, $p<0.05$). Lean mass and the other bone parameters also remained significantly lower in old Pparß/$\delta^{-/-}$ vs Pparß/$\delta^{+/+}$, which was associated with decreased bone formation at endocortical surfaces (BFR/BPm: 0.002±0.001 in Pparß/$\delta^{-/-}$ vs 0.005±0.002 µm2/µm/day in Pparß/$\delta^{+/+}$; MPm/BPm: 0.32±0.10 vs 0.74±0.15 % in Pparß/δ +/+, both $p<0.05$), but not at the periosteum. Compared to SHAM, OVX caused a greater loss in Pparß/δ-/- of muscle volume in the lower leg (-14.9% vs +3.8 in Pparß/$\delta^{+/+}$, $p<0.05$), TB BMD (-13.6% vs 0% in Pparß/$\delta^{+/+}$, $p<0.05$), and CtBV (-9 vs -5.3% in Pparß/$\delta^{+/+}$ ns), whereas changes in TB lean mass, spine and femur BMD, and trabecular BV/TV were similar in Pparß/$\delta^{-/-}$ and Pparß/$\delta^{+/+}$.

These results indicate that Pparß/δ plays an important role on the acquisition and maintenance of muscle and bone mass (particularly cortical) with aging and estrogen-deprivation. Whether Pparß/δ regulates bone remodeling through its effects on muscle and/or directly on bone cells, -as suggested by low bone formation at endocortical rather than periosteal surfaces-, is currently being investigated.

***Disclosures: Nicolas Bonnet**, None.*

1139

Males Recruits with Stress Reaction of the Tibia Exhibit Higher Density and Smaller Geometry than Uninjured Recruits. Rachel Evans*[1], Charles Negus[2], Amanda Antczak[3], Amir Hadid[4], Yael Arbel[4], Ran Yanovich[4], Daniel Moran[4]. [1]U.S. Army Research Institute of Environmental Medicine, USA, [2]L-3 Applied Technologies, USA, [3]US Army Research Institute of Environmental Medicine, USA, [4]Heller Institute of Medical Research, Israel

Susceptibility to bone stress reaction (SR), a painful, debilitating bone overuse injury, has been attributed to parameters of bone that include low BMD, smaller bones (geometry), or a combination of these attributes (bone strength). Specifically, the higher occurrence of SR in women than men during military training has often been attributed to lower BMD. Data supporting this, however, utilized 2-dimensional DXA imaging and may represent smaller bone size in women rather than lower BMD. The purpose of this study was to determine if men and women who sustained a SR over the course of a 4-mo recruit training program differed from uninjured recruits (NSR) in measures of volumetric cortical BMD (vBMD), bone size [total area (TtAr), cortical area (CA), cortical width (CW)], and a bone strength index (BSI). Peripheral QCT was used to obtain cross-sectional images of the tibia from 114 male and 68 female recruits upon entry into the Israeli Defense Forces. MATLAB software assessed whole bone and regional (60° sectors) parameters of the tibia shaft at fracture prone sites (38 and 66% of tibial length). Tibial SR was diagnosed using MRI, bone scan, radiography, and clinical examination.

28 men (24.6%) and 12 women (17.6%) were diagnosed with SR. Women exhibited greater vBMD than men, though their bones were smaller ($p<0.001$). At the 38% site men with SR had higher vBMD than NSR men (1160.7±17.5 vs 1150.9±21.7 mg/cm^3, $p=0.03$), narrower tibial shafts (TtAr 411.0±38.2 vs 451.2±45.1 mm^2, $p<0.001$), and lower BSI (69.7±14.4X106 vs 81.1±6.3X106 mm4, $p=0.001$); similar differences were apparent at the 66% site ($p\leq0.04$). No differences were observed between SR and NSR women. Regional analyses revealed that greater vBMD and smaller area in SR men was most prominent at the anterior and medial-anterior sectors of the tibia. We conclude that male recruits with higher vBMD and smaller tibial geometry, specifically at the anterior/medial-anterior aspect of the tibia (a frequent SR site) may be more susceptible to bone overuse injury. While similar results were not observed in among women, the tibiae of females compared to men exhibited higher vBMD and smaller tibial geometry. Whether the higher incidence of SR in both women and susceptible men is related to higher mineralization that may compensate for smaller bones warrants further exploration. Moreover, previous conclusions that "lower BMD" predisposes healthy women or men to bone overuse injuries should be reconsidered.

***Disclosures: Rachel Evans**, None.*

1140

Reduced Matrix Heterogeneity with Bisphosphonate Treatment in Postmenopausal Women with Proximal Femoral Fractures. Adele Boskey[1], Joseph Lane[1], Brian Rebolledo[1], Brian Gladnick[2], Dennis Meredith[1], Eve Donnelly*[1]. [1]Hospital for Special Surgery, USA, [2]Cornell University, Weill Medical College, USA

Bisphosphonate (BIS) treatment is generally effective in reducing fracture incidence in osteoporotic patients. While no significant association between BIS use and subtrochanteric (ST) fracture risk was detected in analyses of datasets from large trials [Black+ 2010], identification of a rare atypical fracture pattern specifically associated with BIS treatment [Neviaser+ 2008] suggests that BIS use may alter bone quality in a subset of patients. Our objective was to examine the effect of BIS treatment on bone tissue composition near femoral fracture sites.

Bone cores were removed from the lateral aspect of the proximal femur, adjacent to the fracture site, of postmenopausal women admitted for repair of intertrochanteric (IT) and ST fractures in an IRB-approved study. Specimens were allocated to the -BIS group (n=12, age=87$\pm$7y; fracture morphology: 11 IT, 1 ST, 0 atypical) if the patient had never used BIS; all others were allocated to the +BIS group (n=14, age=82$\pm$11y, BIS duration 7.4$\pm$5y; fracture morphology: 9 IT, 1 ST, 4 atypical). Cortices were analyzed with Fourier transform infrared (FTIR) imaging to assess the mineral:matrix ratio, carbonate:phosphate ratio, collagen cross-link maturity (XLR), and mineral crystallinity (XST). Pixel histograms of each parameter were characterized by their mean and full width at half maximum to assess average composition and compositional heterogeneity, respectively.

The XLR distribution width was reduced 29% in the +BIS group vs. the -BIS group (Fig. 1). Trends toward treatment-based effects in the +BIS group were evident in the XST mean (+2%, p=0.055) and width (-22%, p=0.068) but did not reach statistical significance. All other FTIR parameters were similar across groups.

Bisphosphonate treatment was associated with narrowed distributions of collagen maturity in patients with femoral fractures. The average cortical composition was minimally changed. These data are consistent with previous reports of loss of heterogeneity with BIS treatment in perimenopausal women [Boskey+ 2009] and in normal beagles [Gourion+ 2009a]. Our approach comprised analysis of FTIR parameters that are independent predictors of fracture risk [Gourion+ 2009b]. Because reductions in tissue heterogeneity are associated with reduced resistance to crack propagation, our data preliminarily suggest that oversuppression of bone turnover may alter bone quality and contribute to the increased risk of fractures in a subset of patients.

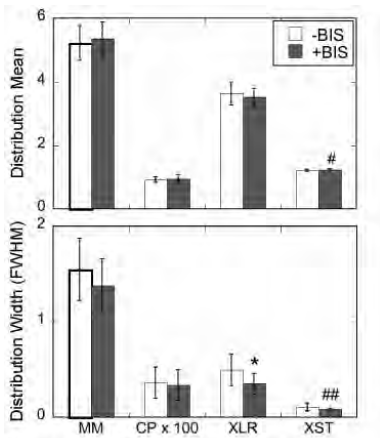

Figure 1: FTIR spectroscopic parameters for each treatment group reported as distribution means (top) and full widths at half maximum (FWHM) (bottom). (MM=mineral:matrix ratio; CP=carbonate:phosphate ratio; XLR= collagen maturity; XST=crystallinity; *p<0.05, #p=0.055, ##p=0.068 by t-test)

Figure 1

***Disclosures: Eve Donnelly**, None.*

1141

Bone Tissue Quality in the Years after Menopause: Micro-hardness is Decreased Independently of Changes in the Degree of Mineralization. Yohann Bala*[1], Susan Bare[2], Georges Boivin[1], Robert R. Recker[2]. [1]INSERM U831, Université de Lyon, France, [2]Osteoporosis Research Center, Creighton University, USA

Bone strength depends not only on bone mass and architecture but also on bone mineralization. The degree of mineralization of bone (DMB) depends on the age of bone structural unit which is influenced by the activity of bone remodeling[1]. Our purpose was to measure bone quality variables reflecting mineralization and microhardness in iliac bone biopsies from 20 women (49$\pm$2 yrs) before and 1 year after menopause (paired samples) and from 20 women (60$\pm$7 yrs) 14$\pm$9 yrs after menopause. DMB (g/cm^3), heterogeneity index (HI, g/cm^3) and Vickers microhardness were measured separately for cortical and cancellous bone[2]. Bone remodeling activity was evaluated with Activation Frequency (Ac.F, #/yr) measured in cancellous bone using tetracycline-based histomorphometry[3]. Ac.F was significantly (p=0.002) increased after 1 year of menopause vs before and was maintained at a high level after 14 yrs of menopause. Among the 3 groups, DMB was not significantly changed neither in cortical nor in cancellous bone. HI was also not significantly changed but lowest values of DMB (0.50-0.75 g/cm^3) were more frequent in bone tissue after 14 yrs of menopause than in other groups. Microhardness of cortical and cancellous bone tissue were significantly ($p<0.04$) decreased one year after menopause vs before. Measured after 14 years past menopause, microhardness of cancellous bone was significantly ($p<10^{-4}$) lower than after 1 year of menopause, this difference was borderline in cortical bone (p=0.07). Thus, menopause was associated with a low microhardness after both 1 and 14 years, independently of changes of DMB. This could be link with the changes in viscoelasticity of bone tissue showed after one year of menopause[4]. Results suggested that the substantial increase in bone remodeling modified the distribution of mineralization. Augmentation in bone formation led to an increase of hypomineralized bone tissue counterbalanced by the increase of resorption which led to an increased frequency of high DMB values. Consequently, DMB and HI were not changed despite of changes in Ac.F. In conclusion, the quality of organic matrix could influence bone strength independently of mineralization[5], and has to be taken into account in further analysis on bone quality.

1-Boivin & Meunier 2002, Connective Tissue Res 43:535 2-Boivin et al 2008, Bone 43:532 3-Recker et al 2004, J Bone Miner Res 19:1628 4-Polly et al 2008, J Bone Miner Res 23:366 5-Fratzl-Zelmann et al 2009, Calcif Tissue Int 85:335

Table: Variables reported as Median [CI 95%]

	Cortical Bone			Cancellous Bone			
	DMB	HI	microhardness	DMB	HI	microhardness	Ac.F
before Menopause	1.09 [1.02-1.12]	0.25 [0.23-0.30]	47.43 [45.34-48.28]	1.09 [1.06-1.14]	0.19 [0.18-0.24]	49.71 [48.39-51.71]	0.13 [0.09-0.20]
1 yr after Menopause	1.06 [1.03-1.11]	0.20 [0.20-0.26]	43.95* [42.73-46.76]	1.11 [1.08-1.15]	0.18 [0.17-0.24]	47.61* [45.91-50.01]	0.24* [0.21-0.37]
14 yrs after Menopause	1.06 [1.02-1.09]	0.22 [0.19-0.26]	42.95* [41.94-43.50]	1.12 [1.08-1.13]	0.18 [0.17-0.21]	43.36*# [42.73-44.15]	0.31* [0.23-0.50]

* p<0.05 vs. before menopause
\# p<0.05 vs. 1 yr after menopause

Table

***Disclosures: Yohann Bala**, None.*

1142

Male Astronauts Have Greater Bone Loss and Risk of Hip Fracture following Long Duration Spaceflights than Females. Rachel Ellman*[1], Jean Sibonga[2], Mary Bouxsein[1]. [1]Beth Israel Deaconess Medical Center, USA, [2]USRA Division of Space Life Sciences, USA

Despite an intense exercise regimen, excellent health, and relatively young age, astronauts experience dramatic bone loss in space. Yet it is not known how this decrement in bone mass influences the risk of fracture in the returning crewmember. Additionally, the sex-specific differences in the skeletal response to microgravity in astronauts have not been investigated, for lack of a sufficient sample size. Thus, our goal was to use a biomechanical approach to determine the risk for hip fracture following long-duration spaceflight in male and female astronauts based on their areal bone mineral density (aBMD) and body composition. To do so, we calculated the factor-of-risk (Φ), defined as the ratio of applied load to bone strength, in long duration astronauts before and after return from a mission on the International Space Station. All NASA long duration astronauts (n=25) from Expedition 1-18, with missions averaging 171 days (range 95-215), were included in the study. The load applied to the hip was calculated for a sideways fall from standing height based on each astronaut's height and weight, minus an attenuating contribution from the soft tissue overlying the greater trochanter. Femoral strength was estimated from trochanteric aBMD measurements by DXA, using a regression derived from a previous study of femoral strength in human cadaveric samples (Roberts et al, Bone 2010). Trochanteric aBMD measurements did not differ between male (n=20) and female crewmembers either at preflight or postflight. However, bone loss was twice as great in men, with 6.9% decrease in BMD ($p < 0.005$) versus 3.3% loss in women ($p = 0.09$). Male crewmembers had a significantly higher factor-of-risk for hip fracture than females, with postflight values of 0.88 $\pm$ 0.14 and 0.36 $\pm$ 0.05, respectively ($p <$

0.005). Three men, but no women, exceeded the theoretical fracture threshold of Φ=1 postflight, indicating that they would likely fracture if they were to fall sideways with impact to the greater trochanter. Altogether, these data indicate that male crewmembers may be at a higher risk for hip fracture than females following spaceflight, primarily due to a greater impact force from a fall. Moreover, the accelerated rate of microgravity-induced bone loss in men is in direct contrast to the greater risk of age-related osteoporosis in women. The mechanisms underlying these different responses warrant further investigation.

***Disclosures: Rachel Ellman**, None.*

1143

High Resolution Peripheral Quantitative CT (HRpQCT) Reveals Preferential Inner Trabecular Bone Loss in Lactating Women. Shannon Kokolus[1], Mary Beth Vrabel[1], Xiaowei Liu[1], Stephanie Boutroy[2], Halley Rogers[3], Donald McMahon[4], Carolyn Westhoff[1], Adi Cohen*[3]. [1]Columbia University, USA, [2]INSERM, Université De Lyon, France, [3]Columbia University Medical Center, USA, [4]Columbia University College of Physicians & Surgeons, USA

Lactation is associated with declines in bone mineral density (BMD) followed by recovery. Rodent studies show loss of trabecular (Tb) BMD with detectable changes in bone microarchitecture and decreases in bone strength. High resolution peripheral quantitative CT (HRpQCT; Xtreme CT, Scanco Medical AG; voxel size 82μm) can image bone microarchitecture *in vivo*, allowing us to examine longitudinal microarchitectural changes in the distal skeleton in lactating women for the first time. We measured BMD by DXA at the lumbar spine (LS), total hip (TH), femoral neck (FN), 1/3 radius (DR) and ultradistal radius (UD) and HRpQCT at the radius and tibia in 12 healthy, exclusively breastfeeding women at baseline and 6 months postpartum. At baseline (38±20 days postpartum), subjects (58% Caucasian) had (mean±SD) age of 34±4 yrs, weight of 62±7 kg, and BMI of 22.6±2.6 kg/m^2. Mean baseline BMD Z scores ranged from -0.68 to 0.28 at the 5 measured sites. By 6 months (190±11 days), subjects had lost 3.5±3.7 kg, a decrease of 5.1±5.0% (p=0.01). BMD also fell by 3.3±3.9% (p=0.01) at the LS, 1.6±3.3% (p=0.1) at the TH, 2.3 ± 4.8% (p=0.1) at the FN, and increased by 1.5±3.0% (p=0.1) at the DR and 0.3±4.1% (p=0.9) at the UD. Greater LS bone loss at 6 months correlated with lower baseline weight (R=-0.7;p=0.01) and greater decrease in weight (R=0.8;p=0.002), while age, baseline BMI and the number of days postpartum at baseline visit were not associated. By HRpQCT at the radius, no significant changes were found in cortical density or thickness, or in total Tb density (Dtrab), number, thickness or separation. However there was a 3.0±4.3% decrease in density of the inner Tb compartment (Dinn; p=0.04) and a 2.9±2.7% increase in the ratio of the outer (Meta) to inner Tb compartment density (Meta/Inn; p=0.004; Table). There were no significant changes in any HRpQCT measure at the tibia. Baseline weight was directly associated with the 6-month change in Dinn (radius: R=0.6; p=0.04; tibia: R=0.6; p=0.06) and inversely associated with the 6-month change in Meta/Inn (radius: R=-0.4; p=NS; tibia: R=-0.8; p=0.004). In summary, at 6 months postpartum, lactating women had expected decreases in LS BMD by DXA. HRpQCT at the radius revealed preferential bone loss in the inner trabecular compartment, similar to the pattern seen in rodent models. The lack of change at the tibia suggests that weightbearing may influence lactation-related bone loss.

	RADIUS		TIBIA	
	Mean % change	p (baseline vs 6mo)	Mean % change	p (baseline vs 6mo)
Dtrab	-1.3± 3.8	0.3	-0.7± 2.0	0.3
Dinn	-3.0± 4.3	**0.04**	-0.4± 3.3	0.9
Dmeta	-0.1 ±4.0	0.9	-1.0± 1.7	0.06
Meta/Inn	2.9± 2.7	**0.004**	-0.7± 2.7	0.7

TABLE

***Disclosures: Adi Cohen**, None.*

1144

Finite Element Analysis of the Hip DXA Scans and Hip Fracture Risk in Older Men. Lang Yang*[1], Annabel Burton[2], Mike Bradburn[2], Eric Orwoll[3], Lynn Marshall[3], Carrie Nielson[3], Richard Eastell[2]. [1]Univesity of Sheffield, United Kingdom, [2]University of Sheffield, United Kingdom, [3]Oregon Health & Science University, USA

Low areal BMD (aBMD) is associated with increased risk of hip fracture, but many hip fractures occur in persons without low aBMD. Finite element (FE) analysis of QCT scans provides a measure of hip strength that predicted hip fractures independently of hip aBMD in MrOS. QCT scans are not widely available. We have developed an FE method for DXA scans of the hip and the aim of the study was to determine whether hip strength estimates predict hip fracture risk independent of aBMD.

This prospective case-cohort study included all first hip fractures (n = 40) and a random sample (n = 210) of non-fracture cases from 3549 community-dwelling men > or =65 yr of age, with a mean follow-up of 5.6 yr. We analyzed the baseline DXA scans of the hip using linear-elastic FE method. Stress and strain within the bone were calculated as a consequence of a sideways fall. A stress-based femoral strength S_s was defined as the impact force that caused the von Mises stress in 100 contiguous elements (24 mm^2) to exceed the element yield stress. A strain-based femoral strength S_e was also calculated similarly with the element yield strain being a constant of 1.45%. Cox regression with Prentice weighting was used to assess the association of the femoral strengths with hip fracture.

The mean femoral strengths S_s and S_e were 1287 (SD 612) and 4659 (SD 2107) N for fractured group, 2054 (SD 1170) and 8072 (SD 3699) N for non-fractured group, respectively. Between-group differences were highly significant ($p<0.0001$). Correlation of total hip (TH) aBMD with S_s: r=-0.44, $p<0.0001$ and with S_e: r=-0.64, $p<0.0001$. S_s and S_e were also positively correlated with one another (r=0.61, $p<0.0001$). The table shows the hazard ratio (HR) of hip fracture per standard deviation (SD) increase in age and decreases in TH aBMD, BMI, S_s and S_e in a variety of Cox regression models. The HRs of S_s and S_e were significant alone and after adjusting for age, BMI and site. When adjusted for age, BMI, site and TH aBMD, the HR of S_e was still significant. The HRs for BMI and site were not significant in any of the regression models.

These results demonstrated that FE analysis of DXA hip scans can provide strength estimates that predict hip fracture independent of aBMD. This finding is consistent with previous work in our group on women and with previous FE analysis using QCT in the same cohort of men.

Hazard ratio (95% CI) of hip fracture for 1 SD change in covariate values in various Cox models

		Adjusted for		
	None	Age	Age, BMI, Site	Age, BMI, Site, TH aBMD
TH aBMD	5.18 (2.76-9.72)	4.69 (2.49-8.83)	5.44 (2.73-10.85)	
S_s	2.80 (1.61-4.89)	2.60 (1.43-4.71)	2.65 (1.44-4.87)	2.01 (0.90-4.47)*
S_e	4.16 (2.32-7.44)	3.64 (1.95-6.79)	3.84 (2.00-7.37)	2.19 (1.03-4.64)**

* HR for TH aBMD in model 4.61 (2.27-9.36); ** HR for TH aBMD in model 3.94 (1.86-8.36)

Table

***Disclosures: Lang Yang**, None.*

1145

Sirtuin1 (*Sirt1*) Regulates Osteoblastogenesis and Represses Sclerostin. Einav Cohen-Kfir*[1], Avi Levin[1], Hanna Artsi[1], Eva Abramowitz[1], Agustina D'Urso[2], Lei Zhong[2], Raul Mostoslavsky[2], Rivka Dresner-Pollak[1]. [1]Hadassah-Hebrew University Medical Center, Israel, [2]The Massachusetts General Hospital Harvard Medical School, USA

The sirtuins are NAD+-dependent enzymes with a prominent role in metabolism and age-related diseases. We have previously reported that *Sirt1*-haploinsuffient (*Sirt1*+/-) adult female mice exhibit a 30% reduction in bone mass (*Sirt1*-/- is lethal). The purpose of this study was to investigate the mechanisms of reduced bone mass in *Sirt1*+/- mice.

Bone formation and resorption were evaluated in vivo and in vitro. A decrease in bone formation was found in *Sirt1*+/- mice as indicated by a 20% reduction in mineral apposition rate and bone formation rate, decreased serum PINP, a 50% reduction in alkaline phosphatase activity in *Sirt1*-derived bone marrow mesenchymal stem cells (BM-MSC) induced to osteogenesis accompanied by fewer Von Kossa positive-stained nodules. On the other hand, no significant changes in bone resorption were observed as indicated by osteoclast number and serum TRAP5b. Osteoclastogenesis upon exposure of marrow machrophages to RANKL and M-CSF was reduced in *Sirt1*+/- mice, resulting in smaller osteoclasts with fewer nuclei. No differences in IGF-1, 25OHvitaminD3 and 17-β estradiol were detected.

To investigate the mechanism by which Sirt1 affects osteoblastogenesis, gene expression in *Sirt1*+/- and WT-BM-MSCs was compared. A 14-fold increase in SOST expression was found in *Sirt1*+/–BM-MSCs. Confirming the gene expression data, sclerostin was increased in *Sirt1*+/- -BM-MSCs and whole bone extracts, and was reduced in *Sirt1*-over-expressing C3HT101/2 cells. Moreover, beta-catenin was increased in *Sirt1*-over-expressing C3HT101/2 cells.

To study how *Sirt1* regulates SOST gene expression, a chromatin immunoprecipitation (ChIP) assay was performed with Sirt1 antibody in mouse embryonic stem (ES) cells. *Sirt1*-/- cells were used as negative control. PCR assay using primers that cover consecutive segments in the regulatory region of the SOST promoter, showed *Sirt1* binding to the 760-1940 region. No binding was detected in Sirt1-/- cells. Next we tested whether *Sirt1* affects the SOST promoter through modification of histone H3K9, a known *Sirt1* target, using a ChIP assay. H3K9 acetylation of the SOST promoter was dramatically increased in *Sirt1*-/- cells in the region of maximal *Sirt1* binding.

Conclusions: This study demonstrates a role for *Sirt1* in bone formation by repressing SOST expression via epigenetic modification of histone 3, and suggests that *Sirt1* is a potential novel target for anabolic therapy for osteoporosis.

***Disclosures: Einav Cohen-Kfir**, None.*

1146

Osteoblast-Specific Deletion of Neuropeptide Y1 Receptors Enhances Bone Formation. Nicola Lee, Ronaldo Enriquez, Amy Nguyen, Kharen Doyle, Amanda Sainsbury, Paul Baldock*, Herbert Herzog. Garvan Institute of Medical Research, Australia

Neuropeptide Y (NPY) has been shown to play a critical role in the central regulation of bone metabolism. However, the peripheral mechanism remains unknown. In-situ hybridisation on femur sections revealed the presence of the NPY, Y1 receptor mRNA in osteoblasts, consistent with a direct role for the Y1 receptor on bone cells.

To investigate the role of the Y1 receptor on osteoblastic cells, we generated mice with selective deletion of the Y1 receptor in osteoblasts ($Y1^{lox/lox,Cre/+}$) by crossing Y1 receptor floxed mice with mice expressing Cre specifically in osteoblasts under control of a 2.3kb fragment of the rat α_1(I)-collagen promoter.

In male mice at 16 weeks of age, osteoblast-specific Y1 receptor deletion resulted in a marked increase in femoral cancellous bone volume ($Y1^{lox/lox,Cre/+}$ 15.2 % $\pm$ 1.4, control 11.0 $\pm$ 0.6; $p<0.01$), trabecular thickness ($Y1^{lox/lox,Cre/+}$ 34.8 µm $\pm$ 2.4, control 29.4 $\pm$ 1.2; $p<0.05$) and trabecular number ($Y1^{lox/lox,Cre/+}$ 4.3 /mm $\pm$ 0.2, control 3.8 $\pm$ 0.1; $p<0.05$). This was the result of elevated osteoblast activity as shown by a significant increase in mineral apposition rate ($Y1^{lox/lox,Cre/+}$ 1.93 µm/day $\pm$ 0.02, control 1.64 $\pm$ 0.05; $p<0.001$) and bone formation rate ($Y1^{lox/lox,Cre/+}$ 0.52 $\mu m^2/\mu m^3$/day $\pm$ 0.02, control 0.41 $\pm$ 0.04; $p=0.01$) with no alterations in bone resorption as measured by osteoclast number and osteoclast surface area. Furthermore, osteoblastic Y1 receptor deletion also led to increased mineral apposition rate on both the endocortical ($Y1^{lox/lox,Cre/+}$ 1.72 µm/day $\pm$ 0.10, control 1.08 $\pm$ 0.08; $p<0.001$) and the periosteal surfaces ($Y1^{lox/lox,Cre/+}$ 1.33 µm/day $\pm$ 0.12, control 0.99 $\pm$ 0.07; $p<0.05$) resulting in significantly increased femoral diameter ($Y1^{lox/lox,Cre/+}$ 5.24 mm $\pm$ 0.10, control 5.00 $\pm$ 0.06; $p<0.05$) and a trend towards increased cortical bone strength as estimated by mean polar moment of inertia ($Y1^{lox/lox,Cre/+}$ 0.42 mm^4 $\pm$ 0.03, control 0.36 $\pm$ 0.02; $p=0.05$).

Together these data demonstrate a direct role for the Y1 receptor on osteoblasts in the regulation of osteoblast activity and bone formation in vivo and suggests that targeting Y1 receptor signalling directly in the bone may have potential powerful therapeutic implications for stimulating bone accrual in diseases such as osteoporosis.

***Disclosures: Paul Baldock**, None.*

1147

Hedgehog Signaling Inhibits Differentiation of Osterix+ Progenitors to Mature Osteoblasts. Kyu Sang Joeng*[1], Fanxin Long[2]. [1]Washington University School of Medicine - St. Louis, USA, [2]Washington University School of Medicine, USA

Although a large number of genetic studies have shown that Indian hedgehog signaling is essential for endochondral bone development in the embryo, the function of Hedgehog (Hh) signaling in postnatal bone formation is not clear. In a previous study, we generated the R26-ΔNGli2 mouse strain which can express a constitutively activated form of Gli2 (termed ΔNGli2) in a CRE-dependent manner. To study the function of Hh signaling in postnatal bones, we initially generated *Col2-CRE; $R26^{\Delta NGli2/+}$* mice by crossing *$R26^{\Delta NGli2/+}$* mice with Col2-CRE mice which express Cre in both osteoblasts and chondrocytes. The *Col2-CRE; $R26^{\Delta NGli2/+}$* animals showed a disorganized growth plate and severe osteopenia at 2 and 4 months of age. However, the disorganized growth plate precluded the analysis of direct effects of Hh signaling on bone. To avoid the growth plate phenotype, we generated *Osx1-GFP::Cre; $R26^{\Delta NGli2/+}$* mice (termed OsxΔNGli2) by crossing *$R26^{\Delta NGli2/+}$* mice with *Osx1-GFP::Cre* mice which specifically express Cre in osteoblasts[1]. The OsxΔNGli2 animals exhibited a dramatic decrease (6-fold by uCT) in bone mass without any obvious growth plate phenotype at 4 and 6 weeks of age. Further analysis showed that the reduced bone mass in OsxΔNGli2 animals was due to decreased osteoblast number and activity. To study the molecular basis for the osteoblast phenotype, we performed in situ hybridization with osteoblast markers in neonatal OsxΔNGli2 animals. Whereas early osteoblast markers, *Runx2* and *Osterix (Osx)*, were expressed normally, the mature osteoblast marker, *Osteocalcin (Oc)*, was rarely detectable in OsxΔNGli2 animals. These data indicate that ectopic activation of Hh signaling by ΔNGli2 inhibits differentiation of Osx+ progenitors to Oc+ osteoblast. To examine the role of physiological Hh signaling in Osx+ progenitors, we generated *SP7-CRE; $Smo^{c/c}$* mice in which *Smoothened (Smo)*, the indispensable mediator for hedgehog signaling, was specifically knocked out in osteoblasts. Remarkably, *Osx1-GFP::Cre; $Smo^{c/c}$* animals showed a notable increase in bone mass (7-fold by uCT). Consistent with the notion that loss of Hh signaling promotes differentiation of Osx+ progenitors, in situ hybridization in neonatal *Osx1-GFP::Cre; $Smo^{c/c}$* animals detected a decrease in Osx signal in the primary spongiosa. Overall, through both gain- and loss-of-function studies, we have uncovered a new function for Hh signaling in osteoblast development. We speculate that the newly identified role of Hh signaling may be important for maintaining an adequate pool of progenitors for osteoblast.

1Rodda SJ, et al. Development. 133 (16), 3231-44 (2006).

***Disclosures: Kyu Sang Joeng**, None.*

1148

Endogenous G_i Signaling in Osteoblasts Restricts Bone Formation in Adult Mice. Susan Millard*[1], Alyssa Louie[2], Nathalie Cotte[3], Bruce Conklin[3], Robert Nissenson[4]. [1]UCSF/VA Medical Center/Northern California Institute for Research & Training, USA, [2]VA Medical Center, USA, [3]Gladstone Institutes, USA, [4]University of California, San Francisco, USA

Blockade of endogenous Gi coupled signaling in osteoblasts throughout development, achieved by transgenic expression of pertussis toxin (PTX), results in increased cortical thickness and a female-specific increase in cancellous fractional bone volume (BV/TV) in femurs of 12wk old mice. Here we report on changes in bone formation rates (BFR) that underlie the Col1(2.3).PTX mouse phenotype and on the effects of blockade of Gi signaling in the adult mouse independent of developmental effects. Increased cortical thickness observed in Col1(2.3).PTX mice results from increased periosteal BFR (Male:1.3$\pm$0.3 vs 2.1$\pm$0.6µm/day $p<0.01$, Female:1.2$\pm$0.3 vs 2.0$\pm$0.8µm/day $p<0.05$). Mineralizing surface (MS) in control mice was primarily restricted to the lateral and anterior surfaces of the femoral midshaft, with little or no active bone formation on the medial and posterior surfaces. In contrast, Col1(2.3).PTX mice displayed an expanded MS with active bone formation evident around the entire circumference of the bone. There was no appreciable change in mineral apposition rate. In cancellous bone at the distal femur, expression of PTX produced no alteration of BFR in male mice (0.68$\pm$0.13 vs 0.77$\pm$0.12µm/day). However, BFR in female Col1(2.3).PTX bones could not be quantified due to the disorganized nature of bone formation which displayed a labeling pattern consistent with the rapid formation of woven bone. To examine the role of endogenous Gi coupled signaling in the adult skeleton we utilized the Tet-regulatable nature of our transgenic model. In these studies, expression of PTX in osteoblasts was delayed until 8wks of age, and the cohort was assessed by in vivo µCT of the distal femur and TFJ. Between 10wks and 6 mths of age, male and female control mice and Col1(2.3).PTX male mice all experienced a 30% decrease in cancellous BV/TV. Col1(2.3).PTX female mice displayed a striking 90% increase in BV/TV. Assessment of the TFJ showed that the percentage increase in cortical thickness to be greater in Col1(2.3).PTX than control mice (Male:5.6$\pm$2.6 vs 9.0$\pm$3.2% $p<0.05$, Female:6.8$\pm$4.1 vs 16.9$\pm$4.5% $p<0.001$). These results indicate that signaling by endogenous Gi coupled receptors in osteoblasts of adult mice: 1) restricts cortical bone formation in both genders; and 2)restricts cancellous bone formation in females. Inhibition of Gi coupled receptor signaling in osteoblasts represents a novel strategy for the development of new anabolic therapies for osteoporosis.

***Disclosures: Susan Millard**, None.*

1149

Intermittent PTH of Short Term can Activate Quiescent Lining Cells to Mature Osteoblasts: Unproven Mechanism of the Anabolic Action of Intermittent PTH. Sang Wan Kim*[1], Paola Divieti Pajevic[2], Martin Selig[3], Henry Kronenberg[2]. [1]Seoul National University Boramae Hospital, South korea, [2]Massachusetts General Hospital, USA, [3]Department of Pathology, Massachusetts General Hospital, USA

Intermittent administration of parathyroid hormone (PTH) increases bone mass, at least in part by increasing osteoblast number, but the molecular and cellular mechanism involved in the anabolic effects have not been completely elucidated. One possible source of osteoblasts might be conversion of inactive lining cells to osteoblasts, and indirect data are consistent with this hypothesis. To better understand the possible effect of PTH on lining cell activation, we conducted a lineage tracing study using an inducible gene system. We used the mouse 10kb DMP1 promoter to drive the expression of the inducible CreERt2 in transgenic mice; this gene is active, upon tamoxifen administration, in osteocytes and some osteoblasts, particularly in the calvarium. DMP1-CreERt2 mice were crossed with Rosa26R reporter mice that contain a conditional LacZ transgene downstream of a floxed stop-cassette inserted into the endogenous Rosa26 locus to render targeted mature osteoblasts and their descendents, lining cells or osteocytes, detectable by X-gal staining. Rosa26R:DMP1-Cre(+) mice were injected with 0.25mg of tamoxifen (TMX) at day 3, 5 and 7 postnatally and then injected with 0.1mg at day 14 and 21. They were sacrificed at day 23, 35 and 42 postnatally (2, 14 and 21 days after the last TMX, respectively). At day 42, some mice were challenged with anabolic injection of human PTH (1-34, 80µg/kg) or vehicle for 3 days, administered subcutaneously. In calvarial and tibia bones of Rosa26R:DMP1-Cre(+) mice at 23 days of age, many cuboidal osteoblasts and osteocytes were positive for X-gal staining. Twenty-one days after the last TMX injection, most of blue cells were found to be very flat on the periosteal surface of both calvaria and tibia. After 3 days of PTH injections, the thickness of blue cells on the inner surface of the calvaria and on the periosteal surface of tibia increased and the number of these cells did not fall as much as with vehicle. Moreover, new blue cells appeared on the outer surface of calvaria, which were not detected with routine light microscopy prior to PTH. Electron microscopy analysis revealed X-gal particles in both blue thin cells prior to PTH and cuboidal cells following PTH administration. PTH did not increased β-galactosidase activity in Rosa26R:DMP1-Cre(-) mice. These data support the hypothesis that short term treatment with intermittent PTH can contribute to the anabolic effect through activating lining cells to mature osteoblasts in vivo.

***Disclosures: Sang Wan Kim**, None.*
This study received funding from: NIH

1150

K-ras Generated Signals in Osteoblasts Increase Trabecular Bone Mass by Stimulating Osteoblast Proliferation and Inhibiting Osteoclastogenesis. Julie Leslie*[1], Ryan Riddle[2], Cassandra R. Zylstra[3], Katia Bruxvoort[3], Thomas Clemens[1], Bart Williams[3]. [1]Johns Hopkins University, USA, [2]Johns Hopkins University School of Medicine, USA, [3]Van Andel Research Institute, USA

K-ras is a GTPase that activates proteins necessary for the propagation of growth factor and receptor-initiated signals. Key among these is the mitogen-activated protein kinase (MAPK) pathway, which is required for osteoblast proliferation and optimal osteogenic gene expression. To directly investigate the role of K-ras signaling in skeletal development *in vivo*, we generated mice expressing a constitutively active form of K-ras in osteoblasts (OB $Kras^{G12D}$). Mice expressing the osteocalcin-Cre transgene were crossed with heterozygous Lox-Stop-Lox $K\text{-}ras^{G12D}$ mice, in which the expression of K-ras with an activating mutation at codon 12 (G12D) is controlled by a removable transcription termination element. Longitudinal analysis of whole body bone mineral density (BMD) by DEXA demonstrated a significant increase in BMD in OB $K\text{-}ras^{G12D}$ mice compared to controls, with the largest increase (14%) evident at 12 weeks of age. Micro-CT measurements of femoral bone structure in OB $K\text{-}ras^{G12D}$ mice revealed no change in cortical bone, but dramatically increased trabecular bone volume (109%). Histomorphometry revealed an increase in the total number of osteoblasts. Consistent with this observation, primary osteoblasts expressing $K\text{-}ras^{G12D}$ exhibited increased rates of proliferation and expression of cyclin D1. Osteoblast differentiation, however, was unaffected by increased activation of MAPK signaling, as alkaline phosphatase expression and matrix mineralization were equivalent in control and mutant osteoblasts. Surprisingly, the number of osteoclasts was reduced by more than 50% in OB $K\text{-}ras^{G12D}$ mice, which suggests that MAPK signaling in the osteoblast indirectly regulates osteoclast development. Indeed, osteoclast differentiation was impaired in co-cultures containing $K\text{-}ras^{G12D}$ expressing osteoblasts compared to cultures containing control osteoblasts, and these cells expressed lower levels of RANKL and higher levels of OPG. Taken together, these results indicate that K-ras-MAPK signaling in the osteoblast plays a dual role in regulating bone acquisition: signals downstream of K-ras directly stimulate osteoblast proliferation and promote additional signals which act in a cell non-autonomous fashion to inhibit osteoclast development. These results support the further development of novel bone anabolic therapies that target the MAPK pathway.

***Disclosures: Julie Leslie**, None.*

1151

Targeted Overexpression of ADAMTS-7 in Chondrocytes Induces Chondrodysplasia in "young" Mice and Osteoarthritis-like Phenotype in "aged" Mice. Yongjie Lai*[1], Xiaohui Bai[1], Yuqing Chen[2], Brendan Lee[2], Chuanju Liu[1]. [1]New York University, USA, [2]Baylor College of Medicine, USA

We previously reported that ADAMTS-7, a metalloproteinase that belongs to ADAMTS family, associated with and degraded cartilage oligomeric matrix protein (COMP) and its level was significantly elevated in arthritis (Liu, et al, FASEB J. 2006; 20(7):988-999). In addition, our recent findings also revealed a physiological, developmental role for ADAMTS-7 in chondrogenesis in vitro (Bai, et al, Mol. Cell. Biol. 2009; 29(15):4201-4219). To define the role of ADAMTS-7 in cartilage development and arthritis in vivo, we generated Col2a1-TS7 transgenic mice overexpressing ADAMTS-7 under the control of a well-characterized Col II promoter. Newborn Col2a1-TS7 mice were significantly smaller. X-ray images revealed remarkable reductions of the skeletal length and bone volumes in transgenic (Tg) mice. Safranin O staining showed that the Tg growth plate was only half the size of that in WT. Staining with alcian blue and alizarin red S of whole body and forelimb skeleton revealed that Col2a1-TS7 mice had hypoplastic limb skeletons and dramatically delayed endochondral bone formation compared with control mice. However, Col2a1-TS7 mice reached to the normal size at about 6 weeks postpartum and no defects were observed in articular cartilage and joints. Interestingly, 8-month old Col2a1-TS7 mice spontaneously developed osteoarthritis (OA)-like phenotype. Micro-CT of the hind knees showed osteophyte formation in aged Tg mice. Safranin O staining demonstrated a remarkable loss of proteoglycan staining, and meniscus ossification in Tg mice. High power photograph revealed clear chondrocyte clustering, and migration of the irregular tide mark to the superficial zone. To further determine the role of ADAMTS-7 in OA development and progression, we established surgically-induced OA model by transecting MMTL (medial meniscotibial ligament) in Col2a1-TS7 and control WT mice. Histological analyses were performed in mice knee joints at 4, 8 and 12 weeks post-surgery. The operated knees of Col2a1-TS7 mice showed moderate loss of Safranin O staining as early as 4 weeks after surgery, while the control mice joints showed minor loss until 8 weeks. The destruction of knee cartilage increased along with time after surgery. Histological score grading indicated higher scores in the operated Col2a1-TS7 knees, with a significant reduction of cartilage thickness and loss of proteoglycan. In addition, COMP degradative fragments were increased in the operated Col2a1-TS7 mice. Collectively, targeted overexpression of ADAMTS-7 in chondrocytes results in defects in chondrogenesis in "young" mice and OA-like phenotypes in "aged" mice, and overexpression of ADAMTS-7 also accelerates surgically-induced OA. These findings not only provide novel insights into the role of ADAMTS-7 in cartilage and arthritis in vivo, but may also lead to the development of novel therapeutic intervention strategies for osteoarthritis.

***Disclosures: Yongjie Lai**, None.*

1152

Mechanisms of Exostosis Formation in Hereditary Multiple Exostoses Syndrome. Julianne Huegel*[1], Christina Mundy[1], Eiki Koyama[2], Yu Yamaguchi[3], Jeffrey Esko[4], Maurizio Pacifici[1]. [1]Thomas Jefferson University, USA, [2]Thomas Jefferson University College of Medicine, USA, [3]Sanford-Burnham Medical Research Institute, USA, [4]University of California, San Diego, USA

Hereditary Multiple Exostoses (HME) syndrome is caused by loss-of-function heterozygous mutations in *EXT1* or *EXT2* that encode glycosyltransferases responsible for synthesis of heparan sulfate (HS), but the *Ext*-dependent mechanisms causing exostosis formation and the origin of exostosis-forming cells remain largely unclear. Interestingly, HME patients produce less than the 50% HS expected of a heterozygous mutation, and heterozygous $Ext2^{+/-}$ mice form exostoses at a very low rate and with atypical characteristics. To test whether exostosis formation requires a steeper drop in HS production, we created double heterozygous $Ext1^{+/-};Ext2^{+/-}$ mice. These mutants did display stereotypic growth plate-like exostoses near their long bones and at high frequency. To identify the origin of exostosis-forming cells, we conditionally deleted *Ext1* in mesenchymal cells near the groove of Ranvier in long bones by mating $Ext1^{fl/fl}$ and *Gdf5Cre* mice. Indeed, this triggered local ectopic chondrogenesis and formation of exostosis-like tissue masses near the epiphyses. To determine whether the responses were cell-autonomous, we prepared micromass cultures of limb bud mesenchymal cells isolated from E11.5 wild type mouse embryos. Treatment of these cultures with the HS antagonist Surfen caused increases in expression in chondrogenic and cartilage matrix genes. As interestingly, Surfen treatment interfered with formation of individual cartilage nodules that became irregularly contoured and often fused with each other. In addition, Surfen-loaded beads placed near the cartilaginous epiphyses in cultured mouse embryo autopods caused similar disruption of the chondro-perichondrial border and formation of ectopic cartilage. Our data reveal that: (i) exostosis formation is inversely related to *Ext1* gene expression; (ii) a specific niche progenitor cell population may be responsible for exostosis formation in long bones; and (iii) exostosis formation involves disruption of mechanisms that control the chondro-perichondrial border. Together, our findings provide major new insights into, and a better understanding of, the pathogenesis of HME.

***Disclosures: Julianne Huegel**, None.*

1153

Schnurri2 Deficiency Increases all of 1,25(OH)2D3, Renal 25-hydroxyvitamin D 1-α Hydroxylase, PTH, FGF23, Serum Calcium and Phosphate in Association with Hypercalcification in Joints. Masashi Nagao*[1], Yoichi Ezura[2], Yoshitomo Saita[3], Kentaro Miyai[1], Ryo Hanyu[1], Tetsuya Nakamoto[1], Hiroaki Hemmi[1], Tadayoshi Hayata[4], Takuya Notomi[5], Shunsuke Ishii[6], Shigeaki Kato[7], Seiji Fukumoto[8], Hisashi Kurosawa[9], Kazuo Kaneko[10], Masaki Noda[1]. [1]Tokyo Medical & Dental University, Japan, [2]Tokyo Medical & Dental University, Medical Research Insititute, Japan, [3]Juntendo University, Department of Ortopedics, Japan, [4]Medical Reserach Institute, Tokyo Medical & Dental University, Japan, [5]GCOE, Tokyo Medical & Dental University, Japan, [6]Laboratory of Molecular Genetics, RIKEN Tsukuba Institute, Japan, [7]University of Tokyo, Japan, [8]University of Tokyo Hospital, Japan, [9]Dept of Orthopedics, Juntendo University, School of Medicine, Japan, [10]Dept of Orthopedics, Juntendo University school of medicine, Japan

Schnurri (Shn)-2 is a zinc finger type transcription factor, regulating adipogenesis and lymphogenesis. In addition, we have shown recently that Shn2 plays an important role in bone remodeling through BMP signaling. Interestingly in that study, we noticed that Shn2 deficient mice exhibited periarticular calcification around the knee joint, as well as high serum phosphate and calcium levels causing high calcium-phosphate product. In this study, we aimed to analyze Shn2 functions in calcium and phosphate metabolism, focusing on the endocrine control. Serum FGF23, intact PTH and 1,25-(OH)2 vitamin D (1,25D) levels were determined in 12-weeks Shn2 deficient (KO) and control mice (WT) fed under the normal condition. Surprisingly, we found that all the hormone levels were significantly higher in KO mice compared to WT mice, indicating the disrupting feed-back systems of blood calcium and phosphate levels in KO mice. We also found that urinary phosphate level was higher in the mutants, as well as the increased serum BUN, and Creatinine levels. Since these clinical phenotypes are similar to human hyper-vitaminosis D, we hypothesized that the disruption of the mechanisms suppressing the 1,25D levels is the primary cause of the mutant phenotypes, and the increased levels of blood FGF23 and PTH are secondary observation caused by functional feed-back system against the hyperphosphatamia. In fact, we found that the 25 hydrodyvitamin D 1-alpha hydroxylase expression in KO mice was about 10 fold higher than those in WT mice, although that of renal 25 hydroxyvitamin D 24-alpha hydroxylase was not changed. Histological analysis revealed no remarkable changes in the parathyroid gland, supporting the notion that the serum PTH level was functionally increased against the increased serum phosphate level. To test this hypothesis, we applied the WT and KO mice under the 0.2% low-phosphate diet, and the endocrine status was followed up. Although a surprising finding was that all KO mice died within a few days due to severe

hypophosphatamia, we could confirm that the blood intact PTH and FGF23 levels are rapidly decreased both in the KO and the control mice, suggesting that the PTH and FGF23 levels are normally regulated for the lower phosphorous intake in these mice. Severe hypophosphatamia of the KO mice might be caused by slow response for declining the FGF23 because of the excessive level from the beginning. These observations indicate a novel function of the Shn2 in the renal tubular cells regulating the serum 1,25D level, that would be beneficial for understanding the mechanism of vitamin D metabolism, as well as understanding the human hypervitaminosis D, or unidentified human diseases caused by disrupting vitamin D regulation.

***Disclosures: Masashi Nagao**, None.*

1154

Proteoglycan-4: A Dynamic Regulator of PTH Actions in Skeletal Anabolism and Arthritic Joints. Chad Novince*[1], Megan Michalski[2], Amy Koh[2], Ben Sinder[2], Jan Berry[2], Kenneth Kozloff[3], Laurie McCauley[1]. [1]University of Michigan, School of Dentistry, USA, [2]University of Michigan, USA, [3]University of Michigan Department of Orthopaedic Surgery, USA

Intermittent parathyroid hormone (PTH) is anabolic via unclear mechanisms, and has been recently reported to protect against arthritic joint remodeling. Proteoglycan-4 (*prg*4) protein products are implicated in articular joint protection, hematopoiesis and megakaryopoiesis. *Prg*4 loss of function mutations result in the human condition camptodactyly-arthropathy-coxa vara-pericarditis syndrome, characterized by precocious joint failure and osteopenia. The purpose of this study was to investigate the role of *prg*4 in the anabolic actions of PTH, and to assess PTH actions on arthritic articular joints in *prg*4 deficient (KO) mice. *Prg*4 KO and wildtype (WT) mice were treated with intermittent PTH from 16-22wks of age and evaluated by histomorphometry and micro-CT. Bone marrow stromal cells (BMSCs) were analyzed for cell autonomous alterations, serum markers were assessed, peripheral blood cells enumerated, bone marrow cells analyzed via flow cytometry, and bone marrow gene expression evaluated by real-time PCR. *Prg*4 KO mice were osteopenic with a significantly blunted PTH anabolic response. BMSCs from *prg*4 KO mice had reduced cell numbers over time in culture, lower proliferation, and less mineralization than WT. KO mice had synovial tissue hyperplasia and arthritic remodeling in the knee joints that was further exacerbated by PTH. *Prg*4 KO mice had significantly lower serum PTH levels, yet serum calcium levels were similar in WT and KO mice. PTH significantly reduced serum FGF-23 in WT but not KO mice, suggesting an altered PTH impact on mineralization in KO mice. KO mice had increased peripheral blood neutrophils and decreased lymphocytes, which were normalized to WT levels with PTH. KO mice had reduced marrow B220+ (B-lymphocytic) cells, which were normalized with PTH. PTH increased hematopoietic progenitor ($Lin^-Sca\text{-}1^+c\text{-}Kit^+$) cells more significantly in WT vs. KO marrow. PTH decreased CD41+ (megakaryopoietic) cells in KO, and PTH increased ploidy status of CD41+ cells more significantly in KO vs. WT mice. KO mice had significantly higher IGF-1 mRNA levels in the marrow. PTH increased osteocalcin mRNA in WT marrow, and increased G-CSF mRNA in KO marrow. In summary, proteoglycan-4 intrinsically regulates BMSC proliferation and differentiation, and mediates PTH actions on immune and hematopoietic cell populations in a favorable physiologic manner. These studies identify proteoglycan-4 as a dynamic regulator of PTH actions in skeletal anabolism and arthritic joints.

***Disclosures: Chad Novince**, None.*

1155

β-Catenin Is A Key Mediator in the Development of Intervertebral Disc Degeneration in Humans and in a β-Catenin Conditional Activation Mouse Model. Bing Shu*[1], Meina Wang[2], Dezhi Tang[2], Baoli Wang[1], Edward Schwarz[2], Paul Rubery[3], Regis O'Keefe[2], Di Chen[1]. [1]University of Rochester Medical Center, USA, [2]University of Rochester, USA, [3]Medical center, University of Rochester, USA

Low back pain is a serious clinical problem that may be related to intervertebral disc (IVD) degeneration. The mechanism responsible for this disease remains unknown. In this study we found that β-catenin protein was up-regulated in IVD tissues from patients with disc degeneration (33 positive from a total of 36 samples analyzed). In contrast, β-catenin was undetectable in disc tissues from normal subjects (n=12). To assess the role of β-catenin on disc degeneration we generated a genetic mouse model in which β-catenin is constitutively expressed specifically in disc cells. These β-catenin conditional activation (cAct) mice expressed high levels of β-catenin in the annulus and endplate cartilage cells in their spine, which led to a 36% reduction in spine length, severe disc space narrowing, and extensive osteophyte formation within 3-months. These structural changes were associated with severe degenerative changes in the cells and extracellular matrix of the IVD. Expression of Mmp13 mRNA and protein was significantly up-regulated in β-catenin cAct mice. Activation of β-catenin with BIO, a GSK-3β inhibitor, enhanced Mmp13 and Runx2 expression in chondrocytes. A 3.4-kb human Mmp13 promoter was cloned and a conserved Runx2 binding site in the Mmp13 promoter (-138/-132) was identified. Mutation of the Runx2 binding site abolished the stimulatory effect of Runx2 as well as BIO on Mmp13 gene transcription. Runx2 siRNA also inhibited BIO-induced Mmp13 transcription. ChIP assay confirmed Runx2 binding to the Mmp13 promoter. These findings suggest that activation of β-catenin induces Mmp13 expression in a Runx2-dependent manner. We have then crossed β-catenin cAct mice with Mmp13-floxed mice and treated the β-catenin cAct mice with a MMP13-specific inhibitor. Micro-CT and histologic data showed that genetic ablation of the Mmp13 gene under β-catenin cAct background (n=8) or treatment of β-catenin cAct mice with the MMP13 inhibitor (n=5) significantly ameliorated the mutant phenotype observed in 3-month-old β-catenin cAct mice. Osteophyte formation was disappeared; disc space was returned to normal; and loss of endplate cartilage and proteoglycan protein was restored. Over 70% rescue was observed based on histomorphometric analysis after deletion of the Mmp13 gene or treatment with the MMP13 inhibitor in β-catenin cAct mice. These findings provide significant insights into the mechanism of disc degeneration.

***Disclosures: Bing Shu**, None.*

1156

Expression of BMP2 in Skeletal Progenitor Cells is Required for Bone Fracture Repair. Giuseppe Intini*, Karen Cox, Vicki Rosen. Harvard School of Dental Medicine, USA

Different from mice lacking Bmp4 or Bmp7, mice lacking Bmp2 are unable to repair fractures. To identify cells in which the expression of Bmp2 is important during fracture repair, we compared mice lacking Bmp2 in osteoblast-committed cells (Bmp2-2.3kbCol1cre mice) with mice lacking Bmp2 in skeletal progenitor cells (Bmp2-Prx1cre mice). We chose this comparison because localization studies using the Rosa26-2.3kbCol1cre mice showed β-gal staining restricted to osteoblast-committed cells whereas localization studies using the Rosa26-Prx1cre mice showed β-gal staining in skeletal progenitors as well as osteocytes, osteoblasts, and chondrocytes.

First, we analyzed the bone mass phenotype of 8-10 week old Bmp2-2.3kbCol1cre mice by μCT (n=7). This analysis showed no difference in terms of bone mass between the Bmp2-2.3kbCol1cre and the wild type mice. Subsequently, we created unilateral femur diaphysal fractures and evaluated the healing process by X-rays in 8-10 week old Bmp2-2.3kbCol1cre and Bmp2-Prx1cre mice (n=3). The X-rays obtained 3, 10, and 20 days after fracture showed normal healing process in Bmp2-2.3kbCol1cre mice and confirmed the lack of healing in Bmp2-Prx1cre mice. Finally, we compared the gene expression profile of the femur diaphyses of 8-10 week old Bmp2-Prx1cre mice to that of 8-10 week old wild type mice. The microarray data, validated by quantitative mRNA analysis, showed increased levels of BMP3, a BMP antagonist, and increased levels of Axin2, Dkk1, Sclerostin, Sfrp2, Sfrp4, and Wif1, inhibitors of the Wnt signaling, in diaphysal bones obtained from the Bmp2-Prx1cre mice (n=6, $p<0.05$).

Results indicate that when Bmp2 is inactivated only in osteoblast-committed cells expressing Col1, no alterations are seen in terms of bone metabolism and fracture healing. However, when Bmp2 is inactivated in skeletal progenitors by means of the Prx1cre recombinase, fracture healing does not occur and a BMP antagonist and Wnt inhibitors are up-regulated in cells of the diaphysal bones.

We conclude that during bone fracture repair expression of Bmp2 is required in the skeletal progenitor cells and that BMP3 and Wnt inhibitors may be responsible for the lack of differentiation of these cells.

***Disclosures: Giuseppe Intini**, None.*

1157

Dentin Matrix Protein 1 Null Mice, a Model of Human Autosomal Recessive Hypophosphatemic Rickets, Exhibit Decreases in Cardiac, Skeletal, and Vascular Smooth Muscle Function. Michael Wacker*[1], Chris Elmore[1], Chad Touchberry[1], Leticia Brotto[2], Neerupma Silswal[1], Nikhil Parelkar[1], Hong Zhao[3], Todd Hall[2], Jon Andresen[4], Jian Feng[5], Marco Brotto[2], Lynda Bonewald[3]. [1]University of Missouri-Kansas City School of Medicine, USA, [2]University of Missouri-Kansas City School of Nursing, USA, [3]University of Missouri-Kansas City School of Dentistry, USA, [4]Universtity of Missouri-Kansas City School of Medicine, USA, [5]Texas A&M Health Science Center, USA

Currently there is little known about cardiac, skeletal, or smooth muscle function in Autosomal Recessive Hypophosphatemic Rickets (ARHR), a disease caused by mutations in Dentin Matrix Protein-1 (DMP1). Patients with Autosomal Dominant Hypophosphatemic Rickets (ADHR) and acquired hypophosphatemia report muscle weakness, while those with X-Linked Hypophosphatemia (XLH) do not. Fibroblast growth factor 23 is much higher in ADHR than XLH and ARHR patients even with phosphate treatment, suggesting that there could be other factors besides simply regulation of phosphate levels that could alter muscle function. As data from our laboratories suggest that a muscle-bone axis may exist in which muscle and bone influence each other in an endocrine manner, we hypothesized that muscle function would be reduced in Dmp1-/- mice. Dmp1-/- and wild-type (WT) mice (16-25 week old) were sacrificed and the heart, extensor digitorum longus muscle (EDL), soleus muscle (SOL), middle cerebral artery (MCA), and aorta were removed. Contractile responses to various stimulatory challenges were studied. Ca^{2+} imaging was also conducted on flexor digitorum brevis (FDB) in order to link ex-vivo contractility to Ca^{2+} homeostatic mechanisms. Dmp1-/- mice displayed an increased heart weight (HW)/body weight (BW) ratio (0.0038 ± 0.0002 vs 0.0045 ± 0.0005) and a decrease in relative maximum heart contraction as compared to WT mice (31.6 ± 11.3 vs 18.9 ± 2.5 mN/g) (n=4; $P<0.05$). The hearts of Dmp1-/- mice also generated weaker

contractions when challenged with high Ca^{2+} and caffeine. EDL and SOL muscles were atrophic. Relative and specific forces were significantly reduced in EDL and SOL muscles from Dmp1-/- mice, indicating that atrophy can only partially explain the force reduction in these muscles (n=4). Intriguingly, caffeine-induced fura-2 Ca^{2+} transients were larger in FDB muscle fibers from Dmp1-/- mice, indicating that the mechanisms for Ca^{2+}-induced Ca^{2+} release might be enhanced in Dmp1-/- mice. Contraction to serotonin was impaired in aortas of Dmp1-/- mice whereas in the MCA agonist induced constriction did not differ between Dmp1-/- and WT mice (n=3). Together, our data suggest that the contractile machinery is compromised in cardiac, skeletal, and vascular smooth muscles from Dmp1-/- mice. The mechanisms underlying the decreased muscle function remain to be elucidated, but may involve endocrine signaling mechanisms triggered by altered osteocyte function.

***Disclosures: Michael Wacker**, None.*

1158

Klotho Lacks a Vitamin D Independent Physiological Role in Aging, Bone, and Glucose Homeostasis. Rene Anour*, Eva Ritter, Reinhold Erben. University of Veterinary Medicine, Austria

Lack of Klotho is known to shorten life span and to cause osteomalacia, hypercalcemia, hyperphosphatemia, elevated circulating vitamin D hormone, and increased peripheral insulin sensitivity in mice. The Klotho gene encodes for a transmembrane protein, acting as a co-receptor for fibroblast growth factor-23 (Fgf-23) which suppresses vitamin D hormone synthesis. In addition, the extracellular fraction of Klotho can be shed and released into circulation. Previous data suggest that circulating Klotho prolongs life span by inhibiting insulin and insulin-like growth factor-1 (IGF-1) signaling. To further explore the role of the vitamin D independent functions of Klotho in the regulation of aging, mineral, and glucose homeostasis, we mated *Klotho* deficient (*Klotho*$^{-/-}$) mice with vitamin D receptor (VDR) mutant mice characterized by a non-functioning VDR. All mice were kept on a rescue diet enriched with calcium, phosphorus, and lactose to prevent secondary hyperparathyroidism in *VDR* and compound mutants, and were killed at 4 weeks of age after double fluorochrome labeling. *Klotho*$^{-/-}$ mice displayed hypercalcemia, hyperphosphatemia, dwarfism, organ atrophy, azotemia, pulmonary emphysema, osteomalacia, and an elevated lumbar volumetric bone mineral density (BMD). In addition, glucose and insulin tolerance tests revealed profoundly increased peripheral insulin sensitivity in *Klotho* deficient mice. Compound mutants were normocalcemic and normophosphatemic, did not show premature aging or organ atrophy, and were phenocopies of *VDR* mutant mice in terms of body weight, BMD, and bone metabolism. Serum calcium and PTH levels as well as urinary calcium and phosphate excretion were not different between *VDR* and compound mutants. Furthermore, ablation of vitamin D signaling in double mutants completely normalized glucose and insulin tolerance, indicating that Klotho has no vitamin D independent effects on insulin and IGF-1 signaling. Histomorphometry of pancreas islets showed similar beta cell area per body weight in all groups of animals. In conclusion, we found no evidence for a physiologically relevant, vitamin D independent, function of Klotho in the regulation of carbohydrate and mineral metabolism in 4-week-old mice.

***Disclosures: Rene Anour**, None.*

1159

Prevention of Chemotherapy Induced Alopecia with a Novel Parathyroid Hormone Fusion Protein. Ranjitha Katikaneni*[1], Tulasi Ponnapakkam[1], Osamu Matsushita[2], Joshua Sakon[3], Robert Gensure[1]. [1]Ochsner Clinic Foundation, USA, [2]Kitasato University Medical School, Japan, [3]University of Arkansas, USA

Chemotherapy is a cancer treatment that causes many side effects, including alopecia, for which there is currently no therapy. Parathyroid hormone agonists and antagonists improve hair growth after chemotherapy; however, rapid clearance and systemic side-effects complicate their usage. To facilitate delivery and retention to the skin, we fused PTH agonists and antagonists to a bacterial collagen binding domain derived from clostridium histolyticum collagenase, and tested these compounds in-vitro and in-vivo. In vitro studies showed no differences in cAMP accumulation in SaOS cells with administration of PTH(1-33)-CBD vs. PTH(1-34). PTH(7-33)-CBD did not stimulate cAMP accumulation, and showed 27% inhibition of PTH(1-34) effect at 20x concentration. In-vivo studies were conducted in 5-week old C57BL/6J mice. 28 mice were divided into 4 groups (No Chemo, Chemo+Vehicle, Chemo+Agonist and Chemo+Antagonist) and depilated to synchronize the stage of the hair follicles. On day 7, No Chemo and Chemo+Vehicle groups received 320 ug/kg sq buffer solution, Chemo+Antagonist received 320 ug/kg sq PTH(7-33)-CBD, and Chemo+Agonist received 320 ug/kg sq PTH(1-33)-CBD. On day 9, cyclophosphamide (150 mg/kg ip) was administered to all animals except those in the No Chemo group. No Chemo mice showed rapid regrowth of hair after depilation. Histological examination showed normal anagen and telogen follicles. Chemo+Vehicle mice showed little hair regrowth and decreased pigmentation. Histological examination showed dystrophic anagen and catagen follicles. Chemo+Antagonist mice showed rapid but partial hair regrowth, only around the site of injection, with little change observed thereafter. Histological examination showed changes indistinguishable from those seen after chemotherapy alone. Chemo+Agonist mice showed regrowth and repigmentation of hair, approaching that seen in No Chemo mice. Histologically, normal follicles predominantly in the anagen phase were seen. Total number of hair follicles was significantly reduced in the Chemo+Vehicle (28+/-1, p=0.12) and Chemo+Antagonist groups (23+/-3, p=0.004) compared to that of the No Chemo group (49+/-7), while the Chemo+Agonist group (42+/-6, p>0.5, NS) showed no reduction in hair follicles. Staging of hair follicles for counts is being performed. Overall, the PTH agonist compounds had the most prominent effects in reducing the damage of chemotherapy on hair follicles, and produced the most cosmetically acceptable results.

***Disclosures: Ranjitha Katikaneni**, None.*

1160

Calcitonin Regulates Bone Formation by Reducing the Extracelluar Levels of Osteoclast-derived Sphingosine 1-phosphate. Thorsten Schinke*[1], Johannes Keller[2], Philip Catala-Lehnen[2], Antje K. Huebner[2], Robert P. Marshall[2], Jerold Chun[3], Michael Amling[2]. [1]University Hospital Hamburg, Eppendorf, Germany, [2]University Medical Center Hamburg-Eppendorf, Germany, [3]Scripps Research Institute, USA

The hormone calcitonin (CT) is long known for its pharmacologic action as an inhibitor of bone resorption, yet its physiologic functions are still not fully clarified. In this regard it was of hallmark importance that the recent analysis of mice lacking either CT or one allele of the CT receptor (CTR) demonstrated a high bone mass phenotype caused by excessive bone formation. Since the CTR is not expressed by bone-forming osteoblasts, these findings have raised the question, how the negative influence of CT on bone formation is explained at the cellular and molecular level. To address this issue we have applied the Cre/lox technology, which enabled us to delete the CTR in specific cell types. While the phenotype of mice with a ubiquitous CTR deletion resembled to one described for CT-deficient mice, we did not observe abnormalities of bone remodelling in mice lacking the CTR specifically in the hypothalamus. In contrast, an osteoclast-specific deletion of the CTR resulted an increased bone formation, thereby demonstrating that CT regulates the production of osteoclast-derived factors that influence osteoblast activities. To identify such factors, we treated wildtype and CTR-deficient osteoclasts with CT and performed a genome-wide expression analysis using Affymetrix Gene Chip hybridization. This approach led us to identify several CT-regulated genes, one of them being Spns2, which encodes a transporter for sphingosine 1-phosphate (S1P). Since others have previously shown that osteoclast-derived S1P promotes an osteoanabolic effect in vitro, we first confirmed that the negative regulation of Spns2 expression by CT resulted in decreased S1P levels in osteoclast-conditioned media. In addition, we were able to identify the serpentine receptor S1pr3 as a functionally relevant S1P receptor on osteoblasts, since S1pr3-deficient mice displayed decreased bone formation, and since the osteoanabolic effect of osteoclast-conditioned medium was fully abrogated, when the osteoblasts were derived from S1pr3-deficient mice. Taken together, our data have helped to identify one of the mechanisms coupling the activities of osteoclasts and osteoblasts. They further raise the possibility that S1P receptor agonists might be useful as osteoanabolic agents for the treatment of bone loss disorders.

***Disclosures: Thorsten Schinke**, None.*

1161

FGF-23 Suppresses Renal 1,25(OH)$_2$D Production and Phosphate Reabsorption via MAP Kinase Activation in *Hyp* Mice. Daniel Ranch*[1], Martin Y.H. Zhang[1], Anthony Portale[1], Farzana Perwad[2]. [1]University of California, San Francisco, USA, [2]University of California San Francisco, USA

X-linked hypophosphatemia (XLH) is characterized by hypophosphatemia due to renal phosphate (Pi) wasting, inappropriately suppressed 1,25(OH)$_2$D production, rickets in children and is caused by a loss-of-function mutation in the *Phex* gene. In XLH and in its murine homologue, the *Hyp* mouse, increased circulating concentrations of fibroblast growth factor-23 (FGF-23) is responsible for the disordered metabolism of Pi and 1,25(OH)$_2$D. We previously showed in cultured renal proximal tubular cells that FGF-23 suppresses 1α-hydroxylase gene expression via activation of the mitogen-activated protein kinase (MAPK) signaling pathway, and such suppression is blocked when MAPK signaling is inhibited. In the present study, we tested the hypothesis that in *Hyp* mice, FGF-23-mediated suppression of renal 1,25(OH)$_2$D production and Pi reabsorption depend upon activation of the MAPK signaling pathway. We fed wild-type (WT) and *Hyp* mice a constant Pi diet (baseline), and then administered either vehicle or the MAPK inhibitor PD0325901 (12.5 mg/kg) orally daily for 4 days. At baseline, the renal abundance of early growth response-1 (egr-1) mRNA, a transcription factor downstream of MAPK pathway activation, was 3-fold greater in *Hyp* mice than in WT mice ($P<0.05$). After treatment with PD0325901, egr-1 mRNA abundance decreased by 94% in both WT and *Hyp* mice ($P<0.05$). In *Hyp* mice, PD0325901 induced a 19-fold increase in renal 1α-hydroxylase mRNA expression ($P<0.05$) and a 4-fold increase in serum 1,25(OH)$_2$D levels (350 ± 41 vs 89 ± 21 pg/ml, mean $\pm$ SEM, $P<0.05$) compared to values in vehicle-treated *Hyp* mice. Compared to WT mice, serum Pi levels in *Hyp* mice were significantly lower at baseline (10.5 ± 0.4 vs 5.8 ± 0.6 mg/dl, $P<0.05$), and increased significantly after treatment with PD0325901 (7.2 ± 0.3 mg/dl, $P<0.05$). The increase in serum Pi levels in *Hyp* mice was associated with increased renal Npt2a mRNA and brush-border membrane Npt2a protein expression. Serum PTH levels were higher in *Hyp* than in WT mice at baseline (54 ± 8 vs 7 ± 5 pg/ml, $P<0.05$) and did not change significantly after treatment. These findings provide evidence that in *Hyp* mice: a) the

MAPK signaling pathway is constitutively activated in the kidneys; and b) inhibition of MAPK signaling reverses FGF-23-dependent suppression of renal $1,25(OH)_2D$ production by up-regulation of renal 1α-hydroxylase gene expression, and partially corrects the hypophosphatemia by increasing renal Pi absorption via Npt2a.

***Disclosures: Daniel Ranch**, None.*

1162

The RANKL Distal Control Region is Required for Cancellous Bone Loss Due to Dietary Calcium Deficiency but not Lactation. Melda Onal*[1], Carlo Galli[2], Priscilla Cazer[1], Jinhu Xiong[1], Xinrong Chen[1], Robert Weinstein[1], Stavros Manolagas[1], Charles O'Brien[1]. [1]University of Arkansas for Medical Sciences, USA, [2]Università Degli Studi Di Parma, Italy

Parathyroid hormone (PTH) controls RANKL gene transcription in part via a distant enhancer, designated the distal control region (DCR). Importantly, deletion of this enhancer from the mouse genome blunts PTH-induced RANKL expression in vivo. Here we assessed the role of the DCR in the control of the bone resorption associated with secondary hyperparathyroidism or lactation, two situations in which the demand for calcium is met by an increase in osteoclastogenesis, at the expense of bone mass, through an increase in the expression of RANKL. In both conditions, activation of the PTH receptor (PTHR1), which binds both PTH (elevated during hyperparathyroidism) and PTH-related protein (PTHrP) (elevated during lactation), is thought to drive the increase in RANKL expression. Secondary hyperparathyroidism was induced by placing 5 month old wild-type (WT) and DCR knock-out (KO) mice on a calcium-deficient diet for 30 days. While secondary hyperparathyroidism led to loss of both cortical and cancellous bone in WT mice, as measured by microCT, only cortical bone was lost in DCR KO mice, demonstrating that the DCR is indispensable for cancellous bone loss in this model. Consistent with this, histological analysis showed that secondary hyperparathyroidism increased the percent of cancellous bone surface covered by osteoclasts in WT, but not KO mice. In contrast to these results, lactation-induced bone loss was not different between 5 month old WT and DCR KO mice, in either the cancellous or cortical compartment. Nonetheless, whereas lactation induced a striking increase in RANKL mRNA in bones from WT mice, as measured by quantitative RT-PCR, this change was abrogated in DCR KO mice. On the other hand, OPG mRNA expression was reduced during lactation in both WT and KO mice. These findings demonstrate that DCR-mediated control of RANKL expression is essential for the cancellous bone loss associated with secondary hyperparathyroidism, but not lactation. Moreover, they suggest that PTH uses different transcriptional enhancers to control RANKL expression in cancellous versus cortical bone. Lastly, the increase in RANKL during lactation also requires the DCR. However, because prevention of this increase does not blunt lactation-induced bone loss, other changes, such as decreases in OPG and estrogen, may be the predominant mechanisms underlying the increase in bone resorption during lactation.

***Disclosures: Melda Onal**, None.*

1163

Risk of Cardiovascular Events with Calcium/Vitamin D - a Re-Analysis of the Women's Health Initiative. Mark Bolland, Andrew Grey, Gregory Gamble, Ian Reid*. University of Auckland, New zealand

Recently, we reported that calcium supplementation was associated with an increased risk of cardiovascular events in the Auckland Calcium Study, and we have now confirmed this in a meta-analysis of studies of calcium monotherapy (IOF, 2010). Previously, the Women's Health Initiative (WHI) reported no effect of calcium/vitamin D supplementation (CaD) on cardiovascular events, but a significant interaction between BMI and the cardiovascular risk associated with CaD allocation. Also, >50% of WHI participants were using non-protocol calcium supplements, which might have obscured any effect of the intervention. Therefore, we re-analyzed the WHI limited access clinical trials dataset to determine whether adverse effects of CaD on cardiovascular events were seen in participants not taking non-protocol calcium supplements and who were not obese. We used Cox proportional hazards models to assess the effect of CaD on incidence of cardiovascular events in these subgroups. 44% of participants (n=15788) were not taking non-protocol calcium supplements at CaD randomisation. In these women, CaD was associated with increases in incidence of myocardial infarction (MI), coronary revascularisation, stroke, and related composite endpoints ranging from 11-19%. For the composite of MI and revascularization, this was significant. In women taking non-protocol calcium supplements, CaD was not associated with altered cardiovascular risk (hazard ratios 0.92-1.08). In non-obese women (BMI<30 kg/m^2), CaD was associated with statistically significant increases in incidence of coronary revascularisation and related composite endpoints ranging from 24-28%, and a non-significant 16% increase in myocardial infarction. In obese women, CaD was not associated with increased incidence of any cardiovascular endpoint. In non-obese women not using non-protocol calcium supplements, revascularizations and composite endpoints including MI were significantly increased, by 21-31% (Table). It is concluded that CaD in the WHI is associated with increased cardiovascular risk, and that this effect was confounded in the previous analysis by non-protocol calcium supplementation. The interaction with obesity might arise from the high incidence of vitamin D deficiency in the obese and a possible protective effect of the vitamin D component of the intervention on cardiovascular risk in those individuals.

Cardiovascular Events in Non-Obese Women Not using Non-Protocol Calcium Supplements

Endpoint	CaD N=4708 n (incidence)[a]	Placebo N=4603 n (incidence)[a]	HR (95% CI)	P
Clinical MI	103 (3.1)	87 (2.6)	1.19 (0.89-1.59)	0.24
Total MI[b]	113 (3.4)	96 (2.9)	1.18 (0.90-1.56)	0.23
Revasc	177 (5.3)	132 (4.0)	1.31 (1.04-1.64)	**0.02**
Stroke	109 (3.2)	85 (2.6)	1.29 (0.97-1.72)	0.08
Total MI/CHD death	135 (4.0)	117 (3.6)	1.17 (0.91-1.50)	0.22
Clinical MI/Revasc	210 (6.3)	167 (5.1)	1.25 (1.02-1.54)	**0.03**
Clinical MI/Stroke	205 (6.2)	168 (5.1)	1.24 (1.01-1.52)	**0.04**
Total MI/CHD death/Revasc	239 (7.2)	197 (6.0)	1.21 (1.00-1.47)	**0.05**

a: Events per 1000 woman-years
b: Includes MI diagnosed from EKG changes alone

Table_IRReid_Cardiovascular Events in Non-Obese Women

***Disclosures: Ian Reid**, None.*

1164

The Efficacy of High-Dose Oral Vitamin D_3 Administered Once a Year: A Randomised, Double-Blind, Placebo-Controlled trial (Vital D Study) for Falls and Fractures in Older Women. Kerrie Sanders[1], Amanda L Stuart[2], Elizabeth J Williamson[2], Julie A Simpson[2], Mark Kotowicz[2], Geoffrey Nicholson*[1]. [1]University of Melbourne, Australia, [2]The University of Melbourne, Australia

Objective

To determine whether a single annual dose of 500,000IU cholecalciferol administered orally to older women in fall or winter would reduce the risk of falls and fracture.

Methods

This single centre double-blind, placebo-controlled trial randomly assigned 2,256 community-dwelling women (median age 76 years, IQR 73, 80.0 years) to receive a single oral dose of cholecalciferol 500,000IU or placebo each autumn/winter for 3 to 5 years. Falls and fractures were ascertained for 4 to 6 years using monthly calendars and details confirmed by telephone interview. Fractures were radiologically confirmed. Biochemistry was done on a sub-study of 137 randomly-selected participants at baseline as well as 12-months post-dose (coinciding with immediate pre-dose for the current year). In 2006 and 2007 blood sampling was also done at one- and three-month post-dose. Serum 25-hydroxyvitamin D (25D) levels were measured in batches using DiaSorin immunoassay.

Results

The vitamin D group had more falls and fractures than the placebo group. The fall rate was 83.4 vs 72.7 per 100 person-years, vitamin D vs placebo groups, respectively and an Incidence Rate Ratio (IRR): 1.15; 95%CI 1.02, 1.30; p=0.025. The rate of fracture was 4.9 vs 3.9 per 100 p-y and the IRR: 1.26; 1.00, 1.59; p=0.047. The increased rate of falling in the vitamin D group was higher in the first three months following dosing (p=0.017). This temporal pattern was also apparent in fracture rates although not significance (interaction p=0.36). The cumulative incidence of first fall and first fracture were both increased in the vitamin D group (hazard ratios; 95% CI: Falls 1.16; 1.05, 1.28 p=0.003; Fractures 1.26; 0.99, 1.59 p=0.057). In the sub-study, the median baseline serum 25D was 49nmol/L. Less than 3% of the sub-study participants had baseline levels <25nmol/L. In the vitamin D group, one-, three- and 12-month median post dose levels were approximately 120nmol/L, 90 nmol/L and 70nmol/L, respectively.

Conclusions

The results indicate that high-dose vitamin D administered orally once yearly to older community-dwelling women increased the risk of falls and fractures.

***Disclosures: Geoffrey Nicholson**, None.*

1165

A Higher Dose of Vitamin D is Required for Hip and Non-vertebral Fracture Prevention: A Pooled Participant-based Meta-analysis of 11 Double-blind RCTs. Heike Bischoff-Ferrari*[1], Endel J Orav[2], Walter Willett[2], Pierre Meunier[3], Ronan Lyons[4], Paul Lips[5], Michael Pfeifer[6], Leon Flicker[7], John Wark[8], Rebecca Jackson[9], Haakon Meyer[10], Jane Cauley[11], Hannes B Staehelin[12], Jana Henschkowski[13], Robert Theiler[14], Bess Dawson-Hughes[15]. [1]University of Zurich, Switzerland, [2]Harvard School of Public Health, USA, [3]Laennec University, France, [4]Swansea University, United Kingdom, [5]VU University Medical Center, The netherlands, [6]Medwiss Bad Pyrmont, Germany, [7]University of Western Australia, Australia, [8]Royal Melbourne Hospital, Australia, [9]The Ohio State University, USA, [10]Norwegian Institute of Public Health, Norway, [11]University of Pittsburgh Graduate School of Public Health, USA, [12]University of Basel, Switzerland, [13]University Hospital Zurich, Switzerland, [14]Triemli City Hospital, Switzerland, [15]Tufts University, USA

Background: Meta-analyses have reached conflicting results regarding vitamin D and fracture reduction, which may be explained by alternative criteria in the inclusion of trials. For efficacy, the focus is on double-blind RCTs.

Methods: Our meta-analysis pooled the individual participant data from 11 of 13 available double-blind RCTs with oral vitamin D supplementation and fracture assessment among seniors age 65 and older. Covariates available in all trials were age, gender, type of dwelling, calcium supplementation, and adherence to supplementation. We used Cox regression analysis to assess hip and any non-vertebral fracture risk by treatment (yes/no) and by quartiles of received dose of vitamin D in the treatment group (received dose = dose*adherence in the treatment group + additional supplement intake in the WHI trial). All analyses adjusted for age, gender, type of dwelling, and study. Due to significant co-linearity between received dose of vitamin D and received dose of calcium supplementation, the main model did not adjust for calcium supplement intake.

Results: The analysis included 29,893 seniors age 65 and older with 1111 hip fractures and 3771 non-vertebral fractures including those at the hip. Mean age was 76 years and 90% were women. For any dose of vitamin D (treatment yes/no), we found a non-significant 10% reduction in hip fracture risk (HR = 0.90; 95% CI: 0.80 -1.01), and a significant 7% reduction for any non-vertebral fracture (HR = 0.93; 95% CI: 0.87-0.99).

For quartiles of received vitamin D dose in the treatment group, fracture reduction was significant only at the highest intake quartile (735 IU+/day) compared to the control group, with a 28% fracture reduction at the hip (HR=0.72; 95% CI: 0.59-0.87) and a 14% fracture reduction at any non-vertebral site (HR = 0.86: 95% CI: 0.77-0.95). The effect of the highest intake quartile of vitamin D was consistent across studies (interaction p-value = 0.71 for hip and 0.35 for non-vertebral fractures). For the hip fracture endpoint, the effect at the highest vitamin D intake quartile stayed significant even when any individual study was removed from the analysis. For the non-vertebral fracture endpoint, statistical significance at the highest vitamin D intake quartile was only lost when the Chapuy 1992 study was removed from the analysis.

Conclusion: Based on this pooled analysis of 11 double-blind RCTs, a received dose of no less than 735 IU per day is required for hip and any non-vertebral fracture reduction.

***Disclosures: Heike Bischoff-Ferrari**, None.*

1166

Ergocalciferol and Cholecalciferol Induce Comparable Increases in Vitamin D Binding Protein and Free 25-hydroxy-itamin D with no Significant Change in Free 1,25-Dihydroxyvitamin D in Hip Fracture Patients. Gerard Chew[1], Charles Inderjeeth[2], Paul Glendenning*[3], Mario Taranto[4], Charles Inderjeeth[2]. [1]School of Medicine & Pharmacology, Australia, [2]Sir Charles Gardner Hospital, Australia, [3]Royal Perth Hospital, Australia, [4]PathWest, Royal Perth Hospital, Australia

Previous data indicate that ergocalciferol 1000 IU daily and cholecalciferol 1000 IU daily have comparable effects on PTH suppression, despite a greater increase in total 25-hydroxyvitamin D (25OHD) with cholecalciferol. The effects of either agent on vitamin D binding protein levels (VDBP), free 25-hydroxyvitamin D index (F25OHD) and free 1,25-dihydroxyvitamin D index (F125OHD) have not been previously examined.

We studied 95 hip fracture patients randomised to 3 months treatment with either cholecalciferol or ergocalciferol therapy. End study serum samples were available in 70 patients. All patients were vitamin D-deficient (25OHD < 50 nmol/L) at baseline. 25OHD was measured by HPLC, VDBP by immunonephelometry, and 1,25OHD by Diasorin radioimmunoassay. F25OHD and F125OHD were calculated from the molar ratios of 25OHD, 1,25OHD and VDBP. Baseline VDBP, F25OHD and F1,25OHD were comparable in the ergocalciferol-treated (n=48) and cholecalciferol-treated (n=47) patients. Mean VDBP increased from 4.4 to 5.1 umol/L with ergocalciferol ($P<0.01$) and 4.4 to 5.3 umol/L with cholecalciferol therapy ($P<0.001$). Mean F25OHD increased from 8.1 to 11.6 ($P<0.01$) with ergocalciferol and 9.7 to 14.2 with cholecalciferol therapy ($P<0.001$). Mean F12OHD declined from 15.1 to 12.8 with ergocalciferol (P= NS) and 18.5 to 15.2 with cholecalciferol therapy ($P<0.05$). Treatment effects were not significantly different between the groups for any of the three outcome parameters ($P>0.1$). There was no difference in outcome measures when the analysis was restricted to treatment-compliant (>80% compliance based on pill count) patients.

In vitamin D-deficient patients, supplementation with cholecalciferol 1000 IU daily produced similar effects on VDBP, F25OHD and F1,25OHD compared with ergocalciferol 1000 IU daily. These findings explain previous data showing no difference in the degree of PTH suppression between treatments.

***Disclosures: Paul Glendenning**, None.*

1167

CYP2R1 is a Potential Candidate for Predicting Serum 25(OH)D Variation as Suggested by Genetic and Epigenetic Studies. Yu Zhou*[1], Fengxiao Bu[1], Joan Lappe[2], Laura Armas[1], Robert Recker[2], Lanjuan Zhao[3]. [1]Creighton University, USA, [2]Creighton University Osteoporosis Research Center, USA, [3]Creighton University Medical Center, USA

Achieving and maintaining an optimal level of serum 25-hydroxyvitmain D [25(OH)D] are important for preventing rickets, osteoporosis and osteoporotic fracture. Oral vitamin D3 supplementation is the best approach to increase serum 25(OH)D levels. However, high variability of serum 25(OH)D in response to a given dose of vitamin D supplementation is widely observed. Factors contributing to the wide variability in serum 25(OH)D are largely unknown.

We first conducted a genetic epidemiology study to identify genes important for prevalent serum 25(OH)D variation. Nine candidate genes (ALPL, CYP24A1, CYP27A1, CYP27B1, CYP2R1, CYP3A4, GC, VDR, and PTH) important for vitamin D metabolism were comprehensively screened using 49 tag SNPs in 156 unrelated healthy Caucasian subjects. Evidence of association was observed at six SNPs in the CYP2R1 and GC gene. We further conducted a replication study for these six SNPs in an independent cohort with 340 unrelated healthy Caucasian subjects. Two SNPs in the promoter region of the CYP2R1 gene, rs10766197 (Pdiscovery = 0.007, Preplication = 0.019) and rs12794714 (Pdiscovery = 0.001, Preplication = 0.016), were confirmed to be significantly associated with prevalent serum 25(OH)D levels.

CYP2R1 was first identified in 2003 as a key vitamin D 25-hydroxylase that converts vitamin D into 25(OH)D. In order to test whether the gene contributes to serum 25(OH)D variability in response to vitamin D3 supplementation, we conducted an epigenetic study. In total, 446 non-Hispanic white postmenopausal women were treated with calcium (1500 mg/day) and vitamin D3 (1100 IU/day) for 12-months. We selected 18 responders and 18 non-responders from the 446 subjects, at the two extreme tails of the distribution of dose-adjusted 12-month increase of serum 25(OH)D. For each subject, genomic DNA before and after 12-month vitamin D3 intervention was extracted from frozen serum. The average methylation ratio of the CYP2R1 promoter in the non-responder group (30%) was significantly higher than that in the responder group (8%) (p=0.004). In both groups, the DNA methylation ratio was unaffected by vitamin D3 intervention. The hypermetylation in the non-responder group may contribute to gene silencing of CYP2R1, leading to lower increase of serum 25(OH)D levels.

These data suggest that CYP2R1 is a strong candidate for the variability in prevalent serum 25(OH)D, and variability in its response to vitamin D supplementation.

***Disclosures: Yu Zhou**, None.*

1168

Effects of Vitamin D Deficiency and High Parathyroid Hormone on Mortality Risk in Elderly Men. Steven Frost[1], Tuan Nguyen[2], Dana Bliuc[2], John Eisman[2], Jacqueline Center[2], Nguyen Nguyen*[2]. [1]University of Western Sydney, Australia, [2]Garvan Institute of Medical Research, Australia

Vitamin D deficiency is common in the elderly. Recent data have suggested that mortality risk is elevated in men with low vitamin D levels; however, the relationship could be confounded by parathyroid hormone (PTH) which had previously been shown to be associated with mortality. Therefore, this study sought to examine the inter-relationship between vitamin D and PTH levels on the risk of mortality in men.

The study was part of the Dubbo Osteoporosis Epidemiology Study, which involved 413 men aged 60+ years as at 1989, whose health status had been continuously monitored for 14 years with biannual visits. During the follow-up period, mortality was ascertained. Vitamin D was measured by 25(OH)D using an in-house pre-extraction competitive binding protein assay with charcoal separation, with an inter-assay CV of 12%. Vitamin D status was classified in 3 groups: deficient (25(OH)D<50nmol/L), insufficient (50-75nmol/L) and sufficient (≥75nmol/L). PTH was measured by a solid phase two-site immunoenzymometric assay also from Diagnostics Products, with an inter-assay CV of 6%. The association between vitamin D and mortality was analyzed by the Cox's proportional hazards model with adjustment for covariates.

The overall prevalence of vitamin D deficiency was 12.6%. During the follow-up period of 4059 person-years, 200 men died, yielding an incidence of mortality of 4.9 per 100 person-years. The prevalence of vitamin D deficiency was 17.5% in the deceased and 8.0% in survivors. Men who died had lower baseline 25(OH)D levels

than those who survived (70.9 ± 22.9 vs. 77.3 ± 23.0 nmol/L, P=0.005), such that each SD (25nmol/L) decreased in 25(OH) D was associated with a 33% increase in the risk of mortality (RR 1.33, 95% CI: 1.12 – 1.57). Higher serum levels of PTH were associated with an increased risk of mortality (+0.5pmol/L, RR 1.16; 95% CI: 1.02-1.32). After adjusting for age and PTH, the association between 25(OH)D and mortality remained statistically significant (1.22; 1.02-1.46). Men with vitamin D deficiency and high levels of PTH were 1.63 (1.01-2.66) fold more likely to die from those with adequate vitamin D and low levels of PTH. Approximately 7% and 4% of mortality risk was attributable to vitamin D deficiency and vitamin D deficiency with high PTH, respectively.

The independent effects of vitamin D and PTH on mortality risk observed in this study suggests that men with vitamin D deficiency and hyperparathyroidism are at increased risk of all-cause mortality.

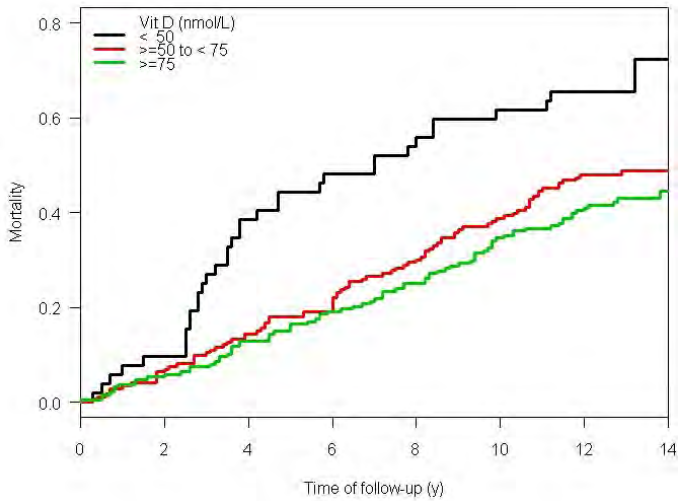

The association between vitamin D and mortality in men

***Disclosures: Nguyen Nguyen**, None.*

1169

Intermittent PTH Treatment Decreases Circulating Sclerostin Levels in Postmenopausal Women. Matthew Drake*[1], Bhuma Srinivasan[1], Ulrike Moedder[1], James Peterson[1], Louise McCready[2], Byron Riggs[3], Denise Dwyer[4], Marina Stolina[4], Paul Kostenuik[5], Sundeep Khosla[6]. [1]Mayo Clinic College of Medicine, USA, [2]Mayo Clinic, USA, [3]Mayo Clinic College of Medicine,Rochester, MN, USA, [4]Amgen Inc, USA, [5]Amgen, Inc., USA, [6]College of Medicine, Mayo Clinic, USA

Intermittent PTH treatment stimulates bone formation (BF) more than bone resorption (BR), but the mechanisms of this stimulation remain unclear. Sclerostin is a recently identified inhibitor of Wnt signaling. Although animal studies have demonstrated that PTH decreases sclerostin production by osteocytes, there are currently no data regarding effects of intermittent PTH treatment on sclerostin production in humans. Thus, we studied 27 postmenopausal women treated with PTH 1-34 (40 μg/d) for 14 days and 28 control women and assessed changes in levels of serum sclerostin (Luminex assay), bone turnover markers, RANKL and OPG. The BF marker CICP increased (by 71%, $P < 0.001$) in PTH-treated women. Concomitant with the increase in BF, serum sclerostin levels decreased significantly in PTH-treated subjects, but did not change in control women (Figure A), and the percent change from baseline in serum sclerostin levels in PTH-treated women was significantly greater than that in control women (Figure B). Bone marrow plasma was obtained in a subset of control and PTH-treated subjects (n = 19 each) at the end of the treatment period, and marrow plasma and peripheral serum sclerostin levels were significantly correlated ($R = 0.64$, $P < 0.0001$). Although marrow plasma sclerostin levels were 24% lower in PTH-treated compared to control women, due to the smaller sample size this difference was not statistically significant ($P = 0.173$). The BR marker, serum CTX, also increased in PTH-treated women (by 59%, $P < 0.001$); while serum or marrow plasma RANKL levels were undetectable in the majority of subjects, marrow plasma (but not peripheral serum) levels of OPG were 33% lower in PTH-treated compared to control women ($P < 0.05$). These studies demonstrate that in humans, the stimulation of BF by intermittent PTH 1-34 treatment is accompanied by a decrease in circulating serum sclerostin levels, which correlate with bone marrow plasma sclerostin levels. Moreover, the observed increase in BR following PTH therapy is accompanied by decreases in bone marrow plasma (but not serum) OPG levels, suggesting that in contrast to circulating sclerostin levels, circulating OPG levels may not reflect changes in the bone microenvironment. Coupled with previous animal studies, our data thus indicate that decreases in bone levels of sclerostin and OPG, potent inhibitors of BF and BR respectively, may contribute to the observed increases in BF and BR following PTH therapy in humans.

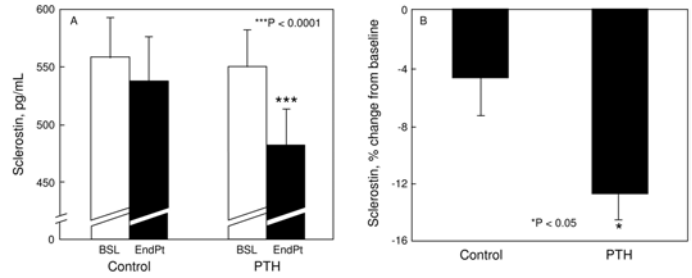

PTH-Sclerostin

***Disclosures: Matthew Drake**, None.*
This study received funding from: Amgen Inc.

1170

Absence of Gut Microbiota Leads to Increased Bone Mass Associated with Low Serum Serotonin Levels. Klara Sjögren*[1], Cecilia Engdahl[2], Marie Lagerquist[2], Fredrik Bäckhed[3], Claes Ohlsson[1]. [1]Centre for Bone & Arthritis Research, GU, Sauhlgrenska Academy, Medicine, Sweden, [2]Centre for Bone & Arthritis Researc, GU, Sauhlgrenska Academy, Medicine, Sweden, [3]The Wallenberg Laboratory, GU, Sahlgrenska Academy, Medicine, Sweden

The gut is inhabited by a microbial ecosystem, the gut microbiota, which consists of 10 times as many cells as our own eukaryotic cells. It is acquired at birth and its composition is modulated by a number of environmental factors throughout life and can thus be considered a dynamic organ that has endowed us with vital metabolic functions such as vitamin synthesis and xenobiotic metabolism. Furthermore, the gut microbiota is involved in the regulation of fat mass and can modulate expression of gut derived hormones[1]. Interestingly, gut-derived circulating serotonin reduces osteoblast proliferation and thereby bone mass, demonstrating that a gut bone connection exists [2,3] The possible impact of gut microbiota for bone metabolism is unknown and we, therefore, evaluated the skeletal phenotype of germ-free (GF)-mice and conventionally raised mice (CONV-R), having normal gut microbiota.

GF mice were kept in sterile flexible film isolators and colonized mice were kept in micro isolator cages in a specified pathogen-free state in a barrier facility. All mice were fed an autoclaved chow diet. At seven weeks of age GF mice had increased proximal tibial trabecular volumetric bone mineral density (vBMD) compared to CONV-R mice (+33%, $p \leq 0.01$) as measured by peripheral quantitative computed tomography (pQCT). To exclude developmental factors we had an extra control consisting of mice that were born germ-free and then colonized at three weeks of age. Colonization reduced the trabecular vBMD compared with GF counterparts (-21%, $p \leq 0.05$). More detailed investigation of the femur with microCT (μCT) showed an increased percent bone volume (BV/TV) in GF compared to CONV-R mice (49%, $p \leq 0.01$). This increase was due to an increased trabecular number (45%, $p \leq 0.01$) and decreased trabecular separation (-33%, $p \leq 0.01$) while trabecular thickness was unaffected in GF compared to CONV-R mice. Cortical thickness was also increased in GF compared to CONV-R mice (+6%, $p \leq 0.05$). Interestingly GF mice had decreased serum serotonin levels compared to CONV-R mice (-67%, $p \leq 0.01$).

In conclusion, absence of gut microbiota leads to increased bone mass associated with reduced serum serotonin. We propose that the gut microbiota modulates gut serotonin synthesis and thereby via an endocrine mechanism also bone metabolism.

1. Backhed, F., et al. Proc Natl Acad Sci U S A 101, 15718-15723 (2004).
2. Yadav, V.K., et al. Nat Med 16, 308-312 (2009).
3. Yadav, V.K., et al. Cell 138, 976-989 (2009).

***Disclosures: Klara Sjögren**, None.*

1171

Comparing the Effects of Odanacatib versus Alendronate on Bone Turnover of Transilial Biopsy in Adult Ovariectomized Rhesus Monkeys. Charles Chen*[1], Brenda Pennypacker[2], David Gilberto[3], Le Thi Duong[2]. [1]Merck & Co., Inc., USA, [2]Merck Research Laboratories, USA, [3]Merck & Co. Inc., USA

Cathepsin K (CatK) is a cysteine protease highly expressed in osteoclasts that degrades bone matrix proteins during resorption. Odanacatib (ODN) is a selective, potent and reversible CatK inhibitor in development for the treatment of osteoporosis. Here, we compared the effects of ODN and alendronate (ALN) on bone turnover in transilial biopsies collected from OVX-rhesus monkeys after 12-months treatment. Monkeys (age 10-22 yrs) were randomized post-OVX into 4 groups (N=16/group): (1) OVX+vehicle (Veh), (2) +ALN (30μg/kg/wk, sc), (3) +2mg/kg/d ODN (L-ODN; 11uM•24hr), or (4) +4mg/kg/d ODN (H-ODN; 49uM•24hr), as compared to estimated daily clinical exposure (~7uM•24hr) from the 50 mg weekly dose. A group of age- and aBMD-matched intact monkeys (Int, N=12) was included

as control. Prior to biopsy, calcein (8mg/kg, sc) was administered with a 15 day interval. Bone formation (BF) was determined in endocortical (Ec) and cancellous surface (Cn) with standard histomorphometric endpoints, including mineralizing surface (MS/BS, %), mineral apposition rate (MAR, μm/d), bone formation rate (BFR/BS). While ALN suppressed Ec BFR/BS ($p=0.01$) with significant reduction ($p<0.05$) of MS/BS and MAR. Neither L-ODN nor H-ODN changed these BF parameters. In the Cn surface, BF parameters tend to be lower in ALN group and were unaffected in ODN groups. In both Ec and Cn surfaces, ODN showed no effects on osteoid thickness (Os.Th, μm) or osteoid surface (OS/BS, %); and ALN treatment reduced Os.Th by 52% ($p<0.05$) and OS/BS by 65% ($p=0.05$). Our previous data indicated while fully blocking osteoclastic bone resorption, ODN increased osteoclast number in the lumbar vertebrae of OVX-monkeys. Here, osteoclast surface (OcS/BS,%) and osteoclast number (OcN/BS, #/mm) in Ec and Cn surfaces of ALN- and H-ODN treated groups were not different from Veh or Int controls. Interestingly, the L-ODN group showed significantly increased Ec OcS/BS and OcN/BS ($p<0.05$) vs. Int, as well as Cn OcS/BS and OcN/BS ($p<0.05$ vs. Veh and Int). In summary, ODN at dose levels exceeding the estimated daily clinical exposure, did not affect bone formation in transilial biopsy of OVX monkeys. This supports earlier findings that ODN differs from the bisphosphonates in sparing bone formation, potentially via uncoupling bone formation from resorption.

***Disclosures: Charles Chen**, None.*

1172

Inhibition of Active TGF-β1 Release by Anti-Resorptive Drugs Blunts PTH Anabolic Effects on Bone Remodeling. Xiangwei Wu*[1], Lijuan Pang[2], Weiqi Lei[2], William Lu[3], Jun Li[2], Zhaoyang Li[3], Frank Frassica[2], Xueling Chen[2], Mei Wan[1], Xu Cao[2]. [1]Johns Hopkins University School of Medicine, USA, [2]Johns Hopkins University, USA, [3]University of Hong Kong, China

Anabolic effects of PTH on bone formation are impaired with concurrent use of anti-resorptive drugs in clinic trials. Here we investigated the cellular mechanism how PTH-induced bone formation was inhibited by concurrent treatment of alendronate. The aged mice were injected with PTH, alendronate or both. PTH or alendronate alone stimulated an increase in bone mass, but additive effects were not observed with both drugs. Osteogenic potential of BMSCs was examined in a CFU-F assay. No significant difference was observed in the numbers of CFU-Fs formed by the bone marrow cells isolated from the different treatment groups, but osteoclast and osteoblast numbers were decreased in mice with concurrent treatment, indicating that reduction of osteoblasts is likely due to the interruption of the BMSCs recruitment.

Active TGF-β1 released during osteoclastic bone resorption induces migration of BMSCs to the bone remodeling sites. Indeed, the levels of active TGF-β1, as measured by ELISA, were significantly higher in the bone marrow of mice treated with PTH than those treated with vehicle or alendronate alone. Concurrent treatment resulted in a reduction in the PTH-stimulated levels of active TGF-β1. Higher numbers of p-Smad2/3-positive cells were found in the microenvironment of TRAP-positive osteoclasts in PTH treatment, but reduced significantly in those with concurrent use of alendronate, indicating that the release of active TGF-β1 from osteoclastic bone resorption sites was inhibited by alendronate. To investigate whether the alendronate-induced inhibition of release of active TGF-β1 impairs the anabolic action of PTH in bone, Tgfb1–/– mice and their wild-type littermates were injected intermittently with PTH or vehicle for 4 weeks. The anabolic effects of PTH on bone were diminished in the Tgfb1–/– mice as compared to their wild-type littermates, indicating that the release of active TGF-β1 during bone resorption is essential for the anabolic effects of PTH on bone formation. In a transplantation experiment, the recruitment of injected mouse Sca-1- and CD29-positive BMSCs stimulated by PTH was inhibited by alendronate. Thus, inhibition of active TGF-β1 release by alendronate reduces the recruitment of BMSCs to the bone sites and impairs PTH anabolic action in bone. Our finding suggests that the additive effects may be achieved by PTH stimulation followed by anti-resorptive drug therapy.

***Disclosures: Xiangwei Wu**, None.*

1173

Selective knock out the membrane-bound Colony Stimulating Factor-1 (mCSF1) results in an increased anabolic response to PTH in mice. Gang-Qing Yao*[1], Jian Jun Wu[2], Karl Insogna[1]. [1]Yale University School of Medicine, USA, [2]Yale University, USA

CSF1 is absolutely required for osteoclastogenesis, and its genetic absence leads to osteopetrosis due to a failure of osteoclast formation. There are two isoforms of CSF1, soluble and membrane-bound (mCSF1), but their individual biological functions are unclear. To better define the role of mCSF1 in vivo, we have generated mCSF1 knock-out (k/o) mice. Bone density, as assessed by PIXImus, was increased by +15.9% ($p<0.01$), +6.8% ($p<0.05$) and +6.9% (NS) in the spine, total body and femur respectively in k/o animals compared to wild-type (wt) littermates. The number of osteoclasts on trabecular bone surfaces was significantly reduced as was the osteoclastogenic potential of bone marrow cells from the mCSF1 k/o mice.

PTH is the only anabolic therapy approved for use in human. However, the anabolic response to PTH is thought to be limited, in part, by the increase in bone resorption that follows the initial increase in bone formation. None-the-less, inhibiting osteoclasts with bisphosphonates does not improve the therapeutic response to teriparatide. Since osteoclasts are present in reduced numbers but phenotypically normal in mCSF1 k/o animals, we hypothesized that the reduced osteoclastogenesis in the genetic absence of mCSF1 would allow for a more robust response to PTH.

To test this idea, adult mCSF1 k/o mice and wt litmates were treated with either a single daily sc injection of human (1-34) PTH (80 ng/g body weight) or vehicle for 4 weeks, and BMD measured after 0 and 4 weeks of treatment. The PTH-treated k/o mice showed a greater increase both in spine and femur BMD compared to vehicle-treated k/o animals than did the PTH-treated wt animals compared to their vehicle-treated controls; $13.7 \pm 2.7\%$ vs. $4.9 \pm 3.3\%$ for the spine and $25 \pm 4.5\%$ vs. $14 \pm 2.2\%$, for the femur, ($M \pm SD$). Further, the PTH-treated mCSF1 k/o mice showed a greater increase in spine and femur BMD compared to baseline than did the wt mice (14.8% vs. 5.2% for the spine and 27.2 vs. 15.2 %; for femur respectively; $M \pm SD$).

Our findings indicate mCSF1 is essential for normal bone remodeling since, in its absence, bone density is increased. Interestingly, the anabolic response to PTH is augmented in mCSF1 k/o mice perhaps because of a reduced resorptive response to this treatment although other mechanisms cannot be excluded. Since the mCSF1 k/o mice do not have phenotypic abnormalities apart from an increase in bone mass, our data suggest that mCSF1 may be a reasonable drug target for low bone mass.

***Disclosures: Gang-Qing Yao**, None.*

1174

Tissue Level Mechanism of Increased Bone Formation by Sclerostin Antibody in Male Cynomolgus Monkeys. MS Ominsky*, Q-T Niu, P Kurimoto, HZ Ke. Amgen Inc, USA

Bone formation can occur with or without prior activation of resorption as part of the remodeling and modeling processes, respectively. In adult humans, the vast majority of bone formation occurs via remodeling, and the increases in histologic bone formation with the anabolic agent teriparatide have been primarily attributed to remodeling. Inhibition of sclerostin by sclerostin antibody (Scl-Ab) has demonstrated robust increases in bone formation and bone mineral density in rodents, monkeys, and humans. In the current study, we quantified the effects of Scl-Ab on modeling- and remodeling-based bone formation in male cynomolgus monkeys. Adolescent (4-5-year-old) monkeys were treated biweekly with subcutaneous vehicle (Veh) or 30 mg/kg Scl-Ab for 10 weeks, as part of a previously reported fibular osteotomy study. Tetracycline (25 mg/kg) was injected on days 14 and 24, and calcein (8 mg/kg) was injected on days 56 and 66. Histomorphometry was performed at the 2nd lumbar vertebra (L2). Calcein-based mineralizing surface (MS/BS) was 68% greater in the Scl-Ab group compared with Veh ($p<0.001$). MS/BS was separated into modeling- and remodeling-based surfaces. The Scl-Ab-mediated increases in MS/BS were almost entirely modeling-based, with an increase from 0.4% of the total bone surface in Veh to 27% in the Scl-Ab group ($p<0.001$). No significant change was observed in remodeling-based MS/BS between the Veh and Scl-Ab groups (17% vs 20%). Interestingly, we observed that mineral apposition rate (MAR) was slower on modeling versus remodeling surfaces in the Veh group (0.6 vs 1.3 μm/day, $p<0.05$), and no treatment-related changes were observed. However, the overall MAR in the Scl-Ab-treated group was lower than in controls (1.3 vs 0.9 μm/day, $p<0.05$), due to the increase in the proportion of modeling-based bone formation surfaces from 3% to 57% of total bone-forming surfaces. Scl-Ab also resulted in a significantly lower eroded surface (2.2% vs 4.6% in controls, $p<0.05$), and a greater proportion of remodeling-based MS/BS which had both underlying tetracycline labels (active from week 2; 52% vs 10% in the control group, $p<0.01$). These results demonstrate that Scl-Ab increased the duration of bone formation at remodeling sites and increased modeling-based bone formation, while reducing bone resorption. Through its unique tissue-level mechanism, sclerostin antibody may provide an efficient way to improve bone mass in conditions with low bone mass such as osteoporosis.

***Disclosures: MS Ominsky**, Amgen Inc., 3; Amgen Inc., 1*
This study received funding from: Amgen Inc.

1175

The Impact of Growth and Development on Bone Mineral Accretion of the Total Body (Less Head) and Lumbar Spine During Childhood and Adolescence; A Report from the Bone Mineral Density in Childhood Study Group. Babette Zemel*[1], Heidi Kalkwarf[2], Andrea Kelly[3], Joan Lappe[4], Mary B. Leonard[3], Struan Grant[3], Soroosh Mahboubi[3], Margaret Frederick[5], Sharon Oberfield[6], John Shepherd[7], Karen Winer[8]. [1]Children's Hospital of Philadelphia, USA, [2]Cincinnati Children's Hospital Medical Center, USA, [3]The Children's Hospital of Philadelphia, USA, [4]Creighton University, USA, [5]Clinical Trials & Survey Corporation, USA, [6]Columbia University Medical Center, USA, [7]University of California, San Francisco, USA, [8]NICHD, USA

Monitoring changes in bone health status to assess disease and/or treatment effects is important for at-risk children. Presently, there are no reference data on bone mass increments to assess adequacy of annual gains, and little is known about factors associated with bone mass increments. This study examined annual increments in bone mineral content (BMC) of the total body less head (TBLH) and lumbar spine

assessed by DXA (Hologic QDR densitometers), and explored the contribution of growth and development to bone accretion during childhood and adolescence.

Healthy subjects, ages 6 to 17years at enrollment, were participants who were measured annually for up to 3 years at 5 U.S. centers in the NICHD Bone Mineral Density in Childhood Study. Growth (initial height and weight, height and weight velocity) and puberty stage were assessed. Analyses were restricted to visits occurring 12 ± 1 month apart. Graphical inspection and backward stepwise multiple regression were used.

BMC accretion peaked at 14-15 and 12-13 y for males and females, respectively. Graphical representation showed strong sex and puberty dependent patterns of BMC accretion, so further analyses were stratified accordingly. For males and females, BMC accretion did not differ for Tanner stages 1 and 2, so they were combined for subsequent analyses. For both sexes and measurement sites, BMC accretion peaked during the year preceding Tanner stage 4, with median BMC accretion values for TBLH of 250 and 188 gm/y and for spine of 7.6 and 6.9 gm/y for males and females, respectively.

The combination of growth variables selected in the stepwise regression analyses varied by sex and puberty stage stratum. The level of explained variance (R2) was generally lower in Tanner 1-2 (0.09 to 0.38) and greater in Tanner 4 & 5 (0.46 to 0.65). Height velocity was significantly associated (all $p<0.001$) with BMC accretion for each stratum, but was the strongest predictor mainly in Tanner stages 4 & 5 for TBLH and spine. The effect of black race was significant mainly at the beginning and end of puberty in males.

These findings suggest that expected gains in BMC are only modestly growth-dependent in pre- and early pubertal children, but growth measures are important predictors during puberty, including children in Tanner stage 5 at follow-up. Evaluation of BMC accretion should be considered according to sex and puberty stage, and should account for growth during the period under examination.

***Disclosures: Babette Zemel**, None.*

1176

Secular Trend for Earlier Skeletal Maturation in US Children. Dana Duren*[1], Ramzi Nahhas[1], Richard Sherwood[2], Miryoung Lee[3], Audrey Choh[1], Bradford Towne[1], Stefan Czerwinski[1], Roger Siervogel[3], Cameron Chumlea[1]. [1]Wright State University, USA, [2]Lifespan Health Research Center,Wright State University, USA, [3]Wright State University Boonshoft School of Medicine, USA

Secular trends have been noted in several markers for maturation in recent childhood cohorts. This is most notable in sexual maturity as indicated by earlier menarche in girls, which has been observed nearly world-wide in industrialized countries. Such trends may also be reflected in processes of skeletal maturation, as indicated by overall bone age and specific bone age endophenotypes such as fusion of the epiphyses of metacarpals and phalanges. The current study examined 1,271 children aged from birth to 18 years for 85 radiographic skeletal maturity indicators (155 maturity levels) in the bones of the hand and wrist. Two cohorts of children from the Fels Longitudinal Study were examined: 690 born 1929-1964 and 581 born 1965-2001. Maturity indicators were sorted into bone type (carpal/long bone) and categories of ossification, fusion, two types of shape change, and appearance of radiopaque densities. By sex, we modeled the proportion of children at a given maturity grade as a function of age using logistic regression, estimated the median age of maturity, and tested for the significance of differences in median age of maturity between the two cohorts ($\alpha=0.05$). The majority of indicator categories showed a general trend for earlier maturation, with some indicator types having both earlier and later maturity transitions in the recent cohort. In boys, 90% of fusion indicators matured significantly earlier in the more recent cohort. Ossification showed less of a tendency for earlier maturation in boys, with only 4.3% of carpal, and 10.2% of long bone, indicators maturing significantly earlier, and 10.2% of long bone ossification indicators maturing later. In girls, 96.7% of fusion indicators matured significantly earlier; ossification also occurred significantly earlier in 68.6% of the carpal and 33.9% of the long bone indicators, with none of the carpal ossification indicators occurring significantly later and only 5.1% of the long bone ossification indicators occurring later. These results demonstrate a significant secular trend for earlier skeletal maturity, especially fusion of the hand long bones, in post-baby-boom generations. The differences in frequency of earlier maturation observed in fusion versus ossification of the bones of the hand and wrist point to a potential shift in timing of pubertal hormone elevation, perhaps reflecting the secular trend in sexual maturity observed in other studies. R01AR055927, R01HD056247, R01HD12252

***Disclosures: Dana Duren**, None.*

1177

Predictors of Skeletal Calcium Accretion in Adolescent Boys and Girls. Kathleen Hill*[1], Berdine Martin[2], Linda McCabe[2], George McCabe[2], Connie Weaver[2]. [1]Indiana University School of Medicine, USA, [2]Purdue University, USA

Purpose: Peak bone mass is a major determinant of osteoporosis risk; maximizing Ca retention during peak bone mineral accrual in adolescence is important for optimizing peak bone mass. The purpose of this study was to determine the relative contributions of diet and physiologic factors on Ca retention in adolescents. Method: A total of 487 observations on 265 10 – 15 y.o. white, black, and Asian boys and girls studied in a series of Ca balance studies were analyzed. Two-phase regression was used to model the relationship between Ca intake and Ca retention in boys and girls. Model building techniques including residual analysis were used to select potential variables for predicting Ca retention. These additional variables included race, BMI, height, weight, body composition, bone parameters, serum 25OHD, serum PTH, serum IGF-1, age, and sexual maturation. Bootstrap resampling was used to determine 95 % confidence intervals. Results: Ca intake explained 31 % and 11 % of the variation in Ca retention in boys and girls, respectively. A model that included Ca intake, BMI, serum 25OHD, and serum IGF-1 explained 40.5 % of the variation in Ca retention in boys. Ca intake, BMI, and serum IGF-1 were positively associated with Ca retention, whereas serum 25OHD was negatively associated with Ca retention. A model that included Ca intake, BMI, age, serum PTH, and race explained 27.9 % of the variation in Ca retention in girls. Ca intake, BMI, and serum PTH were positively associated with Ca retention and age was negatively associated with Ca retention. Black girls retained 147 mg/d Ca across compared to white and Asian girls across the range of Ca intakes studied. Conclusions: Ca intake is a major predictor of Ca retention in boys and girls, and represents a modifiable lifestyle factor. Measures of maturation and regulators of Ca metabolism are predictors of Ca retention in both boys and girls. In girls, the effect of race is evident even after accounting for other predictors of Ca retention, whereas in boys, the effect of race is eliminated by accounting for the other predictors of Ca retention. These results support that adequate dietary Ca during adolescent growth is important for skeletal Ca retention. Predictive models of Ca retention can be used to target interventions to those adolescents most at risk for suboptimal skeletal Ca retention, and lead us in the direction of personalized nutrition.

***Disclosures: Kathleen Hill**, None.*

1178

Gender Differences in Circulating Sclerostin Levels are Established During Puberty and Correlate with Cortical Porosity. Salman Kirmani*[1], Ulrike Moedder[2], Kelley Hoey[1], James Peterson[1], Louise McCready[1], Atkinson Elizabeth[1], Shreyasee Amin[1], L. Joseph Melton[1], Byron Riggs[3], Ralph Müller[4], Sundeep Khosla[5]. [1]Mayo Clinic, USA, [2]Mayo Clinic College of Medicine, USA, [3]Mayo Clinic College of Medicine,Rochester, MN, USA, [4]ETH Zurich, Switzerland, [5]College of Medicine, Mayo Clinic, USA

Sclerostin, produced by osteocytes, is a potent inhibitor of Wnt signaling and bone formation; a neutralizing antibody to sclerostin also reduces bone resorption. However, there is currently no information on possible changes in circulating sclerostin levels during growth in humans. Thus, we used a recently developed ELISA (Biomedica) to measure serum sclerostin levels in 6-21 yr-old girls (n = 62) and boys (n = 56) in whom high-resolution pQCT (XtremeCT, Scanco, voxel size 82 microns) imaging of the wrist was obtained. Markers of bone resorption (CTX) and formation (PINP) were also measured. Subjects were classified into 5 groups by bone age (BA): Group I (pre-puberty, BA 6-8 yrs), Group II (early puberty, BA 9-11 yrs), Group III (mid-puberty, BA 12-14 yrs), Group IV (late puberty, BA 15-17 yrs) and Group V (post-puberty, BA 18-21 yrs). As shown in the Figure, serum sclerostin levels were slightly higher in the girls prior to puberty, tended to decrease in both sexes during puberty, but remained significantly higher in the boys compared to the girls in Groups III-V. After adjusting for BA, sclerostin levels were positively correlated with bone turnover markers in girls ($r = 0.39$, $P = 0.002$ for CTX and $r = 0.29$, $P = 0.02$ for PINP) and in boys ($r = 0.39$, $P = 0.003$ for CTX and $r = 0.38$, $P = 0.004$ for PINP). Trabecular bone parameters showed little association with serum sclerostin levels in either sex; however, cortical thickness and volumetric BMD were inversely associated with sclerostin levels in girls ($r = -0.34$, $P = 0.007$ for both), but not in boys. Interestingly, the cortical porosity index (derived from the Xtreme CT scans), which has previously been shown to increase transiently during adolescent growth and to peak at the time of maximal forearm fracture incidence in both sexes, was positively correlated with serum sclerostin levels in both girls ($r = 0.30$, $P = 0.02$) and boys ($r = 0.41$, $P = 0.002$). We conclude that a gender difference in circulating sclerostin levels is established during puberty, with boys having higher sclerostin levels than girls. The observed associations of sclerostin levels in both sexes with bone turnover markers and with cortical porosity suggest a role for changes in sclerostin production during growth in regulating cortical structure.

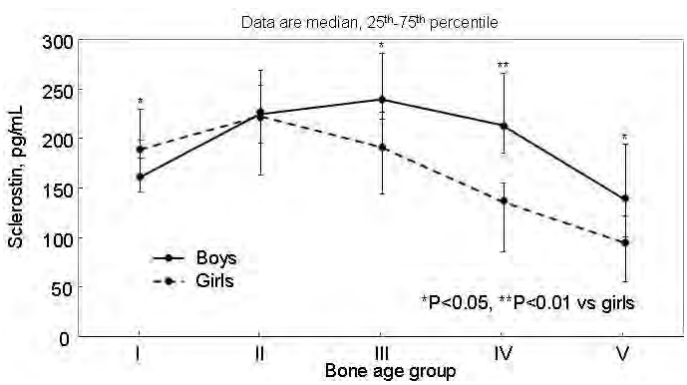

jpeg

***Disclosures: Salman Kirmani**, None.*

1179

Age At Onset Of Puberty Predicts Bone Mass In Young Adulthood. Vicente Gilsanz*[1], James Chalfant[2], Heidi Kalkwarf[3], Babette Zemel[4], Joan Lappe[5], Sharon Oberfield[6], John Shepherd[7], Thomas Hangartner[8], Margaret Frederick[9], Xiangke Huang[9], Soroosh Mahboubi[10], Jean-Claude Desmangles[5], Tishya Wren[2], Karen Winer[11]. [1]Children's Hospital of Los Angeles, USA, [2]Childrens Hospital Los Angeles, USA, [3]Cincinnati Children's Hospital Medical Center, USA, [4]Children's Hospital of Philadelphia, USA, [5]Creighton University Osteoporosis Research Center, USA, [6]Columbia University Medical Center, USA, [7]University of California, San Francisco, USA, [8]Wright State University, USA, [9]Clinical Trials & Surveys Corp., USA, [10]Hand Radiograph Core Laboratory, USA, [11]National Institutes of Health, NICHD, USA

Although the amount of bone gained during puberty is the main contributor to peak bone mass (PBM), the influence that normal variations in sexual development have on bone acquisition are yet to be clearly defined. The purpose of this prospective longitudinal multi-center study was to determine whether the timing of commencement and length of puberty in contemporary children in the United States influence dual x-ray absorptiometry (DXA) values of bone mineral content (BMC) and bone mineral density (BMD) in the axial and appendicular skeletons at skeletal maturity. We identified 78 girls and 85 boys who began puberty (Tanner 2 stage of breast development or greater than 4 mL testes) and completed skeletal maturity (physeal closure of the bones of the hand and wrist) during the duration of the study; 4.4 $\pm$ 0.8 and 4.5 $\pm$ 0.8 years later respectively. Multiple linear regression analyses indicated that the age of onset of puberty was a strong negative predictor of DXA bone measurements at skeletal maturity, independent of bone values at the beginning of puberty and the length of puberty. This negative relation was observed for all BMC and BMD measurements at all skeletal sites, in both boys and girls (all p's < 0.0001). On average, healthy girls starting puberty a year earlier had approximately 5% greater BMC measures and 2.5% greater BMD values at skeletal maturity, while those starting a year later had 5% and 2.5% less. Similar findings of a slightly smaller magnitude were observed in healthy boys. In contrast, length of puberty had no relation to any measures of bone. We conclude that the timing of pubertal commencement is a strong independent negative predictor of bone mass and bone density in healthy young males and females.

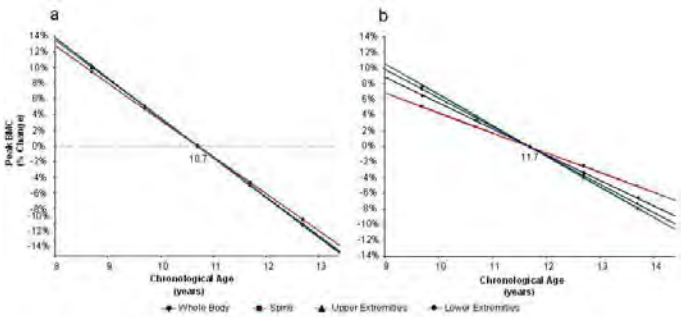

Figure 1. Predicted percent difference in peak BMC as a function of pubertal commencement for girls (a) and boys (b) as compared to the mean peak BMC at mean age of pubertal commencement (10.7 for girls and 11.7 for boys). Data points represent one and two standard deviations from the mean age of pubertal onset.

Predicted percent difference in peak BMC as a function of pubertal commencement

***Disclosures: Vicente Gilsanz**, None.*

1180

The Relationship Between Excess Adiposity and Bone Strength During Growth. Natalie Glass*, James Torner, Kathleen Janz, Elena Letuchy, Trudy Burns, Julie Gilmore, Barbara Broffitt, Steven Levy. University of Iowa, USA

Investigations of the relationship between excess adiposity and pediatric bone strength have yielded conflicting results. Because peak bone mass is attained in early adulthood, evaluation of this relationship may be important for the prevention of osteoporosis later in life. We conducted a longitudinal study in boys and girls to determine whether excess adiposity at age 9 was predictive of bone strength 2 and 4 years later.

Methods: Using peripheral quantitative computed tomography (pQCT), we measured trabecular bone mineral content (tBMC) and density (tBMD) at the 4% site of the distal radius and tibia; cortical bone mineral content (cBMC) density (cBMD), periosteal (peri) and endosteal (endo) circumference at the 20% and 38% distal radius and tibia, respectively; strength strain index (SSI) at the 38% distal tibia; and muscle cross-sectional area (mCSA) at the 66% site of the distal tibia. Data collection in 241 boys and 251 girls was completed at approximately ages 9, 11 and 13 years. Adiposity was ascertained using dual energy x-ray absorptiomety and expressed as fat mass index (FMI, total body fat mass/height^2). Multivariable regression analyses, adjusted for tanner stage, limb length, and mCSA (tibia only), evaluated whether FMI at age 9 predicted bone strength at age 11 and 13.

Results: Age 9 FMI predicted age 11 radial tBMC, tBMD, cBMC, endo, peri and SSI, but not cBMD in girls (p-values: $<$0.0001-0.0088); and radial tBMC, tBMD, endo, peri and SSI, but not cBMC or cBMD in boys (p-values: $<$0.0001-0.0091). Age 9 FMI was positively associated with all tibial bone measures at age 11, except cBMD, in both boys and girls (p-values: $<$0.0001-0.0153). Age 9 FMI was also positively associated with all radial bone measures for age 13 in girls, except cBMD (p-values: $<$0.0001-0.0015); and radial tBMC, cBMC, cBMD, peri, endo, and SSI at age 13 in boys (p-values: 0.0001-0.0495). At the tibia, there was a positive relationship between age 9 FMI and all age 13 bone measures, except cBMD in girls (p-values: $<$0.0001-0.0008), while all age 13 bone measures were positively associated in boys (p-values: $<$0.0001-0.049).

Conclusions: Excess adiposity was predictive of greater bone strength. This relationship was present at both weightbearing and non-weightbearing sites. This may suggest that the effects of excess adipose tissue on growing bone are not completely due to mechanical loading.

***Disclosures: Natalie Glass**, None.*

1181

Osteopontin Plays a Pivotal Role in Sympathetic Control of Bone Mass. Masashi Nagao*[1], Yoichi Ezura[2], Yoshitomo Saita[3], Tetsuya Nakamoto[1], Tadayoshi Hayata[4], Yayoi Izu[1], Ryo Hanyu[1], Hiroaki Hemmi[1], Takuya Notomi[5], Susan Rittling[6], Hisashi Kurosawa[7], Kazuo Kaneko[8], David Denhardt[9], Masaki Noda[1]. [1]Tokyo Medical & Dental University, Japan, [2]Tokyo Medical & Dental University, Medical Research Insititute, Japan, [3]Juntendo University, Department of Ortopedics, Japan, [4]Medical Reserach Institute, Tokyo Medical & Dental University, Japan, [5]GCOE, Tokyo Medical & Dental University, Japan, [6]The Forsyth Institute, USA, [7]Dept of Orthopedics, Juntendo Univ, School of medicine, Japan, [8]Dept of Orthopetics, Juntendo Univ school of medicine, Japan, [9]Department of Cell Biology & Neuroscience, Rutgers University, USA

Sympathetic tone suppresses bone mass levels. However, the link between sympathetic tone and bone metabolism remains obscure. One of the major causes of bone loss is unloading-induced event that is suppressed not only by beta blockers but also by the deficiency of osteopontin (OPN), a cytokine and one of the major components of non-collagenous extracellular matrix proteins of bone. We, therefore, examined whether OPN links sympathetic tone and bone metabolism. First, the activator of sympathetic tone isoproterenol (ISO) treatment increased the levels of plasma OPN. Furthermore, isoproterenol injection increased OPN expression in bone. To elucidate the role of OPN, the effects of OPN-deficiency on sympathetic tone-induced bone changes were examined. In contrast to wild type where isoproterenol treatment reduced the levels of bone volume, OPN-deficient mice were resistant to such isoproterenol-induced bone loss. Isoproterenol treatment suppressed bone formation parameters including mineral apposition rate (MAR) and bone formation rate (BFR) in wild type. However, OPN deficiency mitigated isoproterenol-induced reductions these bone formation parameters. Isoproterenol-treatment also increased the levels of bone resorption parameters such as osteoclast number and osteoclast surface as well as urinary deoxypyridinoline levels in wild type, while these parameters were unaffected by isoproterenol in OPN deficient mice. Isoproterenol treatment enhanced or reduced mRNA expression of osteoclastic or osteoblastic phenotype-related genes respectively, but not in bones from OPN-deficient mice. Though isoproterenol is catabolic and PTH is anabolic to bone, both enhance protein kinase A and CRE dependent luciferase activity. Osteopontin deficiency enhanced isoproterenol-induced CRE-luciferase activity as well as forskolin and IBMX-induced events and this enhancement was blocked by H89. OPN-deficiency enhanced phosphorylation of CRE-binding protein, CREB. Finally anti-OPN antibody treatment suppressed isoproterenol-induced bone loss. Thus, OPN plays a pivotal role in isoproterenol-induced bone loss at least in part via modulating CREB phosphorylation and transcription.

***Disclosures: Masashi Nagao**, None.*

1182

In Vivo Evidence for a Limiting Role of Bone Sialoprotein (BSP) in Primary Bone Formation and Resorption : The Marrow Ablation Model Under PTH Challenge. Ndéyé-Marième Wade-Gueye[1], Maya Boudiffa[2], Arnaud Vanden-Bossche[1], Farida Gueniche[1], Norbert Laroche[1], Jane Aubin[3], Laurence Vico[4], Marie-Helene Lafage-Proust[5], Luc Malaval*[6]. [1]Université de Lyon, INSERM U890, Université Jean Monnet, 42023 Saint-Etienne, France, [2]IRCM, Canada, [3]University of Toronto Faculty of Medicine, Canada, [4]University of St-Etienne, France, [5]INSERM Unit 890, France, [6]INSERM U890-Université de Lyon-Université Jean Monnet, Saint-Etienne, France

Bone sialoprotein (BSP) is highly expressed in early bone deposition and may be involved in primary bone mineralization. We previously showed that BSP-/- mice have

a mild secondary bone phenotype, and are responsive to mechanical and hormonal challenges. However, repair of a cortical bone defect, which involves primary bone deposition, is significantly delayed in these mice. To test whether the mutation more strongly affects newly layed bone, we investigated the role of BSP in a model of primary bone modeling.

Bone marrow was ablated by trans-epiphysis aspiration in the femora of BSP knockout (BSP-/-) and wild type (WT) mice. The femurs were analyzed through microtomography (μCT) and histomorphometry 7 (d7) and 14 days (d14) after ablation. At d7, μCT showed a vigorous new bone formation in the shaft of WT animals (BV/TV=30.2±5.0%, M±SEM, N=4), while medullary bone (MB) building was much reduced in mutants (10.0±0.9%, N=9, $p<0.001$ vs WT). At d14, MB volume was significantly decreased as expected in WT mice (9.8±2.1%, N=9, $p<0.001$), while it remained stable in the BSP-/-. Osteoid thickness and surface was higher in BSP-/- than in WT at d7 (OS/BS=3.6±0.8 vs 1.3±0.2%, N=4, $p<0.05$), suggesting delayed mineralization, while osteoclast surface et number was significantly lower in mutants (Oc.S/BS=8.4±0.8 vs 12.6±0.8%, N=4, $p<0.05$) at d14, during high MB resorption. At d7, mRNA expression of early osteoblast marker genes (runx2, osterix, alkaline phosphatase, osteopontin) did not differ between the two genotypes, while markers of terminal differentiation (MEPE, DMP1, osteocalcin) as well as RANKL and TRAP were significantly lower in mutants.

We investigated whether intermittent PTH treatment, which has been shown to stabilize MB volume in rats (Tissue Eng Part A, 14:237, 2008) could do the same in mice expressing or not BSP. MB volume in WT mice treated with PTH was 3x more abundant than in untreated controls at d8 (28.2±4.2 vs 11.4±2.7%, N=6, $p<0.01$), and 6X at d12 after ablation (39.3±7.6 vs 5.6±1.1%, N=7, $p<0.001$). In contrast, no significant difference between PTH-treated and controls was observed at either time-point in BSP-/- mice (d8: 9.9±3.0 vx 6.3±1.1% ; d12 : 13.7±3.4 vs 7.0±1.0%, N=7). At d12, the MB formed after marrow ablation is partly remodeled (presence of double labeled surfaces after tetracyclin injection). PTH significantly increased the bone formation rate of remodeled surfaces in both genotypes, while it reduced osteoclast numbers and surfaces in the MB of WT (Oc.S/BS=4.5±0.5 vs 10.3±1.2%, N=6, $p<0.001$, d12), but not BSP-/- mice (7.6± 1.0 vs 7.3±0.6%, N=7, d12).

In conclusion, mMB formation after marrow ablation, its subsequent resorption and its stabilization by PTH are blunted in BSP-/- mice. Overall, our findings demonstrate a crucial role for BSP in primary ossification, which has long been suspected for mineralization but here extends to bone deposition and modeling/remodeling.

***Disclosures: Luc Malaval**, None.*

1183

Collagen Extracellular Matrix (ECM) Assembly Dynamics in Living Osteoblasts and Generation of a Collagen-GFP Transgenic Mouse. Suzan Kamel*[1], Yongbo Lu[2], Patricia Veno[1], Charlotte Phillips[3], Vladimir Dusevich[1], Sarah Dallas[4]. [1]University of Missouri, Kansas City, USA, [2]Texas A&M University System Health Science Center, USA, [3]University of Missouri-Columbia, USA, [4]University of Missouri - Kansas City, USA

Type I collagen is the major ECM protein in bone. It is a heterotrimer of two α1(I) and one α2(I) chains encoded by separate genes, mutations in which cause osteogenesis imperfecta (OI). Although much is known about post translational modification of collagen chains and their intracellular assembly into trimers, less is known of the hierarchical process by which collagen trimers are assembled into fibrils followed by larger collagen fibers. To further understand this process and its regulation, live imaging approaches were used to examine collagen assembly dynamics in living bone cells.

We have previously reported the generation of green and red fluorescent collagen probes, in which GFP or mCherry were placed in the pro-α2(I) N-terminus, as well as their stable expression in MLO-A5 late osteoblasts and MEF cells. Further validation of the GFP and mCherry probes confirmed that they are secreted and assembled into extracellular fibrils upon addition of ascorbate, they are localized by immunoEM in banded collagen fibrils and can be co-immunoprecipitated with α1(I) chains from conditioned media or salt extracts of the ECM, suggesting heterotrimer formation. Live imaging of stably expressing MLO-A5 cells showed that assembly of a well organized collagen fiber network is a highly dynamic process, involving migration of collagen to the cell periphery in vesicle-like structures, abundant cell and fibril motions and protrusions of cell processes that appear to align with forming fibers. Imaging of fiber assembly in co-cultures of red collagen and green collagen expressing cells showed co-deposition of red and green collagen within the same fibers, suggesting that multiple cells provide contributions to form fibers. Dual imaging of fibronectin and collagen showed initial deposition of collagen in association with fibronectin followed by turnover of fibronectin, leaving the collagen in place. To examine collagen dynamics in vivo, transgenic mice were generated expressing α2(I)-GFP-collagen driven by the 3.6kb Col1a1 promoter. These mice show GFP-collagen in bone ECM, tail tendon, and intervertebral discs and appear otherwise normal. These data underscore the dynamic nature of collagen assembly, the cooperation of multiple cells in assembly of complex fibril networks and the integration of collagen assembly with fibronectin, which acts as a temporary scaffold. Collagen-GFP mice will allow further delineation of collagen assembly dynamics in vivo and in models of OI.

***Disclosures: Suzan Kamel**, None.*

1184

PHOSPHO1 Is Essential for Mechanically Competent Mineralization and Avoidance of Greenstick Fractures. Carmen Huesa*[1], Manisha Yadav[2], Mikko Finnila[3], Simon Goodyear[4], Simon Robins[5], Katherine E. Tanner[6], Richard Aspden[5], Jose Luis Millan[2], Colin Farquharson[7]. [1]Roslin instituteUniversity of Edinburgh, United Kingdom, [2]Burnham Institute for Medical Research, USA, [3]Department of Medical Technology, University of Oulu, Finland, [4]University of Aberdeem, United Kingdom, [5]University of Aberdeen, United Kingdom, [6]Mechanical Engineering, University of Glasgow, United Kingdom, [7]Roslin Institute, University of Edinburgh, United Kingdom

Bone mineralization is mediated by promoters and inhibitors, of which tissue-nonspecific alkaline phosphatase (TNAP) is recognized to play a central role. TNAP promotes mineralization by restricting the concentration of the calcification inhibitor inorganic pyrophosphate (PPi). TNAP hydrolyses ATP to produce inorganic phosphate (Pi), but the generation of Pi and hydroxyapatite (HA) is unchanged in newborn $TNAP^{-/-}$ mice suggesting the involvement of other phosphatases. A bone specific phosphatase, PHOSPHO1, is hypothesized to be required for Pi generation and the formation of HA within matrix vesicles. $Phospho1^{-/-}$ mice present greenstick fractures in long bones and rib cages at birth. Fracture callus, curved long bones and scoliosis are observed from 10-days of age. Bones from $Phospho1^{-/-}$ mice are undermineralized as determined by BMD and ash weight measurements.

The aim of this study was to investigate the mechanical and material properties of $Phospho1^{-/-}$ bones to confirm the enzyme's specific role in HA formation.

Long bones from 7 wild-type (wt) and 9 $Phospho1^{-/-}$ 1 month old male mice were examined. $Phospho1^{-/-}$ bones did not fracture during 3- point bending but deformed plastically. With dynamic loading nanoindentation the elastic modulus and hardness of $Phospho1^{-/-}$ tibia were significantly lower than wt tibia ($P<0.005$). Raman microscopy showed significantly lower mineral:matrix ratios ($P<0.05$) and lower CO_3^{2-} substitutions ($P=0.005$) in $Phospho1^{-/-}$ tibia. The altered DHLNL:HLNL and PYD:DPD collagen crosslink ratios indicated possible changes in lysyl hydroxylase 1 activity and/or bone mineralization status. Histomorphometry revealed decreased alizarin red staining of trabecular bone and osteoidosis ($P=0.0001$) but no significant differences in the numbers of osteoblasts and osteoclasts. Bone formation (P1NP) and resorption (RatLaps™) markers measured in serum using ELISA were both increased in $Phospho1^{-/-}$ mice ($P<0.001$) indicating higher bone turnover.

In summary these data indicate that $Phospho1^{-/-}$ bones are hypomineralized and, consequently, are softer and more flexible. An inability to withstand physiological loading may explain the deformations noted. We hypothesize that this phenotype is due to the reduced availability of Pi to form HA during mineralization, creating an under-mineralized yet active bone. A higher bone turnover may indicate an attempt to remodel a mechanically competent bone capable of withstanding physiological load.

***Disclosures: Carmen Huesa**, None.*

1185

A Novel Mechanism for Modulation of Canonical Wnt Signaling by the ECM Component, Biglycan. Agnes Berendsen*[1], Tina Kilts[1], Marian Young[2]. [1]NIDCR, National Institutes of Health, USA, [2]National Institutes of Health, USA

Canonical Wnt signaling plays essential roles in the control of bone mass. So far, the role of ECM components of skeletal tissues in modulating Wnt signaling is largely unknown. The ECM of mineralized tissues is enriched in the proteoglycan biglycan (Bgn), which is composed of a core protein and two chondroitin sulfate chains. Previous studies showed that mice deficient in Bgn have a reduced growth rate and decreased bone mass. Considering that Bgn is usually localized in a pericellular space, we hypothesized that it could modulate Wnt availability and function at the cell surface where these proteins are co-localized. To test this possibility, we studied the effects of the canonical Wnt pathway activator, Wnt3a, on the activity of WT and Bgn-KO preosteoblasts obtained from the calvaria of newborn mice. Wnt3a induced nuclear localization of β-catenin in both cell types, indicating activation of the pathway in these cells. However, the Wnt3a-induced expression of several Wnt target genes, including Cyclin D1, Axin2, Myc, WISP1, and MMP14, was blunted in Bgn-KO cells. Bgn-KO cells treated with exogenous Wnt3a had less Wnt3a retained in the cell layer compared to WT cells. Furthermore, the Wnt3a-induced levels of phosphorylation of LRP6 (which is required for activation of β-catenin) appeared reduced in Bgn-KO cells. In addition to a loss of function analysis of Bgn, we studied the effect of adding recombinant Bgn protein on Wnt signaling in cells. Addition of Bgn to HEK cells stably transfected with a luciferase reporter of β-catenin-mediated transcriptional activity, dose-dependently increased the Wnt3a-induced reporter activity. In contrast, activation of the Wnt pathway by LiCl, an inhibitor of intracellular β-catenin degradation, was not affected in the presence of Bgn confirming that the proteoglycan's regulation of Wnt signaling works extracellularly. Bgn depleted of the two chondroitin sulfate chains was also effective in enhancing Wnt signaling indicating that the functional sites likely reside in the core protein and not in the GAG chains. IP analysis revealed that Bgn core protein can prevent the pull-down of Wnt3a, which suggests a direct interaction between these proteins. We propose that the core protein of Bgn may serve as a reservoir for Wnt in the pericellular space and modulate Wnt availability for activation of the Wnt signaling pathway. This study identifies a new role for the ECM protein Bgn in modulating canonical Wnt signaling.

***Disclosures: Agnes Berendsen**, None.*

1186

Collagen XXIV Regulates Osteoblast Differentiation Through Crosstalk of STAT1/Smad7 and TGF-β/Smad3 Signal Pathways. Gang Liang, Shuying Yang*. State University of New York at Buffalo, USA

Collagen XXIV (*Col24α1*) is a new fibrillar collagen, which contains an amino-terminal domain closely related to those of the types V and XI collagen subunits. It is known that mouse col24α1 is predominantly expressed in the forming skeleton of the mouse embryo and the trabecular bone and periosteum of the newborn mouse. However, the role and mechanism of Col24α1 in bone development and formation remain largely unidentified. To gain insight into Col24α1 signaling in osteoblast differentiation, we analyzed expression pattern of Col24α1 gene by Northern blotting and found that col24α1 highly expresses in bone tissue. RT-PCR result further showed that Col24αl transcripts gradually increase during differentiation of osteoblast cells and are undetectable in BMMs induced osteoclast like cells. To demonstrate the importance of Col24α1 function in osteoblast differentiation, we used lentivirus-mediated RNA interference (RNAi) technology to silence (knockdown) Col24α1 expression in MC3T3-E1 clone 4 induced with ascorbic acid (AA)/ β-glycerol-phosphate (β-g-p). In contrast to wild-type cells, we found that the cells infected with Col24α1 shRNA lentivirus contain undetectable Col24α1 protein. Silence of Col24α1 expression significantly decreased ALP activity and cell mineralization at 7days and 14days after induced by AA/ β-g-p. RT-PCR results showed that Col24α1 silencing markedly inhibits expression of mature osteogenic marker such as osteocalcin and Runx2. Transcription of Smad3, the key transcription factor of TGF-β signal pathway, was dramatically decreased; on the contrary, Smad7, a TGFβ type 1 receptor antagonist with function of blocking access to SMAD3, was markedly increased in Col24α1 siRNA-treated MC3T3-E1 cells. Col24α1 contains KGD motifs. Previous reports have shown that KGD-containing peptides is specific and potent inhibitors of intergrin alpha IIb beta 3 function, which inhibits platelet activation and platelet PDGF-AB release via STAT1 signaling pathway, and STAT1 signaling negatively regulates Smad7 expression. Interestingly, we found that silence of Col24α1 increases PDGF-B and STαT1 expression in osteoblast cells. Thus, these results suggested that Col24α1 plays an important role in osteoblast differentiation and activation likely through crosstalk of STAT1/Smad7 and TGF-β/Smad3 signal pathways. Col24α1 knockout model is being generated for further analyzing the role and mechanism of Col24α1 bone development and formation *in vivo*.

***Disclosures: Shuying Yang**, None.*

1187

Activation Function-1 in Estrogen Receptor-α but not Endogenous Estradiol is Required for the Osteogenic Response to Mechanical Loading in Female Mice. Sara Windahl*[1], Leanne Saxon[2], Anna Borjesson[1], Cecilia Engdahl[1], Klara Sjogren[1], M Christina Antal[3], Andrée Krust[3], Pierre Chambon[3], Lance Lanyon[2], Joanna Price[4], Claes Ohlsson[1]. [1]Centre for Bone & Arthritis Research, Sweden, [2]Royal Veterinary College, United Kingdom, [3]Institut de Génétique et de Biologie Moléculaire et Cellulaire, INSERM, France, [4]University of Bristol, United Kingdom

It is hypothesised that with the loss of estrogen, there is a decline in estrogen receptors (ERs) in bone cells, and it is these receptors that are partially responsible for signalling the bones' adaptive response to loading. We have previously shown a reduced response to loading in mice lacking ERα (Lee et al Nature, 2003, 424:389) however these mice still expressed a truncated ERα protein. The aims of the present study were to determine the relative roles of endogenous estradiol and different domains of ERα in the osteogenic response to mechanical loading.

At 17 weeks of age, the right tibia of 8-14 mice in each experimental group were subjected to short periods of cyclic compressive loading three times a week for two weeks (40 cycles, peak strain 1400με). Computed tomography was used to assess the osteogenic response in the cortex of the loaded (right) versus the non-loaded (left) tibia. To evaluate the role of endogenous estradiol, we compared the osteogenic response in intact (sham) and ovariectomized (ovx) mice. Loading increased cortical bone area to a similar extent in sham and ovx mice (sham 24.0±2.2%, ovx 25.7±2.3%). We next evaluated the role of ERα in the loading response using ERα-/- mice with a complete ERα inactivation (Dupont et al Development 2000, 127:4277). The ERα-/- mice displayed a 68±11% ($p<0.01$) lower loading-related increase in cortical area compared with wild type (WT) mice (WT 24.0±2.2%, ERα-/- 7.7±2.6%). The loading-related increase in cortical area was similarly reduced in OVX ERα-/- mice (-51%, $p<0.01$) mice compared with ovx WT mice. To characterize which domains of ERα are involved in this cortical bone response to mechanical loading, mice with specific inactivation of either activation function domain 1 (AF-1; ERαAF-1♂) or AF-2 (ERαAF-2♂) were evaluated. The ERαAF-1♂ mice displayed a 37±8% ($p<0.05$) lower response to mechanical loading in cortical area compared with WT mice while the cortical bone response was mainly unaffected in the ERαAF-2♂ mice compared with WT mice (-11±14%, non significant). These findings demonstrate that AF-1 in ERα but not endogenous ovarian-derived estradiol is required for the osteogenic response to mechanical loading in female mice. We propose that ERα modulates the osteogenic response to mechanical loading in cortical bone in a ligand-independent manner.

***Disclosures: Sara Windahl**, None.*

1188

The Role of Estrogen Receptor-α AF-1 and AF-2 for the Effects of Estradiol in Bone. Anna Borjesson*[1], Sara Windahl[1], Marie Lagerquist[2], Cecilia Engdahl[3], Baruch Frenkel[4], Klara Sjögren[1], Jenny Kindblom[2], Maria Cristina Antal[5], Andrée Krust[5], Pierre Chambon[5], Claes Ohlsson[1]. [1]Centre for Bone & Arthritis Research, Sweden, [2]Sahlgrenska University Hospital, Sweden, [3]Centre for Bone & Arthritis Researc, GU, Sauhlgrenska Academy, Medicine, Sweden, [4]University of Southern California, USA, [5]IGBMC, France

Estrogen exerts a variety of important physiological effects. The bone-sparing effect of estrogen is primarily mediated via estrogen receptor-α (ERα), which stimulates target gene transcription through two activation functions (AFs), AF-1 in the N-terminal and AF-2 in the C-terminal, ligand binding domain. We evaluated the involvement of ERα AF-1 and ERα AF-2 in the effects of estrogen in bone, as well as the immune system and the uterus. Mouse models with inactivation of total ERα (ERα-/-), AF-1 (ERαAF-10) or AF-2 (ERαAF-20) were ovariectomized (ovx) and then treated with either vehicle or estradiol (E2). Both ERαAF-10 and ERαAF-20 mice have a normal expression of ERα, except for the specific deletions of AF-1 and AF-2, respectively. Treatment of ovx mice with E2 increased the trabecular BMD by 334±36% and the cortical thickness (CT) by 27±2% ($p<0.01$). Neither the trabecular nor the cortical bone responded significantly to the E2 treatment in ERα-/- (Trabecular BMD 3±3%, CT -1±11%; of WT E2 response) or ERαAF-20 mice (Trabecular BMD 2±3%, CT -8±7%; of WT E2 response). ERαAF-10 mice displayed a normal estrogenic response in cortical bone (CT 76±11% of WT E2 response, $p<0.01$) but not in trabecular bone (Trabecular BMD 8±3% of WT E2 response, non significant). Although E2 treatment increased bone mass, uterine weight and liver weight, and reduced thymus weight and the frequency of CD19+ cells in bone marrow in ovx WT mice, no effect was seen on these parameters in ovx ERα-/- or ERαAF-20 mice. The effects of E2 in ovx ERαAF-10 mice were tissue dependent, with no response on thymus weight, a weak response on uterine weight (27% of WT E2 response), an intermediate response on bone marrow cellularity and the frequency of bone marrow CD19+ lymphocytes (30-60% of WT E2 response), and a normal response on liver weight (>75% of WT E2 response). In conclusion, ERα AF-2 is required for the estrogenic response in all the parameters evaluated, including the protection of both trabecular and cortical bone. The requirement for AF-1, on the other hand, is tissue specific, with an indispensable role for AF-1 in the E2 response in trabecular, but not cortical bone. These findings demonstrate that the role of ERα AF-1 is tissue dependent and selective ER modulators with minimal activation of ERαAF-1 could, therefore, exert tissue specific effects.

***Disclosures: Anna Borjesson**, None.*

1189

Physiological Impact of Osteoblastic Androgen Receptor in Androgen Anabolic Action. Yuuki Imai*[1], Shino Kondoh[1], Min Ni[2], Kazuki Inoue[1], Takahiro Matsumoto[1], Kunio Takaoka[3], Shigeyuki Wakitani[4], Myles Brown[2], Shigeaki Kato[5]. [1]The University of Tokyo, Japan, [2]Dana-Farber Cancer Institute, USA, [3]Osaka City University Medical School, Japan, [4]Osaka City University Graduate School of Medicine, Japan, [5]University of Tokyo, Japan

Sex steroid hormones play important roles to maintain bone tissues through various mechanisms. It has been clarified that estrogen exerts osteo-protective estrogen action by inducing osteoclast apoptosis through estrogen receptor α (ERα) in both osteoclast and osteoblast. On the other hand, it remains unclear whether androgen directly targets on bone tissue, since male androgen receptor (AR) knockout (KO) mice exhibited bone loss together with systemic endocrine defects. To clarify physiological impact of AR in bone, we generated and analyzed osteoblast specific KO (ObARKO) mice using Col1a1 2.3 kb Cre and AR flox mice. ObARKO did not exhibit systemic endocrine defect regardless of gender. However, male, but not female, ObARKO mice exhibited decreased bone mineral density (BMD) in diaphysis of long bones and calvaria. Micro CT analyses showed decreased cortical thickness in male ObARKO. Moreover, androgen deficiency induced by orchidectomy (ORX) decreased bone mass only in the AR wild-type, not in ObARKO mice. Likewise, ORX-induced bone loss could be recovered by a DHT treatment only in the wild-type mice. Furthermore, by a bone histomorphometry, no apparent change was found in static parameters, however, dynamic parameters such as MAR and BFR were reduced in both cortical and trabecular bone of ObARKO. These results indicated that AR in osteoblasts mediates androgen anabolic actions.

Therefore, to characterize the impact of AR in osteoblasts, a Chromatin Immunoprecipitation sequencing (ChIP-seq) was performed using a next generation single molecule high-throughput sequencer for an osteoblastic cell line, MC3T3E1, treated with DHT. ChIP-Seq analysis revealed 4018 AR binding sites in the mouse genome of MC3T3E1 cells with p value cut off of e-5. About 7.7% and 5.8% of binding sites were be mapped to within 10 kb upstream of the transcriptional start site and 10kb downstream of the transcriptional termination site. Moreover, when ChIP-seq data was merged with the results of gene expression microarray data sets, several genes were identified as candidates of AR direct target genes in osteoblasts.

Taken together, further characterization of AR target genes in osteoblasts to elucidate more precise molecular mechanisms of anabolic actions of androgen will be presented.

***Disclosures: Yuuki Imai**, None.*

1190

Increased Bone VDR Impairs Osteoclast and Osteoblast Activities with Low Dietary Calcium in a Mouse Model. Nga Lam*[1], Peter O'Loughlin[2], Rebecca Sawyer[1], Howard Morris[1], Paul Anderson[1]. [1]Endocrine Bone Research, SA Pathology, Australia, [2]Endocrine Bone Research, SA Pathology, Australia

The vitamin D receptor (VDR) in osteoblasts can mediate mineralization and signal osteoclastogenesis in vitro. While the role for osteoblast VDR in vivo is less clear, the osteoblast-specific VDR over-expressing transgenic mouse (OSVDR) has increased bone volume due to reduced RANKL-mediated osteoclastogenesis and increased bone formation. While the OSVDR bone phenotype can be diminished with reduced dietary calcium, the cellular and molecular mechanisms for this are unclear. Six week old female wild-type (WT) and OSVDR mice were fed either low (0.1%) (WT-LCa, OSVDR-LCa) or high (1%) calcium diet (WT-HCa, OSVDR-HCa) for 4 months, after which animals were killed for biochemical, molecular, histological and structural analyses. In OSVDR-HCa mice, both tibial trabecular and cortical bone volumes were approximately 20% and 15% greater respectively than WT-HCa levels ($P<0.001$). WT-LCa mice did not significantly reduce bone volume compared to WT-HCa mice. In contrast, OSVDR-LCa mice resulted in lower bone volume compared to OSVDR-HCa mice ($P<0.05$). The reduced bone volume in OSVDR-LCa mice occurred without increased serum PTH or induction of RANKL-mediated osteoclastogenesis. Furthermore, the osteoclast marker NFATc1 expression was lower than levels observed in WT-LCa mice ($P<0.001$), suggesting OSVDR mice are less capable of generating osteoclasts under low calcium stress. Importantly, reduced bone volume in OSVDR-LCa mice was also associated with reduced mineralising surface and markedly reduced Runx2, ALP, Col1, and osteocalcin mRNA levels compared to all other groups ($P<0.05$). Thus, unlike WT mice, when OSVDR mice were fed a low calcium diet, bone loss occurs due to a failure of mineralisation rather than increased bone resorption. Interestingly, OSVDR-LCa mice had markedly reduced serum 1,25D levels compared to WT-LCa mice ($P<0.001$), which, as serum PTH was unchanged is likely due to the observed higher serum FGF23 ($P<0.05$). Thus, inappropriately low 1,25D levels in OSVDR-LCa mice may lead to reduced induction of intestinal calcium absorption, reduced osteoclastogenesis and reduced bone mineralisation. In summary, under conditions of low dietary calcium, increased sensitivity to vitamin D in osteoblasts results in direct or indirect suppression of osteoclast and osteoblast activities, increased FGF23 levels and inhibition of renal 1,25D synthesis and possibly intestinal calcium absorption, reducing bone mineral volume.

***Disclosures: Nga Lam**, None.*

1191

Androgen Prevents Hypogonadal Bone Loss Primarily Through Osteocyte-mediated Inhibition of Resorption and is not Anabolic. Anthony Semirale[1], Xiao-Wei Zhang[2], Dawn Olson[3], Urszula Iwaniec[3], Russell Turner[3], Kristine Wiren*[4]. [1]Oregon Health Sciences University, USA, [2]VA Medical Center & OHSU, USA, [3]Oregon State University, USA, [4]Veterans Affairs Medical Center, Oregon Health & Science University Research Ser, USA

Androgen receptor (AR) is expressed throughout the osteoblast lineage, with the highest levels in osteocytes. Using AR-transgenic (tg) mice, we assessed the ability of enhanced androgen sensitivity in mature osteoblasts/osteocytes to ameliorate hypogonadal loss using two different paradigms of steroid replacement following orchidectomy (ORX) in male wild-type (WT) or AR-tg mice. ORX was performed at 3 months with DHT treatment delayed until 5 months (therapeutic, lower turnover), or at 5 months with immediate DHT replacement (preventive, higher turnover), both with treatment for 6 weeks. DXA, microCT and serum analysis were performed. In the preventive model, ORX significantly reduced BMD and BMC in both genotypes compared to sham and DHT was effective at prevention of loss only in AR-tg mice with overexpression in mature osteoblasts. In the therapeutic model, WT mice lost bone mass compared to sham while AR-tg mice lost less bone, and delayed DHT treatment provided no benefit in either genotype. MicroCT analysis of mid-shaft cortical bone in both genotypes generally showed reduced cortical volume and thickness after ORX in both paradigms, changes which were generally prevented with immediate DHT replacement in WT but not AR-tg mice, likely due to expansion of marrow volume. Delayed DHT was ineffective at restoring whole bone volume in either genotype. In cancellous bone, the effect of intevention was more robust. Consistent among 3 sites measured, ORX resulted in significant losses in bone volume/tissue volume (BV/TV) in both genotypes in both paradigms. With delayed treatment, there was no net effect of DHT to restore BV/TV, but when administered at the time of ORX, DHT completely prevented trabecular loss in both genotypes. In both paradigms, trabecular number was decreased with increased spacing with ORX, and improvement was seen with immediate DHT replacement but not after the 2 month delay in both genotypes. Serum osteocalcin and CTX levels revealed anti-resorptive effects of DHT when turnover was high, consistent with DXA and microCT results. In summary, androgen therapy is effective for the prevention of bone loss primarily through its antiresorptive properties, but shows little anabolic action as a therapeutic strategy to restore lost bone as only small improvements are seen. Increased sensitivity in mature osteoblasts/osteocytes does not increase anabolic activity and instead mediates antiresorptive responses.

***Disclosures: Kristine Wiren**, None.*

1192

The 1,25D3-MARRS Receptor/PDIA3/ERp57 is Required for Intestinal Cell Phosphate Uptake. Ilka Nemere*[1], Natalio Garbi[2], Gunter Hammerling[2]. [1]Utah State University, USA, [2]Division of Molecular Immunology, German Cancer Research Center DKFZ, Germany

We have crossed $ERp57^{lfx/flx}$ mice with commercially available mice expressing villin-driven cre-recombinase. Enterocytes isolated from 3-4 wk old littermate (LM) male mice responded to $1,25(OH)_2D_3$ with enhanced phosphate uptake, relative to corresponding controls within 1 min of addition, whereas in cells from targeted knockout (KO) mice the response was severely blunted.

Unlike chick enterocytes, mouse enterocytes did not respond to phorbol ester with enhanced phosphate uptake. However, forskolin, which does not stimulate phosphate uptake in chick intestinal cells did so in enterocytes isolated from either young male LM or KO mice. Intestinal cells isolated from young female LM mice also responded to $1,25(OH)_2D_3$ with enhanced phosphate uptake within 5 min of hormone addition, whereas cells from KO mice did not. Forskolin also stimulated phosphate uptake in enterocytes from either young female KO or LM mice. As with intestinal cells from adult male chickens or rats, cells from adult (8wk) male LM mice lost the ability to respond to $1,25(OH)_2D_3$ with enhanced phosphate uptake. In contrast, intestinal cells from adult female LM mice did respond with enhanced phosphate uptake within 1 min of steroid hormone addition, relative to corresponding controls, and the magnitude of the effect was greater than that observed in enterocytes of young females. Cells isolated from young or adult male or female LM mice failed to respond to $1,25(OH)_2D_3$ with enhanced PKC activity. Finally, we have previously reported that mouse enterocytes have cell surface VDR; however preincubation of such cells with anti-VDR antibodies demonstrated that the classical receptor is not involved in the rapid $1,25(OH)_2D_3$-stimulated uptake of phosphate.

***Disclosures: Ilka Nemere**, None.*

1193

FSH Markedly Increases Bone Mass in Mice via Ovary-dependent Mechanisms. Robert Kalak[1], Charles Allan[1], Kirsten McTavish[1], Colin Dunstan[2], Hong Zhou*[3], David Handelsman[1], Markus Seibel[3]. [1]ANZAC Research Institute, The University of Sydney, Australia, [2]University of Sydney, Australia, [3]Bone Research Program, ANZAC Research Institute, The University of Sydney, Australia

We previously demonstrated that pituitary-independent, transgenic expression of human FSH (tgFSH) increased trabecular bone volume (BV/TV) in female mice (1), contrasting with previous claims that elevated FSH levels cause bone loss (2). Using the tgFSH model to further study the putative FSH actions on bone, we determined i) the dose-dependent effects of FSH in vivo; ii) tgFSH activity on bone in isolation of LH actions, using hypogonadal (hpg) female mice lacking endogenous GnRH and FSH/LH secretion, and iii) the dependence of FSH effects on the presence of intact ovaries, using ovariectomised tgFSH mice.

At circulating levels ranging between 6 and 44 IU/L, human tgFSH dose-dependently increased trabecular bone volume fraction as assessed by μCT. Higher tgFSH levels increased tibial BV/TV by 42-fold and 13-fold in tgFSH hpg and tgFSH non-hpg females (Fig 1), respectively, vs non-tg controls($p<0.001$ for both). Vertebral BV/TV was increased 4-fold ($p<0.001$) in tgFSH females regardless of the presence of LH. Osteoblast surface (Ob.S/BS) was increased in tibial trabecular bone by 1.7-fold ($p<0.001$) and 1.6-fold ($p<0.005$) in tgFSH non-hpg and tgFSH hpg vs control females, respectively. Very high tgFSH levels stimulated de novo bone formation, filling marrow spaces with woven rather than lamellar bone, resembling bone formation induced by strong systemic anabolic stimuli. Uterine weights indicated normal or reduced estradiol activity in tgFSH non-hpg or tgFSH hpg females compared to wildtype mice. However, positive correlations of tibia BV/TV with serum tgFSH ($r=0.65$, $p<0.001$), testosterone ($r=0.62$, $p<0.001$) and inhibin A ($r=0.43$, $p<0.005$) levels in tgFSH females suggests ovarian-derived factors are associated with altered bone dynamics. Ovariectomy completely abolished tgFSH-induced bone formation (Fig 1), proving an ovary-dependent FSH pathway. Furthermore, RT-PCR analysis did not detect any FSH receptor mRNA expression in bone or cultured osteoblast or osteoclast RNA preparations, suggesting FSH does not directly act on bone via local FSH receptor pathways.

Our results indicate that FSH has anabolic effects on bone independent of LH activity. The mechanism of action involves the ovary with no evidence of any direct FSH effects on bone cells.

1. Kalak R., et al. (2008) J Bone Miner Res. 23, S63 Suppl.
2. Sun L, et al. (2006) Cell 125: 247-60.

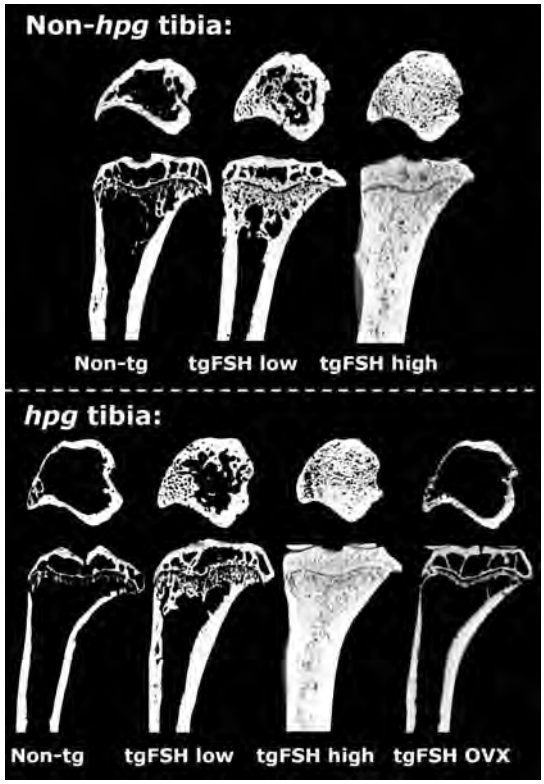

Fig 1

***Disclosures: Hong Zhou**, None.*

1194

Intestinal Calcium Absorption Regulates Serum Calcium by Compensatory Modifications in Bone Mass and Mineralization. Liesbet Lieben*[1], Ritsuko Masuyama[1], Karen Moermans[3], Jan Schrooten[4], Peter Baatsen[5], Roger Bouillon[1], Geert Carmeliet[1]. [1]Laboratory of Experimental Medicine & Endocrinology, Katholieke Universiteit Leuven, Belgium, [2]Department of Metallurgy & Materials Engineering, Katholieke Universiteit Leuven, Belgium, [3]Center for Human Genetics/VIB, Katholieke Universiteit Leuven, Belgium

Calcium is vital to multiple cellular functions and is a crucial component of the mineral phase of bone. Intestinal calcium absorption is critical for calcium acquisition and is mainly controlled by vitamin D [$1,25(OH)_2D_3$]. To genetically confirm the importance of active intestinal calcium absorption, we generated mice with a specific deletion of the vitamin D receptor (VDR) in the intestine (Vdr^{int-}) by mating *Vdr* floxed mice with Villin-Cre mice.

Intestinal calcium absorption was impaired in Vdr^{int-} mice, but serum calcium levels remained normal, which contrasts with the severe hypocalcemia observed in systemic *Vdr* null mice. This finding implies compensatory mechanisms in Vdr^{int-} mice, likely activated by the increase in serum parathyroid hormone (PTH) and $1,25(OH)_2D_3$. Indeed, renal calcium reabsorption was increased and the calcium content of bone was reduced to minimal levels. Hence, Vdr^{int-} mice showed normal skeletal growth, but bone gain was compromised from weaning on due to a hormonally-mediated increase in bone turnover. The high rate of bone modeling was accompanied by osteocyte maturation defects; scanning electron microscopic (SEM) and histological analyses showed that Vdr^{int-} osteocytes were larger with fewer processes and with impaired expression of differentiation markers. In addition to the reduced bone mass, bone mineralization was compromised: excess osteoid was present on all bone surfaces and surrounding the osteocytes. Moreover, the mineral content of the newly formed cortical bone was reduced in Vdr^{int-} mice shown by backscattered SEM. Given that serum calcium and phosphate levels were normal in Vdr^{int-} mice, the decrease in mineral content suggests that mineralization is inhibited. Indeed, increased mRNA levels of mineralization inhibitors, including *Osteopontin* and the pyrophosphate transporter *Ank*, were detected in bones of Vdr^{int-} mice, and *in vitro* data showed a direct regulation of these markers by $1,25(OH)_2D_3$. Bone mass accrual was thus compromised to preserve normocalcemia in Vdr^{int-} mice by increasing bone turnover and decreasing mineralization and these adaptations resulted in bone fractures.

In conclusion, intestinal *Vdr* inactivation impaired intestinal calcium absorption and triggered an increase in PTH and $1,25(OH)_2D_3$, which prevented hypocalcemia, but severely impaired calcium deposition in bone. These findings underline the importance of active intestinal calcium absorption for bone, even during normal calcium intake.

***Disclosures: Liesbet Lieben**, None.*

1195

Resistance to Bone Loss Through Altered Stem Cell Physiology in CMKLR1-Deficient Mice. Christopher Sinal, Shanmugam Muruganandan*. Dalhousie University, Canada

Previously, we reported that decreasing the expression of chemokine like receptor-1 (CMKLR1) in bone marrow stromal stem cells increases osteoblastogenesis in vitro through the abrogation of adipogenesis (J. Bone Miner. Res. 22(2):222-234). In the present study, we examined bone formation in mice deficient for CMKLR1 expression in vivo. A significant increase in bone mineral densities of both homozygous and heterozygous CMKLR1-deficient mice was observed at 16 weeks of age. To induce bone loss, we utilized a diabetic osteopenia mouse model 60 days after the administration of streptozotocin (40 mg/kg, i.p. for 5 days). Bone loss was monitored by Dual-Energy X-Ray Absorptiometry (DEXA), microcomputed tomography (μCT), histological and biochemical analyses. Unexpectedly, heterozygous but not homozygous CMKLR1-deficient mice exhibited a significant and marked resistance to bone loss in both DEXA and μCT analyses. Consistent with this, bone marrow stromal stem cells (BMSCs) derived from heterozygous but not homozygous CMKLR1-deficient mice exhibited a shift to osteoblast phenotype characterized by spontaneous osteoblast differentiation, formation of mineralized nodules and markedly elevated secretion of osteocalcin into the media even in the absence of any differentiation inducer. Furthermore, the osteoblast transcription factors including osterix and runx2 and the osteoblast marker genes, alkaline phosphatase and type I collagen were found to be highly expressed in stem cells from heterozygous CMKLR1-deficient mice. A potentiation of IGF signaling through IGFBP3 was observed in the stem cells derived from heterozygous CMKLR1-deficient mice. Histological analysis revealed a marked induction of bone marrow adipogenesis in homozygous but not heterozygous CMKLR1-deficient animals possibly as a compensatory response to the loss of CMKLR1. These findings of differential stem cell phenotypes with enhanced bone formation in heterozygous vs. homozygous CMKLR1 deficiency suggest a role for CMKLR1 in bone marrow stem cell physiology. Complete loss of CMKLR1 could initiate compensatory adipogenic mechanisms for induced adipogenesis in the homozygous CMKLR1 knockout animals.

***Disclosures: Shanmugam Muruganandan**, None.*

1196

Membrane-type MMPs MT1-MMP and MT3-MMP are Essential for Postnatal Skeletal Homeostasis. Joanne Shi*, Mi-Young Son, Susan Yamada, Pamela Gehron Robey, Kenn Holmbeck. NIDCR, USA

Purpose: The membrane-type matrix metalloproteinases MT1-MMP and MT3-MMP are expressed at high levels in skeletal tissues, including skeletal stem cells, where they facilitate remodeling of unmineralized collagenous matrices such and type I, II and III collagen. Loss of MT1-MMP leads to a severe and progressive disease affecting remodeling of certain unmineralized cartilages and connective tissues associated with the bone and ultimately leads to premature death from fibrosis. In contrast, ablation of MT3-MMP affects skeletal development less severely, although deficient mice display reduced skeletal growth. However, the significance of MT3-MMP function is highlighted by the perinatal demise of MT1-MMP/MT3-MMP double-deficient mice, which display severe skeletal dysmorphism with cleft palate.

Methods: Due to the premature death of MT1-MMP deficient and MT1-MMP/MT3-MMP deficient mice, the role of these proteinases in skeletal homeostasis cannot be assessed. To overcome this impediment, we have generated mice amenable to conditional ablation of MT1-MMP in conjunction with MT3-MMP deficiency using a tamoxifen sensitive ablation strategy.

Results: We report here that postnatal ablation of MT1-MMP and MT3-MMP is compatible with sustained survival. The principal function of MT-MMP activity is therefore associated with proteinase substrate interactions in development and early postnatal growth. Loss of MT-MMP activity in adulthood does however lead to rampant loss of bone mass associated with vigorous osteoclastic activity and a severe progressive fibrosis due to collagen accumulation in skeletal and peri-skeletal tissues.

Conclusion: The results of our analyses demonstrate that MT-MMP activity is essential for viability and development of the skeleton. In addition, sustained postnatal MT-MMP activity is required for fibrosis surveillance and regulation of osteoclast activity in skeletal homeostasis in adulthood. These observations demonstrate the central role of MT-MMPs in pericellular matrix remodeling and signaling modulation in skeletal stem cells and their progeny.

***Disclosures: Joanne Shi**, None.*

1197

Transgenic Over-expression of Human TRPV6 in Intestine Increases Calcium Absorption Efficiency and Improves Bone Mass in Mice. Min Cui*, James Fleet. Purdue University, USA

TRPV6 is a calcium (Ca) channel proposed to mediate basal and 1,25 dihydroxyvitamin D-induced Ca absorption but recent findings in TRPV6 knockout mice suggest this may not be true. To further examine the role of TRPV6 in intestinal Ca absorption we generated transgenic (TG) mice with intestine-specific expression of flag-tagged human TRPV6 driven by the villin promoter. Two TG lines, FT1 (65

copies) and FT2 (6 copies), were characterized; TG mRNA expression was detected from duodenum to distal colon. FT1 mice developed hypercalcemia (15.2 mg/dl), hypercalciuria, bladder stones and systemic soft tissue calcification by 3 mo when fed a chow diet (0.9% Ca). To prevent hypercalcemia in FT1 mice, both FT1 and wild type (WT) mice were fed a 0.25% Ca diet from weaning to 8 wks. TG expression was still elevated in intestine (duodenal total TRPV6 mRNA 2000-fold higher, TRPV6 protein > 300-fold than WT) but serum Ca was only slightly elevated (10.8 mg/dl in FT1 vs. 9.1 mg/dl in WT). Active intestinal Ca absorption (serum $45Ca^{2+}$ accumulation 10 minutes after oral gavage) was increased by > 3-fold in FT1 mice while femur BMD was 26% higher than WT by DEXA. In addition, renal CYP24 mRNA was increased 16-fold and CYP27B1 mRNA was decreased by >95% while high TG expression reduced expression of the transcript for the natural mouse TRPV6 gene in all intestinal segments (<10% WT level). These effects indicate molecular attempts to compensate for high Ca absorption by suppressing vitamin D-regulated calcium absorption. High TG expression was also accompanied by an increase in calbindin-D9K mRNA in duodenum (14-fold) and jejunum (251-fold), suggesting an adaptation to buffer intracellular Ca levels resulting from high calcium absorption efficiency in FT1 mice. FT2 (low TG copy #) mice were indistinguishable from WT in phenotype when fed chow diet. To suppress natural TRPV6 expression, both FT2 and WT mice were fed a 2% Ca diet from weaning to 8 wks. Duodenal total TRPV6 mRNA was 30-fold higher than WT in FT2 mice. This was accompanied by increased serum Ca (11.8 mg/dl vs. 9.0 mg/dl in WT) and 9% higher femur BMD in FT2 mice. Our models demonstrate that TRPV6 is a functional calcium channel important for active intestinal Ca absorption.

***Disclosures: Min Cui**, None.*

1198

***Lrp5* is Required for *Sost* Deficiency Induced Mineral Apposition Rate Increases.** Jonathan Gooi*[1], Ina Kramer[2], Christine Halleux[1], Michaela Kneissel[1]. [1]Novartis Institutes for Biomedical Research, Switzerland, [2]Novartis Institutes for BioMedical Research, Che

Sclerostin, the osteocyte secreted Sost gene product, binds in vitro to Lrp5 and 6 Wnt co-receptors thereby inhibiting canonical Wnt signaling and thus providing a putative molecular mechanism for sclerostin action as a negative regulator of bone formation. To determine whether Sost and Lrp5 interact in vivo we generated Sost;Lrp5 double knockout (KO) mice. We reported previously that bone mass gain was blunted in the long-bones of Sost;Lrp5 double compared to Sost single mutant mice (Kramer et al., J Bone Miner Res 24 Suppl. 1). Here we analyzed the vertebral cancellous bone of 6.5-month-old mutant and wildtype mice by micro computed tomography and histomorphometry.

Sost deficient mice displayed increased cancellous bone volume (females (F): +224%, males (M): +93%) compared to wildtype (WT) mice. Consistently, trabecular number and thickness were dramatically increased. Aged Lrp5 deficient mice showed a moderate reduction in bone volume (Lrp5-/- F: -7%, M: -10%) and other structural parameters compared to WT controls. In heterozygous Sost KO mice bone volume was mildly increased indicating a gene dosage effect (Sost+/- F: +25%, M: +26%). Heterozygous Lrp5 KO mice presented with non-significant changes in bone volume (Lrp5+/- F: -10%, M: +3%). Yet, heterozygous loss of Lrp5 was sufficient to blunt the increase in bone mass induced by Sost deficiency (Lrp5+/-;Sost-/- F: -20% M: -21% compared to Sost-/-). Consistently, homozygous loss of Lrp5 further blunted the bone volume increases of Sost mutants (Lrp5-/-;Sost-/- F: -33%, M: -25% compared to Sost-/-). Evaluation of bone formation dynamics revealed that the blunting of the high bone mass phenotype of Sost deficient mice due to Lrp5 loss-of-function was related to abrogation of mineral apposition rate (MAR) increases. Sost deficient mice displayed a marked increase in MAR (Sost-/- F: +30%, M: +37%) compared to WT controls. Lrp5 single mutant mice had slightly decreased MAR (Lrp5-/- F: -13%, M: -6%). While heterozygous loss of Lrp5 only partially reduced Sost deficiency induced MAR increases (Lrp5+/-;Sost-/- F +24%, M: +17%), homozygous loss of Lrp5 completely abolished MAR increases (Lrp5-/-;Sost-/- F: -16%, M: -4%).

Together, our data demonstrate that Lrp5 is required for Sost deficiency induced increases in mineral apposition rates, reflecting indirectly osteoblastic matrix deposition and hence performance. Thus, Sost targets in part Lrp5 dependent bone anabolic pathways to control bone formation in vivo.

***Disclosures: Jonathan Gooi**, None.*
This study received funding from: Novartis

1199

Does Osteoporosis Therapy Invalidate FRAX® for Fracture Prediction? William Leslie*[1], Lisa Lix[2], Helena Johansson[3], Anders Oden[4], Eugene McCloskey[5], John Kanis[6]. [1]University of Manitoba, Canada, [2]University of Saskatchewan, Canada, [3]Swedish University of Agricultural Sciences, The Biomedical Center, Sweden, [4]Consulting statistician, Sweden, [5]University of Sheffield, United Kingdom, [6]University of Sheffield, Belgium

Ten-year fracture risk assessment with FRAX® is increasingly used to guide treatment decisions. Osteoporosis pharmacotherapy (OTX) reduces fracture risk, but the antifracture effect is greater than can be explained from the increase in BMD. Whether this invalidates predictions from FRAX is uncertain. METHODS: All women age 50 y or older at the time of baseline BMD testing performed during 1996-2008 with retrospectively calculated FRAX probability were included in the analysis (N=35,764). A provincial pharmacy database was used to identify OTX prior to BMD (mean 7.5 y of OTX information) and in the first year after BMD testing (OTX use after the first year was not available). The medication possession (MPR) was calculated for OTX use in the year after BMD testing. Women were categorized as untreated (no OTX in the year after BMD testing, no OTX in the year before BMD testing and <6 m cumulative earlier OTX use), high adherence current OTX users (MPR 0.80 or greater in the year after BMD testing), low adherence current OTX users (MPR < 0.80 in the year after BMD testing), and past users (no OTX in the year after BMD testing with OTX in the year prior to BMD or > 6 months earlier exposure). Ten year major osteoporotic fracture probability from FRAX (Canadian tool) was categorized as low (< 10%), moderate (10-20%), or high (> 20%) in accordance with national guidelines. Fractures outcomes to 10 y (mean 5.3) were established through linkage within a population-based provincial health data repository. For each risk category and OTX subgroup, observed ten year fracture risk was estimated using the Kaplan-Meier (KM) method. Calibration plots (predicted versus observed) were constructed for each OTX group. RESULTS: FRAX stratified major osteoporotic fracture risk in all OTX subgroups (all p<.001) with similar ROC area under curve (untreated 0.66, current OTX [MPR >80%] 0.67, current OTX [MPR <80%] 0.71, prior OTX 0.69; overall 0.70; all p<.001). There was a significant linear trend for higher major osteoporotic and hip fracture rates according to FRAX risk category for all OTX subgroups (all Cochran-Armitage p<.001). Calibration plots did not show significant differences for the four OTX subgroups (see Figure). In particular, there was close agreement in FRAX calibration for the untreated and most highly adherent current OTX users. CONCLUSION: FRAX continues to predict fracture risk in women currently or previously receiving OTX.

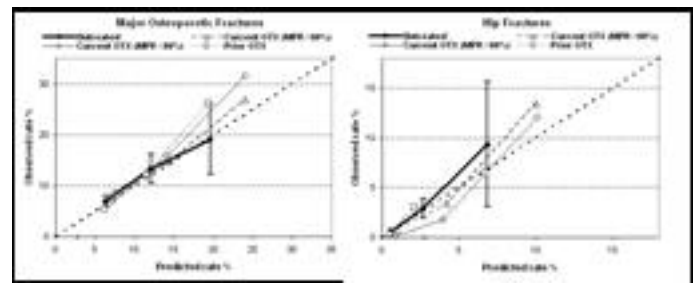

Figure. Predicted 10y fracture risk from FRAX (X-axis) vs observed 10y fracture rates (Y-axis).

***Disclosures: William Leslie**, None.*

1200

Non-Hip Femoral Fractures in Patients on Bisphosphonate Therapy: a Population-Based Study from Olmsted County, Minnesota. Alvin Ng*[1], Matthew Drake[2], Stephen Sems[2], Sara Achenbach[3], Elizabeth Atkinson[4], L. Joseph Melton[5], Bart Clarke[2]. [1]Mayo Clinic Division of Endocrinology, Diabetes, Metabolism, & Nutrition, USA, [2]Mayo Clinic College of Medicine, USA, [3]Mayo Clinic Divsion of Biostatistics, Department of Health Sciences Research, USA, [4]Mayo Clinic Division of Biostatistics, Department of Health Sciences Research, USA, [5]Mayo Clinic Division of Epidemiology, Department of Health Sciences Research, USA

Purpose Long-term bisphosphonate (BP) therapy may be associated with increased risk of minimally traumatic non-hip femoral fractures (NHFF). This study was done to determine incidence rates of NHFF in Olmsted County, MN, before and after introduction of alendronate into clinical practice.

Methods All NHFF events among Olmsted County, Minnesota, residents in 1984-2007 were identified. Incidence rates were assessed before and after 1996, when the oral BP alendronate was approved for clinical practice, and compared to historical incidence rates in Olmsted County from 1965-1984.

Results From 1984-2007, 730 NHFF were observed in 691 residents. Affected residents were 50.8% female, with mean age at first fracture of 59.7 years; and 49.2% male, with mean age 31.5 years. Of the 691 subjects with NHFF, 653 had one, 37 had two, and 1 had 3 fractures. Of these fractures, 20.4% were subtrochanteric, 51.7% were mid-diaphyseal, and 27.9% involved the distal femur. Fractures were due to severe trauma in 51.1%, minimal to moderate trauma in 34.2%, and pathologic causes in 14.8%.

Among 691 residents with a first-ever NHFF, the total cumulative age- and sex-adjusted incidence (ASAI) from 1984-2007 was 26.8 ± 1.0/100,000 person-years, with age-adjusted incidence (AAI) for women 25.0 ± 1.4/100,000 person-years, and AAI for men 26.8 ± 1.6/100,000 person-years. Incidence rates of first-ever NHFF for women increased between 1984 and 1995, and between 1996-2007 (p=0.001), but did not change for men (p=0.125). For 1984-1995, the cumulative ASAI was 21.9 ± 1.4/100,000 person-years, with AAI for women 20.2 ± 1.9/100,000 person-years, and AAI for men 22.0 ± 2.0/100,000 person-years. For 1996-2007, the cumulative ASAI was 30.4 ± 1.5/100,000 person-years, with AAI for women 28.9 ± 2.0/100,000 person-

years, and AAI for men 30.0 ± 2.2/100,000 person-years. The incidence rate of first-ever NHFF from 1984-1995 was lower than the rate of first-ever NHFF from 1965-1984 (37.1/100,000 person-years). Three males and 27 females were taking a bisphosphonate at the time of first-ever NHFF. If patients using bisphosphonates from 1996-2007 were removed from consideration, the AAI rate for first-ever NHFF from 1996-2007 was 25.3/100,000 person-years for females, and 29.5/100,000 person-years for males, with both rates higher than in 1984-1995.

Conclusion The incidence rate of first-ever NHFF increased between 1984-1995 and 1996-2007, driven by a small increase in the rate for women after the introduction of alendronate into clinical practice in 1996.

***Disclosures: Alvin Ng**, None.*

1201

A Retrospective Analysis of all Atypical Femur Fractures Seen in a Large California HMO from the Years 2007 to 2009. Richard Dell[1], Denise Greene[1], Susan Ott*[2], Stuart Silverman[3], Eric Eisemon[4], Tadashi Funahashi[1], Annette Adams[1]. [1]Kaiser, USA, [2]University of Washington, USA, [3]Cedars Sinai, USA, [4]Maimonides Medical Center, USA

Nontraumatic fractures of the femoral diaphysis with an unusual appearance have been recently reported in patients on long term oral bisphosphonates. These case series have not been able to enumerate the population at risk and the incidence of these atypical fractures has not been defined. We therefore conducted a study in a defined population to characterize these fractures and estimate their incidence. Using electronic data sources from a large California health maintenance organization, we identified all subtrochanteric and femur shaft fractures that occurred in patients aged 45 years or older between 1/1/2007 and 12/31/2009. All fractures above the subtrochanteric femur

region and below the distal femoral flair were excluded, as were periprosthetic fractures, pathologic fractures secondary to tumor, and high energy fractures.

The HMO serves 2.6 million patients 45 years or older. Records on over 15,000 femur fractures cases were screened and over 600 radiographs were then reviewed that meet inclusion criteria. We identified those with atypical features that included lateral cortical thickening, a transverse fracture with short oblique extension medially, and flaring of the lateral cortex. For all patients with qualifying fractures, demographic, clinical, and pharmacy data were gathered. 102 patients (99 women, 3 men) had the characteristic radiographic findings. 61% of the fractures occurred in the shaft region and 39% in the subtrochanteric region. 25% of the patients had either a complete fracture or stress fractures on the contralateral femur. The average age was 72 years old (range 45 to 92). Prodromal pain was reported by 70% of the patients. Five patients had not taken a bisphosphonate and 97 patients were on oral bisphosphonates with an average duration of use of 5.5 years. There was no correlation between the duration of bisphosphonate use and the patient age. Based on the number of patients receiving oral bisphosphonate treatment in our HMO (300,000 filled at least one prescription since 2002), preliminary estimates of atypical femur fracture incidence show a progressive increase with longer duration of treatment, from 2:100,000 per year to 78:100,000 cases per year as the duration of treatment went from 2 years to 8 years of oral bisphosphonate treatment.

These preliminary incidence estimates suggest that atypical femur fractures are rare in the general population, but may be more common among patients with longer-term oral bisphosphonate use.

***Disclosures: Susan Ott**, None.*

1202

Long-term Mortality after Low-energy Fractures at Middle-age - a Study of 22 000 Men and 11 000 Women. Anna H Holmberg*[1], Jan-Åke Nilsson[1], Peter M Nilsson[2], Kristina Åkesson[3]. [1]Dpt of Orthopedics, Skåne University Hospital, Malmö, Sweden, [2]Dpt of Internal Medicine, Skåne University Hospital, Malmö, Sweden, [3]Dpt of Clinical Sciences, Malmö, Clinical & Molecular Osteoporosis Research Unit, dpt of orthopedics, Skane University Hospital, Malmö, Sweden

The aim of this study was to examine long-term effects of a low-energy fracture on mortality rates in an urban middle-aged population. How long does the increased mortality risk persist? What types of fractures influence mortality risk? Are there any sex differences in mortality rates?

Methods: The Malmö Preventive Project consists of 10902 women and 22444 men, mean age at inclusion 50 and 44 years respectively.The subjects were followed prospectively regarding fractures and mortality up to 32 years. The subjects were subdivided according to sex and age at first fracture; <50, 50-59, 60-69 and ⩾70 yrs of age and further subdivided according to type of first fracture; forearm, shoulder, hip, clinical vertebral, ankle or other fracture. Standardised mortality rates (SMR), adjusted for age, sex and calendar year, were calculated per 100 person-years (p-yrs) with data from Statistics, Sweden, using the southern region (approx. 1 000 000 inhab) as background population. Dates of death was obtained from the National Board of Health and Welfare, Sweden.

Results: 2069 women and 1800 men sustained fractures and of these 332(16%) women and 648(36%) men died. In women, sustaining any type of fracture increased the 25-yr mortality risk in all ⩾50 yrs (SMR 126-237/100 p-yrs, CI 95% 102-295). A hip fracture at age 60 or more increased the 25-yr mortality risk up to 6 times (SMR 293-601/100 p-yrs, CI 95% 184-852). Vertebral fractures increased the 25-yr mortality risk in women 60-69 yrs (SMR 233/100 p-yrs, CI 95% 101-364).

In men, sustaining any type of fracture increased the mortality risk in all age groups up to 25 yrs (202-284/100 p-yrs, CI 95% 174-329). A hip fracture at age 50 or more increased the 25-yr mortality risk up to 4 times (391-463/100 p-yrs, CI 95% 249-598). Vertebral fractures increased the mortality risk up to 25 yrs post-fracture in all age-groups (SMR 260-375/100 P-yrs, CI 95% 133-607).

In both women and men, shoulder fractures were associated with an increased mortality risk up to 25 yrs, but the effect was small. Ankle fractures did not affect mortality in women, but almost doubled the risk in men aged 50-59 yrs at the fracture event (SMR192/100 p-yrs, CI 95% 126-259).

Conclusions: Any type of low-energy fracture in middle-age significantly influence long-term mortality in both women and men, with a higher impact in men. Hip fractures have the most pronounced effect, but any low-energy fracture in middle-age should be considered a sign of frailty.

***Disclosures: Anna H Holmberg**, Novartis, Amgen, 5*

1203

Bone Age- a Novel Index of Age Based on Bone Mineral Density: A Multi-cohort Analysis. Yahtyng Sheu*[1], Anne Newman[1], Peggy Cawthon[2], Tamara Harris[3], Frances Tylavsky[4], Kristine Ensrud[5], Eric Orwoll[6], Jane Cauley[1]. [1]University of Pittsburgh Graduate School of Public Health, USA, [2]California Pacific Medical Center Research Institute, USA, [3]Intramural Research Program, National Institute on Aging, USA, [4]University of Tennessee, Memphis, USA, [5]Minneapolis VA Medical Center / University of Minnesota, USA, [6]Oregon Health & Science University, USA

Bone mineral density (BMD) and chronological age are strong risk factors for osteoporotic fractures. We investigated "bone age" as an alternative means to understand an individual's biologic age. Data from the Health Aging and Body Composition (HABC, n=3043, aged 68-80 yrs) study, the Osteoporotic Fractures in Men (MrOS, n=5600, aged 65+ yrs) study, and the Study of Osteoporotic Fracture (SOF, n=7546, aged 65+ yrs) was used. To calculate study-specific bone age, we modeled incident risk of non-traumatic and non-spine fracture as a function of chronological age "$h(t|age)=exp(\beta_0+ \beta_1 age)$" and then as a function of femoral neck BMD "$h(t|BMD)=exp(\gamma_0+ \gamma_1 BMD)$" separately using the exponential survival model. We then equated the hazards and solved for age to yield the following estimate of bone age by using in the maximum likelihood estimates for each parameter: $(\gamma_0-\beta_0)+\gamma_1 BMD)/\beta_0$. Bone age is then the risk-equivalent of femoral neck BMD. Results from the Cox regression model (adjusted for race, gender, and/or clinic sites when applicable) showed, in all three studies, that individuals with bone age greater than their chronological age were more likely to experience incident non-spine fracture (Table). Hazard ratios (HRs) for fractures among individuals with bone age 5 yrs older than their chronological age, compared to those with a bone age and chronological age difference within +/- 5 yrs, were 16-36% more likely to have fracture, while the risk was 13-61% lower among individuals with bone age 5 yrs younger than their chronological age (Table). All findings were statistically significant for HABC and SOF, except MrOS studies. Results remained similar when models were further adjusted for weight, height, current smoking status and fracture history. Older adults with younger bone age may have a reduced risk of fracture. Unlike other subclinical measures such as glucose and blood pressure, general public does not comprehend values of BMD or T-score until later in their life. The concept of bone age may provide an easily understandable translation of fracture risk to patients in order to tailor preventive treatments.

	HABC	MrOS	SOF
Follow-up time (yr)	7.7	7.5	13.2
Number of fracture cases	308 (10%)	579 (10%)	3115 (41%)
HR and 95% confidence interval for fractures for "bone age minus chronological age"			
Every +5 yrs difference	1.36 (1.26, 1.47)	1.09 (1.04, 1.14)	1.13 (1.10, 1.16)
< -5 yrs v.s. within ± 5 yrs	0.36 (0.28, 0.54)	0.87 (0.72, 1.06)	0.80 (0.73, 0.87)
> 5 yrs v.s within ± 5 yrs	1.36 (1.06, 1.75)	1.16 (0.95, 1.41)	1.24 (1.14, 1.35)

ASBMR10_BoneAge_Table

***Disclosures: Yahtyng Sheu**, None.*

1204

Direct Comparison of Four National FRAX® Tools for Fracture Prediction. William Leslie*[1], Lisa Lix[2], Helena Johansson[3], Anders Oden[4], Eugene McCloskey[5], John Kanis[6]. [1]University of Manitoba, Canada, [2]University of Saskatchewan, Canada, [3]Swedish University of Agricultural Sciences, The Biomedical Center, Sweden, [4]Consulting statistician, Sweden, [5]University of Sheffield, United Kingdom, [6]University of Sheffield, Belgium

A FRAX® model for Canada was constructed for prediction of osteoporotic and hip fracture risk using national hip fracture data (2005) and mortality data (2004), with and without use of femoral neck BMD. Performance of this model was compared

with FRAX tools from the US (white), UK and Sweden. METHODS: We identified 36,730 women age 50+ with baseline BMD testing in the Manitoba BMD Program database which captures all clinical DXA results for the Province of Manitoba, Canada. FRAX probabilities were calculated based upon age, BMD, BMI and additional clinical risk factors (proxies used for smoking and high alcohol intake, adjustments were made for incomplete parental hip fracture information). Linkage with other provincial health databases allowed for the direct comparison of fracture risk estimates from the FRAX tools with observed fractures up to ten years (506 women with incident hip fractures and 2,380 with major osteoporotic fractures). Kaplan-Meier (KM) estimates of 10 year fracture risk were compared with predicted probabilities in subgroups defined by quintiles in fracture probability to assess fracture discrimination and calibration. RESULTS: The ten year KM estimate of major osteoporotic fractures for all women was 12.1% (95% CI 10.8-13.4%) and for hip fractures was 2.7% (95% CI 2.1-3.4%). The average FRAX probabilities from the Canadian tool were 11.1% and 2.8% respectively, which were within the observed CIs. FRAX estimates with the UK tool were similar to Canada (ratios for major osteoporotic 0.98 and for hip 1.07), were slightly higher with the US tool (ratios 1.11 and 1.09), and were much higher with the Swedish tool (ratios 1.27 and 1.78). The calibration plots (Figure) showed no significant difference in hip fracture discrimination/calibration with the Canada, US or UK tools but poor calibration with the Swedish tool (observed rates lower than predicted). Prediction of major osteoporotic fractures showed clinically insignificant differences between the Canada, US, and UK tools, but again the Swedish tool showed poor calibration (observed rates lower than predicted). CONCLUSION: Although the US and UK FRAX models gave predictions close to the Canadian FRAX model, the Swedish FRAX model significantly overestimated risk in Canadian women. This analysis supports the need for country-specific FRAX models based upon national fracture epidemiology.

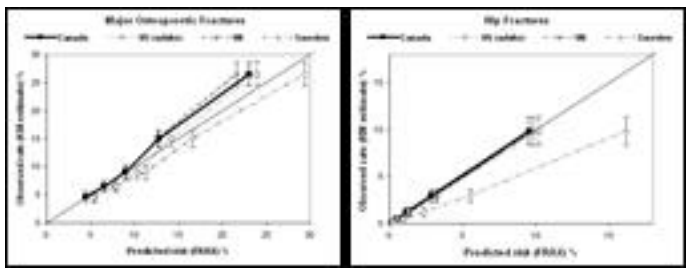

Figure: Predicted 10y fracture risk from FRAX (X-axis) vs observed K-M 10y fracture rates (Y-axis).

***Disclosures: William Leslie**, None.*

1205

Lipoxygenase Alox15 is a Cell Autonomous Amplifier of Oxidative Stress in Osteoblasts and the Skeleton of Estrogen Deficient and Aged Mice. Robert Jilka*, Maria Jose Almeida, Elena Ambrogini, Leslie Climer, Stavros Manolagas. University of Arkansas for Medical Sciences, USA

Loss of bone with advancing age in C57BL/6 mice is accompanied by a progressive increase in reactive oxygen species (ROS) and osteoblast apoptosis, as well as a decrease in osteoblast number and bone formation rate. The increase in ROS is associated with a 5-fold rise in the expression of Alox15, a lipoxygenase that contributes to oxidative stress (OS) in the skeleton by oxidizing polyunsaturated fatty acids to produce the strong pro-oxidant 4-hydroxynonenal. However, the cause of the increased Alox15 expression with age is unknown. Prompted by evidence for high expression of Alox15 in embryonic fibroblasts with increased ROS due to deletion of glutathione peroxidase (Seiler et al, Cell Metab 8:237, 2008), we examined the possibility that ROS stimulate the expression of Alox15. We report that OS caused by addition of H_2O_2, or a xanthine/xanthine oxidase system that generates H_2O_2 continuously, increased the expression of Alox15 by 2-4 fold in murine bone marrow-derived osteoblastic cells. OS also increased Alox15 expression in the vertebrae. Thus, 4 month old mice lacking FoxOs1,3 and 4 (transcription factors that stimulate the expression of anti-oxidant enzymes) exhibited an increase in both OS and Alox15 compared to their control littermates; whereas expression of other lipoxygenases, including Alox12, Alox12b, Alox12e and Alox15b, was unaffected by FoxO deletion. Similar to FoxO1,3,4 deletion, the increased OS caused by ovariectomy in 6 month old mice increased Alox15 expression, and estrogen replacement prevented the increase of both OS and Alox15. On the other hand, suppression of OS by administration of the anti-oxidants N-acetyl cysteine or catalase to 24 month old C57BL/6 mice reduced expression of Alox15 to the level seen in 6 month old mice. Finally, as reported elsewhere in this meeting, the enhanced anabolic efficacy of intermittent PTH in 26 month old mice was associated with a reduction in both OS and Alox15 expression to the levels seen in 6 month old mice. We conclude that ROS stimulates the expression of Alox15 in cells of the osteoblast lineage in a cell autonomous fashion. Because Alox15-mediated lipid oxidation and generation of 4-hydroxynonenal further increases OS, we hypothesize that Alox15 is part of a positive feedback loop that both amplifies and perpetuates OS in the skeleton, thereby contributing to bone loss caused by estrogen deficiency or advancing age.

***Disclosures: Robert Jilka**, None.*

1206

Tissue-Specific Knock-in of Constitutively Active IKKβ Leads to Bone Loss in Mice. Kaihua Zhang*[1], Jesse Otero[1], Muhammad Alhawagri[1], Isra Darwech[1], Yousef Abu-Amer[2]. [1]Washington University, USA, [2]Washington University in St. Louis School of Medicine, USA

Osteoclast differentiation requires stimulation of monocytes/macrophages with receptor activator of NF-κB (RANK) ligand. The ensuing signaling cascade results with activation of multiple pathways, primarily NF-κB. We have reported recently that constitutively active IKKβ ($IKK\beta^{SSEE}$), but not other forms of IKKβ or IKKα, stimulates differentiation of monocytes into *bona fide* functional osteoclasts in a RANK-independent fashion. To validate the physiological relevance of these findings, we generated a tissue-specific knock-in of $IKK\beta^{SSEE}$. Specifically, we utilized the R26Stop$IKK\beta^{SSEE}$ mice in which a cDNA encoding IKKβ containing two serine to glutamate substitutions in the activation loop of the kinase domain, preceded by a loxP-flanked STOP cassette, into the ubiquitously expressed ROSA26 locus. We crossed mice carrying this allele with the CD11b-cre mice in order to express $IKK\beta^{SSEE}$ exclusively in myeloid cells, including osteoclasts. Macrophages and osteoclasts derived from CD11bCre/R26Stop$IKK\beta^{SSEE}$ (Cre+/$IKK\beta^{SSEE}$) express Flag-tagged $IKK\beta^{SSEE}$ detected by Western blot. Real-time PCR showed that $IKK\beta^{SSEE}$ upregulates NFATc1 expression in macrophage/osteoclast lineage (p=0.008). $IKK\beta^{SSEE}$ also significantly enhanced TRAP (p=0.003) and CTR expression (p=0.007) compared to control. Noticeably, heterozygotes and homozygotes Cre+/$IKK\beta^{SSEE}$ mice displayed severe osteopenia due to hyperactive and increased number of osteoclasts which was also reflected by two-fold increase of serum TRACP 5b activity (10.59 U/L vs 4.93 U/L). Micro-CT and histological analyses showed that Cre+/$IKK\beta^{SSEE}$ mice lost half of the trabecular bone compared with control littermates, while marginal reduction of cortical bone was observed. To explore the mechanism underlying enhanced osteoclast activity in Cre+/$IKK\beta^{SSEE}$ mice, we further analyzed the expression and secretion of osteoclastogenic (RANKL and OPG) and inflammatory factors (TNFα and IL1β) in these mice. Serum levels of RANKL and TNFα remain normal, however serum IL1β increased significantly (p=0.018) compared to WT. Interestingly, serum level of OPG also increased dramatically (p=0.019), probably reflecting a negative feedback mechanism in Cre+/$IKK\beta^{SSEE}$ mice. Taken together, our findings indicate that in vivo expression of active IKKβ causes accelerated bone loss and leads to osteopenia in mice. Thus, we surmise that active IKKβ is a key culprit of bone erosion and as such is a promising target for therapeutic intervention.

***Disclosures: Kaihua Zhang**, None.*

1207

Neuropeptide Y, Y6 Receptor, a Novel Regulator of Bone Mass and Energy Homeostasis. Frank Driessler*[1], Ernie Yulyaningshi[2], Ronaldo Enriquez[2], Amanda Sainsbury[2], Herbert Herzog[2], John Eisman[1], Paul Baldock[1]. [1]Garvan Institute of Medical Research, Australia, [2]Garvan Institute, Australia

The view of bone remodelling as an endocrine-paracrine-regulated process is rapidly changing with new evidence demonstrating that neuronal factors also potently modify the activity of bone cells. Neuropeptide Y (NPY) is the most abundant peptides in mammalian brain, inducing a variety of effects through 5 distinct NPY receptors. Hypothalamic Y2 and osteoblastic Y1 receptors are reported to be critical in the regulation of bone homeostasis. However, to date, the role of Y6 receptors is poorly defined. Y6 shares 60% sequence identity with the Y1 receptor, which, in addition to bone effects, is also involved in energy homeostasis. To understand the functional role of Y6 receptors in energy and bone homeostasis we generated Y6 null mice and characterised their phenotype.

$Y6^{-/-}$ mice are viable with equal gender distribution. Deletion of Y6 receptors significantly reduced body weight (11%) through reduced lean (8.6%) and fat mass (32.5%). This is associated with increased in energy expenditure and an elevated respiratory quotient, indicative of decreased preference for lipid as fuel. These metabolic phenotypes are accompanied by significant reduction in BMD (mg/cm^2) and BMC (mg) on a whole body level as well as for isolated femurs (femur BMD: 47.10 ± 1.1 vs. 57.94 ± 2.4, $p<0.01$; femur BMC: 18.58 ± 0.1 vs. 23.71 ± 1.0, $p<0.05$). Importantly, these changes were evident despite no change in femur length.

μCT analyses indicted that cancellous BV/TV (%) was significantly decreased in $Y6^{-/-}$ compared to wt values (7.30 ± 0.5 vs. 10.13 ± 0.7, $p<0.01$), with a significant loss of trabecular number (mm^{-1}) (1.36 ± 0.1 vs. 1.81 ± 0.1, $p<0.01$) albeit no change in trabecular thickness (μm) (wt $55.6. \pm 1$ vs. $Y6^{-/-}$ 53.5 ± 1, ns). A significant loss of cortical thickness (μm) was found in $Y6^{-/-}$ (18.37 ± 1.6 vs. 21.29 ± 6.2, $p<0.01$) accompanied by significant reduction in periosteal surface (mm) (wt: 5.45 ± 0.1 vs. $Y6^{-/-}$ 5.13 ± 0.1, $p<0.05$) with no change in endosteal (mm) surface of the bones (wt: 4.12 ± 0.1 vs. $Y6^{-/-}$ 4.02 ± 0.1, ns).

Together these results suggest an important role of the Y6 receptors in energy and bone homeostasis. The reduction bone mass evident in $Y6^{-/-}$ mice is in contrast to other NPY-mediated models, indicating the potential for a counter regulatory role if Y6 within the NPY system.

***Disclosures: Frank Driessler**, None.*

1208

Brain-derived Neurotrophic Factor Regulates Bone Mass and Energy Homeostasis via the Central Nervous System. Claudia Camerino*[1], Peter Hauschka[2], Majd Zayzafoon[3], Maribel Rios[4]. [1]Center for Advanced Orthopaedic Beth Israel Deaconess Medical Center Boston, USA, [2]Children's Hospital Boston, USA, [3]University of Alabama at Birmingham, USA, [4]Tufts University school of medicine, Department of Neuroscience, USA

Brain-derived Neurotrophic Factor (BDNF) is a member of the neurotrophin family which includes nerve growth factor, neurotrophin-3 and neurotrophin-4/5. BDNF promotes neurite outgrowth and provides trophic support to certain neurons during development and in adulthood. BDNF, and the functional full-length form of its receptor, TrkB, are expressed in various hypothalamic nuclei associated with eating behavior and obesity, which makes it plausible that BDNF may act via the hypothalamic neuronal system. Further, the pharmacological profile of BDNF is strikingly similar to that of leptin, an adipocyte-derived satiety hormone that regulates body adiposity and bone mass in part through activation of the sympathetic nervous system. To determine the effect of BDNF on bone mass and metabolism we evaluated BDNF conditional knock out (KO) mice, in which BDNF expression was deleted from the brain through the use of the Cre-loxP recombination system (Rios et al, 2001). In both males and females, at 3 and 6 mo of age, central BDNF deletion leads to a metabolic phenotype characterized by hyperphagia, increased body weight, elevated serum levels of insulin and glucose, and leptin resistance. The mice are hyperactive with upregulation of UCP1 in brown adipose tissue at older ages. The BDNF conditional KO mice also have 40% greater fat pad weight than wild type littermates, and show evidence of liver steatosis at older ages, thus confirming diabetic status. Regarding the skeletal phenotype, BDNF KO mice have increased femur length (+6%, $p<0.01$) and greater femoral BMD (+30%, $p<0.001$) and BMC (+50%, $p<0.001$). μCT analysis of the femurs and vertebrae of 3 mo old BDNF KO mice reveal significantly greater trabecular BV/TV (+50% for distal femur, $p<0.001$ +35% for vertebral body, $p<0.001$) and mid-femoral cortical thickness (+11 to 17%, $p<0.05$). Bone microarchitecture was also enhanced at 6 mo of age, with more pronounced effect in females than males. Taken together these data identify a novel non-neurotrophic function for neurotrophins and provide evidence that the BDNF-to-TrkB signaling plays a role in the central regulation of bone homeostasis.

***Disclosures: Claudia Camerino**, None.*

1209

PTH Attenuates H_2O_2- and Glucocorticoid-induced Suppression of Wnt Signaling via an Akt-dependent Mechanism: a Mechanistic Explanation for the Efficacy of Intermittent PTH in Old Age- and Glucocorticoid-induced Osteoporosis. Maria Jose Almeida*, Shoshana Bartell, Stavros Manolagas, Robert Weinstein, Robert Jilka. University of Arkansas for Medical Sciences, USA

Intermittent PTH administration is an effective regimen for increasing bone mass and reducing the incidence of fractures in the osteoporosis that occurs with advancing age or with glucocorticoid administration, but the underlying mechanisms are unclear. Studies in mice show that age-related bone loss is due to increased oxidative stress (OS) and a rise in endogenous glucocorticoids, and is associated with reduced Wnt signaling. OS inhibits Wnt signaling by activating FoxOs and diverting β-catenin from Tcf- to FoxO-mediated transcription, whereas glucocorticoids attenuate Wnt signaling in part by inhibiting Akt phosphorylation leading to activation of GSK3β, a negative regulator of β-catenin. Interestingly, PTH activates Akt, and in studies reported elsewhere at this meeting, we show that the increased efficacy of intermittent PTH in old mice is associated with a reduction in oxidative stress and increased Wnt signaling. Therefore, we investigated here whether PTH reverses the negative effects of OS or glucocorticoids on Wnt signaling, and if so whether such effects are mediated by Akt. PTH stimulated β-catenin/Tcf transcriptional activity in UAMS-32P (expressing high levels of PTH receptor) and UMR-106 osteoblastic cells, as measured by a Tcf-luciferase (Tcf-luc) reporter construct. More important, pre-incubation with PTH prevented the H_2O_2- and dexamethasone-induced suppression of basal and Wnt3a-stimulated β-catenin/Tcf transcriptional activity. Moreover, PTH stimulated the phosphorylation of Akt, and attenuated the negative effect of dexamethasone on Akt phosphorylation. Consistent with a role of Akt in this effect of PTH, a dominant negative mutant of Akt abrogated the stimulatory effect of PTH on Tcf-luc activity, and also prevented the protective effect of PTH on H_2O_2-induced suppression of Wnt signaling. Like PTH, overexpression of Akt attenuated the dexamethasone-induced decrease in Wnt signaling. Akt could have promoted β-catenin/Tcf transcriptional activity by phosphorylating and thereby inactivating FoxOs, which would increase levels of β-catenin. Supporting this contention, PTH prevented H_2O_2-induced FoxO activation as measured by a FoxO-luciferase reporter. These findings support the hypothesis that the ability of PTH to attenuate old age- and glucocorticoid-induced bone loss is due at least in part to an Akt-mediated reversal of oxidative stress- and glucocorticoid-induced suppression of Wnt signaling.

***Disclosures: Maria Jose Almeida**, None.*

1210

RAD140: A Novel Non-steroidal SARM with Anabolic Activity in Rats and Non-human Primates. Gary Hattersley*[1], Maysoun Shomali[1], Kyla Gallacher[2], C. Richard Lyttle[3], Chris Miller[2]. [1]Radius, USA, [2]Radius Health, Inc, USA, [3]Radius Health Inc, USA

RAD140 is a novel nonsteroidal selective androgen receptor modulator (SARM) selected for potent oral anabolic activity, tissue selectivity and safety profile. RAD140 binds to the androgen receptor with nanomolar affinity and demonstrates good binding selectivity against a broad panel of molecular targets including nuclear hormone receptors. Muscle anabolism and tissue selectivity were initially evaluated in castrated and intact immature rats by assessing the effects on the levator ani muscle and prostate. In immature rats, castrated 7 days before initiation of treatment, daily oral dosing with 0.3 mg/kg RAD140 resulted in a significant increase in levator ani weight (wt), which was comparable to the wt of intact controls. In contrast, 10 mg/kg was required to restore prostate wt. Treatment with testosterone proprionate at 1 mg/kg resulted in a greater increase in prostate wt than 10 mg/kg RAD140, yet increased levator ani wt less than the maximal stimulation with RAD140. Similar experiments in intact immature rats revealed significant increases in levator ani wt with 0.1 mg/kg RAD140, while prostate wt was significantly increased only at 30 mg/kg. The effects of RAD140 on the male reproductive system were further assessed in a 12-week study in adult intact rats, where RAD140 up to 3 mg/kg did not stimulate but rather reduced prostate size, while maintaining the levator ani. In contrast, DHT administration markedly increased both prostate and levator ani wt. Using ovariectomized (OVX) rats, RAD140 showed positive effects on both trabecular and cortical bone, preventing OVX-induced BMD decrease in both the femur and lumbar spine at doses as low as 0.3 mg/kg. The increase in BMD was associated with improvements in trabecular and cortical bone microarchitecture, including increased cortical thickness in the femoral diaphysis. Consistent with these changes, several parameters of bone quality were also significantly enhanced as shown in femur 3-point bending and lumbar spine compression analysis. The anabolic activity of RAD140 was also demonstrated in male Cynomolgus monkeys, where daily treatment with RAD140 for 28 days at 0.1 mg/kg resulted in an 11% increase in body wt, which was predominantly associated with increased lean tissue mass. These results show potent muscle and bone activity of RAD140 with a low impact on reproductive tissues and could represent a valuable new therapeutic agent for treatment of conditions such as frailty and cachexia.

***Disclosures: Gary Hattersley**, Radius, 3*
This study received funding from: Radius

1211

Oral Contraceptive Use and Change in Bone Density among Adolescent and Young Adult Women: Results from a Prospective Study. Delia Scholes*[1], Laura Ichikawa[2], Rebecca Hubbard[2], Andrea LaCroix[3], Leslie Spangler[2], Jeannette Beasley[2], Susan Ott[4]. [1]Group Health CooperativeGroup Health Research Institute, USA, [2]Group Health Cooperative, USA, [3]Women's Health Initiative, Fred Hutchinson Cancer Research Ctr, USA, [4]University of Washington, USA

Although an estimated 12 million US women use combined oral contraceptives (OCs), the possible adverse impacts of current OC formulations on bone mass gains remain unclear. Particularly needed are evaluations of bone changes that incorporate age, OC dose, duration of use, and potential reversibility of any impacts with discontinuation. The purpose of this study was to compare bone mineral density (BMD) changes in adolescent (14-18) and young adult (19-30) OC users and non-users, examining OC estrogen dose and duration, anatomic site, and changes following OC discontinuation.

In a population-based prospective cohort study, 606 women enrollees of Group Health Cooperative (WA state) were recruited using the plan's computerized databases: 389 were initiating and prevalent OC users (62% were using 30-35 mcg ethinyl estradiol (EE) OCs, 38% were using <30 mcg EE); and 217 were age-similar non-users. Just over half (51%) of the cohort was 14-18 years of age. BMD was measured every 6 months for at least 24 months. We collected data on OC use and other important covariates via interview and survey. Cohort retention was 78% at 24 months of follow-up. Linear regression models were used to compare 24-month mean BMD percent change for OC users vs. non-users by age (14-18 and 19-30 years) and OC dose (30-35 mcg EE and <30 mcg EE) at the hip, spine, and whole body. The models were adjusted for age, race, current smoking, BMI, period regularity, calcium intake, physical activity, baseline BMD, and duration of OC use at baseline.

In these analyses, 14-18 year-olds using 30-35 mcg EE OCs, but not those using <30 mcg EE OCs, had smaller adjusted 24-month mean BMD percent gains than non-users at the spine (0.54% vs. 1.81%, p=0.02) and whole body (1.22% vs. 1.89%, p=0.08) (Fig. A). Differences from non-users increased significantly with increasing duration of 30-35 mcg EE OC use at all anatomic sites. In 19-30 year-olds, mean 24-month percent changes in OC users did not differ from non-users at any anatomic site, regardless of OC EE dose (Fig. B).

These results suggest that use of 30-35 mcg EE OC formulations, particularly longer-term use, is associated with reduced bone accrual in adolescents. In young adult women with more complete bone accrual, bone changes were similar between OC users and non-users.

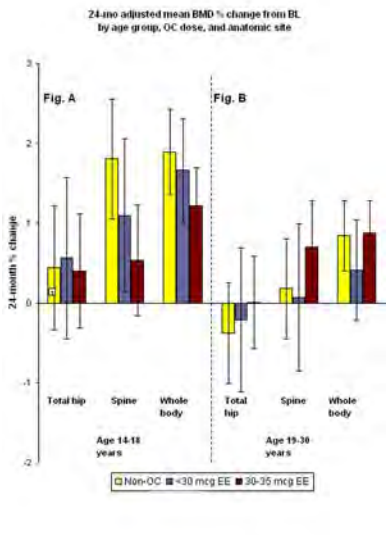

Scholes_OC use and change in BMD, prospective results

***Disclosures: Delia Scholes**, None.*

1212

Effect of Gonadal and Adrenal Steroid Replacement on Bone Cross-Sectional Geometry in Young Women with Anorexia Nervosa: A Hip Structural Analysis Study. Amy DiVasta*[1], Henry Feldman[1], Meryl Leboff[2], Thomas Beck[3], Catherine Gordon[4]. [1]Children's Hospital Boston, USA, [2]Brigham & Women's Hospital, USA, [3]Johns Hopkins Outpatient Center, USA, [4]Children's Hospital Boston & Harvard Medical School, USA

Purpose: Young women with anorexia nervosa (AN) have suppressed concentrations of dehydroepiandrosterone (DHEA) and estrogen that may contribute to the low bone mineral density (BMD) and skeletal fragility seen commonly in these patients. Previous studies have shown that HRT alone does not prevent bone loss in AN. We previously reported that DHEA led to increased areal bone density Z-scores (aBMD-Z), but the effects were offset by accompanied weight gain. In the current study, we aimed to determine the effects of an 18-mo regimen of oral DHEA + hormone replacement therapy (HRT) vs. placebo on bone cross-sectional geometry in young women with AN.

Methods: Eighty women with AN, aged 13-27 yr, received a random, double-blinded assignment to micronized DHEA (50 mg/d) + HRT (20μg ethinyl estradiol/ 0.1mg levonorgestrel) or placebo for 18 mo. Measurements of aBMD at the total hip, lumbar spine, and whole body were obtained by dual-energy X-ray absorptiometry at 0, 6, 12, and 18 mo. We used the Hip Structural Analysis (HSA) Program to determine BMD, cross-sectional area (CSA), and section modulus (Z) at the femoral neck and femoral shaft regions.

Results: Over 18 mo of DHEA+HRT therapy, femoral shaft BMD increased in the treatment group (+3.4% change over 18 mo) while simultaneously dropping in the placebo group (-2.1%) (time x treatment p-value <0.01). Changes in femoral shaft CSA were also significantly different between groups (DHEA+HRT: +2.5% vs. placebo: -1.8%, p<0.01). No difference in shaft section modulus was noted. Shaft buckling ratio, a measure of fracture risk, decreased in the treatment arm, but increased in the placebo arm over 18 mo (-5.9% vs. +2.7%, p=0.02)No difference in hip geometry at the femoral narrow neck was noted between groups.

Conclusions: In young women with AN, a combination regimen of oral DHEA+HRT for 18 mo led to increases in estimates of bone cross-sectional geometry and a decrease in estimated fracture risk compared to placebo therapy. Positive results of treatment were seen at the femoral shaft but not at the femoral narrow neck. Our results indicate that this combination treatment has a beneficial impact on skeletal health in young women with AN.

***Disclosures: Amy DiVasta**, None.*

1213

Altered Bone Composition in Fracture Prone Children With Vertebral Fracture. Inari Tamminen*[1], Mervi K Mäyränpää[2], Mikael Turunen[3], Hanna Isaksson[3], Outi Makitie[4], Jukka S Jurvelin[3], Heikki Kroger[5]. [1]Bone & Cartilage research Unit (BCRU), University of Eastern Finland, Finland, [2]Department of Pediatric Surgery & Department of Pediatrics, Hospital for Children & Adolescents, Helsinki University Hospital, Finland, [3]Department of Physics & Mathematics, University of Eastern Finland, Finland, [4]Hospital for Children & Adolescents, University of Helsinki, Finland, [5]Kuopio University Hospital, Finland

In pediatrics, primary osteoporosis (OP) often leads to vertebral fractures. However, it remains unknown whether these fractures associate with changes in bone composition. This study aimed to determine if the bone composition is different in fracture prone children with and without vertebral fractures, as assessed using Fourier transform infrared spectroscopic imaging (FTIRI) and bone histomorphometry.

Iliac crest biopsies (n=24) were obtained from children with suspected primary osteoporosis based on fracture history and/or low bone mineral density (BMD) in DXA (Table 1) [1]. Samples were analyzed using FTIRI and bone histomorphometry. Phosphate-to-amide I (mineral-to-matrix ratio), carbonate-to-phosphate, carbonate-to-amide I, and cross-link ratios (collagen maturity) were quantified by FTIRI [2]. Additionally, samples were classified into groups based on histomorphometric findings (normal bone volume vs. OP). Mann Whitney U-test was used for statistical comparison.

OP was diagnosed by histomorphometry in 50% of the children with vertebral fracture, and the bone turnover rate was abnormal in 71% of these cases (Table 1). Children with vertebral fractures had lower carbonate-to-phosphate ratio (p<0.05) and higher collagen maturity (p<0.05) than children without vertebral fracture. The children with histomorphometrically diagnosed OP showed lower carbonate-to-phosphate (p<0.05) and carbonate-to-amide I ratios (p<0.05) than the children with normal bone volume.

Our results suggest that the fracture prone children with vertebral fracture history have more frequently osteoporotic trabecular bone and altered bone turnover rate. OP was found in 30 % of cases without vertebral fracture and these children had sustained peripheral fractures (Table 1). The observed changes in bone composition in children with vertebral fracture might explain their greater propensity to develop vertebral fractures.

References:

1. Mäyränpää M et al. Transiliac bone biopsy findings in 24 fracture prone children. XIth Congress of ISBM, 28.-30.5.2009, Austria. An oral presentation.

2. Boskey A, Pleshko Camacho N. FT-IR imaging of native and tissue-engineered bone and cartilage. Biomaterials. 28:2465-2478; 2007.

	No vertebral fracture (n=10)	Vertebral fracture (n=14)
Age (mean ± SD, yrs)	13.8 ± 2.3	10.7 ± 1.9
Males / Females	7 / 3	10 / 4
BMD < -2 SD (%)	10	29
Non-vertebral fracture(s) (%)	100	86
Osteoporosis in biopsy (%)	30	50
Normal turnover in biopsy (%)	40	29

Table 1. Characteristics of the study cohort.

Table 1.

***Disclosures: Inari Tamminen**, None.*

1214

Fractures in Healthy Adolescent Boys are Associated with Reduced Bone Strength as Assessed by Finite Element Analysis at Weight-Bearing Skeletal Site. Thierry Chevalley*[1], Jean-Philippe Bonjour[2], Bert Rietbergen[3], Serge Ferrari[4], Rene Rizzoli[5]. [1]University Hospitals of Geneva Division of Bone Diseases, Switzerland, [2]University Hospital of Geneva, Switzerland, [3]Eindhoven University of Technology, The netherlands, [4]Geneva University Hospital & Faculty of Medicine, Switzerland, [5]University Hospital, Switzerland

In healthy children and adolescent boys, fractures result from trauma of various severity. Whether these fractures are characterized by an intrinsic bone biomechanical fragility remains to be demonstrated. In a cohort of 176 healthy adolescent boys prospectively followed from age 7.5±0.5 to 15.2±0.5 yrs we reported that fracture history (156 fractures recorded in 87/176 boys) was associated with decreased femoral neck (FN) areal (a) bone mineral density (BMD) (-6.0%, p=0.005) measured by dual-energy x-ray absorptiometry (DXA) and lower distal tibia trabecular volumetric (v) density (-5.5%, p=0.029) and number (-4.2%, p=0.040) as determined by high resolution peripheral computerized tomography (HR-pQCT). In the present study we

assessed to what extent this lower trabecular microstructure in the distal tibial among boys with previous fractures was associated with reduced bone strength variables evaluated by micro-finite element analysis (μFEA) based on HR-pQCT measurements. Associations between FN aBMD, distal tibia microstructure and bone strength estimates, and fracture status were evaluated by univariate logistic regression and expressed as odds ratio (OR [95%CI]) per 1 SD decrease. As compared to those without fractures, boys with fractures had a 5.8% lower bone strength of the distal tibia as estimated by stiffness (245 vs. 260 kN/mm, P=0.024) and failure load (11706 vs. 12430 N, P=0.016), after adjustment for age, standing height, body weight, pubertal stage, calcium and protein intakes, physical activity, and calcium supplement or calcium randomization between age 7.5 and 8.5 yrs. As shown in the distal tibia (Figure), the adjusted ORs [95% CI] for fracture per 1 SD decrease were as follows: Stiffness 1.42 [0.96-2.44, P=0.072]; Failure Load 1.60 [0.99-2.60, P=0.056]; Trabecular Density 1.46 [1.02-2.09, P=0.038]; Trabecular Number 1.59 [1.04-2.42, P=0.031]. The corresponding fracture OR for FN aBMD was: 1.80 [95% CI 1.18-2.76, P=0.006]. In conclusion, although trauma plays a non-negligeable role in the occurrence of fractures in healthy children and adolescent boys, our study provides evidence for an intrinsic component of skeletal fragility as assessed by μFEA at weight-bearing site. The measured biomechanical deficit at distal tibia corroborates indirect estimates of fracture risk by assessing macro- and microstructural components of bone mineral density and architecture.

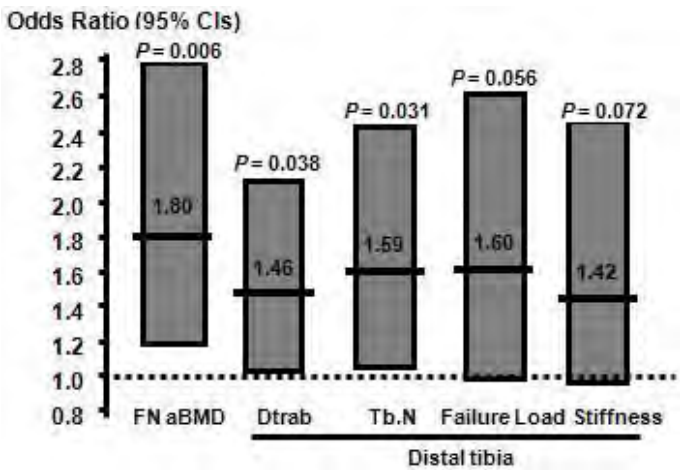

Figure

***Disclosures: Thierry Chevalley**, None.*

1215

High-Resolution pQCT Assessed Trabecular Bone Volume Fraction Is Independently Associated with X-ray Verified Forearm Fractures in Young Men. Robert Rudäng*[1], Anna Darelid[2], Dan Mellstrom[3], Claes Ohlsson[4], Mattias Lorentzon[5]. [1]Center for Bone Research at the Sahlgrenska Academy, Dept. of Internal Medicine, University of Gothenburg, Sweden, Sweden, [2]Gothenburg University, Sweden, [3]Sahlgrenska University Hospital, Sweden, [4]Centre for Bone & Arthritis Research, Sweden, [5]Center for Bone Research at the Sahlgrenska Academy, Sweden

Areal bone mineral density (aBMD) is a well established predictor of fracture risk in adults as well as in children and adolescents. Whether or not measures of trabecular microarchitecture are related to fracture risk in young adults remains unclear. The purpose of this study was to investigate whether indices of trabecular microarchitecture or aBMD, both measured in the forearm, was most strongly associated with distal forearm x-ray verified fractures in young men.

In total, 756 young adult men (age 24.1±0.6 years) were included in this cross-sectional population-based study. The non-dominant radius was measured with dual-energy x-ray absorptiometry (DXA) to obtain aBMD and with an XtremeCT device to measure the trabecular bone volume fraction (BV/TV), trabecular number (Tb.N.), and trabecular thickness (Tb.Th.), cortical volumetric BMD, and cortical thickness. A standardized questionnaire was used to collect information regarding calcium intake, smoking and physical activity. Reported fractures were verified through local hospital X-ray records and national health care registers. In total, 290 (38.4%) men had suffered at least one prevalent fracture and 466 (61.6%) men had no prevalent fractures. There were 395 fractures. The most common fracture sites were at the distal forearm (27.6%, 109/395), the phalangs of the hand (15.7%, 62/395), and the carpals or metacarpals of the hand (13.2%, 52/395). Men with at least one prevalent distal forearm fracture (n=94) had lower radius aBMD (2.1%, p=0.04), and substantially lower trabecular BV/TV (6.9%, $p<0.001$), as a result of reduced Tb.N. (4.1%, $p<0.01$) than men without any fracture. No differences in cortical thickness or cortical volumetric BMD were seen between the groups. Using a logistic regression model (with age, height, weight, calcium intake, smoking and physical activity as covariates), we found that the prevalence of distal forearm fracture was increased for every SD decrease in trabecular BV/TV of the radius (Odds Ratio (OR) 1.47 (1.15-1.88)) but not with aBMD (OR 1.23 (0.96-1.58)) of the same bone. When both aBMD and trabecular BV/TV were included simultaneously, trabecular BV/TV was associated with prevalent radius fracture (OR 1.52 (1.12-2.1) while aBMD was not (OR 0.94 (0.69-1.29). We conclude that trabecular bone volume fraction as measured with high resolution pQCT is more strongly associated with X-ray verified prevalent forearm fractures than aBMD is in a large cohort of young adult men.

***Disclosures: Robert Rudäng**, None.*

1216

Cortical Consolidation Due to Increased Mineralization and Endosteal Contraction in Young Adult Men - a Five Year Longitudinal Study. Anna Darelid*[1], Claes Ohlsson[2], Johanna Melin[1], Dan Mellstrom[3], Mattias Lorentzon[4]. [1]Center for Bone Research at the Sahlgrenska Academy, Dept. of Internal Medicine, University of Gothenburg, Gothenburg, Sweden, [2]Centre for Bone & Arthritis Research, Sweden, [3]Sahlgrenska University Hospital, Sweden, [4]Center for Bone Research at the Sahlgrenska Academy, Sweden

Peak bone mass (PBM) is an important factor for the lifetime risk of developing osteoporosis. Large, longitudinal studies investigating the age of attainment of site specific PBM are lacking.

The aim of the present study was to determine the site specific development of peak bone mass in appendicular and axial skeletal sites, and in the trabecular and cortical bone compartments, using both Dual X-ray Absorptiometry (DXA) and peripheral computed tomography (pQCT). In total, 833 men (aged 24.1±0.6 years (mean±SD)) from the original population-based Gothenburg Osteoporosis and Obesity Determinants (GOOD) Study (n=1068), were included in this follow-up examination at 62.2±2.3 months. Areal bone mineral density (aBMD) was measured with DXA, whereas cortical and trabecular volumetric BMD (vBMD) and bone size were measured by pQCT at baseline and at the five year follow-up. During the five-year follow-up, areal BMD of the total body, lumbar spine, and radius, increased yearly with 0.74%, 0.85%, and 1.55%, respectively ($p<0.0001$). PQCT measurements were used to explore vBMD and bone geometry alterations in the long bones. Yearly increments of 0.43% and 0.13% were seen for cortical vBMD of the radius and tibia, respectively ($p<0.0001$), while cortical thickness gained 0.77% at the radius and 1.30% at the tibia yearly, due to diminished endosteal circumference (radius 0.47% and tibia 0.92% yearly, $p<0.0001$). As a result, the polar stress strain index, a measure of bone strength, increased 0.99% and 1.36% yearly ($p<0.0001$) at the radius and tibia, respectively. During the whole study period, the accumulated increase in polar SSI was 5.0% for the radius and 6.9% for the tibia.

In conclusion, our results indicate that peak aBMD has not yet been attained at the spine and in the long bones between 19 and 24 years of age in men. We demonstrate that between these ages there is a considerable cortical consolidation, that is due to increased mineralization and augmented cortical thickness with endosteal contraction (Figure 1).

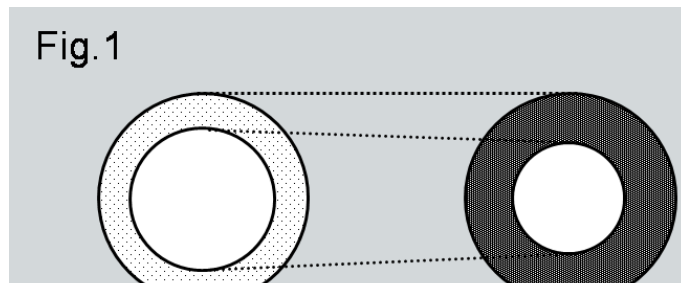

Figure 1

***Disclosures: Anna Darelid**, None.*

1217

microRNA-29 Modulates WNT Signaling in Human Osteoblasts Through a Positive Feedback Loop. Kristina Kapinas*, Catherine Kessler, Gloria Gronowicz, Anne Delany. University of Connecticut Health Center, USA

Our goal was to define the relationship between the microRNA miR-29 and canonical Wnt signaling during the differentiation of human osteoblasts. Wnt signaling is important for the differentiation of human mesenchymal stem cells to osteoblasts and for the maintenance of bone mass in humans. Post-transcriptional regulation of gene expression, mediated by microRNAs, plays an essential role in these processes. Previously we found that miR-29 family members are induced by

canonical Wnt signaling in murine osteoblasts. Here, we first showed by qRT-PCR that miR-29a expression is increased during osteoblastic differentiation of human FOB1.19 mesenchymal precursors and in primary cultures of human osteoblasts derived from bone chips. Knockdown of miR-29a reduced expression of alkaline phosphatase and osteocalcin mRNA, suggesting a role in differentiation, and miR-29a was rapidly induced by Wnt3A. We cloned up to 2 kb of the promoter region of the expressed sequence tag containing the human miR-29a gene into a promoterless luciferase reporter vector. The -982 to -1 region of the promoter contains 2 potential TCF/LEF binding sites. Promoter activity of this region was increased in cells treated with Wnt3A. Mutation of one or both TCF/LEF sites abolished responsiveness to Wnt3A. However, mutagenesis of both TCF/LEF sites increased basal promoter activity, likely due to the repressor function of TCF/LEF, which occurs when nuclear beta catenin is limited.

Since the expression of several antagonists of Wnt signaling are decreased during differentiation, we hypothesized that miR-29a may target these molecules. Based on the potential for miR-29a interaction with the 3' untranslated region (UTR), Dkk1, Kremen2, and sFRP2 emerged as candidates. We generated reporter constructs in which the 3'UTR for Dkk1, sFRP2 or Kremen2 act as the 3'UTR for the luciferase gene, and confirmed repression of these UTRs by miR-29a. Transfection of cells with miR-29a inhibitor increased Dkk1, sFRP2 and Kremen2 protein levels, confirming their regulation by miR-29. Overall, we demonstrate that miR-29 and Wnt signaling are involved in a regulatory circuit that modulates osteoblast differentiation. Canonical Wnt signaling induces miR-29a transcription. The subsequent down regulation of key Wnt signaling antagonists Dkk1, Kremen2, and sFRP2 by miR-29a could potentiate Wnt signaling and further promote a gene expression program necessary for osteoblast differentiation.

***Disclosures: Kristina Kapinas**, None.*

1218

A Regulatory Loop of Runx2 Downregulates Expression of the miR-23a~27a~24-2 Cluster which Targets SATB2 for Control of the Osteoblast Differentiation Program. Mohammad Hassan*[1], Jonathan Gordon[1], Marcio M. Beloti[2], Carlo M. Croce[3], Andre Van Wijnen[1], Janet L. Stein[1], Gary Stein[1], Jane Lian[1]. [1]University of Massachusetts Medical School, USA, [2]University of Massachusetts Medical Schools, USA, [3]Ohio State University, USA

Regulation of osteogenesis includes a program of microRNAs (miRs) to repress the translation of genes that act as inhibitors of bone formation. Yet, how expression of these bone-related miRs is regulated remains a compelling question. Here we report that expression of the miR cluster -23a~27a~24-2 increases continuously during osteogenic differentiation and is directly regulated by Runx2, a transcription factor essential for osteoblastogenesis. Overexpression, reporter and ChIP assays established a functional Runx binding element that mediates downregulation of all 3 miRs (miR-23a, 27a and 24-2) present in the cluster. Consistent with this finding, each of the miRs suppresses osteoblast differentiation, suggesting a role for this cluster in attenuating the late stages of osteoblast differentiation. The biological significance of Runx2 repression of this miR cluster is that each miR directly targets the 3' UTR of SATB2, which is known to synergize with Runx2 to facilitate osteoblast differentiation. These results suggest a Runx2 feed-forward mechanism for negative regulation of multiple miRs in order to cause de-repression of SATB2. Additionally, we find that miR-23a directly targets the 3' UTR of Runx2 and represses its translation, which allows for upregulation of the miR cluster during late differentiation because Runx2 has been downregulated. Thus, this finding defines a miR-mediated negative regulatory loop for attenuation of bone formation at the termination of differentiation. Taken together, we have established a regulatory network with a central role of the miR cluster 23a~27a~24-2 in regulating both progression and attenuation of osteoblast differentiation.

***Disclosures: Mohammad Hassan**, None.*

1219

Exploring Structural and Instructional Features of *CYP24A1* Distal Enhancers. Paul Goetsch*[1], Mark Meyer[2], John Stamatoyannopoulos[3], J. Pike[2]. [1]University of Wisconsin - Madison, USA, [2]University of Wisconsin-Madison, USA, [3]University of Washington, USA

1,25-dihydroxyvitamin D_3 ($1,25(OH)_2D_3$) actions are negatively regulated in target cells via induction of CYP24A1, a cytochrome P450 enzyme that inactivates the hormone and thus limits its transcriptional potential. While early studies suggested that induction of this gene by $1,25(OH)_2D_3$ was controlled by two proximal promoter regulatory elements, our recent studies identified a downstream enhancer cluster that contributes to *CYP24A1* upregulation as well. This region together with the promoter contain functional vitamin D response elements, bind the VDR/RXR heterodimer in response to $1,25(OH)_2D_3$, recruit a series of coregulators and collectively mediate changes necessary for gene activation. However, virtually nothing is known about the origins of such enhancers or what draws the heterodimer to these specific regions. To begin to address these issues, we first asked whether the *CYP24A1* enhancers could be uniquely identified through specific epigenetic marks that may act as beacons for incoming regulatory proteins. To this end, we conducted an extensive ChIP-chip analysis across the *CYP24A1* locus using antibodies specific for various histone acetylation or methylation marks. In the absence of $1,25(OH)_2D_3$, strong H3K4me1 marks were evident at virtually all the *CYP24A1* enhancers but not at the *CYP24A1* promoter. H4K5ac, H4K8ac, H4K12ac and H4K16ac marks were only evident at subsets of these enhancers while H4K12ac and H4K16ac marks could also be seen at the promoter. In contrast, H3K4me3 and H3K36me3 marks were undetectable across the locus. Thus, H3K4me1 and various H4ac marks may highlight enhancers at the *CYP24A1* locus that play a role in *CYP24A1* regulation. We next asked whether these regions were uniquely accessible to entry by regulatory proteins such as VDR/RXR. Accordingly, we examined the patterns of DNaseI hypersensitivity (DHS) generated across an extended series of diverse cell types through deep sequencing analysis as an integral part of the ongoing ENCODE project. Both the *CYP24A1* promoter and virtually all of the gene's enhancers manifested increased hypersensitivity to DNAse I digestion, suggesting that these enhancers maintain structural properties that increase accessibility to incoming VDR. Importantly, these sites are not evident in cells that do not represent targets of vitamin D action. These studies suggest that *CYP24A1* responsiveness to $1,25(OH)_2D_3$ is determined by both preformed regulatory enhancers and a ligand-inducible VDR.

***Disclosures: Paul Goetsch**, None.*

1220

SIRT2 is a Protein Deacetylase Involved in the Regulation of Osteoblastogenesis by Inhibiting Adipogenesis. Jonathan Gordon*, Mohammad Hassan, Hai Wu, Andre Van Wijnen, Janet Stein, Gary Stein, Jane Lian. University of Massachusetts Medical School, USA

Sirtuins are NAD^+-dependent protein deacetylases (HDACs) and are strongly associated with age-related degeneration including decreases in bone mineral density and osteoporosis. Sirt2 is constitutively expressed in mesenchymal cells (C3H10T1/2 fibroblasts, bone marrow stromal cells) and osteoblasts (primary calvarial osteoblasts) during differentiation. Interestingly, shRNA-mediated knockdown of Sirt2 alone had a negative effect on osteogenesis, by significantly increasing adipogenic markers (PPAR gamma) and commitment of mesenchymal progenitor cells to adipocytes. Chromatin immunoprecipitation and co-immunoprecipitation experiments in progenitor cells show that Sirt2 directly interacts with Pbx1, a homeodomain protein that is a negative co-regulator of Hoxa10 mediated transcription. When co-expressed Pbx1 increases the nuclear localization of Sirt2 resulting in increased repression of osteoblast marker genes. Pbx1 and Sirt2 co-localize on osteoblast-related gene promoters (osterix (sp7), osteocalcin (bglap2), bone sialoprotein (ibsp)) while cells are actively proliferating resulting in suppression of these genes. There is a functional relationship between Pbx1 and Sirt2 as knockdown of Sirt2 in Pbx1 overexpressing cells resulted in increased histone acetylation at osteoblast gene promoters and subsequent increased expression of osteoblast-related genes suggesting that Sirt2 is required for Pbx1-mediated repression of osteoblast related genes. These results suggest that cellular levels of Pbx1 and Sirt2 are involved in specifying mesenchymal commitment to the adipocyte or osteoblast lineages and may represent a mechanism regulating age-related changes in osteoblastogenesis and bone formation.

***Disclosures: Jonathan Gordon**, None.*

1221

Contributions of PTH-mediator CREB to Postnatal Bone Mass in Human and Mouse Through Regulation of Osteoblast Function. Hongbin Liu*[1], Rongrong Zhang[1], Shanshan Dong[2], James Edwards[3], Seon-Yle Ko[4], Hong-Wen Deng[5], Ming Zhao[2]. [1]Department of Basic Medical Sciences, UMKC School of Medicine, USA, [2]University of Missouri - Kansas City, USA, [3]Vanderbilt University Medical Center, USA, [4]Dankook University, School of Dentistry, South korea, [5]University of Missouri, Kansas City Medical School, USA

Transcription factor CREB (cAMP-response element binding protein) plays an essential role in osteoblasts to mediate the anabolic signaling of intermittent dosage of PTH in bone. To further investigate the precise physiological role of CREB in maintenance of postnatal bone mass, we have performed human genome-wide association and mouse functional studies. Data from 1000 unrelated US Caucasian subjects have shown that the polymorphisms at multiple positions of CREB gene were significantly associated with bone mineral density (BMD) of spine and ultradistal radius ($p<0.011$~0.042, suggesting that CREB is essential for postnatal bone mass in humans. To validate this relevance of CREB to bone, we created osteoblast-specific CREB knockout mice by crossing CREB floxed mice with Col1a1(3.6)-Cre mice. μCT and histological characterizations have shown that trabecular bone volume of limb bones of two-month-old CREB KO mice was substantially reduced, along with decreased trabecular number and trabecular thickness but increased trabecular separation, compared with those of the control mice. These results validate that normal CREB function in bone is critical for postnatal bone homeostasis. Next, we were interested in exploring the molecular mechanisms by which CREB functions in bone. We found that expression of BMP2, an important growth factor that induces osteoblastogenesis and bone formation, was substantially decreased in the primary CREB-deficient calvarial cells, compared with the control cells. Furthermore, we found that overexpression of CREB up-regulated BMP2 levels in osteoblast MC3T3/E1 cells stably transfected with CREB. DNA sequence analysis has shown that BMP2 promoter contains multiple cAMP response elements (CREs). The subsequent

promoter deletion, EMSA and mutation studies have confirmed that CREB transactivates BMP2 gene expression through these specific CREs in the BMP2 promoter. These results suggest that CREB is a powerful activator of BMP2 transcription in osteoblasts. As expected, we found that transfection of CREB increased ALP activity in various osteoblast cell lines and this action was blocked by noggin, a BMP antagonist, demonstrating that CREB stimulates osteoblast differentiation through BMP pathway. Lastly, we determined the effects of pharmacological manipulation of CREB phosphorylation on CREB activity in osteoblasts. We found that treatment of osteoblast cells with cAMP/PKA activator IBMX or inhibitor KT5720 markedly affected CREB transactivation of the BMP2 expression. Since PTH phosphorylates CREB in osteoblasts, we further examined whether PTH regulates BMP2 transcription. The results showed that BMP2 promoter activity was significantly enhanced when treated with PTH. Together, all the results of these human and mouse studies suggest that PTH-mediator CREB plays an important role in controlling postnatal bone mass by regulating BMP2 production and consequent osteoblast differentiation.

***Disclosures: Hongbin Liu**, None.*

1222

MicroRNA-138 Targets Focal Adhesion Kinase and Regulates I*n Vivo* Bone Formation. Hanna Taipaleenmaki*[1], Tilde Eskildsen[1], Jan Stenvang[2], Basem Abdallah[3], Nicholas Ditzel[4], Sakari Kauppinen[5], Moustapha Kassem[6]. [1]Endocrine Research Laboratory (KMEB), Odense University Hospital, Denmark, [2]MicroRNA Research Unit, Department of Cellular & Molecular Medicine, University of Copenhagen, Denmark, [3]Odense University Hospital, University of South Denmark, Denmark, [4]Endocrine Research Laboratory (KMEB), Department of Endocrinology & Metabolism, Denmark, [5]Santaris Pharma, Denmark, [6]Odense University Hospital, Denmark

MicroRNAs (miRNAs) are short non-coding RNAs that interfere with translation of specific target genes acting as key regulators of diverse cellular processes. Elucidating the mechanisms regulating human mesenchymal stem cell (hMSC) differentiation into osteogenic lineage is of importance to identify novel targets for anabolic therapy of osteoporosis. Through comprehensive analysis of miRNAs expressed during hMSC differentiation into osteoblast we identified miR-138 as a potential modulator of osteoblast differentiation. Microarray analysis and further validation of miRNA expression by qRT-PCR revealed significant down-regulation of miR-138 during osteoblast differentiation of hMSCs. Overexpression of miR-138 inhibited osteoblast differentiation capacity of hMSCs *in vitro*, while silencing miR-138 by anti-miR-138 promoted ALP activity, matrix mineralization and expression of osteoblast specific genes. Furthermore, overexpression of miR-138 reduced ectopic in *vivo* bone formation by 85 % and, conversely, *in vivo* bone formation was enhanced by 60 % when miR-138 was silenced. Target prediction analysis and further experimental validation confirmed focal adhesion kinase (FAK/Ptk2), a kinase playing a role in promoting osteoblast differentiation, as a target of miR-138.

In conclusion, our data demonstrate that miR-138 attenuates *in vivo* bone formation possibly through inhibition of FAK signalling pathway. Inhibition of miR-138 is a potential new strategy for enhancing osteoblast differentiation and bone formation of MSC *in vivo*.

***Disclosures: Hanna Taipaleenmaki**, None.*

1223

Long-Term Lack of Fgf-23 Induces Severe Secondary Hyperparathyroidism in Vitamin D Receptor-Ablated Mice. Carmen Streicher*[1], Olena Andrukhova[1], Ute Zeitz[1], Beate Lanske[2], Reinhold Erben[1]. [1]University of Veterinary Medicine, Austria, [2]Harvard School of Dental Medicine, USA

Fibroblast growth factor-23 (Fgf-23) is an endocrine signal originating from osteocytes which downregulates renal tubular phosphate reabsorption and vitamin D hormone synthesis. Previous studies in 4-week-old *Fgf-23* deficient mice crossed to vitamin D receptor (VDR) mutant mice suggested that the main physiological function of Fgf-23 is the suppression of renal 1α-hydroxlase, the key enzyme in vitamin D metabolism. Due to the short life span of *Fgf-23*$^{-/-}$ mice, data in skeletally more mature mice are lacking. Here, we examined the effects of long-term *Fgf-23* deficiency on mineral and bone homeostasis in 9-month-old wild-type (WT) mice, *VDR* mutant mice, and *Fgf-23*/*VDR* compound mutant mice on both a standard rodent chow and a rescue diet (RD) enriched with calcium, phosphorus, and lactose. As expected, *VDR* and compound mutants on the normal diet showed hypocalcemia and severe secondary hyperparathyroidism (sHPT). *VDR* mutants on RD were normophosphatemic and had normal tibial bone mineral density, but showed slightly reduced ionized blood calcium and increased serum intact PTH (106 ± 87 vs. 15 ± 5 pg/ml in WT). Circulating Fgf-23 was lower in *VDR* mutants relative to WT animals on RD. Relative to *VDR* mutants, compound mutants on RD were characterized by hyperphosphatemia and very high serum PTH (1,432 ± 286 pg/ml). sHPT in compound mutants was associated with bone loss and cortical thinning at the tibial shaft. Analysis of renal handling of minerals revealed additional calcium wasting but unchanged urinary phosphate excretion in compound relative to *VDR* mutants on RD. Quantitative RT-PCR showed that renal calcium wasting in compound mutants was associated with lower expression of calbindin D28k and D9k, but unchanged expression of PTH receptor and up-regulated expression of epithelial calcium channels TRPV5 and 6 mRNA, relative to *VDR* mutants. Collectively, our data suggest that the driving force behind the development of sHPT in compound mutants was hyperphosphatemia and renal calcium wasting. Interestingly, compared with *VDR* mutants, compound mutants showed hyperphosphatemia, renal calcium loss, and unchanged tubular reabsorption of phosphate in the presence of ~13-fold higher serum PTH. Hence, *Fgf-23* deficiency blunts the phosphaturic and calcium-conserving actions of PTH in vivo, suggesting that Fgf-23 and PTH signaling interact in renal tubular cells in a vitamin D independent fashion.

***Disclosures: Carmen Streicher**, None.*

1224

PHEX Has Distinct Roles in Regulating Cancellous and Cortical Bone Mineralization. Peter Rowe*[1], Anne-Marie Hedge[1], Yan Hong[1], Aline Martin[2], Lesya Zelenchuk[1], Valentin David[2]. [1]University of Kansas Medical Center, USA, [2]UTHSC, USA

Mutations in PHEX or DMP1 cause X-linked hypophosphatemic rickets (HYP) and Autosomal Recessive Hypophosphatemic Rickets (ARHR) respectively. Both diseases result in increased FGF23 levels with rickets and hypophosphatemia. DMP1 and MEPE derived ASARM-peptides are physiological substrates for PHEX and are strong inhibitors of mineralization. We described previously a competitive inhibitor of PHEX (SPR4) that binds specifically to ASARM-peptides and reverses the HYP mineralization defect *in vitro*. Here we describe the bone-mineral *in vivo* effects of 28 day osmotic pump infusion of SPR4 peptide in wild type and HYP mice

Wild type and HYP mice (C57BL/6; n=5, male) were infused with vehicle (0.9% NaCl) or peptide (276 nmoles/hr/kg) for 28 days (Alzet Osmotic pumps). Bone mineral Density (BMD) was measured by DEXA at day 0 and 28. Animals were sacrificed on day 28 after overnight metabolic cage housing. Femurs were removed and scanned by micro computed tomography (μCT).

SPR4 peptide treatment significantly reduced the percentage change in total Bone Mineral Density (Δ-BMD) in wild type mice (-22%; $p<0.05$) and this was more marked in femur epiphyses (-60%; $p<0.05$). Detailed μCT analysis revealed a dynamic change in Δ-BV/TV, bone mineral distribution and trabecular structure over the 28 days. Specifically in wild-type mice, segmental analyses of the distal femur head, (epiphyseal region) showed a significant drop in Δ-BV/TV in SPR4 treated animals. In contrast the cortical diaphyseal region contained a 20% increase in Δ-BV/TV (Figure 1A). Treated wild type mice also showed a significant drop in trabecular number, spacing and connectivity as measured by μCT (Figure 1B).

We conclude PHEX plays a major role in maintaining a normal cancellous bone structure. SPR4 disrupts this process by inhibiting competitively PHEX activity. In cortical bone, SPR4 peptide neutralizes free ASARM-peptides and thus positively alters the bone mineralization dynamic. This suggests PHEX plays distinct roles in regulating cancellous and cortical bone. Finally, we speculate SPR4-peptide may be of use in treating the endocortical-osteomalacia that occurs in patients with HYP, ARHR and perhaps ADHR.

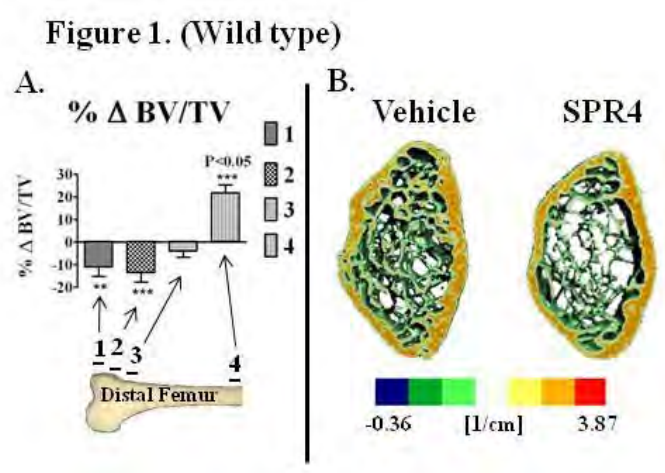

Figure 1

***Disclosures: Peter Rowe**, None.*

1225

Phex Mutations in a Murine Model of X-linked Hypophosphatemia Result in Impaired Phosphate Sensing. Shoji Ichikawa*[1], Anthony M. Austin[2], Amie K. Gray[2], Michael Econs[2]. [1]Indiana University-Purdue University Indianapolis, USA, [2]Indiana University School of Medicine, USA

Fibroblast growth factor 23 (FGF23) is a critical regulator of phosphate homeostasis, which inhibits renal phosphate reabsorption and 1,25-dihydroxyvitamin D (calcitriol) synthesis. Elevated circulating FGF23 concentrations are the main cause of hypophosphatemia in various phosphate wasting disorders, including X-linked hypophosphatemia (XLH). The current standard therapy for XLH is high dose phosphate and calcitriol; however, this therapy further aggravates FGF23 concentrations. This observation suggested that FGF23-producing cells (osteoblasts and osteocytes) in XLH likely have an altered set point for phosphate sensing.

To test this hypothesis, we compared serum biochemistries and femoral Fgf23 mRNA expression between murine models of XLH ($Phex^{K496X}$) and hyperphosphatemic tumoral calcinosis ($Galnt3^{-/-}$), as well as Phex/Galnt3 double mutant mice. Phex mutant mice had increased Fgf23 expression in bone, resulting in markedly elevated serum Fgf23 levels and consequent hypophosphatemia. In contrast, because the secretion of intact, biologically active Fgf23 protein depends on O-glycosylation of Fgf23 by GalNAc transferase 3 (Galnt3), Galnt3 knockout mice had significantly lower circulating concentrations of intact Fgf23, despite markedly increased Fgf23 expression. As a result, Galnt3 knockout mice had hyperphosphatemia.

In the absence of a phosphate sensing defect, Phex/Galnt3 double mutant mice should express Fgf23 mRNA at the similar level as $Phex^{K196X}$ mice, but level of circulating intact Fgf23 protein should be markedly reduced or even normal compared to the single $Phex^{K196X}$ mutant animal and serum phosphate concentrations should be increased compared to $Phex^{K496X}$ mice. Although the double mutant had lower intact Fgf23 concentrations compared to the Phex mutant, these levels were still elevated compared to littermate controls, resulting in hypophosphatemia in the double mutant. Importantly, despite the presence of the marked hypophosphatemia, Fgf23 mRNA expression in the double mutant was 14 fold higher than the Phex mutant and 150 fold higher than controls, consistent with impaired phosphate sensing. In conclusion, these data suggest that Phex mutations lead to intrinsic defects in osteoblasts and osteocytes, which alter their phosphate sensing mechanism.

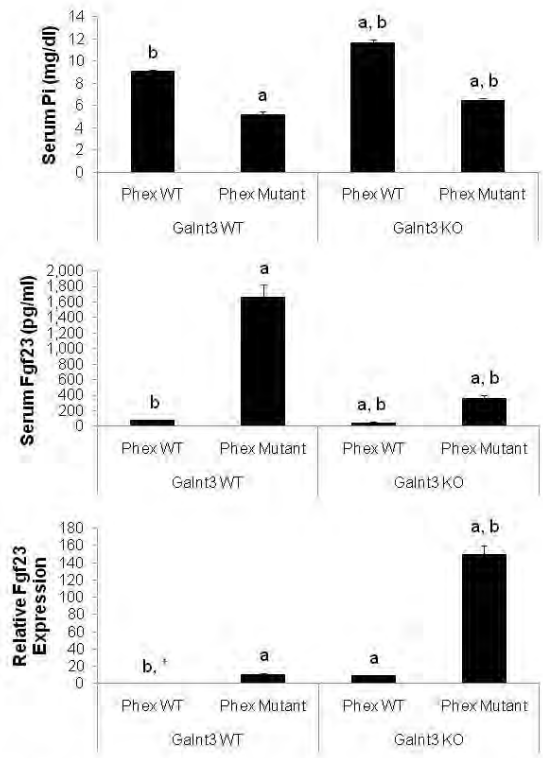

Number of six-week-old mice per group: 6-10. T-test p-values less than 0.01, compared to wild-type controls (a) and to Phex mutant with wild-type Galnt3 (b). *Wild-type controls arbitrarily set at 1.0.

Serum biochemistries and femoral Fgf23 expression

***Disclosures: Shoji Ichikawa**, None.*

1226

Evidence that the Mineralization Defect in *hyp*-mice Results from the Uncoupled Effects of SOST/sclerostin on Osteoblast Mineralization and Proliferation. Baozhi Yuan*[1], Jennifer Meudt[2], Robert Blank[2], Jian Feng[3], Marc Drezner[2]. [1]University of Wisconsin, Madison, USA, [2]University of Wisconsin, USA, [3]Texas A&M Health Science Center, USA

Hyp-mice manifest hypophosphatemia and severe osteomalacia due to a loss of function Phex mutation. Recent studies revealed targeted Phex deletion in osteoblasts (*OC-Cre-*$Phex^{\Delta floxly}$) results in the typical *Hyp* phenotype. However, Phex deletion in osteocytes (*DMP1-Cre-*$Phex^{\Delta floxly}$), while creating *Hyp* biochemical abnormalities, results in a far less severe osteomalacia than in *hyp*- or *OC-Cre-*$Phex^{\Delta floxly}$*-mice*. The less profound mineralization defect in *DMP1-Cre-*$Phex^{\Delta floxly}$-mice occurred despite comparable hypophosphatemia and equal increments in circulating FGF-23, suggesting loss of Phex function in osteocytes causes abnormal mineralization independent of P and FGF-23. Thus, *DMP1-Cre-*$Phex^{\Delta floxly}$-mice provide a model that dissociates increased serum FGF-23 levels and hypophosphatemia from a profound defect in bone mineralization, indicating that Phex may have other unique actions impacting bone calcification. In accord with this hypothesis, we found Sost mRNA expression was significantly increased in the the *hyp*- and *OC-Cre-*$Phex^{\Delta floxly}$-mice with severe osteomalacia, but not in *DMP1-Cre-*$Phex^{\Delta floxly}$-mice with mildly aberrant bone mineralization, consistent with a regulatory effect of Sost on bone mineralization under hypophosphatemic conditions. To create the severe osteomalacia, evident in the *hyp*- and *OC-Cre-*$Phex^{\Delta floxly}$-mice, however, bone remodeling must reflect decreased bone mineralization without a coupled decrement in osteoblast proliferation. To examine if the Sost protein product exhibits such activity, we incubated cultured osteoblasts (TMOB) with sclerostin (0.625 μg/ml) for 14 days. We observed that sclerostin reduced TMOB mineralization (Alizarin stain/destain) compared to that in untreated cells (2.3 ± 0.2 vs 3.2 ± 0.1; $p<0.05$), demonstrating an inhibitory effect of the protein on calcification. Moreover, study of sclerostin action on osteoblast proliferation revealed uncoupled effects. Thus, TMOB cells, cultured with sclerostin (0.625 or 1.25 μg/ml) and harvested at 5, 24, 36, 48, 64, 72, and 82 hrs revealed no changes in cell proliferation (Cyquant assay, Invitrogen). These observations demonstrate sclerostin effects on bone mineralization are uncoupled from actions on osteoblast proliferation. Hence, abnormal bone mineralization evident in *hyp*- and in *OC-Cre-*$Phex^{\Delta floxly}$- mice may manifest due to increased Sost mRNA expression. Studies resulting in inhibition of Sost expression in *hyp*-mice are critical to elucidate this possibility.

***Disclosures: Baozhi Yuan**, None.*

1227

Lrp5 G171V and A214V Knock-in Mice are Protected from the Osteopenic Effects of Sost Overexpression. Alexander Robling*[1], Matt Warman[2], Teresita Bellido[3], Paul Niziolek[3]. [1]Indiana University, USA, [2]Children's Hospital Boston, USA, [3]Indiana University School of Medicine, USA

Several missense mutations in the LRP5 receptor are associated with high bone mass (HBM) in humans. Based on *in vitro* evidence, the HBM mutations are thought to exert their effects on bone mass by providing resistance to binding/inhibition of the soluble LRP5 inhibitor sclerostin, among others. We previously reported the creation of two HBM mouse models, in which we knocked-in the A214V or G171V HBM mutation into the endogenous Lrp5 locus. To determine whether HBM knock-in mice are immune to sclerostin-induced osteopenia, we cross-bred these mice with transgenic mice overexpressing Sost in osteocytes (Dmp1::Sost).

We generated mice that were homozygous for the wild-type Lrp5 allele ($Lrp5^{+/+}$), A214V allele ($Lrp5^{A/A}$), and G171V allele ($Lrp5^{G/G}$). Within each Lrp5 genotype, mice were generated that were positive or negative for the Dmp1::Sost transgene. 8 male and 8 female mice were analyzed in each of the 6 genotype combinations created. Whole body DEXA scans were collected bi-weekly from 4.5 wks to 16.5 wks. At sacrifice (17 wks) the 5th lumbar vertebra was harvested for μCT measurements of trabecular bone properties. Comparisons were made between Dmp1::Sost transgenic and nontransgenic mice within each Lrp5 genotype.

Among $Lrp5^{+/+}$ mice, the Dmp1::Sost transgene lowered L5 vertebral BV/TV by 48-50% ($p<0.05$), compared to non-transgenic $Lrp5^{+/+}$ littermates. The same transgene, expressed in $Lrp5^{A/A}$ mutants resulted in a more mild reduction (10-16% decrease; $p<0.05$) in BV/TV, compared to nontransgenic $Lrp5^{A/A}$ mutants. Conversely, when expressed in the Lrp5 G171V mutants, the Dmp1::Sost transgene produced no significant effect on vertebral BV/TV (2-7% decrease, p=NS), when compared to nontransgenic $Lrp5^{G/G}$ mutants. Whole-body BMC was significantly reduced by the Dmp1::Sost transgene in male but not female $Lrp5^{+/+}$ mice. Among the male mice (where a significant Dmp1::Sost effect was detected), the transgene did not significantly reduce BMC in the $Lrp5^{A/A}$ or $Lrp5^{G/G}$ mutants.

In summary, the HBM mutation G171V imparted immunity to sclerostin-mediated osteopenia in mice. The Lrp5 A214V mutants exhibited immunity to sclerostin in some, but not all measures, suggesting that these two HBM mutations might affect in vivo sclerostin binding and inhibition differently.

***Disclosures: Alexander Robling**, None.*

1228

Augmentation of cAMP Signaling in the Mouse Renal Proximal Tubule by Targeted in vivo Expression of the Extra-large Gsα Variant XLαs. Zun Liu[1], Hiroko Segawa[1], Cumhur Aydin[2], Reinhold Erben[3], Lee Weinstein[4], Vladimir Marshansky[1], Leopold Frohlich[5], Murat Bastepe*[1]. [1]Massachusetts General Hospital, Harvard Medical School, USA, [2]Gulhane School of MedicineAnkara, TURKEY, Turkey, [3]University of Veterinary Medicine, Austria, [4]National Institute of Diabetes & Digestive & Kidney Diseases, USA, [5]Medical University of Graz, Austria

The α-subunit of the stimulatory G protein (Gsα) and its variant XLαs are both encoded by *GNAS*. XLαs, like Gsα, can mediate receptor-activated cAMP generation and, thus, is able to replace the latter in transfected cells. However, it remains unknown whether XLαs can mediate cAMP signaling in vivo. To address this question, we have employed rat type-I γ-glutamyltranspeptidase promoter and generated transgenic mice in which XLαs expression is targeted ectopically to the renal proximal tubule (rptXLαs mice). The transgenic mice were examined regarding renal proximal tubular responses that typically rely on cAMP signaling. Western blots indicated elevated protein kinase A (PKA) activity in renal proximal tubules of rptXLαs mice compared to littermate controls. Quantitative RT-PCR experiments showed that 25-hydroxyvitamin D3 1α-hydroxylase (Cyp27b1) mRNA, a downstream target of cAMP-PKA signaling, was ~2-fold higher in rptXLαs mice than wild-type littermates. In addition, Western blots showed that the expression of sodium-phosphate co-transporter type 2a, which is downregulated upon PKA-mediated mechanisms, was diminished in renal brush border membranes of the transgenic mice. In contrast, Gsα protein and mRNA levels in renal proximal tubules were unaltered, as determined by Western blots and quantitative RT-PCR. Serum calcium and phosphorus in rptXLαs mice were within the normal range, but serum PTH was ~40% lower than in wild-type littermates, consistent with increased PTH sensitivity in rptXLαs mice. When the transgenic mice were crossed to mice heterozygous for maternal ablation of *Gnas* exon 1, a model of pseudohypoparathyroidism, offspring with maternal *Gnas* exon 1 ablation alone had lower levels of 25-hydroxyvitamin D3 1α-hydroxylase mRNA in renal proximal tubules than wild-type mice, whereas offspring carrying both the XLαs transgene and maternal *Gnas* exon 1 ablation showed nearly normal levels of this transcript. These data demonstrate that transgenic XLαs expression in the renal proximal tubule leads to enhanced cAMP signaling, supporting the idea that XLαs can mimic the function of Gsα in vivo. Hence, XLαs may contribute to cAMP signaling and, thereby, play a role in a wide range of biological responses. Changes in XLαs activity may also be involved in the pathogenesis of diseases caused by *GNAS* mutations, including pseudohypoparathyroidism, Albright's hereditary osteodystrophy, and fibrous dysplasia of bone.

***Disclosures: Murat Bastepe**, None.*

1229

Parathyroid Hormone -Related Protein (PTHrP) Gene Ablation in Breast Cancer Cells Inhibits Invasion in vitro and Metastasis in vivo: Role of Akt and CXCR4. Richard Kremer[1], William Muller[2], Peter Siegel[3], Anne Camirand[4], Andrew Karaplis[5], Jiarong Li*[5]. [1]McGill University, Royal Victoria Hospital, Canada, [2]Rosalind & Morris Goodman Cancer Research Centre, Department of Biochemistry, Canada, [3]Goodman Cancer Research Centre, McGill University, Canada, [4]Sir Mortimer B. Davis Jewish General Hospital, McGill University, Canada, [5]McGill University, Canada

An increase in PTHrP circulating levels is associated with breast cancer recurrence and reduced survival. However, a mechanistic link between PTHrP and metastatic spread outside the skeleton has not yet been established. In this study, mice carrying a conditional PTHrP allele were crossed with the PyVMT transgenic mouse mammary tumor model and then with a separate transgenic strain expressing Cre in the mammary epithelium (MMTV/Cre). Tumors from PyVMT-PTHrP$^{flox/flox}$ Cre^{-} animals were harvested, minced, trypsinized and transfected with adeno-Cre GFP (experimental) or adeno-GFP (control) and selected by cell sorting. Cells were analyzed in vitro for invasion by Matrigel assays or reimplanted in vivo into the mammary fat pad (0.5X106 cells) of syngeneic 5-week old FVB mice non-tumor bearing mice of the same strain for analysis of metastatic spread to lung. The invasive ability in vitro of PyVMT-PTHrP$^{flox/flox}$-Cre^{+}cells was reduced by over 80% ($P<0.001$) as compared to control cells (PyVMT-PTHrP $^{flox/flox}$-Cre^{-}).Circulating tumor cells (CTCs) were detectable in animals transplanted into the mammary fat pad with PyVMT-PTHrPflox/flox-Cre-cells but not in animals transplanted with PyVMT-PTHrP $^{flox/flox}$-Cre^{+}cells. Metastatic spread to lungs was seen in 100% of animals transplanted with PyVMT-PTHrP $^{flox/flox}$-Cre^{-} cells when tumor size reached around 1.5cm^{3}. In contrast none of the animals transplanted with PyVMT-PTHrP $^{flox/flox}$-Cre^{+}cells had any evidence of metastatic spread in lungs at the same tumor size. We next assessed AKT1 and CXCR4 expression by Western blot and confocal microscope in both isolated cells and tumors from both genotypes. Akt 1 and CXCR4 expression by Western blot were markedly reduced(over 80% $P<0.001$)in PyVMT-PTHrP$^{flox/flox}$-Cre^{+}cells and tumors as compared to PyVMT-PTHrP $^{flox/flox}$-Cre^{-}cells and tumors. Akt1 and CXCR4 fluorescence intensity was high in PyVMT-PTHrPflox/flox-Cre-cells but almost absent in PyVMT-PTHrPflox/flox-Cre+cells. Furthermore, siRNA knockdown of AKt1 reduced invasion in vitro significantly more in PyVMT-PTHrP$^{flox/flox}$-Cre^{+}cells than in PyVMT-PTHrP$^{flox/flox}$-Cre^{-} cells($P<0.05$) suggesting that PTHrP has Akt dependent and independent effects. Overall, our study demonstrates that PTHrP plays a crucial role in metastatic spread possibly by altering critical checkpoint of cancer progression and suggest its potential usefulness to prevent progression and recurrence of breast cancer.

***Disclosures: Jiarong Li**, None.*
This study received funding from: CIHR

1230

Unveiling Dual Functions of p53 in Preventing Breast Cancer Bone Metastasis by Simvastatin Targeting CD44 and PTEN. Chandi Mandal*[1], Nayana Ghosh-Choudhury[2], Toshiyuki Yoneda[3], Goutam G Choudhury[4], Nandini Ghosh-Choudhury[1]. [1]University of Texas Health Science Center at San Antonio, USA, [2]University of Texas Health Science Center, USA, [3]Osaka University Graduate School of Dentistry, Japan, [4]University of Texas Health Science Center & South Texas Veterans Administration, USA

Metastasis to skeleton is an ominous feature of malignant breast cancer. We used heart injection model to test the effect of simvastatin on breast cancer bone metastasis. Simvastatin prevented osteolytic lesions in mice injected with MDA-MB-231 (MDA) human breast cancer cells, indicating that statin attenuates breast cancer metastasis to bone. To investigate the mechanism, MDA cells were used in an *in vitro* wound healing assay. Simvastatin significantly inhibited the migration of MDA cells. Transwell invasion assay using collagen-coated discs confirmed the inhibitory effect of simvastatin on breast cancer cell invasion. We have recently shown that simvastatin inhibits primary tumor growth in mice by upregulating the tumor suppressor PTEN. Overexpression of PTEN in MDA cells significantly blocked their ability to migrate and invade. To determine the mechanism of PTEN upregulation, we considered the tumor suppressor protein p53, which is known to regulate PTEN expression. Simvastatin-treated mice tumors showed significantly increased levels of p53. Similarly, simvastatin enhanced the expression of p53 in MDA cells. Additionally, simvastatin increased transcription of the reporter plasmids containing the consensus p53-binding element (p53-Luc) or the PTEN promoter (PTEN-Luc). Cotransfection of p53 with these reporter constructs resulted in similar increase in transcription, indicating a role of p53 in PTEN expression by simvastatin. Recent reports indicate a direct correlation between expression of CD44 in breast cancer and their metastasis to other organs including bone. Levels of CD44 were significantly reduced in the tumors of mice treated with simvastatin. In MDA cells, simvastatin decreased the expression of CD44 protein and its transcription, as determined by CD44 promoter-driven luciferase construct (CD44-Luc). p53 acts as transcriptional activator or transcriptional repressor in a cell-type and context-dependent manner. Presence of non-canonical p53-binding elements has been reported in the CD44 promoter. Cotransfection of p53 with CD44-Luc significantly suppressed the transcription of CD44. Furthermore, expression of p53 markedly reduced the expression of CD44 protein. Finally, downregulation of endogenous CD44 by specific shRNA decreased migration of MDA cells. Together these results uncover a novel action of simvastatin, which targets p53 expression to simultaneously increase PTEN and decrease CD44 thus blocking migration and preventing bone metastasis of the human breast cancer cells.

***Disclosures: Chandi Mandal**, None.*

1231

CyclicCHAD is a Novel Biological Agent for the Treatment of Breast Cancer-Induced Bone Metastases Targeting All the Players of the Vicious Cycle. Mattia Capulli*[1], Anna Rufo[2], Marina Alamanou[1], Barbara Peruzzi[2], Marta Capannolo[1], Ole Kristoffer[3], Kaare M. Gautvik[3], Lisbet Haglund[4], Dick Heinegard[4], Anna Teti[1], Nadia Rucci[1]. [1]Department of experimental Medicine, University of L'Aquila, Italy, [2]Department of Experimental Medicine, University of L'Aquila, Italy, [3]Department of Clinical Chemistry, Ullevaal University Hospital & Institute of Biochemistry, University of Oslo, Norway, [4]Department of Experimental Medical Science, Lund University, Sweden

Bone remodeling is based on a virtuous cycle in which osteoblasts and osteoclasts cross-talk and renovate the bone. Cancer cells are able to interfere with this process establishing the so called vicious cycle, in which osteoclasts are over-activated to resorb bone and release tumor-seeking growth factors stored in the bone matrix. Chondroadherin (CHAD) is an integrin binding protein. We observed that a cyclic peptide representing its integrin binding sequence (cyclicCHAD) reduced the mRNA expression of the osteoclastogenic cytokines RANKL IL-1beta and IL-6 by osteoblasts, without affecting their differentiation and function. It also directly inhibited osteoclast formation, adhesion and bone resorption and impaired invasion and migration of the human breast cancer cells, MDA-MB-231. Based on this in vitro evidence that cyclicCHAD targets all the players of the vicious cycle, we tested the efficacy of this peptide in the treatment of bone metastases in an animal model. We first investigated the safety of cyclicCHAD by injecting i.p. Balb-c nu/nu mice with vehicle or with 1 and 10 mg/kg body weight of cyclicCHAD, 5 days/week for 8 weeks. Treatment did not induce macroscopic organ injury, microscopic alteration of liver, kidney and spleen, or derangement of serum markers of tissue damage. Moreover, histomorphometric analysis of tibiae indicated the ability of cyclicCHAD to dose-dependently increase the bone structural parameters. Next we injected the left ventricle of Balb-c nu/nu mice with MDA-MB-231 cells and, starting the day after injection, we treated the animals daily with vehicle, 10 mg/Kg of control peptide, 1 mg/Kg of the reference drug, alendronate, or with 10 mg/kg of cyclicCHAD. Mice

receiving cyclicCHAD showed reduced cachexia (17% incidence) which, in contrast, affected 65% of control and alendronate-treated mice. Similar to alendronate, cyclicCHAD also dramatically reduced the incidence of bone metastases relative to vehicle (18.5% for alendronate and 18% for cyclicCHAD vs. 50% for control). At variance with alendronate, which increased the mean visceral metastasis volume by 2.9 fold vs. control, cyclicCHAD did not induce such adverse effect, thus leading to reduced morbidity and improved quality of life of treated animals. In conclusion, our data indicate that a cyclic peptide representing the integrin binding domain of CHAD could be a potential new drug for the treatment of bone metastases, targeting tumor cells as well as bone cells.

***Disclosures: Mattia Capulli**, None.*

1232

Bone-Targeted Therapy With Zoledronic Acid Combined With Adjuvant Ovarian Suppression Plus Tamoxifen or Anastrozole: 62-Month Outcomes From the ABCSG-12 Trial in Premenopausal Women With Endocrine-Responsive Early Breast Cancer. Michael Gnant*[1], P. Dubsky[1], C. Singer[1], R. Greil[2], B. Mlineritsch[2], H. Stoeger[3], H. Eidtmann[4], R. Jakesz[1], S. Poestlberger[5], G. Luschin-Ebengreuth[3]. [1]Medical University of Vienna, Austria, [2]Paracelsus Medical University Salzburg, Austria, [3]Medical University of Graz, Austria, [4]Universitäts Frauenklinik Kiel, Germany, [5]Hospital of the Sisters of Mercy, Austria

Purpose: The ABCSG-12 trial examined the efficacy of bone-targeted therapy with zoledronic acid (ZOL) in combination with ovarian suppression using goserelin plus anastrozole (ANA) or tamoxifen (TAM) in premenopausal patients (pts) with endocrine-responsive early breast cancer (EBC). The 48-month efficacy analysis presented at ASCO 2008 showed no difference between TAM and ANA; however, adding ZOL significantly reduced the risk of disease-free survival (DFS) events by 36% (P = .01). Longer follow-up is now available.

Methods: 1,803 premenopausal pts with EBC were randomized to goserelin (3.6 mg q28d) and TAM (20 mg/d) or ANA (1 mg/d) ± ZOL (4 mg q6m). The study was approved by each institution's human research committee. Endpoints were DFS and overall survival (OS); both were analyzed using log-rank test and Cox models. Compared with 2008 data, we now report on 34% more DFS events and 55% more deaths, based on data cutoff of December 1, 2009.

Results: With a median follow-up of 62 mo, 183 DFS events and 65 deaths were reported. Overall, adding ZOL reduced the risk of DFS events by 32% (hazard ratio [HR] = 0.68 [95% CI = 0.51-0.91]; P = .009). The risk reduction by ZOL was consistent in the TAM and ANA strata (HR = 0.68 [0.44-1.05] for TAM, HR = 0.68 [0.45-1.02] for ANA), and for N– and N+ pts. ZOL reduced the risk of death by 34% (HR = 0.66 [0.41-1.09]; P = .10), with a trend toward reduced risk of death in the N+ subgroup (HR = 0.61; P = not significant). There was no difference in DFS between pts who received TAM alone vs ANA alone (HR = 1.11 [0.84-1.50]; P = .44). However, ANA pts did worse with respect to OS (HR = 1.74 [1.05-2.87]; P = .03) vs TAM, probably due to differences in postrelapse treatment. Treatments were generally well tolerated. There were no cases of renal failure or osteonecrosis of the jaw.

Conclusions: With longer follow-up of ABCSG-12, adding ZOL (4 mg q6m) consistently improved DFS in the ANA and TAM subgroups, and in N+ and N– pts, with a trend toward better OS. There was no DFS difference between ANA and TAM, but ANA pts had inferior OS vs TAM, probably because ANA pts received second-line therapy off study. Based on these results and the known anticancer activity of ZOL demonstrated in preclinical and clinical studies, adding ZOL to adjuvant therapy should be considered for premenopausal pts with EBC.

***Disclosures: Michael Gnant**, None.*
This study received funding from: Astrazeneca & Novartis

1233

Up-regulation of CGRP Expression by Acid-activated Calcium Channel Nociceptor Trpv1 is Involved in Bone Pain. Masako Nakanishi*[1], Kenji Hata[1], Tomotaka Nagayama[1], Toshihiko Nishisho[2], Toshiyuki Yoneda[1]. [1]Osaka University Graduate School of Dentistry, Japan, [2]BIGLOBE NEC, Japan

Bone pain is one of the most common complications in bone metastases, causing increased morbidity and undermining QOL in cancer patients. The mechanism of bone pain is poorly understood. We reasoned acidic conditions play a role in causing bone pain, since the microenvironment of bone metastases is acidic due to the presence of cancer cells, inflammatory cells and bone-resorbing osteoclasts and acid is a well-known algesic substance. To dissect the role of acid in bone pain, we studied calcitonin gene-related peptide (CGRP) which has been proposed to be critical in pain transmission. Immunohistochemical examination revealed CGRP expression in dorsal root ganglions (DRG), which are cell bodies of the sensory neurons. Moreover, transient receptor potential vanilloid subtype 1 (Trpv1), an acid-sensing calcium channel nociceptor, was co-expressed with CGRP in DRG. In organ cultures of DRG, acidic medium (pH 5.5) increased CGRP mRNA expression and this increase was significantly reduced by the selective Trpv1 antagonist I-RTX. Furthermore, CGRP mRNA elevation by acid was markedly decreased in DRG isolated from Trpv1-null mice. Conversely, Trpv1 introduction increased Ca^{2+} influx and CGRP expression upon acid stimulation in the F11 neuronal cells that are deficient in Trpv1. These results collectively suggest CGRP expression is regulated by acid-activated Trpv1 in the sensory neurons. We next studied the intracellular events that were involved in the up-regulation of CGRP expression by acid-activated Trpv1 with a special focus on CREB. CREB is a pivotal transcription factor in neuronal functions. We found phosphorylated CREB co-expressed with CGRP and Trpv1 in DRG. Acid stimulation increased CREB phosphorylation in the primary neuronal cells, which was inhibited by I-RTX. Knockdown of CREB expression by siRNA and blockade of CREB signaling by A-CREB, a dominant negative form of CREB, diminished acid-induced CGRP mRNA expression. Using the reporter assay and chromatin immunoprecipitation assay, we found acid elevated the transcriptional activity of CREB, thereby directly stimulating CGRP promoter activity. In conclusion, our results suggest that acidic microenvironments created in bone metastases activate Trpv1 in the sensory neurons, which in turn leads to up-regulation of CGRP mRNA expression via activation of CREB transcription activity. These series of events may be involved in the pathophysiology of bone pain.

***Disclosures: Masako Nakanishi**, None.*

1234

Subnuclear Targeting Deficient Mutations of Runx2 Abrogate Cellular Migration and Metastasis in Prostate Cancer Cells. Jacqueline Akech*[1], John J. Wixted[1], Krystin Bedard[1], Margaretha van der Deen[1], Sadiq Hussain[1], Karthiga Gokul[1], Andre Van Wijnen[1], Janet L. Stein[1], Lucia R. Languino[1], Dario C. Altieri[1], Jitesh Pratap[1], Evan Keller[2], Gary Stein[1], Jane Lian[1]. [1]University of Massachusetts Medical School, USA, [2]University of Michigan, USA

The Runx2 bone-specific transcription factor is abnormally expressed in highly metastatic prostate cancer cells (PC3). Human tissue microarray studies of prostate tumors at stages of cancer progression show Runx2 is expressed in both adenocarcinomas and metastatic tumors (*Oncogene, 2010*). Previous studies identified functional activities of Runx2 in facilitating tumor growth and osteolysis in PC3 sublines observing a strong positive correlation between Runx2 cellular levels and increases expression of growth and metastasis-related genes (Survivin, MMP9, MMP13, OP), secreted bone-resorbing factors that promote osteolytic disease (PTHrP, IHH, VEGF) and more aggressive osteolytic bone disease in the intra-tibial metastasis model. Further, shRunx2 expression in PC3 cells blocked their ability to survive in the bone. In these studies, we further analyze the mechanisms by which Runx2 facilitates tumor growth and metastasis in prostate cancer cells. Runx2 is a scaffolding protein that interacts with numerous co-regulatory factors that mediate physiological signaling upregulated in tumor cells including canonical Wnt (TCF/LEF), Src (Yap) and growth factor (TGF, BMP, Smad) pathway responses. Runx2 protein-protein complexes are targeted to subnuclear domains for Runx2 functional activity through these pathways. We characterized PC3 cells knockdown by siRNA and showed decreased cell migration, invasion through Matrigel and downregulated metastasis-related genes. We then analyzed PC3 lines overexpressing functional mutations of Runx2 deficient in subnuclear targeting (C-terminus deletion) and point mutants that disrupted Src and BMP signaling. Runx2 target gene expression by qRT-PCR revealed that mutations of Runx2 abrogated the expression of MMP2, 9 and 13 as well as tumor growth and angiogenesis related markers; survivin, histone H4 and VEGF. In complementary studies, the effects of Runx2 mutations in abrogating tumor metastasis were further verified by invasion and migration assays showing a significant reduction of cellular migration analogous to a complete knockdown. These studies show that Runx2 is a key regulator of events associated with prostate cancer metastatic bone disease. Thus, subnuclear localization and organization of Runx2 is essential in promoting these metastasis events suggesting Runx2 as a molecular target for prostate cancer therapy.

***Disclosures: Jacqueline Akech**, None.*

1235

Evaluation of Blood Flow and Skeletal Kinetics during Loading Induced Osteogenesis using PET Imaging. Ryan Tomlinson*, Kooresh Shoghi, Matthew Silva. Washington University in St. Louis School of Medicine, USA

Mechanical loading of the skeleton stimulates osteogenesis. Angiogenesis is essential to osteogenesis, although its role in loading induced osteogenesis is unknown. Previous studies show loading induced woven bone formation is associated with the production of new blood vessels, whereas lamellar bone formation is not. Our goal was to use positron emission tomography (PET) to examine blood flow and mineral kinetics at the site of loading induced bone formation. Lamellar or woven bone formation was induced by forelimb compression in adult rats using established methods. Right limbs were loaded, and left limbs were used as controls. PET scans were obtained 0, 1, 3, 7, and 14 days after loading and analyzed at the mid-forelimb.

^{15}O water, a freely diffusible radioisotope, was used to evaluate blood flow. Summed images (Fig 1A) show that loaded forelimbs in the lamellar group were not different from control limbs on days 0-7, but had 15% higher uptake on day 14 (after new bone formation). In contrast, loaded forelimbs in the woven group exhibited 30% higher uptake than controls on days 0-7, and remained 15% increased on day 14. Since ^{15}O water diffuses freely throughout the body, this radioisotope was modeled using a one-compartment, two-parameter model (Fig 1B). Modeling results confirm the static analysis.

^{18}F fluoride, a bone-seeking radioisotope, was used to evaluate skeletal kinetics. Summed images (Fig 2A) show no difference between loaded forelimbs in the lamellar group versus control at any time point. In contrast, loaded forelimbs from the woven group had 40-80% increased uptake compared to control limbs. A two-compartment,

three-parameter model was used to model ^{18}F kinetics near the site of bone formation (Fig 2B). At all time points, the macroparameter (K_1) as well as the microparameters (K_1, k_2, k_3) show significant differences in limbs producing woven bone versus lamellar bone (k_2 not significant at day 0 and 14).

In summary, PET imaging provided novel insight into the vascular response and mineral kinetics of osteogenic mechanical loading. There is an immediate and persistent increase in flow rate to the limbs producing woven bone, but only a small, late increase in limbs producing lamellar bone. Modeling of ^{18}F-fluoride indicated decreased vascular clearance during days 1-7, as well as increased incorporation of ^{18}F-fluoride into bone at all time points. We conclude that a strong vascular response precedes woven but not lamellar bone formation.

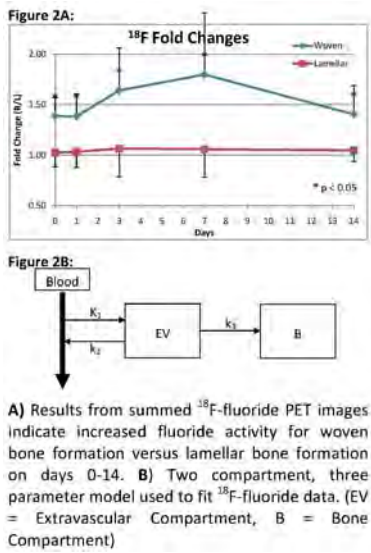

Figure 2

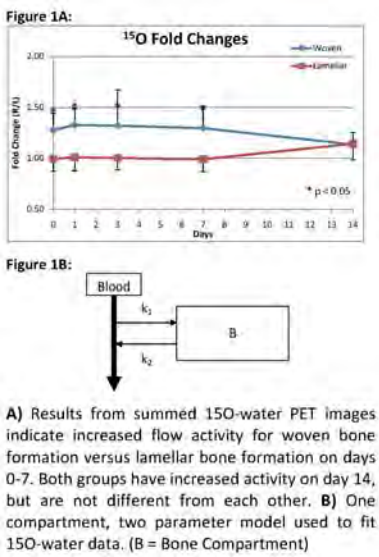

Figure 1

***Disclosures: Ryan Tomlinson**, None.*

1236

The Effect of Age on the Biomechanical Properties of Cortical Bone as a Function of Loading Rate. Daniel Nicolella*[1], Sidney Chocron[1], Arthur Nicholls[1], Don Moravits[1], Travis Eliason[1], Ryan Potter[1], Todd Bredbenner[1], Lorena Havill[2]. [1]Southwest Research Institute, USA, [2]Southwest Foundation for Biomedical Research, USA

The substantial increase in fracture risk with aging is a major clinical problem. With a growing elderly population, much effort has been given to understanding the mechanistic causes of the age-related decline in bone properties. However, the majority of these studies used very slow (e.g. quasi-static) loading rates, contrary to loading rates that are expected in a traumatic event such as a fall, where strain rates can be several orders of magnitudes higher. The objective of this investigation was to determine the effect of age on the biomechanical properties of cortical bone as a function of loading rate.

Cortical bone tensile mechanical properties were determined using specimens from the right femurs of 12 female baboons, part of a breeding colony at the Southwest National Primate Center/Southwest Foundation for Biomedical Research in San Antonio, TX. Animals were divided into two age groups: a young group (n=6, 6.63 ± 0.6 years) and an old group (n=6, 26.96 ± 1.3 years), corresponding to ages of ~20 human years and ~81 human years for young and old baboons, respectively. Two specimens from each femur were used in this study: one for quasi-static testing and one for dynamic testing. Quasi-static specimens were loaded to failure using an electro-mechanical test machine under displacement control at a strain rate of 0.0001 strain/sec to determine their quasi-static mechanical properties. Dynamic tensile tests were performed to failure on a custom built tensile Split Hopkinson Pressure Bar (SHPB) at an average strain rate of 194 strain/sec.

At quasi static strain rates, the mean elastic modulus (EM) for old bone was significantly greater than the mean EM for young bone. However, at dynamic rates, mean EM was greater for young bone compared to old bone. There was no difference in mean yield stress or failure stress between young and old bone at quasi-static loading rates, but at dynamic rates, both mean failure and yield stress were significantly lower in old bone. In contrast, mean failure strain in young bone was significantly greater than in old bone at low rates, but at high rates, there was no difference.

These results indicate that loading rate is a critical factor in determining aging affects on bone biomechanics and fracture risk suggesting that bone quality factors such as microdamage, microstructure, and physicochemical properties of the bone matrix contribute differently when bone is loaded at high strain rates compared to quasi-static strain rates.

***Disclosures: Daniel Nicolella**, None.*

1237

Age-Related Changes in Bone Microarchitecture and Strength of the Distal Radius May Explain Sex Differences in Forearm Fracture Risk. Heather Macdonald*, Kyle Nishiyama, Jane Kang, David Hanley, Steven Boyd. University of Calgary, Canada

High-resolution pQCT (HR-pQCT) provides a non-invasive assessment of bone microarchitecture; however, few population-based data currently exist. In this cross-sectional study, we examined age-related changes in bone microarchitecture and strength at the distal radius (DR) and tibia (DT) in a population-based sample. Participants included 644 adults aged 20-99 yrs recruited from the Calgary, AB cohort of the Canadian Multicentre Osteoporosis Study (n=284 women, 140 men) or randomly selected from the general Calgary population (n=158 women, 62 men). We performed a standard morphological analysis of the DR and DT with HR-pQCT (Scanco Medical, AG), applied a customized segmentation algorithm to quantify cortical porosity (Ct.Po) and used finite element (FE) analysis to estimate bone strength (failure load) and the percentage of load carried by the cortex. In addition, we calculated a DR load-to-strength ratio as the ratio of estimated fall force to bone strength. We used t-tests to compare bone outcomes between young adult (20-29 yrs) women and men, and linear regression to predict change in bone outcomes between 20 and 90 yrs. Bone area, which was 33% larger in young men at both sites, changed similarly with age in women and men at the DT, but increased 22% more in men at the DR ($p<0.001$). Trabecular number and thickness (Tb.Th) were 7-20% higher in young men at both sites, but Tb.Th at the DR declined more with age in men (-16%) than women (-2%, p=0.004). Ct.Po was 31-44% lower in young women than young men at both sites, but women demonstrated 92-176% larger age-related increases in Ct.Po than men at both sites ($p<0.001$, Figure). The cortex carried 13-14% more load in young women at both sites, and the percentage of load carried by the DR cortex did not change with age in women, but declined by 17% in men (p=0.007). FE-estimated bone strength was 34-47% greater in young men at both sites, but the change with age was similar in women and men. In contrast, the load-to-strength ratio, an estimate of forearm fracture risk, was 41% lower in young men and increased more in women (+74%) than men (+47%) with age (p=0.009, Figure). Our results highlight important site- and sex-specific differences in patterns of age-related bone loss. In particular, less periosteal expansion, more porous cortices and a greater percentage of load carried by the cortex at the distal radius in women may underpin the well-documented sex differences in forearm fracture risk.

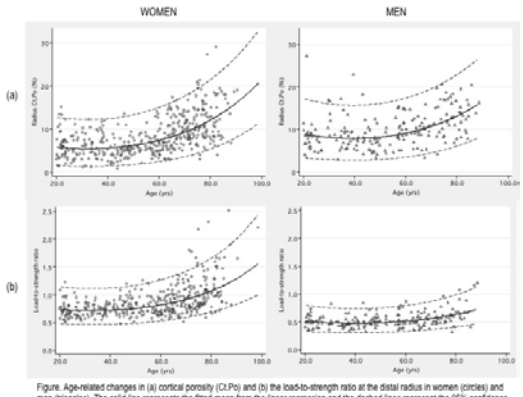

Figure

***Disclosures: Heather Macdonald**, None.*

1238

High-Frequency, Low-Magnitude Mechanical Signals Do Not Prevent Bone Loss in the Absence of Muscle Activity. Sarah Manske*[1], Steven Boyd[1], Craig A. Good[1], Ronald Zernicke[2]. [1]University of Calgary, Canada, [2]University of Michigan, USA

Muscles play a role in transmitting mechanical stimuli to bone, and exogenous high-frequency, low-magnitude mechanical signals (LMMS) may promote bone adaptation by mimicking postural muscle activity. We hypothesized that daily exposure to LMMS would maintain bone structure despite muscle disuse following injection with botulinum toxin type A (BTX). Female 16 wk old BALB/c mice (N = 25) were assigned to (a) BTX + LMMS, (b) BTX + Sham, or (c) Sham. BTX mice were injected with BTX (20 μL; 1 U/100 g body mass) into the posterior musculature of the left hindlimb. For 20 min/d, 5 d/wk, for 3 wk, all mice were anaesthetized and placed on a bed with the left leg strapped to a holder (tibiofemoral angle ~120°). Through the holder, the LMMS group received 45 Hz, 0.6 g acceleration with ~20 με without weight bearing. The sham groups received no mechanical input. The right leg served as an internal control. At baseline and 3 wk, muscle cross-sectional area (MCSA) and tibial bone properties (at metaphysis and diaphysis) were assessed with in vivo microCT (vivaCT40, Scanco Medical). Mice were sacrificed at 3 wk, and muscles were dissected and weighed. MCSA decreased in the BTX + LMMS leg (-47% from baseline) and the BTX + Sham leg (-46% from baseline). The change in MCSA in these groups was different from the Sham (0% from baseline, $p < 0.001$). Similarly, bone volume fraction (BV/TV) decreased in the BTX + LMMS leg (-12% from baseline) and BTX + Sham leg (-7% from baseline) (Figure). The change in BV/TV in these groups was different from the Sham (+34% from baseline, $p < 0.001$). Trends for gastrocnemius mass, soleus mass, trabecular thickness, and diaphyseal cortical area were similar. For all outcomes examined, there were no significant differences between the BTX + LMMS and BTX + Sham groups, nor between-group differences in the contralateral control leg. Our results suggest that LMMS did not prevent bone loss induced by a rapid decline in muscle activity. LMMS, which appears to operate primarily by increasing osteoblastic activity, did not overcome the osteoclastic action triggered by disuse. The daily loading duration was shorter than would be expected from postural muscle activity, and longer exposure may prevent bone loss. However, if LMMS were mimicking postural muscle activity, we would expect a diminished magnitude of bone loss. Understanding the mechanism by which LMMS stimulates bone adaptation will maximize its therapeutic potential.

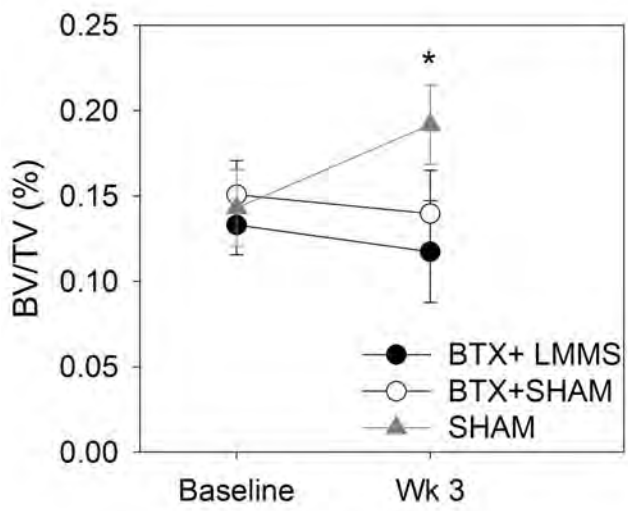

Changes in bone volume fraction (BV/TV) after BTX injection and LMMS or sham in BALB/c mice

***Disclosures: Sarah Manske**, None.*

1239

Increased Cortical Porosity during Puberty May Increase Distal Radius Fracture Risk in Boys: A HR-pQCT Study. Kyle Nishiyama*[1], Heather Macdonald[1], Melonie Burrows[2], Heather McKay[2], Steven Boyd[1]. [1]University of Calgary, Canada, [2]University of British Columbia, Canada

Distal radius fractures peak during puberty and are more common in boys than girls (Cooper et al. JBMR, 2004). A deficiency in cortical bone may underpin the high incidence of forearm fractures in boys (Kirmani et al. JBMR, 2009). For example, cortical density is lower in boys than girls during puberty (Wang et al. JBMR, In Press); however, little is known about the role of cortical porosity. Thus, we aimed to determine the maturity- and sex-related differences in cortical parameters and bone strength, estimated using finite element (FE) analysis and high-resolution pQCT (HR-pQCT). Subjects were healthy girls (N = 174, Age: 14.6 ± 3.9 yrs) and boys (N = 151, Age: 15.6 ± 3.4 yrs) who self-reported their maturity status using the method of Tanner. We grouped the subjects into prepubertal (Tanner I, n=49), pubertal (Tanner II, III, IV, n=155) and postpubertal (Tanner V, n=121) categories. To avoid the growth plate, we scanned the 7% site of the non-dominant distal radius using HR-pQCT (XtremeCT, Scanco Medical AG). We applied a validated automatic segmentation procedure (Buie et al. Bone, 2007; Nishiyama et al., JBMR, In Press) to determine cortical porosity (Ct.Po, %), cortical thickness (Ct.Th, mm) and cortical area (Ct.Ar, mm^2). We used FE analysis to estimate bone strength (ultimate stress, MPa) and determine the percentage of load carried by the cortex. A General Linear Model was applied to determine differences between sexes and across maturity groups. Cortical parameters and bone strength were not significantly different between prepubertal boys and girls (Figure 1). In the pubertal and postpubertal groups, Ct.Po and Ct.Ar were 18-65% lower in girls than boys ($p<0.001$). However, Ct.Th, bone strength, and the load distribution were similar in pubertal and postpubertal boys and girls. Within-sex comparisons indicated that Ct.Po was 35% and 76% lower in pubertal and postpubertal girls compared with prepubertal girls, respectively ($p<0.001$). In contrast, Ct.Po was similar in prepubertal and pubertal boys, but was 35% lower in postpubertal boys compared with prepubertal boys ($p<0.01$). Our results suggest that despite similar bone strength (size adjusted) across puberty, Ct.Po remains higher in boys during puberty, which corresponds to the time of peak forearm fracture incidence. Further investigation may determine whether regional variation in Ct.Po contributes to sex differences in forearm fracture risk during puberty.

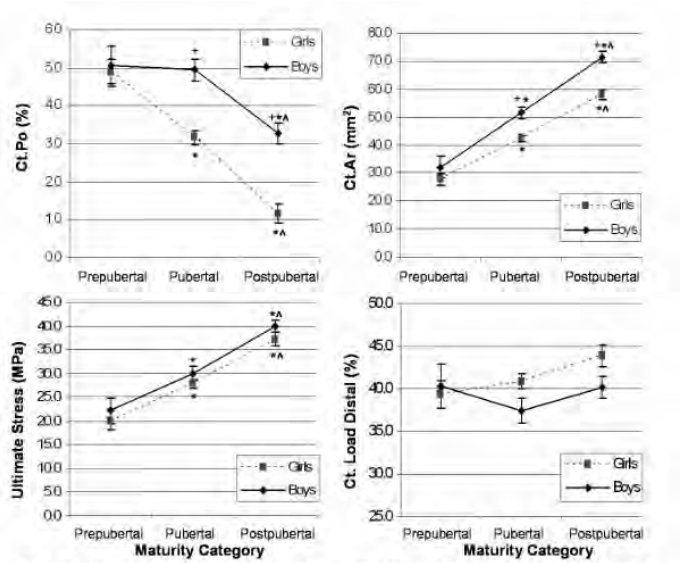

Figure 1: Mean values for boys and girls with standard error bars. ° Difference between sexes, * Difference from prepubertal group, ^ Difference from pubertal group (all p<0.05 after Bonferroni correction)

Figure 1

***Disclosures: Kyle Nishiyama**, None.*

1240

Effects of Non-Enzymatic Glycation on Trabecular Bone Fragility May be Mediated Through Changes in Bone Matrix Quality and Microarchitecture. Deepak Vashishth, Lamya Karim*. Rensselaer Polytechnic Institute, USA

Factors other than reduced bone mass, such as changes in bone quality, may contribute to fracture risk. In addition to changes in the extracellular matrix, alterations in bone quality may be induced by changes in trabecular microarchitecture and microdamage (MDx), which also influence each other. Non-enzymatic glycation (NEG) creates crosslinks known as advanced glycation end products (AGEs) that accumulate and increase bone fragility [1]. The goal of this study was to investigate the interrelationships between NEG, microarchitecture, and MDx, and to determine the dominant factors influencing bone's mechanical integrity. 23 cancellous bone cores from tibiae of human donors (Ages 18 to 97) were imaged with microcomputed tomography to obtain microarchitectural information. Cores were mechanically tested via compression tests, and were subsequently stained with lead-uranyl acetate in order to quantify MDx [2]. From a hydrolyzed bone slice, total AGE content was measured via a fluorometric assay and pentosidine was measured through ultra-high performance liquid chromatography for each specimen. Crosslink content was normalized to collagen content where collagen was calculated based on hydroxyproline quantity measured [3]. Spearman correlations were run for crosslink quantities with microarchitecture, MDx, and mechanical parameters. Forward stepwise regression analysis was used to determine the most significant variables influencing mechanical properties. Mechanical measures related to bone fracture resistance including yield strain, ultimate strain and toughness all decreased with increase in NEG crosslinks (AGEs and PEN). Similarly these variables decreased with transition

to a rod-like from a plate-like structure and increase in microdamage. Stepwise regression, however, yielded only NEG crosslinks (AGEs or PEN) as the significant predictor of bone fragility because NEG crosslinks were also correlated to microarchitectural indexes and microdamage. Our results indicated that NEG depreciates trabecular bone's mechanical integrity and its effects on trabecular bone may be mediated by changes in microarchitecture and bone matrix quality.

1. Tang et al., Bone, 2007
2. Tang and Vashishth, Bone, 2007
3. Gross, J Exp Med, 1958

Funding source: NIH-NIA AG20618 and NIH-NIGMS T32GM067545

***Disclosures: Lamya Karim**, NIH-NIA AG20618, 2*

1241

Contributions of Cortical and Trabecular Bone to Age-related Declines in Vertebral Strength are not the Same for Men and Women. Blaine Christiansen*[1], David Kopperdahl[2], Douglas Kiel[3], Tony Keaveny[4], Mary Bouxsein[5]. [1]University of California - Davis Medical Center, USA, [2]O.N. Diagnostics, USA, [3]Hebrew SeniorLife, USA, [4]University of California, Berkeley, USA, [5]Beth Israel Deaconess Medical Center, USA

Women have a higher incidence of osteoporotic fractures than men, with over 25% of these being vertebral fractures. While this higher incidence of fractures in women is likely partially due to women having a greater decline in vertebral bone density than men, much less is known about compartment-specific changes in vertebral strength. We hypothesize that age-related changes to vertebral structure and strength in the cortical and trabecular compartments differentially affect men and women, ultimately making women more susceptible to vertebral fractures. To investigate these compartment-specific changes, we used finite element analysis of quantitative computed tomography (QCT) scans of the lumbar (L3) and thoracic (T10) vertebral bodies of young and old men and women to characterize bone structure, compressive strength, and bending stiffness. Subjects were selected from participants in the Framingham Heart Study Multidetector CT Study, and consisted of 30 men age 35-42, 30 women age 36-41, 30 men age 73-82, and 30 women age 74-83. We found larger age-related differences in vertebral compressive strength at both vertebral levels for women than for men (Table 1). This was associated with significant age-related differences in trabecular compressive strength in both sexes (with larger differences in women), but cortical strength declined only in women. Bending stiffness behaved similarly, with significant age-related declines at both vertebral levels in women, but no age-related changes in men. Similar changes were also seen for volumetric BMD, which, for women, declined with age in both trabecular and cortical compartments, whereas in men differences were primarily observed in trabecular bone only. This compartment-specific sexual dimorphism is of particular interest since a higher percentage of the total compressive strength of the vertebral body is attributable to the cortical compartment in old vs. young subjects. Altogether, these data point to a differential age-related loss of bone between men and women that is compartment specific — information that provides unique insight into vertebral fracture etiology and which may have relevance for improved sex-specific vertebral fracture risk assessment.

Table 1: Average differences between young and old subjects.

	L3		T10	
	Men	Women	Men	Women
Vert. body strength (N)	**-27.3%**	**-52.4%**	**-19.0%**	**-44.1%**
Trabecular strength (N)	**-40.3%**	**-63.8%**	**-29.3%**	**-52.0%**
Cortical strength * (N)	-9.1%	**-37.3%**	-2.6%	**-33.4%**
Bending stiffness (kNm/rad)	+5.9%	**-33.9%**	-3.0%	**-23.4%**
Vert. body density (mg/cm^3)	**-18.4%**	**-38.2%**	**-11.0%**	**-32.0%**
Trabecular density (mg/cm^3)	**-22.6%**	**-43.4%**	**-16.9%**	**-38.3%**
Cortical density * (mg/cm^3)	**-11.5%**	**-29.8%**	-2.2%	**-23.1%**

Bold – Difference in old vs. young is statistically significant ($p < 0.01$)
* "Cortical" refers to all bone in the CT scan within 2 mm of the periosteal surface and includes the thin cortical shell and adjacent trabecular bone.

Table 1

***Disclosures: Blaine Christiansen**, None.*

1242

Men and Women With Similar Spine aBMD Have Different Bone Size, Volumetric Density, and Strength: The Framingham Study. Kerry Broe*[1], Douglas Kiel[2], Xiaochun Zhang[2], Elizabeth Samelson[3], Blaine Christiansen[4], Ching-An Meng[5], R Manoharan[6], J D'Agostino[6], Thomas Lang[7], Serkalem Demissie[8], LA Cupples[8], Mary Bouxsein[6]. [1]Hebrew Senior Life, USA, [2]Hebrew SeniorLife, USA, [3]Hebrew SeniorLife, Harvard Medical School, USA, [4]University of California - Davis Medical Center, USA, [5]Hebrew SeniorLife, Institute for Aging Research, USA, [6]Beth Israel Deaconess Medical Center, USA, [7]University of California, San Francisco, USA, [8]Boston University School of Public Health, Department of Biostatistics, USA

Areal BMD (aBMD) is commonly used to diagnose osteoporosis and predict fracture risk. However, bone strength depends on bone size, morphology and density – characteristics that aBMD does not distinguish. Thus, the mechanisms underlying sex-specific differences in skeletal fragility may be obscured by aBMD measures. In particular, we hypothesized that men and women with similar spine aBMD would have different vertebral size and volumetric BMD (vBMD). To test this, we compared 3D QCT bone measures among pairs of men and women matched for age and spine aBMD.

Subjects were selected from 1,138 men and 1,086 women from the Framingham Heart Study Multidetector Computed Tomography Study, who had volumetric QCT scans of the thoracic and lumbar spine. QCT scans were analyzed using custom software to measure simulated aBMD (g/cm^2), vertebral body cross sectional area (CSA, cm^2), trabecular volumetric BMD (Tb.vBMD, g/cm^3), integral volumetric BMD (Int.vBMD, g/cm^3), and to calculate the cortical volume ratio (cortex volume/vertebral volume), trabecular volume ratio (trabecular volume/vertebral volume), and compressive strength (Newtons) at L3. From these subjects, we identified 629 male/female pairs (1:1 match) matched on age ($\pm$ 1 yr) and QCT-derived aBMD of L3 ($\pm$ 1%), with an average age of 53 yrs (range: 34-83 yrs), and aBMD of 1.21 $\pm$ 0.58 g/cm^2 (range: 0.57-1.79 g/cm^2). Paired t-tests and multivariate regression were used to assess the sex-specific differences in bone measures.

All QCT bone measures differed significantly between men and women matched for aBMD (see Table, all $p<0.0001$). Differences remained significant after adjusting for height and weight. Matched for aBMD, men had 20% larger vertebral CSA, but lower Int.vBMD (-7%) and Tr.vBMD (-8.6%) than women. Their bigger vertebral bodies compensated for lower density, though, as men had 11% higher predicted compressive strength than women. Further, men had greater trabecular ratios but smaller cortical ratios compared to aBMD-matched women.

In conclusion, vertebral size, morphology, and density differ significantly between men and women matched for spine aBMD, suggesting that men and women attain the same aBMD by different mechanisms, namely a larger vertebral body in men and higher volumetric density in women. These results provide novel information regarding sex-specific differences in mechanisms that underlie skeletal fragility.

Mean spine QCT measures and p-values for paired t-tests for 629 men and women from the Framingham Study matched on age and QCT-derived aBMD

QCT Measures for L3	Men	Women	P-value
Cross-sectional area (cm^2)	12.37 ±1.19	10.29 ±1.31	<0001
Trabecular vBMD (g/cm^3)	0.139 ±0.037	0.152 ± 0.043	<0001
Integral vBMD (g/cm^3)	0.183 ±0.035	0.197 ±0.039	<0001
Cortical volume ratio	0.140 ±0.009	0.156 ±0.009	<0001
Trabecular volume ratio	0.323 ±0.110	0.282 ±0.097	<0001
Compressive strength (N)	4673.74 ±1030.73	4208.25 ±1012.96	<0001

Broe_abstract_table

***Disclosures: Kerry Broe**, None.*

1243

Meta-analysis of Genome-wide Association Studies Identifies 34 loci that Regulate BMD with Evidence of Both Site Specific and Generalized Effects: the GEFOS Consortium. Karol Estrada*[1], Gudmar Thorleifsson[2], Evangelos Evangelou[3], Daniel Koller[4], J. Brent Richards[5], Laura Yerges-Armstrong[6], Liesbeth Vandenput[7], Najaf Amin[8], Nicole Glazer[9], Omar Albagha[10], Ryan Minster[11], Stephen Kaptoge[12], Sumei Xiao[13], Yi-Hsiang Hsu[14], Prof. Andre G. Uitterlinden[8], Annie Kung[15], Candace Kammerer[16], Claes Ohlsson[17], Cornelia M van Duijn[18], David Evans[19], David Karasik[20], Douglas Kiel[20], Elizabeth Streeten[21], Emma Duncan[22], Jane Cauley[16], James F Wilson[23], John Robbins[24], Jonathan Reeve[25], M Zillikens[26], Matthew Brown[27], for the AOGC consortium, Mattias Lorentzon[28], Michael Econs[4], Munro Peacock[29], Pak Sham[30], Scott Wilson[31], Stuart Ralston[10], Tamara Harris[32], Tim Spector[33], Unnur Thorsteinsdottir[2], YongMei Liu[34], John Ioannidis[35], Unnur Styrkarsdottir[2], Fernando Rivadeneira[1], for the GEFOS consortium. [1]Erasmus University Medical Center, The netherlands, [2]deCODE Genetics, Iceland, [3]University of Ioannina School of Medicine, Greece, [4]Indiana University School of Medicine, USA, [5]McGill University, Canada, [6]University of Maryland, USA, [7]University of Gothenburg, Sweden, [8]Erasmus University Medical Center, Netherlands, [9]University of Washington, USA, [10]University of Edinburgh, United Kingdom, [11]University of Pittsburgh, USA, [12]University of Cambridge Bone Research Group, United Kingdom, [13]HONG KONG UNIVERSITY, Peoples republic of china, [14]Hebrew SeniorLife & Harvard Medical School, USA, [15]Department of Medicine, University of Hong Kong, Hong kong, [16]University of Pittsburgh Graduate School of Public Health, USA, [17]Centre for Bone & Arthritis Research, Sweden, [18]Erasmus Univesity Medical Center, Netherlands, [19]University of Bristol, United Kingdom, [20]Hebrew SeniorLife, USA, [21]University of Maryland School of Medicine, USA, [22]University of Queensland, Australia, [23]University of Edinburgh, Teviot Place, United Kingdom, [24]University of California, Davis Medical Center, USA, [25]Strangeways Research Laboratory, United Kingdom, [26]Erasmus MC Rotterdam, The netherlands, [27]University of Queensland Diamantina Institute for Cancer, Immunology & Metabolic Medicine, Australia, [28]Center for Bone Research at the Sahlgrenska Academy, Sweden, [29]Indiana University Medical Center, USA, [30]University of Hong Kong, China, [31]Sir Charles Gardner Hospital, Australia, [32]Intramural Research Program, National Institute on Aging, USA, [33]King's College London, United Kingdom, [34]Wake Forest University of Health Sciences, USA, [35]Sympatico, Canada

BMD is a heritable ($h^2 \asymp 0.60$) complex trait used for the assessment of fracture risk. Genome-wide association studies (GWAS) have identified 22 loci associated with BMD at genome-wide significant (GWS) level. As part of the Genetic Factors of OSteoporosis (GEFOS) Consortium we performed inverse-variance fixed-effects meta-analysis of 17 GWAS for LS-BMD and FN-BMD investigating 2.7 million single nucleotide polymorphism (SNPs) in individuals of Caucasian (n=32,000) and Han Chinese (n=800) ancestry. Traits were analyzed as sex-specific age- and weight-adjusted standardized residuals. Associations were declared GWS at $P<5x10^{-8}$ and suggestive at $5x10^{-6} < P < 5x10^{-8}$ after a conservative double-genomic control correction with an inflation factor of 1.1. In total, we detected 34 GWS and 49 suggestive associated loci. Of the GWS hits, 20 loci replicate previous findings and 14 represent novel loci. Two previously reported loci were significant ($P< 1x10^{-7}$) but not at GWS level (*DCDC5, ARHGAP1*). These 34 GWS hits map within or nearby genes involved in pathways relevant to bone biology; i.e. genes in WNT pathway (*WNT16, AXIN1, WNT4, LRP5, CTNNB1, GPR177, FOXC2*), NF-kB pathway (*AKAP11, TNSFR11B, RANK, OPG*) and/or part of the SOX family of transcription factors (*SOX4, SOX6, SOX9*). Site specificity was observed in six loci based on significant evidence for heterogeneity (Phet): four had significantly stronger effect on LS-BMD (*AKAP11, STARD3NL, KCNMA1, MPP7* with Phet<0.0002) and two loci on FN-BMD (*MEF2C, XKR9* with Phet<0.0006). Such site specificity in ~18% of the GWS loci is consistent with the ~70±6% genetic correlation observed between BMD sites. The 34 GWS loci accounted for ~5% of the phenotypic (~8% of the genetic) variance in BMD. All 83 identified loci will be followed-up by de-novo genotyping in ~50,000 additional samples in association with BMD and with fracture risk including more than 10,000 cases and 40,000 controls. In conclusion, we identified 34 GWS loci associated with LS-BMD and/or FN-BMD. We expect to at least double the number of GWS hits by follow-up replication genotyping and to examine their influence on fracture risk. These findings provide novel insight into relevant factors and biological pathways underlying the complex genetic architecture of BMD variation.

***Disclosures: Karol Estrada**, None.*

1244

Contribution of Genetic Profiling to Individualized Prognosis of Fracture. Bich Tran*[1], Nguyen Nguyen[1], Vinh Nguyen[2], Jacqueline Center[1], John Eisman[1], Tuan Nguyen[1]. [1]Garvan Institute of Medical Research, Australia, [2]School of Electrical Engineering & Telecommunications, University of New South Wales, Australia

While it is well recognized that the fracture risk is determined by multiple genes, each with moderate effect, it is contentious whether a combination of many genes can help the prognosis of fracture for an individual. The present study was designed to examine the contribution of genetic profiling to fracture prognosis. The study was built on the on-going Dubbo Osteoporosis Epidemiology Study, in which fracture and risk factors of 858 men and 1358 women had continuously been monitored from 1989 and 2008. Fragility fracture was ascertained by radiological reports. Bone mineral density at the femoral neck was measured by DXA (GE-Lunar, Madison, WI, USA). Using the actual clinical data, we simulated 50 independent genes with allele frequencies ranging from 0.01 to 0.60 and relative risk from 1.01 to 3.0, such that genes with large effect sizes have lower allelic frequency. Three predictive models were then fitted to the data in which fracture was a function of (I) clinical risk factors only (age, BMD, prior fracture, and falls); (II) genes only; and (III) clinical risk factors and 50 genes. The area under the receiver operating characteristic curve (AUC) was used to assess the degree of discrimination; and reclassification analysis to assess the incremental prognostic value of model with genes. During the follow-up, 17% (n = 149) men and 31% (n = 426) women had sustained a fragility fracture. The distribution of simulated genetic risk score had a median genetic risk score of 13 (range: 4 to 25). Approximately 10% of individuals had <10 risk genotypes; while other 10% had more than 16 risk genotypes. Compared to those with <10 risk genotypes, those with 10-16 risk genotypes had their odds of fracture increased by 5.47 (95% CI: 3.03 – 9.90). Those with >16 risk genotypes had the highest risk of fracture (OR 43.6; 95% CI 22.8 – 83.2). The AUC for model I (clinical risk factors) was 0.77, lower than that of model II with 50 genes (AUC 0.82). Adding genes into the clinical risk factors model (model III) increased the AUC to 0.88, and improved the accuracy of fracture classification by 45%, with most (41%) was the improvement in specificity. In the presence of clinical risk factors, the number of genes required to achieve an AUC of 0.85 was around 25. These results suggest that genetic profiling could enhance the predictive accuracy of fracture prognosis, and help identify high-risk individuals for intervention to appropriate management of osteoporosis.

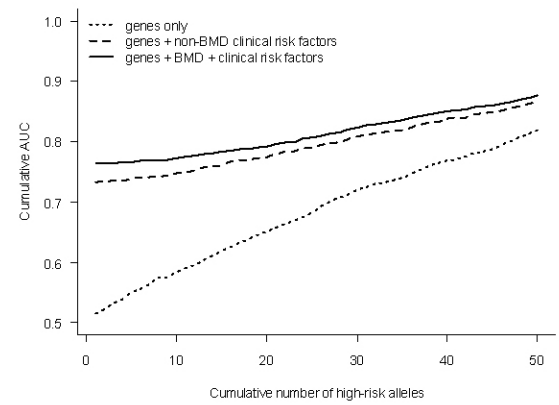

Figure 1. Cumulative AUC as a function of number of genes only (dotted line), with genes + non-BMD clinical risk factors (dashed line), and with genes + BMD + clinical risk factors (solid line).

Figure 1. Cumulative AUC

***Disclosures: Bich Tran**, None.*

1245

Systems Genetics Identifies *Bicc1* as a Regulator of Bone Mineral Density. Charles Farber*[1], Ana Lira[1], Yi-Hsiang Hsu[2], Brian Bennett[3], Luz Orozco[3], Gregory Hong[1], Atila van Nas[3], Hyun Kang[3], Eleazar Eskin[3], Elizabeth Bryda[4], Douglas Kiel[5], Thomas Drake[3], Clifford Rosen[6], Aldons Lusis[3]. [1]University of Virginia, USA, [2]Hebrew SeniorLife & Harvard Medical School, USA, [3]University of California, Los Angeles, USA, [4]University of Missouri, USA, [5]Hebrew SeniorLife, USA, [6]Maine Medical Center, USA

Systems genetics is an approach that combines the genetic analysis of clinical and molecular phenotypes. The advantage of systems genetics is that in addition to discovering genes affecting complex bone traits, it can also provide information on the function of newly identified genes. In the current study, we used systems genetics to identify bicaudal C homolog 1 (*Bicc1*) as a candidate regulator of BMD and predict that it plays a role in osteoblastogenesis. In an F2 mouse cross derived from the C57BL6/J and C3H/HeJ strains, we demonstrated that *Bicc1* transcript levels were regulated by a local expression quantitative trait locus (eQTL). In addition, the *Bicc1* eQTL was

coincident with the BMD QTL, *Bmd42.1*, and based on a causality modeling analysis we predicted that *Bicc1* was responsible for the effects of this locus. In support of this hypothesis, *jcpk*$^{+/-}$ mice which are heterozygous for a null mutation in *Bicc1* had reductions of 4.9% in femoral areal BMD. Moreover, using genome-wide association data from the Framingham Osteoporosis Study we identified a single nucleotide polymorphism in the first intron of human BICC1 that was associated (Bonferroni adjusted P=0.04) with total body BMD. To investigate the function of *Bicc1* we evaluated its expression in a panel of 96 mouse tissues and cell lines and found it to be the most highly expressed in mature osteoblasts. Furthermore, transcriptional network analysis of cortical bone microarray profiles generated in a panel of 97 mouse inbred strains indicated that *Bicc1* was associated with genes involved in osteoblast differentiation. Consistent with these findings the siRNA knockdown of *Bicc1* in primary calvarial osteoblasts resulted in reductions in alkaline phosphatase activity and *in vitro* mineralization in a dose-dependent manner. Similar deficiencies in osteoblast differentiation phenotypes were observed in primary calvarial osteoblasts isolated from *jcpk*$^{+/-}$ mice. These data identify *Bicc1* as a novel BMD gene and suggest that it influences BMD via a role in osteoblast-mediated bone formation. Additionally, our results highlight the strengths of systems genetics for gene discovery and annotating genes of unknown function.

***Disclosures: Charles Farber**, None.*

1246

A Large Meta-Analysis of Genome Wide Association Studies (GWAS) from the "CHARGE" and "GEFOS" Consortia Identifies Several Significant Loci for Lean Body Mass. Serkalem Demissie[1], Tamara B. Harris[2], Lisette Stolk[3], Gudmar Thorleifsson[4], Laura Yerges-Armstrong[5], John Robbins[6], Sophie Van Wingerden[7], Unnur Thorsteinsdottir[4], Liesbeth Vandenput[8], Yongmei Liu[9], Ida Malkin[10], Janina Ried[11], Weihua Zhang[12], Jing Hua Zhao[13], Jian'an Luan[13], Albert Smith[14], Daniel Koller[15], Karol Estrada[16], Andre Uitterlinden[17], Fernando Rivadeneira[16], Braxton Mitchell[18], Jeff O'Connell[19], Nicole Glazer[20], Unnur Styrkarsdottir[21], CM van Duijn[22], David Karasik[23], Yi-Hsiang Hsu[24], Mattias Lorentzon[25], Tamara B. Harris[2], Michael Econs[15], Gregory Livshits[26], Tim Spector[27], Angela Döring[11], H. Erich Wichmann[28], John Chambers[29], Jaspal Kooner[30], Zoltan Kutalik[31], Toby Johnson[32], Dawn Waterworth[33], Ruth Loos[13], Nicholas J. Wareham[13], Tuomas Kilpilainen[13], Vilmundur Gudnason[34], Claes Ohlsson[35], Jane Cauley[36], M Zillikens[37], Douglas Kiel*[23]. [1]Department of Biostatistics, Boston University School of Public Health, USA, [2]National Institute on Aging, USA, [3]Departments of Internal Medicine & Epidemiology, Erasmus Medical Center, Rotterdam, Netherlands, [4]deCODE Genetics, Reykjavík, Iceland, Iceland, [5]University of Maryland, USA, [6]University of California, Davis Medical Center, USA, [7]Department of Epidemiology, Erasmus Medical Center, Rotterdam, Netherlands, [8]University of Gothenburg, Sweden, [9]Wake Forest University of Health Sciences, USA, [10]Sackler Faculty of Medicine, Israel, [11]Institute of Epidemiology, Helmholtz Zentrum München, German Research Center for Environmental Health, Germany, [12]Department of Epidemiology & Public Health, Imperial College, United Kingdom, [13]MRC Epidemiology Unit, Institute of Metabolic Science, United Kingdom, [14]Icelandic Heart Association, Kopavogur, Iceland, University of Iceland, Iceland, [15]Indiana University School of Medicine, USA, [16]Erasmus University Medical Center, The netherlands, [17]Rm Ee 575, Genetic Laboratory, The netherlands, [18]University of Maryland, Baltimore, USA, [19]School of Medicine, University of Maryland, USA, [20]University of Washington, USA, [21]Decode Genetics, Iceland, [22]Department of Epidemiology, Erasmus Medical Center, Netherlands, [23]Hebrew SeniorLife, USA, [24]Hebrew SeniorLife, Harvard Medical Scool, USA, [25]Center for Bone Research at the Sahlgrenska Academy, Sweden, [26]Sackler Faculty of Medicine, Tel Aviv University, Israel, [27]King's College London, United Kingdom, [28]Institute of Epidemiology, Helmholtz Zentrum München, German Research Center for Environmental Health, Neuherberg, Germany, Institute of Medical Informatics, Biometry & Epidemiology, Ludwig-Maximilians-Universität & Klinikum Großhadern, Germany, [29]Department of Epidemiology & Public Health, Imperial College London, United Kingdom, [30]National Heart & Lung Institute, Imperial College London, United Kingdom, [31]Department of Medical Genetics, University of Lausanne, Switzerland, [32]Clinical Pharmacology, William Harvey Research Institute, Barts & The London School of Medicine & Dentistry, Queen Mary, University of London, United Kingdom, [33]Medical Genetics, GlaxoSmithKline, USA, [34]Icelandic Heart Association Research Institute, Iceland, [35]Centre for Bone & Arthritis Research, Sweden, [36]University of Pittsburgh Graduate School of Public Health, USA, [37]Erasmus MC Rotterdam, The netherlands

Lean body mass is a highly heritable trait yet few underlying genes have been identified. The fat and lean soft-tissue compartments of the body can be assessed by relatively simple, accurate methods like DXA and bioelectrical impedance analysis (BIA). Large cohort studies have accumulated such phenotypic information on body composition that permits large-scale GWAS. We performed a meta-analysis of GWAS for total body (TBLM) and appendicular (arms and legs) (aLM) lean mass. In each cohort, ~ 2.5 mil autosomal SNPs were imputed from the International HapMap Project CEU ref panel II. The sample included 39,030 individuals (55% women) of Caucasian ancestry (ages 18 to 100 years) from 20 cohort studies. Lean soft-tissue mass from DXA or BIA were available for the TBLM in all cohorts, while aLM was available in 15 studies (n~28,000) aLM was determined from BIA using a published and validated equation. All cohorts performed GWA analyses on imputed data adjusting for age, age^2, sex, height and total body fat mass. Inverse variance meta-analysis of study-specific results was performed using METAL with fixed effects models. Evidence of genome-wide significance (GWS) was set at $P<5x10^{-8}$ and suggestive evidence (sGWS) at $P<2.3x10^{-6}$ after a conservative double genomic control correction (λ_{GC} 1.03 to 1.06). For TBLM, one locus was associated at GWS (VCAN) and seven at sGWS level (with markers mapping in *PIK3C2B*, *NPSR1*, *RHOC*, and *FTO* and close to the *DCBLD2*, *FRK*, and *ARHGEF4* gene regions). For aLM, one locus was associated at GWS (*PKIB*) while five at sGWS level (with markers mapping in *SERINC1*, *VCAN*, *TNRC6B*, *and HSF2*, and near *ZNF804A*). There was no evidence for significant heterogeneity of results across cohorts. This is the largest GWAS meta-analysis conducted to date for lean body mass identifying novel loci that contribute to this quantitative trait, although only *VCAN*, a large chondroitin sulfate proteoglycan that is a major component of the extracellular matrix, was common to both lean mass phenotypes. Several of the loci were in or near genes that are expressed in skeletal muscle. Further replication by de-novo genotyping is underway for the GWS and sGWS findings. Given the intimate biologic relation between muscle and bone mass, the influence of these loci on fracture risk will also be examined.

***Disclosures: Douglas Kiel**, None.*

1247

Effect of Odanacatib on Bone Density and Bone Turnover Markers in Postmenopausal Women with Low Bone Mineral Density: Year 4 Results. Neil Binkley*[1], Henry Bone[2], John Eisman[3], David Hosking[4], Bente Langdahl[5], Ian Reid[6], Heinrich Resch[7], Jose Rodriguez Portales[8], Romana Petrovic[9], Carolyn Hustad[10], Carolyn DaSilva[10], Arthur Santora[11], Antonio Lombardi[12]. [1]University of Wisconsin, USA, [2]Michigan Bone & Mineral Clinic, USA, [3]Garvan Institute of Medical Research, Australia, [4]Nottingham City Hospital, United Kingdom, [5]Aarhus Sygehus, Aarhus University Hospital, Denmark, [6]University of Auckland, New zealand, [7]Medical University Vienna, Austria, [8]Pontificia Universidad Católica de Chile, Chile, [9]Merck Sharpe & Dohme, Belgium, [10]Merck, USA, [11]Merck Research Laboratories, USA, [12]Merck & Co., Inc., USA

The selective cathepsin K inhibitor odanacatib (ODN) reduced bone resorption markers and progressively increased bone mineral density (BMD) during 3 years of treatment in a Phase 2b study. This study was extended for 2 additional years to further assess ODN efficacy and long-term safety.

In the 2-year base study, postmenopausal women with BMD T-scores between -2.0 and -3.5 at the lumbar spine, femoral neck, trochanter or total hip received placebo or ODN at 3, 10, 25 or 50 mg weekly. In Year 3, participants were re-randomized to ODN 50 mg weekly or placebo. In Years 4/5, women who received placebo or 3 mg ODN in Years 1/2 and placebo in Year 3 were switched to 50 mg ODN for Years 4/5; all others continued with their Year 3 regimen. 141 women entered the extension, and 133 completed 4 years. Endpoints were BMD at the lumbar spine (primary), total hip and hip subregions, and 1/3 radius; levels of biochemical bone turnover markers; and assessments of safety.

Overall, 100 women received 50 mg ODN during Year 4 and 41 received placebo. Continuous treatment with 50 mg ODN for 4 years induced significant BMD increases from baseline at the spine (10.7%), total hip (8.3%), femoral neck (8.9%), and trochanter (10.3%) and maintained BMD (-0.1%) at the 1/3 radius; BMD changes from Year 3 were 2.8% (spine), 2.5% (total hip), 3.9% (femoral neck), and 2.9% (trochanter). Serum CTx remained low at Year 4 (-41%), whereas BSAP was relatively unchanged (-2%) from baseline. Women who received active treatment for 2 years and switched to placebo for 2 years experienced bone loss, with BMD near baseline for most sites and decreased by 4.5% at the 1/3 radius at the end of Year 4. Levels of bone turnover markers in women who discontinued active treatment after 2 years rose in the first month off-treatment, but all levels returned to baseline by the end of Year 4. ODN was generally well tolerated.

In summary, 4 years of ODN treatment increased lumbar spine and hip BMD and was generally well-tolerated in postmenopausal women with low bone mass. Bone formation markers remained relatively unaffected. Discontinuation of ODN after 2 years of treatment was promptly followed by resolution of effects on bone turnover and density such that BMD and bone biomarker levels at Year 4 were at or near baseline.

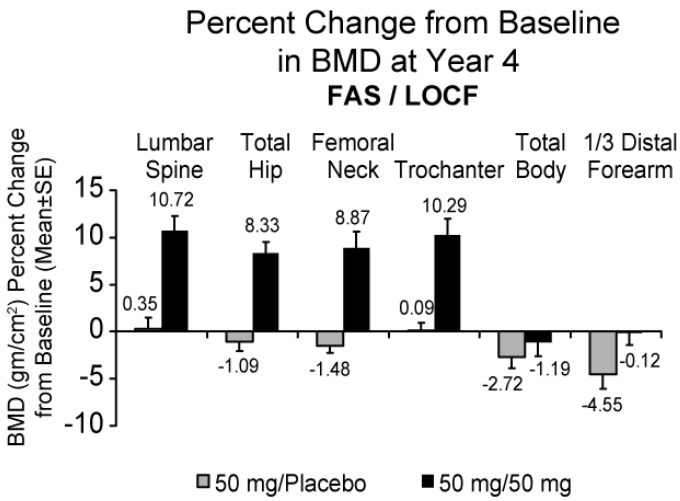

Figure

***Disclosures: Neil Binkley**, Merck, 2*
This study was funded by Merck

1248

A New Active Vitamin D Compound, Eldecalcitol, Is Superior to Alfacalcidol in Preventing Fractures in Osteoporotic Patients. Toshio Matsumoto*[1], Masako Ito[2], Yasufumi Hayashi[3], Takako Hirota[4], Yusuke Tanigawara[5], Teruki Sone[6], Masao Fukunaga[7], Masataka Shiraki[8], Toshitaka Nakamura[9]. [1]University of Tokushima Graduate School of Medical Sciences, Japan, [2]Nagasaki University Hospital, Japan, [3]Tokyo Metropolitan Rehabilitation Hospital, Japan, [4]Kyoto Koka Women's University, Japan, [5]Keio University, Japan, [6]Kawasaki Medical School, Jpn, [7]Kawasaki Medical School, Japan, [8]Research Institute & Practice for Involutional Diseases, Japan, [9]University of Occupational & Environmental Health, Japan

Eldecalcitol, a new active vitamin D compound, has been shown to have superior effects to alfacalcidol in suppressing bone resorption and increasing BMD of the spine and the hip with similar safety profile to alfacalcidol in osteoporotic patients. However, the effect of eldecalcitol on the prevention of osteoporotic fractures has not been evaluated in randomized trials. This randomized, active comparator, double-blind study was undertaken to examine whether eldecalcitol has a superior effect to alfacalcidol in preventing osteoporotic fractures. We assigned 1054 subjects (1030 females and 24 males) with osteoporosis aged from 46 to 92 years to receive either 0.75 μg eldecalcitol or 1.0 μg alfacalcidol once a day for 36 months. Subjects with serum 25-hydroxyvitamin D below 50 nmol/L were supplemented with 400 IU/day vitamin D_3. Vertebral fracture in eldecalcitol group decreased with time, and was significantly less than that in alfacalcidol group during the third year (odds ratio, 0.51; 95% confidence interval [CI], 0.27-0.97), with a reduction in overall vertebral fracture at 36 months (13.4 vs. 17.5%; hazard ratio, 0.74; predefined 90% CI, 0.56-0.97). The anti-fracture effect of eldecalcitol compared with alfacalcidol was more pronounced in patients with BMD T-score -2.5 or less (15.1 vs. 26.6%; hazard ratio 0.56; 95% CI, 0.34-0.90), and in patients with 2 or more prevalent vertebral fractures (23.7 vs. 36.8%; hazard ratio 0.61, 95% CI, 0.40-0.93). Eldecalcitol showed no significant effect on the total non-vertebral fractures, but markedly reduced the incidence of wrist fractures (1.1 vs. 3.6%; hazard ratio 0.29; 95%CI, 0.11-0.77). Eldecalcitol exhibited stronger effects on both serum BALP and urinary NTX, as well as hip (0.4 vs. -2.3%; $p<0.001$) and lumbar BMD (3.4 vs. 0.1%; $p<0.001$) compared with alfacalcidol after 36 month of treatment. Two subjects in eldecalcitol group but no one in alfacalcidol group experienced hypercalcemia over 11.5 mg/dL. Mean postprandial urinary Ca excretion at 36 months was 0.242 and 0.209 mg/dLGF in eldecalcitol and alfacalcidol groups, respectively. It is concluded that eldecalcitol has superior effect over alfacalcidol in preventing vertebral and wrist fractures in osteoporotic patients with sufficient vitamin D supply, with similar safety profiles to alfacalcidol.

***Disclosures: Toshio Matsumoto**, Eli Lilly, 5; Chugai, 5; Asahi Kasei Pharma, 5; Astellas, 5; Ono Pharmaceutical, 2; JT, 5; Daiichi-Sankyo, 5; Teijin Pharma, 5*
This study received funding from: Chugai

1249

Effects of Weight Loss, Exercise, or Combined on Bone Mineral Density and Markers of Bone Turnover in Frail Obese Older Adults. Krupa Shah*[1], Nehu Parimi[2], Suresh Chode[2], David Sinacore[2], Nicola Napoli[3], Reina Armamento-Villarea[4], Dennis Villareal[4]. [1]University of Rochester School of Medicine, USA, [2]Washington University School of Medicine, USA, [3]University Campus Biomedico, Italy, [4]University of New Mexico School of Medicine, USA

Background. Although weight loss therapy ameliorates frailty and improves metabolic coronary heart disease risk factors in obese older adults, weight loss can cause bone loss and increased fracture risk. It is not known whether exercise training can prevent bone loss and increased bone turnover when obese older adults undergo voluntary weight loss.

Methods. We conducted a 1-year randomized-controlled trial to evaluate the independent and combined effects of weight loss and exercise on bone mineral density and markers of bone turnover in 107 obese (BMI≥30 kg/m^2) older (≥65 yrs) adults. They were randomized to one of four groups: Diet-induced weight loss (DIET), Exercise training (EXER), Diet-induced weight loss + exercise training (DIET+EXER) and Healthy-lifestyle (CONTROL). All groups received calcium and vitamin D supplementation to adjust intake to 1200-1500 mg and 1000 IU per day, respectively.

Results. Ninety-four (87%) participants completed the study; adherence was 82 ± 9% for diet and 83 ± 16% for exercise interventions. After one year, body weight decreased in the DIET (-10 ± 5%) and DIET+EXER groups (-9 ± 5%) whereas weight was maintained in the EXER (-1 ± 4%) and CONTROL groups (between-group $P<.05$). Compared with the CONTROL group, total hip BMD decreased in the DIET group (-2.3 ± 0.4%) while it increased in the EXER group (1.3 ± 0.3%) (between-group $P<.05$). Hip BMD did not change in the DIET+EXER group (-0.8 ± 0.5) similar to the CONTROL group (-0.4 ± 0.3%) (between-group $P>.05$). Compared with the CONTROL group, serum markers of bone resorption and formation increased in the DIET group (CTX: 31± 11%, PINP; 9 ± 7%, osteocalcin: 26 ± 9%) while they decreased in the EXER group (serum CTX: -14 ± 7%, and PINP; -13 ± 6%, osteocalcin: -15 ± 7%) (between-group $P<.05$). Markers of bone turnover did not change in the DIET+EXER group (CTX: 15 ± 9%, PINP; 3 ± 8%, osteocalcin:-8 ± .5%) similar to the CONTROL group (CTX: 4 ± 8%, PINP; 1 ± 5%, osteocalcin:-0.4 ± .3%) (between-group $P>.05$).

Conclusions. Regular exercise is effective in preventing bone loss and increase in bone turnover during dietary-induced weight loss in obese older adults with adequate calcium and vitamin D intake. Therefore, exercise should be included as part of a comprehensive weight loss program to offset the adverse effects of dietary-induced weight loss on bone.

***Disclosures: Krupa Shah**, None.*

1250

Teriparatide Treatment of Osteoporotic Women Increases Cortical Bone at Critical Sites in the Proximal Femur: An In Vivo Study using High Resolution Cortical Thickness Mapping. Andrew H Gee[1], Graham M Treece[1], Paul Mayhew[1], Jan Borggrefe[2], Kenneth Poole*[1]. [1]University of Cambridge, United Kingdom, [2]University of Schleswig-Holstein, Germany

Teriparatide treatment of osteoporotic women improved hip bone structure, most likely due to endocortical apposition of new bone since there was no associated increase in periosteal size (Borggrefe et al, JBMR in press). Teriparatide may enhance bone strength by increasing the sensitivity to load stimuli, but evidence for this effect in humans is lacking. In this study, we sought to identify the precise location of teriparatide-stimulated cortical bone growth in the human proximal femur. Women with severe osteoporosis were treated with teriparatide (the EUROFORS study) for 24 months, with QCT scans of the hips performed at baseline, 12 and 24 months. A novel cortical thickness mapping technique (Treece et al, Medical Image Analysis in press) was used to evaluate both proximal femurs of 65 qualifying QCT participants at baseline and 24 months. The surface of each femur was segmented from the CT scans using a semi-automated technique (119 femurs in total, 11 excluded mainly due to metalwork artefacts). This surface was used to automatically guide approximately 7,000 independent measurements of cortical thickness over the femur. Cortical thickness estimates were mapped to a canonical femur surface by non-rigid registration of the 119 femurs. Statistical parametric mapping (SPM) was used to identify significant changes in cortical thickness over time, displayed as a colour map over the canonical femur surface (figure, which shows statistically significant vertices and clusters). Cortical thickness increased significantly at several sites but did not decrease significantly anywhere. Zones that receive a high compressive stress during normal locomotion demonstrated a significant ($p<0.01$) increase in cortical thickness (0.05-0.2mm): the infero-medial cortex, and a posterior inter-trochanteric site where the calcar femorale transmits load from the trabeculae to the cortex. Several sites thought to be under tensile stress during locomotion were significantly thicker after teriparatide: on the greater and lesser trochanters near the attachment sites of the gluteus medius and psoas respectively. Thickness also increased at the head-neck junction of the superior cortex. We conclude that teriparatide treatment for 24 months increases cortical bone thickness at sites of compressive stress during locomotion, near key muscle attachments and in the superior cortex, considered critical for hip fracture susceptibility.

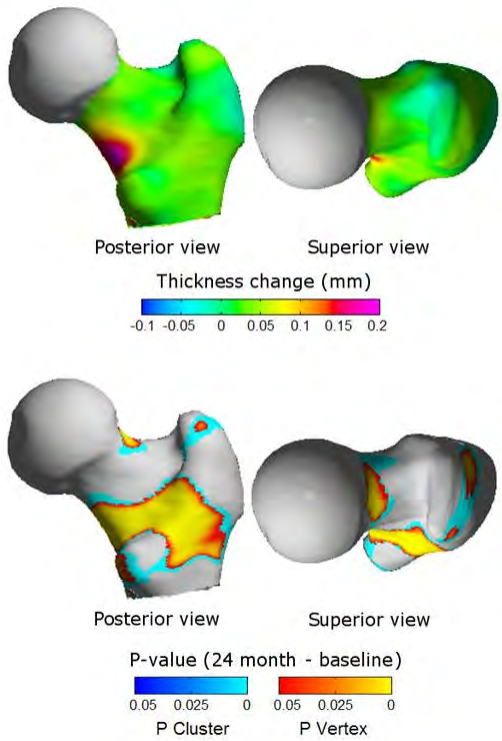

Maps of cortical thickness change (excluding the femoral head) and significance

***Disclosures: Kenneth Poole**, None.*

1251

The Effect of Teriparatide on Bone Material Properties is Not Different in Postmenopausal Women Who Were Previously Treatment-naive or Treated With Alendronate. Birgit Buchinger*[1], Sonja Gamsjaeger[1], Harald Dobnig[2], Jan J. Stepan[3], David B. Burr[4], Helmut Petto[5], Imre Pavo[6], Klaus Klaushofer[1], Eleftherios P. Paschalis[1]. [1]Ludwig Boltzmann Institute of Osteology at Hanusch Hospital of WGKK & AUVA Trauma Centre Meidling, 4th Med. Dept. Hanusch Hospital, Austria, [2]Division of Endocrinology & Nuclear Medicine, Medical University of Graz, Austria, [3]Institute of Rheumatology, Faculty of Medicine, Czech republic, [4]Dept of Anatomy & Cell Biology, Indiana University School of Medicine, USA, [5]Eli Lilly & Company Austria, Austria, [6]Eli Lilly & Company, Austria

Bone material properties are important contributors to bone strength. The purpose of the present study was to investigate the effects of teriparatide (TPTD) treatment on bone material properties (mineral/matrix ratio, carbonate substitution in the apatite lattice, mineral maturity, and relative proteoglycan content), in iliac crest biopsies.

Sixty-six postmenopausal women with osteoporosis (62% with previous fractures) either pre-treated with alendronate (ALN; N=38, mean treatment duration: 64 months) or osteoporosis treatment-naïve (TN, N=28) were treated with daily TPTD for 24 months in a prospective, single-arm, non-randomized study. For 33 patients (ALN, N=18, TN, N=15), valid, paired biopsies (before and after TPTD treatment; double-labelled by tetracycline) were analyzed by Raman microspectroscopy with a spatial resolution of ~1 µm. Spectra were obtained in the area between the second label and the mineralization front (youngest tissue age). Mann-Whitney test were used for between group comparisons and Wilcoxon signed-rank test for within group change in this exploratory analysis. The indices, mineral/matrix ratio, carbonate substitution and proteoglycan/mineral content at baseline and the change from baseline were not significantly different between the two groups (ALN, TN). However, at endpoint, the mineral/matrix ratio was significantly higher in the ALN pre-treated group (0.27 ± 0.2 vs. 0.12 ± 0.08, p=0.03) compared with TN. There was no other significant difference between the two groups (ALN, TN) at endpoint. In the pooled analysis (ALN, TN combined), mineral/matrix ratio, representing ash weight, increased from baseline. The amount of carbonate substitution, indicating mineral maturity, shape, and solubility decreased and relative proteoglycan content expressed as proteoglycan/mineral content decreased significantly (Table).

In conclusion, the observations in the present study indicate that TPTD treatment was associated with increased mineralization (based on mineral/matrix ratio), in formation of less mature crystals and in the formation of more favourable matrix for mineralization commencement (based on proteoglycan content).

	Baseline			Change from baseline		
	ALN N=18	TN N=15	All N=33	ALN N=18	TN N=15	All N=33
Mineral/matrix ratio	0.10 (0.07)	0.11 (0.08)	0.10 (0.07)	0.14* (0.17)	0.02 (0.06)	0.08** (0.14)
Carbonate substitution	6.87 (13.19)	8.75 (10.83)	7.73 (12.03)	-6.57* (15.69)	-5.46 (11.48)	-6.01** (13.48)
Proteoglycan/ mineral content	6.41 (10.85)	8.85 (11.06)	7.52 (10.84)	-4.58 (12.96)	-5.36 (10.81)	-4.97* (11.70)

*p-values <0.05 and **p-values <0.01 for change from baseline

Table: Bone material propterties,mean (SD)

***Disclosures: Birgit Buchinger**, None.*
This study received funding from: Lilly Research Laboratories

1252

Nitroglycerin Improves Bone Mineral Density, Bone Geometry, and Bone Strength: Results from a Two-Year Randomized Controlled Trial. Sophie Jamal*[1], Celeste Hamilton[2], Dennis Black[3], Angela Cheung[4], Steven Cummings[5]. [1]The University of Toronto, Canada, [2]Women's College Hospital/University of Toronto, Canada, [3]University of California, San Francisco, USA, [4]University Health Network, Canada, [5]San Francisco Coordinating Center, USA

Purpose: Nitric oxide stimulates bone formation and inhibits bone resorption. Organic nitrates (such as nitroglycerin; NTG) can act as nitric oxide donors. Observational studies suggest use of organic nitrates is associated with increased bone mineral density (BMD) and decreased fracture risk. However, the effects of nitrates on BMD, geometry and strength have not been tested in a randomized trial. Methods: In a 24 month randomized, blinded trial, we compared the effects of once daily administration of NTG ointment (15mg/day applied at bedtime instead of every 6 to 8 hours as prescribed for angina) or matching placebo in postmenopausal women who had BMD T-scores between 0 and -2.0 at the lumbar spine and above -2.0 at the hip. Participants enrolled if they completed a 1-week run-in period taking the active NTG ointment. All women took at least 1200mg of elemental calcium and 800IU of vitamin D3 daily. We measured BMD at the lumbar spine, femoral neck and total hip at baseline, year 1 and year 2 (GE Lunar Prodigy). We used peripheral quantitative computed tomography (pQCT; Norland/Stratect XCT 2000) to measure bone density, geometry and strength at the radius. We analyzed the data with a modified intention-to treat-approach. Results: We enrolled 243 women; 113 (89%) of the 127 women in the nitroglycerin group and 107 (92%) of 116 in the placebo group completed the 24-month assessments. Compared to placebo, those randomized to NTG had significant ($p<0.001$) increases in BMD at the lumbar spine (6.7%), femoral neck (7.0%) and total hip (6.2%) at 24 months (Figures 1-3). Furthermore, NTG significantly ($p<0.05$) increased trabecular density (11.9%), cortical density (2.2%), cortical area (10.6%), cortical thickness (13.9%), periosteal circumference (7.4%), polar moment of inertia (7.3%) and polar section modulus (10.7%; Table 1). Headache was the most common reason for discontinuing treatment; other adverse events were not significantly different between the groups. Conclusions: Once daily administration of NTG ointment has anabolic effects on cortical bone, increases bone density, and improves indices of bone strength. Nitroglycerin is very inexpensive and widely available. Its efficacy for preventing fractures should be tested in a clinical trial.

Figure 1. Changes in bone mineral density.

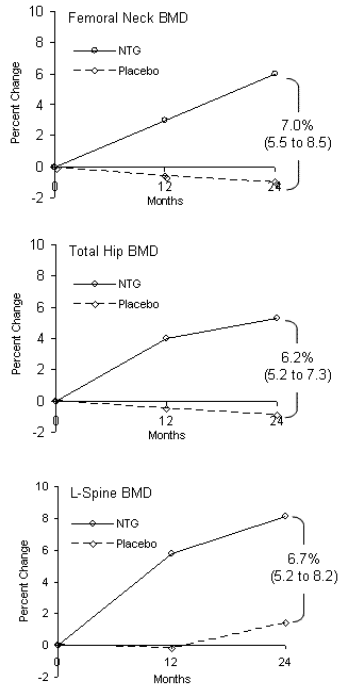

Figure 1

Table 1. Changes in bone geometry, density and strength by pQCT at the radius.

Measurement	Percent Change (95% CI) 0 to Year 1	Year 1 to Year 2	Total 2 Years
Distal radius (4%)			
Trabecular Density			
Placebo	-1.1	0.2	-0.9
NTG	5.3	5.7	11.0
Difference	6.4	5.5	11.9 (8.1, 15.7)
Midshaft radius (20%)			
Cortical Density			
Placebo	0.2	-0.4	-0.2
NTG	1.4	0.4	1.8
Difference	1.3	0.9	2.2 (0.6, 3.7)
Cortical Area			
Placebo	-1.0	-1.2	-2.2
NTG	5.8	2.7	8.5
Difference	6.7	3.9	10.6 (6.9,14.3)
Cortical Thickness			
Placebo	-0.2	-1.2	-1.4
NTG	7.7	4.8	12.5
Difference	7.9	6.0	13.9 (6.0, 21.7)
Periosteal Circumference			
Placebo	-0.4	0.1	-0.3
NTG	3.6	3.5	7.1
Difference	4.0	3.4	7.4 (4.3,10.4)
Polar Moment of Inertia			
Placebo	-0.7	-1.2	-1.9
NTG	4.2	1.2	5.4
Difference	4.9	2.4	7.3 (4.6,10.1)
Polar Section Modulus			
Placebo	-0.3	-1.1	-1.4
NTG	8.2	1.1	9.3
Difference	**8.5**	**2.2**	10.7 (7.5, 13.8)

tablenitrate

***Disclosures: Sophie Jamal**, None.*

1253

Osteogenic Differentiation and In Vivo Complementation of Osteoblast-Deficient Embryos by Induced Pluripotent Stem Cells. James Oh[1], Alyssa Riley[2], Xiaojing Huang[2], Sean Wu[2], Joy Wu*[3]. [1]Endocrine Unit, Massachusetts General Hospital, USA, [2]Cardiovascular Research Center, Massachusetts General Hospital, USA, [3]Massachusetts General Hospital, USA

Induced pluripotent stem cells (iPSCs), like embryonic stem cells (ESCs), are capable of self-renewing and differentiating into cell types of all three germ layers. Furthermore, iPSCs can be derived from individual patients, without the ethical issues associated with ESC derivation, providing a genetically identical source of cells for potential regenerative therapy. To investigate the capacity of iPSCs for differentiating toward the osteogenic lineage, we generated OsxCre-eGFP and constitutively expressing ROSA-YFP iPSC lines by introducing Oct4, Sox2, Klf4, and c-Myc into fibroblasts from transgenic mice carrying these reporter alleles. OsxCre-eGFP iPSCs were differentiated in vitro using the hanging droplet method and cultured in media containing ascorbic acid and β-glycerophosphate. Gene expression analysis demonstrated that markers of pluripotency decreased while markers of osteoblastogenesis increased with differentiation. Alizarin red stain was detected after 14 and 21 days in osteogenic culture, confirming deposition of mineralized matrix. To assess the osteogenic potential of iPSCs in vivo, we employed a model of embryonic osteoblast-deficiency by intermating Runx2 heterozygous mice to generate Runx2 null embryos. These embryos lack bone formation due to a failure of osteoblast differentiation. We introduced wild-type ROSA-YFP iPSCs into blastocysts from Runx2 heterozygous cross-matings and assessed YFP+ cell contribution by whole-mount fluorescence and histological analysis. We observed the presence of YFP+ iPSCs in Runx2 null embryos with partial skeletal contribution. Furthermore, these iPSCs were associated with areas of mineralization. In summary, iPSCs can undergo osteogenic differentiation in vitro and partially reconstitute an osteoblast-deficient skeleton in vivo. Further investigation using genetically modified iPSCs may provide new insights into the molecular pathogenesis of bone disease, and serve as in vitro models for screening of therapeutic agents.

***Disclosures: Joy Wu**, None.*

1254

IGFBP-2 from Mesenchymal Stromal Cells (MSCs) in the Bone Marrow Niche Regulates Hematopoietic Stem Cell Proliferation and Marrow Engraftment. Anne Breggia*[1], Masanobu Kawai[1], Eliza Grlickova-Duzevik[2], David Clemmons[3], Clifford Rosen[1]. [1]Maine Medical Center, USA, [2]Maine Medical Center Research Institute, USA, [3]University of North Carolina, USA

IGFBP2 (BP2) is one of 6 IGF binding proteins that shuttles IGFs to their respective receptors. We previously reported that PTH induces IGFBP2 synthesis in calvarial osteoblasts and that global deletion of BP2 results in small spleens, very low bone formation, impaired bone resorption and increased marrow adiposity. *In vitro*, bone marrow from *bp2*-/- mice show impaired recruitment of both osteoblasts and osteoclasts. BP2 null males also have a hematopoietic phenotype in which increased percentages of lymphoid and myeloid subpopulations are found in both the peripheral blood and spleen. Lodish identified BP2 as a critical factor for hematopoietic stem cell proliferation *ex vivo*. In this study, we hypothesized that BP2 serves a critical role as a proliferative factor in the bone marrow niche. Using RNA from purified mouse mesenchymal stem cells (Stem Cell Technologies), we first found that BP2 gene expression levels were 6-8 times higher than in purified B or T cells. We next performed non competitive bone marrow transplants (BMT) by transplanting LY 5.1+ donor cells into lethally irradiated WT and *bp2*-/- recipients. Donor engraftment was not different between strains as shown by greater than 70% donor cells present in the peripheral blood of recipient mice from both strains. However, in competitive repopulation transplantation using same strain donor-recipient pairs, *bp2*-/- donor cells engrafted *bp2*-/- recipient bone marrow 30% less efficiently (P=0.01) than WT transplants. In addition, there were significantly fewer mature lymphoid (CD3, CD19) and myeloid (CD11b, LY6G and F480) cells in the peripheral blood of bp2-/- recipients ($p \leq 0.05$). In response to administration of a single component of the IGFBP2 molecule, the heparin binding domain (HBD), to *bp2*-/- mice, trabecular bone mass was rescued and osteoblast number increased. Importantly, in vivo administration of the HBD suppressed the percentages of mature monocytes, macrophages and neutrophils in the peripheral circulation, comparable to those found in WT mice. Taken together these data demonstrate that BP2, which is synthesized by MSCs and inducible by PTH, is a potent regulator of hematopoiesis and may specifically control stem cell fate in an IGF binding independent manner within the marrow niche. Niche regulation by IGFBP2 may be therapeutically important to clinical bone marrow transplantation which is currently the only treatment option for many hematologic and solid tissue malignancies.

***Disclosures: Anne Breggia**, None.*

1255

Differentiation of Hematopoietic Cell Lineages is Altered in the Absence of Sclerostin. Corey Cain*[1], Gabriela Loots[2], Randell Rueda[1], Jennifer Manilay[1]. [1]University of California, Merced, USA, [2]LLNLUC Merced, USA

Purpose: Hematopoietic stem cells (HSCs) are in direct contact with osteoblasts (OBs) in the endosteum and trabecular regions of the long bones. OBs are considered "niche" cells that support HSC self-renewal and maintenance and are also important for B cell production in the bone marrow. Sclerostin (SOST) is a negative regulator of bone growth that is secreted by osteocytes and functions to reduce osteoblast proliferation by inhibiting WNT signaling through binding to LRP receptors. SOST-knockout (KO) exhibit generalized hyperosteosis and smaller bone marrow cavities due to an increase in proliferating OBs, osteocytes and excessive mineralization, while LRP5 KO mice are osteopenic. SOST expression is primarily OB and osteocyte-specific, but the effect of absence of SOST on hematopoiesis is unknown. We hypothesized that the increase in OB activity in SOST KO mice would result in increased numbers of self-renewing HSCs and reduce HSC differentiation whereas the decrease in OBs in LRP5 KOs would result in a reciprocal phenotype.

Methods: Bone marrow cells were isolated from SOST KO, LRP5 KO, and wild-type (WT) control mice. Phenotypic characterization of all hematopoietic cell lineages was performed using fluorescent activated cell sorting (FACS). RT-PCR for SOST and LRP5 was assessed in FACS-purified cell populations and digested bone.

Results: Surprisingly, no difference in HSC frequency or absolute number was observed between WT and SOST KO mice. Numbers of common lymphoid progenitors (CLP) and B lymphocytes were also reduced. Furthermore, lack of SOST did not affect myeloerythroid progenitor numbers but reduced the number of mature macrophages and granulocytes in the bone marrow. SOST expression was observed in the HSC, CLP and B cell lineages. Preliminary data showed reduced HSC and CLP numbers in LRP5 KOs.

Conclusions: In SOST KO mice, HSC numbers were unaffected, despite increased OB activity. In contrast, in LRP5 KOs, HSC numbers were reduced. These unexpected results suggest that SOST and LRP5 play different roles in WNT signaling in the OB niche. Lymphoid and myeloid differentiation was blocked in the absence of SOST. Interestingly, SOST is expressed in HSCs, B cells, and granulocytes. Therefore, whether SOST acts in a cell-autonomous or a non-cell autonomous manner on hematopoietic cells is still unclear. These findings have important safety implications for the clinical use of SOST-specific antibodies for the treatment of osteoporosis.

***Disclosures: Corey Cain**, None.*

1256

Gsα-Dependent Signaling in the Osteoblast Lineage Regulates Bone Marrow Hematopoietic Niches. Engin Ozcivici[1], Cris Lo Celso[2], Stefania Lymperi[2], David Scadden[2], Henry Kronenberg[3], Joy Wu*[3]. [1]Mass General Hospital, USA, [2]Center for Regenerative Medicine, Massachusetts General Hospital, USA, [3]Massachusetts General Hospital, USA

Gsα is a heterotrimeric G protein subunit that mediates cyclic-AMP-dependent signaling downstream of G protein-coupled receptors, including the parathyroid hormone (PTH)/PTH-related peptide (PTHrP) receptor (PPR). Deletion of Gsα early in the osteoblast lineage in Osterix-Cre:Gsa(fl/fl) mice results in reduced bone mass with fewer osteoblasts, with impaired differentiation of bone marrow B cell precursors. Since expression of constitutively active PPR in osteoblasts increases trabecular osteoblast number as well as hematopoietic stem cells (HSCs), we hypothesized that ablation of Gsα in osteoblasts would negatively impact HSC number. Eight day-old conditional knockout (KO) mice were sacrificed and their bone marrow analyzed for primitive HSCs. Compared to control littermates, KO mice had 37% fewer long term (LT) HSCs, corresponding to the most primitive and quiescent hematopoietic population. Gsα KO mice have a dramatic reduction in osteoblast number, which may indirectly impact HSC number and function. In an effort to assess the direct effects of Gsα in osteoblasts, sorted $Lin^{-}Sca1^{+}c\text{-}Kit^{+}$ (LKS) cells, a population highly enriched for HSCs, were cultured in the presence of primary calvarial osteoblasts from control or KO mice. Six days later, the frequency of hematopoietic cells was decreased by 17% in wells containing KO osteoblasts. Furthermore, the frequency of B220 positive B cell precursors was reduced by 29%. We have previously shown that B cell precursor development is blocked at the pre-pro-B to pro-B cell transition in Gsα KO bone marrow, and can be rescued by the addition of interleukin (IL)-7. In order to investigate whether Gsα directly regulates IL-7 expression, Gsα was deleted from calvarial osteoblasts by infection with an adenovirus expressing Cre recombinase. IL-7 mRNA levels were reduced in the absence of Gsα. Consistent with this finding, expansion of pre-pro-B cell precursors was significantly inhibited when cultured with Gsα-deficient osteoblasts. Together these results demonstrate that Gsα signaling in cells of the osteoblast lineage plays a direct role in the bone marrow niches for HSCs as well as for more differentiated B cell precursors.

***Disclosures: Joy Wu**, None.*

1257

Ovariectomy Expand the Hemopoietic Stem Cell Pool Through the T cell Costimulators CD40L and OX40. J.-Y. Li*, H. Tawfeek, B. Bedi, J. Adams, M. N. Weitzmann, R. Pacifici. Division of Endocrinology, Metabolism & Lipids, Emory University School of Medicine, USA

Ovariectomy (OVX) leads to a marked increase in bone marrow (BM) hemopoietic cells, primarily by increasing the production of hemopoietic cytokines by BM stromal cells (SCs). Since T cells are known to regulate SC function, we investigated the role of T cells in the pro-hemopoietic effects of ovx. WT mice were immunodepleted of T cells by treatment with anti CD4/8 mAbs, ovx or sham operated, and then sacrificed 4 weeks after surgery. FACS analysis at 2 and 4 weeks showed that OVX induced a 2-3 fold increase in the number of hemopoietic stem cells (HSCs), B cells, and monocytes in T cell replete controls but not in T cell deficient mice. Moreover, T cells induced the expansion of HSCs by upregulating the expression of Jagged1 on SCs. Thus, T cells/SCs cross talk leading to induction of Notch signaling in HSCs is required for OVX to modulate hemopoiesis. Analysis by DXA and μCT confirmed earlier reports that OVX induces a significant trabecular and cortical bone loss in controls, but not in T cell depleted mice. Since the T cell costimulatory molecule CD40L has been shown to regulate SC function by binding to SC expressed CD40, we examined the effect of ovx on HSCs in CD40L-/- mice. At 2 weeks OVX failed to increase the SC expression of Jagged1 and the number of HSCs and mature hemopoietic cells in CD40L-/- mice, while it did so in WT control mice. Therefore, CD40L is a costimulatory molecule by which T cells regulate the capacity of SCs to promote and support hemopoiesis early after ovx. Surprisingly, analysis at 4 weeks revealed that at this time point OVX had equal stimulatory effects on HSCs and mature hemopoietic cells in WT and CD40L-/- mice. These findings suggest that late after ovx T cells regulate SCs through costimulatory molecules other than CD40L. One T cell costimulator, which is known to replace CD40L as driver of skin graft rejection, is OX40. This receptor binds to OX40L, which is expressed on antigen presenting cells. Strikingly, real time PCR analysis showed that OVX upregulated by 3-4 folds the expression of OX40 in T cells and of OX40L in SCs at 4 weeks but not at 2 weeks. Collectively, these data demonstrate that ovx expand the HSCs by upregulating Jagged1 expression in SCs through a T cell costimulatory molecule-dependent mechanism. CD40L is the T cell costimulator that plays a pivotal role in the expansion of HSCs in the early post-ovx period, while OX40 assumes a dominant role later after ovx.

***Disclosures: J.-Y. Li**, None.*

1258

Stem Cell Antigen 1 Positive (Sca-1+) Cell-Based Gene Therapy with a Modified Fibroblast Growth Factor 2 (FGF2) Produces Contrasting Skeletal Effects on Femur as Opposed to Tail Vertebra in Mice. Susan Hall*[1], Shin Tai Chen[1], Suburraman Mohan[1], Jon Wergedal[1], Apurva K. Srivastava[2], Daila S. Gridley[3], Kin-Hing William Lau[1]. [1]Jerry L. Pettis Memorial VA Medical Center, USA, [2]National Institure of Health, USA, [3]Department of Radiation Medicine, Loma Linda University School of Medicine, USA

Administration of FGF2 protein in rats results in large increases in osteoblast (Ob) and osteoid surface at bone sites rich in red (hematopoietic) marrow, but these effects decline rapidly after treatment withdrawal. We have shown that transplantation of Sca1+ cells expressing an FGF2 gene (modified to improve secretion and stability) provides sustained, high dose, local FGF2 expression and results in rapid, robust endosteal bone formation (BF) in red marrow-containing bones of recipient mice (femur, lumbar vertebra). Bone areas that contain yellow (fatty) marrow are known to differ from that of red marrow in their response to stimuli. The current study sought to determine if transplantation of hematopoietic progenitor (Sca-1+) cells and sustained FGF2 expression could also promote BF in yellow marrow bone (tail vertebra). Sublethally irradiated stem cell-deficient mice were injected I.V. with Sca1+ cells transduced with MLV-based vectors expressing FGF2 or GFP genes. At 14 weeks post transplantation, sera, long bones and vertebrae were harvested. Consistent with previous work, serum FGF2 (by ELISA) levels were significantly increased in the FGF2-transplanted group compared to controls. Transduced cell engraftment and transgene expression were confirmed by the finding of high expression levels of human FGF2 mRNA in tibial bone marrow cell extracts in the FGF2 group but not in controls. μCT analyses of femurs revealed significant increases in trabecular bone volume fraction (BV/TV), connectivity density (ConnDens) and trabecular thickness (TbTh) in the FGF2 group compared to controls (243% $p<0.05$, 373% $p<0.03$ and 118% $p<0.02$, respectively) but no significant differences in trabecular number (TbN) or separation (TbSp), suggesting increased BF. In contrast, μCT analyses of tail vertebrae showed that transplantation of FGF2-expressing cells reduced BV/TV, ConDens and TbN (60% $p<0.03$, 42% $p<0.03$ and 62% $p<0.003$, respectively) and significantly increased TbSp (182% $p<0.005$), suggesting increased bone resorption (BR). Based on our data and published findings that FGF2 exerts effects on both osteoblast and osteoclast lineage cells, we conclude that high, sustained expression of FGF2 after transplantation of FGF2-transduced Sca1+ cells produces skeletal site-specific effects to increase BF in the femur and BR in the caudal vertebra. Further work is required to elucidate the mechanisms mediating these contrasting site-specific FGF2 effects.

***Disclosures: Susan Hall**, None.*

1259

Directing Mesenchymal Stem Cells to Bone to Increase Bone Formation. Wei Yao*[1], Min Guan[2], Ruiwu Liu[2], Kit Lam[2], Mohammad Shahnazari[2], Jan Nolta[2], Nancy Lane[1]. [1]University of California, Davis Medical Center, USA, [2]UC Davis Medical Center, USA

Mesenchymal stem cells (MSCs) are the precursors of osteoblasts that form bone. Aging results in a reduction in the number of MSCs in the bone marrow which leads to a reduction in osteogenesis, reduced bone formation and increased bone fragility. Bone regeneration by the means of induction of osteogenesis from MSCs offers a rational therapeutic option. However, this approach is problematic due to the major obstacle of controlling the MSCs' commitment, growth and differentiation into functional osteoblasts on the bone surface. Our research group has developed a method to direct the MSCs to the bone surface. We attached a synthetic peptidomimetic ligand (LLP2A) that has high affinity for activated α4β1 integrin on the MSC surface, to a bisphosphonates (alendronate, Ale) that has high affinity for bone, to direct the MSCs to bone. Experiments. We tested the efficacy of our new hybrid compound (LLP2A-Ale) using two approaches: 1.We evaluated if LLP2A-Ale can guide the MSCs to bone using the Xenotransplantation model. We obtained human MSCs (huMSCs) and injected the cells together with LLP2A-Ale into the immunodeficient mice, NOD/SCID MSPVII. This mouse strain lacks β-glucuronidase (GUSB) so that donor cells could be easily tracked or identified using biochemical detection of GUSB. 2. We performed another study using 2 mos.old female 129SvJ mice that were treated with either PBS, Ale, LLP2A or LLP2A-Ale. The mice received monthly intravenous (iv) injections of the treatments and changes in bone mass were monitored by in vivo microCT scans of the distal femurs. Changes in bone formation were measured by histomorphometry and bone markers. In the NOD/SCID/MSPVII mice that received huMSCs, we found that LLP2A-Ale mobilized MSCs on the bone surface as compared to the control groups (PBS and MSCs) 24 hours after the injection of MSCs (~ 50% in LLP2A-Ale treated group vs. <1% in the control groups). After a single iv injection, mice treated with MSCs + LLP2A-Ale alone had nearly 20% higher cancellous bone than mice treated with MSCs alone or MSC + LLP2A or Ale. In the "normal", 2-mo-old female mice, monthly LLP2A-Ale injection increased cancellous bone mass by > 15% at 4 weeks and > 25% at 8 weeks. Bone formation (serum osteocalcin and BFR/BS) was increased by about 20% from the control groups. In conclusion. our data suggested LLP2A-Ale appears to increase MSC mobility and stimulate the MSCs towards osteoblastogenesis when they are "directed" to bone.

***Disclosures: Wei Yao**, None.*

1260

Lrp5-deficient Mice are Responsive to the Osteo-anabolic Action of Sclerostin Antibody. Alexander Robling*[1], Matthew Warman[2], Chris Paszty[3], Charles Turner[4]. [1]Indiana University, USA, [2]Howard Hughes Medical Institute, Department of Genetics, Harvard Medical School, USA, [3]Amgen, Inc., USA, [4]Indiana University, Purdue University Indianapolis, USA

Wnt signaling through LRP5 is modulated by the osteocytic protein sclerostin. Sclerostin is thought to bind directly to LRP5 and antagonize canonical Wnt signaling. We hypothesized that the osteo-anabolic effects of sclerostin deletion/inhibition would be lost in mice lacking Lrp5. We tested this hypothesis by measuring bone mass in mice lacking both Lrp5 and Sost, and in Lrp5-deficient mice treated with a sclerostin neutralizing antibody. For the genetic crossbreeding experiment, four genotypes were generated by crossing the progeny of an $Lrp5^{-/-}$ $Sost^{-/-}$ mating: $Lrp5^{+/+}$ $Sost^{+/+}$; $Lrp5^{+/+}Sost^{-/-}$; $Lrp5^{-/-}Sost^{+/+}$; and $Lrp5^{-/-}Sost^{-/-}$. In 17-wk old male mice, aBMD was 10.8% lower ($p<0.001$) in $Lrp5^{-/-}Sost^{+/+}$ mice, compared to WT controls ($Lrp5^{+/+}Sost^{+/+}$). $Lrp5^{+/+}Sost^{-/-}$ mice exhibited 38.7% greater ($p<0.001$) aBMD than WT controls. aBMD in the double mutants ($Lrp5^{-/-}Sost^{-/-}$) was significantly greater than in WT controls (17.6% greater; $p<0.001$) but significantly less ($p<0.001$) than in $Lrp5^{+/+}Sost^{-/-}$ mice. Female mice showed similar trends according to genotype. Next, we sought to overcome the developmental effects of Sost deletion (e.g., HBM phenotype effects) on our model by waiting until $Lrp5^{-/-}$ mice were fully adult, then inhibiting sclerostin using a neutralizing antibody (twice-weekly injection with Scl-AbIII, 25 mg/kg., for 3 wks). Whole-body aBMD increased 2-3% over the 3 wk treatment period in both $Lrp5^{+/+}$ and $Lrp5^{-/-}$ mice treated with vehicle. $Lrp5^{+/+}$ mice treated with Scl-AbIII exhibited a 21.1% increase ($p<0.001$) in whole body aBMD, whereas $Lrp5^{-/-}$ mice treated with Scl-AbIII exhibited an 18.7% increase in whole body aBMD. The percent increase induced by the antibody was not statistically different ($p=0.30$) between $Lrp5^{+/+}$ and $Lrp5^{-/-}$ mice. Cortical bone area (CA) at the midshaft femur followed similar trends as the DEXA results; Scl-AbIII improved CA by 22.8% ($p<0.001$) in $Lrp5^{+/+}$ mice and by 18.9% in the $Lrp5^{-/-}$ mice ($p<0.001$), compared to genotype-matched vehicle-treated mice. No difference in antibody mediated improvement was detected between genotypes. Collectively, our data indicate that inhibiting sclerostin can improve bone mass whether Lrp5 is present or not. It remains to be determined how much of sclerostin's action occurs via other receptors, like Lrp4 or Lrp6, and whether there are any compensatory expression mechanisms when one receptor (e.g. Lrp5) is deleted.

***Disclosures: Alexander Robling**, None.*

1261

Sclerostin Inhibition by Monoclonal Antibody Reversed Trabecular and Cortical Bone Loss in Orchiectomized Rats with Established Osteopenia. X Li*[1], KS Warmington[1], Q-T Niu[1], FJ Asuncion[1], M Barrero[1], X Xia[2], M Grisanti[1], E Lee[1], Thomas Wronski[2], MS Ominsky[1], WS Simonet[1], C Paszty[1], HZ Ke[1]. [1]Amgen Inc, USA, [2]University of Florida, USA

Male osteoporosis is becoming an increasingly important public health problem and hypogonadism is a common cause of osteoporosis in men. Sclerostin inhibition has been shown to increase bone formation and BMD in rodents, primates, and humans. In this study, we examined the effects of sclerostin antibody (Scl-AbIII) treatment on bone loss due to androgen deficiency in rats. Six-month-old male SD rats were sham-operated or orchiectomized (ORX) then left untreated for 3 months, allowing for the development of osteopenia. At the age of 9 months, ORX rats were treated with vehicle or Scl-AbIII at 5 or 25 mg/kg (2x/week, s.c.) for 6 weeks (10/group). Sham rats received vehicle. In vivo DXA measurements demonstrated that 3 weeks of Scl-AbIII treatment at both doses fully reversed the significant deficit in lumbar spine BMD caused by 3 months of orchiectomy. Six weeks of Scl-AbIII treatment at 25 mg/kg increased lumbar spine BMD in ORX rats to a level significantly greater than sham controls. Terminal pQCT analysis at the distal femur revealed that the marked loss of trabecular BMD (-41% vs. Sham) in ORX rats was reversed by Scl-AbIII treatment in a dose-dependent manner (Table 1). MicroCT analysis at the mid-femoral diaphysis demonstrated that the significant decreases in cortical vBMC (-12% vs. Sham), cortical thickness (-8% vs. Sham), and cortical area (-11% vs. Sham) in ORX rats were restored by Scl-AbIII treatment in a dose-dependent manner. The three-point bending test at the mid-femoral diaphysis confirmed that Scl-AbIII-treated ORX rats had a dose-dependent greater maximum load and stiffness as compared with ORX controls. Dynamic histomorphometric analysis at the tibial shaft revealed that the marked reduction in periosteal bone formation rate (-95% vs. Sham) in ORX rats was fully restored to the level of sham controls in both Scl-AbIII treatment groups. Endocortical bone formation rate was further increased to a level significantly greater than sham controls in both Scl-AbIII treatment groups. In summary, sclerostin antibody treatment increased bone formation, reversed trabecular and cortical bone loss, and improved cortical geometry in adult rats with androgen deficiency. Furthermore, the increased bone mass was associated with increased bone strength. These results suggest that sclerostin inhibition may be a promising therapeutic approach for increasing both trabecular and cortical bone mass in men with osteoporosis due to androgen deficiency.

Table 1. Selective Endpoints at the Distal Femur, Mid-femoral Diaphysis, and Tibial Shaft After 6 Weeks of Treatment

			ORX		
Site	Endpoints	Sham-Vehicle (n=10)	Vehicle (n=10)	5 mg/kg (n=10)	25 mg/kg (n=10)
Distal Femur	Trabecular BMD (mg/cm^3)	166±16	98±9[a]	154±15	186±18[b]
Mid-Femoral Diaphysis	Cortical Thickness (mm)	0.83±0.02	0.76±0.01[a]	0.82±0.01	0.84±0.02[b]
	Maximum Load (N)	241±9	205±5[a]	230±6	254±14[b]
Tibial Shaft	Ps. BFR/BS ($\mu m^3/\mu m^2/d$)	0.39±0.09	0.02±0.01[a]	0.53±0.13[b]	0.73±0.09[b]
	Ec. BFR/BS ($\mu m^3/\mu m^2/d$)	0.15±0.02	0.13±0.03	0.93±0.09[ab]	0.96±0.06[ab]

Data are mean ± SEM. [a]$p < 0.05$ vs. Sham, [b]$p < 0.05$ vs. ORX-Vehicle

Table 1

***Disclosures: X Li**, Amgen Inc., 1; Amgen Inc., 3*
This study received funding from: Amgen Inc.

1262

PTH Efficacy in a Bone Healing Model with T-Cell Deficient Rats. Masahiko Sato*, M.D. Adrian, Anita Harvey, Q.Q. Zeng, Yanfei Linda Ma. Lilly Research Labs, USA

Previously, T lymphocytes were shown to mediate the skeletal efficacy of PTH, because nude mice exhibited a blunted skeletal response to PTH (M. Terauchi et al. 2008). Therefore, we evaluated the systemic efficacy of PTH in bone healing and non-fractured sites, using NTac:NIH-Whn rats. Male, 14 week old, athymic rats (NIHRNU-M, NTac:NIH-Whn, Taconic) were maintained on a 12hr light/dark cycle at 220C with ad lib access to food (TD 89222 with 0.5% Ca and 0.4%P, Teklad, Madison, WI) and water for 2 weeks, before conducting bilateral cortical defect surgery through both anterior and posterior cortices (D. Komatsu et al. 2009). Animals were weighed and randomized into treatment groups, including vehicle and PTH groups treated with 0, 5 or 30 ug/kg/d sc hPTH1-38 for 7 weeks of treatment, starting 8 days post-surgery. Both PTH doses were efficacious with dose-dependent enhancement of BMD and BMC of the femoral diaphysis at the cortical defect (24%, 20%), intramedullary spaces (95%,95%) compared to controls, but site specific analyses showed no enhanced healing of the anterior cortex or posterior cortex. Load

to failure analyses showed dose dependent enhancement in femoral stiffness (22%) and strength (17%) relative to controls at the site of the cortical defect. PTH systemic efficacy at not affected sites (sites away from the cortical defect) were also observed with dose dependent increases in femoral neck work to failure (70%), strength (38%), serum osteocalcin levels (31%), vertebral BMC (20%), and vertebral BMD (14%). Longitudinal analyses showed that PTH enhances bone healing by stimulating woven bone formation in the intramedullary spaces and stimulating endocortical mineral apposition resulting in stronger femora, but some reductions in mineral apposition of the anterior and posterior cortices were observed relative to other animals. In addition, PTH significantly enhanced mineral apposition at other axial and appendicular sites. Mechanistic studies are in progress to clarify the basis to these PTH effects in athymic nude rats. These data indicate that the T-cell deficient rat skeleton remains responsive to PTH treatment.

***Disclosures: Masahiko Sato**, Eli Lilly & Co, 3*
This study received funding from: Eli Lilly & Co

1263

Elevated Bone Mass in Mice Treated with Anti-Dickkopf-1 Neutralizing Antibodies. Robert Brommage*, Jeff Liu, Dawn M. Bright, Deon D. Smith, Sabrina Jeter-Jones, Christopher M. DaCosta, Sayadeth Khounlo, Melanie K. Shadoan, David R. Powell, David G. Potter. Lexicon Pharmaceuticals, USA

The mutant LRP5 protein in subjects with high bone mass phenotype is resistant to the inhibitory actions of Dickkopf-1 (DKK1). Knockout (KO) of Dkk1 in mice results in embryonic lethality, with heterozygous (HET) mice having increased bone mass. As part of Lexicon's Genome5000^{TM} program to characterize mouse KO phenotypes of pharmaceutically relevant genes, we generated HET Dkk-1 KO mice by targeting exons 2 and 3. BMD and bone architecture were determined by PIXImus DEXA and Scanco μCT40, respectively.

Female wild-type (WT) mice with access to running wheels from 6 to 18 weeks of age had increased bone mass. Dkk1 HET mice have elevated trabecular bone volume (TBV) compared to WTs, and access to running wheels resulted in a synergistic ($P = 0.08$ by two-factor ANOVA) elevation of TBV in the distal femur metaphysis (DFM). These results suggest Dkk1 may be important in mechanical sensing at this bone site.

We identified and characterized two monoclonal mouse antibodies capable of neutralizing Dkk1-mediated inhibition of Wnt signaling in a cell-based reporter assay. Ab-1 recognizes an epitope in the C-terminal half of Dkk1 with sub-nanomolar affinity and prevents Dkk1 from binding to LRP6 while Ab-2 recognizes an epitope in the N-terminal half of Dkk1 with sub-nanomolar affinity and does not affect Dkk1 binding to LRP6.

Treating male WT mice at 4 weeks of age for 4 weeks with neutralizing antibody Ab-2 (30 mg/kg given once per week) produced increases in BMD of the body (11%), spine (19%) and femur (11%). By microCT analyses TBV increased 18% in LV5 and 92% in the DFM. Mice given zoledronate had similar BMD gains, with a 19% increase in LV5 TBV. Whereas zoledronate treatment increased LV5 Tb.N (19%) but not Tb.Th (1%), Ab-2 treatment increased LV5 Tb.Th (10%) but not Tb.N (2%). Ab-1 treatment gave similar results but was less potent. These results indicate treating young mice with neutralizing anti-Dkk1 antibodies increases bone mass through a mechanism distinct from that of zoledronate. Treatment with the Ab-2 antibody also increased bone mass in WT adult mice, but to a lesser extent than in young mice.

Treating male WT mice at 10 weeks of age with dexamethasone (15 mg/kg) for 30 days resulted in an 8-fold elevation of serum Dkk1 levels. Dexamethasone treatment had minimal effects on bone mass but suppressed serum PINP levels (70% on Day 7 and 30% on Day 30) and this suppression was not affected by weekly Ab-2 treatment at 10 mg/kg.

***Disclosures: Robert Brommage**, Lexicon Pharmaceuticals, 3*
This study received funding from: Lexicon Pharmaceuticals

1264

Inhibition of ALK3 (BMPRIA) Signaling Using RAP-661, a Novel Soluble BMP Antagonist, Decreases Sclerostin Expression and Increases Bone Mass. Nicolas Solban*[1], Milton Cornwall-Brady[1], Yoshimi Kawamoto[1], June Liu[1], Benjamin Umiker[1], Shana Walrond[1], Rita Steeves[1], Kathryn Underwood[1], Ravi Kumar[1], Jasbir Seehra[1], Ernesto Canalis[2], R. Scott Pearsall[1]. [1]Acceleron Pharma, USA, [2]St. Francis Hospital & Medical Center, USA

Bone Morphogenetic Proteins (BMPs) induce endochondral bone formation and regulate osteoblastogenesis and osteoclastogenesis. However, the inactivation of the BMP-2 receptor ALK3/BMPRIA, specifically in osteoblasts, causes an increase in bone formation suggesting that the inhibition of endogenous ligands may have different biological consequences then those of the exogenously administered ligands. To investigate new therapeutic strategies for metabolic bone diseases, a soluble ALK3 receptor (RAP-661) with antagonist properties to the endogenous receptor was generated.

Twelve week old C57BL/6 female mice received RAP-661 (10 mg/kg, twice weekly ip) or vehicle (PBS) for 6 weeks and were assessed after 2, 4, and 6 weeks of treatment. RAP-661 treated animals appeared healthy for the duration of the study and their BMD was increased by 3%, 8% and 6% ($p<0.05$) after 2, 4 and 6 weeks of treatment, respectively. After 4 and 6 weeks of treatment, RAP-661 increased serum osteoprotegerin by 38 to 56% ($p < 0.05$), and decreased RANKL by 40 to 52% ($p < 0.05$); TRAP5b levels were decreased at week 2 by 67% ($p < 0.01$), but were equal to control levels by week 6. Histomorphometric analysis of the distal femur determined that RAP-661 increased trabecular bone volume by 63%, 90% and 68% after 2, 4 and 6 weeks, respectively, compared to controls. This increase was due to increased trabecular thickness and not number. While there was no change in osteoblast number, there was a marked increase in the mineralizing surface (67% and 115%, $p < 0.05$) and bone formation rate (80%, $p < 0.05$) after 2 to 4 weeks of treatment with RAP-661. In addition, the eroded surface and osteoclast surface were reduced after 4 weeks (36% and 44%, $p < 0.05$, respectively), indicative of an antiresorptive effect. RAP-661 decreased bone marrow adipocytes by 21 to 36% ($p < 0.05$) and decreased the skeletal expression of sclerostin, a Wnt antagonist, by 61%, 52%, and 43% ($p < 0.05$) after 2 days, 1 and 4 weeks, respectively.

These results indicate that RAP-661 increases trabecular bone volume by increasing bone formation and decreasing bone resorption. The reduction in skeletal sclerostin expression indicates that inhibition of ALK3 signaling may result in increased Wnt signaling leading to increased bone mass. In conclusion, inhibition of BMP signaling using a soluble BMP antagonist offers a promising new alternative for the treatment of bone-related disorders.

***Disclosures: Nicolas Solban**, Acceleron Pharma, 1; Acceleron Pharma, 3*
This study received funding from: Acceleron Pharma

FR0005

Reduced Trabecular Volumetric BMD at Metaphyseal Regions of Weight-bearing Bones is Associated with Prior Fracture in Young Girls. Joshua Farr*[1], Rita Tomas[1], Zhao Chen[2], Jeffrey Lisse[3], Timothy Lohman[3], Scott Going[3]. [1]The University of Arizona, USA, [2]University of Arizona College of Public Health, USA, [3]University of Arizona, USA

Understanding the etiology of skeletal fragility during growth is critical for the development of treatments and prevention strategies aimed at reducing the burden of childhood fractures. Thus, we evaluated the relationship between prior fracture and bone parameters in young girls. Data from 465 girls aged 8–13 from the "Jump-In: Building Better Bones" study were analyzed. Bone parameters were assessed at metaphyseal and diaphyseal sites of the non-dominant femur and tibia using peripheral quantitative computed tomography (pQCT). Dual-energy X-ray absorptiometry (DXA) was used to assess femur, tibia, lumbar spine, and total body areal bone mineral density (aBMD). Binary logistic regression was used to evaluate the relationship between prior fracture and bone outcomes, controlling for maturity, body mass, leg length, ethnicity, and physical activity. Associations between prior fracture and all DXA outcomes and pQCT parameters at diaphyseal sites were non-significant. In contrast, reduced trabecular volumetric BMD (vBMD) at distal metaphyseal sites of the femur and tibia was significantly associated with prior fracture. After adjustment for covariates, every SD decrease in trabecular vBMD at metaphyseal sites of the distal femur and tibia was associated with 1.4 (1.1–1.9) and 1.3 (1.0–1.7) times increased fracture prevalence, respectively. Prior fracture was not associated with metaphyseal bone size (i.e. periosteal circumference). In conclusion, childhood fractures are associated with reduced trabecular vBMD, but not bone size, at metaphyseal sites of the femur and tibia. Reduced trabecular vBMD at metaphyseal sites of long bones may be an early marker of skeletal fragility.

***Disclosures: Joshua Farr**, None.*

FR0009

Girls Accrue More Bone Relative to Lean Mass in Puberty and this Sex-difference Maintains to Young Adulthood: Evidence from 15 - years of Longitudinal Data. Saija Kontulainen*, Donald Bailey, Robert Faulkner, Adam Baxter-Jones. University of Saskatchewan, Canada

Over a century ago the idea of constant interaction between muscles and bones was proposed. During the past decade evidence of sex-specificity in this relationship has been noted from cross-sectional data and theorised to demonstrate accrual of mechanically excess mineral in female skeleton for the reproductive needs. To reliably investigate the sex-specificity in bone mineral content (BMC) accrual in relation to muscle gain from adolescence to adulthood, we examined 15-years of longitudinal data from 127 (66 females) participants of the Saskatchewan Pediatric Bone Mineral Accrual Study (PBMAS). Dual energy x-ray absorptiometry derived BMC (g) and lean body mass (g) of total body (TB), trunk, arms and legs were measured annually from 1991-97 and 2002-2006. Peak height velocity (PHV) was determined for each participant and the age from PHV was calculated to determine biological age at each measurement time. Using random effects models, we analyzed the influence of sex on BMC to lean ratio at each site from adolescence to adulthood while controlling for variations in tempo and timing of body composition development and physical activity.

In the random effects model for BMC to lean ratios in TB, arms and legs, females had 15.3 (SEE 4.8), 54.8 (SEE 8.0) and 17.6 (SEE 7.8) greater values than males, respectively. Sex had no influence on trunk BMC to lean ratio (4.0, SEE 3.1).

When the confounders of maturation, fat mass and physical activity were controlled, females had on average 10% greater total body BMC to lean ratio than males. These longitudinal results support the theory of the mechanically excess bone accrual in pubertal female skeleton and resulting bone mineral reserve in adult females for reproductive needs.

***Disclosures: Saija Kontulainen**, None.*

FR0010

Magnitude and Timing of Peak Bone Mineral Accrual in Young Girls. Joan Lappe*[1], Robert Heaney[2], Michael Davies[2], Diane Cullen[2]. [1]Creighton University Osteoporosis Research Center, USA, [2]Creighton University, USA

Purpose: The greatest lifetime increase in bone mass occurs during adolescence, and the amount accrued affects the risk of osteoporosis later in life. In girls, the fastest accrual occurs around the time of menarche. The purpose of this prospective study is to estimate the time over which this rapid accrual occurs and the magnitude of bone mass accrual.

Methods: Healthy girls, ages 9 -11 years and in Tanner Stage 1-2 at baseline, were participants in 2 randomized trials to determine the effects of optimal dietary calcium intake on bone mineral content (BMC) accrual. This analysis includes 160 girls who were followed for 8-10 years and experienced menarche during follow up. DXA scans were done every 6 months. Each girl's spine BMC at menarche (MABMC) was computed (mean of BMC values immediately prior to and immediately after menarche). All the spine BMC's for one girl were divided by MABMC to yield a sequence of relative BMC's, aggregated at half year intervals from menarche. Then the aggregated average for all girls for each half year step was computed. The times and aggregated averages were fitted to a 4-parameter sigmoid function.

Results:

Descriptives at baseline and end of study - median (min, max)

	Baseline	End of study
Age (yrs)	9.6 (8.7, 11.5)	17.9 (11.9,20.1)
Height (m)	1.38 (1,25, 1.61)	1.65 (1.43, 1.81)
Spine BMC (gm)	22.6 (12.5, 40.8)	57.3 (33.1, 81.8)
Weight (kg)	34.5 (22.5, 56.0)	63.4 (36.4, 112.0)
Menarcheal age (yrs)	12.8 (10.1, 16.7)	N/A

The rapid BMC gain occurred over 4 years (± 2 yrs around menarche). The maximum gain in BMC occurred at menarche, with 21.7% of the rapid gain occurring ± 6 mos around menarche. In aggregate, the gain in spine BMC is about 62% of the value achieved at the end of study (late adolescence).

Discussion: This prospective study expands on and confirms the findings of others that peak BMC accrual in girls is coincident with menarche.[1] Furthermore, this study provides longer follow up than previous studies in a cohort of girls who were very similar in age and pubertal stage at baseline. These data provide a very good estimate of the amount of bone gained during the rapid accrual phase and the time course for this accrual. Our findings can help clinicians evaluate skeletal development in their young female patients.

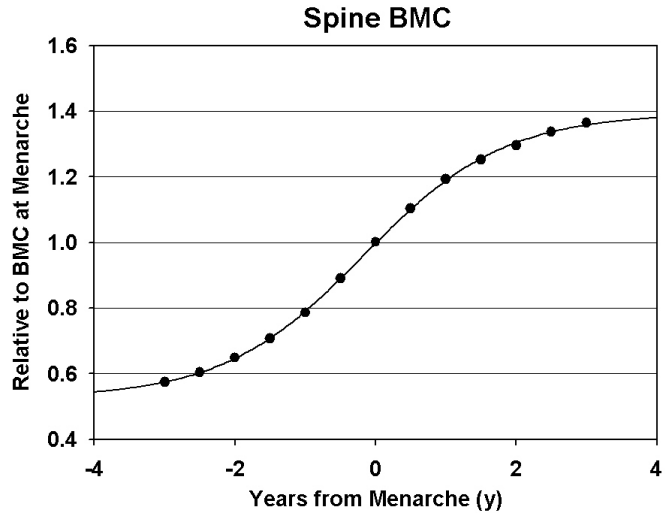

Spine bone mineral accrual

***Disclosures: Joan Lappe**, None.*

FR0012

Maternal Plasma Long Chain Polyunsaturated Fatty Acids Determine Bone Health in their Children at Age of Four: Southampton Women's Survey. Dinesh Dhanwal*[1], Philip Calder[2], Kim Miranda[3], Sian Robinson[3], Hazel Inskip[3], Elaine Dennison[4], Cyrus Cooper[2]. [1]Maulana Azad Medical College, New Delhi andMRC, Southampton UniversityUK, India, [2]University of Southampton, United Kingdom, [3]MRC, United Kingdom, [4]MRC Epidemiology Resource Centre, United Kingdom

Background: Maternal nutrition during pregnancy affects bone health in the children of those pregnancies. Previous studies have shown an association between maternal fatty acid status and offspring bone density in experimental animals and in human infants, but there are no studies in older children.

Objective: To determine the association between maternal long chain polyunsaturated fatty acid (LCPUFA) status in pregnant women and bone mineral density in their children at the age of four years.

Material and methods: The study population included 1455 mothers from the Southampton Women's Survey and their children (763 boys and 692 girls). Maternal dietary intakes of total n3 and n6 PUFA were assessed using a food frequency questionnaire. The concentrations of LCPUFA in maternal plasma phosphatidylcholine (PC) at 34 weeks of gestation were determined by gas chromatography. Bone density measures were made by DXA in the children at the age of four years.

Results: Maternal plasma PC eicosapentaenoic acid (EPA) showed a significant positive association with whole body, spine and hip bone mineral density (BMD) ($r = 0.099$, $p = 0.0009$; $r = 0.096$, $p = 0.011$ and $r = 0.086$, $p = 0.022$ respectively) and with whole body and spine volumetric (V) BMD ($r = 0.092$, $p = 0.015$; and $r = 0.092$, $p = 0.015$ respectively). Maternal plasma PC n-3 docosapentenoic acid (DPA) showed a significant positive correlation with whole body and spine BMD and with spine vBMD ($r = 0.099$, $p = 0.0009$; $r = 0.111$, $p = 0.003$ and $r = 0.104$, $p = 0.009$ respectively). After multivariate analysis, associations between maternal plasma PC EPA and BMD at spine (both total and v BMD) and between maternal plasma PC DPA and whole body BMD, spine BMD and spine vBMD remained significant. There were no significant associations of maternal plasma PC arachidonic acid or docosahexaenoic acid with BMD in the children.

Conclusion: The present study demonstrates a positive association between the status of two n-3 LCPUFA (EPA and DPA) in late pregnancy and BMD in the children of those pregnancies at the age of 4 years. These findings suggest an important effect of early exposure to n-3 LCPUFA and childhood bone development.

***Disclosures: Dinesh Dhanwal**, None.*

FR0021

Impairment of Bone Microarchitecture and Lipodystrophy in Young B6 Mice Treated with the Second Generation Anti-psychotic, Risperidone. Ingrid De Paula*[1], Sutada Lotinun[2], Gavin Welch[3], Sumithra Urs[4], Masanobu Kawai[1], Sheila Bornstein[1], Ann Maloney[4], Mark Horowitz[5], Roland Baron[6], Clifford Rosen[1]. [1]Maine Medical Center, USA, [2]Harvard School of Dental Medicine, USA, [3]Foundation for Blood Research, USA, [4]Maine Medical Center Research Institute, USA, [5]Yale University School of Medicine, USA, [6]Harvard School of Medicine & of Dental Medicine, USA

Risperidone(R) is an atypical antipsychotic widely used in adolescents and children. Adverse effects such as weight gain and hyperprolactinemia can be striking, particularly in young individuals. In this study we hypothesized that R treatment of mice would result in a fat redistribution phenotype and might impair peak bone mass. Young (4 week) male C57BL6 mice were orally (added to food) treated with R at a dose of 1.25mg/kgxdaÿ[1] for 5 weeks. Control mice(C) received a regular 10% fat per calorie diet. During this period food ingestion and body weight were measured daily. At the 5th week, body composition and bone mineral density were analyzed by DXA. In a smaller number of mice body fat content was evaluated by MRI. At sacrifice liver, epididymal and retroperitoneal adipose tissues were weighed. Bone microarchitecture was evaluated by microCT and histomorphometry. Liver oil-red-O staining was performed. T test was used in statistical analysis with a 95% confidence interval. R mice (n=12) tend to gain more weight than C mice (n=11) despite no differences in food intake. Surprisingly, total % body fat by DXA (R:14.6% C:18.6%, $p<0.01$), epididymal (R:14.5mg/gbw C:20.8mg/gbw, $p<0.01$) and retroperitoneal fat weight(R:2.9mg/gbw C:5.0mg/gbw, $p<0.01$) were significantly lower in R than in C mice. R livers were heavier in R than in C ($p<0.008$) and had massive lipid droplet formation. R mice tended to have lower total bone mineral density by DXA, reduced femoral cortical thickness by microCT ($p<0.008$) and lower tibial BV/TV by histomorphometry (R:7.3% C:8.8%,$p<0.05$). All bone resorption parameters such as osteoclast surface per bone surface(R:5.7% C:2.5%, $p=0.01$), osteoclast number per tissue area (R:11.8/mm^2 C:6.4/mm^2, $p<0.02$), osteoclast number per bone perimeter (R:2.3/mm C:1.1/mm, $p=0.009$) and eroded surface per bone surface (R:2.56% C:0.98%, $p=0.002$) were increased in R vs C mice. These results suggest that adipose distribution (visceral vs epididymal and retroperitoneal) is significantly altered by R treatment of pubertal mice, even before excessive weight gain occurs. The detrimental effects of R on bone were principally associated with increased indices of bone resorption with no changes in parameters of bone formation. In sum, R has a profound effect on fat metabolism and the skeletal phenotype. Prolonged use in younger animals and individuals may be associated with the metabolic syndrome as well as impaired peak bone acquisition and maintenance.

***Disclosures: Ingrid De Paula**, None.*

FR0024

High Dose Recombinant Growth Hormone Therapy is More Effective in Pre-pubertal Compared to Pubertal Patients with Growth Failure in Well Controlled Hypophosphatemic Rickets. Agnes Linglart*, Isis Marchand, Pierre Bougneres, Anya Rothenbuhler. AP-HP; Université Paris 5; INSERM, France

Twenty-five to 30% of patients with well controlled X-linked hypophosphatemic rickets (XLHR) show linear growth failure despite optimal treatment with calcitriol and phosphates and have a final height under -2 SDS. Previous studies in small cohorts of patients (maximum N=6) demonstrated improvement in mean height Z-scores under recombinant growth hormone (rGH) therapy. To confirm the benefit of rGH therapy on linear growth we included 18 children and adolescents with hypophosphatemic rickets and growth failure in a controlled clinical trial. The inclusion criteria were the following: XLHR with mutation in the PHEX gene, minimum of one year of optimal oral treatment with phosphate and calcitriol prior to inclusion, insufficient "catch up growth" (height below -2 SDS) after rickets was improved and alkaline phosphates normalized. Patients were put on 80 µg/kg/day of rGH (conventional treatment with phosphate and calcitriol was continued) and monitored every three months (height, weight, growth velocity, metabolic markers of calcium and phosphate metabolism and IGF-1). RGH dose was then adjusted to growth velocity, weight and IGF-1 levels. The study population was divided into two sub-groups: 11 pre-pubertal patients (before and during the rGH trial), 6.0 ± 2.5 years of age, and 7 pubertal patients (Tanner stage 2 or 3 at inclusion) 13.0 ± 1.1 years of age. In pre-pubertal children, both mean height Z-score and mean height velocity Z-score increased significantly at +12 months (M12, N=11) and +24 months (M24, N=7) of the trial (height SDS: baseline -2.3 ± 0.8, M12 -1.5 ± 0.7, M24 -0.98 ± 1.0; height velocity SDS: baseline -1.0 ± 1.1, M12 4.4 ± 1.6, M24 2.3 ± 1.7, respectively). In pubertal patients rGH treatment was a lot less beneficial; mean height SDS went from -2.4 ± 1.1 at baseline to -1.8 ± 1 at M12 and to -1.8 ± 1 at M24. Prepubertal patients displayed low IGF-1 levels prior to rGH therapy (-1.2 ± 0.2 SDS) and increased their IGF-1 levels to 0.05 ± 0.6 SDS (M12) and 0.2 ± 0.4 SDS (M24). Differently, pubertal patients had normal IGF-1 levels (-0.4 ± 0.8 SDS) significantly increased by rGH treatment (1.3 ± 1.0 SDS at M24). Rickets was not modified by rGH treatment.

2- years recombinant GH is effective and safe for treating growth failure in well controlled XLHR when initiated before puberty. IGF-1 levels suggest that XLHR children switch from great IGF-1 sensitivity to IGF-1 resistance. However, follow-up until final height is needed to evaluate the long term benefit of rGH on height.

***Disclosures: Agnes Linglart**, None.*
This study received funding from: novonordisk

FR0028

Age-Related Loss of Hip Bone Strength Varies by Gender and Loading Condition: The AGES-Reykjavik Study. Thomas Lang*[1], Sigurdur Sigurdsson[2], Kristin Siggeirsdottir[2], Diana Oskarsdottir[2], Gunnar Sigurdsson[3], Gyda Karlsdottir[2], Gudny Eiriksdottir[2], Tamara Harris[4], Vilmundur Gudnason[5], Joyce Keyak[6]. [1]University of California, San Francisco, USA, [2]Icelandic Heart Association, Iceland, [3]Landspitali, Iceland, [4]National Institute on Aging, USA, [5]Icelandic Heart Association Research Institute, Iceland, [6]University of California, USA

The risk of incident hip fracture rises rapidly with age, and is particularly high in women. This increase in fracture risk comprises both the age-related increase in the risk of falls and declines in the strength of the proximal femur. To better understand the extent to which proximal femoral strength declines with age as a function of gender and loading condition (fall loading vs normal physiologic loading), we have carried out the first longitudinal analysis of proximal femoral strength in men and women using subject-specific finite element modeling (FEM).

In the AGES-Reykjavik Study vQCT scans of the hip hip (Siemens Somatom 4, 120 kVp, 150 mAs, 1-mm slice thickness sampled at 3 mm) were performed at a baseline visit in 2002-2004 and at a second visit 5.05 ± 0.25 years later. From these, 140 subjects (72 men, 69 women, aged 68-87 years) were randomly selected for longitudinal evaluation using FE models of the left proximal femur, analyzed under single-limb stance loading which simulates normal physiologic loading of the hip. These models incorporated nonlinear material properties and predicted peak fracture load (STANCE); analogous non-linear modeling for fall loading is not yet available, and thus we used linear modeling for a posterolateral fall (FALL). We computed five-year percentage changes in FALL and STANCE. ANOVA was employed to compute compare bone strength loss between genders and the paired Student's T-Test was used to compare between loading conditions.

Results are displayed in Table 1. Significant loss of bone strength occurred for each loading condition within both genders ($p<0.001$). Women tended to lose proximal femoral strength at higher rates than men ($p=0.07$ for FALL, $p=0.03$ for STANCE), and in women, FALL was lost at a sharply higher rate than STANCE ($p<0.001$).

Our longitudinal results indicate that women lose hip bone strength at a rapid rate (nearly 14%/5years for FALL), which is consistent with the sharp age-related increases in hip fracture risk documented for women. The gender difference in hip bone strength loss is consistent with the higher incidence of hip fracture among women. For women, the 40% lesser loss of STANCE compared to FALL strength ($p<0.001$), supports previous findings in animal and human studies that the sub-volumes of bone stressed under normal physiologic loading are relatively protected in aging.

%changes/5 yr	FALL (SD)	STANCE (SD)	p-loading condition
Women	-13.8 (13.5)	-8.6 (8.8)	<0.001
Men	-5.2 (16.0)	-3.2 (7.5)	0.3
p-gender	0.07	0.03	

Table 1

***Disclosures: Thomas Lang**, Merck, 2*

FR0030

Bone Density and Structure of Patients on Bisphosphonates with Atypical Femur Fractures. Angela Cheung*[1], Jonathan Adachi[2], Robert Josse[3], Robert Bleakney[4], Christian Viellette[1], Aliya Khan[5], Moira Kapral[1], Sophie Jamal[6], Heather McDonald-Blumer[7], Earl Bogoch[8]. [1]University Health Network, Canada, [2]St. Joseph's Hospital, Canada, [3]St. Michael's Hospital, University of Toronto, Canada, [4]Mt. Sinai Hospital, Canada, [5]McMaster University, Canada, [6]The University of Toronto, Canada, [7]Mount Sinai Hospital, Canada, [8]St. Michael's Hospital, Canada

Purpose: Atypical femur fractures have been reported recently with bisphosphonate use. We examined the bone density and bone structure of patients on bisphosphonates with atypical femur fractures.

Methods: This is a cross-sectional study of patients referred to the University Health Network Osteoporosis Clinic for assessment of atypical femur fractures. All patients were assessed by an osteoporosis physician. All radiographs were independently reviewed by a musculoskeletal radiologist as well as an osteoporosis expert, and areal BMD by DXA (Hologic Discovery A®, Hologic Inc., Massachusetts, USA) was performed at the lumbar spine, total hip and femoral neck, and HRpQCT (Xtreme CT®, Scanco Medical, Switzerland) at the distal radius and tibia.

Results: Sixteen patients (15 women and 1 man) were included in the study. Six were Chinese, 2 were Indian, 8 were European Canadian. Mean age was 67.2 (range

46.4-88.1) years. Mean duration of bisphosphonate use was 7.5 (range 2 to 10.6) years. Mean serum 25-hydroxyvitamin D level close to the time of fracture was 93nmol/L. Although most patients (11/16) had comorbid conditions or medications (rheumatoid arthritis, pemphigus, liver transplant, diabetes, cancer, steroid or warfarin use), 5 did not. Mean BMD T-score at the lumbar spine, total hip and femoral neck were -0.68, -0.48 and -0.90, respectively. On HRpQCT scans, there is decreased cortical thickness, marked cortical porosity and a lack of trabecular structure with empty ''holes'' on many of the scans (see Table).

Conclusions: Patients on bisphosphonates with atypical femur fractures have poor bone quality and structure as measured by HRpQCT. These results suggest that low bone turnover and increased mineralization may not be the only explanation for these atypical insufficiency fractures.

Table. HRpQCT scans of Patients on Bisphosphonates with Atypical Femur Fractures

Mean	TotalvBMD (mg/cm^3)	CortvBMD (mg/cm^3)	TrabvBMD (mg/cm^3)	CTh (mm)	Tb Th (mm)	Tb N (mm^{-1})	Tb Sp (mm)	BV/TV (%)
Radius	266.8	824.9	101.8	0.65	0.065	1.37	0.918	0.085
Tibia	238.9	791.5	122.6	0.97	0.074	1.46	0.707	0.102

Table

***Disclosures: Angela Cheung**, Amgen, 2; Merck, 2; Novartis, 2; Sanofi-Aventis, 2; Eli Lilly, 2*

FR0031

Collagen Cross-link Concentration Influences the Fatigue Behavior of Human Vertebral Trabecular Bone. Stephanie Viguet-Carrin*[1], David Panus[2], Helene Follet[3], Pierre Delmas[1], Elise Morgan[4], Roland Chapurlat[1], Mary Bouxsein[5]. [1]E. Herriot Hospital, France, [2]Orthopedic Biomechanics Laboratory, Beth Israel Deaconess Medical Center & Harvard Medical School, Boston, USA, USA, [3]INSERM, Université De Lyon, USA, [4]Boston University, USA, [5]Beth Israel Deaconess Medical Center, USA

Although the response of trabecular bone to cyclic loading may contribute to fragility fractures, few studies have investigated the factors that influence this behavior. Thus, the aim of this study was to determine the relative contributions of bone density, microarchitecture, and collagen crosslink content to the fatigue properties of human vertebral trabecular (Tb) bone. L2 vertebrae were obtained from 28 donors (age 54–95; 13 M, 14 F, 1 unknown). We evaluated one Tb core per vertebrae for microarchitecture by μCT and fatigue properties by cyclic testing under a constant strain (0 to 0.4%) at 2 Hz. Outcomes included the initial stiffness (E_0), loss of stiffness at failure (ΔF), number of cycles to failure (Nf), strain at failure and rate of modulus degradation. Collagen crosslink content was assessed by HPLC (pyridinoline (PYD), deoxypyridinoline (DPD) and pentosidine (PEN)). Parametric tests were used except for some non-Gaussian parameters (collagen characteristics and Nf). Results: There were no differences between men and women, and no relationship between age and microarchitecture or collagen characteristics. Among all the parameters characterizing the fatigue tests, only E_0 and ΔF decreased with age ($r = -0.40$; $p=0.04$ and $r = -0.41$; $p=0.03$, respectively). Neither bone volume or microarchitecture were associated with fatigue properties. Enzymatic cross-link content (PYD, DPD) and their combination (PYD + DPD) were associated with fatigue properties. PYD and PYD + DPD content were positively associated with Nf ($rsp = 0.52$, $p=0.004$; $rsp = 0.53$, $p=0.004$, respectively) and negatively associated with the rate of modulus degradation ($rsp = -0.52$, $p=0.005$ for both). PYD, DPD and PYD + DPD content were negatively related to strain at failure ($rsp = -0.57$, $p=0.002$; $rsp = -0.40$, $p=0.04$; $rsp = -0.58$, $p=0.001$, respectively). In contrast, PEN content was not associated with any fatigue properties. These findings indicate that collagen crosslink content, specifically the trivalent mature enzymatic crosslinks of type I collagen, may influence the fatigue behavior of human vertebral trabecular bone.

***Disclosures: Stephanie Viguet-Carrin**, None.*

FR0034

Decreased PTH Secretion is Associated with Low Bone Formation and Vertebral Fracture Risk in Postmenopausal Women with Type 2 Diabetes. Masahiro Yamamoto*[1], Toru Yamaguchi[1], Mika Yamauchi[1], Kiyoko Nawata[2], Toshitsugu Sugimoto[3]. [1]Shimane University Faculty of Medicine, Japan, [2]Department of Health & Nutrition, The University of Shimane, Junior College, Matsue Campus, Japan, [3]Shimane University School of Medicine, Japan

We previously reported that patients with type 2 diabetes (T2DM) had an increased risk of vertebral fractures (VFs) despite higher bone mineral density (BMD) compared to non-T2DM controls (JBMR 2009), and that advanced glycation end-products (AGEs) and its endogenous secretory receptor (esRAGE) were associated with VFs independent of BMD (JCEM 2008 and Diabetes Care 2009), suggesting the existence of poor bone quality in T2DM. Bone turnover is one of the components of bone quality, and bone formation represented by serum osteocalcin (OC) level is decreased in T2DM. Although PTH plays an important role in bone formation, the association of PTH level with bone formation or VFs in T2DM is still unclear. The aim of this study is to clarify the involvement of PTH in decreased bone turnover or increased VF risk in T2DM. We compared parameters including serum levels of intact PTH and N-mid-OC as well as lumbar and femoral BMD values between Japanese T2DM patients (123 postmenopausal women and 132 men over 50 years old) and non-DM controls (189 women and 51 men), who were within normal creatinine levels. PTH and OC levels in T2DM were significantly lower than those in the controls in both genders (women: 22 ± 10 vs. 46 ± 15 pg/ml and 14 ± 6 vs. 23 ± 9 ng/ml, respectively, $P<0.01$; men: 21 ± 10 vs. 46 ± 19 pg/ml and 10 ± 4 vs. 15 ± 5 ng/ml, respectively, $P<0.01$). Multivariate analysis adjusted for age, BMI, serum creatinine, calcium and phosphorus also showed that PTH was significantly and positively correlated with OC in T2DM (women: r=0.32?P<0.01; men: r=0.34, P <0.01). However, PTH levels were not correlated with HbA1c levels in either gender. When T2DM patients were divided into four groups by PTH and OC level, multivariate logistic regression analysis adjusted for age, BMI, serum creatinine level and lumbar BMD showed that the group with both lower PTH and lower OC in T2DM women had a significantly increased risk of VFs than the group with both higher PTH and higher OC (odds ratio 4.3, 95%CI 1.2-16.1, P=0.03). These results showed that suppressed bone formation in T2DM was associated with decreased PTH level irrespective of HbA1c levels, and that the coexistence of diminished PTH and OC levels in postmenopausal T2DM women was a risk factor of VFs independent of BMD. These findings suggest that suppressed PTH secretion may induce low bone formation and reduced bone quality, which may result in VF occurrence in T2DM women.

***Disclosures: Masahiro Yamamoto**, None.*

FR0037

Improved Evaluation of Hip Structure using High Resolution Cortical Thickness Measurement from Clinical CT Data. Graham M Treece, Andrew H Gee, Paul Mayhew*, Kenneth Poole. University of Cambridge, United Kingdom

The distribution of cortical bone in the proximal femur is believed to be critical in determining fracture resistance. Ageing leads to thinning of femoral neck cortical bone, which can become as thin as an egg-shell by the eighth decade in critical areas (0.3mm). In current clinical practice, hip bone mineral density estimates made with 2-dimensional dual-energy x-ray absorptiometry ('DXA') are specific for predicting hip fracture but have low sensitivity. Recent studies have instead utilised multi-detector computed tomography (MDCT) to examine femoral neck cortical thickness and 3-D structure and its potential for in vivo hip fracture prediction. However, existing CT technology is limited in its ability to measure cortical thickness, especially in the sub-millimetre range which lies within the point spread function of today's clinical scanners. We present a novel analysis technique that is capable of producing unbiased cortical thickness estimates down to 0.3mm, considerably outperforming previous methods (referred to here as simple thresholding, and 50% relative threshold). The technique relies on a mathematical model of the anatomy and the imaging system, which is fitted to the data at a large number of sites around the proximal femur, producing around 17,000 independent thickness estimates per specimen. In a series of experiments on sixteen cadaveric femurs, estimation errors were measured as -0.01 ± 0.58mm (mean $\pm$ 1 std. dev.) for cortical thicknesses in the range 0.3mm to 4mm. This compares with 0.25 ± 0.69mm for simple thresholding and 0.90 ± 0.92mm for a variant of the 50% relative threshold method. In the clinically relevant sub-millimetre range, thresholding increasingly fails to detect the cortex at all, whereas the new technique continues to perform well. The many cortical thickness estimates can be displayed as a colour map painted onto the femoral surface. Computation of the surfaces and colour maps is rapid and largely automatic. The technique is ideally suited to the evaluation of cortical bone structure in life, in clinical fracture prediction, and in assessing the structural response of the hip to interventions.

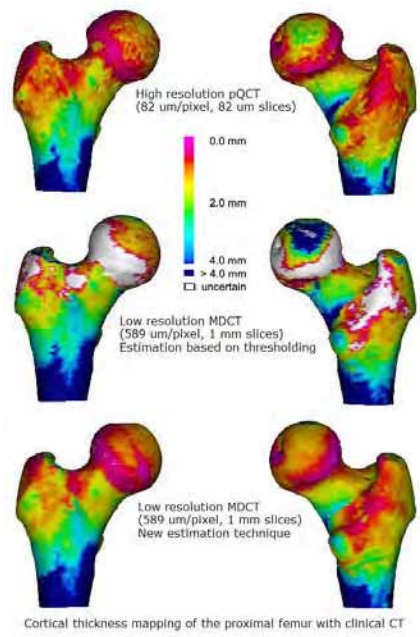

Cortical thickness mapping of the proximal femur with clinical CT

Comparing the high res C.Th map (upper) with low res thresholding (middle) and new technique (lower)

***Disclosures: Paul Mayhew**, None.*

FR0039

Investigation of Statistical Shape and Density Modeling as a Discriminator for Clinical Fracture Risk. Todd Bredbenner*[1], Ryan S. Potter[1], Robert L. Mason[1], Lorena Havill[2], Eric Orwoll[3], Daniel P. Nicolella[1]. [1]Southwest Research Institute, USA, [2]Southwest Foundation for Biomedical Research, USA, [3]Oregon Health & Science University, USA

In this preliminary study, the performance of statistical shape and density modeling (SSDM) methods to predict the risk of future hip fracture was investigated. Baseline QCT data of the right hip was obtained for 40 participants, including 20 who fractured a hip (mean 5.6 year observation, validated by physician review) and 20 who did not, randomly selected from the Osteoporotic Fractures in Men (MrOS) Study.

QCT data was processed to develop a volumetric mesh model of geometry and bone density for each of the 40 proximal femurs. Each model consisted of over 36,000 geometry and density variables (e.g. spatial location and density at each 3D mesh node located at corresponding anatomic positions for all femurs). The set of models was combined and the number of geometry and density variables was reduced using a principal component analysis; individual models were described using the average femur model plus a weighted linear combination of 39 independent and uncorrelated principal components (PCs) that do not have explicit meaning, but rather describe unique features of 3D bone geometry and density. By definition, PC weighting factors cumulatively described the total variance in proximal femur geometry and bone density distribution in a highly compact and efficient manner. Using Wilcoxon rank sum analyses, 3 PCs were found to be significantly different between men with and without subsequent fracture: PC4 ($p = 0.022$), PC15 ($p < 0.05$), and PC18 ($p = 0.037$). These 3 new variables describe the independent, complex, and subtle differences in 3D shape and bone density between participants with and without fracture. Stepwise logistic regression was used to develop a discriminator using PCs against fracture or no fracture group membership. The area under Receiver Operator Characteristic curve for the regression using 5 PCs was significantly greater than for proximal femur aBMD (DXA QDR 4500W; Hologic) (Figure 1) in this small sample.

Statistical shape and density modeling methods compactly and efficiently described the total geometry and bone density distribution variability within this small set of 40 proximal femur models defined from the MrOS cohort. Furthermore, the description of sample variation using SSDM allowed the application of relatively simple statistical tools to investigate important structural differences (e.g. geometry and density distribution traits) that may allow improved prediction of those at risk of subsequent hip fracture.

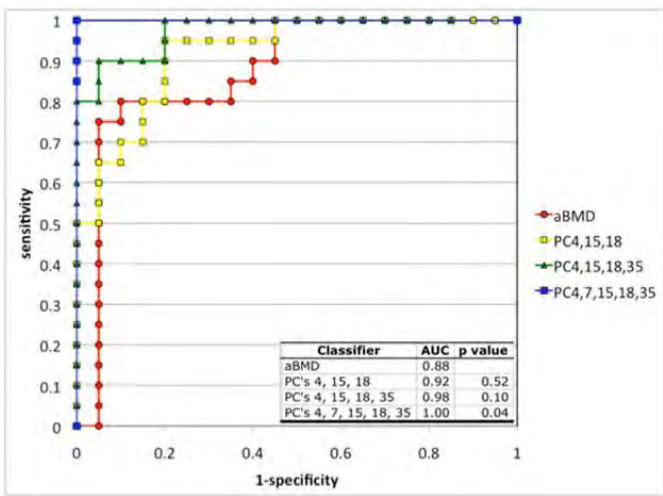

Figure 1: ROC Curves for Hip Fracture Prediction using Total Hip DXA aBMD and Principal Components

***Disclosures: Todd Bredbenner**, None.*

FR0041

Local Topological Analysis at the Distal Radius by HR-pQCT: Application to *In Vivo* Bone Microarchitecture and Fracture Assessment in the OFELY Study. Jean-Baptiste Pialat*[1], Nicolas Vilayphiou[2], Stephanie Boutroy[3], Pierre-Jean Gouttenoire[4], Elisabeth Sornay-Rendu[5], Roland D. Chapurlat[6], Francoise Peyrin[4]. [1]INSERM U831, Université de Lyon & Hospices Civils de Lyon, France, [2]INSERM Unit 831 & Université de Lyon, France, [3]INSERM, Université De Lyon, France, [4]European Synchrotron Radiation Facility (ESRF), France, [5]INSERM, France, [6]INSERM U831 & Université de Lyon, France

Purpose: Local geometric analysis has been developed for high resolution imaging techniques. The aim of our study was to test the feasibility and efficiency of such technique at 82 µm resolution and its ability to detect patients with fracture in a subset of patients from the OFELY cohort.

Methods: 33 women with prevalent wrist fractures were compared with their age and BMI-matched controls. Bone microarchitecture was assessed by HR-pQCT (XtremeCT, Scanco Medical AG, Switzerland), and finite element analysis (FEA) was based on HR-pQCT images of the distal radius [1]. A new local topological analysis method was applied to label each bone voxel as rod, plate or branch [2]. Then the bone volume to total volume (BV/TV), and the rod and plate ratio over bone volume (RV/BV and PV/BV) or total volume (RV/TV, PV/TV) were calculated. These Topological parameters (TPs) were compared to each other, microarchitectural and FEA parameters with Pearson or Spearman correlation tests, depending on the distribution of variables. [2] test was used to evaluate the distribution of wrist fracture in tertiles of RV/TV, PV/TV, RV/BV, and BV/TV (1st & 2nd versus 3rd tertile). Associations between TPs and wrist fractures were computed in a paired logistic regression model, OR [95% CI] per SD change.

Results: Good correlations were found between PV/TV or RV/TV and microarchitectural parameters or bone strength evaluated with FEA (Table 1). In contrast, RV/BV and PV/BV were weakly correlated with TbN ($|r|=0.24$ and 0.31). Moreover, negative correlation between RV/BV and stiffness computed by FEA directly suggested the loss of bone strength related to conversion from plates into rods during bone loss. Individuals with rod-like structure were more likely to have wrist fracture (χ^2 test $p=0.0017$ for RV/BV). We also found an association between wrist fracture and all topological parameters (OR=2.31 [1.18-4.55] per SD increase of RV/BV, $p=0.015$ and OR=2.04 [1.09-3.82] per SD increase of PV/BV, $p=0.025$).

Conclusions: Local topological analysis at 82µm resolution is feasible and improves the microarchitectural description. Further studies might outline how changes from plates to rods impact bone strength.

References:
[1] Boutroy S et al. J Bone Miner Res. 2008;23(3):392-9.
[2] Peyrin F et al. Image Analysis and Stereology. 2007;26(3), 179-185.

Variable	Dtrab	TbN	TbSpSD	ConnD	SMI	Stiffness
PV/BV	0.55***	0.24*	-0.29*	0.37**	-0.75***	0.50***
RV/BV	-0.61***	-0.30*	0.32**	-0.43***	0.78***	-0.54***
BV/TV	0.99***	0.89***	-0.82***	0.94***	-0.92***	0.75***
PV/TV	0.96***	0.77***	-0.75***	0.86***	-0.95***	0.74***
RV/TV	0.96***	0.96***	-0.87***	0.97***	-0.84***	0.71***

* p<0.05; ** p<0.01; *** p<0.001

Table 1: Correlation between topological and microarchitectural parameters (Pearson or Spearman correlation depending on distribution normality).

Table 1

***Disclosures: Jean-Baptiste Pialat**, None.*

FR0042

Non-collageneous Proteins Influence Crystal Orientation and Shape: A SAXS Study. Atharva Poundarik*[1], Ondrej Nikel[2], Caren Gundberg[3], Deepak Vashishth[2]. [1]Rensselaer Polytechnic University, USA, [2]Rensselaer Polytechnic Institute, USA, [3]Yale University School of Medicine, USA

Bone is a complex composite material comprising of mineral (hydroxyapatite) phase, collagen and non-collageneous proteins like osteocalcin (OC) and osteopontin (OPN). Through mechanisms like ligament bridging, diffuse damage and microcracking that aid in energy dissipation, bone averts fracture. Mineral crystals span a few nanometers in either direction and occupy the lowest levels of bone's structural hierarchy [1]. Any modification at this level may alter bone metabolism and affect bone fragility.

Previous studies on OC and OPN knock-out mice (OC-/- and OPN-/-) have demonstrated that these proteins play a key role in crystal structure and organization [2,3]. Here we use small angle X-ray scattering (SAXS) to show that their absence causes a measurable change in crystal orientation and shape. X-ray scattering spectra (Nanostar, Bruker) were obtained from longitudinal femoral cortical sections of three mouse genotypes: wild type (WT), OC-/- and OPN-/-. The 2-D SAXS data [intensity I(q,), scattering vector (q) and polar angle ())]was processed after noise correction to obtain crystal orientation. The spherically averaged intensity function was analysed

based on Porod's law ($I=Pq^{-4}$, at large q) to estimate differences in crystal size and shape [4].

Crystal orientations along the long axis of bone were greater for the knock-out samples (OC-/-, 6.10 deg. and OPN-/-, 5.25 deg.) than WT (4.89 deg.). Greater degree of crystal orientation in both knock-out specimens implied that increased mineral heterogeneity results from the absence of OPN and OC in bone matrix. Furthermore, consistent with previous FTIR studies [2], the Porod analysis revealed a larger surface to volume ratio in OC-/- as compared to WT indicating smaller crystal dimensions. Such differences were not observed in the bones from OPN-/-. Thus, in contrast to the presence of more plate like mineral in WT and OPN-/-, OC-/- mice tend to have more rod-like crystals. We conclude that osteocalcin is a stronger regulator of crystal organization than osteopontin in bone and its absence may alter the organizational hierarchy of bone at higher scales.

References:

[1]: Yerramshetty et al. Bone Vol. 42 2008

[2]: Boskey et al. Bone Vol. 23 1998

[3]: Boskey et al. Calcif. Tissue Int. Vol. 71 2002

[4]: Fratzl et al. Connect. Tissue Res. Vol. 34 1996Acknowledgements: NIH AR 38460 and AR49635

***Disclosures: Atharva Poundarik**, None.*

FR0048

BMD and TBS Micro Architecture Parameters Assessment at Spine in Patients with Primary Hyperparathyroidism (PHPT) before and One Year after Parathyroidectomy. Emilie Maury[1], Renaud Winzenrieth[2], jean-claude Souberbielle[3], Emile Sarfati[4], Catherine Cormier*[5]. [1]Service De Rhumatologie A, AP-HP Groupe Hospitalier Cochin - Saint Vincent De Pa, France, [2]Med-Imaps, PTIB, France, [3]Laboratoire d'Explorations Fonctionnelles, Hopital Necker-Enfants Malades, France, [4]epartment of endocrine surgery,hopital Saint-Louis, APHP, France, [5]AP-HP Groupe Hospitalier Cochin, France

PHPT is a very common endocrinopathy which is often diagnosed during a biological exploration in osteoporotic patients and is considered as a frequent cause of secondary osteoporosis. Increase in bone mineral density (*BMD*) following parathyroidectomy (PTX) has been reported in numerous studies. However, only BMD evaluated by DXA is taken into account. Trabecular bone score (*TBS*) is a grey-level texture measurement, which correlates with 3D parameters of bone micro-architecture. The aim of our study was to examine bone microarchitecture assessed by TBS and BMD in PHPT female subjects assessed before and one year after PTX, and to evaluate theirs associations with clinical variables.

We present a longitudinal study on 29 PHPT Caucasian postmenopausal women with mean age and BMI of 62.1 ± 10.4 years and 25.5 ± 6.5 Kg/m^2 respectively who were all operated on. Before PTX, all patients had a measurement of serum total and ionized calcium, phosphate, PTH, C-telopeptide of type 1 collagen (CTX), as well of 24-hour urine calcium and phosphate reabsorption rate (TRP). BMD and TBS were evaluated at AP Spine (L1-L4) with DXA prodigy (GE-Lunar), QDR 4500 (Hologic), and TBS iNsight® (Med-Imaps) within 6 months before PTX, and one year after PTX. Both DXA were cross-calibrated. Correlations (Spearman rank test) were evaluated between pre-Surgery BMD or TBS or their difference during the study period, and biological variables independently of each other. Differences between pre and post PTX values were assessed using Wilcoxon rank test for paired data.

Pre- and post-Surgery data are presented in Table 1. Before PTX, BMD and TBS were correlated together ($p<0.0001$), with 46% of TBS explained by spine BMD. Before PTX, neither BMD nor TBS was correlated with any of biological parameters. After PTX, BMD and TBS increased significantly by $4,7 \pm 5.4\%$ and $1.6 \pm 4\%$ respectively, without correlation between BMD and TBS gains. Pre-PTX serum total calcium was correlated ($p=0.035$) with the BMD gain one year post-PTX. No other correlation was found between pre-PTX biological parameters and the post-PTX change in BMD or TBS.

The present study is the first to report data on changes in spine BMD and bone microarchitecture both assessed by DXA in PHPT women after PTX. Consistent with previously published data, spine BMD increased after PTX, while TBS increased more slightly. This last result is consistent with what was published when iliac crest biopsies were analyzed longitudinally post-PTX.

	Serum total calcium (mmol/l)	Serum ionized calcium (mmol/l)	Serum Phosphate (mmol/l)	Serum PTH (pg/ml)	Serum CTX (pmol/l)	24-hour urine calcium (mmol/24h)	TRP	Spine BMD (g/cm²)	TBS
Pre-Surgery	2.72±0.22	1.39±0.13	0.85±0.15	117±199	6436±4146	8.5±3.8	77±11	0.765±0.112	1.241±0.088
Post-Surgery	2.36±0.08	1.23±0.04	1.06±0.14	39±20	2614±1525	4.9±2.6	83±4	0.799±0.111	1.261±0.102
p	<0.0001	<0.0001	<0.0001	<0.0001	<0.0001	<0.0001	=0.003	=0.0001	=0.005

Table 1 : Pre- and post-surgery population data

***Disclosures: Catherine Cormier**, None.*

FR0049

Bone Microarchitecture Assessment in Postmenopausal Women with Atypical Fractures and Long Term Bisphosphonate Use. Maria Belen Zanchetta*, Marcelo Sarli, Fabio Massari, Rodolfo Spivacow, Mirena Buttazzoni, Fernando Silveira, Cesar Bogado, Jose Ruben Zanchetta. Instituto de Investigaciones Metabolicas (IDIM), Argentina

Recent reports have suggested a link between atypical fractures and long-term bisphosphonate use. The pathophisiology of these events is unknown.

Our aim was to describe bone microarchitecture in five patients with atypical fractures and long term biphosphonate treatment using High Resolution peripheral computerized Tomography (HR-pQCT).

We identified 5 postmenopausal women who have received bisphosphonate treatment for more than 10 years (mean 14.8 ± 3, 9 years) and who presented with atypical low-energy fractures, defined as fractures occurring in a fall from a standing height or less in atypical sites. Three patients sustained subtrochanteric or proximal diaphyseal fractures and two suffered a pelvic fracture (see table 1). No patient had a history of vertebral fractures. We compared bone volumetric density and architectural parameters measured by HR-pQCT of the radius and tibia in these 5 fractured patients with 54 healthy, ambulatory, postmenopausal, non- treated and non- fractured women selected from our database with similar age and BMD values and with 8 postmenopausal women who have received long term treatment with bisphosphonate (mean 9.6 ± 4.9 years) and who have not suffered an atypical fracture. All women had no conditions or other treatments known to affect bone or mineral metabolism.

ArealBMD at the lumbar spine and femoral neck was measured using DXA (Hologic QDR4500 ;Hologic, Bedford, MA). Volumetric BMD and microarchitecture were measured at the distal radius and tibia using a three-dimensional HR-pQCT system (XtremeCT; Scanco Medical AG, Bassersdorf, Switzerland).Comparisons between groups were assessed by the two-sample T test.

There were no statistically significant differences in age, years since menopause, BMI and BMD T-scores of the lumbar spine and femoral neck between the groups.

In the atypically fractured group cortical density and thickness in radius and tibia seems to be disminished compared with the others two groups. We do not know whether this tendency is due to some atypical response to long term bisphosphonate treatment in a subgroup of women or constitutes a genetic baseline characteristic cortical structure of these five women.Although they are all atypical fractures, pelvic fractures and femoral shaft fractures may not have the same pathophisiology. Additional prospective studies are needed to establish a clear association between atypical fractures and prolonged bisphosphonate treatment.

	Atypical fractures (n=5)	No fractures,long BF treatment (n=8)	P	No fractures, no treatment (n=54)	
Age (years)	74.8 ± 7.0	66.9 ± 6.9	0.0636	70.3 ± 3.1	0.2258
T-score L1-L4	-2.4 ± 0.8	-3.1 ± 0.5 (n=7)	0.0984	-2.5 ± 0.5	0.7304
T-score C.F.	-2.0 ± 0.9	-1.7 ± 0.7	0.9413**	-2.0 ± 0.7	0.6725
Mean treatment time (years)	14.8 ± 3.9	10.0 ± 4.9	0.0944		
Distal radius					
D100 (mg HA/ccm)	226.9 ± 46.2	257.8 ± 75.5	0.6084**	228.5 ± 54.7	0.9517
Dcomp (mg HA/ccm)	781.9 ± 85.0	850.0 ± 50.5	0.1643**	791.4 ± 70.0	0.8383
Ct. Th. (mm)	0.462 ± 0.136	0.625 ± 0.173	0.1027	0.546 ± 0.157	0.2543
Dtrab (mg HA/ccm)	109.8 ± 30.1	94.4 ± 31.3	0.4003	99.9 ± 36.1	0.5543
Distal tibia					
D100 (mg HA/ccm)	190.8 ± 44.2	211.8 ± 57.4	0.5008	208.0 ± 42.3	0.3895
Dcomp (mg HA/ccm)	727.8 ± 81.0	818.8 ± 51.7	0.0339	784.9 ± 52.0	0.1917
Ct. Th. (mm)	0.612 ± 0.247	0.842 ± 0.279	0.1591	0.815 ± 0.205	0.0413
Dtrab (mg HA/ccm)	110.7 ± 18.8	103.7 ± 26.0	0.6150	112.4 ± 30.3	0.9016

table 2

	Atypical Fx (=5)	No fx BP treatment (8)	P	No fx, No treatment (n=54)	P
Age (years)	74.8 ± 7.0	66.9 ± 6.9	0.0636	70.3 ± 3.1	0.2258
T-score L1-L4	-2.4 ± 0.8	-3.1 ± 0.5 (n=7)	0.0984	-2.5 ± 0.5	0.7304
T-score C.F.	-2.0 ± 0.9	-1.7 ± 0.7	0.9413**	-2.0 ± 0.7	0.6725
Mean treatment time (years)	14.8 ± 3.9	10.0 ± 4.9	0.0944		
Distal radius					
D100 (mg HA/ccm)	226.9 ± 46.2	257.8 ± 75.5	0.6084**	228.5 ± 54.7	0.9517
Dcomp (mg HA/ccm)	781.9 ± 85.0	850.0 ± 50.5	0.1643**	791.4 ± 70.0	0.8383
Ct. Th. (mm)	0.462 ± 0.136	0.625 ± 0.173	0.1027	0.546 ± 0.157	0.2543
Dtrab (mg HA/ccm)	109.8 ± 30.1	94.4 ± 31.3	0.4003	99.9 ± 36.1	0.5543
Distal tibia					
D100 (mg HA/ccm)	190.8 ± 44.2	211.8 ± 57.4	0.5008	208.0 ± 42.3	0.3895
Dcomp (mg HA/ccm)	727.8 ± 81.0	818.8 ± 51.7	0.0339	784.9 ± 52.0	0.1917
Ct. Th. (mm)	0.612 ± 0.247	0.842 ± 0.279	0.1591	0.815 ± 0.205	0.0413
Dtrab (mg HA/ccm)	110.7 ± 18.8	103.7 ± 26.0	0.6150	112.4 ± 30.3	0.9016

table 2

***Disclosures: Maria Belen Zanchetta**, None.*

FR0050

Intermittent PTH Treatment Increases Intracortical Osteocyte Density and Decreases Fat Mass in Ovariectomized Rats. Steven Tommasini*[1], Andrea Trinward[2], Alvin Acerbo[3], Lisa Miller[4], Stefan Judex[5]. [1]SUNY Stony Brook, USA, [2]State University of New York at Stony Brook, USA, [3]Brookhaven National Laboratody, USA, [4]Brookhaven National Laboratory, USA, [5]Stony Brook University, USA

Some pharmaceutical treatments for osteoporosis have the potential to deteriorate mechanical properties of the skeleton by altering specific aspects of bone's tissue quality. Here, we hypothesized that PTH and bisphosphonate treatments differ in their effect on intracortical porosity, which has been linked to the stiffness and strength of cortical bone. Further, it is possible that any potential changes in bone porosity are not modulated directly by the specific treatment, but indirectly by altered adiposity. Here, we examined the effects of treatment on intracortical porosity and adiposity in the OVX rat. Six-month old female Sprague-Dawley rats were assigned to either: baseline control, age-matched control, untreated OVX, OVX treated with either 15μg/kg/d hPTH(1-34) (H-PTH) or 0.3μg/kg/d (L-PTH), or OVX treated with either 100mg/kg/2xwk Alendronate (H-ALN) or 1mg/kg/2xwk (L-ALN). Treatments started at 6 mo of age and rats were sacrificed at 6, 8, and 12 mo of age (n=10/group/age). There were no significant differences in femoral diaphysis geomtery or composition among groups as measured via μCT (36μm resolution). Synchrotron CT (0.75μm resolution) detected intracortical microporosities not detected by conventional μCT. Within ages, treatments did not differ in %porosity or avg pore size. However, %porosity decreased with age for all groups. Even though no differences in %porosity were detected, prolonged H-PTH treatment maintained a 54% greater number of osteocyte lacunae (avg vol=250μm^3) and 46% more vascular canals (>1000μm^3) compared to all other groups ($p<0.05$). Tissue mineral density was inversely related to avg pore size (r=-0.83). *In vivo* μCT revealed PTH-treated rats also had significantly lower abdominal fat volume/body weight compared to all other groups ($p<0.01$). The data suggest that the greater number of osteocyte lacunae may be related to changes in metabolic rate, which has been correlated with osteocyte density. The increase in microporosities also may be evidence of ostecytic osteolysis previously reported with continuous PTH treatment. The mechanical consequences of the changes in porosity are yet to be established, but do not necessarily have a negative impact on bone's ability to resist load as very small pores have the potential to delay crack propagation by absorbing shear forces. Therefore, understanding how osteoporosis treatments modulate the interactions between adiposity and bone quality may be critical for reducing fracture risk.

***Disclosures: Steven Tommasini**, None.*

FR0052

A Comparison of Resistance and Aerobic Exercise Training on Physical Ability, Bone Mineral Density and Osteoprotegerin in Older Women. Elisa Marques*[1], Flávia Wanderley[1], Daniel Gonçalves[1], Margarida Coelho[1], João Viana[2], Pedro Moreira[1], Jorge Mota[1], Joana Carvalho[1]. [1]University of Porto, Portugal, [2]Loughborough University, United Kingdom

Purpose: This study compared the effects of a moderate-impact resistance training protocol and a moderate-impact aerobic training protocol on bone mineral density (BMD), physical ability and serum osteoprotegerin (OPG).

Methods: Seventy-one older women were randomly assigned to resistance exercise (RE), aerobic exercise (AE) or control group (CON). RE included 3 sets of 8 repetitions at 70 to 80% of 1 repetition maximum focused on exercises with attachments to the proximal femur and additional complementary upper body exercises. AE program included dynamic activities involving stepping, skipping, walking, jogging, dancing, aerobics and step choreographies at an intensity that gradually increased from 65% to 85% of the heart rate reserve. Both interventions were conducted 3 times per week for 8 months. Outcome measures included proximal femur BMD (by dual X-ray absorptiometry), muscle strength, dynamic balance, handgrip strength, walking performance, fat mass, anthropometric data, and serum OPG. Potential confounding variables included dietary intake, accelerometer-based physical activity and molecularly defined lactase nonpersistence.

Results: After 8 months, the RE group exhibited increases in BMD at the trochanter (2.3%) and total proximal femur (1.9%), and a trend (although nonsignificant) to improve muscle strength. In addition, reduced body mass index was observed. RE and AE decreased the percentage of fat mass and increased walking performance. CON group showed increases in fat mass and maintained or slightly decreased muscle strength. No significant interactions were observed for waist circumference and handgrip strength. Moreover, no significant changes in BMD were observed for AE and CON groups, and no associations were found between lactase nonpersistence and BMD changes. No group differences were apparent in baseline values or change in dietary intakes. Although a significant increase in physical activity level was observed, the change was similar among the groups and did not correlate with any bone and functional adaptations. No significant changes were observed in OPG levels, yet RE group showed the slighter positive mean percent change (0.52%) compared to the negative percent change in AE (-2.7%) and CON (-7.8%) groups.

Conclusion: Data suggest that 8 months of RE may be more effective than AE for inducing favorable changes in BMD, while both interventions demonstrate to protect against the functional weakness that is strongly related to fall-risk.

***Disclosures: Elisa Marques**, None.*

FR0053

Downregulation of Sost/sclerostin Expression is Required for the Osteogenic Response to Mechanical Loading. Xiaolin Tu*[1], Yumie Rhee[2], Racheal Lee[3], Jeffrey Benson[3], Keith Condon[3], Nicoletta Bivi[3], Lilian Plotkin[1], Charles Turner[4], Alexander Robling[3], Teresita Bellido[1]. [1]Indiana University School of Medicine, USA, [2]IUMS, Yonsei University, College of Medicine, South korea, [3]Indiana University, USA, [4]Indiana University, Purdue University Indianapolis, USA

The expression of osteocyte-derived sclerostin is reduced by mechanical loading, raising the possibility that osteocytes coordinate the osteogenic response to mechanical force by locally unleashing Wnt signaling. We investigated herein whether Sost downregulation is a pre-requisite for loading-induced anabolism by examining the response of transgenic mice (TG) overexpressing human Sost in osteocytes (driven by the 8kb-DMP1 promoter) and wild type (WT) littermates at 4-month of age. Loads required to obtain equal strains in TG and WT mice were measured ex vivo in 6 mice/genotype using gauges on ulnar midshafts. Loading induced 14% higher strains in TG (1295.5με/N) compared to WT (1114.8με/N) mice, indicating that TG bones are less resistant to mechanical force. Right ulnae were subjected to in vivo cyclic axial loading at low, medium, and high strains for 1min/d, 2Hz; left ulnae were unloaded controls. Endogenous (murine) Sost mRNA expression measured 24h after 1 loading bout at high strain was similarly decreased in WT and TG mice ($44\pm15\%$ and $47\pm8\%$ respectively, compared to unloaded ulnae; n=3/group). In contrast, human Sost, only expressed in TG mice, was not affected by loading. Six-8 mice/group were loaded on 3 consecutive days and forelimbs were collected 16d after initiation of loading. Dynamic histomorphometric analysis revealed that basal periosteal bone formation rate (pBFR) was similar in WT and TG mice. Loading caused a strain-dependent increase in pBFR in WT mice (0.08 ± 0.05; 0.24 ± 0.16; and 0.50 ± 0.18 um3/um2/d; $p<0.05$ vs unloaded ulnae for low, medium and high strain, respectively), resulting from an increase in both mineralizing surface covered by osteoblasts (MS/BS) as well as activity of individual osteoblasts (MAR). In contrast, loading-induced pBFR was dramatically reduced in TG mice by 70-82% (0.02 ± 0.02, 0.07 ± 0.08, and 0.09 ± 0.05 um3/um2/day), with significant changes only induced by high strains. Reduced pBFR resulted mainly from a marked decrease in MAR, which was not different in loaded vs unloaded ulnae in TG mice at any strain magnitude tested. Loading-induced MS/BS was also reduced in TG mice, with significant increase only induced by high strains. Dose-response curves of pBFR vs strain revealed an overall reduced mechanosensitivity and increased osteogenic threshold in TG bones. Therefore, downregulation of Sost/sclerostin is an obligatory step in the mechanotransduction cascade that directs osteogenesis to where bone is needed.

***Disclosures: Xiaolin Tu**, None.*

FR0055

Modulation of Gene Expression by Mechanical Loading in Mice with Conditional Ablation of the Connexin43 Gene (*Gja1*). Susan Grimston*[1], Marcus Watkins[2], Jin Norris[3], Valerie Salazar[2], Michael Brodt[3], Matthew Silva[2], Roberto Civitelli[2]. [1]Washington University School of Medicine, USA, [2]Washington University in St. Louis School of Medicine, USA, [3]Washington University in St. Louis, USA

We have previously reported attenuated response to anabolic mechanical loading at the endocortical surface in mice with conditional ablation of *Gja1* in osteoblasts. To achieve insights on the mechanisms of such attenuated response, we studied gene expression in cortical bone shortly after application of mechanical loading, using *DM1-Cre;Gja1flox/–* (cKO) mice. These mice, where *Gja1* is selectively ablated in the osteo-chondroprogenitor lineage, have a distinctive cortical bone phenotype characterized by larger cross-sectional area but reduced cortical thickness and decreased bone strength. They also have increases in both endocortical bone resorption and periosteal bone formation. We applied axial compression to the tibia of 2-month-old male mice at 7 N peak force for 120 cycles, with 10 sec rest between cycles. The contralateral tibia was used as an internal control. Tibiae were collected 2 hours post load, and after careful removal of the bone marrow, the bone was pulverized for total RNA extraction and real time qPCR analysis. *Gja1* mRNA was barely detectable in cKO bones, confirming effective *Gja1* deletion. In wild type (WT) littermates, abundance of *Cox2* mRNA, a gene known to be regulated by mechanical stimulation, increased 3-fold ($p<0.01$), as opposed to only 1-fold increase in cKO mice. Interestingly, *Sost* mRNA abundance was dramatically down-regulated (~90%; $p=0.04$) by mechanical loading in WT mice. In cKO mice *Sost* was already about 50% lower relative to WT, and mechanical load down-regulated *Sost* mRNA in cKO, though to a lesser extent (~70%, n.s.) than in WT mice. *BMP-4* mRNA was also significantly down-regulated by mechanical loading in both genotypes, whereas *β-catenin* and *NFATc1* mRNA, also reported to be involved in mechano-responsiveness, were only marginally increased after mechanical stimulation in both groups. Finally, *RANKL* mRNA decreased 50% ($p<0.05$) in loaded WT tibiae, but it did not change in cKO mice. Thus, mechanical skeletal loading rapidly regulates expression of genes involved in BMP-2/4 and Wnt signaling in cortical bone consistent with activation of bone formation, in addition to reduced RANKL expression consistent with suppression of bone resorption. Genetic ablation of *Gja1* in osteogenic cells alters these responses, perhaps reflecting an increased bone turnover state with consequent decreased ability to further activate bone formation upon stimulation.

***Disclosures: Susan Grimston**, None.*

FR0063

Developing an Atlas of GFP Reporters and Cre Drivers of Interest to the Skeletal Biologist. David Rowe*[1], Dong-Guk Shin[2], Peter Maye[1], Xi Jiang[1]. [1]University of Connecticut Health Center, USA, [2]University of Connecticut, USA

Promoter driven GFPs and Cre transgenic mice are widely utilized tools for the skeletal biologist. Unfortunately the characterization of different transgenic lines is highly variable and not widely appreciated, which can limit their utility and can even generate erroneous conclusions. Following the lead of the neuroscience community (http://neurosciencebluprint.nih.gov/factSheet/MouseLines.htm) in which web sites of BAC-GFP and Promoter Cre drivers are presented, we have begun to outline the elements of an atlas of reporter mice of value to the skeletal biology community. This pilot database has been developed to assess if the skeletal biologists would find an appropriately expanded and sophisticated resource to be of value to their research. The database documents a DNA construct map of the transgenic line and provides a survey of tissues where it is expressed and sites where no activity was detected. The images are taken from cryosections of non-decalcified skeletal tissues. GFP reporters were either made in house, submitted by other investigators or acquired from the MMRRC or Jackson Laboratory repositories. The activity is imaged in growing mice or at a site of bone fracture. Currently no histological sections from embryos have been obtained, but whole mounts of intact embryos have been acquired with a stereoscopic fluorescent microscope. In the case of Cre drivers, their activity was obtained by crossing with a recently released Ai9 Cre reporter mouse line (*Nat Neurosci* 13:133, 2010), which uniformly and robustly expresses tomato fluorescent protein in soft and mineralized tissue. Besides depositing the reporter activity in intact tissues, image data of primary cultures derived from various tissues (bone marrow stromal, neonatal calvaria and tendon) can provide additional understanding of the expression properties of the reporter. Strategies for annotating the various image types are being evaluated for their effectiveness for recalling images in response to anticipated queries of the dataset. The value of Cre mediated genetic studies depends on the knowledge of the temporal and cellular pattern of promoter activity, which can be assessed through a well-designed and populated promoter-GFP reporter database. Assembling this information will require a continuing community effort both in contributing existing or newly created transgenic mice and in generating the finances to support the technical efforts to build the database.

***Disclosures: David Rowe**, None.*

FR0068

ALK5, a TGF-beta type I Receptor, Regulates Osteoblast-Dependent Osteoclast Maturation and is Required for Cartilage Matrix Remodeling. Tomoya Matsunobu*[1], Kiyoyuki Torigoe[2], Muneaki Ishijima[3], Ashok Kulkarni[2], Yukihide Iwamoto[1], Yoshihiko Yamada[2]. [1]Graduate School of Medical Sciences, Kyushu University, Japan, [2]National Institute of Dental & Craniofacial Research, NIH, USA, [3]Juntendo University, School of Medicine, Japan

Transforming growth factor-beta (TGF-beta) exerts its diverse activities during development and pathogenesis. TGF-beta forms a specific complex with TGF-beta type I (TbrI/Alk5) and type II (TbrII) receptors, which activates downstream signaling through Smad-dependent and -independent pathways such as MAPK pathways. Previously, we showed that mice lacking ALK5 in chondrocytes and skeletal progenitor cells using Col2a1-Cre ($ALK5^{Col2CKO}$) and Dermo1-Cre ($ALK5^{Dermo1CKO}$), respectively, are perinatally lethal, and display defects in axial skeleton formation such as severe spinal scoliosis. In addition, TGF-beta is required for osteoblast proliferation and differentiation. In this study, we analyzed the limb development of these mutant mice in order to identify the role of TGF-beta signaling in cartilage formation and matrix remodeling. While femurs of $ALK5^{Col2CKO}$ mice were comparable with those of control mice, femurs of $ALK5^{Dermo1CKO}$ mice were significantly shorter than those of control mice. The length of the resting, proliferative and hypertrophic zones in $ALK5^{Dermo1CKO}$ femurs was similar to that in control and $ALK5^{Col2CKO}$ mice. In growth plates of $ALK5^{Dermo1CKO}$ growth plates, chondrocyte proliferation and differentiation were normal, and expression levels of extracellular matrix proteins and GAG (glycosaminoglycan) were similar to those in wild-type growth plates. We found that the cartilage matrix was not degraded and remained in primary spongiosa of E18.5 $ALK5^{Dermo1CKO}$ femurs. Analysis of tartrate-resistant acid phosphatase (TRAP) as a marker for osteoclasts revealed that TRAP-positive osteoclasts were decreased in E18.5 $ALK5^{Dermo1CKO}$ femurs, although osteoclast progenitors formed. We found that RANKL expression by osteoblasts in $ALK5^{Dermo1CKO}$ growth plates was substantially reduced. Since Dermo1-Cre was not expressed in hematopoietic lineage cells, the decreased number of mature osteoclasts in the primary spongiosa of $ALK5^{Dermo1CKO}$ femurs is likely due to reduced RANKL-mediated osteoclast differentiation. Our results suggest that TGF-beta signaling is required for cartilage matrix remodeling during endochondral ossification by promoting osteoclastogenesis in an osteoblast-dependent manner.

***Disclosures: Tomoya Matsunobu**, None.*

FR0069

Directed Differentiation of ES cells to the Chondrocyte Lineage. April Craft*[1], Jason Rockel[2], Gordon Keller[1]. [1]McEwen Centre for Regenerative Medicine, University Health Network, Canada, [2]Stem Cell & Developmental Biology, The Hospital for Sick Children, Canada

Osteoarthritis is a progressively debilitating disease that results from the significant degeneration of cartilage in the weight-bearing joints. The joint-lining chondrocytes (articular) are unable to regenerate upon injury. Defining the signaling pathways that regulate the generation of articular chondrocytes from embryonic stem cells (ESCs) and induced pluripotent stem cells (iPSCs) offers the opportunity to gain new insights into the origins of the disease and will provide a novel unlimited supply of patient-specific cells for transplantation therapies. Our approach to achieve efficient development of chondrocytes from PSCs relies on the stage specific recapitulation of embryonic signaling pathways in serum-free differentiation cultures. Studies in our lab have shown that the development of mesoderm subpopulations can be monitored quantitatively by the expression of the receptor tyrosine kinases Flk1/KDR and PdgfRα, and that it is possible to selectively induce subsets of mesoderm by manipulating two key TGFβ signaling pathways: BMP and activin/Nodal pathways. We have applied these approaches and found that BMP inhibition during activin and Wnt-mediated induction of primitive streak-like populations from mESC differentiation cultures results in the generation of a PdgfRα+ population with enriched somitic and chondrogenic potential, and reduced hematopoietic and cardiac potential. When cultured in appropriate monolayer conditions (containing BMP4 and bFGF), ESC-derived somitic mesoderm cells generated a strikingly homogeneous population of chondrocytes that expressed Sox9 and collagen II, and stained positive with Alcian blue. We have begun to modify the monolayer culture conditions to promote the development of the two chondrocyte subsets, articular and growth plate chondrocytes, which will be distinguished initially based on GDF5, ERG and collagen 10 gene expression. Our preliminary data suggests that the BMP, GDF5, FGF, and Hedgehog signaling pathways may play a role in the specification of articular chondrocytes from ESC-derived somitic mesoderm. Given that these steps represent the earliest stages of commitment to the chondrocyte lineages, these findings will contribute greatly to our overall understanding of how joint-lining cartilage develops which will ultimately lead to the development of novel therapies for the treatment of diseases such as osteoarthritis.

***Disclosures: April Craft**, None.*

FR0073

Lkb1 Regulates Growth Plate Dynamics in the Mammalian Skeleton. Lick Pui Lai*, Andrew McMahon. Harvard University, USA

Liver kinase b1 (Lkb1) is a serine-threonine protein kinase upstream of the AMPK family, and regulates multiple cellular activities, including cell cycle progression and cell polarity. We have removed Lkb1 specifically in chondrocytes, in order to investigate the role of Lkb1 in the chondrocyte development program. Remarkably, the growth plates of the conditional knock-out mice were elongated, and got progressively longer by postnatal day 3. Specifically, the length of the columnar chondrocyte region doubled in comparison to wild type mice. These data indicate that Lkb1 plays a critical role during normal development to control the length of the growth zone. Analysis of a number of molecular determinants of growth plate organization suggests a delay in hypertrophic chondrocyte differentiation in Lkb1 mutants. The mTOR signaling pathway is one of the key pathways regulated by AMPK. To determine the role of mTOR in mediating the effect of Lkb1 in chondrocytes, immunostaining was performed with a specific antibody for mTOR and phosphorylated eukaryotic translation initiation factor 4E-BP1. Elevated level of mTOR in the pre-hypertrophic region of the growth plate was accompanied by enhanced phosphorylation of 4E-BP1, consistent with heightened mTOR signaling when Lkb1 is removed. Taken together, these data suggest that removing Lkb1 in growth plate chondrocytes results in delayed chondrocyte hypertrophic differentiation, and this is mediated by elevated mTOR signaling in chondrocytes. With mTOR being a key convergent point of multiple growth-regulating signaling pathways including AMPK, IGF, and Wnt, Lkb1 regulation of mTOR is likely to have a critical role in mammalian skeletal development.

***Disclosures: Lick Pui Lai**, None.*

FR0075

Postnatal Deletion of the G-protein Subunit Alpha Synergizes with Gq/11 g-Proteins when Mediating PTH Receptor-dependent Fusion of the Epiphyseal Growth Plate. Andrei Chagin*[1], Tatsuya Kobayashi[2], Jun Guo[2], Takao Hirai[3], Min Chen[4], Lee Weinstein[5], Susan Mackem[6], Stefan Offermanns[7], Henry Kronenberg[2]. [1]Karolinska Institutet, Sweden, [2]Massachusetts General Hospital, USA, [3]Kyoto Prefectural University of Medicine, Japan, [4]National Institute of Diabetes, Digestive & Kidney Diseases, National Institutes of Health, USA, [5]National Institute of Diabetes & Digestive & Kidney Diseases, USA, [6]National Cancer Institute, USA, [7]University of Heidelberg, Germany

Recently we showed that ablation of PTH/PTHrP receptor (PPR) from epiphyseal chondrocytes of postnatal mice induced abrupt fusion of the growth plate associated with accelerated chondrocyte hypertrophy, cell death and decreased proliferation. The PPR is a G protein-coupled receptor that activates multiple heterotrimeric G proteins.

To explore the mechanism of this dramatic phenotype, we systemically explored the role of different G proteins in the postnatal growth plate including stimulating G protein subunit alpha (Gsa), extra large isoform of Gsa (XLas), as well as Gq/11 and G12/13 families of G proteins. For this purpose we used mice with collagen-2 (Col2) driven tamoxifen-inducible Cre (Col2-CreERt), mice that also harbor a floxed exon 1 of the *Gnas* gene (Gsa fl/fl), mice with disrupted exon2 of *Gnas*, DSEL mice defective in activation of Gq/11 by the PPR, Ga12-deficient mice and Ga13 fl/fl mice.

We found that ablation of Gsa in the postnatal growth plate dramatically impaired bone growth. This phenotype was associated with permanent disruption of bone epiphyses due to accelerated chondrocyte hypertrophy and growth plate disorganization. In contrast to mice lacking PPR in cartilage, mice missing Gsa in cartilage did not fuse the growth plate completely. The remnant of epiphyseal cartilage consisted of chondrocytes in post-mitotic and prehypertrophic stages that persisted between the epiphysis and metaphysis of long bones. This observation suggests that additional pathways are activated by PPR to cause fusion of the growth plate. Therefore we screened for the other G proteins involved in PPR-dependent growth plate fusion. Preliminary experiments revealed potential involvement of Gq/11 signaling. Indeed, mice without Gsa and with a PPR unable to activate Gq/11 signaling have a dramatically smaller cartilage remnant. Interestingly, neither XLas nor G12/13 G-proteins are involved substantially in postnatal bone growth regulation. The growth plates of mice lacking both Gsa and XLas looked identical to those missing only Gsa. No growth plate phenotype was observed in mice without Ga12, Ga13 or both.

In conclusion, we have shown that Gsa is essential for normal linear growth of postnatal mice and might synergize with Gq/11 to suppress postnatal growth plate fusion. Neither XLas nor G12/13 G-proteins seem to be needed for postnatal bone growth.

***Disclosures: Andrei Chagin**, None.*

FR0078

Zonal Disorganization and Premature Apoptosis of Chondrocytes in the Growth Plate of FGFR3 Mutant Mice. Clair Francomano[1], Zijun Zhang*[2]. [1]Great Baltimore Medical Center, USA, [2]Saint Louis University, USA

Skeletal dysplasia of achondroplasia, featured with disproportional short limbs, includes subtypes of achondroplasia, hydrochondroplasia, thanatophoric dysplasia (TD), and severe achondroplasia with developmental delay and acanthosis nigricans (SADDAN). The type II TD (TDII) patients have severely shortened limbs, macrocephaly, short ribs and hypoplastic thorax and usually die within a few days after birth. Genetically, TDII is caused by a single recurrent mutation (K650E) in the second tyrosine kinase domain of fibroblast growth factor receptor 3 (FGFR3). A mouse model has been created with K644E mutation of FGFR3, using in vivo Cre-loxP system, to simulate the phenotype of TDII. The homozygeous mutants do not survive after birth. The heterozygeous K644E mutants have shortened limbs, especially tibia and humerus. On histology, the ossified diaphysis is particularly short in the mutants, comparing with wild type mice. In this study, Fgfr3/K644E-neo mice mated with Col2a1-Cre mice for a cartilage specific phenotype. The limbs of newborns, which were significantly shorter than the wild type mice, were dissected for histology, immunohistochemistry for type X collagen and transmission electron microscopy (TEM). On histology, the growth plate of the mutants showed typical disorganized chondrocyte columns. In addition, the hypertrophic zone of growth plate defined with chondrocytes that are type X collagen positive was significantly expanded in the mutants, comparing with the wild type mice. TEM revealed apoptotic chondrocytes that are characteristic with a condensed nucleus in the upper level or proliferative zone of the growth plate in the mutants, but not in the normal chondrocyte columns found in the wild type mice. Those apoptotic chondrocytes in the mutant's growth plate were relatively small in size and surrounded by collagen fibrils in a square shape, indicating the cells have not enlarged to an expanded round shape as usually seen in hypertropic chondrocytes. In conclusion, this TDII model demonstrated that a FGFR3 mutation leads to not only disorganization of chondrocyte columns but also disorganization of zonal distribution in the growth plate. Apoptosis of chondrocytes at a premature stage may contribute to the breakdown of chondrocyte columns and expanded "hypertrophic zone" in the growth plate, and eventually causes the disorder of bone growth in TDII.

***Disclosures: Zijun Zhang**, None.*

FR0079

β-Catenin Controls Osteoclast Formation through Regulation of OPG and RANKL Expression in Chondrocytes. Baoli Wang*, Hong-ting Jin, Dezhi Tang, Mei Zhu, Brendan F Boyce, Di Chen. University of Rochester Medical Center, USA

The regulatory mechanism of endochondral bone remodeling remains unclear. In the present studies we generated inducible chondrocyte-specific β-catenin conditional knockout (cKO) and conditional activation (cAct) mice to investigate the role of β-catenin in postnatal skeletal development. Results from Micro-CT showed significant bone destruction in epiphyseal bone area but not the diaphyseal bone area in 3-month-old β-catenin cKO mice. We measured trabecular bone parameters in proximal tibia of 3-month-old mutant mice and found that BV, BMD, and Th.N. were significantly reduced (68, 66 and 58% reduction, respecitively) and SMI was significantly increased (increased 100%) in β-catenin cKO mice. In contrast, BV and BMD were significantly increased (increased 109 and 101%, respectively) in β-catenin cAct mice. Histologic analysis showed that TRAP-positive osteoclast numbers were significantly increased in β-catenin cKO mice, but significantly reduced in the β-catenin cAct mice; while bone formation rates (BFR) were not changed in these mutant mice. Results from chondrocyte/spleen cell co-culture experiments showed that primary chondrocytes isolated from β-catenin cKO mice significantly stimulated multi-nucleated osteoclast formation (increased 2-fold). Addition of OPG significantly inhibited osteoclast formation (72% inhibition). Rankl expression was increased by 2-fold and OPG expression was decreased by 60% in chondrocytes derived from β-catenin cKO mice. In contrast, chondrocytes derived from β-catenin cAct mice inhibited osteoclast formation. To determine if bone marrow (BM) cells are involved in bone loss phenotype observed in the β-catenin cKO mice, BM cells were cultured with M-CSF and 1,25-OH2 vitamin D3. No changes in osteoclast formation were observed. Consistent with this finding, β-catenin protein levels and expression of Rankl and OPG were not changed in BM cells derived from β-catenin cKO mice. These results suggest that BM cells from β-catenin cKO mice did not affect osteoclast formation. We then treated β-catenin cKO mice with bone resorption inhibitor Alendronate (2 mg/kg, once a week, subcutaneous injection) and found that Alendronate significantly reversed the bone destruction phenotype observed in β-catenin cKO mice. In this study, we provide the novel evidence that β-catenin signaling in chondrocytes regulates osteoclast formation through modulation of Rankl and OPG expression.

***Disclosures: Baoli Wang**, None.*

FR0081

Withdrawn

FR0083

Expression Pattern of TgfβR2 and Joint Formation Related Genes in Developing Limbs. Tieshi Li*[1], Lara Longobardi[1], Timothy Myers[1], Froilan Granero-Molto[1], Yun Yan[1], Douglas Mortlock[2], Anna Spagnoli[1]. [1]University of North Carolina at Chapel Hill, USA, [2]University of Vanderbilt, USA

We have previously reported that the*Tgfβr2$^{PRX\text{-}1KO}$* mouse, in which the TGF-β type II receptor (*Tgfβr2*) is conditionally inactivated in developing limbs lacks interphalangeal joints (Spagnoli A et al, J Cell Biol, 2007). To provide a sensitive read-out of *Tgfβr2* expression pattern, a *Tgfβr2-β-Gal-Bac* mouse was generated. A GFP-IRES-β-GEO cassette was inserted into the mouse bacterial artificial chromosome (BAC) clone RP24-317C21 (containing *Tgfβr2*) at the endogenous *Tgfβr2* translational start. Construct was used to generate the *Tgfβr2-β-Gal-Bac* mouse containing β-galactosidase (β-Gal) as an imaginable reporter for *Tgfβr2* expression under the control of endogenous (within 195.8kb) *Tgfβr2* gene regulatory sequences. E12.5 to E18.5 *Tgfβr2-β-Gal-Bac* embryos were subjected to LacZ staining. Transverse, longitudinal and sagittal limb sections were obtained from wild-type and LacZ-stained *Tgfβr2-β-Gal-Bac* embryos and subjected to immunohistochemistry and/or in situ hybridization for Jagged1, Notch1, Notch2, GDF5. We found that in developing autopods, β-gal activity was first evident (E12.5) within the forelimb and then (E13.5) in the hindlimb. An intense temporally and spatially characterized *Tgfβr2-β-Gal* expression/activity was noted in the developing interphalangeal joints. Such expression, which started at E13.5, was initially limited to cells in the dorsal and ventral regions of the interzone and then extended (E15.5- E18.5) laterally and proximally in the perichondrium. β-gal activity was undetectable in the central region of the interzone. Depending on the development stage, *Tgfβr2-β-Gal* expression distinctly over-lapped with expressions of GDF5, Notch1, Notch2 and Jagged1, indicating that essential componβents of the Notch system are co-expressed by TGFβRII+ joints cells and corroborating our previous findings that the TGFβRII signaling is needed to regulate expression of these genes. We also found a peculiar *Tgfβr2-β-Gal* expression/activity that started at E13.5, in the dorsal and ventral perichondrium of middle part of phalange that gradually decreased from E13.5 to E18.5 where it was found primarily surrounding the developing tendons/ligaments. Our findings show a dynamic and spatiotemporally regulated expression pattern of *TgfβR2* during joint/digit formation. Co-expression studies indicate that *TgfβR2* expressing cells provide a signaling niche to promote joint development in synchrony with the GDF5 and Notch pathways.

***Disclosures: Tieshi Li**, None.*

FR0084

MiR-204 and miR-211 Specifically Inhibit Runx2 Expression and Regulate Mesenchymal Stem Cell Differentiation and Bone Formation. Jian Huang*[1], Bing Shu[2], Lan Zhao[1], Di Chen[3]. [1]University of Rochester, USA, [2]Orthopaedics, University of Rochester, USA, [3]University of Rochester Medical Center, USA

Mesenchymal stem cell (MSC) differentiation is controlled by key transcription factors, such as Runx2 and Runx2 expression is tightly regulated at transcriptional and post-transcriptional levels. We found that miR-204 and its homolog miR-211 were expressed in MSCs. Multiple miR-204/211 binding sites were identified in the 3'-UTR of the Runx2 gene by mutation analysis. Over-expression of miR-204 decreased Runx2 protein levels (~50%) in C3H10T1/2 and ST2 progenitor cells. Significant reduction in ALP activity and the expression of osteoblast marker genes such as osteopontin and osteocalcin (40 and 70% reduction) and the mineralized bone nodule formation (75% reduction) were observed in miR-204 over-expressing ST2 cells; while enhancement of adipocyte formation demonstrated by increased Oil red O staining and the adipocyte-specific gene expression such as adipsin and ap2 (increased over 3-fold) was found in ST2 cells over-expressing miR-204. In contrast, retroviral over-expression of a miR-204/211 complementary fragment 'sponge', significantly increased Runx2 protein levels by 3-fold. Inhibition of miR-204/211 promoted osteoblast differentiation by increasing ALP activity, osteopontin and osteocalcin expression, and the mineralized bone nodule formation (increased 2-5 fold), and suppressed adipocyte differentiation (over 75% reduction in Oil red O staining and adipocyte marker gene expression) in ST2 cells. To further determine the role of miR-204/211 in vivo, we generated miR-204/211 sponge conditional transgenic (cTg) mice in which the expression of sponge transgene is activated by Prx1-Cre-mediated recombination. We have analyzed three lines of these cTg mice and found that trabecular bone mass (up 46%) and bone mineral density (up 32%) were significantly increased in these cTg mice by micro-CT and histology analyses. Runx2 protein expression, ALP activity and mineralized bone nodule formation were significantly up-regulated in bone marrow stromal (BMS) cells derived from the sponge cTg mice compared to those from Cre-negative controls. These effects were reversed by transfection of Runx2 siRNA into BMS cells derived from sponge cTg mice. In this study, we demonstrated for the first time that miR-204/211 act as important endogenous negative regulators of Runx2 and regulate mesenchymal stem cell differentiation and bone formation in vitro and in vivo.

***Disclosures: Jian Huang**, None.*

FR0085

MiR-29b Expression Is Dependent of COL1A1 in Bone Marrow Stromal Cells of Osteogenesis Imperfecta Patients During Osteoblast Differentiation. Carla Kaneto*[1], Francisco Jose De Paula[2], Patrícia Lima[3], Dalila Dalila[4], Karen Prata[4], João Pina Neto[5], Sumithra Urs[6], Dimas Covas[4], Wilson Silva[7]. [1]School of Medicine of Ribeirao Preto, University of Sao Paulo, Brazil, [2]School of Medicine of Ribeirao Preto - USP, Brazil, [3]Department of Natural Science, The State University of Bahia, Vitória da Conquista, Bahia, Brazil., Brazil, [4]Regional Blood Center of Ribeirão Preto & National Institute of Science & Technology in Cell Therapy, Brazil, [5]Department of Genetics, Medical School of Ribeirão Preto, University of São Paulo, Brazil, [6]Maine Medical Center Research Institute, USA, [7]Department of Genetics, Medical School of Ribeirão Preto, University of São Paulo., Brazil

The majority of cases of Osteogenesis Imperfecta (OI) are caused by mutations in one of the two genes, COL1A1 and COL1A2 that code for the two chains that trimerize to form the procollagen 1 molecule. However, alterations in gene expression and microRNAs (miRNAs) are responsible by the regulation of cell fate determination and may be evolved in OI phenotype. The mononuclear cell fractions were derived from bone marrow from eight different donors [five patients with Osteogenesis Imperfecta (MOOI1-MOOI5) and three normal donors (MON1-MON3)], who gave consent after full information and approval by the hospital committee. All MNC (mononuclear cells) were isolated and cultivated until the third passage, when the osteogenic differentiation was induced. Eight novel mutations coding region of COL1A1 and COL1A2 genes were identified and four may be responsible for causing OI phenotype. In COL1A1: 1 missense mutation (p. Gly290Glu), 1 nonsense mutation (Arg1026Ter), 1 out-of-frame insertion mutation (p.Leu69GlufsX74) and 2 silent mutations. In COL1A2: 1 missense mutation (p. Gly835Ser) and 2 silent mutations. The distribution of mutations in our patients is similar to that reported in the literature, with glicine substitutions in the helical domain resulting in severe phenotype. In patient MOOI5 with Bruck Syndrome (BS), a very rare disorder characterized by Osteogenesis Imperfecta and arthrogryposis multiplex congenital, 3 mutations were detected which are considered non pathogenic, as they do not alter an amino acid. The RNA was harvested at seven time points during the differentiation period (MSC, D+1, D+2, D+7, D+12, D+17 and D+21) and cDNA was synthesized. qRT-PCR amplification mixtures contained 20 ng template cDNA, 2X Power SYBR Green Master mix buffer (10 µL) (Applied Biosystems) and 400 to 600 nM forward and reverse primers for COL1A1 in a final volume of 20 µL. TaqMan® MicroRNA Assays (Applied Biosystems) were used to assess miR-29b expression levels. Interestingly, miR-29b and COL1A1 expression were severely reduced in both OI type I and type III patients, suggesting miR-29b expression is not a requirement for supporting osteoblast differentiation in OI patients. The data obtained for BS patient showed miR-29b and COL1A1 expression profiles similar to normal samples. Studies of Bruck syndrome have found normal secretion of collagen 1 in three families and mutations in the COL1A1 and COL1A2 genes have not been detected.

***Disclosures: Carla Kaneto**, None.*

FR0086

Repression of Mineralization by the Trps1 Transcription Factor. Dobrawa Napierala*[1], Yao Sun[2], Izabela Maciejewska[3], Elda Munivez[1], Terry Bertin[1], Rena D'Souza[2], Chunlin Qin[2], Brendan Lee[1]. [1]Baylor College of Medicine, USA, [2]Baylor College of Dentistry, Texas A&M Health Science Center, USA, [3]Baylor College of Dentistry, Texas A&M Heatlt Science Center, USA

Trps1 is a transcriptional repressor, whose mutations cause an autosomal dominant craniofacial and skeletal dysplasia tricho-rhino-phalangeal syndrome (TRPS). The *Trps1* expression pattern in mineralizing tissues suggests its involvement in differentiation and/or function of cells destined to produce mineralizing matrix. In perichondrial cells *Trps1* is highly expressed prior to mineralization, and the onset of mineralization of perichondrial cells coincides with decreased expression of *Trps1*. Similarly to perichondrial cells, *Trps1* is expressed in developing preodontoblasts, but not in mature secretory odontoblasts, which produce dentin. Our analyses of *Trps1* mutant mice (*Trps1ΔGT* mice) as well as mice over-expressing *Trps1* in osteoblasts and odontoblasts (*Col1a1-Trps1* mice) suggest that *Trps1* acts as a repressor of mineralization. Our previous studies of *Trps1ΔGT/ΔGT* mice revealed that loss of *Trps1* leads to accelerated perichondrial mineralization. This mutant phenotype was corrected by additional partial deficiency of *Runx2*, which demonstrated genetic interaction between these transcription factors. We confirmed the Trps1-Runx2 interaction at the molecular level and demonstrated that Trps1 acts as a repressor of Runx2. Interestingly, the Trps1 repressive activity is context-dependent; since *Trps1* deficiency has no apparent effect on mineralization of teeth, while over-expression of *Trps1* inhibits dentin mineralization. Only moderately decreases bone mineral density (BMD) in trabecular bone of *Col1a1-Trps1* mice. Using a combination of histological and biochemical analyses of dentin we have demonstrated dramatically reduced levels of major non-collagenous dentin matrix proteins:dentin phosphoprotein (Dpp) and dentin sialoprotein (Dsp), and dramatically decreased expression of the *Dspp* gene. Using chromatin immunoprecipitation (ChIP) assay, we have demonstrated that Trps1 binds to the *Dspp* promoter in odontoblastic cell lines. In summary, our data revealed tissue-specific repression of mineralization by Trps1. Additionally, we have identified the *Dspp* gene as a target of the Trps1 transcriptional repressor.

***Disclosures: Dobrawa Napierala**, None.*

FR0087

TIP39/PTH2R Signalling in Chondrocytes Alters Endochondral Bone Development in vivo. Dibyendu Panda*[1], David Goltzman[2], Andrew Karaplis[1]. [1]McGill University, Canada, [2]McGill University Health Centre, Canada

PTH2 receptor (PTH2R) /TIP39 (tuberoinfundibular peptide of mol wt 39 kD) signalling appears to be a potent inhibitor of chondrocyte proliferation and differentiation in vitro. We have also demonstrated that both TIP39 and PTH2R are present in situ in the newborn mouse growth plate. The receptor localized mainly in the resting zone of periarticular chondrocytes, while the ligand TIP39 was expressed exclusively in prehypertrophic chondrocytes.

To study TIPPTH2R function at the in vivo level, we generated transgenic mice overexpressing human PTH2R in chondrocytes under the control of the rat type II collagen promoter/enhancer. PTH2R transgenic mice revealed impairment of endochondral bone formation associated with reduced expression of type II and type X collagen expression. Chondrocytic cell proliferation in the transgenic mice, as measured by bromodeoxyuridine incorporation, was reduced compared to that of wild-type mice. Mineralization in trabecular bone, as determined by Von Kossa staining, was reduced in transgenic mice both in the primary and secondary spongiosa. Trabecular bone volume, as measured by micro CT analysis, was reduced in the transgenic mice compared to wild type. While examining the mechanism for the observed reduction in trabecular bone, we noted a significant increase in beta-catenin expression at the lower hypertrophic zone and upper primary spongiosa in the PTH2R transgenic mice, as compared to the wild type controls. At the cellular level, TIP39 reduced active glycogen synthetase kinase (phosphorylated GSK) level in the PTH2R expressing CFK2 Cells, thus augmenting beta-catenin signalling.

Moreover, we observed a delay in the development of the secondary ossification center in the PTH2R transgenic mice compared with wild type animals. A significant decrease in the expression of GDF5 and WDR5 proteins was evident in the chondrocytes around the secondary ossification center in the transgenic mice that may explain in part the molecular mechanisms by which TIP39/PTH2R signalling modulates the development of the secondary ossification center.

In summary, our experiments with Col2a-PTH2R transgenic mice indicate that TIP39/PTH2R signalling, through regulation of specific gene expression, contributes, at least in part, to specific events in both endochondral bone formation and in establishment of the secondary ossification site.

***Disclosures: Dibyendu Panda**, None.*

FR0095

Novel Role of CXCR4 in Bone Development and Growth. Wei Zhu*[1], Stephen Doty[2], Adele Boskey[2]. [1]Hospital for Special SurgeryWeill Medical College of Cornell University, USA, [2]Hospital for Special Surgery, USA

Introduction: CXC chemokine receptor 4 (CXCR4) is the primary receptor for stromal derived factor-1 (SDF-1). We previously discovered that blocking of the SDF-1/CXCR4 signal axis inhibited osteogenic differentiation of mesenchymal stem/precursor cells induced by bone morphogenic protein 2 (BMP2). In this study, we aimed to further elucidate the role of CXCR4 in bone development and growth using a transgenic mouse model.

Methods: $CXCR4^{flox/flox}$ mice were interbred with osterix (Osx)-Cre mice to generate conditional knockouts that have CXCR4 deletion in Osx-expressing osteoprogenitor cells (CXCR4-KO). The overall skeletal change and bone quality were determined by high-resolution x-ray and microCT. The CXCR4 effect on osteogenic differentiation was examined by comparing the BMP2-induced alkaline phosphatase (ALP) activity, a marker for preosteoblasts, in osteoprogenitors derived from calvarias of newborn CXCR4-KO mice with that of wild type controls. Moreover, we sequentially injected mice with xylenol orange and tetracycline (4-day interval), and assessed new bone growth by measuring the distance between the two fluoro-labeled mineralization fronts. The CXCR4 effect on growth plate was detected by alcian blue and type X collagen staining for chondrocytes, and pro-collagen I immunohistochemistry for osteoblasts.

Results: The skeletal size of CXCR4-KO mice was ~32% smaller than that of littermate wild types of the same sex and age (1&4-wk-old). Decreased trabecular bone volume fraction, thickness and number were detected in tibias of CXCR4-KO mice, and decreased cortical thickness was found in both tibias and calvarias of CXCR4-KO mice. While BMP2 stimulation increased ALP activities in CXCR4-expressing osteoprogenitors derived from wild type mice, no significant increase in ALP activities was found in osteoprogenitors derived from CXCR4-KO mice. Moreover, the rate of new bone formation (BFR) in CXCR4-KO mice was 31% lower than that of wild type mice (Fig1). Growth plate abnormalities were found in tibias of CXCR4-KO mice, including disorganized proliferating chondrocytes, decreased hypertrophic differentiation, and decreased number and activity of osteoblasts lining the trabecular bone surfaces.

Conclusion: Our data shown that CXCR4 deletion in osteoprogenitor cells led to decreased osteogenic differentiation and bone growth, accompanied by growth plate disorganization. This finding suggests that CXCR4 is an endogenous mediator essential for bone formation.

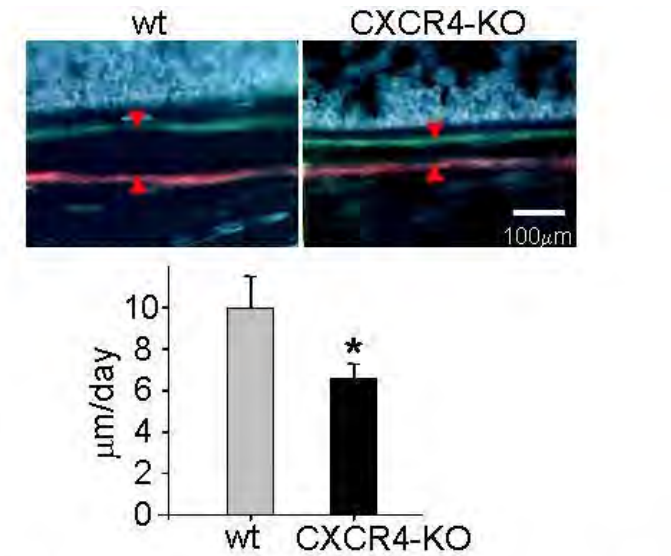

Fig 1. Decreased bone growth in CXCR4-KO mice. BFR was measured by dividing the distance between xylenol orange and tetracycline labels by 4-day time interval. N=5 tibias for CXCR4-KO or wild type control.

Zhu-Fig1

***Disclosures: Wei Zhu**, None.*

FR0096

Procollagen Type III N-Terminal Peptide (P3NP) is Inversely Associated with Lean Mass in Women. Vasan Ramachandran[1], Sarah Berry*[2], Robert McLean[3], Peggy Cawthon[4], Douglas Kiel[5]. [1]Boston University School of Medicine, USA, [2]Hebrew SeniorLife/Beth Israel Deaconess Medical Center, USA, [3]Hebrew SeniorLife, Harvard Medical School, USA, [4]California Pacific Medical Center Research Institute, USA, [5]Hebrew SeniorLife, USA

The discovery of biomarkers associated with muscle mass could lead to improved diagnostic and treatment options for sarcopenia. Type III Procollagen is a major component of skeletal muscle, and Procollagen Type III N-terminal peptide (P3NP) is released during periods of collagen turnover. It is unknown whether elevated levels of circulating P3NP might be associated with low muscle mass. Therefore, we performed a cross-sectional analysis to determine the association between serum P3NP and lean mass (total and appendicular) in men and women of the Framingham Offspring Study. Participants included 251 men and 306 women (106 premenopausal, 330 postmenopausal) with serum P3NP measured during a routine study visit (1995-1998) and lean mass measured by whole body DXA (1996-2001). Total lean mass (kg) was defined as total body soft tissue mass minus total body fat mass, whereas appendicular lean mass included arms and legs only. We examined the association between P3NP and total and appendicular lean mass, using multivariable linear regression. Age, BMI (kg/m^2), current smoking status, alcohol intake (g/week), and for women, hormone replacement, were considered using backwards stepwise models. Because P3NP may be influenced by sex hormones, we performed analyses separately in men, premenopausal women, and postmenopausal women. Mean age of participants was 57 years (range 32-84). Mean total lean mass was 54.7kg in men, 37.0kg in premenopausal women, and 36.3kg in post-menopausal women. Median serum P3NP was 3.2mg/L in men, 3.1mg/L in premenopausal women, and 3.0mg/L in post-menopausal women (range 0.02-53.3 mg/L). In the multivariable analyses, serum P3NP was inversely associated with total and appendicular lean mass in women, although the results were not statistically significant in premenopausal women (Table). No association between serum P3NP and total or appendicular lean mass was observed in men. Results were unchanged when additionally adjusting for indicators of cardiac muscle mass (left ventricular end diastolic diameter and weight). This is the first study to suggest that serum P3NP could potentially be a useful biomarker of muscle mass in postmenopausal women if it is found to have adequate sensitivity and specificity for muscle turnover. Prospective studies of serum P3NP and changes in

Multivariable association between serum P3NP (mg/L) and lean mass (kg) [β coefficient (p-value)]			
	Men	Pre-menopausal women	Post-menopausal women
Total lean mass	-0.04 (0.68)	-0.17 (0.20)	-0.13 (0.006)
Appendicular lean mass	0.00 (0.96)	-0.08 (0.25)	-0.05 (0.03)

Table

***Disclosures: Sarah Berry**, None.*

FR0097

PTH Anabolic Action is Influenced by the Deficiency of TRPV4 in Bone. Paksinee Kamolratanakul*[1], Yoichi Ezura[2], Fumitaka Mizoguchi[1], Tadayoshi Hayata[3], Hiroaki Hemmi[1], Takuya Notomi[4], Teruo Amagasa[1], Masaki Noda[1]. [1]Tokyo medical & dental university, Japan, [2]Tokyo Medical & Dental University, Medical Research Insititute, Japan, [3]Medical Reserach Institute, Tokyo Medical & Dental University, Japan, [4]GCOE, Tokyo Medical & Dental University, Japan

PTH is known as crucial agent for bone remodeling and marked as standard treatment for osteoporosis. TRPV4, as a family of Transient Receptor Potential Vanilloid, plays roles on calcium permeable nonselective cation channel. In addition, TRPV4 deficiency mice showed suppression in unloading-induced bone loss. Either PTH (through PTHR1) or TRPV4 play a role on calcium cascade regulation and have a potential on bone remodeling, however relation of this two molecules remain undiscovered. Accordingly, we challenged the hypothesis whether TRPV4, as a part, effects on PTH/PTHR1-regulated bone metabolism. First, we examined the effect of the intermittent human PTH injection into mice for 4 weeks on bone mineral density (BMD). Intermittent injection of PTH increased BMD by 20% and this increase was statistical significant. Intermittent PTH injection also tended to increase the average value for BMD in TRPV4 knockout mice (8%), however, this difference was not statistical significant. In addition to BMD, we also examined by micro CT as the levels of bone volume per tissue volume (BV/TV) in the femur of the mice. PTH injection increase BV/TV by 18.75% in wild type mice. In case of TRPV4 knockout mice, there was a trend to increase BV/TV value by injection human PTH in intermittent regimen, however, the difference was not statistical significant. With the respect to the histological examination, bone marrow cells and osteoclast appearances were similar regardless of the absence or presence of TRPV4. Upon PTH injection, there was an

increase in osteoblasts and osteoclasts and stromal cells, however, this was similarly observed in TRPV4 knockout mice. Quantification of osteoclastic cells after culturing bone marrow cells taken from wild type or TRPV4 knockout mice in presence of MCSF and RANKL for 5 days exhibited more than 2 folds increase of osteoclast number in wild type mice being exposed to PTH injection. In contrast, number of osteoclasts in culture were similar regardless of the genotype in culture of bone marrow cells, PTH injection did not increase osteoclast cell development in the culture of bone marrow cells. These data suggested that at least for the precursor cells of osteoclasts, TRPV4 is required for the efficient development of osteoclasts in culture in presence of RANKL and M-CSF. Preliminary experiment using TRPV4 knockout mice and constitutively active PTH/PTHrP receptor (H223R mutation) showed some trends of the wild type and heterogeneous TRPV4 that exposed to ca-PPR transgenic mice. Although there was a trend to have some increase in the heterogeneous knockout of TRPV4, p value was 0.25. These data indicated that, at least, in PTH injection models, TRPV4 may interfere the action of PTH receptor signaling in bone.

***Disclosures: Paksinee Kamolratanakul**, None.*

FR0103

Contrasting Osteogenic Response to Mechanical Stimulation Between C57BL/6J and C3H/HeJ Inbred Mice Is In Part Due to Genetic Variations in the Leptin Receptor, Which is a Negative Bone Mechanosensitivity Modulating Gene. Kin-Hing William Lau*[1], Sonia Kapur[2], Chandrasekhar Kesavan[3], Mehran Amoui[2], Subburaman Mohan[1]. [1]Jerry L. Pettis Memorial VA Medical Center, USA, [2]Jerry L. Pettis Mem. VAMC, USA, [3]JLP VA Medical Center, USA

Genetic is a key factor in determining bone response to loading. Accordingly, C57BL/6J (B6) mice respond to in vivo loading with an increased bone formation, but C3H/HeJ (C3H) mice show no such response. Genetic studies of the C3H/B6 pair of mouse strains revealed that bone mechanosensitivity is regulated by genes located in multiple loci on several chromosomes (Chr). Congenic mouse studies have identified a region in Chr 4 that harbors mechanosensitivity modulating genes. Because leptin receptor (Lepr) gene is located inside this Chr 4 region, we sought to show that Lepr plays a key modulating role in bone mechanosensitivity and that genetic variation of Lepr contributes to the different osteogenic responses to loading in C3H and B6 mice. In a previous ASBMR meeting, we reported that leptin-deficient ob/ob mice exhibited enhanced osteogenic response to mechanical loading. In this study, we compared the osteogenic response to loading (2-week four-point bending) in tibia of Lepr-deficient db/db mice [in B6 background] with that in tibia of wild-type (WT) littermates. To adjust for the 6% greater bone size in db/db mice, the load was adjusted to produce the same level of mechanical strain (4603 με at 9N for db/db mice vs. 4549 με at 7N for WT mice). This strain yielded significantly greater osteogenic response in db/db mice compared to WT mice [bone area (21.2% vs.10.6%), periosteal circumference (10.0% vs. 4.9%), BMC (30.9% vs. 12.4%), and vBMD (12.3% vs. 4.9%). We next compared the effects of a 30-min fluid shear (20 dynes/cm^2) on [^{3}H]thymidine incorporation (TdR) and Erk1/2 phosphorylation in db/db osteoblasts (Obs) to WT Obs. While the shear stress increased TdR and Erk1/2 in WT Obs, the stimulations were greater in db/db Obs ($p<0.01$ for each parameter). siRNA-mediated suppression of Lepr expression in B6 Obs enhanced, and in C3H Obs restored, their anabolic responses. These results confirm that Lepr signaling has a negative modulating role in bone mechanosensitivity. In addition, the Lepr signaling (Jak2/Stat3 phosphorylation) was several-fold higher in C3H Obs than in B6 Obs. Of the 3 single nucleotide polymorphisms (SNP) in Lepr between C3H and B6, one yielded an I359V substitution in C3H near the leptin binding region, suggesting that this SNP may contribute to a "hyperactive" Lepr signaling in C3H Obs. In conclusion, genetic variations in Lepr in part contribute to the contrasting osteogenic response to loading between B6 and C3H mice.

***Disclosures: Kin-Hing William Lau**, None.*

FR0105

Identification of Quantitative Trait Loci for Musculoskeletal Mechanosensitivity. Stefan Judex*[1], Engin Ozcivici[2], Weidong Zhang[3], Leah Rae Donahue[4]. [1]Stony Brook University, USA, [2]Mass General Hospital, USA, [3]The Jackson Laboratory, USA, [4]Jackson Laboratory, USA

Bone and muscle are highly sensitive to the removal and application of mechanical signals but little is known about the genetic basis defining the large differences in muscle and bone's mechanosensitivity between individuals. Here, we subjected 450 adult F2 female progeny of BALB and C3H (high- and low-mechanosensitivity) mice to 3wk of disuse (hindlimb unloading) and 3wk of subsequent reambulation to investigate changes in cortical bone and muscle and to define the underlying quantitative trait loci (QTL). *In vivo* μCT quantified longitudinal changes in middiaphyseal cortical bone and muscle surrounding the diaphyseal femur. Genome wide scans determined chromosomal regions with significant ($p<0.01$) QTL. During disuse, the marrow cavity expanded up to 22% in high-responders, concomitant with a 7% smaller cortical bone area. During reambulation, high-responders experienced an 11% contraction of the marrow area and a 9% increase in bone area. Tissue mineral density declined up to 8% during disuse and increased up to 3% during reambulation. Similarly, muscle loss amounted up to 26% during disuse and muscle gain reached 32% during reambulation. For both bone and muscle, low-responders were largely unresponsive during both experimental phases. The loss of cortical bone during disuse was not correlated with bone gain upon reambulation while in muscle, a moderate correlation (R^2=0.32) was observed between the two experimental phases. Further, those mice that experienced the greatest changes in muscle mass did not coincide with those individuals that experienced the greatest changes in cortical bone morphology during disuse or reambulation. For cortical bone area, 6 QTL were identified at baseline, 5 QTL during disuse, and 2 QTL during reambulation. For muscle area, we found 3 QTL at baseline, 1 during disuse, and 2 during reambulation. For both bone and muscle, QTL at baseline were distinct from those associated with unloading and reloading. In addition, there was little overlap between bone and muscle QTL. These data emphasize the strong influence of genetic variations on the mechanosensitivity of the musculoskeleton. They also show that the genetic regulation of the initial response to both the removal or application of mechanical signals is distinct between bone and muscle and that the development of physical interventions for musculoskeletal ailments may have to be optimized independently for bone and muscle.

***Disclosures: Stefan Judex**, None.*

FR0108

ASARM-peptides are Physiological Inhibitors of Renal Calcification. Peter Rowe*[1], Anne-Marie Hedge[1], Yan Hong[2], Aline Martin[3], Lesya Zelenchuk[1], Valentin David[3]. [1]University of Kansas Medical Center, USA, [2]University of Kansas Mecical Center, USA, [3]UTHSC, USA

Acidic-Serine-Aspartate-Rich MEPE-associated (ASARM) peptides are protease resistant mineralization inhibitors released from MEPE and DMP1 (SIBLING proteins). These peptides are present in urine and circulation. MEPE-transgenic mice over expressing ASARM-peptides are resistant to diet induced renal calcification. We described previously a competitive inhibitor of PHEX (SPR4) that binds specifically to ASARM-peptides and reverses the X-linked Hypophosphatemic Rickets (HYP) mineralization defect *in vitro*. Here we describe the renal *in vivo* effects of 28 day osmotic pump infusion of SPR4 peptide in wild type and HYP mice

Wild type and HYP mice (C57BL/6; n=5, male) were infused with vehicle (0.9% NaCl) or peptide (276 nmoles/hr/kg) for 28 days (Alzet Osmotic pumps). Animals were sacrificed on day 28 after overnight metabolic cage housing. Blood was then collected by cardiac exsanguination and chemistries assayed for urine and sera. Kidneys were removed and scanned by micro computed tomography (μCT) or used to prepare mRNA for RT/PCR analysis of gene expression.

In wild type mice, SPR4 treatment induced an increased fractional excretion of phosphate (FEP) (+20%; $P<0.05$), with normophosphatemia. In contrast no significant change was observed with treated HYP mice. FGF23 expression was markedly increased in wild type mice (+50%; $P<0.05$) and was coincident with decreased expression of NPT2a (-35%; $P<0.05$), NPT2c (-47%; $P<0.05$) and renal-Klotho (-73%; $P<0.05$). Circulating PTH levels were also increased in both wild type (+91%; $P<0.05$) and HYP mice (+132%; $P<0.056$ trend). In both wild-type and HYP SPR4 infused mice, a significant and marked increase in osteopontin (OPN) was measured in urine (WT= +166%, $P<0.05$, HYP= +124%; $P<0.05$) and sera (WT=+44%; $P<0.05$, HYP=+ 58%; $P<0.05$). The changes in OPN levels were also coincident with a significant and marked renal calcification with both WT and HYP mice (Figure 1A and B).

This study shows ASARM-peptides play a major role in suppressing renal microcalcification. The secondary increase in osteopontin levels is likely an adaptive response designed to inhibit the larger crystals that occur due to the sequestration of ASARM-peptides. Also, the changes in FGF23, PTH and NPT2a/c are likely due to competitive inhibition of PHEX and a secondary neutralization of ASARM-peptide by SPR4. Finally, ASARM-peptides may play a role in chronic kidney disease and mineralization bone disorders (CKD-MBD). Further studies are necessary to confirm this.

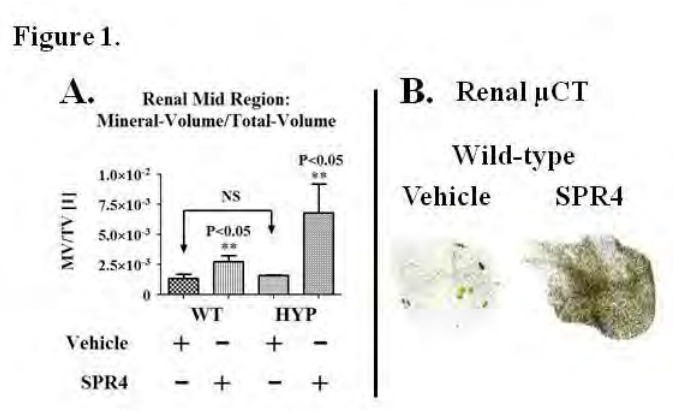

Figure 1

***Disclosures: Peter Rowe**, None.*

FR0110

FGFR1-Mediated Expression of Fgf23 and Dmp1 in Bone Bridges the Local and Systemic Regulation of Mineralization. Emily Farrow*[1], Yumie Rhee[2], Lelia Summers[3], Soo Park[3], Racheal Lee[3], Teresita Bellido[3], Kenneth White[3]. [1]Indiana University, USA, [2]IUMS, Yonsei University, College of Medicine, South korea, [3]Indiana University School of Medicine, USA

FGF23 circulates from bone to the kidneys to control phosphate metabolism, which is critical for normal skeletal mineralization. Local production of FGFs in bone is necessary for proper cell differentiation, as well as for skeletal formation and function. Of note, activating mutations in FGFR1 are uniquely associated with increased FGF23 in patients with the autosomal dominant disorder osteoglophonic dysplasia (OD). Whether paracrine and autocrine FGFs act through FGFR1 to regulate FGF23 and genes associated with elevated FGF23, which then function systemically, is unclear. To examine this question, we first tested for Fgfr1-4 mRNA expression in UMR-106 cells, and determined that these cells predominantly express Fgfr1 mRNA (between 100-10,000 fold over Fgfr2-4), and Fgfr1 protein. FGFs produced in bone, including FGF2 (as positive control, activates Fgfr1-4), and FGF8 (activates Fgfr1), increased phospho-Erk1/2 (p-Erk1/2) and activated Egr1 transcription (50-fold; $P<0.05$ vs. control), a marker of FGF-dependent MAPK signaling. Treatment with FGF8 resulted in a dose- and time dependent increase in Fgf23 mRNA (30-40 fold maximum at 25 nM and time of 24 h; $P<0.05$), which was significantly reduced by the p-Erk1/2 inhibitor U0126 ($P<0.05$). FGF16, which activates Fgfr2-4, showed no effect on Fgf23 mRNA or p-Erk1/2 in UMR-106 cells. Furthermore, differentiated primary cultures of mouse calvarial cells that express Fgfr1-3, treated with FGF2 or FGF8, stimulated Fgf23 mRNA over 200-fold vs. control ($P<0.01$). Loss of function mutations in Dentin matrix protein-1 (Dmp1) are responsible for autosomal recessive hypophosphatemic rickets (ARHR), a disorder associated with increased FGF23. FGF8 dose-dependently elevated Dmp1 mRNA with a 4000-fold increase at a maximum dose of 100 nM in UMR-106, indicating co-regulation with Fgf23 downstream of Fgfr1. To test this relationship in the converse disorder of phosphate wasting, tumoral calcinosis, we used the KL-null mouse, which has markedly elevated Fgf23. Interestingly, Dmp1 mRNA (4-fold; $P<0.005$), as well as protein expression in mature osteocytes were increased in KL-null bone. In sum, local FGF activity through Fgfr1 leads to marked elevation of Fgf23 and Dmp1 in bone cells, and in bone from a TC model. Thus, co-regulation of Fgf23 and Dmp1, likely through both local and systemic factors, is necessary for maintaining the balance of mineral and protein components required for proper bone mineralization.

***Disclosures: Emily Farrow**, None.*

FR0112

Placenta Expresses Klotho and FGFR1 in Syncytiotrophoblast and Might Be a Target Organ of FGF23. Yasuhisa Ohata*[1], Miwa Yamazaki[1], Tomoko Okada[1], Masahiro Nakayama[2], Keiichi Ozono[3], Toshimi Michigami[4]. [1]Department of Bone & Mineral Research, Osaka Medical Center & Research Institute for Maternal & Child Health, Japan, [2]Department of Clinical Laboratory Medicine & Anatomic Pathology, Osaka Medical Center & Research Institute for Maternal & Child Health, Japan, [3]Osaka University Graduate School of Medicine, Japan, [4]Osaka Medical Center, Research Institute for Maternal & Child Health, Japan

Serum levels of phosphate (Pi) in fetus are maintained higher than the maternal levels during late gestation. Although it is suggested an active materno-fetal transport contributes to the high levels of serum Pi in fetus, the mechanism underlying the regulation of serum Pi in fetal stage is poorly understood. In adults, it has been established that fibroblast growth factor (FGF) 23 plays a central role in Pi metabolism as a phosphaturic hormone as well as in vitamin D metabolism, and that Klotho is required as a cofactor for the action of FGF23. Klotho is a single-pass transmembrane protein, and has both transmembrane and soluble forms. We previously reported that human placenta expressed Klotho, and that serum levels of soluble Klotho were about 5-fold higher in cord blood compared with adults (ENDO 2009 meeting). Based on these findings, we tested the hypothesis that placenta might be a target organ of FGF23 in the current study. To address this issue, we first examined the expression of FGF receptors, Na^+/Pi cotransporters, and the molecules involved in vitamin D metabolism in placenta. RT-PCR analyses revealed the expression of *FGF receptor (FGFR) -1*, *-2*, and *-3* as well as *Klotho* both in human and mouse placenta. As to the Na^+/Pi cotransporters, placenta expressed *NPT2b*, *Pit1*, and *Pit2* both in human and mouse. The expression of *1α-hydroxylase*, *24-hydroxylase*, and *vitamin D receptor* was also detected in human and mouse placenta. Then, to investigate whether Klotho and FGFR are co-expressed in the same cells in placenta, we performed immunohistochemical staining, and revealed their co-expression in syncytiotrophoblasts. Syncytiotrophoblast is the main site of feto-maternal interface, and plays the major role in placental functions, including the exchange of ions, gas, and nutrients. An antibody against the phosphorylated FGFR (Y653/Y654) positively immunostained the syncytiotrophoblasts, and so did an antibody against early growth response-1 (EGR-1), a target gene of FGF signaling. We then determined the serum levels of FGF23 in cord blood and found that they were significantly lower than those in adults, suggesting that FGF23 circulating in maternal blood might exert its functions in syncytiotrophoblasts in placenta. Taken together, our results have demonstrated that syncytiotrophoblast in placenta expresses both Klotho and FGFR1 and might be a target of FGF23 signaling, which may play a role in the Pi homeostasis and vitamin D metabolism in fetus.

***Disclosures: Yasuhisa Ohata**, None.*

FR0113

Soluble Klotho Acts as a Coactivator of FGF23 in Bone but not in Kidney to regulate Mineralization. Tomoko Minamizaki*[1], Yuji Yoshiko[2], Yukiko Konishi[1], Hirotaka Yoshioka[1], Katsuyuki Kozai[1], Jane Aubin[3], Norihiko Maeda[4]. [1]Hiroshima University Graduate School of Biomedical Sciences, Japan, [2]Hiroshima University, Japan, [3]University of Toronto Faculty of Medicine, Canada, [4]DHiroshima University Graduate School of Biomedical Sciences, Japan

Fibroblast growth factor 23 (FGF23) is expressed primarily in osteoblasts/osteocytes (Obc cells) and acts on kidney and parathyroid to suppress the type II sodium-phosphate cotransporter and 1α(OH)ase expression and parathyroid hormone production, respectively. Klotho, a senescence-related membrane protein, forms a complex with FGF23-FGF receptor (FGFR), which is necessary for FGF23-specific signaling. In spite of the fact that Klotho is not expressed in bone, accumulating evidence suggests that bone may be an additional target of FGF23. We therefore tested the hypothesis that the extracellular domain of Klotho (KLe), which is truncated and secreted into the circulation, contributes to FGF23 action in bone. Recombinant FGF23 (rFGF23) formed a complex with FGFR only in the presence of rKLe in the rat Obc cell culture model. rFGF23-induced mineralization defects in the rat Obc model were abrogated by blocking FGF23-specific signaling, by removal of soluble Klotho from the fetal bovine serum (FBS) used for the cultures or by substituting serum from *Klotho*-mutant (*kl/kl*) mice for untreated FBS. This model also revealed that neither Wnt signaling nor the calcium channel TRPV5, a known target of KLe, was involved in the rKLe effects. To confirm that KLe and FGF23 act on bone in vivo as we observed in vitro, we intravenously injected rKLe into 4-week-old mice pretreated with $1,25(OH)_2D_3$. $1,25(OH)_2D_3$ increased serum FGF23 and calcium levels with a slight decrease (not significant) in serum phosphorus levels. A single injection of rKLe increased ERK1/2 phosphorylation within 2h in bone but not in kidney, suggesting that KLe contributes to FGF23 signaling in bone. We next injected rKLe subcutaneously and daily for 12 days over the calvaria of 10-day-old *kl/kl* mice, a model that exhibits cryptogenic overproduction of FGF23 with high serum levels of phosphorus, calcium, $1,25(OH)_2D_3$ and FGF23. rKLe treatment did not alter these serum parameters, but did activate ERK1/2 in bone but not in kidney, and increased the number of cells in *kl/kl* bone that were double immunoreactive for FGF23 and phosphorylated ERK1/2. rKLe treatment also increased the amount of unmineralized osteoid in the parietal bone and up- or down-regulated the levels of expression of certain osteoblast marker mRNAs in *kl/kl* bones. Our data suggest that KLe forms a complex with FGF23-FGFR in bone, resulting in mineralization defects through an FGF23-dependent ERK signaling pathway.

***Disclosures: Tomoko Minamizaki**, None.*

FR0116

Endogenous PTH Contributes to Bone Regeneration, Formation and Remodeling by Stimulating Osteoprogenitor Cell Recruitment following Marrow Ablation. Qi Zhu*[1], Lei Shu[1], Jun Yan[2], Andrew Karaplis[3], David Goltzman[4], Dengshun Miao[5]. [1]Nanjing Medical University, China, [2]Second Hospital of Suzhou University, Peoples republic of china, [3]McGill University, Canada, [4]McGill University Health Centre, Canada, [5]Nunjing Medical University, Peoples republic of china

To determine whether endogenous PTH plays a role in stimulating recruitment of osteoprogenotior cells for osteoblastic bone formation and remodeling *in vivo*, marrow ablation was performed in tibiae and femurs of 8-week-old wild-type (WT) and PTH null ($PTH^{-/-}$) mice. Newly formed bone tissues were analyzed from 1-3 weeks postsurgery using micro-CT and histopathology. Bone formation related gene and protein expression levels were evaluated by real-time RT-PCR and Western blots, respectively. At 1 week postsurgery, trabecular bone volume, osteoblast numbers, ALP positive areas, and type I collagen positive areas were all decreased significantly in the diaphyseal regions of bones of $PTH^{-/-}$ mice compared to WT mice, indicating delayed osteoblastic bone formation. Gene expression levels of Cbfa1, ALP, type I collagen and OCN, and protein expression levels of Cbfa1, PTHR, and IGF-1 were also down-regulated significantly in bones of $PTH^{-/-}$ mice compared to WT mice at this time. Bone marrow regeneration was also delayed in $PTH^{-/-}$ mice. In contrast, by 2 weeks postsurgery all parameters related to osteoblastic bone formation were increased significantly in $PTH^{-/-}$ mice compared to WT mice. By 3 weeks postsurgery, trabecular volume had recovered to pre-surgery levels in WT mice, however, remnants of newly formed trabecular bone remained in $PTH^{-/-}$ mice. TRAP positive osteoclast numbers and surface were reduced in $PTH^{-/-}$ mice at 1 week postsurgery. At 2 weeks postsurgery, although TRAP positive osteoclast numbers were increased, the TRAP positive osteoclast surface was still reduced significantly in $PTH^{-/-}$ mice compared to WT mice. The expression of PTHrP in newly formed bone tissues was up-regulated at both gene and protein levels at 1 and 2 weeks postsurgery in $PTH^{-/-}$ mice compared to WT mice. This up-regulation of PTHrP expression may have contributed to new bone formation in PTH deficient mice followed bone marrow ablation by recruiting

osteogenic cells. Long bones from WT mice transplanted 1week after bone marrow ablation into the back muscle of PTH intact β-galactosidase transgenic mice for 1 week, demonstrated Lac-Z positive osteoblastic and fibroblastic cells in the newly formed bone surface and bone marrow cavity, respectively, demonstrating the circulating origin of the repopulating cells. Our study indicates that endogenous PTH is required for optimal bone regeneration, formation and remodeling by stimulating osteoprogenitor cells derived from the circulation.

***Disclosures: Qi Zhu**, None.*

FR0119

Mechanistic Insights into the Dysregulation of PTH Secretion in Hyperparathyroidism: In Vivo Analysis and In Vitro Studies in Parathyroid Glands. Wenhan Chang*[1], Tsui-Hua Chen[1], Nathan Liang[1], Christopher Dinh[1], Viet Pham[1], Hanson Ho[1], Zhiqiang Cheng[1], Chia-Ling Tu[1], Dolores Shoback[2]. [1]University of California, San Francisco, USA, [2]VA Medical Center, USA

Controversy exists as to the basis for PTH hypersecretion in primary and secondary hyperparathyroidism (HPTH) with roles hypothesized for the shift to the right in the set-point for Ca-mediated secretion (Ca-PTH set-point), an expansion of the Ca-nonsuppressible PTH (nonCa-PTH) pools within the gland, and progressive increases in cell number. To test the role of the CaSR in PTH secretion in HPTH, we generated mice with early-onset HPTH by knocking-out one allele of the casr gene conditionally (Het-KO) in the parathyroid glands (PTGs). Het-KO mice displayed HPTH by 2 weeks of age that progressed over time. Serum fibroblast growth factor (FGF)-23 and 1,25-OH vitamin D (1,25-D) levels were also elevated in 2-week-old HET-KO mice. We observed gender- and age-dependent differences in the severity of HPTH in these mice. In male HET-KO mice, serum PTH levels increased progressively from 114±27 pg/mL at 8 weeks of age to 167±18 and 340±39 pg/mL at 12 and 24 weeks of age, respectively. In female HET-KO mice, serum PTH had peaked at 308±47 pg/mL by 8 weeks of age and remained comparably elevated at 12 (264±49 pg/mL) and 24 weeks (250±47 pg/mL) of age. We developed a novel in vitro PTH secretion assay on intact micro-dissected mouse PTGs and compared the Ca-PTH set-points by incubating glands sequentially with media containing different [Ca^{2+}] (0.5–3 mM) and measuring their protein content by BCA assay, as an index of gland mass. At 4 weeks of age, >85% of PTH secretion was suppressed by high [Ca^{2+}] (3 mM) in both Wt and Het-KO PTGs. At 12 weeks of age, we observed an increase in the nonCa-PTH pools – which accounted for ≍40% of the total PTH secretion (Total-PTH) in both Wt male and female mice. The nonCa-PTH pools were further expanded to ≍75 and 60% of the Total-PTH in male and female HET-KO mice, respectively. As expected, Ca-PTH set-points were significantly right-shifted (≍1.2 mM Ca^{2+} in Wt to ≍1.5 mM Ca^{2+} in the HET-KO PTGs) at both time-points. There were no significant changes in gland size in female Het-KO at 4 and 12 weeks of age and in male HET-KO mice at 4 weeks of age. Male HET-KO PTGs, however, doubled in mass by 12 weeks of age. We are assessing gene expression in these PTGs and serum FGF23 and 1,25-D levels in older HET-KO and Wt mice. We conclude that haploinsufficiency of the PTG-CaSR leads to a right-shifted set-point as well as an expanded pool of Ca-nonsuppressible PTH – both hallmarks of HPTH in vivo.

***Disclosures: Wenhan Chang**, None.*

FR0121

Stimulation of Bone Formation and Mineralization Post-Weaning Without Parathyroid Hormone. Beth J. Kirby[1], Andrew Karaplis[2], Christopher Kovacs*[1]. [1]Memorial University of Newfoundland, Canada, [2]McGill University, Canada

The maternal skeleton significantly resorbs and demineralizes during lactation to provide calcium to milk, followed by intense bone formation to reattain the pre-pregnancy bone mineral content (BMC). Osteoclast-mediated resorption and osteocytic osteolysis cause the lactational losses of mineral and are stimulated by low estradiol and mammary-derived PTHrP. In contrast, the mechanisms that stimulate bone formation after weaning are not established. Limited data from humans have shown that PTH increases after weaning; PTH can stimulate bone formation. We therefore hypothesized that PTH stimulates bone formation and skeletal mineralization during post-weaning.

We studied wt and *Pth* null sister mice. In a prior study with a standard 1% calcium diet many *Pth* null mothers died of hypocalcemia in the puerperium, failed to lactate, or culled their litters to an average of 2 pups. To avoid maternal hypocalcemia, in the current study wt and *Pth* null sisters were placed on a 2% calcium with lactose "rescue diet" and mated to the same males. Total body and regional (spine, hindlimb) BMC were measured by DXA (PIXImus, Lunar) during pre-pregnancy baseline, end of pregnancy, end of lactation, and weekly for 21 days post-weaning. Blood and urine were collected at each time point.

On the 2% calcium diet wt mice lost 5.3% of spine BMC during lactation as compared to the expected ~20% loss that wt mice in the same genetic background experience on a 1% calcium diet. *Pth* null mice lost 5.7% of spine BMC and completely restored this within 14 days post-weaning to a value that was 4.1% higher than pre-pregnancy baseline. The BMC excursions did not differ significantly between wt and *Pth* null mice. Two bone formation markers were assessed. Osteocalcin rose in *Pth* nulls from 47.6±6.0 to 79.6±6.0 ng/ml by day 7 post-weaning ($p<0.01$); wt mice showed a similar post-weaning osteocalcin peak of 74.6 ng/ml that did not differ from *Pth* nulls. Wt and *Pth* null mice also achieved similar values of P1NP by day 7 during post-weaning.

In summary, wt and *Pth* null mice lactated normally but the high calcium diet reduced the magnitude of BMC decline during lactation. *Pth* null and wt sisters lost a similar amount of BMC during lactation and restored it fully by day 14 post-weaning. Osteocalcin and P1NP increased in both genotypes by day 7 post-weaning. In conclusion, PTH is not required to stimulate bone formation post-weaning and enable recovery from skeletal losses incurred during lactation.

***Disclosures: Christopher Kovacs**, None.*

FR0122

The Anabolic Action of Parathyroid Hormone on Bone is Mediated by Monocyte Chemoattractant Protein-1. Joseph A. Tamasi*[1], Emi Shimizu[2], Noah Benton[2], Joshua Johnson[2], Nigel Morrison[3], Nicola Partridge[4]. [1]Physiology & Biophysics, University of Medicine & Dentistry of New Jersey, USA, [2]Basic Science & Craniofacial Biology, New York University College of Dentistry, USA, [3]Griffith University, Gold Coast Campus, Australia, [4]New York University College of Dentistry, USA

Parathyroid hormone (PTH) is the major hormone regulating calcium homeostasis, but it also has a significant role as an anabolic hormone in bone when administered by intermittent injection. The mechanisms for the bone anabolic effect of PTH are not understood. However, it has been established that the anabolic effects of PTH require osteoclast activity. PTH acts through a single receptor on the osteoblast to regulate many known genes. Previous microarray studies in our laboratory have shown that the most highly regulated gene, monocyte chemoattractant protein-1 (MCP-1), is rapidly and transiently induced when PTH(1-34) is injected intermittently in rats for 14 days. Through further in vivo studies, we found that rats treated with PTH(1-34) for 14 days showed a significant increase in serum MCP-1 levels 2 h after PTH injection (159 pg/ml) compared to basal levels obtained prior to the last injection (65 pg/ml). Furthermore, serum MCP-1 levels increase with the duration of treatment. Compared to vehicle treatment, PTH(1-34) treatment in rats for 1, 7 and 14 days showed a 24%, 53% and 79% increase in serum MCP-1 levels 2 h after injection, respectively. Using immunohistochemistry, increased MCP-1 expression is evident in trabecular osteoblasts by the second PTH(1-34) injection with peak staining occurring between 3 and 7 days of treatment. Male and female MCP-1 knockout mice injected daily with 80 ug/kg PTH(1-34) for 6 weeks showed significantly reduced anabolic effects of PTH compared to wild type mice as measured by pQCT and micro-CT. PTH-treated male MCP-1 null mice have significantly less trabecular bone mineral density (means, mg/cm^3, vehicle: 454; PTH: 486) than the corresponding PTH-treated wild type mice (means, mg/cm^3, vehicle: 452; PTH: 521). Trabecular bone volume (BV/TV) increased 27% in PTH-treated wild type mice with a corresponding increase in trabecular thickness (Tb.Th), however no increase in BV/TV or Tb.Th was observed in the PTH-treated MCP-1 null mice. Histomorphometric analysis revealed that the 2 fold increase in osteoclast surface and osteoclast number observed with intermittent PTH treatment in the wild type mice was completely eliminated in the MCP-1 null mice. Consequently, the lack of osteoclast activity in the MCP-1 null mice was paralleled by a significant reduction in bone formation rate. We conclude that osteoblastic MCP-1 expression is essential for the anabolic effects of PTH on bone.

***Disclosures: Joseph A. Tamasi**, Bristol-Myers Squibb, 3*

FR0124

Differential Role of Fibronectin Originating from Different Sources in the Bone Marrow on Metastasis Formation. Anja von Au*[1], Christine Hoffmann[1], Matthaeus Vasel[1], Marco Cecchini[2], Inaam Nakchbandi[1]. [1]Max-Planck Institute for Biochemistry & University of Heidelberg, Germany, [2]University of Bern, Switzerland

The extracellular matrix affects tumor cell behavior by binding to surface receptors or modifying growth factor availability. Fibronectin (FN) is expressed in the premetastatic niche, which suggests a critical role for it in tumor development. We sought to examine the role of FN produced by cells of the osteoblastic niche and differentiate it from the effects of other cells in the bone marrow on the formation of bone metastasis.

Mice carrying the Mx or collagen α1(I) promoter attached to cre were mated to nude mice homozygote for a floxed FN gene resulting in mice with deleted FN in the bone marrow (Mx) or in osteoblasts (Col). A bone seeking luciferase expressing MDA-MB-231 tumor cell line was used.

Cardiac injection in Mx-mice resulted in increased median survival from 6.6 in CT to 8.7 weeks ($p<0.05$). Growth assessed using tibia injections was slower at days 14 and 18 after injection (day 18: CT 30±6 $x10^5$ vs. Mx 12±7 $x10^5$ relative luminescence units (RLU), $p<0.05$). This suggested a defect in early angiogenesis that was confirmed (CT 148±10 vs. Mx 89±8 CD31-stained blood vessels/mm^2, $p<0.005$). Histomorphometry revealed an increase in osteoblasts adjusted to tumor-bone interface (CT 44±6 vs. Mx 63±2 Ob/BS, $p<0.05$).

Cardiac injection in Col-mice revealed survival prolongation from 6.6 to 7.6 weeks ($p<0.05$). Tibia injections showed decreased early growth until day 18 (day 7: CT 5±2 $x10^4$ vs. Col 2±0.3 $x10^4$ RLU, $p<0.05$). After that growth was comparable until death at day 40 (1.7±0.5 $x10^8$ vs. 1.7±0.4 $x10^8$ RLU). Despite the lack of difference

in growth histomorphometry showed increased osteoclasts (CT 0.8±0.2 vs. Col 3.6±0.4 OC/BS, $p<0.01$). This presumably resulted from decreased circulating osteoprotegerin levels (CT 4.9±0.4 vs. Col 3.7±0.3 ng/ml, $p<0.05$) that developed in the presence of tumor, because untreated mice had lower and comparable levels (CT 2,4±0.1 vs. Col 2.2±0.2 ng/ml, p=NS). To determine whether osteoblasts lacking FN produce less osteoprotegerin we examined conditioned media from primary osteoblasts and found a significant decrease in osteoprotegerin in Col (CT 3.1±0.4 vs. Col 1.7±0.02 ng/ml, $p<0.05$).

Since osteoblasts produce FN, the increase in osteoblasts could support the comparable early growth in Mx and CT. The increase in osteoclasts in Col is not associated with increased tumor growth raising the possibility that an intermediary involved in the vicious cycle is disturbed in the absence of osteoblast FN.

***Disclosures: Anja von Au**, None.*

FR0125

Enpp1: A Potential Facilitator of Breast Cancer Bone Metastasis. Wen Min Lau[1], Michele Doucet[1], Ryan Stadel[1], Kristy Weber[2], Scott Kominsky*[3]. [1]Johns Hopkins University School of Medicine, USA, [2]Johns Hopkins University, USA, [3]Johns Hopkins School of Medicine, USA

Metastasis is the ultimate cause of mortality in breast cancer patients, developing in the bone more frequently than any other site. Moreover, bone metastasis is frequently incurable and commonly causes significant morbidity in the form of bone pain, pathological fractures, nerve compression, and hypercalcemia. Critical to our ability to prevent and treat bone metastasis is the identification of the key factors mediating its establishment and understanding their biological function. To address this issue we utilized an *in vivo* selection process to generate murine mammary tumor sublines possessing an enhanced ability to colonize either the bone or liver following intracardiac injection. A comparison of gene expression between these sublines by genome-wide cDNA microarray analysis revealed several potential mediators of bone metastasis, including the pyrophosphate-generating ectoenzyme ecto-nucleotide pyrophosphatase/phosphodiesterase I (Enpp1). By qRT-PCR and Western analysis we found that expression of Enpp1 was elevated in human breast cancer cell lines known to produce osteolytic metastasis in animal models compared to non-metastatic and normal mammary epithelial cell lines. Further, mRNA expression was elevated in human breast cancer bone metastasis relative to primary breast tumors and normal mammary epithelium by qRT-PCR and immunohistochemical analysis. To examine the potential role of Enpp1 in the establishment of bone metastasis, we stably increased the expression of Enpp1 in the breast cancer cell line MDA-MB-231 and examined their ability to colonize the bone and induce osteolysis following direct injection into the tibia of athymic nude mice. Interestingly, in two separate experiments, MDA-MB-231 cells with increased expression of Enpp1 demonstrated an enhanced ability to establish osteolytic tumors relative to cells expressing vector alone, as determined by digital radiography. In addition, similar results were observed following intracardiac injection of tumor cells in athymic nude mice. Taken together, these data suggest a potential role for Enpp1 in the establishment of breast cancer bone metastasis.

***Disclosures: Scott Kominsky**, None.*

FR0128

Myeloid-Derived Suppressor Cells Expand During Breast Cancer Progression and Promote Tumor-induced Bone Destruction. Sabrina Danilin*[1], Julie Sterling[2], Alyssa Merkel[2], Josh Johnson[2], Rachelle Johnson[2], James Edwards[2], Gregory R Mundy[2]. [1]Vanderbuilt University, USA, [2]Vanderbilt University Medical Center, USA

Breast carcinoma is a highly metastatic cancer that preferentially metastasizes to bone, causing osteolytic lesions in 70% of patients. Myeloid-Derived Suppressor Cells (MDSC), identified as Gr-1+CD11b+ cells in mice, are a heterogeneous population of myeloid cells at different stages of differentiation that expand in blood, spleen and bone marrow during cancer growth. They are responsible for cancer immunosuppression and are recruited into the primary tumor where they directly promote cancer growth, recurrence and burden. However, little is known about their role at metastatic sites. We hypothesized that MDSCs in bone marrow create a favorable microenvironment for tumor cell and promote cancer cells induced osteolysis. Since immunodeficient mice are used to study breast cancer bone metastasis in vivo, and MDSCs play a critical role in immunosuppression, we first injected nude mice in the mammary fat pad with MDA-MB-231 human cancer cells or immunocompetent balb/c mice with 4T1 cells and assessed MDSCs. FACS analysis and histology demonstrated that MDSCs' expansion and ability to promote tumor growth was similar in both models, validating the use of nude mice for their study. To assess the role of MDSCs in tumor-induced bone disease, we inoculated MDA-MB-231 cells into the left cardiac ventricle of nude mice and monitored metastasis progression by X-ray and GFP fluorescence imaging and MDSCs by FACS weekly. MDSCs were then isolated from normal and tumor-bearing mice, and gene expression and in vitro function assessed. By FACS, we detected an increase in the Gr-1+CD11b+ population as expected, but more importantly, the GR-1lowLy6C+ subpopulation which gives rise to monocytic cells also increased from 6 to 12% in bone marrow of tumor mice. Furthermore, in vitro experiments showed that MDSCs differentiate into osteoclasts when cultured with RANKL and M-CSF and that they increase PTHrP mRNA expression in cancer cells. This enhancement in PTHrP expression is likely due to the 2 fold increase in TGF-ß expression found in MDSCs isolated from tumor mice compared to MDSCs isolated from control mice. Overall, these results demonstrate that MDSCs expand in breast cancer bone metastases in vivo, that they are potential precursors for osteoclasts in vivo and that they are able to influence breast cancer cell behavior. This suggests that MDSCs may help establish a permissive microenvironment for tumor cell metastases to bone and contribute to tumor-induced bone disease.

***Disclosures: Sabrina Danilin**, None.*

FR0133

Treatment with Interleukin 6 Receptor Antibodies Inhibits Breast Cancer Growth in a Murine Model of Bone Metastasis. Katja Boernert[1], Yu Zheng*[1], Hong Zhou[2], Anastasia Mikuscheva[3], Frank Buttgereit[3], Colin Dunstan[4], Markus Seibel[2]. [1]Bone Research Program, ANZAC Research Institute, University of Sydney, Australia, [2]Bone Research Program, ANZAC Research Institute, The University of Sydney, Australia, [3]Humboldt University, Germany, [4]University of Sydney, Australia

In patients with metastatic breast cancer, high circulating interleukin-6 (IL-6) levels are associated with disease progression and poor prognosis. We previously demonstrated in murine models of bone metastasis that increasing or decreasing bone resorption results in corresponding changes of tumor IL-6 expression and tumor progression, indicating that IL-6 may have a role in sustaining metastatic cancer growth in bone1. In the present study, we investigated the effect of blocking IL-6 receptor (IL-6R) signalling on cancer growth in a murine xenograft model, using either the anti-human IL-6R antibody, tocilizumab (Tmab), or the anti-mouse IL-6R antibody, MR16-1.

Five week-old BALB/c nu/nu female mice were inoculated with 50,000 cells each of the human breast cancer cell line, MDA-MB-231, via intra-tibial injection. Tibiae were monitored by x-ray imaging on days 10, 17 and 21 (sacrifice), followed by histological and histomorphometric analysis, including proliferation index, TUNEL staining for apoptosis, and TRAcP staining for osteoclast activity.

In a dose finding study, mice were randomized into 7 groups (n=3 each), receiving Tmab or MR16-1 at doses of 20mg/kg, 50mg/kg and 100mg/kg i.p. every 3 days, or vehicle. The inhibitory effect on cancer growth in bone was most pronounced at a dose of 50mg/kg/3d for Tmab, and 100mg/kg/3d for MR16-1, as assessed by x-ray quantification of osteolytic areas on days 10, 17 and 21, histological measurement of total tumor area, tumor proliferation index and tumor apoptosis rate on day 21.

Further experiments with larger group numbers (n=8) established that both Tmab and MR16-1 were able to inhibit osteolysis on day 10, 17 and 21 ($p=0.066$ for MR16-1 on day 21; $p<0.05$ for all other groups and time points, compared to controls).

The anti-mouse IL-6R antibody, MR16-1, inhibits endogenous IL-6 signalling in the host cell, whereas the anti-human IL-6R antibody, Tmab, not only blocks tumor-induced IL-6 activity, but also affects tumor derived IL-6 which acts on the murine IL-6R as well. Of note, we observed similar effects on tumor progression in bone for treatment with Tmab and MR16-1, suggesting that IL-6 affects tumor progression regardless of species origin. Our data indicate that IL-6 plays an important role in bone metastatic growth and may be a potential treatment target in breast cancer.

Reference

1. Zheng *et al., J Bone Miner Res* 24 (Suppl 1), (2009).

***Disclosures: Yu Zheng**, None.*

FR0135

Activation of Notch Signaling Contributes to the Pathogenesis of Osteoma and Osteosarcoma with a Mouse Model. Jianning Tao*, Shan Chen, Ming ming Jiang, Terry Bertin, Francis Gannon, Brendan Lee. Baylor College of Medicine, USA

Human osteosarcoma (OS) is the most common primary bone cancer, comprising approximately 20% of all bone tumors and about 5% of pediatric tumors overall. Most OS occurs sporadically and our understanding of its molecular basis is still limited. From a signaling perspective, dysregulation of several evolutionally conserved pathways including Wnt, TGF/ BMPs, SHH and FGFs has been found in human OS tumor samples and cell lines. Recently, our and other studies suggest that activation of Notch signaling contributes to the pathogenesis of human OS. Notch signaling plays an important role in the developmental processes and adult tissue homeostasis by regulating cell fate determination, proliferation, differentiation and apoptosis. Notch, a transmembrane receptor, releases its intracellular domain (NICD) into the nucleus to regulate transcription of target genes such as the Hey and Hes family of transcription factors. Altered Notch signaling has been associated with several cancers in which the data suggest that Notch can act both as an oncogene and tumor suppressor gene depending on its expression levels and timing. Our previously established human tumor xenografts in nude mice showed decreased tumor growth after chemical or genetic inhibition of Notch signaling, suggesting that its inhibition may be a therapeutic approach for the treatment of OS. To generate a mouse osteosarcoma model and examine the role of Notch signaling in bone tumorigenesis, we established a bitransgenic mouse line that constitutively expressed a single copy of Notch NICD in osteoblasts. The resulting bitransgenic Notch gain-of-function (GOF) mice developed osteosclerosis at age of two months. Histomorphometric and molecular analysis of cavarial and long bones indicated that Notch could stimulate proliferation of immature osteoblasts while inhibiting their differentiation into mature

osteoblasts. This gain of function phenotype was reminiscent of osteoblastic tumors. Indeed, aging studies of these GOF mice showed that they spontaneously developed osteoma at 100% penetrance. Of 24 aged mice to date, we have detected multifocal malignant tumors in six of them by gross examination. Pathological analysis confirmed that one of them was telangiectatic osteosarcoma, featured by poorly differentiated osteoblast-like cells, tumor osteoid, necrosis and hemorrhage. Together, our preliminary data support our hypothesis that Notch activation may be a dominant mechanism for OS pathogenesis.

***Disclosures: Jianning Tao**, None.*

FR0136

Bone Remodeling Regulated by ARF is a Therapuetic Target for Prevention of Osteosarcoma. Michelle Hurchla*[1], Dan Rauch[2], John Harding[2], Hongju Deng[2], Lauren Shea[2], Mark Eagleton[2], Stefan Niewiesk[3], Michael Lairmore[3], David Piwnica-Worms[2], Thomas Rosol[4], Jason Weber[2], Lee Ratner[2], Katherine Weilbaecher[5]. [1]Washington University in St. Louis, USA, [2]Washington University School of Medicine, USA, [3]Ohio State University, USA, [4]The Ohio State University, USA, [5]Washington University in St. Louis School of Medicine, USA

The ARF tumor suppressor is a critical regulator of ribosomal biogenesis and p53-dependent cell cycle arrest and apoptosis. We have reported that Arf-/- mice have hyperactive osteoclasts (OC). Surprisingly, microCT analysis showed that trabecular bone volume was significantly increased in Arf-/- mice. Further examination revealed that osteoblast (OB) function was also enhanced, resulting in a high bone turnover state with a net increase in bone formation. The in vivo bone formation rate and serum osteocalcin levels of Arf-/- mice were significantly higher than those of Arf+/+. In vitro, we observed significant increases in the progenitor number, proliferation, differentiation and mineralization of OB from Arf-/- mice. We have previously shown that malignancies induced by Tax, an HTLV-1 oncogene, cause the expression of bone-tropic factors that enhance tumor growth. We hypothesized that the increased rate of bone remodeling in Arf-/- mice would facilitate malignant transformation by Tax. Crossing Tax+ and Arf-/- mice resulted in the spontaneous development of osteosarcomas in 100% of the Tax+Arf-/- animals by 7 months of age. Osteosarcoma (OS), characterized by neoplastic bone-forming OB, is the most prevalent form of primary bone cancer. Pathologically, Tax+Arf-/- tumors were well-differentiated OS characterized by abundant woven bone formation and increased OC recruitment. Cell lines established from these tumors consist of a heterogeneous mixture of alkaline phosphatase (ALP)-positive cuboidal OB and ALP-negative fibroblast-like cells. These cell lines express mature OB markers, have the ability to form mineralized nodules in vitro, and grow progressively when transplanted into immunocompromised mice. In addition to mutations or inactivation of ARF, deregulation of the tumor suppressors p53 and Rb and amplification of c-myc are common in human OS. We demonstrate that similar alterations in these pathways are present in Tax+Arf-/- OS. We hypothesized that uncoupling OB and OC would inhibit the high bone remodeling present in Tax+Arf-/- mice and lessen malignant transformation of OB. Treating Tax+Arf-/- mice with the bisphosphonate OC inhibitor zoledronic acid weekly from 1 to 9 months of age prevented or delayed the onset of OS. This discovery reveals an important role for bone remodeling in osteosarcoma and implicates OC-inhibition and bisphosphonates as novel therapeutics for targeted prevention or treatment of OS.

***Disclosures: Michelle Hurchla**, None.*

FR0138

Disruption of Prostaglandin E Biosynthesis and Its Receptor EP4 Attenuated Angiogenesis, Tumor Growth and Bone Metastasis of Cancer. Morichika Takita[1], Satoshi Yokoyama[1], Masaki Inada*[2], Chisato Miyaura[1]. [1]Tokyo University of Agriculture & Technology, Japan, [2]Toyko University of Agriculture & Technology, Japan

Bone metastasis of cancer is accompanied by severe bone destruction with increased bone resorption. We recently found that prostaglandin E (PGE) biosynthesis in bone is mediated by an inducible PGE synthase, membrane-bound PGE synthase-1 (mPGES-1), and PGE production is closely related to the growth and bone metastasis of cancer. In fact, tumor growth and bone metastasis are markedly attenuated in the mice lacking mPGES-1 after injection of malignant melanoma B16 cells. Metastasized tumor is frequently associated with neo-vascularization in various tissues. In this study, we investigate the roles of PGE2 and its receptor EP4 in tumor associated neo-vascularization using mPGES-1-null (mPGES-/-) mice and EP4-null (EP4-/-) mice. When B16 cells were implanted subcutaneously into C57BL/6 wild-type (WT) mice, B16 cells grew rapidly to form solid tumor with angiogenesis. In mPGES-/- mice, however, the tumor volume of B16 was markedly reduced compared with WT mice. Angiogenesis associated with B16 growth was also decreased in mPGES-/- mice. Using the quantitative models of in vivo laser imaging for neo-vascularization, a red fluorescent labeled PEG particle was injected to WT and mPGES-/- mice. In WT mice, neo-vascularization around solid B16 tumor was obviously, but the signal was decreased in mPGES-/- mice. To clear the source cells of PGE2 and angiogenic factors, dermal fibroblasts were obtained from WT and mPGES-/-, and co-cultured with fixed-B16 cells. Production of PGE2 was markedly increased in the conditioned medium from WT fibroblast culture, while dermal fibroblasts from mPGES-/- mice produced negligible amounts of PGE2. Dermal fibroblasts obtained from WT produced vascular endothelial cell growth factor (VEGF)-A and basic fibroblast growth factor (bFGF), and the levels was elevated by adding PGE2. On the other hand, the levels of VEGF-A and bFGF in the conditioned medium were quite low in the culture of dermal fibroblasts collected from mPGES-/- mice. In EP4-/- mice, solid tumor growth and angiogenesis of B16 were markedly attenuated in vivo, and dermal fibroblasts from EP4-/- mice produced only negligible levels of VEGF-A and bFGF. These results suggest that PGE2 produced by host stromal cells elicits the production of VEGF-A and bFGF by fibroblasts via EP4-mediated pathway to induce endothelial angiogenesis and progression of tumor growth.

***Disclosures: Masaki Inada**, None.*

FR0140

Frequent Attenuation of Tumor Suppressor WWOX in Osteosarcomas is Associated With Increased Tumorigenicity and Elevated RUNX2 Levels. Sara Del Mare*[1], Kyle Kurek[2], Zaidoun Salah[1], Suhaib Abdeen[1], Eugenio Gaudio[3], Nicola Zanesi[3], Hussain Sadiq[4], Matthew Warman[5], Gary Stein[6], Janet Stein[4], Jane Lian[6], Rami Aqeilan[7]. [1]The Lautenberg Center for Immunology & Cancer Research, Hebrew University-Hadassah Medical School, Israel, [2]Children's Hospital Boston Department of Pathology, USA, [3]Department of Molecular Virology, Immunology & Medical Genetics, Comprehensive Cancer Center, Ohio State University, USA, [4]Department of Cell Biology, University of Massachusetts Medical School, USA, [5]Department of Orthopaedic Surgery, Howard Hughes Medical Institute, Children's Hospital Boston & Harvard Medical School, USA, [6]University of Massachusetts Medical School, USA, [7]Ohio State University, USA

The WW domain-containing oxidoreductase (*WWOX*) is a *bona fide* tumor suppressor gene that is reduced or absent in most common human malignancies. We recently demonstrated that the short-lived *Wwox*-deficient mice develop periosteal osteosarcomas (OS) and display defects in bone formation. OS are highly aggressive primary bone tumors that commonly affect young patients and frequently metastasize to the lungs, imparting a poor prognosis. Molecular mechanisms underlying OS formation are far from being fully understood. To further investigate the etiology of this aggressive disease and develop new therapeutic targets, we determined expression and tumor suppressor function of WWOX in human OS to shed light on the molecular and signaling pathways in which it is involved. Our analysis revealed that the majority (4/6) of human OS cell lines displayed reduced WWOX expression as assessed by real-time PCR and Western blot analyses. Ectopic expression of WWOX in human OS cell lines having reduced WWOX expression, inhibited proliferation and attenuated invasion *in vitro*, and suppressed tumorgenicity in nude mice. Expression of WWOX was associated with reduced RUNX2 expression in OS cells, whereas RUNX2 levels were elevated in femurs of *Wwox*-deficient mice with accompanying OS formation. Furthermore, we demonstrated that WWOX reconstitution in HOS metastatic OS cells was associated with downregulation of RUNX2 levels and RUNX2 target genes, consistent with the ability of WWOX to suppress RUNX2 transactivation activity. These data are consistent with the observation that WWOX expression is attenuated in the majority of human OS specimens and is associated with aberrant RUNX2 levels. Together, our findings strengthen the evidence of a tumor suppressor role for WWOX in OS and suggest that it is mediated, at least in part, by regulation of RUNX2 levels.

***Disclosures: Sara Del Mare**, None.*

FR0146

Calcitonin Lowers Serum FGF23 Levels in Patients with X-linked Hypophosphatemia. Eva Liu*, Thomas Carpenter, Caren Gundberg, Karl Insogna. Yale University School of Medicine, USA

In X-linked hypophosphatemia (XLH), elevated circulating levels of FGF23 result in renal phosphate wasting and suppression of proximal renal tubular 1-alpha hydroxylase activity. For the past 30 years the cornerstone of medical therapy for XLH has been calcitriol and supplemental phosphorus. However, calcitriol stimulates production of FGF23, which is not desirable. Calcitonin (CT) has been reported to increase circulating levels of $1,25(OH)_2$ D in XLH but whether it affects FGF23 levels is not known. We therefore administered a single, intradermal dose of salmon CT (200 MRC units) to seven subjects with XLH and six normal controls and measured serum FGF23, $1,25(OH)_2$ D and indicies of mineral homeostasis at baseline and serially over the next 24 hrs. Data were analyzed using repeated measures 1-way ANOVA and 2-way ANOVA. In subjects with XLH, CT significantly and rapidly reduced serum FGF23 to a mean value that was $77 \pm 7\%$ of baseline by 4 hours post injection (66 ± 5 pg/mL $\rightarrow$ 52 ± 8 pg/mL; p=0.0002). This decrease was sustained for the next 16 hours. In control subjects, FGF23 did not change significantly following treatment (p=0.16). By 2-way ANOVA, the effect of CT on serum FGF23 was significantly different when subjects with XLH were compared to controls (p=0.01). The decline in FGF23 in subjects with XLH was accompanied by a significant increase in serum $1,25(OH)_2$ D

(45 ± 3 pg/mL $\rightarrow$ 69 ± 5 pg/mL; p=0.0005). There was a comparable increase in $1,25(OH)_2$ D in control subjects and by 2-way ANOVA the response was not different in the two groups (p=0.15). In XLH patients, there was an increase in serum phosphate and the renal phosphate threshold (TmP/GFR) following treatment with CT that was maximal at 10 hours post injection (p=0.0003) while normal subjects had a fall in both these parameters, first noted at 10 hours (p=<0.0001). These results indicate that CT differentially regulates FGF23 in patients with XLH as compared to normal individuals. The rise in $1,25(OH)_2$ D levels in XLH could be due to the known effect of CT to augment proximal renal tubular production of the hormone as well as due to the fall in FGF23. The suppression of FGF23 levels in patients with XLH suggests that CT may be a promising new therapeutic agent for this disease.

***Disclosures: Eva Liu**, None.*

FR0153

***Runx2* haploinsufficiency rescues the craniosynostosis phenotype of *Axin2*-knockout mice.** Meghan McGee-Lawrence*[1], David Razidlo[1], Frank Secreto[1], Xiaodong Li[1], Wei Hsu[2], Jane Lian[3], Jennifer Westendorf[1]. [1]Mayo Clinic, USA, [2]University of Rochester Medical Center, USA, [3]University of Massachusetts Medical School, USA

Runx2 and Axin2 regulate craniofacial development and skeletal maintenance. Deletion of either *Axin2* or *Runx2* causes opposing craniofacial phenotypes in mice: *Runx2* haploinsufficient mice develop cleidocranial dysplasia (CCD) and $Axin2^{-/-}$ mice develop craniosynostosis (CS). We recently showed that Axin2 levels are elevated in $Runx2^{-/-}$ calvarial cells and that Runx2 represses the *Axin2* promoter, suggesting a direct relationship between these two factors *in vivo*. The goal of the current study was to elucidate the molecular interactions between Axin2 and Runx2 and to explore their cooperative effects *in vivo*.

Axin2 is a negative feedback inhibitor of canonical Wnt/beta-catenin signaling. Runx2 represses *Axin2* transcription and its DNA binding domain is necessary for this regulation. In this project, we identified four putative Runx2 binding elements in the *Axin2* promoter and determined that Runx2 specifically bound these sites in gel shift assays. In chromatin immunoprecipitation (ChIP) assays performed on lysates from MC3T3 cells, Runx2 bound *Axin2* promoter regions containing Runx2 binding sites identified in the gel shift experiments. Association of Runx2 with regions of the *Axin2* promoter containing these sites was enriched 5- to 6-fold as compared to a downstream region lacking a Runx2 binding site. Runx2-mediated repression of *Axin2* transcription was blocked by addition of a histone deacetylase (Hdac) inhibitor, trichostatin A. Hdac3 associated with *Axin2* promoter fragments containing Runx2 binding elements in ChIP assays and repressed the *Axin2* promoter. These data suggest that Runx2 and Hdac3 regulate *Axin2 in vivo*.

To determine if Axin2 and Runx2 are components of the same molecular pathway, we mated $Runx2^{+/-}$ and $Axin2^{-/-}$ mice to generate double-mutant $Axin2^{-/-}$:$Runx2^{+/-}$ mice. CS was assessed in skulls of 4 week-old male mice by measuring skull length (nose tip to coronal suture) following microCT (Fig 1). Similar to previous studies, *Axin2* deficiency reduced skull length (-17%) as compared to wildtype animals. Skull lengths were similar in $Runx2^{+/-}$ and wildtype mice. Interestingly, $Axin2^{-/-}$:$Runx2^{+/-}$ mice had skulls that were 10% longer than $Axin2^{-/-}$ mice and were comparable in length to wildtype and $Runx2^{+/-}$ mice. These data indicate that *Runx2* haploinsufficiency rescues the CS phenotype in $Axin2^{-/-}$ mice. Together our data suggest that Runx2 directly regulates *Axin2* expression and is required for enhanced calvarial bone formation in $Axin2^{-/-}$ mice.

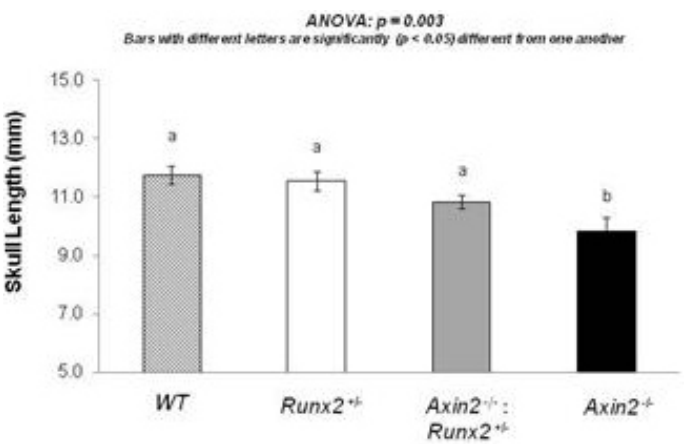

Figure 1: Skull length in 4 wk old male mice

***Disclosures: Meghan McGee-Lawrence**, None.*

FR0154

Age-dependent Arthropathy in Circadian Mutant Mice. Elizabeth Yu*, Sadiq Hussain, Robert Dallmann, Stacey Russell, Jane Lian, David Weaver. University of Massachusetts Medical School, USA

The purpose of this study is to investigate an age-dependent arthropathy observed in circadian mutant mice. In the circadian oscillator, CLOCK and NPAS2 form heterodimers with BMAL1 to drive rhythmic expression of genes that regulate physiology and behavior. $Clock^{-/-};Npas2^{m/m}$ mutant mice lack circadian rhythms. These mice also exhibit progressive arthropathy. To study this arthropathy, $Clock^{-/-};Npas2^{m/m}$ mutant and wild-type mice were subjected to X-ray, micro-computed tomography (micro-CT), and histological analysis to characterize the age of onset, progression, and anatomical distribution of this arthropathy. $Clock^{-/-};Npas2^{m/m}$ mice exhibit site-specific, age-dependent calcification of calcaneal tendon and costosternal junction tissue. These calcifications are detectable by X-ray and micro-CT by 11-12 weeks of age and by histology as early as 6-7 weeks of age. Calcifications enlarge over time and by 40 weeks of age, $Clock^{-/-};Npas2^{m/m}$ mutant mice exhibit extensive calcification of the calcaneal tendon and costosternal junction tissue. These findings are similar to those reported in another arrhythmic circadian mutant mouse, the $Bmal1^{-/-}$ null mouse (Bunger et al., Genesis. 41:122, 2005). $Clock^{-/-};Npas2^{m/m}$ calcaneal tendon and costosternal junction tissue samples are also being analyzed at the age of onset of disease using immunohistochemistry to identify cell types present in those tissues as calcifications begin to form. RNA is additionally being extracted from affected tissues at the age of disease onset to study changes in gene expression between $Clock^{-/-};Npas2^{m/m}$ and wild-type tissues.

From these data we conclude that $Clock^{-/-};Npas2^{m/m}$ and $Bmal1^{-/-}$ mutant mice exhibit similar arthropathy phenotypes. Due to their roles as transcription factor heterodimers in the circadian oscillator, we hypothesize that CLOCK:BMAL1 and NPAS2:BMAL1 heterodimers drive the expression of one or more genes that prevent age-dependent arthropathy.

***Disclosures: Elizabeth Yu**, None.*

FR0155

Conditional Deletion of SKI-1 Using 3.6kb COL1-Cre Leads to Vertebral Fusions, Hind Limb Paralysis, and Impaired Lower Limb Development. Jeffrey Gorski*[1], Nichole Huffman[2], Qian Chen[2], Sarah Dallas[2], Paul Trainor[3], Nabil G. Seidah[4]. [1]University of Missouri, Kansas City, School of Dentistry, USA, [2]University of Missouri - Kansas City, USA, [3]Stowers Institute of Medical Research, USA, [4]Laboratory of Biochemical Neuroendocrinology, IRCM, Canada

Proprotein convertase SKI-1 (subtilisin kexin isozyme1/site-1) activates transmembrane transcription factor precursors including SREBP-1 and -2, CREB-H, OASIS, and ATF-6, facilitating their import into the nucleus. Since the latter three factors have been shown to be required for normal bone formation and the SKI-1 knockout is embryonic lethal, we sought to investigate the skeletal function of SKI-1 by producing a bone-restricted knockout (cKO). Floxed SKI-1 mice were bred with transgenic mice expressing the rat 3.6 COL1 Cre transgene. The cKO [genotype $SKI\text{-}1^{f/f}$:$Cre^{+/-}$] newborns, representing 7% of live births, were paralyzed with severely under-developed lower limbs with reduced musculature and a short curly tail. Ten day old mice were euthanized when average weights of cKO and controls [control genotypes $SKI\text{-}1^{f/f}$:$Cre^{-/-}$; $SKI\text{-}1^{f/+}$:$Cre^{+/-}$; or $SKI\text{-}1^{f/+}$:$Cre^{-/-}$] were 3.8 +/- 0.8 gm and 6.4 +/- 1.6 gm (p=0.025), respectively. MicroCT scans showed that cKO mice exhibited fused lumbar vertebrae, but the central spinal canal remained open. ROSA26 mice were bred with 3.6 COL1 Cre mice to determine the embryonic expression pattern of the Cre transgene. Histological analyses for β-galactosidase (LacZ) revealed a gradient of expression at embryonic day E11.5 with strongest expression occurring distally in the developing spinal column. This region corresponds to where vertebral fusions were observed in cKO newborns. LacZ was expressed in the mantle layer surrounding the neural tube and in discrete cells within the ventricular zone. At this time during spinal column development, neural and cartilage cell precursors at these locations are actively proliferating and differentiating. We have shown elsewhere that SKI-1 is required for mineralization of osteoblastic cultures where it regulates transcription of *fibronectin, Phex, Dmp1, COL1A1* and *COL1A2* by activating transmembrane transcription factor precursors. Our data identify SKI-1 as a major developmental regulator of the spine and lower limbs. The presence of the phenotype at birth and the developmental expression pattern of the Cre transgene suggest that vertebral defects are patterned embryonically during somite segmentation, potentially through altered expression of matrix proteins fibronectin and collagen. SKI-1 deficient mice represent a novel model for mechanistic studies of birth defects altering the coordinated development of the spinal column with the nerves, muscle and cartilage/bone of the lower limbs.

***Disclosures: Jeffrey Gorski**, None.*

FR0161

Molecular Mechanism of the ACVR1^{R206H} Mutation of Fibrodysplasia Ossificans Progressiva. Kyung Woo[1], Hyun-Mo Ryoo[2], Ginah Song*[3], Hyun-Jung Kim[4], Jeong-Hwa Baek[5]. [1]Seoul National University, School of Dentistry, Korea, [2]Seoul National University, School of Dentistry, South korea, [3]Seoul National Univ. School of Dentistry, South korea, [4]BioRunx Co Ltd, South korea, [5]Seoul National University School of Dentistry, South korea

Fibrodysplasia ossificans progressiva (FOP), a rare genetic and catastrophic disorder characterized by progressive heterotopic ossification, is caused by a point mutation, c.617G>A; p.R206H, in the activin A receptor type 1 (ACVR1) gene, one of the bone morphogenetic protein type I receptors (BMPR-Is). Although hyperactivated BMP signaling has been suggested to explain the pathogenesis, the molecular consequences of this mutation are still unknown. Here we studied the impact of ACVR1 R206H mutation on BMP signaling, its downstream signaling cascades and protein expression level in murine myogenic C2C12 cells and human embryonic kidney (HEK) 293 cells. We found that ACVR1 was the most abundant of the BMPR-Is expressed in mesenchymal cells but its contribution to osteogenic BMP signal transduction was minor. The R206H mutant caused weak activation of the BMP signaling pathway, unlike the Q207D mutant, a strong and constitutively active form. The R206H mutant showed a decreased binding affinity for FKBP1A/FKBP12, a known safeguard molecule against the leakage of transforming growth factor (TGF)-β or BMP signaling. The decreased binding affinity of FKBP1A to the mutant R206H ACVR1 resulted in leaky activation of the BMP signal, and moreover, it decreased steady-state R206H ACVR1 protein levels. Interestingly, while WT ACVR1 and FKBP1A were broadly distributed in plasma membrane and cytoplasm without BMP-2 stimulation and then localized in plasma membrane after BMP-2 stimulation, R206H ACVR1 and FKBP1A were mainly distributed in plasma membrane regardless of BMP-2 stimulation. The impaired binding to FKBP1A and translocalization to plasma membrane related with altered receptor internalization by R206H ACVR1 mutation may result in mild hyperactivation of BMP-signaling in extraskeletal sites such as muscle, which lead to progressive ectopic bone formation in FOP patients.

***Disclosures: Ginah Song**, None.*

FR0176

Gremlin is Required for Normal Skeletal Development, but Postnatally it Suppresses Bone Formation. Anna Smerdel-Ramoya[1], Stefano Zanotti[2], Ernesto Canalis*[1]. [1]St. Francis Hospital & Medical Center, USA, [2]Saint Francis Hospital & Medical Center, USA

Bone morphogenetic proteins (BMPs) play a central role in the regulation of bone formation. BMP activity is controlled by secreted BMP antagonists, such as gremlin and noggin, which bind and prevent BMP signaling. The patterning of distal limb skeletal elements is tightly regulated by the reciprocal interactions between BMPs, fibroblast growth factors (FGF) and Sonic hedgehog (SHH). By inhibiting BMP action, gremlin allows for FGF and SHH expression and for proper limb patterning and development. Null mutations of *Gremlin1* (*Grem1*) in mice result in serious developmental abnormalities, leading to newborn lethality. We demonstrated that transgenics overexpressing gremlin under the control of the osteocalcin promoter exhibit decreased bone formation leading to osteopenia and fractures. In contrast, conditional inactivation of *Grem1* in osteoblasts leads to a transient increase in bone formation and bone mass. Recently, we observed that mice carrying the global deletion of *Grem1* in a mixed genetic background (C57BL/6/FVB) survived, allowing for the study of the consequences of the *Grem1* inactivation from development to adulthood. *Grem1* null mice were smaller than littermate controls, and contact radiography revealed a single bone in both forelimbs and hindlimbs. In accordance with the role of gremlin in skeletal development, bone mineral density and bone histomorphometry of the femur revealed osteopenia at 1 month of age in *Grem1* null mice, secondary to decreased trabecular number, without sex distinction. Osteoblast and osteoclast cell number were not altered, but in accordance with the inhibitory effect of gremlin on BMP activity, bone formation was increased leading to a recovery of bone mass in older animals. Therefore, despite their smaller size the osteopenia was reversed at 3 and 6 months of age in *Grem1* null mice. Osteoblast cell cultures from *Grem1* null mice revealed sensitization to the actions of BMP-2 so that BMP had a greater effect on alkaline phosphatase expression and activity and mineralized nodule formation in *Grem1* null cells. Interestingly, noggin expression was increased, suggesting that it may act as a compensatory mechanism in the absence of gremlin. In conclusion, gremlin plays a critical role in limb development, but by opposing BMP activity gremlin decreases bone formation and when in excess it causes osteopenia.

***Disclosures: Ernesto Canalis**, None.*

FR0177

Loss of Bmp2 Impairs Appositional Growth in the Endochondral Skeleton. Luciane Capelo*, Karen Cox, Vicki Rosen. Harvard School of Dental Medicine, USA

Removal of Bmp2 from the early limb has catastrophic consequences on the adult skeleton where bones lacking Bmp2 undergo spontaneous fractures that are not able to heal (Bmp2fl/fl; Prx1::Cre mice). The failure of fracture healing observed in these mice is a direct result of the absence of Bmp2 expression in the periosteum. However, the cause of the spontaneous fractures is unknown. Gross examination of Bmp2fl/fl; Prx1::Cre bones determined they were similar in length to bones of wt mice but greatly reduced in width. As appositional bone growth is controlled by the periosteum, we hypothesized that loss of periosteal Bmp2 expression impairs appositional bone growth in the endochondral skeleton. We focused our attention on mice from birth (NB) to 23 weeks of age. Morphological analysis of Bmp2fl/fl; Prx1::Cre mice showed that the width/length ratio is abnormal in the fore and hind limbs in all ages studied. NB mice exhibit a 20% reduction in cross sectional area at midshaft of radius and ulna in comparison to control mice. At 2 weeks of age, a 50% reduction is observed in cross sectional area at midshaft of the same bones. This difference is maintained over time and is also observed in the hind limb so that by 9 weeks, femurs lacking Bmp2 are half of the width of control mice whereas bone length does not differ significantly between groups. These data suggest that as bones lacking periosteal Bmp2 grow in length but not in width, they become unstable and subsequently fracture. Our data identify a unique role for Bmp2 as a physiological regulator of appositional bone formation during bone growth and also point to a role for Bmp signaling in maintaining bone width proportional to bone length in order to preserve bone strength during growth and aging.

Fig. 1. Morphology of the forelimb of wild-type (control) and Bmp2 deficient mice (Bmp2fl/fl;Prx1::Cre). Dashed lines in the x-rays on the left identify the area of cross sections presented in the right panels.

Morphology of the forelimb of wild-type and Bmp2 deficient mice.

***Disclosures: Luciane Capelo**, None.*

FR0178

A Local Application of Recombinant Human Fibroblast Growth Factor-2 for Tibial Shaft Fractures: A Randomized, Double-Blind, Placebo-Controlled Trial. Hiroshi Kawaguchi*[1], Hiroyuki Oka[2], Seiya Jingushi[3], Toshihiro Izumi[4], Masao Fukunaga[5], Katsumi Sato[6], Takashi Matsushita[7], Kozo Nakamura[8]. [1]University of Tokyo, Faculty of Medicine, Japan, [2]University of Tokyo, Japan, [3]Kyushu Rosai Hospital, Japan, [4]Saihaku Hospital, Japan, [5]Kawasaki Medical School, Japan, [6]Tohoku Rosai Hospital, Japan, [7]Teikyo University, Japan, [8]The University of Tokyo, Japan

Development of synthetic materials is desired to prevent delayed union of bone fractures. Our series of animal studies have shown that a local application of fibroblast growth factor-2 (FGF-2) accelerates fracture healing through its mitogenic activity on mesenchymal cells, and our recent dose-escalation trial has revealed a dose-dependent effect of recombinant human FGF-2 (rhFGF-2; 0.2, 0.4, and 0.8 mg) in a gelatin hydrogel on bone union of patients with surgical osteotomy. Based on these results, we performed a randomized, double-blind, placebo-controlled trial in which patients with fresh and closed tibial shaft fractures of transverse or short oblique type were randomly assigned to three groups receiving a single injection of the gelatin hydrogel containing either 0 (placebo: P), 0.8 mg (low-dosage: L), or 2.4 mg (high-dosage: H) of rhFGF-2 into the fracture gap at the end of an intramedullary nailing surgery. The primary outcome was the time to bone union determined by extracortical bridging calluses on radiographs during 24 weeks. The sample size was calculated to be 23 per group having 90% power to show at least 20% advantage of the agent. Of 194 patients who visited 48 institutions for two years, 85 met the eligibility criteria, and 70 (24 in P, 23 each in L and H groups) completed the study. None of the baseline patient variables was significantly different among the three groups ($p>0.05$). The cumulative percentages of patients with bone union were higher in the rhFGF-2 treated groups ($p=0.031$ and 0.009 in L and H groups, respectively) than in the P group, although there was no significant difference between L and H groups

(p=0.776). The Cox proportional-hazards model showed that rhFGF-2 treatment, but not any of the baseline variables, was the sole significant factor for bone union (hazard ratio=1.94 and 1.85 in L and H groups, respectively). At 24 weeks, 4, 1 and 0 patients in P, L, and H groups, respectively, remained delayed union. The percentage of patients who achieved full-weight bearing without pain showed a tendency to be higher in the rhFGF-2-treated groups, although not statistically significant. There was no significant difference in the profiles of adverse events among the three groups, all of which had recovered before 24 weeks. In conclusion, a local application of the rhFGF-2 hydrogel accelerated healing of tibial shaft fractures with a safety profile. The optimum concentration of rhFGF-2 for clinical use may be around 0.8 mg.

***Disclosures: Hiroshi Kawaguchi**, None.*
This study received funding from: Kaken Pharmaceutical Co. Ltd.

FR0179

Activation of the Kynurenine Pathway of Tryptophan Degradation Plays a Role in Osteoblastogenesis. Wei Li[1], Christopher Vidal*[1], Ralph Nanan[1], Brigitte Nanan[1], Gustavo Duque[2]. [1]Sydney Medical School-Nepean, The University of Sydney, Australia, [2]University of Sydney, Australia

Recent reports suggest that pharmacological inhibition of gut-derived serotonin (GDS), an end product of tryptophan degradation, is a potential bone anabolic treatment for osteoporosis. Since tryptophan degradation may play an important role in bone cells differentiation, in this study, we tested whether other alternative pathways for tryptophan degradation play a role in bone formation. To test our hypothesis, we selected interferon gamma (IFNγ) due to its potent anabolic effect on bone, its well known inhibitory effect on serotonin release and its stimulatory effect on tryptophan degradation in immune and cancer cell models. Human mesenchymal stem cells (MSC) were treated for one week with osteoblastogenesis induction media containing either IFNγ(1,10 and 100 nM) or vehicle alone. Undifferentiating MSC, Jurkat cells and human T lymphocytes were treated under the same conditions. Microarray analysis (Affymetrix), real time PCR, western blots and osteoblastogenesis assays (alizarin red, alkaline phosphatase) were performed. Microarray and real time PCR analysis showed a significant upregulation of the gene of indoleamine 2,3-dioxygenase (IDO), the initial enzyme in the kynurenine pathway of tryptophan degradation, in MSC under osteogenic conditions as compared with the non-differentiating cell types ($p<0.001$). Furthermore,whereas IFNγ treatment increased IDO expression in immune cells (2 fold), IDO expression was not significantly increased by IFNγ treatment in undifferentiating MSC. In addition, the induction of IDO in osteogenic conditions was significantly higher (9 fold) in the osteogenic differentiating MSC treated with an anabolic dose of IFNγ(100 nM)as compared with the untreated osteogenic differentiating MSC (4 fold) ($p<0.001$). This higher induction of IDO was associated with earlier and higher osteoblastogenesis. Finally, no changes in the serotonin synthesis pathway genes, including tryptophan hydroxylase, were identified in any of the cell conditions. In summary, in this study we have identified that tryptophan degradation through the kynurenine pathway is exclusively activated in MSC during osteogenic conditions. The anabolic effect of IFNγ on bone could be partially explained by the very potent stimulatory effect of IFNγ on IDO activity. In conclusion, activation of the kynurenine pathway could constitute a novel anabolic therapy for osteoporosis in the future.

***Disclosures: Christopher Vidal**, None.*

FR0180

Deficiency of Chemokine Receptor CCR1 Causes Osteopenia Due to Impaired Functions of Osteoclasts and Osteoblasts. Tadahiro Iimura[1], Akiyoshi Hoshino*[2], Akira Yamaguchi[1]. [1]Tokyo Medical & Dental University, Japan, [2]National Center for Global Health & Medicine, Japan

Chemokines are characterized by the homing activity of leukocytes to targeted inflammation sites. Recent research indicates that chemokines play more divergent roles in various phases of pathogenesis as well as immune reactions. A chemokine receptor, CCR1, and its ligands are thought to be involved in inflammatory bone destruction, but their physiological roles in the bone metabolism in vivo have not yet been elucidated. In this study, we investigated the roles of CCR1 in bone metabolism using CCR1-deficient mice. *Ccr1*$^{-/-}$ mice have fewer and thinner trabecular bones and low mineral bone density in cancellous bones. The lack of CCR1 affects the differentiation and function of osteoblasts. *Runx2*, *osteopontin*, and *osteonectin* were significantly upregulated in *Ccr1*$^{-/-}$ mice despite sustained expression of *osterix* and reduced expression of *osteocalcin*, suggesting less potency to differentiate mature osteoblasts. In addition, mineralized nodule formation was remarkably disrupted in cultured osteoblastic cells isolated from *Ccr1*$^{-/-}$ mice. Osteoclastogenesis induced from cultured *Ccr1*$^{-/-}$ bone marrow cells also decreased in number and size due to the abrogated cell-fusion. *Ccr1*$^{-/-}$ osteoclasts exerted no osteolytic activity concomitant with reduced expressions of *rank* and its downstream targets, implying that the defective osteoclastogenesis is involved in bone phenotype in *Ccr1*$^{-/-}$ mice. The co-culture of wild-type osteoclast precursors with *Ccr1*$^{-/-}$ osteoblasts failed to facilitate osteoclastogenesis. This result is most likely due to a reduction of the *rankl* expression. These observations suggest that the axis of CCR1 and its ligands are likely to be involved in crosstalk between osteoclasts and osteoblasts through modulating RANK-RANKL-mediated interaction.

***Disclosures: Akiyoshi Hoshino**, None.*

FR0183

Evidence that Osteoclast-derived Osteoactivin is a Novel Bone Coupling Factor: Transgenic Animal and In Vitro Studies. Matilda Sheng*[1], Jon Wergedal[2], Mehran Amoui[3], David Baylink[1], Subburaman Mohan[2], Kin-Hing William Lau[2]. [1]Loma Linda University, USA, [2]Jerry L. Pettis Memorial VA Medical Center, USA, [3]Jerry L. Pettis Mem. VAMC, USA

Our unpublished data suggest that osteoclast(Oc)-derived osteoactivin (OA) could function to couple bone resorption (BR) to bone formation (BF). To test this hypothesis, we first sought to define the effects of Oc-derived OA on BR. Oc produce an abundance of OA, a unique transmembrane protein. Our published in vitro studies indicate that Oc-derived OA stimulates BR activity of Oc. To confirm the effects of OA on BR in vivo, we generated a colony of transgenic (Tg) mice with targeted OA overexpression in cells of Oc lineage using a TRAP promoter. Marrow-derived Oc (md-Oc) of Tg mice showed ~2-fold increases (↑) in OA mRNA and protein ($p<0.05$ for each) compared to md-Oc of wild-type (WT) littermates. At 4 weeks old, Tg mice had significant ($p<0.05$) decrease (↓) in %bone (-21%) and ↑ in Oc # (+18%), %TRAP.PM (+28%), and Oc.BS (+34%). md-Oc of Tg mice were much larger (~2-fold) and had 2-fold ↑ in TRAP activity ($p<0.05$) than WT md-Oc. Resorption pits created by Tg md-Oc were also twice as large ($p<0.03$). Conversely, siRNA-mediated suppression of OA expression (by >60%) in RAW246.7-derived Oc reduced cell size (by 75%), cathepsin K and MMP9 expression (each by ~30%). To fulfill the requirements for a coupling factor (CF), Oc-derived OA should stimulate BF. In this regard, analyses of histomorphometric BF parameters of 8-week old male Tg mice revealed that Tg mice had a significantly ($p<0.05$ for each) ↑ in %TLS (~25%), MAR (~20%), and BF/BS (~25%) in cortical bone. Consistent with the literature that soluble OA is a stimulator of Ob differentiation, attached marrow cells of Tg mice showed >2-fold increase in bone nodule formation compared to WT controls. Condition medium (CM) of Tg md-Oc also produced ~2-fold ↑ on ALP activity of stromal cells compared with CM of WT md-Oc. Together our findings indicate that OA stimulates BR in vivo and in vitro and the OA derived from Oc stimulates BF both in vitro and in vivo, thereby fulfilling the definition of a CF. That the coupling of BF to BR is inherently complex process is supported by several types of evidence, including the fact that several CFs have been validly proposed. This study adds an additional CF candidate and thus places us one step closer to defining the signaling network necessary to understand this exceedingly important regulatory process which acts to promote the adequate structure and function of the skeleton and thereby prevent bone fragility diseases.

***Disclosures: Matilda Sheng**, None.*

FR0186

Muscle Derived Factors Influence the MLO-Y4 Osteocyte Response to Shear Stress. Nuria Lara*[1], Todd Hall[1], Letticia Brotto[1], Joedd Biggs[1], Cheng Lin Mo[1], Sandra Romero-Suarez[1], Marco Brotto[1], Lynda Bonewald[1], Mark Johnson[2]. [1]University of Missouri - Kansas City, USA, [2]University of Missouri, Kansas City Dental School, USA

Sarcopenia and osteoporosis normally manifest as twin diseases of the musculoskeletal system during aging and may be interdependent. We hypothesized that muscle secretory factors enhance the positive effects of physical loading of bone by muscle and that these factors decrease with aging. To begin to test this hypothesis, conditioned media from C2C12 muscle cells and from primary muscle was tested on the activation of the PI3K/Akt pathway in response to fluid flow shear stress (FFSS) in the MLO-Y4 osteocyte cell line. The PI3K/Akt pathway was chosen as it mediates the effects of both the prostaglandin and b-catenin pathways, known to be important in osteocyte signaling. Conditioned media (CM) was collected from C2C12 cells grown in growth media to induce myoblast formation and from C2C12 cells induced to differentiate into myotubes using differentiation media (2.5% horse serum) for 7 days. Intact muscles from 12 month old wildtype mice, extensor digitorum longus (EDL) and soleus (SOL), were dissected, mounted, stretched and electrically stimulated to produce maximal tetanic force and ½ maximal tetanic force using an intermittent stimulation protocol to produce CM from these muscles. All CM was added to MLO-Y4 media at 10% final concentration. MLO-Y4 cells were subjected to FFSS (2 dynes/cm^2) for 2 hours in the presence or absence of CM, the cells collected, and western blotting performed using antibodies against phospho-Akt, Akt and the endogenous control, GAPDH. Activation of the PI3K/Akt pathway in response to FFSS was significantly increased in the presence of myotube CM (2-3 fold) above myoblast CM or MLO-Y4 media. PI3K/Akt activation in the presence of EDL CM was enhanced 2-3 fold above that of SOL CM or control media. These data demonstrate that mature muscle cells release factors that affect the response of MLO-Y4 osteocytes to fluid flow shear stress and that EDL muscle produce greater amounts of these factors compared to SOL muscle. These data suggest that physical loading of bone by muscle may involve more than loading and that factors released by muscle cells may be able to condition and/or regulate the response of osteocytes to loading.

***Disclosures: Nuria Lara**, None.*

FR0188

Skeletal Phenotype of the Leptin Receptor-Deficient db/db Mouse. Garry Williams*[1], Karen Callon[2], Maureen Watson[2], Dorit Naot[2], Jessica Costa[2], Michelle Dickinson[2], Yaoyao Ding[2], Yu Wang[3], Ian Reid[2], Jillian Cornish[2]. [1]University of Auckland, Auckland School of Medicine, New zealand, [2]University of Auckland, New zealand, [3]Hong Kong University, Hong kong

Leptin is a major hormonal product of the adipocyte which regulates appetite and reproductive function through its hypothalamic receptors. It has now become clear that the skeleton has emerged as an important site of action of leptin. The signalling form of the leptin receptor has been found in several cell types including human osteoblasts, rat osteoblasts and human chondrocytes. Previously we have shown leptin to be an anabolic factor in vitro, stimulating osteoblast proliferation and inhibiting osteoclastogenesis. Leptin increases bone mass and reduces bone fragility when administered peripherally but has an indirect inhibitory effect on bone mass via the hypothalamus when administered directly into the central nervous system. The net effect of leptin on bone mass in vivo remains controversial.

Data from animal models where there is an absence of either leptin production (ob/ob) or its receptor (db/db) have been contradictory. In this study we compared the bone phenotype of leptin receptor-deficient (db/db) and wild-type (WT) mice. Micro-CT analysis was done on proximal tibiae using a Skyscan 1172 scanner. Db/db mice had significantly reduced trabecular bone volume (13.0 $\pm$ 1.62% in WT vs 6.01 $\pm$ 0.601% in db/db, p=0.002) and cortical bone volume (0.411 $\pm$ 0.0215mm^3 in WT vs 0.316 $\pm$ 0.00353mm^3 in db/db, p=0.0014), trabecular thickness (0.0484 $\pm$ 0.00107mm in WT vs 0.0451 $\pm$ 0.000929mm in db/db, p=0.041) and trabecular number (2.68 $\pm$ 0.319mm^{-1} in WT vs 1.343 $\pm$ 0.1478mm^{-1} in db/db, p=0.0034). Additionally, we have determined the material properties of db/db cortical bone by three-point bending and at the nanoscale as measured by nano-indentation, showing that the bone strength (13.3 $\pm$ 0.280N in WT vs 7.99 $\pm$ 0.984N in db/db, p=0.0074), and the reduced modulus, a measure of a material's stiffness (28.5 $\pm$ 0.280GPa in WT vs 25.8 $\pm$ 0.281GPa in db/db, p<0.0001) were significantly reduced.

These results demonstrate that in the absence of leptin signalling there is reduced bone mass indicating that leptin indeed acts in vivo as a bone anabolic factor, mimicking the in vitro results. This concurs with the results from peripheral administration of leptin and together with the fact that leptin is produced peripherally by adipocytes in fat tissue and the bone marrow, suggests that the direct effects of leptin on bone cells over-ride the central effects.

***Disclosures: Garry Williams**, None.*

FR0190

The Role of Nell-1 in Cartilage Development and Differentiation. Ronald Siu*[1], Wei Wei Chen[2], Xinli Zhang[1], Benjamin Wu[1], Kang Ting[1], Cymbeline Culiat[3], Chia Soo[1]. [1]University of California, Los Angeles, USA, [2]Zhejiang University, China, [3]Oak Ridge National Laboratory, USA

Nell-1 (a protein strongly expressed in neural tissue encoding EGF-like domain; novel epidermal growth factor (EGF)-like protein) is a potent osteochondrogenic growth factor. We have shown that Nell-1 (1) induces significant bone formation *in vivo*, (2) is a direct target of the master osteogenic transcription factor Runx2, and (3) promotes proliferation and maintenance of the differentiated state of chondrocytes *in vitro* and *in vivo*. Meanwhile, a chemically induced nonsense point mutation in the mouse *Nell-1* gene severely disrupts Nell-1 expression. Homozygous *Nell-1* deficient (ND) mice die perinatally and exhibit numerous skeletal abnormalities associated with cartilage and connective tissue. The purpose of this study is to elucidate the effect of *Nell-1* in cartilage development.

Histology revealed abnormal proximal displacement of the patella from its normal position at the distal end of the femur as well as compression and structural abnormalities in the intervertebral discs (Figure 1). These phenotypes resemble the widespread laxity of connective tissue observed in Ehlers-Danlos syndrome (EDS) in humans, a cartilage disease characterized by extreme flexibility of joints. Indeed, mutations of type V collagen (*Col5a1*) and tenascin X (*Tnxb*) are associated with EDS, and expression of these genes is reduced in ND mice, possibly explaining this phenotype.

To identify molecular mediators of Nell-1 function in chondrocytes, we performed microarray analysis comparing Nell-1 and vehicle-treated ATDC5 prechondrocytic cells, which revealed nuclear factor of activated T-cells cytoplasmic 2 (*Nfatc2*) as a Nell-1 primary response gene. Adenoviral overexpression of wild type or dominant-negative Runx2 revealed that Runx2 is required for *Nfatc2* induction. Recombinant Nell-1 protein inhibits hypertrophy of ATDC5 cells, similar to the function of Runx2 in the perichondrium, but this inhibition is reversed by siRNA knockdown of *Nfatc2* expression. Finally, we found that *Nell-1*, *Runx2*, and *Nfatc2* are co-expressed in the femoral perichondrium of wild type mice, but expression of all three genes were diminished in ND mice (Figure 2), suggesting that Nell-1 is required for *Runx2* and *Nfatc2* expression *in vivo*.

Together, our results suggest important roles for Nell-1 in normal chondrogenesis and cartilage organization during development and possibly also during postnatal tissue repair.

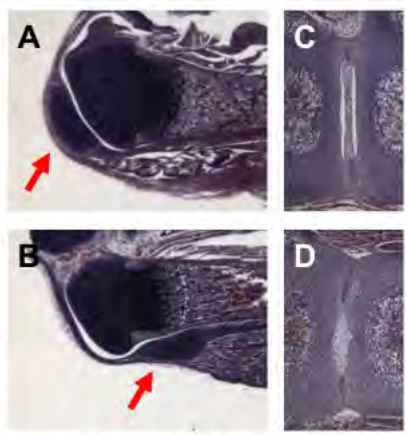

Figure 1. Left: distal femur and patella of newborn wildtype (A) and Nell-deficient (ND) (B) littermates. Arrows indicate abnormal position of patella in ND mouse. Right: L1/L2 intervertebral disc of newborn wildtype (A) and ND (B) littermate, showing reduced size of nucleus pulposus and abnormal compression of disc.

Figure 1

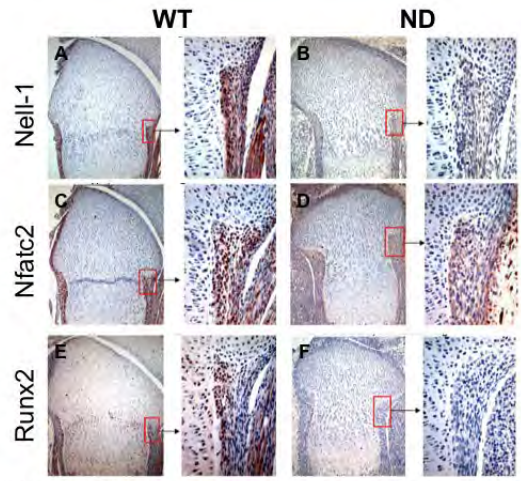

Figure 2. Nell-1, Nfat2, and Runx2 immunohistochemistry in the distal femur in newborn wildtype (WT) and Nell-1 deficient (ND) mice. Inset panels are magnified views of the perichondrium.

Figure 2

***Disclosures: Ronald Siu**, None.*

FR0192

IGF-I Signaling Regulates the Interaction of Osteoblasts and Osteoclasts via the RANKL/RANK and Ephrin B2/EphB4 Signaling Pathways. Yongmei Wang*[1], Hashem ElAlieh[2], Daniel Bikle[1]. [1]Endocrine Research Unit, Division of Endocrinology UCSF, USA, [2]University of California, San Francisco/VA Medical Center, USA

We and others have shown that insulin-like growth factor-I (IGF-I) signaling stimulates both osteoblast (OB) differentiation and osteoclastogenesis and is required for the communication between OBs and osteoclasts (OCLs). However, the mechanisms underlying these processes have not been evaluated. Recent studies found that ephrin B2-EphB4 bidirectional signaling mediates OB and OCL differentiation and communication. To address whether such signaling is involved in IGF-I action, we used knockout mouse models and in vitro culture systems to investigate the mechanism by which IGF-I signaling regulates OB differentiation and their interaction with OCLs focusing on the roles of ephrin B2/EphB4 and RANKL/RANK.

In wild-type (WT) bones, immunohistochemistry demonstrated that ephrin B2 is expressed in OBs and OCLs, while EphB4 is expressed only in OBs. The expression of ephrin B2 and EphB4 was dramatically decreased in OBs and OCLs in global IGF-I knockout (IGF-IKO) mice. In vitro, IGF-I (10 ng/ml) increased the mRNA levels of ephrin B2 and EphB4 in bone marrow stromal cell (BMSC) culture (day 14). Knockdown of EphB4 by siRNA (siEphB4) at day 12 of BMSC culture significantly decreased the mRNA levels of alkaline phosphatase (AP) and osteocalcin (OCN) by 53% and 72%, respectively. Similar results were found for ephrin B2 knockdown (siEphrinB2). IGF-I increased the mRNA levels of AP (68%) and OCN (330%) in control cultures, but induced less or no change in the siEphbrinB2 and siEphB4 cultures. Blocking the interaction of EphB4 and ephrin B2 by TNYL-RAW (a specific antagonist of EphB4) in the OB-OCL co-cultures resulted in the formation of fewer (60% decreased) TRAP positive cells, and the TRAP positive cells that did form contained only one or two nuclei. IGF-I increased OCL number by 40% in control co-cultures, but this effect was abolished in the co-cultures treated by TNYL-RAW. In the control co-cultures, IGF-I increased the mRNA levels of RANKL (49%) RANK (171%) and NFATc1 (30%), respectively, while decreased the mRNA levels of OPG (80%). These effects were likewise blunted in the cultures treated by TNYL-RAW.

Our data indicate that IGF-I promotes OB and OCL differentiation via both ephrin B2/EphB4 and RANKL/RANK signaling by stimulating ephrin B2 production in OBs and OCLs, EphB4 in OBs as RANKL in OBs and RANK in OCLs. These changes enhance OB/OCL communication leading to their mutually dependent differentiation.

***Disclosures: Yongmei Wang**, None.*

FR0194

Thyroid Hormone (T3) Acting via TRα1 is a Key Regulator of IGF-I Transcription in Osteoblasts and Bone Formation in Mice. Weirong Xing*[1], Sheila Pourteymoor[2], Jon Wergedal[3], Carlin Long[4], Graham Williams[5], Subburaman Mohan[3]. [1]Musculoskeletal Disease Center, Jerry L. Pettis Memorial Veteran's Admin., USA, [2]JL Pettis Memorial VA Medical Center, USA, [3]Jerry L. Pettis Memorial VA Medical Center, USA, [4]University of Colorado Health Sciences Center, USA, [5]Molecular Endocrinology Group, Division of Medicine & MRC Clinical Sciences Centre, Imperial College, United Kingdom

It is becoming increasingly established that T3 is essential for normal skeletal development. Since recent Cre/loxP studies reveal a key role for bone-derived IGF-I in regulating peak bone mass, and since IGF-I expression is reduced in mouse models of T3 deficiency, we hypothesized that T3 effects on skeletal growth result from a T3-induced increase in local IGF-I action. Accordingly, T3 treatment increased IGF-I expression (5-15 fold) at both mRNA and protein levels in a dose and time-dependent manner in osteoblasts (Obs). To determine which T3 receptor (TR) isoform is involved in mediating T3 effects, we examined TR expression levels and found greater expression of TRα1 than TRα2 and TRβ1 and no detectable levels of TRΔα1, TRΔα2 or TRβ2 expression in Obs. Transfection of MC3T3-E1 cells with TRα siRNA led to a 70% reduction in TRα1 and TRα2 expression, no effect on TRβ1 expression, and inhibition (>50%, $P<0.01$) of T3-induced IGF-I expression. Adenovirus-mediated overexpression of TRα1 markedly enhanced T3-induced IGF-I expression compared to β-gal control in MC3T3-E1 cells. The rapid effect of T3 on IGF-I expression suggested a direct effect of T3 on IGF-I gene transcription. Accordingly, IGF-I mRNA half-life was not altered in T3 treated cultures in the presence of actinomycin D. Since a putative T3 response element (TRE), located in the first intron 2113-2152 nucleotides from the transcription start site, was highly conserved among rat, mouse and human IGF-I genes, we inserted a 155 bp portion of the mouse Igf-I gene containing the putative TRE upstream of a thymidine kinase promoter (pTAL-Luc reporter) and found increased luciferase activity (2.3 fold, $P<0.01$) after 48h treatment with T3. Furthermore, nuclear extracts from T3 treated MC3TE-E1 cells bound specifically to the putative TRE in gel mobility shift assays. We next evaluated the role of IGF-I in mediating T3 biological responses using metatarsal organ cultures derived from newborn conditional IGF-I knockout (KO) mice in which IGF-I is disrupted in type I collagen producing Obs and corresponding wild type (WT) mice. Lack of IGF-I expression in Obs caused a marked reduction in 10 ng/ml T3-induced increase in mineralized length (25% in WT vs 8% in KO vs vehicle, $P<0.01$) after 10 days. Conclusions: 1) T3 via TRα1 regulates IGF-I gene transcription in Obs; and 2) T3 effects on skeletal growth are mediated in part via T3-induced local IGF-I expression.

***Disclosures: Weirong Xing**, None.*

FR0195

Bone-specific Calibration of Extracellular Matrix Material Properties by TGF-β and Runx2 is Required for Hearing. Jolie Chang*[1], Delia Brauer[2], Carol Chen[1], Omar Akil[1], Guive Balooch[3], Mary Beth Humphrey[4], Alexandra Porter[2], Robert Ritchie[5], Sally Marshall[1], Grayson Marshall[1], Lawrence Lustig[1], Tamara Alliston[1]. [1]University of California, San Francisco, USA, [2]Imperial College, United Kingdom, [3]LBNL, USA, [4]University of Oklahoma Health Sciences Center, USA, [5]UC Berkeley, USA

The mineralized collagen matrix of bone has unique material properties that are anatomically distinct, such that the elastic modulus of bone matrix ranges from 15 GPa in calvariae to 30 GPa in cochleae. In addition to their structural importance, the material properties of the extracellular matrix (ECM) are powerful determinants of cell function. Like biochemical signals, properties such as elastic modulus direct cell lineage selection, differentiation, and gene expression. Stiff matrices drive mesenchymal stem cells to undergo osteogenic differentiation, while compliant matrices promote neurogenic differentiation. Conversely, subtle changes in a tissue's ECM material properties disrupt cell proliferation and drive disease progression and tumorigenesis. Therefore, mechanisms that regulate ECM material properties are critically important in development and in disease. However, the molecular mechanisms that establish tissue-specific material properties and couple them to healthy tissue function are largely unknown.

Because healthy bone exhibits a range of material properties, the skeleton serves as an ideal model system to define mechanisms that establish ECM material properties, and to test the hypothesis that ECM material properties are calibrated for tissue-specific function. Using nanonindentation of bone from *Runx2*+/- mice, we identify Runx2 as a lineage-specific transcription factor that helps to establish the material properties of the ECM. We find that Runx2 regulates the material properties of bone matrix through the same TGF-β-responsive pathway that controls osteoblast differentiation. In the ear, inadequate levels of Runx2 activity compromise the unique material properties of cochlear bone and cause hearing loss, likely providing a basis for the unexplained cause of sensorineural hearing loss in human cleidocranial dysplasia. Remarkably, osteoblast-specific inhibition of TGF-β signaling rescues both the material properties and hearing loss of $Runx2^{+/-}$ mice. While this work advances our understanding of the control of bone matrix quality and the role of bone in hearing, it also suggests a paradigm by which signaling pathways and lineage-specific transcription factors cooperate to define the functionally essential material properties of a specific tissue.

***Disclosures: Jolie Chang**, None.*

FR0196

Classical TGFβ Signaling in Osteoclasts is Not Required for Maintenance of Bone Volume and Architecture: Evidence from Osteoclast-Specific TGFβRII Null Mice. Daniel Perrien*[1], Jeffry Nyman[1], Ying X. Wang[2], Chad S. Boomershine[2]. [1]Vanderbilt University Medical Center, USA, [2]Vanderbilt University, USA

Transforming growth factor beta (TGFβ) is a critical regulator of osteoblast differentiation and bone turnover and has been implicated in postmenopausal osteoporosis and cancer induced osteolysis. Numerous *in vitro* studies have reported direct, but often contradictory, effects of TGFβ on osteoclast (OCL) differentiation and apoptosis. However, the physiological relevance of TGFβ signaling in OCL to bone volume and density *in vivo* has not been demonstrated. TGFβ has two known signaling pathways: the well characterized classical pathway that requires binding of both TGFβRI and TGFβRII to activate Smad signaling, and the poorly characterized nonclassical pathway utilizing TGFβRIII/betaglycan. Based on cell culture studies, it was hypothesized that loss of TGFβ signaling via the classical TGFβRI/II pathway in OCL would inhibit osteoclast differentiation, thereby increasing bone volume and reducing turnover,. To test this hypothesis, LysM-cre mice were crossed with $TGF\beta RII^{flox/flox}$ mice to delete the gene encoding TGFβRII specifically in OCL and macrophages ($TGFRII^{OCL-/-}$). Skeletal effects were determined by microCT and histomorphometric evaluation of metaphyseal trabecular and diaphyseal cortical bone in the femora of 3 month old female wildtype (WT) and $TGFRII^{OCL-/-}$ mice (n=10 and 15, respectively). Surprisingly, deletion of TGFβRII in OCL's did not significantly alter trabecular bone volume (BV/TV, 0.060 +/-0.034 vs. 0.050 +/- 0.015; p=0.306), number, thickness, separation, or connectivity density (all $p>0.10$). Similarly, cortical thickness, cross sectional area, and polar moment of inertia were not significantly altered in $TGF\beta RII^{OCL-/-}$ mice. However, the material BMD of cortical, but not trabecular, bone was significantly increased ($p<0.025$) in $TGF\beta RII^{OCL-/-}$ mice (1283.1 mgHA/ccm +/-26.6) compared to WT (1258.2 mgHA/ccm +/-21.6). The bending strength and modulus of the femoral diaphysis, as determined by three point bending, were also not significantly altered in $TGF\beta RII^{OCL-/-}$ mice. These data demonstrate that classical TGFβ signaling via the receptor I/II complex in cells of the macrophage lineage is not required for normal skeletal development and homeostasis and calls into question the physiological relevance of previous *in vitro* studies concerning the effects of exogenous TGFβ on OCL development, function, and apoptosis. However, the effect on cortical mineral density suggests that TGFβ signaling in OCL may have an indirect effect on osteoblast activity and matrix mineralization.

***Disclosures: Daniel Perrien**, None.*

FR0198

Tamoxifen-Induced Deletion of Smad4 in Osteoblasts Enhances Proliferation in the Periosteum, Growth Plate, and Bone Marrow. Valerie Salazar*[1], Gabriel Mbalaviele[2], Roberto Civitelli[1]. [1]Washington University in St. Louis School of Medicine, USA, [2]Washington University School of Medicine, USA

Smad4, a transcription factor of the TGFβ/BMP pathway, can physically interact with components of the canonical Wnt pathway. We previously reported that siRNA-mediated knockdown of Smad4 in C3H10T1/2 cells synergistically enhances the ability of Wnt3a or activated β-catenin to stimulate *Cyclin-D1* transcription. We also find that Smad4 antagonizes pro-mitotic signals from canonical Wnts or activated β-catenin. To assess how Smad4 affects osteoblast proliferation *in vivo*, we mated $Smad4^{flox/flox}$ mice to *Osx-CreERT2* (kindly provided by T Kobayashi and H Kronenberg, Massachusetts General Hospital, Boston, MA. USA) and then evaluated BrdU incorporation in bone following Tamoxifen-induced, conditional ablation of *Smad4* in Osterix^{+} cells. Macroscopic examination of β-galactosidase activity in bones from $ROSA26^{fl(LacZ)}$; *Osx-CreERT2* mice indicates that 5 doses of Tamoxifen (2 mg/day, i.p.) are sufficient to induce substantial gene recombination in femurs and tibias of 6 week old male mice. On histology, we find strong β-galactosidase activity in a high percentage of cuboidal cells lining cortical and trabecular bone surfaces. By contrast, Tamoxifen treatment activates recombination in very few osteocytes or chondrocytes, and virtually no bone marrow cells. Thus, *Osx-CreERT2* represents a good model to achieve inducible and post-natal gene recombination in osteoblasts. We used immunofluouresence to detect BrdU incorporation in Tamoxifen-treated control (*Osx-CreERT2*) or *Smad4 cKO* (*Smad4flox/flox; Osx-CreERT2*) mice. Proliferation was altered in several compartments within the bone marrow microenvironment of *Smad4 cKOs*. Tamoxifen-induced ablation of *Smad4* in osteoblasts greatly increased the number of BrdU-positive cells in the primary and secondary spongiosa, as well as proliferating chondrocytes in the growth plate. Surprisingly, acute loss of *Smad4* affected proliferation of osteoblasts depending on resident location within the bone. While proliferation greatly decreased on the endosteum, it was markedly activated on the periosteum. In summary, the *Osx-CreERT2* mouse model efficiently induces post-natal gene recombination in osteoblasts. Tamoxifen-induced ablation of *Smad4* in osteoblasts alters proliferation in the osteogenic, chondrogenic, and bone marrow compartments. These data suggest Smad4 functions in osteoblasts to regulate the proliferative capacity of discrete populations within the bone marrow microenvironment, potentially through indirect mechanisms.

***Disclosures: Valerie Salazar**, None.*

FR0200

Absence of Bone Remodeling Compartment Canopies Correlates with an Arrested Reversal Phase and Deficient Bone Formation in Post-menopausal Osteoporosis. Ellen Hauge[1], Thomas Andersen*[2], Jens Bollerslev[3], Per Kjærsgaard-Andesen[4], Jean-Marie Delaisse[5]. [1]Aarhus University Hospital, Denmark, [2]Vejle Hospital, IRS-CSFU, University of Sourthern Denmark, Denmark, [3]National University Hospital, Norway, [4]Department of Orthopaedic Surgery, Vejle Hospital, University of Sourthern Denmark, IRS-CSFU, Denmark, [5]Vejle Hospital, University of Southern Denmark, Denmark

The reason why bone reconstruction is deficient during bone remodeling in post-menopausal osteoporosis (PMO) remains poorly understood, despite intensive research on osteoclasts (OC) and osteoblasts (OB), and despite detailed histomorphometry of bone surfaces (BS). Based on observations on normal, primary hyperparathyroidism (PHPT), myeloma, and Cushing patients, we showed recently that bone remodeling compartments (BRC) are critical for bone reconstruction during remodeling. BRCs are formed by a canopy of flattened OB-like cells separating the remodeling area from the marrow cavity, and associated with capillaries. Here we investigated whether the BRC concept can be extended to PMO.

Masson trichrome-stained sections of cancellous bone from 23 PMO patients and respectively 10 and 4 aged-matched controls and PHPT were assessed for ES, OS, BS, Oc.S, Ob.S, and Reversal cell surfaces (Rvc.S), identified as mononucleated cells on ES. Each parameter was related to the presence or absence of BRC canopies.

Controls and PHPTs showed more than 75% of ES/BS under BRC canopies, 8 of the 23 PMOs were similar to controls and PHPTs (PMO+ group), whereas the other 15 PMOs showed less than 75% of ES/BS under BRC canopies (PMO- group). Interestingly, the PMO- showed significantly less Ob.S/BS (8.8 vs. 14.3 %) and more Rvc.S/BS (13.6 vs. 8.3 %) than the PMO+, which were similar to controls and PHPTs. Oc.S/BS was unaffected. This thus indicates that in the absence of BRC, bone reconstructing OBs are decreased, even if RVCs were recruited to the remodelling sites. Interestingly also, when analyzing specifically the Rvc.S away from any visible resorption or reconstruction event, PMO- showed an increased extent of these specific Rvc.S compared to PMO+, controls, and PHPTs (6.6 vs. below 3.1 %). This observation can best be explained by an increased frequency of remodelling events that had stopped at the level of the reversal phase. Since RVCs are commonly considered as the OB progenitors, this would mean that RVCs are arrested and do not differentiate into bone forming OBs

In conclusion, there is a strict link between BRCs and formation of new bone during bone remodeling in PMO. The bone remodeling step that is most critically affected by the absence of BRCs is the reversal phase, which is arrested, and does not progress to OB differentiation and bone formation. Prevention of reversal phase arrest could be a future target for PMO treatment.

***Disclosures: Thomas Andersen**, None.*

FR0203

Bone-resorbing Osteoclasts Secrete A Factor That Stimulates Osteoblastic Differentiation. Sunao Takeshita*[1], Toshio Fumoto[1], Kyoung-ae Park[1], Hiroyuki Aburatani[2], Shigeaki Kato[2], Masako Ito[3], Kyoji Ikeda[1]. [1]National Center for Geriatrics & Gerontology, Japan, [2]University of Tokyo, Japan, [3]Nagasaki University Hospital, Japan

Bone is constantly remodeled through resorption of old bone by osteoclasts and deposition of new bone by osteoblasts. The net bone mass is regulated through a balance between preceding resorption and subsequent formation; however, the factor(s) and mechanism that couple the two processes are not fully understood. We hypothesized that such coupling factor is secreted or presented by osteoclasts and stimulates osteoblastic differentiation. Through global gene expression analysis during osteoclastogenesis, we have identified a protein, named couplin, that is secreted specifically by mature osteoclasts actively engaged in bone resorption and acts on marrow stromal cells to stimulate osteoblastic differentiation *in vitro* and bone formation *ex vivo*. The expression of couplin in bone decreases with aging and alendronate treatment, and increases in a high bone turnover state, such as PTH treatment. Loss- and gain-of function experiments by mouse genetics revealed that the deletion of the couplin gene in osteoclasts results in low bone mass due to insufficient bone formation, while mice overexpressing couplin are protected from bone loss with aging. Thus, couplin is a factor that relays from bone-resorbing osteoclasts to osteoblastic bone formation, thereby regulating the rate of bone turnover.

***Disclosures: Sunao Takeshita**, None.*

FR0204

Co-translocation of the Osteoclastogenic Estrogen Element Binding Protein and ß-Catenin to the Nucleus of Osteoblasts is Regulated by Wnt Signaling. Hong Chen*[1], Mark Nanes[2], Linda Gilbert[3], Martin Hewison[4], John Adams[5]. [1]VA / Emory University School of Medicine, USA, [2]VA Medical Center & Emory University, USA, [3]VA Medical Center GA, USA, [4]UCLA, USA, [5]University of California, Los Angeles, USA

The heterogeneous nuclear ribonucleoprotein (hnRNP)-like estrogen response element binding protein (ERE-BP) is a nucleic acid binding protein that functions as a competitor with estrogen receptor α (ERα) for occupancy of target gene estrogen response elements (ERE). Here we report that in bone, ERE-BP can also act independently of estradiol-ERα to stimulate osteoclastogenesis. Overexpression of ERE-BP promotes osteoclastogenesis by stimulating RANKL (7-fold) and RANK expression (3-fold) in osteoblasts(OB) and osteoclast precursor RAW cells, respectively. ERE-BP directly stimulates RANKL transcription 2 fold as shown in transient transfection assays utilizing a mouse RANKL promoter luciferase reporter. In contrast, silencing ERE-BP decreases osteoblastic RANKL promoter activity. Co-cultures of bone marrow cells with ERE-BP lentevirus-transducted ST-2 stromal cells induced formation of multinucleated, TRAP+, calcitonin receptor-expressing cells and increased calcium resorption from bone slices by 22% ($p<0.01$). Osteoprotegerin(OPG) expression and ratio of OPG/RANKL were decreased in the ERE-BP co-culture system. Wnt signaling has been suggested to influence osteoclastogenesis in genetic models that silence β-catenin and concomitant effects on the regulation of RANKL. To determine if ERE-BP interacts with Wnt/β-catenin signaling, immunofluorescent staining of β-catenin and ERE-BP was performed in preosteoblastic MC3T3 cells. ERE-BP and β-catenin were co-localized in the cytoplasm of unstimulated cells. Co-immunoprecipitation with either anti-ERE-BP or anti-β-catenin antibody resulted in reciprocal pull-down from whole OB cell extracts. Stimulation with Wnt3a-conditioned medium or the GSK3β inhibitor LiCl for 4 hours resulted in translocation and co-localization of β-catenin and ERE-BP in the nucleus. ERE-BP overexpression in OBs also stimulated the movement of β-catenin to the nucleus. ERE-BP expression did not affect β-catenin mRNA levels. Taken together, these results indicate that: 1] ERE-BP stimulates osteoclastogenesis and bone resorption, 2] ERE-BP and β-catenin co-chaperone one another to the nuclear compartment of OBs; 3] the co-translocation of ERE-BP and ß-catenin to the nucleus is regulated by Wnt signaling. We therefore hypothesize that ERE-BP can influence bone turnover not only via disruption of ERα signaling, but also via interaction with the Wnt/β-catenin pathway.

***Disclosures: Hong Chen**, None.*

FR0206

Genetic Dissection of the Molecular Events Taking Place in Osteoblasts and Triggered by Leptin Signaling in the Brain. Gerard Karsenty, Daisuke Kajimura*. Columbia University, USA

A large body of evidence has identified leptin as an important, negative regulator of bone mass accrual that acts through a neural relay to eventually affect bone

formation. A major mediator linking leptin signaling in the brain to bone cells is the sympathetic nervous system acting through the *Adrb2* expressed in osteoblasts. Although some aspects of the sympathetic signaling in osteoblasts have emerged, there are still many steps that are unknown. To address this question, we generated and analyzed an allelic series of cell-specific gene deletion in the mouse. Extending previous results, we show here that an osteoblast-specific deletion of the *Adrb2*, the only adrenergic receptor expressed in osteoblasts, results in a high bone mass phenotype caused by an increase in bone formation and a decease in bone resorption parameters. Moreover and unlike what is observed in wild type mice, intracerebroventricular (ICV) infusion of leptin could not decrease bone mass in the $Adrb2_{osb}$ -/- mice. These results demonstrate formally that the sympathetic tone, acting through *Adrb2* expressed in osteoblasts, is a mediator of leptin regulation of bone mass. Next, we generated an osteoblast-specific deletion of *Creb*, a transcription factor and a major downstream target of sympathetic signaling in many cell types. $Creb_{osb}$ -/- mice were also resistant to the deleterious effect of leptin ICV infusion on bone mass. *cMyc* is a well characterized downstream target of Creb that also regulates cell proliferation. As expected, deletion of *cMyc* in osteoblasts decreased their proliferation, but also abrogated the deleterious effect of leptin ICV infusion on bone formation. Lastly, through the generation and studies of several compound heterozygous mice, we could establish the existence of a genetic cascade taking place in osteoblasts, downstream of leptin signaling in the brain and that includes *Adrb2*, *Creb and cMyc*. Hence, this study provides a complete molecular road maps explaining how, under the control of leptin, sympathetic signaling in osteoblasts regulates osteoblast proliferation and bone formation.

***Disclosures: Daisuke Kajimura**, None.*

FR0207

Histone Deacetylase Inhibition Causes Bone Loss. Meghan McGee-Lawrence*[1], Angela L. McCleary-Wheeler[1], Minzhi Zhang[1], Bridget A. Stensgard[1], Jane Lian[2], Jennifer Westendorf[1]. [1]Mayo Clinic, USA, [2]University of Massachusetts Medical School, USA

Histone deacetylase inhibitors (HDIs) are used clinically to treat cancer, epilepsy, and other conditions. Their effects on the mineralized skeleton are not well understood. In vitro, histone deacetylase inhibition accelerates osteoblast maturation and induces osteoclast apoptosis. Paradoxically, long-term in vivo administration of the HDI valproate, such as for the treatment of epilepsy, reduces bone mineral density and increases fracture risk. The purpose of this study was to determine the effects of the clinically relevant pan HDI, suberoylanilide hydroxamic acid (SAHA; Vorinostat), on bone mass and cellular activity in vivo.

Seven week-old male C57BL/6 mice received daily SAHA (100 mg/kg) or vehicle (PEG400/DMSO) intraperitoneal injections for 4 weeks. All animals also received dual calcein injections prior to sacrifice. Western blots on spleen lysates for acetylated histone 3 confirmed HDI activity in the SAHA-treated mice. Micro-computed tomography revealed that SAHA induced significant trabecular bone loss in the distal femoral metaphysis, as evidenced by decreases in bone volume fraction (-22%), trabecular number (-9%), and apparent mineral density (-21%), and an increase in trabecular separation (+11%) (Fig 1). Cortical bone at the femoral midshaft was not affected by SAHA. Serum levels of P1NP, a global marker of bone formation, were decreased (-23%) in SAHA-treated mice. Expression levels of osteoblastic genes including osteocalcin and osteopontin were also lower following SAHA treatment. SAHA reduced histological measures of osteoblast number; however, it increased local indices of osteoblast activity including mineral apposition rate (MAR) and bone formation rate (BFR/BS). Neither serum (TRAcP 5b) nor histological (Oc.S/BS) markers of osteoclast number were affected by SAHA. Our data suggest that SAHA causes bone loss by reducing overall osteoblast number, even while increasing activity of pre-existing committed osteoblasts. These data support the hypothesis that HDIs negatively affect the proliferation, survival and/or pluripotency of mesenchymal stem cells while simultaneously promoting differentiation and increased activity of cells already committed to the osteoblastic lineage. This effect could contribute to the bone loss observed both in our study and seen clinically after long-term administration of HDIs.

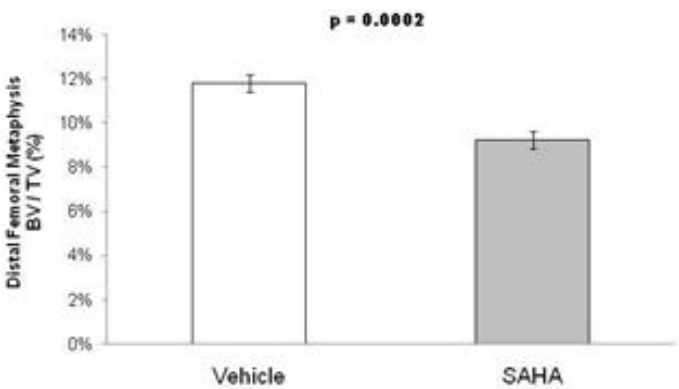

Figure 1: SAHA reduced trabecular bone volume fraction (BV/TV) in mice

***Disclosures: Meghan McGee-Lawrence**, None.*

FR0209

Loss of *Connexin43* in Mature Osteoblasts and Osteocytes Results in Delayed Mineralization and Bone Remodeling During Fracture Healing. Alayna Loiselle*[1], Andrew Billingsley[1], Emmanuel Paul[1], Yue Zhang[2], Henry Donahue[3]. [1]Penn State Hershey, USA, [2]Penn State University, USA, [3]The Pennsylvania State University College of Medicine, USA

Connexin 43 (*Cx43*) is the most abundant gap junction protein in bone, and regulates osteoblast differentiation. Mice with osteoblast/osteocyte specific (Osteocalcin-Cre) loss of Cx43 display decreased gap junctional intercellular communication, bone density and cortical thickness. The purpose of this study was to examine the role of *Cx43* in mature osteoblasts during fracture healing, and test the hypothesis that loss of *Cx43* results in decreased osteoblast differentiation, and a delay in fracture healing. A closed fracture was produced by three-point bending in Osteocalcin-Cre+; $Cx43^{flox/flox}$ (KO) and Cre- $Cx43^{flox/flox}$ (WT) mice. Healing was assessed by μCT, histology and *in situ* hybridization.

A bridging callus was present in WT and KO mice 14 days after fracture, with Alcian blue staining of the cartilaginous callus in both groups. By 21 days, Alcian Blue and *Col2* positive cells were still present in the fracture callus of KO mice indicating a persistence of cartilage. In contrast, the callus in WT mice had been mineralized, and had abundant *Osteocalcin* expression indicating mature osteoblasts. The total volume of KO fractures was significantly greater than WT fractures at this time (KO: 9.47 ± 0.37; WT: 4.15 ± 0.17; $p=0.017$) consistent with a larger callus volume. Using a novel μCT analysis to identify remodeling bone, we found that high density BV/TV was decreased in WT mice compared to KO (0.05 ± 0.02; 0.157 ± 0.012, $p=0.014$), indicating more remodeling in WT bones.

At 28 days a large mineralized callus was still present around the fracture site of KO animals, while the callus had been remodeled in WT mice. Additionally, there was still expression of *RANKL* and *OPG* in KO callus, indicative of osteoclastogenesis and active bone remodeling, whereas *RANKL* and *OPG* expression had decreased in WT fractures. At 35 days after fracture, the callus in KO mice had been nearly completely remodeled, however areas of woven bone remained.

These data indicate that loss of *Cx43* in mature osteoblasts results in delayed completion of endochondral bone formation and bone remodeling during fracture healing. These studies identify a novel role for the gap junction protein *Connexin 43* during fracture healing, suggesting that loss of *Cx43* can result in delayed mineralization and remodeling due to decreased osteoblast differentiation. Therefore, enhancing *Cx43* expression or gap junctional intercellular communication may provide a novel means to enhance fracture healing.

***Disclosures: Alayna Loiselle**, None.*

FR0211

Osteoclast Secretion of the Chemokine Sphingosine-1-Phosphate is Crucial for Recruitment of Osteoblast Lineage Cells. Patrick Quint*[1], Moustapha Kassem[2], Jennifer Westendorf[3], Sundeep Khosla[4], Merry Jo Oursler[3]. [1]Mayo Clinic Rochester, USA, [2]Odense University Hospital, Denmark, [3]Mayo Clinic, USA, [4]College of Medicine, Mayo Clinic, USA

Bone is a dynamic tissue that continuously remodels and, under most conditions, resorbed bone is nearly precisely replaced in location and amount by new bone. This laboratory is investigating how preosteoblastic cells are recruited to the site of bone degradation following the resorption phase of bone turnover. Using ten-fold concentrated osteoclast conditioned medium, we observed that osteoclasts release factors that stimulate preosteoblastic stromal cells' mineralization. To determine candidate osteoclast coupling factors, we compared gene expression between preosteoclasts and mature osteoclasts and determined that Sphingosine-1-phosphate 1 (SPHK1) was upregulated during differentiation, and thus may contribute to osteoclast influences on stromal cells. The enzymatic product of SPHK1 is the chemokine sphingosine-1-phosphate (S1P), which is too small to be concentrated in the conditioned media in the above experiment. To determine whether low molecular weight coupling factors contribute to mineralization stimulation, we compared effects of concentrated verses unconcentrated conditioned media on mineralization of mouse calvarial cells and human bone marrow stromal cells overexpressing telomerase (hMSC-TERT cells). Mineralization stimulation by unconcentrated conditioned medium was nearly the same as concentrated conditioned medium (Figure 1). As an early step in preosteoblast recruitment, stromal cells move to the vicinity of the bone surface. Cell movement can be either random (chemokinesis) or directed toward a stimulus (migration). We therefore compared calvarial cells for chemokinesis and migration responses to concentrated and unconcentrated osteoclast conditioned media. Both conditioned media stimulated chemokinesis and migration. Interestingly, the unconcentrated conditioned medium stimulation level was over 80% of that of the concentrated conditioned medium. These data supported that much of the stimulatory effect was due to a small molecule and we therefore examined the role of S1P in hMSC-TERT cell chemokinesis and migration. A S1P receptor agonist stimulated chemokinesis and migration in both osteoclast conditioned media and control media (osteoclast precursor conditioned media) whereas the receptor antagonist suppressed chemokinesis and migration when added to osteoclast conditioned media.

These data support that the chemokine S1P is likely to contribute coupling of bone formation to bone resorption.

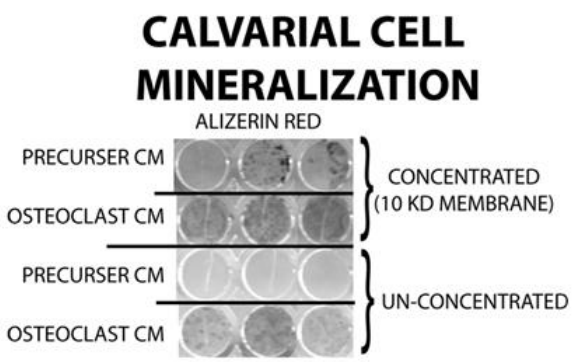

Figure 1. Un-concentrated or 10-fold concentrated conditioned media (CM) from either osteoclast precursors or mature osteoclasts were used to feed calvarial cells for 14 days. Cells were then fixed and stained with Alizerin red to visualize mineralization.

Figure 1: Mineralization of Calvarial Cells

***Disclosures: Patrick Quint**, None.*

FR0213

Retinaldehyde Dehydrogenase 1 Deficiency Promotes Osteoblastogenesis and Increases Trabecular and Cortical Bone Mass. Shriram Nallamshetty*[1], Sheila Bornstein[2], Masanobu Kawai[2], Yougen Xi[3], Mark Horowitz[3], Clifford Rosen[2], Jorge Plutzky[1]. [1]Brigham & Women's Hospital, USA, [2]Maine Medical Center, USA, [3]Yale University School of Medicine, USA

The retinoid X receptor (RXR) mediates the pleotropic effects of retinoids -the biologically active structural derivatives of vitamin A (retinol). The nuclear receptor peroxisome proliferator activated receptor-gamma (PPARγ), a key regulator of bone remodeling and stromal cell fate in the marrow, requires heterodimerization with RXR for its transcriptional activity. As such, RXR and retinoids represent critical nodal points in PPARγ pathways. Despite this, the role of RXR and its ligands in determining PPARγ responses in the skeleton remains undefined. Recently we reported that retinaldehyde (Rald), a retinol metabolite with no previously documented role outside of the retina, inhibited the PPARγ-RXR complex and repressed adipogenesis *in vivo*. Mice lacking retinaldehyde dehydrogenase 1 (Raldh1), which converts Rald to retinoic acid (RA), had high Rald levels in adipose tissue and were protected against diet-induced obesity. We hypothesized that global Raldh1 deletion (*Raldh1-/-*) would impair PPARγ activation in bone marrow stromal cells (MSCs) and increase bone mass. Therefore, we performed developmental phenotyping of female *Raldh1-/-* and wild-type (WT) mice on a C57B6 background. DXA scans showed higher femoral bone mineral density as early as 8 weeks of age in *Raldh1-/-* mice (BMD 0.062 vs. 0.049; $p < 0.001$). These differences persisted at 12, 18, 26, and 36 weeks of age. On μCT, *Raldh1-/-* mice had significantly higher trabecular bone density at 8, 12, and 18 weeks of age (BV/TV of 0.11 vs. 0.05; 0.034 vs 0.093; 0.038 vs 0.101 respectively [$p<0.001$]). *Raldh1-/-* mice also had significantly higher trabecular numbers and lower SMI at these ages. To investigate the molecular basis of these skeletal changes in *Raldh1-/-* mice, we performed *in vitro* osteoblastogenesis assays using MSCs from 12-week-old WT and *Raldh1-/-* mice. *Raldh1-/-* MSCs demonstrated enhanced osteoblastogenesis and mineralization as measured by alkaline phosphatase and alizarin red staining respectively. MSC-derived osteoblasts from *Raldh1-/-* mice demonstrated increased gene expression of Runx2, Osx, osteocalcin, and collagen. In addition, Wnt 10b expression was higher in osteoblasts derived from *Raldh1-/-* MSCs, suggesting that the shift in retinoids that occurs in *Raldh1-/-* mice drives canonical wnt/β catenin signaling and a pro-osteoblastogenic differentiation program. These data provide insight into the potential role of Rald/RXR in regulating PPARγ within the marrow niche.

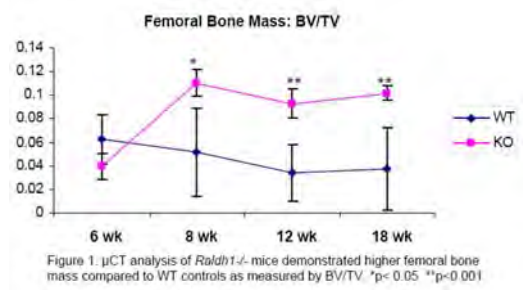

Figure 1. μCT analysis of *Raldh1-/-* mice demonstrated higher femoral bone mass compared to WT controls as measured by BV/TV. *p< 0.05 **p<0.001

Femoral Bone Mass of Raldh1-/- Mice

***Disclosures: Shriram Nallamshetty**, None.*

FR0217

Vascular Development during Distraction Osteogenesis Proceeds by the Sequential Arteriogenesis Exterior to Bone Followed by Angiogenesis within the Bone. Elise Morgan[1], Bader Al-Awadhi[2], Daniel Hogan[3], Amira Hussein[1], Zainab Al-Aql[2], Jennifer Fitch[3], Billy Andre[1], Louis Gerstenfeld*[3]. [1]Boston University, USA, [2]Boston University School of Dental Medicine, USA, [3]Boston University School of Medicine, USA

Distraction osteogenesis (DO) is a surgical method of applying mechanical tension within an osteotomy in order to promote bone regeneration. Osteogenesis during DO has been shown to be dependent on the formation of blood vessels. The spatial interactions by which vascular and osseous tissues integrate their development were assessed by quantifying the temporal and spatial characteristics of these two tissues across the time course of DO. Following perfusion of the vasculature with a radio-opaque contrast agent, image registration and subtraction procedures were applied to sequential micro-computed tomography scans obtained before and after demineralization in order to quantitatively asses vascular and osteogenic tissues in the same sample. Immunohistological assessments were made to discriminate arteriogenesis (large vessel) from angiogenesis (small vessel) formation. Within the gap region, vessel volume was greater at the end of the consolidation period (31 days post surgery) as compared to both the baseline (end-latency; 7 days post surgery) and 7 days after distraction was initiated (14 days post surgery). Total vessel thickness was largest at the end of the active distraction period (17 days post surgery). At all timepoints, total vessel volume was greater in the extraosteal region while vessel connectivity was greater in the intraosteal region. Analysis of vessel volume in the proximal to distal orientation always showed larger values in the proximal and central regions in both intra- and extraosteal regions. Vessel formation proceeded from muscle outside into bone regenerate. Immunohistology validated the structural assessments that arteriogenesis occurred primarily during the period of active distraction while angiogenesis occurred during the consolidation phase. Regional differences in vessel formation suggest that non-uniform mechanical strains within the regenerate may play a role in providing the signals that direct the spatial orientation of new vessel formation in the DO regenerate. The intense period of angiogenesis that precedes and is concurrent with mineralized bone formation is consistent with the prevailing view that the infiltration of blood vessels promotes bone mineralization. However, the spatial association of vascular and osseous tissues within the intraosteal region also suggests a feedback loop wherein biological factors produced during the maturation of bone tissues during consolidation in turn promote angiogenesis.

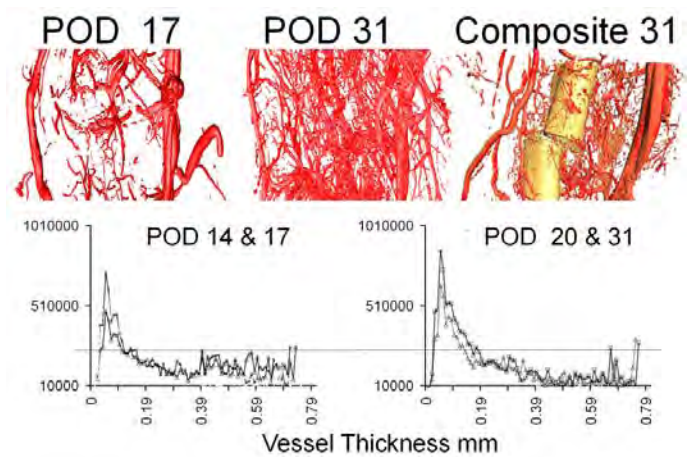

Vessel Volume and Thickness

***Disclosures: Louis Gerstenfeld**, None.*

FR0218

AP-1 Proteins Affect Bone Formation Negatively via both AP-1 Transcriptional Activity and Interaction with β-Catenin whereas Truncated Isoforms (FosB/2FosB) Do Not. Ilana Platt*[1], Glenn C. Rowe[2], Sutada Lotinun[1], William Horne[1], Azeddine Atfi[1], Roland Baron[3]. [1]Harvard School of Dental Medicine, USA, [2]Beth Israel Medical Center, USA, [3]Harvard School of Dental Medicine, Harvard Medical School, MGH Endocrine Unit, USA

Several genes that regulate osteoblast (OB) differentiation and function are activated by AP-1 transcription factors (TFs), composed of dimers of Fos and Jun proteins. We have demonstrated that the naturally truncated AP-1 protein, Δ2ΔFosB, which lacks FosB's Fos homology (FH) and transactivating (TA) domains, increases bone mass when overexpressed in OBs in mice. Since Δ2ΔFosB antagonizes FosB's AP-1 TA potential, we hypothesized that inhibition of FosB and AP-1 activity is critical to the anabolic actions of Δ2ΔFosB on bone. To test this hypothesis, we used

the osteocalcin (OG2) promoter to target overexpression of a dominant negative (DN) truncated form of JunD to OBs in mice. Like Δ2ΔFosB, DNJunD lacks the TA domain but can still dimerize with Fos and Jun proteins and bind to DNA, antagonizing AP-1 activity. Compared to littermate controls, calvarial OBs from 1 day old OG2-DNJunD pups have higher alkaline phosphatase activity, and tibia from 6 week old mice have significantly higher bone volume (BV/TV) and bone formation rates (BFR/BS). These results support the hypothesis that inhibition of AP-1 activity is overall anabolic to bone, possibly explaining the bone phenotype in ΔFosB/Δ2ΔFosB mice.

Since AP-1 TFs modulate Wnt target gene expression, and Wnt proteins promote OB differentiation, we then hypothesized that inhibition of AP-1 TA by Δ2ΔFosB may enhance Wnt signaling. FosB, but not Δ2ΔFosB, was immunoprecipitated with β-catenin and inhibited β-catenin-induced TOPFlash activity. Interestingly, FosB constructs in which the leucine zipper (required for dimerization) and/or the DNA binding domain are disabled prevented FosB's AP-1 TA in the AP-1 luciferase reporter assay, but did not prevent the inhibition of TOPFlash reporter activity, indicating that this effect is likely due to direct interaction of the N-terminal and/or FH domains with β-catenin, independent of the formation of the AP-1 complex and TA activity. These results suggest that AP-1 proteins negatively regulate bone formation by both AP-1 dependent and β-catenin-dependent mechanisms. ΔFosB/Δ2ΔFosB and DNJunD may therefore increase bone formation by preventing both AP1 TA and the negative effects of FosB interactions with β-catenin.

***Disclosures: Ilana Platt**, None.*

FR0220

Epigenetic Control of Osteoblastogenesis by Pbx1 Repressing Hoxa10-Mediated Recruitment of Activating Chromatin Remodeling Factors. Jonathan Gordon*[1], Mohammad Hassan[1], Matthew Koss[2], Sharanjot Saini[3], Martin Montecino[4], Licia Selleri[5], Andre Van Wijnen[1], Janet Stein[1], Gary Stein[1], Jane Lian[1]. [1]University of Massachusetts Medical School, USA, [2]Cornell University Weil Medical School, USA, [3]University of California-San Francisco, USA, [4]Universidad de Concepcion, Chile, [5]Cornell University Weill Medical school, USA

Homeobox (HOX) factors have been demonstrated to be potent transcriptional and epigenetic regulators of osteogenesis. Abdominal-class homeodomain-containing (Hox) factors form multimeric complexes with TALE-class homeodomain proteins (Pbx, Meis) to regulate tissue morphogenesis and skeletal development. Here we have identified components of a Pbx1 complex that is associated with osteoblast-related gene promoters and established that Pbx1 negatively regulates Hoxa10-mediated gene transcription in mesenchymal cells. Expression of Pbx1 impaired osteogenic commitment of C3H10T1/2 pluripotent cells and differentiation of MC3T3-E1 pre-osteoblasts. Conversely, targeted depletion of Pbx1 by shRNA increased expression of osteoblast-related genes. Studies using wild type and mutated osteocalcin and bone sialoprotein promoters revealed that Pbx1 acts through a Pbx-binding site that is required for attenuation of Hoxa10 gene activation. Chromatin-associated Pbx1 and Hoxa10 were present at osteoblast-related gene promoters preceding gene expression, but Pbx1 was absent from promoters during induced transcription of osterix, osteocalcin and bone sialoprotein. Pbx1 was associated with histone deacetylases normally linked with chromatin inactivation and loss of Pbx1 from osteoblast promoters in differentiated osteoblasts was associated with increases in histone acetylation and CBP/p300 recruitment, as well as decreased H3K9 methylation. We propose Pbx1 plays a central role in attenuating the activity of Hoxa10 as an activator of osteoblast-related genes and functions to establish proper timing of gene expression during osteogenesis. These novel in vitro epigenetic mechanisms regulating the onset of bone formation are currently being addressed in an in vivo context, by osterix-Cre-mediated conditional deletion of Pbx1 during osteogenesis.

***Disclosures: Jonathan Gordon**, None.*

FR0221

ER Stress Response Mediated by PERK-eIF2α-ATF4 Pathway is Involved in Osteoblast Differentiation Induced by BMP2. Kimiko Ochiai*[1], Atsushi Saito[2], Douglas Cavener[3], Kazunori Imaizumi[2]. [1]University of Miyazaki, Japan, [2]Division of Molecular & Cellular Bioligy, Dapartment of Anatomy, Faculty of Medicine, University of Miyazaki, Japan, [3]The Pennsylvania State University College of Medicine, USA

Various stresses conditions lead to accumulation of unfolded proteins in the endoplasmic reticulum (ER) lumen (ER stress). Eukaryotic cells have the potential to deal with unfolded proteins to avoid cellular damage. This system is termed the ER stress response. PKR-like endoplasmic reticulum kinase (PERK) is one of major transducers of ER stress response, and can phosphorylate eukaryotic initiation factor 2α (eIF2α), resulting in translational attenuation. Phosphorylated eIF2α specifically promotes the translation of transcription factor 4 (ATF4). ATF4 is well known to play important roles in osteoblast differentiation and bone formation. Recently, PERK deficient mice has been reported to exhibit severe osteopenia, and the phenotypes observed in bone tissues are very similar to those of ATF4 deficient mice. However, it is unclear that the PERK-eIF2α-ATF4 signaling pathway and/or ER stress itself are involved in osteogenesis. We examined the expression levels of many genes and proteins in bone tissues of PERK deficient mice. Phosphorylated eIF2α and ATF4 proteins were decreased in PERK deficient calvaria at postnatal day 4, and the gene expression levels of osteocalcin (OCN) and bone sialoprotein (BSP), that are targets for ATF4, were also down-regulated. Treatment of WT primary calvarial immature osteoblasts with BMP2, which is required for osteoblast differentiation, induced expression of ATF4 protein. In contrast, that in PERK deficient primary culture was severely inhibited and the levels of OCN and BSP were also decreased. There results indicate that activation of ATF4 is required for PERK signaling pathway in osteoblast differentiation. PERK deficient osteoblast culture exhibited a decrease in collagen fibers, alkaline phosphatase activities, and delayed mineralized nodule formation relative to WT culture. There abnormalities were almost completely restored by the introduction of ATF4 into PERK deficient osteoblasts. We previously reported that treatment of calvarial primary osteoblast culture with BMP2 leads to ER stress due to the production of abundant proteins during osteoblast differentiation. Taken together, physiological ER stress occurs during osteoblast differentiation and activates PERK-eIF2α-ATF4 signaling pathway followed by promotion of gene expression essential for osteogenesis such as OCN and BSP. However, further detailed investigation is required for clarifying the relationship between osteogenesis and PERK-ATF4 pathway in vivo.

***Disclosures: Kimiko Ochiai**, None.*

FR0223

KLF10 is a Critical Mediator of Wnt Signalling in Osteoblasts. John Hawse*[1], Elizabeth Bruinsma[2], Sarah Grygo[2], Frank Secreto[3], Nalini Rajamannan[4], Thomas Spelsberg[3], Malayannan Subramaniam[3]. [1]Mayo Clinic College of Medicine, USA, [2]Mayo Clinic College of Medicine, USA, [3]Mayo Clinic, USA, [4]Northwestern University Medical School, USA

We have previously demonstrated that KLF10 plays important roles in bone as knockout (KO) mice display a gender specific osteopenic phenotype defined by decreased bone mineral density, bone mineral content and overall loss of bone strength in female animals. Recent studies indicate that KLF10 may be involved in mediating Wnt signaling, a pathway critical for proper bone development, growth and skeletal maintenance. Therefore, we analyzed the expression levels of multiple Wnt pathway genes in calvarial osteoblasts (OBs) isolated from KLF10 KO mice relative to wildtype (WT) controls. These analyses revealed significant decreases in the basal expression levels of LRP6, cMyc, Wnts 2b, 3, 5a, 5b, 9a, 10a, 10b, and 11, as well as increased expression of the inhibitory DKK1 gene, in KO OB cells. During the course of OB differentiation, the expression levels of Wnt 10b and 11 increased significantly in WT cells but not in KLF10 KO cells. Expression of Lef, a Wnt-dependent transcription factor involved in mediating β-Catenin gene regulation, increased in WT but not KO OBs during late stages of differentiation, while expression of LRP5 was significantly decreased in KO cells. We next demonstrated that Lef was not able to activate a Lef/Tcf reporter construct (Top-Flash) when transfected into KLF10 KO OBs. However, when KLF10 was co-expressed with Lef, a significant increase in reporter activity was observed. Additionally, KLF10 alone could activate the Top-Flash reporter in both U2OS cells and calvarial OBs, and interestingly, such activation was equivalent to or exceeded that observed with Lef alone. Expression of both KLF10 and Lef led to co-activation of the Top-Flash reporter. Similarly, co-expression of KLF10 and β-catenin led to enhanced Top-Flash activity relative to either alone, and this activation was further enhanced by the addition of Lef. These data suggested that KLF10, Lef and β-catenin interact with each other to form a transcriptionally active protein complex. Indeed, co-immunoprecipitation assays demonstrated that KLF10 does interact with both Lef and β catenin in OBs. Taken together, these data implicate a previously unidentified role for KLF10 in mediating Wnt signaling and Lef transcriptional activity in OBs, and imply an important role for the Wnt pathway in the observed osteopenic bone phenotype of KLF10 KO mice.

***Disclosures: John Hawse**, None.*

FR0224

NF-kB RelB-/- Mice Have Age-Related Trabecular Bone Gain in their Diaphyses, Indicating that RelB negatively Regulates Bone Formation. Zhenqiang Yao*[1], Chen Zhao[2], Yanyun Li[1], Lianping Xing[1], Brendan Boyce[2]. [1]University of Rochester, USA, [2]University of Rochester Medical Center, USA

NF-κBp50/p52 expression is required for osteoclast (OC) formation. RelB interacts with p52 and is required for RANKL-mediated OC formation in vitro but not for basal OC formation in vivo: no bone phenotype was reported in RelB KO mice. However, we have found that RelB-/- mice develop age-related increased diaphyseal trabecular bone volume starting at 6-8 wks-old, bone volume (BV/TV, %) being 10± 2 vs. 5±2.5, $p<0.01$ in WT mice. At 12-15 wks-old, BV/TV remained unchanged in WT mice but increased to 23.5±4.6 in the KO mice with increased Tb.N (7.6±0.5 vs 5.8±0.4/mm, $p<0.01$), no change in Tb.Th., but significantly reduced OC# in vivo (45±16 vs 70±23/mm ($p<0.01$) and RANKL and TNF mediated OC formation in vitro. c-Fos is critical for OC formation down-stream from NF-κB. We found that both RANKL and TNF-induced c-Fos mRNA expression depends on RelB and that over-expression of c-Fos rescued OC formation induced by these cytokines in KO OC precursors. Surprisingly, osteoblast (OB) surface (8±2 vs 25±9 %, $p<0.01$) and bone formation rate (BFR: 0.37±0.15 vs 1.07±0.47 um3/um2/d, $p<0.05$) were significantly reduced in the KO mice due to decreased mineral

apposition rate (MAR, 1.13±0.15 vs 1.72±0.4 um/d, $p<0.05$) and mineralizing surface (16.7±5.1 vs 35.1±9.6%, $p<0.01$) in 6-8 wk-old mice. However, KO bone marrow cells (BMC) formed more mineralized nodules earlier than WT BMCs associated with increased osteocalcin mRNA expression. In summary, 1) RelB-/- mice have age-related bone gain in their diaphyses characterized by increased trabecular number, decreased bone resorption and formation in vivo, but accelerated bone nodule formation in vitro; 2) RelB targets c-Fos to mediate OC differentiation. We conclude that RelB negatively regulates diaphyseal bone mass and helps to maintain bone homeostasis by balancing bone resorption and formation, but the precise mechanism whereby RelB regulates osteoblastic bone formation remains to be determined.

***Disclosures: Zhenqiang Yao**, None.*

FR0225

Osteoblast-targeted Overexpression of TAZ Results in Increased Bone Mass. Jee Hyun An*[1], Jae Yeon Yang[1], Sun Wook Cho[1], Ju Yeon Jung[1], Yenna Lee[1], Sang Wan Kim[1], Seong Yeon Kim[1], Jung Eun Kim[2], Jung Ho Hong[3], Chan Soo Shin[1]. [1]Department of Internal Medicine, Seoul National University College of Medicine, South korea, [2]Department of Molecular Medicine, Kyungpook National University, South korea, [3]College of Life Science, Korea University, South korea

Osteoblasts are derived from mesenchymal progenitors and differentiation to osteoblasts and adipocytes are reciprocally regulated. Transcriptional coactivator with PDZ-binding motif (TAZ) is a transcriptional coactivator that induces differentiation of mesenchymal cells into osteoblasts while blocking differentiation into adipocytes. To investigate the role of TAZ on bone metabolism in vivo, we have generated transgenic mice that overexpress TAZ under the control of procollagen type 1 promoter (Col1-TAZ). Whole body bone mineral density (BMD) measurement by DXA showed that Col-TAZ mice exhibited significant increase in BMD by 7.0% at 8 weeks of age and the difference was maintained up to 20 weeks of age. Furthermore, micro-CT analysis of distal femur at 16 weeks of age demonstrated significant increase in trabecular bone volume (14.5%), trabecular number (12%) and trabecular thickness (2%) in Col1-TAZ mice compared with WT littermate. In addition, dynamic histomorphometric analysis of lumbar spine revealed increased bone formation rate. When primary calvaria cells were cultured in osteogenic medium, the induction of alkaline phosphatase (ALP) activities were significantly increased in Col1-TAZ mice compared with WT littermate with consistent increase in mineralizing nodule formation assessed by Alizarin Red stain. Finally, quantitative real-time PCR analysis showed that the expression of Runx2, Col type 1, ALP and osteocalcin was significantly increased in calvaria cells from Col1-TAZ compared to those from WT littermate. Taken together, these results suggest that TAZ is a positive regulator of bone mass in vivo.

***Disclosures: Jee Hyun An**, None.*

FR0228

Sclerostin Is a Direct Target of Osteoblast-Specific Transcription Factor Osterix. Fan Yang[1], Wanjin Tang[2], Sarah So[2], Benoit de Crombbrugghe[3], Chi Zhang*[2]. [1]Bone Research Laboratory,Texas Scottish Rite Hospital, USA, [2]Bone Research Laboratory, Texas Scottish Rite Hospital, USA, [3]Dept of Genetics, University of Texas M.D. Anderson Cancer Center, USA

Bone formation is a developmental process involving the differentiation of mesenchymal stem cells to osteoblasts. Osterix (Osx) is an osteoblast-specific transcription factor required for bone formation and osteoblast differentiation. Osx knock-out mice lack bone completely and cartilage is normal. Our recent observations that Osx inhibits Wnt pathway provide a novel concept of feedback control mechanism involved in bone formation. Mechanisms of Osx inhibition on Wnt pathway are not fully understood. In this study Microarray was carried out to compare the RNA expression profiles of wild type and Osx-null calvarial cells at E18.5 in mice embryos. Our results revealed that Sclerostin (Sost) expression was abolished in Osx-null calvarial cells, and this was confirmed by quantitative real-time RT-PCR, suggesting Osx is required for Sost expression. We hypothesize that Osx may target Sost directly. Sost is a Wnt signaling antagonist and plays a role on bone remodeling. Overexpression of Osx in stable C2C12 mesenchymal cell line using Tet-off system was found to result in Sost expression upregulation. To test Osx regulation of Sost expression in vitro, we made a luciferase reporter construct driven by 1kb Sost promoter. Transient transfection assay showed that Osx activated Sost promoter activity in a dose-dependent manner. To define minimal region of Sost promoter activated by Osx, we made a series of deletion mutants of Sost promoter constructs, and narrowed down the minimal region to the proximal 250bp by transfection assay. Gel Shift Assay indicated that Osx bound to one GC-rich binding site within this minimal region of Sost promoter, and that point mutations of this binding site disrupted Osx binding. Moreover, the same point mutations in 250bp Sost promoter reporter disrupted the promoter activation by Osx, suggesting that the GC-rich binding site was responsible for Osx activation of Sost 250bp region promoter. To further examine physical association of Osx with Sost promoter in vivo, quantitative Chromatin immunoprecipitation (ChIP) assays were carried out. We observed the Osx association with endogenous Sost promoter in primary osteoblasts from mouse calvaria. Taken together, these findings support our hypothesis that Sost is a direct target of Osx. This provides a new additional mechanism through which Osx inhibits Wnt pathway during bone formation.

***Disclosures: Chi Zhang**, None.*

FR0232

G Proteins Differentially Regulate Wnt/β-catenin Signaling in Skeletal Development and Disease. Jean Regard*[1], Michael Collins[1], Pamela Robey[2], Lee Weinstein[3], Yingzi Yang[4]. [1]National Institutes of Health, USA, [2]National Institute of Dental & Craniofacial Research, USA, [3]National Institute of Diabetes & Digestive & Kidney Diseases, USA, [4]NIH/NHGRI, USA

Wnts are a family of secreted glycoproteins that control many aspects of skeletal development and homeostasis. The "canonical" Wnt signaling pathway is transduced through the stabilization of β-catenin. Despite their central importance in development and diseases, the mechanisms regulating Wnt signaling remain incompletely understood. The Frizzled family of Wnt receptors are 7 transmembrane-containing proteins with homology to G protein-coupled receptors (GPCRs), though the precise roles of G proteins in transducing Wnt signals are not known. Through a series of in vitro and in vivo experiments we have explored the interactions of the four major Gα protein families ($G\alpha_s$, $G\alpha_{i/o}$, $G\alpha_{q/11}$, $G\alpha_{12/13}$) with the Wnt/β-catenin signaling pathway. Gain-of-function experiments suggest activated $G\alpha_s$ potentiates Wnt/β-catenin signaling, though $G\alpha_s$ is not itself sufficient to activate this pathway. Similar activation of $G\alpha_q$ or $G\alpha_{13}$ inhibits Wnt/β-catenin signaling while activation of $G\alpha_{i/o}$ has no effect. Activated forms of $G\alpha_s$, $G\alpha_q$ and $G\alpha_{13}$ (but not $G\alpha_{i2}$) co-immunoprecipitate with Axin while wildtype forms either fail to bind or bind less robustly, demonstrating activity-dependent enhanced binding. Thus, Gα proteins may act through Axin, a core component in this pathway that assembles the β-catenin destruction complex. Importantly, removal of $G\alpha_s$, $G\alpha_{i/o}$, $G\alpha_{q/11}$ or $G\alpha_{12/13}$ from cells has no effect on the ability of Wnt to activate β-catenin, suggesting Gα proteins are not required for signaling. To test the functional significance of these Gα/Wnt/β-catenin interactions in vivo, we utilized a combination of mouse genetics and human disease samples. Removal of $G\alpha_s$ from the developing mouse limb leads to a profound decrease in Wnt/β-catenin signaling and decreased bone formation, demonstrating a physiologically important interaction in vivo during skeletal development. Also, activating mutations of human $G\alpha_s$ known to cause McCune-Albright Syndrome (MAS) potentiate Wnt/β-catenin signaling and β-catenin is upregulated in fibrous-dysplastic bone and thyroid tissues from MAS patients. This observation indicates that dysregulation of Wnt/β-catenin signaling may be at least partially responsible for the pathophysiology of this debilitating human syndrome. In conclusion, our data suggests that Gα proteins are playing physiologically significant regulatory roles in Wnt/β-catenin signaling during both skeletal development and disease.

***Disclosures: Jean Regard**, None.*

FR0234

Insulin Receptor Signaling in Osteoblasts Regulates Bone Acquisition and Glucose Metabolism. Ryan Riddle*[1], Keertik Fulzele[2], Douglas Digirolamo[3], Xuemei Cao[4], Chao Wan[5], Marie-Claude Faugere[6], Mehboob Hussain[3], Jens Bruning[7], Thomas Clemens[3]. [1]Johns Hopkins University School of Medicine, USA, [2]Massachusetts General Hospital; Harvard Medical School, USA, [3]Johns Hopkins University, USA, [4]University of Alabama at Birmingham, USA, [5]University of Alabama, Birmingham, USA, [6]University of Kentucky Medical Center, USA, [7]University of Cologne, Germany

Management of constant energy supply in an environment of variable food intake is critical for the survival of all terrestrial species. Mammals have evolved intricate networks of local and circulating factors that coordinate energy expenditure. Bone is increasingly recognized for its role in coordinating global energy utilization via the insulin secretagogue, osteocalcin. For this putative bone-pancreas hormonal network to function efficiently, we reasoned that insulin should regulate osteoblast activity. To test this idea, we generated mice lacking the insulin receptor (IR) specifically in the osteoblast (Ob-ΔIR). Six-week-old Ob-ΔIR mice demonstrated reduced (47%) trabecular bone volume and reduced osteoblast numbers. *In vitro*, primary ΔIR osteoblasts failed to differentiate and demonstrated reduced Runx2 and osteocalcin mRNA expression. Insulin treatment induced a 3-fold increase in osteocalcin promoter activity and a 2.5-fold increase in Runx2 occupancy of the OSE2 element (CHIP). Transcriptional profiling and immunoprecipitation experiments conducted in insulin-treated and ΔIR osteoblasts indicated that insulin regulates osteoblast differentiation by suppression of the Runx2 inhibitor, Twist2. Surprisingly, as Ob-ΔIR mice aged, they developed marked peripheral adiposity and biochemical changes indicative of insulin resistance. Insulin and glucose tolerance tests showed that the Ob-ΔIR mice exhibited profound glucose intolerance and insulin resistance accompanied by lowered energy expenditure but normal food intake. Pancreatic β-cell mass and *Ins1* and *Ins2* expression were reduced in the pancreas of Ob-ΔIR mice compared to controls, suggesting that insulin resistance is accompanied by reduced insulin secretory reserves. Importantly, both total and undercarboxylated osteocalcin serum levels were decreased significantly in Ob-ΔIR mice compared to controls. Finally, we measured the effect of a 2-week infusion of undercarboxylated osteocalcin on glucose

and insulin sensitivity. Osteocalcin infused Ob-ΔIR mice had blunted glucose excursions and more pronounced reductions in serum glucose following a bolus of insulin relative to controls. These results suggest the existence of a bone-pancreas endocrine loop, through which insulin signaling in the osteoblast ensures osteoblast differentiation and stimulates osteocalcin production, which in turn regulates insulin sensitivity and pancreatic insulin secretion to control glucose homeostasis.

***Disclosures: Ryan Riddle**, None.*

FR0235

Insulin Signaling in Osteoblasts is a Positive Regulator of Bone Resorption. Jianwen Wei*, Tatsuya Yoshizawa, Mathieu Ferron, Patricia Ducy, Gerard Karsenty. Columbia University, USA

Insulin is one of the most important hormones in vertebrates. This is explained in large part because insulin acts on numerous cell types and has pleiotropic functions in these cells. The classical insulin target tissues are liver, muscle and white adipose tissue, where it regulates glucose and energy metabolism. However, the fact that the insulin receptor is expressed in many cell types suggests that the spectrum of insulin target tissues and of insulin functions is broader than that. In particular, that the insulin receptor is expressed in osteoblasts along with the fact that injection of a bolus of insulin increases phosphorylation of the insulin receptor in bone suggests that insulin may regulate aspects of bone physiology. In order to address this question, we generated mice lacking the insulin receptor in the osteoblast lineage only. Unexpectedly, *InsR osb-/-* mice develop a severe low turnover, low bone mass phenotype. Histomorphometric and biochemical analyses revealed that insulin signaling in osteoblasts normally favors bone resorption by osteoclasts. A molecular analysis of this latter phenotype revealed that insulin signaling in osteoblasts is a powerful regulator of *Osteoprotegerin* expression. Co-culture assays followed by a thorough gene expression analysis demonstrated that the main osteoclast function regulated by insulin signaling in osteoblasts is the acidification of the extracellular matrix. This occurs through its regulation of the expression of *Cathepsin K* and *Tcirg1,* two genes mutated in of human skeletal dysplasia. These results identified a signaling cascade downstream of insulin signaling in osteoblasts leading to acidification of the bone extracellular matrix by osteoclasts. As such, they revealed that insulin is a major hormonal regulator of bone remodeling.

***Disclosures: Jianwen Wei**, None.*

FR0236

PIN1 Mediates The Effects of Notch on The Stability of NFATc2 Transcripts. Stefano Zanotti*[1], Anna Smerdel-Ramoya[2], Ernesto Canalis[2]. [1]Saint Francis Hospital & Medical Center, USA, [2]St. Francis Hospital & Medical Center, USA

Notch are transmembrane receptors that determine cell fate decisions. Interactions of Notch with its ligands result in the release of its intracellular domain (NICD), which is the mediator of Notch signaling. Nuclear Factor of Activated T-Cells (NFAT) are a family of four transcription factors that determine cell differentiation and function. NFATc1 and NFATc2 are expressed by osteoblasts. Notch is a suppressor of osteoblastogenesis, whereas the role of NFATc1 and NFATc2 in osteoblast differentiation is controversial. We have shown that Notch regulates NFAT transactivation in osteoblasts, but the mechanisms involved are not known. To investigate the actions of Notch on NFATc1 and NFATc2 expression, osteoblasts from $Rosa^{Notch}$ mice, where NICD is induced following the deletion of a STOP cassette by CRE recombination, were used. Notch downregulated NFATc1 mRNA by suppressing its transcription. In contrast, Notch induced NFATc2 by a post-transcriptional mechanism, without affecting NFATc2 transcription. To determine the rate of decay of NFATc1 and NFATc2 mRNA, osteoblasts were treated with 5,6-dichloro-1-β-D-ribofuranosylbenzimidazole (DRB) to inhibit RNA polymerase II. Notch did not modify the half-life of NFATc1 mRNA, confirming that it downregulated NFATc1 exclusively by transcriptional mechanisms. In contrast, Notch extended the half-life of NFATc2 transcripts from 2 h to 8 h, demonstrating that Notch stabilizes NFATc2 mRNA. To study the mechanisms involved, we explored the role of Peptidyl-Prolyl Cis/Trans Isomerase Nima-Interacting Protein (PIN1), an isomerase that regulates the mRNA stability of secreted proteins. PIN1 acts on mRNA-binding proteins and catalyzes the cis/trans isomerization of the peptide bond between a phosphorylated Serine/Threonine and a Proline residue. To test whether PIN1 mediated the effects of Notch on NFATc2 mRNA stability, PIN1 was down regulated in $Rosa^{Notch}$ osteoblasts by RNA interference, in the context, or not, of NICD overexpression. Downregulation of PIN1, as well as the use of a specific inhibitor of PIN1 activity, reversed the stabilizing effect of Notch on NFATc2 mRNA. This is the first report demonstrating post-transcriptional regulation of NFATc2 mRNA and documenting that the role of PIN1 extends beyond the control of mRNA stability of secreted proteins. In conclusion, Notch stabilizes NFATc2 transcripts through a PIN1 dependent mechanism.

***Disclosures: Stefano Zanotti**, None.*

FR0238

Age-related Declines in Expression of CYP27B1 and in Osteoblast Differentiation in Human MSCs. Shuo Geng*, Shuanhu Zhou, Julie Glowacki. Brigham & Women's hospital, USA

Human marrow contains adherent cells with potential to differentiate to osteoblasts and other cell lineages. We and others showed that there is an age-related decline in osteoblast potential and that osteoblast differentiation can be stimulated by 1,25-dihydroxyvitamin D ($1,25(OH)_2D$). We recently reported that human marrow stromal cells (hMSCs) have vitamin D hydroxylases and that expression of CYP27B1/1α-hydroxylase (1α) is related to clinical features of the subject from whom the hMSCs were obtained (Endocrinology 2010;151:14). This study tests the hypothesis that 25-hydroxyvitamin D (25OHD) stimulates osteoblast differentiation in hMSCs that express 1α and that there may be effects of age. Human MSCs were prepared from bone marrow that was discarded from subjects undergoing joint replacement. Low-density mononuclear cells were isolated by centrifugation on Ficoll/Histopaque 1077; after overnight culture in phenol red-free αMEM, 10% fetal bovine serum, and antibiotics, non-adherent cells were removed and the adherent MSCs were expanded and studied. Osteoblast differentiation was assessed by measurement of alkaline phosphatase activity. Osteoblastogenesis of hMSCs (n=33 subjects, ages from 27 to 83 years) was stimulated by 10 nM $1,25(OH)_2D_3$ with a significant age-related decrease in response with age (r=-0.381, p=0.029). In a series of 20 samples from elders (66 ± 11), $1,25(OH)_2D_3$ stimulated osteoblastogenesis in 55%. In 30% of those samples, both $1,25(OH)_2D_3$ and $25OHD_3$ stimulated osteoblastogenesis. Expression of 1α in 27 subjects (57 ± 12) was inversely correlated with age (r=-0.498; p=0.008, Figure). The constitutive expression of 1α in the younger group (<50 years, n=12) was 1.8-fold greater than in the older group (>55, n=15, p=0.007). To test for a role of 1α in the stimulation of osteoblastogenesis by $25OHD_3$, a cytochrome P450 inhibitor ketoconazole (10 μM) was added to some cultures. Osteoblastogenesis was stimulated by $25OHD_3$ ($p<0.05$), but there was no stimulation in the presence of ketoconazole. This suggests that 1α-hydroxylation of $25OHD_3$ may be needed for its stimulation of osteoblastogenesis. The age-related decline in constitutive expression of 1α may account for the age-related decline in osteoblast differentiation in hMSCs.

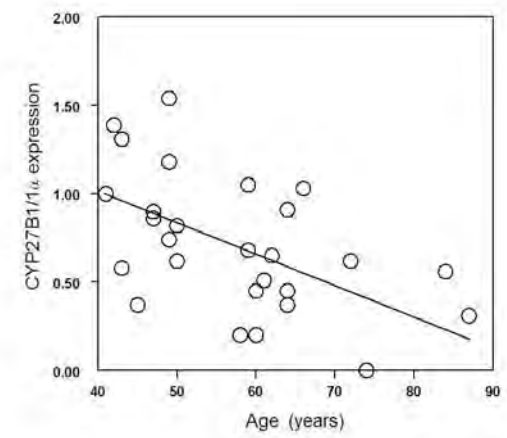

Figure

***Disclosures: Shuo Geng**, None.*

FR0240

Dicer Excision in Mature Osteoblasts in the Postnatal Skeleton Induces High Bone Mass by Inactivating miR that Attenuate Bone Formation. Tripti Gaur*[1], Sadiq Hussain[1], Stacey Russell[1], Lammy Kim[2], Jennifer Colby[1], Dana Frederick[1], Andre Van Wijnen[1], David Eyre[3], Janet Stein[1], Gary Stein[1], Stephen Jones[1], Jane Lian[1]. [1]University of Massachusetts Medical School, USA, [2]University of Washington, USA, [3]University of Washington Orthopaedic Research Labs, USA

Studies have reported the requirement of miRNA (miR) processing by a ribonuclease enzyme, Dicer, for the control of gene expression to regulate cell growth and differentiation in mammalian tissues. We established a requirement for miRs and Dicer in bone development and homeostasis by conditional deletion of Dicer in mature osteoblasts using Osteocalcin-Cre. Analysis of the ratio of precursor miR to mature miR for selected miRs was higher in $Dicer^{\Delta oc/\Delta oc}$ bone samples as expected, confirming reduced miR biogenesis following Dicer ablation. Our microCT results show that $Dicer^{\Delta oc/\Delta oc}$ induces an increase in the mass of long bones in adult mice beginning at 1 month and progressing up to up to 8 months of age. Cortical porosity was reduced significantly in $Dicer^{\Delta oc/\Delta oc}$ mice. The membranous calvarial bone had increased BMD without excessive bone formation. Dynamic histomorphometry by calcein labeling revealed more than a 2-fold increase in bone matrix apposition in both cortical and trabecular region in $Dicer^{\Delta oc/\Delta oc}$ femurs compared to the control mice, rendering a thickened bone from the periosteal side. However, normal bone

architecture and cellular organization with similar osteocyte density was observed. With increased rate of bone formation, lamellar bone but not woven bone, was revealed by polarizing microscopy. Mature collagen crosslinks (hydroxylysyl pyridinoline and lysyl pyridinoline) were comparable between $Dicer^{c/c}$ and $Dicer^{\Delta oc/\Delta oc}$ when examined at 2 and 4 months of age, again suggesting normal collagen fibril organization. Biomechanical and mineral property studies are in progress to evaluate the bone quality. To further explore the molecular basis for the unusual bone phenotype of $Dicer^{\Delta oc/\Delta oc}$ mice, we examined collagen levels in affected bone. In agreement with a previous report indicating that miRs expressed in osteoblasts/osteocytes negatively regulate bone matrix proteins and collagens, we observed a 5-fold increase in gene expression for Type I collagen in Dicer-ablated bone, and a decrease for Types III and V, typically higher in immature bone. Furthermore, in silico analysis of miRs in osteoblasts suggests that upregulation of canonical Wnt components in $Dicer^{\Delta oc/\Delta oc}$ bone, contribute to the high bone mass phenotype. We conclude that miRs regulate osteoblastogenesis and the acquisition of bone mass, in part by targeting bone matrix genes and the canonical Wnt pathway.

***Disclosures: Tripti Gaur**, None.*

FR0245

Mechanical Inhibition of Adipogenesis Achieved via a Regenerated β-catenin Signal is Amplified by Incorporating a Refractory Period. Buer Sen*[1], Zhihui Xie[2], Natasha Case[3], Maya Styner[3], Clinton Rubin[4], Janet Rubin[3]. [1]University of North Carolina At Chapel Hill, USA, [2]UNC-CH, USA, [3]University of North Carolina, Chapel Hill, School of Medicine, USA, [4]State University of New York at Stony Brook, USA

Mechanical signals are recognized as anabolic to bone and inhibitory to fat. Evidence indicates that both low intensity vibration (LIV) and high magnitude strain (HMS) achieve these outcomes by directly biasing mesenchymal stem cell (MSC) lineage towards osteoblastogenesis and away from adipogenesis. To understand the molecular cues and the "idealized" mechanical requirements for direct mechanical control of MSC lineage selection, we studied the effects of daily LIV or HMS in cultures of C3H10T1/2 or bone marrow derived MSCs cultured in adipogenic conditions for 7-10 days. LIV (0.6g, 90 Hz) delivered for 20 or 40 minutes 1X day failed to repress adipogenesis, as measured by increased fat marker proteins (adiponectin, aP2). LIV significantly and robustly reduced acquisition of fat phenotype when a second 20 min LIV treatment was added each day. The second treatment achieved efficacy only if delivered after a rest period of >1 hour between mechanical treatments. The ability of the second LIV treatment to suppress adipogenesis was enhanced by increasing the rest period to more than 3 h. The addition of a third LIV treatment each day, again following a 3h rest period, further augmented repression of adipogenesis (30% decrease in adiponectin with 2x LIV/day, 75% with 3x/day - see Fig). Similarly, 400 cycles of HMS (2% strain, 0.17 Hz, 40 min), showed increased efficacy when the HMS was divided into 2 x 20 min (200 cycles) sessions separated by >1 h. These results are consistent with the presence of a biological refractory period independent of the type of mechanical input. The signal cascade triggered by LIV exposure involved inhibition of GSK3β with subsequent activation of β-catenin: siRNA silencing of β-catenin negated LIV's effect on adipogenesis. Finally, MSCs treated with 2 x LIV daily for 7 d showed increased induction of osteocalcin mRNA by BMP 100 ng/ml compared to MSC that were not exposed to LIV: osteocalcin increased by $62 \pm 12\%$ after LIV and $38 \pm 9\%$ in control. Our data suggests that mechanical input triggers a burst of signaling in MSCs, where the extent of cellular response depends more on treatment scheduling than magnitude of the mechanical signal. Once the MSC response is triggered via LIV or HMS, the biological system must "reset" before it can fully respond again. As such, incorporating a biological refractory period into a treatment regimen should enhance the response to repeated high or low magnitude mechanical signal.

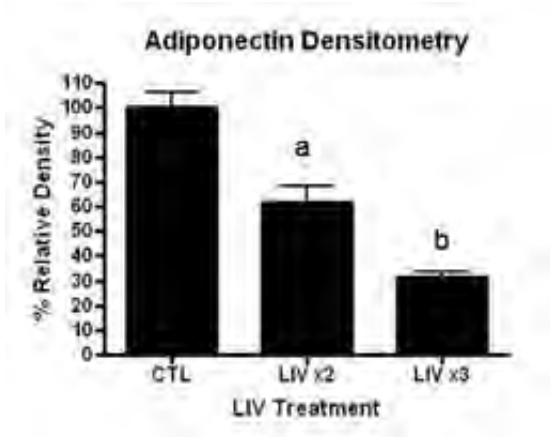

SenJPG

***Disclosures: Buer Sen**, None.*
This study received funding from: NIAMS

FR0246

Mechanical Signals Protect the Bone Marrow Stem Cell Niche from Damage due to a High Fat Diet. Benjamin Adler*[1], Danielle E. Green[1], Ete M. Chan[1], Stefan Judex[1], Clinton Rubin[2]. [1]Stony Brook University, USA, [2]State University of New York at Stony Brook, USA

Obesity is widely thought to compromise bone quality and bias the differentiation of bone marrow stromal cells (BMSCs) towards adipogenesis. Obesity also increases lifetime susceptibility to illness, implicating a compromised immune system perhaps due to impaired hematopoiesis as marrow adiposity increases. Hematopoietic stem cells (HSC) occupy a complex niche in which they are co-localized, interact with, and are regulated by osteoblasts, BMSCs, bone structure and vasculature. Low intensity vibration (LIV) has been shown to stimulate proliferation of BMSCs and bias their differentiation towards osteoblastogenesis and suppress adiposity. In this study, we hypothesize that animals fed a high fat diet will suffer impaired hematopoiesis, and considering LIV's influence on BMSCs, that these mechanical signals may also serve to protect the HSC niche and hematopoiesis from this diet-induced impairment. To test this hypothesis, 7 wk old male C57Bl/6J mice were fed either a high fat (45% Kcal from fat-FDC,FDV) or regular diet (RDC) and subject to LIV (90Hz, 0.25g)(FDV), or sham handling (FDC, RDC) for 15min/day, 5 days/wk for 6 weeks (n=7 per group). At sacrifice, marrow was extracted from the left leg and stained for flow cytometry. Side population cells which are c-kit+, Lin-, and Sca-1+ (SPKLS) are highly enriched for HSC's, whereas the c-kit+, Lin-, and Sca-1+ (KLS) compartment contains both HSC's and progenitor cells. Means were compared with one-way ANOVAs and Tukey post hoc tests. High fat feeding increased the proportion of SPKLS cells in both FDC and FDV animals by 23 and 21% compared to RDC (NS). In contrast, the proportion of KLS cells in the FDC group dropped by 28% (p=0.03 to RDC), whereas FDV KLS cells fell by only 14% (NS to RDC). Although HSC proportions were almost identical in both the FDC and FDV groups, the drop in FDC KLS cells, which represent early progenitors, implies that the high fat diet compromised HSC differentiation. LIV resulted in 19% more KLS cells than the fat diet controls, suggesting that these mechanical signals mediated a partial rescue of HSC function. That even a short term increase in dietary fat can result in significant negative effects on HSC function is alarming and intimates the effects of chronic changes to the bone marrow niche on hematopoiesis and health. The partial rescue of HSC function by LIV suggests that the systemic chronic complications of obesity may ultimately be checked by non-pharmacologic means.

***Disclosures: Benjamin Adler**, None.*

FR0248

Peptide-mediated Disruption of N-cadherin-LRP5/6 Interaction Stimulates Wnt Signaling, Osteoblast Replication and Differentiation. Eric Haÿ*[1], Thibault Buczkowski[1], Pierre Marie[2]. [1]Inserm U606 & University Paris Diderot, France, [2]INSERM Unit 606 & University Paris Diderot, France

Canonical Wnt signalling plays an important role in the control of osteoblastogenesis. We previously showed that N-cadherin interacts with the Wnt co-receptors LRP5/6 and downregulates osteoblast proliferation, differentiation and bone formation via attenuation of Wnt, ERK and PI3K/Akt signalling. In this study, we investigated the functional domains of N-cadherin that interact with LRP5/6. To this goal, MC3T3-E1 osteoblastic cells were transfected with full length N-cadherin or N-cadherin constructs lacking the last 153 (Delta 153), 114 (Delta 114) or 62 (Delta 62) aminoacids (AA) that interact with axin, cyclin D1, casein kinase 1 (CK1) or GSK3. The expression of truncated N-cadherin constructs was confirmed by western blot analysis and immunocytochemistry. Immunoprecipitation analysis showed that transfection with Delta 62 abolished the physiological interaction between N-cadherin and LRP5. In contrast to full length N-cadherin, transfection with Delta 62 N-cadherin did not affect beta-catenin transcriptional activity. Interestingly, transfection with Delta 62 N-cadherin increased cell replication, alkaline phosphatase (ALP) activity and osteoblast gene expression (Runx2, ALP, Col1A1) in MC3T3-E1 cells. This indicates that deletion of the Delta 62 domain abolishes N-cadherin-LRP5 interaction, and thereby promotes osteoblast proliferation and differentiation. We previously showed that N-cadherin interacts with the 28 last AA in the LRP5/6 intracellular domain in osteoblasts. We therefore hypothesized that blocking this interaction may promote Wnt signaling. Immunoprecipitation analyses showed that a synthetic cyclic peptide containing the last 28 AA of LRP5 abolished the functional interaction between N-cadherin and LRP5 in MC3T3-E1 osteoblasts. Strikingly, this peptide increased beta-catenin nuclear translocation and transcriptional activity, and enhanced ERK and PI3K/Akt signalling in MC3T3 cells, resulting in increased cell proliferation and osteoblast gene expression. The results show that 1) the 28 last AA in the LRP5/6 intracellular domain physiologically interacts with the 62 last amino acids of N-cadherin, and 2) peptide-mediated disruption of the interaction between LRP5/6 and N-cadherin intracellular domains results in increased osteoblast proliferation and differentiation, thus providing a novel potential target to promote osteoblastogenesis.

This work was sponsored in part by the FP7 Program Talos.

***Disclosures: Eric Haÿ**, None.*

FR0253

Disruption of Cathepsin K in the Osteoclast Lineage Increased Bone Formation through Coupling-dependent Mechanism. Sutada Lotinun*[1], Riku Kiviranta[2], Lynn Neff[1], Jean Vacher[3], Eero Vuorio[2], William Horne[1], Georgios Sabatakos[4], Roland Baron[5]. [1]Harvard School of Dental Medicine, USA, [2]University of Turku, Finland, [3]Institut De Recherches Cliniques De Montréal, Canada, [4]Procter & Gamble Pharmaceuticals, Inc., USA, [5]Harvard School of Medicine & of Dental Medicine, USA

Loss of function mutation of cathepsin K (CathK) in humans causes pycnodysostosis. It has been shown that CathK-null mice have high bone formation rate (BFR) and high numbers of poorly functional osteoclasts (OCs) (Kiviranta et al., 2005; Pennypacker et al., 2009). We have reported that ablation of CathK in hematopoietic cells using Mx1-cre-LoxP (Mx1-cre;CKLP$^{fl/fl}$ mice) eliminated most of CathK mRNA expression in OCs but not in osteoblasts (OBs). Mx1-Cre-induced CathK deficiency resulted, as expected, in moderate osteopetrosis with increases in cancellous bone volume (+163%) and number of poorly functional OCs (+178%). Interestingly, BFR and OB number were also markedly increased (+188% and +214%, respectively). Both ALP and mineralized bone nodules were increased in Mx1-Cre;CathK$^{fl/fl}$ OBs cultured *in vitro*. In contrast, targeted deletion of CathK in OB lineage had no effect on bone formation or bone resorption, suggesting that deletion of CathK in OC induces the increased BFR. However, the mechanism leading to increased BFR in Mx1-cre;CKLP$^{fl/fl}$ mice remains undefined. We proposed that deletion of CathK in OCs causes a release of coupling factors, recruiting osteoprogenitors to the remodeling sites and stimulating bone formation. To test this hypothesis, we specifically deleted CathK in the OC lineage by crossing with CD11b-cre mice. CD11b-Cre-induced CathK deficiency increased OC number but also resulted in increases in several indices of bone formation (MS, MAR, BFR, and OB number), demonstrating that the increased BFR is OC-mediated. Steady-state levels of OB marker genes osterix and osteocalcin also increased. We measured *in vitro* gene expression of OC-derived coupling factors, including wnt10b, ephrin b2, and sphingosine kinase (SPHK), an enzyme that catalyzes the phosphorylation of sphingosine to sphingosine 1-phosphate (S1P). Ablation of CathK in OCs increased SPHK1 but not SPHK2, wnt10b or ephrin b2. Immunostaining confirmed the increased SPHK1 in OCs. Our data provide evidence that the increased BFR in CathK-null mice is due to changes in OCs and that S1P may be one of the coupling factors that induce this increase.

***Disclosures: Sutada Lotinun**, None.*
This study received funding from: Procter & Gamble

FR0254

CD68 Regulates Osteoclast Function via Mediation of Attachment to Bone. Jason Ashley*, Zhenqi Shi, Xu Feng. University of Alabama at Birmingham, USA

Adhesion of osteoclasts to the bone surface by way of the sealing zone has long been recognized as an important feature of their bone resorptive activity; however, how osteoclasts form this strong attachment at the sealing zone has not been fully elucidated. In an effort to identify mediators of osteoclast/osteoclast precursor attachment to bone, we developed a phage-display library from cDNA derived from bone marrow macrophages (BMMs) grown on bone slices and screened that library in a bio-panning assay with a selection bias towards phages with high affinity for bone matrix. Sequencing of cDNA from an adherent phage identified CD68 as a candidate bone adhesion molecule. CD68, a heavily-glycosylated transmembrane protein belonging to the Lysosome Associated Membrane Protein (LAMP) family, is highly expressed by macrophages and osteoclasts. Unlike most LAMPs, CD68 possesses a largely O-glycosylated mucin-like domain that faces either the lumen of the lysosome or the extracellular space depending on its localization. *In vitro* antibody blockade and RNAi experiments revealed that, in the absence of functional CD68, BMM attachment to bone slices is reduced. Furthermore, osteoclasts formed *in vitro* from shRNA-silenced BMMs do not spread properly and fail to efficiently resorb bone. These data indicate that CD68 plays an important role in osteoclast function by mediating their attachment to bone. Interestingly, during osteoclastogenesis there is an increase in CD68 expression concomitant with a decrease in apparent molecular weight (MW), which is likely due to a decrease in glycosylation. We found that M-CSF alone increases CD68 expression, while RANKL is required for the change in MW. This shift is apparent within 36 hours of initial RANKL treatment and becomes more pronounced as osteoclastogenesis progresses. RANK signals through multiple intracellular TRAF-binding and non-TRAF-binding motifs. Using human Fas/mouse RANK chimeric receptors that allow specific activation of TRAF versus non-TRAF motifs, we found that stimulation of receptors with functional TRAF motifs, but not those without, induces a reduction in CD68 MW that parallels the shift seen in BMMs treated with RANKL, indicating that the RANKL-induced change in CD68 MW is mediated through TRAF signaling. The findings described above show that CD68 plays a role in bone resorption by mediating osteoclast attachment and this function likely depends upon a RANKL-induced reduction in CD68 glycosylation.

***Disclosures: Jason Ashley**, None.*

FR0255

Osteoclast Attachment and Motility are Regulated by Nitric Oxide Through the Dual Effects of IRAG on Calcium Release and Cytoskeletal Protein Interactions. Lisa Robinson*, Harry Blair, Beatrice Yaroslavskiy. University of Pittsburgh, USA

Control of osteoclast activity is critical to the maintenance of skeletal mass. Previous studies showed that nitric oxide (NO), a negative regulator of bone resorption, promotes detachment and motility of osteoclasts: we observed disassembly of the cytoskeletal complexes required for specialized osteoclast attachments at resorption sites after NO signals, and found that NO-stimulated osteoclast motility required inositol-1,4,5-trisphosphate receptor (IP3R) controlled calcium release. In the present studies, using human osteoclasts in vitro, we further explored the molecular mechanisms of osteoclast regulation by NO, focusing on the roles of the IP3R1-associated cGMP-dependent protein kinase substrate (IRAG). Two isoforms of IRAG exist, resulting from alternative splicing; both are expressed by the osteoclast. As in other cell types, the larger (endosomal) form of IRAG is found at the endoplasmic reticulum, where it is proposed to act as a scaffold facilitating phosphorylation of IP3R1 by PKG1beta. Co-immunoprecipitation and Western blot studies revealed specific binding of the endosomal IRAG to IP3R1 in osteoclasts and serine phosphorylation of both by the cGMP-dependent protein kinase (PKG). Unexpectedly, we found that IRAG-IP3R1 association was not static in osteoclasts: NO stimulated dissociation of the complex. Both NO antagonists and PKG inhibitors stabilized the IRAG-IP3R1 complex. NO-dependent Src activation, which by phosphorylating IP3R1 enhances calcium release, also promoted dissociation of IRAG from IP3R1. When IRAG was suppressed by siRNA, basal calcium levels increased, and calcium regulation by NO was lost, consistent with IRAG as a link between NO and IP3R1. Immunofluorescence studies also showed IRAG localization to podosomes but the predominant form at this site was the smaller isoform, hitherto of unknown function. Using co-immunoprecipitation and Western blotting we detected binding of IRAG to cytoskeletal regulatory proteins migfilin and VASP. Inhibition of IRAG expression by siRNA reduced cell spreading and attachment, and altered podosome distribution, the resulting pattern resembling that of osteoclasts with attachment defects associated with osteopetrosis. Together these results identify IRAG as a mediator of NO effects on osteoclast attachment involved both in the regulation of IP3R1 calcium release and in interactions with cytoskeletal proteins critical to osteoclastic bone resorption.

***Disclosures: Lisa Robinson**, None.*

FR0258

Bone Marrow Stromal Cells Suppress TACE-mediated M-CSFR and RANK Shedding to Facilitate Osteoclastogenesis and Suppress DC Differentiation from Monocytes. Masahiro Hiasa*[1], Masahiro Abe[2], Ayako Nakano[3], Asuka Oda[2], Hiroe Amou[2], Keiichiro Watanabe[4], Shingen Nakamura[2], Hirokazu Miki[2], Kyoko Takeuchi[2], Kumiko Kagawa[2], Shuji Ozaki[2], Eiji Tanaka[1], Kenzo Asaoka[1], Toshio Matsumoto[5]. [1]University of Tokushima Graduate School, Japan, [2]University of Tokushima, Japan, [3]University of Tokushima Graduate School of Medicine, Japan, [4]The University of Tokushima Graduate School of Oral Science, Japan, [5]University of Tokushima Graduate School of Medical Sciences, Japan

Multiple myeloma (MM), a malignancy of plasma cells, arises and expands in the bone marrow and generates devastating osteoclastic bone destruction. In contrtast to enhanced osteoclastogenesis, dendritic cells (DCs) decrease in number and function in MM, suggesting the dysregulation of OC and DC differentiation from their precursor, monocytes. We recently reported that GM-CSF and IL-4, an inducer of DC differentiation, up-regulate TNF-alpha converting enzyme (TACE) expression in monocytes to cleave their surface M-CSF receptor (M-CSFR) and RANK and disrupt osteoclastogenesis (Blood, 2009). Because bone marrow stromal cells (BMSCs) play an important role in osteoclastogensis in MM, we explored the role of BMSCs in the regulation of monocyte differentiation into OCs and DCs. BMSCs suppressed DC induction and resumed osteoclastogenesis from monocytes along with the restoration of surface M-CSFR and RANK expression on monocytes in the presence of GM-CSF and IL-4. BMSCs secreted a large amount of TIMP-3, an inhibitor for TACE. The suppression of TIMP-3 production in BMSCs by TIMP-3 siRNA significantly increased M-CSFR ectodomain shedding in monocytes and resumed GM-CSF and IL-4-mediated DC differentiation from monocytes in the presence of BMSCs, suggesting the regulation of TACE activity in monocytes and monocyte differentiation by BMSC-derived TIMP-3. The TIMP-3 production by BMSCs was further enhanced by IL-6 and TGF-beta which are known to be over-produced in MM bone lesions. Interestingly, RANK ligand induced TIMP-3 mRNA expression in RAW264.7 cells; TIMP-3 expression was robustly up-regulated in OCs compared to that in their precursor monocytes while TACE expression showed no appreciable change. These results suggest that BMSCs up-modulate M-CSFR and RANK on monocytes through TIMP-3 elaborated by BMSCs to facilitate osteoclastogenesis and suppress DC differentiation, and that TIMP-3 expression is induced in OCs by themselves during osteoclastogenesis to further block TACE activity and enhance the surface expression of these receptors. Besides the up-regulation of RANK ligand expression in BMSCs by MM cells, the suppression by BMSCs of TACE-mediated shedding of M-CSFR and RANK may dysregulate monocyte differentiation towards OCs to cause extensive bone destruction and immunodeficiency in MM.

***Disclosures: Masahiro Hiasa**, None.*

FR0261

Identification of a Novel Osteoclastogenic Co-activator for Nfatc1, OCAN. Min-Young Youn*[1], Sally Fujiyama-Nakamura[1], Shigeaki Kato[2]. [1]IMCB, University of Tokyo, Japan, [2]University of Tokyo, Japan

Osteoclastogenesis is the highly regulated process governed by diverse factors. Among them, Nfatc1 is a prime transcriptional factor throughout osteoclastogenesis. With differentiation signal, Nfatc1 is dramatically induced by auto-amplification with its unique promoter status, suggesting involvement of specialized epigenetic regulation. However, epigenetic complexes assisting Nfatc1 expression and/or function during osteoclastogenesis remain to be identified. To address this issue, we tried to biochemically purify epigenetic regulators associating with Nfatc1. Nuclear extracts prepared from RANKL-induced Raw264 cells were applied into Nfatc1-antibody column, and then candidate proteins were identified by MALDI-TOF/MS analysis. Among several identified factors, we focused on an uncharacterized protein 'osteoclastogenic co-activator for Nfatc1 (designated as OCAN)', simultaneously purified with Brg1 and Baf protiens of SWI/SNF-type chromatin remodeler complex. These interactions were also confirmed by co-immunoprecipitation experiment, suggesting that OCAN is a novel component of SWI/SNF-type chromatin remodeler complex to support Nfatc1 function. To understand the role of OCAN, transcriptional activity of Nfatc1 was detected by luciferase assay. Interestingly, its transcriptional activity was enhanced by OCAN overexpression. Consistently, OCAN knockdown resulted in decreased expression of osteoclast-specific genes such as CtsK and TRAP with inhibited osteoclast formation. These results indicate that OCAN plays a role as a co-activator of Nfatc1 during osteoclastogenesis. To define the molecular mechanism of OCAN, the recruitment of Nfatc1 on promoters of its target genes was detected with ChIP assay. Nfatc1 could not be recruited on its target genes without OCAN protein. Similarly, recruitment of Brg1 was reduced in OCAN-knockdown cells. Taken together, OCAN can be considered as a novel component of a SWI/SNF-type chromatin remodeler complex to reorganize the chromatin status for DNA-binding ability of Nfatc1.

***Disclosures: Min-Young Youn**, None.*

FR0263

MicroRNA-21 Has a Central Critical Role in Osteoclastogenesis. Keith Hruska, Toshifumi Sugatani*. Washington University in St. Louis School of Medicine, USA

MicroRNAs, integral elements in the post-transcriptional control of gene expression, are implicated in many physiological cellular processes and contribute to molecular alterations in pathophysiological conditions. Our previous studies have demonstrated that conditional deletion of Dicer with a cre-lox strategy employing a cre directed to the myeloid-osteoclast lineage, CD-11b-Cre mice, produced mild osteopetrosis due to decreased osteoclast numbers and bone resorption, indicating that microRNA biogenesis is obligatory for osteoclastic control of bone metabolism. Dicer is an endoribonuclease in the RNase III family that cleaves double-stranded RNA and precursor-microRNA into short double-stranded RNA fragments called small interfering RNA. However, the mechanisms of microRNA action and the biological roles of specific microRNAs in osteoclastic control of bone metabolism are not fully understood. We found that two microRNAs of 617 mouse microRNAs are robustly expressed during osteoclastogenesis using a high-throughput analysis. In the analysis of the role of one of these, microRNA-21 (miR-21), we demonstrated that its expression and function was critical in osteoclastogenesis. Gene silencing of miR-21 significantly inhibited TRAP-positive osteoclast formation. In investigating the biological function of miR-21 in osteoclastogenesis, we focused explicitly on the function of programmed cell death 4 (PDCD4), one of the targets of miR-21, in osteoclastogenesis. Forced expression of PDCD4 significantly suppressed TRAP-positive osteoclast formation numbers due to attenuated c-Fos activity and expression of NFATc1. Moreover, the expression of osteoclast-specific markers such as cathepsin K and integrin beta-3 was inhibited by PDCD4 overexpression. In addition, forced expression of PDCD4 robustly induced the expression of nuclear factor I-B (NFIB) which is a target of miR-21, and additionally, a transcriptional repressor of the miR-21 promoter. Also, c-Fos overexpression triggered miR-21 transcription through several binding sites of AP-1 in the miR-21 promoter, and the expression of miR-21 was extremely attenuated in c-Fos deficient osteoclast precursors. On the basis of these results, we conclude that mir-21 is central to a novel mechanism regulating osteoclast development beginning with pro-osteoclastogenic cytokines triggering c-Fos expression and stimulation of microRNA-21 gene expression due to suppression of PDCD4.

***Disclosures: Toshifumi Sugatani**, None.*

FR0266

Regulatory Role of Osteoactivin/Gpnmb in Osteoclast Differentiation and Function In Vivo. Joyce Belcher*[1], Fabiola Del Carpio- Cano[2], M. Alexandra Monroy[3], Steven Popoff[4], Fayez Safadi[4]. [1]Temple University, School of Medicine, USA, [2]Temple University School of Medicine, Department of Anatomy & Cell Biology, USA, [3]Temple University School of Medicine, Department of Anatomy & Cell Biology & Department of Surgery, USA, [4]Temple University School of Medicine, USA

Osteoactivin/Gpnmb (OA/Gpnmb) is a glycoprotein initially identified in bone and later found to be strongly expressed in bone-forming osteoblasts. Recent literature suggests that OA/Gpnmb is also expressed in bone-resorbing osteoclasts; therefore, we sought to elucidate a role for OA/Gpnmb in osteoclast differentiation and function. We first examined osteoclast differentiation in response to M-CSF and RANKL in culture. Non-adherent mouse bone marrow hematopoietic stem cells (HSCs) were cultured in the presence of 50ng/ml of M-CSF for two days and then with M-CSF and 100 ng/ml of RANKL in the presence or absence of 50ng/ml recombinant OA/Gpnmb. We observed a dramatic increase in multinucleated TRAP-positive osteoclasts and the number of nuclei per osteoclast in OA/Gpnmb-treated compared to control cultures. Additionally, analysis of HSCs showed increased cell proliferation in response to exogenous OA/Gpnmb treatment. Next, we assessed osteoclast differentiation using a mouse model with a natural mutation in the OA/Gpnmb gene caused by a premature stop codon that results in the generation of a truncated OA/Gpnmb protein. These mice exhibit a skeletal phenotype associated with decreased bone mass. Histomorphometric analysis of femoral sections revealed increased numbers of TRAP-positive osteoclasts in OA/Gpnmb mutant compared to WT mice. Although the number of osteoclasts was higher in OA/Gpnmb mutant mice, ELISA assessment of serum levels of C-terminal collagen telopeptide (CTx), a marker for osteoclast activity, showed a significant reduction in OA/Gpnmb mutant compared to WT mice. These data suggest that although osteoclasts are increased in number they appear to be functionally defective in the OA/Gpnmb mutant mice in vivo. When osteoclasts were differentiated in ex vivo cultures of hematopoietic progenitors derived from OA/Gpnmb mutant and WT mice, we observed decreased osteoclast number and size in OA/Gpnmb mutant compared to WT cultures. This decrease was abrogated when cultures were treated exogenously with recombinant OA/Gpnmb. Western blot analysis of HSCs revealed decreased PU.1 and CSF-receptor expression in OA/Gpnmb mutant in comparison to WT, suggesting that the mutation in OA/Gpnmb affects early commitment to the osteoclast lineage. Collectively, these data implicate a regulatory role for OA/Gpnmb in osteoclast differentiation and function.

***Disclosures: Joyce Belcher**, None.*

FR0268

Vitamin E Induces Osteoclast Fusion and Decreases Bone Mass. Koji Fujita*[1], Makiko Iwasaki[2], Takako Koga[3], Hiroshi Takayanagi[4], Kimitaka Takitani[5], Hiroshi Tamai[5], Hiroyuki Arai[6], Hiroshi Ito[7], Kenichi Shinomiya[8], Shu Takeda[9]. [1]Dept. of Orthopedics, Tokyo Medical & Dental University,Global Center of Excellence (GCOE) Program, International Research Center for Molecular Science in Tooth & Bone Diseases, Japan, [2]Dept. of Orhopedics, Tokyo Medical & Dental University, Japan, [3]Dep of Cell Signaling, Graduate School of Medical & Dental Sciences, Tokyo Medical & Dental University, Japan, [4]Tokyo Medical & Dental University, Japan, [5]Department of Pediatrics, Osaka Medical College, Japan, [6]Department of Health Chemistry, Graduate School of Pharmaceutical Sciences, The University of Tokyo, Japan, [7]Dept. of Nephrology, Endocrinology & Metabolism Keio Univ., Japan, [8]Dept. of Orthopedics, Tokyo Medical & Dental University, Japan, [9]Keio University, Dept. of Nephrology, Endocrinology & Metabolism, Japan

Vitamin E, a fat-soluble vitamin, is well known as an antioxidant. Of eight forms of food-derived vitamin E, only α-tocopherol is secreted into the general circulation through the action of α-tocopherol transfer protein (α-TTP) expressed in the liver. Therefore, α-TTP knockout (KO) mice develop severe vitamin E deficiency. To clarify the role of vitamin E in bone metabolism, we analyzed bone phenotype of α-TTPKO mice.

At three months of age, α-TTPKO mice showed high bone mass. Histomorphometric analysis revealed that bone resorption of α-TTPKO mice was increased, which is also confirmed by an increase in serum TRAP5b. In contrast, no change in bone formation was observed in α-TTPKO mice. Interestingly, when we cultured osteoclast using serum from α-TTPKO mice, osteoclast differentiation was markedly hampered, indicating that lack of α-tocopherol in the serum is responsible for the high bone mass in α-TTPKO mice. In line with that, addition of α-tocopherol to the culture media during the maturation phase of osteoclastic differentiation significantly induced osteoclast fusion. In contrast, α-tocopherol did not affect proliferation of osteoclast precursors or osteoclast apoptosis. Molecular analysis revealed that *DC-STAMP*, essential molecule for osteoclast fusion, was specifically increased by α-tocopherol treatment, while expression of *Atp6v0d2*, *Meltrin-α*, *CD44*, *CD47* and important molecules for cell fusion was unchanged. Moreover, induction of osteoclast fusion by α-tocopherol was abolished in *DC-STAMP* knockdown osteoclasts or osteoclasts

generated from DC-STAMPKO mice, demonstrating that α-TTP regulates osteoclast fusion through DC-STAMP.

Finally, wild type mice fed a high-α-tocopherol diet developed low bone mass phenotype due to increase in bone resorption. Taken together, these results demonstrated that α-tocopherol regulates osteoclast fusion and bone resorption in a DC-STAMP-dependent manner and excessive intake of vitamin E may cause osteoporosis.

***Disclosures: Koji Fujita**, None.*

FR0270

Deficiency of Dok-1 and Dok-2, Ras-Erk Pathway Inhibitors, Enhances Bone Loss in Postmenopausal Osteoporosis Model of Mice. Daisuke Miyajima*[1], Aya Kawamata[2], Akane Inoue[3], Yoichi Ezura[4], Tetsuya Nakamoto[1], Tadayoshi Hayata[5], Takuya Notomi[6], Teruo Amagasa[7], Yuji Yamanashi[8], Masaki Noda[1]. [1]Tokyo Medical & Dental University, Japan, [2]Medical Research Institute, Tokyo Medical & Dental University, Japan, [3]Division of Genetics & Department of Cancer Biology, Institute of Medical Science, University of Tokyo, Japan, [4]Tokyo Medical & Dental University, Medical Research Insititute, Japan, [5]Medical Reserach Institute, Tokyo Medical & Dental University, Japan, [6]GCOE, Tokyo Medical & Dental University, Japan, [7]Maxillofacial Surgery, Tokyo Medival Dental University, Japan, [8]Division of Genetics, The Institute of Medical Science, The University of Tokyo, Japan

Dok-1 and Dok-2 are adaptor proteins and act as negative regulators of the Ras-Erk pathway downstream of M-CSF signaling system. These two molecules are preferentially expressed in hematopoietic cell lineage and are involved in the regulation of macrophages. Dok-1 and Dok-2 promote recruitment of p120 rasGAP and this action is critical for their negative regulation of the Ras-Erk pathway. Although osteoclasts are derived from hematopoietic stem cells and share similarities with macrophages regarding the developmental processes, the molecular mechanisms of Dok protein function in osteoclastic regulation in pathophysiological condition have not yet been fully understand. Double deficiency of Dok-1 and Dok-2 reduces the levels of bone mass (bone volume per tissue volume, BV/TV) in mice, although the levels of the number of TRAP positive cells per bone surface were similar between Dok-1 and Dok-2 double knockout mice compared to wild type, leaving a possibility that the function of osteoclastic cell may be enhanced by the deficiency of these two molecules. With regard to the development of osteoclasts in vitro in the presence of M-CSF and RANKL, the deficiency of Dok-1 and Dok-2 enhances sensitivity of the osteoclast progenitor cells in the bone marrow to M-CSF to develop into TRAP positive osteoclastic cells. Therefore, Dok-1/2 may play a role in M-CSF dependent activation during osteoclast differentiation in vitro. To further examine whether such characteristics of Dok-1/2 would be involved in the pathophysiological situation, we examined the effects of Dok-1 and Dok-2 deficiency on bone loss in postmenopausal osteoporosis model. In wild type mice, ovariectomy reduced bone mass and also the uterine weight. In Dok-1/2 double deficient mice, uterine weight loss was similarly observed compared to wild type mice. In contrast, however, ovariectomy-induced bone loss was enhanced in the region of the secondary trabecular bone. These observations suggest a role of Dok-1/2 in establishing osteopenic situation in the postmenopausal osteoporosis model of the ovariectomised mice.

***Disclosures: Daisuke Miyajima**, None.*
This study received funding from: GCOE

FR0273

LIS1, a Plekhm1 Binding Protein, Regulates Microtubule Organization/ Transportation and Cathepsin K secretion in Osteoclasts and is indispensable for Osteoclast Formation and Function. Shiqiao Ye*[1], Yunfeng Feng[2], Kanan Vyas[3], Stavros Manolagas[1], Haibo Zhao[1]. [1]University of Arkansas for Medical Sciences, USA, [2]Department of internal medicine, Washington University School of medicine, USA, [3]Center for Osteoporosis & Metabolic Bone Diseases, University of Arkansas for Medical Sciences & Central Arkansas Veterans Healthcare System, USA

Osteoclasts (OCs) secret protons and cathepsin K to resorb mineralized bone matrix through lysosome exocytosis. Mutations or deletion of PLEKHM1 is responsible for osteopetrosis in the ia/ia rat as well as a subset of patients with intermediate osteopetrosis. Moreover, we and others have demonstrated that Plekhm1 is associated with lysosomes in OCs and regulates cathepsin K secretion. However, the precise function of plekhm1 in OCs remains unknown. To better understand how Plekhm1 might regulate OC activity we searched for potential Plekhm1 binding proteins. GST-Plekhm1 was used to pull-down associated proteins from mature murine OC lysate followed by mass spectrometry analysis. By this method, we have identified LIS1 as a novel Plekhm1 binding protein in OCs. The interaction between LIS1 and Plekhm1 was further confirmed by co-immunoprecipitation of endogenous LIS1 with HA-tagged Plekhm1 from mature OCs. Mutations or deletion of the LIS1 gene has been documented in patients with lissencephaly, a severe human developmental brain disorder that is caused by incomplete neuronal migration. LIS1 is part of a highly conserved evolutionary pathway that regulates microtubule dynamics and cytoplasmic dynein motor function. When expressed as V5-tagged protein, LIS1 co-immunoprecipitates and co-localizes with cytoplasmic dynein independent of Plekhm1 in OCs. To elucidate the role of LIS1 in OC we knocked down its expression by lenti-viral vector mediated shRNA expression. LIS1 protein levels were decreased by 90% in the LIS1 shRNA transduced BMMs, pre-Ocs, and mature OCs as compared with control cells. Decreased LIS1 expression dramatically attenuated the formation of multinucleated, TRAP+ OCs. Additionally, both the size and total area of resorption pits were decreased in LIS1 shRNA expressing OCs as compared with control OCs. Furthermore, the medium level of CTx, a marker of bone resorption, was 10 times lower in LIS1 knockdown OCs. Knockdown of LIS1 also induced aggregation of microtubules and lysosomes around nuclei and caused a decrease in cathepsin K secretion and the labeling of lysosomal membrane protein LAMP-2 at the ruffled border membrane. Taken together, these findings demonstrate for the first time that LIS1 regulates OC microtubule organization, transportation and lysosome secretion by binding to and modulating dynein and Plekhm1. We, therefore, conclude that because of these functions LIS1 is essential for osteoclast formation and bone resorption.

***Disclosures: Shiqiao Ye**, None.*

FR0278

Rac Deletion in Osteoclasts Causes Severe Osteopetrosis. Monica Croke*[1], F. Patrick Ross[2], Steven Teitelbaum[3]. [1]Washington University School of Medicine, USA, [2]Hospital for Special Surgery, USA, [3]Washington University in St. Louis School of Medicine, USA

The unique ability of the osteoclast to normally resorb bone requires the αvβ3 integrin. Liganding this heterodimer induces a canonical signaling complex which transits the small GTPase, Rac, from its inactive GDP- to its active GTP-bound form. While the molecular mechanisms by which αvβ3 activate Rac, are in hand, whether the GTPase meaningfully impacts osteoclast function is unknown. We find that deletion of Rac1 or Rac 2, alone, does not alter skeletal structure. However, variable reduction of Rac1 in osteoclastic cells of Rac2-/- mice, yields osteopetrosis more severe than occurs with deletion of other members of the integrin-activated signaling complex, save c-src. Osteoclasts lacking Rac1 and 2 (RacDKO), in combination, fail to effectively resorb bone. On the other hand, osteoclasts are abundant in RacDKO osteopetrotic mice and normally express the cells' maturation markers. These data indicate that the osteopetrotic lesion of RacDKO mice largely reflects impaired function and not arrested differentiation of the resorptive polykaryon. The dysfunction of RacDKO osteoclasts represents failed cytoskeleton organization as evidenced by reduced motility and inability to spread or generate the key resorptive organelles, actin rings and ruffled borders. The ability of Rac to organize the osteoclast cytoskeleton is regulated by binding of effector proteins to specific amino acids in its Switch 1 domain. Multiple Rac effectors likely cooperate to assemble and maintain the dynamic actin ring. Supporting this hypothesis, expression of Rac1 constructs containing point mutations that target separate Rac-effector interactions (T35S, F37A or Y40C) fail to rescue actin ring formation and bone resorption activity. Additionally, activation of p21 activated kinase (PAK), a Rac effector that activates several actin modifying proteins, is diminished in the Rac dKO OCs both in response to c-Fms and αvβ3 activation. Thus, Rac1 and Rac2 are mutually compensatory and while their combined absence does not impact differentiation, it promotes severe osteopetrosis by dysregulating the osteoclast cytoskeleton.

***Disclosures: Monica Croke**, None.*

FR0279

The Distinct Roles of Cbl and Cbl-b in Osteoclast Differentiation, Survival and Function are Due to Unique Phosphorylation-dependent Interaction of Cbl with PI3K. Naga Suresh Adapala*[1], Alexander Tsygankov[1], Mary Barbe[2], Archana Sanjay[2]. [1]Temple University, USA, [2]Temple University School of Medicine, USA

Cbl and Cbl-b proteins are E3 ubiquitin ligases and adaptor proteins that are expressed in osteoclasts (OCs). Although both proteins share domain organization and significant homology their absence in mice results in disparate skeletal phenotypes: adult Cbl-/- mice are normal whereas deficiency of Cbl-b results in osteopenia due to hyperactivity of OCs. Interaction of Cbl with PI3K depends on phosphorylation of tyrosine737 within YEAM motif of Cbl, which is not present on Cbl-b. Previously we have demonstrated that in contrast to Cbl-/-, ablation of PI3K binding site on Cbl in mice (YF mice) results in increased bone volume due to defective OC function despite two-fold increase in OC numbers. We also showed that YF OCs have increased survival in response to RANKL due to increased AKT activation. These data suggested that Cbl and Cbl-b have different roles, thus while Cbl-b negatively regulates bone resorption, Cbl positively mediates OC function. To investigate the distinct roles of Cbl and Cbl-b we generated YF mice in the Cbl-b$^{-/-}$ background (CYB mice). Micro CT analysis of the tibiae from 12 wk old male mice showed that in the absence of Cbl-b, the decrease in OC function due to YF Cbl mutation is lost and the mice showed decreased bone volume similar to Cbl-b KO (BV/TV% WT 8.1 ± 0.10, CYB: 6.4 ± 0.11, Cbl-b-/-: 4.9 ± 0.08). On the other hand, TRAP staining of long bones showed that similar to YF samples the OCs numbers were increased in CYB mice (OC/mm^2, WT: 6 ± 0.4, YF: 12.8 ± 2.04, CYB: 10.5 ± 0.2).

We also examined osteoclast differentiation, survival and pit formation in *ex vivo* culture system among the five genotypes. Our data showed that compared to the Cbl-/- and Cbl-b-/- which had normal differentiation and survival, in YF and CYB OCs both differentiation and survival in response to RANKL was increased 2 and 3 fold respectively. At the molecular level AKT phosphorylation was unchanged in the absence of Cbl or Cbl-b protein. However, in YF and CYB OCs, in response to RANKL sustained and enhanced AKT phosphorylation was seen. The enhanced AKT activation in YF and CYB OCs was further confirmed by increased phosphorylation of GSK a AKT substrate. Cumulatively, these in vivo and in vitro results confirm that Cbl and Cbl-b perform distinct non-redundant roles in osteoclast biology. Thus while bone resorption is negatively regulated by Cbl-b, Cbl by binding to PI3K positively modulates osteoclast function while negatively regulating differentiation and survival.

***Disclosures: Naga Suresh Adapala**, None.*

FR0281

A Marrow 'Guardian' Cell inhibits Marrow Space Mineralization and Trabecularization through Sost/sclerostin Expression. Jian Feng[1], Xianglong Han*[2]. [1]Texas A&M Health Science Center, USA, [2]Baylor College of Dentistry, TX A&M Health Science Center, USA

It is well known that bone marrow ablation leads to rapid new bone formation within the marrow space and that this bone is gradually removed and replaced with marrow. We hypothesize that a 'guardian' cell exists in the marrow space that inhibits bone formation to maintain normal marrow function. It has been shown that Sost/Sclerostin is a major negative regulator of bone formation. This factor is highly expressed in osteocytes embedded in bone, but we sought to test if also present in marrow cells. To accomplish this goal, we compared Sclerostin expression by both Western blot and real-time RT-PCR of flushed bone marrow cells to extracted mineralized bone. In Western immunoblotting, the identical 24 kDa bands were detected in protein extracts from both the bone marrow cell and the cortical bone matrix by using a monoclonal anti-SOST antibody. A quantitative real-time PCR assay showed a ratio of Sost mRNA in long bone to bone marrow as 2:1. In situ hybridization further confirmed expression of Sost mRNA in a mesenchymal-like bone marrow cell with a slightly lower expression intensity than that in osteocytes embedded in bone matrix. Next, we generated a Sost-cre mouse line where the Cre is under control of a Sost BAC clone containing the entire cis-regulatory region of murine Sost gene. Both lacZ positive osteocytes and bone marrow cells were detected when Sost-cre mice were crossed with Rosa 26-lacZ reporter mice similar to the in situ hybridization data. We have also generated mouse models where either the BMP receptor 1a was deleted or ?-catenin was constitutively activated in progenitor cells using either 3.6 Col 1a1-cre or inducible Mx1-cre. Characterization techniques include radiographs, micro-CT, scanning electron microscope, H&E and TRAP assays. Surprisingly, in both of these models (3.6 Col-cre x Bmpr1a fl/fl or Mx1-cre x mutant ?-catenin exon 3 fl/fl) over 80% of bone marrow space was filled with trabecular bone with little changes in osteoclast numbers. In the BMP receptor 1a conditional knockout mice, there was a decrease in Sost/sclerostin expression and an increase in ?-catenin signaling. Taken together, the above data support a hypothesis that an early marrow progenitor cell expresses Sost to prevent ectopic marrow bone formation, and that trabecular versus cortical bone mass is differentially regulated. Identification and characterization of this marrow 'guardian' cell will provide further information on how bone mass is differentially controlled. (This study was supported by NIH grants to JQF for DE015209, AR051587; and LFB/JQF/SEH for AR046798)

***Disclosures: Xianglong Han**, None.*

FR0282

Bone-Muscle Crosstalk is Demonstrated by Morphological and Functional Changes in Skeletal and Cardiac Muscle Cells in Response to Factors Produced by MLO-Y4 Osteocytes . Nuria Lara[1], Todd Hall*[1], Chad Touchberry[1], Jon Andresen[1], Marco Brotto[1], Mark Johnson[2], Michael Wacker[3], Christopher Elmore[1], Sandra Romero - Suarez[1], Cheng Lin Mo[4], Lynda Bonewald[1], Neerupma Silswal[1]. [1]University of Missouri - Kansas City, USA, [2]University of Missouri, Kansas City Dental School, USA, [3]University of Missouri-Kansas City School of Medicine, USA, [4]Univsity of Missouri - Kansas City, USA

Osteocytes, which compose 90-95% of all bone cells, are mechanosensory cells that also function in an endocrine fashion to target the function of other organs such as kidney. We hypothesized that osteocytes could target muscle and that the effects of muscle induced mechanical loading of bone could regulate muscle signaling factors produced by osteocytes. To begin to examine this hypothesis, we tested the effects of conditioned media (CM) from MLO-Y4 osteocytes with and without fluid flow shear stress (FFSS) on C2C12 muscle cells, HL-1 cardiac muscle cells and A7R5 vascular smooth muscle cells.

CM was obtained from static MLO-Y4 osteocytes and cells subjected to FFSS (2 or 16 dynes/cm^2) for 2 hours. CM was applied to C2C12 myoblasts and replaced the complete growth media (CGM) that stimulates proliferation of myoblasts, to HL-1 cardiac myocytes serum starved for 48 hours in Claycomb's minimal media, and to A7R5 vascular smooth muscle cells grown in DMEM with 10% FBS. All muscle cells were monitored for morphological changes for up to 4 days. As PGE2 is a major osteocyte signaling factor induced by FFSS, PGE2 (5μM) was tested on morphology and intracellular calcium (Ca^{+2}) homeostasis in C2C12 muscle cells.

CM from static or 2 dynes/cm^2 FFSS treated MLO-Y4 cells promoted robust differentiation of C2C12 myoblasts into myotubes (~13-15 myotubes in CM vs. 3-5 myotubes in CGM per random field of view, n=3). PGE2 had no effect on myotube formation suggesting this effect was not due to PGE2, but to other osteocyte factors. In C2C12 myotubes induced by normal differentiation media with 2.5% horse serum, caffeine challenge produced a single peak calcium transient whereas PGE2 induced 4-6 oscillatory calcium waves. This suggests that PGE2 produced by osteocytes could have an effect on gene expression as this oscillatory pattern of Ca^{+2} waves has been linked with modulation of gene activity. MLO-Y4 FFSS (16 dynes/cm^2) CM increased HL-1 cardiac myocyte cell area by 28.4 $\pm$ 14.2% (n=3), indicative of cardiac hypertrophy. In contrast, MLO-Y4 CM had no effects on A7R5 vascular smooth muscle cells.

Our data suggest that factors released from osteocytes can influence muscle cell morphology and function. By promoting the differentiation of myoblasts into myotubes, osteocytes may modulate muscle repair and regeneration. Our results support the hypothesis that osteocytes might act as an endocrine organ that modulates the function of striated muscles.

***Disclosures: Todd Hall**, None.*

FR0283

Cx43 in Osteocytes, but not in Osteoblasts, Is Required to Preserve Osteocyte Viability, Bone Geometry and Material Stiffness. Nicoletta Bivi*[1], Mark Nelson[2], Racheal Lee[3], Jeffrey Benson[3], Keith Condon[3], Jiliang Li[2], Matthew Allen[3], Teresita Bellido[3], Lilian Plotkin[3]. [1]Indiana University, USA, [2]Indiana University, Purdue University Indianapolis, USA, [3]Indiana University School of Medicine, USA

Mice lacking connexin (Cx)43 in osteoblasts and osteocytes (Cx43^{fl};OCN-Cre mice, named Cx43$^{\Delta OB/OT}$) exhibit increased prevalence of cortical osteocyte apoptosis, higher endocortical resorption and periosteal apposition leading to wider femoral cross-sections, as well as decreased material stiffness (Young's modulus) likely resulting from the reduced collagen crosslinking detected by FTIR. Deletion of Cx43 in osteoblastic cells has been shown to delay differentiation, abolish pro-survival signaling induced by bisphosphonates and parathyroid hormone, and impair prostaglandin/ATP release and the osteogenic response to mechanical loading. To distinguish the individual contribution of osteocytes vs. osteoblasts to the Cx43$^{\Delta OB/OT}$ mouse phenotype, we removed Cx43 exclusively from osteocytes by mating Cx43^{fl} mice with 8kb-DMP1-Cre mice (Cx43$^{\Delta OT}$). The deleted form of Cx43 was found in genomic DNA by PCR and Cre mRNA was detected by qPCR in bone from Cx43$^{\Delta OT}$ mice, but not from control Cx43^{fl} littermates. Deleted Cx43 or Cre transcripts were not found in heart or kidney from either mouse. Moreover, Cre mRNA expression was detected in green fluorescent protein (GFP)-expressing cells (osteocytes) and not in GFP negative cells (osteoblasts) isolated from calvaria of 8kbDMP1-Cre mice crossed with 10kbDMP1-GFP mice, confirming osteocyte-specific expression of Cre recombinase. Cx43$^{\Delta OT}$ mice exhibited a marked increased in the prevalence of osteocyte apoptosis (12.6$\pm$7.4% vs. 1.1$\pm$1.4%) as well as empty lacunae, an additional sign of cell death, (13.1$\pm$6.9% vs. 0.8$\pm$0.5%) in femoral middiaphysis (n=5/group, $p<0.05$). This was associated with an increase of 26% in femoral marrow cavity area and 20% in total cross-sectional area by μCT, likely the result of increased endocortical resorption and periosteal apposition, respectively. In addition, Young's modulus was 22% lower in Cx43$^{\Delta OT}$ mice as measured by femoral 3-point bending. Therefore, Cx43 deletion only from osteocytes is sufficient to induce osteocyte apoptosis, and to alter bone geometry and material stiffness. We hypothesize that Cx43 is required to sense and transmit physiological survival signals in osteocytes and that, in its absence, apoptotic osteocytes trigger resorption resulting in larger bones. In addition, Cx43 expressed in osteocytes is required to maintain proper bone material stiffness, a function attributed to osteoblasts, but, unexpectedly, not fulfilled by Cx43-expressing osteoblasts in our Cx43$^{\Delta OT}$ mice.

***Disclosures: Nicoletta Bivi**, None.*

FR0284

Homozygous Deletion of the *SOST* Gene Results in Enhanced Union and Increased Hard Callus Formation in Healing Fractures. Michelle McDonald*[1], Alyson Morse[2], Lauren Peacock[2], Kathy Mikulec[2], Ina Kramer[3], Michaela Kneissel[4], David Little[2]. [1]The Childrens Hospital Westmead, Australia, [2]The Kids Research Institute, The Children's Hospital Westmead, Australia, [3]Novartis Institutes for BioMedical Research, Che, [4]Novartis Institutes for Biomedical Research, Switzerland

Sclerostin, transcribed by the *Sost* gene, is expressed by osteocytes and is a negative regulator of bone formation. Sclerostin antagonizes Wnt/β-catenin signaling activity via interaction with the Lrp5/6 co-receptor, negatively regulating osteoblast differentiation. Therefore the complete deletion of S*ost* in mice results in an extensively high bone mass. We sought to examine bone repair in the absence of *Sost* in these mice, hypothesizing that the complete loss of the *Sost* gene would result in enhanced bone repair with increased bone volume and content within the repairing callus.

Homozygous-null mice (*Sost* -/-) were compared to wildtype (*Sost* +/+, WT) littermates after tibial closed fracture stabilized by external fixation. Time points examined were 2 weeks (cartilage callus) and 4 weeks (hard callus). Outcome measures were plain X-ray for union, QCT, Micro CT (μCT), and histology.

At 2 weeks there was a 79% decrease in cartilage content in the *Sost* -/- calluses compared to WT ($p<0.05$), consistent with a trend to an increase in the rate of union. At 2 weeks QCT revealed increases of 88% in BMC, 25% in BMD and 50% in bone volume in the *Sost* -/- calluses compared to WT ($p<0.01$). At 4 weeks all fractures had united and BMD was increased by 31% in *Sost* -/- compared to WT ($p<0.01$). μCT of the *Sost* -/- calluses showed a 51% and 44% increase in 3 dimensional BV/TV at 2 weeks and 4 weeks respectively ($p<0.01$).

At the early stage of repair *Sost* -/- mice showed enhanced cartilage removal and earlier hard callus union, along with increased bone content, density, volume and BV/TV. During hard callus remodelling *Sost* -/- mice continued to have increased bone density and BV/TV. This suggests that the absence of sclerostin resulted in enhanced endochondral ossification to union resulting in a denser hard callus.

***Disclosures: Michelle McDonald**, None.*
This study received funding from: Novartis Pharma

FR0285

Role of Histone Deacetylases (HDACs) in PTH-mediated Repression of MEF2-dependent Sost Expression in UMR-106 Cells. Stefan Baertschi*, Heidi Jeker, Simone Degen, Hansjoerg Keller. Novartis Institutes for BioMedical Research, Switzerland

Previously, we have shown that parathyroid hormone (PTH) treatment leads to suppression of sclerostin (SOST) expression by inhibiting myocyte enhancer factor 2 (MEF2), which activates the SOST gene bone enhancer. However, the molecular mechanisms of MEF2 inhibition by PTH in osteocytes are yet unknown. In muscle, MEF2 activity is repressed by direct binding of class IIa histone deacetylases (HDACs 4, 5, 7 & 9), which shuttle between cytoplasm and nucleus, regulated by phosphorylation of conserved serines. To study a role of class IIa HDACs in MEF2-mediated SOST expression we first determined their RNA expression levels in SOST-expressing UMR106 cells using quantitative RT-PCR (qPCR). HDAC5 and 7 were strongly expressed, HDAC4 much less and HDAC9 only marginally. High Content Analysis was used to analyze class IIa HDACs nucleo-cytoplasmic shuttling in response to PTH using GFP fusion-proteins. Only HDAC5 showed a rapid nuclear import upon PTH stimulation within 20 minutes. Mutating two conserved serines, which are involved in nuclear export, to alanines we generated a nuclear enriched HDAC5 mutant (S2A) that mimicked PTH-induced nuclear accumulation of wt HDAC5. S2A inhibited MEF2-dependent bone enhancer activity in transient transfections by 52% whereas wt HDAC5 was inactive. Accordingly, the nuclear export inhibitor Leptomycin B led to a strong nuclear retention of HDAC5 and inhibited endogenous Sost expression by 62%. Next, we analyzed the effect of HDAC enzyme inhibition on SOST expression. The pan-HDAC inhibitor Trichostatin A repressed SOST expression similarly as PTH indicating that SOST expression requires HDAC enzymatic activity. Furthermore, the class I HDAC2,3,8 inhibitor Apicidin also led to full inhibition of SOST expression suggesting a specific activating role for class I HDACs. Compared to class IIa HDAC5, HDAC1 and 2 were similarly expressed, HDAC3 much lower and HDAC8 only marginally. Finally, we analyzed the effect of PTH on nucleo-cytoplasmic localization of HDAC3, which is the class I HDAC known to shuttle. In contrast to PTH-induced nuclear import of HDAC5 PTH led to nuclear export of HDAC3. In summary, these data suggest that the PTH-mediated SOST repression involves nuclear import of HDAC5 inhibiting MEF2 and nuclear export of HDAC3. The catalytic activity of HDAC2,3 may be required for SOST expression. Hence, HDAC2,3 inhibitors might have a potential as bone formation stimulators.

***Disclosures: Stefan Baertschi**, Novartis, 3*

FR0286

Tracking Osteocyte Lineage Plasticity In Vitro. Slavica Pejda*[1], Tomislav Kizivat[1], Mohammad fatahi[1], John Igwe[2], Ivo Kalajzic[3]. [1]Department of Reconstructive Sciences, University of Connecticut Health Center, USA, [2]Department of Orthopedic Surgery,University of Connecticut Health Center, USA, [3]University of Connecticut Health Center, USA

Presently, there is no evidence that mature osteoblast and osteocytes are able to dedifferentiate. However, dedifferentiation of these cells could provide an additional source of cells for skeletal reconstruction/repair. The use of visual transgenes, such as GFP, has been instrumental in identifying cells at different stages of maturation. However, markers that are under the control of specific promoters that are no longer expressed after the cell reaches a point when promoter activity ceases, or when a cell transitions to an alternative differentiation state cannot be used to track cell histories. It is then necessary to to use a tool like the Cre/loxP system for lineage tracing. In this study we present evidence that preosteocytes/osteocytes can undergo dedifferentiation, accompanied by dramatic changes in gene expression. We have utilized previously developed transgenic mice in which Dmp1 promoter had been used with GFP as a visual marker of current stage of differentiation (DMP-GFP) or to drive Cre recombinase and turn on an historical marker in osteocytes and odontoblasts (DMP-Cre).

Primary bone chip outgrowth cell (BCOC) cultures were prepared after surface osteoblasts have been removed using enzymatic digestion. When we utilized a DMP-GFP transgene, outgrowth cells were GFP negative by epifluorescence and by immunofluorescent staining using GFP antibody. Using DMP-Cre mice, floxed GFPreporter+ cells emerged from bone chips after 48-72 hours, where GFP expression iindicates their previous osteocytic phenotype. In addition, a large proportion of BCOC's began to express a-SMA-GFP. Preliminary results obtained by microarray analysis of BCOC isolated 7 days after plating and compared to the RNA of marrow stromal cells showed large increases in markers characteristic of mature osteoblast/osteocytes, including Bglap, Ibsp, Phex, Osterix, BMP8a, and Pthr1. Expanded BCOC's in vitro were transplanted by intra-bone marrow cavity injection. Four weeks after transplantation, GFP-labeled donor cells were detected as numerous osteocytes deeply embedded in newly formed bone.

Our results indicate that under certain conditions cells embedded in the matrix can emerge out and begin to proliferate. This process does not preclude the ability of outgrowth cells to differentiate again into mature osteocytes. Future studies should be aimed at evaluating factors that affect the process of dedifferentiation with the goal of increasing bone formation in vivo and in vitro.

***Disclosures: Slavica Pejda**, None.*

FR0287

Use of a Sost-GFP Mouse Model to Determine the Role of the AKT-GSK3β in Osteocyte Function and to Map Local Strain Fields around Osteocytes with Loading. Stephen Harris*[1], Marie Harris[1], Jelica Gluhak-Heinrich[1], Wuchen Yang[1], Yong Cui[2], Ryan S Potter[3], Lynda Bonewald[4], Daniel Nicolella[3]. [1]University of Texas Health Science Center at San Antonio, USA, [2]U. of Texas Health Science Center at San Antonio, USA, [3]Southwest Research Institute, USA, [4]University of Missouri - Kansas City, USA

Sost/sclerostin is primarily expressed in mature osteocytes and negatively responds to mechanical loading in osteocytes. The Akt-GSK3β pathway is central to the mechanical load response of MSC, osteoblasts and osteocytes. Using a recombineering approach, we placed an EGFP reporter construct into a 189kb mouse DNA fragment containing the Sost gene with all the cis-regulatory regions. Tranasgenic mice generated with Sost-GFP showed GFP selectively in most osteocytes, as well as an unknown population of cells in the bone marrow. We used an ex vivo culture of long bones, femur and tibia, from 2 month old animals, in which the growth plate region and bone marrow and osteoblasts are removed by collagenase-trypsin digestion. These ''bone tubes'', containing primarily osteocytes in their ''natural'' home of cortical bone were then used for experiments. The bones were treated ex vivo for 4hrs with the GSK3 specific inhibitor, BIOS, for microarray analysis and network reconstruction. This is the first database derived from cortical long bone osteocytes in older animals. The gene expression signature in these long bone osteocytes overlap with primary calvarial osteocytes and with a subset that is unique to the long bone osteocytes. From over 1200 genes, a gene regulatory network, centered on β-catenin and Mef2 action was constructed using Ingenuity Pathway Analysis and other bioinformatic tools. This system proved useful for determining for the first time the genes upregulated in osteocytes downstream of GSK3β node which include DMP1, Mepe, Osterix, Myogenin, Mef2c, Tcf7, BMP3, BMP2, and Wnt7b. To determine how these genes may be regulated by loading, strain-mapping around osteocyte lacunae was performed. Using Dismap, the strain field distribution was determined using the Sost-GFP osteocytes as landmarks. The intact, digested, tibial 'bone tubes' were loaded in 3-point bending at 3N and images of the GFP positive osteocytes were captured. The load was then removed and the osteocyte distribution again captured. We observed extremely variable local strain distribution with the strains around the osteocytes reaching up to 10-20,000 microstrain around some lacunae. These observations with ''live'' osteocytes confirm previous observations with polished pieces of hydrated ''dead'' bone and support the concept that regions around osteocytes are strain concentrators. This Sost-GFP model will be useful to perform correlations of strain with GFP and gene expression.

***Disclosures: Stephen Harris**, None.*

FR0289

Late Osteoblastic/Osteocytic Cell Line IDG-SW3 Expresses Dmp1-GFP, SOST and FGF23 *in vitro* and Promotes New Bone Formation *in vivo*. Stacey Woo*[1], Lianxiang Bi[1], Mark Johnson[2], Lynda Bonewald[1]. [1]University of Missouri - Kansas City, USA, [2]University of Missouri, Kansas City Dental School, USA

Limitations of existing cell lines reflect the need for additional model systems to study osteocyte biology and function. The Immortomouse/Dmp1-GFP (IDG)-SW3 osteoblastic/osteocytic cell line was previously shown to generate an extensive mineralizing matrix containing Dmp1-GFP positive cells, suggesting differentiation towards the osteocyte phenotype. To further characterize these cells and determine their capacity to mimic primary bone cells, *in vitro* 2D and 3D culture was compared, and the capacity of these cells to support new bone formation in non-healing calvarial defects was examined. The cells maintained viability for at least 35 days in culture. On 2D collagen surfaces, IDG-SW3 expresses the osteocyte-selective genes Dmp1, SOST,

and FGF23. Expression of the early osteocyte marker, Dmp1, is first detectable by qRT-PCR at day 3, rises dramatically, plateaus at day 14, and is maintained to day 21 and 35. The GFP fluorescence pattern mirrors Dmp1 mRNA expression. Expression of the late osteocyte marker, SOST, is first detectable at day 14 and increases by day 21 and 35 by qRT-PCR. FGF23 expression is maintained at low levels, first detectable at day 14 and increasing from day 21-35 by PCR.

In 3D collagen gels and sponges, the cells both penetrate the collagen and grow on the surface, forming multilayers containing cells and extracellular matrix as shown by transverse histological sections. Cells within the gels and sponges show a dendritic morphology and dramatic GFP expression. Cells cultured for 14 days on 3D collagen sponges were placed into calvarial defects, and bone healing was monitored at 2, 4, and 6 weeks by *in vivo* μCT analysis. At week 6, fractional bone volume (BV/TV) was significantly greater in IDG-SW3-filled calvarial defects compared to controls, with empty and sponge-filled defects showing negligible healing at all time points (0.100 ± 0.027 versus 0.007 ± 0.002 and 0.018 ± 0.001, respectively; $p<0.05$). Our results suggest that IDG-SW3 cells trigger events leading to bone formation *in vivo*. We conclude that IDG-SW3 is a promising new model system for osteocytes with unique advantages over existing osteocyte cell lines, namely expression of an osteocyte-selective lineage marker, an osteocyte selective gene profile, embedding in a mineralized extracellular matrix, penetration of cells in 3D matrices, and accelerated bone healing *in vivo*.

***Disclosures: Stacey Woo**, None.*

FR0290

Calcimimetics Regulate FGF23, Sclerostin and Dkk1 Expression in Bone in a Rat Model of Chronic Kidney Disease-Mineral and Bone Disorder with Secondary Hyperparathyroidism. Victoria Shalhoub*[1], Eliane Valente[1], Edward Shatzen[1], Sabrina Ward[1], Charles Henley[1], Xuechun Xia[2], Xiaodong Li[1], Thomas Wronski[2], William Richards[1]. [1]Amgen Inc, USA, [2]University of Florida, USA

Renal osteodystrophy affects patients with chronic kidney disease-mineral and bone disorder (CKD-MBD) and secondary hyperparathyroidism (SHPT). Calcimimetics, documented allosteric activators of the parathyroid gland calcium sensing receptor, suppress parathyroid hormone (PTH) synthesis, thereby lowering serum calcium and phosphorus in CKD-MBD dialysis patients. However, little is known about calcimimetic regulation of osteoblast/osteocytic genes in CKD-MBD. This study examined regulation of fibroblast growth factor 23 (FGF23), sclerostin and Dkk1 in 5/6 nephrectomized (Nx) rats, a model of CKD-MBD. Male SD rats (250g, 2 months) were placed on a high phosphate diet post Nx surgery. Three weeks post-Nx, sham operated and Nx rats were given 14 days of vehicle (sham-veh, Nx-veh) or R-568 (Nx-R568) (30 mg/kg, po, daily) (n = 10/group). Blood was drawn pre- and 4 hrs post-dose on days 0, 7 and 14. On day 14 (5 weeks post-Nx), bones were harvested for in situ hybridization (ISH) and cancellous histomorphometry. Serum PTH and FGF23 levels were measured using intact ELISAs (Immutopics, San Clemente, CA and Kainos, Japan). Five weeks post-Nx, Nx-veh rats had elevated serum BUN, creatinine, iPTH, and FGF23; increased osteoid surface (32.6+11.9 vs 12.5+5.1, P<0001), higher surface based bone formation rate (0.76+0.17 vs 0.45+0.16, P<0.01), and osteoblast surface (32.9+12.1 vs 12.7+4.7, P<0001) compared with sham-veh. ISH localized FGF23 mRNA to growth plate chondrocytes and osteoblast-like cells near the growth plate in sham-veh and Nx-veh. Nx-veh rats also expressed FGF23 in osteoblast-like cells lining metaphyseal trabecular bone. In sham-veh rats low/moderate sclerostin mRNA levels were found in osteocytes of metaphyseal and diaphyseal cortical bone. Dkk1 was expressed at low levels in osteoblast-like cells near the growth plate, osteocytes of metaphyseal trabecular bone and few osteocytes of diaphyseal cortical bone. In Nx-veh rats with SHPT sclerostin and Dkk1 expression was diminished. After 14 day R568 treatment FGF23 mRNA was not detectable in Nx rat bones, whereas sclerostin (but not Dkk1) expression recovered. Failure to detect FGF23 and recovery of sclerostin transcripts paralleled R568-induced declines in serum PTH. FGF23 expression was up-regulated and sclerostin was down-regulated in bones of CKD-MBD rats with SHPT. These changes, which were prevented by 14 day calcimimetic treatment, may be related to regulation of serum PTH levels.

***Disclosures: Victoria Shalhoub**, Amgen Inc, 3; Amgen Inc, 1*

FR0299

Construction and Validation of a Simplified Fracture Risk Assessment Tool for Canadian Women and Men: Results from the CaMos and Manitoba BMD Cohorts. William Leslie*[1], Claudie Berger[2], Lisa Langsetmo[3], Jonathan Adachi[4], David Hanley[5], George Ioannidis[6], Robert Josse[7], Christopher Kovacs[8], Tan Towheed[9], Stephanie Kaiser[10], W.P. Olszynski[11], Jerilynn Prior[12], Sophie Jamal[13], Nancy Kreiger[14], David Goltzman[15]. [1]University of Manitoba, Canada, [2]McGill University, Canada, [3]Canandian Multicenter Osteoporosis Study, Canada, [4]St. Joseph's Hospital, Canada, [5]University of Calgary, Canada, [6]Sympatico, Canada, [7]St. Michael's Hospital, University of Toronto, Canada, [8]Memorial University of Newfoundland, Canada, [9]Queen's University, Canada, [10]Dalhousie University, Canada, [11]Midtown Medical Center (#103), Canada, [12]University of British Columbia, Canada, [13]The University of Toronto, Canada, [14]University of Toronto, Canada, [15]McGill University Health Centre, Canada

Using data from a new Canadian FRAX® model, we updated risk tables for the Canadian Association of Radiologists and Osteoporosis Canada (CAROC) fracture risk assessment system. CAROC is based on sex, age, BMD and two clinical risk factors (prior fragility fracture and corticosteroid use). CAROC provides a simple semi-quantitative alternative to FRAX but does not require computer or web access, and categorizes 10 year fracture probability for major osteoporotic fractures as low (<10%), moderate (10-20%) or high (>20%). METHODS: Risk tables for women and men were constructed from Canadian FRAX estimates for major osteoporotic fractures using the Manitoba BMD cohort (36,730 women and 2,873 men age 50+ years) after removing the effect of prior fragility fracture and corticosteroid use. We then determined sex- and age-specific femoral neck T-score cutoffs corresponding to fracture probabilities of 10% and 20%. This defined the basal CAROC risk categories, which were subsequently increased (low to moderate, moderate to high) for each clinical risk factor. We independently validated the new risk tables in the CaMos cohort (4,778 women and 1,919 men age 50+ years). RESULTS: The new CAROC cutoffs are substantially lower than the old cutoffs which were based on Swedish fracture data (most notably for women 50-75 years and men 70-85 years). The new CAROC system demonstrated a high level of overall concordance (89% and 88%) with FRAX in both the CaMos and Manitoba cohorts when the FRAX risk category was defined using the same cutoffs (10% and 20%). Concordance was highest in individuals without additional risk factors (92% and 93%), followed by those with both risk factors (100% and 76%), and lowest for those with a single risk factor (61% and 74%). Ten year fracture outcomes (Kaplan-Meier estimates) in the CaMos and Manitoba cohorts showed similarly good discrimination and calibration for both CAROC (6.1-6.5% in low risk, 13.5-14.6% in moderate risk, 22.3-29.1% in high risk individuals) and FRAX systems (6.1-6.6% in low risk, 14.4-16.1% in moderate risk, 23.4-31.0% in high risk individuals). Recategorization of the CAROC risk category under FRAX was <5% for low risk, 20-24% for moderate risk and 27-30% for high risk. CONCLUSION: The new CAROC system is well calibrated to the Canadian population and shows a high overall degree of concordance with the FRAX. The CAROC system is a simple alternative when it is not feasible/possible to use the full FRAX tool.

***Disclosures: William Leslie**, None.*

FR0300

Enhancement of Hip Fracture Prediction Using Finite Element Analysis of CT Scans. David Kopperdahl*[1], Paul Hoffmann[1], Sigurdur Sigurdsson[2], Thor Aspelund[2], Kristin Siggeirsdottir[2], Gudny Eiriksdottir[2], Tamara Harris[3], Vilmundur Gudnason[2], Tony Keaveny[4]. [1]O.N. Diagnostics, USA, [2]Icelandic Heart Association Research Institute, Iceland, [3]Intramural Research Program, National Institute on Aging, USA, [4]University of California, Berkeley, USA

Finite element modeling of the proximal femur has potential for improved fracture risk assessment over areal BMD, particularly for subjects in the osteopenic range, since there is evidence that some osteopenic individuals have femoral strength values more typical of those with severe osteoporosis. In this study, we assessed the ability of finite element analysis to enhance prediction of hip fractures in both women and men, with a focus on those in the osteopenic range.

The study used a case-cohort design of 199 incident hip-fracture cases (131 women; 68 men) and 724 no-hip-fracture controls (412 women; 312 men), taken from the 3088 subjects of the AGES-Reykjavik study aged 65-93 years who had quantitative computed tomography (CT) scans of the hip at baseline and 5-year follow-up. Average follow-up was 5.7 years. Non-linear 3D finite element analysis of the CT scans, performed blinded to fracture status, simulated a sideways fall to provide measures of strength and a strength-to-density ratio. Load-to-strength ratios were calculated based on patient weight, height, and the thickness of soft tissue over the trochanter. Since DXA was not available, femoral neck areal BMD as measured from the CT scans was used to classify subjects as osteopenic (-2.5<-1.0) or osteoporotic (T<-2.5). Cox proportional hazards analysis was performed to estimate hazards ratios per SD change. Multivariable survival analysis was used to assess if adding any biomechanical outcomes to areal BMD improved overall prediction. This was done for the entire study sample (n=923) and a subset of osteopenic subjects (n=377).

We found that all finite element outcomes, and the strength-to-density ratio, were predictive of fracture in both women and men, as was femoral neck areal BMD (Figure). In multivariable models including both age and sex, the biomechanical predictors where chosen instead of areal BMD when using stepwise selection. In multivariable models forced to include age, sex, and areal BMD, stepwise selection added body mass index and two additional biomechanical terms ($p<0.05$) to the model. For the osteopenic group, the AUC for this latter model (0.77) was significantly higher ($p=0.04$) compared to the AUC (0.75) for the same model without the additional biomechanical terms; this enhancement did not reach significance for the full cohort ($p=0.08$).

We conclude that finite element analysis can enhance prediction of hip fracture, particularly for those with low bone density.

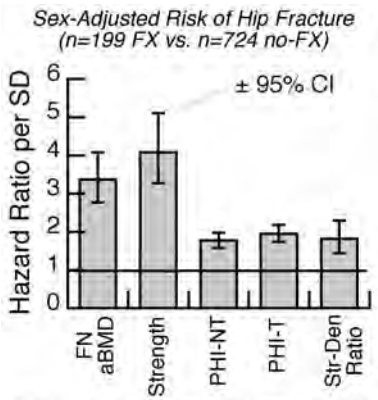

Figure: Strength: from the finite element analysis; FN aBMD: areal BMD of the femoral neck, measured from the CT scan; PHI-NT and PHI-T: load-to-strength ratios, excluding and including patient-specific trochanteric soft tissue thickness, respectively; Str-Den ratio: ratio of femoral strength to volumetric BMD (cortical plus trabecular).

Figure 1

***Disclosures: David Kopperdahl**, O.N. Diagnostics, 3*
This study received funding from: NIH AR052234

FR0301

Fracture Prediction and Calibration of a Canadian FRAX® Tool: A Population-Based Report From CaMos. Lisa-Ann Fraser[1], Lisa Langsetmo[2], Claudie Berger[3], George Ioannidis[4], David Goltzman[5], Jonathan Adachi[6], Alexandra Papaioannou[7], Robert Josse[8], Christopher Kovacs[9], Wojciech P. Olszyynski[10], Tanveer Towheed[11], David Hanley[12], Stephanie Kaiser[13], Jerilynn Prior[14], Sophie Jamal[15], Nancy Kreiger[16], Jacques Brown[17], Helena Johansson[18], John Kanis[19], William Leslie*[20]. [1]University of Western OntarioMcMaster University, Canada, [2]Canandian Multicenter Osteoporosis Study, Canada, [3]McGill University, Canada, [4]Sympatico, Canada, [5]McGill University Health Centre, Canada, [6]St. Joseph's Hospital, Canada, [7]Hamilton Health Sciences, Canada, [8]St. Michael's Hospital, University of Toronto, Canada, [9]Memorial University of Newfoundland, Canada, [10]University of Saskatchewan, Canada, [11]Queen's University, Canada, [12]University of Calgary, Canada, [13]Dalhousie University, Canada, [14]University of British Columbia, Canada, [15]The University of Toronto, Canada, [16]University of Toronto, Canada, [17]Laval University, Canada, [18]Swedish University of Agricultural Sciences, The Biomedical Center, Sweden, [19]University of Sheffield, Belgium, [20]University of Manitoba, Canada

PURPOSE: To validate a new Canadian WHO fracture risk assessment (FRAX®) tool in a prospective, population-based Canadian cohort, the Canadian Multicentre Osteoporosis Study (CaMos).

METHODS: Ten year estimates of major osteoporotic fracture and hip fracture were derived from observed CaMos data using the Kaplan-Meier method for women (N=4,778) and men (N=1,919). These rates were compared with predicted ten year fracture rates based on the FRAX tool (both without and with BMD) developed by the WHO and calibrated for the Canadian population. Predicted and observed fracture risks were compared in men and women for each quintile of predicted fracture risk. Fracture prediction, using FRAX with BMD, FRAX without BMD, and BMD alone, was compared using ROC analysis. Cox proportional hazards models were used to investigate the contribution of individual FRAX variables within this population.

RESULTS: FRAX-estimated ten year risk for major osteoporotic fracture was not significantly different from the actual rates in men (predicted 5.4% vs. observed 6.4% [95% CI 5.2-7.5%]), and was very similar in women (predicted 10.8% vs.observed12.0% [95% CI 11.0-12.9%]). FRAX was well calibrated for hip fracture risk in women (predicted 2.7% vs. observed 2.7% [95% CI 2.2-3.2%]) but underestimated risk in men (predicted 1.3% vs. observed 2.4% [95% CI 1.7-3.1%]). There was close correlation between predicted and observed risk in women with a regression slope for major osteoporotic fractures of 1.07 (95% CI 0.97-1.17) and for hip fractures 0.93 (95% CI 0.83-1.03), where a slope of 1.00 indicates perfect calibration. The corresponding slopes in men were 1.26 (95% CI 1.04-1.48) and 1.83 (95% CI 1.39-2.27) respectively, but were based on fewer numbers of fractures with wide CIs. FRAX with BMD was more predictive of fracture risk than FRAX without BMD or BMD alone for both major osteoporotic fractures and hip fracture (Table). Age, body mass index, prior fragility fracture and femoral neck BMD were significant independent predictors for major osteoporotic fracture; sex, age, prior fragility fracture and femoral neck BMD were significant independent predictors of hip fractures.

CONCLUSION: The Canadian FRAX tool generally provides fracture risk estimates that agree closely with observed fracture rates in Canadian women (though less well in men), thereby providing a valuable tool for Canadian clinicians assessing patients at risk of fracture.

ROC analysis for FRAX measures vs BMD alone.

	Major Fractures		Hip Fractures	
	ROC Area	Std. Error	ROC Area	Std. Error
FRAX with BMD	0.687	0.011	0.799	0.016
FRAX without BMD	0.657	0.011	0.766	0.017
Femoral neck T-score	0.664	0.011	0.760	0.018
Minimum T-score	0.675	0.011	0.746	0.018

Table.

***Disclosures: William Leslie**, None.*
This study received funding from: Merck Frosst Canada Ltd.; Eli Lilly Canada Inc.; Novartis Pharmaceuticals Inc.; The Alliance: sanofi-aventis & Procter and Gamble Pharmaceuticals Canada Inc.; Servier Canada Inc.; Amgen Canada Inc.; The Dairy Farmers of Canada

FR0302

FRAX or Fiction: Should We Treat All Long Term Care Residents for Osteoporosis? Julie Wagner*[1], Kimberly Zukowski[1], MaryAnne Ferchak[1], Carroll Lee[1], Sherry L. Knoblock[1], Donna Medich[1], Gail Fiorito[2], Megan Miller[1], Subashan Perera[1], David Nace[1], Neil Resnick[1], Susan Greenspan[1]. [1]University of Pittsburgh, USA, [2]University of Pittsburgh, USA

Purpose: Although osteoporosis and clinical fractures are common in long term care (LTC) residents, little data are available on screening or treatment strategies for such patients. Our aims were to examine different screening strategies for LTC residents and to determine their impact on therapeutic recommendations.

Methods: We examined the prevalence of osteoporosis and vertebral fractures (VF) using bone mineral density (BMD) and DXA-derived VF assessments in 96 frail women LTC residents with no previous history or diagnosis of osteoporosis. Classification of osteoporosis included a spine, total hip, or femoral neck T-score <-2.5 SD (+BMD) or the presence of a VF (+VF). We determined if patients were eligible for treatment using 2008 NOF clinical guidelines by BMD alone (+BMD), VF alone (+VF), a combination of +BMD plus +VF, FRAX with hip BMD alone (+FRAX), a combination of +BMD plus +FRAX, or FRAX using body mass index (BMI) only (+FRAX BMI).

Results: Age and BMI were similar among the groups (Table). 44% of patients were classified with osteoporosis by BMD T-scores alone. 55% of all residents had vertebral fractures by VFA. Using combination +BMD and +VF, 71% of residents would be treated. This means that 38% of residents with osteoporosis would have been missed by BMD alone. If FRAX were utilized for patients without osteoporosis by BMD or VF criteria, 33% would be eligible for treatment. Using NOF criteria for those with +BMD plus +FRAX, 75% would be treated. However, if BMD and VF were unknown and only +FRAX BMI used, 99% of patients would be eligible for treatment.

Conclusions: We conclude the recommended treatment criteria would suggest therapy in 44 to 99% of LTC residents depending on the screening strategy employed. Using BMD plus VF knowledge or BMD plus FRAX would lead to recommended treatment of 71 to 75% of such women. BMD alone would miss 38% of residents with osteoporosis. FRAX without BMD (using BMI alone) likely overestimates the need for treatment. Further studies are needed to determine the appropriate screening strategy for these patients.

Table: Patients Eligible for Treatment Based on Screening Strategy (Mean ± SEM unless otherwise noted)

	+ BMD only	+VF only	+BMD plus +VF	+FRAX alone	+BMD plus +FRAX	+FRAX BMI alone
N (%)	42/96 (44%)	53/96 (55%)	68/96 (71%)	30/91 (33%)	72/96 (75%)	95/96 (99%)
Age (years)	87.6 ± 0.7	87.0 ± 0.6	87.3 ± 0.6	86.3 ± 0.8	87.0 ± 0.5	86.6 ± 0.5
BMI (kg/m^2)	26.5 ± 0.7	26.5 ± 0.7	26.6 ± 0.6	26.9 ± 0.9	26.7 ± 0.5	27.1 ± 0.5
Spine T-score	-1.5 ± 0.2	-0.7 ± 0.3	-0.8 ± 0.2	-0.3 ± 0.2	-1.0 ± 0.2	-0.7 ± 0.2
Total Hip T-score	-2.9 ± 0.1	-2.1 ± 0.2	-2.3 ± 0.1	-1.7 ± 0.1	-2.4 ± 0.1	-2.1 ± 0.1
Femoral Neck T-score	-2.9 ± 0.1	-2.0 ± 0.2	-2.2 ± 0.2	-1.7 ± 0.1	-2.4 ± 0.1	-2.0 ± 0.1

Table

***Disclosures: Julie Wagner**, None.*

FR0305

Underestimated Fracture Risk in Patients with Unilateral Hip Osteoarthritis as Calculated by FRAX. Nithya Setty*, Giulia Rinaldi, Julie Glowacki, Thomas Thornhill, Meryl Leboff. Brigham & Women's Hospital, USA

Osteoporosis (OP) and osteoarthritis (OA) are two age-related degenerative diseases previously believed to be mutually exclusive (Br J Rheumat. 1996, 35:813). We found however, that 25% of women with advanced OA had occult OP (J Bone Joint Surg Am. 2003,85A:2371), and that femoral neck (FN) bone mineral density T-scores were higher in hips with OA than in contralateral ones, likely attributable to reactive bone, osteophytes, subchondral osteosclerosis, and larger area (J Clin Densitom. 2010,13:24). The recently developed FRAX calculator (http://sheffield.ac.uk/FRAX) makes it possible to estimate age and gender-specific, 10-year absolute total (clinical spine, hip, forearm and humerus) and hip fracture risk on the basis of clinical risk factors and FN T-score. OP treatment is recommended for patients with a calculated fracture risk of ⩾20% for total fractures and ⩾3% for hip fractures (National Osteoporosis Foundation. 2008,Clinician's Guide). The objective of this study was to determine, for subjects with unilateral hip OA, whether the calculated FRAX fracture risk was underestimated in subjects when using the OA vs. the contralateral FN T-score, and whether the calculated risk could impact clinical decisions regarding OP therapy. We determined clinical risk factors and bilateral hip T-score for 40 subjects (26 women and 14 men, age ⩾40 years) scheduled for hip replacement due to unilateral advanced hip OA. We compared FRAX 10-year probability risks of total and hip osteoporotic fracture using the FN T-score of the OA vs. the contralateral hip. We found significant differences in FRAX total fracture ($p=0.00044$) and hip fracture ($p=0.0089$) risk using the OA vs. the contralateral FN T-score, where the mean difference ± SEM in total fracture risk was 2.53 ± 0.66, and hip fracture risk was 1.41 ± 0.51. The mean difference ± SEM in FN T-scores between the OA vs. the contralateral hip was 0.75 ± 0.18 ($p=0.00013$). The fracture risk differences resulted in OP treatment recommendations for 10% vs. 22% of subjects at risk for total fractures and for 20% vs. 33% of subjects at risk for hip fractures when using the OA vs. contralateral hip BMD, respectively. These data indicate that subjects with advanced OA are at risk for osteoporotic fractures, and that fracture risk with FRAX is underestimated when calculated with the FN T-score in an OA hip. Recommendations for OP diagnosis should avoid BMD testing of OA hips for fracture risk prediction and OP treatment decisions.

***Disclosures: Nithya Setty**, None.*

FR0310

In Vivo Quantification of Intracortical Porosity and Cortical Remnants Adjacent to Marrow Identifies Individuals at Risk for Fracture Better than Prevailing Methods. Ali Ghasem-Zadeh[1], Sandra Iuliano-Burns[1], Ego Seeman[1], Roger Zebaze*[2]. [1]Austin Health, University of Melbourne, Australia, [2]Austin Health, Australia

Background

We reported that ~ 50% of bone lost during ageing occurs by remodelling in cortex adjacent to marrow enlarging and coalescing pores leaving a transitional zone (TZ) of trabecular-appearing cortical remnants. We hypothesized that quantification of this TZ of cortical remnants identifies individuals with fracture.

Methods

We studied 20 women with forearm fracture and 47 age, height and weight matched controls. Images were collected at the distal radius using HRpQCT (Scanco Medical). Total, cortical and trabecular volumetric density (T, Ct, and Tr vBMD) were analyses using a newly developed software (Strax1.0) which assesses the compact-appearing cortex (CC) and the layer of cortical remnants. Thicknesses of the compact-appearing cortex (Th. CC) and cortical remnants of the TZ were measured. We further separated the TZ into inner (ITZ) and outer (OTZ) zones, the ITZ being adjacent to marrow, a location of higher remodeling than in the OTZ and CC. The proportion of the total cortical thickness (CC + TZ) occupied by the CC and the ITZ were measured and denoted %CC and %ITZ. Porosity (Po) was measured in each zone.

Results

Total cortical thickness was similar in cases and controls (952.9 ± 39.7 vs 986.3 ± 28μm; NS)(mean ± SEE). However, the % CC was reduced in fracture cases relative to controls (70.91 ± 1.03 vs 72.85 ± 0.40; $p=0.038$), mostly due to an increase in the % ITZ (12.82 ± 0.43 vs $15.59 \pm 1.1\%$; $p=0.01$). In absolute terms, the thickness of the CC in fracture cases was reduced (664.1 ± 39 vs 710.3 ± 28μm; NS) and the thickness of the ITZ was increase (155.8 ± 74 vs 129.6 ± 36; $p=0.05$) compared to controls. Porosity in compact-appearing cortex was similar in cases and controls (2.4 ± 0.52 vs $2.89 \pm 0.43\%$, NS) but Po in the ITZ was higher in cases than controls (48.32 ± 2.93 vs 42.02 ± 1.48; $p = 0.03$). Po ITZ correlated modestly with density parameters with r2 respectively 0.03, 0.17 and 0.47 for Ct D, vBMD and Tr D suggesting density does not fully capture porosity. Differences in Ct vBMD (262.5 ± 12.79 vs 288.54 ± 9.5), vBMD (853.6 ± 4.59 vs 858.94) and Tr vBMD (111.8 ± 7.84 vs 132.2 ± 5.55; $p=0.04$) were smaller and/or non-significantly different.

Conclusion

Porosity producing trabecularization is an important indicator of structural decay and fragility. Quantification of this process in vivo identifies individuals at risk for fracture beyond currently existing measurements.

***Disclosures: Roger Zebaze**, None.*

FR0316

A Four Years Exercise Intervention Program in Pre-Pubertal Children Increases Bone Mass and Bone Size But Do Not Affect the Fracture Risk. Bjarne Lofgren*[1], Jan Åke Nilsson[2], Magnus Dencker[2], Magnus Karlsson[3]. [1]Clinical & Molecular Osteoporosis Research Unit Dept. of Clinical Sciences, Lund University, Dept of Orthopaedics, Skåne University Hospital, Sweden, [2]Skane University Hospital, Sweden, [3]Skåne University Hospital Malmö, Lund University, Sweden

Abstract

Introduction: Pediatric exercise intervention studies, that evaluate if exercise could be used as a prevention of fragility fracture, span at maximum 24 months and uses bone traits as surrogate endpoints for fractures. But reports have inferred that increased training may possibly lead to more trauma and more fractures. Therefore we designed a 48 months controlled exercise intervention study with also fracture as endpoint.

Material and Methods: The intervention group achieved 40 minutes/day of school physical education and the controls 60 minutes/week. Included were 2395 children aged 7-9 years, 446 boys and 362 girls in the intervention (2675 person-years) and 807 boys and 780 girls in the control group (5661 person-years). Fractures were prospectively registered. In 73 boys and 48 girls in the intervention and 52 boys and 48 girls in the control group, skeletal development was followed by dual energy X-ray absorptiometry (DXA). Bone mineral content (BMC; g) in lumbar spine (LS), femoral neck (FN) and trochanter, bone width (cm) in third lumbar vertebra (L3) and FN and hip structural analyses (HSA) variables were included.

Results: The rate ratio (RR) for fractures in the intervention group was 1.11 (0.78, 1.57) (mean (95% CI)). In the DXA measured children, there were at baseline no group differences in age, anthropometrics or bone parameters. The mean annual gain in both BMC and bone width was higher in the interventions than in the controls groups, for LS BMC 0.6 standard deviations (SD) higher in both girls ($p<0.01$) and boys ($p<0.05$), in trochanter BMC 0.5 SD higher in girls ($p<0.01$), in femoral neck width 0.5 SD higher in girls ($p < 0.05$) and 0.3 SD higher in boys ($p <0.05$) and in L3 width 0.5 SD higher in girls ($p<0.05$).

Conclusion: Increased duration of moderate intense exercise in 7-9 year old children could be used on population based level as to improve bone mass and bone size without increasing the fracture risk.

***Disclosures: Bjarne Lofgren**, None.*

FR0320

DXA Self-Scheduling Improves Osteoporosis Screening. Amy Warriner*[1], Ryan Outman[2], Kenneth Saag[2], Elizabeth Kitchin[2], Sarah Morgan[2], Jeffrey Curtis[2]. [1]UAB, USA, [2]University of Alabama at Birmingham, USA

Purpose: U.S. guidelines recommend bone density screening with central dual energy x-ray absorptiometry (DXA) in all women 65 years or older. However, less than one-third of eligible U.S. women undergo DXA testing. The main barrier in achieving greater rates of osteoporosis screening is identifying a systematic, effective and generalizable way for healthcare providers and patients to schedule and receive DXA results.

Methods: We conducted a group randomized, controlled trial involving 39 primary care physicians at the University of Alabama at Birmingham. Women 65 years or older with no DXA scan in the past 4 years cared for by these physicians were identified using administrative billing data. Randomization was performed in two waves, each forming a cohort. In each cohort, 30 patients per physician were randomized to the intervention (sent mailed materials twice); the remaining patients comprised the control group (received no mailing). The intervention included a patient brochure regarding osteoporosis and fracture risk and a letter providing patients the opportunity to self-schedule a DXA. Results from the two cohorts were similar and pooled for analysis. Stratified results compared receipt of DXA among women receiving primary care proximate to the site where the DXA scanner was located (62% of study population) vs. more distant satellite clinics which required additional travel to the DXA scanner.

Results: Of 5122 identified women meeting inclusion criteria, 978 women were randomized to the intervention group and 4,144 to the control group. A total of 19.5% of women in the intervention group received a DXA, compared to 6.3% women receiving DXA in the control group (risk difference [RD] for DXA receipt 13.2%, 95% CI 10.8 – 16.0%), Figure 1. Comparing intervention to control group patients, receipt of DXA in main clinic patients was greater (22.7% for intervention group vs. 7.6% for control group, RD = 15.1%, 95% CI 11.9 – 18.7%) compared to satellite clinic patients (13.4% for intervention group vs. 4.3% for control group, RD = 9.1%, 95% CI 5.7 – 13.3%).

Conclusions: DXA scheduling and receipt was improved significantly through the use of a simple mailed osteoporosis brochure and the availability for patients to self-schedule their own DXA scans. This modality may be an effective component of a multi-faceted quality improvement program to increase rates of osteoporosis screening.

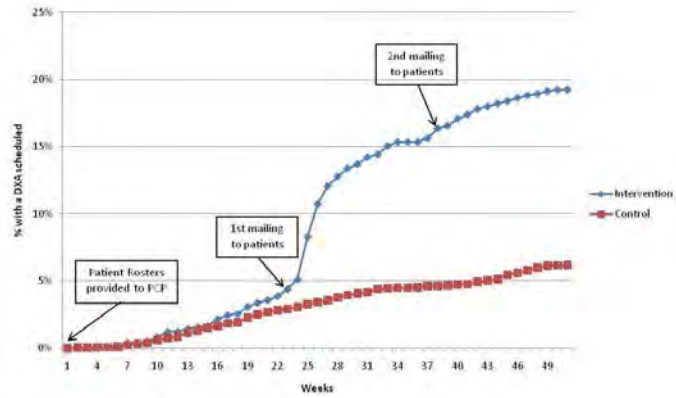

Figure. DXA Screening by Treatment Arm

***Disclosures: Amy Warriner**, None.*
This study received funding from: Procter & Gamble

FR0321

Evaluation of the Risk of Fracture in Early Postmenopausal Women: Predictive Value of Baseline BMD and Development of Prognosis BMD T-score Thresholds. Jean-Michel Pouilles[1], Florence Tremollieres*[2], Patricia Dargent[3], Nicolas Drewniak[4], Claude Ribot[2]. [1]Menopause Center. Hôpital Paule de Viguier, France, [2]Hopital Paule De Viguier, France, [3]INSERM Unit 953 (ex 149), France, [4]Inserm U953, France

Osteopenia (op) is common in healthy early postmenopausal (PM) women. It is still not clear how those women should be managed with regard to their long-term risk of osteoporosis (OP) and we lack suitable algorithms for identifying higher-risk subgroups for fracture. The aim of this study was (1) to determine the number of healthy early PM women who had progressed from normal/op to OP over a 12-year follow-up period of time and (2) to identify the baseline T-score thresholds associated with less than 10% risk of developing OP and/or incident OP fracture. We analyzed DXA of the lumbar spine (LS) and femoral neck (FN) from 713 women ⩾45 years of age (mean:54±4 yrs) from the MENOS cohort with at least 2 BMD measurements (using the same Lunar GE DPX-IQ) at baseline and the final follow up time point examination. None of the women were or had taken OP medication or HRT throughout the follow-up. We only considered major incident fractures that occurred with minimal trauma. The lowest LS or FN T-score was used to classify women as having OP or op. We derived T-score thresholds associated with a 90% probability of not developing OP and/or a 1st incident fracture over the follow-up period (NPV:90%).

At baseline, 28.8% of the women were classified as normal and 50.2% and 21% as having op and OP, respectively. Over an average follow-up period of time of 12.4 yrs (± 2), 5 (2%) normal women and 118 (33%) with op developed densitometric OP. 73 women sustained a 1st low-energy fracture including 41 wrist, 15 symptomatic spine, 12 humerus and 5 hip fractures. At baseline, 82% of the women with fracture had either op (n=30) or OP (n=30). Women with a baseline T-score at the lower of the 2 sites above -1.9 (75% of the population) and -1.5 (55%) exhibited a risk of less than 10% of developing pure densitometric OP and/or incident fracture, respectively. Women with OP and/or fracture had significantly lower mean baseline BMD values, a higher FRAX score, a higher rate of vertebral (but not femoral) bone loss (-0.21±0.7 vs -0.43±0.7%/yr, $p<0.001$) and higher serum osteocalcin levels. Baseline BMD was associated with a better discriminative value than the rate of vertebral bone loss to predict OP and/or incident fracture (AUC: 0.80 vs 0.66, $p<0.001$).

In conclusion, about 33% of early PM women with op will develop OP within the 1st PM decade. Women with a minimum T-score above -1.5 had a 90% probability of avoiding OP and/or a low-trauma major fracture in the next 10 years.

***Disclosures: Florence Tremollieres**, None.*

FR0322

FRAX and UK-Based Diagnostic and Therapeutic Decisions the Day Before a Fracture in the Netherlands. Tineke van Geel*[1], Sandrine Bours[2], Kirsten Huntjens[2], Geert-Jan Dinant[1], Joop van den Bergh[3], Piet Geusens[2]. [1]Maastricht University/Caphri, Netherlands, [2]Maastricht University Medical Centre, Netherlands, [3]VieCuri Medical Centre Noord-Limburg, Netherlands

Objective: To investigate the predictive value of FRAX to assess the short-term fracture risk using the cut-off points as prescribed by the National Osteoporosis Guideline Group (NOGG).

Methods: In total, 509 patients aged between 50 and 90 years, who attended the emergency room at a hospital in the Southern part of the Netherlands at the time of a low trauma fracture, were included in this study. All risk factors prescribed in the FRAX were assessed, including the femoral neck bone mineral density (FN-BMD) measurement by dual energy X-ray absorptiometry (DXA). Using FRAX, the 10-year fracture risk was calculated and diagnostic and therapeutic decisions according to NOGG before the current fracture, with and without BMD.

Results: The FRAX was completed for 482 patients with a fracture (75% women) of whom 8% sustained a hip fracture, 58% a major fracture (clinical spine, forearm or shoulder) and 34% a minor fracture (all other fractures).

Before the fracture and based on major fracture risk of FRAX without FN-BMD, 44% would not have required treatment, 43% would have needed a BMD measurement, and 14% would have required treatment. If FN-BMD was included, 17% would and 83% would not have required treatment. Of the patients with osteoporosis before the fracture 70% were considered at low risk and 30% of them would have been advocated treatment.

In women (n = 362) after their fracture and based on major fracture risk of FRAX without FN-BMD, 1.4% would not have required treatment, 66% would have required a BMD measurement, and 33% would have required treatment. If FN-BMD was included, 30% would and 70% would not require treatment. Similar results were found if 10-year hip fracture risk was used.

Conclusion: Most patients with a fracture would have been considered at low risk the day before a low trauma fracture occurred and would not have been advocated treatment according to UK-FRAX and NOGG. This indicates that this treatment decision algorithm is not useful for short term fracture prediction and prevention in the Netherlands. Extrapolating these results to the Netherlands, without BMD, only 11.200 of the 80.000 patients older than 50 years yearly presenting with a fracture would have required treatment before the fracture and 34.400 would have needed a DXA measurement. With BMD, 13.600, instead of 11.200, would have been advocated treatment the day before the fracture.

***Disclosures: Tineke van Geel**, None.*

FR0327

Dual Effect of Adipose Tissue on Bone Health during Growth. Heli Viljakainen*[1], Minna Pekkinen[2], Elisa Saarnio[2], Christel Lamberg-Allardt[2], Outi Mäkitie[3]. [1]Helsinki University Central Hospital for Children & Adolescents, Finland, [2]University of Helsinki, Finland, [3]Helsinki University Central Hospital for for Children & Adolescents, Finland

Recent studies suggest association between body fat and childhood bone health, although conflicting findings have also been reported. The aim of the present study was to examine the association between body fat content and BMD, bone turnover markers, and calcitropic factors in apparently healthy children and adolescents in a cross-sectional setting.

The study was carried out as a school based cross-sectional cohort study with 186 subjects (61% girls) aged from 7 to 19 years. Background characteristics, including medical history and lifestyle factors, were collected by a questionnaire. Anthropometry, BMD and body composition measurements with DXA and pQCT, a fasting blood sample and a second morning void urine sample were obtained.

Body mass index exceeded 25 kg/m^2 and 30 kg/m^2 in 6 and 2 subjects, respectively. Relative weight (height-adjusted weight) was calculated for 176 subjects, of whom 31 (19%) had relative weight above 20% (=overweight) and 3 above 40% (=obesity). Girls were on average significantly older and had more advanced puberty than the boys. Girls had a higher fat percent than boys, but age and gender specific Z-scores for fat percent did not differ between the genders. The subjects were divided into three groups, representing low, intermediate and high adiposity, based on age and gender specific fat percentage Z-scores. Multivariate analysis was performed to all bone variables using lean body mass, pubertal development, dietary intake of calcium and intensity of physical activity as covariates. In pQCT, a significant difference between the groups was observed in cortical BMD (MANOVA; p=0.02) in proximal radius, the intermediate group having the highest values. Similarly, DXA-derived LS and WB BMD Z-scores differed significantly between the groups (MANOVA; p=0.026 and p=0.036, respectively), with highest values in the intermediate group. High body fat content associated also with low bone turnover markers, low PTH, high S-Ca and high urinary calcium excretion.

These findings suggest that normal body fat content is beneficial for bone health in growing children and adolescents while both low and high body fat content have adverse skeletal effects.

***Disclosures: Heli Viljakainen**, None.*

FR0332

A Population-Based Analysis of the Post-Fracture Care Gap 1996-2008: The Situation Is Not Improving. William Leslie*[1], Marina Yogendran[1], Mahmoud Azimee[1], Suzanne Morin[2], Colleen Metge[1], Patricia Caetano[1], Lisa Lix[3]. [1]University of Manitoba, Canada, [2]McGill University Health Centre, Canada, [3]University of Saskatchewan, Canada

Previous reports have documented low rates of BMD testing and/or osteoporosis treatment in older individuals who have sustained a non-traumatic fracture. We previously reported improvement in testing and treatment rates between 1997/98 and 2001/02, but even in the final study year only 20.5% of women post-fracture underwent an intervention (*Can Fam Physician 2008;54:1270*). OBJECTIVE: To characterize temporal changes in post-fracture BMD testing and/or osteoporosis treatment initiation from 1996/97 to 2007/08. METHODS: A population-based

administrative data repository for the province of Manitoba, Canada, was accessed to identify non-traumatic fractures in men and women age 50 years and older. High-trauma fractures, residents of personal care homes, and those with recent BMD testing (preceding three years) were excluded. The outcomes of interest were BMD testing and/or dispensation of an osteoporosis medication in the twelve months post-fracture (with/without exclusion of those on treatment at the time of fracture). RESULTS: 33,578 fracture events met the inclusion criteria (30,920 after exclusion of individuals on treatment at the time of fracture). Post-fracture BMD testing in increased from 0.7% in 1996/97 to 8.9% 2007/08. Osteoporosis medication use increased from 9.9% in 1996/97 to 19.1% in 2001/02 and then declined to 11.9% in 2007/08 (6.1%, 12.3%, 5.9% respectively after exclusion of those already on treatment). Based on either BMD testing or treatment initiation, rates increased from 10.1% in 1996/97 to 21.8% in 2001/02 and have been stable thereafter (maximum 15.3% after exclusion of individuals already on treatment). Other factors associated with any intervention were sex (men 4.4% vs women 24.5%), area of residence (lower in the rural north), socioeconomic status (least in lower income quintile groups), and fracture site (hip 15.1%, spine 37.5%, humerus 15.8%, forearm 18.9%, pelvis 20.9%, other 15.4%). CONCLUSIONS: The post-fracture ''care gap'' has not narrowed in recent years. Following an initial improvement, rates of medication initiation have actually declined since 2001/02. Novel strategies are required to disseminate and implement best practices at the point of care to reduce the risk of recurrent fractures and the associated morbidity and mortality.

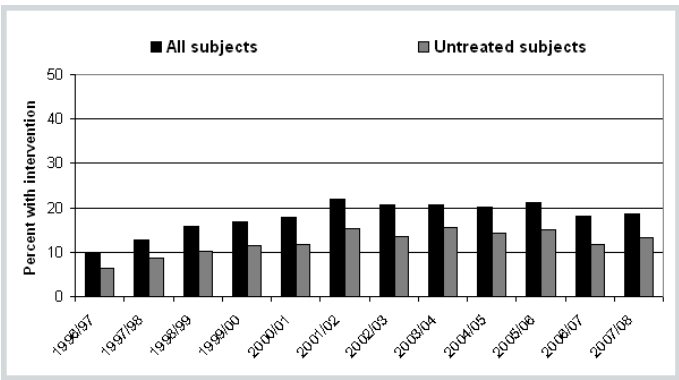

Figure: Percent with either BMD testing or osteoporosis medication use in the year post-fracture

***Disclosures: William Leslie**, Amgen, 2*
This study received funding from: Amgen

FR0338

In COPD Inhaled Glucocorticoids, but not β2-Agonist are Associated with Vertebral Fracture Risk. Stefano Gonnelli*[1], Carla Caffarelli[1], Stefania Maggi[2], Stefania Rossi[1], Paola Siviero[2], Gaetano Crepaldi[2], Ranuccio Nuti[1]. [1]University of Siena, Italy, [2]CNR - Center on Aging, Italy

Although inhaled glucocorticoids (GCs) are being more frequently prescribed in the managements of COPD, their role in the reduction of bone mineral density (BMD) and in fracture risk still remains controversial. Also inhaled β2-adrenergic agonists have been associated with an increased fracture risk.

The EOLO (Evaluation of Obstructive Lung disease and Osteoporosis) study enrolled a total of 3,030 ambulatory COPD patients (1,778 men and 1,262 women) aged 50 years or over. Of COPD patients, 68.3% were treated with GCs (55.0% inhaled GCs, 3.9% oral GCs and 9.5% oral + inhaled GCs) 16.8% were not treated with specific COPD medications and the remaining 14.7% were treated with short-or long-acting β2-agonists, xanthines or antimuscarinics but not with GCs. The COPD patients treated with inhaled GCs (n=1653) were divided in to 3 groups on the basis of the daily dose of inhaled GCs expressed as beclometasone equivalents: ≤ 750 μg; 750 – 1500 μg; ⩾ 1500 μg. Beta2-agonists (long-acting and short-acting) was expressed as albuterol equivalents. Spirometry and the presence of vertebral fractures on lateral chest X-ray were evaluated. Ultrasound parameters at calcaneous, namely Stiffness were also measured by Achilles apparatus (GE, Lunar).

The risk of fractures was markedly increased in patients with very severe or severe COPD, (OR=2.05; CI 1.28- 3.28 and OR=1.40; CI 1.06- 1.82, respectively). Moreover, the risk of vertebral fractures was significantly increased in patients taking the highest dose (>1500 μg) of inhaled GCs (OR=1.4; CI 1.04 - 1.89). The use of inhaled GCs at doses ranging from 750 and 1500 μg was associated to a positive, but not significant, increase in vertebral fracture risk. On the contrary, the different daily doses of β2-agonists were not associated with an increased risk of vertebral fractures. Both COPD severity and inhaled GCs at daily dose > 1500 μg were associated to Stiffness value lower than 57%. On the contrary the daily dose of inhaled β2-agonists was not associated to a reduction in Stiffness values.

In conclusion, in COPD patients the highest doses of inhaled GCs, but not inhaled β-adrenergic agonists, are associated with to an increased risk of vertebral fractures and to a reduction of QUS at calcaneous.

***Disclosures: Stefano Gonnelli**, None.*

FR0339

Inhibition of the Serotonin Transporter and Risk of Fracture in Older Women. Susan Diem*[1], Terri Blackwell[2], Katie Stone[3], Jane Cauley[4], Elizabeth Haney[5], Kristine Ensrud[6]. [1]University of Minnesota, USA, [2]California Pacific Medical Center Research Institute, USA, [3]California Pacific Medical Center-Research Institute, USA, [4]University of Pittsburgh Graduate School of Public Health, USA, [5]Oregon Health & Science University, USA, [6]Minneapolis VA Medical Center / University of Minnesota, USA

Recent work has suggested a possible role for circulating serotonin in the regulation of bone mass, raising the possibility that use of medications that inhibit the serotonin transporter and raise extracellular serotonin levels may have effects on bone health. To test the hypothesis that degree of serotonin transporter inhibition is associated with risk of non-spine fracture, we assessed current use of antidepressant medications and incident fractures over a 12 year period in a cohort of 7024 older women participating in the Study of Osteoporotic Fractures. We categorized specific antidepressant medications by degree of serotonin transporter inhibition (low, intermediate, and high). Antidepressant use status was updated at each follow-up visit (an average of 4.9 and 9.8 years after initial assessment) using time-dependent methods. The hazard ratio (HR) and 95% CI for risk of fracture was calculated by category of serotonin transporter inhibition using Cox regression models. All results were adjusted for the following characteristics, which were updated at each follow-up visit: age, race, BMI, health status, history of fall in previous 12 months, cognitive function, depression, and neuromuscular function.

Average length of follow-up was 7.87± 3.45 years. Of the 7024 women (average age 80 years at initial visit), 1992 (30%) women experienced ⩾ 1 non-spine fracture during the follow-up period, including 670 (10.1%) with a hip fracture and 383 (5.5%) with a wrist fracture. Below are the age- and multivariable-adjusted HRs for risk of fracture by level of serotonin transporter inhibition use. After adjustment for multiple confounders, use of medications with the highest level of serotonin inhibition was associated with an increased risk of non-spine fracture (table), including hip and wrist fractures. However, there was no evidence of a graded association between degree of serotonin transporter inhibition and risk of these fractures as risk of fracture appeared to be greater among women using medications with a low degree of serotonin transporter inhibition than that among women using medications with an intermediate degree of inhibition. These results suggest that degree of inhibition of the serotonin transporter may not explain the observed association between use of antidepressant medications and higher risk of fractures.

Fracture Type	Hazard Ratio (95% CI) by Degree of Serotonin Transporter Inhibition			
	No Use (N=6382)*	Low† (N=152)*	Intermediate† (N=206)*	High† (N=272)*
Non-spine Fracture				
Age-adjusted	1.00 (referent)	1.43 (1.10, 1.88)	1.15 (0.90, 1.47)	1.68 (1.41, 2.01)
MV model	1.00 (referent)	1.32 (1.00, 1.76)	1.10 (0.85, 1.41)	1.53 (1.26, 1.84)
First Hip Fracture				
Age-adjusted	1.00 (referent)	1.94 (1.29, 2.92)	0.76 (0.46, 1.25)	1.64 (1.22, 2.20)
MV model	1.00 (referent)	1.73 (1.13, 2.66)	0.75 (0.46, 1.24)	1.46 (1.07, 2.00)
Wrist Fracture				
Age-adjusted	1.00 (referent)	1.92 (1.13, 3.28)	1.12 (0.64, 1.94)	1.58 (1.06, 2.36)
MV model	1.00 (referent)	1.75 (0.98, 3.14)	1.10 (0.61, 1.96)	1.59 (1.05, 2.42)

*N refers to use status at initial visit
†Inhibition constant in nM: low >10, intermediate >1 ≤10, high ≤1

Table 1

***Disclosures: Susan Diem**, Eli Lilly, Inc., 2*

FR0342

Reduced Rate of Bone Loss Predicts Survival Post-Fracture and May Mediate Mortality Risk Reduction Associated With Bisphosphonate Treatment: Data From An 18-Year Prospective Study From Dubbo Osteoporosis Epidemiology Study. Dana Bliuc*, Nguyen Nguyen, Tuan Nguyen, John Eisman, Jacqueline Center. Garvan Institute of Medical Research, Australia

Mortality risk is increased following all osteoporotic fractures, but factors contributing to this risk are poorly defined. Bone loss is associated with mortality risk, but its role in mortality post-fracture is unclear. Bisphosphonates (BP) also reduce mortality post-fracture but the mechanism is unknown. The aims of this study were to: 1) examine the association between bone loss and mortality risk in the presence of fracture and 2) determine whether the effect of BP on mortality risk is mediated by a reduction in bone loss.

All low trauma fractures and mortality data were collected from 777 women and 514 men aged 60+ from the Dubbo Osteoporosis Epidemiology Study who had at least 2 bone mineral density (BMD) measurements (April 1989-May 2007). Bone loss was the difference between the first and last BMDs, and for those with fractures, was measured post-fracture. Co-morbidities, muscle strength and medication obtained at baseline and updated 2-yearly. Cox proportional hazards models used to determine mortality risk.

There were 226 fractures in women and 68 in men over 15 (IQR: 9-17) and 14 years (IQR: 7-16) with 284 deaths (101 post-fracture) in women and 246 (43 post-fracture)

in men. A 3%/yr increase in bone loss increased mortality risk by 47% in women and 29% in men, after adjusting for fracture (time dependent) and other frailty markers. In those with fractures, post-fracture bone loss ⩾1%/year increased mortality risk by ⩾50% in both genders after confounder adjustment compared with <1% bone loss.

The relationship between bone loss and BP was explored in 65 subjects on BP, and 1285 on no treatment. BP was independently associated with a 71% mortality risk reduction after adjustment for frailty markers. Bone loss was non-significantly less in the BP group compared to non-treated group (-0.44g/cm^2 vs -0.63g/cm^2; p= 0.37). However, when bone loss was added to the model, BP and bone loss were independent mortality risk predictors, and the effect size of BP on mortality reduction increased by 20%, suggesting a greater effect of BP on mortality in the presence of bone loss. This effect was driven by those on BP and calcium ± vitamin D, where bone loss was significantly less ($p<0.05$) and fewer deaths occurred.

Thus, reduced bone loss is associated with better survival in the presence of fracture and may play a role in the mortality risk reduction observed with bisphosphonates.

***Disclosures: Dana Bliuc**, None.*

FR0343

The Impact of Two Educational Interventions on Osteoporosis Diagnosis and Treatment After a Fragility Fracture: a Randomized-controlled Trial. Louis Bessette*[1], Sonia Jean[2], Sophie Roy[3], K. Shawn Davison[4], Louis-Georges Ste-Marie[5], Jacques Brown[1]. [1]Laval University, Canada, [2]Institut National De Sante Publique, Canada, [3]Institut national de santé publique du Québec, Canada, [4]Centre de recherche du CHUQ, Canada, [5]Hospital Saint-LucCHUM, Canada

Purpose: To investigate the utility of two education-based interventions for increasing the diagnosis and treatment of osteoporosis in women (>50y old) after fragility fracture (FF).

Methods: This study was part of the Recognizing Osteoporosis and its Consequences in Quebec (ROCQ) programme. Women who recently suffered a FF were recruited from hospitals and from an administrative database-generated list of women who had recently suffered a FF (Quebec Ministry of Health). Six to eight months after FF, women were randomized into one of three groups: 1.) usual care, 2.) documentation group, or 3.) documentation and video group. Documentation consisted of information for both the patient and their respective primary care physician regarding osteoporosis, FF and the need for treatment following FF. The 15-minute video consisted of similar information as the documentation, but went into greater depth. Rates of osteoporosis diagnosis and treatment at randomization and after 12 months were compared.

Results: At randomization, a total of 1,174 women had neither a diagnosis nor treatment for osteoporosis and 1,314 women were without osteoporosis treatment. No significant baseline differences existed among groups for any investigated variable. In the group of women without diagnosis and treatment for osteoporosis at randomization, diagnosis of osteoporosis 12 months after randomization occurred in 12% of the control group, 15% of the documentation group (p=0.07) and 16% ($p<0.05$) of the video group (all vs. control group). Treatment rates for this group were 8% for the control group, 12% for the documentation group (p=0.052) and 11% for the video group (p=0.06). In the group of women with no treatment at randomization, osteoporosis therapy was initiated in 10% of the control group, 13% of the documentation group (p=0.11), and 13% of the video cohort (p=0.12). The greatest impact on diagnosis and treatment was whether a woman passed on the documentation to her primary care physician (18% for receiving diagnosis and 14-15% for receiving appropriate treatment).

Conclusions: Educational interventions alone are not satisfactory to significantly increase diagnosis or treatment for osteoporosis in women over the age of 50y who have recently suffered a FF. Having the patient provide their primary care physician with documentation had the largest impact on both receiving a diagnosis of osteoporosis and in obtaining appropriate treatment.

***Disclosures: Louis Bessette**, Roche, 8; Roche, 2; Pfizer, 5; Novartis, 8; Merck, 2; Amgen, 8; Pfizer, 2; Amgen, 5; Bristol-Myers-Squibb, 2; Amgen, 2; Eli Lilly, 2; Abbott, 2; Abbott, 5; Merck, 5; Pfizer, 8; Warner Chilcott, 8; Roche, 5; Merck, 8; Novartis, 5 This study received funding from: Warner Chilcott, sanofi-aventis, Merck, Novartis, Eli Lilly*

FR0344

Validation of Diagnostic Codes for Subtrochanteric, Diaphyseal, and Typical Hip Fractures Using Administrative Claims Data. Pongthorn Narongroeknawin[1], Nivedita Patkar[1], Bita Shakoory[1], Archana Jain[2], Jeffrey Curtis[1], Elizabeth Delzell[1], Philip Lander[1], Robert Lopez-Ben[1], Michael Pitt[3], Monika Safford[1], David Volgas[1], Kenneth Saag*[1]. [1]University of Alabama at Birmingham, USA, [2]University of Alabama, USA, [3]Radiology, University of Alabama at Birmingham, USA

Purpose:

Recent studies have raised concern about a possible association of subtrochanteric and diaphyseal fractures of femur (SFF and DFF) with long-term bisphosphonate use. Administrative claims databases provide large sample sizes and high generalizability to test these associations if these fractures can be accurately identified. To develop and validate claims-based algorithms for identification of SFF and DFF, we assessed the accuracy of hospital and physician diagnosis codes to identify these fractures.

Method:

We identified adults with an ICD-9 code for femoral fracture (820.xx, 821.xx, 733.14, 733.15) at University of Alabama at Birmingham Hospital from 01/04 to 12/08. All patients with SFF and random sample of other femoral fracture types were selected, medical records and radiology reports were reviewed independently by two physician reviewers, providing a gold standard for SFF and DFF. Discordance among record reviewers was adjudicated by consensus of an expert panel of radiologists and an orthopedic trauma surgeon. We assessed diagnostic properties of algorithms based on ICD-9 diagnosis codes appearing on hospital discharge and surgeons' fracture repair records to identify a SFF or DFF.

Results:

We identified 137 persons with suspected SFF and randomly selected 55 persons with suspected DFF. The positive predictive value (PPV) to identify SFF ranged from 69% to 89% based on the level and source of diagnosis codes (Table). PPVs for DFF were slightly greater, ranging from 81 to 97%. Case algorithms that accepted SFF or DFF primary or secondary diagnosis code on hospital discharge record had PPVs of 69% and 89% for SFF and DFF respectively. Algorithms that required both primary hospital discharge diagnosis code and the same diagnosis code from the surgeon who performed the fracture repair had highest PPVs.

Conclusion:

Administrative claims data-based algorithms that combined hospital discharge with surgeon's diagnosis codes to identify cases of SFF and DFF yielded relatively high PPVs, particularly for DFF. A more specific case algorithm that required SFF diagnosis code both as the primary discharge diagnosis and as the surgeon's diagnosis resulted in the highest PPV. Work is underway to identify atypical fractures with ''beaking'' and transverse morphology. These claims algorithms will be useful in future population-based observational studies to evaluate the association between osteoporosis medications and subtrochanteric and diaphyseal fractures.

Positive Predictive Value (PPV) of Various Case Identification Algorithms for Subtrochanteric and Diaphyseal Femoral Fractures

Case Identification Algorithm	Number of identified cases by different algorithms (%)*	PPV (95% CI)
Subtrochanteric Femoral Fractures (n=137)		
• Any position on hospital discharge diagnosis list (primary or other)	137 (100)	69 (61-76)
• Primary hospital discharge diagnosis	107 (78)	74 (66-82)
• Surgeon's diagnosis on administrative claim	87 (64)	80 (71-88)
• Both primary discharge diagnosis AND surgeon's diagnosis	81 (59)	89 (81-97)
Diaphyseal Femoral Fractures (n=55)		
• Any position on hospital discharge diagnosis list (primary or other)	55 (100)	89 (81-97)
• Primary hospital discharge diagnosis	35 (64)	94 (87-100)
• Surgeon's diagnosis on administrative claim	46 (84)	81 (72-90)
• Both primary discharge diagnosis AND surgeon's diagnosis	44 (80)	97 (90-100)

*Compared to a case finding algorithm that accepted any SFF or DFF diagnosis on any position of hospital discharge diagnosis list

Table

***Disclosures: Kenneth Saag**, None.*

FR0350

Association of Stressful Life Events with Incident Falls and Fractures in Older Men: the Osteoporotic Fractures in Men (MrOS) Study. Howard Fink*[1], Michael Kuskowski[1], Lynn Marshall[2]. [1]GRECC, Minneapolis VA Medical Center, USA, [2]Oregon Health & Science University, USA

In case-control analyses, major life events have been associated with hip fracture, but such studies are prone to bias. Therefore, using a prospective cohort design, we examined the association of stressful life events with risk of incident falls and fractures. We hypothesized that any observed risk would be moderated by evidence of social support.

We used data from MrOS, a longitudinal cohort study of men aged >=65 yrs. Approximately 2 yrs after MrOS baseline (V1), subjects reported by interim questionnaire (IQ) whether they'd experienced stressful life events in the past 12 months (e.g. wife/partner serious illness, loss of/separation from other close relative or friend, serious financial trouble) and regarding their level of social support (e.g. live with spouse/partner, number of living children, presence of confidant). Self-reported incident falls and fractures occurring after IQ were collected every 4 months, with fractures confirmed by radiology reports. Total hip BMD was measured at V1 and history of falls in the past year was measured by IQ. Log binomial regression and Cox proportional hazards regression were used to model risk (and 95% confidence intervals (CI)) of falls and fracture outcomes, respectively.

Of 5705 men completing the IQ, 55% reported >=1 stressful event in the past year. In the year after the IQ, 13% (n=779) of men reported 2+ falls and 2% (n=107) had a confirmed clinical fracture. After adjustment for age and past falls, compared to men with no stressful events, those with stressful events had a small increased risk of multiple falls in the following year (any stressful event: RR=1.09 [95%CI: 1.01-1.18]; 1 event: RR=1.05 [0.97-1.14]; 2 events: RR=1.16 [1.05-1.29]; 3+ events: RR=1.19 [1.03-1.38]). After adjustment for age and BMD, compared to men with no stressful events, those with stressful events had a modestly increased risk of clinical fracture in the following year (any stressful event: HR=1.44 [95%CI: 0.97-2.16]; 1 event: HR=1.35 [0.88-2.09]; 2 events: HR=1.36 [0.75-2.48]; 3+ events: HR=2.61 [1.25-5.42]). Results were unchanged after adjustment for social support variables.

In this older male cohort, stressful life events were independently associated with a small risk of subsequent falls and a modest increase in fracture risk. This risk was not moderated by social support. Further studies should examine mechanisms through which stressful events increase risk of these adverse outcomes.

***Disclosures: Howard Fink**, None.*

FR0351

Baseline Serum Interleukin-6 (IL-6), Tumor Necrosis Factor-α (TNF-α) and C-reactive Protein (CRP) Do Not Predict Subsequent Hip Bone Loss in Men or Women: The Framingham Osteoporosis Study. Robert McLean*[1], Xiaochun Zhang[2], James Meigs[3], Joao Fontes[4], L. Adrienne Cupples[5], Douglas Kiel[2], Marian Hannan[6]. [1]Hebrew SeniorLife, Harvard Medical School, USA, [2]Hebrew SeniorLife, USA, [3]Massachusetts General Hospital, USA, [4]Framingham Heart Study & Boston University, USA, [5]Boston University School of Public Health, USA, [6]HSL Institute for Aging Researchand Harvard Medical School, USA

In vitro studies suggest that several pro-inflammatory cytokines increase bone resorption and that their activity is amplified following estrogen withdrawal. Yet there is little epidemiologic evidence that circulating concentrations of inflammatory markers predict bone loss in men and women, or that estrogen status may influence this relation. We therefore examined the associations of serum concentrations of the cytokines IL-6 and TNF-α, and CRP, a marker of systemic inflammation, with bone loss among men and women in the Framingham Offspring Study. We hypothesized that increased baseline concentrations of inflammatory markers would be associated with greater bone loss, and that this association would be strongest among postmenopausal women not using hormone replacement therapy (HRT). Baseline fasting blood samples were obtained (1998-2001) from 501 men, 106 premenopausal women, 206 postmenopausal using HRT at baseline, and 334 postmenopausal not using HRT. Serum IL-6 (pg/mL) and TNF-α (pg/mL) were measured using ELISAs and CRP (mg/L) using a high-sensitivity assay. Total femur bone mineral density (BMD; g/cm^2) was measured at baseline with a Lunar DPX-L (1996-2001) and at follow-up using a Lunar Prodigy (2002-05), accounting for equipment change. Bone loss was calculated as percent BMD change per year. Within each of the 4 groups defined by sex, menopause status and HRT use, participants were categorized into tertiles of inflammatory markers. We used analysis of covariance to compare mean bone loss in each of the upper 2 tertiles to the lowest tertile and test for a linear trend across tertiles, adjusting for baseline age (y), BMI (kg/m^2), height (in), physical activity, and current smoking (y/n). Mean age at baseline was 61 y (range 29-85 y), and mean follow-up time was 4.6 y (range 1.5-7.9 y). There were no statistically significant associations between inflammatory markers and total hip bone loss in any of the sex/menopause/HRT groups (Table). Our findings suggest that circulating biomarkers of inflammation are not associated with hip bone loss in men or groups of women categorized by menopause status and HRT use. Future investigations of inflammation and BMD should address limitations of our study by including longitudinal measures of inflammatory markers, more precise measures of estrogen status (e.g. sex hormones), and larger samples that could detect the small bone loss effects suggested by our results.

Least squares-adjusted mean annual % change (SE) in total femur BMD for tertiles of inflammatory biomarkers in Framingham Offspring men and women.

	T1 (Low)	T2	T3 (High)	P trend
Men				
IL-6	-0.01 (0.08)	0.12 (0.07)	-0.03 (0.08)	0.90
TNF-α	0.08 (0.09)	-0.04 (0.09)	-0.05 (0.09)	0.34
CRP	0.04 (0.08)	-0.03 (0.07)	0.07 (0.08)	0.79
Premenopausal women				
IL-6	-0.46 (0.16)	-0.15 (0.16)	-0.02 (0.18)	0.07
TNF-α	-0.08 (0.18)	-0.29 (0.18)	0.05 (0.18)	0.62
CRP	-0.44 (0.17)	-0.13 (0.16)	-0.07 (0.19)	0.16
Postmenopausal women				
HRT users				
IL-6	0.17 (0.12)	0.22 (0.12)	-0.13 (0.13)	0.12
TNF-α	0.31 (0.13)	-0.05 (0.14)	0.11 (0.14)	0.29
CRP	0.09 (0.13)	-0.02 (0.12)	0.19 (0.13)	0.60
HRT non-users				
IL-6	-0.23 (0.12)	-0.20 (0.11)	-0.29 (0.11)	0.72
TNF-α	-0.19 (0.13)	-0.23 (0.12)	-0.47 (0.12)	0.12
CRP	-0.37 (0.12)	-0.23 (0.11)	-0.13 (0.12)	0.18

Table

***Disclosures: Robert McLean**, None.*

FR0355

Incidence of Subtrochanteric and Diaphyseal Fractures in Older White Women: Data from the Study of Osteoporotic Fractures. Michael Kelly[1], Rosanna Wustrack*[1], Douglas Bauer[1], Lisa Palermo[1], Shane Burch[1], Katherine Wilt[2], Jane Cauley[3], Kristine Ensrud[4], Dennis Black[1]. [1]University of California, San Francisco, USA, [2]California Pacific Medical Center, USA, [3]University of Pittsburgh Graduate School of Public Health, USA, [4]Minneapolis VA Medical Center / University of Minnesota, USA

Purpose: Recent case reports have raised concerns for an increasing incidence of low energy subtrochanteric and diaphyseal femur fractures, which may be associated with long-term bisphosphonate therapy. The incidence of these fractures has not been well defined. The goal was to determine the incidence of low energy, subtrochanteric and diaphyseal femur fractures in the Study of Osteoporotic Fractures (SOF). Methods: 9704 women over age 65 were recruited in 1986 and have been followed for up to 23 years. Radiographic reports for all femur fractures occurring in the intertrochanteric region and below were independently reviewed by two orthopaedic surgeons to determine location of the fracture. These fractures were originally classified as hip (HP) or upper leg. Fractures were reclassified as intertrochanteric (IT), intertrochanteric with subtrochanteric extension (ITST), subtrochanteric or diaphyseal (SH), and distal metaphyseal(DM). Fractures previously classified as femoral neck (FN) were included for analysis without review. Any SH fractures of a high energy mechanism, that were periprosthetic or were pathologic were excluded. The risks per person-year for HP and SH fractures were calculated. Results: 1,396 women with HP fractures were identified in 9704 women. 78 SH fractures were identified in 74 women. After exclusions, there were 48 SH fractures in 45 women. The overall incidence of HP fractures was 103/10,000, and SH fractures was 3/10,000 person-years. The SH fractures represented less than 2% of all hip fractures. For all 3 fractures, incidence increased with age. Conclusions: Subtrochanteric and diaphyseal femur fractures were rare occurrences, far outnumbered by femoral neck and intertrochanteric hip fractures, in this prospective cohort. Those patients greater than 85 years old sustained more fractures of all subtypes.

***Disclosures: Rosanna Wustrack**, None.*

FR0356

Increasing Kyphosis Predicts Worsening Mobility Among Older Community-Dwelling Women: A Prospective Cohort Study. Wendy Katzman, DSc*[1], Eric Vittinghoff[2], Kristine Ensrud[3], Dennis Black[4], Deborah Kado[5]. [1]University of California San Francisco, USA, [2]University of California, USA, [3]Minneapolis VA Medical Center / University of Minnesota, USA, [4]University of California, San Francisco, USA, [5]University of California, Los Angeles, USA

Purpose: Although hyperkyphosis has been associated with impaired mobility in cross-sectional studies, no one has determined whether increasing kyphosis has a detrimental effect on mobility over time. We performed a prospective cohort study to determine whether increasing kyphosis angle is independently associated with worsening mobility, as measured by the Timed Up and Go test. Methods: We used data from 11 clinical centers in the United States including 3,223 women age 55-80 years who were randomized to the placebo arms of the Fracture Intervention Trial, a randomized controlled trial of the effect of alendronate on risk for osteoporotic fractures in osteoporotic and osteopenic women. The primary predictor, change in kyphosis angle, was measured using the Debrunner Kyphometer at baseline and an average of 4.4 years later; the outcome was change in mobility measured as performance time on the Timed Up and Go test that was assessed over the same time interval. Covariates included baseline age, kyphosis angle, body mass index, self-reported health status, grip strength, the number of baseline vertebral fractures, incident vertebral fractures, and change in total hip bone mineral density (BMD). Results: The mean kyphosis angle at baseline was 48.0, SD = 11.9 degrees. Over an average of 4.4 years of follow-up, the kyphosis angle increased a mean of 4.0, SD = 9.4 degrees. Increasing kyphosis angle was associated with increase in mobility performance time $p<0.0005$, independent of other significant predictors of worsening mobility including age, baseline kyphosis, health status, grip strength, body mass index, change in hip BMD, and new vertebral fractures. For every standard deviation increase in kyphosis angle, Timed Up and Go performance times increased by 0.16 seconds (95% C.I.:0.08,0.25), that is more than the expected increase in mobility time over one year. Conclusion: In older women, increasing kyphosis angle was independently associated with worsening mobility over time. If this association is confirmed in other cohorts, randomized controlled trials should be conducted to determine whether reducing hyperkyphosis preserves mobility in older community-dwelling women.

***Disclosures: Wendy Katzman, DSc**, Merck, Roche, Novartis, 2; Medtronic, Kyphon, 5*

FR0360

Previous Fractures Increase Risk for Subsequent Fractures at Multiple Sites: Global Longitudinal Study of Osteoporosis in Women. Stephen Gehlbach*[1], Kenneth Saag[2], Jonathan Adachi[3], Silvano Adami[4], Steven Boonen[5], Susan Greenspan[6], Coen Netelenbos[7], Philip Sambrook[8], Stuart Silverman[9], Julie Flahive[10], Ethel Siris[11]. [1]University of Massachusetts, USA, [2]University of Alabama at Birmingham, USA, [3]St. Joseph's Hospital, Canada, [4]University of Verona, Italy, [5]Center for Metabolic Bone Disease, Belgium, [6]University of Pittsburgh, USA, [7]VU Medical Center, The netherlands, [8]Royal North Shore Hospital, Australia, [9]Cedars-Sinai/ UCLA, USA, [10]COR, UMass Medical School, USA, [11]Columbia University College of Physicians & Surgeons, USA

Background: History of fracture is a potent predictor of future fracture in postmenopausal women. We assessed the relationship between 10 prior fracture locations and incident fractures. Methods: The Global Longitudinal study of Osteoporosis in Women (GLOW) is an observational cohort study of women ⩾55 years recruited by 723 primary physician practices (17 sites, 10 countries). All non-institutionalized patients visiting the practices within the previous 2 years were eligible. Self-administered questionnaires were mailed (2:1 over-sampling of women ⩾65). At baseline, patients reported any prior fractures since age 45 at 10 specified locations (clavicle, upper arm, wrist, spine, rib, hip, pelvis, upper leg, lower leg, ankle). At 1-year follow-up, patients reported the frequency and location of incident fractures sustained in the past year. Results: Complete baseline and 1-year fracture data were available for 50,332/60,393 women (83%); 23% reported a prior fracture since age 45 (1 bone, n=8883, 17.6%; 2 bones, n=2065, 4.1%; ⩾3 bones, n=808, 1.6%). Overall, 1958 patients reported incident fractures at 1-year follow-up; rates of incident fractures are shown in the Table, by location of prior fracture. In logistic regression analyses, adjusting for age and multiple prior fractures, 7/10 prior fracture locations were associated with any incident fracture; the greatest odds ratios (ORs) were for rib (2.3), spine (2.0) and wrist (1.7). Prior fracture locations varied in their predictive implications for incident fracture. The strongest predictors of hip and spine incident fracture were prior fracture of spine (OR 4.17), hip (OR 2.96) or rib (OR 2.06). Major incident fracture was significantly associated with prior fracture of the upper leg (OR 3.45) and upper arm (OR 3.04). Minor incident fracture was significantly associated with prior fracture of the rib (OR 2.42), wrist (OR 1.72) and ankle (OR 1.42). Having ⩾1 prior fracture added substantially to the likelihood of incident fracture: the OR for incident fracture increased from 2.0 for 1 prior fracture to 3.6 for 2 prior fractures and 5.5 for ⩾3 prior fractures. Conclusion: A broader range of prior fracture sites should be considered in both clinical assessments and risk model development.

Prior fracture location	Incident fracture rate (%)				
	Any bone* (n=1958)	Previous bone (refracture) (n=241)	Hip, spine (n=227)	Major bone† (n=333)	Minor bone‡ (n=1170)
No previous fracture	2.9		0.3	0.5	2.0
Prior fracture location					
Rib	10.9	2.4	1.4	1.3	5.8
Hip	10.0	2.1	2.7	1.8	3.3
Wrist	8.0	1.8	1.0	1.3	4.2
Spine	11.3	2.5	2.9	1.8	3.8
Upper arm	9.3	1.6	1.1	2.7	3.2
Ankle	6.8	1.3	0.8	1.0	3.8
Lower leg	7.8	0.7	0.7	1.4	4.0
Upper leg	11.2	1.4	1.4	3.6	3.2
Clavicle	7.4	0.5	1.2	1.9	3.0
Pelvis	11.0	1.2	1.0	2.6	4.5

Includes: *10 fracture types listed at baseline+foot, hand, shoulder, knee, elbow, sternum, finger, toe+multiple fractures with unspecified bone type; †pelvis, upper leg, lower leg, upper arm, shoulder; ‡clavicle, wrist, rib, ankle, hand, foot, sternum, elbow, knee, finger, toe.

Rates of incident fracture

***Disclosures: Stephen Gehlbach**, The Alliance for Better Bone Health (sanofi-aventis and Warner Chilcott), 2*
This study received funding from: The Alliance for Better Bone Health (sanofi-aventis and Warner Chilcott)

FR0363

Abnormal Microarchitecture and Decreased Stiffness Suggest That Postmenopausal Ankle Fractures Reflect Bone Fragility. Emily Stein*[1], Xiaowei Liu[2], Thomas Nickolas[3], Adi Cohen[3], Dionisio Ortiz[4], Valerie Thomas[3], Perry Yin[2], Felicia Cosman[5], Jeri Nieves[5], Donald McMahon[1], X Guo[2], Elizabeth Shane[1]. [1]Columbia University College of Physicians & Surgeons, USA, [2]Columbia University, USA, [3]Columbia University Medical Center, USA, [4]SUNY Downstate College of Medicine, USA, [5]Helen Hayes Hospital, USA

Ankle fractures are not typically considered osteoporotic fractures. However, bone quality in patients with low trauma ankle fractures has not been explored.

Women with a history of low trauma ankle fracture after menopause (FX; n=19) and women with no history of fragility fracture (C; n=110) had aBMD of lumbar spine (LS), total hip (TH), femoral neck (FN) and 1/3 radius (1/3R) measured by DXA. Trabecular (Tb) and cortical (Ct) volumetric BMD (vBMD) and Tb microarchitecture were measured by HRpQCT (Xtreme CT, voxel size ~82 μm) of the radius (DR) and tibia (DT). Finite element analysis (FEA) of HRpQCT scans was performed to estimate bone mechanical properties. Individual trabeculae segmentation (ITS) based morphological analysis was performed to assess plate (P) and rod (R) structure of the bone.

Women with fractures tended to be older (71±2 vs 68±1 years; $p<0.07$) but were similar with respect to time since menopause, race, and BMI. Mean T-scores of FX were above the osteoporotic range (LS:-1.4±0.2; TH:-1.2±0.2; FN:-1.8±0.2; 1/3R:-1.4±0.3) and did not differ from C; only 26% of FX had osteoporosis at any site. In contrast, HRpQCT, FEA, and ITS measurements at both DR and DT differed between FX and C (Table). At DR, FX had lower Tb number, increased Tb separation and network heterogeneity, and a striking loss of central (inner) trabeculae relative to outer subcortical trabeculae compared to C. At DT, FX had lower total and Tb density and tended to have lower Ct density; FX had lower Tb number, increased Tb separation and network heterogeneity and tended to have lower Ct thickness. Tb dropout was more uniformly distributed across the Tb compartment than at the radius. Whole bone stiffness was ~15% lower at DR and DT in FX ($p<0.05$). ITS revealed that FX had lower R bone volume fraction(rBV/TV:-10%,$p<0.05$) R number(-4%,$p<0.05$), and R-R junction density(-13%,$p<0.05$) at DR and tended to have lower rBV/TV(-9%,$p<0.09$), P number(-4%,$p<0.08$), R number(-4%,$p<0.08$), R-P junction density(-11%,$p<0.06$) and P-P junction density(-11%,$p<0.07$) at DT.

Postmenopausal women with ankle fractures have microarchitectural deterioration and decreased stiffness compared to women with no fracture history. The occurrence of these changes at both the radius and tibia provides evidence for a generalized decrease in bone quality. These findings suggest that low trauma ankle fractures should be considered similarly to other more classical osteoporotic fractures.

HRpQCT at the radius (DR) and tibia (DT) in postmenopausal women by fracture history (mean±SE)

	DR Fracture	DR Non-fracture	DT Fracture	DT Non-fracture
Total density (mgHA/ cm³)	278 ± 19	299 ± 7	218 ± 11	244 ± 5*
Ct. density (mgHA/ cm³)	836 ± 17	852 ± 7	762 ± 21	784 ± 6#
Tb. density (mgHA/cm³)	117 ± 10	130 ± 4	129 ± 9	146 ± 3*
Outer/Inner trabecular density	16.7±9.9	2.6±0.1**	3.4±0.7	2.5±0.2
Ct. thickness (mm)	0.65 ±0.03	0.72 ± 0.02	0.73 ±0.06	0.86 ± 0.03#
Tb. Number (1/mm)	1.57 ± 0.10	1.77 ± 0.03*	1.55 ± 0.07	1.74 ± 0.03*
Tb. Separation (mm)	0.58 ± 0.07	0.54 ± 0.02*	0.60 ± 0.03	0.53 ± 0.01*
Network Heterogeneity	0.41 ± 0.09	0.27 ± 0.02*	0.32 ± 0.04	0.25 ± 0.01*

**p<0.001; *p<0.05; #p<0.08 vs fracture subjects

Stein_table_leg fractures

***Disclosures: Emily Stein**, None.*

FR0365

Bone Microstructure During and After Lactation. Åshild Bjørnerem*[1], Ali Ghasem-Zadeh[2], Thuy Vu[3], Ego Seeman[2]. [1]Department of Community Medicine, University of Tromsø, Norway, [2]Austin Health, University of Melbourne, Australia, [3]Endocrine Centre, Austin Health, University of Melbourne, Australia

Estrogen deficiency increases bone turnover and bone loss. Lactation is an estrogen deficient state believed to be associated with reversible bone loss. As bone loss assessed using DXA may partly be the result of changes in marrow composition, we assessed the effects of lactation on volumetric bone mineral density (vBMD) and microarchitecture from baseline 14.6 days (2-25) after delivery, with follow-up during 5.2 months (2-7) of breastfeeding, and with the third measurement more than 6 months after weaning in 82 women aged 20-42 years. Total, cortical and trabecular vBMD, cortical and trabecular cross-sectional area (CSA), cortical and trabecular thickness, and trabecular number were measured at the distal tibia and radius using high-resolution 3-D peripheral quantitative computed tomography (HR-3D-pQCT XtremeCT; Scanco Medical, Switzerland).

During lactation, tibia total and cortical vBMD diminished by 0.6 and 0.3% at distal tibia ($p<0.05$), whereas tibia trabecular vBMD was unchanged. Cortical CSA was reduced by 1.8 and 1.4%, cortical thickness was reduced by 1.8 and 1.3%, while trabecular CSA increased by 0.2 and 0.3%, trabecular thickness increased by 5.9 and 4.5% and trabecular number diminished by 4.4 and 2.1% at tibia and radius, respectively (all $p<0.05$). After weaning, cortical vBMD was 0.7 and 0.8% lower than baseline at tibia and radius, whereas trabecular vBMD was 3.1 and 4.0% higher than at baseline at tibia and radius.

We infer that intracortical and endocortical bone loss occurred during lactation as reflected in lower cortical vBMD and thinner cortices perhaps due to trabecularization of cortex. The lack of decline in trabecular vBMD during lactation may be an underestimation of trabecular bone loss because of cortical trabecularization erroneously inflating trabecular vBMD. Lactation may cause a deleterious effect on cortical structure as cortical bone loss was not completely restored after weaning in humans.

***Disclosures: Åshild Bjørnerem**, None.*

FR0368

Estradiol Replacement Therapy Lowers Serum Sclerostin Levels in Postmenopausal Women. Faryal Mirza*[1], Pamela Taxel[1], Yun Ey Chung[2], Sandra Jastrzebski[3], Lawrence Raisz[1], Joseph Lorenzo[1]. [1]University of Connecticut Health Center, USA, [2]Univ. of Connecticut Health Center, USA, [3]Univ of Connecticut Health Center, USA

Purpose: Sclerostin is a negative regulator of Wnt signaling and bone formation. We previously reported that serum estrogen levels inversely correlate with serum sclerostin levels in postmenopausal women. In this study, we examined the effect of short-term estradiol replacement therapy on serum sclerostin levels in postmenopausal women.

Methods: We evaluated 18 postmenopausal women at baseline, ten of whom received 1 mg of micronized 17-β estradiol (E2) daily and were re-evaluated at 3 weeks. Serum sclerostin levels were measured along with levels of E2, estrone (E1), sex hormone binding globulin (SHBG) and serum and urine bone formation and resorption markers. Free estrogen index was calculated as (E2+E1 (pmol/l)/SHBG, FEI) The Wilcoxon Ranks test was used to compare differences with treatment. Spearman product moment correlations were used to evaluate the relationships between changes in sclerostin, sex hormones and bone markers.

Results: Mean age of the subjects was 56 ± 3 years. E2 treatment significantly changed the serum levels of the following: E2 (10 ± 1 to 89 ± 19 pg/ml, $p<0.005$), E1 (26 ± 2 to 344 ± 54 pg/ml, $p= 0.005$), SHBG (62 ± 8 to 106 ± 14 nmol/l, $p <0.005$) and FEI (3 ± 1 to 16 ± 2 pmol/nmol, $p <0.005$). Serum sclerostin level decreased significantly with E2 treatment (24 ± 3 to 19 ± 2 ng/ml, $p = 0.005$). When the ratio of bone specific alkaline phosphatase (BSAP) to urine deoxypyridinoline (DPD) and BSAP to urine N-telopeptide (NTX) were used as measures of relative bone formation to resorption at baseline, we found significant inverse correlations with serum sclerostin ($r = -0.854$, $p = 0.007$and $r = -0.737$, $p = 0.015$, respectively), consistent with an association between decreasing serum sclerostin and an increasing bone formation to resorption ratio. In addition, with E2 treatment, the decline in sclerostin correlated positively with increases in the BSAP to NTX ratio ($r = 0.812$, $p = 0.01$), further supporting this relationship.

Conclusions: E2 replacement in postmenopausal women significantly lowered serum sclerostin levels. Moreover, baseline serum sclerostin levels show a strong inverse correlation with the ratio of basal bone formation to resorption. The change in serum sclerostin levels with E2 treatment is also inversely associated with changes in the ratio of bone formation to resorption. We conclude that estrogen decreases serum sclerostin levels by mechanisms that are linked to the ratio between bone formation and resorption.

***Disclosures: Faryal Mirza**, None.*

FR0369

Oxytocin Mediates the Anabolic Action of Estrogen on the Skeleton. Graziana Colaianni[1], Adriana DiBenedetto[2], Roberto Tamma[2], Giovanni Greco[2], Stefania Dell'Endice[2], Concetta Cuscito[2], Lucia Mancini[2], Ling-Ling Zhu[3], Xuan Liu[3], Yuanzheng Peng[3], Jianhua Li[3], Jammel Iqbal[3], Li Sun[4], Alberta Zallone[1], Mone Zaidi*[5]. [1]University of Bari Medical School, Italy, [2]Department of Human Anatomy & Histology, University of Bari, Italy, [3]The Mount Sinai Bone Program, Mount Sinai School of Medicine, USA, [4]Mount Sinai School of Medicine, USA, [5]Mount Sinai Medical Center, USA

We have shown that the posterior pituitary hormone oxytocin directly regulates bone mass by acting on its receptor, Oxtr, on osteoblasts and osteoclasts (Tamma et al., PNAS, 2009). Here we demonstrate that oxytocin is produced peripherally by osteoblasts, and is required for the anabolic action of estrogen on the skeleton. Thus, mice lacking the Oxtr failed to respond to 17ß-estradiol (50 µg/mice/day, s.c.) in terms of the increases in bone mineral density (Piximus) and mineral apposition rate (histomorphometry) noted in wild type littermates. Impressively, the decline in bone mineral density at the spine post-ovariectomy was not reversed by 17ß-estradiol, whereas a robust reversal of this drop was noted in wild type, sham-operated littermates. This in vivo insensitivity to estrogen was accompanied ex vivo by an attenuated ability of Oxtr-/- bone marrow stromal cells to form mineralizing CFU-ob colonies in response to 17ß-estradiol (10-8 M). To study this lack of responsiveness further, we knocked down the Oxtr using siRNA, which resulted in a marked reduction in Oxtr expression on Western immunoblotting. In Oxtr-sufficient cells, 17ß-estradiol (10-8 M) stimulated the expression of osteoblast genes, namely osteocalcin, Runx2, osterix, BMP-2, bone sialoprotein, and schnurri2; these responses were either strongly attenuated or abrogated in Oxtr siRNA-treated osteoblasts. We next explored the peripheral source of oxytocin. Quantitative PCR and Western immunoblotting showed that both Oxtr and oxytocin were expressed in osteoblasts, and that 17ß-estradiol (10-8 M) stimulated the expression of both molecules in a time-dependent manner. This is consistent with an autocrine function of locally produced oxytocin in mediating the osteoblastic action of estrogen. Interestingly, however, the effect of estrogen on oxytocin synthesis was exerted via a non-genomic route. We found that, for estrogen-induced oxytocin synthesis, estrogen must act extracellularly at a membrane site to activate the MAP kinase Erk. Thus, cell impermeant BSA-conjugated 17ß-estradiol produced as robust an increase in oxytocin and oxtr mRNA as did free 17ß-estradiol. However, the estrogen-mediated increase in oxytocin mRNA, but not Oxtr mRNA was sensitive to PD98059, an inhibitor of Erk phosphorylation. Overall, the study not only expands our premise for a novel pituitary bone axis, but also, in revealing a new bone marrow location for oxytocin production, strengthens the notion of the skeleton serving as a hormone-producing endocrine organ.

***Disclosures: Mone Zaidi**, None.*

FR0370

High Seretonin Levels and High Platelet Count are Associated with Low Bone Mineral Density in Elderly Men, MrOs Sweden. Dan Mellstrom*[1], Malin Aronsson[2], Mattias Lorentzon[3], Osten Ljunggren[4], Magnus Karlsson[5], Ulf Lerner[6], Claes Ohlsson[7]. [1]Sahlgrenska University Hospital, Sweden, [2]Center for Bone & Arthritis Research at the Sahlgrenska Academy, Institute of Medicine & Geriatrics, University of Gothenburg, Sweden, Sweden, [3]Center for Bone Research at the Sahlgrenska Academy, Sweden, [4]Uppsala University Hospital, Sweden, [5]Skåne University Hospital Malmö, Lund University, Sweden, [6]Center for Bone Research at the Sahlgrenska Academy, Dept. of Internal Medicine, University of Gothenburg, Sweden, Sweden, [7]Centre for Bone & Arthritis Research, Sweden

Recent experimental studies demonstrate a role of circulating serotonin in the regulation of bone mass (Yada et al. Cell 2008). One previous cross-sectional study evaluating 275 women showed an indirect association between serum serotonin and BMD in total body and spine (Mödder et al JBMR 2009). Circulating serotonin is to a large extent bound to platelets. The relative role of platelet count and serum serotonin for BMD is unknown. We measured serum serotonin (155±77 ng/ml) in 1010 elderly men (70-80 year) in the Gothenburg part of MrOS Sweden, using a competitive enzyme-linked immunosorbent assay (ELISA) (Immuno-Biological lab, Inc, Minneapolis, MN). BMD was measured with a Hologic 4500.

Serum serotonin associated inversely with BMD in the hip (total hip $r = -0.08$, $p<0.01$; neck -0.08, $p<0.02$; trochanter $r = -0.08$, $p<0.02$). However, serum serotonin also associated with body weight $r = -0.09$ ($p<0.01$) and body fat mass $r = -0.13$ ($p<0.01$) and after adjustment for BMI and age, no significant association between serotonin and BMD was found. Serum serotonin associated strongly directly with platelet count $r = 0.28$ ($p<0.001$). Interestingly, platelet count was independently (adjusting for serum serotonin, BMI and age) associated with BMD at all investigated bone sites (Standardized β = -0.08 for total BMD, -0.14 for spine BMD, -0.16 for total hip total, -0.14 for femoral neck and -0.14 for trochanter BMD; $p< 0.01$).

In conclusion, although serum serotonin in univariate analyses associated with BMD at hip bone sites, no significant association was seen after adjustment for BMI. Serum serotonin associated strongly with platelet count and we made the novel observation that platelet count was an independent predictor of BMD at all investigated bone sites.

***Disclosures: Dan Mellstrom**, None.*

FR0371

Neural and Endocrine Signalling Interact to Control Bone and Adipose Homeostasis. Ayse Zengin*, Ronaldo F Enriquez, Amy D Nguyen, Amanda Sainsbury, Herbert Herzog, John Eisman, Paul Baldock. Garvan Institute of Medical Research, Australia

The coordinated control of bone and fat mass is now well appreciated. Endocrine and neural pathways that regulate bone and fat mass have a similar origin within the hypothalamus, suggesting the potential for interaction between them. Here we show interaction between androgens and neuropeptide Y (NPY) in control of osteoblast and adipocyte activity. NPY, a critical component of efferent neural signalling, acts through central Y2 and peripheral Y1 receptors to regulate bone and fat mass. In bone, the anabolic phenotype of NPY Y1 receptor deficient mice ($Y1^{-/-}$) was completely attenuated by orchidectomy (ORX), however, this attenuation was not evident following ORX in wild type or $Y2^{-/-}$ mice. In adipose tissue, ORX increased white adipose tissue mass of $Y1^{-/-}$, but not in wild type or $Y2^{-/-}$ mice. These differential responses between $Y1^{-/-}$ and $Y2^{-/-}$ mice suggest a receptor-specific interaction between androgens and NPY.

In order to further investigate this interaction, the skeletal response to ORX was examined in NPY deficient mice ($NPY^{-/-}$) in comparison with $Y1^{-/-}$ and $Y2^{-/-}$ mice. Mice underwent ORX or sham-operation at 8 weeks of age; skeletal and adipose responses were examined at 16 weeks of age.

White adipose tissue (WAT, g) was decreased post-ORX in wild type (0.98 ±0.08 vs 0.47 ±0.05, $p<0.0001$). This loss was absent in $NPY^{-/-}$ (0.73 ±0.06 vs 0.72 ±0.09), this is in contrast to $Y1^{-/-}$ which gained WAT post ORX (0.81 ±0.02 vs 1.28 ±0.14, $p<0.01$). Cancellous bone volume (BV/TV) was reduced by ORX in wild type (7.7 ±0.9 vs 3.5 ±0.2, $p<0.0001$) and $NPY^{-/-}$ (11.6 ±1.6 vs 6.7 ±0.4, $p=0.003$) however, BV/TV in ORX-$NPY^{-/-}$ mice remained greater than ORX-wt ($p<0.0001$), in contrast to *ORX-*$Y1^{-/-}$. The NPY-mediated anabolic phenotype involves greater mineral apposition rate (MAR µm/d). MAR in wild type mice was not affected by ORX (1.1±0.05 vs. 1.2±0.07, $p=0.28$) but was increased in $NPY^{-/-}$ (1.8 ±0.1 vs 2.2 ±0.1, $p=0.006$). This is in contrast to the loss of MAR post-ORX in $Y1^{-/-}$ compared to ORX-wild type mice.

Bone and fat mass are regulated by interactions between NPY and androgens. The similarity between $NPY^{-/-}$ and $Y2^{-/-}$ responses, indicates that Y2 signalling regulates the loss of bone and fat post-ORX. However, the unique post-ORX responses involving Y1 receptors indicate a complex relationship between central and peripheral signalling between androgens and the NPY system.

***Disclosures: Ayse Zengin**, None.*

FR0376

Comparison of Transdermal and Subcutaneous Teriparatide Pharmacokinetics and Pharmacodynamics of Bone Markers in Postmenopausal Women.

Yael Kenan[1], Efrat Kochba[1], Michal Shahar[1], Hana Gadasi[1], Galit Levin[1], Ajit Suri[2], Kyoungah See[2], A. Joseph Foldes[3], Sophia Ish-Shalom*[4], Toshio Matsumoto[5], Robert Lindsay[6], Claus Christiansen[7], Robert Neer[8]. [1]TransPharma-Medical, Israel, [2]Eli Lilly & Company, USA, [3]Hadassah-Hebrew University Medical Center, Israel, [4]Rambam Health Care Campus, Technion Faculty of Medicine, Israel, [5]University of Tokushima Graduate School of Medical Sciences, Japan, [6]Helen Hayes Hospital, USA, [7]Nordic Bioscience, Denmark, [8]Massachusetts General Hospital, USA

TransPharma-Medical has developed a system for transdermal (TD) delivery of teriparatide to alleviate the discomfort of subcutaneous (SC) injections and to improve acceptance and compliance. The TD delivery of teriparatide utilized radiofrequency ablation to create microchannels in the skin, allowing rapid diffusion into systemic circulation from a subsequently applied drug patch. In a phase 1 study, TD 50, 70, and 90 µg teriparatide demonstrated significant increases in bone turnover, similar to SC 20 µg teriparatide[1]. The aim of this phase 2 study was to compare efficacy (bone turnover markers), safety, and teriparatide pharmacokinetics (PK) in a 3-month, randomized, multicenter study in postmenopausal women with osteoporosis (mean ± SD, age 65.1 ± 6.8 yr). Patients were randomly assigned to either open-label SC 20 (n=36) or double-blind TD 50 (n=34) or 80 µg (n=34) once-daily teriparatide. Blood samples for PK analysis were taken at 0 (pre-dose), 0.25, 0.5, 1, 1.5, 2, 2.5, 3, 4, 6, and 8 hours post-dose. PK parameters ($AUC_{0\text{-}t}$, Cmax, Tmax, and T1/2) were evaluated at days 1 and 96. PINP and CTX increased from baseline to day 96 with TD 50, 80, and SC 20 µg teriparatide ($p<0.05$); TD increases were dose-dependent (PINP, p=0.02; CTX, p=0.007)[2]. There was a dose-proportional increase in Cmax and AUC for TD 50 and 80 µg (Table). Cmax and AUC values at days 1 and 96 were similar for TD, indicating no accumulation of drug or temporal change in PK (Table). The Tmax for PK profile following TD treatment, similar to that reported in phase 1[1], was shifted to the right ($p<0.0001$) for TD 50 and 80, compared with the SC injection group, indicating a delayed time to peak concentration and a slower absorption of TD than SC teriparatide. Compared with SC 20 µg on day 1, the TD 50 and 80 µg geometric mean (95% CI) AUC-ratios were 1.65 (1.03-2.64, p=0.037) and 2.48 (1.51-4.08, p=0.0005, respectively. The Cmax-ratios were 0.64 (0.47-0.88, p=0.0068) and 0.98 (0.65-1.47, p=0.92) for TD 50 and 80 µg, respectively. No clinically significant differences across study groups or time were observed for hypercalcemic, dermatologic, or other adverse events. In conclusion, the TD system of microchannels and subsequently applied drug patch to facilitate diffusion of teriparatide into systemic circulation, may be an effective alternative to SC injection delivery of teriparatide.

[1]Ish Shalom et al. J Bone Miner Res. 2008;23(abstracts):S207
[2]Kenan et al. IOF WCO-ECCEO 2010, P440

	AUC 0-t (h*pg/mL)[a]	Cmax (pg/mL)[a]	Tmax (h)[b]	T 1/2 (h)[b]
TD 50 µg				
Day 1	200 [159,252] (n=34)	55.3 [47.2,65.0] (n=34)	3.0 [2.5,4.0] (n=34)	2.2 [1.7,2.6] (n=14)
Day 96	192 [158,232] (n=31)	57.9 [49.2,38.0] (n=32)	2.8 [2.5,3.0] (n=32)	1.8 [1.5,2.4] (n=15)
TD 80 µg				
Day 1	300 [226,399] (n=34)	84.2 [62.0,114.5] (n=34)	3.0 [2.5,3.0] (n=34)	2.2 [1.9,2.8] (n=22)
Day 96	292 [201,425] (n=28)	84.2 [58.8,120.5] (n=30)	2.8 [2.0,3.0] (n=30)	1.7 [1.5,2.3] (n=18)
SC 20 µg				
Day 1	121 [79,185] (n=33)	85.9 [65.1,113.3] (n=34)	0.4 [0.3,0.5] (n=34)	1.1 [0.8,1.8] (n=31)
Day 96	222 [185,265] (n=33)	134.7 [114.7,158.1] (n=34)	0.3 [0.3,0.5] (n=34)	1.1 [0.9,1.7] (n=34)

[a]Geometric mean (95% confidence intervals); [b]Median [25th, 75th percentile]

Table. Teriparatide PK for Days 1 and 96 by treatment group

***Disclosures: Sophia Ish-Shalom**, TransPharma-Medical, 1; TransPharma-Medical, 3*
This study received funding from: Eli Lilly and Company

FR0377

Does Anabolic Therapy Correct the Homogeneity In Bone Composition Associated With Osteoporosis?

Adele Boskey*[1], Lyudmila Spevak[1], David Dempster[2], Anthony Hodsman[3]. [1]Hospital for Special Surgery, USA, [2]Columbia University, USA, [3]St. Joseph's Health Care, Canada

Treatment with intermittent PTH(1-34) (Teriparatide) is reported to stimulate new bone formation in osteopenic/osteoporotic patients and animal models of osteoporosis. Previously we reported that Fourier Transform Infrared Imaging (FTIRI) of iliac crest biopsies at 6.25 um spatial resolution (54 untreated patients with and without fractures) revealed significant differences in material properties (mineral crystal size and composition and collagen maturity) in both cortical and cancellous regions that, based on multiple logistic regressions were predictive of fracture risk. We also have limited data (17 patients) that the pixel distribution of values (heterogeneity) of these parameters was significantly reduced in fracture cases. The present pilot study compared FTIRI compositional analyses of iliac crest biopsies obtained after treatment from 10 PTH treated osteoporotic women who had fractures at base-line (and were treated for 1 month with 50 ug daily subcutaneousl compared to age, and sex-matched non-treated fracture controls. Results showed that in two age groups (53-70 and 71-80) the mean mineral:matrix, collagen maturity, crystallinity, and carbonate content did not differ among treated and non-treated controls in cortical or cancellous bone, although the cancellous bone parameters were always less than the age-matched parameters for the same age group. Global averages over all age ranges for cancellous bone (figure 1) showed slight but significant decreases in mineral/matrix (Min/Mat) ratio and increases in collagen maturity (XLR) with no change in crystallinity (Cryst) or carbonate/phosphate (CO3/PO4) content with PTH(1-34) treatment. Additionally, the pixel heterogeneity based on the line-width at half maximum for each of these parameters in each bone area was significantly greater for the PTH(1-34)-treated subjects than for controls, although the mean BMDs for each age group were not different. Since increased tissue heterogeneity has recently been correlated with reduced micro-crack propagation in Finite Element Models, these data suggest that an anabolic therapy can correct the loss of heterogeneity in bone composition that is associated with osteoporosis, thereby improving the structural integrity of the bone.

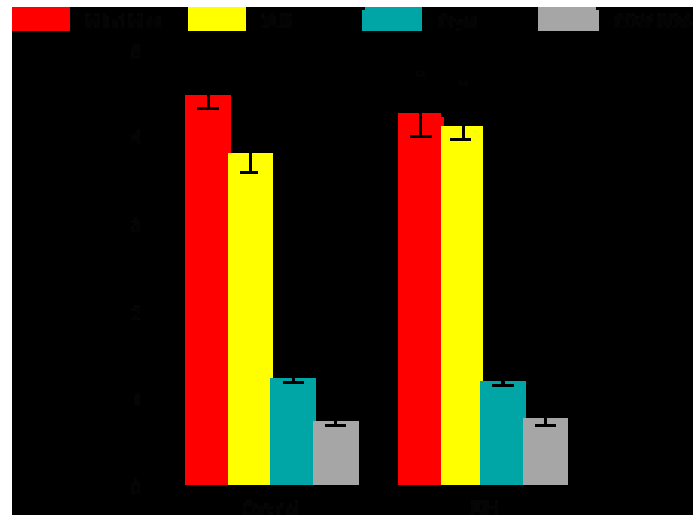

Figure 1

***Disclosures: Adele Boskey**, None.*

FR0378

Effects of Teriparatide and Strontium Ranelate on Periosteal Bone Formation in the Ilium of Postmenopausal Women with Osteoporosis.

Robert Recker*[1], Fernando Marin[2], Jan Stepan[3], Qing Q. Zeng[2], Xiahoai Wan[2], Sophia Ish-Shalom[4], Federico G. Hawkins[5], Georgios Kapetanos[6], M Pilar de la Peña[7], Jordi Farrerons[8], Yanfei Ma[9]. [1]Creighton University Osteoporosis Research Center, USA, [2]Lilly Research Labs, USA, [3]Charles Univ., Czech republic, [4]Bone Metabolism Unit, Technion Univ., Israel, [5]Endocrinology, Hospital 12 de Octubre, Spain, [6]Orthopedic Surgery, Aristotelion Univ., Greece, [7]Clínica Médica Monraz, Mexico, [8]Internal Medicine, Hospital Sant Pau, Spain, [9]Eli Lilly & Company, USA

The periosteum contains osteogenic cells that regulate bone size, the outer shape of the bone and its cortical thickness. Periosteal expansion serves to improve the biomechanical properties of bone. Our purpose is to describe the bone envelope-specific effects of daily subcutaneous injection of teriparatide (TPTD, 20 µg/d) or oral strontium ranelate (SrR, 2 g/d) in postmenopausal women with osteoporosis using biopsy specimens from a completed study[1]. Transiliac crest biopsies were obtained

after tetracycline double labeling from 49 subjects (TPTD: 27; SrR: 22) at the end of 6 months of treatment. The specimens were examined for single and double-labeled surfaces, mineralized surfaces as a percent of bone surfaces (MS/BS %), bone formation rate per bone surface (BFR/BS), and mineral apposition rate (MAR). Histomorphometric results were analyzed using an exact permutation test as a safeguard against potential non-normality of the data (Table).

The percent of specimens that exhibited double labels was higher in the TPTD (70%) than the SrR group (27%) ($p<0.005$, Fisher's exact test). Specimens that showed single label were also more frequent in the TPTD (93%) than in the SrR (64%) group ($p<0.05$). The endocortical results were similar to those for the periosteal envelope (data not shown).

Conclusion: Bone formation and mineralization variables, including MS/BS% and MAR, were statistically significantly higher for TPTD than SrR treated women at periosteal and endosteal combined cortices after 6 months of treatment. These findings provide new insights into the structural basis by which TPTD improves cortical bone geometry in patients with osteoporosis.

[1]Recker RR et al. J Bone Miner Res (2009); 24:1358.

Dynamic histomorphometric variables, both periosteal surfaces combined [mean (SE)]

	Teriparatide	SrR	p-value
MS/BS %	8.08 (1.22)	3.22 (1.05)	0.003
BFR/BS ($mm^3/mm^2/yr$)	0.01 (0.00)	0.00 (0.00)	0.057
Single-labeled perimeter (%)	12.17 (2.08)	4.97 (1.66)	0.009
Double-labeled perimeter (%)	1.99 (0.51)	0.73 (0.49)	0.086
MAR (µm/d)	0.35 (0.06)	0.14 (0.06)	0.012

Table

***Disclosures: Robert Recker**, Lilly, 8*
This study received funding from: Lilly Research Center, Europe

FR0387

Bisphosphonates and Glucocorticoid Osteoporosis in Men: Results of a Randomized Controlled Trial Comparing Zoledronic Acid With Risedronate. Philip Sambrook*[1], Christian Roux[2], Jean-Pierre Devogelaer[3], Kenneth Saag[4], C Lau[5], Jean-Yves Reginster[6], C Bucci-Rechtweg[7], G Su[7], David Reid[8]. [1]Royal North Shore Hospital, Australia, [2]Hospital Cochin, France, [3]St. Luc University Hospital, Belgium, [4]University of Alabama at Birmingham, USA, [5]University of Hong Kong, Hong kong, [6]CHU Centre Ville, Belgium, [7]Novartis Pharmaceuticals Corporation, USA, [8]University of Aberdeen, United Kingdom

Purpose: There are limited data available on the effect of bisphosphonates in men receiving glucocorticoid therapy. We studied 265 men, mean age 56.4 yrs (range 18 – 83), among the patients enrolled in two arms of a double-blind, double dummy, 1-year study comparing the effects of Zoledronic acid (ZOL) *vs.* Risedronate (RIS) in patients either commencing glucocorticoid treatment at a dose of at least 7.5 mg per day of prednisone or equivalent (prevention arm, n=88) or continuing long-term treatment of glucocorticoid at that dose (treatment arm, n=177).

Methods: Patients received either ZOL 5 mg infusion at study entry or RIS 5 mg daily, along with calcium (1000 mg) and vitamin D (400-1200 IU) supplementation daily. The primary endpoint was difference in bone mineral density (BMD) at the lumbar spine (LS) at 12 months. Secondary endpoints were changes in BMD at other sites such as total hip (TH) and femoral neck (FN), changes in biochemical markers of bone turnover (β-C-terminal telopeptides of type 1 collagen [β-CTx] and procollagen type 1 aminoterminal propeptide [PINP]), and overall safety.

Results: In the treatment arm, ZOL increased LS BMD by 4.7% compared with 3.3% for RIS and at TH the changes were 1.8% *vs.* 0.2%, respectively. In the prevention arm, bone loss was prevented by both treatments. At the LS the changes were 2.5% *vs.* -0.2% for ZOL *vs.* RIS and at TH the changes were 1.1% *vs.* -0.4%, respectively. The differences between ZOL and RIS were significant at the LS in the treatment ($p<0.025$) and prevention ($p<0.0025$) arms as well as at TH (p=0.0004 and $p<0.025$ for treatment and prevention, respectively). In the treatment sub-group, ZOL demonstrated a significantly greater reduction in serum β-CTx and PINP relative to RIS at all time-points. In the prevention sub-group, ZOL demonstrated a significantly greater reduction in β-CTx at all time-points, and in PINP at Month 3 (p=0.0297) only. Both treatments were well tolerated in men, albeit with a higher incidence of influenza-like illness and pyrexia events post-infusion with ZOL.

Conclusion: Once yearly IV infusion of ZOL preserves or increases bone density within 1 year to a greater extent than daily oral RIS in men receiving glucocorticoid therapy.

***Disclosures: Philip Sambrook**, Roche, Merck, Sanofi - Aventis, Servier, and Novartis, 8; Australian National Health and Medical Research Council, 2; Roche, Merck, Sanofi - Aventis, Servier, and Novartis, 5*
This study received funding from: Novartis Pharma AG, Basel, Switzerland

FR0388

BMD Response to a Novel Delayed-release Risedronate 35 mg Once-a-Week Formulation Taken With or Without Breakfast: One Year Results. Michael McClung*[1], Michael Bolognese[2], Paul Miller[3], Joseph Sarley[4], Leigh McCullough[5], Jacques Brown[6], Robert Recker[7]. [1]Oregon Osteoporosis Center, USA, [2]Bethesda Health Research, USA, [3]Colorado Center for Bone Research, USA, [4]Procter & Gamble Pharmaceuticals Health Care Research Center, USA, [5]Warner Chilcott Phamaceuticals, USA, [6]Laval University, Canada, [7]Creighton University Osteoporosis Research Center, USA

Bisphosphonates (BPs) are the standard of care for postmenopausal osteoporosis. The dosing instructions of oral BPs per their approved labels require that they be taken on an empty stomach at least 30 to 60 minutes before the first food or drink or other medications. One year efficacy and safety results of a novel delayed release (DR) formulation of risedronate 35 mg once-a-week (OaW) that can be taken with or without breakfast will be presented.

This phase III study was a randomized, double blind, active controlled study conducted at 43 study centers across North America, Europe and South America. The primary efficacy analysis was to test the non-inferiority, based on the percent change in lumbar spine BMD from baseline at Endpoint (last observation carried forward at Week 52), of the risedronate 35 mg OaW DR formulation taken before or after breakfast compared to the 5 mg daily immediate release (IR) dose taken per label. Participants were postmenopausal women at least 50 years of age, ⩾ 5 years since last menses, with a lumbar spine or total hip BMD corresponding to a T-score < -2.5 or a T-score < -2.0 with at least one prevalent vertebral fracture (T4 to L4). Patients were randomly assigned to risedronate 35 mg OaW DR following breakfast (FB) (n=307), or risedronate 5 mg IR daily (n=307) or risedronate 35 mg OaW DR at least 30 minutes before breakfast (BB) (n=308).

At one year, the risedronate 35 mg OaW DR formulation, whether taken before or after breakfast, was shown to be non-inferior to the 5 mg IR daily. The mean percent changes in BMD at the hip (total proximal femur, femoral neck, and femoral trochanter) were similar across groups. Both the 5 mg IR daily and the 35 mg OaW DR regimens were well tolerated, and the overall frequency of adverse events was similar.

At one year, Risedronate 35 mg OaW DR, whether taken before or after breakfast, provided similar efficacy and tolerability to risedronate 5 mg/day IR taken per the label.

***Disclosures: Michael McClung**, Warner Chilcott Pharmaceuticals, 5*
This study received funding from: Warner Chilcott Company, LLC

FR0389

Comparison of Risedronate and Alendronate on Bone Remodeling, Architecture and Material Properties; a Cross-sectional Study in Women with Postmenopausal Osteoporosis. Eleftherios Paschalis[1], Roger Phipps*[2], Frank Ebetino[3], Babul Borah[4]. [1]Ludwig Boltzmann Institute for Osteology, Austria, [2]Husson University School of Pharmacy, USA, [3]Procter & Gamble Pharmaceuticals, Inc., USA, [4]Procter & Gamble Pharmaceuticals, USA

The effects of risedronate and alendronate on bone architecture, remodeling, and material properties were analyzed in transiliac crest biopsies collected from a non-randomized cross-sectional sample of 100 women with postmenopausal osteoporosis. Subjects recruited at 8 sites were at least 5 yr postmenopause and had been treated for >3 years with daily or weekly alendronate (n=68, mean age 70 yr) or risedronate (n=32, mean age 70 yr). Subjects received standard tetracycline labeling, and biopsies were placed in 70% ethanol and were embedded in methylmethacrylate. Complete biopsies were scanned at 8 µM resolution using a Scanco MicroCT40 scanner. After thresholding and masking, architecture measurements were derived from 3-D data sets, and grey level images were calibrated against HA standards to allow for measurement of mineralization. Five-µm thick sections were prepared for static and dynamic histomorphometry. Five-µm thick sections were also prepared for FTIR analysis of mineral crystallinity and collagen cross-links ratio for assessment of bone material properties and maturity of the bone matrix. All analyses were performed blinded. Values are medians, and groups were compared with the Wilcoxon Rank Sum test.

There were no significant differences in patient demographics including lumbar spine and total hip T-scores, and previous fractures. Mineralizing surface, bone formation rate and activation frequency (histomorphometry), and the low:high mineralization ratio in trabecular and cortical bone (micro-CT) were all significantly higher in risedronate-treated subjects than in alendronate-treated subjects. While trabecular architecture parameters (bone volume, trabecular thickness, trabecular number) were all higher in risedronate treated subjects, most differences were not statistically significant. There was no significant difference in cortical porosity between the 2 treatment groups. By FTIR, there were no statistically significant differences between the two drugs, although a trend towards younger (tissue-age wise) bone matrix at forming surfaces in risedronate treated subjects was consistent with published data from non head to head studies. These results support that long-term treatment with risedronate suppresses bone remodeling less than treatment with alendronate, but provides corresponding preservation of trabecular and cortical bone architecture and material properties.

Parameter	Alendronate	Risedronate	P-value
Trabecular bone volume (%)	15.4	17.5	0.12
Trabecular thickness (µm)	123	138	0.04
Mineralizing surface (%)	1.32	2.55	0.01
Activation frequency (#/yr)	0.12	0.20	0.01
Low high mineralization ratio - trabecular	0.26	0.41	0.01
Low high mineralization ratio - cortical	0.22	0.30	0.02
Collagen cross link ratio – trabecular forming surfaces AUC 0-49 µm depth	182	132	0.70

Table 1

***Disclosures: Roger Phipps**, Warner Chilcott Pharmaceuticals, 5*
This study received funding from: Warner Chilcott Pharmaceuticals

FR0390

Disintegration Times of Brand and Generic Bisphosphonates Available in Canada. W.P. Olszynski*[1], Jonathan Adachi[2], Jana Davison[3], K. Shawn Davison[4]. [1]Midtown Medical Center (#103), Canada, [2]St. Joseph's Hospital, Canada, [3]a priori medical sciences inc., Canada, [4]Laval University, Canada

Purpose: The purpose of this investigation was to compare the disintegration times among Canadian-marketed brand (Fosamax 70mg, Fosavance 70mg, Actonel 35mg) and generic (Novo-Alendronate 70mg and Apo-Alendronate 70mg) bisphosphonates. Differences in disintegration times among brand and generic versions of bisphosphonates may translate into differences in tolerability, safety and effectiveness between brand and generic formulations.

Methods: All tests were performed with the use of a Vanderkamp Disintegration Tester as per the United States Pharmacopeia guidelines. The time to tablet disintegration was recorded for each tested tablet. All tests were performed over a three day period, with an approximate third of each group tested daily. Between 18 and 20 samples were tested for each bisphosphonate group (n=18 for Novo-alendronate, n=20 for all others). Basic descriptive statistics were completed for all tablet groups. Analysis of variance was used to assess whether there were significant differences in disintegration time among the tablets tested and the Tukey post-hoc procedure was used to establish whether significant differences existed between specific tablet groups. Alpha was set at $p<0.05$ for all tests.

Results: The mean $\pm$ SD disintegration times were significant faster for the Apo-Alendronate (26 ± 5.6 seconds) and the Novo-Alendronate (13 ± 1.1 seconds) as compared to the brand alendronate (150 ± 50.5 seconds), the brand alendronate plus vitamin D (378 ± 60.5 seconds) and the brand risedronate (101 ± 20.6 seconds). There was no significant difference in disintegration time between the two generic forms of alendronate. Brand alendronate with vitamin D had a significantly slower disintegration time than all other tablets tested.

Conclusions: Generic formulations of alendronate were found to disintegrate significantly faster than brand versions of alendronate or risedronate. The rapid disintegration of the generic compounds were found to be similar to those reported for tablets specifically-engineered for disintegration in the mouth (<30 seconds). The rapid disintegration of generic alendronate as compared to brand versions of the alendronate or risedronate may have important safety implications, particularly for adverse events in the oesophagus. Further, the potential for quick-disintegrating alendronate to come into contact with food or drink while adhered to the oesophagus may be higher, thereby decreasing its effectiveness.

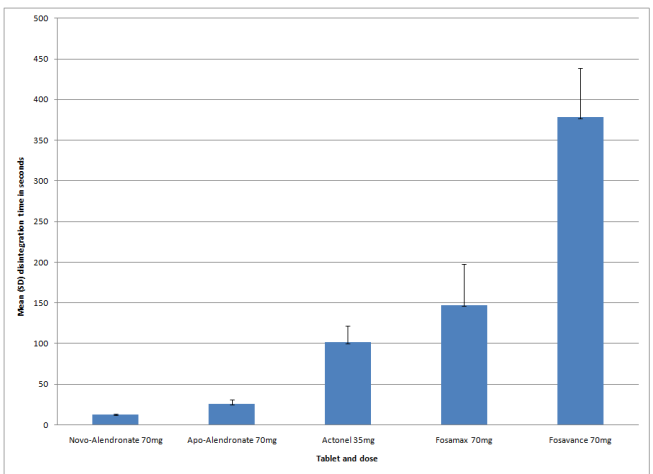

Figure

***Disclosures: W.P. Olszynski**, None.*

FR0393

The Effect of Long Term Bisphosphonate Therapy on Cortical Thickness Ratio of the Proximal Femur. Quang Ton*[1], Kashif Ashfaq[2], John Kleimeyer[3], Aasis Unnanuntana[2], Joseph Lane[2]. [1]Englewood Hospital & Medical Center, USA, [2]Hospital for Special Surgery, USA, [3]Weill Cornell Medical College, USA

There is little in the literature which attempts to prove a causal relationship between long-term bisphosphonate (BP) use and alteration of bone strength. Previous studies identified typical radiographic characteristics of patients with a so-called "BP fracture'' that include cortical thickening at the subtrochanteric (ST) area [Neviaser+2008]. A small subset of these patients develop low energy proximal femoral fractures. These patients have cortical thickness of >30%, while osteoporotic patients with similar fractures not on BP have cortical thickness of < 25%. Our hypothesis was that long term BP therapy results in progressive thickening of the proximal femoral cortex.

This study was a retrospective review of 49 patients from 1996-2010. Patients included were post-menopausal women on BP for at least 5 years and had serial dual energy X-ray absorptiometry (DXA) before and after treatment. Baseline and most recent hip DXA were uploaded into an imaging system and standard technique was used to measure the proximal femur. Measurement was intially standardized by first doing calibration and then measuring the medullary and femoral diameter at a level 3.5 cm and 4.0 cm from the tip of greater trochanter (GT) downwards which represented the ST area. These measurements allowed us to derive the cortical thickness ratio (CTR), periostal, and endosteal growth. The data was compared by using a paired t-test of the initial and last DXA.

The baseline average CTR 3.5 cm below the tip of GT was 0.40 + 0.06 mm. This ratio was decreased to 0.38 + 0.06 mm after 5 years of BP therapy. The difference was not statistically significant before and after treatment ($p = 0.108$). The baseline average CTR 4.0 cm below the tip of GT was decreased from 0.44 + 0.06 mm to 0.42 + 0.07 mm, when compared before and after 5 years of BP treatment ($p = 0.0005$). The difference was statistically significant. The average periosteal thickening ratio was -0.03 + 0.10; while the endosteal thickening ratio was -0.03 +0.10.

This study suggests that the cortical thickness of the proximal femur does not change over long-term BP of at least 5 years. There is neither periosteal nor endosteal growth after the treatment. Our hypothesis that patients on prolonged BP treatment get increased cortical thickness was thus disproved, therefore patients with ST fractures may have had thickened cortices at the onset of their BP treatment and these BP may not have resulted in further thickening of the cortices.

***Disclosures: Quang Ton**, None.*

FR0396

Zoledronic Acid Improves Health-related Quality of Life in Patients with Hip Fracture: Results of HORIZON-RFT. Jonathan Adachi*[1], Kenneth Lyles[2], Cathleen Colon-Emeric[2], Steven Boonen[3], C Pieper[2], Carlos Mautalen[4], Lars Hyldstrup[5], Christopher Recknor[6], L Nordsletten[7], C Bucci-Rechtweg[8], G Su[8], Erik Fink Eriksen[9], Jay Magaziner[10]. [1]St. Joseph's Hospital, Canada, [2]Duke University Medical Center, USA, [3]Center for Metabolic Bone Disease, Belgium, [4]Centro de Osteopatías Médicas, Argentina, [5]Hvidovre Hospital, Denmark, [6]United Osteoporosis Center, USA, [7]Ullevål University Hospital, Norway, [8]Novartis Pharmaceuticals Corporation, USA, [9]Oslo University Hospital, Norway, [10]University of Maryland, Baltimore, USA

Purpose: In HORIZON-RFT, annual i.v. zoledronic acid (ZOL) 5 mg infusion significantly reduced the rate of new clinical fractures and all-cause mortality compared with placebo.[1] A pre-defined exploratory objective of the same study was to analyze the benefits of ZOL *vs.* placebo on Health-related quality of life (HRQoL) using the EQ-5D health questionnaire in selected countries.

Methods: In this randomized, double-blind, placebo-controlled trial 2127 patients were randomized to single infusion of ZOL 5 mg (n=1065) or placebo (n=1062) within 90 days after surgical repair of low-trauma hip fracture, followed by annual infusions up to 3 years, with a median follow-up time of 1.9 years. HRQoL was measured using EQ-5D-Visual Analogue Scale (VAS) and -utility scores (EuroQol instrument) at end of the study. Analysis of covariance model included baseline EQ-5D status, region and treatment as explanatory variables.

Results: At baseline, patients (mean age: 75 years; 24% men and 76% women) were well-matched between treatment groups with mean EQ-5D VAS of 65.82 in ZOL group and 65.70 in placebo group. At the end of the study, mean change from baseline in EQ-5D VAS was greater for ZOL *vs.* placebo in all patients (7.67 ± 0.56 *vs.* 5.42 ± 0.56), and in subgroups of patients experiencing clinical vertebral fractures (8.86 ± 4.91 *vs.* -1.69 ± 3.42), non-vertebral fractures (5.03 ± 2.48 *vs.* -1.07 ± 2.16), and clinical fractures (5.19 ± 2.25 *vs.* -0.72 ± 1.82) with treatment difference significantly in favor of ZOL (Figure). EQ-5D utility scores were comparable for ZOL and placebo groups but more patients on placebo consistently had extreme difficulty in mobility (1.74% for ZOL *vs.* 2.13% for placebo; p=0.6238), self-care (4.92% *vs.* 6.69%; p=0.1013) and usual activities (10.28% *vs.* 12.91%; p=0.0775).

Conclusion: In addition to reducing the risk of vertebral, hip, and non-vertebral fractures, treatment with ZOL significantly improved overall quality of life in patients with low-trauma hip fracture.

References: 1. Lyles KW *et al. N Engl J Med.* 2007;357:1799-809.

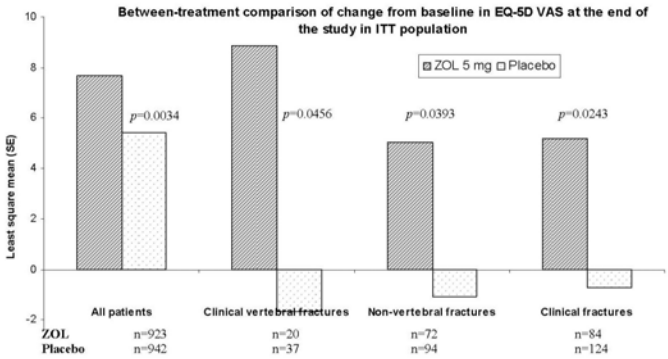

Figure

***Disclosures: Jonathan Adachi**, Amgen, Eli Lilly, GlaxoSmithKline, Merck, Novartis, Pfizer, Procter & Gamble, and Roche, 2; Amgen, AstraZeneca, Eli Lilly, GlaxoSmithKline, Merck, Novartis, Pfizer, Procter & Gamble, Roche, Sanofi-Aventis, and Servier, 8; Amgen, AstraZeneca, Eli Lilly, GlaxoSmithKline, Merck, Novartis, Pfizer, Procter & Gamble, Roche, Sanofi-Aventis, and Servier, 5*
This study received funding from: Novartis Pharma AG, Basel, Switzerland

FR0402

Efficacy and Safety of Bazedoxifene in Postmenopausal African American Women. Amy B. Levine*[1], Monika Ciesielska[1], Arkadi Chines[2]. [1]Pfizer Inc, USA, [2]Wyeth Research, USA

The results of 2 global, double-blind, placebo- and active-controlled, phase 3 studies (2-year prevention study [mean age, 58 y]; 3-year treatment study [mean age, 66 y]) have demonstrated the efficacy and safety of bazedoxifene (BZA) in the prevention and treatment of postmenopausal osteoporosis. The purpose of this analysis was to evaluate the effects of BZA on bone mineral density (BMD), bone turnover, and safety parameters in African American women enrolled in these studies. The data from these 2 studies were pooled and an integrated analysis was performed. Five hundred and five African American women were randomly assigned to receive daily treatment with BZA 20 mg (n=119), BZA 40 mg (n=141), raloxifene (RLX) 60 mg (n=120), or placebo (PBO; n=125); they also received supplementation with calcium and vitamin D. Mean lumbar spine BMD T-scores at baseline were –2.3, –2.6, –2.3, and –2.7 in the BZA 20- and 40-mg, RLX 60-mg, and PBO groups, respectively. At 24 months, the mean (±standard error) percent changes from baseline in BMD at the lumbar spine were significantly greater with BZA 20 or 40 mg and RLX 60 mg (0.88±0.64%, 1.14±0.60%, and 1.42±0.63%, respectively) versus PBO (–0.25±0.62%; P <0.05). Similar results were seen at the total hip, femoral neck, and femoral trochanter (BZA 20 mg: 1.24±0.53%, 2.14±0.61%, 1.01±0.73%, respectively; BZA 40 mg: 1.18±0.49%, 2.39±0.58%, 1.23±0.68%, respectively; RLX 60 mg: 1.06±0.51%, 2.46±0.60%, 0.99±0.71%, respectively; PBO: –0.06±0.51%, 0.61±0.59%, –0.36±0.71%, respectively; P <0.05 vs PBO for all). BZA 20 or 40 mg and RLX 60 mg significantly reduced serum C-telopeptide (–47%, –57%, and –57%, respectively) and osteocalcin (–42%, –44%, and –45%, respectively) levels versus PBO (–35% [P <0.05] and –24% [P <0.001], respectively) at 12 months. There was a small number of vertebral fractures among African American women in the treatment study (BZA 20 mg [n=2]; BZA 40 mg [n=3]; RLX 60 mg [n=1]; PBO [n=2]). The overall incidence of treatment-emergent adverse events (95%) and serious adverse events (16%) in African American women was not different among the BZA, RLX, and PBO groups. The incidence of cerebrovascular and venous thromboembolic events was low and similar among groups. In conclusion, BZA preserved BMD, reduced bone turnover, and showed a favorable safety profile in postmenopausal African American women, which was consistent with findings observed in the entire integrated phase 3 populations.

***Disclosures: Amy B. Levine**, Pfizer Inc, 3*
This study received funding from: Pfizer Inc

FR0403

The effect of Raloxifene on Vertebral and Non-vertebral Fracture Risk Is Independent of Baseline FRAX® Probability. John Kanis[1], Helena Johansson[2], Anders Oden[2], Eugene McCloskey*[3]. [1]University of Sheffield, Belgium, [2]WHO Collaborating Centre for Metabolic Bone Diseases, United Kingdom, [3]University of Sheffield, United Kingdom

A major application of FRAX® has been in the clinical assessment of patients, but there is also interest emerging in its application to clinical trials. The Multiple Outcomes of Raloxifene Evaluation (MORE) study, a placebo controlled phase III trial of raloxifene in postmenopausal osteoporosis, showed that both doses tested (60mg and 120mg daily) reduced the risk of vertebral fracture with no significant effect on non-vertebral fractures. The aim of the present study was to evaluate the distribution of fracture risk assessed at baseline using the FRAX® tool in MORE and to determine the efficacy of raloxifene as a function of baseline fracture risk.

The effects of raloxifene (60 and 120 mg daily combined) compared to placebo on the risk of all clinical fractures (including clinical vertebral fractures) as well as the risk of morphometric vertebral fracture were examined as a function of baseline fracture risk. Baseline clinical risk factors and BMD were entered in country specific FRAX® models to compute the 10-year probability of major osteoporotic fractures. No information was available on parental history of hip fracture and this variable was simulated. The interaction between fracture probability and treatment efficacy was examined by Poisson regression.

The mean ± SD 10-year probability of major osteoporotic fractures (with BMD) was 21±11% (range 0.9-77.2%). Treatment with raloxifene was associated with an 18% decrease in all clinical fractures compared to placebo treatment (hazard ratio HR = 0.82; 95% CI = 0.71-0.95; p = 0.0063) and a 42% decrease in incident morphometric vertebral fractures (HR = 0.58; 95% CI = 0.48-0.69; p < 0.001). Efficacy was shown over the whole range of fracture probability and the interaction between fracture probability and treatment was not significant. The efficacy or raloxifene on vertebral fracture risk was significantly greater at lower ages. At the 90th percentile of age (75 years) vertebral fracture risk was reduced by 31% irrespective of FRAX® probabilities. In contrast at younger ages, efficacy was higher and increased further still with decreasing fracture probability.

Raloxifene (60 and 120 mg doses combined) significantly decreased the risk of all clinical fractures and morphometric fractures in women. Overall, there was no significant interaction between efficacy and fracture probability. In the case of morphometric vertebral fractures efficacy decreased significantly with increasing age.

***Disclosures: Eugene McCloskey**, None.*
This study received funding from: Lilly

FR0404

Impact of Comorbidities on Hospitalization Costs Following Hip Fracture. Lucas Nikkel*[1], Christopher Hollenbeak[2], Kevin Black[2], Edward Fox[2]. [1]Pennsylvania State University College of Medicine, USA, [2]Pennsylvania State Hershey Medical Center, USA

INTRODUCTION: Hip fractures are common in elderly populations and have important implications for healthcare costs and health-related quality of life. Patients with hip fractures frequently present with comorbid illnesses. However, little is known about the relationship between comorbid illness and hospital costs or length of stay (LOS) following hip fracture in the United States. We hypothesized that specific individual comorbid illnesses and the presence of multiple comorbid illnesses would be directly related to the cost of hospitalization and the length of stay for older patients following hip fracture.

METHODS: Using ICD-9-CM diagnosis codes, 35,221 patients age 55 or older were identified from the 2007 Nationwide Inpatient Sample (NIS) database with an isolated femoral neck or intertrochanteric fracture. Using generalized linear models, we estimated the impact of comorbidities on hospitalization costs and LOS, controlling for patient, hospital, and procedure characteristics.

RESULTS: Hypertension, deficiency anemias, and fluid and electrolyte disorders were the most common comorbidities. The mean number of comorbidities was 2.9. Only 5.1% of patients presented without comorbidities. The average cost for a hospitalization following hip fracture in our reference patient (no comorbidities, age 55-64, white, female from the Northeast, undergoing open reduction with internal fixation (ORIF) at a medium-sized, non-teaching, urban hospital) was $13,739 (p<0.001). Patients presenting with weight loss or malnutrition had the largest increased hospitalization costs (+$5,928; p<0.001), followed by pulmonary circulation disorders (+$3,444; p<0.001). Most other comorbidities significantly increased the cost of hospitalization. In comparison, partial hip arthroplasty added $2,190 (p<0.001) to the cost relative to ORIF, and total hip arthroplasty added $4,966 (p<0.001). Male and non-white patients also had elevated hospitalization costs. There was a general trend of increasing number of comorbidities associated with increased hospitalization costs and LOS. Comorbidities and patient characteristics that elevated costs also increased the LOS.

CONCLUSIONS: Comorbidities significantly affect the cost of hospitalization and length of stay following hip fracture in older Americans, even while controlling for other variables. These findings have important implications for hospital cost savings through better management of comorbidities in this population.

***Disclosures: Lucas Nikkel**, None.*

FR0405

Physician Notification From Administrative Health Data Is A Cost-Effective Post-Fracture Intervention: Interim Report From A Randomized Controlled Trial. William Leslie*, Patricia Caetano. University of Manitoba, Canada

Post-fracture care is suboptimal and strategies to address this major ''care gap'' are urgently required. Case management is effective but is resource-intensive and difficult to deliver to a widely scattered population. HYPOTHESIS: Post-fracture notification of physicians and/or patients will lead to improved osteoporosis care. METHODS: An RCT (NCT00594789) was conducted across the Province of Manitoba, Canada, in which men and women age 50 or older with recently reported fracture (hip, spine, humerus, and forearm) from medical claims data, and without recent BMD testing

(three years) or osteoporosis therapy (last year), were randomized to three groups: Group 1 received usual care; Group 2 (MDs only) had mailed notification to the reporting and primary care physicians (alert letter, BMD requisition, management flow chart); Group 3 (MDs and patient) had physician notifications and patient notification (alert letter). BMD testing and/or osteoporosis treatment initiation in the next six months was documented from a population-based data repository. RESULTS: During the initial ten months (June 2008 to March 2009), 2,901 fracture patients meeting the inclusion criteria were randomized. Groups were well balanced. Group 1 (usual care) intervention rates were all less than 10%. There was a significant improvement in all outcome measures for groups 2 (MDs only) and 3 (MDs and patient). There was no additional benefit in patient notification in addition to physician notification. The adjusted odds ratio (OR) for treatment initiation in group 2 was 7.2 (95% CI 4.9-10.5) and in group 3 was 8.0 (95% CI 5.4-11.7). In addition to randomized group, factors associated with treatment initiation included age and sex, but not fracture site (Table). Direct costs related to the initiative (programming, case identification, mailings) were $12,379 CDN. The incremental cost per individual started on osteoporosis therapy (net above usual care treatment rates) was $31 CDN. CONCLUSIONS: This post-fracture intervention, based upon medical claims data, provides an easy way to enhance post-fracture care. The approach is scalable, can be delivered to a widely scattered population, and requires minimal infrastructure. This low cost intervention may complement more resource-intensive programs based on case managers.

		BMD Testing		Drug Treatment		Either	
		OR (95% CI)	P	OR (95% CI)	P	OR (95% CI)	P
Group	Usual care	Reference	.	Reference	.	Reference	.
	MDs only	1.7 (1.2-2.6)	0.008	7.2 (4.9-10.5)	<.001	3.9 (2.9-5.2)	<.001
	MDs and patient	2.3 (1.6-3.5)	<.001	8.0 (5.4-11.7)	<.001	4.6 (3.4-6.1)	<.001
Sex	Male	0.5 (0.3-0.7)	<.001	0.4 (0.3-0.5)	<.001	0.4 (0.3-0.5)	<.001
Age	50-59	Reference	.	Reference	.	Reference	.
	60-69	2.1 (1.2-3.7)	0.006	1.8 (1.4-2.4)	<.001	1.9 (1.5-2.4)	<.001
	70-79	4.1 (2.5-6.8)	<.001	1.6 (1.2-2.1)	<.001	2.0 (1.5-2.6)	<.001
	80+	3.7 (2.2-6.0)	<.001	0.6 (0.4-0.8)	0.002	1.0 (0.8-1.4)	0.734
Fracture	Forearm	Reference	.	Reference	.	Reference	.
	Hip	1.6 (1.0-2.5)	0.042	0.7 (0.5-1.0)	0.029	0.8 (0.6-1.0)	0.094
	Humerus	1.6 (1.1-2.4)	0.021	0.8 (0.6-1.1)	0.144	0.9 (0.7-1.1)	0.401
	Spine	1.9 (1.2-2.9)	0.003	0.9 (0.7-1.1)	0.308	1.1 (0.9-1.5)	0.279

Table: Adjusted odds ratios (OR) for post-fracture intervention.

***Disclosures: William Leslie**, None.*

FR0408

Effects of the Cathepsin K Inhibitor, ONO-5334, on BMD as Measured by 3D QCT in the Hip and the Spine After 12 Months Treatment. Klaus Engelke*[1], Shinichi Nagase[2], Thomas Fuerst[3], Richard Eastell[4], Harry Genant[5], Maria Small[2], Tomohiro Kuwayama[2], Steve Deacon[2]. [1]University of Erlangen, Germany, [2]ONO PHARMA UK LTD, United Kingdom, [3]Synarc, Inc., USA, [4]University of Sheffield, United Kingdom, [5]UCSF/Synarc, USA

Purpose: To evaluate the efficacy of the Cathepsin K inhibitor, ONO-5334 in a randomized, double-blind, parallel-group study using quantitative computed tomography (QCT).

Methods: 285 post-menopausal female subjects (age: 55-75) with osteoporosis (with no fragility fractures) or osteopenia (with a fragility vertebral fracture) were equally randomized to five study arms: three doses of ONO-5334 (50mg bd, 100 or 300mg qd), placebo (PBO) or Alendronate (ALN, 70mg qw). Calcium and vitamin D were given to all subjects. 3D QCT scans of the spine (L1 and L2) and of the proximal femur were taken at baseline and after 1 year. QCT (exploratory endpoint) analysis was performed for those patients who provided informed consent for this assessment, with MIAF (Medical Image Analysis Framework) in various integral, cortical and trabecular volumes of interest. 188 subjects had baseline and follow-up femur scans, 193 subjects had baseline and follow-up spine scans.

Results: Percentage BMD changes in total vertebral body of L1 plus 2 and total femur after 12 months relative to baseline are shown in the table. In the spine, analysis of mid, superior and inferior sub volumes showed very similar results compared to those for the total vertebral body. Vertebral volume did not change in any treatment. In the femur, results for the neck were very similar to those of the total femur but in the trochanter integral %BMD changes were slightly higher for the ONO-5334 and ALN groups. In all hip regions, trabecular %BMD changes were higher for ONO-5334 50mg, 300mg and ALN groups. Total volume and cortical thickness of the hip did not change significantly in any group.

Conclusions: In the spine ONO-5334 50 mg bd and 300 mg qd demonstrated similar increases from baseline that were consistently superior to 100 mg qd and roughly equivalent to alendronate (ALN). As expected, percentage increases were larger in the integral and trabecular VOIs compared to the cortical VOIs. In the hip the three doses of ONO-5334 showed a similar pattern as in the spine with 50 mg bd and 300 mg qd showing similar increases from baseline that were consistently superior to 100 mg qd. Compared to ALN, ONO-5334 showed nearly equivalent increases in integral BMD and numerically superior increases in trabecular BMD in the femur. Cortical increases were similar between ONO-5334 and ALN.

VOI		PBO	ONO-5334 50mg bd	ONO-5334 100mg qd	ONO-5334 300mg qd	ALN 70mg qw
Total vertebral body	Int BMD	-1.1 ± 0.8	7.0 ± 0.7***	5.2 ± 0.8***	7.4 ± 0.8***	7.1 ± 0.8***
	Trab BMD	-1.8 ± 1.2	8.3 ± 1.1***	7.0 ± 1.2***	7.5 ± 1.2***	8.3 ± 1.2***
	Cort BMD	-0.7 ± 0.8	5.3 ± 0.8***	3.4 ± 0.9***	6.2 ± 0.8***	5.6 ± 0.8***
Total femur	Int BMD	-0.7 ± 0.5	3.1 ± 0.5***	1.3 ± 0.5**	3.0 ± 0.5***	3.0 ± 0.5***
	Trab BMD	1.0 ± 1.5	7.0 ± 1.4**	3.8 ± 1.4	7.5 ± 1.3***	5.0 ± 1.4*
	Cort BMD	-0.4 ± 0.5	2.0 ± 0.5***	0.7 ± 0.5	1.8 ± 0.5**	2.3 ± 0.5***

Mean +/- SE, Full Analysis Set was used, *<0.05, **<0.01, ***<0.001 vs. placebo

Table: Percentage change from baseline in volumetric BMD

***Disclosures: Klaus Engelke**, ONO PHARMA UK LTD, 5; Ono Pharmaceutical Co., Ltd., 5*
This study received funding from: Ono Pharmaceutical Co., Ltd.

FR0410

Hip QCT Results From the FREEDOM Trial: Evidence for Positive BMD/ BMC Changes in Integral, Trabecular, and Cortical Bone With Denosumab. Harry Genant*[1], Klaus Engelke[2], Jose Ruben Zanchetta[3], Arne Hoiseth[4], Chui Kin Yuen[5], Sigitas Stonkus[6], Michael Bolognese[7], Edward Franek[8], Thomas Fuerst[9], Hoi-Shen Radcliffe[10], Cesar Libanati[11], Michael McClung[12]. [1]UCSF/Synarc, USA, [2]Synarc, Germany, [3]Instituto de Investigaciones Metabolicas (IDIM), Argentina, [4]Curato Røntgen, Norway, [5]Manitoba Clinic, Canada, [6]Kaunas University of Medicine, Lithuania, [7]Bethesda Health Research, USA, [8]Central Clinical Hospital MSWiA, Poland, [9]Synarc, Inc., USA, [10]Amgen Inc, United Kingdom, [11]Amgen Inc, USA, [12]Oregon Osteoporosis Center, USA

Denosumab, a fully human monoclonal antibody to RANKL, decreased bone resorption, increased bone mineral density (BMD), and reduced vertebral, nonvertebral, and hip fractures in postmenopausal women with osteoporosis in the FREEDOM trial (Cummings SR et al., NEJM, 2009:361:756). In FREEDOM, subjects received 60 mg denosumab or placebo every 6 months for 3 years; all subjects received daily supplements of calcium and vitamin D. Hip QCT scans were obtained at baseline and at months 12, 24, and 36, in a subset of women and were analyzed using Medical Image Analysis Framework (MIAF) software (University of Erlangen, Germany), in a blinded-to-treatment manner. MIAF allows the determination of integral, trabecular, subcortical, and cortical BMD for the hip (proximal femur) as well as various sub-regions with precision errors of 1.5% to 2.5%. These analyses enable thorough evaluations of compartmental changes which may have different relevance to bone strength. This exploratory analysis evaluated the magnitude of changes from baseline and from placebo in denosumab-treated subjects with hip QCT at baseline and month 36 who completed 36 months of treatment (denosumab n=45; placebo n=36). Data from month 36 were excluded for 19 subjects due to CT scanner malfunction at 1 site. Baseline mean age was 74 years, mean years since menopause was 25, and mean aBMD T-score of the total hip was –1.85 for all subjects. Denosumab resulted in significant improvements in vBMD and bone mineral content (BMC) from baseline by 12 months. Over 36 months, the improvements from baseline in integral hip BMD reached 6.3% and 4.8% for BMC (both $p<0.0001$). These gains were accounted for by significant and consistent increases in cortical, subcortical, and trabecular BMD and BMC (Table). In the placebo group, integral hip BMD and BMC decreased at 36 months from baseline by –1.4% and –2.8%, respectively (both $p\leq0.0231$), mainly attributable to losses in both the subcortical and trabecular compartments. The differences between denosumab and placebo were highly significant ($p\leq0.0008$) at 12, 24, and 36 months for integral, cortical, and trabecular BMD and BMC, except for cortical BMD at 12 months ($p=0.0661$). In summary, denosumab results in significant improvements in both vBMD and BMC from baseline and placebo across integral, cortical, subcortical, and trabecular hip compartments. These changes support the clinical effect of denosumab to reduce hip fractures as observed in the FREEDOM trial.

Table. Mean Percent Change and 95% CI from Baseline

		Bone Mineral Content			Bone Mineral Density		
		Month 12	Month 24	Month 36	Month 12	Month 24	Month 36
Cortical	Pbo	-1.0 (-2.2, 0.2)	-1.6 (-3.7, 0.5)	-1.4 (-2.7, -0.1)	1.5 (0.4, 2.6)	0.2 (-1.4, 1.7)	0.2 (-1.0, 1.4)
	DMAb	2.2 (1.1, 3.4)	3.2 (1.9, 4.6)	4.0 (2.9, 5.2)	2.6 (1.9, 3.4)	3.3 (2.2, 4.4)	5.3 (4.4, 6.3)
Subcortical	Pbo	0.9 (-1.7, 3.5)	0.3 (-2.7, 3.4)	-3.0 (-5.2, -0.9)	1.3 (-0.9, 3.4)	0.6 (-1.8, 3.1)	-1.5 (-3.4, 0.5)
	DMAb	2.9 (1.8, 3.9)	4.4 (3.0, 5.9)	4.7 (3.1, 6.3)	3.1 (2.2, 4.0)	4.5 (3.3, 5.6)	6.2 (4.8, 7.6)
Trabecular	Pbo	-0.3 (-3.2, 2.6)	-3.8 (-8.5, 0.8)	-8.9 (-12.9, -4.9)	-0.3 (-2.9, 2.3)	-4.1 (-8.6, 0.4)	-7.7 (-11.5, -4.0)
	DMAb	5.4 (3.7, 7.0)	8.9 (5.4, 12.5)	8.3 (6.0, 10.6)	5.7 (4.2, 7.2)	9.0 (5.7, 12.2)	9.8 (7.8, 11.9)

Pbo = placebo; DMAb = denosumab. Values are mean (95% confidence intervals).

Table

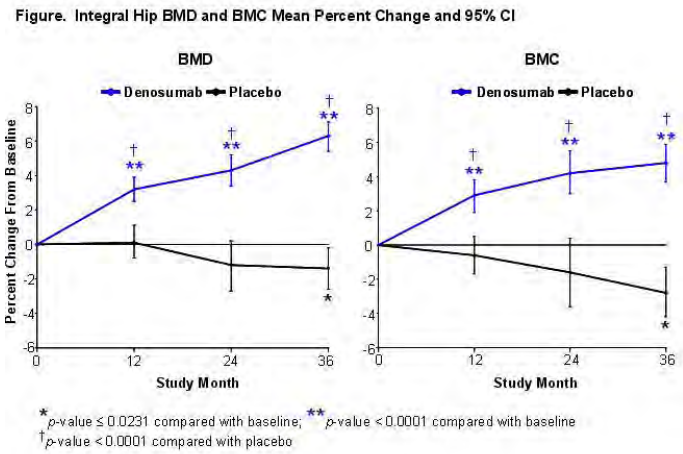

Figure

***Disclosures: Harry Genant**, Amgen, Merck, GSK, Roche, Servier, BMS, Lilly, 8; Synarc, 1; Amgen, Merck, GSK, Roche, Servier, BMS, Lilly, 5*
This study received funding from: Amgen Inc.

FR0413

Effect of Vertebroplasty on the Quality of Life of Patients with Pain Related to Osteoporotic Vertebral Fractures. Preliminary Results of a Randomized Trial. Angels Martinez-Ferrer*[1], Pilar Peris[2], Jordi Blasco[3], Josep-LLuís Carrasco[4], Ana Monegal[5], Jaume Pomés[6], Nuria Guanabens[7]. [1]Hospital Clinic Barcelona, Spain, [2]Hospital Clinic of Barcelona, Spain, [3]Department of Radiology. Hospital Clinic, Spain, [4]Hospital Clinic, Spain, [5]Department of Rheumatology. Hospital Clinic Barcelona, Spain, [6]Department of Radiology. Hospital Clínic Barcelona, Spain, [7]Universitat De Barcelona, Spain

The aim of the study was to compare the effects of vertebroplasty vs conservative approach in the quality of life and pain of patients with painful osteoporotic vertebral fractures, as well as to analyze the secondary adverse effects and the development of new fractures in both treatment groups during a 12-months follow-up period.

Methods: Randomized, controlled trial of subjects with acute painful osteoporotic vertebral fractures (less than 12 months duration and unhealed, as confirmed by magnetic resonance imaging [MR]). At baseline, complete anamnesis and evaluation of quality of life (by Qualeffo-41questionnaire) and pain (by VAS measurement) were performed as well as MR of whole column and dorsolumbar X-rays. Outcomes, secondary effects and complications were assessed at 2 weeks and at 2, 6 and 12 months. X-rays were performed at baseline and at 12 months and also when symptoms suggested a new vertebral fracture or when a significat height loss was observed (>2 cm).

Results: A total of 121 patients were enrolled, and 77 (37 of 59 in the vertebroplasty group and 40 of 62 in the placebo group) completed the 12-month follow-up. The baseline clinical characteristics of the participants were similar in both groups. There was a significant improvement in overall pain and quality of life in both study groups at each follow-up assessment. When compared with conventional therapy the improvement in VAS was greater in patients treated with vertebroplasty at 2 (p=0.026) and at 12 months (p=0.045). Similar improvements were seen in both groups of patients with respect to quality of life measurements. Patients treated with vertebroplasty presented a higher incidence of vertebral fractures than those with conservative approach (20.3% vs 4.8%, p=0.0087).

Conclusions: Vertebroplasty and conservative treatment are both associated with a significant improvement in pain and quality of life in patients with painful osteoporotic vertebral fractures throughout a one-year follow-up period. Patients treated with vertebroplasty showed greater pain relief at 2 and 12 months after treatment, although this procedure was associated with a significant increase in the incidence of vertebral fractures.

***Disclosures: Angels Martinez-Ferrer**, None.*

FR0415

Alfacalcidol Improves Muscle Power, Muscle Function and Balance in Elderly Patients with Reduced Bone Mass. Erich Schacht[1], Johann Diederich Ringe*[2]. [1]ZORG (Zurich Osteoporosis Research Group), Switzerland, [2]Medical Clinic 4, Klinikum Leverkusen (University of Cologne), Germany

Objective: In an open, multi-center, uncontrolled, prospective study on a cohort of patients with reduced bone mass, we investigated the effect of daily therapy with 1 mcg alfacalcidol* on muscle power, muscle function and balance performance.

Subjects and methods: Out of the 2097 participants, who were recruited for this study in Germany, 87.1% were postmenopausal women and 12.9% were men. The patients had a mean age of 74.8 years and a mean BMI of 26.3 kg/m^2. Out of the total number of patients, 75.3% had osteoporosis (87.1% in women), 81% had a diagnosis of ''increased risk of falls'' and 70.1% had a creatinine clearance (CrCl) of < 65ml/min. At onset and after 3 and 6 months participants underwent muscle function and muscle power tests: the Timed-Up and Go Test (TUG) and the Chair Rising Test (CRT), as well as a balance test: the Tandem Gait Test (TGT), the latter performed only at baseline and at 6 months.

Successful performance in these tests is associated with a significantly lower risk for falls and non-vertebral fractures in elderly patients (successful test performance: TUG ≤ 10 sec., CRT ≤ 10 sec., TGT ≥ 8 steps)♂.

Results: After 3 months of treatment with alfacalcidol, participants already showed a statistically significant improvement in the performance of the two muscle tests. This effect (n =1970 for TUG; n = 1857 for CRT) had further increased by the end of the therapy period. We observed a significant increase in the number of participants able to successfully perform the different tests: 24.6% at baseline and 46.3 % at the end for the TUG (p< 0.0001) and 21.7% at baseline and 44.2% at the end for the CRT (p=0.0001). After treatment, the mean time used for the TUG was decreased by 3.0 sec (17.0 sec at the onset) and by 3.1 sec (16.5 sec at the onset) for the CRT.

At the end of the observation time the percentage of participants (n=1933) able to perform the balance test (8 steps in the TGT) increased from 36.0% to 58.6% (p<0.0001).

No cases of hypercalcemia were registered.

Conclusion: We conclude that treatment with alfacalcidol increases muscle power, muscle function and balance. The significant improvement in the risk tests for falls TUG, CRT and TGT may have a preventative effect on falls and fractures. We suggest that the quantitative risk tests used in this study are reliable surrogate parameters for the risk of falls and fractures in elderly patients.

* (Doss®- TEVA/AWD.pharma)

♂ Zhu K et al, J Bone Miner Res 2008:23;119.

***Disclosures: Johann Diederich Ringe**, TEVA/AWD.phama, 5*
This study received funding from: TEVA/AWD.pharma

FR0418

Efficacy of Rapid Oral Replacement of Vitamin D: 300,000 IU and 150,000 for Severe and Moderate Deficiency. Muhammad Javaid*[1], Kerri Rance[2], Vicki Toghill[2], William Fraser[3], John Wass[4]. [1]University of Oxford, United Kingdom, [2]Nuffield Orthopaedic Centre, United Kingdom, [3]Royal Liverpool University Hospital, United Kingdom, [4]Holmby House, United Kingdom

Purpose: Vitamin D deficiency is a risk factor for falls and fracture. While in clinical trials, daily calcium and vitamin D replacement is effective in normalizing the vitamin D levels, adherence to daily preparations is very poor and unlikely to be effective. Whilst higher dose replacement regimens have been tested, the sample sizes are typically small. We therefore audited the effectiveness of rapid oral replacement of vitamin D in a pragmatic clinical setting.

Methods: Patients referred to secondary care metabolic bone unit for assessment and treatment of osteoporosis have a baseline serum level of 25(OH)D measured using HPLC with MS. Patients were loaded with either 300,000 IU (50,000 IU D3 daily for 6 days) if severe deficiency (25(OH)D less than 25 nM) and 150,000 IU (50,000 IU D3 daily for 3 days) if moderate deficiency 25(OH) D between 25 and 50 nM). We used 50,000 IU cholecalciferol capsules (Biotech). Patients were contacted by letter if they required treatment and invited to collect their prescription from the hospital pharmacy or have the supplement posted to their house. We also asked patients to have a serum calcium and in a subset a serum 25(OH)D measured between 2 and 4 weeks after the loading dose. We defined biochemical repletion as more than 50 nM 25(OH)D and hypercalcaemia as a albumin adjusted serum calcium of greater than 2.65 mM.

Results: Between August and December 2009, 201 patients identified as requiring vitamin D supplementation, collected the supplement and had a recorded measured at 2- 4 weeks. Of those with severe deficiency, 92% had biochemical repletion afterwards and of those with moderate deficiency 97% were replete (Figure). No patient had post loading concentrations of more than 250 nM. Using a higher threshold of repletion (> 75nM), only 14% of severe deficient (after 300,000 iu loading) and 32% of moderate deficient (after 150,000 IU) achieved this level. We could not exclude an effect of season or adherence to therapy. Of those with hypercalcaemia, one had pre-existing primary hyperparathyroidism and the other was established on daily teriparatide. In both the hypercalcaemia was asymptomatic. No patient contacted the helpline with side-effects, however these were not systematically assessed.

Conclusion: In patients with osteoporosis and vitamin D deficiency, oral loading of cholecalciferol was effective at achieving repletion using a threshold of 50 nM but not 75 nM. Further studies demonstrating the target level in patients with osteoporosis and the clinical rather than biochemical effectiveness of high dose replacement are urgently required.

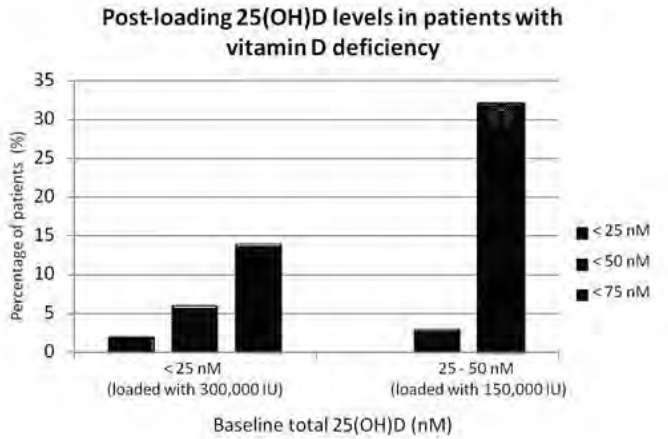

Figure

***Disclosures: Muhammad Javaid**, None.*

FR0420

A Catechol-derivative Inhibits Tph1 Synthesis and Cures Osteoporosis in Ovariectomized Mice. Vijay Yadav*, Yuli Xie, Gerard Karsenty, Patricia Ducy. Columbia University, USA

Tryptophan hydroxylase 1 (Tph1) catalyzes the rate-limiting step in the biosynthesis of gut-derived serotonin, a molecule that affects a variety of physiological processes. Recently it was demonstrated that gut-derived serotonin negatively regulates osteoblasts proliferation and bone formation. Here we report the identification of a novel catechol-derivative, Catechol-3,6-bismethyleneiminodiacetic acid (CBMIDA) as a Tph1 inhibitor that can selectively reduce serotonin levels in the serum after oral administration without any significant effect on brain serotonin content. Furthermore, oral administration of this small molecule once daily for up to 6 weeks prevents the development of and fully rescues, in a dose-dependent manner, osteoporosis in ovariectomized mice because of an isolated increase in bone formation. These molecules add to the emerging class of Tph1 inhibitors that have the potential to become novel anabolic treatments for low bone mass diseases such as osteoporosis.

***Disclosures: Vijay Yadav**, None.*

FR0421

Decreased Oxidative Stress and Greater Bone Anabolism in the Aged, as Compared to the Young, Murine Skeleton by Parathyroid Hormone. Robert Jilka*, Maria Jose Almeida, Elena Ambrogini, Li Han, Paula Roberson, Robert Weinstein, Stavros Manolagas. University of Arkansas for Medical Sciences, USA

Intermittent administration of PTH is an effective anabolic therapy in the elderly but the underlying mechanisms are poorly understood. Studies in mice have revealed that age-related bone loss is associated with increased levels of reactive oxygen species (ROS) and phosphorylated $p66^{Shc}$ (an amplifier of oxidative stress), decreased glutathione, and decreased Wnt signaling, osteoblast survival and bone formation rate (BFR). The reduction in Wnt signaling is due to activation of FoxO transcription factors by ROS, resulting in diversion of β-catenin from Tcf- to FoxO-mediated transcription; and to activation of PPARγ by oxidized lipids produced by Alox15, leading to proteasomal degradation of β-catenin. Increased expression of Alox15 also contributes to oxidative stress by producing the pro-oxidant 4-hydroxynonenal. Based on these advances, we investigated whether PTH antagonizes the cellular and molecular mechanisms leading to age-related bone loss. Daily injections of 100 ng/g of PTH(1-34) produced a greater increase in vertebral trabecular bone mineral density and cancellous bone volume, and a greater expansion of the endocortical bone surface in the femur, in 26 as compared to 6 month old female C57BL/6 mice. PTH increased trabecular connectivity in vertebrae and the toughness of both vertebrae and femora in old, but not young, mice; and increased BFR and reduced osteoblast apoptosis to a greater extent in old mice. Most strikingly, PTH reduced ROS, phosphorylated $p66^{Shc}$ and Alox15, and increased glutathione, in bone of old mice. PTH also increased Wnt signaling in old mice as indicated by the expression of 8 Wnt target genes. Moreover, PTH attenuated the H_2O_2-induced increase in ROS, phosphorylated $p66^{Shc}$, as well as H2O2-induced suppression of Wnt signaling in cultured osteoblastic cells; and increased expression of the anti-oxidant enzyme aldehyde dehydrogenase 3a1 by 10-fold in vitro and in vivo. These findings suggest that PTH-stimulated Wnt signaling is augmented in aged mice by the ability of the hormone to attenuate pathways that would otherwise reduce β-catenin, i.e. activation of FoxOs by ROS, and activation of PPARγ by oxidized lipids. We propose that the increased efficacy of intermittent PTH in the aged skeleton is due to a novel anti-oxidant effect that increases osteoblast survival and enhances the ability of the hormone to stimulate Wnt signaling. Thus, PTH represents a mechanistically rational therapy for osteoporosis in the elderly.

***Disclosures: Robert Jilka**, Radius Health, Inc., 1*

FR0425

Sclerostin Antibody Treatment Enhances Fracture Healing and Increases Bone Mass and Strength in Non-fractured Bones in an Adult Rat Closed Femoral Fracture Model. CY Li*, HL Tan, M Barrero, E Lee, FJ Asuncion, MS Ominsky, HZ Ke. Amgen Inc, USA

Inhibition of sclerostin with a sclerostin antibody (Scl-Ab) significantly increased bone formation, resulting in increased bone mass and bone strength in animal models of osteoporosis. Bone formation also plays an important role in fracture healing, and Scl-Ab was shown to increase bone mass and bone strength in the fractured bones of adolescent mice, rats, and monkeys. In this study, we further examined the effect of Scl-Ab on fracture healing in skeletally mature rats.

Seven to 7.5-month-old male SD rats underwent a standard closed femoral mid-diaphyseal fracture stabilized with an intramedullary pin. Animals were subcutaneously injected with saline (Veh, n=18) or Scl-Ab at 25 mg/kg (n=14), twice per week for 7 weeks. Both fractured and intact contralateral femurs were collected for densitometry (DXA and micro-CT) and bone strength testing (3-point bending) at the end of the study.

In the central 30% of the fractured femurs, Scl-Ab significantly increased DXA BMD and BMC by 11% and 19%, respectively, compared with Veh (both $p<0.05$). The fracture callus was isolated from the original cortex by micro-CT, and a 1mm region at the fracture line was analyzed. Scl-Ab significantly increased callus region area (+16%), callus vBMC (+26%), and callus bone volume/total volume (+41%) compared with Veh (all $p<0.05$). The Scl-Ab-mediated increase in bone mass at the fracture site was associated with increased bone strength, as demonstrated by a 76% increase in peak load and a 125% increase in stiffness compared with Veh (both $p<0.05$).

Scl-Ab also increased bone mass in the intact contralateral femur, as demonstrated by significant increases in micro-CT vBMC at the cortical diaphysis (+10%) and the trabecular region of the distal metaphysis (+39%) compared with Veh (both $p<0.05$). The increase in diaphyseal vBMC with Scl-Ab was associated with a significant increase (+17%) in peak load in the contralateral femurs compared with Veh ($p<0.05$).

In summary, systemic administration of a sclerostin antibody improved bone mass and bone strength in the fractured and intact long bones of skeletally mature rats. These results support the potential use of sclerostin antibody as a therapeutic to enhance fracture healing in adults.

***Disclosures: CY Li**, Amgen Inc., 1; Amgen Inc., 3*
This study received funding from: Amgen Inc.

FR0427

The Osteoanabolic Effect of Systemic Dkk1 Inhibition is Associated with Canonical Lrp5/6 and Erk Signaling in Bone and is Modulated by N-cadherin in Osteoblasts. Valerie Salazar*[1], Jin Norris[2], Lisa Huang[2], Gabriel Mbalaviele[2], Roberto Civitelli[1]. [1]Washington University in St. Louis School of Medicine, USA, [2]Washington University School of Medicine, USA

Neutralizing antibody to Dkk1, a natural antagonist to Lrp5/6, increases bone mass. We previously reported that mice lacking the *N-cadherin* gene specifically in osteoblasts (*$Cdh2^{flox/flox}$; Col1α1Cre*) require 4-fold less Dkk1 neutralizing antibody (αDkk1) to generate a bone anabolic response (5mg/kg compared to 20mg/kg for *wild type* controls). To understand the mechanism of enhanced sensitivity in *$Cdh2^{flox/flox}$; Col1α1Cre* (*Ncad cKO*) mice, we investigated the molecular mechanism of action of αDkk1. Western blot analysis on protein from tibias of *wild type* (*WT*) mice indicates that a bone anabolic dose of αDkk1 (20mg/kg) stimulates phospho-inhibition of GSK3β, accumulation of β-catenin, and phospho-activation of Jnk. Thus, systemic inhibition of Dkk1 leads to rapid activation of canonical Lrp5/6 signaling in bone. In *WT* mice, this signal cascade peaks 30 minutes post-injection, returns to baseline at 60 min, and is reactivated at 2 hrs. By contrast, accumulation of β-catenin is sustained in tibias from *Ncad cKOs*, and only 5mg/kg αDkk1 is required for Lrp5/6 pathway activation. Thus, osteoblast N-cadherin antagonizes activation of, and prevents prolonged signaling through, the Lrp5/6 pathway in bone. This may be partially explained by increased mRNA expression of *Lrp5* in *Ncad cKO* mice. *Dkk1*, *SOST*, and *β-catenin* mRNA are unchanged. Systemic inhibition of Dkk1 also regulates Erk1/2 in bone. In *WT* tibias, a sub-anabolic dose of αDkk1 (5mg/kg) is sufficient to stimulate Erk1/2, which peaks at 45 min and returns to baseline by 2 hrs. By contrast, Erk1/2 phosphorylation cycles are weaker and more rapid in *Ncad cKOs*, yielding 2 distinct peaks in 2 hrs. Thus, N-cadherin promotes high and sustained levels of Erk1/2 activity in bone. Moreover, the strength and kinetics of Erk1/2 activity in *WT* mice following an anabolic dose of αDkk1 (20mg/kg) more closely

resemble that of *Ncad cKOs*. Hence, Dkk1 inhibition generates dose-dependent Erk1/2 activity profiles in bone that are sensitive to expression of N-cadherin in osteoblasts. In summary, accrual of bone mass in response to systemic inhibition of Dkk1 is accompanied by bone-specific signaling through canonical components of the Lrp5/6 pathway and Erk1/2. Removing *Cdh2* selectively in osteoblasts modulates local signaling through Lrp5/6 and Erk1/2, resulting in enhanced sensitivity to the osteoanabolic effect of Dkk1 inhibition.

***Disclosures: Valerie Salazar**, None.*

FR0430

Prolonged Bisphosphonate Release after Treatment in Women with Osteoporosis. Relationship with Bone Turnover. Pilar Peris*[1], Merce Torra[2], Ana Monegal[2], Varinia Olivares[3], Raquel Reyes[3], Angels Martinez-Ferrer[2], Nuria Guanabens[4]. [1]Hospital Clinic of Barcelona, Spain, [2]Hospital Clinic Barcelona, Spain, [3]Hospital Clinic, Spain, [4]Universitat De Barcelona, Spain

Bisphosphonates (BP), especially alendronate and risedronate, are the most commonly used drugs for osteoporosis treatment. These compounds are incorporated into the skeleton, where they inhibit bone resorption. Thereafter BP are slowly released during bone turnover. However, at present, there are few data on the release of BP in patients who have received treatment with these drugs for osteoporosis. This information is essential for evaluating the possibility of BP cyclic therapy in these patients and for controlling their long-term presence in bone tissue. Therefore, the aim of the study was to evaluate the urinary excretion of alendronate and risedronate in patients who have been treated with these drugs for osteoporosis and to analyze its relationship with bone turnover, time of previous drug exposure and time of treatment discontinuation.

Methods: we included 43 women (aged 65±9 years) who had been previously treated with alendronate (n=36) or risedronate (n=7) for osteoporosis and had not been treated with other antiosteoporotic treatment prior to the analysis. Both BP were detected in 24-hour urine by HPLC. Weight, height, length of treatment, time of treatment cessation and renal function were recorded in all patients. In addition, coincident with BP determination, bone formation (PINP) and bone resorption (NTX) markers were analyzed. Both BP were also determined in urine in a control group of 7 women during alendronate or risedronate treatment.

Results: Alendronate was detected in 41 % of women who had been previously treated with this drug whereas no patient previously treated with risedronate showed urinary detectable values of this BP. All control group patients showed detectable values of both types of BP. In patients with detectable alendronate levels the time of drug cessation was shorter than in patients with undetectable values of this BP (11.8±3.8 vs 30.7±19.9 months, $p<0.001$). No patient with more than 19 months from cessation of alendronate treatment showed detectable values of the drug. Alendronate levels were inversely related to time of treatment discontinuation ($r=-0.403$, $p=0.01$) and the latter was directly related to the bone resorption marker NTX ($r=0.394$, $p=0.02$). No relationship was observed with age, length of drug exposure, renal function or weight.

Conclusions: Contrary to risedronate, which was not detected in patients after cessation of treatment, alendronate was frequently detected in women previously treated with this agent up to 19 months after discontinuation of therapy. The relationship between alendronate levels and both bone resorption and time of treatment cessation further indicates a residual effect of this drug in bone despite treatment discontinuation.

***Disclosures: Pilar Peris**, None.*

FR0431

Skeletal Uptake and Desorption of Fluorescently Labeled Bisphosphonate is Anatomic Site-Dependent. Demin Wen[1], Liu Qing[2], Gerald Harrison[1], Ellis Golub[3], Sunday Akintoye*[1]. [1]University of Pennsylvania, USA, [2]The Fourth Military Medical University, China, [3]University of Pennsylvania School of Dental Medicine, USA

Objectives. Bisphosphonates commonly used to treat osteoporosis, Paget's disease, multiple myeloma and hypercalcemia of malignancy have been associated with bisphosphonate-associated jaw osteonecrosis (BJON). A potential etiological factor is disproportionate concentration of bisphosphonate in the jaws; but it is unclear if regional biodistribution and bioavailability of bisphosphonates is site-dependent. Using a rat model, we tested the hypothesis that skeletal uptake and release of pamidronate (a nitrogen-containing bisphosphonate) is anatomic site-dependent.

Methods. Four female nude rats received tail vein injection of 80 nmol/kg body weight of fluorescently-tagged pamidronate (OsteoSense^{TM}680) followed by optical imaging after 24 hours. On sacrifice, individual bone parts were recovered and re-scanned using similar *in vivo* imaging parameters. Bound bisphosphonate in bone parts was desorbed using sequential EDTA decalcification. Bisphosphonate signal intensity per unit area normalized to adjacent background intensity was expressed as relative fluorescence units (RFU) after defining specific regions of interest (ROI) correlating with bone sections subjected to bisphosphonate desorption. Recovered labeled bisphosphonate was measured with a fluorometer while calcium released in solution was measured with a flame atomic absorption spectrophotometer. Mean site-specific RFU was correlated with bisphosphonate and calcium amounts from corresponding bone sections. Skeletal site differences of ROIs were analyzed and compared based on oral, axial and appendicular regions. Data expressed as mean ± standard deviation was analyzed by one-way ANOVA followed by Dunn-Sidak post hoc multiple comparisons with statistical significance set at $p < 0.05$.

Results. Bisphosphonate signal intensity was similar in oral and appendicular bones but lower in axial bones. However, liberation of hydroxyapatite-bound bisphosphonate following sequential EDTA decalcification resulted in significantly higher bisphosphonate release from oral bones relative to axial and appendicular sites ($p < 0.05$).

Conclusions. This study demonstrated regional site-disparity in rat skeletal uptake and release of bisphosphonate in oral, axial and appendicular bones that suggest possible preferential bisphosphonate uptake in the jaw bone. (Work supported by NIH/NIAMS research grant AR050950, University of Pennsylvania Research Foundation and USPHS/NIH/NCI grant 5K08CA120875-03).

***Disclosures: Sunday Akintoye**, None.*

FR0432

Insulin like Growth Factor and Bone Mass is Influenced by Higher Protein Intake During One Year of Caloric Restriction. Deeptha Sukumar*[1], Hasina Ambia- Sobhan[1], Robert Zurfluh[1], Theodore Stahl[2], Sue Shapses[1]. [1]Nutritional Sciences, Rutgers University, USA, [2]Department of Radiology, University of Medicine & Dentistry/Robert Wood Johnson Medical School, USA

Weight (wt) reduction induces bone loss by several factors including reduced Ca absorption and serum insulin-like growth factor-1 (IGF-1). The role of high protein (HP) diets on bone is controversial; the negative effects mediated by higher urinary Ca excretion and acid load, and positive effects by increasing serum IGF-1 and Ca absorption. Previous studies examining the effect of protein intake on bone during wt loss have not controlled for Ca intake (diets either being deficient or excessive in Ca intake). Our goal was to examine how bone responds to caloric restriction during a 1 year randomized trial using 2 levels of protein intake with controlled Ca intake of 1.2 g/day. We screened 182 women (2006-2009) and after drop-outs/exclusion, 47 (58.0 ± 4.4 years; body mass index of 31.4 ± 4.6 kg/m^2) were allocated to either a normal (NP, 18%, n = 21) or higher (HP, 30%, n = 26) protein and a lower fat intake (28%). We measured bone mineral density and content (BMD, BMC), fat and lean mass using dual energy x-ray absorptiometry and serum and urine were analyzed for bone regulating hormones and turnover markers. After 1 year, subjects lost 6.4 ± 4.7 % of body wt, 11.8% of fat mass and 2.8 % of lean mass with no differences between the groups. Protein intake was 18% (60 g/d) and 24% (86 g/d) of total calories in the NP and HP groups, respectively. Intake of Ca, vitamin D and other nutrients were not significantly different between the groups. Repeated measures ANOVA using diet (HP and NP) and time (0, 6 and 12 months) showed a significant interaction resulting in greater loss of BMD at ultra distal radius, lumbar spine and hip in the NP compared to HP diet. There was also a greater increase in bone resorption (deoxypyridinoline) in the NP than HP group ($p < 0.05$; trend for PYD). The HP diet resulted in greater increases in IGF-1 and its binding protein (IGFBP-3) ($p < 0.05$), and tended to increase estradiol ($p=0.06$) more than the NP group. Interestingly, caloric restriction (in both groups) reduced serum parathyroid hormone ($p < 0.05$), increased 25-hydroxy-vitamin D by 2.6 ± 5.2 ng/mL ($p<0.001$) and pyridinoline crosslinks (PYD) ($p<0.02$). These data show that the positive effect of dietary protein on bone is not due to higher Ca intake. In summary, a higher dietary protein- calorie restricted diet that increases serum IGF-1 and IGFBP-3 may be responsible for attenuating bone loss at certain sites in postmenopausal women.

***Disclosures: Deeptha Sukumar**, None.*

FR0435

A Multi-Modality Imaging Comparison of Odanacatib to Alendronate in the Ovariectomized Rhesus Monkey. Paul McCracken*[1], Richa Jayakar[2], Mona Purcell[1], Parker Mathers[1], Alan Savitz[1], John Szumiloski[1], Jacquelynn Cook[1], Bernie Dardzinski[2], Thomas Hangartner[3], Sherri Motzel[1], Richard Hargreaves[1], Jeffrey Evelhoch[1], Le Thi Duong[1], Donald Williams[1]. [1]Merck Research Laboratories, USA, [2]Merck & Co., Inc., USA, [3]Wright State University, USA

The aim of this study was to evaluate efficacy of the Cathepsin K inhibitor, odanacatib (ODN), and compare to alendronate (ALN) in the estrogen-deficient model of the ovariectomized (OVX) rhesus monkey by multiple imaging modalities. Macro- and micro-architectural imaging markers relevant to bone strength were measured at multiple anatomic locations at baseline, 3, 6, 9, 12, and 18 months of treatment in OVX-monkeys (16/group, age 10-22 yrs) treated with either vehicle (VEH), ODN (2 mg/kg/d) or ALN (30 ug/kg/week) for 20-months. BMD, cortical and cancellous parameters were interrogated in the ultradistal radius, ultradistal tibia, distal radius and distal tibia by hr-pQCT (XtremeCT, Scanco Medical), similar regions by MRI (Siemens TIM Trio), lumbar vertebrae and proximal femur by quantitative CT (GE-DST), and in standard locations by DXA (GE Lunar iDXA). QCT analysis was done using QCTPro (Mindways Software, Inc.), modified for non-human primate analysis. QCT trabecular vBMD of the spine increased by 11% and 9.9% for ODN and ALN, respectively, by 18 months of therapy and were significantly ($p<0.001$) higher than VEH. QCT integral vBMD taken from a 1.5mm region in the

femoral neck increased by 11% for ODN and 6.8% for ALN, where ODN was significantly higher than ALN (p=0.028) and VEH (p<0.001). VBMD by hr-pQCT (D100) in the ultradistal radius and ultradistal tibia increased by 13.9% and 12.7% respectively for ODN and 2% and 8.2% for ALN, where ODN was significantly higher than ALN (R p<0.001, T p<0.001) and VEH (R p<0.001, T p=0.031). Cortical thickness by hr-pQCT in the ultradistal radius and ultradistal tibia increased by 25.1% and 17%, respectively, for ODN and 1% and 8.2% for ALN, where ODN was significantly higher than ALN (p<0.001, p=0.003) and VEH (p<0.001, p=0.012). Cortical thickness by hr-pQCT in the distal radius and distal tibia increased by 6.7% and 5.6%, respectively, for ODN and 2.9% and 2.4% for ALN, where ODN was significantly higher than ALN (p=0.039, p=0.014) and VEH (p=0.001, p=0.030). In summary, in-vivo imaging markers have demonstrated the positive therapeutic effects of ODN and differentiated ODN from ALN on vBMD in the hip, radius and tibia, and cortical thickness in the radius and tibia of OVX rhesus monkeys. The translational application of imaging parameters relevant to fracture risk at multiple skeletal sites will be evaluated in odanacatib clinical trials.

***Disclosures: Paul McCracken**, None.*

FR0438

Efficacy of ONO-5334, a Cathepsin K Inhibitor, on Bone Mass and Strength in Ovariectomized Cynomolgus Monkeys. Hiroyuki Yamada*, Hiroshi Mori, Akiko Kunishige, Satoshi Nishikawa, Yasuaki Hashimoto, Makoto Tanaka, Tsutomu Shiroya. ONO Pharmaceutical Co., Ltd., Japan

ONO-5334 is a small molecule and an orally-active inhibitor of cathepsin K, which plays an important role in osteoclast-mediated bone resorption. We have previously reported that ONO-5334 increased lumbar areal BMD (L3-5) compared with ovariectomized (OVX) control in cynomolgus monkey 1). Therefore, we evaluated the efficacy of ONO-5334 on integral, trabecular and cortical BMC, separately, and bone strength in the lumbar vertebra in this study.

Female cynomolgus monkeys were assigned to one of the following 6 groups (20 per group): sham operated, OVX control treated with vehicle, ONO-5334 1.2, 6 or 30 mg/kg, or alendronate (ALN) 0.05 mg/kg. ONO-5334 was administered orally once daily from the day following OVX surgery for 16 months. ALN was administered intravenously once every 2 weeks. After necropsy, bone mass (volumetric BMC) and strength (maximum load) at the 4th lumbar were measured by pQCT and compression test, respectively.

OVX caused a significant decrease in cortical vBMC (p<0.05 vs sham). ONO-5334 at 6 and 30 mg/kg significantly increased integral and cortical vBMC (both p<0.05 vs OVX) and increased trabecular vBMC to sham level. ALN tended to increase cortical vBMC. Maximum load and ultimate strength (maximum load divided by cross sectional area) tended to decrease due to OVX and significantly increased by ONO-5334 at 6 and 30 mg/kg (both parameters p<0.01 vs OVX). ALN tended to increase ultimate strength. Maximum load was significantly correlated with integral vBMC in OVX + ONO-5334 groups (r=0.80, p<0.0001).

These results suggest that ONO-5334 increases bone mass by affecting cortical bone as well as trabecular bone in the lumbar vertebra. In addition, ONO-5334 has a positive effect on bone strength. A good linear relationship between bone mass and strength was confirmed, and suggests that the increase in bone mass with ONO-5334 treatment corresponds to a parallel increase in bone strength.

1) Yamada H, et al. ASBMR, 2009, FR0420.

***Disclosures: Hiroyuki Yamada**, None.*

FR0439

N-Butyryl Glucosamine (GlcNBu) Preserves Bone in the Ovariectomised Rat Model: Possible Mechanism through Serotonin Reuptake Inhibition. Karen Rees_Milton*[1], Marc Grynpas[2], Tassos Anastassiades[3]. [1]Dept of Medicine, Queen's University, Canada, [2]Samuel Lunenfeld Research Institute, Canada, [3]Queen's University, Canada

Purpose: Studies in bone homeostasis in post-menopausal OP have emphasized primarily osteoclastic rather than osteoblastic (OB) regulation. We have been using a model of post-menopausal OP, the ovariectomised (Ovx) rat, for pre-clinical studies of N-butyryl glucosamine (GlcNBu), as an agent for preventing OP in this model. We had reported that secreted phosphoprotein 24 (spp24) was significantly up-regulated in the livers of the Ovx rats, suggesting an indirect protective effect of GlcNBu on the bone through the liver. Here we report on a possible direct mechanism of action of GlcNBu at the OB level, through serotonin (SR or 5-hydroxytryptamine, 5HT) reuptake inhibition (SSRI). The skeletal effects of SSRIs are uncertain but functional 5HT and 5HTT (5HT transporter) receptors in bone cells have been identified.

Methods: The groups of mature female rats were: Glucose (Glc)-fed, non-OVX (control); GlcNBu-fed, non-OVX; Glc-fed, OVX; GlcNBu-fed, OVX. At 6 months, animals were euthanized and the bones evaluated for bio-mechanical properties and bone mineral densities (BMD). We quantified spp24 in the sera by immunoassay, utilizing chitosan coated plates, permitting preliminary isolation of the spp24 (Anal. Biochem. (2010) 396(2):310-2). The proliferation of the OB cell line, UMR-106, in the presence and absence of SR and the SSRI fluoxetine hydrochloride was studied, using the quantitative Perkin Elmer ATPlite chemiluminescence assay.

Results: Ovariectomy resulted in lower femoral and spinal BMDs. GlcNBu-fed OVX rats demonstrated maintenance of femoral head, total femur and spine BMDs. Orally administered GlcNBu, preserved bone biomechanical properties in the OVX rat. There was a strong positive correlation between serum spp24 and IGF-1 concentrations. Experiments with UMR-106 indicate that OB proliferation and alkaline phosphatase activity is suppressed by SR, and more so by the SSRI, fluoxetine hydrochloride, in a dose-dependent fashion. Pre-incubating the UMR-106 cells with GlcNBu significantly reverses the SSRI-dependent inhibition, but less so SR-dependent inhibition.

Conclusions: 1. Orally administered GlcNBu, preserves BMD and bone biomechanical properties in the OVX rat. 2. At the OB level, GlcNBu may be acting through the re-uptake mechanism of SR. 3. At the level of the liver, GlcNBu's protective effect on bone may be indirectly mediated by spp24, possibly through IGF-1.

***Disclosures: Karen Rees_Milton**, None.*

FR0440

Quantitative Computed Tomography Based Finite Element Analysis to Estimate *In-Vivo* Bone Strength of Proximal Femur in Odanacatib Treated Rhesus Monkeys. Antonio Cabal*[1], Seetha Ramudu Kummari[2], Stephen Krause[1], Mona Purcell[1], Paul McCracken[3], Le Thi Duong[3], Bernard Dardzinski[1], Sherri Motzel[1], Donald Williams[1]. [1]Merck & Co., Inc., USA, [2]Case Western Reserve University, USA, [3]Merck Research Laboratories, USA

Preclinical evaluation of disease burden and treatment efficacy is critical to the development of new therapies for osteoporosis. Clinically translatable imaging modalities beyond DXA, such as quantitative computed tomography (QCT) has the potential to estimate bone strength *in-vivo* using image-based finite element analysis (FEA). The effects of Cathepsin K inhibitor, odanacatib (ODN), on *in-vivo* estimates of bone strength in the proximal femur was quantified using QCT (GE Healthcare) of the hip based fall loading configuration FEA in the estrogen-deficiency induced osteopenia of the ovariectomized (OVX) rhesus monkey. QCT data were obtained for three OVX groups of monkeys treated with vehicle (VEH), 2 mg/kg ODN (daily oral), and alendronate (ALN, subcutaneous 15 ug/kg twice weekly; n=16/group, age 11-18 years at study start). ODN was dosed with a novel VEH (different from our previous monkey study) which significantly improved bioavailability of ODN to approximately 13 uM per 24 hours. Longitudinal QCT measurements were made at 0, 12, and 18 months post-treatment, with the treatment starting within 10 days of OVX. Strength of the proximal femur was defined as 4% deformation of the (non-linear force-deformation curve) femoral head with respect to the greater trochanter. Percent change of strength from baseline (pre-treatment) for the ODN, ALN, and VEH groups at 18 months were 17.1%, 6.4%, and 3.2%, respectively, with ODN group showing statistically significant differences (p<0.05) from the VEH and ALN groups. Measurable differences were observed in the geometry, average volumetric BMD, and FEA estimated hip bone strength between the ODN-treated group as compared to ALN- and VEH-treated estrogen deficient non-human primates.

***Disclosures: Antonio Cabal**, None.*

FR0442

Increased Bone Cell Vitamin D Activity: The Basis for Synergy between Dietary Calcium and Vitamin D for Bone Health? Howard Morris*[1], Alice Lee[2], Rebecca Sawyer[3], Shunji Iida[4], Peter O'Loughlin[5], Paul Anderson[3]. [1]SA Pathology, Australia, [2]Discipline of Physiology, University of Adelaide, Australia, [3]Endocrine Bone Laboratory, Hanson Institute, Australia, [4]Oral Functional Science, Hokkaido University, Japan, [5]Chemical Pathology, SA Pathology, Australia

Clinical studies indicate that the combination of vitamin D and dietary calcium supplementation reduces the risk of fracture to a greater extent than either supplement alone. Preclinical dietary studies indicate that an adequate vitamin D status reduces osteoclastogenesis and increases trabecular bone volume.[1] We now report data from further preclinical dietary studies of high dietary calcium increasing 25-hydroxyvitamin D (25D) metabolism by bone cells associated with increased cortical and trabecular bone volumes and increased bone strength. Female Sprague-Dawley rats aged 6 or 9 months of age were fed either 0.1% or 1% calcium supplemented AIN-93-VX diets containing 0, 100, 600, or 1000 IU vitamin D3/kg for 3 or 6 months following which they were killed and blood, kidney, femora and tibia collected for analyses. 25D-1α-hydroxylase (CYP27B1) mRNA was analysed in bone and kidney by quantitative RT-PCR. Cortical and trabecular bone regions were analysed by micro-CT and Ultimate Load measurement was obtained from 3-point bending at the tibia. Bone CYP27B1 mRNA levels were 3 to 4 fold higher in animals fed 1% compared to 0.1% calcium diets (P<0.05) independent of vitamin D status which was opposite to these mRNA levels in kidney. Mean serum 25D levels ranged from 14.0($\pm$1.5) to 161($\pm$38.8) nmol/L. Regression analyses demonstrated significant positive relationships between serum 25D and proximal femoral trabecular bone volume (R^2 =0.23, P<0.01) and femoral cortical bone volume (R^2 =0.22, P<0.01). The increase in femoral cortical bone volume with increasing serum 25D level was significant with animals fed 1% calcium (P<0.05) with no change in animals fed the 0.1% calcium diet. Mechanical testing demonstrated that Ultimate Load measurement was highest on tibiae from animals fed 1% calcium and the highest vitamin D diets (P<0.05). An adequate vitamin D status (serum 25D levels >80 nmol/L) is required to maintain cortical and trabecular bone volumes in mature rats fed a 1% calcium diet but these levels of vitamin D cannot maintain these bone volumes in animals fed 0.1% calcium

diet. The maintenance of bone volume is independent of serum 1,25D and PTH levels. The increased bone volume with 1% diet calcium is associated with increased mRNA levels for bone CYP27B1 responsible for bone cell conversion of 25D to 1,25D.

[1]Anderson et al JBMR 2008; 23: 1789-97

***Disclosures: Howard Morris**, None.*

FR0445

PTH and ALN reduce fractures and alter bone mechanical properties in the *oimloim* mouse model of OI. Cesare Ciani*[1], Kirsten Stoner[2], Michael Cross[1], Liza Osagie[1], Bettina Willie[1], Marjolein Van Der Meulen[2], Mathias Bostrom[1]. [1]Hospital for Special Surgery, USA, [2]Cornell University, USA

Osteogenesis Imperfecta (OI), a genetic disorder typically caused by a mutation in Type I collagen, manifests with defective connective tissue resulting in multiple skeletal fractures. Intermittent bisphosphonate therapy is the standard treatment, while parathyroid hormone (PTH) is currently under evaluation as an alternative. This study investigated the effects of PTH, both individually and in combination with alendronate (ALN) in the oim/oim mouse model of OI.

68 oim/oim mice and 68 wild type (WT) mice were randomized into 4groups: saline, ALN, PTH and PTH+ALN, each for 12weeks. A baseline untreated OI group was euthanized at 4weeks (Table 1). Outcome measurements included fracture incidence, cancellous histomorphometry and three-point bend testing.

Fracture number was reduced in all OI treated groups compared to the OI saline group ($p<0.05$), with ALN causing the greatest reduction (2.5 compared to 5.4 of the saline group), and PTH+ALN the least (Figure 1). ALN increased trabecular number in both OI and WT mice (9.1 and 9.4 respectively compared to 2.9 and 4.8 in OI and WT saline groups). ALN and ALN+PTH significantly increased bone volume fraction (BV/TV) in OI mice compared to OI PTH group, resulting in BV/TV values equal to untreated WT levels (Figure 2). PTH did not alter any cancellous histomorphometry. ALN decreased energy to failure and increased bending stiffness in all groups. In OI mice PTH+ALN restored strength and energy to failure to WT saline levels. ALN and PTH+ALN treatments increased bending strength in OI mice.

While PTH alone did not alter cancellous histomorphometry, fracture incidence was reduced comparable to ALN treatment. PTH+ALN improved cancellous architecture and reduced fracture number. Reduction in fracture number can be attributed to increased bone volume fraction when OI bone was treated with ALN. Individual ALN treatment produced brittle behavior in both OI and WT femora, but used in combination with PTH strength and ductility were rescued to WT levels. Ultimately, PTH and ALN's effect on fracture number, and their synergistic effect on mechanical properties cannot solely be ascribed to morphological changes, but reflects changes in intrinsic bone tissue material properties to be assessed in future studies.

Table 1: PTH and saline were injected daily at a dose of 30 µg/kg. Alendronate was injected weekly at a dosage of 0.03 mg/kg.

Genotype – age	Baseline	12 weeks Saline	12 weeks PTH	12 weeks ALN	6 weeks PTH +6 weeks ALN
oim/oim – 4 weeks	n = 13	n = 17	n = 17	n = 17	n = 17
+/+- 4 weeks	n = 0	n = 17	n = 17	n = 17	n = 17

Figure 1: Fracture number in OI mice; * p < .05 vs baseline; ** p < .05 vs saline.

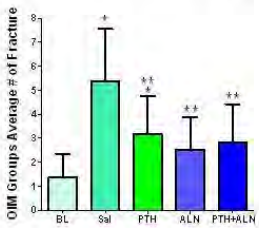

Figure 2: Trabecular bone volume fraction (BV/TV); * p < .05 vs OI baseline, saline and PTH; # p < .05 vs wt saline and PTH; ## p < .05 vs WT ALN.

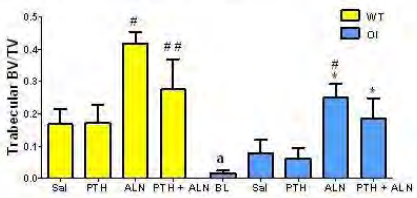

Tables_figures

***Disclosures: Cesare Ciani**, None.*
This study received funding from: Osteogenesis Imperfecta Foundation

FR0446

Bone turnover and 1,25-dihydroxyvitamin D are independent determinants of circulating FGF23: a sub-analysis of CHIBA (Coronary Heart Disease of Ischemia and Bone Association) study. Daisuke Inoue*[1], Toshihiro Amaki[1], Yuichiro Shimizu[2], Seiji Fukumoto[2], Yusuke Nakatsu[1], Kengo Ayabe[1], Jun-ichi Ohashi[1], Tadanao Higaki[1], Nobuyuki Tai[1], Fumitaka Nakamura[1], Ryo Okazaki[1]. [1]Teikyo University Chiba Medical Center, Japan, [2]University of Tokyo Hospital, Japan

FGF23 is a phosphaturic hormone physiologically secreted by cells of the osteoblast lineage. Despite accumulating knowledge on its function and mode of action, little is known about in vivo regulators of FGF23 production. We previously reported that in 301 male subjects who visited the cardiovascular unit of our department for coronary angiography, bone turnover markers, particularly MMP-dependent ICTP, was a good predictor of both cardiac damage (proBNP) and dysfunction (LVEF). In the present study, we aimed to identify determinants of circulating levels of FGF23 in a part of this cohort. Subjects included in this sub-analysis were 168 males (64±11y.o.) with normal renal function (eGFR>60 ml/min).

We found that intact FGF23 levels were significantly correlated most strongly with ICTP (r=.254, p=0.001), and also with TRACP-5b and N-mid osteocalcin, but not with βCTX, BAP, PICP, Ca, P, hsCRP or proMMP-9. 1,25D was also negatively correlated with FGF23 as expected. There was a positive correlation between 25D and 1,25D, and a negative association between PTH and 25D, but neither 25D nor PTH showed a correlation with FGF23. And the correlation between ICTP and FGF23 remained significant even after adjusted for PTH, 25D, 1,25D, Ca, P, parameters of glucose and lipid metabolism, hsCRP, proMMP-9, proBNP and LVEF. Interestingly, stepwise multiple regression analysis revealed ICTP, 1,25D and blood sugar (BS) as independent determinants of FGF23. HbA1c and C-peptide correlated with BS, but not with FGF23. These results were intriguing in light of the fact that osteocalcin secreted by osteoblasts regulates glucose metabolism. However, we were unable to find any association of undercarboxylated osteocalcin (ucOC) with BS or FGF23 in this population. And although the association between BS and FGF23 seemed stronger in those with high BS, exclusion of the highest extremes resulted in loss of statistical significance. Thus, a possible association between FGF23 and high BS in a diabetic range remains an open question.

Collectively, these results demonstrate a novel link of FGF23 secretion to bone turnover, and possibly blood glucose as well. Our observations further suggest that FGF23 production by osteoblasts and osteocytes may be under the influence of the same regulatory mechanism that controls their endocrine and paracrine function governing bone and glucose metabolism.

***Disclosures: Daisuke Inoue**, None.*

FR0451

Effect of Vitamin D Nutrition on Indices of Disease in Patients With Primary Hyperparathyroidism. Sudhaker Rao, Joanna Miragaya*, Sara Ahmadi, Liliana Garcia, Nayana Parikh, Mahalakshmi Honasoge, Arthur Carlin, Gary Talpos, Meredith Mahan, Sudhaker Rao. Henry Ford Hospital, USA

Vitamin D nutrition has been implicated in the clinical expression of primary hyperparathyroidism (PHPT) in most, but not all studies. However, very little is known about the effect of vitamin D nutrition on biochemical indices of disease severity. Accordingly, we determined the effect of vitamin D nutrition, as assessed by serum 25-OHD (the best available index of vitamin D nutrition) on adenoma weight, and on biochemical indices of disease severity, as assessed by serum calcium (Ca), PTH, alkaline phosphatase (AP) and phosphate (P) in a large cohort of 933 patients with surgically verified PHPT and normal renal function.

Materials & Methods: All patients with normal renal function, defined as serum creatinine <1.5 mg/dl, operated between January 1, 1992 and December 31, 2007 were included. Patients with familial PHPT, renal failure, failed surgery, and persistent PHPT were excluded. Parathyroid pathology was based on the report. Vitamin D status was defined by serum 25-OHD level. A level <20ng/ml was considered deficiency in the initial analyses, and the analyses were repeated with cut-off levels of <15 ng/ml and <30 ng/ml.

Results: Among the 933 patients there were: 461 blacks and 845 women with a mean age of 61 ± 12y. Other relevant data are in the Table. Adenoma weights are shown both in arithmetic mean ± SD and geometric mean ± multiplicative SD. As a group, patients with 25-OHD <20 ng/ml had larger tumors, and greater effect on disease indices (higher PTH, AP (total and bone specific), and lower P). Serum Ca, creatinine and 1,25DHCC were similar in the 2 groups. There was a highly significant inverse correlation between gland weight and serum 25-OHD level (r= -0.26; p<0.0001). In a multiple regression model only the 25-OHD level was a significant predictor of gland weight with the expected significance for the relationship between gland weight and Ca & PTH. In the ROC analysis to predict tumor weight of either >500 mg or >1000 mg, the AUC for 25-OHD was 0.72 (for both with p<0.001). Results were almost identical for the 25-OHD cut-off level of <15 or <30 ng/ml.

Conclusions: Vitamin D nutrition adversely affects parathyroid adenoma size (growth?) and disease expression as assessed by biochemical markers. Restriction of vitamin D intake for fear of aggravating hypercalcemia in PHPT is not warranted.

Variable	25-OHD <20 ng/ml	25-OHD >20 ng/ml	P Value
25-OHD (ng/ml)	13.2 ± 4.3	27.6 ± 7.3	--
Ca (mg/dl)	11.0 ± 0.8	10.9 ± 0.8	n.s
P (mg/dl)	2.8 ± 0.5	3.0 ± 0.6	0.007
AP (IU/L)	110 ± 63	98 ± 43	0.001
PTH (pg/ml)	168 ± 290	111 ± 90	<0.0001
Adenoma (g)	1.43 ± 4.6	0.84 ± 1.3	0.004
Adenoma (g)*	0.62 ± 3.6	0.45 ± 3.2	0.0007

* Geometric mean and multiplicative SD; Ca is adjusted for albumin

Table: Comparison of Relevant Variables in the Two Groups

***Disclosures: Joanna Miragaya**, None.*

FR0459

Osteocyte Proteins Regulating Mineralization and Systemic Phosphate Homeostasis are Altered Early in CKD-MBD in Humans and *Jck* Mice. Fabiana Graciolli*[1], Luciene dos Reis[1], Yves Sabbagh[2], Wen Tang[3], Stephen O'Brien[3], Shiguang Liu[3], Aluizio Carvalho[4], Rosa Moysés[1], Susan Schiavi[2], Vanda Jorgetti[5]. [1]Universidade de São Paulo - Nephrology Division, Brazil, [2]Genzyme Corp, USA, [3]Genzyme Corporation, USA, [4]Federal University of São Paulo, Brazil, [5]University of São Paulo, Brazil

Disturbances in mineral and bone metabolism occur early in CKD, as illustrated by the early increase in the phosphaturic hormone FGF23 with subsequent elevation of PTH. The relationship of these hormonal changes with the progression of bone disease in CKD is not understood. Additionally, the recent finding that FGF23 expression is regulated by proteins associated with mineralization suggest that osteocyte specific pathways may play a role in coordinating bone mineralization with systemic mineral metabolism in normal physiology that may become deranged during the disease state. As a first step in addressing the natural history of CKD-MBD and the potential role of the osteocyte in the mineral dysregulation associated with CKD progression, we examined the expression of key osteocyte proteins using immunostaining in bone biopsies from patients with early CKD pre-dialysis patients (CKD; n=9; creatinine clearance = 49 ± 17 ml/min), CKD patients on hemodialysis (HD; n=8), and age, sex matched normal individuals (n=4). As shown in Table 1, the total number of osteocytes (Ost) was higher in HD than in CKD patients. We also observed significant increases in percentage of osteocytes expressing SOST, PTHR1 and both total and phosphorylated β-catenin in trabecular bone. As CKD progressed, the number of SOST and PTHR1 expressing cells decreased, whereas the number of of osteocytes expressing phosphorylated β-catenin continued to increase. Interestingly, an increase in the number of FGF23 expressing cells was observed only in stage 5 CKD bones. In order to confirm these findings, we evaluated bones from Jck mice, which is a progressive preclinical CKD model, and we found similar results. Taken together, our data suggest that in CKD, bone changes occur very early, before the detection of biochemical disturbances. The molecular mechanisms involved in CKD bone disease and a causal effect of these proteins expression should be elucidated in further studies.

Table 1. Proteins expression

	Ost	SOST	FGF23	PTHR	β-cat	pβ-cat	MEPE	Phex
Control	391 ± 92	4 ± 2*	9 ± 5*	7 ± 3	4 ± 2	1 ± 1*	5 ± 3*	7 ± 4*
CKD	331 ± 119*	46 ± 25* *	10 ± 5*	19 ± 8*	3 ± 2*	7 ± 6	n.a.	n.a.
HD	508 ± 147	19 ±14	27 ±15	14 ± 10	8 ± 5	13 ± 7	22 ± 19	15 ± 11

*p< 0.05 vs. HD; * p< 0.05 vs. Control; n.a.= not available

Table 1

***Disclosures: Fabiana Graciolli**, Genzyme Corporation, 2*
This study received funding from: Genzyme Corporation

FR0461

Circulating Osteogenic Cells are Decreased in Type 2 Diabetes Mellitus. John Manavalan[1], Aruna Kode[1], Jayesh Shah[1], Daniel Donovan[1], Carlos Lopez-Jimenez[1], James Sliney[1], Rebecca Ives[2], Pat Kringas[1], Lauren Golden[1], Matthew Freeby[1], Stavroula Kousteni[2], Mishaela Rubin*[1]. [1]Columbia University, USA, [2]Columbia University Medical Center, USA

Type 2 Diabetes Mellitus (T2D) is associated with an increased fracture incidence despite normal bone mineral density (BMD). Previous data show suppressed bone formation in T2D, but the mechanisms for this are poorly understood. We hypothesized that the supply of osteogenic cells is decreased in T2D, possibly via effects of insulin resistance on oxidative stress and osteocalcin. Osteogenic cells can be detected in the peripheral blood (PB) by flow cytometry using antibodies for osteoblast-specific ligands, such as osteocalcin (OCN), and the early stem cell markers CD34 and CD146. To evaluate the effects of T2D on these cells, we studied 28 T2D subjects (19 female; 52 ± 14 yrs; fasting plasma glucose: 179 ± 66 mg/dl; HgbA1c 8.9 ± 3%) and 28 matched non-diabetic controls (Cntls). Expression profiling of the cell populations using real time PCR was performed in a small sub-group of T2D (n=3) and matched Cntls (n=3) for OCN, insulin receptor and superoxide dismutase 2 (SOD2), a transcriptional target of the oxidative stress marker forkhead box O1 (FOXO1). The percentage of PB cells that expressed osteocalcin (OCN+) on the cell surface was significantly lower in T2D vs. Cntls (0.7 ± 0.4 vs. 1.3 ± 0.6%; p<0.0001). Although overall OCN+ cells were lower, T2D subjects had more cells that co-expressed the early markers CD34 and CD146. The sub-population of OCN+ cells that co-expressed CD146 was increased in T2D (53.7 ± 40 vs, 6.5 ± 6%; p<0.0001) and there were more OCN+ cells that co-expressed CD34 and CD146 (5.8 ± 7 vs. 2.9 ± 3%; p=0.06) in T2D. In T2D, higher levels of OCN+/CD146+ were significantly correlated with higher HgbA1c levels (r=+0.62, p=0.008) in males. Expression profiling of the OCN+/CD34+ cell populations showed decreased expression in T2D of OCN by more than 2-fold (p<0.05) and of insulin receptor by more than 2-fold (p<0.05), while SOD2 expression was increased more than 2-fold (p<0.05).

These data suggest that T2D subjects have a significant decrease in circulating osteogenic cells, along with a disproportionate increase in the expression of early cell markers. Worsening glycemic control was associated with an increase in early osteogenic cells in diabetic men. Decreased insulin receptor expression may lead to an increase in the FOXO1 target SOD2, which in turn suppresses osteocalcin expression. Alterations in insulin sensitivity and oxidative parameters may be associated with an arrested development of osteogenic cells in T2D.

***Disclosures: Mishaela Rubin**, None.*

FR0462

Deletion of the MDS1 Gene in Mice Results in Disk Degeneration and Kyphosis Through Mis-regulation of Matrix Protein Synthesis by Tendon/ligament Cells. Lianping Xing*[1], Subhash Juneja[2], Caroline Zeiss[3], K Lezon-Geyda[1], D Reynolds[1], Zhenqiang Yao[1], S Lin[1], G Perkins[1], T Ardito[1], W Philbrick[1], H Awad[1], Brendan Boyce[2], Archibald Perkins[1]. [1]University of Rochester, USA, [2]University of Rochester Medical Center, USA, [3]Yale University, USA

Intervertebral disk degeneration (IVDD) and kyphosis frequently accompany osteoporosis in the elderly. However, the causes of IVDD and kyphosis remain poorly understood, and there are few animal models to study these conditions. Here, we generated myelodysplasia syndrome 1 null mice (Mds1-/-) using a lacZ knock-in approach. Mds1-/- mice are viable and at 2 weeks-old exhibit slight lumbar lordosis, reduced vertebral bones and narrowed intervertebral space. The spine abnormalities progress with aging and by 8 weeks-old, their thoracic column becomes extremely kyphotic, which is associated with IVD collapse, vertebral fusion, bone loss (BV/TV (%) in L2: 8+2 vs 40+8 in WT), and reduced vertebral biomechanical strength (Max load (N): 1+0.2 vs 6+1 in WT). Interestingly, long bones of Mds1-/- mice are normal. To investigate the cellular and molecular mechanisms leading to the spine defects, we examined the distribution of Mds1-expressing cells by LacZ staining. We found LacZ+ cells in the sclerotome and developing limbs at E9.5 and within the cartilaginous anlagen of developing vertebral bodies and their processes at E14.5. In newborns, LacZ+ cells were only seen in the tendinous layer surrounding vertebral bodies and anchoring the intercostal muscles to the ribs and in ligaments between vertebral processes. Ultrastructural analyses of sacral and tail tendons and the IVDs of Mds1-/- mice revealed marked disarray of the collagen fibrils with small diameters (Fibril diameter: 74+19 vs 224+61 nM in WT). Because tendon and ligament are closely related and derived from the same lineage in sclerotomes and express scleraxis (scx), a distinct marker for tendon and ligament cells, we cultured tendon cells from Mds1-/- and WT mice and compared the expression levels of tendon and extracellular matrix genes. Mds1-/- tenocytes expressed 10-20-fold less scx, tenomodulin and decorin; 5-10-fold less cartilage oligomeric matrix protein; 2-fold less biglycan and fibromodulin than WT cells, but similar levels of collagens 1, 2, 3, and 8, tissue inhibitor of metalloproteinase 3 and lysyl oxidase. In summary, Mds1-/- mice develop progressive IVDD, kyphosis and osteoporosis associated with dysfunctional tendon and ligament cells. Our findings indicate that the transcription factor, Mds1, not only regulates hematopoiesis, but also plays an important role in maintaining spine integrity by regulating the functions of tendon/ligament cells and affecting extracellular matrix production.

***Disclosures: Lianping Xing**, None.*

FR0470

Type 1 Diabetes Mellitus Effects Bone: Results of Histomorphometric Analysis. Robert Recker[1], Laura Armas*[2]. [1]Creighton University Osteoporosis Research Center, USA, [2]Creighton University, USA

Diabetes Mellitus has a detrimental effect on the body's microvascular system effecting the kidneys, eyes and nerves. The effect on bone is less well known. Patients with Type 1 diabetes have lower bone mass and higher fracture risk than age and sex matched controls. The effect of diabetes on bone micro-architecture and turnover is not well elucidated. We report here preliminary results of eighteen subjects (10 females, 8 males, age 21-47) with Type 1 diabetes for a median of 16 years. The subjects were otherwise healthy without diabetic complications and the females were premenopausal. Two subjects had experienced low trauma fractures. A transilial bone biopsy was obtained after tetracycline labeling. The biopsy specimens were fixed, embedded, sectioned, and evaluated as previously described by Baron et al. Two sections, >250 μm apart, were read from the central part of each biopsy. Mann-Whitney U test was used to compare the results with an existing set of premenopausal controls. Structural measures such as bone volume (BV/TV) and trabecular thickness (TbTh) were lower in the diabetic subjects compared to premenopausal controls (Table 1). The dynamic data showed increased remodeling rates with greater mineralizing surface, mineral apposition rate and activation frequency. The two subjects that had experienced low trauma fractures had lower activation frequencies of 10 and 19 /yr respectively. Histomorphometry in diabetics demonstrates a decrease in bone volume and an increase in remodeling to levels similar to postmenopausal women. This is consistent with the results obtained from microCT and DXA measurements. The increased remodeling may not be related to increased fracture risk though, as the 2 subjects that fractured had lower activation frequency.

Table 1

Variable	Diabetic	Control	P value
Bone Volume (BV/TV %)	18.6(14.8-23.9)	21.9(19.4-26.1)	0.035
Trabecular Number (1 /mm)	1.6(1.4-1.8)	1.5(1.3-1.6)	0.039
Trabecular Thickness (mm)	120.7(102.2-138.8)	151.4(133.7-183.8)	<0.0001
Trabecular Separation (mm)	611.9(548.2-702.6)	669.6(624.7-737.8)	0.049
Mineralizing Surface (%)	4.6(3.4-9.9)	3.2(1.5-5.0)	0.006
Mineral Apposition Rate (μm/d)	0.55(0.48-0.60)	0.41(0.37-0.50)	<0.0001
Activation Frequency (/yr)	0.31(.23-.62)	0.14(0.06-0.21)	<0.0001

Table 1

***Disclosures: Laura Armas**, None.*

FR0472

Prevention of Fractures After Solid Organ Transplant: A Meta-analysis. Emily Stein*[1], Dionisio Ortiz[2], Zhezhen Jin[3], Donald McMahon[1], Elizabeth Shane[1]. [1]Columbia University College of Physicians & Surgeons, USA, [2]SUNY Downstate College of Medicine, USA, [3]Columbia University, USA

Bone loss and fracture are serious sequelae of organ transplantation, particularly in the first year post-transplant. The majority of interventional studies designed to prevent transplant bone loss have been inadequately powered to detect effects on fracture.

We performed a meta-analysis to determine whether treatment with bisphosphonates (BPs) or active vitamin D analogues (vitD) during the first year after transplant reduced fracture risk, and to provide an accurate estimate of the effect of these interventions on rates of bone loss. A systematic review of the literature was conducted using MEDLINE/Pubmed, Cochrane database, and abstracts from scientific meetings. Randomized clinical trials of BPs or vitD compared to placebo that assessed incidence of fracture during the first year following solid organ transplantation were included. For each study, log odds ratio (OR) of fractures was estimated along with its standard error (SE). The relative percentage change in 12 month in lumbar spine (LS) and femoral neck (FN) bone density from baseline between groups was calculated along with its SE. Heterogeneity was examined by Cochran Chi-square tests. Fixed-effects (FEM) and random-effects models (REM) were used.

Ten studies of 817 transplant recipients (135 fractures) were included. Treatment with BPs or vitD reduced the number of subjects with fracture compared to placebo using FEM (OR 0.56, 95% CI of 0.32-0.96, see figure below); the results by REM did not reach significance (OR 0.56, 95% CI 0.28-1.11). No reduction was seen in total number of fractures (OR 0.33, 95% CI 0.10-1.02; REM) or number of vertebral fractures (OR 0.28, 95% CI 0.07-1.03; REM). A significant increase in LS BMD was found by both FEM (2.87, 95% CI 2.05-3.68) and REM (3.15, 95% CI 1.39-4.92). Similarly, a significant increase in FN BMD was observed by FEM (3.07, 95% CI 2.16-3.98) and REM (3.24, 95% CI 1.82-4.66). When BP trials were examined separately, there was no significant reduction in any fracture outcome with treatment, but significant increases in LS BMD and FN BMD were still observed.

Treatment with BPs or vitD during the first year following solid organ transplant was associated with a reduction in the number of subjects with fractures, though this reduction was only significant using FEM. In contrast, significant improvements in LS and FN BMD were observed with treatment. Additional studies are required to demonstrate a consistent effect of treatment on fracture reduction.

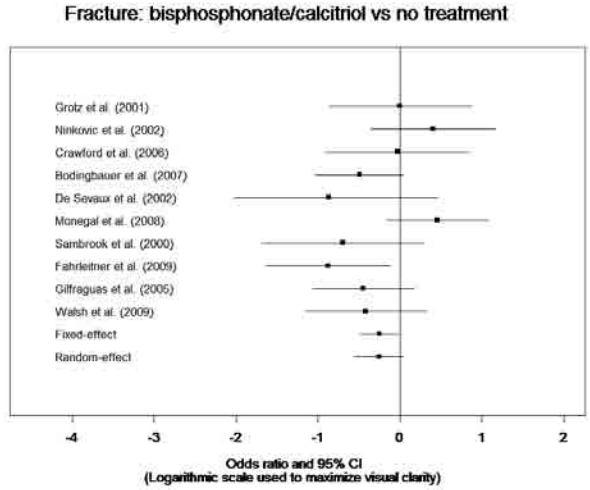

Stein_meta-analysis_figure

***Disclosures: Emily Stein**, None.*

FR0478

Mechanical Loading Increases Estrogen Receptor Alpha Expression in Osteocytes and Osteoblasts Despite Chronic Energy Restriction. Sibyl Swift*[1], Joshua Swift[2], Elizabeth Greene[1], Susan Bloomfield[1]. [1]Texas A&M University, USA, [2]United States Navy, USA

Moderate energy restriction (40% EnR) in young, exercising women can attenuate the positive effects of exercise on bone. We sought to determine whether 40% EnR limits the bone response to mechanical loading (LOAD) through a down-regulation of estrogen receptor alpha (ERα) in osteocytes and/or osteoblasts, resulting in an attenuation of the cancellous bone response to loading. After an 8 wk acclimation, 12 female Sprague-Dawley rats (7-mo-old) were sacrificed as baseline controls (BC). The remaining 48 rats were randomized to control groups (ADLIB-SHAM and ADLIB-LOAD) and fed AIN-93M rat diet ad lib for 12 wks. EnR groups (EnR40-SHAM and EnR40-LOAD) were fed modified AIN-93M with 40% less energy but 100% of all other nutrients provided. At wk 12, rats in both LOAD groups were anesthetized and subjected to muscle contractions once every 3 days (75% peak isometric strength; 4 sets of 5 reps; 1000ms isometric + 1000ms eccentric contraction). SHAM groups were anesthetized and fine wire electrodes implanted without any muscle contraction. Histomorphometric analyses revealed that 40% EnR resulted in significantly lower proximal tibia Tb.Th (-6-fold), higher Tb.Sp (+127.4%), and lower BV/TV (-2-fold) in SHAM but not LOAD rats (vs ADLIB-SHAM). ObS/BS (+23-fold) and OS/BS (+13-fold) were greater in both LOAD groups vs. ADLIB-SHAM. Mechanical loading prevented reductions in mineralizing surface (MS/BS) and bone formation rate (BFR/BS) resulting from EnR; EnR40-LOAD was 5-fold higher vs. SHAM groups. EnR significantly blunted cancellous bone's response to mechanical loading. BFR/BS and MS/BS were -33 and -52% lower, respectively, in the EnR40-LOAD vs. ADLIB-LOAD group. Immunostaining revealed that osteoblast and osteocyte expression levels of ERα protein were +6 and +26-fold greater, respectively, in EnR40-LOAD vs. EnR40-SHAM. However, EnR did not diminish these LOAD-induced increases in ERα expression. These data suggest that a brief period of mechanical loading is able to mitigate losses in cancellous bone microarchitecture related to 40% energy restriction. Chronic energy restriction does limit the bone formation response to mechanical loading, but this may not be the result of a dowregulation in ERα protein on osteoblasts and osteocytes (mechanosensors in bone).

Funded by the Sydney and J.L. Huffines Institute for Sports Medicine and Human Performance and by Dept. of Defense grant #WSIXWH-06-1-0479.

***Disclosures: Sibyl Swift**, None.*

FR0479

A Key Role for CARM 1 Arginine Specific Methylation in Vitamin D Receptor Mediated Transcription. Leila Mady*, Yan Zhong, Puneet Dhawan, Sylvia Christakos. University of Medicine & Dentistry of New Jersey, USA

Hormone dependent transcriptional regulation involves chromatin remodeling by coactivator proteins. Although roles of acetylation and phosphorylation in chromatin remodeling have been widely studied, recent findings have also indicated an important role for methylation. Little is known however about the exact role of methyltransferases and their regulation by different physiological signaling pathways. Using

MDCT renal distal tubule cells or VDR transfected COS-7 and the rat 24(OH)ase promoter (-298/+74) we found that CARM1 (co-activator associated arginine methyltransferase 1) cooperates with the p160 coactivator GRIP1 to enhance $1,25(OH)_2D_3$ induced transcription. Transfection of GRIP1 (0.05 ug) enhanced $1,25(OH)_2D_3$ induced transcription 2 fold and co-expression of GRIP (0.05 ug) + CARM1 (0.2 ug) resulted in a 4 fold enhancement. All activity was dependent on $1,25(OH)_2D_3$. When a CARM1 mutant lacking methyltransferase activity or when the GRIP1 mutant ΔAD2, which lacks the binding site for CARM1, was used, cooperative activation was not observed. Thus, the coactivator function of CARM1 requires methyltransferase activity and coexpression of GRIP1. When PRMT2A, another arginine methyltransferase, was substituted for CARM1, cooperative transactivation with GRIP1 was not observed, suggesting a preferential role for CARM1. ChIP analysis using methyl (R17)H3 antiserum indicated that dimethylation of histone H3 at arginine 17, which is mediated by CARM1, occurs in a $1,25(OH)_2D_3$ dependent manner, further supporting the participation of CARM1 in VDR mediated gene activation. Western blot analysis of MDCT cells indicated a 9.6 ± 1 fold induction of methyl(R17)H3 (the CARM1 methylated form of H3) 30 minutes after $1,25(OH)_2D_3$ treatment. This induction was completely inhibited when the cells were co-treated with 1mM 8 bromo cAMP and $1,25(OH)_2D_3$ for 30 minutes. These findings suggest that the PKA signaling pathway may serve as a molecular switch for controlling CARM1 enzymatic activity, at least in distal tubule cells. Our findings are the first to describe $1,25(OH)_2D_3$ regulation of the CARM1 methylated form of histone 3 and inhibition of the $1,25(OH)_2D_3$ induction by the cyclic adenosine monophosphate signaling pathway. Our findings suggest an interplay between acetylase and methylase in VDR mediated regulation of gene transcription and that CARM1 methylation may play a key role in activation and modulation of $1,25(OH)_2D_3$ induced transcription.

***Disclosures: Leila Mady**, None.*

FR0481

Identification of Novel Vitamin D Receptor Target Genes in Osteoblasts Based on Promoter Interaction with the Vitamin D Response Element Binding Protein. Thomas Lisse*[1], Ting Liu[1], John Adams[2], Martin Hewison[3]. [1]UCLA/Orthopaedic Hospital Research Center, USA, [2]University of California, Los Angeles, USA, [3]UCLA, USA

Heterogeneous nuclear ribonucleoprotein (hnRNP) C1/C2 plays a pivotal role in vitamin D receptor (VDR) signaling by acting as a vitamin D response element-binding protein (VDRE-BP). Transcriptional regulation by the active form of vitamin D_3, 1,25-dihydroxyvitamin D_3 ($1,25(OH)_2D_3$) involves occupancy of VDRE by VDRE-BP or $1,25(OH)_2D_3$-bound VDR; this relationship is disrupted by over-expression of VDRE-BP and can result in a form of human hereditary vitamin D-resistant rickets (HVDRR). To characterize the impact of VDRE-BP on bone function we carried out DNA array analyses using B-lymphoblastic cells from an HVDRR patient and an age and sex-matched normal (wild type; WT) human subject. Data defined a sub-cluster of 114 genes induced or suppressed (>1.5-fold) in WT cells after exposure to 10 nM $1,25(OH)_2D_3$. Of these, 113 were rendered insensitive to $1,25(OH)_2D_3$ by over-expression of VDRE-BP in the HVDRR cells. Using a selection of these genes, further studies were carried out to determine whether over-expression of VDRE-BP also suppressed $1,25(OH)_2D_3$-mediated transcription in human osteoblastic cells. Prominent amongst the VDRE-BP-regulated, $1,25(OH)_2D_3$-responsive genes identified in osteoblast-like cells was the DNA-damage-inducible transcript 4 (DDIT4), an inhibitor of the mammalian target of rapamycin (mTOR) signaling pathway. Chromatin immunoprecipitation (ChIP) assays using $1,25(OH)_2D_3$-treated osteoblasts confirmed that liganded VDR and VDRE-BP compete for binding to the proximal promoter region of the DDIT4 gene in a similar fashion to that observed for other $1,25(OH)_2D_3$ target genes such as CYP24A1. A role for $1,25(OH)_2D_3$-induced DDIT4 expression in regulating mTOR signaling was confirmed by $1,25(OH)_2D_3$-induced suppression of phosphorylated $S6K1^{T389}$ protein (a downstream target of mTOR). The functional importance of this $1,25(OH)_2D_3$-action in osteoblasts was underlined by the fact that rapamycin inhibition of mTOR suppressed antiproliferative responses to $1,25(OH)_2D_3$. These data confirm that VDRE-BP is an important component of the transcriptional apparatus required for normal $1,25(OH)_2D_3$-VDR-mediated transcription and cell function. Conversely, over-expression of VDRE-BP exerts a dominant-negative effect on transcription of many $1,25(OH)_2D_3$-target genes. Characterization of VDRE-BP action in $1,25(OH)_2D_3$-treated osteoblasts highlights an entirely novel role for vitamin D as a regulator of mTOR – a known 'master regulator' of cell function.

***Disclosures: Thomas Lisse**, None.*

FR0482

MBD4 Is an Epigenetic Regulator In the Vitamin D Metabolism. Takeshi Kondo*[1], Mi-sun Kim[1], Yuuki Imai[2], Shino Kondoh[2], Yoko Yamamoto[1], Takahiro Matsumoto[1], Ken-ichi Takeyama[1], Shigeaki Kato[3]. [1]IMCB, University of Tokyo, Japan, [2]The University of Tokyo, Japan, [3]University of Tokyo, Japan

We have previously reported that 1α,25(OH)2D3 (VD) is potent to induce HDAC/VDR co-repressor complex and negatively regulates transcription in the CYP27B1 gene promoter by direct DNA binding of VDIR (bHLH transcription factor) to a specific negative vitamin D response element, while parathyroid hormone (PTH) induces gene expression of CYP27B1 at the transcription level (Murayama A *et al*., EMBO J, 2004). More, recently, we have also reported that VD -dependent transrepression of this gene was regulated by DNA methytransferases associating with liganded-VDR/VDIR co-repressor complex through repressive histone modification and epigenetic DNA methylation. Conversely, MBD4 (methyl-CpG binding domain-4) in the co-respressor complex was phosphorylated by PTH-activated protein kinase C and phosphorylated MBD4 facilitated demethylation of the methylated CpG sites in the CYP27B1 promoter (Kim MS *et al*., Nature, 2009). Although these findings have clarified a part of functions of VDR and MBD4 in the transcriptional mechanisms, the roles of MBD4 in vitamin D metabolism remain unknown. In this study, we tried to characterize the physiological role of MBD4 in bone and mineral metabolisms using $MBD4^{-/-}$(KO) mice. Endogenous Cyp27b1 gene expressions in kidneys of both wild-type (WT) and MBD4KO mice were significantly suppressed by vitamin D treatment. However, subcutaneous injection of PTH significantly recovered Cyp27b1 gene expression only in VD-pretreated WT mice, not in VD-pretreated MBD4KO mice. In addition, the Cyp27b1 gene expression of MBD4KO mice was also significantly reduced by changing calcium content in the diet, compared with WT mice. These findings indicate that the responsiveness against PTH stimulation in kidneys is impaired in MBD4KO mice, at least on the transcriptional level of Cyp27b1 gene. Moreover, from the results of radiological analysis such as soft X-ray and μCT, twenty four week-old MBD4KO mice exhibited bone loss in the diaphyseal area of long bones and calvaria compared to WT mice. Interestingly, this bone loss of MBD4KO mice was rescued by feeding with high calcemic diet. Taken together, these results suggested that MBD4 plays a physiological role in bone metabolism. However, it is still unclear whether the bone mass alteration in MBD4KO mice is due to loss of direct MBD4 functions in bone cells or the results from loss of responsiveness to PTH in the kidney. Further characterization of MBD4 functions in bone metabolism will be presented.

***Disclosures: Takeshi Kondo**, None.*

FR0485

The VDR/RXR Cistrome in Intestinal/Colonic Cells Regulates Genes Involved in Proliferation and Differentiation, Calcium and Phosphate Transport and Xenobiotic Metabolism. Mark Meyer*, J. Pike. University of Wisconsin-Madison, USA

1,25-Dihydroxyvitamin D_3 ($1,25(OH)_2D_3$) plays a central role in calcium and phosphorus homeostasis. In the intestine, these actions regulate calcium and phosphate transporter genes, xenobiotic-metabolizing genes and genes involved in development, growth and differentiation. To explore potential targets of vitamin D action in intestinal/colonic cells, we conducted a ChIP analysis linked to deep sequencing (ChIP-seq) of VDR/RXR in LS180 cells and correlated genome-wide binding to changes in histone modification and gene expression. While VDR binding was detected at 728 sites under basal conditions, VDR bound to over 8150 sites following activation by $1,25(OH)_2D_3$. A similar analysis revealed that RXR binding at 8902 sites was comparable. While some sites were located near gene promoters, most were located within introns and/or at distal intergenic regions. Many sites contained one or more VDRE-like sequences. Genome-wide ChIP-seq analysis also revealed that many of these sites were marked by histone H4 acetylation (H4ac) and that occupancy by VDR/RXR increased this histone mark. RNA polymerase II density was also increased. Importantly, $1,25(OH)_2D_3$ induced VDR/RXR binding at target genes identified previously including *CYP24A1*, *TRPV6* and *SLC34A3*, and at *CYP3A4* and *CYP3A7* in the xenobiotic-metabolizing multigene locus. Perhaps most interesting was the observation that VDR/RXR binding was also observed at genes involved in intestinal epithelial cell proliferation and differentiation, including genes involved in Wnt/b-catenin activation and at β-catenin targets such as *c-MYC*. At this gene, VDR bound to not only the proximal enhancers located at both ends of the gene, but also to upstream regions known to mediate β-catenin activation, including a distal site at -335 kb. Analysis of the CDX2 homeobox, C/EBPβ and β-catenin ChIP-seq cistromes revealed that these transcription factors also play roles in $1,25(OH)_2D_3$-regulated gene expression. In fact, while generally pre-bound, CDX2 binding overlapped 1255 sites to which activated VDR was associated. Direct gene expression studies confirmed that many but not all of these genes were regulated in LS180 cells by $1,25(OH)_2D_3$. These studies indicate that $1,25(OH)_2D_3$ exerts complex actions in intestinal/colon cells that impact not only calcium/phosphorus homeostasis and xenobiotic metabolism, but intestinal cell proliferation as well. This latter activity may be useful therapeutically in colon cancer.

***Disclosures: Mark Meyer**, None.*

SA0001

Axial and Appendicular Bone Properties in Ambulatory Children with Cerebral Palsy. Tishya Wren*[1], David Lee[1], Robert M. Kay[1], Frederick J. Dorey[1], Vicente Gilsanz[2]. [1]Childrens Hospital Los Angeles, USA, [2]Children's Hospital of Los Angeles, USA

Children with cerebral palsy (CP) have deficient bone growth and an increased propensity for non-traumatic fractures. However, most studies of bone in children with CP have been limited to individuals with moderate to severe involvement (GMFCS levels 3-5). Higher functioning children with CP (GMFCS 1-2) may also be at risk for deficient bone acquisition due to muscle weakness and mobility limitations. The purpose of this study was to examine the relationship of axial and appendicular bone properties in ambulatory children with CP to functional (GMFCS) level.

Quantitative computed tomography (QCT) measurements were compared among 37 children with CP (N = 12, 5, 18, 2 for GMFCS levels 1, 2, 3, 4; age 9.3 $\pm$ 1.5 years; 18 male) and 37 controls with the same age and sex distribution. Vertebral (L3) properties were compared between CP and control and across GMFCS levels. Tibia properties were compared only across GMFCS levels because tibia data were not available for the controls. The primary method of analysis was linear regression. Simple and multivariable regression produced similar results, and only the multivariable results are presented here. The final multivariable model included height, weight, sex as covariates since height, weight, and their respective percentiles decreased with increasing disease severity ($P<0.03$).

There was no difference in vertebral cancellous bone density based on diagnosis (95% CI for coefficient: -15 to 7; P=0.49) or GMFCS level (CI: -12 to 8; P=0.68). The control group had larger vertebrae (CI: -81 to 9; P=0.02) than the children with CP, primarily due to smaller vertebral size in GMFCS levels 3 and 4 (CI: -98 to -7; P=0.02). In the tibia, geometric properties of the diaphysis decreased with increasing GMFCS level (CI: 35 to -1 for CSA, -25 to -6 for CBA; $P<0.05$). Cancellous density of the metaphysis also decreased with increasing GMFCS level (CI: -16 to -2 for entire metaphysis, -35 to -6 for slice; $P<0.02$) although values were similar between GMFCS levels 1 and 2.

This study is among the first to examine bone in higher functioning children with CP. The results suggest that children with CP of all levels may have reduced bone mass in their tibias, while spine deficits differentially affect more involved children. Since the lifespan of persons with CP is increasing and even small bone deficits may manifest as osteoporosis later in life, it is important to study bone acquisition in all children with CP.

***Disclosures: Tishya Wren**, None.*

SA0002

Effect of Vitamin D2 and D3 Supplementation in Healthy Adolescents from a Risk Region of Vitamin D Deficiency in Argentina. Cristina Tau*[1], Edit Scaiola[2], Juliana Castagneto[1], Marina Rodriguez[3], Carina De Roccis[4], Zulma Pellisa[1]. [1]Metabolismo Cálcico y Óseo, Endocrinología, Hospital de Pediatría J.P.Garrahan, Buenos Aires, Argentina, [2]Servicio de Pediatria,Hospital Regional de Ushuaia, Tierra del Fuego, Argentina, [3]Servicio de Clínica Médica, Hospital Regional de Ushuaia,Tierra del Fuego, Argentina, [4]Laboratorio, Hospital Regional de Ushuaia,Tierra del Fuego, Argentina

In order to improve vitamin D status of healthy adolescents from Ushuaia (55˚S), in the south of Argentina, three periodic vitamin D2 or vitamin D3 supplementations of 100,000 IU were administered every three months: at the beginning of Winter (March), during winter (June), and in spring (September). Serum 25-hydroxyvitamin D (25OHD) was measured before the study, a month after the first supplementation, and two months after receiving the third supplementation (September 2008, April, and November 2009). After informed consent was signed by the parents, we studied 34 healthy adolescents, age (mean $\pm$ SD) 18.5$\pm$2 years old (range 14.7 to 21.6), 21 girls and 13 boys. An inquiry was made in reference to sun exposure, calcium intake by dairy products. Weight, height, and type of skin of each individual were considered. None had received previous vitamin D. Serum calcium(SCa), phosphate(SP), and alkaline phosphatase(AP) were measured at the beginning of the study. Weight was 0.16$\pm$0.74 (Z-Score), height was 0.2$\pm$0.81. Seventeen adolescents received vitamin D2 or ergocalciferol and 17 received vitamin D3 or cholecalciferol. SCa was 9.35$\pm$0.37 mg/dl, SP was 4.3$\pm$0.73 mg/dl, AP: 91$\pm$63 mg/dl. Basal levels of serum 25OHD were 13$\pm$6.3 ng/ml (range 2-26) in september/spring 2008 (D2 group: 14.4$\pm$6.4, D3 group: 11.8$\pm$6.1). One month after the first supplementation, 25OHD increased significantly in both groups: 29$\pm$7 range 16-44 ng/ml ($p< 0.01$), but was higher in the D3 than in the D2 group (31.6$\pm$5.4 vs 25.7$\pm$7.3 ng/ml, $p<0.012$). At the end of the study, 14 months after the beginning of the study, 25OHD decreased significantly: 22$\pm$5.3 range 12-32 ng/ml ($p<0.018$). However, although 25OHD decreased in both groups when compared with the one-month peak, they did not differ between them (D3: 23.9$\pm$5.1 and D2: 20.2$\pm$5ng/ml). None of the adolescents had vitamin D intoxication (>50 ng/ml). Values less than 15 ng/ml were seen at the end of the study in 2 individuals who received D2. Calcium intake was below FDA recommendations: 570$\pm$320 mg/day. These results indicate that to prevent vitamin D deficiency in risk zones, three supplementations of 100,000 IU of vitamin D during fall, winter and spring, would be adequate and safe to increase 25OHD levels. Morever, vitamin D2 or D3 are efficient to prevent vitamin D deficiency.

***Disclosures: Cristina Tau**, None.*

SA0003

Increased Bone Turnover in Preterm Infants Assessed by Serial Measurements of Urinary Osteocalcin and C-terminal Telopeptides of Type I Collagen (α-CTX-I and β-CTX-I). Kaisa Ivaska*[1], Leena Kilpelainen[2], Mikko Hakulinen[3], Tiina Lyyra-Laitinen[3], Esko Vanninen[3], Natalia Habilainen-Kirillov[1], Tanja Kuiri-Hanninen[2], Ulla Sankilampi[2], Kalervo Vaananen[1], Leo Dunkel[2]. [1]University of Turku, Department of Cell Biology & Anatomy, Finland, [2]Kuopio University Hospital, University of Eastern Finland, Department of Pediatrics, Finland, [3]Kuopio University Hospital, Department of Clinical Physiology & Nuclear Medicine, Finland

Moderate prematurity and rapid postnatal growth in preterm infants may have an impact on bone metabolism and development. The purpose of the present study was to evaluate bone metabolism in preterm infants during the first six months of life and compare them with full term infants.

Bone turnover was analyzed in 67 preterm infants (gestational age 24.7-36.7 weeks, median 32.9) and in 58 full term infants (gestational age 37.0-42.1 weeks, median 39.7) at postnatal day 7 (D7) and thereafter monthly until the age of six months (M1-M6). Bone turnover was assessed by measuring urinary osteocalcin midfragments (U-OC) and urinary concentrations of C-terminal telopeptides of type I collagen (α-CTX-I and β-CTX-I, indicative for resorption of native and aged type I collagen, respectively). All results were corrected for urinary creatinine. Bone mineral content was assessed by dual energy x-ray absorptiometry at the corrected age of 14 months.

U-OC was significantly higher ($p<0.001$) in preterm group compared with the full term group at all time points analyzed (D7-M6). Similarly, α-CTX-I concentration was significantly higher in preterm group from time point M2 to M6 (all $p<0.001$). β-CTX-I concentrations were similar in preterm and full term infants. In preterm infants, median U-OC concentration increased by two fold by M2 ($p<0.001$) and then started to decline, reaching the initial level by M6. Similar postnatal increase in median α-CTX-I concentration was seen in both preterm and full term groups by the age of one month. Bone mineral content at the age of 14 months did not differ between the two groups and there were no gender differences.

In conclusion, urinary OC and α-CTX-I concentrations reflect bone metabolism in infants and are suitable markers for serial monitoring of bone turnover in early postnatal life. Bone turnover, as assessed by urinary OC or α-CTX-I, was faster in preterm infants than in full term infants. Increased bone turnover in preterm infants resulted in normal bone mineral content by the age of 14 months.

***Disclosures: Kaisa Ivaska**, None.*

SA0004

Measuring Trabecular Density in the Peripheral Pediatric Skeleton: How Well Does pQCT Compare to QCT? Babette Zemel*[1], Keenan Brown[2], Soroosh Mahboubi[3], Rohama Khadija[4], Krista Whitehead[3], Mary Leonard[1]. [1]Children's Hospital of Philadelphia, USA, [2]Mindways Software, USA, [3]The Children's Hospital of Philadelphia, USA, [4]University of Texas, USA

Appendicular sites are preferred for QCT measures of trabecular density (TrabDen) in children due to lower radiation exposure compared with spine scans. However, open growth plates complicate reference line placement, and differences in TrabDen distribution along the metaphysis and changes in bone dimensions during growth present additional challenges. This study compared distal tibia TrabDen measured at a single 2.3 mm slice by peripheral QCT (pQCT, Stratec XCT 2000) vs. QCT TrabDen averaged across the entire distal metaphysis (Siemens Somatom Sensation, Mindways QCT Pro Software) taken at two study visits, 12$\pm$1 months apart.

Subjects (n=40, ages 9 to 21y) were participants in an ongoing blinded randomized control trial to treat low TrabDen in youth with Crohn disease. Tibia length was measured anthropometrically and from the QCT scan. Metaphyseal length (MetLength) was defined using density values along a central ellipse as the distance from the distal peak (just proximal to the growth plate) to the zero density point where trabecular bone was no longer detectable (see Figure). QCT TrabDen was calculated using a threshold of 450mg/cm^3 and averaged across the MetLength. pQCT TrabDen was measured at 3% from the proximal edge of the distal physis (threshold 600 mg/cm^3). Correlation analysis and paired t-tests were used for cross-sectional and longitudinal comparisons.

TrabDen by pQCT vs. QCT at baseline (r=0.76) and 12 months (r= 0.78) showed excellent agreement. Baseline vs. 12 month correlations for TrabDen were high and not significantly different for pQCT (r=0.68) and QCT (r=0.79), respectively. MetLength was consistent over time (r=0.77) and varied modestly as a function of tibia length and sex (p for interaction=0.03, overall R2=0.20). pQCT TrabDen (but not QCT TrabDen) was significantly associated with MetLength (r=0.33 & 0.42, for baseline and follow-up, respectively). pQCT Trabden increased significantly over 12 months ($p<0.01$) but not QCT TrabDen.

These findings demonstrate good agreement between a single slice 3% distal tibia pQCT TrabDen measurement and QCT TrabDen averaged across the entire metaphysis at multiple time points, and stability in both measures over time. However, longitudinal changes in pQCT TrabDen may be related to bone growth and re-distribution of trabecular bone along the MetLength. Further research is needed to optimize the use of pQCT in the assessment of TrabDen for bone health in children.

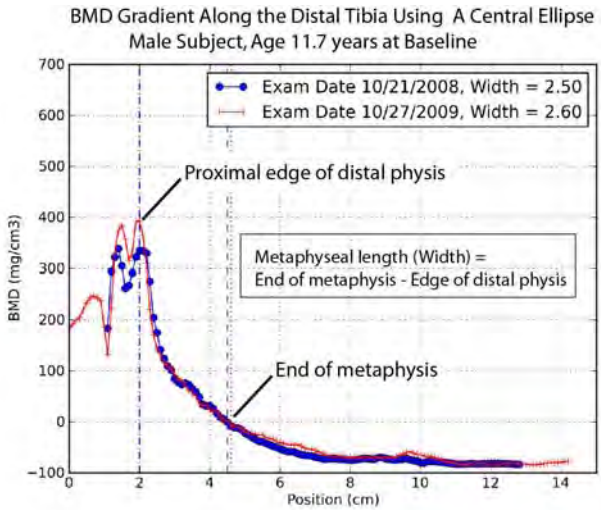

figure

***Disclosures: Babette Zemel**, None.*

SA0005

See Friday Plenary number FR0005.

SA0006

Systemic Biomarker Profiling of Metabolic and Dysplastic Skeletal Diseases Using Multiplex Serum Protein Analyses. Michael Whyte*[1], Deborah Wenkert[1], Denise C. Dwyer[2], David L. Lacey[2], Marina Stolina[2]. [1]Shriners Hospital for Children, USA, [2]Amgen Inc, USA

Understanding the etiology and pathogenesis of dysplastic and metabolic bone diseases has come from both genetic and biochemical investigation. Here, we describe our approach to systemic biomarker profiling using multiplex serum protein analyses to study age- and disease–mediated changes in healthy controls and patients as well as family members with these disorders.

The Research Center at Shriners Hospital for Children, St. Louis, Missouri, serves as a national referral center for inpatient diagnosis, treatment, and investigation of pediatric dysplastic, nutritional, and metabolic bone disorders where collection of fasting blood is routine. At Amgen (Thousand Oaks, California), Luminex-based, micro-bead, multiplex kits are used for osteopontin, osteocalcin, ligand of receptor activator NF-κB (RANKL), osteoprotegerin (OPG), fibroblast growth factor 23 (FGF23), matrix metalloproteinases (MMP 1, 3, 7, 8, and 13), and cytokine quantitation. ELISA kits are used for prostaglandin E_2 (PGE_2), bone-specific alkaline phosphatase (BAP), tartrate-resistant acid phosphatase (TRACP 5B), and collagen formation/degradation markers. Serum levels of sclerostin (SOST) and dickkopf (DKK1) were evaluated by custom ELISAs (developed at Amgen, Inc).

All sera were obtained after donors fasted at least 4 hours. To establish reference ranges, we studied 9 healthy children and 18 healthy adults (ages 6-60 yrs). MMPs (1, 3, 7, 8, and 13) correlated positively with age (R^2 0.26 - 0.64, $p<0.05$), whereas osteocalcin, BAP, c-terminal propeptide of collagen type I (CICP), and TRACP 5B correlated negatively (R^2 0.23 - 0.71, $p<0.05$). The patients represented 30 established and 14 unique diagnoses. Affected family members (dominant disorders) and obligate carriers (recessive disorders) were also studied, reflecting a total of 110 individuals. Our analyses revealed that serum concentrations of FGF23 were significantly increased in x-linked hypophosphatemia (XLH), TRACP 5B in osteopetrosis, and RANKL in juvenile Paget's disease, whereas decreases in BAP were documented for hypophosphatasia, validating our array strategy.

Hence, our multiplex serum protein analyses could reveal unique markers for specific bone disorders, and enhance understanding for a wide range of skeletal diseases.

***Disclosures: Michael Whyte**, Amgen, Incorporated, 3*
This study received funding from: Amgen, Incorporated

SA0007

To Asses the Incidence of Low Vitamin D Levels in Children with Osteogenesis Imperfecta and to Determine its Effect on Bone Healing and Number of Fractures. Antony Kallur*, Richard Kruse, Lauren Davey, Michael Bober. A.I. DuPont Hospital for Children, USA

Purpose: The prevalence of Vitamin D insufficency inchildren with OI is unknown.The aims of this study are to determine the correlation between low vitamin D level on bone quality and number of fractures. Low vitamin D levels in children with Osteogenesis Imperfecta negatively affects bone quality and increases fracture risk, requiring routine monitoring of vitamin D levels and supplementation.

Methods: We retrospectively reveiwed the medical records of patients on our database with diagnosis of Osteogenesis Imperfecta. All the patients with Vitamin D levels done were included in the study. We reveiwed the database and extracted the first ever value of Vit D assayed.

The treatment, number of fractures, surgeries and whether Bisphonates were used and complications were analysed.

Results: We had 61 patients who met our inclusion criteria. The average levels were 32.4ng/ml with 30 patients (50%) with levels less then 30ng/ml. 9 of the 61 patients had levels less then 20ng/ml (15%). The values ranged from 61ng/ml to 14ng/ml with a standard deviation of 11.66.

Conclusions: Children with O.I. have significant incidence of Vitamin D insufficency and defficency futher putting them at riskl for fractures. This has to be addressed when assessing and treating patients with OI.

***Disclosures: Antony Kallur**, None.*

SA0008

Effects of Repetitive Loading on the Growth-Induced Changes in Bone Mass and Cortical Bone Geometry: A 12-Month Longitudinal Study in Pre- and Post-Menarcheal Tennis Players. Gaele Ducher*[1], Shona Bass[2], Leanne Saxon[3], Robin Daly[4]. [1]Penn State University, USA, [2]Deakin University, Australia, [3]Royal Veterinary College, United Kingdom, [4]The University of Melbourne, Western Hospital, Australia

Pre- and early-puberty may be the most opportune time to strengthen the skeleton, but there is little longitudinal data to support this claim. The aim was to study longitudinal growth and exercise-induced skeletal benefits relative to menarche in young female tennis players. Competitive players (n=45) aged 10-17 yrs were followed over 12 months. At baseline, 13 players were pre-menarcheal, of which 10 had menarche during follow-up (PRE/PERI). The remaining 32 players were post-menarcheal at baseline (POST). All players started playing tennis before menarche (mean 6.9 ± 1.9 yrs); PRE/PERI had similar training volume than POST (11 ± 5 vs. 12 ± 6 hrs/wk) but shorter playing history (5.7 ± 2.0 vs 7.5 ± 2.0 yrs, $p<0.05$). The osteogenic response to loading was studied by comparing the playing and nonplaying humeri for DXA BMC and MRI total bone area (ToA), medullary area (MedA), cortical area (CoA) and muscle area (MCSA) at the mid and distal humerus. Growth effects: Over 12 months, growth-induced gains (nonplaying arm) in BMC, ToA and CoA at the mid and distal humerus were greater in PRE/PERI (9-19%, $p<0.001$) than in POST (2-7%, $p<0.05$-0.001). There were no within group changes in MedA, with the exception that mid humerus MedA decreased in POST. Exercise effects: At baseline, BMC, ToA, CoA and MCSA were 7-19% greater in the playing vs. nonplaying arm in both PRE/PERI and POST ($p<0.001$); MedA was smaller in the playing vs. nonplaying arm in POST only ($p<0.05$). Over 12 months, these side-to-side differences increased further for mid ToA and CoA and distal ToA in PRE/PERI, and BMC, distal ToA and CoA in POST ($p<0.05$). When comparing the annual gains in the playing arm after accounting for the corresponding changes in the nonplaying arm, the increases in mid ToA, CoA, and MCSA were greater in PRE/PERI than POST ($p<0.05$). At both skeletal sites, the smaller the side-to-side differences in BMC and CoA at baseline, the larger the exercise benefits at 12 months ($r=-0.36$ to -0.48, $p<0.01$). Training parameters and exercise-induced changes in MCSA were not predictive of the exercise benefits in BMC, ToA or CoA. In conclusion, both pre- and post-menarcheal tennis players showed significant exercise-induced skeletal benefits within a year, but these benefits tended to be greater in pre-menarcheal girls. Accelerated rates of growth and smaller pre-existing bone asymmetries due to past training were associated with greater skeletal responsiveness to loading.

***Disclosures: Gaele Ducher**, None.*
This study received funding from: National Health and Medical Research Council, Australia

SA0009

See Friday Plenary number FR0009.

SA0010

See Friday Plenary number FR0010.

SA0011

Maternal Perinatal Diet Induces Developmental Programming of Bone Architecture. Maureen Devlin*[1], Corinna Grasemann[2], Alison M. Cloutier[1], Mark R. Palmert[2], Mary Bouxsein[1]. [1]Beth Israel Deaconess Medical Center, USA, [2]The Hospital for Sick Children, Canada

The discovery of complex interactions of bone, fat, and brain suggests that osteoporosis and obesity may share common origins. Prior work has shown maternal diet in gestation and lactation triggers developmental programming that raises metabolic disease risk, but potential skeletal effects are unknown. We hypothesize that maternal diet induces perinatal programming that alters postnatal skeletal acquisition, bone mass and strength. Given recent evidence for central hypothalamic mediation of skeletal homeostasis, we predict that such programming alters central regulation of bone mass. Methods: To test this hypothesis and establish a contribution of developmental programming to skeletal acquisition, we compared postnatal skeletal acquisition in pups from mothers fed high fat (HF, 45% kCal/fat) or normal (N, 18% kCal/fat) diet. Female (F) C57Bl/6J mice were fed N or HF diet ad lib. from 6 wks prior to breeding through gestation and lactation. At 3 wks of age we weaned F pups from HF mothers (HF-N) and N mothers (N-N) onto N diet ad lib. Outcomes at 14 and 26 wks of age included body mass, body length, %body fat, total body bone mineral density (BMD, g/cm^2) via pDXA, cortical (Ct) and trabecular (Tb) architecture at the midshaft and distal femur via μCT, and glucose tolerance. Results: At 14 and 26 wks of age, body mass, body length, %body fat and glucose tolerance did not differ in F HF-N vs. N-N. Total body BMD increased by 50% more in N-N vs. HF-N from 14-26 wks of age (+12% vs. +8%), suggesting impaired skeletal acquisition. Thus HF-N had 3% lower BMD at 26 wks and 5-9% lower BMC at 14 and 26 wks vs. N-N ($p<0.05$ for all). In the midshaft femur, Ct.Th was 6% lower in HF-N vs. N-N at 14 wks of age ($p<0.03$), but Ct.BA/TA (%) did not differ between HF-N and N-N at either timepoint. Most provocatively, in the distal femur, Tb.BV/TV (%) was 19-26% higher in HF-N vs. N-N F at 14 and 26 wks ($p<0.05$ for both). Conclusion: These data reveal complex effects of perinatal diet on postnatal skeletal acquisition. Female HF-N pups show lower bone acquisition from 14-26 wks of age, with lower Ct.Th at 14 wks of age, but higher distal femur Tb. bone volume vs. N-N at both timepoints. We propose that maternal HF diet may impair postnatal BMC acquisition in pups, but also slow age-related Tb. bone loss. Our data support the hypothesis that maternal diet alters postnatal skeletal homeostasis, and highlight the need for further work to identify the mechanisms involved.

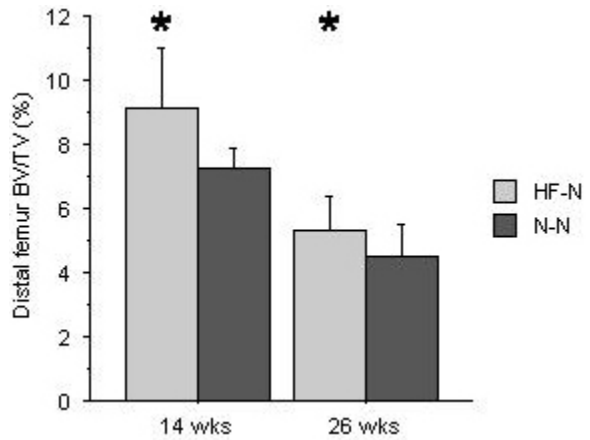

Distal femur BV/TV (%)

***Disclosures: Maureen Devlin**, None.*

SA0012

See Friday Plenary number FR0012.

SA0013

Physical Activity is Associated with Increased Volumetric Bone Density and Bone Strength in Early Childhood. Zoe Cole*[1], Nick Harvey[2], Miranda Kim[2], Keith Godfrey[2], Hazel Inskip[2], Nick Wareham[3], Ulf Ekelund[3], Elaine Dennison[2], Cyrus Cooper[4]. [1]MRC Epidemiology Resource Centre, Southampton General Hospital, United Kingdom, [2]MRC Epidemiology Resource Centre, United Kingdom, [3]MRC Epidemiology Unit, United Kingdom, [4]University of Southampton, United Kingdom

Introduction: Both femoral geometry and bone mass have been shown to independently to predict both hip strength and fracture risk in adults. Whereas intrauterine and early postnatal life has been shown to influence bone mass, the relationship between hip geometry and strength is poorly understood. We therefore used a large prospective cohort study to explore the relationships between growth and lifestyle in early life and hip geometry, strength and volumetric density at 6 years old.

Methods: Children were recruited at 6 years old from the Southampton Women's Survey. Their mothers diet lifestyle and anthropometry had previously been characterised before and during pregnancy. The children underwent measurement of bone mass by DXA (Hologic), including hip structure analysis (HSA), and by pQCT at the tibia (Stratec). Physical activity (PA) was assessed by accelerometry (Actiheart, Cambridge Neurotechnology Ltd, Cambridge, UK) for 7 continuous days. Diet was assessed using a validated food frequency questionnaire and detailed anthropometric data was also collected.

Results: There were 215 children with PA data who underwent a DXA scan, of these 49 children also underwent pQCT assessment. Mean daily time spent in vigorous activity (VPA) was positively associated increased measures of volumetric BMD for whole body ($r=0.32$, $p<0.001$), lumbar spine ($r=0.16$, $p=0.02$) and hip ($r=0.15$, $p=0.03$). In the subset that underwent pQCT, VPA was positively related to cortical volumetric bone mineral density ($r=0.29$, $p=0.05$). Increased daily time in VPA was also positively associated with femoral neck and intertrochanteric section modulus ($r=0.23$, $p=0.001$; $r=0.23$, $p=0.001$ respectively), cross sectional area (CSA) ($r=0.26$, $p=0.0002$; $r=0.24$, $p=0.0009$) and cortical thickness ($r=0.17$, $p=0.02$; $r=0.19$, $p=0.009$). These relationships were independent of maternal and childhood dietary, lifestyle and anthropometric factors. Similar associations for VPA with section modulus ($r=0.17$, $p=0.02$) and CSA ($r=0.16$, $p=0.02$) were observed at the femoral shaft.

Conclusions: Higher levels of vigorous physical activity in childhood are associated with increased femoral neck strength, both in terms of geometric shape and volumetric mineral density. This work supports the notion that increasing physical activity in childhood is likely to be a potential public health strategy to improve childhood skeletal development and reduce the burden of osteoporotic fracture in later life.

***Disclosures: Zoe Cole**, None.*

SA0014

Skeletal Deficits and Recovery in Methylphenidate Treated Rats. Michelle Mary*[1], Haden Janda[1], Christine Snearly[1], Winfred Abrams[2], Nora Volkow[3], Gene-Jack Wang[4], Lisa Robinson[4], Mala Ananth[4], Tim Wigal[5], James Swanson[5], Panayotis Thanos[4], Michael Hadjiargyrou[6], David Komatsu[1]. [1]InMotion Orthopaedic Research Center, USA, [2]University of Tennessee, USA, [3]Laboratory of Neuroimaging, NIAAA, NIH, USA, [4]Behavior Neuropharmacology & Neuroimaging Lab, Medical Dept. Brookhaven National Laboratory, USA, [5]Child Development Center, University California Irvine, USA, [6]State University of New York at Stony Brook, USA

Up to 9% of American youths are diagnosed with Attention Deficit Hyperactivity Disorder (ADHD), 90% of which are treated with methylphenidate (MP). This study examined the effects of MP in adolescent rats to test the hypotheses that long-term treatment is detrimental to skeletal development and cessation of treatment leads to recovery of normal skeletal characteristics.

Four-week old male Sprague-Dawley rats were randomized to 3 groups (n=24/grp): low-dose (MP low), high-dose (MP high), and vehicle (Veh). MP was administered daily via drinking water with MP high and MP low rats receiving 30 or 4 mg/kg, respectively, for 1 hour followed by 60 or 10 mg/kg, respectively, for 1 hour. Veh rats received water with no MP. After 3 months, half of the rats (n=12/grp) were sacrificed. The remaining rats (Recovery) were taken off treatment and sacrificed 5 weeks later. Femora and tibiae were harvested for: DXA determination of BMD, BMC, and area; caliper measurements of length, anterior-posterior (AP) and medial-lateral (ML) diameter; and 3-point bending tests for energy to failure (EF), stiffness (SF), and ultimate force (UF), as well as histologic and gene expression analyses. Serum was also collected for biomarker analyses. One-way ANOVA and Dunnett's tests were used to identify significant differences ($p<0.05$).

Weight gain during treatment in MP high rats was 15% less than Veh rats. Femoral and tibial BMD and BMC were lower in MP high compared to Veh (femur: 6% & 9%; tibia: 5% & 9%, respectively). In addition, femoral AP diameter was smaller in MP low (5%) and MP high (9%) as compared to Veh. Biomechanically, EF was lower in MP low (25%) and MP high (31%) compared to Veh, and UF was 14% lower in MP high. In the Recovery rats, none of these parameters were significantly different. Serum ALP was 31% higher in MP high rats compared to Veh, and similarly elevated in Recovery rats.

In summary, MP treatment resulted in less weight gain and weaker, less mineralized, smaller bones, particularly at high doses. However, these effects were ameliorated within 5 weeks. Higher serum ALP in MP high rats suggests increased osteoblast activity, but bone specific ALP remains to be quantified. Also, ongoing experiments to assess osteoclast activity, histology, and gene expression need to be completed to determine how MP impairs skeletal development. Clinically, these data suggest that adolescents treated with high dose MP may have weaker bones and an increased fracture risk.

***Disclosures: Michelle Mary**, None.*

SA0015

The Lifetime OsteoGenic Exercise Score: A Method to Estimate Bone Status in Young Adult Women. Tara Dahn, Jo Welch*. Dalhousie University, Canada

A simple tool to predict bone status would have both clinical and public health applications. Furthermore, if bone status was known to women when they were young adults, early adoption of lifestyle choices that favor better bone health could minimize future age-related bone deterioration. The purpose of the study was to develop a tool based on exercise history to predict the category of bone status in young adult women. For this study, 80 non-smoking women, aged 18-25, mean height, 67 cm, mean weight 63 kg, were recruited. They completed a simple questionnaire that included their exercise history and age at menarche. A Lunar Achilles InSight bone ultrasonometer was used to measure Stiffness Index (SI) at the calcaneus. An equation that could quantify impact loading from exercise was then developed. The Lifetime OsteoGenic Exercise Score (LOGES) uses the following formula to score each exercise reported in an exercise history questionnaire: LOGES = $(AR^2*D*F*M)/ [(YS/2)+1]$, where AR = activity rating; activities were divided into 5 categories based on published effects on bone, D = duration of participation (y), F = frequency of participation (hr/wk), M = developmental period multiplier, based on whether activity occurred before, during or after puberty, and YS = years since cessation of activity (y). The score for each exercise activity was then summed to provide a total score for each subject. Subjects were ranked by their total scores. The list of ranked subjects was then partitioned into five equal groups, based on activity levels, which resulted in mean SI per group of 99.8, 105.9, 108.2, 110.5, and 114.3. The relationship between group mean activity level and SI was strong ($R^2 = 0.96$). To test the reliability of the scoring system, 8 people unfamiliar with exercise and bone health were provided with 5 minutes of verbal explanation and a short written description of the scoring system. Each novice rater then scored the same 5 randomly selected subjects from their initial questionnaires. The Pearson's correlation coefficient for inter-rater reliability was R = 0.996. In conclusion, the LOGES system enabled the classification of young women into categories of bone status based on exercise and pubertal history. This system of estimating bone status is reliable and offers a method to screen young women, who rarely receive bone tests, for bone status.

***Disclosures: Jo Welch**, None.*

SA0016

IBD Causes Greater Bone Loss in Male Compared to Female Mice. Regina Irwin, Laura McCabe*. Michigan State University, USA

Inflammatory bowel disease (IBD) is the most common chronic gastrointestinal disease in the United States. Nearly 1.4 million males and females are affected with one of the two major forms of IBD which are Crohn's disease and ulcerative colitis. One complication of IBD is bone loss. Purpose: To examine the influence of gender on IBD induced bone loss. Method: *Helicobacter hepaticus* was used to induced IBD in male compared to female IL-10 knockout mice. This model effectively simulates Crohn's disease. Mice, at 14 weeks of age, were gavaged with bacteria and after 6 weeks bone parameters were examined. Results: Both sexes experienced significant decreases in bone parameters, however, the losses were less in females. Specifically, IBD decreased bone mineral content and denisty by 26% in males, but only by 15% in females. Similarly, IBD caused a decrease in bone volume fraction and trabecular thickness, by 37% and 19%, in males and only by 16% and 10% in females. In contrast, osteocalcin expression in bone was reduced to a similar extent (50%) in both males and females. Histomorphometry demonstrated similar changes in osteoblast and osteoclast numbers in male and female mouse bones. Conclusion: Our findings suggest that the female skeleton is partially protected from IBD induced bone loss. A potential beneficial role for estrogen is currently being investigated.

***Disclosures: Laura McCabe**, None.*

SA0017

PTH Increases and Serum NTX is Associated with Maternal Bone Loss in Pregnant Adolescents. Bridget Essley*[1], Allison McIntyre[2], Beth Cooper[2], Thomas McNanley[2], Tera Kent[1], Frank Witter[3], Z. Leah Harris[3], Kimberly O'Brien[1]. [1]Cornell University, USA, [2]University of Rochester Medical Center, USA, [3]Johns Hopkins University, USA

Bone turnover increases during pregnancy and a net loss of bone can occur over the course of pregnancy. Pregnant adolescents may be at increased risk for bone loss as the calcium (Ca) demands of the developing fetus are added to the demands of adolescent growth. Pregnant teens are also at increased risk for insufficient Ca intakes and vitamin D insufficiency. To assess the relationships between vitamin D status, parathyroid hormone (PTH), and Ca intake on maternal bone health across gestation, pregnant adolescents ($\leq$ 18 y) were recruited at $\geqslant$ 12 weeks of gestation and followed at 3 points across pregnancy (at approximately 16, 25 and 34 wks gestation). At each visit an ultrasound of the calcaneus was performed and a 24-hr dietary recall and FFQ were obtained. Blood samples were collected at mid-gestation (25.3 $\pm$ 3.4 weeks) and maternal and cord blood were obtained at delivery (39.2 $\pm$ 2.8 weeks). 25(OH)D, intact PTH, osteocalcin (OC: a marker of bone formation) and N-telopeptide (NTX: a marker of bone resorption) were measured in all blood samples. Teens were 17.1 years of age at entry into the study (n=141). Vitamin D insufficiency (25(OH)D $\leq$ 20 ng/mL) was found in 49% of teens at mid-gestation, 48% at delivery, and 46% of neonates were D insufficient at birth. In adolescents, 25(OH)D was inversely related to PTH at mid-gestation (p=0.034, n=93) and delivery (p=0.066, n=76). PTH increased across gestation ($p<0.05$, n=76) and was elevated (PTH $\geqslant$ 46 pg/mL) in 13% of teens at mid-gestation (n=93) and 32% of teens at delivery (n=81). Ca intake averaged 874 $\pm$ 379 mg/day (recall) and 975 $\pm$ 484 mg/day (FFQ) and was not related to PTH or changes in maternal calcaneus measures. Markers of bone turnover increased across gestation and the increases in OC and NTX per week were positively correlated (p=0.002, n=57). The average change in ultrasound bone measures were negative (n=120) indicative of maternal bone loss across gestation. The increase in NTX per week was positively associated with changes in bone ultrasound measures (SOS, QUI, BMD; $p<0.05$, n=94). This population exhibited a high prevalence of vitamin D insufficiency, net loss of maternal bone across gestation and unexpected increases in PTH across gestation. Calcitriol analyses are underway and a model will be constructed to elucidate the main determinants of maternal bone loss and fetal bone growth in this population of pregnant adolescents.

***Disclosures: Bridget Essley**, None.*

SA0018

Acute Mandibular Lesion in a 12 year old Girl with McCune Albright Syndrome and Fibrous Dysplasia. Nancy Dunbar*[1], David Ebb[2], Ksenia Tonyushkina[3], Thomas Carpenter[4], Leonard Kaban[2]. [1]Baystate Medical Center, USA, [2]MassGeneral Hospital for Children, USA, [3]Baystate Children's Hospital, USA, [4]Yale University School of Medicine, USA

McCune Albright Syndrome (MAS) is caused by activating, somatic mutations of GNAS, resulting in fibrous dysplasia (FD) of bone, café-au-lait skin markings and precocious puberty. Only two mutations have been reported in MAS (commonly, at R201 and also at Q227). No genotype/phenotype correlations are known. Fibrous dysplasia in MAS can be severe, causing significant disfigurement, pain and restriction of function. Uncommonly, aggressive cystic lesions arise, usually in the craniofacial area, and are associated with disfigurement and pain. These lesions have been shown to produce excessive amounts of FGF23.

We report a 12 year old girl with MAS, severe polyostotic fibrous dysplasia, and a 5x5cm mandibular lesion, which had acutely expanded in one week. The superior aspect of the lesion was bony to palpation but ballotable inferiorly; the overlying skin was yellowed. The lesion stabilized after 10 further days and the pain remitted. Radiographic studies revealed an expansile lesion with fluid-fluid levels eroding through the inferior cortex of the mandible (see images below). Widespread fibrous dysplasia occurred throughout the mandible and skull base. Bone pain had been treated during the previous year with intravenous pamidronate at 3-month intervals, last administered 10 weeks prior to the observation of the lesion. Of interest, an acutely expanding lesion involving her right orbit led to surgical excision in Kyrgystan at age 7.

During the preceding several months, serum alkaline phosphatase activity increased from 513 to 686 IU/L, circulating PTH increased from 31 to 60 pg/ml, and circulating 1,25(OH) decreased from 64 to 24 pg/ml. Serum 25-OHD, calcium and phosphorus levels were stable within the normal range. Surgical enucleation of the mandibular lesion was performed. Gross inspection was consistent with an aneurysmal bone cyst. Histopathology and pre/post-operative serum FGF23 levels are pending. Treatment with interferon to stabilize the vasculature is under consideration pending the histopathology.

This case presents the clinical course and therapeutic response to an aggressive cystic lesion in the mandible of a 12-year-old girl with severe MAS/FD presumed to be an aneurysmal bone cyst. The role of FGF23 in the pathogenesis of acute cystic lesions in FD, and the role of interferon in their treatment are currently unknown.

***Disclosures: Nancy Dunbar**, None.*

SA0019

Bone Health in Children with Neurofibromatosis Type 1 - a High Incidence of Abnormal Vertebral Morphology and Altered Skeletal Geometry. Peter Simm*[1], Julie Briody[2], Aaron Schindeler[2], Christopher Cowell[2], David Little[2], Kathryn North[2], Craig Munns[2]. [1]Royal Children's Hospital, Melbourne, Australia, [2]The Children's Hospital At Westmead, Australia

There is increasing evidence that some young people with Neurofibromatosis Type 1 (NF1) have an abnormal bony phenotype, however this is yet to be fully characterized. We performed a bone health assessment on 23 patients with NF1 (11 female) aged between 5 and 16 years (mean age 9.5 yrs).

Results showed that this is a highly heterogenous group, however there is a subgroup who have an abnormal bone phenotype. Dual energy absorptiometry (DXA) scanning showed a mean lumbar spine bone mineral density (BMD) Z score of 0.1 SD (corrected for height), with a wide spread (+/-1.43).

Peripheral quantitative computerised tomography (pQCT) showed a distinct phenotype, with the mean results showing a low trabecular BMD (-0.89 SD, +/-0.61, p <0.001) at the 4% site and reduced bone area (-0.73 SD, +/-1.31, p = 0.02), cortical thickness (-0.51 SD, +/- 0.81, p = 0.009) and a trend towards reduced stress strain index (-0.38 SD, +/- 1.15, p = 0.14), but normal cortical BMD (0.65 SD, +/-1.23, p = 0.03), at the 66% site of the tibia. Muscle cross sectional area was also reduced (-0.63 SD, +/- 1.06, p = 0.01) which may be contributing to the observed skeletal geometry.

Of the 21 patients who had spinal Xrays, 7 (33%) had significant anterior wedge deformity by Genant criteria with greater than 15% loss of anterior height compared with posterior height, predominantly in the mid thoracic region. A further 4 patients had abnormal shaped vertebrae without meeting the Genant criteria. Therefore over 50% of our patients showed vertebral body changes. The significance of these findings is unclear as there was no correlation between low BMD on DXA scan and vertebral changes. Whether the vertebral changes reflect bone weakness and fragility, or rather dysplasia, remains to be determined.

Metacarpal index was reduced (1.91, N >2.0), with 8 pts (35%) having a score less than 1.75. 4 patients had a vitamin D level of <50 nmol/L, despite no patients having established risk factors for Vitamin D deficiency. Only 3 patients reported a previous fracture. The subjects had mean height Z score of -0.4 SD but had increased body mass index Z score (0.4 SD).

Our results confirm that there is a subset of patients with NF1 who have an abnormal bone phenotype. We plan to follow our cohort longitudinally to obtain data on prospective incidence of fracture and to follow the vertebral body changes in the more severely affected individuals.

***Disclosures: Peter Simm**, Pfizer, 2*
This study received funding from: Pfizer

SA0020

Impact of Weight Gain on Bone Mineral Content in Adolescents with Type 1 Diabetes. Sowmya Krishnan*[1], Brianna Bright[2], Mary Murray[3], Kenneth Copeland[2], David Fields[2]. [1]The University of Oklahoma Health Sciences Center, USA, [2]University of Oklahoma health science center, USA, [3]University of Utah, USA

Background: Lower spine and whole body bone mineral content (BMC) has been reported in adolescents with type 1 diabetes, while overweight status in adolescents without diabetes has been shown to be associated with higher BMC. It is not known if being overweight is protective for the bones of adolescents with type 1 diabetes. The following is a cross sectional study examining the influence of weight status on BMC in overweight and normal weight adolescents with type 1 diabetes.

Methods: A total of 31 adolescents with type 1 diabetes (HbA1c range 6.5% to 10.7% with a mean of 8.5%) participated in the study. All were Tanner stage 3 or above. 16 were overweight (mean BMI = 28.3 $\pm$ 3.6) and 15 were normal weight (mean BMI = 20.6 $\pm$ 2.0). All adolescents underwent a whole body DXA scan (Hologic QDR 4500, Waltham, MA). Additionally 21 wore a step activity monitor and 18 completed a detailed 4-day food recall.

Results: Adolescents with type 1 diabetes who were overweight had higher total BMC and subtotal BMC than adolescents with type 1 diabetes who were normal weight, though this difference did not reach statistical significance (p=0.0692 and 0.0594 respectively). As expected, both total BMC and subtotal BMC correlated significantly with age (r=0.55, p=0.0014 and r=0.50, p=0.0038 respectively). BMC measures (both total and subtotal) did not significantly correlate with any other variables, including physical activity measures (total steps/day, sedentary time/day) or vitamin D and calcium intake.

Conclusion: Overweight adolescents with type 1 diabetes had higher total and subtotal BMC values compared to normal weight adolescents with type 1 diabetes, indicating a similar relationship of BMC to overweight and normal weight status as that reported in non-diabetic adolescents. These observations pertain to adolescents with relatively well-controlled type 1 diabetes; whether they can be generalized more broadly to all diabetic patients regardless of glycemic control remains to be demonstrated.

***Disclosures: Sowmya Krishnan**, Novo Nordisk, 2*
This study received funding from: Novo Nordisk

SA0021

See Friday Plenary number FR0021.

SA0022

Paternal Deletion of the GNAS Imprinted Locus in a Girl Presenting with AHO, Severe Obesity and ACTH-independent Adrenal Hyperplasia. Caroline Kannengiesser[1], Stéphanie Maupetit-Méhouas[2], Sabine Rouleau[3], Régis Coutant[3], Agnes Linglart[4], Caroline Silve*[5]. [1]Assistance Publique-Hôpitaux de Paris; Université Paris 7. Hôpital Bichat Claude Bernard, Service de Biochimie hormonale et génétique, France, [2]INSERM U986, France, [3]Department of Pediatric Endocrinology, University Hospital, France, [4]INSERM U986; Assistance Publique-Hôpitaux de Paris. Endocrinologie-diabétologie pédiatrique et Centre de référence des maladies rares du métabolisme du calcium et du phosphore, Hôpital St-Vincent de Paul, France, [5]INSERM Unit 986, France

Diseases due to GNAS genomic or epigenomic alterations include : 1. pseudohypoparathyroidism (PHP) 1a characterized by Albright Hereditary Osteodystrophy (AHO) with multi-hormonal resistance due to maternally inherited Gsa loss of function (LOF) mutations; 2. pseudoPHP, characterized by AHO without hormonal resistance due to paternally inherited Gsa LOF mutations; 3. PHP1b usually presenting with selective PTH resistance without AHO due to maternal epimutations of the GNAS differentially methylated regions (DMRs); and 4. McCune-Albright syndrome characterized by hyperplasia and increased function of endocrine glands, including the adrenal, due to somatic Gsa gain of function mutations. Patients with Gsa LOF mutations usually present with ectopic mineralization, which are more severe when the mutation are paternally inherited. We investigated a girl who presented with AHO, no ectopic ossification, severe obesity (as in PHP1a), no hormonal resistance (as in PPHP), bilateral adrenal hyperplasia and increased function (as in McCune Albright) as indicated by hirsutism, amenorrhea, acne, elevated circulating androgens (testosterone, SDHA) and elevated cortisol cycle albeit normal urinary cortisol and no Cushing syndrome. She was the only child born to healthy parents. Systematic sequencing of the GNAS coding exons 1 to 13 did not show any mutation nor heterozygous polymorphism. Methylation analysis of the GNAS DMRs using enzymatic digestion after bisulfite treatment or methylquantification showed a maternal pattern of methylation of the entire GNAS locus. Genome wide CGH-array analysis (Nimblegen 12*385K) demonstrated the presence of a ~1.575 Mb genetic deletion encompassing the entire GNAS locus. The deletion was confirmed by allelic quantification of genomic DNA; microsatellites analysis of the parents and proband DNAs demonstrated the paternal origin of the deletion. In summary we describe a new case of constitutional paternal deletion of chromosome 20 encompassing the entire GNAS locus and associated with a paradoxical phenotype. While the short stature and the bone features defining AHO are likely due to Gsa haploinsufficiency, the mechanisms leading to the severe obesity and adrenal gland bilateral hyperplasia need to be elucidated. Because a defect in none of the genes included in the deleted genetic interval are likely to be associated with the phenotype, it is tempting to speculate that the absence of XLS and/or AB and AS transcript expression due to the paternal deletion contributes to the phenotype.

***Disclosures: Caroline Silve**, None.*

SA0023

Evidence of Metabolic Bone Disease in Young Infants with Multiple Fractures Misdiagnosed as Child Abuse. Chuck Hyman[1], Marvin Miller[2], David Ayoub*[3]. [1]Pediatrician, USA, [2]Wright State University Boonshoft School of Medicine, USA, [3]Clinical Radiologists, SC, USA

Purpose: Assess the presence of clinical and evidence of metabolic bone disease in young infants presenting with multiple unexplained fractures (MUFs) undergoing an investigation for child abuse.

Methods: We have evaluated the radiographs and pertinent medical records of 40 infants with MUFs and their mothers for signs and risk factors of impaired bone metabolism.

Results: The average age of presentation was 12.6 $\pm$ 9.0 weeks (range 2-52). Twelve of thirteen (92.3%) mothers tested had subnormal 25OH vitamin D. Ten were deficient (<20 ng/ml) and two within the insufficient (<30 ng/ml) range. Ten of seventeen (58.8%) infants had subnormal 25OH vitamin D. Most infants with normal vitamin D levels were tested many weeks after presentation and had been supplemented. Twenty-seven mothers (68%) had 2 or more risk factors for VDD. There was evidence of decreased fetal bone loading in 17/40 (43%) pregnancies. Twenty percent of women had gestational diabetes. Acid lowering drugs which can decrease calcium absorption were used in at least 16 (40%) mothers while pregnant and in 11 (27.5%) of infants.

There were 14.1 $\pm$ 9.0 fractures, including classic metaphyseal lesions (CMLs), per infant (range 3-47). One hundred eighty-nine CMLs were encountered in 37 infants (5.1 per infant; range 0-15). Epiphyseal separations were suspected in 5.8% of CMLs. All other CMLs were clinically silent and healed without callus or periosteal reaction. Multiple rib fractures were seen in 33 infants (7.8 per infant; range 2-20). Infants had at least one non-CML fracture at these sites: skull (20.0%), which was always linear and usually diastatic, clavicle(32.5%), thoracolumbar spine(17.5%), appendicular diaphysis (40.0%) or metaphysis (15.0%), scapula (5.0%), and small bones of hands/feet (20.0%). All infants displayed multiple radiographic signs of metabolic bone disease (Table 1).

Conclusions: This study reports a large series of infants with MUFs who had clinical and radiographic evidence of metabolic bone disease likely of multifactorial etiology overlooked during an investigation for child abuse. While metabolic bone disease is a

known cause of increased bone fragility and MUFs, its differentiation from inflicted or accidental injury remains challenging. Careful review of the radiographs with attention to the unappreciated signs or risk factors that impair fetal and infant bone mineralization is critical to avoid an erroneous diagnosis of child abuse and its consequences.

Table 1. Radiographic signs* in 40 infants with MUFs

radiographic sign	n	%
metaphyseal hypermineralization	38	95.0%
metaphyseal clubbing	37	92.5%
calvarial mineralization defects	31	77.5%
trabecular thickening	30	75.0%
bowing deformity of lower leg	30	75.0%
ulnar cupping	24	60.0%
rachitic rosary	23	57.5%
periosteal neostosis	19	47.5%
subperiosteal resorption	18	45.0%
Looser Zone	18	45.0%
kyphoscoliosis	16	40.0%
intrasutural bone	9	22.5%

*per infant basis

Table 1

***Disclosures: David Ayoub**, None.*

SA0024

See Friday Plenary number FR0024.

SA0025

New Case of Infantile Generalized Arterial Calcification: Evolution from Prenatal Diagnosis to 12 Months of Age under Bisphosphonates' Therapy. Thomas Edouard*[1], Nathalie Alos[2], Joaquim Miro[1], Chantal Lapierre[1], Jacques Michaud[1], Gilles Chabot[3]. [1]CHU Sainte-Justine - Université Montréal, Canada, [2]CHU Sainte Justine, Canada, [3]Hopital Saint Justine, Canada

Background: Generalized arterial calcification of infancy (GACI, OMIM 208000) is a rare autosomal recessive disease characterized by extensive calcification of large- and medium-sized muscular arteries. The diagnosis is prenatal or in early infancy, with variable clinical presentations including heart failure, hypertension or failure to thrive. This disease is linked to mutations in the ENPP1 gene which encodes an enzyme that generates inorganic pyrophosphate (PPi), a potent inhibitor of hydroxyapatite crystal formation. Treatment with bisphosphonates, which are synthetic PPi analogues, has been proposed as a means to reduce arterial calcifications in GACI patients. GACI has been reported to be frequently lethal, and the efficiency of any therapy, including bisphosphonates, remains unknown.

Case report: We report on a girl who was diagnosed prenatally at 32 weeks gestation with GACI when a routine fetal ultrasonographic examination revealed arterial calcification and pericardial effusion. The parents were healthy and non consanguineous without relevant family history. The newborn baby was born by vaginal delivery at 364/7 weeks gestation with normal birth weight and length but no pulses were palpable. Secondary to pericardial effusion, he developed mild respiratory distress in the first hour of her life and required pericardial fluid drainage and respiratory support for 6 days. Ultrasonographic and tomodensitometric evaluations confirmed diffuse arterial calcification that involved the coronary, main and branch pulmonary and aorta arteries. Mutational screening demonstrated mutations in ENNPP1 gene, which correspond to c.583T/C.

Evolution: Intravenous disodium pamidronate (3 infusions at days 8, 15, 18 of 0.25mg/kg, 0.50 mg/kg and 0.50mg/kg respectively) was changed to oral disodium etidronate (starting dose of 20 mg/kg daily: 50 mg die) at 3 weeks of age. Follow-up included 3-monthly clinical reviews and assessments of mineral homeostasis, 6-monthly DEXA, ultrasonography and tomodensitometric studies, and annual x-rays of the wrists and knees. Progressive resolution of arterial calcifications was seen by 3 months of age and etidronate dosage was kept at 50 mg daily. At 12 months, under 6mg/kg of etidronate, growth and development, serum mineral homeostasis and areal bone mineral densitometry of the lumbar spine remained normal. X-rays of the wrist and knees didn't show any sign of rickets.

***Disclosures: Thomas Edouard**, None.*

SA0026

The Use of Intravenous Bisphosphonate Therapy to Treat Vertebral Fractures due to Osteoporosis among Boys with Duchenne Muscular Dystrophy. Anne Marie Sbrocchi*[1], Frank Rauch[2], Pierre Jacob[1], MaryAnn Matzinger[1], Leanne M. Ward[1]. [1]University of Ottawa, Canada, [2]McGill University, Canada

Purpose: Boys with Duchenne Muscular Dystrophy (DMD) are at risk for vertebral fractures. Bisphosphonates have been used to treat the spine fragility; however, detailed analyses of the response to therapy are lacking. The objective of this study was to assess the efficacy and safety of IV bisphosphonate treatment for painful vertebral fractures among boys with DMD.

Methods: This was a one-year, retrospective observational study of 7 boys (age 7.9-14.0 years) with DMD who had received either IV pamidronate (9 mg/kg/year) or zoledronic acid (0.1 mg/kg/year) to treat painful vertebral fractures. The co-primary outcomes were back pain status and change in vertebral morphometry (with categorization as per the Genant score) at 12 months post-bisphosphonate initiation. Changes in vertebral heights were deemed to be statistically significant if they exceeded the Least Significant Change at the 99% confidence level. Secondary outcomes included development of new vertebral fractures, changes in lumbar spine areal bone mineral density (BMD), and adverse events.

Results: A description of the cohort at baseline and 12 months is presented in the Table. Pubertal development was Tanner stage 1 (n=6), and Tanner stage 2 (n=1). All but one boy had received glucocorticoids prior to treatment initiation (average cumulative steroid exposure per patient 16,058 mg/m^2 in prednisone equivalents), and only one was fully ambulatory. There were 27 fracture events noted in the 7 patients at baseline; 3 fractures in 1 patient, 2-4 in 2 patients and >5 in 2 patients. Of the 27 fracture events, 14 improved, 11 stabilized and 2 deteriorated (30% to 37% and 15% to 32% loss in vertebral height). All but one Grade 2 (moderate) and Grade 3 (severe) vertebral fractures improved (n=11) or stabilized (n=6) at 12 months. There were 3 new Grade 0.5 fractures in 2 boys apparent after 1 year of therapy. Back pain either resolved completely (n=4) or improved (n=3). The mean ± SD spine BMD also increased (see Table). First-dose side effects were present in 4 patients and included fever and malaise (N=4), and hypocalcemia (N=2).

Conclusion: In boys with spinal osteoporosis and DMD, IV bisphosphonate therapy administered over 12 months was associated with improvements not only in spine BMD, but also in the more clinically relevant back pain and vertebral morphometry. The therapy was generally well-tolerated.

Clinical Characteristics	Results 12 Months Post Bisphosphonate Initiation (N=7)	
	Pre-Treatment	12 Months Post
Anthropometry		
Height Z-score	-1.7 (-4.2, -0.5)	-2.0 (-3.5, -0.1)
Weight Z-score	0.4 (-2.4, 1.8)	-1.7 (-1.9, 1.9)
BMI Z-score	1.2 (0.2, 2.3)	0.4 (-1.6, 2.3)
Vertebral Morphometry of existing fractures		
Genant Grade for VF Events, N (%)		
Grade 0: Normal	0 (0%)	8 (30%)
Grade 0.5: >15-20% loss in VH	5 (18%)	7 (26%)
Grade 1: >20-25% loss in VH	4 (15%)	5 (18%)
Grade 2: >25-40% loss in VH	14 (52%)	7 (26%)
Grade 3: >40% loss in VH	4 (15%)	0 (0%)
Lumbar spine BMD		
aBMD Z-score	-2.1 (-4.9, -0.4)	-1.4 (-2.6, -0.2)
vBMD Z-score	-1.0 (-3.0, 0.9)	-0.1 (-2.6, 1.4)

Median (min, max) values reported unless otherwise specified.
VF = Vertebral fracture, VH=Vertebral height, BMD= Bone mineral density; a=areal, v=volumetric.

Table. Clinical Parameters Pre- and 12 Months Post-Treatment

***Disclosures: Anne Marie Sbrocchi**, None.*

SA0027

***In vivo* Microstructural Quantification of Finger Joints using High-Resolution pQCT.** Christoph Kolling[1], Kathryn S Stok*[2], Thomas L Mueller[2], Ralph Müller[2], Jörg Goldhahn[2]. [1]Schulthess Clinic, Switzerland, [2]ETH Zurich, Switzerland

Fingers are a primary target of destructive processes like rheumatoid arthritis (RA) leading to bony erosions, destruction of the subchondral bone and local osteopenia, and results in loss of hand function. Evaluation of treatment success is limited to measures such as counting of swollen joints or scoring of X-rays. In contrast, high-resolution peripheral quantitative computed tomography (HR-pQCT) can detect small changes in bone microarchitecture and is established for analysis of peripheral joints in vivo (distal tibia and radius). High-resolution structural measurements of finger joints, however, have not been performed to-date. The goal of this study was to quantify structural parameters in finger bones from a group of healthy volunteers, and to correlate this with established parameters at the ipsilateral radius.

A group of 19 healthy volunteers (aged 39 to 69) underwent clinical assessment to ensure the absence of any systematic disease. HR-pQCT measurements (Scanco Medical AG) in conjunction with a fixation device (Pearltec AG) were performed at the metacarpal-phalangeal (MCP) and proximal interphalangeal (PIP) joints of the right hand (Fig 1a) with an isotropic nominal resolution of 82 μm. Two volumes of interest were defined; the trabecular bone of the epiphyseal region, and the cortical shell surrounding it (Fig 1b). Morphometric parameters were computed, and Wilcoxon Rank-Sum and Spearman correlation coefficient were used to test statistical relationships.

Significant differences were seen for all parameters between fingers and between joint parts for average bone density, D100, and cortical thickness, Ct.Th. In the MCP, D100 and Ct.Th increased in the distal region. From finger 2 to 3 to 4, D100 decreased in the MCP and increased in the PIP. Strong correlations were observed in finger joints between the proximal and distal aspects, and strong correlations were also found between the fingers themselves. Finally, the ipsilateral radius correlated weakest to finger 2, and strongest to fingers 3 and 4, especially in the PIP distal region.

In conclusion, the data show distinct structural relations between joint parts, between joints of the same finger, and within the same region of different fingers. These findings indicate that HR-pQCT has the potential for analysing structural changes in small finger bones with the onset of RA. The healthy cohort will now be used as a normative database for examining subchondral bone changes with the onset of RA.

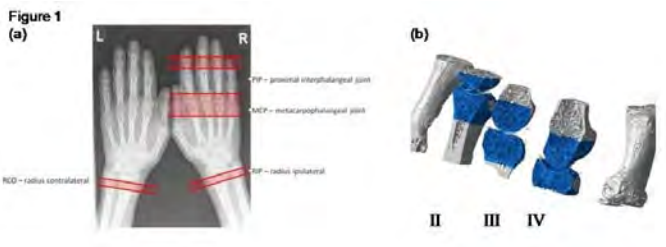

Figure 1. (a) Measurement regions for HR-pQCT scans, and (b) Specific joint volumes of interest.

***Disclosures: Kathryn S Stok**, None.*

SA0028

See Friday Plenary number FR0028.

SA0029

Agreement between pQCT and DXA-derived indices of bone geometry, density and theoretical strength in females of varying age, maturity and physical activity. Portia Flowers*[1], Jodi Dowthwaite[2], Rebecca Hickman[1], Tamara Scerpella[3]. [1]SUNY Upstate Medical University, USA, [2]State University of New York, Upstate Medical University, USA, [3]State University of New York Upstate Medical University, USA

Purpose

DXA is commonly used to assess bone but does not specifically measure cross-sectional geometry, compartmental density or skeletal strength. Indices of bone geometry and strength can be derived from DXA output (Sievanen 1996). Previously, we used pQCT as a standard to validate these DXA-derived indices in post-menarcheal females (Dowthwaite 2009). In the current study, we validate these indices across a broader maturational range.

Methods

Contemporaneous pQCT and DXA scans of the distal radius were performed in 97 females, aged 8.0 to 22.8 yrs, mean=15.1 yrs (premenarche n=42; postmenarche n=55). Ultradistal (UD) and 1/3 DXA indices were compared to 4% and 33% pQCT results, using Pearson correlations and mean differences (Bland-Altman plots). The original Sievanen formulae were modified to improve inter-method agreement for UD output.

Results

DXA and pQCT indices were significantly positively correlated with stronger correlations at 1/3 (R=0.85–0.93, $p<0.001$) than at UD (R=0.64–0.97, $p<0.001$). At UD, all DXA indices exceeded pQCT measures except periosteal cross-sectional area (CSA). At 1/3, DXA indices exceeded pQCT measures for all CSA indices. DXA indices were lower than pQCT results for bone mineral apparent density (BMAD), cortical thickness, section modulus, and fall strength ratio. Inter-method agreement was only affected by maturity level for UD BMAD and fall strength; DXA vs. pQCT differences were positive premenarche and negative postmenarche.

Conclusion

Across a broad age and maturity range, DXA-derivations for the distal radius yield useful indices of bone geometry, density and strength, providing a valuable supplement to traditional DXA assessments of the distal radius during growth.

References

Sievanen, H., P. Dannus, V. Nieminen, A. Heinonen, P. Oja, I. Vuori. 1996 Estimation of various mechanical Characteristics of human bones using dual energy x-ray absorptiometry: methodology and precision. Bone 18:17S – 27S.

Dowthwaite, J.N., R.M. Hickman, J.A. Kanaley, R.J. Ploutz-Snyder, J.A. Spadaro, T.A. Scerpella. 2009 Distal Radius Strength: A Comparison of DXA-Derived vs pQCT-Measured Parameters in Adolescent Females. J CLin Densitom 12: 42 – 53.

DXA vs. pQCT-derived indices:Pearson correlation coefficients and mean differences (95% confidence intervals)

UD (n= 94)				1/3 (n=97)			
DXA	pQCT	r	DXA-pQCT index Mean Difference (95% CI)	DXA	pQCT	r	DXA-pQCT index Mean Difference (95% CI)
BMAD (g/cm^3)	Total vBMD (g/cm^3)	0.64	0.017 (-0.118 to 0.152)	BMAD (g/cm^3)	Total vBMD (g/cm^3)	0.77	-0.281 (-0.396 to -0.166)
Total CSA (mm^2)	Total CSA (mm^2)	0.86	-5.2 (-71.6 to 61.1)	Total CSA (mm^2)	Total CSA (mm^2)	0.96	30.55 (5.64 to 55.46)
IBS (g^2/cm^4)	IBS (g^2/cm^4)	0.97	0.002 (-0.092 to 0.095)	Cortical CSA (mm^2)	Cort/Sub CSA (mm^2)	0.98	2.63 (-4.44 to 9.70)
Fall Strength Ratio	Fall Strength Ratio	0.90	1.25 (-7.90 to 10.0)	Cortical CSA (mm^2)	Cortical CSA (mm^2)	0.98	4.29 (-2.51 to 11.10)
				Intramedullary CSA (mm^2)	Intramedullary CSA (mm^2)	0.85	27.92 (3.61 to 52.23)
				Cortical Thickness (mm)	Cortical Thickness (mm)	0.90	-0.51 (-0.98 to -0.04)
				Section Modulus (mm^3)	Polar SSI (mm^3)	0.95	-20.31 (-68.36 to 27.74)
				Fall Strength Ratio	Fall Strength Ratio	0.80	0.12 (0.05 to 0.19)

Table 1

***Disclosures: Portia Flowers**, None.*

SA0030

See Friday Plenary number FR0030.

SA0031

See Friday Plenary number FR0031.

SA0032

Comparison between Clinical Diagnostic Tools and QCT-based Finite Element Models for Predicting Human Vertebral Apparent Strength In Vitro. Enrico Dall'Ara*[1], Dieter Pahr[1], Peter Varga[1], Franz Kainberger[2], Philippe Zysset[1]. [1]Vienna University of Technology, Austria, [2]Medical University of Vienna, Austria

Vertebral fracture is a common medical problem in osteoporotic individuals. Bone Mineral Density (BMD) is nowadays the gold standard to evaluate fracture risk *in vivo*. Quantitative computer tomography (QCT)-based finite element analysis (FE) may be an attractive method to predict vertebral strength. The aim of this study was to compare the ability of FE and clinical diagnostic tools to predict vertebral strength *in vitro* using an improved testing protocol.

Soft tissues and endplates were removed from 37 vertebral bodies (level T12-L5, gender 7M-3F, age 44-82). The obtained sections were scanned with QCT (0.39x0.39x0.45 mm^3) and the images calibrated with a phantom. Bone mineral content (BMC), total BMD (vBMD), areal BMD from lateral (aBMD-lat) and anterior-posterior (aBMD-ap) projections were evaluated. Wedge shape fractures were then induced in each section with a novel testing setup [1]. FE models were generated from QCT images coarsened to 1.3^3 mm^3 by converting voxels directly to hexahedral elements. The boundary conditions were well controlled during the test and accurately reproduced in the models. For both experiments and nonlinear FE, both strength (defined as maximal load: Exp_FM and FE_FM) and apparent strength (defined as maximal load divided by mean cross section area: Exp_App_FM and FE_App_FM) were computed. Density-based (vBMD) and mass-based (BMC) measurements were used to predict Exp_App_FM and Exp_FM, respectively. FE and mixed variables (aBMD-ap and aBMD-lat) were used to predict both.

FE was found to better predict Exp_App_FM and Exp_FM (R^2=0.80 and R^2=0.79) than diagnostic tools (Exp_App_FM: R^2=0.74 for vBMD, R^2=0.41 for aBMD-lat and R^2=0.48 for aBMD-ap; Exp_FM: R^2=0.70 for BMC, R^2=0.67 for aBMD-lat and R^2=0.63 aBMD-ap). In particular, prediction of Exp_App_FM with FE was quantitatively correct without fitting and significantly better than the ones found for aBMD-ap and aBMD-lat (Fischer's z-test: $p<0.01$ for both).

Due to the normalization with area that accounts for bone dimension, Exp_App_FM may be the most relevant parameter for vertebral fracture risk. It should also be emphasized that our aBMD measurements were free of the artifacts that are usually generated by the posterior elements and iliac crest during standard DEXA. Nevertheless, it remains to be tested if significantly improved FE prediction of vertebral strength enhances significantly the determination of vertebral fracture risk.

[1] Dall'Ara et al., Bone, 44: P325, 2009

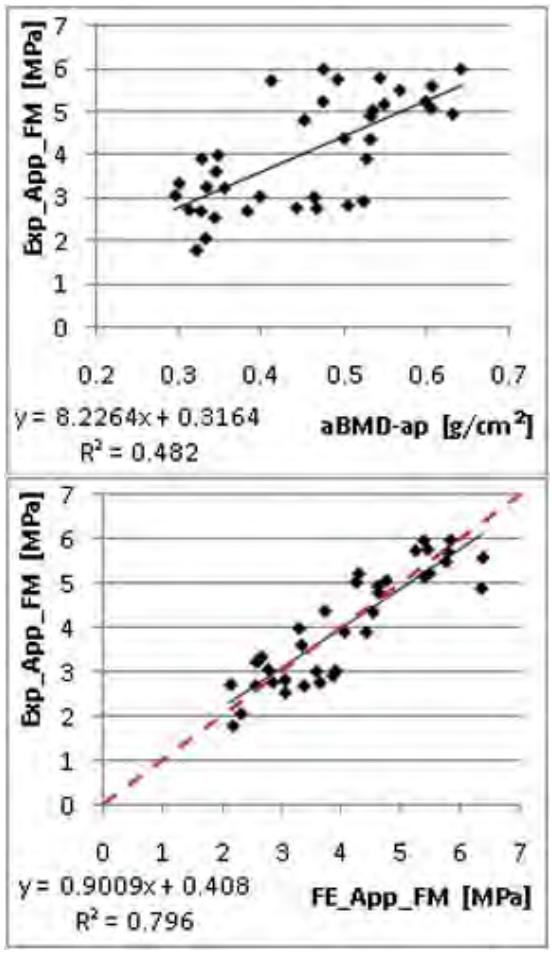

Exp_App_FM predictions with aBMD-ap and FE_App_FM. Red dashed line represents 1:1 relation.

***Disclosures: Enrico Dall'Ara**, None.*

SA0033

CT-based Structural Rigidity Analysis Can Alter the Course of Treatment in Patients with Skeletal Metastasis. Brian Snyder*[1], Ara Nazarian[2], Vahid Entezari[3], John Hipp[4], Nathan Calderon[5], Richard Terek[6], Edward Cheng[7], Albert Aboulafia[8], Megan Anderosn[3], Mark Gebhardt[3], Timothy Damron[9]. [1]Children's Hospital BostonHarvard Medical School, USA, [2]Beth Israel Deaconess Medical Center, USA, [3]BIDMC, USA, [4]Baylor College of Medicine, USA, [5]UT Austin, USA, [6]Brown University, USA, [7]University of Minnesota, USA, [8]Sinai Hospital, USA, [9]State University of New York Upstate Medical University, USA

The skeleton is the 3rd most common site of metastatic cancer, and a third to half of all cancers metastasize to bone. Clinicians make subjective assessments regarding fracture risk using clinical guidelines now recognized to be inaccurate. We have developed and validated a CT-based structural rigidity analysis (CTRA) method to monitor the fracture risk associated with metastatic lesions. We hypothesize that introduction of CTRA to the physicians' decision making process will alter the management of patients with skeletal metastasis. The aim of this study was to evaluate whether patient's treatment based on clinical guidelines was changed by CTRA.

X-rays and CT scans of the involved bones were obtained on all patients with a hydroxyapatite phantom included in the image to convert the X-ray attenuation for each pixel to bone mineral density. The elastic and shear moduli of elasticity were calculated from bone mineral density using empirically derived constitutive relationships. The cross-section through the affected bone that has the largest reduction in rigidity is the weakest and assumed to govern failure of the entire bone. The orthopaedic oncologist was asked to select between: Observation, chemo/radiation, non-invasive surgical stabilization and tntercalary allograft/prosthetic replacement based on the fracture risk assessment using Mirels' score and then again after reviewing the CTRA report. Treatment plans based initially on clinical guidelines and then again after CTRA were compared to identify cases where the treatment plan was changed as a result of CTRA.

Forty seven patients with 56 metastatic lesions to the appendicular skeleton were enrolled into the study. Based on Mirels' criteria (score ⩾9), 43 (78.2%) lesions needed prophylactic fixation, while CTRA-based fracture threshold identified 28 (50.9%) lesions at risk for fracture and suggested prophylactic surgery. Treatment based on CTRA would have changed the initial treatment plan for 19 (34.5%) lesions. In 43 lesions, the clinician did not deviate from the original treatment plan, although in 11 of them CTRA indicated a different course of treatment, which of those 3 out of 11 (27.3%) were at high risk for fracture.

The results of the study suggest that CTRA has the potential to alter treatment plan based on clinical guidelines in 35% of the time. CTRA was most valuable in cases where bone destruction was moderate or osteoporosis was coexistent.

***Disclosures: Brian Snyder**, None.*

SA0034

See Friday Plenary number FR0034.

SA0035

Effects of Rosiglitazone on Bone: Assessing QCT Parameters in a Mechanistic Study in Postmenopausal Women with type 2 Diabetes Mellitus. John Bilezikian*[1], Barbara Kravitz[2], E. Michael Lewiecki[3], Colin Miller[4], Allison R. Northcutt[5], Gitanjali Paul[5], Alexander R. Cobitz[5], Antonio Nino[6], Lorraine Fitzpatrick[7]. [1]Columbia University College of Physicians & Surgeons, USA, [2]GlaxosmithKline Pharmaceuticals, USA, [3]University of New Mexico School of Medicine, USA, [4]BioClinica, Inc. (formerly Bio-Imaging Technologies, Inc.), USA, [5]CVM/MDC, GlaxoSmithKline, USA, [6]GSK, USA, [7]GlaxoSmithKline, USA

Abstract

This mechanism-of-action study assessed the effect of rosiglitazone (RSG) on bone mass and structure through imaging modalities including areal bone mineral density (BMD) and hip structural analysis (HSA) with dual-energy X-ray absorptiometry (DXA) of the lumbar spine and hip, high resolution magnetic resonance imaging (hr MRI) of the wrist, digitized hip radiography and volumetric BMD of the lumbar spine and hip with quantitive computerized tomography (QCT) . Serum biomarkers of bone formation and resorption, calcium homeostasis and selected sex hormone changes over time were assessed. Parameters of glucose control included measurement of hemoglobin A1C (HbA1C), fasting plasma glucose (FPG) and serum insulin. Here we present the effect of RSG on volumetric BMD at the hip and lumbar spine as measured by QCT (CT.gov.NCT00679939).

Methods

This was a Phase IV, 52 week, double-blind, multicenter study. A total of 226 postmenopausal women were randomized in a 1:1 ratio of RSG or metformin (MET). At baseline mean age was 63.8 $\pm$ 6.5 years while mean years post-menopause was 16.9 $\pm$ 8.4. Median duration of diabetes was 3.5 (1.8 -7.8) years. Other baseline characteristics were: mean body mass index (BMI) 31.4 $\pm$ 5.9 kg/m^2; mean FPG and HbA1c were 111.7$\pm$ 23.4 mg/dl and 6.4 $\pm$ 0.65% respectively. Femoral neck BMD was 0.83 g/cm$^2\pm$ 0.141, at total hip 0.98 g/cm$^2\pm$ 0.123, and at total spine 1.05 g/cm^2 $\pm$ 0.161. Femoral neck T-score was -0.95$\pm$ 0.908, total hip -0.02$\pm$ 0.970, and total spine was -0.55 $\pm$ 1.247.

Using spiral multi-detector scanners, a subset of 79 subjects underwent QCT scans of the lumbar spine and hip at baseline and after 52 weeks of treatment. All scans were centrally evaluated and read. The change in integral, cortical and trabecular BMD at the lumbar spine and hip from baseline to week 52 was estimated within and between the two treatment groups.

Conclusion:

Volumetric trabecular, cortical and integral BMD at the hip and the lumbar spine may provide insight on the effect of RSG on bone and may help explain the increased risk of fracture reported in long-term controlled clinical trials.

***Disclosures: John Bilezikian**, GlaxoSmithKline, 5*
This study received funding from: GlaxoSmithKline

SA0036

Effects of Rosiglitazone on Bone: Understanding its Effects through Assessment of Bone Structure using Digitized x-rays in a Mechanistic Study of Postmenopausal Women with type 2 Diabetes Mellitus. Antonio J. Nino*[1], Claude Arnaud[2], Rene Vargas-Voracek[3], Cesar Bogado[4], Barbara Kravitz[5], Allison R. Northcutt[1], Gitanjali Paul[1], Alexander R. Cobitz[1], Lorraine Fitzpatrick[6]. [1]CVM/MDC, GlaxoSmithKline, USA, [2]University of California at San Francisco, USA, [3]Imaging Therapeutics, USA, [4]Instituto De Investigaciones Metabolicas (IDIM), Argentina, [5]GlaxosmithKline Pharmaceuticals, USA, [6]GlaxoSmithKline, USA

Abstract:

The study objective was to characterize the effects of rosiglitazone (RSG) on bone mass and structure in postmenopausal women with type 2 diabetes mellitus through different imaging modalities including dual-energy X-Ray absorptiometry (DXA) of the lumbar spine and hip region, hip structural analysis (HSA), high resolution magnetic resonance imaging (hr MRI) of the wrist, quantitative computerized tomography (QCT) of the lumbar spine and structural assessment using hip

radiographs (ImaTx). Serum biomarkers of bone formation and resorption, calcium homeostasis and selected sex hormone changes over time were assessed. Parameters of glucose control included measurement of:hemoglobin A1C (HbA1C), fasting plasma glucose (FPG),and serum insulin. Here we present findings from assessment of hip radiographs.

Methods:

This was a phase IV, double-blind, multi-center study (CT.gov. NCT00679939) of 52 weeks duration. A total of 226 postmenopausal women were randomized to RSG or metformin (MET) in a 1:1 ratio. At baseline mean age was 63.8 ± 6.5 years while mean years post-menopause was 16.9 ± 8.4. Median duration of diabetes was 3.5 (1.8 -7.8) years. Other baseline characteristics were: mean body mass index (BMI) 31.4 ± 5.9 kg/m^2; mean FPG and HbA1c were 111.7 ± 23.4mg/dl and 6.4 ± 0.65% respectively. Femoral neck BMD was 0.83 g/cm^2 ± 0.141, at total hip 0.98 g/cm^2 ± 0.123, and at lumbar spine 1.05 g/cm^2 ± 0.161. Femoral neck T-score was -0.95 ± 0.908, total hip -0.02 ± 0.970, and lumbar spine is -0.55 ± 1.247.

All subjects underwent hip radiographs at Baseline and Week 52. All radiographs were read centrally. A total of 30 femoral geometry and cortical macro-anatomical-parameters were measured including hip axis length, neck-shaft angle, neck cortical thickness and shaft cortical thickness.

Conclusion:

Trends and differences, observed between relevant group comparisons of bone structure measurements from hip radiographs of postmenopausal women followed during the study,may provide insight on the effect of RSG on bone and its relation to the risk of bone fractures.

***Disclosures: Antonio J. Nino**, GlaxoSmithKline, 3*
This study received funding from: GlaxoSmithKline

SA0037

See Friday Plenary number FR0037.

SA0038

In Vivo Evaluation of an Anatomical Subject-specific FE-model to Predict Hip Fracture Load. Erwan Jolivet*[1], Marie-Astrid DUCOBU[2], Valérie Bousson[3], Klaus Engelke[4], Jean-Denis Laredo[5], David Mitton[2], Wafa Skalli[6]. [1]Arts et métiers ParisTech, France, [2]Arts et Metiers ParisTech, CNRS, LBM, France, [3]Hôpital Lariboisière, France, [4]University of Erlangen, Germany, [5]Service de Radiologie ostéo-articulaire, Hôpital Lariboisière, Assistance Publique des Hôpitaux de Paris et Faculté de Médecine Diderot, Université Paris 7, France, [6]Arts et Metiers ParisTech, CNRS, France

Finite element models have proved their ability to predict bone strength better than DXA and several author have developed and validated in vitro subject specific finite element models. However there is still no validation on in vivo data. Using a previously validated finite-element model of the proximal femur, this study investigated first whether contra lateral femur strength could be an appropriate indicator for in-vivo model evaluation and secondly if such finite element model is able to discriminate fractured patients from controls.

The model was applied to 22 patients, 11 controls and 11 with a hip fracture. All subjects were women with age ranged from 71 to 96 years and data were collected during the 3D-QCT European project.

The CTscan acquisition and reconstruction parameters were 1 mm contiguous slices, B40s convolution kernel and 0.293 mm in-plane pixel size. First, periosteal and endosteal surfaces were semi-automatically segmented using MIAF software (Kang et al. 2004) and hexahedral patient-specific mesh was automatically generated. Bone was considered as a heterogeneous isotropic material with a Poisson's ratio of 0.4. A Young's modulus and an ultimate stress were attributed to each element based on Hounsfield Units (Duchemin et al. 2008) and a stress based criterion was defined to assess fracture load . For simulation, the boundary conditions reproduced a stance configuration.

To validate the hypothesis of using the contra lateral femur for patient analysis, both right and left femurs in the control groups were modelled. No significant difference of the fracture load was observed using a paired t-test ($p<0.05$).

Considering three range of the fracture load (low < 5000 N, middle 5000-7000 N and high fracture load > 7000 N), 55%of the patients were classified in the low level group and only 18% in the high level group. On the contrary, 14% of the control subjects were in the low level group and 55% were classified in the high level group.

These results are promising as for the identification of subjects with high risk of hip fracture. Taking into account clinical parameters, such as defined by Frax index, should still improve the accuracy to go towards fracture risk estimation.

Duchemin, L., et al. Med Eng Phys 30(3): 321-8, 2008.

Duchemin, L., et al. Comput Methods Biomech Biomed Engin 11(2): 105-11, 2008.

Kang, Y., et al. Med Image Anal 8(1): 35-46, 2004.

***Disclosures: Erwan Jolivet**, None.*

SA0039

See Friday Plenary number FR0039.

SA0040

Lean mass predicts bone mineral density and estimates of hip strength in middle-aged individuals with non-insulin-requiring type 2 diabetes mellitus. Kendall Moseley*[1], Devon Dobrosielski[2], Kerry Stewart[2], Deborah Sellmeyer[2], Suzanne Jan De Beur[3]. [1]The Johns Hopkins Hospital, USA, [2]The Johns Hopkins Bayview Medical Center, USA, [3]Johns Hopkins University, USA

Purpose: Individuals with type 2 diabetes mellitus (T2DM) typically have higher bone mineral density (BMD), but higher fracture risk, than non-diabetics. Our aim was to examine the independent contributions of fat and lean mass to BMD and estimates of hip strength in those with T2DM.

Methods: Subjects for this cross-sectional analysis were men (n=78) and women (n=56) aged 56 ± 6 years with uncomplicated, non-insulin-requiring T2DM. Total body fat and lean mass as well as total body, hip, and lumbar spine BMD were measured with dual energy x-ray absorptiometry (DXA). Abdominal visceral, subcutaneous (SQ) and total abdominal fat were measured with magnetic resonance imaging. Averaged bilateral femoral neck strength measures including section modulus (SM), cross sectional area (CSA) and buckling ratio (BR) were estimated from DXA using validated hip structure analysis (HSA) formulae.

Results: Participants had normal BMD at all sites and were overweight to morbidly obese (BMI 29 to 41 kg/m^2) with well controlled T2DM (HbA1C in women 6.6 ± 1.2%, men 6.7 ± 1.6 %). In bivariate analysis, higher lean mass was associated with higher total body, femoral neck and hip BMD and higher SM and CSA across both sexes (r=0.36-0.55). In men only, lean mass was inversely correlated with BR (r=-0.27, $p<0.05$). Increased total body fat mass and abdominal SQ fat correlated with increased total body and hip BMD as well as increased SM and CSA in women (r=0.34-0.57). In men, these fat measures correlated with only total body BMD and no estimates of hip strength. In multiple regression analyses, lean mass remained a significant predictor of total body, hip and femur BMD in men and women, while fat mass predicted only total body BMD ($p<0.05$). In a separate model including both sexes, lean mass significantly contributed to all three measures of hip strength.

Conclusions: In middle-aged men and women with non-insulin-requiring T2DM, lean mass was a significant predictor of BMD at the total body, hip and femoral neck. Lean mass predicted measures of hip strength including SM, CSA and BR. Fat mass may additionally contribute to BMD and HSA in women. These data suggest that maintenance of lean mass may preserve BMD and maintain hip integrity in those with T2DM who lose weight to improve insulin sensitivity. Strengthening exercises may be an intervention for hip fracture prevention in T2DM.

***Disclosures: Kendall Moseley**, None.*

SA0041

See Friday Plenary number FR0041.

SA0042

See Friday Plenary number FR0042.

SA0043

Predicting Subchondral Bone Structural Properties Using a Depth-Specific CT Topographic Mapping Technique in Normal and Osteoarthritic Proximal Tibiae. James Johnston*[1], Saija Kontulainen[1], Bassam Masri[2], David Wilson[3]. [1]University of Saskatchewan, Canada, [2]University of British Columbai, Canada, [3]University of British Columbia, Canada

Altered subchondral bone mechanical properties are undoubtedly involved in the initiation and/or progression of osteoarthritis (OA). To better understand the role of bone in OA we developed a 3D *in vivo* imaging tool: computed tomography topographic mapping of subchondral density (CT-TOMASD). CT-TOMASD employs quantitative CT (QCT) and surface projection image processing to characterize and map subchondral bone mineral density in relation to depth from the subchondral surface. The main objective of this study was to determine if CT-TOMASD could predict the structural stiffness of proximal tibial subchondral bone. A secondary objective involved assessing whether factors such as compartment (medial/lateral), age or cartilage degeneration (an indicator of OA disease) affected these predictions.

Fourteen proximal tibial compartments (4 medial, 10 lateral) from 10 donors (10M; age: 73+/-11 years) were CT scanned (0.5mm isotropic voxel) with a QCT bone density phantom. CT-TOMASD averaged subchondral bone density to depths of 1.5, 2.5, 5 and 10mm from the subchondral surface (Fig. 1). We performed indentation testing (3.5mm diameter flat indentor, 2mm/minute rate, 0.5mm displacement, 250N max load) directly at the subchondral surface (4-6 sites per compartment, 68 sites in total). Prior to indentation, cartilage degeneration was graded using ICRS scoring. Test sites were classified as normal (ICRS<2; n=39) or OA (ICRS>=2; n=29). We

related structural stiffness to CT-TOMASD measures using power-law regression models (SPSS). We adjusted the models for compartment, age and cartilage status to test effect on model prediction. If no effect was observed, we tested the coincidence of separate regression models using F tests.

CT-TOMASD measures across the 0-1.5mm layer explained 54% of the variance in stiffness (p=0.000) (Fig. 2). After adjustments, the model explained 61% of the variance in stiffness (p=0.004). Density was the primary predictor (beta=0.77; p<0.001) while side (beta=0.24; p=0.005) improved model prediction. Age (beta=0.01; p=0.859) did not improve model prediction nor did cartilage status (beta=0.13; p=0.087). F tests revealed that separate normal and OA regression models exhibited similar stiffness-density relationships. CT-TOMASD measures to depths of 2.5, 5 and 10mm from the subchondral surface explained less variation in stiffness than across the 0-1.5mm layer. CT-TOMASD has potential to predict subchondral bone stiffness *in vivo*.

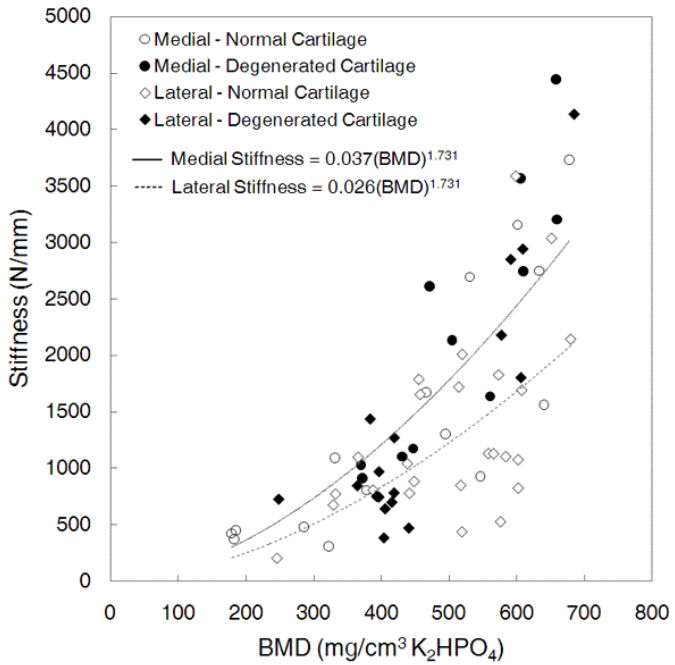

Figure 2 - Stiffness-density plots for medial and lateral plateaus.

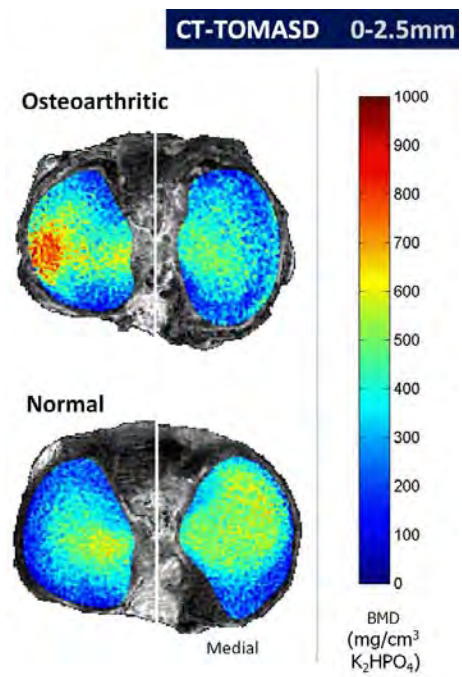

Figure 1 - CT-TOMASD images subchondral density from OA and normal knees.

***Disclosures: James Johnston**, None.*

SA0044

Predicting Trabecular Bone Elastic Properties from MRI-derived Measures of Bone Volume Fraction and Fabric. Michael Wald*[1], Jeremy Magland[1], Chamith Rajapakse[2], Ed Guo[3], Felix Werner Wehrli[1]. [1]University of Pennsylvania Medical Center, USA, [2]University of Pennsylvania School of Medicine, USA, [3]Department of Biomedical Engineering, Columbia University, USA

Significant effort has been expended on predicting bone strength through in vivo assessment of its structure. Even though bone volume fraction (BVF) is predictive of bone strength, the variation in mechanical properties with test direction requires inclusion of measures of structural orientation. Here, we examine whether the inclusion of trabecular bone (TB) fabric can improve the BVF-based prediction of the elastic constants derived from linear μFE analysis of μMR images acquired with resolution and signal-to-noise (SNR) characteristics achievable in vivo.

Thirty demarrowed, cadaveric human distal tibia specimens were fixed in 1 mM aqueous Gd-DTPA/10% formalin solution. Images with a 160 μm isotropic voxel size were acquired using a two-channel phased-array ankle coil and a custom-designed 3D spin-echo sequence at 1.5T field strength. Micro-MR datasets were processed to yield BVF images with pure bone and pure marrow corresponding to intensities of 100 and 0, respectively. Two 7.5x7.5x7.5mm^3 sub-regions of TB were extracted from the posterior (P) and lateral (L) portions of the tibia where the TB orientation is known to be different (Figure a). Each sub-region was subjected to orientation analysis via the mean-intercept-length (MIL) algorithm where angularly-sampled MIL measurements were fit to an ellipsoid with axes λ_1, λ_2, λ_3. Six stress/strain simulations were performed via μFE analysis where each element was assigned a modulus proportional to its BVF with pure bone having 15GPa. The nine orthotropic elastic constants (three Young's moduli - E_{ii} (i=1, 2, 3), three shear moduli - G_{ij} (j=1, 2, 3), and three Poisson's ratios - v_{ij}) were fit to a model [Cowin, 1985] of the normalized fabric eigenvalues λ_1, λ_2, λ_3 and power-law functions of BVF where the exponent α was allowed to vary from 1 to 3.

Each sub-region's E_{ii} were best predicted by separate power-law functions of BVF (R^2s=0.92-0.98, Figures b and c - P and L sub-regions, respectively). Adding fabric into the model predicted the pooled data for both analysis regions and all testing directions with high accuracy (R^2=0.986, Figure d). Model agreement for pooled G_{ij} and v_{ij} were also good when fabric information was considered (R^2s=0.99 and 0.68). Non-pooled models of BVF explained variations in G_{ij}, but not in v_{ij} (P: R^2s=0.92-0.97 and 0.08-0.51, L: R^2s=0.92-0.96 and 0.04-0.42). Inclusion of fabric information established a general model between BVF and elastic constants independent of sub-region and test direction. The data emphasize (1) the importance of fabric as a predictor of bone mechanical properties, and (2) that these relationships can be assessed in the limited resolution and SNR regime of μMRI.

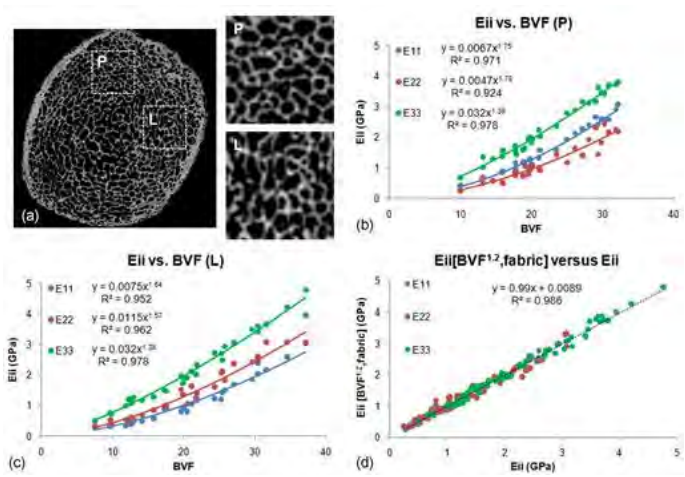

Figure

***Disclosures: Michael Wald**, None.*

SA0045

Quantitative Characterization of Motion Artifact in HR-pQCT Images of the Distal Radius and Tibia. Miki Sode*[1], Andrew Burghardt[2], Jean-Baptiste Pialat[3], Thomas Link[2], Sharmila Majumdar[2]. [1]University of California San Francisco & Berkeley, USA, [2]University of California, San Francisco, USA, [3]INSERM U831,Université de Lyon & Hospices Civils de Lyon, France

Motion artifacts are commonly seen in in vivo high-resolution peripheral quantitative computer tomography (HR-pQCT) images, especially at the radius. Compromised image quality confounds the accuracy of cortical and trabecular

densitometric and structure indices. It often leads to repeating the acquisition, thereby exposing the subject to more radiation. Criteria for accepting/rejecting an image are highly subjective. Therefore, the objective of this study was to develop a technique to measure motion and estimate error.

A total of 54 sets of HR-pQCT images of the distal radius (N=33) and tibia (N=21) acquired for various studies conducted in our laboratory were reviewed. Each set consisted of 2 acquisitions of the same site before and after repositioning. At least one image was graded 1 (no visible motion) according to the manufacturer-suggested quality grading system. The cortical and trabecular densitometric and structure indices were calculated for each image, and the % difference between paired was calculated. The amount of motion during a single acquisition was quantitatively measured in the following manner. First, the raw cone beam projection images were parallelized and corrected for dark and flat field intensity. Next the projected bone region at 0˚ and at 180˚ flipped with respect to the detector center were compared using i) normalized mutual information (MI), ii) sum of squared intensity difference (SSD), iii) entropy (E), iv) ratio image uniformity (RIU), and v) maximum normalized cross correlation (NXC). The mean % difference between paired acquisitions was calculated for each measure. A linear regression analysis was performed for the correlation (Spearman's ρ) between the % differences in each index and the similarity measure. Radius and tibia data were pooled.

The % differences in E, RIU, and NXC positively and significantly correlated with the % differences in cortical and trabecular densitometric and structure indices (ρ=0.27-0.58; all $p \leq 0.04$). Cortical area and thickness as well as trabecular bone volume fraction, -number and -spacing had strong correlations with these similarity measures (all $\rho \geq 0.36$ and $p \leq 0.007$) (Figure 1).

The result of this study provides a basis for quantitative characterization of motion artifact.

Figure 1

***Disclosures: Miki Sode**, None.*

SA0046

Radiation Therapy Causes a Rapid Loss of Bone Mineral Density of Thoracic Vertebra in Women and Men Lung Cancer Patients. Michael Lawrence*[1], Jeffrey Willey[2], Mert Saynak[1], Ted Bateman[3], Lawrence Marks[1]. [1]University Of North Carolina, USA, [2]Clemson University, USA, [3]Univesity of North Carolina, USA

Cancer patients receiving radiation therapy (RT) for pelvic tumors are at greater risk of hip fractures. The mechanisms are unknown, but recent preclinical studies have identified a rapid activation of osteoclasts. We hypothesize that RT also causes atrophy of thoracic vertebra (ThV) during lung cancer treatment. A retrospective analysis of 25 lung cancer patients was performed. Change in volumetric bone mineral density (vBMD) was examined using pre- and 6 months post-RT thoracic CT scans. Ten women (mean age of 61 years) and 15 men (72 years) were studied; no patients received chemotherapy or antiresorptive treatment.

Patients typically received a total RT dose of ~66 Gy in 2.0Gy/day fractions to the tumor. The trabecular bone of 6 vertebral bodies were contoured using UNC's RT treatment planning system (PlanUNC); the average CT density was calculated for pre- and post-RT contours. The mean dose for each ThV was determined by PlanUNC, permitting assessment of the dose-dependent nature of vBMD changes. All density changes were normalized to tissue changes well outside the treatment beam. Significance was determined by paired t-test.

The average loss of ThV vBMD for each patient was -21% ($p<0.001$), with no difference in the degree of loss for women (-21%,$p<0.001$) and men (-21%,$p<0.001$). Linear regression analysis showed no correlation with patient age and vBMD decline. By calculating RT dose to each vertebra within a patient, we were able to examine the relative radiation sensitivity of ThV trabecular bone. Significant loss of vBMD occurred across dose ranges: 45+ Gy (-24%,$p<0.001$); 35-45 Gy (-23%,$p<0.001$); 25-35 Gy (-15%,NS); 15-20 Gy (-16%,$p=0.047$); and 5-10 Gy (-20%,$p=0.003$). No differences were observed between doses using a 1-way-ANOVA.

Lung cancer patients receiving RT lost ThV vBMD in incidentally irradiated bone at a rapid rate of ~3% per month. Trabecular bone within the ThV appears to be a radiation-sensitive tissue, occurring with only a total dose of5-15 Gy. This rate of TrV bone loss confirms other clinical data from pelvic tumor RT. This rate of loss also conforms to preclinical reports showing early osteoclast activation from RT. Past studies showing bone loss or fractures from RT have only examined women. In this study, men and women were equally susceptible to bone loss. Future studies need to examine subsequent recovery of vBMD and strength. Antiresorptive therapies may be appropriate to prevent this RT-induced bone loss.

***Disclosures: Michael Lawrence**, None.*

SA0047

Relationship Between Age, Mineral Characteristics, Mineralization, Microhardness, And Microcracks In Human Vertebral Trabecular Bone. Delphine Farlay*[1], Yohann Bala[2], Brigitte Burt-Pichat[3], Roland Chapurlat[3], Georges Boivin[4], Helene Follet[5]. [1]University of Lyon, France, [2]Université De Lyon, France, [3]INSERM U831, Université de Lyon, France, [4]INSERM, France, [5]INSERM, Université De Lyon, USA

Relationship between mineralization and microcracks has been mainly studied on the same Bone Structural Units in cortical bone (1). Our purposes were to analyze at tissue level the contribution of bone mineralization and mineral characteristics in the development of microcracks in trabecular bone. Human vertebrae trabecular cores (L2, Ø 8.2mm, height 10mm) from 53 cadavers (54-95 yrs) were embedded in PMMA for analysis of pre-existing microcracks by bulk staining in xylenol (2), Crack length (Cr.Le) and crack density (Cr.Dn) were measured. Fourier Transform Infrared Microspectroscopy was performed on 2µm-thick sections (mean of 20 areas by sample, 30*100µm each). Mineral maturity (MM) was the ratio between apatitic/non apatitic phosphates, and mineralization index (MI) the ratio between mineral/organic matrix. Crystallinity index (CI) reflected size/perfection of bone crystals (3-4). Quantitative microradiography performed on 100µm-thick sections allowed the measurement of the degree of mineralization (DMB), and microhardness (Hv) was calculated on the surfaced block (5). Normality of the distributions was tested, and logarithmic transformation was performed for Cr.Le and Cr.Dn. Relationships between variables were tested using Pearsons' correlations. A positive correlation between age of donor and CI was found. DMB, Hv and MM were positively associated with MI. Interestingly, a positive correlation was found between Cr.Le and DMB, MI, MM, but not with CI (Table). The more mature the mineral was, the higher were the degree of mineralization and the crystallinity, and the harder was bone tissue. Moreover, the length of microcracks increased with the mineralization (degree and maturity), whereas crystals size/perfection had no influence. Thus, propagation of microcracks was more influenced by the age of mineral than by crystals dimension and composition. Finally, the density of microcracks was not influenced by mineralization, suggesting that their propagation and density are not linked. In conclusion, in vertebral bone, crystallinity (crystal size/perfection) increased with age of donor, and could explain partly bone fragility.

1 Wasserman et al Eur J Morph 2005, 42 : 43.
2 Arlot et al J Bone Miner Res 2008, 23 : 1613.
3 Farlay et al J Bone Miner Metab 2010 Epub
4 Bala et al Bone 2010, 46 : 1204.
5 Boivin et al Bone 2008, 43 : 532

Table : Pearsons' coefficient correlations

Variables	CI	MI	Cr.Le	Cr.Dn
Age of donor	0.35*	NS	NS	0.40**
CI	-	0.71**	NS	NS
MM	0.51**	0.65**	0.28*	NS
MI	0.71**	-	0.33*	NS
DMB (g/cm^3)	NS	0.28*	0.29*	NS
Hv (kg/mm^2)	NS	0.30*	NS	NS

*:$p<0.05$; **:$p<0.005$

Table

***Disclosures: Delphine Farlay**, None.*

SA0048

See Friday Plenary number FR0048.

SA0049

See Friday Plenary number FR0049.

SA0050

See Friday Plenary number FR0050.

SA0051

The Effects of Simulated Microgravity and Return to Weightbearing on Densitometric and Mechanical Properties of the Femoral Neck in the Adult Rat HU Animal Model. Joshua Kupke, Scott Morgan*, Yasaman Shirazi-Fard, Joshua Davis, Joseph Marchetti, Alyssa McCue, Susan Bloomfield, Harry Hogan. Texas A&M University, USA

Microgravity-induced bone loss is one of the primary concerns for astronaut health on long duration spaceflights. However, bone mineral density (BMD) does not always provide accurate predictions of changes in bone quality and strength. Thus, bone strength indices based on CT scans have been devised using various combinations of both geometric and densitometric properties The objective of the current study was to characterize the effects of microgravity, and recovery, on the femoral neck (FN) using the adult hindlimb unloaded (HU) rat model. An additional important goal was to compare calculated strength indices to mechanical testing results at the FN.

Adult male Sprague-Dawley rats (6-mo) were grouped into baseline (BL), weightbearing cage control (CC), and hindlimb unloaded (HU). HU animals were further divided into sub-groups (n=15 each): HU euthanized after 28d of suspension, and HU euthanized after 28, 56, and 84 days of recovery. CC groups were euthanized at the same four end points. The excised right femur was scanned ex vivo at the FN using peripheral quantitative computed tomography (pQCT). Mechanical testing was performed with the femur oriented vertically and quasi-static loading applied to the femoral head in a proximal-to-distal direction. This conventional approach creates a combination of compression, bending, and shear in the FN.

HU exposure gave rise to 6.3% lower bone mineral content (BMC) compared to BL and 7.8% lower total volumetric (integral) bone mineral density (vBMD) at the FN. The most dramatic effect was for the neck compression strength index (NCSI), defined as $vBMD^2$ times the minimum cross-sectional area. The mean NCSI was 13.4% lower for HU compared to BL. By contrast, the neck bending strength index (NBSI) was only 3.9% lower. As an estimator of bone strength, NCSI corresponds more closely to the actual maximum breaking force for the femoral neck, which was 17.1% lower after 28d HU. Considering recovery after return to weightbearing, BMC was only 2.5% lower than BL after 28d of recovery and returned to the same level as BL after 56d. After 28d of recovery, vBMD was 5.1% lower than BL but was higher after 56d. The NCSI remained 10.5% and 5.8 % lower after 28d and 56d recovery, respectively. However, the measured breaking force returned to BL levels after only 28d of recovery. Thus, the NCSI is a reasonable predictor of strength for the initial exposure to HU, but underestimates actual strength values during recovery.

***Disclosures: Scott Morgan**, None.*

SA0052

See Friday Plenary number FR0052.

SA0053

See Friday Plenary number FR0053.

SA0054

Mechanically-induced Signaling Events in Loaded Bones In-vivo Include Activation of ERK1/2 During Functional Adaptation. Jason Bleedorn*[1], Susannah Sample[2], Troy Hornberger[3], Peter Muir[4]. [1]University of Wisconsin-Madison, USA, [2]UW-Madison School of Veterinary Medicine, USA, [3]School of Veterinary Medicine - UW Madison, USA, [4]University of Wisconsin, Madison, USA

Purpose: Mechanical stimuli play an important role in the regulation of bone mass. Failure of the skeleton to maintain bone mass contributes significantly to patient morbidity and mortality in conditions such as osteoporosis. The mechanisms involved in converting biophysical signals into the molecular events that regulate functional adaptation have not been defined. The present study was designed to determine activation of mechanically-induced signaling events in bone in an in-vivo bone loading model.

Methods: 22 male rats aged 10-12 weeks were used. 8 rats were used to determine the timeline of signaling events after mechanical loading. 4 rats were used as controls, 2 of which received insulin treatment (5 IU/kg Humulin R) as positive control, and 2 which were sham loaded. The remaining 4 rats had their right ulna loaded at 4Hz for 1,500 cycles at -3,750με (-18N). Individual rats were euthanatized and both right and left ulnas were collected at 0, 15, 30 and 60 minutes after in vivo loading. The remaining 14 rats were used for further investigation of specific time points after bone loading using the same loading protocol. Right and left ulnae were collected at 15 minutes (n=4 loaded, n=3 sham) and at 60 minutes (n=4 loaded, n=3 sham) after right ulna loading. Bones were immediately frozen in liquid nitrogen, ground to a powder with a pestle and mortar, and the proteins extracted. Phosphorylation of p70S6k, PKB, p38, JNK and ERK was examined using Western blot analysis.

Results: Mechanical loading resulted in a cascade of protein phosphorylation evident at various time points in the first phase of the study. Activation of p70S6k(389) PKB(308) PKB(473), JNK1/2 and ERL1/2 were detected in the loaded right ulna after mechanical loading. Activation of p38 was not detected at the time points examined. In the second phase of the study, activation of the ERK signaling pathway (p-ERK1/2) was consistently (n=4) seen in loaded bone at 15 minutes after mechanical loading.

Conclusion: These results confirm that it is possible to detect mechanically-induced signaling events in loaded bone during functional adaptation in-vivo. Load-induced bone formation is associated with activation of p70S6k, PKB, ERK1/2 and JNK1/2 at distinct time points in loaded bones. Further work is needed to determine whether additional mechanically-induced signaling events are evident to further characterize the molecular mechanisms that regulate functional adaptation of the skeleton.

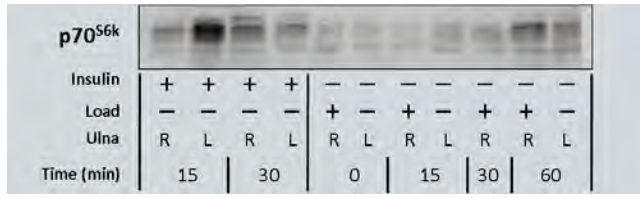

Signaling time line for p70S6k(389) after mechanical loading of the right ulna

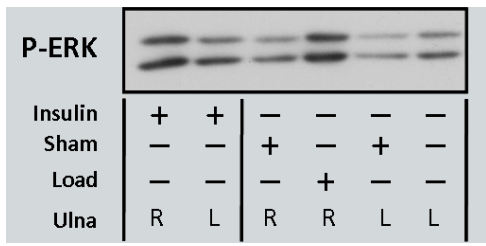

ERK signaling at 15 minutes following mechanical and sham loading of the right ulna

***Disclosures: Jason Bleedorn**, None.*

SA0055

See Friday Plenary number FR0055.

SA0056

Are Exercise-induced Gains in Lumbar Spine vBMD Driven by Changes in Back Extensor and Psoas Muscle Size in Older Men? An 18-month Randomised Controlled Trial. Christine Bailey*[1], Sonja Kukuljan[2], Riku Nikander[3], Caryl Nowson[2], Robin Daly[3]. [1]The University of Melbourne, Australia, [2]School of Exercise & Nutrition Sciences, Deakin University, Melbourne, Australia., Australia, [3]The University of Melbourne, Western Hospital, Australia

Since muscle and bone are inextricably linked, it is often assumed that changes in muscle size and strength should affect bone strength predictably and correspondingly. For older adults, progressive resistance training (PRT) can markedly improve muscle mass and strength, but its effects on LS BMD are mixed. In addition, from the limited Ex trials that have reported a positive effect on LS BMD, few have examined whether the changes in bone are predominantly mediated by gains in back muscle CSA. The aims of this study were to examine: 1) the effects of a multi-component Ex program incorporating PRT and weight-bearing impact Ex on erector spinae (ErSp) and psoas muscle CSA, and CT-measured lumbar spine vBMD in older men; 2) whether any exercise-induced changes in bone were mediated by changes in muscle CSA; and 3) the effects of training load on muscle and bone. Men (n=180) aged 61 ± 7 years ($\pm$SD) were randomised to an Ex or non-Ex group with or without additional Ca-Vit D3. The Ex consisted of high intensity (60-85% 1RM) PRT and weight-bearing impact Ex performed 3 d/wk for 18 mo. QCT was used to assess L1-L3 total and trabecular vBMD (TrvBMD), and muscle CSA. Ex led to a significant 2.3% net gain in TrvBMD and 1.6-4.9% net increase in ErSp and psoas muscle CSA relative to no-Ex (all $p<0.05$). The Ex-induced gains in ErSp, psoas and total back muscle CSA were correlated with the changes in TrvBMD (r=0.26-0.33, $p<0.05$-<0.001). Similar significant correlations were observed in the no-Ex group (r=0.33-0.41, $p<0.01$-<0.001). However, further analysis revealed that there were no differences in the slopes nor intercepts for the changes in muscle and bone between the Ex and no-Ex group. This suggests that the Ex-induced gains in vBMD were not mediated by the changes in muscle size. When we examined the influence of training load on the skeletal changes, we found that the average RT load and number of impacts per session were related to the changes in TrvBMD (r=0.38 and 0.43, respectively, $p<0.001$). When both parameters were entered into the regression model, only the number of impacts per session remained significantly related to the changes in TrvBMD ($p<0.05$). In conclusion, an 18-month Ex program consisting of PRT and impact training was effective for improving both back muscle size and lumbar spine

BMD, but these skeletal changes appeared to be related to the number of impacts per session and not the gains in muscle size.

***Disclosures: Christine Bailey**, None.*

SA0057

Effects of Pulsed Electromagnetic Field Stimulation on Gene Expression Related to Bone Formation in Spontaneously Hypertensive Rats. Hiroaki Takekura[1], Hiroyuki Tamaki*[2], Hideaki Onishi[2], Tomie Nishizawa[3], Kengo Yotani[1], Atsumu Yuki[1], Futoshi Ogita[1], Hikari Kirimoto[2], Kounosuke Tomori[1]. [1]National Institute of Fitness & Sports, Japan, [2]Niigata University of Health & Welfare, Japan, [3]Chukyo Women's University Junior College, Japan

Pulsed magnetic stimulation (PMS) has been used to treat bone disorders and reportedly modifies differentiation, proliferation and mineralization of osteoblasts in vitro. The spontaneously hypertensive rat (SHR) displays a disorder characterized by cancellous bone deficit in the skeleton. We examined the temporal effects of repetitive PMSs (rPMS) on bone formation in vivo for SHR tibiae and femora and investigated magnetic field mapping in bone during PMS. The magnetic sensor was placed in the distal metaphysis of the femur to determine maximum magnetic field strengths during PMS. Measurements were made at 9 positions (X-Y axis) and 9 distances (Z axis) from the sensor during PMS supplied at 10 stimulation intensities in increments of 10% of the maximal output of the stimulator. One hindlimb of male SHR and normal rats at 6 and 33 weeks old was held on the table in the prone position and the PMS probe was placed 10-20 mm from the thigh and leg. A stimulation intensity of 60-80% was used for rPMS at a frequency of 0.5-1 Hz, for 3-5 min. After sacrifice, tibiae were analyzed by quantitative histomorphometry and femora were used for analysis of bone morphogenetic protein (BMP)-2, transforming growth factor (TGF)-β2, osteocalcin (OC), and collagen (Col)-I mRNA expressions by real-time reverse transcriptase-polymerase chain reaction (RT-PCR). Magnetic field strength in the bone during PMS showed a nonlinear hyperbolic decrease and a linear increase depending on probe distance and stimulation intensity, respectively, within the range of 250-450 mT at a distance of 10-20 mm and 60-80% stimulation intensity. Lower trabecular bone volume (BV/TV) was observed in old SHR compared to normal old rats. RT-PCR showed that rPMS stimulated mRNA levels of BMP2 and TGF-β2 after 24-h of treatment compared to the contralateral hindlimb. These findings suggest that temporary local rPMS on the bone provides potent stimulation of bone formation in vivo for SHR by promoting BMP-2, and TGF-β2 production.

***Disclosures: Hiroyuki Tamaki**, None.*

SA0058

Loaded Physical Activity Predicts Bone Strength, but not bone microstructure, at the Distal Radius in Adolescents. Heather McKay*, Danmei Liu, Deetria Egeli, Melonie Burrows. University of British Columbia, Canada

Physical activity (PA) has a positive effect on bone mineral content and bone geometry in male and female adolescents across a range of skeletal sites. There is also evidence for the beneficial effects of PA on bone strength and bone microstructure at the distal tibia, an inherently loaded site, in adolescents during growth. However, no studies have examined the relationship between PA, bone strength and bone microstructure in adolescents at inherently unloaded sites. Our aims in this cross-sectional study were to evaluate the independent contribution of PA to bone strength and bone microstructure in adolescent males and females at the radius. We assessed the distal radius using XtremeCT (Scanco Medical) at the 7% site in 113 males (Age 17.4 ±1.6yrs; Height 175.6 ± 7.3cm; Weight 69.0 ± 15.4kg), and 97 females (Age 17.9 ±1.8yrs; Height 162.8 ± 6.9cm; Weight 59.5 ± 11.3kg). We assessed PA (loaded and unloaded) using the modified PA Questionnaire for Adolescents [1]. Our primary outcome was bone strength index (BSI, mg^2/mm^4; ToA (mm^2) x $ToD^2(mg/cm^3)$ [2]. We also assessed cortical bone density (CoD, mg/cm^3), cortical thickness (Cort.Th, mm), trabecular bone density (TrD, mg/cm^3) and trabecular number (Tb.N, 1/mm). We used multiple regression (STATA, Version 10.1) to evaluate the independent contribution of PA (PA, hours per week) to bone outcomes after adjusting for maturation (Tanner), height (cm), weight (kg), radius length and calcium intake (mg/day). Loaded PA was a significant predictor of BSI, ToA and TrD in males ($P<0.001$; Table 1). Loaded PA was a significant predictor of BSI only in females ($P<0.05$; Table 1). There was no influence of loaded PA on bone microstructure in either sex ($P<0.05$). There was no influence of unloaded PA on BSI or bone microstructure in either sex ($P<0.05$). Our results suggest that whilst loaded PA has a positive effect on bone strength at the radius in both sexes, it has no significant effect on bone microstructure. These findings are at odds with the reported beneficial effects of PA on bone microstructure at the distal tibia. Data are required to further assess the influence of PA on inherently loaded and unloaded skeletal sites across growth.

1. Crocker PR, Bailey DA, Faulkner RA et al.(1997) Measuring general levels of physical activity. Medicine and Science in Sports and Exercise 29:1344-1349

2. Martin RB (1991) Determinants of the mechanical properties of bones. J Biomech 24 Suppl 1:79-88.

Table 1 Multiple regression results for HR-pQCT variables at the distal radius (7% site) for male and female participants

	Variables	β (SE)	P value	R^2
MALES				
Bone strength index	Loaded physical activity	0.56 (0.14)	<0.001	0.30**
	Body weight	0.29 (0.06)	0.001	
	Radius bone length	-0.25 (0.12)	0.036	
	Tanner (Breast stage)	6.96 (2.22)	0.002	
Total area	Loaded physical activity	2.21 (0.54)	<0.001	0.29**
	Body weight	3.50 (0.92)	<0.001	
Trabecular bone density	Loaded physical activity	1.42 (0.43)	0.001	0.21**
	Body weight	0.52 (0.24)	0.033	
	Calcium intake	0.10 (0.004)	0.025	
FEMALES				
Bone strength index	Loaded physical activity	0.45 (0.20)	0.024	0.07*

Note: Only models and variables with significance p<0.05, are shown. β = estimated regression coefficient, SE = standard error. * R^2 change significant at $P<0.05$, ** R^2 change significant at $P<0.001$

Table 1

***Disclosures: Heather McKay**, None.*

SA0059

Maturity-specific Differences Attributed to Gymnastic Loading at the Distal Radius. Jodi Dowthwaite*[1], Portia Flowers[2], Rebecca Hickman[2], Paula Rosenbaum[2], Tamara Scerpella[3]. [1]State University of New York, Upstate Medical University, USA, [2]SUNY Upstate Medical University, USA, [3]State University of New York Upstate Medical University, USA

Purpose: Loading exposure during growth is linked to high bone mineral indices, but few studies address maturity and tissue-specific adaptations in bone geometry and density. The current study tests for an interaction between gymnastic loading and menarche status.

Methods: Contemporaneous pQCT (pQ) and DXA (DX) scans were performed at the radial metaphysis (4%, Ultradistal (UD)) and diaphysis (33%, 1/3) in 113 females aged 8-25 yrs (mean 14.9 yrs). Premenarcheal (PRE) subjects included 24 nongymnasts (NON), 30 gymnasts (GYM, exposure >4 h/wk). Post-menarcheal subjects (POST) included 5 gymnasts and 26 exgymnasts (EX/GYM exposure >2yrs at >6h/wk); all others were defined as NON (n=28). Two factor analysis of covariance evaluated gymnastic exposure and menarche status, adjusting for age and height.

Results: EX/GYM and NON differed in height and % body fat (NON>EX/GYM)($p<0.02$); POST exceeded PRE means for all but % body fat ($p<0.05$). At both sites, DX area, aBMD, all BMC, all periosteal and cortical areas were greater in EX/GYM than NON ($p<0.05$), as was 4% trabecular vBMD. However, diaphyseal cortical vBMD was higher in NON than EX/GYM ($p<0.05$). Interactions were influential at both sites. EX/GYM emphasized greater periosteal and trabecular/intramedullary dimensions in late puberty, whereas POST NON emphasized only thickened cortices, yielding higher total vBMD/BMAD than EX/GYM ($p<0.05$). Fewer interactions were detected by DXA.

Conclusion: Distal radius differences attributed to gymnastic loading during growth are maturity-specific. POST EX/GYM advantages emphasize bone geometry rather than density; this may reflect pubertal loading and/or training cessation (84% ex). High adjusted bone outcomes in POST NON suggest pubertal acceleration of cortical growth. Generally, DXA and pQCT results agreed. However, pQCT detected more significant interactions, potentially reflecting greater sensitivity, accuracy or positional influence.

Adjusted means for bone parameters by gymnastic exposure (two-factor ANCOVA).
For significant interactions, results are presented by menarche status.

		Gym	Non	Pre Gym	Pre Non	Post Gym	Post Non
METAPHYSIS	DX aBMD (g/cm²)	0.429***	0.379				
	DX Area (cm²)	2.99***	2.75				
	DX BMC (g)	1.28***	1.04				
	pQ BMC (mg)	Interaction*		67.9***	50.6	107.2***	91.2
	pQ tot vBMD (g/cm³)	Interaction*		0.354**	0.313	0.450	0.472 NS
	DX BMAD (g/cm³)	Interaction*		0.272**	0.242	0.270	0.279 NS
	pQ trab vBMD (mg/cm³)	0.223***	0.190				
	pQ pCSA (mm²)	219.0***	176.3				
	DX pCSA (mm²)	313.6***	264.3				
	pQ cscCSA (mm²)	Interaction**		67.7***	50.1	99.9***	88.5
	pQ trabCSA (mm²)	131.8***	105.3				
	pQ trab/total CSA (%)	Interaction*		63.3%	68.1% NS	57.3% *	53.2%
	pQ IBS (g²/cm⁴)	Interaction*		0.241***	0.158	0.482 NS	0.430
	DX IBS (g⁴/cm⁴)	0.230***	0.180				
	pQ fall strength ratio	Interaction***		0.32***	0.20	0.34 NS	0.31
	DX fall strength ratio	0.21***	0.17				
		Gym	**Non**	**Pre Gym**	**Pre Non**	**Post Gym**	**Post Non**
DIAPHYSIS	DX aBMD (g/cm²)	0.629***	0.590				
	DX Area (cm²) (int.p=0.05)	2.48***	2.28	2.24*	2.13	2.70***	2.44
	DX BMC (g)	1.56***	1.35				
	pQ BMC (mg)	80.96***	68.79				
	pQ cort BMC (mg)	77.3***	65.8				
	pQ cort vBMD (mg/cm³)	1109.9	1126.6*				
	pQ tot vBMD (g/cm³)	Interaction***		0.885 NS	0.869	0.961	1.035***
	DX BMAD (g/cm³)	Interaction*		0.633NS	0.622	0.670	0.718*
	pQ pCSA (mm²)	Interaction*		70.60*	62.99	104.69***	79.84
	DX pCSA (mm²) (int.p=0.05)	118.51***	100.18	96.83*	87.44	140.47***	84.61
	pQ cCSA (mm²)	69.69***	58.44				
	DX cCSA (mm²)	74.37***	63.88				
	pQ IMCSA (mm²)	Interaction***		11.09	11.82 NS	19.55***	11.34
	DX IMCSA (mm²)	Interaction*		34.67 NS	32.17	52.30**	38.44
	pQ cort thick (mm)	Interaction**		2.62***	2.33	3.14	3.17 NS
	DX cort thick (mm)	2.40**	2.26				
	pQ SSI (mm²)	167.34***	133.89				
	DX Z (mm³)	156.02***	122.36				
	pQ fall strength ratio	0.0165***	0.0129				
	DX fall strength ratio	0.142**	0.117				

Means are adjusted for age and height. All variables were analyzed as natural logarithms; results are antiln.
Two-factor ANCOVA *p<0.05; **p<0.01; p<0.001

DX=Dual energy X-ray Absorptiometry; aBMD= areal bone mineral density; Area= projected area;
BMC= bone mineral content; pQCT= peripheral quantitative computed tomography;
vBMD= volumetric bone mineral density; BMAD= bone mineral apparent density; trab= trabecular;
pCSA= periosteal cross-sectional area; cscCSA= cortical/subcortical cross-sectional area;
cCSA= cortical cross-sectional area; IMCSA= intramedullary cross-sectional area; cort th= cortical thickness;
SSI= strength-strain index; Z= section modulus; fall strength ratio= strength index/forearm length*weight

Table 1

***Disclosures: Jodi Dowthwaite**, None.*

SA0060

Normal Masticatory Function Protects the Rat Mandibular Bone from Estrogen Deficiency-related Bone Loss. Anestis Mavropoulos[1], René Rizzoli[2], Stavros Kiliaridis[1], Patrick Ammann*[2]. [1]University of Geneva, Switzerland, [2]University Hospital, Geneva, Switzerland

Purpose. In a previous investigation we showed that mandibular alveolar (trabecular) bone appears to be less sensitive to estrogen-related osteoporosis than the proximal tibia spongiosa. We hypothesized that the heavy mechanical loading during mastication may protect the alveolar bone from the detrimental effects of estrogen deficiency observed in other skeletal sites. In this study we tested this hypothesis by comparing the effect of ovariectomy on the mandibular alveolar bone of Sprague-Dawley rats fed either a normal (hard) or a soft diet. Methods. Forty six-month-old female Sprague-Dawley rats underwent transabdominal ovariectomy (OVX) or sham operation (SHAM). Half of the animals received their food in the usual form of pellets (hard food), while the other half received a soft, porridge-like, isocaloric food. The experiment lasted 16 weeks. Micro-computed tomographic histomorphometry was used in order to evaluate the effect of estrogen deficiency on the mandibular alveolar bone. Results. Both experimental manipulations (OVX, soft diet) had a significantly negative impact on the micro-architecture of the mandibular alveolar bone. Soft diet led to a reduction of BV/TV (p=0.02), and trabecular thickness (p=0.03) and number (p<0.03). The conjunction of soft diet and OVX led to a significant reduction of BV/TV (p<0.001), and trabecular thickness (p<0.001), number (p<0.001), and separation (p<0.001). Ovariectomy led to 21.2% reduction of BV/TV in rats fed the soft diet (p<0.001), whereas a non significant change (-8.2%) was observed in those receiving the hard diet. Conclusions. Estrogen-deficiency seems to only minimally influence rat mandibular alveolar bone under normal masticatory mechanical loading, at least for the duration of this experiment. Soft diet and the ensuing hypofunction of the masticatory system significantly accentuated the negative effects of estrogen deficiency on the mandibular alveolar bone.

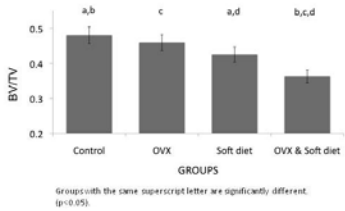

figure

***Disclosures: Patrick Ammann**, None.*

SA0061

Site and Frequency Specific Effects of Whole Body Vibration on Axial and Appendicular Structural Bone Parameters in Aged Rats. Marion Pasqualini*[1], Norbert Laroche[1], Arnaud Vanden Bossche[1], Laurence Vico[2]. [1]Inserm U890 - Lyon University, France, [2]University of St-Etienne, France

Mechanical stimulation of bone by Whole Body Vibration (WBV) was shown to have osteogenic effects. Most studies of WBV in rodents were done in growing, or gonadectomized animals. There is a lack of reports of WBV in aged adult animals and thus no preclinical evidence to support WBV in the prevention of bone loss. The goal of this study was to test the skeletal effects of different WBV frequencies, applied with the same acceleration, in aged rats. Our hypothesis was that high frequencies (90Hz) are more anabolic than low frequencies (8Hz). We exposed 48 male Wistar, 10-month rats to 4 weeks of vertical vibrations for 10 min/day, 5 days/week at 0.5g at frequencies of 8Hz, 52Hz or 90Hz. Trained rats stood free on the vibrating platform, control rats stood on the unmoving platform. Proximal tibia metaphyses were scanned in vivo by micro-CT (VIVA CT40, Scanco Medical) at the initiation and the end of the training period. At sacrifice, we measured trabecular and cortical bone parameters in the distal femur and L2 vertebral body. Post-hoc multiple comparisons were done when ANOVA results were significant. Rats vibrated at 8 and 52Hz lost body weight, while weight increased under a 90Hz training. Longitudinal follow up of the trabecular proximal tibia showed no significant effect of WBV. At sacrifice however, the trabecular compartment of the distal femur showed larger trabeculae (+11%, n=12, p<.0001) and an increased degree of anisotropy (+29%, n=12, p<.0001) at 90Hz vs controls. In contrast, these parameters were decreased at 52 Hz and even more at 8Hz vs 90Hz. Bone volume, trabecular number and connection density were all increased at 90Hz as compared to 52 and 8Hz. At 90Hz vs control, the cortical thickness is increased (+11%, p<0.01) and the porosity is reduced (-50%, p<0.05). In the L2 vertebra, all trabecular parameters were improved at 90Hz vs controls, bone volume and density connection were also increased at 52Hz, while no effect was observed at 8Hz. We showed that 0.5g WBV at 8Hz and 52Hz is either deleterious or inefficient in long bones. The anabolic effects of the 90Hz regimen observed in the vertebrae suggest that bone volume would also increase in the femur and tibia after a longer training period. The cortical effects also suggest improved biomechanical properties. This study showed that in WBV, in addition to the acceleration level, frequency is an important parameter with site-specific effects.

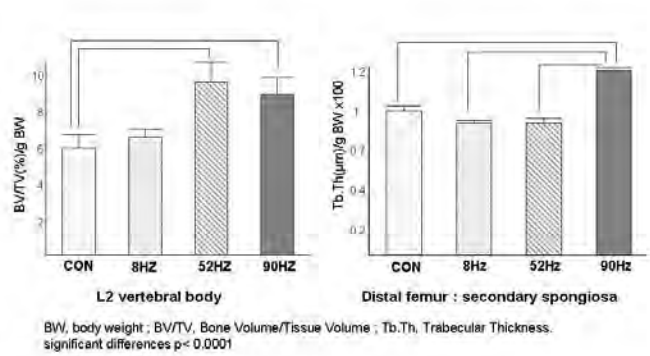

Figure 1

***Disclosures: Marion Pasqualini**, None.*

SA0062

A New Urinary Bio Marker of MMP-derived Cartilage Degradation. Anne-Christine Bay-Jensen[1], Jianxia Wang[2], Inger Byrjalsen[3], Yi Li[4], Qinlong Zheng[4], Kim Henriksen[5], Per Qvist[5], Morten Karsdal*[5]. [1]Nordic Bioscience, Denmark, [2]Nordic Bioscience China, Denmark, [3]CCBR-Synarc, Denmark, [4]Nordic Bioscience Beijing, China, [5]Nordic Bioscience A/S, Denmark

Joint degenerative disease is characterized as progressive damage of the joint tissue, which includes cartilage erosion, osteophyte formation, subchondral sclerosis, and synovial alterations. The turnover of cartilage is normally maintained by a balance between catabolic and anabolic processes. However, in the case of pathological matrix destruction, the rate of cartilage degradation exceeds the rate of formation, resulting in a net loss of cartilage matrix. The specific products of tissue formation and degradation can be measured in serum and urine, as markers of pathology. A monoclonal antibody was raised against a MMP9-derived neoepitope in type II collagen, which was identified mass spectrometry (N-terminal-GRDGAAG1053). An ELISA assay, called CIIM, was developed and optimized. The level of CIIM fragments was measured in urine samples from a normal population of men and women (N=145, age range 22 – 84 years). Immunohistochemistry was done to validate the presence of the neoepitope OA cartilage samples from patients undergoing knee replacement. The technical performance of the assay was accepted, giving inter- and intra-assay CV below 6%. We verified that the neoepitope was actually MMP-dependent by adding MMP-inhibitor (GM6001) to cartilage cultures and measuring the release of the fragment to the medium. GM6001 could inhibit the release of CIIM from catabolic active cartilage when compared to catabolic active control. Next, we measured the level of CIIM in urine of a normal population and found that there was a significant difference between men (84.8 pg/mmol creatinine, n=82) and women (126.4 pg/mmol creatinine n= 74, $p<0.01$). We also found that post-menopausal women (153.2 pg/mmol creatinine, n=47) had a higher level than pre-menopausal women (83.0 pg/mmol creatinine, n=27, $p<0.01$). We found the neoepitope to be immunolocalized to OA pathological features of the cartilage: 1) to eroded surface of the cartilage; 2) to the calcified cartilage; 3) to lesions. We developed a new biomarker assay that measures type II collagen degradation by MMP. We believed that this new markers could be a new and valuable tool for measuring cartilage breakdown observed in joint degenerative disease such as OA.

***Disclosures: Morten Karsdal**, Nordic Bioscience, 3*

SA0063

See Friday Plenary number FR0063.

SA0064

Exercise May Prevent Regional Bone Loss Induced By Monosodium Iodoacetate Osteoarthritis Model. Arnaud Boudenot*[1], stephane pallu[2], Eric Dolleans[2], Eric Lespessailles[3], Christelle Jaffre[2], Claude Laurent Benhamou[4]. [1]Inserm Unit U658Hopital Porte MadeleineOrléansFrance, France, [2]INSERM UNIT U 658, France, [3]Centre Hospitalier Regional, France, [4]INSERM Orléans-France, France

Knee injuries (i.e. anterior cruciate ligament tear or menisectomy surgery) are frequent in contact sports and may lead to early knee osteoarthritis. Monosodium iodoacetate (MIA) injection into joints is a validated animal model of induced osteoarthritis. This study aims to demonstrate the possible protective effect of exercise (treadmill running) on the subchondral bone changes at the proximal tibia (PT) and distal femur (DF) in the MIA-induced osteoarthritis model.

Male Wistar rats aged of 13 weeks (n=47) were divided into two groups: exercise (Ex) (n=24) or non exercise (NEx) (n=23). Ex rats were subjected to intermittent progressive training one hour per day, 5 days per week for 10 weeks. At the end of the training period, each group was divided into two subgroups and underwent either MIA injection (1mg/100µL NaCl) or NaCl (100µL) into the right knee joint leading to 4 groups: 1) Ex-NaCl, 2) Ex-MIA, 3) NEx-NaCl and 4) NEx-MIA. Bone Mineral Density (BMD) was evaluated on specific regions of interest (PT and DF) at baseline, after training (10 weeks) and at sacrifice (14 weeks). All data are expressed as mean ± SD. Mann-Whitney U test was used to determine the statistical significance of the differences between groups, p values lesser than 0.05 were considered significant *.

Before the MIA or NaCl injection we did not observed any significant differences between groups in BMD at the PT or DF subregions. Mean PT-BMD in the Ex-MIA group before injection was 0.429 ± 0.030 and 0.435 ± 0.021 g/cm^2 at sacrifice (p = NS). In contrast, in the NEx-MIA group we observed significantly lower values of mean TP-BMD at sacrifice than before injection (0.409 ± 0.022 vs 0.429 ± 0.025 g/cm^2; p=0.03). At sacrifice, we did not observed significant differences in BMD at DF between groups. In contrast PT-BMD of the injected knees was significantly lower in the NEx-MIA group compared to the other groups (Fig.).

These results suggest that physical activity could prevent the MIA deleterious effects on the BMD at proximal tibia in this rat model of osteoarthritis.

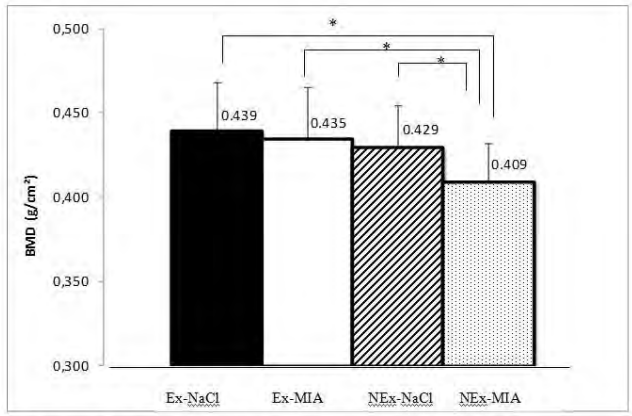

Fig. Proximal tibia BMD differences between groups at sacrifice

Proximal tibia BMD differences between groups at sacrifice

***Disclosures: Arnaud Boudenot**, None.*

SA0065

Preservation Effects on Bone Tissue Mechanical Properties. Sasha Rosen*[1], Bryan Kaye[2], Omar Ahmady[2], Connor Randall[3], Paul Hansma[1]. [1]University of California, Santa Barbara, USA, [2]UCSB Hansma Lab, USA, [3]UCSB, USA

Recently, The Reference Point Indentation (RPI) instrument has been shown to distinguish patients with and without fractures[(1)]. Patients with fractures tended to have larger values of Total Indentation Distance (TID) and Indentation Distance Increase (IDI)[(1-3)]. For laboratory work on cadaver bone, the bone must typically be preserved. Freezing is a commonly preferred method of bone preservation, as it prevents lysis and, thus, helps maintain the *in vivo* spatial arrangement of the bone proteins[(4)]. Another accepted approach is via chemical (namely ethanol) fixation. The advantages of chemical storage are primarily twofold; tissue decay is reduced and cell structure is preserved. In this study, the effects of these preservation techniques were evaluated using the Reference Point Indentation (RPI) instrument which performs Bone Microindentation Testing (BMT)[(1)]. Specifically, we studied the dependence of Indentation Distance Increase (IDI) and Total Indentation Distance (TID) on preservation technique.

The effects of preservation techniques were investigated on bovine femur. Baked and control samples of bovine femur were used to contrast weakened (baked) versus strong (control) organic extracellular matrix. Samples were frozen at -20℃. IDI and TID did not change after freezing baked bone. However, a 15% increase ($P<0.001$) in IDI was noted after the initial freeze cycle of control bone, but there was no difference in TID. Subsequent freeze-thaw cycles did not affect IDI or TID in both, baked and control bone. This leads us to postulate that a bone with less organic matrix will have a smaller degradation due to the first freeze-thaw cycle. Furthermore, subsequent freeze-thaw cycles no longer diminish the bone. Samples were stored in 70% ethanol at 5℃ and 25℃ for 40 days. The IDI of the samples that were stored at 5℃ increased by 18% ($P<0.001$), compared to a 35% increase ($P<0.001$) in IDI of the samples stored in 25℃. Ethanol fixation in bone and its corresponding degradation of the extracellular matrix is likely responsible for the deterioration in the mechanical properties. After exploring these common preservation techniques, we were able to determine statistically significant changes in the mechanical properties that were determined with the RPI instrument, revealing that these preservation techniques cannot maintain the mechanical properties investigated in this study.

***Disclosures: Sasha Rosen**, None.*
This study received funding from: National Institutes of Health

SA0066

Assessment of Bone Mineralization in Rats Treated with Sclerostin Antibody. Lindsey Edwards*[1], Amarjit Virdi[2], Kotaro Sena[2], D. Rick Sumner[2]. [1]Rush University, USA, [2]Rush University Medical Center, USA

Sclerostin antibody is being developed for the treatment of postmenopausal osteoporosis because of its robust efficacy in increasing bone volume. Generally, sclerostin, the protein product of the SOST gene, maintains bone surfaces quiescent. Neutralizing sclerostin with an antibody up-regulates Wnt signaling and activates quiescent surfaces into bone forming surfaces. While studies show that antibody treatment in animals and humans increases bone volume, little data has been published describing the quality of the newly formed bone. We hypothesize that treatment with sclerostin antibody will lead to a short-term depression in overall bone mineralization because of the anticipated increase in bone volume and the lag time associated with full mineralization. In the present experiment, the femurs of 10 Sprague Dawley rats that had received titanium implants in their contralateral limbs

were used. The rats were treated with saline or sclerostin antibody (Scl-Ab III: 25mg/kg, twice weekly) for 8 weeks. Positive effects of sclerostin antibody treatment on implant fixation were reported previously. In the present investigation, the intact femurs were harvested, formalin-fixed and scanned using micro-computed tomography (microCT) to assess bone volume and mineral density. The bones were then embedded in polymethyl methacrylate, sectioned, polished, carbon-coated and imaged using quantitative backscatter electron imaging (qBEI) as a second assessment of mineral density. Cortical bone area increased by 29% ($p < 0.001$) and trabecular BV/TV increased by 3-fold ($p<0.001$) in the sclerostin antibody-treated group. The mineral density of the cortical and trabecular bone, whether assayed by microCT or qBEI showed no statistical difference between groups (Table 1). The skewness, kurtosis and variance of the mineral frequency distributions were similar in each group. Thus, in addition to increasing bone volume, sclerostin antibody may also increase the rate of mineralization.

Table 1: Assessment of mean bone tissue mineralization at 8 weeks (n = 5). None of the differences between groups were significant, in contrast to the expectation that sclerostin antibody treatment would lead to an overall pattern of depressed mineralization.

	qBEI (calibrated grayscale units)		microCT (mg HA/cc)	
	Control	Scl-Ab Treated	Control	Scl-Ab Treated
Trabecular Bone:				
Mean ± SD	11.6 ± .14	11.6 ± .05	984 ± 21.2	1000 ± 13.3
Cortical Bone:				
Mean ± SD	11.9 ± .23	12.0 ± .19	1188 ± 13.7	1184 ± 7.0

Table 1

***Disclosures: Lindsey Edwards**, None.*
This study received funding from: Amgen

SA0067

***Runx2* Overexpression in Hypertrophic Chondrocytes Delayed Chondrocyte Maturation and Endochondral Ossification.** Ming Ding*[1], Qiping Zheng[2]. [1]Rush University, USA, [2]Rush University Medical Center, USA

Runx2 Overexpression in Hypertrophic Chondrocytes Delayed Chondrocyte Maturation and Endochondral Ossification

Ming Ding1, Sam Abbassi1, Jun Li2, Yaojuan Lu1, Rick D. Sumner1, Vale'rie Geoffroy3, Feifei Li1, Anna. Plaas2, and Qiping. Zheng1, *

Runx2, a member of the Runt domain protein family, has been demonstrated to be an essential transcription factor for osteoblast differentiation as well as a critical regulator for chondrocyte maturation. The type X collagen gene (Col10a1) is a specific molecular marker of hypertrophic chondrocytes during endochondral bone formation. It has been shown that type X collagen plays a critical role during skeletal development and maintenance by impacting the supporting properties of the growth plate and the mineralization process. Recently, a growing body of evidence suggests that Runx2 regulates type X collagen gene expression during chondrocyte maturation in different species. To investigate how Runx2 regulates murine Col10a1 gene expression and impacts chondrocyte maturation during skeletal development, we have generated transgenic mice in which Flag-tagged Runx2 cDNA was under the control of the 300-bp cell-specific Col10a1 regulatory element. Real-time PCR using total RNAs prepared from mouse limbs at the E17.5 and P1 stages showed that both Runx2 and Col10a1 mRNA were significantly increased in transgenic mice compared to their wild-type littermate controls. Histological analysis of long bone sections showed elongated hypertrophic zone with disorganized chondrocytes in transgenic mice. Skeletal staining suggests delayed ossification in craniofacial, long bone digits and the tails from embryonic day 14.5 (E14.5) till postnatal day 3 (P3). microCT analysis of the mice at 1 month stage suggests that the transgenic mice have shorter femur length. We have also performed expression analysis of marker genes for chondrocyte differentiation, maturation or apoptosis. The results showed that Sox9, Ihh (Indian Hedgehog), Mmp13 (Collagenase-3), Bcl-2 (the anti-apoptotic marker gene), and Osx (Osterix) were all significantly increased in transgenic mice. No expression level change was observed for Vegf (Vascular endothelial growth factor). Our data suggest that Runx2 regulates cell-specific Col10a1 expression and chondrocyte maturation in vivo. The Runx2 transgenic mice that have enhanced Runx2 and Col10a1 expression may trigger Ihh and Sox9 expression which dominantly arrest chondrocyte maturation. This may lead to matrix environment change and impact chondrocyte apoptosis during skeletal development and maintenance.

***Disclosures: Ming Ding**, None.*

SA0068

See Friday Plenary number FR0068.

SA0069

See Friday Plenary number FR0069.

SA0070

Dual Action of Von Hippel Lindau (VHL) in Limb Bud Mesenchyme. Elisa Araldi*[1], Richa Khatri[1], Amato Giaccia[2], Ernestina Schipani[3]. [1]MGH, USA, [2]Stanford University, USA, [3]Massachusetts General Hospital & Harvard Medical School, USA

Numerous lines of evidence suggest that the genetic program activated by hypoxia has a critical role in endochondral bone developmentt in vivo. Consistent with its avascularity, the murine fetal growth plate displays a gradient of oxygenation with a central, hypoxic region. Genetic experiments in vivo have shown that the transcription factor Hypoxia-inducible factor-1α (Hif-1α), which is a major mediator of the cellular adaptation to hypoxia, is necessary for chondrocyte survival and for differentiation of mesenchymal precursors into chondrocytes, by triggering a complex homeostatic response that involves, at least in part, the accumulation of a proper extracellular matrix.To expand our understanding of the role of the Hif family of transcription factors (Hifs) in chondrogenesis, in this study we genetically deleted Von Hippel Lindau protein (pVHL), the E3 ubiquitin ligase responsible for degradation of Hifs under normoxia, in whole limb bud mesenchyme, i.e. both in mesenchymal cells that differentiate into chondrocytes and in mesenchymal cells that give origin to the vascularized soft tissue surrounding the avascular cartilaginous primordia. Lack of pVHL in chondrocytes caused a severe shortening and thinning of the mutant cartilaginous elements, which were markedly deformed and hypocellular, and eventually collapsed, possibly as a result of cellular growth arrest and death. Conversely, lack of pVHL in the soft tissue surrounding the chondrocytic growth plates led to formation of foci of ectopic cartilage, to massive fibrosis, and to appearance of fibromyxoid tumor-like structures, which expanded into and replaced the collapsed cartilaginous structures. We are currently investigating the molecular mechanisms of this apparent dual action of pVHL in cartilage and in the surrounding mesenchyme, with particular emphasis on the role of the Hif family of transcription factors. Taken together, our findings indicate that lack of pVHL may have differential biological effects in cells of mesenchymal origin, depending on their phenotypical identity.

***Disclosures: Elisa Araldi**, None.*

SA0071

Histological, Functional and Contrast-based çCT Evaluation a Novel Osteoarthritis Model in Mice. Zhechao Merry Ruan*[1], Frank Gannon[1], Michael Heggeness[1], Brian Dawson[1], Ming-ming Jiang[1], Jennifer Black[2], Brendan Lee[1]. [1]Baylor College of Medicine, USA, [2]Vanderbilt Univeristy, USA

Osteoarthritis (OA) is common clinical condition characterized by degeneration of articular cartilage, limited intraatricular inflammation with synovitis, and changes in peri-articular and subchondral bone. Current well-characterized animal models of OA include spontaneous models in larger animals, genetics models in mice, and surgery models in rats and rabbits. However, none of these models are optimal for genetics and therapeutic studies that are clinically relevant. Patients with anterior cruciate ligament (ACL) tearing usually develop OA within 1 to 2 years after injury. And, the progression of the disease is similar to spontaneous development of OA in elder patients. Therefore, we hypothesize that ACL transected mice will provide an OA model of great genetic and therapeutic relevance. To test this, we developed a microsurgical procedure to transect the ACL in hind limbs of mouse with minimal damage to the surrounding tissues. We developed a scoring system for mouse OA based on the human OA grading system published by Priztker et. al. in 2006. Samples collected 24 hours after surgery confirmed that little damage were caused directly by the surgery to surrounding tissues. 4 weeks after surgery, histological scoring of ACL transected mouse joint samples by blinded observers showed significantly different scores in transected vs. mock surgery groups (N=10). We also observed synovitis, mast cells recruitment, and neovascularization in cartilage in the ACL transected group. To evaluate the motor skills of mice in this model, ACL transected and mock mice were subjected to various behavior tests before surgery and 4 weeks after surgery. While the walking speed and active/rest time remains similar in ACL transected group and mock, the former showed decreased rotarod running time and increased hotplate response time compared to the latter (N=15). We also observed gait changes in the ACL transected group. Finally, we established a method to evaluate mouse cartilage quantitatively and qualitatively by contrast-based micro-computed tomography (μCT). We are testing whether this method could differentiate ACL transected group from mock surgery. This model will facilitate the study of genetic manipulations in cartilage in the pathogenesis and treatment of OA.

***Disclosures: Zhechao Merry Ruan**, None.*

SA0072

Hypophosphatemia-independent Changes in Extracellular Matrix Proteins in Hyp Mice may Underlie the Articular Cartilage Degeneration of X-linked Hypophosphatemia. Carolyn Macica*[1], Ali Nasiri[2], Guoying Liang[3]. [1]Yale University School of Medicine, USA, [2]Yale Univeristy, USA, [3]Yale University, USA

The two major sites of paradoxical hypermineralization in patients with X-linked hypophosphatemia (XLH) occur in cartilaginous tissues; the fibrocartilaginous tendon/ligament insertion sites and at the margins of synovial joints resulting in formation of enthesophytes and osteophytes, respectively. Despite effective treatment of rickets/osteomalacia, this complication dominates the adult clinical picture. We have previously demonstrated that the Hyp mouse, a murine XLH model, develops an enthesopathy at sites most commonly affected in patients, characterized by a significant expansion of mineralizing fibrocartilage (Liang et al., 2009). Osteophyte formation is an adaptive response that occurs secondary to articular cartilage (AC) degeneration. We now identify alterations in the articular surface of Hyp mice (12 wks) that may predispose patients with XLH to AC degeneration.

We identified a significant reduction in the expression of two matrix proteins normally confined to the mineralized zone of AC; the matrix-degrading enzyme, matrix metalloproteinase-13 (MMP13) and osteopontin (OPN), a mineral-binding secreted glycoprotein. This is accompanied by a significant loss of the mineralized hypertrophic zone of AC (von Kossa), despite elevated alkaline phosphatase activity. EPIC-microCT analysis of hexabrix-labeled-AC (6 micron isometric voxel size, threshold applied to include unmineralized AC but exclude mineralized AC/bone) confirmed an increase in unmineralized AC (wt 0.096 ± 0.01 mm vs. Hyp 0.158 ± 0.01 mm, $p<0.05$). SafO staining revealed a redistribution of proteoglycans from above the tidemark into the entire articular surface. In contrast, secreted osteoblast MMP13 and OPN were unaffected in subchondral and trabecular bone, underscoring potential regulatory differences between mineralizing osteoblasts and chondrocytes in Hyp mice despite an identical metabolic backdrop.

The cellular cues for these changes likely include both mechanical and biochemical factors and may be unique to cartilaginous tissues. We thus measured markers of mineralizing hypertrophic AC of Hyp mice treated with or without oral P/vitamin D to determine the impact of correcting the abnormal phosphorous and mechanical forces of rickets/osteomalacia. We found that while the rickets was effectively treated, the AC abnormalities persisted. These data suggest a local role of biochemical factors unique to XLH in mediating changes to the architecture of the zonal arrangement that defines AC.

***Disclosures: Carolyn Macica**, None.*

SA0073

See Friday Plenary number FR0073.

SA0074

Muscular Function and Bone Strength Related Variables after Knee Replacement. Ari Heinonen*[1], Timo Rantalainen[2], Anu Valtonen[3], Tapani Pöyhönen[4], Sarianna Sipilä[5]. [1]Department of Health Sciences, University of Jyväskylä, Finland, [2]Neuromuscular Research Centre, Department of Biology of Physical Activity, University of Jyväskylä, Finland, [3]Rehabilitation & Pain Unit, Kymenlaakso Central Hospital & Department of Health Sciences, University of Jyväskylä, Finland, [4]Rehabilitation & Pain Unit, Kymenlaakso Central Hospital, Finland, [5]Gerontology Research Centre, Department of Health Siences, University of Jyväskylä, Jyväskylä, Finland

The bone loss after total knee replacement is apparently stress shielding related and may lead to loosening of the prosthesis. In order to provide more information for rehabilitation after knee replacement to prevent this bone loss, a sample of 29 women and 19 men who were 55 to 75 years old and had undergone unilateral knee replacement surgery an average of 10 months (range 4-17) earlier were recruited. Muscular function was assessed with maximal torgue in knee extension and flexion with an isokinetic dynamometer at an angular velocity of 60°/s. A single computed tomography (QCT) slice was obtained from femoral mid-shaft comprising both legs. The Hounsfield units provided by the QCT device were converted to volumetric bone mineral density (vBMD) values by scanning (K2HPO4) phantom liquids and calculating the linear conversion equations. Cortical cross-sectional area (CoA), cortical volumetric BMD (CoD) and density weighted section modulus (SSI) were calculated from the QCT slices for the operated and the non-operated femurs. The bones were compared to each other with ANOVA having the leg as a within subject factor. The operated thigh CoA was 3% smaller ($393 + 82$ mm^2 vs. $405 + 75$ mm^2; $p = 0.003$) and CoD 1% lower ($991+ 39$ mg/ cm^3 vs. $999 + 37$ mg/ cm^3; $p < 0.001$) than that in the operated thigh, whereas no side-to-side difference was observed in SSI ($2560 + 690$ mm^3 vs. $2600 + 630$ mm^3; $p = 0.120$). In the stepwise regression analyses knee extension and flexion torque, age, height, body mass, pain score (VAS, mm) and time since operation explained 44% of the variance in the CoA, 33% in CoD and 52 % of the variance in SSI on the operated side. Body mass explained independently 7% ($p = 0.020$) of the CoA variation, 14 ($p < 0.001$) of the CoD and 7% ($p = 0.015$) of the SSI variation. In addition, maximal knee flexion torque turned out to be the strongest independent predictor, explaining 37% ($p < 0.001$) of CoA variation, 7% ($p = 0.043$) in CoD and 45% ($p<0.001$) of the SSI variation. Further, time since operation explained independently 12% ($p=0.020$) of the CoD variation. In conclusion, the operated thigh had less cortical bone, and muscle force of the operated leg is a strong independent predictor of the femoral mid-shaft bone strength in subjects undergone unilateral knee replacement surgery. This indicates indirectly that after total knee replacement, early and efficient rehabilitation should be emphasized.

***Disclosures: Ari Heinonen**, None.*

SA0075

See Friday Plenary number FR0075.

SA0076

The Potential Role of Gas6 in Growth Plate Chondrocytes. Phillip Newton*[1], Ann Canfield[1], Colin Farquharson[2]. [1]University of Manchester, United Kingdom, [2]Roslin Institute & R(D)SVS, University of Edinburgh, United Kingdom

During endochondral ossification mesenchymal cells differentiate into chondrocytes and further differentiate to a state of hypertrophy. In the developing bone, the chondrocytes align to form the highly organized mature growth plate. At each stage the chondrocytes secrete specific extracellular matrix (ECM) components and ultimately this ECM becomes mineralized allowing vascular invasion and the formation of the primary spongiosa. Gas6 has previously been detected in growth plate chondrocytes by microarray analysis and recombinant Gas6 has been shown to influence chondrocyte differentiation in vitro, although a precise function and mechanism is yet to be elucidated. Signaling within the growth plate has been suggested via interactions between Gas6 and its receptors Axl and most recently, Mer. Axl and Gas6 have also been reported in chondrocytes of articular cartilage and their signalling has been shown to prevent ectopic mineralization within the vasculature via anti-apoptotic mechanisms.

To determine the spatial expression of Gas6 in the growth plate, 28-day old murine tibial growth plates were analysed by immunohistochemistry. Also, an in vitro model using chondrocyte-like ATDC5 cells was used to determine the temporal expression patterns of Gas6, Axl, Mer and chondrocyte markers by Western blot and qPCR during chondrocyte differentiation and ECM mineralization.

Gas6 was detected by immunohistochemistry in the resting, proliferating and hypertrophic zones of the growth plate but expression was concentrated in the proliferating zone. Analysis of ATDC5 cells confirmed that they underwent the expected stages of differentiation as demonstrated by the expression of collagen types II and X; ECM mineralization began at day 14 of culture. Gas6 mRNA expression was minimal at day 6 of culture and was maximally expressed at day 13 before decreasing. Total Axl protein and mRNA expression both peaked at day 8 and decreased thereafter, whereas phosphorylation of Axl was prolonged throughout culture. Mer mRNA expression was determined from day 6 and peaked at day 8 before decreasing. This data shows the spatial and temporal distribution of Gas6 within the growth plate and in addition, the detection of phosphorylated Axl within differentiating ATDC5 cells. This strongly suggests a role for Gas6 signaling in the growth plate.

The consequences of Gas6 signaling within the growth plate are unknown and further studies are required to determine Gas6 mediated events.

***Disclosures: Phillip Newton**, None.*

SA0077

The Role for CTGF and Src in Mesenchymal Stem Cell Condensation Induced by TGF-β1. Fabiola Del Carpio-Cano*[1], Steven Popoff[2], Raul DeLa Cadena[3], Fayez Safadi[2]. [1]Temple University, USA, [2]Temple University School of Medicine, USA, [3]Temple University School of Medicine, Department of Physiology, USA

The aggregation/condensation of mesenchymal cells (MSC) is a critical step for chondrocyte differentiation. TGF-β1 has been shown to promote MSC migration, proliferation, and condensation. Connective tissue growth factor (CTGF) is a matricellular protein expressed during MSC condensation where regulates matrix production. Previous studies have shown that CTGF acts as a downstream mediator of TGF-β1-induced MSC condensation. Silencing of CTGF expression inhibits MSC condensation induced by TGF-β1. In the present study, we further examined the role of CTGF in TGF-β1-induced MSC condensation. We assessed MSC migration, proliferation, condensation, and other markers of chondrogenesis induced by TGF-β1 in C3H10T1/2 cells infected with adenovirus expressing either CTGF-GFP (Ad-CTGF-GFP) or GFP alone (Ad-GFP; control), both in the presence or absence of exogenous TGF-β1 (5ng/ml) treatment. CTGF overexpression inhibited TGF-β1-induced MSC condensation compared to control cultures. Overexpression of CTGF inhibited the migration and proliferation that is normally observed in cells treated with TGF-β1. We also evaluated gene expression for extracellular matrix and chondrogenesis markers (aggrecan, Col 1α2, Col 2α1, fibronectin and Sox-9) by qPCR analysis. The overexpression of CTGF inhibited the expression of all markers compared to the control infected cultures and also prevented up-regulation of markers induced by TGF-β1. Next, we examined whether Src activation plays a role in MSC condensation induced by TGF-β1. Src was activated upon TGF-β1 treatment of MSC cells. In the presence of PP2, a Src family kinase inhibitor, TGF-β1 failed to induce MSC condensation. In the Ad-CTGF-GFP overexpressing cells, Src was constitutively activated at very high levels despite the fact that these cells did not condense or

respond to TGF-β1 treatment. These results suggest that although CTGF and Src play essential roles in the induction of MSC condensation when induced by TGF-β1 in a temporal fashion, the continuos overexpression of CTGF has the opposite effect and prevents TGF-β1 induction of MSC condensation.

***Disclosures: Fabiola Del Carpio-Cano**, None.*

SA0078

See Friday Plenary number FR0078.

SA0079

See Friday Plenary number FR0079.

SA0080

***RANKL* Expression in Mouse and Human T-Lymphocytes is Regulated by a Set of Cell-Type Specific Enhancers Designated the T-Cell Control Region.** Kathleen Bishop*, Xiaohua Wang, Heidi Coy, Robert Nerenz, Mark Meyer, Jenny Gumperz, J. Pike. University of Wisconsin-Madison, USA

Chronic activation of the immune system is directly linked to systemic bone loss. Excess bone resorption is likely due to elevated expression of receptor activator of NF-κB ligand (RANKL), a key osteoclastogenic factor synthesized by both osteoblasts and T-lymphocytes. In osteoblasts, RANKL expression is controlled through multiple distal elements marked by increased transcription factor occupancy, histone acetylation and RNA polymerase II recruitment. In T-cells, however, the mechanisms that underlie the expression of *RANKL* remain undefined. To explore this process, we confirmed that *RANKL* was induced in both mouse and human primary T-cells and then scanned over 400 kb surrounding the *RANKL* locus for regulatory enhancers using ChIP-chip analysis for histone H3/H4 acetylation. We identified potential *Rankl* enhancers at several regions previously characterized in osteoblasts, including the D5 enhancer, and identified a unique set of regulatory regions located over 120 kb upstream of the mouse *Rankl* TSS which we designated the T-cell control region (TCCR). Further studies showed that both DNA sequences and epigenetic modifications within the TCCR were highly conserved in both mouse and human and that histone H3/H4 acetylation levels were increased at the TCCR following activation. Inhibition of both MEK1/2 and calcineurin by U0126 and cyclosporine-A, respectively, resulted in decreased *RANKL* expression, suggesting that multiple T-cell signaling pathways are involved. Accordingly, we found that c-FOS, an effector of MEK1/2, was recruited to both the D5 enhancer and the TCCR, suggesting that c-FOS may mediate *RANKL* upregulation. The human and mouse D5 enhancers and segments of the TCCR mediated robust inducible luciferase activity following activation in Jurkat T-cells that was abrogated following mutation of the putative c-FOS response elements. Importantly, both D5 and segments of the TCCR were shown using 3C analysis to be in direct contact with the *Rankl* TSS and thus able to influence the gene's promoter directly. Finally, we note that SNPs linked to bone mineral density in both hip and spine are located within the TCCR, providing additional evidence that RANKL expression by T-cells may contribute to both normal bone remodeling as well as disease-related bone loss. We conclude that both the D5 and TCCR regions represent control segments within the *RANKL* locus that play an integral role in the transcriptional regulation of this gene in T-cells.

***Disclosures: Kathleen Bishop**, None.*

SA0081

Withdrawn

SA0082

Effects of Inorganic Phosphate on the Dento-alveolar Complex, In Situ and I*n Vitro*. Yuri Yamamoto*[1], Sunao Sato[2], Brian Foster[3], Kenji Takada[2], Takashi Takata[4], Martha Somerman[3], Satoru Toyosawa[2]. [1]Osaka University, Japan, [2]Osaka University Graduate School of Dentistry, Japan, [3]University of Washington School of Dentistry, USA, [4]Hiroshima University Graduate School of Biomedical Sciences, Japan

Objectives: The genes and associated proteins that regulate phosphate/pyrophosphate homeostasis, e.g., Ank or ENPP-1, are associated with protection from ectopic calcification. Hypercementosis has been reported in mice with mutations/knock-out of Ank and ENPP-1, where tissue pyrophosphate (PPi) levels are decreased and phosphate (Pi) to PPi ratio is increased. The aim of this study was to examine the effect of Pi/PPi imbalance on gene expression in cells associated with periodontal tissues, i.e., osteoblasts, cementoblasts and the precursor cell, follicle cells, *in vitro*.

Material and Methods: Incisors and molars obtained from mice with Ank and ENPP-1 mutations were examined at the light microscopic level. Osteoblasts, cementoblasts and follicle cells, previously isolated from mouse tissues, were cultured under different concentrations of Pi/PPi as a model to mimic the animal conditions for Ank/ ENPP-1 mutations. Changes in expression of specific genes, osteopontin (OPN), type ?collagen (Col?), dentin matrix protein 1 (DMP1), osteocalcin (OCN) and bone morphogenetic protein 2 (BMP-2), were examined by real-time reverse-transcriptase polymerase chain reaction (RT-PCR) at designated times from 12 hours to 72 hours and dose of 0, 1, 3, 5, 7mM Pi.

Results: Histological observations indicated that not only the molars but also the incisors from Ank and ENPP-1 mutant mice showed a marked increase in the amount of cementum when compared to wild-type. In ENPP-1 mutant mice, the thickened cementum was positively stained with OPN and DMP1.

BMP-2 was up-regulated 3-fold in dose and time dependent manner in the follicle cells, but wasn't changed in the osteoblasts and the cementoblasts. In contrast, DMP1 was up-regulated by 7mM Pi more than 200-fold in cementoblasts by 48 hrs and osteoblasts by 72 hrs, but was not changed in follicle cells. OCN was downregulated about 0.1 fold in dose and time dependent manner in the cementoblasts and about 0.2 fold in dose and time dependent manner in the follicle cells, but not in osteoblasts. OPN was up-regulated in all three cells.

Conclusion: These results suggest that functional changes in proteins such as ANK and ENPP-1, by affecting Pi/PPi ratio, may in turn affect mineralized tissue formation by altering expression of key genes and associated proteins in osteoblasts and cementoblasts, and further, may impact differentiation potential in follicle cells.

***Disclosures: Yuri Yamamoto**, None.*
This study received funding from: NIH/NIDCR RO1 DE15109 (MJS)

SA0083

See Friday Plenary number FR0083.

SA0084

See Friday Plenary number FR0084.

SA0085

See Friday Plenary number FR0085.

SA0086

See Friday Plenary number FR0086.

SA0087

See Friday Plenary number FR0087.

SA0088

Amino Acids Differentially Regulate Bone Formation and Resorption. Carlos Isales*[1], Kehong Ding[1], Qing Zhong[1], Michael Cain[1], Xing-Ming Shi[1], Byung Rho Lee[1], Richard Robbins[1], Mark Hamrick[1], Wendy Bollag[1], Clare Bergson[1], Crystal Perkins[1], Justin Cowart[1], Monte Hunter[1], Brandon Scott[1], Norman Chutkan[1], Karl Insogna[2]. [1]Medical College of Georgia, USA, [2]Yale University School of Medicine, USA

The impact of dietary protein on bone mass has been controversial. Posited mechanisms for dietary protein's influence on the skeleton have focused on nutrient effects (e.g. the need for protein to model and remodel bone) or metabolic effects (e.g. the metabolic acid load imposed by sulfur-containing amino acids). However, recent data from a number of laboratories suggests that an underappreciated mechanism of nutrient action is directly on bone cells, a paradigm in which nutrients act as signaling molecules. In pursuing the possibility of direct nutrient effects on bone cells we examined individual amino-acid effects on osteoprogenitor/bone marrow stromal cells (BMSCs), a key target for bone anabolism and on osteoclasts, a key target for bone catabolism. Using BMSCs isolated from C57Bl6 mice and exposed individually to twenty of the common amino-acids we found that: (1) tyrosine, tryptophan and phenylalanine induced the largest increases in intracellular calcium as measured by single cell calcium measurements with Fura-2; (2) the same AA's that increased intracellular calcium, also led to a time-dependent increase in ERK phosphorylation, peaking at 10 minutes and returning to baseline by 30 minutes. ERK phosphorylation was not inhibited by Rapamycin (mTOR inhibitor) suggesting that the observed effects were not due to AA uptake and metabolism; and (3) tyrosine and tryptophan resulted in the greatest increases in BMSC proliferation (as measured by thymidine uptake). When the effects of all twenty common AAs were examined on primary osteoclasts isolated from C57Bl6 mice we found that: (1) cysteine, serine, methionine and arginine had the largest effect on early markers of osteoclastic differentiation while cysteine, proline, serine and arginine had the largest effects on late markers of differentiation as quantified by real time RT-PCR (vitronectin, MMP9, cathepsin K and calcitonin receptor); and (5) when osteoclastic activity was examined measuring pit resorption with Osteologic discs, the AAs: arginine, serine and proline were found to be most pro-resorptive. In summary our data

demonstrate that individual AAs can selectively activate either bone formation or breakdown. Our data also suggests that the observed differences may account for some of the discrepancies in the literature on dietary protein effects on bone since the AA composition may vary from one dietary source to another.

***Disclosures: Carlos Isales**, None.*

SA0089

Arthroplasty Patients with Diabetes Mellitus Have Higher Bone Pentosidine Levels and Greater Immunohistochemical RAGE and MMP-1 than Patients without Diabetes. Karen King*[1], Allison Williams[2], Trevor Oren[1], Allan Bucknell[2]. [1]University of Colorado School of Medicine, USA, [2]VA Eastern Colorado Health Care System, USA

We previously identified a higher rate of total joint replacement surgeries (arthroplasty) in patients diagnosed with diabetes mellitus compared to patients without diabetes mellitus in a Veterans Affairs database.[1] The purpose of the present study was to identify an effect, if any, of diabetes on joint tissue metabolism.

With IRB-approval, cartilage and bone tissues were obtained as surgical wastes from total knee arthroplasty surgeries of osteoarthritis patients diagnosed with diabetes (N=10) or not diagnosed with diabetes (N=10). Osteochondral cores (5 mm dia.) were taken from the tibia plateau and either separated to cartilage and bone samples for collagen analysis or fixed whole for histology. Levels of collagen cross-links (HP, LP, and pentosidine) and total collagen were measured using HPLC. Osteochondral thin-sections were probed with monoclonal antibodies for RAGE or MMP-1.

Overall, cartilage had higher pentosidine levels than bone in both groups ($P < 0.001$). Bone pentosidine levels were higher in the group with diabetes compared to the group without diabetes (9.153×10^{-3} mol pentosidine/mol collagen vs. 6.945×10^{-3}, $P < 0.05$). Cartilage pentosidine levels were higher, but not statistically significant, in the diabetes group (2.624×10^{-2} mol pentosidine/mol collagen vs. 2.167×10^{-2}, $P = 0.075$). There were no differences between groups in the levels of HP or LP in bone or cartilage ($P > 0.05$). Immunostaining for RAGE was greater in the thin-sections obtained from the diabetes group. Immunostaining for MMP-1 was also greater in the diabetes group. Furthermore, the cells positive for RAGE and MMP-1 were located in the same regions, the cartilage superficial and mid zones and at the bone-cartilage interface.

These results support the hypothesis that hyperglycemia leads to increased pentosidine and other advanced glycation end-products in diabetes mellitus patients and that AGE-RAGE signaling causes inflammatory events such as increased MMP activity.[2] We propose that this hypothesis is applicable to the joint tissues and may be a factor (along with others such as BMI) in the increased rates of arthroplasty surgeries.

[1]King et al. Diabetics receive joint replacements more frequently and at a younger age. Orthopaedic Research Society 56th Annual Meeting, New Orleans, 2010. [2]Yan et al. Receptor for AGE (RAGE) and its ligands-cast into leading roles in diabetes and the inflammatory response. J Mol Med. 87:235, 2009.

***Disclosures: Karen King**, Cerapedics, Inc., 5; Cerapedics, Inc., 2; DePuy Orthopaedics, Inc., 2*

SA0090

Delayed Healing and Efficient *In Vivo* Retroviral Transgene Transduction in a Mouse Segmental Defect Model of Bone Healing. Charles H. Rundle*, Nicoleta L. Popa, Jon Wergedal, Subburaman Mohan, Kin-Hing William Lau. Jerry L. Pettis Memorial VA Medical Center, USA

Approximately 10% of bone fractures display severely impaired healing that is resistant to current therapeutic approaches. Because the closed three-point bending rodent fracture model traditionally used in fracture studies heals well without intervention, its utility for investigations of impaired bone healing is limited. It is imperative to develop a rodent model that can be used to identify therapeutic approaches for severely impaired bone healing. Ideally, this model should: 1) exhibit non-union healing, and 2) permit efficient delivery of molecular therapy to the injury. To determine whether such a model of impaired bone healing is feasible in the mouse, we compared healing and transgene expression in the three-point bending fracture model with a segmental defect model. In each model, the femur was stabilized with an intramedullary pin; a drill was used to produce a 1-2 mm defect around the entire cortical circumference of the segmental defect model. Healing was monitored by radiology and by histology at 7 and 28 days healing. The segmental defect developed a callus of fibrous tissue during healing, but X-ray examination revealed that the hard callus failed progress to bony union (i.e., healing). Histomorphometry of the callus tissues at 7 days healing (N=4 to N=7 mice per group) established that the callus area of the segmental defect was reduced (38.7 ± 10.5 mm^2 vs 34.1 ± 4.8 mm^2, $p<0.05$), as was the proportion of cartilage area per callus area ($9.2 \pm 5.0\%$ vs $3.2 \pm 2.4\%$, $p<0.03$). There were no significant differences in these two parameters between models at 28 days healing, but the three-point bending fracture model had progressed to bony union, while the segmental defect model retained fibrous tissue within the defect. This model therefore exhibits bone repair with severely delayed union. To determine whether transgenes of potential benefit can be expressed from these tissues *in vivo*, we compared the closed fracture and segmental defect models (N=3 each) for expression of a ß-galactosidase gene delivered in retroviral-based vector. ß-galactosidase staining at 7 days healing demonstrated comparable transgene expression between models. Despite the loss of bony tissue in the segmental defect model, direct injection of viral vector to the injury was effective in transducing resident cells. It is therefore a valuable model to assess the therapeutic efficacy of gene therapy strategies to promote the healing of more clinically challenging bone defects.

***Disclosures: Charles H. Rundle**, None.*

SA0091

Folate Supplementation During Pregnancy and Lactation Improves Bone Health of Female Mouse Offspring at Adulthood. Jovana Kaludjerovic*, Wendy Ward. University of Toronto, Canada

Supplementation with folic acid during the perinatal period is advocated for women of childbearing age as a prevention strategy against neural tube defects. However, the effects of folate supplementation on bone development have not been well characterized. The objective of this study was to determine if exposure to low (0 mg of folate/kg diet), adequate (2 mg of folate/kg diet) and supplemental (8 mg of folate/kg diet) amounts of dietary folate during perinatal life (defined as the period 1 week before conception to 3 weeks post conception) programs bone health at young adulthood in female mice. CD-1 mice (n = 12-16 pups/group) were randomly assigned to receive an amino acid based diet fortified with 0, 2 or 8 mg of folate/kg diet during pregnancy and lactation. At weaning, all pups were switched to an amino acid diet containing 2 mg of folate/kg diet, as this is the basal dietary requirement for rodents, and were studied to young adulthood (4 months of age). Body weight was measured weekly. Bone mineral density (BMD) and biomechanical strength at femur and lumbar vertebrae were measured at 4 months of age. There were no differences in body weight from postnatal day 1 to 10 among groups, but from postnatal day 10 to 120, mice fed a diet fortified with 2 or 8 mg of folate had significantly higher ($p<0.05$) body weights compared to folate deficient mice who grew at a significantly lower rate. Females fed a diet containing 8 mg of folate/kg diet had significantly higher ($p<0.05$) BMC and BMD at the femur and lumbar vertebrae (LV1-3) compared to those fed a folate deficient diet. Moreover, peak load of the femur midpoint, femur neck and LV2 was significantly higher ($p<0.05$) in mice fed 8 mg of folate compared to those fed a diet devoid of folate. In conclusion, exposure to dietary folate (2 or 8 mg/kg diet) during perinatal life results in normal growth and bone development in CD-1 mice. Future research should determine if the higher BMC, BMD and greater bone strength with supplemental levels of folate in utero and during suckling protect against deterioration of bone tissue during aging.

***Disclosures: Jovana Kaludjerovic**, None.*

SA0092

Large Scale Destabilization of Type I Collagen Triple Helix may Explain Increased Severity of Osteogenesis Imperfecta Caused by Mutations Near the Collagenase Cleavage Site. Elena Makareeva[1], Sejin Han[1], Juan Carlos Vera[1], Nydea Aviles[1], Wayne A. Cabral[1], Joan Marini[2], Robert Visse[3], Hideaki Nagase[3], Sergey Leikin*[1]. [1]National Institutes of Health, USA, [2]National Institute of Child Health & Human Development, USA, [3]Imperial College London, United Kingdom

Most cases of severe and lethal osteogenesis imperfecta (OI) are caused by substitutions of obligatory Gly residues in the triple helical region of type I collagen. Years of studies and hundreds of reported substitutions revealed no simple relationship between OI genotypes and phenotypes, probably because many different factors contribute to the disease severity. One such factor appears to be regional variations in structural and functional properties of the collagen triple helix. In the present study we focused on characterizing the region surrounding the collagenase cleavage site, in which virtually all α1(I) and many α2(I) Gly substitutions were found to be lethal. Analysis of structural changes in this region caused by various mutations revealed reversible unfolding of a significant fraction of the triple helix, clearly detectable by circular dichroism and susceptibility to different enzymes. For instance, we observed not only faster cleavage of mutant molecules by collagenases but also their efficient cleavage by a gelatinase (MMP-2) and the catalytic domain of MMP-1, which have only residual collagenase activity. Our earlier findings suggested that procollagen triple helix folding within this region may be challenging for cells even in the absence of mutations. The large scale triple helix destabilization observed in the present study suggests that mutations within this region may be particularly detrimental for procollagen folding, resulting in severe ER stress and malfunction of osteoblasts, potentially explaining the lethal OI phenotype. Further testing of this hypothesis is currently under way.

***Disclosures: Sergey Leikin**, None.*

SA0093

Micro-Computerized Tomographic Assessment of Zebrafish Skeleton. THEODORE CRAIG*[1], Glenda Evans[2], Theresa Hefferan[1], Michael Yaszemski[3], Stephen Ekker[4], Rajiv Kumar[3]. [1]Mayo Clinic, USA, [2]Orthopedics Research, Department of Orthopedics, Mayo Clinic, USA, [3]Mayo Clinic College of Medicine, USA, [4]Department of Biochemistry & Molecular Biology, Mayo Clinic, USA

Skeletal development in the zebrafish (*Danio rerio*) is similar to that observed in mammals. The expression of genes that might play a role in skeletal development can be readily manipulated in zebrafish, and genetic screens can be used to identify novel genes important in skeletal morphogenesis in this organism. Methods to assess bone architecture and bone mineral content in zebrafish are needed. Bone specific dyes such as alizarin red and calcein can be used to assess skeletal morphology but do not yield quantitative data regarding mineralization. Assessment of skeletal structure, development and mineralization using micro-computerized tomography (μCT), a non-invasive method with high spatial resolution, has not been standardized in this organism. Thirty day-old, juvenile, zebrafish were euthanized and fixed in formalin/phosphate buffered saline. Fish were scanned with a Scanco 35 μCT instrument (integration time 300; isotropic resolution of 3.5 μm; Vasquez et al, Anat. Rec. 291:475-487, 2008) to assess skeletal morphology and bone characteristics. The data were analyzed using the Scanco software. The architecture of mandibular and pharyngeal bones and the components of the dorsal skull was clearly visualized. In the vertebrae of the spine, structure and bone density were readily determined. Data from male and female zebrafish at each of the following ages will be presented: 10 day post fertilization (dpf), 20 dpf, 30 dpf, 60 dpf and 90 dpf. For purposes of comparison skeletal architecture in fish stained with 0.1% alizarin red in 3% potassium hydroxide (Quatro and Longaker, Cells Tissues Organs 181:109-118, 2005) and 0.2% calcein in de-ionized water (Du *et al*, Dev. Biol., 238:239-246, 2001) will be presented.

Results: Micro-computerized tomography assessed the structure and bone mineral density of the zebrafish skeleton with exceptional clarity and accuracy at ~30 dpf. In the skull, cranial sutures were readily visualized and bone density determinations were readily performed on bones of the skull and vertebrae. Bone structure was visualized as early as 10 dpf. Micro-computerized tomography is more easily performed and more sensitive than the dye based methods.

Conclusions: Micro-computerized tomography can be used to assess zebrafish skeletal development and bone mineral density and should serve as a powerful tool to assess skeletal defects and changes in mineralization.

***Disclosures: THEODORE CRAIG**, None.*
This study received funding from: NIH

SA0094

Morphological Comparison of the Skulls of Mice Mimicking Human Apert Syndrome Resulting From Gain-of-function Mutation of FGFR2 Ser252Trp and Pro253Arg. Xiaolan Du, Tujun Weng, Qifen He, FengTao Luo, Lin Chen*. State Key Laboratory of Trauma, Burns & Combined Injury, Center of Bone Metabolism & Repair, Trauma Center, Institute of Surgery Research, Daping Hospital, Third Military Medical University, China

Apert syndrome is caused mainly by two gain-of-function mutations in FGFR2, Ser252Trp and Pro253Arg. Slaney,et al found that patients with Apert syndrome resulting from FGFR2 Pro253Arg mutation have more severe syndactyly and less common cleft palate. Von Gernet found that patients with Apert syndrome resulting FGFR2 Ser252Trp, in general, have more severe craniofacial phenotypes than those of patients with FGFR2 Pro253Arg. There is, however, no well-controlled comparison of the difference in the skull morphology between Apert syndrome resulting from these two FGFR2 mutations. Taking the advantage of the mouse models mimicking these two syndromes, we did this comparison. The three-dimensional coordinate locations of 27 biologically relevant landmarks located on the skulls of mice mimicking human Apert syndrome resulting from FGFR2 Ser252Trp (Fgfr2+/S252W) and Pro253Arg (Fgfr2+/P253R) and their wild-type (WT) littermates (8w) were collected by using three-dimensional coordinate measuring machine. The euclidean distance matrix analysis (EDMA) was used to statistically characterize the three dimensional form of 10 biologically relevant landmark subsets that were designed to represent the skull shapes of the Fgfr2+/S252W and Fgfr2+/P253R mutants. In general, compared with that in WT littermates, Fgfr2+/S252W mutant mice have more shallow and wider orbit, wider anterior neurocrania, more shortened premaxilla and face height than that in Fgfr2+/P253R mice. We further found that there were significant differences in the biologically relevant landmark subsets for maxilla, orbit and anterior neurocrania ($P<0.01$). Differences were also found in face height and neurocranium($P<0.05$). There were, however, no differences in the landmark subsets for the nasal, frontal, midface, smaller midface and vault ($P>0.05$). Our results indicate that there are subtle differences in the skull morphology between Apert syndrome caused by FGFR2 Ser252Trp and FGFR2 Pro253Arg mutation. Further studies are needed to confirm these findings in detail and in patients with Apert syndrome. This work was supported by the Major State Basic Research Development Program of China (2005CB522604) and National Natural Science Foundation of China (30971607, 30530410)

***Disclosures: Lin Chen**, None.*

SA0095

See Friday Plenary number FR0095.

SA0096

See Friday Plenary number FR0096.

SA0097

See Friday Plenary number FR0097.

SA0098

Tgf-beta in the Development of the Intervertebral Disc. Rosa Serra[1], Philip Sohn[2], Megan Cox*[2]. [1]University of Alabama at Birmingham, USA, [2]UAB, USA

Transforming growth factor β (Tgf-β) signaling plays an integral part in skeletal development. Conditional deletion of Tgf-β type II receptor (Tgfbr2) from type II Collagen expressing cells has been shown to cause defects in vertebrae and intervertebral disk (IVD) development. To determine how Tgf-β affects differentiation of mesenchymal progenitor cells in the axial skeleton, we performed an RNA microarray analysis on sclerotome cells that had been cultured with or without Tgf-β1. A separate microarray screen was done using RNA collected from vertebrae and IVD tissue isolated by laser dissection from e13.5 mice. From the microarray data, we determined through hierarchical clustering analysis that Tgfbr2 deleted IVD more closely resembled developing vertebrae than developing IVD. Furthermore, scatter-plot analysis was used to show that the genes that are up-regulated by TGF-ß are primarily expressed in the IVD, supporting the hypothesis that TGF-ß can promote the IVD phenotype at the molecular level. We selected several transcription factors that were regulated by Tgf-β treatment, differentially expressed in the IVD versus the vertebrae, and/or decreased in IVD with Tgfbr2 deletion, for further study: Erg, Nfatc1, Ebf1, and cMaf. Regulation by Tgf-β was confirmed by semi-quantitative RT-PCR on RNA from primary sclerotome cells treated with Tgf-β1. In situ hybridization analysis and database searches were done to determine the expression pattern of genes in vivo. This analysis showed that Erg1 and Nfatc1 are specifically localized to the IVD and Ebf1 and c-maf are preferentially localized to the vertebrae. To study the effects of Tgf-β overexpression in axial skeleton development, we used the chick model system. Tgf-β soaked Affi-gel beads were placed into the lumbar region of the axial skeleton at stage HH 22- HH 25. Within 48h post-implantation, we are able to see an inhibition of cartilage formation as determined by Alcian blue staining in the area surrounding the bead. This suggested that Tgf-β acts to suppress cartilage formation in the sclerotome. Overall, the data support a model in which Tgf-β acts to maintain the IVD and prevent differentiation into cartilage. These experiments help to address fundamental questions about development of the axial skeleton and provide a basis for future studies aimed at disc repair or replacement.

***Disclosures: Megan Cox**, None.*

SA0099

The Role of Tgfbr2 in Sclerotome Migration During Vertebrae Development. Ying Wang*, Rosa Serra. University of Alabama at Birmingham, USA

The vertebral column develops from somites. During vertebrae development, sclerotome, a population of undifferentiated mesenchymal cells, differentiates and migrates to give rise to distinct parts of the vertebrae and ribs. Spina bifida occulta is one of the most common congenital malformations in humans leading to disability. Our laboratory has shown that deletion of TGFβ type II receptor (Tgfbr2) in Col2a expressing tissue in mice results in alterations in the formation of the vertebrae. The dorsal vertebrae of these mice failed to fuse, which mimics the symptom seen in patients with spina bifida occulta. Since sclerotome cell (SC) migration plays a key role during dorsal structure formation, we hypothesized that signaling through Tgfbr2 mediates the development of the dorsal vertebrae by regulating migration of SC. We first crossed the Col2aCre mice to the Rosa26 reporter strain to track SC migration *in vivo*. There was no observable difference between control and experimental group at E15.5. However, migration defects were seen in the mutant mice by E17.5, suggesting that TGFβ signaling is required for sclerotome migration during later stages of dorsal vertebrae development. To determine the underlying mechanism of TGFβ regulation of SC migration, we isolated SC from E11.5 embryos and performed migration assay using a chemotaxis chamber. TGFβ greatly induced wild-type cell migration, while migration of cells lacking Tgfbr2 was disrupted. Since platelet-derived growth factor (PDGF) has been shown to play a central role in regulating sclerotome migration, and it is one of the downstream effectors of the TGFβ signaling pathway, we then determined the direct effect of PDGF on SC migration. Both ligands AA and BB induced migration at distinct concentrations. The expression of PDGF-BB was greatly increased in cells treated with TGFβ, while that was decreased in cells lacking Tgfbr2. These data suggest that the action of TGFβ on SC migration may be mediated by the downstream effector PDGF-BB. The changes of PDGF-BB expression in the mutant mice will be examined by in situ hybridization analysis. To identify additional target genes involved in SC migration, we performed a microarray assay comparing

untreated and TGFβ treated SC and found that chemokine CCL21 was upregulated by TGFβ. Preliminary studies showed that CCL21 promoted SC migration. Taken together, our data suggest that PDGF-BB may mediate TGFβ induced SC migration along with other chemokines.

***Disclosures: Ying Wang**, None.*

SA0100

Hypoxia Promotes Myotube Formation and Fusion via AKT-FoxO3a Pathway. Yoshitaka Kawato*[1], Makoto Hirao[1], Yui Honjo[1], Hiroki Oze[1], Kenrin Shi[1], Akira Myoui[2], Hideki Yoshikawa[1], Jun Hashimoto[1]. [1]Osaka University Graduate School of Medicine, Japan, [2]Osaka University Hospital, Japan

Muscle is a very important organ in musculoskeletal system. There are two major pathways to create adenosine triphosphate(ATP) in skeletal muscle tissue. Change of oxygen levels is one of major determinant for skeletal muscle bioenergetics; oxidative phosphorylation and glycolysis, however it remains unknown that oxygen level also influence on myogenesis. It has been reported that normal O_2 levels in skeletal muscle tissue is relatively low (2-5%) (Kunze 1976; Heinrich 1987; Evers 1997). So, we hypothesized that myogenesis might be promoted when low oxygen tension condition. The murine myoblast C2C12 was induced to differentiate using DMEM supplemented with 2% horse serum and cultured under normoxia (20%O_2) for 4days. After that, we separated to normoxia and hypoxia (5%O_2) and cultured another 6days. We performed immunocytochemistry using mouse monoclonal anti-myosin MF20 primary antibody. Fusion index (the number of nuclei within myotubes/ total number of nuclei) was increased by hypoxia (85.7 ± 3.7%) (mean ± S.D.) compared to normoxia (34.8 ± 2.7%). Hypoxia also increased the percentage of myotubes with over six nuclei (82.4 ± 6.2%) compared to normoxia (37.8 ± 11.2%). Western blot analysis revealed the increase of myosin heavy chain protein expression under hypoxia in day7 and 10. Next, we checked the influence of p38MAPK and PI3K-AKT pathway on the hypoxia-induced promotion of myogenesis, because these pathways have been reported to play important role in the myogenesis, furthermore to be activated by hypoxia stimulation. SB203580 (p38MAPK inhibitor) blocked myotube formation dose dependently, however, hypoxia-induced influence was clearly still remained. On the other hand, LY294002 (PI3K-AKT inhibitor) abolished the myotube formation induced by hypoxia. Then, we focused on FoxO3a, which is downstream of AKT pathway and an important transcriptional factor for muscle atrophy-related genes. In fact, *atrogin-1* expression was down-regulated by hypoxia. Luciferase reporter assay revealed that FoxO3a transcription activity was down-regulated by hypoxia, and phosphorylation of AKT and FoxO3a was clearly up-regulated. Furthermore, overexpression of FoxO3a using constitutively active form FoxO3a (TM-FoxO3a) almost completely blocked hypoxia-induced myotube formation and fusion. Taken together, although further confirmation is required, down-regulation of FoxO3a activity due to phosphorylation of AKT-FoxO3a pathway is an important mechanism in hypoxia-induced myotube formation and fusion.

***Disclosures: Yoshitaka Kawato**, None.*

SA0101

Impairment of Long Bone Growth and Progressive Establishment of High Trabecular Bone Mass in Mice Lacking Bone Sialoprotein (BSP). Maya Boudiffa[1], Ndéyé-Marième Wade-Gueye[2], Marco Cardelli[3], Norbert Laroche[2], Arnaud Vanden-Bossche[2], Jane Aubin[4], Laurence Vico[5], Marie-Helene Lafage-Proust[6], Luc Malaval*[7]. [1]IRCM, Canada, [2]Université de Lyon, INSERM U890, Université Jean Monnet, 42023, France, [3]Dept. of Molecular Genetics, University of Toronto, Canada, [4]University of Toronto Faculty of Medicine, Canada, [5]University of St-Etienne, France, [6]INSERM Unit 890, France, [7]INSERM U890-Université de Lyon-Université Jean Monnet, Saint-Etienne, France

Bone sialoprotein (BSP) is strongly expressed by osteoblasts, osteoclasts and hypertrophic chondrocytes, and is particularly abundant in sites of primary bone formation. We previously showed that adult mice with a knockout of the bsp gene (BSP-/-) present with low bone formation and resorption parameters but a higher trabecular bone mass than their wild type counterparts. This raises the question of the mechanisms of trabecular bone accumulation in the mutants. In this study we analysed bone development in BSP-/- mice.

Newborn BSP-/- mice do not show any general skeletal abnormality. However, microtomographic (μCT) analysis reveal a delay in membranous primary ossification, with wider sutures in BSP-/- than in BSP+/+ fetuses, as well as thinner femoral cortical bone (-/- vs +/+, M±SEM, 31.4±3.3 vs 56.4±5.3μm, N=4, $p<0.01$) and lower tissue mineral density (367±5.5 vs 400±11.0, N=5, $p<0.05$). Histomorphometric measurements on newborns show that trabecular bone volume and osteoclast parameters do not differ between genotypes (BV/TV=8.6±0.7 vs 9.9±2.8%, N=10). However, as early as 3 weeks after birth, osteoclast number (not shown) and surface drop in mutant mice of both sexes (males: 8.6±0.9 vs 6.4±0.7%, females: 7.2±1.4 vs 3.6±0.4%, N=5, $p<0.001$, 2way ANOVA), concomitant with trabecular bone accumulation (m: 15.9±1.0 vs 11.6±1.6%, f: 18.6±1.6 vs 6.8±1.3%, N=6, $p<0.001$).

Mutant mice are smaller than wild type since birth and throughout life. The growth plates are thinner in newborn BSP-/- (564±18 vs 655±36μm, N=5, $p<0.05$), with a thinner hypertrophic zone (204±10 vs 218±8μm, N=5, $p<0.05$), suggestive of lower activity. At 3 weeks of age, there is no difference in total growth plate thickness, but the proliferating zone of either sex is thinner and the hypertrophic zone thicker in BSP-/- than in BSP+/+ mice (m: 131±14 vs 94±10μm, f: 98±4 vs 84±8μm, N=5, $p<0.05$), maybe reflecting a combination of lower proliferation and impaired resorption. No differences in growth plate parameters were observed in older (10, 16, 40, 48 week) mice.

In conclusion, lack of BSP alters long bone growth through early growth plate kinetics, as well as membranous/cortical primary bone formation and mineralization. Endochondral development is however normal in mutant mice and the accumulation of trabecular bone observed in adults develops progressively in the weeks following birth, concomitant to a drop in osteoclast numbers/surfaces. Further studies are needed to clarify the impact of BSP deficiency on growth plate chondrocytes and the compensatory mechanisms that allow normal endochondral development in BSP-/- mice.

***Disclosures: Luc Malaval**, None.*

SA0102

A Novel Mechanism for Dose-to-Duration Encoding: ATP Concentration Determines the Persistence of Ca^{2+}/NFATc1 Signaling through Distinct P2 Receptor Subtypes in Osteoblasts. Matthew Grol*, Alexey Pereverzev, Stephen Sims, S. Jeffrey Dixon. The University of Western Ontario, Canada

Cellular responses typically vary with the strength of the stimulus. Thus, underlying transduction mechanisms must relay quantitative information about the intensity of the signal. We and others have shown that ATP, released in response to mechanical stimuli, signals through cell-surface P2 receptors expressed in many cell types including osteoblasts. P2Y are G protein-coupled receptors that classically signal through release of calcium from intracellular stores; whereas, P2X are ATP-gated channels that permit influx of calcium from the extracellular milieu. The calcium-regulated transcription factor NFATc1 (which upon activation translocates from the cytoplasm to the nucleus) plays an essential role in the differentiation of osteoblasts; however, mechanisms leading to activation of NFATc1 during osteoblastogenesis are unknown. Our preliminary studies revealed dramatic differences in the duration of NFATc1 signaling encoded by the concentration of extracellular ATP. Thus, our purpose was to investigate the mechanisms underlying this "dose-to-duration" encoding. Live- and fixed-cell confocal microscopy were used to localize enhanced green fluorescent protein-tagged NFATc1 in osteoblasts. Both low (10-100 μM) and high (1-3 mM) concentrations of ATP induced nuclear translocation of NFATc1 that peaked at 15 min. Notably, NFATc1 returned to the cytoplasm 1 h following stimulation with low [ATP], whereas nuclear translocation induced by high [ATP] persisted for 2-3 h in duration. Since ATP activates P2Y at low concentrations and P2X7 receptors at concentrations equal to and exceeding 1 mM, we tested the contribution of these receptor subtypes. UTP (exclusively activates P2Y) mimicked responses observed with low [ATP], whereas BzATP (P2X7 agonist) induced prolonged NFATc1 translocation. Consistent with these findings, fluorescence measurements revealed that ATP or UTP (10-100 μM) cause only transient increases in cytosolic calcium concentration, whereas BzATP and ATP (1-3 mM) elicit more sustained elevations. Taken together, these findings demonstrate for the first time that the presence of multiple receptor subtypes with different affinities increases the range of ATP concentrations for which dose-dependent responses are possible. This phenomenon provides a novel mechanism by which osteoblasts may transduce differences in the intensity of mechanical stimuli over a wide dynamic range, otherwise unattainable through a single subtype of cell-surface receptor.

***Disclosures: Matthew Grol**, None.*

SA0103

See Friday Plenary number FR0103.

SA0104

Hyper-occlusal Force Induced the Expression of Type XII Collagen in Periodontal Tissue. Tetsuomi Nemoto[1], Kazuko Goto[1], Hiroshi Kajiya[1], Yutaka Takahashi[1], Tsuzuki Takashi*[2], Koji Okabe[1]. [1]Fukuoka Dental College, Japan, [2]fukuoka dental college, Jpn

It is well known that excessive mechanical force by hyper-occlusion is induced to occlusal trauma. In clinical, traumatic force produce disorganization of cells and fibers, resorption of bone and cementum, resulting in tooth mobile. However, the mechanism in the process remains to be understood. In the present study, to examine morphological and biological mechanisms in occlusal trauma on periodontal ligament tissue we employed in vivo hyper occlusion model rodents.

Five weeks-old wester rats or ddy mice were kept in hyperocclusion for 0, 2, 4, and 7 days with bonding steel wire on the occlusal surface of the upper light molars. To investigate alveolar bone resorption induced by the hyper-occlusion the sections of the lower right first molar were stained with tartrate-resistant acid phosphatase (TRAP) as a maker for osteoclasts. In parallel experiments, the three parts of tooth, buccal cervix, furcation, and lingual cervix were stained with TRAP. To investigate the relationship between hyper-occlusion and regeneration of cell matrix, we examined

the effect of hyper-occlusal force on the expression of type I and type XII of collagens using immunohistochemistry and real time PCR methods.

On control animals (day 0), the furcation of teeth and arrangement of collagens fibers were in order. Type I collagen was localized in the extracellular area at furcation in teeth root. The expression and localization of type I collagens were no effects on the hyper-occlusion treatment. On contrast, the expression and localization of type XII collagen was unclear in periodontal ligament tissues.

On day 4 after the hyper-occlusion treatment, a number of TRAP-positive cells significantly increased in the furcation and lingual cervical parts of teeth compared to control animals. The type XII collagens were gradually up-regulated by hyper-occlusion treatment in time-dependent manner and localized in around periodontal ligament cells. Using real time PCR method, type I collagen mRNA expression was not up-regulated in periodontal tissues during hyper-occlusion treatment, while type XII collagen mRNAs significantly up-regulated on day 2 and 4 after hyper-occlusion treatment.

The results indicated the hyper-occlusal force significantly up-regulated the expression of type XII collagen in periodontal tissue, but not type I collagen, suggesting in the regeneration of periodontal tissues for prevention of occlusal trauma.

***Disclosures: Tsuzuki Takashi**, None.*

SA0105

See Friday Plenary number FR0105.

SA0106

Toughness of Human Cortical Bone under Realistic Loading Conditions. Elizabeth Zimmermann*[1], Maximilien E. Launey[2], Robert O. Ritchie[1]. [1]University of California, Berkeley, USA, [2]Lawrence Berkeley National Lab, USA

Cortical bone invariably contains cracks and fracture mechanics provides the best methodology to characterize their resistance to fracture, or toughness. Fracture studies on the behavior of human cortical bone have provided much information on how the hierarchical microstructure of bone is able to resist the initiation and growth of incipient cracks at numerous length scales. In particular, the toughness of bone originates from a combination of plasticity mechanisms below the micron length scale (i.e., collagen uncoiling, fibrillar sliding, etc.) and crack tip shielding mechanisms at the micron scale (i.e., crack deflection, crack bridging, crack twisting, etc.).

In vivo, these cracks are subject to combinations of tension, in-plane shear and out-of-plane shear at the crack tip, which is called mixed-mode loading. To date, measurements of cortical bone toughness have only been performed under tensile loading conditions because they were assumed to be the limiting value.

In this study, human cortical bone samples were taken from three male donors. The hydrated, notched samples were tested under symmetric and asymmetric four-point bend, which allows the relative amount of tension and shear at the crack tip to be tuned. The tests were performed in an environmental scanning electron microscope to simultaneously image crack growth. Further investigations into the mixed-mode crack growth behavior and the effects of out-of-plane shear were performed.

Our results reveal that in the longitudinal orientation (crack is parallel to the osteons), bone is tougher under in-plane shear. However, in the transverse orientation (crack is perpendicular to the osteons), bone is 25% tougher in tension. This result is a consequence of both the bone matrix's ability to control the crack path through the highly mineralized cement lines, which are oriented along the longitudinal orientation, and the applied mechanical loads that drive the crack forward in tension and cause deflections under in-plane shear.

Thus, when assessing the toughness of bone, the mode I value is not always the limiting value; in addition, one orientation does not sample the same intrinsic and extrinsic mechanisms that control crack propagation in bone. Testing methods to assess the resistance to fracture in bone will be discussed in this context, especially with applications to small animal studies, which are mostly done under tensile loading conditions in the transverse orientation.

***Disclosures: Elizabeth Zimmermann**, None.*

SA0107

Synthesis, Characterization, and Evaluation of Bone Targeting Salmon Calcitonin Analogues in Normal and Osteoporotic Rats. Michael Doschak, Madhuri Newa, Krishna Bhandari*. University of Alberta, Canada

Purpose: To synthesize, characterize & evaluate the efficacy of bone-targeting salmon calcitonin (sCT) analogues.

Introduction: sCT elicits an antiresorptive effect by acting upon its receptors (CTRs) on bone-resorbing osteoclasts (OC). However, antiresorptive therapy utilizing conventional sCT is severely hampered by its short t1/2 (17–57 min) due to rapid systemic clearance & degradation in kidneys, liver & blood resulting in poor & variable bioavailability. Pegylation, the attachment of polyethylene glycol, improves the pharmacokinetic parameters of sCT by increasing its circulation time, & by reducing proteolysis & immunogenicity. However, as CTRs are also widely distributed in kidneys, lung, and other tissues, the competitive uptake of sCT (or pegylated sCT) by non-bone tissue resident CTRs may not always lead to optimal sCT bioavailability at bone resident OC– the desired site of action for osteopenic bone diseases. Thus, we sought to target sCT & pegylated sCT to bone by conjugation to a bisphosphonate (BP) carrier.

Methods: BP conjugates of pegylated & non-pegylated sCT analogues were synthesized, characterized by MALDI-TOF, Tris-Tricine SDS-PAGE & number of BP/sCT, & evaluated for sCT secondary structure by circular dichroism, in vitro bone mineral affinity & specificity by different calcium salt binding affinity assays, cytotoxicity in OC precursor RAW 264.7 cells by MTT assay, continued sCT bioactivity & CTR binding potential by intracellular cAMP stimulation assay in T47D breast cancer cells, sCT antibody binding ability by ELISA on calcium phosphate coated osteologic cell culture plates, & for their duration of action & effect on plasma calcium & phosphate levels in normal (n=20) & osteoporotic (OP) (n=18) rats.

Results: BP & PEG-BP conjugated sCT resulted in a stable & desirable α-helical form without altered receptor & antibody binding specificity. They exhibited significantly greater bone mineral affinity & specificity over unmodified sCT, retained strong sCT bioactivity, were non-toxic & exhibited an improved duration of action & a comparable reduction in serum calcium to that of parent sCT.

Conclusion: We report the synthesis of a new class of antiresorptive bone drug that has not previously been attempted & neither has a bone targeting formulation of the antiresorptive peptide hormone Calcitonin. These compounds hold great promise for clinical utility in the treatment of osteopenic bone disease & other related indications.

***Disclosures: Krishna Bhandari**, None.*

SA0108

See Friday Plenary number FR0108.

SA0109

Differential Gene Expression in Osteoblast/Osteocyte Lineage Cells between *Hyp* Mouse and Wild-type Mouse. Kazuaki Miyagawa*[1], Keiichi Ozono[2], Kanako Tachikawa[1], Yuko Mikuni-Takagaki[3], Mikihiko Kogo[4], Toshimi Michigami[5]. [1]Department of Bone & Mineral Research, Osaka Medical Center & Research Institute for Maternal & Child Health, Japan, [2]Osaka University Graduate School of Medicine, Japan, [3]Kanagawa Dental College & Graduate School of Dentistry, Japan, [4]Department of 1st Oral Surgery, Osaka University Graduate School of Dentistry, Japan, [5]Osaka Medical Center, Research Institute for Maternal & Child Health, Japan

Among the molecules responsible for hereditary hypophosphatemic rickets, FGF23, PHEX and DMP1 are expressed in osteoblast/osteocyte lineage cells. In X-linked hypophosphatemic rickets (XLH) and its murine homolog *Hyp* caused by mutations in *PHEX*/*Phex* gene, serum levels of FGF23 are elevated, although the underlying mechanism is not fully understood. Therefore, in the current study, we isolated primary osteoblasts and osteocytes from *Hyp* and wild-type mice to analyze the gene expression by real-time PCR. Long bones obtained from female *Hyp* mice or wild-type mice were minced and subjected to sequential digestion with collagenase and decalcification with EGTA for fractionation of osteoblasts and osteocytes. We confirmed the high levels of serum FGF23 in female *Hyp* mice. Among the 9 fractions isolated from wild-type bones, *alkaline phosphatase* was expressed in fractions 3-5 and attenuated in the later fractions, while strong expression of *Dmp1* and *Sost* was detected in fractions 6-9, suggesting that fractions 3-5 and fractions 6-9 from wild-type mice were considered as osteoblast-rich and osteocyte-rich fractions, respectively. *Phex* and *Fgf23* were expressed in both osteoblast-rich and osteocyte-rich fractions, and the expression of *Fgf23* was more intense in osteocyte-rich fractions. Then, we analyzed gene expression in osteoblast/osteocyte lineage cells isolated from *Hyp* bones, which was compared with that in wild-type cells. The expression of *Fgf23* was stronger in *Hyp* cells, and interestingly, it was relatively high even in the early fractions (fractions 3 and 4) in *Hyp*. As to the expression of *Dmp1*, it was also higher in *Hyp* cells, and its level in fraction 5 was almost comparable to that in fractions 6-9. We also found the slight increase in *Hyp* cells in the levels of mRNA corresponding to 5'portion of *Phex* gene retained in *Hyp* allele. Next, since we have previously demonstrated that extracellular Pi triggers signal transduction via type III Na^+/Pi cotransporter *Pit1*, we determined its expression. In all the fractions, it was almost 2-fold stronger in *Hyp* cells compared to wild-type cells, suggesting the altered response to extracellular Pi. These results indicate that molecules responsible for hereditary hypophosphatemic rickets are differentially expressed in osteoblast/osteocyte lineage cells between *Hyp* and wild-type mice, which might involve the difference in responsiveness to extracellular Pi as well as that in the composition of extracellular matrix.

***Disclosures: Kazuaki Miyagawa**, None.*

SA0110

See Friday Plenary number FR0110.

SA0111

Increased MEPE Protein Expression in Rat Bone Tissue after a Single Bout of Mechanical Loading. Nathalie Bravenboer*[1], Maartje Broeders[2], Huib Van Essen[3], Christianne Reijnders[4], Paul Lips[1]. [1]VU University Medical Center, The netherlands, [2]dept Endocrinology, VU University Medical Center, Netherlands, [3]VU Medical Center, The netherlands, [4]Dept Dermatology, VU University Medical center, Netherlands

Skeletal integrity in humans and animals is maintained by daily mechanical loading. It has been widely accepted that osteocytes function as mechanosensors. Many biochemical signaling molecules are involved in the response of osteocytes to mechanical stimulation. One of these molecules is matrix extra cellular phosphoglycoprotein (MEPE). It has been shown that MEPE gene expression was up regulated in response to 4 point bending load. MEPE plays a role in the regulation of bone mineralization, dentin mineralization, renal phosphate handling and vitamin D metabolism. The aim of this study was to detect MEPE protein expression after mechanical loading in order to elucidate the role in the translation of mechanical stimuli into bone formation. The 4-point-bending model of Forwood and Turner (1) was used to induce a single or a repeated period of mechanical loading on the right tibia shaft, whereas the contra-lateral left tibia served as control. Repeated loading consisted of 10 loading periods in 12 days. Rats were sacrificed 6 hours after the last loading period. MEPE was detected by immunohistochemistry. MEPE positive area relative to total cortical area (PosCo %) was measured in longitudinal bone sections from loaded and unloaded tibiae. A single bout of loading resulted in doubling of PosCo in the loaded right tibia (1.17 $\pm$ 0.79%) compared to the contra-lateral control (0.60 $\pm$0.50 %, p= 0.0137). After repeated loading PosCo was unchanged in the loaded right tibia (0.61 $\pm$ 0.38 %) compared to the contra-lateral control tibia (0.61 $\pm$ 0.35 %). In rats that received no mechanical loading no difference between the right and the left tibia was observed. In conclusion MEPE protein expression is stimulated by mechanical loading, which confirms the data on MEPE gene expression. This indicates MEPE could play an important role in the translation of mechanical stimuli into bone formation.

(1) Forwood MR, Owan I, Takano Y, Turner CH Increased bone formation in rat tibiae after a single short period of dynamic loading in vivo. Am J Physiol. 1996: 270:E419-23.

***Disclosures: Nathalie Bravenboer**, None.*

SA0112

See Friday Plenary number FR0112.

SA0113

See Friday Plenary number FR0113.

SA0114

Activation of Vascular Smooth Muscle Parathyroid Hormone Receptor Inhibits Wnt/β-Catenin Signaling and Aortic Fibrosis and Calcification in Diabetic Arteriosclerosis. Su-Li Cheng*[1], Jian-Su Shao[1], Linda Halstead[2], Oscar Sierra[1], Kathryn Distelhorst[3], Dwight Towler[2]. [1]Washington University in St. Louis School of Medicine, USA, [2]Washington University in St. Louis, USA, [3]Wahsington University in St. Louis School of Medicine, USA

Vascular fibrosis and calcification contribute to diabetic arteriosclerosis, impairing Windkessel physiology necessary for distal tissue perfusion. Wnt family members – up-regulated in arteries by the low-grade inflammation of ''diabesity'' – stimulate type I collagen expression and osteogenic mineralization of mesenchymal cells via β-catenin. Conversely, intermittent administration of parathyroid hormone (PTH) inhibits Wnt/ β-catenin signaling and calcification in aorta of LDLR (low density lipoprotein receptor) -deficient mice fed with high fat diabetogenic diets (HFD). To better understand PTH type 1 receptor (PTH1R) - Wnt/β-catenin interactions in diabetic arteriosclerosis, we generated SM-caPTH1R transgenic mice, a model in which the constitutively active PTH1R variant H223R (caPTH1R) is expressed only in vasculature by employing minimal SM22 promoter. When fed with HFD, SM-caPTH1R+;LDLR+/- mice become obese and diabetic, with no improvements in fasting serum glucose, cholesterol, body weight, body composition, or bone mass vs. LDLR+/- siblings. Moreover, serum PTH and calcium levels were unaltered and urinary calcium clearance was unaffected by the transgene. However, the expression of SM-caPTH1R transgene decreased aortic β-catenin protein accumulation and aortic β-galactosidase activity in TOPGAL+ (TCF/LEF optimal promoter – β-galactosidase reporter); LDLR+/- mice on HFD. Although TNF, Msx2, Wnt7a, and Wnt7b mRNA levels were not altered, Col1A1, alkaline phosphatase, osteopontin, MMP9, Runx2, Osx, and Nox1 were down-regulated in SM-caPTH1R aorta. In contrast, p21 level was increased. Aortic calcification and collagen and Nox1 protein accumulation were also reduced in SM-caPTH1R mice. Moreover, levels of aortic superoxide – a reactive oxygen species upregulated with calcific arteriosclerosis – were concomitantly reduced by caPTH1R. Ex vivo aortic plethysmography revealed that expression of caPTH1R increased aortic compliance. In vitro, the caPTH1R suppressed myofibroblast proliferation, inhibited Wnt3a, Wnt7a, and Wnt7b -induced TopFlash and Col1A1 promoter activity, and decreased MMP9. Matrix mineralization was also reduced in caPTH1R myofibroblasts. In conclusion, cell-autonomous VSMC PTH1R inhibits arteriosclerotic Wnt/β-catenin signaling and reduces vascular oxidative stress, thus limiting type I collagen and calcium accrual in aortas of diabetic LDLR-deficient mice.

***Disclosures: Su-Li Cheng**, None.*

SA0115

Circulating Sclerostin Levels in Disorders of Parathyroid Function: Primary Hyperparathyroidism (PHPT) and Hypoparathyroidism (HypoPT). Aline Costa*[1], Serge Cremers[1], Mishaela Rubin[1], Elzbieta Dworakowski[1], Donald McMahon[2], Shonni Silverberg[1], John Bilezikian[2]. [1]Columbia University, USA, [2]Columbia University College of Physicians & Surgeons, USA

Sclerostin is a protein product of osteocytes that is encoded by the SOST gene. It plays an important regulatory role in anabolic signaling pathways and, unimpeded, sclerostin inhibits the osteoanabolic Wnt signaling pathway. An attractive hypothesis to account for the anabolic actions of PTH is an osteocyte interaction that leads to the inhibition of sclerostin. However, the data supporting this idea comes from animal studies in which SOST gene expression is measured by mRNA, sclerostin-positive osteocytes (by immunocytochemistry), and sclerostin protein (by Western-blot analyses of bone lysates). To test the hypothesis that sclerostin is regulated by PTH in human subjects, we used a new highly specific and sensitive ELISA for sclerostin (TECOmedical, Sissach, Switzerland) to measure circulating sclerostin levels in serum of 25 subjects with PHPT and HypoPT and compared them with historical controls as reported by the manufacturer. The standard detection range is 0.25 to 4.0 ng/mL and sensitivity is 0.15ng/mL; intra-assay CV 1.3-1.6%, inter-assay CV 1.8-2.7%. Thirteen subjects had PHPT (11F/2M, median age 64 yrs) and twelve subjects had HypoPT (7F/5M, median age 49 yrs). All patients had their disease for at least 3 years. Sclerostin levels were markedly higher in hypoparathyroid subjects as compared to those with PHPT (mean$\pm$SD: 1.13$\pm$0.37 vs 0.46$\pm$0.10ng/mL, p=<0.0001) and to historical controls (mean$\pm$SD: 0.45$\pm$0.23ng/mL, p=<0.0001). Sclerostin levels in PHPT patients did not differ from historical controls p=0.68). These data suggest that sclerostin levels can be accurately measured in the circulation of human subjects. The results are consistent with the hypothesis that low PTH levels appear to favor SOST gene expression, and provide support for the hypothesis that PTH inhibits sclerostin production. The finding of normal levels of sclerostin in PHPT suggests that in a chronic state of PTH excess, sclerostin function is not perturbed, or any perturbation is not reflected in the circulation. Studies to track these levels after intervention with PTH (hypoparathyroidism) or removal of PTH (parathyroidectomy in PHPT) are currently ongoing.

***Disclosures: Aline Costa**, None.*

SA0116

See Friday Plenary number FR0116.

SA0117

Heterozygosity in the VDR Gene Influences Body Composition more than Bone Mass. Francisco Jose De Paula*[1], Sheila Bornstein[2], Ingrid Dick-de-Paula[3], Phuong Le[4], Bahman Rostama[4], Clifford Rosen[2]. [1]School of Medicine of Ribeirao Preto - USP, Brazil, [2]Maine Medical Center, USA, [3]School of Medicine of Ribeirao Preto, University of Sao Paulo, Brazil, [4]Maine Medical Center Research Institute, USA

The influence of modest vitamin D deficiency on bone and body composition in animal models is not clear. Vitamin D receptor null mice (VDR) not only have very low bone mass but also have a lean phenotype and increased insulin sensitivity. We hypothesized that mice with loss of one allele of the VDR gene (VDR+/-) might have moderate skeletal and body composition phenotypes. Female VDR+/- mice on a B6 background and B6 controls (+/+) were raised on a regular chow diet until 12 weeks (wk) of age. VDR+/- and VDR+/+ mice were treated either with PTH (sc, bovine PTH 50 μg/kg daily x 4 wk) or vehicle (VH) x 4 wk. The study comprised 4 female groups of mice: VDR+/+ VH (+/+VH, n=5), VDR+/+ PTH (+/+PTH, n=7), VDR+/- VH (+/-VH, n=10) and VDR+/- PTH (+/-PTH, n=11). Basal PTH serum levels were determined by enzyme immunoassay (Immunotopics), bone mass (aBMD) and body composition were determined by PIXIMUS before and after treatment. Bone microstructure (BV/TV) was determined by μCT in the lumbar spine (L5) and femur; MRI assessed percent body fat and femoral fat after treatment. Baseline PTH serum levels were modestly higher in VDR+/- mice (+/+= 67.7$\pm$10 vs +/- = 74.8$\pm$7 pg/ml). At 12 wk of age femoral aBMD in VDR+/+ did not differ from VDR +/- mice. Four weeks of PTH treatment for both genotypes showed a 12.2% increase in femoral aBMD from baseline (p<0.01 vs baseline, NS by genotype). With PTH treatment, total body aBMD increased slightly more in VDR+/- than VDR+/+ mice (+7 vs +6%, p=NS), whereas strikingly the VDR+/+ gained more fat mass (+0.32 $\pm$ 0.20 g) than

the VDR+/- group (-0.022 ± 0.18g). A similar trend in fat mass was noted for the PTH treated groups of VDR+/- and VDR+/+ mice (VDR +/+= +0.44 ± 0.17g vs VDR +/-= +0.28 ± 0.16 g). By μCT, L5 Trabecular thickness was higher in +/-PTH than +/-VH (+/-= 0.05676 μm ± 0.0006656 vs +/+= 0.06092 ± 0.001614 μm). Our results suggest that VDR heterozygote mice respond normally to an anabolic stimulus (PTH) and have a very mild skeletal phenotype associated with slight increases in PTH and reduced trabecular bone volume. Remarkably during continued growth at 16 weeks female VDR+/- mice with or without PTH remained leaner than VDR +/+ mice suggesting that the body composition phenotype is more pronounced than the skeletal one. Further studies to delineate the role of vitamin D in energy metabolism and its relationship to skeletal acquisition are needed.

***Disclosures: Francisco Jose De Paula**, None.*

SA0118

Irradiation Primes the Skeleton for PTH Anabolic Actions. Teresa Wang[1], Amy Koh*[2], Chad Novince[3], Russell Taichman[3], Hector Rios[2], Laurie McCauley[3], Xin Li[2]. [1]U of M, USA, [2]University of Michigan, USA, [3]University of Michigan, School of Dentistry, USA

PTH is an anabolic agent used clinically to treat osteoporosis and is in investigational use for increasing hematopoietic stem cells (HSCs). Irradiated (IRR) mice have increased PTH anabolic actions compared to non-IRR mice (30% bone area increase). The purpose of this study was to identify mechanisms responsible for enhanced PTH actions in IRR mice. C57B6 mice were IRR (310-325cGy; 2 fractions 3h apart) then administered PTH (0.05μg/g/d) for 21d. Flow cytometric analysis, microarray, real-time PCR gene expression, serum assays, immunohistochemistry and bone histomorphometry were performed along with primary cell isolation and analyses. IRR reduced bone marrow (BM) cellularity with retention of osteoblastic cells lining trabeculae. IRR decreased cell numbers in calvarial cell cultures in vitro suggesting against a cell autonomous benefit of irradiation. BM added to bone marrow stromal cell (BMSC) monolayers restricted mineralization which was less restrictive with IRR vs. non-IRR BM. IRR co-culture increased BMSC numbers, and IRR BM contained more adipocytes than non-IRR BM. FGF2 and IL-6 mRNA was increased in IRR BM in vivo. IRR decreased, and PTH increased periostin mRNA in the bone marrow with greater and more widespread periostin positivity throughout the marrow. PTH significantly increased serum OCN and P1NP in IRR mice despite lower baseline levels versus non-IRR. IRR decreased B220 cells, while the % of LSK cells (lin-,sca-1+,c-kit+) was increased. IRR mice had increased % BrdU positive cells and PTH increased total numbers of BrdU positive cells in IRR mice. Osteoclast number was not altered with IRR but was increased with PTH in both groups. Megakaryocytes (vWF stain) were reduced yet were located more closely to trabecular surfaces with IRR, and PTH treatment resulted in increased megakaryocyte ploidy status. PTH anabolic activity was augmented evidenced by increased bone area, serum OCN and P1NP in IRR mice. These results suggest IRR increased osteoblastic proliferation in an indirect manner and that PTH acted in the IRR mice by increasing bone active cell populations. IRR via increased IL-6 and FGF2 may prime the skeleton for anabolic actions of PTH. Furthermore, reduced cellularity and the retention of MKs, LSKs and/or adipocytes with IRR may increase osteoblast exposure to these cells to support anabolic actions. Alternatively, irradiation may decrease inhibitory cell types that negatively affect anabolic actions of PTH.

***Disclosures: Amy Koh**, None.*

SA0119

See Friday Plenary number FR0119.

SA0120

PTH but not 25(OH)D is Directly Associated with Blood Pressure and Inversely Associated with Carotid-femoral Artery Pulse Wave Velocity. Ashley Davidson*[1], Kathy Ryan[2], Alan Shuldiner[3], Elizabeth Streeten[1]. [1]University of Maryland School of Medicine, USA, [2]Department of Endocrinology, Diabetes & Nutrition, USA, [3]Department of Endocrinology, Diabetes & Metabolism, USA

Background: Both 25-hydroxyvitamin D (25-D) and PTH have been reported to be associated with cardiovascular (CV) phenotypes in some, but not all, studies. Pulse wave velocity (PWV) is a measurement of arterial stiffness and has been shown to be associated with PTH in populations receiving hemodialysis but has not been reported in healthy individuals with normal renal function. The purpose of this study was to investigate the associations of PTH and 25(OH)D with blood pressure and other subclinical vascular disease markers in the Amish, a population with a relatively homogeneous diet, levels of physical activity and low levels of smoking which can be confounders in other populations.

Methods: This observational study included participants in the Amish Family Osteoporosis and Amish Family Calcification Studies. Generally healthy participants with normal serum calcium and creatinine had the following measured: PTH, 25(OH)D, blood pressure, coronary artery calcification (CAC by electron beam computed tomography), carotid intimal medial thickness (cIMT) and PWV [carotid-femoral (C-F) and carotid-radial (C-R)]. Association analyses were performed between both 25(OH)D and PTH and: BP (n=1108), CAC (n = 650), cIMT (n = 220), C-R PWV (n = 257) and C-F PWV (n = 249). The relations of 25(OH)D and PTH levels, adjusted for season, age and sex, with subclinical vascular disease measures were assessed by comparing mean levels by Pearson's correlation.

Results: The mean age was 51.18 ± 13.02 years (range 18-91). 59.1% of the subjects were female (n = 655). The mean 25(OH)D was 22.32 ± 5.87 ng/ml, mean PTH 55.38 ± 14.27 pg/ml, mean systolic BP 119 ± 12.9 and mean diastolic BP 74.18 ± 7.37. A positive association was found between PTH and systolic (p = 0.04) and diastolic (p = 0.0004) BP. No association was shown between 25(OH)D and BP (systolic p=0.11, diastolic p=0.11). PTH and C-F PWV were inversely associated (p = 0.03). There was no association of PTH with CAC, cIMT or C-R PWV (p = 0.85, 0.4, 0.54), nor of 25(OH)D with CAC, cIMT, C-F or C-R PWV (p= 0.8. 0.52, 0.05, 0.6). The correlation between PTH and 25(OH)D was -0.30 (p<0.0001).

Conclusions: PTH level was directly associated with systolic and diastolic BP, and inversely associated with C-F PWV. 25(OH)D was not associated with these phenotypes. These results suggest that PTH may play a direct role in cardiovascular health. Alternatively, PTH may be a surrogate marker for 1,25-dihydroxyvitamin D in these associations.

	n	Correlation Coefficients	P-value
PTH			
Systolic Blood Pressure	1108	0.06135	0.04
Diastolic Blood Pressure	1106	0.10639	0.0004
25OH Vitamin D			
Systolic Blood Pressure	1097	-0.04828	0.11
Diastolic Blood Pressure	1095	-0.04853	0.11

*adjusted for age and sex
†PTH and 25OH Vitamin D adjusted for season

Quartile of seasonally-adjusted iPTH

	n	Q1	Q2	Q3	Q4	p-value for trend*
CAC score (Agatston units) †	650	0 (0, 66.3)	0 (0, 106.1)	4.8 (0, 148.9)	39 (0, 151.8)	0.85
Has CAC (%)	650	43.8	46	51.5	56.2	0.93
cIMT (mm)	220	0.59 (0.52, 0.71)	0.62 (0.51, 0.75)	0.65 (0.55, 0.73)	0.67 (0.54, 0.73)	0.4
Carotid-Radial Artery PWV	257	7.42 (6.71, 8.58)	7.09 (6.30, 8.01)	7.27 (6.84, 8.12)	7.61 (6.51, 8.13)	0.54
Carotid-Femoral Artery PWV	249	5.65 (4.79, 7.27)	5.3 (4.60, 6.15)	5.12 (4.64, 5.96)	5.3 (4.71, 6.73)	**0.03**

*adjusted for age and sex
†p-value based on log-transformed values

Table 1

***Disclosures: Ashley Davidson**, None.*

SA0121

See Friday Plenary number FR0121.

SA0122

See Friday Plenary number FR0122.

SA0123

Combined *In Vivo* MicroCT and Near-Infrared Imaging Allows for Quantitative Analyses of the Tumor Microenvironment. Rachelle Johnson*[1], Lindsay Johnson[2], Don Nolting[3], Steve Munoz[1], Gregory Mundy[1], H. Charles Manning[1], Todd Peterson[1], Julie Sterling[1]. [1]Vanderbilt University Medical Center, USA, [2]Department of Biomedical Engineering, Vanderbilt University, USA, [3]Institute of Imaging Science, Vanderbilt University, USA

The majority of breast cancer and prostate cancer patients with metastatic disease will go on to develop bone metastases, which contribute largely to patient morbidity and mortality. Numerous small animal models of cancer metastasis to bone have been developed in order to study tumor-induced bone destruction, but the advancement of imaging modalities utilized for these models has lagged significantly behind clinical imaging, particularly in the bone microenvironment in response to tumor cell establishment and treatment. We hypothesized that a combination of *in vivo* micro-Computed Tomography (μCT) and Near-Infrared (NIR) imaging can be utilized to perform quantitative longitudinal and end-point analyses of bone volume and monitor protein-level changes in the tumor-bone microenvironment. We utilized the MDA-MB-231 intratibial breast cancer model and imaged mice weekly by Faxitron, *in vivo* μCT, and Maestro (fluorescence, NIR). We found that *in vivo* μCT can significantly detect individual and group level changes in bone destruction over time in a bisphosphonate drug treatment model without altering tumor cell growth (tumor-bearing v. control limb, p<0.0001; tumor limb treated v. un-treated p<0.0001). This imaging method was validated by ex-vivo μCT and histological analyses at end-point with comparable findings. In addition, we found a significant accumulation of NIR-labeled TGF-β neutralizing antibody in the hind limbs when compared to a NIR-labeled control IgG (p<0.05), and we found significantly more NIR-labeled TGF-β antibody in the tumor-bearing limb when compared to the contra-lateral PBS-injected limb (p<0.05), indicative of increased bone remodeling at sites of tumor metastasis. More importantly, this technique offers the potential for real-time, non-invasive imaging of protein changes at the tumor-bone interface, such as increased secretion of osteolytic factors. Taken together, these data

present a comprehensive analysis of the tumor-bone microenvironment, in which imaging techniques provide an accurate method of monitoring changes in bone destruction and protein expression in the vicious cycle of tumor-induced bone disease.

***Disclosures: Rachelle Johnson**, None.*

SA0124

See Friday Plenary number FR0124.

SA0125

See Friday Plenary number FR0125.

SA0126

Influence of Connexin43 Expression on the Metastatic Phenotype and the Bone Impact of Prostate Cancer Cells. Coralie Lamiche*[1], Jonathan Clarhaut[1], Pierre-olivier Strale[1], Sophie Crespin[1], Norah Defamie[1], Marc Mesnil[1], Francoise Debiais[2], Laurent Cronier[3]. [1]CNRS - UMR 6187, Institut de Physiologie et Biologie Cellulaires, France, [2]Hopital Jean Bernard, France, [3]University of Poitiers, France

Prostate cancer (PCa) has the highest incidence in men with bone metastasis occurring in 80% of cases and mainly characterized by osteoblastic lesions. The mechanisms by which prostate cancer cells are induced to metastasize to bone are variable and complex, implicating oncogenes, pro-angiogenic factors and adhesion molecules. Among them, transmembrane proteins named connexins (Cxs) involved in gap junctional intercellular communication (GJIC) are known to permit coordinated cellular activities during development and differentiation processes. PCa cells are deficient in Cx isoforms however recent studies suggest that Cx43 could be implicated in the last stages of the tumorigenic process. Moreover, cumulated data support the involvement of Cx43 in the differentiation process of bone-forming osteoblastic cells and bone turnover. Therefore, we have investigated the role of Cx43 on the metastatic potential of PCa cells and on their impact on the osteoblastic phenotype.

To examine the effects of increased expression of Cx43 gene in PCa cells, we have performed retroviral infection in two well characterized cells lines representing different stages of cancer progression: PC3 (aggressive) and LNCaP (less metastatic). The impact on proliferation and differentiation of osteoblastic (OB) cells was evaluated in vitro by means of cocultures with OB cells from murine calvarias. In LNCaP-Cx43 cells, the Cx43 was mainly observed in plasma membrane and a functional GJIC was demonstrated by gap-FRAP and preloading assays between PCa cells as well as in the heterocellular configuration (between LNCaP and OB cells). In PC3-Cx43 cells, Cx43 was restricted to the cytoplasmic part and no cell-to-cell communication was measured. In addition, phenotypic characterization of both cell types demonstrated significant differences in adhesion, invasion and proliferation. Finally, proliferation and differentiation abilities were significantly modified by cocultures with PCa cells. The increased proliferation rate due to contact with PCa cells was not linked to the Cx43 expression level. In contrast, the impact on OB differentiation potential, revealed by alkaline phosphastase activity and qPCR analyses of differentiation markers (Cbfa-1, OCN, OPN), seems to depend on the Cx43 level.

Our *in vitro* study demonstrates that Cx43 could influence the metastatic status of prostate cancer cells. *In vivo*, preliminary data confirm the potential implication of this connexin in the bone impact.

***Disclosures: Coralie Lamiche**, None.*

SA0127

Inhibition of ATP6V1C1 (a Subunit of the V-ATPase) Expression Decreases 4T1 Mouse Breast Cancer Cell Invasion and Bone Destruction. Shengmei Feng*[1], Lianfu Deng[2], Guochun Zhu[1], Wei Chen[3], Yi-Ping Li[3]. [1]The Forsyth Institute, Shanghai Institute of Trauma & Orthopaedics, USA, [2]Shanghai Institute of Trauma & Orthopaedics, Ruijin Hospital, China, [3]The Forsyth Institute, Harvard School of Dental Medicine, USA

Vacuolar H+-ATPases (V-ATPases) located at the plasma membrane of highly metastatic human breast cancer cells are involved in the acquisition of a more metastatic phenotype, and V-ATPase inhibitors decrease the invasion and migration of highly metastatic cells. Importantly, the ATP6V1C subunit (C) of the V-ATPase complex is primarily responsible for its enzymatic function through the control of a reversible dissociation of the V0 and V1 domains. ATP6V1C1 (C1), an isoform of the C subunit, is highly expressed in oral squamous cell carcinoma. Furthermore, we recently reported that C1 is an essential component of the osteoclast proton pump and that it is important for F-actin ring formation in osteoclasts. Nonetheless, the role and mechanisms of the C subunit in breast cancer growth and metastasis remain unknown. To reveal the role of V-ATPase subunit C1 in breast cancer, we selected single subclones of 4T1 mouse breast cancer cells after transfection with lentivirus (Lenti)-GFP and Lenti-LacZ (control; siRNA targets LacZ) or Lenti-c1s3 (siRNA targets C1). Immunohistochemistry and Western blot showed that C1 expression was significantly reduced in C1-knockdown 4T1 cells, while ATP6V1C2 (C2) was not expressed in 4T1 cells with or without C1-knockdown. Furthermore, acridine orange staining showed that C1-knockdown 4T1 cells have reduced acidification, which is similar to C1-knockdown osteoclasts. Remarkably, C1-knockdown 4T1 breast cancer cells also exhibited decreased proliferation, migration, and invasion through matrigel. PBS or one of the different 4T1 clones (i.e. 4T1, 4T1-Lacz, 4T1-c1s3-1, or 4T1-c1s3-11) was implanted into the left femur of female BALB/C mice. After 16 days, X-rays and micro-CT scanning revealed that there was reduced bone destruction compared with the control mice in the femurs and tibiae of mice in which C1-knockdown 4T1 cells were implanted. All assays were done in triplicate, and all animals were maintained according to the Guide for the Care and Use of Laboratory Animals. We report here for the first time, that C1 not C2 is an essential subunit of the V-ATPase complex in 4T1 mouse breast cancer cells and that inhibition of C1 expression in 4T1 breast cancer cells decreased their growth and invasion in vitro and in vivo. Though these data suggest that the inhibition of C1 expression can decrease the invasive properties of 4T1 cells, additional studies are needed to define the molecular mechanisms of how C1 influences 4T1 migration.

***Disclosures: Shengmei Feng**, None.*

SA0128

See Friday Plenary number FR0128.

SA0129

Sympathetic Nervous System Activation Increases Breast Cancer Metastasis to Bone. J. Campbell*[1], Julie Sterling[2], Yun Ma[2], GR Mundy[2], Florent Elefteriou[2]. [1]Vanderbilt Center for Bone Biology, USA, [2]Vanderbilt University, USA

Depression, while not associated with breast cancer incidence, is linked to increased recurrence and decreased survival. Increased Sympathetic nervous (SNS) outflow, a hallmark of mental stress, controls multiple processes in the bone, such as hematopoietic stem cell trafficking, osteoblast proliferation and osteoclastogenesis via β-adrenergic receptors (βAR) and cytokines also involved in cancer metastasis, such as SDF-1 and RANKL. These observations suggested a possible involvement of SNS activation in cancer cell osteotropism, tumor burden and the formation of osteolytic lesions. To address this question, we used an established model of lytic bone metastasis in which MDA-MB-231 human breast cancer cells are injected via left cardiac ventricle in athymic nude mice. Isoproterenol (Iso), a (βAR) agonist, was used as a surrogate for SNS activation. Faxitron, 3D-microtomography and histomorphometric measurements were used to quantify number and size of lytic lesions, tumor burden and BV/TV. We observed that Iso treatment before MDA-MB-231 inoculation increased the number of bone lytic lesions and lesion area ($p<0.05$). Treating with Iso after bone metastasis increased the size of the lytic lesions ($p<0.05$) but not lesion number. These results suggested that sympathetic activation alters the bone microenvironment to make it favorable for cancer cell homing and growth. Although it did not affect lytic lesion number in a model without chronic depression, βAR blockade by propranolol decreased lesion area ($p<0.05$). *In vitro*, direct stimulation of the β2AR in MDA-MB-231 cells produced no effect on migration, cell growth or *PTHrP, Rank* and *CXCR4* expression. In contrast, stimulation of the β2AR in bone marrow stromal cells, calvaria and MC3T3 osteoblasts increased *Rankl* but not *Sdf1* expression ($p>.005$). The conditioned media of Iso-treated osteoblasts increased MDA-MB-231 cell transwell migration ($p<0.005$), which could be blocked by OPG but not by the CXCR4 antagonist AMD300. These results suggest that the increase in osteolysis and metastasis observed following Iso treatment *in vivo* are due to a predominant effect on the bone marrow stroma rather than a direct effect on cancer cells. These findings support the hypothesis that depression, via sympathetic activation, make the bone marrow environment permissive to cancer metastasis, growth, or recurrence, and imply that β-blockers may reduce both bone tumor burden and relapse in breast cancer patients.

***Disclosures: J. Campbell**, None.*

SA0130

The Effect of Various Vitamin D Supplementation Regimens on 25-OH Vitamin D Levels in Breast Cancer Patients Undergoing Treatment. Alissa Huston*, Luke Peppone, Kristin Skinner, Michelle Janelsins, Gary Morrow. University of Rochester Medical Center, USA

Vitamin D (VID) deficiency is linked to decreased bone mineral density (BMD), increased breast cancer incidence, recurrence, and mortality. Breast cancer treatment, specifically hormonal therapy (HT), reduces BMD and increases fracture risk. Our study aims include: 1) determining the prevalence of VID deficiency among women receiving treatment, 2) evaluating the effect various VID supplementation regimens on deficiency, and 3) determining the association between VID levels and BMD. Serum 25-OH VID levels were obtained from approximately 224 women and BMD from 75 women undergoing treatment (HT, radiation, chemo, or any combination) for non-metastatic breast cancer (ages 24-88). The proportion of patients with VID deficiency was determined for the total sample, and compared across race and stage of disease at baseline. VID and BMD were compared using ANCOVA models. Severely VID deficient patients (<25 ng/mL) were prescribed high-dose VID (≥50,000 IU/week),

mildly deficient patients (26-31 ng/mL) were prescribed low-dose VID (≥2,000 IU/day), and patients with normal VID levels (≥32 ng/mL) were not given any prescription. The change in 25-OH VID levels was compared across the 3 supplementation levels. At baseline, 23% of all women were considered VID deficient (<20 ng/mL), while 43% were considered VID insufficient (20-31 ng/mL). Lower baseline 25-OH VID was observed in Non-Caucasian patients (Caucasian: 28.2 ng/mL vs. Non-Caucasian: 19.3 ng/mL; $p<0.01$) and patients with later-stage disease (Stage I: 29.7 ng/mL vs. Stage III: 22.9 ng/mL; $p<0.01$). Weekly high-dose VID resulted in a significant increase (+27 ng/mL; $p<0.01$) in 25-OH VID, while there was no difference between low-dose VID supplementation (+14 ng/mL; p=0.28) and no supplementation (+9 ng/mL). Among women not on bisphosphonates, spinal BMD was lower for those with deficient (<20 ng/mL: 0.99 g/cm^2; p=0.01) and insufficient follow-up VID levels (20-31 ng/mL: 1.18 g/cm^2; p=0.07) compared to those with normal VID levels (≥32 ng/mL:1.26 g/cm^2). VID deficiency was extremely prevalent in women being treated for breast cancer, and more common in breast cancer patients who presented with later-stage disease and were Non-Caucasian. Weekly high-dose VID is required to significantly increase 25-OH VID levels, as opposed to conventional low-dose VID. Lower VID levels were also significantly associated with reduced spinal BMD among women not using bisphosphonates.

***Disclosures: Alissa Huston**, None.*

SA0131

The Histone Deacetylase Inhibitor, Vorinostat, Reduces Metastatic Cancer Cell Growth and Associated Osteolytic Disease, but Promotes Normal Bone Loss. Jitesh Pratap*[1], Jacqueline Akech[1], John J. Wixted[1], Gabriela Szabo[1], Robinder J. Dhillon[2], Xiaodong Li[2], Krystin Bedard[1], Sadiq Hussain[1], Andre Van Wijnen[1], Janet L. Stein[1], Gary Stein[1], Jennifer Westendorf[2], Jane Lian[1]. [1]University of Massachusetts Medical School, USA, [2]Mayo Clinic, USA

Vorinostat, an oral histone deacetylase inhibitor with anti-tumor activity, is in clinical trials for hematological and solid tumors that metastasize and compromise bone structure. Consequently, there is a requirement to establish the effects of vorinostat on tumor growth in the bone microenvironment. Metastatic cancer cells were injected into tibias of SCID mice and the effects of vorinostat on tumor growth and osteolytic disease were assessed by radiography, μCT, histological and molecular analyses. Vorinostat-treated and control mice without tumors were also examined. Vorinostat significantly decreased tumor cell proliferation and promoted apoptosis of prostate and breast cancer cells. Tumor growth in bone was reduced ~33%. Bone osteolysis was significantly reduced in the first weeks of tumor growth, but then increased with continued vorinostat treatment. The non-tumor bearing contra-lateral femurs showed significant bone loss (50% volume density of controls) after four weeks of vorinostat therapy. This same extent of bone loss occurred in vorinostat-treated normal mice (without tumors). We show that vorinostat mediated bone loss is caused by a 2 to 3 fold upregulation of factors promoting bone resorption (PTHrP, IL-8 and osteopontin); factors secreted by tumor cells to induce osteoclast activity. Thus, our studies indicate that vorinostat effectively inhibits tumor growth in bone, but has a negative systemic effect on the integrity of normal trabecular bone and thereby contributes to osteolysis independent of tumor cell activity. Vorinostat treatment reduces tumor growth but can promote osteopenia throughout the skeleton. Our studies indicate therapeutic regimens should be considered that combine vorinostat with anti-resorptive agents to prevent treatment-induced bone loss.

***Disclosures: Jitesh Pratap**, None.*

SA0132

The Role of Tumor Derived Interleukin 6 in a Murine Model of Breast Cancer Bone Metastasis. Yu Zheng*[1], Anastasia Mikuscheva[2], Hong Zhou[3], Katja Boernert[1], Frank Buttgereit[2], Colin Dunstan[4], Markus Seibel[3]. [1]Bone Research Program, ANZAC Research Institute, University of Sydney, Australia, [2]Humboldt University, Germany, [3]Bone Research Program, ANZAC Research Institute, The University of Sydney, Australia, [4]University of Sydney, Australia

Breast cancer has a high propensity to metastasise to the skeleton. The bone microenvironment plays a central role in metastatic cancer growth as reduced bone resorption inhibits and increased bone turnover accelerates cancer growth in bone[1,2]. In patients with metastatic breast cancer, high circulating interleukin-6 (IL-6) levels have been associated with disease progression/ poor clinical outcomes. We found in animal studies that increasing or decreasing bone resorption results in corresponding changes in tumor IL-6 expression and tumor proliferation, indicating that IL-6 expression by cancer cells may play a role in sustaining breast cancer growth in bone[3]. However, it is unclear whether tumor-derived IL-6 affects cancer cell behavior *in vitro* and *in vivo*.

To investigate this question, IL-6 expression was silenced in MDA-MB-231 cells via a lentiviral-based expression system driving the production of short hairpin RNA species (shRNAs). Knock-down efficacy was 80% as assessed by real-time RT-PCR (mRNA) and ELISA (secreted protein).

In vitro characterization of control vs. knock-down MDA-MB-231 cells demonstrated that silencing of IL-6 expression significantly reduces invasiveness without affecting proliferation.

In vivo studies: Control and IL-6 knock-down MDA-MB-231 cells (50000 cells per injection) were implanted via intra-tibial inoculation into 4-week-old BALB/c nu/nu female mice (n=7/group) kept on a low (0.1%) calcium diet to induce high bone turnover[1, 2]. Tumor growth was monitored using X-ray imaging on days 10, 17 and 21, and bones were analysed by histology and histomorphometry following sacrifice on day 21 post inoculation. Compared to controls, IL-6 knock-down resulted in significantly smaller osteolytic lesions on day 10, 17 and 21 ($p< 0.05$, by X-ray analysis), and significantly reduced total tumor area on day 21 ($3.20 \pm 0.76mm^2$ *vs.* $5.57 \pm 0.98mm^2$, $p<0.05$, by histology). Growth of subcutaneously implanted tumors was similar in animals injected with IL-6 silenced or normal MDA-MB-231 cells.

We conclude that IL-6 knock-down in MDA-MB 231 cells reduces cancer cell invasiveness *in vitro* and intraskeletal tumor growth *in vivo*, supporting the conecpt that tumor-derived IL-6 has an important role in the biology of metastatic breast cancer and may be a potential therapeutic target.

References
1. Zheng *et al., Cancer Res* 67, 9542 (2007).
2. Zheng *et al., Clin Exp Metastasis* 25, 559 (2008).
3. Zheng *et al., J Bone Miner Res* 24 (Suppl 1), (2009).

***Disclosures: Yu Zheng**, None.*

SA0133

See Friday Plenary number FR0133.

SA0134

A Role for the ARF Tumor Suppressor in Osteoclasts. Crystal Winkeler*[1], Monica Croke[2], Emanuella Heller[1], Michelle Hurchla[1], Chan Lee[1], Katherine Weilbaecher[3], Jason Weber[1]. [1]Washington University in St. Louis, USA, [2]Washington University School of Medicine, USA, [3]Washington University in St. Louis School of Medicine, USA

In response to oncogenic stress, the ARF tumor suppressor is able to halt both cell proliferation and growth. ARF stabilizes and activates p53 through the inhibition of Mdm2, the E3 ubiquitin ligase for p53. More recently, ARF has been ascribed p53-independent functions through its ability to inhibit ribosome biogenesis. However, there is an inherent difficulty in separating these two functions of ARF by the fact that cell growth is intimately tied to cell proliferation. To resolve this, we have chosen to study the function of ARF in osteoclasts. Osteoclasts provide a unique model in that they are post-mitotic and function independent of p53. Furthermore, understanding the growth control of osteoclasts is important in understanding diseases such as osteoporosis and osteolytic bone metastasis.

To assess osteoclastogenesis and osteoclast function *in vitro*, BMMs were harvested from wildtype or *Arf-/-* mice. Osteoclastogenesis was assessed by TRAP-staining under various concentrations of RANKL. Mature wildtype and *Arf-/-* osteoclasts were used to assess the role of ARF in ribosome biogenesis, actively-translating ribosomes, protein synthesis, and cell growth. Additionally, we crossed $Arf^{fl/fl}$ mice with mice containing *Cre* under the control of the *Cathepsin K* promoter. Resultant mice were used to assess osteoclast-specific *Arf* loss *in vivo* by vivaCT, serum CTX, and histological analysis. *Arf* loss caused enhanced osteoclastogenesis and increased osteoclast size, resulting in greater osteoclast activity. This hyperactivity was most evident in our novel osteoclast-specific *Arf*-null mice, which exhibited a decrease in bone volume and density compared to control mice. Thus, we propose a teleological function for ARF, distinct from its classical role as a tumor suppressor, in the regulation of osteoclast activity.

***Disclosures: Crystal Winkeler**, None.*

SA0135

See Friday Plenary number FR0135.

SA0136

See Friday Plenary number FR0136.

SA0137

Controlled Bone Tissue Ablation using Novel Navigational RF Device. Andreas Kurth*[1], Dirk Proschek[2], Aaron Germain[3], Robert Poser[3]. [1]Goethe-Universität Frankfurt, Germany, [2]Dep. Orthopaedic Surgery, University Medical Center, Germany, [3]Dfine Inc., USA

Purpose: Bone metastasis is a debilitating complication that result in severe pain, pathologic fractures, dysfunction, cord compression and decreased quality of life. Radiation and surgery are the common local treatment options, along with systemic treatment for the underlying primary cancer. Radiofrequency (RF) ablation

has been successfully used in radiation resistant tumors or small localized disease. Clinical advantages of RF ablation in spinal metastasis are more immediate pain relief and less systemic toxicity. However, clinical limitations of RF ablation in treatment of vertebral lesions include lack of minimally invasive (MI) navigation in hard tissue and accurate ablation zones. The present study evaluates a novel RF ablation device for local treatment of bone metastates.

Methods: A 10 gage, bipolar, RF ablation instrument with a navigational articulating tip containing thermocouples and a proprietary RF generator were used. Based on strategically located thermocouples, the software automatically controls ablation zones using tissue (adjacent to ablation zone) temperature control. Sixty ex-vivo ablations were performed in bovine liver at each power settings for a total of 180 ex-vivo ablations. Infrared thermography recorded tissue temperature gradients during ablation at three power settings (5W, 15W, 25W). Using a porcine in-vivo model, similar ablations were performed in both liver (n=20) and cancellous bone (n=8) sites followed by gross examination, histologic processing and histomorphometric analysis.

Results: Discrete thermal profiles measured by IR and reproducible ablation zones (20x8 mm) were identified in all ex-vivo specimens. While the rate of ablation was dependent on the power setting, the size of ablation was extremely consistent across power settings. In-vivo ablation zone dimensions were within those recorded in extensive ex-vivo tests. Histomorphometric confirmation of effective, reproducible, site specific in-vivo ablation of both liver and cancellous bone were confirmed in a porcine model.

Conclusion: Site and size specific ablation zones are extremely important in treating bone metastasis that can be close to neural elements. These data demonstrate the unique ability to create reproducible ablation zones in hard tissue at variable rates, based on real time temperature mapping controlled software.

***Disclosures: Andreas Kurth**, None.*
This study received funding from: Dfine Inc, San Jose, CA, USA

SA0138

See Friday Plenary number FR0138.

SA0139

Epigenetic Silencing of the Homeobox-containing Transcription Factor Dlx2 Promotes Chemoresistance in Human Osteosarcoma Cells. Erik Sampson*[1], Vinit Amin[2], Laurence Donahue[2], Edward Schwarz[1], Regis O'Keefe[1], Randy Rosier[2]. [1]University of Rochester, USA, [2]University of Rochester Medical Center, USA

Osteosarcoma (OS) is the most common primary paediatric bone tumor. Greater than ninety percent of patients who present with metastatic OS and thirty to forty percent of patients with nonmetastatic disease will experience relapse. Drug resistance is one underlying mechanism contributing to the failure of chemotherapy to elicit a lasting response in these patients. Expression of the homeobox-containing transcription factor Dlx2 is associated with chemotherapy sensitivity in various cancer cell lines. In addition, several Dlx family members are expressed early during osteogenesis, raising the possibility that loss of Dlx2 expression during osteosarcomagenesis concomitantly renders OS cells insensitive to chemotherapy. Indeed, the expression of Dlx2 protein is decreased in OS cell lines compared to immortalized human osteoblasts. Retrovirus-mediated expression of Dlx2 in OS cell lines did not affect cell proliferation, basal apoptosis levels or *in vitro* clonogenicity a surrogate assay for *in vivo* tumorigenicity. However, OS cell lines stably expressing Dlx2 were up to ten-fold more sensitive to doxorubicin, a chemotherapeutic commonly used to treat OS, as determined by flow cytometric analysis of caspase 3 activation. Numerous homeobox genes, including several Dlx family members are potentially silenced in cancer cells via aberrant promoter DNA methylation. Epigenetic mechanisms of gene silencing including DNA methylation, histone deacetylation and histone methylation are emerging targets for novel cancer therapeutic development. The histone deacetylase inhibitor (HDACi) suberoylanilide hydroxamic acid (SAHA; vorinostat (Zolinza)) is approved by the Food & Drug Administration for the treatment of cutaneous T-cell lymphoma. The expression of Dlx2 message and protein was increased in OS cell lines treated either with SAHA or another HDACi, valproic acid (VA). Pre-treatment with SAHA or VA followed by doxorubicin had a striking, synergistic effect on apoptosis in OS cells. This synergistic increase in cell death was in part rescued by RNA interference with HDACi-mediated Dlx2 induction. Dlx2 induction therefore partially mediates rather than simply correlates with OS chemosensitization by HDACi. While future studies will be required to determine whether Dlx2 is a bona fide OS-related tumor suppressor gene, strategies to increase Dlx2 expression including HDACi or DNA methyltransferase inhibitors may overcome chemotherapy resistance in relapsed OS patients.

***Disclosures: Erik Sampson**, None.*

SA0140

See Friday Plenary number FR0140.

SA0141

Identification of Novel Molecule for Melanoma Malignancy -Role of CIZ -. Kentaro Miyai[1], Masaki Noda[1], Tadayoshi Hayata[2], Tomomi Sakuma*[3], Yoichi Ezura[4]. [1]Tokyo Medical & Dental University, Japan, [2]Medical Reserach Institute, Tokyo Medical & Dental University, Japan, [3]Tokyou Medical & Dental University, Japan, [4]Tokyo Medical & Dental University, Medical Research Insititute, Japan

Metastasis of tumor to bone is one of the serious complications during tumor treatment. One of the possible key molecules for the establishment of bone metastasis would be those for cell attachment and transcription of the genes. Cas-Interacting-Zinc finger protein, CIZ, posses these two properties as it is localized at the site of focal adhesion plaque and it could trans locate into nuclei. B16, a malignant melanoma cell, are highly metastatic tumor. Therefore, we examined the possible roles of CIZ for the establishment of tumor metastasis of bone. In B16 cells, CIZ protein was expressed and localized in nuclei and cytosol. Cell migration to wild-type (WT) serum was inhibited by knockdown of CIZ, suggesting that CIZ would be one of factor for cell movement in B16. Treatment of BMP, which is involved in both cancer promotion and inhibition, suppressed migration of B16 to WT serum. Treatment with BMP suppressed CIZ expression in B16, suggesting that down regulation of CIZ by BMP may be involved in this cell migration process CIZ knock down revealed that CIZ interferes with the increase of the transcription through BMP response element by BMP treatment in Luciferase assay. Taken together, these results suggest that CIZ and BMP antagonize each other. In the host side, to examine the difference of local proliferation in bone microenvironment between WT and CIZ KO mice, we inoculated B16 into bone. After 5 weeks, CIZ KO mice suppressed cancer cell proliferation. To investigate whether CIZ-deficient microenvironment also affects cancer cell migration, migration assay was performed. B16 migrated to the side of medium containing the serum derived from WT mice, whereas migration of B16 was suppressed when serum from CIZ KO mice was used. And the size of cells that barely migrated to CIZ KO serum was significantly small compared to WT serum. These results suggest that certain factors under the control of CIZ are required for regulation of migration and morphology of B16. To investigate the molecular mechanism underlying this migration defects in CIZ KO serum, we focused on Cxcl12 involved in tumor growth and metastasis. We analyzed expression level of Cxcl12 in bone marrow, but there is no change between WT and CIZ KO mice. These results suggest that CIZ regulates tumor growth and progression in both sides of the cancer cell and host microenvironment. Breakdown of the balance between BMP and CIZ may be involved in tumor progression.

***Disclosures: Tomomi Sakuma**, None.*

SA0142

Leukemia Blasts Compromise Osteoblast Function in a Mouse Model of Acute Myelogenous Leukemia. Barbara Silva*[1], Yoshihiro Yoshikawa[2], Charles Duncan[2], Linda Johnson[3], John Manavalan[2], Ellin Berman[4], Stavroula Kousteni[1]. [1]Columbia University Medical Center, USA, [2]College of Physicians & Surgeons, Columbia University, USA, [3]Cornell University & Memorial Sloan-Kettering Cancer Center, USA, [4]Memorial Sloan-Kettering Cancer Center, USA

The bone marrow niche has been implicated in the pathogenesis of leukemia, as a permissive microenvironment required for its emergence or progression. Yet, few studies have shown how the malignant cells influence specific cell populations within the bone niche or characterized signals that orchestrate their crosstalk. In this context, we aimed to define specific bone cell populations and signals that are involved in the changes occurring in the niche after the disease is established. We injected WEHI-3b murine myelomonocytic leukemia cells into immunocompetent Balb/C mice, and compared them to a control group that had not been injected with leukemia cells. Fourteen days later, tumor engraftment was present in both femur and spine of the leukemic mice as observed by histopathological analysis. Leukemic mice showed a marked, 68%, and significant decrease in osteoblast numbers, 50% decrease in bone formation rate, and a less pronounced, 14%, but also significant, trabecular bone loss. Osteoclast numbers were not affected. The decrease in osteoblast numbers appeared to be caused by a decrease in differentiation as evidenced by reduced expression of osteoclacin, Runx2, osterix and alkaline phosphatase. A specific subset of non-hematopoietic (CD45- and CD34- negative) bone marrow cells expressing the endothelial cell marker CD105 were affected, as determined by flow cytometry. This was evidenced by a negative correlation between the tumor burden and the CD45-/CD34-/CD105+ subset of bone marrow cells. wInterestingly, gene expression studies and mineralization assays showed that this particular population of CD45-/CD34- cells has the highest osteogenic potential. Additionally, osteoblastic expression of OPG was decreased, whereas RANKL was increased, leading to a marked increase in the RANKL:OPG ratio, probably explaining the maintenance of osteoclast numbers in the presence of reduced osteoblast numbers. Expression of SDF-1, a gene implicated in normal hematopoietic cell homing in the bone marrow niche, was reduced in osteoblasts, which could contribute to derangements in normal hematopoiesis during the course of the disease. In summary, 1) osteoblastogenesis was decreased, 2) osteoblast- osteoclast uncoupling was noted, and 3) a CD45-/CD34-/CD105+ subset of bone marrow cells was identified as the osteogenic population affected by leukemic engraftment. These data demonstrate that leukemia blasts influence osteoblast growth and functional characteristics.

***Disclosures: Barbara Silva**, None.*

SA0143

Targeting Wnt or BMP Pathways Differentially Modulates Osteoclast-inducing Activity of Giant Cell Tumor Stromal Cells: Biologic and Therapeutic Implications. Matthew Steensma*[1], Wakenda Tyler[2], John Healey[3], F. Patrick Ross[4], Steven Goldring[4], Ed Purdue[4]. [1]Memorial Sloan-Kettering Cancer Center/Hospital For Special Surgery, USA, [2]Rochester University, USA, [3]Memorial Sloan-Kettering Cancer Center, USA, [4]Hospital for Special Surgery, USA

Giant Cell Tumor of Bone(GCT) is an osteolytic tumor comprised of three cell populations: fibroblast-like stromal cells(SC); myeloid mononuclear cells; and multi-nucleated osteoclast(OC)-like giant cells. The SC is thought to represent the neoplastic element based on a sustained, high proliferation rate in culture and the presence of cytogenetic abnormalities. SC's express genetic markers consistent with an arrest in an early stage of osteoblast(OB) differentiation that is associated with high expression levels of the OC-inducing factor, RANKL. We aimed to test the hypothesis that SC's could be reprogrammed to undergo OB differentiation by targeting the Wnt or BMP pathways resulting in modulation of key regulators of OCgenesis, including osteoprotegerin(OPG). 6 GCT specimens were obtained in accordance with an approved IRB protocol. SC's were isolated from collagenase-dispersed tumor cells using negative selection with a CD14 magnetic bead column. Purity was assessed based on morphology, the absence of CD14 expression (FACS and IF microscopy), and the absence of OC-specific genes, including cathepsin K. SC's were cultured for 10-12 d in the presence or absence of BMP-2, SB415286(a specific GSK-3beta inhibitor and Wnt mimetic), or osteogenic medium (OGM). Differential expression of OB differentiation markers was assessed by qPCR. OPG production was determined by ELISA. The OCgenic activity of SC's was assessed using a human monocyte co-culture system. OC formation was quantified by TRAP stain cell counts done in triplicate. SC's exposed to BMP-2, SB415286, or OGM demonstrated >2-fold induction of OB-associated genes, including Runx2 and osterix. Wnt pathway activation or growth in OGM was accompanied by a marked increase in the OPG/RANKL ratio and loss of SC OC-inducing activity. Conversely, treatment with rhBMP-2 resulted in a *decreased* OPG/RANKL ratio, and *enhanced* OC formation. The capacity of Wnt and BMP pathway activation and OGM to induce SC's to undergo OB differentiation provides further evidence of their OB lineage. Surprisingly, the induction of OB differentiation by BMP or Wnt pathway activation produced differential effects on OC-inducing activity. This effect may be attributed to the differential effects of the Wnt and BMP pathways on OPG/RANKL production. The ability to manipulate the OCgenic phenotype of SC's provides a potential novel approach for treatment and insight into the mechanisms by which OB lineage cells regulate OCgenesis.

***Disclosures: Matthew Steensma**, None.*

SA0144

Unraveling the Molecular Connections between Anti-Cancer and Anti-Osteoporosis Drugs Using the Connectivity Map. Jameel Iqbal*[1], Xuan Liu[1], Ling-Ling Zhu[1], Jianhua Li[2], Yuanzhen Peng[3], Zuhong Lu[4], Guangyu Zhu[1], Alberta Zallone[5], Li Sun[6], Mone Zaidi[7]. [1]The Mount Sinai Bone Program & Department of Medicine, Mount Sinai School of Medicine, USA, [2]Tount Sinai School of Medicine, USA, [3]The Mount Sinai School of Medicine, USA, [4]State Key Laboratory of Bioelectronics, Southeast University, Nanjing China, China, [5]University of Bari Medical School, Italy, [6]Mount Sinai School of Medicine, USA, [7]Mount Sinai Medical Center, USA

Cancer is the second leading cause of death, and osteoporosis the leading cause of morbidity in the aging population. There is mounting evidence that bisphosphonates, the mainstay of osteoporosis therapy, have anti-carcinogenic properties. While it is known that bisphosphonates prevent bone metastases for breast, prostate and lung cancers, recent evidence suggests that these drugs can prevent the growth of breast cancer lesions. We therefore investigated the molecular mechanisms underlying the anti-resorptive and putative anti-carcinogenic actions of bisphosphonates. Human osteoclasts were treated with alendronate or risedronate to generate a unique bisphosphonate gene signature by combining affymetrix datasets from the respective drugs. We then interrogated the Connectivity Map (CMAP, Broad Institute), a powerful genetic database comprising gene expression profiles that define functional connections between drug actions, genetic perturbations, and disease states. Non-parametric, rank-based pattern-matching using the Kolmogorov-Smirnov statistic examined shared mechanisms of action to reveal both mimics and anti-mimics of the bisphosphonates. The bisphosphonate gene signature identified two anti-cancer drugs, the EGF signaling inhibitor tyrphostin AG1478 and the PARP inhibitor 1,5-isoquinolinediol. Both these anti-cancer drugs displayed potent anti-resorptive properties in vitro identical to bisphosphonates, thus attesting to their use as potential candidates for osteoporosis therapy. Given the molecular connectivity of bisphosphonates to EGFR inhibitors, we tested the effects of alendronate and risedronate on the proliferation of lung cancer cells harboring EGF receptor mutations. Both bisphosphonates potently inhibited cell proliferation. Because breast, lung, and prostate cancers are all known to have aberrant EGFR signaling, often with a dependence on Akt, we tested whether the bisphosphonates could inhibit EGF-induced Akt activation. We found that both alendronate and risedronate suppressed Akt phosphorylation: this represents a novel mechanism for bisphosphonate action that may be utilized for inhibiting cancer growth, especially for cancers with known EGFR/Akt mutations. In conclusion, CMAP could be a powerful new alternative to drug discovery, particularly as it unravels new actions of 'old' drugs. Its use could conceivably reduce the often prohibitive costs and lengthy time intervals that underpin modern drug development.

***Disclosures: Jameel Iqbal**, None.*

SA0145

Zoledronic Acid Prolongs Time to First Skeletal-Related Event (SRE), Progression-Free Survival (PFS), and Overall Survival (OS) Versus Clodronate in Patients With Newly Diagnosed Multiple Myeloma (MM): Results of the Medical Research Council (MRC) Myeloma IX Trial. W. Gregory[1], A. Szubert[1], R. Owen[2], J. Child[1], A. Ashcroft[3], M. Drayson[4], N. Navarro Coy[1], Faith Davies[5], Graham Jackson[6], K Cocks[1], Gareth Morgan*[7], S. Bell[1]. [1]University of Leeds, United Kingdom, [2]St. James's University Hospital, United Kingdom, [3]Mid-Yorkshire Hospitals NHS Trust, United Kingdom, [4]University of Birmingham, United Kingdom, [5]Institute of Cancer Research, United Kingdom, [6]University of Newcastle, United Kingdom, [7]Royal Marsden Hospital, United Kingdom

Purpose: Myeloma cells grow within the bone marrow, and patients (pts) with MM are at high risk for SREs such as pathologic fracture or spinal cord compression. In addition to prolonging OS, an important goal is preventing these potentially debilitating SREs. Bisphosphonates (BPs) are standards of care for reducing the risk of SREs in pts with bone metastases from solid tumors or bone lesions from MM. In addition, several BPs have demonstrated anticancer activity in preclinical models. In particular, zoledronic acid (ZOL) has shown anticancer activity in preclinical models and clinical studies in various cancer types, including MM. In pts with early breast cancer, adding ZOL improved disease-free survival by 36% (P = .01) vs endocrine therapy alone (Gnant et al. *N Engl J Med.* 2009).

Methods: In the MRC Myeloma IX trial (ISRCTN68454111), pts with newly diagnosed MM were randomized to IV ZOL (4 mg q 21-28 days) or oral clodronate (CLO; 1,600 mg/d) plus antimyeloma therapy. Treatment continued at least until disease progression. All pts provided written informed consent, were evaluated for disease outcomes and safety, and the study was approved by institutional review boards. OS, PFS, and SREs were evaluated in adjusted Cox models. OS was also evaluated in an exploratory Cox model adjusted for time-dependent SRE effects.

Results: A total of 1,960 pts were evaluable, with median follow-up of 3.7 yr. In the ZOL and CLO groups, mean age was 65 yr, IgG was the predominant subtype, and ~70% of pts had bone lesions. Overall, ZOL significantly reduced the risk of first SRE by 26% vs CLO (hazard ratio = 0.74; 95% CI: 0.62, 0.87; P = .0004). Pts treated with ZOL had a significant 2-mo increase in PFS (19.5 vs 17.5 mo, respectively; P = .0179) and a 5.5-mo increase in OS (50 vs 44.5 mo, respectively; P = .0118) vs CLO. Moreover, ZOL's survival benefit remained statistically significant after adjusting for potential effects of SREs on OS (P = .0178). Both BPs were generally well tolerated. There was no significant between-group difference in the rate of acute renal failure (ZOL, 6.1%; CLO, 5.8%), and the incidence of confirmed osteonecrosis of the jaw was low (ZOL, 3.5%; CLO, 0.3%).

Conclusions: The results of the MM IX Trial demonstrate a beneficial effect of ZOL on OS and PFS, and superior SRE prevention vs CLO, in pts with MM. Moreover, ZOL OS benefits remained significant after readjustment for SREs, supporting potential anticancer activity.

***Disclosures: Gareth Morgan**, None.*
This study received funding from: Novartis, Boehringer Ingelheim, Pharmion, and Celgene for the clinical trial.

SA0146

See Friday Plenary number FR0146.

SA0147

Coexpressions of FGF-23 and MEPE in Causative Tumors of Oncogenic Osteomalacia. Yuki Nagata*[1], Yasuo Imanishi[1], Jun Hashimoto[2], Wataru Ando[2], Keisuke Kobayashi[1], Takafumi Ueda[3], Akimitsu Miyauchi[4], Hajime Koyano[5], Hiroshi Kaji[6], Takatoshi Saito[7], Koichi Oba[8], Yasato Komatsu[9], Hitoshi Goto[1], Takami Miki[10], Masaaki Inaba[1], Yoshiki Nishizawa[10]. [1]Osaka City University Graduate School of Medicine, Japan, [2]Osaka University Graduate School of Medicine, Japan, [3]Osaka National Hospital, Japan, [4]Omura municipal Hospital, Japan, [5]Juntendo University, School of Medicine, Japan, [6]Kobe University, Japan, [7]Jikei University School of Medicine, Japan, [8]Graduate School of Medical Sciences, Kyushu University, Japan, [9]Kyoto City Hospital, Japan, [10]Osaka City University Medical School, Japan

Purpose Oncogenic osteomalacia (OOM) is a rare disease characterized by renal phosphate wasting and osteomalacia, and is caused by the secretion of fibroblast

growth factor 23 (FGF-23) from causative tumors. Matrix extracellular phosphoglycoprotein (MEPE) as well as its proteolytic ASARM peptide elevate FGF-23 expression in bone. Although the expression of MEPE was reported in some OOM tumors, little is known whether MEPE contributes to the FGF-23 expression in OOM tumors. In this study, we attempt to determine the expressions of FGF-23 and MEPE in OOM tumors.

Subjects and Methods Eleven causative OOM tumors were examined for expressions of FGF-23 and MEPE by quantitative real-time RT-PCR and immunohistochemistry. Two hemangiopericytomas and 4 giant cell tumors, obtained from non-osteomalacic patients, were used as controls, which pathological diagnoses are common among OOM.

Results The expression levels of FGF-23 in OOM tumors were 10^5 times higher than those in non-OOM tumors. The expression levels of MEPE in OOM tumors were also 10^5 times higher than those in non-OOM tumors. Immunohistochemical examinations revealed the presence of FGF-23 in all OOM tumors, and that of MEPE in 10 of 11 OOM tumors.

Conclusions The coexpressions of FGF-23 and MEPE in OOM tumors suggest that MEPE or its proteolytic ASARM peptide may contribute to the FGF-23 overexpression in OOM tumors.

***Disclosures: Yuki Nagata**, None.*

SA0148

Combined Effects Of Exercise And Alcohol On Bone Status In Rats. Delphine Maurel*[1], Christelle Jaffre[2], Eric Dolleans[2], Nathalie Boisseau[3], Claude-Laurent Benhamou[2]. [1]Inserm Unit 658, Hopital Porte Madeleine, Orléans, France, [2]Inserm Unit U658, France, [3]LAPHAP Laboratory, France

Chronic alcoholism is known to alter bone balance by a decrease of bone remodeling, bone mineral density (BMD), bone mineral content (BMC) and bone resistance in rats and in men. Nowadays most of the treatments to manage bone loss are drug treatments. However, positive effects of exercise on bone are well known. To date and to our knowledge, no study has been driven to determine the possible beneficial effects of regular exercise on bone loss induced by chronic alcohol consumption. To address this question, we designed a study in rats to determine the effects of combined alcohol and exercise on bone.

Thirty-six 2-month old male Wistar rats were divided in 3 groups: Control (C), Alcohol (10 g/kg) (A) and Alcohol+Exercise (AE). The rats were alcoholised for 17 weeks, trained for 14 weeks and then sacrificed. BMC and BMD were assessed by DXA (Hologic, Discovery) and the micro architecture of cortical and trabecular bone has been measured by microCT (Skyscan 1072).

Ethanol consumption decreased significantly the BMC (19.68 ± 0.98; 15.61 ± 1.06 and 16.67 ± 1.73 g respectively for C, A and AE; $p<0.0001$) and BMD (0.205 ± 0.006; 0.189 ± 0.006 and 0.196 ± 0.008 g/cm^2; p=0.0005) of the total body and right femur (BMC: 0.88 ± 0.07; 0.70 ± 0.05 and 0.73 ± 0.08 g for C, A, and AE; $p<0.0001$; BMD: 0.389 ± 0.020; 0.337 ± 0.019 and 0.359 ± 0.019 g/ cm^2 for C, A and AE; $p<0.0001$) compared to Controls. The BV/TV parameter (15.61 ± 5.49; 11.28 ± 3.05 and 16.43 ± 3.86 % for C, A, and AE; p=0.02), the trabecular thickness (0.096 ± 0.012; 0.084 ± 0.007 and 0.101 ± 0.009 mm for C, A, and AE; p=0.0002) and the trabecular number (1.61 ± 0.44; 1.34 ± 0.29 and 1.62 ± 0.31 1/mm for C, A and AE; p=0.01) were also decreased by alcohol compared to Controls while the cortical porosity (1.01 ± 0.27; 1.39 ± 0.33 and 1.06 ± 0.31% for C, A and AE; p= 0.015) and pore number (0.24 ± 0.05; 0.34 ± 0.08 and 0.25 ± 0.06 1/µm for C, A and AE; p=0.001) increased.

The Alcohol+Exercise group had significantly higher femoral BMD, BV/TV, and trabecular thickness compared to A group as well as better cortical porosity and pore number. The maximal strain supported by the bone was also significantly higher in the AE group compared to the A group (182.73 ± 35.10 vs 144.65 ± 18.02 N/mm^2 for AE and A; p=0.017).

In conclusion, regular exercise partly prevents the bone loss and deterioration of the trabecular, cortical microarchitecture and BMD induced by chronic alcoholism.

***Disclosures: Delphine Maurel**, None.*

SA0149

Gene by Diet Interactions in the *Alox5* Knockout Mice (*Alox5-/-*) Is Associated with Significant Bone Loss. Phuong Le*[1], Masanobu Kawai[2], Sheila Bornstein[2], Mark Horowitz[3], Clifford Rosen[2]. [1]Maine Medical Center Research Institute, USA, [2]Maine Medical Center, USA, [3]Yale University School of Medicine, USA

Lipoxygenase 5 encoded by *Alox5* gene catalyzes the generation of leukotriene B4 from arachidonic acid, and the loss of *Alox5* has been postulated to result in the increased enzymatic conversion of prostaglandin (PG) D2 into PGJ2, an endogenous ligand for PPARγ. Polymorphisms in the *Alox5* gene and its associated protein have been linked to cardiovascular disease; intriguingly, *Alox5* is also a candidate gene regulating peak bone mass in mice. These findings led us to hypothesize that a high fat diet (HFD) in association with deletion of the *Alox5* gene could result in a major bone loss in part through activating PPARγ expression. To test our hypothesis, we fed 3 week old male C57BL/6J (B6, control) and *Alox5-/-* mice either a regular chow diet (10% fat/kcal) or a HFD (45% fat/kcal) for 13 weeks post weaning. We then examined skeletal phenotype by DXA, µCT, serum bone turnover markers, histomorphometry, and cell culture. We also examined PPARγ gene expression in 8-12 week old mice by qPCR. After 13 weeks of treatment, whole body and femoral areal bone mineral density (BMD) were significantly higher in *Alox5-/-* than in B6 ($p<0.01$). Similar phenotypic differences were noted by µCT in the femur. *Alox5-/-* mice had higher serum osteocalcin and PINP levels ($p<0.001$) than B6. *In vitro* bone marrow stromal cell cultures from *Alox5-/-* mice demonstrated greater ALP and von Kossa staining positive colonies compared to cells from B6. Osteoclast number was decreased by histomorphometry in *Alox5-/-* vs. B6 (p=0.06). On the HFD, there were marked strain differences such that B6 showed increased bone mass in the spine and femur. In contrast, *Alox5-/-* mice on a HFD had lower whole body BMD, femoral and vertebral trabecular BV/TV than *Alox5-/-* mice on a regular diet, which was accompanied by reduced trabecular number and increased osteoclast number. Serum Trap5b in the *Alox5-/-* mice was greater on the HFD while P1NP decreased significantly (p=0.04) compared to mice on a regular diet. qPCR results showed marked increase of PPARγ levels in femur from *Alox5-/-* vs. B6 on HFD. In summary, PPARγ gene associated with diet interactions in *Alox5-/-* mice causes significant bone loss by suppressed bone formation and increased bone resorption. This line of evidence may provide an insight into the important interaction between dietary fat intake and genetic predisposition to osteoporosis.

***Disclosures: Phuong Le**, None.*

SA0150

Potent Inhibition of Heterotopic Ossification by a Selective RARγ Agonist. Kengo Shimono*, Wei-en Tung, Hsu-Tsai Chi, Chrissy Mundy, Johanna Jasinski, Daine Pilchak, Julie Williams, Motomi Enomoto-Iwamoto, Maurizio Pacifici, Masahiro Iwamoto. Thomas Jefferson University, USA

Heterotopic ossification (HO) consists of formation of ectopic bone masses following trauma and involves recruitment of progenitor cells, differentiation into chondrocytes and replacement by endochondral bone. Available HO treatments such as irradiation are not fully effective and do not target any of the above HO-formation steps. Differentiation of mesenchymal cells into chondrocytes requires decreases in both retinoic acid (RA) signaling and nuclear retinoic acid receptor α (RARα) action. Indeed, we previously showed that treatment with a synthetic RARα agonist inhibits HO formation in a mouse model. Here, we asked whether another family member – RARγ- represents a previously unsuspected and possibly more powerful regulator of chondrogenesis and HO. Micromass cultures of wild type E11.5 mouse embryo limb mesenchymal cells were treated with RA (that activates every RAR isoform) or a selective RARγ agonist (γ-agonist). Numerous cartilage nodules formed in untreated cultures, but few formed in RA-treated cultures and nearly none in γ-agonist-treated cultures. When the micromass cultures were prepared with double RARα/RARβ-null limb bud cells, the same results were obtained. However, when RARγ-null cells were used, inhibition of cartilage nodule formation by RA was only about 25-30%, strongly indicating that RARγ is the major anti-chondrogenic regulator. Next, we tested whether the γ-agonist acts via a blockage of the key pro-chondrogenic BMP/Smad signaling pathway. It did but, surprisingly, it not only inhibited Smad1 nuclear translocation, but also caused rapid Smad1 degradation via proteasome action. To determine γ-agonist effectiveness in vivo, we induced HO formation by implantation of BMP-2-loaded collagen sponges in mouse calf muscles. Large ectopic HO-like cartilaginous masses formed in control mice and were replaced by bone by day 14. However, cartilage and bone formation was nearly prevented in mice receiving γ-agonist (0.4 to 4.0 mg/kg/day) by gavage; inhibition was about 95% measured by BV/TV ($p<0.01$). There were no appreciable γ-agonist side effects in terms of body weight, liver and kidney function and articular cartilage phenotype. As expected, we observed partial HO inhibition in mice receiving RA (12 mg/kg/day), but this treatment had side effects including severe skin and articular cartilage damage. In sum, our study shows that selective pharmacologic activation of RARγ represents a novel, powerful and seemingly safe treatment against HO.

Suppression of Heterotopic Ossification By Selective RARγ Agonist

Suppression of Heterotopic Ossification By Selective RARg Agonist

***Disclosures: Kengo Shimono**, None.*
This study received funding from: NIH, US Army

SA0151

Studies of Type I Collagen Mutations in Type I and IV Osteogenesis Imperfecta (OI) Patients Induced Pluripotent Stem (iPS) Cells. Xiaonan Xin*, Mary Louise Stover, Dr. Yongxing Liu, Dr. Liisa Kuhn, David Rowe, Dr. Alexander Lichtler. University of Connecticut Health Center, USA

Osteogenesis imperfecta (OI) is a heritable bone disease caused by mutations in the type I collagen genes. Severe have defective collagen fibers with inherently unstable structures causing bone fragility. Previously we reported initial derivation of iPS cells from patients with severe and mild IO, with the long term goals of investigating OI pathogenic mechanisms, and testing therapeutic strategies. In the current studies we have further characterized the cells we produced, and we are in the process of investigating the mutant collagen that they produce. The mutations in the two cell lines have been identified; as expected, the Type I OI cells contain a premature termination codon that leads to mRNA instability, and the Type III/IV cells have an alanine substituted for the glycine at amino acid position 491. RNA analysis using an ABI pluripotency low density array PCR plate showed a similar gene expression profile of the iPS cells to H9 hES cells. With the goal of identifying defined, non-human factor-free culture conditions for the iPS cells, we have showed that our cells have similar gene expression profiles when cultured in Stemgent NutriStem media compared to standard mouse embryo fibroblast conditioned media. We have developed a method for differentiating our iPS cells into a mesenchymal stem cell-like population that is over 95% CD73+ and CD44+, and negative for hematopoietic cell markers. Low density array PCR analysis demonstrated expression of mesodermal markers in the differentiated cells, and Type I collagen mRNA is also expressed. We are currently assessing the ability of the iPS cells to produce teratomas that contain bone, and we will analyze the mutant collagen produced by the differentiated cells. We are also working to develop methods to induce differentiation of these cells into osteoblasts, and also to test the zinc-finger methodology for mutation correction.

***Disclosures: Xiaonan Xin**, None.*

SA0152

Suppression of Bone Quality by Diet-induced Obesity Correlates with Increase in Insulin Resistance and Suppression of Immune Cells. Ete M. Chan*[1], Elizabeth M. Fievisohn[1], Ada H. Tsoi[1], Mario E. Botros[1], Benjamin Adler[2], Danielle E. Green[1], Clinton Rubin[3]. [1]Department of Biomedical Engineering, Stony Brook University, USA, [2]Stony Brook University, USA, [3]State University of New York at Stony Brook, USA

Obesity is a serious condition leading to diseases such as Type II diabetes (T2D) which is known to affect bone quality, but the underlying mechanisms of this relationship are still unclear. To investigate the effect of obesity on bone quality, twenty 7w male C57BL/6J mice were randomly assigned to either a high fat (HF) diet (45% kcal) or a regular chow diet group (RD) (n=10) for ~6 months following which the trabecular bone compartment in the proximal tibia was evaluated using micro-computed tomography (microCT). Furthermore, to assess characteristics of T2D and any downstream effects resulting from obesity, 1) abdominal adipose tissue load was evaluated with microCT, 2) glucose tolerance test (GTT) was performed, 3) levels of fasting insulin and fasting glucose in blood were measured and 4) proportional changes in cells from myeloid and lymphoid lineages within bone marrow and blood (subgroup, n=4) were evaluated using flow cytometry. The HF diet treatment induced significant changes in the trabecular bone compartment in the HF group (Fig 1): As compared to the RD group, the HF group has 11% higher trabecular thickness Tb.Th ($p=.026$), but 24% lower trabecular number Tb.N ($p=.023$) and 39% larger trabecular separation Tb.Sp ($p=.05$). Accompanying changes in trabecular bone are increases in body mass (42%, $p<.001$), adipose tissue volume (56%, $p<.001$) and fasting insulin (354%, $p=.03$), indicating the prominent role of obesity in inducing insulin resistance. While body mass is positively correlated to the Tb.Th ($r=.63$, $p=.009$) and negatively correlated to the Tb.N ($r=-.54$, $p=.032$), glucose intolerance as measured by GTT is also negatively correlated to Tb.N ($r=-.61$, $p=.012$) and positively correlated to Tb.Sp ($r=.60$, $p=.014$). This indicates that glucose intolerance could contribute to the compromised bone quality. Interestingly, the HF group showed a significant reduction in the B cell proportion both in bone marrow (66.9%, $p=.011$) and blood (36.5%, $p=.045$) indicating an impairment of hematopoiesis in the bone marrow. We conclude that obesity upregulated T2D and compromised the bone marrow cells, disrupting the ability of the bone to adapt to the increased load bearing challenges.

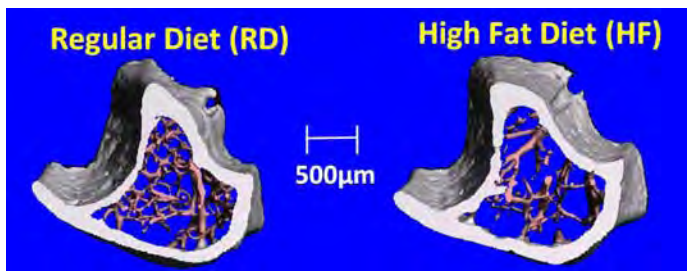

Fig 1

***Disclosures: Ete M. Chan**, None.*

SA0153

See Friday Plenary number FR0153.

SA0154

See Friday Plenary number FR0154.

SA0155

See Friday Plenary number FR0155.

SA0156

Genetic Variation in the *LRP4* Gene Influences Bone Mineral Density and Hip Geometry while Missense Mutations Cause Sclerosteosis. Elke Piters*[1], Eveline Boudin[2], Olivier Leupin[3], Fenna de Freitas[2], Karen Jennes[2], Manuel Bueno-Lozano[4], Feliciano J Ramos-Fuentes[4], Peter H Itin[5], Torben Leo Nielsen[6], Marianne Andersen[6], Kristian Wraae[6], Kim Brixen[7], Michaela Kneissel[3], Wim Van Hul[1]. [1]University of Antwerp, Belgium, [2]Department of Medical Genetics, University of Antwerp, Belgium, [3]Novartis Institutes for Biomedical Research, Switzerland, [4]Departmento de Pediatría, Universitad de Zaragoza, Spain, [5]Department of Dermatology, University Hospital Basel, Switzerland, [6]Department of Endocrinology, Odense University Hospital, Denmark, [7]Institute for Clinical Research, Denmark

Some of us have recently reported a role for low density lipoprotein-related protein (LRP)-4 in binding to and facilitating sclerostin in its inhibition of both Wnt signaling and bone mineralization (1). In the scope of these findings, we performed mutation analysis of an extensive set of patients with different high bone mass disorders and additionally carried out an association study with a selection of *LRP4* polymorphisms in a population-based cohort from the Odense Androgen Study. Mutation analysis revealed the existence of two missense mutations in the *LRP4* gene in two unrelated patients of Mediterranean origin that both showed several typical sclerosteosis features such as an increased bone mineral density (BMD), facial asymmetry and syndactyly. The first patient was homozygous for a p.Arg1170Trp mutation while the other showed a heterozygous p.Trp1186Ser substitution. Both the mutations were absent in a large control set of mixed European origin and completely blocked the interaction with sclerostin and the concomitant sclerostin-enhancer action. The mutations occur adjacent to each other at the surface of the third extracellular β-propeller, which corresponds with the assumption that this domain is involved in sclerostin interaction and function. In another effort to implicate *LRP4* in human bone disease, we studied 2 non-synonymous coding polymorphisms in the region encoding the third extracellular β-propeller. BMD measurements of the hip and the spine as well as different hip geometry parameters were available for a total of 1404 Danish men from two age groups ([20-29 y]: n= 804; [60-74 y]: n= 600). Using linear regression analysis adjusted for age, height and weight, we were able to replicate previous associations (2, 3) between rs6485702 and BMD at all sites. The most significant association was found with whole body BMD ($p= 4.7*10^{-5}$). In addition, we found this SNP to be associated with different hip geometry parameters suggesting that LRP4 is able to regulate bone structure in addition to BMD. However, another SNP in the same region (rs2306033) did not show association with any of the studied phenotypes. Ongoing genetic and functional studies with additional SNPs will aid in delineating the region of *LRP4* that partly explains the natural variance in BMD. In conclusion, genetic variation in the *LRP4* gene determines BMD both in human bone disease and in the general population. This again illustrates the importance of LRP4 in bone homeostasis.

(1) Leupin et al, J. Bone Miner. Res. 24 (S1): 1250, 2009.
(2) Styrkarsdottir et al, N. Engl. J. Med. 358: 2355, 2008.
(3) Styrkarsdottir et al, Nat. Genet. 41: 15, 2009.

***Disclosures: Elke Piters**, None.*

SA0157

Low Bone Mass and Turnover Phenotype in a Mouse Model of Down Syndrome. Tristan Fowler*, John W. Bracey, Nisreen Akel, Robert A. Skinner, William R. Hogue, Frances L. Swain, Dana Gaddy, Kent D. McKelvey, Galen R. Wenger, Larry Suva. University of Arkansas for Medical Sciences, USA

Down syndrome (DS) is a human aneuploidy resulting from the presence of a third chromosome 21. It occurs in the human population at a rate of approximately 1 per 1,000 live births in all ethnic groups. This condition is associated with a number of physical characteristics and clinical conditions including a degree of mental retardation, thrombocytosis, and a 500-fold increased risk of developing megakaryocytic leukemia. Recently, DS has also been associated clinically with a dramatically increased rate of fracture in adolescent and adult patients. Since individuals with DS are reported to have a survival rate of >50% to age 50, skeletal complications should be considered in these patients. However, the specific effects of trisomy 21 on the skeleton remain poorly defined. To study this question, we determined the skeletal phenotype of the Ts65Dn mouse model of DS. Ts65Dn mice are trisomic for 104 orthologs of human Chr 21 (HSA21) genes and this model is the most widely used and accepted mouse model for DS. The mice are characterized by segmental trisomy for the region of mouse Chr 16 (MMU16) that extends from just proximal to the amyloid precursor protein (App) gene to the distal telomere and contains about 75% of the HSA21-homologous genes present in the mouse. We have discovered that adult Ts65Dn mice display a profound low bone mass phenotype, with significant decreases in bone volume fraction of the tibia and femur. Interestingly, Tb.N. was dramatically decreased whereas Tb.Sp. and Tb.Th are increased compared with euploid control littermates. The low bone mass in Ts65Dn mice is associated with a dramatic reduction in bone biochemical markers, with an approximately 50% decrease in serum P1NP and TRAP5b levels, indicative of a mechanism for low bone mass involving decreased bone turnover. In addition, the effects of trisomy 21 are not limited to trabecular bone, as the cortical geometric parameters of cortical cross sectional area, cortical thickness, total cross sectional area and periosteal perimeter are all significantly decreased in Ts65Dn mice. These dramatic changes in cortical bone were translated into significant decreases in mechanical strength and stiffness of the Ts65Dn femur. Our studies demonstrate the potential of DS mouse models to improve our understanding of chromosome 21 gene dosage effects in the skeleton and provide novel insight into the causes of the clinical observations of the extraordinary bone fragility in Down's patients.

***Disclosures: Tristan Fowler**, None.*

SA0158

Low Bone Mass in Genetic Hypercalciuric Stone-Forming (GHS) Rats is Associated with Higher RANKL Expression in Bone Marrow Stromal Cells. Hongwei Wang*[1], Randal Zhou[1], David Bushinsky[2], Murray Favus[1]. [1]University of Chicago, USA, [2]University of Rochester, USA

GHS rats are a useful model to study human idiopathic hypercalciuria (IH) as both share increased intestinal Ca absorption and bone resorption, decreased renal Ca reabsorption, low bone mass, and Ca nephrolithiasis. We investigated low bone mass in male and female GHS rats and normocalciuric (NC) controls. Rats were fed a diet adequate in Ca (0.8%) diet. MicroCT scanning showed reduced tibial bone density (BD) in GHS vs NC rats. Microarray analysis of GHS rat bone marrow stromal cells (BMSCs) showed reduced expression of genes that enhance bone formation (BMP2, SPP1 and SOST) while gene expressions that stimulate bone resorption (RANKL, RANK, GM-CSF, TNFα and IL1) were increased. Real time PCR confirmed the microarray results. The numbers of osteoclasts (OCs) in primary cultures of GHS rat bone marrow were increased 2-3 fold. GHS rat OCs were larger by volume, and the BMSCs contained greater RANKL expression by immunostaining. In conclusion, the data strongly suggest that GHS rats have low bone mass due to greater expression of genes of the resorptive stimulatory pathway and suppression of genes that modulate the bone formation pathway. The molecular basis for the dysregulated resorption and formation genes remains to be determined.

***Disclosures: Hongwei Wang**, None.*

SA0159

Mandible Length Quantitative Trait Loci (QTLs) in HcB-8 x HcB-23 Intercross. In Kyu Han[1], Gurpreet Sandhu[1], Suzanne J. Litscher[1], Neema Saless[2], Peter Demant[3], Robert Blank*[1]. [1]University of Wisconsin, USA, [2]University of California, San Francisco, USA, [3]Roswell Park Cancer Institute, USA

We previously mapped quantitative trait loci (QTLs) for femoral biomechanical performance and anatomy in a reciprocal intercross of HcB-8 and HcB-23. In that work, we determined that a robust QTL on chromosome 4 acts by altering the proliferative response to mechanical loading and that the additional affected phenotypes are secondary consequences of the modeling difference. Further, we inferred that the gene underlying the chromosome 4 QTL is *Ece1*, encoding endothelin converting enzyme 1. To further test our model, we hypothesized that there would be a mandibular size phenotype linked to the chromosome 4 QTL, related to the insertion of the masseter muscle. Here we report mapping of QTLs for mandibular length in our cross.

We subdivided the mandible into 3 segments with boundaries defined by the mentum, the posterior margin of the 3rd molar, the coronoid process, and the angle. We measured the projected distance between the landmarks from digital photographs of the hemimandibles, averaging the left and right sides. We performed linkage analysis using R/qtl and QTL Cartographer. Experiment-wide $\alpha = 0.05$ significance thresholds varied between 2.8 and 3.0.

The entire F2 progeny included 603 animals. QTLs for the mentum-molar segment are located at 67 cM on chromosome 1 with LOD = 3.8 and at 28 cM on chromosome 6 with LOD 7.5. The molar-coronoid segment has QTLs at 41 cM on chromosome 1 with LOD = 3.8 and at 67 cM on chromosome 4 with LOD = 5.7. No QTLs for coronoid-angle length were detected. There were no significant sex x QTL or cross x QTL interactions. Larger subsets of the mandible did not detect additional QTLs. The chromosome 6 QTL accounts for 8% of the mentum-molar length variance. The chromosome 4 QTL accounts for 7% of the F2 molar-coronoid length variance.

The data support our hypothesis that the chromosome 4 QTL mediates response to mechanical loading. There are no muscle of mastication insertions anterior to the molars, while the masseter inserts primarily in the region between the coronoid process and the 3rd molar. The proximal chromosome 1 QTL may also act via modeling. The chromosome 6 QTL for the anterior jaw is distinct from the male-specific QTL we identified for femoral size and mechanical performance. To the best of our knowledge, this is the first instance in which a skeletal QTL's existence has been predicted on the basis of the affected phenotypes at a remote anatomical site.

***Disclosures: Robert Blank**, None.*

SA0160

Modelling Bone Healing Deficiencies in Type 1 Neurofibromatosis. David Little[1], Aaron Schindeler[1], Ian Alexander[2], Jad El-Hoss*[1]. [1]The Children's Hospital at Westmead, Australia, [2]The Children's Medical Research Institute, Australia

Congenital tibial dysplasia (CTD) involves bowing and weakness of the tibia that leads to fracture and poor subsequent bone healing. CTD and scoliosis are key diagnostic features of the autosomal dominant genetic condition Neurofibromatosis Type 1 (NF1). Based on some compelling new evidence that CTD is associated with local double inactivation of *NF1*, we are developing advanced murine systems to model the genetics of *Nf1* inactivation in mice. We have previously shown deficient bone healing in the $Nf1^{+/-}$ mouse. We are now using a Cre-expressing adenovirus (Ad-Cre) to generate local double inactivation of *Nf1* in $Nf1^{flox/-}$ and $Nf1^{flox/flox}$ mice. Briefly, Cre-expressing adenovirus will infect local cells and excise crucial exons of the *Nf1* gene in $Nf1^{flox/flox}$ and $Nf1^{flox/-}$ mice. These mice were generated by crossing *Nf1* null ($Nf1^{+/-}$) and *Nf1* conditional ($Nf1^{flox/flox}$) strains. In the context of fracture healing we anticipate this will further impair union compared to the traditional $Nf1^{+/-}$ mouse. Cultured bone marrow cells from $Nf1^{flox/+}$ mice were exposed to Ad-Cre and this led to efficient *Nf1* excision as measured by PCR on genomic DNA. *Nf1* gene excision was also detected by PCR in a tibial fracture model where the Ad-Cre was locally injected at the time of surgery. The Z/AP reporter mice were examined to histologically track the efficiency and distribution of Cre-mediated recombination. Alkaline phosphatase positive stain confirmed virus mediated recombination of cells lining the fracture site. In $Nf1^{flox/flox}$ mice, fractures treated with Ad-Cre displayed poor fracture healing compared to Ad-GFP treated controls. Ad-Cre treated fractured where characterised by a fibrocartilaginous plug that impaired further fracture healing. These results show that local knockout of *Nf1* impairs fracture healing. Furthermore, we have generated a novel model for the local double inactivation of *Nf1* in a fracture setting using the Ad-Cre virus system. This new model will prove beneficial to test novel therapeutics and better mirror the clinical condition.

***Disclosures: Jad El-Hoss**, None.*
This study received funding from: National Health and Medical Research Council

SA0161

See Friday Plenary number FR0161.

SA0162

New Mouse Model for Type IV Osteogenesis Imperfecta – Cellular and Molecular Changes in Long Bone Precede Post-Pubertal Adaptation. Frieda Chen*[1], Ruolin Guo[2], Shousaku Ito[3], Luisa Moreno[4], Esther Rosenthal[1], Tanya Zappitelli[1], Ralph Zirngibl[1], Ann Flenniken[5], William Cole[6], Marc Grynpas[4], Lucy Osborne[7], Wolfgang Vogel[1], Lee Adamson[4], Janet Rossant[8], Jane Aubin[9]. [1]University of Toronto, Canada, [2]University of Rochester, USA, [3]Osaka University Graduate School of Dentistry, Japan, [4]Samuel Lunenfeld Research Institute, Canada, [5]Toronto Centre for Phenogenomics, Canada, [6]University of Alberta Hospital, Canada, [7]Toronto General Research Institute, Canada, [8]Hospital for Sick Children, Canada, [9]University of Toronto Faculty of Medicine, Canada

Mutations in type I collagen or in proteins involved in its processing have been shown to cause the genetic bone disease Osteogenesis Imperfecta (OI). By a genome-wide N-ethyl-N-nitrosourea (ENU)-induced mutagenesis screen in mice, we identified a founder mouse with the classic clinical manifestations of OI. Mapping and sequencing identified a T to C transition in a splice donor of the collagen alpha1 type I (Col1a1) gene resulting in the skipping of exon 9 and an 18 amino acid deletion in the main triple helical domain of Col1a1. $Col1a1^{Jrt/+}$ mice are smaller in size and have lower bone mineral density (BMD), decreased bone volume/tissue volume, reduced trabecular number and weaker, more brittle bones than their +/+ (wild type (WT)) littermates. Bone fractures occur at multiple sites at all ages, but with a high incidence of fractures of the pelvis and olecranon process of the ulna, in young $Col1a1^{Jrt/+}$ mice. Biochemical analyses of matrices in dermal fibroblast cultures indicated that total collagen content of the $Col1a1^{Jrt/+}$ matrices was ~40% that of WT, with the content of type I collagen only ~30% of that in WT cultures, suggesting that mutant collagen chains exert a dominant negative effect on type I collagen biosynthesis. Electron microscopic analysis of tendon and bone samples, as well as extracellular matrices deposited by dermal fibroblasts *in vitro*, indicated that collagen fibrils are markedly smaller in diameter in $Col1a1^{Jrt/+}$ versus WT mice and cell cultures. *In vitro* analysis of stromal cells indicated that the size of the osteoprogenitor population is unaffected, but osteoblast differentiation as assessed by marker expression and mineralization are reduced in stromal cell cultures from age-matched young (5-week-old) versus older (20-week-old) $Col1a1^{Jrt/+}$ versus WT mice. Expression of Col1a1 and Ocn mRNAs was increased in bones of 5 week-old $Col1a1^{Jrt/+}$ versus WT mice, while that of Opn was decreased and Alp increased in 20 week animals. Thus, $Col1a1^{Jrt/+}$ mice are a new model of dominantly-inherited type IV OI. Differences observed in the bone phenotype and osteoblasts at different ages suggest that the $Col1a1^{Jrt/+}$ model will be useful to explore further the mechanisms by which OI bone adapts during growth and adulthood and other aspects of OI pathophysiology and treatment.

***Disclosures: Frieda Chen**, None.*

SA0163

Superoxide Dismutase Deficiency in Cytoplasm Exacerbated Bone Loss Under Reduced Mechanical Loading. Daichi Morikawa*[1], Yoshitomo Saita[2], Hidetoshi Nojiri[2], Chizuru Tsuda[1], Yoshinori Asou[3], Kazuo Kaneko[2], Takahiko Shimizu[1]. [1]Molecular Gerontology, Tokyo Metropolitan Institute of Gerontology, Japan, [2]Department of Orthopaedics, Juntendo Univ., Japan, [3]Section of Regenerative Therapeutics for Spine & Spinal Cord, Tokyo Medical & Dental Univ., Japan

Cu/Zn-superoxide dismutase (*Sod1*) is one of the major antioxidant enzymes in mammals. *Sod1*-deficient ($Sod1^{-/-}$) mice has been reported to present a variety of aging-like pathological changes (muscle atrophy, skin thinning, age-related macular degeneration). Last year, we have reported that $Sod1^{-/-}$ mice exhibit low turnover osteopenia via suppressed osteoblastic bone formation.

In order to clarify the cause of osteoblastic dysfunction, we compared gene expression profile between $Sod1^{-/-}$ and $Sod1^{+/+}$ osteoblasts isolated from neonates using DNA microarray. This analysis identified the down-regulated genes involved in cell adhesion in $Sod1^{-/-}$ osteoblasts. Among them, we confirmed that osteomodulin (Omd), Comp, chadherin 11, and osteopontin were significantly decreased by real-time PCR analyses in $Sod1^{-/-}$ both *in vitro* (osteoblast) and *in vivo* (whole bone). These results suggest that *Sod1* might be involved in cell adhesion and sensing of mechanical stress in osteoblast, and that oxidative stress could relate to mechanical loading in bone. Therefore, we performed hindlimb unloading (HU) in $Sod1^{-/-}$ mice.

Ten-weeks-old $Sod1^{-/-}$ and $Sod1^{+/+}$ mice were conducted in HU for 14 days. Bone mineral density by DEXA was decreased by unloading in both $Sod1^{-/-}$ and $Sod1^{+/+}$ mice compared to loading group. Interestingly, three dimensional micro CT showed that trabecular bone volume (BV/TV) was decreased more than twice in $Sod1^{-/-}$ (55% loss vs. loading) compared to $Sod1^{+/+}$ (24% loss vs. loading), however, the decrease of cortical bone volume was not significantly different between $Sod1^{-/-}$ (16.3% loss vs. loading) and $Sod1^{+/+}$ (15.8% loss vs. loading). In bone marrow cell culture after unloading, the development of TRAP positive osteoclast-like cells were increased in unloading group both in $Sod1^{-/-}$ and $Sod1^{+/+}$ mice and it tended to be accelerated in $Sod1^{-/-}$ mice.Finally, we examined whether hindlimb unloading increased reactive oxygen species (ROS) in bone marrow cells. Interestingly, ROS production was significantly increased after unloading and it peaked one week after unloading, suggesting that reduced mechanical loading increases oxidative stress in bone marrow.

Our data revealed that cytoplasmic oxidative stress could exacerbate trabecular bone loss under reduced mechanical loading.

***Disclosures: Daichi Morikawa**, None.*

SA0164

Genome Wide Linkage of Osteocalcin to Chromosome 18 in Multi-generational Families of African Ancestry. Allison Kuipers*[1], Caren Gundberg[2], Amy Dressen[3], Candace Kammerer[1], Clareann H. Bunker[3], Ashely Edwards[3], Alan L. Patrick[4], Victor W. Wheeler[4], Anne Newman[3], Joseph Zmuda[1]. [1]University of Pittsburgh Graduate School of Public Health, USA, [2]Yale University School of Medicine, USA, [3]University of Pittsburgh, USA, [4]Tobago Health Studies Office, Trinidad & tobago

Osteocalcin (OC), synthesized by osteoblasts, is an important protein constituent of bone matrix, and is a marker of bone turnover. Emerging evidence suggests that OC may also be a novel hormonal regulator of energy metabolism. We sought to identify genomic regions involved in regulating total and uncarboxylated OC using genome-wide linkage analysis in 458 individuals from seven large multi-generational families of African ancestry residing on the island of Tobago (mean family size, 56; 4,206 relative pairs; mean age, 42.7 years). We genotyped 5361 single nucleotide polymorphisms with minor allele frequency >0.05 and spaced ~1 centimorgans apart using the Illumina Infinium II Human Linkage 12 panel. We estimated residual heritability (after adjusting for age, sex, height, and weight) and conducted multipoint quantitative trait linkage analyses using pedigree-based maximum likelihood methods. Means (and residual heritabilities) of total OC, uncarboxylated OC and percent uncarboxylated OC were 4.47μg/L (0.63 ± 0.09), 1.53μg/L (0.83 ± 0.09) and 35.53%(0.41 ± 0.09), respectively. We detected significant evidence of linkage on chromosome 18 (maximum LOD=4.17, 92cM) and suggestive evidence of linkage on chromosomes 9 (maximum LOD=2.16) and 20 (maximum LOD=2.15) for total OC. Suggestive evidence of linkage for percent uncarboxylated OC was observed on chromosome 12 (maximum LOD=2.23). Interestingly, the structural locus for OC resides on chromosome 1, outside of the linked regions. The linked region on chromosome 18 contains 15 known and predicted genes. A potential candidate gene of interest in this region is the melanocortin 4 receptor (MC4R), which regulates appetite and energy expenditure and is expressed in osteoblasts. Further studies of the linked chromosomal regions may reveal novel insight into the regulation of osteocalcin and bone metabolism.

***Disclosures: Allison Kuipers**, None.*

SA0165

Heritability of Densitometric, Structural and Strength Properties of Bones: Results from the GAO (Genetic Analysis of Osteoporosis) Project. Jorge Malouf*[1], Ana Laiz-Alonso[1], Ana Marin[1], Angel Martinez-Perez[2], Leonor Rib[2], Raquel Perez[2], Alfonso Buil[2], Jordi Casademont[1], Jordi Farrerons[1], Jose Manuel Soria[2]. [1]Hospital de la Santa Creu i Sant Pau, Spain, [2]Institut de Recerca (IR-HSCSP), Spain

Osteoporosis is a skeletal disorder characterized by compromised bone mass and strength that increases the risk of fracture. The genetic basis of primary osteoporosis is complex with multiple genes and environmental factors acting jointly to determine risk. However, recent advances in genetic analyses permit the identification of the genetic determinants of complex diseases. Towards this end, we designed a family-based study of the genetics of osteoporosis in a Spanish population, called GAO (Genetic Analysis of Osteoporosis).

A total of 110 individuals in 5 Spanish extended families (at least three-generation families) were included. All of the families were recruited through a proband with osteoporosis and all of them signed an informed consent. After filling a questionnaire, a spine, femur and whole body densitometry was performed using a Discovery densitometer with the APEX 2.3 software, from HOLOGIC® Bedford, Massachusetts, USA. The strength and geometrical properties of the hip were analyzed using the HSA® software included in the Apex 2.3 software.

Maximum likelihood-based covariance decomposition analysis was used to assess heritabilities (h2) and the genetic and environmental correlations (ρG and ρE) between phenotypes. Table 1 shows the h2 found among the phenotypes.

This is the first study that quantifies the genetic component of several important parameters involved in osteoporosis and fracture risk in extended pedigrees. The high heritability of the majority of them indicate that genetic effects account for a significant proportion of the observed phenotypic variation of these parameters. Thus, a strategy based on a family-based study through a genome scanning can be used to identify the specific genes involved in osteoporosis and fracture risk. Additionally, this knowledge will greatly facilitate the search for genes involved in osteoporosis, and ultimately find its way into the clinic.

Heritability among phenotypes

Trait	mean	sd	h^2	P-value
Bone Density				
Trochanteric BMD	0.69	0.91	0.56	***0.001**
Interthrocanteric BMD	1.14	0.90	0.28	**0.560**
Femoral Neck BMD	0.79	0.89	0.41	**0.068**
Total Hip BMD	0.96	0.89	0.34	**0.178**
Lumbar Spine BMD	0.93	0.96	0.45	0.243
Structural traits				
Axis Length	115.40	5.96	0	**1**
Shaft Neck Angle	125.72	6.02	0.57	**0.314**
Strength properties				
Narrow Neck CSMI	3.50	0.85	0.09	1
Narrow Neck Z	1.79	0.81	0.21	1
NN cortical Thickness	0.18	0.94	0.40	0.106
Narrow Neck BR	10.86	1.99	0.58	***0.013**
Narrow Neck CSA	3.16	0.87	0.20	**1**
Intertrocantheric CSMI	16.42	4.08	0.36	0.102
Intertrocantheric Z	4.92	1.06	0.40	***0.031**
IT Cortical thickness	0.44	0.87	0.45	***0.015**
Intertrocantheric BR	7.66	1.52	0.23	**0.991**
Intertrocantheric CSA	5.49	1.01	0.48	***0.005**
Shaft CSMI	4.17	1.02	0.22	**0.764**
Shaft Z	2.67	0.71	0.27	**0.484**
Shaft Cortical thickness	0.65	0.90	0.17	**1**
Shaft BR	2.48	0.87	0.21	1
Shaft CSA	4.86	0.80	0.18	1

h^2: Heritability; sd: standard deviation; *p-value at significant level <0.05 (using bonferroni correction for multiple testing).

Table 1. Heritability among phenotypes

***Disclosures: Jorge Malouf**, None.*

SA0166

A Significant Interaction between Simple Nucleotide Polymorphism (SNP) in *NFKB* and *RANK* is Associated with Women BMD in the Framingham Osteoporosis Study. Bi Hua Cheng*[1], Xing Chen[2], YanHua Zhou[3], Serkalem Demissie[3], Adrienne Cupples[3], David Karasik[4], Douglas Kiel[4], Yi-Hsiang Hsu[5]. [1]Chang Gung Memorial Hospital - Kaohsiung Medical Center, Chang Gung University, USA, [2]HSL, USA, [3]BUSPH, USA, [4]Hebrew SeniorLife, USA, [5]Hebrew SeniorLife & Harvard Medical School, USA

The RANK/RANKL/OPG signaling pathway plays a crucial role in signal transduction in osteoblasts and osteoclasts. Previous GWAS have shown that SNPs in TNFRSF11A (*RANK*), TNFSF11(*RANKL*), and TNFRSF11B(*OPG*) genes are associated with BMD. Although NFKB gene is known to mediate osteoclastogenesis via the RANK/RANKL/OPG signaling pathway, its interactions with RANK, RANKL, or OPG genes in relation to BMD have not been examined in human populations. Therefore, we performed a gene-gene interaction study to investigate this relationship. Femoral neck (FN) and L2-L4 lumbar spine (LS) BMD were measured by a Lunar DPX-L. Genotyping was performed using the Affymetrix 550K SNP chips. A total of 1,813 women and 1,375 men (mean age 62.5 yrs) with both phenotypes and genotypes in the Framingham Osteoporosis Study were in the final analysis. Genotyped SNPs were selected with (1)minor allele frequency $\geq$ 1% and (2) HWE test p-value $\geq$ 0.0001 and (3) located in the gene and within 20 kb 5' upstream flanking region (38 SNPs in *NFKB*, 37 in *RANK*, 61 in *RANKL*, and 58 in OPG). Sex-specific linear mixed-effect models were performed to determine the single SNP-phenotype associations with LSBMD and FNBMD. Covariates adjusted in the models included age, height, BMI, alcohol consumption, smoking status and principal component for their ancestral genetic background. The most significant association (the lowest p-value) with LS BMD were found for *NFKB* rs7685474,*RANK* rs2980973,*RANKL* rs7334307,and OPG rs7014574 in women and NFKB rs17032779, *RANK* rs17069956, *RANKL* rs7989838, and *OPG* rs11992072 in men. No SNP with association p-value less than 0.01 was found for FN BMD in women or men; therefore we did not perform gene-gene interaction for FN BMD. Six pair-wise interactions between the most associated SNPs in these four genes were performed in each gender. Bonferroni correction was used to adjust for multiple testing (α level=0.00416). A significant interaction between NFKB rs7685474 and RANK rs2298073 (p=0.0039) was found in women only at LSBMD. Individuals with polymorphic alleles in the RANK rs2298073(C)and the NFKB rs7685474(G)had a higher BMD compared to individuals without polymorphic alleles in both of the genes or in one of the genes (Fig 1). No significant gene-gene interactions were found in relation to LS BMD in men. This is the first genetic epidemiological study to reveal an interaction between NFKB and the RANK pathway at genetic level with LSBMD in a Caucasian population.

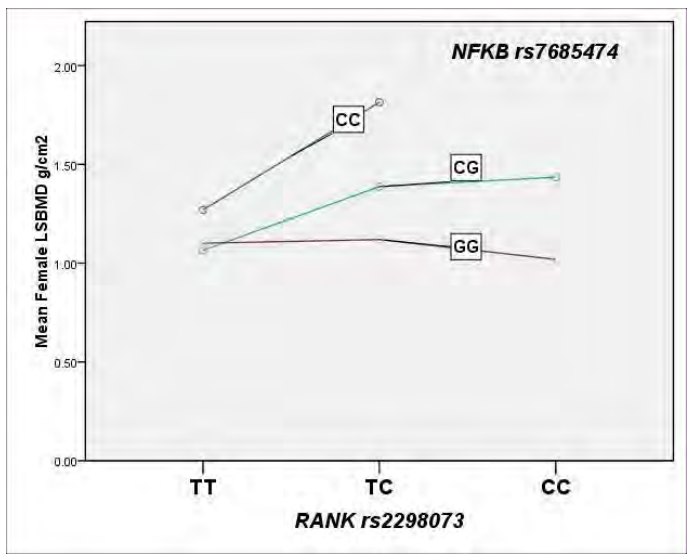

Fig 1 . Interaction between NFKB rs7685474 and RANK rs2980973 in relation to LSBMD in women

***Disclosures: Bi Hua Cheng**, None.*

SA0167

Association of LRP4 Polymorphisms to Bone Properties and Fracture in Women. Maria Swanberg*[1], Jitender Kumar[2], Fiona McGuigan[3], Kristina Akesson[4]. [1]Lund University, Sweden, [2]Lund University, Sweden, Sweden, [3]University of Lund, Malmö Skane University Hospital, Malmö, Sweden, [4]Malmo University Hospital, Sweden

LRP4 and LRP5 are structurally similar members of the low density lipoprotein-receptor gene family that may regulate osteogenesis as co-receptors in the Wnt signaling pathway. Experimental data supports a role for LRP4 and -5 in regulating bone mass, growth and turnover. Genetic association to BMD and fracture has been reported for LRP4 and has been confirmed for LRP5 in several cohorts.

In this study, we examined the association of single nucleotide polymorphisms (SNPs) in LRP4 (rs3816614, rs6485702, rs2306033, rs7926667) and LRP5 (rs68242, rs498832, rs373622) to bone properties and fracture risk. Two cohorts living in Malmö, Sweden, were studied with regard to bone mineral density (BMD) and bone architecture; the PEAK-25 cohort representing 1002 young (25 years old) women, and the OPRA cohort representing 1002 elderly (75 years old) women. The OPRA cohort was followed for 5 years and additional phenotypes studied in this cohort were BMD at age 80, bone loss between age 75 and 80, femoral neck (FN) bone geometry and acquired fractures until age 80.

In the OPRA cohort, LRP4 was associated to BMD corrected for smoking and weight for total body and FN at age 75 (rs2306033 $p<0.05$) and at age 80 (rs2306033 $p<0.01$; rs3816614 $p<0.01$) and for lumbar spine at age 80 (rs6485702, $p<0.05$). Similarly, in the PEAK-25 cohort, LRP4 (rs6485702) was associated to BMD corrected for smoking and weight at the FN ($p<0.05$), lumbar spine ($p<0.05$) and total body ($p<0.01$).

In the OPRA cohort, LRP4 was also associated with the rate of total body bone loss between age 75 and 80 (rs3816614 $p<0.05$), bone quality measurements taken through ultrasound (rs3816614 $p<0.05$) and bone geometry for FN width (rs648570 $p<0.01$) and moment of inertia (rs648570 $p<0.05$).

Until age 80 in the OPRA cohort, 609 individuals had suffered at least one fracture, including 139 women with hip fractures, while 329 women had not suffered any fracture. LRP4 was associated to any fracture (rs3816614 $p<0.05$, rs2306033 $p<0.01$, rs6485702 $p<0.05$) and to hip fracture specifically (rs2306033 $p<0.01$), with more carriers of the variant alleles in the no-fracture group.

In conclusion, non-synonymous polymorphisms in the LRP4 gene were consistently associated with various bone properties i.e. BMD, bone geometry, quality, rate of bone loss and, importantly, to fracture in elderly women. In addition, LRP4 was also associated to BMD in young women, thereby having probable effects on bone throughout life.

***Disclosures: Maria Swanberg**, None.*

SA0168

Association of Non-coding Variants in the 3′-UTR of the Frizzled-1 Gene with Skeletal Geometry Among Afro-Caribbean Men. Yingze Zhang*[1], Allison Kuipers[2], Cara Nestlerode[1], Clareann Bunker[1], Victor Wheeler[3], Alan Patrick[3], Joseph Zmuda[2]. [1]University of Pittsburgh, USA, [2]University of Pittsburgh Graduate School of Public Health, USA, [3]Tobago Health Studies Office, Trinidad & tobago

The Wnt/β-catenin pathway is important in osteoblast differentiation, proliferation and apoptosis. Frizzled 1 (FZD1) is a member of the Wnt/β-catenin pathway and is a trans-membrane co-receptor with LRP5 for Wnt molecules. We previously demonstrated a novel association between two common single nucleotide polymorphisms (SNP) in the promoter region of frizzled-1 (FZD1) and bone geometric properties.

In the current analysis, we tested whether SNPs in the 3′ untranslated region (UTR) of FZD1 are independently associated with measures of bone geometry. Three SNPs (rs2232163, rs3750145 and rs1052015) in the 3′-UTR of the FZD1 were analyzed in 1844 Afro-Caribbean men aged 40 years and older. The minor allele frequencies of these 3 SNPs were: 8.6%, 6.6%, and 5.2%, respectively. Haplotype analysis identified 4 haplotypes GTA, ATA, GCC, and GCA with frequencies of 84.5%, 8.6%, 5.3% and 1.5%, respectively. Association analyses of the SNPs and haplotypes with peripheral quantitative computed tomography measures were performed under an additive model adjusting for age, height and body weight and the two promoter SNPs (rs2232157, rs2232158) to test the independent association of the 3′-UTR variants. The minor allele of rs2232163 was associated with decreased ($P=0.005$) whereas the minor allele of rs3750145 was associated with increased ($P=0.04$) cortical thickness at the radius. The ATA haplotype was associated with decreased ($P=0.008$) whereas the GCA haplotype was associated with increased ($P=0.002$) cortical thickness. Interestingly, these 3′-UTR variants encompass several predicted microRNA binding sites. Functional analysis of these SNPs and haplotypes will be important to elucidate the significance of these regulatory region variants.

***Disclosures: Yingze Zhang**, None.*

SA0169

BMD-associated Variation at the *Osterix* Locus is Correlated with Pediatric BMI in Females. Jianhua Zhao[1], Jonathan Bradfield[1], Mingyao Li[2], Haitao Zhang[1], Frank Mentch[1], Kai Wang[1], Patrick Sleiman[1], Cecilia Kim[1], Joseph Glessner[1], Edward Frackelton[1], Rosetta Chiavacci[1], Robert Berkowitz[1], Babette Zemel[3], Hakon Hakonarson[1], Struan Grant*[3]. [1]Children's Hospital of Philadelphia, USA, [2]University of Pennsylvania, USA, [3]Children's Hospital of Philadelphia, USA

Recent genome wide association studies (GWAS) have revealed a number of genetic variants robustly associated with bone mineral density (BMD) and/or osteoporosis. Evidence from epidemiological and clinical studies has shown an association between BMD and body mass index (BMI), presumably as a consequence of bone loading. We investigated the 34 previously published BMD GWAS-derived loci in the context of pediatric BMI by leveraging our existing genome-wide genotyped European American cohort of 1,106 obese children (BMI$\geq 95^{th}$ percentile) and 5,997 controls (BMI$<95^{th}$ percentile). Evidence of association was only observed at one locus, namely *Osterix* (*SP7*), with the G allele of rs2016266 being significantly over-represented among childhood obesity cases ($P=2.85\text{x}10^{-3}$). When restricting these analyses to each gender, we observed strong association between rs2016266 and childhood obesity in females (477 cases and 2,867 controls; $P=3.56\text{x}10^{-4}$). However, no evidence of association was observed among males. Similar observations were made when treating BMI as a quantitative trait in the same cohort. Interestingly, Osterix is the only GWAS locus uncovered to date that has also been previously implicated in the determination of BMD in childhood. In conclusion, these findings indicate that a well established variant at the *Osterix* locus associated with increased BMD is also associated with childhood obesity primarily in females. These results are in keeping with the bone loading impact on BMD through increased BMI.

***Disclosures: Struan Grant**, None.*

SA0170

Bone Mineral Density Locus Associated with Coronary Artery Calcification. Laura Yerges-Armstrong*[1], Xinggang Liu[1], Elizabeth Streeten[2], Alan Shuldiner[1], Braxton Mitchell[3]. [1]University of Maryland, USA, [2]University of Maryland School of Medicine, USA, [3]University of Maryland, Baltimore, USA

Epidemiologic and in vitro studies support a relationship between calcification of bone and vascular tissue, although the nature of the relationship is unclear. To identify genes having pleiotropic effects on these two traits, we tested whether SNPs found by previous genome wide association (GWA) studies (Rivadeneira et al.: Nat Gen 2009) to be robustly associated with BMD were also associated with coronary artery calcification (CAC). Our study was carried out in a population of Old Order Amish individuals in whom we had measured BMD at the hip and spine by DXA (N=889) and calcification of the coronary arteries (N=506) by electron beam CT. On average participants were 56 years of age and 47% of the population was male. The BMD loci were extracted from a recent meta-analysis of Caucasian reference data that identified loci for BMD at the lumbar spine (LS) or femoral neck (FN). We created a genotype score for LS (15 loci) and FN (10 loci) by summing the number of copies of the high BMD allele across all loci. As expected, genotype scores were associated with BMD in the Amish (p=7.7x10-7 for FN and p=0.013 for LS) although the scores explained very little of the total variation in BMD ($r^2=0.03$ and 0.01 respectively for LS and FN). We then evaluated associations of the genotype scores with CAC quantity adjusting for the effects of age and gender. FN genotype score was not significantly associated with CAC. In contrast, analysis of the LS genotype score revealed that an increasing number of high BMD alleles was associated with lower CAC quantity ($p = 0.046$). Further analyses of the individual SNPs identified an association ($p=0.02$) between a SNP on 13q14 and CAC in our sample. These results extend previous studies suggesting a relationship between cardiovascular disease and lower bone mineral density by showing a common genetic link between the two disorders. These analyses also reveal a specific BMD variant (rs9533090 downstream of AKAP11) that is also associated with cardiovascular health.

***Disclosures: Laura Yerges-Armstrong**, None.*

SA0171

Cooperative Effect of Serum 25-Hydroxyvitamin D Concentration and a Polymorphism of Transforming Growth Factor β-1 Gene on the Prevalence of Vertebral Fractures in Postmenopausal Osteoporosis. Kazuki Kobayashi*[1], Seijiro Mori[2], Noriyuki Fuku[3], Yuko Chiba[2], Fumiaki Tokimura[2], Takayuki Hosoi[4], Yoshiyuki Kimbara[2], Yoshiaki Tamura[2], Atsushi Araki[2], Masashi Tanaka[3], Hideki Ito[2]. [1]Tokyo Metropolitan Geriactic Hospital, Japan, [2]Tokyo Metropolitan Geriatric Hospital, Japan, [3]Tokyo Metropolitan Institute of Gerontology, Japan, [4]National Center for Geriatrics & Gerontology, Japan

Purpose: A T869→C polymorphism of the transforming growth factor β1 (TGF-β1) gene is reported to be associated with genetic susceptibility to both osteoporosis and vertebral fracture. Low serum 25-hydroxyvitamin D [25(OH)D] level is known to be associated with a higher risk for hip fracture. This study aimed to assess a possible cooperative effect of the gene polymorphism and vitamin D status on vertebral fracture risk.

Methods: Prevalence of vertebral fracture in 168 postmenopausal female patients with osteoporosis was analyzed, and its association with the TGF-β1 gene polymorphism and serum 25(OH)D concentration was assessed cross-sectionally.

Results: The fracture prevalence increased according to the rank order of the TGF-β1 genotypes CC < CT < TT, as expected. A significant difference was found not only between the CC and TT genotypes ($p = 0.005$) but also between the CC and CT genotypes ($p < 0.05$) when the patients with serum 25(OH)D of more than the median value [22 ng/mL (55 nmol/L)] were analyzed. On the other hand, when those with serum 25(OH)D of less than the median value were analyzed, a protective effect of the C allele against the fracture was blunted; statistical significance in the difference of the fracture prevalence was lost between the CC genotype and the other genotypes.

Conclusion: These data suggest that vitamin D fulfillment is prerequisite for the TGF-β1 genotype in exerting its full effect on the fracture prevalence.

Effect of Serum 25(OH)D Level on the Relationship between TGF-β1 Genotype and Prevalence of Vertebral Fracture

		Vertebral Fracture	n
25(OH)D ≥ 22 ng/mL			
	CC	2 (9)	23
	CT	16 (31)*	52
	TT	8 (47)**	17
25(OH)D < 22 ng/mL			
	CC	7 (32)	22
	CT	14 (35)	40
	TT	8 (57)	14

Number (percent) of patients is presented.
*$p < 0.05$ and **$p = 0.005$ versus *CC* with 25(OH)D ≥ 22 ng/mL.

Table

***Disclosures: Kazuki Kobayashi**, None.*

SA0172

Genetic Association Study of Common Mitochondrial DNA Variants in Osteoporosis. Shufeng Lei*[1], Yan Guo[1], Tielin Yang[2], Hui Shen[1], Xianghong Xu[3], Shanshan Dong[1], Yao-zhong Liu[1], Yong-Jun Liu[1], Hong-Wen Deng[4]. [1]University of Missouri - Kansas City, USA, [2]The University of Missouri-Kansas City, USA, [3]University of Missouri-Kansas City, School of Medicine, USA, [4]University of Missouri, Kansas City Medical School, USA

Many lines of evidence suggest that mitochondrial DNA (mtDNA) variants are involved in the pathogenesis of human complex diseases, especially for age-related disorders. Osteoporosis is a typical age-related complex disease, however, the role of mtDNA variants in the susceptibility of osteoporosis is largely unknown. In this study, we reported a mitochondrial genome-wide association study for bone mineral density (BMD) in Caucasians.

A total of 445 mitochondrial single nucleotide polymorphisms (mtSNPs) were genotyped in a sample of 2,286 unrelated Caucasian subjects (558 males and 1728 females) by using the Affymetrix Genome-Wide Human SNP Array 6.0. SNPs were tested for association with hip BMD by the quantitative association tests implemented in PLINK, while controlling for potential confounding factors, such as age, gender, height and weight.

A SNP within the NADH dehydrogenase 2 gene (ND2), rs28571027 (C/A), was strongly associated with hip BMD ($p = 3.63 \times 10\text{-}4$). The C allele was associated with reduced hip BMD values and the effect size (ß) was estimated to be ~0.022. Our results highlighted the importance of mtDNA variants in influencing BMD variation and risk to osteoporosis. Further genetic and molecular functional investigations for the relationship between mtDNA variants and osteoporosis are warranted.

***Disclosures: Shufeng Lei**, None.*

SA0173

BMP2 Binds Preferentially to BMP Receptors Localized in Caveolae and Initiates Smad Signaling. Oleksandra Moseychuk*[1], Beth Bragdon[2], Jeremy Bonor[1], Anja Nohe[1]. [1]University of Delaware, USA, [2]University of MaineUniversity of Delaware, USA

Bone Morphologic Proteins (BMPs) are growth factors that regulate skeletal development and repair. They are used as therapeutics in spinal fusion and fracture repair but little is known about the initiation of signaling on the receptor level. BMP receptors (BMPRs) are found on the plasma membrane, in caveolae and clathrin coated pits (CCPs). Current literature suggests that BMP2 mediated signaling by Smad 1,5 and 8 is initiated on the plasma membrane followed by endocytosis of receptors through CCPs, however our studies demonstrate that ligand binding, BMP receptor type-Ia (BMPRIa) phosphorylation and Smad 1,5 and 8 activation occurs in caveolae within 10 min.

Combination of Atom Force Microscopy (AFM) and advance confocal imaging were used to determine the binding affinity of ligand with receptors on the surface of live cells. Biologically active AFM tip was designed by covalently linking BMP2, to an AFM tip and live C2C12 cells were transfected with Caveolin-1 GFP conjugated plasmid (protein that is responsible for the flask shape structure of caveolae) as a marker to visualize caveolae. Our AFM data together with high resolution confocal images and retraction curve data demonstrated that BMP2 binds predominantly to BMPRs localized in caveolae. Since BMPR phosphorylation is the first step of the signaling cascade, we performed fractionation of the plasma membrane based on the lipid composition to determine the location of phosphorylated form of BMPRIa in C2C12 cells. We observed phosphorylation in the lipid raft fractions, namely caveolae. Additionally, Smad 1, 5, and 8 phosphorylation was probed at different time points during BMP2 stimulation. It showed the initial phosphorylation takes place in caveolae as early as 10 min post stimulation, followed by endocytosis. After 45 min stimulation with BMP2, the phosphorylated form of Smad 1, 5, and 8 is degraded in the lysosome. Taken together, these data show that BMP2 dependent phosphorylation of BMPRIa and activation of regulatory Smads takes place predominantly in caveolae, not CCPs.

***Disclosures: Oleksandra Moseychuk**, None.*

SA0174

BMP2 Gene as an Organizer Coordinating Osteogenesis and Angiogenesis Postnatally and Roles in Mechanical Properties of Bone. Wuchen Yang*[1], Jeffry Nyman[2], Yong Cui[1], Jelica Gluhak-Heinrich[1], Marie Harris[1], Ivo Kalajzic[3], David Rowe[3], Gregory Mundy[4], James Edwards[2], Barbara Kream[3], Alexander Lichtler[3], Xiao-Dong Chen[1], Yuji Mishina[5], Stephen Harris[1]. [1]University of Texas Health Science Center At San Antonio, USA, [2]Vanderbilt University Medical Center, USA, [3]University of Connecticut Health Center, USA, [4]Vanderbilt University, USA, [5]University of Michigan, USA

Coordination between osteogenesis and angiogenesis is important for proper bone remodeling and repair postnatally. Our previous study using the 3.6Col1a1-Cre;BMP2 cKO mice showed that the postnatal deletion of the BMP2 gene from collagen producing osteoblasts inhibits latter stages of osteoblast differentiation and causes an intrinsic 80% reduction in the Mesenchymal Stem Cells (MSCs) population, as determined by CFU-F assays. The long bones of the 3.6Col1a1-Cre;BMP2cKO mice appeared to be less red, suggesting a decrease in vascularization. Since perivascular cells are potentially one of the MSCs niches that associated with blood vessels, we further evaluated the bones by CD146 immunohistochemistry (IHC) and confirmed that the perivascular cells are indeed reduced in vivo in the BMP2 cKO relative to control littermates. Using α-SMA-Cherry transgene, in which the perivascular candidate MSCs are labeled red on microvasculature, we confirmed a reduction of this MSCs population in vivo in the BMP2cKO mice. To address whether this reduction of the MSCs population is caused by a reduction of angiogenesis leading to the reduction of MSCs niches, collagen IV IHC was then performed for both femur and tibia. This revealed that blood vessel density is reduced 20 to 50% in the 3.6Col1a1-Cre;BMP2cKO mice at different ages up to 6 month. These results suggest that the angiogenesis is reduced after BMP2 deletion from osteoblasts. To explore the mechanism by which BMP2 in osteoblasts regulates angiogenesis, the expression level of VEGFA, an angiogenesis stimulator that is secreted by mature osteoblasts, was assayed by IHC and VEGFA association with osteoblasts was reduced 50% in the BMP2 cKO animals. Thus, ablation of BMP2 gene from osteoblasts interferes drastically with the late stage of osteoblast maturation that in turn leads to reduction

of VEGF production and results in defective angiogenesis and reduced MSCs niche availability. These phenotypes in the BMP2 cKO lead to altered geometric and mechanical properties of the long bones. There was an over 50% reduction in Work-to-fracture in the femur. A greater than 80% reduction in Post Yield toughness in the BMP2 cKO also suggests these bones are much more brittle than control bones, possibly due to the decreased vascularization and reduced MSCs population.

***Disclosures: Wuchen Yang**, None.*

SA0175

Dullard, a Novel BMP Inhibitor, Targets Smad1 to Suppress BMP-dependent Transcription in Mammalian Osteoblastic Cells. Tadayoshi Hayata*[1], Yoichi Ezura[2], Makoto Asashima[3], Ryuichi Nishinakamura[4], Masaki Noda[5]. [1]Medical Reserach Institute, Tokyo Medical & Dental University, Japan, [2]Tokyo Medical & Dental University, Medical Research Insititute, Japan, [3]University of Tokyo, Japan, [4]Kumamoto University, Japan, [5]Tokyo Medical & Dental University, Japan

BMP plays crucial roles during osteoblast differentiation and its signaling effect is negatively regulated to maintain the appropriate signaling levels. However, mechanism of signal regulation by BMP inhibitors during osteoblast differentiation has not been fully understood. Dullard encodes a phosphatase preferentially localized in caveosome and has been reported to suppress BMP signaling pathway primarily by promoting degradation of BMP receptor complex via the lipid raft-caveolar pathway and secondarily by dephosphorylation of activated BMPR1. In osteoblasts, Dullard limits BMP responsiveness. With regard to BMP antagonistic activity in ''Xenopus animal cap assay'', Dullard does not suppress constitutively active BMPR1a (caALK3) signaling. However, in the current study, we unexpectedly found that Dullard suppresses constitutively active BMPR1 in ''mammalian osteoblastic cells''. To refine at what level Dullard can suppress BMP signaling pathway in ''mammalian cells'', BMP responsive element (BRE)-luciferase assay was performed using MC3T3-E1 cell line. Overexpression of Dullard inhibits caALK3-induced activation of BRE-reporter independently of its phosphatase activity. Furthermore, overexpression of Dullard inhibits the activity of both constitutively active phospho-mimetic Smad1 (SMAD1-EVE), in which two serine residues at C-terminal phosphorylated by receptor kinase are mutated into glutamic acid, and more potent SMAD1-EVE-MM, in which MAPK phosphorylation sites in the linker region are mutated. These epistatic experiments indicate that Dullard can suppress BMP signaling pathway at or downstream of the Smad1 level. We also tested whether Dullard affects TGF-ß signaling pathway. Dullard suppresses TGFß-induced reporter activity and constitutively active TGFBR1 (caALK5)-induced TGFß signaling independently of its phosphatase activity. In BMP-induced osteoblast differentiation, siRNA-mediated knockdown of Dullard decreases alkaline phosphatase production as well as expression of marker genes including Id3, Osterix, osteocalcin, and alkaline phosphatase. Although Dullard was previously identified as a modulator of BMP receptor degradation, it plays more extensive role as a general suppressor of BMP/TGF-ß signal transduction downstream of type I receptor/SMAD and promotes BMP-induced osteoblast differentiation. In conclusion, we identified Smad1 and TGF-ß signaling pathway as novel targets of Dullard.

***Disclosures: Tadayoshi Hayata**, None.*

SA0176

See Friday Plenary number FR0176.

SA0177

See Friday Plenary number FR0177.

SA0178

See Friday Plenary number FR0178.

SA0179

See Friday Plenary number FR0179.

SA0180

See Friday Plenary number FR0180.

SA0181

Delayed Fracture Healing in Protease Activated Receptor-2 Deficient Mice. Kevin O'Neill*[1], Christopher Stutz[1], Mignemi Nicholas[1], Jeffry Nyman[2], Gregory Mencio[1], William Obremskey[1], Conor Lynch[1], Jonathan Schoenecker[1]. [1]Vanderbilt University, USA, [2]Vanderbilt University Medical Center, USA

Objectives: Extracellular proteases and inflammation are essential elements of fracture repair. Protease activated receptors (PARs) allow proteases to behave like traditional hormones. It is known that PAR-2 provides an important link between extracellular protease activation and regulation of cellular inflammation. Although PAR-2 is expressed by developing osteoblasts, its function in fracture healing is unknown. The purpose of this study was to compare fracture healing between wild-type (WT) and PAR-2 deficient (PAR-$2^{-/-}$) mice. We hypothesized that PAR-$2^{-/-}$ mice will demonstrate delayed fracture healing relative to WT mice.

Methods: With IUCUC approval, unilateral transverse mid-shaft femur fractures were created in 10 PAR-$2^{-/-}$ and 11 WT mice after intramedullary fixation. Mice were sacrificed at 7 weeks, fractured and contralateral intact femurs were harvested, and axial micro-computed tomography (µCT) images were obtained. Torsional rigidity and ultimate strength were calculated from torque versus angular displacement curves obtained by torsion testing. Bone volume fraction (BV/TV), bone mineral density (BMD), and polar moment of inertia (pMOI) were determined from µCT images.

Results: For WT mice, the torsional rigidity and ultimate strength of fractured femurs were not significantly different from intact femurs. In contrast, for the PAR-$2^{-/-}$ mice, significant differences were noted between the fractured and intact femurs for both torsional rigidity ($p=0.04$) and ultimate strength ($p=0.04$). Significant differences were also noted in PAR-$2^{-/-}$ mice between pMOI, BV/TV, and mBMD (all $p<0.001$) values of fractured compared to intact femurs (Figure 1).

Conclusions: The PAR-$2^{-/-}$ mice demonstrated delayed fracture healing measured by both biomechanical torsion testing and radiographic µCT imaging. Future studies are needed to determine if the delayed healing observed is secondary to a diminished inflammatory response in the fracture environment. Unveiling this mechanism has potential impact on the basic science of fracture healing and the development of novel pharmaceuticals that, through PAR-2, may enhance fracture healing.

Figure 1 - Ultimate torque (A) and bone volume fraction (B, BV/TV) of intact and healing femurs 7 weeks after fracture for PAR-2 knockout and wild type (WT) mice.

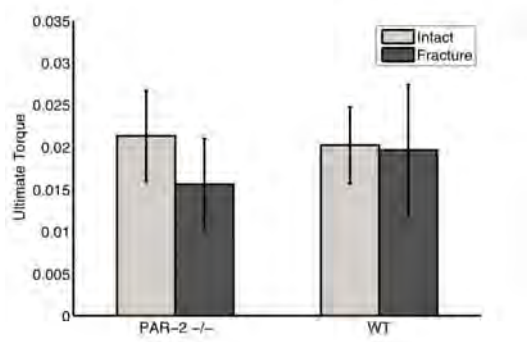

Figure 1 - A

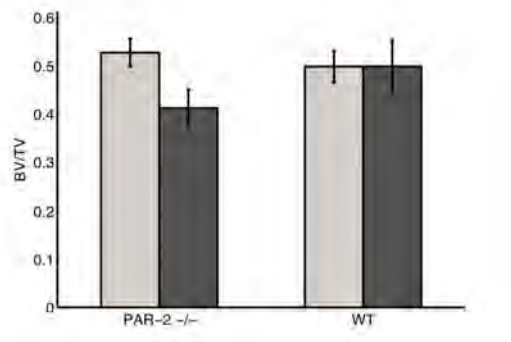

Figure 1 - B

***Disclosures: Kevin O'Neill**, None.*

SA0182

Effect of Infection on Bone Marrow Stromal Cells (MSCs): a Role for IL-6 in Erythropoiesis. Brian Sworder*[1], David Chou[2], Michael Grigg[2], Yasmine Belkaid[2], Pamela Robey[3]. [1]National Institutes of Health, USA, [2]NIAID/NIH, USA, [3]National Institute of Dental & Craniofacial Research, USA

Inflammation induces and necessitates changes in hematopoiesis (HP). Previous studies have examined the HP alterations that occur in the bone marrow (BM) during an immune response. However, despite the critical role that BM stroma plays in supporting HP, its function during inflammation remains largely unexplored. This study seeks to determine how BM stromal cells (BMSCs) and their influence on HP are altered during an immune response.

Mice were orally infected with the intracellular parasite, Toxoplasma gondii. This infection model causes severe systemic T helper type 1 inflammation and results in anemia and potential death. Eight days after infection, total cell number in the BM fell to half that of naïve mice. Flow cytometry analysis showed significant changes in the percentages of lymphoid, myeloid, and erythroid constituents. Notably, the fraction of nucleated cells contributing to erythropoiesis was reduced 5-fold. Conversely, there was no apparent change in the number of CFU-Fs (a subset of BMSCs) after infection.

A variety of knockout mice (IFNg receptor, iNOS, TCRa, IL-1, TNFa receptor, IFN-a/B receptor, IL-15, and IL-6) were screened to determine which molecules were important in mediating the pathogenic anemia induced by T. gondii infection. Only IL-6 KO mice were found to have better maintenance of erythropoiesis and a significantly larger erythroblast population than WT mice. IL-6 is known to play an important role in anemia associated with inflammation. However, the relative importance of IL-6 production by various cellular sources in mediating anemia is not known. To determine whether IL-6 from BM stroma might contribute, BMSCs were isolated from naïve and infected mice by FACS (VCAM+/CD45-/Ter119-). Strikingly, analysis by ELISA showed a 2-fold increase in IL-6 secretion by BMSCs after T. gondii infection. Using bone marrow transplants and ectopic ossicle models with WT and IL-6 KO cells, experiments are currently underway to more directly determine the contribution of IL-6 from BM stroma to infection-induced anemia.

Our results demonstrate that IL-6 is a key mediator of erythropoietic collapse during T. gondii infection and that BMSCs may be the relevant source of IL-6. This study also suggests that the bone marrow stroma is functionally different during an immune response, and that BMSCs are potential mediators of changes in HP composition as a consequence of inflammation.

***Disclosures: Brian Sworder**, None.*

SA0183

See Friday Plenary number FR0183.

SA0184

Human Blood Eosinophils: An Extrarenal Source of Converting Inactive Vitamin D to Its Active Form and Potential Role in Inflammation. Devendra Agrawal*[1], Divya Pankajakshan[1], J. Christopher Gallagher[2]. [1]Creighton University School of Medicine, USA, [2]Creighton University Medical Center, USA

Rationale: Vitamin D, especially its most active metabolite 1,25-dihydroxyvitamin D3 or calcitriol, is essential in regulating calcium homeostasis, immune modulation, cell proliferation and differentiation. Although extra-renal synthesis of calcitriol associated with inflammatory diseases is known to occur in macrophages and epithelial cells, little is known on the existence of enzymes involved in vitamin D synthesis and metabolism in circulating immune cells. In this study, we examined such enzymes in human blood eosinophils and also investigated the effect of calcitriol, administered in vivo or added exogenously, on the expression of intracellular molecules involved in inflammation in purified white blood cells (WBCs).

Methods: Peripheral blood was drawn from healthy volunteers and WBCs were purified (purity >97%; viability >98%) and stimulated in vitro with calcitriol (100 nM) for 24 hrs. We also purified WBCs from the blood of vitamin D-deficient (25-OHD levels <20ng/ml) subjects (n= 78) before and after treatment with 800-4,200 IU/d vitamin D for 1 year. The mRNA expression of importin-alpha3 (KPNA4), CYP27B1 and CYP24A1 was examined by real-time PCR.

Results: The mRNA transcripts for CYP27B1, CYP24A1, cathelicidin, and KPNA4 were found in human blood eosinophils. In vivo administration of vitamin D for 1 yr in vitamin D-deficient subjects significant increased the mRNA transcripts of CYP27B1, CYP24A1 and cathelicidin, but significantly decreased the mRNA transcripts of KPNA4. Under in vitro conditions, stimulation of human WBCs of healthy volunteers with calcitriol decreased mRNA transcripts of KPNA4 with more pronounced reduction (60-70%) in neutrophils and eosinophils. Calcitriol increased the mRNA transcripts of CYP24A1 in human blood eosinophils.

Conclusions: Presence of both CYP27B1 and CYP24A1 in human blood eosinophils suggest their role in converting inactive vitamin D to its active form and decreased expression of KPNA4 in response to vitamin D could be one of the underlying mechanisms for the anti-inflammatory and immunoregulatory effects of vitamin D in inflammatory diseases involving eosinophils.

***Disclosures: Devendra Agrawal**, None.*

SA0185

Meox2Cre-CSF-1 Knockout Mice: A Novel Osteopetrosis Model. Sherry Abboud Werner*, Kathleen Woodruff, Diane Horn, Marie Harris, Stephen Harris. University of Texas Health Science Center at San Antonio, USA

CSF-1, a key regulator of mononuclear phagocytes, is expressed in most tissues and exerts pleiotropic effects. This is supported by studies in spontaneous mutant op/op B6C3 mice where absence of CSF-1 leads to osteopetrosis as well as defects in fertility, mammary development and neural function. However, the biologic effect of CSF-1 knockout(KO) in specific tissues has not been explored. To determine whether Cre-lox technology provides a useful strategy for producing CSF-1KO mice, a targeting vector for generating a conditional KO allele for CSF-1(deleting exons4,5,6)was electroporated into ES cells. Heterozygous C57BL/6 mice harboring the floxed construct containing a 5' loxP site in intron 3 of the CSF-1 gene and a 3' loxP site with a FRT-polII-neo-FRT-loxP cassette in intron 6 were established. The neo cassette was removed by crossing CSF-$1^{flox+neo}$mice with heterozygous beta-actin-Flip recombinase mice and the CSF-$1^{flox-neo}$(fx) allelle was confirmed by Southern blot. CSF-1fx/CSF-1fx mice were then bred with Meox2Cre mice to produce heterozygous CSF-1KO mice that were subsequently interbred to generate mice homozygous for the KO allele(hCSF-1KO). At 3 weeks, CSF-1 was analyzed; bones were x-rayed and histological sections were examined using histomorphometry. Offspring showed the expected ratio of genotypes. Mice heterozygous for the KO allele resembled wt controls, whereas hCSF-1KO showed an osteopetrotic phenotype similar to op/op mice. hCSF-1KO showed CSF-1 deficiency, failure of tooth eruption, domed skull, stunted growth and reduced weight compared to wt. hCSF-1KO radiographs showed marked skeletal sclerosis with dense radioopaque bone in tibia and femoral metaphysis, vertebrae and pelvis. Compared to wt, hCSF-1KO hindlimbs showed an expanded growth plate with thick irregular calcified cartilage extending into the metaphysis obliterating the marrow cavity. Numerous TRAP-positive osteoclasts were identified in wt, whereas rare small weak TRAP-positive osteoclast-like cells were detected in hCSF-1KO. These findings provide the first evidence that global CSF-1KO can be achieved using a Cre-based system and that the osteopetrotic phenotype is reproducible in C57BL/6. Development of conditional CSF-1KO mice will be crucial for elucidating the mechanisms by which CSF-1 mediates its effect in targeted tissues. Results may lead to novel approaches for improving reproductive defects and regulating osteoclastogenesis in fracture repair and bone metastasis.

***Disclosures: Sherry Abboud Werner**, None.*

SA0186

See Friday Plenary number FR0186.

SA0187

Serum Osteocalcin is Negatively Correlated to Insulin and Adiponectin in Hibernating Bears. Rachel Bradford[1], Patricia Buckendahl[2], Caren Gundberg[3], Kim Henriksen[4], Michael Vaughan[5], Seth Donahue*[6]. [1]Michigan Technological University, USA, [2]Rutgers University, USA, [3]Yale University School of Medicine, USA, [4]Nordic Bioscience A/S, Denmark, [5]Virginia Tech, USA, [6]Michigan Tecnological University, USA

Hibernating bears do not lose cortical or trabecular bone despite being physically inactive for up to 6 months per year. Histomorphometry shows decreased bone turnover with balanced bone formation and resorption during hibernation. The purpose of hibernation is to conserve metabolic energy when food is unavailable. Fat is the primary energy source during hibernation; bears lose 30-40% of their body mass (almost exclusively fat mass) during hibernation. Bears also experience markedly decreased kidney function and do not urinate or defecate during hibernation, but maintain eucalcemia. The purpose of this study was to quantify seasonal bear serum markers of bone formation (BSAP) and osteoclast number (TRAP), which do not accumulate with decreased kidney function. To assess bone/fat/energy relationships, we also quantified serum osteocalcin (OC), adiponectin, NPY, insulin, and glucose. Serum was collected every 10 days from black bears before, during, and after hibernation. Serum BSAP and TRAP decreased ($p<0.0001$) during hibernation by 57% and 29% respectively, supporting the histomorphometric findings of decreased bone turnover. Serum total OC, which is also a bone formation marker, increased 59% during hibernation ($p<0.0001$). This increase could possibly be explained by the accumulation of OC due to reduced renal function. Serum NPY was not significantly different in hibernating and active bears. Adiponectin decreased 30%, insulin decreased 20%, and glucose decreased 31% ($p<0.0009$) during hibernation relative to non-hibernation periods. Total OC was negatively correlated ($p<0.0001$) with adiponectin, unlike the positive association in humans. Insulin was negatively correlated ($p=0.008$) to total OC only during the pre-hibernation period. We are currently investigating seasonal changes in uncarboxylated OC. Reduced bone turnover contributes to energy conservation in hibernating bears, but the relationships between osteocalcin, adiponectin, insulin, and glucose may be different in bears than other species since bears rely on lipids for metabolic fuel nearly exclusively during hibernation (fasting). Hibernating bears are a unique model for understanding bone/fat/energy relationships and the prevention of disuse osteoporosis (i.e., bone loss due to prolonged physical inactivity); the biological mechanisms may have implications for human medicine.

***Disclosures: Seth Donahue**, None.*

SA0188

See Friday Plenary number FR0188.

SA0189

The Effect of Vitamin K Supplementation on Glucose Metabolism. Hyung Jin Choi*[1], Juyoun Yu[1], Hosanna Choi[1], Jee Hyun An[1], Yenna Lee[1], Hwa Young Cho[1], Sun Wook Cho[2], Sang Wan Kim[3], Chan Soo Shin[1]. [1]Department of Internal Medicine, Seoul National University College of Medicine, South korea, [2]University of Michigan School of Dentistry, USA, [3]Seoul National University Boramae Hospital, South korea

Vitamin K has been known to regulate glucose metabolism via modulating osteocalcin and/or inflammation pathway. However, the exact mechanisms for this regulation in vivo have not been fully investigated. We have investigated the effects of vitamin K on beta-cell function and insulin sensitivity in healthy young male volunteers using frequently sampled intravenous glucose tolerance test (FSIGT) before and after 4 weeks of vitamin K treatment. Twenty-two healthy young male subjects (age 28.2±4.5; BMI 24.4±2.5) were given menatetrenone (Vitamin K2) 30mg tid for 4 weeks and FSIGT were performed before and after the vitamin K treatment and carboxylated/undercarboxylated osteocalcin, interleukin-6, CRP, and adiponectin concentrations were measured. Vitamin K treatment significantly decreased and increased undercarboxylated and carboxylated osteocalcin, respectively (both, $P < 0.05$). However, there were no significant changes in the levels of inflammation markers, ie., interleukin-6 and CRP. Vitamin K treatment significantly increased disposition index (DI), which indicates beta-cell function in relation to insulin action, compared with baseline (baseline: 2507±1448, 4 week treatment: 3468±1584; $P = 0.003$). There were no significant changes in acute insulin response to glucose (AIRg) and insulin sensitivity (SI). Change in undercarboxylated osteocalcin was significantly associated with change in AIRg after adjusting for confounding factors, including baseline AIRg, age, BMI and weight change ($P < 0.05$). There was no significant change in body weight and adiponectin concentration. Taken together, these results suggest that vitamin K treatment for 4 weeks increased beta-cell function in healthy young men, which appears to be related to the modulation of osteocalcin metabolism rather than systemic inflammation.

***Disclosures: Hyung Jin Choi**, None.*

SA0190

See Friday Plenary number FR0190.

SA0191

***Igfb2-/-* Mice Exhibit Age-related Changes in Skeletal Mass, Body Composition and Metabolic Status.** Victoria Demambro*[1], Kathryn Shultz[2], Harold Coombs[2], Jane Maynard[2], David Clemmons[3], Wesley Beamer[2], Clifford Rosen[4]. [1]Maine Medical Research Institute, USA, [2]The Jackson Laboratory, USA, [3]University of North Carolina, USA, [4]Maine Medical Center, USA

We have previously reported on a global *Igfbp2* null mouse on a C57BL/6J background in which the male mice at 16 weeks of age had significantly decreased bone volume and turnover and increased adiposity (Endocrinology 149:2051, 2008). To test the effect of IGFBP-2 absence over time, we aged Igfbp2 null (-/-) and control (+/+) males to 24 months of age. Body composition was examined by PIXImus DEXA at 2, 4, 6, 12, 18 and 24 months. Femurs were analyzed by pQCT at 4, 12 and 24 months for vBMD and MicroCT for structural changes at 4 and 12 months. Mice were evaluated for metabolic changes by ITT and GTT and serum insulin at 12 months. The -/- males were found to be heavier with increased fat mass at all time points. Whole body BMC was significantly reduced in -/- mice compared to +/+ control mice through 18 months. Remarkably, between 12 to 24 months, +/+ males had a dramatic loss in weight (-19%), whole body BMC (-13%), and fat mass (-27%), while -/- male mice appeared protected from these age related decreases by showing a significant increase in BMC (+7%) and a trend towards increased fat mass (+5%). Reductions in femoral vBMD (+/+ = -30%, -/- = -18%) and cortical thickness (+/+ = -22%, -/- = -6%) were observed, however to a lesser extent in the -/- femurs. Due to this differential rate of loss by 24 months -/- femurs were significantly increased for both measures compared to +/+ femurs. MicroCT analysis of distal femurs revealed similar decreases in trabecular BV/TV and number from 4 to 12 months of age. Interestingly there was no change in trabecular thickness in the +/+ mice with the mutants exhibiting a 16% increase during this same period. At 12 months of age, -/- mice were found to be hyperinsulinemic in both the fasted and fed states compared to +/+ mice. When glucose challenged, -/- mice exhibited higher glucose values and ITT results showed a decrease in the hypoglycemic response to exogenous insulin. Taken together, these results are indicative of a mild but significant insulin resistance. In summary, *Igfbp-2* null males appear to be protected from age related loss of bone with minor reductions in cortical mass and increased trabecular thickness. On the other hand, they seem to be more susceptible to age related increases in obesity and insulin resistance.

***Disclosures: Victoria Demambro**, None.*

SA0192

See Friday Plenary number FR0192.

SA0193

The Skeletal Effect of Parathyroid Hormone Treatment after Ovariectomy is Diminshed when Circulating Growth Hormone is Elevated. J. Fritton*[1], Devendra Bajaj[1], Hui Sun[2], Yinjgie Wu[2], Mary Bouxsein[3], Shoshana Yakar[2]. [1]New Jersey Medical School, USA, [2]Mount Sinai School of Medicine, USA, [3]Beth Israel Deaconess Medical Center, USA

Parathyroid hormone (PTH) is routinely prescribed to postmenopausal women to restore bone and prevent osteoporotic fracture. However, the effects of the PTH therapy are quite variable in both these women and after ovariectomy (OVX) of animals. Both growth hormone (GH) and insulin-like growth factor (IGF-1) are potent regulators of bone remodeling processes. Previous investigations utilizing OVX have revealed that a serum balance in mice that favors GH over IGF-1 diminishes the effects of ablated ovarian function and leads to reduced endosteal resorption and greater bone formation. We utilized the liver IGF-1 deficient (LID) mouse to study the possible additional effects of PTH treatment. OVX surgery was performed on 12-week-old mice followed by 4 weeks of daily (7d/wk) PTH (50 ng/g body weight) intraperitoneal (i.p.) injection. 12-μm μCT (Scanco) scans were completed for femurs and vertebrae. Whole-bone mechanical properties were quantified for mid-diaphyseal femurs by loading to failure in 4-point bending. Bone formation histomorphometry measurements were made on sections from double-labeled, calcein-injected (i.p.) mice. Contrary to the expected gains with PTH observed in controls, very small effects were found in LID mice with PTH treatment after OVX (Δ cross-sectional moment of inertia of mid-shaft femur: WT – 25%; LID – < 1%, Δ trabecular thickness: WT – 3%; LID - < 1%). One explanation for this lack of effect is that cancellous and cortical bone structures may reach homeostasis due to the previously reported enhanced expansion of cross-sectional structures in LID mice that exhibit 3-fold greater circulating GH. Our data suggest little synergism of PTH during estrogen deficiency when GH is elevated and offer a possible insight into the variability of response to PTH treatment for bone loss in postmenopausal women.

***Disclosures: J. Fritton**, None.*

SA0194

See Friday Plenary number FR0194.

SA0195

See Friday Plenary number FR0195.

SA0196

See Friday Plenary number FR0196.

SA0197

Runx2 Stimulation of HSP70/HSPA1B Gene Transcription Decreases Runx2 Protein Stability in Osteoprogenitors. Nadiya M. Teplyuk[1], Jennifer Cotton[1], Jonathan Gordon[1], Viktor I. Teplyuk[1], Mario Galindo[2], Di Chen[3], Suk-Chul Bae[4], Jane Lian[1], Janet L. Stein[1], Gary Stein[1], Andre Van Wijnen*[1]. [1]University of Massachusetts Medical School, USA, [2]University of Chili, Chile, [3]University of Rochester Medical Center, USA, [4]Chungbuk National University, South korea

Inactivation, haplo-insufficiency and dosage insufficiency of Runx2 have been linked to skeletal defects during mammalian development and in human skeletal diseases. Reduced levels of Runx2 in osteoblasts are linked to different skeletal phenotypes, including symptoms of Cleidocranial Dysplasia (i.e., craniofacial abnormalities, supernumerary teeth), as well as absence of clavicles and delayed ossification of cranial sutures in mouse models. Elevation of Runx2 levels in transgenic mouse models is associated with an osteoporotic phenotype. Consequently, it is necessary to establish how osteoblasts succeed in continuously calibrating Runx2 levels to maintain a non-pathological state. Here we show that Runx2 transcriptionally stimulates expression of HSP70, which is a key specificity factor of the C-terminal HSP70 Interacting Protein (CHIP), as well as HSP40 and other HSP proteins, in the absence of external stress signals (e.g., heat shock) in osteoprogenitor cells. Expression of a functionally defective Runx2 protein does not alter HSP70 gene expression. Importantly, we find that HSP70 interacts with Runx2 protein by co-immunoprecipitation and that down-regulation of HSP70 by siRNA depletion increases steady-state levels of Runx2, while forced expression of HSP70 decreases Runx2 levels. We propose that Runx2 controls the levels of HSP70 as a component of an auto-inhibitory rheostat that maintains Runx2 proteins levels within a physiological range that is required for normal skeletal development and bone homeostasis. Interestingly, mutations in the chaperonin function of HSPs have been linked to skeletal dysplasias.

***Disclosures: Andre Van Wijnen**, None.*

SA0198

See Friday Plenary number FR0198.

SA0199

A Tentative Role of S100A6 in Regulation of Osteoblastogenesis. Weida Lu*[1], Yingchun Zhao[2], Jing Xiao[2], Robert Recker[3], Gary Guishan Xiao[1]. [1]Creighton University, USA, [2]Creighton University Medical Center Osteoporosis Research Center, USA, [3]Creighton University Osteoporosis Research Center, USA

A progressive adipogenesis with age in bone marrow is associated with reduced bone formation and loss of bone mass. In elderly adults and osteoporotic patients at all ages, increase of bone marrow adipose tissue and decrease of matrix structure are often observed. However, the role of bone marrow adipocytes in the aging bone tissues remains unknown. In our previous study, we used two different modes of co-cultures of adipocytes and osteoblasts, which were derived from human mesenchymal stem cells (hMSC), to study the effects of hMSC-derived adipocytes on osteoblastogenesis. We identified S100A6 in osteoblastogenesis, which is regulated by hMSC-derived adipocytes, suggesting the possible role of S100A6 in the regulatory effects of adipocytes on osteoblastogenesis. In this research, we aimed to study the mechanism of the inhibitory effects of adipoctyes on osteoblastogenesis. S100A6 is one of the members in S100 calcium-binding protein family, and is reported to be an oncogenic transcriptional factor playing a major role in cancer metastasis. However, the role of S100A6 in bone formation is unknown. We hypothesized that S100A6 may play a crucial role in regulation of osteoblastogensis by hMSC-derived adipocytes. To confirm the involvement of S100A6 in osteoblastogenesis, we transfected hMSC with siRNA of S100A6 during osteoblastogenesis, and found that the number of pre-osteoblasts decreased in cells transfected with siRNA of S100A6 compared to cells subjected to negative control. The alkaline phosphatase (ALP) positive area and ALP activity also decreased significantly after transfection of siRNA of S100A6. These suggest that S100A6 may be involved in osteoblastogenesis. To further study the mechanism of S100A6 regulating bone formation, we examined expression of bone formation marker such as Runx2, and found that Runx2 expression was significantly reduced in the transfected cells compared to the non-transfected cells. We also found that the reduced osteogenesis activity, measured by ALP positive area, its activity, and Runx2 expression level, was associated with the decreased expression level of β-catenin after transfection with siRNA of S100A6. Data from this study suggest that S100A6 may play an important role in adipocytes regulatory process of osteoblastogenesis through Wnt signaling pathway. This is the first study that tackles the mechanism of S100A6 regulating osteoblastogenesis.

***Disclosures: Weida Lu**, None.*

SA0200

See Friday Plenary number FR0200.

SA0201

Bone Anabolic Factors are Specific to Osteoclasts and the Release of These Factors is Altered by Osteoclast Substrate. Catherine Cruger Hansen*[1], Anita Neutzsky-Wulff[2], Kim Andreassen[3], Morten Karsdal[1], Kim Henriksen[1]. [1]Nordic Bioscience A/S, Denmark, [2]Nordic Bioscience & University of Copenhagen, Denmark, [3]Nordic Bioscience, Denmark

Normal bone remodeling is a coupled process in which bone formation by osteoblasts succeeds bone resorption by osteoclasts, ensuring the amount of resorbed bone is replaced by an equal amount of new bone. However, in osteopetrotic patients suffering from Autosomal Dominant Osteopetrosis II (ADOII) and Autosomal Recessive Osteopetrosis (ARO), an uncoupling phenomenon occurs in which bone resorption is decreased while bone formation remains normal or increased. Additionally, the number of non-resorbing osteoclasts is increased; suggesting bone anabolic factors derive from osteoclasts independent of bone resorption. The aim of this study was to investigate the specificity of the osteoclasts ability to induce bone formation.

Human monocytes were isolated from blood and differentiated into mature osteoclasts using M-CSF and RANKL. For some experiments, RANKL was substituted with OPG to prevent osteoclast differentiation. The cells were then cultured on different substrates including decalcified and non-remodeled substrates. Conditioned medium (CM) and corresponding non-conditioned medium (non-CM) were collected during culture. TRAP activity and bone resorption were used as measurements of osteoclast quality. The pre-osteoblastic cell line 2T3 was subsequently treated with 50% of CM or non-CM in addition to relevant controls. Induction of bone nodule formation was assessed by Alizarin Red-S staining / dye extraction.

CM collected from differentiating osteoclasts was shown to induce bone nodule formation 7+ days after initiation of differentiation while CM collected from macrophages did not. This indicates that secretion of bone anabolic factors is specific to osteoclasts. On non-remodeled dentin and decalcified bone, the osteoclasts were comparable to osteoclasts on calcified bone with respect to number and activity, yet the CMs collected from mature osteoclasts cultured on decalcified bone and dentin showed a 90% reduction in anabolic activity compared to calcified bone.

In conclusion, the secretion of bone anabolic factors is specific to osteoclasts. Furthermore, the secretion of bone anabolic factors by mature osteoclasts is attenuated by altered and non-remodeled substrates. Hopefully these findings, along with further investigations, can lead to a better understanding of the uncoupling between bone resorption and bone formation.

***Disclosures: Catherine Cruger Hansen**, Nordic Bioscience, 3*

SA0202

Bone Formation Is Predicted by Triiodothyronine and Lean Body Mass in Exercising Women with Hypothalamic Amenorrhea. Jennifer Scheid*[1], Nancy Williams[2], Gaele Ducher[1], Mary Jane De Souza[3]. [1]Penn State University, USA, [2]The Pennsylvania State University College of Medicine, USA, [3]Pennsylvania State University, USA

Decreased bone formation is related to an energy deficiency in exercising women with functional hypothalamic amenorrhea (FHA), but the underlying mechanism is unclear. This impact of energy deficiency on bone formation occurs despite an apparent osteogenic impact of exercise. The purpose of this study was to examine the relative contributions of energy related factors and factors reflective of the exercise stimulus to bone formation in exercising women with FHA. In this cross-sectional study, regularly exercising women were divided according to menstrual status: 1) Ovulatory (ExOV, n= 31), 2) Amenorrheic (ExAMEN, n=21). Menstrual status was assessed by daily urinary reproductive hormones for a menstrual cycle, or 28-day monitoring period if AMEN. Type I procollagen amino-terminal propeptide (PINP), bone-specific alkaline phosphatase (BSAP), ghrelin, triiodothyronine (TT3), peptide YY (PYY), and leptin were measured in the serum. Exercise minutes per week were assessed by exercise logs. Resting metabolic rate (RMR) was assessed by indirect calorimetry and adjusted for lean body mass. Lean body mass and BMD were assessed by DXA. The ExAMEN group had similar age (23.2 ± 0.8yr), weight (57.9 ± 1.1kg), lean body mass (41.7 ± 0.9kg), and exercise minutes (336.4 ± 44.3min) compared to ExOV, but lower BMI (20.3 ± 0.4 vs. 21.5 ± 0.3 kg/m^2, $p=0.020$). ExAMEN also had lower BMD at the lumbar spine and hip ($p<0.01$). No differences were found in bone formation markers between the two groups. TT3 was lower ($p=0.060$) and PYY was higher ($p<0.001$) in the ExAMEN compared to the ExOV group. All other parameters of energy status were not different between the two groups. Independent variables in a regression model predicting PINP included TT3 and lean body mass which accounted for 34.3% of the variance in PINP ($R^2=0.371$, $p<0.001$). In the ExAMEN group alone the proportion of variance in PINP explained by TT3 and lean body mass went up to 67.6% ($R^2=0.710$, $p<0.001$). Adjusted RMR ($r=0.303$, $p=0.038$) was the only energy related variable related to BSAP in the whole sample. Energy status, measured by TT3 and adjusted RMR, and lean body mass are independent predictors of bone formation in exercising women with FHA. Combining an exercise program that improves muscle mass and an adequate energy environment could potentially optimize the skeletal benefits in exercising women with FHA.

Disclosure: Supported by US DoD (PR054531) and CIHR.

***Disclosures: Jennifer Scheid**, None.*

SA0203

See Friday Plenary number FR0203.

SA0204

See Friday Plenary number FR0204.

SA0205

Enhancing Effects of HDAC Inhibitors on Osteoblastic Differentiation. Rabia Islam*[1], Hyun-Jung Kim[2], Won-Joon Yoon[3], Hyun-Mo Ryoo[3]. [1]School of Dentistry, Seoul National University, South korea, [2]BioRunx Co. Ltd., South korea, [3]Seoul National University, South korea

Recently HDACs have been proven to be associated with endochondral bone formation, osteoblast maturation as well as osteoclast survival. In addition to histone proteins, many non-histone proteins including Runx2 are also reported as substrates for HDACs resulting in regulation of cell growth and differentiation. Although HDAC inhibitors (HDI) including SAHA and depsipeptide are recently approved by FDA as anti-cancer therapy and have been extensively studied for cancer treatment, the studies of HDI for bone diseases are rare. The purpose of this study is to observe the effect of HDIs including SAHA and MS-275 on osteoblast differentiation using C2C12 and MC3T3E1 cells in order to give some clues to the therapeutic usage of HDIs in bone diseases. Firstly, treatment with SAHA or MS-275 induced ALP activity and showed synergistic effect with BMP2 in C2C12 cells. To investigate their effects on bone marker gene expressions during osteoblast differentiation, C2C12 and MC3T3E1 cells were treated with SAHA or MS-275 in doses optimized after cytotoxicity and efficacy observation with cytotoxicity assay and ALP staining, respectively, and then qRT-PCR was performed for cells in different stages of

differentiation. Both SAHA and MS-275 significantly increased Runx2, Alp, and collagen type(I) gene expression. We also examined Runx2 protein level in MC3T3-E1 cells treated with or without SAHA or MS-275. Both HDIs also increased Runx2 protein expression. Further studies showed that SAHA and MS-275 increased Runx2 stability and acetylation, leading to transcriptional activation of Runx2. Taken together, SAHA and MS-275 has enhancing effect on osteoblast differentiation, indicating that they might be applicable for therapeutic usage in bone diseases.

***Disclosures: Rabia Islam**, None.*

SA0206

See Friday Plenary number FR0206.

SA0207

See Friday Plenary number FR0207.

SA0208

Human Bone Resorption Lacunas Contain Specific Glycan Epitopes. Meeri Keinänen*[1], Jarkko Räbinä[2], Leena Valmu[2], Petri Lehenkari[1], Juha Tuukkanen[1]. [1]University of Oulu, Finland, [2]Finnish Red Cross Blood Service, Finland

The aim of this study was to characterize the glycan epitopes in human bone located at the resorption lacunas. We hypothesize that the glycans have a particular function in the regulation of bone remodeling.

Human bone slices resorbed with human bone marrow –derived osteoclasts were stained with various lectins. The affinity of various fluorescently labeled lectins towards resorption pits was studied before and after cleaving the glycan epitopes by enzymatic treatments. Results were visualized using confocal microscopy.

Resorption lacunas were positively labeled when treated with sialic acid binding lectins. Also, treatment with N-acetylglucosamine-, mannose- and galactose-specific lectins gave positive result in stainings. Treatment of the resorbed human bone slices with two different sialidases and N-glycosidase changed the binding of lectins, which was observed as weaker signals in confocal microscopy.

These observations show that resorption lacunas contain various glycan epitopes that might have an effect on the subsequent cellular attachment and regulation of the bone formation process.

***Disclosures: Meeri Keinänen**, None.*

SA0209

See Friday Plenary number FR0209.

SA0210

Osteoblast Targeted Disruption of Kremen Increases Bone Accrual in Mouse. Zhendong Zhong*[1], Cassandra R. Zylstra[2], Bart Williams[2]. [1]Van Andel Institute, USA, [2]Van Andel Research Institute, USA

Kremen proteins are single-pass transmembrane proteins encoded by two genes in mammals. The molecular functions of Kremens are still being elucidated, although some studies have linked its function to regulation of the Wnt/B-catenin signaling pathway. Recently, Ellwanger et al. (Mol. Cell. Biol., 28:4874, 2008) created mice homozygous germline deletions in Kremen1 and Kremen2 and found that mice lacking both genes, both not either one singly, developed increases in bone volume and bone formation. To gain insight what cell type was responsible for this increase in bone mass, we created mice homozygous for a germline inactivation of Kremen1 that also carry an osteoblast-specific deletion in Kremen2. Analysis of these mice reveals depletion of Kremens in osteoblast can significantly increase the whole body bone density, tibia cortical bone thickness and BV/TV ratio. Thus, our data supports the idea that functions of Kremen within the osteoblast are associated with regulation of normal bone mass.

***Disclosures: Zhendong Zhong**, None.*

SA0211

See Friday Plenary number FR0211.

SA0212

Recapturing Fracture Repair and Bone Formation using a Periosteal Derived Cell Population. Scott Roberts*[1], Eline Desmet[1], Jan Schrooten[1], Frank Luyten[2]. [1]K.U.Leuven, Belgium, [2]University Hospitals KU Leuven, Belgium

Fracture repair involves several key processes including inflammation, callus formation and bone remodeling. It has previously been shown that the integrity of the periosteum, a fibrous tissue which covers all bones, is required for successful bone repair. This is mainly due to populations of osteo/chondro progenitors being resident within the periosteum which mediate bone healing. In this study a population of human periosteal derived cells (hPDCs) was isolated and pooled from six healthy donors by collagenase digestion. These cells were shown, by FACS, to be positive for the mesenchymal stem cell markers CD73, CD90 and CD105 (100%) as well as the endothelial progenitor cell marker CD146 (4.9%) and the hematopoietic progenitor marker CD34 (45%) indicating the heterogeneous nature of this population. To mimic the environment which these cells would be exposed to during fracture healing, five different commercially available orthopedic 3D matrices composed of calcium phosphate particles in an open collagen network (NuOss^{TM}, CopiOs^{TM}, Bio-Oss$^{®}$, Collagraft^{TM} and Vitoss$^{®}$) were selected. Cells were successfully seeded onto the matrices with efficiencies of greater than 90%. Gene expression analysis for the osteo/chondro transcription factors Runx2 and Sox9, following cell seeding and 24 hours and 7 days of passive culture *in vitro*, showed similar levels of expression, indicating the persistence of bone forming progenitors. Bone formation was observed after eight weeks following implantation, subcutaneously in NMRI nu/nu mice, with hPDCs loaded on NuOss^{TM}, Bio-Oss$^{®}$, Collagraft^{TM} and Vitoss$^{®}$ matrices. NuOss^{TM} provided the most optimal environment for bone formation with 13% bone observed within the total volume of implant, when compared to Bio-Oss$^{®}$ (5.3%), Vitoss$^{®}$ (3.2%) and Collagraft^{TM} (1.9%). Interestingly CopiOs^{TM} combined with hPDC cells did not exhibit any bone formation. The formation of bone marrow sinusoids were observed throughout the NuOss^{TM}/hPDC implant, in contrast to other tested cell/matrix combinations, suggesting bone formation through a chondrogenic route as seen during fracture repair. No bone formation was observed when these matrices were implanted in the absence of cells. This study highlights the importance of optimizing the cell-matrix combination, whilst also considering the host interaction when investigating bone forming potential of progenitor cell populations.

***Disclosures: Scott Roberts**, None.*

SA0213

See Friday Plenary number FR0213.

SA0214

Sodium/Proton Exchange is a Major Regulated Mechanism Supporting Bone Mineral Deposition. Li Liu*[1], Peter A. Friedman[1], Paul H. Schlesinger[2], Harry Blair[1]. [1]University of Pittsburgh, USA, [2]Washington University, USA

The osteoblast regulates bone deposition in part by secretion of nucleating proteins for hydroxyapatite, but mineralization proceeds when these proteins are absent. Because bone mineral evolves ~ 1.5 moles of protons per mole of Ca^{2+} precipitated, we hypothesized that facilitated acid transport supports mineralization. Using genome-wide expression in mineralizing human osteoblasts, we identified candidate H^+ transporters; databases on protein interactions were used to identify potential transport systems. Acid transport and expression of proteins was measured in mineralizing osteoblasts. We find that osteoblast H^+ transport involves at least two types of membrane transport. To facilitate mineral deposition at the zone of mineral deposition, there is vectorial H^+ uptake by vesicles, possibly a subset of matrix vesicles, which also express alkaline phosphatase to elevate phosphate. This transport was demonstrated by weak base accumulation by intact membrane vesicles isolated from mineralizing bone. Transport requires a K^+ gradient but it is independent of ATP; H^+ uptake is sensitive to Zn^{2+} but not to H^+ pump inhibitors; the identity of this H^+ transporter is uncertain. Bulk acid flux at the osteoblast basolateral surface proceeds by a second mechanism, vectorial facilitated H^+ transport mediated by Na^+/H^+ exchanger-6 (NHE6). NHE6 mediates cation exchange at high capacity across the gap-junction connected osteoblasts during bone synthesis. Osteoblasts express both NHE6, a specialized NHE, and NHE1, widely expressed. A chaperon protein, RACK-1, trafficks NHE6 to the cell membrane in osteoblasts. Nonmineralizing MG63 osteoblasts express low levels of NHE6 and have low Na^+-dependent H^+ transport, shown by whole cell pH in response to 40 mM proprionate, while mineralizing osteoblasts exhibit rapid Na^+/H^+-exchange and high levels of NHE6. When MG63 is transfected with NHE6, Na^+/H^+-exchange is similar to mineralizing osteoblasts. Knockdown of NHE1 has minimal effects on pH change with acid loading. Osteoblasts also express the PDZ domain-containing Na^+/H^+ exchange regulatory factor-1 (NHERF-1), a PTH-receptor binding organizing protein that complexes with SLC9-family NHEs including NHE6, and RACK-1, regulating them. In NHERF-1$^{-/-}$ mice an unusual osteomalacia with broadened mineral deposition zones and ~30% defect in matrix and mineral synthesis occur. We conclude that NHE-dependent H^+ transport, mediated mainly by NHE6, supports hydroxyapatite deposition in bone.

***Disclosures: Li Liu**, None.*

SA0215

Stimulation of Bone Formation in Cortical Bone of the Mice Treated with a Novel Bone Anabolic Peptide with Osteoclastogenesis Inhibitory Activity. Hisataka Yasuda[1], Atsushi Inagaki[2], Kaoru Mori[2], Yuriko Furuya*[2]. [1]Oriental Yeast Company, Limited, Japan, [2]Oriental Yeast Co., Ltd., Japan

In spite of making every effort in developing bone anabolic drugs the only clinically available one is PTH. The major difficulty is lack of clarification of mechanisms regulating osteoblast (Ob) differentiation and bone formation. Here we report that a peptide known to abrogate osteoclast (Oc) differentiation *in vivo* via blocking RANKL-RANK signaling surprisingly exhibited bone anabolic effect *in vivo*. In the previous study administration of the peptide significantly inhibited bone loss by reducing NOc/BS and OcS/BS in trabecular bone in OVX mice. To investigate the effects of the peptide it was administered subcutaneously to mice three times per day for 5 days at a dose of 10mg/kg. DXA and pQCT analysis showed that the peptide augmented BMD significantly in cortical bone not in trabecular bone. Histomorphometrical analysis showed that the peptide had little effect on NOc/BS and OcS/BS in distal femoral metaphysis but markedly increased MAR and BFR in femoral diaphysis. Our findings were inconsistent with the previous report that the peptide acted as an inhibitor of bone resorption and suggested that the peptide exerted its activity through unknown mechanisms. To clarify them, we investigated the effects of the peptide on Ob differentiation/mineralization with MC3T3-E1 (E1) cells and those on Oc differentiation with RAW264 cells and sRANKL. The peptide markedly increased ALP activity and decreased TRAP activity in each cell culture in a dose-dependent manner, respectively. In addition, the peptide stimulated mineralization evaluated by alizarin red staining. Increases in ALP activity and mineralization were similarly observed in human mesenchymal cell culture under osteoblastic conditions. Increases in mRNA expression of BMP4, CTGF, IGF1, IGF2, ALP, and osteoclacin were observed in E1 cells treated with the peptide for 96 h in GeneChip analysis. Addition of p38 MAP kinase inhibitor reduced ALP activity in E1 cells treated with the peptide, suggesting a signal through p38 was involved in the mechanisms. Taken together, the peptide abrogated osteoclastogenesis by blocking RANKL-RANK signaling and stimulated Ob differentiation/mineralization at the same concentration with unknown mechanism *in vitro*. However, in our experimental conditions the peptide exhibited bone anabolic effect dominantly in vivo. Since the peptide was known to bind RANKL, we hypothesized that the peptide shows the bone anabolic activity with reverse signaling through RANKL in Obs.

***Disclosures: Yuriko Furuya**, Oriental Yeast Co., Ltd., 3*
This study received funding from: Oriental Yeast Co., Ltd.

SA0216

Suppression of NADPH Oxidases Prevents Chronic Ethanol-Induced Bone Loss. Jin-Ran Chen*[1], Oxana P. Lazarenko[2], Kelly Mercer[3], Kartik Shankar[2], Michael L. Blackburn[2], Thomas M. Badger[2], Martin J. Ronis[2]. [1]University of Arkansas for Medical Science, Arkansas Children's Nutrition Center, USA, [2]University of Arkansas for Medical Sciences/ Arkansas Children's Nutrition Center, USA, [3]Arkansas Children's Nutrition Center, USA

Since the molecular mechanisms through which chronic excessive alcohol consumption induces osteopenia and osteoporosis are largely unknown, potential treatments for prevention of alcohol-induced bone loss remain unclear. We have previously demonstrated that, chronic ethanol (EtOH) treatment leads to accumulation of reactive oxygen species (ROS) in osteoblasts dependent on NADPH (nicotinamide adenine dinucleotide phosphate) oxidase (Nox). EtOH-induced ROS production might mediate both inhibition bone formation and increases in bone resorption. Using total enteral nutrition in a cycling female Sprague-Dawley rat model, we found that EtOH infusion for 4 weeks reduced bone mass ($P<0.05$) assessed by peripheral quantitative computerized tomography (pQCT) analysis. Co-administration of diphenylene iodonium chloride (DPI) a pan Nox inhibitor by daily s.c. injection of 1 mg/kg/d, abolished EtOH-induced bone loss. Static histomorphometric analysis revealed that EtOH effected both osteoblast and osteoclast indices ($P< 0.05$). EtOH decreased bone volume and the number of osteoblasts, whereas it increased osteoclast number, bone surface covered by osteoclasts and the eroded bone surface characteristic of increased osteoclastic activity. DPI was able to normalize both osteoblast and osteoclast indices affected by EtOH. EtOH-induced bone loss was associated with up-regulation of mRNA levels of all three Nox subtypes 1, 2, 4 and RANKL (receptor activator of NF-kB ligand) in bone, and EtOH-induced RANKL promoter activity in vitro ST2 cell culture ($P<0.05$). To confirm Nox activation is truly associated with EtOH-induced bone loss, we fed a 36 % alcohol containing liquid diet to nicotinamide dinucleotide phosphate oxidase-deficient p47phox-/- female mice for 6 weeks. In vivo systemic CT scan analysis revealed that, in wild type animals, EtOH reduced bone mineral density (BMD) compared to a pair fed group ($P<0.05$). In contrast, EtOH failed to down-regulate BMD in p47phox-/- female mice compared to their pair fed controls. Bone marrow cells taken from p47phox-/- female mice cultured with 50 mM EtOH for 24 h failed to induce RANKL gene expression but EtOH was able to induce RANKL gene expression in cells from wild type animals ($P< 0.05$). These data suggest that inhibition of Nox expression or activity may be new target for prevention or treatment of chronic EtOH-induced bone loss, and perhaps other conditions resulting in oxidative stress associated bone resorption such as aging. This study was supported by NIH grant RO1 AA18282 to MJR.

***Disclosures: Jin-Ran Chen**, None.*

SA0217

See Friday Plenary number FR0217.

SA0218

See Friday Plenary number FR0218.

SA0219

Duality of TRIP-1 Function in Regulating Osteoblast Activity In Vitro. Diana Metz-Estrella*[1], Tzong-jen Sheu[2], J. Edward Puzas[3]. [1]University of Rochester School of Medicine & Dentistry, USA, [2]Univesity of Rochester School of Medicine & Dentistry, USA, [3]University of Rochester School of Medicine, USA

The importance of the "TGFβ receptor interacting protein" (TRIP-1) in bone remodeling was first recognized when it was found to interact with tartrate resistant acid phosphatase (TRAP). It has been suggested that the interaction of these two proteins activate the TGFβ pathway and increase markers of osteoblast differentiation. Interestingly, TRIP-1 may also have another role inside the cell since it shares a perfect homology to a subunit of the eukaryotic initiation factor 3 complex (i.e. eIF3i). Therefore, we believe that during bone remodeling TRIP-1 integrates extracellular signals in osteoblasts and mediates regulation of protein translation. Consequently, this would lead to a control over osteoblast proliferation and differentiation. To evaluate the role of TRIP-1 in osteoblasts we transiently transfected siRNA against TRIP-1 into primary rat calvarial osteoblasts in vitro. These cells were then cultured in osteoblast differentiation media for 5 days. Cells transfected with TRIP-1 siRNA show an 84% decrease in TRIP-1 protein levels at day 3 after transfection compared to cells transfected with a control siRNA. In addition, cells transfected with TRIP-1 siRNA presented reduced alkaline phosphatase staining and exhibited a 60% decrease in alkaline phosphatase activity when compared to control cells. Using qRT-PCR we found that cells transfected with a TRIP-1 siRNA have decreased expression of osteoblast differentiation markers (i.e., collagen I, alkaline phosphatase, osteopontin and osteocalcin). Interestingly, TRIP-1 siRNA visibly reduced cell number in this assay. In relation to this, cyclin D1 protein levels were dramatically decreased in cells transfected with the TRIP-1 siRNA. These data suggested a role for TRIP-1 in cell cycle regulation. To address this possibility, cells transfected with control or TRIP-1 siRNA were labeled with BrdU and sorted by flow cytometry to assay for possible cell cycle arrest. The results suggested that cells transfected with a TRIP-1 siRNA are arrested in the S and G2M phases of the cell cycle. Moreover, luciferase reporter assays showed that knocking down TRIP-1 interferes with the normal signaling of TGFβ and BMP pathways. In conclusion, our data show that TRIP-1 is an essential protein for normal osteoblast differentiation and proliferation and through its interaction with TRAP may be one mechanism by which site-directed bone formation can occur.

***Disclosures: Diana Metz-Estrella**, None.*

SA0220

See Friday Plenary number FR0220.

SA0221

Withdrawn

SA0222

Fibroblast Growth Factor Receptor 2 Expression in Pre-osteoblasts Requires the PBAF Chromatin-remodeling Complex. Fuhua Xu*, Stephen Flowers, Elizabeth Moran. Department of Orthopaedics, NJMS-UH Cancer Center, UMDNJ, USA

Unfolding of the gene expression program that converts precursor cells to osteoblasts is critically dependent on the nucleosome remodeling activity of the mammalian SWI/SNF complex. This ATPase-powered complex regulates stage-specific gene expression in all tissues. Understanding how it acts to maintain or advance specific stages of differentiation is basic to understanding molecular mechanisms of tissue development. The complex can be powered by either of two ATPases: BRM or the BRM-related gene product BRG1. We have recently shown that BRM-specific complexes restrain osteoblast differentiation, helping to maintain the committed precursor state until the pre-osteoblasts receive appropriate signals for differentiation (Flowers et al. 2009. J. Biol. Chem. 284:10067-75). In contrast, BRG1-containing SWI/SNF (also called BAF) generally acts to induce osteogenic genes.

BRG1 also participates in a related complex, designated PBAF. BAF and PBAF share most subunits, but can be distinguished by the choice of another component that also occurs as related alternatives: the ARID family subunits. These are large proteins containing interactive domains for associated proteins, as well as the ARID-motif, which specifies a DNA binding domain of loose specificity. SWI/SNF complexes contain ARID1A or ARID1B. PBAF contains ARID2. To determine whether the PBAF complex is required in osteoblast differentiation, we used an shRNA approach to target ARID2 in MC3T3-E1 pre-osteoblasts.

Cells stably depleted of ARID2 are sharply impaired for induction of the osteoblast specific marker alkaline phosphatase, and show delayed progression to a mineralization phenotype. BRG1-depleted cells are more severely impaired, showing essentially complete failure to differentiate. The results indicate that both BAF and PBAF complexes contribute to induction of the osteoblast phenotype.

Gene array analysis suggests that the BRG1-containing nucleosome remodeling complexes also play an important role in precursor cell commitment to the osteoblast lineage. Analysis of osteogenic gene expression in BRG1-depleted MC3T3-E1 cells reveals several genes expressed in pre-osteoblasts whose expression declines without BRG1. These include BMP4 and fibroblast growth factor receptor type-2 (FGFR2). Preliminary analysis of FGFR2 suggests that maintenance of its expression in pre-osteoblasts requires the PBAF complex.

***Disclosures: Fuhua Xu**, None.*

SA0223

See Friday Plenary number FR0223.

SA0224

See Friday Plenary number FR0224.

SA0225

See Friday Plenary number FR0225.

SA0226

Phosphorylation-Dependent SUMOylation Regulates the Activity of the αNAC Transcriptional Coactivator. Omar Akhouayri[1], Rene St-Arnaud*[2]. [1]Shriners Hospital for Childrent, Canada, [2]Shriners Hospital for Children & McGill University, Canada

To act as a transcriptional coactivator of c-Jun-dependent osteocalcin gene transcription in osteoblasts, αNAC shuttles between the cytoplasm and the nucleus. It has been shown that the subcellular localization of the protein is regulated through differential phosphorylation. We have identified an additional mode of post-translational modification of αNAC through covalent attachment of the Small Ubiquitin-like MOdifyer, SUMO. Since sumoylation has been shown to differentially impact on the stability, localization, and activity of transcriptional regulators, we have characterized the SUMO acceptor site on the protein and examined which parameters are affected by sumoylation of αNAC. We first used a commercial assay providing the components of the sumoylation cascade to show that recombinant αNAC could be sumoylated in vitro. Immunoprecipitation followed by immunoblotting with anti-SUMO antibodies then confirmed that αNAC is conjugated to SUMO1 in cultured osteoblasts and in calvarial tissue. The amino acid sequence of αNAC contains one copy of the composite 'phospho-sumoyl switch' motif, ΨKxExxS (where Ψ is a hydrophobic amino acid and K is the site of SUMO conjugation), that couples sequential phosphorylation and sumoylation. We have engineered site-specific mutants in which the putative lysine sumoylation site (K127) and the potential serine phosphoregulation site (S132) were mutated alone or in combination. Mutation K127R inhibited sumoylation, demonstrating that it is the primary SUMO conjugation site. Interestingly, mutation S132A reduced the sumoylation of αNAC, while the phosphomimetic S132D mutation increased it, confirming that the sumoylation of αNAC is regulated through differential phosphorylation of serine 132. The subcellular localization, half-life, or DNA-binding activity of αNAC were not affected by mutation at residues K127 or S132. Non-sumoylatable forms of αNAC (K127R, S132A, and K127R/S132D) were unable to coactivate c-Jun-mediated transcription, while the hyper-sumoylated S132D mutant had increased coactivating potential. Our studies characterized a novel post-translational modification of the αNAC coactivator and identified one of the rare transcriptional regulators whose activity is potentiated, not inhibited, by sumoylation. The characterization of the upstream kinase involved in the regulation of αNAC sumoylation will identify an additional pathway involved in the regulation of osteoblastic gene transcription.

***Disclosures: Rene St-Arnaud**, None.*

SA0227

Runx2 Is Necessary for Smurf1 Expression in Osteoblastic Cells. Jeong-Hwa Baek[1], Gwan-Shik Kim[2], Hyun-Mo Ryoo[3], Kyung Mi Woo[2], Kyunghwa Baek[2], Hye Lim lee*[2]. [1]Seoul National University School of Dentistry, South korea, [2]Seoul Nat'l University, South korea, [3]Seoul National University, School of Dentistry, South korea

Smurf1 is an E3 ubiquitin ligase and involved in degradation of BMP signaling molecules such as Smad1, Smad5 and Runx2. Previously we have reported that TNF-α stimulates Smurf1 expression via JNK activation and subsequent AP-1 binding to Smurf1 promoter in C2C12 cells. However, TNF-α–induced Smurf1 expression was not observed in Runx2-nulled mouse calvarial cells. Therefore, we investigated the role of Runx2 in Smurf1 expression. Runx2 overexpression induced basal Smurf1 expression and rescued TNF-α-mediated induction of Smurf1 in Runx2-nulled cells. In addition, neither Smurf1 nor Runx2 was expressed in C3H10T1/2 cells. However, Smurf1 expression was induced by exogenous Runx2 expression, not by c-Jun overexpression nor by TNF-α in these cells. Runx2 increased Smurf1 reporter activity in a dose-dependent manner. Studies using Smurf1 promoter mutants have shown that among 4 putative Runx2 binding sites (~2.7 kb) the most proximal one is important to Runx2-mediated Smurf1 expression. Runx2 directly bound to Smurf1 promoter region, and TNF-α enhanced Runx2 binding to Smurf1 promoter region, which was confirmed by ChIP assay. These results suggest that Runx2 is necessary for Smurf1 expression in osteoblastic cells.

***Disclosures: Hye Lim lee**, None.*

SA0228

See Friday Plenary number FR0228.

SA0229

The Osteocyte marker, Podoplanin, is Expressed in Transformed Osteoblasts and is Regulated by AP-1. Takeshi Kashima*[1], Akiko Kunita[2], Masashi Fukayama[2], Agamemnon Grigoriadis[3]. [1]Nuffield Orthopaedic Centre, United Kingdom, [2]University of Tokyo, Japan, [3]King's College London, United Kingdom

Podoplanin (E11 antigen) is a type-I transmembrane sialomucin-like glycoprotein that has been shown to be highly expressed in osteocytes both in vivo and in vitro, but not in active bone forming-osteoblasts or chondrocytes. The regulation of podoplanin expression is not well understood, although it has been reported recently that the c-Fos proto-oncogene directly regulates podoplanin expression in a skin cancer model. In this study, we aim to examine whether or not the AP-1 protein, c-Fos, upregulates podoplanin expression in transformed bone and cartilage cells, using previously isolated c-Fos-inducible MC3T3-E1 osteoblastic cells (AT9.2) and ATDC5 chondrogenic cells (DT12.4) as well as osteosarcoma cells derived from c-Fos transgenic tumors.

Induction of exogenous c-Fos in AT9.2 cells resulted in a stimulation of podoplanin expression as well as TGF-b1, a known c-Fos/AP-1 target gene. Western blot analysis of c-Fos transgenic osteosarcoma cell lines confirmed high podoplanin levels in cells overexpressing c-Fos. Further, immunohistochemical analysis showed that podoplanin was intensely positive in c-Fos osteosarcoma xenograft tumor cells. To clarify the cell type specificity of podoplanin expression, immunohistochemistry was performed in normal bone and primary c-Fos transgenic osteosarcomas. Podoplanin was expressed in osteogenic tumor cells and in cells within the tumor bone matrix resembling osteocytes. All tumor cells strongly expressed c-Fos protein as well as TGF-b1. Interestingly, no podoplanin expression was observed in chondrogenic areas within the tumors, and this was confirmed by the lack of correlation between c-Fos and podoplanin expression in c-Fos-inducible DT12.4 chondrocytes.

These data imply that c-Fos and TGF-b1 play a role in the regulation of podoplanin expression in c-Fos overexpressing / transformed osteoblasts, and suggest that the specificity of podoplanin expression is expanded along the osteogenic lineage in pathologic osteoblasts.

***Disclosures: Takeshi Kashima**, The Japanese Ministry of Education, Culture, Sports, Science and Technology, 2*

SA0230

The RUNX2 Cistrome Defines a Regulatory Target Genome Responsible for the Osteoblast Phenotype. Mark Meyer*, J. Pike. University of Wisconsin-Madison, USA

RUNX2 is a master regulator of osteoblast differentiation and function whose primary role is to integrate the complex activities of a collection of transcription factors through target genes and multiple signaling pathways. While many osteoblast genes are targets of RUNX2, the RUNX2 regulome in osteoblast precursors has not been assessed. To define this set of RUNX2-responsive genes, we conducted a ChIP coupled to microarray (ChIP-chip) and sequencing (ChIP-seq) analysis of RUNX2

binding activity on a genome-wide level in mouse MC3T3-E1 cells and correlated these sites of RUNX2 action with enhancer-specific histone marks. RUNX2 was found to be pre-bound to approximately 4822 sites on the mouse genome. While 15% of these sites were within 5 kb of promoters, most were located within introns (36%) or at striking distances (41%) from transcriptional start sites of regulated genes. Two or more binding sites were frequently observed at target genes and over 70% contained a RUNX2 response element. The majority of these sites correlated with elevated levels of histone H4 acetylation, a covalent mark of regulatory activity. Interestingly, RUNX2 binding was specifically observed at both RUNX2 promoters, suggesting that RUNX2 auto-regulates its own expression in osteoblasts. RUNX2 binding was also evident at known sites on genes that were previously characterized as RUNX2 targets, including *Bglap2*, *Spp1*, *Alkp*, *Col1a1* and *Fgf18*, thereby validating the many additional sites found to be direct targets of RUNX2 action. RUNX2 was also found at genes involved in cell cycle control, including *Ccnd1*, *Ccnd2* and *Cdk1a*. Perhaps most interesting was the finding that RUNX2 localized directly to a surprisingly large repertoire of downstream transcription factor genes involved in osteoblast function. These include genes for *Sox9* (but not *Sox5* or *6*), *Sp7* and *Atf4* (but not *Atf1* or *2*) but also genes for *Clebpα,* β and δ, *Runx2* isotype genes *1* and *3*, *Vdr*, *c-Fos*, *c-Jun* and *Nfatc1*. We also conducted genome-wide ChIP-seq analysis for C/EBPβ and the $1,25(OH)_2D_3$-activated VDR/RXR heterodimer, two transcription factors known to interact directly with RUNX2. Interestingly, while C/EBPβ bound to over 6440 sites in the genome, 1704 of those sites were associated with pre-bound RUNX2. A similar relationship was found with VDR/RXR. We conclude that RUNX2, through its actions on multiple target genes, is indeed a master regulator of the osteoblast phenotype.

***Disclosures: Mark Meyer**, None.*

SA0231

Cell Surface ATP Synthase: A Novel Mechanism for Extracellular ATP synthesis in Osteoblasts. Shyama Majumdar*[1], Vimal Gangadharan[1], Kirk Czymmek[2], Randall Duncan[1]. [1]University of Delaware, USA, [2]University of Delaware & Delaware Biotechnology Institute, USA

ATP, the energy currency of a cell, has many functions other than providing cellular energy; including extracellular signaling in a variety of tissues. We, and others, have previously demonstrated that osteoblasts, osteocytes and osteoclasts use vesicular ATP release to respond to numerous stimuli, including mechanical loading. In addition, these cells have significant basal release of ATP. However, the mechanism for basal release, as well as packaging of ATP into vesicles, remains unknown. We hypothesize that F_1F_oATP synthase is present on the cell membrane of osteoblasts and is functionally active for basal signaling in unstimulated osteoblasts. Furthermore, we hypothesize that ATP synthase is present in cytosolic vesicular membranes to package ATP in preparation for stimulated release. Immunofluorescence, cell surface protein isolation and membrane fractionation techniques were employed to demonstrate the presence of cell surface ATP synthase in MC3T3-E1 pre-osteoblasts as well in primary mouse calvarial osteoblasts. Using a luminescence based ATP assay to measure extracellular ATP synthesized in the presence of varying doses of extracellular ADP, we found that ATP synthase produces ATP in a dose dependent manner and that this synthesis is attenuated when the functional α and β subunits are blocked using blocking antibodies or angiostatin. We have demonstrated that membrane ATP synthase uses a similar hydrogen ion gradient to the mitochondrial ATP synthase by creating a hydrogen ion gradient across the cell membrane. Reducing extracellular pH significantly increased ATP synthesis. To determine the role of membrane ATP synthase during mechanical stimulation, we subjected MC3T3-E1 cells to fluid shear stress (FSS). ATP synthase protein levels increased within 1 to 5 minutes of application of fluid shear stress indicating a mechanism whereby additional ATP synthase is incorporated into the membrane in response to FSS. These data suggest that ATP synthase is present on the cell membrane of osteoblasts and is functionally active. We also predict ATP synthase is present on the vesicular membrane and may be responsible for ATP packaging into vesicles. These data suggest a novel mechanism for the basal release of ATP and the regulation of purinergic signaling in bone cells.

***Disclosures: Shyama Majumdar**, None.*

SA0232

See Friday Plenary number FR0232.

SA0233

Heterodimerization of Purinergic ATP Receptors in Osteoblasts. Roy Choi*, Gallant Chan, Karl Tsim. The Hong Kong University of Science & Technology, Hong kong

Purinergic ATP receptor superfamily contains P2Y (G-protien-coupled receptor) and P2X (ligand-gated ion channel) subfamilies. The metabotropic P2Y receptors have been shown to involve numerous physiological processes, such as neurotransmission, neuromodulation, immunomodulation, and bone formation. Among them, activation of P2Y1 receptor (one subtype of P2Y subfamily) indirectly increases osteoclast formation and bone resorption via the stimulation of RANKL in osteoblasts, while application of P2Y2 receptor agonist blocks bone formation process, suggesting that the extracellular nucleotides can function locally as a crucial negative modulator in bone metabolism. In the present study, we focused on the interaction of P2Y1 and P2Y2 receptors in osteoblasts. Specifically, the possibility of forming P2Y1-P2Y2 receptor heterodimer in osteoblasts would be discussed, which could be used to support the significance and physiological function of receptor dimerization within P2Y receptor subfamily.

Acknowledgement: This study was supported by the RGC grant (660409) to RCYC.

***Disclosures: Roy Choi**, None.*

SA0234

See Friday Plenary number FR0234.

SA0235

See Friday Plenary number FR0235.

SA0236

See Friday Plenary number FR0236.

SA0237

Adipogenic Cells as Primary Target of Strontium? Carole FOURNIER*[1], Anthony Perrier[2], Laurence Vico[3], Alain Guignandon[1]. [1]INSERM U890, France, [2]Laboratoire de Biologie du Tissu Osseux, France, [3]University of St-Etienne, France

Strontium Ranelate is used to treat osteoporosis and its ability to reduce fracture risks is clearly established. If Strontium (Sr) effects are late and positive on osteoblastogenesis and/or early and negative on adipogenesis is still an open question. Our work hypothesis is that SR inhibits commitment of stromal cells towards adipogenesis by regulating the balance between Runx2 and PPARy2 master genes. We treated multipotent mesenchymal cell (C3H10T1/2) with various doses of Sr (0 to 3mM) for limited durations (max 5 days) in various differentiation media (neutral, osteoblastic, adipogenic, or both). Whatever the conditions, we found that Sr inhibits PPARy2 expression without major Runx2 alteration. After a one-day-culture PPARy2 inhibition was dose-dependent and reached 80% of inhibition at 3mM of Sr in an adipogenic context. This observation may explain why Sr could be particularly efficient in physiological challenges enhancing bone marrow adiposity and/or oxidative stress such as aging, ovariectomy, and immobilisation. In an attempt to mimic such challenges we treated our cells with rosiglitazone (Rosi) a potent PPARy2 co-activator. We confirmed that Sr (3mM) was able to reduce Rosi-induced adipogenic differentiation by downregulating PPARγ2 expression by 50%. We also showed by immunodetection that PPARγ2 located in the nucleus of preadipocytes, remains in the cytoplasm under 3mM of Sr. At day 5, C3H10T1/2 treated with both Rosi and 3 mM Sr showed expression levels of adipogenic genes (PPARγ2 and C/EBP) and osteoblastic genes (Runx2 and PAL) similar to those of uncommitted cells as seen in C3H10T1/2 cultivated in αMEM alone. We also showed that Rosi alone stimulates catalase (a PPARγ-dependent gene reducing oxidative stress) expression by 300%. Further treatment with 3 mM strontium reduces catalase expression to the level of uncommitted cells. In the same culture conditions, we observed that Rosi induces an upregulation of SOD1 and 2 (cytosolic and mitochondrial antioxidant enzymes, respectively) and that further strontium treatment normalizes these alterations. The upregulation of antioxidant enzymes under Rosi likely reflects the important production of reactive oxygen species, which is counteracted by Sr treatment. These complex changes suggest that strontium acts in part through PPARγ2, key controller of the osteoblastic/adipogenic balance in which actors of oxidative stress is involved.

***Disclosures: Carole FOURNIER**, None.*

SA0238

See Friday Plenary number FR0238.

SA0239

Withdrawn

SA0240

See Friday Plenary number FR0240.

SA0241

Differences in Oxygen Consumption Rate of Osteoblast Lineage Cells in Rats Bred for High and Low Aerobic Capacity. Riyad J. Tayim*[1], Jacqueline Cole[2], Neil R. Halonen[1], Grant C. Goulet[1], Lauren G. Koch[3], Steven L. Britton[3], Ronald Zernicke[2], Andrea Alford[2], Kenneth Kozloff[1]. [1]University of Michigan Department of Orthopaedic Surgery, USA, [2]University of Michigan, USA, [3]University of Michigan Department of Anesthesiology, USA

Cells of the osteoblast lineage are particularly responsive and sensitive to their local oxygen environment, and their ability to improve their intracellular aerobic metabolism in response to exercise may have important downstream effects on bone cell function and skeletal phenotype. In this study, we tested the influence of inherent aerobic capacity on bone metabolism independent of applied mechanical loading. Using the Koch-Britton selective breeding rat model of high capacity (HCR) and low capacity (LCR) runners, an intrinsic 5-to-7 fold functional genomic difference in aerobic exercise capacity exists between non-trained animals after 20 generations of selection. HCR have consistently demonstrated heightened skeletal mineralization and osteoblast activity correlated with their inherent aerobic capacity. In the present study, we compared cellular oxygen metabolism between HCR and LCR osteoblast lineage cells during osteoblast differentiation in vitro. Bone marrow stromal cells (BMSCs) were harvested from the femora and tibiae of 8.5 month, female, generation 25 rats (N=3), and were cultured under standard conditions for 12 days followed by osteoblast differentiation. The Seahorse Bioscience XF24 Analyzer was used to assess cellular aerobic capacity on Day 0, 3, 7, 10, 14, 21, and 28 of the differentiation time course. Basal respiration and glycolysis were assessed and normalized to cell number through time-resolved measures of oxygen consumption rate (OCR) and extracellular acidification rate (ECAR). OCR and OCR/ECAR ratios in both HCR and LCR cells suggested less glycolytic and more aerobic cell metabolism with differentiation and matrix production followed by a return to glycolysis as cells became engulfed in their ECM. HCR cells consumed less oxygen per cell than LCR through Day 14, suggesting a more efficient phenotype. With the addition of oligomycin, HCR cells showed an increase in percent oxygen consumed for ATP production at Day 14 vs. LCR, but this pattern was reversed by Day 28. The HCR/LCR selective breeding rat model allows us to investigate how intrinsic differences in aerobic metabolism result in differences in cellular aerobic metabolism within osteoblast lineage cells. Thus we are able to define cellular parameters that may be responsible for the heightened mineralization and osteoblast activity found in these animals.

***Disclosures: Riyad J. Tayim**, None.*

SA0242

Generation and Characterization of iPS Cells from CMD Patients and Healthy Controls. I-Ping Chen*[1], Xiaonan Xin[1], Mary-Louise Stover[2], Shuning Zhan[2], Jonathan Kantor[3], Ernst Reichenberger[1], Alexander Lichtler[1]. [1]University of Connecticut Health Center, USA, [2]UCHC, USA, [3]North Florida Dermatology, USA

Studying rare genetic bone disorders is clinically significant due to the lifetime debilitating impact they have on patients and limited treatment options for these disorders because little of their pathogeneses is known. Research on rare disorders is not only beneficial for future treatment of patients, but contributes to the understanding of important biological mechanisms in bone development and remodeling. Obstacles for research in this field include unavailability of tissue specimens and lack of animal models. Rapid advances in induced pluripotent stem (iPS) cell biology opened new avenues to study bone cells from such patients.

We propose to use patient-specific iPS cells to investigate craniometaphyseal dysplasia (CMD), a rare genetic bone disorder characterized by progressive thickening of craniofacial bones and widening of metaphyses in long bones. Here, we report our first success of generating and characterizing iPS cells from human skin fibroblasts and from SHEDs (stem cells from human exfoliated deciduous teeth) of CMD patients and healthy controls. Methods for generating human iPS cells from fibroblasts and SHEDs are well established. Reprogramming of somatic cells into iPS cells was performed by retroviral transduction of Oct3/4, Sox2, Klf4 and c-Myc with the addition of a vector expressing Lin28, which contains a GFP cassette to monitor transduction efficiency. Both fibroblasts and SHEDs were reprogrammed into iPS cells. Reprogrammed cells had an indistinguishable morphology from H1 and H9 human embryonic stem (hES) cells. These iPS cells expressed hES cell markers SSEA-4, TRA-1-60, TRA-1-81, Oct4 and Nanog, as shown by RT-PCR and immunocytochemistry. The pluripotency of these iPS cells is further supported by in vitro embryoid body (EB) formation. Assays for testing in vivo differentiation capability of these iPS cells by teratoma formation are in progress.

Previously, we have presented the first CMD knock-in mouse model replicating many characteristics of human CMD. We use this mouse model to generate hypotheses for subsequent iPS-based human studies. Ultimately, we plan to investigate the cellular and molecular basis of CMD in the human system, which is only possible with a sufficient supply of human cells. We expect that combining mouse data with findings generated from the use of human iPS cell technology will significantly add to our understanding of CMD pathology and will establish a system to study other craniotubular disorders.

***Disclosures: I-Ping Chen**, None.*

SA0243

Integrin-linked Kinase Contributes to Mechanical Regulation of GSK3β in Mesenchymal Stem Cells. Jacob Thomas[1], Natasha Case*[1], Maya Styner[1], Buer Sen[2], Zhihui Xie[1], Janet Rubin[1]. [1]University of North Carolina, Chapel Hill, School of Medicine, USA, [2]University of North Carolina At Chapel Hill, USA

GSK3β is emerging as a critical mediator of mechanical responses in mesenchymal stem cells (MSC). Mechanical strain causes inactivation of GSK3β, resulting in stabilization of β-catenin levels and indirectly increasing COX2 expression via NFATc1. Importantly, both β-catenin and COX2 influence MSC differentiation. The signaling molecules required for mechanical inhibition of GSK3β activity via phosphorylation are unknown. AKT, known to decrease GSK3β activity in response to insulin, may also participate in mechanical effects as strain rapidly activates this molecule. Integrin-linked kinase (ILK) can also directly inhibit GSK3β activity, in addition to indirect effects via activation of AKT. Here we wished to define proximal events whereby mechanical stimulation regulates both AKT and GSK3β activity in marrow-derived MSC. We compared strain to insulin, which is known to activate PI3K. Mechanical strain (2%, 0.17Hz, 30 min) caused phosphorylation of AKT at both Thr 308 and Ser 473. In the presence of the PI3K inhibitor LY294002 (20 μM), strain induction of T308~P was inhibited, but S473~P was unimpaired. Importantly, mechanical inactivation of GSK3β, measured by Ser9~P, was not blocked by PI3K inhibition, nor was the effect of strain to induce a 3X increase in COX2 mRNA. This suggested that strain regulation of GSK3β was largely PI3K independent. This contrasts with effects of insulin, which also phosphorylates AKT at both T308 and S473: inhibition of T308~P with LY294002 almost completely ablated insulin-induced GSK3β phosphorylation. To assess whether ILK was involved in PI3K independent effects of strain, siRNA (100 nM) to ILK was used. When ILK was decreased by ~70%, strain still induced AKT T308~P, but phosphorylation of S473 was absent. This may indicate that ILK is largely responsible for strain induced GSK3β inhibition, and may explain the persistence of strain effects in the presence of PI3K inhibition. In further work we hope to confirm that ILK activation is a primary response to strain, and plays a critical role in regulating MSC lineage selection.

***Disclosures: Natasha Case**, None.*

SA0244

Lamin A/C is Required during Osteoblast Differentiation to Facilitate Nuclear Mobility and Function of Runx2. Gustavo Duque*[1], Christopher Vidal[1], Lee Wei Li[2], Li Sze Yeo[3], Diane Fatkin[3]. [1]University of Sydney, Australia, [2]University of Sydney, Nepean Clinical School, Australia, [3]Molecular Cardiology & Biophysics Division, Victor Chang Cardiac Research Institute, Australia

We have recently demonstrated that inhibition of the lamin A/C (lmna) gene inhibits osteoblastogenesis *in vitro* and results in severe osteoporosis *in vivo*. However, the mechanism by which lamin A/C regulates osteoblastogenesis remains unknown. Lamin A/C is a protein of the nuclear envelope, which interacts with multiple nuclear proteins including Runx2, an important transcription factor in osteoblastogenesis. Low levels of lamin A/C are associated with impaired Runx2 transcriptional activation *in vitro*. Using lmna knockout (*lmna-/-*) mice, we undertook studies to characterize the changes in protein interactions in the nucleus in the absence of lamin A/C activity and their potential effect on Runx2 activation *in vivo*. We focused on MAN1, an inner nuclear membrane protein that not only physically interacts with lamin A/C but also has been associated with osteopoikilosis, a rare type of hyperostosis found after loss of function of the MAN1 gene. Antibodies against MAN1 were able to co-immunoprecipiate Runx2 from marrow cells extracts obtained from *lmna-/-* mice demonstrating that, in the absence of lamin A/C, they reside in the same complex. In contrast, co-immunoprecipitation between MAN1 and Runx2 was not found in bone marrow cells obtained from WT controls. Furthermore, absence of Lamin A/C determined a reduction in Runx2 nuclear complex activity identified by ELISA and co-immunoprecipitation analyses. We further examined the consequences of lamin A/C knockout on in situ nuclear organization of MAN1 and Runx2 in bone marrow cells using three dye staining confocal microscopy. We established that in WT mice lamin A/C and MAN1 expression closely overlap and the subnuclear distribution of Runx2 shows a clearly punctuated pattern. In contrast, in bone marrow cells of *lmna-/-* mice, Runx2 lacks a punctuated pattern and closely overlaps the distribution of MAN1. In summary, in absence of lamin A/C, MAN1 and Runx 2 are structurally inseparable thus affecting Runx2 function in osteoblastogenesis. We conclude that the role of lamin A/C in osteoblastogenesis is mediated by a novel molecular mechanism in which the presence of lamin A/C is required to prevent the sequestration of Runx2 by MAN1 in the subnuclear region, thus facilitating Runx2 mobility and function.

***Disclosures: Gustavo Duque**, None.*

SA0245

See Friday Plenary number FR0245.

SA0246

See Friday Plenary number FR0246.

SA0247

Withdrawn

SA0248

See Friday Plenary number FR0248.

SA0249

Revitalization of Bone Allografts by Murine Periosteal Cells Expressing BMP2 and VEGF. Nick van Gastel*[1], Maarten Depypere[2], Scott Roberts[3], Ingrid Stockmans[1], Sophie Torrekens[1], Jan Schrooten[4], Frederik Maes[2], Frank Luyten[5], Geert Carmeliet[6]. [1]Laboratory of Experimental Medicine & Endocrinology, Katholieke Universiteit Leuven, Belgium, [2]Department of Electrical Engineering (ESAT/PSI), Katholieke Universiteit Leuven, Belgium, [3]K.U.Leuven, Belgium, [4]Department of Metallurgy & Materials Engineering, Katholieke Universiteit Leuven, Belgium, [5]University Hospitals KU Leuven, Belgium, [6]Katholieke Universiteit Leuven, Belgium

To date, autologous bone transplantation remains the therapy of choice to treat large bone defects. Despite numerous advantages, its use is restricted by major drawbacks, including limited availability and donor site morbidity. Bone allografts lack these shortcomings and provide the strength and flexibility needed in load-bearing applications. However, allografts are not osteogenic, due to their acellular nature, which prevents integration into the host bone. Here, we show that murine periosteal cells, transiently expressing bone morphogenetic protein 2 (BMP2) and vascular endothelial growth factor (VEGF) and seeded on a segmental allograft, can substitute for the absent periosteum and improve callus formation and allograft incorporation.

First, a protocol was established to isolate periosteal cells from long bones of adult mice. Flow cytometric analysis revealed a substantial higher number of mesenchymal stem cells (MSCs) in the periosteal population as compared to bone marrow stromal cells. In addition, periosteal cells showed trilineage differentiation potential (osteogenic, chondrogenic and adipogenic) and when implanted ectopically in mice they formed a substantial amount of bone.

To enhance their therapeutic potential, periosteal cells were transduced with adenoviral vectors encoding BMP2, VEGF or GFP. Increased secretion of growth factors in the culture medium persisted for at least 14 days, as demonstrated by ELISA. Cells expressing BMP2 and VEGF were seeded onto 4mm cortical allografts and implanted into femoral defects in mice. Autografts, empty allografts and allografts with GFP-transduced cells served as controls. After 4 weeks, bone healing was analyzed using μCT and histology. Defects treated with empty allografts or grafts with GFP-transduced cells showed little callus formation and little to no remodeling of the graft. Grafts seeded with BMP2- and VEGF-transduced periosteal cells however induced the formation of a large callus, comparable to autografts, accompanied by manifest graft remodeling.

In conclusion, the successful isolation of adult mouse periosteal cells could help to further explore the role of this cell population using the available genetic mouse models. Moreover, establishing an artificial periosteum consisting of periosteal cells expressing BMP2 and VEGF considerably improves allograft incorporation into large bone defects in mice.

***Disclosures: Nick van Gastel**, None.*

SA0250

Role of GILZ in TNF-α-Mediated Inhibition of Marrow Mesenchymal Stem Cell Osteogenic Differentiation. Xing-Ming Shi, Nianlan Yang, Linlin He*. Medical College of Georgia, USA

Tumor necrosis factor-alpha (TNF-α) is a potent proinflammatory cytokine and it inhibits osteoblast differentiation while stimulating osteoclast differentiation and bone resorption. TNF-α activates MAP kinase pathway leading to inhibition of osterix (Osx) expression. TNF-α also induces the expression of E3 ubiquitin ligase protein Smurf1 and Smurf2 and promotes degradation of Runx2, another key transcription factor regulating osteoblast differentiation and bone formation. We showed previously that overexpression of glucocorticoid (GC)-induced leucine zipper (GILZ) enhances osteogenic differentiation of bone marrow mesenchymal stem cells (MSCs). We and others also demonstrated that GILZ is a GC effect mediator and it mimics GCs' antiinflammatory actions. In this study, we asked whether GILZ retains its osteogenic activity while mediating GC antiinflammatory action. We infected MSCs with GILZ-expressing retroviruses and exposed the cells to TNF-α in an osteogenic environment. Our results show that overexpression of GILZ can override the inhibitory effect of TNF-α on MSC osteogenic differentiation as determined by Alizarin red staining of mineralized bone nodules. Real-time qRT-PCR and Western blot analyses show that overexpression of GILZ antagonized the inhibitory effect of TNF-α on Osx and Runx2 mRNA and protein expression. Finally, we demonstrate that GILZ antagonizes TNF-α effect on Osx expression by inhibiting TNF-α-induced MAP kinase activation. Together, these results indicate that GILZ is capable of dissociating the desired anti-inflammatory GC effects from its adverse bone effects and suggest that GILZ may have therapeutic potential for preventing bone loss caused by chronic inflammation such as rheumatoid arthritis.

***Disclosures: Linlin He**, None.*

SA0251

Zolendronate Induce Expression of Runx2 to Promote Osteogenic Commitment of Human Periodontal and Pulp Cells. Harunur Rashid*[1], Nachiket Saoji[1], Somsak Sittitavornwong[1], Haiyan Chen[1], Farah Ghori[1], Huw Thomas[1], Soraya Gutierrez[2], Amjad Javed[1]. [1]University of Alabama at Birmingham, USA, [2]Universidad de Concepcion, Chile

Bisphosphonates (BP) are widely used to treat osteoporosis and malignant bone metastasis but osteonecrosis of the jaws and musculoskeletal pain has recently emerged as a significant complication in a subset of patients receiving these drugs. BP inhibits osteoclast mediated bone resorption however its action on other skeletal cells remains largely unknown. We established primary PDL and Pulp cells from non-infected, impacted third molars of healthy individuals to explore the impact of PB treatment on cell growth and differentiation. We determined that a 14-fold dilution of clinically used dose of zolendronate is non cytoxic in exvivo cultures. Exposure of PDL and pulp cells to BP caused a significant inhibition of cell proliferation consistent with its action on osteoclast. However, BP strongly enhanced osteogenic differentiation of both PDL and Pulp cells as evidenced by progressive increase in ALP activity, matrix synthesis and mineral deposition. For a molecular understanding of how BP stimulated osteoblast differentiation, we analyzed gene expression profile by microarray analysis. Interestingly, 70% (78 of 112) of the osteogenic genes were significantly induced and 14% were down regulated upon BP treatment. These changes were noted for all the key ECM genes, considered markers of specific stages of osteoblast differentiation (ALP; 19-fold, Col1a; 19-fold, BSP; 11-fold, DSPP 42-fold, OC; 48-fold, SOST; 103-fold). BP also enhanced the expression of osteogenic regulatory molecules (FGF2; 20-fold, BMP7; 43-fold, TGFβ; 8-fold), their receptors and transducers (TGFβR; 102-fold, BMPR; 12-fold, SMAD9; 18-fold). Moreover, expression of essential transcription factors and regulators of osteoblast differentiation were robustly increased (Runx2; 21-fold, Sox9; 41-fold, Msx2; 3-fold). Similar pattern of gene profile was noted in Pulp cells, indicating BP target a common regulatory pathway in tooth derived mesenchymal progenitors. The upregulation of selected osteoblast marker genes was further confirmed by RT-PCR from primary PDL and Pulp cells of three independent individuals. EMSA and Immunofluorescence studies demonstrated that BP enhanced both DNA binding and nuclear accumulation of Runx2 protein. Finally, BP stimulated Runx2 mediated activation of the OC promoter. Taken together, our studies demonstrate that, bisphosphonate activate program of osteoblast differentiation by enhancing functional competency of Runx2 in tooth derived mesenchymal cells.

***Disclosures: Harunur Rashid**, None.*

SA0252

Glucocorticoids Attenuate Bone Turnover, but do not Appear to Affect Chondrocytes In Vitro. Kim Henriksen*[1], Kim Vietz Andreassen[1], Morten Karsdal[1], Anne-Christine Bay-Jensen[2]. [1]Nordic Bioscience A/S, Denmark, [2]Nordic Bioscience, Denmark

Glucocorticoids are known to attenuate bone formation in vivo leading to decreased bone volume and increased risk of fractures, whereas effects on the joint tissue are not known. This study aimed at characterizing the effect of glucocorticoids on osteoclasts and osteoblasts, as well as the closely related chondrocytes. We used CD14+ monocytes cultured in the presence of M-CSF and RANKL to investigate the effect of glucocorticoids on different osteoclastic parameters. We measured TRACP activity and Calcium release as indices of osteoclast number and activity. 2T3 preosteoblastic cells we used to characterize the effects of glucocorticoids on bone formation, either in the presence or absence of BMP-2. Alizarin Red was used to measure nodule formation, ALP activity as an indicator of osteoblastogenesis. Bovine full depth cartilage explants were cultured with or without TNF-a, OSM and IGF-1 to characterize the effects of glucocorticoids on cartilage turnover. Collagen type II degradation was measured by CIIMB, and aggrecan degradation by 373-G1. Safranin O staining was used to investigate proteoglycan content in sections of the cultured explants. In all assays Alamar Blue was used as an indicator of viability. DEX and PRED dose-dependently inhibited osteoclastogenesis by promoting cell death. For mature osteoclasts, low doses of GLUC induced bone resorption short term, whereas high doses and continued exposure led to osteoclast death. In osteoblasts glucocorticoids induced cell death in the non-stimulated cells. For BMP-2 stimulated cells; we found that GLUCs augmented nodule formation, while still reducing cell viability. In cartilage we found that GLUCs were unable to alter cartilage turnover, although at high concentrations a minor reduction in safranin O staining intensity was observed. In summary, using highly robust models of bone and cartilage turnover, we have shown that the effects of glucocorticoids on bone depend very much in the cell targeted, i.e. activated osteoblasts are further activated by GLUC, whereas non-activated cells undergo cell death. In cartilage no apparent effects were observed, indicating that cartilage may not possess glucocorticoid receptors, or that these are

not active. We believe that these model systems are highly relevant for the continued development of glucocorticoid analogues without the detrimental effect on bone.

***Disclosures: Kim Henriksen**, Nordic Bioscience, 3*

SA0253

See Friday Plenary number FR0253.

SA0254

See Friday Plenary number FR0254.

SA0255

See Friday Plenary number FR0255.

SA0256

Bone-wasting Cytokines are Up-regulated in Fragility Fractures: Role of Bone and Bone Marrow Cells. Patrizia D'Amelio*[1], Ilaria Roato[2], Lucia D'Amico[2], Luciana Veneziano[3], Elena Suman[3], Francesca Sassi[3], Giuseppina Bisignano[3], Giancarlo Isaia[1]. [1]University of Torino, Italy, [2]CeRMS (Centre for Research & Medical Studies), San Giovanni Battista Hospital, Italy, [3]Gerontology Section, Department of Surgical & Medical Disciplines, University of Torino, Italy

The roles of bone and bone marrow cells in bone turnover control and the amounts of cytokines they produce are not clear. This study compares cytokines production in patients with a fragility fracture and those with osteoarthritis (OA).

We evaluated 52 femoral heads from women subjected to hip-joint replacement surgery for femoral neck fractures due to low-energy trauma (37), or for OA (15). Total RNA was extracted from both bone and bone marrow, and quantitative PCR was used to identify RANKL, OPG, M-CSF, TGFβ, DKK-1 and SOST expression.

We found an increase of RANKL/OPG in bone marrow from fractured patients (Fig 1 A), as previously reported for the early post-menopause (1), whereas this parameter was similar in the bone (Fig.1B). It may thus be supposed that bone marrow cells are the main drivers of osteoclast formation and activity. Both RANKL and OPG were up-regulated in bone marrow from the fractured patients. The increase in OPG may be interpreted as an attempt to inhibit RANKL, and as a sign of increased bone turnover.

This pro-osteoclastogenic cytokine profile was accompanied by an increase in the Wnt pathway inhibitor DKK-1 in bone (Fig.2A) and bone marrow (Fig.2B), which reduces osteoblast activity in fractured patients. Osteoporosis may perhaps be regarded as both an osteoblast and an osteoclast disease.

TGFβ was slightly (about 1.5%) increased in OA bone (Fig.3 A). The role of TGFβ in controlling bone turnover is not completely clear. As expected, more was produced by bone marrow (Fig.3 B) with no significant difference between the two sets of patients (data not shown). Since OA chondrocytes produce more TGFβ, the small increase observed in OA bone may be due to their contribution.

We observe no difference in fractured as respect to OA patients in M-CSF and SOST expression.

In conclusion, we have demonstrated the important contribution of bone marrow cells in the regulation of bone turnover. Bone marrow from fractured patients produces more RANKL than that from patients with OA, whereas bone from fractured patients expresses more DKK-1. The cytokine pattern is thus shifted towards osteoclast activation and osteoblast inhibition in patients with a fragility fracture.

REFERENCES.
1. Eghbali-Fatourechi G, et al. J Clin Invest. 2003; 111:1221-30.

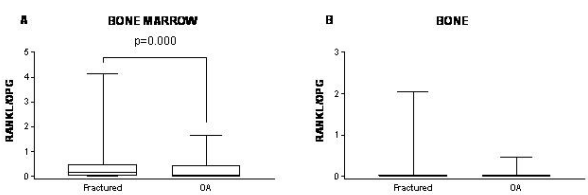

Figure 1. RANKL/OPG is higher in fractured patients.
A. Box and whisker plot represents RANKL/OPG measured in bone marrow in fractured compared to OA patients. The p value indicated was calculated with the Mann-Whitney U test after correction for age
B. As in A: RANKL/OPG measured in bone
Graphs represent the median, the upper and the lower quartile and the interquartile range calculated for all the data set.

Figure 1

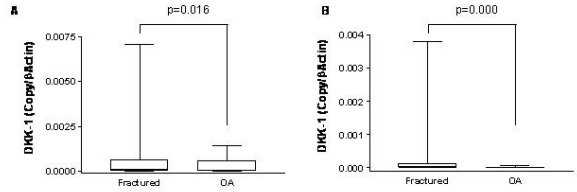

Figure 2. DKK-1 production in bone and bone marrow from fractured and OA patients.
A. Box and whisker plot represents DKK-1 measured in bone in fractured as respect to OA patients. The p value indicated was calculated by means of Mann-Whitney U test after correction for age
B. As in A: DKK-1 measured in bone marrow.
Graphs represent the median, the upper and the lower quartile and the interquartile range calculated for all the data set.

Figure 2

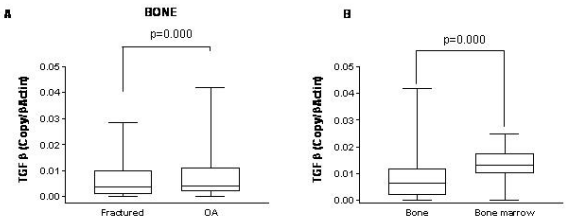

Figure 3. TGFβ production in bone and bone marrow from fractured and OA patients.
A. Box and whisker plot represents TGFβ measured in bone in fractured as compared to OA patients. The p value indicated was calculated by means of the Mann-Whitney U test after correction for age
B. Box and whisker plot represents TGFβ measured in bone marrow and in bone of all the samples. The p value indicated was calculated by means of Wilcoxon's test.
Graphs represent the median, the upper and the lower quartile and the interquartile range calculated for all the data set.

Figure 3

***Disclosures: Patrizia D'Amelio**, None.*

SA0257

Role of T Cells in the Activation of Osteoclastogenesis in Phenylketonuria Patients. Ilaria Roato*[1], Lucia D'Amico[2], Francesco Porta[3], Alessandro Mussa[3], Marco Spada[4], Riccardo Ferracini[5]. [1]CeRMS, Center for Experimental Research & Medical Studies, A.O.U. San Giovanni Battista, Italy, [2]CeRMS, Italy, [3]Department of Pediatrics, University of Turin, Italy, [4]Department of Pediatrics, University of Torino, Italy, [5]Department of Orthopaedics, A.O.U. San Giovanni Battista, Italy

Phenylketonuria (PKU) is a rare inborn error of metabolism commonly complicated by a progressive bone impairment of uncertain etiology, as documented by both ionizing and non- ionizing techniques. We studied osteoclastogenesis and T cell activation state in 40 PKU patients, considering their bone condition and metabolism in an attempt to elucidate the pathogenesis of bone damage. Peripheral blood mononuclear cell (PBMC) cultures were performed to study osteoclastogenesis, adding or not recombinant human monocyte-colony stimulating factor (M-CSF) and receptor activator of NFκB ligand (RANKL). TNF-a, RANKL and OPG were dosed in cell culture supernatants by ELISA. RANKFc and anti-TNF-a were added in some experiments to investigate their ability to inhibit osteoclastogenesis. T cell activation state was analyzed evaluating CD69 and CD25 expression by flow citometry. Bone conditions and the phenylalanine levels in PKU patients were clinically evaluated.

PKU patients disclosed an increased osteoclastogenesis compared to healthy controls, both in unstimulated and M-CSF/RANKL stimulated PBMC cultures. These OCs formed resorbing lacunae on the mineralized supports used to test OC activity. We dosed higher TNF-a levels in PKU patients than in healthy controls. RANKL levels were detected both in PKU patients and in healthy controls cultures, but they were higher in patients than in controls. OPG levels were not statistically different between patients and controls, but the RANKL/OPG ratio was higher in PKU patients, explaining the spontaneous osteoclastogenesis in the unstimulated cultures of patients. The addition of the specific antagonist RANK-Fc inhibited osteoclastogenesis, whereas anti-TNF-a failed to inhibit it. RANKL was produced by T and B cells both in patients and in controls, but T cells from patients resulted more active than ones from controls. Osteoclastogenesis in PKU patients was inversely related to bone condition assessed by Quantitative Ultrasound and directly related to non-compliance to therapeutic diet reflected by hyperphenylalaninemia.

Spontaneous osteoclastogenesis is present in PKU patients and correlates with hyperphenylalaninemia, suggesting its role in the pathogenesis of bone impairment in PKU. Osteoclastogenesis is dependent on RANKL, which is produced by T and B cells, suggesting a direct involvement of immune system in the bone damage of PKU patients.

***Disclosures: Ilaria Roato**, None.*

SA0258

See Friday Plenary number FR0258.

SA0259

Comprehensive Analysis of Epigenetic Role of TGF-beta in RANKL-induced Osteoclastogenesis by ChIP-seq Approach. Tetsuro Yasui*[1], Takumi Matsumoto[2], Hironari Masuda[2], Jun Hirose[2], Yasunori Omata[2], Yuho Kadono[2], Hisataka Yasuda[3], Daizo Koinuma[2], Shuichi Tsutsumi[2], Kozo Nakamura[2], Hiroyuki Aburatani[2], Sakae Tanaka[2]. [1]University of Tokyo, Japan, [2]The University of Tokyo, Japan, [3]Oriental Yeast Company, Limited, Japan

Osteoclast differentiation from monocyte-macrophage lineage precursor cells is regulated by two essential cytokines, receptor activator of NF-κ B ligand (RANKL) and macrophage colony-stimulating factor (M-CSF). TGF-β is a cytokine with ubiquitous proliferation and differentiation activity in many types of cells, and we recently demonstrated that TGF-β is essential for RANKL-induced osteoclastogenesis. In this study, we analyzed the role of TGF-β in osteoclastogenesis through comprehensive epigenetic approach.

To identify TGF-β-regulated genes in osteoclast precursors (OCPs), chromatin immunoprecipitation using anti-Smad2/3 antibody and massively parallel DNA sequencing was performed (ChIP-seq). 2,786 Smad2/3 binding sites were identified, and 903 genes were extracted as Smad2/3 target genes. Microarray analysis demonstrated that expression of these genes was in fact upregulated by TGF-β treatment.

To further specify the key regulatory genes of osteoclast differentiation, we analyzed histone modification profiles of OCPs. It has been recently recognized that trimethylation of histone H3 lysine 4 (H3K4me3) is associated with active transcription of a gene and trimethylation of histone H3 lysine 27 (H3K27me3) is associated with gene silencing. Dynamic changes in the histone modification pattern of cell lineage-specific genes from H3K4me3/H3K27me3 bivalent to H3K4me3 monovalent are known to be involved in the differentiation of stem cells to terminally differentiated cells. We therefore analyzed histone methylation patterns by ChIP-seq approach using anti-H3K4me3 antibody or anti-H3K27me3 antibody. We found that histone modification pattern was converted from K4/K27 bivalent to K4 monovalent by TGF-β treatment in 85 genes, with 18 of them being Smad2/3 target genes. Expression of these 18 genes was significantly upregulated by TGF-β treatment, while none of them was upregulated more than 2-fold by RANKL treatment. Interestingly, in as many as 6 out of the 18 genes, treatment of OCPs with RANKL for 72 hrs converted histone modification pattern to be H3K27me3 monovalent and gene expression was downregulated less than 1/4 fold. These findings indicate that RANKL epigenetically silences transcription of TGF-β-regulated key osteoclastogenic genes.

Combined with our finding that TGF-β most strongly promoted RANKL-induced osteoclastogenesis when TGF-β was applied to OCPs prior to RANKL stimulation, it is suggested that the role of TGF-β in osteoclastogenesis is to maintain OCPs in undifferentiated state and thus support RANKL-induced osteoclastogenesis.

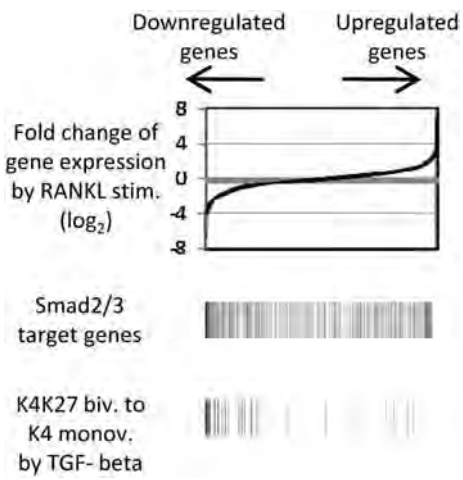

TetsuroYasui

***Disclosures: Tetsuro Yasui**, None.*

SA0260

Elucidating the Mechanism of Impaired Osteoclastogenesis in Cultures of Cells from +/R740S Osteopetrotic Mice. Irina Voronov*[1], Noelle Ochotny[1], Morris Manolson[1], Jane Aubin[2]. [1]University of Toronto, Canada, [2]University of Toronto Faculty of Medicine, Canada

Osteoclasts are multinucleated cells responsible for bone resorption. Vacuolar H^+-ATPases (V-ATPases), the multimeric enzymes present at the ruffled border of osteoclasts, are necessary for acidification of the resorption lacunae. V-ATPases consist of fourteen subunits, one of which, the "a3" subunit, is highly enriched in osteoclasts. Heterozygous mice with an R740S mutation in "a3" (+/R740S) have defective V-ATPase activity resulting in a higher bone density. Osteoclast number is increased in +/R740S bones, but in cultures of either bone marrow- or spleen-derived +/R740S cells, osteoclastogenesis is decreased compared to wild type (+/+) cells. We hypothesize that "a3" not only is important for acidification, but also plays a role in osteoclast differentiation.

To characterize osteoclastogenesis *in vitro*, +/R740S and +/+ bone marrow cells were cultured in the presence of RANKL and M-CSF for 6 days; the expression of osteoclast markers was analyzed by RT-PCR and apoptosis was assessed by TUNEL labeling. Gene expression levels of all osteoclast-specific markers, including tartrate resistant acid phosphatase (TRAP), osteoclast associated receptor (OSCAR), dendritic cell specific transmembrane protein (DC-STAMP), and the "d2" subunit of V-ATPase, were decreased in +/R740S cells *in vitro*, while "a3" expression was not changed compared to +/+ cells. "a3" and "d2" protein expression levels showed a similar pattern as determined by Western blotting. TUNEL assay results demonstrated that there was no difference in the number of apoptotic osteoclasts in +/R740S versus +/+ cell cultures, indicating that decreased osteoclast numbers in +/R740S cell cultures were not due to increased cell death. The expression levels of both the pro-apoptotic marker Fas and the anti-apoptotic marker Bcl2 were unexpectedly higher in +/R740S versus +/+ cultures. Besides acidification of extracellular spaces, the V-ATPases are known to play an important role in vesicular trafficking. Our results to date indicate that there is no difference in "a" subunit localization between +/R740S and +/+ cells grown on non-resorbing surface as assessed by immunofluorescence. Future experiments will determine whether the R740S mutation affects vesicular trafficking in osteoclasts. These studies will help to elucidate precise roles of the V-ATPase "a3"subunit in osteoclast maturation and activity.

***Disclosures: Irina Voronov**, None.*

SA0261

See Friday Plenary number FR0261.

SA0262

Live-Cell Microscopy of Osteoclast Precursor Fusion and Osteoclast Fission. Ineke Jansen*[1], Veerle Bloemen[2], Jan Stap[3], Ton Schoenmaker[4], Teun De Vries[5], Vincent Everts[5]. [1]ACTA, The netherlands, [2]Vrije Universiteit Medical Center, The netherlands, [3]Department of Cell Biology & Histology, Netherlands, [4]Dept. of Oral Cell Biology & Periodontology, Netherlands, [5]ACTA, Vrije Universiteit, The netherlands

Purpose: Osteoclasts are specialized cells with the unique capacity to resorb bone. The formation of these cells is a multistep process in which migration is essential for both the precursors and the osteoclast itself. Yet, surprisingly little is known about the dynamics of cell migration throughout the process of osteoclast formation. In this study we investigated the migratory behavior and cell-cell interaction of osteoclast precursors and mature osteoclasts.

Methods: Human peripheral blood mononuclear cells (PBMCs) were cultured with the osteoclastogenic cytokines macrophage colony-stimulating factor (M-CSF) and receptor activator of NF-KB-ligand (RANKL). The cultures were analyzed by live cell microscopy during 96 hours, both after one week and after two weeks of culture. In addition, we analyzed the migratory behavior of mature osteoclasts isolated from rabbits.

Results: At an early stage the osteoclast precursors were actively migrating over relatively long distances and migrated further away from their initial position compared to the later stage. At the two weeks time point, just prior to fusion, the cells were motile, but did not travel long distances. We next monitored isolated osteoclasts and showed for the first time a unique phenomenon: osteoclasts can undergo fission to generate functional multinucleated compartments as well as compartments that contained apoptotic nuclei.

Conclusions: These findings indicate important differences in the dynamics of cell migration during osteoclastogenesis: First, the osteoclast precursor explores the environment in search for fusion partners whereas in a later stage the osteoclast precursor moves in a much more localized area, possibly preparing for an interaction with neighboring cells. The most intriguing observation of dividing osteoclasts suggest that the osteoclast divides into several multinucleated cells in order to simultaneously control bone resorption at different sites and shed apoptotic nuclei to free the cell from non-functional elements. Our observations provide new information on the cellular behavior of multinucleated cells and open a new prospective for controlling bone resorption.

***Disclosures: Ineke Jansen**, None.*

SA0263

See Friday Plenary number FR0263.

SA0264

Osteocyte Apoptosis Directly and Indirectly Regulates Osteoclast Formation In Vitro. Lidan You, Axel Guenther, Saja Al-Dujaili*. University of Toronto, Canada

Introduction:

Microdamage is believed to disrupt interstitial fluid flow in bone, thereby reducing solute transport and causing osteocyte apoptosis. Osteocyte apoptosis in microdamage areas was shown to precede increased local osteoclast formation and activity, thereby initiating targeted bone remodeling in vivo. Osteocytes have been demonstrated to release RANKL, M-CSF and VEGF as pro-osteoclastogenic factors in vivo. However, the mechanisms for osteoclast formation and resorption in microdamage areas are unknown. We hypothesize that: a) apoptotic osteocytes localized near microdamage are directly responsible for initiating targeted bone remodeling, and b) apoptotic osteocytes indirectly regulate bone remodeling by sending cues to nearby healthy osteocytes, which then initiate targeted remodeling.

Methods:

We serum-starve MLO-Y4 osteocyte-like cells for 24hr to achieve similar apoptosis effect associated with bone microdamage. Conditioned medium was obtained at 2hr and 24hr post-apoptosis to represent early stages in the initiation of bone remodeling in the following groups:

A) Apoptotic osteocytes (i.e. osteocytes at microdamage)

B) Healthy osteocytes treated with apoptosis conditioned medium (i.e. healthy osteocytes sensing apoptosis cues from microdamage)

C) Healthy osteocyte treated with non-apoptosis conditioned medium (i.e. healthy osteocytes in the absence of microdamage)

We measured soluble concentrations of RANKL, VEGF and M-CSF in conditioned medium, and conditioned medium effect on osteoclast formation/size.

Discussion:

Our findings indicate that both apoptotic osteocytes and apoptosis-conditioned healthy osteocytes are involved in regulating osteoclast formation, as was demonstrated by elevated soluble RANKL and VEGF concentrations in conditioned medium. Moreover, our results suggest that healthy osteocytes near apoptosis are not only responsible for initiating the resorption response, but also for confining osteoclasts to the apoptosis area, thereby creating a ''halo'' around the microdamage. These findings are first to provide a mechanism linking osteocyte apoptosis with bone microdamage, and suggest that osteocyte apoptosis both directly and indirectly regulates the initiation of targeted bone remodeling.

***Disclosures: Saja Al-Dujaili**, None.*

SA0265

Regulation of Osteoclast Formation by Pyruvate Kinase M2. Seong Sik Kim*[1], Ryan Ricofort[2], Eric Serrano[2], Jian Zuo[2], Alan Jenkins[2], John Neubert[2], Mathew Boxer[3], Douglas Auld[4], Craig Thomas[5], Lexie Holliday[2]. [1]Department of Orthodontics, College of Dentistry, Pusan National University, Pusan, Korea., South korea, [2]University of Florida College of Dentistry, USA, [3]NIH Chemical Genomics Center, National Human Genome Research Institute, National Institutes of Health, USA, [4]NIH Chemical Genomics Center, USA, [5]NIH Chemical Genomics Center, National Institutes of Health, USA

Recent studies suggest that a physical link occurs between the vacuolar H^+-ATPase (V-ATPase) and several glycolytic enzymes, and that these interactions are required for assembly of the V-ATPase (1). Given that osteoclasts express very high levels of V-ATPase, this predicts that increases in levels of glycolytic enzymes might be expected during osteoclast formation in order to support V-ATPase assembly. This study was initiated to test this prediction. By quantitative immunoblotting we found that aldolase, glyceraldehyde 3-phosphate dehydrogenase and phosphofructokinase all increased by approximately 10-fold relative to the level of actin during osteoclastogenesis. Because high levels of glycolytic enzymes are expressed in cancer cells and this is associated with a switch from utilization of pyruvate kinase M1 (PKM1) to the use of PKM2, we used an anti-PKM2 antibody in immunoblots to demonstrate high level expression of PKM2 in osteoclasts. RT-PCR was used to confirm the expression of PKM2 and PKM1. A small molecule activator of PKM2 (NCGC00185916-01; ref. 2) at a concentration of 1 micromolar increased the number of osteoclasts (tartrate-resistant acid phosphatase expressing multinuclear cells) formed during differentiation of RAW 264.7 cells stimulated by RANKL and mouse marrow osteoclasts stimulated by calcitriol by from 1.5 to 5-fold. Stimulaton was concentration-dependent with highest stimulation achieved at 1 micromolar of the activator. These data suggest that osteoclastogenesis is associated with expression of increased levels of several glycolytic enzymes and with the expression of PKM2. Osteoclast formation was significantly increased by a small molecule activator of PKM2. The unusual expression of glycolytic enzymes and the presence of PKM2 represent potential therapeutic targets for the treatment of osteoclast-mediated disease processes.

1. Lu, M., Ammar, D., Ives, H., Albrecht, F., and Gluck, S. L. (2007) *J. Biol. Chem.* 282, 24495-24503

2. Boxer, M. B., Jiang, J. K., Vander Heiden, M. G., Shen, M., Skoumbourdis, A. P., Southall, N., Veith, H., Leister, W., Austin, C. P., Park, H. W., Inglese, J., Cantley, L. C., Auld, D. S., and Thomas, C. J. (2010) *J. Med. Chem.* 53, 1048-1055

***Disclosures: Seong Sik Kim**, None.*

SA0266

See Friday Plenary number FR0266.

SA0267

The RANK IVVY$^{535\text{-}538}$ Motif Plays a Critical Role in Tumor Necrosis Factor-α-mediated Osteoclastogenesis by Rendering Osteoclast Genes Responsive to Tumor Necrosis Factor-α. Joel Jules*, Zhenqi Shi, Xu Feng. University of Alabama at Birmingham, USA

Tumor necrosis factor-α (TNF), a proinflammatory cytokine, is implicated in bone loss stemming from various bone disorders, but its precise role in osteoclast (OC) formation remains controversial. While several groups showed that TNF can promote OC formation independent of RANKL, others demonstrated that TNF-mediated OC formation needs permissive levels of RANKL. To address this discrepancy, we independently examined the role of TNF in OC formation in culture dish and bone slices using primary bone marrow macrophages (BMMs). Our data indicate that OC formation in both conditions requires permissive levels of RANKL. Moreover, we show that TNF can stimulate OC formation from BMMs previously exposed to RANKL for as short as 6h. These data indicate that RANKL plays a critical role in TNF-mediated OC formation by priming BMMs into OC lineage. RANKL induces OC formation by activating the expression of numerous genes, including those encoding metallopeptidase 9, carbonic anhydrase 2, cathepsin K and tartrate resistant acid phosphatase. To investigate the molecular basis of the RANKL-mediated lineage commitment, we studied the effect of TNF on the expression of these genes. While TNF alone cannot activate the four genes, TNF is able to do so either in the presence of permissive levels of RANKL or from BMMs previously exposed to RANKL, indicating that the RANKL-mediated lineage commitment involves reprogramming of OC genes into an inducible state. We have previously shown that the RANK IVVY$^{535\text{-}538}$ motif plays a critical role in mediating OC lineage commitment. Hence, we examined whether this motif is involved in reprogramming of OC genes into an inducible state. To this end, we used 2 chimeras: Ch1 & Ch2. Ch1 comprises the human Fas external domain linked to the transmembrane & intracellular domains of normal RANK and Ch2 has inactivating mutations in the IVVY motif. The chimeras were activated by a human Fas activating antibody (Fas-AB), specific to human Fas, without affecting endogenous RANK or Fas. BMMs expressing Ch1 or Ch2 were pretreated with Fas-AB/M-CSF for 18h, followed by TNF/M-CSF for 96h. BMMs expressing Ch1, but not Ch2, formed OCs. More importantly, the expression of the four genes in BMMs expressing Ch1, but not Ch2, was activated by TNF stimulation. Taken together, we conclude that the RANK IVVY motif plays a crucial role in TNF-mediated OC formation by reprogramming of OC genes into an inducible state in which they can be activated by TNF.

***Disclosures: Joel Jules**, None.*

SA0268

See Friday Plenary number FR0268.

SA0269

Characterization of the V-ATPase *a3*-B2 Subunit Interaction. Norbert Kartner*[1], Yeqi Yao[2], Keying Li[3], Morris Manolson[1]. [1]University of Toronto, Canada, [2]Faculty of Dentisty, University of Toronto, Canada, [3]Faculty of Dentistry, University of Toronto, Canada

V-ATPases are highly expressed in ruffled borders of bone-resorbing osteoclasts, where they play a crucial role in skeletal remodeling. V-ATPases are composed of at least 14 subunits, some of which have multiple isoforms. Mammalian cells have 4 isoforms of the a subunit (a1-a4) and two isoforms of the B subunit (B1 and B2). To discover protein-protein interactions with the a subunit in mammalian V-ATPases, a GAL4 activation-domain fusion library was constructed from an in vitro osteoclast model, RANKL-differentiated RAW 264.7 cells. This library was screened with a bait construct consisting of GAL4 binding-domain fused to the 50 kDa N-terminal cytoplasmic domain of V-ATPase a3 subunit (NTa3), the a subunit isoform that is highly expressed in osteoclasts. One of the prey proteins identified was the V-ATPase B2 subunit, which is also highly expressed in osteoclasts. Further characterization, using affinity pulldowns and solid-phase binding assays, revealed an interaction of apparent high affinity between NTa3 and C-terminal domains of both B1 and B2 subunits. Dual B-binding domains of equal apparent affinity were observed in NTa3, suggesting a possible model for interaction between these subunits in the V-ATPase complex. There did not appear to be any discrimination between binding of B1 or B2 subunits by the four mouse isoforms of the a subunit; however, the a3-B2 interaction appeared to be favored over a1, a2 and a4 interactions with B2, suggesting a

mechanism for the specific subunit assembly of plasma membrane V-ATPase in osteoclasts. We present here a novel model for interaction of the NTa domain with the catalytic headpiece of V-ATPase, which takes into account all known intra-complex interactions with NTa. Further understanding of these interactions could aid in the design of targeted therapeutics for bone loss disorders, such as osteoporosis and rheumatoid arthritis. With this goal in mind, we have used the a3-B2 solid-phase binding assay to screen synthetic chemical compound libraries for inhibitors of the interaction. One inhibitor of the a3-B2 interaction was useful in inhibiting acid secretion by osteoclasts in vitro, suggesting that the a3-B2 interaction is of importance in maintaining V-ATPase proton-translocating activity at the osteoclast ruffled border (see abstract, The benzohydrazide derivative KM91104 inhibits osteoclast mineral resorption at μM concentrations that do not affect osteoclast differentiation or fusion. Crasto et al.).

***Disclosures: Norbert Kartner**, None.*

SA0270

See Friday Plenary number FR0270.

SA0271

Dissociation of Bone Resorption and Bone Formation in Adult Mice Transplanted with *ocloc* Hematopoietic Stem Cells. Christian Thudium*[1], Carmen Flores[2], Anita Neutzsky-Wulff[3], Vicki Jensen[4], Geerling Langenbach[5], Annemarie Brüel[6], Jesper Skovhus Thomsen[6], Natalie Sims[7], Maria Askmyr[8], Thomas John Martin[7], Vincent Everts[9], Morten Karsdal[4], Johan Richter[2], Kim Henriksen[4]. [1]Nordic Bioscience, Denmark, [2]Molecular Medicine & Gene Therapy, Lund University, Sweden, [3]Nordic Bioscience & University of Copenhagen, Denmark, [4]Nordic Bioscience A/S, Denmark, [5]Dept. Oral Cell Biology, Academic Centre of Dentistry Amsterdam (ACTA), Universiteit van Amsterdam & Vrije Universiteit, Netherlands, [6]Department of Connective Tissue Biology, Institute of Anatomy, University of Aarhus, Denmark, [7]St. Vincent's Institute of Medical Research, Australia, [8]St. Vincent's Institute for Medical Research, Australia, [9]ACTA, Vrije Universiteit, The netherlands

Patients and mice with mutations reducing the ability of the osteoclasts to secrete acid have osteopetrosis, characterized by defective bone resorption, increased osteoclast numbers, and interestingly normal or even increased bone formation. However, the developmental nature of these phenotypes limits the general applicability of these findings.

To shed light on bone turnover and coupling in osteopetrosis, independent of bone development, we transplanted three-month old mice with hematopoietic stem cells from wt or oc/oc mice, which have defective acid secretion and bone resorption. Changes in bone turnover and structure were investigated in detail during a three month period, which was followed up by a six month study, to allow time for a more drastic change in bone phenotype.

Adult mice were irradiated and transplanted with fetal liver cells from wt or oc/oc mice (Ly5.2 background) by IV injection into wt mice (Ly5.1 background). Engraftment levels were assessed using flow cytometry of the Ly5.2/Ly5.1 ratio. Serum samples were collected every sixth week for measurement of bone turnover markers (CTX-I, PINP, ALP and TRACP 5b). At 12 and 28 weeks the animals were euthanized and bones were collected for histomorphometry, μCT and mechanical tests.

An engraftment level >95% was obtained. The resorption marker CTX-I was reduced in both 3 and 6 month cohorts throughout the timeline, while TRACP 5b was increased in the oc/oc group compared to wt/wt. The bone formation markers PINP and ALP were elevated, when comparing the oc/oc group to wt/wt. μCT analyses of femurs and vertebrae showed a 50% increased bone volume in trabecular and 20% in cortical compartments of oc/oc mice compared to wt. Bone histomorphometry confirms the increased bone volume found in μCT analysis. Furthermore, mechanical tests showed a 35% increase in bone strength in the femoral neck and diaphysis of oc/oc mice compared to wt, as well as a trend in the vertebrae. Bonestrength and volume continue to increase from 3 to 6 months.

In conclusion, we here present data showing that bone formation is uncoupled from bone resorption in adult mice, when the osteoclasts are unable to acidify the resorption lacunae. The observed increase in non-resorbing osteoclasts strongly suggests that bone formation is controlled by the osteoclasts, but not their resorptive activity, and that this uncoupling leads to increased bone quality.

***Disclosures: Christian Thudium**, Nordic Bioscience, 3*

SA0272

Expression and Activity of Cholinergic Receptors in Osteoclasts. Arik Bar*[1], Alon Bajayo[1], malka Attar[1], Alberta Zallone[2], Itai Bab[1]. [1]The Hebrew University, Israel, [2]University of Bari Medical School, Italy

Acetylcholine receptors have been reported in osteoblasts but not in osteoclasts. In the present study we have systematically scanned mouse bone marrow-derived monocytes and osteoclasts cultures for the expression and activity of these receptors. RT-PCR analysis revealed the absence of mRNA transcripts for neither of the five known muscarinic receptors. mRNA expression was found mainly for the nicotinic acetylcholine receptor (nAChR) α2 and β2 subunits. Quantitative mRNA analysis indicated a marked increase in the expression of these subunits during osteoclastogenesis. In addition, weaker signals were noted for the nAChR γ, δ and α10 subunits in monocytes and β1, δ and β4 in osteoclasts. The presence of α2 and β2 subunits in osteoclasts was confirmed by immunocytochemistry and in vivo immunohistochemistry. To assess the effect of nAChR activation on osteoclastogenesis and bone resorption, osteoclastogenic cultures (grown in the presence of M-CSF and RANKL) were challenged with the cholinergic agonists nicotine or carbamylcholine. Three-day cultures showed a dose dependent increase in the number of TRAP-positive multinucleated cells. The maximal increase (60 %) was at 10^{-8}-10^{-6} M agonist concentration. By contrast, four-day cultures showed a decrease (60 %) in the number of intact osteoclasts at the same agonist dose range. This decrease was associated with a more than 15-fold increase in the number of apoptotic osteoclasts. Resorption analysis on dentine slices demonstrated no effect on pit number, but a 50 % reduction in pit size. Taken together, these data suggest a significant role for nAChR signaling in the inhibition of bone resorption, which results from the early formation of immature osteoclasts and their enhanced death.

***Disclosures: Arik Bar**, None.*

SA0273

See Friday Plenary number FR0273.

SA0274

Osteoclast Inhibitory Peptide-1 Binding to the FcγRIIB Modulates ITIM and ITAM Signaling in Preosteoclast Cells. Srinivasan Shanmugarajan*[1], Craig C. Beeson[2], Sakamuri Reddy[1]. [1]Charles P. Darby Children's Research Institute, USA, [2]Medical University of South Carolina, USA

Osteoclast inhibitory peptide-1 (OIP-1/hSca) is an autocrine/paracrine inhibitor of osteoclast differentiation, and mice that over-express OIP-1 in osteoclast lineage cells develop an osteopetrosis bone phenotype. We recently demonstrated that OIP-1 binding to the FcγRIIB inhibits osteoclast differentiation, however the underlying molecular mechanism is unclear. Immunoreceptor tyrosine-based activation motif (ITAM)-bearing common γ subunit of FcRs (FcγRI and FcγRIII) and DAP12 are crucial for osteoclast development. Further, Immunoreceptor tyrosine-based inhibitory motif (ITIM) bearing FcγRIIB adapter proteins known to inhibit ITAM signaling in immune cells. Therefore, we examined the OIP-1 inhibition of FcR signaling during osteoclast differentiation. Total cell lysates obtained from the OIP-1 mice derived preosteoclast cells stimulated with RANKL demonstrated increased levels (4-fold) of (ITIM) phosphorylation of FcγRIIB compared to wild-type (WT) mice. In contrast, OIP-1 mouse derived preosteoclasts cells stimulated with RANKL demonstrated inhibition of ITAM phosphorylation of FcRγ but not DAP12. Also, OIP-1 c-peptide treatment to preosteoclast cells obtained from FcγRII$^{-/-}$ deficient mice showed no significant change in the phosphorylation of ITAM. Moreover, evidence suggesting that the tyrosyl-phosphorylated ITIM has affinity with cytoplasmic SH2 domain-containing phosphatases like SHP1, SHP2 and SHIP proteins. Further studies indicate that these inhibitory proteins dephosphorylate tyrosines in ITAM bearing Fc receptors. Total cell lysates obtained from OIP-1 mice derived preosteoclast cells stimulated with RANKL demonstrated a 3-fold increase in phosphorylation of SHP1 but not SHP2. Also, there is no significant change in the levels of phospho-SH2 inositol 5-phosphatases (pSHIP1 and pSHIP2). Interestingly, preosteoclast cells from OIP-1 mice stimulated with RANKL had a 4.5-fold decrease in the levels of ITAM activating phospho-Syk compared to WT mice. These results suggest that cross-regulation of ITIM and ITAM bearing Fc receptors may play a role in OIP-1 suppression of Syk activation and inhibition of osteoclast differentiation. Thus, OIP-1 may have therapeutic utility for bone diseases with high bone turnover.

***Disclosures: Srinivasan Shanmugarajan**, None.*

SA0275

Peroxiredoxin II Negatively Regulates LPS-induced Differentiation and Bone Resorption. Mijung Yim[1], Hyojung Park*[2]. [1]Sookmyung Women's University, South korea, [2]Sookmyung Women's University, South korea

Lipopolysaccharide (LPS) is pathogen that causes inflammatory bone loss. LPS has been known to induce the osteoclast formation from osteoclast precursors, which mediates NF-kB and other signaling molecules. Recent study showed that peroxiredoxin II (Prx II) is an essential negative regulator of LPS-induced inflammatory signaling. Prx II is a member of antioxidant enzyme family and plays a protective role against oxidative damage caused by reactive oxygen species (ROS). In this study, we investigated the role of Prx II in LPS induced-osteoclast formation using Prx II-deficient mice. We cultured wild-type and Prx II-deficient spleen cells with RANKL for 48 hours and used as osteoclast precursors throughout the study. When 2 types of cell were treated with LPS, as compared to wild-type cells, osteoclast formation was enhanced in PrxII-deficient cells. To gain molecular insight, we examined the effect of PrxII-deficiency on signaling pathways and transcription factors. The expression of NFATc1, a master regulator of osteoclast differentiation, was enhanced in Prx II-deficient cells. Although LPS did not show different activation patterns of IkB, ERK 1/2, p38 MAPK pathways between wild-type and PrxII-deficient cells, LPS increased the expression of proinflammatory cytokines, IL-1 and

IL-6. Furthermore, NO production and iNOS expression is accelerated in PrxII-deficient cells. Also, ROS production is enhanced in PrxII-deficient cells, interestingly, activation of signal transducers and activators of transcription 3 (STAT3) is promoted in PrxII-deficient cells. These results show that PrxII modulates LPS-induced osteoclast differentiation through controlling ROS-related signaling. Consistent with the in vitro result, PrxII-deficient mice showed increased LPS-challenged bone loss. Taken together, PrxII negatively regulates LPS-induced osteoclast differentiation and bone loss. For further study, we continue to make progress in studies about the precise mechanism of Prx II in LPS-induced osteoclastogenesis.

***Disclosures: Hyojung Park**, None.*

SA0276

Spontaneous Rythmic Fluctuations of Osteoclasts Intracellular pH. Raif Musa-Aziz, Priscilla Morethson*. University of Sao Paulo, Brazil

Large amounts of acid are secreted into the resorption lacuna by the osteoclasts to promote bone mineral dissolution. This extracellular acidification is mediated by a vectorial proton secretion, one of the key elements of the osteoclast activity (Bruzzaniti A & Baron R, 2006) and may have an impact on osteoclast pH regulation. The vacuolar H^+-ATPase is the known mechanism related to the proton secretion; however, other proteins, such as Na^+/H^+ exchanger, the voltage-gated proton channel and a proton-coupled chloride transporter (CLC-7), are also expressed in osteoclasts and may be implicated in the proton secretion process. The role of the aforementioned mechanisms and their interplay during the osteoclast proton secretion are still poorly understood.

This work was performed to evaluate which are the mechanisms involved with proton transport at the osteoclast plasma membrane and their function in the intracellular pH (pHi) regulation. To address these questions, we worked with freshly isolated osteoclasts from long bones or osteoclast-like (OCL) cells generated from bone marrow precursor cells (using M-CSF and RANK-L) of Wistar rats. The cells were plated on glass or plastic coverslips in α-MEM + 10% FBS, pH 7.4, placed in a 5% CO_2 incubator at 37°C. At the time of the experiments, osteoclasts and OCL-cells were identified by their morphology using enhanced contrast microscopy and, for some experiments, a further confirmation of the cell phenotype was done by cytochemistry for TRAP or immunocytochemistry for calcitonin receptor. The pHi was measured using the probe BCECF. The emitted fluorescence ratios (R) after excitation of intracellular BCECF at 490 and 440 nm (R = 490/440) were converted to pHi using the high-K^+ nigericin technique. The experiments were performed in the presence of standard HEPES solution free of CO_2/HCO_3^-, pH 7.4, 37°C, without perfusion (''basal conditions'').

Under these conditions, our preliminary data show that the osteoclasts exhibit cyclic pHi variations characterized by repeated periods of spontaneous acidification and alkalinization. These cyclic pHi variations seem to be regular, with a frequency of 14.5 ± 1.1 min, n=11, and an amplitude—difference between maximal and minimal pHi—of 1.59 ± 0.02 pH units, n=3.

Our data suggest that, at ''basal conditions'', osteoclasts do not maintain a constant pHi but, instead, these cells seem to exhibit an oscillatory pHi pattern that may be independent of any stimulus or acid challenge.

***Disclosures: Priscilla Morethson**, None.*
This study received funding from: CNPq, Fapesp

SA0277

P62, PKCzeta and NF-kappaB Signaling in Human Osteoclasts: a Link With Paget's Disease of Bone. Estelle Chamoux*[1], Martine Bisson[2], Laetitia Michou[3], Jacques Brown[4], Sophie Roux[2]. [1]Centre Hospitalier Universitaire Sherbrooke, Canada, [2]University of Sherbrooke, Canada, [3]Centre De Recherche Du Chuq-Chul, Canada, [4]Laval University, Canada

In Paget's Disease of Bone (PDB), osteoclasts (OCs) are larger, more numerous and more active than healthy ones. PDB has been linked to mutations of the sequestosome1 (SQSTM1) gene encoding the protein p62. The most prevalent p62 P392L mutation promotes an active OC phenotype, with a basal and constitutive activation of PKCζ and NF-κB (Chamoux et al, Mol Endocrinol 2009). However, the mechanisms by which the P392L mutation alters p62-associated pathways remain to be investigated. In the present work, OCs generated from cord blood monocytes were transfected with vectors containing the wild-type or mutated p62 gene. Using immunoprecipitations, we determined that p62 associates time-dependently with IκB and that significant degradation of IκB occurs after RANKL stimulation, an effect enhanced by the over-expression of p62WT but prevented by a preincubation with MG-132, a proteasome inhibitor. However, in cells expressing the $p62^{P392L}$ variant, increased expression of IκB was detected in non-stimulated cells, which remained relatively high in the presence of MG132. In addition, we showed that p62/IκB interactions were less consistent in these cells, thus indicating that the p62 mutation may alter the function of p62 in NF-κB signaling by decreasing its capacity to bind IκB, and thus to shuttle this factor towards the proteasome. In order to reconcile these results with our previous observations showing that $p62^{P392L}$ expression lead to over-active OCs, we evaluated the role of PKCζ as a potential intermediate between p62 and NF-κB. The use of a myristoylated PKCζ inhibitor prior to RANKL stimulation significantly decreased NF-κB activation in non-transfected OCs. Moreover, the PKCζ inhibitor abolished both the baseline and RANKL-induced increase in NF-κB activation observed in OCs expressing $p62^{P392L}$ but had only limited effects in $p62^{WT}$-expressing cells, and tended to decrease the area of bone resorbed by $p62^{P392L}$-expressing OCs. Thus, our results suggest that the reduced proteasomal degradation of IκB and the increased PKCζ activation both contribute to the resulting NF-κB activation. While the P392L mutation in p62 renders the proteasomal pathway inefficient, it over-activates the PKCζ pathway leading to uncontrolled NF-κB functions and increased bone resorption. The present study highlights for the first time a double function of p62 and clearly points out the importance of PKCζ in the phenotypic changes specific to the P392L mutation in human OCs.

***Disclosures: Estelle Chamoux**, None.*

SA0278

See Friday Plenary number FR0278.

SA0279

See Friday Plenary number FR0279.

SA0280

The Dynamin GTPase-induced Dephosphorylation of Pyk2 is Mediated by PTP-PEST and Regulates Osteoclast Bone Resorption. Pierre Eleniste*[1], Angela Bruzzaniti[2]. [1]Indiana University-Purdue University Indianapolis, USA, [2]Indiana University School of Dentistry, USA

Osteoporosis is a bone disease that affects millions of people worldwide and is characterized by low bone mass and structural deterioration of bone tissue, which increases the risk of bone fracture, frailty, morbidity and mortality. Excessive bone loss is caused by the activity of osteoclasts which degrade the bone matrix. The specific aim of this study is to identify and characterize the signaling proteins in osteoclasts that regulate the bone resorbing activity of these cells. The non-receptor tyrosine kinase Pyk2is highly expressed in osteoclasts, and mice lacking Pyk2 have an increase in bone mass due to impairment in the cytoskeletal organization and bone resorbing activity of osteoclasts. Following integrin activation, Pyk2 is activated by phosphorylation at Y402, which is necessary for its full kinase activity, and consequently for osteoclast spreading and bone resorption. We previously reported that the GTPase dynamin regulates osteoclast bone resorption in part by leading to the dephosphorylation of Pyk2 at Y402, thus decreasing Pyk2's kinase activity and its ability to bind to Src and downstream signaling proteins. In the current study we examined the intracellular mechanism by which dynamin leads to the dephosphorylation of Pyk2. We report that Pyk2 associates with dynamin via a unique mechanism involving Pyk2's N-terminal domain, most likely its FERM domain, and dynamin's plextrin homology domain. In addition, Pyk2 dephosphorylation requires dynamin's GTPase activity since expression of specific dynamin mutants that have either reduced affinity for GTP or exhibit defective GTPase activity significantly rescue Pyk2-Y402 phosphorylation. Moreover, we find that Pyk2 phosphorylation is rescued in the presence of chemical inhibitors of the tyrosine phosphatases and we identified PTP-PEST as a major phosphatase involved in the dynamin-mediated dephosphorylation of Pyk2. Together, our studies suggest that dynamin and PTP-PEST associate with Pyk2 and regulate the cyclic phosphorylation and dephosphorylation of Pyk2, which is critical for integrin signaling, podosome turnover and osteoclast attachment, migration and bone resorbing activity. Understanding the role of Pyk2 and dynamin and the intracellular mechanism that regulates osteoclast function may lead to the identification of novel therapeutic targets for the treatment of bone-related diseases such as osteoporosis.

***Disclosures: Pierre Eleniste**, None.*

SA0281

See Friday Plenary number FR0281.

SA0282

See Friday Plenary number FR0282.

SA0283

See Friday Plenary number FR0283.

SA0284

See Friday Plenary number FR0284.

SA0285

See Friday Plenary number FR0285.

SA0286

See Friday Plenary number FR0286.

SA0287

See Friday Plenary number FR0287.

SA0288

Evidence that Sclerostin is a Locally Acting Regulator of Osteoblast to Osteocyte Transition and a Master Regulator of Mineralization. Gerald Atkins*[1], Asiri Wijenayaka[1], Katie Welldon[1], Peter Rowe[2], David Findlay[1], Hui Peng Lim[1]. [1]University of Adelaide, Australia, [2]University of Kansas Medical Center, USA

Sclerostin is a product of mature osteocytes embedded in mineralised bone and is a negative regulator of bone mass and osteoblast differentiation. The identity of the cells that respond to sclerostin has not been identified, although the localized expression of sclerostin implies that it may have local paracrine or autocrine activities. We tested the hypothesis that sclerostin would regulate the behaviour of the cells actively involved in mineralisation, the late osteoblast or pre-osteocyte. First, long-term cultures of differentiating human primary osteoblastic cells (HO) were exposed to chronic levels of recombinant sclerostin. Significant inhibition of in vitro mineralization occurred in a dose-dependent manner. Analysis of gene expression revealed that sclerostin decreased the expression of mature osteocyte markers, DMP1 and that of SOST itself, whereas the expression of the pre-osteocyte marker E11 was increased. E11 expression was also increased by sclerostin in the MLO-Y4 osteocyte cell line. To separate possible effects on immature cells, primary HO were cultured for 5 weeks, a process that served to differentiate the cells to a post-proliferative and more uniformly mature, pre-osteocyte stage. Cultures were then exposed acutely to sclerostin and gene expression analysed. These cells were exquisitely sensitive to sclerostin and concentrations of 1 – 50 ng/ml consistently increased the expression of E11, while decreasing the expression of the mature markers DMP1 and SOST. Concomitantly, the expression of MEPE was increased by sclerostin, at both the mRNA and protein levels and PHEX mRNA was decreased. This implies that mature osteocytes, by virtue of their expression of sclerostin, are able to impede differentiation of pre-osteocytes as well as alter levels of key regulators of bone mineralization. Consistent with this, MEPE protein levels were increased by sclerostin and immunostaining revealed that sclerostin promoted an increase in the levels of the MEPE-ASARM peptide, shown previously to bind to and inhibit the growth of nascent bone mineral. Our results suggest that sclerostin acts through regulation of the PHEX/MEPE axis and behaves as a master regulator of physiological bone formation, in a local paracrine fashion. The regulation by sclerostin that we have identified of both pre-osteocyte and osteocyte activity is consistent with its localization in the bone and its established role in the inhibition of bone formation.

***Disclosures: Gerald Atkins**, None.*

SA0289

See Friday Plenary number FR0289.

SA0290

See Friday Plenary number FR0290.

SA0291

Effect of Intermittent PTH (1-34) Treatment on Osteocyte Lacunae in Ovariectomized Rats. Donald Kimmel*[1], Susan Candell[2], Tiffany Fong[3], Jack Coats[4], Mohammed Akhter[5], Thomas Wronski[6]. [1]Kimmel Consulting Services, USA, [2]Xradia Inc., USA, [3]Xradia Inc, USA, [4]Xradia, USA, [5]Creighton University Osteoporosis Research Center, USA, [6]University of Florida, USA

Parathyroid hormone (PTH) increases serum calcium by several mechanisms including osteocyte (Ocy) activity that may release mineral from bone and increase Ocy lacunar (Ocy.La) size. The purpose of this work is to quantify Ocy.La density and volume in mineralized bone tissue of PTH-treated rats by 3D Xray microscopic imaging.

Female rats aged 13wks were ovariectomized (OVX) (N=24). After 6wks, rats were treated subcutaneously for 16wks with 0 [Veh] or 0.05 mg/kg PTH (1-34) (Bachem) 5d/wk. Tibiae and L2 vertebrae (L2V) were fixed in 10% PO4-buffered formalin for 24hrs, then stored in 70% ethanol. Histomorphometric studies showed typical PTH-related increases in proximal tibial cancellous bone volume and bone formation rate. L2V (4/grp) were trimmed of posterior and transverse processes, leaving whole L2 body (L2VB) samples measuring 12mm diameter X 8mm long. These were scanned (5μm pixel resolution [PR]; 125μm^3 voxel resolution [VR]) with a 3D Xray microscope (XCT-200). 3D images were reconstructed and a 1.5mm diameter subregion (0.5-1.3mm distal to the cranial growth plate) rich in trabecular bone was identified and re-scanned (0.9μm PR; 0.729μm^3 VR). 3D images were reconstructed and multiple 0.9μm PR 2D slices from each rat were reviewed (Figures). While Ocy.La were more visible in some (Fig 2) than others (Fig 1), automated quantitation of Ocy.La density and volume by segmentation software could not be completed due to insufficient resolution. Blind-coded, randomized 2D slices from all rats were ranked [0-3 semi-quantitative scale (Figs 1 and 2)] independently by all authors for Ocy.La visibility. Combined scores (mean $\pm$ SD) were respectively, 0.63 ± 0.46 [Veh] and 2.23 ± 0.50 [PTH] ($P < .001$, Mann-Whitney U).

The semi-quantitative data indicate that each author considered Ocy.La more visible in PTH than Veh rats, perhaps suggesting that Ocy.La are larger in PTH rats than in Veh rats. We also conclude that while images acquired at 0.9μm PR seem acceptable for qualitatively evaluating Ocy.La, images with better than 0.9μm PR are required to facilitate automated analysis of Ocy.La density and volume by segmentation software. Trabecular bone rich specimens from all rats, cut from plastic-embedded L2VBs and measuring 2mmX2mmX8mm, are being re-scanned at 0.125μm^3 VR (0.5μm PR), a resolution that was previously proven sufficient to allow automated analysis of Ocy.La properties in human bone.

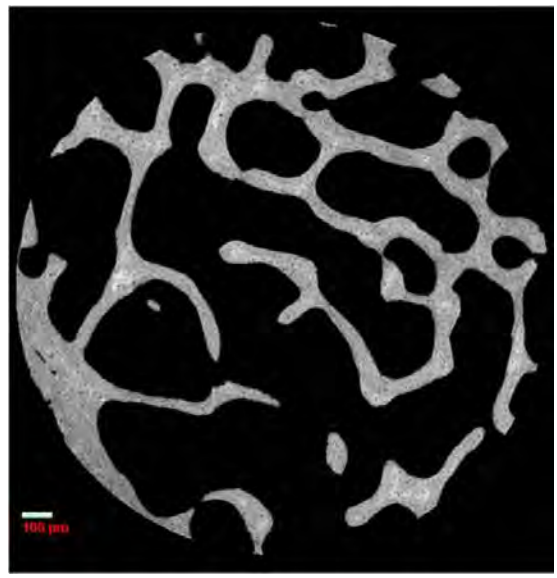

Fig. 1. 2D Xray microscopic image of rat vertebral trabecular bone. Few Ocy.La are visible (Rank=0).

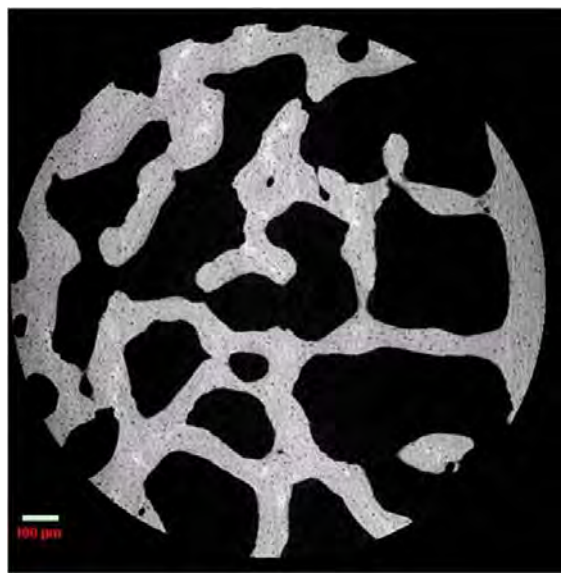

Fig. 2. Many Ocy.La are visible (black dots) (Rank=3).

***Disclosures: Donald Kimmel**, Xradia, Inc., 5*
This study received funding from: Xradia Inc.

SA0292

Association of Changes in Serum Levels of Intact Parathyroid Hormone with Changes in Biochemical Markers of Bone Turnover and Bone Mineral Density: A 10-year Follow-up of the Taiji Cohort. Noriko Yoshimura*[1], Shigeyuki Muraki[1], Hiroyuki Oka[1], Hiroshi Kawaguchi[2], Kozo Nakamura[3], Toru Akune[1]. [1]University of Tokyo, Japan, [2]University of Tokyo, Faculty of Medicine, Japan, [3]The University of Tokyo, Japan

The aim of this 10-year prospective cohort study is to evaluate changes in the serum levels of intact parathyroid hormone (iPTH) in the general population, and to assess the association of these changes with changes in biochemical bone-turnover markers (BTMs) and bone mineral density (BMD). We randomly selected 400 individuals (aged 40–79 years; 50 men and women in each of 4 age groups) from a list of registered residents of Taiji in 1993 (baseline). The BMD and various serum markers, namely, iPTH, total osteocalcin (OC), beta-C-terminal cross-linking telopeptide of type I collagen (beta-CTX), and N-terminal cross-linking telopeptide of type I collagen (NTX), were measured in the lumbar spine and femoral neck of the participants, at baseline and in the 10-year follow-up survey. The blood and BMD examinations could be performed at both time points in 317 of the 400 subjects (79.3%; 149 men and 168 women). The mean (standard deviation) serum levels of iPTH at baseline were 26.9 (11.0) pg/mL in men and 28.8 (12.6) pg/mL in women. Six individuals (1 man and 5 women) whose iPTH levels were higher than 65 pg/mL (65.02-79.1 pg/mL) at baseline were included in the follow-up analysis. After 10 years, the mean iPTH levels were 32.1 (12.3) pg/mL in men and 32.3 (12.9) pg/mL in women. The serum iPTH levels tended to increase over 10 years in both genders ($p < 0.0001$ in men, $p = 0.059$ in women). Multivariate regression analysis after adjustment for age, body mass index (kg/m^2), and menstrual status in females (0: normal menstruation, 1: irregular, 2: menopause) at baseline revealed that the changes in the serum iPTH levels were significantly positively associated with the changes in the levels of total OC (men: $\beta = 0.25$, $p = 0.002$; women: $\beta = 0.19$, $p = 0.03$), beta-CTX (men: $\beta = 0.44$, $p = 0.000$; women: $\beta = 0.27$, $p = 0.002$), and NTX in women ($\beta = 0.22$, $p = 0.01$). Multivariate regression analysis after adjustment for the above-mentioned confounders revealed a significant inverse relationship between changes in the serum iPTH levels and changes in the BMD of the femoral neck in women ($\beta = -0.19$, $p = 0.02$). An increase in the serum iPTH levels was found to be related to an increase in all BTM levels in both genders, with the exception of NTX in men. These findings confirmed that the serum iPTH levels were associated with bone metabolism, while they had a limited effect on changes of BMD over 10 years.

***Disclosures: Noriko Yoshimura**, None.*

SA0293

Is Bone Turnover Adequately Suppressed in Osteoporotic Patients, Treated with Bisphosphonates, in Daily Practice? Danielle Eekman*[1], Ben A.C. Dijkmans[2], Willem Lems[3], Annemieke C. Heijboer[2], Irene E.M. Bultink[2]. [1]VU University Medical Center, The netherlands, [2]VU University Medical Center, Netherlands, [3]Vrije Universiteit Medical Centre, The netherlands

Purpose: In patients with osteoporosis persistence is generally poor. It has been suggested that monitoring therapy by measurement of bone turnover markers (BTM) after 3 months of anti-resorptive therapy might improve persistence.

Methods: We investigated serum bone marker levels in two groups. The first group consisted of patients newly diagnosed with osteoporosis and starting treatment with bisphosphonates. We observed which proportion shows a decrease of BTM of $\geqslant 30\%$ (the least significant change). Serum levels of procollagen type 1 N-terminal propeptide (P1NP) and C-terminal crosslinking telopeptide (CTX) were determined before the start of treatment and after > 2 months of treatment. Secondly, P1NP and CTX levels were measured cross sectionally in a group of patients who were already treated with bisphosphonates for $\geqslant 3$ months. We observed which proportion reached the biological goal of therapy, BTM in the lower half of the normal premenopausal range. We also measured P1NP and CTX in a reference population of 34 healthy premenopausal women.

Results: In the first group 32 patients were included (23 women) mean age 66. During a mean treatment period of 4 months the P1NP and CTX level decreased significantly with 50% and 63% respectively. In 26 patients (81%) levels of both markers decreased with $\geqslant 30\%$. In 6 patients bone turnover was not adequately decreased, probably related to non-compliance (1), prednisone use (1), alcohol abuse (1), decreased mobility (1), paraproteinemia (1) and low calcium intake (1).

In the second group 96 patients were included, mostly women, aged 67. In 95% the serum P1NP levels and CTX levels were in the lower half of the premenopausal range. In 6 of the 7 patients with a level above the premenopausal range a possible explanation could be found: non-adherence (1), non-compliance (2), immobility (1), rheumatoid arthritis (1) and polymyositis and phenytoin use (1).

Conclusion: Our data illustrate that a decrease in bone turnover greater than the LSC can be observed in the majority (81%) of newly treated patients. Of chronically treated patients 95% have a BTM in the premenopausal range. In most patients an explanation for inadeqauate suppression of bone turnover was available. Monitoring treatment effect with bone turnover markers is in daily practice is feasible, and might be an additive tool in improving compliance.

***Disclosures: Danielle Eekman**, None.*

SA0294

Is Isolated serum 25-Hydroxyvitamin D Measurement to assess Vitamin D Nutritional Status Clinically Relevant? Nayana Parikh*, Tarlisha Eskridge, Leila Idi, Shijing Qiu, Sudhaker Rao. Henry Ford Hospital, USA

There has been growing interest in assessing vitamin D nutrition (VDN) in patients in general and those with bone & mineral disorders in particular. However, there are no guidelines for screening in the general population. Nevertheless, the number of 25-OHD measurements has increased exponentially in the last 2 years especially the number with isolated 25-OHD measurements. The clinical relevance of such practice is yet to be established. Accordingly, we reviewed serum 25-OHD testing in the lab over 5 years to determine the prevalence of 25-OHD measurements with and without simultaneous measurement of serum PTH levels and the relationship between the two, and develop guidelines for appropriate interpretation of serum 25-OHD levels in clinical practice.

Methods: We included all measurements from 2005 to 2009 for both PTH and 25-OHD. The relevant data are summarized in the Table.

Results: While the number of PTH testing remained relatively constant over the 5 years, the number of 25-OHD measurements increased by 9 folds, mostly in the last 2 years. More importantly, the number of isolated 25-OHD measurements as a fraction of total 25-OHD measurements increased from 28% in 2005 to 80% in 2009, again mostly in the last 2 years. However, the fraction of 25-OHD tests <30 ng/ml, a consensus cut-off for optimal VDN, remained constant throughout the 5 year period. There was the expected significant inverse relationship between 25-OHD and PTH both within each year and for the entire cohort, without significant difference between the 5 yearly slopes.

Conclusions: The exponential increase in 25-OHD measurements suggests increased awareness of VDN among clinicians. However, the relevance of isolated 25-OHD measurement without PTH may overestimate vitamin D depletion (because of seasonal or recent vitamin D deficiency) and the need for pharmacologic vitamin D supplementation. Further studies are needed to determine the clinical implications of an isolated 25-OHD measurement to assess VDN.

Measurement	2005	2006	2007	2008	2009
PTH Tests (Total #)	10937	12810	15426	17149	18209
25-OHD Tests (Total #)	7530	11762	19644	35687	64993
25-OHD <30ng/ml (% Total)	67	72	66	68	64
25-OHD <30ng/ml with PTH (% Total)	72	63	52	34	20

Table: Testing Trends for 25-OHD & PTH from 2005-2009

***Disclosures: Nayana Parikh**, None.*

SA0295

Serum Levels of Cathepsin K and Bone Turnover Markers are Decreased in Patients with Type 2 Diabetes. Pedro Rozas*[1], Rebeca Reyes[2], Antonia García-Martín[3], Maria Dolores Perez-Avilés[3], Mariela Vasavsky[3], Manuel Munoz-Torres[4]. [1]Hospital General, Spain, [2]Bone Metabolic Unit., Spain, [3]Bone Metabolic Unit. Endocrinology Division. San Cecilio University Hospital., Spain, [4]University Hospital, Spain

Background: Studies of bone resorption in diabetes are limited, and the results are conflicting. Aim: To analyse serum levels of bone turnover markers (BTM), cathepsin K, PTH-i and 25 OH vitamin D in patients with type 2 diabetes mellitus (T2DM) and the relationship with bone mineral density (BMD). To compare BTM and cathepsin K levels between T2DM and controls. Patients and methods: Case-Control study including 133 subjects, 78 patients with T2DM and 55 healthy controls. Lumbar spine and femoral BMD were measured by dual X-Ray absorptiometry (Hologic QDR 4500). We measured: bone alkaline phosphatase (b-ALP) (OCTEIATM IDS Ltd Boldon UK), osteocalcin (OC) (DiaSorin, Stillwater, Minnesota USA; tartrate resistant acid phosphatase (TRAP) (Bone TRAP ® Assay IDS Ltd); CTX (Elecsys ß Cross-Laps,Roche Diagnostics SL, Barcelona, Spain); Serum cathepsin K levels by ELISA (Biomedica Medizinprodukte GhbH & Co KG Wien, Austria). PTH-i (Intact PTH, Roche Diagnostics SL); 25 OH vitamin D (25-Hydroxyvitamin D 125I RIA DiaSorin). Results: Mean age was 56,7$\pm$ 6,8 yr (57.8$\pm$ 6.4 and 55,1$\pm$ 7,1 in T2DM and control group respectively; p=0.024). Among the T2DM patients (n=78), 47.2% were females (n=35) and 52.8% males (n=43). Serum levels of bone resorption markers were lower in T2DM compared with controls (TRAP: T2DM 1.39$\pm$0.99 UI/l vs controls 1.85$\pm$0.81 UI/l, p<0.05; CTX: T2DM 0.20$\pm$0.12 ng/ml vs controls 0.33$\pm$0.15 ng/ml, p<0.05). There were no differences in bone formation markers (b-ALP: T2DM 14.83$\pm$6.5 ug/L vs controls 12.96$\pm$6.73 ug/L, p 0.11; OC: T2DM 1.48$\pm$1.25 ng/ml vs controls 1.45$\pm$1.2 ng/ml, p 0.91). In the subgroup of patients where cathepsin K serum levels were measured (27 T2DM, 11 controls), T2DM presented lower levels although this difference was not significant (T2DM 4.36$\pm$5.46 pmol/l vs controls 6.56$\pm$10.13 pmol/l, p 0.39). PTH-i serum levels were lower in T2DM (PTH-i: T2DM 38.35$\pm$18.20 pg/ml vs controls 50.22$\pm$18.99 pg/ml, p<0.05). T2DM have lower levels of 25 OH vitamin D with respect to controls, although differences were not significant (T2DM 17.81$\pm$11.14 ng/ml vs controls 21.30$\pm$11.05 ng/ml, p 0.07). In T2DM there was a negative correlation between CTX levels and BMD at different sites (p<0.001). Conclusions: T2DM patients have lower levels of bone resorption markers and PTH-i compared with controls. Cathepsin K serum levels seem to be lower in T2DM, although larger studies are needed to clarify this significance of this finding.

***Disclosures: Pedro Rozas**, None.*

SA0296

Assessment of Tibial and Radial Peripheral Quantitative Computed Tomography: Precision Measurements. Charles Wisniewski*, Giulia Rinaldi, Nithya Setty, Meryl Leboff. Brigham & Women's Hospital, USA

Purpose: Peripheral Quantitative Computed Tomography (pQCT) measures true volumetric (3-dimensional) bone mineral density (vBMD) at the radius and tibia, with minimal radiation exposure. In addition, this technique discriminates cortical and trabecular compartments and cortical thickness. Assessment of the reproducibility of pQCT depends on the machine, technician and testing procedures. Sources of imprecision not related to the instrument are inexact repositioning of the subject in follow-up scans, anatomic site, reference line placement and movement artifacts. Methods: To determine the reproducibility of pQCT, we performed 3 repeated measurements in normal subjects ages 22-35 years within 2 months at the tibia (N=18) and at the radius (N=20) using pQCT (XCT 3000, Stratec, Germany). To minimize extremity movement and discomfort, customized arm and leg holders were used (Bone Diagnostic Inc, WI). We determined the percent coefficient of variation (%CV; standard deviation divided mean BMD times 100) and the least significant change (LSC; root mean square standard deviation times 2.77 for a 95% confidence level) for total area, total density and cortical thickness at each site (4% and 33% radius and 4% and 38% tibia), for trabecular density at the distal sites and for cortical density at the proximal sites of both limbs. Results: At all the tibial sites and proximal radius, the reproducibility (%CV) ranged from 0.34% to 2.41% (Tables 1 and 2). In contrast, the %CV at the 4% metaphyseal site at the radius was $>$ 5% in total area and density; %CV and LSC measures improved when cross sectional area (CSA) at the 4% radial site was within ± 10 mm^2 on repeated measures for each subject (J Musculoskelet Neuronal Interact. 2009 Jan-Mar;9(1):18-24) (Table 2). Cortical thickness at all sites, except at the radial 4%, showed a %CV below 1% and LSC of 0.082-0.42 (Tables 1 and 2). Conclusions: These data show that pQCT is a precise technique for measurements of vBMD and skeletal compartments of the extremities, but the 4% metaphyseal, radial site has the greatest variability. Thus, with standardized measurement procedures, pQCT is a valuable and precise clinical research tool for assessment of the therapeutic benefits of new treatment interventions on bone.

Table 1: Reproducibility at the Tibia

TIBIA	%CV	LSC
Total Area 4%	1.93	51.18 mg/cm^2
Total Density 4%	1.16	9.88 mg/cm^3
Trabecular Area 4%	2.41	51.34 mg/cm^2
Trabecular Density 4%	0.72	4.73 mg/cm^3
Cortical Thickness 4%	0.86	0.42 mm
Total Area 38 %	1.11	11.98 mg/cm^2
Total Density 38%	0.34	8.72 mg/cm^3
Cortical Area 38%	1.24	10.32 mg/cm^2
Cortical Density 38%	0.37	12.24 mg/cm^3
Cortical Thickness 38%	0.76	0.12 mm

Table 1: Reproducibility at the Tibia

Table 2: Reproducibility at the Radius

RADIUS	%CV	LSC
Total Area 4%	5.39 (1.60*)	44.46 (13.15*) mg/cm^2
Total Density 4%	5.77 (2.28*)	57.80 (21.51*) mg/cm^3
Trabecular Area 4%	4.42 (1.55*)	7.99 (2.90*) mg/cm^2
Trabecular Density 4%	1.94	9.53 mg/cm^3
Cortical Thickness 4%	2.64	18.98 mm
Total Area 33%	1.42	3.70 mg/cm^2
Total Density 33%	0.60	17.18 mg/cm^3
Cortical Area 33%	1.28	3.12 mg/cm^2
Cortical Density 33%	0.84	28.28 mg/cm^3
Cortical Thickness 33%	0.97	0.082 mm

* = Cross Sectional Area ± 10 mm^2

Table 2: Reproducibility at the Radius

***Disclosures: Charles Wisniewski**, None.*

SA0297

Combination of Bone Mineral Density and Trabecular Bone Score for vertebral fracture prediction in secondary osteoporosis. Sophie Bréban*[1], Sami Kolta[2], Karine Briot[3], Simon Paternotte[4], Mirieme Ghazi[4], Jacques Fechtenbaum[2], Maxime Dougados[4], Christian Roux[5]. [1]Cochin HospitalParis Descartes University, France, [2]Centre D'Evaluation, Des Maladies Osseuses, France, [3]Cochin Hospital, France, [4]Paris Descartes University, Cochin Hospital,Rheumatology Department, France, [5]Hospital Cochin, France

Rationale and objective: The relationship between decreased BMD and fracture risk is less clear in secondary osteoporosis than in post menopausal osteoporosis. The Trabecular Bone Score (TBS) is determined from a grey-level analysis of Dual X-ray Absorptiometry image and is thought to provide non quantitative information on bone. The aim of this study was to test the combination of TBS and BMD for vertebral fracture risk detection in a rheumatoid arthritis (RA) population treated (CS) or not (NCS) with glucocorticoids. Patients: 140 women aged 55.9 $\pm$ 14.0 years, with RA since 15.2 $\pm$ 10.2 years; 94 were receiving glucocorticoids (mean dose of 6.7 $\pm$ 4.7 mg/day) and 129 a disease modifying drug. Lumbar spine and hip BMD (g/cm^2) were assessed by DXA and TBS was applied to anteroposterior image of lumbar spine. Vertebral fractures from T4 to L4 were evaluated using Vertebral Fracture Assessment (VFA) software on DXA device.

Results: Mean spine and hip Tscores were -0.9 $\pm$ 1.4 and -1.6 $\pm$ 1.0, and -0.8 $\pm$ 1.5 and -1.5 $\pm$ 1.1, in patients with and without CS respectively. There was no difference in BMD between both groups, but TBS was 1.19 $\pm$ 0.11 and 1.23 $\pm$ 0.09 in CS and NCS groups respectively (p=0.03). TBS was significantly correlated to spine and hip BMD in all groups (r=0.52 to 0.61; p$<$0.0003). The vertebral fractures prevalence was 16.7% in the whole population, 23.9% in NCS group and 13.0% in CS group. In the whole population, the Area under the Curve (AUC) in the vertebral fracture risk prediction was higher in the TBS model (0.736) compared to the BMD model (0.670 for spine BMD; 0.705 for hip BMD; 0.708 for femoral neck BMD). We calculated a threshold of TBS (1.173) which corresponds to the best sensitivity (75%) and specificity (66%) according to ROC curves. Among patients without osteoporosis (n=97), 13 had vertebral fractures and 8 of them had a TBS lower than 1.173. Conclusion: Trabecular Bone Score provides additional information compared to BMD alone in vertebral fracture risk assessment, in RA population, with or without glucocorticoids. The bone parameters assessed by TBS need to be identified.

***Disclosures: Sophie Bréban**, None.*

SA0298

Comparison of a Prototype and Current DXA Whole Body Phantoms Provide Inconsistent Relationships. Cassidy Powers*[1], Bo Fan[2], Colin Miller[3], John Shepherd[2]. [1]Bone & Breast Density Group, University of California San Francisco, USA, [2]University of California, San Francisco, USA, [3]BioClinica, Inc. (formerly Bio-Imaging Technologies, Inc.), USA

PURPOSE: This study was conducted to determine if available whole body phantoms give consistent cross-calibration and quality control relationships between two DXA systems.

METHODS: A BioClinica whole body phantom prototype, the Hologic Whole Body Phantom (each containing an aluminum skeleton), and the BioImaging Variable Composition Phantom (VCP) were scanned 10 times (BioClinica and Hologic) and 5 times in three configurations (VCP) on the Lunar Prodigy and Hologic Discovery DXA scanners using whole body mode (smartscan off). Analysis was performed using Hologic Apex v3.0 (Hologic, Inc.) and Encore v13.2 (GE Healthcare, Inc.) software. Whole body and subregion ROIs were used on the BioClinica and Hologic phantoms to provide BMD, total mass, fat mass, lean mass, percent fat (pfat), BMC and area values. A centered subregion ROI was used to find pfat values for the VCP. Precision was described using means, SDs and %CVs.

RESULTS: The best precision was found using the Hologic WB phantom on both DXA systems. The total mass was very precise for both the BioClinica (17407.08 $\pm$ 42.03g, 16893.05 $\pm$ 53.40g) and Hologic (29147.17 $\pm$ 28.67g, 28274.97 $\pm$ 77.79g) phantoms. The Discovery produced better precision for BMD (0.98 $\pm$ 0.01, 1.10 $\pm$ 0.01) and area (516.44 $\pm$ 10.76, 651.21 $\pm$ 9.08) measures for the BioClinica and Hologic phantoms. It also gave better precision for total fat, lean, mass, and pfat for BioClinica (6413.86 $\pm$ 70.88, 10484.64 $\pm$ 81.01, 17407.08 $\pm$ 42.03, 36.84 $\pm$ 0.41, respectively). Total BMC (489.55 $\pm$ 7.58, 699.88 $\pm$ 6.07) was more precise on the Prodigy. The assumed single-point cross calibration between the Discovery and Prodigy was in good agreement for mass, BMD, and BMC, but soft tissue variables differed from 6.7 % (lean) to 18.0% (pfat) depending which phantom was used. However, the VCP showed a significant offset (7.4%) between the systems for pfat that could not have been predicted by the other two phantoms. Although small (n$\leq$30) in vivo cross calibration populations would provide some adjudication, the power is generally too poor to discern these calibration differences.

CONCLUSIONS: None of the phantoms tested were shown to be superior to the others. A universal standard of accuracy is greatly needed to determine truth in calibration for whole body DXA bone and soft tissue results. However, the phantoms may be useful for evaluation of consistent calibration on a single instrument.

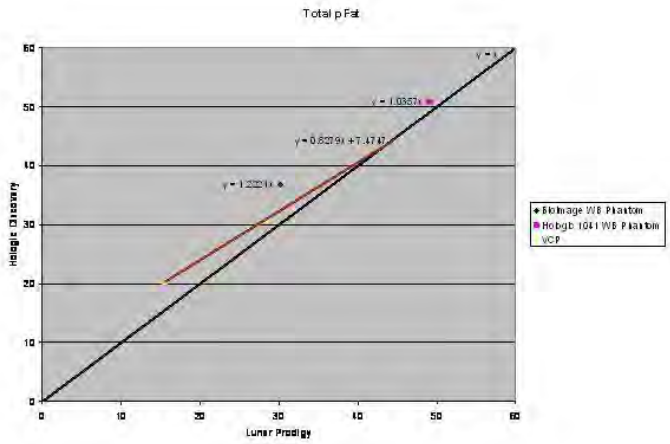

Figure 1: Mean percent fat values of the BioClinica, Hologic and VCP phantoms.

***Disclosures: Cassidy Powers**, None.*

SA0299

See Friday Plenary number FR0299.

SA0300

See Friday Plenary number FR0300.

SA0301

See Friday Plenary number FR0301.

SA0302

See Friday Plenary number FR0302.

SA0303

Reducing Unneccessary BMD Testing in Healthy Women at Menopause. Gillian Hawker*[1], Susan Jaglal[2], Jacob Cancino-Romero[1], Arielle Mendel[1], Samra mian[1], Esther Waugh[1], Sophie Jamal[3]. [1]Women's College Hospital, Canada, [2]University of Toronto, Canada, [3]The University of Toronto, Canada

Purpose: Bone mineral density (BMD) testing rates are highest in women at menopause, when fracture risk is low. No BMD testing guidelines exist for this group. Thus, we determined risk factors for low BMD and their ability to discriminate those with/without low BMD in this group.

Methods: Women aged 40-60 years having their first BMD at an academic centre were assessed for osteoporosis (OP) risk factors and spine and hip BMD by dual x-ray absorptiometry. Risk factors were: age, weight, physical activity, smoking, alcohol, caffeine and calcium intake, age at menarche, parity, breastfeeding and menopausal status, and family/personal history of fracture > age 40. We excluded women with medical conditions linked to OP. Using logistic regression and bootstrap technique, we determined the model that best discriminated (using area under the curve, AUC) women with/without low BMD (any site t-score ≤ -2.0). For ease of use, continuous risk factors were then dichotomized at cut-points that best discriminated women with/without low BMD. We compared the AUC of these models with that of the Osteoporosis Self-Assessment Tool (OST score=[weight(kg)-age(yrs)]x 0.2), developed to identify women 65+ years for BMD testing.

Results: Of 958 healthy women sent for a first BMD test, 944 with complete data were included; 87/944 (9.2%) had low BMD. Low BMD was significantly associated with older age, > years post menopause, lower weight, prior fracture, older age at menarche, and physical inactivity in adolescence. In multivariable analysis, older age, lower weight, > years post menopause, and prior fracture were significant independent predictors of low BMD (AUC 0.75 versus OST AUC 0.70, p=0.01). Dichotomizing weight (≤71/>71 kg), years post menopause (≥2 /<2), and age (>52/≤52) gave similar discrimination (AUC=0.745). Using the 4 dichotomous risk factors and setting sensitivity to detect low BMD at 95%, 258 women with normal BMD and 4 with low BMD would *not have been* recommended for testing. None of the 944 women had OST scores < -3 (high OP risk); 41 *with low* BMD and 205 *without low* BMD had OST scores between 1 and -3 (moderate OP risk). Using an OST score ≤1 to recommend testing would identify only 47.1% with low BMD.

Conclusions: In healthy women at menopause <10% had low BMD, supporting the need for guidance about testing. Assessment of 4 risk factors was superior to the OST in discriminating women with versus without low BMD.

***Disclosures: Gillian Hawker**, None.*

SA0304

The Influence of Exogenous Fat and Water on Lumbar Spine Bone Mineral Density in Healthy Volunteers. KYU-NAM KIM*. Ajou University, South korea

Background Changes in human body composition can affect the accuracy of spine bone mineral density (BMD) measurements. The purpose of this study was to evaluate whether fat and water in the soft tissue of the abdomen influence lumbar spine BMD measurements obtained using dual energy X-ray absorptiometry (DEXA).

Methods Healthy volunteers (10 male, 10 female) had duplicate BMD measurements on the same day before and after placement of the following 3 materials in the abdominal area: lard 900g, 1.5cm thick; oil 1.4 liters in a vinyl bag; and water 1.2 liters in a vinyl bag. Duplicate BMD measurements were also made using the Hologic anthropomorphic spine phantom under the same conditions.

Results In the case of human participants, following the placement of exogenous water to mimic extracellular fluid (ECF), there was a significant decrease in lumbar spine BMD (-0.012 g/cm^2, P = 0.006); whereas, placement of exogenous lard and oil to mimic abdominal fat, produced a slight increase in lumbar spine BMD (0.006 g/cm^2, P = 0.301; 0.008 g/cm^2, P = 0.250, respectively). The average percentage of lumbar spine BMD change with and without exogenous lard, oil, and water increased 0.51% and 0.67% and decreased 1.02%, respectively. Using the phantom, BMD decreased with placement of both lard (-0.002g/cm^2, P = 0.699) and water (-0.006 g/cm^2, P = 0.153); however, there was no difference in BMD after oil placement (0 g/cm^2, P = 0.870). Differences in lumbar BMD between lard and oil, representing solid fat and liquid fat respectively, were not significant (P = 0.607).

Conclusions These results suggest that in cases where changes in fat and ECF volume are similar, ECF exerts a greater influence than fat on DXA lumbar BMD measurements.

***Disclosures: KYU-NAM KIM**, None.*

SA0305

See Friday Plenary number FR0305.

SA0306

Which Limb to Scan? Revisiting the Relationship Between Skeletal and Functional Limb Dominance. Benjamin Weeks, Belinda Beck*. Griffith University, Australia

Purpose: The typical referral for clinical or research bone densitometry requests a ''non-dominant'' limb exam. While hand dominance reliably predicts upper extremity skeletal dominance, our experience suggests that functional dominance does not predict lower limb skeletal dominance. In the absence of a single reliable technique to determine lower extremity functional dominance, the extrapolation of the upper extremity rule is widespread; to the extent that scanning devices such as densitometers are generally designed to facilitate scanning of the left hip rather than the right to accommodate the preponderance of right handed individuals in the population. The aim of the current work was to determine the true nature of the association between functional and skeletal dominance of the lower limb. The ultimate goal is to establish a simple and reliable determinant of lower extremity skeletal dominance. Methods: 100 healthy men and women (age 32.5 ±10.2 years) were recruited for anthropometry and bilateral hip densitometry (BMD; Norland XR-800), calcaneal quantitative ultrasonometry (BUA; QUS-2, Quidel) and tibial peripheral quantitative computed tomography (cortical and trabecular density and area, cortical width and stress strain indices [SSI]; XCT3000 Stratec). Side dominance questionnaires and physical tasks were completed including the Waterloo Footedness Questionnaire(Revised) (WFQ-R), hop distance test, step test, handedness and footedness questions, and side preference for a number of common postures (e.g. folding arms). Correlation analyses and chi square tests with crosstabs were run on all bone and functional dominance parameters using SPSS(17). Results: Significant negative relationships were found for handedness and WFQ-derived dominance with femoral neck BMD dominance (r = -0.35, p = 0.01 and r = -0.32, p = 0.03 respectively), as well as arm folding dominance with tibial SSI dominance at the 14% site (r = -0.62, p = 0.003). While significance was not reached for other measures, a consistent trend for lower limb skeletal dominance in the functionally non-dominant limb was observed for 70% of all bone parameters. Conclusions: Contrary to conventional thinking, the functionally dominant lower extremity exhibits lower bone mass than the functionally non-dominant lower limb. Findings bring into question the standard practice of scanning left lower extremity regions of right handed individuals when skeletally non-dominant lower limb measures are desired.

***Disclosures: Belinda Beck**, None.*

SA0307

Bone Density and Bone Size in Older Men and Women Assessed by High Resolution pQCT: Contributions of Growth, Consolidation and Aging. Richard Eastell[1], Margaret A. Paggiosi[2], Jennifer Walsh*[2]. [1]University of Sheffield, United Kingdom, [2]NIHR Bone Biomedical Research Unit, United Kingdom

Bone size and density are major determinants of bone strength. HR-pQCT (Xtreme CT, Scanco) measures size-independent volumetric density (vBMD) and structure. The aims of this study were to 1) identify gender differences in bone density and size in older men and women, 2) determine the contributions of growth, consolidation and aging to bone density and size in older men and women 3) identify site-specific changes in bone density and size with aging. We conducted a cross-sectional observational study of 171 male and female healthy volunteers ages 16-18 (end of growth), 30-32 (peak bone mass) and >70 (aging). We measured BMD at the spine and hip with DXA, and the distal radius and tibia with HR-pQCT. HR-pQCT results were analysed by ANOVA with gender, age group and gender*age group interaction as fixed factors. ANOVA with linear contrast was used to compare groups and differences between groups. The table shows subject characteristics, DXA BMD and selected HR-pQCT results.

Radius total density was similar in older men and women, and was similar in men and women at the end of growth and peak bone mass. Density decreased with aging in men and women (M -18%, W -20%, $p<0.001$). Radius cortical perimeter was greater in older men than older women, and was also greater in men at the end of growth and peak bone mass ($p<0.001$). Cortical perimeter increased with aging in men and women (M 10%, W 6%). Cortical perimeter increased from the end of growth to peak bone mass in men, but not women (M 7%, W -1%, $p<0.05$).

Tibia total density was higher in older men than older women ($p<0.001$). Density decreased with aging in men and women (M -14%, W -23%, $p<0.001$). Women had slightly lower peak density, and greater loss with aging. Tibia cortical perimeter was higher in older men than older women, and was also higher in men at the end of growth and peak bone mass ($p< 0.001$). However, cortical perimeter did not differ by age in men or women.

We conclude: 1) radius vBMD does not differ by gender, 2) older men have larger radius size than women due to greater size at the end of growth and a gender-specific increase between the end of growth and peak bone mass, 3) older women have lower tibia vBMD than men due to lower peak values and greater loss with aging, 4) older men have larger tibia size than women due to greater size at the end of growth, 5) weight-bearing and non-weight-bearing bones differ in density and size variation due to gender and age.

	age 16-18		age 30-32		age 70+	
	F = 30	M = 30	F = 29	M = 24	F = 28	M = 30
Age years	17.5 (0.8)	17.4 (0.8)	31.2 (0.8)	31.5 (0.8)	75.0 (3.5)	75.5 (3.5)
Height cm	164.8 (5.1)	178.9 (7.2)	165.1 (5.9)	179.4 (5.8)	158.2 (6.7)	175.2 (6.0)
BMI kg/m^2	22.2 (3.6)	24.5 (5.9)	24.3 (4.0)	26.3 (3.6)	28.1 (5.0)	27.0 (3.1)
Lumbar spine BMD g/cm^2	0.962 (0.083)	0.995 (0.106)	1.040 (0.108)	1.090 (0.197)	0.965 (0.176)	1.111 (0.149)
Total hip BMD g/cm^2	0.959 (0.088)	1.082 (0.153)	0.974 (0.126)	1.087 (0.129)	0.871 (0.138)	1.019 (0.123)
Radius density[2] mg/cm^3	292.8 (52.4)	293.1 (53.8)	314.8 (62.1)	324.6 (46.0)	250.1 (60.1)	267.3 (48.4)
Radius perimeter[123] cm	70.8 (7.1)	81.3 (9.1)	70.1 (5.5)	87.0 (10.3)	75.3 (6.0)	95.7 (10.0)
Tibia density[12] mg/cm^3	295.3 (48.7)	308.9 (55.0)	324.1 (61.5)	349.0 (44.2)	248.6 (49.9)	300.2 (42.7)
Tibia perimeter[1] cm	105.7 (14.7)	123.9 (18.8)	99.9 (8.5)	116.8 (8.4)	105.2 (7.7)	121.5 (8.7)
values are mean (SD) multifactor ANOVA p<0.01: [1]gender, [2]age, [3]gender*age interaction						

Table

***Disclosures: Jennifer Walsh**, None.*

SA0308

Detection of Vertebral Fractures in Lateral Scout Views from Computed Tomography Using Statistical Models of Shape and Appearance. Jane Haslam[1], Yoo Mee Kim[2], Douglas Kiel[3], Elizabeth Samelson[3], Joes Staal[4], Peter Steiger*[5], Mary Bouxsein[2]. [1]Optasia Medical Ltd, United Kingdom, [2]Beth Israel Deaconess Medical Center, USA, [3]Hebrew SeniorLife, USA, [4]Optasia Medical Ltd., United Kingdom, [5]Optasia Medical, USA

Purpose: Vertebral fractures (VFx) are underdiagnosed worldwide. New methods that improve reliable VFx assessment are needed. Thus, the aim of this study was to develop and test algorithms which detect osteoporotic vertebral fractures in lateral CT scout view images.

Methods: Subjects included 50 men and 50 women (aged 50-87 yrs, mean 70 yrs) selected from the Framingham Heart Study Offspring and Third Generation cohorts. Vertebral shape was captured by a non-radiologist on CT lateral scout views from T4 – L4 using a novel semi-automated software tool (SpineAnalyzer, Optasia Medical), which captures vertebral shape with 95 points per vertebra. Scout films were also read by two trained radiologists using Genant SQ scores. Machine learning techniques were used to develop classification algorithms (or classifiers) for automatically detecting vertebral fractures given vertebral shape, for two definitions of VFx: 1) SQ grades 1-3 vs. grade 0, and 2) SQ grades 2-3 vs. grades 0-1. The classifiers were evaluated against consensus SQ readings for each definition of VFx in terms of their equal error rates (EERs), area under the Receiver Operator Characteristic (ROC) curve, and kappa score. Classifier testing was performed using ''leave one out'' cross-validation in order to give very nearly unbiased performance estimates.

Results: Based on radiologists' consensus SQ readings 977 vertebrae were normal and 44 fractured: 25 grade 1 (mild), 16 grade 2 (moderate) and 3 grade 3 (severe). For the two definitions of VFx, classifiers yielded EERs of 8.7% and 0.7%, areas under the ROC curves of 0.97 and 0.998, and maximum kappa scores of 0.57 (95% CIs: 0.42-0.71) and 0.83 (0.70-0.97) respectively. In comparison, for SQ 1-3 vs. SQ 0, radiologist inter-reader kappa scores were 0.56-0.59. For SQ 2-3 vs. SQ 0-1 radiologist inter-reader kappa scores were 0.68-0.72.

Conclusions: These initial results indicate the potential feasibility of developing algorithms which allow non-radiologist operators to use vertebral shape measurements, determined using a highly automated algorithm, to distinguish VFx in lateral CT scout view images. The algorithms' agreement with ''gold-standard'' SQ scores is similar to the agreement between experienced radiologists for the same data-set. These data provide strong rationale to validate the results on a larger data-set.

***Disclosures: Peter Steiger**, Optasia Medical Ltd., 3; Optasia Medical Ltd., 1*

SA0309

Effects of Antiresorptive Agents on Bone Micro-Architecture Assessed by Trabecular Bone Score in Women Age 50 and Older: The Manitoba Prospective Study. Marc-Antoine Krieg*[1], Andrew Goertzen[2], William Leslie[2], Didier Hans[3]. [1]University Hospital, Switzerland, [2]University of Manitoba, Canada, [3]Lausanne University Hospital, Switzerland

Antiresorptive agents such as biphosphonates induce a rapid increase of BMD during the 1st year of treatment and a partial maintenance of bone architecture. Trabecular Bone Score (TBS), a new grey-level texture measurement that can be extracted from the DXA image, correlates with 3D parameters of bone micro-architecture.

AIM: To evaluate the longitudinal effect of antiresorptive agents on spine BMD and on site-matched spine micro-architecture as assessed by TBS.

METHODS: From the BMD database for Province of Manitoba, Canada, we selected women age >50 with paired baseline and follow up spine DXA examinations who had not received any prior HRT or other antiresorptive drug. Women were divided in two subgroups: (1) those not receiving any HRT or antiresorptive drug during follow up (=non users) and (2) those receiving non-HRT antiresorptive drug during follow up (=users) with high adherence (medication possession ratio >75%) from a provincial pharmacy database system. Lumbar spine TBS was derived by the Bone Disease Unit, University of Lausanne, for each spine DXA examination using anonymized files (blinded from clinical parameters and outcomes). Effects of antiresorptive treatment for users and non-users on TBS and BMD at baseline and during mean 3.7 years follow-up were compared. Results were expressed % change per year.

RESULTS: 1,150 non-users and 534 users met the inclusion critera. At baseline, users and non-users had a mean age and BMI of [62.2 ± 7.9 vs 66.1 ± 8.0 years] and [26.3 ± 4.7 vs 24.7 ± 4.0 Kg/m^2] respectively. Antiresorptive drugs received by users were bisphosphonates (86%), raloxifene (10%) and calcitonin (4%). Significant differences in BMD change and TBS change were seen between users and non-users during follow-up ($p<0.0001$). Significant decreases in mean BMD and TBS (-0.36 ± 0.05 % per year; -0.31 ± 0.06 % per year) were seen for non-users compared with baseline ($p<0.001$). A significant increase in mean BMD was seen for users compared with baseline ($+1.86 \pm 0.0$ % per year, $p<0.0018$). TBS of users also increased compared with baseline ($+0.20 \pm 0.08$ % per year, $p<0.001$), but more slowly than BMD.

CONCLUSION: We observed a significant increase in spine BMD and a positive maintenance of bone micro-architecture from TBS with antiresorptive treatment, whereas the treatment naïve group lost both density and micro-architecture. TBS seems to be responsive to treatment and could be suitable for monitoring micro-architecture.

***Disclosures: Marc-Antoine Krieg**, None.*

SA0310

See Friday Plenary number FR0310.

SA0311

Measuring Bone Quality using Peripheral Quantitative Computed Tomography at the Tibia in Individuals with SCI: Reproducibility and Methodological Considerations. Lora Giangregorio[1], Deena Lala*[1], Kayla Hummel[1], Christopher Gordon[2], B. Catharine Craven[3]. [1]University of Waterloo, Canada, [2]McMaster University, Canada, [3]Toronto Rehabilitation Institute, Canada

Background: Measurements of trabecular connectivity and hole size can be obtained at the radius using the Stratec pQCT device despite the limited resolution. There are no reports of the same pQCT-based trabecular structure measurements at the tibia. It would be important to establish whether they could be measured reliably, particularly in individuals with low BMD.

Objective: To investigate the reproducibility of bone structure measurements in individuals with spinal cord injury (SCI) obtained using peripheral quantitative computed tomography (pQCT).

Design: Cross-sectional study

Participants/methods: Eleven individuals with SCI (C5-L1) were recruited to participate; 1 was excluded due to contractures. Mean (±SD) age was 43 (10) years and years post injury was 18 (14). pQCT scans were performed twice on the same day at the ultra-distal tibia, with repositioning between scans. The following bone structure variables were determined using in-house software: average and maximum hole size [mm^2]; connectivity index; average cortical thickness [mm]; bone volume to total volume (BVTV) ratio. For each outcome, the root mean squared coefficients of variation (RMSCV) were calculated.

Results: Mean (±SD) and RMSCV (in %) for bone structures variable were: average hole size 9.5 (9.7) mm^2, 7.0%; maximum hole size 663.1 (253.0) mm^2, 5.4%; connectivity index 0.16 (0.06), 2.9%; cortical thickness 0.94 (0.1) mm, 1.8%; BVTV 0.28 (0.12), 0.7%. Variability observed across participants may be attributable to factors such as age, impairment (AIS) or duration of injury. Potential sources of within subject variability include variations in positioning, or movement during scanning.

Conclusions: Although pQCT is a novel and feasible tool for measuring tibia bone structure, the RMSCV for some variables may necessitate multicentre studies with large sample sizes to determine treatment efficacy.

***Disclosures: Deena Lala**, Merck Frosst, 2*
This study received funding from: Canadian Institutes of Health Research, #86521

SA0312

Reliability of Semi-Automated Vertebral Morphometry Measurements using Lateral Scoutviews from Computed Tomography. Yoo Mee Kim*[1], Serkalem Demissie[2], Rahel Eisenberg[1], Douglas Kiel[3], Mary Bouxsein[1]. [1]Beth Israel Deaconess Medical Center, USA, [2]Boston University School of Public Health, USA, [3]Hebrew SeniorLife, USA

The presence of vertebral fracture (VFx) is among the strongest risks for future fracture. Despite this, underdiagnosis and undertreatment of VFx is a well-known problem worldwide. New methods are needed to improve the accuracy and efficiency of identifying VFx. Thus, the aim of this study was to determine intra- and inter-reader reliability of vertebral morphometry measurements performed using a new semi-automated algorithm that is based on shape-based statistical modeling (SpineAnalyzer, Optasia Medical, Cheadle, UK). Methods: 100 subjects (50 men and 50 women, aged 50-87 yrs, mean: 70.3±8.9 yrs) were selected from the Framingham Heart Study Offspring and Third Generation Multi-Detector Computed Tomography Study. Two non-radiologist readers independently assessed vertebral morphometry from the CT lateral scoutviews for T4-L4 at 2 time points. Deformities were classified as mild (≥20%), moderate (≥25%) or severe (≥40%) based on Genant's criteria. Intraclass correlation coefficients (ICCs), root mean squared CV (RMS-CV) and kappa (k) statistics were used to assess reliability. Results: Four subjects were excluded due to poor image quality. Of 1248 individual vertebrae from T4-L4 in 96 subjects, 1246 were analyzed. The time per subject needed to conduct morphometry measurements averaged 5 min 22 sec (range: 3:13 to 9:06 min:sec). Intra- and inter-reader ICCs for anterior, mid and posterior vertebral heights for all vertebral levels combined were excellent, ranging from 0.96 to 0.98. ICCs were also excellent at distinct spinal regions (T4-9, T10-12, and L1-4), ranging from 0.87 to 0.96. Intra- and inter-reader RMS-CV ranged from 2.5 to 3.9% and 3.3 to 4.4%, respectively. Based on morphometry measurements alone, Reader A and B identified 51-52 and 46-59 subjects, with at least one prevalent VFx, respectively. Examining all vertebral levels together, we found good intra- (k =0.59 to 0.69) and inter-reader agreement (k= 0.67) for VFx defined by a deformity of ≥ 20%. Conclusions: This new semi-automated method for assessing vertebral morphometry has excellent intra- and inter-reader reliability for vertebral height measurements on lateral CT scoutviews, and requires less time than conventional 6-point morphometry. Reliability for VFx assessment was comparable to previous reports for SQ grading by radiologists. Altogether, this semi-automated technique using CT lateral scoutviews is a convenient and reproducible method to facilitate assessment of VFx.

***Disclosures: Yoo Mee Kim**, None.*

SA0313

Vertebral Bone Loss Quantified by Normalised Mean Vertebral Area in Lateral Radiographs. Erik B Dam[1], Mads Nielsen[2], Martin Lillholm*[3]. [1]Nordic Bioscience & CCBR-Synarc, Denmark, [2]University of Copenhagen, Denmark, [3]Nordic Bioscience, Denmark

Osteoporosis drug trials often use incident vertebral fractures as markers of disease progression and treatment efficacy. The purpose of this study was to investigate bone loss through a continuous measure of vertebral area as a supplement to established progression markers.

The case-control study population consisted of 126 postmenopausal women; a subset of the community recruited PERF study. Case and control groups were matched with respect to age, height, weight, and BMD. Fracture status at baseline and follow-up (6.3 years) was determined from lateral radiographs by an experienced radiologist using Genant's semi-quantitative method. All subjects were fracture-free at baseline and the 101 controls remained fracture-free. The 25 cases developed at least one incident fracture in the lumbar region. The lumbar vertebrae had the corner and mid points marked using a computer tool. The vertebral bone area was calculated as the area of the hexagon defined by the six points. Radiographic scaling invariance was approximated through normalization with the square of the average width of vertebrae (T12-L5). Width was defined as the distance between the midpoints of the anterior and posterior heights. The normalised average vertebral area of the lumbar region was defined as the mean of the six areas. This area was calculated at baseline and follow-up for all 126 subjects. Results are given as mean ± SEM and significance tested using the Wilcoxon ranksum test for unpaired samples and the signed variant for paired.

The mean vertebral areas for the case group at baseline and follow-up and were 0.83 ± 0.01 and 0.77 ± 0.01, $p=1\times10^{-5}$. Similarly for the control group at baseline and follow-up: 0.84 ± 0.01 and 0.82 ± 0.01, $p=2\times10^{-12}$. The difference between cases and control was significant at follow-up $p=2\times10^{-5}$ whereas the difference between cases and controls at baseline was not p=0.35. The average vertebral bone area loss was significantly larger for the case group, $p=7\times10^{-12}$.

Several intuitive results were confirmed: The matched case and control groups had comparable vertebral bone area at baseline. Both groups individually suffered significant bone area loss from baseline to follow-up and the case group with fractures lost significantly more bone area than the fracture-free control group. Most promising is, however, the significant bone area loss in the fracture-free control group – a continuous and significant progression that is not registered by fracture readings.

***Disclosures: Martin Lillholm**, CCBR-Synarc, 3; CCBR-Synarc, 1*
This study received funding from: Nordic Bioscience and CCBR-Synarc

SA0314

Preliminary Comparison of FRAX™ (excluding BMD) with FRAX™ (including BMD calcaneal QUS T-Score) Screening Tool for Estimating Long-term Fracture Risk. Simon Dyall[1], Daphne Bird[1], Ian Drysdale*[2], Heather Hinkley[2]. [1]British College Osteopathic Medicine, United Kingdom, [2]British College of Osteopathic Medicine, United Kingdom

The aims of this study were to compare FRAX™ (excluding BMD) with FRAX™ (including calcaneal QUS T-Score) predictions for fracture risk and assess the ability of each to predict actual fracture over the long-term (10 years). Osteoporosis remains a major public health concern and accurate assessment of the associated bone fracture risk should enable appropriate targeting of vulnerable individuals with interventions intended to reduce this risk. Fracture risk may be predicted using simple non-invasive screening techniques that ensure patient safety at relatively low cost such as quantitative ultrasound (QUS) or the WHO fracture risk assessment tool, FRAX™, an algorithm of hip and other major osteoporotic fracture risk over 10 years.

180 Caucasian females, aged 40 to 79 at baseline were randomly selected from a cohort of 900 subjects screened using calcaneal QUS (McCue Cubaclinical). Relevant patient details were retrospectively entered into the FRAX™ assessment tool, either with or without BMD calcaneal QUS T-score, and indices of fracture risk were compared. Subjects completed a follow up questionnaire to ascertain details of any fracture and level of trauma within the subsequent 10 years, and fragility fractures were abstracted. Scores were classified into low, medium and high risk based on FRAX™ criteria, and the results analysed by Chi-squared statistic.

The FRAX™ scores were significantly different when calculated with and without BMD ($P<0.05$), and although not significant the Chi-squared analysis indicated a far closer relationship between fragility fracture and high risk with BMD QUS T-score (P=0.08 vs. P=0.93). Furthermore, ten year follow up (mean 10.1 years) revealed that 26 of the 180 subjects sustained fragility fractures, 9 of which were predicted by FRAX™ (18%) and 13 by FRAX™ (with BMD) (28%). There were two spine fractures which were in the high risk category for both techniques, of the 17 wrist fractures 5 were in the high risk category for FRAX™ and 8 for FRAX™ (with BMD), the hip fracture was predicted by both techniques as was one of the two elbow fractures.

It should be noted that the predictive ability of the techniques may have been confounded by increased interim use osteoporosis treatments taken following the initial screen. However, these preliminary findings suggest that the addition of calcaneal QUS T-score improves the ability to predict fragility fractures in women.

***Disclosures: Ian Drysdale**, None.*

SA0315

Prognosis of Fracture Risk by Quantitative Ultrasound Measurement and Bone Mineral Density. Nguyen Nguyen[1], Jacqueline Center[1], John Eisman[1], Tuan Nguyen[1], Mei Chan*[2]. [1]Garvan Institute of Medical Research, Australia, [2]Osteoporosis & Bone Biology, Australia

Quantitative ultrasound measurement (QUS) or bone mineral density (BMD) has been shown to predict fracture risk in women. However, whether a combination of QUS and BMD can improve the predictive value of fracture remains unclear. In this study, we sought to determine whether the combined use of calcaneal QUS and BMD measurements could improve the accuracy in fracture risk prediction, and to develop a nomogram based on the predictive model to predict the 5-year and 10-year fracture risk for individual men and women.

The study was designed as a population-based prospective investigation, which involved 407 women and 421 men aged 62-89 year, who had been followed for a median of 13 years (range 11-15 years) during the period of 1994-2009. BMD was measured at femoral neck by DXA using GE Lunar DPX-L densitometer and BUA was measured at the calcaneus using CUBA sonometer. The Cox's proportional hazards regression model was used to assess the association between fracture risk and the predictive variables. Reclassification analysis was used to compare the prognostic performance of the model including age, BMD and fall with the model including BUA.

During the follow-up period, 18% men (n=77) and 38% women (n = 154) had sustained a fragility fracture. Each standard deviation decrease in BUA was associated with a hazard ratio [HR] of fracture 1.86 (95%CI, 1.57-2.27) in women and 1.50 (95% CI, 1.19-1.94) in men. After adjustment for BMD, BUA remained significantly associated with fracture risk in women and men with reduced magnitude (HR 1.57, 95%CI, 1.26-1.95 in women; HR 1.32, 95% CI, 1.03-1.69 in men). For the model with BUA and BMD combined, the AUC increased from 0.71 to 0.74 in women, and from 0.695 to 0.697 in men. Reclassification analysis also yielded a total net reclassification improvement (NRI) of 9.7% (p = 0.02) and 3% (p = 0.69) for women and men respectively. Overall, 21% of women and 33% of men were reclassified into a different risk category.

Based on the estimated parameters of the final model (i.e. BUA, BMD fall and age), two nomograms were constructed for predicting fracture risk for an individual man and woman. These results suggest that calcaneal QUS was significant and independent predictor of fracture risk in both men and women. The combination of QUS and BMD in form of a nomogram can enhance the accuracy of categorizing individuals according to their risk of fracture, supporting the potential role of QUS in the prognosis of fracture.

***Disclosures: Mei Chan**, None.*

SA0316

See Friday Plenary number FR0316.

SA0317

Association Between Fat and Lean Distributions with Bone Mineral Density in KNHANES. Woong-Hwan choi[1], Sangmo Hong*[2]. [1]Hanyang university hospital department of internal medicine, South korea, [2]Hanyang University, South korea

It is uncertain whether obesity is protective or harmful to bone. There were many limitations due to collinearitis between BMD, Fat mass, muscle mass, and body weight in ths studies for role of fat to BMD.

The aim of this study was to define the role of muscle and fat distributions to BMD.

We analyzed body composition and BMD data of 1172 Male and 1546 female from KNHANES IV. Body composition and BMD were measured by DXA. Metabolic syndrome (Mets) modified to define any two of four factors except waist circumference by IDF definition due to conventional Mets has collinearity with central obesity. The relations of [Appendicular lean/Trunk lean; AM] for muscle, [Appendicular fat /Trunk lean; AF] for subcutaneous fat, [Trunk fat/Trunk Lean; CO] for central obesity, age, body weight (BW) and Mets with sub-total BMD analyzed by multiple regressions. We also generated the Z score of each factors by LMS method with LMS chartmaker pro 2.3.

In men, BMD (R2=0.275) had positive relations with AM (B=0.193) and BW (B=0.006) but had negative correlations with AF (B=-0.229), CO (B=-0.111), and Mets (B=-0.016). BMD (R2=0.258) of ⩾50 yr men only showed relation with CO (B=-0.187) and BW (B=0.006). Z score of BMD (BMDz, R2=0.251) showed relations with Z score of AF (AFz, B=-0.027), AMz (0.009), BWz (B=0.059) and Mets (B=-0.025) but Coz had no relation with BMDz. In ⩾50yr men, BMDz (R2=0.237) showed negative correlation with COz (B=-0.014) and AFz (B=-0.014), but AMz and Mets had no relation with BMD of ⩾50yr men. In women, BMD (R2=0.322) had negative relations with AF (B=-0.095), CO (B=-0.045), age (B=-0.002) and Mets (B=-0.009), and positive relations with AM (0.135) and BW (B=0.005). In ⩾50 women, BMD (R2=0.202) only had relation with CO (B=-0.043), BW (B=0.004), age (B=-0.004) and AM (B=1.124) but AF had no relations with BMD. BMDz (R2=0.219) in women had negative relations with AFz (B=-0.128), and COz (B=-0.096), and positive relations with AMz (B=0.135) and BWz (B=0.524). In ⩾50yr women, BMDz (R2=0.177) only had relation with COz (B=-0.098), BWz (B=0.457) and AMz (B=0.087) and AFz had no relations with BMDs.

We found that central obesity and subcutaneous fat had negative effects to bone except ⩾50 women. And muscle mass had relations with BMD, but its significant was disappeared (in men) or weaken [in women AMz B=0.131(<50yr) → 0.087(⩾50yr)] in older subjects.

***Disclosures: Sangmo Hong**, None.*

SA0318

Association of calcaneal QUS BMD and DEXA BMD at the femoral neck, lumbar spine and whole body in American Indian Men and Women. Maureen Murtaugh*, Molly McFadden, Khe-ni Ma, Tracy Frech, Laurie Moyer-Mileur, Martha Slattery, Tom Greene. University of Utah, USA

Little information is available about bone density, osetoporosis, and fracture risk in American Indian populations in the United States. The feasibility of dual energy s-ray absorptiometry (DEXA) screening among American Indian populations living in remote areas of reservations is met with challenges including cost, radiation exposure, and proximity to a DEXA table. Quantitative ultrasound (QUS) is attractive because it is portable, non-invasive, and does not involve exposure to radiation. Anecdotal reports from Alaska Native healthcare providers suggested that BMD estimated by QUS had a high false positive rate for osteopenia and osteoporosis determined by DEXA at the hip. Therefore, we explored the association of QUS measures as a predictor of DEXA measured BMD (g/cm^2) at the femoral neck, lumbar spine and whole body in American Indians living in the southwest. Participants were recruited randomly from the Education and Research Toward Health (EARTH) study to fill age and gender strata. Bone density of the hip, lumbar spine (L1-L4) and whole body were measured using a Hologic Discovery W DEXA machine following standard protocols in 925 men and women. Bone density at the heel was estimated using a Hologic Sahara QUS device in men and women ranging from 18 to 81. We explored the association of estimates of BMD from QUS as a predictor of femoral neck BMD using linear regression analyses stratified by gender. Calcaneal BMD, estimated using QUS, accounted for approximately 26% of the variation of femoral neck, lumbar spine and whole body BMD in women. In men, 15% of the variation of femoral neck BMD but only 4% of lumbar spine BMD and 8% of whole body BMD was explained by QUS BMD. A joint model including age, BMI and QUS BMD accounted for 51% of the variation in measured femoral neck BMD in women and 37% in men (Table 1). Associations with spine and whole body were lower, particularly among men. Using speed of sound (SOS), broadband ultrasound attenuation (BUA) and quantitative ultrasound index (QUI) in place of QUS BMD, resulted in similar associations with DEXA BMD at the three sites. In separate regression models, mean differences between estimates of BMD from calcaneal QUS vs. DEXA at the femoral neck, spine and whole body were systematically related to BMI, suggesting a BMI-dependent bias (Table 2). Population characteristics may be an important consideration in the utility of calcaneal QUS in estimation of BMD and bone health screening.

Table 2: DEXA minus Calcaneal QUS BMD (N=925)

		Femoral Neck	Spine	Whole Body
Gender	BMI	Mean ± SE		
Men	24	0.19±0.01	0.12±0.02	0.1±0.01
	30	0.24±0.02	0.15±0.02	0.13±0.02
	36	0.28±0.02	0.18±0.02	0.15±0.02
Women	24	0.11±0.02	0.06±0.02	0.01±0.02
	30	0.16±0.02	0.09±0.02	0.03±0.02
	36	0.2±0.02	0.12±0.03	0.06±0.02

Table 2

Table 1. R^2 for Models predicting DEXA BMD measurements From Calcaneal QUS BMD, BMI and age

		Femoral Neck	Spine	Whole Body
Model	SEX	R^2		
Calcaneal QUS BMD (g/cm)	F	0.256	0.284	0.262
Calcaneal QUS BMD	M	0.151	0.036	0.080
Calcaneal QUS BMD + BMI + Age	F	0.510	0.390	0.368
Calcaneal QUS BMD + BMI + Age	M	0.374	0.129	0.186

Table 1

***Disclosures: Maureen Murtaugh**, None.*

SA0319

Bone Density Following Long-Duration Spaceflight and Recovery. Shreyasee Amin*[1], Sara Achenbach[1], Elizabeth Atkinson[1], Elisabeth Spector[2], HJ Hartnett[2], L. Joseph Melton[1], Sundeep Khosla[3], Jean Sibonga[4]. [1]Mayo Clinic, USA, [2]Wyle Integrated Science & Engineering Group, USA, [3]College of Medicine, Mayo Clinic, USA, [4]NASA-Johnson Space Center, USA

Rapid bone loss in the weight-bearing skeleton is well recognized during long-duration spaceflight, but the implications on long-term bone health remain unclear. How bone mineral density [BMD] in US crew members serving on long-duration missions in space [US crew] compare with what would be expected had they not been exposed to microgravity, is unknown.

We therefore examined the observed changes in BMD (g/cm^2) among 28 US crew (immediately post-flight and following ~12 months recovery) relative to comparable age- and gender-expected changes derived from 348 men (age range at baseline: 22-90 yrs) and 351 women (range: 21-93 yrs) representing an age-stratified, random sample of the adult community population. BMD measurements (Hologic QDR 2000) were made at the total hip, lumbar spine, ultradistal and midshaft radius, and total body (sites also measured in US crew). Men were measured at baseline, 2, and 4 yrs; women were measured at baseline, 1, 2, and 4 yrs. Linear mixed effects models were used to predict follow-up BMD using baseline BMD, age, gender, and follow-up time, adjusting for the fact that most people were measured more than once. Models including body mass index (BMI) or lean mass were also considered. In US crew (24 men, age range at pre-flight scan: 36-53 yrs; 4 women, age: 41-53 yrs), BMD was measured pre-flight, immediately post flight and at ~12 months post-flight using Hologic QDR 2000, QDR 4500 and Discovery scanners. The majority had pre- and post-flight BMD on similar machines. Immediate post-flight BMD was performed a median of 6 (range: 3-33) days after return, with a median flight duration of 167 (range: 95-215) days. 22 men and 4 women had a scan within 6-18 months post-flight; median days from landing to ~12 months scan was 376 (range: 184-534) days.

The table shows the predicted and observed BMD and rates of change immediately and ~12 month post-flight for US crew. Findings were similar using prediction models which included BMI or lean mass. Due to microgravity exposure, the observed immediate post-flight BMD at all sites was significantly lower than predicted. However, at ~12 months post-flight, BMD at most sites in US crew were still lower than would be expected had they not been exposed to microgravity.

These findings have implications on potential long-term adverse effects on bone health of US crew serving on long-duration spaceflight missions.

	Mean BMD (g/cm²) (% change in BMD per month) [95% Confidence Interval]					
BMD Site	Immediate Post Flight			~12 Month Post Flight		
	Predicted	Observed	p-value	Predicted	Observed	p-value
Total Hip	1.082 (-0.00) [-0.05, 0.04]	1.012 (-0.87) [-1.04, -0.71]	<0.001	1.086 (0.01) [-0.01, 0.02]	1.062 (-0.10) [-0.15, -0.06]	<0.001
Spine	1.078 (0.12) [0.10, 0.13]	1.028 (-0.48) [-0.61, -0.34]	<0.001	1.086 (0.05) [0.05,0.06]	1.068 (-0.03) [-0.01, 0.03]	0.004
Ultradistal Radius	0.519 (-0.02) [-0.05, -0.00]	0.511 (-0.21) [-0.34, -0.09]	0.01	0.512 (-0.07) [-0.07, -0.06]	0.517 (-0.02) [-0.07, 0.02]	0.03
Mid Shaft Radius	0.710 (0.17) [0.11, 0.23]	0.695 (-0.06) [-0.17, 0.04]	0.001	0.705 (0.06) [0.03, 0.09]	0.694 (-0.01) [-0.06, 0.04]	0.02
Total Body	1.264 (-0.05) [-0.05, -0.04]	1.240 (-0.26) [-0.37, -0.16]	0.002	1.264 (-0.02) [-0.03, -0.02]	1.248 (-0.08) [-0.15, -0.01]	0.08

Table

***Disclosures: Shreyasee Amin**, None.*

SA0320

See Friday Plenary number FR0320.

SA0321

See Friday Plenary number FR0321.

SA0322

See Friday Plenary number FR0322.

SA0323

25-Hydroxyvitamin D-Levels in Community-Dwelling Postmenopausal Women Differ Between Swiss Mountain and Plain Areas During Winter. Jotinder Schuematschek-Kainth*[1], David Kissner[1], Albrecht Popp[1], Günter Menz[2], Raphael Kessler[3], Matthias Stahl[4], Christoph Senn[1], Spiros Arampatzis[1], Antonella Berlingieri[1], Romain Perrelet[1], Kurt Lippuner[1]. [1]Osteoporosis Policlinic, University of Bern, Switzerland, [2]Hochgebirgsklinik Davos, Switzerland, [3]HFR Tafers, Switzerland, [4]Kantonsspital Olten, Switzerland

Background: Adequate vitamin D supply plays a critical role in the maintenance of optimal musculoskeletal health. Since dietary vitamin D sources are scarce, sunlight exposure is an important determinant of Vitamin D status which therefore could differ among geographic regions. Little is known about differences in vitamin D status between plain and mountain areas in Switzerland, a country where 25% of the population lives in mountain sites.

Methods: In 150 randomly selected, community-dwelling women, aged 65-80 years, from 3 different regions, serum levels of 25-hydroxyvitamin D (25[OH]D) were assessed using the DiaSorin LIAISON "25-OH Vitamin D Total Assay" kit (Diasorin, Stillwater, MN, USA). One third of the women were living in a mountain area (Davos, 1600 m.a.s.l., n=50), one third in a plain rural area (Tafers, 651 m.a.s.l., n=50) and one third in a plain urban area (Olten, 396 m.a.s.l., n=50). All blood samples were taken during wintertime (February). Current intake of vitamin D supplements were recorded.

Results: Mean ($\pm$ SD) 25(OH)D levels were highest in Davos (49.9 $\pm$ 24.7 nmol/L), followed by Tafers (43.4 $\pm$ 23.6 nmol/L) and Olten (38.9 $\pm$ 19.2 nmol/L, p=0.015 vs. Davos). The respective rates of women with vitamin D inadequacy (<75nmol/L), insufficiency (<50 nmol/L) and deficiency (<22.5 nmol/L) were: 90%, 64%, and 20% (overall population), 84%, 56%, and 10% (Davos), 88%, 68%, and 18% (Tafers), and 98%, 68%, and 30% (Olten). The rates of inadequacy and deficiency were significanly higher in Olten than in Davos (p=0.015). One third of the women indicated to take current vitamin D-supplements in all three areas.

Conclusions: In Switzerland during wintertime, the prevalence of vitamin D inadequacy in community-dwelling postmenopausal women was high despite intake of supplements. People living in mountain areas may have some advantage over those in plain areas, possibly due to higher sun exposure.

***Disclosures: Jotinder Schuematschek-Kainth**, None.*

SA0324

A Bout of Resistance Exercise Increased Osteoprotegerin in Healthy Young Men. Katherine Brooke-Wavell*[1], James King[1], Stephen Burns[2], David Stensel[1]. [1]Loughborough University, United Kingdom, [2]National Institute of Education, Singapore

Purpose: The binding of receptor activator nuclear factor κB ligand (RANKL) to its receptor promotes osteoclast differentiation, activation and attachment to bone. The soluble decoy receptor osteoprotegerin (OPG) binds to RANKL, preventing the binding of RANKL to RANK, so reducing or preventing bone resorption. In vitro studies have reported increased production of OPG, and reduced production of RANKL, in response to loading. Increases in OPG have also been reported in humans following endurance running but there is little information as to the effects of resistance exercise. The purpose of the study was thus to determine whether a bout of resistance exercise influences serum OPG.

Methods: Participants were 16 healthy young men, who each completed a resistance exercise trial, and a control trial, in random order. The resistance exercise trial consisted of 3 sets of 12 repetitions of 10 resistance exercises, at 80% of 12-repetition maximum. During the control trial participants undertook sedentary activity in the laboratory. Food intake was matched for 48 hours before, and during the trials. A venous blood sample was collected before exercise and after 2.5 hours (30 minutes after the exercise bout). Changes in plasma volume were estimated from haemoglobin and haematocrit concentrations. OPG was analysed using a commercially available enzyme immunoassay from serum in seven participants and plasma in nine. Comparisons between trials were made with paired t-tests and repeated measures analysis of variance.

Results: Participants' mean +/- SD age was 24.1 +/- 3.2 y, height 1.79 +/- 0.06m and weight 77.6 +/- 9.3 kg. Resting OPG concentration did not differ between control and exercise trials (2.9 +/- 0.7 versus 3.2 +/- 0.9 pmol/l respectively). Changes in plasma volume did not differ between trials (p=0.591). OPG increased by mean (standard error) 7.3 (4.0) % after the exercise trial but decreased by 5.1 (3.6) % after the control trial. This difference between trials was statistically significant (p=0.040).

Conclusion: A bout of resistance exercise of an intensity that may be expected to increase bone mineral density increased serum OPG in healthy young men. The OPG/RANKL/RANK system may be involved in bone response to mechanical loading.

***Disclosures: Katherine Brooke-Wavell**, None.*

SA0325

Age-related Cortical Bone Loss and Fracture Patterns in the Neolithic Community of Çatalhöyük, Turkey. Sabrina Agarwal[1], Bonnie Glencross*[2]. [1]University of California, USA, [2]University of Toronto, Canada

The Neolithic (from 10,000 to 5,000 cal BC) is broadly characterized by population increase, sedentism, crowding and the adoption of an agricultural lifestyle. Typically prehistoric populations that follow a change in subsistence and lifestyle, show a decline in health as indicated by disruptions in bone remodeling, low cortical bone mass for age, poor bone quality and fragility fracture. The focus of this study is to examine age and sex-related patterns of cortical bone loss as well as skeletal fragility fracture in a Neolithic archaeological skeletal sample from Çatalhöyük, Turkey. Using metacarpal radiogrammetry, a method with specific advantages for investigating cortical bone loss in archaeological remains, 50 adult metacarpals (f=28 m=22) were examined. Measurements of total bone width (TW) and medullary width (MW) were taken and used to calculate cortical thickness (CT) and cortical index (CI). These parameters were then standardized for comparison with historic and modern European data. Çatalhöyük males and females demonstrate an inverse relationship where CI decreases as age and MW increase. Analyses indicate statistically significant age-related change in MW, CT and CI amongst the oldest females. Further, both Çatalhöyük males and females have significantly more compact bone across the entire adult life course than males and females from a medieval historic sample while maintaining similar amounts of compact bone in comparison to recent Europeans. Despite age-related loss of bone, no typical fragility fractures are observed. We discuss possible growth and lifestyle factors at Çatalhöyük that may have contributed to improved skeletal strength and reduction in the risk of fragility fracture, and the implications for understanding age-related bone loss in modern populations.

***Disclosures: Bonnie Glencross**, None.*

SA0326

Dietary Patterns and Bone Health in Women. Sarah McNaughton[1], Tikky Wattanapenpaiboon[1], John Wark*[2], Caryl Nowson[1]. [1]Centre for Physical Activity & Nutrition Research, School of Exercise & Nutrition Sciences, Deakin University, Australia, [2]Royal Melbourne Hospital, Australia

Increasingly, measures of dietary patterns have been used to capture the complex nature of dietary intake. Dietary patterns have been shown to be associated with health but few studies have investigated the impact of specific dietary patterns on bone health. The aim of this study was to examine the association between dietary patterns and measures of bone health in a sample of Australian women aged 18-65 years (n=527) recruited through the Twin and Sister Bone Research Program at the Royal Melbourne Hospital.

Bone mineral density (BMD; g/cm^2) at the lumbar spine (L2-L4) and total hip was measured from site-specific scans and total body bone mineral content (BMC; g) was measured from a total body scan using dual energy X-ray absorptiometry. Diet was assessed using a 4-day food diary. Dietary patterns were identified using principal components analysis (PCA). Scores were calculated based on the amount of each food consumed in the pattern and the weightings determined by the PCA. Participants were categorised into quintiles according to the scores. Analysis was conducted using generalised estimating equation methods and adjusted for clustering associated with twin and sister pairs and covariates.

PCA revealed 5 dietary patterns. Pattern 1 was characterised by high consumption of refined cereals, soft drinks, hot chips, sausages and processed meat, vegetable oils, beer and takeaway foods and low consumption of other vegetables, vegetable dishes, tea, coffee, fruit, wholegrain breads and breakfast cereals. This pattern was significantly inversely associated with total body BMC (adjusted for age, height, energy intake, physical activity, smoking, education and calcium intake). Each quintile increase in consumption of this pattern was associated with a 0.7% lower total body BMC. Pattern 4 (high consumption of legumes, seafood, seeds, nuts, wine, rice and rice dishes, other vegetables and vegetable dishes and low consumption of bacon and ham) was directly associated with BMD at both sites and total BMC in adjusted models. Each quintile increase was associated with an average higher bone density of 0.2% at the hip, 0.3% at the spine and 0.6% with total body BMC. The remaining dietary patterns, including those containing dairy foods, were not consistently associated with BMD or total body BMC.

This study identified specific dietary patterns associated with BMD and total body BMC among women and potential food-based strategies for improving bone health.

***Disclosures: John Wark**, None.*

SA0327

See Friday Plenary number FR0327.

SA0328

Evidence for an Association Between Seasonal Fluctuation of 25(OH)D and Serum C-telopeptide (CTx): Preliminary Evidence from the D-FINES study. Andrea Darling*[1], Fatma Gossiel[2], Rosemary Hannon[2], Debra Skene[1], Jacqueline Berry[3], Richard Eastell[2], Susan Lanham-New[1]. [1]University of Surrey, United Kingdom, [2]University of Sheffield, United Kingdom, [3]University of Manchester, United Kingdom

The purpose of this study was to assess whether there is a difference in bone resorption by degree of seasonal change in 25(OH)D and whether this varies by ethnicity. In the recent D-FINES study, (Vitamin D, Food Intake, Nutrition and Exposure to Sunlight in Southern England, 2006-2007), a subset of n=65 from the 293 participants (South Asian (n 30) and Caucasian (n 35)) had blood taken in four seasons for determination of 25(OH)D and serum c-telopeptide (sCTX). sCTX was measured using an electrochemiluminescent immunoassay (Roche cobas e411). Seasonal fluctuation of 25(OH)D was assessed by calculating differences between the winter (nadir) and summer (peak) 25(OH)D. For ease of interpretation these changes were expressed as positive values. This enabled investigation of the absolute change in 25(OH)D but not its direction. This variable was then split into quartiles within ethnicity. The dependent variables were absolute concentration of sCTX in each season as well as summer to winter change in sCTX. ANCOVA was run with absolute summer and winter 25(OH)D status, age, BMI, socioeconomic status, physical activity, and dietary calcium as covariates. In the Asian group there was no clear trend between degree of seasonal fluctuation and absolute sCTX. Indeed, only the autumn data was statistically significant (F=5.93; p= 0.01) and with no consistent pattern among the quartiles. No data were significant for change in summer to winter sCTX in Asians or Caucasians despite a trend in both ethnic groups for lower sCTX in the middle quartiles relative to the highest and lowest. Last, in Caucasians, there was a non-statistically significant ($p>0.05$) inverse trend between cycling of 25(OH)D and absolute serum C-telopeptide levels. These data suggest lower bone resorption in all seasons in Caucasians with increased cycling, and a reduction in sCTX between summer and winter in both ethnic groups in the middle quartile relative to the other quartiles. As the values were covariate adjusted, these findings are not likely to be due to other variables. However, it must be borne in mind that these results are only trends, which is likely due to the small numbers of subjects. Further research is required to analyse banked urine samples from the D-FINES study (n 293) which would enable us to see if these results are statistically significant with increased statistical power.The D-FINES study was funded by the UK Food Standards Agency. All views are those of the authors alone

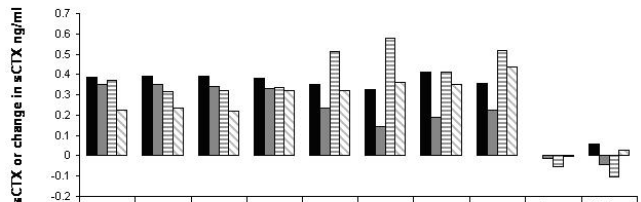

	Cauc Summer	Cauc Autumn	Cauc Winter	Cauc Spring	Asian Summer	Asian Autumn	Asian Winter	Asian Spring	Cauc change in sCTX	Asian change in sCTX
1st Quartile	0.387	0.391	0.39	0.382	0.352	0.327	0.41	0.356	0.003	0.058
2nd Quartile	0.351	0.353	0.34	0.331	0.235	0.146	0.189	0.223	-0.011	-0.045
3rd Quartile	0.373	0.318	0.32	0.335	0.514	0.58	0.41	0.519	-0.053	-0.104
4th Quartile	0.223	0.233	0.221	0.32	0.319	0.363	0.349	0.439	-0.002	0.03

Serum CTX by quartile of seasonal change in 25(OH)D

***Disclosures: Andrea Darling**, None.*

SA0329

Middle-aged Men with Dietary Intake of Omega-3 Long Chain Polyunsaturated Fatty Acids above the Median have Higher Bone Mass for Age. Nour Makarem*[1], Jason DeGuire[1], Catherine Vanstone[1], Suzanne Morin[2], Hope Weiler[1]. [1]McGill University, Canada, [2]McGill University Health Centre, Canada

Background: Dietary eicosapentaenoic (EPA) and docosahexaenoic acid (DHA) are associated with improved bone health in postmenopausal women and in animals, but evidence is scarce in men.

Objective: To determine if the dietary intake of EPA and DHA and their subsequent levels in erythrocytes are associated with higher BMD in healthy middle aged men.

Methods: This analysis represents the first 27 participants in a cross-sectional sample of healthy men between 37 and 53 years. Measures included: anthropometry, dietary intake of EPA and DHA using the validated Harvard/Willett food frequency questionnaire (FFQ), assessment of serum 25-hydroxy vitamin D using an automated immunoassay (Liaison, Diasorin), and assessment of BMD at the whole body, spine, total left hip and femoral neck using DXA. The Paffenbarger physical activity questionnaire was used to capture total and weight-bearing activity. BMD of

participants with dietary intake of EPA and DHA below (group 1: G1) and above (group 2: G2) the median was compared using t-tests. The results were then confirmed with a multiple regression analysis using EPA and DHA intake, calcium intake, serum 25-hydroxy vitamin D, height, and BMI as independent variables and whole body BMD and spine, hip, and femoral neck BMD z-scores as the dependent variables.

Results: There were no differences between the groups for age (G1: 43.6 ± 1.3 vs G2: 45.9 ± 1.4 y, P=0.259), BMI (G1: 25.7 ± 1.2 vs G2: 28.1 ± 1.1 kg/m^2, P=0.149), serum 25-hydroxy vitamin D (G1: 67.0 ± 6.6 vs G2: 67.0 ± 5.0 nmol/L, P=0.497), or calcium intake (G1: 1255 ± 116 vs G2: 1169 ± 103 mg/d, P=0.584). By design, mean intakes of EPA plus DHA were higher in group 2 (P=0.009). Group 2 had higher BMD for whole body (P=0.019), spine (P=0.012), and femoral neck (P=0.040), but not total hip (P=0.074) plus higher BMD z-scores at the spine (P=0.005), total hip (P=0.033), and femoral neck (P=0.016). Multiple regression analysis confirmed that EPA and DHA intake was the only significant independent predictor of whole body BMD (P= 0.014) and regional BMD z-scores (P<0.024).

Conclusion: These data suggest that men with higher intakes of EPA and DHA have improved bone health. This is consistent with evidence from other population groups. Future investigation using a larger sample will include assessment of EPA and DHA using erythrocyte membrane fatty acid analyses, confirm present results, and provide clarification as to whether benefits are also evident for the hip BMD.

	Group 1	Group 2	P-value
Whole Body BMD (g/cm^2)	1.268 ± 0.037	1.380 ± 0.025	0.019
Lumbar Spine BMD (g/cm^2)	0.998 ± 0.043	1.131 ± 0.024	0.012
Hip BMD (g/cm^2)	1.016 ± 0.046	1.114 ± 0.026	0.074
Femoral Neck BMD (g/cm^2)	0.874 ± 0.049	1.000 ± 0.030	0.040
Lumbar Spine BMD z-score	-0.814 ± 0.361	0.529 ± 0.239	0.005
Hip BMD z-score	0.036 ± 0.035	0.800 ± 0.190	0.033
Femoral Neck BMD z-score	0.007 ± 0.320	0.993 ± 0.211	0.016

Data are mean ± SEM

Group 1 and Group 2 BMD and BMD z-scores

***Disclosures: Nour Makarem**, None.*

SA0330

Temporal Trends and Determinants of Longitudinal Change in 25-Hydroxyvitamin D Levels in a Population-based Study. Claudie Berger*[1], Lisa Langsetmo[2], Nancy Kreiger[3], Linda Greene-Finestone[4], Christopher Kovacs[5], Brent Richards[6], Nick Hidiroglou[7], Kurtis Sarafin[7], K. Shawn Davison[8], Jonathan Adachi[9], Jacques Brown[8], David Hanley[10], David Goltzman[11]. [1]McGill University, Canada, [2]Canandian Multicenter Osteoporosis Study, Canada, [3]University of Toronto, Canada, [4]Public Health Agency of Canada, Canada, [5]Memorial University of Newfoundland, Canada, [6]Jewish General Hospital, McGill University, Canada, [7]Health Canada, Canada, [8]Laval University, Canada, [9]St. Joseph's Hospital, Canada, [10]University of Calgary, Canada, [11]McGill University Health Centre, Canada

Vitamin D plays a clear role in skeletal health and in other diseases. We examined vitamin D intake, sun-exposure, and body mass index (BMI) and subsequent changes in serum 25(OH)D over a five-year period among CaMos participants in 2 centres.

We studied 481 women and 213 men aged 30+ years with available 25(OH)D levels drawn in 2000-02 (year 5) and 2005-07 (year 10). Blood samples were all analyzed in the same laboratory using Diasorin Liaison. Our main outcome was change in serum 25(OH)D levels (nmol/L). Potential predictors were vitamin D intake from supplements and drugs (year 10 and change), BMI (year 10 and change), and sun exposure. We used multiple linear regression adjusting for sex, age, season of blood draw, centre (Quebec City and Calgary), and physical activity. Interactions between change in vitamin D intake and season of blood draw and centre were considered.

Vitamin D supplement intake was 174.3 (SD=279.3) IU/day at year 5 and 336.9 (SD=408.6) IU/day five years later. Average BMI increase was 0.27kg/m^2 (95% CI: 0.10; 0.44). More than two-thirds of participants reported direct sunlight exposure (>30 minutes) as never or seldom at both time points, while 7.6% reported regular or frequent exposure. 66% of the participants had both draws done in the same season. Average difference between year 5 and 10 in 25(OH)D levels was 3.24 (1.64; 4.83) nmol/L. Those who had their blood drawn in the same season showed an average increase of 3.6 (1.6; 5.7) nmol/L and those who had them drawn in a different season showed a trend toward an increase with a mean of 2.5 (-0.2; 5.1) nmol/L. At year 5, only 33.3% of men, 32.4% of women, and 32.7% overall had 25(OH)D levels >75 nmol/L. By year 10, 38.4% of men, 42.7% of women and 39.6% overall had levels >75nmol/L. Increase in vitamin D supplements, older age, and being from Quebec city were among the variables associated with an increase in 25(OH)D levels over time. BMI (year 5 or change) was not associated with changes in 25(OH)D levels.

The results, in a longitudinal population-based cohort, indicate a trend toward increasing 25(OH)D levels over the 5-year period. This trend appears to be due to changes in vitamin D intake but indicate that more than 400 IU per day will be required to increase levels in the population above 75nmol/L.

***Disclosures: Claudie Berger**, None.*

SA0331

50 Year Predicted Changes in BMD Distribution and Hip Fracture Incidence in Canada. Lisa Langsetmo*[1], David Hanley[2], Claudie Berger[3], Nancy Kreiger[4], Christopher Kovacs[5], Alexandra Papaioannou[6], David Hanley[2], K. Shawn Davison[7], Jerilynn Prior[8], Robert Josse[9], David Goltzman[10]. [1]Canandian Multicenter Osteoporosis Study, Canada, [2]University of Calgary, Canada, [3]McGill University, Canada, [4]University of Toronto, Canada, [5]Memorial University of Newfoundland, Canada, [6]Hamilton Health Sciences, Canada, [7]Laval University, Canada, [8]University of British Columbia, Canada, [9]St. Michael's Hospital, University of Toronto, Canada, [10]McGill University Health Centre, Canada

Background: The age distribution in the Canadian population is expected to change over the next 50 years, with a consequent increase in the burden of hip fracture. Our objective was to predict the burden of hip fracture based on estimated distribution of age and bone mineral density (BMD) over the period 2006-2056 assuming a) sex-age-specific fracture rates remain constant and b) sex-age-specific fracture rates change according to changes in sex-age-specific BMD.

Methods: Study participants (2590 men, 5740 women) were members of CaMos, an on-going population-based cohort study of Canadians ages ⩾ 25 years. We assessed the distributions of BMD at baseline (1995-1997) and year 10 (2005-2007), as well as the mean 10-year longitudinal rate of change by sex and five-year age categories. We assumed constant peak bone mass and constant sex-age-specific rates of change to forecast the future distribution of BMD. Multiple imputation was used to account for missing data. Our base fracture model assumed the sex-age-specific hip fracture rates remain constant over time. Our second model incorporated the expected changes in BMD together with the established relationship between BMD and hip fractures to estimate a predicted fracture rate. Future population age distributions were based on Statistics Canada forecasts.

Results: For men over 50 years, the mean total hip BMD was 0.997 g/cm^2 in 2006, 0.979 g/cm^2 with same BMD distribution but 2056 age weights, and 0.963 g/cm^2 using the predicted 2056 age and BMD distribution. For women over 50 years, the mean total hip BMD was 0.858 g/cm^2 in 2006, 0.833 g/cm^2 using the same BMD distribution and 2056 age weights, and 0.880 g/cm^2 using the predicted 2056 age and BMD distribution. Assuming constant rates, the crude incidence rate of fracture over 50 years would increase by 153% in men and 133% in women, due to estimated changes in age (see Figure). Assuming the predicted changes in BMD distribution, the crude incidence rate of fracture over 50 years would increase by 177% in men, but would increase by only 54% in women.

Conclusion: A simple model based on age alone predicted decreases in mean BMD in both men and women, as well as dramatic increases in hip fracture incidence between 2006 and 2056. However, the predicted increases in hip fracture due to changes in age distribution may be partially mitigated by secular increases in BMD in women, but not in men.

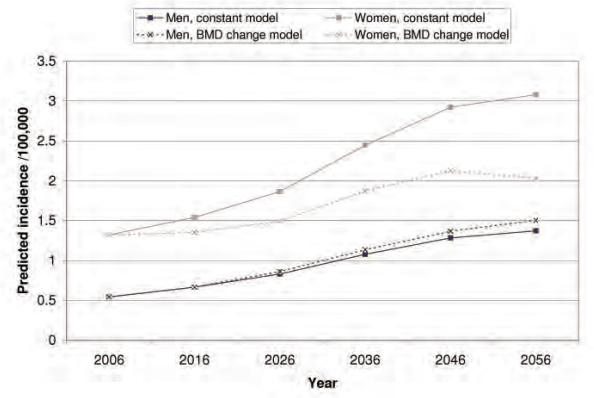

Figure

***Disclosures: Lisa Langsetmo**, None.*

SA0332

See Friday Plenary number FR0332.

SA0333

Association Between Beta-blocker use and Fracture Risk: the Dubbo Osteoporosis Epidemiology Study. Shuman Yang*[1], Nguyen Nguyen[2], Jacqueline Center[2], John Eisman[2], Tuan Nguyen[2]. [1]Garvan Institute, Australia, [2]Garvan Institute of Medical Research, Australia

Mice treated with beta-blockers (BB) had increased bone mass. Low bone mass is a predictor of fracture risk. The present study sought to examine the association between BB use and fracture risk in elderly men and women.

Data from 3536 participants (1293 men) aged 50 years and above in the Dubbo Osteoporosis Epidemiology Study were analyzed. Baseline characteristics of participants were obtained at the initial visit which had taken place between 1989 and 1993. Bone mineral density (BMD) at the lumbar spine and femoral neck was measured by dual energy X-ray absorptiometry (GE-LUNAR Corp, Madison, WI). Two hundred and seventy (21%) men and 451 (20%) women had been on BB, as ascertained by direct interview and verification with medication history. The incidence of fragility fractures was ascertained during the follow-up period (1989-2008). Propensity score analysis was used to adjust for potential differences in covariates between BB users and non-BB users.

During the follow-up period, 237 men and 681 women had sustained a fragility fracture. As expected, men and women with a fracture were older and had lower BMD than those without a fracture. Men who used only beta-blocker had a significantly lower risk of fracture than those not on beta-blocker (odds ratio [OR]: 0.63; 95% CI: 0.43-0.92). A similar trend was observed in women, but it was not statistically significant (0.96; 0.77-1.21). These associations did not change after adjusting for age, BMD and common risk factors. A combination of the use BB and thiazide was non-significantly associated with lower fracture risk in both sexes (0.94; 0.37-2.47 for men and 0.95; 0.61-1.49 for women). Men on BB had higher BMD at the femoral neck (0.96 versus 0.92 g/cm^2, $P<0.01$) after adjustment for propensity score.

These data suggest that use of beta blockers was associated with reduced fracture risk in men, and the association is likely to be mediated by BMD. Given the high prevalence of osteoporosis and hypertension in the general population, this finding raises the possi-
bility that these anti-hypertensive agents may have materially affected osteoporosis in many populations with high incidence of hypertension, such as the US, Europe and Japan.

***Disclosures: Shuman Yang**, None.*

SA0334

BMD Enhances Clinical Risk Factors in Predicting Ten-Year Risk of Osteoporotic Fractures in Chinese Men: The Hong Kong Osteoporosis Study. Cora Bow*[1], Shirley Tsang[2], Sze Sze Soong[1], Siu Ching Yeung[1], Annie Kung[3]. [1]Department of Medicine, The University of Hong Kong, Hong kong, [2]University of Hong Kong, Peoples republic of china, [3]Department of Medicine, University of Hong Kong, Hong kong

Introduction: Clinical risk factors with or without bone mineral density (BMD) measurements are increasingly recognized as reliable predictors of absolute fracture risk. Clinical risk factors may be population specific. The purpose of this prospective study was to determine the risk factors for osteoporotic fractures and to predict the 10-year risk of fractures in Southern Chinese male population.

Materials and Methods: This is a part of the Hong Kong Osteoporosis Study. 1,525 community-dwelling, treatment-naive Southern Chinese men aged 50 or above were recruited. Baseline demographic characteristics and clinical risk factors were obtained, and BMD at the spine and hip were measured. Subjects were prospectively followed for incident low trauma fractures. Ten-year risks of major osteoporotic fracture and hip fracture were calculated using Cox proportional hazards models.

Results: The mean age of subjects was 68 $\pm$ 10 years. After 3.5 $\pm$ 3 (1–14) years of follow-up, 36 non-traumatic incident fractures were reported. The incident rates for osteoporotic fractures and hip fractures were 676/100,000 and 132/100,000 person-years respectively. The most significant predictors of osteoporotic fracture were history of fall (odds ratio 14.5) and fragility fracture (odds ratio 4.4). Other predictive factors included outdoor activity <60 minutes per day, body mass index (BMI) < 20 kg/cm^2, difficulty bending forward, use of walking aid, and age $\geq$ 65 years. Each SD reduction in BMD at spine or hip was associated with 1.7 to 2.6-fold increase in fracture risk. Subjects with 5 or more clinical risk factors had an absolute 10-year risk of osteoporotic fracture of 6.2%, which increased to 18.2% if they also had total hip BMD T-score $\leq$ -2.5. Addition of BMD information (total hip T-score $\leq$ -2.5) significantly enhanced fracture risk prediction when compared to clinical risk factors only (omnibus test p=0.001). Men with multiple risk factors and low BMD T-scores have a higher absolute fracture risk, while men with no risk factors and normal BMD have a lower fracture risk than that predicted by FRAX.

Conclusions: Clinical risk factors are population specific and the addition of BMD measurement to risk factor assessment improves fracture risk prediction in Southern Chinese men.

***Disclosures: Cora Bow**, None.*

SA0335

Clinical Utility of Combined Femoral Neck and Lumbar Spine Bone Mineral Density Measurements in the Individualized Prognosis of Fracture. Tuan Nguyen*[1], Nguyen Nguyen[1], Steven Frost[2], Dana Bliuc[1], Jacqueline Center[1], John Eisman[1]. [1]Garvan Institute of Medical Research, Australia, [2]University of Western Sydney, Australia

Femoral neck bone mineral density (FNBMD) has been used as the principal predictor of fracture risk in men and women, even though more than 50% of women and ~70% of men who fracture do not have low FNBMD. Lumbar spine BMD (LSBMD) has also been used in the prognosis of fracture risk, but there is a concern over its predictive value due to degenerative change that affects spinal BMD measurement. The present study sought to address that question by examining the contribution of FNBMD and LSBMD to the prediction of fracture.

The Dubbo Osteoporosis Epidemiology Study was designed as a community-based prospective study, with 1358 women and 858 men aged 60+ years as at 1989. Baseline measurements included femoral neck bone mineral density (FNBMD and LSBMD), prior fracture, a history of falls and body weight. The Cox's proportional hazards model was used to assess the contributions of BMD and clinical risk factors to the prediction of fracture risk.

During the follow-up period, 426 women and 149 men had sustained a low-trauma fracture. There were 77 first hip fractures in women and 26 in men. For predicting any fracture and hip fracture, LSBMD was not a significant and independent predictor in the presence of FNBMD. The area under the ROC (AUC) of the model including FNBMD, age, prior fracture and falls was 0.75; when LSBMD was added to the model the AUC was still 0.75. For hip fracture, the AUC value of the model with FNBMD and the model combined FNBMD and LSBMD were the same of 0.85. When the lower value of either LSBMD or FNBMD was used in the model, these results remained unchanged. Further re-classification analysis revealed that while the use of lower LSBMD did not improve the AUC over and above that of FNBMD, value of LSBMD was useful in ruling out fracture (i.e., increase specificity by ~17% to 38%).

These data suggest that although lumbar spine BMD may not be an independent predictor of fracture risk, its use in conjunction with femoral neck BMD could be useful for ruling out fracture cases, particularly hip fracture. This "ruling-out" utility can be very valuable in the individualization of fracture prognosis.

***Disclosures: Tuan Nguyen**, None.*

SA0336

Creation of an Electronic Order Set to Improve the Care of Patients with Osteoporotic Fractures. Beatrice Edwards*[1], Andrew Bunta[2], Nikolas Kazmers[3], Kenzie Cameron[4], Lidia Andruszyn[3], Nicole Dillon[3], Gabrielle Edwards[3], Allison Hahr[5], Mark Williams[6]. [1]Northwestern University Medical School, USA, [2]Northwestern University Feinberg School of Medicine, USA, [3]Northwestern University, USA, [4]Division of Internal Medicine, Northwestern University, USA, [5]Division of Endocrinology, Northwestern University, USA, [6]Division of Hospital Medicine, Northwestern University, USA

Background: Patients with osteoporotic fractures are rarely assessed and treated for osteoporosis

Goal: creation of Information technology based intervention to assist physicians in providing medical care for osteoporosis to individuals hospitalized with fractures.

Methods: Study conducted at Northwestern Memorial Hospital (NMH) Chicago from Jan 2008- Dec 2009. Physician focus groups explored attitudes about osteoporosis and secondary prevention in patients with fractures. Physicians provided feedback on their ideal EMR intervention in order to improve care of patients with fractures. Information technology: based on physician recommendation a Powerchart (Cerner) based order set was created for clinical use. Creation of list of patients hospitalized with fractures was performed via text "parsing". Parsing is the visual recognition of specific terms in radiologic report. Terms searched included: fractures, compression deformity, and insufficiency fracture. A list of patients with fractures was created. Exclusion: patients under the age of 50 yrs, with metastatic cancer, other metabolic bone disorders, or CKD stage 5 . Dissemination: conferences were held for medical staff and trainees on secondary prevention of osteoporosis and review of the order set (4 sessions) Evaluation: Medical records of patients hospitalized in the Medicine service were reviewed for the following 9 months. Monthly treatment rates were calculated

Results: Four focus groups were conducted with six physicians per group, participants were General Internal Medicine (N= 10) Hospital Medicine (n=14). All were attendings at NMH. Physicians noted that lack of radiologist emphasis on presence of fracture, time constraints, competing demands, need for brief hospitalization, and lack of IT-based reminders limited their ability to provide care for such patients. 278 cases were reviewed, diagnosis and anti-resorptive treatment rate varied from 2-12%, mention of need for outpatient osteoporosis care with PCP varied from 3-14% over the next 12 months. Figure 1 Pelvic fractures were readily identfied and treated (n=14/21, 67%)

Conclusion: The creation of an order set was recommended by clinicians but rarely used in practice. Low level of clinician/radiologist awareness, competing demands, need for brief hospitalizations, limit clinicians' ability to address osteoporosis in practice. Other interventions must be explored in an effort to overcome this gap in medical care.

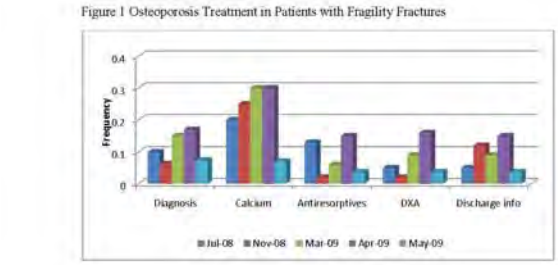

Figure 1 OSTP in Patients with fractures

***Disclosures: Beatrice Edwards**, Amgen,5; Procter and Gamble, 2; Eli Lilly,5; Novartis,5*

SA0337

Has the Cost Burden of Incident Fractures Changed Over Time? A Longitudinal Analysis from 1996-2008. Colleen Metge*[1], Mahmoud Azimee[1], Lisa Lix[2], Suzanne Morin[3], Patricia Caetano[4], William Leslie[1]. [1]University of Manitoba, Canada, [2]University of Saskatchewan, Canada, [3]McGill University Health Centre, Canada, [4]Manitoba Health, Canada

Cost-of-illness (COI) analysis is used to evaluate the economic burden of illness in terms of health care resource (HCR) consumption and production losses. Incidence-based COI is useful when considering fracture prevention measures and post-fracture management from a cost distribution perspective.

AIM: To estimate costs over time related to incident fractures in older women and men and to describe the incremental costs of fracture in Canada.

METHODS: We used the Population Health Research Data Repository for Manitoba—a comprehensive collection of databases including physician visits, hospitalization and pharmaceutical prescriptions—to identify incident fractures (Apr 1997-Mar 2007) and HCR costs (Mar 1996-Apr 2008). An incidence approach was used to count fracture numbers by site/mechanism (hip, wrist, spine, humerus, other and trauma) and sex in Manitobans aged 50 y and older; a bottom-up approach was used to estimate costs (quantity x unit costs) in the year pre- and post-fracture. Incremental fracture-related costs were calculated as the difference between the year pre- and post-fracture. Costs were expressed in constant dollars (2006 CDN) and evaluated for linear trends over time.

RESULTS: Over the 10 years, adjusted post-hip fracture costs in women changed minimally for hospitalization ($24,863 to $20,085, -1.6% per y, p=.12) and personal care home residence ($11,980 to $12,485, +1.7% per y, p=.15), significantly for physician costs ($2,149 to $3,447, +6.7% per y, p<.0001) and drug costs ($792 to $1974, +14.3% per y, p<.001); home care costs did not change significantly over time ($3,456 to $3,433, -0.5% per y, p=.55). Total costs in the year post-hip fracture were stable in women (+0.1% per y, p=.87) and men (-0.6% per y, p=.58). Incremental costs (the difference between pre- and post-hip fracture costs) increased significantly for physician services (p<.001) and decreased significantly for drug costs (p<.001) in both women and men. Total incremental cost changes over time were variable and depended on type of fracture and sex (see Table); a significant reduction was seen for wrist fractures in women (-4.4% per y, p<.001) with increases for trauma fractures in women (+7.9% per y, p=.003) and men (+8.4% per y, p=.018).

CONCLUSION: Post-fracture costs have changed over time in a site-dependent manner. Identifying projected cost-of-illness including health care resource use will help to estimate the future cost burden of fracture.

		Hip	Wrist	Spine	Humerus	Other	Trauma
	N=	5217	6295	2128	3326	15997	924
Women	Annual % Change	+0.3%	-4.4%	+1.3%	-0.5%	+2.6%	+7.9%
	p for Linear Trend	0.801	<.001	0.484	0.792	0.255	0.003
Men	Annual % Change	-1.3%	-0.4%	-4.8%	-0.6%	+1.7%	+8.4%
	p for Linear Trend	0.659	0.915	0.189	0.769	0.338	0.018

Table: Change in incremental total costs over time (1996-2008)

***Disclosures: Colleen Metge**, Bayer Inc, 5; sanofi-aventis, 5; Amgen, 2*
This study received funding from: Amgen Canada

SA0338

See Friday Plenary number FR0338.

SA0339

See Friday Plenary number FR0339.

SA0340

Ontario Osteoporosis Strategy: Three Year Evaluation of Quality Indicators. Gillian Hawker[1], Susan Jaglal*[2], Cathy Cameron[1], Ruth Croxford[3]. [1]Women's College Hospital, Canada, [2]University of Toronto, Canada, [3]Institute for Clinical Evaluative Sciences, Canada

Purpose: In February 2005, the Ontario Osteoporosis Strategy was launched to address the gaps in care with the overall goal to reduce fractures, morbidity, mortality and costs from osteoporosis through an integrated and comprehensive approach aimed at health promotion and disease management in the population. The province of Ontario, Canada has 11 million inhabitants. The purpose of this research is to evaluate the impact on health system indicators after the first 3 years of implementation of the strategy. Methods: A literature review followed by a Delphi process was used to identify and refine quality indicators for osteoporosis and post-fracture care. Quality indicators using administrative data sources were selected for the three year evaluation due to data availability. Data sources included hospital discharge abstracts and emergency department visits to identify fractures; physician billings for BMD testing and drug plan data which only includes individuals 65 years and older. Time trends for each indicator were calculated from 2002 to 2008. Indicators examine fracture rates, BMD testing, treatment rates and adherence. Results: For the primary indicator, fracture rate there was no significant change in fracture rates between 2002 and 2008. The rate of BMD testing was constant over the time period with a greater proportion of patients at "high risk" being tested. The number of BMD tests was constant at about 500,000 per year until 2008 when it dropped to 480,000. The indicator BMD testing one year after a fracture showed an increasing proportion among those who fractured from 2002 to 2007. In 2005 12.7% of hip fracture patients had a BMD test compared to 16.6% in 2007 compared to 24.9% in 2005 and 26.5% in 2007 for wrist fractures. However, over the time period there was no difference in one year adherence rates among those 66+ years who initiated an osteoporosis medication. Conclusions: In the first three years of implementation of the Ontario Osteoporosis Strategy the emphasis was on improving post-fracture care where fracture clinic coordinators were placed in high volume hospitals. This 3 year evaluation suggests that the strategy is successful in targeting these high risk individuals for osteoporosis care. More time is needed before conclusions can be drawn about the impact on fracture rates.

***Disclosures: Susan Jaglal**, None.*

SA0341

Questionnaire Survey to Validate an Educational Program Intended for Orthopaedic Surgeons to Improve the Management of Severe Osteoporosis. Irene Cerocchi*[1], Giuseppina Resmini[2], Antonio Capone[3], Giovanni Iolascon[4], Alfredo Nardi[5], Umberto Tarantino[6]. [1]PTV Foundation - University of Tor Vergata, Italy, [2]Treviglio Hospital, Italy, [3]University of Cagliari, Italy, [4]Second University of Naples, Italy, [5]Rovigo General Hospital, Italy, [6]Azienda Ospedaliera PTV, Italy

The GOST (Management of Severe Osteoporosis in Traumatology) project was intended for orthopaedic surgeons, whose knowledge about osteoporosis and fragility fractures is known to be often poor and superficial, as widely documented in the literature. During 18 educational events the 510 participants were invited to fill in a questionnaire both at the beginning and at the end of the course, in order to verify if its structure and content had brought an improvement in the understanding of osteoporosis and related arguments. The questionnaire was made of 36 multiple choice questions: 7 about basic science, 12 about the clinical aspects of osteoporosis and metabolic bone diseases, 7 about diagnostic tools, 6 about pharmacological therapy and 4 about surgical treatment. There was an overall improvement of 18,77%, and for each question the percentage of right answers was higher at the end of the course compared to the beginning. The data obtained were also compared based on the subject treated. The best results were achieved in the clinical field (62,76% right answers before versus 84.64% after the meeting, with a 21,88% improvement). The percentage of right answers increased by 20,84% in the diagnosis field, and by 16,83% and 16,81% for the questions about medical treatment and basic science, respectively. The lower percentage of improvement in the surgical field (12,21%) was probably due to the already good knowledge about bone implants and the treatment of osteoporotic fractures, as the courses were attended by orthopaedic surgeons only. Moreover, the finality of the educational events was to focus on the biological, clinical and therapeutical aspects of osteoporosis, that are usually poorly considered by surgeons, who tend to focus on the surgical treatment of the fracture, often forgetting the pathophysiology, characteristics and consequences of poor bone quality. In conclusion, the GOST courses proved to be an useful tool in the improvement of orthopaedic knowledge about effective diagnosis and management of metabolic bone diseases.

***Disclosures: Irene Cerocchi**, None.*

SA0342

See Friday Plenary number FR0342.

SA0343

See Friday Plenary number FR0343.

SA0344

See Friday Plenary number FR0344.

SA0345

What was the FRAX® Value the Day Before the Fracture? Karine Briot*[1], Frédéric Sailhan[2], Antoine Babinet[2], JP Courpied[2], Philippe Anract[2], Christian Roux[1]. [1]Paris Descartes University, Rheumatology Department, Cochin hospital, France, [2]Paris Descartes University, Orthopaedics Department, Cochin hospital, Paris, France, France

Rationale and objectives

FRAX® is a fracture prediction algorithm to determine a patient's absolute fracture risk, and to select patients who should receive the highest priority for treatment. FRAX® calculates the 10-year probability of hip (H-FRAX®) and major osteoporotic (clinical spine, forearm, hip and shoulder) fractures (MO-FRAX®). The aim of this study was to calculate the FRAX® in a population of patients with a recent fracture.

Patients and methods

We calculated the FRAX® with femoral neck BMD for all the patients hospitalized for low trauma hip and major osteoporotic fracture over 1 year from February 2009. Bone mineral density (BMD) was measured by DXA and the number of vertebral fractures (VF) were defined using vertebral fracture assessment (VFA) performed during the same exam. The FRAX® was calculated from the data of the day before the fracture, without taking into account the current fracture. All the patients receiving an anti-osteoporotic treatment were excluded.

Results

435 patients were hospitalized over 1 year in the Orthopaedic Department for a non traumatic non vertebral fracture. 134 were excluded because of cognitive disorders, poor general health and ongoing antiosteoporotic treatment and 59 because of non major osteoporotic fracture. Assessment was thus performed in 242 patients (75.2 $\pm$11 years); 134 with hip and 108 with other major osteoporotic fractures (clinical spine fractures excluded). Mean femoral neck T score was -2.3 ($\pm$1.1), and 53% of patients were osteoporotic according to spine and/or hip T scores. Mean MO-FRAX® in patients with incident MO fractures was 13.5 $\pm$9.5% and 44.6% and 62% had a MO-FRAX® $\leq$10% and 15% respectively. Mean H-FRAX® in patients with a hip fracture was 7.2 $\pm$5.8% and 28.2% and 50% had a FRAX® $\leq$3 and 7% respectively. Prevalence of VF by VFA was 42.2% and 50.7% in patients with MO and hip fracture respectively, and 6.3% of these VF were known. Adding these prevalent fractures in the FRAX® calculation increases it to 11.5 % and 22.1% for hip and MO fracture.

Conclusion: this study suggests that following the threshold, 25 to 60 % of patients with recent fracture would not have been detected by the FRAX® before their fracture. Adding prevalent vertebral fracture in the calculation increases the scores, and thus VFA tool should be consider for fracture prediction improvement.

***Disclosures: Karine Briot**, None.*
This study received funding from: Novartis Laboratory

SA0346

Decreased Risk Of Vertebral Fracture Is Associated With Low-Moderate Amount Of Alcohol Intake In A Random Sample Of Mexicans. Laura Paola Bernal-Rosales*[1], Patricia Clark[2], Juan O Talavera-Piña[3], Margarita Deleze[2], Fidencio Cons-Molina[4]. [1]Hospital Infantil de México "Federico Gómez", Mexico, [2]Laboratorios Clinicos De Puebla, Mexico, [3]Centro Médico Nacional Siglo XXI, Mexico, [4]Unidad de Diagnóstico de Osteoporosis, Mexico

Purpose: The present study analyzed the potential risk factors in a random sample of Mexicans with vertebral fractures. Methods: A total of 820 subjects were evaluated (406 women and 414 men) aged 50 and over. The sample was randomized and stratified according to four age groups (50–59, 60–69, 70–79, and those over 80) from both sexes.A questionnaire containing information on demographic characteristics, gynecologic history, lifestyle habits, calcium intake, alcohol intake, and physical activity was applied to all participants. Lateral X-rays of the lumbar and thoracic spine and BMD by DXA were obtained in all cases. The protocol was submitted and approved by the Institutional Review Board and written consent was obtained from all participants once the implications of their participation in the study was explained in detail and before the application of questionnaires and/or interviews. A bivariate analysis was performed to estimate the odds ratio and the 95% confidence interval for every risk factor related with the presence of a vertebral fracture; this was followed by a multivariate analysis where each variable was adjusted by the rest of them in a global index. Results: The average age for study group was 69.3 years. Age, gender, and physical inactivity were related to vertebral fracture as follows: age of 70–79 years (OR=2.40, IC95% 1.04–5.68), age over 80 years (OR=6.83, IC95% 3.15–15.16), sedentary lifestyle (OR=1.63, IC95% 0.97–2.72) and female gender (OR=2.28, IC95% 1.40–3.73). A low and moderate intake of alcohol (1–40 g/day) was protective factor for vertebral fracture (OR=0.51, IC95% 0.30–0.87). In the multivariate analysis, low and moderate consumption of alcohol remained as a protective factor (OR=0.56, IC95% 0.33–0.92). Conclusion: Moderate alcohol consumption (1–40g/day) presented a protective effect for vertebral fracture, and, as other studies have showed, an association between the age and gender was observed as risk factors of vertebral fracture.

***Disclosures: Laura Paola Bernal-Rosales**, None.*

SA0347

Effects of Cigarette Smoke Cadmium on Urine Calcium Excretion in Postmenopausal Women. Maryka Bhattacharyya, Shahram Bozorgnia*. Medical College of Georgia, USA

Low-level cadmium (Cd) exposure in humans is significantly correlated with decreased bone density and increased susceptibility to fractures. In addition, cigarettes are a major source of Cd exposure, with individual smokers having blood Cd concentrations up to 10-fold above those of non-smokers. As part of a larger project, this study investigates if the Cd component of cigarettes is associated with increased calcium excretion from the kidneys of persons who smoke. Eighteen postmenopausal women who smoke cigarettes and 11 non-smokers were studied. From each participant, 2 blood and 11 urine samples were collected over 7 weeks: the first 3 weeks during which smokers smoked at their customary rate; the next 4 days when all smokers ceased smoking; the next 4 weeks when smokers, to different degrees, returned to their previous smoking status. Blood was collected at the beginning and end of the 7 weeks. A first-of-morning (FOM) urine specimen was collected 1- to 2-times per week during the 7 weeks. Smoking status was documented with a daily diary and verified with a carbon monoxide breath test. Analyses included blood Cd concentration (CdB), urine Cd concentration (CdU), and urine calcium concentration (CaU). Results demonstrate that mean values of CdB and CdU were significantly higher in smokers than non-smokers (3.5-fold and 2.6-fold, respectively, $p<0.05$). In addition, prior to smoking cessation, Cd exposure did not increase mean levels of Ca in FOM urine, with 57$\pm$7, 60$\pm$14, and 54$\pm$10 mg Ca per sample for high-Cd smokers (CdB, 1.0-2.7 ng Cd/ml, n=9), lower-Cd smokers (CdB, 0.5-0.9 ng Cd/ml, n=8), and non-smokers (CdB, 0.2-0.6 ng Cd/ml, n=11), respectively (mean $\pm$ SE). However, effects of smoking cessation, measured longitudinally in each subject, did depend upon Cd exposure. During 4 days of smoking cessation, FOM CaU decreased in lower-Cd smokers (-16$\pm$5 mg Ca), showed no change in high-Cd smokers (3$\pm$4 mg Ca), and increased in non-smokers (32$\pm$14 mg Ca). These results indicate that subjects with higher CdB values maintained elevated levels of CaU during the short period of smoking cessation, while CaU values decreased in the lower Cd group. For subjects taking Ca supplements, effects of smoking cessation on CaU were also diminished. Results confirm smoking as a significant source of cadmium exposure and demonstrate that the Cd component of cigarettes may maintain elevated calcium excretion by the kidney, which may play a direct role in osteoporosis.

***Disclosures: Shahram Bozorgnia**, None.*

SA0348

Should Risk of Osteoporosis Restrict Weight Control for Other Health Reasons Among Postmenopausal Women ? - 10-year Follow-up Study. Joonas Sirola*[1], Toni Rikkonen[2], Marjo Tuppurainen[3], Risto Honkanen[4], Heikki Kröger[3]. [1]University of Eastern Finland / Kuopio, Finland, [2]University of Eastern Finland, Campus of Kuopio, Finland, [3]Kuopio University Hospital, Finland, [4]University of Kuorio, Finland

Introduction: High body mass index (BMI) is a risk factor for several morbidities but may be protective against osteoporosis. The aim of the present study was to investigate the effects of overweight and obesity on postmenopausal co-morbidity.

Methods: 1970 Finnish women from the OSTPRE cohort were measured with DXA of femoral neck (FN) and lumbar spine (LS) at baseline (1994) and at 10-year follow-up (2004). Women were categorized according to BMI into normal (under 25 kg/m^2), overweight (25-29 kg/m^2) and obese (over 30 kg/m^2). Weight change (WC) during the follow-up was categorized into tertiles: 1) < 1 kg 2) 1-6.2 kg 3) > 6.2 kg. The definition of osteoporosis in the present study was 10-year follow-up FN or LS T-score under -2.5 SD or under -2.0 SD + low trauma energy follow-up fracture. Information about other co-morbidities was based on self-reports. The end-point morbidities were not allowed to be present at baseline. The risk of each co-morbidity was obtained with multivariate logistic regression, adjusted for age, alcohol intake and smoking.

Results: The incidence of co-morbidities during the follow-up were: hypertension (HT) 25.7 %, cardiac insufficiency 6.2 %, coronary artery disease (CAD) 10.3 %, stroke 5.0 %, diabetes mellitus (DM) 7.3 %, osteoarthritis (OA) 22.3 %, breast cancer (BC) 2.8 %, depression 2.8 %, osteoporosis (OP) 8.2 %, chronic back pain (BP) 17.1 % and poor self-rated health (SRH) 4.3 %. Obesity / overweight predicted higher 10-year risk of HT (OR=2.6 / OR=1.7, $p<0.001$ compared to normal BMI), CAD (OR=1.6, $p<0.05$ / OR=1.2, p=NS), DM (OR=11.7 / OR=5.3, $p<0.001$), OA (OR=1.4, $p<0.05$ / OR=1.1, p=NS), BP (OR=1.6, p=0.007 / OR=1.2, p=NS) and poor SRH (OR=2.4, $p<0.05$ / OR=1.5, p=NS) and lower risk of OP (OR=0.13 / OR=0.41, $p<0.001$). The combined 10-year risk for any co-morbidity significantly associated with BMI, other than SRH and OP, was 2.2 for obese and 1.7 for overweight women (p=0.001). In

comparison to the third WC tertile, the first had 1.8 and 2.6 times ($p<0.001$) and the second 1.6 and 2.9 times ($p<0.05$) lower risk of having HT and BC, respectively.

Conclusions: The health related risks of obesity, especially DM, outweigh its protective effects on bone health. Weight loss has no significant effect on OP but may protect from HT and BC. Patients with BMI under 25 kg/m^2 should be screened for OP, because the risk is over two times higher than the reduction in combined risk of HT, CAD, DM, BP and OA.

***Disclosures: Joonas Sirola**, None.*

SA0349

Assessing Bone Health in Adult Premenopausal Females in Karachi - A Preliminary Report from Pakistan. Aysha Khan*, Farhan Dar, Romaina Iqbal, Imran Siddiqui, Farooq Ghani. Aga Khan University, Pakistan

Objective: To assess the bone health status in healthy females by using biochemical markers of bone metabolism

Material and Methods:

Study Design: A cross- sectional study.

Place and Duration: The study was conducted at Section of Chemical Pathology, Department of Pathology & Microbiology, The Aga Khan University Hospital, Karachi, Pakistan, from November 2007 to June 2008.

Methodology: 174 healthy premenopausal female volunteers were recruited through convenient, non-purposive sampling after informed consent. Females taking vitamin D or calcium supplements or any medicine or disease altering bone turnover were excluded. A questionnaire addressing the demographic details was filled; NTx, 25OHD and iPTH were measured in blood in fasting. NTx value >19 nMBCE/L was considered high bone turnover. 25OHD levels were stratified as deficient <20 ng/ml, 21-29 ng/m insufficient, and >30 ng/ml sufficient. Plasma iPTH level of > 87 pg/ml was considered high. Data was analyzed using the Statistical Package for Social Sciences SPSS (Release 16.0, standard version, copyright SPSS). A p-value of <0.05 was treated as significant.

Results: Mean age and BMI of the participants was 29.06 ± 6.89 (18 – 48 years) and 23.12 ± 4.58 (13.84 – 41.2) kg/m^2 respectively. 82.8% of the females were identified as D deficient, 16.1% had insufficient levels and 1.1% had optimal levels. High bone turnover as depicted by NTx was seen in 36.8% cases. Secondary hyperparathyroidism was present in 25.9% volunteers while others had blunted PTH response. NTx associated with 25OHD ($r = 0.198$; P-value=0.009); 25OHD associated with iPTH ($r = –0.199$; P=0.009). Major determinant of high serum NTx were 25OHD, sun exposure and purdah observation. High bone turnover coexists with both low 25OHD (hypovitaminosis D; <30ng/ml) and optimal 25OHD (>30ng/ml).

Conclusion: Vitamin D deficiency is highly prevalent in adult females. Bone turnover is high regardless of vitamin D status. There is a need to develop strategies to understand further, the bone biomechanics and bone quality for Pakistani females.

***Disclosures: Aysha Khan**, None.*

SA0350

See Friday Plenary number FR0350.

SA0351

See Friday Plenary number FR0351.

SA0352

Comparison Between Logistic Regression and Artificial Neural Networks for Morphometric Vertebral Fractures Risk Assessment: New Data from GISMO Lombardia Database. Cristina Eller Vainicher*[1], Ivana Santi[2], Marco Massarotti[3], Luca Pietrogrande[4], Matteo Longhi[5], Valter Galmarini[6], Giorgio Gandolini[7], Maurizio Bevilacqua[8], Iacopo Chiodini[1], Enzo Grossi[9]. [1]Fondazione IRCCS Cà Granda Ospedale Maggiore Policlinco Milano, Italy, [2]Istituto Geriatrico ASP IMMeS e Pio Albergo Trivulzio Milano, Italy, [3]IRCCS Humanitas Clinical Institute, Italy, [4]Ospedale S.Paolo - Università degli Studi di Milano, Italy, [5]IRCCS Galeazzi Milano, Italy, [6]AO Fatebenefratelli e Oftalmico Milano, Italy, [7]Don C. Gnocchi Foundation IRCCS Milan, Italy, [8]Ospedale L. Sacco - Polo Universitario, Italy, [9]Centro Diagnostico Italiano, Italy

Background: There is growing interest in the development of algorithms, like FRAX™, using traditional statistical approach, for predicting osteoporotic fractures. Nevertheless, some studies suggest their poor sensitivity. Artificial Neural Networks (ANNs), computer algorithms inspired by the highly interactive processing of the human brain, could represent an attractive alternative to this approach. So far, no reports have investigated the ability of ANNs in predicting osteoporosis fracture.

Aim: To evaluate the capacity of ANNs, compared with Logistic Regression (LR), to recognise patients with or without morphometric vertebral fractures (MVF+ and MFV- respectively) on the basis of classical bone osteoporotic risk factors and other clinical information.

Methods: We compared the prognostic performance of ANNs with that of LR in predicting MFV in 372 female patients affected with postmenopausal osteoporosis (MVF+ n=176; MVF- n=196), described by 42 independent variables. ANNs where allowed to choose the relevant input data automatically (Twist system-Semeion).

Results: 18 variables were selected, as most relevant, among 42 by TWIST system. Using this set of variables the mean sensitivity of LR and ANNs in test data sets was 35.8% and 72.47% respectively, the mean specificity was 76.53% and 78.50% respectively, the overall accuracy was 56.17% and 75.48% respectively.

Age, BMI, years since menopause, smoking habit, hypertension, dislipydemia, calcium intake, bone mineral density, family history of femoral fracture, resulted to be the most relevant variables for the best performing model.

Conclusions: ANNs showed a better performance than LR in predicting the presence of MVF, in particular ANNs showed a higher sensitivity in respect with LR. These results suggest a promising role of ANNs in the development of algorithm for predicting osteoporotic fractures.

***Disclosures: Cristina Eller Vainicher**, None.*

SA0353

Differences in Skeletal and Non-Skeletal Factors in a Diverse Sample of Men With and Without Type 2 Diabetes Mellitus. Ann Schwartz[1], Gretchen Chiu[2], Julia Dixon[2], Andre Araujo*[2]. [1]University of California, San Francisco, USA, [2]New England Research Institutes, USA

Purpose: While fracture risk is higher in patients with type 2 diabetes mellitus (T2DM), patients with T2DM tend to have higher bone mineral density (BMD) than their non-diabetic counterparts. These observations motivate comparisons of both skeletal and non-skeletal factors in subjects with and without T2DM.

Methods: The Boston Area Community Health/Bone (BACH/Bone) Survey is a population-based cross-sectional survey of skeletal health in a random sample of 1,219 Boston men aged 30-79 y. Diabetes status, age and race/ethnicity were obtained via self-report. BMD and body composition were measured by DXA. Physical function was assessed via a composite physical function score derived from walk and chair stand tests. Grip strength was measured with a hydraulic hand dynamometer. Multivariate linear regression was used to examine the association of T2DM status with skeletal and non-skeletal factors.

Results: Of the 1137 men with complete data included in this analysis, the mean age was 48 y. Prevalence of T2DM was 12.5%, with an average duration of disease of 7.4 y. Of the skeletal factors considered, only lumbar spine BMD was significantly higher in men with T2DM. Of the non-skeletal factors considered, both the composite physical function score and maximum grip strength were significantly lower in men with T2DM. As shown in the table, skeletal factors were no longer significantly associated with T2DM status in multiple regression models. Non-skeletal factors including appendicular lean mass, arms lean mass, and maximum grip strength were negatively associated with T2DM after adjustment.

Conclusion: These results suggest that non-skeletal factors such as body composition and muscle strength, which may influence fall risk, could explain higher fracture rates among patients with T2DM.

		T2DM		
Subgroup	Outcomes	β	SE	p-value
Skeletal Factors	Femoral neck BMD (g/cm^2)	-0.01	0.02	0.46
	Lumbar spine BMD (g/cm^2)	0.01	0.02	0.56
Non-Skeletal Factors	Lean mass (kg)	-0.54	0.82	0.51
	Appendicular lean mass (kg)	-1.04	0.50	0.04
	Arms lean mass (kg)	-0.42	0.15	0.006
	Legs lean mass (kg)	-0.62	0.37	0.097
	Composite score	-0.48	0.26	0.07
	Maximum grip strength (kg)	-3.02	1.25	0.02

Adjusted for age, race/ethnicity, and body mass index

Multiple regression models showing the association between T2DM and outcomes

***Disclosures: Andre Araujo**, None.*

SA0354

Gender Differences in Factors Associated with Falls in a Population-Based Cohort Study in Japan: The ROAD Study. Shigeyuki Muraki*[1], Toru Akune[1], Hiroyuki Oka[1], Kozo Nakamura[2], Hiroshi Kawaguchi[3], Noriko Yoshimura[1]. [1]University of Tokyo, Japan, [2]The University of Tokyo, Japan, [3]University of Tokyo, Faculty of Medicine, Japan

Fall is the most serious factor for fractures in the elderly; therefore, it is important to identify subjects with factors associated with fall. The objective of the present study was to determine factors associated with falls in elderly men and women. From the 3,040 participants in the ROAD study, the present study analyzed 1,180 subjects aged more than 60 years from the mountainous and coastal cohorts (431 men and 749

women; mean age, 71.7 years). At the baseline, physical ability was estimated by measuring grip strength, 6-m walking time, normal step length (NSL), and chair stand time. Further, vertebral fracture (VFx) was assessed by lateral radiographs of the lumbar spine. Lumbar spondylosis and knee osteoarthritis (OA) were defined as a Kellgren/Lawrence grade of ≥3. Falls during the preceding year were evaluated by a self-reported questionnaire. During 1 year, 63 men (14.7%) and 153 women (20.5%) fell once or several times. In men, logistic regression analysis without adjustment revealed that NSL and radiographic VFx at the baseline were significantly associated with falls (odds ratio [OR], 0.94 and 2.21; 95% confidence interval [CI], 0.90–0.99 and 1.19–4.00, respectively), but grip strength, 6-m walking time, chair stand time, knee OA, and lumbar spondylosis were not associated with falls (OR: 0.98, 1.01, 1.03, 0.77, and 1.13; 95% CI: 0.94–1.02, 0.91–1.10, 0.96–1.10, 0.36–1.54, and 0.66–1.94, respectively). Multiple logistic regression analysis after adjustment for age revealed that NSL and radiographic VFx were independently associated with falls (OR, 0.94 and 2.08; 95% CI, 0.89–0.98 and 1.08–3.88, respectively). In women, logistic regression analysis without adjustment revealed that grip strength and knee OA were significantly associated with falls (OR, 0.96 and 1.52; 95% CI, 0.92–0.99 and 1.05–2.20, respectively), but 6-m walking time, NSL, chair stand time, VFx, and lumbar spondylosis were not associated with falls (OR: 1.03, 0.99, 1.02, 1.47, and 1.23; 95% CI: 0.97–1.08, 0.94–1.03, 0.98–1.05, 0.86–2.42, and 0.86–1.75, respectively). Multiple regression analysis after adjustment for age revealed that grip strength and knee OA were independently associated with falls (OR, 0.95 and 1.56; 95% CI, 0.91–0.99 and 1.05–2.30, respectively). In conclusion, this study revealed distinct factors associated with falls in men and women. In men, NSL and VFx were associated with falls, whereas in women, grip strength and knee OA were associated with falls.

***Disclosures: Shigeyuki Muraki**, None.*

SA0355

See Friday Plenary number FR0355.

SA0356

See Friday Plenary number FR0356.

SA0357

Lack of Association Between Osteoporosis and Coronary Artery Disease in Korean Men and Women. Se Hwa Kim[1], Soo-Kyung Kim[2], Deok-Kyu Cho[1], Yun-Hyeong Cho[1], Sun-Ok Song*[1]. [1]Kwandong University College of Medicine, Myongji Hospital, South korea, [2]Pochon CHA University College of Medicine, South korea

Background: Coronary artery disease (CAD) and osteoporosis are major causes of morbidity and mortality in the elderly. The aim of this study was to investigate whether osteoporosis or osteoporotic fractures was associated with CAD independent of traditional risk factors. Subjects and Methods: Study population consisted of Korean men and women who underwent coronary angiography. The following clinical and demographic parameters were recorded: age, sex, body mass index (BMI), hypertension, diabetes mellitus, coronary artery disease, smoking status. Bone mineral density (BMD) and T-L spine lateral X-ray were taken. Of 485 patients, 250 were taken T-L spine lateral X-ray to assess the vertebral fractures and BMD was assessed using dual energy X-ray absorptiometry (DXA) in 110 patients. Results: Patients were grouped according to the BMD (normal, osteopenia, and osteoporosis). Patients with vertebral fractures were regard as osteoporosis group. Patients with osteoporosis were older and had lower BMI than those with normal or osteopenia. There were not significant differences between three groups in respect to diabetes mellitus, hypertension, hypercholesterolemia, BMD. Prevalence of CAD was not different between the 3 groups. However, prevalence of CAD involving more than 2 coronary arteries in patients with osteoporosis or vertebral fractures was higher than in patients with normal BMD (26% vs. 56% in women, 36% vs. 69% in man). In the logistic regression analysis showed that age and diabetes mellitus were independently associated with CAD. Conclusions: Age and diabetes mellitus were independent predictors of CAD in our study population. However, osteoporosis or vertebral fracture did not show any association with CAD in Korean men and women.

***Disclosures: Sun-Ok Song**, None.*

SA0358

Modification of the Osteoporosis Patient Assessment Questionnaire Using Item Response Theory Methods. April Naegeli*[1], Russel Burge[1], Steven Watts[1], Timothy Stump[2], Deborah Gold[3], Stuart Silverman[4]. [1]Eli Lilly & Company, USA, [2]Indiana University School of Medicine, USA, [3]Duke University Medical Center, USA, [4]Cedars-Sinai/UCLA, USA

The purpose of this study was to develop a modified version of the Osteoporosis Patient Assessment Questionnaire (OPAQ 3.0) that reduces respondent burden and specifically assesses the impact of osteoporosis on physical function and mobility for use in clinical trials evaluating drug therapy for the prevention of vertebral fracture.

This study was conducted using the Multiple Outcomes of Raloxifene Evaluation (MORE) trial database. At baseline, 1478 patients were administered the OPAQ 2.0. The OPAQ 2.0 is an 18-domain, 60-item patient reported outcome (PRO) measure used in clinical trials to evaluate health-related quality of life in patients with fractures related to their osteoporosis. Items were evaluated based on the application of a unidimensional, polytomous Item Response Theory (IRT) model and clinical relevance founded on expert judgment. Dimensionality was assessed with a factor analysis considering eigenvalues. A large drop from the first to second eigenvalue with the rest following the scree plot was indicative of a unidimensional scale. Items were retained based on their relatedness to the underlying construct and ability to discriminate through analysis of Item Information and Item Characteristic Curves, respectively. All analyses were conducted using Mplus statistical software.

OPAQ 3.0 contains 6 domains with 21 items retained from OPAQ 2.0: walking and bending (6 items), sitting and standing (3 items), transfers (4 items), backache and pain (2 items), fear of falls (3 items), and independence (3 items). Slight modifcations to item wording and response options were necessary to improve clinical relevance and to capture descriptions as depicted by patients with osteoporosis.

OPAQ 3.0 was developed based on clinical trial responses to OPAQ 2.0 to decrease respondent burden by reducing the number of items from 60 to 21, and to assess the impact of osteoporosis, specifically on physical function and mobility. Next steps for OPAQ 3.0 include confirmation of content validity, and evaluation of psychometric properties (factor structure, reliability, validity, and responsiveness) in targeted clinical trial patient populations for drug therapy aimed to prevent fracture related to osteoporosis.

***Disclosures: April Naegeli**, Eli Lilly and Company, 3; Eli Lilly and Company, 1*
This study received funding from: Eli Lilly and Company

SA0359

Obesity in Adolescence and Bone Strength in Adulthood. Kirsti Uusi-Rasi*[1], Marika Laaksonen[2], Olli Raitakari[3], Jorma Viikari[4], Mika Kähönen[5], Harri Sievänen[1]. [1]UKK Institute for Health Promotion Research, Finland, [2]University of Helsinki, Finland, [3]University oh Turku, Finland, [4]University of Turku, Finland, [5]University of Tampere, Finland

While obese children have been reported to have lower bone mass for a given weight, obese adults have greater bone mineral density compared with normal weight adults. In this prospective cohort study we evaluated differences in bone cross-sectional size and density in relation to the age of gaining excess body mass.

328 women from the population-based cohort of The Young Finns Study were divided into 4 groups by body mass index (BMI) at the age of 12-15 years (healthy body weight, C-, or overweight/obese, C+) and 24 years later (healthy weigh in adulthood A-, or overweight/obese in adulthood A+). Of 162 overweight women, 49 had been obese since childhood (C+A+) and 113 had gained extra weight in adulthood (C-A+). Of 166 healthy weight women, 24 had been overweight in childhood (C+A-) and 142 had always been healthy weight (C-A-).

Total cross-sectional area (ToA, mm^2) and cortical (shaft CoD, mg/cm^3) and trabecular (distal TrD, mg/cm^3) bone density of the radius and tibia were measured with pQCT at the mean age (SD) of 38 (1.5) years. Between-group differences were evaluated with analysis of covariance.

Mean body height was 166 (6) cm without between-group differences. In healthy weight groups, mean body mass was similar being 62 (6) and 61 (6) kg, but those women who had been obese since childhood weighted more than women who had become obese in adulthood, the mean weights being 89 (18) and (80 (10) kg, respectively. Childhood obesity was associated with larger ToA especially at the tibia, whilst obesity in adulthood predicted higher TrD and lower CoD (Table).

Childhood obesity was associated with larger cross-sections at long bone diaphyses and distal tibia, but not distal radius. Being obese since childhood or gaining excess weight in adulthood may lead to lower cortical and higher trabecular density both at weight-bearing and nonweight-bearing bones. In contrast, it seems that temporary obesity in adolescence, while being associated with increased bone size, may lead to lower trabecular density.

	C-A+, n=113	C+A+, n=49	C+A-, n=24	p for group differences
Distal radius TrD	2.7 (-1.6 to 6.9)	3.4 (-2.3 to 9.0)	-3.5 (-11.7 to 4.3)	0.073
Distal radius ToA	1.4 (-3.0 to 5.8)	2.3 (-3.5 to 8.0)	4.1 (-3.8 to 11.3)	0.450
Radial shaft CoD	-0.7 (-1.4 to -0.2)	-0.9 (-1.6 to 0)	0.0 (-1.2 to 0.9)	0.002
Radial shaft ToA	2.3 (-1.9 to 6.5)	5.6 (0 to 10.7)	2.3 (-5.2 to 9.4)	0.057
Distal tibia TrD	6.2 (2.3 to 10.1)	6.5 (1.1 to 11.3)	-4.0 (-11.9 to 3.2)	<0.001
Distal tibia ToA	1.4 (-2.3 to 4.9)	4.5 (-0.2 to 9.0)	5.2 (-1.2 to 11.1)	0.026
Tibial shaft CoD	-1.2 (-1.6 to -0.5)	-1.4 (-2.1 to -0.7)	0.0 (-0.9 to 0.9)	<0.001
Tibial shaft ToA	5.2 (1.8 to 8.2)	8.2 (4.1 to 12.1)	6.9 (1.4 to 12.1)	<0.001

Height adjusted between-group mean differences (95% CI) compared with the C-A- group (n=142)

***Disclosures: Kirsti Uusi-Rasi**, None.*

SA0360

See Friday Plenary number FR0360.

SA0361

Serum 25-Hydroxyvitamin D Levels, Mortality and Risk of Non-spine and Hip Fractures in Older White Women: Data from the Study of Osteoporotic Fractures. Marc Hochberg*[1], Li-Yung Lui[2], Dennis Black[3], Jane Cauley[4], Peggy Cawthon[2], Kristine Ensrud[5], Lisa Fredman[6], Teresa Hillier[7], Steven Cummings[8]. [1]University of Maryland School of Medicine, USA, [2]California Pacific Medical Center Research Institute, USA, [3]University of California, San Francisco, USA, [4]University of Pittsburgh Graduate School of Public Health, USA, [5]Minneapolis VA Medical Center / University of Minnesota, USA, [6]Boston University School of Public Health, USA, [7]Kaiser Center for Health Research, USA, [8]San Francisco Coordinating Center, USA

Objective: The associations between low serum vitamin D levels and mortality and fracture risk are inconsistent. The objective of the current analysis was to determine whether low serum levels of 25-hydroxyvitamin D (25[OH]D) were associated with higher mortality and an increased risk of non-spine, including hip, fractures in older white women. Methods: Serum 25(OH)D levels were measured by liquid chromatography-tandem mass spectroscopy in frozen specimens from 5915 white women (mean [SD] age: 76.7 [4.8] years) who completed Visit 4 in the Study of Osteoporotic Fractures between August 1992 and July 1994. Cox proportional hazards models were used to test the association of serum 25(OH)D levels, as either a continuous or categorical variable, with all-cause mortality, and the incidence of non-spine and hip fractures; results are expressed as hazard ratios (HR) with 95% confidence intervals (CI).Results: Mean (SD) serum 25(OH)D level was 23.2 (11.7) ng/ml; quartiles were defined as <=16, 17-22, 23-28 and >=29 ng/ml. 3199 women died during a mean 11.1 (4.5) years of follow-up. There was a significant trend for increasing mortality in lower quartiles of 25(OH)D in age-adjusted but not multivariate (MV)-adjusted models (Table). Women in the lowest quartile of serum 25(OH)D levels had a significantly increased risk of mortality in age-adjusted models compared with women in Q2-4 combined: HR 1.10 (1.02, 1.19). This association was stronger with shorter length of follow-up: HR 1.29 (1.10, 1.51) and 1.15 (1.04, 1.27) after 5 and 10 years of follow-up, respectively. 2174 women sustained a non-spine fracture, including 768 with a hip fracture, over a mean 8.7 (5.0) years of follow-up. Lower serum 25(OH)D levels were significantly associated with a decreased risk of both non-spine and hip fractures in both age- and MV-adjusted models as a continuous but not as a categorical variable (Table). There was a significant trend for decreasing hip fracture risk in lower quartiles of 25(OH)D levels in MV-adjusted models (Table). Similar results were found when data were analyzed using clinically relevant cutpoints (deficient, insufficient and sufficient) for 25(OH)D levels.Conclusion: These data suggest a relationship between low serum 25(OH)D levels and an increased risk for all-cause mortality while, paradoxically, providing evidence for a reduced risk of hip fractures in these older white women with lower 25(OH)D levels.

Serum 25(OH)D	All-cause Mortality	Non-spine fractures	Hip fractures
Per SD decrease			
Age-adjusted	1.00 (0.96, 1.03)	0.92 (0.88, 0.96)	0.93 (0.87, 0.99)
Multivariate adjusted	0.98 (0.95, 1.02)	0.92 (0.88, 0.96)	0.92 (0.86, 0.99)
Quartiles (Age-adjusted)			
Q 1 (<=16 ng/ml)	1.09 (0.99, 1.20)	0.98 (0.87, 1.10)	0.86 (0.71, 1.05)
Q 2 (17-22 ng/ml)	1.01 (0.91, 1.11)	0.99 (0.88, 1.12)	0.83 (0.68, 1.01)
Q 3 (23-28 ng/ml)	0.97 (0.87, 1.07)	1.00 (0.88, 1.12)	0.93 (0.76, 1.14)
Q 4 (>=29 ng/ml)	1.00 (ref)*	1.00 (ref)	1.00 (ref)
Quartiles (multivariate adjusted)			
Q 1 (<=16 ng/ml)	0.98 (0.89, 1.09)	0.96 (0.85, 1.08)	0.83 (0.68, 1.01)
Q 2 (17-22 ng/ml)	1.00 (0.90, 1.10)	0.99 (0.87, 1.12)	0.77 (0.63, 0.95)
Q 3 (23-28 ng/ml)	0.93 (0.83, 1.03)	0.95 (0.84, 1.08)	0.88 (0.71, 1.08)
Q 4 (>=29 ng/ml)	1.00 (ref)	1.00 (ref)	1.00 (ref)*

*P value for trend = 0.04

Adjusted HR (95% CI) for the Association of Serum 25(OH)D Levels with Mortality and Fractures

***Disclosures: Marc Hochberg**, None.*

SA0362

The Effect of Biological Aging On Bone Mineral Density and Fracture. Kyoung Min Kim*[1], Kwang Joon Kim[2], Su-Jin Park[3], Gadi Jogeswar[3], Jami Ajita[3], Yumie Rhee[4], Sung-Kil Lim[5]. [1]Yonsei University, South korea, [2]Severance Hospital, South korea, [3]Yonsei university colleage of medicine, South korea, [4]IUMS, Yonsei University, College of Medicine, South korea, [5]Yonsei University College of Medicine, South korea

Introduction: Bone mineral density is influenced by the dynamics of aging, inflammation and bone remodeling processes. Admittedly, chronological age (CA) being a major determinant of BMD. However, this CA simply measures the amount of time that has gone by since birth. Thus, CA provides only limited information about matters such as declining functional capacity and other properties we associate with aging. Therefore, several previous reports have tried to search the correlations between telomere length, as a marker of biological aging, and BMD. Purpose : We sought to identify the useful candidate biomarkers of aging for evaluation of individual biological capacity, and using these to develop an equation measuring biological age (BA), then to investigate the relationships between individual biological aging with BMD. Results : Among 4763 men and 5275 women aged 39~70 years-old, we selected 1509 subjects who met the normality criteria of each biochemical variables. Variables showing significant correlations (correlation coefficient >0.15, $p<0.05$) with CA were selected. 5 variables were selected including systolic blood pressure (SBP), forced expiratory volume in 1 s (FEV1), glycosylated hemoglobin (HbA1c), red blood cell count(RBC) and waist/hip ratio(W/H). Then, Biological aging calculating equation was obtained by multiple regression analysis with using these 5 variables. We calculated each one's BA and the differences between these two ages (BA-CA, Biological Aging Score(BAS)). Individual BAS showed significant correlations with glucose metabolism, pulmonary function, hematological variables, lipid profile and anthropometric parameters after adjusting CA. However, BAS was not associated with BMD, osteoporosis or fracture after adjusting CA unlikely other clinical parameters. Conclusions : No association was observed between BAS and BMD in Korean. This finding can tell us that BMD will be strongly afftected by not BA but CA, the time after birth.

***Disclosures: Kyoung Min Kim**, None.*

SA0363

See Friday Plenary number FR0363.

SA0364

Better Skeletal Microstructure Confers Greater Mechanical Advantages in Chinese-American Women than Caucasian Women. Xiaowei Liu*[1], Marcella Walker[1], Bini Zhou[1], Donald McMahon[2], Julia Udesky[1], George Liu[3], John Bilezikian[2], X Guo[1]. [1]Columbia University, USA, [2]Columbia University College of Physicians & Surgeons, USA, [3]New York Downtown Hospital, USA

Despite lower areal BMD (aBMD) by DXA, Chinese-American (CH) women have fewer fractures (Fx) than Caucasian (CA) women. We hypothesized that better skeletal microstructure in CH women could account for this paradox. To address this hypothesis, we applied individual trabeculae segmentation (ITS), a novel image analysis technique, and micro finite element analysis (μFEA), to high-resolution peripheral quantitative computed tomography (HR-pQCT) images of premenopausal CH and CA women.

Age was similar (36 ± 7 *vs.* 35 ± 4), but height (64 ± 2 *vs.* 65 ± 3 inches; p=0.02) and weight (125 ± 22 *vs.* 139 ± 38 lbs; p=0.03) were lower in the CH (n=46) *vs.* CA (n=49) group. aBMD by DXA did not differ at the spine, hip and 1/3 radius. ITS analysis was applied to trabecular sub-volumes of HR-pQCT (XtremeCT, Scanco Medical; voxel size 82 μm) images at the distal radius (DR) and distal tibia (DT) to quantify trabecular plate- and rod-microarchitecture. Remarkably, CH women had 94% (DR) and 80% (DT) higher plate bone volume fraction (pBV/TV) and 20% (DR) and 18% (DT) higher plate number density (pTb.N) as compared to CA women ($p<0.0001$). In contrast, rod-like characteristics {*i.e.* the amount and number of trabecular rod (rBV/TV and rTb.N)} were similar. Thus, the plate/rod ratio was much greater in CH than in CA trabecular bone. Additionally, plate thickness (pTb.Th) was 9% (DR) and 4% (DT) greater in CH women ($p<0.001$). Plate-rod and plate-plate junction densities (P-R & P-P Junc.D), parameters indicating the trabecular network connections, were 37% and 56% (DR) and 29% and 49% (DT) greater in CH women ($p<0.01$). These striking differences in trabecular bone translate into 55%-69% (DR, $p<0.001$) and 29%-54% (DT, $p<0.05$) higher Young's and shear moduli in the CH vs. CA groups, as estimated by μFEA of HR-pQCT images. Moreover, although CH women have 9% (DR, p=0.03) and 6% (DT, p=0.08) smaller bone size than CA women, thicker cortices (18% and 10% higher in CH vs. CA, $p<0.05$) and more plate-like trabecular bone lead to 14% (DR) and 8% (DT) greater whole bone stiffness ($p<0.05$).

Greater microstructural advantages in CH, as shown by these results, may help to account for lower Fx rates in CH women as compared to CA women.

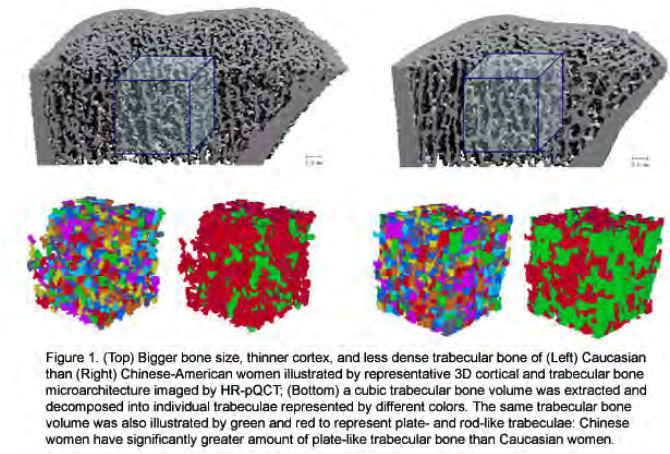

Figure 1. (Top) Bigger bone size, thinner cortex, and less dense trabecular bone of (Left) Caucasian than (Right) Chinese-American women illustrated by representative 3D cortical and trabecular bone microarchitecture imaged by HR-pQCT; (Bottom) a cubic trabecular bone volume was extracted and decomposed into individual trabeculae represented by different colors. The same trabecular bone volume was also illustrated by green and red to represent plate- and rod-like trabeculae: Chinese women have significantly greater amount of plate-like trabecular bone than Caucasian women.

Figure 1

***Disclosures: Xiaowei Liu**, None.*

SA0365

See Friday Plenary number FR0365.

SA0366

Association of Homocysteine, Folate and Vitamin B12 with Bone Mineral Density and Biochemical Bone Turnover in Young Healthy Indians; A Cross Sectional Study. Sushil Gupta[1], Nisha Nigil Haroon*[2]. [1]Sanjay Gandhi Post Graduate Institute of Medical Sciences, India, [2]University of Toronto, Canada

Purpose: Indians have lower peak bone mass, higher bone turnover and higher prevalence of osteoporosis compared to Caucasians. Hyperhomocysteinemia (HHcy) is linked to fractures. But the association of homocysteine (Hcy), folate and vitamin B12 to bone mineral density (BMD) is controversial. The role of these factors in determining bone health of young adults is not clear. We studied the effect of Hcy, folate and vitamin B12 on BMD and bone turnover in young healthy Indians.

Methods: This cross sectional study was conducted at a tertiary care centre in Lucknow,India and involved 151 young healthy adults.Data regarding demographic, dietary and lifestyle factors were obtained using a questionnaire. Serum chemistry (calcium, phosphorus, albumin, creatinine, total alkaline phosphatase (ALP) and haematocrit), 25(OH)D3, PTH, vitamin B12, folate, Hcy, bone formation (N-MID-Osteocalcin (OC), bone specific alkaline phosphatase (BAP)) and resorption markers (cross laps (CTx)) were measured. BMD was assessed at hip (total hip, femoral neck and trochanter), lumbar spine (L1-L4) and forearm using DXA (Hologic QDR 4500A). Correlations were assessed with Spearman's correlation coefficient. Linear regression was used to find predictors of BMD. Comparisons between males and females were done using Student's t test or Mann-Whitney U test.

Results: The subjects (n=151) had a mean age of 26+5 years. Table 1 depicts baseline data.Only 6% had a recommended B12 intake of 2.4mcg/day. Most subjects (75%) were vegetarians and took less vitamin B12 than non vegetarians (0.6 vs.1.4 mcg, $p<0.01$). Low BMD was noted in 17% of subjects. The prevalence of biochemical osteomalacia (ALP >150 IU/L), vitamin B12 deficiency (<200 pmol/L), HHcy (>15µmol/L) and hypovitaminosis D (< 20 ng/ml) were 27%, 68%, 71% and 83% respectively. Serum Hcy inversely correlated with vitamin B12 and folate ($r=-0.327$, -0.224, $p<0.05$) levels. Vitamin B12, Hcy and folate levels did not correlate with ALP, BAP, OC, CTx and BMD at total hip, femoral neck, trochanter, lumbar spine and forearm. Even in those with Hcy levels in the highest quartile, no correlation was found between Hcy and BMD or bone markers.On multiple linear regression, height, BMI and calcium intake were independent and significant predictors of BMD.

Conclusion: Young North Indian adults have high prevalence of HHcy and vitamin B12 deficiency. Hcy, folate and vitamin B12 are not predictors of bone turnover and BMD in young adults.

Table 1: Baseline characteristics of study subjects.

Parameter	Total (n=151)	Males (n=51)	Females (n=100)
25(OH) vitamin D3 (ng/ml)	9 (7-17)	16 (9-25)*	9 (6-14)
iPTH (pg/ml)	29 (21-35)	27 (19-32)	29 (22-36)
Vitamin B12 (pmol/L)	140 (72-230)	91 (55-186)	152 (81-244)
Homocysteine (µmol/L)	18 (14-32)	24 (16-40)*	16 (13-25)
Serum Folate (ng/ml)	5 (4-8)	4 (3-6)	5 (4-9)
BAP (U/L)	24 (20-28)	27 (23-34)*	22 (18-27)
N-MID-Osteocalcin (ng/ml)	11 (8-15)	13 (10-20)*	11 (8-13)
Serum crosslaps (ng/ml)	0.4 (0.3-0.6)	0.7 (0.4-0.9)*	0.4 (0.3-0.5)

*p <0.01 (males vs. females).Data are mean ± SD or median (IQ).BAP: Bone specific alkaline phosphatase.

Table 1: Baseline characteristics of study subjects.

***Disclosures: Nisha Nigil Haroon**, None.*

SA0367

Vitamin K Deficiency in Subjects with Severe Motor and Intellectual Disabilities. Akiko Kuwabara[1], Akiko Nagae[2], Naoko Tsugawa[3], Kunihiko Tozawa[4], Mari Kitagawa[2], Hiroaki Kohno[5], Masakazu Miura[6], Toshio Okano[3], Masao Kumode[2], Kiyoshi Tanaka*[7]. [1]Osaka Shoin Women's University, Japan, [2]Biwako Gakuen Kusatsu Medical & Welfare Center for Children or Person with Severe Motor & intellectual disabilities, Japan, [3]Kobe Pharmaceutical University, Japan, [4]Sanko Junyaku Co., Ltd, Japan, [5]Orthopaedics, Japan, [6]Hokuriku University, Japan, [7]Kyoto Women's University, Japan

Purpose: Subjects with severe motor and intellectual disabilities are at high risk of fracture. High incidence of vitamin D deficiency and BMD increase after vitamin D intervention have been reported in these subjects. Regarding vitamin K; another bone-active vitamin, however, only few papers are available. Therefore, we have studied the vitamin K status in these subjects by measuring serum levels of protein induced by vitamin K absence (PIVKA-II) and undercarboxylated osteocalcin (ucOC) as sensitive markers for hepatic and skeletal vitamin K deficiency, respectively.

Methods: Eighty-two subjects with severe motor and intellectual disabilities, mostly due to cerebral palsy, were evaluated for their serum levels of PIVKA-II and ucOC, and their 7-day vitamin K intake.

Results: Serum concentrations of PIVKA-II and ucOC were 60.9 ± 106.5 mAU/mL (median: 29.0) and 5.44 ± 5.70 ng/mL (median: 3.49), respectively. Subjects with oral intake had approximately 3 times higher vitamin K intake (median; 208.5 µg/day) and significantly lower serum levels of PIVKA-II and ucOC than those under enteral feeding. Serum levels of PIVKA-II and ucOC were significantly higher, and vitamin K intake was significantly lower in those with antibiotics use than those without it. Next, subjects were divided into four groups depending on the presence or absence of enteral feeding and antibiotics treatment. In those with both of them, median serum PIVKA-II and ucOC concentrations were 67.0 mAU/mL and 7.02 ng/mL, respectively, which were significantly higher than those in other three groups.

Conclusions: The current subjects had high prevalence of vitamin K deficiency both in the bone and liver, to which enteral feeding and antibiotics use were the contributing factors, and these two risk factors were additive. Thus, subjects with both enteral feeding and antibiotics use were at the highest risk of vitamin K deficiency. Although this is a preliminary cross-sectional study evaluating only the surrogate markers, attention should be paid on the vitamin K deficiency in subjects with severe motor and intellectual disabilities with its possible involvement in the increased fracture risk in these subjects.

***Disclosures: Kiyoshi Tanaka**, None.*

SA0368

See Friday Plenary number FR0368.

SA0369

See Friday Plenary number FR0369.

SA0370

See Friday Plenary number FR0370.

SA0371

See Friday Plenary number FR0371.

SA0372

Endogenous Opioid Effects on Bone Reveal a Critical Role of Hypothalamic Neuropeptide Y. Frank Driessler*[1], Iris Wong[1], Ronaldo Enriquez[2], Brigitte Kieffer[3], Christoph Schwarzer[4], Amanda Sainsbury[2], Herbert Herzog[2], Jacqueline Center[1], John Eisman[1], Paul Baldock[1]. [1]Garvan Institute of Medical Research, Australia, [2]Garvan Institute, Australia, [3]IGBMC, France, [4]Institut für Pharmakologie, Austria

Exogenous opioids are known to exert powerful effects on bone mass via endocrine and non-endocrine effects, increasing hip fracture by around 2-fold. We examined a component of endogenous opioid system, the dynorphins, for skeletal effects and the signaling pathway involved. Dynorphins are predominantly expressed within the central nervous system, with actions on pain, addiction and depression. In the hypothalamus, dynorphin and pre-prodynorphin is co-expressed with neuropeptide Y (NPY) and NPY expression is reduced in $Dyn^{-/-}$ mice.

We examined the bone phenotype of Dynorphin knockout mice ($Dyn^{-/-}$) and the potential involvement of NPY.

Cancellous bone volume was elevated in $Dyn^{-/-}$ mice compared to wild type (wt: 8.8%±0.6 vs Dyn-/-: 11.9%±1, $p<0.02$). Osteoclast surface (7.9%±0.7 vs 11.9%±0.7, $p<0.01$) and osteoclast number (3.3/mm±0.3 vs 4.4/mm± 0.2, $p<0.05$) were elevated in $Dyn^{-/-}$ mice. However, these changes were overridden by an increased mineral apposition rate (MAR) in $Dyn^{-/-}$ (1.6µm/d±0.1 vs 2.4µm/d±0.2, $p<0.02$).

Dynorphins signal through the kappa opioid receptor (KOR or), however, this receptor does not appear involved in the skeletal changes. There was no skeletal phenotype in $KOR^{-/-}$ mice (wt: 18.3%±1.6 vs $KOR^{-/-}$: 20.2%±1.8, ns) or those treated with the KOR antagonist norBNI. Moreover, KOR was expressed in brain but not in bone tissue and KOR agonist treatment induced a response in primary neurons but not primary osteoblasts *in vitro*, thereby indicating an indirect action.

Loss of dynorphin signalling is known to reduce neuropeptide Y expression in the hypothalamus, a change known to elevate bone formation. Both $NPY^{-/-}$ and $Dyn^{-/-}$ mice have elevated bone volume and bone formation, however, $NPY^{-/-}/Dyn^{-/-}$ double mutant mice showed no further increase compared to single mutant mice (MAR wt: 1.3µm/d±0.06, $NPY^{-/-}$: 1.5µm/d±0.06, $Dyn^{-/-}$: 1.6µm/d±0.08, $NPY^{-/-}/Dyn^{-/-}$: 1.5µm/d±0.04). This indicates a critical role for NPY in the transmission of the central dynorphin pathway.

The endogenous opioid system is required for normal bone homeostasis. The dynorphin system, acting via NPY, may represent a pathway by which higher processes including stress, reward/addiction and depression influence skeletal metabolism. Understanding of these interactions may also enable modulation of the adverse effects of exogenous opioid treatment.

***Disclosures: Frank Driessler**, None.*

SA0373

Reduced Bone Density Concomitant with Metabolic Abnormalities in Type 1 Diabetic (T1D) Patients. Priscille Masse*[1], Carole C. Tranchant[2], Maisha B. Pacifique[2], Karen Ericson[3], Sharon M. Donovan[4], Edgard Delvin[5]. [1]University of Moncton, Canada, [2]Université de Moncton, Canada, [3]Indiana University-Purdue University, USA, [4]University of Illinois, USA, [5]Hopital Sainte-Justine, Canada

Type 1 diabetic (T1D) patients are at risk of osteoporosis and nutritional deficiencies. These risks have never been investigated in parallel. Nutritional deficiencies can aggravate T1D complications. The present study aimed at fully investigating T1D-induced bone disorder by densitometry combined with blood chemistry after the attainment of peak bone mass. Twenty seven (27) insulin-treated T1D female patients, without renal complication, and 32 healthy controls, aged 30-40 yrs, were rigorously recruited. Exclusion criteria were vegetarianism, pregnancy or lactation, BMI>30 and use of drugs susceptible to influence bone metabolism, including estrogen. Bone mineral density (BMD, g/cm^2) was measured by Lunar DEXA on trabecular and cortical sites of lumbar vertebrae and femur. Diagnosis of low BMD (osteopenia + osteoporosis cases) was made according to WHO T-scores. The two groups of women were homogenous and comparable. Kidney functions, assessed by urinary albumin/creatinine, did not differ between them. T1D, diagnosed since 21 yrs in average, was fairly well-controlled with HbA1c (7.8%) only slightly above limit. BMD was significantly reduced in the T1D group at 4 lumbar sites (L1, $P<0.02$; L2, $P<0.03$; L1-L2, $P<0.02$; L1-L3, $P<0.05$) and at the Ward triangle ($P<0.04$). There was no significant difference for the cortical bone of the diaphyseal femur. The proportion of low BMD (≤ -1.1 SD) cases, when averaging all trabecular sites, was 1.75 greater ($P<0.01$) in the T1D group. This group had lower protein status for serum transferrin ($P<0.02$) and IGF-I ($P<0.001$) but not for serum albumin. Contrarily to other reports, serum Mg and plasma (P) pyridoxal phosphate (PLP), coenzyme in collagen maturation, were not reduced. P-PLP, used as a biomarker of vitamin B6 nutritional status, was near cut-off limit of deficiency in both groups. Serum iron concentration was also reduced in T1D group ($P<0.03$) although body stores (ferritin) and hemoglobin level were not affected. Whereas serum phosphate was unchanged, serum Ca (adjusted for albumin) was increased ($P<0.0003$) despite the reduction of 1,25(OH)2D3 ($P<0.001$). Vitamin D nutritional status, assessed by 25(OH)D3, was adequate in both groups. Significant blood differences were correlated with %HbA1c indicating that the changes evidenced were disease-induced. This study demonstrated metabolic abnormalities associated with T1D that could not jeopardize the quality of bone collagenous matrix, nor explain bone mineral loss.

***Disclosures: Priscille Masse**, None.*

SA0374

Disuse Osteopenia of the Forearm: What Accounts for Response Variability Following Immobilization? Joseph Spadaro*[1], Christina Centore[2], Rebecca Hickman[3], Jennifer Kelly[1]. [1]State University of New York Upstate Medical University, USA, [2]Department of Biomedical & Chemical Engineering, Syracuse University, USA, [3]Upstate Medical University, USA

Changes in bone density and geometry, as a result of immobilization, was more closely examined as part of an ongoing study of bone loss after disuse. Although on average a substantial loss of bone density occurs (5-20%) soon after injury/immobilization, a large variability among individuals is observed. In an attempt to better understand and predict individual responses, we examined the "responders" in our cohort and some of the factors that might be involved. Data was available on the extent of loss of bone mineral density (BMD) in the forearm bones during the six months period following forearm immobilization due to Colles' fracture or carpal surgery in 82 subjects, 30 males and 52 females, age 18 - 80 (the e-Bone Study). No subjects had conditions or medications known to affect bone density. Measurements of BMD (DXA) in the forearm were categorized by the amount of bone loss at 8, 16, and 24 weeks since completion of immobilization (baseline). Here we focused on the distal ulna, which was not fractured, to help eliminate the extra variability inherent in the radius BMD in these individuals.

Those individuals who had subsequent bone BMD loss between >3% at week 8 were considered "responders" to disuse (57% of the subjects) and 26% >10% loss (figure 1). By 24 weeks, this increased to 39% with > 10% losses. On average, the females lost more bone early (8 weeks), while the males had increased losses by 24 weeks. Those whose dominant hand was casted had more delayed ulna bone loss: 7 individuals at week 8 vs. 20 at weel 24. Dietary calcium does not appear to be a strong factor, and increasing age has previously been identified as increasing disuse bone loss.

It appears that using the "responder" approach to study disuse bone loss can be useful in identifying susceptible individuals disposed to larger losses after disuse, but so far the etiological variables appear to be numerous and a combinatorial approach may be beneficial.

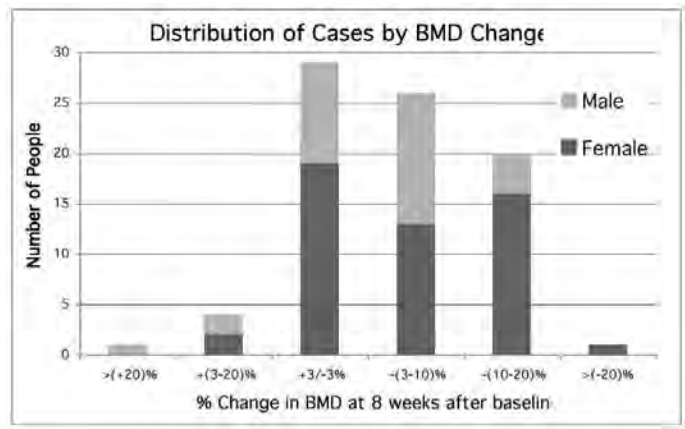

Figure 1: Disuse BMD loss in the distal ulna by gender

***Disclosures: Joseph Spadaro**, None.*

SA0375

Skeletal Changes in Type 2 Diabetic Goto-KaKizaKi Rats and Their Relationship with Expression of Bone Formation and Resorption Genes. José L. Pérez-Castrillón*[1], Jose A. Riancho[2], Daniel De Luis[3], David Guede-Garcia[4], José Ramon Caeiro[5], Manuel Gonzalez-Sagrado[6], María Domingo-Andres[7], David Primo-Martin[6]. [1]Hospital Universitario Río Hortega. Instituto Endocrinología. Reticef, Spain, [2]Hospital Universitario Marques de Valdecilla.Reticef.Univiversidad de Cantabria, Spain, [3]Hospital Rio Hortega. Instituto de Endocrinologia.Reticef, Spain, [4]Trabeculae., Spain, [5]Trabeculae. Reticef, Spain, [6]Hospital Universitario Río Hortega. Reticef, Spain, [7]Reticef, Spain

It has been suggested that the risk of fracture is increased in diabetic patients. However, studies on type 2 diabetes have demonstrated decreased, normal or even increased BMD. Overweight and obesity are prevalent in individuals with type 2 diabetes. Obesity per se tends to be associated with increased bone mass and is thus a confunding factor. We used Goto-KaKizaKi rats, a non-obese animal model of spontaneous type 2 diabetes, to characterize the bone properties in type 2 diabetes.

This study was performed to characterize the bone metabolism in five Goto-KaKizaKi (GK) rats, a spontaneous type 2 diabetic model. Bone samples from 5 GK rats and 5 age-matched, non-diabetic Wistar rats were analyzed. All specimens were

analyzed by μ-CT at a 9.0 μm nominal resolution with a Skyscan 1172 scanner and associated analysis software. The following parameters were measured in cancellous bone region: bone volume fraction (BV/TV), trabecular thickness (Tb.Th), trabecular separation (Tb.Sp), structure model index (SMI) and trabecular bone pattern factor (Tb.Pf). Parameters in cortical bone region included cross-sectional thickness (Cs.Th) and 3D cortical thickness (C.Th). Additionally, volumetric bone mineral density (vBMD) was measured in both regions. RNA was isolated from the femoral heads and the expression of several genes involved in bone formation or resorption (BGP, RANKL, OPG, SOST and DKK1) was measured by real-time qPCR. Structural studies showed a significantly decreased trabecular bone volume and interconnectivity of the trabeculae. In addition, the expression of osteocalcin gene was significantly decreased whilst SOST and DKK1 gene expression was significantly increased. In conclusion, the GK non-obese diabetic rat shows a decreased bone mass associated with decreased expression of the osteoblast-derived osteocalcin gene and might be a useful model to unravel the effects of diabetes on bone independent of obesity.

***Disclosures: José L. Pérez-Castrillón**, None.*
This study received funding from: RETICS. RETICEF

SA0376

See Friday Plenary number FR0376.

SA0377

See Friday Plenary number FR0377.

SA0378

See Friday Plenary number FR0378.

SA0379

Interactions of Nitric Oxide and Insulin-Like Growth Factor I, in Prevention of Bone Loss. Sunil Wimalawansa*. Robert Wood Johnson Medical School, USA

Many therapeutic advances have been made over the past decade in the prevention and treatment of osteoporosis. However, these are expensive and some also have significant adverse effects, and hence simple, cost-effective therapeutic options are warranted. The beneficial effects of estrogen on bone maintenance is at least in part mediated via nitric oxide (NO)/cGMP pathway, and perhaps also via IGF-1. At appropriate doses, nitroglycerin (NG) as a nitric oxide donor was shown to favorably affect both osteoblasts and osteoclasts (i.e., uncoupling these two cell types), and prevention of estrogen as well as glucocorticoid-induced bone losses.

A three-year randomized, doubled-blind, controlled clinical trial was conducted to assess the efficacy NG in preventing bone loss in early postmenopausal women. This study, Nitroglycerin as an Option: Value in Early Bone Loss (NOVEL) was funded by NIAMS. Women were randomized to receive either nitroglycerin ointment or placebo ointment. All women received calcium and vitamin D supplementation. There were no differences in the BMD in the treatment vs. calcium and vitamin D arms. However, taking compliance (~75%) into consideration, the dose actually used by the study participants was only ~50% of that was originally intend to use in this study; i.e., a sub-therapeutic dose that would not have even expected to have positive effect on the skeleton.

Nevertheless, a significant increase of serum IGF-1 levels was observed in women who had positive BMD response following NG therapy, but not in the placebo-treated subjects who had gain in BMD. NG-treated subjects with increased BMD had increase of serum IGF-1 levels, 201 $\pm$ 25.6 vs. non-responders, 40.2 $\pm$ 16.9 ng/mL ($p<0.001$), and the BMD changes was significantly correlated with the change of serum IGF-1 levels from the baseline ($r = 0.5$; $p<0.01$). Whereas, those who were in the placebo group with increased BMD had no change in serum IGF-1 levels (-2.6 $\pm$ 24.6 vs. 10.8 $\pm$ 13.5 ng/mL, NS; responders vs. non-responders). Previously, we have demonstrated that estrogenic effects on bone can be completely blocked with nitric oxide synthase (NOS) inhibitors such as L-NAME. Current data suggest that NG, in addition to be one of the key final common pathways for positive effect of estrogen in bone, may also involved in enhancing the local production of IGF-1, thereby assisting bone formation that is observed with nitric oxide therapy.

***Disclosures: Sunil Wimalawansa**, None.*

SA0380

Teriparatide Treatment in Japanese Subjects with Osteoporosis at High Risk of Fracture: Effect on Bone Mineral Density and Bone Turnover Markers during 12-Month, Randomized, Placebo-Controlled, Double-Blind and 12-Month Open-Label Study Periods. Toshio Matsumoto*[1], Toshitsugu Sugimoto[2], Hideaki Sowa[3], Mika Tsujimoto[4], Miho Hatano[4], Takao Awa[4], Noriko Iikuni[4], Akimitsu Miyauchi[5], Margaret R Warner[6], Toshitaka Nakamura[7]. [1]University of Tokushima Graduate School of Medical Sciences, Japan, [2]Shimane University School of Medicine, Japan, [3]Eli Lilly Japan K.K., Japan, [4]Eli Lilly Japan KK, Japan, [5]Omura municipal Hospital, Japan, [6]Eli Lilly & Company, USA, [7]University of Occupational & Environmental Health, Japan

This multicenter study was conducted to assess the safety and efficacy of teriparatide 20 μg/day in Japanese men and women with osteoporosis at high risk of fracture during a 12-month, randomized, double-blind, placebo-controlled treatment period followed by a 12-month, open-label treatment period with all subjects receiving teriparatide. Subjects (93% female; median age 70 years) were randomized 2:1 to teriparatide versus placebo (teriparatide, n=137; placebo-teriparatide, n=70). In the open-label treatment period, 119 subjects continued teriparatide and 59 placebo-treated subjects switched to teriparatide (placebo-teriparatide group). For subjects with measurements at the 12-month timepoint, bone mineral density (BMD) at the lumbar spine (L2-L4), femoral neck, and total hip increased from baseline by 10.04 $\pm$ 5.23% (mean percent change $\pm$ SD), 2.01 $\pm$ 4.63%, and 2.72 $\pm$ 4.04% in the teriparatide group and 0.19 $\pm$ 4.33%, 0.44 $\pm$ 3.97%, and -0.26 $\pm$ 3.42% in the placebo-teriparatide group. At the last available measurement through 12 months (LOCF), teriparatide significantly increased BMD compared with placebo at the lumbar spine ($P<0.001$), at the femoral neck ($P=0.015$), and at the total hip ($P<0.001$). For subjects with measurements at the 24-month timepoint, BMD at the lumbar spine, femoral neck, and total hip increased from baseline by 13.42 $\pm$ 6.12%, 3.26 $\pm$ 4.25%, and 3.67 $\pm$ 3.98% in the teriparatide group and 9.11 $\pm$ 5.14%, 2.19 $\pm$ 4.81%, and 2.46 $\pm$ 3.54% in the placebo-teriparatide group. In the teriparatide group, serum procollagen I N-terminal propeptide (PINP) increased significantly from baseline within 1 month and remained elevated at 24 months (median percent change 49.24%, $P<0.001$); in the placebo-teriparatide group PINP change was -17.23% at 12 months and 76.12% at 24 months (for both times, $P<0.001$ versus study baseline). The incidence of treatment-emergent adverse events (TEAEs), serious TEAEs, and discontinuations due to TEAEs was comparable in the teriparatide and placebo-teriparatide groups. These lines of evidence suggest that teriparatide 20 μg/day was well tolerated and stimulated bone formation in Japanese subjects with osteoporosis at high risk of fracture during 24 months of treatment.

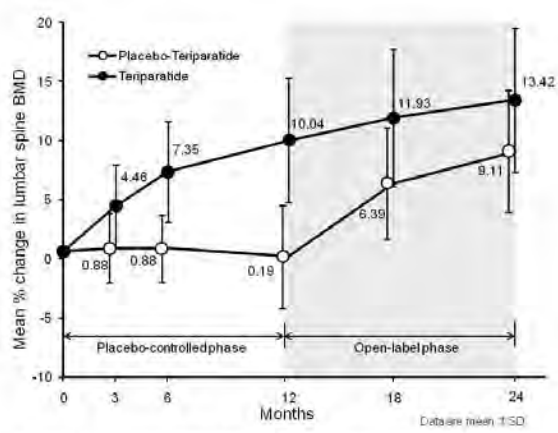

Forteo 24month figure_ASBMR

***Disclosures: Toshio Matsumoto**, Ono Pharmaceutical, 2; JAPAN TOBACCO INC, 5; Teijin Limited, 5; Chugai Pharmaceutical Co., Ltd., 5; Eli Lilly Japan KK, 5; Astellas Pharma Inc, 5; Asahi Chemical, 5; Daiichi Sankyo Company, 5*

SA0381

Vitamin D Insufficency as a Possible Explanation for Lack of BMD Increase in Bisphosphonate Pretreated Male Patients with Fractures and PTH 1-84 Therapy. Friederike Kühne[1], Judith Haschka[1], Miriam Putz[1], Astrid Fahrleitner-Pammer[2], Heinrich Resch[1], Roland Kocijan[1], Christian Muschitz*[3]. [1]Medical Department II - The VINFORCE Study Group, Austria, [2]Department of Endocrinology - Medical University of Graz, Austria, [3]St. Vincent's Hospital, Austria

Purpose: The aim of this prospective open label study is the evaluation of efficacy and tolerability of PTH (1-84) in men at high risk for first or further osteoporotic fracture. Methods: A total of 15 men with a mean age of 60.6 ± 16.2 years was prospectively assigned to PTH (1-84) 100 µg sc daily for 24 months. All patients received 1000mg calcium and 800IE vitamin D supplementation daily. 13 had prior bisphosphonates with a mean duration of 7.6 ± 3.8 years, 9 of them had major osteoportic fractures an, 2 had a bone biopsy (low connectivity). 12 patients had prior vertebral fractures (mean 3 fractures) and 3 patients had prior hip fracture. We investigated DXA (spine & hip), BTMs, fracture status, improvement of daily activities and reduction of pain. Results: For evaluation baseline and 12 months results were compared. Mean levels of PTH decreased from 49.6 ± 16.7 to 36.3 ± 21.0 ng/ml (P=0.030); P1NP increased from 26.38 ± 9.64 to 148.13 ± 35.45 µg/l (P=0.005) and S-CTX increased from 0.29 ± 0.16 to 0.75 ± 0.44 ng(ml (P=0.002). BMD L1-L4 increased 3.6% (P=0.097) while BMD at hip did not change. Subjects were divided into two groups according to the initial vitamin 25OHD3 levels (cut off: 30 ng/ml). 7 out of 15 subjects had vitamin D insufficiency, only 4 of them reached levels above 30 ng/ml during therapy. 2/8 subjects with physiological levels at baseline decreased within 12 months. The mean increase of vitamin D in the group <30 was 4.75 ng/ml while the mean decrease of vitamin D in the group >30 was 12.8 ng/ml (P=0.032). In the group with evidence of vitamin D insufficiency there was no change in lumbar spine BMD while there was a slight decrease of -1.8% in the other group (P=0.044). No hypercalcaemia was observed and no new vertebral fracture occurred in the 15 patients. Patients reported a significant reduction of back pain resulting in an improvement of daily activities (P<0.05). Conclusions: There is a rapid and sustained change in markers of bone turnover and spine BMD indicating an anabolic effect. The majority of the male patients had an initial vitamin D insufficiency and also a large number of patients with initialy sufficient levels decreased during therapy. Our data show that Vitamin D is as important as the osteoinductive effect of PTH for the increase of mineralsation of bone and deficiency leads to a release of the osteoanabolic effect of PTH. An initial boost phase with high dose vitamin D is essential prior to PTH therapy.

***Disclosures: Christian Muschitz**, None.*

SA0382

A Systematic Review of the Risk of Bisphosphonate-related Osteonecrosis of the Jaw in Osteoporosis. Emileigh Mercer*[1], Sook-Bin Woo[2], Nathaniel Treister[2], Jerry Avorn[3], Sebastian Schneeweiss[3], Daniel Solomon[4]. [1]Brigham & Women's Hospital, USA, [2]Division of Oral Medicine & Dentistry, Brigham & Women's Hospital, USA, [3]Division of Pharmacoepidemiology, Department of Medicine, Brigham & Women's Hospital, USA, [4]Harvard Medical School, USA

Purpose: We reviewed the epidemiological literature regarding bisphosphonate (BIS) treatment for osteoporosis and its association with osteonecrosis of the jaw (BRONJ) to both understand the methodologies used and describe the results.

Methods: The literature was reviewed for all English language articles using the search terms "osteonecrosis of the jaw," or one of each "alendronate," "etidronate," "ibandronate," "pamidronate," "risedronate," or "zoledronic acid," and "epidemiology." We also searched for "bisphosphonate-related osteonecrosis of the jaw" and "epidemiology." After excluding articles without primary data on the prevalence of BRONJ in patients with osteoporosis, 4 articles were examined for their methodology, including study design, population source, BRONJ definition, treatment type, exclusion criteria, BRONJ confirmation, and treatment duration, as well as their final prevalence estimate of BRONJ.

Results: Of the 4 articles, 2 were from the United States, one from Korea and one from Australia. All 4 studies defined the inclusion for BRONJ cases similarly; either using the AAOMS definition or other broadly accepted criteria. When needed, confirmation of BRONJ was obtained by some combination of medical chart review and follow-up to reaffirm cases. The methods varied widely particularly with respect to the definition of the denominator of BIS-users: 1 study used an insurance database, 1 used hospital medical records, 1 study used an electronic medical record from a dental clinic and 1 used pharmaceutical marketing data. Various methods for collecting cases were used as 2 queried electronic medical records, 1 surveyed dental surgeons and specialists known to treat BRONJ, and 1 surveyed BIS users for dental symptoms. Treatment type also varied across the studies: 2 simply considered alendronate, while 2 others focused on alendronate, risedronate, and ibandronate. The results of each of the studies are shown in the Table. The incidence rate of BRONJ ranged from 0.1 to 1.0 per 1,000 persons based on the 3 strongest studies.

Conclusions: The epidemiologic literature on BRONJ is inconsistent in rigor, possibly explaining the great variation in reported incidence rates. The best studies suggest rates much higher than original estimates. Further work should use standard definitions for BRONJ, utilize appropriately defined denominators, and examine populations not using BIS to determine whether these drugs are truly the primary risk factor.

Study	N-value (Min/Max)	Cases Used for Calculation	Prevalence Estimate (per 1,000)
Hong, 2009	9,882/12,752	7	0.5–0.7
Lo, 2009	8,572/13,835	9	0.7-1.0*
Mavrokokki, 2007	304,900 on BIS for osteoporosis	36	0.1-0.4 on BIS
			0.9-3.4 on BIS with extractions
Sedghizadeh, 2009	208 alendronate users	9	40

*28 per 100,000 person-years of oral BIS treatment

Table 1: Epidemiologic Results of Studies Presenting a Prevalence Estimate for BRONJ in BIS Users

***Disclosures: Emileigh Mercer**, None.*

SA0383

Analgesic Effect of Minodronate, a New Bisphoshonate, on Back and Knee Pain in Elderly Subjects with Osteoporosis and/or Osteoarthritis. Takuo Fujita*[1], Mutsumi Ohue[1], Yoshio Fujii[2], Akimitsu Miyauchi[3], Yasuyuki Takagi[4]. [1]Katsuragi Hospital, Japan, [2]Calcium Research Institute Kobe Branch, Japan, [3]Omura Municipal Hospital, Japan, [4]National Hyogo Chuo Hospital, Japan

Purpose In addition to increasing bone mineral density and reducing occurrence of fracture, bisphosphonates were reported to be effective on back and knee pain associated with osteoporosis and osteoarthritis in elderly subjects. The analgesic effect of minodronate, a new bisphosphonate, was tested by electroalgometry (EAM)measuring fall of skin impedance and recording subjective pain by visual rating scale (VRS).

Methods In 22 patients with a mean age of 70±4 years (20 females and 2 males), complaining of back and knee pain both back and knee pain in 21 and back pain alone in 1), 1 mg minodronate was orally administered once daily 30 minutes before breakfast. Osteoporosis by lumbar BMD < 70% of YAM was seen in 27%, possibly underestimated because of osteoarthritic changes (Nathan Score of 2 or higher) was seen in 63% and Kellgren Score for knee osteoarthritis of 2 or higher for spinal osteoarthritis in 77%. Pain was estimated before and after exercise loading; knee bending, walking on a flat surface and up and down stairs and lying down supine on bed and standing up, by measuring the fall of skin impedance using Impedance Meter made by General Devices, Richfield, New Jersey (EAM) and recording subjective pain by VRS scale dividing the distance between unbearable pain and no pain into a 0 to 100.

Results The fall of skin impedance (% of the preload value) employed as an EAM pain index showed a significant positive regression over subjective pain recorded on VRS scale with r=0.484, Y=3.58X + 15.75, p= 0.0221. Paired comparison of pain indices between pre- and post-minodronate treatment revealed a significant analgesic effect 28 day treatment by EAM (p=0.0248) and 56 day treatment by VRS (p=0.0269). Overall paired comparison of pain indices between pre-test and 14~56 day post-treatment indicated a highly significant decrease of pain by both EAM (p=0.0009) and VRS (p=0.0004).

Conclusion Minodronate significantly alleviated back and knee pain in 22 elderly subjects according to EMS measurement of the fall of skin impedance and VRS recording of subjective pain, the former effect noted after 28 days and the latter after 56 days of treatment

***Disclosures: Takuo Fujita**, None.*

SA0384

Biphosphonate-associated osteonecrosis of the jaw: An Ontario Survey. Aliya Khan*, Lorena Rios Stange, Nazir Khan. McMaster University, Canada

Purpose: To evaluate the period prevalence of bisphosphonate (BP)-associated osteonecrosis of the jaw (ONJ) seen by oral surgeons in Ontario between 2004 and 2006.

Methods: A survey developed by representatives of the Ontario Society of Oral and Maxillofacial Surgeons was mailed to Ontario oral and maxillofacial surgeons (OMFSs) in December 2006 asking oral surgeons to provide information on cases of ONJ seen in the previous three calendar years (2004 to 2006). OMFSs were subsequently contacted by phone if they had not responded or if they had reported cases of ONJ. The frequency of ONJ in association with BP use was estimated from the number of patients with filled prescriptions in Ontario between 2004 and 2006. The incidence of ONJ was calculated separately for both iv BP use in cancer related bone disease as well as oral or iv BP use for osteoporosis or other metabolic bone diseases

Results: Forty-one cases of ONJ were identified of which 32 cases occurred between 2004 and 2006. Nineteen patients were receiving intravenous BP for cancer related skeletal disease and 13 patients were receiving oral or intravenous BP for osteoporosis or metabolic bone disease. The average annual incidence of BP associated ONJ was 4 per 1000 for cancer patients and 2/100000 for patients with osteoporosis or other metabolic bone disease on oral or intravenous BP. Other risk factors for ONJ were present in all five cases in whom detailed assessment was available. In osteoporosis patients the median duration of BP use was 42 months (36 to 120 months). In patients receiving intravenous BP for cancer related skeletal disease the median duration of exposure to intravenous bisphosphonate therapy was 42 months (11 to 79 months).

Conclusions: The average annual incidence for BP associated ONJ was 4/1000 in cancer patients. In people receiving oral or iv BP for osteoporosis or metabolic bone disease, the average annual incidence was 1/100,000. This study provides an

approximate frequency of BP associated ONJ in Canada. These numbers need to be quantified prospectively with accurate assessment of coexisting risk factors.

***Disclosures: Aliya Khan**, NPS, 2; MERCK, 2; Novartis, 2; Aventis, 2; Amgen, 2*
This study received funding from: Novartis, Proctor & Gamble, MERCK

SA0385

Bisphosphonate Use in Women and Men Who Are at High Risk for New Fractures and Living in Long-Term Care Homes: The Vitamin D Osteoporosis Study (ViDOS). Alexandra Papaioannou*[1], Sharon Marr[2], George Ioannidis[3], Courtney Kennedy[2], Lora Giangregorio[4], Laura Pickard[2], Jenna Johnson[1], Glenda Campbell[5], Jackie Stroud[5], Suzanne Morin[6], Robert Josse[7], Anna Sawka[8], Richard Crilly[9], Lehana Thabane[2], Lisa Dolovich[2], Mary Lou van der Horst[2], Norm Flett[2], Lynn Nash[2], Jonathan Adachi[10]. [1]Hamilton Health Sciences, Canada, [2]McMaster University, Canada, [3]Sympatico, Canada, [4]University of Waterloo, Canada, [5]Medical Pharmacies Group Inc, Canada, [6]McGill University Health Centre, Canada, [7]St. Michael's Hospital, University of Toronto, Canada, [8]Toronto General Hospital, Canada, [9]University of Western Ontario, Canada, [10]St. Joseph's Hospital, Canada

Aim: The ViDOS study is an integrated knowledge translation initiative designed to improve the management of falls and fracture in the long-term care (LTC) setting. One of the study objectives is to increase appropriate prescribing of bisphosphonates in high-risk residents.

Methods: The ViDOS study is a clustered randomized control trial involving a multifaceted integrated disease management process that consists of a small group of physicians, nurses, and pharmacists employed by LTC homes who regularly meet to examine resident care and quality improvement objectives. In intervention homes, these groups attend 3 problem-based learning sessions occurring 5-months apart and led by an Osteoporosis Expert. Control homes receive standard materials given to all LTC homes in the province. The planned recruitment is 40 LTC homes randomized into either intervention (n=20) or control (n=20). Prescribing, falls and fracture data will be collected for both the control and intervention LTC homes in 3 time periods (baseline, follow-up 1 and follow-up 2). Demographic, medications, and disease conditions are collected from the central pharmacy database that has records for all residents living in each home. Medication and co-morbidity data are based on the medication administration records (MAR). This analysis evaluated baseline data and examined the use of bisphosphonate therapy in women and men who are at high risk for new fracture in 16 LTC homes. High risk was defined as residents who had osteoporosis or a prior hip fracture recorded on their MAR sheets. Descriptive statistics are presented for women and men separately.

Results: A total of 1559 medical records for women and 688 for men were analyzed. The mean (SD) age was 83.8 (10.3) years for women and 78.1 (11.8) years for men. Results revealed that 15% (n=236) and 8% (n=119) of women and 4% (n=29) and 2% (n=17) of men had documented osteoporosis or a prior hip fracture, respectively. A total of 50% (118/236) of women and 55% (16/29) of men with documented osteoporosis were taking a bisphosphonate. Furthermore, 40% (47/119) of women and 0% (0/17) of men with a prior hip fracture were taking a bisphosphonate.

Conclusions: A large number of women and men at high risk of fracture in LTC, particularly for those with a prior hip fracture, were not taking bisphosphonate therapy. Ensuring optimal osteoporosis management may reduce the probability of future fractures and the negative consequences associated with fracture.

***Disclosures: Alexandra Papaioannou**, Amgen, 2; Amgen, 8; Merck Frosst, 8; Novartis, 2; Procter and Gamble, 2; sanofi-aventis, 8; Merck Frosst, 2; Eli Lilly, 8; Servier, 8; Eli Lilly, 2*

SA0386

Bisphosphonate-related Osteonecrosis of the Jaw; Clinical and Radiographical Difference Between the Conventional Chronic Osteomyelitis of the Jaw. Tae-Geon Kwon*[1], So-Young Choi[2], Chang-Hyeon An[3]. [1]Kyungpook National University, School of Dentistry, South korea, [2]Kyungpook National University, School of Dentistry, Oral & Maxillofacial Surgery, South korea, [3]Kyungpook National University, School of Dentistry, Oral & Maxillofacial Radiology, South korea

There had been various reports concerning the osteonecrosis of the jaw after receiving the intravenous or oral bisphosphonates. Bisphosphonate-related osteonecrosis of the jaw (BRONJ) is mainly related with various degree of infection of the jaw bone. With the use of antibiotics and improved dental care, conventional osteomyelitis of the jaw is less common these days, but BRONJ is newly emerged in oral and maxillofacial surgery field. PURPOSE: The present study was intended to compare the conventional osteomyelitis and BRONJ on the features of clinical and radiographic finding so that we can establish the optimized treatment for BRONJ. PATIENTS AND METHODS: The CT, Panorama, Bone scan data of 83 BRONJ patients (Male 6, Female 77, and mean age 70.3 years) and 98 conventional chronic osteomyelitis patients (Male 54, Female 44, Mean age 58.0 years) were compared. Destruction of trabeculae or cortex, size of the sequestra, invasion of adjacent structure such as inferior alveolar nerve or sinus, periosteal new bone formation, intramedullary osteosclerosis were investigated. Also correlation of the radiographic or clinical symptoms with biochemical markers CTX (C-terminal telopeptide), Alkaline phosphatase, Osteocalcin, C-reactive protein were evaluated in 32 patients. RESULTS: BRONJ and conventional chronic osteomyelitis (C-OM) showed similar proportion of systemic disease whereas BRONJ occurred more multiple sites than C-OM. Larger sequestrum ($\geq$15mm), adjacent bone destruction ($p<0.05$) were more frequent in BRONJ patients. BRONJ patient showed significant lower CTX value ($p<0.05$). However the biochemical markers used in the study did not correlate with disease severity and or stage of the BRONJ. CONCLUSIONS: According to the previous treatment protocol (AAOMS), conservative treatment was recommended if possible. However, as the BRONJ showed more destructive pattern than C-OM, these results implies the surgery at the proper time might be more effective. Moreover, CTX value can be used as one of the clinical reference but cannot be regarded as a standard for BRONJ progression.

***Disclosures: Tae-Geon Kwon**, None.*
This study received funding from: Brain Korea 21, MRC

SA0387

See Friday Plenary number FR0387.

SA0388

See Friday Plenary number FR0388.

SA0389

See Friday Plenary number FR0389.

SA0390

See Friday Plenary number FR0390.

SA0391

Histologic Analysis of the Lateral Femoral Cortex in Two Patients, One with a Biphosphonate Related Femoral Fracture and the Other with a Pending Fracture. Richard Dell[1], Eric Eisemon*[2], Vincent Vigorita[2]. [1]Kaiser, USA, [2]Maimonides Medical Center, USA

Purpose: Several case reports have demonstrated a specific type of femur fracture seen in patients on bisphosphonates. The hallmark of these fractures is a thickened lateral cortex with a lateral projection at the fracture line, which is transverse on the lateral cortex and oblique on the medial cortex. Pre-fracture signs are focal thickening, lateral projections and a radiolucent line on the lateral cortex. The purposed underlying pathology of these fractures is a low turnover state induced by long term bisphosphonate use. We performed a histological analysis of the cortex where the fractures occur.

Methods: Inclusion criteria for our study were atypical appearing femur fractures or pending fracture as described above, low energy mechanism of injury or focal pain, and a documented history of bisphosphonate use. One patient with pre-fracture (Fig 1A) and fracture (Fig 2A) were included in our study. Specimens were obtained during surgery of the lateral cortex at the level of the fracture, along with intramedullary reamings. The specimens were processed in a non-decalcified manner and treated with hematoxylin and eosin, Goldner, and Von Kossa stains.

Results: Specimens consisted of fragments of both cancellous and cortical bone. Samples showed focal osteoblast activity and focal osteoid deposition indicating bone formation activity. In the pre-fracture patient with pre-fracture there was little identifiable osteoclast activity (Fig 1B) and in the patient with fracture osteoclasts were present but appeared detached from the bone surface (Figure 2B). The osteoclasts in both cases appeared rounded, without ruffled borders. There was no evidence of frank osteomalacia in either specimen.

Conclusions: Our findings demonstrate limited osteoclast remodeling but some osteoblast remodeling activity in the cancellous bone but demonstrable abnormal remodeling in the cortical bone. The most interesting finding was the lack of cortical osteoclast activity in one case (Fig 2A) and the abnormal appearance of the cortical osteoclasts in the other case (Fig 2B). Detached from the bone surface and rounded in appearance, the oseoclasts appear dysfunctional. These findings are significant in that they demonstrate abnormal bone remodeling at the fracture and pre-fracture site and are consistent with some known long term effects of biphosphonate therapy which, in part, are felt to cause interference with osteoclast linkage (ligand) to the bone surface.

Figure 1A

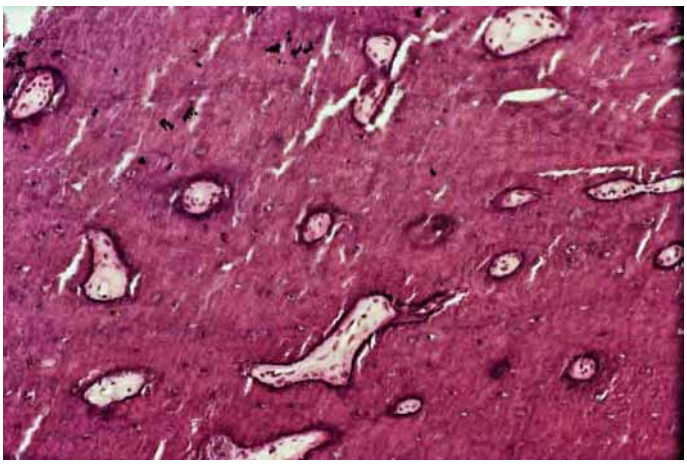

Figure 1B

Figure 2A

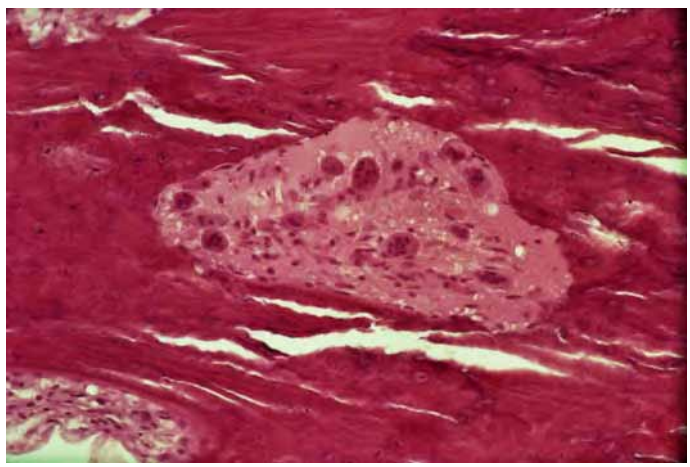

Figure 2B

***Disclosures: Eric Eisemon**, None.*

SA0392

Randomized Placebo-controlled Trial of Risedronate in Patients with Crohn's Disease and Osteopenia. Marieke Pierik[1], Daan W Hommes[2], Gerard Dijkstra[3], Ruud A van Hogezand[2], Paul Lips*[4], Maurice Russel[5], Ad A. van Bodegraven[6], C.J. van der Woude[7], Lex Van De Langerijt[8], Pieter Stokkers[9], Geeske M.E.E. Peeters[6], Bas Oldenburg[10], Coen (J.C.) Netelenbos[6]. [1]Academisch Ziekenhuis Maastricht, Netherlands, [2]Leiden University Medical Center, Netherlands, [3]Academisch Ziekenhuis Groningen, Netherlands, [4]VU University Medical Center, The netherlands, [5]Medisch Spectrum Twente, Netherlands, [6]VU University Medical Center, Netherlands, [7]Erasmus Medical Center, Netherlands, [8]Sanofi-aventis, The netherlands, [9]Academic Medical Center, Netherlands, [10]University Medical Center, Netherlands

Purpose:
Crohn's disease (CD) is associated with increased bone resorption inducing low bone density and increased fracture risk. To assess the efficacy of bisphosphonates to increase bone density in Crohn's disease associated osteopenia, a prospective, randomized, double-blind trial was conducted with risedronate 35 mg weekly versus

placebo. The patients originated from clinics of all 8 university hospitals, and one referral hospital in The Netherlands.

Methods:

Bone mineral density was assessed by dual energy absorptiometry (DXA) in 123 patients with established CD that was in remission. Patients were between 18-60 years of age and had no recent use of glucocorticoids or bisphosphonates, and all were vitamin D sufficient. Crohn's disease Activity Index (CDAI) was calculated, and C-reactive protein was measured to ascertain clinically inactive disease at baseline. DXA was measured at baseline, 12 and 24 months using Hologic densitometers. Daily calcium and vitamin D supplements were provided along with risedronate 35mg or placebo once per week. Activity of CD was evaluated during the 2-years study period. The primary endpoint of study was the change in BMD, expressed as T-score between baseline and 24 months of treatment

Results:

Baseline demographics included a patient mean age of 42.7 (SD 13.0) yrs, 46 % were male, and at inclusion CRP levels and CDAI were 3 mg/L and 86 in the placebo and 4 mg/l and 76 in the risedronate group, respectively. Patients groups with risedronate and placebo were comparable.

DXA in the lumbar spine at baseline was median 0.93 (IQR 0.88-1.01) g/cm^2, T-score –1.28 (SD 0.77) in the placebo group, and 0.93 (IQR 0.89-1.00) g/cm^2, T-score –1.30 (SD 0.61) in the risedronate group. The median lumbar BMD change at 24 months was 0.01 (IQR –0.02 – 0.03) g/cm^2 in the placebo and 0.03 (IQR 0.00 – 0.07) g/cm^2 in the risedronate group (P= 0.006). The T-score increased at 24 months 0.08 (SD 0.42) in the placebo group and 0.33 (SD 0.46) in the risedronate group (P=0.005). Changes in BMD of the femur were not significant.

Conclusion:

Risedronate improves lumbar bone mineral density in CD-patients suffering from CD- associated low bone mass as assessed by DXA.

***Disclosures: Paul Lips**, Sanofi-Aventis, 2*
This study received funding from: Sanofi-Aventis

SA0393

See Friday Plenary number FR0393.

SA0394

Validation of Electronic Coding in Women with Diaphyseal Femur Fractures in a Defined Population. Susan Ott*[1], Leslie Spangler[2], Delia Scholes[3]. [1]University of Washington Medical Center, USA, [2]Group Health Cooperative, USA, [3]Group Health CooperativeGroup Health Research Institute, USA

Recent reports have questioned whether non-traumatic fractures of the diaphyseal femur are associated with long-term bisphosphonate use. Automated database studies may be useful in evaluating this and estimating incidence. Our study was undertaken to validate electronic coding for femur fractures and was conducted in a non-profit managed care plan that provides comprehensive health care, including medications. We used automated data for 2007 to identify the first occurrence of a relevant ICD9 code in women >45 years (n = 95,765). The ICD9 codes were those for fractures of the subtrochanteric region (820.22, 820.32), the shaft (821.01, 821.11), unspecified part of femur (821, 821.0, 821.00, 821.1, 821.10) or stress fracture, femur (733.97). Medical records were reviewed. Of the 161 women identified by the ICD9 codes, charts had enough data to verify fracture location in 157. This showed that diaphyseal fractures (subtroch or shaft) occurred in 58 cases; 64% of them had a code for either subtroch or shaft, and the remaining 36% had a code for non-specified part of the femur. The code for subtroch was accurate in 11 of 21 cases and shaft in 16 of 32 cases. We also evaluated timing of the fracture. The fracture date was prior to 7/1/06 in 12 of the 161 cases. Altogether, of the cases identified by an electronic search of ICD-9 codes, only 49 (30%) were classed as incident diaphyseal fractures.

In the 49 diaphyseal fractures, we viewed all available images; the following patterns were seen: trauma, periprosthetic, thin "osteoporotic", thick, and thick with beaking. In 6 cases images were unavailable but radiology reports clearly defined thin or comminuted pattern, and in 4 cases there were no images or detailed descriptions. Of 5 with the thick, beaked pattern, 4 had been taking bisphosphonates (mean 3.8 yrs). In the other 44 cases, 9 had received bisphosphonates (2.4 yrs). Approximately 4500 women had > one oral bisphosphonate prescription filled in 2007. These results from a defined population are consistent with an association between long-term bisphosphonate use and a pattern of transverse femoral fractures with thick cortices and beaking. This relationship was found only if radiographs were viewed.

In this study use of ICD9 codes alone resulted in unsatisfactory confirmation rate of femoral diaphyseal fractures. Our findings support validating ICD9 codes before they are used as a surrogate for the occurrence of a femoral diaphyseal fracture.

PATTERN	N	Mean Age	N using bisphosphonates
Severe trauma	2	57	0
Periprosthetic	12	84	4
Thin "osteoporotic"	22	81	4
Thick, not beaked	4	69	1
Thick and beaked	5	72	4

Table

***Disclosures: Susan Ott**, None.*

SA0395

Zoledronate Prevents Tibial Bone Loss in Postmenopausal Women with Osteoporosis. Albrecht Popp*, Helene Buffat, Christoph Senn, Isolde Okere, Romain Perrelet, Kurt Lippuner. Osteoporosis Policlinic, University of Bern, Switzerland

Background: Zoledronate (ZOL 5mg i.v., once yearly) reduces the risk of fractures in postmenopausal women with osteoporosis (PMO). In the pivotal HORIZON trial, a gain of bone mineral density (BMD) was demonstrated at the lumbar spine and the hip compared to placebo. Little is known about the effects of zoledronate on BMD at peripheral sites.

Methods: An ancillary investigator-initiated substudy was performed in patients who participated in the PMO-HORIZON-core study at the Osteoporosis Policlinic, University of Bern, Switzerland. Bone density measurements of the distal tibial epiphysis (T-EPI) and diaphysis (T-DIA) were performed at month 0, 6, 12, 24 and 36 according to a previously validated method (Casez JP, J Bone Miner Res 1994; Popp AW, Osteoporos Int 2009) using a Hologic QDR 4500 A^{TM} scanner.

One hundred seventeen women consented to participate in the substudy and were randomised to ZOL or placebo (PLB). Treatment allocation was recently unblinded for fifty-one women (ZOL 23/ PLB 28) who did not participate to the extension study (E1) of HORIZON (drop-outs, unsuitable for or unwilling to participate to the extension study). This preliminary analysis includes all patients who received at least one dose of the study medication and had at least one follow-up DXA measurement (ZOL 22/ PLB 25). Changes in BMD were compared using ANOVA for repeated measurements. Missing values were imputed by carrying forward the last observation. Values are indicated as means $\pm$ SEM.

Results: Baseline characteristics of included patients were comparable with those in the core study and were similar in ZOL and PLB. After 36 months, BMD at lumbar spine increased by 7.5 $\pm$ 1.6% ($p<0.0001$) vs baseline in ZOL and did not change significantly in PLB (+1.9 $\pm$ 1.0%). At the total hip, BMD increased in ZOL (+2.6 $\pm$ 0.9%, $p<0.001$) and decreased in PLB (-1.4 $\pm$ 0.7%, $p< 0.05$). Peripheral bone loss at T-EPI and T-DIA was prevented by ZOL (+ 0.9 $\pm$ 0.8%; -0.1 $\pm$ 0.4%, both n.s. vs baseline), while a significant loss was observed at both tibial sites under PLB (-3.2 $\pm$ 1.2%; -1.2 $\pm$ 0.5%, both $p<0.01$ vs baseline).

Conclusion: ZOL prevented peripheral bone loss at the distal tibial sites in postmenopausal women with osteoporosis. This finding may differ from the reported effects with other bisphosphonates.

***Disclosures: Albrecht Popp**, Received speaker's fees of andl or was member of a advisory board of Amgen, Daiichi Sankyo, Eli Lilly, MSD, Synthes., 9*

SA0396

See Friday Plenary number FR0396.

SA0397

Compliance and Efficacy of Ibandronate 3 mg iv Quarterly vs. Oral Alendronate - Real World Data with the Non-interventional Study VIVA. Peyman Hadji*. Philipps-University of Marburg, Germany

Purpose: Numerous clinical trials have demonstrated the efficacy of Bisphosphonates in the treatment of postmenopausal osteoporosis. Bisphosphonates have been shown to be an effective treatment with regard to risk reduction of bone loss, osteoporosis related fractures, bone pain and as such are currently the standard of care treatment. However, the translation of clinical study results to real world experience is dependent on treatment compliance which in RCTs is generally high while in clinical practice significantly lower. This is generally true for many chronic diseases where patient adherence to treatment has been shown to be poor, which is particularly the case for oral bisphosphonates. Oral formulations of bisphosphonates are associated with poor gastrointestinal absorption and an increase in gastrointestinal adverse events necessitating complicated dosing regimens. It is well known that suboptimal adherence to bisphosphonate therapy is associated with an increased

risk of fracture. In contrast to the poor adherence with oral bisphosphonates, the treatment with Ibandronate iv seems to guarantee an optimal absorption and adherence, because it is applied directly by the physician.

The objective of this non-interventional study is to investigate compliance and persistence of patients with Ibandronate 3 mg iv quarterly vs. alendronate 70 mg weekly in a real world setting. Additionally the management and controllability of intravenous Ibandronate vs. oral alendronate is assessed. Furthermore the impact of compliance and persistence and of intravenous or oral therapy on important factors reflecting real life efficacy like pain intensity, quality of life, mobility and incidence of new osteoporotic fractures will be investigated. Additionally, for the first time relating to PMO, patient questionnaires for the prospective assessment of probable compliance (SSAS and BMQ) are used in this study.

Methods: This non-interventional study has started in Germany end of March 2010. Overall 6.000 patients with postmenopausal osteoporosis will be enrolled by 1.500 to 2.000 office based physicians. Since the interest of this study is focused mainly on Ibandronate, a 3:1 ratio Ibandronate iv : alendronate has been chosen. The observation period per patient is 12 months. Final results are expected in autumn 2012. Together with more details on the study outline first insights on progression of recruitment of this important study will be presented.

***Disclosures: Peyman Hadji**, None.*
This study received funding from: Roche Pharma AG, Germany

SA0398

Identifying Factors Associated with Patients Making the link Between a Fragility Fracture and Osteoporosis. Rebeka Sujic*[1], Monique Gignac[2], Rhonda Cockerill[3], Dorcas Beaton[4]. [1]St. Michael's Hospital, Canada, [2]Toronto Western Research Institute, Canada, [3]University of Toronto, Canada, [4]Keenan Research Centre, St Michael's Hospital, Canada

Introduction: Patients who associate their fragility fracture with osteoporosis (OP) are more likely to initiate first-line OP treatment. It is not known, however, who is more likely to make this association. The purpose of this study is to examine baseline factors associated with patients making the link between their fragility fracture and OP at follow up.

Methods: Data on a population-based cohort were collected as part of a provincial OP screening initiative targeting low trauma fracture patients over the age of 50. OP screening coordinators collected data at baseline and treatment-naïve, previously undiagnosed patients were followed up at 3 and/or 6 month. Logistic regression was used to identify which modifiable (e.g., patient perception) and non-modifiable (e.g., previous fracture) factors are predictive of patients making an association between their fragility fracture and OP at follow up.

Results: At baseline, 93% (853/916) of patients were unsure or did not believe their fracture was caused by OP. Of these, only 8.8% changed this perception at follow up. Adjusted analyses showed that those who changed were more likely to have a previous fracture OR 2.3 (1.3-4.1), be uncertain about maternal history of fractures OR 2.5 (1.1-5.7), perceive their bones as thin OR 6.9 (3.5-13.4) or be unsure about the quality of their bones OR 2.7 (1.4-5.3) at baseline.

Discussion: Many fragility fracture patients do not associate their fracture with having OP. We identified the baseline characteristics predictive of making the OP-fracture link at follow up. These findings should be incorporated in post-fracture OP interventions to better communicate to patients their risk of future fractures and OP. Future research should support increasing awareness in the patient group likely to make the OP-fracture link and consider using other approaches in those not fitting this profile.

***Disclosures: Rebeka Sujic**, None.*

SA0399

Influence of a Written or Oral Patient Support Program on Adherence with a Weekly Bisphosphonate in Comparison to Standard Information – Results of the COMBI-Study. Volker Ziller*[1], Karina Höntsch[2], Ioannis Kyvernitakis[2], Berna Seker-Pektas[2], Peyman Hadji[3]. [1]Philipps-University-Marburg, Germany, [2]Philipps-University Marburg, Germany, [3]Philipps-University of Marburg, Germany

Background

In long term medical treatment of postmenopausal osteoporosis an issue of increasing relevance is reduced adherence using oral bisphosphonates. Because reasons for non-adherence are multiple and complex, we designed two interventions intending to inform, motivate and remind patients about osteoporosis, treatment options, side effects problems and solutions and provided counseling contact to health care professionals. The COMBI-Study (Compliance in Osteoporosis treatment in Marburg using Bisphosphonates) was designed as a monocentric, prospective, randomized, partially blinded three armed parallel group study to evaluate the effect of a written versus oral versus standard patient support program on adherence to weekly bisphosphonates.

Material and Methods

180 postmenopausal women with diagnosed osteoporosis according to German guidelines and treatment with a weekly bisphosphonate had been randomized in the three intervention arms. The intervention groups received personalized letters and information leaflets or phone calls by a specially trained study nurse in predefined patterns for one year. Adherence and persistence were measured with a combination of self-report, prescription refill counts and bone marker changes (CTX). For the primary endpoint the three adherence measurements were combined to classify adherent versus non-adherent patients.

Results

Baseline characteristics showed a well balanced randomisation with no significant differences in age, weight, bone mineral density, prevalent fractures, back pain, loss of height and others. In the standard group 53,0%, in the phone group 52,7% and in the letter group 52,6% of patients were classified adherent. The differences were not statistically significant. Furthermore, there were no significant differences in persistence or diverse clinical parameters among the groups.

Discussion

Improving adherence to medical treatment in osteoporosis treatment is of upmost importance to the individual as well as to health care economic aspects.

The COMBI-Study showed no significant effect on adherence with a complex and multifaceted letter or phone based patient support program in a prospective, randomized setting. More understanding of factors influencing adherence is needed to design and evaluate effective interventions in the future

***Disclosures: Volker Ziller**, Procter and Gamble Pharmaceuticals, 8; Daichi Sankyo Germany, 8; Lilly Germany, 8; Novartis, 8*
This study received funding from: Procter and Gamble Pharmaceuticals

SA0400

Secondary Fracture Prevention in Home Health Care: Initial Results from a Group Randomized Trial. Meredith Kilgore*[1], Ryan Outman[2], Kenneth Saag[2], Julie Locher[2], Jeroan Allison[3], Jeffrey Curtis[2]. [1]University of Alabama At Birmingham School of Public Health, USA, [2]University of Alabama at Birmingham, USA, [3]University of Massachusetts School of Medicine, USA

Purpose: To develop and evaluate a multimodal intervention to increase rates of osteoporosis treatment in high risk patients receiving home health services.

Methods: We developed and tested an intervention to improve preventive care, particularly use of prescription osteoporosis drugs, among patients with a history of fracture receiving home health services. The intervention included an educational component for nurses, a computerized care plan that prompted the nurse to initiate specific actions related to osteoporosis management, easy reference materials for physicians, prepared order sheets to facilitate osteoporosis drug prescription, and patient education materials focused on osteoporosis, fracture risks, fracture prevention, and medication adherence. Field offices (n=23) of a home health agency operating throughout Alabama were randomized to receive the intervention or serve as controls. The primary outcome measure was the rate of osteoporosis medications prescribed among patients with a fracture history. A t-Test of proportions was used to assess difference between groups

Results: We found an absolute difference of 3.9% (NS) between the treatment and control group in post-intervention osteoporosis care. The figure shows the monthly distribution of treatment rates by office before and after the intervention. While all but one of the treatment offices showed an improvement, overall rates were low, and the corresponding rates in the control arm improved as well.

Pre- & Post-Intervention Osteoporosis Medication Prescription Rates in Intervention and Control Groups

A secondary analysis tested whether treatment rates increased when the nursing care plan was activated. In this case the difference was 15.3% ($p < 0.0001$).

Conclusions: Preliminary results do not demonstrate significant efficacy of the intervention overall, but suggest that improvements in processes of care could have significant effects on appropriate osteoporosis care delivery. The trial is continuing with a reinforcement of the nursing in-service training with audit and feedback to field offices on their relative performance rates, particularly with respect to activating the nursing care plan.

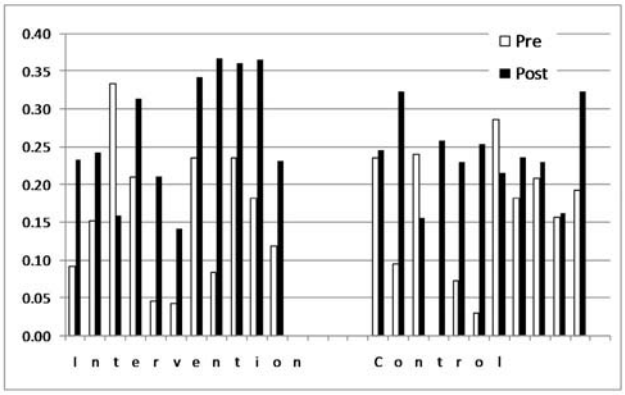

Figure

***Disclosures: Meredith Kilgore**, Amgen, Inc., 2; Eli Lilly, 2; Amgen, Inc., 5*
This study received funding from: Amgen, Inc.

SA0401

What Predicts Inititation of Osteoporosis Treatment after Fracture: Education, Organisation, Socio-economic Status. Nathalie Saidenberg-kermanac'h*. avicenne hospital (AP-HP), France

Purpose
The reasons of the limited success of initiatives aimed at increasing osteoporosis (OP) care after fragility fractures are still poorly understood. To answer this question we studied a population of patients entering our hospital for fragility fracture that underwent a dedicated intervention program of education on OP and organisation of further OP care. We then analysed patients- and intervention program-related factors predictive of OP investigation and treatment initiation as evaluated 6 months after the fracture event.
Methods
349 patients entering Avicenne Hospital (Bobigny, France) for fragility fracture underwent a dedicated program of OP education (structured interview with a trained nurse) and proposition of further OP care: either with their general physician (or private rheumatologist) or at the hospital. In the latter case, the patients were given a date for OP-centred investigation and consultation. Six months after the fracture they were telephonically contacted to know whether they had been investigated and had started a treatment for OP. The patients- and intervention program-related factors predicting the outcome were analysed.
Results
The organisation of further OP care at the hospital yielded the highest probability of being treated, at both univariate (OR 26,74; 95%CI [11,99-59,57) and multivariate analysis (OR 118,09; 95%CI [13,93-1000,92]), while patient's education on OP had a slighter effect (OR 4.74; 95%CI [2,15-10,44]). A low socio-economic status was the patient-related strongest negative predictor of further treatment (OR 0,22 [95%CI 0,09-0,47]).
Conclusions
The organisation of patient's OP care is the strongest determinant of OP investigation and treatment after fracture, and this aspect should be taken care of when attempting to increase OP care in everyday practice. Patients having a low socio-economic status are less likely to be investigated and treated, and additional effort to properly organise their care are warranted.

***Disclosures: Nathalie Saidenberg-kermanac'h**, None.*
This study received funding from: MSD

SA0402

See Friday Plenary number FR0402.

SA0403

See Friday Plenary number FR0403.

SA0404

See Friday Plenary number FR0404.

SA0405

See Friday Plenary number FR0405.

SA0406

A Randomized Controlled Trial of Music-Based Multitask Training on Gait, Balance and Falls Risk. Andrea Trombetti*[1], Mélany Hars[1], Silvia Del Bianco[2], François Herrmann[1], Serge Ferrari[3], Rene Rizzoli[4]. [1]University Hospital of Geneva, Switzerland, [2]Jaques-Dalcroze Institute, Switzerland, [3]Geneva University Hospital & Faculty of Medicine, Switzerland, [4]University Hospital, Switzerland

PURPOSE
Fracture prevention aims at reducing both bone loss and fall risk. Fall prevention includes a large variety of measures with inconsistently demonstrated efficacy. We assessed the effects of a 6-month music-based multitask training program (Jaques-Dalcroze eurhythmics) on gait, balance, and falls risk in community-dwelling elderly at increased risk of falling.
METHODS
We randomized 134 community-dwellers aged 65 or older (76 ± 7 years), to either a 1-hour weekly eurhythmics (Jaques-Dalcroze) program (n=66) or no intervention (control, n=68) for 6 months. The intervention consisted of multitask exercises performed to the rhythm of improvised piano music. The primary endpoint was the change in gait variability as assessed by quantitative gait analysis recorded on a 10 meter electronic walkway under single and dual task conditions, and balance analysis with a sway measuring portable device, together with a battery of functional tests. Falls were prospectively ascertained using a monthly diary. A carryover effect was measured at 12 months. Analysis was by intention-to-treat.
RESULTS
112 participants (84%) completed the first 6-month period. At that time, the intervention group exhibited significant improvements in gait as compared with controls, with an increase in usual gait speed (adjusted mean difference: 4.7cm/s, 95%CI:0.5-8.8, p=0.03) and a reduction in step and stride length variability (-1.8%, 95%CI:-2.8–0.9, p<0.001; -1.4%, 95%CI:-2.3–0.6, p<0.002, respectively) under dual-task. One-legged stance duration and medio-lateral angular velocity in the intervention group were significantly improved after the exercise program (+0.9s, 95%CI:0.3-1.6, p<0.006; -4.6, 95%CI:-8.6–0.6, respectively), as compared with controls. In the intervention group, there were improvements in the Tinetti score and the Timed Up and Go test. During the intervention period, there were fewer falls in the intervention group (Incidence Rate Ratio: 0.46, p=0.005) and a reduction in the risk of falling (Relative Risk=0.61, p=0.03). Two fractures occurred in the intervention group and 3 in the controls. Benefits of intervention were retained 6 months after the program has ended on gait, balance and fall risk.
CONCLUSIONS
This randomized controlled trial in community-dwelling elderly, indicates that a music-based multitask training program improves gait performance under single and dual-task conditions, and balance, as well as reduces both rate of falls and the risk of falling.

***Disclosures: Andrea Trombetti**, None.*

SA0407

Analysis of Response to Denosumab in Postmenopausal Osteoporosis. Richard Eastell*[1], Li-Yung Lui[2], Douglas Bauer[3], Cesar Libanati[4], Steven Boonen[5], Ian Reid[6], Steven Cummings[7]. [1]University of Sheffield, United Kingdom, [2]California Pacific Medical Center Research Institute, USA, [3]University of California, San Francisco, USA, [4]Amgen Inc, USA, [5]Center for Metabolic Bone Disease, Belgium, [6]University of Auckland, New zealand, [7]San Francisco Coordinating Center, USA

Denosumab is an investigational human monoclonal antibody to RANKL and it reduced the risk of new vertebral, non-vertebral and hip fracture in the FREEDOM Trial. The aim of the present study was 1) to define patterns of response according to total hip BMD change and 2) to identify the characteristics associated with greater or lesser response. FREEDOM was a randomised, placebo-controlled trial of denosumab 60 mg sc or placebo every 6 months in women ages 60 to 90 years with postmenopausal osteoporosis defined as a T-score less than -2.5 at the spine or hip and not less than - 4 at either site. All received daily calcium (1000 mg) and vitamin D supplement (400 to 800 IU). We measured 2 bone resorption markers, serum CTX (ELISA, Osteometer) and TRACP5b (immunocapture activity assay, Suomen Bioanalytiikka Oy, Oulu, Finland) in baseline fasting serum samples from 3906 in the placebo and 3902 in the denosumab group. We defined responder thresholds in subjects receiving all six injections (and so were 100% compliant) by calculating the 20th and 80th percentiles respectively for percentage change in total hip BMD in the treated group (80% increased by more than 2.8%) and for the placebo group (80% changed by <1.9%). These numbers were rounded and lesser responders were defined as change less than or equal to 2%, and greater responders more than 2% at 3 years. This threshold was then applied to all patients treated with denosumab in the trial who had hip BMD measurement at 3 years and the table shows that greater responders by BMD were characterised by better compliance and higher baseline bone resorption markers (p<0.01), any associations with age or BMD were small or not significant.

Table 1. Baseline characteristics of women with postmenopausal osteoporosis treated with denosumab; change in hip BMD over 3 years in lesser responders ≤2% and in greater responders >2%.

	Lesser responders N = 483 (15.5%)	Greater Responders N = 2631 (84.5%)
Compliance, % with 6 injections	71.0%	95.8%
Age, years, mean (SD)	72.6 (5.2)	71.9 (5.0)
T-score, % < -2.5		
Lumbar spine	74.3%	75.1%
Total hip	18.8%	21.6%
Femoral neck	32.7%	28.2%
CTX baseline, ng/mL, median, IQ Range	0.46, 0.32 – 0.63	0.55, 0.40 – 0.72
TRAP5b, baseline, IU/L, median, IQ Range	3.89, 3.05 – 4.65	4.50, 3.56 – 5.68

Table 1

***Disclosures: Richard Eastell**, Amgen, Inc., 5*
This study received funding from: Amgen, Inc.

SA0408

See Friday Plenary number FR0408.

SA0409

Glucocorticoid Use Cancels the Positive Effects of Biologics on Bone Metabolism in Patients with Active Rheumatoid Arthritis. Tadashi Okano*, Masahiro Tada, Yuko Sugioka, Shigeyuki Wakitani, Hiroaki Nakamura, Tatsuya Koike. Osaka City University Medical School, Japan

Rheumatoid arthritis (RA) is associated with systemic bone loss, subchondral bone erosion and cartilage degradation. Biologics therapy has proven efficacious in improving both disease activity and focal bone erosions in patients with RA. We investigated the effects of biologics on bone mineral density (BMD) and biochemical markers in Japanese RA patients. To examine whether treatment with biologics prevents loss of BMD in patients with RA, and to study the changes in markers of bone metabolism during biologics treatment. One hundred and twenty three (103 women, 20 men, 55.8±12.9 years old) patients with active RA, who were treated with biologics (Infliximab:93, Etanercept:27, Tocilizumab:3) during 1 year, were included in this open cohort study. The BMD of the lumbar spine and total hip (DXA: QDR-4500, Hologic) and bone metabolic marker (urinary NTX) were measured at baseline and after at least more than one year. Thirty three patients received bisphosphonates while 84 patients were under oral prednisolone, we also assessed these effect. The BMD of the lumbar spine and hip was unchanged during treatment with biologics. The BMD of the hip in patients who have received predonisolone without bisphosphonates (n=55) showed significant decreases ($p<0.01$) compared with patients not receiving predonisolone or receiving predonisolone with bisphosphonates. Moreover, the BMD of lumbar spine has increased (p=0.02) in patients who were administered with bisphosphonates (n=32). In whole patients, NTX was significantly decreased from 66.0±67.9 to 51.9±37.7 nmol/mmol CRE ($p<0.01$). To maintain BMD, dose reduction of prednisolone or the introduction of bisphosphonate should be required, even if biologics are administered.

***Disclosures: Tadashi Okano**, None.*

SA0410

See Friday Plenary number FR0410.

SA0411

Postmenopausal Women with PON1 172TT Genotype Respond to Lycopene Intervention With a Decrease in Oxidative Stress Parameters and Bone Resorption Marker NTx. Leticia Rao*[1], Erin Mackinnon[2], Ahmed El-Sohemy[3], Robert Josse[4], Venketeshwer Rao[3]. [1]University of Toronto, St. Michael's Hospital, Canada, [2]Department of Medicine, St Michael's Hospital & University of Toronto, Canada, [3]Department of Nutritional Sciences, University of Toronto, Canada, [4]St. Michael's Hospital, University of Toronto, Canada

We have shown recently that lycopene may decrease the risk of osteoporosis through its antioxidative properties, but the mechanism remains unknown. Paraoxonase 1 (PON1) is an HDL-associated, enzyme that contributes to the antioxidant properties of HDL by hydrolyzing the reactive oxygen species hydrogen peroxide that contributes to oxidative stress in the body. Polymorphisms of PON1 have been associated with chronic diseases associated with oxidative stress including osteoporosis. Our objective is to determine whether a polymorphism of PON1 172T→A modifies the effect of lycopene intervention on oxidative stress parameters and bone turnover markers in postmenopausal women. Following a one-month washout period, 45 postmenopausal women between 50-60 years of age were supplemented for 4 months with regular tomato juice, lycopene-enriched tomato juice, or lycopene capsules (30, 70 and 30 mg lycopene/day, respectively). Serum samples were analyzed for lycopene, total antioxidant capacity (TAC), the oxidative stress parameters, protein thiols and thiobarbituric acid reactive substances (TBARS), and the bone resorption marker crosslinked N-telopeptides of type I collagen (NTx). Genotyping was performed and carriers of the A allele were compared with those with the TT genotype. Repeated-measures ANOVA was used to determine change over time. Regardless of genotype and type of supplementation, lycopene resulted in significantly increased serum lycopene (both genotypes: $p<0.0001$), and significantly decreased protein (TT genotype: $p<0.005$ and A allele carriers: $p<0.05$) and lipid peroxidation biomarkers (TT genotype: $p<0.005$ and A allele carriers: $p<0.0005$). However, in participants with the TT genotype lycopene supplementation resulted in increased TAC ($p<0.01$) and significantly decreased NTx ($p<0.001$); an effect not observed among A allele carriers. The decrease in NTx in the TT genotype was inversely correlated with TBARS ($p<0.05$). This suggests that supplementation with lycopene decreases lipid peroxidation, which may result in decreased NTx in the TT genotype only ($p<0.05$ for interaction between change in TBARS and PON1 genotype). These findings provide preliminary evidence of how lycopene decreases biomarkers of lipid peroxidation, which may result in decreased bone resorption, and thus may reduce the risk of osteoporosis in postmenopausal women.

***Disclosures: Leticia Rao**, Research Grants, 2*

SA0412

Relevance of Serum Undercalboxylated Osteocalcin(ucOC) in the Treatment of Women with Osteoporosis. Humiki Hirahara[1], Hiromi Yoshikata[2], Rituko Kikuchi[1], Yoshiyuki Nomura*[1], Kentaro Kurasawa[1], Osamu Chaki[3]. [1]Yokohama City Univ., Japan, [2]Yokohama City Univ., USA, [3]Yokohama City University, Japan

Backgroud

Undercarboxylated osteocalcin (ucOC) levels are regarded as a marker of vitamin K status. Recently it was reported that vitamin K status is associated with vertebral fracture of Japanease postmenopausal eldely women, as well as hip fracture. We usually use N-telopeptide of type ?collagen (NTX), Bone alkaline phosphatase (BAP), Deoxypyridinoline (DPD) as bone makers for osteoporosis treatment. Moreover we tried to measure serum ucOC concentration for postmenopausal women with treatment of osteoporosis.

Method

We studied 145 osteoporotic postmenopausal women were treated (mean age, 64.4±9.7 yrs, range, 36-77yrs.) We measured the serum ucOC, urinary NTX, and BMD (Lumber 2~4) by 6 months. And we were scoring dietary guestionnaire of vitamin K. Then we administered vitamin K2 or guided diet for patients was over 4.5(ng/ml) of serum ucOC.(high level of serum ucOC).

After 3 months from supply by vitamin K, we research serum level of ucOC again.

Results

Serum ucOC level was low by taking drug which is strong suppressive born absorption, bisphosphonate. High serum level of ucOC (over 4.5 ng/ml) was 26.3% of all. Dietary score of vitamin K was correlative to serum level of ucOC. The patients which was low level of urinary NTX and high level of serum ucOC, was 23% of all. This result was discrepant established theory. Therefore we considerd BMD in this group, and it was deceased the percent change of BMD for 3 years. After 3 months from the vitamin K2 intake, serum level of ucOC was decreased and the percent change of BMD was increased.

Conclusion

This study suggests that the vitamin K intake affect to get the bone quantity as for the patients are treating by Bisphosphonate, but serum level of ucOC were high .

***Disclosures: Yoshiyuki Nomura**, None.*

SA0413

See Friday Plenary number FR0413.

SA0414

Health-related Quality of Life after Vertebral or Hip Fracture in Women - Short Health Scale Useful for Clinical Practice? Inger Hallberg*, Göran Toss, Anna-Christina Ek, Henrik Hjortswang, Margareta Bachrach-Lindström. Linköping University, Sweden

Introduction: Health-related quality of life (HRQOL) is an important part in clinical practice of osteoporotic fracture assessment. Numerous HRQOL questionnaires are currently at use. However, there is a need for a simple and short questionnaire that still covers the major important health domains. The aim of the study was to validate the Short Health Scale (SHS) in women after vertebral or hip fracture.

Methods: Out of 91 invited women 67 (mean age 75.5, SD 4.6) completed the SHS and 2 other HRQOL questionnaires in a seven-year follow-up after vertebral or hip fracture. SHS was validated and compared with the generic SF-36 and disease-specific Qualeffo-41 questionnaires. The SHS is a four-item self-administered disease-specific health measurement (six-point scale, no problem to very severe problem). Each item represents one of the subjective health dimensions: Distress/Symptoms, Daily function, Worry and General well-being. High scores in SF-36 and low scores in Qualeffo and SHS indicate better HRQOL.

Results: The convergent validity were supported by the correlations (r2) between the SHS and the more extensive SF-36 and Qualeffo-41 corresponding dimensions, such as SHS-Distress/symptoms vs SF-36-Bodily pain (-.71***) and Qualeffo-Backache (.65***); SHS-Daily function vs SF36-Physical function (-.64***), Role physical (-.60***) and Qualeffo-Jobs (.67***) and Mobility (.60***). SHS General well-being correlated well to SF-36-General health (-.72***), Mental health (-.66***) and to Qualeffo-General Health (.79***). The SHS-Worries covers a domain that is less well monitored by the SF-36 or Qualeffo-41. Construct validity using the known-groups approach was supported by the significantly worse score in SHS-distress/symptoms and SHS-daily function in women with vertebral fracture compared to women without vertebral fracture. Similarly women who had suffered new osteoporotic fracture during the last five years had significantly worse score in SHS-Distress/symptoms, SHS-Daily function and SHS-Worry than those without new fracture(s). In conclusion, SHS seems to be valid, is easy and quick to complete and gives a comprehensive overview of the main aspects of the women's subjective health perception after vertebral or hip fracture. It could be a useful tool in clinical practice, but further evaluation in larger study groups is still needed.

***Disclosures: Inger Hallberg**, None.*

SA0415

See Friday Plenary number FR0415.

SA0416

Concentrations of the C-3 epimer of 25-hydroxyvitamin D3 in Adult, Child and Neonate Serum Samples. Gary Lensmeyer*[1], Michael Poquette[2], Donald Wiebe[2], Anita Iwanski[2], Neil Binkley[3]. [1]GLensmeyer@uwhealth.org, USA, [2]University of Wisconsin Hospital & Clinics Clinical Toxicology Laboratory, USA, [3]University of Wisconsin, USA

Epimers have identical molecular structure but differ in stereochemical congfiguration. Currently, it is accepted that the C-3 epimer of 25-hydroxyvitamin D3 (3 epi-25(OH)D3), is found primarily in neonates. Yet, recently this epimer was detected in a limited number of adult serums but concentrations were not reported. The physiological importance of 3 epi-25(OH)D3 is uncertain, although, it has been reported that the 1,25 dihydroxy metabolite of this epimer is relatively inactive in calcium metabolism but inhibits parathyroid cells in vitro. Importantly, the influence of 3 epi-25(OH)D3 on 25(OH)D test results obtained with various immunochemical and chromatographic assays, and ultimately on the reliability of "25(OH)D" measurement, remains to be defined. We have observed a peak consistent with 3 epi-25(OH)D3 in serum tested with a high-performance liquid chromatography (HPLC) method we developed. Here we report serum 25(OH)D3 and 3 epi-25(OH)D3 concentrations in a cohort (n = 200+; 60% female) ranging in age from neonates to age 80+. To simplify data presentation and analysis, only sera with 25(OH)D3 and no 25(OH)D2 were included. HPLC with ultraviolet detection (HPLC/UV) and tandem mass spectrometry (LC/MS/MS) equipped with cyanopropyl analytical columns were used to baseline-separate and quantitate 25(OH)D3 and its C-3 epimer. Authentic C-3 epimer substance and NIST reference materials were employed to validate the identity of the C-3 epimer chromatographic peak. Between-run precision for the assays was $<$ 7%; the assays were linear up to at least 300 ng/mL. Lower limit of detection for the C-3 epimer on LC/MS/MS was 0.2 ng/mL. The C-3 epimer was detected in $>$95% of these samples. Concentrations ranged from 3-610 ng/mL for 25(OH)D3 and 0.2-70 ng/mL for 3 epi-25(OH)D3. The relative amounts of the epimer to 25(OH)D3 ranged from 2.5-14%. The relative amount of epimer to 25(OH)D3 increased as 25(OH)D3 increased; the regression analysis relationship was not linear. In sera with the same 25(OH)D3 concentration, the ratio of epimer to 25(OH)D3 varied. In conclusion, 3 epi-25(OH)D3 is present in the majority of serum specimens regardless of age or gender. Importantly, 3 epi-25(OH)D3 is not limited to neonates. Further work must investigate the impact of 3 epi-25(OH)D3 on the various 25(OH)D assays and ultimately what information, if any, the C-3 epimer can afford clinically.

***Disclosures: Gary Lensmeyer**, None.*

SA0417

Effects of Risedronate with Cholecalciferol in Osteoporosis: Results of a Multicenter, Randomized Controlled Trial. Hoyeon Chung*[1], Jung-Min Koh[2], Sung-hwan Moon[3], Yoon-Sok Chung[4], Byung-koo Yoon[5], Moo-Il Kang[6], Hyun-Koo Yoon[7], Hyoung-moo Park[8]. [1]Kyung Hee University, South korea, [2]Asan Medical Center, South korea, [3]Yonsei University, South korea, [4]Ajou University School of Medicine, South korea, [5]Sungkyunkwan University, South korea, [6]Seoul St. Mary's Hospital, South korea, [7]Cheil Hospital & Women's Healthcare Center, South korea, [8]Chung-ang University, South korea

Introduction: A randomized, double-blind, prospective, 16-week clinical trial in osteeoporosis was performed to evaluate the efficacy and safety of risedronate with and without cholecalciferol on vitamin D status and bone markers.

Methods: A total of 164 women and men with osteoporosis were randomly assigned to one of two treatment group; risedronate 35mg with cholecalciferol 5600 IU(RIS plus) or risedronate(RIS). Serum 25OH D, PTH, bone markers and muscle function tests were performed at baseline and after 8 and 16 weeks of treatment.

Results: Serum 25OH D increased from 15.9 to 28.2 ng/ml with RIS plus and declined from 16.3 to 14.0 ng/mL with RIS after 16-week treatment. Both treatment groups had significant increase in serum PTH during the study. The RIS group had a significantly greater increase of PTH from baseline at 16-week versus RIS plus group(13.7 ± 17.6 vs 4.7 ± 13.8; p=0.0004). In both groups, serum BSAP and CTX declined rapidly, and to a similar extent and there were no significant differences between the two groups. The result of muscle function test, 8-foot walking test and sit-to-stand test were also no significant differences between the two group after 8 and 16 weeks of treatment. The overall incidence of clinical adverse events was not significantly different between treatment groups.

Conclusion: In osteoporosis patients, this once-weekly risedronate with cholecalciferol provided equivalent anti-resorptive efficacy, improved vitamin D status over 16 week treatment without significant adverse events.

***Disclosures: Hoyeon Chung**, None.*
This study received funding from: Hanlim pharmaceutical Co.Ltd

SA0418

See Friday Plenary number FR0418.

SA0419

Weekly Alendronate Plus Vitamin D_3 5600 IU vs. Usual Care: Effect on Serum Hydroxyvitamin D in Osteoporotic Postmenopausal Women with Vitamin D Inadequacy - 6-month Results of a Randomized Trial. Stuart Ralston*[1], Neil Binkley[2], Steven Boonen[3], Douglas Kiel[4], Christian Roux[5], Suvajit Samanta[6], Elizabeth Rosenberg[6], Arthur Santora[7]. [1]University of Edinburgh, United Kingdom, [2]University of Wisconsin, USA, [3]Center for Metabolic Bone Disease, Belgium, [4]Hebrew SeniorLife, USA, [5]Hospital Cochin, France, [6]Merck & Co., Inc., USA, [7]Merck Research Laboratories, USA

Purpose: To compare effects on serum 25-hydroxyvitamin D [25(OH)D] and bone turnover markers in postmenopausal osteoporotic women with low 25(OH)D after treatment with either weekly combination tablets of alendronate 70 mg plus vitamin D3 5600 IU (ALN+D) or referred care (prescribed by patients' personal physicians).

Methods: Postmenopausal women age $\geq$65 years with osteoporosis (BMD T-score $\leq$2.5, or $\leq$1.5 with a prior fragility fracture), 25(OH)D $\leq$20 ng/mL but $\geq$8 ng/mL, and increased risk of falls (past history of falls, functional performance, low 25(OH)D) were randomly assigned to receive ALN+D weekly (and 500 mg elemental calcium daily if daily intake was $<$1000 mg) or referred (provided with a letter stating they had osteoporosis needing treatment) to their personal primary or specialist physicians (who were not investigators in the trial) for osteoporosis drugs and nutritional support with marketed vitamin D and calcium supplements. The primary evaluation reported here is the proportion of patients in each group with 25(OH)D $<$20 ng/mL after 26 weeks of treatment. Secondary evaluations compare bone turnover markers. Safety was monitored through adverse experience reporting.

Results: Participants receiving ALN+D (n=257) and referred care (n=258) had similar baseline characteristics (mean age=73 years, 72% Caucasian, mean 25(OH)D=15 ng/mL, and 56% with 25(OH)D$\leq$15 ng/mL). At 6 months, the proportion of women with 25(OH)D$<$20ng/mL was 7.8% with ALN+D and 31.2% with referred care (P$<$0.001). Least squares (LS) mean changes from baseline in 25(OH)D at week 26 were 14.1 and 10.7 ng/mL, respectively. Geometric LS mean changes from baseline for serum BSAP were -46% and -39%, and for urine NTX were -58% and -50% with ALN+D and referred care, respectively (P$\leq$0.004 for each

difference). Incidence of adverse events and discontinuations due to adverse events were similar among treatments, and consistent with recognized safety profiles.

Conclusions: ALN+D reduced the proportion of postmenopausal, osteoporotic women with 25(OH)D<20 ng/mL more than did referred care (that might have included vitamin D supplementation) prescribed by physicians not directly involved with the investigation. Patients in the ALN+D group had lower BSAP and NTX than did patients in referred care.

***Disclosures: Stuart Ralston**, Merck, 5*
This study received funding from: The study was funded by Merck, the sponsor of the study

SA0420

See Friday Plenary number FR0420.

SA0421

See Friday Plenary number FR0421.

SA0422

Exploring the LRP5 SOST Interacting Surface to Identify Small Molecule Inhibitor of SOST Action. David Halladay*[1], Amy Sato[2], Yanfei Ma[1], Pamela Shetler[1], Heather Bullock[1], Venkatesh Krishnan[1]. [1]Eli Lilly & Company, USA, [2]DePauw University, USA

The Wnt signaling pathway has been shown to be important in bone formation. Specific mutations of the Wnt co-receptor LRP5 results in a high bone mass (HBM) phenotype in humans. Additionally, nonsense mutations within the sclerostin gene (SOST), an inhibitor of the Wnt signaling pathway, resulted in sclerosteosis, characterized by progressive skeletal overgrowth. We have utilized a Fluorescence Resonance Energy Transfer (FRET) based assay to study the interacting surface of LRP5 and SOST. Using a MYC-tagged hLRP5 and HA-tagged hSOST and/or FLAG-tagged hSOST we show specific interactions between these two proteins. We also show specific interactions between Wnt1 and LRP5 using similar methods. Using a stably transfected TCF/LEF reporter cell line transiently transfected with either pSOST-HA or pSOST-FLAG we show a dose dependent inhibition of Wnt3a-CM induced activity and this inhibitory activity was reversed by an anti SOST Ab. To confirm that SOST bound the first propeller domain of LRP5 we tested three HBM mutants located in the first propeller domain of LRP5 (tagged with MYC) and clearly demonstrate decreased ability to bind SOST as compared to wt hLRP5. In order to explore what regions of SOST were important for LRP5 binding we created mutant SOST-FLAG plasmids with various deletions in the second loop. We demonstrate that more pSOST-HA was needed to compete with pSOST-FLAG for MYC-LRP5 binding compared to the pSOST(-ΔLoop2)-FLAG, the largest deletion, indicating that pSOST(ΔLoop2)-FLAG has a lower affinity for MYC-LRP5 than the wild-type pSOST-FLAG. Smaller deletions within the loop 2 of hSOST showed intermediate affinity for hLRP5. Transient transfection of the TCF/LEF reporter stable cell line with wt pSOST-FLAG dose dependently reduced Wnt3a-CM induced luciferase activity, whereas pSOST(ΔLoop2)-FLAG increased Wnt3a-CM induced luciferase activity. The shorter deletions of SOST loop 2 had no inhibitory or stimulatory effect. Here we also show, for the first time, that a small molecule was able to dose dependently disrupt the binding of SOST to LRP5 via this specific interacting surface and as expected this disruptor led to the stimulation of the TCF/LEF reporter activity. Additional characterization of this agent as a potential bone anabolic agent in rodent animal models will be discussed.

***Disclosures: David Halladay**, None.*

SA0423

Monitoring of Intermittent PTH(1-34) Treatment by Serum PINP in Adult Ovariectomized Osteopenic Rats. Jussi Halleen*[1], ZhiQi Peng[1], Katja Fagerlund[1], Tiina A. Suutari[1], Jukka Vääräniemi[1], Mari Suominen[1], Jukka Rissanen[2], Harrie C.M. Boonen[3], Trine S.R. Neerup[4], Hanne H. Bak[4], Jukka Morko[5]. [1]Pharmatest Services Ltd, Finland, [2]Pharmatest Services,Limited, Finland, [3]University of Copenhagen, Denmark, [4]Zealand Pharma A/S, Denmark, [5]Pharmatest Services Ltd, Fin

Procollagen I N-terminal propeptide (PINP) is a sensitive marker of bone formation for monitoring the efficacy of treatment with recombinant human parathyroid hormone (1-34) analog [PTH(1-34)] in osteoporotic patients. Recently, a new immunoassay has been developed for serum PINP in rodents, allowing measurement of serum PINP in preclinical rodent osteoporosis models. The purpose of this study was to evaluate the use of serum PINP for monitoring intermittent PTH(1-34) treatment in adult ovariectomized (OVX) osteopenic rats. Study groups included a sham-operated control group and an OVX-operated control group receiving vehicle, and OVX-operated groups receiving daily subcutaneous injections of 1.2, 4.0, 12.0, 40.0 and 120.0 μg/kg human PTH(1-34). Each group contained 12 animals that were 6 months of age at the time of the operations. Dosing was started at 7 weeks after OVX and continued for 6 weeks. Before the start of treatment, the animals were randomized to groups based on their body weights and trabecular bone mineral density values obtained by peripheral quantitative computed tomography (pQCT). PINP values were determined from serum samples collected before the start of treatment, at 2 weeks after the start of treatment and at the end of the study. The PINP values obtained at 2 weeks and at the end of the study were divided by the values obtained in the same animal before the start of treatment to determine the change of PINP in each animal during the treatment. PTH(1-34) treatment showed strong anabolic effects in tibial metaphysis, tibial diaphysis and vertebra based on bone parameters determined by pQCT measurements and static and dynamic histomorphometry. Serum PINP values showed a strong dose-dependent increase by PTH(1-34) treatment both at 2 weeks after start of treatment and at the end of the study. We conclude that serum PINP is a reliable marker for monitoring the effects of anabolic treatment with PTH(1-34) in the rat OVX model, and short-term changes in serum PINP values predict long-term changes in bone parameters obtained by pQCT measurements and histomorphometry.

***Disclosures: Jussi Halleen**, IDS Ltd, 5*
This study received funding from: ZEALAND Pharma A/S

SA0424

Osteoporosis from type 1 Diabetes is Reversed by Intermittent Parathyroid Hormone Stimulation of Bone Formation. Katherine Motyl*, Laura McCabe. Michigan State University, USA

Type 1 diabetic osteoporosis results from impaired osteoblast activity and osteoblast death. Because diabetes does not affect or reduces resorption, antiresorptive bisphosphonates may not be the most appropriate therapy. Anabolic intermittent parathyroid hormone (PTH) stimulates bone remodeling and increases bone density, although the exact mechanism of its action is unknown and could be altered/defective in type 1 diabetes. Here, we examined the ability of daily 8 μg/kg and 40 μg/kg PTH to counteract bone loss in streptozotocin-induced diabetic BALB/c mice. We found a significant elevation of tibia trabecular bone density parameters with the 40 μg/kg dose in control mice and diabetic mice (compared to their metabolic-state matched vehicle treated controls), and elevation of trabecular bone parameters in diabetic 8 μg/kg treated mice. In particular, bone mineral density (BMD) was increased 17% in 40 μg/kg PTH treated control mice (compared to untreated euglycemic control mice), and 26% in equivalently treated diabetic mice (compared to untreated diabetics). Increased bone density in diabetic PTH-treated mice was due to increased bone formation, mineral apposition, and osteoblast surface, all of which are defective in type 1 diabetes. We also determined that 40 μg/kg PTH treatment reversed preexisting bone loss from diabetes, such that diabetic PTH treated BMD was not significantly different from that of untreated controls. We conclude that intermittent PTH is capable of promoting bone formation under diabetic conditions, even after bone loss has already occurred. Thus, this work warrants further investigation into the use of PTH as an osteoporosis therapy for patients with type 1 diabetes.

***Disclosures: Katherine Motyl**, None.*

SA0425

See Friday Plenary number FR0425.

SA0426

Strontium Stabilizes β-catenin by Activating Wnt Signaling. Zhaoyang Li*[1], Tao Qiu[2], Mei Wan[2], Xu Cao[3], William Lu[4]. [1]The University of Hong Kong, Peoples republic of china, [2]Johns Hopkins University School of Medicine, USA, [3]Johns Hopkins University, USA, [4]The University of Hong Kong, Hong kong

Strontium (Sr) compounds stimulate bone formation by promoting differentiation of osteogenic bone marrow stromal cells and are used in prevention and treatment of osteoporosis, but the precise mechanisms responsible for their responses in osteoblasts are not known. LRP6-mediated stabilization of ?-catenin has been shown to play an important role in bone cell function. Particularly, PTH induces the association of LRP6 with PTH/PTHrP receptor PTH1R to stabilize β-catenin and its translocation into the nucleus. Here we show that Sr treatment increased the abundance of β-catenin in osteoblastic MC3T3 cells. Calcium sensing receptor (CaSR), a seven-trans-membrane receptor like PTH1R, regulates calcium metabolism. We further examined whether strontium stabilizes β-catenin by activating Wnt signaling. Preosteoblast MC3T3 cells were treated with 6.0 mM SrCl2 and harvested at 0, 5, 15, 30 and 60 minutes after treatment. Sr stimulated the level of β-catenin in a time dependent manner with 10 fold increase at 60 min after treatment, whereas Ca2+ had modest effect on β -catenin stabilization. Phosphorylation of β-catenin by Glycogen synthase kinase (GSK)-3β leads to constantly degradation of β-catenin via the ubiquitin-proteosome pathway and activation of LRP6 results in phosphorylation of GSK3β and stabilizes β-catenin. Western blot analysis revealed that Sr induced phosphorylation of GSK3β, indicating activation of Wnt signaling for β-catenin stabilization. In summary, our data suggests that Sr likely increased the osteoblast differentiation and bone formation through activating Wnt signaling pathway. The stabilized β-catenin protein may accumulate in the nucleus and complex with the TCF/LEF family of DNA-binding transcription factors to enhance gene expression and stimulate bone formation.

***Disclosures: Zhaoyang Li**, None.*

SA0427

See Friday Plenary number FR0427.

SA0428

A Novel Bisphosphonate with Potent Anabolic Action. Hisashi Shinoda*[1], Keiko Suzuki[2], Mirei Chiba[1], Shinobu Murakami[1], Sadaaki Takeyama[3], Yuka Narusawa[1], Hiroaki Hirotani[1], Shogi Yamada[2], Kaoru Igarashi[1], Paula Stern[4]. [1]Tohoku University Graduate School of Dentistry, Japan, [2]Showa University Graduate School of Dentistry, Japan, [3]Hokkaido University Graduate School of Dentistry, Japan, [4]Northwestern University Medical School, USA

Bisphosphonates (BPs) are potent inhibitors of osteoclastic bone resorption and have been used for the treatment of various metabolic bone diseases that are accompanied by excessive bone resorption. BPs are chemically characterized by a P-C-P bond and this structure allows us to create a great number of variations by changing two lateral side chains on the carbon atom. Many BPs have been synthesized and investigated with respect to their effects on bone. The data show that the pharmacological characteristics of bisphosphonates, such as their potency, mechanism of action, and side effects, vary depending on the structure of the side chains.

[4-(Methylthio)phenylthio] methanebisphosphonate (MPMBP) is a novel synthetic bisphosphonate with an anti-oxidant side chain on the carbon atom of the P-C-P bond. During the course of our studies on the structure-activity relationships of various bisphosphonates, we recently found that MPMBP has not only anti-bone-resorbing action, but also potent anabolic action on bone.

Our observations and findings can be summarized as follows: (1) MPMBP dose-dependently increased alkaline-phosphatase activity in a culture of osteoblastic MC3T3-E1 cells. (2) MPMBP increased the synthesis of collagen (type-I) in an organ culture of mouse calvaria. (3) Topical injection of MPMBP to alveolar bone induced prominent increases in both the bone mass and thickness of alveolar bone at the local site of injection in both rats and rabbits. (4) MPMBP increased the mRNA expression of alkaline-phosphatase, type-I collagen, osteocalcin, and bone sialoprotein in MC3T3-E1 cells. (5) In osteoblasts from cultured mouse calvaria, MPMBP inhibited the translocation of NF-κB to the nuclei and enhanced the expression of Fos-related antigen-1(Fra-1), an essential transcription factor involved in bone matrix formation *in vivo* and *in vitro*.

Taken together, our findings show that MPMBP can promote bone formation both in vitro and in vivo, and suggest that this compound could be used for the treatment of various bone diseases associated with excessive bone loss, such as periodontitis and osteoporosis. It may also be useful for the promotion of fracture healing, for the maintenance of implants, for the treatment of cleft palate and for various conditions that require the regeneration of bone tissues.

***Disclosures: Hisashi Shinoda**, None.*

SA0429

Active Site Mutants of Farnesyl Pyrophosphate Synthase Help to Characterise Inhibition by Nitrogen Containing Bisphosphonates. Maria Tsoumpra*[1], Bobby L. Barnett[2], Richard L. Walter[3], Frank H. Ebetino[4], Robert G.G. Russell[5], Udo Oppermann[5], James E. Dunford[5]. [1]Oxford University, United Kingdom, [2]Chemistry Department, University of Cincinnati, USA, [3]Shamrock Structures, USA, [4]Warner Chilcott, USA, [5]Botnar Research Centre, Nuffield Department of Orthopaedics, Rheumatology & Musculoskeletal Sciences, Oxford University, United Kingdom

Farnesyl Pyrophosphate Synthase (FPPS) is a key branch point enzyme in the mevalonate pathway. Selective inhibition of FPPS impairs osteoclast survival and forms the basis of antiresorptive treatment by nitrogen containing bisphosphonates (N-BPs). Crystallographic and kinetic studies suggest that potent N-BPs compete for and finally occupy the allylic substrate binding site. Subsequent binding of isopentenyl pyrophosphate (IPP) results in FPPS isomerization and formation of a tight bound enzyme-inhibitor complex. The present study aimed to investigate the role of FPPS amino acid residues that are strongly implicated in i)stabilization of the carbocation intermediate (lysine 200 or K200) ii)conformational switch upon IPP binding (phenylalanine 239 or F239) and iii)formation of a tight enzyme-inhibitor complex (tyrosine 204 or Y204). Disrupted interactions between the N-BP phosphonate group and the amino group of K200 might be responsible for the increased inhibition constants (Ki) for risedronate (Ris) from 0.34 to 62.9 nM, ibandronate (Ibn) from 3.6 to 18.2 nM, alendronate (Aln) from 56.9 to 82.7 nM and pamidronate (Pam) from 52.2 nM to 460.8 nM in K200 to glycine (K200G) mutant. Replacement of K200 with Leucine (K200L) led to further reduction of N-BP potencies with increased Ki for Ris (75.1 nM), Ibn (140.2 nM), Aln (239.8 nM) and Pam (3717.4 nM). The F239 to alanine mutation (F239A) led to increased inhibition constants for all N-BPs examined (Ris: 65.5 nM, Ibn:15.5 nM, Aln: 75.4 nM, Pam: 945.7 nM), revealing inability to form a tight enzyme: inhibitor complex. Removal of Y204 reduced the Ris potency in phenylalanine mutant (Y204F, Ki= 2.22) as well as alanine mutant (Y204A, Ki=5.18), possibly due to abolishing hydrophobic interactions between the heterocyclic ring of Ris and the phenyl ring of Y204. Furthermore, the decreased Ki for Aln (6 nM) and Pam (19 nM) in Y204F but not in the Y204A mutant suggests formation of novel interactions between the amino group of N-BPs and the phenyl ring of Y204F, previously inhibited due to interference by the hydroxyl group in Y204. Finally, determination of kinetic parameters for all mutants revealed unaltered binding of the FPPS with respect to the allylic substrate geranylpyrophosphate (GPP) but reduced catalytic activity and affinity for IPP. In conclusion, data highlight important aspects of the multiple interactions between N-BPs and side chain FPPS residues that determine the strength of N-BP binding.

***Disclosures: Maria Tsoumpra**, None.*
This study received funding from: Procter & Gamble

SA0430

See Friday Plenary number FR0430.

SA0431

See Friday Plenary number FR0431.

SA0432

See Friday Plenary number FR0432.

SA0433

A Comparison of the Effects on Bone, Muscle and Fat Tissue between a more Potent Synthetic Androgen 7α-methyl-19-nortestosterone (MENT) and Testosterone: Evidence from a Preclinical Hypogonadal Rat Model. Filip Callewaert[1], Maarten Morreels[1], Narender Kumar[2], Regine Sitruk-Ware[2], Frank Claessens[1], Steven Boonen[3], Dirk Vanderschueren*[1]. [1]Catholic University of Leuven, Belgium, [2]Population Council, USA, [3]Center for Metabolic Bone Disease, Belgium

Orchidectomy-induced hypogonadism results in muscle frailty, bone loss and gain of fat mass. In contrast with testosterone (T), a synthetic androgen 7α-methyl-19-nortestosterone (MENT) is not amplified in the male reproductive tract since it does not undergo 5α-reduction. In this study, the potential curative properties of MENT as anabolic agent was evaluated and compared with T in a preclinical hypogonadal male rat model. Aged male Wistar rats (11 months) were either orchidectomized (orch) or sham-operated (sham) and left untreated during a period of two months. As expected these orch animals experienced a significant loss of trabecular bone volume (-58% vs. sham) as well as lean mass (-8% vs. sham). On the other hand, cortical bone and fat mass were not significantly altered following 2 months castration. Subsequently, these 13-month-old orch rats were treated with either vehicle, MENT (12 μg/day) or T (72 μg/day) subcutaneously for 4 months via mini-osmotic pumps. Results were compared with age-matched sham or vehicle-treated orch rats (orch). Despite a 6-fold difference in dose, MENT and T equally restored the weight of the ventral prostate to sham level, but MENT increased the weight of the seminal vesicles and the musculus levator ani above sham levels (+20% and +44%, resp.). At the end of the study, trabecular bone volume and lean mass remained significantly lower in orch vs. sham rats (-60% and -16%, resp.). Yet, also cortical bone area was significantly decreased in orch rats at sacrifice (-23% vs. sham), through a lower periosteal but higher endocortical bone formation. MENT and T both fully restored lean mass and trabecular bone volume to sham level. The cortical bone loss was also prevented by MENT and T, however without full recovery to sham level. However, MENT restored periosteal and endocortical bone formation to sham level, while T normalized endocortical bone formation but stimulated periosteal bone formation above sham level (+94%, $p = 0.06$). MENT and T also normalized the higher fat mass in orch rats, but MENT decreased fat tissue even below sham levels (-24%) and this correlated with lower leptin levels (-43%).

In conclusion, MENT appears a more potent androgen than T in a preclinical model of male hypogonadism, with significantly more of an effect on fat mass. Both MENT and T restore trabecular bone loss and prevent cortical bone loss in aged hypogonadal rats. T showed a superior effect on periosteal bone formation compared with MENT.

***Disclosures: Dirk Vanderschueren**, None.*
This study received funding from: The Population Council, Inc

SA0434

Equol Decreased Bone Resorption in Equol Non-producing Postmenopausal Japanese Women: a Pilot Randomized Placebo-Controlled Trial. Tomomi Ueno[1], Yoshiko Ishimi[2], Junko Ezaki[3], Shigeto Uchiyama[4], Yasuhiro Fujii[4], Yuko Tousen*[2], Mamoru Nishimuta[5]. [1]Otsuka Pharmaceutical Co., Ltd., Japan, [2]National Institute of Health & Nutrition, Japan, [3]Food Function & Labeling Program, National Institute of Health & Nutririon, Japan, [4]Saga Nutraceutricals Research Institute, Otsuka Pharmaceutical Co., Ltd., Japan, [5]Chiba Prefectural University of Health Sciences, Japan

Objective: Equol, a metabolite of isoflavone daidzein, obtained from soy isoflavones may play a critical role in the prevention of bone loss in postmenopausal women. However, clinical trials on the use of equol have not yet been published. This study aimed to investigate the effects of equol on bone metabolism, as well as on serum sex and thyroid hormone levels, in postmenopausal Japanese women.

Methods: We performed a 1-year double-blind, randomized placebo-controlled trial using natural S-equol supplementation in 93 equol non-producing postmenopausal Japanese women at less than 5 years after the onset of menopause. Subjects aged 41–62 years were randomly assigned to the following 4 groups: placebo, 2 mg of S-equol (EQ-2), 6 mg of S-equol (EQ-6), and 10 mg of S-equol (EQ-10); subjects were required to take the supplements once per day.

Results: The mean body weight and height of the subjects were 54.1 ± 8.2 kg and 156.8 ± 4.9 cm, respectively. There were no major differences in body weight and height among the different groups at baseline and after 12 months of equol intervention. Equol intervention increased the concentration of equol in the serum and urine of subjects in a dose-dependent manner. After 12 months of the intervention, urinary deoxypyridinoline (DPD) level significantly decreased to -23.94% in the EQ-10 group compared with that in the placebo group (-2.87%) ($p = 0.020$). This showed that 10 mg per day of equol supplementation markedly inhibited bone resorption. Additionally, the percent change in the whole body bone mineral density (BMD) in the EQ-10 group was -1.10%, which was significantly different from that in the placebo group (1.88%) ($p = 0.027$). Thus, a 12-month supplementation of 10 mg per day of equol prevented the decrease in the whole body BMD in postmenopausal women. Serum sex and thyroid hormone concentrations did not differ among the 4 groups after the equol intervention.

Conclusions: This is the first report providing specific evidence of the effect of equol on bone metabolism in humans. The findings of this study suggest that supplementation of 10 mg of equol per day may contribute to the amelioration of bone health in equol non-producing postmenopausal women without causing any adverse effects. Further research is needed to determine the effects of equol on bone metabolism and safety.

***Disclosures: Yuko Tousen**, None.*
This study received funding from: Otsuka Pharmaceuticals Co., Ltd.,

SA0435

See Friday Plenary number FR0435.

SA0436

Atorvastatin Attenuates Lrp5/Wnt3a in the eNOS null mouse experimental hypercholesterolemic femurs. Jeffrey Park*[1], Malayannan Subramaniam[2], John R. Hawse[2], Amy Flores[1], Thomas C. Spelsberg[2], Nalini Rajamannan[3]. [1]Northwestern University, USA, [2]Mayo Clinic, USA, [3]Northwestern University Medical School, USA

Atorvastatin Attenuates Lrp5/Wnt3a in the eNOS null mouse femurs after experimental hypercholesterolemia Osteoporosis(OP) is the most common cause of morbidity secondary to the increased risk of bone fractures. This study hypothesizes that OP develops secondary to activation of Wnt3a/LRP5 via endochondral bone turnover in experimental hypercholesterolemia in the eNOS null mouse. We tested this hypothesis in the eNO null mouse as a model of oxidative stress. In this study, we utilized eNOS null mice as a model system to determine if a high cholesterol diet leads to osteoporosis and if this process could be revered by the addition of Atorvastatin. The following groups of eNOS null mice were used in this study: control (n=80), cholesterol (n=80), cholesterol + Atorvastatin (n=80) . Treatments began at 2 months of age and were continued for a duration of 6 months. At this time, the femurs of all mice were analyzed for the development of osteoporosis using Li-Cor Infrared Imaging Li-Cor imaging uses an infrared technique to determine if a hydroxyapatite bone probe is taken up in active bone turnover. The bone probe is injected 48 hours prior to analysis of the femurs. . Additionally, the femurs of 240 mice were isolated and mRNA was extracted for RT-PCR analysis of, Lrp5, Wnt3a, Cbfa1, Osteocalcin, OPN, and Sox 9. RNA isolated from the femurs of cholesterol treated eNOS mice revealed increased expression of Cbfa1, Sox9, OPN, Lrp5 and Wnt3a relative to control mice. Increased expression of these genes was attenuated with atorvastatin therapy. LiCor infrared imaging revealed an increase in bone probe uptake 48 hours after injection into the cholesterol mouse with attenuation with the atorvastatin therapy($p<0.05$). (Quantification of results are in Table 1.)Taken together, these data demonstrate that eNOS null mice develop an osteoporotic phenotype following administration of a high cholesterol diet which is reversible by the addition of Atorvastatin. Furthermore, we have shown evidence for an important role for the Wnt3a/Lrp5 pathway in mediating this bone phenotype.

Table 1

	Control	Cholesterol	Cholesterol + Atorvastatin
Quantification of Gene Expression: Femurs			
CBFA	0.118 ± 0.00952	0.160 ± 0.0305*	0.116 ± 0.0196**
Sox9	0.532 ± 0.0696	0.707 ± 0.202*	0.611 ± 0.207**
Cyclin	0.752 ± 0.424	0.763 ± 0.436	0.529 ± 0.245
Osteopontin	0.406 ± 0.0889	0.524 ± 0.0391*	0.455 ± 0.100
Lrp5	0.241 ± 0.0895	0.213 ± 0.0479*	0.334 ± 0.100**
Wnt3a	0.196 ± 0.0126	0.256 ± 0.0222*	0.180 ± 0.0539**
Quantification Li-Cor Molecular Imaging			
Femurs	3120 ± 0.02	4265 ± 0.02*	3105 ± 0.09 **

*p<0.05 control versus cholesterol
**p<0.05 cholesterol versus cholesterol + Atorvastatin

Table 1

***Disclosures: Jeffrey Park**, None.*

SA0437

Differential Effects of Odanacatib Compared to Alendronate on Bone Turnover Markers in Adult Ovariectomized Rhesus Monkeys. Le Thi Duong[1], Sherri Motzel[2], Gregg Wesolowski[3], Maureen Pickarski*[3]. [1]Merck Research Laboratories, USA, [2]Merck & Co., Inc, USA, [3]Merck & Co., Inc., USA

Odanacatib (ODN) is a selective, potent and reversible inhibitor of cathepsin K (CatK) currently in development for the treatment of postmenopausal osteoporosis. ODN (at 2-4μM•24hr) was previously demonstrated to fully prevent bone loss and resulted in normal biomechanical properties in ovariectomized (OVX) rhesus monkeys post treatment for 21-mo. Here, the effects of ODN on bone turnover markers were directly compared to that of Alendronate (ALN) in the same preclinical model. OVX-rhesus monkeys (10-22 yr-old) were randomized post-surgery into four groups (N=16/group), and dosed daily by oral gavage with HPMC-AS vehicle (Veh), ODN at 2mg/kg (L-ODN; 11μM•24hr), ODN at 8mg/kg (H-ODN; 140μM•24hr), or ALN (15μg/kg; 2X/wk, s.c.) in prevention mode for 20 mo. The H-ODN dose was reduced to 4mg/kg (49μM•24hr) approximately 7-months post dosing. Treatment with both doses of ODN and ALN resulted in rapid suppression of bone resorption markers, uNTx and sCTx, to 65-75% below baseline levels. ALN consistently reduced serum bone formation markers, BSAP and P1NP, by 60% and 80% of baseline, respectively. ODN displayed significantly less reduction in a dose-reversal manner of BSAP (40% in L-ODN and <10% in H-ODN) and P1NP (60% in L-ODN and 40% in H-ODN) compared to ALN for the first 7-mo. post-dosing. As the H-ODN dose group was switched from 8 to 4mg/kg/d, the degree of reduction in BSAP and P1NP reversed to 30% and 45% reduction from baseline, closer to that of the L-ODN group. The serum marker 1-CTP, a metalloproteinase-generated C-terminal peptide of Col type I and a substrate of CatK, was not responsive to Veh or ALN treatment. Steady state levels of 1-CTP increased by 70% and 120% in the L-ODN and H-ODN groups versus Veh. The selective induction of 1-CTP supported the target engagement of Cat K by ODN in bone. ALN rapidly suppressed Trap-5b levels by 30% within 1.5 mo. post-dosing. However, Trap-5b levels trended to elevate in L-ODN and increased 80% in H-ODN above Veh within 6-mo. post-dosing. Hence, ODN is as effective as ALN in suppressing the bone resorption markers. However, ODN clearly works differently from ALN in displaying significantly less reduction of bone formation markers and increased a marker for osteoclast number. These findings on the effects of ODN on bone turnover markers in OVX-monkeys are consistent with previous observations on the bone formation sparing effects of odanacatib in a PhII study with osteoporotic women.

***Disclosures: Maureen Pickarski**, Merck & Co., Inc, 3*
This study received funding from: Merck & Co., Inc

SA0438

See Friday Plenary number FR0438.

SA0439

See Friday Plenary number FR0439.

SA0440

See Friday Plenary number FR0440.

SA0441

Bone Quality in Monkeys Treated with ED-71, a Vitamin D Analogue. Marc Grynpas*[1], Richard Cheung[2], Susan Y. Smith[3], Hitoshi Saito[4]. [1]Samuel Lunenfeld Research Institute, Canada, [2]Lunenfeld Research Institute, Canada, [3]Charles River Laboratories, Canada, [4]Chugai Pharmaceutical Company, Limited, Japan

Bone quality was assessed in femurs and vertebrae (verts) by density fractionation, and illustrated by electron backscattering imaging (BSE) on selected tibia and verts. Trabecular connectivity (trab conn) was evaluated in verts by strut analysis of BSE images.

Bones were from 2 groups (10 animals/group) in 2 separate studies. Following OVX, monkeys (China, 9+ years) were gavaged daily with vehicle or ED 71 for 26 weeks at 0.1 or 23 weeks at 0.3μg/kg/day. In vivo results showed ED-71 preserved bone mass due to prevention of OVX-induced increases in the rate of bone remodeling.

Verts/femora were ground and sieved to separate bone particles <20 μm. Bone powder was chemically "fractionated" (<1.6->2.1 g/ml) for verts and (<2.0->2.2 g/ml) femora in a bromoform-toluene mixture by stepwise centrifugation (Grynpas & Hunter 1988). The contribution of each fraction, relative to original unfractionated bone weight, was calculated to determine a mineralization profile.

Tibia cross-sections and verts were fixed, dehydrated, embedded in Spurr resin, polished, carbon coated and examined by BSE. Images from verts were skeletonized and quantified for # of nodes, free-ends and different types of struts to determine trab conn.

To estimate if 2 distributions differ the logit function (LF) of each distribution was calculated. LF: ln= (proportion X) where X is the density cut-off for each group. There was no significant difference between LF of controls vs 0.3 ($p=0.144$) while a shift in LF between controls and 0.1 was significant ($p=0.015$) for femurs indicating an increase in mineralization. This was confirmed by BSE of tibiae. The shift in LF for verts was significant between controls and 0.3 ($p<0.001$) while there was no difference between LF of 0.1 and controls ($p=0.294$). Results were consistent with increased trab conn as demonstrated by increases in # of multiple points, node-node struts and decreased end points and free-free struts at 0.3. Similar trends were seen at 0.1.

In general, OVX-induced increases in bone turnover results in a shift of the mineralization profile to lower densities due to an increase in newly formed bone. Cortical porosity also increases markedly. Drugs like ED 71 that slow bone turnover tend to shift the mineralization profile to higher density due to an increase in secondary mineralization. In addition, we see decrease trab conn due to loss of trabeculae, a consequence of OVX; this was prevented at the 0.3 dose.

***Disclosures: Marc Grynpas**, contract, 5*
This study received funding from: Chugai Pharmaceutical

SA0442

See Friday Plenary number FR0442.

SA0443

Vitamin D Malnutrition is Associated with a Substantially Lower Bone Mass in Northern Chinese Older Postmenopausal Women. Qian Zhang*[1], Xiaoqi Hu[2], Cuixia Wang[2], Ying Liu[2], Yifan Duan[2], Richard Prince[3], Kun Zhu[4]. [1]Institute of Nutrition & Food Safety, Chinese Center for Disease Control & P, Peoples republic of china, [2]National Institute for Nutrition & Food Safety, Chinese Centre for Disease Control & Prevention, China, [3]Sir Charles Gardner Hospital, Australia, [4]University of Western Australia, Sir Charles Gairdner Hospital, Australia

Background: Low vitamin D status may lead to osteoporosis or osteomalacia. There are few data in Northern Chinese older people on the prevalence and predictors of low vitamin D status and its association with bone mass.

Objective: The aims of this study were to examine the prevalence of hypovitaminosis D, to identify predictors of vitamin D status and to evaluate its association with bone mass in Chinese older postmenopausal women.

Design: A total of 446 healthy community-dwelling postmenopausal women aged over 60 years (mean age 68.2± 5.6 yrs) living in Beijing, China were recruited from May to July 2008. Serum 25-hydroxyvitamin D [25(OH)D] concentration was determined by RIA in duplicates. Bone mineral density (BMD) at lumber spine, proximal femur, and whole body, and body composition of whole body were measured by a dual-energy X-ray absorptiometry (DXA). Information on lifestyle was elicited by questionnaires.

Results: The average serum 25(OH)D concentration was 15.6± 7.0 ng/mL, 19.5% had vitamin D deficiency (25(OH)D<10 ng/mL), 59.0% insufficiency (25(OH)D 10-20 ng/mL) and only 4.9% of subject had 25(OH)D above 30 ng/mL. Predictors of low 25(OH)D in regression analysis (overall $R^2=0.31$) included poor education ($\beta=-4.6$, $P<0.001$), city and apartment living ($\beta=-7.43$, $P<0.001$ and $\beta=-3.8$, $P<0.001$), low dairy intake ($\beta=-1.6$, $P=0.05$), overweight ($\beta=-1.1$, $P=0.07$) and an early summer sample date ($\beta=-2.3$, $P=0.003$), but not out door time, physical activity level, age, height, waist circumstance, body composition indices, smoking and alcohol consumption. Compared to women with vitamin D insufficiency and deficiency, those with 25(OH)D concentrations above 20 ng/mL had significantly higher total hip (5.8-10.1%), femoral neck (6.9-10.4%), total body (4.8-5.9%) and lumber spine (6.3-7.5%) BMD after accounting for confounding variables including age, sample date, living area, height, weight, physical activity level and calcium intake (all $P<0.05$).

Conclusions: The prevalence of hypovitaminosis D is alarmingly high in older community-dwelling postmenopausal women living in Beijing. Importantly unlike European population studies low vitamin D status predicted a substantially lower bone mass (5-10%). These findings require urgent investigation to understand the nature of the relationship between vitamin D status and bone structure in Chinese populations.

***Disclosures: Qian Zhang**, None.*

SA0444

Osteopenia in Gaucher Disease Develops Early in Life: Response to Imiglucerase Enzyme Therapy in Children, Adolescents and Adults. Thomas Hangartner*[1], Neal Weinreb[2], Paige Kaplan[3], J. Alexander Cole[4], Andrea Gwosdow[4], Pramod Mistry[5]. [1]Wright State University, USA, [2]University Research Foundation for Lysosomal Storage Diseases, Inc., USA, [3]Children's Hospital of Philadelphia, USA, [4]Genzyme Corporation, USA, [5]Yale University School of Medicine, USA

Purpose: To analyze the bone mineral density (BMD) of children, adolescents, young and older adults with type 1 Gaucher disease (GD1) at baseline and after treatment with imiglucerase. Methods: The analysis included all patients between the ages of 5 and 50y with GD1 treated with imiglucerase and enrolled in the ICGG Gaucher Registry. Lumbar spine BMD was assessed by dual-energy x-ray absorptiometry (DXA) and expressed as Z-scores. BMD data at baseline and up to 10y on imiglucerase were analyzed in each age group. Correlations were evaluated between BMD and other phenotypic characteristics, i.e., hemoglobin, platelet counts, spleen and liver volumes, bone pain and bone crises. Descriptive statistics were used to calculate mean DXA Z-scores at baseline according to 5-year age categories. Non-linear mixed effects models were used to analyze DXA Z-scores over time. Results: Baseline hematological and visceral manifestations in the 4 age groups were similar. The most common genotype of patients with bone manifestations was N370S/Other. At baseline, DXA Z-scores were below ≤-1 in 44% of children (ages ≥5 to <12 years; n=43), 76% of adolescents (≥12 to <20 years; n=41), 54% of young adults (≥20 to <30 years; n=56) and 52% of adults (≥30 to <50 years; n=171). Among children with DXA Z-scores below -1 at baseline (n=19), regression models revealed the median DXA Z-scores improved from baseline -1.38 (95% CI -1.73 to -1.03) over 6y of imiglucerase to -0.73 (95% CI -1.25 to -0.21). A similar response was observed in adolescents and both adult groups. Among young adults with DXA Z-scores below -1 at baseline (n=30), regression models revealed that imiglucerase resulted in improvement of bone density from baseline Z-scores of -1.95 (95% CI -2.26 to -1.64) to -0.67 (95% CI -1.09 to -0.26) after 10y of imiglucerase. Conclusions: Low bone density is prevalent in all age groups with GD; it is even more prevalent during adolescence, a developmental period critical to attainment of peak bone mass. Imiglucerase results in amelioration of osteopenia in all age groups but the effect is greater in younger patients. The early onset of osteopenia in young untreated GD patients, with resultant failure to achieve optimal bone mass, and the good response to treatment in these patients suggest that early therapeutic intervention is the best strategy for achieving maximal skeletal outcomes.

***Disclosures: Thomas Hangartner**, None.*
This study received funding from: Genzyme Corporation

SA0445

See Friday Plenary number FR0445.

SA0446

See Friday Plenary number FR0446.

SA0447

Effect of a Single Oral Dose of 600,000 IU of Cholecalciferol on Serum Calciotropic Hormones in Young Subjects With Vitamin D Deficiency: a Prospective Intervention Study. Cristiana Cipriani*[1], Elisabetta Romagnoli[1], Alfredo Scillitani[2], Iacopo Chiodini[3], Romano Del Fiacco[4], Vincenzo Carnevale[5], Maria Lucia Mascia[6], Claudia Battista[5], Luciano Carlucci[6], Cristina Eller Vainicher[7], Salvatore Minisola[1]. [1]University of Rome, Italy, [2]Casa Sollievo Della Sofferenza Scientific Institute, Italy, [3]Department of Medical Sciences, University of Milan, Fondazione Policlinico IRCCS, Italy, [4]University "Sapienza" - Rome, Italy, [5]Department of Internal Medicine & Endocrinology Casa sollievo della Sofferenza Hospital, Italy, [6]Department of Clinical Sciences, University of Rome Sapienza, Italy, [7]Fondazione IRCCS Cà Granda Ospedale Maggiore Policlinco Milano, Italy

Purpose: Vitamin D depletion has been reported as a very common condition among adult general population. Neverthless, the effect of vitamin D repletion in young people with low vitamin D status has not been investigated so far. We carried out a prospective intervention study to evaluate short and long-term serum changes of the main parameters of calcium metabolism inducend by a single oral dose of cholecalciferol (600,000 IU) in a sample of young subjects with vitamin D deficiency.

Methods: Forty-eight young subjects (35 females and 13 males; mean age 36.04 ± 8.46 SD yrs, range 25-56 yrs; BMI 24 ± 3.52 kg/cm^2) with vitamin D deficiency received a single oral dose of 600,000 IU of cholecalciferol. Serum levels of 25-hydroxyvitamin D [25(OH)D], total calcium [Ca], phosphorus [P], magnesium [Mg] and parathyroid hormone [PTH] were measured at baseline, and at 3, 15 and 30 d. A subgroup of 20 female subjects (mean age 33.15 ± 6.02, range 25-50; BMI 23.8 ± 4.01) were also assessed at 60 and 90 d. In this subgroup serum calcitriol (1,25-dihydroxyvitamin D [1,25$(OH)_2$D]) levels were also measured.

Results: We found a significant change in 25(OH)D levels throughout the entire observation period ($p<0.001$). 25(OH)D serum levels were significantly increased at 3 d (77.16 ± 30.52 ng/ml; $p<0.001$) and up to 30 d (62.46 ± 26.12; $p<0.001$) compared to baseline. A significant concomitant decrease in serum PTH concentration was found ($p<0.001$). This decrease was already significant at 3 d (-14.47 ± 13.89 pg/ml; $p<0.001$) and up to 30 d (-9.69 ± 16.01; $p<0.001$). These trends were mantained in the subgroup followed up to 90 d ($p<0.001$). Mean serum Ca, P and Mg values significantly changed throughout the entire period ($p<0.05$, $p<0.01$ and $p<0.001$ respectively). Ca and P levels were significantly higher at 3 d compared to baseline (9.46 ± 0.32; 4 ± 0.56 mg/dl; $p<0.01$ for both). On the contrary, mean serum Mg values were significantly reduced at the same time point (1.91 ± 0.18 mg/dl; $p<0.01$). Serum 1,25$(OH)_2$D concomitantly increased ($p<0.001$) and was significantly higher than baseline as soon as 3 d of observation (51.03 ± 41.08 pg/ml; $p<0.001$) and up to 60 d (12.77 ± 24.48; $p<0.05$).

Conclusions: A single very large oral dose of 600,000 IU of cholecalciferol is useful in rapidly and safely enhancing serum 25(OH)D and in reducing serum PTH in young people with vitamin D deficiency. Serum 25(OH)D seems to play a direct role in modulating PTH secretion, regardless of 1,25$(OH)_2$D and calcium levels.

***Disclosures: Cristiana Cipriani**, None.*

SA0448

Prevalence and Risk Factors of Low Vitamin D Status among Inuit Adults. Jessy Hayek*, Hope Weiler, Grace Egeland. McGill University, Canada

Background: Low vitamin D status may be a risk factor for many health conditions, including osteoporosis, cardiovascular disease, and cancer. Evidence since the Nutrition Canada Survey (1973) suggests that Aboriginal people have low intakes of vitamin D and are shifting away from the consumption of traditional foods. Further risk factors including age, higher body mass index (BMI), ethnicity, elevated parathyroid hormone (PTH) concentrations and low socio-economic status predispose Aboriginal populations to low vitamin D status.

Objectives: 1) Determine the prevalence of vitamin D deficiency and insufficiency in Inuit adults and 2) Identify risk factors for low vitamin D status (gender, age, vitamin D intake, BMI, household crowding, and socio-economic status.) Methods: 2207 Inuit adults (18 - 90 y) participated in the 2007-2008 Inuit Health Survey. Households were selected randomly from communities in Nunavut, Nunatsiavut and Inuvialuit Settlement Region. All data were collected in the field and through a mobile research laboratory, the Amundsen Research Ship. Dietary intake was assessed through the administration of a 24 h recall and a Food Frequency Questionnaire (FFQ). Anthropometric measurements and information about household living conditions, supplement use and health status were collected through interviews. Nurses collected blood samples and serum 25(OH)D and PTH were measured by Chemiluminesent technology (Diasorin, Liaison). Statistical analysis, including student t test, ANOVA, chi-square and logistic regression were performed using STATA 10.

Results: At the end of the summer, 72% of Inuit adults had insufficient 25(OH)D concentrations (> 75nmol/L) with a weighted mean of 58.5 ± 33.3 nmol/L. Older adults (> 50 years old) had higher vitamin D concentrations and intake than younger adults (47.6 ± 27.2 vs 83.8 ± 32.4 nmol/L, $p<0.05$). Men had better vitamin D status and intake than women (60.6 ± 34.2 vs 57.2 ± 32.7 nmol/L, $p<0.05$). The strongest predictors of vitamin D status among Inuit adults were age and BMI.

Conclusions: This is the first population assessment of vitamin D status in Inuit adults. Based on our results, there is a need for interventions promoting the consumption of traditional foods rich in vitamin D particularly among young adults. Further, assessment of vitamin D status in the winter across wider age ranges is advised.

***Disclosures: Jessy Hayek**, None.*

SA0449

Propagation of Paget's Disease of Bone after Reaming and Intramedullary Rod Placement for a Fracture. Joseph Shaker*[1], David King[2], Mercedes Gacad[3], Frederick Singer[3]. [1]Medical College of Wisconsin, USA, [2]Medical College of Wiconsin, USA, [3]John Wayne Cancer Institute, USA

Paget's disease of bone (PDB) has rarely been reported to develop in a new bone after inadvertent use of pagetic bone in a bone graft. We now report a case of PDB developing in the distal tibia after surgery on a pagetic proximal tibia. A 49 year old man developed pain in the right tibia in 1/07. Radiographs suggested mixed lytic/sclerotic PDB involved the proximal tibia. There was no family history of PDB or other bone disease. In 4/07, while playing soccer he turned and fractured the proximal right tibia. He underwent a biopsy and intramedullary rod placement with reaming. Because of postoperative deformity he had a revision with repeat intramedullary rod placement as well as a plate in 5/07. In early 2009 he developed right lower leg pain. In 4/09 his pain became more severe and radiographs revealed new lytic lesions more distally in the right tibia. On examination there was slight warmth over the right tibia with mild tenderness distally. Laboratory data included total serum alkaline phosphatase 144 U/L (40-129), bone specific alkaline phosphatase 37.5 µg/liter (0-20.1), 25-hydroxy vitamin D 21 ng/ml, creatinine 0.74 mg/dl, and urinary calcium 295 mg per 24 hours. A total body bone scan demonstrated increased uptake in the proximal right tibia as well as in the new lytic lesions more distally located in the right tibia. The initial biopsy (4/07) as well as a biopsy of one of the new lytic areas (8/09) revealed numerous large multi-nucleated osteoclasts, numerous osteoblasts and a fibrovascular marrow characteristic of PDB. Immunohistochemical evaluation of the 4/07 biopsy with an anti-measles virus nucleocapsid protein antibody demonstrated staining of the osteoclasts.

After repletion of vitamin D in 11/09 he was treated with zoledronic acid 5 mg intravenously. Approximately 2 months later, the right tibia symptoms had improved 30-40% and the bone specific alkaline phosphatase had decreased to 12.1 µg/liter (0-20.1).

This patient presented with PDB in the proximal right tibia and developed lytic PDB in the distal tibia after reaming and intramedullary rod placement for a fracture. The new lytic lesions developed much faster than would be expected from the normal progression of a lytic lesion in PDB. This suggests that the PDB was propagated by the procedure. The explanation for the spread of PDB could be the transposition of bone cells containing measles virus nucleocapsid protein from the proximal to the distal tibia.

***Disclosures: Joseph Shaker**, None.*

SA0450

Cinacalcet Treatment in Patients with Primary Hyperparathyroidism. Claudio Marcocci*, Luisella Cianferotti, Chiara Banti, Feredica Saponaro, Edda Vignali, Silvia Chiavistelli, Giuseppe Viccica, Filomena Cetani. University of Pisa, Italy

Primary hyperparathyroidism (PHPT) is an endocrinopathy diagnosed by chronically elevated serum calcium and PTH. Parathyroidectomy usually cures the disease, but few treatment alternatives exist for patients who fail surgery, have contraindication or refuse surgery, or do not meet current operative guidelines. Medical therapies capable of reducing serum calcium and PTH and increasing bone mass in PHPT patients are needed. Calcimimetics binding the calcium-sensing receptors (CASR) quickly and directly reduce serum calcium level.

The aim of the present study was to evaluate efficacy, safety, and long-term tolerability of cinacalcet in women with PHTP. We studied 13 patients with PHPT. All subjects had serum calcium levels higher than 11.2 mg/dl. In Europe cinacalcet is approved for reduction of hypercalcemia in patients with PHPT for whom parathyroidectomy is indicated on basis of calcium levels but in whom surgery is clinically inappropriate or is contraindicate. Subjects requiring drugs metabolized by cytochrome P450 were excluded because of cytochrome P450 inhibition by cinacalcet. Women on treatment with bisfosphonate were included in the study. During the initial dose-titration phase, cinacalcet dose increase from 30 mg daily to 60 mg daily. In the maintenance phase, visits were approximately every 4-5 wk and then every 12 -24 wk, during which doses could be adjusted. If a patient developed hypocalcemia (serum calcium <8 mg/dl), cinacalcet treatment was withheld for approximately 1 wk until the next serum calcium measurement was at least 8,4 mg/dl. Blood was drawn after an overnight fast the morning dose of cinacalcet and adverse events recorded. Blood was collected for measurement of serum calcium, ionized calcium, PTH, bone alkaline phosphatase, osteocalcin, urinary and serum cross laps, and 24 h urinary calcium. These parameters were evaluated at baseline and after 6-8 months.

Three out of 13 patients withdrew cinacalcet due to adverse effects (nausea, vomiting and heartburn), and underwent surgery. In the remaining patients, compared with baseline, cinacalcet treatment improved measures of PHPT including

reducing serum calcium, ionized calcium and PTH. No changes in bone markers and 24 h urinary calcium were seen.

Treatment of PHPT patients with cinacalcet maintained normocalcemia, reduces plasma PTH, and was well tolerated

***Disclosures: Claudio Marcocci**, None.*

SA0451

See Friday Plenary number FR0451.

SA0452

Mutational Analysis of GCMB, a Parathyroid-Specific Transcription Factor, Suggests That it is Not a Frequent Cause of Primary Hyperparathyroidism. Michael Mannstadt*[1], Emily Holick[2], Wenping Zhao[2], Harald Jueppner[3]. [1]Massachusetts General Hospital Harvard Medical School, USA, [2]Endocrine Unit, Massachusetts General Hospital, USA, [3]Massachusetts General Hospital, USA

Purpose of the study: Primary hyperparathyroidism (PHPT) is a common endocrine disorder characterized by hypercalcemia and elevated PTH levels. In a small subset of parathyroid adenomas, activating mutations of the cyclin D gene have been identified. Many parathyroid adenomas are monoclonal in origin, but the somatic or germ-line mutations that lead to an adenoma have not been identified in the majority of cases. GCMB is a parathyroid specific transcription factor, which causes hypoparathyroidism when inactivated before parathyroid gland development. It continues to be expressed in adult parathyroid glands where its post-natal function remains unknown. However, overexpression of GCMB mRNA has been reported in parathyroid adenomas, and we tested the hypothesis whether acquired activating mutations of GCMB can be found in parathyroid adenomas.

Methods: We studied 30 surgically resected parathyroid adenomas from 30 patients with HPTH. Genomic DNA was extracted and all exons and exon-intron borders of the gene encoding GCMB were sequenced. Nucleotide sequence variations were compared to public databases and novel amino acid changes were tested in vitro by Western blot analysis and Luciferase assay using transfected DF-1 cells.

Results: Several polymorphisms were identified that were previously reported or can be found in public databases. In one of the 30 glands, a novel heterozygous missense mutation, c1144G>A, was identified leading to the substitution of an evolutionary conserved valine at position 382 to methionine (V382M). The presence of this mutation, which was not found in public databases, was confirmed by restriction site analysis. Western blot analysis using mutant GCMB (GCMB-V382M) from lysates from transiently transfected DF-1 fibroblasts demonstrated a protein band that was identical in size and similar in intensity to the wildtype protein indicating that the identified amino acid change does not significantly impair GCMB expression. Transient transfection of DF-1 cells with plasmids encoding wildtype and GCMB-V382M showed a similarly robust, 16-fold increase in luciferase activity. Cotransfection of wildtype and mutant proteins did not change luciferase activity.

Conclusions: In 30 analyzed parathyroid adenomas from patients with primary hyperparathyroidism, functionally important mutations in GCMB were absent. This suggests that mutations in this transcription factor do not seem to play a major role in the pathogenesis of PHPT.

***Disclosures: Michael Mannstadt**, None.*

SA0453

No Improvement in Carotid Vascular Abnormalities with Parathyroidectomy in Mild Primary Hyperparathyroidism. Tatjana Rundek[1], Marcella Walker*[2], Chiyuan Zhang[2], Donald McMahon[2], James Lee[2], Jessica Fleischer[2], Tamara Taggart[2], Julia Udesky[2], Ralph Sacco[1], Shonni Silverberg[2]. [1]University of Miami, USA, [2]Columbia University, USA

We have reported that mild primary hyperparathyroidism (PHPT) is associated with subclinical cardiovascular (CV) abnormalities. This study seeks to determine whether carotid vascular abnormalities are reversible with parathyroidectomy (PTX).

Results: Patients (N=43) with mild PHPT (79% female, age 62 ± 7 yrs, serum calcium 10.6 ± 0.5 mg/dl, PTH 97 ± 47 pg/ml; blood pressure 121 ± 15/74 ±10 mmHg) had carotid ultrasound prior to and 1-YR post-PTX. BP did not change after PTX. Carotid plaque was present in 42% at baseline and did not regress after PTX (present in 49%, p=0.66). Maximum plaque thickness (MCPT) increased post-operatively (0.86 ± 1.08 to 1.03 ± 1.11: p=0.01). This increase was not associated with baseline calcium or PTH or predicted by postoperative changes in calcium or PTH levels. Mean carotid intima-media thickness [(IMT): 0.96 ± 0.09; normal < 0.90 mm; elevated in 74%] and stiffness (6.3 ± 3.1; normal < 6; elevated in 42%), were increased at baseline. Neither measure, however, was linearly associated with baseline calcium, PTH, 25-hydroxyvitamin D or 1, 25-dihydroxyvitamin D levels, nor did they improve 1 yr after PTX. Other indices of decreased vessel compliance (strain and distensibility) also did not change after PTX. None of the carotid measures improved after PTX in the subsets of patients that were abnormal at baseline.

Conclusions: Patients with mild PHPT have evidence of increased carotid stiffness and IMT, a structural indicator of subclinical CV disease associated with an increased risk of deleterious CV outcomes. These abnormalities did not improve in the first postoperative year after PTX. Plaque thickness increased after PTX, but the increase is not clearly associated with cure of PHPT. Without improvement in these indices, there is no clear suggestion that the presence of carotid vascular abnormalities should be an indication for surgery in PHPT. It will, however, be important to evaluate whether there are beneficial changes in other aspects of the CV system after PTX.

Carotid Test	Normal Range	Baseline Mean ± SD n=43	12 month Mean ± SD n=43	p-value* Baseline vs. 12 months
IMT (mm)	0.7-0.9	0.96 ± 0.09	0.97 ± 0.07	0.35
STRAIN (%)	6-12%	9 ± 3	8 ± 3	0.16
STIFFNESS	< 6	6.3 ± 3.1	6.5 ± 2.7	0.79
DISTENSIBILITY	>0.425	1.2 ± 0.5	1.1 ± 0.4	0.57
MCPT (mm)	<1.9	0.86 ± 1.08	1.03 ± 1.11	0.01

Carotid Studies

***Disclosures: Marcella Walker**, None.*

SA0454

Parathyroidectomy Does Not Affect Flow-Mediated Vasodilation in Mild Primary Hyperparathyroidism. Angela Carrelli*[1], Marcella Walker[2], Marco Di Tullio[3], Shunichi Homma[3], Chiyuan Zhang[2], Donald McMahon[3], Shonni Silverberg[2]. [1]New York Presbyterian- Columbia University, USA, [2]Columbia University, USA, [3]Columbia University College of Physicians & Surgeons, USA

Purpose: Severe primary hyperparathyroidism (PHPT) has been linked to impaired endothelial function, which normalizes after parathyroidectomy. Endothelial dysfunction is an important early event in the pathogenesis of atherosclerosis. It is not known if endothelial dysfunction occurs in mild PHPT and if so, whether it is reversed following parathyroidectomy. To address this issue, we measured flow-mediated dilation (FMD) by ultrasound imaging in patients with mild PHPT prior to and 12 months after parathyroidectomy. FMD, a non-invasive technique that estimates endothelial function, quantifies the brachial artery response to reactive hyperemia by measuring the percent change in vessel diameter before and after inflation of a forearm cuff to supra-systolic pressure for 5 minutes.

Results: We studied 43 patients who were typical of those with mild PHPT (79% female, age ± SD 62±7 yrs, serum calcium 10.6±0.5 mg/dl, PTH 97±47 pg/ml). Baseline blood pressure was normal (Table).

At baseline, FMD in these PHPT patients was normal (4.59±3.19 %; age matched control population: mean 4.92±3.93%, 25th percentile 2.55, 75th percentile 6.77). Baseline FMD was not associated with serum calcium or PTH levels (calcium: r=0.16, p=0.29; PTH: r=-0.057, p=0.72). Baseline brachial artery diameter prior to cuff inflation was positively associated with PTH levels (r=0.34, p=0.03). Although this finding is consistent with known vasodilatory effects of PTH, this association did not persist after controlling for height and weight.

One yr after parathyroidectomy, FMD remained normal (5.13±4.71 %) and was not significantly changed compared to baseline (difference: 0.54%, p=0.49). The change in FMD was not predicted by baseline calcium or PTH levels (calcium: r=-0.28, p=0.06; PTH: r=-0.16, p=0.30), nor was it associated with the change in serum calcium or PTH following parathyroidectomy (calcium: r=0.20, p=0.19; PTH: r=0.21, p=0.17).

Conclusions: FMD is normal in patients with mild PHPT and is unchanged one year after parathyroidectomy. We conclude that mild PHPT does not appear to be associated with the endothelial dysfunction seen in severe PHPT.

	Baseline Mean ± SD N=43	12 month Mean ± SD N=43
Systolic BP (mm Hg)	121 ± 15	122 ± 14
Diastolic BP (mm Hg)	74 ± 10	76 ± 9
Baseline vessel diameter (mm)	3.46 ± 0.66	3.47 ± 0.73
Vessel diameter post-hyperemia (mm)	3.61 ± 0.64	3.63 ± 0.69
FMD (%)	4.59 ± 3.19	5.13 ± 4.71

Table

***Disclosures: Angela Carrelli**, None.*

SA0455

PTH Reverses the Imbalance between Cortical and Trabecular Bone Compartments in Hypoparathyroidism: A Three-Year Longitudinal HR-pQCT Study. Xiaowei Liu*[1], Mishaela Rubin[1], Jim Sliney Jr[2], Donald McMahon[3], David Dempster[1], John Bilezikian[3]. [1]Columbia University, USA, [2]Columbia University Medical Center, USA, [3]Columbia University College of Physicians & Surgeons, USA

Hypoparathyroidism (HypoPT), a disorder of PTH deficiency, is associated with increased bone density and microstructural abnormalities. To address the hypothesis that these skeletal abnormalities of HypoPT can be reversed by PTH administration, we evaluated cortical (Ct) and trabecular (Tb) skeletal microstructure in HypoPT by high resolution peripheral quantitative computed tomography (HR-pQCT; Xtreme CT, Scanco Medical) before and after PTH treatment. This represents the first prospective longitudinal HR-pQCT study of a disorder of defective parathyroid function.

In comparison to age- and sex-matched controls, subjects with untreated hypoPT (n=42, 9 male, 33 female, 46±13 yrs) had significantly ($p=0.03$) higher Ct area (Ct.Area, +13%) and thickness (Ct.Th, +12%) at the distal radius (DR), but not at the distal tibia (DT). While Ct volumetric BMD (DComp) was similar to controls, Ct perimeter (Ct.Pm) was 14% and 8% higher at DR and DT ($p<0.05$). Tb area (Tb.Area), Tb vBMD (Dtrab), and Tb microstructure measurements were similar between HypoPT and controls while integral vBMD tended to be higher in HypoPT at DR and DT.

100 μg of hPTH(1-84) was administered every other day for 36 months. HR-pQCT scans were obtained at baseline and after 3, 6, 12, 24, and 36 months. Reductions were found in Ct.Area at DR (24mo, -2%, $p=0.08$) and DT (36mo, -2%, $p=0.03$), Dcomp at DR (24&36mo, -1-2%, $p<0.02$) and DT (24&36mo, -1-2%, $p<0.01$), Ct.Th at DR (36mo, -3%, $p=0.11$) and DT (24&36 mo, -2%, $p<0.02$). In contrast, Dtrab significantly increased at DR (24&36mo, +2-3%, $p<0.05$), but remained unchanged at DT. As a result, at DR, integral vBMD remained unchanged with Dcomp and Dtrab changing in opposite directions; at DT, vBMD significantly decreased (24mo, 1%, $p=0.02$). In addition, Tb.Area did not change with PTH. Other Tb microstructure measures, such as Tb number, thickness and spacing, showed no significant change.

In conclusion, PTH deficiency in HypoPT is associated with normal Tb indices but abnormal increases in the Ct bone compartment in the peripheral skeleton as compared to matched controls. PTH treatment is associated with normalization in the area and thickness of the Ct compartment at both DR and DT, along with concomitant decreases in Tb bone density at DR. These data suggest that PTH administration reverses microstructural skeletal abnormalities in HypoPT by restoring the balance between Ct and Tb indices.

***Disclosures: Xiaowei Liu**, None.*

SA0456

Accumulation of Maillard Reaction Products Involve Bone Fragility in Adynamic Bone Disease. Yoshiko Iwasaki*[1], Hideyuki Yamato[2], Masafumi Fukagawa[3]. [1]Oita University of Nursing & Health Sciences, Japan, [2]Kureha Corporation, Japan, [3]Tokai University School of Medicine, Japan

It is well known that adynamic bone disease (ABD) is highly prevalent in dialysis patients. Although patients with ABD have normal bone mineral density (BMD), they have a high incidence of fracture rates. However, it still remains unknown why fracture rates increase in ABD. In this meeting last year, we presented that rat models with ABD have reduced bone strength despite having normal BMD. It was a possibility that this reduction was affected by changing bone chemical composition. On the other hand, several studies determined Maillard reaction products, such as pentosidine, carboxymethyl-lysine (CML), contribute collagen properties. The purpose of this study is to clarify whether Maillard reaction products affect bone strength. As for the ABD model, after male SD rats underwent thyroparathyroidectomy (TPTx), they underwent 5/6 nephrectomy (Nx) or sham operations. These rats were continuously infused with rat PTH and injected with L-thyroxin subcutaneously to maintain physiological levels. Therefore TPTx-Nx rats can simulate ABD, because of their low turnover bone associated with the suppression of renal function. Groups were ABD (TPTx-Nx) and control (TPTx-sham). Recently, it has became easier to obtain spectroscopic properties from bone with a laser raman spectroscopy system (Nicolet Almega XR, Thermo Fisher Scientific Co.). We can obtain much information about the matrix in bone and we can also evaluate local change of bone composition by this system. As the results, by means of Raman, pentosidine, which is a non-enzymatic collagen crosslink, and CML revealed higher level in ABD group compared with control group. In comparison to the control group, the accumulation level in ABD of pentosidine and CML was 10% and 15% higher, respectively. And also, enzymatic crosslink was accumulated in the ABD group. In addition, the levels of Pentosidine, CML, and crosslink were correlated with bone viscoelasticity measured by DMA system.

These results suggest that accumulation of Maillard reaction products induced by kidney dysfunction were deterioration mechanical properties of bone. Those matrix changes affect bone fragility and could lead to increased fracture risk without bone loss.

***Disclosures: Yoshiko Iwasaki**, None.*

SA0457

Anti-Diabetes Drug Class of SGLT1 Inhibitors Increases Bone Mass in Young and Adult Female Sprague-Dawley Rats by Decreasing Bone Turnover. Rana Samadfam*[1], Nancy Doyle[1], Martin Heinrichs[2], Thomas Kissner[2], Eckart Krupp[2], Susan Y. Smith[1]. [1]Charles River Laboratories, Canada, [2]Sanofi-Aventis, Germany

Diabetes mellitus is a chronic metabolic disorder characterized by hyperglycemia caused by defective insulin secretion, resistance to insulin action, or a combination of both. Due to the important role of bone in energy balance and the cross-talk between nutritional hormones and the skeleton, it is likely that anti diabetic compounds affect bone mass. Treating hyperglycemia with drugs that block intestinal glucose uptake and renal glucose reabsorption via the sodium-glucose transporters (SGLT1, SGLT2) represents a novel approach to diabetes treatment. These studies were designed to investigate the effect of SGLT1 inhibitors on bone and electrolytes in serum and urine. Rats were treated daily with either vehicle control or SAR474832, a selective SGLT1 inhibitor and SAR7226, a mixed SGLT1/2 inhibitor for 28 days. Blood and urine were collected for calciotropic hormone and bone turnover analysis. In addition, bone densitometry (DXA, pQCT) and bone quality (three point bending test and compression test) were assessed. Histology was also performed on excised bones. Treatment with SAR7226 resulted in dose-related, marked glucosuria (the anticipated pharmacological effect), polyuria, and calciuria. Normal serum calcium was maintained while serum phosphorus was slightly increased. PTH and 1,25 vitamin D3 were markedly suppressed as well as markers of bone turnover. These effects were associated with increases in bone mineral density (BMD). Increases in BMD at the spine were positively associated with increases in bone strength. Effects on bone mass were characterized microscopically by increases in trabecular bone. The SGLT1/2 inhibitor SAR7226 markedly influences calcium and phosphorus homeostasis with positive effects on bone mass and strength. Similar effects were observed with the low-absorbable selective SGLT1 inhibitor SAR474832. From these results it is concluded that calciuria observed following treatment with SAR7226 and SAR474832 is not associated with calcium release from bone. These studies highlight the importance of considering evaluations of the skeleton in the safety assessment of compounds affecting calcium homeostasis to provide important safety data. Calciuria and increased trabecular bone was found in toxicity studies in rats with the mixed SGLT1/2 inhibitor SAR7226 and the low-absorbable and selective SGLT1 inhibitor SAR474832.

***Disclosures: Rana Samadfam**, Contract Research, 3*
This study received funding from: Sanofi-Aventis

SA0458

Assessment of Bone Tissue Composition in Patients Undergoing Dialysis Therapy Using Raman Spectrometry. Shozo Yano*[1], Yoshiko Iwasaki[2], Akihide Tokumoto[3], Hideyuki Yamato[4], Toru Yamaguchi[1], Toshitsugu Sugimoto[5]. [1]Shimane University Faculty of Medicine, Japan, [2]Oita University of Nursing & Health Sciences, Japan, [3]Kamifukubara Medical Clinic, Japan, [4]Kureha Corporation, Japan, [5]Shimane University School of Medicine, Japan

BACKGROUND: It is well-known that adynamic bone disease (ABD) is common in patients undergoing dialysis therapy, and recent findings suggest that low turnover of bone metabolism might decrease the quality of the bone. Although bone biopsy is gold standard for the assessment, the examination is invasive. Thus, FT-IR and Raman spectrometry would be candidates for the substitutive and non-invasive methods, if they can extracorporeally assess the bone characteristics. OBJECTIVE: To analyze bone tissue composition in dialysis patients using Raman spectrometry. SUBJECTS and METHODS: Bone specimen was obtained from 43 patients with maintainance dialysis (HD 37and PD 6). According to the histomorphometrical analysis, ABD, mild lesion (ML) and osteitis fibrosa (OF) were shown in 14, 16 and 13 patients, respectively. Bone composition was analyzed by Raman spectrometry (Nicolet Almega XR: Thermofisher Scientific Co) . RESULTS: Mineral matrix ratio, which was expressed as (PO_4^{3-})/Amide I ratio, was the highest in the ABD group among 3 groups. The hydroxyproline/proline ratio implying the maturation of collagen was similar result. Collagen crosslink, a marker of mature crosslink, was shown in ABD>ML>OF whereas the pentosidine/Amide I ratio, a marker of senile crosslink, had a similar tendency. CONCLUSION: Reduced bone mineral content was observed in OF and ML, which was consistent with clinical findings such as decreased bone density associated with secondary hyperparathyroidism. In contrast, in ABD, mature as well as senile crosslink accumulation was found in the highest level among 3 groups. These results were also compatible with clinical findings where the fracture frequency was elevated in patients with lower serum PTH levels, suggesting the association of ABD with skeletal fragility.

***Disclosures: Shozo Yano**, None.*

SA0459

See Friday Plenary number FR0459.

SA0460

Volumetric Bone Mineral Density, Geometry and Stiffness Discriminate Vertebral Fracture Status in Patients with Chronic Kidney Disease. Thomas Nickolas*[1], Xiaowei Liu[2], Valerie Thomas[1], Emily Stein[3], Adi Cohen[1], Ryan Chauncy[1], Donald McMahon[3], Mary Leonard[4], X Guo[2], Elizabeth Shane[3]. [1]Columbia University Medical Center, USA, [2]Columbia University, USA, [3]Columbia University College of Physicians & Surgeons, USA, [4]Children's Hospital of Philadelphia, USA

Introduction: In chronic kidney disease (CKD), dual energy X-ray absorptiometry (DXA) measures of lumbar spine (LS) areal BMD (aBMD) provide poor discrimination of vertebral fracture (VFx) status. Discrimination of VFx in CKD patients by high resolution peripheral quantitative computed tomography (HRpQCT, Xtreme CT, voxel size ~82 microns) has not been evaluated.

Methods: Patients with (n=10) and without (n=38) VFx were enrolled from an ongoing observational study of adults ⩾50 years with CKD stages 3-5 not on dialysis. DXA aBMD was measured at LS, total hip (TH), femoral neck (FN) and ultradistal radius (UDR). Total, Cortical (Ct) and Trabecular (Tb) volumetric BMD (D100, Dcort and Dtrab); Ct thickness (CtTh) and periosteal perimeter (CtPm); total, Ct and Tb area (TotArea, CtArea and TbArea); and Tb microarchitecture were measured by HRpQCT at the distal radius (RAD) and tibia (TIB). Bone stiffness and both proximal and distal Ct load share (PCLS and DCLS) were measured by finite element analysis (FEA) of HRpQCT datasets. Results are expressed as Means ± SD, percent differences and areas under the receiver operating characteristic curves (AUC) with 95% confidence intervals (CI).

Results: Age, estimated glomerular filtration rate and BMI were 71 ± 9 years, 34 ± 16 mL/minute and 29 ± 5 kg/m^2, respectively. Twenty-one percent were women and 54% were white. Mean T-Scores were above the osteoporotic range (LS: -0.2 ± 1.6; TH: -0.9 ± 1.1; FN: -1.5 ± 1.0; UDR: -1.5 ± 1.4). There were no significant differences in demographics or T-Scores between groups with/without VFx. By HRpQCT of the RAD, patients with VFx had 20% lower D100 (p=0.03), 9% lower Dcort (p=0.01), 27% lower CtTh (p=0.01) and 17% greater TbArea (p=0.006). At the TIB, patients with VFx had 9% lower Dcort (p=0.05), 8% greater CtPm (p=0.0008), 14% greater TotArea (p=0.007), 15% greater TbArea (p=0.006), 31% lower DCLS (p=0.03) and 16% lower PCLS (p=0.01). AUCs for VFx discrimination at the RAD for Dcort (0.74; 0.58-0.91) and CTh (0.76; 0.59-0.92) and at the TIB for Dcort (0.69; 0.49-0.90), CtPm (0.80; 0.67-0.93), TbArea (0.70; 0.55-0.85), PCLS (0.76; 0.60-0.92) and DCLS (0.72; 0.54-0.90) were all significantly better than LS aBMD (0.53; 0.34-0.73).

Conclusions: Volumetric BMD, geometric parameters and whole bone stiffness measured by HRpQCT and FEA provide better discrimination of VFx than LS aBMD in pre-dialysis CKD patients. Longitudinal studies are needed to determine whether HRpQCT can predict VFx in CKD patients

***Disclosures: Thomas Nickolas**, None.*

SA0461

See Friday Plenary number FR0461.

SA0462

See Friday Plenary number FR0462.

SA0463

Gene Analysis To Elucidate the Mechanisms of Tenofovir Mediated Osteopenia. Kim Mansky*, Iwen Grigsby, Lan Pham, Ann Emery, Louis Mansky, Raj Gopalakrishnan. University of Minnesota, USA

Clinical observations have revealed a strong correlation between loss of bone density in HIV-infected individuals, particularly in conjunction with the antiretroviral drug tenofovir, a nucleotide analog that inhibits HIV reverse transcriptase. The most compelling correlations have been observed in clinical studies involving young children and adolescents. The goal of this study was to investigate the in vitro effects of tenofovir exposure on primary osteoblast and osteoclast gene expression in order to gain insights into the potential mechanisms for the loss of bone density as well as to identify potential biomarkers. Primary osteoblasts and osteoclasts were generated from calvaria and bone marrow of wild type mice, respectively. Osteoblast and osteoclast cultures were either untreated or treated with the tenofovir prodrug, tenofovir disoproxil fumarate (TDF) and total RNA were extracted and used for microarray analysis to assess TDF-associated changes in gene expression profiles. Hierarchical clustering and Gene Ontology analysis were performed of the gene expression data from both osteoblasts and osteoclasts. Data from osteoblasts showed broad changes in gene expression profiles, including alterations in genes associated with osteoblast function. Inspection of these results led to the identification of genes that are associated with the Wnt, TGF-beta, Hedgehog, VEGF, B cell receptor, and the Fc epsilon RI signaling pathways. Data from osteoclasts revealed downregulation of Gnas, Got2 and Snord32a in TDF-treated cells. Microarray results were validated by confirming expression of the identified genes by qPCR analysis. To our knowledge these are the first studies, which demonstrate the impact of tenofovir on osteoblast and osteoclast gene expression. Understanding the functions of these genes should help explain the basis for tenofovir-associated loss of bone density in HIV-patients as well as identify potential biomarkers for diagnosis.

***Disclosures: Kim Mansky**, None.*

SA0464

Hyperkyphosis and Decline in Functional Status in Older Community Dwelling Women: The Study of Osteoporotic Fractures (SOF). Mei-Hua Huang[1], Wendy Katzman, DSc[2], Steven Cummings[3], Deborah Kado*[1]. [1]University of California, Los Angeles, USA, [2]University of California San Francisco, USA, [3]San Francisco Coordinating Center, USA

Maintaining physical functional ability is an important prerequisite for preserving independence in later life. Hyperkyphosis, or an increased thoracic curvature, is commonly observed in older persons and has been associated with worse self-reported and objectively measured physical function in multiple cross-sectional studies, including the Study of Osteoporotic Fractures. However, it is unknown whether hyperkyphosis may predict worse physical function over time. Therefore, we sought to determine whether hyperkyphosis precedes worse self-reported and objectively measured physical function over an average follow-up of 15 years. The digitized Cobb angle (T4-T12) derived from supine lateral thoracic spine plain films was used to calculate the degree of kyphosis in 1196 older women aged 65 and older who were randomly selected from the original cohort of 9,704 women because they had 15 year clinic visit data available for analyses. Participants were an average of 68.8 years old (SD= 3.3) and had a mean kyphosis angle of 44.6 degrees (SD = 12.1). Multivariable linear regression models were used to evaluate the association between kyphosis measured at baseline and change over 15 years in: 1) self-reported functional status (any difficulty in performing six tasks: walking 2-3 blocks, climbing or descending 10 steps, preparing meals, heavy housework, and shopping); 2) measured walking speed; and 3) grip strength. With each 10 degree increase in kyphosis, women were more likely to decline in functional status15 years later (β estimate = 0.086, p = 0.04), after adjustment for age, clinic, weight, height, physical activity, baseline functional status, baseline vertebral fracture, heel bone mineral density, health status, and arthritis. In similarly adjusted models, with each 10 degree increase in kyphosis, women had a decline in walking speed of 1.4 cm/sec (p = 0.017). There was no significant association between kyphosis and worsening grip strength. Interestingly, in these multivariable models, having a baseline vertebral fracture was not predictive of functional decline (β estimate = -0.023, p = 0.87) nor decline in walking speed (β estimate = -0.006, p = 0.74). Although the effect of hyperkyphosis on future physical functional decline is small in magnitude, in this select group of women survivors followed for 15 years, having hyperkyphosis was a stronger predictor of physical functional decline than was having a baseline prevalent vertebral fracture.

***Disclosures: Deborah Kado**, None.*

SA0465

Regulation of Energy Metabolism By Osteocytes. Ronald Kwon*, Diana Meays, Natalie Kardos, John Frangos. La Jolla Bioengineering Institute, USA

Bone has been discovered to exert endocrine control of energy metabolism [1], however the cellular mediators of this process have not been fully explored. Recently, Lee et al. implicated osteoblasts in regulating energy metabolism via a mechanism that involves the hormone osteocalcin (OCN) and the enzyme OST-PTP, which alters OCN bioactivity [1]. Given that osteocytes outnumber osteoblasts in vivo and produce high levels of OCN in culture, we hypothesized that osteocytes also exert endocrine control of energy metabolism through this mechanism. In this study, we used mice possessing a diphtheria toxin (DT) receptor transgene driven by the DMP1 promotor (DMP1-DTR) [2] to investigate the effects of DT-induced osteocyte ablation on energy metabolism. 8wk M wildtype (WT) and transgenic (Tg) DMP1-DTR mice were administered a single dose of DT (10ug/kg), and various indices of energy metabolism were quantified 4wk later. By focusing on long-term effects and using a relatively mild DT dose [2], we minimized the potential for confounding effects on energy metabolism by short-term inflammatory processes associated with osteocyte ablation. In the 4wks following DT administration, Tg mice gained significantly less weight per day compared to WT mice (WT: 0.18 ± 0.03g/day, Tg: 0.08 ± 0.03g/day; p=0.03, n=17 per group) despite consuming a similar amount of food (WT: 4.3 ± 0.5g/day, Tg: 5.6 ± 1.5g/day; p=0.47, n=7-9 per group). Fasted levels of blood glucose (WT: 161.3 ± 4.4mg/dl, Tg: 175.1 ± 3.8mg/dl; p=0.03, n=7-9 per group) and serum insulin (WT: 0.18 ± 0.01ng/ml, Tg: 0.24 ± 0.01ng/ml; p=0.02, n=5-7 per group) were significantly elevated in Tg mice. Unexpectedly, serum levels of OCN were not significantly different in Tg mice (WT: 28.8 ± 2.4ng/ml, Tg: 28.5 ± 1.8ng/ml; p=0.93, n=6-7 per group); nor were serum levels of adiponectin (WT: 8.5 ± 0.4ug/ml, Tg: 8.3 ± 0.6ug/ml; p=0.75, n=6-7 per group), which has been shown to be reduced as a result of osteoblast specific-deletion of OCN [1]. This suggests that effects of osteocyte ablation on energy metabolism were not due to reduced levels of circulating OCN. Finally, serum levels of leptin were not significantly different in Tg mice (WT: 3.8 ± 1.0ng/ml, Tg: 4.5 ± 0.9ng/ml; p=0.64, n=7 per group). Together, these data suggest that osteocytes regulate energy metabolism via an unidentified mechanism, either through endocrine signaling, or regulating a cellular intermediary such as osteoblasts.

[1] Lee et al., Cell 2007; [2] Tatsumi et al., Cell Metab 2007

***Disclosures: Ronald Kwon**, None.*

SA0466

Sex-related Differences in Skeletal Phenotype in a Rat Model of Type 2 Diabetes Mellitus. Maxime Gallant*[1], Kathleen Hill[1], Jennifer M. Doyle[1], Susan Reinwald[1], Richard G. Peterson[2], David Burr[1]. [1]Indiana University School of Medicine, USA, [2]PreClinOmics, Inc., USA

Type 2 diabetes mellitus (T2DM) is a complex metabolic disease that leads to various comorbidities. T2DM is known to increase the risk of fractures with little change in BMD. Men with T2DM are at higher risk for fractures than women with T2DM, and post-menopausal women are at greater risk than pre-menopausal women. We hypothesized that gender differences in bone structure that reduce bone mechanical properties may explain these differences in fracture risk in T2DM.

This study investigates sex differences in bone phenotype in a model of spontaneous T2DM, the ZDSD rat, with non-diabetic CD rats as controls. Animals were fed a high-fat diet to induce T2DM onset. Fourteen weeks after T2DM onset, animals were euthanized and bone phenotype was investigated using dual-energy X-ray absorptiometry, micro-CT imaging and mechanical testing. T-tests were used to test for differences between ZDSD and controls within each sex, and two-way ANOVAs were used to detect main effects for sex, diabetes and their interaction.

Femur and lumbar BMD were lower in male and female ZDSD rats compared to controls. However, when corrected for weight, lumbar BMD was not different between ZDSD and control females. Micro-CT analyses revealed that lumbar spine and femur trabecular bone architecture was compromised in ZDSD rats compared to controls (reduced BV/TV and Tb.Th, increased SMI and Tb.Sp), this deterioration being predominant in males compared to females. Lumbar ventral Ct.Th was lower in ZDSD rats compared to controls, but to a larger extent in males versus females (50 and 15% decreases, respectively). These architectural changes were reflected in vertebrae material properties where ultimate stress and toughness were lower in male ZDSD rats only. Cortical bone analyses showed that only ZDSD male rats had smaller (i.e.: Area/length) bone than their controls and significantly thinner cortices than ZDSD females. The material properties of cortical bone were reduced in ZDSD males but not females, as shown by lower UF, yield force, stiffness, post-yield displacement, toughness and post-yield toughness, indicating a more brittle phenotype in ZDSD males.

These results indicate that, as seen in humans, T2DM exerts a more detrimental effect on bone in males compared to females, suggesting that female sex hormones might play a protective role for bone in T2DM.

***Disclosures: Maxime Gallant**, None.*

SA0467

The Impact of type 2 Diabetes on Bone Microarchitecture: A Cross-sectional Evaluation in Postmenopausal Women. Janet Pritchard*[1], Lora Giangregorio[2], Stephanie Atkinson[1], Karen Beattie[1], Jonathan Adachi[3], Dean Inglis[4], Alexandra Papaioannou[5]. [1]McMaster University, Canada, [2]University of Waterloo, Canada, [3]St. Joseph's Hospital, Canada, [4]Centre for Appendicular MRI Studies, Canada, [5]Hamilton Health Sciences, Canada

PURPOSE: In adults with type 2 diabetes (T2D), fracture risk is elevated despite normal or elevated areal bone mineral density (aBMD). The primary objective of this study was to compare trabecular bone microarchitecture in postmenopausal women with long-standing T2D, to that of postmenopausal women without T2D. The secondary objective was to compare aBMD between groups.

METHODS: Participants with T2D had a self-reported diagnosis of T2D ($\geqslant$ 5 years), and were recruited from out-patient diabetes clinics. Participants without T2D were recruited through community advertisements. The non-dominant distal radius was imaged using a 1T peripheral magnetic resonance imaging (pMRI) system (OrthOneTM, ONI Inc.). A sagittal localizer scan was performed, followed by a coronal localizer scan to plan the final transaxial slices of the distal radius. The axial MR images (in-plane resolution =195 μm) were segmented at the endosteal surface and parameters of microarchitecture (marrow pore size, BV/TV, Tb.Th, Tb.N, Tb.Sp, free ends) were derived using in-house software. Body composition, lumbar spine aBMD, and proximal femur aBMD were measured using DXA (Hologic, Discovery QDR4500A). The characteristics of participants and all bone variables are reported as mean $\pm$ SD for continuous variables, and variables were compared using an unpaired t-test (SPSS v.17.0). A p-value of <0.05 was considered significant for this study.

RESULTS: Participants with T2D (n=29) were similar in age (71.0 ± 4.8 yrs vs. 70.7 ± 4.8 yrs, p=0.87) and number of years since menopause (21.7 ± 6.6 yrs vs. 22.1 ± 7.7 yrs, p=0.84) compared to the participants without T2D (n=26). Participants with T2D had greater body mass index (BMI) (34.6 ± 7.6 kg/m^2 vs. 27.9 ± 5.6 kg/m^2, p=0.00), but not percent body fat (40.3 ± 6.1% vs. 37.2 ± 6.5%, p=0.06) compared to participants without T2D. The average number of years with a diagnosis of T2D was 16.6 ± 11.1 yrs, and 62.1% (18/29) of participants with T2D were taking exogenous insulin. Table 1 displays bone densitometry and microarchitecture data for the participants.

CONCLUSIONS: Hole size has been shown to be a good predictor of fracture. We have shown for the first time that the average marrow pore size is greater in postmenopausal women with T2D. Therefore, skeletal fragility in postmenopausal women with T2D may be due in part to enlarged perforations between trabecular units in cancellous bone, which constitutes about 50% and 90% of the bone at the hip and spine, respectively.

Parameter, mean (SD)	**Diabetes n= 29**	**Control n=26**	*P-value*
Lumbar spine (L1-L4) aBMD, g/cm^2	1.09 (0.17)	0.98 (0.18)	0.045
Femoral neck aBMD, g/cm^2	0.74 (0.12)	0.69 (0.10)	0.229
Marrow pore size, mm^2	2.25 (0.44)	1.99 (0.39)	0.023
BV/TV, %	47.5 (1.1)	48.0 (1.2)	0.095
App. Tb.Th, μm	71.1 (3.5)	70.2 (2.7)	0.282
App. Tb. Sp, μm	79.1 (6.1)	104.3 (143.1)	0.356
App. Tb. N, per mm	6.7 (0.4)	6.9 (0.4)	0.143
No. free ends/area, per mm	0.50 (0.07)	0.47 (0.06)	0.109

Values are expressed as mean (SD) and compared using an unpaired 2-tailed t-test.
Abbreviations: BV/TV: bone volume-to-total volume ratio; App: apparent; Tb.Th: trabecular bone thickness; Tb.Sp: trabecular bone separation; Tb.N: trabecular bone number

Table 1. A comparison of bone-related parameters in women with T2D and controls

***Disclosures: Janet Pritchard**, None.*

SA0468

The Multifunctional Role Of Osteopontin In Diabetic Arteriosclerosis. Jian Su Shao[1], Oscar Sierra[1], Su-Li Cheng[1], Linda Halstead[2], Dwight Towler*[2]. [1]Washington University in St. Louis School of Medicine, USA, [2]Washington University in St. Louis, USA

Calcification and fibrosis reduce vascular compliance in diabetic arteriosclerosis, increasing lower extremity ischemia. To better understand the role of osteopontin (OPN), a multifunctional protein upregulated in diabetic arteries, we evaluated contributions of OPN in male LDLR-/- mice fed high fat Western diet (HFD), a model of diabetic arteriosclerosis and vascular calcification. OPN deficiency had no impact on HFD-induced hyperglycemia, dyslipidemia, or body composition. However, OPN-/-;LDLR-/- mice exhibited an altered time-course of aortic calcium accrual – reduced during disease initiation but increased with progression – vs. OPN+/+; LDLR-/- controls. Moreover, diabetic OPN-/-;LDLR-/- mice exhibited reduced aortic compliance and diminished hind-limb blood flow. Collagen accumulation, fragmented elastin, and wall thickness were significantly increased in aortas of diabetic OPN-/-;LDLR-/- mice, as were serum levels of P1NP, a biomarker of type I collagen synthesis. VSMC-specific expression of OPN (SM22-OPN transgene) did reduce aortic elastin fragmentation and Col2A1 expression in OPN-/-;LDLR-/- mice, but did not significantly impact aortic calcification, collagen protein accumulation, or arterial stiffness. However, pharmacologic dosing with the pro-inflammatory OPN fragment SVVYGLR upregulated aortic Wnt3a, Wnt7a, and Wnt7b, increased aortic β-catenin protein, induced osteochondrocytic gene expression (Runx2, COL2A1, COL10A1, OSC), and restored early-phase aortic calcification in OPN-/-;LDLR-/- mice on HFD. Thus, OPN has stage- specific roles in diabetic arteriosclerosis. Pro-inflammatory actions promote vascular osteochondrocytic differentiation and calcification with disease initiation – but other actions limit elastin fragmentation, chondroid metaplasia, vascular calcification and fibrosis with disease progression. Complete OPN deficiency yields a net increase in arteriosclerotic disease severity, reducing distal hind limb tissue perfusion in diabetic LDLR-/- mice.

***Disclosures: Dwight Towler**, None.*

SA0469

The Prevalence of Low Muscle Mass (Sarcopenia) in Individuals with HIV. Bjoern Buehring*, Elisabeth Kirchner, Zhiyuan Sun, Leonard Calabrese. Cleveland Clinic, USA

Purpose: The introduction of highly active antiretroviral therapy to treat HIV infections has turned this disease from a fatal to a chronic process. With the increasing life span changes in bone and fat tissues have became more important. Low bone mineral density (BMD) is common in individuals with HIV and associated with increased fracture risk. Lipodystrophy syndrome leads to metabolic and morphological abnormalities. Less attention has been given to changes in muscle mass in this population. Growing evidence exists that low muscle mass and poor muscle function is associated with increased disability, morbidity, and mortality in older adults. This study aimed to examine the prevalence of low muscle mass as well as low BMD and lipodystrophy in persons with HIV using current DXA definitions. Methods: We invited individuals with HIV on therapy or treatment naïve to undergo DXA whole body composition. We used WHO T-score criteria to assess BMD, a % central fat / % lower extremity ratio to define lipodystrophy and previously proposed sarcopenia criteria (appendicular lean mass / (height)2 and lowest 20% of residuals from regression analysis) to identify persons with body composition abnormalities. Potential risk factors (HIV medication, Age, BMI, length of illness, CD4 count, viral load, testosterone levels, and tobacco use) were assessed through chart review.

Results: 66 males (56 with treatment, 10 treatment naïve) volunteered. Treated individuals were older than naïve (44 vs 34 years) and had HIV longer (108 vs 14 months). In all 66 males prevalence of sarcopenia was 21.2% and 18.2% depending on the definition used. Low BMD was present in 68.2% (60.6% osteopenia, 7.6% osteoporosis). 53% had lipodystrophy. Persons on treatment had higher prevalence of lipodystrophy than treatment naïve (61.1% vs 20%, p=0.034). Lower BMI was related to presence of sarcopenia. Sarcopenia and lipodystrophy were negatively associated (OR 0.11-0.18, p≤0.012). Risk factors for abnormal BMD were treatment with thymidine analogues and non-nucleoside reverse transcriptase inhibitors. Development of lipodystrophy was associated with multiple HIV drugs. Conclusions: To our knowledge this is the first study to estimate the prevalence of low muscle mass based on DXA definitions in persons with HIV. Sarcopenia is common considering the age of our study population. More research is necessary to reproduce these results and to obtain measures of muscle function as well as outcomes data.

***Disclosures: Bjoern Buehring**, None.*

SA0470

See Friday Plenary number FR0470.

SA0471

Low Incidence of Clinical Fractures after Liver Transplantation: An Audit of 531 Consecutive Patients. Melissa Premaor[1], Tapas K Das[2], Irene Debiram[3], Graeme Alexander[3], Juliet Compston*[4]. [1]Addenbrooke's Hospital, United Kingdom, [2]Liver Unit, Addenbrookes Hospital, Cambridge & Peterborough & Stamford Hospitals NHS Foundation Trust, United Kingdom, [3]Department of Medicine - University of Cambridge, United Kingdom, [4]University of Cambridge School of Clinical Medicine, United Kingdom

In earlier studies high rates of fracture were reported in patients following liver transplantation. Subsequently, lower doses of glucocorticoids for immunosuppression and the use of bone protective therapy for patients at high risk of fracture have become standard practice. The aim of this study was to document clinical fracture incidence after liver transplantation during the period 1998-2008 in a single transplant centre, following the introduction of a protocol for bone protective therapy in patients at risk. An audit was performed in all patients with a first liver transplant between Jan 1998 and Jan 2008. Records were retrieved from 531 of 592 eligible patients (89.7%), 327 male and 204 female, mean age 51.7 yrs. The median(IQR) duration of prednisolone therapy was 3(3,5) months. Spine X-rays were obtained before transplant in 432 patients and after transplant when clinically indicated. All fractures were recorded and verified radiologically. Bone mineral density was assessed pre-transplant by DXA in 67.4% of patients. The mean follow-up period was 61.4 months (range 0-131). 5.6% of the patients had a history of fracture prior to transplant (76% spine, 8% wrist, 8% lower leg, 8% other). After transplantation, incident clinical fracture was recorded in 15 patients (3.5%) of which 46.7% were vertebral. The median time since transplant to fracture was 26 months (range 2-83). Patients with an incident clinical fracture were significantly older than those without (p=0.002) and significantly more likely to be female (p=0.007). Pre-transplant spine and hip BMD T-scores were lower in patients with fracture [-1.74(2.0) vs -1.16(1.6) and -1.08(1.2) vs -0.65(1.2); p=ns]. A previous fracture was not significantly more common in patients with than without previous fracture [13.3% vs 5.1%]. The median(IQR) duration of prednisolone post-transplant was 4(3,36) months in patients with incident fracture and 3(3,5) months in those without (p=0.016). 60% of patients with incident fracture and 28.3% of those without had received bone protective therapy post-transplantation. Our results demonstrate low rates of fracture in patients undergoing liver transplantation in our centre over the last ten years. Lower doses of prednisolone and administration of bone protective therapy in high risk patients are both likely to have contributed. In addition, the low rate of fractures prior to transplant indicates better bone health prior to transplant.

***Disclosures: Juliet Compston**, None.*

SA0472

See Friday Plenary number FR0472.

SA0473

Weekly Alendronate versus Zoledronic Acid For Prevention of Bone Loss During the First Year After Heart or Liver Transplantation. Adi Cohen*[1], Emily Stein[2], Halley Rogers[1], Donald J. McMahon[3], Shannon Kokolus[3], Polly Chen[3], Chiyuan Zhang[3], Ronald B. Staron[3], Susan Restaino[3], Donna M. Mancini[3], Robert S. Brown[3], Elizabeth Shane[2]. [1]Columbia University Medical Center, USA, [2]Columbia University College of Physicians & Surgeons, USA, [3]Columbia University, USA

The first year after heart (CTX) or liver transplantation (LTX) is characterized by high rates of bone loss and fractures. Bone mineral density (BMD) declines by 3-10% and vertebral fracture rates vary from 5-30%. Daily alendronate (ALN) reduces rates of bone loss in CTX recipients and quarterly infusions of zoledronic acid (ZA) reduce rates of bone loss in LTX recipients.

We conducted a 1-year, double-masked, active comparator, non-inferiority, randomized clinical trial (RCT) in which we compared rates of bone loss in CTX and LTX recipients assigned to receive ALN (70 mg/week) for the first year or a single infusion of ZA (5 mg). We hypothesized that ZA, administered within 1 month of transplantation (TX) would provide similar protection from bone loss as weekly ALN initiated at the same time. Subjects (n=84) were randomized to ALN or ZA, 25+8 (SD) days after TX. A nonrandomized reference (REF) group of TX recipients (n=25) with BMD T scores >-1.5 was enrolled to provide data on rates of bone loss in TX recipients not treated with bisphosphonates (BP). As vitamin D deficiency was very common (>70% of participants), all received ergocalciferol 50,000 IU daily for 5 days before the ZA/placebo infusion. All received immunosuppressive therapy (prednisone, calcineurin inhibitors) and daily calcium (945 mg) and vitamin D (1000 IU) during the study. The primary efficacy variable is percent change from baseline in total hip (TH) BMD at 1 year in the ALN and ZA groups. Secondary efficacy variables include percent change from baseline in lumbar spine (LS) and femoral neck (FN) BMD at 1 year, and serum bone resorption markers. Secondary analyses will compare rates of bone loss in the ALN and ZA groups to the REF group.

At baseline, REF and randomized subjects were similar with respect to age (48+15 vs 54+10 respectively, P=0.07); gender (% Male: 77 vs 80; P=NS), race (% Caucasian: 60 vs 68; P=NS); transplant type (% CTX: 63 vs 64; P=NS). Baseline BMD (g/cm^2) was significantly higher (all $p<0.001$) in the REF group at the TH (1.078+0.13 vs 0.923+0.14), LS (1.123+0.15 vs 0.964+0.14), and FN (0.924+0.11 vs 0.793+0.12). The study remains blinded at the writing of this abstract. The last patient will complete the study in July 2010. One-year results comparing rates of bone loss between the ALN and ZA groups, and between the ALN and ZA groups and the REF group will be available and presented at the time of the meeting.

***Disclosures: Adi Cohen**, None.*
This study received funding from: Novartis

SA0474

N-linked Glycosylation Sites Required for Normal Calcium-sensing Receptor Expression and/or Function. Sarah Brennan*[1], Karolina Windloch[1], Arthur Christopoulos[2], Arthur Conigrave[1]. [1]University of Sydney, Australia, [2]Monash University, Australia

The extracellular calcium-sensing receptor (CaR) is a class C G-protein coupled receptor (GPCR) that provides feedback control of calcium homeostasis by inhibiting parathyroid hormone secretion and renal calcium reabsorption. CaRs are activated not only by Ca_o^{2+}, but also by L-amino acids and type II calcimimetics, including cinacalcet (Sensipar).

The CaR has eight recognised *N*-linked glycosylation sites in the extracellular Venus Fly Trap (VFT) domain and loss of 3 or more of these sites has been reported to markedly impair receptor expression [1]. Further investigation of the roles of specific glycosylation sites has led to the identification of two mutants that exhibit notable aberration in calcium-sensing - an inactivating mutation, N468Q and an activating mutation, N130Q.

When transiently transfected in HEK-293 cells, N468Q exhibited a marked reduction in the complex glycosylated 160kDa form of the receptor but apparently normal levels of the immature high mannose 140kDa form, as determined by Western blotting, indicative of retention in the endoplasmic reticulum. In addition, cell surface expression of the mutant was significantly decreased (by ~70%) compared to wild type in an ELISA-based assay. The proteasome inhibitor, MG132, partially increased surface expression (to ~50%), implying that proteasomal-dependent degradation may be involved.

The N468Q mutant also showed a marked reduction in potency and maximal agonist effect in response to Ca_o^{2+}-mediated Ca_i^{2+}mobilization, with a complete loss of oscillatory behaviour. Neither L-Phe (10 mM) nor the type II calcimimetic NPS R-467 (1 μM) were able to rescue this loss of function to Ca_o^{2+}.

In contrast, the N130Q mutation increased the Ca_o^{2+} potency, with an EC_{50} for Ca_o^{2+} of 2.90 ± 0.2 mM (n = 6). In comparison, the apparent EC_{50} for Ca_o^{2+} in the wild type receptor was 4.0 ± 0.4 mM (n=9) despite similar levels of surface expression. N130 lies in a region, close to the dimer interface between VFT domains, that has been shown to be particularly susceptible to activating mutations (residues 116 - 131)

In conclusion, individual disruption of the N-linked glycosylation sites at 130 and 468 disturbs the normal Ca_o^{2+}-sensing properties of the CaR in HEK-293 cells.

1. Ray K., et al., J Biol Chem, 1998. 273: 34558-67

***Disclosures: Sarah Brennan**, None.*

SA0475

Glucocorticoids Suppress Bone Formation by Attenuating Osteoblast Differentiation via the Monomeric Glucocorticoid Receptor. Alexander Rauch*[1], Ulrike Baschant[1], Sebastian Seitz[2], Thorsten Schinke[3], Michael Amling[4], Ulf Lerner[5], Jean-Pierre David[6], Guenther Schuetz[7], Jan P. Tuckermann[1]. [1]FLI Jena, Germany, [2]Center for Biomechanics & Skeletal Biology, Germany, [3]University Hospital Hamburg, Eppendorf, Germany, [4]University Medical Center Hamburg-Eppendorf, Germany, [5]University of Umea, Sweden, [6]University Erlangen-Nuremberg, Germany, [7]DKFZ Heidelberg, Germany

It has been hypothesized that many side effects of glucocorticoid (GC) therapy, such as osteoporosis, depend on dimerization of the glucocorticoid receptor (GR). Using a novel Cre-transgenic mouse line, we now demonstrate that repression of bone formation by GCs is abrogated in the absence of GR expression in osteoblasts since they become refractory to hormone-induced apoptosis and inhibition of proliferation and differentiation. In contrast, mice carrying a dimerization-defective GR mutation (GRdim) display reduced bone formation upon GC treatment, resulting in bone loss in vivo and enhanced apoptosis and suppressed differentiation in vitro. GCs potently suppress osteoclast activity in vivo independent of GR dimerization or GR ablation in the osteoblasts. Therefore GCs act in a cell autonomous manner in the osteoblasts to decrease bone mass and bone formation. The inhibitory effects by GCs on osteoblasts were found to be due to a novel mechanism involving inhibition of cytokines such as interleukin-11 via the monomer GR recruitment to AP-1 responsive elements in the promoter. Moreover supplementation of GC-treated osteoblasts with interleukin-11 in vitro abrogates the suppression of differentiation. Taken together, attenuation of osteoblast differentiation by GR dimerization-independent suppression of osteoblast-derived cytokines contributes, at least in part, for bone loss during GC therapy.

***Disclosures: Alexander Rauch**, None.*

SA0476

25-Hydroxyvitamin D Reduces Secondary Hyperparathyroidism in Mice with Chronic Kidney Disease Independent of Circulating 1,25-Dihydroxyvitamin D *In Vivo*. Loan Nguyen-Yamamoto*[1], Isabel Bolivar[2], Miren Gratton[2], Raymonde Gagnon[2], Richard Kremer[1], Geoffrey Hendy[1], David Goltzman[3]. [1]McGill University, Royal Victoria Hospital, Canada, [2]McGill University, Canada, [3]McGill University Health Centre, Canada

Increases in serum 25-hydroxyvitamin D (25OHD), are associated with reductions in serum parathyroid hormone (PTH) due to the renal and/or local conversion of 25OHD to 1,25 dihydroxyvitamin D [1,25$(OH)_2$D]. However, *in vivo* evidence of extra-renal conversion of 25OHD to modulate PTH levels is lacking. We examined the influence of vitamin D metabolites on parathyroid and mineral homeostasis in an adenine-treated mouse model of chronic kidney disease (CKD) where renal production of 1,25$(OH)_2$D was severely diminished. We compared this to results in mice expressing the null mutation for the 25OHD-1αhydroxylase enzyme (1αOHase$^{-/-}$) which exhibit tissue-wide inability to synthesize 1,25$(OH)_2$D. Compared to normal controls, CKD mice had 2.3-fold increases in serum creatinine, 4-fold increases in blood urea nitrogen (BUN), normal serum calcium (Ca)(2.56 ± 0.09mM), elevated serum phosphorus (P)(3.78 ± 0.25mM), and markedly reduced serum 1,25$(OH)_2$D (80.40 ±12.51pM compared to normal levels of 248 ± 35.21 pM). In 1α OHase$^{-/-}$ mice on a normal diet, serum creatinine and BUN were normal, serum Ca (1.58 ± 0.12mM) and P (2.13 ± 0.07mM) were low and serum 1,25$(OH)_2$D was undetectable (<25pmol/L). Serum PTH levels were extremely elevated in 1αOHase$^{-/-}$ mice (22-fold), and in CKD mice (11-fold) . Administration of 1,25$(OH)_2$D3 (50 pg/g/thrice weekly) for 6 weeks, normalized serum Ca, P and PTH in 1αOHase$^{-/-}$mice, and increased serum Ca (2.93 ± 0.07) and normalized serum PTH in CKD mice. A very high dose of 25OHD_3 (75 ng/g/thrice weekly) also increased serum calcium (2.78 ± 0.09 mM) increased serum P (3.89 ± 0.36 mM) and normalized PTH in 1αOHase$^{-/-}$ mice. This dose of 25OHD_3 in CKD mice normalized serum P and PTH with no increase in circulating 1,25$(OH)_2$D. Administration of a lower dose(10ng/g/thrice weekly) of 25OHD_3, did not affect the abnormal serum Ca, P and PTH in 1αOHase$^{-/-}$mice, however in CKD mice, serum P was normalized and serum PTH was reduced by 50% with no increase in circulating 1,25$(OH)_2$D. The *in vivo* PTH-lowering efficacy of the very high administered dose (75ng/g) of 25OHD_3 in mice with tissue-wide absence of the 1αOHase enzyme reflects the capacity of 25OHD_3 to cross react with low affinity at the VDR. The *in vivo* PTH-lowering efficacy of the lower dose (10ng/g) of 25OHD_3 in CKD mice with severely impaired renal 1αOHase activity but with intact extra-renal 1αOHase activity indicates that local extra-renal conversion of 25OHD_3 is significant *in vivo*.

***Disclosures: Loan Nguyen-Yamamoto**, None.*

SA0477

Estrogen Ameliorates Synovial Inflammation and Joint Erosivity in mBSA Induced Monoarthritis. Cecilia Engdahl*, Anna Börjesson, Alexandra Karlström, Catharina Lindholm, Hans Carlsten, Marie Lagerquist. Center for Bone & Arthritis Research, Institution of Medicine, Sahlgrenska Academy at the University of Gothenburg, Sweden

Objective. Estrogen ameliorates the development and progression of collagen II induced polyarthritis, a systemic animal model for postmenopausal rheumatoid arthritis (RA). The aim of this study was to determine whether estrogen ameliorates mBSA induced monoarthritis in the same manner and to elucidate the mechanism behind these protective effects of estrogen.

Methods. Female C57/Bl6 mice were ovariectomized at 3 months of age and mBSA monoarthritis was induced. One knee was injected with mBSA and the control knee with saline. Mice were treated with estradiol (0,9µg/day) or placebo using subcutaneous pellets. At termination, knees were collected for histology, synovial cells were investigated using flow cytometry and serum was analyzed for mBSA specific antibodies.

Results. Treatment with estradiol decreased synovitis (-22%, $p<0.05$) and dramatically reduced the grade of bone erosion (-60%, $p<0.05$) in the mBSA-injected knee as compared to placebo treatment. In both estradiol and placebo treated mice, mBSA-injection resulted in an increase in the frequency of lymphocytes (+61% and 83%, respectively, $p<0.05$) as well as macrophages (+29% and +107%, respectively, $p<0.05$) in the synovium compared to saline-injection. Interestingly, a tendency to decrease in the frequency of macrophages was found in the synovium of mBSA-treated knees after estradiol treatment as compared to placebo treatment (-40%, $p=0.058$). The serum levels of mBSA specific antibodies were not affected by estradiol treatment.

Conclusion. In a model of monoarthritis, estrogen ameliorates the disease by significantly decreasing both the synovitis and the bone erosions. Induction of arthritis by injection of mBSA increases the frequency of inflammatory cells (lymphocytes and macrophages) in the synovium. Interestingly, estrogen reduces the induction of macrophages resulting in decreased frequency in macrophages after estradiol-treatment as compared to placebo treatment. This reduction might be part of the mechanism behind the protective effects of estrogen on synovitis and bone erosions. Increased knowledge about the mechanisms behind the beneficial effects of estrogen is useful in the search for novel treatment against inflammation triggered bone loss.

***Disclosures: Cecilia Engdahl**, None.*

SA0478

See Friday Plenary number FR0478.

SA0479

See Friday Plenary number FR0479.

SA0480

A Transgene Containing the Human Vitamin D Receptor Gene Locus Recapitulates Endogenous Tissue-specific Expression of the Receptor in the Mouse. Seong Min Lee*[1], Kathleen Bishop[1], Mark Meyer[1], Robert Nerenz[1], Charles O'Brien[2], J. Pike[1]. [1]University of Wisconsin-Madison, USA, [2]University of Arkansas for Medical Sciences, USA

The vitamin D receptor (VDR) is a primary determinant of target tissue response to 1,25-dihydroxyvitamin D_3 (1,25$(OH)_2D_3$). In recent studies, we have characterized key regions that regulate both basal and inducible expression of the mouse VDR gene by hormones such as 1,25$(OH)_2D_3$, PTH and retinoic acid. These studies led to the development of a mouse transgene capable of recapitulating endogenous VDR gene expression *in vivo*. While the human VDR gene is highly conserved, several important differences are evident. They include the presence of an additional promoter, synthesis of two gene products, and the presence of novel phosphorylation sites. A number of single nucleotide polymorphisms (SNPs) have also been identified within the locus that are associated with altered bone mineral density and/or increased cancer risk. To explore the human VDR gene, we searched for control regions across the gene locus using ChIP-chip and ChIP-seq analyses and employed antibodies capable of detecting epigenetic histone marks that correlated directly with active regulatory regions. These studies highlighted the two VDR promoters, one near the annotated TSS and the second over 30 kb upstream. They also revealed potential enhancers that were shared in the mouse gene. Additional studies demonstrated that specific regulatory regions bound VDR in bone cells, the estrogen receptor in MCF-7 cells, and c-FOS in activated T cells. To explore determinant of tissue-specific VDR gene expression, we created a BAC clone containing the extended human VDR locus, an HA tag inserted at the VDR translational start site and a luciferase reporter in the last exon, and prepared mouse strains containing germ-line copies of this transgene for subsequent tissue analysis. We contrasted luciferase expression as well as both endogenous and BAC clone-derived VDR expression using immunohistochemical staining procedures. Expression from the VDR BAC clone recapitulated endogenous sites of VDR

expression in all tissues examined, including segments of the intestinal tract and sections from the kidney, parathyroid glands, pancreatic islets, hair follicles and the epidermis. Liver and muscle expression of endogenous and recombinant VDR was not detected. These studies support the identification of key regulatory regions within the human VDR gene essential for factor-regulate and tissue-specific expression of the VDR gene both *in vitro* and *in vivo* and should permit humanization of the VDR-null mouse.

***Disclosures: Seong Min Lee**, None.*

SA0481

See Friday Plenary number FR0481.

SA0482

See Friday Plenary number FR0482.

SA0483

Phospholipase A2 Activating Protein (PLAA) is Required for 1α,25(OH)2D$_3$-Induced Rapid Membrane Response in Osteoblasts. Maryam Doroudi*, Zvi Schwartz, Barbara Boyan. Georgia Institute of Technology, USA

We have previously reported that phospholipase A2 activating protein (PLAA) is required for 1α,25-dihydroxyvitamin D3 (1,25D3) signaling in growth zone chondrocytes in a rat costochondral growth plate model. After 1,25D3 binds its membrane-associated receptor, Pdia3 (ERp60, ERp57, 1,25-MARRS), PLAA is activated. Cytosolic PLA2 is stimulated, resulting in production of arachidonic acid, which can activate PKC directly. We also shown that caveolae and caveolin-1 are required for rapid 1,25D3-dependent PKC signaling and Pdia3 is co-localized with Cav-1 in the plasma membrane and in lipid rafts. PLAA exhibits homology with the G-protein beta subunit, suggesting that it is also membrane-associated. However, it is not clear whether PLAA is present in caveolae and if it interacts with Cav-1 and Pdia3. MC3T3-E1, a pre-osteoblastic cell line, and MC3T3-E1 cells silenced for PLAA (shPLAA) were treated for 9 or 90 minutes with either vehicle (0.001% ethanol) or 10-8M 1,25D3. Whole cell lysates were collected for immunoprecipitation, caveolae isolation, and analyzed by Western blot. Subconfluent cultures of MC3T3-E1 cells were immunostained against PLAA, Cav-1 and Pdia3, and imaged with confocal microscopy. The effect of 1,25D3 on PLA2 activity was examined by measuring total PLA2 activity in cell lysates using a PLA2 assay kit. Although PLAA, Pdia3, and Cav-1 were detected in the plasma membrane by Western blot, just Pdia3 and Cav-1 were detected in caveolae. Whole cell lysates treated with either vehicle of 1,25D3 for 9 and 90 minutes were immunoprecipitated using PLAA antibody. Cav-1 was detected in all samples analyzed, but Pdia3 was present only after treatment with 1,25D3. Cav-1 was found when immunoprecipitated with anti-Pdia3 antibodies. These observations were confirmed by immunofluorescence staining for Pdia3, Cav-1 and PLAA. shPLAA cells failed to activate PLA2 with 1,25D3 treatment at 9 minutes. Taken together, our results show that PLAA is present in plasma membranes, but not in caveolae, in the absence of 1,25D3. PLAA and Pdia3 interact with Cav-1 in both the control and 1,25D3-treated groups. PLAA interacted with Pdia3 only in the presence of 1,25D3. shPLAA cells did not activate PLA2 with 1,25D3 treatment at 9 minutes. Thus, 1,25D3 initiates conformational changes in membrane proteins, recruiting PLAA to caveolae and initiating the Pdia3 signaling pathway.

***Disclosures: Maryam Doroudi**, None.*

SA0484

Role of Parathyroid Hormone and Vitamin D Insufficiency in Bone Resorption. Adarsh Sai*[1], Xiang Fang[2], J. Christopher Gallagher[1]. [1]Creighton University Medical Center, USA, [2]Creighton University, USA

Background: Vitamin D deficiency, defined as serum 25-hydroxyvitamin D (25OHD) < 12 ng/ml, is associated with osteomalacia and vitamin D insufficiency with 25OHD < 20ng/ml is associated with increased fractures. There is disagreement about the definition of Vitamin D insufficiency; according to the WHO definition it is a serum 25OHD < 20ng/ml, however others suggest that vitamin D insufficiency is less than 30ng/ml because serum parathyroid hormone (PTH) which is inversely associated with serum 25OHD reaches a plateau at a serum 25OHD between 20 - 40ng/ml in various studies. We examined the relationship between serum 25OHD, PTH and bone markers in elderly women.

Methods: 489 postmenopausal women with osteopenia and osteoporosis, mean (SD) age 71.5(3.6) yrs were enrolled in an interventional treatment study (STOP IT). These results are from the baseline data. Serum PTH was measured by an intact assay (Nichols), serum 25OHD by competitive protein binding assay (Haddad), 24h urine N-telopeptides (Ntx/cr) and serum osteocalcin by Elisa. Calcium absorption was measured with 100 mg calcium and 5 μCi Ca^{45}. The variables were analyzed using linear and piece-wise regression.

Results: Serum 25 OHD was inversely correlated with serum PTH (r = -0.32, p < 0.001)(Figure 1). There was a continuous decrease in mean (±SE) serum PTH from 57.9 (±5.1) pg/ml to 23.4 (±2.8) pg/ml as serum 25 OHD increased from < 10 ng/ml to > 60 ng/ml respectively (p<0.0001) and there was no sign of a plateau effect. There was a decrease in the bone markers, serum osteocalcin and urine NTx as serum 25OHD increased but the response plateaued at ~ 20 ng/ml (p= 0.0001, Figure 1).

Conclusion: The data suggests that Vitamin D insufficiency contributes to increased bone resorption at serum 25OHD < 20 ng/ml. The continuing decrease in serum PTH as serum 25 OHD increases >20 ng/ml is not associated with increased bone resorption. There is no evidence that vitamin D insufficiency should be defined as a serum 25OHD of <30ngml for bone. It may be that the continuing decrease in serum PTH at serum 25OHD levels between 20-60 ng/ml reflects the pharmacologic effect of vitamin D on the Vitamin D response element in the PTH gene.

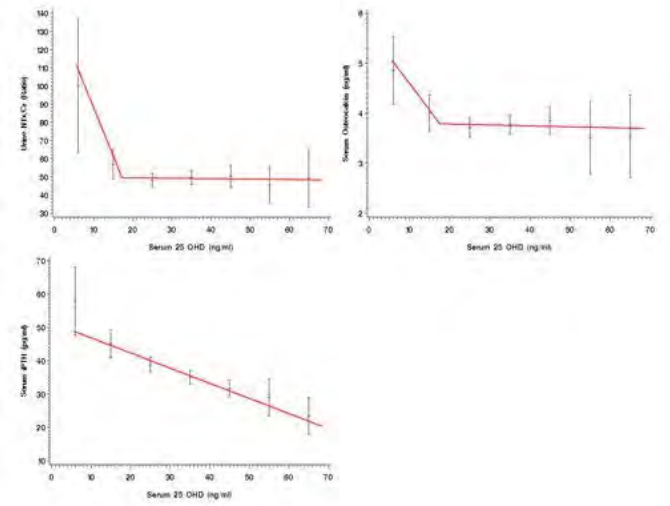

Figure 1

***Disclosures: Adarsh Sai**, NIH Grants AG28168, UO1-AG10373 and RO1-AG10358, 2*

SA0485

See Friday Plenary number FR0485.

SU0001

Adiponectin is Reciprocally Related to Bone Mass in Children with Chronic Diseases. Mohamad Maghnie[1], Giovanni Melioli[2], Natascia Di Iorgi*[1], Flavia Napoli[3], Giuliana Cangemi[2], Anna E.M. Allegri[1], Linda Ambrosini[1]. [1]Department of Pediatrics, IRCCS, Giannina Gaslini-University of Genoa, Italy, [2]Laboratory of Biochemical Analyses, IRCCS, Giannina Gaslini-University of Genoa, Italy, [3]IRCCS, Giannina Gaslini-University of Genoa, Italy

In vitro and animal models have demonstrated a multi-faceted relationship between serum values of adiponectin and bone, while in humans adiponectin has been negatively associated with bone mineral density (BMD) both in healthy subjects and diabetic adults. However, data in the pediatric population are scarce. Aim of the study is to evaluate the relation between bone, fat and adiponectin concentrations in a large cohort of pediatric patients referred to a single Pediatric Bone Centre. Dual X-ray absorbiometry (DXA-Lunar, GE) measures of total body (TB) without head and lumbar (L) BMD Z-scores and of TB fat mass were obtained in 291 subjects with chronic diseases at a mean age of 11.9 ± 4.2 yrs (136 F, 155 M). All subjects underwent anthropometric evaluation for height, body weight, Body Mass Index (BMI), pubertal Tanner staging (mean B3 for females and mean G2 for males) and serum adiponectin measurement. Females showed higher values of adiponectin (P=0.03) and of percentage of fat mass compared to males (P=0.002). Adiponectin was negatively and significantly related to age in both females and males (r= -.18 and -.17, P's 0.05, respectively); inverse relations emerged between adiponectin and all anthropometric measures, Tanner stage and bone parameters (r's between -.33 and -.50, all P's 0.0001). Anthropometric and fat mass measures were associated with TB and LBMD Z-scores in females and with LBMD Z-score in males. TBBMD Z-score was related to anthropometric values, but not with fat mass in males. In multivariate regression analyses, adiponectin predicted independently and reciprocally bone parameters (TB βcoeff -1.989 and -1.579, P's0.0001 and L βcoeff -1.979, P0.001 and -1.170, P=0.001 in females and males, respectively) after correction for age, BMI and Tanner stage. Adiponectin is reciprocally related to DXA bone measures in pediatric subjects with chronic diseases independently of adiposity, age and determinants of bone.

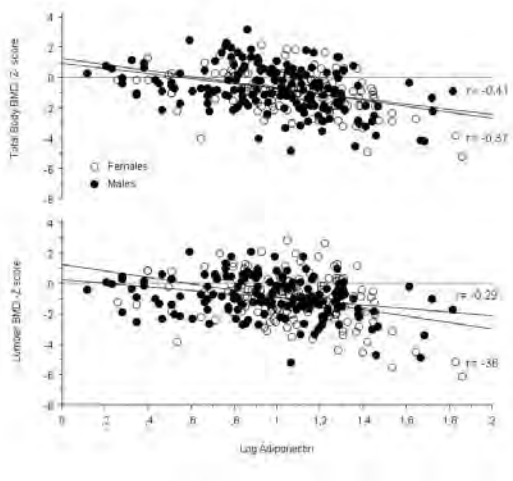

Table1

***Disclosures: Natascia Di Iorgi**, None.*

SU0002

Bone Strength And Geometry Are Compromised In A Mouse Model of Duchenne Muscular Dystrophy: Can Vibration Prevent or Reverse this Response. Susan Novotny*[1], David J. Nuckley, PhD[2], Moira Petit[3], Kristen A. Baltgalvis, PhD[4], Gordon L. Warren, PhD[5], Dawn A. Lowe, PhD[2]. [1]University of Minnesota, Department of Kinesiology, USA, [2]University of Minnesota, Program in Physical Therapy & Rehabilitation Science, USA, [3]University of Minnesota, USA, [4]University of Minnesota, Department of Biochemistry, Molecular Biology & Biophysics, USA, [5]Georgia State University, Division of Physical Therapy, USA

Muscle degeneration in Duchenne muscular dystrophy (DMD) reduces the frequency and magnitude of mechanical loads applied to bone. Consequently, boys with DMD have reduced bone mass and elevated fracture incidence, suggesting compromised bone strength; however this as well as bone geometry have been minimally assessed. Traditional exercise modalities to improve bone strength and geometry are not advisable because dystrophic muscle is prone to injury. Thus, low-magnitude, high-frequency vertical vibration is an attractive alternative to improve bone in this population while minimizing damage to muscle. The purpose of this research was two-fold. Study 1 aimed to confirm that tibial bone strength and geometry were compromised in the *mdx* mouse model of DMD, and Study 2 explored the efficacy of vibration in *mdx* mice to initiate bone formation. In Study 1, tibias from *mdx* and wildtype mice (n=8 and 7) were excised and 66 sequential μCT (Scanco Medical) images at the midshaft were assessed for total cross-sectional area (CSA, mm^2), cross-sectional moment of inertia (CSMI, mm^4) and volumetric bone density (vBMD, mg/cm^3). Bone strength was assessed by 3-point bending (Mecmesin) at the midshaft by assessing ultimate load (UL, N) and stiffness (N/mm). In the second study, *mdx* mice were vibrated for 7 days (15min/d at 45Hz) at accelerations of 0*g* (sham), 0.5*g* or 1*g* (n=6 each). Plasma osteocalcin (OC) levels were measured and RNA isolated from tibias were analyzed with an osteogenic gene array (SABiosciences). Independent *t*-tests were used in Study1 and one-way ANOVAs for Study 2; significance was set at $P<0.05$. Three-point bending results confirmed that *mdx* bones were compromised, as indicated by ~17% reductions in UL and stiffness. These decrements were attributed to *mdx* mice having smaller CSA and CSMI (14 and 25%, respectively), rather than altered vBMD (P=0.32). Vibration exposure in *mdx* mice elevated OC levels by 48% in the 1.0*g* group compared to sham. Upregulated gene expression was only apparent in mice vibrated at 0.5g and these genes were predominately associated with chondrogenesis (i.e. collagen X and XI, Integrin alpha2, and Sox9). These data establish that *mdx* mice are a suitable model to research methods aimed at improving skeletal health and decreasing fracture risk. Furthermore, these data suggest that vibration has potential to improve dystrophic bone; however, further studies are warranted to optimize vibration parameters to elicit the greatest benefit.Funding: Muscular Dystrophy Association Research Grant #114071

***Disclosures: Susan Novotny**, None.*

SU0003

Evaluation of Bone Strength and Response to Bisphosphonate Therapy in a Child with McCune - Albright Syndrome Using Peripheral Quantitive Computed Tomography (pQCT) of the Tibia. Erato Atsali*[1], Konstantinos Stathopoulos[2], Pelagia Katsimbri[3], Elephteria Metania[4], Anna Papadopoulou[5], Anastasios Papadimitriou[6], Polikseni Nikolaidou[6], Aristidis Zoubos[4], Grigoris Skarantavos[4]. [1]3rd Pediatric University Clinic "Attikon" University Hospital, Greece, [2]"Attikon" Athens University Hospital, Greece, [3]Bone Metabolic Unit, 1st Orthopedic University Clinic,"Attikon" University Hospital, Greece, [4]Bone Metabolic Unit,1st Orthopedic University Clinic,"Attikon" University Hospital, Greece, [5]3rd Pediatric University Clinic, "Attikon" University Hospital, Greece, [6]3rd Pediatric University Clinic,"Attikon" University Hospital, Greece

Purpose : The evaluation of bone strength and response to treatment in a girl with McCune -Albright syndrome using tibia pQCT.

Material and Methods : We present the case of a 14 years old girl referred to our department 3 years ago with cystic lesions consistent with fibrous dysplasia (right humerus, femur and tibia, bone skull), precocious puberty (7.5 years) and café au lait spots (lower abdomen). McCune-Albright syndrome was diagnosed using clinical and imaging (radiographs, MRI) findings and confirmed by genetic testing (heterozygous c.601C>T mutation in exon 8 of the GNAS1 gene). We commenced therapy with iv pamidronate followed by iv zolendronic acid and performed pQCT (Stratec XCT-2000 scanner, Stratec Medizintechnik, Pforzheim, Germany) of right and left tibia before and during treatment.

3 slices (1mm each) were obtained (4%, 14% and 38% of tibia length sites). The 38% site of the right tibia corresponds anatomically to the location of the cystic lesion. For each slice we assessed trabecular (Trab_Cont) and cortical mass (Cort_Cont) and trabecular (Trab_Den) and cortical density (Cort Den) and for 14% and 38% slices Stress Strength Indexes (SSI) . We compared pQCT variables between right and left tibia at baseline and through follow-up and estimated therapy-induced changes (%) prospectively.

Results: Cort Den of the right tibia at the 38% site was significantly decreased compared to the left at baseline (916.53 mg/cm^3 vs 1154.47 mg/cm^3, - 20,62%), and throughout treatment. SSI (38% site) was similarly reduced at baseline (941 vs 1110,35, -15,22%) and during treatment. All parameters (mass, density, strength) increased at the 38% site between 2006 and 2009 at both legs using bisphosphonates: Cort Cont left [2.85g/cm vs 3.18, + 10.37%], Cort Den left: [1154.47 vs 1247.57 mg/cm^3, +8.05%], SSI left: [1110.35 vs 1236.30, +11,35%], Cort Cont right [2.13 vs 2.27 g/cm,+6.6%], Cort Den right [916.53 vs 1022.16 mg/cm^3,+11.5%], SSI right [941.14 vs 1151.67,+22%]. Similar changes were observed in the other 2 pQCT slices of both legs.

Conclusions: 1) With 3 dimensional densitometry we can practically see the, characteristic for McCune-Albright syndrome, loss of cortical and trabecular bone and strength.

2) iv bisphosphonates improved bone mass and strength in this child. Tibia pQCT may be the easiest and safest non invasive way for monitoring disease progress.

***Disclosures: Erato Atsali**, None.*

SU0004

Growth Hormone Therapy in Former Premature Very Low Birth Weight Infants Promotes Catch-up Growth Pre-puberty. Susan Docherty Skippen, Dawei Wang, Stephanie Atkinson*, John Van dermeulen. McMaster University, Canada

Purpose: Former very low birth weight premature infants (PI) are known to have short stature and low bone mass for age even at 7 years or older (Wang et al, Pediatr Res 2007;61:11). This study was designed to test whether growth faltering and low bone mass in former PI would benefit from 1 y of therapy with recombinant human growth hormone (rhGH) by stimulating height, lean and bone mass growth. Methods: Pre-pubertal children (n=10, 9 males/1 female) with height < 10th %ile (treatment) or > 10th %ile (reference) were identified from subjects previously studied (Pediatr Res 2007:61;11). Consenting treatment subjects (age 10±2.1 y) entered a non-randomized trial of rhGH (HUMATROPE, Eli Lilly, CA) at 0.05 mg/kg/d for 1 y. Serial measures included anthropometry and bone mass (Hologic QDR4500 Discovery) as lumbar spine bone mineral density (LSBMD) and whole body bone mineral content (WBBMC), and fat and lean mass as well as blood assays for IGF-I, osteocalcin, C-terminal telopeptide of type 1 collagen (CTx) and glucose.

Results: During the year of GH therpy compared to the following year, growth velocity was accelerated for height (12.6±2.0 vs 4.6±1.8 cm/y, p<0.0001), WBBMC (90±15 vs 49±54, g/y, p<0.003) and LSBMD (0.05±0.0 vs 0.02±0.0 g/cm^2/y, p<0.05). Over the year of GH therapy, mean height %ile rose from 3.3 to 10.1 (Reference=42.2±7.1 %ile), lean mass index increased from 12.2±0.9 to 13.0±1.1 kg/height cm^2 (p<0.001) and % body fat declined (18.1±3.6 to 16.3±5.1 %, p<0.003). Baseline z-scores for LSBMD (-2.0 ± 0.9) or WBBMC (-1.10 ± 0.9) did not change. In response to GH, serum IGF-I rose (78.8±25.2 to 209.6±69.0 ng/ml, p<0.001) and CTx declined (17.3 ± 2.3 to 1.6±0.2 nmol/L, p<0.01). Plasma ostecalcin rose from baseline of 11.9±2.7 to 34.0±19.2 ng/ml over 1 yr GH but declined to baseline by 1 year off GH (p=0.293, NS). Mean blood glucose following GH was 5.2±0.6 mmol/L but was elevated above normal range in only one child.

Conclusions: GH for 1 y stimulates height, lean and bone mass growth in former very low birth weight PI without metabolic consequences but does not provide for complete catch-up to 50th %ile values for gender and age.

***Disclosures: Stephanie Atkinson**, None.*
This study received funding from: Eli Lilly

SU0005

Simple Equations To Correct For Height Using Dual Energy X-ray Absorptiometry (DXA) In Pre-Pubescent Children. Fan Zhang[1], Michael Whyte[2], Deborah Wenkert*[2]. [1]Shriners Hospt for Children, USA, [2]Shriners Hospital for Children, USA

Height-adjusted DXA bone mineral content (BMC) and density (BMD) Z-scores in children reveal relationships to fractures. Bone size correlates with BMC and impacts areal (g/cm^2) BMD. Practitioners use height growth curves together with DXA printouts to visually "adjust" pediatric BMD Z-scores. Recently, numerous formulas for Hologic DXA, at multiple bone sites, spanning ages 7-17 yrs, were published whereby Z-scores for BMC or BMD and for height generate height-adjusted BMC and BMD Z-scores[1]. However, adjusting for height first, to be entered for DXA should: i) simplify correction for bone size, ii) apply to any DXA instrument, and iii) evaluate young children. For DXA, we developed 2 simple equations to adjust for height in prepubescent (Tanner stage I) girls and boys.

We defined "height-age" as the age a child would be if height were average (50th percentile). The equations were derived from 1-mo interval, sex-specific, "smoothed", 2000 CDC growth data tables (www.cdc.gov/growthcharts/data/zscore/statage.xls). To avoid pubertal effects on growth and on BMC and BMD, data included only ages 2-12 yr (girls) and 2-13 yr (boys). We performed polynomial regression analysis using SAS 9.1 with 50th percentile height (cm) as the independent variable (X) and age as the dependent variable (Y). The resulting equations are seen in the figure.

Height-ages calculated at one-year intervals for the 10th and 90th percentile isopleths were consistent with visual inspection, R^2 = 0.9997 for girls, and 0.9973 for boys. DXA (Hologic QDR-4500A) of 61 prepubertal children with hypophosphatasia, which compromises stature and bone mineralization, validated the equations. Patient height-adjusted L_1-L_4 BMC and BMD Z-scores were calculated using our 2 equations and contrasted with the methods of Zemel B.S. et al.[1] using the same normal range[2]. The results correlated well (R^2=0.97 and 0.98 respectively) showing no difference (P=0.83 for BMC, and 0.68 for BMD, paired T-test).

Regression analysis showed the height-effect, prior to height adjustment, on Z-scores for BMC (R^2=0.29, P<0.0001) and BMD (R^2=0.07, P=0.0056), was removed (R^2=0.026, and 0.0, P= 0.133 and 0.97 respectively) using our equations.

Two simple equations for height-age improve DXA interpretation in healthy children and pediatric patients with bone disease.

1. Zemel B.S., et al., Clin. Endocrinol. Metab. 95:1265-73; 2010
2. Kalkwarf H.J., et al., J. Clin. Endocrinol. Metab. 92:2087-99; 2007

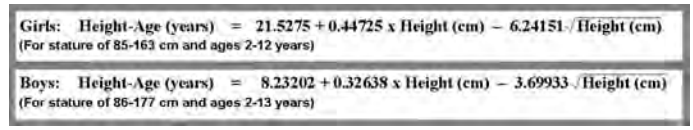

Simple Equations

***Disclosures: Deborah Wenkert**, None.*
This study received funding from: Enobia Pharma

SU0006

Structural Bone Deficits and Body Composition Abnormalities after Pediatric Bone Marrow Transplantation. Sogol Mostoufi-Moab*[1], Jill Ginsberg MD[2], Babette Zemel PhD[3], Justine Shults PhD[4], Nancy Bunin MD[5], Meena Thayu[1], Rita Herskovitz[3], Mary Leonard[6]. [1]The Children's Hospital of Philadelphia, USA, [2]Department of Pediatrics; Division of Oncology; The Children's Hospital of Philadelphia, USA, [3]Department of Pediatrics, The Children's Hospital of Philadelphia, USA, [4]Department of Biostatistics & Epidemiology, University of Pennsylvania School of Medicine, USA, [5]Department of Pediatrics; Division of Oncology, The Children's Hospital of Philadelphia, USA, [6]Children's Hospital of Philadelphia, USA

BACKGROUND & AIMS: Children requiring bone marrow transplant (BMT) for leukemia have multiple risk factors for impaired bone accrual. The long-term effects on volumetric bone mineral density (vBMD), bone structure, and body composition have not been established. The objective of this cross-sectional study was to assess musculoskeletal outcomes and body composition in children and young adult long-term survivors after BMT using peripheral quantitative computed tomography (pQCT) and whole body DXA, respectively. METHODS: Tibia pQCT was performed in 29 BMT subjects (ages 5-25 yrs) a median of 5 yrs (range 3-11) after BMT for leukemia. pQCT outcomes were converted to sex-, race-, and age or tibia length specific Z-scores based on reference data in over 650 controls. DXA whole body lean mass (LM) and fat mass (FM) results were converted to sex- and race-specific Z-scores relative to height, compared to 987 healthy controls. Multivariate linear regression models were used to compare BMT subjects to controls. RESULTS: BMT survivors had significant deficits in trabecular vBMD (-1.1± 1.1; p< 0.001), cortical stress strain index (SSI, a composite measure of geometry and vBMD) (-0.4±0.8; p=0.01), and section modulus (-0.3 ± 0.8; p=0.02) Z-scores, compared with controls. The lower SSI and section modulus were due to smaller endosteal and periosteal circumferences. Although BMI Z-scores did not differ between BMT survivors and controls, BMT survivors had significantly lower LM-ht (-0.5±1.4; p=0.002) and greater FM-ht (1.2 ±1.0; p< 0.01) Z-scores compared with controls. In addition, BMT survivors had significant growth impairment: height Z-scores averaged (-0.9±1.1) and 16% were <3rd %ile for height relative to age and sex. Only one participant was on glucocorticoids at the time of the study. CONCLUSIONS: Substantial deficits in trabecular vBMD, cortical bone geometry, and lean muscle mass were observed in BMT survivors of childhood leukemia. BMT survivors had significantly elevated fat mass despite normal BMI Z-scores. Future studies are needed to identify therapies to improve bone accrual and determine the clinical significance of these bone and body composition abnormalities in survivors of childhood leukemia after BMT.

***Disclosures: Sogol Mostoufi-Moab**, None.*

SU0007

Transient Hyperphosphatasaemia of Infancy and Early Childhood - Review and Evaluation of Published Data. Stepan Kutilek*. Pardubice Hospital; Faculty of Health Studies; University of Pardubice, Czech republic

Introduction: THI is characterized by transiently increased S-ALP, predominantly its bone and/or liver isoform, in children under 5 years of age. Following criteria apply: (1)age of below 5 years; (2)unrelated symptoms; (3)no bone or liver disease;(4)ALP analysis showing elevations in bone and liver activity; (5) return to normal S-ALP in four months. The cause is most likely impaired clearance of ALP from the circulation. In case of infrequently encountered and incidentally detected condition, large studies are impossible to perform. A systematic review of the published data is helpful. Methods: Data from 127 papers published in peer-reviewed journals/monographies were reviewed and analysed. Results: 930 patients with THI have been reported in the literature; gender in 721 with male:female ratio 405:316 (1.28:1.0). Age range 1-144 months, mean 18 ±14 mo; median 15 mo. Incidence was 0.3–2.8%. Duration 7-365 days; mean 80 ± 60 d. Seasonal clustering: most frequent in Autumn-Winter. Infectious origin probable; THI observed in siblings or patients hospitalised together in 30 cases.Most frequent primary diagnoses in 764 patients; included: diarrhea 29.1%, respiratory infections 19.1%, failure to thrive 8.8%. Frequently encountered viral infections: ECHO virus, Epstein-Barr virus, cytomegalovirus, rotavirus. adenovirus. S-Ca and S-P were always normal. Wrist X-ray was performed in: 204 cases (22.6%) and was always normal. 99Tc bone scan was performed in 20 cases (2.2%); always normal. The serum parathyroid hormone levels were assessed in 70 patients(7.7%), always with normal results. The bone turnover markers have been assessed in 176 patients (19%): U-hydroxyprolin (n=65), S-ICTP

(n=33), S-TRACP (n=15), S-osteocalcin (n=17), S-ICTP (n=33), lysylpyridinolin(n=7), hydroxylysylpyridinolin(n=6). Bone resorption markers (S-TRACP) and U-hydroxyprolin were only mildly elevated in 40% and 23% of evaluated subjects, respectively, while formation markers (S-ICTP and osteocalcin) were never elevated in the course of THI. Where elevation in bone turnover markers occurred, this was only mild-to-moderate, never related to the S-ALP magnitude. Conclusions: (1)THI occurrs in children with various diagnoses, most frequently in patients with gastrointestinal symptoms and infections. (2)There is not a common infectious agent. (3)THI occurs even in children above 5 years of age and can last above 4 mo. (5)Changes in bone turnover are not likely. (6)THI is a benign state.

***Disclosures: Stepan Kutilek**, None.*

SU0008

A Prospective Analysis Of Body Fat And Bone Mineral Accrual During Pubertal Growth. Katherine Harris*[1], Emma Laing[1], Daniel Hall[1], Norman Pollock[2], Clifton Baile[3], Richard Lewis[1]. [1]The University of Georgia, USA, [2]Medical College of Georgia, USA, [3]University of Georgia, USA

The effects of fat mass on bone mineral accrual from early childhood to adolescence are unclear. The purpose of this prospective investigation was to determine the effects of fat mass accumulation on changes in bone mineral content (BMC) in young females (N=191; aged 4 to 8 years at baseline), over a period of up to 11 years. Total body, lumbar spine, total proximal femur, and forearm BMC, as well as total body percent fat and fat mass, were determined by dual-energy X-ray absorptiometry. A mean annual increment (MAI), given as the slope of the regressions of each subject's repeated measurements over time, was calculated for each subject and for each measurement site. Pearson and partial correlations were calculated between the MAI for BMC at each bone site and the MAI for either percent body fat or fat mass. Partial correlations were corrected for the MAIs in total body lean mass and height. Both percent body fat and total body fat mass, respectively, were positively correlated to BMC at the total body ($R=0.42$, $p<0.0001$ and $R=0.69$, $p<0.0001$), lumbar spine ($R=0.23$, $p=0.003$ and $R=0.47$, $p<0.0001$), non-dominant total proximal femur ($R=0.38$, $p<0.0001$ and $R=0.60$, $p<0.0001$), and non-dominant forearm ($R=0.37$, $p<0.0001$ and $R=0.61$, $p<0.0001$). When corrected for height and total body lean mass, the relationships between lumbar spine BMC and total body percent fat ($p=0.99$) or fat mass ($p=0.552$) attenuated. Significant associations remained at the other bone sites even when height and total body lean mass were accounted for in the analyses. In summary, this longitudinal analysis of females ranging from early childhood through adolescence indicates a significant positive impact of adiposity on BMC accrual. It is unclear why adiposity is favorably impacting BMC accrual in this study, but examination of body fat distribution, structural and geometric bone parameters and assessment of hormonal factors, such as adipocytokines, warrant further consideration.

***Disclosures: Katherine Harris**, None.*

SU0009

Architectural Compromise is Greater in the Tibia than the Femur in the Involved Lower Extremity of Individuals with Hemiplegic Cerebral Palsy. Christopher Modlesky[1], Jacques Riad[2], Freeman Miller[3], Brianne Mulrooney*[1], Joshua Kirby[1]. [1]University of Delaware, USA, [2]Department of Orthopaedics Astrid Lindgrens Children's Hospital, Sweden, [3]AI duPont Hospital for Children, USA

The architecture and strength of the femur and tibia are severely underdeveloped in nonambulatory children with quadriplegic cerebral palsy (CP); however, bone status is poorly studied in individuals with less involved CP. The aim of this study was to assess the level of architectural compromise in the femur and tibia of ambulatory individuals with mild hemiplegic CP. Adolescents and young adults with mild hemiplegic CP (n = 36; 13 to 23 years) and a Gross Motor Function Classification of I or II participated in the study. Magnetic resonance images of the femur and tibia (0.5 cm thick and 1.0 cm apart) were collected in the involved and uninvolved lower extremities (Philips, 1.5 T). Images at the level of the middle-third of the femur and the middle-third of the tibia were identified and total, medullary and cortical bone volume and estimates of bone strength [polar moment of inertia (J; reflects resistance to torsion) and section modulus (Z; reflects resistance to bending)] were determined using custom software developed with Interactive Data Language (IDL; Research Systems, Inc, Boulder CO). The involved side compared to the uninvolved side had lower cortical volume, total volume, J and Z in the midfemur (8 ± 7, 4 ± 5, 22 ± 12, 9 ± 9 %, respectively, $p < 0.05$) and midtibia (11 ± 13, 8 ± 8, 25 ± 22, 15 ± 15 %, respectively, $p < 0.05$). A significant bone by side interaction for total volume, J and Z ($p < 0.05$), indicates a greater compromise in the architecture and strength of the tibia than the femur in the involved lower extremity. There was also a significant bone by side interaction for medullary volume with the involved side having higher medullary volume in the femur but lower medullary volume in the tibia. The findings suggest that the femoral and tibial shafts in the involved lower extremity of individuals with hemiplegic CP have an underdeveloped architecture and lower estimates of bone strength; however, the level of compromise is greater in the tibia. Future studies are needed to identify the primary factors that limit the development of the tibia and femur in individuals with hemiplegic CP.

***Disclosures: Brianne Mulrooney**, None.*

SU0010

Babies Have Bones Too: Development of Reference Values for Bone Mass and Density of the Lumbar Spine of Infants and Toddlers Considering Age, Size, Sex and Race. Heidi Kalkwarf*, Kimberly Yolton, Gemma Uetrecht, Arin Fletcher, James Heubi. Cincinnati Children's Hospital Medical Center, USA

Purpose: Assessment of bone mass and density of infants and toddlers has been problematic owing to movement during DXA scanning and poor detection of very low density bone during scan analysis. New software has been developed by Hologic, Inc. to analyze lumbar spine DXA scans of individuals < 36 mo of age. The advantage of measuring the spine is that infants can be restrained during scanning to prevent movement without interfering with the scan image. The objectives of this study were to describe age, sex, race and size effects on bone mass and density of the lumber spine in healthy infants and toddlers, and to determine the precision of measurements. Our goal is to develop reference data that will aid the clinical evaluation of bone health of infants and toddlers.

Methods: Lumbar spine DXA scans were acquired on 269 healthy infants (130 female, 139 male; 60 black, 209 non-black) ages 1 to 36 mo using the Hologic QDR densitometer. A second scan was obtained on 32 infants age < 24 mo and 31 infants age > 24 mo for precision determination. Scans were analyzed with the new infant spine software, and then visually inspected to assess the quality of the software-derived bone map. Data were analyzed by multiple regression.

Results: The software produced a good bone map of L1-L4 on all scans. BMC and BMD increased with age ($R^2 = 0.86$ and 0.74, $p < 0.001$). Predicted BMC at ages 6 mo and 36 mo were 3.38 g and 11.27 g, and BMD were 0.252 mg/cm^2 and 0.435 mg/cm^2, respectively. Similar increases in BMC and BMD occurred with increasing weight and length with R^2 ranging from 0.74 to 0.90 (all $p < 0.001$). When accounting for age, males had a 6% greater BMC than females ($p < 0.0001$), but there was no difference in BMD between males and females. No sex differences in BMC or BMD were evident when statistically adjusting for age, length and weight. There were no differences in BMC or BMD by race ($p > 0.20$). Precision (%CV) of BMC and BMD measurements was 4.2% and 2.5% for infants age < 24 mo, and 1.6% and 1.2% for infants > 24 mo, respectively.

Conclusions: Measurement of lumbar spine BMD of infants and toddlers can be obtained with good precision. Age specific reference values for lumbar spine BMC, but not BMD, need to be sex specific. There is no apparent need to develop race specific reference data for infants and toddlers.

***Disclosures: Heidi Kalkwarf**, None.*

SU0011

Bone Health in Children with Chronic Kidney Disease: A 5-Year Follow-Up Study. Diana Swolin-Eide*[1], Sverker Hansson[2], Per Magnusson[3]. [1]Queen Silvia Children's Hospital, Sweden, [2]The Gothenburg Unit For Child & Adolescent Psychiatry, Sweden, [3]Linkoping University Hospital, Sweden

Children with chronic kidney disease (CKD) are at risk of developing skeletal problems with long-term consequences such as growth retardation and low peak bone mass and longitudinal studies have been warranted. This prospective study was designed to investigate the development of bone mass and biochemical markers of bone turnover in children with CKD over a 5-year period. Areal bone mineral density (BMD) was measured by DXA (Lunar Progidy) and DXL (Demetech AB). Fifteen Swedish children and adolescents, 5 boys and 10 girls, 4.2–15.0 years, were included with a median glomerular filtration rate (GFR) of 48 (range 8–94) mL/min/1.73 m^2. The mean follow-up time was 5.2 years.

The median height SDS was –0.65 at start and 0.1 after 5 years, with a range from –1.7 to 1.7, which implies that growth was acceptable. Body mass index SDS did not change significantly during the study period. Median GFR decreased from 48 to 42 mL/min/1.73 m^2 during the study period. Both total body BMD and lumbar spine BMD increased during the study period, ($p<0.0001$). None had total body BMD Z-scores and lumbar spine Z-score below –2.0 at follow-up. Total femoral neck BMD increased significantly ($p=0.001$) over the study period. Calcaneal BMD, which reflects mostly trabecular bone, increased ($p= 0.0015$) during the study period, but the bone mineral apparent density did not change. Two fractures occurred during the course of the study. Most patients had normal total ALP, PINP and TRACP5b levels. Eleven out of the 15 CKD patients had increased PTH levels at baseline and 10 patients after 5 years.

In conclusion, this is one of the few prospective 5-year studies of bone health in children with CKD. Growth was satisfactory but a delayed bone age was observed. A normal BMD does not exclude mineral bone disorder in patients with CKD, yet the BMD Z-scores were well preserved and most markers of bone turnover were within the reference intervals.

***Disclosures: Diana Swolin-Eide**, None.*

SU0012

Can Total Body DXA Scans Be Used To Estimate Cortical Bone Strength? Adrian Sayers*[1], J.H. Tobias[2]. [1]University of Bristol, United Kingdom, [2]Avon Orthopaedic Centre, United Kingdom

Introduction

Although total body DXA scans are used to assess skeletal integrity in children clinically, how these results relate to bone strength and fracture risk is currently unclear. Conversely, peripheral quantitative computerised tomography (pQCT) directly assesses cortical size, thickness and density, which may have a closer relationship with bone strength compared to DXA measures, yet this technique is only available as a research tool. To clarify the relationship between total body DXA scan results in children and cortical bone strength, we examined associations between bone mineral density (BMD $g.cm^{-2}$), bone mineral content (BMC g) and bone area (BA cm^2) as measured by total body DXA, and periosteal circumference (PC mm), cortical thickness (CT mm), and volumetric cortical bone mineral density (CBMD $mg.cm^{-3}$) as measured by pQCT.

Methods

Using 4006 adolescents (boys= 1851), with a mean age of 15.5 years from the Avon Longitudinal Study of Parents and Children (ALSPAC), we compared total body DXA scans and matched pQCT scans of the mid (50%) right tibial shaft. Using linear regression we estimated the predictive ability (r^2) of DXA bone phenotypes (BMD, BA, and BMC) and pQCT bone phenotypes (PC, CT and CBMD). We also compared the predictive ability of more complex models using multiple variables acquired from the DXA scanning procedure.

Results

Single TBLH DXA based measures were strongly positively predictive of PC and CT. DXA BMC was the strongest predictor of PC, and DXA BMD the strongest predictor of CT, explaining 51.4% and 56.1% of the variation respectively. Conversely, single DXA measures were only very weakly predictive of CBMD (eg DXA BA explained 0.5% of the variation in CBMD). Using multi variable models the predictive ability of DXA measures in relation to pQCT improved: DXA BMC, BA and sex together explained 63.4% of the variability in PC; DXA BMC, BMD and sex explained 58.2% of the variation in CT; DXA BMD, BA and sex explained 50.5% of the variation in CBMD. Adding fat mass, lean mass, and height improved the predictive ability of these models by less than 1.5%.

Conclusion

Parameters obtained from total body DXA scans can be used to explain a substantial portion of the variation in measures of cortical bone geometry such as PC and CT. These findings imply that total body DXA scans can be used to estimate bone strength variables such as section modulus, which are derived from measures of cortical bone perimeter and thickness.

***Disclosures: Adrian Sayers**, None.*

SU0013

Hypocalcemia Induced Seizures in Pregnancy Complicated by New Hypoparathyroidism. Loren Greene[1], Ayse Mohyuddin*[2]. [1]New York University School of Medicine, USA, [2]NYU School of Medicine, USA

Lowered calcium levels are often found in pregnancy due to hypoalbuminemia and pregnancy, as well as changing levels of hormones, such as calcitonin responsible for regulation of calcium homeostasis. True hypocalcemia due to de novo primary hypoparathyroidism during pregnancy is a rare condition.

We report the case of a 37 year old woman with a history of hypothyroidism who had mild hypocalcemia, but normal corrected calcium levels adjusted for albumin, during her first pregnancy. She soon became pregnant again. Fifteen weeks into her second pregnancy, she complained of fatigue and was found to have with hypocalcemia with inappropriately low levels of PTH. She was treated with calcium supplements, vitamin D and calcitriol 0.5mg daily, further increased to 0.5 bid at 25 weeks. At 28 weeks into her pregnancy, she fell. At 29 weeks, she had a seizure documented by EEG and she and had a serum calcium level of 7.7mg/dL. Her seizure was presumed to be due to hypocalcemia., and she was restarted on D4 2000 IU/day and calcitriol 0.5 bid. She had a premature delivery at 37 weeks, complicated by toxemia, and her child had a pneumothorax at delivery.

Pregnancy is responsible for a multitude of changes in the female body. An increase in circulating blood volume causes a decrease in albumin and a fall in total calcium. Under normal conditions, ionized calcium remains relatively constant throughout pregnancy. Parathyroid hormone falls to a low-normal range during pregnancy Other hormones that affect serum calcium level are also altered in pregnancy. Serum calcitonin levels are increased during pregnancy and may derive from maternal thyroid, breast and placenta, and has been proposed to protect the maternal skeleton against excessive resorption during times of increased calcium demand. Parathyroid hormone-related protein is secreted from the placenta and breast, so its level increases in pregnancy and lactation, but its role in calcium homeostasis in pregnancy is not well understood

Even when it is a known pre-existing condition, hypoparathyroidism can exhibit variable effects that can present management challenges during pregnancy. Case reports show that some hypoparathyroid pregnant women may require higher doses of calcitriol to avoid severe hypocalcemia. Paradoxically, other women with prior hypoparathyroidism have fewer hypocalcemic symptoms during pregnancy, perhaps because 1,25-dihydroxy-vitamin D production and calcium absorption may increase, regardless of PTH levels.

Lab Work

Date	Ca	Albumin	Corr. Ca	iCa	25-VitD	1,25-VitD	PTH	PTH-ip	Mg	PO4
	8.6-10.2	3.6-5.1	8.6-10.2	4.8-5.6	20-100	19-67	10-65	14-27	1.5-2.5	2.5-4.5
5/25/2005	9.4									
11/2/2005	9.5	4.8								
2/17/2006	9.7	4.9								
9/29/2006	8.8	4								
2/5/2007	9.2									
10/10/2007	8.1	3	8.58							
11/6/2007	8.9	3.6	8.9		43	91	17		1.8	3.5
11/24/2007	8.4				62	106	14.8		1.85	2.9
11/17/2007	8.3					91	17			
1/3/2008	8.5	2.8	9.14						1.7	3.5
1/19/2008	8.5	2.9	9.06	4.7	57	54	9.16		1.6	3.8
11/23/2008	9.8	4.7	9.8	5.1	37	32	10.3		2.2	3.4
2/3/2009	8.5			5	20		9		1.9	
2/22/2009	8.5	3.7	8.5	5	33	63	13.1		1.8	3.9
4/29/2009	8.6				39		<3		1.8	
5/12/2009	8.5				49		3.7			
5/28/2009	8.8	2.7	9.52	5.3	38	130	7.94	15		3.1
5/29/2009	8.5	3.1	8.74	5.3		78	3.7			
6/24/2009	8.2	3.2	8.52	5.2	60	146	3.3		1.8	
7/8/2009	7.7	3	8.18	4.4					1.8	

Lab data

***Disclosures: Ayse Mohyuddin**, None.*

SU0014

Induced Bone Formation by a Novel Calcium Phosphate-calcium Sulfate Composite in a Rat Model. Xu Yang*, Liza Osagie, Antonia Hille, Mathias Bostrom. Hospital for Special Surgery, USA

Infection is a complex orthopedic problem, where debridement and localized antibiotic delivery is the standard treatment. Calcium phosphate is a bone substitute commonly used as an antibiotic vehicle, yet investigated elution rates are variable. Calcium sulfate is a well tolerated and non-immunogenic antibiotic carrier; studies suggest more favorable elution characteristics. This study investigated treatment and preventative efficacy of a vancomycin impregnated calcium phosphate-calcium sulfate composite (CaP/CaS), (CERAMENT^{TM}, BONESUPPORT AB), in comparison to polymethyl methacrylate (PMMA).

32 male rats (treatment arm) received a drill hole on the medial side of right proximal tibia. 10 µl of 1.5 x 108 CFU/ml of Staphylococcus Aureus was inoculated into the medullary canal to induce osteomyelitis. After 3 weeks, osteomyelitis was confirmed in all rats with faxitron imaging. Defects were debrided and irrigated and rats randomly allocated into two groups. Group I received a plug of CaP/CaS and group II a plug of PMMA. Another 32 rats (prevention arm) underwent the same inoculation procedure and divided into two groups. Plugs of CaP/CaS (Group III) and PMMA (Group IV) were introduced immediately after inoculation. All cement plugs were 3mm x 3mm (D x H), impregnated with 10% (weight/weight) vancomycin and press-fit into the hole. Six weeks after cement insertion, animals were euthanized; right tibiae were harvested at 5 mm distal to cement. Outcome measures included bacterial colony count, histological analysis and micro-computed tomography. Two-way ANOVA was used for statistical analysis.

No signs of infection were found in any animals to date. No bacterial colony was found on culture plates. Treatment and prevention groups using CaP/CaS showed partial resorption of the plug, and increased formation of new bone (figure 1). In both PMMA treated groups, the volume of the PMMA did not change and minimal new bone formed around the cement plug (figure 2). Histological analysis is in process.

A cement that is an efficacious antibiotic vehicle, and biologically favorable-is essential for the treatment of periprosthetic infections. PMMA is currently the mainstay of localized antibiotic delivery, yet our results suggest that the CaP/CaS composite has comparable treatment efficacy, and in addition demonstrates superior resoptive properties over 6 weeks (figure 3); thus, outlining a favorable material with a number of orthopedic implications.

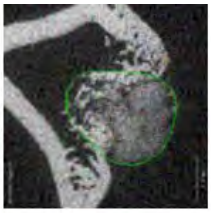

Figure 1. CaP/CaS was partially resorbed and replaced by new bone.

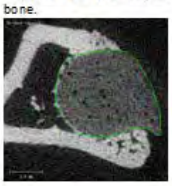

Figure 2. PMMA plug with minimal bone formation.

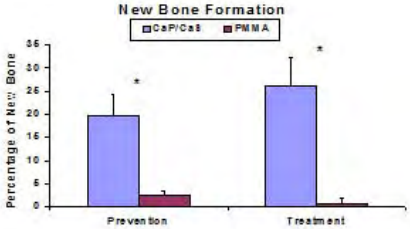

Figure 3. In both Treatment and Prevention arms, more than 20% of the CaP/CaS was replaced by new bone while minimal new bone formed around PMMA.

ASBMR FIGURES1,2,3

***Disclosures: Xu Yang**, None.*

This study received funding from: Bone Support

SU0015

Recreational Gymnastics: Strengthening the Musculoskeletal System in Young Girls. Lauren Burt*[1], Geraldine Naughton[1], David Greene[1], Gaele Ducher[2]. [1]Centre of Physical Activity Across the Lifespan, School of Exercise Science, Australian Catholic University, Australia, [2]Noll Laboratory, Department of Kinesiology, Penn State University, USA

Purpose: Recreational gymnastics may enhance the upper body musculoskeletal structure and function of young girls without engaging in elite-level, injury-prone sport. The purpose of this study was to quantify the musculoskeletal benefits in non-elite pre-pubertal artistic gymnasts in comparison with age and gender matched non-gymnasts.

Methods: Eighty-two girls (8.6 years, range 6-11) were divided into three groups based on their participation in gymnastics: high training volume (HGYM), 6 to 16 hr.wk^{-1}, low training volume (LGYM), 1 to 5 hr.wk^{-1} and non-gymnasts (NONGYM). Peripheral QCT was used to assess bone strength and strength/weight index (risk of fracture from a fall) at the 4 and 66% non-dominant radius. In addition, radial measures of bone area and density as well as muscle cross sectional area (CSA) were analyzed. Muscle function was estimated with grip strength, seated medicine ball throw, a weighted arm sequence and a static body weight support.

Results: Greater radial bone strength was found in HGYM compared with NONGYM after adjustment for height (Z-scores: bone strength index (BSI) 4% site, +0.84 SD; strength strain index (SSI) 66% site, +0.59 SD, $p<0.05$). Gains in bone strength were only significant for training volumes greater than 5 hrs.wk^{-1}. The strength/weight index was greater in HGYM than NONGYM at both measured sites (Z-scores: 4% site, +1.00 SD; 66% site, +1.07 SD, $p<0.01$). Skeletal benefits were also found in LGYM who displayed larger total (radius and ulna) bone area (ToBA) at the 66% site (Z-score +0.39 SD, $p<0.05$) than NONGYM, although they had lower cortical density (CoD) (Z-score -0.71 SD, $p<0.05$). Muscle CSA was larger in HGYM than NONGYM (Z-score +0.82 SD, $p<0.01$). Both HGYM and LGYM performed better than NONGYM in all muscle function tasks, except grip strength (Z-scores: LGYM, +0.48 to +0.63 SD; HGYM, +0.93 to +1.30 SD, all $p<0.05$). No differences were observed in muscle function between HGYM and LGYM.

Conclusions: Recreational gymnastics was associated with musculoskeletal benefits in young girls. Given observations of greater between-group differences in Z-scores for muscle than bone, it is possible that muscle adaptations may precede bone. Longitudinal data are needed to confirm that the sequence of adaptation occurs first through muscle function, then muscle size, and finally through to bone.

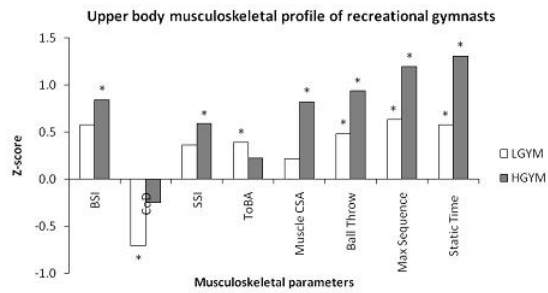

Musculoskeletal profile of recreational gymnasts

***Disclosures: Lauren Burt**, None.*

SU0016

The Use of Intranasal Calcitonin in Improving Bone Mineral Density in Young Patients with Inflammatory Bowel Disease. Helen Pappa*[1], Catherine Gordon[2], Tracee Saslowsky[3], Rajna Filip-Dhima[4], Diane Difabio[5], Richard Grand[3]. [1]Children's Hospital Boston, USA, [2]Children's Hospital Boston & Harvard Medical School, USA, [3]Department of GI & Nutrition, Children's Hospital Boston, USA, [4]Clinical Research Program, Children's Hospital, USA, [5]Clinical & Translational Study Unit, Children's Hospital, USA

Background & Aims

Bone health is compromised in children with inflammatory bowel disease (IBD), and there are sparse data regarding factors that affect bone accrual and therapeutic options for these patients. Our study aim was to investigate the efficacy and safety of intranasal calcitonin in improving bone mineral density (BMD) in pediatric patients with IBD and to examine clinical variables that affect bone mineral accrual.

Methods

A double-blind, randomized, placebo-controlled clinical trial was conducted in the Children's Hospital Boston Clinical and Translational Study Unit. After screening 222 outpatients, ages 8 to 21 years, with IBD using dual energy X-Ray absorptiometry (DXA), 63 participants with a lumbar spine BMD Z-score $\leq$ -1.0 SD were randomized to receive 400 IU intranasal calcitonin (n=31) or placebo (n=32) daily, and age-appropriate calcium and vitamin D supplements for 18 months. Follow up measurements were obtained at 18 months. Laboratory values, anthropometrics and disease and patient-related data were collected every 3 months.

Results

Intranasal calcitonin was well-tolerated. The change in BMD Z-score at the whole body was: a) placebo: 0.0 ($\pm$.51), b) calcitonin: -0.21 ($\pm$.59), p = 0.3; at the spine: a) placebo = 0.18 ($\pm$.5), b) calcitonin = 0.19 ($\pm$.53), p = 0.9. In multivariable regression models adjusted for age, gender, race, pubertal stage, height (Ht) and bone mineral content (BMC) at screening, percent change in whole body BMC was related to: change in height (ΔHt) (β = 1.65 (0.82, 2.48), p = 0.00), lean body mass by DXA (β = 0.89 (0.11, 1.67), p = 0.03), lifetime glucocorticoids (β = -0.46 (-0.88, -0.04), p = 0.04), weight bearing activity (β = 1.06 (0.43, 1.69), p = 0.0), caloric intake (β = 0.38 (0.02, 0.74), p = 0.04) and C-reactive protein (CRP) (β = -4.32 (-6.48, -2.16), p = 0.00) during the study. Percent change in spinal BMC was related to: ΔHt (β = 2.53 (1.36, 3.71), p = 0.0), vitamin D intake (β = 1.78 (0.58, 3.04), p = 0.01), lifetime glucocorticoid use (β = -0.73 (-1.40, -0.07), p = 0.03), pubertal stage (β = 10.43 (-0.39, -20.47), p = 0.04) and CRP (β = -4.23 (-7.62, -0.84), p = 0.02) after the same adjustments.

Conclusions

In this randomized controlled trial, intranasal calcitonin did not improve BMD in children and adolescents with IBD. Linear and lean mass improvement, caloric intake, weight-bearing activity and vitamin D intake, appear to benefit, whereas glucocorticoid exposure and increased inflammation appear to hinder bone mineral accrual.

***Disclosures: Helen Pappa**, None.*

SU0017

The Role of Muscle Properties in Predicting pQCT Estimated Bone Strength at the Radius in Midlife. Amanda Lorbergs*, Jon Farthing, Adam Baxter-Jones, Saija Kontulainen. University of Saskatchewan, Canada

Muscular activity is suggested to modify properties of bone, including architecture and strength (Frost 1987). In midlife the incidence of wrist fracture increases in both men and women (Larsen & Lauritsen 1993). Our purpose was to examine the relationship between forearm muscle area (MCSA), muscle force, or rate of torque development (RTD) with two radius bone strength indices; compressive bone strength index (BSI) at the wrist and strength strain index in torsion (SSIp) at the shaft, in healthy middle-aged adults.

Distal (4%) and shaft (65%) sites of non-dominant forearms were scanned using pQCT (Stratec XCT2000) in a sample of 40 adults (49.5 $\pm$ 2.3 yrs) to obtain estimated

bone strength indices and MCSA. Muscle force was measured by grip dynamometry (Jamar) and RTD was obtained using isokinetic dynamometry (Norm). We used linear regressions adjusted for sex and weight to assess the muscle-bone association.

Muscle properties, sex and weight explained 63% to 71% of variance in BSI at the 4% site ($p<0.05$) and 73% to 78% of variance in SSIp ($p<0.05$) at the 65% site. MCSA explained 10% of BSI ($p<0.05$) and 3% of SSIp ($p<0.05$) total variance. Grip force was a significant predictor of SSIp ($p<0.05$), but not for BSI ($p>0.05$). RTD explained a significant amount of variance in BSI ($p<0.05$), but not in SSIp. Body weight emerged as a significant predictor ($p<0.05$) in models that did not account for MCSA.

Our results indicate that muscle properties might stimulate distal and shaft sites of the radius differently. Muscle size appears to be a better predictor of radius bone strength than muscle function. Whether training these muscle properties would improve radius bone strength warrants further research.

***Disclosures: Amanda Lorbergs**, None.*

SU0018

A Survey on Vitamin D Deficiency in Children in Japan. Kohji Miura*, Noriyuki Namba, Keiichi Ozono. Osaka University Graduate School of Medicine, Japan

Reemergency of vitamin D deficiency has been recognized as threat to the world-wide public health. Insufficient vitamin D intake and avoid of sunshine exposure are two main causes. To investigate the present condition of vitamin D deficiency in children, we carried out the study based on questionnaire about patients with vitamin D deficiency in Japan. The questionnaire was sent to pediatricians in 535 major hospitals which have resident training program for pediatric practice approved by the Japanese Society of Pediatrics. We obtained response from 257 hospitals (48%) and found 531 cases of vitamin D deficiency in 86 hospitals during 5 years (2003-2007). The hospitals were located in almost all prefectures and did not show geographic preference. 276 cases had rickets and 37 cases showed convulsion or tetany. Convulsion or tetany was often observed in infancy and school-age children. Malnutrition, restriction of food intake due to food allergy and limitation of sun exposure were suspected to main cause. Mothers milk without supplementation of vitamin D was a risk factor. Clinical data were provided in 41 patients. 32% patients showed short stature (height less than -2 S.D.). Most patients showed hypocalcemia, elevated ALP and intact PTH. However, serum phosphate levels were various, ranging from 1.6 to 8.3 mg/dl. Serum intact FGF23 levels were checked in some patients with vitamin D deficiency and were constantly low (6.4 +/- 5.1 pg/ml). Serum 25-hydroxyvitamin D levels were lower than 20 ng/ml (50 nmol/l) in all patients and less than 10 ng/ml was found in more than half of them. The levels of 1,25-dihydroxyvitamin D were significantly correlated to 25-hydroxyvitamin D levels in this survey. Currently in Japan, alfacalcidol was most common medicine to treat vitamin D deficiency and its average dose was 0.1 microgr/kg/day since ergocalciferol and cholecalciferol are not available as prescribed medicine. The median duration of alfacalcidol administration was nealy one year. Calcium supplementation was associated in 40% patients. The survey reveals the relatively high prevalence of vitamin D deficiency in pediatric practice in Japan. FGF23 levels may be helpful to make differential diagnosis in patients with rickets. Note: this study was done as members of Japanese study group for vitamin D deficiency in children.

***Disclosures: Kohji Miura**, None.*

SU0019

Clinical Regulators of FGF23 in X-linked Hypophosphatemic Rickets: A Cohort Level Analysis. Mary Ruppe*. University of Texas Health Science Center at Houston, USA

X-linked hypophosphatemic rickets (XLH) is the most common disorder of renal phosphate wasting affecting 1 in 20,000 children. Resulting in short stature, bone pain, lower extremity deformities and dental abscesses, XLH is characterized by abnormal regulation of phosphate homeostasis and vitamin D metabolism. It is a disease of great clinical diversity with some patients having severe bone disease and extreme short stature while others are only mildly affected. Fibroblast Growth Factor 23 (FGF23) has been implicated as a leading contributor to the renal phosphate wasting but its regulation in XLH is poorly understood. The objective of the study was to create a prediction model of FGF23 levels in an XLH cohort. Subjects with XLH were recruited. At outpatient visits, a history was taken, a clinical examination was performed and laboratory evaluation was obtained. Data on mutational status, inheritance pattern, kindred membership, sex, growth velocity, medication doses along with measurements of serum calcium, creatinine, phosphorus, alkaline phosphatase, intact parathyroid hormone level and urinary calcium, creatinine and phosphorus were obtained. FGF23 levels were measures using an intact assay (Kainos). A mixed effects model was developed to explore the relationship between FGF23 level and familial, clinical, treatment and laboratory parameters. The model utilized clustering at the level of the subject and the kindred. To date, thirty-one subjects from 22 kindreds have been included. At the time of initial recruitment, there were 9 males and 22 females ranging in age from 18 months to 17 years and 6 months. During the study period, each subject visited the clinic between two and eight times. Utilizing the developed statistical model, the model revealed a significant relationship between serum phosphorus ($p= < 0.001$) and inheritance status ($p= 0.02$) and FGF23 levels. There was a predicted increase in FGF23 of 262 pg/mL (95% CI 151-373 pg/mL) for every unit increase in serum phosphorus. For individuals with sporadic as opposed to familial inheritance, there was a predicted increase in FGF23 of 384 pg/mL (95% CI 33-735 pg/mL). There appeared to be no relationship between either phosphorus dose in mg/kg/day ($p = 0.41$) or calcitriol dose in ng/kg/day ($p= 0.37$). This data underlines the complex factors that contribute to the regulation of FGF23 in a clinical setting and highlights our need to better understand the complex pathophysiology of XLH.

***Disclosures: Mary Ruppe**, None.*

SU0020

GBA1 Deficient Mice Recapitulates Gaucher's Disease Displaying System-wide Cellular and Molecular Dysregulation Beyond the Macrophage. Pramod Mistry*[1], Jun Liu[1], Mei Yang[1], Timothy Nottoli[1], James McGrath[1], Dhanpat Jain[1], Kate Zhang[2], Joan Keutzer[2], Wei-Lein Chuang[2], Wajaha Mehal[1], Aiping Lin[1], Shrikant Mane[1], Yuanzhen Peng[3], Jianhua Li[3], Ling-Ling Zhu[3], Harry Blair[4], Lisa Robinson[4], Jammel Iqbal[3], Li Sun[5], Mone Zaidi[6]. [1]Departments of Pediatrics, Medicine, Comparative Medicine, Genetics, & Pathology, Yale School of Public Health, Keck Center for Genomics, Yale School of Medicine, USA, [2]Genzyme Corporation, USA, [3]The Mount Sinai Bone Program, Mount Sinai School of Medicine, USA, [4]University of Pittsburgh, USA, [5]Mount Sinai School of Medicine, USA, [6]Mount Sinai Medical Center, USA

In non-neuronopathic type 1 Gaucher's disease, mutations in the GBA1 gene result in the deficiency of glucocerebrosidase and the accumulation of its substrate, glucocerebroside, along with minor lipids, in the lysosomes of mononuclear phagocytes. This metabolic defect leads to a complex phenotype involving visceral organs, bone marrow and the skeleton. The prevailing macrophage-centric view, however, does not explain emerging aspects of the disease, such as malignancies, autoimmune diathesis, Parkinson's disease and, importantly, osteoporosis, all of which are resistant to macrophage-directed enzyme replacement therapy. To understand the pathophysiology of the multi-system involvement in Gaucher's disease, we conditionally deleted the GBA1 gene in the hematopoetic and mesenchymal cell lineages using an Mx1 promoter. We fully recapitulated human Gaucher's disease, in particular, the severe osteoporosis that we found unexpectedly arose from a defect in osteoblastic bone formation. Micro-CT revealed significant decrements in trabecular volume, with evidence of trabecular thinning and loss, accompanied, on calcein labeling, with reduced mineral apposition rates in GBA1 mice compared with control littermates. This was associated with reduced osteoblastoid colony forming units, CFU-ob, in bone marrow stromal cell cultures, consistent with an autonomous defect in osteoblast maturation. Contrary to the prevailing view, osteoclastic resorption in vivo and TRAP-positive osteoclast formation ex vivo remained unaffected in GBA1 deficiency. Cytokine measurements, microarray, and immunophenotyping together revealed a widespread dysfunction not only in macrophages, but also in thymic T- and B-cell, as well as dendritic cell populations. Our study provides the first demonstration for the involvement of cell lineages other than mononuclear phagocytes, most notably osteoblasts, lymphocytes, and dendritic cells, in the pathophysiology of Gaucher's disease. Important therapeutic implications may eventually follow from these studies.

***Disclosures: Pramod Mistry**, None.*

SU0021

Hypoxia-inducible Factor-1 Is a Positive Regulator of Sox9 Activity in the Cartilage Following Femoral Head Ischemia. Chi Zhang*[1], Fan Yang[2], Reuel Cornelia[2], Wanjin Tang[2], Harry Kim[3]. [1]Bone Research Laboratory, Texas Scottish Rite Hospital, USA, [2]Texas Scottish Rite Hospital, USA, [3]Scottish Rite Hospital for Children, USA

Legg-Calve-Perthes disease (LCPD) is a juvenile form of ischemic osteonecrosis of femoral head caused by blood supply disruption to the femoral head which results in the hypoxic injury. Hypoxia-inducible factor-1α (Hif-1α) is a master regulator of cellular response to hypoxia. Piglet model of ischemic osteonecrosis of the femoral head involves surgically disrupting the blood supply to the femoral head. The model has been shown to have radiographic and histopathologic changes resembling LCPD. In LCPD and the piglet model, the articular cartilage of the femoral head continues to grow and thicken after ischemia. The mechanism underlying this cartilage response is not known. We hypothesize that hypoxia stimulates chondrocyte activity following femoral head ischemia. To explore this hypothesis, a porcine microarray was performed to determine hypoxia-induced downstream gene activity following femoral head ischemia in the cartilage. In the ischemic cartilage, the expression of Sox9, a required factor for chondrocyte differentiation, was upregulated along with Hif-1α. The expressions of Sox9 target genes, the type II collagen and aggrecan, were also increased. Microarray results were confirmed by quantitative real-time RT-PCR. In addition, immunohistochemistry assay demonstrated that both Hif-1α and Sox9 immunostaining were increased in the ischemic cartilage compared with controls. To further investigate the possible molecular mechanisms of hypoxia on Sox9 activity, we examined the effect of Hif-1α on Sox9 expression in vitro. A luciferase reporter construct for Sox9 was made driven by 2kb Sox9 promoter. Transient transfection

assay showed that Hif-1α activated Sox9 promoter activity in a dose-dependent manner. Since Sox9 is known to activate type II collagen gene expression, Hif-1α was cotransfected with Sox9 in type II collagen reporter assay to test the effect of Hif-1α on Sox9-mediated transcription. Hif-1α was found to enhance Sox9-mediated transcriptional activity. Moreover, co-immunoprecipitation assay demonstrated that Hif-1α associated with Sox9 directly. Taken together, these findings indicate that Hif-1α activates Sox9 expression and enhances Sox9-mediated transcriptional activity by physical association with Sox9. We speculate that Hif-1α regulation of Sox9 activity may have a chondroprotective role following femoral head ischemia.

***Disclosures: Chi Zhang**, None.*

SU0022

The Relationship of Intestinal Calcium Absorption with Serum 25-Hydroxyvitamin D Levels in Children on Low Calcium Intakes. Tom Thacher*[1], Steven Abrams[2]. [1]Mayo Clinic, USA, [2]Baylor College of Medicine, USA

Aims: Calcium absorption is inconsistently related to serum 25(OH)D values in children with adequate calcium intake. Vitamin D-dependent calcium absorption may be more critical when calcium intakes are low. Our objective was to determine if fractional calcium absorption was related to serum 25(OH)D in children with low calcium intakes.

Method: We pooled data from calcium absorption studies using dual-isotope techniques in Nigerian children (ages 2-14 years) with calcium deficiency rickets (n=49) and healthy control children (n=23) on low calcium diets.

Results: The mean ± SD dietary calcium intakes in rachitic and control children were 181 ± 70 and 227 ± 103 mg/d, respectively (P=0.07). Serum 25(OH)D concentrations were 16 ± 7 and 25 ± 5 ng/ml (P<0.001), and fractional calcium absorption values were 61 ± 22% and 61 ± 22% (P=0.95) in rachitic and control children, respectively. The relationship of fractional calcium absorption with serum 25(OH)D concentrations was marginally inverse in rachitic children (r=-0.26, P=0.06) and absent in control children (r=0.00). In a multiple regression analysis, calcium absorption values were unrelated to age, usual dietary calcium intake, anthropometric variables, serum calcium, phosphorus, PTH, $1,25(OH)_2D$, urinary calcium excretion, forearm bone density, or the severity of radiologic rickets. Fractional calcium absorption was greater in girls (66 ± 21%) than in boys (52 ± 20%, P=0.002). Results of the analysis were unchanged by the exclusion of three children over the age of 8 years.

Conclusion: There was no positive relationship of fractional calcium absorption with serum 25(OH)D concentrations in children on low calcium diets.

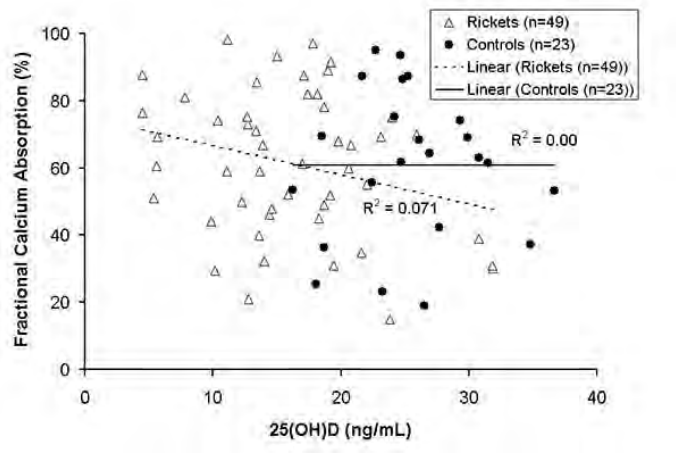

Figure 1

***Disclosures: Tom Thacher**, None.*

SU0023

Vertebral Fractures, Tibial Muscle-Bone Structural Changes and Muscle Hypofunction in Children with Crohn's Disease. Leanne M. Ward*[1], Frank Rauch[2], Nazih Shenouda[3], David R. Mack[1]. [1]Department of Pediatrics, Children's Hospital of Eastern Ontario, University of Ottawa, Canada, [2]Department of Pediatrics, Shriners Hospital for Children, McGill University, Canada, [3]Department of Diagnostic Imaging, Children's Hospital of Eastern Ontario, University of Ottawa, Canada

In pediatric Crohn's disease (CD), the consistently observed bone mass deficit is associated with reductions in total body lean mass and suppression of bone turnover. The impact of these findings to muscle and vertebral strength has not been described. We examined whether the sarcopenia is associated with reductions in leg muscle function among recently diagnosed children with CD. Changes in tibia/fibula bone and muscle structure as well as the potential for vertebral fractures (VF) were also assessed.

Forty children with CD underwent a bone health evaluation within 2 weeks of diagnosis (23 boys, 17 girls; mean age 13.7 ± 2.8 years). Muscle function was measured by peak jump power on a single, two-legged jump using a mechanography force plate (Leonardo?). Bone and muscle structural indices were measured by peripheral quantitative computed tomography (pQCT) at the 4, 38 and 66% tibia/fibula sites. Peak jump power and pQCT results were compared to age- and gender-matched healthy controls. Lateral spine radiograph for VF assessment according to Genant semi-quantitative (GSQ) and Algorithm-Based Qualitative (ABQ) methods was carried out at a median of 3 months (range 0 to 16 months) post-diagnosis.

Ninety-two percent of children had a severe pediatric Crohn's disease activity score (PCDAI), the rest were moderate. Nine children (23%) reported a single extremity fracture each; 6/40 (15%) showed 9 ABQ VF events (loss of endplate parallelism in all cases). Peak jump power (W/kg) was significantly reduced (mean 34 ± 9 compared to 43 ± 8 in the controls, p<0.001). Distal tibia trabecular density (mg/cm^3) was normal (197 ± 44 compared to 206 ± 29 in controls, p=0.999), while cortical density at 38% was increased (1106 ± 37 vs 1032 ± 49, p<0.001). The ratio between total tibia and fibula BMC at 38% and muscle cross-sectional area (mCSA) at 66% ($mg*mm^{-1}*cm^{-2}$) was elevated (6.2 ± 1.0 compared to 5.6 ± 0.6 in controls, p<0.001). At the diaphysis (66%), total mCSA (mm^2) was reduced (4320 ± 1123 versus 5335 ± 1258 in controls, p<0.001).

Leg muscle mass and function were reduced in recently diagnosed children with CD. In addition, ABQ VF were present in 15%, highlighting that vertebral strength can also be impaired in this context. The leg structural findings of preserved trabecular density, elevated cortical density and high BMC per muscle cross-sectional area suggest a relatively recent insult affecting muscle development that was associated with low intra-cortical remodeling activity.

***Disclosures: Leanne M. Ward**, None.*

SU0024

Calcitriol Administration in Type 1 Diabetic Adolescents: Does It Improve or Impair Bone Health? Nicola Napoli*[1], Dario Pitocco[2], Carla Bizzarri[3], Rocky Strollo[1], Reina Villareal[4], Elisa Cipponeri[1], Antonella Lo Rubbio[1], Silvia Manfrini[1], Paolo Pozzilli[1], IMDIAB group[1]. [1]University Campus Biomedico, Italy, [2]Università Cattolica del Sacro Cuore, Italy, [3]Ospedale Pediatrico Bambino Gesù, Italy, [4]University of New Mexico, USA

Purpose: In recent onset Type 1 Diabetes (T1D), the lack of anabolic effect of insulin and amylin may disturb bone remodelling, particularly in puberty, a critical period for bone mass increment. Aims of the study were to determine the effect of metabolic control and 1 year treatment with calcitriol on bone turnover in subjects with T1D and to analyze the role of Osteocalcin (OC) on pancreatic function and metabolic control.

Methods: In a double blind study, 25 subjects with recent-onset T1D and baseline C-peptide > 0.25 nM, were randomized to calcitriol at 0.25 μg daily dose or placebo and followed-up for 1 year. OC and β-CrossLaps (β-CL), were evaluated by ECLIA (Roche Diagnostics, Germany) at diagnosis and at 1 year follow-up.

Results: At onset, OC and β-CL levels were not different respect to literature-derived values for healthy subjects. OC positively correlated with insulin requirement (r=0.48, P<0.01), while no significant correlation were found in relation to HbA1c and C-peptide. At 1 year follow-up OC and β-CL dropped by 38.6% and 47.3%, respectively in the calcitriol treated group but their levels were not significantly different compared to diagnosis due to high variability. No significant differences were also found at 1 year comparing calcitriol vs. the placebo group for both OC and β-CL. No significant differences were observed between calcitriol and placebo groups for C-peptide, HbA1c and insulin requirement. By stratifying patients according to age, we found that at 1 year follow-up as compared to diagnosis, calcitriol treated patients ≤18 years of age showed statistically significant 61% drop of OC, (p=0.04) and a 67% reduction in β-CL (p=0.09). In this age range, patients on calcitriol therapy vs. placebo showed at 1 year follow-up a trend for lower OC (p=0.08) and significantly lower β-CL (p=0.03). Differences were not statistically significant in patients >18 years of age.

Conclusions: In contrast to what expected, OC was not associated with residual pancreatic β-cell function or metabolic control in recently diagnosed T1D patients. Calcitriol had no effect on residual β-cell function, insulin dose, reduced bone markers in the adolescent cohort showing that may contrast the physiological increasing in bone turnover during puberty. At this stage of study, we don't know whether this effect of calcitriol is good to preserve bone mass or in T1D, a condition of anabolic deficiency for the bone, it disturbs pubertal bone mass increment.

***Disclosures: Nicola Napoli**, None.*

SU0025

Effectiveness of Bisphosphonates as Treatment of Symptomatic Osteonecrosis occurring in Children Treated for Acute Lymphoblastic Leukemia. Coralie Leblicq*[1], Caroline Laverdière[1], Jean-Claude Décarie[1], Albert Moghrabi[1], Julie Dubé[1], Marc Isler[1], Gilles Chabot[2], Nathalie Alos[3]. [1]CHU Sainte-Justine - Université Montréal, Canada, [2]Hopital Saint Justine, Canada, [3]CHU Sainte Justine, Canada

Introduction: Osteonecrosis (ON) is recognized as a severe complication of treatments for Acute Lymphoblastic Leukemia (ALL). Risk factors have been identified: age≥ 11 yrs, female gender, increased dose of corticoids. ON diagnosis usually leads to discontinuation of corticoid therapy, support care and in some case, surgery. Recent studies had suggested that the use of bisphosphonates might reduce pain and loss of motor function.

Patients and Methods: Symptomatic ON, as complication of primary ALL treatment, was diagnosed in 23 children at our center, between April 2000 and September 2008. 18 patients were treated with pamidronate, administered by infusions of 1 mg/kg, weekly for the first 2 doses, then every 6 to 8 weeks. ON diagnoses were confirmed by MRI. Clinical and radiological evolution as well as reintroduction of corticoid treatment were followed and analyzed.

Results: Out of 242 patients diagnosed with ALL, only 23 (9.5%) developed ON secondary to the ALL treatment. All patients were in their first marrow remission at the time of ON diagnosis. 18/23 patients (78.3%) received pamidronate for severe pain or loss of motor function. The 18 patients' median age, at the ALL diagnosis, was 9.2 yrs (2.6 – 14.9), (7F/11M; 9HR/9SR) and ON occurred at a median time of 14.7 months (2.5 – 19.0) after the initiation of ALL treatment. In 14 patients, ON was bilateral or multifocal. Lesions were distributed as follows: 5 (27.8%) at the hip; 2 (11.1%) at the knee; 15 (83.3%) at the ankle or foot. All 18 patients were treated with pamidronate during a median period of 8 months (3.2-27.0). Clinical improvement (pain and motor function) generally appeared after the first 2 doses of pamidronate (except for one patient). 10/18 patients (55.6%) continued corticoids after ON diagnosis, their median age at the ALL diagnosis was 6.8 yrs (2.6 – 13.5), (2F/8M; 2HR/8SR), and ON occurred in a median time of 14.3 months (2.5 – 19.0). In 6 patients, ON was bilateral or multifocal. Lesions were distributed as follows: 1 at the knee; 10 at the ankle or foot. Clinical and radiological improvement was noted in this subgroup despite the reintroduction of the corticoids.

Conclusion: Pamidronate seems to be effective in the management of pain and motor function loss in ON as a complication of childhood ALL therapy. Treatment of these patients with pamidronate might lead to rapid decrease of pain and improvement of motor function while allowing continuation of corticoids.

***Disclosures: Coralie Leblicq**, None.*

SU0026

Vitamin D Supplementation in Breastfed Infants: Results of A Prospective Trial in the Southern United States. Tulasi Ponnapakkam*, Elease Bradford, Robert Gensure. Ochsner Clinic Foundation, USA

Breastfeeding has become popular because of known benefits to mother and baby; however, there are concerns if breast milk has sufficient vitamin D to prevent rickets. The American Academy of Pediatrics has recommended that breastfed infants receive vitamin D (200 IU/day) from 2 months of age; this recommendation recently increased to 400 IU/day from birth. However, there are few studies of universal supplementation, none of which were conducted in the southern United States. We therefore conducted a placebo-controlled clinical trial of vitamin D supplementation in breastfed children at our hospital in New Orleans, LA. After obtaining institution review board approval, normal newborns (> 50% breast milk intake for at least 3 months) were recruited and randomized into one of three groups: no supplementation, 200 IU/day vitamin D2 from 2 months, and 200 IU/day from birth. Blood samples and questioners were collected at birth, two, four, and six months of age. We recruited 80 subjects, 24 of which completed the study. The most common reason for dropping out of the study was premature cessation of breast feeding. Statistically significant differences in 25-vitamin D levels were observed at the 4 month time point (Vit.D 137+/-37 nmol/l, placebo 63+/-9 nmol/l, $p<0.05$), but by 6 months the 25-vitamin D levels in the placebo group had risen to those of the treatment groups (Vit.D 132+/-29 nmol/l, placebo 117+/-28 nmol/l, NS). No study subjects developed rickets, and alkaline phosphatase did not differ significantly between the placebo and treatment groups at any of the measured time points. Serum calcium, phosphate, and PTH did not differ between groups at any time point. Compliance with the study medication, assessed by questionnaire, was poor, with less than 50% of subjects receiving >90% of the study medications. Our data does not show evidence of benefit from vitamin D supplementation in breastfed infants in the southern United States. Importantly, 75% of the subjects completing the study were at low risk to develop rickets; the study is ongoing to determine if high risk subjects might benefit from supplementation.

***Disclosures: Tulasi Ponnapakkam**, None.*

SU0027

Automated and Dynamic Image-guided Failure Assessment of Bone Ultrastructure and Bone Microdamage. Philipp Schneider*[1], Alina Levchuk[1], Ralph Müller[2]. [1]Institute for Biomechanics, ETH Zurich, Switzerland, [2]ETH Zurich, Switzerland

Recently, it has been suggested that ultrastructural bone phenotypes, such as the cortical canal network, could be directly linked to the mechanical failure behavior of bone tissue. Moreover, the amount of microdamage and the rate of its accumulation were reported as being important factors that reduce bone post-yield properties. Specifically, high accumulation of microdamage significantly increased cortical bone brittleness and thus, is a precursor of mechanical failure. On this account, we recently developed an automated micro-compression device (MCD) for dynamic image-guided failure assessment (DIGFA) of bone ultrastructure and bone microdamage. Here, we present a first biological study using DIGFA. Mouse femora were extracted from one C57BL/6 (B6) and one C3H/He (C3H) mouse each, embedded in PMMA and aligned along their longitudinal axis. A reduced areal cross section was simulated by introducing a notch in the transverse plane of the mid-diaphysis, which created a weakened region of bone to stimulate crack formation. Samples were then stored in 70% ethanol and rehydrated in PBS for 24 hours before testing. DIGFA was performed at TOMCAT beamline of the Swiss Light Source using SR CT. All tests were done in compression until failure, where each compressive step (0.5% strain interval) was visualized using synchrotron radiation-based computed tomography (SR CT) at a nominal resolution of 740 nm. The intracortical porosity was separated into osteocyte lacunae, the canal network, and microcracks (Figures 1 & 2) for subsequent morphometric evaluation. The thicker cortex of C3H was penetrated by a dense network (canal volume density Ca.V/Ct.TV = 3.83%, canal spacing Ca.Sp = 126 µm) of thick canals (canal thickness Ca.Th = 28.9 µm), whereas in B6, only few scattered (Ca.V/Ct.TV = 0.26%, Ca.Sp = 187 µm) and fairly small canals (Ca.Th = 7.5 µm) were present. For B6, the first occurrence of crack was noted at 3% strain, while for C3H, crack initiation took place at 4% strain only. In addition, microcracks preferentially initiated at large canal units in C3H and they ran parallel to the canal network, whereas in B6, initiation took place exclusively at the periosteal surface. In conclusion, initiation and propagation of microcracks was investigated for two different mouse strains, demonstrating that DIGFA in combination with SR CT is a suitable technique for concomitant dynamic 3D assessment of bone morphology and bone fracture behavior down to the cellular level.

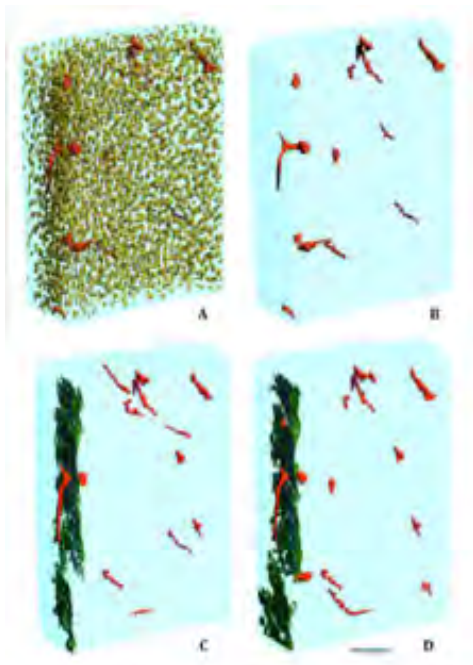

Figure 1: Porosity within the femoral mid-diaphysis of a B6 mouse: (A) Canal network (tubes in red), osteocyte lacunae (prolate ellipsoids in yellow), and cortical bone (semitransparent shell in blue) at 0% strain. (B) Same as A, showing only canals and cortical bone. (C) Microcracks (green clefts) initiating at 3% strain. (D) Propagation of microcracks at 3.5% strain. (A-D) Scale bar denotes 100 µm.

Figure 1

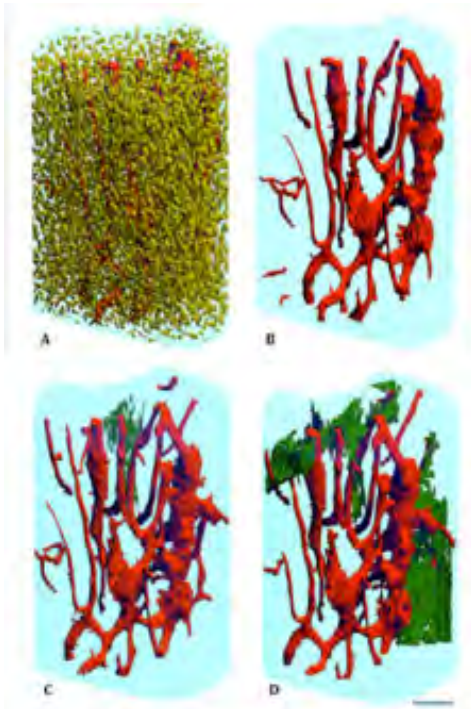

Figure 2: Porosity within the femoral mid-diaphysis of a C3H mouse. (A) Canal network (tubes in red), osteocyte lacunae (prolate ellipsoids in yellow), and cortical bone (semitransparent shell in blue) at 0% strain. (B) Same as A, showing only canals and cortical bone. (C) Microcracks (green clefts) initiating at 4% strain. (D) Propagation of microcracks at 5.5% strain. (A-D) Scale bar denotes 100 µm.

Figure 2

***Disclosures: Philipp Schneider**, None.*

SU0028

Bone Turnover During Pregnancy in Horses. Claudia Greiner[1], Etienne Cavalier[2], Benoit Remy[3], Annick Gabriel[4], Frédéric Farnir[4], Zdzislaw Gajewski[5], Bianca Carstanjen*[1]. [1]Freie Universität Berlin, Germany, [2]CHU de Liège, Belgium, [3]Reprobiol, Belgium, [4]Université de Liège, Belgium, [5]Warsaw University of Life Sciences, Poland

Pregnancy is associated with several physiological and anatomical changes that essentially affect musculoskeletal conditions. However, the influence of pregnancy on equine bone metabolism has not been studied to great detail. This study is intended to longitudinally evaluate the effect of pregnancy on bone turnover markers in clinically normal mares.

Venous blood samples were collected 11 times from 19 multiparous mares at 36 weeks pre-parturition (-36w pp), -32w pp, -28w pp, -24w pp, -20w pp, -16w pp, -12w pp, -8w pp, 4w pp, as well as in the week of parturition (0w) and one week post parturition (+1w). All horses had normal gamma glutamyl transferase and creatinine values. Serum concentrations of osteocalcin and carboxy-terminal cross-linking telopeptide of type I collagen (CTX-I) were determined using an equine specific osteocalcin radioimmunoassay and an automated CTX-I electrochemiluminescent sandwich antibody assay. Serum CTX-I values significantly ($P<0.05$) increased during the last trimester of pregnancy. Serum osteocalcin concentrations decreased between -28w pp and -12w pp and increased thereafter until parturition. Both bone markers significantly ($P<0.0001$) increased between -4w pp and 0w.

In conclusion, changes in bone turnover seem to depend on the stage of pregnancy. Peak values of serum CTX-I and osteocalcin were obtained directly around the time of parturition.

***Disclosures: Bianca Carstanjen**, None.*

SU0029

Contribution of Trabecular Microarchitecture and its Heterogeneity to the Mechanical Behavior of Human L3 Vertebrae. Julien Wegrzyn*[1], Jean-Paul Roux[2], Monique Arlot[3], Stephanie Boutroy[4], Nicolas Vilayphiou[5], Olivier Guyen[6], Pierre Delmas[7], Roland Chapurlat[8], Mary Bouxsein[9]. [1]INSERM U831 - Université de Lyon, France, [2]INSERM, France, [3]Faculte de Medecine Laennec, France, [4]INSERM, Université De Lyon, France, [5]INSERM Unit 831 & Université de Lyon, France, [6]Department of Orthopedic Surgery - Pavillon T. Hopital Edouard Herriot, Lyon, France, France, [7]INSERM U 831, France, [8]E. Herriot Hospital, France, [9]Beth Israel Deaconess Medical Center, USA

Low BMD is a strong risk factor for vertebral fracture, though many fractures occur in people with moderately decreased BMD. Along with BMD, trabecular microarchitecture influences vertebral strength, although there is little information about the contribution of microarchitecture heterogeneity to vertebral fragility. Our aim was to assess the influence of microarchitecture and its heterogeneity on the mechanical behavior of human L3 vertebrae.

21 L3 vertebral bodies (75 ± 10 years) were obtained fresh-frozen, analyzed for BMD by DXA and for microarchitecture by HR-pQCT (82 µm voxel size, XTreme CT Scanco®), and then tested in axial compression. The following microarchitectural parameters were measured: BV/TV, SMI, Tb.Sp*, Tb.Th* and Tb.N*. Heterogeneity was assessed using 2 vertically oriented virtual biopsies (anterior (Ant) and posterior (Post)) – each divided into 3 zones (superior, middle and inferior), and using the whole trabecular volume for Tb.Sp*SD (Figure 1). Heterogeneity parameters were defined as 1) ratios of Ant/Post microarchitecture parameters and 2) the coefficient of variation (CV) of microarchitecture from the 3 vertical zones.

BMD ($r = 0.66$, $p = 0.001$) and microarchitecture were significantly correlated with failure load ($|r| = 0.44 – 0.81$, $p = 0.04 – <0.0001$), with parameters of the Ant biopsy being the best predictors of mechanical behavior ($r = 0.56 – 0.74$, $p = 0.009 – <0.0001$). Using stepwise regression, the combination of BMD (3rd step, $p = 0.004$), SMI (1st step, $p < 0.0001$) and DA_{ratio} (2nd step, $p = 0.001$), was strongly associated with failure load ($R = 0.93$, $p <0.0001$). Also, the combination of BV/TV (p = n.s.), SMI (2nd step, $p = 0.008$) and DA_{ratio} (1st step, $p = 0.003$) was correlated to failure load ($R = 0.89$, $p < 0.0001$).

In conclusion, BMD alone explained up to 44% of the variability in vertebral mechanical behavior, BV/TV up to 53% and microarchitecture up to 66%. Importantly, the combination of bone mass (BMD or BV/TV) with microarchitecture and its heterogeneity improved the prediction of vertebral mechanical behavior, together explaining up to 86% of the variability in vertebral failure load. Our data indicate that regional variation of microarchitecture assessment expressed by heterogeneity parameters may enhance prediction of vertebral fracture risk.

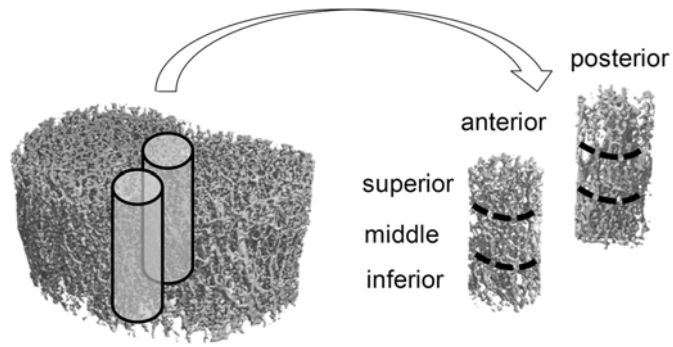

Figure 1: Whole trabecular volume of L3 vertebra and the 2 virtual biopsies

***Disclosures: Julien Wegrzyn**, None.*

SU0030

Differences in Bone Quality as Determined by HRpQCT in Postmenopausal Chinese and Caucasian Women. Marcella Walker*[1], Xiaowei Liu[1], Donald McMahon[1], Julia Udesky[1], George Liu[2], John Bilezikian[1]. [1]Columbia University, USA, [2]New York Downtown Hospital, USA

Chinese American (CH) women have lower hip and forearm fractures (fx) rates than Caucasian (CA) women despite lower areal bone density (aBMD) by dual x-ray absorptiometry (DXA). We recently reported higher trabecular (Dtrab) and cortical (Dcomp) bone density as well as greater trabecular (TbTh) and cortical thickness (CTh), but smaller bone area (CSA), as measured by high resolution peripheral QCT (HRpQCT) in premenopausal CH compared to CA women. The current study extends these investigations to postmenopausal women. The CH (n=29) & CA (n=30) groups did not differ in age (mean ± SD) (61 ± 2 vs. 62 ± 3 yrs; p=0.13) or in physical activity level. Height (62 ± 2 vs. 64 ± 2 inches; $p<0.0001$), weight (128 ± 17 vs. 151 ± 29

lbs; p=0.0004), as well as daily calcium (901 ± 544 vs. 1449 ± 625 mg; p=0.0008) and vitamin D (460 ± 354 vs. 988 ± 686 IU; p=0.0006) intake were lower in CH women. Serum 25-hydroxyvitamin D (31 ± 10 vs. 38 ± 14 ng/dl; p=0.03) was lower, but PTH was similar (37 ± 11 vs. 39 ± 12 pg/ml; p=0.57) in the CH versus the CA group. aBMD by DXA did not differ at any site (LS: 0.901 ± 0.13 vs. 0.967 ± 0.13 g/cm^2; p=0.06); (FN: 0.700 ± 0.08 vs. 0.706 ± 0.10 g/cm^2; p=0.47); (TH: 0.829 ± 0.09 vs. 0.865 ± 0.11 g/cm^2; p=0.18) and (1/3 RAD: 0.618 ± 0.06 vs. 0.641 ± 0.06 g/cm^2; p=0.16). Major differences, however, were detected by HRpQCT. At the radius, CSA was smaller in the CH vs. CA group (201 ± 33 vs. 227 ± 38 mm^2, p=0.006). CTh (0.86 ± 0.14 vs. 0.75 ± 0.21 mm, p=0.03) and Dcomp was greater (916 ± 54 vs. 865 ± 86 mgHA/ccm; p=0.01) in CH compared to CA women but there was no difference in Dtrab (118 ± 36 vs. 132 ± 34 mgHA/ccm; p=0.13) or BV/TV (9.8 ± 3.0 vs. 11.0 ± 3.0 %; p=0.13). Trabecular number (TbN) was lower (1.6 ± 0.3 vs.1.8 ± 0.3 1/mm, p=0.05) and separation (TbSp) was greater (0.597 ± 0.17 vs. 0.520 ± 0.11 mm, p=0.04) in CH compared to CA women. There was no difference in TbTh (0.061 ± 0.01 vs. 0.062 ± 0.01 mm, p=0.76). At the tibia results were similar though TbTh (0.078 ± 0.015 vs. 0.069 ± 0.012 mm, p =0.02) was also greater while Dtrab (138 ± 29 vs. 158 ± 25 mgHA/ccm, p=0.008) and BV/TV (0.115 ± 0.024 vs. 0.131 ± 0.021, p=0.008) were lower in CH compared to CA women. The results suggest that the racial differences in Dcomp and CTh persist after menopause and provide further evidence to support the idea that bone quality in CH women as determined by HRpQCT may help to account for their lower fracture risk in comparison to CA women.

***Disclosures: Marcella Walker**, None.*

SU0031

Effects of an Ulna Critical Size Defect on Ipsilateral Radius in Rabbit. Rana Samadfam*[1], Susan Y. Smith[1], Nancy Doyle[2], Aurore Varela[1], Luc Chouinard[3]. [1]Charles River Laboratories, Canada, [2]Charles River, Canada, [3]Charles River Laboratories, PCS Montreal, Canada

The replacement and repair of bone lost due to trauma, cancer or congenital defects is a major clinical challenge. Several critical size defect models have been developed and used for skeletal tissue engineering over the last decades. The rabbit ulna critical size defect is one of the most widely used long bone defect model. The model is reproducible, does not require fixation and allows imaging, histology and biomechanic testing. The model has been well characterized and used to evaluate various bone substitute and/or biological agents to improve healing. However, the effect of increase biomechanical loading on the ipsilateral radius has not been described. A 20 mm unilateral, mid-diaphyseal defect was created on the right ulna of skeletally mature New-Zealand White Rabbit. The defect site was closed without other intervention .Following a 12 week observation period, animals were sacrificed and ulna-radius was collected. High resolution radiographs (Faxitron) were taken for all defect sites to determine the mid callus for pQCT analysis . For the right ulna, five slices were obtained: one at the middle of defect site and the other two below and above the middle of the defect site (5 and 10 mm apart from the middle). MicroCT analyses included the whole defect site (24-27mm). As expected for a critical size defect model, the untreated ulnae defect did not show bridging 12 weeks post surgery for majority of the specimens, however the proximal and distal ulna segments were focally fused to the radius at the extremities of the defect. PQCT analysis indicated marked increases in total slice area and periosteal circumference for the right radius at the level defect site compared to the left intact radius, consistent with marked increases in cortical area, cortical BMC and CSMI. These increases were considered related to the increased biomechanical loading following defect creation on the ulna. MicroCT analysis confirmed these observations. In conclusion, bone geometry and bone mass of the radius at the defect site were statistically significantly increased in response to the increased mechanical loading due to the ulna defect. These data suggest that ulna critical size defect model can be useful to evaluate the effect of increased loading on radius.

***Disclosures: Rana Samadfam**, Contract Research, 3*

SU0032

Effects of Rosiglitazone on Bone Microarchitecture as Assessed by High Resolution MRI Scans in a Mechanistic Study of Postmenopausal Women with type 2 Diabetes Mellitus. Cesar Bogado*[1], Fabio Massari[1], Barbara Kravitz[2], Antonio J. Nino[3], Allison R. Northcutt[3], Gitanjali Paul[3], Alexander R. Cobitz[3], Lorraine Fitzpatrick[4]. [1]Instituto De Investigaciones Metabolicas (IDIM), Argentina, [2]GlaxosmithKline Pharmaceuticals, USA, [3]CVM/MDC, GlaxoSmithKline, USA, [4]GlaxoSmithKline, USA

Abstract:

In this prospectively designed mechanism-of-action study, the effect of RSG on bone mass and structure will be studied through different imaging modalities: dual-energy X-Ray absorptiometry (DXA) of the lumbar spine and hip regions, hip structural analysis (HSA), high resolution magnetic resonance imaging (hr MRI) of the wrist, Quantitative Computerized Tomography (QCT) and structural assessment of the hip using digitized hip radiographs (ImaTx). Serum biomarkers of bone formation and resorption, calcium homeostasis and selected sex hormone changes over time were assessed. Parameters of glucose control included measurement of: hemoglobin A1C (HbA1C), fasting plasma glucose (FPG), and serum insulin. Here we present findings from hr MRI measurements to help characterize the effects of RSG on bone microarchitecture in a population of postmenopausal women with type 2 diabetes mellitus.

Methods:

This was a Phase IV, 52 Week, double-blind, multi-center study where 226 postmenopausal women were randomized to RSG or metformin (MET) in a 1:1 ratio. At baseline mean age was 63.8 ± 6.5 years while mean years post-menopause was 16.9 ± 8.4. Median duration of diabetes was 3.5 (1.8 -7.8) years. Other baseline characteristics were: mean body mass index (BMI) 31.4 ± 5.9 kg/m^2; mean FPG and HbA1c were 111.7 ± 23.4 mg/dl and 6.4 ± 0.65% respectively. Femoral neck BMD (g/cm^2) was 0.83 ± 0.141, at total hip 0.98 ± 0.123, and at lumbar spine 1.05 ± 0.161. Femoral neck T-score was -0.95± 0.908, at total hip -0.02± 0.970, and at lumbar spine -0.55 ± 1.247.

Using a 1.5 Tesla GE scanner, a subset of 37 subjects underwent hr MRI scans of the distal radius. Multi-slice, fat gradient-echo localizer images in the sagittal, coronal and axial planes were obtained initially, followed by the high resolution imaging sequence. The following variables were obtained: trabecular number, volume, thickness and spacing, apparent bone volume fraction, cortical area, volume and thickness.

Conclusion:

Comparison of the effects on bone microarchitecture between treatment groups may provide insight on the effect of RSG on bone and help to understand its relationship with the increased risk of fracture reported in long term clinical trials.

***Disclosures: Cesar Bogado**, GlaxoSmithKline, 5*
This study received funding from: GlaxoSmithKline

SU0033

Fewer Trabecular Plates and Decreased Connectivity Between Plates and Rods Is Associated with Reduced Bone Stiffness in Postmenopausal Women with Fragility Fractures. Xiaowei Liu*[1], Emily Stein[2], Bin Zhou[1], Ervis Bezati[1], Thomas Nickolas[3], Adi Cohen[3], Valerie Thomas[3], Chiyuan Zhang[1], Donald McMahon[2], Elizabeth Shane[2], X Guo[1]. [1]Columbia University, USA, [2]Columbia University College of Physicians & Surgeons, USA, [3]Columbia University Medical Center, USA

Osteoporosis is typically diagnosed by measuring areal BMD (aBMD) by dual energy x-ray absorptiometry (DXA). However, many women with postmenopausal fractures (Fx) have aBMD measurements above the osteoporotic threshold. To improve understanding of the contribution of bone microarchitecture to Fx susceptibility in postmenopausal women, we applied micro finite element analysis (μFEA) and a recently developed image analysis technique, individual trabeculae segmentation (ITS), to high-resolution peripheral quantitative computed tomography (HR-pQCT) images of the distal tibia (DT) and distal radius (DR). We hypothesized that ITS and μFEA would discriminate between postmenopausal women with and without fragility Fx.

Women (68 ± 7 years) with (n=68) and without (n=101) a history of postmenopausal Fx had aBMD of the spine, hip and forearm by DXA and HR-pQCT scans (XtremeCT, Scanco Medical; voxel size 82 μm) of the DR and DT. ITS analyses were applied to the whole trabecular compartment of HR-pQCT images to calculate plate and rod bone volume fraction (pBV/TV and rBV/TV), plate and rod number (pTb.N and rTb.N, 1/mm), plate and rod thickness (pTb.Th and rTb.Th, mm), rod length (rTb.l, mm), and rod-rod, plate-rod and plate-plate junction densities (R-R, P-R and P-P Junc.D, 1/mm^3). Whole bone and trabecular bone stiffness were estimated by μFEA of HR-pQCT scans.

Mean DXA T-scores were in the osteopenic range at all sites, and similar in women with and without Fx at the spine, hip and 1/3 radius. At the DR, pBV/TV and rBV/TV were 26% and 10% lower, and pTb.N 8% lower in Fx subjects ($p<0.002$). In contrast, rTb.l, a measure of trabecular spacing, was 3% higher and R-P and P-P Junc.D were 24% and 22% lower in Fx subjects ($p<0.001$). rTb.N, pTb.Th, rTb.Th, and R-R Junc.D were similar between groups. The pattern was similar at the DT, but differences were less pronounced. In Fx subjects, whole bone stiffness was 14% and 7% lower, and trabecular bone stiffness 29% and 11% lower at the DR and DT, respectively ($p<0.002$). All significant differences remained so before and after adjustment for aBMD.

In conclusion, despite similar aBMD by DXA, women with postmenopausal Fx have fewer trabecular plates and decreased connectivity between rods and plates at both the DR and DT, leading to lower volumetric BMD and bone stiffness. Application of ITS and μFEA to HR-pQCT scans of the DR and DT can discriminate postmenopausal women with fragility FX independent of aBMD by DXA.

***Disclosures: Xiaowei Liu**, None.*

SU0034

Fracture Surface Analysis to Understand the Failure Mechanisms of Collagen Degraded Bone. Chrystia Wynnyckyj[1], Lisa Wise-Milestone[2], Marc Grynpas*[3], Sidney Omelon[4]. [1]University of Toronto, Canada, [2]Sunnybrook Research Institute, Canada, [3]Samuel Lunenfeld Research Institute, Canada, [4]Chemical & Biological Engineering, University of Ottawa, Canada

Fracture surface analysis is a powerful technique to investigate failure mechanisms of bone. Previously, male and female emu tibiae were endocortically treated with 1 M

potassium hydroxide (KOH) solution for 1-14 days. This treatment caused *in situ* collagen degradation and resulted in negligible mass loss (0.5%), collagen loss (0.05%), no significant differences in geometrical parameters but significant changes in mechanical properties. Specifically, male and female tibiae showed significant decreases in failure stress and icnreased failure strain and toughness with increasing KOH treatment time. The fracture surfaces of untreated and 14-day KOH treated failed specimens were examined to further identify differences in the failure process between KOH treated and untreated male and female bones in order to explain the previously observed increase in toughness. Areas of 'tension', 'compression' and 'transition' were identified using digital images of the fracture surfaces. Within these areas, the degree of roughness and smoothness were identified and estimated, using Scanning Electron Microscopy (SEM). All groups exhibited significantly more percent areas of tension compared to compression, typical of bending tests. In terms of 'roughness', the fracture surfaces of 14-day male and female KOH treated bones showed a significantly higher 'roughness' compared to untreated bones, indicating that more energy was consumed in the 14-day KOH treated samples. For untreated groups, the tensile surfaces showed a 'smooth' surface compared to the complex fracture surface of interlamellar cleavage and longitudinal splitting seen on the compressive side. These features were present in the KOH treated samples but to a higher degree of 'roughness' on the tensile side and disorder and fragmentation on the compressive side for both sexes. Furthermore, additional toughening mechanisms, which are important features for dissipating energy during the failure process, were observed in the KOH treated samples, but were absent in the untreated samples for both sexes. This suggests that these mechanisms slowed propagation of the fatal crack. These results indicate that the significant increase in toughness of KOH treated bones is due to structural alterations that enhanced the ability of the microstructure to dissipate energy during the failure process, thereby slowing crack propagation.

***Disclosures: Marc Grynpas**, None.*

SU0035

Geometrically-Equivalent Models for Femoral Neck Bone Cross-Sections. Alia Khaled*[1], Ben Schafer[1], Felix Eckstein[2], Thomas Beck[3]. [1]Johns Hopkins University, USA, [2]Paracelsus Private Medical University (PMU), Austria, [3]Johns Hopkins Outpatient Center, USA

CT is commonly used to generate engineering models of the hip but scanners capable of scanning the hip blur bone details especially in osteoporosis. Blurred trabecular regions may be adequately handled by using the density/modulus relationship to account for partial volume averaging. Cortices which bear most of the load in osteoporotic femurs are not well depicted by density/modulus relationships and continuum models do not simulate local buckling failure. Towards a more accurate model of the femoral neck cortex we have developed an approach for generating geometrically-equivalent models from CT cross-sections. Methods: Fundamentally the method assumes that 1) the outer cortical boundary can be accurately defined, and 2) any variation in apparent cortical density is due to partial volume averaging not increased porosity. Six cadaver femurs from German subjects were scanned in a water bath using a 16-slice Siemens CT scanner with a slice spacing of 0.5 mm. Specialized software was used to extract the cross-section at the minimum neck diameter then the Canny algorithm was used to extract the outer boundary from surrounding tissues. An estimate of maximum cortical thickness was used to define an inner contour approximately concentric to the actual inner cortex. The inner and outer boundaries were then modeled by non-uniform rational B-spline (NURBS) curves. To generate the shell model, a mask traced the original shell image and the inner boundary was defined such that the center of mass and the cross-sectional area (CSA) of the original shell are preserved. To generate the trabecular core model, each column and row in the core image assumed its mean value modeling a uniform distribution. The column and row models were then averaged to obtain the final model. CSA, principal moments of inertia and the principal angle of the original cross-section were used to judge the model accuracy. Results: Fig. 1 shows the original femoral neck images vs. the generated models, and table 1 lists errors in the geometrical measurements of the model cross-sections. The models are geometrically equivalent to the original cross-sections with error $\leq$ 6%. Conclusions: We have developed a reliable method to generate smooth, geometrically accurate models of the femoral neck cross-sections from CT data, without employing the density/modulus relationship in the cortex. These models can be used in structural and mechanical analysis of femoral neck using advanced finite element methods.

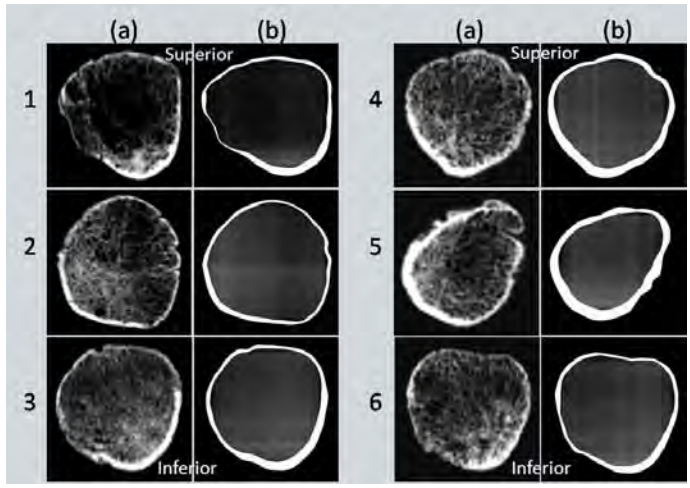

Fig.1: Original femoral neck cross-sections (a) versus the generated models (b) for the 6 subjects

Subject	Cross-sectional area (Absolute relative error)	Principal angle (Absolute error)	Principal moments of inertia (Absolute relative error)
1	0.007	3.0°	0.039, 0.003
2	0.004	0.8°	0.050, 0.024
3	0.003	4.8°	0.019, 0.061
4	0.001	6.8°	0.014, 0.032
5	0.005	0.2°	0.013, 0.019
6	0.003	4.2°	0.033, 0.064

Table 1: Errors in the geometrical measurements between the original and the model cross-sections

***Disclosures: Alia Khaled**, None.*

SU0036

In Situ Mechanical Measurements of Rat Tibia. Alexander Proctor*. Active Life Technologies, USA

Here we evaluate the consistency and reproducibility of the BioDent^{TM} 1000 Reference Point Indentation (RPI) instrument for measuring rat tibia in situ. To evaluate the consistency and reproducibility of this instrument, age matched male Sprague-Dawley rat tibia (n=19) were measured. The rats were sacrificed as part of an unrelated behavioral study which maintained a controlled diet and habitat for the duration of their lives. The tibiae were not excised and were measured immediately after sacrifice. 20 measurements were made on left tibiae using a commercial BP1 Probe Assembly. Each measurement consisted of 20 indentation cycles loading the bone up to 3.5 Newtons for each cycle at 2 Hz. Each in situ measurement was made by penetrating the fur and skin covering the left tibia on each rat with the Probe Assembly. Measurements started at the proximal condyle and ended at the distal side of the tibia-fibia junction. No other preparation was made to the bone prior to measurement. Hydration was maintained on the bones from natural fluids in the specimen. Hank's Balanced Salt Solution was applied if the tissue appeared to be drying out. Indentation Distance Increase (IDI), Creep Indentation Distance (CID) and Total Indentation Distance (TID) were calculated for each measurement. The average values for the population of rats were: IDI =9.80μm $\pm$2.11μm; CID =3.32μm $\pm$0.56μm; TID = 36.43μm $\pm$4.77μm. Minor ($p<0.15$) differences were measured between rats. Individual measurements on each rat deviated from the mean by 9.5% to 37% for IDI, 7.6% to 32.4% for CID, and 4.5% to 24% for TID. The consistency of the inter-animal measurements and reproducibility of intra-animal measurements indicates that RPI is an adequate technique for measuring the mechanical properties of rat tibia, in situ. However, the BioDent^{TM} 1000 was only moderately capable of measuring small differences in the mechanical properties of bones between rats of the same strain and age. Future studies could improve the standard deviation by ensuring the bone samples are measured in one location (e.g. mid-diaphysis), comparing site specific measurement results (e.g. distal measurement 1 on bone 1 compared to distal measurement 1 on bone 2) or using improved fixation devices. The relative ease of measurement and minimal invasiveness of this technique indicates that RPI may be a suitable technique for in vivo rat studies.

***Disclosures: Alexander Proctor**, Active Life Technologies, 4*

SU0037

Influence Of Femoral Head Trabecular Arch On The Ostoporotic Femoral Strength: A Finite Element Analysis. Wafa Skalli*[1], Guillaume Salmon-Legagneur[2], Erwan Jolivet[3], Sandra Guerard[4], Valérie Bousson[5], Jean-Denis Laredo[6]. [1]Arts et Metiers ParisTech, CNRS, France, [2]Arts et Métiers Paristech, LBM, France, [3]Arts et métiers ParisTech, France, [4]Arts et Métiers ParisTech, LNM, France, [5]Hôpital Lariboisière, France, [6]Service de Radiologie ostéo-articulaire, Hôpital Lariboisière, Assistance Publique des Hôpitaux de Paris et Faculté de Médecine Diderot, Université Paris 7, France

Using femoral head BMD for femoral strength estimation has been recently suggested (reference). Such information is difficult to investigate on routine DXA images, so its relevance is an important issue. The aim of this study is to use a finite element model in order to investigate the role of the femoral head trabecular arch in the estimation of the proximal femur strength.

The study is based on an existing non linear model of the proximal femur built from QCT data for geometry and material properties, with a stress criterion to estimate fracture load. The model was previously validated with 30 human femurs in stance configuration. This model was used with three different analyses (figure 1): (a) initial model (I model) with subject specific attribution of material properties for each element of cortical and spongy bone from QCT Hounsfield units; (b) same model with simplification for the spongy area by using two media, one for the femoral head trabecular arch and one for the remaining spongy area, each with mean values of Young modulus and yield stress, called TA (trabecular Arch) model; (c) same model with an oversimplification for the spongy area by neglecting the effect of trabecular arch, i.e. using for the trabecular arch the same material properties as the remaining spongy area, called S(simplified) model; Predicted fracture loads were compared to experimental reference (Exp), and among models using signed wilcoxon tests and correlation analysis. For the 11 analysed femurs, results are presented in table 1. There was no statistical significant difference between Exp and initial model (p=0.13, r2 =0.92), nor between I and TA, and Exp and TA (respectively p=0.60 and p=0.09, r2 = 0.92 and 0.89). A significant difference was found between TA and S. Considering the spongy area as a homogeneous medium without taking into account the trabecular arch effect (S model) lowered the fracture load by 12% to 36 % with regard to TA model). The decrease was inversely correlated to initial value of fracture load. For those femurs with low fracture loads, trabecular arch was often already weak and disrupted, and therefore could be less contributive to the femoral strength. Other parameters could play a role, such as the arch orientation and geometry.

This study suggests that the femoral head trabecular arch plays a significant role in increasing femoral strength, and therefore a femoral head BMD could increase relevance of femur strength estimation.

Femurs	Experimental	I model	TA model	S model	Difference TA-S
1	3994	4900	4500	3200	1300
2	6034	5400	6500	5300	1200
3	6949	5600	4800	3800	1000
4	7235	7900	6800	6000	800
5	7894	7100	8800	6000	2800
6	8946	7800	8500	6400	2100
7	8963	9900	9300	7100	2200
8	9774	8500	8500	5400	3100
9	10645	9100	8700	6900	1800
10	12791	12900	11800	9700	2100
11	15886	15900	15000	11100	3900

Table 1 : Experimental fracture load (N), predicted fracture for I model, TA model and S model and d

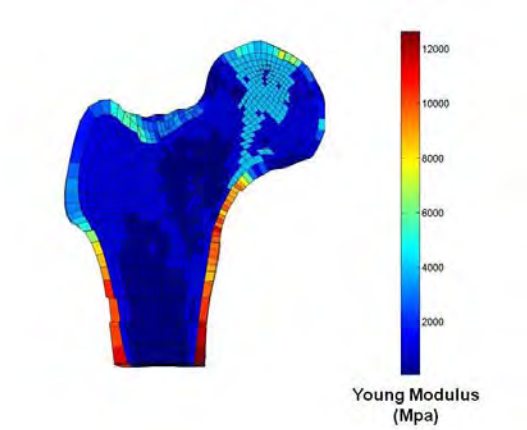

Young Modulus distribution for a femur with a weak trabecular arch

***Disclosures: Wafa Skalli**, None.*

SU0038

Longitudinal Study of the Bone Strength in the Proximal Femur in Patients with Glucocorticoid-induced Osteoporosis by DXA-based Hip Structural Analysis. Ikuko Tanaka*[1], Shigenori Tamaki[2], Jyunichi Ishii[3], Hisaji Oshima[4]. [1]National Institute for Longevity Science, Japan, [2]Department of Rheumatology, Mie Chuou Medical Center, Japan, [3]Fujita Health University School of Medicine, Japan, [4]Tokyo Medical Center, Japan

[Background] Hip structural analysis (HSA) has demonstrated as a useful tool to evaluate the bone strength from dual-energy X-ray absorptiometry (DXA) data. The data for primary osteoporosis have been accumulating, but there are still few study about secondary osteoporosis. Actually, the prevalence of osteoporosis (bone loss) is high in patients under glucocorticoid (GC) therapy. Thus, further data for GC-induced osteoporosis will be required. [Purpose] We evaluated the influences of GC therapy on the bone strength using DXA-based HSA. [Objects] 245 subjects with collagen diseases (mean age 55 year old, mean PSL dosage 5.8 mg/day) were recruited in rheumatology clinic. [Methods] Bone mineral density (BMD) of proximal femur was calculated from pixel distribution parameters using DXA and quantified bone geometric parameters; cross-sectional area (CSA), cross-sectional moment of inertia (CSMI, cm4), the section modulus (SM, cm3), the buckling ratio (BR) at femoral narrow neck (NN), intertrochanter (IT) and Femoral shaft (FS) regions. DXA was performed at interval of 6 months and the changes in the bone parameters were evaluated in subjects with or without GC therapy. [Results] (1) Subjects without GC therapy showed no significant changes in BMD at all three regions. However, a significant decrease in BMD at NN (-2.8%) was observed in the subjects with GC therapy during this study. (2) CSA values were significantly decreased at both NN (-2.0%) and IT (-1.8%) in subjects with GC therapy. (3) BR values at NN in subjects with GC therapy were significantly changed during this study (6.5%). [Discussion] (1) The influence of GC on the bone strength was observed at NN within only 6 months. Especially, the loss of the bone strength was observed in BR. These data suggested that the follow-up at NN was important in subjects with GC therapy. (2) HAS is a convenient tool since the bone strength was calculated as a strength in 3D using 2D DXA scans. Thus, HSA is still useful even in GC-induced osteoporosis, although HSA is calculated using femoral neck as a simplified structural model and mainly assess the cortical bone.

***Disclosures: Ikuko Tanaka**, None.*

SU0039

Maximum Stress Peaks after Growth while Volumetric Bone Mineral Density does not. Jesper Thomsen*[1], Annemarie Brüel[2], Kim Brixen[3], Annie Charles[4], Ellen Hauge[5]. [1]Institute of Anatomy,University of Aarhus, Denmark, [2]University of Aarhus, Denmark, [3]Institute for Clinical Research, Denmark, [4]University of Aarhus, Denmark, Denmark, [5]Aarhus University Hospital, Denmark

Purpose: Peak bone mass is a major determinant of fracture risk in senescence. During childhood the growth-related increase in areal bone mineral density (aBMD) and in maximum load (F_{max}) are related to a concomitant increase in bone size. In contrast, volumetric measurement of BMD (vBMD) and maximum stress (σ_{max}) are independent of bone size. Consequently, the purpose of the study was to investigate the age-related changes in vBMD and σ_{max} and their relationship in childhood and adulthood.

Methods: Age-related changes in σ_{max} and vBMD were investigated using second lumbar vertebral bodies obtained during routine autopsy procedures. The study

comprised 108 individuals (50 women, 58 men), aged 0.2–95 years (median 56 years). The individuals had died suddenly from accidents or acute diseases. Individuals with known malignant, renal, or metabolic bone diseases were excluded from the study as were vertebral bodies with known fractures. The endplates of the vertebral bodies were sawn off using a diamond parallel precision saw, and the volume was determined using Archimedes principle. Then the samples were pQCT scanned at a voxel size of $0.689 \times 0.689 \times 1$ mm^3, and compression tested in a materials testing machine at a constant deformation rate of 5 mm/min. Data were analyzed by linear regression.

Results: During the period from birth to peak bone mass (0–25 years) σ_{max} increased (r^2; B, p) (0.52; 0.181 MPa/year, $p<0.001$), whereas vBMD remained constant, and was therefore not correlated with age (0.03; -0.52 mg/cm^3/year, $p=0.45$). After peak bone mass was reached, vBMD decreased significantly with age for women (0.63; -2.0 mg/cm^3/year, $p<0.001$) and men (0.51; -1.2 mg/cm^3/year, $p<0.001$). This senescent decrease in vBMD was paralleled by a decrease in σ_{max} for both women (0.62; -0.11 MPa/year, $p<0.001$) and men (0.42; -0.05 MPa/year, $p<0.001$). The σ_{max} and vBMD were correlated from the second decade in women (0.82; 0.05 MPa/mg/cm^3, $p<0.001$) and men (0.62; 0.04 MPa/mg/cm^3, $p<0.001$), whereas this relationship was not present in the first decade (0.16; 0.01 MPa/mg/cm^3, $p=0.51$).

Conclusions: In the adult population σ_{max} and vBMD are tightly correlated, making bone mass a major determinant of fracture risk. The absence of correlation between σ_{max} and vBMD during childhood suggests that other factors such as bone structure may play a significant role for vertebral bone strength during early growth.

***Disclosures: Jesper Thomsen**, None.*

SU0040

Radiation Therapy Causes Rapid Loss of Proximal Femur Bone Strength and Density in Women with Gynecological Tumors. Ted Bateman*[1], Thomas Lang[2], Dana Carpenter[2], Michael Lawrence[3], Varun Sehgal[4], Nilam S. Ramsinghani[4], Jeffrey V. Kuo[4], Muthana Al-Ghazi[4], Jeffrey Willey[5], Joyce Keyak[6]. [1]Univesity of North Carolina, USA, [2]University of California, San Francisco, USA, [3]University Of North Carolina, USA, [4]University of California, Irvine, USA, [5]Clemson University, USA, [6]University of California, USA

Postmenopausal women receiving radiation therapy (RT) for pelvic tumors have a 65-200% increased risk of hip fracture compared to women receiving non-RT cancer treatment. It is generally accepted that RT damages local osteoblasts and vasculature resulting in a low-turnover, gradual decline in bone mass. However, it has recently been observed in rodent models that ionizing radiation activates osteoclasts. To test the hypothesis that early osteoclastic resorption may cause a rapid loss of bone, changes in proximal femur strength, bone density, and mineral content were examined in women receiving RT for gynecological tumors.

Eight women (age 36-71 years) with cervical (n=6), vaginal, or uterine cancer provided informed consent. CT scans were performed pre-RT and on the last day of RT (6 weeks later). Patients received 50.4 Gy in 28 days (M-F). Total dose to the proximal femur was ~25.0 Gy. CT scans were used for finite element strength and volumetric quantitative CT (vQCT) analyses. Proximal femur strength was calculated for models representing a single-limb stance load (SL) and a fall load (FL) onto the posterolateral aspect of the greater trochanter. Volumetric bone mineral density (vBMD) and bone mineral content (BMC) were calculated via vQCT for trabecular (Tr), cortical (Co) and integral (Tr + Co) compartments of the proximal femur. Significance was determined by paired t-test.

All patients lost proximal femur strength for both SL and FL conditions (-5%, -10% $p<0.05$). vBMD was reduced in both the Tr and integral (-17%,-6% $p<0.01$), but not the Co, compartments. BMC was reduced for all regions: Tr -24%, Co -14% and integral -16% ($p<0.02$). Co BMC decline is accompanied by a loss of Co, and integral volume (-14%,-1-% $p<0.05$) indicating periosteal resorption and a thinning of the cortex. Linear regression analysis shows a greater loss of Tr BMC with decreasing age ($p=0.03$), but there was no correlation of age with BMD or strength changes.

RT caused rapid decline of bone strength, density and mineral content in the proximal femur. Only an early activation of osteoclasts can account for this rate of loss (BMC decline >2%/wk). For context, the bone loss from 6-wks of RT is roughly equivalent to 3 years of bone loss in women due to menopause. Future studies will examine later time points to determine the degree of recovery. As more data are available, prophylactic treatment of radiation-induced bone loss with antiresorptives should be considered.

***Disclosures: Ted Bateman**, Procter and Gamble Pharmaceuticals, 2*

SU0041

Reduced Bone Mineral Density is not Associated with Reduced Bone Quality in Men and Women Practicing Long-term Calorie Restriction with Adequate Nutrition. Dennis Villareal[1], John Kotyk[2], Reina Armamento-Villarea*[1], Venkata Kenguva[3], Pamela Seaman[4], Allon Shahar[4], Michael Wald[5], Michael Kleerekoper[6], Luigi Fontana[2]. [1]University of New Mexico School of Medicine, USA, [2]Washington University School of Medicine, USA, [3]St. Lukes Hospital, USA, [4]MicroMRI Inc, USA, [5]University of Pennsylvania School of Medicine, USA, [6]MicroMRI Inc., USA

Purpose: Calorie restriction (CR) without malnutrition reduces bone quantity but not bone quality in rodents. Nothing is known regarding the long-term effects of CR with adequate intake of vitamin and minerals on bone quantity and quality in middle-aged lean men and women. The objective of this study is to evaluate body composition, bone mineral density (BMD), and serum markers of bone turnover and inflammation in patients practicing CR.

Methods: Participants included 32 subjects eating a CR diet for an average of 6.8 ± 5.2 years (mean age 52.7 ± 10.3 years) and 32 age- and sex-matched sedentary controls eating Western diets (WD). Bone mineral density (BMD) and body composition were measured using dual energy x-ray absorptiometry (DXA), while markers of bone turnover and highly-sensitive C-recative protein (Hs-CRP) were measured by Elisa. In a subgroup of 10 CR and 10 control volunteers, we also measured trabecular bone (TB) microarchitecture of the distal radius using high-resolution magnetic resonance imaging.

Results: We found that the CR volunteers had significantly lower body mass index than the WD volunteers (18.9 ± 1.2 vs. 26.5 ± 2.2 kg/m^2; P=0.0001). BMD of the lumbar spine and hip was lower in the CR; serum markers of bone turnover (C-terminal peptide and bone-specific alkaline phosphatase) were similar between groups; while serum Hs-CRP was lower in the CR than the WD group (Table 1). TB microarchitecture parameters such as the erosion index and surface-to-curve ratio were not significantly different between groups (Table 2).

Conclusion: Our findings demonstrate that long-term CR with adequate nutrition is associated with normal bone turnover markers and well-preserved TB micro-architecture, despite markedly low BMD in middle-aged men and women.

Table. 1 Subject characteristics, body composition, bone mineral density, and markers of bone turnover and inflammation

	CR group (n=32)	WD group (n=32)	P value
Age (years)	52.7 ± 10.3	53.4 ± 9.4	0.761
Sex (M/F)	28/4	28/4	
BODY COMPOSITION			
Body weight (kg)	57.5 ± 5.3	84.8 ±11.4	0.0001
Body mass index (kg/m^2)	18.9 ± 1.2	26.5 ± 2.2	0.0001
Body composition			
Fat mass (%)	10.6 ± 6.6	25. 4 ± 7.7	0.0001
Lean mass (kg)	49.2 ± 7.3	60.0 ± 9.3	0.0001
BONE MINERAL DENSITY			
Lumbar spine (g/cm^2)	0.870 ± .111	1.138 ± .120	0.0001
T score	-2.1 ± 1.0	0.36 ± 1.0	0.0001
Total hip (g/cm^2)	0.806 ± .118	1.047 ± .118	0.0001
T score	-1.47 ± 0.78	0.12 ± 0.73	0.0001
Femoral neck (g/cm^2)	0.677 ± .110	0.856 ± 0.118	0.0001
T score	-1.8 ± 0.8	-0.53 ± 0.83	0.0001
Trochanter (g/cm^2)	0.611 ± .102	0.809 ± 0.123	0.0001
T score	-1.3 ± 0.80	0.26 ± 0.90	0.0001
MARKERS OF BONE TURNOVER AND INFLAMMATION			
S-CTX (ng/mL)	0.595 ± .288	0.508 ± .179	0.152
S-BSAP (U/L)	17.6 ± 5.8	18.1 ± 4.5	0.691
HsCRP (mg/L)	0.19 ± 0.26	1.46 ± 1.56	0.0001

Values are mean ± SD. S-CTX = serum C-terminal telopeptide; S-BSAP = serum bone-specific alkaline phosphatase, HsCRP = high sensitivity C-reactive protein

Table 1

Table 2. Hr-MRI Parameters

	CR group (n=10)	WD group (n=10)	P value
BV/TV	0.092 ± .019	0.102 ± .022	.318
Trabecular thickness (mm)	0.089 ± .007	0.097 ± .008	.023
Volume (cc)	1.706 ± .314	1.877 ± .424	.320
Skeleton density	0.051 ± .011	0.056 ± .012	.353
Surface-to-curve ratio	10.3 ± 4.3	12.2 ± 6.7	.440
Erosion index	0.917 ± 0.276	0.876 ± 0..278	.739

Values are mean ± SD. BV/TV = Bone volume to total volume ratio

Table 2

***Disclosures: Reina Armamento-Villarea**, Alliance for Better Health, 2*
This study received funding from: MicroMRI, Alliance for Better Bone Health

SU0042

Short-term Implications of Renal Transplantation on Stiffness of Distal Tibia Estimated by MRI-Based Finite Element Modeling. Chamith Rajapakse*[1], Yusuf Bhagat[2], Mary Leonard[3], Wenli Sun[2], Jeremy Magland[2], Felix Werner Wehrli[4]. [1]University of Pennsylvania School of Medicine, USA, [2]University of Pennsylvania, USA, [3]Children's Hospital of Philadelphia, USA, [4]University of Pennsylvania Medical Center, USA

The short-term structural and mechanical effects of renal transplantation (RTxp) are not known. Here, we examined the hypothesis that temporal changes in trabecular and cortical bone mechanical competence following RTxp can be assessed with the aid of micro-finite-element (μFE) modeling based on high-resolution magnetic resonance (MR) images to create the μFE mesh. Images were acquired from 31 subjects (median 42, range 20-60) before and six months after RTxp at the distal tibial metaphysis along with sex-matched healthy 34 controls (median 34, range 23-52). Images were processed to yield three sets of 3D μFE models corresponding to a transaxial slab of 5 mm thickness, referred to as whole-bone (WB) section, trabecular-bone (TB) compartment, and cortical bone (CB) compartment. Axial stiffness was computed via simulated compressive loading in the axial direction. At the time of RTxp, WB and TB stiffness were 18.1% ($p<0.0001$) and 20.1% ($p<0.0001$) lower, respectively, than controls. Six months following transplantation, mean WB and TB stiffness decreased significantly by 6.7% ($p<0.05$) and 11.9% ($p<0.005$), respectively. The mean difference in CB stiffness between TRxp and controls at baseline did not reach statistical significance. The CB stiffness decreased marginally by 5.2% ($p=0.05$) from baseline to follow-up in the TRxp recipients. The mean CB stiffness was lower by 15.1% ($p<0.05$) in the TRxp recipients at 6-mo follow-up compared to controls. The data show that MRI-based μFE analysis is suited for assessing short-term mechanical implications of intervention in patients.

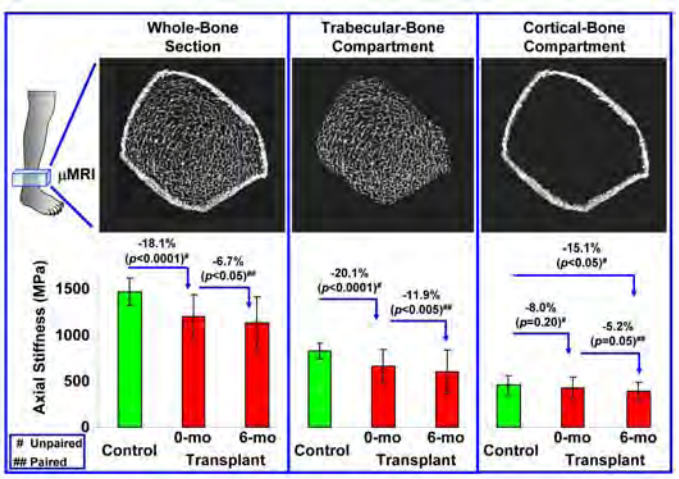

Figure 1

***Disclosures: Chamith Rajapakse**, None.*

SU0043

Structural Changes of Bone Influence Bone Quality in Ovariectomized Rats. ZhiQi Peng*[1], Jukka Morko[2], Jukka Rissanen[3], Jukka Vääräniemi[1], Jussi Halleen[1]. [1]Pharmatest Services Ltd, Finland, [2]Pharmatest Services Ltd, Fin, [3]Pharmatest Services,Limited, Finland

The rat ovariectomy (OVX) model is the most extensively used preclinical animal model of osteoporosis. Similarly to human postmenopausal osteoporosis, OVX increases bone turnover and induces trabecular bone loss in rats. However, mechanical properties, like bending strength, of femoral or tibial diaphysis and femoral neck may be either decreased, unchanged or increased in OVX rats, suggesting that OVX-induced changes in bone quality are unstable in rats. The purpose of this study was to clarify these controversial changes in bone quality in OVX rats. Female Sprague-Dawley rats were either ovariectomized or sham-operated at the age of 12 weeks and 11 months, and their femora and tibiae were harvested for bone analyses at 5 and 6 weeks after the operations, respectively. Mechanical properties of bone were determined from tibial diaphysis by three-point bending test and from femoral neck by cantilever bending test. In addition, tibial diaphysis, femoral neck and femoral distal metaphysis were studied by bone histomorphometry. OVX did not induce changes in bone material properties of tibia and in bending strength of tibial diaphysis in either young or aged rats. However, OVX decreased maximal load of femoral neck in young OVX rats, but not in aged rats. At the upper part of the femoral neck, bone histomorphometry revealed a lack of functional bone formation, and an OVX-induced increase in longitudinal bone growth rate in young rats. This OVX-induced effect was associated with increased longitudinal length of the femoral neck, influencing the bone load, but the moment of maximal load remained unchanged in the femoral neck of these young OVX rats. In addition, OVX-induced increase in bone turnover and bone formation in association with OVX-induced bone loss demonstrated increased bone resorption in marrow cavity, especially in young OVX rats. This increased endosteal bone resorption was compensated by increased periosteal bone formation, maintaining the cross-sectional moment of inertia in tibial diaphysis. These results suggest that OVX induces high bone turnover and further changes in bone structural properties, which influence the bone quality. OVX does not decrease the bending strength of tibial diaphysis, but it decreases the load of femoral neck in young rats. This effect, however, disappears gradually when the local growth plate in the femoral neck closes.

***Disclosures: ZhiQi Peng**, None.*

SU0044

The Pattern of Compensatory Trait Interactions Defining Variation in Skeletal Function among Individuals is Recapitulated within a Single Bone. G. Felipe Duarte[1], N. Remi Gendron[1], Philip Nasser[1], Richard Ghillani[1], Rachel Evans[2], Charles Negus[3], Karl Jepsen*[1]. [1]Mount Sinai School of Medicine, USA, [2]U.S. Army Research Institute of Environmental Medicine, USA, [3]L-3 Applied Technologies, USA

Complex systems like bone rely on compensatory interactions among morphological and tissue-quality traits to buffer genetic and environmental factors that compromise system function. Although critical for bone strength, these complex interactions complicate the search for simple traits that predict fracture risk. Prior studies reported that traits covaried in a predictable way when viewed across a population of genetically distinct individuals with diverse life histories. Specifically, slender bones are compensated by an increase in relative cortical area and tissue-mineralization, whereas robust bones are compensated by reduced relative cortical area and mineralization. We wanted to know whether this pattern holds within an individual, where genetic background and life histories are controlled.

The trumpet-shaped tibia was used as a model to test whether the proximal-to-distal variation in external bone size was functionally correlated with tissue-mineralization. Peripheral quantitative computed tomography, pQCT, scans of 25 cadaveric human tibiae (16 male, 9 female, aged 17-49) at sites 25%, 38%, 50%, 66% and 75% from the distal end plate (0.1mm voxel size), were analyzed for cross-sectional geometry and tissue mineral density (TMD). In addition, sections were cut and ashed from 12 of the tibiae to confirm the correlation between TMD derived by pQCT and mineralization.

As expected TtAr/Le decreased nearly two-fold from proximal to distal and CtAr was only lower for the distal two sites ($p<0.0001$, repeated measures ANOVA). TMD, which correlated significantly with ash content ($R2=0.4$, $p<0.0001$), varied 1.8 $\pm$ 0.9% from proximal (low) to distal (high) ($p<0.0001$). Multiple regression analysis revealed that 78 $\pm$ 20% of the intra-bone variation was explained by TtAr/Le and CtAr for 19 of the 26 individuals (e.g. TMD = 1332 - 0.086*CtAr - 51.4*TtAr/Le, $R2=0.996$, $p<0.002$). Similar correlations were found for ash content, confirming that the associations between morphology and TMD represent a biological phenomenon and not an artifact of pQCT.

The negative correlation between TMD and CtAr and TtAr/Le indicated that higher TMD compensated for smaller CtAr and TtAr/Le along the tibial length. Finding the association that morphology and tissue quality are functionally related among individuals as well as along tibial length provides further evidence in support of phenotypic covariation playing a central role in establishing mechanical function in bone.

***Disclosures: Karl Jepsen**, None.*

SU0045

Understanding the Effects of Rosiglitazone on Bone as Measured by DXA and HSA: a Mechanistic Study in Postmenopausal Women with Type 2 Diabetes Mellitus. Lorraine A. Fitzpatrick*[1], Antonio J. Nino[2], Barbara Kravitz[3], Allison R. Northcutt[2], Gitanjali Paul[2], Alexander Cobitz[2]. [1]Biopharm R&D, GlaxosmithKline, USA, [2]CVM/MDC, GlaxoSmithKline, USA, [3]GlaxoSmithKline Pharmaceuticals, USA

Abstract

This was a phase IV, double-blind, multi-center study (CT.gov.NCT00679939) of 52 weeks of duration, to characterize the effects of rosiglitazone (RSG) on bone parameters related with mass, structure, and remodeling. In this mechanism-of-action study, the effect of RSG on bone mass and structure will be studied through different imaging modalities including dual-energy X-ray absorptiometry (DXA), hip structure analysis (HSA), high resolution magnetic resonance imaging (hr MRI) of the wrist, Quantitative Computerized Tomography (QCT) and digitized hip radiography. Serum biomarkers of bone formation and resorption, calcium homeostasis and selected sex hormone changes over time were assessed. Parameters of glucose control included measurement of: hemoglobin A1C (HbA1C), fasting plasma glucose (FPG), and serum insulin. Here, we present the change in bone mineral density (BMD) as measured by DXA at the femoral neck, lumbar spine, total hip and trochanter. Change in Hip Structural Analysis (HSA) parameters were assessed in a subset of 140 subjects.

Methods

Following a screening period of two weeks, subjects were randomized to RSG or metformin (MET) in a 1:1 ratio. All randomized subjects (226) underwent a DXA scan at baseline and at weeks 16, 28, and 52. All DXA scans were centrally read. At baseline mean age was 63.8 $\pm$ 6.5 years while mean years post-menopause was 16.9 $\pm$ 8.4. Median duration of diabetes was 3.5 (1.8 -7.8) years. Other baseline characteristics were: mean body mass index (BMI) 31.4 $\pm$ 5.9 kg/m^2; mean FPG and HbA1c were 111.7 $\pm$ 23.4 mg/dl and 6.4 $\pm$ 0.65% respectively. Femoral neck BMD was 0.83 g/cm^2 $\pm$ 0.141, at total hip 0.98 g/cm^2 $\pm$ 0.123, and at total spine 1.05 g/cm^2 $\pm$ 0.161. Femoral neck T-score was -0.95 $\pm$ 0.908, total hip -0.02 $\pm$ 0.970, and total spine is -0.55 $\pm$ 1.247.

HSA method used cross-sectional dimensions measured on DXA hip scans. Specific HSA measurements include BMD, average buckling ratio, section modulus, and shaft angle at shaft, intertrochanter, and narrow neck. Changes from baseline in BMD via DXA and HSA parameters were estimated between and within the two treatment groups at each anatomical site and time points.

Conclusion

Changes in BMD by DXA and HSA parameters will be presented. These changes may provide insight into the mechanism of action of RSG on bone.

***Disclosures: Lorraine A. Fitzpatrick**, GlaxoSmithKline, 3*
This study received funding from: GlaxoSmithKline

SU0046

Effects of Soy Isoflavone Supplements on Bone Turnover Markers in Menopausal Women: Systematic Review and Meta-analysis of Randomized Controlled Trials. Kyoko TAKU*[1], Melissa K. Melby[1], Mindy S. Kurzer[2], Shoichi Mizuno[1], Shaw Watanabe[1], Yoshiko Ishimi[1]. [1]National Institute of Health & Nutrition, Japan, [2]University of Minnesota, USA

Introduction: Effects of soy isoflavone supplements on bone turnover markers remain unclear. This up-to-date systematic review and meta-analysis of randomized controlled trials (RCTs) was performed primarily to more completely and precisely clarify the effects on urinary deoxypyridinoline (DPD) and serum bone alkaline phosphatase (BAP) and secondarily to evaluate the effects on other bone turnover markers, compared with placebo in menopausal women.

Methods: PubMed, CENTRAL, ICHUSHI, and CNKI were searched in June 2009 for relevant studies of RCTs. Data on study design, participants, interventions, and outcomes were extracted and methodological quality of each included trial was assessed.

Results: From 3740 identified relevant articles, 10 (887 participants), 10 (1210 participants), and 8 (380 participants) RCTs were selected for meta-analysis of effects on DPD, BAP, and serum osteocalcin (OC), respectively, using Review Manager 5.0.22. Daily ingestion of an average 56 mg soy isoflavones (aglycone equivalents) for 10 weeks to 12 months significantly decreased DPD by 14.1% (95% CI: -26.8% to -1.5%; $P = 0.03$) compared to baseline (heterogeneity: $P < 0.00001$; $I^2 = 93\%$; random effects model). The overall effect of soy isoflavones on DPD compared with placebo was a significant decrease of -18.0% (95% CI: -28.4% to -7.7%, $P = 0.0007$; heterogeneity: $P = 0.0001$; $I^2 = 73\%$; random effects model). Subgroup analyses and meta-regressions revealed that isoflavone dose and intervention duration did not significantly relate to the variable effects on DPD. Daily supplementation of about 84 mg and 73 mg of soy isoflavones for up to 12 months insignificantly increased BAP by 8.0% (95% CI: -4.2% to 20.2%, $P = 0.20$; heterogeneity: $P < 0.00001$; $I^2 = 98\%$) and OC by 10.3% (95% CI: -3.1% to 23.7%, $P = 0.13$; heterogeneity: $P = 0.002$; $I^2 = 69\%$) compared with placebo (random effects model), respectively.

Conclusions: Soy isoflavone supplements moderately decreased the bone resorption marker DPD, but did not affect bone formation markers BAP and OC in menopausal women. The effects varied between studies, and further studies are needed to address factors relating to the observed effects of soy isoflavones on DPD and to verify effects on other bone turnover markers.

***Disclosures: Kyoko TAKU**, None.*

SU0047

In Vivo Longitudinal Assessment of Microarchitecture and Biomechanical Properties in Women With or Without Treatment: An HR-pQCT Study. Nicolas Vilayphiou*[1], Stephanie Boutroy[1], Emmanuelle Vignot[2], Elisabeth Sornay-Rendu[1], Françoise Munoz[1], Bert Rietbergen[3], Pierre Delmas[1], Roland Chapurlat[1]. [1]INSERM Unit 831 & Université de Lyon, France, [2]Department of Rheumatology, Hôpital Edouard Herriot, France, [3]Eindhoven University of Technology, The netherlands

Evolution of bone microarchitecture and mechanical properties assessed by finite element analysis (FEA) under treatment is poorly known. We have performed a case control longitudinal study to determine their evolution in treated and untreated women.

Our study involved 89 women: 39 untreated women without fracture (CTRL - 69 $\pm$ 4yrs, all from the OFELY cohort); 39 women with history of vertebral fracture ($\geq$2), treated for 18 months with teriparatide (TPD - 69 $\pm$ 10yrs), after treatment by bisphosphonates; and 11 women with other osteoporotic fractures treated by bisphosphonates (BP - 71 $\pm$ 7yrs). Follow-up times were 22 $\pm$ 2m in CTRL group, 20 $\pm$ 4m in BP women and 18 $\pm$ 1m in TPD women. Treated women were recruited via the department of Rheumatology.

Areal BMD was measured by DXA, total volumetric BMD (vBMD), cortical thickness (CTh) and trabecular number (TbN) were assessed by HR-pQCT, and for treated women only, estimated bone stiffness was obtained by FEA. Paired t-tests were used to assess differences during the follow-up within each group, and ANCOVA for longitudinal variation explained by treatment, with the baseline value as covariate, assessed differences between groups. HR-pQCT data are presented for the tibia only (see Table), as patterns at the radius were similar.

At baseline, differences in hip or spine aBMD among the 3 groups were not significant, and remained stable in all groups. At the tibia TPD-women had lower total vBMD and an impaired microarchitecture when compared to BP or CTRL women ($p<0.05$). Bone stiffness in TPD women tended to be lower than in the BP group ($p=0.10$). After 18 months of treatment in TPD women, total vBMD decreased significantly by 3%, whereas in other groups it remained stable ($p<0.01$). A cortical thinning was observed (-2% to -6%), that was not different across the 3 groups. In contrast, TbN increased in treated groups (+6% in BPP, +3% in TPD), whereas CTRL women had stable microarchitecture. However, this effect was not sufficient to counterbalance the loss in cortical bone despite the treatment. Indeed, bone stiffness was lower after the treatment period, in TPD women (-3%, $p<0.01$) and in BP women (-1.5%, $p=0.11$), but these 2 groups did not differ significantly ($p=0.08$).

In conclusion, we found weak benefits of anti-osteoporotic treatments were obtained at the peripheral sites, where unexpected loss of cortical bone dominated the gain in trabecular bone.

Table: Longitudinal evolution of HR-pQCT parameters at the tibia according to treatment.

	CTRL n=39		BP n=11		TPD n=39		ANCOVA Δ by TTT with Baseline
	Baseline Mean ± SD	Mean Δ %	Baseline Mean ± SD	Mean Δ %	Baseline Mean ± SD	Mean Δ %	p value
Age [yrs]	70 ± 4	NA	71 ± 7	NA	69 ± 10	NA	NA
aBMD Hip [g/cm²]	0.715 ± 0.031	-0.07	0.720 ± 0.084	1.02	0.697 ± 0.120	0.21	NS
Total vBMD [g/cm³]	216 ± 42	-0.66	222 ± 57	-0.85	192 ± 43	-3.04 **	0.010
CTh [mm]	0.75 ± 0.20	-2.40 **	0.71 ± 0.32	-3.25	0.71 ± 0.25	-6.45 **	NS
TbN [1/mm]	1.43 ± 0.23	-0.62	1.50 ± 0.23	6.19 *	1.15 ± 0.33	3.11 *	0.003
Stiffness [kN/mm]	NA	NA	286 ± 33	-1.49	259 ± 47	-3.64 **	0.083

Differences are indicated for differences from baseline value
*p<0.05 ; **p<0.01

Longitudinal evolution of HR-pQCT parameters at the tibia according to treatment.

***Disclosures: Nicolas Vilayphiou**, None.*

SU0048

Variations in Cancellous Bone Tissue Composition and Mechanical Properties with a Model of Osteoporosis and Treatment in Sheep. Jayme Burket*[1], Jennifer MacLeay[2], Shefford Baker[1], Adele Boskey[3], Marjolein Van Der Meulen[1]. [1]Cornell University, USA, [2]Hill's Pet Nutrition, Inc., USA, [3]Hospital for Special Surgery, USA

The reduced bone strength occurring with osteoporosis is not only a function of bone mass and architecture, but also tissue properties. Osteoporosis reduces tissue mineralization, alters the collagen matrix, and decreases tissue heterogeneity, but the effects of these compositional changes on the tissue mechanical properties are unclear. Metabolic acidosis (MA) in sheep produces similar mineral changes as human osteoporosis, allowing us to examine disease and treatment effects on cancellous tissue composition and mechanical properties.

Cancellous bone was obtained from the distal femur of skeletally mature ewes. Controls were fed a normal diet for 12 months, whereas treatment groups were fed a diet to induce MA for 6 months and then treated with either Raloxifene (RAL), Alendronate (ALN) or vehicle, while maintaining the diet for another 6 months (n=2/group). Three trabeculae were characterized per sample by nanoindentation and Raman. Indentation modulus (Ei) and hardness (H) were assessed along lines

spanning the width of the trabeculae, with indents placed at the center of lamellae (n=10-17/trabecula). Mineral:matrix ratio (M:M, degree of mineralization), carbonate:phosphate ratio (C:P, carbonate substitution into the hydroxyapatite crystal lattice) and crystallinity (XST, crystal size and perfection) were measured at the indent locations. Treatment effects were assessed by one-factor ANOVAs with Tukey post-hoc tests.

MA decreased Ei below control values. RAL and ALN treatment increased Ei and H over MA+vehicle, with ALN increasing Ei by 9% more than RAL. H increased 10% more with ALN than RAL, achieving a 17% increase over control. MA did not alter M:M. ALN increased M:M by 13% relative to MA+vehicle and 12% relative to control. C:P decreased in all MA groups relative to control, with the greatest reduction by ALN. In all MA groups, XST was 3% greater than control.

MA reduced stiffness and altered mineral properties. Treatment with RAL and ALN restored tissue stiffness and hardness to levels found in healthy tissue, with ALN producing greater increases than RAL. However, crystallinity and carbonate substitution were not restored to normal with either treatment. Increased stiffness and hardness corresponded with increased tissue mineralization. The greater increases in mineralization and stiffness with ALN likely reflect that ALN reduces bone turnover more than RAL.

Table 1. Mean ± SD of the mechanical and compositional parameters.

	Indentation Modulus	Hardness	Mineral:Matrix	Carbonate:Phosphate	Crystallinity
Control	27.8 ± 0.5	1.12 ± 0.03	7.72 ± 0.18	0.200 ± 0.002	0.0595 ± 0.0002
MA + Vehicle	25.5 ± 0.5^{A}	1.08 ± 0.03	7.68 ± 0.20	0.183 ± 0.003^{A}	0.0618 ± 0.0002^{A}
MA + RAL	27.2 ± 0.5^{B}	1.20 ± 0.03^{B}	7.85 ± 0.23	0.181 ± 0.003^{A}	0.0619 ± 0.0002^{A}
MA + ALN	29.5 ± 0.6^{BC}	1.31 ± 0.03^{AB}	8.65 ± 0.21^{AB}	0.173 ± 0.003^{AB}	0.0618 ± 0.0002^{A}

^{A} = Different from Control, ^{B} = Different from MA + Vehicle, ^{C} = Different from MA + RAL

Table 1

***Disclosures: Jayme Burket**, None.*

SU0049

Recovery of Abdominal Adiposity and Vertebral Bone after Multiple Exposures to Mechanical Unloading. Shikha Gupta*[1], Gunes Uzer[2], Stefan Judex[2]. [1]State University of NY, Stonybrook, USA, [2]Stony Brook University, USA

Reduced levels of mechanical loading, as experienced during bedrest, space flight, or injury, result in marked bone atrophy. The loss of functional weightbearing also has other systemic and cellular consequences which may affect the onset of obesity or diabetes, including altered tissue adiposity and a disruption of fat metabolism. In light of the complex relationship between bone and fat, here, we hypothesize that single and multiple exposures to disuse will affect the ratio of abdominal adiposity to bone. Adult (16wk) male C57BL/6J mice were allowed to ambulate normally or were exposed to 2wk of hindlimb unloading (HLU) once, twice, or thrice at age 28wk (1x-HLU), at 22wk and 28wk (2x-HLU), or 16wk, 22wk, and 28wk (3x-HLU), respectively. Each HLU cycle was followed by 4wk of reambulation (RA). Longitudinal *in-vivo* microCT scans of the abdominal region were performed at 28, 30, and 34wk to quantify total (TF), subcutaneous (SF), and visceral (VF) fat and vertebral apparent density. At baseline, all mice had comparable body mass and bone density. Prior to HLU at 28wk, SF was about 30% of TF for all groups. HLU mice experienced weight loss, which was accompanied by a greater concomitant % loss of TF, SF, VF and vertebral density after HLU. Despite the decrease in SF volume, the % SF of TF increased to 40% post-HLU. The changes in adiposity and vertebral density after HLU were similar, irrespective of whether they had 0, 1, or 2 prior exposures to disuse. Changes in bone density and all three fat compartments after HLU were significantly correlated. Though all HLU groups largely recovered bone after 4wk of RA, with % change from 28wk comparable to age-matched animals, only multiple HLU groups achieved full recovery of TF, SF, and VF at 34wk. Regardless of the extent of recovery, the ratio of SF to TF returned to 30% for all groups. In contrast to clinical studies of bed rest or spinal injury, in which abdominal and marrow fat increase, a decrease in adiposity was observed during HLU. This may be attributed in part to lower food intake during HLU, which preferentially reduced visceral fat and thereby altered the composition of abdominal adiposity. While all indices returned to values comparable to age-matched control for 2x- and 3x-HLU mice, TF did not fully recover post-RA in 1x-HLU mice. Together, the results suggest that only the initial cycle of HLU reduces adiposity permanently, with complete recovery after multiple exposures that matches the recovery of vertebral bone.

***Disclosures: Shikha Gupta**, None.*

SU0050

Serum 25(OH)D Levels and Tibia Volumetric Bone Mineral Density (vBMD) in Patients with Chronic Spinal Cord Injury (SCI). Kayla Hummel*[1], B. Catharine Craven[2], Lehana Thabane[3], Jonathan Adachi[4], Alexandra Papaioannou[5], Neil McCartney[3], Milos R. Popovic[6], Lora Giangregorio[1]. [1]University of Waterloo, Canada, [2]Toronto Rehabilitation Institute, Canada, [3]McMaster University, Canada, [4]St. Joseph's Hospital, Canada, [5]Hamilton Health Sciences, Canada, [6]University of Toronto/Toronto Rehabilitation Institute, Canada

Purpose: Low vBMD of the tibia is shown to predict lower extremity fractures post-SCI. Additional fracture predictors may include vitamin D status and trabecular bone structure. We explored the relationships between serum 25(OH)D levels and vBMD and bone structure outcomes (connectivity, mean and maximum hole size) in individuals with chronic SCI.

Methods: Adults with chronic SCI (>2 years post-injury) were recruited into this cross-sectional study and had serum 25(OH)D levels measured at the time of consent. PQCT scans of the tibia were obtained at the ultra-distal tibia (4% site), where trabecular vBMD, connectivity, and mean and maximum hole sizes were evaluated, and at the tibia shaft (66% site), where total vBMD and cortical thickness were assessed. Stratec XCT commercial software was used for analysis, except for trabecular structure parameters, which were determined using software designed in-house. Spearman correlation coefficients were calculated between serum 25(OH)D and each bone outcome.

Results: Mean (SD) age and injury duration of participants (N=25; 19 males, 6 females) were 50 (12.4) and 15.4 (9.4) years, respectively. Fifteen participants had motor complete SCI and 10 motor incomplete SCI of whom 8 were tetraplegic and 17 paraplegic. Mean (SD) serum 25(OH)D was 88.0 (45.0) nmol/L; 52% of levels were in the sufficient range (>75nmol/L), 32% insufficient (51-74nmol/L), and 16% deficient (<50nmol/L). Participants with sufficient/insufficient ranges of 25(OH)D levels were taking supplements. The mean (SD) for each bone outcome was: trabecular vBMD 138.9 (50.0) mg/cm^3, connectivity 0.189 (0.075) nodes/unit of connected network, mean hole size 7.85 (10.62) mm^2, maximum hole size 628.27 (327.41) mm^2, and shaft total vBMD 1081.0 (63.1) mg/cm^3 and cortical thickness 3.12 (1.14) mm. No significant correlations between 25(OH)D levels and trabecular vBMD (r=-0.039 p=0.863), connectivity (r=0.036 p=0.899), mean hole size (r=0.032 p=0.910) or maximum hole size (r=0.014 p=0.960), or shaft vBMD (r=-0.275 p=0.216) and cortical thickness (r=-0.177 p=0.431) were observed.

Conclusion: Vitamin D levels were not associated with vBMD or trabecular structure outcomes; relationships which have not been explored previously. Serial assessments of vitamin D status among a larger sample with adjustment for likely confounders (age, impairment, injury duration) may elucidate reasons for the lack of observed association.

***Disclosures: Kayla Hummel**, None.*

SU0051

Biphasic Transport Characteristics of Various Molecular Weight Tracers Through the Osteocyte LCS of Mechanically Loaded Bone. Christopher Price*[1], Xiaozhou Zhou[2], Wen Li[2], Bin Wang[2], Liyun Wang[1]. [1]University of Delaware, USA, [2]University of Delaware, Center for Biomedical Engineering Research, Department of Mechanical Engineering, USA

Since proposed by Piekarski and Munro in 1977, load-induced fluid flow through the lacunar-canalicular system (LCS) has been accepted as critical for bone metabolism, mechanotransduction, and adaptation. However, direct observation and quantification of load-induced fluid and solute convection in bone has been lacking. Recently, barriers to the direct observation of solute transport in the LCS were overcome using a novel approach combining fluorescence recovery after photobleaching (FRAP) with synchronized mechanical loading. This allowed us to quantify the transport kinetics of sodium fluorescein, a small molecular weight fluorescent tracer, in mouse tibiae subjected to *ex vivo* mechanical loading.

The goal of the current investigation was to investigate the relationship between mechanical loading and transport kinetics for fluorescent tracers over a range of sizes. Adult B6 male mice received either sodium fluorescein (376Da, n=5 mice) or one of the following AlexaFluor488 conjugated molecules via tail-vein injection; dextran (3kDa n=5), parvalbumin (12.3kDa n=6), or ovalbumin (45kDa n=6). After the tracer equilibrated within the LCS, intact left tibiae were harvested for transport studies using a combined FRAP imaging and mechanical loading protocol. Sub-periosteal osteocyte lacuna were selected for FRAP imaging over consecutive paired, rest-inserted (-3N, ~400με, 0.5Hz, 4s rest) cyclic axial end-loaded [loaded] and -0.2N static end-loaded [diffusive] tests. FRAP data were used to quantify the characteristic solute transport rates under loaded (k_{load}) and diffusive (k_{diff}) conditions and the solute transport enhancement due to load-induced fluid convection (k_{Load}/k_{Diff}).

Application of rest-inserted cyclic loading significantly enhanced the transport of solutes of all sizes within the tibial LCS (k_{Load}/k_{Diff} =1.18-1.45). Further, a biphasic relationship between transport enhancement and molecular weight was observed; with intermediate sized molecules (12.3kDa) exhibiting the greatest enhancements. These results provided direct evidence supporting load-induced convective solute transport and have allowed us to begin to elucidate the relationships between loading and the perfusion/microfluidics of the LCS *in vivo*. Ongoing studies will explore the effects of loading magnitude and frequency on LCS solute convection. These studies provide a

framework for the future study of bone fluid flow and the response of osteocytes to loading/fluid flow *in vivo*.

***Disclosures: Christopher Price**, None.*

SU0052

Effects of Regular Physical Activity in Osteocyte Apoptosis and Bone Strength Following Ovariectomy. Helder Fonseca*[1], Daniel Moreira-Gonçalves[2], Maria Paula Mota[3], José Alberto Duarte[2]. [1]CIAFEL, Faculty of Sport Sciences, University of Porto, Portugal, [2]CIAFEL, Faculty of Sport, University of Porto, Portugal, [3]CATED, Department of Sport, University of Trás-os-Montes e Alto Douro, Portugal

Purpose: Osteocytes are the most prevalent cells on bone tissue and form a syncytial network through matrix canaliculus. Their importance in mechanotransduction, is widely accepted. Osteocyte death by apoptosis was recently shown to be closely associated with subsequent osteoclast bone resorption and increased intracortical bone porosity and fragility. Osteocyte apoptosis has been shown to be linked with estrogen deficiency hence being a possible contributor to post-menopausal bone fragility. While there is in-vitro evidence that mechanical stimulation reduces osteocyte apoptosis in cultured cells, in-vivo evidence is still lacking.

The objective of this study was to determine if regular physical activity, after ceasing estrogen production by ovariectomy, effectively modifies the rate of osteocyte apoptosis and the bone resistance to fracture.

Methods: Twenty-five female Wistar rats (aged 5 months) were either ovariectomized (OVX, n=13) or sham operated (Sham; n=12) and further housed in cages either with running wheel allowing them to freely exercise (OVXEX, n=7; SHAMEX, n=6) or in identical cages without wheel imposing them a sedentary behavior (OVXSED, n=6; SHAMSED, n=6), during 9 months. After sacrifice, apoptotic osteocytes were identified on left femur by TUNEL assay and by transmission electron microscopy. Intrinsic bone resistance to fracture was determined by 3-point bending of right femur diaphysis. Estradiol was assayed by ELISA in serum. Owing the normality of data distribution the statistical analysis was performed by two-way ANOVA.

Results: Both OVXEX and SHAMEX animals showed a significantly smaller number of apoptotic osteocytes compared to sedentary counterparts. Significantly less femoral diaphysis stiffness and maximal stress was only observed in OVXSED group compared to OVXEX and not between SHAMSED and SHAMEX.

Conclusions: Our results suggest that regular physical activity significantly counteracts the typical increase of osteocyte death following estrogen ceasing. This decrease was accompanied by a decrease in bone fragility in physically active OVX animals. However in animals with normal estrogen levels, the decrease of apoptotic osteocytes seen in physically active animals was not accompanied by increased mechanical resistance.

Regular physical activity seems therefore to be a successful strategy for delaying bone matrix osteocyte loss following menopause, with beneficial effects on bone resistance to fracture.

Figure

Quantitative analyses of apoptotic osteocytes ($Oc.N^+$/Total Oc.N) revealed a significantly reduced number in EX animals on both OVX and SHAM animals. EX-exercised; SED-sedentary; OVX-ovariectomized; SHAM-sham operated; * $p<0.05$

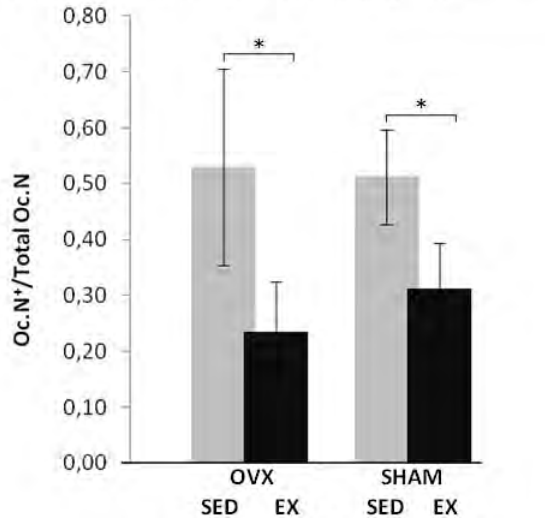

Figure

***Disclosures: Helder Fonseca**, None.*
This study received funding from: FCT, Fundação para a Ciência e Tecnologia

SU0053

Prostaglandin E_2 Released by Osteocytes after Sustained Mechanical Loading Activates ERK Signaling that Directly Phosphates Connexin 43 Leading to the Closure of Hemichannels. Sirisha Burra[1], Xuechun Xia[2], Paul Lampe[3], Lynda Bonewald[4], Eugene Sprague[2], Jean Jiang*[5]. [1]University of Texas, USA, [2]University of Texas Health Science Center, USA, [3]Fred Hutchinson Cancer Research Center, USA, [4]University of Missouri - Kansas City, USA, [5]University of Texas Health Science Center at San Antonio, USA

Mechanical stimulation of bone cells is known to cause the release of bone modulators, such as prostaglandin E_2 (PGE_2), important for bone formation and remodeling. We have previously shown that connexin (Cx) 43 hemichannels abundantly expressed in osteocytes mediate the release of PGE_2 in response to mechanical loading. Importantly, hemichannels in MLO-Y4 osteocytes are adaptively regulated and the hemichannel opening induced by fluid flow shear stress (FFSS) is closed after long, sustained FFSS. However, the molecular mechanism that modulates the closure of the hemichannels is unknown. Here, we show that activation of ERK upon continuous FFSS leads to Cx43 phosphorylation at S279/282, the sites characterized to be phosphorylated by ERK. Incubation of MLO-Y4 cells with conditioned media (CM) collected after continuous FFSS for 24 hours resulted in an increased phosphorylation of Cx43 and inhibition of Cx43 hemichannel opening induced by FFSS. The effect of 24 hour-FF CM on closure of Cx43 hemichannels was abolished when the cells were pre-treated with PD98059, a MAPK pathway inhibitor. As an attempt to identify the factors present in the FF-CM that cause ERK activation and consequent Cx43 phosphorylation, we probed for PGE_2 in the CM media collected after 0, 0.5, 2, 4, 8 and 24 hours of FFSS. We observed a time-dependent accumulation of PGE_2 in the conditioned media during continuous FFSS. MLO-Y4 cells treated with PGE_2 showed an increase in pERK levels and also Cx43 phosphorylation at S279/282 sites. Depletion of PGE_2 from conditioned media and treatment with U0126, a MAPK pathway specific inhibitor, resulted in a complete inhibition of Cx43 phosphorylation. Together, our results suggest that extracellular PGE_2 accumulated after continuous FFSS is responsible for activation of ERK signaling and subsequent phosphorylation of Cx43 by activated ERK leads to hemichannel closure. This adaptive, feedback regulation of Cx43 hemichannel function is most likely crucial in the regulation of the extracellular anabolic/catabolic signaling factors, including prostaglandins and other small molecules in response to mechanical loading.

***Disclosures: Jean Jiang**, None.*

SU0054

A Six-Month Vibration Intervention Did Not Enhance Bone Adaptation in Healthy Young Females. Charles Negus*[1], Rachel Evans[2], Mark Lester[2], Amanda Antczak[3], Kathleen Galloway[4]. [1]L-3 Applied Technologies, USA, [2]U.S. Army Research Institute of Environmental Medicine, USA, [3]S. Army Research Institute of Environmental Medicine, USA, [4]School of Physical Therapy, Belmont University, USA

Previous studies have shown that low-magnitude, high frequency vibration therapy can improve muscle performance in animals and humans, and bone mass in animals. Though such an intervention could be an attractive alternative to pharmacological antiresorptive therapies, bone quality outcomes in human studies have been mixed. The purpose of this study was to determine if six months of vibration therapy improved measures of tibial quality and geometry in a cohort of healthy, young women.

Eighty-one untrained female volunteers (23.7 ± 2.9 yrs) were randomly assigned to an intervention or control group. The intervention group used a vibration platform, designed to induce a peak vertical acceleration of 0.2g, at 30 Hz, for two 10-min sessions per day (separated by $\geq$ 3 hours), 5 days a week, for six months. Compliance was monitored by sensors in the devices and a written log kept by the subject. Neither group participated in physical conditioning programs during the course of the study. The bone adaptation response was measured at 0 and 6 mos using peripheral quantitative computed tomography (pQCT) and bone turnover markers. Image analysis software written in MATLAB was used to assess both whole bone and regional (six 60° sectors) parameters of the tibia at sites 4%, 38% and 66% of tibial length from the distal end plate. Quality was assessed by trabecular density (TrDn) at the 4% site and cortical density (CtDn) at the 38% and 66% sites. Geometric measures included cortical area (CtAr) and cortical thickness (CtTh). Bone alkaline phosphatase (BAP), procollagen type 1 amino-terminal propeptide (P1NP), and tartrate-resistant acid phosphatase (TRAP 5B) were used to assess bone turnover. Measures from pQCT images with minimal motion artifacts and pre-post alignment error were analyzed using ANOVA for subjects who completed >75% of the training regimen.

Significant changes in the intervention group were limited to a small increase in CtTh at the medial-anterior sector of the 66% site and a decrease in BAP (see Table).

Changes in bone quality and geometry are subtle in adults, even over a six month period, and may be difficult to ascertain using pQCT. Nevertheless, because there were also no observed increases in any of the bone biomarkers -a reliable sentinel of remodeling activity- we conclude that this intervention is insufficient to produce a measureable enhancement of bone quality or geometry in the tibia of healthy young women.

	Control			Intervention			Group*Time
pQCT Measures	n	Pre	Post	n	Pre	Post	P-Value
4% TrDn (mg/cm^3)	35	278.9 ± 30.6	280.1 ± 30.1	23	284.3 ± 23.1	286.4 ± 23.3	P=0.194
4% TrAr (mm^2)	35	867.4 ± 130.9	867.1 ± 129.3	23	841.2 ± 126.1	834.4 ± 125.3	P=0.384
38% CtDn (mg/cm^3)	33	1198.2 ± 16.6	1203.2 ± 17.6	21	1197.2 ± 16.9	1199.6 ± 17.7	P=0.088
38% CtAr (mm^2)	33	261.4 ± 34.9	261.9 ± 35.6	21	265.3 ± 16.5	266.2 ± 17.4	P=0.638
38% CtTh (mm)	33	4.80 ± 0.55	4.83 ± 0.55	21	4.90 ± 0.39	4.92 ± 0.40	P=0.961
66% CtDn (mg/cm^3)	24	1164.0 ± 17.1	1167.6 ± 17.6	16	1165.6 ± 15.8	1171.5 ± 15.8	P=0.118
66% CtAr (mm^2)	24	280.1 ± 43.2	280.6 ± 42.6	16	279.2 ± 22.2	279.9 ± 22.7	P=0.876
66% CtTh (mm)	24	3.96 ± 0.64	3.95 ± 0.63	16	3.92 ± 0.41	3.94 ± 0.39	P=0.089
66% CtTh-MedAnt(mm)	24	3.09 ± 0.54	3.08 ± 0.54	16	3.11 ± 0.44	3.17 ± 0.44	P=0.049
Biomarkers							
BAP	40	20.61 ± 5.39	21.04 ± 5.35	27	21.86 ± 7.44	20.68 ± 7.50	P=0.042
P1NP	40	51.08 ± 16.17	46.71 ± 15.02	27	48.80 ± 15.4	42.35 ± 13.1	P=0.457
Trap 5B	40	2.93 ± 1.47	2.91 ± 1.57	27	2.80 ± 0.87	2.71 ± 0.987	P=0.761

Table

***Disclosures: Charles Negus**, None.*

SU0055

Effects of Animal Enclosure Module Spaceflight Hardware on the Skeletal Properties of Ground Control Mice. Shane Lloyd*[1], Virginia Ferguson[2], Steven Simske[3], Alexander Dunlap[4], Eric Livingston[5], Ted Bateman[6]. [1]The Pennsylvania State University College of Medicine, USA, [2]University of Colorado, USA, [3]BioServe Space Technologies, University of Colorado, USA, [4]National Aeronautics & Space Administration Headquarters, USA, [5]Clemson University, USA, [6]Univesity of North Carolina, USA

Spaceflight experiments utilizing rat and mouse models require habitats that are specifically designed for the microgravity environment. Currently, rodents are housed in specially designed meshed cages with gravity-independent support systems. These Animal Enclosure Modules (AEMs) have been utilized for over two decades, however little is known about their effects on skeletal physiology in mice. It is important to characterize these effects in order to optimize ground controls and accurately evaluate countermeasures to spaceflight-induced bone loss.

We examined the effect of NASA's AEMs on the skeletal properties of 8-week-old female C57BL/6J mice. This 13-day ground-based study paralleled the CBTM-01 animal payload on space shuttle flight STS-108, with standard vivarium-housed mice compared to AEM (n = 12/group).

The microarchitectural effects of the AEM were most pronounced in the trabecular compartment of the proximal tibiae. AEM mice had greater bone volume fraction (+44%) and connectivity density (+144%). There were reductions in both AEM osteoblast surface (-79%) and osteoclast surface (-65%), accompanied by a greater bone formation rate (+185%) and mineralizing surface of trabecular bone (+295%). Overall changes in femoral cortical bone formation were primarily due to changes at the endocortical surface (-36%). AEM mice experienced changes in percent mineral composition at the femur diaphysis (-1.7%) and metaphyses (+5.6%). AEM mice had reduced levels of serum osteocalcin (-35%) and alkaline phosphatase (-25%), with no change in TRAP-5b. There was little effect of AEM housing on femoral mechanical properties.

With only modest effects at select cortical sites, AEM housing was found to produce its most dramatic effects on trabecular bone. These changes were accompanied by reductions in osteoblasts and osteoclasts, representing a decline in bone turnover at this site. Overall, these results suggest that there is an important, confounding effect of the AEM hardware on the trabecular bone of mice. It is reasonable to hypothesize that altered skeletal loading, with mice living and climbing on the six wire-meshed walls, makes a significant contribution to these effects. While the AEM remains an integral part of animal experimentation in space, it would be prudent to consider a two-week preflight acclimation period in order to help negate some of the early effects as mice adjust to this unique housing environment.

***Disclosures: Shane Lloyd**, None.*

SU0056

Evidence for Increased Tibial Posterior Bone Remodeling in Elite Male Recruits with Bone Overuse Injury. Amanda Antczak*[1], Rachel Evans[2], Charles Negus[3], Amir Hadid[4], Yael Arbel[4], Ran Yanovich[4], Daniel S. Moran[4]. [1]US Army Research Institute of Environmental Medicine, USA, [2]U.S. Army Research Institute of Environmental Medicine, USA, [3]L-3 Applied Technologies, USA, [4]Heller Institute of Medical Research, Sheba Medical Center, Israel

Bone adaptation begins early following the onset of strenuous training. At times these changes can be detrimental, as evidenced in the occurrence of stress reaction injuries (SR). It is unclear if the rapid onset of mechanical stimulus on un-adapted bone or the modeling process bone undergoes following strenuous stimulus is cause for SR. The purpose of this study was to determine the bone adaptation response at the tibia among recruits during 16-wks of elite military training with a specific focus on individuals who sustained SR.

Ninety-five males entering basic recruit training in the Israeli Defense Forces volunteered for this study. Peripheral quantitative computed tomography scans were taken at sites 4%, 38% & 66% from the distal tibial endplate prior to training (pre) and after 16 weeks (post). MATLAB software analyzed images to identify trabecular and cortical bone and calculate volumetric BMD. Images were then divided into six 60♂ sectors and analyzed. Tibial SR were diagnosed using MRI, bone scan, radiography or clinical examination. A 2x2 ANOVA was conducted to determine pre-post changes in whole bone periosteal (PPm) & endosteal (EPm) perimeter, and in whole and regional trabecular density (TrDn), area (TrAr), and cortical density (CtDn), area (CtAr), and thickness (CtTh) between SR and non SR (NSR) males. Significance was set at $p<0.05$.

The incidence rate of tibial SR was 26.3%. Increases were observed in 4% TrDn (pre=316.47$\pm$25.97mg/cm^3, post=319.42$\pm$25.89mg/cm^3, $p<0.001$) and 38% CtTh (pre=5.41$\pm$0.58mm, post=5.45$\pm$0.59mm $p<0.03$) in both groups. At 38%, the increase in CtTh was greater in the SR group (pre=5.38$\pm$0.37mm, post=5.45$\pm$0.36mm) compared to the NSR group (pre=5.43$\pm$0.64mm, post=5.45$\pm$0.66mm). This increase was specific to the posterior region in the SR group (pre=5.80$\pm$0.61mm, post=5.89$\pm$0.71mm, p=0.02). While both groups increased 66% CtAr ($p<0.02$), in SR males these increases were specific to the posterior region (pre=66.86$\pm$8.37mm^2, post=69.91$\pm$7.42mm^2, $p<0.001$). In SR males, a 1.68% decrease in 66% EPm ($p<0.03$) and 1.47% increase in 66% CtTh was observed. Increased CtTh was specific to the medial-anterior and posterior regions (increased by 3.35% and 5.63% respectively, $p<0.003$).

As a response to mechanical loading, unique tibial bone adaptations can occur in recruits who develop SR during 16 weeks of elite military training. These changes may only be evident at discrete locations and detected by specific methodologies such as sector analysis.

***Disclosures: Amanda Antczak**, None.*

SU0057

Identification of Novel Microanatomical Structures in Bone from a Patient with Alkaptonuria. Adam Taylor*[1], Alan Boyde[2], John Davidson[3], Jonathan Jarvis[1], Lakshminarayan Ranganath[1], James Gallagher[1]. [1]University of Liverpool, United Kingdom, [2]Institute of Dentistry, Barts & The London School of Medicine & Dentistry, United Kingdom, [3]Royal Liverpool & Broadgreen University Hospital Trust, United Kingdom

Alkaptonuria (AKU) is a rare autosomal recessive condition caused by a single enzyme deficiency in tyrosine metabolism. This results in high circulating levels of homogentisic acid, which undergoes polymerisation and deposition as a melanin-like pigment in cartilage matrix leading to early onset arthropathy similar to OA. To investigate the effects on bone microstructure, we obtained tissue from AKU patients undergoing joint replacement. Samples were processed for histology and for topographical 3D scanning electron microscopy (SEM) and quantitative back scattered electron SEM (qBSE-SEM). These analyses revealed an extraordinary bone phenotype including novel microanatomical structures. Pigment was progressively deposited in uncalcified cartilage starting in the deep layers; there was no deposition in calcified cartilage or bone, yet these latter tissues underwent significant structural modelling. The most striking feature was the resorption of subchondral bone and calcified cartilage such that in advanced stages there was complete loss of the subchondral bone plus calcified cartilage plate. The underlying trabecular bone also contained idiosyncratic architecture. Trabecular surfaces had numerous outgrowths that we have termed "trabecular excrescences" of which three distinct types were recognized. The first type arose from the incomplete resorption of branching trabeculae and they were characterized by scalloped surfaces and rugged edges. The second type arose in a similar way but had been smoothed over by new bone deposition. The third type which resembled coarse stucco probably arose from resting surfaces that had been focally reactivated. These were poorly cemented to the prior trabecular wall. They had a disorganized arrangement of collagen fibres and contained poorly mineralised and hypermineralised regions. We propose that these distinctive microanatomical structures do not arise as a result of pigmentation *per se* but because of abnormal osteoclast/osteoblast modelling secondary to altered mechanical loading or other aberrant signalling. The distinctive subchondral environment underneath pigmented cartilage in AKU provides a unique model to investigate the response of bone to altered mechanical loading.

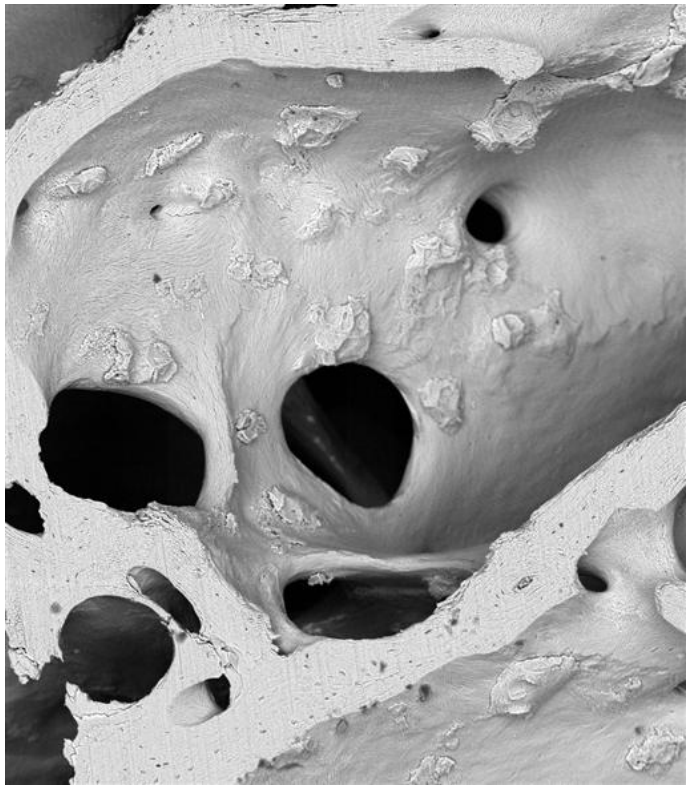

3D SEM image showing numerous type 3 trabecular excrescences

***Disclosures: Adam Taylor**, None.*

SU0058

In Vivo Mechanical Loading of the Skeletal Mature Rabbit Tibia Model. Thomas Willett*[1], Jian Wang[2], Richard Renlund[2], Marc Grynpas[3]. [1]Mount Sinai Hospital, Canada, [2]University of Toronto, Canada, [3]Samuel Lunenfeld Research Institute, Canada

Stress fractures can result from intensive exercise, typically occur in the lower limbs, and are not solely the result of bone material fatigue; rather they may be due to lack of adaptation and repair. College athletes and military recruits have the highest incidence. Female have an estimated 3.5-10 higher incidence than males under the same training conditions. Few animal models using physiological levels of loading (1000-2000 microstrains) have been studied. We have developed an experimental model for applying axial loading to the right tibiae of rabbits (applied using a custom-built mechanical testing device) in order to study biological response to physiological, reportedly osteogenic levels of loading in osteonal bone. Each rabbit lies prone with its right leg in flexion while under anaesthesia (1 litre O2/min + 2.5% isoflurane). The foot is attached via a rigid brace to an actuator and the knee is restrained allowing loading. We have previously determined experimentally in skeletally mature rabbits (4.5-5 kg; >28 weeks old) that the loading method is highly linear and repeatable. A load of approximately 250N (5 times body weigh; 5xBW) resulted in strains at the anterior and posterior surfaces of the mid-diaphysis of approximately 1600 and -1900 microstrains respectively. Six male and 6 female rabbits were loaded for 15 minutes Monday, Wednesday, and Friday for 4 weeks. Each loading cycle (10s total) consisted of a ramp to 5xBW at 600N/s, a 330ms dwell, a ramp return to 50N at 600N/s and then a static load of 50N (1xBW) was held for 9s. Each rabbit received a Calcein Green (CG) injection 3 days before the start of loading. This was followed by Xylenol Orange injection two weeks later and a second CG injection on the final day of loading. The tibiae were analysed for adaptation and intracortical remodelling using computed tomography and dynamic histomorphometry. The unloaded left tibiae acted as paired controls. Data were analysed using non-parametric statistical tests comparing loaded to unloaded and the difference in the sexes. These physiological levels of loading seem to increase the number of labelled osteons indicating an intra-cortical repair response rather than the adaptive response by periosteal expansion often reported for superphysiolgical loading in rats and mice.

***Disclosures: Thomas Willett**, None.*

SU0059

Intramedullary Pressure Induced by Dynamic Hydraulic Pressure Stimulation and Its Potential in Bone Adaptation. Yi-Xian Qin*[1], Minyi Hu[2], Frederick Serra-Hsu[3], Suzanne Ferreri[2], Jiqi Cheng[2], Zongkang Zhang[2], Yunkai Huang[2], Denis Evangelista[2]. [1]State University of New York at Stony Brook, USA, [2]Stony Brook University, USA, [3]State University of New York, Stony Brook, USA

Mechanotransductive signals through bone fluid flow induced by intramedullary pressure (ImP) are effective in bone adaptation. Previous *in vivo* studies showed that dynamic muscle stimulation can generate ImP to mitigate disuse osteopenia in a frequency-dependent manner. As a direct fluid flow coupling method to potential new treatments for osteoporosis, it was hypothesized that external oscillatory hydraulic pressure stimulation can generate ImP with minimal strain in a frequency-dependent manner. The aim of this study was to evaluate the immediate effects on ImP and bone strain induced by a novel, non-invasive dynamic external pressure stimulus in response to a range of loading frequencies. Three 15-month old female Sprague-Dawley virgin rats with a mean body weight of 425 ± 11g were used to measure the ImP and bone strain simultaneously under dynamic hydraulic pressure stimulations. For the ImP measurement, a 1mm hole was carefully drilled into the right tibial marrow cavity from the proximal end of the tibia. A micro-cardiovascular pressure transducer (Millar Instruments, TX) was inserted into the tibial marrow cavity, guided by a 16-gauge catheter. The drill hole was completely sealed with the catheter and the pressure transducer apparatus. For bone strain measurement, a single element strain gauge (120?, factor 2.06) was firmly attached to the surface of the same tibia at the mid-diaphyseal region. The pressure stimulation was achieved by an inflatable cuff placed around the right mid-tibia with 40mmHg static+30mmHg dynamic pressure at a range of frequencies from 1Hz to 4Hz over 0.1Hz intervals, then from 4Hz-10Hz over 1Hz intervals. For each animal, the entire frequency spectrum was repeated six times. Dynamic hydraulic stimulation has shown noticeable effect in increasing ImP. Approximately 1mmHg tibial ImP was generated by normal heart beat. The ImP values (p-p) values was increased in a nonlinear fashion by gradual increases with frequencies and peaked at 2.7Hz. The ImP increased on the order of 11.3 ± 8.4mmHg at 1Hz, 34.4 ± 22.3mmHg at 2.7Hz, 21.3 ± 17.8mmHg at 6Hz, and 12.2 ± 10.1mmHg at 10Hz (Fig. 1). No detectable bone strain ($<5\mu\varepsilon$) was observed. These results imply that external oscillatory hydraulic stimulation can significantly induce ImP, which may further trigger adaptive response.

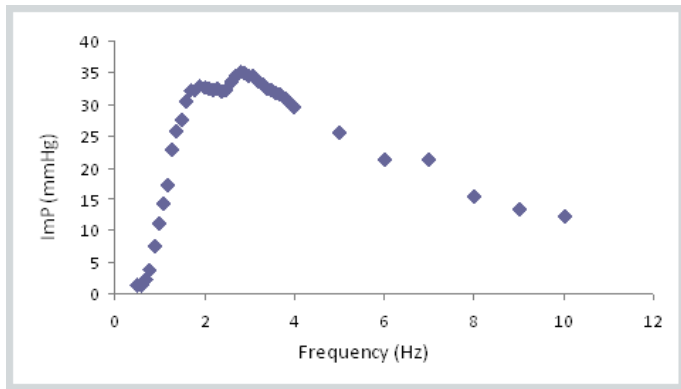

Fig. 1. Measurement of ImP under oscillatory hydraulic pressure

***Disclosures: Yi-Xian Qin**, None.*

SU0060

Relationship Between Appendicular Bone Structural Measurements and Functional Capacity in Women. Andy Kin On Wong*[1], Karen Beattie[1], Colin Webber[2], Laura Pickard[1], Dean Inglis[3], Angela Cheung[4], Christopher Gordon[1], Alexandra Papaioannou[2], Jonathan Adachi[5]. [1]McMaster University, Canada, [2]Hamilton Health Sciences, Canada, [3]Department of Civil Engineering, McMaster University, Canada, [4]University Health Network, Canada, [5]St. Joseph's Hospital, Canada

Objectives: 1) To determine the relationship between appendicular bone structure and physical function in postmenopausal women; 2) To examine how the dependence of bone structure on physical function is modulated by age and body mass index (BMI)Methods: Women $\geq$ 50 years of age and enrolled in the Hamilton cohort of the Canadian Multicentre Osteoporosis Study (CaMos) between 1994 to 2009 were scanned on a high-resolution peripheral quantitative computed tomography scanner at the ultradistal radius and ultradistal tibia. Appendicular bone structural parameters: cortical thickness (C.Th) and trabecular separation (Tb.Sp) were computed. Timed "up-and-go" (TUG) and grip strength tests were performed during study visit. Each participant completed a 36-item short form medical outcomes (SF-36) questionnaire between two to three years ago and the physical function score was

obtained. A multivariate linear regression analysis was used to determine the relationship between bone structure and each of TUG, grip strength and SF-36 physical function scores with adjustment for age and body mass index (BMI). Regression coefficients were compared between weight-bearing and non-weight-bearing skeletal sites, and between analyses with and without covariate adjustment by using an independent samples standardized test after Fisher transformation.

Results: 54 participants, mean (SD) age 71.5 (8.5) years and BMI 28.2 (6.1) kg/m^2 were studied. Consistent with SF-36 physical function scores, there was wide variance in TUG and grip strength measurements. A small amount of variance in ultradistal radius C.Th was explained by functional capacity measures and the SF-36 physical function component (Table I). However, only the relationship with SF-36 physical function remained significant after adjustment for age and BMI. An increasing Tb.Sp at the distal radius was modestly correlated with decreased grip strength independent of age. No bone structural parameters were explained by TUG times after covariate adjustment. Neither covariate adjustment nor weight-bearing significantly changed the strength of the correlations observed.

Conclusions: Functional capacity measures are indicative of muscular performance. A modest relationship between bone structure and each of physical function and grip strength was observed here. These results support the notion that muscle strength may be a determinant of bone quality affected by age and BMI but not mediated by weight-bearing.

Table I. *Appendicular bone structure versus physical function and functional capacity*. **SF-36 physical function and grip strength were entered as independent variables in a multivariate linear regression with bone structural parameters obtained at the ultradistal radius and tibia. Bold indicates significance at the 95% confidence level.**

Variables	R^2	Beta	p-value
SF-36 Physical Function			
Tibial C.Th	0.020	0.143	0.303
Radial C.Th	0.122	0.350	**0.010 ****
Grip Strength			
Tibial Tb.Sp	0.127	-0.356	**0.008 ****
Radial Tb.Sp	0.117	-0.343	**0.011***

*** remained significant after adjusting for age**
**** remained significant after adjusting for age and BMI**

Table I.

***Disclosures: Andy Kin On Wong**, None.*

SU0061

Timing Skeletal Loading to Optimally Enhance Bone Formation. Sundar Srinivasan*[1], Dewayne Threet[1], Jitendra Prasad[2], Brandon Ausk[1], Steven Bain[1], Ted Gross[1]. [1]University of Washington, USA, [2]University of Washington, Seattle, USA

Repeated activation of signaling pathways underlying bone mechanotransduction can lead to sustained downstream synthesis of auto-regulatory repressors (e.g RCAN1, ICER). As such, mechanical loading strategies that subject bone to bouts of loading every 24 or 48 hrs may be sub-optimal, as loading events following the first few bouts would necessarily operate upon signaling pathways under active suppression. We therefore hypothesized that increasing the duration between loading bouts would achieve equivalent loading-induced bone formation despite fewer loading events. To test this hypothesis at the in vivo level, the right tibiae of two groups of mice underwent a 50 c/d, 10-s rest-inserted loading protocol calibrated to induce 2000 με peak strain in the tibia mid-shaft. The first group received loading on M, W, F for three weeks (9 bouts total, n = 7), while the second group received loading only on M for each of three weeks (3 bouts total, n = 4). As a control for loading bout number, a third group of animals received loading on M, W, F of the first week only (n=4). All animals received calcein labels (d 10, 19) and dynamic histomorphometry measures were determined at the tibia mid-shaft upon sacrifice (d 22). Subjecting mice tibiae to three bouts of loading within the first week did not significantly increase periosteal bone formation rate (p.BFR) compared to contralateral controls (p = 0.14). As was anticipated, mice receiving loading 9 times demonstrated significantly more relative periosteal bone formation rate (rp.BFR) than mice receiving loading 3 times during the first week of a 3 wk experiment (0.73 $\pm$ 0.21 vs 0.21 $\pm$ 0.17 μm3/μm2/d; p = 0.04). Interestingly, rp.BFR induced by 3 bouts of loading provided once weekly was not significantly different from that induced by 9 bouts of loading over the 3 wks (0.54 $\pm$ 0.15 μm3/μm2/d, p = 0.24). In effect, a 7-day separation between loading bouts was recognized by the bone cell syncytium as a statistically equivalent, robust osteogenic stimulus despite a 3-fold reduction in the number of loading bouts. These experiments begin to bracket the time course over which negative regulators of pathways activated by mechanical stimuli would be expected to return to normal, baseline levels. An explicit understanding of these dynamics could yield critical insights regarding when to mechanically load bone in order to both efficiently and maximally enhance bone adaptation.

***Disclosures: Sundar Srinivasan**, NIH, 2*

SU0062

Comparison of Bone Mineralization using Microcomputed Tomography and Transmission X-ray Microscopy. Grace Kim*[1], Garry Brock[1], Florian Meirer[2], Eduardo Almeida[3], Joy Andrews[4], Marjolein Van Der Meulen[1]. [1]Cornell University, USA, [2]Technical University of Vienna, Austria, [3]NASA Ames Research Center, USA, [4]Stanford Synchrotron Radiation Lightsource, USA

Bone is a hierarchical tissue with structure and organization on multiple length scales. Associated with these features are compositional and mechanical heterogeneities that change with aging and disease and ultimately affect whole bone resistance to fracture. Commonly used techniques such as vibrational spectroscopy and bench top microcomputed tomography (μCT) can resolve mineralization changes on the micron scale. However, a hard transmission X-ray microscope (TXM) with synchrotron radiation source has the capability to acquire density information of mineralized tissue with 30-40nm resolution [Andrews et al. in press]. The goal of this study was to compare nanometer and micron scale mineralization of longs bones. To ensure a range of bone mineralization, a vitamin D deficiency model in rats was used.

Weanling male Sprague Dawley rats were divided into three groups and put on either a control, mild, or severe vitamin D/Ca deficient diet regimen. After 10 weeks animals were euthanized and femurs and 3rd metacarpals were removed (n=3/group). Femurs were scanned using μCT (GE Healthcare, eXplore CT120, voxel size= 25μm). The mean attenuation value (HU) was calculated for a 0.5mm thick region of cortical bone at the mid-diaphysis for each sample. 1mm thick transverse sections were cut from the metacarpals and polished to a thickness of <50um using silicon carbide polishing paper lubricated with ethylene glycol. Metacarpal samples were imaged in absorption contrast using a TXM operating on beamline 6-2 at SSRL (5.4KeV,voxel size = 0.0157μm). Using the Beer-Lambert law the mean attenuation coefficient for a 1200-1800μm^2 area was calculated for each sample.

μCT mean attenuation values were higher for control animals than both vitamin D deficient groups. For the TXM data, controls were larger only compared to the mild vitamin D deficient group. Mean μCT attenuation values correlated well with mean attenuation coefficients from TXM (r^2=0.51).

μCT scans of the entire cross section of the femur revealed heterogeneous mineral distribution radially and circumferentially. The small sample area used for TXM showed good correlation with larger scale μCT data while at the same time providing additional information about finer scale mineralization heterogeneities.

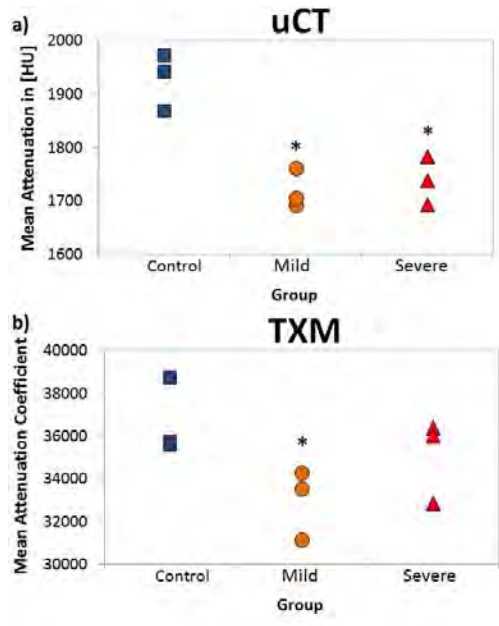

Figure 1 a) Mean attenuation from çCT. b) Mean attenuation coefficient from TXM. *p<0.05 vs Control

***Disclosures: Grace Kim**, None.*

SU0063

Fluorescence Based, Observer Independent Dynamic Bone Histomorphometry. Seung-Hyun Hong*[1], Xi Jiang[2], Li Chen[2], Dong-Guk Shin[1], David Rowe[2]. [1]University of Connecticut, USA, [2]University of Connecticut Health Center, USA

Dynamic and cellular histomorphometry of trabecular bone is the most biologically relevant assessment of steady state bone health. While the measured and calculated values are clearly defined, the identification of the visual features that form the basis of the measurements is subjective to the analyst which reduces inter-observer reliability. In addition, the time and cost involved in sectioning and data generation limits its wide application to many laboratories. Here we report our progress in developing a lower cost, rapid and observer-independent method for dynamic histomorphometry of the distal femur and vertebral bone of the mouse. Mice are administered calcein and alizarin red complexone 7 and 2 days prior to sacrifice. Excised bones are fixed for 2-3 days in paraformaldehyde. After washing, the mineralized tissues are cryosectioned using a tape transfer protocol in which the tape side of the section is immobilized on a glass slide and the sample side is temporally covered with glycerol and a cover slip. Three sections, separated by 50 microns, are taken per bone. A sequential work flow is implemented in which endogenous fluorescent signals (bone mineral, green and red mineralization lines), TRAP identified by ELF97 and AP identified by Fast Red are captured as individual tiled image files of the section for each fluorescent color. Subsequently, the section is treated with a chromogenic stain to generate a traditional view of the histology. All of the image files are submitted to an image analysis pipeline that identifies the mineralized regions of bone and selects a region of interest (ROI). Analysis of this image provides the static measurements of bone volume (BV), trabecular number (TN) and TT (trabecular thickness). The remaining files are aligned to the mineralized file through the use of fluorescent registration beads that were placed adjacent to the tissue at the time of sectioning. The program thresholds each fluorescent signal and relates it to the bone surface within the ROI from which the mineral apposition rate (MAR), bone formation rate (BFR), osteoclast and osteoblast surface measurements are calculated. The method has been used to generate a dataset from 8 and 16 week old male and female CD1 and C57Bl6 mice and revealed a significantly greater bone turnover rate in female vs male animals irrespective of age or strain. Power analysis indicates that 6 mice per group will yield a 90% power to detect a 30% difference.

***Disclosures: Seung-Hyun Hong**, None.*

SU0064

New Fluorescent Protein Reporter Animal Models to Study Skeletal Biology. Peter Maye*, Yu Fu, Xi Jiang, Yaling Liu, Mary Louise Stover, David Rowe. University of Connecticut Health Center, USA

The generation of fluorescent protein reporter mice to mark distinct cell types has increasingly become a powerful strategy to explore the biology of different cell populations. Past methodologies have exploited the use of BACs, bacterial recombination techniques, and fluorescent protein reporters as a high throughput and accurate strategy to generate reporter gene mice, relative to using conventional defined promoter DNA constructs. Our past studies have capitalized on these advances in transgenic technologies and have applied these approaches to study cells of the osteogenic lineage. Here we report on our expanded efforts to mark additional skeletal cell populations including cell populations of the joint, growth plate, tendon, insertion sites, and osteoclast. Specifically, we have generated or have obtained and characterized reporter gene mice for Collagen II, Collagen X, GDF-5, Lubricin, Sox9, Dkk-3, Tenascin C, and TRAP. In many cases we have generated these different transgenic lines with different fluorescent protein spectral variants allowing for the intercrossing of multiple transgenic lines to further resolve, define, and investigate the interactions between various cell populations. Reporter gene expression of these different transgenic animal models at different stages of skeletal development will be presented.

***Disclosures: Peter Maye**, None.*

SU0065

Relevance of Enzymatic Collagen Crosslinks Analysis by Infrared Microspectroscopy in Bone Tissue. Delphine Farlay*[1], Marie-Eve Duclos[2], Cindy Bertholon[1], Evelyne Gineyts[1], Stephanie Viguet-Carrin[3], Ganesh D Sockalingum[4], Dominique Bertrand[5], Thierry Roger[6], Daniel J Hartmann[2], Roland Chapurlat[7], Georges Boivin[8]. [1]INSERM U831, Université de Lyon, France, [2]Université de Lyon, France, [3]E. Herriot Hospital, France, [4]CNRS UMR6237, Université de Reims, France, [5]INRA, France, [6]Ecole Nationale Vétérinaire de Lyon, France, [7]INSERM U831, Hopital Edouard Herriot, France, [8]INSERM, France

Fourier Transform Infrared (FTIR) spectroscopy has been used to show that the ratio of 2 bands in amide I region (1660/1690 cm^{-1}) was linked to collagen maturity, mainly to enzymatic crosslinks (ECL), as PYR/DeH-DHLNL[1]. A previous study on 53 human trabecular vertebral bones has shown that the ratio 1660/1690 was not associated with biochemical ECL (unpublished). So, we studied a model of lathyritic rats with decreased ECL formation by inhibition of lysil oxydase (LOX)[2-3]. Fourteen female Wistar rats, divided into 2 groups, were injected twice daily during 30 days with 666 mg/kg/day of ß-aminopropionitrile or vehicle. After 30 days, animals were euthanized. Left radius were embedded for FTIR Microspectroscopy (FTIRM). Measurement of ECL by HPLC was performed on right radius. FTIRM was performed on 2µm sections (10-20 measurements/sample; 35*35µm). The area ratios 1660/1690[1] and 1030/1110 cm^{-1} (mineral maturity)[4] were calculated. FTIR Imaging, combining both spectral and spatial informations (6.25µm/pixel), was performed on control and lathyritic bones. Principal Components Analysis (PCA), which visualizes high-dimensional data by transforming them into a very low-dimensional space, was performed on infrared images by randomly selecting 1000 spectra/image. The whole collection of sampled spectra was used as principal observations in PCA and projected in the corresponding single PCA-space. The lathyritic group exhibited a decrease of 80% of pyridinoline (PYD) compared to the control group whereas FTIRM showed no difference in the 1660/1690 area ratio (Table). However, the increase in 1660/1690 area ratio was correlated with an increase in mineral maturity. Thus, 1660/1690 area ratio was only related to collagen maturity but not to ECL. PCA showed identical results, indicating that the 1660/1690 area ratio increased with mineral maturity, as a function of bone age, but had no link with ECL. A limitation of our study is that we have only measured the mature but not immature ECL. However, inhibition of LOX produced a decrease of both mature and immature ECL. In conclusion, the 1660/1690 ratio increased with bone age, but was not related to enzymatic crosslinks, suggesting that a modification of this ratio could be due to a modification of secondary structure of collagen in relation with the mineralization.

1 Paschalis et al. J Bone Miner Res 2001, 16
2 Oxlund et al. Bone 1995, 17
3 Knott and Bailey Bone 1998, 22
4 Farlay et al. J Bone Miner Metab 2010 Epub

Table. Control and lathyritic rats

			Control rats	Lathyritic rats	Difference
Mean ±SD	***Biochemical dosage*** (mmol/mol coll)	**PYD**	206 ±30	42 ±10	-80%, p=0.009
	FTIRM (Area ratio)	**1660/1690**	2.85 ±0.73	2.66 ±0.63	Not significant
Spearman correlation between: **1660/1690 & Mineral Maturity**			r_{sp}=0.659 p<0.0001	r_{sp}=0.421 p<0.0001	
PCA on Infrared Images (1000 spectra/image)			No significant difference		

Table

***Disclosures: Delphine Farlay**, None.*

SU0066

Screening Bone for Collagen Content Using MicroCT. Maria Squire*[1], Jennifer A. Tripp[2], Matthew Mariyampillai[1], Julie Hamilton[3], Robert E.M. Hedges[3]. [1]Department of Biology, The University of Scranton, USA, [2]Department of Chemistry, The University of Scranton, USA and San Francisco State University, USA, [3]Research Laboratory for Archaeology & the History of Art, University of Oxford, United Kingdom

Sufficient protein preservation in archaeological bones is critical for techniques including radiocarbon dating, stable isotope analysis, and extraction of ancient DNA, yet collagen isolation is a time-consuming process that can sometimes result in insufficient collagen yields. Identifying a technique that could be used to screen bones for protein preservation prior to isolating the collagen would therefore be ideal. The degree of bone preservation, based on protein content, has been found to correlate well with bone microarchitecture and, in particular, porosity. In the current study, we sought to examine whether microcomputed tomography (mCT) could serve as a suitable prescreening method for bone preservation. Sheep and cattle long bones (n=4) of varied preservation that were collected from the site of Etton, United Kingdom were scanned at a resolution of 60 mm using the mCT 80 scanning system (Scanco Medical, Switzerland). Cortical porosity (Ct.Po), calculated as 1- bone volume fraction (BV/TV), was determined for a 9-mm region of each bone and compared with previously determined collagen recovery values. Upon visual inspection of the images, there were striking differences in the appearance of the well preserved versus poorly preserved bones. Bones with generally good preservation had lower cortical porosities as compared to the poorly preserved bones. In addition, when compared to collagen recovery rates, a trend was observed in which cortical porosity was higher in bones with poor collagen recovery than in bones with good collagen recovery. These results suggest that this microCT method has the potential to be an appropriate prescreening tool for determining protein preservation in bones. Analysis of a larger subset of variably preserved bones is currently underway to further explore the efficacy of this technique for evaluating the collagen content of archeological bones.

***Disclosures: Maria Squire**, None.*

SU0067

Linear Polyphosphates (PolyP5 and PolyP65) Inhibit MC3T3-E1 Osteoblast Culture Mineralization via Direct Binding to Mineral. Betty Hoac, Marc McKee*. McGill University, Canada

Studies on various states of inorganic phosphate, as well as on organic phosphate added by post-translational phosphorylation of proteins, all demonstrate a central role for phosphate in biomineralization processes. Inorganic polyphosphates (polyPs) are chains of orthophosphates linked by phosphoanhydride bonds that can be up to hundreds of orthophosphates (Pi) in length. The role of polyPs in mammalian systems, where they are ubiquitous in cells and tissue fluids, and at particularly high levels in osteoblasts, is not well understood. In cell-free systems, polyPs inhibit hydroxyapatite nucleation, crystal formation and growth, and solubility. In animal studies, polyP injections inhibit vitamin D-induced vascular calcification. While recent work has proposed an integrated view of polyP function in bone (Omelon et al Plos One 4:e5634, 2009), little experimental data for bone are available. Here we show in osteoblast cultures producing an abundant collagenous matrix that two polyPs (polyP5 and polyP65) are potent mineralization inhibitors. Twelve-day MC3T3-E1 osteoblast cultures with added ascorbic acid (for collagen matrix assembly) and β-glycerophosphate (a source of phosphate for mineralization) were treated with polyP5 and polyP65 from 0-6 days, 6-12 days, and 0-12 days. Von Kossa staining and calcium quantification revealed that mineralization was inhibited in a dose-dependent manner by both polyPs, with complete mineralization inhibition at 10 μM polyP (as measured by Pi molarity). Cell proliferation (MTT assay) and collagen assembly (picrosirius staining) were unaffected by polyP treatment, indicating that polyP inhibition of mineralization results not from cell and matrix effects but from direct inhibition of mineralization. This was confirmed by showing that polyP5 and polyP65 bound to synthetic hydroxyapatite in a concentration-dependent manner. Finally, at physiologic concentrations, both polyPs were not substrates for tissue-nonspecific alkaline phosphatase. We conclude that polyP acts as an inhibitor of induced mineralization in MC3T3-E1 cultures by binding to hydroxyapatite.

***Disclosures: Marc McKee**, None.*

SU0068

Raman Spectroscopy of Neonatal Murine Calvaria Reveals Periodic Mineralization in Fontanel. Michael Morris*, John-David McElderry, Guisheng Zhao, Renny Franceschi. University of Michigan, USA

Bone formation is affected by clock gene-mediated pathways, and systemic markers of bone formation such as osteocalcin are known to exhibit diurnal fluctuations. However, direct detection of cyclical, local changes in bone formation has not been previously reported. Using a custom Raman microscope and stage incubation chamber, we tracked the kinetics of first mineral formation in the fontanel region on *ex vivo* calvarial tissue cultures of neonatal mice. With a time resolution of 20-30 minutes we observed mineral dynamics occurring on the hour time scale. Mineral phosphate levels in the collagenous tissue increased in short (1-4 hour) intervals several times during the first 6 days after birth. Time between mineralization bursts varied from 8 to 12 hours. We simultaneously probed a series of points 25 μm apart in a line perpendicular to the edge of the interparietal plate within the suture region. Mineral was detected sequentially along the line. The mineral nearest the interparietal plate displayed a linear propagation rate similar to values previously reported for osteoblast cell culture mineral formation [1]. Earliest measurements of the mineral contain a phosphate ν_1 Raman band centered at 958 cm^{-1} which matches values for apatitic mineral in mature murine long bones. Changes in mineralization were also compared with levels of osteoblast and clock gene mRNAs. Based on these studies, we conclude that mineralization in developing bone tissue undergoes periodic step-wise increases in mineral content driven by local factors in the bone. This is the first reported evidence for periodic biomineralization in bone development. Our findings suggest a more complex mechanism for intramembranous mineralization than previously thought.

1. Dallas et al. Cells Tissues Organs 189:6, 2009.

***Disclosures: Michael Morris**, Kaiser Optical Systems, Inc., 5*

SU0069

A 30-bp Murine *Col10a1* Distal Promoter is Responsible for Its Hypertrophic Chondrocyte-specific Expression In Vivo. Feifei Li*[1], Yaojuan Lu[1], Sam Abbassi[1], Yuqing Chen[2], Ming Ding[1], Siying Wang[3], Brendan Lee[4], Qiping Zheng[1]. [1]Rush University Medical Center, USA, [2]Baylor College of Medicine, China, [3]Anhui Medical University, China, [4]Baylor College of Medicine, USA

Chondrocyte maturation, a process characterized by expression of the hypertrophic chondrocyte-specific type X collagen gene (Col10a1), is a critical stage of chondrocyte terminal differentiation during endochondral bone formation. Therefore, understanding the molecular regulation of Col10a1 expression may contribute to the understanding of the molecular processes of skeletal development as well as the pathogenesis of diseased skeletal conditions that show abnormal chondrocyte maturation. We have previously shown that a 150-bp (-4296 to -4147) Col10a1 distal promoter is sufficient to mediate its hypertrophic chondrocyte-specific expression in transgenic studies. To further localize the cis-enhancer in this 150-bp Col10a1 distal promoter, we recently generated two additional transgenic mouse lines that use different lengths of the 5¢-sequences (-4296 to -4255 bp and -4296 to -4214 bp) upstream of the same Col10a1 basal promoter each to drive LacZ as a reporter. No reporter expression (blue staining) was observed in the hypertrophic chondrocytes of either of these two transgenic mouse lines. This result, together with our previous transgenic studies using a 90-bp (-4296 to -4280 and -4238 to -4171) deletion mutant reporter construct, suggests the importance of a 45-bp (-4215 to -4171) Col10a1 distal promoter in mediating its cell-specific expression in vivo. Interestingly, detailed sequence analysis of this region identified two tandem repeat putative Runx2 core binding sites (TGTGGG-TGTGGC, -4187 to -4176). Electrophoretic mobility shift assay (EMSA) using DNA oligos (-4201 to -4163 bp and -4197 to -4171 bp) covering these Runx2 binding sites demonstrated that these Runx2 core binding sites are required to form the specific DNA/protein complexes with hypertrophic MCT cell nuclear extracts. Moreover, in vitro transfection using reporter constructs containing these Runx2 binding sites shows upregulated reporter activity. Taken together, our results further localize the cis-enhancer to 30 base pairs of the Col10a1 distal promoter and suggest that Runx2 or other candidate factors may regulate Col10a1 expression via these Runx2 binding sites. This short cis-enhancer allows us to identify Runx2 as well as novel molecules that regulate cell-specific Col10a1 expression during chondrocyte maturation and therefore, potentially provides novel targets for therapeutic intervention and treatment of multiple skeletal disorders that have abnormal chondrocyte maturation.

***Disclosures: Feifei Li**, None.*

SU0070

Carbonic Anhydrase 9 Suppresses Hypertrophic Differentiation of Chondrocytes. Toshifumi Maruyama*[1], Yoichi Miyamoto[1], Atsushi Yamada[2], Gou Yamamoto[3], Kentaro Yoshimura[1], Tomohito Akiyama[4], Tetsuo Suzawa[1], Masamichi Takami[1], Tetsuhiko Tachikawa[3], Kazuyoshi Baba[4], Ryutaro Kamijo[5]. [1]Showa University School of Dentistry, Japan, [2]Showa University School of Dentistry, Japan, [3]Department of Oral Pathology, Showa University School of Dentistry, Japan, [4]Department of Prothodontics, Showa University School of Dentistry, Japan, [5]Department of Biochemistry, Showa University School of Dentistry, Japan

Carbonic anhydrase (CA)-9 (CA9) is one of the transmembrane isoforms of CAs which catalyze reversible hydration of CO_2 to HCO_3^- and H^+. The catalytic domain of CA9 locates outside of cells, and hence CA9 is believed to be involved in regulation of extracellular pH. It is known that the expression of CA9 is up-regulated by hypoxia-inducible factor-1. Recently, CA9 attracts attention for its high expression in hypoxic tumors and contribution to malignant progression. While it was reported that CA9 is also distributed in human articular cartilage, its role in development of cartilage has not been explored. Here we investigated the expression of CA9 in mouse epiphyseal cartilage and its role in growth and differentiation of chondrocytes in vitro. Resting, proliferating, and hypertrophic zones of epiphyseal cartilage were isolated from frozen sections of tibiae of one-day postnatal ddY mice by laser capture microdissection. Total RNA was extracted from each dissected specimen, and expression of mRNAs for type II collagen (Col II), type X collagen (Col X), and CA9 was analyzed by real-time RT-PCR. CA9 mRNA was expressed in the resting and proliferating cartilage where Col II is expressed, but it was not detected in the Col X-expressing hypertrophic zone. The same results were obtained in an immunohistochemical analysis using specific antibodies for Col II, Col X, and CA9. Consequently, we investigated the role of CA9 in growth and differentiation of chondrocytes in vitro. Interestingly, introducing siRNA for CA9 to mouse primary chondrocytes from costal cartilage potently induced the expression of Col X mRNA, while it suppressed those of Col II and aggrecan. CA9 knockdown also lowered alcian blue deposition to the chondrocytes. These results indicate that the reduced expression of CA9 is one of the triggers of hypertrophic differentiation of chondrocytes in growth plates. On the other hand, introduction of CA9 siRNA to mouse chondrogenic ATDC5 cells suppressed their proliferation, indicating CA9 is involved in chondrocyte proliferation in earlier stage of their differentiation. Collectively, it is plausible that CA9 positively regulates proliferation of resting and proliferating chondrocytes and inhibits further differentiation into hypertrophic chondrocytes, and hence the transcriptional silencing of CA9 induces hypertrophic differentiation.

***Disclosures: Toshifumi Maruyama**, None.*

SU0071

Chronology of Growth Hormone (GH) Receptor, Insulin-like Growth Factor (IGF) Type I Receptor, IGFI and IGFII Expression in Human Fetal Epiphyseal Chondrocytes from 7-20 Weeks Fetal Age. Cynthia Goodyer, Marcel Edwards*. McGill University, Canada

GH, IGFs and their receptors (GHR, IGFIR) play essential roles in growth of the long bones by promoting chondrocyte proliferation and differentiation. Developmental studies of their expression have been carried out in growth plates (GP) of several animal models, but not the human. Thus, we have undertaken an ontogenic study in human femoral epiphyses at the earliest stage of bone development (7-20wks fetal age [wFA]).

GPs were fixed, decalcified and paraffin-embedded. Sections underwent citrate-buffer antigen retrieval and were incubated with antibodies for GHR, IGFIR and a

series of chondrocytic, ECM and vascular markers followed by AlexaFluor conjugated secondary antibodies. Fluorescent *in situ* hybridization assays were performed for IGFI and IGFII mRNA. The distribution of GHR, IGFIR, IGFI and IGFII expressing chondrocytes relative to resting zone (RZ), proliferative (PZ) and hypertrophic (HZ) subpopulations was assessed by parallel characterization of COLII and PCNA (RZ/PZ), PTHR1 (late PZ/early HZ), RUNX2 (late PZ/HZ), COLX (HZ) and CD31 (vascular).

At 7wFA, when the GP consists of condensed mesenchymal precursors and early differentiated chondrocytes, all cells were GHR^+ and $IGF\text{-}IR^+$ and demonstrated IGFI/II mRNA expression. By 9-10wFA, a primary ossification zone was visible within the cortical shaft while the two GPs displayed three distinct chondrocytic subpopulations all GHR^+ and $IGF\text{-}IR^+$; IGFI/II were expressed in RZ and PZ cells, while IGFI was also found in periosteal and periarticular cells. At 11wFA, when vascularization of the GP was first consistently detected, GHR and IGFIR expression decreased significantly in the RZ and was almost completely undetectable in the HZ, but was maintained at high levels in cells rapidly proliferating (PZ and perivascular chondrocytes). Between 11-16wFA, IGFI expression remained in RZ, PZ and periosteal cells, but with decreased expression in periarticular cells. IGFII expression persisted across the RZ and PZ. From 16wFA, following major vascular invasion in the GPs, GHR and IGFIR were expressed predominantly in PZ and perivascular chondrocytes and at low levels in RZ cells, while previous patterns for the IGFs were maintained.

These data demonstrate parallel localization of GHR, IGFIR, IGFI and IGFII in the human fetal femoral GP, suggesting these receptors and their ligands act in concert to regulate chondrocyte proliferation and differentiation beginning at the earliest stage of human bone formation.

***Disclosures: Marcel Edwards**, None.*

SU0072

Dynamic Effects of Nfat1 and Sox9 on Articular Chondrocyte Function Associate with their Age-related Expression and Epigenetic Histone Modifications. Marianna Rodova[1], Qinghua Lu[1], Ye Li[1], Brent Woodbury[1], Jamie Crist[1], Brian Gardner[1], John Yost[1], Xiao-bo Zhong[1], H Clarke Anderson[1], Jinxi Wang*[2]. [1]The University of Kansas Medical Center, USA, [2]University of Kansas Medical Center, USA

Multiple factors are involved in cartilage formation, and transcription factor Sox9 is considered a master regulator of chondrocyte differentiation during skeletal development. However, transcriptional regulation of adult articular chondrocyte function remains unclear. To determine whether Nfat1, one of the nuclear factor of activated T cells (NFAT) transcription factors, regulates the function of differentiated adult articular chondrocytes, we examined the age-dependent effects of Nfat1 and Sox9 on articular chondrocyte function in Nfat1-deficient and wild-type mice by morphology, gene/protein expression, and chromatin immunoprecipitation (ChIP) assays. Nfat1 expression in wild-type articular chondrocytes was lowest at the embryonic stage and elevated in adults; deletion of Nfat1 did not induce osteoarthritis (OA)-like dysfunction of articular chondrocytes until the adult stage. Sox9 expression in articular chondrocytes was highest at the embryonic stage and decreased in adulthood; the presence of Sox9 was not sufficient to prevent OA-like changes in adult Nfat1-deficient articular cartilage. RNA interference-mediated knockdown of Sox9 significantly reduced the expression of chondrocyte marker genes in articular chondrocytes during development, with relatively mild changes in adults. ChIP assays demonstrated that increases in Nfat1/Sox9 expression were associated with an increase in Nfat1/Sox9 DNA-specific H3K4me2 dimethylation (a histone code for activation of gene transcription), whereas decreases in Nfat1/Sox9 expression were correlated with an increase in Nfat1/Sox9 DNA-specific H3K9me2/H3K27me3 (histone codes for repression of gene transcription) modifications. The results suggest that Sox9 is essential for articular chondrocyte function during development, whereas Nfat1 is a key factor that may act together with Sox9 for maintaining chondrocyte homeostasis in adult articular cartilage. Age-dependent expression of these two factors in articular chondrocytes is associated with age-related histone modifications, one of the epigenetic mechanisms that regulate gene transcription by altering histone-DNA interactions and chromatin structure in the nuclei of eukaryotic cells.

***Disclosures: Jinxi Wang**, None.*

SU0073

IL-6 is Stimulant for Initial Chondrocytic Differentiation in Chondrogenic Condition of Hypoxia. Yui Honjo*[1], Makoto Hirao[2], Yoshitaka Kawato[1], Hiroki Oze[1], Kenrin Shi[1], Akira Myoui[3], Hideki Yoshikawa[2], Jun Hashimoto[2]. [1]Department of Orthopaedics,Osaka University Graduate School of Medicine, Japan, [2]Osaka University Graduate School of Medicine, Japan, [3]Osaka University Hospital, Japan

The effects of interleukin 6(IL-6) on chondrocytic differentiation were shown in several previous in vitro studies. These earlier invesitigations revealed the inconsistency of its effects on chondrocytic differentiation, and it remains to be clarified whether IL-6 plays as stimulus or inhibitor in chondrogenesis and as anabolic or catabolic in cartilage remodeling. Our previous data showed that hypoxia is favorable condition in chondrocytic differentiation and preserves chondrocytic phenotype by inhibiting hypertrophy of chondrocyte (J Biol. Chem. 281(41), 2006). Oxygen concentration in vivo is hypoxic compared with the 20% O2 concentration widely used in vitro cell culture. We speculate, therefore that one of the reasons of inconsistency of the previously reported data is O2 condition of cell culture which does not reflect the condition in vivo. So the recent study was focus the effects of IL-6 on chondrocytic differentiation in hypoxia condition and furthermore aimed to clarify the phase specific influences of IL-6.At first, we evaluated the effect of IL-6 and monoclonal antibody against IL-6 receptor (IL-6R mAb) on initial stage of chondrogenesis using N1511 murine chondrocyte. N1511 cells were cultured with rh-BMP2 (100ng/ml), and at the same time stimulation of IL-6(10ng/ml) was also added. These cultivations were performed under hypoxia (5% O2). IL-6 stimulation caused dramatic increase of cartilaginous matrix synthesis in alcian blue staining after 16days. Real time RT-PCR analysis revealed that Col2a1 gene expression was up-regulated by IL-6 on day8, however addition of IL-6R mAb completely blocked this IL-6-induced phenomenon. There was no Col10a1 gene expression regardless of IL-6 stimulation. IL-6 clearly promoted Sox9 gene expression, while suppressed Runx2 gene expression on day4. Addition of IL-6R mAb abolished IL-6-induced Sox9 gene expression, on the other hand, restored IL-6-induced suppression of Runx2 expression. Next, we focused on p38MAPK pathway, because p38MAPK is activated by IL-6 stimulation, furthermore plays pivotal role in BMP-induced chondrogenesis. Ten micro molar of SB203580 (a specific p38MAPK inhibitor) also abolished IL-6-induced Sox9 gene expression, on the other hand, restored IL-6-induced suppression of Runx2 expression. Taken together, IL-6stimulation is important for initial chondrocytic differentiation, and p38MAPK pathway plays major part in such IL-6-induced phenomena.

***Disclosures: Yui Honjo**, None.*

SU0074

Lack of Pericyte Contribution to BMP4-induced Heterotopic Ossification. Eileen Shore[1], Frederick Kaplan[2], Vitali Lounev*[1]. [1]University of Pennsylvania, USA, [2]University of Pennsylvania Hospital, USA

Heterotopic ossification (HO) is extra-skeletal bone formation that can occur in response to trauma, burns, and hip replacement surgery as well as in rare genetic disease such as fibrodysplasia ossificans progressiva (FOP), the most severe form of heterotopic ossification in humans. A fundamental question in the cellular pathogenesis of HO is the identity of cells responsible for formation of new postnatal chondro/osseous tissue. We have previously shown that cells of Tie2 cell origin contributed abundantly to BMP4 induced HO, giving rise to ~50% of cells at fibroproliferative, chondrogenic, and osteogenic stages of BMP4 inducible HO. In order to identify additional cell lineages that contribute to HO, we investigated the participation of pericytes since this cell type was reported in several recent studies as contributing to mesenchymal stem cell population. Therefore we examined whether the cells of NG2 cell lineage contribute to HO. NG2 chondroitin sulfate proteoglycan is expressed by pericytes, chondrocytes and glial cells. To tag cells of NG2 cell origin, we crossed NG2-Cre mice with a floxed IRG reporter mouse line. Tie2-Cre mice crossed with IRG served as positive controls. Double positive NG2-Cre;IRG and Tie2-Cre;IRG mice were implanted with BMP4 in matrigel into skeletal muscle of hindlimb - a model that we have previously shown to induce an inflammatory muscle reaction followed by heterotopic endochondral ossification. This process is physiologically similar to the events experienced by patients who have FOP. Samples of skeletal muscle tissue from site of injection were examined histologically at selected time points (day 1 to day 14) to monitor HO formation and contribution of pericytes to HO. In contrast to cells of Tie2 cell origin that differentiate through an endochondral pathway to form heterotopic bone and contribute to all stages of HO, we found that cells of NG2 cell origin did not contribute to any stage of HO. Insight into the cellular pathophysiology of HO has important implications for the development of cell-targeted therapies for FOP and other conditions of dysregulated BMP-induced heterotopic ossification.

***Disclosures: Vitali Lounev**, None.*

SU0075

Mechanical Response of Chondrocytes to Cyclic Loading is Age Dependent. Craig Blanchette*[1], Cynthia Thomas[1], Todd Sulchek[2], Nadeen Chahine[3], Gabriela Loots[4]. [1]Lawrence Livermore National Laboratories, USA, [2]Georgia Tech Research Institute, Georgia, [3]Feinstein Institute for Medical Research, USA, [4]LLNLUC Merced, USA

Chondrocytes are responsible for the elaboration and maintenance of the extracellular matrix in articular cartilage. The biosynthetic responses of chondrocytes are known to be regulated by mechanical loading; therefore, mechanical properties of the cells play a pivotal role in the regulation of articular cartilage. Cartilage is unlike any other tissue in the human body since it lacks blood supplies and has low intrinsic regenerative properties. As a result, cartilage structure and function is more likely to degenerate in response to aging. We have hypothesized that functional deterioration observed in adult tissue is due in part to age-dependent changes in mechanical stiffness. To test this we: 1) investigated the indentation-dependent response of bovine chondrocytes to mechanical cyclic loading at different resting intervals using atomic force microscopy; 2) measured the effects of age on this response. Indentation-dependent curves were fit to the Hertzian model, which assumes a constant compressive stiffness, and a non-Hertzian model, where the indentation dependent compressive stiffness was empirically calculated. When the mechanical properties of single chondrocytes isolated from 1 day (1d) and 32 month old (32m) bovine were evaluated as a function of the resting time between successive cyclic indentations

(relax time), the compressive modulus of both cell types was shown to drastically decrease between a relax time of 0.5s and 2s. However, the magnitude of the compressive modulus varied between these two cells. At a 0.5s relax time, the compressive modulus of the 32m chondrocytes (n=12) was 1.57 +/- 0.253 and 1.09 +/- 0.21 kPa (Hertzian and non-Hertzian model), which decreased to 0.77 +/- 0.23 and 0.57 +/- 0.1 kPa when the relax time was greater than 2s. In contrast, the compressive modulus at a 0.5 s relax time for 1d old chondrocytes (n=87) was 1.2 +/- 0.21 and 0.88 +/- 0.21 kPa (Hertzian and non-Hertzian models) and these values decreased to 0.37 +/- 0.84 and 0.26 +/- 0.53 kPa at relax times greater than 2s. These results suggest that immediately after cyclic indentation, chondrocytes experience a higher stiffness that decreases with increasing relaxation time. This relaxation behavior may be due to fluid pressurization inside the cell or viscoelastic elements in the membrane or organelles. In addition, the mechanical response of chondrocytes was dependent on age, where 1d old chondrocytes had a lower stiffness than 32m old chondrocytes.

***Disclosures: Craig Blanchette**, None.*

SU0076

Over-expression of VEGF164 is Not Sufficient to Fully Prevent the Cell Death of HIF-1α Deficient Growth Plates. Christa Maes*[1], Elisa Araldi[2], Katharina Haigh[3], Richa Khatri[2], Riet Van Looveren[1], Amato J. Giaccia[4], Jody J. Haigh[3], Geert Carmeliet[5], Ernestina Schipani[2]. [1]Laboratory of Experimental Medicine & Endocrinology, K.U.Leuven, Belgium, [2]Massachusetts General Hospital & Harvard Medical School, USA, [3]Vascular Cell Biology Unit, VIB & University Ghent, Belgium, [4]Department of Radiation Oncology, Stanford University, USA, [5]Katholieke Universiteit Leuven, Belgium

Vascular endothelial growth factor (VEGF-A) is a classical downstream target of the family of hypoxia-inducible transcription factors (HIF). In the fetal growth plate, VEGF-A is expressed both in late hypertrophic chondrocytes, where it is a critical modulator of cartilage replacement by bone, and in the center of the proliferative layer and in the upper hypertrophic zone, i.e in the hypoxic regions of the growth plate. Fetal growth plates from mice in which all VEGF-A isoforms are genetically ablated exclusively in chondrocytes show massive central cell death, indicating that VEGF-A is critical for the survival of hypoxic chondrocytes. This phenotype has a striking similarity to the cell death observed in HIF-1α deficient growth plates. In this study, we used a genetic approach to assess whether VEGF-A is the prime downstream component of the Hif-1α-dependent survival pathway in chondrocytes.

Col2a1-Cre;ROSA26-VEGF(Tg/+) transgenic mice, which conditionally over-express the VEGF164 isoform in chondrocytes, were bred with Hif-1α(f/f) mice to generate double mutant mice that over-express VEGF164 and lack HIF-1α in chondrocytes. Of note, over-expression of VEGF164, which is the most abundant isoform in normal chondrocytes, does not cause any detectable fetal growth plate abnormality per se. Fetal growth plates of double mutant mice lacking Hif-1α and over-expressing VEGF164 displayed an obvious central cell death phenotype, which, however, was delayed and less severe compared with that in mutant mice exclusively lacking Hif-1α. This finding indicates that over-expression of VEGF164 only partially prevented the central cell death phenotype of fetal growth plates deficient in Hif-1α. Conversely, in a parallel series of control experiments VEGF164 over-expression was able to fully correct the spatially localized loss of cell viability observed in growth plates of embryos conditionally lacking all VEGF-A isoforms in chondrocytes.

In conclusion, our findings indicate that VEGF-A is not the main mediator of the HIF-1α survival function in chondrocytes, and that additional molecular mechanisms are likely to be involved. Moreover, our data demonstrate the VEGF164, when expressed at sufficiently high levels, can fully compensate for the lack of all VEGF isoforms, at least in mediating the VEGF-A-dependent survival of chondrocytes.

***Disclosures: Christa Maes**, None.*

SU0077

Primary Cilia are Required for Ihh Signal Transductioon in Response to Hydrostatic Loading of Growth Plate Chondrocytes. Lai Wang[1], Yvonne Shao*[1], Jean Welter[2], Robert Ballock[3]. [1]Cleveland Clinic, USA, [2]Case Western Reserve University, USA, [3]The Cleveland Clinic Foundation, USA

Objective: Indian hedgehog is a key component of the regulatory apparatus governing chondrocyte proliferation and differentiation in the growth plate. Recent studies have demonstrated that the primary cilium is also the site of Indian Hedgehog (Ihh) signaling within the cell. Although it is well established that mechanical forces can influence the behavior of growth plate chondrocytes (the Hueter-Volkmann principle of physeal growth), little is known about the response of growth plate chondrocytes to mechanical forces at the molecular level. The hypothesis of this study was that primary cilia are required for Ihh signal transduction in response to mechanical loading in growth plate chondrocytes.

Methods and Results: Growth plate chondrocytes were collected from the epiphyseal growth regions of two day-old Sprague Dawley rats and transiently transfected with an Ihh-responsive Gli-luciferase reporter plasmid. Cells were cultured as three dimensional cell pellets for four days, then subjected to hydrostatic compression forces (1 hour on, 1 hour off) for 48 hours at 37 degrees C. Control pellets were cultured under the same conditions without compression loading. During the 48 hours loading, cell pellets were treated with or without cyclopamine (an Ihh inhibitor), or chloral hydrate (a reagent that destabilizes primary cilia).

The effects of hydrostatic compression on Ihh signaling was analyzed by measuring Gli-luciferase reporter activity. After 48 hours of compression, Gli-luciferase activity increased three-fold compared to unloaded pellets. This increase in Gli-reporter activity was blocked by addition of either cyclopamine or chloral hydrate.

To visualize morphologic changes in primary cilia as a result of chloral hydrate treatment, immunostaining of alpha-tubulin was performed. Chloral hydrate treatment caused deformation of cilia structure, and also reduced gene expression of Ihh to 57% of control levels and reduced expression of Smo to 44% of control levels as measured by quantitative real-time PCR. Western blotting demonstrated that Ihh protein was decreased to 61% of controls and Smo protein reduced to 73% of controls following chloral hydrate treatment.

Conclusion: We conclude that mechanical forces are transduced into biological signals at cellular level through Ihh signaling at the primary cilia on growth plate chondrocytes, and that primary cilia are required for this mechano-biological signal transduction to occur.

***Disclosures: Yvonne Shao**, None.*

SU0078

Recombinant Myostatin (GDF-8) Treatment Decreases Chondrogenesis *In Vitro* and Decreases Fracture Callus Bone Volume *In Vivo*. Moataz Elkasrawy*, Phonpasong Arounleut, Mark Hamrick. Medical College of Georgia, USA

Myostatin (GDF-8), a member of the transforming growth factor β superfamily, is a negative regulator of skeletal muscle growth and development. Loss of myostatin leads to doubling in muscle mass. We recently demonstrated that mice lacking myostatin also show an increase in fracture callus volume. Although myostatin is immediately expressed during the early phases of fracture healing, its role is poorly understood. The purpose of this study is to investigate the direct role of myostatin in bone repair and regeneration. First, we examined the effects of myostatin on bone marrow-derived mesenchymal stem cell (BMSC) chondrogenic differentiation, a key step in fracture healing. To this end, we collected BMSCs from Collagen type 2 (Col2)-GFP reporter mice. Bone marrow cells were expanded in culture and hematopoietic cells removed using anti-CD11b/CD45 magnetic beads. BMSCs were then isolated using anti-sca-1 magnetic beads, and purity was analyzed by high-speed flow cytometry. A high mass aggregate culture was treated in the presence or absence of 100ng/ml of recombinant myostatin delivered at 0 or 48-hour in defined chondrogenic medium for 6 days. Relative Col2 expression was quantified from fluorescent images of mounted aggregates using ImageJ software. Results show a decrease in Col2 expression of 31% with early myostatin treatment, and a decrease of 25% with later myostatin treatment. Next, we assessed the direct role of myostatin in fracture healing using a fibular osteotomy procedure in 18 wild type mice. A skin incision was made along the lateral side of the leg, and a transverse fracture was induced at the middle of the fibula using microtenotomy scissors. Mice received 30μl of re-absorbable hydrogel loaded with 0, 10, or 100μg/ml recombinant myostatin injected directly into the open fracture site. Forelegs were collected 15 days post-surgery and total bone volume of the fracture callus was calculated using microCT imaging. Results show a dose-dependent decrease in fracture callus total bone volume of 47% and 23%, respectively, with the higher dose of recombinant myostatin yielding the greatest decrease in callus bone volume. Together, these findings suggest that myostatin can regulate the initial differentiation of chondrogenic progenitors, ultimately influencing the size and volume of the fracture callus. Funding for this research was provided by the National Institute of Health (AR049717), and the Office of Naval Research (N000140810197).

***Disclosures: Moataz Elkasrawy**, None.*

SU0079

Regulation of the CamkII Node Determines Proliferative Potential in Growth Plate Chondrocytes. Yuwei Li, Andrew Dudley*, Molly Ahrens. Northwestern University, USA

For tissues that develop throughout embryogenesis and into post-natal life, the generation of differentiated cells to promote tissue growth is at odds with the requirement to maintain the stem cell/progenitor cell population to preserve future growth potential. In the growth plate cartilage, this balance is achieved in part by establishing a proliferative phase that amplifies the number of progenitor cells prior to terminal differentiation into hypertrophic chondrocytes. Here we combine three powerful tools - retroviral expression of epitope tagged proteins, a phospho-specific antibody, and potent chemical inhibitors - to show that activation of endogenous calcium/calmodulin-dependent protein kinase II (CamkII) activity in chick and mouse chondrocytes is both sufficient and required for chondrocyte hypertrophy. Studies in chick additionally demonstrated that CamkII activity is under negative regulation by the Wnt and the Pthrp signaling pathways, which regulate CamkII activity via distinct mechanisms. Furthermore, upregulation of CamkII activity promotes multiple independent, dosage-sensitive effector pathways that compose the terminal differentiation (hypertrophy) program. In this manner, CamkII functions as a node which integrates information from signaling pathways to place strict limits on the growth potential of proliferative chondrocytes. We present an integrated model for the regulation of proliferative potential that has important implications for studies of adult stem cells.

***Disclosures: Andrew Dudley**, None.*

SU0080

Wnt5b Regulates Mesenchymal Cell Aggregation and Chondrocyte Differentiation through the Planar Cell Polarity Pathway. Elizabeth Bradley*, Hicham Drissi. University of Connecticut Health Center, USA

Emerging genetic evidence demonstrated a role for Wnt5b in modulating cartilage development. However, little is known about the mechanisms underlying non-canonical Wnt5b-regulated chondrocyte differentiation. We therefore investigated the signal transduction pathways induced by Wnt5b during chondrocyte differentiation and maturation. Using our high-density micromass culture model, we found that over-expression of Wnt5b promoted Sox9 expression and inhibited chondrocyte maturation. In addition, expression of Wnt5b disrupted the cellular aggregation associated with mesenchymal condensation. This loss of aggregation was not observed when cells were treated with the highly related growth factor, Wnt5a. Although Wnt5b and Wnt5a activated known calcium-dependent signaling pathways, Wnt5b exclusively induced activation of JNK, as assayed by increased phosphorylation of JNK. We observed a marked increase in the wound closure using a scratch assay analysis with Wnt5b expression. This effect was blocked by inhibition of JNK, but not by inhibition of other Wnt5b responsive factors. These data indicate that Wnt5b may promote chondrocyte migration potentially through the JNK-dependent planar cell polarity pathway. We therefore also assessed the effects of Wnt5b on chondroprogenitor cell aggregation. Wnt5b expression decreased aggregation of chondroprogenitor cells. This decrease in aggregation was associated with a decrease in cadherin expression as well as an increase in cadherin receptor turnover. In this study we describe a potential mechanism for effects of Wnt5b on chondrocyte differentiation. Our data demonstrate for the first time that not only does Wnt5b inhibit chondrocyte hypertrophy, but also that Wnt5b modulates cellular adhesion and migration through the JNK-dependent planar cell polarity pathway.

***Disclosures: Elizabeth Bradley**, None.*

SU0081

Differential and Site Specific Gene Expression of Adult Rodent Long Bones Following Hindlimb Unloading and Periods of Reloading Adaptation. Daniel Martinez*[1], Laura Gutierrez[1], Kristin Reddoch[1], Meaghen Krebsbach[1], Yasaman Shirazi-Fard[2], Susan Bloomfield[2], Harry Hogan[2]. [1]University of Houston, USA, [2]Texas A&M University, USA

Cortical and trabecular bone are sensitive to the deprivation of ground reaction forces as evidenced by decreases in mineral density and organic extracellular matrix (ECM). The cellular and molecular responses of osteoblasts, osteocytes and osteoclasts to decreased load bearing occur at the onset of load reduction. However, the temporal component to re-establish gene expression profiles to the pre-unloaded state is not known. Therefore, the first objective was to determine the regional differences in bone gene expression markers essential for formation (Col1a2), differentiation (Osteocalcin, Runx2, Osterix) and resorption (MMP-2) following 28d of hindlimb unloading (HLU). The second objective was to determine if these genes are expressed equally following 3-periods of re-loading recovery after HLU. Our working hypothesis is that HLU causes a decrement in Col1a2, Osteocalcin, Runx2 and Osterix expression and an increase in MMP-2 expression. Recovery of the gene expression markers after HLU is postulated to achieve baseline values once the adaptation to reduced loads has been offset.

Materials and Methods: Adult male rats (6-10 months) were randomly assigned to 5 groups, n=10 each: 1.) baseline (t=0), 2.) 28d of HLU, and 3 recovery groups following HLU, 3.) Rec28, 4.) Rec56, and 5) Rec84. Following euthanasia, bilateral femurs and tibias were isolated and cleaned of soft tissue. Total RNA was procured from the distal femoral metaphysis (DFM), proximal tibial metaphysis (PTM) and tibial diaphysis (TD) sites. RT Q-PCR analysis was performed in triplicate cDNA, and then compared to known quantities of sDNA standard oligomers.

Results: HLU induced gene expression patterns favoring the greatest turnover in the PTM site with decreases in Col1a2, Osterix (-16% each) and increases in MMP-2 levels (38%). Interestingly, HLU Osteocalcin gene expression was 50%-113% greater than controls in all bone sites. The gene expression profile favoring the greatest bone formation during recovery was Rec28. Runx2 levels were highest in the Rec28 and Rec56 in DFM and TD bone sites. During recovery, gene expression patterns were differentially expressed dependent on the bone site and length of re-loading.

Summary: Gene expression patterns are differentially expressed in rat long bones and within the same bone at different sites after HLU. Initial reloading of 28d after HLU demonstrated the greatest change in collective gene expression compared to longer durations of recovery from HLU.

***Disclosures: Daniel Martinez**, None.*

SU0082

Dlk1/FA1 Regulates the Early Chondrocyte Differentiation in Limb Bud Micromass Culture and its Expression is Modulated by TGF-beta Singaling Pathway. Basem Abdallah*[1], Linda Harkness[2], Hanna Taipaleenmaki[3], Moustapha Kassem[4]. [1]Odense University Hospital, University of South Denmark, Denmark, [2]Department of Endocrinology (KMEB Lab.), Odense University Hospital, Denmark, [3]Department of Medical Biochemistry & Molecular Biology, University of Turku, Turku, Finland, Denmark, [4]Odense University Hospital, Denmark

Recently, we have identified Dlkl/FA1 (delta like 1/fetal antigen1) as a novel marker of chondroprogenitor cells that undergo embryonic lineage progression from proliferation to the prehypertrophic stage (Harkness L, et al., Stem Cell Rev and Rep, 2009 Dec;5(4):353-68). We aimed in this study to investigate the regulatory role of Dlk1/FA1 in chondrogenesis. For that purpose, we used the mouse embryonic limb mesenchymal micromass culture as an in vitro system that recapitulates the sequential stages of chondrogenesis. In this culture system, we examined the possible regulation of dlk1/FA1 expression in response to different signal pathways and their antagonists that involved in the entire program of cartilage development. Real-time PCR, immunostaining and ELISA (for active soluble form of Dlk1/FA1) assays showed that Dlk1/FA1 started to be expressed at stages of mesenchyme condensation (day 1-3) and peaked up through chondrogenesis (Day 3-6) in parallel with the expression of *Sox9* and type 2 collagen, while dramatically down-regulated after day7 to be abolished completely upon the expression of ColX by hypertrophyic chondrocyte at day 10. Interestingly, TGF-b1 (an early signal for condensation/differentiation) treatment delays chondrocyte hypertrophy and inhibits matrix mineralization in parallel with marked down-regulation of *Dlk1* expression (by 80%) with maintaining the expression of early chondrogenic markers *Sox9* and *Col2a1*. In contrast to the inhibition of *Dlk1* expression by TGFb1 to maintain chondrocyte in premature stage, blocking of TGF-b signal using SB431542 (a selective inhibitor of ALK-2,-5 and -7 receptors) strongly inhibits mesenchyme condensation and chondrogenesis in parallel with marked stimulation of *Dlk1* expression (by 4 folds). Furthermore, *Dlk1*$^{-/-}$ mouse embryonic fibroblast cells (MEFs) showed to differenetiate efficently into mature chondrocyte when cultured as micromass pellets in the presence of TGFb1 as compared to WT-MEFs cells. In conclusion, our data identified Dlk1/FA1 as a regulatory marker that regulating early events of endochondral bone development, at chondrogenic condensation and proliferation stages. The down-regulation of Dlk1/FA1 expression by TGF-b signaling, suggest a plausible mechanism by which the stimulatory effect of TGF-b on chondrogenesis is mediated at least in part by Dlk1/FA1.

***Disclosures: Basem Abdallah**, None.*
This study received funding from: NovoNordisk Foundation

SU0083

Elucidation of WISP1 Protein Function in Chondrocytes. Katrin Schlegelmilch[1], Viola Monz[1], Alexander Keller[2], Ludger Klein-Hitpass[3], Norbert Schuetze*[1]. [1]University of Wuerzburg, Orthopedic Center for Musculoskeletal Research, Germany, [2]University of Wuerzburg, Biocenter, Department of Bioinformatics, Germany, [3]University of Duisburg-Essen, Institute of Cell Biology (Tumor Research), Germany

WISP proteins (wnt1 inducible signaling pathway proteins 1-3, CCN4-6) are matrix associated secreted signal molecules that belong to the CCN family. These proteins are characterised by an identical modular structure and act in a cell-specific and partly non redundant manner. The proteins play a role in development, angiogenesis, proliferation, adhesion, migration and other fundamental cell processes. Molecular data on WISP functions are limited, but their association with the wnt/ß-catenin pathway indicates an important role during skeletal development. Here we aim to elucidate the role of WISP1 in chondrocytes.

shRNA analyses were performed to reduce the endogenous WISP1-level in the chondrocyte cell line Tc28a2. Different shRNA- and control constructs (scrambled and GFP) were transfected into human embryonic kidney cells (HEK 293-T) via lipofectamine. Lentivirus supernatant was used to infect the target cell line Tc28a2. After 4-8 days, total RNA was isolated and analysed by RT-PCR. As a second functional tool recombinant WISP1-Fc protein was expressed in baculovirus infected insect cells and purified using protein G-sepharose. Western blotting and silver staining were applied to verify size and purity. WISP1 gene expression was analysed at the mRNA level by RT-PCR.

RT-PCR analysis revealed a remarkable decrease of WISP1 (both isoforms) expression in the knock-down experiments, whereas the RT-PCR signal intensity remained unchanged in control cells (scrambled- and GFP constructs as well as the plko.1 vector without insert). Subsequent Affymetrix array analyses using the HG-U133plus2.0 chip revealed the reproducible regulation of 790 genes due to the knock down compared to controls (n=5 pairwise comparisons). A striking cluster of apoptosis-, chemokine- and Jak-STAT-signal transduction related MAP kinases was identified. WISP1 protein was functionally expressed in SF-21 cells. Treatment of Tc28a2 cells with 500 ng/ml isoform T1 and T2 resulted in an increase of only the respective isoform of WISP1 as measured by RT-PCR, indicating a self regulatory role.

The knock down of WISP1 in chondrocytes resulted in gene regulation changes associated with apoptosis, proliferation and inflammation. Data indicate that this

protein appears to be an important regulator within the musculoskeletal system. Recombinant proteins as well as efficient knock-down approaches are fundamental tools to further elucidate the function of WISP1 in cells of the musculoskeletal system.

chrondrocytes,

***Disclosures: Norbert Schuetze**, None.*

SU0084

Gene Transfer of RUNX-2, Osterix Transcription Factor Promotes Osteogenesis of Adipose Tissue-derived Mesenchymal Stem Cells. Gun Il Im[1], Jai Sun Lee*[2]. [1]Department of Orthopaedics, Dongguk university international hospital, South korea, [2]Dongguk University International Hospital, South korea

INTRODUCTION Large bone defects that occur as a result of major trauma or tumor resection have been treated by allogeneic bone grafting. However, the technique has inherent disadvantages such as high cost, the risk of infection and slow bone remodeling. Recently, cell therapies using mesenchymal stem cells are being developed as an alternative treatment. Although bone marrow makes the most known source of adult stem cells, the available volume of bone marrow is limited. In contrast, the adipose tissue provides an alternative and abundant source of adult stem cells. The objective of this study was to examine the feasibility of using Runx-2, Osterix gene transfer to enhance the osteogenic differentiation of adipose tissue-derived stem cells (ATMSCs).

METHODS To create non-viral expressing RUNX-2, Osterix, full-length human RUNX-2, Osterix complementary DNA (cDNA) was amplified by polymerase chainreaction (PCR) and cloned into pEGFPC1 mammalian expression vector (Clontech, Palo Alto, CA). The microporatorTM (Invitrogene) and the buffer system were utilized for gene delivery. Microporator transfersgenes into living cells by means of high voltage electric pulses. Approximately 3 × 105 ATMSCs and 0.5 g plasmid DNA were used for a single transfer. After microporation, the osteogenic differentiation was carried out using 2.5 x 105 ATMSCs in osteogenic medium. After one week, cells were analyzed for real time PCR, western blotting, ALP assay and alizarin-red staining. ATMSCs to which empty vector was transferred was used as the negative control.

RESULTS To confirm the protein expression of RUNX-2, Osterix, we attempted to western blotting. Expression of the Osterix gene was significantly increased by RUNX-2, Osterix overexpression. Real-time PCR analysis showed that the mRNA levels of OCN, ALP, Col1A1, and BSP increased several fold in ATMSCs to which RUNX-2, Osterix genes were transferred. RUNX-2, Osterix overexpression induced ALP activity in ATMSCs. Alizarin-red staining demonstrated that ATMSCs to which the RUNX-2, Osterix genes were transferred exhibited greater accumulation of the calcium contents than negative control.

DISCUSSION The nonviral method for gene transfer shown here demonstrated a high efficiency not preceded by other studies. Gene transfer of RUNX-2, Osterix was effective in promoting osteogenesis. This nonviral gene transfer system for RUNX-2, Osterix may provides potent new means to achieve osteogenic differentiation from ATMSCs.

ACKNOWLEDGEMENT This work was supported by a grant from the Korea Ministry of E ducation, Science and Technology (Grant No S 2009 A0004 00041).

***Disclosures: Jai Sun Lee**, None.*

SU0085

Investigating the Developmental Origins of the Meniscus. Dorothy Pazin*[1], Laura Gamer[2], Karen Cox[2], Vicki Rosen[3]. [1]Harvard School of Medicine, USA, [2]Department of Developmental Biology, Harvard School of Dental Medicine, USA, [3]Harvard School of Dental Medicine, USA

The meniscus is a fibrocartilagenous disk found in the knee that serves to transmit and distribute forces, and acts as a cushion to protect the tibia and femur from damage during movement. Meniscal injuries are common, and predispose individuals to development of osteoarthritis. Efforts to repair damaged menisci are often unsuccessful largely due to an incomplete understanding of the signals required to initiate meniscal repair. We hypothesize that the regulatory molecules that control meniscal morphogenesis may be effective meniscal repair agents. However, the embryonic origins of the meniscus, as well as the genes and signaling pathways that are involved in its differentiation have yet to be identified. To collect this information, the expression pattern of known joint markers was examined by in situ hybridization (ISH) in knee regions isolated from E14, E16, and E18 mice. Our data confirm that Gdf5 marks the interzone cell population at E14 and reveals that Gdf5 is not expressed in the meniscus at E16. Expression of Wnt9a was not detected in the meniscus at any of the stages tested. A few TOPGAL positive cells could be detected at the periphery of the meniscus at E18 indicating that WNT signaling may be involved in the differentiation of some meniscal cells. Expression of Col2 was detected in a subset of meniscal cells only at E18 and a few Lubricin-expressing cells were detected at the periphery of the meniscus at E18. Overall, this data suggests that the meniscus arises from a cell population with a unique gene expression signature. To identify meniscus-specific markers, RNA from E15 and E16 mouse elbow (no meniscus) and knee (meniscus present) joints will be isolated and run on separate microarrays, and a comparative approach will be used to identify genes that are meniscus-specific. Meniscal cells will also be isolated using laser capture microdissection and their transcriptome deciphered using next-generation sequencing technology. Once meniscus-specific genes have been identified, their spatiotemporal expression will be examined using ISH. Additionally, bioinformatic analysis of the microarray and sequencing results will provide insight into the signaling pathways involved in meniscus development. By determining the morphological signals required for meniscus development, we hope to find effective repair agents for adult meniscal tissue.

***Disclosures: Dorothy Pazin**, None.*

SU0086

PERP Regulates Ameloblast Adhesion and Is Critical for Proper Enamel Formation. Andrew Jheon*[1], Malcolm Snead[2], Rebecca Ihrie[1], Eli Sone[3], Pasha Mostowfi[1], Laura Attardi[4], Ophir Klein[1]. [1]University of California, San Francisco, USA, [2]USC, USA, [3]University of Toronto, Canada, [4]Stanford, USA

Enamel is the hardest mineralized tissue in the body and is unique in its epithelial origin. Relatively little is known about the role(s) of cell-cell adhesion during enamel formation (amelogenesis). Here we report that PERP, a desmosome-associated tetraspan membrane protein involved in epithelial development, is a critical regulator of amelogenesis. *Perp* is expressed in the ectoderm-derived epithelial cells during embryonic tooth development, and its expression is controlled by p63, a master regulator of stratified epithelial development. In neonatal mouse teeth, PERP is localized at the interface of the ameloblasts and the stratum intermedium (SI), a layer of cuboidal cells that subtends the ameloblasts. *Perp* homozygous null mice display dramatic defects in enamel matrix and mineralized enamel. There is an uneven distribution of enamel matrix, which subsequently results in major alterations in mineralization. Our data suggest that the enamel defects are caused by detachment of ameloblasts from the SI due to a compromise in desmosome structure. This process of detachment results in changes in expression of amelogenesis-related genes, such as *Ameloblastin*, *Enamelin*, and *Mmp20*, but not *Amelogenin*, *Tuftelin*, and *Apin*. Thus, the interaction between ameloblasts and SI via PERP and desmosomes is necessary for proper ameloblast gene expression and enamel formation.

***Disclosures: Andrew Jheon**, None.*

SU0087

The Function of Sox4 Transcription Factors in Zebrafish Bone Development and Homeostasis. Jessica Aceto*, Patrick Motte, Martial Joseph, Marc Muller. University of Liege, Belgium

Small fish models, such as zebrafish (Danio rerio) and medaka (Oryzias latipes) present many advantages and are increasingly used to study vertebrate development and physiology. In mammals, the Sox4 gene is known to be involved in the development of several tissues, such as brain, teeth, lymphocytes and endocardial crest. Moreover, Sox4 was shown to control bone mass and mineralization in mice. The *sox4* gene is well conserved among all vertebrate species, however two homologs for the mammalian *Sox4* gene are present in zebrafish, *sox4a* and *sox4b*.

In this study, we focus on the first bone to be formed during embryogenesis in zebrafish, the head skeleton. We show that both *sox4* genes are expressed in the pharyngeal region, but not at the same stage of the development. Double *in situ* hybridization experiments were performed to define exactly the tissues where they are expressed. To better understand their function during bone development, we used microinjection of morpholino antisense oligonucleotides to block the translation of each specific gene. Knock-down of Sox4a or Sox4b leads to morphological modifications in the jaw, suggesting that both genes are important for correct formation of the mandible and hyoid. In addition, we treated larvae with chemicals such as PTH or Vitamin D3, known to decrease or increase, respectively, bone formation. We observe a correlation between bone formation and expression of *sox4* genes.

In conclusion, our results show that both Sox4a and Sox4b homologs are involved in the control of bone formation in zebrafish.

***Disclosures: Jessica Aceto**, None.*

SU0088

A Non-cell Autonomous Role for *rpz* in Skeletogenesis. Matthew Goldsmith*[1], Douglas Oppedal[2], Bendi Gong[2]. [1]Washington University School of Medicine, USA, [2]Washington University, USA

Purpose: Mechanisms that regulate vertebrate skeletal development and homeostasis are protean and incompletely understood. The zebrafish mutant *rapunzel* has heterozygous defects in bone development, resulting in skeletal overgrowth. The mutant phenotype results from a gain of function mutation in the novel *rpz* gene, however the mechanistic basis of the skeletal overgrowth phenotype remains unresolved.

Methods: *rapunzel* was previously identified through an ENU-based forward genetic screen. *In situ* hybridization (ISH) and quantitative RT-PCR (qPCR) were used to characterize gene expression in wild type and mutant embryos. Blastula

transplantation was GFP-marked cells was used to create mosaic zebrafish and determination whether the mutant *rapunzel* phenotype was cell autonomous or non-cell autonomous in nature.

Results: The zebrafish mutant *rapunzel* has heterozygous defects in skeletogenesis, resulting in overgrowth of the appendicular skeleton and hyperossification of the axial skeleton. ISH and qPCR demonstrate that *rapunzel* expression precedes the formation of definitive skeletal elements, suggesting a non-cell autonomous role for *rpz* in skeletogenesis, data that are supported by transplantation studies and analyses of mosaic fish. We also demonstrate that heterozygous *rapunzel* mutants have increased expression of the osteoblast-specific markers *col1a1* and *osx*, ultimately resulting in an almost 2-fold increase in bone mineral density.

Conclusions: We previous cloned *rapunzel* and identified a gain of function mutation in a novel gene (*rpz*) of unknown function. Here we report that mosaic analyses suggest a non-cell autonomous role for *rpz* in skeletogenesis and furthermore, that heterozygous *rapunzel* mutants have an increase in expression of osteoblast-specific markers, suggesting either an increased recruitment of bone-forming cells from the mesenchymal anlage or an increase in activity of bone-forming cells. These data regarding *rapunzel* provide new insight into the mechanisms underpinning vertebrate skeletal biology.

***Disclosures: Matthew Goldsmith**, None.*

SU0089

A Novel OI Mouse Model with *Col1A1* Splicing Site Mutation. Joan Marini[1], Weizhong Chang*[2]. [1]National Institute of Child Health & Human Development, USA, [2]National Institutes of Health, USA

Splice site mutations comprise 15-20% of type I collagen helical mutations in the OI Mutation Consortium Database, but their splicing and matrix abnormalities have not been well-studied. We characterized the first mouse model with Osteogenesis Imperfecta (OI) caused by a collagen splicing defect. The mouse was generated by ENU-induced mutagenesis (Beutler laboratory, Scripps Institute) and has a point mutation in the *col1a1* exon 36 splice donor site (c.2526+2T->A). Heterozygous mice are superficially normal. Homozygous mice are about 15% smaller than wt littermates at age 2 months. Most homozygous mice display normal locomotion, but some have a "waddling gait" of unclear etiology. Interestingly, type I collagen synthesized by cultured dermal fibroblasts from heterozygous or homozygous mice has α1 chains with normal gel migration, but slower migration of α2 chains. In addition, reduction of the type I/type III collagen ratio in the cell layer of both heterozygous and homozygous mice suggests partial insufficiency of type I collagen. However, *col1a1* transcript levels are normal in heterozygous and homozygous mice on real-time RT-PCR. To determine the effect of the mutation on splicing of *col1a1* transcripts, we amplified the cDNA spanning exons 34 to 38 from total RNA of emitine-treated fibroblasts of homozygous mice. Sequencing of 16 subclones of PCR products revealed that most (81%) have normal sequences. Three alternatively spliced isoforms were detected: (1) skipping of exon 36, (2) retention of 4 nt of intron 36, (2) use of a cryptic donor site within exon 36, 53 nt upstream of normal donor site. The proportions of the splicing isoforms are being determined by RNA-protection assays. While two isoforms are out-of-frame and lead to PTC and NMD, exon 36 skipping produces in-frame transcripts. Incorporation of shortened α1 chains into collagen triple helix will cause register shift among the chains. The murine splicing patterns are similar to those in some OI patients with splice site defects, who have a complex mixture of normal splicing, exon skipping and use of alternative splice sites. Homozygosity for the exon 36 donor site mutation would be expected to increase the proportion of abnormal collagen chains and increase matrix heterogeneity, which may be the basis of the more severe homozygous phenotype. This new OI mouse model will be important for studying the complex effects of collagen splice site defects and the mechanism of their bone dysplasia.

***Disclosures: Weizhong Chang**, None.*

SU0090

Bio-composite Microfluidic Platforms for Bone Cell Mechanobiology Study. Dina Badawy*[1], Yan Zhao[2], Lidan You[3], Hani Naguib[1]. [1]University of Toronto, Canada, [2]China Everbright Bank, Beijing Department, China, [3]Mechanical & Industrial Engineering, University of Toronto, Canada

Bone and joint diseases affect millions of people worldwide. However, due to the limited understanding of the cellular and molecular mechanism underlying these diseases, effective strategies in treatment and prevention of these bone disorders are yet to come. To date, most in vitro bone cellular studies are conducted in 2D environment which lacks the critical ultrastructure elements existing in in-vivo extracellular environment which may potentially result misleading information on bone cell behaviour under normal physiological conditions. Currently, our lab uses microfluidic technology facilitates the study of bone cell metabolism in controlled 3D engineered platforms.

Our microfluidic chamber structure is designed to maximally simulate the in vivo lacunar-canalicular network. Fig. 1 shows Single MLO-Y4 cell adhesion on our device, 3 h after cell seeding with Chamber diameter: 30 μm.

The purpose of this research is to prepare two bio-composite materials that potentially mimicking bone matrix characteristic. A Twin screw extruder Mini-Compounder is used to blend the polymer with the desired ceramic ratio (zero, 2, 5, 10 wt %). Hot embossing machine is used to replicate the micro chamber design to our bio-composite material.

Material selection for the current study is Polylactic acid (PLA) which is a biocompatible biodegradable approved polymer with good mechanical properties (2-7 GPa) [1]. However, PLA is a hydrophobic material which weakens cell attachment. Both nHA and βTCP are bio-ceramics that is known for its osteoconductive properties that support osteogenesis.

Hydroxyapitite (nHA) (< 200 nm) and β-tricalcium phosphate (βTCP) (≂ 60 μm) are used as filler material to improve the mechanical properties and cell attachment. Fig.2 shows an SEM Image for our device using PLA. And Fig. 3 and 4 shows an SEM sample for topography observation for PLA/nHA with composition of 2 and 5 wt % respectively. Mechanical, thermal and biodegradation evaluation for the two composites are currently carried out.

In summary, filler ceramics improve the mechanical properties of PLA and make it suitable surface for bone cell study. Additionally, our lab believes that the incorporation of bio-composite in microfluidic devices provides cells with similar environment to native tissue. We expect that cellular response to mechanical stimuli will be different than the previously reported data.

[1] T. Kasuga, Y.Ota, M.Nogami, Y. Abe, Biomaterials 22:1, 2001.

Fig. 1: Single MLO-Y4 cell adhesion on our device, 3 h after cell seeding

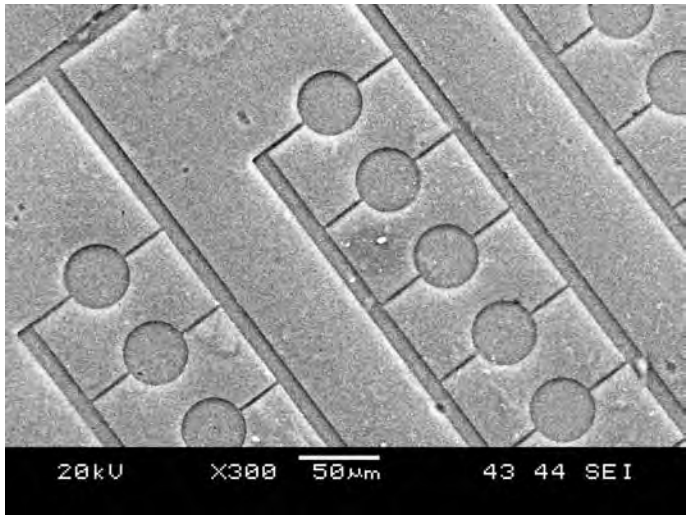

Fig. 2: SEM image for our microfluidic device using PLA

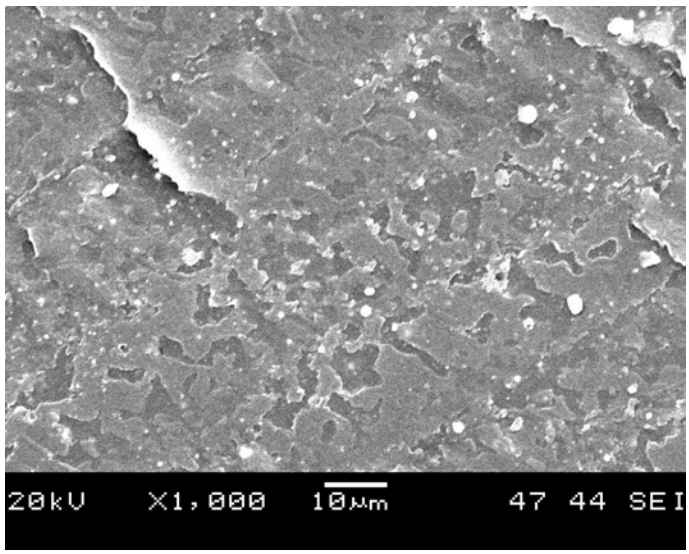

Fig. 3: SEM observation of PLA/nHA composite 2 wt%

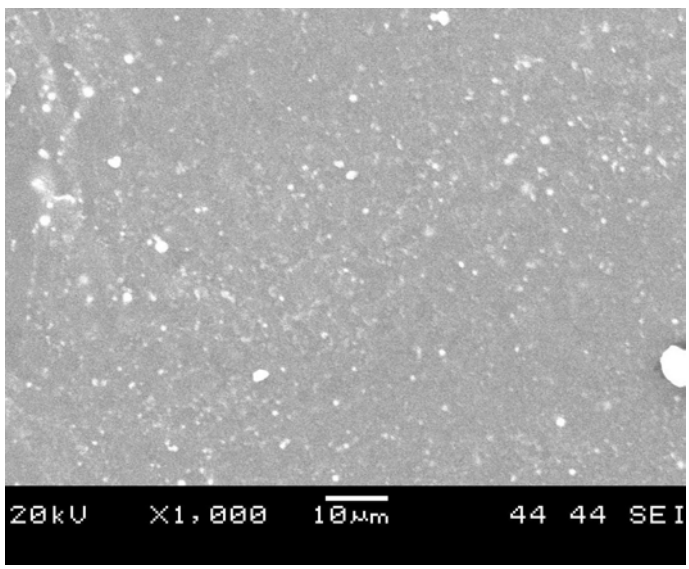

Fig. 4: SEM observation of PLA/nHA composite 5 wt%

***Disclosures: Dina Badawy**, None.*

SU0091

Effect of Low Dose Ionizing Radiation on Bone Microarchitecture and Bone Marrow Progenitor Differentiation. Florence Lima*[1], Joshua Swift[2], Elisabeth Greene[1], Matthew Allen[3], David A Cunningham[1], Leslie Braby[1], Susan Bloomfield[1]. [1]Texas A&M University, USA, [2]United States Navy, USA, [3]Indiana University School of Medicine, USA

Exposure to ionizing radiation has deleterious effects on bone health. Therapeutic radiation involves exposure to photon (gamma/X-ray), electron, or proton radiation. Humans in space are exposed to high-energy heavy ions and proton radiation from cosmic and solar sources but at lower doses (0.5 to 1.0G during shuttle, Skylab and Apollo missions) and dose rates and for prolonged periods as compared with radiotherapy. The purpose of this study was to determine the effect of low-dose ionizing radiation on bone microarchitecture in adult mice and bone marrow stromal cell (BMSC) differentiation. Methods: Female BALB/cByJ mice (4-mo, n= 9 /group) were exposed to one acute dose of 0.17Gy, 0.5Gy, or 1Gy on Day 0 using a X-ray beam (Norelco MG300 X-ray industrial radiograph). SHAM groups were placed in the X-ray box without activation of the x-ray source. Mice were sacrificed at 3 and 21 days after exposure. Trabecular microarchitecture was determined with MicroCT scans (Skyscan 1172) of excised distal femurs; traditional 2D bone histomorphometry of the distal femur quantified cancellous bone formation rate. Flushed BMSC from tibia were cultured in presence of different differentiation media and analyzed for osteogenic differentiation capability: alkaline phosphatase activity (ALP), osteoblast-Colony Forming Unit (OB-CFU) and calcified nodule number (No), adipocyte differentiation (AC) and osteoclast differentiation (OC). Results: No changes to bone microarchitecture or bone formation rate at 3 days after radiation were observed at any dose. However, at 21 days post-radiation while there is no change in bone formation, with 1Gy X-ray exposure we saw the biggest decrease in trabecular number, separation, and material density in femur (by uCT) compared to all other groups, and a highest increase in the structural model index and trabecular pattern factor ($p<0.01$). No significant differences in any parameters were observed between the SHAM controls and the 0.17 and 0.5 Gy dose groups at 21 days. BMSC harvested 3 days after radiation showed impaired OB differentiation (decrease in ALP, OB-CFU, No) with no change in OC or AC differentiation. BMSC differentiation from irradiated mice 21 days after radiation exposure at 0.17 Gy were impaired, whereas at 0.5 Gy and 1.0 Gy cells exhibited an increased ALP, OB-CFU, OC and AC numbers. Conclusion: Low dose radiation affects cell progenitors at both 3 and 21 days and impairs bone microarchitecture.

***Disclosures: Florence Lima**, None.*
This study received funding from: Funded by NSBRI through NASA Cooperative Agreement NCC 9-58 and the Sydney and JL Huffines Institute for Sports Medicine and Human Performance.

SU0092

ERbeta Antagonist PHTPP Promotes Bone Repair in Osteoporotic Mice: A microCT and Biomechanical Study. Yixin HE*[1], Ge Zhang[2], Zhong Liu[3], Xiaohua Pan[4], Xinhui Xie[5], Chun-Wai Chan[6], Kwong-Man Lee[7], Gang Li[8], Ling Qin[9]. [1]The Cuinese University of Hong Kong, Hong kong, [2]Price of Wales Hospital, Peoples republic of china, [3]Musculoskeletal Research Laboratory, Department of Orthopaedics & Traumatology, The Chinese University of Hong Kong, Hong Kong SAR, China, China, [4]Department of Orthopedics, Second Hospital of Medical College of Ji Nan University, Shenzhen People's Hospital, Shenzhen, China, [5]The Chinese University of Hongkong, Hong kong, [6]Musculoskeletal Laboratory, Department of Orthopedics & Traumatology, The Chinese University of Hong Kong, China, [7]Lee Hysan Clinical Research Laboratory, The Chinese University of Hong Kong, China, [8]The Chinese University of Hong Kong, Peoples republic of china, [9]Chinese University of Hong Kong, Peoples republic of china

Introduction: Orthopedic surgeons are challenged by impaired or delayed fracture repair in osteoporotic bone. In terms of bone physiology, intramembranous ossification and endochondral ossification are the two important processes during fracture repair for callus mineralization. Both callus neovascularization and mineralization is impaired during osteoporotic fracture repair in ovariectomized (OVX) animals. Clinical biopsy data has demonstrated that the number of estrogen receptor beta (ERbeta) positive proliferative chondrocytes within fracture callus was increased in postmenopausal women. In addition, it has been report that, ERbeta expression at both protein and mRNA levels in bone was significantly increased by relieving from estrogen's inhibitory effect in OVX-induced osteoporotic animals. which implying that activated ERbeta signaling might play an important role in osteoporotic fracture repair. Further, evidence from ERbeta gene knockout female mouse study with longitudinal experimental design has demonstrated that ERbeta signaling participates in inhibiting both intramembranous and endochondral ossification during bone development. The objective of this study was to test whether ERbeta antagonist PHTPP can promote osteoporotic bone healing in mice.

Methods: Total 16 3-month-old female C57BL/6 mice were randomizely divided into Control group and Treatment group. A cortical bone defect on right femur was created six weeks after ovariectomy operation in all the mice. The mice were oral feed with vehicle or PHTPP (10ug/kg body weight/day) accordingly. High resolution micro-CT (VivaCT 40, Scanco) was employed to in-vivo monitoring the repair process

at day 0,3,7,10,14 and 21. Mice callus contralateral intact femur were collected for mechanical testing at day 21.

Results: With regard to microCT measurement, control (vehicle) and treatment (PHTPP) mice differed significantly in the pattern of the change in the volumetric bone mineral density (BMD) over time in both defect region and intra-medulla space ($P<0.05$ for the interaction between time and group by the repeat measure ANOVA) (Figure 1 and Figure 2). For callus mechanical testing at day 21, Treatment mice recovered 80% of ultimate load and 70% of energy to failure to their intact bone while control mice only recover 67% and 58% accordingly. (Figure 3). Conclusion: ERbeta antagonist PHTPP could promote bone repair in osteoporotic mice, inhibit ERbeta may be a good approach to promote osteoporotic fracture repair.

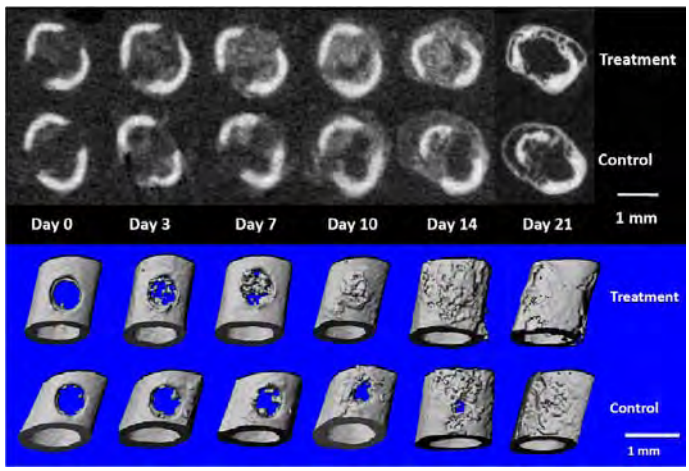

Figure 1.Time course changes in both 2-D (upper) and 3-D structure (lower) within bone defect region

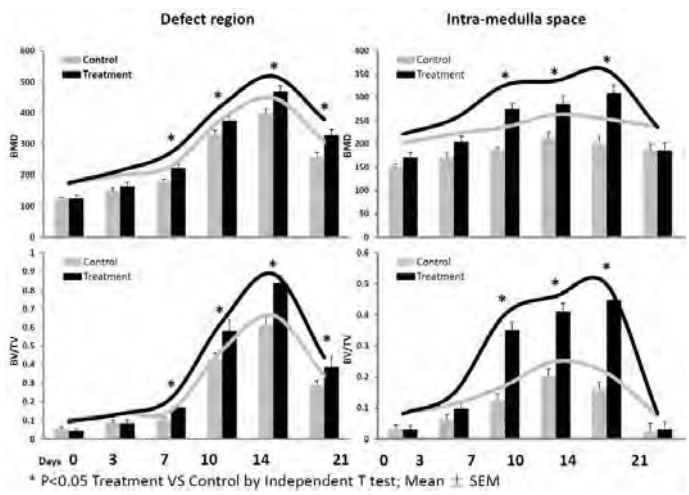

Figure 2. Time course changes in BMD and BV/TV within defect region and intra-medulla space

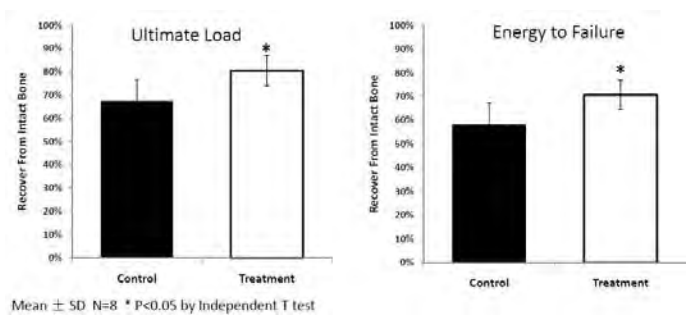

Figure 3. Recovery of mechanical property in the callus

***Disclosures: Yixin HE**, None.*

SU0093

Estradiol Treatment Increases Cortical Vascularisation in Ovariectomized Mice. Phil Salmon*[1], Anna Borjesson[2], Sara Windahl[2], Claes Ohlsson[2]. [1]Skyscan N.V., Belgium, [2]Centre for Bone & Arthritis Research, Sweden

What is generally referred to as cortical porosity consists largely of blood vessel canals which pervade cortical bone in the mouse. There has been little research into blood vessel density within cortical bone in murine models of bone disease, and still less consideration of how cortical vascularisation responds to biochemical stimuli.

In this study three-month-old mice were ovariectomized (ovx) and then treated with either vehicle or estradiol (E2, 167 ng/mouse and day) for four weeks (n=7 for both groups). Animals were then sacrificed and tibias harvested for micro-CT analysis. Micro-CT imaging of the proximal half of the tibia was done with a pixel size of 1.7 microns for clear visualization of blood vessel canals. The morphometry of cortical bone and the contained blood vessel canals was assessed in cortical volumes of interest referenced to the growth plate (the VOIs commenced 3mm distal of the growth plate and comprised a ring 0.5mm in axial length).

Cortical bone volume increased by 14% in the E2 treated compared to the vehicle treated OVX group ($p<0.01$). Cortical porosity – the blood vessel percent space – increased sharply by 190% in the E2 treated compared to the vehicle group ($p<0.001$). The mean diameter of blood vessel pores was not significantly affected by E2 treatment, at 17-18 microns. The density of blood vessels expressed as length of vessels per mm^3 of cortical bone was 55 and 146 mm-2, respectively in the vehicle and E2 treated groups ($p<0.001$).

Treatment with E2 resulted in gain in cortical volume and also a marked increase in vascularisation of the cortical bone (figure 1). The mechanism of this relatively rapid change in vascularisation including the intracortical remodeling required, is not well understood.

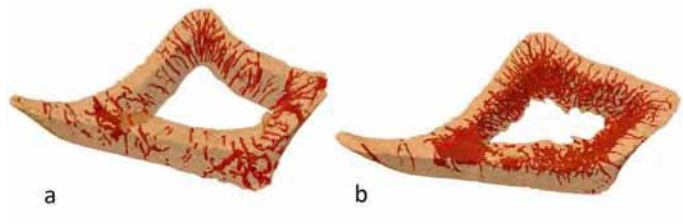

Figure 1. Cortical vascularisation (micro-CT) in OVX mice treated with vehicle (a) and E2 (b)

***Disclosures: Phil Salmon**, SkyScan NV, 3*

SU0094

Higher Occurrence of Knee OA in Older Female Baboons and the Value of the Baboon in Studies of Naturally Occurring Human Knee OA. Daniel Araujo[1], Tanya Lerma[1], Thomas Macrini[1], Todd Bredbenner[2], Daniel Nicolella[2], Lorena Havill*[3]. [1]St. Mary's University, USA, [2]Southwest Research Institute, USA, [3]Southwest Foundation for Biomedical Research, USA

Osteoarthritis (OA), the leading cause of disability in the U.S., involves breakdown and eventual loss of cartilage and other joint tissues resulting in joint stiffness, pain and loss of movement. Though OA clearly runs in families, very little progress has been made in identifying the genes that underlie OA risk and pathogenesis due in large part to the absence of an appropriate animal model in which to conduct such investigations. The baboon is an established non-human primate model for studies of bone health. The natural occurrence of OA in this animal model and the baboon's genetic proximity to humans make it an invaluable model system in which to investigate the etiology, pathogenesis, and genetic basis of OA. We are developing a long term research program to establish the baboon as a model for studies of OA genetics and for pre-clinical trials of osteoarthritis therapies. Here we focus on knee OA due to the clinical relevance of this site in patient disability. We test the hypothesis that, as in humans of post-reproductive age, older baboon females show higher rates of knee OA than do males. We assessed presence and severity of knee OA by gross visual inspection of the distal right femur (obtained at necropsy) of 44 female baboons over the age of 19 years and 16 male baboons over the age of 17 years. Each specimen was categorized as ''unaffected,'' moderate OA (clear cartilage degradation), or advanced OA (cartilage degeneration and eburnation). 59% of females and 44% of males showed either advanced or moderate OA. The average age of individuals with knee OA was 23.45 years for females and 20.45 years for males. Chi-square analysis indicates significantly higher occurrence of naturally occurring (non-induced) knee OA in female baboons ($p=0.03$). This sex trend in knee OA in older baboons is consistent with the trend in humans. This result and the pedigreed nature of the baboon colony in which the study was performed, provide unique research opportunities regarding naturally occurring knee OA in humans.

***Disclosures: Lorena Havill**, None.*

SU0095

Programming of Bone Tissue by Early Exposure to Soy Isoflavones: Comparison of Two Dosing Protocols. Wendy Ward, Jovana Kaludjerovic, Elsa Dinsdale*. University of Toronto, Canada

Background: We previously reported that neonatal exposure to soy isoflavones, at levels that are present in soy protein based infant formula, can favorably program female bone health at adulthood. These programming effects include higher bone mineral density (BMD), improved bone structure (greater trabecular thickness and connectivity) and stronger bones. The previous study used a 5-day dosing protocol, starting at postnatal day (PND) 1. However, to more accurately reflect the duration of exposure to human infants we have since lengthened the protocol such that mice are exposed to isoflavones throughout suckling (the first 21 days of life). Objectives: To determine if administering isoflavones throughout suckling results in an enhanced effect on bone outcomes at young adulthood (4 months of age) compared to the previously used 5-day exposure. Study Design: Female CD-1 mice (n = 8-16 pups/group) were randomized to subcutaneous injections of soy isoflavones (7 mg/kg body weight/d) or corn oil from postnatal day (PND) 1-5, representing the first four months of human life, or throughout suckling (PND 1-21), representing the first year of human life. BMD and bone strength were measured at the femur and lumbar spine at 4 months of age and were compared to their respective control groups. Results: Females treated with soy isoflavones for either the first 5 or 21 days of life had higher ($p<0.05$) BMC, BMD and peak load at the lumbar spine (LV1-3) compared to their control groups. The percent change in BMC and BMD at the lumbar vertebrae between the 5 and 21 day isoflavone treatment relative to their respective control was similar (Table 1), but the percent increase in the peak load was markedly higher with 21 day compared to 5 day treatment. Only females treated with soy isoflavones from PND 1-21 had higher ($p<0.05$) whole femur BMC, BMD and peak load at femur midpoint at adulthood compared to their control group. Summary: Exposure to isoflavones throughout suckling versus the first 5-days of life results in greater effects on lumbar spine, and unlike 5-day exposure, also has favorable effects on femur outcomes.

Table 1: Percent increase in BMC, BMD and peak load at three different skeletal sites with two different dosing protocols of isoflavone in females

	Isoflavone Exposure PND 1-5			Isoflavone Exposure PND 1-21		
	Lumbar vertebrae	Femur Neck	Femur Midpoint	Lumbar vertebrae	Femur neck	Femur Midpoint
BMC	29%	5%		26%	26%	
BMD	21%	0%		23%	25%	
Peak Load	21%	14%	11%	35%	14%	24%

*Expressed as percentage increase relative to the respective control group.

Table 1

***Disclosures: Elsa Dinsdale**, None.*

SU0096

The Role of *Hox11* Genes in the Formation and Integration of the Musculoskeletal System. Ilea Swinehart*[1], Deneen Wellik[2]. [1]University of Michigan, USA, [2]University of Michigan Medical Center, USA

Proper development and function of the musculoskeletal system requires the coordinated action of multiple tissues. An exciting area of current research is studying how muscles, tendons, and skeletal elements are patterned during development to form and integrated and functional system. Recent data from our lab suggest that *Hox* genes play a key role in the formation and integration of these cell types *in vivo.*

Hox genes are well known regulators of skeletal morphology. Loss-of-function mutation of *Hox11* paralogous genes results in dramatic malformation of zeugopod elements (the radius and ulna of the forelimb and tibia and fibula of the hindlimb). Expression analyses show that *Hox11* genes are expressed in multiple tissues of the developing limb including distal chondrocytes, perichondrium, tendons, and connective tissue. Interestingly, our analyses have also revealed that Hox genes are specifically down regulated in differentiating tissues and remain expressed only in the non-differentiated stromal compartment during the establishment of limb morphology. As suggested by the expression patterns, these mutants also have severe defects in the formation and patterning of the associated tendons and muscle groups. Using 3 dimensional reconstruction on serial sections of the limb to clearly define the muscle and tendon phenotype in *Hox11* mutants, and conditional deletion approaches, our goal is to determine the functional contribution of *Hox11* genes in musculoskeletal integration during development.

Elucidating the *in vivo* factors required for musculoskeletal development is a key goal of our research. Regeneration and repair mechanisms often closely mirror developmental pathways and, given the clear role for *Hox* genes in the patterning of many organ systems, especially the developing skeleton, our work may have important implications for tissue engineering strategies.

***Disclosures: Ilea Swinehart**, None.*

SU0097

Osteoblast Attachment to Fibronectin Regulates Calcium Signaling. James Knox, Patricia Jones*, Randall Duncan. University of Delaware, USA

During bone remodeling, osteoblast adhesion to the extracellular matrix (ECM) is a critical event necessary for proper function of the osteoblast and the response of these cells to hormonal and mechanical stimuli. We postulate that intracellular calcium (Ca^{2+}) signaling is essential to the regulation of osteoblast adhesion to ECM proteins. To delineate the Ca^{2+} pathways important in adhesion, we used Ca^{2+} imaging techniques to determine the global $[Ca^{2+}]_i$ response of MC3T3-E1 preosteoblastic cells elicited by soluble ECM proteins. Addition of soluble fibronectin to MC3T3-E1 cells produced a slow, sustained increase in $[Ca^{2+}]_i$, whereas type I collagen and the ECM-associated peptide RGDS caused a smaller, more rapid increase in $[Ca^{2+}]_i$. Focusing on the response to fibronectin, we found that this Ca^{2+} response is dependent upon both extracellular and intracellular Ca^{2+}. However, inhibition of the L-type voltage sensitive Ca^{2+} channel (L-VSCC) with nifedipine decreased the number of responding cells to soluble fibronectin as compared to controls. This suggests a role for the L-VSCC in osteoblasts in the regulation of signaling events triggered by binding to the ECM. The cytoskeleton may provide a tonic control of this Ca^{2+} response as disruption of the actin cytoskeleton or microtubules increases the cell's response to soluble fibronectin. Inhibition of the second messenger, protein kinase C, with the inhibitor GF109203X decreased the peak calcium response, as did inhibition with PP2, an inhibitor of focal adhesion associated Src tyrosine kinases. These data suggest that integrin binding to specific ECM proteins directly controls Ca^{2+} signaling in osteoblasts and is dependent on both an intact cytoskeleton and the function of multiple focal adhesion associated kinases. We postulated that, because an increase in $[Ca^{2+}]_i$ is required for cell attachment, the Ca^{2+} increase we see in response to soluble fibronectin is necessary for formation of adhesion complexes upon osteoblast attachment to the bone matrix. Using immunofluorescence to visualize the focal adhesion protein vinculin, we found that treatment of MC3T3-E1 cells with soluble fibronectin during attachment increased focal adhesion formation as compared to untreated cells. Our results suggest that $[Ca^{2+}]_i$ mediates attachment of osteoblasts to fibronectin to regulate osteoblast attachment to the bone surface during bone remodeling.

***Disclosures: Patricia Jones**, None.*

SU0098

Osteocalcin Gene and Protein Expression in Rat Neural Tissues. Daniel Benjamin[1], Christopher Franz[2], Patricia Buckendahl*[2]. [1]Cenoxsys Corporation, USA, [2]Rutgers University, USA

Many studies have shown that osteocalcin (OC) is involved with mineralization of bone; most have focused on osteoblast function and bone turnover. Relatively little has been done to find and identify the presence and function of OC outside of the skeleton, though recent work with mice identified hormone-like activity of OC in regulation of energy metabolism. Osteocalcin gene expression was also reported in rat and mouse brain, yet its specific location was not elucidated. However, evidence of OC protein in rat sensory ganglia and spinal cord was demonstrated via immunolocalization. Those studies suggested that ganglia and afferents in the rat spinal cord and brain should be targets for further investigation of OC gene expression in neural tissue. The purpose of our study is to assess both gene expression and local concentrations of OC in the rat superior cervical (SCG) and dorsal root ganglion (DRG) and in various sections of rat brain. We analyzed tissues from adult and embryonic rats. Total RNA was extracted from tissues and treated with DNase to eliminate genomic DNA prior to conversion to cDNA. Specific expression was detected by semi-quantitative RT-PCR with probes from Applied Biosystems (Bglap, Rn01455285_g1). Results indicted the presence of OC mRNA in E14.5 rat hindbrain, forebrain, SCG, spinal cord, DRG, and adult rat DRG. Embryonic mRNA expression was approximately 100-fold lower than adult DRG. OC protein was quantified by ELISA using a guinea pig anti-OC antibody and goat anti-guinea pig HRP conjugate with TMB substrate. The OC protein concentrations in adult tissues, ng/mg soluble protein, were: posterior hypothalamus, 8.5; DRG, 90.1; amygdala, 6.3; hippocampus, 11.2; cortex, 7.2. In day 14.5 embryos, OC protein concentrations, ng/mg soluble protein, were: forebrain, 104; hindbrain, 118; cortex (avg 3 embryos) 120; spinal cord, 288. SCG and DRG had detectable OC, but exceedingly low total protein. CNS concentrations were several-fold greater than blood; therefore, OC was not from plasma. Our data indicate for the first time that OC gene expression and protein production in neural tissues is widespread and differs by tissue location and age. Of considerable interest is that embryonic neural production of OC precedes bone mineralization, and its concentration in embryonic tissues exceeds that of the adult. These data suggest that potential functions for OC in neural development should be investigated further.

***Disclosures: Patricia Buckendahl**, None.*

SU0099

Proteomics Approach to Study Proteins from Laser Microdissected Bone Tissue. Deepak Vashishth, Grazyna Sroga*. Rensselaer Polytechnic Institute, USA

In adult vertebrates, bones are constantly renewed due to bone remodeling. Bone remodeling processes change over a life-time and influence the amount of bone mass in a body. Mechanical strain plays an important role in adaptive responses that occur in bone and is a factor in defining the thresholds for bone remodeling activity in normal bone1. Therefore, strain histories differ between regions of the same bone and as such, bone may be able to adjust its structural/material organization at the local level leading to increased heterogeneity. As recent studies done in our laboratory and by others have demonstrated the role of proteins and/or protein modifications in age-related and other fragility fractures2-4, we hypothesized that local bone adjustment to mechanical strain should be reflected by relative differences between younger osteonal and older interstitial tissue. We developed a methodology that permits separation and measurement of very small amounts of proteins from samples obtained via laser-capture microdissection (LCMD) of bone tissues. To this end selected areas of osteonal and interstitial human cortical bone tissues were LCMD and analyzed using a combination of 2-D SDS-PAGE with MALDI-TOF/TOF-MS and MS/MS. This analysis permitted identification of proteins that differed between sub-proteomes of the young osteonal and old interstitial bone tissue. For example, the 2-D SDS-PAGE revealed several differences between osteonal and interstitial tissue at the sub-proteome level. Submission of the m/z data to a Protein Prospector (UCSF, CA) search of the SwissProt.2008.06.10 database revealed the identity of two proteins. The searches yielded a match to peptides of human osteopontin precursor (Pre-OPN; an MOWSE score of 58.6 and a MOWSE P factor of <0.4 as a descriptive of a random match) and human osteocalcin precursor (Pre-OC; with an MOWSE score of 35.4 and a MOWSE P factor of <0.4 as a descriptive of a random match). Subsequent quantification of two proteins that significantly differed between the two tissues was performed using enzyme-linked immunosorbent assay (ELISA). Our data indicate that there is more osteocalcin (OC) and osteopontin (OPN) in younger osteonal tissue. We hypothesize that in certain combination, OC and OPN may act to regulate bone remodeling, and thus, influence bone response to mechanical strain and microdamage accumulation. Currently, more detailed study is conducted to test this hypothesis. [1] Rubin, C.T. et al. Nature 412, 603-604 (2001). [2] Vashishth, D. Curr Ostep Rep 5, 62-66 (2007). [3] Fantner, G.E. et al. Nano Lett. 8, 2491-2498 (2007). [4] Poundarik, A. et al. Proceedings of the 55th Meeting of the Orthopedic Research Society, p. 724, Las Vegas Feb. 22-25, 2009.

***Disclosures: Grazyna Sroga**, None.*

SU0100

Compositional and Material Properties of Rat Bone after Bisphosphonate and/or Strontium Ranelate Drug Treatment. Yuchin Wu*, David Munoz-Paniagua, Samer Adeeb, M. John Duke, Michael Doschak. University of Alberta, Canada

Purpose: To investigate the chemical element distribution and corresponding material properties of bone after antiresorptive drug treatments in rats developing Osteoporosis (OP).

Methods: Sixteen 6-month old female SD rats were ovariectomized (OVX), and divided into 4 groups (n=4/group); OVX-control, OVX-RIS (Risedronate bisphosphonate [BP] treated), OVX-SrR (Strontium Ranelate [Protos®] treated), OVX-RIS+SrR, and compared with Sham-operated controls (n=3). After 16 wk of treatment (RIS 0.06 mg/kg q3.5d; SrR 308mg/kg qd p.o), rats were euthanized and dissected lumbar vertebrae (L4, L5, L6) were scanned by micro-CT to measure bone mass, morphometry and BMD. The L4 vertebral body was cut coronally and nano-indentation testing undertaken using the TI 900 TriboIndenter. Reduced modulus (Er) and hardness (H) values were used to calculate Young's modulus. Samples were then embedded in epoxy resin and electron probe microanalysis (EPMA) was undertaken using a Cameca SX100 electron probe to map and quantify the distribution of Ca, P and Sr. L5 and L6 samples were loaded in compression to failure using an Instron 4443 mechanical testing system.

Results: Mean Bone Volume (BV; mm^3) was significantly reduced ($p<0.05$) in the OP control group (132.80 ± 9.50) compared with BP (168.58 ± 22.30), SrR (145.27 ± 2.06), and BPs+SrR (172.49 ± 8.39) groups. However, 3D fractal dimension (FD) values of trabecular bone quality was superior only for both BP and BP+SrR treatment groups (7.4%, $p<0.05$), compared to the OP control group. EPMA mapped elemental Sr deposition to the periosteal surface of cortical bone (50~100 μm thick), and to endosteal trabecular surfaces (20 μm thick), as well as to both vertebral growth plates. The atomic ratio of (Ca+Sr)/P were similar (~1.667) for all non-SrR treatment groups (including OP control), but significantly reduced with SrR treatment (2.4%~6.6%, $p<0.05$), indicating Sr incorporation into bone mineral as Sr-HA. Using nano-indentation, we did not measure any differences in Young's modulus or hardness in either longitudinal or circumferential directions after 16 wk of drug treatment. Conversely, compression stiffness in L5 and L6 vertebral bodies showed that all BP groups had increased structural bone strength compared with other groups.

We conclude that BP drugs dominate the conservation of trabecular geometry and structural bone strength in OP rats, whereas SrR may influence bone volume and material composition locally.

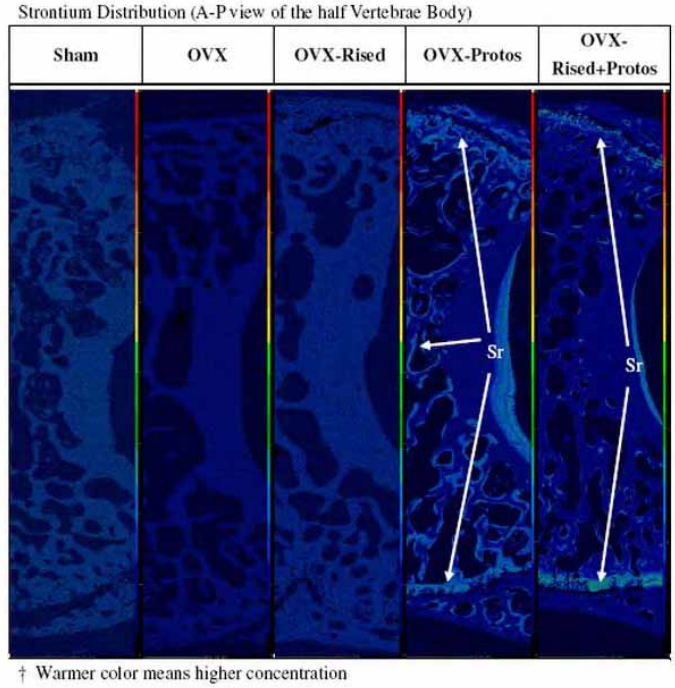

Bone Sr distribution by EPMA

***Disclosures: Yuchin Wu**, None.*

SU0101

Development of an Arrayed Platform for the Investigation of Matrix Control of Stem Cell Osteogenic Differentiation. Wen Li Chen*, Craig A. Simmons. University of Toronto, Canada

Background: The ability to control stem cell differentiation to produce clinically-relevant cell types is important for connective tissue regeneration. Stem cell differentiation can be modulated by a multitude of microenvironmental signals, including the biochemical and physical properties of the extracellular matrix (ECM). Although cell-based arrays have been developed to study mixtures of biochemical factors, similar platforms to systematically investigate the combinatorial effects of biochemical and physical signals on cell function do not exist. To meet this need, we developed an array platform to facilitate the study of ECM-derived signals (i.e., ECM composition and substrate stiffness) in driving stem cell osteogenic specification.

Methods: Combinations of type I collagen (col I), fibronectin (Fn), and laminin (Lm) at different concentrations (50, 100, or 200 μg/mL) were patterned onto polyacrylamide substrates of various elasticities (3, 21, or 144 kPa) according to statistical design of experiment. Mouse mesenchymal stem cells (MSCs) were seeded onto these ECM arrays and were cultured in basal or osteogenic media, and the expression of a bone-specific transcription factor, osterix, was quantified by immunofluorescence. The effects, interactions and dose-responses of the matrix signals on osterix expression were determined by regression analysis.

Results and Discussion: In basal media, osterix expression was positively modulated by substrate stiffness ($\beta_{stiffness}= 0.22$, $P<0.01$) and laminin ($\beta_{Lm*Lm}=0.35$, $P=0.02$; $\beta_{Lm}=0.21$, $P=0.01$); synergistically promoted by substrate stiffness and fibronectin ($\beta_{stiffness*Fn}=0.20$, $P=0.02$); and inhibited at high fibronectin concentration ($\beta_{Fn*Fn}=-0.32$, $P=0.03$). In osteogenic media, osterix expression was positively regulated by substrate stiffness ($\beta_{stiffness}=0.31$, $P<0.001$); synergistically promoted by substrate stiffness and laminin ($\beta_{stiffness*Lm}=0.23$, $P=0.01$); and inhibited at high collagen concentration ($\beta_{Col\ I*Col\ I} =-0.22$, $P=0.07$; $\beta_{Col\ I}= -0.21$, $P=0.01$). These results confirm that MSC osteogenic specification is differentially modulated by multiple microenvironmental cues.

Conclusion: We have developed ECM arrays on mechanically tunable substrates to study stem cell differentiation. The use of this novel screening platform together with statistically modeling not only improves the understanding of matrix control of osteogenic differentiation, but also has practical relevance in biomaterial design.

***Disclosures: Wen Li Chen**, None.*

SU0102

Effects of Tamoxifen and ICI 182,780 on Bone's Response to Mechanical Loading in Female Mice. Toshihiro Sugiyama*[1], Gabriel Galea[2], Lance Lanyon[2], Joanna Price[1]. [1]University of Bristol, United Kingdom, [2]Royal Veterinary College, United Kingdom

Estrogen receptors (ERs) regulate bone's osteogenic response to mechanical strain, by which mechanism adequate functional levels of bone mass are maintained. It is unknown whether the ER modifiers tamoxifen and ICI 182,780 (fulvestrant), used clinically for breast cancer, influence this adaptive response. We therefore assessed the effect of these drugs using the mouse unilateral tibia axial loading model. At 16 weeks of age (day 1), female C57BL/6 mice were weight-matched into sham-ovariectomised (SHAM) and ovariectomised (OVX) groups. On day 11, these groups were randomly sub-divided into 7 groups (n=7 per group): SHAM + vehicle, SHAM + tamoxifen, SHAM + ICI, OVX + vehicle, OVX + tamoxifen, OVX + ICI and OVX + tamoxifen + ICI. Vehicle (peanut oil), tamoxifen citrate (1 mg/kg/day) and ICI (10 mg/kg/day) were given in 5 subcutaneous injections on days 11, 13, 15, 18 and 21. On the same day the right tibiae were subjected to a single period of non-invasive axial dynamic loading (peak load 12N, peak 2400 microstrain, 40 cycles, 10s between cycles). Mice were euthanized on day 25 and both tibiae evaluated by high-resolution micro-computed tomography. Outcomes were assessed by mixed model analysis. In left control tibiae, no treatments significantly changed cortical bone volume (CBV) compared with vehicle, but trabecular bone volume/tissue volume (BV/TV) was decreased by OVX, increased by tamoxifen, and unchanged by ICI alone or tamoxifen + ICI. In all loaded tibiae there was a significant osteogenic response to loading in both trabecular and cortical regions. OVX was associated with a slight enhancement of this response in BV/TV but not CBV. Independently of OVX, tamoxifen enhanced loading-related increases in BV/TV and CBV by increasing trabecular thickness and periosteally enclosed volume, respectively. ICI alone did not significantly modify loading-related increase in BV/TV or CBV but abrogated the effect of tamoxifen on BV/TV with and without loading. These data confirm that tamoxifen alone has a potent osteogenic effect on trabecular bone in female mice. They also demonstrate, for the first time, that tamoxifen enhances the osteogenic response to mechanical loading. That both these effects were blocked by ICI indicates that they are ER modulated. These findings suggest that modification of ER activity may enhance the osteogenic workings of the mechanostat. This carries the possibility of influencing bone mass in a structurally appropriate manner.

***Disclosures: Toshihiro Sugiyama**, None.*

SU0103

Genetic Loci that Define Trabecular Bone's Plasticity during Unloading and Reambulation. Stefan Judex*[1], Engin Ozcivici[2], Weidong Zhang[3], Leah Rae Donahue[4]. [1]Stony Brook University, USA, [2]Mass General Hospital, USA, [3]The Jackson Laboratory, USA, [4]Jackson Laboratory, USA

Disuse induced osteopenia and the associated loss of bone strength present a major socio-economical burden and can lead to major complications both on earth as well as in space, in particular because bone morphology and strength may never fully recover upon reambulation. Changes in trabecular morphology during un- and re-loading are marked by large variations between individuals, implicating a strong influence of genetic make-up on the magnitude of the response. Here, we subjected 450 adult second generation (BALBxC3H) mice to 3wk of disuse (hindlimb suspension) followed by 3wk of reambulation to identify the quantitative trait loci (QTL) that define an individual's propensity to either lose trabecular bone when weightbearing is removed or to gain trabecular bone when weightbearing is reintroduced. Longitudinal *in vivo* μCT scans demonstrated that some mice lost as much as 72% in trabecular BV/TV in the distal femur (average: 42%). Changes in trabecular BV/TV during the initial 3wk reambulation period ranged from a continuation of bone loss (-18%) to large additions (73%) of tissue (average: 10%). Finite element modeling (FEM) of each individual trabecular structure determined the mechanical consequences of changes in trabecular quantity and micro-architecture. During disuse, peak stresses increased on average by 27% and decreased by 10% during reambulation. Genome wide two-dimensional scans identified QTL at $p<0.01$. During disuse, 6 major QTL accounted for 23% of the total variability in changes in BV/TV while 4 major QTL accounted for 17% of the variability in the changes in peak trabecular stresses. For reambulation, 6 QTL accounted for 13% of the variability in changes in BV/TV and 2 QTL accounted for 8% of the variability in the changes in peak trabecular stresses. Most of the QTL defining changes during disuse or reambulation did not overlap with those QTL identified at baseline, suggesting that these QTL harbor mechano-sensitive genes. The lack of overlap in QTL between disuse and reambulation also emphasizes that the genes modulating the trabecular response to unloading are distinct from those regulating tissue recovery during reloading. These data demonstrate the strong genetic regulation of trabecular mechanosensity. The novel identification of the underlying QTL may ultimately define the regulatory genes and serve towards the identification of those individuals that are most susceptible to disuse induced bone loss and/or the least capable of recovering.

***Disclosures: Stefan Judex**, None.*

SU0104

Hyper-occlusion Stimulated Osteoclast Recruitment Though Chemokines Expression. Tetuomi Nemoto, Takashi Tsuzuki, Hironobu Sato, Hiroshi Kajiya, Kazuko Goto*, Koji Okabe. Fukuoka Dental College, Japan

The mechanical forces produced by normal occlusion have an inhibitory effect on unopposed eruption and physiological drifting of teeth. In contrast, excessive occlusal force has known to induce disappearance of alveolar hard line, enlargement of periodontal ligament space and the destruction of periodontal tissues and alveolar bone, leading to occlusal traumatism. Recently, Ccl-2 (MCP-1), Ccl-3 (MIP-1α), and Ccl-5 (RANTESE) have reported to be involved in osteoclast chemotaxis and differentiation during osteoclastogenesis. However, little is known to whether hyper-occlusal force was involved chemokines expression and its function of role in periodontal ligament (PDL) tissue. In the present experiments, we studied the effects of excessive mechanical stress by hyper-occlusal force on chemokines expression and alveolar bone resorption using in vivo and in vitro hyper-occlusion models. In vitro hyper-occlusion model; Human PDL cells were obtained from healthy human wisdom teeth of three donors with informed consent. The human PDL cells were cultured onto silicon chamber and the chamber bottom applied uniaxial sinusoidal stretch for 1-7 days. We examined the expression of chemokine on human PDL cells using microarray analysis, real time PCR method, ELISA and Western blot analysis. In vivo hyper-occlusion model;To create a hyper-occlusive state, the three right maxillary molars in eight weeks-old Wister rats were bonded with stainless steel wire using a superbond. We also investigated the expression of chemokines and TRAP positive cells in 1-7days after hyper-occlusion stimulation. Using DNA microarray analysis continuous mechanical stretch (MS) up-regulated the expression of typical osteoclastogenesis-associated chemokines, Ccl-2, -3 and -5 in human PDL cells. Excess mechanical stress loading in vivo hyper-occlusion model rat, stimulated Ccl-2 expression in periodontal tissue and TRAP positive cells in alveolar bone. The Ccl-2 expression was localized in force-loading periodontal tissue around teeth furcations and roots. In summary, hyper-occlusion by MS dominantly up-regulated Ccl-2 expression in the human PDL cells and promoted pre-osteoclasts migration, resulting in non-inflammatory and mechanical-dependent alveolar bone resorption.

***Disclosures: Kazuko Goto**, None.*

SU0105

Neonatal Mechanical and Tactile Stimulation (MTS) Improves Markers of Bone Growth in Adult Rats from a Neonatal Stress Model. Shannon Haley*[1], Shannon O'Grady[2], Kristy Gulliver[2], Roberto Baldassarre[2], Brett Barrett[3], Robert Lane[2], Laurie Moyer-Mileur[2]. [1]University of Utah School of Medicine, USA, [2]University of Utah, USA, [3]Univeristy of Utah, USA

Purpose: Premature infants experience stressful events in the newborn intensive care unit (NICU). Neonatal stress impairs postnatal bone mineralization. Clinical studies demonstrate that mechanical and tactile stimulation (MTS) in early life improves bone mineralization. Our animal model for neonatal stress was used to test the hypothesis that neonatal MTS intervention improves bone mineral density (BMD), trabecular bone micro structure, circulating markers of bone turnover, and growth plate morphometry in adult rats.

Methods: Timed pregnant dams were delivered at term (E21). Litters were culled to 10 pups (5 M, 5 F) and divided into 3 groups: control (CTL; maternal separation), neonatal stress control (Stress-CTL; maternal separation + injection + hypoxia/hyperoxia) and Stress-MTS (stress treatment with 10 min of stroking and limb movement). Treatments were given from Day 6 to Day 10 and tissue was harvested on Day 120 (D120) of life. Dual energy x-ray absorptiometry (DXA) measures of bone mineral density, bone growth plate morphometry, microcomputed tomography (micro-CT) of bone structure, and circulating levels of bone turnover markers, tartrate-resistant acid phosphatase (TRAP), type I procollagen N-terminal propeptide (PINP), and osteocalcin were measured.

Results: Stress with MTS (Stress-MTS) increased bone mineral density (BMD) by 8% compared to CTL and Stress-CTL ($p=0.02$). Tibial growth plate width was approximately 20% larger in Stress-MTS treated male rats compared to CTL and Stress-CTL males ($p=0.01$). Neonatal stress treatment resulted in changes to the bone trabecular microarchitecture compared to CTL in male rats. Male Stress-CTL rats had greater bone volume ($p=0.047$) and greater BV/TV ratios ($p=0.036$) compared to male CTL. There were no differences in circulation levels of bone turnover markers.

Conclusion: MTS during neonatal stress in early postnatal life improves long-term bone mineral density in male and female rats. We speculate that the alterations in bone microarchitecture in Stress-CTL males but not females suggest a gender specific mechanism in regards to MTS, neonatal stress, and adult bone structure.

***Disclosures: Shannon Haley**, None.*

SU0106

Trabecular Bone Homeostasis is Modulated by Neuromuscular Proprioception. Steven Bain*[1], Sandra Poliachik[2], DeWayne Threet[1], Sundar Srinivasan[1], Ted Gross[1]. [1]University of Washington, USA, [2]Seattle Children's Hospital, USA

Trabecular bone loss in the proximal tibia following transient calf paralysis with botulinum toxin A (BTxA) is rapid and profound. The rate and magnitude of this loss exceeds that induced by hindlimb suspension but is comparable to sciatic neurectomy (SCX) or spinal cord injury (SCI). As BTxA induced calf paralysis induces only a mild gait dysfunction compared with SCX or SCI, we reasoned that reduction of gait induced bone deformations arising secondary to motor impairment were not the sole driver of acute bone loss in the model. Because BTxA also impairs sensory signaling arising from the paralyzed limb, we speculated that BTxA-induced sensory disruption was causally linked to acute bone resorption following transient muscle paralysis. To address this question we used high-resolution *in vivo* microCT to assess bone morphology of the proximal tibia metaphysis in two genetic models of disrupted sensory signaling; the vanilloid (capsaicin) receptor knockout mouse (VR1), and the radiation induced Sprawling mouse (Swl +/-). VR1 mice have impaired nociception (with normal proprioception and motor function), while Swl +/- mice display a hindlimb proprioceptive neuropathy (with normal nociception and motor function). Baseline trabecular bone morphology (TBM; BV/TV, Tb.N, Tb.Th, Tb.Sp) in VR1 WT mice (n=5), was equivalent to that of VR1 KO mice (n=7). At baseline, Swl +/- mice (n=6) had -43.6% less BV/TV in the proximal tibia ($p<0.01$), reduced Tb.N (-18.8%) and Tb.Th (-12.5%), and increased Tb.Sp (23.0%; all $p<0.05$) vs WT mice (n=4). After imaging, the right calves of all mice were paralyzed with BTxA (2 U/100 g) with BV/TV of the proximal tibia assessed at d 5 and d 12. WT VR1 and SWL mice demonstrated significant loss of BV/TV at d 5 and d 12 following calf paralysis (both $p<0.05$), with VR1 KO mice demonstrating the same loss of BV/TV as WT mice (d 5: -21.2 $\pm$ 6.8 %; d 12: -72.4 $\pm$ 1.8 %). In contrast, Swl +/- mice demonstrated no loss of BV/TV at d 5 (1.1 $\pm$ 6.6 % vs d 0). By d 12, loss of BV/TV was significant in Swl +/- (-34.7 $\pm$ 13.0 % vs d 0, $p = 0.03$), but the magnitude was significantly less than that observed in VR1 or Swl WT mice ($p = 0.02$). Taken together, we believe these initial findings implicate neuromuscular proprioception as a novel pathway that directly modulates trabecular bone homeostasis. As such, targeting this pathway may have therapeutic potential in mitigating bone loss pathologies associated with neuromuscular dysfunction.

***Disclosures: Steven Bain**, None.*

SU0107

Mice Over-expressing Salmon Calcitonin have Strongly Attenuated Bone and Cartilage Changes after Destabilization of the Medial Meniscus. Bodil Sondergaard[1], Catherine Cruger Hansen[2], Thorsten Schinke[3], Suzi Madsen[2], Anne-Christine Bay-Jensen[1], Morten Karsdal*[2]. [1]Nordic Bioscience, Denmark, [2]Nordic Bioscience A/S, Denmark, [3]University Hospital Hamburg, Eppendorf, Germany

The pathogenesis of osteoarthritis (OA) involves both bone and cartilage changes. Calcitonin is well known for its inhibitory actions on osteoclasts. We investigated the effect of endogenous increased levels of salmon calcitonin (sCT) on the articular cartilage and subchondral bone, after destabilization of the medial meniscus (DMM) in normal and sCT over-expressing mice. Mice over-expressing sCT and wild-type (WT) littermates were used for the experiments. Genotype determination was performed by measuring the circulating serum levels of sCT by ELISA. For evaluation of cartilage and subchondral bone changes, forty-four 10 week old mice were divided into four groups and subjected to DMM or sham operation. After 7 weeks the study was terminated and the knee joints isolated for histolophatological analysis and biochemical markers were measured in serum. sCT mice had >800 pg/mL serum sCT and WT mice had no detectable levels. Previously presented data show, analyzed by Von Kossa staining, an increase in trabecular bone volume (BV/TV) of 100% after 6 month and 150% after 12 month in sCT mice when compared to WT ($P<0.05$). WT DMM operated mice had major damage to the articular cartilage, compared to DMM operated sCT mice. In wild-type animals a 5-fold increase in the quantitative erosion index was observed after DMM, and the semi-quantitative score showed more than 400% ($P<0.001$) increase, compared to WT sham. DMM operated sCT mice were protected against cartilage erosion and showed a 65% and 64% ($P<0.001$) reduction, respectively, for the two histopathological evaluation methods, compared to DMM WT. sCT over-expressing mice had higher subchondral bone volume compared to WT, and were protected against cartilage erosion compared to wild-type litter mate controls. These data was supported by quantitative stereology. This suggest that increased levels of sCT may hamper the pathogenesis of OA however more studies are necessary to confirm these preliminary results.

***Disclosures: Morten Karsdal**, None.*

SU0108

Is there a Potential Role of FGF-23 in Regulation of Fracture Healing? Ulla Stumpf*[1], Birgit Willmann[2], Joachim Windolf[1], Walter-Josef Fassbender[3]. [1]Dept. of Traumatology & Hand Surgery, University Clinic Duesseldorf, Germany, [2]Hospital zum Hl. Geist Kempen, Germany, [3]Hospital Zum Hl. Geist, Chefarzt Der Inneren Abteilung, Germany

The role of FGF-23 in fracture healing process has not been fully cleared yet. The aim of our longitudinal study was to investigate relations and correlations between clinical fracture healing and the phosphatonine FGF-23 (intact and c-terminal) and other calciotropic parameters.

In a prospective, ethical comittee approved study we investigated 55 persons admitted to the Department of trauma surgery of Duesseldorf University hospital for diagnostic and treatment of peripheral fractures of the upper and lower extremities. At timepoint 0 (within 24 hours after fracture), 3, 6, 9 days serum and urine samples were collected in the acute phase following fracture. Also data from timepoints 42 and 90 days after fracture were collected, these laboratory values were not all obtainable yet. FGF 23 intact and c-terminal were measured by ELISA (c-terminal and intact, "Human Intact FGF-23 ELISA kit " and "Human FGF-23 (C-Term) ELISA kit", Immutopics).

To date 19 complete patient data sets were obtainable and calculated. Arithmetic mean values of FGF-23 (intact) at timepoint 0 were 85.9 ng/,l, at day 3 63.3 ng/ml, at day 6 69.1 ng/ml and at day 9 after fracture 57.8 ng/ml (all $p< 0.05$ vs. timepoint 0).

FGF-23 c-terminal arithmetic mean values at timepoint 0 were 271.9 U/ml, at day 3 98.1 U/ml, at day 6 91.0 U/ml and at day 9 after fracture 69.8 U/ml (all $p< 0.05$ vs timepoint 0). Parameters of renal function were within the normal range in all patients. Serum phosphate levels showed inverse correlations to measured FGF-23 intact as also to FGF-23 c-terminal values.

We conclude, that the phosphatonine FGF-23 plays a role in the acute phase of fracture healing by lowering renal phosphate excretion in the early phase after fracture to allow adequate retention of phosphate probably to support physiological tissue mineralization processes in the fracture area.

***Disclosures: Ulla Stumpf**, None.*

SU0109

Measurement of Serum KLOTHO, a Co-receptor for FGF23, in X-linked Hypophosphatemic Rickets. Erik Imel*[1], Amie Gray[1], Hisashi Hasegawa[2], Yuji Yamazaki[2], Michael Econs[1]. [1]Indiana University School of Medicine, USA, [2]Kyowa Hakko Kirin, Japan

Background: X-linked hypophosphatemia is the most common renal phosphate wasting disorder caused by excess circulating fibroblast growth factor 23 (FGF23). Klotho is a critical cofactor for FGF23 signaling. Klotho exists in both membrane bound and soluble forms. The purpose of this study was to test the hypothesis that serum klotho concentrations are altered in XLH.

Methods: This was a cross-sectional study of 34 XLH subjects (16 children, 18 adults) and 41 healthy control subjects (22 children, 19 adult). Nine XLH subjects were receiving treatment with calcitriol and phosphate at the time of sampling and the rest were not on treatment. We measured serum klotho concentrations using an ELISA (Immunobiological Laboratories Co. Ltd. (Japan)). Intact FGF23 was measured using an ELISA (Kainos, Japan). Serum phosphate, calcium, creatinine and alkaline phosphatase were measured using standard clinical methods. To normalize distribution, klotho concentrations were log-transformed for statistical analysis. T-test was used for analysis.

Results: Subject ages for control subjects ranged from 1.3 to 54.1 years. Ages for XLH subjects were 1.1 to 69.4 years. Mean serum klotho concentrations were 1051 $\pm$ 599 pg/ml for healthy children, 282 $\pm$ 134 in healthy adults, 707 $\pm$ 280 pg/ml for XLH children and 311 $\pm$ 125 for adults. LogKlotho was not significantly different between adult XLH patients and controls, but there was a trend for children with XLH to have lower Logklotho than controls ($p=0.07$). LogKlotho was not significantly different between treated and untreated XLH subjects. Serum klotho concentrations were higher in children than adults for both controls and XLH ($p<0.001$). In both healthy controls and in subjects with XLH, LogKLotho correlated significantly with age ($r=-0.664$ and $r=-0.653$, respectively), creatinine ($r=-0.465$, $r=-0.464$), phosphate ($r=0.501$, $r=0.461$), and alkaline phosphatase ($r=0.512$, $r=0.526$) (for listed correlations, $p<0.01$). LogKlotho correlated with FGF23 in controls but not in XLH ($r=0.358$). However after adjusting for age, the correlations with creatinine, phosphate, alkaline phosphatase and FGF23 were no longer significant for either group.

Conclusions: Serum klotho concentrations did not differ between control subjects and subjects with XLH, but klotho concentrations were higher in children and did not correlate with FGF23. Alterations in circulating klotho concentrations are not involved in the pathophysiology of XLH.

***Disclosures: Erik Imel**, None.*

SU0110

Novel Insight of Phosphate-overload on Atherosclerosis: Self-limiting Process of Arterial Calcification in Type III Na-dependent Pi Transporter-over-expressing Rats. Atsushi Suzuki*[1], Sahoko Sekiguchi[2], Megumi Shibata[2], Shogo Asano[1], Junichi Yasutake[3], Hiromi Takanashi[3], Teruyuki Sakai[3], Mitsuyasu Itoh[1]. [1]Fujita Health University Division of Endocrinology, Japan, [2]Fujita Health University, Division of Endocrinology, Japan, [3]Kyowa Hakko Kirin Co., Ltd, Drug Discorvery Research Lab, Japan

Background: Phosphate (Pi) overload plays a crucial role for the initiation of ectopic calcification in artery, especially in end-stage renal diseases (ESRD). Pi has been reported to change arterial smooth muscle cells (ASMC) to osteoblastic phenotype through the induction of type III Na-dependent Pi transporter, Pit-1. Although the elevation of serum Pi and Ca levels contribute a lot on arterial calcification, the amount of ectopic calcification on arterial wall does not show linear accordance with serum Ca and Pi concentrations. In the present study, we investigated the role of extracellular Pi in arterial calcification by using 5/6-nephrectomized (5/6Nx) Pit-1-overexpressing transgenic rats (TG).

Methods: 5/6Nx was performed on TG and their wild type littermates (WT) at their 8th weeks old. They were fed with normal diet for 2 weeks, and then with 1.2% high-Pi diet supplemented with 20% lactose for 4 weeks.

Results: Both WT and TG rats showed the elevation of serum creatinine, BUN, and Pi levels two weeks after 5/6Nx. In TG rats, serum Ca, albumin and 1,25(OH)2D3 levels were lower than those in WT rats. Serum concentrations of Pi and FGF23 in TG were not different from those in WT. Increased accumulation of Ca and Pi in thoracic aorta was seen in 8 cases in 10 TG rats, while 5 cases in 10 WT rats. However, the amount of Ca and Pi accumulation in TG rats was limited compared with WT rats. The expression of Runx-2 (x 21.1), osteocalcin (x 3.59) and Col1a1 (x 6.12) in sham-operated TG rats were higher than in sham-operated WT rats (x 1.0). However, there were little difference of Runx-2 and Col1a1 expression in 5/6Nx WT and TG. The expression of osteocalcin in 5/6Nx WT (x 9.42) was higher than that in 5/6Nx TG (x 4.11). The expression of Matrix Gla protein (MGP) in 5/6Nx WT rats (x 10.2) was higher than those in 5/6 Nx TG (x 5.68), and sham-operated TG (x 3.95) and WT (x 1.0). Conclusion: These findings suggest us that extracellular Pi influx in ASMC induces its osteoblastic trans-differentiation, but also keeps ASMC from the terminal differentiation as mature osteoblasts, and limits the progress of further progress of arterial calcification.

***Disclosures: Atsushi Suzuki**, Kyowa Hakko Kirin Co,ltd, 2*

SU0111

Overexpression of the Type III Sodium-dependent Phosphate Transporter Pit1 Markedly Perturbs Enamel Formation during Tooth Development. Hirotaka Yoshioka*[1], Yuji Yoshiko[2], Tomoko Minamizaki[1], Asako Nobukiyo[2], Yusuke Sotomaru[2], Atsushi Suzuki[3], Mitsuyasu Itoh[4], Norihiko Maeda[1]. [1]Hiroshima University Graduate School of Biomedical Sciences, Japan, [2]Hiroshima University, Japan, [3]Fujita Health University Division of Endocrinology, Japan, [4]Fujita Health University School of Medicine, Japan

Inorganic phosphate (Pi) is required in many biological processes including signaling cascades, skeletal development, tooth mineralization, and nucleic acid synthesis. The type II sodium-dependent phosphate transporter (NPT2) contributes to renal Pi reabsorption and intestinal Pi absorption. The type III NPT (NPT3) is thought to serve a housekeeping role in cellular Pi homeostasis, but its exact function remains controversial. Recently, we showed that NPT3 family member Pit1-mediated Pi transport in osteoblasts is indispensable for osteoid mineralization in rapidly growing rat bones. Also, aged (over 4-month-old) transgenic (Tg) rats overexpressing mouse Pit1 show a slight decrease in bone mineral density with systemic disturbances in mineral metabolism, such as hyperphosphatemia, hypocalcemia, and hyperparathyroidism. Because bone and tooth formation share some common molecular features, we assessed tooth development in the Tg rats. Around weaning, there was no significant difference in skeletal growth and serologic parameters between wild type (WT) and Tg rats. However, as early as 4 weeks of age, Tg rats displayed white spot lesions in the enamel of mandibular incisors. X-ray analysis revealed that the mandibular incisor apex in Tg rats was located distinctly anterior to that in age-matched WT controls. By histological analysis, no detectable differences were seen in Tg vs WT enamel, dentin and pulp including enamel rods, dentinal tubules, odontoblasts and pulp cells. Tg ameloblasts were normally arrayed from immature to the more differentiated (secretory) stage, but some ameloblastin-positive cells formed clusters at the basolateral side during transition and maturation stages. These pathologies became more severe with age, and included formation of cyst-like or multi-layer structures of ameloblasts, accompanied by a chalky white appearance with abnormal attrition and fracture in 5-month-old Tg rats; abnormal serological parameters were also observed in the aging Tg rats. μCT and electron probe microanalysis revealed impairments in enamel, such as delayed mineralization and hypomineralization of the enamel surface. Our results suggest that enamel formation is more sensitive to imbalances in Pit1-mediated signaling than is bone formation but that both processes are under the control of systemic factors.

***Disclosures: Hirotaka Yoshioka**, None.*

SU0112

Transrepression of Renal 25-hydroxyvitamin D_3 1α-hydroxylase (CYP27B1) Gene Expression by Thyroid Hormone Receptor β1. Mina Kozai*[1], Hironori Yamamoto[2], Masashi Masuda[1], Yuichiro Takei[3], Sarasa Tanaka[1], Yutaka Taketani[1], Ken-Ichi Miyamoto[4], Shigeaki Kato[5], Eiji Takeda[6]. [1]University of Tokushima, Japan, [2]University Tokushima, Japan, [3]The University of Tokushima School of Medicine, Japan, [4]Tokushima University School of Medicine, Japan, [5]University of Tokyo, Japan, [6]University of Tokushima School of Medicine, Japan

The renal 25-hydroxyvitamin D_3 1α-hydroxylase enzyme (CYP27B1), is implicated in the control of serum 1,25-dihydroxyvitamin D ($1,25(OH)_2D$) levels. Previously, it has been demonstrated that the low levels of plasma $1,25(OH)_2D$ in hyperthyroidism patients and the decrease of CYP27B1 synthesis in perfused kidneys treated with 3, 5, 3'-tri-iodothyronine (T_3). However, it has never been reported about the regulation of renal CYP27B1 expression by direct effect of thyroid hormones. To address whether thyroid hormones regulates CYP27B1 gene expression in the kidney, mice were rendered pharmacologically hypo- and hyperthyroid. Hyperthyroid mice showed low levels of plasma $1,25(OH)_2D$ and marked decrease in renal CYP27B1 mRNA and protein levels. In addition, T_3 inhibited the renal CYP27B1 mRNA expression highly induced in mice given low-phosphorus diet or low-calcium diet, vitamin D receptor-knockout mice and klotho mutant mice. Promoter analysis of the CYP27B1 gene with a luciferase assay using opossum kidney proximal tubular cells revealed that the CYP27B1 promoter activity was thyroid hormone receptor β1 (TRβ1)-dependently inhibited by T_3 and its analog and the transrepression of CYP27B1 gene promoter by T_3 involves a negative vitamin D response element (1αnVDRE) and VDR interacting repressor (VDIR). The gel shift analysis demonstrated that the binding of VDIR to 1αnVDRE was reduced by TRβ1/retinoid X receptor α. Furtheremore, the inhibitors of histone deacetylase and DNA metyltransferase completely abrogated T_3-dependent transrepression of CYP27B1 gene premoter. These results suggest that T_3 down-regulates renal CYP27B1 mRNA expression *in vivo* and directly suppresses the CYP27B1 gene transcription via TRβ1/VDIR/1αnVDRE in renal proximal tubular cells *in vitro*.

***Disclosures: Mina Kozai**, None.*

SU0113

Cytoplasmic Polyadenylation Element Binding Protein is a Conserved Target of Tumor Suppressor *HRPT2/CDC73*. Jianhua Zhang[1], Leelamma Panicker[1], Erica Seigneur[1], William Simonds*[2]. [1]Metabolic Diseases Branch/ NIDDK, USA, [2]National Institute of Diabetes & Digestive & Kidney Diseases, USA

Parafibromin, a tumor suppressor protein encoded by *HRPT2/CDC73* and implicated in parathyroid cancer and the hyperparathyroidism-jaw tumor familial cancer syndrome, is part of the PAF1 transcriptional regulatory complex. Parafibromin has been implicated in apoptosis and growth arrest, but the mechanism by which its loss of function promotes neoplasia is poorly understood. We report here that a hypomorphic allele of *hyrax (hyx)*, the *Drosophila* homolog of *HRPT2/CDC73,* rescues the loss-of-ventral-eye phenotype of *lobe (Akt1s1,* also called *PRAS40)*. Such rescue is consistent with previous reports that hyx/ parafibromin is required for the nuclear transduction of Wingless/Wnt signals and that Wingless signaling antagonizes *lobe* function. A screen employing double *hyx/lobe* heterozygotes identified an additional interaction with *orb* and *orb2*, homologs of mammalian cytoplasmic polyadenylation element binding protein (CPEB), a translational regulatory protein. *Hyx* and *orb2* heterozygotes lived longer and were more resistant to starvation than controls. In mammalian cells knockdown of parafibromin expression reduced levels of *CPEB1*. Chromatin immunoprecipitation demonstrated occupancy of *CPEB1* by endogenous parafibromin. Bioinformatic analysis revealed a significant overlap between human transcripts potentially regulated by parafibromin and CPEB. These results show that parafibromin may exert both transcriptional and, through CPEB, translational control over a subset of target genes and that loss of parafibromin (and CPEB) function may promote tumorigenesis in part by conferring resistance to nutritional stress.

***Disclosures: William Simonds**, None.*

SU0114

Determinants of Plasma PTH and Their Implication for Defining a Reference Interval. Lars Rejnmark*[1], Peter Vestergaard[1], Lene Heickendorff[2], Leif Mosekilde[1]. [1]Aarhus University Hospital, Denmark, [2]Dept of Clinical Biochemistry, Denmark

At the Third International Workshop on Asymptomatic Hyperparathyroidism, 2008, more data on the upper limit of the reference ranges for PTH levels were requested in order to improve the diagnostic sensitivity of PTH measurements. As PTH levels vary inversely with plasma 25-hydroxyvitamin D (25OHD) levels and as vitamin D-insufficiency is widespread, special attention was requested on the effects of

low vitamin D levels on the PTH reference range as measured by isotope dilution liquid chromatography–tandem mass spectrometry (LC-MS/MS).

Aim, design, and methods: In a cross-sectional design, including 2316 solely free-living women aged 17-84 years, we studied effects of different indices on plasma PTH levels and determined 95% reference ranges using a non-parametric approach.

Results: PTH was a positive function of age, body weight, and BMI, and inversely associated with total daily calcium intake, smoking, plasma calcium- and 25OHD-levels, which explained 29% of the variability in plasma PTH levels. The threshold value for 25OHD levels below which PTH levels started to rise was 95 nmol/l. Plasma PTH levels varied inversely with the seasonal variations in 25OHD levels. Mean PTH level was 4.1 pmol/l with a reference range equal to 2.0 - 8.6 pmol/l. Restricting the population in whom the reference interval was calculated to only women with 25OHD levels above 25 or 100 nmol/l lowered the upper limit of the reference interval to 8.4 and 7.7 pmol/l, respectively. Similar, stratification according to age, body mass index, smoking, and calcium intake had only minor impact on the reference interval.

Conclusion: Indices with known effects on plasma PTH levels have only a moderate impact on the upper levels of the normative reference interval. As several studies have indicated harmful effects of PTH levels in the upper range of the normative reference interval, it needs to be considered whether the upper acceptable limit for plasma PTH should be defined according to a biological algorithm in terms of a decision limit rather than in terms of a statistical derived normative reference range.

***Disclosures: Lars Rejnmark**, None.*

SU0115

Development of a 1-84 Specific Parathyroid Hormone Assay for the LIAISON Analyzer. Kim Paulsen*, Scott Bergmann, Cindy Zuo, Christa Klatt, Trent Kowalchyk, Frank Blocki, Joshua Soldo, John Walter. DiaSorin Inc., USA

Parathyroid hormone (PTH) plays a critical role in the regulation of bone and mineral metabolism by regulating extracellular calcium homeostasis through direct action on bone and kidney, and by indirect action on the intestine. Three key regulators of PTH secretion and synthesis are extracellular calcium, phosphate, and 1,25-dihydroxyvitamin D. Low serum calcium, high serum phosphate and/or reductions in 1,25-dihydroxyvitamin D either directly or indirectly stimulate the parathyroid gland to excrete PTH. The 1-84 PTH molecule stimulates ionized calcium release from bone, re-absorption of calcium by the kidney, and hydroxylation of 25-hydroxyvitamin D to1,25-dihydroxyvitamin D up-regulation which stimulates intestinal absorption of calcium. We report here on the new DiaSorin LIAISON® 1-84 PTH assay intended for the quantitative determination of 1-84 PTH without cross-reaction to 7-84 PTH fragment in human serum and plasma.

Second generation or 'intact' PTH immunoassays were initially believed to detect only active 1-84 PTH molecules. These assays utilized capture antibodies specific to the 39-84 C-terminal portion and tracer antibodies specific to the 1-34 N-terminal portion of the 1-84 PTH molecule. In fact, second generation PTH immunoassays cross react with 7-84 PTH fragments, and the extent of the reaction depends upon the assay. Third generation assays like the DiaSorin LIAISON® 1-84 PTH assay provide superior performance for direct measurement of 1-84 PTH without cross-reaction to the 7-84 PTH fragment.

The LIAISON® 1-84 PTH assay consists of 150 µL of patient sample mixed with ABEI conjugated 1-84 PTH N-terminal specific antibody and incubated for 20 minutes. A C-terminal antibody coated on paramagnetic particles is subsequently added and incubated for an additional 20 minutes. The particles are washed and the chemiluminescent signal is proportional to the quantity of 1-84 PTH in the sample.

The LIAISON® 1-84 PTH assay measuring range is 4 to 1800 pg/mL with 0% cross reactivity to the 7-84 PTH fragment. The assay demonstrates good correlation to the Scantibodies Whole PTH™ (1-84) Specific IRMA assay: LIAISON® = 1.02 (IRMA) – 5.2 pg/mL, R = 0.981. The analytical sensitivity is ≤ 1.7 pg/mL, functional sensitivity is ≤ 4 pg/mL, and inter-assay precision is ≤ 10%. Dilution Linearity yields a regression equation of Observed = 1.00 (Expected) – 18.8, R = 1.0 for serum, and Observed = 1.00 (Expected) – 15.9, R = 1.0 for plasma.

***Disclosures: Kim Paulsen**, DiaSorin, Inc., 3*
This study received funding from: DiaSorin, Inc.

SU0116

MKP-1 Knockout Mice Reveal Sexual Dimorphism in Bone Mass and Disparate PTHrP Responsiveness of Primary Calvarial Osteoblasts. Nabanita Datta*[1], Chandrika Mahalingam[1], Jaclynn Kreider[2], Keith Kirkwood[3], Steven Goldstein[4], Abdul Abou-Samra[5]. [1]Wayne State University School of Medicine, USA, [2]University of Michigan, USA, [3]Medical University of South Carolina, USA, [4]University of Michigan Orthopedic Research Labs, USA, [5]Wayne State University, School of Medicine, USA

Cell signaling mediated by Parathyroid hormone (PTH) and PTH related peptide (PTHrP), via PTH 1 receptor (PTH1R), is an essential component of bone physiology and involves cAMP, PKC and MAPK pathways. MAPKs are negatively regulated by a family of dual-specificity phosphatases known as the MAPK phosphatases (MKPs). The role of MKP-1 in PTH and PTHrP anabolic action in bone is yet to be investigated. Our previous study demonstrated an increase in MKP-1 expression in differentiated osteoblasts following PTH1R induction both in vitro and in vivo. In this report, we have determined the in vivo effect of MKP-1 on bone, using knockout (KO) mice developed by Bristol Meyer Squibb, in which exon 2 of MKP-1 was deleted. H and E staining and microCT analyses identified sex-dependent differences in the tibiae and femoral bone of 12 week old male and female MKP-1 KO mice compared to their wild-type (WT) strain. Relative to WT animals, female MKP-1 KO bones show a significant reduction ($p<0.02$-0.001) in BV/TV (40%), Tb. Th. (22%), Tb. N (24%), BMD (25%), TMD (8%); and an increase ($p<0.002$) in BS/BV (28%) and Tb. Sp (30-40%). Strikingly, at the basal state, male MKP-1 KO mice display higher bone parameters ($p<0.03$-0.001) from their wild type counterparts in BV/TV (50-60%), Tb. Th (8-11%), Tb. N (35%), BMD (36%), TMD (3-5%) and a decrease in BS/BV (16%) and Tb. Sp (37%). Von kossa assay of primary cell cultures originating from MKP-1 KO calvarial osteoblasts suggests that MKP-1 acts as a positive regulator of osteoblast mineralization in female mice. Following differentiation of primary osteoblasts with ascorbic acid (50 µg/ml) for 7 days and treatment with 100 nM PTHrP, Western blot analysis on whole cell lysates also demonstrate a gender difference in the molecular regulation on KO mice. PTHrP down-regulation of pERK1/2 and cyclin D1 expression in differentiated calvarial osteoblasts is attenuated in female but not in male MKP-1 KO osteoblasts compared to WT osteoblasts. Taken together, these results suggest that MKP-1 is important for maintaining bone homeostasis in females and may be a target gene in the treatment of osteoporosis.

***Disclosures: Nabanita Datta**, None.*

SU0117

Normocalcemic Primary Hyperparathyroidism in Patients With Low Bone Mass: Biochemical and Clinical Characteristics. Muriel Babey*[1], Spiros Arampatzis[2], Albrecht Popp[2], Jotinder Schuematschek-Kainth[2], Peter A Kopp[3], Kurt Lippuner[2]. [1]Endocrine Research Unit, USA, [2]Osteoporosis Policlinic, University of Bern, Switzerland, [3]Division of Endocrinology, Metabolism & Molecular Medicine, USA

Background: Widespread clinical use of PTH assays has identified patients with elevated PTH levels in absence of hypercalcemia in whom secondary causes such as Vitamin D insufficiency and renal failure for increased PTH levels were ruled out, thus leading to the diagnosis of normocalcemic primary hyperparathyroidism (nPHPT).

Methods: To further determine the phenotype of nPHPT patients, we analyzed densitometric, biochemical and clinical characteristics in nPHPT patients (n=36) in comparison to patients with hypercalcemic primary hyperparathyroidism (hPHPT) (n=58). All patients had been referred to the Osteoporosis Policlinic, University Hospital of Bern, Switzerland for evaluation of bone metabolism.

Results: Bone mineral density (T-scores/Z-scores) measured by DXA was not significantly different at lumbar spine and femoral neck between nPHPT and hPTHP patients. Serum intact parathyroid hormone (PTH), alkaline phosphatase and osteocalcin levels were significantly higher in hPTHP patients (mean ± SD 112 ± 50 pg/ml; 93 ± 37 U/l; 43 ±24 ng/ml) compared to nPHPT patients (83 ± 13 pg/ml; 77 ± 24 U/l; 32 ± 10 ng/ml, $p<0.001$, $p=0.023$, $p=0.02$). Serum 1,25-hydroxyvitamin D levels were similar for nPHPT (127 ± 32 nmol/l) and hPHTP (154 ± 67 nmol/l) patients, but serum 25-hydroxyvitamin D levels showed higher values in nPHPT patients (68 ± 16 pmol/l) than in hPHPT patients (53 ± 23 pmol/l, $p<0.001$). Serum phosphate levels were lower in hPHPT patients (0.85 ± 0.14 mmol/l) compared to nPHPT patients (1.09 ± 0.18 mmol/l, $p<0.001$). Arterial hypertension presented more often in hPHPT patients (39%) than in nPHPT (26%) patients. Similar prevalences of nonvertebral and vertebral fractures, based on medical history were observed in nPHPT (18%;29%) and hPTHP patients (18%;25%).

Conclusion: Our findings indicate that nPHPT in the absence of secondary causes such as Vitamin D insufficiency and renal failure is not an uncommon condition and presents as a milder form of PHPT.

***Disclosures: Muriel Babey**, None.*

SU0118

Osteocytes do not Mediate the Stimulatory Effect of Parathyroid Hormone (PTH) on the Bone Marrow Hematopoietic Stem Cell Niche. Laura Calvi*[1], Olga Bromberg[2], Yumie Rhee[3], Jonathan Weber[2], Julianne Smith[2], Racheal Lee[4], Miles Basil[2], Benjamin Frisch[1], Teresita Bellido[5]. [1]University of Rochester School of Medicine, USA, [2]Department of Medicine, Division of Endocrinology & Metabolism, University of Rochester School of Medicine, USA, [3]IUMS, Yonsei University, College of Medicine, South korea, [4]Department of Internal Medicine, College of Medicine, Yonsei University, South korea, [5]Indiana University School of Medicine, USA

The bone marrow microenvironment instructs hematopoietic stem cell (HSC) fate choices. Parathyroid hormone (PTH), through its action on osteoblastic cells, expands HSC. Still, the maturation stage of the osteoblastic cells on which PTH acts to expand HSC is unknown. Recent evidence demonstrates that activation of the PTH receptor in osteocytes recapitulates the increase in bone mass and remodeling induced by the hormone. To establish whether osteocytes mediate the stimulatory effect of PTH on HSC, we studied mice expressing a constitutively active PTH1R in osteocytes (DMP1-caPTHR1 mice, hereafter named TG). Trabecular bone as well as osteoblast

and osteoclast number was increased in femur, tibia, and spine as assessed by histomorphometry. Even though hematopoietic cells were visualized within the bone marrow, TG mice had mild peripheral neutropenia, suggesting impaired hematopoiesis. HSC-enriched lineage-Sca1+cKit+ (LSK) cells were increased, and even Flt3-CD48-CD150+Long-Term HSC (LT-HSC), barely detectable in WT spleens, were strongly increased in TG spleens. These data suggest that bone marrow LT-HSC niches are insufficient in TG mice, displacing LT-HSC to the spleen. Evaluation of 4-5 wk old mice identified litter-specific variability of the TG phenotype: some litters had decreased marrow cellularity, decreased LSK per limb and increased spleen LSK; others had normal bone marrow cellularity and normal LSK number per limb despite a robust bone increase. In the latter group, competitive repopulation, the gold standard in HSC quantification, demonstrated similar early engraftment of cells from WT or TG mice, while the rate of long term engraftment (24 wks) was decreased, suggesting decreased HSC activity in TG bone marrow. Since HSC may be tightly bound to trabeculae, bone marrow was also obtained by crushing the long bones. By this method we have confirmed a significant increase in phenotypic HSC after PTH treatment in vivo. In crushed long bones from 3.5-wk old TG mice with a strong bone phenotype and normal bone marrow cellularity, we confirmed that there were no changes in bone marrow LSK or LT-HSC. Moreover, by competitive repopulation there was no increase in bone marrow HSC in TG vs WT. Together, these data demonstrate that activation of the PTHR1 in osteocytes, in spite of dramatic osteoblastic cell expansion, does not increase HSC in the bone marrow, thus pointing to a less mature osteoblastic cell as the stimulatory component of the HSC niche.

***Disclosures: Laura Calvi**, None.*

SU0119

Withdrawn

SU0120

Vitamin D Status and its Association with Vitamin D Intake in Finnish Children and Adolescents. Minna Pekkinen*[1], Heli Viljakainen[2], Elisa Saarnio[1], Christel Lamberg-Allardt[1], Outi Makitie[3]. [1]University of Helsinki, Finland, [2]Helsinki University Central Hospital for Children & Adolescents, Finland, [3]Hospital for Children & Adolescents, University of Helsinki, Finland

Vitamin D is important for calcium metabolism and for bone mass accrual during growth. Recent studies have demonstrated that vitamin D insufficiency is common among children and adolescents. This may have long-term skeletal consequences as peak bone mass accrued during childhood is one of the most important predictors for osteoporosis and osteoporotic fractures later in life. In the present study we investigated vitamin D status and its association with vitamin D intake in Finnish children and adolescents.

This school-based study included 202 healthy children and adolescents (126 girls, 76 boys) aged 7-19 years, who were assessed for bone health and its determinants. Dietary vitamin D intake was evaluated with a validated food frequency questionnaire. The concentrations of serum 25-hydroxyvitamin D (25-OHD) was determined by HPLC and PTH by EIA. Statistical analyses were performed with SPSS.

We observed that 72% of the study population had serum 25-OHD concentration below 50 nmol/L, the median 25-OHD being 41 nmol/L for girls and 45 nmol/L for boys (range 17-82 nmol/L). The median vitamin D intakes were 9.1 and 10 µg/day in girls and boys, respectively. The average dietary vitamin D intake was thus in accordance and even exceeded the Scandinavian recommendation (7.5 µg/day). There was a positive correlation between dietary intake of vitamin D and serum 25-OHD concentration ($r=0.322$, $p<0.001$), and an inverse association between serum 25-OHD and PTH concentrations after controlling for calcium intake ($r=-0.196$, $p=0.02$). The average vitamin D intake in those with vitamin D sufficiency was 12.3 µg/day.

Vitamin D insufficiency is common in normal healthy children and adolescents in Finland, in the winter, even in subjects whose vitamin D intake exceeds the recommended daily intake. The intake of vitamin D have to be increased to assure adequate vitamin D status in all children.

***Disclosures: Minna Pekkinen**, None.*

SU0121

A Cross-sectional Study Evaluating Bone Quantity and Quality in Women with Bone Metastases from Breast Cancer. Orit Freedman*[1], Eitan Amir[2], Mark Clemons[3], Esther Lee[2], Hanxian Hu[4], George Dranitsaris[2], Angela Cheung[4]. [1]Durham Regional Cancer Centre, Canada, [2]Princess Margaret Hospital, Canada, [3]The Ottawa Hospital Cancer Centre, Canada, [4]University Health Network, Canada

Background: Approximately 1/3 of patients with metastatic breast cancer (MBC) and bone disease will sustain a skeletal related event (SRE) despite use of a bisphosphonate; there is therefore an urgent unmet need in this large population to better assess individual SRE risk and develop more effective bone protective agents. In a retrospective study, osteoporosis was the main risk factor identified in the development of SRE. Using novel tools to assess bone quality may therefore help guide individual patient treatment choices as well as future trial design. Methods: Women with MBC and bone metastases were recruited. Bone metastases were diagnosed based on bone scan. Baseline bone assessments were performed using dual-energy X-ray absorptiometry (DXA) [areal bone mineral density (BMD) and vertebral fracture assessment (VFA)], high-resolution peripheral quantitative computed tomography (HR-pQCT), and serum markers of bone turnover [serum CTX and bone-specific alkaline phosphatase (BAP)]. Risk factors for osteoporosis and fractures were then recorded. Results: 49 baseline assessments were completed. Mean age and body mass index were 53.6 (range 30-80) and 27 (range 17-45) respectively. One in four women had an ECOG 2-3, and 24% had a clinical fracture since the diagnosis of MBC. 94% had estrogen positive disease, 11% were HER2+. 53% had prior radiation therapy to bone; 90% received bisphosphonate therapy. Bone assessments are outlined in Table 1. Vertebral compression deformity (VCD) using VFA was most strongly associated with clinical fracture ($p = 0.003$). Conclusions: This is the first study to describe bone quantity and quality in women with MBC. Women with MBC have multiple factors that may effect bone quality; breast cancer treatment can induce early menopause, aromatase inhibitors can cause significant decrease in bone density, and bisphosphonate therapy may influence bone remodelling. Prospective evaluation of the effect of bone quantity and quality to an individual's SRE risk will enable improved patient-centred care and allow more rational use of bone targeted therapies. VFA may better inform treatment decisions and choice of agents in women with MBC. Future follow-up of these patients will help determine the optimal assessment modality.

Table 1: Bone quantity and quality assessments

Indicators	Results
*DXA**	
aBMD	
Hip T-score	0.12 (-3.5-+2.8)
Femoral neck T-score	-0.74 (-3.4-+1.9)
Lumbar Spine T-score	0.53 (-3.0-+6.6)
VFA (n)	
No VCD	40
Grade 1 VCD	1
Grade 2-3 VCD	5
Bone turnover markers Median (range)	
CTX (nM/L)	214 (10-1,300)
BAP (U/L)	20 (11-137)
HRpQCT* Mean (range)	
Total vBMD (mgHA/ccm)	276 (160-402)
Trabecular vBMD (mg HA/ccm)	150 (84-222)
Cortical vBMD (mg HA/ccm)	838 (616-953)
Trabecular thickness (mm)	0.06 (0.04-0.10)
Number of trabeculae	1.8 (1.18-2.67)
Cortical thickness (mm)	1.08 (.6-1.83)

* Three patients were not assessable.

Table 1: bone quantity and quality assessments

***Disclosures: Orit Freedman**, None.*

SU0122

CD68 Plays a Role in Mediating Attachment of Breast Cancer Cells to Bone. Erin McCoy*, Zhenqi Shi, Jason Ashley, Xu Feng. University of Alabama at Birmingham, USA

The most common site of distant metastases in breast cancer (BC) is bone. While not as lethal as visceral metastases, bone metastases account for the worst morbidities of the disease. The precise molecular mechanisms regulating this preferential metastasis of breast cancer to bone have not yet been fully elucidated, but it has been hypothesized that local conditions in the bone create an environment conducive to colonization by BC cells. These conditions can relate to recruitment of BC cells to bone via chemotactic gradients and the ability of BC cells to attach to bone matrix. Our laboratory recently identified and validated macrosialin as a key molecule mediating the interaction between murine osteoclast precursors and bone. In the current study we seek to determine if CD68, the human homologue of mouse macrosialin, plays a role in BC bone metastasis by mediating BC tumor cell attachment to bone. To this end, we first examined protein expression levels of CD68 in four BC cell lines (MCF7, MDA-MB-231, MDA-MB-435, and MDA-MB-468). We found that CD68 is expressed abundantly in MDA-MB-231 and MDA-MB-435, BC cell lines capable of metastasizing to bone in animal models. Consistently, semi-quantitative RT-PCR shows increased CD68 mRNA levels in the MDA-MB-231 and MDA-MB-435 cell lines as compared with the others. More importantly, flow cytometry data show that CD68 is expressed on the surface of MDA-MB-231s and, to a lesser degree, on the surface of MDA-MB-435s. To determine if CD68 expression levels positively correlate with the BC cells capacity to attach to bone, we performed in vitro bone adhesion assays and found that CD68 expression levels correlate with greater capacity to attach onto bone. Moreover, we incubated MDA-MB-435 or MDA-MB-231 on bone slices for 1 hour with either anti-CD68 antibody or control IgG and found that the anti-CD68 antibody can block attachment onto bone by MDA-MB-231, which express high levels of CD68 on the cell surface. Furthermore, transient knockdown of CD68 using siRNA significantly blocks attachment of MDA-MB-231 to bone in vitro. We are currently optimizing stable shRNA-mediated knock down of CD68 expression in BC cells in order to further explore the significance of

CD68 expression with respect to in vitro and in vivo metastatic characteristics. Taken together, these in vitro findings suggest that surface expression of CD68 may play an important role in BC bone metastasis by mediating BC cell attachment on bone.

***Disclosures: Erin McCoy**, None.*

SU0123

High Resolution MRI, Vertebral Fractures and Misclassification of Osteoporosis in Men with Prostate Cancer. Julie Wagner, Donna Medich, Megan Miller, Joel Nelson, Neil Resnick, Subashan Perera, Susan Greenspan*. University of Pittsburgh, USA

Androgen deprivation therapy (ADT), a common treatment for prostate cancer, is associated with increased bone loss and fracture. Although bone mineral density (BMD) assessed by conventional dual energy x-ray absorptiometry (DXA) is the gold standard to determine fracture risk, BMD only explains 60% of fracture risk and does not assess for vertebral fractures (VF). High resolution microMRI (HR-MRI) is a new technique to assess bone microarchitecture and may provide additional information on fracture risk. We postulated that 1) assessment for VF would increase the diagnosis of osteoporosis in men with prostate cancer on ADT and 2) assessment of trabecular microstructure by HR-MRI could demonstrate skeletal deterioration in men with VFs, not assessed by conventional BMD.

Methods: 53 men ⩾ 60 years with nonmetastatic prostate cancer on ADT for ⩾6 months were recruited. BMD of the spine and hip were assessed by DXA and classified using standard WHO criteria for osteoporosis. Each patient underwent vertebral fracture assessment (VFA) by DXA confirmed with conventional lateral x-ray and HR-MRI of the wrist.

Results: The duration of ADT was greater in men with vertebral fracture (VF+) (Table, mean ± SE). For each additional year of ADT, the odds of vertebral fracture increased by 16% ($p<0.05$). 13% of total participants were classified as having osteoporosis by standard DXA. 49% of men without osteoporosis by DXA had VF assessed by VFA and conventional x-rays. This suggests that 29% of patients with clinically defined osteoporosis would have been misclassified by DXA alone. Indices of HR-MRI including bone volume to total volume (BV/TV), surface density (represents trabecular plates) were significantly lower in VF+ patients ($p<0.05$, Table) with similar trends for surface/curve ratio (plates/rods) and higher for erosion index (higher depicts deterioration). Conventional BMD was lower in VF+ patients (Table). Indices of HR-MRI were associated with BMD at the ultra distal radius ($r=0.69$-0.75, $p<0.001$), total hip ($r=0.59$-0.64, $p<0.001$) and spine ($r=0.30$-0.52, $p< 0.05$). We conclude that assessment for vertebral fracture should be performed in men on ADT to avoid misclassification of osteoporosis. The longer the duration of ADT, the greater the odds of a VF. HR-MRI provides a novel technique to assess the deterioration of structural integrity in men with VFs and adds additional information to conventional BMD.

	VF + (n=17)	VF – (n=36)
Age (years)	50 ± 10	65 ± 4
BMI (kg/m^2)	28 ± 1	29 ± 1
Duration ADT (months)	73 ± 19†	36 ± 6
BMD spine (g/cm^2)	1.009 ± 0.046 *	1.136 ± 0.036
Total hip (g/cm^2)	0.892 ± 0.032†	0.974 ± 0.025
Femoral neck (g/cm^2)	0.699 ± 0.027*	0.803 ± 0.023
High Resolution MicroMRI		
BV/TV	12.2 ±0.5*	13.4 ± 0.3
Surface density	0.058 ± 0.003*	0.065 ± 0.002
Surface/curve	9.734 ± 0.879 †	11.810 ± 0.719
Erosion index	0.932 ± 0.47 †	0.829 ± 0.029
* p<0.05, † p≤0.08, vertebral fractures (VF+) vs no vertebral fractures (VF-)		

Table

***Disclosures: Susan Greenspan**, None.*

SU0124

Inhibition of Breast Cancer Bone Metastasis and Osteolysis by Omega-3 Docosahexaenoic Acid. Gabriel Fernandes*[1], Ganesh Halade[2], Md M Rahman[2], Jyothi M Veigas[2], Yoneda Toshiyuki[3], Paul J Williams[2]. [1]University of Texas Health Science Centre, USA, [2]University of Texas Health Science Center at San Antonio, USA, [3]Osaka University Graduate School of Dentistry, Japan

An estimated 192,370 women in USA will be diagnosed with breast cancer and 40,170 will die in 2009. Further, there were approximately 2,533,193 women in USA living with breast cancer in 2006. Among them, many will develop bone metastasis and will have poor quality of life each year. Metastatic bone disease is a major cause of morbidity in breast cancer patients. It is suspected that the microenvironment of the bone may be influenced by dietary factors and adiposity in the bone marrow may influence bone metastasis and osteolysis. We have observed that corn oil enriched diet increases obesity and also adipocytes in bone marrow while omega-3 fatty acids show reduced adipocytes and inflammation. We therefore carried out studies using omega-3 fatty acids both in vitro and in vivo. Our recent studies on proliferation of MDA-231BO cells demonstrated a dose dependent inhibition of tumor cells in vitro by EPA and DHA, the latter being more pronounced in its activity. Similarly, matrigel invasion of MDA-231BO breast cancer cells showed significant reduction of tumor cell invasion by eicosapentaenoic acid (EPA) and docosahexaenoic acid (DHA). Based on these encouraging observations, we carried out a new study using concentrated EPA (EPA 55% and DHA 5%) and DHA (DHA 60% and EPA 5%) obtained from Ocean Nutrition, Canada. We fed 4 week old nude mice with regular control chow diet, 10% EPA and 10% DHA for 1 month (n=10). Mice in each group were injected with 1x105 MDA-231BO breast cancer cells intracardially. After four weeks, all mice were scanned by X-ray to measure bone osteolysis followed by histomorphology of both leg joints to evaluate tumor proliferation. It was noted that mice fed DHA show very minimal proliferation and osteolysis. Also, osteolysis in the tibial metaphysis was significantly lower in DHA fed mice. The tumor cell proliferation in tibial metaphysis was measured and tumor cell proliferation was markedly lower in DHA fed mice. Further, CD44 expression in bone section was also found lower in DHA fed mice. Thus we are very encouraged to see these results for the first time using intracardial injection of tumor cells, which selectively metastasizes in bone, and the inhibition of its metastasis and osteolysis by DHA. This finding may lead to set up clinical studies in breast cancer patients to prevent onset of metastasis and bone pain in later years. This work is supported by DOD-CDMRP (Grant number BC096459) under Breast Cancer Research Program.

***Disclosures: Gabriel Fernandes**, None.*

SU0125

Ovarian Failure and Body Composition Changes in Women with Breast Cancer Treated with Adjuvant Chemotherapy. Angela M. Gordon*[1], Shelley Hurwitz[1], Charles L. Shapiro[2], Meryl Leboff[1]. [1]Brigham & Women's Hospital, USA, [2]Ohio State University Medical Center, USA

Purpose: Weight gain occurs commonly in breast cancer patients receiving adjuvant chemotherapy. We reported accelerated bone loss in pre-menopausal women with early stage breast cancer who developed chemotherapy-induced ovarian failure (CIOF).[1] The objective of this study was to evaluate weight and body composition changes in pre-menopausal women with early stage breast cancer undergoing adjuvant chemotherapy and to determine whether these changes are related to CIOF.

Methods: Body composition of 43 pre-menopausal women with stage I or II breast cancer was measured by dual-energy x-ray absorptiometry within 4 weeks prior to beginning chemotherapy and at 12 months from baseline. At 12 months, CIOF was determined by history of amenorrhea for 3 or more months and an elevated serum FSH.

Results: Median weight gain for all 43 women was 2.7 kg ($p=0.0002$) over 12 months, and consisted of increased fat, but not lean mass, in the trunk and legs. Thirty-four women (79%) gained weight, 35 (81%) gained fat mass, and 23 (53%) lost lean mass. There was no significant correlation between weight gain and weight at baseline ($r=0.17$, $p=0.27$). Weight, total body fat, and leg fat increased similarly in women with and without CIOF. In the 30 women (70%) who developed CIOF, there was an increase in truncal fat (median 1.8 kg, $p=0.0004$) with a decrease in truncal lean mass (median -0.6 kg, $p=0.02$). Women without CIOF also gained truncal fat (median 0.9 kg, $p=0.06$). Though this was a smaller increase compared to women with CIOF, the difference between groups was not significant. Caloric intake decreased similarly in women with and without CIOF (-184 vs. -290 kcals, respectively; $p=0.77$). The associations between changes in body composition and bone density will be presented.

Conclusions: CIOF may affect compositional changes in the trunk, though overall, body composition changes were similar in women with and without CIOF and included significant accumulation of fat in the trunk and legs. Further research is needed to investigate whether a gain in body fat, particularly truncal fat, during adjuvant chemotherapy affects breast cancer and other outcomes and, if so, how it can be minimized or prevented.

1. Shapiro CL, Manola J, LeBoff M. Ovarian failure after adjuvant chemotherapy is associated with rapid bone loss in women with early-stage breast cancer. J Clin Oncol. 2001;19(14):3306-11.

***Disclosures: Angela M. Gordon**, None.*

SU0126

Profiling of Genes Expressed in Breast Cancer Cells Colonized in Bone Identified NEDD9 as a Novel TGF-β Target Gene. Yoshihiro Morita*[1], Kenji Hata[2], Masako Nakanishi[2], Toshihiko Nishisho[3], Yoshiaki Yura[1], Toshiyuki Yoneda[2]. [1]Osaka Univ Grad Sch Dent, Japan, [2]Osaka University Graduate School of Dentistry, Japan, [3]BIGLOBE NEC, Japan

Bone is one of the most preferential metastatic sites of cancers including breast, prostate and lung cancers. It has been well-recognized that the crosstalk between cancer cells and bone microenvironments is critical to the development and progression of bone metastases. To determine the molecular basis of bone metastasis, we attempted to uncover the molecules that are expressed in breast cancer cells under the influences of bone microenvironments.

The bone-seeking MDA-MB-231 cells stably transfected with GFP were inoculated into the left cardiac ventricle (HI) or the marrow cavity of tibiae (TI) to expose cancer cells to the bone microenvironments via circulation or directly,

respectively. MDA-MB-231 cells that were inoculated into the mammary fat pads were used as control (SC). Two weeks after the inoculation, MDA-MB-231 cells were enzymatically dissociated and GFP-positive cancer cells were then sorted using FACS Aria without expansion in culture. Microarray analysis between FACS-sorted HI or TI and SC cells revealed 1,382 or 226 genes that were elevated more than 2-fold compared to SC cancer cells. In those genes there were 158 genes that overlapped between HI and TI cancer cells. Detection of PTHrP and COX-2, both of which were shown to play important roles in bone metastasis, suggests that our gene profiling was valid.

Out of these genes, we focused on NEDD9 (neural precursor cell expressed developmentally down-regulated protein 9). NEDD9 is a scaffold protein involved in varieties of biological activities such as cell migration and integrin-dependent cell adhesion. Real-time PCR showed NEDD9 mRNA expression in MDA-MBA-231 cells was increased by TGF-β and this increase was reduced by the TβR-I inhibitor LY364947. We found strong NEDD9 expression in bone metastases by immunohistochemistry. Importantly, knockdown of NEDD9 using shRNA decreased bone metastases following intracardiac inoculation. Of interest, MDA-MB-231 cancer cells isolated from tibia of mice treated with the bisphosphonate zoledronic acid showed reduced NEDD9 mRNA expression. In conclusion, our results suggest that NEDD9 expression in breast cancer cells that is up-regulated by TGF-β released from bone is critical to the development of bone metastasis. Further profiling of genes expressed in cancer cells colonized in bone may lead to new therapeutic approaches for the treatment of bone metastasis at molecular levels.

***Disclosures: Yoshihiro Morita**, None.*

SU0127

PTHrP Suppression by Novel Bis-Cyclic Thioureas Identified by Combinatorial Chemistry Inhibits the Proliferation of Cancer Cells. Leonard Deftos*[1], Adel Nefzi[2], Douglas Burton[1], Su Tu[1], Rick Quintana[1], Randolph Hastings[1]. [1]Veterans Administration San Diego Healthcare System & University of California, USA, [2]Torrey Pines Institute for Molecular Studies, USA

Background: PTHrP (parathyroid hormone related protein) is abnormally expressed in the aggregate majority of breast, lung, and prostate cancers. This oncoprotein plays a key role in tumor progression for many of these cancers, especially those that metastasize to bone. Since PTHrP is a signal of both the tumor and its invasiveness, this oncoprotein could be a reasonable target for treating patients with PTHrP-expressing cancers. However, PTHrP antibody studies notwithstanding, modalities involving PTHrP have received little attention as treatments for these malignancies. We have recently conducted in vitro studies that posit a novel role for bis-cyclic thioureas in tumor management.

Methods: These in vitro studies were conducted using a panel of human lung and prostate cancer cells. We screened combinatorial libraries of small molecule heterocyclic amines for effects on PTHrP expression, on PTHrP promoter specific mRNA transcripts, and on cell proliferation, as measured by immunoassays, qPCR, and MTT assays.

Results: After the initial screens of the combinatorial libraries, we identified six lead bis-cyclic thiourea compounds that demonstrated > 60% inhibition on PTHrP expression as measured by immunoassays from BEN, PC-3 and NCI-H727 cancer cells compared to vehicle control treatment. Another tumor biomarker, calcitonin, was reduced by the bis-cyclic thioureas to a much smaller degree. The compounds decreased PTHrP mRNA levels, particularly promoter P3-specific transcripts, but had no effect on message stability in cells treated with actinomycin D. The lead bis-cyclic thioureas were next assayed for the effects on cancer cell proliferation in a 6 day time course study. 5/6 and 6/6 compounds significantly inhibited ($P < 0.01$) BEN and NCI-H727 cell proliferation, respectively, at days 2, 4 and 6.

Conclusions: Contemporary combinatorial chemistry procedures identified PTHrP inhibitory bis-cyclic molecules that inhibited the PTHrP expression and the growth in vitro of PTHrP-producing cancers. These inhibitory effects may act on PTHrP transcription. This family of compounds has the potential for innovative treatments of PTHrP expressing cancers that involve many organ systems, including breast, lung and prostate tumors.

***Disclosures: Leonard Deftos**, None.*

SU0128

Reduced Risk of Breast Cancer and Breast Cancer Death in Postmenopausal Women Prescribed Alendronate - National Register Based Cohort Study. Bo Abrahamsen*[1], Michael Pazianas[2], Pia Eiken[3], Richard Eastell[4], R Graham Russell[2]. [1]Copenhagen University Hospital Gentofte, Denmark, [2]University of Oxford, United Kingdom, [3]Cardiology & Endocrinology, Hillerød Hospital, Denmark, [4]University of Sheffield, United Kingdom

Background: We have been studying cancer incidence in large cohorts of ALN users and matched controls, and have reported a 40% reduction in colon cancers. A 31% reduction in the risk of invasive breast cancer in 2,200 women who received alendronate (ALN) was recently observed within the BMD sub-study of the Women's health initiative (WHI)[1]. We have independently investigated BrCa incidence and mortality in a larger, national cohort of ALN users and matched controls.

Methods: Restricted cohort study. We used national health registers to identify all women aged 50+ without a prior cancer diagnosis, who began ALN in the years 1996-2005. Observations were linked to the national cause of death registers and the hospital discharge register. We identified 30,606 incident ALN users and assigned 4 age, sex and prescription year-matched controls to each ALN user, covering 520,000 patient years. Cox proportional hazards analysis was used.

Results: ALN users had a lower BrCa incidence (crude HR 0.75, 0.66-0.84, adjusted HR 0.74, 0.66-0.84, controlled for HRT, Charlson co-morbidity index, and number of co-medications, both models $p<0.001$). The median survival after a diagnosis of BrCa was also longer with ALN (all cause, 2.3 y vs 1.9 y, $p=0.03$). The risk of BrCa death was lower in ALN users (crude and adjusted HR both 0.53 (0.40-0.68, $p<0.001$).

Limitations: Because of the observational, non-randomized setting drug channelling bias remains possible.

Conclusion: This national register based cohort study shows a significantly lower risk of developing and dying from BrCa in postmenopausal women who receive ALN, compared with age and sex matched control subjects.

1 Chlebowski R, et al "Oral bisphosphonates and breast cancer: Prospective results from the Women's Health Initiative" SABCS 2009

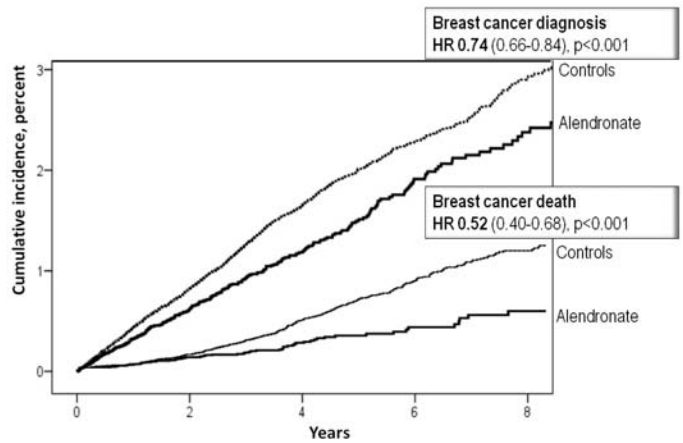

Fig 1

***Disclosures: Bo Abrahamsen**, Novartis, 2; Eli Lilly, 8; Merck, 8; Amgen, 5; Nycomed, 5*

SU0129

Role of Prostaglandin E Receptor EP4 in Breast Cancer Growth and Osteolysis Due to Bone Metastasis. Satoshi Yokoyama[1], Morichika Takita[1], Takayuki Maruyama[2], Chisato Miyaura[1], Masaki Inada*[3]. [1]Tokyo University of Agriculture & Technology, Japan, [2]Ono Pharmaceutical Co. Ltd, Japan, [3]Toyko University of Agriculture & Technology, Japan

Breast cancer preferentially metastasized to bone which accompanied by severe bone destruction with increased bone resorption. We have shown that prostaglandin E (PGE) and its receptor EP4, one of the receptor subtypes of PGE (EP1-EP4), are involved in the mechanism of osteolysis due to bone metastasis of malignant melanoma. In this study, we focused on the roles of PGE in breast cancer metastasis. Mouse breast cancer 4T1 was introduced to mice by i.v. injection. By the soft X-ray analysis, osteolysis was clearly observed in distal femurs and proximal tibiae on day 14 after the injection of 4T1. We first characterized the profiles of cell growth and bone malignancy of 4T1. Adding PGE2 stimulated the proliferation of 4T1 and its invasive activity measured by collagen substrates. 4T1 expressed both EP1 and EP4, but EP2 and EP3 could not be detected. The treatment of EP4 antagonist suppressed the proliferation and invasive activity elevated by PGE2 in dose-dependent manner. To examine the effect of EP4 antagonist on osteolysis induced by breast cancer, we performed ex vivo organ culture of mouse calvaria co-cultured with 4T1. 4T1 induced bone resorption in mouse calvarial cultures, and the treatment of EP4 antagonist clearly attenuated the bone resorption induced by 4T1 breast cancer. In co-culture of host cells and cancer cells (4T1, osteoblasts and bone marrow cells), osteoclast formation was observed without exogenous bone resorbing factor, and EP4 antagonist inhibited the formation of osteoclasts. To clear the source cells of PGE2 production in the co-culture, we measured PGE2 level in the circumstances of reversible living cells and fixed cells. PGE2 production and RANKL expression were enhanced in the culture of living osteoblasts with fixed-4T1, however, 4T1 cultured on fixed-osteoblasts did not induce PGE2 and RANKL expression, suggesting PGE2 is mainly produced by host osteoblasts after cell-cell contact with breast cancer cells. The cell-cell interaction between breast cancer cells and osteoblasts induces the production of PGE which stimulates the growth and invasive activity of cancer cells, and also induces RANKL-dependent osteoclast formation. Therefore, EP4 antagonist is a possible candidate for the therapy of bone metastases of breast cancer.

***Disclosures: Masaki Inada**, None.*

SU0130

Runx2 Transcriptome of Prostate Cancer Cells: Insights into Invasiveness and Bone Metastasis. Sanjeev Baniwal*[1], Omar Khalid[2], Yankel Gabet[1], Ruchir R Shah[3], Daniel J Purcell[1], Deepak Mav[3], Alice E. Kohn-Gabet[1], Yunfan Shi[1], Gerhard A Coetzee[1], Baruch Frenkel[1]. [1]University of Southern California, USA, [2]Univeristy of Southern California, USA, [3]SRA International, USA

Prostate cancer (PCa) cells preferentially metastasize to bone at least in part by acquiring osteomimetic properties. Runx2, an osteoblast master transcription factor, is aberrantly expressed in PCa cells, and promotes their metastatic phenotype. The transcriptional programs regulated by Runx2 have been extensively studied during osteoblastogenesis, where it activates or represses target genes in a context-dependent manner. However, little is known about the gene regulatory networks influenced by Runx2 in PCa cells. We therefore investigated genome wide expression changes in PCa cells in response to Runx2. We engineered a C4-2B PCa sub-line called C4-2B/Rx2^{dox}, which conditionally expresses Runx2 upon Doxycycline (Dox) treatment. Transcriptome profiling using whole genome expression array followed by in silico analysis indicated that Runx2 upregulated a multitude of genes with prominent cancer associated functions. They included secreted factors (CSF2, SDF1), proteolytic enzymes (MMP9, CST7), cytoskeleton modulators (SDC2, Twinfilin, SH3PXD2A), intracellular signaling molecules (DUSP1, SPHK1, RASD1) and transcription factors (SOX9, SNAI2, SMAD3) functioning in epithelial-mesenchymal transition (EMT), tissue invasion, as well as homing and attachment to bone. Consistent with the gene expression data, induction of Runx2 in C4-2B cells enhanced their invasiveness through Matrigel in vitro and growth in the bone microenvironment in vivo (Figure 1). Interestingly, Runx2 promoted cellular quiescence by blocking the G1/S phase transition during cell cycle progression in vitro, suggesting that Runx2-positive tumors must acquire additional properties in vivo to maximize their oncogenic potential. In line with this juncture, the Runx2-mediated cell cycle block was reversed as Runx2 levels declined after Dox withdrawal from C4-2B/Rx2^{dox} cells. The Runx2 transcriptome in PCa cells highlights plausible mechanisms underlying their metastatic phenotype, including tissue invasion, homing to bone and promotion of high bone turnover. Runx2 is therefore an attractive target for the development of novel diagnostic, prognostic and therapeutic approaches to PCa management. Targeting Runx2 may prove more effective than focusing on its individual downstream genes and pathways.

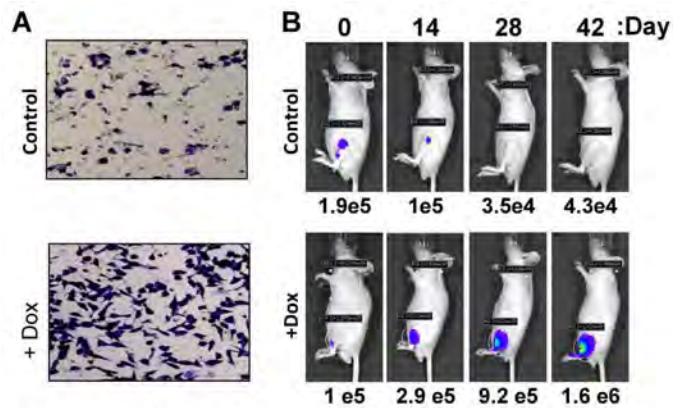

Figure 1 Runx2 enhances tissue invasion. **A**, Matrigel invasion assay; **B**, growth of C4-2B-Rx2^{dox}/LUC tumor cells in bone.

Figure 1

***Disclosures: Sanjeev Baniwal**, None.*

SU0131

Side Population in Human Breast Cancer Cells Exhibits Cancer Stem Cell-like Properties but Does Not Have Higher Bone-metastatic Potential. Toru Hiraga*[1], Susumu Ito[2], Hiroaki Nakamura[1]. [1]Matsumoto Dental University, Japan, [2]Shinshu University, Japan

Accumulating evidence suggests that cancers contain a small subset of their own stem-like cells called cancer stem cells (CSCs). This concept has recently been adapted for a growing number of tumors, including breast cancer. CSCs, which are characterized by the extensive self-renewal and proliferative capacity and the resistance to chemotherapy and radiotherapy, are emerging as an important target for cancer therapy. However, the role of CSCs in cancer metastasis, especially to bone, has not been extensively studied yet. Side population (SP), which is identified based on efficient Hoechst dye 33342 efflux, has been found in several kinds of cancer cells and shown to enrich CSCs. In the present study, we characterized the SP cells isolated from human breast cancer MDA-MB-231 cells in comparison to the non-SP (NSP). Fluorescence-activated cell sorter analysis demonstrated the existence of SP in MDA-MB-231 cells (3.40 $\pm$ 0.60%). The SP fraction was markedly reduced in the presence of fumitremorgin C, a specific inhibitor of ATP-binding cassette sub-family G member 2 (ABCG2/BCRP1), but not in the presence of verapamil, an ABCB1/MDR1 inhibitor. Quantitative RT-PCR analysis showed that ABCG2 mRNA expression was significantly higher in SP cells compared with NSP cells, while ABCB1 mRNA was undetectable. These results suggest that ABCG2 expression is likely responsible for the SP phenotype of MDA-MB-231 cells. SP cells formed increased numbers of tumorsphere in suspension culture, whereas the cell proliferation of SP cells in monolayer culture was similar to that of NSP cells. Furthermore, the tumor growth in the orthotopic mammary fat pad in nude mice was significantly accelerated in SP cells, although the tumor formation rate was similar between SP and NSP cells. Then, we examined the bone-metastatic potential of SP cells by intracardiac injection into nude mice. The incidence and number of metastases and the metastatic tumor burden in bone showed no difference between SP and NSP cells. Furthermore, SP abundance in the tumor cells isolated from the bone metastases was not increased compared with that in the mammary tumors and in the parental cells in culture. These results suggest that the SP of MDA-MB-231 cells possesses some of the CSC-like properties but does not have higher metastatic potential to bone. However, since definite markers for CSCs have not been established yet, further studies are required to determine the bone metastatic potential of CSCs.

***Disclosures: Toru Hiraga**, None.*

SU0132

The Role of Gamma-secretase Mediated Cleavage of Notch and Amyloid Precursor Protein in Breast Cancer Cell Attachment to Osteoblasts. Jenna Fong*, Osama Hussein, Svetlana Komarova. McGill University, Canada

Skeletal metastasis is a major complication of breast cancer, leading to hypercalcemia, bone fractures, and considerable pain burden. Osteoblasts contribute to the regulation of the hematopoietic stem cell niche and control osteoclastogenesis through the production of pro-resorptive cytokine RANKL, however their role in cancer metastases to bone is not fully understood. To study the effects of breast cancer cells on osteoblasts, we used C57BL/6J mouse bone marrow cells treated for 3-12 days with ascorbic acid (AA; 50 ug/mL), in the presence or absence of medium conditioned by MDA-MB-231 human breast carcinoma cells (10%) or 4T1 mouse breast carcinoma cells (10%). We have found that treatment with 231 CM inhibits osteoblast differentiation while promoting osteoclastogenesis. Importantly, exposure of bone cells to breast cancer-derived factors also stimulated subsequent attachment of cancer cells to immature osteoblasts. Since Notch signalling has been previously shown to expand an immature osteoblast population, we have considered its role in the observed effects using inhibitors of the activator of Notch signalling, gamma-secretase. Inhibition of gamma-secretase reversed osteoclastogenic effects of breast cancer derived factors and prevented breast cancer cell attachment to osteoblasts, but could not fully rescue breast cancer-induced inhibition of osteoblast differentiation. To explore alternative targets of gamma-secretase activity, we assessed the involvement of amyloid precursor proteins (APP), which were recently shown to play a role in osteoblast attachment. We have found that exposure of osteoblastic cultures to breast cancer factors resulted in decrease in the high molecular weight APP, as assessed by immunoblotting, which corresponded with an increase in immunofluorescence intensity of APP labelling in non-permeabilized cultures. These cancer-induced changes in APP amount and localization were reversed by the inhibition of gamma-secretase. These data suggest that cleavage of APP may play a role in a breast cancer factors-induced breast cancer cell attachment to immature osteoblasts. Thus, our data uncovered osteoblasts as critical intermediary of pre-metastatic signaling by breast cancer cells and suggest that gamma-secretase is a robust target for developing therapeutics potentially capable of reducing both homing and progression of cancer metastases to bone.

***Disclosures: Jenna Fong**, None.*

SU0133

Vitamin D Deficiency Promotes Human Prostate Cancer Growth in a Murine Model of Bone Metastasis. Yu Zheng*[1], Hong Zhou[2], Li Ooi[3], Daniel Snir[4], Colin Dunstan[3], Markus Seibel[2]. [1]Bone Research Program, ANZAC Research Institute, University of Sydney, Australia, [2]Bone Research Program, ANZAC Research Institute, The University of Sydney, Australia, [3]University of Sydney, Australia, [4]University od Sydney, Australia

Prostate cancer has a high propensity to metastasise to the skeleton where the bone microenvironment plays a pivotal role in supporting metastatic cancer cell growth. Vitamin D (vitD) deficiency has recently been shown to enhance breast cancer growth in an osteolytic model of breast cancer bone metastasis [1]. In the current *in vivo* study, we investigated the effect vitD-deficiency on prostate cancer cell growth in bone.

Three-week old male nude mice were either weaned onto a vitD-free diet or kept on normal chow. Animals on a vitD-free diet developed hypovitaminosis D within 6 weeks (mean serum 25OH-vitD level 6.9 $\pm$ 1.8nmol/L vs. 97.9 $\pm$ 10nmol/L in controls; $p<0.01$). At steady state, 50000 cells of the prostate cancer cell line PC-3 were injected intra-tibially into vitD-deficient and vitD-replete mice (n=9). Animals were monitored for lytic/sclerotic skeletal lesions by x-ray on days 21, 28 & 35, and tibiae were

analysed by micro-CT and histological analyses at endpoint (day 35). Osteoprotegerin (OPG) was co-administered at a dose of 3mg/kg every 3 days in a subset of mice (n=9) to determine the contribution of the bone microenvironment to tumor growth.

Inoculation of PC-3 cells into mouse tibiae caused predominantly osteolytic lesions with a smaller osteosclerotic component. At endpoint, all outcome measures were significantly increased in vitD-deficient compared to vitD-replete mice: osteolytic lesion area (2.88 ± 0.38 mm^2 *vs.* $1.71 \pm 0.17 mm^2$, $p < 0.05$); total tumor area ($3.53 \pm 0.47 mm^2$ *vs.* $2.13 \pm 0.17 mm^2$, $p<0.05$); sclerotic lesion area ($0.57 \pm 0.08 mm^2$ *vs.* $0.38 \pm 0.05 mm^2$, $p<0.05$). Compared to vitD-replete mice, tumors in vitD-deficient animals demonstrated a higher mitotic activity (+56%) but no alteration in cell apoptotic rate. Co-treatment with OPG completely prevented osteolysis, significantly reduced tumor burden, sclerotic lesion area and mitotic activity, and increased cell apoptosis in both vitD-deficient and replete mice compared to untreated controls. The growth of subcutaneously implanted tumors was similar in vitD-deficient and replete mice.

In conclusion, vitD-deficiency promotes intra-tibial prostate cancer growth in mice. Anti-resorptive treatment with OPG significantly inhibits tumor growth, indicating that changes in the bone microenvironment secondary to vitD deficiency play a critical role in stimulating tumour growth.

Reference

1. Ooi *et al. Cancer Res* 70:1835 (2010).

***Disclosures: Yu Zheng**, None.*

SU0134

Biomarkers of Bone Remodeling Associate with Osteolysis in Bisphosphonate-treated Bone Metastasis. Marta Martín-Fernández[1], Carolina Zandueta[2], Karmele Valencia[3], Diego Luis-Ravelo[2], Iker Anton[3], Susana Martínez[2], Concepcion De La Piedra Gordo*[1], Fernando Lecanda[2]. [1]Instituto de Investigación Sanitaria Fundación Jiménez Díaz, Spain, [2]Center for Applied Medical Research, Spain, [3]Foundation for Applied Medical Research, Spain

Bone represents a frequent target organ of metastasis in a variety of solid tumors including lung. We have recently developed several models of lung cancer bone metastasis. After intracardiac inoculation (i.c.) in nude mice, highly metastatic subpopulations (HMS) were selected with increase prometastatic activity. We have used a HMS of lung adenocarcinoma inducing rapid and selective model with specific bone tropism inducing marked osteolytic lesions. The aim of this study was to investigate the sensitivity of serum biomarkers, isoenzyme 5b of tartrate resistant acid phosphatase (TRAP5b) and aminoterminal propeptide of procollagen I (PINP), during the development of osteolytic lesions during treatment with bisphosphonates. Osteolytic lesions were monitored by X-ray image analysis and microCT scans. Cells were transduced with a luciferase reporter to assess tumor burden and tropism by in vivo bioluminescence imaging. Mice were treated with a single dose of zoledronic acid (ZA, 70μg/kg) or vehicle alone (control), and 10 animals of each group were sacrificed at 7, 14, 21, and 28 days postinoculation.

Osteolytic lesions were detected at 2 weeks after i.c. by X-ray image analysis and microCT scans in control mice. Interestingly, ZA-treated mice showed a significant decrease in tumor burden and osteolytic lesions between day 14 and 28. TRAP5b levels in serum decreased significantly in ZA-treated mice as compared to control mice. Consistent with the antiresorptive effects of ZA, serum PINP showed a marked decrease in ZA-treated mice as compared to control mice. These data indicate that TRAP5b and PINP biomarkers correlate with tumor burden by bioluminescence imaging, osteolytic lesions by X-ray image analysis and osteolytic activity, assessed by the number of TRAP+ cells at tumor bone interphase.

These studies suggest the validity of these biomarkers to monitor the degree of osteolysis during ZA-treatment.

***Disclosures: Concepcion De La Piedra Gordo**, None.*

SU0135

Chemotherapy Induced Changes in WWOX and RUNX2 Expression as a Potential Prognostic Tool in Human Osteosarcoma. Kyle Kurek*[1], Sara Del Mare[2], Zaidoun Salah[2], Suhaib Abdeen[2], Hussain Sadiq[3], Suk-hee Lee[3], Kevin Jones[4], Barry DeYoung[5], Gail Amir[6], Mark Gebhardt[7], Matthew Warman[8], Gary Stein[9], Janet Stein[3], Jane Lian[9], Rami Aqeilan[10]. [1]Children's Hospital Boston Department of Pathology, USA, [2]The Lautenberg Center for Immunology & Cancer Research, Hebrew University-Hadassah Medical School, Israel, [3]Department of Cell Biology, University of Massachusetts Medical School, USA, [4]Department of Orthopaedics, University of Utah, USA, [5]Department of Pathology, University of Iowa Hospital & Clinics, USA, [6]Department of Pathology, IMRIC, Hebrew University-Hadassah Medical School, Israel, [7]Department of Orthopaedic Surgery, Children's Hospital Boston & Harvard Medical School, USA, [8]Department of Orthopeadic Surgery, Howard Hughes Medical Institute, Children's Hospital Boston & Harvard Medical School, USA, [9]University of Massachusetts Medical School, USA, [10]Ohio State University, USA

Osteosarcoma (OS) is an aggressive bone tumor with a poor prognosis that frequently metastasizes to the lungs. Aside from chemotherapy-induced tumor necrosis, predictors of overall response and metastatic potential are lacking. After demonstrating that mice deficient in the tumor suppressor *Wwox* develop OS, we sought to examine the status of WWOX and RUNX2, which is regulated by WWOX, in primary OS, and to follow their levels in post-chemotherapy resections and metastases. Expression was determined by immunohistochemistry in representative paraffin tissue sections, whereby WWOX was scored as strong/reduced/absent and RUNX2 as positive/negative, as compared to normal osteocyte controls. Eighty-three OS samples were identified from 51 patients, including 34 pre-chemotherapy biopsies, 34 post-chemotherapy resections, and 15 post-chemotherapy metastases. Overall, 59% (20/34) of primary tumor biopsies were reduced or absent for WWOX, and 60% (12/20) were positive for RUNX2; however, individual cases displayed a range of abnormal patterns of WWOX and RUNX2 expression. In 12 patients examined before and after chemotherapy, WWOX increased in 50%, while RUNX2 was absent in 92% of resections. Interestingly, most metastases had either unchanged (33%; 3/7) or reduced (45%; 4/7) WWOX levels as compared to matched pre-treatment biopsies. The majority (71%, 5/7) of metastases had persistent RUNX2 positivity. In conclusion, WWOX is lost or reduced in the majority of OS cases, and is accompanied by an aberrant relationship with RUNX2. That some tumors increased WWOX levels and lost RUNX2 expression following chemotherapy suggests a subset of patients may have an improved prognosis due to tumor cell normalization. Furthermore, lack of normalization may be predictive of metastatic development. Our findings suggest potential prognostic value in examining WWOX and RUNX2 in OS specimens.

***Disclosures: Kyle Kurek**, None.*

SU0136

c-Myc is a Downstream Target of CXCL13 to Stimulate RANK Ligand Expression in Bone Marrow Stromal/Preosteoblast Cells. Yuvaraj Sambandam*[1], James S. Norris[1], William Ries[1], Sakamuri Reddy[2]. [1]Medical University of South Carolina, USA, [2]Charles P. Darby Children's Research Institute, USA

Chemokine ligand-13 (CXCL13) has been implicated in oral squamous cell carcinoma (OSCC) tumor progression and osteolysis. We recently demonstrated that NFATc3 transcription factor plays a role in CXCL13 stimulated RANK ligand (RANKL) expression, a critical osteoclastogenic factor in OSCC cells. We hypothesized that CXCL13 production by OSCC cells stimulates RANKL expression in stromal/preosteoblast cells in the bone microenvironment. Interestingly, treatment of human bone marrow derived stromal cells (SAKA-T) and murine preosteoblast cells (MC3T3) with conditioned media (20%) obtained from SCC14a cells significantly increased RANKL expression while incubation with an antibody against CXCL13 specific receptor, CXCR5 markedly decreased RANKL expression in these cells. Western blot analysis demonstrated that recombinant hCXCL13 treatment (0-15 ng/ml) of SAKA-T and MC3T3 cells for a 6 h period increased (5-fold) RANKL expression. Real-time RT-PCR analysis identified a dose-dependent stimulation of CXCR5 mRNA expression in these cells. CXCL13 stimulation of SAKA-T and MC3T3 cells transiently transfected with hRANKL gene promoter-Luc reporter plasmid demonstrated a 3.5 and 3.0-fold increase in RANKL gene promoter activity, respectively. Further, CXCL13 stimulation significantly increased p-ERK1/2 levels in SAKA-T and MC3T3 cells. Transcription factor array screening by real-time RT-PCR identified high levels of c-Myc and NFATc3 mRNA expression in CXCL13 stimulated SAKA-T cells. Western blot analysis revealed that CXCL13 dose-dependently increased the levels of c-Myc and NFATc3 expression in these cells. We also showed that CXCL13 increased the phosphorylation of c-Myc in SAKA-T (10-fold) and MC3T3 (7-fold) cells. Furthermore, siRNA suppression of c-Myc expression markedly decreased CXCL13 stimulated RANKL and NFATc3 expression in bone marrow stromal cells. Chromatin-immuno precipitation (ChIP) assay confirmed c-Myc binding to the hRANKL promoter region (-1315 bp to -1435 bp). In summary, CXCL13 production by OSCC cells stimulates RANKL expression in bone

marrow stromal/preosteoblast cells and that c-Myc is a downstream target of the CXCL13/CXCR5 axis to stimulate RANKL expression. Thus, our results implicate CXCL13 as a potential therapeutic target to prevent OSCC bone invasion/osteolysis.

***Disclosures: Yuvaraj Sambandam**, None.*

SU0137

Controlled Delivery of 2-Methoxyestradiol in Osteosarcoma Cells. Avudaiappan Maran*[1], Mahrokh Dadsetan[2], Kristen Shogren[2], Michael Yaszemski[2]. [1]Mayo Clinic College of Medicine, USA, [2]Mayo Clinic, USA

Controlled-release devices consisting of biocompatible polymers have been shown to maximize the therapeutic effect and minimize the systemic toxicity of drugs. The anti-tumor compound, 2-methoxyestradiol (2-ME), kills osteosarcoma cells, but does not affect normal osteoblasts. In order to effectively target osteosarcoma and improve the bioavailability of the drug 2-ME, we have encapsulated 2-ME in a biodegradable oligo (polyethylene glycol) fumarate /poly (lactic-co-glycolic acid) (OPF/PLGA) polymeric composite and studied the effect of polymer-mediated 2-ME delivery. We have investigated the drug release and the osteosarcoma cell survival. The in vitro release profile of 2-ME from the OPF/PLGA composite was compared to the release of 2-ME encapsulated directly within the OPF polymer. We have shown that 2-ME can be released in a controlled manner over a 50-day time interval, and that the burst release of 2-ME at day 1 was reduced from 50% for release from the OPF alone to 22% for release from the microspheres embedded within the OPF. Cell cycle analysis using flow cytometry shows that OPF-released 2-ME induced a 2.6-fold increase in G1 phase and a 6-fold decrease in S phase cells in MG63 osteosarcoma cells, compared to the appropriate vehicle controls. 2-ME released from PLGA and OPF/PLGA composite increased the number of cells in G2 phase to 2.3-fold and 2-fold, respectively, compared to the vehicle controls. This suggests that burst release of 2-ME from OPF polymer causes G1 arrest, whereas slow release from the PLGA and OPF/PLGA composite causes G2 arrest in osteosarcoma cells. Also, comparison of the direct one-time administration of 2-ME to the OPF-mediated controlled delivery in cultured MG63 osteosarcoma cells shows that direct treatment has no effect after 6 days in culture, whereas controlled delivery produces an anti-tumor effect that is sustained. Thus, our findings show that 2-ME delivered via a controlled release system induces cell cycle arrest and cell death in osteosarcoma cells. The OPF/PLGA polymeric delivery system may prove to be useful in sustained delivery of 2-ME with reduced side effects and increased bioavailability, and could be further explored in the treatment of osteosarcoma and other cancers.

***Disclosures: Avudaiappan Maran**, None.*

SU0138

Decreased Bone Mineral Density in Patients With Invasive Cervical Cancer. Heung Yeol Kim*[1], Hoon Choi[2], Min Hyung Jung[3], Tak Kim[4], Byung Ick Lee[5], Hyoung Moo Park[6]. [1]Department of Obstetrics & Gynecology, School of Medicine, Kosin University, South korea, [2]Inje University Sanggyepaik Hospital, South korea, [3]School of Medicine, Kyung Hee University, Kyung Hee Medical Center, South korea, [4]Department of Obstetrics & Gynecology, School of Medicine, University Anam Hospital, Korea University, South korea, [5]Department of Obstetrics & Gynecology, School of Medicine, Inha University Hospital, Inha University, South korea, [6]Department of Obstetrics & Gynecology, School of Medicine, Chungang University Yongsan Hospital, Chungang University, South korea

Background: In women, osteoporosis is a common chronic disease that induces spinal compression and femoral neck fractures, resulting in life-threatening complications. It is very important to identify risk factors in order to prevent this disorder. Bone destruction is a well-recognized complication in a variety of neoplasms without bone metastasis. Therefore, in the present study, we investigated the spinal bone mineral density (BMD) in patients with cervical cancer without bone metastases.

Methods: We measured spinal bone mineral densities by dual-photon absorptiometry is 119 patients with invasive uterine cervical cancer and compared them with measurements from 135 control women.

Results: When adjusted for age and menopause duration, mean bone mineral density in patients with uterine cervical cancer was 13.9% lower (p=.0003) and age-matched percentiles were 9.2% lower (p=.0003) than in control women. The deficits in bone mineral density and age-matched percentiles were confined to the uterine cervical cancer patients in their fifties, ie, less than 5 years' menopause duration.

Conclusion: Our study results suggest that patients with invasive cervical cancer have a lower BMD, resulting in an increased risk of osteoporosis.

***Disclosures: Heung Yeol Kim**, None.*

SU0139

Development of a Clinically Relevant Murine Model with a Biomarker to Monitor the Longitudinal Effect of Radiation on Bone Remodeling. Gregory Fairchild*[1], Luke Arentsen[2], Louis Kidder[2], Manju Sharma[2], Kathleen Coghill[2], Seymour Levitt[2], Douglas Yee[2], Susanta Hui[1]. [1]University of Minnesota, USA, [2]Univ of Minnesota, USA

Purpose: To develop a clinically relevant murine radiation model and to study the longitudinal effects of radiation with a non-invasively measured 45Ca isotope marker to determine whether bone damage is a slow, chronic process or is an acute problem with decreasing severity over time.

Methods: Six groups (n=7 in each group) of skeletally mature BALB/c mice were used. Groups were differentiated by whether they were intact (I) or ovariectomized (X), the number of days between 45Ca IV and radiation (10 or 30) and whether or not they received radiation (R): I30, I30R, X10, X10R, X30 and X30R. All mice were radiolabelled with 15 microcuries 45Ca. Feces and urine were collected for 24 hours periods in metabolic cages at different time points. The hind limbs of the mice receiving radiation were exposed to 16 Gy of X-ray radiation (using a Phillip Orthovoltage) while all critical organs were shielded. Delivered dose was verified by microTLD. This exposure was the radiobiological equivalent of a clinical radiation treatment of 50 Gy, 2Gy/fraction. The X10R group was used to test the effectiveness of the 45Ca marker to detect bone loss at the pre-equilibrium or washout period. The disintegrations per minute (dpm) of 45Ca were measured using a liquid?scintillation counter (Beckman Coulter LS 6500).

Results: All mice tolerated the radiation dose well as exhibited by minimal weight loss, a rapid return to normal behaviors, and excreta with normal traits. High rate of 45Ca excretion was observed in the early days. In the group that was irradiated during the washout period, variances in 45Ca excretion were immediately discernible. 45Ca in feces and urine from the X10R mice increased by an average of 14% compared to their control (Figure 1). Quasi-steady states of 45Ca for all other groups were attained between days 25-28 post-IV. Radiation effect in the I30R and X30R groups was rapid with the rate of turnover decreasing after 20-30 days.

Conclusions: We developed a clinically relevant murine model with an effective, non-invasive isotope marker to monitor skeletal effects of radiation therapy over time. 45Ca isotope allows for the non-invasive evaluation of the temporal effect of radiation during its pre-equilibrium (or washout time period) and equilibrium state.

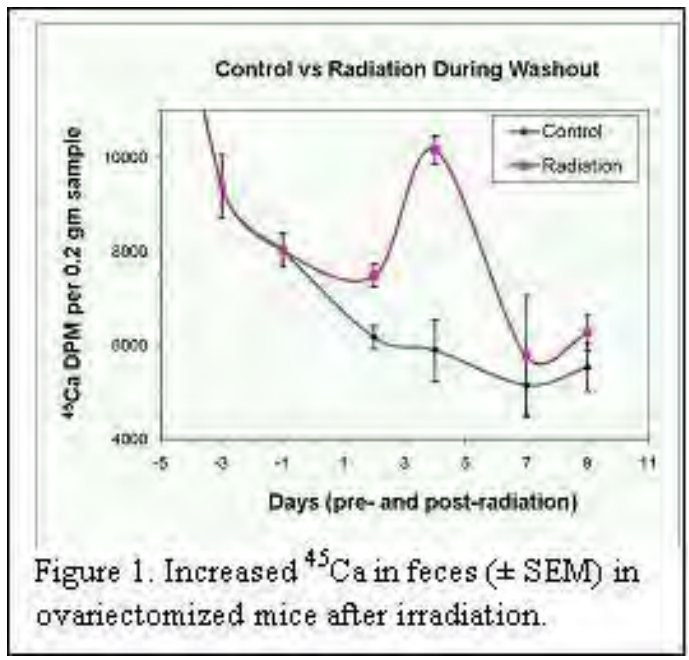

Figure 1. Increased ^{45}Ca in feces (± SEM) in ovariectomized mice after irradiation.

45Ca Excretion in Feces During Pre-Equilibrium

***Disclosures: Gregory Fairchild**, None.*

SU0140

Impact of Changes in Bone Resorption on Bone Mineral Density in Children after Hematopoietic Cell Transplantation. Matthew Deyo*[1], K. Scott Baker[2], Anna Petryk[1], Lynda Polgreen[1]. [1]University of Minnesota, USA, [2]Fred Hutchinson Cancer Research Center, USA

Purpose: We have previously reported a decrease in bone mineral density (BMD) associated with decreased bone formation over the first 12 months following hematopoietic cell transplantation (HCT) in pediatric patients. However, it was not clear if increased bone resorption also contributed to bone loss in children after HCT.

The objectives of this prospective pilot study were to assess bone resorption in children over the first 6 months after HCT, and to determine if bone resorption correlates with changes in BMD following HCT.

Methods: BMD was measured by dual-energy x-ray absorptiometry (DXA) at baseline and at day 180 after HCT. Urine deoxypyridinoline (DPD) and pyridinoline (PYD) corrected for urine creatinine, and plasma C-telopeptide (CTX) and N-telopeptode (NTX), were collected at baseline, day 30, 100 and 180 after HCT. Paired t-tests were used to evaluate change in BMD Z-scores (adjusted for age and gender). Bone markers were correlated (Pearson) with BMD Z-scores.

Results: Seven participants, 5 with leukemia and 2 with aplastic anemia, were included in analysis; mean age at HCT was 11.5 ± 3.7 years. By day 180, BMD Z-scores decreased for total body less head from 0.5 ± 0.8 to 0.2 ± 0.7 (N=7 p=.002), and for lumbar spine (L2-L4) from -0.6 ± 0.7 to -0.9 ± 0.8 (N=7 p=.005). A larger gain in total body BMD Z-score from day 0 to day 180 correlated with a greater increase in PYD from day 0 to 180 (r=.88 p=.047). Higher total body BMD Z-scores at day 180 correlated with a greater increase in bone resorption from day 30 to 180: PYD (r=.96 p=.008), DPD (r=.95 p=.01), and NTX (r=.97 p=.001). In contrast, decreased bone resorption over the first 30 days correlated with higher BMD Z-scores at day 180: PYD (r=-.82 p=.047), DPD (r=-.94 p=.005), and NTX (r=-.87 p=.02). Changes in CTX did not significantly correlate with BMD Z-scores.

Conclusions: Children treated with HCT for hematologic and oncologic diseases show decreasing BMD during the 6 months following HCT. Our pilot data suggest that an early attenuated decrease in bone resorption, without a subsequent rise in bone turnover contributes to bone deficits in children 6 months after HCT. It is likely that a decrease in bone resorption combined with the previously observed decrease in bone formation causes an adynamic bone state, with impaired bone remodeling, which results in BMD deficits in children after HCT. The long-term clinical implications of this early decrease in BMD and bone turnover have yet to be determined.

***Disclosures: Matthew Deyo**, None.*

SU0141

IP-10 Amplification Loop is an Important Therapeutic Target to Treat Bone Metastasis. Jong Ho Lee*, Hyunil Ha, Zang Hee Lee. Seoul National University School of Dentistry, South korea

IP-10 is a chemokine, which takes a significant role in migration and proliferation of T cells. It binds to the receptor CXCR3 and is induced in a wide variety of cell types. We have reported in our previous study that RANKL promotes the expression of IP-10 in osteoclast precursors and, in turn, IP-10 mediates RANKL expression in T cells in the synovium. Auto-amplification loop of IP-10 has been acknowledged to be involved in bone destruction of rheumatoid arthritis. However, the role of IP-10 in bone metastatic destruction remains largely unknown. We are currently conducting further research on the potential role of IP-10 in bone resorption and bone metastasis. In this study, the synergistic production of IP-10 was found in co-culture of bone marrow cells and cancer cells in the presence of RANKL. In addition, the serum level of IP-10 was increased in bone metastatic mice. The IP-10 deficient mice showed less metastatic lesions in long bone compared to wild mice. Furthermore, treatment with neutralizing antibody to IP-10 and antagonist for IP-10 and CXCR3 interaction significantly inhibited the infiltration of tumor cells into long bone and increased the mice survival rate. It is highly possible that IP-10 amplification loop might be one of the therapeutic targets in bone metastasis, and blockade of this loop may be an important therapeutic target in the prevention of bone destruction in bone metastasis.

***Disclosures: Jong Ho Lee**, None.*

SU0142

Osteoclastogenic and Metalloproteolytic Activities Configure Bone Metastatic Colonization. Diego Luis-Ravelo*[1], Iker Anton[2], Silvestre Vicent[1], Karmele Valencia[2], Susana Martinez[1], Carolina Zandueta[1], Fernando Lecanda[1]. [1]Center for Applied Medical Research, Spain, [2]Foundation for Applied Medical Research, Spain

Lung cancer comprises a large variety of histological subtypes with a frequent proclivity to form bone metastasis. The purpose of this study was to identify common mechanisms in the development of osteolytic lesions in lung cancer. Using a systematic strategy, we developed three different models with common proclivity to form osseous metastasis after intracardiac inoculation (i.c.) of athymic nude mice. Comparative analysis revealed different incidences and latency times indicating distinct patterns of bone metastatic colonization. These differences were highly associated with cell-type specific secretion of prosteoclastogenic factors, including MIP-1a, IL-8 and PTHrP some of which were exacerbated in conditions mimicking tumor-stroma interactions. Consistently, osteoclastogenic induction *in vitro* using the conditioned media derived from each cell model strongly associated with the time of latency of in vivo bone lesions. Interestingly, using a combination of fluorogenic peptides to assess MMP activities and specific qPCR in coculture with murine ST-2 cells, we found that the extent of tumor-induced MMP-3 and stromal-derived MMP-2 activities *in vitro* were closely associated with the degree of tumor burden and osteolytic metastasis *in vivo*. Therefore, osseous colonization was also associated with a distinct signature of metalloproteolytic (MMP) activities derived from tumor and reactive stroma upon cell-cell interactions. Likewise, each tumor model cell-autonomously contributed to a different pattern of cachexia development. Since TGF-β plays a critical role in bone microenvironment, we tested its implication in vivo. After i.c. of lung tumor cells, anti-TGF-β treatment severely reduced tumor burden (X-rays image analysis) and osteolytic activity of tumor cells (osteoclast number) compared to scrambled peptide and vehicle control treated animals in one model. In contrast, TGF-ß had a marginal effect in the other two models, indicating that the contribution of TGF-ß to the severity of bone lesions *in vivo* was only cell model-specific. Mechanisms of bone colonization and tumor-induced osteolysis are thus unique for each different lung histological subtype. These mechanisms share, although each to a different extent, dual MMP and osteoclastogenic activities differentially enhanced upon tumor-stromal interactions.

***Disclosures: Diego Luis-Ravelo**, None.*

SU0143

Purinergic Signaling between Osteocytes and Neurons: Potential Mechanism for Nociception. Mary Boggs*[1], Mary Farach-Carson[2], Thomas Beebe[1], Randall Duncan[1]. [1]University of Delaware, USA, [2]Rice University, USA

Bone pain is a devastating complication in patients with advanced cancer with bone metastases that significantly impacts the quality of life of the patient. Nociception in bone, particularly in bone cancer, is not well understood and treatment is relatively ineffective. Osteocytes are likely candidates for bone-to-neuron pain communication because these cells are found throughout bone and their location in bone provides many sites for osteocytes to associate with neurons. Because both mechanical loading in bone and nociception in the nervous system have been shown to utilize purinergic signaling, we postulate that bone pain is transduced through an osteocyte-neuron purinergic functional synapse. We further propose that metastatic cancer cells can potentially communicate with nociceptive neurons in a similar manner, but to a greater degree, since cancer cells injected into mice have been shown to release large quantities of ATP. To study communication between bone cells and neurons, we developed a unique patterned surface to co-culture MLO-Y4 osteocyte-like cells with dorsal root ganglia (DRG). This co-culturing system presents itself as an ideal method for culturing MLO-Y4 and DRG in close proximity to mimic the in vivo anatomy and to study bone-neuron communication. When subjected to mechanical loads, MLO-Y4 cells increase release ATP 6-fold after 10 min of stimulation and continually increase this release up to 12-fold over basal release after 15 min. The prostate cancer metastatic cell line C4-2B4 exhibited greater basal release of ATP and were significantly more sensitive to loading than MLO-Y4 cells. To determine if ATP induced action potentials in neurons, we used patch clamp techniques to current clamp freshly isolated DRG neurons from mice. We found that these neurons responded to ATP within seconds with a rapid depolarization of approximately 20 mV from resting membrane potentials, followed by multiple action potentials. These studies suggest that purinergic signaling may be central to communication between nociceptive neurons and osteocytes. Further, innervation near a bone metastatic tumor may elicit an even stronger pain response due to the increased ATP release from the tumor in response to the increased strains caused by loading the weaken bone.

***Disclosures: Mary Boggs**, None.*

SU0144

TGF-b and IL-1a in Jaw Tumor Fluids Participate in Bone Resorption Through the Stimulation of Osteoclastogenesis. Tomonao Aikawa*[1], Chiaki Yamada[1], Ikuko Tsujimoto[1], Katsuhiko Amano[1], Noriyuki Namba[2], Seiji Iida[3], Mikihiko Kogo[1]. [1]Osaka University Graduate School of Dentistry, Japan, [2]Osaka University Graduate School of Medicine, Japan, [3]Okayama University Graduate School of Medicine, Dentistry, & Pharmaceutical Science, Japan

Odontogenic tumor and odontogenic cyst, arising in jaw bone, grow with resorption and destruction of jaw bones. However, the mechanisms of bone resorption by odontogenic tumor and odontogenic cyst are still unclear. These odontogenic tumor and cyst consist of odontogenic epithelial cells and stroma fibroblasts. It has been demonstrated that odontogenic epithelial cells of developing tooth germ induce osteoclastogenesis to prevent tooth germ from invasion of developing bone. Thus we hypothesized that odontogenic epithelial cells in odontogenic tumor and cyst induce osteoclastogenesis, and then that would play potential roles in tumor outgrowth into jaw bones. Purpose of this study is to examine osteoclastogenesis by cytokines, focusing on TGF-b and IL-1a, produced by odontogenic epithelial cells.

Osteoclastogenesis of CD-14(+) human peripheral blood monocytes (PBMCs) and RAW cells were assessed by TRAP staining. Concentration of TGF-b, IL-1a in fluids of odontogenic tumor and cyst (ameloblastoma, keratocystic odontogenic tumor, and follicular cyst) was measured by ELISA, and expression of TGF-b and IL-1a, were examined by immunohistochemistry. Expression of RANKL, OPG, and COX-2 in stroma fibroblasts in culture was assessed by RT-PCR and/or western blotting, and PGE2 synthesis was measured by ELISA.

Fluids of jaw tumor and cyst increased expression of RANKL in stroma fibroblasts isolated from odontogenic tumor, but did not change expression of OPG. Induction of RANKL-expression was further enhanced by acidified fluids, and the fluids phosphorylated Smad-3 in stroma fibroblasts, suggesting the fluids contain TGF-b. TGF-b increased RANKL expression in stroma fibroblasts, and induction of

RANKL was completely disappeared by pretreatment of stroma fibroblasts with SB-505124, a selective inhibitor of TGF-b receptor kinase.

Fluids of tumor and cyst contained TGF-b and IL-1a, which were positive in epithelial cells of odontogenic tumor/cyst. Both TGF-b and IL-1a induced expression of COX-2, and synthesis of PGE2, and then RANKL expression in stroma fibroblasts. On the other hand, TGF-b and IL-1a induced osteoclastogenesis of RAW cells and CD-14(+) PBMCs in vitro.

These data suggest that Odontogenic jaw tumor/cyst produce TGF-b and IL-1a, and these cytokines induce osteoclastogenesis, via direct action to osteoclast precursor cells and via indirect action to increased RANKL expression of stroma fibroblasts.

***Disclosures: Tomonao Aikawa**, None.*

SU0145

Zoledronic Acid and Calcitriol in Malignancies with Bone Involvement. Genaro Miguel Palmieri*[1], L.S. Schwartzberg[1], T.D. Hodgkiss[1], M.S. Walker[2], A.M. Pallera[1], B.M. Wheeler[1], K.W. Tauer[1], R.E. Imseis[1], D. McCommon[1], T.B. Stewart[1]. [1]The West Clinic, USA, [2]ACORN Research, LLC, USA

Zoledronic acid (Z) and calcitriol (C) have in vitro anti-cancer effects. In patients (pts) with malignant bone involvement (BI), Z reduces skeletal related events (SREs) and C is controversial. Since Z and C have different, potentially additive mechanisms of action, we performed a 12 month (mo) pilot trial to investigate the effects of Z+C in 20 pts with BI: 9 breast and 7 prostate cancers and 4 multiple myeloma, none with a history of hypercalcemia (HCa), renal or liver insufficiency. Treatment (Rx): Z, 4mg IV every 4 wks; C, 1μg iv biweekly for 2 weeks followed by oral C 0.75 μg/d; and Ca, 1g/d po. All pts continued their ongoing chemo/hormonal Rx. Evaluation: Skeletal surveys (Ss) were performed by MRI in 19 pts or x-rays (XR) in 1pt and DXA bone densitometry (BMD) of femoral neck (FN), total hip (TH), lumbar spine (LS) and whole body (WB) were determined at baseline and at 3 mo intervals (Tri). Each Tri MRI/XR was compared with the previous Tri and labeled as non-responders (progression of old lesions or appearance of new lesions) or responders (stable lesions or signs of healing). Serum parathyroid hormone (PTH), bone alkaline phosphatase (BAP), urine N-telopeptide (NTX) were measured every 3 mo and, serum Na, K, Cl, Ca, Mg, creatinine (cr), albumin, and C and Ca/cr ratio in urine every 1-2 mo. Results: Combination of Z+C was well tolerated. No clinical SREs were noted. 13 pts completed their 1st Tri Ss and 10 completed the 2nd, 3rd and 4th Tri. 61% of pts were Ss responders and 39% were non-responders. BMD increased at all sites relative to baseline, which was normal: FN 4.44% (P=.031), TH 7.59% (P=.011), LS 12.87% (P=.004) and WB 2.78% (P=.019); with significant or near significant progressive increase during Rx (FN, P=.071; TH, P=.007, LS, P=.006; WB, P=.079. Urine NTX fell by 54.5% (P=0.001), BAP fell by 23.8% (P=.023). PTH fell by 15.3% (NS). Serum C was within normal range before and during Rx, but increased by 34.6% during Rx (P=.036). Analysis of covariance of Ss and C data during Rx showed responders had lower serum C than non-responders (P=.018). There were no significant changes in serum Ca, Na, Cl, Mg, albumin, cr and urine Ca/cr ratio. Conclusion: The addition of a relatively low dose of C to Z in the Rx of cancer pts with BI is well tolerated and could add additional benefits to Rx compared with Z alone.

***Disclosures: Genaro Miguel Palmieri**, None.*
This study received funding from: Novartis

SU0146

Development of a High-throughput Screening (HTS) Assay for the Identification of Small Molecule Modulators of Gsα. Nisan Bhattacharyya*[1], Catherine Chen[2], Wei Zheng[2], John K. Northup[3], Susanne Neumann[4], Michael T. Collins[5]. [1]NIDCR, NIH, USA, [2]CSA, NHGRI, NIH, USA, [3]NIDCD, NIH, USA, [4]CEB, NIDDK, NIH, USA, [5]CSDB, NIDCR, NIH, USA

Mis-sense mutations in the small subunit of the G-protein, Gs?, are directly correlated with the occurrence of fibrous dysplasia of bone/McCune-Albright syndrome (FD/MAS), a disease that is defined by skeletal abnormalities that can be associated with various forms of hyperfunctioning endocrinopathies. The biochemical outcome of these mutations (R201H or R201C) is increased cAMP levels due to the impaired GTPase negative feedback regulatory step that converts active GTP-bound adenylate cyclase to the inactive GDP-bound form. This ligand-independent increased cAMP level poses serious physiological problems. The aim of this study is to isolate small molecule modulators that will be useful in regulating cAMP levels mediated by the mutated Gsα. Specially engineered CHO cells were stably transfected with either wild-type or mutated versions of Gsα (R201 and R201H). Several stable cells from each set were tested for cAMP levels using a cAMP ELISA method. Selected cell-lines were then examined by western blotting to check for equivalent Gsα expression levels. One cell line from each set (WT9, C6 and H2), which had equivalent Gsα protein expression and robust cholera toxin-indifferent elevation in cAMP level, were then selected for further studies. C6 cells looked more fibroblastic compared to the WT9 cells, whereas the H2 cells had a mixed morphology. The cAMP levels from the C6 and H2 cells were also tested by a fluorescence resonance energy transfer (FRET)-based cAMP assay method. Different adenylyl cyclase and adrenergic receptor inhibitors were used with these two lines to check for the dose- and time-dependent inhibition of cAMP levels. Results indicated that 10μM 2',5'-Dideoxyadenosine (ddA) could suppress 90% of total cAMP levels as early as 15 minutes after treatment. SQ 22536, another specific adenylyl cyclase inhibitor, also had similar but slightly less inhibitory effects on the cAMP levels. These cell lines have characteristics necessary for HTS of molecular libraries to identify molecules with specific activity at Gsα. A LOPAC small molecule library (Sigma-Aldrich) consisting of 1,280 small molecules was tested on the C6 cells using the high-throughput screening method. This screen identified 2 molecules (0.16% hit rate) with specific activity on C6 cells. Compounds identified in HTS will be further tested in different cell culture and animal models, and eventually may be useful in treating FD and other human diseases that are caused by mutations in the Gsα protein.

***Disclosures: Nisan Bhattacharyya**, None.*

SU0147

Efficacy of Cinacalcet Therapy in Patients Affected by Primary Hyperparathyroidism Associated to Multiple Endocrine Neoplasia Syndrome Type 1 (MEN1). Preliminary Results of the Florentine Study. Francesca Giusti*[1], Alberto Falchetti[2], Laura Masi[2], Debora Strigoli[1], Gigliola Leoncini[1], Francesco Franceschelli[1], Maria Luisa Brandi[2]. [1]Department of Internal Medicine, University of Florence, Italy, [2]University of Florence, Italy

Primary hyperparathyroidism (PHPT) is the main endocrinopathy associated with MEN1, more than 90% of individuals, with a complete penetrance within 50 years of age. Generally, its age of onset is 3 decades earlier than nonsyndromic PHPT. MEN1-PHPT is generally supported by multiglandular disease, clinically manifesting with hypercalcemia, even if it may remain asymptomatic for a long time or occur with a precocious reduction in bone mass. Neck surgery still represents the elective care of MEN1-PHPT. Recently, cinacalcet, successfully used in secondary hyperparathyroidism and nonsyndromic PHPT, may represent a medication also for MEN1-PHPT. To date, an extensive clinical experience on a prolonged use of cinacalcet in hereditary forms of PHPT does not exist. Our study aims to evaluate whether cinacalcet can be considered an effective therapy in MEN1-PHPT by analyzing: A) tolerability profile; B) reduction/normalization of PTH and serum calcium levels; and C) stabilization of the mass of affected parathyroids. Currently, we have enrolled 7 patients with MEN1-PHPT [2 M and 5 F, mean age 46.1 years, range 39-63; 5 familial cases (71%) from 4 MEN1 families and 2 simplex cases (29%)]. PHPT was the first clinical manifestation in 6/7 patients (85%) (2 M and 4 F, mean age 37.5 years, range 23-60). At baseline, all patients showed elevated PTH (mean 16.7 pmol/L, range 8.1-26, reference values 1.3-7.6 pmol/L) and total serum calcium levels (mean 9.9 mg/dl, range 9.0-10.0, reference values 8.2-10.2 mg/dl). Specifically, 4 patients (57%) started cinacalcet in alternative to surgery and 3 patients (43%) opted for the drug due to persistence of MEN1-PHPT after surgery. Currently, 3 patients (42%) have completed 3 months of cinacalcet therapy, 2 patients (28%) 6 months, 1 patient (15%) 9 months, and 1 patient (15%) 18 months. Apart from mild transient gastrointestinal effects, to date none of the patients has shown side effects that discontinue treatment. In 4 patients (57%) at 6 months of cinacalcet we found a 28% decrease of PTH values (mean 12.2 pmol/L, range 6.5-13.1), although not falling down to the reference range, and normalization of serum calcium values with a reduction of 26% (average 9.0 pmol/L, range 9.0-10.0). Preliminary data obtained from clinical monitoring of these patients confirm that treatment with cinacalcet is well tolerated and already at 6 months of therapy calcium homeostasis is stabilized together with a reduction of PTH secretion also in MEN1-PHPT. We are currently still build up the case series through the clinical biochemistry screening of 4 new MEN1 patients.

***Disclosures: Francesca Giusti**, None.*

SU0148

Evaluation of Serum FGF23 in Juvenile Onset Systemic Lupus Erythematosus (JSLE): A Possible Link with Renal Involvement. Laura Masi*, Francesco Franceschelli, Gigliola Leoncini, Loredana Cavalli, Antonietta Amedei, Alberto Falchetti, Maria Luisa Brandi. Metabolic Bone Diseases Unit, Italy

Phosphatonins are hormones involved in the regulation of phosphate homeostasis. FGF23 acts through FGF receptor 1 present in target tissues including kidney, vessels and heart. FGF23 levels are elevated in subjects with chronic kidney disease and an association between serum FGF23 levels and increased mortality independently of established risk factors has been demonstrated in these patients. Previous reports have shown that JSLE is associated with an increased risk of atherosclerosis. Renal disease represents the main risk of poor outcome in JSLE. We have evaluated the serum level of intact FGF23 in JSLE patients and we have correlated FGF23 values to lipid profile (total cholesterol, LDL, HDL, tryglicerides), renal function (serum creatinine, creatinine clearance, proteinuria, microalbuminuria), renal biopsy results in pts with renal damage, and cardiac data. A group of 53 consecutive pts (46 F, 7 M, mean age 13.3? 5.6) fulfilling the ACR criteria for SLE, with disease onset before 18 yrs, entered randomly in the study. 12/53 had signs of renal disease at onset and 13 at different time from disease onset. All pts with glomerulonephritis underwent renal biopsy within the first 6 months from onset: 4 WHO IIA, 6 IIB, 10 III, 5 IV. 35 sex and age matched acted as controls. The serum intact FGF23 concentration was measured with an ELISA assay (Immunotopics, USA). FGF23 serum levels resulted significantly higher in SLE pts than in controls (t-student: 67.1 ± 40SD vs 5 ± 3.2SD pg/ml). By Mann-Whitney U Test we showed that pts with renal disease had serum FGF23 values significantly higher than those without (45.3 ± 20 vs 13,77 ± 9.2 SD pg/ml;

p=0.0001). By Ancova analysis we observed that pts with severe renal disease (WHO III-IV) had higher levels when compared to WHO IIA-IIB (52,5±21 and 58,5±15 pg/ml respectively vs 13.7±9 and 35±10 pg/ml p=0.004). No significant correlation was found among serum FGF23 levels, lipid profile and cardiac function. However a trend characterized by an inverse correlation between FGF23 and HDL was found by Pearson's correlation test (r-0.07; p=n.s.) In conclusion, serum FGF23 is higher in pts with JSLE and appears to be correlate with renal damage. It may be a helpful biomarker for assessing the risk of renal damage and may be especially useful in patients with early kidney disease in whom FGF23 levels increase first. Data in a larger cohort of pts are needed to better define the role of FGF23 in renal disease in JSLE pts.

***Disclosures: Laura Masi**, None.*

SU0149

Genomewide Association Study Using Extreme Truncate Selection Identifies Novel Genes Controlling Bone Mineral Density. Emma Duncan*[1], Patrick Danoy[1], John Kemp[2], Paul Leo[1], Brent Richards[3], Tim Spector[4], Fernando Rivadeneira[5], Andre Uitterlinden[6], John Wark[7], Elaine Dennison[8], Graeme Jones[9], Richard Prince[10], John Eisman[11], Philip Sambrook[12], Geoffrey Nicholson[13], Richard Eastell[14], Eugene McCloskey[14], David Evans[2], Matthew Brown[15]. [1]University of Queensland, Australia, [2]University of Bristol, United Kingdom, [3]McGill University, Canada, [4]King's College London, United Kingdom, [5]Erasmus University Medical Center, The netherlands, [6]Rm Ee 575, Genetic Laboratory, The netherlands, [7]Royal Melbourne Hospital, Australia, [8]MRC Epidemiology Resource Centre, United Kingdom, [9]Menzies Centre for Population Health Research, Australia, [10]Sir Charles Gardner Hospital, Australia, [11]Garvan Institute of Medical Research, Australia, [12]Royal North Shore Hospital, Australia, [13]University of Melbourne, Australia, [14]University of Sheffield, United Kingdom, [15]Diamantina Institute of Cancer, Immunology & Metabolic Medicine, Australia

BMD is strongly correlated with fracture risk, and is highly heritable. This study aimed to identify genes associated with BMD, using a unique design of extreme truncate selection in a cohort ascertained for BMD at one skeletal site (total hip (TH)), and one gender and age/menopausal status group (postmenopausal women age 55-85 years).

A GWAS was performed in a cohort of 2073 women of white western European descent, with either high (z=+1.5 to +4, n=1129) or low (z=-1.5 to -4, n=944) TH BMD, using Illumina Infinium genotyping chips. Following imputation, 2,543,109 SNPs were tested for association with TH BMD. Minimal evidence of inflation of test statistics was observed, with a genomic inflation factor (λ) of 1.04. 127 SNPs were studied in replication cohorts including 10000 women from Australia, England and Europe (AOGC-replication), and in-silico from the TwinsUK and Rotterdam GWAS.

Three novel loci associated with BMD were identified in the discovery at $P<10^{-4}$ and confirmed ($P<0.05$) in the AOGC-replication set and the TwinsUK/Rotterdam cohorts, and mapped to strong candidates: GALNT3, LTBP3, CLCN7. Mutations of GALNT3 cause familial tumoral calcinosis and hyperostosis-hyperphosphataemia syndrome through effects on FGF23 glycosylation. Mutations of LTBP3 cause dental agenesis and high BMD, thought through effects on TGFB1 bioavailability. Mutations of CLCN7 cause osteopetrosis due to effects on osteoclastic bone resorption.

Our dataset also replicated at $P<0.05$ previously associated SNPs in 21 of 26 BMD genes reported from previous GWAS (ARHGAP1, CTNNB1, ESR1, FAM3C, FLJ42280, FOXL1, GPR177, HDAC5, JAG1, LRP5, MARK3, MEF2C, MEPE, OPG, RANK, RANKL, STARD3NL, SOST, SOX6, SP7 (Osterix) and ZBTB40). Fracture association was observed ($P<0.05$) with SNPs at GALNT3, CLCN7, FLJ42280 and GPR177 loci. Our study also strongly confirms the previously reported suggestive association of TGFBR3 with BMD ($P=6.7x10^{-5}$), indicating that this is a true BMD-associated gene.

The extreme-truncate ascertainment scheme used in this study resulted in markedly increased study power, with similar statistical power to studies of ~16,000 unselected cases; and gains further power relative to previous screens through its site, gender and age focus.

In summary, we report identification of three novel, and confirmation of 21 of 26 previously reported, BMD-associated genes. This study design is efficient and effective for gene discovery in quantitative traits such as BMD.

***Disclosures: Emma Duncan**, None.*

SU0150

Hindlimb Skeletal Muscle Function and the Impact of Weight-bearing Exercise on Bone Biomechanical Integrity in the Osteogenesis Imperfecta Model (*oim*) Mouse. Stephanie Carleton, Charlotte Phillips*, Bettina Gentry, J. Andries Ferreira, Marybeth Brown. University of Missouri-Columbia, USA

Osteogenesis imperfecta (OI), a heritable connective tissue disorder commonly due to type I procollagen gene defects, is characterized by bone deformity and fragility. Though it is well established that physical activity improves exercise tolerance and strengthens bone biomechanical integrity there is paucity in exercise studies and related functional outcomes in OI patients, who report exercise intolerance, muscle fatigue and weakness. Using the *oim* mouse model, which harbors a functional null col1a2 gene defect, we examined skeletal muscles for inherent pathology and investigated if a weight-bearing exercise (treadmill) regimen would impact skeletal muscle and improve bone biomechanical integrity. Homozygous *oim* mice (*oim*/*oim*) model moderately severe OI type III with reduced bone mineral density and strength. Heterozygous mice (+/*oim*) model mild OI type I and have an intermediate phenotype between oim/oim and wildtype (Wt) mice. In the following study, Wt, +/*oim* and *oim*/*oim* mice participated in an 8 week treadmill exercise regimen, beginning at 7 weeks of age. Mice were weighed daily prior to exercising for 30 min/day, 5 days/week at 10 m/min. At 4 months of age, hindlimb muscles and femurs of non-exercised (control) and treadmill mice were analyzed.

Skeletal muscles from control *oim*/*oim* mice were unable to maintain or reach the same level of muscle contraction as Wt mice at either 7 weeks or 4 months of age, indicating *oim*/*oim* mice have inherent muscle weakness. *Oim*/*oim* mice poorly tolerated the treadmill exercise, with 7/11 mice experiencing hindlimb fractures, necessitating their removal from the protocol. However, both male and female +/*oim* mice were able to complete treadmill exercise and their muscles had similar responses to exercise as Wt mice (Table 1). To examine whole bone biomechanical and material properties control and exercise femora were evaluated by μCT (geometry) and torsional loading to failure. Female Wt and +/*oim* femurs demonstrated positive responses to treadmill exercise, with gains in whole bone and material strength. The response of male Wt and +/*oim* femurs was less clear. Taken together, these data suggest that muscle weakness reported by OI patients may reflect inherent skeletal muscle pathology and/or inactivity. Additionally, +/*oim* mice with mild osteogenesis imperfecta can tolerate weight-bearing exercise and female +/*oim* bones appear to respond positively to weight-bearing exercise.

Table 1. Response of Wildtype (Wt) and Heterozygote (+/*oim*) Gastrocnemius Muscle (P_o) and Femoral Geometric and Biomechanical Parameters to 8 Week Treadmill Regimen Relative to Non-exercise Controls

	Females				Males			
	Wt		+/*oim*		Wt		+/*oim*	
	Controls (n=10-14)	Exercise (n=10-13)	Controls (n=11-13)	Exercise (n=3-8)	Controls (n=12-22)	Exercise (n=9-11)	Controls (n=12-17)	Exercise (n=12-14)
Weight (g)	22.12±0.39	22.01±0.26	23.38±0.53	21.24±0.68[a]	29.53±0.55[b]	29.55±0.75[b]	28.94±0.92[b]	27.50±0.41[ab,c]
P_o/CSA[1]	0.062±0.007	0.054±0.007	0.051±0.006	0.055±0.007	0.062±0.006	0.053±0.007	0.066±0.006	0.060±0.007
J (mm⁴)[2]	0.56±0.02	0.58±0.02	0.49±0.01	0.76±0.04[c]	0.79±0.04[b]	0.86±0.06[b]	0.76±0.04[b]	0.75±0.04[b]
U (Nmm)[3]	3.76±0.44	5.04±0.44	2.89±0.47	4.74±1.08	6.15±0.56[b]	5.69±0.41	5.55±0.78[b]	4.18±0.46[c]

Mean±standard error (n)
[1]Contractile generating capacity of the gastrocnemius muscle normalized to the muscle fiber cross sectional area
[2]Polar moment of area (K; mm⁴) is a relative measure of the amount of bone as determined by μCT analysis
[3]Energy to failure (U; Nmm) describes the amount of energy the femur can absorb prior to fracture; the area under the stress-strain curve
[a]p<0.05 compared to control (same genotype and gender)
[b]p<0.05 compared to female (same genotype and treatment)
[c]p<0.05 compared to Wt (same gender and treatment)

Table

***Disclosures: Charlotte Phillips**, None.*

SU0151

Impact Of Chronic Alcohol Consumption On The Osteocytes And Bone Marrow Adipocytes In A Wistar Rat Model. Delphine Maurel*[1], Stéphane Pallu[2], Priscilla C Aveline[2], Nathalie Boisseau[3], Gael Rochefort[2], Eric Dolleans[2], Christelle Jaffre[2], Claude Laurent Benhamou[4]. [1]Inserm Unit 658Hopital Porte MadeleineOrléansFrance, France, [2]Inserm Unit U658, France, [3]LAPHAP Laboratory, France, [4]INSERM Orléans-France, France

Recently, osteocytes have been more studied and it has been shown that they have a mechanosensory function, detecting fluid flow pressure and modifying bone remodeling in function of the mechanical strain. Chronic alcohol consumption is known to have a detrimental effect on bone mass through changes in bone cell activity. However little is known about the mechanism of action of ethanol on osteocytes. This study was designed to assess the effects of chronic alcohol consumption on osteocytes in rats.

Twenty-four 2-month old male Wistar rats were divided in 2 groups: Control(C) and Alcohol(A). Alcohol (35% v/v =14 mL/kg) was mixed to water and separated from the food. The rats were alcoholised for 17 weeks and sacrificed. Tibias were dissected and fixed in formalin 4% (v/v) before being cut in thin slices, demineralized and stained. The osteocyte morphology was assessed by transmission electron

microscopy and osteocyte apoptosis by epifluorescence microscopy after immunolabeling of the bone slices by caspase-3 Rabbit mAb (Cell Signaling Technology, USA). Bone marrow adiposity was assessed by photonic microscopy on bone slices stained by toluidine blue.

Chronic ethanol consumption increased significantly the cells stained with caspase-3 (5.85±2.32 vs 0.57±0.67 cells for 30000µm2 in A vs C; p<0.0001). Osteocytes of the alcoholized rats presented intracellular fat deposits. There was also significantly more empty osteocyte lacunae in the alcoholized rats (20.76±6.86 vs 15.56±9.44 empty lacunae for 60000µm2 for A and C; p=0.03) while the areas of the lacunae were higher in this alcohol group (29.29±6.67 vs 21.31±6.15 µm2 for A and C; p<0.0001). Regarding the marrow adiposity, we found more adipocytes in the A group (73.1±35.3 vs 16.2±21.0 adipocytes per 100000µm2 for A and C; p<0.0001) and the adipocytes had a larger area in the A group compared to the Control group (414.15±167.37 vs 188.93±149.16 µm2 for A and C; p=0,0005). The percentage of bone marrow represented by adipocytes was 7 fold higher in the A group compared to the control group (29.00±13.77 vs 4.35±5.91 vs % for A and C; p<0.0001).

In conclusion, chronic alcohol consumption damages osteocytes with an increase of their apoptosis (in parallel to the known anti osteoblastic effect) and may further worsen bone status via bone marrow increased adipogenesis.

***Disclosures: Delphine Maurel**, None.*

SU0152

Mechanism of Inflammation in Cherubism. Yasuyoshi Ueki*[1], Tomoyuki Mukai[2], Teruhito Yoshitaka[3]. [1]University of Missouri-Kansas CitySchool of Dentistry, USA, [2]University of Missouri - Kansas City, USA, [3]University Missouri-Kansas CitySchool of Dentistry, USA

Cherubism is an autosomal dominant craniofacial disorder that occurs in children at 4-6 years of age. It is characterized by a severe fibrous/inflammatory lesion in the jaw leading to extensive bone resorption and disruption of bone architecture and is accompanied by severe facial swelling. We have reported that mutations in the signaling adaptor protein, SH3BP2, are responsible for this disease. Using a homozygous knock-in mouse model that mimics human disease, we have previously shown that macrophages carrying the SH3BP2 mutation are hypersensitive to macrophage colony stimulating factor (M-CSF) and receptor activator of nuclear factor kappa B ligand (RANKL), leading the mice to develop TNF-alpha dependent systemic macrophage inflammation and bone loss. However, it remains unclear why the bone disease in Cherubism is primarily restricted to the orofacial skeleton, with much lesser effects on the rest of the skeleton.

We hypothesized that restriction of Cherubism to the orofacial skeleton occurs because of the high bacterial load in the oral cavity and associated host response to damage-associated molecular patterns (DAMPs) and/or pathogen-associated molecular patterns (PAMPs). To test this hypothesis, homozygous Cherubism mice lacking MyD88, an adaptor protein that functions downstream of toll-like receptors (TLRs) and interleukin-1 receptor (IL-1R) in mediating host responses to DAMPs and PAMPs, were generated. MyD88 deficiency in homozygous cherubism mice greatly reduced the swollen appearance of the face and microCT analysis showed an improvement of the bone destruction. Histological analysis showed reduced amounts of inflammatory infiltrates in liver, lung and lymph nodes and a marked improvement in the inflammatory bone erosion and joint destruction in these mice. Taken together, these data suggest an important role for MyD88-mediated signaling in the development of inflammation in Cherubism and suggest that DAMPs or PAMPs may act as potential triggers in the disease pathogenesis. These findings have implications not only for Cherubism, but for other inflammatory diseases of the skeleton.

***Disclosures: Yasuyoshi Ueki**, None.*

SU0153

Rare Activating Mutation (S33C) of CTNNB1 in Parathyroid Adenoma. Vito Guarnieri*[1], Filomena Baorda[2], Claudia Battista[3], Michele Bisceglia[4], Michelangelo Fiorentino[5], Sabrina Corbetta[6], Anna Spada[7], Geoffrey Hendy[8], David E. C. Cole[9], Massimo Carella[2], Alfredo Scillitani[10]. [1]Medical Genetics Service, IRCCS Casa Sollievo della Sofferenza Hospital, Italy, [2]Medical Genetics Service, IRCCS "Casa Sollievo della Sofferenza" Hospital, Italy, [3]Unit of Endocrinology, IRCCS "Casa Sollievo della Sofferenza" Hospital, Italy, [4]Unit of Pathology, IRCCS "Casa Sollievo della Sofferenza" Hospital, Italy, [5]Laboratorio di Patologia Molecolare Oncologica e dei Trapianti, Istituto Oncologico "F.Addarii", Policlinico S.Orsola-Malpighi, Italy, [6]Endocrinology & Diabetology Unit, University of Milan, IRCCS Policlinico S.Donato, Italy, [7]Endocrinology & Diabetology Unit, University of Milan, IRCCS Policlinico S.Donato, S.Donato M.se & IRCCS Fondazione Ospedale Maggiore Policlinico, Mangiagalli & Regina Elena, Italy, [8]McGill University, Royal Victoria Hospital, Canada, [9]Banting Institute, University of Toronto, Canada, [10]Casa Sollievo Della Sofferenza Scientific Institute, Italy

Altered Wnt/beta-catenin signaling occurs in many tumor types. Activating mutation (S37A) of CTNNB1 that encodes beta-catenin has been found in a small subset of parathyroid adenomas in a Swedish study. However, screening of additional cohorts in Japanese, North-American and Italian studies has failed to confirm this result. We initially screened 70 adenoma samples from primary hyperparathyroid patients of southern and northern Italian origin. Exon 3 of CTNNB1 was amplified and directly sequenced. In a single case, a somatic heterozygous mutation of serine 33 (S33C) was identified. To confirm this finding, we sequenced the DNA from individual colonies of the cloned PCR product. The S33C mutation has been identified previously in ovarian and endometrial cancer. Recently, in brain tumours, it has been demonstrated to affect in vitro the Cyclin D1 transcriptional activity. Immunostaining for b-catenin and Cyclin D1 proteins did not reveal any difference between mutated tissue vs not-mutated/control ones. While the results of our preliminary study confirm that CTNNB1 activating mutations are rare in parathyroid adenoma, further analyses are ongoing to establish the mutation frequency in Italian population.

***Disclosures: Vito Guarnieri**, None.*

SU0154

A Model of Osteopetrosis Using shRNA Knock-down of Tcirg1 in Osteoclasts from Human CD34+ Cells. Ilana Moscatelli*[1], Christian Thudium[2], Carmen Flores[1], Kim Henriksen[3], Johan Richter[1]. [1]Lund University, Sweden, [2]Nordic Bioscience, Denmark, [3]Nordic Bioscience A/S, Denmark

Gene/protein function studies in human osteoclasts have been hampered as these terminally differentiated cells are hard to manipulate genetically. The aim of this study was to derive functional osteoclasts from CD34+ human cord blood cells and investigate whether lentiviral vectors can be used to overexpress and/or knock down genes in these cells.

First, human cord blood CD34+ cells were cultured with M-CSF, GM-CSF, IL-6, SCF and Flt3L. After 2 weeks the CD34+ cells expanded approximately 500 fold, and FACS analysis revealed gradual loss of CD34 expression while 50% of cells became CD14+. Non-adherent cells were then incubated with M-CSF and RANKL on bone for 10 days. Osteoclasts derived from these cells expressed TRAP and released calcium into the media. They exhibited the actin-ring characteristic of osteoclasts and generated resorption pits on bone slices. The cells treated with the V-ATPase inhibitor diphyllin developed into osteoclasts, but resorption was severely impaired.

Next, CD34+ cells were transduced on day 0 using a SIN lentiviral vector expressing GFP under a SFFV promotor at MOI of 5 resulting in GFP expression in 20-25% of the cells at day 2. Expression was retained throughout differentiation to functional osteoclasts. At this stage the frequency of GFP-marked cells was increased but GFP intensity of individual osteoclasts was lower, due to the fusion of GFP+ and GFP- monocytic cells to form mature osteoclasts.

Finally, a human model of infantile malignant ostepetrosis (IMO) was generated by transducing cord blood CD34+ cells using lentiviral vectors with the puromycin resistance gene and shRNAs targeting TCIRG1. After transduction and selection with puromycin (1 µg/ml puromycin for 48 h) approximately 20% of cells survived and were differentiated to mature osteoclasts. qPCR analysis revealed decreased levels of Tcirg1 mRNA and western blot revealed decreased protein levels compared to controls. When compared to scramble the osteoclasts had a 40% increase in TRAP expression whereas calcium release, pit formation on bone slices and CTX-1 levels in the medium were all lower, in line with the known phenotype of IMO.

In conclusion osteoclast differentiation from lentivirally transduced CD34+ cells poses a way to generate and manipulate osteoclasts in vitro, providing a novel tool to study osteoclast development and function. Furthermore the knock-down of TCIRG1 in CD34+ cord blood cells provides a human model of IMO.

***Disclosures: Ilana Moscatelli**, None.*

SU0155

Abnormal Tooth Development in a Mouse Model for Craniometaphyseal Dysplasia. Eliane Dutra*, I-Ping Chen, Ernst Reichenberger. University of Connecticut Health Center, USA

Mice carrying a knock-in mutation (Phe377del) in the Ank gene develop skeletal and dental phenotypes seen in human craniometaphyseal dysplasia (CMD). A known function of the transmembrane protein ANK is to transport intracellular pyrophosphate (PPi) into the extracellular environment. Characterization of the tooth phenotype in homozygous Ank knock-in (AnkKI/KI) mice revealed abnormal cervical loop positioning of the lower incisors and excessive cementum deposition in molars. Cementum formation in molars appears to be especially sensitive to altered Pi/PPi equilibrium, which may be the reason for excessive cementum formation in AnkKI/KI mice. Incisors erupt, but the cervical loops, which sustain the continuous incisor growth fail to progress backwards with age from a position close to the 2nd molar in 1-week-old mice to a position close to the mandibular foramen of the ramus in adult mice. Mechanisms that control the repositioning of the cervical loop in rodent incisors are poorly understood. The AnkKI/KI mouse is therefore a good model to study the prerequisites for apical movement of mouse incisors.

Here, we describe the effects of this Ank KI mutation in tooth development. Micro-CT, radiographic, and histological evaluations show that mandibular incisors of AnkKI/KI mice have a 33% decreased volume, are 20% shorter when compared to Ank+/+ incisors and have abnormal positioning of the cervical loop, which remains at the level of the 3rd molar. Dynamic histomorphometry and axial growth measurement revealed slower dentin deposition in the incisor of AnkKI/KI mice as well as a reduced eruption rate, suggesting decreased cell proliferation or differentiation. In addition, we observed less and smaller TRAP-positive cells at the apical end, which indicates reduced bone resorption in the mandibles of AnkKI/KI mice. The cervical loop of the lower incisor in heterozygous adult Ank+/KI mice is positioned in an intermediate position between the cervical loop location of Ank+/+ and AnkKI/KI mice suggesting a dose-dependent effect. We believe that two possible mechanisms may contribute to the abnormal cervical loop position observed in AnkKI/KI mice: reduced apical bone resorption and impaired function of stem cells in the cervical loop.

***Disclosures: Eliane Dutra**, None.*

SU0156

Elevated Activation of BMP Signaling by ACVR1 Variant Mutations Occurring in Patients with Atypical FOP. Meiqi Xu*[1], Frederick Kaplan[2], Eileen Shore[1]. [1]University of Pennsylvania, USA, [2]University of Pennsylvania Hospital, USA

Fibrodysplasia ossificans progressiva (FOP) is a human disorder of bone formation that causes developmental skeletal defects and extensive debilitating bone formation within soft connective tissues (heterotopic ossification) during childhood. All patients with classic clinical features of FOP (great toe malformations and progressive heterotopic ossification) have previously been found to carry the same heterozygous mutation (c.617G>A; R206H) in the GS activation domain of activin A type I receptor/activin-like kinase 2 (ACVR1/ALK2), a bone morphogenetic protein (BMP) type I receptor. Among patients with FOP-like heterotopic ossification and/or toe malformations, we have also identified patients with clinical features unusual for FOP. Patients described as FOP variants have major variations in one or both of the two classic defining features of FOP, and instead of the recurrent R206H mutation that is found in all cases of classic FOP, all FOP variant patients that we have examined have novel heterozygous *ACVR1* missense mutations in either the GS or protein kinase domains. Protein structure homology modeling predicts that each of these amino acid substitutions activates the ACVR1 protein to enhance receptor signaling. In order to test these models, we generated a series of V5-tagged mutant *ACVR1* constructs (n=6) for use in *in vitro* BMP signaling activity assays. Expression of each construct in COS-7 cells were confirmed by western blot using an anti-V5 antibody. Using assays to detect BMP pathway activation through phosphorylation of Smad1/5/8, all FOP variant mutations show higher levels of activation in the absence of added BMP ligand in comparison to a wild-type *ACVR1* control construct, but also increase signaling in response to ligand, similar to the R206H mutation. Further, these levels of enhanced basal BMP signaling are lower than levels induced by a constitutively active ACVR1 mutation (Q207D). Luciferase activity assays from a reporter construct with the ID1 promoter containing the Smad binding site also showed increased activation of BMP signaling from the ACVR1 variant mutations. In conclusion, our data show that FOP variant mutations activate BMP signaling similarly as the classic FOP R206H ACVR1 mutation suggesting that mild hyperactivation of BMP signaling leads to induction of heterotopic ossification in FOP.

***Disclosures: Meiqi Xu**, None.*

SU0157

FKBP10 mutations cause both Osteogenesis Imperfecta and Bruck syndrome. Brian Kelley*[1], Fransiska Malfait[2], Luisa Bonafe[3], Dustin Baldridge[1], Sofie Symoens[2], Nursel Elcioglu[4], Christine Verellen[5], Yves Gillerot[6], Deborah Krakow[7], Dobrawa Napierala[1], Peter Beighton[8], Andrea Superti-Furga[9], Anne De Paepe[2], Lionel Van Malderghem[2], Brendan Lee[1]. [1]Baylor College of Medicine, USA, [2]Ghent University, Belgium, [3]Centre Hospitalier Universitaire Vaudois, Switzerland, [4]Marmara University Medical Faculty, Turkey, [5]University of Louvain Medical School, Belgium, [6]Cliniques universitaires St Luc, Belgium, [7]Cedars-Sinai Hospital, UCLA, USA, [8]University of Capetown, South africa, [9]University of Freiburg, Germany

Osteogenesis imperfecta (OI) is a heritable disorder of connective tissue characterized by bone fragility and alteration in synthesis and post-translational modification of collagen type I. Autosomal dominant OI is caused by mutations in the genes (COL1A1 or COL1A2) encoding the chains of type I collagen. Bruck syndrome is a recessive disorder featuring congenital contractures in addition to bone fragility; one variant associated with pterygia (Bruck syndrome type 2) is caused by mutations in PLOD2 encoding collagen lysyl hydroxylase, while the other variant (Bruck Syndrome type 1) has been mapped to 17q12 but the gene has remained elusive so far. Recently, the molecular spectrum of OI has been expanded with the description of the mechanistic basis of a unique post-translational modification of type I collagen, i.e., 3-prolyl-hydroxylation. Three proteins, cartilage-associated protein (CRTAP), prolyl-3-hydroxylase-1 (P3H1, encoded by the LEPRE1 gene), and the prolyl cis-trans isomerase Cyclophilin-B (PPIB) form a complex that is required for fibrillar collagen 3-prolyl-hydroxylation and mutations in each gene have been shown to cause recessive forms of OI. Recently, an additional putative collagen chaperone complex, composed of FKBP10 (also known as FKBP65) and SERPINH1 (also known as HSP47), has also been shown to be mutated in recessive OI. Here, we performed a Sanger sequencing screen for FKBP10 in 67 patients with known recessive OI, after excluding other known OI causing genes. We identified 5 families with mutations in the coding region of FKBP10. The phenotype in 4 probands was consistent with Bruck syndrome, while the other two affected individuals had phenotypes consistent with OI type III. This is especially interesting since one sibling set with identical mutations presented with different phenotypic disorders - a brother with Bruck syndrome and sister with OI type III. Given the previous mapping of Bruck syndrome type 1 to the chromosomal region containing FKBP10, we conclude that FKBP10 mutations may be the cause of Bruck syndrome type 1 and may further present with a variable phenotype between type III OI and Bruck syndrome.

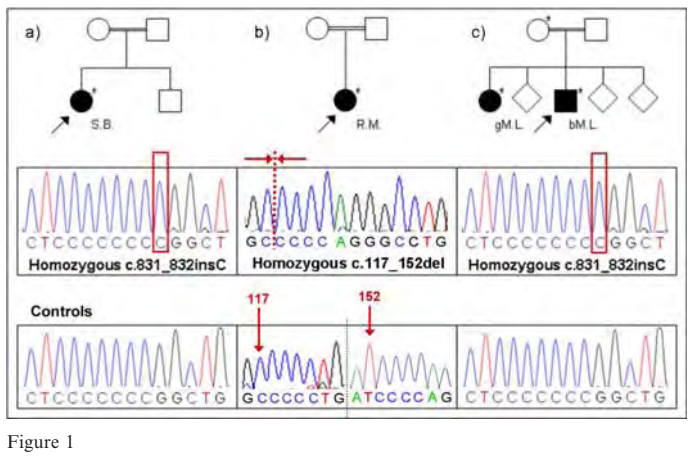

Figure 1

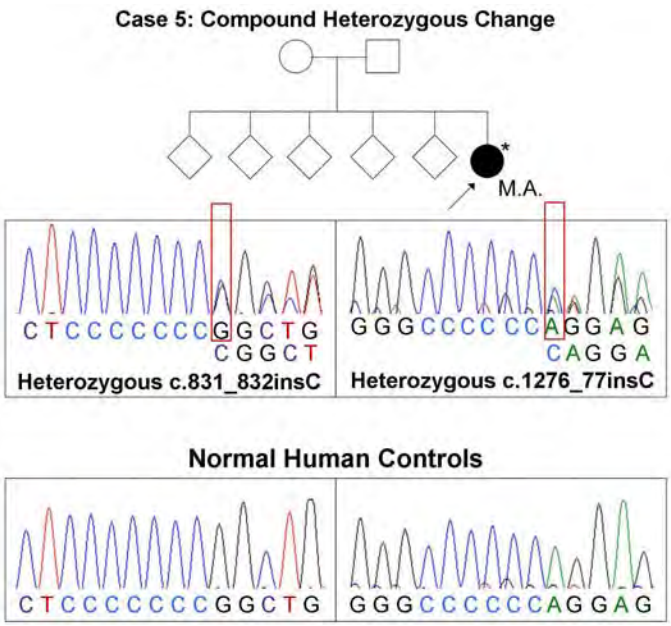

Figure 2

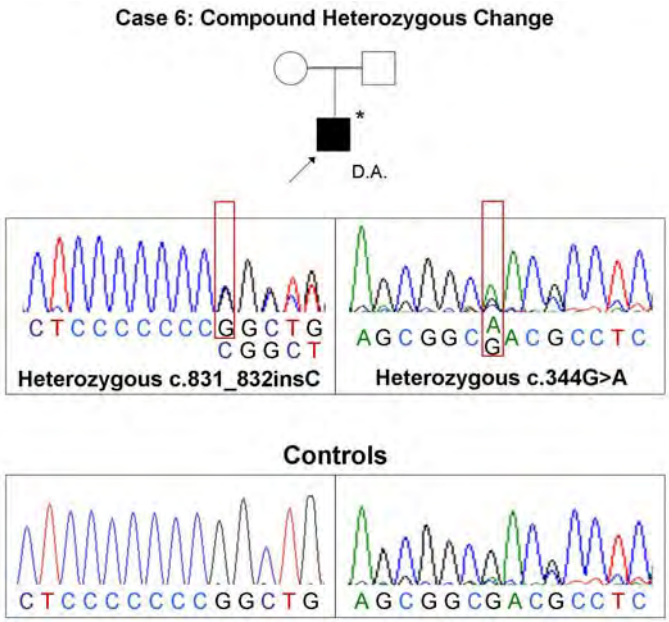

Figure 3

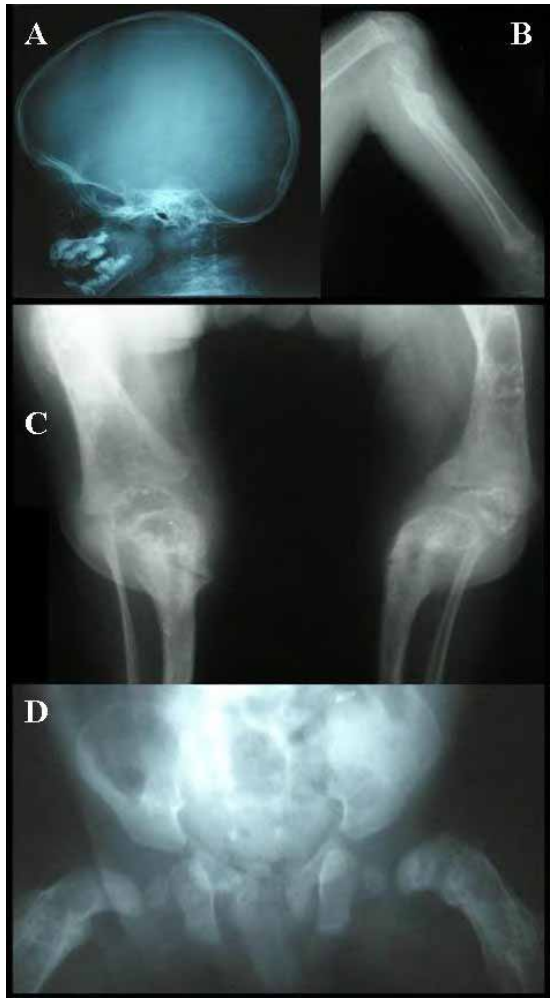

Figure 4

Disclosures: ***Brian Kelley****, None.*

SU0158

Gja1*Jrt*/+ - A Connexin43 Mutation Affecting Bone. Tanya Zappitelli*[1], Frieda Chen[1], Marc Grynpas[2], Janet E. Henderson[3], Luisa Moreno[2], Ralph Zirngibl[1], Jane Aubin[4]. [1]University of Toronto, Canada, [2]Samuel Lunenfeld Research Institute, Canada, [3]McGill University, Canada, [4]University of Toronto Faculty of Medicine, Canada

Oculodentodigital dysplasia(ODDD) is a human disease caused by a mutation in the gap-junction alpha 1 gene(GJA1) which encodes Connnexin43(Cx43). Through a genome-wide ENU-mutagenesis screen for dominant mutations, we isolated a mutant mouse line, Gja1Jrt/+, with a dominant negative missense mutation leading to a G60S amino acid substitution in Cx43(Flenniken A et al.,2005). In addition to having the classical symptoms of ODDD, Gja1Jrt/+ mice are osteopenic, but the differences in BMD compared to wild type(WT) littermates become less pronounced with age and, indeed, Gja1Jrt/+ mice appear to be protected from age-related bone loss. To elucidate the mechanisms underlying the bone anomalies, we performed histomorphometric and cell and molecular biology experiments. Histomorphometry confirmed that Gja1Jrt/+ mouse bones exhibit significantly lower bone volume:tissue volume, trabecular number and thickness than WT bones at 2 and 4 months, but differences diminished to non-significance by 12 months of age, concomitant with significant increases in cortical bone in Gja1Jrt/+ but not WT mice. No difference was detected in the number or size (number of nuclei) of osteoclasts formed in Gja1Jrt/+ versus WT bone marrow or spleen cell cultures supplemented with M-CSF and RANKL, but osteoclasts from 4 month old Gja1Jrt/+ spleens resorb more bone in vitro than their WT counterparts. qPCR quantification of RANKL and OPG expression indicated an increase the RANKL:OPG ratio in trabecular but not cortical bone and in stromal cultures of Gja1Jrt/+ compared to WT mice. No differences were seen in osteoblast or osteocyte number in bones from Gja1Jrt/+ versus WT mice. Although no differences were seen in expression at early differentiation times, expression of several mature osteoblast-osteocyte markers, most notably BSP and OCN, were significantly higher at late differentiation time points in stromal cell cultures and in RNA from trabecular bone, but not in calvarial bone, of Gja1Jrt/+versus WT mice, suggesting that Gja1Jrt/+ osteoblasts from a subset of anatomical sites are hyperactive. We conclude first that the G60S allele has differential effects on osteoblasts at different anatomical sites.

Second, we conclude that hyperactivity of osteoclasts leads to osteopenia in young Gja1Jrt/+ mice, but the increased activity of osteoblasts in the appendicular skeleton leads to significant new bone accrual, protecting Gja1Jrt/+mice from the age-related bone loss that occurs in WT mice.

***Disclosures: Tanya Zappitelli**, None.*

SU0159

Intracellular Superoxide Dismutase Deficiency Decreased Bone Mass *In Vivo* by Impairment of Cell Viability and Redox Balance in Osteoblasts. Yoshitomo Saita*[1], Hidetoshi Nojiri[1], Chizuru Tsuda[2], Tsuyoshi Miyazaki[3], Daichi Morikawa[2], Kazuo Kaneko[1], Takahiko Shimizu[2]. [1]Department of Orthopaedics, Juntendo Univ., Japan, [2]Molecular Gerontology, Tokyo Metropolitan Institute of Gerontology, Japan, [3]Geriatric Medicine, Tokyo Metropolitan Institute of Gerontology, Japan

Oxidative damage contributes to many age-related diseases, such as cancer, heart disease, diabetes, and Alzheimer's disease, however, its contribution to age-related osteoporosis remains to be elucidated. We previously reported that mice lacking in Cu/Zn-superoxide dismutase (*Sod1*), the essential enzyme for dismutation of intracellular superoxide anion to H_2O_2 and O_2, exhibit osteopenia due to low turnover bone remodeling (Nojiri et al. 2009). However, the physiological role of SOD1 in bone was not fully understood and it was uncertain whether this model mouse caused an oxidative damage to bone tissue. Here we further explored the biological significance of SOD1 in bone.

In bone histomorphometry, *Sod1* deficiency markedly suppressed mineralized surface and osteoblast number per bone surface, therefore, we hypothesized that *Sod1* deficiency *in vivo* would increase oxidative stress in osteoblasts leading to osteoblastic disability. To confirm this, isolated osteoblasts derived from *Sod1*$^{-/-}$ mice were examined. *Sod1*-deficient osteoblasts increased the production of dichlorohydrofluorescein diacetate (DCFH-DA) oxidation, a direct indicator of reactive oxygen species, compared to osteoblasts from wild-type mice. In addition, TUNEL and BrdU assay showed increased cell apoptosis and decreased cell proliferation in *Sod1*$^{-/-}$ osteoblasts. These data indicated that *Sod1* is an essential determinant of bone mass by regulating cell viability of osteoblasts.

Next, we analyzed bone resorption, which the other aspects of bone remodeling. As previously reported, the number of osteoclasts was decreased in *Sod1*$^{-/-}$ mice, while *in vitro* osteoclast development, survival and pit-formation were not dysregulated in *Sod1* insufficiency, indicating that *Sod1* deficiency fails to impair osteoclast differentiation and function in cellular level. Therefore, we hypothesized that decreased number of osteoclasts *in viv*o was caused by the suppressed ability of osteoblast-dependent osteoclastogenesis. As expected, the expression level of Rankl mRNA was down-regulated in bones of *Sod1*$^{-/-}$ mice.

These results indicate that SOD1 is required for the maintenance of physiological bone metabolism by controlling osteoblastic cell viability, suggesting that oxidative stress would be one of the determinants of age-related osteoporosis.

***Disclosures: Yoshitomo Saita**, None.*

SU0160

Mechanisms of Inhibition of Heterotopic Ossification by a RARγ Agonist. Hsu-Tsai Chi*[1], Kengo Shimono[1], Wei-en Tung[1], Johanna Jasinski[1], Christine Macolino[1], Satoru Otsuru[2], Maurizio Pacifici[1], Masahiro Iwamoto[1]. [1]Thomas Jefferson University, USA, [2]The Children's Hospital of Philadelphia, USA

Heterotopic ossification (HO) involves formation of ectopic bone masses within soft tissues and is triggered by trauma or major surgical interventions. Though its exact pathogenesis is unclear, HO often involves a recapitulation of endochondral bone formation. Recruitment of progenitor cells and their differentiation into chondrocytes occurring during that process are known to be blocked by retinoid signaling. Indeed, we show elsewhere at this meeting that the retinoic acid receptor γ (RARγ) is a major negative regulator of chondrogenesis and that oral administration of a selective RARγ agonist (γ-agonist) effectively blocks BMP-induced HO in mice. To clarify the mechanisms of inhibition, we tested the effects of the γ-agonist on BMP signaling by Id-luc reporter assays and Smad protein analyses, using ATDC5 chondrogenic cells treated with rhBMP2 in presence or absence of γ-agonist. This compound dose-dependently inhibited Id-luc reporter activity, and immunoblots of whole cell lysates revealed that γ-agonist treatment had decreased not only Smad 1, 4 and 5 phosphorylation but also their respective protein levels. In contrast, Smad 3 content was slightly increased by 24 hrs of γ-agonist treatment. Such decrease of Smad 1, 4 and 5 protein levels was prevented by co-treatment with proteasome inhibitors. Real-time PCR analysis revealed that γ-agonist treatment for 24 hrs did not significantly change gene expression of Smad 1, 4 and 5, suggesting that the decrease of Smad levels was due to accelerated protein degradation. Next, we studied the effects of the γ-agonist on skeletogenic differentiation of mouse derived bone marrow mesenchymal stem cells (BMSCs) established from GFP expressing mice. When the BMSCs were treated with the γ-agonist for three days, they failed to express alkaline phosphatase in response to rhBMP2. In a last set of experiments, control or γ-agonist -treated BMSCs were mixed with Matrigel and 1μg rhBMP2 and then transplanted into nude mice. In controls, the Matrigel explants developed into endochondral bone masses by 2 weeks, and GFP immunostaining confirmed that the majority of the bone-forming cells were GFP-positive. In contrast, the Matrigel explants containing γ-agonist-treated BMSCs had very little bone and the very small amount of bone present was GFP-negative. Our findings indicate that the γ-agonist exerts its potent inhibitory effects on HO by selectively blocking and destabilizing the canonical BMP signaling pathway.

***Disclosures: Hsu-Tsai Chi**, None.*
This study received funding from: NIH, US Army

SU0161

Melorheostosis - Polyostotic Affection of Skeleton. Vaclav Vyskocil*[1], Karel Koudela[2]. [1]Center for Metabolic Bone Diseases, Czech republic, [2]Department of Orthopaedic Surgery & Traumatologic Clinic, Czech republic

Melorheostosis together with osteopoikilosis, ostepathia striata and Buschke-Ollendorfov's syndrom belongs to mesodermal sclerotic dysplasia. Melorheostosis is a very rare disease with an incidence of 1:1 000 000, which was firstly described by French neurologist Léri in 1922. Hyperdense bands prominent upon the outer cortex niveau are visible on X-Rays of long bones diaphysis reminding flowing wax of a candle. This disease is connected with contractures of soft tissues, limited motion, intermittent edemas of joints, limb deformities and especially algesia. Etiology is still unknown. Dysfunction of gene LEMD3 with simultaneous inhibition of TGF-beta and BMP is considered. On the contrary, couples of cases were reported without detection of mutation or gene function impairment.

It is possible to detect 3 forms of melorheostosis: monostotic, monomelic and polyostotic. Polyostotic form is sometimes described as a generalized form. It represents combined monomelic and osteopoikilotic affection of other parts of skeleton. Standard X-Ray is very important tool for differential diagnosis. For the further examination 3-phase scintigraphy, CT and MRI are needed. CT and MRI are necessary for surgery extend planning, which is used especially when oppression of central neurovasal or release of extreme joint restriction is desirable.

Authors present a case of 26-year old female. Despite the severe restriction of shoulder and elbow joint movement, palmar flexion of the wrist and concomitant affection of vertebral body of cervical spine and collarbone the diagnosis was confirmed as late as her age of 25 as a consequence of accidental injury. Differential diagnosis, conservative as well as surgery treatment is further discussed.

***Disclosures: Vaclav Vyskocil**, None.*

SU0162

Modeling Genetic Skeletal Diseases in ES and iPS Cells. Edward Hsiao*[1], Trieu Nguyen[2], Mark Scott[2], Chris Schlieve[2], Bruce Conklin[2], Robert Nissenson[1]. [1]University of California, San Francisco, USA, [2]Gladstone Institutes, USA

Skeletal tissues derived from embryonic stem (ES) and induced pluripotent stem (iPS) cells are promising routes for generating replacement tissues and for studying human genetic diseases. However, our understanding of how stem cells can be guided to form skeletal tissues is rudimentary. We have established models of chondrocyte and osteoblast differentiation based on mouse ES and human iPS cell cultures. Our initial studies show that both of these cell culture models can express markers for osteoblasts and chondrocytes after culturing for 2 weeks in osteogenic media containing ascorbic acid, dexamethasone, and beta glycerol phosphate. In addition, cell culture density plays an important role in directing differentiation of mouse ES cells towards chondrocytes or osteoblasts. Increasing cell culture density by 10-fold decreased collagen I (a marker of osteoblasts) expression 3-fold while increasing collagen II and sox9 expression (markers of chondrocytes) 9-fold and 3-fold, respectively, even in the presence of osteogenic media. To further validate our ES cell culture system, we established human iPS cell lines from patients with two diseases with dramatically increased skeletal tissue formation: Fibromyositis Ossificans Progressiva (FOP) and Multiple Hereditary Exostosis (MHE),. Multiple iPS cell lines were successfully generated by viral transduction of four pluripotency-inducing factors (Oct4, Sox2, Klf4, and cMyc) into skin fibroblasts of FOP and MHE patients with confirmed genetic mutations characteristic of these diseases. Preliminary differentiation studies of the FOP and MHE iPS cells into the osteoblast lineage indicate that ossifying MHE cells express higher levels of chondrocyte markers. This finding may indicate fundamental differences in the osteogenic mechanisms between FOP and MHE patients. In conclusion, we are establishing ES and iPS cell models for studying human skeletal tissue formation in vitro. Our results indicate that stem cell-based models could be valuable for identifying genetic mechanisms regulating osteoblast and chondrocyte differentiation. Further, this approach may facilitate a molecular understanding of the pathogenesis of genetic disorders of bone development, and thus provide the basis for the development of novel therapies for diseases of abnormal skeletal growth.

***Disclosures: Edward Hsiao**, None.*

SU0163

Panostotic High Turnover Bone Disease with Massive Jaw Tumor Formation.

Anne Schafer*[1], Ivan El-Sayed[1], Steven Mumm[2], Mark Anderson[1], Edward Hsiao[1], Frederick Schaefer[3], Michael Collins[4], Panagiota Andreopoulou[4], Michael Whyte[5], Dolores Shoback[6]. [1]University of California, San Francisco, USA, [2]Washington University School of Medicine, USA, [3]Center for Genetic Testing at Saint Francis, USA, [4]National Institutes of Health, USA, [5]Shriners Hospital for Children, USA, [6]VA Medical Center, USA

A 27-year-old man was transferred to the UCSF Otolaryngology Service for management of a bleeding basketball-sized mandibular tumor. Born in Mexico, he was deaf and mute, and was ''bow-legged'' but active as a child. Family history was negative for bone disease. Puberty occurred normally, but he developed difficulty straightening his limbs, multiple fractures, and a bony tumor on his chin. At age 18 years, all limbs were misshapen. As the mandibular mass grew, the diagnosis of McCune-Albright syndrome (MAS) was considered. The mass was deemed inoperable, and he was provided hospice. Later, in California, the lesion bled, and he was transferred to UCSF. The mass protruded from the oral cavity and extended to the lower ribs. Other bony defects included a maxillary mass and serpentine limbs (Fig. 1). There were no café-au-lait spots. Labs included serum Ca 7.1 mg/dL, PO_4 2.4 mg/dL, albumin 1.7 g/dL, PTH 91 ng/L, 25(OH)D 11 ng/mL, and alkaline phosphatase 1760 U/L (nl 29-111). There was no clinical or biochemical hyperfunctioning endocrinopathy. Radiography of the limbs showed medullary expansion and cortical thinning with severe bowing (Fig. 2). The patient underwent mandibular mass excision, 5 months later partial maxillectomy, and subsequently further maxillary debulking. Histopathology showed curvilinear trabeculae of woven bone on a background of hypocellular fibrous tissue. After surgery and vitamin D supplements, labs showed bone-specific alkaline phosphatase >575 mcg/L (nl 8.4-29.3), C-telopeptide 1644 pg/mL (nl 87-1200), $1,25(OH)_2D$ 45, and intact FGF23 60 pg/mL (nl 10-50). In samples of affected bone and leukocyte DNA, site-specific enrichment mutation analysis followed by sequencing for codon 201 of *GNAS* showed no mutation, making MAS and panostotic fibrous dysplasia of bone unlikely. Sequencing is in progress for mutations in receptor activator of nuclear factor-κB (RANK) pathway. Preliminary results show no exon or splice site mutations in the genes encoding RANK-L or OPG, but they suggest a unique duplication in the signal peptide of RANK. The elevated bone turnover, reflected in the markers and disorganized bone histology, could be due to amplified RANK signal transduction, even though this case seems different from those reported previously with increased RANK signaling (e.g., familial expansile osteolysis). This finding may have implications for targeted therapy for our patient and may enhance understanding of osteoclast activation.

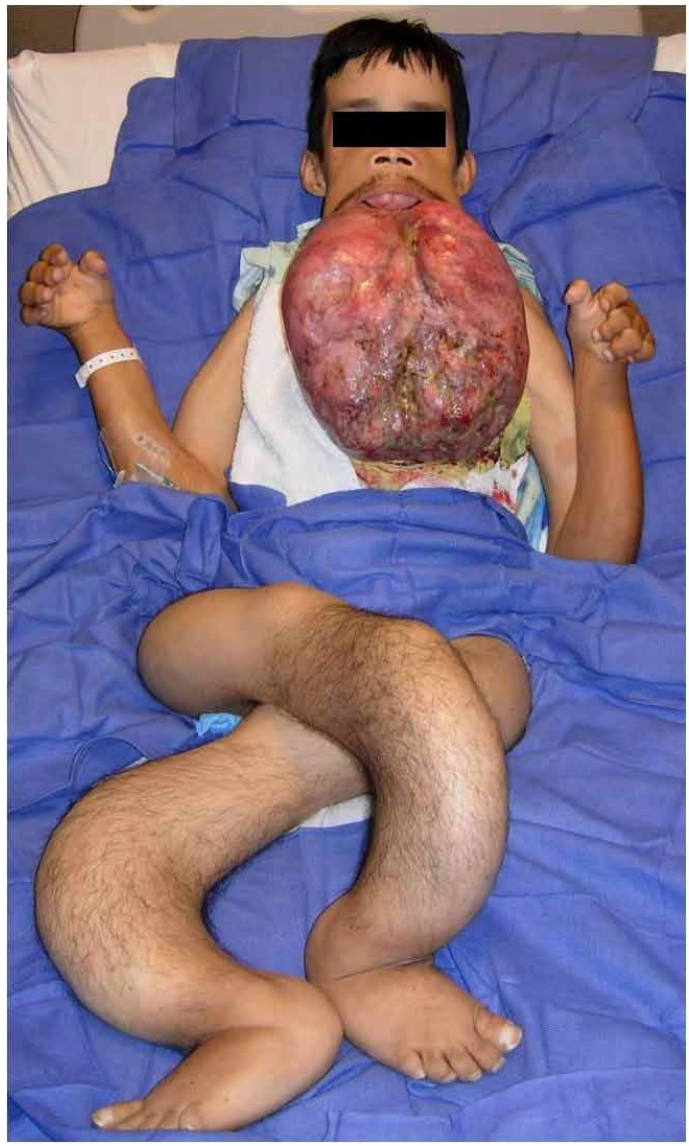

Figure 1

Figure 2

***Disclosures: Anne Schafer**, None.*

SU0164

Genome-Wide Scan for Bone Mineral Density in Multi-Generational Families of African Ancestry: The Tobago Family Health Study. Joseph Zmuda*[1], Victor Wheeler[2], Amy Dressen[3], Allison Kuipers[1], Cara Nestlerode[3], ClareAnn Bunker[3], Alan Patrick[2], Victor Wheeler[2], Anne Newman[3], Candace Kammerer[1]. [1]University of Pittsburgh Graduate School of Public Health, USA, [2]Tobago Health Studies Office, Trinidad & tobago, [3]University of Pittsburgh, USA

Although considerable research has been done to identify the genetic factors that underlie bone mineral density (BMD), the vast majority of this research has been conducted on populations of European and Asian ancestry. Considerably less is known about the genetics of BMD in African ancestry populations, who have substantially higher BMD and lower osteoporotic fracture rates compared to other population groups. We sought to identify genomic regions that may harbor genetic variants contributing to BMD in 430 African ancestry individuals aged ⩾18 years who were members of 7 large, multi-generational pedigrees on the Caribbean island of Tobago (family size, 18-130; 4581 relative pairs). BMD was measured with dual energy x-ray absorptiometry at the proximal femur, lumbar spine and whole body. We genotyped 5,361 single nucleotide polymorphisms (minor allele frequency >0.05; mean, 0.31) distributed across the autosomal genome with approximately 1cM spacing (Illumina Infinium HumanLinkage-12 BeadChip). Pedigree-based maximum likelihood methods were used to calculate multipoint logarithm of odds (LOD) scores for a polygenic model after accounting for significant covariates. Residual heritabilities for all BMD traits were highly significant ($P<0.00001$). We obtained strong evidence that a region on chromosome 12 (65 cM) influenced lumbar spine and whole body BMD (LOD=4.30 and 2.06, respectively). We also detected suggestive evidence of linkage for whole body BMD on chromosomes 13 (87 cM; LOD=2.29); trochanteric BMD on chromosome 16 (49 cM; LOD=2.16); and wards BMD on chromosome 11 (49 cM; LOD=2.57). Our results suggest that loci on chromosomes 11, 12, 13 and 16 may harbor genes influencing BMD in African ancestry individuals. Of interest, the region of strongest linkage on chromosome 12 includes the vitamin D receptor, wnt1 and wnt10b genes which have been implicated in the regulation of bone metabolism.

***Disclosures: Joseph Zmuda**, None.*

SU0165

The Role of Sex and Diet in the Quantitative Genetics of Osteoporosis-Related Traits. Jane Kenney-Hunt*[1], Heather Lawson[1], E. Ann Carson[1], Hattie Hiler[1], Priya Nagarajan[1], Matthew Silva[2], James Cheverud[1]. [1]Washington University School of Medicine, USA, [2]Washington University in St. Louis School of Medicine, USA

Key risk factors for osteoporosis, in which bones have low mass and are brittle and fracture-prone, include family history, sex, age, and obesity. Women, those with a family history of low bone mass, and older adults are all at increased risk of bone fracture, while obesity decreases risk. The relationship between these risk factors is currently unclear. This project investigated the effects and interactions of sex, obesity, and genetic architecture on cortical bone properties in mice and identified quantitative trait loci (QTL) with effects on cortical bone.

The LG/J X SM/J intercross has been previously characterized as a good non-mutant model for the study of obesity and related complex traits. Males and females from the F34 generation of the LG/J X SM/J Advanced Intercross Line (Wustl:LG,SM-G34) were fed either a high-fat (42% calories from fat) or low-fat (15% calories from fat) diet for 20 weeks. One femur and one radius from each individual (n=1139) was collected. This design allowed the osteoporosis risk factors of obesity, genetics, and sex to be addressed. We used micro-computed tomography (microCT) to examine properties of cortical bone including cross-sectional diaphyseal area, moments of inertia with respect to the x- and y-axis, and cortical thickness. A genome-wide scan for quantitative trait loci (QTL) was performed.

The heritabilities of bone properties and genetic correlations to body fat, body mass, and leptin levels were calculated. Sex and diet cohorts were considered individually, as well as pooled across the population, to identify effects specific to a cohort. QTL and positional candidate loci were identified, many with significant sex, diet, or sex-and-diet interactions. Some QTL were replicated from an earlier pilot study. For example, a significant QTL on mouse chromosome 4 with effects on femoral area and y-axis moment of inertia was fine-mapped from a previously identified 97 Mb region to a 3.8 Mb region containing 14 positional candidate genes. QTL were also examined to determine overlap with QTL for dietary obesity related traits. In conclusion, results indicate that bone properties are affected by a complex interaction of genetic and environmental effects. Future research will examine candidate genes and their relationship to bone properties, obesity, and leptin levels in more detail to elucidate the genetic architecture of osteoporosis.

***Disclosures: Jane Kenney-Hunt**, None.*

SU0166

24 Hydroxylase Polymorphism as a Possible Explanation for the Higher Level of 1, 25 (OH)2 Vitamin D in African American Ethnicity. Shadab Salehpour*[1], Laleh Ardeshirpour[2], Bethy Wong[3], Thomas Carpenter[4]. [1]University of Toronto, Canada, [2]Yale University Pediatric Endocrinology, USA, [3]Sunnybrook Health Sciences Center, Canada, [4]Yale University School of Medicine, USA

Context: States of vitamin D insufficiency are important determinants of rickets, as well as osteoporosis and other common complex disorders like diabetes, cancer and infectious diseases. Although serum concentrations of the vitamin D metabolites are primarily driven by vitamin D supply (by diet or cutaneous synthesis), there is emerging evidence to suggest that single nucleotide variants (SNVs) are important genetic determinants.

Objective: The aim of this study was to determine whether a functional SNV in the 24-hydroxylase gene promoter (c.-686A>G in CYP24A1) shows significant association with blood levels of vitamin D metabolites

Methods: Genomic DNA from 776 inner-city New Haven children aged 6 mon to 3 yr with different ancestries (African American, Caucasian, and Hispanic) was genotyped for the c.-686A>G SNV. Serum 25-hydroxy vitamin D and 1,25-dihydroxy vitamin D [1,25(OH)2D] were measured by RIA. Ancestry was assessed using a validated panel of 108 Ancestry Informative Markers (AIMs) and data from well-characterized African, Native American, and European population samples.

Main outcome measures: The main outcome measures were significance of associations between the c.-686A>G CYP24A1 SNV and vitamin D metabolites, with modeling to adjust for age, season, vitamin D intake and other co-variates. Secondarily we examined the strength of these associations in relation to SNV frequency in the three major ancestral groups.

Results: Subjects with the variant allele of CYP24A1(and decreased 24-hydroxylase activity) had a significantly higher mean 1, 25 (OH)2D ($p<0.001$), but all variants were found in African-Americans who, as a group, had higher mean 1, 25(OH)2D ($p<0.0001$). Since the effect was not significant when the association was AIMs-adjusted for ancestry, we cannot exclude confounding by stratification.

Conclusion: Further studies of the CYP24A1 SNV are warranted, but the 24-hydroxylase polymorphism may be considered as one possible contributor to the increased 1, 25(OH)2D that is widely observed in African Americans.

***Disclosures: Shadab Salehpour**, None.*

SU0167

Association Analysis between Polymorphisms of the Coagulation Factor V Gene and the Risk of Osteonecrosis of Femoral Head in Korean Population. Tae-Ho Kim*[1], Jung Min Hong[1], Hyun-Ju Kim[1], Eui Kyun Park[2], Shin-Yoon Kim[3]. [1]Kyungpook National University School of Medicine, South korea, [2]Kyungpook National University School of Dentistry, South korea, [3]Kyungpook National University Hospital, South korea

Osteonecrosis of the femoral head (ONFH) is a debilitating bone disease characterized by necrosis of the bone tissue, which results in the collapse of the joint cartilage and femoral head. Although the precise pathophysiology of ONFH has not been completely elucidated, the disruption of the blood supply to the femoral head seems to be the major risk factor. Some studies have investigated the associations between osteonecrosis and genes related to the coagulation and fibrinolytic system. In Caucasians, the G1691A mutation of factor V (factor V Leiden), the G20210A mutation of prothrombin, and the *PAI*-1 4G/5G polymorphism have been associated with osteonecrosis. To study a possible genetic effect of the *F5* (Coagulation factor V) gene on susceptibility to ONFH, we directly sequenced the *F5* gene (promoter, 25 exons and boundaries) in 24 Korean individuals and identified 16 known sequence variants. The factor V Leiden mutation (G1691A) was not found in our study agreement with previous report. According to LDs and allele frequencies, six polymorphisms were selected and genotyped in ONFH patients (n=427) and controls (n=350), using the TaqMan 5' allelic discrimination assay. Comparison of ONFH and control subjects using logistic regression models revealed no statistically significant differences in the frequencies of the *F5* polymorphisms and haplotypes. Further analysis stratified by etiology (idiopathic, steroid and alcohol) also showed no association. Contrary to the previous studies with Caucasian, these results suggest that *F5* polymorphisms play no significant role in the susceptibility to ONFH in the Korean population. Further studies, with larger sample size and detailed coagulation profile, would be necessary to fully assess the significance of this gene in ONFH.

***Disclosures: Tae-Ho Kim**, None.*

SU0168

Identification of Gender-Specific BMD Candidate Genes in Chromosome 1. Bouchra Edderkaoui*, Yan Hu, Anil Kapoor, Subburaman Mohan. Jerry L. Pettis Memorial VA Medical Center, USA

Bone mineral density (BMD) achieved in early adulthood is a major determinant of osteoporosis risk. Studies in mouse model have revealed several quantitative trait loci (QTL) that exert gender-specific effects on femoral structure and peak BMD. The

presence of sex specific variations in skeletal phenotypes implies that skeletal responses to therapies that aim on preventing or treating metabolic bone diseases could vary with gender. Therefore, studies on identification of genetic basis for male-female differences in peak BMD are obviously important. In our previous studies using linkage analyses and generation of congenic mice followed by subcongenic lines to narrow down the size of the QTL, we have identified a gender specific BMD1-4 locus in Chr 1. The female congenic mice that carry CAST BMD1-4 locus in C57BL/6J (B6) background showed significantly greater volumetric (v) BMD compared to gender and age-matched B6 mice, but no difference was observed between male congenics and corresponding B6 mice. In this study to determine if the vBMD variation is due to trabecular and/or cortical bone changes, we performed micro-CT measurements at the mid-diaphysis and the distal femur metaphysis derived from 16 week-old mice. No difference in cortical bone parameters was found between female or male congenics and corresponding B6 mice. However, trabecular bone volume/total volume was significantly greater in female (24%, $P<0.05$) but not male congenics compared to corresponding B6 mice which was due to increased trabecular thickness (15%, $P<0.01$) but not reduced trabecular separation, thus suggesting that bone formation but not bone resorption difference is responsible for the BMD variation between the female congenics and the corresponding B6 mice. In order to screen for the gender BMD QTL candidate genes, we have used public database to identify the sequence variations between B6 and Cast within the BMD1-4 locus. Among the 30 genes located in the QTL region only 2 ESTs and 6 known genes show non-synonymous SNPs (nSNPs) between B6 and CAST mice. Among the known genes, Efcab2, Kif26b and Smyd3 genes exhibit significant differences in the expression in the femurs between 14 week-old male and female B6 mice. Conclusions: 1) QTL1-4 regulates BMD by influencing trabecular bone density in a gender-specific manner. 2) Based on the SNP differences and gender differences in expression, we consider Efcab2, Kif26b and Smyd3 as potential candidate genes for BMD1-4 locus.

***Disclosures: Bouchra Edderkaoui**, None.*

SU0169

Lack of Association of Functional Polymorphisms of *RANK* and *RANKL* With BMD In BARCOS Cohort of Postmenopausal Women. Guy Yoskovitz[1], Natalia Garcia-Giralt[1], Xavier Nogues*[1], Susana Jurado[1], Roberto Güerri[1], Roser Urreizti[1], Leonardo Mellibovsky[1], Luis Perez-Edo[2], Lidia Agueda[3], Patricia Sarrión[3], Daniel Grinberg[3], Susana Balcells[3], Adolfo Diez-Perez[4]. [1]Institut Municipal d'Investigació Mèdica, Spain, [2]Hospital Ntra Sra Del Mar, Spain, [3]The University of Barcelona, Spain, [4]Hospital del Mar-IMIM-Autonomous University of Barcelona, Spain

Osteoporosis has a complex genetic basis which is incompletely defined. Bone Mineral Density (BMD) measurements have been defined as the osteoporosis gold standard. The bone remodelling equilibrium, which determines BMD, is dominated by a set of protein reactions known as the RANK/RANKL/OPG system. The special importance of the Receptor Activator of NF-kappa-B (RANK) and its interaction with its ligand (RANKL) is that the RANK/RANKL complex is one of the main triggers of osteoclast differentiation and survival. Hence, in depth analysis of variants in the *RANK* (*TNFRSF11A*) and *RANKL* (*TNFSF11*) genes may contribute to the understanding of the genetic of the disease.

The aim of this study was to evaluate putative functional SNPs of the RANK and RANKL genes. The SNPs were selected according to evolutionary conservation. Genomic sequences of mouse, rat, dog, cow and human were compared. Using the ENSEMBL multiple alignment tool we defined a region as 'conserved' only when all species presented the same nucleotide but the human SNP. Other SNPs were selected in case of non-synonymous changes. Thirty three SNPs were chosen (15 for *RANK*, 17 for *RANKL*). In 17 cases there was no data regarding minor allele frequency (MAF) among Caucasian and these SNPs were validated in our laboratory either by sequencing or by RFLP, only to include those with a MAF>0.1. Nine SNPs were excluded. A total of 820 postmenopausal women from Hospital del Mar, Barcelona (BARCOS cohort) were available, with anthropometric features together with Lumbar Spine (LS) and Femoral Neck (FN) BMD were recorded.

Genotyping of the 23 SNPs was performed by SNPlex. Three SNPs failed to genotype. Association to BMD was assayed by ANCOVA using height, weight, menarche age, month of breast-feeding and years since menopause as covariates. General, recessive and dominant models were considered in all cases; In general no association was found for any of the SNPs with the only exception of SNP rs12150741 (intron 1) which yielded a significant statistical result (p value=0.032) for LS BMD (dominant model). However, this result does not stand correction for multiple tests.

In conclusion, none of the putatively functional SNPs in the proximal regulatory and coding regions of *RANK* and *RANKL* show association to BMD in the BARCOS cohort of Spanish postmenopausal women.

***Disclosures: Xavier Nogues**, None.*
This study received funding from: FIS.RETICEF.INSTITUTO CARLOS III. Spanish Ministry of Science and Technology

SU0170

Osteonectin 3' Untranslated Region Single Nucleotide Polymorphisms Differentially Regulate Gene Expression: microRNAs Target SNP Regions. Kristina Kapinas, Tiziana Franceschetti*, Catherine Kessler, Anne Delany. University of Connecticut Health Center, USA

In this study we determined whether osteonectin 3' untranslated region (UTR) single nucleotide polymorphisms (SNPs) differentially regulate gene expression, and characterized microRNAs (miRNAs) that may interact with these SNP regions. We previously reported that haplotypes consisting of 3 SNPs in the 3'UTR of osteonectin/SPARC, at cDNA bases 1046(C/G), 1599(C/G) and 1970(T/G), are associated with bone mass in a cohort of men with idiopathic osteoporosis. Osteonectin is abundantly expressed by osteoblasts, regulating collagen fibril assembly and supporting osteoblast maturation and survival. Osteonectin-null and –haploinsufficient mice develop progressive low-turnover osteopenia, indicating that gene dosage is important for normal bone remodeling.

We generated luciferase-osteonectin 3'UTR reporter constructs, which were transiently transfected into hFOB1.19 human osteoblastic cells. The function of each haplotype was assayed in the context of the entire 3'UTR (cDNA bases 1018-2123). We found that haplotype A, which was associated with the lowest bone densities in osteoporosis patients, allowed the least luciferase expression compared with the other 5 haplotypes tested. These data suggest that individuals with osteonectin 3'UTR haplotype A may have lower osteonectin expression in bone cells.

The function of individual SNPs was assayed in the context of the 25 bases on either side of the SNP. We found that the activity of constructs carrying 1046G or 1046C was not different. In contrast, luciferase activity from constructs carrying 1599G was ~2 fold higher compared with 1599C constructs. Transfection of inhibitor for miR-135b relieved repression of the 1599 constructs, suggesting that miR-135b acts on this UTR region. For 1970, constructs carrying 1970T had 4-6 fold greater activity than those carrying 1970G. Transfection of miR-98 inhibitor relieved repression of the 1970 constructs, suggesting that miR-98 targets this region. Osteonectin decreases during human osteoblastic differentiation. During differentiation, miR-135b was induced ~4 fold, whereas miR-98 was decreased ~3 fold. Osteonectin is also a target for miR-29, which was increased 2 fold with differentiation. Overall, we show that osteonectin 3'UTR SNPs can contribute to differential regulation of gene expression, and may interact with specific miRNAs. Polymorphisms in key genes, resulting in small functional or regulatory differences, may affect bone mass over the lifetime of an individual.

***Disclosures: Tiziana Franceschetti**, None.*

SU0171

The Association Between BMD and Polymorphisms in SOST and PTH Is Dependent on Physical Activity in Perimenopausal Women. Lise Husted*[1], Torben Harsløf[2], Kim Brixen[3], Pia Eiken[4], Jens-Erik Beck Jensen[5], Leif Mosekilde[6], Lars Rejnmark[6], Bente Langdahl[7]. [1]Aarhus Amtssygehus, Aarhus University Hospital, Denmark, [2]Århus University Hospital, Aarhus Sygehus, Denmark, [3]Institute for Clinical Research, Denmark, [4]Hillerød Hospital, Denmark, [5]Hvidovre Hospital, Denmark, [6]Aarhus University Hospital, Denmark, [7]Aarhus Sygehus, Aarhus University Hospital, Denmark

PTH inhibits the expression of SOST and it has been shown that part of the anabolic effect of PTH treatment is mediated by SOST. Recently, SNPs in the SOST and PTH genes have been shown to be associated with BMD in genome wide association studies. The aim of this study was to investigate the effect of three of these SNPs on perimenopausal BMD, postmenopausal bone loss and osteoporotic fracture risk. Furthermore, we wanted to examine whether there is an interaction between the effect of these SNPs and physical activity on perimenopausal BMD and whether the SNP in PTH has an effect on p-PTH levels.

The study involved 1712 perimenopausal women participating in the Danish Osteoporosis Prevention Study (DOPS). The SNPs were genotyped using iPLEX genotyping assays or TaqMan assays and BMD was determined by DXA at baseline and after 5 and 10 years. Physical activity was recorded at baseline and grouped into high and low after the median value. p-PTH was measured at baseline in a subgroup of 928 women. For the association analyses with p-PTH levels women with hypercalcaemia and women with diseases or use of drugs known to increase p-PTH were excluded (n=59).

All SNPs were in Hardy-Weinberg equilibrium and had minor allele frequencies between 36 and 40%. We found that rs1107748 in SOST was associated with increased BMD at the lumbar spine and femoral neck (additive model: p=0.006 and p=0.04, respectively). The other SOST SNP rs1513670 was borderline significantly associated with decreased femoral neck and total hip BMD (dominant model: p=0.07 and p=0.06, respectively). Rs2036417 in PTH was associated with increased BMD at the total hip (additive model: p=0.047) and carriers of the variant allele had decreased levels of p-PTH (p=0.02).

For all three SNPs there was an interaction between the effects of the SNP and physical activity. Both SOST SNPs were significantly associated with BMD at the lumbar spine, femoral neck and total hip in women with low physical activity but not in women with high physical activity. The PTH SNP was associated with increased BMD at the total hip (p=0.03) in physically active women but not in physically inactive women.

None of the SNPs were associated with postmenopausal bone loss or osteoporotic fracture risk.

In conclusion we found that SNPs in SOST and PTH were associated with perimenopausal BMD and that the effects on BMD were dependent on physical activity. Furthermore, the SNP in PTH was associated with p-PTH levels.

***Disclosures: Lise Husted**, None.*

SU0172

"Same Day" *Ex Vivo* Regional Gene Therapy: A Novel Strategy to Heal Large Bone Defects. Mandeep Virk*[1], Osamu Sugiyama[1], Sang Park[2], Hicham Drissi[1], Douglas Adams[1], Sanjiv Gambhir[3], jay lieberman[1]. [1]University of Connecticut Health Center, USA, [2]University of California at Los Angeles, USA, [3]Stanford University School of Medicine, USA

Ex vivo regional gene therapy involves culture expansion of donor cells for weeks prior to implantation and this process is expensive, inconvenient and time consuming. The purpose of this study was to develop "same day" strategy of ex vivo gene therapy that will bypass the step of culture expansion so that the harvest, viral transduction and implantation of transduced cells can be performed in a short period of time on a single day. In the "same day" strategy, buffy coat cells (SD-RBMCs) were harvested from the rat bone marrow and transduced with lentiviral vector expressing BMP-2 for duration of one hour. In order to enhance BMP-2 production following short duration of viral transduction, we modified the standard lentiviral vector using two step transcriptional amplification (TSTA) system and achieved ten fold higher BMP-2 production (Fig.1). Using a rat critical sized femoral defect model (8 mm), a total of eighteen femoral defects were divided into two groups: Group I (n=13): 15 x 106 transduced SD-RBMCs; Group II (n=5): 15 x 106 non-transduced SD-RBMCs. The healing rates and quality of new bone formed was compared using plain radiogaphs, histology and histomorphometry. There was consistent BMP-2 production by the SD-RBMCs following one hour transduction period which was significantly higher ($p<0.05$) when compared to the nontransduced SD-RBMCs, which did not produce any significant amount of BMP-2. At 8 weeks, all of the thirteen femoral defects in Group I (SD-RBMCs + LV-TSTA-BMP-2) demonstrated bridging new bone formation across the femoral defect and complete radiographic healing. Two animals in Group I demonstrated heterotopic new bone formation that extended into the surrounding muscle. None of the defects (0/5) in Group II demonstrated osseous continuity on plain radiographs. On histologic analysis, a continuous cortex was present at the proximal and distal host defect interface and in the middle of the defect in Group I femora. In contrast, the defects in Group II demonstrated sparse periosteal new bone formation on either the proximal and/or the distal host defect interface. The bone area to tissue area fraction (BA/TA) in Group I defects (0.15 ± 0.02) was significantly higher ($p<0.01$) than Group II defects (0.04 ± 0.02). The results of this study demonstrate the potential clinical application of a novel "same day" gene therapy strategy, which offers a solution for the culture expansion process required in the traditional ex vivo gene therapy.

Fig.1

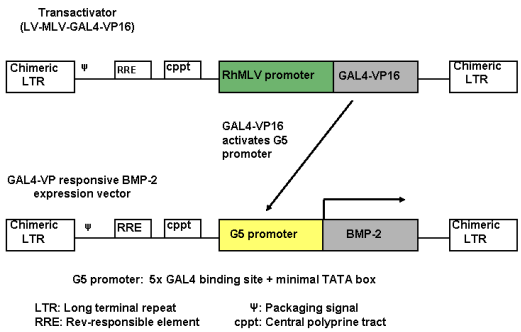

Two step transcriptional activation (TSTA) system

***Disclosures: Mandeep Virk**, None.*

SU0173

Alx3, a Paired-type Homeodomein Containing Transcription Factor, Regulates Osteoblast Differentiation Induced by BMP-2. Takashi Matsumoto*[1], Atsushi Yamada[2], Dai Suzuki[3], Masamichi Takami[4], Tetsuo Suzawa[4], Yoichi Miyamoto[4], Kazuyoshi Baba[5], Ryutaro Kamijo[4]. [1]Showa University, School of Dentistry, Japan, [2]Showa University School of Denistry, Japan, [3]Showa University, Japan, [4]Showa University School of Dentistry, Japan, [5]Departments of Prosthodontics, School of Dentistry, Showa University, Japan

Alx3 (aristaless like homeobox 3) is a homeobox gene related to the Drosophila aristaless gene and a group of vertebrate genes that includes Prx1/2, Cart1 and Alx4. Alx3 is expressed in frontonasal head mesenchyme and the first and second pharyngeal arches, which are derived from neural crest-derived mesenchyme, as well as in the limbs, which are derived from the lateral plate mesoderm. Alx3 has been linked to developmental functions in craniofacial structures and limb development. However, little is known about its direct relationship with bone formation. In the present study, we focused on the mechanisms of Alx3 gene expression and function during osteoblast differentiation induced by BMP-2. In C2C12 cells, Alx3 mRNA levels were enhanced in the presence of 10 ng/ml of BMP-2 and then increased in a dose-dependent manner, with a plateau reached at 300 ng/ml. Next, the time course for Alx3 mRNA induction by BMP-2 was determined with a fixed concentration of 300 ng/ml at various time points between 1 and 4 days. Increased Alx3 expression was detected 1 day after addition of BMP-2, then gradually increased up to 4 days. These results demonstrated that the BMP-2-induced increase of Alx3 gene expression occurs in both time- and dose-dependent manners. To determine whether induction of Alx3 gene expression by BMP-2 is dependent on the Smad signaling pathway, we performed ablation of Smad4 in C2C12 cells using an siRNA knockdown system. Ablation of Smad4 in C2C12 cells abrogated the induction of Alx3 gene expression by BMP-2. Finally, we examined whether Alx3 is involved in BMP-2-induced osteoblast differentiation in C2C12 cells. Following knockdown of Alx3 by siRNA in C2C12 cells, BMP-2-induced the gene expressions of alkaline phosphatase, osteocalcin and osterix were significantly decreased. Together, our results indicate that Alx3 expression is enhanced by BMP-2 via a mechanism that is dependent on Smad signaling and also involved in osteoblast differentiation of C2C12 cells induced by BMP-2.

***Disclosures: Takashi Matsumoto**, None.*

SU0174

Modulation of Proprotein Processing Enhanced Recombinant hBMP-2 Secretion. Aileen Zhou*[1], Cameron Clokie[2], Sean Peel[3]. [1]University of Toronto, Canada, [2]Faculty of Dentistry, Canada, [3]Induce Biologics Inc, Canada

Purpose: Bone morphogenetic proteins (BMPs) are key regulators of bone growth and differentiation. BMP-2 is synthesized as a precursor protein, proBMP-2, which undergoes enzymatic cleavage at two sites (S1 and S2) to form mature BMP-2. Several studies on proteins of the BMP family showed that the pro-domains can affect intracellular processing and secretion of the mature proteins. This study investigated the role of pro-domain processing on BMP-2 secretion. Methods: To modulate BMP-2 processing, the S1 site of the hBMP-2 gene was mutated to make it resistant to enzymatic cleavage. The mutated (mS1) or wild-type (wt) gene was transfected into HEK cells. In a second series of experiments, two stable cell lines (CHO and HEK) expressing hBMP-2 gene were cultured in the presence of pro-protein convertase (PC) inhibitor IND-1 in short-term (24-hr, multi-well) and long-term (two-month, bioreactor) cultures. The secreted BMP-2 was characterized by Western blot. Mature BMP-2 and proBMP-2 were quantified by ELISA. The activity of the rhBMP-2 was assessed in vitro using the C2C12 cell based assay. Results: HEK-hBMP2(mS1) secreted rhBMP-2 migrated at 22 kDa; whereas CHO-hBMP2(wt) and HEK-hBMP2(wt), secreted a mixture of 18 kDa and 22 kDa isoforms. HEK-hBMP2(mS1) showed 15-fold and 1000-fold increases in mature and proBMP-2 secreted (respectively) compared to the cells expressing the wild type hBMP-2. In addition, IND-1 treated cells secreted significantly greater amounts of pro- and mature rhBMP-2 in short-term (by 6-fold and by 10-fold, respectively) and long-term cultures, without any negative effects on cell growth or viability. The rhBMP-2 secreted by either mS1 cells or IND-1 treated cells induced differentiation of myogenic cells, suggesting the rhBMP-2 was biologically active. Conclusions: Modulation of proprotein processing resulted in greater amounts of both pro- and mature BMP-2 secretion compared to the untreated cells expressing wild type hBMP-2. These results suggest that proprotein processing can affect mature BMP-2 secretion.

***Disclosures: Aileen Zhou**, Induce Biologics Inc., 3*
This study received funding from: Induce Biologics Inc.

SU0175

Platelet Factor 4 is a Novel Potentiator of BMP-induced Osteoblastic Differentiation and Bone Formation. Takenobu Katagiri*[1], Toru Fukuda[2], Akihiro Tomoyasu[1], Masaaki Goto[3], Kunihiko Kodaira[3], Shoichiro Kokabu[4], Satoshi Ohte[4], Kazuhiro Kanomata[1], Tohru Tsukui[1], Hidefumi Fukushima[5], Hiroko Serizawa[1], Junya Nojima[4], Atsushi Nakamura[4], Katsumi Yoneyama[1], Hiroki Sasanuma[1], Masashi Shin[1], Keiko Fujita[4], Masumi Akita[4], Anna Kowalska[6], Eijiro Jimi[7], Hiromitsu Toyoda[8], Kunio Takaoka[8], Tatsuya Koike[8], Kanji Higashio[9], Tatsuo Suda[10]. [1]Saitama Medical University Research Center for Genomic Medicine, Japan, [2]Keio University School of Medicine, Japan, [3]Chugai Pharmaceutical Co., Ltd., Japan, [4]Saitama Medical University, Japan, [5]Beth Israel Deaconess Medical Center, USA, [6]The Children's Hospital of Philadelphia, USA, [7]Kyushu Dental College, Japan, [8]Osaka City University Medical School, Japan, [9]Metabolome Pharmaceuticals, Inc, Japan, [10]Research Center for Genomic Medicine Saitama Medical School, Japan

We previously reported that heparin, a highly sulfated polysaccharide, stimulates BMP activity both in vitro and in vivo. We also found that platelet-rich plasma, which is clinically used as an autologous blood product to stimulate tissue regeneration,

contains a novel potentiator activity for BMPs. In the present study, we purified and identified tetramer of platelet factor 4 (PF4) as a body of BMP potentiator activity in bovine serum. Recombinant human PF4 expressed in E. coli also stimulated ALP activity induced by BMP-4 in C2C12 myoblasts, but PF4 mutants which were substituted its C-terminal basic residues or lacked its tetramer-forming capacity did not. In contrast to heparin, PF4 stimulated early events induced by BMP-4 within 1 h (accumulation of phospho-Smad1/5/8 in nuclei and expression of Id genes) in C2C12 cells. Implantation of BMP-2 with increasing amounts of PF4 in mice dose-dependently induced ectopic bones with high BMC and BMD. Simultaneous treatment of C2C12 cells with PF4 and heparin in the presence of BMP-4 reduced the stimulatory capacities of both PF4 and heparin, suggesting that positive and negative charges of PF4 and heparin may be important to stimulate BMP activity. PF4 KO mice showed a delay of fracture healing in aged animals. Taken together, these findings suggest that PF4 is a novel circulating potentiator of BMP-induced osteoblastic differentiation and bone formation.

***Disclosures: Takenobu Katagiri**, Chugai Pharmaceutical Co., Ltd., 2; Metabolome Pharmaceuticals, Inc., 2*
This study received funding from: Chugai Pharmaceutical Co., Ltd.

SU0176

Functional Characterization of a Novel FGFR2 Mutation, E731K, in Craniosynostosis. Hyun-Mo Ryoo, Won-Joon Yoon*. Seoul National University, School of Dentistry, South korea

We had genetic analysis of six Korean patients who have craniosynostosis as a phenotype. Two of them were Crouzon syndrome and the rest were Apert syndrome as a phenotype. All patients had at least one mutation in FGFR2 gene; five of those mutations have already been reported elsewhere while only one mutation is novel, and that might lead to Apert syndrome. In this study, we functionally analyzed the novel FGFR2 mutation, E731K. The mutation is in the 2nd tyrosine kinase domain in the C-terminal cytoplasmic part of the molecule. The mutation caused an enhanced phosphorylation of E731KFGFR2 and ERK MAP kinase, the stimulation of transcriptional activity of Runx2 and consequently enhancement of osteogenic marker gene expression. Thus, we can conclude that E731K substitution of FGFR2 is a novel mutation that resulted in a constitutive activation of the receptor and finally resulted in premature suture obliteration.

***Disclosures: Won-Joon Yoon**, None.*

SU0177

Wnt/β-Catenin Pathway Members in the Elephant Shark *(Callorhinchus milii)*. Damian D'Souza[1], Kesha Rana[2], Samantha Richardson[1], Justin Bell[3], Terence Walker[3], Helen Maclean[2], Jeffrey Zajac[4], Sydney Brenner[5], Byrappa Venkatesh[6], Janine Danks*[1]. [1]School of Medical Sciences, RMIT University, Australia, [2]University of Melbourne, Dept of Medicine, Australia, [3]Marine & Freshwater Research Institute, Australia, [4]Austin & Repatriation Medical Centre, Australia, [5]Institute of Molecular & Cell Biology, A*STAR., Singapore, [6]Institute of Molecular & Cell Biology, A*STAR, Singapore

The development of bone was a major step in the evolution of vertebrates. A bony skeleton provided the structural support essential for the movement from an aquatic to a terrestrial environment and a reservoir for calcium. Cartilaginous fishes are the oldest living group of jawed vertebrates. In this study, we have identified two members of the Wnt/β-catenin Pathway members in a cartilaginous fish, the elephant shark (*Callorhinchus milii)*. Data mining of the elephant shark genome assembly identified sequences with similarity to the mammalian genes, *CTNNB* (encoding β-catenin) and *SFRP* (encoding secreted frizzled related protein). These genes and their corresponding proteins are members of the Wnt/β-catenin pathway - a major signalling pathway - and play an important role in the development of the skeleton.

Our aim was to examine tissue specific mRNA expression of each of these genes, and β-catenin localization in the elephant shark tissue based on the hypothesis that the elephant shark contains the genes and proteins necessary for carrying out the Wnt/β-catenin pathway in its cartilaginous skeleton.

Primers designed to amplify conserved regions within each of the *β-catenin* and *SFRP* genes were designed and used to observe the mRNA expression of these genes in different tissues in the elephant shark using reverse transcription PCR analysis (RT-PCR). PCR amplification and sequencing showed that these genes are indeed expressed in the elephant shark. *β-catenin* was expressed in cartilage, kidney and gills and *SFRP* was expressed in cartilage, kidney, spleen and gills. β-catenin protein was localized using anti-human β-catenin antibody, in different elephant shark tissues, including intestine, skin, uterus, kidney tubules, testis, pancreas, spleen, heart, liver and cartilage surrounding the spinal cord and showed similar patterns of localization seen in human tissue sections.

Our data supports the proposed hypothesis and consequently further research into the other genes and proteins of the Wnt/β-catenin pathway will be undertaken in order to understand the role this pathway plays in elephant shark, why they maintain their cartilaginous skeleton and do not replace it with bone, and the differential regulation of these genes within the elephant shark compared to humans. These studies will provide valuable insight into the function of this pathway in a basal vertebrate.

***Disclosures: Janine Danks**, None.*

SU0178

A Novel Vascular Function for Osteoclast-associated Receptor (OSCAR). Claudia Goettsch*[1], Susann Helas[1], Martina Rauner[2], Nadia Al-Fakhri[3], Michael Schoppet[4], Lorenz Hofbauer[5]. [1]Department of Medicine III, Technical University, Dresden, Germany, [2]Medical Faculty of the TU Dresden, Germany, [3]Department of Clinical Chemistry & Molecular Diagnostics, Philipps-University, Marburg, Germany, [4]Department of Internal Medicine & Cardiology, Philipps-University, Marburg, Germany, [5]Dresden Technical University Medical Center, Germany

Cross-talks between bone and vascular biology and the immune system play a crucial role in vascular diseases such as atherosclerosis or vascular calcification, both frequently linked to osteoporosis. The osteoclast-associated receptor (OSCAR) has been implicated as a modulator of osteoimmunology as it was identified as a co-stimulatory regulator of osteoclast differentiation and regulator of dendritic cell maturation. Microarray analysis identified OSCAR expression in vascular smooth muscle cells. Thus, we hypothesized that OSCAR may play a novel role in the regulation of vascular biology. We identified OSCAR in human primary endothelial cells and vascular smooth muscle cells by real time PCR and Western blot analysis. Human mature osteoclasts served as positive control. Furthermore, immunohistochemistry revealed endothelial cells and smooth muscle cells in arteries from the umbilical cord that stained positive for OSCAR. At the subcellular level, OSCAR was found to be located in the membrane fraction. Consistent with these data, OSCAR co-localized with VE-cadherin and PECAM, two membrane-bound endothelial markers. To further assess the regulation of OSCAR by proatherogenic factors, HCAEC were exposed to oxidized low density lipoprotein (oxLDL). OSCAR mRNA and protein levels were induced in a time- and dose-dependent manner by up to 2-fold. Consistent with these findings, OSCAR was transcriptionally regulated by oxLDL, as shown by OSCAR promoter analysis. The oxLDL-induced OSCAR expression was blocked by a neutralizing antibody against the lectin-like oxLDL receptor LOX-1. Next, we examined the role of nuclear factor of activated T cells (NFAT), a known transcription factor, which regulates OSCAR. OxLDL induced NFATc1 translocation into the nucleus 1.8-fold. Furthermore, specific inhibition of the NFAT pathway using VIVIT peptide prevented the oxLDL-mediated increase of OSCAR mRNA and protein expression. Electrophoretic mobility shift assays revealed an interaction of the OSCAR promoter region containing a NFAT binding site and protein from human endothelial cells. In addition, mice on a high-fat diet showed increased OSCAR levels in the aorta and the heart. In conclusion, OSCAR is expressed in human primary endothelial cells and regulated by oxidative stress. This suggests that OSCAR may have a dual role at the intersection of bone metabolism and vascular biology.

***Disclosures: Claudia Goettsch**, None.*

SU0179

Doubling the Dosage of Vitamin D Supplementation During Pregnancy Reduces Bone Mineral Content Adjusted for Body Weight in Male Guinea Pig Offspring at Birth. Negar Tabatabaei*[1], Celia Rodd[1], Richard Kremer[2], Hope Weiler[1]. [1]McGill University, Canada, [2]McGill University, Royal Victoria Hospital, Canada

Introduction: Dietary vitamin D intake recommendations for women of reproductive age vary among institutions and societies. In 1996 the Institute of Medicine recommended an adequate intake of 200 IU to prevent deficiency with the tolerable upper level set at 2000 IU/d; these values are under review. A healthy diet including vitamin D fortified milk and milk products, fatty fish, fortified margarine, and small amounts from other foods plus a pregnancy supplement (400 IU) may approach a total intake of 1000 IU/d. Recently the Canadian Paediatric Society recommended that pregnant and lactating women consume 2000 IU/d to provide for sufficient transfer to their offspring. The effects of doubling intakes on maternal and fetal bone have not clearly been investigated.

Objective: To determine if dietary intake of vitamin D twice the recommended value has implications for fetal bone mineral acquisition using the guinea pig model for human reproduction and development.

Methods: Twelve female pigmented guinea pigs 16 weeks of age were randomized to diets with adequate vitamin D (1 IU/g diet; G1) for guinea pigs or double that amount (2 IU/g; G2), and then mated. These diets were isocaloric and only differed in vitamin D3 content. The 1 IU/g diet is known to support vitamin D status with serum 25-hydroxy vitamin D values > 90 nmol/L throughout pregnancy. Pups born to these sows were anaesthetized using isoflurane inhalant 24-36 h after birth to immobilize them for measurement of whole body BMC (g) and BMD (g/cm^2) using DXA. To adjust for body size, BMC was divided by weight (g/kg). Statistical analyses were performed using a mixed ANOVA model with a fixed effect of diet and a random effect of litter and gender. No differences were observed in body weight (125.5 $\pm$ 4.0 vs 129.9 $\pm$ 4.1 g, P=0.24), BMC (3.9 $\pm$ 0.1 vs 3.9 $\pm$ 0.1 g, P=0.63) or BMD (0.119 $\pm$ 0.002 vs 0.119 $\pm$ 0.002 g/cm^2, P=0.84) according to diet groups and no interaction with gender was observed. However for BMC/kg, diet interacted with gender such that values were lower in the males of the 2 IU group (see Table 1).

Conclusions: These preliminary data suggest that intakes of vitamin D above those proven to support vitamin D do not offer benefit to bone in female offspring. In contrast, exceeding the recommendations for guinea pigs appears to reduce BMC adjusted for body size in male offspring. Whether these observations reflect changes in bone structure remain to be investigated.

Table 1. The effect of 1 vs. 2 IU of vitamin D/g of diet during pregnancy on BMC (g/kg) in female and male guinea pig offspring at birth.

Diet (vitamin D content)	Females(n)	Males(n)
G1 (1 IU/g)	31.18± 0.66ª (9)	30.80± 0.58ª (12)
G2 (2 IU/g)	30.27± 0.69ª (8)	28.50± 0.59ᵇ (11)

Values with different superscripts are significantly different (P<0.02).

Table 1

***Disclosures: Negar Tabatabaei**, None.*

SU0180

Evidence that the "High" Vertebral Bone Mass in Leptin Deficient *ob/ob* Mice is Due to Defective Skeletal Maturation. Kenneth Philbrick*, Russell Turner, Urszula Iwaniec. Oregon State University, USA

Despite morbid obesity, there is an overall reduction in bone mass in leptin-deficient *ob/ob* mice. However, *ob/ob* mice develop greater cancellous bone volume/tissue volume (BV/TV) in the lumbar vertebrae (LV) compared to wild type (WT) mice. It has been suggested that the mosaic skeletal phenotype of *ob/ob* mice results from the balance between direct bone anabolic actions of systemic leptin and indirect antiosteogenic actions mediated through the hypothalamus. Our observation that hypothalamic leptin gene therapy results in increased serum osteocalcin and rescues the *ob/ob* bone phenotype in both the cortical and cancellous compartments (Peptides, 28:1012-9, 2007; and Peptides, 30:967-73, 2009) does not support this hypothesis. To further investigate the underlying mechanism responsible for the *ob/ob* vertebral bone phenotype we randomized C57BL/6 *ob/ob* and WT mice into two groups, fed them *ad libitum,* and sacrificed them at 7 and 15 weeks of age. Total femur and cancellous bone in the LV5 were analyzed by μCT. The main and interactive effects of age and genotype were identified by two-way ANOVA with a Tukey post hoc test. As expected, *ob/ob* mice were heavier, had greater abdominal white adipose tissue (WAT) mass, lower femoral BV, and greater LV5 BV/TV than WT mice. The effect of leptin deficiency on body weight, WAT and LV5 BV/TV increased with age. Analysis of changes in vertebral architecture revealed that trabecular thickness (Tb.Th) increased with age in both genotypes. In contrast, trabecular number (Tb.N) decreased with age in WT but not *ob/ob* mice. As a consequence, the age-related increase in BV/TV in leptin-deficient *ob/ob* mice is explained by preservation of trabeculae that would normally be resorbed during growth. These findings suggest that the *ob/ob* mosaic skeletal phenotype results from defective skeletal maturation associated with well described reductions in growth plate cartilage and reductions in bone formation and resorption. These results further support the hypothesis that leptin is a permissive factor required for normal skeletal growth and maturation.

	Age = 7 Weeks		Age = 15 Weeks		Interaction
	WT (n = 9)	ob/ob (n = 11)	WT (n=8)	ob/ob (n=5)	P-Value
Body Mass (g)	16.0 ± 0.3	33.1 ± 1.4*	21.4 ± 0.5	50.4 ± 2.1*	P < 0.0001
WAT (g)	0.37 ± 0.02	3.35 ± 0.19*	0.42 ± 0.02	6.12 ± 0.33*	P < 0.0001
Femur BV (mm^3)	12.5 ± 0.2	10.9 ± 0.4	16.2 ± 0.2	13.5 ± 0.5	P = 0.14
LV5 BV/TV (%)	15.1 ± 0.4	16.7 ± 0.8	14.5 ± 0.5	24.4 ± 1.2*	P < 0.0001
LV5 Tb.Th (μm)	37.8 ± 0.4	37.1 ± 0.6	42.7 ± 0.4	44.3 ± 0.9	P = 0.049
LV5 Tb.N (1/mm)	5.3 ± 0.1	5.9 ± 0.1*	4.0 ± 0.1	5.6 ± 0.1*	P < 0.0001

Mean = SE; Main effects for age and genotype were significant (P < 0.05) for all endpoints. *Different from WT within age, P < 0.05.

Table: Effects of age and ob/ob genotype on bone (LV5 & Femur), body mass, and WAT mass

***Disclosures: Kenneth Philbrick**, None.*

SU0181

Expression of Adiponectin Receptors in Osteoblastic Cells. Takashi Ikeo*, Aiko Kamada, Yoshihiro Yoshikawa, Eisuke Domae, Seiji Goda, Isao Tamura. Osaka Dental University, Japan

Adiponectin (AN), an adipocyte-derived biologically active molecule, is abundantly present as a plasma protein, and exhibits various biological functions. Two types of adiponectin receptor (AdipoR1 and AdipoR2) have recently been cloned and found to be expressed ubiquitously. More recently, T-cadherin (CDH13) has been characterized as a novel adiponectin receptor on vascular endothelial cells and smooth muscle. Previously, we demonstrated the gene expressions of the two receptors in osteoblasts and their involvement with osteoblastic differentiation. In this study we investigated effects of adiponectin on gene expression profiles during osteoblast differentiation using DNA microarray analysis, and analyzed exclusively the clusters including adiponectin receptors.

Osteoblastic differentiation of a murine pro-osteoblastic cell line, MC3T3-E1 cells, was induced by differential medium including ascorbic acid and β-glycerophosphate with or without recombinant murine full-length type (AN) and globular type (gAN) adiponectin. Three days after stimulation, RNA was extracted and reverse-transcribed. Gene expression profiles were obtained by DNA microarray analysis, and applied to hierarchical clustering with correlation centered similarity metrics. Functional cluster annotations for the selected clusters were generated based on the significant gene ontology terms.

The significant genes up-regulated by differential medium were related to osteoblast differentiation and cell growth. The cluster AdipoR1 belonged to included the genes which were down-regulated by differential medium, although the cluster AdipoR2 belonged to included the genes up-regulated by the medium. CDH13 was also belonged to the cluster including the genes up-regulated during osteoblastic differentiation.

Our study suggests that AdipoR2 and CDH13 rather than AdipoR1 may be involved in osteoblastic differentiation.

***Disclosures: Takashi Ikeo**, None.*

SU0182

FGF2 Upregulates Dmp1 in the Osteoblast Lineage through the ERK MAPK Pathway. Shunichi Murakami, Zhufeng Ouyang, Ai Kyono*. Case Western Reserve University, USA

Recent studies have indicated that the extracellular signal-regulated kinase (ERK) mitogen-activated protein kinase (MAPK) pathway plays an essential role in osteoblast differentiation. To examine the roles of the ERK MAPK pathway and its upstream FGF signaling in the late stages of osteoblast differentiation, we performed microarray analyses using the osteocyte cell line MLO-Y4 treated with FGF2 and the MEK inhibitor U0126. This microarray experiment indicated that FGF2 regulates a number of mineralization-related genes in an ERK MAPK dependent manner, including *Dmp1*, a gene that plays an essential role in matrix mineralization and phosphate homeostasis. Real time PCR indicated that FGF2 increases *Dmp1* mRNA levels up to 6 fold in MLO-Y4 cells at 8h after treatment. Dmp1 upregulation by FGF2 was also confirmed at the protein level in the culture supernatant of MLO-Y4 cells by Western blot analysis. In addition, U0126 strongly inhibited both basal expression of *Dmp1* mRNA and FGF2-induced *Dmp1* mRNA upregulation, suggesting that *Dmp1* expression depends on ERK MAPK signaling. Similar results were also obtained in preosteoblastic MC3T3E1 cells and primary calvaria osteoblasts. Furthermore, PD173074, a selective FGF receptor inhibitor, decreased *Dmp1* mRNA expression in primary calvaria osteoblasts, suggesting that endogenous FGFs regulate *Dmp1* expression. FGF2-induced upregulation of *Dmp1* was strongly inhibited by cycloheximide in MLO-Y4 cells, suggesting that the FGF2 regulation of *Dmp1* expression requires new protein synthesis. To investigate the roles of ERK1 and ERK2 in *Dmp1* expression in vivo, we examined skeletal elements in which *ERK2* was inactivated in the *ERK1*-null background using the *Prx1-Cre* transgene. Real time PCR indicated that *Dmp1* expression was remarkably decreased in the tibia, femur, and humerus of *ERK1*$^{-/-}$; *ERK2*^{floxflox}; *Prx1-Cre* embryos at E16.5 compared with littermate embryos with an intact allele of either *ERK1* or *ERK2*. Consistent with this observation, immunohistochemical analysis showed reduced Dmp1 deposition in the bone matrix of *ERK1*$^{-/-}$; *ERK2* ^{floxflox}; *Prx1-Cre* mice compared with littermate control mice. Collectively, our observations indicate that FGF signaling upregulates *Dmp1* expression in the osteoblast lineage through the ERK MAPK pathway. Given the importance of Dmp1, these observations strongly suggest that FGF and ERK1ERK2 play an important role in the late stages of osteoblast differentiation and mineral metabolism.

***Disclosures: Ai Kyono**, None.*

SU0183

IL-23 Induces Osteoclastogenesis In Vivo and is Required for Osteoclast Maturation. Iannis Adamopoulos*[1], Cheng-Chi Chao[2], Wei Yao[3], Nancy Lane[3], Eddie BOWMAN[2]. [1]Schering Plough, USA, [2]Schering Plough Biopharma, USA, [3]University of California, Davis Medical Center, USA

IL-23 is a pro-inflammatory cytokine implicated in arthritis development and the resulting bone erosion. In this paper we utilized overexpression of IL-23 in adult mice using hydrodynamic delivery of IL-23 minicircle DNA to study IL-23 in vivo. IL-23 minicircle DNA induces histopathologic features consistent with an autoimmune arthritis and induces severe bone loss. Depletion of CD4+ cells, gamma deltaTCR cells and NK cells, had little effect in the inhibition of arthritis progression but depletion of macrophage and dendritic cells showed a marked decrease in paw swelling. Moreover bone marrow macrophages derived from IL-23p19-/- mice were evaluated for their ability to form functional osteoclasts. A slower maturation of osteoclasts is observed in mice deficient in IL-23 signalling with reduced TRAP+ cells, and reduced dentine resorption capacity. Finally bone mineral density was calculated in 8 and 26 week old male mice deficient in IL-23 signalling with physiological RANKL/OPG ratio. 26 week old male mice had a decreased number of multi-nucleated osteoclast-like cells and had 30% more trabecular bone volume and number compared to controls. Collectively our data suggest that IL 23 plays a direct role in osteoclast differentiation and bone resorption

***Disclosures: Iannis Adamopoulos**, IE. ADAMOPOULOS, 3*
This study received funding from: Merck

SU0184

Nell-1 Delivered From Heat-Inactivated Demineralized Bone Matrix Enhances Bone Growth and Quality in a Sheep Spinal Fusion Model. Ronald Siu*[1], Steven Lu[2], Janette Zara[1], Xinli Zhang[1], Benjamin Wu[1], Kang Ting[1], Chia Soo[1]. [1]University of California, Los Angeles, USA, [2]Cedars-Sinai Medical Center, USA

Nell-1 (Nel-like molecule-1; Nel: a protein strongly expressed in neural tissue encoding epidermal growth factor like domain) is a growth factor that operates downstream of Runx2-mediated osteochondral commitment and thus may act more specifically toward osteoblasts. The aim of this study is to evaluate the osteogenicity of Nell-1 and determine an optimal dosage concentration in a sheep spinal fusion model, one of the phylogenetically highest mammalian platforms for osteogenic studies with quantitative biomechanical similarities to human spines.

For implantation, Nell-1 protein was mixed with DBX, an easily molded putty of hyaluronic acid and sheep demineralized bone matrix which can conform to the shape of a defect. As demineralized bone matrix has been reported to contain residual growth factors that may remain active after material processing, we heat-inactivated DBX to isolate the osteogenic effect of Nell-1 from these factors. All mixtures were added to intervertebral spacers, and the spacers were implanted between L3/L4 and L5/L6 of sheep spines thereby creating two data points per sheep. Four experimental groups were used (n=4 sites each, 16 total): (1) DBX only; (2) DBX+0.3 mg/ml Nell-1; (3) DBX+0.6 mg/ml Nell-1; and (4) DBX+1.5 mg/ml Nell-1. Fusion was assessed by a series of radiographic, microcomputed tomography (microCT), and histologic techniques.

Spines treated with Nell-1 exhibited increased frequency of bone fusion and accelerated bone formation within the spacers compared to Nell-free controls. Nell-1 also improved bone volume and bone mineral density in the newly formed bones in a dose-dependent manner. Histologic staining of vertebral bone tissue supports our radiographic and microCT findings of increased fusion rate and bone quality.

In conclusion, we demonstrated dose-dependent enhancement of bone formation when Nell-1 protein is delivered from an inactivated DBX carrier, indicating that Nell-1 is an independently potent osteogenic molecule. Thus, Nell-1 may be a more advantageous adjunctive osteoinductive molecule due to its specificity to cells already committed toward the osteochondrogenic pathway and could minimize adverse effects associated with current therapies, such as ectopic bone formation, inflammation, and soft tissue swelling.

***Disclosures: Ronald Siu**, None.*

SU0185

Positive Regulation of Osteogenesis by Bile Acid through Farnesoid X Receptor (FXR). Sun Wook Cho*[1], Jee Hyun An[2], Jae-Yeon Yang[3], Ju Yeon Jung[2], Hyung Jin Choi[2], Yenna Lee[2], Sang Wan Kim[4], Young Joo Park[2], David D Moore[5], Jung-Eun Kim[6], Chan Soo Shin[2]. [1]University of Michigan School of Dentistry, USA, [2]Department of Internal Medicine, Seoul National University College of Medicine, South korea, [3]Department of Internal Medicine, Seoul National University College of Medicine, South korea, [4]Seoul National University Boramae Hospital, South korea, [5]Department of Molecular & Cellular Biology, Baylor College of Medicine, USA, [6]Kyungpook National University School of Medicine, South korea

Metabolic bone disease represents one of the major health problems of chronic cholestatic liver disease. Although pathogenetic mechanism of this condition is poorly understood, it may be possible that bile acids per se can regulate the function of osteoblast. Bile acid is mainly metabolized by Farnesoid X receptor (FXR), a member of the nuclear receptor superfamily that is mainly expressed in liver, intestine, kidney and adipose. We have investigated the role of bile acids in regulating bone metabolism in vitro and in vivo. Immunohistochemical staining showed that primary calvaria cells express endogenous FXR especially in the nucleus and treatment with deoxycholic acid (dCA) and chenodeoxycholic acid (CDCA) has increased the expression level of FXR. When calvaria cells were treated with dCA and CDCA, alkaline phosphatase (ALP) activities were significantly increased in a dose-dependent manner. In addition, in vivo deletion of FXR (FXR(-/-)) has resulted in significant reduction in whole body bone mineral density (BMD) by 10% ($p<0.001$) and 5% ($p<0.05$) in both female and male, respectively, at 8 weeks of age compared with wild-type (WT) littermate and the difference was maintained up to 20 weeks of age. No significant difference in body weight was observed between FXR(-/-) and WT littermate. Furthermore, micro-CT analysis of distal femur at 16 weeks demonstrated significant reduction of trabecular bone volume (-34%), trabecular number (-23%), trabecular thickenss (-15%) and cortial thickenss (-30%) in FXR(-/-) mice compared with WT littermate. Induction of ALP activities upon treatment with dCA and CDCA was also blunted in primary calvaria cells from FXR(-/-) mice compared with those from WT littermate. Expression of RunX2, ALP and Osteocalcin was significantly suppressed in calvaria cells from FXR(-/-) mice compared with WT littermate. In addition, bone marrow macrophage culture showed that osteoclastogenesis was also significantly increased in FXR(-/-) mice compared with WT littermate. Taken together, these results suggest that bile acid is a positive regulator of bone mass and FXR plays a critical role in this regulation.

***Disclosures: Sun Wook Cho**, None.*

SU0186

Systemic Inflammation Impairs Fracture Healing. Daniel Toben*[1], Alessandro Serra[2], Ireen Schroeder[3], Thaqif El Khassawna[3], Manav Mehta[3], Likit Rugpolmuang[3], Katharina Schmidt-Bleeck[3], Hanna Schell[3], Jasmin Lienau[3], Andreas Radbruch[2], Georg Duda[3]. [1]Charité Universitätsmedizin Berlin, Germany, [2]German Arthritis Research Center, Germany, [3]Julius Wolff Institute & Center for Musculoskeletal Surgery, Charité Universitätsmedizin, Germany

Purpose: This project was aimed at further elucidating how activation of the host immune system influences the process of bone regeneration following fracture. The hypothesis of this study was that fracture healing would be impaired due to lipopolysaccharide (LPS) induced activation of the innate immune system.

Methods: A standard closed femoral fracture was created in 8-10 weeks old wildtype (WT) mice and mice receiving LPS. Repeated intraperitoneal injections of LPS (2 mg/kg body weight) 24 h before fracture that were repeated every 3 days induced activation of the innate immune system. For biomechanical testing and µCT analysis, animals were sacrificed after 14 and 21 days (N=8/time point). Statistical comparisons between groups were performed using the Mann-Whitney U-test.

Results: Biomechanical testing demonstrated a significantly lower torsional stiffness at day 14 (25 (15/31) % vs. 47 (33/58) %; [median (25/75 percentile)], $p=0.01$) in the LPS injected mice in comparison to the WT group. µCT evaluation of LPS specimens (FIG. 1) at day 21 showed a lower bone volume of the callus (BV) (8.0(7.7/9.1) mm^3 vs. 10.5(9.7/14.7) mm^3, $p=0.001$) and higher tissue mineral density (TMD) (945(927/994) vs. 903(857/943), $p= 0.014$).

Conclusion: The results of this study have shown impaired bone regeneration in mice following induction of immune responses by LPS. The morphometric and biomechanical analyses provide strong evidence for this conclusion supporting the results of Reikeras et al. (2005). Cells of the innate immune system including macrophages and neutrophils are key players in the response to LPS. LPS signals are transduced via toll like receptor-4 (TLR-4) and potently induce the release of proinflammatory cytokines including TNF-α. This could potentially lead to impaired healing. Further analyses are necessary to identify the underlying molecular and cellular mechanisms.

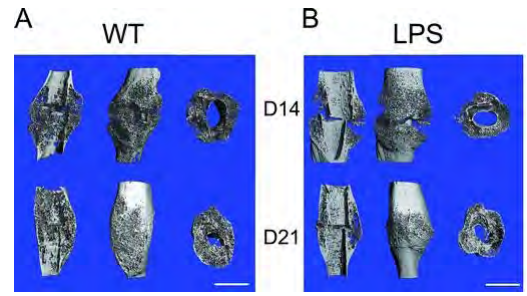

FIG. 1

***Disclosures: Daniel Toben**, None.*

SU0187

Th17- and RANKL$^+$Th1-cells Compete for Regulating Alveolar Bone Loss in T1D. Tien-Yu Shieh[1], Yen-Tung (Andy) Teng*[2], Yen-Chun G Liu[1], Deeqa Mahamed[3]. [1]Center for Osteoimmunology & Biotechnology Research, College of Dental Medicine, Kaohsiung Medical University, Taiwan, [2]Kaohsiung Medical University, Taiwan, [3]Lab. of Molecular Microbial Immunity, Div. of Periodontics, Eastman Dental Center & Dept. of Microbiology & Immunology, University of Rochester, USA

Background: Diabetes imposes a high risk of developing severe periodontitis and we have shown that diabetic non-obese diabetic (NOD) mice, an analogue of human type-1 diabetes (T1D), manifest more severe periodontal breakdown than that of non-diabetics controls (Diabetes 54:1477, 2005). IL-17 is known to implicate on arthritic bone loss; however, its role in periodontitis under T1D remains unclear. Objective: To study the mechanism of T-cell-mediated immunity, IL-17 and RANKL-RANK signaling to enhancing periodontal breakdown in diabetic NOD mice orally infected with Aggregatibactor actinomycetemcomitans (Aa), a G(-) anaerobe responsible for aggressive and severe chronic periodontitis. Materials & Methods: Pre-diabetic (5-6-weeks-old), non-diabetic (14-16-weeks-old) and diabetic (>16-18 weeks-old) NOD mice were orally inoculated with Aa (ATCC-29523) 2x/wk for 3 wks, and followed till 8-wks. Subsequently, molars were quantified for alveolar bone loss by histomorphometry and local CD4+Th-cells were purified for responses to Aa stimulation in vitro, RANKL-vs.-IL-17 expressions by flow-cytometry, real-time PCR and cytokines in culture supernatant by ELISA. Results: i) Aa-reactive CD4+T-cells from diabetic mice exhibit significantly higher proliferation and RANKL expressions than those from pre- & non-diabetic controls; ii) in parallel, diabetic Th-cells have a 3.5-fold increase in RANKL vs. a 3.4-fold increase in IL-17 mRNA expression, along with higher IL-17 secretion, via ELISA; iii) through FACS analyses, Aa-reactive CD4+Th-cells from diabetic mice maintain similar

subsets of RANKL+IL-17+Th(17)-cells, despite higher IL-17 production. In conclusion: Microbes-reactive RANKL(+) diabetic CD4+Th(17)-cells do not express higher amount of IL-17, whose contribution during the enhanced periodontal breakdown in T1D awaits further determination and are likely different from those in arthritic bone loss. Ongoing study of RANKL and IL-17/Th17 interactions are discussed to reveal the underlying mechanisms in T1D. This project was supported by grants from NIH-DE018356 & -014473, USA & EX99-S34199N, NHRI, Taiwan.

***Disclosures: Yen-Tung (Andy) Teng**, None.*

SU0188

The Environmental Contaminant and Potent PPARγ Agonist Tributyltin Stimulates Aging-Like Alteration of the Bone Marrow Microenvironment and Impairs Lymphopoiesis. Amelia R. Haas*[1], David H. Sherr[2], Louis Gerstenfeld[1], Jennifer J. Schlezinger[2]. [1]Boston University School of Medicine, USA, [2]Boston University School of Public Health, USA

The bone marrow is a multifunctional organ that supports bone formation and lymphopoiesis, both of which are compromised during aging. Aging also is associated with increased fat mass within the marrow. Recent literature showed that: 1) there is a reciprocal relationship between adipocyte and osteoblast differentiation, 2) osteoblasts are necessary for optimal lymphopoiesis and 3) adipocytes are negative regulators of lymphopoiesis. The environmental contaminant tributyltin (TBT) is a highly potent agonist for PPARγ, the master regulator of adipocyte differentiation (~10 nM EC_{50}) and, uniquely, can activate PPARγ as well as its dimerization partner RXRα. Detection of organotins in humans suggests that use in plastics, wood preservatives, and pesticides has resulted in significant environmental exposure. We hypothesize that TBT can alter bone marrow mesenchymal stromal cell differentiation through its activation of PPARγ and impairs B lymphopoiesis by both compromising the bone marrow microenvironment and activating apoptosis. This hypothesis was explored in primary mouse bone marrow cultures, a mouse pro/pre-B cell line, and an *in vivo* exposure study. Treatment of primary cultures with TBT at concentrations relevant to human exposures and with the therapeutic PPARγ agonist rosiglitazone stimulate adipocyte differentiation (Nile Red staining), but the RXRα agonist bexarotene did not. In contrast, TBT and bexarotene had a more substantial effect on suppressing osteoblast differentiation (alkaline phosphatase, mineralization, and nodule number) than did rosiglitazone. Hematopoietic cells in the primary cultures were negatively affected by PPARγ and RXRα agonist exposure. There was a significant reduction in cell number, including the loss of B220+ progenitor B cells. The most substantial suppression was seen with TBT and was likely enhanced by the direct activation of apoptosis in hematopoietic cells, as TBT is a highly potent activator of apoptosis in a developing B cell model (cytochrome c release and caspase 3 activation). Long term, low-dose exposure to TBT *in vivo* significantly reduced peripheral B cell numbers, possibly resulting from altered bone marrow physiology. Thus, therapeutic and environmental PPARγ ligands may suppress lymphopoiesis by accelerating aging-like adipocyte differentiation and compromise of the bone marrow microenvironment, an effect that may be exacerbated by simultaneous induction of apoptosis by toxic environmental ligands.

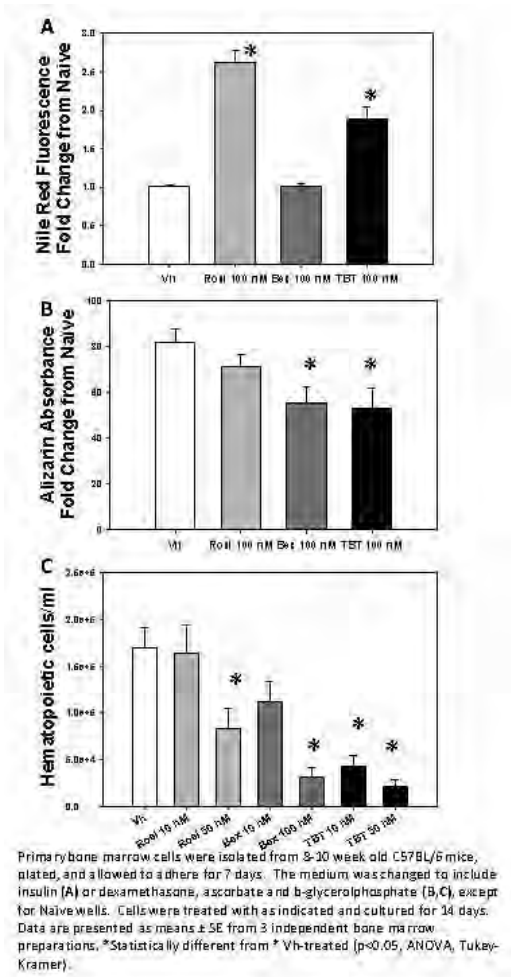

Primary bone marrow cells were isolated from 8-10 week old C57BL/6 mice, plated, and allowed to adhere for 7 days. The medium was changed to include insulin (A) or dexamethasone, ascorbate and b-glycerolphosphate (B,C), except for Naïve wells. Cells were treated with as indicated and cultured for 14 days. Data are presented as means ± SE from 3 independent bone marrow preparations. *Statistically different from * Veh-treated (p<0.05, ANOVA, Tukey-Kramer).

Distinct Effects of PPAR, RXR, and Dual Ligands on Marrow Microenvironment

***Disclosures: Amelia R. Haas**, None.*

SU0189

Distinct Growth Hormone Receptor Signaling Modes Regulate Skeletal Muscle Development and Insulin Sensitivity. Douglas Digirolamo*[1], Mahendra Mavalli[2], Yong Fan[3], Ryan Riddle[4], Kenneth Campbell[5], Mark Sperling[3], Thomas van Groen[2], Stuart Frank[2], Karyn Esser[5], Marcus Bamman[2], Thomas Clemens[1]. [1]Johns Hopkins University, USA, [2]University of Alabama at Birmingham, USA, [3]University of Pittsburgh, USA, [4]Johns Hopkins University School of Medicine, USA, [5]University of Kentucky, USA

The growth hormone (GH) / insulin-like growth factor-1 (IGF-1) axis is critical for normal postnatal growth and the development of bone and skeletal muscle. Mammals with large muscles also have large bones, indicating the presence of a mechanism for crosstalk between these anatomically adjacent tissues that serves to "synchronize" their mass. Our previous work has shown that both bone and cartilage formation requires IGF-1 receptor (IGF-1R) signaling, but that GH receptor (GHR) is dispensable for normal longitudinal growth and acquisition of bone mass. Thus, GH appears to exert its anabolic effects on the skeleton primarily through increased IGF-1 production. To identify the mechanisms responsible for the anabolic actions of GH in skeletal muscle, we determined the impact of skeletal muscle-restricted disruption of GHR (ΔGHR), IGF-1 (ΔIGF-1) and IGF-1R (ΔIGF-1R) on skeletal muscle development and function in mice. Both ΔGHR and ΔIGF-1R mice exhibited impaired skeletal muscle development characterized by profound reductions in myonuclei numbers and myofiber cross-sectional area, as well as accompanying functional deficiencies assessed by grip strength and rotarod. Mice with skeletal muscle-restricted disruption of IGF-1, by contrast, had no detectable phenotype. In primary myoblasts, GH increased IGF-1 production, stimulated myoblast fusion, and induced nuclear localization and activity of NFAT, a transcription factor known to be required for myoblast fusion. Disrupting GHR did not alter basal myoblast fusion *in vitro*, but as expected, eliminated GH-stimulated fusion. However, disrupting the IGF-1R abolished GH-induced fusion, which suggests that the anabolic effect of GH is mediated by IGF-1. Surprisingly, mature ΔGHR mice developed a metabolic phenotype not seen in the ΔIGF-1R mice, including marked peripheral adiposity, insulin resistance and glucose intolerance, measured by insulin and glucose tolerance tests. *In vitro*, glucose uptake was virtually abolished in myoblasts lacking GHR.

Impaired glucose uptake was accompanied by decreased insulin receptor protein abundance and significantly increased phosphorylation of IRS-1 on Serine 1101, an inhibitory site previously shown to be phosphorylated in nutrient excess-induced obesity. These results identify distinct signaling pathways through which GHR regulates skeletal muscle development and modulates nutrient metabolism.

***Disclosures: Douglas Digirolamo**, None.*

SU0190

Genetic Evidence that Thyroid Hormone is Indispensable for Prepubertal Rise in IGF-I Expression and Bone Accretion in Mice. Subburaman Mohan*[1], Kristen Govoni[2], Heather Davidson[3], Leah Rae Donahue[4]. [1]Jerry L. Pettis Memorial VA Medical Center, USA, [2]University of Connecticut, USA, [3]JL Pettis Memorial VA Medical Center, USA, [4]Jackson Laboratory, USA

It is now well established that disruption of IGF-I in both mice and humans leads to a dramatic reduction in peak BMD. Based on the findings that the magnitude of deficit in BMD and bone size is several-fold greater in IGF-I knockout mice compared to growth hormone (GH) deficient mice at the end of prepubertal growth period, we predicted that IGF-I regulation of bone accretion during prepubertal growth period is mediated by a GH-independent mechanism. Accordingly, we found no significant difference in serum IGF-I level between GH-deficient and control littermates during prepubertal growth (21 days) but a >75% reduction in adult GH-deficient mice. Because the rapid increase in serum IGF-I levels during prepubertal growth period were preceded by increased serum T3 and correlated highly ($r=0.82$, $P<0.001$) with serum T3, we proposed that the increase in IGF-I expression during the prepubertal growth period is predominantly mediated by TH, independent of GH. To demonstrate a cause and effect relationship between changes in serum T3 and IGF-I levels, we induced hypothyroidism in newborn mice by treating pregnant mice with 0.05% methimazole in drinking water. We found serum T3, serum IGF-I, femur IGF-I mRNA and femur BMD were reduced by 32%, 36%, 33% and 15% respectively (all $P<0.01$) at day 14 in methimazole treated mice compared to control mice. Serum IGF-I levels in methimazole treated mice showed significant positive correlation ($r=0.76$, $P<0.05$) with serum T3 levels. Furthermore, IGF-I mRNA levels were significantly decreased in the femurs of methimazole treated mice. To obtain further experimental proof that the increase in IGF-I production during prepubertal growth period is dependent on TH, we used two mutant mouse models, *Tshr*$^{hyt/hyt}$ and *Duox2*$^{-/-}$, that exhibit TH deficiency. In both of these mutant models, neither serum IGF-I nor femur BMD were affected at day 7. However, at day 21, serum IGF-I and femur BMD were decreased by >50% ($P<0.01$) and >25% ($P<0.01$), respectively, in *Tshr*$^{hyt/hyt}$ and *Duox2*$^{-/-}$ mice. Treatment of *Tshr*$^{hyt/hyt}$ mice during prepubertal growth period (day 5-14) with daily administration of replacement doses of T3/T4 for 10 days rescued deficits in serum IGF-I, skeletal IGF-I and femur BMD. Based on our findings, we conclude that: 1) IGF-I expression during prepubertal growth is predominantly mediated by TH in mice, and 2) TH and not GH is indispensable for bone accretion that occurs during prepubertal growth in mice.

***Disclosures: Subburaman Mohan**, None.*

SU0191

Hypoxic Treatment of Preadipocyte 3T3-L1 Cells Leads to the Inhibition of Adipogenesis from Pre-adipocyte to Mature Adipocyte. J. Edward Puzas[1], Tian-Fang Li[2], yi-jang lee[3], Hsin Chiu Ho[2], Tzong-Jen Sheu*[2]. [1]University of Rochester School of Medicine, USA, [2]University of Rochester, USA, [3]National Yang Ming Medical university, Taiwan

Our previous works have demonstrated that hypoxic treatment of preadiopocyte 3T3-L1 cell model leads to inhibition of adipogenesis induced by differentiating stimuli (IDM). The differentiated 3T3-L1 fibroblasts exhibited accumulated lipid drops stained by Oil Red O lipophilic dyes. The morphology showed significant different between pre-induction of and post-induction of adipocyte differentiation. Based on this phenomenon, hypoxic treatment of cells (0.5% of oxygen) during induction of adipogenesis greatly inhibited by oxygen existance. We also compared the timing of hypoxic treatment during induction of adipogenesis. DFO was added concomitantly with IDM or one day after IDM to 3T3-L1 cells, and the immediate DFO treatment showed better inhibitory effect on adipocyte differentiation. This observation lead us hypothesize that hypoxia can preserve the undifferentiating state of stem cells or progenitor cells instead the whole phases of differentiation. The mRNA expression of the preadipocyte marker (pref-1) did not change under hypoxia during adipogenesis, compared to normoxia. Given that hypoxia mainly up-regulates HIF-1a protein, we examine whether knockdown of HIF-1a expression can compromise the inhibitory effects of hypoxia in adipcyte differentiation. The position of siRNA was chosen based on the mouse HIF-1a sequence. Two siRNAs (S11 and S18) were prepared and transfected into 3T3-L1 cells. The results showed that S11 but not S18 siRNA can efficiently repress HIF-1a expression under hypoxia. These two siRNAs differentially compromise the hypoxia-mediated inhibition of adipocyte differentiation in 3T3-L1 cells (S11 siRNA has greater effect than S18 siRNA). These results suggest HIF-1a can directly affect the adipogenesis. To better understand the effect of HIF-1a on inhibition of adipogenesis, a mutant HIF-1a cDNA with deletion of oxygen dependent degradation fragment (HIFODD) was constructed in the pBIG2i autoregulatory bidirectional tet-on gene expression system including a IRES-EGFP for monitoring the expression of target gene. The results show that HIFODD can co-express with EGFP in the stable 3T3-L1 cells by fluorescence microscopic detection and Western Blot analysis. We also started to use the Hif-1a conditonal knockout mice to further understand this adipogenesis inhibt effect.

***Disclosures: Tzong-Jen Sheu**, None.*

SU0192

Inhibition of c-Src Reduces IL-6 Expression *In Vivo* and *In Vitro*. Implication for Therapy. Barbara Peruzzi*[1], Alfredo Cappariello[2], Nadia Rucci[3], Fabrizio De Benedetti[2], Anna Teti[3]. [1]University of L'Aquila, Bambino Gesù Children Hospital, Italy, [2]Bambino Gesù Children Hospital, Italy, [3]University of L'Aquila, Italy

The pro-inflammatory cytokine IL-6 has a pivotal role in inflammation and bone turnover. In transgenic mice overexpressing IL-6 (IL-6 TG) bone formation is impaired. The non-receptor tyrosine kinase c-Src also inhibits bone formation and we have identified a loop between IL-6 and c-Src that maintains osteoblasts in a poorly differentiated status. We observed that in osteoblasts in which c-Src was inhibited by PP1, siRNA or dominant negative construct, IL-6 expression was time-dependently reduced vs. vehicle-treated osteoblasts with a mechanism involving STAT3, which is a component of the IL-6 pathway, a transcription factor for IL-6 itself and a substrate of c-Src. Prolonged treatment of osteoblasts with IL-6 induced c-Src activation likely mediated by the IGF-I pathway through the IGFBP -3 and -5, which were induced in osteoblasts by c-Src inhibition. According to the observation that the IGFBP-3 and -5 promoters have consensus sequences for Runx-2 and that c-Src inhibition upregulates Runx-2, the overexpression of Runx-2 in osteoblasts led to increased IGFBP-3 and -5 mRNAs, suggesting a role for this transcription factor in the link between the two IGFBPs and the IL-6/c-Src loop. To establish whether the interplay between IL-6 and c-Src is relevant in vivo, we used three established animal models. Firstly, we treated WT and IL-6 TG mice with a c-Src inhibitor. While this treatment mildly affected the bone structural parameters of WT mice, in IL-6 TG mice it had a robust effect increasing bone volume and trabecular thickness/number, and decreasing trabecular separation of the distal femur secondary spongiosa vs. vehicle-treated IL-6 TG mice. This outcome correlated with increased osteoblast and decreased osteoclast parameters, and with significant reduction of IL-6 mRNA in the whole long bones. Secondly, we treated WT mice with the IL-6 inducing agents, LPS or turpentine, and with the c-Src inhibitor, resulting again in a reduction of IL-6 mRNA in the whole long bones. Thirdly, we treated with the c-Src inhibitor immunodeficient mice previously injected in the left ventricle with the human breast cancer cell line MDA-MB-231 to develop experimental bone metastases. This treatment reduced the incidence of the osteolytic lesions and decreased both tumor-derived (human) and bone-derived (mouse) IL-6 production. In conclusion, we have identified a loop between IL-6 and c-Src that is active also in vivo and could have important implications for therapy.

***Disclosures: Barbara Peruzzi**, None.*

SU0193

A New Approach to Osteoblast Induction with RGD and /or BMPs Mimetic Peptides. Marie-christine Durrieu[1], Omar El Farouk Zouani*[2]. [1]INSERM U577, France, [2]Inserm, France

The bone morphogenetic proteins (BMPs) are cytokines of the transforming growth factor beta family. Some BMPs such as BMP-2, BMP-7 and BMP-9 play a major role in the bone and cartilage formation. After having designed a mimetic peptide of these growth factors, we immobilized these peptides as well as a peptide of adhesion (GRGDSPC) on polyethylene terephthalate (PET) surfaces and we evaluated the state of differentiation of pre-osteoblastic cells. The behavior of these cells on various functionalized surfaces highlighted the activity of the mimetic peptides immobilized on surfaces. The induced cells (observed in the case of surfaces grafted with BMP-2, 7 or 9 mimetic peptides) were characterized on several levels. First of all, we focused on the evaluation of the osteoblastic markers such as the transcriptional factor Runx2, which is a critical regulator of osteoblastic differentiation. Secondly, the results obtained showed that these induced cells take a different morphology compared to the cells in a state of proliferation or in a state of extracellular matrix production. Induced cells were characterized by an increased thickness compared to non-induced cells. Thus, our studies prove a direct correlation between cell morphology and state of induction. Thereafter, we focused on characterizing the extracellular matrix formed by the cells on various surfaces. The extracellular matrix thickness was more significant in the case of surfaces grafted with mimetic peptides of the BMP-2, 7 or 9, which once again proves their activity when immobilized on material surface. In this study, we showed synergy between two pathways induced by the surfaces bifunctionalized with two mimetic peptides (GRGDSPC and mimetic peptides of BMP-2, 7 or 9 immobilized in a homogeneous way): the first pathway ensured by the presence of the peptide of adhesion (GRGDSPC), which acts at the level of actin filaments via the integrins; the second pathway via the BMP receptors, which act on the expression of osteogenic markers.

***Disclosures: Omar El Farouk Zouani**, None.*

SU0194

TGF-β Suppressed the Expression of *Odd-skipped related 2* in Mesenchymal Cells. Shinji Kawai*, Atsuo Amano. Osaka University Graduate School of Dentistry, Japan

Several intercellular messengers properly regulate cellular proliferation, migration, and differentiation. Transforming growth factor-beta (TGF-β) is one of these messengers and regulates multiple biological processes from early development to maintenance of adult homeostasis.

Zinc-finger transcription factor *Odd-skipped related 2* (*Osr2*) is one of the regulators in osteoblast proliferation and bone formation. We previously reported its regulatory role using dominant-negative *Osr2* transgenic mice. The transgenic mice revealed the characteristic features, including 1) delayed mineralization in calvarial and cortical bone tissues, 2) distinctly increased radiolucency in soft X-ray analysis, 3) reduced staining intensities with alcian blue and alizarin red in the skull and skeletal elements, and 4) markedly thinner parietal and cortical bones. Differentiation and proliferation of alvarial osteoblasts oftransgenic mice were also found to be highly attenuated. In addition, *Osr2*-deficient mice revalidated that *Osr2* play a critical role in the secondary palate and teeth development.

In this study, we found that TGF-β dose-dependently suppressed *Osr2* expression and *Osr2* was involved in cellular migration in mesenchymal C3H10T1/2 cells. The suppression of *Osr2* expression by TGF-β was mediated by Smad3/Smad4 and p38 signaling molecules. The *Osr2* promoter possessed Smad3/4 binding element (SBE) between -647 and -64 of promoter. Ikzf1 (Ikaros) binding element existed just downstream of SBE. Ikzf1 acted as co-repressors of *Osr2* promoter with Smad3/4. We first identified Ikzf1 as Smad cofactor. Moreover, TGF-β induced cellular migration, but Osr2 inhibited migration.

We propose that TGF-β elicites migration via repression of Osr2 expression and activation of a Ikzf1-Smad3/4 transcriptional complex represents a mechanism of gene repression during cellular migration.

***Disclosures: Shinji Kawai**, None.*

SU0195

Sensitivity of Human Osteoblasts to TRAIL Induced Apoptosis. Silvia Colucci*[1], Giacomina Brunetti[1], Francesca Sardone[1], Angela Oranger[1], Giorgio Mori[2], Matteo Centonze[1], Alberta Zallone[3], Maria Grano[4]. [1]Department of Human Anatomy & Histology, University of Bari, Italy, [2]Department of Biomedical Science, University of Foggia, Italy, [3]University of Bari Medical School, Italy, [4]University of Bari, Italy

The number of osteoblasts (OBs), the bone forming cells, plays a critical role in bone turnover, and the control of their survival and/or apoptosis is finely regulated by apoptotic molecules. Conflicting data in the literature demonstrated that osteoblastic cells show different sensitivity to the apoptotic effect of TNF-related apoptosis-inducing ligand (TRAIL). However, these studies did not take into account the profound functional changes to which these cells undergo during their differentiation. Thus, in the present work we investigated the sensitivity of OBs to TRAIL-mediated apoptosis during their differentiation process as well as the expression of the death (DR4, DR5) and the decoy (DcR1, DcR2) TRAIL receptors in undifferentiated and differentiated normal human OBs. Our results showed that only undifferentiated OBs are sensitive to TRAIL apoptotic effect, in which TRAIL treatment induced the upregulation of the death receptor DR5 and the downregulation of the decoy receptor DcR2 respect untreated OBs at both mRNA and protein levels. In parallel experiments, we show that the stimulation of TRAIL induce a decrease of the expression of two intracellular inhibitors of apoptosis such as FLIP and XIAP in cells at the same differentiation status. On the contrary, differentiated OBs were resistant to TRAIL apoptotic effect. In these cells, TRAIL treatment induce a decrease of DcR2 receptor expression and an increase of FLIP and XIAP mRNA levels. In conclusion, our data highlight an important role for the TRAIL/TRAIL-receptor system in the regulation of OB apoptosis during the differentiation process.

***Disclosures: Silvia Colucci**, None.*

SU0196

Clopidogrel, a $P2Y_{12}$ Receptor Antagonist, Inhibits Osteoblast Differentiation and Function. Andrea Brandao-Burch[1], Timothy Arnett[2], Isabel Orriss*[1]. [1]University College London, United Kingdom, [2]University College, London, United Kingdom

There is mounting evidence that extracellular nucleotides, signalling through P2 receptors, play a significant role in bone, modulating both osteoblast and osteoclast function. We have shown previously that bone cells express multiple P2 receptor subtypes. ATP and UTP, signalling via the $P2Y_2$ receptor, selectively inhibit *in vitro* bone mineralization. In this study, we have investigated the expression of the $P2Y_{12}$ receptor by osteoblasts and the effects of Clopidogrel treatment on osteoblast formation, differentiation and function. Clopidogrel (Plavix®) is a selective $P2Y_{12}$ receptor antagonist and, currently, is the only P2 receptor antagonist available for therapeutic use. It is an antithrombotic, prescribed to reduce the risk of heart attack and stroke, acting via inhibition of platelet aggregation; at present its effects on bone cells are unknown. Osteoblasts were obtained from rat calvaria by trypsin/collagenase digestion and $P2Y_{12}$ receptor expression was studied at 4, 7 and 14 days using qPCR and western blotting. Osteoblasts were cultured with Clopidogrel (1-50μM) for up to 14 days and bone nodule formation was measured by image analysis of alizarin red-stained cell layers. Cell number, viability, alkaline phosphatase (ALP) activity and collagen formation were assessed colorimetrically. The progression of osteoblast differentiation was shown by 2.5-fold and 5-fold increases in ALP mRNA expression at days 7 and 14, respectively (and bone formation at day 14). $P2Y_{12}$ receptor mRNA expression increased 2-fold and 6.5-fold at days 7 and 14, respectively; similar increases in $P2Y_{12}$ receptor protein expression were also observed. ADP, the primary agonist at the $P2Y_{12}$ receptor had no effect on osteoblast differentiation and function. In contrast, Clopidogrel at 5μM and 10μM inhibited bone nodule formation by 50% and > 95%, respectively. At day 7 of culture, Clopidogrel caused dose-dependent decreases in cell number (25-40%) at concentrations of ⩾ 1μM; by day 14 no differences in osteoblast number were seen. ALP activity was reduced 65% and 90% in cultures treated with ⩾10μM Clopidogrel at days 7 and 14, respectively. Treatment with ⩾10μM Clopidogrel dose-dependently decreased collagen formation by up to 35% and 50% at days 7 and 14 of culture. These findings raise the possibility that long-term exposure of osteoblasts to Clopidogrel *in vivo* could directly impact bone health.

***Disclosures: Isabel Orriss**, None.*

SU0197

Effects of Direct Inhibition of Geranylgeranyl Pyrophosphate Synthesis on Osteoblast Differentiation. Megan Moore-Weivoda*, Huaxiang Tong, Raymond Hohl. University of Iowa, USA

Cholesterol-lowering statin drugs stimulate bone morphogenetic protein-2 (BMP-2) expression and osteoblast differentiation. Statins also deplete farnesyl pyrophosphate (FPP) and geranylgeranyl pyrophosphate (GGPP); addition of GGPP prevents statin-stimulated osteoblast differentiation. We hypothesized that direct inhibition of GGPP synthase (GGPPS) with digeranyl bisphosphonate (DGBP) leads to BMP-2 expression and osteoblast differentiation. MC3T3-E1 pre-osteoblasts and primary rat calvarial osteoblasts were studied. Intracellular FPP and GGPP were quantified by reverse phase HPLC to assess inhibition of GGPPS by DGBP. Western blot was used to evaluate perturbations of protein prenylation. Osteoblast differentiation cultures were set-up to assess the effects of DGBP on BMP-2 expression and mineralization. Cultures were exposed to 5-25μM DGBP for 24 hrs followed by replacement of differentiation media alone. qPCR was used to quantify BMP-2 expression and Alizarin red was used to analyze mineralization. Treatment of MC3T3-E1 and primary osteoblasts with DGBP for 24 hrs led to a dose-dependent depletion of GGPP, EC50=0.51 and 1.22 μM, respectively. Protein geranylgeranylation, but not farnesylation, was reduced. Ten and 25 μM DGBP increased mineralization of primary osteoblasts (65% and 87%, respectively). In contrast, 5-10μM DGBP dose-dependently reduced mineralization of MC3T3-E1 cultures (33% and 49%, respectively) although there was the expected increase in BMP-2 expression (3-fold with 5μM DGBP at day 8). The reduced mineralization was not prevented by GGPP addition. By inhibiting GGPPS, DGBP also increases the substrate FPP. Baseline FPP was significantly lower in MC3T3-E1 cells (1.76 pmol/mg protein) compared to primary cells (3.76 pmol/mg protein) making them potentially more sensitive to DGBP-induced increases in FPP. Five μM DGBP increased FPP by 73% in MC3T3-E1 cells; this remained elevated until 72 hrs following pulse removal. To determine whether the increase in FPP could explain the effects of DGBP on mineralization in MC3T3-E1 cultures, lovastatin (Lov) co-treatments were performed. 1μM Lov inhibited the increase in FPP by DGBP. A combination pulse of 1μM Lov and 5μM DGBP prevented inhibition of mineralization by DGBP in MC3T3-E1 cultures, whereas 1μM Lov alone had no effect. Our work suggests that FPP, in addition to GGPP, is important in osteoblast differentiation and this may more completely explain statins' effects on bone.

***Disclosures: Megan Moore-Weivoda**, None.*

SU0198

Enhanced Healing of Rat Calvarial Critical Size Defects with Beta-tricalcium Phosphate Discs Associated with Dental Pulp and Adipose-derived Stem Cells. Roberto Fanganiello*[1], Felipe Ishy[2], Christhiane Ribeiro[3], Daniela Bueno[4], Ana Helena Bressiani[3], Maria Rita Passos-Bueno[2]. [1]Institute of Biosciences, University of Sao Paulo, Brazil, Brazil, [2]Institute of Biosciences, University of Sao Paulo, Brazil, [3]IPEN, University of Sao Paulo, Brazil, [4]São Paulo University, Brazil, Brazil

Development of biomaterials to replace bone implants is fundamentally important in the field of tissue engineering and an ideal scaffold to support bone regeneration must have both osteoconductive and osteoinductive properties. The osteoconductive characteristics can be fine-tuned controlling the macro-structure and the micro-architecture of the biomaterial to be used as a scaffold. On the other hand the osteoinductive properties might be enhanced associating the scaffold with cells harboring osteogenic potential. In this study we screened for micro-macro configurations of 5 different biomaterials to heal rat calvarial critical size defects when associates with adult stem cells of 2 origins. Stem cell populations were isolated from dental pulp of human deciduous teeth (DPSCs) and of human adipose tissue (ASCs) and cell culture was established. These cell populations were mainly positively

marked for mesenchymal stem cell antigens (CD29, CD90, CD105, SH3 and SH4) while negative for hematopoietic cell markers (CD14, CD34, CD45, CD117) and for endothelial cell marker (CD31). After in vitro induction these populations were capable to undergo osteogenic differentiation, as evidenced by alkaline phosphatase and alyzarin red staining. Both populations were independently associated (10e5) to 4.5 mm discs of different types of biomaterials: equine trabecular bone (Bioteck), processed porcine bone (BioOSS), powdered hidroxiapatite (HA) (OsteoSynt), biphasic synthetic beta-TCP / HA and monophasic beta-TCP. In vivo ossification was accessed using a rat (Wistar) model of paired critical size defects. Control groups were performed transplanting the cell free biomaterials. Through histological hematoxylin / eosin staining we compaired the in vivo bone formation induced by the different kinds of biomaterials paired with their control groups and we attested an enhanced ossification of the monophasic beta-TCP when associated with DPSCs or with ASCs as early as 1 month after the surgical intervention, with new bone formation and osteoblast linings surrounding several pores of the scaffold. In this work we showed that this screening and the successful association of adult stem cell to monophasic beta-TCP are solid starting points in order to test both the in vivo potential of stem cells from other origins and the clinical applications of these associations with monophasic beta-TCP.

CAPES /CEPID / FAPESP/ CNPq robertofanganiello@yahoo.com

***Disclosures: Roberto Fanganiello**, None.*
This study received funding from: CAPES

SU0199

Functional Adaptation in Female Rats: The Role of Estrogen Signaling. Susannah Sample*[1], Molly Racette[2], Zhengling Hao[2], Cathy Thomas[2], Mary Behan[2], Peter Muir[3]. [1]UW-Madison School of Veterinary Medicine, USA, [2]University of Wisconsin - Madison, USA, [3]University of Wisconsin, Madison, USA

Purpose: Osteoporosis is characterized by low bone mass and reduced fracture resistance. Ovariectomy (OVX) induces selective loss of sensory innervation from bone. In male rats load-induced bone formation is locally and neuronally-regulated. In female rats, estrogen receptor-α (ER-α) is thought to regulate functional adaptation at the level of bone cells, but it is unclear whether estrogen signaling in the nervous system is also important. The purpose of this study was to determine whether estrogen is involved in the neuronal regulation of load-induced bone formation.

Methods: 42 ovariectomized female 4 month old Sprague-Dawley rats were divided into the following groups based on the contents of a subcutaneous pellet implanted after OVX: Sham, Estrogen (17β-estrodiol), and G-1, an agonist that selectively targets the non-genomic estrogen receptor GPR-30. 14 days after OVX, the right ulna of each rat was loaded for 1,500 cycles at 2Hz and -17N. Half the loaded rats had temporary brachial plexus anesthesia of their right thoracic limb during loading. To label new bone formation calcein green was given after loading and alizarin red 7 days later; euthanasia occurred at 10 days. Transverse sections of ulnae were made. New bone formation was determined by standard methods. Brachial intumescence dorsal root ganglia (DRG) were dissected at euthanasia and expression of the ER-α, ER-β and GPR-30 genes was determined.

Results: Treatment with estrogen suppressed labeled bone formation in both loaded and contralateral ulnae, although neither estrogen nor G-1 treatment altered mechanosensitivity. Temporary brachial plexus anesthesia did not alter load-induced periosteal bone formation in any groups. Estrogen replacement increased ER-α expression in loaded limb DRG of rats that did not undergo brachial plexus anesthesia.

Conclusion: This study suggests that GPR-30 signaling does not influence load-induced bone formation. In this model the suppressive action of estrogen is likely via ER-α or ER-β. Bone loading in rats supplemented with estrogen resulted in increased expression of ER-α in the ipsilateral DRG suggesting a means by which estrogen may act on the skeleton via neuronal signaling. In experiments using a single period of loading, the adaptive response with and without neuronal blocking appears different male and female rats. The skeleton of male rats is more responsive to mechanical loading; the mechanism underlying this difference is unclear.

***Disclosures: Susannah Sample**, None.*

SU0200

H1-calponin Negatively Regulates Bone Mass in Mice. Nan Su, Maomao Chen, Siyu Chen, Can Li, Lin Chen*. State Key Laboratory of Trauma, Burns & Combined Injury, Center of Bone Metabolism & Repair, Trauma Center, Institute of Surgery Research, Daping Hospital, Third Military Medical University, China

H1-calponin (basic calponin) is known as a smooth muscle–specific, actin-binding protein which regulates smooth muscle contractile activity. Previous study showed that h1-calponin also plays a role in bone development, however the mechanism about the effects of h1-calponin on bone formation is not well clarified. To study the role of h1-calponin in bone formation, we first generated a transgenic mouse model (Col1-CNN1) in which the expression of h1-calponin is driven by the osteoblast-specific Col1a1 promoter. We found that the BMD (bone mineral density) of ColI-CNN1 mice detected by DEXA was decreased. Micro-computed tomography and histomorphometric analyses showed that ColI-CNN1 mice had decreased BMD and trabecular number compared with that in wild-type mice at 2 and 4 month. Three-point bending test revealed decreased biomechanical properties of femurs of 2 and 4-month-old ColI-CNN1 mice. To further explore the mechanism for the altered bone formation in ColI-CNN1 mice, we cultured primary osteoblasts to evaluate their proliferation and osteogenic differentiation. The proliferation of ColI-CNN1 osteoblasts was decreased compared with that in wild-type mice. On day 21 after osteogenic differentiation, ColI-CNN1 osteoblasts had fewer mineralized colonies, but there was no significant difference between the alkaline phosphatase activity of both ColI-CNN1 and wild-type osteoblasts. These data suggest that h1-calponin may inhibit the proliferation and mineralization of osteoblasts. Bone mass is maintained through the close microanatomical coupling of osteoblastic and osteoclastic activities, so we also detected the osteoclast formation using osteoblast:osteoclast co-culture system. The result showed that the number and size of osteoclasts co-cultured with ColI-CNN1 osteoblasts were increased compared with wild-type osteoblasts, which was caused by increased level of RANKL and decreased level of OPG in ColI-CNN1 osteoblasts. All the results indicated that the reduced bone mass of ColI-CNN1 was caused by impaired osteogenesis and enhanced osteoclastogenesis.

[The work was supported by the Special Funds for Major State Basic Research Program of China (973 program) (No.2005CB522604), National Natural Science Foundation of China (No.30425023, No.30530410, No.30901527)]

***Disclosures: Lin Chen**, None.*

SU0201

High Fat Diet-Induced Obesity Reduces Bone Formation through Activation of PPARγ to Suppress Wnt/β-catenin Signaling in Prepubertal Rats. Jin-Ran Chen*[1], Oxana P. Lazarenko[2], Kartik Shankar[2], Xianli Wu[2], Thomas M. Badger[2], Martin J. Ronis[2]. [1]University of Arkansas for Medical Science, Arkansas Children's Nutrition Center, USA, [2]University of Arkansas for Medical Sciences/Arkansas Children's Nutrition Center, USA

The effects of a high fat diet (HFD) and of obesity on skeletal development, maturation and remodeling remain largely unclear particularly in children. In this report, we utilized a total enteral nutrition (TEN) model to examine the direct effect of HFD feeding on bone prior to puberty. We chronically fed HFD containing 25% or 45% fat calories via TEN to male Sprague-Dawley rats for 4 weeks beginning at weaning. Body weight gains were matched between HFD-fed rats and rats fed a low fat chow diet (LFD) ad libitum. Both gonadal and abdominal fat mass were increased in HFD-fed animals compared to the LFD group ($P<0.05$). In addition, leptin and total non-esterified fatty acids (NEFA) were elevated in the HFD groups ($P<0.05$). HFD-feeding reduced total bone mineral content (BMC) and trabecular bone mineral density (BMD) compared to LFD-fed animals ($P<0.05$). This was accompanied by decreases in the serum bone formation marker osteocalcin, but increases in the bone resorption marker RatLaps ($P<0.05$). NEFA composition in serum from HFD and LFD-fed rats was characterized and quantified by a Shimazu QP-2010 GC-MS system after TLC separation. We found that five major free fatty acids, palmitic, stearic, oleic, linoleic and arachidonic acid in the ratio of 5:3:1:3:1 were 5 times higher in concentration in rat serum from 45% fat HFD-fed compared to LFD-fed rats. Consistent with an increase in bone marrow adiposity, increased adipogenic gene PPARγ and AP2 expression was measured in bone from HFD-fed compared to LFD-fed rats ($P<0.05$). In contrast osteoblastogenic gene osteocalcin and Runx2 expression was reduced in bone tissue from the HFD-fed group compared to HFD-fed group ($P<0.05$). Impaired osteoblastogenic stromal cell differentiation in the HFD-fed rats stemmed from down-regulation of the key canonical Wnt signaling molecule β-catenin protein and reciprocal up-regulation of nuclear PPARγ expression in bone ($P<0.05$). In a set of in vitro studies using pluripotent ST2 mesenchymal stem cells (MSCs) treated with serum from rats on the different diets or using a mixture of free fatty acids based on the ratio appearing in serum from HFD-fed rats, we were able to recapitulate our in vivo findings These observations strongly suggest that increased NEFA in serum from HFD-fed rats directly impaired bone formation due to stimulation of bone marrow adipogenesis. These effects of HFD-feeding on bone in early life may result in impaired attainment of peak bone mass and therefore increase the prevalence of osteoporosis later on in life. This study was supported by ARS CRIS #6251-51000-005-03S.

***Disclosures: Jin-Ran Chen**, None.*

SU0202

Inhibition of EphA-ephrinA Interaction Induces Acute Bone Formation in an Adult Bone Organ Culture and in Mice. Naoko Irie*, Koichi Matsuo. School of Medicine, Keio University, Japan

To maintain bone homeostasis, functions of osteoclasts and osteoblasts are tightly regulated through communication between and within these two cell lineages. Previously we showed that the cell surface ligand ephrinA2 and the receptors EphA2 and EphA4 are expressed in these bone cells. The purpose of this study is to investigate the roles of ephrinA-EphA interaction in bone homeostasis by loss-of-function experiments using EphA2/4 inhibitors and knockout mice lacking EphA2.

As EphA2/4 inhibitors, we used 2,5-dimethylpyrrolyl benzoic acid and its isomer, which bind selectively to the ligand binding domains of EphA2/4 receptors, and block the ligand-receptor interaction. Mice lacking EphA2 were provided by Dr. M. Asano

(Kanazawa Univ). In addition to conventional osteoclast and osteoblast cultures, we employed a novel organ culture procedure using adult mouse long bones.

We first examined M-CSF/RANKL-induced osteoclast formation from mouse bone marrow-derived macrophages in the presence of EphA2/4 inhibitors, and found that osteoclastogenesis was suppressed dose-dependently (day 6). Bone marrow-derived macrophages lacking EphA2 also showed less efficient osteoclast differentiation compared with wild-type controls. On the other hand, in neonatal mouse calvarial osteoblast cultures, EphA2/4 inhibitors enhanced alkaline phosphatase activity (day 6) and calcium deposition (day 13) in a dose dependent manner.

Next, we cultured intact adult mouse long bones in the presence or absence of EphA2/4 inhibitors. Micro computed tomography (μCT) measurement revealed that bone mineral density was increased in the secondary spongiosa of the distal femur by EphA2/4 inhibitors within 24 hrs and was further increased upto 72 hrs. The calcium concentration in the culture supernatant of the bone organ culture was decreased by EphA2/4 inhibitors with concomitant increase in bone mineral density. We observed calcein labeling in secondary spongiosa upon EphA2/4 inhibitor treatment within 72 hours. These data suggest that EphA2/4 inhibitors rapidly induced calcium uptake and deposition from the extracellular environment to bone formation surface. Finally, we injected EphA2/4 inhibitors into adult mice in every 24 hrs for 3 days. EphA2/4 inhibitors induced high bone mineral density of the entire femur compared to control. In conclusion, inhibition of epnrinA-EphA interaction induces unexpected "acute" bone matrix formation/mineralization in both organ culture and in mice.

***Disclosures: Naoko Irie**, None.*

SU0203

Intravenous, Low Dose, Short Interval Double Labels Analyzed by Confocal Microscopy Optimise Precise Quantitation of Mineral Apposition and Bone Formation Rate. Moira Cheung*[1], Alan Boyde[2], John Bassett[3], Graham R. Williams[1]. [1]Molecular Endocrinology Group, Imperial College London, United Kingdom, [2]Bart's & London School of Medicine, Queen Mary University of London, United Kingdom, [3]Imperial College London, United Kingdom

Bone formation can be investigated following administration of fluorochrome labels separated by a defined interval. The mineral apposition rate (MAR) is calculated as the distance between the labels divided by the time between their administration. The product of MAR and extent of surface mineralizing activity represents the bone formation rate (BFR). Unfortunately, the lack of standardized protocols has resulted in unreliable comparisons of BFR between laboratories. Furthermore, results obtained from analysis of thin undecalcified bone sections using fluorescence microscopes should be corrected for plane of section in order to obtain accurate BFR estimates. Mineralizing surfaces of littermate mice were labelled with intravenous or intraperitoneal administration of calcein or alizarin at 22 hour intervals at doses of 2.5mg/kg, 25mg/kg and 100mg/kg. The width of label incorporated into dentine was determined by confocal laser scanning microscopy (CSLM) of transverse sections of mandibular incisors and effects of route of administration and fluorochrome concentration compared. Incorporated calcein and alizarin labels were narrower following intravenous administration (calcein: $0.95 \pm 0.2\mu m$ vs 5.4 ± 0.5***; alizarin: 1.7 ± 0.3 vs 6.5 ± 0.8***; mean width $\pm$ SEM, intravenous versus intraperitoneal, ***$p<0.001$, student's unpaired t-test). Labels were also narrower after intraperitoneal administration of low (2.5mg/kg alizarin and calcein) compared to high (25mg/kg calcein, 100mg/kg alizarin) doses of fluorochrome (calcein: $2.1 \pm 0.3\mu m$ vs 5.9 ± 0.9***; alizarin: 2.2 ± 0.3 vs 8.3 ± 0.7***, low dose vs high dose, ***$p < 0.001$). In trabecular bone, double labels were undetectable following intraperitoneal administration of fluorochrome whereas multiple discrete sites of double labeling were resolved following intravenous administration. CSLM improves accuracy by allowing selection of only those labeled surfaces lying parallel to the optic axis for analysis, thereby eliminating measurement artefacts resulting from variable planes of sectioning. These data indicate that sharp, discrete labeling can be obtained by intravenous short interval administration of low doses of fluorochromes, resulting in much more precise determination of MAR and BFR.

***Disclosures: Moira Cheung**, None.*

SU0204

KLF10/KLF11 Double Knockout Mice Exhibit an Osteopenic Skeletal Phenotype. John Hawse*[1], Urszula Iwaniec[2], Kevin Pitel[3], Elizabeth Bruinsma[3], Kenneth Peters[3], Nalini Rajamannan[4], Russell Turner[2], Malayannan Subramaniam[5], Thomas Spelsberg[5]. [1]Mayo Clinic College of Medicine, USA, [2]Oregon State University, USA, [3]Mayo Clinic College of Medicine, USA, [4]Northwestern University Medical School, USA, [5]Mayo Clinic, USA

KLF 10 and 11 are members of the Krüppel family of transcription factors. Previously, we have shown that female KLF10 knockout (KO) mice exhibit a gender-specific osteopenic bone phenotype which diminishes with age (5-12 months). This observation led to the hypothesis that another closely related gene may be compensating for loss of KLF10 expression. Since KLF11 is the most closely related gene which is also expressed in osteoblasts, we generated KLF10/KLF11 double KO mice to determine if a more severe and prolonged bone phenotype would be observed. Indeed, pQCT analysis revealed that deletion of both KLF10 and KLF11 leads to a more pronounced osteopenic phenotype which affects both male and female mice and persists throughout age. Significant decreases in multiple bone parameters were detected including femur length, and total bone mineral content and area. Micro-CT analysis confirmed that the femurs and vertebrae of double KO mice had lower bone volume relative to WT littermates. Interestingly, over 50% of the double KO mice also displayed a trabecularization of cortical bone in vertebrae. Since we have previously shown that KLF10 can directly regulate Runx2 and osterix expression as well as mediate TGFβ and Wnt signalling through repression of Smad7 and activation of Lef consensus elements respectively, we sought to determine if KLF11 also regulates these important osteogenic genes and pathways. Unlike KLF10, KLF11 is not able to repress Smad7 promoter activity, or induce Runx2 or osterix promoter activity. However, KLF11 is able to induce a Lef reporter construct to a greater degree than that of KLF10 and is also a more potent co-activator of Lef transcriptional activity in osteoblasts. Co-immunoprecipitation studies revealed that like KLF10, KLF11 protein also interacts with both Lef and β catenin. Taken together, our results suggest that KLF11 may compensate for KLF10 in bone during the aging process. These data also reveal that loss of both KLF10 and KLF11 triggers a more severe osteopenic phenotype which affects both male and female animals and persists with age. At the molecular level, the transcriptional actions of KLF11 are similar to that of KLF10 only with regard to activation and co-activation of a Lef reporter construct suggesting that the Wnt pathway may be one of the more prominent mechanisms through which KLF11 compensates for loss of KLF10 in bone.

***Disclosures: John Hawse**, None.*

SU0205

Low Intensity Ultrasound Increase Rate of Mineralization in Stimulated Microgravity. Sardar Uddin*[1], Yi-Xian Qin[2], Minyi Hu[1], Shu Zhang[1], Jiqi Cheng[3], B Huang[4]. [1]Stony Brook University, USA, [2]State University of New York at Stony Brook, USA, [3]Stony Brook Univeristy, USA, [4]Stony Broo Univeristy, USA

Microgravity causes bone loss in skeleton potentially due to decrease in bone mineralization by osteoblast cells. *In vitro* studies using stimulated microgravity has shown significant decrease in expression of osteoblastic transcription factors and low of alkaline phosphatase activity (ALP). Low-intensity pulse ultrasound (LIPUS) has shown capability in promoting bony ingrowth and accelerating rate of mineralization in osteoblast cells by up regulating expression of different osteoblastic transcription factors, matrix proteins and ALP activity. Ultrasound has been known to increase calcium deposition in the osteoblast cells. The objective of this study was to study the effects of LIPUS on osteoblast mineralization in stimulated microgravity.

Human fetal osteoblast (hfob 1.19) was cultured in DMEM:F12 media supplemented with 15% FBS and 0.3mg/ml G418 with initial seeding density of 50,000 cell per Opticell cartilage. Cells were allowed to grow to confluency, and stimulations were started at day 7 of post confluency. Cells were distributed into four groups (n=4 each), gravity, gravity + LIPUS, simulated microgravity, and microgravity + LIPUS. Stimulated microgravity environment was created by putting Opticells into an *in vitro* rotary system, with rotation set at 15 RPM. LIPUS groups were stimulated daily for total of 14 days with $30mW/cm^2$ for 20 min. Cells were kept at 37C, 5% CO_2 environment during experiment and medium was changed every second day. After 14 days of stimulations cells were analyzed for calcification by staining with Alizarin red stain and cytoskeleton changes with antibodies against actin and microtubules. Only the area stimulated with ultrasound was used for analyses.

Alizarin red (AZ) staining (Fig 1) shows significant increase in calcification in microgravity + LIPUS group (2.70 ± 0.03 mM AZ/ 10^6 Cells) compare to microgravity group (2.16 ± 0.24 mM AZ/10^6 Cells, p=0.023). Significant decrease of calcification was also observed (47%) from gravity (3.18 ± 0.21 mM AZ/ 10^6 Cells) group to the microgravity group (2.16 ± 0.24 mM AZ/10^6 Cells, p=0.009). Higher mineralization was observed in gravity + LIPUS group (3.69 ± 0.31 mM AZ/10^6 Cells) compare to gravity group (3.18 ± 0.21 mM AZ/ 10^6 Cells, p=0.08). It was also observed that microgravity samples had lesser number of cells.

These results imply that LIPUS increases mineralization in osteoblast cells in microgravity environment. Further experiments will look at cytoskeleton and transcription factors.

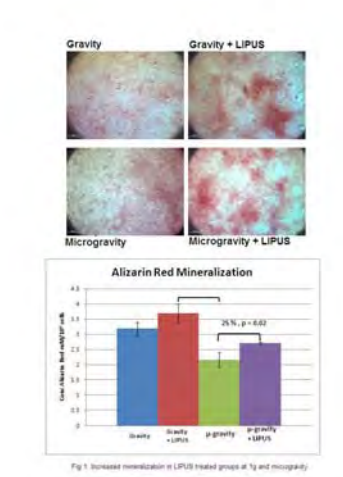

Matrix Mineralization

***Disclosures: Sardar Uddin**, None.*

SU0206

Nck1, a Molecular Adaptor Prerequisite for Cell Motility, is Stimulated by Bone Morphogenetic Protein and Contributes to Maintain Bone Mass. Ryo Hanyu[1], Tetsuya Nakamoto[1], Kentaro Miyai[1], Masasi Nagao[1], Smriti Aryal A.C*[2], Masaki Noda[1], Yoichi Ezura[3], Tadayoshi Hayata[4], Takuya Notomi[5], Hiroaki Hemmi[1], Tony Pawson[6]. [1]Tokyo Medical & Dental University, Japan, [2]Department of molecular pharmacology, Tokyo medical & dental university, Japan, [3]Tokyo Medical & Dental University, Medical Research Insititute, Japan, [4]Medical Reserach Institute, Tokyo Medical & Dental University, Japan, [5]GCOE, Tokyo Medical & Dental University, Japan, [6]Mount sinai hospital, samuel lunenfeld research institute, Canada

Bone remodeling is determined by the precise coordination of bone resorption and subsequent bone formation. Negative balance of bone remodeling process results in osteoporosis. Cell motility is critical for proper bone remodeling as cells in osteoblastic lineages are migrating into the sites of remodeling after bone resorption has been taken place. Regulation of the actin cytoskeleton, i.e the dynamic assembly and disassembly of filamentous actin, governs essential aspects for cell motility such as the formation of membrane protrusions and cell adhesion to other cells or to the substrate. Extracellular signals including the attachment of the cells to the bone and cartilage can induce remodeling of the actin cytoskeleton through changes in tyrosine phosphorylation. Nck proteins are adaptor molecules and regulate actin organization. Mammals carry 2 related Nck genes Nck1 and Nck2 (collectively termed Nck) each of which encodes a protein with three SH3 domains and a C terminal SH2 domain. Nck, is a critical link in transducing signals from tyrosine phosphorylation to the cytoskeleton. However, the role of Nck and its mechanism of action in bone metabolism is not known. In vivo, Nck1 single knockout mice reduce trabecular BV/TV, bone formation rate (BFR), Mineral apposition rate (MAR) is also reduced in Nck1 knock out mice in comparison to the control. The expression of bone phenotypic markers of primary osteoblastic culture such as type I collagen and osteocalcin is reduced in Nck1 deficient osteoblasts compared to the wild type. We examined how Nck1 deficiency causes such osteoblastic dysfunction and bone loss. In vitro, Nck1 is expressed in MC3T3E1 osteoblastic cells based on RT PCR. Fluorescence immunostaining was performed using antibody against Nck1 and we found that Nck1 is localized in the cytoplasm and nucleus of MC3T3E1 osteoblastic cells. The expression of Nck1 in these cells after exposure to BMP2 was increased. In Nck1 overexpressing MC3T3E1 osteoblastic cells, Nck1 overexpression no longer affected Nck1 expression compared to the control. Our preliminary data indicates that the expression of osteoblast differentiation marker, type I collagen was increased in Nck1 overexpressing MC3T3E1 cells more than that in control after BMP2 treatment. In conclusion, these results indicate molecular adaptor Nck1 that acts on cell motility, is under the control of BMP and stimulates osteoblastic bone matrix production.

***Disclosures: Smriti Aryal A.C**, None.*
This study received funding from: 21st century GCOE program

SU0207

Osthole Stimulates Osteoblast Differentiation by Activation of Beta-Catenin-BMP Signaling. Dezhi Tang*[1], Wei Hou[2], Quan Zhou[2], Minjie Zhang[3], Jonathan Holz[3], Tzong-Jen Sheu[4], Tian-Fang Li[3], Shaodan Cheng[2], Qi Shi[2], Di Chen[3], Yongjun Wang[2]. [1]Spine Research Institute, Shanghai University of Traditional Chinese Medicine, Peoples republic of china, [2]Spine Research Institute, Shanghai University of Traditional Chinese Medicine, China, [3]University of Rochester Medical Center, USA, [4]University of Rochester, USA

Osteoporosis is defined as reduced bone mineral density with high risk of fragile fracture. Current available treatment regimens include antiresorptic drugs such as estrogen receptor analogues and bisphosphates and anabolic agents such as PTH. However, neither option is completely satisfactory because of adverse effects, some of them life-threatening. It is thus highly desirable to identify novel anabolic agents to improve future osteoporosis treatment. Osthole, a coumarin-like derivative extracted from Chinese herbs, has been shown to stimulate osteoblast differentiation. However, its effect on bone formation in vivo and underlying mechanism remain unclear. In the present studies, we found that local injection of Osthole significantly increased new bone formation on the surface of mouse calvaria. Bone histomorphometric analysis demonstrated that bone formation rates (BFR) were significantly increased after Osthole treatment by using double calcein labeling. Ovariectomy caused evident bone loss in rats, while Osthole largely prevented such loss demonstrated by improved bone microarchietecture, histomorphometric parameters and biomechanical properties. In vitro studies demonstrated that Osthole stimulated osteoblast differentiation in a dose-dependent manner. To determine the signaling mechanism during Osthole-induced osteoblast differentiation, we found that Osthole significantly upregulated Bmp2 expression at both mRNA and protein levels. Western blot analysis and immunofluorescent labeling showed that Osthole induced the phosphorylation of Smad1/5/8 and a rapid nuclear translocation of p-Smad1/5/8. Osthole also increased BMP reporter (12xSBE-OC-Luc) activity demonstrated by luciferase assay. Except the Bmp2 signaling, Osthole also activated the Wnt/β-catenin signaling, which was demonstrated by increased the expression of Wnt1, Wnt3a and Wnt4, the activative β-catenin protein level and the topgal reporter activity. Targeted deletion of the β-catenin and Bmp2 gene abolished the stimulatory effect of Osthole on osteoblast differentiation. Since deletion of the Bmp2 gene did not affect β-catenin expression and the deletion of the β-catenin gene inhibited Bmp2 expression in osteoblasts, we propose that Osthole acts through β-catenin-BMP signaling to promote osteoblast differentiation. Our findings demonstrate that Osthole could be a potential anabolic agent to stimulate bone formation and prevent estrogen deficiency-induced bone loss.

***Disclosures: Dezhi Tang**, None.*

SU0208

Rab27a and Rab27b are Involved in Stimulation-dependent RANKL Release from Secretory Lysosomes in Osteoblastic Cells. Yoshiaki Kariya*[1], Masashi Honma[1], Akiko Hanamura[1], Shigeki Aoki[1], Tadashi Ninomiya[2], Yuko Nakamichi[2], Nobuyuki Udagawa[2], Hiroshi Suzuki[1]. [1]The University of Tokyo Hospital, Japan, [2]Matsumoto Dental University, Japan

The amount of RANKL on the osteoblastic cell surface is considered to determine the magnitude of the signal input to osteoclast precursors and the degree of osteoclastogenesis. Previously, we have shown that most of the newly synthesized RANKL is transferred from the Golgi apparatus to the lysosomal storage compartment via the route involving Vps33a in osteoblastic cells. We have also shown that RANKL is relocated to the cell surface from secretory lysosomes in response to RANK stimulation. However, physiological meaning of the stimulation-dependent RANKL release process has not been elucidated. Here, we addressed the physiological significance of stimulation-dependent RANKL release process through the investigation of the molecular mechanisms behind it. Firstly, we focused on small GTPase members, Rab27a and Rab27b, as candidates for regulatory mechanisms involved in the RANKL release pathway. RNAi suppression of either Rab27a or Rab27b in osteoblastic cells resulted in the marked reduction in the amount of RANKL released upon stimulation. Confocal microscopic analyses showed that the suppression of Rab27a/b did not inhibit accumulation of RANKL residing lysosomal vesicles around the stimulation sites, but did inhibit the fusion of these vesicles to the plasma membrane. These observations suggested that Rab27a/b are involved in the membrane fusion events in RANKL release process. Subsequently, we have identified the effector molecules which coordinately function with Rab27a/b. Among the known effector molecules, Slp1, Slp2-a, Slp4-a, Slp5 and Munc13-4 were expressed in osteoblastic cells. While the suppression of Slp1 and Slp2-a did not affect the stimulation-dependent RANKL release, the suppression of Slp4-a, Slp5 and Munc13-4 inhibited the RANKL release in a manner similar to the cases of Rab27a/b suppression. The co-culture assay with bone marrow cells showed that, the suppression of these effector molecules in osteoblastic cells resulted in reduced osteoclastogenic ability. Furthermore, Jinx mice, which lack a functional Munc13-4 gene, exhibited a phenotype of increased bone volume and decreased serum NTx level, suggesting that Munc13-4 dysfunction *in vivo* resulted in the decreased bone resorptive activity. Conclusively, stimulation-dependent RANKL release is mediated by Rab27a/b and their effector molecules, Slp4-a, Slp5 and Munc13-4, and the pathway is considered physiologically important for maintaining bone homeostasis *in vivo*.

***Disclosures: Yoshiaki Kariya**, None.*

SU0209

Strontium Ranelate Promotes Osteoblast Differentiation and Increases OPG/RANKL Ratio in Osteoblast-osteoclast Co-cultures. Johannes Van Leeuwen[1], Marjolein Van Driel*[2]. [1]Erasmus University Medical Center, The netherlands, [2]Erasmus Medical Center, The netherlands

In the treatment of osteoporosis Strontium Ranelate (SrRan) is unique in its dual effect on bone remodeling, on the one hand stimulating osteoblasts (OB) and on the other hand inhibiting osteoclasts (OC). The calcium sensing receptor has been reported to be involved in the action of SrRan. In vitro evidence of the dual effect of SrRan has been obtained in cultures of OB and OC separately. Here we present the first study in which the effects of SrRan are shown in a co-culture of OB and OC, an experimental condition closer to the in vivo situation.

OC precursors (RAW 264.7) were co-cultured for 7 days with human pre-osteoblasts (SV-HFO) during early and late (mineralization) stage of OB differentiation (9-16 days or 23-30 days of OB culture, respectively). Cells were treated with different concentrations of SrRan (0.1 - 10 mM). Continuous SrRan treatment occurred from start of OB culture.

The effects of SrRan on OB and OC cultured separately were first assessed. When OB were cultured alone, SrRan dose-dependently increased in early as well as late stage of differentiation the expression of collagen type I (Col1A1) and alkaline phosphatase (ALP) by 1.5 fold. In the late stage of osteoblast differentiation SrRan increased the OPG/RANKL ratio by about 2-fold. When OC were cultured alone, OC differentiation was inhibited by 10 mM SrRan, as shown by an inhibition of fusion of mononuclear cells and a decrease in gene expression of TRAP by 1.5-fold. Importantly, in OB-OC co-culture, SrRan increased both ColA1 and ALP gene expression 1.5-fold. OPG/RANKL ratio was increased 3-fold. TRAP expression in osteoclasts tended to be further reduced by SrRan treatment.

In conclusion, these results show for the first time the beneficial effect of SrRan on the osteoblastic (Col1A1 and ALP) and osteoclastic-related differentiation markers (OPG/RANKL ratio) in OB-OC co-culture, which is closer to the in vivo situation where OB and OC are found in the same environment.

***Disclosures: Marjolein Van Driel**, None.*
This study received funding from: Servier

SU0210

The Forkhead Transcription Factor Foxc2 promotes Osteoblastogenesis via Regulation of Integrin Beta1 Expression. SU JIN PARK*[1], Kyoung-Won Cho[1], Se Hwa Kim[2], Kyoung Min Kim[1], Yumie Rhee[3], Han-Sung Jung[1], Sung-Kil Lim[4]. [1]Yonsei University, South korea, [2]Kwandong University College of Medicine, Myongji Hospital, South korea, [3]IUMS, Yonsei University, College of Medicine, South korea, [4]Yonsei University College of Medicine, South korea

The forkhead box C2 (Foxc2) protein is a member of the forkhead/winged helix transcription factor family, playing an important role in regulation of metabolism, arterial specification, and vascular sprouting. However, the roles of Foxc2 on the osteoblastogenesis have not been understood fully yet. In this study, we show that in mouse calvarial organ culture, significant reduction of the basal expression of Foxc2 by siFoxc2 remarkably inhibited cell proliferation and induced cell death in suture mesenchyme. Moreover, osteoblast differentiation in suture mesenchyme was significantly decreased after siFoxc2 treatment. And, in vitro study, knock-down of Foxc2 expression by siFoxc2 significantly suppressed the proliferation and differentiation, and induced the cell death in both of MC3T3-E1 and primary mouse calvarial cells. In addition, the resistance to apoptosis induced by serum deprivation was also significantly reduced after siFoxc2 treatment. The activation of Akt and ERK was also reduced by siFoxc2 treatment. Conversely, overexpression of Foxc2 increased the proliferation of MC3T3-E1 and primary mouse calvarial cells. Interestingly, we found Foxc2 directly regulates expression of Integrin beta 1, one of important modulators on osteoblastogenesis, by activating its promoter. Taken together, these results indicate that Foxc2 plays an important role in osteoblastogenesis by promoting osteoblast proliferation, survival and differentiation.

***Disclosures: SU JIN PARK**, None.*

SU0211

The O-glycosylation Site in the Variable Region of Fibronectin Affects Osteoblast Differentiation. Nina Kawelke, Anja von Au*, Inaam Nakchbandi. Max-Planck Institute for Biochemistry & University of Heidelberg, Germany

Osteoporosis associated with cholestatic liver disease results mostly from a defect in osteoblast function. We have shown that a glycosylated fibronectin (FN) isoform that we identified by the presence of an O-glycosylation in the variable region is increased in these patients and that this isoform inhibits nodule formation by osteoblasts *in vitro* and bone formation *in vivo* (Kawelke et al. JBMR 2008). The following studies were performed to identify the glycosylation type and site responsible for this effect.

Two types of glycosylations have been reported for FN: N- and O-glycosylation. There are 7 N-glycosylation sites and two O-glycosylation sites, one of which is localized in the variable region and the other one close to the N-terminus. The O-glycosylation that defines oncofetal fibronectin (oFN) is located in the variable region. The other O-glycosylation site is present in both oFN and plasma FN (pFN).

Deglycosylation of both pFN and oFN were performed for either the O-, the N-or the combination of both glycosylation sites using sialidase A followed by O-glycanase and/or N-glycanase PNGase F (PROzyme). Deglycosylation was confirmed based on Western blotting for the O-glycoslyation site at the variable region and the GelCode glycoprotein staining kit for the remaining glycosylation sites.

Nodule formation assay of primary calvarial mouse osteoblasts using the resulting substances at 100 μg/ml every other day added to differentiation media showed the following for pFN: O-deglycoslyation: no change in nodule formation (p=NS); N-deglycoslyation: decrease to 47% ($p<0.0005$), and O- + N-deglycosylation: decrease to 81% ($p<0.05$). For oFN the following was found: control: inhibition to 39% of pFN control ($p<0.0001$), O-deglycoslyation: normalization of nodule formation to become equivalent to pFN control with 107% ($p<0.0001$), N-deglycoslyation: similar to control oFN with 45% (p=NS), and O- + N-deglycosylation: similar to control oFN with 54% (p=NS at 0.08).

In summary, the O-glycosylation site in the variable region of oncofetal fibronectin is responsible for the inhibition of nodule formation. The N-glycoslyation site seems to also affect osteoblast behavior if the O-glycosylation site in the variable region is absent. Since the only integrin that is known to bind to the variable region of fibronectin is α4β1-integrin it seems likely that modification of fibronectin binding to α4β1-integrin via an O-glycosylation changes osteoblast behavior.

***Disclosures: Anja von Au**, None.*

SU0212

The Role of Ascorbate in Bone Homeostasis. Roy Morello*[1], Kurt Bohren[2], Peter Vogel[3], Kenneth Gabbay[2]. [1]University of Arkansas for Medical Sciences, USA, [2]Baylor College of Medicine, USA, [3]Lexicon Pharmaceuticals, Inc, USA

We have generated knockout mice for aldehyde reductase (GR) and aldose reductase (AR) and identified these enzymes as responsible for conversion of D-glucuronate to L-gulonate, a key step in the ascorbate (ASC) synthesis pathway. While the double knockout mice cannot synthesize ASC and develop scurvy, the single knockout mice for GR (GRKO) and AR (ARKO) are about 85% and 15% ASC deficient, respectively. The GRKO mice develop and grow normally when fed a regular diet (no ASC) but develop severe osteopenia and spontaneous fractures following a pregnancy or castration which increase their ASC requirement. Castration greatly increases osteoclast parameters in GRKO mice and promotes further bone loss as compared to WT controls, and additionally induces proliferation of immature dysplastic osteoblasts. This is likely due to an ASC-sensitive block(s) in early osteoblast differentiation as suggested by staining with Osterix and Runx2 antibodies. ASC as well as other antioxidants block osteoclast proliferation and bone loss, but only ASC seems to fully restore osteoblast differentiation while preventing their proliferation. To our knowledge this is the first in vivo demonstration of two independent roles for ASC, as an antioxidant suppressing osteoclast activity and number and as a cofactor promoting osteoblast differentiation. Thus, ASC may play an earlier role in osteoblast differentiation than its widely accepted importance for collagen matrix post-translational modification. These studies support the concept that ASC deficiency in the general population may play a hitherto unrecognized role in the development of human osteoporosis.

***Disclosures: Roy Morello**, None.*

SU0213

The Uncoupling of Bone Formation from Bone Resorption: Decreased BMP6 and Increased BMP Signaling Antagonist Expression in Osteoclasts with Aging. Sundeep Khosla[1], Larry Pederson[2], Kuniaki Ota*[2], Jennifer Westendorf[2], Merry Jo Oursler[2]. [1]College of Medicine, Mayo Clinic, USA, [2]Mayo Clinic, USA

Osteoclast-mediated bone resorption leads to subsequent osteoblast-mediated bone formation and this process is tightly coupled in young adults. With aging, coupling of bone resorption to bone formation breaks down in that bone formation does not keep pace with the increase in bone resorption. We have demonstrated that osteoclasts secrete factors that promote osteoblast mineralization and that BMP6 produced by osteoclasts is involved this response. In this study, we tested the hypothesis that the uncoupling of bone formation from bone resorption with aging may be due to altered BMP6 production by osteoclast. Osteoclasts were differentiated from marrow from 6-8 week old mice and from 12 month old mice. The cells differentiated comparably. Conditioned media were assessed for support of stromal cell mineralization. The conditioned medium from the aged mouse cells was unable to support mineralization compared to conditioned media from young mice (Figure 1).Comparing gene expression between these two cell origins, BMP6 was significantly suppressed whereas the BMP antagonist Sostdc1 was elevated in the cells from old mice compared to young mice. Because the osteoclasts are generated in identical media, differences in gene expression between the cells from the young and old mice are likely due to epigenetic modifications. To explore this, we treated osteoclasts from old mouse marrow with the histone deacetylase inhibitor suberoylanilide hydroxamic

acid (SAHA) and found that BMP6 expression increased 5-fold with treatment. These data indicate epigenetic suppression of BMP6 in osteoclasts from aged animals.

With aging, circulating estrogen (E) levels are lower. It has been postulated that E may sustain bone density in part through stimulating TGF-β expression in osteoblasts and osteoclasts. We examined the effects of E and TGF-β on gene expression in osteoclasts from old mouse marrow. TGF-β rapidly stimulated BMP6 expression. E stimulation of BMP6 required longer treatment, supporting that E stimulation is indirect, perhaps through increasing TGF-beta expression.

We conclude that the breakdown in coupling of bone formation to bone resorption that occurs with aging may be due, at least in part, to loss of circulating E and epigenetic suppression of BMP6.This is combined with age-related enhanced expression of a BMP antagonist in osteoclasts. These events contribute to age-related decreased coupling of bone resorption to subsequent bone formation.

Figure 1

***Disclosures: Kuniaki Ota**, None.*

SU0214

TRPV4 (Transient Receptor Potential Vanilloid 4), a Mechanosensor for Bone Is Required for the Maintenance of Bone Mineral Density of Mandible Exposed to Occlusal Force. TAKAFUMI SUZUKI*[1], Takuya Notomi[2], Yoichi Ezura[3], Tetsuya Nakamoto[1], Tadayoshi Hayata[4], Hiroaki Hemmi[1], Atsuko Mizuno[5], M Suzuki[6], Fumitaka Mizoguchi[1], Y Izumi[1], Masaki Noda[1]. [1]Tokyo Medical & Dental University, Japan, [2]GCOE, Tokyo Medical & Dental University, Japan, [3]Tokyo Medical & Dental University, Medical Research Insititute, Japan, [4]Medical Reserach Institute, Tokyo Medical & Dental University, Japan, [5]Jichi Medical University, Japan, [6]Jichi Medical School, Japan

Mechanical stress is an important factor to regulate alveolar bone homeostasis, and plays an important role in maintaining the structure and mass of alveolar bone throughout life. TRPV4 is a Ca2+ and Mg2+ permeable non-selective cation channel, and activated by a variety of physical stimulation (cell swelling, heat, mechanical stress) and chemical reagents (endocannabinoids, arachidonic acid). TRPV4 is involved in bone formation and remodeling as deficiency of TRPV4 suppresses unloading-induced osteoclast activation and osteoblast suppression. TRPV4 is expressed in osteoblasts and osteoclasts and plays a role in sensing mechanical stress and controlling bone remodeling in long bone. Alveolar bone is exposed to occlusal force. However, the function of TRPV4 in alveolar bone is not known. The aim of our study is to investigate the possible role of TRPV4 in alveolar bone in steady state. Quantitative real-time PCR analysis revealed that TRPV4 is detected in RNA from extracted tooth including periodontal ligament. We focused on alveolar bone around molar of mandible, because alveolar bone around molar is under mechanical stress in steady state. We first examine the levels of Bone mineral density (BMD) in mandible. BMD was reduced in mandible and tooth area of TRPV4 deficient mice compared to WT mice, suggesting that abnormality of bone remodeling could be involved in the reduction of BMD in steady state. Using micro computed tomography (micro CT), we examined bone structure of three areas including furcation area, interradicular area and periodontal space in mandibular. Bone structure in all these areas of TRPV4-deficient mice was similar to WT mice. Therefore, reduction of BMD in TRPV4 deficient mice appears to be due to the overall bone mass reduction rather than bone resorption in particular sites. In conclusion, we identified that the presence of TRPV4 is critical to maintain alveolar bone mineral density.

***Disclosures: TAKAFUMI SUZUKI**, None.*

SU0215

Vps33a Mediates RANKL Storage In Secretory Lysosomes In Osteoblastic Cells. Masashi Honma*[1], Yoshiaki Kariya[1], Shigeki Aoki[1], Hiroshi Suzuki[2]. [1]The University of Tokyo Hospital, Japan, [2]Department of Pharmacy, The University of Tokyo Hospital, Japan

Previous studies have shown that osteoclast activation in response to stimulation by RANKL takes place predominantly through cell-to-cell contact between osteoblastic cells and osteoclasts. In addition, the extracellular portion of RANKL is cleaved by matrix metalloproteinase 14 and a disintegrin and metalloproteinase 10, which are proteases localized on the plasma membrane, and suppression of these proteases results in increased osteoclastogenesis. Based on these facts, we can assume that the amount of RANKL expressed on the cell surface of osteoblastic cells is an important factor determining the magnitude of the signal input to osteoclast precursors and the degree of osteoclastogenesis in vivo. However, subcellular trafficking of RANKL and its regulatory mechanisms in osteoblastic cells were unclear, and we addressed this point here. Using confocal laser scanning microscopic analyses, we have shown that RANKL is predominantly localized in lysosomal organelles, but little is found on the cell surface of osteoblastic cells. We have also shown that RANKL is relocated to the plasma membrane in response to stimulation with RANK-Fc coated beads, indicating that the lysosomal organelles where RANKL is localized function as secretory lysosomes. In addition, using a protein pull-down method, we have identified vacuolar protein sorting (Vps) 33a as interacting with the cytoplasmic tail of RANKL. Furthermore, siRNA knockdown of Vps33a expression reduced the lysosomal storage of RANKL and caused the accumulation of newly synthesized RANKL in the Golgi apparatus, indicating that Vps33a is involved in transporting RANKL from the Golgi apparatus to secretory lysosomes. We have also shown that suppression of Vps33a resulted in the increase of the cell surface expression level of RANKL, resulting in the increased osteoclastogenesis in the co-culture assay system with bone marrow macrophages. This result also indicated that there exists the minor pathway transporting RANKL from the Golgi apparatus directly to the plasma membrane. Conclusively, RANKL storage in secretory lysosomes is important to control osteoclast activation and to maintain bone homeostasis.

***Disclosures: Masashi Honma**, None.*

SU0216

Canonical Wnt Signaling Regulates CXCL12 Expression in Stromal Osteoblasts. Masato Tamura*, Mari Sato. Biochem & Molecular Biol, Grad Sch Dent Med, Hokkaido University, Japan

Wnt signaling plays important roles in the skeletal system during many stages of embryonic development and adult homeostasis. We previously demonstrated that OPG, a key regulator of bone turnover, is a target gene for canonical Wnt signaling in osteoblasts. Chemokines that bind to specific G-protein coupled receptors on target cell membranes are the major regulators of cell trafficking. CXCL12 (stromal cell-derived factor-1, SDF-1), produced by stromal and endothelial cells including bone marrow, binds to its receptor CXCR4 and this axis regulates hematopoietic and tumor cell homing to bone. Recently, osteoclast precursor cells were found to express several chemokine receptors including CXCR4 and a potential role for the CXCL12-CXCR4 axis during osteoclast precursor cell recruitment/retention and development was proposed as a regulator of bone resorption. We examined the role of Wnt signaling in regulating the expression of CXCL12 in stromal osteoblasts. In mouse stromal ST2 cells, CXCL12 mRNA was expressed, while its expression was dramatically reduced in Wnt3a over-expressing ST2 (Wnt3a-ST2) cells not but Wnt5a-ST2 cells. Wnt3a decreased CXCL12 levels in the culture supernatant from ST2 cells or mouse bone marrow stromal cells (BMSC) measured by ELISA. CXCL12 expression was also reduced after lithium chloride treatment in these cells. The culture supernatant from Wnt3a-ST2 cells reduced migration activity of bone marrow derived cells in a transwell migration assay. Silencing of glycogen synthase kinase-3β by siRNA or sgRNA (tRNaseZL-utilizing gene silencing method) also decreased CXCL12 expression, suggesting that the canonical Wnt signaling pathway regulates CXCL12 expression. To investigate the mechanisms involved in the inactivation of CXCL12 gene transcription by canonical Wnt signaling, we cloned an approximately 1.8-kilobase-pair genomic DNA fragment corresponding to the 5'-flanking promoter region of the murine CXCL12 gene. Treatment of lithium chloride resulted in a decrease in reporter gene transcription activity in a transient transfection assay performed in ST2 cells. Deletion mutation analyses revealed that a proximal 420-base pair promoter region was required for lithium chroride responsiveness and a functional β-catenin response element was identified in this region. These results show that canonical Wnt signaling regulates CXCL12 gene expression, and this is the first study linking chemokine expression to Wnt signaling in osteoblasts.

***Disclosures: Masato Tamura**, None.*

SU0217

Dlx3/5 and Runx2 are required for Transcriptional Regulation of Osteoactivin/Gpnmb by BMP-2 in Osteoblasts. Maneet Singh*[1], Fabiola Del Carpio-Cano[1], Alexandra M. Monroy[1], Steven Popoff[2], Fayez Safadi[2]. [1]Temple University, USA, [2]Temple University School of Medicine, USA

Our laboratory identified Osteoactivin (OA)/Gpnmb in bone, a secreted glycoprotein that promotes osteoblast (OB) differentiation and function. Previous studies suggest that OA expression is regulated by Bone Morphogenetic Protein-2 (BMP-2), an osteogenic growth factor, through Smad1 signaling. Furthermore, we have shown that OA acts as a downstream mediator of BMP-2 effects on OB differentiation and function. BMP-2 is required for the initial commitment of OB progenitor cells and promotes their differentiation into mature OBs. BMP-2 mediates these osteogenic effects by recruiting transcription factors (TFs) including, Runx2, Homeodomain (HD) proteins namely Dlx3 and Dlx5, Smad1 and Smad4 to the promoter region of OB specific genes and induces their transcription. The goal of this study is to identify TFs that regulate BMP-2 induced OA transcription. In order to study the regulatory effects of BMP-2 on OA promoter activity, we cloned 1kb upstream of rat OA gene in a luciferase expression vector and have shown that BMP-2 stimulated OA promoter activity in a dose- and time-dependent manner. Using deletion mutants of this OA promoter lacking one or more of the consensus binding sites for Runx2, HD, Smad1 and Smad4, we have shown that loss of TF binding sites significantly decreased both basal and BMP-2-induced OA promoter activity. Similarly, site-directed mutagenesis of Runx2 and HD binding sites decreased both basal and BMP-2-induced OA promoter activity. Both these studies suggested that Runx2, Dlx3/Dlx5, Smad1 and Smad4 binding sites are important for OA transcriptional regulation. These results were further confirmed by mobility shift assay. Specific roles of TFs on OA promoter regulation were studied by evaluating the effect of knockdown and over expression of Runx2, Dlx3 and Dlx5, Smad1 and

Smad4, respectively on OA promoter activity. Lastly, OA promoter occupancy by Runx2, Dlx3, Dlx5, Smad1 and Smad4 during OB differentiation was evaluated by ChIP assay. BMP-2 treatment significantly induced differential association of Runx2, Dlx3/ Dlx5, Smad1 and Smad4 with OA promoter during different stages of OB differentiation. Collectively, our results suggest that Dlx3/Dlx5, Runx2, Smad1 and Smad4 are involved in both basal and BMP-2-induced regulation of OA transcription. The information gained from studies of the transcriptional regulation of OA may help in developing potential anabolic factors that can promote bone formation in the treatment of osteoporosis.

***Disclosures: Maneet Singh**, None.*

SU0218

HDAC7 Represses Proliferation and Differentiation of Osteoblasts. Eric Jensen*[1], Ali Khammanivong[2], Jennifer Westendorf[3], Kim Mansky[2], Raj Gopalakrishnan[2]. [1]University of Minnesota School of Dentistry, USA, [2]University of Minnesota, USA, [3]Mayo Clinic, USA

Histone deacetylase 7 (HDAC7) is an important regulator of osteoblast differentiation through repressive effects on Runx2. We previously showed that the key osteogenic growth factor BMP2 promotes PKD1-dependent phosphorylation of HDAC7 and transient export of HDAC7 from the nucleus to the cytoplasm.

The goal of the present study is to further characterize the effects of HDAC7 expression and subcellular localization on osteoblastic differentiation. We find that HDAC7 expression significantly decreases during BMP2-stimulated osteoblastic differentiation as compared to proliferating cells. This suggests a novel mechanism through which BMP2 inhibits HDAC7 repression and promotes osteoblast formation. To better test the involvement of HDAC7 nuclear-cytoplasmic shuttling for osteoblastogenesis, we generated lines of osteoblastic cells that stably overexpress either wild-type or constitutively nuclear mutant forms of HDAC7. Consistent with an antagonistic effect on differentiation, overexpression of either HDAC7 protein inhibits BMP2-stimulated induction of osteoblastic markers. Interestingly, we find that constitutive nuclear localization of HDAC7 significantly reduces apoptosis and delays progression through G1 phase of the cell cycle by increasing expression of cyclin dependent kinase inhibitors. Collectively, these data indicate that HDAC7 inhibits osteoblast formation by inhibiting the proliferation and differentiation of osteoblastic cells.

***Disclosures: Eric Jensen**, None.*

SU0219

Identification of Zranb2, a Novel R-Smads Binding Protein, as a Suppressor of BMP Signaling. Satoshi Ohte*[1], Shoichiro Kokabu[1], Toru Fukuda[2], Shunichiro Iemura[3], Hiroki Sasanuma[4], Katsumi Yoneyama[4], Masashi Shin[4], Eijiro Jimi[5], Toru Natsume[3], Takenobu Katagiri[6]. [1]Saitama Medical University, Japan, [2]Keio University School of Medicine, Japan, [3]National Institute of Advanced Industrial Science & Technology, Japan, [4]Saitama Medical University, Research Center for Genomic Medicine, Japan, [5]Kyushu Dental College, Japan, [6]Saitama Medical University Research Center for Genomic Medicine, Japan

Smad 1/5/8 are critical transcription factors activated by BMP receptors. To reveal the molecular mechanism of BMP signaling, we analyzed Smad1-binding proteins by a proteomics technique. We identified ZRANB2, zinc finger, RAN-binding domain containing 2, as one of the Smad1-binding proteins in HEK293 cells. Zranb2 interacted with R-Smads but not Smad4. Over expression of Zranb2 inhibited osteoblastic differentiation of C2C12 myoblasts induced by BMP-4 or transient transfection of constitutively active BMPR-IA with Smad1. Zranb2 suppressed a BMP specific IdWT4F-luciferase activity induced by the constitutively active BMPR-IA or a constitutively active Smad1. Knockdown of Zranb2 in C2C12 cells by siRNA transfection stimulated both osteoblastic differentiation and IdWT4F-luciferase activity induced by BMP-4. Deletion analysis of Zranb2 indicated that C-terminal serine/arginine rich (SR) domain, but not N-terminal two zinc finger (ZF) domains, was essential for the suppressive capacity of Zranb2 on BMP signaling. Immunohistochemical analysis showed that wild-type and ZF-deleted Zrnab2 were co-localized with phosphorylated Smad1/5/8 in nucleus. In contrast, SR-deleted Zranb2 localized cytoplasm, suggesting that the SR domain is essential for the nuclear localization to suppress Smads. Taken together, these findings suggested that Zranb2 is a novel suppressor of BMP signaling that forms a complex with BMP-regulated R-Smads in nucleus.

***Disclosures: Satoshi Ohte**, None.*

SU0220

Influence of Glucose and Advanced Glycation End-product Levels (AGEs) in Human Osteoblasts Gene Expression. Cristina Miranda*[1], Merce Giner[2], M José Montoya[1], M Angeles Vazquez[1], Ramon Perez-Temprano[3], M Jose Miranda[3], Ramon Perez-Cano[1]. [1]University of Seville, Spain, [2]University Hospital " Virgen Macarena", Spain, [3]University Hospital Virgen Macarena, Spain

Introduction: Type 2 diabetes mellitus is associated with a major risk of osteoporotic fractures. Multiple factors have been pointed out as responsible mechanisms, such as blood glucose levels and the presence of Advanced Glycation End-Products (AGEs) which may induce alterations in bone remodelling.

Aim: To assess if these different conditions in osteoblastic cell culture media have an influence on gene expression in genes related to cell differentiation and osteoblastic activity.

M&M: We have studied 12 patients belonging to three groups: 4 patients with osteoarthritis (OA), 4 osteoporotic patients with fractures (OP) and 4 diabetic patients with osteoporotic fractures (OP DM), with ages: 66.13 ± 11.18 (OA), 79.84 ± 8.42 (OP) and 83.83 ± 10.1 (OP DM). All biopsies were obtained from patients who had undergone surgery. Ethical approval had been obtained from the local Research Ethic Committee. We obtained primary osteoblast cultures (hOB) from fragments of trabecular bone and after reaching cellular confluence, cells were incubated with different osteogenic media: low glucose (4,5mM) similar to normal glycemia range, high glucose (25 mm), manitol (25 mm), and 0.1 mg/ml of AGE during 24h. Osteoprotegerin (OPG), RANKL, AGE receptors (RAGE), Runx2 and ribosomal 18S (control) mRNA expression were determined by qPCR. Trypan Blue was used to screen out dead cells after harvesting. Statistical analysis was performed using the ANOVA test (SPSS 17.0).

Results: Significant differences were not observed in cell viability in any of the studied conditions. Only the hOB enriched with AGEs medium showed differences in the expression of osteogenic genes. We observed an increase in mRNA RANKL (OA= 1.2 ± 0.72; OP DM= 5.57 ± 2.79), RANKL/OPG ratio (OA= 0.93 ± 0.64_; OP DM= 3.05 ± 1.55) and Runx2 expression (OA = 1.08 ± 0.43 r.u.; OP DM = 3.33 ± 0.73 r.u. ($p = 0.039$)) in the group of diabetic patients (OP DM). We didnt find any differences in AGER and OPG gene expression in any of the studied conditions nor between the groups of patients.

Conclusion: These results suggest a major effect of the high levels in AGEs on the gene expression of hOB, mainly from diabetic patients.

***Disclosures: Cristina Miranda**, None.*

SU0221

Inhibition of Osteoblast Function in Hypothermia: A Microarray Analysis. Jessal J. Patel*[1], Della Hyliands[2], Fei-Ling Lim[2], Dawn J. Mazzatti[2], Duncan C.S. Talbot[2], Kavita Karnik[2], Timothy R. Arnett[1]. [1]Department of Cell & Developmental Biology, University College London, United Kingdom, [2]Unilever Discover, Unilever PLC, United Kingdom

Core body temperature declines with aging due to a reduction in heat production and peripheral vasoconstriction. Core temperatures of ≤35.5℃ are common in the elderly population. We have found that hypothermia (34℃ - 35.5℃) inhibits in vitro bone formation by osteoblasts, whilst stimulating osteoclast formation and bone resorption. Here, we used gene array to investigate further the effect of mild hypothermia (35.5℃) on osteoblast function. Primary osteoblasts were derived from neonatal rat calvaria by trypsin/collagenase digestion. Cells were cultured at 35.5℃ and 37℃ for up to 14 days in medium (DMEM) supplemented with 2mM β-glycerophosphate, 50μg/ml ascorbate and 10^{-8}M dexamethasone. Samples were analysed at days 7 and 14, representing early and late osteoblast differentiation, respectively, using Agilent whole genome arrays. Microarray analysis of day 7 cultures identified 192 down-regulated and 90 upregulated transcripts at 35.5℃. Downregulated genes included PAK1 and transcripts involved in the NFκB pathway, and PLOD2 and transcripts involved in the TGFβ1 pathway; both pathways known to promote osteoblast proliferation and differentiation. Upregulated transcripts included FGF21. Though predominantly expressed in the liver, over-expression of FGF21 in mice has been associated with a fall in core body temperature, greater sensitivity to insulin, and resistance to diet-induced obesity. At day 14 however, 274 transcripts were upregulated and only 77 were down-regulated at 35.5℃. In contrast to day 7, transcripts included in the NFκB and TGFβ1 pathways were up-regulated. Klotho, which is required for normal bone formation in mice, and may slow ageing, was also upregulated. The shift in gene expression patterns between days 7 and 14 is consistent with the observed effects of chronic mild hypothermia on osteoblast function (strong initial inhibition, followed by a pronounced recovery). These data indicate that hypothermia exerts complex actions on osteoblast function that warrant further investigation.

***Disclosures: Jessal J. Patel**, None.*
This study received funding from: Unilever PLC

SU0222

P38 Regulates Expression of Osteoblast-specific Genes by Phosphorylation of Osterix. María José Ortuño*[1], Silvia Ruiz-Gaspà[2], Edgardo Rodriguez-Carballo[3], Antonio R G Susperregui[3], Francesc Ventura[3]. [1]Universitat Barcelona, Spain, [2]CIBERehd, Spain, [3]L'Hospitalet de Llobregat, Spain

Osterix, a zinc-finger transcription factor, is specifically expressed in osteoblasts and osteocytes of all developing bones. Since no bone formation occurs in osterix null mice, Osterix is thought to be an essential regulator of osteoblast differentiation. We report that, in several mesenchymal and osteoblastic cell types, BMP-2 induces an increase in expression of the two isoforms of Osterix arising from two alternative promoters. We identified a consensus Sp1 sequence (GGGCGG) as Osterix binding regions in the fibromodulin and the bone sialoprotein promoters *in vitro* and *in vivo*. Furthermore, we show that Osterix is a novel substrate for p38 MAPK *in vitro* and *in vivo*, and that Ser73 and Ser77 are the regulatory sites phosphorylated by p38. Our data also demonstrate that Osterix is able to increase recruitment of p300 and Brg1 to the promoters of its target genes fibromodulin and bone sialoprotein *in vivo* and that it directly associates with these cofactors through protein-protein interactions. Phosphorylation of Osterix at Ser 73/77 increases its ability to recruit p300 and SWI/SNF to either fibromodulin or bone sialoprotein promoters. We therefore propose that Osterix binds to Sp1 sequences on target gene promoters and that its phosphorylation by p38 allows efficient recruitment of coactivators to form stable, transcriptionally active complexes.

***Disclosures: María José Ortuño**, None.*

SU0223

Risedronate Increases Osteoblastic Differentiation and Up-regulates Connexin43 Promoter Activity In Vitro. Dong Jin Chung*[1], Kwang Youl Lee[2], Hyung Min Jeong[2], Dong Hyeok Cho[1], Jin Ook Chung[1], Min Young Chung[1], Roberto Civitelli[3]. [1]Chonnam National University Medical School, South korea, [2]College of Pharmacy, Chonnam National University, South korea, [3]Washington University in St. Louis School of Medicine, USA

Bisphosphonates are potent antiresorptive drugs which have good antifracture efficacy by reducing bone turnover rate and increasing bone mineral density. Clinical studies suggest some differences in effectiveness among bisphosphonates, possibly due to differences in mineral binding affinities and in inhibitory potency on farnesyl pyrophosphate synthase in osteoclast. There is also evidence suggesting that bisphosphonates have some effect on osteocytes or osteoblasts. Specifically, inhibition of osteocyte apoptosis by bisphosphonates has been proposed to be mediated through the opening of connexin43 (Cx43) hemichannels. In this study, we investigated the effect of risedronate on osteoblast differentiation and Cx43 expression using the cell line C2C12. Risedronate increased OSE–luciferase (Runx2 response element) activity in a concentration-dependent manner with highest activity at 50 μM. The activities of osteocalcin and bone sialoprotein (BSP) promoters were also increased at 25 μM of risedronate with peak activity at 50 μM. Likewise, alkaline phosphatase (ALP) activity was also increased by risedronate dose-dependently. When risedronate and 5 ng/ml of BMP2 were used in combination, ALP activity increased to a larger extent than when BMP2 was used alone. These results suggest that risedronate may facilitate the differentiation of osteoblasts, synergizing with BMP-2. Co-transfection of expression vectors and luciferase-reporter constructs revealed that Runx2 increased Cx43-promoter activity in a concentration-dependent manner. Similar findings were observed with Dlx5 expression. Likewise, Cx43 promoter activity was up-regulated by osterix overexpression, though to a lesser degree than for Runx2 transfection. As the concentration of risedronate was increased, Cx43-promoter activity was increased by 2.5 fold. Furthermore, the combination of Runx2 (0.5 μg) and risedronate up-regulated Cx43 promoter activity to a far larger extent than did either Runx2 or risedronate alone, suggesting an interaction between the bisphosphonate and Runx2 in activating the Cx43 promoter. A similar interaction was observed between Dlx5 and risedronate (10 μM). Finally, we found that risedronate increased Cx43 protein abundance and up-regulated expression of Runx2, Osterix, and Dlx5 proteins. These results suggest that risedronate promotes osteoblast differentiation and regulates Cx43 expression in C2C12 cells.

***Disclosures: Dong Jin Chung**, None.*

SU0224

The Transcriptional Activity of Osterix Requires the Recruitment of Sp1 but not Sp3 to the Osteocalcin Proximal Promoter. Corinne Niger*[1], Florence Lima[2], David Yoo[1], Rishi Gupta[1], Carla Hebert[1], Joseph Stains[1]. [1]University of Maryland School of Medicine, USA, [2]Texas A&M University, USA

Osterix, a member of the Sp family of transcription factors, is required for osteogenic differentiation and bone formation in vivo. This zinc-finger protein has been shown to act at Sp1 DNA binging elements and has been shown to stimulate osteocalcin (OCN) transcription. Previously, we characterized a C/T rich element (-70/-57) in the OCN proximal promoter that binds the transcriptional activator Sp1 or the repressor Sp3. Further, we have shown that the recruitment of Sp1/Sp3 to the OCN promoter is altered by the presence of the gap junction protein connexin43, which promotes occupancy of the promoter by Sp1. In the present study, we examine if Osterix can stimulate transcription from this gap junction responsive, Sp1/Sp3-binding region of the OCN promoter.

Using rat OCN proximal promoter-luciferase reporter constructs and transient transfections with Sp1, Sp3 or Osterix expression vectors, we show that Osterix alone is an insufficient activator of OCN transcription. Conversely, Sp1 and Osterix act cooperatively to increase transcription from the -92/+32 OCN promoter. In contrast, Sp3 does not support activation of the OCN promoter by Osterix. By chromatin immunoprecipitation (ChIP), we show that expression of Sp1, but not Sp3, dramatically enhances the recruitment of Osterix to the OCN promoter. By co-immunoprecipitation, we show that Sp1 and Osterix may physically interact. In total these data suggest that Osterix is an insufficient transactivator, requiring Sp1 but not Sp3 for targeting to the OCN promoter.

Additionally, we examine the influence of gap junctions on the recruitment of Osterix, Sp1 and Sp3 to the OCN promoter, since this region of the OCN promoter is affected by alteration in the expression of the gap junction protein connexin43. By luciferase reporter assays, we show that expression of connexin43 can increase transcription from the osteocalcin promoter. By ChIP, we show that the expression of connexin43 dramatically enhances the recruitment of both Osterix and Sp1 to the OCN promoter, while reducing the presence of Sp3. These findings not only reinforce the reported role of gap junctions as a regulator of osteogenic genes via Sp1/Sp3 specific activation, but also provide insight on how gap junctions may modulate osteoblast differentiation via alteration of Osterix recruitment during bone formation.

***Disclosures: Corinne Niger**, None.*

SU0225

Transcriptional Regulation Mechanisms in Bone Following Mechanical Loading. Sara Mantila Roosa*[1], Yunlong Liu[2], Charles Turner[3]. [1]Purdue University, USA, [2]Indiana University School of Medicine, USA, [3]Indiana University, Purdue University Indianapolis, USA

The time course of bone formation after initiating mechanical loading is well characterized. However, the regulatory activities governing the loading-dependent changes in gene expression are not well understood. Predictive bioinformatics algorithms offer ways to predict important regulatory mechanisms using gene expression data. The goal of this study was to determine the time-dependent regulatory mechanisms that govern mechanical loading-induced gene expression in bone. A standard model for bone loading was employed in rats in which the right forelimb was loaded axially for three minutes, while the left forearm served as a non-loaded control. Animals were subjected to loading sessions every day, with 24 hours between sessions. Ulnae were sampled at 11 time points, from 4 hours to 32 days after beginning loading. The time points are referenced to the number of hours or days after the first bout of bone loading was applied. RNA was isolated and mRNA abundance was measured at each time point using Affymetrix exon arrays (GeneChip® Rat Exon 1.0 ST Arrays). Gene expression data from arrays were analyzed using a modeling algorithm, MotifModeler, to predict which transcription factor binding motifs and microRNA binding sites most likely regulated gene expression across the time course.

MotifModeler predicted 44 transcription factor binding motifs and 29 microRNA binding sites across the time course. Transcription factor binding motifs and associated transcription factors known to be important in bone were predicted, such as STAT and CREB, which were predicted at early and later time points, respectively. Novel motifs were identified as well, including SREBP-1, which seems to be important in regulating expression of matrix-related genes and osterix. In addition, several microRNA binding sites were predicted to regulate loading-induced gene expression. Our data suggest that microRNAs function in a stimulatory rather than inhibitory capacity in loading-induced bone formation. In conclusion, we predicted several transcription factor binding motifs and microRNA binding sites that may be important in controlling the loading-induced bone formation process. To our knowledge, the role of microRNA regulation in bone formation has not yet been investigated and the list of predicted microRNAs could include several novel regulatory mechanisms for loading-induced bone formation.

***Disclosures: Sara Mantila Roosa**, None.*

SU0226

WW Domain-Containing Proteins Regulate RUNX2 Functional Activity and Osteoblast Differentiation. Marcio M. Beloti*[1], Mohammad Hassan[1], Yang Lou[2], Andre Van Wijnen[1], Gary Stein[1], Jane Lian[1], Rami Aqeilan[3], Janet L. Stein[1]. [1]University of Massachusetts Medical School, USA, [2]University of Massachusetts, USA, [3]The Hebrew University-Hadassah Medical School, Israel

WW (tryptophan-tryptophan) domain-containing proteins are expressed in many tissues and act as coregulators of transcription factors. Based on its ligand recognition motifs, the WW domain family is classified into four groups, the largest of which recognizes ligands with the PPxY motif (P is proline, *x* is any amino acid and Y is tyrosine). WW domains of several proteins bind to the PP*x*Y motif of RUNX2, the principal transcriptional regulator of osteoblast phenotype development, and regulate RUNX2 activity. Here, we focused on how interactions between RUNX2 and WW

domain-containing proteins, including WWP1, WWOX, YAP and TAZ, control osteoblast differentiation. These WW domain-containing proteins exhibited distinct patterns of expression (mRNA and protein) during osteoblast differentiation in MC3T3 cells. Real-time RT-PCR assays revealed peak expression of WWP1 (8-fold), TAZ (6-fold), and WWOX (3-fold) in mature osteoblasts at day 12, whereas YAP was maximal (3-fold) from days 10 to 15. Protein-protein interactions between RUNX2 and WW domain-containing proteins were detected by co-immunoprecipitation assays. RUNX2 interacts with each of these proteins overexpressed in HeLa cells and endogenously in osteoblasts. We examined the biological relevance of the regulation of RUNX2 functional activity by introducing a mutation into the PP*x*Y motif of RUNX2 (RUNX2 Y433A), which inhibited RUNX2 binding to WW domain-containing proteins. Furthermore, binding of WWP1 and WWOX, but not TAZ and YAP, resulted in significant degradation of RUNX2 protein as observed by western blot analysis, and such degradation was blocked by the RUNX2 Y433A mutation. Using short hairpin RNAs (shRNA) in MC3T3 cells, we found that knockdown of WWP1 increased and YAP decreased the mRNA levels of RUNX2 and osteocalcin, both markers of osteoblast differentiation. These results indicate that different WW domain-containing proteins interact with RUNX2 either to repress (WWP1 and WWOX) or to enhance (TAZ and YAP) its activity. We conclude that WW domain-containing proteins contribute to regulation of osteoblast differentiation, and consequently of bone formation, by affecting RUNX2 functional activity.

***Disclosures: Marcio M. Beloti**, None.*

SU0227

αNAC Exerts Dual Functions as a Co-activator and a Co-repressor in the Transcriptional Control of Myogenin and Osteocalcin Gene Expression. Toghrul Jafarov*[1], Rene St-Arnaud[2]. [1]Shriners Hospitals for Children,McGill University, Canada, [2]Shriners Hospital for Children & McGill University, Canada

In the nucleus of differentiated osteoblasts, αNAC has been shown to act as a transcriptional co-activator of the osteocalcin gene by providing a protein bridge between the homodimeric c-Jun transcription factor and the basal transcriptional machinery. αNAC can bind DNA but is not capable of regulating transcription on its own. We used a Chromatin Immunoprecipitation-Microarray assay (ChIP-chip) to identify DNA-bound targets of αNAC in osteoblastic cells. As expected, we found that αNAC binds the osteocalcin promoter but also identified the myogenin promoter as an αNAC target. We confirmed these array data using conventional ChIP assay and further detected that αNAC binds to these same promoters in myoblasts. These results suggest cell- and promoter-context specific functions for αNAC since osteocalcin expression is up regulated and myogenin expression is inhibited in osteoblasts during maturation, while osteocalcin is not expressed and myogenin is up-regulated during myogenesis. We hypothesized that αNAC dynamically recruits co-repressors to inhibit myogenin expression in cells committing to the osteoblastic lineage or to inhibit osteocalcin expression in differentiating myoblasts. Using co-immunoprecipitation assays, we detected complexes between αNAC and basic co-repressors such as HDAC1, HDAC3, Sin3a and N-Cor, both in C2C12 myoblasts and MC3T3-E1 osteoblastic cells. Treatment with the non-specific HDACs inhibitor sodium butyrate decreased interaction between αNAC and the co-repressors. Quantitative ChIP assays showed that binding of αNAC to the myogenin promoter was detectable in pre-osteoblasts but decreased as the cells commit to osteoblastogenesis. We also observed binding of αNAC to the osteocalcin promoter in myoblasts that decreased as the cells progressed through myogenesis. Overexpression of αNAC in myoblasts disrupts their differentiation into myotubes, leading them to acquire a fibroblastic phenotype. Structure-function analysis revealed that overexpression of an N-terminus truncated αNAC mutant allowed myoblasts to differentiate in myotubes, suggesting that this region of the protein is involved in the interaction with co-repressors. This study identified additional DNA-binding targets and novel protein-protein interactions for αNAC. We propose that αNAC plays a role in regulating mesenchymal cell differentiation by adopting the functions of a co-repressor or co-activator in a cell- and promoter-specific context.

***Disclosures: Toghrul Jafarov**, None.*

SU0228

1,25-Dihydroxyvitamin D_3 Affects Pulsating Fluid Flow-Induced Nitric Oxide Production by Osteoblasts Dependent on the VDR Pathway Activated. Hubertine M.E. Willems*[1], Ellen G.H.M. van den Heuvel[2], Astrid Bakker[3], Jenneke Klein-Nulend[4]. [1]ACTA-University of Amsterdam & VU University Amsterdam, Dept Oral Cell Biology, Research Institute MOVE, Netherlands, [2]Life Science, Royal FrieslandCampina Research, Netherlands, [3]Academic Centre for Dentistry Amsterdam, UvA & VU, Research Institure MOVE, The netherlands, [4]ACTA-VU University Amsterdam, The netherlands

Local bone remodeling is regulated by mechanical usage, but the overall level of remodeling is determined by systemic (pro)hormones such as 1,25-dihydroxyvitamin D_3 ($1,25(OH)_2D_3$). Elevated circulating $1,25(OH)_2D_3$ levels counteract disuse-induced bone loss, which suggests interaction of $1,25(OH)_2D_3$ and strain at the tissue level. $1,25(OH)_2D_3$ affects cells either via the nuclear receptor (nVDR), or via a non-genomic membrane receptor (mVDR). Therefore we investigated whether 1) $1,25(OH)_2D_3$ modulates bone cell mechanotransduction, and 2) whether this occurs via mVDR and/or nVDR.

MC3T3-E1 osteoblasts were subjected to mechanical load by pulsating fluid flow (PFF; 0.7 $\pm$ 0.3 Pa at 5 Hz) for 30 min, in the presence or absence of 10^{-9},10^{-11}, or 10^{-13} M $1,25(OH)_2D_3$ to allow binding of $1,25(OH)_2D_3$ to mVDR. Controls were kept under static culture conditions. Medium samples were taken at 5 and 30 min after start of PFF, and NO production was determined as parameter of bone cell responsiveness. Some cultures were pre-incubated before PFF with or without 10^{-9}, 10^{-11}, or 10^{-13} M $1,25(OH)_2D_3$ for 24 h to allow binding of $1,25(OH)_2D_3$ to nVDR.

Within 10 min, PFF increased NO production by 8-12 fold. $1,25(OH)_2D_3$ (10^{-9}-10^{-13} M) for 30 min and 24 h abolished this response, but via different pathways. NO production by PFF-stimulated cells was lower in cells incubated for 30 min with $1,25(OH)_2D_3$ (10^{-9}-10^{-13} M) than in cells subjected to PFF without $1,25(OH)_2D_3$ (4-2 fold reduction at 10 min). $1,25(OH)_2D_3$ (10^{-9}-10^{-13} M) for 30 min did not affect NO production by cells under static culture. In contrast, NO production by PFF-stimulated cells was similar in cells pre-incubated for 24 h with $1,25(OH)_2D_3$ (10^{-9}-10^{-13} M) and in cells without $1,25(OH)_2D_3$. 24 h $1,25(OH)_2D_3$ (10^{-9}-10^{-13} M) increased NO production by cells under static culture (2-7 fold increase at 5 min).

Our results suggest that mechanical loading and $1,25(OH)_2D_3$ interact at the level of mechanotransduction. The similar effects of PFF and 24 h $1,25(OH)_2D_3$ treatment on NO production by MC3T3-E1 osteoblasts as found in this *in vitro* study may relate to similar effects of PFF and $1,25(OH)_2D_3$ on bone metabolism *in vivo*. We conclude that $1,25(OH)_2D_3$ differentially affects the NO response to mechanical loading dependent on the VDR pathway activated.

***Disclosures: Hubertine M.E. Willems**, None.*
This study received funding from: Royal FrieslandCampina Research

SU0229

Calcium Signaling Induced by Lysophosphatidic Acid in Osteoblasts. Karen Ann Bridge*, S. Jeffrey Dixon. University of Western Ontario, Canada

Mechanical stimuli induce the release of ATP, which can then activate cell surface P2 nucleotide receptors. Our laboratory has shown that stimulation of P2X7 receptors on osteoblasts leads to the production of lysophosphatidic acid (LPA), which in turn stimulates osteogenesis (J Cell Biol 181:859-71, 2008). LPA is a potent lipid mediator that has been shown to regulate cell proliferation, survival and migration in other systems. Recently, others have provided additional evidence of a role for LPA in regulating osteoblast differentiation (J Cell Biochem 109:794-800, 2010). Our purpose was to investigate LPA signaling in osteoblasts. The effects of LPA can be mediated by at least five G protein-coupled receptors (GPCRs), termed LPA1-5, activation of which often elicits elevation in the concentration of cytosolic free calcium. Calcium is a ''universal'' second messenger that contributes to control of numerous cell functions including proliferation, differentiation, apoptosis and motility. To examine the effects of LPA on cytosolic calcium, UMR-106 osteoblast-like cells and primary rat calvarial cells were loaded with the calcium-sensitive fluorescent probe indo-1. LPA induced transient elevation of calcium, lasting ~100 s. The amplitude of the calcium transient was concentration dependent, with half-maximal effects observed at ~20 nM LPA in both UMR-106 cells and primary osteoblasts. Interestingly, the response in UMR-106 cells was abolished by VPC-32183, a selective LPA1/3 antagonist. In contrast, VPC-32183 only partially blocked LPA-induced calcium signaling in primary rat osteoblasts, consistent with expression of multiple calcium-mobilizing LPA receptors. LPA still induced transient elevation of cytosolic calcium in the absence of extracellular calcium. Moreover, pretreatment with the SERCA (sarco/endoplasmic reticulum calcium-ATPase) inhibitor thapsigargin abolished the response, indicating that LPA induces release of calcium from intracellular stores. Finally, pretreatment with pertussis toxin suppressed LPA-induced elevations in calcium, consistent with signaling through Gi. These data establish that LPA signals through Gi-coupled, calcium-mobilizing GPCRs in osteoblasts. Stimulation of P2X7 nucleotide receptors on osteoblasts leads to the production of LPA, which may then act through these GPCRs to stimulate osteogenesis in an autocrine or paracrine manner.

***Disclosures: Karen Ann Bridge**, None.*

SU0230

Effects of Hydroxyapatite Released Calcium Ion on Osteoblast Differentiation. Gil-Yong Jung*[1], Jung-Suk Han[2], Yoon-Jeong Park[3]. [1]Seoul national university, South korea, [2]School of dentistry, Seoul National University, South korea, [3]Interdisciplinary program for Bioengineering & School of dentistry, Seoul National University, South korea

Hydroxyapatite (HA) is a widely used calcium phosphate implant substitute and has dissolution property. Although HA has been shown a beneficial effect on osteoblast differentiation, the exact mechanism is still unclear. In the present study, we proposed that Ca2+ released from HA activated the expression bone associated proteins, OPN and BSP, mediated by L-type calcium channel and calcium/calmodulin-dependent protein kinase (CaMK) 2 which resulted into improved osteoblast differentiation. Results showed that HA elevated ALP expression as well as OPN and BSP expression in MC3T3-E1 cells. The result from western blot of CaMK2α indicated that HA released Ca2+ activated CaMK2 through L-type calcium channel. Furthermore, upregulation of OPN and BSP mRNA expression was significantly inhibited when blocking the L-type calcium channel or CaMK2. These

results suggest that property of dissolvability of HA provide more suitable environment in osteoblast differentiation through L-type calcium channel which triggered CaM-CaMK2 pathway.

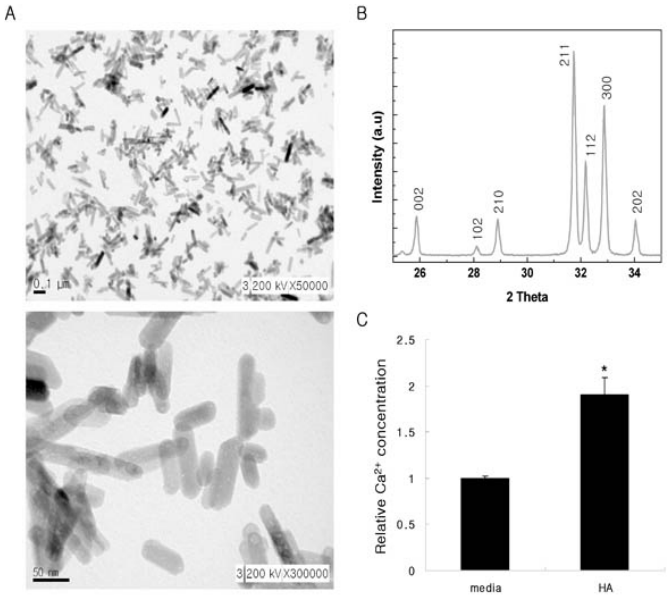

figure1

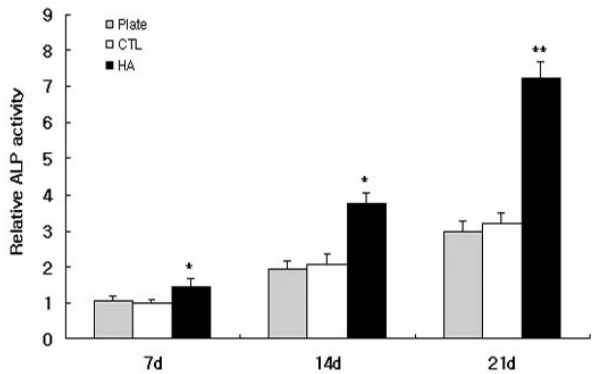

figure2

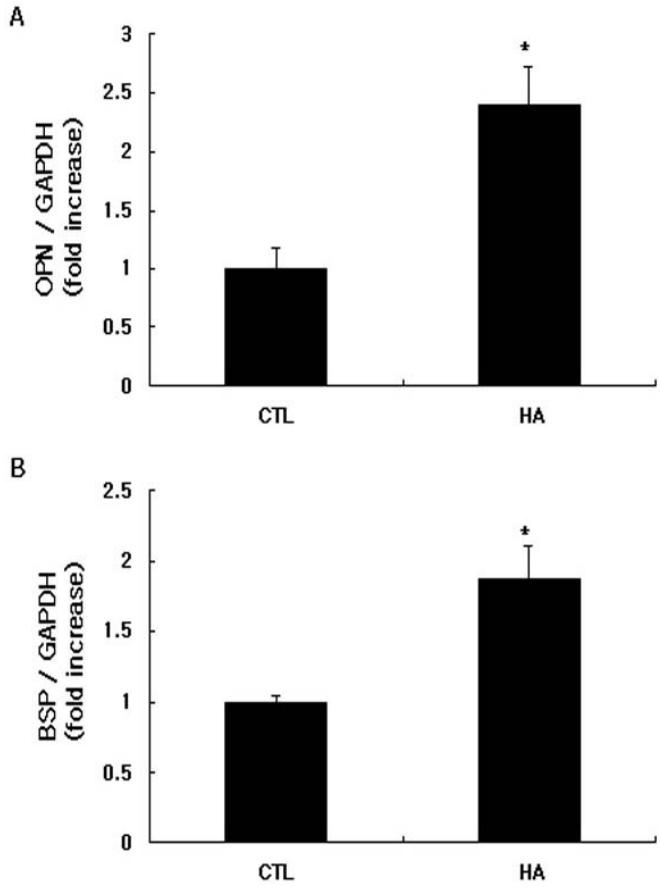

figure3

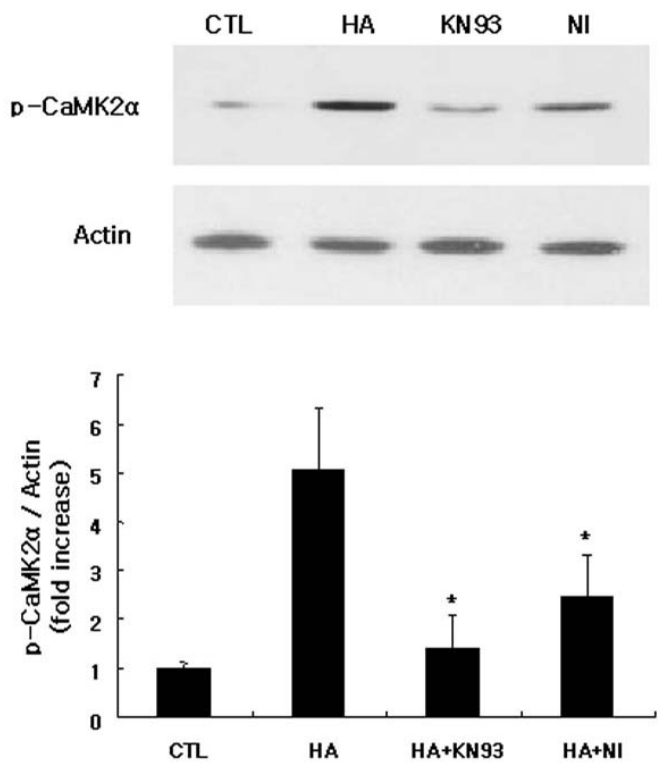

figure4

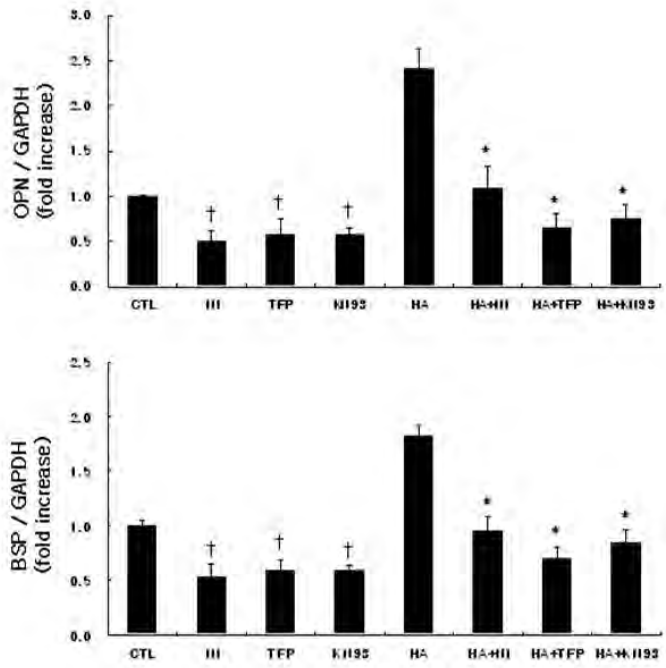

figure5

***Disclosures: Gil-Yong Jung**, None.*

SU0231

Short-term Activation of Liver X Receptors Inhibits Osteoblasts, but Long-term Activation does not have an Impact on murine Bone In Vivo. Janne Prawitt[1], Wolfgang Ruether[2], Joerg Heeren[2], Robert Matshall[2], Alexander Bartelt[2], Michael Amling[2], Bart Staels[2], Andreas Niemeier*[2], Timo Beil[2]. [1]Univ Lille Nord de France, France, [2]University Medical Center Hamburg-Eppendorf, Germany

Liver X receptors (LXRs) are nuclear receptors that play a crucial role in the transcriptional control of lipid metabolism. Pharmacological LXR activation is an attractive concept for the treatment of atherosclerosis. Genetic LXR deficiency in mice has been shown to have an influence on bone turnover and structure and LXR activation is known to stimulate the osteogenic differentiation of bone marrow stromal cells. Therefore, therapeutic pharmacological LXR activation may have relevant effects on bone.

Here, using two synthetic LXR ligands, T0901317 and GW3965, we investigated the effect of LXR activation on murine osteoblasts and the influence of long-term LXR activation on bone in vivo in mice. Short term (48-hour) in vitro treatment of primary murine osteoblasts with T0901317 resulted in a dose-dependent decrease of osteocalcin and alkaline phosphatase mRNA and protein. In vivo, a six-day treatment of C57BL/6 mice with T0901317 led to a 40% reduction of serum osteocalcin concentrations. Long-term (12-week) oral administration of T0901317 and GW3965 influenced the expression of established LXR target genes in liver and intestine, but did not alter trabecular and cortical bone structure or bone turnover as determined by total skeleton radiography, histomorphometric analysis of lumbar vertebral trabecular bone, micro CT analysis of femur cortical bone and biochemical determination of bone formation and resorption markers.

We conclude that short-term pharmacological LXR activation has the potential to profoundly influence osteoblast function, but that long-term LXR activation in vivo has no adverse effects on the murine skeleton.

***Disclosures: Andreas Niemeier**, None.*

SU0232

The Role of Focal Adhesion in Primary Cilia-mediated Mechanotransduction in MC3T3-E1 Pre-osteoblastic Cells. Ok Hee Jeon*, Yeong-Min Yoo, Chi Hyun Kim. Yonsei University, South korea

Fluid flow-induced shear stress (FSS) is an important anabolic mechanical signal that results in the upregulation of cyclooxygenase2 (COX2) and prostaglandin E2 (PGE2) in bone cells. Primary cilium is a microtubule-based structure that may be responsible for the sensing of mechanical signals. It has been shown that primary cilia are required for the induction of COX2 and PGE2 in bone cells in response to FSS. In this study, we hypothesized that primary cilia leads to COX2 and PGE2 release in osteoblasts via increases in focal adhesion when subjected to FSS. MC3T3-E1 pre-osteoblastic cells were removed of primary cilia using 4mM chloral hydrate for 72 hours and allowed to adhere in glass slides for 1 hour in fresh medium. Then FSS of 1 Pa was applied to the cells for 2 hours. First, mRNA levels of COX2 and focal adhesion kinase (FAK) were determined using real-time RT-PCR and protein levels of PGE2 were determined using an ELISA kit. Second, vinculin-positive focal adhesion was visualized to determine the role of FAK in cilia-mediated upregulation of COX2 and PGE2. Third, ras, ERK, p-ERK, Akt, and p-Akt were analyzed using Western blot to investigate the cilia-mediated mechanosensing pathway. Both COX2 and FAK decreased by over 90% in the loading group without cilia (CX-L) compared with the loading group with cilia (CO-L). Also, immunofluorescence images showed that the CX-L group formed a significant lack of focal adhesion compared to the CO-L group which resulted in an active regeneration of focal adhesion. Finally, there were no differences in ras and p-ERK levels between the CX-L and CO-L groups, whereas p-Akt decreased by approximately 50% in the CX-L groups compared with the CO-L group. Our results suggest that primary cilia may be a critical factor that is related to focal adhesion in response to FSS during the early cell spreading and adhesion periods in osteoblasts. Also, primary cilia may control FSS-induced upregulation of PGE2 release and COX2 gene expression via focal adhesion by the activation of Akt in osteoblasts.

***Disclosures: Ok Hee Jeon**, None.*
This study received funding from: National Research Foundation of Korea

SU0233

Uch-l3 Knock-out Induces Osteopenia Through the Destabilization of Smad1. Ji Young Kim*[1], Hey-Sim Cho[1], Kyung-Ae Yoon[1], Keiji Wada[2], Je-Yoel Cho[1]. [1]School of Dentistry, Kyungpook National University, South korea, [2]National Institute of Neuroscience, National Center of Neurology & Psychiatry, Japan

Deubiquitination, the reversal of ubiquitination, is a critical regulatory process. It is performed by the action of deubiquitinating enzymes (DUBs). Mutations in genes expressing DUBs have been implicated in a number of diseases including osteoporosis, cancer, and neurodegeneration. Our recent report showed that ubiquitin C-terminal hydrolase l3 (Uch-l3) a DUB was founded as a BMP2 signaling modulator in the global proteomic study for identifying targets in BMP2-induced osteoblast differentiation. In this study, we confirmed the physical interaction between Uch-l3 and Smad1. Its deubiquitination activity decreased the ubiquitinated Smad1. The exogenous expression and knock-down of Uch-l3 modulated the BMP signaling as analyzed by osteoblast markers ALP, OPN, and OC etc. We also studied the specific function of Uch-l3 in bone metabolism *in vivo*. For the first time, we found Uch-l3 knock-out mice have the osteopenic phenotype by the analysis of micro-CT and Von Kossa staining. The expressions of bone marker genes were also decreased in the bone from Uch-l3 knock-out mice, compared to that of wild-type. In contrast, the activity of osteoclast is not affected by the deficiency of Uch-l3, as analyzed by TRAP staining. These results suggest Uch-l3 is might be an important regulator that controls bone metabolism in osteoblast differentiation. This work was supported by the National Research Foundation of Korea (NRF) grant funded by the Korea government (MEST) (No. 2009-004608 and 2010-0011231) and the Korea Health 21 R&D Project, Ministry of Health & Welfare (No. A010252 and A090610).

***Disclosures: Ji Young Kim**, None.*
This study received funding from: National Research Foundation of Korea (NRF) grant funded by the Korea government (MEST) (No. 2009-004608) and the Korea Health 21 R&D Project, Ministry of Health & Welfare (No. A010252 and A090610)

SU0234

A Role for LIM kinase 1 in Osteoblast Differentiation. Robert Botta*, Karl Insogna. Yale University School of Medicine, USA

LIM kinase 1 (LIMK 1) controls actin remodeling by phosphorylating and deactivating the actin-severing protein, cofilin. We found that the LIMK $1^{-/-}$ mice are osteopenic due, in part, to a reduction in the number of osteoblasts, as compared to controls when quantified by histomorphometry. The number of CFU-Ob was markedly reduced in LIMK $1^{-/-}$ animals as compared to controls, and the ability of LIMK $1^{-/-}$ osteoblasts to mineralize in vitro was significantly impaired. The cytoskeleton has been shown to have a role in determining the differentiation of osteoblasts, but the connection between the molecular regulators of the cytoskeleton and osteoblastic differentiation is not understood. To determine if cytoskeletal abnormalities existed in LIMK $1^{-/-}$ osteoblasts, we imaged the actin cytoskeleton of neonatal calvarial osteoblasts using immunofluorescent confocal microscopy. Cells were plated on type 1-A collagen-coated slides and cell area was quantified 5-9 days later. The spread area of the the LIMK $1^{-/-}$ osteoblasts was 2.3 times greater than that of wild type cells (1902 ± 164 vs. 836 ± 110 μm^2; $p < 0.0001$).

Actin is required for the normal assembly of focal adhesions, which contain integrins, FAK, and other signaling and adhesion proteins. Since it has previously been reported that the signaling from integrins to FAK is required for osteoblast differentiation (JBC 272:29309), we examined FAK activation in LIMK $1^{-/-}$ and wild type osteoblasts over a 120'' time course following adherence to collagen-coated plates. FAK activation was measured using a commercially available ELISA kit that measures phosphorylation at Tyr397 (Millipore, cat # 17-480).

FAK activation was significantly impaired in LIMK $1^{-/-}$ osteoblasts plated on collagen. In wild type cells FAK activity was increased 3.0-fold over baseline at 60'' and remained 2.2-fold elevated at 120'', while the LIMK $1^{-/-}$ cells showed only a 1.5

fold increase in FAK activity at 60" with no subsequent significant change. By 2-way ANOVA there was a significant effect of genotype and the values at 60" were different by post hoc testing ($p < 0.001$). These results indicate that in the absence of LIM 1, FAK activation in osteoblasts is impaired, suggesting that this is part of the mechanism by which LIMK 1 exerts an important and hitherto unappreciated effect on osteoblast differentiation and function.

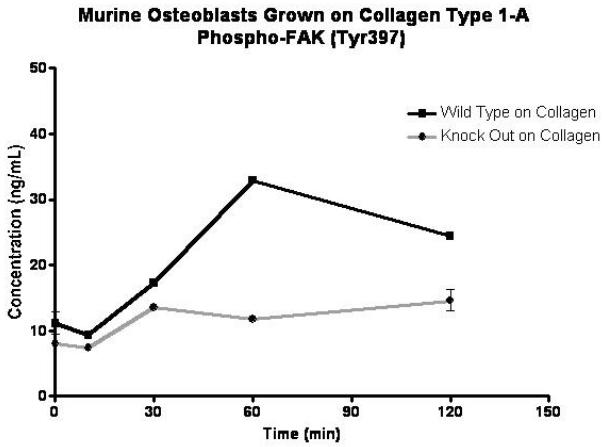

LIMK 1 Osteoblast Graph

***Disclosures: Robert Botta**, None.*

SU0235

Attenuation of Adipogenesis by Mechanical Strain Involves Downregulation of C/EBPβ. Maya Styner*[1], Natasha Case[1], Zhihui Xie[2], Buer Sen[3], Jacob Thomas[2], Janet Rubin[1]. [1]University of North Carolina, Chapel Hill, School of Medicine, USA, [2]University of North Carolina, USA, [3]University of North Carolina At Chapel Hill, USA

Mechanical strain's ability to directly limit adipogenesis of mesenchymal stem cells (MSC) has important implications for exercise treatment of osteoporosis and obesity. Prior work in our lab demonstrated that strain's repression of adipogenesis is partially dependent on inhibition of GSK3β as well as preservation of β-catenin. However, silencing of β-catenin does not entirely prevent mechanical repression of adipogenesis. As well, strain also decreased PPARγ expression, a step presumably proximal to effects on β-catenin. We asked here whether strain might have effects upstream of PPARγ and β-catenin. We concentrated on the leucine zipper transcription factor C/EBPβ, which is a necessary signal upstream to PPARγ, and is activated by GSK3β. C3HT101/2 MSCs and marrow derived MSCs were cultured in adipogenic media (± indomethacin) for up to 6 days. Indomethacin caused a rapid induction of PPARγ and fat markers adiponectin and aP2 by d 3 preceded by robust upregulation of C/EBPβ at d 2. In the absence of indomethacin, adipogenesis was not evident until at least d 4. The application of a daily strain regimen (2%, 3600 cycles/d) decreased adipogenesis by more than 50%, as expected. Importantly, we found that strain also blunted the early rise in C/EBPβ in proportion to its repression of both adiponectin and aP2. In addition to its role in adipogenesis, C/EBPβ is implicated in ER stress in pancreatic beta cells as well as in stress induced hepatic steatosis. Addition of the ER stress inducer tunicamycin (≤3.5 μg/ml) here caused an increase in C/EBPβ protein in MSC. As recent data suggests that mechanical factors can decrease hepatic steatosis, and our data shows that mechanical strain limits C/EBPβ, we speculate that mechanical factors limit ER stress through this pathway. In summary, our findings indicate that C/EBPβ is a transcription factor key in the induction of MSC adipogenesis, and is subject to regulation by mechanical strain. The association between strain and C/EBPβ activity suggests that mechanical factors may have an unexplored role in regulating ER stress, and as such contribute to the salutary effects of exercise.

***Disclosures: Maya Styner**, None.*

SU0236

Effects of TGFβ-family Members on hMSC. Barbara Klotz*[1], Martina Regensburger[2], Ludger Klein-Hitpass[3], Regina Ebert[4], Franz Jakob[2]. [1]Orthopädisches Zentrum Für Muskuloskelettale Forschung, Denmark, [2]Orthopedic Center for Musculoskeletal Research Experimental & Clinical Osteology, Germany, [3]Institut für Zellbiologie (Tumorforschung), Germany, [4]University of Wuerzburg, Orthopedic Center for Muskuloskeletal Research, Germany

Myoststin (GDF8), Activin A (AA) and Folliststin (FST) are members of the TGFβ-βfamily. Serum levels of GDF8, a negative regulator of skeletal muscle growth, are enhanced during ageing, which is associated with the development of age-related sarcopenia. GDF8 inactivation leads to an increase in skeletal muscle mass. Bone cells express AA, which inhibits the mineralization process in osteoblast cultures, while an AA antagonist showed anabolic and antiresorptive effects in monkeys. FST inhibits other TGFβ-family proteins by dimer formation. The influence of GDF8, AA and FST on basal cell-function was investigated in human mesenchymal stem cells (hMSC), which play a role in bone regeneration and osteoblastic differentiation. HMSC (n=3) were stimulated with 0.01 or 0.1 μg/ml rhGDF8, rhAA and rhFST for 48 and 72 h, and apoptosis and proliferation rates were determined. To identify GDF8-responsive genes in hMSC microarray hybridizations were performed (HG U133 Plus 2.0 array, Affymetrix) and the array results were calculated with SAM (Significance Analysis of Microarrays). RT-PCR validation of Array results were performed by using hMSC of 3 human donors. RhGDF8 incubation of hMSC for 72 h shows an inhibition of apoptosis (up to 33%; 0.01 μg/ml and up to 25%; 0.1 μg/ml), only minimal effects were seen on proliferation. 72 h AA incubation decreases cell proliferation up to 21% (0.1 μg/ml) and the apoptosis rate up to 22% (0.01 μg/ml) and 10% (0.1 μg/ml), respectively. 72 h rhFST cultured hMSC show a 13% decline in proliferation and a 14% decrease in apoptosis (both 0.1 μg/ml). A costimulation with rhFST and rhGDF8 inhibits proliferation (14%; 0.1 g/ml) and apoptosis (20%; 0.1 g/ml). GDF8 did not show significant effects on the expression of stem cell markers cmyc, klf4, oct4 and sox2 as detected by RT-PCR. SAM calculations resulted in 102 probesets, which were significantly upregulated, and 172 probesets, which were significantly downregulated in rhGDF8 treated hMSC. Primarily, cell cycle associated genes were affected. Analysis of selected candidate genes revealed donor variability in newly established hMSC populations. Single donors showed an enhanced expression of pbx1, pbx2, sod2 and hgf as a result of rhGDF8-stimulation. The investigated morphogenes of the TGFβ-family show an inhibiting effect on proliferation and apoptosis after 72 h stimulation. Pbx1 and oct4 affect central processes of stemness and morphognesis. The expression of cmyc, klf4, oct4 and sox2 was detected by RT-PCR, but no significant modulating effects of rhGDF8 on stemness were observed. The evaluation of the array analysis displays high donor variability although we found interesting candidate genes, which require further functional investigations.

***Disclosures: Barbara Klotz**, None.*

SU0237

Evaluation of Osteogenic Differentiation by Embryonic Stem Cells. Dario Repic*[1], Tiziana Franceschetti[1], Ivo Kalajzic[2]. [1]Department of Reconstructive Sciences, University of Connecticut Health Center, USA, [2]University of Connecticut Health Center, USA

Recent studies reported the successful differentiation of mouse or human ES cells into osteoblasts. To achieve osteogenic differentiation, some procedures utilize generation of embryoid bodies, while others use a direct differentiation protocol. It has been reported that ES cells can be induced to express a mature osteoblastic phenotype by culture in the presence of various osteo-inductive molecules (Vit D3, dexamethasone, ascorbic acid, ß-glycerol phosphate and/or BMP2). It is conceivable that osteogenic differentiation requires that ES cells undergo differentiation through an intermediary step involving a mesenchymal lineage precursor. These cells are known as ESC-derived, mesenchymal stem cells (ES-MSCs) and they can be identified by functional and morphological criteria. To identify ES-MSC we have generated ES cells from previously developed transgenic mice in which an α-SMA promoter directs the expression of red fluorescent protein (RFP) to adult mesenchymal progenitor cells. To track the transition of ES-MSC into mature osteoblast lineage cells we have utilized a Col2.3 promoter driving green fluorescent protein (GFP). Osteogenic differentiation in the ES cells derived from dual transgenic mice was evaluated. Following osteogenic induction we have observed expression of alkaline phosphatase and subsequent mineralization as detected by von Kossa staining. However, gene expression analysis of the time course during the differentiation period showed an absence of markers of the mature osteoblast lineage (osteocalcin, bone sialoprotein). After one week of osteogenic induction, ES cells begin to express αSMA-RFP. This expression was localized to the peripheral area encircling a typical ES cell colony. Nevertheless, these α-SMA-RFP positive cells did not show activation of the Col2.3-GFP promoter even after 4 weeks of osteogenic differentiation. Our results indicate that expression of alkaline phosphatase and mineralization occuring during induction of ES cells are not sufficient critera to detect osteogenic maturation using ES cells. The procedures utilizing protocols for differentiation without the step of embryoid bodies formation require further studies. In addition, we are currently examining the activation of Col2.3GFP using an in vivo assay of teratoma formation. This would provide us with assurance that we can identify two steps during osteogenic differentiation of murine ES cells.

***Disclosures: Dario Repic**, None.*

SU0238

Withdrawn

SU0239

Identification of a Novel Cell Population in the Adult Mouse Bone Marrow. Wanida Ono*[1], Masanobu Ohishi[2], Noriaki Ono[3], Richa Khatri[1], Henry Kronenberg[4], Hector Aguila[5], Louise Purton[6], Ernestina Schipani[3]. [1]MGH-Harvard Medical School, USA, [2]National Kyushu Medical Center, Japan, [3]Massachusetts General Hospital & Harvard Medical School, USA, [4]Massachusetts General Hospital, USA, [5]University of Connecticut Health Center, USA, [6]St. Vincent Hospital, Australia

In order to gain insights into the complexity of the bone marrow stroma, we have recently generated a double transgenic mouse expressing both a constitutively active PTH/PTHrP receptor (PPR*Tg) and green fluorescent protein (GFP) in osteoblasts. These mice (PPR*Tg/GFP), were generated by crossing hemizygous PPR*Tg and hemizygous GFP mice, in which the respective transgenes were expressed under the control of a 2.3 kb fragment of the a1(I) collagen gene promoter. Confocal microscopy analysis of frozen sections of adult tibias isolated from PPR*Tg/GFP revealed the presence in the bone marrow of GFP(+) fibroblastoid cells that were also positive for the hematopoietic marker CD45. As expected, mature osteoblasts expressed GFP but were negative for CD45. Osteoclasts, i.e TRAP+ cells adjacent to bony surfaces, were negative for GFP. To further characterize the GFP(+)CD45(+) cells identified in the bone marrow of PPR*Tg/GFP, we performed flow cytometry analysis of bone marrow cells isolated from either WT/GFP or PPR*Tg/GFP mice, upon crushing of the long bones. To minimize the number of mature osteoblasts in our samples we did not use enzymatic digestion. Flow cytometry analysis confirmed the presence of GFP(+)CD45(+) cells in the bone marrow of both mutant and control mice. This population was significantly expanded in the bone marrow of PPR*Tg/GFP animals, and was still measurable upon hematopoietic lineage depletion achieved using a cocktail of antibodies specific against Gr1, Ter119, CD5, F4/80 and B220 antigens. In addition, the vast majority of GFP(+)CD45(+) cells was positive for CD11b, a marker of cells belonging to the monocyte lineage. RT-PCR analysis of total RNA extracted from sorted GFP(+)CD45(+) indicated that these cells expressed both collagen type I and GFP mRNAs. Moreover, the native PTH/PTHrP receptor (PPR), which is a mesenchymal lineage marker, and RANK, expressed in osteoclast and in dendritic cells, were also detectable in GFP(+)CD45(+) cells, confirming that these cells had indeed features of both mesenchymal and hematopoietic lineages. In summary, our data indicate that the adult bone marrow contains a novel cell population with mixed features of mesenchymal and hematopoietic cells; this population is also significantly expanded in a model of high bone turnover due to activation of PPR in osteoblasts. Its role in bone homeostasis is currently under investigation.

***Disclosures: Wanida Ono**, None.*

SU0240

Ionizing Radiation Alters the Bone Marrow Microenvironment by Inducing Senescence of Stromal Cells. Cynthia Carbonneau*[1], Geneviève Despars[1], Audrey Fortin[1], Oanh Le[1], Trang Hoang[2], Christian Beauséjour[1]. [1]Centre de recherche du CHU Ste-Justine, Université de Montréal, Canada, [2]IRIC, Université de Montréal, Canada

The extent to which the integrity of the bone marrow stroma contributes to the success of hematopoietic stem cell (HSC) transplantation is not well known. Alterations of the bone marrow microenvironment, which has been shown to occur during aging or following genetic manipulations of telomere length, impair HSC functions and engraftment. These results suggest that an increased number of senescent marrow stromal cells could affect the niche functions. Exposure to ionizing radiation (IR), by inhibiting marrow stromal cells colony forming unit (CFU) potential, is believed to severely impair the bone marrow microenvironment, but the direct effects of such damage on transplantation is unknown. Using immunohistochemistry and qPCR, we demonstrated that exposure to IR induces an upregulation in marrow stromal cells of the senescence-associated beta-galactosidase and $p16^{INK4a}$, two well established senescence markers. A $Cdkn2a^{-/-}$ mouse model was used to identify p16 as an important inducer of the senescence phenotype. However, alterations to the proliferative potential of marrow stromal cells and to the bone marrow homing of HSC were p16-independent. Indeed, we observed a comparable reduction in CFU-F from wild type and $Cdkn2a^{-/-}$ mice one week following exposure to IR. Bone marrow homing was also altered in both groups compared to non-irradiated mice but returned to baseline 8 weeks following exposure to IR and went even better than controls in $Cdkn2a^{-/-}$ irradiated mice. This could be related to the higher number of bone marrow stromal cells in those mice. All together, our results provide a mechanistic link as to how irradiation, by inducing senescence of the stroma, impairs the function of the hematopoietic niche. Morever, p16 isn't responsible for altered stromal cells functions, but is implicated in the induction of their senescence phenotype.

***Disclosures: Cynthia Carbonneau**, None.*

SU0241

Irradiation-induced DNA Damage Interferes with Mesenchymal Stem Cell Plasticity. Cynthia Carbonneau[1], Geneviève Despars*[1], Oanh Le[2], Christian Beauséjour[1]. [1]Centre de recherche de l'Hôpital Sainte-Justine, Université de Montréal, Canada, [2]Centre de recherche du CHU Ste-Justine, Université de Montréal, Canada

Exposure to ionizing irradiation (IR) can lead to the induction of cellular senescence, a process by which cells undergo growth arrest and secrete a specific pattern of cytokines and inflammatory factors. The cellular effectors for senescence are the transcription factors p53 which upregulates $p21^{CIP}$and the cell-cycle regulating protein $p16^{Ink4a}$ through Rb hypophosphorylation.

Multipotent stromal cells (MSCs) give rise to chondrocytes, osteoblasts and adipocytes. Several transcription factors positively regulate osteoblastogenesis, such as Dlx5, Runx2, and Sp7/Osx. Furthermore, cooperation between the basic helix-loop-helix factors E2A and Twist and the zinc finger protein Snail regulate $p21^{CIP}$ expression during bone formation. Members of the nuclear receptor family either positively, such as PPARγ, or negatively, like RORα, regulate adipogenesis. Other key transcriptional regulators of adipogenesis are the C/EBP family of proteins.

We found that IR-induced senescent MSCs were unable to differentiate into adipocytes and osteoblasts *in vitro*, indicative of a cell-autonomous defect which could be due to aberrant expression of lineage-specific transcription factors.

We investigated whether there could be a functional link between the $p53/p21^{CIP}$ and the $p16^{Ink4a}$ signalling pathways and the expression of selected transcription factors from the adipogenic and osteogenic lineages following the induction of senescence. Steady-state and IR-induced senescent MSCs derived from wild-type, $Trp53^{-/-}$, $Cdkn1a^{-/-}$ and $Cdkn2a^{-/-}$ mice were tested for the expression of lineage-specific transcription factors and their ability to differentiate into adipocytes and osteoblasts *in vitro*. Using a heterotypic bone formation we will also investigate the re-programming potential of irradiated MSCs when exposed to a non-irradiated host. Altogether our work provides a framework to investigate the cell-autonomous effects of irradiation on the mesenchymal cell system, and the effects of irradiation on bone homeostasis. Our results will contribute to the development of novel strategies aimed at improving engraftment following irradiation-induced bone marrow conditioning.

***Disclosures: Geneviève Despars**, None.*

SU0242

Mechanical Stress to Integrins Induces Biological Responses in Mesenchymal Stem Cells. Annika Kasten[1], Petra Müller[1], Ulrike Bulnheim[1], Jürgen Groll[2], Martin Möller[2], Joachim Rychly*[1]. [1]University of Rostock, Germany, [2]RWTH Aachen, Germany

Regeneration of bone depends on the control of mesenchymal stem cells by environmental factors, which involve mechanical forces. Because integrins are regarded as mechanotransducers, we applied forces to integrins using magnetic microbeads attached to integrin subunits on the apical surface of bone marrow derived human mesenchymal stem cells. Using an inhomogeneous magnetic field, integrins were pulled by the beads in parallel to the cell surface for 15 min. We studied the expression of proteins which are related to cell differentiation and were interested in the release of VEGF, a factor which plays a role in vascularization. When MSC were cultured on plastic, both the magnetic field alone and a mechanical stress to the β1-integrin subunit induced an increased expression and release of VEGF, detected by real time RT-PCR. Concerning the expression of different markers for cell differentiation, the magnetic field and the short time application of physical forces was sufficient to induce Sox9, a marker for chondrogenic differentiation within 48 h, whereas other differentiation markers remained unaffected. We further revealed that the matrix to which the cells adhere determined the cellular responses due to physical forces. When cells were cultured on fibronectin or RGD peptides, mechanical load to integrins induced an increased expression of collagen I, which was not detectable on plastic. To see, whether different integrin subunits specifically induce a biological response of the cells, we tested the effect of mechanical forces to different integrin-α subunits. In Western blots we found that mechanical stress to integrin-α subunits and most obviously to the fibronectin receptor α5 induced the expression of collagen I, which was less obvious when stressing the β1-integrin subunit.

In summary, mechanical forces applied to integrin subunits, but also a magnetic field are able to induce the expression of markers of differentiation as well as growth factors, like VEGF in mesenchymal stem cells. The cellular responses due to mechanical forces depend on matrix of adhesion and the integrins, which were stressed. The results have significant impact for tissue engineering strategies, e. g. in the design of physical and chemical characteristics of implants for tissue regeneration.

***Disclosures: Joachim Rychly**, None.*

SU0243

Monocytes and Macrophages Promote Osteogenic Differentiation of Human Mesenchymal Stem Cells via Cyclooxygenase 2 and Lipoxygenase. Vicky Nicolaidou*[1], Andrew P. Cope[2], Nicole Horwood[3]. [1]Imperial College London, GBR, [2]Academic Department of Rheumatology, King's College London, United Kingdom, [3]Kennedy Institute of Rheumatology, United Kingdom

Bone loss is a characteristic of many chronic inflammatory and degenerative diseases such as rheumatoid arthritis and osteoporosis. A major challenge for regenerative medicine is to replace bone once it's lost. Mesenchymal stem cells (MSC) are multipotent progenitors that can be induced in culture to form osteoblasts (OB). Recent findings suggest that macrophages (M) are an integral part of bony tissue and can regulate OB function (Chang et al., 2008) however the mechanisms for these cellular interactions are not understood. Cycloxygenases (COX) and lipoxygenases (LOX) are enzymes that catalyze the synthesis of endogenous mediators such as prostaglandins and more recently identified lipoxins and resolvins. A growing body of evidence concerning the use of these molecules in *in vivo* disease models suggests that they have a role in bone regeneration (Hasturk et al., 2009). To investigate the mechanism of MSC/M interactions in osteogenesis we established co-cultures of human MSC with either peripheral blood monocytes or M-CSF derived Ms. To inhibit COX-2 and LOX we used specific inhibitors, NS-398 and baicalein, respectively. Osteogenic differentiation of MSC was assessed by measuring alkaline phosphatase (ALP) activity and bone nodule formation. Monocytes and Ms induced MSC differentiation towards OBs as shown by ALP staining and bone nodule formation. Differentiation required cell contact but could also take place when conditioned media from another co-culture was added directly onto MSCs. In the presence of NS-398, cell contact mediated differentiation was abolished but this could be rescued by the exogenous addition of PGE2 or agonists of the EP2/4 receptors. NS-398 addition did not affect the ability of conditioned media to induce differentiation but in the presence of baicalein both cell contact and conditioned media induced differentiation was abolished. These findings indicate that COX2 expression is required in the monocyte/M whilst LOX is required in the MSC for the induction of differentiation. We present novel findings that monocytes can direct differentiation of MSC to OB via COX and LOX pathways. Initial contact between MSCs and monocytes leads to COX2 induction and PGE2 production which can then act via EP2 and EP4 receptors. Once PGE2 is produced it can activate LOX leading to the production of the lipoxins and resolvins which in the presence of osteogenic stimuli will enhance MSC osteogenic differentiation in a LOX–dependent manner.

***Disclosures: Vicky Nicolaidou**, None.*

SU0244

Msx2 Expression Is Positively Associated With the Osteoblastic Potential of Adipose-derived Stromal Cells. William Ferris*[1], Stephen Hough[2], Hanel Sadie-Van Gijsen[2]. [1]University of Stellenbosch., South africa, [2]University of Stellenbosch, South africa

Purpose: We wished to compare the *in vitro* osteoblastic differentiation of adipose-derived stromal cells (ADSCs) from subcutaneous and visceral adipose depots from lean and diet-induced obese rats, to assess whether metabolic status affects osteoblast differentiation. In addition, we wished to determine whether expression levels of osteoblast-associated transcription factors Runx2 and Msx2 could serve as an indicator of osteoblast differentiation potential in ADSCs.

Methods: ADSCs were isolated from subcutaneous and visceral adipose tissue from lean and diet-induced obese adult male Wistar rats. Cultured cells were treated with osteoblast differentiation media (OM) and examined for alkaline phosphatase activity and matrix mineralization, both indicative of the osteoblastic phenotype. The expression of the osteoblast-associated transcription factors Runx2 and Msx2 was measured using semi-quantitative RT-PCR.

Results: For both lean and obese rats, OM treatment induced osteoblast differentiation in subcutaneous ADSCs (scADSCs), but not in visceral ADSCs (vADSCs). However, the up-regulation of alkaline phosphatase activity and matrix mineralization in response to OM was less pronounced in scADSCs from obese rats, compared to scADSCs from lean rats. In naïve cells, basal Msx2 expression was found to be higher in osteogenic scADSCs than in non-osteogenic vADSCs. Msx2 expression was up-regulated during osteoblastic differentiation of scADSCs from lean rats, and to a lesser extent in scADSCs from obese rats. Msx2 was not up-regulated in response to OM in vADSCs, which do not differentiate into an osteoblastic phenotype. Msx2 expression is therefore positively associated with osteogenesis in ADSCs. Runx2 was expressed in all cells, but was not associated with the potential of ADSCs to differentiate into osteoblasts.

Conclusions: The potential of cultured ADSCs to differentiate into osteoblasts is influenced by the adipose tissue depot from which the cells were originally isolated, as well as the metabolic status of the donor animal. These cells retain a ''memory'' of their origin after *in vitro* expansion. In addition, the expression of Msx2 may be considered as a marker of *in vitro* osteoblast differentiation potential in ADSCs.

***Disclosures: William Ferris**, None.*

SU0245

Withdrawn

SU0246

Osteogenic Potential of Side Population Cells in Periodontal Ligament. Tadashi Ninomiya*, Toru Hiraga, Akihiro Hosoya, Hiroaki Nakamura. Matsumoto Dental University, Japan

Periodontitis, one of sever infectious periodontal diseases, is characterized by decreases of alveolar bone mass and is a most common cause for tooth loss in adult. Then, regeneration of periodontal tissue is essential for maintenance of tooth and preventable disease. The studies of regeneration of oral tissue have been performed using several cells, such as periodontal ligament cells, dental pulp cells, and mesenchymal stromal cells. Especially, periodontal ligament cell (PDL) is attracted notice in oral tissue regeneration, because periodontal tissue such as alveolar bone and cementum is formed by osteoblasts and cementoblasts differentiated from PDL. In previous studies, we showed that alveolar bone is formed between branches of the bifurcated root in transplanted tooth into the subcutaneous tissues and that PDL contains stem cells with the ability to regenerate alveolar bone. On the other hand, it is well known that stem cells are abundantly contained in side population (SP) cells which possess the capability to strongly efflux drug and dye. In this study, we examined the existence of SP cell in PDL and the osteogenic potential of SP cell in PDL. We harvested SP cells from PDL of rats using a fluorescence activated cell sorting (FACS) system. Flow cytometric analysis of rat PDL suspensions with Hoechst treatment revealed that approximately 2% of total cells were found distinctly in the tail of the curve. RT-PCR analysis showed that the expression of MDR-1 in SP cells was higher level than that in Non-SP (NSP) cells. The functions of osteoblast differentiation and calcification in SP cells were studied in vitro. ALPase staining showed that SP cells possessed higher levels of ALPase activity, compare with that of NSP cells. Alizarin red staining demonstrated that SP cells induced mineralization in osteogenic medium for 10 days, however, NSP cells were not induced. With differentiation into osteoblasts, the genes of osteoblast marker such as ALPase, osteocalcin, and osterix, in SP cells were higher than that in NSP cells. In addition, osteogenic potential of SP cells was investigated by transplantation examination in vivo. As result, it was revealed that SP cells have ability which forms mineralized tissue, in consistency with in vitro studies. In conclusion, SP cells which contains in PDL have abilities that be differentiated into osteoblasts and form mineralized tissue. These results suggest that SP cells is effective in regeneration of alveolar bone.

***Disclosures: Tadashi Ninomiya**, None.*

SU0247

Overexpression of HEY1 and HEY2 Induces Osteoblastic Differentiation and Suppresses cGMP-Dependent Protein Kinase (cGK)II Activity *in vitro*. Ernesto Canalis[1], Anna Smerdel-Ramoya[1], Maria Monarca[1], Stefano Zanotti*[2]. [1]St. Francis Hospital & Medical Center, USA, [2]Saint Francis Hospital & Medical Center, USA

Hairy and Enhancer of Split-related with a YRPF motif (HEY) are evolutionary conserved basic helix-loop-helix transcription factors. HEY proteins are homologues of *Drosophila Hey* and were first identified as targets of the Notch signaling pathway. cGMP-dependent protein kinase (cGK)II, the product of *Protein kinase cGMP-dependent type II*, phosphorylates glycogen synthase kinase (GSK)3β, favoring its degradation. GSK3β phosphorylates cytosolic β-catenin, and induces its degradation by the proteasome. Notch suppresses the expression of cGKII in osteoblastic cells, and as a consequence decreases phospho-GSK3β and enhances the levels of active GSK3β, suppressing the cytosolic levels of β-catenin. This mechanism partially explains the inhibitory effects of Notch on osteoblastic differentiation and function. To define the role of HEY1 and HEY2 in osteoblastic cell fate, ST-2 stromal cells were transduced with pLPCX retroviral vectors expressing either HEY1 or HEY2 under the control of the cytomegalovirus promoter, or with pLPCX as a control. In contrast to the previously reported effects of Notch, overexpression of HEY1 or HEY2 induced mineralized nodule formation, alkaline phosphatase and osteocalcin mRNA levels. Accordingly, alkaline phosphatase activity was induced by both HEY paralogues. We asked whether the divergent effects of the HEY proteins and Notch on osteoblastic differentiation could be due to differential regulation of cGKII mRNA levels and activity. ST-2 cells transduced with HEY1 and HEY2 expressed increased cGKII mRNA levels and suppressed protein levels of GSK3β. These results demonstrate that cGKII is central to the effects of Notch signaling on osteoblastic cell differentiation and that divergent effects of Notch signaling can be explained by its regulation of cGKII. In conclusion, HEY1 and HEY2 can induce osteoblastic cell differentiation by stimulating cGKII expression.

***Disclosures: Stefano Zanotti**, None.*

SU0248

Pyk2 Regulates Megakaryocyte-Induced Osteoblast Proliferation *In Vitro* and Bone Formation *In Vivo*. Angela Bruzzaniti*[1], Ying-Hua Cheng[2], Su Huang[1], Khanh Nguyen[3], Brahmananda R. Chitteti[2], Edward F. Srour[2], Lindsey D. Mayo[2], Melissa Kacena[2]. [1]Indiana University School of Dentistry, USA, [2]Indiana University School of Medicine, USA, [3]Purdue University, USA

Megakaryocytes (MKs) are hematopoietic cells responsible for the production of platelets. A growing body of evidence also suggests that MKs play a key role in regulating skeletal homeostasis. In support of this, mice deficient in GATA-1 or NF-E2, transcription factors required for normal MK development, exhibit an increase in immature MKs, a dramatic decrease in platelet number, and a striking 300% increase in trabecular bone volume. The cellular mechanisms underlying this increase in bone mass remain unclear. Histological evaluation of GATA-1 and NF-E2 deficient mice reveals higher numbers of osteoblasts (OBs) on trabecular surfaces, most likely due to increased numbers of MKs. Consistent with these studies, our in vitro data demonstrate that MKs significantly enhance OB proliferation by direct cell-to-cell contact involving integrin engagement and resulting in the temporal expression of two isoforms of Pyk2 in OBs. Pyk2 is a key tyrosine kinase involved in signaling downstream of activated integrins. Here we show that the relative expression of the Pyk2 isoforms is differentially regulated during OB differentiation, with full-length Pyk2 decreasing and the shorter alternatively spliced Pyk2 isoform increasing with differentiation. In addition, we found that in Pyk2-/- OBs, alkaline phosphatase, type I collagen, osteocalcin and calcium deposition are enhanced, suggesting that Pyk2 negatively regulates OB differentiation and mineralization. Using OBs from Pyk2-/- and wild-type mice, we further show that Pyk2 is required for the MK-mediated increase in OB number and cell cycle progression through the S-G2M phases. Furthermore, Pyk2 forms a complex with the cell cycle arrest protein Retinoblastoma (Rb) and the murine double minute-2 (Mdm2), an E3 ubiquitin ligase that regulates proteosome mediated degradation. Finally, using spleen cells from GATA-1 deficient mice, we adoptively transferred the high bone mass phenotype (increased trabecular density) of GATA-1 deficient mice into wild-type recipient mice but not Pyk2-/- recipient mice, demonstrating in vivo the essential role of Pyk2 in MK-induced increase in bone volume. Taken together, our data demonstrate that Pyk2, via its association with the cell cycle proteins Mdm2 and Rb, regulates OB proliferation in response to MKs, and that down regulation of full-length Pyk2 during OB differentiation is required for mineralization and bone formation by mature OBs.

***Disclosures: Angela Bruzzaniti**, None.*

SU0249

Risedronate on Osteoblast and Adipocyte Differentiation from Human-Mscs. Antonio Casado-Díaz*[1], Raquel Santiago-Mora[2], Jose Manuel Quesada Gomez[3]. [1]Hospital Reina Sofía, Spain, [2]Universidad De Córdoba, Spain, [3]Gabinete Quesper, Spain

Risedronate reduces bone loss by regulating osteoclastic activity and it is one of the most widely used drugs in the treatment of osteoporosis. It is effective in the reduction of fractures in the elderly in whom adipocyte formation in bone marrow overrides osteoblastogenesis. Our objective is to evaluate the effect of risedronate on adipocyte and osteoblast differentiation from mesenchymal stem cells.

Human mesenchymal stem cells (MSCs) from bone marrow were transferred into plates containing MSC media composed of α-MEM, 10% foetal bovine serum, 2 mM of glutamine, antibiotic and 1 ng/ml of bFGF. When the culture reached confluence, the bFGF was removed from the MSC media and adipocyte and osteoblast differentiation inductors were added, whit or without risedronate (10-8 or 10-9 M). Alkaline phosphatase activity, extracellular matrix formation on osteoblasts and lipid vesicle formation on adipocytes were monitored at timed intervals. Moreover, the expression of different genetic markers of adipogenesis and osteoblastogenesis were measured by the mRNA quantitation through real time PCR.

Osteoblastogenesis was modified by risedronate: alkaline phosphatase and mineralization of the extracellular matrix formation increased. Adipogenesis was not modified by risedronate.

Our findings reflect the additional effects of risedronate increasing the osteoblastogenesis. This stimulation of the osteoblastogenic differentiation from MSCs could represent a new way of bone loss prevention by risedronate.

***Disclosures: Antonio Casado-Díaz**, None.*

SU0250

Effects of Odanacatib Treatment on Osteoclast Vesicular Trafficking during Bone Resorption. Le Thi Duong[1], Ya Zhuo[2], Patrick Leung[2], Maureen Pickarski*[3]. [1]Merck Research Laboratories, USA, [2]Merck & Co., Inc, USA, [3]Merck & Co., Inc., USA

Cathepsin K (CatK) is the major osteoclast (Oc) collagenase responsible for degrading demineralized bone matrix. Odanacatib (ODN) is a selective, reversible inhibitor of CatK currently in development for the treatment of postmenopausal osteoporosis. Previously, ODN was shown to fully prevent bone loss in OVX-monkeys. This treatment led to typical accumulation of enlarged intracellular granules in the Oc cytoplasm. The aim of this study is to characterize the cellular mechanism of ODN-mediated inhibition of bone resorption. In vitro, ODN inhibits human Oc bone resorption, without affecting cell polarization or differentiation. We demonstrate that human Oc generate typical trail-like resorption pits, while ODN treated cells make shallow discrete pits. Confocal microscopy detects punctate staining of CatK and its substrate TRAP in intracellular vesicles of resorbing osteoclasts. ODN treatment increases the number of intracellular vesicles which are intensely stained for CatK and TRAP. Interestingly, CatK and TRAP are not co-localized in the same vesicles in ODN-treated Oc. While TRAP(+) vesicles are evenly distributed in the cytoplasm, Cat K(+) vesicles localize toward the apical membrane of the polarized Oc. The intracellular accumulation is further validated in Oc lysates by Western blot. Both precursor and active TRAP increase ~2-fold in treated vs. untreated cells. Similarly, the levels of pre-pro and mature CatK increase by 6- and 2-fold in ODN-treated Oc, respectively, demonstrating that ODN also effectively inhibits auto-catalytic activation of CatK. By directly labeling bone surface matrix proteins with tetramethylrhodamine (TAMRA), we examine the effects of ODN on Oc vesicular trafficking of degraded bone matrix proteins. ODN treatment also leads to an increased number of TAMRA-labeled vesicles compared to that in untreated cells. Moreover, only a subpopulation of TAMRA(+) vesicles are co-localized with CatK, suggesting ODN disrupts multiple vesicular trafficking pathways during Oc resorption. Taken together, ODN treatment of human Oc in vitro results in significantly increased numbers of intracellular vesicles containing CatK and its substrates, similar to that observed in ODN-treated monkeys. Our findings suggest that via blocking CatK-mediated protein degradation in the resorption lacunae, ODN also retards intracellular vesicular trafficking and bone matrix processing in Oc, leading to overall reduction of bone resorption efficiency.

***Disclosures: Maureen Pickarski**, Merck & Co., Inc, 3*
This study received funding from: Merck & Co., Inc

SU0251

Bone is not Essential for Osteoclast Activation. Karen Fuller[1], Jade Ross[2], Kinga Szewczyk[2], Ray Moss[2], Timothy Chambers*[3]. [1]St. George's University of London, United Kingdom, [2]St George's, University of London, United Kingdom, [3]St. George's Hospital Medical School, United Kingdom

It has been considered that bone mineral is essential for the recognition of bone as the substrate appropriate for resorption, although the underlying mechanisms have never been clarified. We used correlates of resorptive behavior to identify the characteristics of substrates that are responsible for activation of osteoclasts. Osteoclasts incubated on bone secrete tartrate-resistant acid phosphatase (TRAP) into the culture supernatant. We found that they also do this if they are incubated on glass coverslips coated with vitronectin, but not fibronectin, even though both ligands enable adhesion. Osteoclasts likewise expressed podosome belts only on vitronectin, and podosome belts were modulated by resorption-regulating cytokines in the manner expected if they reflect resorptive behavior. We found that the greater circumference of podosome belts on glass versus actin rings on bone might have a trivial explanation: podosome belt diameter was substantially reduced on roughened versus smooth Perspex. To further assess whether osteoclasts are activated by non-mineralized surfaces, we developed a method whereby their undersurface can be inspected in the scanning electron microscope after incubation. We found that after incubation on vitronectin, but not fibronectin, osteoclasts showed a densely folded, ruffled undersurface, with exocytotic vesicles and circumferential adhesion structures clearly visible. In the presence of the cathepsin inhibitor E64 the ruffled border was obscured by a protein film. Analogously, osteoclasts formed resorption-like trails in this protein film on vitronectin- but not fibronectin-coated glass coverslips. Like bone resorption, these trails were dependent upon RANKL and were inhibited by E64. Bone mineral induced podosome belts and resorption only if coated with vitronectin. Last, we found that a rigid substrate was not necessary for osteoclasts to form podosome belts: they were seen on vitronectin-coated flexible substrates. These results suggest that podosome belts are reliable markers for resorptive behavior in osteoclasts. The results also suggest that integrin αvβ3 ligands are not only necessary but also sufficient for the induction of resorptive behavior in osteoclasts; that it is these ligands, rather than bone itself, that induce resorption; and that bone is recognized through the ability of bone mineral to bind to these ligands, rather than through its mechanical attributes, or through a putative 'mineral receptor'.

***Disclosures: Timothy Chambers**, None.*

SU0252

CIZ Expression is Enhanced by Inflammatory Stimulation and Transcriptionally Regulates the RANKL Promoter. Tetsuya Nakamoto*[1], Takayuki Motoyoshi[2], Tasuku Hada[2], Tomomi Sakuma[3], Tadayoshi Hayata[4], Yoichi Ezura[5], Riko Kitazawa[6], Sohei Kitazawa[7], Masaki Noda[1]. [1]Tokyo Medical & Dental University, Japan, [2]Department of Molecular Pharmacology, Medical Research Institute, Tokyo Medical & Dental University, Japan, [3]Tokyou Medical & Dental University, Japan, [4]Medical Reserach Institute, Tokyo Medical & Dental University, Japan, [5]Tokyo Medical & Dental University, Medical Research Insititute, Japan, [6]Kobe University, Japan, [7]Ehime University, Japan

Rheumatoid arthritis deteriorates the quality of life in a large number of patients but its causes have not yet been fully understood. CIZ (Cas interacting zinc finger protein) is a nucleocytoplasmic shuttling transcription factor that is present in cell adhesion plaque and in nuclear matrix. CIZ is expressed in the articular cartilage and the expression is enhanced in K/BxN serum induced rheumatoid arthritis model. CIZ deficiency suppressed the inflammatory cell infiltration, cartilage destruction, osteoclast number, and urine deoxypiridinolin excretion in serum-induced arthritis model. Arthritis-induced enhancement in RANKL, MMP-3, and IL-1 beta mRNA expression was also suppressed by CIZ deficiency. Based on the above observations in mice, we utilized cell lines and primary cell culture to obtain further insights to the function of CIZ in arthritis.

Primary chondrocytes from newborn mouse ribs expressed CIZ and the levels of the expression correlated with the chondrocyte differentiation. When chondrocytes were stimulated with IL-1 beta, the expression of CIZ increased by 60% dose-dependently. In addition, overexpression of CIZ in chondrocytes induced the upregulation of MMP-3 by more than 50%.

Next we used bone marrow stroma cell line, ST2 cells, to examine the effectS of CIZ ON RANKL promoter. ChIP assay using anti-CIZ antibody confirmed that CIZ bound to sequences in the RANKL promoter, which include CIZ-binding consensus sequences "CAAAAA" and "CTTTTT". Furthermore, overexpression of CIZ enhanced the promoter activity from the RANKL promoter up to 2.5 folds. Similar results were obtained in the osteoblastic cell line, MC3T3-E1 cells. These data indicate that CIZ expression is induced by IL-1 beta in arthritis and the overexpressed CIZ enhances the expression of MMP-3 and RANKL explaining in vivo phenotypes that CIZ plays an exacerbating role in mouse arthritis model.

***Disclosures: Tetsuya Nakamoto**, None.*

SU0253

Novel Mechanisms Underlying Low Bone Density in Muscular Dystrophy. Anna Rufo*[1], Andrea Del Fattore[1], Maria Luisa Bianchi[2], Enrico Bertini[3], Antonio Musarò[4], Serge Ferrari[5], Dominique Pierroz[6], Mattia Capulli[1], Nadia Rucci[1], Lucia Morandi[7], Fabrizio De Benedetti[8], Anna Teti[1]. [1]Department of Experimental Medicine, University of L'Aquila, Italy, [2]Bone Metabolic Unit, Istituto Auxologico Italiano, Italy, [3]Ospedale pediatrico "Bambino Gesù", Italy, [4]Department of Histology & Medical Embriology, University "La Sapienza", Italy, [5]Geneva University Hospital & Faculty of Medicine, Switzerland, [6]University Hospital of Geneva, Switzerland, [7]Neurologic Institute "C. Besta", IRCCS, Italy, [8]Ospedale pediatrico "Bambino Gesù", Italy

Muscular dystrophies are characterized by myofiber necrosis and presents with inflammation, osteoporosis and increased risk of fractures. We observed muscular atrophy and bone loss in mice overexpressing the pro-inflammatory cytokine IL-6 and propose that IL-6 may link the muscular and the bone phenotype in muscular dystrophies. Duchenne Muscular Dystrophy (DMD) is a X-linked disease due to various mutations in the dystrophin gene. In DMD patients, we observed increased IL-6 in muscle biopsies and in sera. Similar to osteoblasts from IL-6 overexpressing mice and to osteoblasts treated with IL-6, human osteoblasts exposed to DMD sera failed to mineralize the extracellular matrix and showed reduced Osterix and Osteocalcin mRNA expression, despite normal alkaline phosphatase activity and Runx2 mRNA. The circulating RANKL/OPG protein ratio was low in DMD patients and inversely correlated with bone density. Transcriptional analysis revealed a similar reduction in RANKL/OPG ratio and increased IL-6, IL-11, activin A and TGFB2 in osteoblasts exposed to DMD sera, along with up-regulation of further 23 genes and down-regulation of further 90 genes associated with osteoblast function and osteoblast-osteoclast cross-talk. Despite low RANKL/OPG ratio, but in agreement with the increased cytokine levels, peripheral blood monocytes from patients and those from healthy donors exposed to DMD sera exhibited increased osteoclastogenesis similar to that observed in IL-6 overexpressing mice. Consistently, single or combined treatments with these cytokines significantly stimulated osteoclast formation in bone marrow cell cultures. By microCT and histomorphometry we noted that dystrophin-deficient (MDX) mice showed reduced tibial trabecular and cortical bone compared to WT, with decreased osteoblast and increased osteoclast activity, this latter also confirmed by high C-terminal telopeptide of type I collagen in MDX sera. Interestingly, similar alterations, especially for the osteoclast lineage, were observed in calvariae from MDX mice, in which muscular traction is negligible. Finally, high serum IL-6 underlined the involvement of this circulating cytokine in the bone phenotype of MDX mice. In conclusion we propose that, besides mechanical failure, additional factors induce low bone density in DMD patients and MDX mice, among which we underlined a relevant role for circulating IL-6 and for other local cytokines.

***Disclosures: Anna Rufo**, None.*

SU0254

Prostaglandin D_2 Induces Apoptosis of Human Osteoclasts by Interaction with the CRTH2 Receptor. Artur De Brum-Fernandes[1], Li Yue*[2]. [1]Universite De Sherbrooke, Canada, [2]University of Sherbrooke Medical School, Canada

Prostaglandin D_2 (PGD_2) is a lipid mediator synthesized from arachidonic acid that directly activates two specific receptors, the prostanoid DP1 receptor and chemoattractant receptor homologous molecule expressed on T-helper type 2 cells (CRTH2). PGD_2 can affect bone metabolism by influencing both osteoblast (OB) (J. Bone Min. Res. 20:672, 2005.) and osteoclast (OC) functions (J. Bone Min. Res. 23:1097, 2008.), and these effects are probably relevant in in vivo fracture repair (J. Rheumatol. 37:644, 2010.). The mechanisms of OC apoptosis are tightly regulated and of great clinical interest, but the effects of PGD_2 and its receptors in the regulation of OCs apoptosis are unknown. Our objective in the present study was to determine if OC apoptosis was affected by PGD_2. Human peripheral blood mononuclear cells were differentiated into OCs after 21 days culture in the presence of RANKL and M-CSF. The apoptosis of differentiated OCs after incubation with PGD_2, DP antagonist, DP agonist, CRTH2 antagonist or CRTH2 agonist (0.1 nmol/L-10 μmol/L, Cayman Chemical) was determined by using the TACS Blue Label kit (R&D Systems) under a light microscope. To inhibit endogenous prostaglandin production Naproxen was used in some assays. Blue multinucleated (three or more nuclei) cells were counted as apoptotic OCs and pink ones as live OCs. Treatment with PGD_2 for 24 hours in the presence of naproxen (10 μM) increased the percentage of apoptotic OCs in a dose-dependent manner as compared to naproxen treatment alone. To further study the contribution of receptors in PGD_2-induced apoptosis, differentiated OCs were incubated with a DP antagonist (BW A868C, 24 hours) or CRTH2 antagonist (CAY10471, 24 hours) in the absence of naproxen, or with a DP agonist (BW 245C, 24 hours) or CRTH2 agonist (13,14-dihydro-15-keto-Prostaglandin D2, 24 hours) with naproxen. Treatment with the CRTH2 agonist in the absence of endogenous prostaglandins increased whereas the CRTH2 antagonist – in the absence of naproxen - reduced OC apoptosis. Treatment with either agonist or antagonist of DP receptor did not change OC apoptosis compared to control condition. In conclusion, these results show that PGD2 induces human OCs apoptosis in vitro through activation of CRTH2 receptor. Further study is required to investigate the pathways implicated in this effect.

***Disclosures: Li Yue**, Pfizer Canada, 2*

SU0255

CD47 (Integrin Associated Protein) and its Receptor SIRPα Are Not Required for Osteoclast Differentiation or Adult Bone Homeostasis. Julia Charles*[1], Joseph Simonton[2], William E. Seaman[3], Mary Nakamura[4]. [1]University of California, San Francisco & VA Medical Center, USA, [2]VA Medical Center, USA, [3]University of California & VA Medical Center, USA, [4]University of California, San Francisco, USA

Osteoclast (OC) differentiation requires co-stimulatory signals from innate immune receptors associated with the immunoreceptor tyrosine-based activation motif (ITAM)-adapter molecules DAP12 and Fcγ. OC also express immunoreceptor tyrosine-based inhibitory motif (ITIM)-receptors, which are known to oppose the action of ITAM-mediated signaling in myeloid cells and have been implicated in regulation of osteoclasts. We studied CD47 and its receptor, signal regulatory protein-α (SIRPα), an ITIM receptor of the immunoglobulin superfamily. Both SIRPα and CD47 participate in multi-nucleation of macrophage giant cells. SIRPα also associates with the tyrosine phosphatase SHP-1, and SHP-1 deficient mice have marked osteopenia. Although antibodies to SIRPα and CD47 are reported to inhibit OC formation, both increased and decreased bone mass phenotypes have been reported for the $CD47^{-/-}$ mouse and a modest decrease in cortical bone was reported for C57BL/6 mice lacking the cytoplasmic signaling domain of SIRPα (SIRPmut mice). We find that cell surface expression of CD47 and SIRPα by flow cytometry increases during OC differentiation. We examined adult female BALB/c CD47-/- and SIRPmut mice by micro-computed tomography and found no difference in trabecular and cortical bone parameters compared with wild-type littermates. *In vitro* assays of OC differentiation and resorptive capacity also showed no significant differences between wild-type and mutant mice. Preliminary studies also failed to detect a difference in osteoblast formation from bone marrow stromal cells. To determine if differences in reported bone phenotypes could be due to strain differences, we also examined the bone phenotype of C57BL/6 $CD47^{-/-}$, SIRPmut and $CD47^{-/-}$ SIRPmut mice. Consistent with prior reports, we found that C57BL/6 SIRPmut mice have a modest decrease in cortical thickness, but we also found these mice to have decreased body weight. C57BL/6 $CD47^{-/-}$ have been reported to have a modest increase in trabecular bone mass, but in contrast we found cortical and trabecular bone parameters from C57BL/6 $CD47^{-/-}$ and combined CD47-/- SIRPmut mice be similar to wild-type. In summary, our studies suggest that neither CD47 nor SIRPα intracellular signaling are essential for OC differentiation or normal bone mass and homeostasis. It is possible that the effects of SIRPα-CD47 on OC are

evident only under certain conditions and we are currently testing this in models of stimulated bone loss.

***Disclosures: Julia Charles**, None.*

SU0256

Extracellular L-Serine Regulates Intracellular Amino Acid Levels and mTORC1 Activation in Mouse Osteoclast Precursors. Takuya Ogawa*, Orie Nishida, Yoshie Matoba, Toshiki Sakai, Koichi Kishida, Naoki Fujii, Anton Bahtiar, Norihiro Ishida-kitagawa, Tatsuo Takeya. Nara Institute of Science & Technology, Japan

Previously, in the investigation of the mechanism underlying the cell density-dependent suppression of murine osteoclast differentiation *in vitro*, we found the indispensability of L-serine (Ser) for RANK expression in precursors and their subsequent differentiation. However, since Ser is generally classified as nutritionally non-essential and most cells are capable of synthesizing Ser *de novo*, the mechanism how the osteoclast precursors sense extracellular Ser level remains totally unclear. To address this issue, we examined the expression of Ser *de novo* synthetic enzymes and the effect of extracellular Ser on the intracellular and extracellular amino acid levels in osteoclast precursors by using primary cultures of murine bone marrow macrophages. RT-PCR analysis demonstrated that all three enzymes constituting *de novo* Ser biosynthesis from 3-phosphoglyserate (*phgdh*, *psat1*, *psph*) were expressed in osteoclast precursors at comparative levels to other types of cells examined. Then, intracellular and extracellular content of individual amino acids were determined. Culture at high cell density or Ser withdrawal from culture medium caused depletion of intracellular Ser. In addition, intracellular levels of some essential amino acids (EAAs) were also dramatically decreased by Ser withdrawal. In contrast, extracellular Ser level still remains almost constant regardless of cell density. Moreover, phosphoserine, the immediate precursor of Ser in its *de novo* biosynthesis, was detected at an almost constant level under Ser starved condition. Overexpression of three Ser biosynthetic enzymes failed to compensate for the intracellular Ser depletion in the absence of extracellular Ser. Finally, the activation status of a key nutrient sensor mTOR complex 1 (mTORC1) exhibited strong dependency on extracellular Ser. These results suggest that, in osteoclast presursors, extracellular Ser is an essential and rate-limiting factor for mTORC1 activation by other amino acids including EAAs, which is probably attributed to high metabolic demands for Ser exceeding the cellular ability to synthesize it *de novo*.

***Disclosures: Takuya Ogawa**, None.*

SU0257

Genetic Conversion of Osteoclast Precursor to be Responsive to Light-controlled Cation Channel Activation Enhances Differentiation Upon Modulation of their Membrane Potential. Takuya Notomi*[1], Miyuki Kuno[2], Yoichi Ezura[3], Masaki Noda[4]. [1]GCOE, Tokyo Medical & Dental University, Japan, [2]Osaka City University, Japan, [3]Tokyo Medical & Dental University, Medical Research Insititute, Japan, [4]Tokyo Medical & Dental University, Japan

Osteoclasts express many kinds of ion channels and transporters including ClC-7, VSOP, and HCN. Their function and gating mechanism are modulated by membrane potential (MP). Thus MP could regulate osteoclast function. However, little is known about the role of MP itself on bone physiology, because temporal patterns of MPs were not able to be controlled. To challenge this difficulty, we developed a genetic strategy to evoke light-inducible modulation of MP in osteoclast precursors and found a novel mechanism of osteoclast differentiation via controlled activation of MP.

For controlling MP, we genetically converted osteoclast precursors by permanently transfecting Channel rhodopsin Wide Receiver with Venus fluorescence protein (ChWR) which is activated by blue light and causes the permeation of cations. After establishing the stable cell lines of ChWR (WR) or control vector (C) expressing RAW267.4, the light-induced changes of MP and currents were recorded under the whole cell clump configuration. These cells were exposed to series of blue light stimulus (BLS; Excitation wave length 475/30 nm, (2 sec of stimulus - 1 sec of rest) $\times$ 10 times). MPs in WR cells were depolarized from various potentials to around -10 mV immediately ($<$ 50 msec) after the on-stimulus and were returned to the pre-stimulus potential after the off-stimulus. The BLS evoked inward currents (170 $\pm$ 25 pA) at -60 mV within 5 msec. No changes were recorded in C cells upon exposure to BLS. Thus, this illumination system enables us to control the temporal patterns of MP strictly.

To investigate the relationships between the modulation of MP and osteoclast differentiation, we stimulated WR and C cells by BLS once a day for 5 days in the presence of suboptimal RANKL (50 ng/ml). BLS increased TRAP activities in WR cells 5- to 6- fold, but not in C cells. The number of osteoclast like cells (OCLs) was also increased by BLS. Occasionally, BLS induced the formation of OCLs without RANKL. These results suggest that modulation of MP promotes osteoclast differentiation. Considering the pathway of osteoclast differentiation, the expression of NFATc1 was analyzed. The BLS increased the expression level of NFATc1 4- to 8-fold, suggesting that the light-controlled cation channel activation (LCCA) system activates calcium signaling.

In conclusion, LCCA system promotes osteoclast differentiation by increasing the expression of NFATc1 via MP. Our LCCA system could potentially help identify novel pharmacological targets to find drug candidates for osteoporosis.

***Disclosures: Takuya Notomi**, None.*

SU0258

Highly-Requirement of Exogenous Cholesterol and Positive Role of Lipid Raft for Osteoclast Differentiation. Mari Okayasu*[1], Naoto Hada[2], Chiyomi Hayashida[3], Takuya Sato[4], Yoshiyuki Hakeda[2]. [1]Meikai University Graduate School of Dentistry, Japan, [2]Meikai University School of Dentistry, Japan, [3]Meikai University Graduate School of Dentistry, Japan, [4]Meikai University School of Dentistry, Jpn

To search molecules that are induced by RANKL in osteoclastogenesis, we employed fluorescent differential display method using cDNAs derived from osteoclast precursors treated with or without RANKL, and we identified caveolin-1 (Cav-1) as a RANKL-inducing gene. Cav-1 is a major structural protein of lipid rafts in plasma membrane that are the microdomains containing enriched cholesterol. However, osteoclast formation from bone marrow cells of Cav-1-knockout mice was comparable to that of wild-type littermates, and the KO mice exhibited no obvious changes of phenotypes. However, the destruction of lipid rafts by deletion of cholesterol from the plasma membrane with methyl-ß-cyclodextrin (MCD) caused disordered molecular signaling for osteoclastogenesis such as constitutive hyper-activation of Erk, JNK and NF-κB without RANKL-stimuli. Inversely, the MCD treatment resulted in low basal level of phosphorylated Akt and no activation by RANKL. The abnormal signal transduction system for osteoclastogenesis also occurred when osteoclast precursors were cultured in lipoprotein-deficient serum (LPDS); that is, the hyper-activation of Erk and inactivation of Akt. In addition, even in the presence of RANKL, osteoclast formation was depressed under the culture condition with LPDS, and the depression was rescued by exogenous addition of low-density lipoprotein (LDL) and oxidized LDL (oxLDL). The effect of LDL and oxLDL was additive, suggesting positive roles of LDL receptors (LDLR) and scavenger receptors in osteoclast differentiation. In fact, osteoclast precursors expressed the both receptors while the expressions were independent of RANKL. When osteoclast precursors were cultured with LPDS, the expression of c-fos mRNA increased constitutively and RANKL-independently. However, the induction of expression of NFATc1 by RANKL was greatly delayed compared to that in the cells cultured with normal serum. The amount of FcRγ in lipid rafts of the cells cultured with LPDS decreased compared to that in cells cultured with normal serum, and consistently the amount of NFATc1 translocated into nuclei was decreased, causing the accumulation of NFATc1 in cytosol. Furthermore, osteoclast formation in cultures of bone marrow cells from LDLR-KO mice was delayed compared to that of wild-type mice. In conclusion, this study indicates that osteoclast differentiation is highly dependent on exogenous cholesterol while involvement of Cav-1 in osteoclastogenesis still remains unclear.

***Disclosures: Mari Okayasu**, None.*

SU0259

Interferon-inducible p204 Protein Inhibits Osteocalstogenesis Through Direct Interaction with NF-κB Transcription Factor. Wei Tang*, Yi Luan, Nabeel Syed, Chuanju Liu. New York University, USA

We previously reported that p204, an interferon-inducible p200 family protein, serves as a cofactor of Cbfa1 and mediates osteoblast differentiation and chondrocyte hypertrophy (Liu CJ, et al J. Biol. Chem., 2005; 280(4):2788; Zhang Y., et al, Cell Death Differ. 2008; 15(11):1760); in addition, p204, Cbfa1, pRb, and Id proteins form a regulatory circuit and act in concert in the course of osteogenesis (Luan Y., et al, J. Biol. Chem. 2007; 282(23):16860; Luan Y., et al, Mol. Biol. Cell, 2008; 19(5):2113). Here we report the expression and function of p204 in osteoclastogenesis as well as the molecular mechanisms involved. p204 mRNA was quickly induced and reached its peak level at 4 hour in RANKL-induced osteoclastogenesis of RAW264.7 cells, indicating it is early responsive gene of osteoclastogenesis. p204 mRNA was then quickly reduced to basal level. Intriguingly, p204 protein was induced and remained higher level until day 4. In addition, nuclear p204 was shown to shuttle to the cytoplasm in the course of osteoclastogenesis. We next determined the effects of alternations in p204 level on osteoclast formation. RAW264.7 cells transfected with either pCMV-p204 for overexpressing p204, pSuper-p204 that encodes a siRNA against p204, or corresponding controls, were cultured for 4 days in the presence of 100ng/ml RANKL, and the cells were stained for TRAP. TRAP-positive multi-nucleated cells (TRAP+ MNCs) containing three or more nuclei were then counted. Overexpression of p204 significantly inhibited formation of TRAP+ MNCs in RAW-264.7 cells, but repression of p204 markedly increased the size and number of TRAP+ MNCs. In addition, overexpression of p204 led to robust decrease in the expressions of osteoclast marker genes, including β3 integrin, cathepsin K, calcitonin receptor, matrix metalloproteinase 9, and TRAP, whereas knockdown of p204 increased the expression of these genes. Molecular mechanistic studies demonstrated that p204 directly associated with NF-κB p65, and the C-terminal b fragment of p204 (aa 436-635) was required for its interaction with p65. p204 inhibits NF-κB-mediated osteoclastogenesis at two levels: (i) p204 blocks the binding of NF-κB to DNAs of its target genes; and (ii) p204 inhibits the nuclear accumulation of NF-κB. In conclusion,

this study provides evidence showing that p204, whose level was induced and bulk of p204 translocated to the cytoplasm in the course of osteoclastogenesis, inhibits osteoclast differentiation via associating with and inhibiting NF-κB, a transcription factor known to play the central role in osteoclastogenesis.

***Disclosures: Wei Tang**, None.*

SU0260

Negative Feedback Control of Osteoclast Formation Through Ubiquitin-mediated Down-regulation of NFATc1. Jungha Kim*[1], Nacksung Kim[2], Hye Mi Jin[2], Bang Ung Youn[2], Kabsun kim[2]. [1]Chonnam National University Medical, South korea, [2]Chonnam National University, South korea

The regulation of NFATc1 expression is important for osteoclast differentiation and fuction. Herein, we demonstrate that macrophage-colony-stimulating factor induces NFATc1 degradation via Cbl proteins in a Src kinase-depenednt manner. NFATc1 proteins are ubiquitinated and rapidly degraded during late stage osteoclastogenesis, and this degradation is mediated by Cbl-b and c-Cbl ubiquitin ligases in a Src-dependent manner. In addition, NFATc1 interacts endogenously with c-Src, c-Cbl, and Cbl-b in osteoclasts. Overexpression of c-Src induces down-regulation of NFATc1, and depletion of Cbl proteins blocks NFATc1 degradation during late stage osteoclastogenesis. Taken together, our data provide a negative regulatory mechanism by which macrophage-colony-stimulating factor activates Src family kinases and Cbl proteins, and subsequently, induces NFATc1 degradation during osteoclast differentiation

***Disclosures: Jungha Kim**, None.*

SU0261

Pim-1 Regulates RANKL-induced Osteoclastogenesis via NF-kB Activation and NFATc1 Induction. Bangung Youn[1], Kabsun Kim*[2], Nacksung Kim[1], Jung Ha Kim[1], Hye Mi Jin[1]. [1]Chonnam National University Medical School, South korea, [2]Chonnam National University Medical School, South korea

Pim kinases are emerging as important mediators of cytokine signaling pathway in hematopoietic cells. Here, we show that Pim-1 positively regulates RANKL-induced osteoclastogenesis. Expression levels of Pim-1 are increased by RANKL during osteoclast differentiation. The silencing of Pim-1 by RNA interference or over-expression of Pim-1 dominant negative (DN) in bone marrow-derived macrophage cells attenuates RANKL-induced osteoclast formation. Overexpression of Pim-1 DN blocks RANKL-induced activation of TAK1 and NF-κB as well as induction of NFATc1 during osteoclastogenesis. The inhibitory effect of NF-κB activation by Pim-1 DN is rescued by overexpression of TAK1. In addition, Pim-1 interacts with RANK as well as TAK1, indicating that Pim-1 is involved in RANKL-induced NF-κB activation via TAK1. Furthermore, Pim-1 also regulates NFATc1 transcription activity, subsequently induces OSCAR, an osteoclast-specific gene. Taken together, our results suggest that Pim-1 plays an important role in RANKL-induced signaling pathway via NF-κB activation and NFATc1 induction during osteoclastogenesis.

***Disclosures: Kabsun Kim**, None.*

SU0262

SLAT Negatively Regulates RANKL-mediated Osteoclast Differentiation. Jung Ha Kim[1], Hye Mi Jin[1], Kabsun Kim[1], Nacksung Kim[2], Bang Ung Youn*[1]. [1]Chonnam National University, South korea, [2]Chonnam National University Medical School, South korea

Receptor activator of nuclear factor κB ligand (RANKL) induces osteoclast formation from hematopoietic stem cell. Here, we show that SWAP-70-like adapter of T cells (SLAT) negatively regulates RANKL-induced osteoclast differentiation. Expression levels of SLAT are reduced during RANKL-induced osteoclastogenesis. Overexpression of SLAT in bone marrow-derived monocyte/macrophage lineage cells (BMMs) inhibits TRAP positive multinuclear osteoclast formation and attenuates the expression of NFATc1 and OSCAR, which are important modulator in osteoclastogenesis. Furthermore, silencing of SLAT by Si-RNA in BMMs enhances osteoclast formation as well as gene expression of NFATc1 and OSCAR. Taken together, our results suggest that SLAT can act as an negative modulator in RANKL-mediated osteoclastogenesis.

***Disclosures: Bang Ung Youn**, None.*

SU0263

The Osteoclastogenesis in The Alteration of Bone Marrow Cells during Medullary Bone Formation in Estrogen-Treated Male Japanese Quails. Shinji Hiyama*[1], Yuichi Akagi[2], Mineo Watanabe[1], Takashi Uchida[1]. [1]Hiroshima University Graduate School of Biomedical Sciences, Japan, [2]Hiroshima University, Faculty of Dentistry, Japan

Medullary bone (MB) is a unique tissue of female birds, which is remodeled in the bone marrow cavity of long bones to reserve and provide for calcium of egg-shell during the reproductive period. Interestingly, estrogen administration induces MB formation by osteoblasts that are developed from bone lining cells in male birds, and then this bone is resorbed immediately by osteoclasts. Until now, we reported that osteoclast precursor cells are increased and the differentiation of osteoclasts from precursor cells is controlled under RANK/RANKL/OPG system during MB formation period. However, it is not clear what happens in bone marrow cell (BMC) population after E2 administration. To address this question, we examined the alteration of BMC population during MB formation using estrogen (E2)-treated male Japanese quails. After E2 administration, the expressions of RANKL and OPG mRNAs in bone lining cells and osteoblasts on the surface of MB were examined by RT-PCR analysis at 3 (Day 3), 2 (Day 2), 1 (Day 1) and 0 (Day 0) days. There was no difference in the expression level of RANKL mRNA between each Day. However, OPG mRNA indicated high expression at Day 2 and 3. Additionally, there was the high expression of c-fms mRNA in BMC of Day 2 as compared to BMC of other Days. Following this, when lymphocyte/monocyte isolated BMC by Ficoll-Paque were cultured, these cells of Day 2 and 3 were formed many osteoclasts. In CFU-assay using BMC of each Day, although many CFU-GM were formed at Day 2 and 3, many other colonies were formed at Day 0 and 1. These results suggest that the population of BMC may shift from undifferentiated cells to osteoclast precursor cells during MB formation period. Therefore, the appearance of osteoclasts may not be recognized during these period in spite of the presence of RANKL-expressed osteoblasts. Additionally, when these precursor cells increased, osteoclastogenesis may be transiently inhibited by OPG that secreted by osteoblasts until adequate MB formation.

***Disclosures: Shinji Hiyama**, None.*

SU0264

The Role of Calcium Release Activated Calcium Channels in Osteoclast Differentiation In Vitro and In Vivo. Jonathan Soboloff*[1], Lisa J. Robinson[2], Yandong Zhou[1], Tricia Lewis[3], Salvatore Mancarella[1], Li Liu[4], Lida Guo[2], Irina Tourkova[2], Kathy Brundage[3], Rosana Schafer[3], Karen Martin[3], Donald L. Gill[1], Harry Blair[4], John Barnett[3]. [1]Temple University, USA, [2]University of Pittsburgh School of Medicine, USA, [3]West Virginia University School of Medicine, USA, [4]University of Pittsburgh, USA

Ca^{2+} oscillations have been widely reported to occur during osteoclast differentiation although both the identities of their molecular mediators and their role precise contribution to osteoclast formation remain poorly understood. Examination of the expression and function of the Ca^{2+}-Release-Activated Ca^{2+} (CRAC) channel components STIM1 and Orai1 in vitro revealed significant changes over the course of m-CSF/RANKL-mediated differentiation from both human and murine monocytic precursors. Studies included cytosolic Ca^{2+} measurement, Western blot and mRNA analysis of CRAC components, and analysis of cell membrane punctae formation associated with STIM1-mediated activation of Orai1. Inhibition of CRAC using either the pharmacological agent 3,4 dichloropropioanilide (DCPA), controlled with an inactive congener DFPA, or by knockdown of Orai1 expression using a pool of four siRNAs, severely inhibited formation of multinucleated osteoclasts while scrambled RNA controls were unaffected. Surprisingly, multinucleation was severely reduced without affecting protein tartrate resistant acid phosphatase (TRAP) expression. Further, characterization of Orai1-/- mice revealed extensive skeletal changes and near absence of osteoclasts. Interestingly, the animals do not develop osteopetrosis because of a corresponding severe defect in bone formation, seen as gracile shells of bone in sites with appositional growth, such as the ribs. In sites normally converted into trabecular bone, e.g., the vertebral bodies, trabeculae fail to develop or are greatly decreased in number. TRAP activity is found in mononuclear cells in the marrow, but multinucleated osteoclasts were rare, with these patterns being congruent with results of in vitro differentiation. This pattern is consistent with a role for STIM1 and Orai1 in osteoclast differentiation in vivo. Additionally, by analysis of whole cell calcium currents and STIM1-dependent Orai1 activity, we show that DCPA functions by interfering with STIM1-dependent activation of calcium channels. We conclude that CRAC channel activity is not only required for osteoclastic differentiation but that loss of CRAC also leads to defects in bone growth via unclear mechanisms. Further, DCPA is known to have low toxicity, and thus is a CRAC channel inhibitor with therapeutic potential for treatment of osteoporosis.

***Disclosures: Jonathan Soboloff**, None.*

SU0265

A Novel Murine Model of Osteopetrosis by Administration of a Denosumab-like anti-Murine RANKL Neutralizing Monoclonal Antibody (OYC1). Hisataka Yasuda*[1], Kaoru Mori[2], Yoshiya Tomimori[2], Tadashi Ninomiya[3], Nobuyuki Udagawa[3], Naoyuki Takahashi[3], Yuriko Furuya[2]. [1]Oriental Yeast Company, Limited, Japan, [2]Oriental Yeast Co., Ltd., Japan, [3]Matsumoto Dental University, Japan

A fully human anti-RANKL monoclonal antibody named denosumab (the trade name: Prolia) is almost ready for clinical use for the treatment of osteoporosis. Since denosumab does not cross react with rodent RANKL, its evaluation in preclinical studies has been done only by using cynomolgus monkeys or human RANKL-knock-in mice (HuRANKL mice) in which the exon 5 in murine *rankl* was replaced with that in human *RANKL*. To investigate the effect of RANKL inhibition in normal mice we prepared anti-murine RANKL neutralizing monoclonal antibody (OYC1) and established a novel murine model of osteopetrosis by administration of OYC1 to normal mice. One subcutaneous injection of the antibody increased bone mass markedly with remarkable decrease in OcS/BS and NOc/BS after two weeks. In addition, ObS/BS, MAR, and BFR were also reduced markedly. These results were consistent with the recent report treating HuRANKL mice with denosumab. Decreases in bone resorption marker (TRAP-5b) and formation marker (ALP) were observed in the OYC1-treated mice. Serum TRAP-5b activity in the treated mice was almost zero for 4 weeks and OYC1 was detected in serum of the treated mice even after 4 weeks. Histological and micro CT analyses showed that the OYC1-treated mice exhibited osteopetrotic phenotype in analogy to OPG-treated mice. The phenotype was evident 4 days after the single injection of OYC1 to normal mice and the bone mass was gradually increased in a time-dependent manner for 4 weeks. In comparison to the previous report, the effect of single injection (5 mg/kg) of OYC1 for 2 weeks on bone mass was roughly equivalent to that of three-daily injections (24 mg/kg) of OPG for 2 weeks, indicating that the efficacy and stability of the anti-RANKL antibody *in vivo* was much higher than those of OPG. Osteopetrosis is generally caused by failure of osteoclast-mediated resorption of skeleton. There are numerous murine models of osteopetrosis without osteoclasts, including *RANKL*-deficient mice. The OYC1-treated mouse is a simple inducible osteopetrosis model with only one injection. Since OYC1 acts as a denosumab-like antibody in mice, it is possible to investigate the difference between bisphosphonates and anti-RANKL antibody in normal mice. It is also possible to test the effects of switching pharmaceutical candidates, e.g. PTH to anti-RANKL antibody and to test the effects of their combinations. The anti-RANKL antibody, OYC1 is also useful to investigate unknown functions of RANKL *in vivo*.

***Disclosures: Hisataka Yasuda**, Oriental Yeast Co., Ltd., 3*
This study received funding from: Oriental Yeast Co., Ltd.

SU0266

Bis-enoxacin: A novel Anti-Bone Resorptive Bisphosphonate. Edgardo Toro*[1], Vivian Bradaschia-Correa[2], Victor Arana-Chavez[3], David A. Ostrov[1], Thomas Wronski[1], Lexie Holliday[4]. [1]University of Florida, USA, [2]University of Sao Paulo, Brazil, [3]University of São Paulo, Brazil, [4]University of Florida College of Dentistry, USA

By using computational chemistry and in vitro screening, we identified enoxacin as an inhibitor of the interaction between the B2-subunit of vacuolar H+-ATPase (V-ATPase) and microfilaments. Enoxacin reduced osteoclast formation and bone resorption in mouse marrow cultures in vitro without affecting osteoblast function [1]. We tested the hypothesis that a bisphosphonate constructed by linking enoxacin to a bisphosphonate backbone would target enoxacin's unique anti-osteoclastic activity to bone. A chemical derivative of enoxacin was synthesized by adding a bisphosphonate to the piperazine group of enoxacin. An intermediate carbon between enoxacin and the carbon of the bisphosphonate backbone was added yielding bis-enoxacin. The purpose of the study was to characterize the anti-resorptive activity of the bisphosphonate-linked derivative of enoxacin. Mouse marrow osteoclasts were differentiated by treatment with calcitriol and loaded onto bone slices, in the presence of varying concentrations of bis-enoxacin, alendronate as a positive control, or vehicle. Raw 264.7 cells were stimulated with recombinant RANKL in the presence or absence of inhibitors. Osteoclasts were identified by staining for tartrate-resistant acid phosphatase activity, or by staining with phalloidin to detect actin rings. Osteoblasts were detected by alkaline phosphatase activity or the presence of mineralized nodules. Bone resorption was measured by quantitative scanning electron microscopy. We found that bis-enoxacin had similar anti-osteoclastic activity compared with enoxacin in cultures that did not contain bone slices. Both inhibited osteoclast formation with an IC 50 of approximately 10 μM. Neither blocked osteoblast proliferation or mineralization at 100 μM. Bis-enoxacin bound bone tightly, and was able to inhibit bone resorption when bound to bone. We confirmed that alendronate inhibited osteoclasts by triggering cell death, but we did not detect increases in apoptotic cells in the presence of bis-enoxacin. Rather, bis-enoxacin retained osteoclasts alive in a non-resorptive state. In conclusion, a novel anti-resorptive bisphosphonate (bis-enoxacin) was identified. Bis-enoxacin inhibited osteoclast activity by a different mechanism than currently available therapeutic bisphosphonates like alendronate. Bis-enoxacin holds potential as a novel tool for studying the molecular mechanisms by which osteoclasts function, and may prove useful for the treatment of diseases of excess bone resorption. 1.Ostrov, D.A., et al. 2009. *J.Med.Chem.*Jul 24. 52:5144-5151

***Disclosures: Edgardo Toro**, None.*

SU0267

Elucidating Specific Interacting Domains Between a3-B2 and a3-d2 Vacuolar H^+-ATPase Subunits. Natoosha Azizi*[1], Norbert Kartner[1], Yeqi Yao[2], Keying Li[2], Morris Manolson[1]. [1]University of Toronto, Canada, [2]University of Toronto, Faculty of Dentistry, Canada

Osteoclasts are multinucleated cells that resorb bone by expressing the proton-pumping vacuolar type H^+-ATPases (V-ATPases) on their cell surfaces to acidify their resorption lacunae. Mammalian V-ATPases are multimeric complexes composed of a hydrophobic transmembrane sector (V_0) consisting of subunits a, c, c'', d and e responsible for translocation of H^+ across the membrane, and a hydrophilic, cytoplasmic sector (V_1) consisting of subunits A, B, C, D, E, F, G and H which is responsible for ATP hydrolysis. There exist tissue/cell specific isoforms of some subunits, with a3, d2, and B2 isoforms being highly enriched in osteoclasts. Though the overall organization of the complex is understood, the exact subunit-subunit interactions remain largely unknown. Determining precise subunit interactions could be a first step in developing therapeutics that would block these interactions for the treatment of osteolytic diseases such as osteoporosis and periodontal disease. We have shown that a3 interacts with B2, and we and others have shown that a3 interacts with d2, but we believe that these two a3 interactions are mutually exclusive; we hypothesize that the 50 kDa N-terminal domain of a3 (NTa3) interacts with B2 only when the V_1 and V_0 complexes are associated while the NTa3-d2 interaction only occurs when V_1 and V_0 are disassociated. To test this hypothesis we intend to determine the precise interacting sites between a3-B2 and a3-d2 by creating constructs that consecutively cut B2 and d2 in half. ELISA binding assays with purified NTa3 will determine the interaction site(s). Preliminary data show that NTa3 interacts with the C-terminal domain of B2 (CTB2) and that both the N and C-terminal halves of CTB2 interact with NTa3. All three B2 constructs have the same apparent affinity for NTa3, suggesting that there may be more than one interaction site between NTa3 and B2. NTa3 is predicted to have two finger-like projections and analysis of electron microscopy images of the V-ATPase suggests that these finger-like projections might interact in two consecutive AB grooves. One explanation for our data might be that one of the NTa3 fingers interacts in an AB groove, but that the other finger interacts in the subsequent BA groove, making two interaction sites in subunit B possible.

***Disclosures: Natoosha Azizi**, None.*

SU0268

Latent Osteoclasts After Alendronate Treatment During Rodent Molar Eruption *versus* Bone Resorption *in vitro*. Vivian Bradaschia-Correa[1], Edgardo Toro[2], Lexie Holliday[3], Victor Arana-Chavez*[4]. [1]Universidade de São Paulo, Brazil, [2]University of Florida, USA, [3]University of Florida College of Dentistry, USA, [4]University of São Paulo, Brazil

Recent studies in which sodium alendronate (ALN) was daily administered to newborn rats at a dose of 2.5mg/kg inhibited resorption of the bony crypt by osteoclasts to establish the eruption pathway. The present study compares the ultrastructural features of osteoclast activity in alveolar bone of newborn rats treated with ALN (*in vivo*) with the response of cultured osteoclasts to several doses of ALN (*in vitro*). Newborn Wistar rats were daily injected with 2.5mg/kg ALN during 4, 14 and 30 days, while controls (CON) received saline. At the mentioned time points, the animals were killed and the maxillae were fixed in 0.1% glutaraldehyde and 4% formaldehyde under microwave irradiation, decalcified in 4.13% EDTA and embedded in JB-4 historesin or Spurr epoxy resin. JB-4 sections were incubated for TRAP histochemistry and Spurr ultrathin sections were examined in a JEOL 1010 transmission electron microscope (TEM). For the *in vitro* experiment, mouse marrow cultures were obtained from femurs and tibiae of Swiss Webster mice, and grown over bone slices in 24 well plates with alpha MEM medium supplemented with 1,25-dihydroxy vitamin D3, and treated with ALN at 10uM, 1uM, 100nM, 10nM, 1nM and only vehicle (VEH). After 5 days, the bone slices were removed and washed thoroughly in 2% SDS, dehydrated, gold coated and analyzed in a JEOL JSM 6200 scanning electron microscope (SEM). The cells remaining on the plate were stained for TRAP. The TRAP staining of ALN revealed, at 14 and 30 days, numerous multinucleated TRAP-positive osteoclasts in alveolar bone. However, the bone surrounding the tooth germs was not resorbed by the latent osteoclasts at all time points. Ultrastructurally, most of the cells were not adhered to the bone surfaces and did not present clear zones and ruffled border. Some of them presented a short podosome adhering to the bone matrix, but resorption signals were not detectable. The *in vitro* experiment showed presence of multinucleated and giant TRAP-positive osteoclast-like cells in all experimental groups; however, SEM of the bone slices revealed few shallow resorption lacunae on ALN specimens at higher doses, while VEH presented numerous larger and deeper resorption pits. Thus, ALN inhibited bone resorption and impeded tooth eruption in rats, because osteoclasts formed but remained latent. The *in vitro* experiment additionally showed that, even at the higher doses of ALN, some resorption occurs.

***Disclosures: Victor Arana-Chavez**, None.*

SU0269

Measurement of Chloride Transport in Relation to Lysosomal Acidification in Osteoclasts. Vicki Jensen*, Morten Karsdal, Kim Henriksen. Nordic Bioscience A/S, Denmark

Lysosomal acidification is essential for a range of cellular processes, such as bone resorption. In the bone resorbing osteoclast a resorption lacuna is formed towards the bone surface by exocytosis of lysosomes. Two essential proteins for the osteoclastic acidification of the lysosomes and resorption lacuna are the proton pumping V-ATPase and the chloride transporting ClC-7. Various studies have shown that ClC-7 is the primary chloride transporter of the resorption lacuna membrane in osteoclasts, and thereby it plays an important role in bone resorption by maintaining the electroneutrality of the lacunae.

Previously, lysosomal acidification of the osteoclast was measured using the influx assay, which does not provide direct information on chloride transport. Since compounds inhibiting ClC-7, are promising agents for treatment of osteoporosis we focused on developing an assay specifically measuring chloride transport in osteoclastic vesicles.

Using human osteoclastic microsomal vesicles, the dye MEQ, which emits fluorescence that is quenched by Cl^-, an assay detecting chloride transport was developed. Through freeze/thawing cycles followed by water sonication MEQ was incorporated in the membranes together with a low pH citrate-potassium buffer. The buffer is externally exchanged to a higher pH citrate-sodium buffer using ultra-spin columns. The potassium ionophore Valinomycin was used to activate the system. To validate the assay a range of commercial chloride channel inhibitors were tested, and Cl^- was substituted with other anions.

Using a combination of a pH and a K^+ gradient the assay was shown to be independent of V-ATPase activity, and the sensitivity of the assay was improved by using valinomycin as activator, which was 90% better than increasing pH. Addition of chloride ionophore dose-dependently attenuated chloride transport, confirming chloride sensitivity.

Overall using the dye MEQ has led to a successful implementation of a chloride sensitive assay in human osteoclast derived membranes. The fact that the assay measures the chloride transport independent of the osteoclastic V-ATPase provides a promising foundation for the finding of a compounds directly hitting the osteoclastic chloride transport. Furthermore, since the technology is based on membrane vesicles, it can readily be implemented to study chloride transport in other cell types of interest, i.e. the parietal cells of the stomach, which are involved in secretion of hydrochloric acid.

***Disclosures: Vicki Jensen**, Nordic Bioscience, 3*

SU0270

Non-steroidal Anti-inflammatory Drugs Inhibit Osteoclast Activation by Inhibiting Nuclear Translocation of NFκB. Hitoshi Amano, Akiko Karakawa*, Keiko Suzuki, Shoji Yamada. Showa University School of Dentistry, Japan

Non-steroidal anti-inflammatory drugs (NSAIDs) act efficiently analgesic and against inflammation; however, adverse effect of NSAIDs on bone remodeling has raised concerns. The effect of NSAIDs on bone remodeling is still controversial. In clinical use, NSAIDs are known to progress bone repair as a result of their inhibitory effects on inflammatory factors; in contrast, there are some reports showing that NSAIDs delay bone fracture healing in animal models. To elucidate the mechanism of NSAIDs on bone remodeling, the effects of NSAIDs on osteoclastogenesis and nuclear translocation of NFκB were examined.

To clarify the direct effect of NSAIDs on osteoclasts, three types of NSAIDs were added to the culture, in which more than 99% of cells were differentiated to tartrate-resistant acid phosphatase (TRAP) positive pre-osteoclasts. SC-560, SC-58125, and diclofenac sodium (Diclofenac) were used as a prostaglandin H synthase (PGHS)-1 selective inhibitor, PGHS-2 selective inhibitor and a non-selective inhibitor, respectively.

After 48-hours of culture, each type of NSAIDs significantly decreased TRAP-positive multinucleated cell numbers in a dose-dependent manner. Level of cathepsin K transcripts, a marker for mature osteoclast, was almost completely down-regulated in osteoclasts treated with 10 nM SC-560, Diclofenac, and SC-58125. Pit assay showed a significant reduction in bone resorbing activity in cultures treated with SC-560 and Diclofenac, while SC-58125 exhibited limited inhibition.

To identify the inhibitory mechanisms of NSAIDs, transcriptional factor NFκB expression was examined. Diclofenac, an NSAID which inhibits both PGHS-1 and -2, induced the accumulation of inhibitor of kappa B (IκB) in cytosol, suggesting that decrease of IκB degradation led to suppression of the nuclear translocation of NFκB. Phosphorylated NFκB expression was examined as the index of NFκB activity. Diclofenac suppressed phosphorylated NFκB expression in the nucleus while the expression in cytosol showed normal levels.

In summary, we identified that NSAIDs have direct effect on osteoclast differentiation and bone resorptive activity. Selective PGHS-1 inhibitor showed more potent inhibitory effect on osteoclast activation than PGHS-2 inhibitor did. Moreover, the results in the Western blot analysis showed that Diclofenac, a non-selective inhibitor, decreased the expression level of both intact and phosphorylated NFκB in nucleus.

***Disclosures: Akiko Karakawa**, None.*

SU0271

Ovariectomy Induced Bone Loss in Mice Requires Intact Cbl-PI3K Interaction. Nagasuresh Adapala*[1], Mary Barbe[1], Alexander Tsygankov[2], Archana Sanjay[1]. [1]Temple University School of Medicine, USA, [2]Temple university, USA

Cbl and Cbl-b are ubiquitously expressed proteins with E3-ligase and adaptor functions. Absence of Cbl in mice resulted in delayed bone development although adult mice had no overt bone phenotype. In contrast, deficiency of Cbl-b resulted in osteopenia due to hyperactivity of osteoclasts (OCs). Ovariectomy (OVX) in rodents reduces trabecular bone volume by increasing both bone formation and resorption. To determine if there was inherent defect in the ability of Cbl-/- OCs to respond we attempted to increase bone resorption by OVX. In WT mice, OVX resulted in increased OC activity (serum CTX levels ng/ml SHAM 9.59 ± 2.5, OVX 14.1 ± 2.1) and μCT analysis of L2 vertebra revealed 39.5% decrease in bone volume. In contrast in Cbl-/- mice, CTX levels were unaltered following OVX (CTX SHAM 9.3 ± 1.8, OVX 9.5 ± 1.6) and correspondingly, only 15.2% bone volume loss was observed. Previously, we have demonstrated that in contrast to Cbl-/-, CblYF/YF mice (knock-in mice in which the PI3K binding site in Cbl is ablated) results in increased bone volume due to defective OC function. In accordance with decreased functionality of YF OCs in basal conditions, even in dynamic conditions of bone remodeling induced by OVX serum CTX levels and BMD also did not change significantly (CTX ng/ml SHAM 8.4 ± 1.25, OVX 7.38 ± 1.87; BMD WT SHAM 0.54 ± 0.01, OVX 0.41 ± 0.06, YF SHAM 0.6 ± 0.16, OVX0.42 ± 0.11) suggesting that Cbl-PI3K interaction is required for bone resorption and possibly it is the lack of this interaction in the absence of Cbl, which confers protection from bone loss in Cbl-/- mice. We also examined the effect of OVX-induced bone loss in Cbl-b-/- mice and found that OVX increased OC activity (CTX: Sham 11.8 ± 0.37, OVX 15.2 ± 1.4, p=0.01) and resulted in 33.3% bone volume loss. Since estrogen loss results in cytokine mediated inflammatory response and Cbl proteins are known to participate in immune responses, we measured serum levels of pro-inflammatory cytokines IL-1b, IL-6 and TNF-a and found that in both Cbl-/- and Cbl-b-/- mice cytokines levels were upregulated to similar extents due to OVX suggesting that the differential response of OVX-induced bone loss in Cbl-/- and Cbl-b-/- mice is not due to altered levels of these cytokines. In conclusion, our data demonstrates that OVX increases bone resorption in Cbl-b-/- mice. Our results also suggest that during dynamic conditions of bone remodeling, Cbl regulates OC function, which is determined by its ability to interact with PI3K.

***Disclosures: Nagasuresh Adapala**, None.*

SU0272

Generation of Osteoclasts and Characterization of their Progenitors from Human Pluripotent Stem Cells. Hector Aguila, Sierra Root*. University of Connecticut Health Center, USA

The study of osteoclastogenesis and identification of osteoclast progenitors in humans have been centered predominantly on peripheral blood progenitors. Because the distribution of myeloid progenitors in periphery is dependent on the physiological conditions of each individual, this limits reproducibility and does not allow the study of osteoclastogenesis from primordial progenitors. Human pluripotent stem cells could serve as a novel and renewable source of progenitors to study osteoclastogenesis from the earliest stages of commitment and differentiation. We have designed differentiation protocols co culturing human embryonic stem cells (hESCs) with mouse stroma cell lines. We have optimized culture conditions and using antibodies against CD44 and CD34 we have been able to characterize, using flow cytometry and genomic approaches, several cell populations with predictable developmental potentials. Fractions with hematopoietic potential were isolated by fluorescence activated cell sorting (FACS), expanded in early hematopoietic cytokines and further cultured in osteoclastogenic conditions (M-CSF+RANKL). This protocol generated efficiently *bona fide* human osteoclasts represented by TRAP positive multinucleated cells with the ability to resorb mineral matrix when developed over bovine bone slices. Using antibodies against cell surface markers expressed in early monocytic lineage, we have been able to identify intermediate stages, that could represent osteoclast committed progenitors. These include: CD45, CD14, CD34, CD38, CD45RA, CD115 and CD117. The combination of these antibodies dissected several phenotypes with osteoclast progenitor potential including: $CD45^+$ $CD34^+$ $CD38^-$ $CD45RA^+$ $CD115^+$, and $CD45^+$ $CD14^+$ $CD115^+$ $CD117^+$. We are currently isolating these populations by FACS and evaluating their individual potential to generate osteoclasts *in vitro*. In future studies we will refine the phenotype of progenitors, we will perform clonal studies and we will evaluate the ability of these progenitors to form osteoclasts *in vivo* upon transfer them into immunodeficient animal models. With a defined and unlimited supply of progenitor cells, we would be well positioned to understand mechanisms of osteoclast commitment in humans, to study the role of mediators of osteoclastogenesis and to generate novel models of bone disease.

Supported by State of Connecticut Stem Cell Program (Grants 06SCC04 and 08-SCD-UCHC-003)

***Disclosures: Sierra Root**, None.*

SU0273

Identification and Characterization of a Common Progenitor for Osteoclasts, Macrophages and Dendritic Cells in Murine Bone Marrow. Christian Jacome*, Sun-Kyeong Lee, Joseph Lorenzo, Hector Aguila. University of Connecticut Health Center, USA

Osteoclasts (OCL) are unique bone-resorbing multinuclear cells of hematopoietic origin. Previously, we defined the phenotype and isolated bone marrow progenitors with the ability to efficiently form OCL *in vitro* (Jacquin et al. 2006). These cells have the phenotype $CD45R^{-}$ $CD3^{-}$ $CD11b^{lo}$ $CX3CR1^{+}$ $CD115^{+}$ $CD117^{+}$. Here we tested if this population could also form functional macrophages- and dendritic-like cells when cultured with M-CSF and GM-CSF/IL-4, respectively. Using flow cytometry we isolated progenitors that produced colonies from a single cell when cultured in 96 well plates. Their cloning efficiency to generate OCL, macrophages- or dendritic-like cells *in vitro* was 94%. When treated with RANKL and M-CSF, these single cells produced colonies with as many as 100 multinuclear cells. These were TRAcP + and formed characteristic resorption pits on bovine bone. Cells cultured in conditions favoring macrophage or dendritic-like cell development, showed differential expression of lineage specific markers (CD11b, CD11c, F4.80, MHCI and MHCII) and were functionally active as macrophages- and dendritic-like cells by phagocytosis and antigen presentation assays, respectively. These results suggested a common developmental pathway for OCL, macrophages- and dendritic-like cells from a monocyte progenitor with the above-described phenotype. Using similar approaches, we looked for cells with osteoclastogenic potential in spleen and peripheral blood. In the spleen, we found that cells negative for lymphoid markers (CD3, CD45R and NK1.1) and positive for CD11b generated a higher number of multinuclear TRAcP+ OCL than the CD11b negative fraction (113 ± 6 vs 9 ± 7 $p=0.0001$). Interestingly this population expresses low levels of Gr-1, a phenotype associated with peripheral circulating monocytes. Further dissection of this population, using CD115 and CD117 identified a double positive population with higher efficiency to generate OCL *in vitro,* compared to the $CD115^{+}$ $CD117^{-}$ fraction (147 ± 4 vs 62 ± 6 $p=0.001$). A similar progenitor was also identified in peripheral blood. These experiments suggested that circulating OCL progenitors are derived from a common bone marrow osteoclasts/ macrophage/dendritic cell progenitor, which we have now characterized at a clonal level. Our findings will be important to identify equivalent populations in humans to study their correlation with pathologies associated with abnormal bone resorption.

***Disclosures: Christian Jacome**, None.*

SU0274

Cytoskeletal Dysfunction and not Arrested Differentiation Dominates in DAP12-Deficient Osteoclasts. Wei Zou*[1], Tingting Zhu[2], Clarissa S. Craft[3], Thomas J. Broekelmann[3], Robert P. Mecham[3], Steven Teitelbaum[1]. [1]Washington University in St. Louis School of Medicine, USA, [2]Department of Pathology & Immunology, Washington University School of Medicine, USA, [3]Department of Cell Biology, Washington University School of Medicine, USA

Despite evidence that the co-stimulatory molecule, DAP12, regulates the osteoclast, mice lacking the ITAM-bearing protein exhibit only a mild osteopetrotic phenotype indicating in vivo compensation. The fact that DAP12-/- mice, also lacking FcRγ (DKO), are severely osteopetrotic suggests the latter is a substituting molecule. Controversy exists, however, as to whether the resorptive properties of these co-stimulatory molecules reflect osteoclast formation or function and if osteoblasts are the activators of osteoclastic FcRγ in vivo. We find DAP12 and WT bone marrow macrophages differentiate into equal numbers of osteoclasts when generated with WT osteoblasts. On the other hand, DAP12 deficient cells fail to spread and organize their cytoskeleton. Cytoskeletonal dysfunction is further substantiated by the fact that collagenase treatment of these co-cultures yields few osteoclasts attached to plastic indicating inability of the mutant cells to transmigrate through the osteoblast layer. The capacity of retroviral-expressed DAP12, but not FcRγ, to rescue spreading and transmigration of DKO osteoclasts establishes DAP12 as the dominant co-stimulatory molecule involved in cytoskeletal organization, To determine if FcRγ mediates osteoclast function in the absence of DAP12, we overexpressed a hybrid consisting of the FcRγ co-receptor, OSCAR, fused to Flag (OSCAR-FLAG) in DAP12-/- osteoclasts. The construct is activated by culturing the tranduced osteoclasts on anti-Flag mAb. OSCAR-FLAG fail to normalize the actin cytoskeleton in cells resident on glass but induces formation of atypical actin rings on bone and its degradation. On the other hand, OSCAR-FLAG overexpression fails to impact the abnormal cytoskeleton of DAP12-/- osteoclasts generated with osteoblasts. These findings indicated that cytoskeletal disorganization is the dominant consequence of DAP12-deficiency in osteoclasts. While activated, overexpressed OSCAR modifies the DAP12-/- osteoclast cytoskeleton phenotype on bone, the failure of osteoblasts to do so., indicates the functionally relevant quantities of OSCAR ligand do not reside in the bone forming cells.

***Disclosures: Wei Zou**, None.*

SU0275

Osteoclast-specific NIK Stabilization Causes Osteoporosis. Chang Yang*[1], Kathleen McCoy[1], Jennifer Davis[1], Roberta Faccio[1], Deborah Novack[2]. [1]Washington University in St Louis School of Medicine, USA, [2]Washington University in St. Louis School of Medicine, USA

NF-κB inducing kinase (NIK) dominates the activation of the alternative NF-κB pathway in response to RANKL in the osteoclast (OC) lineage. Under basal conditions, TRAF3-mediated NIK degradation prevents downstream signaling to RelB. NIKΔT3, a constitutively active form of NIK lacking the TRAF3 binding domain, is not degraded and thereby turns on the alternative pathway. In order to investigate the effects of constitutive NIK activation in OCs, we characterized mice in which OC-specific expression of the NIKΔT3 transgene (tg) is mediated by CathepsinK-cre. OC precursors expressing NIKΔT3 (tg+) exhibited accelerated differentiation, forming OCs earlier and in greater number than their tg- counterparts. This was accompanied by increased nuclear translocation of RelB and up-regulation of several OC differentiation markers. Moreover, OC activity was enhanced by expression of NIKΔT3. When plated on bone, tg+ OCs showed enlarged actin rings, increased resorption area and significantly enhanced medium CTX from 4-14 days. Additionally, OC life span was prolonged, likely contributing to the enhanced OC activity. These results indicate that the sustained activation of the alternative pathway due to NIK stabilization leads to increased OC differentiation, which mirrors our previous finding that NIK and RelB-deficient precursors have defective OCgenesis. Furthermore, we now demonstrate an additional, novel effect of NIK activation on OC function. Next, we characterized the basal bone phenotype of NIKΔT3 x CathepsinK-cre mice. In contrast to our finding that NIK deficiency causes only a small increase in BV/TV, with no effect on Oc.S/BS, in unmanipulated mice, the effects of OC-specific NIK activation are dramatic. At 9 weeks of age, tg+ mice showed a 57% decrease in BV/TV and a 35% decrease in BMD by μCT (both $p<0.01$). Strikingly, histomorphometric analysis showed a 98% increase in Oc.S/BS ($p<0.01$) in tg+ mice. To examine the secondary effect of the NIKΔT3 transgene on osteoblasts (OB), we monitored OB activity and found no significant differences in N.Ob/BS or mineral apposition rate. In summary, sustained activation of the alternative NF-κB pathway in the OC lineage, achieved by NIK stabilization, results in osteoporosis due to enhanced formation and function of OCs. Thus, manipulation of NIK activity provides a potential clinical target for pathological bone conditions.

***Disclosures: Chang Yang**, None.*

SU0276

$P2X_7$ Receptor Involvement in Human Osteoclast Activity and Survival. Melissa Barron*[1], Rory Clifton-Bligh[2], James S. Wiley[3], Rebecca Mason[4]. [1]The University of Sydney, Australia, [2]Northern Clinical School & Kolling Institute of Medical Research, The University of Sydney, Australia, [3]Nepean Clinical School, The University of Sydney, Australia, [4]University of Sydney, Australia

The $P2X_7$ receptor is a purinergic receptor expressed by both osteoblasts and osteoclasts. It has recently been proposed that $P2X_7$ signalling may be a component of a new bone regulatory system. This plasma membrane receptor is an ATP-gated ion channel, potently activated by the long-acting ATP analog, benzoylbenzoyl-ATP (BzATP). In a recent report, two types of inactivating $P2X_7$ receptor polymorphisms were associated with an increased fracture risk in postmenopausal women (Pharmacogenetics & Genomics 17(7): 555-67, 2007). In preliminary studies, patients with $P2X_7$ receptor mutations show a decrease in bone density, supporting the proposal that this receptor is involved in bone turnover (Abstract from the 30th ASBMR meeting: S296, 2008). We have previously shown that activation of the $P2X_7$ receptor resulted in a decrease in human osteoblast proliferation and alkaline phosphatase activity. In this current study, the aim was to determine a role for the $P2X_7$ receptor in human primary osteoclasts. Treatment of human osteoclast precursors, derived from buffy coats of blood, with varying concentrations of BzATP altered osteoclastogenesis. A 4-7 fold increase in pits on dentine were found in the groups treated with 0.01-0.1mM BzATP compared to controls ($p<0.001$), suggesting an involvement of the $P2X_7$ receptor in osteoclast activity. In addition, a nearly 2-fold increase in the number of multinucleated osteoclasts at late stages of culture with 1mM BzATP ($p<0.01$) indicates a potential role for the $P2X_7$ receptor in regulating osteoclast lifespan. It is planned to extend these investigations to precursor osteoclasts derived from blood samples of postmenopausal women with loss-of-function $P2X_7$ receptor polymorphisms, to further our understanding of its role in bone cell function. The data presented here raise the possibility that the $P2X_7$ receptor may have the potential to become a therapeutic target for novel treatments for bone diseases, such as osteoporosis.

***Disclosures: Melissa Barron**, None.*

SU0277

Serum Calcium-decreasing Factor, Caldecrin, Suppresses Osteoclastogenesis by Antagonizing RANKL-stimulated PLCγ and Ca^{2+} Oscillation. Mineko Tomomura[1], Akito Tomomura*[2], Hiroya Hasegawa[3]. [1]Meikai Pharmaco-Medical Laboratory, Meikai University School of Dentistry, Japan, [2]Meikai University, School of Dentistry, Japan, [3]Department of Orthodontics, Graduate School of Dentistry, Meikai University, Japan

Purpose: Hypocalcemia occurs in patients with acute pancreatitis, suggesting that there is a hypocalcemic factor in the pancreas. We have isolated caldecrin/chymotrypsin C as a serum calcium-decreasing factor from the pancreas, which is a novel secreting- type serine protease. Caldecrin dose-dependently suppressed serum calcium without protease activity. To investigate the calcium-lowering mechanism of caldecrin, we focused the function of caldecrin on the bone metabolism. We previously reported that caldecrin suppressed the mature osteoclastic bone resorption. Here, we investigated the effect of caldecrin on the osteoclast differentiation induced by M- CSF and RANKL from the monocyte/ macrophage cell lineage of bone marrow cells in mice and on the intracellular signaling pathway of osteoclast precursors.

Results: Wild type and protease-deficient mutant caldecrin dose-dependently inhibited RANKL- stimulated TRAP-positive osteoclast formation from bone marrow cells. Caldecrin did not affect the macrophage colony formation from monocyte/ macrophage lineage nor osteoclast progenitor generation in cultures of bone marrow cells. Caldecrin inhibited accumulation of the RANKL-stimulated NFATc1 mRNA in bone marrow cells. Caldecrin also suppressed RANKL- induced differentiation of the RAW264.7 cells into osteoclasts. Caldecrin reduced the transcriptional activity of NFATc1 in RAW264.7 cells, while those of NF-κB and c-Fos were unaffected. Caldecrin inhibited RANKL-stimulated nuclear translocation of NFATc1 by the suppression of calcium/calmodulin dependent phosphatase, calcineurin. Caldecrin inhibited PLCγ1-mediated Ca^{2+} oscillation upstream of calcineurin-NFATc1 evoked by RANKL stimulation.

Conclusions: Caldecrin inhibits osteoclastogenesis, without its protease activity, by preventing PLCγ1- mediated Ca^{2+}oscillation - calcineurin- NFATc1 activity.

***Disclosures: Akito Tomomura**, None.*
This study received funding from: Ministry of Education, Culture, Sports, Science and Technology of JAPAN

SU0278

Autophagy, an Intracellular Recycling Process, Opposes Osteocyte Death Induced by Glucocorticoids, Reactive Oxygen Species, and Hypoxia In Vitro and May Become Less Efficient with Age. Haibo Zhao*, Kanan Vyas, Jinhu Xiong, Stavros Manolagas, Charles O'Brien. University of Arkansas for Medical Sciences, USA

Autophagy is a process in which cellular components, such as mitochondria and proteins, are enveloped by a double-membrane structure, termed the autophagosome, and are delivered to lysosomes for degradation and reuse of the components. Inhibition of autophagy in long-lived cells such as neurons, hepatocytes, and myocytes leads to increased numbers of damaged mitochondria, oxidative stress, and cell death. Importantly, the accumulation of damaged cellular components that occurs with old age has been attributed to a decrease in the efficiency of autophagy. Autophagy is also required for the adaptation of cells to hypoxic environments by reducing the number of mitochondria to avoid oxidative stress. Because osteocytes are the longest-lived bone cell, and because they likely exist in a relatively hypoxic environment, we examined the role of autophagy in the MLO-Y4 osteocytic cell line and measured expression of autophagy related genes in young and old DBA/2 mice. To monitor and quantify autophagosome formation, we transduced MLO-Y4 cells with a GFP-LC3 fusion protein, a widely used marker of autophagy. Inhibition of mTOR with rapamycin, a maneuver known to induce autophagy in other cell types, dramatically increased the number of GFP-LC3 positive autophagosomes in MLO-Y4 cells. We next suppressed autophagy in these cells by short hairpin-mediated suppression of ATG7, which is essential for autophagy. Knock-down of ATG7 increased the sensitivity of the cells to death induced by dexamethasone or H2O2, as measured by trypan blue staining and caspase 3 activity. Culturing the MLO-Y4 cells in a hypoxic environment (1% oxygen) induced expression of critical genes for autophagy such as BNIP3, LC3, and ATG12, as well as autophagosome formation. Moreover, knock-down of ATG7 not only inhibited autophagosome formation during hypoxia, but also increased the rate of cell death under these conditions. Lastly, we found that expression of BNIP3 and LC3 mRNA was significantly reduced in femoral cortical bone from 21 month old mice, compared with 6 month old mice. Based on these results, we conclude that autophagy is an important survival process that helps osteocytes resist the death induced by stressors such as glucocorticoid excess, reactive oxygen species, and hypoxia. Moreover, the reduced expression of autophagy-related genes in aged bone suggests that reduced efficiency of this process over time contributes to the elevated osteocyte death that occurs with age.

***Disclosures: Haibo Zhao**, None.*

SU0279

Distinct Intracellular Calcium Waves in Osteocytic Networks under Fluid Flow Are Due to T-Type Voltage-Gated Calcium Channels in Osteocytes. Xin Lu*, Andrew Baik, X Guo. Columbia University, USA

Osteocytes are believed to comprise a sensory network in bone that monitors *in vivo* physical loading and triggers adaptive responses from osteoblasts and osteoclasts. Osteoblasts can also directly respond to mechanical stimuli. However, it is poorly understood whether intracellular calcium $[Ca^{2+}]_i$ waves, one of the early signaling fingerprints in mechanotransduction, in osteocytic networks under fluid flow are different from those in osteoblastic networks. If they are different, investigation into the underlying biochemical mechanism of these differences is warranted.

Two types of cell networks were constructed *in vitro* with either MLO-Y4 (osteocyte-like) or MC3T3-E1 (osteoblast-like) cells using micro-fabrication techniques. Each cell was physically connected with four neighboring cells through gap junctions in a square grid network. Cells were stimulated with steady fluid flow at four different physiologically relevant levels (0.5, 1, 2, and 4 Pa). The $[Ca^{2+}]_i$ responses of cells were recorded and analyzed. At the 2 Pa level, the two types network were further divided into separate groups, and treated with inhibitors blocking the ATP pathway, gap junction connection, intracellular calcium store, extracellular calcium source, T- or L-type voltage-gated calcium channel (VGCC), or ryanodine receptor.

The responsive rate of MLO-Y4 cells was consistently high (~95%) regardless of fluid flow strength, while that of MC3T3 cells steadily increased from 59% at 0.5 Pa to 99% at 4 Pa. Most MC3T3 cells released a major $[Ca^{2+}]_i$ spike at the onset of flow followed by a few weaker peaks. MLO-Y4 cells, however, demonstrated dramatically distinct $[Ca^{2+}]_i$ waves with numerous, unattenuated multiple spikes. Blocking either the ATP pathway or the intra- or extracellular calcium sources abolished multiple responses in both cell types, while the gap junction inhibitor only reduced the number of peaks. Inhibition of the ryanodine receptor had no effect on either cell type. However, treatment with the T-type VGCC blocker abolished the multiple spikes in MLO-Y4 cells but had no effect on osteoblasts.

In conclusion, osteocytic networks under fluid flow stimulation demonstrated distinct oscillatory $[Ca^{2+}]_i$ waves. The oscillatory $[Ca^{2+}]_i$ responses in osteocytes are related to the T-type VGCC (not expressed in osteoblasts), which acts as an important mediator of $[Ca^{2+}]_i$ oscillation in many cell types.

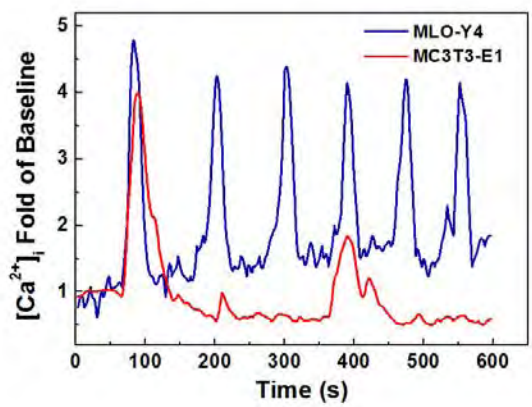

Typical Calcium Responses from Osteoblast and Osteocyte

***Disclosures: Xin Lu**, None.*

SU0280

High Glucose Medium Prevents the Pro-Survival Effect of Mechanical Stimulation on MLO-Y4 Osteocytes. Marta Maycas*[1], Luis Fernandez de Castro[2], Alvaro G. Romero[2], José Manuel Pozuelo[2], Pedro Esbrit[3], Arancha Gortazar[4]. [1]Fundación Jiménez Díaz (Capio Group), Spain, [2]Universidad San Pablo-CEU, Spain, [3]Fundacion Jimenez Diaz (Capio Group), Spain, [4]Universidad San Pablo-CEUSchool of MedicineMadrid Spain, Spain

Osteocytes respond to mechanical stimuli by modulating their survival. Changes in the Wnt/β-catenin pathway appear to play a key role in the underlying mechanisms of osteocyte protection. Various studies also indicate that diabetes mellitus induces deleterious effects in osteoblastic growth and function by poorly defined mechanisms. Our recent preliminary studies show an increased osteocyte apoptosis in cortical bone of mice with type 1 diabetes. However, to our knowledge no previous studies have explored the possibility that high glucose (HG) itself might prevent the positive effects of mechanical stimuli on osteocyte survival. In the present study, we aimed to address this issue in well characterized mouse MLO-Y4 osteocytes (generously supplied by L. Bonewald, Kansas City, MO) in vitro. These cells were pre-exposed to HG (25 mM) or normal glucose medium for 24 h, and then were submitted or not (controls) to

mechanical stress by either laminar fluid flow (16 dyn/cm^2) or exposure to a hypotonic medium (230 mOsm) for 15 min, followed by 1 μM dexamethasone for 6 h in serum-depleted medium. Cell viability was assessed by nuclear morphology (apoptosis) in GFP-transfected MLO-Y4 cells (kindly provided by T. Bellido, Indianapolis, IN) and trypan blue exclusion. We found that both mechanical stimuli prevented cell death induced by dexamethasone in normal glucose but not HG medium. Moreover, HG alone significantly induced a decrease in these cells' viability. This deleterious effect of HG was not reproduced by the same concentration of mannitol (osmotic control). Mechanical stimuli were found to increase β-catenin stabilization within 1 h, related to glycogen synthase kinase and extracellular signal-regulated kinase phosphorylation in MLO-Y4 cells. Gene expression of the canonical Wnt pathway inhibitor dickkopf-1 (which was barely detectable in these cells) was unaffected by either mechanical stimuli or HG. Moreover, the former failed to change the gene expression of the PTH receptor 1 -an important modulator of bone mass in part through downregulation of the Wnt inhibitor Sost-, but this expression was decreased (30%) by HG. Albeit the latter failed to affect basal or PTH-inhibited Sost expression in osteoblastic UMR-106 expressing this gene in contrast to MLO-Y4 cells. In conclusion, our findings demonstrate that a diabetic medium exerts a negative effect on the capacity of osteocytes to respond to mechanical loading, apparently interacting with β-catenin.

***Disclosures: Marta Maycas**, None.*

SU0281

Ift88 Function in the Murine Skeleton. Bradley Yoder[1], Courtney Haycraft*[2], P. Darwin Bell[2]. [1]University of Alabama at Birmingham, USA, [2]Medical University of South Carolina, USA

Primary cilia are found on most mammalian cells including the osteoblasts and osteocytes. Ift88/polaris is one of the proteins essential for formation and maintenance of primary cilia and its loss in the embryonic limb mesenchyme results in defects in skeletal patterning and endochondral bone formation. While cilia have been shown to play a mechanosensory role in the kidney, their function in the remodeling and maintenance of the skeleton remains elusive. We have shown that Ift88/polaris is expressed in osteocytes in vivo and co-localizes with the primary cilium marker acetylated α-tubulin using confocal microscopy. Recent work has identified a role for polycystin-1, known for its mechanosensory role in the renal tubule primary cilium, in the skeleton suggesting that the primary cilium may serve as a mechanosensory organelle in the osteoblasts and osteocytes. To address this possibility, we have generated mice lacking Ift88/polaris, and subsequently cilia, specifically in the osteoblasts and osteocytes using transgenic mice expressing Cre recombinase under the control of the osteocalcin promoter (OC-cre) and a conditional allele of Ift88/polaris. Preliminary analyses of adult Ift88;OC-cre conditional mutant mice on a mixed genetic background showed decreased trabecular number and cortical thickness at 9 months of age when analyzed by microCT. Conditional mutant mice also had decreased numbers of osteoblasts. We have begun to confirm these results using Ift88;OC-cre conditional mutant mice on an inbred C57BL/6J genetic background to minimize variability of the observed phenotype. Surprisingly, at one month of age Ift88;OC-cre conditional mutant mice show an increase in trabecular bone volume/total volume ratio (BV/TV) and increased trabecular thickness in the proximal tibia but no change in cortical thickness. These preliminary results are being confirmed in additional samples but suggest that primary cilia play an important role in remodeling of the skeleton during postnatal development. Analyses are also being extended to include older mice. We anticipate that the increased BV/TV and trabecular thickness will be lost as the mouse ages as seen in mice on the mixed genetic background. Overall these results suggest that primary cilia play a complex role in the remodeling and maintenance of the mammalian skeleton.

***Disclosures: Courtney Haycraft**, None.*

SU0282

Perlecan/HSPG2 Helps Maintain the Pericellular Space of the Lacuno-Canalicular System Surrounding Osteocytic Processes in Murine Cortical Bone. William Thompson*[1], Shannon Modla[1], Brian Grindel[2], Kirk Czymmek[1], Catherine Kirn-Safran[1], Liyun Wang[1], Randall Duncan[1], Mary Farach-Carson[2]. [1]University of Delaware, USA, [2]Rice University, USA

Osteocytes project long, slender processes throughout the mineralized matrix of bone where they connect and communicate with effector cells. The interconnected cellular projections form the functional lacuno-canalicular system that allows fluid to pass for cell to cell communication and nutrient and waste exchange. Prevention of bone mineral intrusion into the pericellular space of the lacuno-canalicular pericellular space is crucial to maintain unimpeded interstitial fluid movement. Factors that prevent the clear pericellular space of the lacuno-canalicular system and keep it open to fluid movement remain unclear. Because of their activity in inhibiting hydroxyapatite formation, heparan sulfate containing macromolecules are viable candidates to perform this function.

In this study, we examined osteocyte lacuno-canalicular morphology in mice deficient in the large heparan sulfate proteoglycan perlecan/HSPG2 in this tissue. Immunohistochemical imaging demonstrates perlecan/HSPG2 expression localized to the osteocyte lacuno-canalicular system of cortical bone and electron micrograph immunogold data reveal the presence of this proteoglycan in the pericellular space of the lacuno-canalicular system. In contrast, PLN expression was severely decreased in cortical bone of perlecan/HSPG2 deficient mice. Ultrastructural measurements using electron micrograph images of perlecan/HSPG2 deficient mice demonstrate a significant decrease in osteocyte canalicular pericellular area, resulting from a reduction in the total canalicular area, when compared to controls. Additionally, perlecan/HSPG2 deficient mice show significantly diminished canalicular density and a significant reduction in the number of transverse tethering elements per canaliculus.

These data indicate that perlecan/HSPG2 is present in the pericellular space of the osteocytic processes in the lacuno-canalicular system in a location where it could function to help maintain clear fluid path. Additionally, as shown with perlecan/HSPG2 deficient mice, perlecan/HSPG2 contributes to the integrity of the osteocyte lacuno-canalicular system by maintaining the size of the pericellular space, an essential task to promote uninhibited interstitial fluid movement in this mechanosensitive environment. This work thus identifies a new barrier function for perlecan/HSPG2 in murine cortical bone.

***Disclosures: William Thompson**, None.*

SU0283

Simulated Microgravity Induces SOST/Sclerostin Upregulation in Osteocytes. Jordan Spatz*[1], Jean Sibonga[2], Honglu Wu[2], Kevin Barry[3], Mary Bouxsein[4], Paola Divieti Pajevic[5]. [1]Harvard-MIT Dvision of Health Sciences & Technology (HST), USA, [2]NASA, USA, [3]MGH, USA, [4]Beth Israel Deaconess Medical Center, USA, [5]Massachusetts General Hospital, USA

Osteocytes are theorized to be the mechanosensors and transducers of mechanical forces in bone, yet the biological mechanism of this action remains elusive. Recent evidence suggests that SOST/Sclerostin is an important regulator of mechanotransduction. To investigate the molecular mechanisms of SOST/Sclerostin regulation under in vitro and ex-vivo unloading we used the NASA Rotating Wall Vessel (RWV) Bioreactor. For in-vitro experiments, MLOY-4 osteocytic cells were seeded at a concentration of 250,000 cells onto 3D collagen scaffold (BD). Scaffolds (4 per condition) were either rotated in a vertical 50ml NASA/bioreactor vessel at 18 rpm (unloaded), cultured in a horizontal 50 ml NASA bioreactor vessel at 18 rpm (control for the sheared environment of vertical rotating vessel), or cultured in a static T-75 cm dish (static condition) for 7 days. For ex-vivo experiments, calvaria bones were harvested from 12-week old C57/Bl6 mice and sequentially digested with type I/II collagenase to remove periosteal osteoblasts. Calvaria halves (10 per condition) were then exposed to the same set of culture conditions described above. Simulated unloading, as achieved in the NASA RWV, resulted in enlarged, round osteocytes, as assessed by H&E staining, that was reminiscent of prior reports of unloading causing loss of osteocyte morphology and dendritic network connectivity. Semiquantitative realtime qPCR and immunohistochemistry from both in-vitro and ex-vivo RWV experiments demonstrated a four-fold up-regulation of SOST/Sclerostin. Furthermore, mRNA of the transcriptional SOST enhancer Mef2C was upregulated 1.4 fold in ex-vivo calvaria subjected to unloading conditions of the NASA RWV, suggesting that Mef2C might be an important regulator of mechano-sensation. These findings are consistent with results from seven day hindlimb unloading experiments, C57/Bl6 females, conducted in our laboratory and validate the use of the NASA RWV as a tool to study osteocyte mechnotransduction. Improved understanding of the fundamental mechanisms of mechanotransduction at the osteocyte cellular level may lead to novel treatment options to mitigate the effects of disuse osteoporosis.

***Disclosures: Jordan Spatz**, None.*

SU0284

The Decrease in the Rate of Osteocyte Apoptosis in OVX Rats Treated with Two Different Doses of Risedronate. Shijing Qiu*[1], Frank Ebetino[2], Saroj Palnitkar[1], D. Sudhaker Rao[1]. [1]Henry Ford Hospital, USA, [2]Procter & Gamble Pharmaceuticals, Inc., USA

Both clinical and empirical data indicate that estrogen deficiency would accelerate osteocyte apoptosis. Recently, it has been reported that risedronate can inhibit osteocyte apoptosis induced by bone microdamage. However, it remains unknown whether risedronate is able to inhibit osteocyte apoptosis resulting from estrogen depletion. Ovariectomy (OVX) was performed on 24 female SD rats aged 6 months. The animals were divided into 3 groups with risedronate (higher dose: 2.4 μg/kg; lower dose: 0.24 μg/kg, s.c.) and placebo treatment. Another 8 rats underwent sham ovariectomy (S-OVX) and were treated with placebo. The treatments started 3 days before surgery and continue every 3 days until the rats were sacrificed at 15th day after surgery. The middle diaphysis of the right tibia was removed from each rat. The bone segments were fixed, decalcified, dehydrated, embedded in paraffin and sectioned into 5 μm for immunohistochemical examinations. TUNEL assay was used to determine the amount of apoptotic osteocytes, and Bcl-2 and Bax assays were used to determine the changes in apoptosis control proteins. The percentage of TUNEL, Bcl-2 and Bax positive osteocytes and the ratio between Bax and Bcl-2 positive osteocytes (% Bax positive osteocytes divided by % Bcl-2 positive osteocytes) were calculated. The results are shown in Table 1. Compared to S-OVX, TUNEL and Bax positive osteocytes were significantly increased but Bcl-2 positive osteocytes was significantly decreased in OVX rats, resulting in a significant increase in Bax/Bcl-2 ratio. Risedronate treatment, either high or low dose, significantly reduced TUNEL and Bax positive osteocytes and

increased Bcl-2 positive osteocytes in OVX rats. In addition, low dose risedronate caused a higher reduction in osteocyte apoptosis than high dose. Estrogen depletion is a contributing factor in promoting osteocyte apoptosis, which is associated with increased Bax (pro-apoptosis) and decreased Bcl-2 (anti-apoptosis). Both higher and lower doses of risedronate can inhibit osteocyte apoptosis resulting from OVX, but the lower dose has a stronger beneficial effect than higher dose. The possible mechanism is that risedronate increases Bcl-2 expression and inhibites Bax in osteocytes.

Table 1. Comparison of immnohistochemistric variables between different groups

Group	TUNEL (%)	Bcl-2 (%)	Bax (%)	Bax/Bcl2
S-OVX	8.28 (1.21)	17.7 (1.69)	10.9 (1.20)	0.618 (0.098)
OVX	22.1 (1.45)[1]	10.8 (0.632)[1]	38.4 (4.14)[1]	3.55 (0.380)[1]
OVX+Low Ris	11.9 (1.02)[1,2]	43.5 (1.21)[1,2]	29.5 (3.17)[1,2]	0.678 (0.078)[2]
OVX+High Ris	13.8 (0.71)[1,2,3]	31.9 (1.81)[1,2,3]	32.3 (3.79)[1,2,3]	1.02 (0.134)[2]
p	<0.001	<0.001	<0.001	<0.001

Significant difference between groups - 1: vs S-OVX; 2: vs OVX; 3: vs OVX+Low Ris

Table 1. Comparison of immunohistochemistric variables between different groups

***Disclosures: Shijing Qiu**, Procter & Gamble, 2*
This study received funding from: Procter & Gamble

SU0285

The Role of the Sphingosine-1-Phosphate Signaling Pathway in Osteocyte Mechanotransduction. Jia Ning Zhang*, Yan Zhao, Elizabeth S. Han, Chao Liu, Xue Yu, Steffen-Sebastian Boltz, Darcy Lidington, Lidan You. University of Toronto, Canada

During the process of bone adaption under mechanical loading, osteocytes have been proposed to be the mechanosensory cells that translate mechanical loading into biochemical signals, which in turn regulate other bone cells in bone remodeling. However, the exact mechanism of how mechanical loading is transduced into biochemical signals in osteocytes is unclear. Lipid mediator sphingosine-1-phosphate (S1P) has been reported to play a role not only in the mechanotransduction process in blood vessels, but also in the dynamic control of bone mineral homeostasis. Nevertheless, the potential role of S1P in bone mechanotransduction has yet to be elucidated. Hypothesis: S1P cascade is involved in the activation of osteocytes in response to loading-induced oscillatory fluid flow (OFF) in bone. Methods: we firstly demonstrated that MLO-Y4 osteocyte-like cells express most components of S1P cascade. To examine the involvement of S1P signaling in osteocyte mechanotransduction, we applied OFF (1 Pa, 1 Hz) on MLO-Y4 cells while some of the components of S1P signaling pathway were modulated. Results: we found that decreased endogenous S1P level significantly suppressed OFF-induced intracellular calcium response. Addition of extracellular S1P not only enhanced the synthesis and release of prostaglandin E2 (PGE2) in static cells, but also amplified OFF-induced effects in MLO-Y4 cells. The stimulatory effect of OFF on the gene expression levels of receptor activator for nuclear factor κ B ligand (RANKL) and osteoprotegerin (OPG) was shown to be S1P independent. Furthermore, S1P receptor S1P2 was shown to be involved in OFF-induced PGE2 synthesis and release, as well as down-regulation of RANKL/OPG ratio at the gene expression level. Conclusion: our data suggest that S1P cascade is involved in OFF-induced mechanotransduction in MLO-Y4 cells, and extracellular S1P exerts its effect partly through S1P2 receptors. A deeper understanding of the osteocyte mechanotransduction may lead to advancement cures in musculoskeletal diseases such as osteoporosis.

***Disclosures: Jia Ning Zhang**, None.*
This study received funding from: NSERC

SU0286

Detection of Sclerostin Epitopes in Zebrafish Skeleton and Kidney. THEODORE CRAIG*[1], Rajiv Kumar[2]. [1]Mayo Clinic, USA, [2]Mayo Clinic College of Medicine, USA

Sclerostin (scl), a secreted cystine-knot protein, is a potent inhibitor of osteoblast function. To better understand scl physiology, we examined the distribution of scl in the adult zebrafish, Danio rerio. We used a monoclonal antibody generated against scl peptide, corresponding to amino acids 168-183 in human scl (168-KRLTRFHNQSELKDFG-183) that is very similar in human, mouse, or fish scl for immunohistochemical (IHC) studies. Adult zebrafish (~5 mo of age) were raised under standard conditions in fish water and were de-calcified and fixed using Dietrich's solution. The fish were embedded in paraffin and sectioned to obtain 4-μm sections. Scl c-terminal antibody was used for IHC. 4μm-thick sections from fish were placed on silanized slides and were deparaffinized, rehydrated, and rinsed in water. Endogenous peroxidase activity was blocked. 10 mM citric acid, pH 6.0 was used to enhance epitope detection. Sections were treated with anti-scl antibody (C-term), at a dilution of 1:100, at room temperature. After rinsing, sections were treated with biotinylated anti-mouse immunoglobulin G (1:200; Dako), followed by peroxidase-labeled streptavidin (1:500; Dako) for 30 min at room temperature. Sections were developed by adding 0.1 M sodium acetate, pH 5.2, containing aminoethyl carbazole and H2O2 for 15 min. Sections were counterstained with hematoxylin and placed on a coverslip with aqueous mounting media. Negative controls for nonspecific staining were done on tissue sections using preimmune mouse serum diluted 1:100 in place of primary antibodies. To assure specificity, slides were also stained using primary antibodies that were preadsorbed with scl antigen or scl buffer (as control) prepared as described above.

Results: Scl epitopes were detected in osteoblasts within the vertebral column, dorsal spine, and bones of the skull. Additionally, strong scl staining was observed in osteocytes within bone. Reduced staining was observed when non–immune serum was used. In addition, scl epitopes were detected in the renal tubules. No staining was observed in glomeruli or the interstitium. Scl epitopes were not detected in the liver, intestine, heart, or striated muscle.

Conclusion: Scl is detected in osteoblasts and osteocytes of bones within the adult zebrafish skeleton. In addition, scl epitopes are found in tubular structures of the zebrafish kidney. Our data suggests that scl may play a role not only in skeletal function but in renal function as well.

***Disclosures: THEODORE CRAIG**, None.*

SU0287

Structural Basis for Bone Resorption within the Cortical Bone. Nobuhito Nango*[1], Shogo Kubota[1], Yoshihiro Takeda[2], Wataru Yashiro[3], Atsushi Momose[3], Koichi Matsuo[4]. [1]Ratoc System Engineering Co., Ltd., Japan, [2]Department of Advanced Materials Science, School of Frontier Sciences, The Universtity of Tokyo, Japan, [3]Department of Advanced Materials Science, School of Frontier Sciences, The University of Tokyo, Japan, [4]School of Medicine, Keio University, Japan

Bone releases and stores calcium and phosphate to maintain homeostasis. However, resorption by osteoclasts at the surface of trabecular and endosteal bone may not fully account for calcium and phosphate release from bone. In this study, we hypothesized that cells responsible for resorption reside inside bone, and we employed three-dimensional imaging with an X-ray microscope using synchrotron radiation to detect and analyze them.

Tibiae and femurs were isolated from mice at 8, 14, 16, and 28 weeks of age. The central 3 mm of diaphysis was cut out and further sectioned longitudinally into 300μm-diameter square pillars. The X-ray microscope was operated using optical configurations to generate differential phase contrast and defocus refraction contrast. Monochromatic X-rays (9 keV) were used with a magnification of 20.2. Cortical bone samples were observed by CT scans, and 3D images were reconstructed at a pixel size of 0.25 μm with an image matrix of 1200x1200x500. Differences in calcification of bone matrix surrounding bone cells were imaged by differential phase contrast. Osteocytes and osteocytic canaliculi were visualized with defocused refraction contrast. The two types of reconstructed CT images were aligned three-dimensionally and analyzed using 3D image analysis software TRI/3D-BON (Ratoc).

We observed that osteoclast-like cells of 10-15 μm diameter were located mostly at the end of blood capillaries in cortical bone(Fig.1a). We also found that osteocytes under endosteal and periosteal surfaces were aligned largely parallel to the long axis of the bone, and their size, orientation, and proximal distance from osteocyte to osteocyte were comparable. By contrast, in the area surrounding osteoclast-like cells, the size and orientation of osteocytes were more variable and irregular. Finally, a high-calcium bands in bone matrix were detected close to osteoclast-like cells and canaliculi(Fig.1b). These bands could be the result of mineral resorption or deposition by osteoclast-like cell or canaliculi.

In conclusion, three-dimensional analysis suggests that blood capillaries, osteoclast-like cells and osteocytic canaliculi in cortical bone may form the structural basis for resorption of bone mineral inside bone.

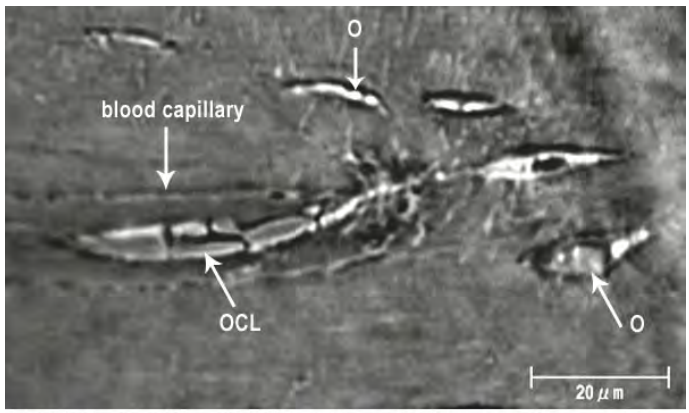

(a) Osteoclast-like cell (OCL) at the end of blood capillary

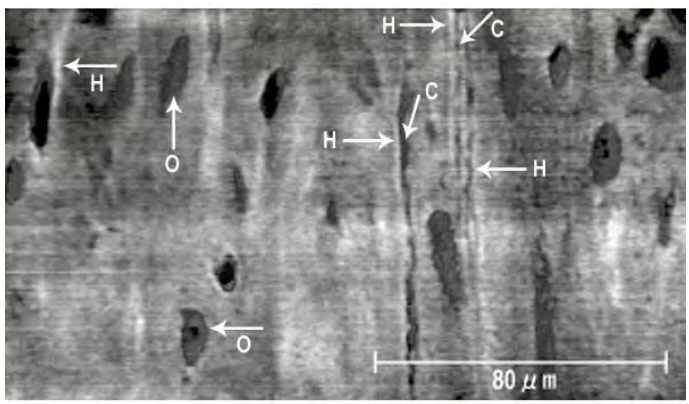

(b) Canaliculi and the surrounding High-calcium band

C: Canaliculus H: High-culcium band O: Osteocyte

Fig.1

***Disclosures: Nobuhito Nango**, None.*

SU0288

A New Automated Method for Measuring Intact Amino-terminal Propeptide of Type I procollagen (P1NP). Karl Insogna[1], Christine Simpson*[2]. [1]Yale University School of Medicine, USA, [2]Yale University, USA

Measuring intact P1NP is a useful clinical method for monitoring bone formation and assessing the response to anti-osteoporotic therapy. Used in conjunction with markers of bone resorption, P1NP can be used to estimate the rate of skeletal turnover. The IDS-iSYS® Intact P1NP assay is a recently developed automated chemiluminescent method in which an unknown is sample is incubated with a biotinylated anti-P1NP monoclonal antibody, an acridinium labeled monoclonal antibody, streptavidin labeled magnetic particles and an assay buffer. The particles are captured using a magnet prior to washing. Trigger reagents are added and the resulting light emitted by the acridinium label is directly proportional to the concentration of intact P1NP in the unknown sample, based on a master standard curve.

The results using this automated method were compared to those in the UniQ P1NP RIA (Orion Diagnostica), a widely used RIA assay for P1NP determination. Sera from 73 subjects were analyzed using both methods. The samples were from postmenopausal Caucasian women (ages 59-87 mean age=70 years) not receiving therapy for osteoporosis, who typically consume low protein diets (mean intakes between 0.6 - 1.0 g/kg/d). These women are participating in the SPOON trial, which seeks to determine the impact of a whey protein supplement on bone mass. Blood was drawn fasting between 9 and 11 am. There was excellent correlation between the two assays over a wide range of values (from 13 to 141 ng/mL, see Figure). Pearson's correlation (r) was 0.98 and the coefficient of determination (r2) was 0.95. Intra and inter coefficients of variation for the IDS-iSYS method were 1.8% and 5.8% respectively. The time to first result for the IDS-iSYS P1NP was < 60 min. vs. 3-4 hrs for the RIA. The iSYS can accommodate 64 samples per run with future plans to increase sample capacity. Since the iSYS reagents, are non-radioactive they have a relatively long shelf life and an on-board stability of 7 days. These data indicate that the IDS-iSYS analyzer offers a reliable, fast and convenient new method for measuring P1NP that provides comparable results to the Orion Diagnostica P1NP RIA.

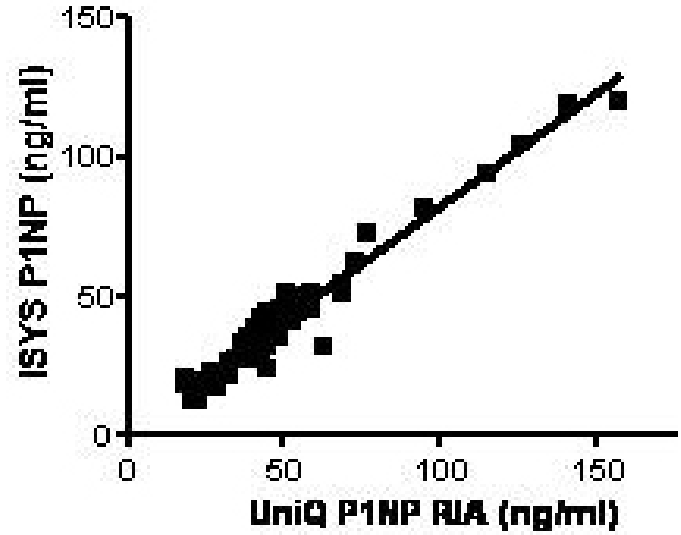

Fig.Simpson

***Disclosures: Christine Simpson**, None.*

SU0289

Seasonal Variation of Serum Markers of Bone Turnover and 25-Hydroxyvitamin D in Irish Patients attending an Osteoporosis Clinic. Joseph Browne*[1], Florence O Connell[2], Martin Healy[3], Kara Fitzgerald[2], James Walsh[4], Miriam C Casey[2]. [1]St James's Hospital, Ireland, [2]Bone Health & Osteoporosis Unit, Mercer's Institute of Research on Ageing, St James's Hospital, Ireland, [3]Department of Biochemistry, St James's Hospital, Ireland, [4]Trinity College Dublin, The University of Dublin, Ireland

Background: Biochemical markers of bone turnover have been shown to provide invaluable information for the diagnosis and monitoring of underlying metabolic disease. However, long-term physiological variations, such as seasonal variations, need to be clearly identified to improve their clinical usefulness.

Methods: Consecutive patients >50 yrs attending an Irish osteoporosis clinic had baseline assessments performed over a 24 month period between January 2008 to December 2009. Our clinic is located in Dublin, Ireland with the latitude of 53°N. Serum markers of bone turnover including Parathyroid Hormone (PTH), 25-hydroxy-vitamin D (25(OH)D), C-Telopeptide (CTx), Procollagen Type 1 Intact N Terminal Propeptide (P1NP) and Osteocalcin (Osc) were collected. Baseline assessment included current medications, age, gender, previous fracture history and BMD measurements.

Results: 631 patients were assessed over a 24-month period. Mean age (+/-StdDev) was 70.9 (+/-10.6) yrs with 85.1% being female. Mean vitamin D was 54.98 (+/- 28.58) nmol/L. Mean Serum 25(OH)D was significantly lower in spring (February, March, April) compared to autumn (August, September, October) with mean serum 25(OH)D of 45.8(+/-26.6) and 63.4(+/- 29.9) nmol/L respectively ($p<0.001$). This was observed in patients taking and naïve to vitamin D supplementation ($p<0.005$ in both groups).

525 patients had bone markers performed with 294 (56%) patients not on anti-resorptive treatment at the initial assessment. Mean levels of CTx, Osteocalcin, and P1NP were observed to be lower in autumn when compared to spring ($p=0.02$, 0.09 and 0.12, respectively). This trend was also noted in patients on anti-resorptive treatment, particularly in P1NP levels ($p=0.02$). PTH levels showed some slight variation with season, however this was non-significant.

Conclusions: Seasonal changes in serum vitamin D and bone turnover markers follow an orderly sequence throughout the year. The seasonal variation in serum vitamin D is closely associated with changes in bone metabolism. Lower 25(OH)D levels coincided with higher levels of bone turnover. This was observed in patients on anti-resorptive therapy or naïve to treatment. Higher vitamin D levels appear to reduce bone turnover and may enhance bone marker responses to osteoporosis medications.

	Spring	Summer	Autumn	Winter	P-value
Combined Groups (nmol/L) (n=631)	45.8 (+/-26.6)	56.5 (+/-27.4)	63.4 (+/-29.9)	56.2 (+/-28.1)	0.0001
No Calcium/Vitamin D (nmol/L) (n=264)	31.3 (+/- 18.2)	39.6 (+/- 22.3)	41.9 (+/- 21.7)	42 (+/- 22.5)	0.0047
Calcium and Vitamin D Supplementation (nmol/L) (n=367)	59.2 (+/- 25.8)	65.1 (+/- 25.8)	75.6 (+/-26.9)	70.2 (+/-26)	0.0002

Seasonal Variation in Serum Levels of 25(OH)D in Patients based on Vitamin D Supplementation

***Disclosures: Joseph Browne**, None.*

SU0290

Serum Osteocalcin Exerts Beneficial Effects on Insulin Sensitivity and Secretion. Ippei Kanazawa*[1], Toru Yamaguchi[2], Yuko Tada[2], Masahiro Yamamoto[2], Mika Yamauchi[2], Shozo Yano[2], Toshitsugu Sugimoto[3]. [1]McGill University, Canada, [2]Shimane University Faculty of Medicine, Japan, [3]Shimane University School of Medicine, Japan

Previous animal studies have shown that osteocalcin (OC) is related to glucose and lipid metabolism. Our clinical study has previously shown that serum OC was negatively correlated with plasma glucose and visceral fat mass in type 2 diabetes mellitus (JCEM 2009). Although the animal studies showed that OC stimulated the expression of insulin in islets as well as of adiponectin in adipocytes with increased insulin secretion and sensitivity, the associations of serum OC with those parameters remains unclear in humans.

We employed 101 postmenopausal women and 152 men with type 2 diabetes, who have never taken drugs for diabetes or osteoporosis, in a cross-sectional study. We also examined 75g oral glucose tolerance test (OGTT) in 18 postmenopausal women and 20 men who visited our clinic for medical check-up for diabetes. We analyzed the association of serum OC with parameters of insulin resistance (HOMA-IR) and insulin secretion (HOMA-β), adiponectin, and body composition.

In the cross-sectional study, multiple regression analysis adjusted for age, body mass index, and serum creatinine showed that, in both women and men, OC was negatively associated with HbA1c, %Trunk fat, and HOMA-IR (women; HbA1c β=-0.27, $p<0.01$; %Trunk fat β=-0.22, p=0.04; and HOMA-IR β=-0.22, p=0.02, respectively: men; HbA1c β=-0.27, $p<0.01$; %Trunk fat β=-0.21, p=0.02; and HOMA-IR β=-0.25, $p<0.01$, respectively), and positively with HOMA-β (women; β=0.23, p=0.03: men; β=0.16, p=0.04). In addition, a positive association of OC with adiponectin was found in women (β=0.16, p=0.04). In men, OC was negatively associated with visceral/subcutaneous fat ratio (β=-0.20, p=0.03) although the association of OC with adiponectin was not significant. In the OGTT examinations, subjects were divided into tertiles by their serum OC concentrations. Women in the lowest tertile showed hyperglycemia ($p<0.05$) and hyperinsulinemia ($p<0.05$) compared to the highest tertile after oral glucose loading. Men in the lowest tertile also indicated hyperinsulinemia ($p<0.05$) while hyperglycemia was not found.

In conclusion, OC was negatively associated with blood glucose and trunk fat mass, and positively with insulin sensitivity and its secretion in the cross-sectional study. In addition, OGTT examinations showed that insulin resistance existed in the lowest OC tertile group. Taken together, these findings indicate that serum OC has beneficial effects on glucose homeostasis by enhancing insulin action.

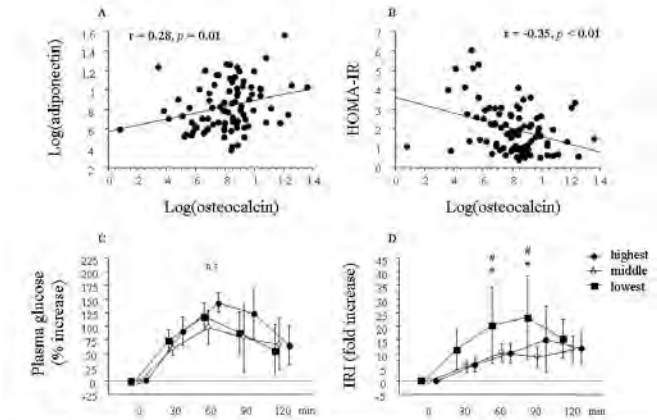

Figure. Simple regression analysis showed that serum osteocalcin levels were significantly and positively associated with serum adiponectin levels (A) and negatively with HOMA-IR (B) in postmenopausal women. 75g OGTT in men showed hyperinsulinemia (D), but not hyperglycemia (C), in the lowest tertile after glucose loading. IRI, immunoreactive insulin. *; $p<0.05$ v.s the highest group, #; $p<0.05$ v.s middle group.

Simple regression analysis and 75gOGTT

***Disclosures: Ippei Kanazawa**, None.*

SU0291

A New Approach to Time-based Bone Mineral Density Differences. Lin Ling*[1], Carl Wesolowski[2]. [1]Memorial University, Canada, [2]Nuclear Medicine Physician, Canada

Objectives: The purpose of this study is to calculate and apply total detectable difference (TDD) of bone mineral density (BMD) from longitudinal measurements, where TDD includes same-day machine error and long-term biological variation of individual patient's bone density, to reduce the overestimation of significance of BMD differences known to occur using least significant change (LSC).

Methods: A sample size of 5359 to 5533 females and males, aged 18 to 103 years old, having three sequential BMD studies over an average period of 7 years, was identified. Ordinary least squares linear regression was applied to each patient's serial BMDs to find scaled standard deviations and these deviations were used to create frequency distribution histograms, which, in turn, were fitted with half-normal distributions. TDD was then defined as 2SD for an approximate 95% confidence interval.

Results: Females and males have statistically indistinguishable TDD values allowing the results to be grouped. The TDD values of the combined female and male group are 0.042 for total hip, 0.047 for femoral neck, 0.059 for lumbar spine L1-L4 and 0.063 g/cm^2 for L2-L4 (see Table). Use of TDD reduced the frequency of detecting differences in BMD by approximately one-half.

Conclusions: TDD should be used to replace LSC because LSC does not account for natural patient's biological variation in BMD over time.

Support Information:

Total detectable difference (TDD) of bone density in g/cm^2 from female, male and female+male groups.

3 samples	Female			Male			Female + Male		
	n	TDD	R^{2*}	*n*	TDD	R^{2*}	*n*	TDD	R^{2*}
Total hip	5020	0.042	0.998	339	0.042	0.982	5359	0.042	0.997
Femoral neck	5138	0.047	0.996	345	0.051	0.969	5483	0.047	0.995
L1-L4	5146	0.059	0.997	348	0.061	0.983	5494	0.059	0.998
L2-L4	5183	0.062	0.997	350	0.066	0.985	5533	0.063	0.997

R^{2*} is the adjusted coefficient of determination of half-normal distribution fits to frequency histograms.

Support Information

***Disclosures: Lin Ling**, None.*

SU0292

Accuracy of Vertebral Fracture Assessment by Dual-Energy X-Ray Absorptiometry Using GE iDXA Compared to Conventional Radiography. Daniele Diacinti[1], Romano Del Fiacco*[2], Daniela Pisani[3], Elisabetta Romagnoli[4], Stefania Russo[5], Jessica Pepe[5], Emilio D'Erasmo[5], Salvatore Minisola[4]. [1]Dept. of Radiological Sciences - University "SAPIENZA" Rome, Italy, [2]University "Sapienza" - Rome, Italy, [3]Dept. of Medical Sciences - Azienda Ospedaliera Sant'Andrea - University "SAPIENZA" Rome, Italy, [4]University of Rome, Italy, [5]Dept. of Clinical Sciences - University "SAPIENZA" Rome, Italy

Purpose: This prospective investigation was carried out in order to evaluate the accuracy of vertebral fracture assessment by dual-energy X-ray absorptiometry using GE iDXA device (GE Medical Systems Lunar, Madison, WI, USA) compared to conventional radiography.

Subjects and methods: We enrolled 180 subjects (133 females and 47 males, age range 35-82 years) consecutively studied at our Mineral Metabolism Centre, which were undergoing a spine vertebral X-ray evaluation. Lateral images of the spine, from T4 to L4, by both conventional X-ray and DXA with a double row of detectors (GE Lunar iDXA), were acquired in each subject on the same day, after informed consent was obtained. The conventional radiographs were evaluated by an experienced skeletal radiologist (D.D.), using the Genant semiquantitative (SQ) technique. Deformities were identified by a trained operator, unaware of the SQ assessment results, by visual assessment of the iDXA scans using a specific software (enCORE).

Results: By means of SQ radiological technique, we evaluated 2295 (98%) of the 2340 available vertebrae, and identified 90 vertebral deformities (52 mild and 38 moderate or severe). By means of iDXA we evaluated 2219 (95%) of the 2340 vertebrae and identified 87 vertebral deformities (49 mild and 38 moderate or severe). Forty-nine subjects (27.2% of the total sample) were identified as having 1 or more vertebral fractures by SQ technique and 47 subjects (26.1%) were recognized by iDXA (χ^2 = n.s.). A single fracture was detected in 33 patients (18.3%) by conventional radiographs and in 31 subjects (17.2%) by iDXA; 16 subjects (8.9%) had multiple vertebral fractures detected by both techniques. Considering radiological SQ assessment as the gold standard, iDXA sensitivity was 96% and the specificity was 99% (Positive Predictive Value 98%; Negative Predictive Value 98%). Agreement between radiographs and iDXA was 98% with a kappa statistic of 0.96 (confidence interval 0.91-1.0).

Conclusion: According to the results obtained, iDXA and SQ radiological technique demonstrated good agreement in classifying vertebrae as normal or deformed. Therefore, since iDXA performs spine images with good resolution and lower dose, it proves to be useful in the clinical evaluation of patients at risk of osteoporosis or for the selection of patients for osteoporosis-related clinical trials.

***Disclosures: Romano Del Fiacco**, None.*

SU0293

Bone Loss and Fracture Risk after High Level of Physical Activity in Adolescence and Young Adulthood. Magnus Tveit*[1], Henrik Ahlborg[2], Bjorn Rosengren[3], Jan-Åke Nilsson[4], Magnus Karlsson[3]. [1]Skåne University Hospital Malmö, Lund University, Sweden, Sweden, [2]Malmo University Hospital, Sweden, [3]Skåne University Hospital Malmö, Lund University, Sweden, [4]Skane University Hospital, Sweden

Purpose: Physical activity is associated with high peak bone mass and may, if residual skeletal benefits remain in old age, prevent osteoporosis and fragility fractures. Therefore we designed a controlled study in which we cross-sectional evaluated fracture risk after exercise career in former athletes and for 39 years prospectively followed changes in bone mass from active career into long term retirement.

Method: Fracture incidence was by a mailed questionnaire registered in 709 former male athletes aged 69 years (range 50-93) and 1368 matched controls aged 70 years (range 51-93). In 46 of the former athletes aged 61 years (range 53-79) and 24 of the controls aged 63 years (range 53-76), bone mineral density (BMD; g/cm^2) was measured by the same single photon absorbtiometry (SPA) apparatus in distal femur at active career and in distal radius after a follow-up period of mean 39 years (range 38-40) and a retirement period of mean 29 years (range 10-58). At follow-up, BMD was also measured by dual energy X-ray absorbtiometry (DXA) in lumbar spine, femoral neck and legs, by quantitative ultrasound in calcaneus (SOS and BUA) and by peripheral computed tomography in tibia. Data is presented as mean with 95% CI.

Results: After retirement, there were 28 fractures/10000 person-years among the former athletes and 40 fractures/10000 person-years in the control group, leading to a Rate Ratio (RR) after active career of 0.70 (0.52, 0.93). The RR for fragility fractures sustained after age 50 years was 0.50 (0.27, 0.89) and for distal radius fractures 0.29 (0.09, 0.74). The BMD Z score was during active career in distal femur 1.0 (0.7, 1.4). The BMD Z scores at retirement were in distal radius 0.7 (0.2, 1.1), lumbar spine 0.5 (0.3, 0.7), femoral neck 1.2 (0.8, 1.7), legs 1.0 (0.6, 1.4), calcaneus SOS 1.0 (0.4, 1.7), calcaneus BUA 0.6 (0.2, 1.1), tibia trabecular vBMD 1.0 (0.5, 1.5). There were no changes in BMD Z scores during the follow-up period, neither when BMD was estimated by the same SPA apparatus (at active career in a loaded and at follow-up in an unloaded region); delta Z score was then -0.3 (-0.8, 0.2), nor when BMD was estimated in the same region at both occasions (at active career by SPA and at follow-up by DXA); delta Z score was then 0.0 (-0.4, 0.4).

Conclusions: Physical activity in younger years is associated with lower fracture risk later in life, at least partly due to residual exercise induced retained skeletal benefits.

***Disclosures: Magnus Tveit**, None.*

SU0294

Clinical Risk Factors as Predictors of Bone Mass in a Brazilian Women Population. Maria Marta Sarquis Soares*[1], Alessandra P. G Dias[2], Marcio W. Lauria[3], Bárbara Campolina Carvalho Silva[4], Eduardo Pimentel Dias[5], Bruna Galvão Marinho[1], Bruno Camargos[6]. [1]Federal University of Minas Gerais, Brazil, [2]Hospital Felicio Rocho, Brazil, [3]Hospital Felcio Rocho, Brazil, [4]Columbia University - Federal University of Minas Gerais, Brazil, [5]Felicio Rocho Hospital - Endocrine Department, Brazil, [6]Rua Padre Francisco Arantes, USA

Early identification of patients at risk for osteoporosis is of great clinical importance and essential to the implementation of effective strategies for prevention, diagnosis, and treatment of the disease, helping to avert the ultimate consequence of osteoporosis: the bone fractures. Purpose: We aim to evaluate the association between the presence of clinical risk factors for osteoporosis and the result of bone densitometry (BMD) in a population of Brazilian women. Methods: A cross sectional study was conducted in 170 patients, selected between January 2009 and January 2010, from a general endocrine clinic at Felicio Rocho Hospital, in Brazil. The patients submitted to bone densitometry were screened for the presence of clinical risk factors for osteoporosis through a questionnaire. We assessed the following parameters: age, body mass index (BMI), calcium intake, sun exposure, physical activity, smoking, age at menarche, age at menopause, number of pregnancies, breastfeeding duration, hysterectomy, oophorectomy, nephrolithiasis, previous fractures events, family history of osteoporosis, clinical conditions and medications that might interfere with bone metabolism as Cushing, primary or secondary hyperparathyroidism, hyperthyroidism, use of bisphosphonates, hormone replacement therapy (HRT) and calcium or vitamin D supplementation.Results: Among the 170 patients evaluated, 22.4% had normal BMD, 40% osteopenia and 37.6% osteoporosis. Only 30% of patients engaged in regular physical activities, 41.8% had adequate calcium intake and 24.8% reported regular exposure to sunlight. Osteoporotic patients, compared to normal or osteopenic, were older, had earlier menopause age, greater number of pregnancies, lower BMI, higher frequency of nephrolithiasis and more frequent family history of osteoporosis. Osteopenic patients did not statistically differ from patients with normal BMD in relation to the presence of risk factors.Conclusions: Our findings suggest that clinical factors may correlate with decreased bone mass and could be used to identify patients at higher risk for osteoporosis. Early detection of some modifiable risk factors could also lead us to advice the correction of inappropriate habits that negatively influence bone metabolism.

Risk factors and its association with bone densitometry

Risk Factors	BMD N=38 Normal	BMD N=68 Osteopenia	BMD N=64 Osteoporosis	P
Age (years)	58,1 ± 10,6 A	60,8 ± 10,1 A	67,4 ± 10,4 B	P<0,000
Menopause (years)	48,7 ± 5,7 A	48,3 ± 5,6 A	46,2 ± 6,1 B	P=0,008
Pregnancy	3,1 ± 3 Median: 2 A	2,8 ± 1,9 Median: 3 A	3,9 ± 2,6 Median: 4 B	P=0,01
Nephrolithiasis (%)	YES: 17,9 NO: 82,1 A	YES: 8,5 NO: 91,5 A	YES: 33,3 NO: 66,7 B	P=0,008
Family History (%)	YES: 45,7 NO: 54,3 A	YES: 39,7 NO: 60,3 A	YES: 62,7 NO: 37,3 B	P=0,03
BMI (Kg/m²)	27,6 ± 3,6 A	27 ± 4,5 A	25 ± 3,6 B	P=0,002

ABC, p<0,05

Risk factors and BMD

Distribution of patients according to the result of bone densitometry

BMD	N	%
Normal	38	22,4
Osteopenia	68	40
Osteoporosis	64	37,6
TOTAL	170	100

Patient Distribution and BMD

***Disclosures: Maria Marta Sarquis Soares**, None.*

SU0295

Influence of Fat Layering on Bone Mineral Density Measurements by DXA and QCT. Elaine Yu*, Robert Neer, Bijoy Thomas, Joel Finkelstein. Massachusetts General Hospital, USA

Purpose: Alterations in body composition appear to have complex effects on the measurement of bone mineral density (BMD) by dual-energy x-ray absorptiometry (DXA), and may lead to spurious results when body composition is changing, such as occurs with weight loss. We sought to determine the effect of fat layering on *in vitro* and *in vivo* BMD measurements by DXA and to explore whether similar changes occurred when BMD is measured using quantitative computed tomography (QCT).

Methods: We scanned an anthropomorphic spine phantom by DXA and QCT at baseline and after successive layers of rectangular fat bags (up to 10 kg) were placed circumferentially. In addition, we measured lumbar spine and proximal femur BMD by DXA and trabecular spine BMD by QCT in 13 adult volunteers both at baseline and after 7.5 kg of circumferential fat layering. In the human volunteers, DXA lumbar spine scans were repeated with rectangular fat bags placed in a vertical orientation (long axis parallel to the individual's torso, covering 2/3 of torso width).

Results: With the spine phantom, DXA BMD increased linearly with successive fat layers ($p<0.01$), and its reproducibility progressively worsened. QCT BMD increased slightly ($p=0.06$) although reproducibility did not change significantly with additional fat layers on the spine phantom. In humans, circumferential fat layering had no significant impact on mean spine and hip DXA BMD although the reproducibility deteriorated, particularly for hip measurements (Table). When fat bags were placed vertically, however, DXA spine BMD decreased ($p<0.01$), and reproducibility worsened. As with the phantom, circumferential fat layering of human volunteers caused a small but statistically significant increase in QCT trabecular BMD ($p=0.05$).

Conclusions: These results suggest that fat layering simulations with spine phantoms approximate *in vivo* conditions reasonably well for QCT but not for DXA. In human volunteers, fat layering leads to inaccuracy and poor reproducibility, particularly for DXA hip measurements. The orientation of fat layers has profound effects on DXA spine BMD, perhaps due to irregularities in fat:lean tissue calculations. Caution must be used when interpreting BMD results of clinical studies in which body composition is changing.

Table. Changes in BMD and reproducibility after 7.5 kg of fat layering on spine phantoms and human volunteers

	Mean BMD Change (%)	Reproducibility (RMS CV%)[a]
DXA spine phantom	+5.5 [b]	3.8
QCT spine phantom	+1.4 [c]	1.5
DXA spine (V)[d]	-8.1 [b]	6.6
DXA spine	-1.9	2.7
DXA total hip	-2.6	7.9
DXA femoral neck	+0.7	3.9
QCT trabecular spine	+1.5 [e]	2.0

Fat layers placed circumferentially unless otherwise noted;
[a] RMS CV = root mean square coefficient of variation;
[b] p<0.01; [c] p=0.06; [d] Fat layers placed vertically; [e] p=0.05

Fat Layering Study Table

***Disclosures: Elaine Yu**, None.*

SU0296

Is Regional Bone Density in a Hip Scan Reflected by Traditional Hip Scan DXA Assessments. Tom Sanchez*[1], Jing Mei Wang[2], Kathy M Dudzek[3], Chad A Dudzek[3]. [1]Norland - A Cooper Surgical Company, USA, [2]Norland–a CooperSurgical Company, Peoples republic of china, [3]Norland–a CooperSurgical Company, USA

The hip is a complex structure with bone mineral routinely distributed in response to the biomechanical needs of this structure. This study examined if bone density in four biomechanically sensitive regions—the principle compressive and tensile regions and the secondary compressive and tensile regions–is reflected by measurements made in the traditionally DXA-evaluated regions of the Femur Neck, Trochanter, Ward's and Total Hip.

Hip scans from 150 Caucasian female subjects underwent evaluation of traditional scan sites (Total Hip, Femur Neck, Trochanter and Ward's) and four operator defined regions sampling bone in the principle and secondary compressive and tensile regions using analysis with Norland Illuminatus software.

Linear regressions showed significant correlations (between 0.9325 and 0.6675) and tight standard deviation of residuals between the traditionally evaluated hip regions (Femur Neck, Trochanter, Ward's and Total Hip) and the principle and secondary compressive and tensile regions. Results between these traditionally evaluated hip regions and these operator defined regions are provided in the results table.

The study has shown that in this population of women bone density in traditionally evaluated regions of the hip reflect bone density in mechanically significant regions. Bone density in traditional scan regions can reflect risk in particularly susceptible mechanical areas of the hip.

	Principle Compressive Region	Principle Tensile Region	Secondary Compressive Region	Secondary Tensile Region
Femur Neck	0.9325 0.0598	0.9219 0.0555	0.8296 0.1059	0.7468 0.1032
Trochanter	0.8054 0.0981	0.7201 0.0995	0.7915 0.1160	0.8781 0.0742
Ward's	0.7761 0.1044	0.8614 0.0728	0.7738 0.1202	0.6675 0.1155
Total Hip	0.8635 0.0835	0.8932 0.0854	0.8770 0.0927	0.8521 0.0812

Correlation and Standard Deviation of Residuals Between Sites

***Disclosures: Tom Sanchez**, None.*

SU0297

Lower Extremity BMD Measurement Methodology in Chronic Spinal Cord Injury Populations. Lisa Streff*[1], Thomas Schnitzer[2], Dorian Samuels[1], Benjamin Grover[1]. [1]Rehabilitation Institute of Chicago, USA, [2]Northwestern University, USA

Aims: To compare different methods of BMD measurement by DXA at the distal femur and proximal tibia of people with spinal cord injuries (SCI).

Method: A convenience sample of 15 individuals aged 21-63 with chronic SCI underwent bone density evaluation using a Hologic QDR-4500A densitometer. BMD was measured at the distal femur (DF) and proximal tibia (PT) using both the AP spine and forearm acquisition software. Initial studies evaluated varying the size and position of the global ROI (GROI) as well as comparing the smaller ROIs at the sites of interest (areas within the DF and PT); later studies used optimized GROIs to examine precision of measurements at both sites with each acquisition software by obtaining repeat scans. All included BMDs were averaged within each ROI and across scan acquisition type and standard deviations of the differences between repeat scans were calculated.

Results: The mean age of subjects was 40 $\pm$ 12 years, 12 males and 3 females, with duration since SCI of 7.9 $\pm$ 7.7 years. BMD measurements were found to be affected by size of GROI chosen and its position, as well as the size and positioning of the targeted ROIs. Larger GROI resulted in more stable measurements; positioning of the GROI was critical to obtaining meaningful and reproducible data, with BMD values being highly dependent on placement; large variability was observed with minor changes (single pixel) in position, unrelated to any identifiable parameter (e.g., air, external markers). Utilizing optimal GROIs and standard DF and PT ROIs, the forearm acquisition software provided more precise BMD estimates (SD of difference = 0.0068 gm/cm^2) than spine software (SD of difference = 0.0233 gm/cm^2) at both the DF and PT. Precision was independent of the site being scanned (DF or PT) or the specific ROI within that site. Interestingly, the absolute BMD measurements at each ROI were also affected by type of acquisition software with higher values seen with forearm vs. spine at most ROIs evaluated.

Conclusions: BMD measurement by DXA at the DF and PT in people with SCI is highly dependent on measurement technique. Better standardization is needed before this procedure can be utilized effectively in either clinical practice or research settings.

***Disclosures: Lisa Streff**, None.*
This study received funding from: Proctor and Gamble

SU0298

Osteoporosis Screening with a New Volumetric Evalauation of Dental Alveolar Bone Density. Yoshitomo Takaishi*[1], Aiko Kamada[2], Takashi Ikeo[2], Takami Miki[3], Takuo Fujita[4]. [1]Takaishi Dental Clinic, Japan, [2]Osaka Dental University, Japan, [3]Osaka City University Medical School, Japan, [4]Katsuragi Hospital, Japan

< Background >

In order to prevent and treat osteoporosis, a global health problem threatening millions with impending fracture, simple, readily accessible screening method is required, especially in view of the low participation rate to the current survey method based on sophisticated methods such as DXA. By utilizing dental X-ray apparatus under wider distribution, a new volumetric method of alveolar bone mineral density (BMD) was developed. By taking X-ray picture of alveolar bone on a dental film pasted with an aluminum step wedge and computerized standardization (Bone Right System) and measurement of bone thickness for correction, it became possible to measure volumetric alveolar bone density.

< Methods >

In 35 postmenopausal females with a mean age of 59.7 years (50 - 69), volumetric alveolar bone mineral density (alBMD) was measured by Bone Right System (Dentalgraphic.Com, Himeji, Japan) at a site 6 mm lower than neck of the right mandibular first premolar along with lumbar BMD (LBMD) measurement by DXA and survey on history of fracture and body height shortening by more than 3 cm. Volumetric alveolar BMD was measured by correcting conventional BMD with the bucco-lingual distance at 6 mm lower than the cement-enamel junction of the right mandibular first premolar to be expressed as alveolar BMD / mm (ValBMD).

< Results >

Even within the narrow age range of postmenopausal period, a significant negative correlation was found between age and alBMD ($r = -0.652$, $p<0.01$). A significant positive correlation was noted between ValBMD and LBMD ($r = -0.644$, $p<0.01$). Fracture increased with age exhibiting a significant positive correlation ($r = 0.379$, $p<0.05$). Negative correlation was noted between fracture and both LBMD ($r = -0.442$, $p<0.01$) and ValBMD ($r = -0.484$, $p<0.01$). In ROC curves, alBMD and ValBMD exhibited AUC (0.941 and 0.842) better than those by lumbar bone mineral density (LBMD) (0.770) indicating a high capability of alBMD and ValBMD in fracture prediction.

< Conclusion >

In order to overcome the drawbacks of two-dimensional densitometry for alBMD previously reported influenced by body, attempts were made to measure ValBMD, which appeared to be compared favorably with LBMD in the diagnosis of generalized osteoporosis.

***Disclosures: Yoshitomo Takaishi**, None.*

SU0299

Relationship Between Body Composition and the Skeleton. Xiaohai Wan[1], John Krege[1], Yebin Jiang*[2]. [1]Eli Lilly & Company, USA, [2]Osteoporosis & Arthritis Lab, University of Michigan, USA

Purpose: Body composition is known to impact the skeleton, since lower areal bone mineral density (aBMD) is often observed in the setting of lower body mass index (BMI). Alternatively, inverse correlations between fat and bone have been described after adjustment for confounding factors such as mechanical loading.

Methods: To study the effect of body composition on bone, we analyzed baseline data from the teriparatide Fracture Prevention Trial (I) and the Multiple Outcomes of Raloxifene Evaluation study (II). The studies enrolled a small number of women with low BMI (<19 kg/m^2): 30 (1.9%) in study I (N = 1609) and 280 (3.6%) in study II (N = 7705). The majority of women had moderate (19 - <25 kg/m^2) or high (25 - <30 kg/m^2) BMI: 1257 (78.1%) in study I and 6545 (85.0%) in study II. There were 322 (20.0%) and 877 (11.4%) obese (30+ kg/m^2) osteoporotic women in study I and II, respectively. The relationship between pairs of variables was assessed using Spearman's rank correlation test (Table).

Results: Weight and BMI correlated positively with aBMD at all skeletal sites measured. Weight and BMI were weakly positively correlated with parathyroid hormone (PTH) and weakly negatively correlated with 25-hydroxyvitamin D (25(OH)D) and bone formation marker procollagen type 1 amino-terminal propeptide (P1NP). The overall findings suggest that postmenopausal women with lower weight and BMI in these two trials had lower aBMD, associated with lower PTH and higher calcium, albumin, 25(OH)D, and P1NP.

Conclusions: These findings may be consistent with postmenopausal women with lower weight and BMI, and hence lower contribution of adipose tissue, having a lower capacity to aromatize androgen precursors to estrogen. This work provides some insights into the relationship between body composition and the skeleton.

		aBMD			Laboratory Assessments				
		LS	Hip	FN	Calcium	Albumin	PTH	25(OH)D	P1NP
Weight	I	0.41*	0.51*	0.41*	-0.02	-0.06**	0.08	-0.18*	-0.06
	II	0.27*		0.24*	-0.03***	-0.08*	0.12*	-0.12*	-0.15*
BMI	I	0.32*	0.44*	0.34*	-0.06	-0.05***	0.12	-0.22*	-0.08***
	II	0.21*		0.23*	-0.02	-0.08*	0.15*	-0.18*	-0.14*

* p-value<0.0001, ** p-value<0.01, *** p-value<0.05
BMI = Body Mass Index, aBMD = Areal Bone Mineral Density, LS = Lumbar Spine, FN = Femoral Neck, PTH = Parathyroid Hormone, 25(OH)D = 25-Hydroxyvitamin D, P1NP = Procollagen Type 1 Amino-Terminal Propeptide

Table 1

***Disclosures: Yebin Jiang**, Eli Lilly and Company, 1; Eli Lilly and Company, 3*
This study received funding from: Eli Lilly and Company

SU0300

Teriparatide and Risk of Nonvertebral Fractures in Women with Postmenopausal Osteoporosis. Xiaohai Wan, John Krege*. Eli Lilly & Company, USA

Purpose: To examine the impact of teriparatide (TPTD) on a variety of nonvertebral fracture outcomes in postmenopausal women treated with TPTD versus placebo. Methods: The Fracture Prevention Trial (FPT) was a double-blind trial of postmenopausal women randomly assigned to TPTD 20 mcg/day (N=541), TPTD 40 mcg/day (N=552), or placebo (N=544) by daily self-injection, for a median of 19 months and a median follow-up of 21 months. All patients received calcium and vitamin D supplementation. Reports of nonvertebral fractures were collected from patients at each visit and confirmed by a written radiology report or review of the x-ray films. Nonvertebral fracture sites captured included: hip, wrist, pelvis, humerus, ribs, ankle, foot, and other. Pathological fractures and fractures of the face, skull, metacarpals, fingers and toes were excluded. Fracture outcomes are shown (table). Results: The risk of nonvertebral fragility fracture was significantly reduced in the TPTD versus placebo group when all fracture sites were considered, and also when major sites and 5 nonvertebral (NV5) sites were considered. However, significant reductions in traumatic fractures were not observed. Conclusion: In the FPT, the risk reduction for nonvertebral fracture in patients treated with TPTD versus placebo depended on the set of nonvertebral fractures included in the analysis; lower relative risks were observed for nonvertebral fractures more likely to be osteoporotic in origin.

Table. Number of Patients with Fractures (Relative Risk versus Placebo)

	Fragility[1]			Traumatic[2]			Fragility or Traumatic		
	Placebo	TPTD 20	TPTD 40	Placebo	TPTD 20	TPTD 40	Placebo	TPTD 20	TPTD 40
All	30	14 (0.47*)	14 (0.46*)	23	19 (0.83)	16 (0.69)	53	34 (0.65*)	32 (0.60*)
Major[3]	21	8 (0.38*)	9 (0.42*)	14	9 (0.65)	8 (0.56)	35	18 (0.52*)	19 (0.54*)
Non-major	12	7 (0.59)	7 (0.57)	11	10 (0.91)	8 (0.72)	24	17 (0.71)	15 (0.62)
NV5[4]	19	6 (0.32*)	8 (0.42*)	9	8 (0.89)	7 (0.77)	28	15 (0.54*)	17 (0.60)
Non-NV5	13	8 (0.62)	7 (0.53)	14	11 (0.79)	10 (0.70)	28	19 (0.68)	17 (0.60)

1. Not classified by investigators as traumatic
2. Defined by the investigators and included those fractures resulting from automobile accidents or falling from greater than standing height
3. Major sites included hip, wrist, pelvis, humerus, and ribs.
4. NV5 sites included hip, wrist, pelvis, humerus, and ankle.

* P<0.05
TPTD 20 = teriparatide 20 mcg/day, TPTD 40 = teriparatide 40 mcg/day

Table 1

***Disclosures: John Krege**, Eli Lilly and Company, 3; Eli Lilly and Company, 1*
This study received funding from: Eli Lilly and Company

SU0301

Bone Geometry and Strength in Obese Adults. Lesley M. Scibora*[1], Amanda J. Smock[1], Beth C. Kaufman[1], Mindy S. Kurzer[2], Thomas Beck[3], Moira Petit[1]. [1]University of Minnesota, USA, [2]University of Minnesota, USA, [3]Johns Hopkins Outpatient Center, USA

Few studies have explored the relationship between body weight and bone strength in morbidly obese adults. Purpose: To describe tibial and radial bone geometry, volumetric density, and estimates of bone strength in obese adult women. Methods: Bone geometry and strength were assessed by peripheral quantitative computed tomography (pQCT) in obese (mean BMI 41.8 $\pm$ 10.3 kg/m^2, n = 21) and healthy weight (mean BMI 21.5 $\pm$ 1.5 kg/m^2, n = 71) women. Total volumetric bone mineral density (ToD, mg/mm^3), total bone area (ToA, mm^2), and bone compressive strength (bone strength index (BSI)) were assessed at the distal (4%) sites of the tibia and radius. ToA and cortical bone area (CoA, mm^2), cortical volumetric density (CoD, mg/mm^3), cortical thickness (CoTh, mm), and bone bending strength (polar strength strain index (SSIp), mm^3) were measured at the midshaft sites of the tibia (66%) and radius (50%). Results: Compared to healthy weight females, bone strength was higher (8-14%, $P < 0.05$) in the obese women at all sites except the distal radius. The greater bone strength was due primarily to a greater ToA (+7-10%, $P < 0.05$). Interestingly, ToD and CoD were significantly lower in obese women at the proximal radius (-4-5%, $P < 0.05$). Simple correlations suggested a negative association between CoD and body weight (r = -0.59, $P < 0.01$). After adjustment for bone length and body weight, differences remained significant at the distal sites (all $P < 0.05$), but bone strength was significant *lower* in obese women at the cortical sites of the radius (-2%, $P < 0.01$) and tibia (-9%, $P < 0.05$). Conclusions: Obese women had greater bone strength compared to healthy weight women, due to greater bone area, at both weight bearing and non-weight bearing sites. However, these differences reversed at cortical bone regions after adjusting for bone length and body weight. Similar to findings in pediatric studies, these data suggest that bone strength may be low for body weight in obese women. Future studies should further explore the relationship of body weight, and its components, to parameters of bone strength in morbidly obese populations.

***Disclosures: Lesley M. Scibora**, None.*

SU0302

Comparison Between Vertebral Body Height Ratios Assessed by X-ray Based and Norland Illuminatus DXA-based Vertebral Fracture Assessments. Terry W Schwalenberg[1], JC Liu[2], George Ekker[1], Tom Sanchez[3], Jingmei Wang*[4]. [1]Norland–a CooperSurgical Company, USA, [2]Department of Nuclear Medicine, PLA 304th Hospital, China, [3]Norland - A Cooper Surgical Company, USA, [4]Norland–a CooperSurgical Company, China

Vertebral fracture assessment which used to be conducted using x-ray based measurements of vertebral body heights is being applied using DXA-based measurements. This study compared vertebral body height ratios using X-ray based and the Norland Illuminatus DXA-based technologies.

Twenty-seven subjects underwent measurement of vertebral body heights in lateral x-ray based film and in a DXA-based study of the thoracic and lumbar spine in decubitis recumbency on a Norland scanner fitted with dynamic filtration. These studies underwent measurement of the posterior, mid and anterior vertebral body

heights of all vertebrae from T-9 to L-4. Vertebral body height ratios (H_a/H_p, H_m/H_p, H_m/H_a and H_p/H_{pa}) were calculated for the two sets of measured vertebrae and difference was assessed by t-test.

When clinical assessment of a fracture was conducted 95.5% (825 of 864) of the assessments made by DXA-based studies and x-ray based studies were similar. Of the 39 pair of studies that were not similar, 13 pairs (33.3% of the dissimilar–1.5% of the total sample) showed DXA-based studies identifying a fracture when x-ray based studies did not show fractures. A Fisher's Test showed the results not to be significantly different.

The study shows that Norland DXA-based vertebral body height ratios appear similar to those obtained from height ratios calculated from x-ray based vertebral body heights and that vertebral fracture assessment from the two methods does not differ.

***Disclosures: Jingmei Wang**, None.*

SU0303

Cortical Bone Water Measured by UTE MRI Far Exceeds Variations in Mineral Density. Felix Werner Wehrli*[1], Hamidreza Saligheh Rad[2], Mary Leonard[3], Jeremy Magland[2], James Love[2], Hee Kwon Song[2], Helen Peachey[2]. [1]University of Pennsylvania Medical Center, USA, [2]University of Pennsylvania, USA, [3]Children's Hospital of Philadelphia, USA

Cortical bone water concentration (BWC) has emerged as a new metric of bone quality (Techawiboonwong et al, Radiology 2008). Here we quantify CBW in healthy subjects with BMD Z-scores at the hip within ± 1 (N=66, age range 30-80 years, M=29, F=47). Proton images were acquired with a 3D hybrid-radial dual-TR ultra-short TE (UTE) pulse sequence at 3T field strength that also measures the longitudinal relaxation time (T1) of BWC. Measured proton density, representative of water in various compartments, was quantified with respect to a reference phantom of manganese chloride in 80% D_2O/20% H_2O. BWC was not associated with age in men but increased 2.0%/decade in women ($p<0.001$). In contrast, neither hip or spine areal BMD showed any age dependence in this sample of subjects with normal DXA hip BMD Z-scores. Fig. 1 displays parametric images of BWC and T1 relaxation times in two subjects highlighting age-related increases in BWC and T1. Fig. 2 shows an inverse correlation of BWC with 3D BMD measured by pQCT at the same anatomic location. The slope of the correlation indicates the fractional change to be five-fold greater for BWC than for BMD. The data thus suggest BWC to be a potentially sensitive metric of bone quality. CBW is primarily composed of pore and collagen-bound fractions and the age-related increase in this parameter is consistent with the known increase in microporosity with age (Bousson, et al, Radiol 2000). Increased proportion of larger pores manifests in increased T1, which was found to strongly correlate with BWC ($R=0.72$, $p<0.0001$).

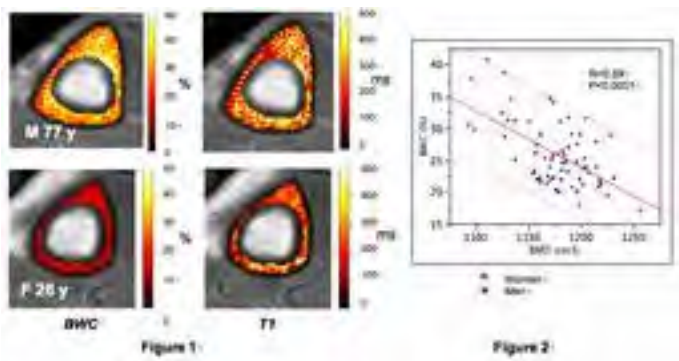

Figures 1 and 2

***Disclosures: Felix Werner Wehrli**, None.*

SU0304

Evaluation of an Automated Morphometry Software Program (SpineAnalyzer™) on VFA Images. Diane Krueger*[1], Joes Staal[2], Peter Steiger[3], Bjoern Buehring[4], Harry Genant[5], Neil Binkley[6]. [1]University of Wisconsin, Madison, USA, [2]Optasia Medical, United Kingdom, [3]Optasia Medical, USA, [4]Cleveland Clinic, USA, [5]UCSF/Synarc, USA, [6]University of Wisconsin, USA

Prior vertebral fracture increases fracture risk. Thus, knowledge of fracture status is necessary for therapeutic decisions, making densitometric vertebral fracture assessment (VFA) valuable. However, VFA limitations include difficulties in mild (grade 1) fracture identification; a weaknesses that may be reduced by imaging improvements. As such, this study evaluated the utility of SpineAnalyzer™, software which utilizes a 95-point morphometry approach on VFA DXA images acquired with a GE Healthcare iDXA.

In a prior study, VFA was performed on 103 individuals and read by two clinicians from printed images, twice on separate dates, applying the Genant VSQ system without morphometry. In 55/103 cases for which the clinician's interpretations were not concordant, images were sent to a recognized expert (HKG) whose interpretation was defined as our "gold standard." Many of these 55 patients had substantial degenerative disease, scoliosis or other anatomic variation making fracture identification challenging. The mean age and lowest T-score in these 55 subjects (14 men/41 women) was 72.4 years and -1.6 respectively.

The main outcome parameter was vertebral fracture number and grade from T4-L4 using SpineAnalyzer™, as analyzed by an ISCD-certified technologist, in comparison to the gold standard and non-radiologist physician experienced in VFA interpretation. Some manual adjustment of morphometry point placement was required on the majority of these images. This primarily was required for abnormal or upper thoracic vertebral bodies. For analysis as normal (VSQ grade 0) or fracture (VSQ grade 1, 2 or 3), moderate agreement was observed between the gold standard and both SpineAnalyzerTM and the clinician (kappa 0.60 and 0.55 respectively). When limiting evaluation to just grade 2 and 3 fractures (VSQ = 0, 1 together vs. VSQ = 2, 3 together) moderate agreement with the gold standard was again observed; kappa of 0.56 for both SpineAnalyzer™ and clinician.

In conclusion, when evaluating VFAs in a cohort with substantial degenerative disease and/or anatomical abnormalities, SpineAnalyzer™ with morphometry performed by a technologist is similar to an experienced clinician when comparing to a gold standard reader. Studies evaluating more representative populations are needed to better characterize the utility of SpineAnalyzer™ application to VFA images.

***Disclosures: Diane Krueger**, None.*

SU0305

Generation of an Atlas of the Proximal Femur for Automatic Placement of Identical VOIs for the Analysis of Trabecular Bone. Julio Carballido-Gamio[1], Dimitrios C. Karampinos[2], Jenny Folkesson[2], Thomas Link[2], Sharmila Majumdar[2], Roland Krug*[2]. [1]Grupo Tecnológico Santa Fe, S.A. de C.V., Mexico, [2]University of California, San Francisco, USA

Purpose: To automatically place volumes of interest (VOIs) to analyze identical regions of trabecular bone micro-architecture from high-spatial resolution (HR) MR images of the proximal femur.

Methods: Coronal HR-MR images of the proximal femur of 12 subjects were acquired on a 3T MR750 scanner (GE Medical Systems, Milwaukee, WI) using an 8 channel phased-array coil and a fully-balanced steady-state free-precession pulse sequence. Spatial resolution was 0.234x0.234x0.5mm with a matrix size of 512x512x96. IDEAL (Iterative Decomposition of water and fat with Echo Asymmetry and Least-squares estimation) water-only (W) images were also acquired with half the spatial resolution and half the matrix size.

An IDEAL scan was randomly selected as reference (R) and 9 IDEAL scans were automatically registered to it using 3D multiresolution affine registrations (4 scales) followed by 3D free-form deformations[1] (FFDs; 3 scales; control point spacing (CPS)=20 voxels; smoothness regularization) using in-house developed software to create a W-IDEAL atlas. A dilated contour of the upper-R femur was used to restrict the volume to compute the optimization metric (mean squared differences) and to restrict the number of active control points. Transformations were applied to the HR images and a HR atlas was created where a spherical (S) VOI was prescribed. Using affine registrations and FFDs, the W-IDEAL atlas was automatically registered to the 2 scans which were not used to build the atlas. A rectangular parallelepiped based on a box in the middle slice of each of the 2 scans was used to restrict the transformations which were later applied to the HR atlas to place the S-VOI in the 2 subjects.

Results: Fig. 1a shows a slice of the W-IDEAL atlas, and Fig. 1b shows the corresponding slice of the HR atlas with a cross-section of the S-VOI. Edges in both atlases are clearly visible indicating that the anatomical variability was well accommodated and explained by the FFDs. Automatic placement of the S-VOI in the 11th and 12th subjects is shown in Fig. 1c and 1d where anatomical correspondence with Fig. 1b can be easily appreciated.

Conclusions: The feasibility of constructing an atlas of the proximal femur to prescribe VOIs and automatically place them in other subjects has been demonstrated. Current work is in progress to reduce the CPS without substantially increasing the computational time to make the HR-atlas edges more pronounced.

References: [1]Rueckert et al. IEEE-TMI, 22(8)-2003.

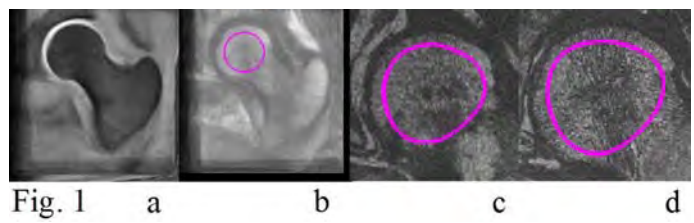

Figure 1

***Disclosures: Roland Krug**, None.*
This study received funding from: NIH R01AR057336 and NIH 1P30AR058899

SU0306

Intra-sample Variability in Bone Volume in Bone Iliac Crest Biopsies Evaluated by Fast Fourier Transform (FFT). Jean-Paul Roux*, Brigitte Burt-Pichat, Nathalie Portero-Muzy, Roland Chapurlat, Pascale Chavassieux. INSERM U831, Universite de Lyon, France

Introduction: Bone biopsy is an important tool for diagnosis and research in bone diseases. Bone histomorphometry remains the only procedure allowing for assessment of bone turnover at both the tissue and cellular level and other bone quality determinants, including the bone matrix texture and mineralization defects The aim our study was to investigate the intra-sample variability inside bone biopsies and to determine how many 2D slices must be needed to have representative histomorphometric values of bone volume (BV) referent parameters.

Methods: 28 Iliac crest biopsies taken with a 7.5-mm inner diameter Bordier-Meunier trephine from long term bisphosphonate treated osteoporotic patients were studied. BV/TV was measured by 1) 2D-histomorphometry using an automatic image analyzer (Bone, Explora Nova, La Rochelle, France) on three 8 µm thick sections cut at 3 different planes 300 µm apart; 2) 3D-µCT with 18 µm nominal isotropic voxel size (Skyscan 1076 microtomograph, Aartselaar, Belgium) and by 2D-µCT on the full stacks to evaluate the intra-sample variability. We analyzed the profile curves of the intra-sample variability of 2D BV/TV using fast Fourier transform (FFT) (PEAS software, J. Grecner, CZ) in order to determine the main half-periods (i.e. maximum to minimum BV/TV) (figure 1).

Results: BV/TV 3D-µCT and BV/TV 2D-histomorphometry measurements (graph 1) were significantly correlated (r' = 0.54; p = 0.005). No significant difference was found between BV/TV measured by 3D-µCT and by 2D-histomorphometry. The intra-sample coefficients of variation of the 2D BV/TV values measured by 2D-µCT on the stacks across the biopsies ranged from 7.20 to 53.50% with a mean of 15.64%. The mean value of the half periods by FFT was 554µm ± 237.

Conclusions: In conclusion, the intra-sample variability of BV/TV was characterized by a mean half period of 554 µm. This result confirms that histomorphometric measurements of BV referent parameters must be performed on at least 3 different planes with a minimum 554 µm between the first and third planes.

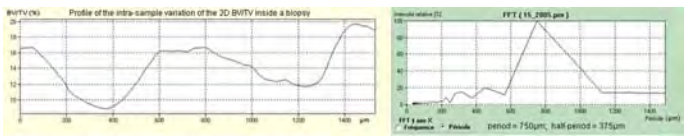

figure1

	BV/TV 3D-µCT (%)	BV/TV 2D-histomorphometry (%)
Mean ± SD	13.13 ± 5.30	12.83 ± 4.75
minimum	3.47	5.03
maximum	33.30	24.90

graph1

***Disclosures: Jean-Paul Roux**, None.*

SU0307

Reproducibility of Volumetric Topological Analysis for Trabecular Bone via Multi-Detector CT Imaging. Punam Kumar Saha*. University of Iowa, USA

Several studies have demonstrated association of skeletal diseases including osteoporosis and osteoarthritis with trabecular bone (TB) architectural changes. Multi-detector CT scanner (MDCT) is clinically widely available, less expensive, easy to use and fast to perform and has a low effective dose of about 0.05 mSv. Here, we present a new approach for volumetric topological analysis (VTA) of TB via MDCT imaging and examine its reproducibility under in vivo conditions.

VTA uses several novel methods related to digital topological analysis, manifold topology and scale, and volumetric feature propagation and computes local TB bone width in mm allowing classification plates and rods on their continuum (Figure 1). Also, VTA provides bone mineral distribution at different pate widths which may be a unique tool for understanding micro-structural effects in disease progression and treatment process.

Five cadaveric ankle specimens were scanned using a Siemens Somatom Definition Flash 128 MDCT scanner at 120 kVp and 160 mAs. After scanning in a helical mode with a slice thickness of 0.4 mm, data was reconstructed at 0.3 mm slice thicknesses and 0.21 pixel size utilizing a very sharp kernel of U70u to achieve high-resolution. For each specimen, three scans were acquired after repositioning the specimen each time. Each image was processed through the following steps – (1) computation of bone volume fraction (BVF) image, (2) resampling of BVF images at 0.15 mm isotropic voxel, (3) registration of BVF images from three repeat scans, and (4) application of VTA methods.

Repeat CT scans have shown high visual agreement in TB structures and VTA based micro-structural classification (Figure 1). For each image, a cylindrical ROI of 10 mm radius and 15 mm height was chosen over TB region at 8 mm above distal cortical endplate. Bone volume/total volume (BV/TV) and two VTA-derived parameters, surface width (SWVTA) and surface-to-curve ratio (SCRVTA) were measured. For three repeats scans, intra class correlations found experimentally are 0.98, 0.97, and 0.96 for BV/TV, SWVTA, and SCRVTA, respectively. Preliminary results of this study show high potential of the new VTA method for TB micro-structural analysis via MDCT imaging.

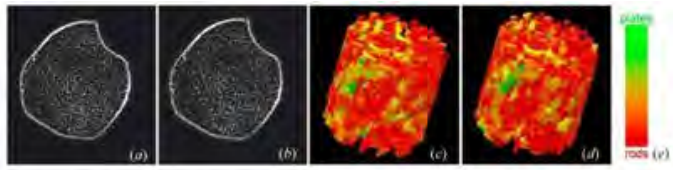

Figure 1 Micro-structural classification of TB in repeat MDCT scans. (a,b) Matching axial slices from BVF images in two repeat scans. (c-d) VTA-based classifications of two repeat scans over matching ROIs. (e) The common color coding bar used in (c-d).

Figure 1

***Disclosures: Punam Kumar Saha**, None.*

SU0308

Short Term In Vivo Precision of BMD and Parameters of Trabecular Architecture at the Distal Forearm and Tibia. Thomas Fuerst[1], Klaus Engelke*[2], Paul McCracken[3], Bernd Stampa[4], Wolfram Timm[4], Bernie Dardzinski[5], Harry Genant[6], Anne De Papp[5]. [1]Synarc, Inc., USA, [2]University of Erlangen, Germany, [3]Merck Research Laboratories, USA, [4]Synarc Inc, Germany, [5]Merck & Co., Inc., USA, [6]UCSF/Synarc, USA

Purpose:

To evaluate the short term in vivo precision of high resolution peripheral QCT at the forearm and tibia in a multi center trial of odanacatib 50mg once weekly oral administration.

Methods:

42 postmenopausal women (age: 64.4 ± 6.8 y) with spine or hip T-score ≤ -1.5 and > -3.5 recruited at 10 different imaging centers underwent double baseline scans at the tibia and the radius using the XtremeCT scanner (SCANCO Medical, Switzerland). After training and standardization, patients were scanned twice with repositioning on the same day. In addition to the standard ultradistal locations (tib_{ud} and rad_{ud}) scans ≍ 2 cm more proximal were performed (tib_d and rad_d) to more reliably assess the cortex. The scans were analyzed centrally (Synarc, Hamburg) and quality was graded perfect (G1), slight (G2) or pronounced (G3) movement artifacts, or unacceptable (G4). Root mean square (RMS) % coefficients of variation (CV) were calculated for integral (BMD_i), trabecular (BMD_t) and cortical BMD (BMD_c), cortical thickness (Ct.Th), BV/TV, Tb.Sp, Tb.Th, Tb.N, and mean cortical pore diameter (Po.D). Trabecular structure parameters were only measured at the ultradistal and Po.D at the distal locations.

Results:

The precision errors varied widely ranging from 0.56 for tib_{ud} BMD to 6.30 for rad_{ud} Tb.Sp (Table). Some patients (rad_{ud}: 0, rad_d: 5, tib_{ud}: 1. tib_d: 2) could not be measured twice at all four locations. Scans with G4 (rad_{ud}: 4, rad_d: 5, tib_{ud}: 0. tib_d: 2) were excluded from analysis. The table shows the CVrms values of the analyzable pairs including scans with quality in the range G1-G3 or G1-G2. Double baseline scans both with grade G1 were rare (rad_{ud}: 0, rad_d: 6, tib_{ud}: 4. tib_d: 5). The ultradistal radius was affected most by patient movement. In 17 (20%) patients at least one of the double scans was graded G3 or G4, whereas at the other three locations less than 10% of patients had at least one scan graded G3 or G4.

Conclusions:

Overall the precision error was lower at the tibia than at the radius and BMD errors were smaller than those for architecture. Scan quality had no effect on BMD but at the ultradistal radius precision errors of trabecular architecture parameters were lower for scans with fewer movement artifacts. Motion artifacts remain a challenge, particularly at the forearm, and care must be taken to evaluate each scan before accepting the measurement results. Precision in the context of a clinical trial with standardized procedures and training was comparable to single center results previously reported.

Table – Root mean square (RMS) % coefficients of variation (CV) by location, parameter and grade.

	Patients >75 years		
	Baseline	18 mths	36 mths
EQ-5D Health State Value (median, IQR)	0.53 (0.00, 0.69)	0.69 (0.52, 0.80)	0.69 (0.52, 0.80)
EQ-VAS mean (SD)	49.3 (22.01)	63.8 (20.87)	65.4 (22.24)
Back pain			
	N = 584	N = 444	N = 589
Every day / almost every day*	68.8%	28.8%	22.5%
	N = 551	N = 388	N = 262
Moderate / severe*	92.6%	61.3%	61.5%
VAS (mm)* mean (SD)	59.8 (26.12)	34.7 (24.29)	31.4 (26.13)

table

***Disclosures: Klaus Engelke**, Synarc, 3*
This study received funding from: Merck

SU0309

Trabecular Bone Score Helps Classifying Women at Risk of Fracture: A Prospective Analysis within the OFELY Study. Stephanie Boutroy*[1], Didier Hans[2], Elisabeth Sornay-Rendu[1], Nicolas Vilayphiou[1], Renaud Winzenrieth[2], Roland Chapurlat[1]. [1]INSERM U831 & Universite de lyon, France, [2]Department of Bone & Joint Diseases, Lausanne University Hospital, Switzerland

Trabecular Bone Score (TBS, Med-Imaps, France) is an index of bone microarchitecture calculated from antero-posterior spine DXA scan and reported to be associated with fracture in prior case-control studies and in a large prospective study on Prodigy DXA device. The aim of our study was to assess the ability of TBS to predict incident fracture and improve the classification of fracture prospectively in the OFELY study.

TBS was assessed in 564 postmenopausal women (66±8 years old) from the OFELY cohort, who had a lumbar spine DXA scan (QDR 4500A, Hologic, USA) between year 2000 and 2001. During a mean follow up of 7.8±1.3 years, 94 women sustained a fragility fracture (30 wrists, 29 vertebral fractures, 15 tibia, 5 hip, 4 humerus, 6 ribs, 3 metatarsal, 1 scapula and 1 elbow).

At the time of baseline DXA scan, women with incident fracture were significantly older (70±9 vs 65±8 yrs), had a lower lumbar spine BMD (T-score: -1.9±1.2 vs -1.3±1.3, $p<0.001$) and spine TBS (-3.1%, $p<0.001$) than women without incident fracture.

The magnitude of fracture prediction was similar for spine BMD (OR = 1.6[1.2;2.0] per SD decrease [95% CI].) and TBS (OR = 1.7[1.3;2.1]). After adjustment for age, BMI and the presence of prevalent fracture, the combination of TBS to spine BMD was not significant (AUC Curve increased by 0.003). Spine BMD and TBS were both correlated with age (respectively r=-0.17 and -0.49, $p<0.001$) and correlated together with 39% of TBS explained by spine BMD (r=0.63, $p<0.001$).

When using the WHO classification, 38% of the fractures occurred in osteoporotic (n=36/123, fracture rate = 29%), 47% in osteopenic (n=44/280, fracture rate = 16%) and 15% in women with T-score > -1 (n=14/161, fracture rate = 9%). By classifying our population in tertiles of TBS, we found that 39% of the fractures that occurred in osteopenic women were in the lowest tertile of TBS (n=17/89). 47% of the fractures occurred in the lowest tertile of TBS, regardless of BMD, with a fracture rate of 23%.

In conclusion, spine BMD and TBS predicted fractures equally well. The addition of TBS to age and spine BMD added only limited information to fracture risk prediction in our cohort. Nevertheless combining the osteopenic T-score and the lowest TBS may help defining a subset of osteopenic women at higher risk of fracture.

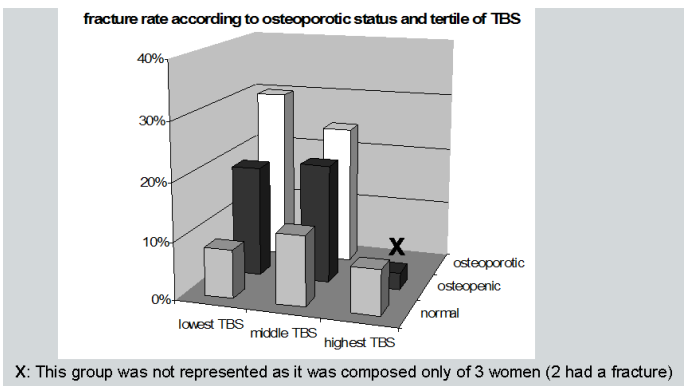

Fracture rate according to osteoporotic status and tertile of TBS

***Disclosures: Stephanie Boutroy**, None.*

SU0310

Longitudinal Effects of a Vegan Diet on Bone Mineral Density as Assessed by Calcaneal Quantitative Ultrasound. Simon Dyall*[1], Daphne Bird[1], Ian Drysdale[2], Heather Hinkley[2]. [1]British College Osteopathic Medicine, United Kingdom, [2]British College of Osteopathic Medicine, United Kingdom

It has been frequently suggested that vegans may have inadequate calcium and vitamin D intakes due to the lack of dairy products in their diet and insufficient calcium and vitamin D rich foods that could effectively substitute for these. This low dietary intake may subsequently have a negative effect on their bone mineral density (BMD). The aim of this study was to assess the long-term effects of changing to a vegan diet on BMD.

The BMD of 9 new mature female vegans was assessed using calcaneal QUS (McCue Cubaclinical). The subjects had a mean age of 33.3 years (S.D. 10.3 years) at baseline. All the subjects had adopted a vegan diet within 18 months (mean 11 months) prior to the initial screening. Following this initial assessment the subjects were then re-assessed at an annual vegan fair (May/June) to monitor changes in BMD.

Interim analysis at 3 years revealed a significant decrease of 7.8% in the mean left calcaneal scores ($P<0.05$). This trend was also seen with the right calcaneal scores, although it was not statistically significant (mean decrease 7.1%). Interestingly, at 4 years analysis of a subset of these scores revealed a partial restoration in mean BMD scores, such that the values were no longer significantly different from the baseline scores.

The results of this study suggest that when initially changing to a vegan diet there is an apparent initial detrimental effect on BMD; however, this effect appears transient in nature as restoration of BMD is achieved within a fairly short time-frame. It should be noted that due to the small sample size these results can only be considered exploratory in nature and this work is part of an ongoing longitudinal same-subject study.

***Disclosures: Simon Dyall**, None.*

SU0311

Ultrasonic Assessment of the Radius. Jonathan Kaufman*[1], Gangming Luo[1], Mark Lieberman[2], Stanley Rosenfeld[2], Alfred Rosenbaum[2], Robert Siffert[3]. [1]CyberLogic, Inc., USA, [2]Computerized Diagnostic Scanning Associates, Inc., USA, [3]The Mount Sinai School of Medicine, USA

The long-term objective of this research is to establish ultrasound as a safe, effective, and non-invasive method for assessing osteoporotic fracture risk. The purpose of this study was to design, fabricate and test a novel device that can assess the radius at the 1/3rd location. A new ultrasound device (*UltraScan 650*, CyberLogic, Inc., shown below) was used in this study. The device emits a 3.5 MHz broadband ultrasound signal from a single element rectangular source that propagates through the radius and soft tissue to a 64-element linear array rectangular receiver. Computer simulations and *in vitro* experiments were used to determine the specifications and expected performance of the device[1,2]. In brief, nineteen radii were used in a thru-transmission configuration in a water tank and analogously in computer simulations (*Wave2000*, CyberLogic, Inc.). Time delays associated with three distinct ultrasound propagation pathways were evaluated, and two net time delay (NTD) parameters were defined. Both *in vitro* and computer simulated data demonstrated a high correlation ($R>0.9$) between a non-linear function of the NTDs and the cortical cross-sectional area. A clinical study using seven subjects was also carried out. Both arms were measured with DXA (Hologic QDR 4500) and with ultrasound. Short term precision was also evaluated and found to be better than three percent. The data showed that the linear correlation coefficient between radial bone mineral density (BMD) and an ultrasound based estimate was $R=0.92$ ($P<0.01$). A different non-linear combination of the NTDs produced similar results for radial bone mineral content (BMC). These results are consistent with the *in vitro* and computational studies. The UltraScan 650 therefore has the potential to become a simple, safe and effective screening tool for bone loss and fracture risk assessment. 1. Le Floch V et al. (2008) Ultrasound in Med & Biol 34:1972-1979, 2008. 2. Kaufman JJ et al. (2008) IEEE Trans Ultrason Ferroelectr Freq Control 55:1205-18.

UltraScan 650 Radius Assessment Device

***Disclosures: Jonathan Kaufman**, CyberLogic, Inc., 3*
This study received funding from: CyberLogic, Inc.

SU0312

A Comparison of Case-Finding Strategies for the Management of Osteoporosis. Eugene McCloskey*[1], Helena Johansson[2], Juliet Compston[3], Anders Oden[2], John Kanis[4]. [1]University of Sheffield, United Kingdom, [2]WHO Collaborating Centre for Metabolic Bone Diseases, United Kingdom, [3]University of Cambridge School of Clinical Medicine, United Kingdom, [4]University of Sheffield, Belgium

The aim of this study was to compare the effectiveness of the Royal College of Physicians (RCP) case-finding strategy previously used in the UK and the updated guideline published by the National Osteoporosis Guideline Group (NOGG), which incorporates the FRAX® tool to calculate fracture probability.

Comparisons were made by simulating population samples of 1000 women at ages ranging from 50 to 85 years, using age-specific prevalence of risk factors and UK-derived rates for fracture and mortality. Comparators comprised the number of women identified at high risk, the incidence of hip fracture and the femoral neck bone mineral density (BMD) in those identified, the number of BMD tests required to identify a prospective hip fracture case, the acquisition cost and the cost per hip fracture averted

Compared with the RCP strategy, NOGG identified similar or slightly reduced numbers of women at high risk (average 34.6% vs. 35.7% across all ages), but with lower numbers of scans required at each age. For example, NOGG required only 3.5 scans at the age of 50 years to identify one case of hip fracture, whereas RCP required 13.9. At the age of 75 years, the corresponding numbers needed to scan were 0.9 and 1.5. The lower number of BMD tests meant that the acquisition costs for identifying a hip fracture case and the total costs (acquisition and treatment) per hip fracture averted were also lower.

Compared to the RCP strategy, the FRAX-based NOGG strategy makes more efficient use of BMD resources with lower acquisition costs and lower costs per hip fracture averted.

***Disclosures: Eugene McCloskey**, None.*

SU0313

Association between Bone Mineral Density and Metabolic Syndrome in Korean women. Yun Kyung Jeon*, Jung Eun Huh, Ji Young Mok, Mi Ra Kim, Sang Su Kim, Bo Hyun Kim, In Ju Kim. Pusan National University Hospital, South korea

Metabolic syndrome (MS) has two conflicting factors, such as an obesity known to have a protective effect against osteoporosis and an inflammation that has been suggested to activate bone resorption. The aim of this study was to evaluate the difference of bone mineral density (BMD) in women with or without metabolic syndrome according to menopausal state. This is a cross sectional study of 2,265 women (1,234 premenopausal and 931 postmenopausal) aged over 20 years old who had visited the Health Promotion Center from January 2006 to December 2009. We measured BMD at lumbar and femur neck. Metabolic syndrome was defined by the American Heart Association/National Heart, Lung, and Blood Institute (AHA/NHLBI). The prevalence of MS was 5.5% in premenopausal women and 13.5% in postmenopausal women according to the AHA/NHLBI definition. BMD of lumbar and femur neck decreased as the number of MS components increased (for trends $p<0.001$, $p=0.003$, respectively). After adjustment for all covariates, mean lumbar BMD were significantly lower in subjects with MS in both premenopausal ($p=0.014$) and postmenopausal group ($p=0.013$). Mean femur neck BMD was also lower in women with MS in postmenopausal group ($p=0.011$) but was not different in premenopausal group ($p=0.177$). When multiple linear regression models were applied to each BMD with MS components, lumbar and femur neck BMD were correlated with age and waist circumference ($p<0.001$, respectively) and only femur neck BMD was correlated with HOMA-IR ($R2=0.156$, $p=0.001$). These findings suggest that MS was associated with a lower lumbar BMD in Korean women regardless of menopausal state. Femur neck BMD was affected by menopause than lumbar BMD. There might be a relationship between femur neck BMD and insulin resistance.

***Disclosures: Yun Kyung Jeon**, None.*

SU0314

Change in Hip Bone Mineral Density (BMD) and Risk of Fractures in Older Men. Peggy Cawthon*[1], Susan Ewing[2], Dawn Mackey[3], Howard Fink[4], Steven Cummings[5], Kristine Ensrud[6], Cora Lewis[7], Douglas Bauer[8], Jane Cauley[9], Eric Orwoll[10]. [1]California Pacific Medical Center Research Institute, USA, [2]University of California, USA, [3]CPMC Research Institute, USA, [4]GRECC, Minneapolis VA Medical Center, USA, [5]San Francisco Coordinating Center, USA, [6]Minneapolis VA Medical Center / University of Minnesota, USA, [7]University of Alabama at Birmingham, USA, [8]University of California, San Francisco, USA, [9]University of Pittsburgh Graduate School of Public Health, USA, [10]Oregon Health & Science University, USA

Low hip BMD is a risk factor for fractures in older men. However, there is little information about change in hip BMD and subsequent risk of fracture in men. Using data from the Osteoporotic Fractures in Men study (MrOS), we tested the hypothesis that greater femoral neck BMD loss was associated with increased risk of subsequent non-spine and hip fractures.

Change in femoral neck BMD was assessed in 4,470 MrOS participants who had a baseline and at least one repeat dual x-ray absorptiometry scan over an average of 4.6 $\pm$ 0.4 SD years between the baseline and final BMD measure. Change in BMD was estimated using mixed effects models, and analyzed as a continuous variable. Men were also categorized into three categories of BMD change: *maintenance* [N=1,113; change$\geq$0 g/cm^2]; *expected loss* [N=2,806; change between 0 g/cm^2 and $>$ - 1 SD below mean change ($>$-0.034 g/cm^2)]; and *accelerated loss* [N=551; change -1 SD below mean change (-0.034 g/cm^2) or worse]. Proportional hazards models were used to estimate the risk of fracture over the 3.4 $\pm$ 0.8 SD years that followed assessment of BMD change. Fracture adjudication was completed by centralized physician review of radiology reports.

The average BMD loss over 4.6 years was -0.013 $\pm$ 0.022 SD g/cm^2. During 3.4 years of subsequent follow-up, men who had maintained BMD during the BMD change period experienced fewer subsequent non-spine (N=64, 5.8%) and hip fractures (N=4, 0.4%) than men who had accelerated loss (N=57, 10.3% non-spine and N=15, 2.7% hip fractures) ($p<.002$). Compared to men who had maintained BMD, men who had accelerated BMD loss had a 1.8-fold increased risk of any subsequent non-spine fracture and a 5.8-fold increased risk of hip fracture in multivariate-adjusted models. (Table) Each additional SD of BMD loss during the BMD change period was associated with a subsequent 1.2-fold increased risk of any non-spine fracture and a 1.4 fold-increased risk of hip fracture. Exclusion of men who experienced a fracture during the BMD change period (data not shown) or adjustment for baseline BMD (table) did not substantially alter results.

In conclusion, change in femoral neck BMD is a strong risk factor for subsequent non-spine fractures, in particular hip fracture. Men with accelerated loss of BMD have a very high risk of hip fracture compared to men who maintain BMD over time.

Table. Hazard ratios (95% confidence intervals) for fracture by change in femoral neck BMD

	Risk of hip fracture		Risk of any non-spine fracture	
BMD change category	Multivariate model	Multivariate model + baseline BMD	Multivariate model	Multivariate model + baseline BMD
Maintenance	1.0 (reference)	1.0 (reference)	1.0 (reference)	1.0 (reference)
Expected loss	3.1 (1.1, 8.7)	3.0 (1.1, 8.5)	1.2 (0.9, 1.5)	1.1 (0.8, 1.5)
Accelerated loss	5.8 (1.9, 17.8)	6.2 (2.0, 19.4)	1.8 (1.2, 2.6)	1.8 (1.3, 2.6)
Per SD decrease	1.4 (1.1, 1.7)	1.6 (1.2, 2.1)	1.2 (1.1, 1.4)	1.3 (1.2, 1.4)

Multivariate models are adjusted for baseline age, weight, physical activity, self-reported heath and self-reported diabetes status, concurrent change in weight and concurrent change in physical activity

Table

***Disclosures: Peggy Cawthon**, None.*

SU0315

Circadian Clock Gene Associations with Bone Density In Older Men. Elizabeth Haney*[1], Carrie Nielson[1], Greg Tranah[2], Joseph Zmuda[3], Katie Stone[4], Eric Orwoll[1]. [1]Oregon Health & Science University, USA, [2]California Pacific Medical Center, USA, [3]University of Pittsburgh Graduate School of Public Health, USA, [4]California Pacific Medical Center-Research Institute, USA

Background: Markers of bone metabolism show circadian rhythmicity. We evaluated whether variants in circadian rhythmicity candidate genes are associated with bone traits.

Methods: We evaluated 621 haplotype tagging (HapMap phase II) and coding region SNPs in 51 genes in 2260 Caucasian men from the U.S. Osteoporotic Fractures in Men Study (IIllumina Bead Array). All had BMD measured by DXA; 1293 also had volumetric BMD measurements at the femoral neck. None reported use of bone-altering medications. Linear regression was used to test the additive model, with adjustment for age, clinic site, population substructure, height and weight. The recessive model was tested for single nucleotide polymorphisms (SNPs) in which $\geq$10 men were in the homozygous recessive category. The adjusted r2 for each SNP was also calculated to determine the amount of variation in the bone trait accounted for by

each genotype. Experiment-wide significance was set at alpha=1.0 x 10-4 to account for multiple testing, incorporating linkage disequilibrium among SNPs.

Results: Participants had a mean age of 73 years (SD 5.6). After adjustment for multiple comparisons, only retinoid X receptor alpha (RXRA) and trabecular BMD were significantly associated (Table). SNPs in DDC, PPARGC1B, RORA, NPAS2, and TPH1 were associated with DXA femoral neck BMD with p ≤0.01 (selected results in Table). SNPs in ARNTL, CRY1, RORA, RORC, and RXRA were associated with QCT femoral neck trabecular BMD. SNPs in NPAS2, NR1D, NR1D2, RPL31, DDC, and NPAS2 were associated with QCT femoral neck cortical BMD.

Conclusion: In this cohort of older men, circadian clock gene variation was associated with BMD. The retinoid X receptor forms heterodimers with vitamin D receptor, and RXRA genotype has been reported to be associated with circulating levels of vitamin D. This association may explain its association with BMD in this study. These results require validation but support emerging evidence of the involvement of clock genes in the regulation of bone phenotypes. Further research will be important to understand how circadian clock gene variants may influence bone.

Table: Circadian genes with the strongest association with femoral neck traits.

	Gene (SNP)	Minor allele frequency	B	p value	r^2
BMD (DXA)	PPARGC1B (rs1030176)	0.15	-0.017	0.001	0.005
	PPARGC1B (rs11167483)	0.16	-0.013	0.002	0.004
	DDC (rs735274)	0.24	0.012	0.002	0.004
	TPH1 (rs623580)	0.33	0.024	0.002	0.004
Trabecular BMD (QCT)	RXRA (rs11103633)	0.03	-0.020	1.9×10^{-3}	0.014
	RXRA (rs7039190)	0.04	-0.014	5.2×10^{-3}	0.009
Cortical BMD (QCT)	NPAS2 (rs9653467)	0.08	-0.053	7.0×10^{-4}	0.009
	NPAS2 (rs6729727)	0.11	0.038	7.0×10^{-4}	0.009

Analyses adjusted for age, clinic site, population substructure, height, weight. NPAS2 results are from a recessive model; others are from an additive model.
Experiment-wide significance was set at alpha=0.00014 after correction for multiple testing that incorporates linkage disequilibrium among SNPs.

Table

***Disclosures: Elizabeth Haney**, None.*

SU0316

Depressive Symptoms and Rates of Hip Bone Loss in Men. Susan Diem*[1], Stephanie Harrison[2], Elizabeth Haney[3], Katie Stone[4], Jane Cauley[5], Kristine Ensrud[6]. [1]University of Minnesota, USA, [2]San Francisco Coordinating Center, USA, [3]Oregon Health & Science University, USA, [4]California Pacific Medical Center-Research Institute, USA, [5]University of Pittsburgh Graduate School of Public Health, USA, [6]Minneapolis VA Medical Center / University of Minnesota, USA

Depression is associated with low bone mineral density (BMD) and higher rates of bone loss in some, but not all, studies. To test the hypothesis that elderly men with depression, as defined by a Geriatric Depression Scale (GDS) score of 6 or greater, have increased rates of hip bone loss, we assessed depressive symptoms using the Geriatric Depression Scale and obtained serial hip BMD measurements in a subset of 2460 older men (mean age 75.7 yrs) participating in the Osteoporosis in Men study, a prospective cohort study of community dwelling men. Hip BMD was measured in 2003-05 and an average of 3.4 years later in 2007-09.

We categorized men according to their GDS score at the first visit as not-depressed (GDS $<$ 6) and depressed (GDS $\geqslant$ 6). Using least squares means from linear regression, the adjusted mean annual percentage change in total hip BMD and two subregions of the hip were calculated for the non-depressed vs. depressed men. All results were adjusted for the following characteristics measured at the first exam: age, clinic site, race, health status, functional status, physical activity, cognitive function, calcium supplement use, vitamin D supplement use, smoking, bisphosphonate use, BMI, oral steroid use, antidepressant use, and selected comorbidities.

Age- and multivariate-adjusted mean annual percentage changes in hip BMD appear in the table below. While depression was associated with higher rates of hip bone loss in age-adjusted models, this association was largely explained by characteristics associated with depression status and no longer reached significance in multivariable models.

	Mean Annualized Rate of Hip Bone Loss by Depression Status		
Fracture Type	GDS <6 (n=2324)	GDS >6 (n=136)	p-value
Total Hip			
Age-adjusted	-0.39	-0.69	0.0017
MV model	-0.39	-0.57	0.097
Femoral Neck			
Age-adjusted	-0.45	-0.72	0.031
MV model	-0.45	-0.53	0.55
Trochanter			
Age-adjusted	-0.34	-0.64	0.0075
MV model	-0.34	-0.52	0.14

Table 1

***Disclosures: Susan Diem**, Eli Lilly, Inc., 2*

SU0317

Low Calcaneal Stiffness Index Is a Predictor of Physical Impairment Among Japanese Women: The Hizen-Oshima Study. Kiyoshi Aoyagi, Yasuyo Abe*. Nagasaki University, Japan

Decreased activities of daily living (ADL) have been reported as one of the lifestyle factors of osteoporosis. However, there is sparse data regarding the prospective association between bone mass and future decrease in ADL.

We explored the prospective associations of low calcaneal stiffness index with physical impairment among 375 Japanese women ages 40 to 87 years. Quantitative ultrasound (QUS) was performed at the right calcaneus (stiffness index), and spine radiograph was obtained between 1998 and 1999 (baseline examination). Participants were also asked if they had back pain and other painful joints at non-spine sites at baseline.

Follow-up examination was conducted in 2008. A self-administered questionnaire was used to survey participants about difficulty in performing selected basic and instrumental ADL.

Overall, 37% of women had low stiffness index, defined as t-score <-2.5, and the prevalence of low stiffness index increased progressively with age.

After adjusting for age, low stiffness index was significantly associated with bending-, spine-extension-, walking-related activity, standing endurance and heavy activity. Impaired function was defined as difficulty performing 3 or more ADLs. After adjusting for age, the odds of impaired function increased by 2.4 times (95% CI: 1.5, 4.0) in women with low stiffness index. Additional adjustment for number of prevalent vertebral deformities, back pain, number of painful joints and body mass index did not significantly alter these findings.

In conclusion, low bone mass may lead to long-term physical impairment, independent of confounding factors. Clinicians should take appropriate treatment, to prevent worsening of osteoporosis, and associated disability.

***Disclosures: Yasuyo Abe**, None.*

SU0318

Prevalence of osteoporosis in Korean population based on 2008 Korean National Health and Examination Survey(KNHANES) IIII. ILWOO JOO*[1], JunHyung Cho[2], Ji-hyun Ko[3], HanJin Oh[4]. [1]Cheil General Hospital, Kwandong University, South korea, [2]Korean society of neurosurgery, South korea, [3]Korean Society of Osteoporosis, South korea, [4]Korean Societyof Osteoporosis, South korea

Introduction : An available large-scaled epidemiologic study with representative samples of South Korean popultaion about the prevalence rate of osteoporosis and osteopenia have not been investigated extensively because of economic limitation of 'Ministry for Health, Welfare and Family Affairs' in Korea.Now we present the 2008 Korean National Health and Examination Survey(KNHANES) IIII data about the bone mineral density and prevalence of osteoporosis among the South Korean populaton aged 20 years or older. Subjects and methods : Subjects were excluded who present involved any disease that affect bone metabolism, including hyperthyroidism, hyperparathyroidism, chronic renal failure, bronchial asthma, rheumatoid arthritis and cancer. Thus, total of 3135 subjects (1367 men and 1768 women) were included without exclusion criteria. Result : Regarding the gender differences in bone mineral density, BMD at femoral neck, femoral trochanter and total hip were significantly lower in women than in men. At the lumbar spine, BMD was lower in men aged 30 to 49 than women aged 30-49. According to residential area, BMD was lower in urban 20-39 aged subjects than in rural 20-39 aged subjects, while BMD was lower in rural population than in urban population aged 40 and older at every skeletal sites. In 5 year interval, the peak bone mineral density was reached in Korean men aged 20-24 at the lumbar spine, femoral neck, femoral trochanter and total hip. However, in women, the peak bone mineral density was reached differently according to skeletal sites(20-24 at femur neck, 35-39 at lumbar spine, 40-44 at femur trochanter and total hip). The standardized prevalence of osteoporosis in Korea is 4.8% in men and 31.9% in women aged 50 years and older. Discussion : The fact that this study is the first nationwide cross-sectional survey under supervision of Ministry for Health, Welfare and Family Affairs preformed in Korea is worthwhile to focus on. The standardized prevalence of osteoporosis in Korea is 4.8% in men and 31.9% in women aged 50 years and older.

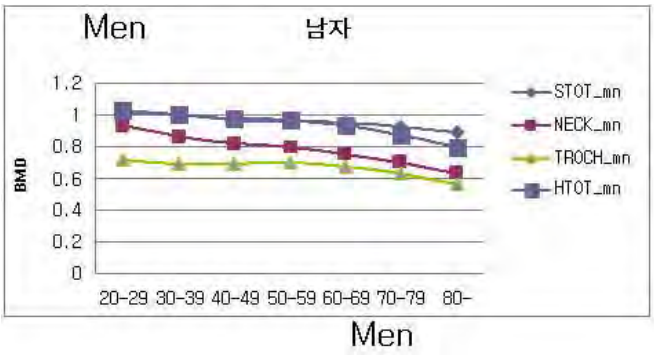

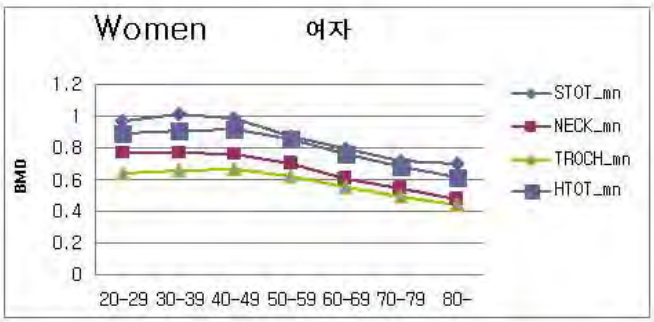

Prevalence of osteoporosis in Korean population 50 year and older according to age group

Prevalence of osteoporosis in Korean population

***Disclosures: ILWOO JOO**, None.*

SU0319

Relationships between OPG, RANKL, Bone Turnover Markers and Bone Mineral Density in Men and Women Following Hip Fracture. Julia Chan*[1], Ram Miller[1], Michelle Shardell[1], Elizabeth Streeten[2], Marc Hochberg[2], Jay Magaziner[3], Denise Orwig[3]. [1]University of Maryland Baltimore, USA, [2]University of Maryland School of Medicine, USA, [3]University of Maryland, Baltimore, USA

Objective: The RANK/RANKL/OPG system is critical to bone remodeling. However, little is known about the relationships among OPG, RANKL, bone turnover markers (BTM) and bone mineral density (BMD) in persons with hip fracture (HipFx). The objective of the present analysis was to examine the relationships between serum OPG, RANKL and BTM and BMD after HipFx and compare these relationships between men and women.

Methods: The Baltimore Hip Studies Cohort 7 (BHS7) is a longitudinal study of sex differences in functional, physiologic, and metabolic consequences of HipFx. Frozen serum from 151 BHS7 participants was analyzed for OPG, RANKL, the bone formation marker, PINP, and the bone resorption marker, CTX-I. BMD was measured by DXA. Assessments were made at baseline (within 15 days of hospitalization) and 2- and 6-months after fracture. OPG concentrations were divided into tertiles, RANKL was categorized as detectable or undetectable levels, and RANKL/OPG ratio was grouped as participants with high OPG levels and undetectable RANKL and those not fitting these criteria. Generalized estimating equations (GEE) modeled the association of OPG, RANKL, and RANKL/OPG with BTM and BMD over time, adjusting for covariates.

Results: Analyses included 151 participants (75 men and 76 women) aged 65 years and older (mean [SD] = 81.5 [7.6] years). Higher levels of OPG were associated with higher femoral neck (p=0.0084) and total hip (p=0.0017) BMD. After stratification by sex, this relationship remained significant in both men and women with total hip BMD (p=0.0008 and 0.0136, respectively) and in women only with femoral neck BMD (p=0.0014). Detectable RANKL values were not significantly associated with BTM or BMD either overall or in sex-specific analyses. The relationship between RANKL/OPG ratio and BMD followed similar patterns as OPG, whereas a relationship between the RANKL/OPG ratio and BTM was non-evident.

Conclusions: Data demonstrate that serum OPG is positively associated with BMD, with lower OPG concentrations contributing to the excess decline in BMD after HipFx. Although not significant, differences seen in the relationship between RANKL, BTM, and BMD suggest that men and women experience variations in the hip fracture recovery process.

	Femoral Neck BMD (95% CI)				Total Hip BMD (95% CI)			
	β	95% CI		p-value	β	95% CI		p-value
All Participants								
Baseline	0.04	0.02	0.06	0.0002	0.05	0.02	0.07	<0.0001
2 month	0.05	0.02	0.09	0.0047	0.06	0.02	0.10	0.0048
6 month	0.05	0.00	0.09	0.0326	0.03	-0.01	0.07	0.18
GLOBAL P	*0.0084*				*0.0017*			
Males								
Baseline	0.03	0.00	0.06	0.07	0.05	0.02	0.08	0.0019
2 month	0.03	0.00	0.07	0.06	0.05	0.02	0.08	0.0005
6 month	0.03	-0.02	0.08	0.32	0.02	-0.01	0.06	0.16
GLOBAL P	*0.22*				*0.0008*			
Females								
Baseline	0.04	0.02	0.07	0.0008	0.03	0.00	0.06	0.0429
2 month	0.07	0.04	0.11	0.0002	0.08	0.03	0.13	0.0012
6 month	0.07	0.01	0.13	0.0341	0.05	0.00	0.11	0.0496
GLOBAL P	*0.0014*				*0.0136*			

Mean difference in BTM and BMD per tertile of OPG (higher versus lower) at each time point

***Disclosures: Julia Chan**, ALPCO Diagnostics, 9; Biomedica Inc., 9*

SU0320

Sex Differences in the Fracture Prediction by Bone Mineral Density Assessed at Peripheral Sites. Diane Claflin*[1], Denise Von Muhlen[2], Heather Hofflich[3], Elizabeth Barrett-Connor[3]. [1]UCSD, USA, [2]Unoversity of California San Diego, USA, [3]University of California, San Diego, USA

Background: Osteoporotic fractures are a major public health problem. It is estimated that 1 in 2 women and 1 in 4 men over the age of 50 will have an osteoporosis-related fracture in their lifetime. Bone mineral density (BMD) at the hip is currently the preferred test to predict an osteoporotic fracture.

Method: We compared sex specific BMD measured at the heel (Hologic-Sahara), distal arm (DTX-200 DexaCare) and finger (Accudexa) with BMD of the total hip (Hologic QDR 1000) in 430 men and 620 women aged 71 +/- 9 years participants from the Rancho Bernardo Study to determine: 1) the cross-sectional clinical value of BMD assessed at peripheral sites to identify older men and women with osteoporosis, and 2) whether these peripheral measurements are associated with non-vertebral prevalent and incident osteoporotic fractures.

Results: The correlations between hip and each peripheral site BMD were r=0.55 for heel, r=0.67 for finger and r=0.72 for the distal arm, all p<0.001. Agreements between osteoporosis at the hip and finger were Kappa = 0.35; between hip and arm were Kappa=0.28, and between hip and heel were kappa=0.32, all p<0.001. Overall 17% of the men and 20% of the women reported an osteoporotic fracture at baseline, and 6.2% of the men and 4.2% of the women had an incident osteoporotic fracture during the follow up (mean 3.5, range 2 to 6 years). Sex specific multiple adjusted logistic regression models (age, BMI, exercise, current smoke and alcohol intake) showed that BMD at any of the sites measured was associated with prevalent osteoporotic fractures in women (OR=0.56, 95% CI 0.42-0.76 for hip; OR=0.51, 95% CI 0.34-0.75 for distal arm; OR=0.62, 95% CI 0.47-0.83 for finger and OR=0.54, 95% CI 0.42-0.70 for the heel), but only total hip BMD was associated with OP fractures in men (OR=0.72, 95% CI 0.52-0.99). None of the BMD sites was associated with a new (incident) OP fracture in men or women

Conclusion: In this community-based population of older men and women bone mineral density measured at the hip and peripheral sites was equivalent in identifying of women at risk for an osteoporotic fracture, but only hip BMD was a good tool to identify men with an osteoporotic fractures

***Disclosures: Diane Claflin**, None.*

SU0321

The Association Between Serum Thyrotropin (TSH) Levels and Bone Mineral Density in Healthy Euthyroid Men. Sung Jin Bae*[1], Beom-Jun Kim[2], Seung Hun Lee[3], Hong Kyu Kim[4], Jae Won Choe[4], Ha Young Kim[5], Jung-Min Koh[1], Ghi Su Kim[6]. [1]Asan Medical Center, South korea, [2]Division of Endocrinology & Metabolism, Asan Medical Center, University of Ulsan College of Medicine, South korea, [3]Asan Medical Center, University of Ulsan College of Medicine, South korea, [4]Health Promotion Center, Asan Medical Center, University of Ulsan College of Medicine, South korea, [5]Wonkwang University Sanbon Medical Center, Korea, [6]University of Ulsan, South korea

Objective : Although osteoporosis is increasingly shown to occur in a considerable proportion of men, data on risk factors for male osteoporosis are limited. In the present study, we investigated the association between serum thyrotropin (TSH) concentration and bone mineral density (BMD) in healthy euthyroid men.

Design : A cross-sectional community (health promotion center)-based survey.

Subjects and measurements : For 1,478 apparently healthy euthyroid men who participated in a routine health screening examination, we measured BMD at the lumbar spine and femoral neck using dual energy X-ray absorptiometry, and serum TSH concentrations using immunoluminometry.

Results : Lumbar spine BMD linearly increased with TSH level after adjustment for age, weight, and height (P for trend = 0.002), and statistical significance persisted after additional adjustment for smoking and drinking habits (P for trend = 0.010). When serum alkaline phosphatase was added as a confounding variable, the relationship was still significant (P for trend = 0.016). Femoral neck BMD also tended to increase in higher TSH concentration after adjustment for age, weight, and height (P for trend = 0.042), but this association disappeared after additional adjustment for smoking and drinking habits. The odds of lower BMD (i.e., osteopenia and osteoporosis combined) was significantly increased in subjects with low-normal TSH (i.e., 0.4-1.2 mU/l), as compared to high-normal TSH (i.e., 3.1-5.0 mU/l), after adjustment for confounding factors (odds ratio = 1.45, 95% CI = 1.02-2.10).

Conclusion : These results suggest that a serum TSH concentration at the lower end of the reference range may be associated with low BMD in men.

***Disclosures: Sung Jin Bae**, None.*

SU0322

Determinant of Bone Mineral density in Korean Men - A Nation wide study. Kwang Joon Kim*[1], Kyoung Min Kim[2], Sung-Kil Lim[1], Yumie Rhee[1], Han Seok Choi[3]. [1]Severance Hospital, South korea, [2]Yonsei University, South korea, [3]Dong-Kuk University hospital, South korea

Male osteoporosis is a serious health problem that cannot be overlooked. To determine the hormonal and lifestyle risk factors for low BMD in Asian men, we studied 1452 community-dwelling Korean men aged 30 years and above. Medical history and lifestyle habits were obtained with a structured questionnaire. Dietary calcium, educational status, smoking and alcohol habits, weekly activities were assessed by a semi-quantitative questionnaire. Geometry and BMD at the spine and hip were measured by dual-energy X-ray absorptiometry(DXA). Fasting blood was analyzed for 25(OH)D, parathyroid hormone (PTH), lipid profile, HbA1c and other laboratory parameters. The mean age of the cohort was 48.3 $\pm$ 16.1 (30 — 92) years. We divided subjects into 2 different groups based on the BMD. The proportion of OSteoporosis is 30.6% when we used young average mean (YAM) of Korean BMD. However, when we use the YAM of Japam, the ratio is just 4.3%. It might be caused by the difference between peak BMD of Korean and Japan. These discrepancy need to be addressed. Univariate logistic regression analysis showed that age, body mass index (BMI), Audit score, cigarette smoking, energy intake, weight bearing exercise, level of education, all of geometry data independently associated with osteoporosis. In the linear regression model, weight, age, body mass index (BMI) were signi?cant determinants of total hip and femur neck BMD. Body mass index being the most important determining factor. After adjusting for age and body mass index (BMI), weight bearing exercise was identified as additional determinants of total hip and femur neck BMD. In the linear regression model, weight, age, body mass index (BMI) were signi?cant determinants of total hip BMD. Strategies to prevent bone loss and osteoporosis in Asian men should include lifestyle modi?cation such as weight bearing exercise regulary and quit smoking. Furthermore, the diagnostic criteria of osteoporosis should be based on the YAM of their own county, especially developing country such as Korea.

***Disclosures: Kwang Joon Kim**, None.*

SU0323

Development and Validation of a Food Frequency Questionnaire for Assessing Macronutrient and Calcium Intake in Women Residing in Karachi, Pakistan. Romaina Iqbal, Gulshan Bano, Mujtaba Bilgrami, Farhan Dar, Aysha Khan*. Aga Khan University, Pakistan

Introduction:

Culture or region specific Food Frequency Questionnaires (FFQ) are developed to assess nutrient intake because foods vary between culture and region. Here we report the development and validation of an FFQ against multiple 24 hour recalls.

Methods:

The list of food items for the FFQ was developed through 24 hour recalls conducted on (n=70) participants visiting AKUH pathological labs collection points in 5 different areas of Karachi. The final FFQ had 57 food items, 7 categories for frequency of intake and a fixed portion size column. We validated the FFQ against 4 24 hour recalls conducted over a period of one year in healthy women residing in Karachi. We also looked at the agreement between quartiles of nutrients estimated by FFQ versus quartiles of nutrient estimates of mean 24 hour recalls using kappa statistics. Furthermore we validated nutrient estimates against certain indirect measures of nutrient intake i.e. BMI and serum NTX levels.

Results:

The mean estimate of energy 1644 and 1399(kcal), Protein 55.0 and 45.6(g), Fat 61.7 and 52.7(g), and calcium 610.7 and 468.7 (mg) for FFQ and mean of 4 24 hour recalls, respectively. All of the correlations between mean of 24 hr recalls estimates and FFQ were significant and ranged between 0.15-0.36. All macronutrients had a strong correlation with BMI but we did not observe a significant correlation between calcium intake measured by the FFQ and serum NTX.

Conclusion:

We developed a FFQ for assessing macro nutrient intake of Pakistani women residing in Karachi.

***Disclosures: Aysha Khan**, None.*

SU0324

Lean Mass is a Stronger Determinant of BMD than Fat Mass in Young Women with a History of Anorexia Nervosa. Esther Waugh*, Cheryl Chase, Gillian Hawker. Women's College Hospital, Canada

In healthy young women, evidence indicates that lean mass has a greater effect than fat mass on bone density. This cross-sectional study examined whether this relationship persists in the setting of anorexia nervosa (AN) where the adaptation of bone mass to muscle loading may be altered due to an abnormal hormonal environment. Participants were women aged 17-40 yrs who had received inpatient treatment for AN. Illness history was obtained using a Life History Calendar interview. DXA was used to measure fat mass (FM), lean mass (LM) and BMD at the lumbar spine L1-L4 (LS), femoral neck (FN) and total body (TB). Participants were considered recovered if they had achieved a BMI $\geq$ 18.5 kg/m^2 and resumed regular menstruation for $\geq$ 1 yr. Linear regression was used to examine the association between BMD (g/cm^2) and FM (kg) and LM (kg) adjusting for height (cm), age, duration and severity (lowest BMI) of illness and duration of recovery.

We recruited 190 participants: 77recovered, 113 ill. At interview, mean age was 27.2 $\pm$ 5.6 yrs, age at onset was 18.2 $\pm$ 4.2 yrs, duration of illness was 5.2 $\pm$ 4.4 yrs and lowest BMI was 13.2 $\pm$ 2.3 kg/m^2. Compared to recovered participants, those ill had lower mean BMI (17.9 vs 21.6), % fat (22.2 vs 32.1%), FM (10.9 vs 17.9 kg) and LM (35.3 vs 37.1 kg). In ill patients, LM was associated with illness duration (r = -0.43, p<0.0001) and lowest BMI (r=0.36, p<0.0001); FM was not associated with any illness characteristic. In recovered participants, no associations were seen between LM or FM and illness characteristics. In ill patients, LM had a greater effect than FM on BMD at each skeletal site; LM was significantly associated with FN (LM: 0.009, p=0.03; FM: 0.0009, p=0.67) but not LS (LM: 0.005, p=0.22; FM 0.003, p=0.19) or TB (LM: 0.004, p=0.06; FM: 0.002, p=0.08). In recovered patients, LM had a greater effect than FM and was significantly associated with FN (LM: 0.01, p=0.01; FM: -0.002, p=0.53) and TB (LM: 0.006, p=0.01; FM: 0.003, p=0.09); FM had a greater but non-significant effect at LS (LM: -0.002, p=0.62; FM: 0.003, p=0.27).

We conclude that, as in healthy women, LM contributes more strongly than FM to BMD in both ill and recovered AN patients, particularly at the FN. This suggests that strategies such as exercise may be beneficial in certain patients to preserve or increase lean mass, potentially reducing fracture risk.

***Disclosures: Esther Waugh**, None.*

SU0325

Premenopausal BMD Loss and its Relationship to Prolonged Lactation and Poor Nutrition: A Study Using Mediaeval Skeletons. Gordon Turner-Walker[1], Simon Mays*[2]. [1]School of Cultural Heritage, National Yunlin University of Science & Technology, Taiwan, [2]English Heritage for Archaeology, United Kingdom

During lactation there is normally a decrease in maternal bone mineral density (BMD) but this is normally quickly recovered once lactation ceases. However, some studies suggest that recovery of lactational loss of BMD may not occur in women in developing countries where lactation is prolonged and nutrition poor, but that their loss in BMD is permanent. At a population level this leads to depressed BMD in the later reproductive years. It is unclear whether women in populations of European ancestry show a similar decline in BMD in their reproductive years if lactation is prolonged and nutrition poor. This work attempts to address this question using skeletons (N=129) of Mediaeval peasants from an English churchyard. BMD is measured at the femur neck using DXA. Duration of breastfeeding was estimated using nitrogen stable isotopic analysis of bone collagen. Nutritional level of the population was assessed using skeletal growth in children. We have previously speculated a link between premenopausal BMD loss in archaeological populations and prolonged lactation in poor living conditions, but this study is the first time in which data on BMD, duration of lactation, and nutrition have been available for a single archaeological population, enabling close investigation of that hypothesis.

The nitrogen stable isotopic analyses suggests breastfeeding in this community normally continued for about 18 months post partum. Child growth resembles that of 19th century urban slum children, indicating that nutrition was poor. In Mediaeval males, age-related loss in BMD resembles that seen in modern European men. In females, although post-menopausal BMD loss resembles that in modern European women (age at menopause in the past was similar to that today), there was evidence for loss of BMD in the reproductive years: in the 30-50 yr age group, mean BMD=0.920gcm^{-2} vs 1.102 gcm^{-2} for 18-30 yr age group, p=<0.001. The decrease in female BMD in Mediaeval women's later reproductive years resembles that reported in populations in the developing world today where prolonged breastfeeding occurs in conditions of poor nutrition. Although determinants of BMD in women are complex, it may be that BMD losses in Mediaeval English women during lactation were not regained due to poor living conditions. This suggests that non-recovery of BMD lost during lactation may be a potential problem for poorly nourished women of European ancestry as well as for those in the developing world.

***Disclosures: Simon Mays**, None.*

SU0326

Skin Colour Change in Caucasian Postmenopausal Women Predicts Seasonal Change in 25-hydroxyvitamin D: Findings from the ANSAViD Cohort Study. Helen Macdonald*[1], Alexandra Mavroeidi[2], Lorna A. Aucott[2], Brian Diffey[3], Anthony Ormerod[2], William D. Fraser[4], David Reid[2]. [1]University of Aberdeen Bone & Musculoskeletal Research Programme, United Kingdom, [2]University of Aberdeen, United Kingdom, [3]University of Newcastle, United Kingdom, [4]University of Liverpool, United Kingdom

UV radiation is responsible for vitamin D synthesis and skin tanning. There are no longitudinal data relating skin colour to vitamin D status. The aim of this study was to determine whether seasonal changes in facial skin colour are related to changes in vitamin D status in women living at 57♂N latitude.

314 Caucasian women aged 60-65 y (mean age±SD 62.3±1.4 years) from the Aberdeen Nutrition Sunlight and Vitamin D (ANSAViD) study attended 5 visits over 15-months, starting spring 2006. At 3-monthly intervals, skin colour was assessed on both cheeks and the forehead, using a CM-2600d spectrophotometer, and expressed as the individual topographical angle [ITA] (higher number indicates paler skin). Total 25-hydroxyvitamin D [25(OH)D] was measured by immunoassay. Use of sunscreen and cosmetic products containing UV filters was evaluated.

Most women had Fitzpatrick sun-reactive skin type III (43%), followed by skin types II (32%), and I, the most sun-sensitive skin type (always burns, never tans) (25%). Skin colour [ITA] showed significant seasonal variation for all skin types, with skin type III having the greatest spring-summer (or summer-winter) colour difference. Overall, mean (SD) ITA in degrees were 36.6 (7.7), 38.2 (6.5) and 42.8 (5.3) respectively for summer, autumn and winter ($P<0.001$). Linear regression adjusting for confounders showed that for each 1° summer-winter change in ITA, there was a corresponding increase of 0.8 nmol/L 25(OH)D ($p<0.001$). Skin colour did not change according to quartile of BMI but mean 25(OH)D (nmol/L) was significantly lower for the top BMI quartile (Q4, BMI>30.9 kg/m^2) compared to the other quartiles (spring: p=0.014, Q1 41.1, Q4 33.7; summer: p=0.010, Q1 57.1, Q4 49.7).

Figure.

These longitudinal data show that seasonal skin colour changes predict 25(OH)D changes. Low vitamin D status in obese women was not due to reduced sun exposure compared to lean women, suggesting that it may be due to increased requirements or inaccessibility of vitamin D stores. Further work is required to determine whether tissue stores accumulated in the summer months are sufficient for optimum health in the winter.

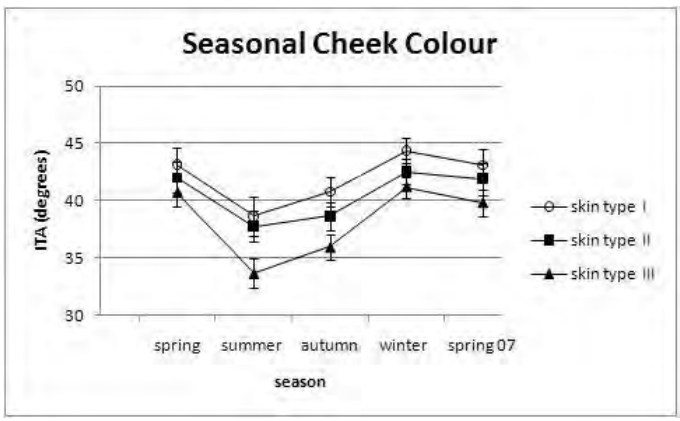

Seasonal changes in skin colour according to skin type

***Disclosures: Helen Macdonald**, None.*

SU0327

Study about Relationships between Young Age's Body Mass Index (BMI) and Postmenopausal BMI for Bone Mineral Density (BMD) in Postmenopausal Osteoporosis Patients. Dongwon Byun*, Jioh Mok, Heeja Ko, Jiyon Kim, Chanhee Jung, Sungwan Jeon, Younhee Park, Wonson Jeon, Hyeongkyu Park, Yeoju Kim, Chulhee Kim, Sangjin Kim, Kyoil Suh, Myunghi Yu. Soon Chun Hyang University Hospital, South korea

Background: Among the various kinds of osteoporosis's risk factor, body weight (BW) is one of the most important factor for osteoporotic fracture. But young age's BW or body mass index (BMI) is not studied for the relationship with BMD in postmenopausal patients. So author investigated the relationships between young age's BMI and postmenopausal BMI for BMD in postmenopausal Korean women.

Subjects and methods: From Jan. 2005 to Sep. 2009, total 109 postmenopausal women who visited endocrinology department of Soonchunhyang University Hospital were enrolled. All the subjects were checked current and young age's BW, BMI and BMD. Patients were devided by 2 groups, one was osteoporosis group (OS, n=38) and the other was normal and osteopenia group (OP, n=37).

Results: Total 75 subjects who's mean age was 61.07 years and BMI was 23.5 kg/m^2 were included. BMI at young age was 20.29 kg/m^2 in osteoprosis (OS) group and 20.30 kg/m^2 in normal and osteopenia(OP) group which showed no statistical difference. BW after postmenopausal period showed significant correlations with lumbar spine (r=0.292, p=0.011), femur neck (r=0.283, p=0.014), total hip (r=0.271, p=0.019). But BW at young age showed significant correlations only with lumbar spine (r=0.265, p=0.021).

BW change from young age to postmenopausal period showed significant difference (p=0.03) between OS group (5.23 ± 7.21 kg) and normal and OP group (9.81 ± 10.31 kg).

Conclusion: Young age's BW was only correlated with lumbar spine BMD and young age's BMI were not correlated with BMD. BW changes are bigger in normal and OP group than OS group which means that weight gain after peak bone mass formation to menopausal period is more important than young age's BW for prevention of osteoprosis.

***Disclosures: Dongwon Byun**, None.*

SU0328

The Relationship between Body Mass Index and the Risk of Peripheral Fragility Fracture. Louis Bessette*[1], Sonia Jean[2], Sophie Roy[3], K. Shawn Davison[1], Louis-Georges Ste-Marie[4], Jacques Brown[1]. [1]Laval University, Canada, [2]Institut National De Sante Publique, Canada, [3]Institut national de santé publique du Québec, Canada, [4]Hospital Saint-LucCHUM, Canada

Purpose: The objective of this analysis was to evaluate the association between body mass index (BMI) and the occurrence of peripheral fragility fracture (FF).

Methods: ROCQ is an ongoing prospective cohort study of women over 50y of age who have sustained a FF or traumatic fracture (TF). Women who recently suffered a FF or TF were recruited from hospitals and from an administrative database-generated list of women who had recently suffered a FF or TF (Quebec Ministry of Health). All subjects were contacted by phone 6-8 months following fracture to complete a questionnaire on demographic features, clinical characteristics, and risk factors for osteoporosis. FF was defined as a fracture occurring spontaneously or following a minor trauma, such as a fall from standing height, a fall from the sitting position or a fall from laying down on a bed or a reclining deck chair from less than a meter high, a fall after having missed 1 to 3 steps in a staircase, after a movement outside of the typical plane of motion, or coughing. Few women with vertebral fractures were recruited, thus this site was not considered in this analysis. BMI was calculated using self-reported weight and height and was validated via weight and height from clinic records of 100 women randomly selected from the cohort (r=0.96).

Results: The questionnaire was completed by 2712 women (2079 FF and 633 TF). Mean (SD) age of FF and TF was 64.1y (9.5) and 60.8y (7.6), respectively. The most frequent fracture sites for both FF and TF were wrist, ankle, humerus, and the hip region, with all sites having similar proportions of FF (80-90%). Women with a BMI ⩾25kg/m^2 experienced 59% of the FF and 56% of the TF. In univariate analyses, being underweight (BMI<18.5kg/m^2) was a significant risk factor for FF at the wrist (OR: 1.43 95% CI 0.45-6.38) or hip (OR: 1.96 95% CI 0.42-14.0), but a decreased risk for FF at all other fracture sites (OR: 0.40 95% CI 0.16-1.06), all as compared to obese women (BMI ⩾30kg/m^2). Multivariate analyses are underway to understand the association between BMI, bone mineral density results, and risk of FF by fracture site.

Conclusions: Few studies have evaluated the effect of BMI on fracture risk. The effect of BMI on FF risk may vary depending on fracture site with those being underweight having a greater risk of wrist or hip fracture and those overweight or obese having a greater risk at all other osteoporotic sites.

***Disclosures: Louis Bessette**, Bristol-Myers-Squibb, 2; Pfizer, 8; Warner Chilcott, 8; Novartis, 8; Roche, 5; Eli Lilly, 2; Amgen, 8; Abbott, 5; Abbott, 2; Merck, 8; Amgen, 5; Pfizer, 2; Pfizer, 5; Novartis, 5; Merck, 5; Roche, 2; Roche, 8; Merck, 2*
This study received funding from: Warner Chilcott, sanofi-aventis, Merck, Amgen, Eli Lilly, Novartis

SU0329

Vitamin K and Bone Health: An Updated Systematic Review and Meta-analysis. Joanna Wadsworth[1], Andrea Darling*[1], Martin Shearer[2], Michelle Gibbs[1], Joy Adamson[3], David Torgerson[3], Susan Lanham-New[1]. [1]University of Surrey, United Kingdom, [2]St Thomas's Hospital, United Kingdom, [3]University of York, United Kingdom

Previous research suggests vitamin K may increase bone mass, prevent loss of bone mineral density (BMD), and possibly reduce fracture incidence. The purpose of this study was to update the systematic review and meta-analysis of the effect of both vitamin K1 and vitamin K2 (menaquinone-4 and menaquinone-7) on bone turnover, BMD and fracture risk that we published in 2007 in the light of key vitamin K supplementation studies completed in the last 30 months. The Cochrane Library (1994-2009) and EMBASE (1980-2009) databases were searched for relevant cross-sectional, longitudinal and intervention studies. Thirty three studies were included in the systematic review and seven in the meta-analysis.

Results from the systematic review for vitamin K1 suggested a significant negative correlation with undercarboxylated osteocalcin (ucOC), but mixed results for total OC, bone resorption markers and fracture, and no association with BMD. The meta-analysis supported these results, showing a significant effect of vitamin K1 supplementation on reducing ucOC ($p<0.00001$, Z=15.59, weighted mean differ-

ence=-21.23 95% CI (-23.90 to-18.57)), but no significant effect on BMD at any site (P=0.78, Z=0.28, weighted mean difference=0.00, 95%CI (0.00 to 0.01)). There was insufficient data to analyse fracture incidence, bone resorption or OC in the K1 meta-analysis.

Results from the systematic review of K2 studies showed a significant negative association of K2 on ucOC in intervention studies. The intervention studies, but not cross-sectional studies, independently associated vitamin K2 with fracture risk. No effect of vitamin K2 supplementation on bone resorption was found for any study type, but the intervention studies were associated with increased BMD. This was supported by results from the vitamin K2 meta-analysis for a reduction in ucOC ($p<0.00001$, Z=8.75, weighted mean difference=95% CI (-68.54 to-43.45)) and increased BMD from combined sites (p=0.004, Z=3.86, weighted mean difference=95% CI (1.24-6.48)).

These findings suggest vitamin K; especially K2, may be beneficial for bone health, as ucOC is an independent risk factor for osteoporotic fracture. In this analysis, K2, but not K1 supplementation, was associated with increased BMD. However, overall the results from the studies were too conflicting to recommend routine supplementation. Further, higher quality and more homogenous studies are needed before any clear conclusions can be made about vitamin K and bone health.

***Disclosures: Andrea Darling**, None.*

SU0330

Clinical Vertebral Fractures Result in More of a Health Burden and Hospitalization than Other Osteoporotic Fractures. The AGES-Reykjavik Study. Kristin Siggeirsdottir*[1], Thor Aspelund[1], Brynjolfur Y Jonsson[2], Brynjolfur Mogensen[3], Anna H Bjornsdottir[1], Lenore Launer[4], Tamara B Harris[4], Gunnar Sigurdsson[5], Vilmundur Gudnason[1]. [1]Icelandic Heart Association Research Institute, Iceland, [2]Malmo University Hospital, Department of Orthopedics, Sweden, [3]National University Hospital, Department of Orthopedics, Iceland, [4]National Institute on Aging, USA, [5]Landspitali, Iceland

In aging populations an understanding of the determinants of decline of function after fracture is of importance. The aim was to investigate decline in health after clinical fractures, especialy vertebral with respect to function, quality of life and hospitalization.

5764 free living individuals born between 1907 and 1935 from the population based cohort study Age, Gene/Environment Susceptibility (AGES)-Reykjavik Study were examined between 2002 and 2006 and followed until April 2009 for an average of 4.8 years. The impact of sustained fracture on future hospitalization was prospectively assessed using the Cox proportional hazards model in individuals with history of any vertebral fractures, other osteoporotic fractures and without fractures as a control group. The main outcome was the relative risk (RR) for hospital admission, by reason for hospitalization, duration of hospitalization, and cross sectional association between fracture status and mobility, strength, activities of dayly living (ADL) and quality of life (QoL). Prior osteoporotic fractures conferred an increased risk of hospitalization compared with the controls; RR;1.3 ,95% confidence interval (CI), 1.2-1.5, (P=0.0002), for vertebral fractures and RR; 1.1, (95% CI, 1.1-1.2), (P=0.002), for other osteoporotic fractures. This was seen for all the most common hospitalization diagnosis. Furthermore those with previous vertebral fracture had on average 60% longer hospital stay than those in the control group ($P<0.0001$). History of osteoporotic fractures was reflected in a consistently worse performance assessed by functional tests and ADL in both sexes and QoL for women only. This was especially pronounced for those with vertebral fractures. Individuals with clinical vertebral fractures carried more of a health burden than those with other types of osteoporotic fractures. It is thus important to pay greater attention to the care of those with osteoporotic fractures and in particular vertebral fractures with regard to complication and consequent diseases.

***Disclosures: Kristin Siggeirsdottir**, None.*

SU0331

Confounding in Pharmacoepidemiologic Studies of Fracture Risk. Suzanne Cadarette, Lindsay Wong*. Leslie Dan Faculty of Pharmacy, University of Toronto, Canada

Background: Pharmacoepidemiologic studies are essential in post-marketing surveillance to assess the real-world effects of pharmacotherapy. Results of studies that rely on healthcare utilization (administrative claims) databases, however, may be prone to residual confounding due to missing information. An independent risk factor for osteoporotic fracture is a confounder when its prevalence is imbalanced between drug exposure groups under comparison. If a confounding factor is not controlled for, its effect on fracture risk is falsely attributed to drug effects. Thus, better understanding of missing data that may lead to residual confounding will help assess the validity of pharmacoepidemiologic results. We therefore sought to identify major risk factors for fracture that are unmeasured in claims data.

Methods: We used MEDLINE literature, Statistics Canada documentation and results from an Ontario community study about osteoporosis to identify risk factors for osteoporotic fracture and their prevalence among female Ontario seniors. Risk factors were categorized as major or minor according to their strength of association with osteoporotic fracture based on estimates of relative risk (RR), and their prevalence among Ontario women aged 65 or more years. We focused on identifying major risk factors for osteoporotic fracture that are not captured by Ontario claims data.

Results: Low bone mineral density (T<-2.5; RR=2.6, prevalence=30%), prior adult fracture (RR=2.2, prevalence=25%), a marker of frailty/strength (use of arms to stand from a chair, RR=2.6, prevalence=41%), and history of falls (RR=1.8, prevalence=26%) were identified as major independent risk factors unmeasured in claims data. Although clinical fractures are available using claims data, most pharmacoepidemiologic studies only consider fractures within a 1-year lookback from treatment initiation. Failure to control for these four major risk factors may lead to biased results if imbalance exists between comparison drug exposure groups.

Conclusions: We identified four major independent risk factors for osteoporotic fracture unmeasured in claims data that are prevalent in female Ontario seniors. Controlling for these potential unmeasured confounders may strengthen the validity of estimated drug effects on fracture risk. Supplementing claims data with external data sources that contain these unmeasured risk factors is a promising method to adjust for residual confounding. Our results may also be useful in theoretical sensitivity analyses that consider the potential residual confounding effects of these unmeasured factors.

***Disclosures: Lindsay Wong**, None.*

SU0332

Economic Burden of Osteoporosis-related Fracture Hospitalizations in France. Milka MARAVIC*[1], Alexandre VAINCHTOCK[2], Baptiste JOUANETON[2], VALERIE TOCHON[3]. [1]Département d'Information Médicale, Hôpital Léopold Bellan, France, [2]HEVA, France, [3]Amgen, France

Objective. To estimate the number and costs of hospitalizations associated with postmenopausal osteoporosis-related fractures in France.

Methods. Data were extracted from the 2008 Hospital National Database (PMSI). Inclusion criteria were established according to ICD-10 codes related to osteoporosis as the primary or secondary diagnosis (if the primary diagnosis was dorsalgia, dorsopathy or fractures others than of the skull, cervical vertebra, fingers or toes). Hospital stays were selected for women aged ⩾50 years. Hospitalizations associated with chemotherapy were excluded (N = 19,461 hospitalizations). As the rules of coding are not strictly followed in real practice, an additional database analysis was performed to include stays related to surgical management of hip fractures, coded as primary diagnosis after exclusion of polytrauma or fracture related to cancer (N = 50,848 hospitalizations). Duplicate hospitalizations were excluded (N = 2502). We assessed number of hospitalizations, number of patients, type of hospital and management, and length of stay and costs. Hospital costs were calculated according to the public and private hospital tariff (2009€)[1].

Results. There were 67,807 hospitalizations (64,793 patients) associated with osteoporosis-related fractures; 83% of the patients ⩾75 years and 83% of the total hospitalizations were in patients ⩾75 years. A total of 76% of the hospitalizations occurred in public care hospitals and 80% were associated with the surgical management of fractures. The overall cost of hospitalizations was 415,429,993€ of which 4.2% was related to medical devices. Women aged ⩾75 years accounted for 88% of the total costs for hospitalizations. The mean (SD) length of stay was 12.1 ± 7.89 days. The mean (SD) hospital cost including medical devices was 6127€ ± 2352€.

Conclusion. In 2008, postmenopausal osteoporosis-related fracture hospitalizations were associated with a substantial economic burden in France. Patients aged ⩾75 years accounted for 88% of the total costs.

[1] Arrêté du 27 février 2009 fixant pour l'année 2009 les ressources d'assurance maladie des établissements de santé exerçant une activité de médecine, chirurgie, obstétrique et odontologie, French Official Journal. Feb 28th, 2009.

***Disclosures: Milka MARAVIC**, AMGEN France SAS, 5*
This study received funding from: AMGEN SAS, Paris, France

SU0333

Fragility Fractures and the Osteoporosis Care Gap in Women: the Canadian Multicentre Osteoporosis Study. Lisa-Ann Fraser*[1], George Ioannidis[2], Jonathan Adachi[3], Laura Pickard[4], Stephanie Kaiser[5], Jerilynn Prior[6], Jacques Brown[7], David Hanley[8], Wojciech P. Olszynski[9], Tassos Anastassiades[10], Sophie Jamal[11], Robert Josse[12], David Goltzman[13], Alexandra Papaioannou[14]. [1]University of Western OntarioMcMaster University, Canada, [2]Sympatico, Canada, [3]St. Joseph's Hospital, Canada, [4]McMaster University, Canada, [5]Dalhousie University, Canada, [6]University of British Columbia, Canada, [7]Laval University, Canada, [8]University of Calgary, Canada, [9]University of Saskatchewan, Canada, [10]Queen's University, Canada, [11]The University of Toronto, Canada, [12]St. Michael's Hospital, University of Toronto, Canada, [13]McGill University Health Centre, Canada, [14]Hamilton Health Sciences, Canada

Purpose: A history of prior fragility fracture is strongly predictive of future fracture risk. Previous studies have indicated that, despite good evidence for the efficacy of osteoporosis therapies, women with fragility fractures are not receiving the indicated treatment. However, most previous reports involve follow-up of post fracture clinics and acute care visits and cover only a relatively short period of time. We aimed to describe post fracture care in Canadian women using a large, population-based prospective cohort that began in 1995-1997.

Methods: We followed 5566 women over 50 years of age from across Canada over a period of 10 years in the Canadian Multicentre Osteoporosis Study. Information on medication use and incident clinical fragility fractures was obtained during a yearly questionnaire or interview and fractures were confirmed by radiographic/medical reports.

Results: Over the 10 year study period, 42-56% of women with yearly incident clinical fragility fractures were not treated with an osteoporosis medication. During year 1 of the study, 22% of the women who had experienced a fragility fracture were on treatment with a bisphosphonate and 26% were on estrogen+/-progesterone (hormone) therapy (HT). We were not able to differentiate HT use for menopause symptoms vs osteoporosis. Use of bisphosphonate therapy increased over time; odds ratio (OR) for use at year 10 compared to use at year 1 was 3.65 (95%CI 1.83-7.26). In contrast, HT use declined, with an OR of 0.07 (95%CI 0.02-0.24) at year 10 compared to year 1 of the study. By year 10 of the study, 46% of women with incident fragility fractures were on therapy with a bisphosphonate and 4% were on HT. In women with a bone mineral density (BMD) T-score <-2.5, independent of fracture status, 51% were on therapy for osteoporosis at year one, with a trend towards higher rates of treatment (65% at year 10) over time.

Conclusion: In a large population-based cohort study we found a therapeutic care gap in women with osteoporosis and fragility fractures. Although bisphosphonate therapy usage in women with fragility fractures and those with BMD T-scores <-2.5 improved over time, probably reflecting increased osteoporosis care, a substantial gap remains.

Odds of a woman with an incident fragility fracture being on medical treatment for osteoporosis in year one versus subsequent years, prospectively documented in women aged 50 and older in the Canadian Multicentre Osteoporosis Study

Year of CaMos Study	Any Osteoporosis Therapy[a]		Bisphosphonate Therapy		Hormone Therapy	
	OR[b]	95% CI	OR	95% CI	OR	95% CI
2	1.15	0.66-2.00	1.69	0.90-3.2	0.82	0.45-1.52
3	0.95	0.53-1.73	1.74	0.88-3.42	0.60	0.35-1.04
4	1.42	0.77-2.61	2.72	1.31-5.62	0.68	0.33-1.41
5	1.09	0.64-1.84	1.90	0.97-3.70	0.60	0.32-1.11
6	1.21	0.70-2.10	2.25	1.19-4.27	0.76	0.43-1.35
7	1.51	0.85-2.69	3.57	1.79-7.15	0.27	0.10-0.72
8	1.67	0.94-2.98	3.94	1.99-7.80	0.28	0.11-0.70
9	1.50	0.88-2.55	4.14	2.21-7.74	0.15	0.06-0.36
10	1.16	0.65-2.07	3.65	1.83-7.26	0.07	0.02-0.24

[a]Hormone therapy, calcitonin, SERM, or bisphosphonate
[b]Odds ratio controlled for BMD, age, smoking and early menopause status

Table 1.

***Disclosures: Lisa-Ann Fraser**, None.*
This study received funding from: Merck Frosst Canada Ltd.; Eli Lilly Canada Inc.; Novartis Pharmaceuticals Inc.; The Alliance: sanofi-aventis & Procter and Gamble Pharmaceuticals Canada Inc.; Servier Canada Inc.; Amgen Canada Inc.; The Dairy Farmers of Canada

SU0334

FRAX: Does Fracture Prediction Differ by Race/Ethnicity? Jane Cauley*[1], Andrea Z. LaCroix[2], Chunyuan Wu[2], Beth Lewis[3], Jean Wactawski-Wende[4], Kamal Masaki[5], Karen Johnson[6], Mary Jo O'Sullivan[7], Rebecca Jackson[8], Susan Hendrix[9], John Robbins[10]. [1]University of Pittsburgh Graduate School of Public Health, USA, [2]Fred Hutchinson Cancer Research Center, USA, [3]University of Alabama, USA, [4]University at Buffalo, USA, [5]University of Hawaii at Manoa, USA, [6]University of Tennessee Health Science Center, USA, [7]Leonard M Miller School of medicine at the University of Miami, USA, [8]The Ohio State University, USA, [9]Wayne State College, USA, [10]University of California, Davis Medical Center, USA

A web-based risk assessment tool (FRAX) using clinical risk factors with and without femoral neck bone mineral density (BMD) has been incorporated into clinical guidelines for the treatment of osteoporosis. The majority of the cohorts used to develop this tool were Caucasian. FRAX calculations for US ethnic groups make assumptions about the relative risk of hip fractures in these ethnic groups in comparison to Caucasians. The objective of the current analysis is to examine whether fracture prediction with FRAX is similar across ethnic group. The FRAX tool (US version 3) was calculated for 133,533 Caucasian; 14,627 African American; 6,512 Hispanic; 715 American Indian and 4,192 Asian women enrolled in either the Clinical Trials (CT) or Observational Study (OS) of the Women's Health Initiative. BMD was available on a subset of 8,819 Caucasian; 1,574 African American; 738 Hispanic; 149 American Indian and 36 Asian women. Fractures were identified over an average follow-up of 10.3 years; all fractures were confirmed by radiographic reports in the CT women. For OS women, hip fractures and all fractures in the 3 BMD clinics were confirmed; we relied on self-report of fractures at the remaining clinical sites. The FRAX algorithm calculates 4 fracture probabilities for each participant: the 10-year probability of hip fracture (with and without BMD) and the 10 year probability of major osteoporotic fracture (defined as hip, clinical spine, wrist or humerus) with and without BMD. Because of a small number of hip fractures in non-whites, we focused on the FRAX score for major osteoporotic fractures. Outcomes included major osteoporotic fractures and all clinical fractures (except fingers, toes, face, skull and sternum). Areas under the curve (AUC) statistics from receiver operating characteristic curve analyses were compared across ethnicity. Women ranged from an average age of 60.3 to 63.6 years at baseline. The AUCs were higher for FRAX models with BMD and for FRAX models predicting the 4 major osteoporotic fractures in all women, irrespective of their ethnicity, Table.

The AUC for African American women for FRAX models without BMD was significantly lower that the AUC for Caucasian women. Our results suggest that there may be ethnic differences in the sensitivity and specificity of FRAX for fracture prediction.

Table: AUC for FRAX 10-year probability of major osteoporotic fracture across ethnicity

	Caucasian		African American		Hispanic		American Indian		Asian		
	# fx	AUC	# fx	AUC	# fx	AUC	# fx	AUC	# fx	AUC	P value
Major osteoporotic fractures (hip, wrist, spine, humerus)											
FRAX w/o BMD	12476	0.64	358	0.61*	252	0.63	40	0.61	208	0.67	0.11
FRAX with BMD	580	0.71	20	0.69	22	0.68	7	0.63	1	---	0.92
	Caucasian		African American		Hispanic		American Indian		Asian		
All clinical fractures											
	# fx	AUC	# fx	AUC	# fx	AUC	# fx	AUC	# fx	AUC	P value
FRAX w/o BMD	26693	0.58	1271	0.54*	687	0.57	110	0.61	484	0.58	<0.001
FRAX with BMD	1496	0.62	113	0.58	69	0.61	20	0.69	6	----	0.42

*Pairwise comparisons: P<0/001 vs. Caucasians

Table

***Disclosures: Jane Cauley**, None.*

SU0335

Functional Capacity and Survival after One Year of Hip Fracture in Brazilian Older People: A Prospective Study. Adriana Machado*, Gilberto Pereira, Jose Eduardo Corrente. Univ Estadual Paulista, Brazil

Due to its high morbidity, mortality and cost, hip fracture is considered to be the most dramatic consequence of osteoporosis. In Brazil, there is a lack of prospective studies to evaluate function and survival in such patients. In this study, functional capacity and survival in older patients with proximal femur fractures (caused by low trauma or spontaneous) were evaluated during a one-year follow-up at a university hospital in a medium-sized city in São Paulo state, Brazil. Follow-up occurred during hospitalization, 1, 3, 6 and 12 months after the fracture. Function capacity was studied by using the activities of daily living (ADL) scale, which ranges from 0 to 6 (0 to 4 classified as dependent and 5 and 6 as independent). Pre-fracture functional status was considered to be that in the week prior to fracture. Sixty-four patients (44 females and 20 males) consecutively admitted to our hospital from April to December 2008 were studied. Mean age was 80 years (SD, 8, range 60 to 98). After 12 months, 41 patients survived (64%). Survival rates were 50% for males and 70% for females. As estimated by the Kaplan-Meier method and the log-rank test, survival rates were 85% for females <85 years old and 47% for those ⩾85 years old (p=0.005). For males, survival rates were 53% for <85 and 33% for those ⩾85 (p=0.427). A significant difference (p=0.019) was observed between genders for the group <85, and a non significant difference was found between genders for ⩾85-year-old individuals. Survival time did not show proportional hazard when taking gender and age into account. Then, a model was fitted for the survival time by considering a gamma

distribution controlled by gender and age. Time between fracture and surgery (p=0.038), number of comorbidities (p=0.0014) and time of surgery (p<0.0001) were significantly related to survival time. When comparing the pre-fracture dependence status with that at 12 months, 17.1% of the survivors became dependent. Walking ability was preserved after one year in 89% of the survivors that could walk before the fracture (only 3 could not), although 70% with help of a walking device. We concluded that the functional capacity (including walking without help) of a reasonable percentage of the survivors was affected. Regarding survival, elderly men, at any age and very old women are specially affected. Strategies to focus on these special groups should be ensured in order to improve high-quality survival.

***Disclosures: Adriana Machado**, None.*

SU0336

Hospitalizations of Major Osteoporotic Fractures in Switzerland between 2000 and 2007. Kurt Lippuner[1], Albrecht Popp*[1], Patrick Schwab[2], Matt Gitlin[3], Thilo Schaufler[4], Christoph Senn[1], Romain Perrelet[1]. [1]Osteoporosis Policlinic, University of Bern, Switzerland, [2]Swiss Federal Statistical Office, Switzerland, [3]Amgen (Europe) GmbH, Switzerland, [4]Amgen Switzerland GmbH, Switzerland

Purpose: An increase in the socio-economic impact of osteoporosis in Switzerland has been forecasted until 2020, using a Markov Model and fracture data from the year 2000[1]. The aim of the present study was to verify these underlying epidemiological assumptions using the latest available data on major osteoporotic fracture (MO-Fx) hospitalizations in our country from 2000 to 2007.

Methods: Administrative and medical data (age, sex, number of hospitalized fractures, and duration of hospitalization) from the Swiss Federal Statistical Office (FSO) was obtained for analysis. Representativeness of the data ranged from 81.2% of all Swiss hospitals in 2000 to 98.6% in 2007. The crude incidence of hospitalizations due to MO-Fx (hip, spine, distal radius, and proximal humerus, defined through ICD-10 diagnosis codes) and the mean length of hospital stay (LOS) were calculated by 10-year age groups and sex. The average cost per day of hospitalization was obtained from the yearly hospital statistics database of the FSO (CHF 996.00 per day in 2000 to 1543.00 per day in 2007). To estimate the total cost burden of hospitalized MO-Fx we multiplied the average cost per day by the LOS of each MO-Fx hospitalization.

Results: Compared to the year 2000, the number of women and men aged ⩾45 years had increased by 11.1% and 14.6%, respectively. The incidence of hospitalizations due to hip fractures decreased from 2000 to 2007. In contrast, the incidence of hospitalizations due to the other three MO-Fx increased within the same period of time (Table). Mean LOS decreased from 16.1 days (men: 15.3 days) in 2000 to 11.4 days (men: 11.2 days) in 2007. The total yearly cost of hospitalizations for MO-Fx increased from CHF 223 million (men: CHF 71 million) to CHF 285 million (men: CHF 97 million). For hip fractures, the yearly costs increased from CHF 146 million (men: CHF 48 million) to CHF 171 million (men: CHF 58 million).

Conclusions: Between 2000 and 2007, there was an overall increase in hospitalizations associated with MO-Fx as well as a rise in daily hospitalization costs. These factors have contributed to an increased socio-economic burden of the disease in Switzerland.

1. Schwenglenks, et al. Osteoporos Int 2005;16:659-671.

Incidence of fracture hospitalizations per 100'000 persons aged ≥45 years

	Women				
	Total	Hip	Spine	Distal Radius	Proximal Humerus
2000	901	496	84	187	134
2007	939	438	107	246	148
% Change	4.2%	-11.7%	27.4%	31.6%	10.4%
	Men				
	Total	Hip	Spine	Distal Radius	Proximal Humerus
2000	351	191	64	48	48
2007	367	172	75	63	57
% Change	4.6%	-9.9%	17.2%	31.3%	18.8%

Table

***Disclosures: Albrecht Popp**, Through the Osteoporosis Policlinic, Univ. of Bern from Amgen, Novartis, Roche, Servier, MSD., 2; Recived speaker's fees and/or was a member of a paid advisory board for Amgen, Daiichi Sankyo, Eli Lilly, MSD, Novartis, Nycomed, Roche, and Servier, 9*
This study received funding from: Amgen Switzerland GmbH

SU0337

Incidence of Hip Fracture and Mortality after Hip Fracture in South Korea. Yong-Chan Ha[1], Hyung-Jin Choi[2], Hyun-Koo Yoon*[3], Young-Kyun Lee[4], Chan-Mi Park[5], Deog-Yoon Kim[4]. [1]Seoul National Universtiy Bundang Hospital, South korea, [2]Department of Internal Medicine, Seoul National University Hospital, South korea, [3]Cheil Hospital & Women's Healthcare Center, South korea, [4]Kyung Hee University Hospital, South korea, [5]Health Insurance Review & Assessment Service, South korea

Introduction: Hip fracture is the most important sequelae of the osteoporosis with regards to the impact on mortality. We evaluated nationwide the incidence and mortality following hip fracture in South Korea using data from the Health Insurance Review Agency (HIRA), which includes nationwide information.

Methods: We designed a population based, retrospective cohort study, using HIRA data and identified hospitalized patients who were 50 years of age or older between January 1, 2005 and December 31, 2008 and who had a new study-defined fracture diagnosis code with the ICD10 (S720 and S721) within that period. Following hospitalization for hip fracture we followed each patient by code concordance to identify deaths. The standardized mortality ratio (SMR; observed/expected deaths) was calculated. Expected number of death was calculated on the basis of age and gender-specific rated from the general population.

Results: The total number of hip fractures was 16,866 in 2005 and 20,432 in 2008. The crude rate of hip fractures in women and men increased from 191.9/100,000 in 2005 to 200.0/100,000 in 2008 and from 94.8/100,000 in 2005 to 97.8/100,000 in 2008. The crude incidence of mortality following hip fractures within 12 months was 18.8% (3166/16866) in 2005 and 17.7% (3299/18610) in 2007. Mortality for men and women was 22.6% and 17.3%, respectively. The SMR was 4.64 in 6 months and 3.30 in 12 months follow-up period. The highest SMR was observed among men aged 70-80 years, and both men and women aged 70-80 had persistently elevated SMR for 2 years.

Conclusion: This observational study is the 1st nationwide evaluation for the epidemiology of the hip fracture in Korea (South). Incidence of hip fracture had increased and mortality was higher among men than women. High mortality after hip fracture is possible to be serious socioeconomic problems in the near future.

***Disclosures: Hyun-Koo Yoon**, None.*
This study received funding from: Health Insurance Review & Assessment Service

SU0338

Prevalence and Risk Factors of Fragility Fracture in Brazilian Community-dwelling Elderly. Jaqueline B Lopes*[1], Camille Danilevicius[2], Valeria F Caparbo[1], Liliam Takayama[1], Rosa Pereira[1]. [1]Faculdade de Medicina da Universidade de São Paulo, Brazil, [2]Universidade De São Paulo, Brazil

Purpose: Epidemiological study to estimate the prevalence of fragility fractures and investigate factors associated with this condition in Brazilian community-dwelling elderly.

Methods: 1075 elderly subjects (659 women/416 men) from São Paulo, Brazil were evaluated using specific questionnaire including risk factors for osteoporotic fractures. Fragility fractures were defined as that resulting of a fall from standing height or less after 50 years of age at sites characteristic of bone fragility. Traumatic fractures and those occurring at the face, skull, ankle, elbow and finger were not considered. Anthropometric data was obtained by physical examination and body mass index (BMI) was calculated. Bone mineral density (BMD) was measured by DXA in hip and lumbar spine. Laboratory tests were also performed.

Results: The prevalence of fragility fractures was of 11.9% (127) and the main fracture sites were forearm (50.4%), humerus (19.7%), femur (11.2%) and ribs (8.7%). Women had higher prevalence (15.3%; 95%CI 12.6-18.1) than men (6.5%; 95%CI 4.1-8.9) (P<0.001). In women, the main factors associated with fractures were Caucasian race (OR=1.7; 95%CI 1.1–2.8; P=0.027), BMI (OR=0.9; 95%CI 0.89–0.98; P=0.002) and femoral neck T-score (OR=0.7; 95%CI 0.5–0.9; P<0.001). After adjustment for these significant variables, the logistic-regression analyses revealed that Caucasian race (OR=1.7, 95%CI 1.03-2.7 P=0.038) and femoral neck T-score (OR=0.7, 95%CI 0.51-0.86; P=0.002) remains a significant factor for fragility fractures in women. In men, the main factors associated with fragility fractures were current smoking (OR=3.2; 95% CI 1.4–7.6; P=0.007), diabetes mellitus (OR=3.1; 95%CI 1.3–7.1; P=0.008), chronic faller (OR=2.9; 95% CI 1.1–7.6; P=0.033) and femoral neck T-score (OR=0.4, 95% CI 0.2-0.6; P<0.001). The logistic-regression analyses revealed that current smoking (OR=2.5, 95% CI 1.2-6.2; P=0.048), diabetes mellitus (OR=4.5; 95% CI 1.8–11.1; P=0.001) and femoral neck T-score (OR=0.4, 95% CI 0.2-0.6; P<0.001) were independent factors in predicting fragility fractures in men.

Conclusions: Our results suggest that fragility fractures are common in Brazilian community-dwelling elderly and, a low hip BMD is an important risk factor for this condition in both genders. In men, diabetes and smoking are also related to this comorbity.

***Disclosures: Jaqueline B Lopes**, None.*
This study received funding from: FAPESP, CAPES, CNPQ

SU0339

Prevalence of Clinical Risk Factors for Fracture in Postmenopausal Women in 5 European Countries: The POSSIBLE EU® Study. Christian Roux*[1], Cyrus Cooper[2], Adolfo Diez-Perez[3], Luc Martinez[4], Sergio Ortolani[5], Matt Gitlin[6], Gerd Moeller[6], Susan Shepherd[7], Nick Freemantle[8]. [1]Hospital Cochin, France, [2]University of Southampton, United Kingdom, [3]Hospital del Mar-IMIM-Autonomous University of Barcelona, Spain, [4]Société Francaise de Médecine Générale, France, [5]Istituto Auxologico Italiano, Italy, [6]Amgen (Europe) GmbH, Switzerland, [7]Amgen Ltd, United Kingdom, [8]Birmingham University, United Kingdom

Aims: Risk factors can be used for assessing patient status and treatment needs for osteoporosis although the guidelines for reimbursement may differ across Europe. The POSSIBLE EU® study (Prospective Observational Study Investigating Bone Loss Experience in Europe) describes the characteristics and experience of postmenopausal women receiving or initiating medication for osteoporosis (N = 3,402) in France, Germany, Italy, Spain and the UK.[1] In this analysis, we explore risk factors for fracture among patients in these 5 European countries at baseline and during the 12-month follow-up period.

Methods: Patients were recruited by their general practitioner from December 2005 until March 2008. Data collected at study entry included bone loss diagnosis (yes, no, unknown), the diagnosis (osteoporosis or osteopenia), the method used at time of diagnosis (eg, DXA), fracture history during adulthood (≥18 years of age) and information pertaining to additional risk factors, such as parental history of hip fracture and glucocorticoid use.

Results: Of the 3,402 women enrolled (mean age [SD] 68.2 [9.8]), 3,260 had a bone loss diagnosis, with 1,784 being diagnosed using DXA (osteoporosis 68%, osteopenia 31%, unknown 1%) and 1,476 being diagnosed by other means. Median minimum T-score at diagnosis (25th, 75th percentile) was -3.0 (-3.5, -2.7) and -2.1

(-2.3, -1.7) for osteoporosis and osteopenia patients, respectively. Previous fractures were recorded in 39% of the overall patient population. The percentage of patients with previous fractures varied by country (highest: UK [52%] and lowest: Italy [28%]) as did other risk factors (Figure).

Conclusions: The findings showed differences in risk factors for fracture across Europe in patients initiating or receiving medication, which may be, in part, due to the various local reimbursement guidelines. This may have important implications for disease management strategies across Europe.

Reference

1. Freemantle N, et al. Arch Osteoporos 2010. In press.

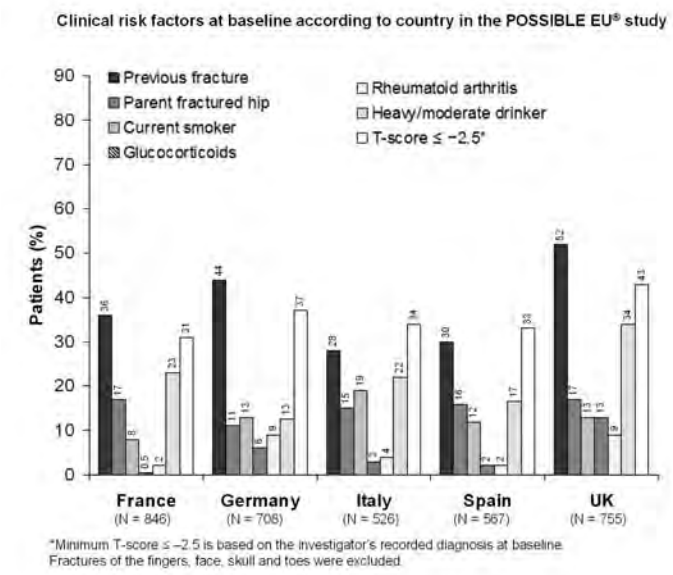

Figure

***Disclosures: Christian Roux**, Amgen, 5; Amgen, 8; Amgen, 2*
This study received funding from: Amgen (Europe) GmbH

SU0340

Risk Factors for in-hospital Post-hip Fracture Mortality. John Eisman[1], Nguyen Nguyen[1], Tuan Nguyen[1], Steven Frost*[2]. [1]Garvan Institute of Medical Research, Australia, [2]University of Western Sydney, Australia

Approximately 20% of individuals with a hip fracture die during the first year following fracture, with a substantial number of patients die during hospitalization. However, risk factors of in-hospital mortality among hip fracture patients are not clear. This study sought to identify risk factors and to develop models for the prognosis of in-hospital mortality among hip fracture patients.

The study setting was a large teaching hospital in the Sydney, Australia. Between 1997 and 2007, 1504 patients (410 men and 1094 women) with hip fracture (ICD-10-AM S72.0-S72.2) aged 50-years or older were admitted to the hospital for treatment. Clinical data, including concomitant illnesses, were obtained from inpatient data. These data were used to derive the Charlson co-morbidity index. The outcome of interest was in-hospital mortality. A log-binomial regression model was used estimate the risk of in-hospital death and a nomogram was developed to individualize this risk.

The rate of in-hospital mortality was 9% in men and 4% in women. The risk of in-hospital mortality was significantly associated with advancing age (rate ratio [RR] for each 10-year increase: 1.91 95% confidence Interval [CI]: 1.47 to 2.49), being male (RR 2.13; 95% CI 1.41 to 3.22) and the presence of comorbid conditions on admission (RR for one or more comorbid conditions versus none: 2.30; 95% CI 1.52 to 3.48). After adjusting for age and sex, a history of congestive heart failure (RR 3.02, 95% CI 1.65 to 5.54), liver disease (RR = 4.75, 95% CI 1.87 to 12.10) were significant risk factors for in-hospital mortality. A history of cerebral vascular disease, cancer, and renal disease were also significantly associated with increased risk of mortality. The area under the ROC for the final model (incorporating age, sex and specific Charlson co-morbidity index conditions) was 0.76. A prognostic nomogram was developed (Figure 1) for predicting the risk of mortality for an individual man and woman. Approximately a third of the risk of in-hospital mortality was attributable to the presence of at least one co-morbid condition at admission.

These data suggest that advancing age, gender, and pre-fracture concomitant diseases were main risk factors of in-hospital mortality. The nomogram developed from this study can be used to convey useful prognostic information to patients and help guide treatment decision.

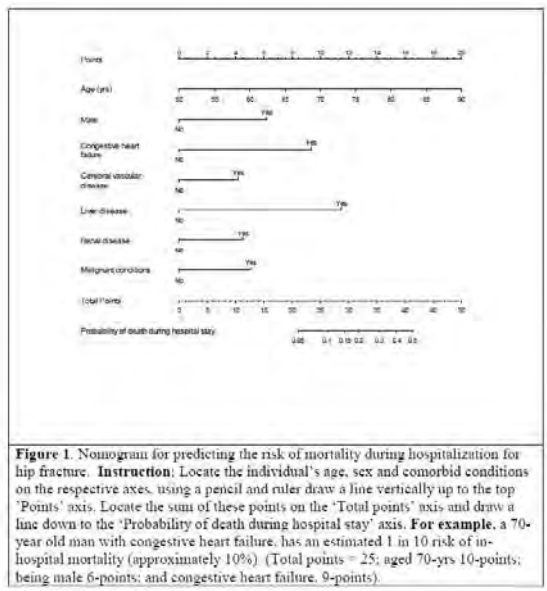

Figure 1. Nomogram for predicting the risk of mortality during hospitalization for hip fracture. **Instruction**: Locate the individual's age, sex and comorbid conditions on the respective axes, using a pencil and ruler draw a line vertically up to the top 'Points' axis. Locate the sum of these points on the 'Total points' axis and draw a line down to the 'Probability of death during hospital stay' axis. **For example**, a 70-year old man with congestive heart failure, has an estimated 1 in 10 risk of in-hospital mortality (approximately 10%). (Total points = 25; aged 70-yrs 10-points; being male 6-points; and congestive heart failure, 9-points).

Figure 1.

***Disclosures: Steven Frost**, None.*

SU0341

Systematic Review of Osteoporosis Interventions in Pharmacy Practice. Mary Elias*[1], Andrea Burden[1], Suzanne Cadarette[2]. [1]University of Toronto, Canada, [2]Leslie Dan Faculty of Pharmacy, University of Toronto, Canada

Purpose: Complete a systematic review of the literature to examine the impact of pharmacist interventions in narrowing the two main gaps in osteoporosis management: identifying at-risk individuals, and improving adherence to therapy.

Methods: We searched the electronic databases of EMBASE, HealthStar, International Pharmaceutical Abstracts, and MEDLINE from inception to December 2009, examined grey literature and completed manual searches to identify English-language research that examined osteoporosis management interventions in pharmacy practice. Titles and abstracts were reviewed for significance by two independent reviewers and articles were excluded if no reference to osteoporosis or pharmacist interventions was made. We did not exclude studies based on quality, yet focus on the evidence of effects from controlled studies.

Results: We identified 21 eligible studies: 3 cross-sectional, 1 historical/ecological control, 14 cohort (3 controlled), and 3 randomized controlled trials. Interventions varied from simple educational programs for patients and/or health care professionals, to patient-file review and consultation, to screening based on risk factors or bone mineral density testing and subsequent physician referrals or contact. Results suggest that pharmacy interventions can increase patient awareness of osteoporosis, improve calcium and vitamin D supplementation, identify high risk patients and

improve pharmacoprevention. No study examined the impact of pharmacist intervention on treatment adherence or fracture reduction.

Conclusions: Few high-quality studies have examined osteoporosis interventions within pharmacy practice. Data support potential benefits, such as increased patient awareness and calcium/vitamin D supplementation, as well as improved identification of high-risk patients and subsequent treatment. Pharmacists are well-positioned to reduce the burden of osteoporosis by identifying at-risk individuals and improving patient adherence to therapy. More high-quality research/evidence is needed to determine the comparative effectiveness of different pharmacy intervention strategies.

***Disclosures: Mary Elias**, Canadian Institutes of Health Research, 9*

SU0342

The Incidence and Lifetime Risk of Major Osteoporotic Fracture in South Korea. Yong-Chan Ha[1], Chan-Mi Park[2], Young-Kyun Lee[3], Deog-Yoon Kim*[3]. [1]Chung-Ang University, South korea, [2]Health Insurance Riview & Assessment Service, South korea, [3]Kyung Hee University Hospital, South korea

Purpose: Although South Korea dose not belongs to high-risk countries for osteoporosis, according to the demographic projection scenarios, the considerable human, social, and economic burden represented by osteoporotic fractures will increase. The purpose of this study was to determine the annual incidence and lifetime risk of major osteoporotic fracture in South Korea, with using data from the Health Insurance Review Agency (HIRA), which includes nationwide information entrusted by Korean government. Methods: All new visit or admissions to Korean hospitals for fracture were recorded prospectively in nationwide cohort by the Korean HIRA using ICD-10 code. These data were retrospectively evaluated to determine the annual incidence and lifetime risk of major osteoporotic (hip, spine, distal radius, proximal humerus) fracture, in men and women aged 50 years or more between the years of 2005 and 2008. Results: The annual incidence of major osteoporotic fractures was 19.1, 18.9, 18.7, and 18.7 per 100,000 person-years in men and women aged 50 years or more from 2005 to 2008. The annual incidence of osteoporotic fracture in women was three times as much as men. Incidence of osteoporotic fracture among women and men aged 50-59, 60-69, 70-79, and 80-100 was approximately 8, 18, 35, 50 per 10,000 person-years respectively. At the age of 50 years, in South Korea, the remaining lifetime probability of suffering an osteoporotic fracture is 28.97% for women and 10.68% for men, which are lower than western countries, but higher than Japan, one of Asian countries. Conclusion: This observational study shows that the incidence of osteoporotic fracture increased with advancing age and lifetime risk for osteoporotic fracture is 2.7 times higher among women than men. This study could partly provide the basic data for treatment and research on osteoporosis in South Korea

***Disclosures: Deog-Yoon Kim**, None.*
This study received funding from: Health Insurance Review and Assessment Service

SU0343

Pinto Beans as a Course of Bioavailable Selenium to Support Bone Structure in Mice. Jay Cao*[1], Brian Gregoire[2], Huawei Zeng[2]. [1]USDA ARS, USA, [2]USDA/ARS/Grand Forks Human Nutrition Research Center, USA

Selenium (Se) is an essential trace mineral for animals and humans. The deficiency of Se has been linked to increased oxidative stress with increased levels of reactive oxygen species (ROS). Oxidative stress and ROS have been shown to stimulate bone resorption and osteoclast activity. Selenium, a chemical component of selenoproteins (such as glutathione peroxidases and thioredoxin reductase), plays a major role in cellular redox status and may have beneficial effects on bone health. The objective of the study was to determine whether Se deficiency affects bone microarchitecture and whether Se from pinto beans (SeB) is bioavailable as compared to that of Se in the form of selenomethionine (SeM) in supporting normal bone development in a mouse model. Thirty-three male C57BL/6J mice, 18-wk-old, were assigned randomly to three groups. Mice were fed either purified Se-deficient diet (SeD) containing ~0.005 ppm Se, or diets containing ~0.1 ppm Se in the form of SeM or SeB for four months. Selenium concentration in liver and glutathione peroxidase activity in red blood cells were higher in mice fed SeM or SeB diet than those fed SeD diet ($P < 0.0001$). Mice fed SeM or SeB diet had higher femoral trabecular bone volume/total volume and trabecular number and lower trabecular separation than mice fed SeD diet. Selenium deficiency did not affect any mid-shaft cortical bone parameters of the femur ($P > 0.05$). Interestingly, mice fed SeB diet had higher liver Se concentration ($P < 0.05$) but similar glutathione peroxidase activity in red blood cells as compared to mice fed SeM diet. There were no significant differences in bone structural parameters between SeM and SeB groups ($P > 0.05$). Taken together, this study demonstrates that Se plays a critical role in supporting bone structure and Se from pinto beans is equally bioavailable to support normal bone development in mice as compared to Se in the form of selenomethionine.

***Disclosures: Jay Cao**, None.*

SU0344

Bone Mineral Density and Serum Osteoprotegerin Levels in Pre- and Postmenopausal Women. Cora Bow*[1], Ching-Lung Cheung[2], Yi Gao[1], Kam Shing Lau[1], Sze Sze Soong[1], Siu Ching Yeung[1], Annie Kung[3]. [1]Department of Medicine, The University of Hong Kong, Hong kong, [2]Hebrew SeniorLife, Institute for Aging Research, Singapore, [3]Department of Medicine, University of Hong Kong, Hong kong

Introduction: Osteoprotegerin (OPG) is an essential regulator of bone turnover through its suppression on osteoclastogenesis. Findings from previous studies of serum OPG and bone mineral density (BMD) in humans have been conflicting. The objective of this study was to identity factors associated with serum OPG levels and to determine its effect on BMD in pre- and post- menopausal women.

Methods: This is a part of the Hong Kong Osteoporosis Study. 2,343 community-dwelling, treatment and hormonal therapy naive female subjects aged 18 or above were recruited (679 premenopausal women, mean age 36.7 ± 8.8 years; 1,664 postmenopausal women, mean age 62.6 ± 8.5 years). Baseline demographic characteristics, serum biochemistry, hormonal profile and fasting serum OPG levels were obtained. Baseline BMD at the spine and hip were measured.

Results: Serum OPG levels was correlated with age in both pre- and post-menopausal women(premenopause $r=0.208$, postmenopause $r=0.258$, both $p<0.0001$). After adjusting for age, OPG levels were positively correlated with serum estradiol ($r=0.100$, $p<0.05$) and negatively with follicular stimulating hormone (FSH) ($r=-0.114$, $p<0.01$) in premenopausal but not postmenopausal women. In premenopausal women, higher serum OPG levels were associated with higher age- and BMI-adjusted BMD (spine $r=0.147$, $p<0.05$; femoral neck $r=0.138$, $p<0.05$; total hip $r=0.148$, $p<0.05$). In postmenopausal women, age-adjusted OPG showed no correlation with BMD in the linear regression model. However, a negative correlation was observed between OPG in quartiles and hip BMD (p-tread <0.01), but not spine BMD.

Conclusions: Serum OPG level is an independent factor associated with higher BMD in pre-menopausal women. However it's protective effect on BMD is not significant in post-menopausal women with low bone mass.

***Disclosures: Cora Bow**, None.*

SU0345

Are Rib Fractures Osteoporotic? Sara Achenbach[1], Shreyasee Amin[1], Sundeep Khosla[2], L. Joseph Melton[1], Lisa-Ann Wuermser*[3]. [1]Mayo Clinic, USA, [2]College of Medicine, Mayo Clinic, USA, [3]Mayo Clinic Medical Center, USA

Purpose: This study looks at the association between rib fractures in both low and high velocity trauma and risk factors for osteoporosis in a representative population.

Methods: An age stratified population was evaluated at baseline for risk factors for osteoporosis including alcohol use, smoking, prior fractures and secondary causes of bone loss. Areal bone density as well as bone formation and resoprtion markers were also collected at baseline. The subjects were then followed for an average of 14 years. Data on subsequent fractures were collected by subject report as well as review of the medical record. Circumstances surrounding the onset of new fractures were collected when available. All rib fractures included in this analysis were confirmed radiologically. Cumulative incidence was calculated and compared with expected incidence using a log-rank test statistic. Andersen-Gill time to fracture regression models were to used to test the impact of covariates.

Results: Fifty six of the 699 subjects had 67 rib fracture episodes (more than 1 rib could be fractured per episode) during 8560 person-years of follow up. The majority (73%)occurred during moderate trauma including falls from standing. Severe trauma was the etiology in 25%, while only a small number resulted from little to no trauma. The cumulative incidence of rib fracture was 9.5% at fifteen years, compared to expected incidence of 6.7%. Rib fracture risk increased with age (HR per 10 years 1.7, 95% CI 1.5-2.0). After adjustment for age, only prior fracture remained a risk factor for rib fracture (RR 1.95, 95% CI 1.11-3.44). Physical activity (RR 0.40, 95% CI 0.16-0.97) and higher serum osteocalcin levels (RR per 1SD decrease 1.72, 95% 1.19-2.47) were protective after age adjustment. There was no difference in the predictive value of any covariate when restricting to only those fractures occurring with mild-moderate trauma.

Conclusions: Rib fracture risk increases with age. Physical activity and higher bone formation markers are protective. Bone density more than a decade earlier is not predictive, unlike other typically osteoporotic fractures. Rib fractures may represent an early sign of bone frailty, prior to the occurrence of other osteoporotic fractures.

***Disclosures: Lisa-Ann Wuermser**, None.*

SU0346

Are Women with Thicker Cortices in the Femoral Shaft at Higher Risk of Subtrochanteric/diaphyseal Fractures?: The Study of Osteoporotic Fracture. Nicola Napoli[1], Jane Cauley[2], Aldric Chau[3], Dennis Black[4], Michael Kelly[4], Shane Burch[5], Rosanna Wustrack*[4], Katherine Wilt[6], Kristine Ensrud[7]. [1]University Campus Biomedico, Italy, [2]University of Pittsburgh Graduate School of Public Health, USA, [3]UCSF Department of Epidemiolgy & Biostats, USA, [4]University of California, San Francisco, USA, [5]UCSF Department of Orthopaedic Surgery, USA, [6]California Pacific Medical Center, USA, [7]Minneapolis VA Medical Center / University of Minnesota, USA

Background:

Thickened cortices are commonly mentioned as a feature in recent reports of "atypical" femur fractures, but it is unclear if thickened cortices are a risk factor or the result of preceding stress fracture and what role bisphosphonates might play in cortical thickening. We aimed to examine the relationship of femoral shaft cortical thickness to the risk of femur fractures in the subtrochanteric or diaphyseal region using a large population-based cohort of older women.

Methods:

We evaluated cortical thickness as a risk factor for femoral shaft fractures in the Study of Osteoporotic Fractures: 9704 women aged > 65 years recruited in 1986 who are still being followed. X-ray reports form all femur and intertrochanteric hip fractures (n=897) were reviewed to identify fractures that occurred below the lesser trochanter but above the metaphyseal flare (designated SH). Morphology, howerve, could not be assessed from the reports. AP pelvic radiographs obtained at baseline were used to measure cortical thickness (CW) 3 cm below the lesser trochanter in a random sample of the cohort (used as controls) and all relevant fracture cases. We then examined the relationship of CW to SH as well as femoral neck fractures (FNF) using a Cox regression model. We present analysis of the medial cortex (R/L mean) although results were similar using medial plus lateral cortices.

Results:

45 women with SH fractures were found over 140,000 person-years of follow up. 33 had evaluable baseline AP pelvis radiographs and were compared to 388 random controls. We found that women with the thickest medial cortices were at lower risk of SH compared to those with the thinnest cortices, with a relative hazard (RH) of 0.18 (95% CI 0.06-0.56) in thickest compared to the thinnest quartile. The relationship of quartiles of medial CW to risk of FNF was similar to SH fractures (figure 1). A relatively small number of women (9/45) had taken bisphosphonates and the results were similar when restricted to non-users.

Conclusion:

Recent case studies have suggested that thicker cortices might be a risk factor for SH fractures in bisphosphonate users. However, in a cohort of women who were primarily bisphosphonate naive, we found no evidence that thicker cortices placed women at higher risk of SH fractures: those with thicker cortices were at lower risk. Whether cortical thickness among bisphosphonate users plays a role in atypical SH fractures remains to be determined.

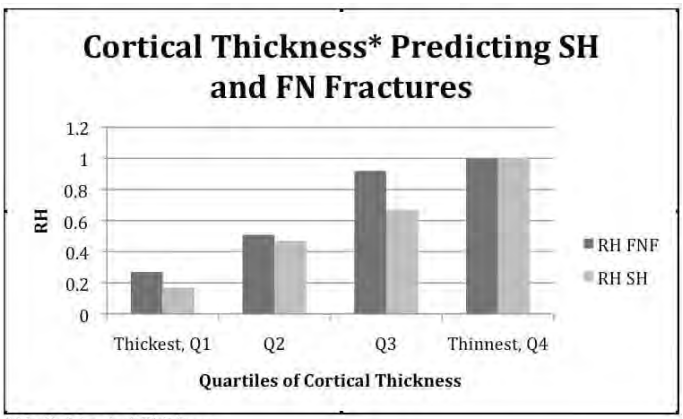

* Medial Cortical Thickness

Figure 1: The RH is the lowest for the thickest medial cortices.

Figure 1

***Disclosures: Rosanna Wustrack**, None.*

SU0347

Association of Quantitative Calcaneal Ultrasound with Long-term Care Service Utilization in Elderly Women: A Cross-sectional Population-based Study. Takao Suzuki*[1], Hideyo Yoshida[2], Shuji Yoshida[3], Kiichi Nonaka[4]. [1]National Institute for Longevity Sciences, Japan, [2]Tokyo Metropolitan Institute of Gerontology, Japan, [3]Nippon Dental University, Japan, [4]ELK Corporation, Japan

Aim: A number of studies in the world including USA, Europe, and Japan have demonstrated that quantitative ultrasound (QUS) measurements have a certain association with osteoporosis and its associated fractures. To our knowledge, however, very few studies have shown the association of QUS with frailty or loss of independence among the elderly living in the community.

We performed a cross-sectional population-based study to investigate the relationship between calcaneal QUS measurements and utilization of care services provided by the long-term care insurance, which can be regarded as an indicator of frailty or loss of independence.

Methods: In 2007 and 2008, a total of 2,388 elderly women aged 78.2 +/- 3.53 (mean +/-standard deviation) years living in an urban community underwent mass comprehensive health check-ups at the Tokyo Metropolitan Institute of Gerontology (TMIG), for the prevention of health degeneration ultimately requiring long-term care. In the mass health check-ups, calcaneal QUS (CM-200) and forearm DXA (DTX-200) were used for the evaluation of bone health.

Utilization of care services provided by the long-term care insurance was confirmed by interview survey, and other general health information such as activity of daily living (ADL) and self-rated health was obtained. QUS was evaluated by CM-200 that measures speed of sound (SOS) at the calcaneus, and DXA was assessed by DTX-200 that measures bone mineral density (BMD) at the proximal regions of the radius and ulna.

Results: Multiple regression analysis was conducted to determine the odds ratio (OR), using utilization of care services as dependent variable and the tertiles of SOS and BMD as independent variables. After adjustment for age, body mass index (BMI), and major chronic diseases including hypertension, stroke, cardiac diseases, diabetes, and osteoporosis, the OR for the lowest tertile of SOS was 2.61 [95% confidence interval (CI): 1.80-3.79] ($p<0.001$) and that for the middle tertile was 1.51 (CI: 1.02-2.26) ($p<0.05$). There was no significant correlation for the tertiles of BMD.

Conclusion: Calcaneal QUS measurement is associated with the risk of frailty or loss of independence, indicated by utilization of care services provided by the long-term care insurance, among the community-dwelling elderly women in Japan. The challenge now is to identify the relationship by conducting a longitudinal follow-up study.

***Disclosures: Takao Suzuki**, None.*

SU0348

Bone Loss in Chronic Spinal Cord Injury: Effect of Age and Duration Since Injury. Lisa Streff[1], Benjamin Grover[1], Victoria Lent[2], Meghan Romba[3], Thomas Schnitzer*[4]. [1]Rehabilitation Institute of Chicago, USA, [2]University of Medicine & Dentistry of New Jersey, USA, [3]University of Illinois, USA, [4]Northwestern University, USA

Aims: To determine the bone density by DXA at various regions of interest in patients with chronic spinal cord injury, correlate bone loss with age, gender, time since injury, and degree of motor impairment, and compare to non-impaired controls.

Methods: A convenience sample of 37 individuals with chronic spinal cord injury and 21 controls underwent bone density evaluation using a Hologic QDR-4500A densitometer. BMD was measured by standard techniques at the lumbar spine, total hip, femoral neck, radius, distal femur and proximal tibia. Demographic and clinical data were obtained from the patients by soliciting their history.

Results: BMD at the total hip and femoral neck of the SCI patients was significantly lower than that of the controls (0.732+0.163gm/cm^2 and 0.729+0.171gm/cm^2 vs 0.975+0.881gm/cm^2 and 0.881+0.185gm/cm^2, $p<0.001$ and $p=0.003$ respectively). Because the age of the SCI patients was somewhat older than the controls (42.3+12.4yr vs 34.5+14.7yrs, $p=0.04$), BMD was compared within each of 3 age strata between SCI patients and controls: 18-29yr, 30-49yr, and >50 yrs. A statistically significant difference between SCI patients and controls was observed for the 2 younger strata but not the oldest strata (Table 1). Interestingly, the expected age-related decrease in BMD seen in the controls was not observed in the SCI patients, and BMD at the lumbar spine showed an increase with age in patients with SCI. BMD at all sites measured decreased with increasing duration since injury but did not reach statistical significance ($p>0.05$).

Conclusions: Individuals with SCI have lower hip BMD than age-matched controls. However, BMD at the hip appears to be largely independent of age in SCI individuals, not showing the normal age-related decrease seen in healthy normals. This may be the consequence of BMD homeostasis being controlled by different mechanisms in people with SCI compared to healthy controls.

Acknowledgements: This research was supported in part by an unrestricted educational grant from Proctor and Gamble Pharmaceuticals.

BMD (mg/cm2) in Different Age Strata

	18-29 yr	30-49 yr	50+ yr
Total Hip - SCI	0.732	0.709	0.777
Total Hip - Control	1.039	0.960	0.822
Fem Neck - SCI	0.732	0.709	0.777
Fem Neck - Control	0.973	0.826	0.710
Lumbar Spine - SCI	1.039	1.101	1.177
Lumbar Spine - Control	1.060	1.041	0.960

Table 1

***Disclosures: Thomas Schnitzer**, None.*
This study received funding from: Proctor and Gamble

SU0349

Comparison of Bone Mass and Biochemical Markers in Patients with Obstructive Airway Diseases and Healthy Controls in Taiwan. Yi-Chin Lin*[1], Wei-Shan Chang[2], Hui-Lun Hsiao[2], Tzu-Ching Wu[3]. [1]Chung Shan Medical University, Taiwan, [2]School of Nutrition, Chung Shan Medical University, Taiwan, [3]Chung Shan Medical Univ. Hospital, Taiwan

Patients with obstructive airway diseases (asthma and chronic obstructive pulmonary disease, COPD) may have poorer bone health. The baseline data of patients with obstructive airway diseases who have been recruited for a currently ongoing interventional trial was analyzed and compared to healthy controls. Data of ninety-seven patients with confirmed diagnosis of obstructive airway diseases (54.6% with COPD; 45.4% with asthma) and have completed baseline questionnaire interview and bone density examination by dual-energy x-ray were included. The data of the control group (n=35) is recruited in the same university hospital as were the patients. The results showed that in general, the patients have lower body mass index, bone mineral contents (BMC, in g) and bone mineral density (BMD, in g/cm^2) at all sites measured (total body, femoral neck, spine L2-L4) than the healthy controls, and the differences were statistically significant for TBBMD (t=-2.22, p=0.03), TBBMC (t=-2.00, p=0.05), and FNBMD (t=-3.31, p=0.02). The body composition also differs between patients and controls such that body fat percentage was significantly lower in the patient group (28.01% vs. 31.85%, p=0.03). In the patient group, the prevalence rates of osteoporosis (t-score for BMD lower than -2.5) at femoral neck (41.24% vs. 14.71% in the controls), lumbar spine (31.96% vs. 11.76%), or either of the two sites (49.48% vs. 17.14%) were higher than in the control group. The patients were higher in serum levels of parathyroid hormone (27.57 vs. 23.73 pg/mL, p=0.08), bone resorption marker ICTP (5.19 vs. 3.72 microgram/L, p<0.001), and c-reactive protein (CRP)(0.34 vs. 0.18 mg/L, p=0.08). The results of correlation analyses, partialled for age, showed positive relations between pulmonary function parameters (FEV1, forced expiratory volume in 1 second and FVC, forced vital capacity) and BMD and BMC at total body, LS1-4 and femoral neck. A negative correlation was observed between serum level of CRP and TBBMC (r=-0.195, p=0.083) in the patients. The insignificance of the relations between serum levels of PTH and ICTP to bone measurements may be partially attributed to the unequal distribution of age (mean age: 72.7$\pm$10.3 in COPD vs. 61.4$\pm$13.4 in asthma subgroup vs. 58.1$\pm$12.6 years in the controls) and gender (males/females is 48/5 in COPD vs. 19/25 in asthma subgroup vs. 19/16 in the controls) in the groups of patients versus the controls. Patients with obstructive airway diseases may have higher risk of osteoporotic fractures.

***Disclosures: Yi-Chin Lin**, None.*

SU0350

Dose Hepatic Steatosis Affect the Risk of Osteoporosis In Korean Postmenopausal Women? Hee-Jeong Choi*[1], HJ Oh[2], BY Yu[3], BI Lee[4]. [1]Department of Family Medicine, Eulji University School of Medicine, South korea, [2]Department of Family Medicine, Kwandong University School of Medicine, South korea, [3]Department of Family Medicine, Konyang University School of Medicine, South korea, [4]Department of Obstetrics & Gynecology, Inha University Colleage of Medicine, South korea

Background: Non-alcoholic fatty liver disease, the common chronic liver disease in Korea, is associated with obesity and metabolic syndrome. Obesity-induced chronic inflammation is a key component in the pathogenesis of insulin resistance and metabolic syndrome. Also, it might be another risk factor for osteoporosis and related fractures. The objective of this study was to determine the relationship between non-alcoholic fatty liver and bone mineral density (BMD) in postmenopausal women whose daily alcohol consumption less than 20 g. Methods: Subjects are postmenopausal women who had visited Health Promotion Center. Medical history and lifestyle data were collected by a questionnaire and history taking. Laboratory tests include fasting blood glucose, lipid profile, C-reactive protein, and uric acid. Body composition including fat mass% was measured by body composition analyzer. Lumbar spinal BMD was measured by dual-energy X-ray absorptiometry. Also, to evaluate liver steatosis and its grade, abdominal ultrasonography was conducted. Multivariate logistic regression analysis was used to determine the grade of steatosis affecting lumbar spinal BMD. Results: A total of 1,245 postmenopausal women were selected for this study. Mean age was 58.3$\pm$6.3 years old. The lumbar spinal BMD were significantly different according to the grade of steatosis, after adjusting for age; no steatosis (0.819$\pm$0.004 g/cm^2), mild (0.846$\pm$0.007 g/cm^2), moderate (0.844$\pm$0.009 g/cm^2) and severe steatosis (0.779$\pm$0.031 g/cm^2). The proportion of osteoporosis (L_{1-4} T-score $\leq$2.5) was 39.1% in no steatosis group. Otherwise, in mild, moderate, and severe steatosis group, each proportion of osteoporosis was 30.3%, 31.6%, and 56.3%, respectively. Also, women with severe steatosis were significantly increased risk of osteoporosis (OR=3.65, 95% CI; 1.217-10.920) compared to those with no steatosis after adjusting for age, body mass index, current smoking, and exercise. Conclusion: In postmenopausal women with severe hepatic steatosis, the lumbar spinal BMD is lower than those with no steatosis. Also, the risk of osteoporosis is 3.56-fold higher in these women compared to those without steatosis.

***Disclosures: Hee-Jeong Choi**, None.*

SU0351

Falls and Fractures in Elderly Men Can Be Predicted by Physical Ability Tests – Up to 7 Years Prospective MrOS Data. Bjorn Rosengren*[1], Eva L. Ribom[2], Osten Ljunggren[2], Claes Ohlsson[3], Dan Mellstrom[4], Jan-Åke Nilsson[1], Magnus Karlsson[1]. [1]Skåne University Hospital Malmö, Lund University, Sweden, [2]Uppsala University Hospital, Sweden, [3]Centre for Bone & Arthritis Research, Sweden, [4]Sahlgrenska University Hospital, Sweden

If we could identify fallers, or better frequent fallers, or at the best fallers who will sustain fractures, we could identify individuals in need for fall and fracture preventive interventions. The purpose of this prospective study was to report fall epidemiology and evaluate if simple clinical tests of physical ability could be used to identify elderly male fallers and fracture patients both in a short and long term perspective.

Included was a population-based sample of 3014 randomly selected men in Sweden aged 69-81 years who participated in the MrOS Study. At baseline, physical ability was estimated by handgrip strength test, time stand test, 6-meter walking test and 20-cm narrow walking test. Self-reported falls and fractures were registered every 4th month for up to 84 months through repeated mailed postcards. All fractures were verified by radiographs.

During the first 12 months there were 19.0% fallers, 8.7% frequent fallers and 1.8% fallers with fractures. During the 36 month period following baseline there were 37.4% fallers, 22.6% frequent fallers and 15.7% fallers with fractures. During the median 64 month period following baseline there were 53.7% fallers, 31.3% frequent fallers and 12.8% fallers with fractures. The physical ability tests predicted fallers during the first 12 months so that each Z-score lower test score for grip strength and higher for time stand and walking tests was associated with an odds ratio (OR) varying between 1.16-1.31 (95% CI 1.06-1.43). The tests discriminated multiple fallers from single and non fallers, so that each Z-score lower grip strength and higher time stand and walking tests was associated with an OR varying between 1.20-1.34 (95% CI 1.05-1.49). Finally, the tests (except 6 meter walking test) also discriminated individuals who were to sustain a fracture from individuals who would not, so that each Z-score lower grip strength and higher time stand and walking tests was associated with an OR varying between 1.25-1.82 (95% CI 1.03-2.38). The same predictive ability was found for the tests when instead evaluating a 36 month or a median 64 month period.

This study infers that simple clinical tests of physical ability could identify elderly men with high risk for falls, multiple falls and fall related fractures both in a short and long term perspective. As the traits are possible to target, these could in elderly men be a potential source for intervention as to reduce the fall and fracture risk.

***Disclosures: Bjorn Rosengren**, None.*

SU0352

Involving Patients in the Osteoporosis Care Gap and the Research Agenda: the Canadian Osteoporosis Patient Network. Anh, Anne Le-Gnoc[1], Angela Cheung[2], Jacques Brown[3], Famida Jiwa[4], Alexandra Papaioannou[5], Suzanne Morin*[6]. [1]McGill University, Canada, [2]University Health Network, Canada, [3]Laval University, Canada, [4]Osteoporosis Canada, Canada, [5]Hamilton Health Sciences, Canada, [6]McGill University Health Centre, Canada

Purpose: The role of the patient in the development of healthcare policies and delivery is becoming essential. The Canadian Osteoporosis Patient Network (COPN), of Osteoporosis Canada, is a virtual network created by patients with goals of education and advocacy. This network communicates electronically and its members receive educational material on a bi-weekly basis. The objectives of our study were to 1) to describe the characteristics of the COPN members 2) to assess their knowledge about osteoporosis care and their perception of research needs.

Methods: We conducted a survey of all members of COPN in April 2009. The questionnaire included 39 questions and was distributed electronically (1,267) or by mail (584) in French and in English.

Results: We received 563 completed surveys (30% response rate). Respondents were mostly women (87.2%) of an average age of 67.4 (SD 11.1) years. Seventy four % reported a diagnosis of osteoporosis and 242 (43%) reported a fracture after the age of 40 (Table 1). Of those with fractures, 78% were somewhat/very afraid of a recurrent fracture and 16% claimed that their daily activities were very much limited because of osteoporosis, as compared to those without fractures (67% and 6.1% respectively, P<0.0001). Respondents scored a mean of 78% (CI 95% ± 10) on a 12-point questionnaire assessing knowledge. "People most at risk for breaking bones have low bone density, are older and have already broken a bone" (true or false) was the question missed most frequently. Most reported they obtained their information from the COPN newsletter (68%) and their primary care physician (41%); 57.5% considered the newsletter as a very/extremely useful source of information whereas only 23.4% considered their primary care professional as such. Top ranked areas for research include improvement in knowledge dissemination to healthcare professionals, development of treatment and ways to improve quality of life in patients with osteoporosis. 2.5% respondents were concerned about chronic pain associated with osteoporosis (Table 2).

Conclusions: Ensuring patient involvement in the knowledge dissemination cycle and the development of the research agenda is key to improving the osteoporosis care gap.

COPN_tables 1and2

***Disclosures: Suzanne Morin**, None.*

SU0353

Is There an Increased Risk of Hip Fracture in Parkinson Disease (PD)? Analysis of the Nationwide Inpatient Sample (NIS). Rajib Bhattacharya*[1], Richard Dubinsky[2], Sue Min Lai[2]. [1]KU Medical Center, USA, [2]University of Kansas, USA

Objective: To determine if people with PD have a higher rate of hip fractures and to explore the discharge disposition of PD patients vs. non-PD admitted for acute hip fracture.

Background: Frequent falls in people with PD combined with the higher rate of osteoporosis in people with PD should lead to an increased risk of hip fracture. Yet this is still controversial.

Methods: Retrospective cohort analysis 20 years of the NIS (HCUP, AGRQ.gov), a 20% stratified sample of US hospital admissions. Admissions with a primary diagnosis of acute hip fracture were identified, as was the subset with a secondary diagnosis of PD. Indirect adjustment was used to compare the prevalence of PD in this population, to that from the Copiah County study (Schoenberg B, Neurology, 1985). Because of the large number of records and multiple comparisons, *p* was set a priori at .0001.

Results: 3.56% of 1,079,626 hip fracture admissions were for PD. Hip fracture occurred more often in men than in women, there was a trend for lesser mortality for PD (2.76 vs. 3.02%, p= .0003) yet discharge to nursing home was greater for PD (70.3% vs. 60.6%, p < .0001). When compared to the population prevalence the prevalence of PD among the patients with hip fracture was 3.41 (95% confidence interval; 3.40, 3.42) predicted when age adjusted and 3.52 (3.51,3.53) when adjusted for gender and age. When adjusted for race (white, black) the prevalence was 2.97 (2.96,2.98). Race was specified for 65% of the sample.

Conclusions: In this nationwide sample of 20 years of US hospital admissions the rate of hip fracture was three times more than predicted. These osteoporotic hip fractures in PD patients lead to higher rates of long-term care admissions. While the risk of falls can be partially mitigated through medication management, efforts are needed to further understand and to treat osteoporosis in people with PD.

***Disclosures: Rajib Bhattacharya**, Novartis, 8; Novartis, 1*

SU0354

Non-vertebral Fractures in Obese Postmenopausal Women: Are They Fragility Fractures? Melissa Premaor[1], Juliet Compston*[2], Li-Yung Lui[3], Richard Parker[4], Steven Cummings[5], Kristine Ensrud[6]. [1]Addenbrooke's Hospital, United Kingdom, [2]University of Cambridge School of Clinical Medicine, United Kingdom, [3]California Pacific Medical Center Research Institute, USA, [4]The General Practice & Primary Care Research Unit, Department of Public Health & Primary Care, Institute of Public Health, University of Cambridge, United Kingdom, [5]San Francisco Coordinating Center, USA, [6]Minneapolis VA Medical Center / University of Minnesota, USA

Body mass index (BMI) is a major determinant of bone mineral density (BMD) and higher BMD in obese individuals is widely believed to protect against fracture. Rather than being protective, however, higher BMD associated with obesity may reflect adaptation to increased mechanical demands on the skeleton and BMD in obese women with fracture, although often normal according to the WHO classification, may be low relative to obese women without fracture. We tested this hypothesis by comparing BMD in obese postmenopausal women with and without fracture.

Characteristics of obese women with and without fracture were investigated using the Study of Osteoporotic Fractures (SOF) database. SOF is a prospective population-based study of 9704 Caucasian postmenopausal women followed up for a mean(SD) of 12.8(5.4) years. BMD was measured by dual energy X-ray absorptiometry. Fractures were confirmed by X-ray report.

1480 (18.6%) women in the cohort were obese (BMI ⩾30kg/m^2) of whom 516 (34.8%) suffered a non-vertebral fracture during the follow-up period. The mean(SD) age at baseline in obese women with and without fracture was 72.8(4.6) and 72.3(4.4) years and mean weight 83.0(8.8) and 83.8(9.1) kg respectively. BMD T-scores in the spine, femoral neck and total hip were significantly lower in the women with fracture than in those without fracture [odds ratio (OR) (95% CI) -1.26 (1.48) vs -0.70(1.53), -1.52(0.89) vs -1.05(0.96), and -1.12(1.03) vs -0.60(1.03); p<0.0001]. 50.2% of obese women with fracture had a previous history of fracture compared to 33.1% of obese women without fracture (p<0.0001). Tobacco use, alcohol intake, menopausal age, parental fracture and physical activity were similar in the fracture and non-fracture group. Falls were more common in obese women with fractures (34% vs 28% in the year prior to baseline; p<0.05). In a logistic regression model a previous history of fracture and femoral neck BMD were independently associated with incident non-vertebral fracture (1.69(1.33-2.14); p<0.0001) and 1.62(1.42-1.85) per 1SD decrease in BMD; p<0.0001) respectively. In conclusion, obese postmenopausal women who sustain non-vertebral fractures have significantly lower BMD and are more likely to have a past history of fracture than obese women without fracture. Fractures in obese postmenopausal women thus exhibit some characteristics of fragility fractures. However, the effects of bone protective therapy in this population are unknown.

***Disclosures: Juliet Compston**, None.*

SU0355

The Association of Serum 25-Hydroxyvitamin D with Indices of Bone Strength in Older Men of Caucasian and African Descent. Kamil Barbour*[1], Joseph Zmuda[1], Mara Horwitz[2], Elsa Strotmeyer[3], Robert Boudreau[3], Kristine Ensrud[4], Moira Petit[5], Christopher Gordon[6], Jane Cauley[1]. [1]University of Pittsburgh Graduate School of Public Health, USA, [2]University of PittsburghDiv of Endocrinology - EMRC, USA, [3]University of Pittsburgh, USA, [4]Minneapolis VA Medical Center / University of Minnesota, USA, [5]University of Minnesota, USA, [6]McMaster University, Canada

There are limited data on serum 25-hydroxyvitamin D [25(OH)D] and bone density and geometry in older black men.To better understand if there are racial differences in vitamin D status and indices of bone strength we determined the association of 25(OH)D with peripheral quantitative computed tomography (pQCT) parameters including trabecular and cortical volumetric bone mineral density (vBMD),bone mineral content (BMC), bone geometry and polar and axial strength strain index (SSIp and SSIx) among Caucasian (N=446) men living in the US and men of African (N=496) descent living in Tobago aged ⩾65 years. Serum concentrations of total (D2 +D3) 25(OH)D were measured using liquid chromatography and tandem mass spectrometry and categorized using clinical categories defined as sufficient (⩾30 ng/ml),insufficient (20-<30 ng/ml) and deficient (<20 ng/ml). Surprisingly,men of African descent had higher 25(OH)D concentrations than Caucasians (34.7 vs. 27.6 ng/ml, p<0.001). Possibly due to higher ultraviolet (UV) light exposure and lower BMI in the Tobago cohort. In Caucasians, higher 25(OH)D levels were associated with higher cortical vBMD (p trend=0.042), total BMC (p trend=0.007),cortical thickness (p trend=0.004),SSIp (p trend=0.028) and SSIx (p trend =0.012) at the distal radius after adjusting for covariates including age, BMI, season of blood draw, and history of fracture. These associations were also significant at the distal tibia, with the exception of cortical vBMD and SSI parameters. There was also greater total BMC among 25(OH)D sufficient versus deficient men at the distal radius and tibia. In contrast, in men of African descent, 25(OH)D was not associated with pQCT parameters with the exception that higher levels were associated with lower total bone area (p trend=0.005) and SSIx (p trend=0.048). There was strong evidence that the association between 25(OH)D and pQCT parameters depended on race. Race

modified the association between 25(OH)D and total BMC (p =0.003), total bone area (p=0.006), SSIp(p=0.006), SSIx (p=0.002), and trabecular vBMD (p=0.015) of the radius. In Caucasians, there was evidence of a threshold effect on tibial total BMC and cortical thickness at 19 and 18 ng/ml of serum 25(OH)D, respectively. Beyond this 25(OH)D level, effects of higher 25(OH)D levels on bone parameters appeared to be minimal. Prospective studies in diverse populations are needed to evaluate the association of 25(OH)D with trabecular and cortical bone loss.

25(OH)D and pQCT

***Disclosures: Kamil Barbour**, None.*

SU0356

The Non-Linear Association between Percentage Body Fat and Fracture Risk: The European Prospective Investigation into Cancer-Norfolk Study. Alireza Moayyeri*[1], Robert Luben[2], Nicholas J Wareham[3], Kay-Tee Khaw[2]. [1]University of Cambridge, United Kingdom, [2]Department of Public Health & Primary Care, University of Cambridge, United Kingdom, [3]MRC Epidemiology Unit, United Kingdom

Body fat mass, an important index of obesity, has been linked to osteoporosis and fracture risk in different directions. This inconsistency between studies can be a result of ignoring potential non-linear nature of association between fat mass and bone health as well as use of surrogate outcomes (e.g. BMD) for fractures. We aimed to examine the association between percentage body fat (%BF) and prospective risk of fracture in the European Prospective Investigation into Cancer (EPIC)-Norfolk study.

%BF was measured using a validated bio-impedance technique in 1997-2000 and participants were followed for any incident fracture up to 2008. From 14,789 participants (6,470 men) aged 42-82 years at baseline, 556 suffered a fracture (184 hip fractures) during 122,330 person-years of follow-up (mean 8.7 $\pm$ 0.8 years). Fractional polynomial modelling was used to determine the shape of association between %BF and fracture risk with adjustment for known risk factors of fracture (age, height, history of fracture, smoking status, alcohol intake and broadband ultrasound attenuation of the heel) with and without adjustment for body mass index (BMI).

The prospective risk of hip fracture decreased linearly (in logarithmic scale) with rising %BF values among women. Effects of 10% decrease in %BF on risk of hip fracture was almost equal to 5 years increase in age and 1 standard deviation (16 dB/MHz) lower BUA. In model without adjustment for BMI among women, the association between %BF and risk of 'any type of fracture' was a second-degree fractional polynomial curve with the lowest hazard seen around mean %BF of 40%. After adjustment for BMI, the association turned to a first-degree fractional polynomial with continuous but altering decrease in fracture risk with higher %BF (Figure). There was no significant association among men.

In conclusion, this study shows that increased body fat mass is associated with lower risk of fracture among women but not in men. The association is linear for hip fractures but of a non-linear nature for other types of fracture. While low values of %BF are accompanied with substantially high risk of any fracture, high values of %BF are associated with moderately lower risk of fracture among women. Understanding differences in relationships between different indices of obesity (such as %BF and BMI) as well as sex interaction may help elucidate the metabolic and other underlying mechanisms involved in bone health and fracture risk.

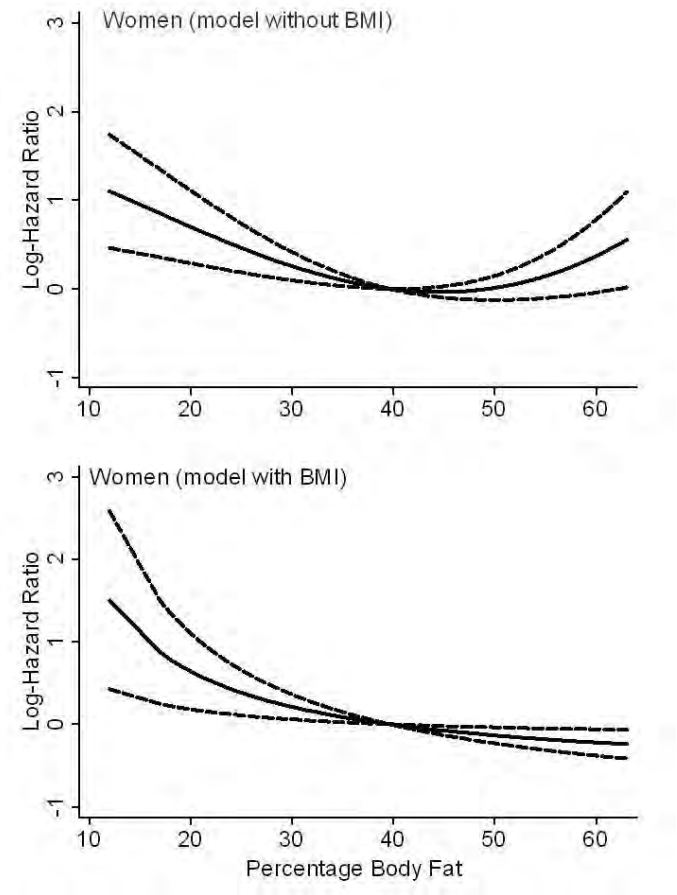

Association between %BF and risk of 'any type of fracture' among female participants of EPIC-Norfolk

***Disclosures: Alireza Moayyeri**, None.*

SU0357

Which FRAX® for French Women? Evaluation in a General Population of the Riviera and Contribution of Vertebral Fracture Assessment by DXA (VFA). Veronique Breuil*, Virginie Da Silva, Christian Hubert Roux, Nicolas Rijo, Christine Albert-Sabonnadière, Philippe Flory, Christian Grisot, Pascal Staccini, Liana Euller-Ziegler. CHU de nice, France

Introduction: we have no recent evaluation of osteoporotic (OP) fracture risk in the general French population. The FRAX® algorithms give the 10-year probability of fracture. Often not diagnosed, vertebral fractures (VF) represent however an important factor in FRAX® calculation. Aim of the study: to evaluate in a general population sample hip fracture risk and major OP fractures risk using the FRAX® tool, without and with VFA. Subjects and methods: the FRAX® was calculated in women who declared they never took drugs for OP (including estrogens) in a sample of 519 women, aged 50 to 85 y, randomly choosen in the list of social security and representative of general population. For all subjects, we performed a questionnaire, a DXA (hip, femoral neck (FN) and spine) and a high resolution VFA, read by 2 independent medical doctors (Genant scoring method). Results: the 341 women evaluated had the following characteristics: mean age 63 $\pm$ 9 y., BMI 26 $\pm$ 5.2 kg/m^2 and FN T-score -1.19 $\pm$ 0.99, parent fractured hip in 11.7% of the cases, previous clinical fracture 11.1% (including 3 VF), current smoking 2.9%, alcohol $\geqslant$ 3 units 4.4%, glucocorticoids 8.8% and rheumatoid arthritis 0.6%. 13.5% of the subjects had a T-score below -2.5DS at one of the sites. Without VFA, the mean value of hip FRAX® was 1.85% $\pm$ 4.42 and major FRAX® 6.26% $\pm$ 6.13. VFA identified 207 VF in 83 women (23.32%): 111 Genant 1, 84 Genant 2 and 12 Genant 3. In fractured women, the mean number of fracture was 2.2 (range 1-8). Taking in account the VFA ($\geqslant$Genant 1), the mean value of the major FRAX® was 7.24%$\pm$7.03, significantly higher than without VFA (p=0.027), and hip FRAX® was 2.10%$\pm$4.91, similar to FRAX® without VFA . If we considered cost effective to treat for a major FRAX® $\geqslant$ 7%, in our population, without VFA, 28.7% women had to be treated and with VFA 34.6%. If we considered cost effective to treat for a minor FRAX® $\geqslant$ 3%, in our population, without VFA, 16.42% women had to be treated and with VFA 20.52%. Conclusion: this study provide for the first time an quantitative evaluation of the FRAX® in the general French population and underline the high number of undiagnosed VF and the interest of VFA in fracture risk assessment, that may be an important factor for the therapeutic decision. Moreover, it shows the limits of the

FRAX® tool, which doesn't take into account the number of prevalent fracture and spine BMD.

***Disclosures: Veronique Breuil**, None.*

SU0358

Influence of Vitamin D levels on Bone Mineral Density and Osteoporosis. Mir Sadat-Ali*[1], Haifa Al-Turki[2], AbdulMohsen Al-Elq[3]. [1]King Fahd University Hospital, Saudi arabia, [2]Department of Obstetrics & Gynecology, College of Medicine, Dammam University, King Fahd University Hospital, Saudi arabia, [3]Department of Internal Medicine, College of Medicine, Dammam University, King Fahd University Hospital, Saudi arabia

Background and Objectives: The effect of vitamin D on bone mineral density (BMD) remains underevaluated. With the objective to look critically the influence of 25 hydroxy Vitamin D (25HOD) on BMD this study was conducted.

Patients and Methods: Healthy men and women in the peak bone mass (PBM) age group and over ⩾50 years of age were recruited from the outpatient at King Fahd University Hospital, Al Khobar, Saudi Arabia, between February 1st 2009 and May 31st 2009. Patients age and sex were documented and body mass index (BMI) was calculated. Routine hematological tests and serum 25OHD was performed. Bone mineral density (BMD) was done using dual energy X-ray absorbptiometry (DEXA) at upper femur and lumbar spine.

Results: In the Peak bone mass (PBM) age group with normal 25OHD levels 50% of the women had low bone mass compared to 26.6% of males of the same age group of 4.8% (P=<0.001). With normal vitamin D levels in women of Postmenopausal Age group (PMA) group 26.4% women had abnormal BMD while 49.2% of men had abnormal BMD indicating low bone mass (P=0.001). In PBM age group with insufficiency of 25OHD, 84.2 % had low bone mass and in males of the same age had 88.9% had low bone mass. With deficiency of 25OHD none of the men and women irrespective of age had normal BMD. Regression Co-efficient analysis for 25OHD, Parathormone (PTH) and BMD showed that in Postmenopausal Women ⩾50 years, insufficiency and deficiency of 25OHD correlated negatively with PTH and BMD (r=0.758, p<0.000 and r=0.25, p=0.031). In women of PBM age group, deficiency of 25OHD correlated negatively with PTH, and significantly positive with BMD (r=0.634, p=0.03). In men ⩾50 years insufficiency of 25OHD correlated significantly only with PTH (r=0.582, P<0.009). Deficiency of 25OHD correlated negatively with PTH, positively significantly with significantly positive with BMD (r=0.92, p=0.001), while in men aged ⩽35 years insufficiency of 25OHD correlated significantly only with PTH (r=0.582, P<0.009). Deficiency of 25OHD correlated negatively with PTH, and significantly positive with BMD (r=0.92, p=0.001).

Conclusions: In the assessment of bone health, normal vitamin D levels or bone mineral density on their own are not enough. Our study shows that even with normal levels of 25OHD, men and women can have low bone mass while with insufficiency and deficiency of 25OHD there is consistently low bone mass.

***Disclosures: Mir Sadat-Ali**, None.*
This study received funding from: Deanship of scientific Research, Dammam University

SU0359

Bone Changes in Systemic Mastocytosis: An Histomorphometric Approach. Béatrice Bouvard*[1], Maurice Audran[2], Erick Legrand[3], Emmanuel Hoppé[1], Charles Masson[1], Daniel Chappard[4]. [1]INSERM, U922 - LHEA, France, [2]Université et CHU Angers; INSERM U922, France, [3]Centre Hospitalier d'Angers, France, [4]INSERM, U922- LHEA, France

Systemic mastocytosis (SM) is a disorder characterized by mast cell proliferation and accumulation within various organs, most commonly the skin and bone. SM, although rare, should be included in the differential diagnosis of idiopathic osteoporosis. Increased serum tryptase level is a good marker of the disease, but in the absence of cutaneous manifestation, the diagnosis may be very difficult. In the past 17 years, diagnosis of SM was confirmed in 98 patients from our department by means of histomorphometric analysis of transiliac bone biopsies and microCT analysis of the bone cores. 33 patients had also a bone marrow biopsy. ~ 30% of the patients suffering from ''unexplained osteoporosis'' or ''unusual presentation of bone fragility'' as assessed by DEXA, had negative clinical investigations (no cutaneous manifestation, no organo-megaly nor digestive disorder...) and extensive and negative biological tests. Accumulation of mast cells was confirmed on bone biopsies by toluidine blue staining, tryptase and c-kit immunohistochemistry. Atypical mast cells (with a spindle-like shape) were arranged in nodules and sometimes contained few granules. A marked number of mast cells was applied onto the osteoblasts and lining cells and always contained an increased number of granules. In the unexpected cases, the initial diagnosis was: idiopathic osteoporosis, MGUS, and primary hyperparathyroidism. Microarchitectural analysis and parameters of bone turnover (BV/TV_{2D} and BV/TV_{3D}, number of osteoclasts, bone formation rate, active eroded surfaces, star volume of marrow spaces) were analyzed. There was an important range of these values in patients.~ 8% of the patients had normal active eroded surfaces values. In conclusion, transiliac bone biopsy is a better tool than bone marrow biopsy for the diagnosis of systemic mastocytosis in patients with presumed idiopathic osteoporosis after thorough, but negative clinical and biological investigations. In our study, analysis of histological parameters of bone remodeling showed frequently an increased bone turn-over (increased eroded surfaces, number of osteoclasts), as well as a marked deterioration of bone quality (decreased bone star volume).

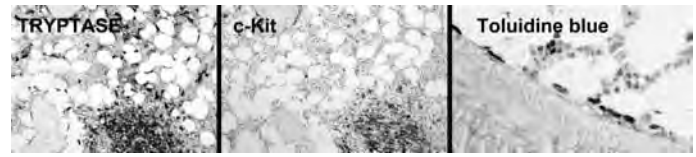

fig 1

***Disclosures: Béatrice Bouvard**, None.*

SU0360

A Comparative Study of the Metabolic Response in Three Mouse Strains to Diet-induced Obesity and The Implications on Skeletal Health. Elizabeth Rendina*, Yan Wang, Kristen Hester, Kelsey Hembree, McKale Davis, Krista Shawron, Stephen Clarke, Edralin Lucas, Brenda Smith. Oklahoma State University, USA

Diet induced obesity (DIO) and the metabolic changes associated with glucose intolerance have been shown to increase long-term fracture risk; however the mechanisms that lead to compromised bone quality remain elusive. This study was designed to examine the metabolic response to a high fat (HF) diet in three mouse strains to provide insight into the mechanism by which bone metabolism is altered. Male 8-wk old C57BL/6, C57BL/6J, and C3H/HeJ mice were fed a control (AIN-93M) or HF diet (45% fat kcal) for 24 wks. Body weight, fasting blood glucose and plasma insulin were monitored over time, and an oral glucose tolerance test (OGTT) and micro-CT analysis were performed at the end of the study. C57BL/6 and C3H/HeJ mice on the HF diet experienced an increase ($p<0.05$) in body weight during the first 2-3 wks and after 5 wks in the C57BL/6J strain. Percent body fat and epididymal fat pad weights increased in all 3 mouse strains on the HF diet. In the C57BL/6 and C57BL/6J strains fat deposition was increased in visceral regions, whereas, in the C3H/HeJ strain greater subcutaneous fat accumulation was observed. Fasting blood glucose was elevated beginning at 8 and 16 wks in C57BL/6 and C57BL/6J on the HF diet, and in the C3H/HeJ strain at 24 wks only. Plasma insulin of the C57BL/6 and C3H/HeJ mice was increased ($p<0.05$) after 2 months of the HF diet compared to their respective controls, while in the C57BL/6J mice insulin was only elevated at 24 wks. OGTT showed that all HF groups had a higher area under the curve compared to mice on the control diet, but by 120 min no differences in blood glucose were observed in the C3H/HeJ strain due to diet. Vertebral BV/TV was decreased in the C57BL/6 (-14.5%) and C57BL/6J (-13.6%) mice fed the HF diet. In these strains TbN and TbSp tended to be reduced ($p<0.1$), but did not reach statistical significance. Structural model index was increased in these two strains indicating, a more rod-like trabecular structure but no differences were detected in cortical bone parameters. No alterations in trabecular or cortical bone were observed in the C3H/HeJ mice consuming the HF diet. These results suggest that C3H/HeJ is not susceptible to bone loss associated with DIO, despite the fact that blood glucose and insulin levels increased in the HF group. Due to the C3H/HeJ strain point mutation in the toll-like receptor (TLR)-4, further studies are warranted to evaluate the role of TLR-4 signaling in bone loss associated with DIO.

***Disclosures: Elizabeth Rendina**, None.*

SU0361

The Effects of Diacylglycerol Oil on Bone Metabolism of C57BL/6J Mice. Hanseok Choi*[1], Kwang Joon Kim[2], Kyoung Min Kim[3], Se Hwa Kim[4], Sung-Kil Lim[5]. [1]Dongguk University Ilsan Hospital, South korea, [2]Severance Hospital, South korea, [3]Yonsei University, South korea, [4]Kwandong University College of Medicine, Myongji Hospital, South korea, [5]Yonsei University College of Medicine, South korea

Background: In epidemiologic and animal studies, a high fat diet (HFD) has been reported to be associated with lower BMD and higher risk of osteoporotic fractures. Meanwhile, consuming HFD containing diacylglycerol (DAG) instead of triacylglycerol (TAG) has been reported to have metabolically beneficial effects such as reduction in body weight and abdominal fat. In this study, we investigated the effects of HFD containing DAG on oxidative stress and bone metabolism in mice.

Methods: 36 four-week-old male C57BL/6J mice were divided into 3 groups: the chow diet group (n=12), HFD with TAG group (n=12), and HFD with DAG group (n=12). After 16 weeks of treatment, bone density and microstructure were analyzed using DXA and micro-CT. Oxidative stress in bone marrow cells was measured using dihydroethidium staining. Real-time PCR of bone marrow cells was performed to investigate the expression of osteoblastogenic or adipogenic transcription factors.

Results: Compared to HFD with TAG group, HFD with DAG group had lower body weight (30.5 $\pm$ 1.1g vs. 35.7 $\pm$ 3.8g), higher BMD (0.0546 $\pm$ 0.0025g/cm^2 vs. 0.0511 $\pm$ 0.0022g/cm^2), increased trabecular thickness and number, and decreased trabecular separation. Oxidative stress in bone marrow was lower in HFD with DAG group than in HFD with TAG group. HFD with DAG group showed increased

expression of Runx2 and decreased expression of PPARγ compared to HFD with TAG group.

Conclusions: Compared to HFD with TAG, HFD with DAG induced a lower oxidative stress in bone marrow and had a beneficial effect on bone metabolism of C57BL/6J mice.

***Disclosures: Hanseok Choi**, None.*

SU0362

Effect of Body Mass Index on Bone Metabolism and Bone Mineral Density: Role of Endogenous Sex Hormones. Adarsh Sai*[1], Xiang Fang[2], J. Christopher Gallagher[1]. [1]Creighton University Medical Center, USA, [2]Creighton University, USA

Introduction: Few studies have examined the association of body mass index (BMI) with bone metabolism and bone mineral density (BMD).

Methods: 489 postmenopausal women with osteopenia and osteoporosis, mean (SD) age 71.5(3.6) yrs were enrolled in an interventional treatment study (STOP IT). These results are from the baseline data. Serum parathyroid hormone (PTH) was measured by an intact assay (Nichols), serum 25-hydroxyvitamin D (25OHD) by competitive protein assay (Haddad), 24h urine N-telopeptides (NTx/Cr) and serum osteocalcin by Elisa and serum 1,25-dihroxyvitamin D ($1,25(OH)_2D$) by radioreceptor assay (Incstar, USA). Serum bioavailable estradiol, testosterone and sex hormone binding globulin (SHBG) were measured by radioimmunoassay. BMD measurements were done on DPXL scanner. Calcium absorption was measured with 100 mg calcium and 5 μCi Ca^{45}. We divided study population into tertiles of BMI and compared the groups with one-way ANOVA.

Results: BMD at all sites was significantly higher in the highest BMI group compared to the lowest ($p< 0.001$,Table 1). Serum 25OHD and PTH were significantly different among BMI tertiles (Table 1). Serum $1,25(OH)_2D$ and serum osteocalcin were significantly lower in tertile 3 versus 1 of BMI (33 ± 6.9 pg/ml vs 35.28 ± 8.3 pg/ml for $1,25(OH)_2D$ and 3.50 ± 1.2 ng/ml vs 4.1±1.3 ng/ml for osteocalcin, p for both < 0.001). Serum bioavailable estradiol and testosterone were significantly increased in higher BMI tertiles (Table1, $p<0.01$) and serum sex hormone binding globulin was significantly lower in tertiles 2 and 3 vs 1 (181.8 ±73.7 nmol/L in tertile 1 vs 146.6 ± 54.6 nmol/L in 2 and 112.5 ± 54.3 nmol/L in 3; $P<0.001$). Calcium absorption (weight adjusted) at 2 hours was significantly greater in higher BMI tertiles (23.27 ± 6.1 % AD/liter in tertile 1 vs 25.48 ± 6.8 in 2 and 29.80 ± 8 in tertile 3; $p<0.001$).

Conclusions: Women with higher BMI have increased levels of bioavailable sex hormones. They have lower bone resorption, higher calcium absorption and higher BMD. Despite the higher serum PTH in the highest tertile, bone resorption was lower and BMD higher suggesting that endogenous sex hormones protect bone.

Tertiles of BMI		1 (14.12-24.72)	2 (24.73-28.67)	3 (28.68-46.61)
L2-4 BMD	(g/cm^2)	0.94±0.16	1.00±0.17**	1.09±0.18**
Femoral neck BMD	(g/cm^2)	0.73±0.10	0.77±0.08**	0.79±0.08**
Urine NTx/Cr (nmolBCE/mmolCr)		57.0±28.4	49.0±22.7*	46.4±27.9**
Serum PTH	(pg/ml)	33.76±12.9	36.10±13.5	41.79±16.7**
25OHD	(ng/ml)	33.83±11.5	31.07±10.1	28.94±9.3**
Bio-Estradiol	(pg/ml)	2.69±1.60	3.52±1.9**	4.48±2.3**
Bio-testosterone	(ng/ml)	20.88±12.8	24.93±14.7	34.22±20.1**

*P<0.05 and **p<0.01 as compared to tertile 1 after Scheffe post-hoc correction
Data expressed as Mean ± SD

Table 1

***Disclosures: Adarsh Sai**, NIH Grants AG28168, UO1-AG10373 and RO1-AG10358, 2*

SU0363

Menstrual Cycle History but not Percent Body Fat Predicts Bone Mineral Density in Exercising Women. Rebecca Toombs*[1], Nancy Williams[2], Gaele Ducher[1], Jennifer Scheid[1], Mary Jane De Souza[3]. [1]Penn State University, USA, [2]The Pennsylvania State University College of Medicine, USA, [3]Pennsylvania State University, USA

Amenorrheic exercising women typically present with low bone mineral density (BMD) when compared to their ovulating counterparts. These women are also observed to have lower percent body fat (%BF) than ovulatory exercising women, serving as a possible contributing factor to low BMD due to the effects of the adipocyte-derived hormone leptin on BMD. The purpose of this study was to determine the respective roles of the number of menstrual cycles in the past year and %BF in predicting BMD among exercising women. Exercising ovulatory (ExOv, n=31) and amenorrheic (ExAmen, n=18) women (18-35 yrs) completed a questionnaire about menstrual history. Body composition and BMD at the lumbar spine (L1-L4) and hip were assessed using DXA. ExAmen women weighed less (55.4±1.5 vs 59.3±0.9 kg, p=0.018) and had a lower BMI (20.1±0.4 vs 21.6±0.3 kg/m^2, p=0.005) than ExOv women. %BF was significantly lower among the ExAmen women compared to ExOv women (21.8±1.22 vs 25.9±0.7%, p=0.004) and leptin showed a trend to be lower in ExAmen compared to ExOv women (5.7±1.3 vs 8.7±0.8 ng/ml, p=0.055); there was, however, a large overlap in %BF (10.1-29.0% vs 16.9-32.7%) and leptin (0.3-18.1 vs 1.2-17.2 ng/ml) between the groups. The two groups of exercising women were similar with respect to lean body mass (41.5±1.1 vs 41.6±0.7 kg, p=0.936). ExAmen women presented with lower L1-L4 ($p<0.001$) and hip (p=0.017) BMD than ExOv women. In all subjects, the number of menstrual cycles in the last 12 months was positively correlated with BMD at L1-L4 and the hip independent of %BF and was a significant linear predictor of BMD at these sites ($p<0.05$), explaining 18.8% and 7.2% of the variance in L1-L4 and hip BMD, respectively. Neither %BF nor leptin significantly predicted BMD at L1-L4 or the hip. Among exercising women displaying a wide range of %BF and leptin, the number of menstrual cycles in the past year, but not %BF and leptin, was a positive predictor of BMD at multiple sites, suggesting that menstruation is a stronger predictor of BMD than %BF. The low BMD observed in amenorrheic exercising women is due to the uncoupling of bone formation and resorption that occurs in an environment of low energy availability, suppressed estrogen activity, and the resulting absence of menses. Longitudinal research that explores changes in hormonal, metabolic, and menstrual status and the effects on BMD is warranted.

Supported by the U.S. DoD (PR054531)

***Disclosures: Rebecca Toombs**, None.*

SU0364

Morphological Changes in Osteocyte Lacunae in Paired Iliac Crest Biopsies of Men with Primary Idiopathic Osteoporosis after 2 year- intravenous Ibandronate Treatment. Heinrich Resch*[1], Janina Patsch[2], Martin Stauber[3], Philipp Schneider[4], Paul Roschger[5], Andrea Berzlanovich[6], Peter Pietschmann[2]. [1]Medical University Vienna, Austria, [2]Medical University of Vienna, Austria, [3]b-cube AG, Switzerland, [4]Institute for Biomechanics, ETH Zurich, Switzerland, [5]L. Boltzmann Institute of Osteology, Austria, [6]Department of Forensic Medicine, Medical University of Vienna, Austria

Male osteoporosis is a major but largely underestimated health concern. Current treatment options increase bone density and reduce fracture risk, but it is unclear if a more gender-specific approach might improve treatment response. Considering the pathophysiological background of primary male osteoporosis potentially involving a functional defect of the osteoblastic lineage, our aim was to analyze the morphological properties of cortical osteocyte lacunae in men with primary idiopathic osteoporosis and non-osteoporotic controls. Furthermore, we aimed at studying the effects in lacunar properties induced by intravenous ibandronate treatment. After written informed consent and the exclusion of secondary or malignant causes of bone loss, 14 men underwent iliac crest biopsy. Five men had a follow-up biopsy after 2 years of treatment. Iliac crest specimens from age-matched men with sudden death and consecutive forensic autopsy served as controls (n=4). One cortical subsection per sample was cut from PMMA-embedded biopsies and scanned at the TOMCAT beamline of the Swiss Light Source using synchrotron radiation based micro-computed tomography at a nominal resolution of 740 nm. Data were filtered using a 3-dimensional constrained Gaussian filter to partially suppress noise. An advanced segmentation technique was applied to separate bone (Ct.TV) and osteocyte lacunae. The mean volume of osteocyte lacunae (<Lc.V>), the osteocyte lacunar number density (N.Lc/Ct.TV) and the lacunar volume density (Lc.V/Ct.TV) were determined and statistically compared. Overall, the relative lacunar volume (Lc.V/Ct.TV) was in the same range for all three groups. Paired biopsies revealed a non-significant decrease in the number of cortical osteocyte lacunae (N.Lc/Ct.TV) upon ibandronate treatment. However, a significant increase in the mean single lacunar volume (+13.3%; p=0.02) was observed. We interpreted the treatment dependent increase in single lacunar size as a sign of bone adaptation to possibly altered matrix strain due to a potentially increased matrix stiffness.

***Disclosures: Heinrich Resch**, None.*

SU0365

Altered Bone Matrix Composition in Premenopausal Women With Idiopathic Osteoporosis as Determined by Raman and FTIR Microspectroscopy. Birgit Buchinger[1], Sonja Gamsjaeger[1], Adi Cohen[2], Emily Stein[3], David Dempster[4], Halley Rogers[2], Robert Recker[5], Joan Lappe[5], Thomas Nickolas[2], Hua Zhou[6], Donald McMahon[3], Eleftherios Paschalis*[7], Elizabeth Shane[3], Klaus Klaushofer[8]. [1]Ludwig Boltzmann Institute of Osteology, Hanusch Hospital of WGKK, & AUVA Trauma Centre Meidling, Hanusch Hospital, Austria, [2]Columbia University Medical Center, USA, [3]Columbia University College of Physicians & Surgeons, USA, [4]Columbia University, USA, [5]Creighton University Osteoporosis Research Center, USA, [6]Helen Hayes Hospital, USA, [7]Ludwig Boltzmann Institute for Osteology, Austria, [8]Hanusch Hospital, Austria

Idiopathic osteoporosis (IOP) in premenopausal (PreM) women is an uncommon disorder in which fragility fractures and/or low bone mineral density (BMD) occur in otherwise healthy women with normal gonadal function. It is widely accepted that several aspects of bone quality are important contributors to bone strength. In this regard, we have reported that PreM women with IOP have thin cortices and cancellous microarchitectural deterioration and we have also found reduced

mineralization of bone matrix by quantitative backscattered electron imaging (qBEI). The purpose of this study was to examine bone mineral and collagen quality in IOP. Included were 59 PreM women, 31 healthy Controls with normal BMD (Z-score >-1.0) at all sites and 28 with IOP, 17 with Fractures and 11 with Low BMD (Z-score <-2.0 at spine and/or hip) who have not fractured. Transiliac bone biopsies were examined by Raman and FTIR microspectroscopy for lamellar organization, mineral to matrix ratio, relative proteoglycan content, mineral maturity/crystallinity, and collagen pyridinoline/divalent cross-link ratio on actively bone forming trabecular surfaces. Both techniques allow the analysis of thin tissue sections with a spatial resolution of ~1 μm in the case of Raman, and ~6.3 μm in the case of FTIR. Bone forming sites were selected based on the presence of tetracycline double labels (for the Raman analysis; data were obtained within the double labels), or primary mineralized areas (for the FTIR analysis). Since the analysis was performed at anatomical sites of similar tissue age, the reported results are independent of bone turnover. Lamellar organization was similar among the three groups (data not shown). While there was no difference in mineral to matrix ratio between Controls and IOP Fracture, the Low BMD group was significantly lower than either of the other groups (Table). Both IOP Fracture and Low BMD groups had significantly higher proteoglycan content than Controls, noteworthy as proteoglycans are reported to inhibit initiation of mineralization. Finally the pyridinoline/divalent collagen cross-link ratio was significantly higher in both groups of IOP patients than Controls, suggesting that there are alterations in post-translational modification of collagen in IOP. The results of the present study indicate that bone matrix composition is abnormal in PreM women with IOP, a factor that may contribute to increased skeletal fragility in this uncommon disorder.

Table: Bone Material Properties in IOP (Mean ± SE)	Control N=31	IOP Fracture N=17	IOP Low BMD N=11
Mineral/Matrix Ratio	0.29 ± 0.03	0.36 ± 0.04	0.17 ± 0.03 * #
Relative Proteoglycan content	1.84 ± 0.72	6.59 ± 1.43 *	5.93 ± 1.65 *
Pyridinoline/divalent collagen cross-links ratio	1.96 ± 0.15	10.52 ± 0.65 *	5.26 ± 0.48 * #
* p<0.05 vs Control; # p<0.05 vs IOP Fracture			

FTIR Table

***Disclosures: Eleftherios Paschalis**, None.*

SU0366

Association of Serum Leptin with Bone Mineral Density in an Ethnically-Diverse Population. Naim Maalouf*[1], Alex Tessnow[2], Colby Ayers[2], Alice Chang[2], Ugis Gruntmanis[1]. [1]University of Texas Southwestern Medical Center, Dallas, USA, [2]University of Texas Southwestern Medical Center, USA

Background: Previous studies have found a variable association of leptin and bone mineral density (BMD). Whether the association of leptin and bone density is independent of obesity is not clearly established. Circulating levels of leptin vary by ethnicity, which could potentially explain some of the ethnic differences in BMD.

Purpose of Study: To assess whether the relationship between leptin and BMD is independent of fat mass in a multi-ethnic population-based cohort.

Methods: We examined the association between serum leptin concentration and BMD in the Dallas Heart Study, a probability-based cohort over-sampled for African-Americans. Subtotal body BMD (BMD of whole body excluding head) and fat mass were measured by DXA scan, while serum leptin was measured using a commercial radioimmunoassay. Analyses were stratified by ethnicity, gender and menopausal status. Multiple linear regression analysis was performed with BMD as the dependent variable and independent variables of serum leptin (log-transformed to correct for skewed distribution), fat mass, age, tobacco, alcohol use, estrogen use and family history of osteoporosis.

Results: 1,565 participants were included in this analysis (47% African-American, 35% Caucasian, 18% Hispanic). Within each gender, BMD, fat mass and serum leptin were highest in African-Americans, intermediate in Caucasians, and lowest in Hispanics. In unadjusted analysis, leptin was positively associated with BMD only in Caucasian and African-American men and African-American and Hispanic pre-menopausal women. Adjusting for fat mass and in multivariate adjustment, leptin was significantly and inversely associated with BMD among African-American men, Caucasian premenopausal women, and Caucasian and African-American postmenopausal women.

Conclusions: Leptin is significantly and independently associated with BMD, after adjusting for fat mass and other BMD–related factors. The significance of the racial and gender differences in this association need to be further explored.

			Unadjusted		Fat Mass-Adjusted		Multivariate-adjusted*	
			Estimate	p-value	Estimate	p-value	Estimate	p-value
Men	C	N=289	0.018	0.005	-0.007	0.485	-0.005	0.660
	AA	N=359	0.015	0.012	-0.025	0.006	-0.022	0.020
	H	N=128	0.002	0.841	-0.021	0.080	-0.021	0.092
Pre-menopausal Women	C	N=117	0.014	0.054	-0.037	0.006	-0.037	0.008
	AA	N=169	0.013	0.024	-0.013	0.089	-0.010	0.167
	H	N=108	0.017	0.010	0.000	0.986	-0.001	0.928
Postmenopausal Women	C	N=125	0.012	0.130	-0.028	0.049	-0.028	0.045
	AA	N=197	0.014	0.066	-0.030	0.005	-0.031	0.003
	H	N=38	0.000	0.984	0.010	0.621	0.015	0.522

Estimate for each standard deviation change in log (leptin)

C = Caucasian, AA = African-American, H = Hispanic

*Adjusted for age, fat mass, smoking, alcohol use, history of diabetes, family history of osteoporosis, and estrogen use

Association of Serum Leptin (Log-transformed) and BMD by Gender and Ethnicity

***Disclosures: Naim Maalouf**, None.*

SU0367

Comparison of Two Different Test Platforms to Assess Motor Performance Relevant to Bone's Health and Risk of Falling. Claudia Kneitz[1], Peter Schneider*[2]. [1]University Clinic Würzburg, Germany, [2]Clinic for Nuclear Medicine, Germany

Purpose: Two devices designed to assess muscle force and power non-invasively were compared to gain information about factors influencing bone degradation and increased risk of fall.

Methods: Two different ground-reaction force platforms were used for force-vector tracing in different test situations. The Balance-Exercise-Explorer (BXP), developed at the University of Würzburg, Germany, was used to measure force, power and stance parameters. The Leonardo (LEO) jump plate (Novotec Medical GmbH, Pforzheim, Germany) designed to measure simple maximum power was used for quad jump and stance testing. Sway area [cm^2] during a tandem stance was tested in 303 male and female subjects (6-84years). Out of these, 208 subjects were able to perform both, continuous knee bending on the BXP (not designed for jumping) and quad jumps on the LEO. The maximum anaerobic motor force and power was normalized to body weight for better comparison. Each test took 10 seconds.

Results: Age depending decline of power and maximum force were more pronounced in knee bending than in jumping (r=-0.60 vs. -0.42 and r=-0.36 vs. -0.33, resp., $P>0.001$). The correlation between the two methods was r=0.74 for power and 0.55 for force ($P<0.001$). Average max. force was 14% higher on the LEO. Power showed a more pronounced age related decline on the LEO than on the BXP (r=-0.57 vs. -0.34, $P<0.001$). The peak power correlated higher than peak to continuous power between the 2 devices. Sway area was smaller on the BXP platform than on the LEO (54 ± 64 vs. 216 ± 299 cm^2). Age showed a greater influence on sway on the BXP than on the LEO platform (r=0.27 vs. 0.19, $P<0.001$ and $P=0.004$).

Conclusion: The LEO calculates the max. power during the steepest force gradient within a fraction of a second which is different from the continuous anaerobic power measured with the BXP. Thus, the methods may be useful to illuminate the proposed impact of continuous high cyclic forces versus short peak forces on bone stimulation. The sway area differences observed between the two platforms suggest a better test reliability of the BXP, perhaps due to a very simple x*y multiplication of maximum vector elongations implemented in the LEO. However, both methods may provide useful tools to assess motor training status, performance and ageing of fall relevant muscles. Quad jumps in elderly must be advised with great care.

***Disclosures: Peter Schneider**, None.*

SU0368

LPS Stimulates RANKL Expression in Bone Marrow Stromal Cells but Suppresses RANKL Expression in T Cells. Xinrong Chen*, Priscilla Cazer, Jinhu Xiong, Melda Onal, Stavros Manolagas, Charles O'Brien. University of Arkansas for Medical Sciences, USA

Inflammation-associated bone loss due to increased osteoclast number is common in conditions such as rheumatoid arthritis and periodontal disease. Osteoclastogenesis requires the cytokine RANKL and is directly proportional to the amount of RANKL available. In healthy remodeling bone, RANKL is supplied by stromal cells, which may be of the osteoblast lineage, and by osteocytes, as shown elsewhere at this meeting. While the source of RANKL in inflammatory conditions is unclear, activated T cells have been proposed as a major contributor. However, some studies have shown that activated T cells can directly inhibit osteoclast differentiation. Thus, the role of T cells in the control of bone resorption during inflammation is unclear. T cells may promote bone resorption either by expressing RANKL or by stimulating other cell types, such as stromal cells or osteocytes, to do so. To clarify the contribution of RANKL produced by T cells during inflammation, we developed a model in which LPS administration (10 mg/kg body weight) to adult C57BL/6 mice every 4 days for 16 days resulted in significant bone loss in the lumbar spine.

Quantification by realtime RT-PCR 4 days after the last injection revealed only a mild (2-fold) increase in RANKL mRNA expression in CD3+ T cells isolated from the spleen, compared to vehicle injected mice. However, no increase was observed in CD3+ T cells isolated from the bone marrow. Moreover, there was no change in RANKL expression in the spleen as a whole or in vertebral bone. The lack of increased expression in bone at day 16 suggested that LPS may have induced a transient rise in RANKL at an earlier time after injection. Therefore, we quantified RANKL expression 6 hr after a single LPS injection and found that it was increased by 6- to 8-fold in vertebrae and calvaria. In contrast, RANKL mRNA was decreased by 8-fold in the spleen. RANKL was also suppressed by 3- to 5-fold in CD3+ T cells derived from the bone marrow and spleen. Other cytokines, such as IL-6 and TNF-α, were robustly stimulated by LPS in CD3+ T cells from the bone marrow and spleen, as well as in whole spleen and bones. In vitro LPS treatment of primary bone marrow cultures, highly enriched in stromal cells, stimulated RANKL expression by more than 6-fold. These results suggest that LPS control of RANKL expression is different in stromal cells versus T cells and that stromal cells are likely to be a more significant source of the RANKL that drives LPS-induced bone loss.

***Disclosures: Xinrong Chen**, None.*

SU0369

Sitagliptin Does Not Exacerbate Loss of Bone Mineral Density Mediated by Pioglitazone in the Ovariectomized Rat. Tara Cusick*[1], Helmut Glantschnig[2], James Mu[2], Zhihua Li[2], Ku Lu[2], Xiaolan Shen[2], Nan Wei[2], Chris Johnson[2], Nancy Thornberry[2], Bei Zhang[2]. [1]Merck & Co., Inc., USA, [2]Merck Research Laboratories, USA

The insulin-sensitizing thiazolidinedione pioglitazone (PIO) at doses necessary to achieve glycemic control in patients with type 2 diabetes (T2D) has been linked to an accelerated loss of bone and an increased risk of fracture. Sitagliptin (SITA) is a potent, selective and reversible inhibitor of the DPP-4 enzyme representing a new class of antihyperglycemic agents that increase glucose-dependent insulin secretion and glucose tolerance. The combination therapy of SITA with PIO potentially offers improved glycemic control of inadequately controlled T2D, but the inherent risks of adverse skeletal events observed with PIO need to be examined. In this head-to-head study, we investigated the effects of SITA, PIO and combination treatments with SITA+PIO on ovariectomy (OVX)-induced bone loss and bone-turnover markers in Sprague Dawley rats. Following OVX, rats were treated immediately once daily by oral gavage for 3 months with vehicle (Veh), SITA (100, 300 and 500 mg/kg), PIO (5 and 30 mg/kg), or SITA+PIO (300+5, 500+5, 300+30 and 500+30 mg/kg). At trough drug levels, all SITA groups demonstrated ≥ 80% DPP-4 inhibition and showed significantly decreased glucose excursion during an oral glucose tolerance test. Dose dependent lowering of plasma triglyceride and insulin by PIO was observed. OVX induced significant loss in areal bone mineral density (BMD) in lumbar vertebra (LV; $p<0.01$; ANOVA Fisher's PLSD) and all analyzed regions of the femur ($p<0.05$) except the central femur. Under the same conditions, PIO treatment dose-dependently exacerbated OVX-induced loss of LV-BMD; by 3.8% ($p<0.2$, 5 mg/kg) and 9.7% ($p<0.01$, 30 mg/kg) vs. OVX-Veh. Exacerbated loss in BMD by PIO at 30 mg/kg was also evident in the proximal ($p<0.001$; 8.7%) but not in the distal and central femur. In contrast, SITA treatment alone did not reduce LV- and femoral-BMD at any dose tested. Consistently, reduction in LV- and femoral-BMD in SITA+PIO combination groups was not exacerbated when compared to the effects seen in the respective PIO-alone treatment groups. In summary, SITA, at dosages which achieve near complete inhibition of plasma DPP-4, did not exacerbate loss in BMD when administered alone or in combination with PIO at all skeletal sites analyzed. The data in this rodent model of high bone turnover suggest that SITA is neutral towards PIO-mediated effects on bone.

***Disclosures: Tara Cusick**, Merck, 3*
This study received funding from: Merck & Co.

SU0370

Effects of Cerclage Wiring on Cancellous Bone Union After Osteomy at the Proximal Tibia in Ovariectomized (OVX) Rats. Hiroyuki Tsuchie*, Naohisa Miyakoshi, Yuji Kasukawa, Hiroshi Aonuma, Yoichi Shimada. Akita University Graduate School of Medicine, Japan

Osteoporotic fractures often occur at cancellous bone-rich sites such as the vertebral body and femoral neck. However, most animal models of fracture healing following surgical intervention or antiosteoporotic agents have been established using cortical bones including the femoral shaft. The fracture healing process at the cancellous bone area following surgical intervention in animals has not been reported. We thus evaluated the effects of cerclage wiring on cancellous bone union at the osteotomy site in the proximal tibia of ovariectomized (OVX) rats.

Seven-month-old female Sprague-Dawley rats underwent OVX. Four weeks after OVX, all rats underwent complete mid-sagittal osteotomy of the proximal tibia and were divided into the wiring group and non-wiring group (n=14 each). In the wiring group, cerclage wiring was performed at the osteotomy site. The rats were sacrificed at 2 and 4 weeks after osteotomy (n=7 each, in both groups), and decalcified hematoxylin and eosin attained sections of the operated tibiae were prepared. Bone histomorphometry at the osteotomy site was performed to evaluate the percentage of the cancellous bone union and fibrous union.

After 2 weeks, none of the rats in the wiring group, but 3 of 7 rats in the non-wiring group showed fibrous tissue at the osteotomy site. The percentage of bone union was significantly higher in the wiring group than in non-wiring group ($p=0.004$) 2 weeks after osteotomy. However, there was no significant difference between the groups in terms of the percentage of bone union at 4 weeks. Although wiring procedure tended to show less fibrous tissue at the osteotomy site, there was no significant difference in the percentage of fibrous union between the groups both at 2 and 4 weeks after osteotomy ($p=0.062$, $p=0.063$, respectively).

Cerculage wiring technique improved cancellous bone union at the osteotomy site of the proximal tibia in OVX rats by 2 weeks. Potential effect of wiring for cancellous bone union was the maintenance of close contact bone at the bone interface and reduction of fibrous tissue intervention. However, the effect of wiring on bone union was not obvious 4 weeks after osteotomy in OVX rats.

***Disclosures: Hiroyuki Tsuchie**, None.*

SU0371

Serum Sclerostin is Inversely Associated With Bone Remodeling in Normal Premenopausal Women But Not in Premenopausal Women With Idiopathic Osteoporosis. Elizabeth Shane[1], Adi Cohen*[2], Serge Cremers[3], Emily Stein[1], Halley Rogers[2], Donald McMahon[1], Joan Lappe[4], Robert Recker[4], Clifford Rosen[5], Thomas Kohler[6], Thomas Nickolas[2], Thomas Kohler[6], Elzbieta Dworakowski[3], Ralph Müller[6], David Dempster[3]. [1]Columbia University College of Physicians & Surgeons, USA, [2]Columbia University Medical Center, USA, [3]Columbia University, USA, [4]Creighton University Osteoporosis Research Center, USA, [5]Maine Medical Center, USA, [6]ETH Zurich, Switzerland

Idiopathic osteoporosis (IOP) in premenopausal (PreM) women is an uncommon disorder in which fragility fractures (FX) and/or low bone mineral density (BMD) occur in otherwise healthy women with intact gonadal function. Using high resolution imaging and transiliac bone biopsy, we have reported that PreM women with IOP have thin cortices and cancellous (Cn) microarchitectural deterioration compared to age-matched PreM Controls with normal BMD. We have also found reduced osteoid seam width (OWi) and wall thickness (WTh) of completed osteons in women with IOP, suggesting osteoblast dysfunction. However, bone remodeling activity, assessed by serum bone turnover markers (BTMs), mineralized perimeter (MdPm) and bone formation rate (BFR/BS), was heterogeneous and did not differ between PreM women with IOP and normal Controls. Sclerostin is an inhibitor of Wnt signalling secreted by osteocytes. Hypothesizing that sclerostin might be a negative regulator of bone formation in IOP, we compared serum sclerostin measured by ELISA (Tecomedical, Sissach, Switzerland) in 64 PreM with IOP (44 FX, 19 LowBMD) and 40 Controls, mean age 37 for both groups, and also assessed relationships among serum sclerostin and BMD, BTMs and bone histomorphometry. Serum sclerostin did not differ between Controls and IOP FX (0.81+0.44 vs 0.68+0.37 ng/mL; $p=0.12$). BMD was not associated with serum sclerostin in either IOPs or Controls. Serum BTMs were not related to serum sclerostin in either group (Table). Serum IGF-1 was inversely and significantly related to serum sclerostin in Controls but not in IOPs. There was no relationship between serum sclerostin and serum PTH, 25-OHD or follicular phase serum estradiol in either group (data not shown), although serum sclerostin was inversely related to serum 1,25(OH)2D in Controls but not IOP. In Controls, serum sclerostin was inversely related to cancellous bone volume fraction (BV/TV by μCT) and MdPm, BFR/BV and remodeling activation frequency (ActF). In contrast, there was no relationship between serum sclerostin and these parameters in IOP subjects. In summary, serum sclerostin is inversely related to serum IGF-1 and histomorphometric remodeling parameters in normal PreM Controls, but not in women with IOP. The absence of any relationship between remodeling and serum sclerostin in PreM with IOP may suggest that Wnt signalling is disrupted in IOP.

Table: Correlation coefficients between Serum Sclerostin (r)	Controls	IOP
Serum C-telopeptide	-0.270	-0.108
Serum Osteocalcin	-0.102	0.032
Serum IGF-1	-0.411*	-0.240
Serum 1,25(OH)$_2$D	-0.338**	0.110
BV/TV (μCT; %)	-0.321*	-0.135
Mineralized perimeter (MdPm)	-0.570**	-0.077
Bone formation Rate (BFR/BS)	-0.526**	-0.125
Activation Frequency (ActF)	-0.509**	-0.115
*p<0.05 and **p<0.001		

Sclerostin_Abstract_Table.gif

***Disclosures: Adi Cohen**, None.*

SU0372

A 4-week Study of AXT914, a Novel Calcilytic Compound for Oral Bone Anabolic Osteoporosis Therapy, in Postmenopausal Women. Markus John*[1], Evita Harfst[1], Juergen Loeffler[1], Rossella Belleli[1], Julia Zack[2], Jon Ruckle[3], Leo Widler[4], Linda Mindeholm[1]. [1]Novartis Pharma AG, Switzerland, [2]Novartis Pharma AG, USA, [3]Hawaii Clinical Research Center, USA, [4]Novartis Institutes for Biomedical Research, Switzerland

Antagonism of the calcium-sensing receptor in parathyroid glands leads to parathyroid hormone (PTH) release via stimulation of an endogenous hormone-release mechanism. Calcilytics are a new class of molecules which aim to exploit this mechanism. In order to mimic the known bone-anabolic PK profile of s.c. administered PTH, a drug must release PTH transiently and robustly. In this 4-week, repeat-dose clinical study we evaluated the safety and pharmacodynamic efficacy of AXT914, a quinazolin-2-one derivative, which had previously been evaluated as part of an exploratory IND.

42 healthy postmenopausal women were randomized in parallel into the lowest 45 and 60 mg AXT914 dose cohorts in this double-blind, active comparator, placebo-controlled 4-week repeat-dose study.

Blood samples for safety, PK, and pharmacodynamic analyses were obtained at short intervals.

Both AXT914 doses demonstrated reproducible, robust and sharp PTH-release profiles. After 28 days of dosing - for 45mg AXT914, 60mg AXT914, 20 µg Forteo or Placebo respectively - the anabolic biochemical marker PINP increased 12.9%, 9.3%, 72.1% and 8.4% (geometric means) from baseline. Osteocalcin increased 10%, 7.9%, 60.5% and -4.6%. The bone resoprtion marker CTX1 increased 20.1%, 14.9%, 7.4% and -9.3%. Interestingly, the lower AXT914 dose had a more pronounced biochemical marker response compared to 60mg. The 45 and 60 mg AXT914 treatment groups did show a mean relative increase of 8.0% and 10.7% respectively in pre-dose total serum calcium values from Baseline to day 29, as compared to the Forteo and Placebo groups, with mean pre-dose changes of 1.3% and 1.0%, respectively. AXT914 was well tolerated at all doses. Adverse event frequency, safety laboratory values, vital signs or 12-lead ECG intervals did not suggest any clinically significant compound-related adverse effects. The trial was terminated early due to lack of efficacy following an interim analysis after these initial two dose levels.

In conclusion, the observed transient and reproducible PTH-release after repeat administration of AXT914 had an exposure profile close to that observed with s.c. PTH and was well tolerated. However, it did not translate into a biochemical anabolic window and was associated with a robust, persistent dose-dependent increase in serum calcium levels the mechanism of which is unknown.

***Disclosures: Markus John**, Novartis, 3*
This study received funding from: Novartis

SU0373

Does Acute Fracture Influence The Anabolic Activity of Teriparatide. Quang Ton*, Aasis Unnanuntana, Joseph Nguyen, Joseph Lane. Hospital for Special Surgery, USA

Teriparatide is the only anabolic agent in the United States for treatment of osteoporosis. Some conditions however may adversely affect the anabolic response of teriparatide such as a catabolic state from fracture. Studies have shown that fractures lead to a change in protein metabolism resulting in a negative nitrogen balance [Patterson+1992]. This study aims to compare the percent changes of bone mineral density (BMD) and biochemical bone markers at 1- and 2-year post teriparatide treatment between acute fracture and non-fracture groups.

We retrospectively reviewed patients treated with teriparatide during 2003 to 2009. Patients were included if they had teriparatide for at least 12 months. All patients had a history of antiresorptive therapy prior to teriparatide. Patients were divided into 2 groups based on indication: acute fracture and non-fracture. The acute fracture group included patients treated because of fragility fractures (n=77); while the non-fracture group (n=64) was those who had declining BMD or low turnover osteoporosis. The BMD at lumbar spine and hip was determined at baseline, 12 and 24 months after treatment. The bone markers (osteocalcin, urine NTX, bone specific alkaline phosphatase [BSAP]) were also measured at pre-treatment, 3, 12 and 24 months.

The lumbar spine BMD was increased at all visits in both groups with an average of 5.9% at 1 year and 9.0% at 2 years for acute fracture group, while being 6.2% at 1 year and 8.6% at 2 year for non-fracture group. There was no difference between groups. The average hip BMD in acute fracture group increased with a mean of 1.3% and 4.1% at 1 and 2 years, respectively. Hip BMD in non-fracture group however, had a transient decrease at 1 year after treatment (-0.3%), which was reversed at 2 years (3.8%). Again there was no difference between groups. Significant increases of osteocalcin and urine NTX were found in both groups at each time point of the study; however, there were no differences between groups. Similarly, there were no differences of BSAP levels between groups.

Acute fracture does not affect the anabolic activity of teriparatide. Teriparatide induces a positive effect on BMD in both hip and spine, and in ostoecalcin at 3 months, and urine NTX, at 3, 12 and 24 months, regardless of the presence of acute fracture. Therefore, clinicians should anticipate comparable anabolic responses when treating patients with teriparatide after recent osteoporotic fractures or for other indications.

***Disclosures: Quang Ton**, None.*

SU0374

Fracture Incidence, Quality of Life and Back Pain in Elderly Women (age >75 years) with Osteoporosis Treated with Teriparatide: 36 Month Results from the European Forsteo Observational Study (EFOS). James Walsh*[1], Willem Lems[2], Dimitrios Karras[3], Bente Langdahl[4], Osten Ljunggren[5], Clare Barker[6], Astrid Fahrleitner-Pammer[7], Annabel Barrett[6], Gerald Rajzbaum[8], Franz Jakob[9], Fernando Marin[10]. [1]Trinity College Dublin, The University of Dublin, Ireland, [2]Vrije Universiteit Medical Centre, The netherlands, [3]Veterans Administration Hospital, Greece, [4]Aarhus Sygehus, Aarhus University Hospital, Denmark, [5]Uppsala University Hospital, Sweden, [6]Lilly, United Kingdom, [7]Medical University Graz, Austria, [8]Hopital St. Joseph, France, [9]Julius-Maximilians-Universitat, Germany, [10]Eli Lilly & Company, Spain

Aim: To describe clinical fractures (Fxs), health-related quality of life (HRQoL) and back pain in the subset of postmenopausal women with osteoporosis aged 75 or more, who were treated with teriparatide (TPTD) in normal clinical practice. Methods: A prospective, observational study in 8 countries. Data on incident clinical vertebral and non-vertebral Fxs were collected, back pain assessed using a 100mm VAS and a questionnaire, and HRQoL measured using EQ-5D. Changes in incident Fx rates were calculated using logistic regression with repeated measures (RM). Changes from baseline in back pain VAS and EQ-VAS were analysed using an RM model and EQ-5D HSV (health state values) using Wilcoxon's signed rank test. Results: 1581 patients from EFOS had follow-up data, 589 women (37%) were ⩾75 yrs old. In the ⩾ 75 yrs cohort 80.2% of the patients had sustained ⩾2 Fxs after age 40 yrs, 75.6% had prior bisphosphonate use. Post-TPTD follow-up data were available for 298 patients, 95.6% received OP medication after stopping TPTD, 63.4%receiving bisphosphonates. During the 36 mths of follow-up, 87 women ⩾75 yrs (14.8%) sustained a total of 111 incident Fxs (33.3% clinical vertebral, 66.7% non-vertebral). A significant reduction from 0-6 mths in the odds of fracture was observed after 24 and 36 mths, odds ratios 0.42, $p<0.05$, and 0.20, $p=0.01$, respectively. The reported median EQ-5D HSV showed statistically significant improvements at all visits compared with baseline ($p<0.001$). Back pain frequency and severity was significantly reduced compared with baseline. The improvements in back pain and HRQoL were first seen after 3 mths of treatment (Table). Conclusion: Patients with severe postmenopausal osteoporosis aged 75 or older treated with TPTD in EFOS showed an early and significant reduction in back pain and improvements in HRQoL. These outcomes lasted for at least 18 mths after TPTD discontinuation under consolidating anti-osteoporotic treatment. Overall fracture incidence was markedly reduced by 36 mths compared with baseline. These results should be interpreted in the context of an uncontrolled observational study.

	Patients >75 years		
	Baseline	18 mths	36 mths
EQ-5D Health State Value (median, IQR)	0.53 (0.00, 0.69)	0.69 (0.52, 0.80)	0.69 (0.52, 0.80)
EQ-VAS mean (SD)	49.3 (22.01)	63.8 (20.87)	65.4 (22.24)
Back pain			
	N = 584	N = 444	N = 589
Every day / almost every day*	68.8%	28.8%	22.5%
	N = 551	N = 388	N = 262
Moderate / severe*	92.6%	61.3%	61.5%
VAS (mm)* mean (SD)	59.8 (26.12)	34.7 (24.29)	31.4 (26.13)

Table

***Disclosures: James Walsh**, None.*
This study received funding from: Eli Lilly and Company

SU0375

May Teriparatide Prevent Subsequent Vertebral Fractures After Vertebroplasty? Marco Massarotti*[1], Flavio Tancioni[2], Gianluigi Fabbriciani[3], Laura Belloli[3], Riccardo Rodriguez y Baena[2], Bianca Marasini[3]. [1]IRCCS Humanitas Clinical Institute, Italy, [2]Neurosurgery Unit, IRCCS Humanitas Clinical Institute, Italy, [3]Rheumatology Unit, IRCCS Humanitas Clinical Institute, Italy

Background - Percutaneous vertebroplasty (VP) is a minimally invasive, radiologically guided, therapeutic procedure for the treatment of pain caused by a vertebral body compression fracture (VF). In the last few years this procedure has gained popularity in the treatment of VF associated with osteoporosis (OP). Altough VP seems to be a good option for the treatment of acute VF with a prompt pain relief, some studies raised concerns that this procedure may increase the risk of fracture at an adjacent level. Low BMI, shorter distance from the treated vertebrae, advanced age of the patient, treatment of multiple vertebrae, and severe wedge deformity have been proposed as risk factors for subsequent VF after VP. However VF may increase per se the risk of new VF and the risk seems to be significantly greater in adjacent than in nonadjacent vertebrae. Data from the Fracture Prevention Trial showed that teriparatide (TPTD) may reduce the risk of any new, new adjacent, and new nonadjacent VF by 72%, 75%, and 70%, respectively, compared with the placebo group.

Objective – To evaluate if TPTD may prevent subsequent VF after VP.

Methods – We retrospectively evaluated a cohort of 110 OP patients treated in our center with TPTD between september 2005 and march 2010. We selected a sample of 20 consecutive patients who started TPTD after VP. We examined the patients that completed at least 12 months of TPTD treatment recording any VF occurring during such treatment.

Results - One patient discontinued TPTD after a few days because of side effects (nausea). Four patients completed only few months of treatment at the moment of our analysis. Fifteen patients completed at least 12 months of treatment and were included in our analysis (1 M and 14 F; mean age 71 ± 11 yrs.). Nine patients underwent more than one VP procedure (range, 2-4) due to multiple VF diagnosed concurrently (n=4 patients) or to a new VF subsequent to a first VP (n=5 patients). None of the patients experienced a new VF during the period of treatment with TPTD and back pain was significantly reduced at the end of the observation (VAS baseline vs VAS at 12 months = 55.4 ± 30.4 vs 27.5 ± 17.5).

Conclusion – Subsequent VF is known to be a major limitation to VP in OP patients. TPTD seems to reduce the risk of a refracture in patients treated with VP. Our preliminary report needs to be confirmed in a larger and controlled trial.

***Disclosures: Marco Massarotti**, None.*

SU0376

Monthly Cholecalciferol Supplementation and Intermittent PTH(1-84): Acute Effects on 25(OH)D Levels in Postmenopausal Osteoporotic Women. Stefania Boldini*[1], Serena Pancheri[1], Sonia Zenari[1], Anna Avesani[1], Luca Dalle Carbonare[1], Sandro Giannini[2], Francesco Bertoldo[1]. [1]Dept of Biomedical & Surgical Sciences, University of Verona, Italy, [2]University of Padova, Italy

Purpose: Optimal vitamin D levels are necessary to obtain the expected results in the treatment of postmenopausal osteoporosis. Indeed 1,25(OH)2D levels explain roughly the 20% of the variability in change of lumbar BMD over the first 12 months of PTH(1-84) treatment. A very large portion of osteoporotic women has low or deficient levels of vitamin D and supplementation with cholecalciferol is mandatory when therapy with PTH(1-84) begins. Intermittently injected or continuously infused PTH consumes 25(OH)2D by increasing its conversion in 1,25(OH)2D and 24,25(OH)2D. The aim of the study was to investigate the acute effects of PTH(1-84) on 25(OH)2D, calcium (Ca) and PTH in vitamin replated women (monthly doses of cholecalciferol).

Methods: 10 postmenopausal women (mean age 72+3 y.o.) with severe osteoporosis were treated with PTH(1-84) 100 ug/day. Fasting serum samples were taken at 8.00 am before the daily PTH(1-84) dose at baseline (T0) and at days 1, 3, 7 and 30 of therapy (T1,T3,T7,T30). All subjects were supplemented with oral cholecalciferol 30 days before starting PTH(1-84), (300,000 IU for 2 days consecutively) followed by 100,000 IU every 60 days (1600 IU/day).

Results: At T0 25(OH)2D was 48.55+26.82 ng/ml (n.v. >30 ng/mL), PTH 42.10+4.20 ng/L (n.v. 8-60 pg/mL) and Ca 9.00+0.50 mg/dL (n.v. 8-10 mg/dL). The 71% of patients have normal vitamin D levels. 25(OH)2D decreased progressively from baseline (T1 -4%, T3 -6%, T7- 8%, T 30 -43%, $p<0.005$), reaching the nadir at T30 (27.98+14.26 ng/ml -43%, $p<0.05$). After 7 days of treatment patients with normal vitamin D shifted from 71% to 42%. We observed a biphasic change in Ca which increased within the first 7 days (T6 +6%, T30 + 3%, n.s.) (without hypercalcemia) and then decreased slightly till T30 with consequent opposite changes of PTH (T7 -43%, T 30 + 56%, $p<0.01$).

Conclusions: our data suggest that PTH(1-84) dose acutely enhances the physiological turnover of 25(OH)2D, increasing the risk of hypovitaminosis D notwithstanding normal baseline levels of 25(OH)2D and generous vitamin D supplementations (more than 1000 IU daily of cholecalciferol).

The biphasic changes of PTH and Ca reflects the transient increase of 1,25(OH)2D till normal levels of 25(OH)2D are maintained and the following decrease of 1,25(OH)2D when 25(OH)2D became insufficient. The observed changes could be influenced by the monthly schedule of vitamin D administration, suggesting that more frequent doses should be preferred.

***Disclosures: Stefania Boldini**, None.*

SU0377

Prior Bisphosphonate Treatment Doubles the Likelihood of Attenuated Teriparatide Response and Blunts the Gain in Bone Mineral Density. Guan Choon Chan*[1], Ingrid Borovickova[2], Martin Healy[2], Nessa Fallon[1], James Walsh[3], Miriam Catherine Casey[1]. [1]Bone Health & Osteoporosis Unit, St James's Hospital, Ireland, [2]Clinical Biochemistry, St James's Hospital, Ireland, [3]Trinity College Dublin, The University of Dublin, Ireland

Purpose

Teriparatide has been shown to reduce the risk of vertebral fractures by exerting an anabolic bone effect. On the other hand bisphosphonates are potent antiresorptive agents which suppress bone remodeling. The primary aim of this study was to determine whether prior bisphosphonate treatment increased the likelihood of an attenuated Teriparatide response (≤3% Least Significant Change in Spinal BMD). The secondary aim was to determine whether Spinal BMD change differs in the 2 groups (prior bisphosphonate vs bisphosphonate naïve) after Teriparatide treatment.

Methods

This is a retrospective study of 110 patients who had completed 18mths of Teriparatide treatment in our Osteoporosis Clinic. Information obtained included patients' DXA at baseline and 18mths, baseline bone markers (P1NP, Osteocalcin, CTX) and exposure to significant bisphosphonate therapy (at least 6mths) before Teriparatide therapy. Patients were divided into Good Responders (> 3%LSC BMD Spine) and Attenuated Responders (≤3%LSC BMD Spine).

Results

Of the 110 patients, 103 were female, 7 were male. Mean age 71.5 +/- 10.2. In total 16 patients (15%) were deemed Attenuated Responders (≤ 3%LSC BMD Spine). 38 patients were on prior bisphosphonate treatment, 72 were bisphosphonate naive. Of those on bisphosphonate, 8 (21%) were Attenuated Responders and 30 (79%) were Good Responders. Of those who were bisphosphonate naïve 8 (11%) were Attenuated Responders while 64 (89%) were Good Responders. The mean baseline Spinal BMD of the Good Responders were 0.73 +/- 0.14 and Attenuated Responders were 0.79 +/- 0.08 (p=0.03)

Patients with prior bisphosphonate treatment had a mean gain in lumbar spine BMD of 9.4% +/- 8.0 compared to 14.6% +/- 11.2 (p= 0.02) in the bisphosphonate naïve group. Overall the bone markers of those with prior bisphosphonate group compared to bisphosphonate naïve group were lower at baseline ($p<0.05$)

Conclusion

Compared to bisphosphonate naïve patients, those on bisphosphonate prior to Teriparatide treatment were almost twice as likely (21% vs 11%) to have an attenuated Teriparatide response (≤ 3% BMD Spine gain) at 18mths. In addition patients with prior bisphosphonate also had a blunted Spinal BMD gain at 18 months (9.4% vs 14.6%). Patients who have an attenuated response also have higher Spinal BMD at baseline (0.79 vs 0.73) with lower bone turnover. Overall 85% of our patients treated with Teriparatide had a good response with 12% +/- 9.6 gain on Spinal BMD.

Total n=110	Good Responders (> 3%LSC BMD Spine)	Attenuated Responders (≤ 3%LSC BMD Spine).
Prior Bisphosphonate (n=38)	30 (79%)	8 (21%)
Bisphosphonate Naïve (n= 72)	64 (89%)	8 (11%)
Age	71.5 +/- 10.3	71.4 +/- 10.0
Baseline Spinal BMD (g/cm^2)	0.73 +/- 0.14	0.79 +/- 0.08*
Baseline CTX (ng/ml)	0.30 +/- 0.36	0.17 +/- 0.10*
Baseline P1NP (ng/ml)	49.4+/- 43.6	23.1+/- 11.3*
Baseline Osteocalcin (ng/ml)	23.7 +/- 16.4	15.9 +/- 6.4*

*$p<0.05$

Comparison of Good Responders to Attenuated Responders

***Disclosures: Guan Choon Chan**, None.*

SU0378

Teriparatide and Risedronate In Sequence After Proximal Femoral Fracture In Severe Osteoporosis. Costantino Corradini*[1], luca parravicini[2], marcello macchia[2], calogero crapanzano[2], fabio massimo ulivieri[3], cesare verdoia[2]. [1]Orthopaedic Institute G. Pini, Italy, [2]AO Orthopaedic Institute G. Pini, Italy, [3]Fondazione Policlinico, Italy

BACKGROUND: The efficacy of teriparatide in multi-fractured elderly patients to reduce significantly the rate of complications and the relative risk of new fracture has been recognized. Recently the prolonging of these beneficial effects with sequential use of bysphosphonates has been debated. The purpose of the present study was to evaluate bone turnover markers, compliance and persistence to treatment and relative risk of new fracture in severe osteoporotic patients who are managed with teriparatide and risedronate in sequence. METHODS: 28 compliant female between 59 and 91 years-old presenting a proximal femoral fracture treated surgically associated to a previous vertebral compression fracture were recruited. During hospitalization they were undergone to a routinary instrumental examines completed by biochemical bone turnover markers and BMD by DXA. From day 15 by recovery they received a standard supplementation of calcium carbonate and colecalciferol plus daily subcutaneous teriparatide per day for 18 months and then risedronate weekly or monthly for other 12 months. All the patients repeated: xrays of affected segments at 1 and 3 months; DEXA at first, second, third year; biochemical bone turnover markers within control visit at 1, 3, 6, 12, 18, 24, 30 months. RESULTS: The healing was detected with radiograms. The vitamin D was under minimum levels at admission in all patients but the supplementation was sufficient to normalize in one month. The other biochemical variables of bone formation and resorption peaked within the consolidation processes completed in 3 months. At 6 month they were indistinguishable from baseline and maintained for 30 months. Lumbar and contralateral femoral BMD were increased in the first year and maintained for another year. At 30 month follow-up the rate of survival was 100%, persistence was decreased to 93.9% because of discontinuation of risedronate in two patients for epigastralgy; none have needed a re-operation or was afflicted by new vertebral or non vertebral fracture. CONCLUSIONS: In severe osteoporosis the sequential therapy with teriparatide in the first 18 months after femoral fracture followed by risedronate for other 12 months may contribute to recover and maintain balanced the bone turnover markers without occurence of new fragility fractures or mobilization of implants.

***Disclosures: Costantino Corradini**, None.*

SU0379

The Anabolic Effect of Teriparatide in Postmenopausal Women with Osteoporosis Measured Using Nuclear Scintigraphy During and After Therapy. Amelia Moore*[1], Glen Blake[2], Kathleen Taylor[3], Asad Rana[3], Ignac Fogelman[2]. [1]Kings College London, United Kingdom, [2]Guy's Hospital, United Kingdom, [3]Eli Lilly & Company, USA

Purpose: Teriparatide (TPTD) therapy has been reported to cause visual changes on bone scintiscans. Methods: We quantified the metabolic effect of TPTD on bone by measuring ^{99m}Tc-MDP skeletal plasma clearance in 10 postmenopausal women with osteoporosis (mean age, 68 years; mean baseline lumbar spine T-score, –3.2) who had radionuclide bone scans at baseline, 3, and 18 months (m) after starting therapy with subcutaneous TPTD 20 mcg/day and after 6 m off therapy. Participants were injected with 600 MBq ^{99m}Tc-MDP and whole body bone scan images were acquired at 10 minutes (min), 1, 2, 3, and 4 hours (h). Multiple blood samples were taken between 5 min and 4 h and free ^{99m}Tc-MDP was measured using ultrafiltration. ^{99m}Tc-MDP plasma clearance (Kbone) was evaluated using the Patlak plot method. Regional differences in Kbone were studied by measuring the whole skeleton and 6 subregions (calvarium, mandible, spine, pelvis, upper extremities, lower extremities). Serum concentrations of procollagen type I N-terminal propeptide (PINP), bone-specific alkaline phosphatase (BSAP), and urinary excretion of N-terminal telopeptide (NTX) were also measured at each visit. Results: The median increase from baseline in whole skeleton Kbone was 22% (P=0.004) at 3 m and 34% (P=0.002) at 18 m, decreasing to 0.7% after 6 m off therapy. In other subregions Kbone value increases were statistically significant at 3 m, and in all subregions except the pelvis at 18 m. After 6 m withdrawal from teriparatide therapy, whole skeleton Kbone and subregional Kbone values returned toward baseline. Bone markers increases from baseline were statistically significant at 3 m and 18 m (BSAP, 15% and 36%; PINP, 137% and 192%; NTX, 109% and 125%). After 6 m off therapy, PINP and NTX values had declined, though remained above baseline. (BSAP, -3%; PINP, 43%; NTX, 56%). Increased Kbone values in the whole body and lower extremities were correlated with increases in most bone markers at 3 and 18 m of treatment. Increased skeletal uptake of ^{99m}Tc-MDP during treatment with teriparatide is indicative of increased bone formation and is supported by increases in bone turnover markers and bone mineral density. At 6 m off therapy, patients experienced a diminution of metabolic activity as measured by bone scan and bone turnover markers. Conclusion: These data may provide physicians with useful clinical insights into the total and regional skeletal effects of teriparatide as measured by radionuclide bone scans.

***Disclosures: Amelia Moore**, Eli Lilly and Company, 9*
This study received funding from: Eli Lilly and Company

SU0380

A Comparison of the Effects of Raloxifene and Hormon Therapy on Lipid Profile and Bone Mineral Density in Postmenopausal Osteopenia Women. Min Hyung Jung*[1], Heung Yeol Kim[2], Hoon Choi[3], Tak Kim[4], Byung Ick Lee[5], Hyoung Moo Park[6]. [1]School of Medicine, Kyung Hee University, Kyung Hee Medical Center, South korea, [2]Department of Obstetrics & Gynecology, School of Medicine, Kosin University, South korea, [3]Inje University Sanggyepaik Hospital, South korea, [4]Department of Obstetrics & Gynecology, School of Medicine, Korea University Anam Hospital, Korea University, South korea, [5]Department of Obstetrics & Gynecology, School of Medicine, Inha University Hospital, Inha University, South korea, [6]Department of Obstetrics & Gynecology, School of Medicine, Chungang University Yongsan Hospital, Chungang University, South korea

Objectives: To compare the effects of raloxifene on lipid profile and bone mineral density to those of estrogen therapy in postmenopausal osteopenia women.

Methods: The effects of raloxifene (Evista® 60 mg/day, N=42) and estrogen therapy (Premarin® 0.625 mg/day, N=84) were compared in terms of lipid profile (total cholesterol, low-density lipoprotein cholesterol (LDL-C), high-density lipoprotein cholesterol (HDL-C), and triglyceride (TG)) change and bone mineral density change over 24 months. Lipid profile and bone mineral density (BMD) measurements were performed at every 12 months.

Results: Women treated with raloxifene for 24 months experienced decrease in total cholesterol and TG level by 4.8 % and 5.5 %, increase in LDL-C and HDL-C level by 1.7 % and 7.1 %, respectively, which did not show statistical significance. Women treated with estrogen for 24 months experienced decrease in total cholesterol level by 1.1 %, increase in TG, LDL-C and HDL-C level by 2.5 %, 6.1 %, and 5.3 %, respectively, which did not show statistical significance. Women treated with estrogen for 24 months experienced decrease in bone mineral density of lumbar spine by 2.7 % and increase in bone mineral density of femur neck by 0.7 %, respectively, which did not show statistical significance. There was no statistical difference in total cholesterol, LDL-C and HDL-C, and TG, and bone mineral density between raloxifene and estrogen therapy.

Conclusion: There was no statistical difference in effects of raloxifene and estrogen on lipid profile and bone mineral density in postmenopausal women for 24 months.

***Disclosures: Min Hyung Jung**, None.*

SU0381

Atypical Femur Fractures and Bisphosphonate Use in a Canadian Tertiary-Care Academic Hospital. Angela Cheung*[1], Christian Viellette[1], Robert Bleakney[2], Khalid Syed[1], Christina Young[1], Heather McDonald-Blumer[3], Lianne Tile[1], Savannah Cardew[1], Rajiv Gandhi[1], Moira Kapral[1], Rod Davey[1], Nizar Mahomed[1], Rowena Ridout[4]. [1]University Health Network, Canada, [2]Mt. Sinai Hospital, Canada, [3]Mount Sinai Hospital, Canada, [4]Toronto Western Hospital, Canada

Purpose: Bisphosphonate use has been associated with atypical femur fractures. We conducted a retrospective review of patients who presented with atypical femur fractures at a Canadian tertiary-care academic hospital.

Methods: We examined the records of all patients admitted to the Toronto Western Hospital, University Health Network with femur fractures from April 1, 2007 to May 31, 2009. During this period, all subtrochanteric and mid-diaphyseal fractures were fixed with intramedullary gamma or trigen antegrade femoral nails. Using computerized records of these implants, we identified all patients with such fractures who were surgically fixed. Radiographic images of these femurs were independently reviewed by two experts (an orthopaedic surgeon and a musculoskeletal radiologist) to assess for features consistent with an atypical femur fracture such as clean transverse break in subtrochanteric, mid-diaphyseal or distal femoral shaft area, focal or diffused cortical thickness of the femoral shaft, beaking, and small lesion on contralateral side. The radiographic reviewers were blinded to clinical characteristics including bisphosphonate use. Clinical charts were then reviewed by two other individuals to determine demographic and clinical characteristics. Descriptive statistics were performed to summarize the data.

Results: Four hundred and fifty-two patients presented with femur fractures over the 25 months of study. Fifty-one of these (11.2%) were classified as subtrochanteric or femoral shaft fractures and were fixed with intramedullary nails. Only 6 (5 women, 1 man) of the 51 (1.3%) were classified as classic atypical femur fractures. Of the remaining subtrochanteric or femoral shaft fractures, most were subtrochanteric extension of intertrochanteric or femoral neck fractures, spiral fractures or comminuted fractures with multiple fragments, and nine were pathological fractures from malignancy. Mean age of patients with classic atypical fractures was 65.3 (range 49.4 – 80.6) years. Five were women, one man. All had fragility fractures. Two of the six had lesions on the contralateral side. Four of the six patients with atypical fractures were on bisphosphonates; two have never used any bone mitigating agents.

Conclusions: Atypical femur fractures are uncommon and can occur in bisphosphonate-naive patients. Further studies are required to determine the relationship of these unusual insufficiency fractures to bisphosphonate use.

***Disclosures: Angela Cheung**, Amgen, Eli Lilly, 2; Merck, Novartis, 2; Sanofi-Aventis, 2*

SU0382

Characteristics of U.S. Medicare Enrollees With the New ICD9 Code For Osteonecrosis of the Jaw. Jeffrey Curtis*, Robert Matthews, Huifeng Yun, Tarun Arora, Kenneth Saag, Elizabeth Delzell. University of Alabama at Birmingham, USA

Purpose: In October, 2007, a new International Classification of Diseases, 9th edition (ICD-9) code was introduced to more specifically identify osteonecrosis of the jaw (ONJ). We evaluated characteristics of patients with healthcare claims associated with this code.

Methods: Using a national 5% random sample of Medicare beneficiaries, we identified individuals with $\geq$ 1 medical claim with the new ICD9 for ONJ (733.45). Patients eligible for this analysis must have had Medicare part A+B and not be enrolled in Medicare Advantage (i.e. full coverage) in the 12 months prior and 3 months following the first claim of any type for ONJ, which defined a suspected ONJ case. Characteristics of these individuals were identified in the one year prior to the first ONJ claim. A sensitivity analysis evaluated medical claims using all antecedent data for each individual, which extended a median of 8.0 years with full coverage prior to the ONJ claim.

Results: From October 2007 to December 2008 (the most recent Medicare data available), a total of 122 individuals had at least 1 ONJ claim. Of these, 69% had $\geq$ 2 claims. A total of 74 patients (61%) had at least 1 ONJ hospitalization claim or ONJ outpatient physician evaluation and management claim. Characteristics of the 122 patients were: 77% women, median age 76 years. Twenty four percent (24%) of suspected ONJ cases had no evidence for cancer in the 1 year prior, and 20% had no evidence for cancer at any time. Among the cancer patients, the most common primary cancer types were breast and myeloma.

Of the suspected ONJ cases identified using inpatient hospital claims or outpatient physician claims, 64% did not use intravenous (IV) bisphosphonates (BPs) in the year prior to the first ONJ claim, and 38% never used IV BPs at any time. Among individuals with no evidence for cancer in the year preceding the ONJ claim, 63% had a previous inpatient or physician claim for osteoporosis at any time.

Conclusions: A new ICD-9 code introduced in late 2007 is available to more specifically identify ONJ in large, population-based data sources that use administrative claims data. Although most cases of suspected ONJ had evidence of cancer, a notable minority had no cancer or exposure to IV BPs. Ongoing efforts are underway to examine the validity of this diagnosis code compared to a gold standard of medical record review and to evaluate associations between ONJ and other risk factors of interest.

***Disclosures: Jeffrey Curtis**, Eli Lilly, 8; Merck, 2; Novartis, 2; Novartis, 8; Procter & Gamble, 2; Eli Lilly, 2; Merck, 5; Procter & Gamble, 5*
This study received funding from: Amgen

SU0383

Effect of Once Yearly Zoledronic Acid versus Once Weekly Generic Alendronate in Men with Established Osteoporosis. Johann Ringe*[1], A Dorst[2], H FAber[2], P Farahmand[2]. [1]Klinikum Leverkusen, University of Cologne, Germany, [2]West German Osteoporosis Center & Medizin. Klinik IV, Klinikum Leverkusen, University of Cologne, Germany

Purpose: Oral once weekly generic Alendronate (ALN) is associated with significant increase in the incidence of adverse events (AEs), and poorer compliance leading to impaired therapeutic results as compared with other oral bisphosponates (BPs). Once-yearly intravenous (IV) infusion of zoledronic acid (ZOL), however, has a safety profile different from oral BPs and the mode of administration guarantees 100% compliance at least for the first year. This study compared the efficacy and safety of IV ZOL vs. oral generic ALN in men with established osteoporosis.

Methods: In this retrospective patient chart review analysis, 92 men with established osteoporosis and bone mineral density (BMD) T-scores =–2.5 SD at both lumbar spine (LS) and total hip (TH) and at least one prevalent vertebral fracture were included. All patients were recruited from the out-patient department based on their treatment choice of either once yearly IV infusion of ZOL 5 mg, or once weekly generic oral ALN 70 mg. All patients also received calcium (1200 mg) and vitamin D (800 IU) daily. Primary endpoints were study drug-related AEs, compliance with BP, calcium and vitamin D therapy, and changes in LS- and TH-BMD after 12 months of therapy.

Results: The two groups had different patterns of AEs with significantly more gastrointestinal (GI) complaints in patients on ALN. After 12 months, compliance to treatment was higher in patients on ZOL vs. ALN (100% vs. 54%) with significantly higher persistence on calcium and vitamin D. After 12 months, mean LS-BMD significantly increased with ZOL vs. ALN (7.6% vs. 2.6%; $p<0.01$). The mean change from baseline in TH-BMD with ZOL vs. ALN was 4.7 vs. 1.3% ($p<0.03$). The incidence of new vertebral or non-vertebral fractures were similar between the two treatment groups, but both fractures taken together, there were fewer new fractures with ZOL vs. ALN (5 vs.12; p=0.041). Furthermore, back pain score significantly decreased with ZOL vs. ALN (58% vs. 22%; $p<0.01$).

Conclusions: In men with established osteoporosis, once yearly IV ZOL significantly increased the LS- and TH-BMD compared to those treated with once weekly generic oral BP. Additionally, ZOL improved the overall fracture rate and significantly ameliorated back pain. The lower therapeutic efficacy of oral generic ALN may be associated with lower potency and significantly lower compliance, which may be mainly due to higher incidence of GI-AEs

***Disclosures: Johann Ringe**, Novartis, 8*
This study received funding from: Novartis

SU0384

Effects of Bisphosphonate on Bone Mineral Density, Bone Metabolic Markers and Vertebral Fractures in Young-old and Old-old Osteoporotic Patients. Yuji Kasukawa*[1], Naohisa Miyakoshi[1], Toshihito Ebina[2], Akira Horikawa[3], Toshiaki Aizawa[2], Yoichi Shimada[1]. [1]Akita University Graduate School of Medicine, Japan, [2]Kakunodate General Hospital, Japan, [3]Yuzawa Clinic, Japan

It has been well known that bisphosphonate improves bone mineral density (BMD) in osteoporotic patients and shows preventive effects on newly occurred osteoporotic fractures. Most of the effects of bisphosphonate have demonstrated in post-menopausal osteoporotic women, but not in over young-old osteoporotic patients, who have high risk of osteoporotic fractures. The purpose of present study was to evaluate the effects of bisphosphonate on BMD, bone metabolic markers, and number of newly occurred vertebral fractures in young-old and old-old osteoporotic patients.

Forty-eight osteoporotic women (average age; 76 years) were enrolled in this study. They divided into following two groups: 1) young-old group (n=23), the ages were between 65 to 74 years; and 2) old-old group (n=25), the ages were over 75 years, at the beginning of treatment. Before and after one year treatment of bisphosphonate, following parameters were evaluated. BMD was measured by dual-energy X-ray absorptiometory at the distal third of forearm. Serum markers of bone resorption [cross-linked N-telopeptide of type 1 collagen (NTx)] and formation [bone alkaline phosphatase (BAP)] were measured. Vertebral fractures of thoracic and lumbar spine were detected by plain X-ray film.

There were no significant difference of average serum NTX and BAP between young-old and old-old groups [19.1 (nmolBCE/L) and 29.3 (U/L) respectively in young-old group, and 16.9 (nmolBCE/L) and 26.2 (U/L) respectively in old-old group] before treatment. Average BMD [0.27 (g/cm^2), young adult mean (YAM) 56.3%] in old-old group before treatment was lower than the BMD [0.24 (g/cm^2), YAM 54.7%] in young-old group (p=0.05). The average serum NTX and BAP were significantly decreased in young-old group ($p<0.05$ and $p<0.0001$, respectively) and in old-old group ($p<0.01$ and $p<0.01$, respectively) after one-year treatment. Although BMDs did not show significant difference before and after treatment in both young-old and old-old groups, the BMD in old-old group after treatment was significantly lower than that in young-old group ($p<0.05$). No new vertebral fracture occurred in young-old group, but 5 new vertebral fractures were observed in old-old group.

Bisphosphonates suppressed the serum bone metabolic markers and maintained the BMD in both young-old and old-old groups. However, new vertebral fractures were occurred only in old-old patients.

***Disclosures: Yuji Kasukawa**, None.*

SU0385

Factors Associated with the Prevention of Glucocorticoid-Induced Osteoporosis using a Large U.S. National Pharmacy Database. Ryan Outman*[1], Ronald Aubert[2], Jeffrey Curtis[1], Robert Epstein[2], Felix Frueh[2], Mona Khalid[2], Christopher Sanders[2], Eric Stanek[2], Amy Steinkellner[2], Amy Warriner[3], Kenneth Saag[1]. [1]University of Alabama at Birmingham, USA, [2]Medco Health Solutions, Inc., USA, [3]UAB, USA

Purpose: Despite a growing scientific literature supporting efficacy and the widespread dissemination of guidelines supporting preventive therapies, use of prescription anti-osteoporosis therapies among chronic glucocorticoid users has been historically low. Examining a large US pharmacy benefits manager, we evaluated recent patient factors associated with the use of therapies to prevent glucocorticoids (steroid)-induced osteoporosis.

Methods: Using a de-identified database from a national pharmacy benefits manager, we identified members who had been prescribed glucocorticoids (> 90 days of use) during a one-year period, July 2008 through June 2009. We also ascertained the presence of two or more prescriptions for anti-osteoporosis medications during the same period. Factors associated with anti-osteoporosis therapies were identified and included member demographics, and utilization of drugs used to treat rheumatoid arthritis (RA).

Results: We identified 328,880 patients who were prescribed glucocorticoids in 2008-2009. Of these patients, 61.8% were female, 42.9% were between the ages of 50-70, and 38.9% were age >70. Only 19.1% of patients prescribed glucocorticoids also filled a prescription for an anti-osteoporosis medication. Of patients prescribed an anti-osteoporosis medication (n=62,820), 98% were prescribed a bisphosphonate, 6% raloxifene, 3% teriparatide, and 7% calcitonin with 13% of patients being prescribed more than one anti-osteoporosis medications between July 2008 and June 2009. Persons over the age of 70 (n=31,580) were nearly four-times more likely to be prescribed an anti-osteoporosis medication (OR=3.90, CI: 3.78 – 4.02; $p<0.001$). Also, women (n=48,921) were 2.5 times more likely than males to be prescribed anti-osteoporosis medications (OR=2.50; CI: 2.45-2.56; $p<0.001$) as were patients (n=13,373) prescribed RA medications (OR=1.48; CI: 1.44-1.51; $p<0.001$); rates were lowest for patients less than 50 years of age (7.7%).

Conclusions: Treatment rates of glucocorticoid-induced osteoporosis remain low, especially among those under age 50.

***Disclosures: Ryan Outman**, None.*

SU0386

First Cases of Osteonecrosis of the Jaw in two Metabolic Bone Diseases Services. Alicia Bagur[1], Silvina Mastaglia*[2]. [1]Sección Osteopatías Médicas, Hospital de Clínicas, Universidad de Buenos Aires & Centro de Osteopatías Médicas Dr. Carlos Mautalen, Argentina, [2]Sección Osteopatías Médicas, Hospital de Clínicas, Universicad de Buenos Aires, Argentina

Bisphosphonates (BP) are the choice therapeutic agents for osteoporosis, bone metastasis, and Paget's disease. They have been associated with a condition known as bisphosphonate related osteonecrosis of the jaw (BRONJ). We saw no case of osteonecrosis of the jaw related or unrelated to BP over our 25 years' experience in BP use until 2009. We report the first two cases of BRONJ seen at two reference centers: a university hospital and a metabolic bone diseases center.

Case 1: A 60-year old woman with a ten-year history of osteoporosis treated with oral alendronate (70mg/week) for 5 years, calcium and vitamin D. She received 3 dental implants which were successful, but developed BRONJ after receiving another 2 in the maxilla. She exhibited exposed bone for over 8 weeks, which prompted consultation and immediate suspension of BP. Menopause occurred at age 50; dairy intake was 1000mg calcium/day. She reported regular exercising, hand fracture and colon cancer surgery 7 years earlier. She had no history of pathology or of taking medication affecting bone. Laboratory results were normal except for slight hypovitaminosis D: Ca 9.0 mg/dl, P 3.5 mg/dl, PTH 38 pg/ml, CTX 290 ng/L, 25OHD 27 ng/ml, BGP 23 ng/ml, Bone alkaline phosphatase 72 IU/L and Cr 0.7 mg/dl. Bone mineral density (BMD) on presentation of BRONJ was low (Hologic, DXA): Lumbar spine 0.866 (Tscore -1.6), Femoral neck 0.607 (Tscore -2.4) and Total femur 0.706 (Tscore -1.9). The jaw lesion improved with local dental treatment but failed to remit. Dietary calcium and Vitamin D were prescribed.

Case 2: A 71-year old woman with severe osteoporosis (wrist and hip fracture), type II insulin-dependent diabetes with inadequate metabolic control, retinopathy, and diabetic foot. Physical examination: 158cm height; 62.500 Kg weight; 25 Kg/m^2 body mass index (BMI), dorsal kyphosis and scoliosis. She received 70mg/week of oral alendronate and 320mg/day of calcium. Four years later she suffered fractures in D7, L1, and L3, thus requiring a walking aid. The patient did not show for follow-up for 2 years, during which she developed a necrotic lesion in the jaw. Biopsy confirmed BRONJ. She received adequate treatment for the lesion and alendronate was suspended; 18 months later the lesion had not healed completely.

Conclusion: 1- Though unusual, BRONJ is a complication that must be taken into account in BP treated osteoporosis patients. 2- Our patients had potentially associated factors, i.e. diabetes and invasive dental treatments.

***Disclosures: Silvina Mastaglia**, None.*

SU0387

Rapid Onset and Sustained Efficacy (ROSE) Study of Zoledronic Acid *Vs* Alendronate In Postmenopausal Women With Osteoporosis: Quality of Life (QoL), Compliance and Therapy Preference. Peyman Hadji*[1], Dieter Gamerdinger[2], Wolfgang Spieler[3], Peter Kann[4], Helena Loeffler[5], Konstantin Articus[5], Monika Baier[5], Rüdiger Moericke[6], Volker Ziller[7]. [1]Philipps-University of Marburg, Germany, [2]Orthopedic Practise, Germany, [3]Reseach Center for Osteology & Rheumatology, Germany, [4]Philipps University Marburg, Germany, [5]Novartis Pharma GmbH, Germany, [6]Endocrinologic Practice, Germany, [7]Philipps-University-Marburg, Germany

Purpose: Annual iv infusion of zoledronic acid 5 mg (ZOL) is an effective and well-tolerated therapy for patients with osteoporosis and in patients with a recent low-trauma hip fracture[1]. Improved compliance was observed with ZOL when used in the treatment of osteoporosis[2]. ROSE study compared ZOL 5mg with alendronate 70 mg (ALN) in postmenopausal women with osteoporosis or osteopenia. Here we describe QoL, compliance and therapy preference in patients enrolled in ROSE study.

Methods: ROSE study was a 1-year, open label, multicenter, randomized, controlled trial in postmenopausal women (n=604) aged 55-59 years, with documented osteopenia/osteoporosis (T-score ≤-2.0 at total hip or spine measured by DXA). Exclusion criteria were prior bisphosphonate therapy, calculated creatinine clearance <35mL/min, secondary osteoporosis, primary hyperparathyroidism, and contraindications to study drugs, calcium or vitamin D. Patients were randomized (2:1) to receive either once-yearly i.v. ZOL or once-weekly oral ALN. All patients received daily doses of 1200 mg calcium and 800 I.U. vitamin D. Changes in health status, QoL and therapy preference were assessed using visual analogue scale (VAS), Qualeffo-41 questionnaires, preference questionnaire, respectively. Compliance with ALN was assessed by investigator or study personnel at each visit.

Results: At Month 12, improvement in health status, was similar in both treatment groups (ZOL *vs.* ALN; 1.3 *vs.* 1.2). Using Qualeffo-41 questionnaires, significant improvement in QoL was observed with ZOL in total score, as well as in 3 subscales (Table). In the ALN treatment group only the pain domain showed a significant improvement as compared to baseline. The differences between treatments were not significantly different. 80.9% patients were compliant with ALN therapy. The majority of patients (68.8%) would prefer treatment with a once-yearly infusion compared with weekly, oral therapy. In the ZOL group, 80.9% of patients preferred an annual i.v. infusion whereas 48.7% preferred weekly oral therapy in the ALN group.

Conclusion: Treatment with once-yearly ZOL 5 mg i.v. infusion significantly improves overall patient QoL. Moreover, annual i.v. infusion with ZOL has the potential to improve patient compliance and, as such, is a promising treatment option for postmenopausal women with osteoporosis.

References: 1. Lyles KW *et al. N Engl J Med* 2007; 357: 1799- 1809. 2. Owens G *et al. Am J Manag Care* 2007; 13: S290-S308.

Table Changes in QoL from baseline to Month 12 assessed using the Qualeffo-41 questionnaire (ITT population)

Change from baseline to month 12, mean ± SD	ZOL(n=408)	ALN (n=191)
Total score	–1.2 ± 8.8 p=0.0053	–0.6 ± 9.0 N.S.
Pain	–5.5 ± 21.9 p<0.0001	–4.3 ± 21.9 p=0.0084
Activities of daily living	–1.9 ± 14.1 p=0.0088	0.1 ± 17.1 N.S.
Jobs around the house	–1.8 ± 14.0 N.S.	–1.3 ± 13.2 N.S.
Mobility	–0.5 ± 10.4 N.S.	0.4 ± 10.5 N.S.
Leisure, social activities	–0.8 ± 16.2 N.S.	0.7 ± 17.6 N.S.
General health perception	–2.1 ± 16.3 p=0.0098	–1.2 ± 16.5 N.S.
Mental function	0.8 ± 11.1 N.S.	0.5 ± 11.8 N.S.

Scoring of the domain scales: 1= very good, 100 = very bad quality of life. Negative changes indicate improvement in quality of life. P-values: student's t-test for change from baseline to month 12

Table: Changes in QoL from baseline to Month 12 assessed using the Qualeffo-41 questionnaire

***Disclosures: Peyman Hadji**, None.*
This study received funding from: This research was funded by Novartis Pharma AG, Basel, Switzerland

SU0388

Response Rates to Bisphosphonate Therapy for Low Bone Mineral Density In A Primary Care Setting. Amanda Carmel*[1], Stasi Lubansky[1], Richard Bockman[2]. [1]Weill Cornell Medical College, USA, [2]Hospital for Special Surgery, Weill Medical College, USA

Many large randomized controlled trials (RCT's) have shown bisphosphonates improve bone mineral density (BMD) and decrease fracture risk. For example, in the Fracture Intervention Trial (FIT), clinical fractures occurred in 12% of patients treated with alendronate, and after 3 years significant increases in hip BMD occurred in 97.5% of patients. In the extension of the FIT trial, on average patients on persistent bisphosphonate treatment for 10 years maintained their BMD. Purpose: We sought to determine the rate of bisphosphonate response in a primary care setting as well as to determine whether vitamin D level and other clinical variables were associated with response status. Methods: The study was conducted in the internal medicine ambulatory care practice affiliated with an urban academic medical center [Weill Cornell Internal Medicine Associates (WCIMA)]. Those patients who met the eligibility criteria and agreed to participate were enrolled. Patients were considered "inadequate responders" if they: 1) Sustained a low trauma fracture despite treatment with a bisphosphonate > 12 months, 2) Had a lumbar spine, total hip, or femoral neck BMD T-score of −3.0 or less after documented prior bisphosphonate treatment > 24 months, 3) Experienced a decrease of >3.0% in BMD between scans. Along with BMD at various sites, fracture data, vitamin D level, urine N-telopeptide level, intact PTH, a basic metabolic panel, as well as self reported data on diet, activity level, sun exposure, and compliance with bisphosphonate treatment were collected for each subject. Results: Since January 2009, of approximately 60,000 visits to WCIMA, 250 patients were identified based on initial screening of the electronic medical record, 56 of these met the eligibility criteria, and 36 patients have been enrolled. The mean age was 67 (SD 9yrs), mean duration of bisphosphonate treatment was 6 years (SD 3 yrs), 36% have been characterized as adequate responders, and 64% as inadequate responders. 19% of the patients sustained a new low trauma fracture. Our data suggest that among inadequate responders there were a greater proportion of patients who had vitamin D < 33ng/ml (78% vs. 28% P value = 0.15). Conclusion: An important role of the academic general internist is to translate data from large clinical trials to the management of primary care patients. Our preliminary data suggest lower response rates of bisphosphonate therapy for this group of patients in a primary care setting than that seen in large RCT's with bisphosphonates. The reason for the discrepancy between response rates in our study and larger trials is unknown. A trend in our data suggests that vitamin D sufficiency may play a role in response to bisphosphonate therapy. These data present an important opportunity for larger studies, which may inform quality improvement in the management of low bone density in primary care.

***Disclosures: Amanda Carmel**, None.*

SU0389

Risedronate Improves Proximal Femur Bone Density and Geometry in Patients with Osteoporosis or Osteopenia and Clinical Risk Factors of Fractures: A Practice-Based Observational Study. Jun Iwamoto[1], Masayuki Takakuwa*[2]. [1]Keio University School of Medicine, Japan, [2]Takakuwa Orthopedic Nagayama Clinic, Japan

Advanced Hip Assessment (AHA) software from Dual Energy X-ray Absorptiometry (DXA, GE-Lunar) can be used to perform bone strength analysis of the proximal femur as well as bone mineral density (BMD) measurement. Femur Strength Index (FSI), which is the corresponding strength parameter, is calculated from structural geometric properties, neck shaft angle, height, and body weight. We investigated the effects of risedronate on AHA parameters of the proximal femur and BMD of the lumbar spine and proximal femur in patients with increased risk of fractures. In total, 172 patients (mean age 67.9 + 9.9 yrs; 165 females and 7 males) with osteoporosis or osteopenia and clinical risk factors of fractures were treated with risedronate for 20 months in our out-patients clinic. AHA parameters of the proximal femur and BMD of the proximal femur and lumbar spine (L1-L4) were evaluated after 4, 8, 12, 16 and 20 months of treatment with risedronate. The percentage change from baseline in FSI after 4 months of risedronate treatment was 7.5±19.7%($p<0.001$)for the right femur and 4.5±18.3%($p<0.01$) for the left femur. After 8, 12, 16 and 20 months of treatment, the respective values for the right femur were 5.8±17.5%, 10.0±17.7%, 12.6±19.6%, 13.6±24.9%($p<0.001$) and those for the left femur were 7.7±18.8%, 8.2±22.9%, 11.5±20.4%, 10.2±18.4%($p<0.001$). Cross-sectional moment of inertia (CSMI), cross-sectional area (CSA), mean neck width in the femoral neck ROI, and BMD of the right and left proximal femur and BMD of the lumbar spine also continued to increase during 20 months of treatment. The increases in FSI and CSMI at each time point were apparently greater than those in the proximal femur and lumbar spine BMD. These results indicate that risedronate may rapidly improve femoral strength parameters as well as BMD of the proximal femur and lumbar spine, and that these improvements were at least sustained over 20 months. Thus, risedronate not only increases BMD, but also, more significantly, may improve bone quality, thereby contributing to prevention of fractures in patients with increased risk of fractures.

***Disclosures: Masayuki Takakuwa**, None.*

SU0390

Risk Reduction for Falls and Fractures by a Combined Therapy with Alfacalcidol and Alendronate: A Real Life Short Term Trial on 2579 Patients. Erich Schacht[1], Parvis Farahmand[2], Johann Diederich Ringe*[2]. [1]ZORG (Zurich Osteoporosis Research Group), Switzerland, [2]Medical Clinic 4 & West German Osteoporosis Center, Klinikum Leverkusen (Univ. of Cologne), Germany

Background: A previous study proved a significant superiority of alendronate once weekly combined with daily 1 mcg alfacalcidol over alendronate plus plain vitamin D substitution (1). Recently a combination package containing 4 self explaining one week blisters, each with one tablet of 70mg alendronate and 7 capsules of 1 mcg alfacalcidol, was introduced primarily in Germany (Tevabone® -TEVA/AWD.pharma).

Methods: 825 practicing physicians all over Germany recruited 2579 patients for a 12 week phase 4 observational trial with the above new combination pack. 92% were women; the average age was 74 years. 55% had a history of falls. Prevalent vert. and non-vert. fractures were documented in 62% and 63% of the patients resp. and a creatinine clearance below 65ml/min was documented in 65%. Main outcome parameters were CRT (Chair Rising Test) and TUG (Timed Up and Go test) and back pain at onset and after 3 months.

Results: The percentage of patients able to perform the CRT within 10 sec. increased from 26% at onset to 43% after 3 months (increase 63%, $p<0.001$) while the successful performance within 10 sec of TUG increased by 54% ($p<0.001$).The average overall improvement of CRT was 2.3 sec. and of TUG amounted to 2.4 sec. It was shown in another recently published study that a mean increase of 2.6 sec. in the performance of TUG results in a 24% increased risk for non-vert. fractures (2). Mean back pain measured by the Visual Analogue Scale (VAS 0 - 10) decreased significantly from 5.9 to 3.5 ($p<0,001$).

Conclusion: With the new combined regimen of alfacalcidol and alendronate highly significant ameliorations in back pain, CRT and TUG could be reached already after 3 months. This may contribute to the previously shown significant effects on falls and fractures with the same regimen during a long-term trial (1).

1. Ringe JD et al.: Rheumatol Int. 2007;27:425-34
2. Zhu K et al.: J Bone Miner Res 2008:23;119

***Disclosures: Johann Diederich Ringe**, TEVA/AWD.pharma, 5*
This study received funding from: TEVA/AWD.pharma

SU0391

Safety and Efficacy of Risedronate in Osteoporosis Patients with Diabetes Mellitus, Hypertension or Dislipidemia -A Pooled Analysis of Three Clinical Trials in Japan. Ryo Okazaki*[1], Daisuke Inoue[1], Yoshiki Nishizawa[2], Ryoichi Muraoka[3], Toshitsugu Sugimoto[4]. [1]Teikyo University Chiba Medical Center, Japan, [2]Osaka City University Medical School, Japan, [3]Ajinomoto Phamaceuticals Co, Ltd., Japan, [4]Shimane University School of Medicine, Japan

The number of patients with osteoporosis who also have metabolic syndrome has been increasing in developed countries. Risedronate(RIS) has been shown to inhibit osteoporotic fractures and widely used in the world. However, it is unknown whether this agent is equally efficacious in patients with metabolic syndrome. Thus, we did post-hoc analyses of RIS Japanese phase III trials to see whether the presence of diabetes mellitus(DM), hypertension(HTN) or dyslipidemia(HL) affect its efficacy and safety.

Data from subjects who were administered RIS in three Phase III clinical trials conducted in Japan were pooled and analyzed. The analysis included 885 subjects who received 48-week treatment with RIS (636 patients, once-a-day 2.5mg tablets; 249 patients, once-a-week 17.5 mg tablets). They were divided into two groups according to the presence or absence of each comorbid condition and evaluated: DM group (n=53) vs. non-DM group (n=832), HTN group (n=278) vs. non-HTN group (n=607), and HL group (n=292) vs. non-HL group (n=593). Bone mineral density (BMD), urinary type1 collagen N-telopeptide (uNTX) and serum bone-specific alkaline phosphatase (BAP) were measured at baseline and after 48 weeks.

There were no significant differences in baseline BMD between any of the two groups. Overall BMD was increased by 5.52%, whereas u-NTX and BAP were decreased by 35.4 %, and 33.8 %, respectively. Their changes in each subgroup are shown in the Table. Although BMD and uNTX responses appeared to be blunted in DM group, overall, there were no statistically significant differences in the responses to RIS between any two groups. As for the adverse event incidence, there were no significant differences except that HL showed more events than non-HL with a marginal significance (84.9% in the DM group against 87.3% in the non-DM group; relative risk [RR], 0.97, 95% CI, 0.87 to 1.09, 88.9% in the HTN group against 86.3% in the non-HTN group; RR, 1.03, 95% CI, 0.98 to 1.08, 90.4% in the HL group against 85.5% in the non-HL group; RR, 1.06, 95% CI, 1.01 to 1.11). A few serious adverse drug reactions were observed, but there was no difference of incidence between any two groups

The present study demonstrates that RIS is safe and effective in suppressing bone turnover and thereby increasing BMD in osteoporosis patients regardless of comorbid DM, HTN, or HL. Further studies are needed to verify that RIS is equally efficacious for fracture prevention in patients with metabolic syndrome.

		DM	non-DM	HTN	non-HTN	HL	non-HL
BMD	% increase	5.22 ± 4.01	5.53 ± 4.46	5.33 ± 4.02	5.59 ± 4.51	5.34 ± 4.24	5.61 ± 4.45
	difference	-0.31		-0.25		-0.28	
	95% confidence interval [CI]	-2.01 to 1.39		-1.10 to 0.60		-1.08 to 0.53	
u-NTX	% decrease	25.5 ± 44.0	36.0 ± 37.6	35.7 ± 44.5	34.8 ± 40.1	36.5 ± 33.7	34.8 ± 40.1
	difference	-10.5		0.4		1.7	
	95% confidence interval [CI]	-22.1 to 1.1		-5.9 to 6.5		-4.2 to 7.6	
BAP	% decrease	33.7 ± 16.7	33.6 ± 20.9	31.6 ± 20.2	34.7 ± 20.9	32.7 ± 21.5	34.4 ± 20.1
	difference	-0.1		-3.1		1.7	
	95% confidence interval [CI]	-8.1 to 8.0		-7.3 to 1.2		-2.3 to 5.8	

Effects of Risedronate on BMD and Bone Markers

***Disclosures: Ryo Okazaki**, None.*

SU0392

Subtrochanteric Fractures: A complication of prolonged bisphosphonate use? Beatrice Edwards*[1], Andrew Bunta[2], Clarita Odvina[3], Sudhaker Rao[4], Joseph Lane[5], Dennis Raisch[6], Allison Hahr[7], June McKoy[7], Steve Belknap[7], Dennis West[7], Paula Stern[1]. [1]Northwestern University Medical School, USA, [2]Northwestern University Feinberg School of Medicine, USA, [3]University of Texas Southwestern Medical Center, Dallas, USA, [4]Henry Ford Hospital, USA, [5]Hospital for Special Surgery, USA, [6]8VA Cooperative Studies Program Clinical Research Pharmacy, USA, [7]Northwestern University, USA

Background:

Bisphosphonates, effective agents preventing osteoporosis related fractures and consequent morbidity, have been associated with sporadic cases of atypical subtrochanteric fractures. Fractures are typically atraumatic, occasionally preceded by prodromal thigh pain, and have characteristic findings on radiographs with thickened cortices and a transverse fracture with a ''beak'' appearance, are often bilateral and exhibit delayed healing.

Methods:

Case reports, case series, systematic reviews of the literature with search terms bone disease, osteoporosis, adverse drug reaction, subtrochanteric fracture, bisphosphonate associated osteopetrosis, alendronate, risedronate, ibandronate, zoledronate. Review of the FDA Adverse events reporting series (FDA AERS) from January 1996-December 2008.

Results:

Between 2005-2009, academic investigators reported on 109 cases of atypical subtrochanteric fractures in patients on alendronate with a median duration of therapy 6 years. In the FDA adverse events reporting system (AERS) 210 cases of pathological or non union fractures mostly associated with alendronate use had been reported. The proportional reporting ratio (PRR) was 6.19 (95% C.I. 5.88, 6.42). Co-morbidity and concomitant drug use was noted in less than 10% of cases. The incidence appears to be less than 1:100,000. A safety notification was issued by the FDA on March 10, 2010. No safety hearings at the FDA, European Medicines Agency (EMEA), Canada Health, or the Adverse Drug Reactions Advisory Committee (ADRAC) in Australia have been held.

Conclusions:

Bisphosphonate therapy for osteoporosis is an effective intervention for preventing morbidity related to osteoporotic fractures . Possible etiologies for atypical fractures include bisphosphonates' suppression of bone turnover, depletion of osteoblasts at the fracture site, and alterations of collagen and mineral metabolism. Subtrochanteric fractures may represent a rare complication of prolonged bisphosphonate therapy.

***Disclosures: Beatrice Edwards**, Eli Lilly, 5; Novartis, 5; P&G, 2; Roche, 5; Amgen, 5*

SU0393

Subtrochanteric Hip Fracture in Edmonton, Alberta, Canada - Case Reports. Stephanie Davis[1], Angela Juby*[2]. [1]University of Alberta Hospital, Canada, [2]University of Alberta, Canada

Purpose

The purpose of this study was to evaluate the prevalence of subtrochanteric fractures in Edmonton, Alberta, and to examine for any association with osteoporosis or osteoporosis treatment.

Methods

This was a retrospective chart review of all cases with an ICD 10 code for subtrochanteric fracture or unspecified hip or femur fracture referred to a tertiary care hospital over a one year period (2007-2008). Demographic, radiological and orthopaedic data was collected. Information on current medication and past medication was captured. Bone mineral density was recorded if this had been evaluated. Data is being gathered for other years. Ethics approval was obtained from the regional ethics review board.

Results

Five cases of subtrochanteric fracture were identified in the charts reviewed. All were women with an average age of 68years (62-74years). Four were associated with

falls, one occurred while rolling over (in a previously fractured hip). Four had diagnoses of osteoporosis. Two were taking alendronate and two were taking etidronate currently, and one had taken etidronate prior to alendronate. One had no history of bisphosphonate (BSP) exposure, and the other had just recently started the alendronate. One had 5 years of etidronate followed by 5 years of alendronate, another had 17 years of etidronate, another 4 years of etidronate. Two had been taking oral prednisone (for COPD and hypopituitarism). The COPD patient was not on BSP treatment. Four had treated hypothyroidism. Femoral neck BMD was 0.646g/cm^2, T -1.8 and 0.704g/cm^2, T -1.3 in the two cases in which it was evaluated.

Conclusions

Subtrochanteric fractures are rare fractures, that can occur in those patients with osteoporosis, whether it is primary or secondary (such as steroid therapy). In these five cases there was an association with bisphosphonate therapy and hypothyroidism. The associated BSP was etidronate but this is likely a reflection of formulary guidelines in Alberta that dictate that etidronate is the first line of osteoporosis therapy.

***Disclosures: Angela Juby**, None.*

SU0394

Underuse of Treatment for Osteoporosis Among High Risk Older Adults Living in the Community Receiving Home Health Services. Amy Mudano*[1], Ryan Outman[1], Meredith Kilgore[2], Liana Fraenkel[3], Elizabeth Kitchin[1], Julie Locher[1], Kenneth Saag[1], Amy Warriner[4], Jeffrey Curtis[1]. [1]University of Alabama At Birmingham, USA, [2]University of Alabama At Birmingham School of Public Health, USA, [3]Yale University, USA, [4]UAB, USA

Purpose: To examine characteristics, estimated fracture risk (using FRAX), and medication usage among community-dwelling individuals with osteoporosis or a previously diagnosed fracture receiving home health services from a state-wide home health care agency.

Methods: Using electronic health record data, we identified patients with either an osteoporosis or a fracture diagnosis that received home health services. Potentially eligible patients were contacted by phone; those agreeing to participate completed a computer assisted telephone interview. Data collected included information on demographics, medical history, fall risk, fracture history, osteoporosis treatment (current and past), and dietary supplements (i.e. calcium and vitamin D). We used the FRAX WHO Fracture Risk Assessment calculator to calculate the 10-year probability of hip fracture and the 10-year probability of a major osteoporotic fracture.

Results: Among 554 patients called, contact was made with 78%; 189 (34% of total) agreed to participate. Survey participants were 83% female with an average age of 75.2+9.9 years and predominantly white (92%). Among patients with a history of fracture (78% of total), 47% reported that they had been given a diagnosis of osteoporosis. Of those reporting a fracture (n=101), the most common type was hip (39%). The median (IQR) estimated 10-year probability of hip fracture was 7.6(14.8) and 23.0(22.5) for 10-year probability of any osteoporotic fracture. Less than half of participants reported taking calcium (41%) or vitamin D (43%) supplements. Only 24% of participants reported current use of an osteoporosis medication; 18.5% reported use of bisphosphonates and 5% reported other osteoporosis medications. The following table shows the use of calcium + vitamin D supplements and osteoporosis medications based on fracture and a healthcare provider-reported diagnosis of osteoporosis . Use of osteoporosis medications was highest among those with a known osteoporosis diagnosis and no history of fracture.

Conclusions: Use of supplemental calcium and vitamin D and osteoporosis medications was low in this group of high-risk, elderly home health patients, regardless of fracture history and osteoporosis diagnosis. More patients with hip fractures had previously used osteoporosis drugs but stopped using them than were currently using them, emphasizing the need for better strategies to improve adherence.

	Prescription Osteoporosis Medications		Calcium + Vitamin D use
	Current Use	Past, Not Current Use	
Prior Hip Fracture	18%	28%	64%
Prior Other Fracture	23%	18%	60%
Osteoporosis Diagnosis with no history of Fracture	59%	18%	35%
Prior Hip Fracture and Osteoporosis Diagnosis	33%	39%	72%
Prior Other Fracture and Osteoporosis Diagnosis	34%	28%	72%

Proportion of High Risk Home Health Care Patients Receiving Osteoporosis Rx, Calcium and Vit D

***Disclosures: Amy Mudano**, None.*
This study received funding from: Eli Lilly

SU0395

A Dedicated Intervention Program Reduces Refracture Rates in Patients with Incident Non-Vertebral Osteoporotic Fracture: Results of a 4-Year Prospective Controlled Study. Anna Lih*[1], Haren Nandapalan[1], Michael Kim[1], Markus Seibel[2]. [1]Department of Endocrinology & Metabolism, Concord Hospital, The University of Sydney, Australia, [2]Bone Research Program, ANZAC Research Institute, The University of Sydney, Australia

The risk of refracture, disability and death significantly increases following an osteoporotic fracture. There is limited good-quality data on the effectiveness of dedicated clinical programs to reduce refracture rates in patients with osteoporotic fractures. The current analysis measured the effect of a coordinated management and intervention program on refracture rates during the study period of May 2005 to October 2009.

Methods: Within the framework of a prospective controlled cohort study, a preventative care program was established to identify, investigate and treat patients presenting with an osteoporotic fragility fracture to a large tertiary referral hospital in Sydney, Australia. Patients aged 45+ with a recent non-vertebral minimal trauma fracture (MTF) were identified and referred to the MTF program. Patients attending the service were assessed for a) clinical risk factors, b) bone mineral density (DEXA), c) prevalent vertebral fractures (TL spine X-ray), and d) secondary causes of osteoporosis (biochemistry, bone scans as indicated). If a diagnosis of osteoporosis was made, patients were commenced on appropriate therapy and followed-up every 6-12 months. Patients who did not attend the service formed the concurrent control group and underwent an extensive telephone interview at study completion.

Results: There were 246 patients in the MTF group and 157 in the control group. At baseline, both groups were balanced for anthropometric, socio-economic and clinical risk factors. During a mean post-fracture follow-up period of 37.7 months, 10 patients (4.1%) in the MTF group suffered a further fragility fracture. In the control group, 31 patients (19.1%) re-fractured within a mean follow-up time of 35.2 months, translating into a 5.3-fold risk of refracture in the control group (95% CI 2.61-10.7; $p<0.01$). In women, there was a 6.6 fold increase in refracture compared to the control group (95% CI 2.98-14.4, $p<0.01$). The median time to refracture was 23 months in the MTF group and 13 months in the control group ($p<0.01$). Group assignment ($p<0.001$), age ($p<0.01$), and BMI ($p<0.001$) were all significant predictors of refracture.

Conclusion: A dedicated post-fracture program greatly reduces the risk of further fracture. The results from this prospective controlled study prove that active identification and management of patients with osteoporotic fracture prevent further fractures and hence disability associated with osteoporosis.

***Disclosures: Anna Lih**, None.*

SU0396

Bisphosphonate Prescribing in Ontario, Canada 1996/7-2008/9. Suzanne Cadarette*[1], Andrea Burden[2], M. Alan Brookhart[3], Susan Jaglal[2], David Juurlink[2], Muhammad Mamdani[2], J. Michael Paterson[4], Daniel Solomon[5]. [1]Leslie Dan Faculty of Pharmacy, University of Toronto, Canada, [2]University of Toronto, Canada, [3]University of North Carolina, USA, [4]Institute for Clinical Evaluative Sciences, Canada, [5]Harvard Medical School, USA

Background: Three oral bisphosphonates are available for treating osteoporosis in Canada: alendronate, etidronate and risedronate. Access to these agents through the Ontario public drug plan changed over time: etidronate has been available without restriction since 1996 and alendronate and risedronate were subject to various limited access criteria until 2007. Since 2007, all three agents have been open listed without restriction. We sought to characterize trends in bisphosphonate prescribing in Ontario from 1996/97 to 2008/09.

Methods: We identified all new users of alendronate (10mg, 70mg), cyclical etidronate, and risedronate (5 mg, 35 mg) through the Ontario public drug plan that covers all residents aged 65 or more years, 1996/97-2008/09. Patients younger than age 66 years, as well those with Paget's disease or use of any bisphosphonate, calcitonin, raloxifene or teriparatide within the 365 days prior to the index date were excluded. We summarized the number of new users by fiscal year, sex and index drug, and compared descriptive characteristics (age, fracture history and bone mineral density [BMD] testing within the past year) over time.

Results: We identified 451,113 eligible new bisphosphonate users. Their mean age was 76 years (SD=6.9) and 84% were female. The total number of new users rose steadily over the first few years, from 12,953 in 1996/97 to 37,296 in 1999/00 with 99.8% dispensed etidronate. Etidronate prescribing declined steadily after 1999/00, reaching a low of 10% of new users in 2008/09. The percentage of new users that were female also declined over time, from 94% in 1996/97 to 74% in 2008/09. Besides sex and index drug, we document little difference in the characteristics of new bisphosphonate users over time: mean age=76 years (SD=6.9), 6% fracture history and 62% prior BMD test. In 2008/09, 90% of new bisphosphonate users in Ontario were prescribed alendronate or risedronate (98% weekly), and 74% were female.

Conclusions: Prescribing practices changed over time as access to second generation bisphosphonates improved: etidronate prescribing declined and a larger percentage of males were treated over time. However, little difference between new users was observed over time by age, fracture history or prior BMD testing. In 2008/

09, 90% of new bisphosphonate users were prescribed alendronate or risedronate and 26% were male.

***Disclosures: Suzanne Cadarette**, None.*

SU0397

Compliance with Bisphosphonate Therapy and Change in Bone Mineral Density in Clinical Practice. Derek Weycker[1], Lois Lamerato[2], Susan Schooley[2], Tiffany Siu Woodworth[1], David Macarios*[3], Nicole Yurgin[3], Gerry Oster[1]. [1]Policy Analysis Inc, USA, [2]Henry Ford Health System, USA, [3]Amgen Inc, USA

Background. In randomized trials, bisphosphonates have been found to increase bone mineral density (BMD) and to decrease fracture risk in women with postmenopausal osteoporosis. Change in BMD in typical clinical practice, where patients may be less compliant with prescribed treatment than in clinical trials, is largely unknown.

Methods. The study was conducted at Henry Ford Health System, a large integrated health system in Detroit, MI. Study subjects were women, aged ≥45 years, who began treatment with an oral bisphosphonate between 2002 and 2007, and who had ≥1 BMD value at the (total) hip during the 12-month period preceding treatment and ≥1 such BMD thereafter. Change in BMD was calculated as the difference between the most recent pretreatment scan and first follow-up scan. Compliance with bisphosphonate therapy was measured using the medication possession ratio (MPR; total days of therapy/total days of follow-up), evaluated between date of therapy initiation and date of first follow-up scan. Change in BMD was examined in the overall cohort, and within strata defined on MPR and time from therapy initiation to first follow-up scan.

Results. A total of 1040 women were identified who met study entry criteria; average age (±SD) was 64 (±10) years, pretreatment BMD was 0.80 (±0.11), and T-score was -1.3 (±0.9). Mean follow-up was 2.3 (±1.0) years. Mean MPR was 0.58 (±0.36). On an overall basis, BMD increased by 1.1% (95%CI: 0.8, 1.4); change in BMD was -0.3% (-0.7, 0.1) for subjects with MPR <50% (n=430), 1.7% (1.1, 2.2) for those with MPR from 50-80% (n=198), and 2.2% (1.8, 2.7) for those with MPR >80% (n=412). Among patients whose first follow-up scan occurred ~2 years after therapy initiation (n=503), BMD increased by 1.4% (0.99, 1.8); change in BMD was 0.03% (-0.60, 0.66) for subjects with MPR <50% (n=192), 1.5% (0.68, 2.40) for subjects with MPR from 50-80% (n=103), and 2.6% (1.95, 3.29) for those with MPR >80% (n=208). Across all strata, the smallest change in BMD was observed among patients with MPR <50%.

Conclusions. "Real-world" benefits of bisphosphonate therapy, as measured by change in BMD, are highly correlated with adherence. Patients with low adherence derive little clinical benefit from such therapy.

***Disclosures: David Macarios**, Amgen Inc, 5*
This study received funding from: Amgen Inc

SU0398

Medication Adherence and Fracture Risk Among Patients Using Osteoporosis Medications in a Large U.S. Health Plan. Sally Wade*[1], Jeffrey Curtis[2], Jingbo Yu[3], Jeffrey White[4], Brad Stolshek[5], Claire Merinar[5], Akhila Balasubramanian[5], Joel Kallich[5], John Adams[6], Hema Viswanathan[5]. [1]Wade Outcomes Research & Consulting, USA, [2]University of Alabama at Birmingham, USA, [3]HealthCore, Inc., USA, [4]WellPoint, USA, [5]Amgen Inc, USA, [6]RAND Corp, USA

Purpose

Osteoporosis (OP) poses a significant economic and clinical burden. Low adherence may mitigate treatment efficacy including fracture risk reduction. This study examines the association between OP medication adherence during the first year on therapy and subsequent fracture risk using recent data from a commercially insured population.

Methods

Patients were identified from a large, commercially insured U.S. population with integrated pharmacy and medical claims. Patients were included if they were ≥ age 45, new to OP therapy (no OP medication claims in prior year) with first (index) OP medication claim between 1/1/2005 and 4/30/2008, and had continuous coverage for ≥12 months pre- and post-index. Patients were excluded if they had: pre-index Paget's disease or malignant neoplasm, or were in a skilled nursing facility or on combination therapy at index. Patients who had a fracture in the first year on therapy were excluded. This ensured that the time periods for assessing exposure (medication) and outcome (fracture) did not overlap. Logistic regression was used to assess the association between the medication possession ratio (MPR) during the 12 months post-index and fracture risk thereafter in bisphosphonate users. Covariates included baseline demographic and clinical characteristics including comorbidities and prior fracture.

Results

The analysis included 38,243 patients who were new to OP therapy, had a mean age (± SD) of 59.5 ± 9.3 years, and had a mean post-index follow up of 834 days; 94% were female. At index, 87.8% used a bisphosphonate. Over 12 months post-index, the MPR=0.57 (95% CI: 0.57, 0.58). The 22,882 patients with 24 months of follow up had a mean MPR=0.49 (95% CI: 0.49, 0.49) over that period. Mean 12-month MPR was lower among patients with fracture (n=1,093) compared with those without fracture (n=37,150; 0.54 vs 0.57, respectively; $p<0.001$). In multivariate modeling, bisphosphonate users with a MPR>0.8 over 12 months had a 14% lower risk of subsequent fracture compared with those with a MPR<0.5, even after controlling for demographic characteristics, insurance type, prior fracture, select comorbidities, and other potential confounders.

Conclusion

In this study, patients in a large, commercial health plan had a mean 12-month MPR of 0.57 for OP medications. Patients with low adherence (MPR<0.5) experienced an increased fracture risk even after controlling for a large number of fracture-related covariates.

***Disclosures: Sally Wade**, Amgen Inc., GE Healthcare, 5*
This study received funding from: Amgen Inc.

SU0399

Methods to Examine the Impact of Real-world Adherence to Osteoporosis Pharmacotherapy on Fracture Risk: Systematic Review and Recommendations. Milica Nikitovic*[1], Daniel Solomon[2], Suzanne Cadarette[1]. [1]Leslie Dan Faculty of Pharmacy, University of Toronto, Canada, [2]Harvard Medical School, USA

Objective: To review methods of prior studies that estimate the association between compliance to osteoporosis pharmacotherapy on fracture risk, and make recommendations to guide future research.

Methods: We supplemented prior reviews with a systematic search of MEDLINE to identify all English language non-experimental studies that examined the impact of adherence to osteoporosis pharmacotherapy on fracture risk. Studies that measured compliance were eligible and those that only examined persistence were excluded. We summarized the methodology of each study and make recommendations for future research.

Results: We identified fourteen eligible articles: nine cohort and five nested case-control. Length of baseline periods ranged between three months and two years, with nearly all studies (n=12) restricting inclusion to treatment naïve users. A threshold of 80% was most commonly used to define compliance (n=10), with few studies providing a more thorough analysis through categorical (n=3) or continuous (n=1) measures. All nine cohort studies adjusted for sex, age, prior fracture, and comorbidities; however, only one of the five case-control studies controlled for drug exposure, sex, age, event date and length of follow-up. One study considered a theoretical sensitivity analysis to account for potential healthy adherer bias, yet all mentioned limitations related to possible residual confounding.

Conclusions: We identify great variability in methods of prior studies that evaluate the impact of compliance to osteoporosis pharmacotherapy on fracture risk, and make recommendations for future research.

***Disclosures: Milica Nikitovic**, None.*

SU0400

Relationships Between Osteoporosis Medication Adherence, Surrogate Marker Outcomes and Non-Vertebral Fracture Incidence. Richard Eastell*[1], Bernard Vrijens[2], David Cahall[3], Christian Roux[4], Johann Ringe[5], Patrick Garnero[6], Nelson Watts[7]. [1]University of Sheffield, United Kingdom, [2]AARDEX Ltd, Belgium, [3]sanofi-aventis Pharmaceuticals, USA, [4]Hospital Cochin, France, [5]Klinikum Leverkusen, University of Cologne, Germany, [6]Synarc SAS, France, [7]University of Cincinnati Bone Health & Osteoporosis Center, USA

Purpose: Response to osteoporosis treatments may be reduced by poor adherence. Treatment response can be monitored by using surrogate markers of fracture risk, bone turnover markers (BTMs) and bone mineral density (BMD). The relationships between adherence and 1) non-vertebral fracture (NVF) incidence, 2) BTM and BMD responses and 3) BTM and BMD changes and NVF outcomes were evaluated in this study.

Methods: Secondary analysis of the Improving Measurements of Persistence on Actonel Treatment (IMPACT) study, a multinational prospective, open-label, cluster randomized study of postmenopausal women on oral risedronate 5 mg daily for 1 year. Electronic drug monitors were used to assess adherence. Urinary N-terminal and serum C-terminal cross-linked telopeptide of type I collagen (uNTX and sCTX, respectively) were assessed at baseline and week 22. BMD was assessed at baseline and 1 year.

Results: Among 2302 women, 1) no association was observed between adherence and NVF outcomes at 1 year. 2) The number of patients on risedronate with significant reduction (>30%) in uNTX and sCTX was positively related to the number of doses taken at week 22 ($p<0.001$). Adherence was positively associated with BMD increase at 1 year ($p<0.001$, spine; $p=0.02$, hip). 3) BTM and spine BMD responses were related to NVF outcomes. At week 22, NVF incidence was lower in patients with >30% reduction in uNTX and sCTX than in those with BTM reduction ≤30% (1.6 vs 3.2%/yr, $p=0.02$ and 1.7 vs 4.3%/yr, $p=0.002$, respectively). At 1 year, NVF rate was also lower in patients with >3% increase in spine BMD than in those with ≤3% change (1.4 vs 3.1%/yr, $p=0.01$).

Conclusions: Adherence to osteoporosis therapy is related to reductions in BTM and BMD, which are consecutively associated with a reduction in fracture risk. The

relationship between fracture outcomes emphasizes the importance of monitoring these surrogate markers during treatment.

*Disclosures: **Richard Eastell**, Procter & Gamble Pharmaceuticals, 2; Sanofi-Aventis, 5; Sanofi-Aventis, 2; Procter & Gamble Pharmaceuticals, 5*
This study was funded by The Alliance for Better Bone Health (a partnership between Warner Chilcott plc and its affiliates, and sanofi-aventis US, Inc.)

SU0401

Who is Not Treated Following the Implementation of Optimus, a Successful Initiative to Treat Osteoporosis Following a Fragility Fracture. Gilles Boire*[1], François Cabana[2], Michèle Beaulieu[3], Sawsan Mikhail[4], Dominique Lambert[5]. [1]Centre Hospitalier Universitaire De Sherbrooke, Canada, [2]Centre hospitalier universitaire de Sherbrooke, Division of Orthopaedics, Canada, [3]Medical Liaison, Merck Canada, Canada, [4]Medical Liaison, Novartis Pharmaceuticals Canada, Canada, [5]Medical Liaison, Warner Chilcott, Canada

Background: Underlying osteoporosis (OP) is inconstantly treated after a fragility fracture (FF). To decrease this treatment gap, we established the OPTIMUS program to evaluate 2 interventions prompting primary care practitioners (PCPs) to treat OP following a FF: a Minimal (MI) and an Intensive Intervention (II) differing by the frequency of intervention (0, 4 and 8 months vs 0 and 6 months) targeting the patient and the PCP, and in the amount and personalization of patient data and treatment recommendations given to the PCP.

Objectives: To improve our future interventions, we compared the characteristics of treated and untreated patients at 12 months.

Methods: Consenting outpatients ⩾50 years seen by orthopedists for an incident FF were randomized to Standard Care (SC; no intervention, phone FU at 6 and 12 months) or to either MI or II. Baseline characteristics of patients and PCPs were compared.

Use of OP treatments was collected at inclusion and at each FU and was confirmed with patients' pharmacists at 1 year. Appropriate treatment was defined as calcium and vitamin D supplements plus an effective OP treatment (aminobisphosphonates in >95%).

Results: Over 3 years, we recruited 670 patients from 258 PCPs, with no differences in baseline characteristics between groups. By January 15 2010, 197/200 SC, 177/247 MI and 165/223 II patients had achieved 12 months of FU, of which 10 had died. Phone FU at 12 months was obtained from 500/529 (94.5%) survivors, with no significant differences between groups. Among patients untreated at the time of FF, 21% (31/148) in SC were treated 12 months after FF, and 42% (50/119) and 53% (61/115) after MI and II, respectively. Being part of an intervention, history of osteoporosis or previous FF, and ever having a BMD performed were all significant predictors of being treated ($p<0.0001$). Relative to treated patients, patients untreated at 12 months were more frequently male ($p<0.005$), active smokers ($p = 0.011$) and trended to be younger (63.0 vs 66.7 y.o.; $p<0.06$). PCP characteristics also influenced treatment rates.

Conclusion: Both our interventions at least double rates of treatment at 1 year in previously untreated patients, but the more intensive one works better (half the patients) and faster (not shown). Males, smokers and younger patients were the least likely to be treated for OP after a FF. Specific interventions to target subsets of FF patients and PCPs are likely to improve our current interventions.

*Disclosures: **Gilles Boire**, Alliance for Better Bone Health (Warner Chilcott and sanofi aventis Canada); Merck Canada; Novartis Canada, 2*
This study received funding from: Alliance for Better Bone Health (Warner Chilcott and sanofi aventis Canada); Merck Canada; Novartis Canada

SU0402

Comparison of FRAX® and German DVO Osteoporosis Guidelines for Cost-Effective Selection of Patients in Need of Therapy: Prospective Fracture Data from the OPUS Study. Claus-C Glueer*[1], Reinhard Barkmann[2], Christian Graeff[3], Richard Eastell[4], Dieter Felsenberg[5], David Reid[6], Christian Roux[7]. [1]Christian Albrechts Universitaet zu Kiel, Germany, [2]Universitaetskinikum Kiel, Germany, [3]University Clinic Schleswig-Holstein, Germany, [4]University of Sheffield, United Kingdom, [5]Charité - Campus Benjamin Franklin, Germany, [6]University of Aberdeen, United Kingdom, [7]Hospital Cochin, France

Selection of patients in need of treatment should be based on their risk of fracture. FRAX® provides estimates of fracture risk for major fractures or hip fractures but an intervention threshold is not given. The German S3 DVO osteoporosis guidelines follow a similar approach but are based on 10-year risk of vertebral (clinical or radiological) or hip fracture; therapy is indicated if this risk exceeds 30%. The set of clinical risk factors is more extensive compared to FRAX® and both BMD of spine and hip are considered. We compared the performance of FRAX®, DVO guidelines, and DVO guidelines with Quantitative Ultrasound (QUS) instead of DXA in identifying patients in need of therapy.

Methods. Probability of fracture was modeled for the three approaches based on baseline data from the OPUS study. In the OPUS study random population samples were recruited in 5 European centers and followed over 6 years. Here we analyzed fracture incidence data of 1415 women age 55 or older. We tested whether those subjects who fractured during the follow-up time would have been correctly selected by the three risk assessment approaches as being subjects at risk at baseline. The intervention threshold for FRAX® was selected by matching its sensitivity with that of the DVO guidelines.

Results. Based on matched sensitivity, the 30% 10-year risk level for vertebral and hip fractures of the DVO guidelines, a FRAX® intervention threshold of 3.6% for 10 year hip fracture risk and 14.1% for risk of major fracture all resulted in identification of 301 women as being in need of therapy. 178 women suffered a fracture including 62 vertebral or hip fractures and 81 major fractures. Compared to women who did not fracture women with fractures had a 2.5 times higher DVO probability to be categorized as in need of therapy (FRAX® hip: 2.2 times higher, FRAX® major: 2.2). Assuming a fracture risk reduction effect of therapy of 50% for vertebral fractures and 30% for non-vertebral fractures the number needed to treat (NNT) for one year was 54.6 for DVO, 62.4 for FRAX® major fractures, and 61.2 for FRAX® hip fractures (for other fracture types see fig). QUS based data were almost identical to the DVO guidelines based on DXA.

We conclude that all approaches were effective in identifying subjects in need of treatment. Assuming annual costs of treatment of 200 Euros, 1 fracture of any kind, 1 vertebral or 1 hip fracture could be prevented by investing 10,000 to 20,000 Euros on medication.

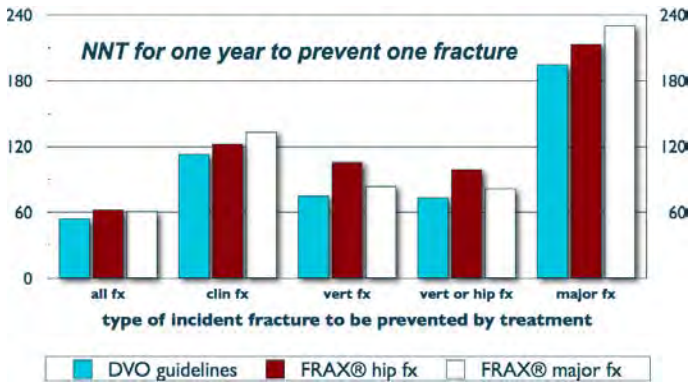

Comparison of number needed to treat for DVO and FRAXÛ

*Disclosures: **Claus-C Glueer**, None.*
This study received funding from: Sanofi-Aventis, Eli Lilly, Novartis, Pfizer, Proctor and Gamble Pharmaceuticals, Roche

SU0403

Raising the Bar on Secondary Fracture Prevention. Richard Dell*, Denise Greene, Shireen Fatemi, Nora Strick, Tadashi Funahashi, Annette Adams, Brenda Thomason. Kaiser, USA

Aims: To evaluate the effectiveness of a secondary fracture prevention program run by care mangers using reports generated from an electronic medical record to identify patients who received DXA scan and/or anti-osteoporosis treatment.

Methods: All patients aged 65 years or older who sustained a fragility fracture (any low energy fracture excluding face, skull, fingers, and toes) in 2008 were identified from the inpatient and ambulatory care records of a large health maintenance organization in Southern California. Qualifying fractures were identified by ICD9 codes. Electronic medical records were used to ascertain additional information on patient demographics and clinical characteristics, fracture type, DXA scan reports, anti-osteoporosis treatment, and eligibility. Proportions of patients screened and/or treated for osteoporosis were described by sex and age group, as were proportions of patients for whom screening or treatment was ordered, but not implemented.

Results: In 2008, 3037 men and 7351 women aged 65 years or more sustained a new fragility fracture. DXA scans and/or pharmacologic treatment had been administered to 2439 men (80.3%) and 6796 women (92.5%). DXA scans and/or treatment had been ordered, but not carried out for an additional 237 men and 238 women. The combined rate of DXA scan and/or treatment and intended to treat was 88.1% in men and 95.7% in women. Only 186 patients who did not receive a DXA scan and/or treatment or had a DXA scan and/or treatment ordered remain active members of the SCAL HMO. Of the 10,388 initial fragility fracture patients, that leaves 1.8% of these patients that still have a care gap on secondary fracture prevention.

Conclusion: Our goal was to get to as close to 100% of DXA scanning and/or treatment in patients over 65 years old with a fragility fracture as possible. We came close to achieving that goal by utilizing care managers and an electronic medical record to target all patients with a fragility fracture who had not received a DXA scanning and/or treatment and then acting the behalf of the patient's primary care physician to order a DXA scan and/or treatment.

*Disclosures: **Richard Dell**, None.*

SU0404

The Economic Consequences of Hip Fractures: Impact of Home Exercise and High-dose Vitamin D. Heike Bischoff-Ferrari*[1], Bess Dawson-Hughes[2], Endel Orav[3], Walter Willett[3], Andreas Egli[4], Andreas Maetzel[5], Hannes B Staehelin[6], Robert Theiler[7]. [1]University of Zurich, Switzerland, [2]Tufts University, USA, [3]Harvard School of Public Health, USA, [4]Centre on Ageing & Mobility, Switzerland, [5]University of Toronto, Canada, [6]University of Basel, Switzerland, [7]Triemli City Hospital, Switzerland

Background: Economic consequences of hip fractures extend beyond its repair.

Methods: Health care resource utilization was assessed in monthly phone calls to 173 acute hip fracture patients enrolled in a factorial design 12-month RCT comparing the effects of high-dose vitamin D (2000 IU versus 800 IU vitamin D per day) and an unsupervised exercise home program instructed during acute care (home program versus standard care), with 79% women, mean age 84 years, 77% living at home. The total cost included hip fracture repair, and inpatient and outpatient costs in the first 12 months after hip fracture (acute care, rehabilitation, physiotherapy, MD visits, home care). Health care utilization was validated against insurance claims data available in 46 of 173 hip fracture patients. Median regression analysis was used to determine the effects of the two strategies, controlling for age, gender, body mass index, type of dwelling prior to hip fracture, 25-hydroxyvitamin D level at baseline, and time of follow-up.

Results: The median total cost of hip fracture care over 12 months for 173 hip fracture patients was 31,221 CHF (95% Cl: 16,606-83,622): 20,282 CHF (95% Cl: 11,228-52,997) for hip fracture repair and 9,214 CHF (95% Cl: 510-37,225) for post-hip fracture inpatient and outpatient care (CHF are Swiss Francs = 0.94 USD). Based on insurance claims data from a subgroup of 46 hip fracture patients, the median total health care cost in the year prior to the hip fracture was 4,448 CHF (95% Cl: 578-20,345), median hip fracture repair cost was 20,359 CHF (95% Cl: 10,721-71,257) and post hip fracture care was 11,469 CHF (95% Cl: 1,911-37,225). Median costs did not differ by the tested interventions, however the tail of the cost distribution was brought in with savings on the 75th ($p = 0.07$) and 90th percentile ($p = 0.02$) of cost distribution among those randomized to the home exercise program. With the exercise home program, the total cost were 17,751 CHF lower per hip fracture patient in the 90th percentile of cost distribution. The higher versus standard dose of vitamin D was cost-neutral.

Conclusion: Health care costs increase by a factor of 2.5 in the first year after hip fracture excluding the cost of hip fracture repair. Thus hip fractures have important economic and clinical consequences that extend beyond its repair. The interventions tested in this trial didn't alter median costs, but the instructed home program reduced costs significantly at the high end of the cost distribution.

***Disclosures: Heike Bischoff-Ferrari**, None.*

SU0405

Assessing the Efficacy of Melatonin on Bone Health in Perimenopausal Women. Mary Kotlarczyk*[1], Judith Balk[2], Holly Lassila[3], Christine O'Neil[3], Hildegarde Berdine[3], Paula Witt-Enderby[1]. [1]Duquesne University Graduate School of Pharmaceutical Sciences, USA, [2]University of Pittsburgh School of Medicine, USA, [3]Duquesne University Mylan School of Pharmacy, USA

Current osteoporosis therapies primarily target osteoclasts to prevent further bone loss. The problems with these approaches lie in their inability to build bone and their adverse effects. The pineal hormone melatonin has been shown to modulate bone activity in cell and animal models via inhibition of osteoclasts and stimulation of osteoblasts; however, little is known about the effects of melatonin on bone in humans. The purpose of this study was to test the efficacy of melatonin to improve bone health in perimenopausal women, a population of women at high risk for bone loss. Besides effects on bone, the efficacy of melatonin on secondary measures of health including sleep quality and overall well-being was examined. It was hypothesized that daily nocturnal supplementation with melatonin would improve bone health and overall quality of life in perimenopausal women. Eighteen women were recruited to participate in a preliminary, randomized, double-blind study. Five subjects were given placebo, and thirteen were given melatonin (3mg, p.o.) daily for six months. Bimonthly serum levels of type I collagen cross-linked N-telopeptide (NTX) and osteocalcin were monitored to evaluate changes in osteoclast and osteoblast activity, respectively. Overall health, including blood pressure measurement, was assessed each month by a nurse. Patient-perceived health was monitored through the use of daily journals kept by the participants. Two validated surveys, Menopausal Quality of Life-Intervention (MEN-QOL-Intervention) and Pittsburgh Sleep Quality Index (PSQI), were administered to the study subjects before and following the six month trial to assess any melatonin-induced effects on quality of life. Women treated with melatonin are expected to have decreased NTX and increased osteocalcin levels, indicating improved bone health. Additionally, women taking melatonin are expected to show improvements in sleep/wake patterns and general well-being as compared to participants receiving placebo. This study will provide important information regarding the potential use of melatonin as a preventative therapy for improving both bone health and quality of life in perimenopausal women. Moreover, this translational study will be the first of its kind to examine the relationship between melatonin and bone health in a human population.

***Disclosures: Mary Kotlarczyk**, None.*

SU0406

Bone Metabolism, Oxidative Stress and Biochemical Evaluation of Perimenopausal Women under Treatment with Lipoic Acid. Rodrigo Barbosa*[1], Francisco Paulo Freire-Neto[1], Maria do Socorro Medeiros Morais[1], Karla Simone da Costa Oliveira[1], Yonara Monique da Costa Oliveira[1], Heglayne Pereira Vital Silva[1], Luciana Cristina Alves de Souza[1], Leandro Vinicius F. de Morais[1], Marcela Abbot Galvão Ururahy[1], João Felipe Bezerra[1], Raul Hernandes Bortolin[1], André D. Luchesi[2], Sonia Quateli Doi[3], Rosário Dominguez Crespo Hirata[2], Mario Hiroyuki Hirata[2], José Brandão Neto[1], Maria das Graças Almeida[1], Adriana Rezende[4]. [1]Universidade Federal Do Rio Grande Do Norte, Brazil, [2]Universidade de São Paulo, Brazil, [3]Uniformed Service of Healthy Science, USA, [4]Federal University of Rio Grande De Norte-UFRN, Brazil

Purpose: The present study aimed to evaluate the biochemical changes that women in the menopausal transition are subject to, their bone metabolism, and the relationship between them. The influence of an alternative therapy with lipoic acid (LA) in these changes was also investigated. Methods: A double-blind study was carried out in perimenopausal women that underwent a three month treatment with 600 mg of LA compared with another group that received placebo during the same period. Results: The women that took part in this study had a waist circumference and body mass index above the values recommended by World Health Organization (WC $\geqslant$ 80 cm; BMI $>$ 25kg/m^2). Moreover, these women had increased concentrations of total cholesterol and triglycerides, and borderline LDL (Total Cholesterol>200mg/dL; Triglycerides>150mg/dL; LDL>130mg/dL). These values were not affected by treatment with LA. There were no detectable shifts in the concentration of liver markers (ALT, AST and GGT), kidney markers (urea, creatinine, total protein and albumin), mineral markers (Total Calcium, Ionized Calcium, Phosphorus and Magnesium) and in bone markers (Osteocalcin, Total Alkaline Phosphatase and Tartrate Resistant Acid Phosphatase) after treatment with LA. The results of the oxidative markers showed that treatment with LA decreased GPx activity ($p<0,01$), while TBARS, GSH and SOD activity presented no differences. The expression of RANKL mRNA was reduced ($p<0,05$) whereas RANK expression was increased ($p<0.001$) after treatment with LA. The expression of IL-6 and TNF-α genes showed no changes. Conclusions: Taking these results all together, it's possible to conclude that women in the perimenopause stage may show changes in lipid profile and body composition that can induce shifts in oxidative and bone metabolism. LA treatment may have a positive effect in the oxidative and bone metabolism since GPx activity, and mRNA expression of RANKL were reduced. The results also suggest a beneficial and protective effect of LA, indicating it as a potential alternative treatment to help preventing the complications associated with estrogen deficiency.

***Disclosures: Rodrigo Barbosa**, None.*

SU0407

Clinical Evaluation of Percutaneous Vertebral Augmentation Procedures using Radiofrequency Kyphoplasty in Treatment of 68 Vertebral Compression Fractures. Luke Sewall*, Steven Smith, Vlahos Athanasios. Vascular & Interventional Radiology, USA

Purpose: Recent reports suggest percutaneous vertebral augmentation (PVA) may be no better than placebo in treatment of vertebral compression fractures (VCF). This U.S. multicenter study evaluates safety and clinical efficacy of a new vertebral augmentation procedure and system.

Methods: 68 vertebra were treated in 56 patients. Patients with confirmed acute/subacute fractures based on MRI or bone scans underwent RF Kyphoplasty using a novel non-balloon PVA system. The system uses an articulated navigational osteotome for vertebral cavity creation, instead of 2 balloons, enabling unipedicular as opposed to bipedicular access. The cement reaches ultrahigh viscosity (UHV) prior to entering the vertebra by radiofrequency (RF) treatment. RF energy modulates the viscosity of PMMA cement immediately prior to entering the patient allowing for unique combination of extended working times and UHV cement delivery. Radiographic outcomes: fracture plane/cleft filling and percent patients with cement extravasation. Clinical outcomes: pain assessment using a 10cm visual analog pain scale and patient's subjective response. Preoperative and procedural imaging was reviewed by 3 certified interventional radiologists. Cement extravasation or venous leakage was assessed. Improvement was categorized as none, minimal, moderate or complete.

Results: Fracture etiology was 50 osteoporosis; 4 trauma; 2 neoplasia. All 68 levels were treated successfully with no complications. 94% of procedures were unipedicular with the articulated osteotome able to be navigated across vertebral midline. Bipedicular access was used in 4 levels due to severely sclerotic bone. Average cement used per level was 4.8cc. 90% of patients had no extravasation. Of patients with cement leakage, 8% had non-venous leaks into the disc space or paravertebral tissues and 4% had venous leaks. No leaks were clinically significant. 94% of patients had excellent vertebral body and fracture plane filling. 93% of patients experienced complete or moderate pain relief. 3% patients had minimal relief and 4% patients had no pain relief.

Conclusion: This novel PVA system evaluated in 68 VCF's in a multicenter analysis of 56 patients resulted in excellent safety and clinical efficacy using a unipedicular approach and RF treated UHV cement. This may allow patients a potentially less invasive procedure.

***Disclosures: Luke Sewall**, DFine Inc, 5*
This study received funding from: DFine Inc

SU0408

Fractional Absorption of Active Absorbable Algal Calcium (AAACa) and Calcium Carbonate Measured by a Dual Stable - Isotope Method. Kazuhiro Uenishi[1], Takuo Fujita*[2], Hiromi Ishida[1], Yoshio Fujii[3], Mutsumi Ohue[2], Hiroshi Kaji[4], Midori Hirai[4], Mikio Kakumoto[4], Steven Abrams[5]. [1]Kagawa Nutrition University, Japan, [2]Katsuragi Hospital, Japan, [3]Calcium Research Institute Kobe Branch, Japan, [4]Kobe University, Japan, [5]Baylor College of Medicine, USA

With the use of stable isotopes, this study aimed to compare the bioavailability of active absorbable algal calcium (AAACa), oyster shell powder heated to a high temperature, with an additional heated seaweed component (Heated Algal Ingredient, HAI), with that of calcium carbonate. In 10 postmenopausal women volunteers aged 59 to 77 years (Mean ± SD, 67 ± 5.3), the fractional calcium absorption of AAACa and CaCO3 was measured by a dual stable isotope method. After a fixed menu breakfast and pre - test urine collection (Urine 0), 42Ca - enriched CaCl2 was intravenously injected and 44Ca - enriched CaCO3 orally administered without carriers 15 minutes later, followed by a complete urine collection for the next 24 hours (Urine 24). The fractional calcium absorption was calculated as the ratio of " augmentation of 44Ca from Urine 0 to Urine 24 / augmentation of 42Ca from Urine 0 to Urine 24 ". Differences and changes of 44Ca and 42Ca were corrected by comparing each with 43Ca. Fractional absorption of AAACa, 23.1 ± 6.4 (Mean ± SD) was distinctly and significantly higher than that of CaCO3 14.7 ± 6.4, p = 0.0060 by paired t - test. The mean was approximately 1.57 times as high in AAACa as CaCO3. The serum 25 (OH) vitamin D level was low (Mean ± SD, 14.2 ± 4.95 ng/ml), as is common among this age group in Japan. Among the parameters of the bone and mineral metabolism measured, none displayed a significant correlation with the fractional absorption of CaCO3 and AAACa. Higher fractional absorption of AAACa compared with CaCO3 supports previous reports on the more beneficial effect of AAACa than CaCO3 on osteoporosis.

***Disclosures: Takuo Fujita**, None.*

SU0409

Using Quantitative Ultrasonography to understand Reduction in Fractures due to Vitamin K1 Supplementation in Postmenopausal Women with Osteopenia. Tayyab Khan*[1], George Tomlinson[2], Lianne Tile[3], Yuna Lee[4], Maryam Hamidi[5], Irene Ho[1], Brooke Stewart[1], Suzanne Cohen[1], Claudia Chan[1], Angela Cheung[6]. [1]Osteoporosis Programs, University Health Network, Canada, [2]Institute of Medical Science & the Department of Medicine, University of Toronto, Canada, [3]Osteoporosis Programs, University Health Network, & the Department of Medicine, University of Toronto, Canada, [4]St. Michael's Hospital, & the Department of Medicine, University of Toronto, Canada, [5]Osteoporosis Programs, University Health Network, & the Institute of Medical Sciences, University of Toronto., Canada, [6]Osteoporosis Programs, University Health Network, St. Michael's Hospital, & the Department of Medicine, University of Toronto., Canada

Background: Traditionally known as an important player in the hemostatic pathway, Vitamin K has recently gained attention for its role against postmenopausal bone loss. Our single centre, placebo-controlled, double-blind trial aimed to Evaluate the Clinical use of vitamin K supplementation in women with Osteopenia (ECKO). We found that vitamin K supplementation reduced fractures without any corresponding changes in areal bone mineral density), suggesting that other factor(s) may be underlying the reduction in fractures.

Methods: We used data from the ECKO trial which involved 440 postmenopausal women; 217 receiving 5mg vitamin K1 daily and 223 receiving placebo, for up to four years. We evaluated bone quality parameters such as Broadband Ultrasound Attenuation (BUA), the Speed of Sound (SOS) and BMD equivalent (QUS BMD) as measured by the Sahara bone sonometer (Hologic, MA) at 12 and 24 (duration of original study), and 36 and 48 months (study extension) and compared them to readings obtained at baseline.

Findings: While no differences were observed between the two groups at the 12 month time point, women receiving vitamin K supplements showed a 1.81% increase in BUA at 24 months compared to baseline; which was significantly greater than the 0.21% decrease shown by the placebo group (p=0.045). This difference between responses of the two groups was most marked at 36 months where the treatment group displayed smaller losses in both QUS BMD (-0.29% for treatment versus -2.75% for placebo group; p=0.038) and SOS (-0.23% for treatment versus -0.45% for placebo group; p=0.037) compared to placebo. These differences did not persist until 48 months, which could, at least partly, be due to the substantial decrease in the number of study participants by this time point.

Interpretation: Quantitative ultrasound parameters may partially explain the reduced number of fractures observed with long-term daily supplementation of vitamin K1 in postmenopausal women with osteopenia. Further studies are required to understand the effect of vitamin K1 supplementation on bone quality.

***Disclosures: Tayyab Khan**, None.*
This study received funding from: Wyeth Foundation

SU0410

Association of Fracture Risk and Quality of Life as Measured by the Osteoporosis Patient Assessment Questionnaire. Stuart Silverman[1], Steven Watts*[2], Deborah Gold[3], April Naegeli[2], John Kanis[4], Russel Burge[2]. [1]Cedars-Sinai/UCLA, USA, [2]Eli Lilly & Company, USA, [3]Duke University Medical Center, USA, [4]University of Sheffield, Belgium

Health related quality of life (HRQoL), as measured by disease-targeted instruments such as the Osteoporosis Patient Assessment Questionnaire (OPAQ), decreases following incident clinical fracture. The HRQoL effect of clinical vertebral fracture depends on the number and location of fractures (Silverman, QoL Res, 2000; Olesik, JBMR, 2000). Our goal in osteoporosis therapy is to prevent osteoporosis fracture and subsequent decrease in HRQoL. Patients are identified for treatment based on both bone mineral density (BMD) T-score and absolute fracture risk algorithms such as FRAX®, which provides 10-year probabilities of a major osteoporotic fracture, calculated using several clinical risk factors. The relationship between BMD and HRQoL is unclear. Our objective, therefore, was to examine the relationship between a comprehensive measure of fracture risk, based on FRAX®, and HRQoL as measured by OPAQ.

Patients in the Multiple Outcomes for Raloxifene Evaluation trial who completed OPAQ at baseline were studied. We examined the relationship between both OPAQ dimension and domain scores and baseline FRAX® risk for a major osteoporotic fracture (version 3.0 with BMD). Baseline FRAX® and OPAQ scores were statistically signficantly correlated in 11 of 14 domains and in all 4 dimensions. Statistically significant domain coefficients ranged from ≍-0.05 to -0.19. All correlations were negative except for 'support from family and friends'. The Physical Function, Emotional Status, and Symptoms dimensions yielded negative correlations, whereas the Social Interactions dimension had a positive correlation. Four domains - 'household/self-care', 'fear of falls', 'usual work', 'independence' - were statistically significant in both the No Fracture and the Fracture subgroups; correlation coefficients were larger in the No Fracture subgroup vs. Fracture subgroup. The 'social activity' domain was statistically significant in the No Fracture subgroup but not in the Fracture subgroup, while the reverse was true for 'support from family and friends'.

For most OPAQ dimensions and all domains, there were statistically significant correlations with baseline FRAX® score, though the magnitudes were somewhat modest. Not surprisingly, higher risk of fracture was associated with lower OPAQ scores in most domains and dimensions. Among patients with prevalent fractures, a higher risk of fracture was correlated with higher OPAQ scores for support by family and friends and social interactions.

***Disclosures: Steven Watts**, Eli Lilly and Company, 8; Eli Lilly and Company, 5; Eli Lilly and Company, 2*
This study received funding from: Eli Lilly and Company

SU0411

Effects of a Simple, Low-intensity Back Extension Exercise on Quality of Life and Back Extensor Strength in Patients with Osteoporosis and Vertebral Fractures: A 6-month Randomized Controlled Trial. Naohisa Miyakoshi*[1], Akira Horikawa[2], Michio Hongo[3], Yuji Kasukawa[1], Yoichi Shimada[1]. [1]Akita University Graduate School of Medicine, Japan, [2]Igarashi Memorial Hospital, Japan, [3]Akita University School of Medicine, Japan

Back extensor strength is of considerable importance in patients with osteoporosis. Back-strengthening exercises, particularly from a prone position and using a backpack, are effective in increasing back extensor strength, decreasing the risk of vertebral fractures, and improving quality of life (QOL). However, reductions in exercise intensity may be beneficial for patients with prevalent vertebral fractures and severe spinal deformity who cannot perform exercises while prone and/or under loading. We thus conducted a 6-month, prospective, randomized trial of simple and low-intensity back extension exercises on QOL and back extensor strength. Subjects comprised 31 postmenopausal women ⩾70 years old with osteoporosis who had ⩾1 osteoporotic vertebral fracture. Subjects were randomized to either a control group (n=15) or an exercise group (n=16). Instruction was provided in 2 simple, low-intensity back extension exercises in this study. In one exercise, patients were instructed to stand facing a wall with feet 30 cm from the wall. Then, with arms elevated and touching the wall, the subject had to lower the chest as close to the wall as possible to extend the back. In the other exercise, the subject sat in a sturdy chair or sofa with hands behind the neck, then extended the back while leaning on the backrest to extend the back as much as possible. Patients in the exercise group repeated these exercise 10 times each, twice a day, 7 days/week, for 6 months. Isometric back extensor strength and QOL were evaluated at baseline and 6 months. QOL was evaluated using the Japanese Osteoporosis QOL Questionnaire (JOQOL). The control group showed no significant differences in terms of total JOQOL score or domain scores between baseline and 6 months. In the exercise group, total JOQOL score and all domain scores except for posture and figure were significantly higher at 6 months than at baseline ($p<0.001$). Total JOQOL score was significantly higher in the exercise group than in the control group at 6 months ($p=0.026$). Back extensor strength was significantly increased in the exercise group after 6 months ($p<0.001$), and significantly decreased in the control group after 6 months ($p=0.005$). In conclusion, 6 months of simple, low-intensity back extension exercises improved QOL and back extensor strength in patients with postmenopausal osteoporosis and vertebral fractures.

***Disclosures: Naohisa Miyakoshi**, None.*

SU0412

Spinal Proprioceptive Extension Exercise Dynamic (S.P.E.E.D.) Program for relief of back pain and iliocostal friction syndrome: A painful challenge of spinal osteoporosis. Mehrsheed Sinaki*. Mayo Clinic, USA

Background: Axial posture is not static but rather a dynamic process represented by alignment of the body's anatomical units in relationship to one another at any given time. Posture affects body locomotion and risk of falls. Posture can be influenced by multiple factors: i.e. aging, gender, bone loss, and muscle strength. The thoracic spine suffers the most disfiguring effect of osteoporosis due to vertebral anterior wedging and the effects of gravity on the natural thoracic curve.

We regularly treat patients with back pain and/or flank pain in our outpatient Rehabilitation of Osteoporosis Program Exercise (ROPE). The majority of these patients are not seen again as their pain subsides or they are geographically unable to return.

Fifty cases of individuals diagnosed with flank pain (36/50) or back pain (14/50) are reported here. All had thoracic hyperkyphosis (> 50♂) with or without osteoporosis. All had tried other measures for pain relief without success. All had neurological and musculoskeletal evaluations as well as assessment of gait and physical activity.

Intervention: All subjects reported reduction of pain after initial trial with Weighted Kypho-Orthosis (WKO). This device was developed for reduction of kyphosis and consists of shoulder straps with a weighted pouch suspended below the scapulae. After the trial, all subjects were started on the S.P.E.E.D. Program. The goal of S.P.E.E.D. is to reduce kyphosis without bracing or spinal immobilization with subsequent strengthening of back muscles.

Results: Fourteen of 50 subjects returned after one month, and reported significant reduction of pain using a standardized pain scale ($P<0.001$). Formal gait analysis showed statistically significant changes in fall risk at obstacles ($P<0.05$), disequilibrium through computerized posturography ($P<0.003$), back strength ($P<0.001$), physical activity score ($P<0.001$), and improvement in height ($P<0.001$).

Conclusion: The S.P.E.E.D. Program uses kinematics and proprioceptive feedback of the spine to reduce kyphosis and facilitate the use of paraspinal muscles to improve posture. This pilot program has been successful in reducing back and iliocostal pain related to kyphotic spinal deformities.

***Disclosures: Mehrsheed Sinaki**, None.*

SU0413

Has the Prevalence of 25-hydroxyvitamin D (25(OH)D) Inadequacy Decreased at Latitude 43°. Matthew J Davis[1], Frances Budden*[2]. [1]Technion Israel Institute of Technology - American Medical Program, Israel, [2]St Joseph's Health Centre, Toronto, Canada

Has the prevalence of 25-hydroxyvitamin D (25(OH)D) inadequacy decreased at latitude 43°?

1512 25(OH)D levels measured on inpatients and outpatients of a community hospital from January - December 2009, inclusive, were reviewed. The 25(OH)D levels were the only data that were collected.

Collections of 25(OH)D levels ranged from 75 to 161 patients monthly. The annual average 25(OH)D level was 80.36 nmol/L, with the lowest being December, 70.45 nmol/L, and the highest being July, 95.02 nmol/L. The monthly average of patients with deficient 25(OH)D, < 25 nmol/L, was 4, range 0 - 6, or 2.9%, range 0 - 7.2%. The monthly average of patients with insufficient 25(OH)D, 25 to 74 nmol/L, was 53, range 37 - 84, or 42.9%, range 30.9 - 53.8%. The monthly average of patients with adequate 25(OH)D, > 74 nmol/L, was 69, range 36 - 101, or 54.2%, range 42.3 - 69.1%.

From R Vieth et al, Eur. J. Clin. Nutr. 55:1091-1097, 2001, serum 25(OH)D level is the objective measure of vitamin D nutritional status. Hepatic synthesis of 25(OH)D is loosely regulated and blood levels of this molecule largely reflect the amount of vitamin D produced in the skin or ingested. In this group, because they live at latitude 43°, only a small amount of vitamin D is produced in the skin from sun exposure. In our data, the 25(OH)D levels varied little from season to season. When compared to the annual 25(OH)D level average of 80.36 nmol/L, the lowest month varied by 9.92 nmol/L and the highest month varied by 14.66 nmol/L. In Vieth's study, there were significant seasonal variations compared to the annual average. In addition, Vieth's study showed that the % prevalence of <40 nmol/L in the winter months of December - April increased to >25%. In our study, the % prevalence in winter months did not differ from that of the summer months, fluctuating from 5 - 16% throughout the year.

We were unable to reproduce a seasonal variation even using Vieth's frames of reference. It appears that the prevalence of 25(OH)D inadequacy has decreased since this 2001 study. In our group, there were definitely those who had deficient or insufficient 25(OH)D levels, but there has been an increase in the number of people taking adequate vitamin D.

This study was retrospective, looking only at 25(OH)D levels. A population study with adequate clinical information needs to be done to determine if our data is reproducible in the general population, reflecting an improved daily intake of vitamin D.

***Disclosures: Frances Budden**, None.*

SU0414

Relationship between Fasting Glucose, Vitamin D and PTH in Early Postmenopausal Women. Susanna Streym Thomsen*[1], Lars Rejnmark[1], Peter Vestergaard[1], Christine Brot[2], Pia Eiken[3], Pernille Hermann[4], Leif Mosekilde[1]. [1]Aarhus University Hospital, Denmark, [2]Osteoporosis & Metabolic Bone Unit, Hvidovre Hospital, Denmark, [3]Department of Cardiology & Endocrinology, Hillerød Hospital, Denmark, [4]Department of Endocrinology, Odense University Hospital, Denmark

Background: Studies have shown an increased risk of type 2 diabetes with low 25-hydroxyvitamin D (25OHD) levels.

Hypothesis: Low vitamin D is associated with a high level of blood glucose.

Aim: To investigate any association between blood glucose and 25OHD adjusted for Body Mass Index (BMI), body composition, PTH and physical activity in postmenopausal women.

Design: Cross-sectional study in postmenopausal women.

Material and Methods: Data are based on analyses from the Danish Osteoporosis Prevention Study (DOPS), which is a cohort study in early postmenopausal Caucasian women (n=2016) aged 45 to 58 years old.

Measurements: Fasting blood glucose was measured after an overnight fast by standard laboratory methods. Serum levels of 25OHD were measured by a competitive assay using rachitic rat binding protein. The fat and lean mass was measured by DXA-scan. Serum intact parathyroid hormone was measured by DPC Immulite (chemilucens) with an inter-assay CV of 11% and an intra-assay CV of 6%. Data on physical activity was collected through a questionnaire.

Results: Results from bivariate analysis are shown in the table, indicating a significant relation between fasting blood glucose and 25OHD and all studied indices. In a multivariate linear regression analyzing fasting blood glucose was significantly associated with BMI ($\beta=0.038 \pm 0.007$ (SE), $2p<0.001$), PHT ($\beta=0.035 \pm 0.015$ (SE), $2p=0.021$and total physical activity ($\beta=-0.005 \pm 0.002$ (SE), $2p=0.036$, but not with 25OHD ($\beta=0.001 \pm 0.002$ (SE), $2p=0.643$).

The mean and SEM for Glucose was 4.72 mmol/l ($\pm$ 0.02) and 25OHD 25.1 ng/ml ($\pm$ 0.3).

Conclusion: The apparent relationship between fasting blood glucose and serum 25OHD seems to be mediated by serum PTH, BMI and physical activity. As 25OHD is known to lowering PHT levels interventional trials with vitamin D supplements are warranted in order to term whether improvement of vitamin D status may improve glucose tolerance.

Table: Pearson correlation

	Blood Glucose	25 OHD	BMI	Fat	Lean	Physical activity	PTH
Blood Glucose	-						
25 OHD	-0.069**	-					
BMI	0.238**	-0.134**	-				
Fat	0.178**	-0.119**	0.920**	-			
Lean	0.1752**	-0.059**	0.905**	0.836**	-		
Physical activity	-0.653**	0.091*	-0.020	-0.065**	0.022	-	
PTH	0.106**	-0.142**	0.219**	0.221**	0.097**	0.012	-

* = p<0.05
** = p<0.01

Table - Pearson correlation

***Disclosures: Susanna Streym Thomsen**, None.*

SU0415

The Vitamin D in Osteoporosis Study (ViD*OS*): A Novel Knowledge Translation Initiative in Canadian Long-Term Care Homes. Courtney Kennedy[1], Alexandra Papaioannou*[2], George Ioannidis[3], Lora Giangregorio[4], Laura Pickard[1], Jenna Johnson[1], Campbell Glenda[5], Jackie Stroud[5], Sharon Marr[1], Suzanne Morin[6], Robert Josse[7], Anna Sawka[8], Richard Crilly[9], Lehana Thabane[1], Lisa Dolovich[1], Mary-Lou van der Horst[1], Norm Flett[1], Lynn Nash[1], Jonathan Adachi[10]. [1]McMaster University, Canada, [2]Hamilton Health Sciences, Canada, [3]Sympatico, Canada, [4]University of Waterloo, Canada, [5]Medical Pharmacies Group Inc., Canada, [6]McGill University Health Centre, Canada, [7]St. Michael's Hospital, University of Toronto, Canada, [8]Toronto General Hospital, Canada, [9]University of Western Ontario, Canada, [10]St. Joseph's Hospital, Canada

Despite good evidence that vitamin D can prevent falls and fractures in the frail elderly, there is a clear gap in the application of knowledge in the long-term care (LTC) setting. It is estimated that up to 70% of LTC residents in Ontario, Canada are

not receiving adequate vitamin D supplementation; calcium and bisphosphonates are also being underutilized. Challenges faced by LTC professionals include managing large caseloads of residents with multiple co-morbidities and medications and often isolation from academic settings. Previous work suggests that barriers to falls and fracture care are modifiable and could be overcome through education and modifications to local care delivery systems.

To address potential barriers and facilitators for integrating "knowledge into practice", the Vitamin D in Osteoporosis Study (ViD*OS*) was recently initiated as a novel, integrated knowledge translation intervention informed by a research synthesis and via consultation with a broad range of LTC stakeholders. The target audience is pre-existing Professional Advisory Committees who meet quarterly at each LTC home consisting of: the Medical Director, the Director of Care, consultant pharmacist, nutritionist, and other physicians, nurses, and rehabilitation staff.

The ViD*OS* study design is a multi-centered cluster Randomized Controlled Trial consisting of 20 control homes and 20 intervention homes. The primary objective is to increase the rate of vitamin D prescribing (≥800 IU/daily) by at least 20% in intervention homes. Secondary objectives include: to increase the appropriate prescribing of calcium and bisphosphonates in high-risk individuals. Control homes will only receive an LTC Osteoporosis Tool-kit and a 10-minute DVD that is provided to all LTC homes in Ontario. Intervention homes will participate in three problem-based learning sessions occurring approximately 5-months apart. Sessions occur at the LTC site and are led by an Osteoporosis Expert Opinion Leader and Research Coordinator. Via a collaborative learning approach, session components include: presentation of best practices; watching a 10-minute DVD; performance reports/ benchmarking with other LTC homes (on vitamin D, calcium, bisphosphonate, falls, fractures indicators); and action planning including completion of a work-sheet to set implementation goals. In between sessions, teams are given time and support to implement their action plans. Assessment of outcomes occurs at baseline, month 5, and month 10.

***Disclosures: Alexandra Papaioannou**, None.*

SU0416

Vitamin D and Calcium Supplementation in Women and Men Living in Long Term Care (LTC) Homes: The Vitamin D Osteoporosis Study (ViDOS). George Ioannidis*[1], Alexandra Papaioannou[2], Courtney Kennedy[3], Lora Giangregorio[4], Laura Pickard[3], Jenna Johnson[2], Glenda Campbell[5], Jackie Stroud[5], Sharon Marr[3], Suzanne Morin[6], Robert Josse[7], Anna Sawka[8], Richard Crilly[9], Dr. Lehana Thabane[3], Lisa Dolovich[3], Mary Lou van der Horst[3], Norm Flett[3], Lynn Nash[3], Jonathan Adachi[10]. [1]Sympatico, Canada, [2]Hamilton Health Sciences, Canada, [3]McMaster University, Canada, [4]University of Waterloo, Canada, [5]Medical Pharmacies Group Inc, Canada, [6]McGill University Health Centre, Canada, [7]St. Michael's Hospital, University of Toronto, Canada, [8]Toronto General Hospital, Canada, [9]University of Western Ontario, Canada, [10]St. Joseph's Hospital, Canada

Purpose: The ViDOS study is an integrated knowledge translation initiative designed to improve the management of falls and fracture in the long-term care (LTC) setting. The study objectives are 1) to increase the number of all residents prescribed the appropriate dose of vitamin D (≥800IU daily) and 2) to increase appropriate prescribing of calcium and bisphosphonates particularly in high-risk individuals.

Methods: ViDOS is a clustered randomized control trial involving a novel "knowledge into practice" initiative. The planned recruitment is 40 LTC homes randomized into either intervention (n=20) or control (n=20). The ViDOS intervention consists of 3 problem-based learning sessions led by an Osteoporosis Expert and occurring 5-months apart. Control homes receive standard materials given to all LTC homes in the province. The target audience is the Professional Advisory Committee (e.g. medical and nursing directors; other medical, nursing, rehabilitation, pharmacy, nutrition staff) at each home who already meet quarterly to examine resident care and quality improvement objectives. Prescribing, falls and fracture data is collected at 3 time periods for each home (baseline, follow-up 1 and follow-up 2). Performance reports, benchmarked to other homes in the study, are provided to intervention homes at each session. Complete medication records are retrieved from a central pharmacy database. In this baseline analysis, we evaluated the use of vitamin D and calcium supplements for all of the residents in the first 16 LTC homes recruited. Individuals were categorized as using or not using vitamin D and calcium (yes/no) and by the dose (vitamin D ⩾ 800 IU/day; calcium: ⩾ 500 mg/day). Descriptive statistics are presented for women and men separately.

Results: A total of 2247 medical records were analyzed; 1559 women and 688 men. Results showed that 53% (n=820) and 37% (n=577) of women and 39% (n=266) and 24% (n=168) of men were taking vitamin D or calcium, respectively. A total of 36% (n=564) of women and 23% (n=157) of men were taking vitamin D ⩾ 800 IU/day. Furthermore, 35% (n=553) of women and 23% (n=157) of men were taking calcium ⩾ 500 mg/day.

Conclusions: Numerous residents living in LTC homes were not taking vitamin D or calcium, and for many residents who were taking supplements, the doses were inadequate. This care gap appears more pronounced in men. Enhancing optimal vitamin D and calcium nutrition among residents in LTC may improve health care outcomes.

***Disclosures: George Ioannidis**, None.*

SU0417

Vitamin D Supplementation in Vitamin D Deficiency/Insufficiency increases Circulating Fibroblast Growth Factor -23 (FGF-23) Concentrations. Geeta Hampson*[1], Ignac Fogelman[2], Joseph Cheung[3]. [1]St. Thomas' Hospital, United Kingdom, [2]Guy's Hospital, United Kingdom, [3]St Thomas' Hospital, United Kingdom

1, 25 dihydroxy vitamin D plays a central role in bone metabolism and up-regulates the production of fibroblast growth factor-23 (FGF-23) by bone cells. Recent data suggest that FGF-23 is implicated in bone mineralisation, independently of its effect on phosphate homeostasis. Vitamin D deficiency/insufficiency is prevalent in patients with osteoporosis and leads to bone loss and mineralisation defects. The aim of the study was to assess the effects of vitamin D supplementation on circulating FGF-23 in patients with low vitamin D status.

Fifteen patients, 6 M aged mean[SD] 54[15.5] and 9 F aged 57[18] years with vitamin D deficiency/insufficiency (25 (OH)vitamin D < 50nmol/L) were studied over 3 months. Thirteen patients had osteoporosis and were treated with bisphosphonates. They were administered a bolus intra-muscular injection of 300,000 I.U of ergocalciferol (vitamin D2) and asked to take daily supplements of Calcium (1.2 gram) and 800 I.U of colecalciferol (vitamin D3) as maintenance for 3 months. Blood samples were obtained at baseline, 1, 2 and 3 months for measurement of total calcium, phosphate, 25 (OH)vitamin D, PTH, serum CTX and FGF-23. Circulating FGF-23 was measured by the human FGF-23 C-terminal second generation ELISA.

Serum calcium increased from (mean [SD]) 2.29 [0.14] mmol/L to 2.35 [0.12] mmol/ L (p= 0.03) and PTH decreased from 85 [95] ng/L to 46 [34] ng/L (p=0.04) at 3 months. No change in serum phosphate or e GFR was seen. Serum 25 (OH)vitamin D increased significantly from 34 [15] nmol/L at baseline to 78 [46] nmol/L at 3 months ($p < 0.001$). No significant change in serum CTX was observed. A significant correlation was seen between baseline circulating FGF-23 and serum phosphate (r= 0.56, p=0.02). FGF-23 concentrations increased significantly from a basal level of 84 [41] RU/ml to 120 [53] RU/ml at 3 months ($p < 0.01$).

These preliminary data demonstrate that correction of vitamin D deficiency leads to increased production of FGF-23 and confirm that vitamin D is an important stimulator of FGF-23. Further interventional studies are needed to confirm our findings and to assess whether the rise in FGF-23 production following vitamin D supplementation has a direct biological effect on the skeleton.

***Disclosures: Geeta Hampson**, None.*

SU0418

A Novel Cyclic PTH(1-17) Analog with Bone Anabolic Activity and Efficacy Sufficient to Treat Established Osteopenia in Adult Ovariectomized Rats. Jukka Morko*[1], ZhiQi Peng[2], Jukka Vääräniemi[2], Jukka Rissanen[3], Mari Suominen[2], Katja Fagerlund[2], Tiina A. Suutari[2], Harrie C.M. Boonen[4], Trine S.R. Neerup[5], Hanne H. Bak[5], Jussi Halleen[2]. [1]Pharmatest Services Ltd, Fin, [2]Pharmatest Services Ltd, Finland, [3]Pharmatest Services,Limited, Finland, [4]Department of Pharmacology & Pharmacotherapy, University of Copenhagen, Denmark, [5]Zealand Pharma A/S, Denmark

Recombinant human parathyroid hormone (PTH) analogs [PTH(1-34) and PTH(1-84)] are used as bone anabolic agents in clinical practice. Hitherto, bone anabolic activity has not been observed with PTH analogs shorter than 28 amino acids in vivo. The purpose of this study was to characterize effects of a novel, cyclic PTH(1-17) analog, ZP2307, on the treatment of established osteopenia in adult ovariectomized (OVX) rats. ZP2307 has been developed at Zealand Pharma A/S. Female Sprague-Dawley rats were ovariectomized at the age of 6 months. After 6 weeks without treatment, the development of metaphyseal osteopenia was confirmed by peripheral quantitative computed tomography (pQCT). Treatment was started at 7 weeks after the operations and continued for 6 weeks. The osteopenic rats were treated subcutaneously, once a day with ZP2307 at doses of 2.0, 6.0, 20.0, 60.0 and 200.0 μg/kg/d, and with PTH(1-34) used as a reference compound at doses of 1.2, 4.0, 12.0, 40.0 and 120.0 μg/kg/d. Treatment effects were analyzed by pQCT, bone histomorphometry, bone ash weight determination, and biomechanical testing in long bones and vertebra. During the treatment period, osteopenic changes of metaphyseal trabecular bone exacerbated in OVX rats treated with vehicle. Treatment with ZP2307 reversed the development of osteopenia in tibial metaphysis and lumbar vertebra at all doses in a dose-dependent manner, and enhanced bone formation on their trabecular bone surface at the dose of 200.0 μg/kg/d. Treatment with ZP2307 also reversed OVX-induced reduction in lumbar vertebral strength at the doses of 6.0-200.0 μg/kg/d and increased cortical thickness in tibial diaphysis at the doses of 60.0-200.0 μg/kg/d. Treatment with PTH(1-34) induced similar dose-dependent effects although stronger than treatment with ZP2307. Maximal effects of ZP2307 treatment were observed at the dose of 200 μg/kg/d and these effects corresponded mainly to effects induced by PTH(1-34) treatment at the doses of 4.0-40.0 μg/kg/d, depending on bone site studied and parameter used. This study demonstrated that the novel, cyclic PTH(1-17), ZP2307, is the shortest PTH analog reported hitherto to exhibit bone anabolic activity and efficacy sufficient to treat established osteopenia in adult OVX rats. Due to its mild efficacy, ZP2307 may be very tolerable and have a broad therapeutic window and a better safety/efficacy profile than the PTH analogs currently used in clinical practice.

***Disclosures: Jukka Morko**, None.*
This study received funding from: Zealand Pharma A/S

SU0419

Bone Anabolic Effects of PTH treatment in Streptozotocin Induced Diabetes Bone Loss Rats. Yanfei Ma*[1], Qinggiang Zeng[1], Leah Porras[1], Ricky Cain[1], Mervyn Michael[1], Amy Cox[1], Liao Cui[2], Bilian Xu[2], Masahiko Sato[1], Leah Helvering[1]. [1]Eli Lilly & Company, USA, [2]Depart of Pharmacology, Guangdong Medical College, China

Patients with diabetes mellitus have been shown to be at increased risk for fractures and may have bones of inferior quality. We evaluated the effects of PTH in diabetic rats to determine the responsiveness to bone in the face of uncontrolled glucose levels. Male, 4.5 month old rats were subjected to STZ-induced diabetes with Zanosar Streptozotocin (STZ) and allowed to continue in this state for 8 weeks prior to treatment initiation. Rats were randomized into 4 groups according to plasma glucose levels and subcutaneously administered with PTH (1-38) at 0, 3, 10, or 30μg/kg/d for 21 days. Compared to aged-match normal rats, STZ rats had nearly 3 fold higher serum glucose, and had significantly lower distal femur -BMD (-20%), mid femur-BMD (-6%), proximal tibial metaphysis-trabecular area (-62%), trabecular width (-21%),trabecular number (-52%) and femoral neck peak load (-38%). Bone biomarkers and histomorphometric analyses indicated that the diabetes-induced bone loss was primary due to suppression bone formation and increase bone resorption. PTH treatment dose-dependently restored the bone mass and micro architecture in cancellous bone sites of lumbar vertebrae, and proximal tibiae as compared to the normal control levels. However, PTH treatment was only partial efficacious in restoring cortical bone in the diabetic rats. PTH dose responsively improved bone strength in femoral neck but the changes in lumbar vertebrae and mid femur did not reach statistical significant. Bone histomorphometry showed that PTH increased bone formation indices of mineralizing surface, mineral appositional rate, and bone formation rate on trabecular, endocortical and periosteal surfaces indicating that a longer treatment duration may be required to influence cortical structure. In summary, severely diabetic rats experienced substantial bone loss over a 8 week period, but the bone retained it responsiveness to an anabolic PTH stimulus as exhibited by increases in bone formation at all examined sites.

***Disclosures: Yanfei Ma**, Eli Lilly Company, 3*

SU0420

Effect of Cathepsin K Inhibition on PTH, CTX-I and Ionized Calcium Levels in Cynomolgus Monkeys. Erik Lindstrom[1], Lotta Vrang[1], Susanne Sedig[1], Ylva Terelius[1], Britt-Louise Sahlberg[1], Kristina Wikstrom[1], Bertil Samuelsson[1], Timothy Chambers[2], Urszula Grabowska*[3]. [1]Medivir AB, Sweden, [2]St. George's Hospital Medical School, United Kingdom, [3]Medivir, United Kingdom

Inhibition of cathepsin K has anti-resorptive effects on bone. It has been suggested that cathepsin K inhibition also leads to transient increases in circulating PTH levels. This is of interest since PTH has anabolic effects on bone, at least when levels increase in a transient manner. The aim of the current study was to examine the effect of the selective cathepsin K inhibitor MIV-711, a clinical development candidate, (formerly MV076159) on circulating PTH, CTX-I and ionized calcium levels in intact cynomolgus monkeys. Animals received MIV-711 (10 or 30 μmol/kg) or vehicle by oral gavage (n = 3-5). Plasma levels of MIV-711 increased in a dose-dependent manner with Tmax occurring at 2 hrs. MIV-711 reduced CTX-I levels in a dose-dependent manner with maximal reductions occurring 4-8hrs after dose (70% and 78% inhibition in response to 10 and 30 μmol/kg MIV-711 respectively). CTX-I levels were still reduced by 46 and 48% respectively, 24h after dose but returned to baseline levels by 48h. By comparison, CTX-I levels declined by a maximum of 41% in vehicle-treated animals. At 4 and 8h after dose, ionized calcium levels were in general lower in the MIV-711-treated animals compared to vehicle-treated (4h data: vehicle: 1.21 ± 0.01 mM; 10 μmol/kg MIV-711: 1.19 ± 0.01 mM; 30 μmol/kg MIV-711: 1.15 ± 0.02 mM). At 4 and 8h after dose, PTH levels were higher in the MIV-711-treated animals compared to vehicle-treated (4h data: vehicle: 1.06 ± 0.25 pmol/L; 10 μmol/kg MIV-711: 2.73 ± 0.41; 30 μmol/kg MIV-711: 3.27 ± 0.22). There were no obvious differences in PTH levels between the different groups 12-24hrs after dose. In summary, the cathepsin K inhibitor MIV-711 reduces CTX-I levels in cynomolgus for at least 24h after a single oral dose. Ionized calcium levels were transiently reduced and PTH levels were transiently increased between 4–8hrs after dose. MIV-711 affords sustained anti-resorptive effects on bone and transient increases in PTH levels which may result in maintained or even enhanced anabolic effects on bone. The effect of MIV-711, orally q.d. dosing over 5 days, on PTH, CTX-I and ionized calcium levels are being studied.

***Disclosures: Urszula Grabowska**, None.*
This study received funding from: Medivir AB

SU0421

Maintenance of Bone Strength after Discontinuation of Bone Active Agents is Different for Cortical and Cancellous Bone. Mohammad Shahnazari*[1], Wei Yao[2], Brian Panganiban[3], Robert Ritchie[3], Nancy Lane[2]. [1]UC Davis Medical Center, USA, [2]University of California, Davis Medical Center, USA, [3]Lawrence Berkeley National Laboratory, USA

Introduction: Osteoporotic patients treated with bone active medications experience an increase in bone mass and a reduction in incident fractures. In clinical medicine, anti-resorptive agents are now discontinued after 5 years. The anabolic agent, rhPTH (1-34), is discontinued after 2 years, with sustained vertebral fracture risk reduction reported for up to 18 mo. after treatment withdrawal (Lindsay et al, 2004). We evaluated the changes in bone quality and bone strength in an osteopenic rat model after a prolonged discontinuation of bone active agents.

Methods: Six mo. old ovariectomized (OVX) rats were treated with placebo, alendronate (Aln, 2μg/kg), PTH (1-34) (20ug/kg), or raloxifene (Ral, 2mg/kg) 3x/week for 4 mo. and withdrawn from the treatments for 8 mo. The study endpoints included changes in cancellous and cortical bone mass, biochemical and surface-based measures of bone turnover (BFR/BS), degree of bone mineralization, and cortical and trabecular bone strength. Multiple regression analyses were performed to determine variables that predicted bone strength.

Results: Treatment with Aln, PTH, and Ral increased the vertebral trabecular bone volume (BV/TV) by 47, 53, and 31%, with corresponding increases in vertebral maximum compression load by 27, 51, and 31%, respectively, vs. OVX controls ($p<0.001$). The resulted bone strength were similar to Sham with Aln and Ral and higher than Sham ($p<0.001$) with PTH treatment. At 4 mo. after treatment withdrawal, bone turnover remained suppressed in the Aln group, nearly 40% lower than OVX controls ($p<0.001$), and vertebral strength was higher than OVX ($p<0.05$) and similar to the Sham only in Aln-treated group. The vertebral BV/TV remained 25% higher than OVX controls up to 8 mo. after withdrawal of Aln ($p<0.05$) but returned to OVX control level in both the PTH and Ral groups 4 mo. after withdrawal. Interestingly, cortical bone mineralization increased only with PTH treatment. At 4 mo. after treatment withdrawal, only the PTH-treated group showed a higher maximum load of bending vs. OVX controls ($p<0.05$). Animals in the Aln group lost another 16% of vertebral strength from 4 to 8 mo. treatment withdrawal ($p<0.05$), and at this time point none of the treatment groups were different from the OVX control for cortical or cancellous bone strength.

In summary, both Aln and PTH maintained bone strength (maximum load) 4 mo. after discontinuation of the treatment despite changes in bone mass and bone turnover; however, PTH maintained cortical bone strength while Aln maintained the cancellous bone strength. Additional research on the long-term effects on bone strength after discontinuation of osteoporosis medications is needed to improve our long-term treatment of osteoporosis.

***Disclosures: Mohammad Shahnazari**, None.*

SU0422

No synergistic effect of PTH and strontium on immobilisation-induced loss of bone strength in rats. Annemarie Brüel*[1], Jesper Thomsen[2]. [1]University of Aarhus, Denmark, [2]Institute of Anatomy,University of Aarhus, Denmark

Aim

PTH and strontium (Sr) have both been shown to reduce bone loss induced by immobilisation. PTH is a potent bone anabolic agent and Sr has been shown to be antiresorptive. The aim of the study was to investigate whether a combination of PTH and Sr would have additive or synergistic effect on bone strength in a rat model of immobilisation-induced bone loss.

Materials and methods

Immobilisation was obtained by injecting 2 IU Botox (BTX) into the muscles of the right hind limb, thereby inducing a bone loss. Seventy-two female Wistar rats, 3-months-old, were divided into the following groups: Baseline, controls, BTX, BTX+PTH, BTX+Sr, and BTX+PTH+Sr (n=12 in each group). PTH was given as s.c. injections at a dosage of 60 μg/kg/d, and Sr as 900 mg/kg/d in the food. The experiment lasted for 4 weeks. The rectus femoris muscles were isolated and weighed. Fracture strength (F_{max}) of the femoral mid-diaphysis, femoral neck, and distal femoral metaphysis was determined using a materials testing machine.

Results

In all groups, BTX induced a weight loss of ~10% (vs. controls, $P<0.001$), and reduced the right rectus femoris muscle wet weight by ~55% (right vs. left, $P<0.001$). However, no difference in femur length was found in BTX rats compared with controls, indicating that BTX did not induce growth retardation.

Total cross-sectional area (bone+marrow) (tCSA) of the femur was reduced by 3.4% (right vs. left, $P<0.001$) in the BTX group. No significant difference between right and left femoral tCSA was found in the rats treated with PTH, Sr, or PTH+Sr. F_{max} of the right femoral diaphysis was reduced by 8.3% (right vs. left, $P<0.001$) by BTX. This reduction was significantly counteracted by both PTH and Sr, but not by PTH+Sr. The right femoral neck F_{max} was reduced by 27% (right vs. left, $P<0.001$) by BTX, and this effect was not counteracted by PTH, Sr, or PTH+Sr. However, F_{max} of the right femoral neck was increased by 24% ($P<0.05$) in BTX+PTH compared with BTX. F_{max} of right femoral metaphysic was reduced by 13% (right vs. left, $P<0.001$) by BTX, and this effect was not counteracted by PTH, Sr, or PTH+Sr. However, F_{max} of the right femoral metaphysis was increased by 15% ($P<0.05$) in BTX+PTH+Sr compared with BTX.

Conclusion

Both PTH and Sr partly inhibited the effect of immobilization induced loss of bone strength. Furthermore, PTH and Sr prevented the reduction in femoral tCSA. However, no synergistic effect of PTH and Sr on bone strength was found.

***Disclosures: Annemarie Brüel**, None.*

SU0423

Strontium Exerts In Vivo Anabolic Effect on Trabecular Bone through Modulating Osteogenic and Osteoclastogenic Potential of Bone Marrow Cells. William Lu*[1], Songlin Peng[1], Xiaowei Liu[2], Ting Wang[1], Zhaoyang Li[1], KDK Luk[1], X.Edward Guo[2]. [1]The University of Hong Kong, Hong kong, [2]Columbia University, USA

Purpose: The present study aims to investigate the dual effect of strontium (Sr) on trabecular bone and the possible cellular mechanisms by examining the osteogenic and osteoclastogenic potential of bone marrow cells.

Methods: Thirty 3-month-old female Sprague-Dawley rats were randomly divided into three groups (n=10 in each group): Sham operated and treated with Vehicle (0.9% saline) (Sham), ovariectomized and treated with either vehicle (OVX) or Sr phosphate (4 mmol/kg/d) (Sr). All animals were supplied with calcium supplements (1.8 mmol/kg/d). Both Veh and Sr compound were daily orally administrated for 12 weeks. The effect of Sr on trabecular bone microstructure was analyzed by microCT on proximal tibiae. Static and dynamic histomorphometric analysis was performed to evaluate the bone formation and resorption markers in trabecular bone. Osteogenic and osteoclastogenic genes in the bone marrow were analyzed with real-time PCR assay. Bone marrow cells were cultured and colony formation assays (CFU-F and CFU-ALP) and tartrate-resistant acid phosphatase (TRAP) staining were evaluated.

Results: Trabecular bone microstructure was improved after Sr treatment. Bone volume (BV/TV), trabecular number (Tb. N) and connectivity density (Conn. D) were greater in Sr-treated versus Veh-treated OVX rats ($p<0.05$ for all). At the tissue level, mineral apposition rate (MAR) and bone formation rate (BRF/BS) were greater while osteoclast surface (N. Oc/BS) was less in Sr-treated versus Veh-treated OVX rats ($p<0.05$ for all). Bone sailoprotein and osteocalcin genes were significantly up-regulated while cathepasin K gene was significantly down-regulated in Sr-treated versus Veh-treated OVX rats ($p<0.05$ for all). Colony formation assays demonstrated that bone marrow cells from Sr-treated group exhibited higher osteogenic colony (CFU-ALP, $p<0.05$) while fibroblast colony (CFU-F) was comparable between these two groups ($p>0.05$). Number of TRAP positive multinucleated cells was less in Sr-treated versus Veh-treated OVX rats ($p<0.05$).

Conclusion: Our study confirmed the dual effect of Sr on trabecular bone by providing the static and dynamic parameters of bone formation and resorption. The modulation of osteogenic and osteoclastogenic potential of bone marrow cells may contribute to the dual action of Sr on bones, which may shed light on cellular mechanisms for the dual action of Sr on postmenopausal women.

***Disclosures: William Lu**, None.*

SU0424

Treatment With a Sclerostin Antibody Increased Osteoblast-derived Markers of Bone Formation and Decreased Osteoclast-related Markers of Bone Resorption in Ovariectomized Rats. M Stolina*, D Dwyer, Q-T Niu, X Li, K Warmington, C-Y Han, H Salimi-Moosavi, MS Ominsky, WS Simonet, PJ Kostenuik, HZ Ke. Amgen Inc, USA

We previously reported that treatment of aged, ovariectomized (OVX) osteopenic rats with a sclerostin antibody (Scl-Ab) increased bone formation and restored vertebral bone mass. In the present study, we examined the molecular mechanisms by which Scl-Ab increased bone mass in OVX rats. Six-month-old female SD rats were either Sham- or OVX-operated. Five months later, OVX rats were treated with vehicle (Veh) or a murine Scl-Ab (Scl-AbII, 25mg/kg, 2x/wk, SC) for 5 weeks. BMD of the femur/tibia was measured weekly by DXA, and trabecular histomorphometry of the proximal tibia was performed at the end of the study (week 5). Markers of bone formation and resorption were measured in terminal serum (osteocalcin, PINP, CTX1, TRACP 5B), and at the mRNA level in whole tibia mRNA extracts (*Col1A, Osteocalcin, Cathepsin K, TRAP5*). After 5 weeks of Scl-AbII treatment, bone formation rate (BFR/BS) was 5-fold greater in the OVX-Scl-AbII group compared with OVX-Veh controls ($p<0.05$), and the 15% deficit in femur/tibia BMD caused by 5 months of OVX was fully reversed. Other anabolism-related changes with Scl-AbII treatment included significantly greater serum osteocalcin (+68% vs OVX-Veh) and PINP (+66%), tibial osteoblast numbers (+275%), and tibial mRNA expression of *Osteocalcin* (+133%) and *Col1a* (+145%). The bone resorption markers serum TRACP 5B and CTX1 were reduced with Scl-AbII by 60% ($p<0.05$) and by 11% ($p=0.39$), respectively, compared with OVX-Veh controls. Scl-AbII treatment was also associated with significant reductions in tibial osteoclast surface (OcS/BS, -53%), and 50% lower mRNA expression of the osteoclast-specific genes *TRAP5* and *Cathepsin K* in whole tibia extracts ($p<0.05$ vs OVX-Veh). Both of these osteoclast mRNA species correlated in a positive linear manner with tibial osteoclast number (N.Oc/T.Ar) across all groups. Positive linear correlations were also observed between local *Osteocalcin* mRNA and serum osteocalcin, and between *TRAP5* mRNA and serum TRACP 5B, suggesting that Scl-AbII-mediated changes in serum levels of these proteins reflected changes in their skeletal RNA expression. In summary, OVX rats treated with sclerostin antibody exhibited an increase in osteoblast number and activity, and a decrease in the number of mature osteoclasts. These results suggest that BMD restoration under these experimental conditions was mediated by increased bone formation and reduced bone resorption.

***Disclosures: M Stolina**, Amgen Inc., 1; Amgen Inc., 3*
This study received funding from: Amgen Inc.

SU0425

Whole Body Autoradiography of a Fusion Protein [35S]hPTH-CBD in Mice. Robert Gensure[1], Shigeru Miyata[2], Osamu Matsushita[3], Joshua Sakon*[4], Kentaro Uchida[3], Yoko Komatsu[3], Hirofumi Suda[2]. [1]Ochsner Clinic Foundation, USA, [2]Kagawa University, Japan, [3]Kitasato University, Japan, [4]University of Arkansas, USA

Single intraperitoneal (IP) injection of a fusion protein of hPTH(1-33) and collagen binding domain (CBD) segment of Clostridial collagenase increased bone mineral density in normal mice and in ovariectonized osteoporotic animal models as presented by Gensure et al. Single subcutaneously (SC) injected PTH-CBD can also prophylactically prevent chemotherapy induced alopecia and reverses chemotherapy induced osteoporosis. The purpose of the present investigation is to trace the fate of PTH-CBD injected into mice by the two different administration routs, i.e. IP vs. SC.

Male ddY mice weighing 32-35g each (7 weeks old) were injected with purified [35S]PTH-CBD. Then sacrificed at 1, 12 or 24 hours after injection. Either IP or SC injected [35S]-PTH-CBD accumulated in bone, skin, liver, kidney and intestine. Importantly the distribution of PTH-CBD is distinct from that of [3H]PTH or [125I]PTH published by Barling and Biddy and by Rouleau et al. and by Kretser, Martin and Melick. PTH showed little accumulation in the bone but accumulated mostly in kidney and liver. When PTH-CBD is injected by IP route, some remains in the peritoneal cavity, but significant amounts migrate to skin, bone, kidney, liver and intestine within the 1st hour. Much less PTH-CBD remains in the peritoneal cavity after 24 hours. PTH-CBD is taken up by the skeletal system at 24 hrs. The highest concentrations of the PTH-CBD are in the bladder and intestinal lumen, particularly at 24 hours, this likely represents the excretion route. Similarly when PTH-CBD is injected by SC route, some remains at the site of injection, but significant amounts migrated to skin, bone, liver, kidney and intestine within the 1st hour. Within 12 hrs, it migrated mostly to skeletal system and intestine. Interestingly the PTH-CBD is taken up on either side of the disks in the vertebral column. The region has the thickest cortical bone. The distribution could explain why PTH-CBD dramatically increased spinal bone mineral density in mice (>30%). PTH-CBD is also taken up in the area of growth-plate and cortex in tibia and fibula. Very little is found in marrow. In summary, CBD alters the distribution of fused PTH. PTH-CBD accumulated in tissues where physiological effects were seen, i.e. bone and skin.

***Disclosures: Joshua Sakon**, BiologicsMD, 1*

SU0426

Frequent Administration of High-Dose Zoledronate Safely Prevents Ovariectomy-Induced Loss of Jaw Alveolar Bone In A Genetic Mouse Model of Osteoporosis and Periodontal Disease. Nicolas Bonnet*[1], Philippe Lesclous[2], Serge Ferrari[3]. [1]Geneva University Hospital, Switzerland, [2]Equipe d'accueil EA 2496, France, [3]Geneva University Hospital & Faculty of Medicine, Switzerland

Osteoporosis and periodontitis are frequently associated in the elderly, both concurring to the loss of alveolar bone. Bisphosphonates may prevent/reverse bone loss due to estrogen-deficiency but could also precipitate ONJ triggered by local inflammation. We investigated the efficacy and safety of high-dose Zoledronate (Zol) on ovariectomy (OVX)-induced alveolar and systemic bone loss in the periostin (Postn)-deficient mouse, characterized by severe periodontitis and osteoporosis. Ten month-old female Postn-/- and Postn+/+ mice were OVX or Sham-operated and administered Zol (100µg/kg/week) or vehicle (Veh) for 3 months. Trabecular and cortical microarchitecture of the femur, as well as alveolar and basal bone volume fraction (BV/TV) in the jaw was analyzed by microCT. The distance between enamel-cement and alveolar bone (DEA), an index of apparent bone in the oral cavity, was measured at the root of M1 by microCT. Compared to Postn+/+, intact Postn-/- mice had significantly lower BMD, trabecular BV/TV, and cortical bone volume (CtBV); lower alveolar BV/TV and basal BV/TV, and higher DEA (all $p<0.01$), -the latter consistent with the effects of periodontitis-. Compared to sham, OVX significantly decreased femur BMD (-10.4%, $p<0.05$), BV/TV (-72%, $p<0.05$) and CtBV (-12.8%, $p<0.05$) in Postn+/+. OVX also reduced jaw basal BV/TV (-24%, $p<0.05$) and less so alveolar BV/TV, and increased DEA (+12%, $p<0.01$) in Postn+/+. In Postn-/-, OVX did not cause further bone loss but their skeletal phenotype remained significantly worse than in OVX Postn+/+, both systemically and in the jaw. Compared to Veh, Zol significantly improved BMD, femur BV/TV and CtBV in both OVX Postn+/+ and Postn-/- (all $p<0.01$). Zol also improved jaw alveolar and basal BV/TV independently of the genotype ($p<0.01$), although it did not fully restore Postn-/- to Postn+/+ levels. In contrast Zol did not modify DEA post-OVX, which remained higher in Postn-/- than Postn+/+. In summary, following estrogen-deprivation Zol improved trabecular and compact bone mass in the femur and jaw, both in absence and presence of peridontitis. Although Zol did not entirely rescue the poor alveolar bone microstructure in Postn-/-, perhaps due to the periodontal inflammation, it did

not either aggravate their index of apparent bone in the oral cavity. This mouse model of osteoporosis and periodontitis suggests that the latter does not prevent the efficacy nor safety of high-dose, frequent zoledronate on the skeleton.

***Disclosures: Nicolas Bonnet**, None.*

SU0427

Structure-activity Relationships of Bisphosphonates with Respect to their Effect on the LPS-induced Increase in the Synthesis of Prostaglandin E_2 and Nitric Oxide. Hisashi Shinoda*[1], Shinobu Murakami[1], Keiko Suzuki[2], Mirei Chiba[1], Sadaaki Takeyama[3], Yuka Narusawa[1], Hiroaki Hirotani[1], Shoji Yamada[2], Kaoru Igarashi[1], Paula Stern[4]. [1]Tohoku University Graduate School of Dentistry, Japan, [2]Showa University Graduate School of Dentistry, Japan, [3]Hokkaido University Graduate School of Dentistry, Japan, [4]Northwestern University Medical School, USA

Recent studies have shown that therapy with nitrogen-containing bisphosphonates (NBPs) is associated with the development of osteonecrosis of the jaw (ONJ), and have suggested that the ONJ might be related to inflammatory conditions in the jaw bone or oral tissues. However, there seemed to be no systemic study on the relationship between bisphosphonates and inflammatory condition. The current study was carried out to investigate whether bisphosphonates affect the inflammation induced by lipo-polysaccharide (LPS) and if so, by what mechanism. We investigated the effect of various BPs on the LPS-induced-increase in the synthesis of prostaglandin E_2 (PGE_2) and nitric oxide (NO) using organ cultures of neonatal mouse calvaria, and cultures of osteoblast-like MC3T3-E1 cells and calvarial cells. The following results were obtained. (1) All of the NBPs examined (zoledronate, risedronate, incadronate, alendronate, and pamidronate) dose-dependently promoted the LPS-induced increase in PGE2 synthesis and increased the mRNA expression of cyclooxygenase-2 (COX-2) in 24-72 hour calvarial cultures. In contrast, bisphosphonates which do not contain nitrogen in their side chain (non-NBPs) (clodronate, etidronate, tiludronate and [4-(methylthio)phenylthio] methanebisphosphonate (MPMBP)) dose-dependently inhibited LPS-stimulated-increases in PGE_2 synthesis and mRNA expression of COX-2. (2) NBPs stimulated the LPS-induced-increase in NO (NO_2/NO_3) synthesis and mRNA expression of inducible NO synthase (iNOS), while non-NBPs inhibited LPS-stimulated-increases in NO synthesis and mRNA expression of iNOS. (3) In the cultures of neonatal mouse calvaria and osteoblastic MC3T3-E1 cells, a NBP (zoledronate) enhanced the translocation of cytosolic NF-κB to the nucleus, while a non-NBP (MPMBP), in contrast, inhibited the translocation of the NF-κB to the nucleus. The above results suggest that the effect of BPs on inflammation differs depending on the structure of side chain; NBPs can enhance LPS-induced inflammatory reactions, while non-NBPs can inhibit the reactions. Since LPS is an essential bacterial factor causing inflammation in oral tissues, the currently observed effects of NBPs on LPS-induced inflammatory actions in bone might be relevant for the onset and development of ONJ associated with NBPs.

***Disclosures: Hisashi Shinoda**, None.*

SU0428

The Effects of pH on the Relative Bone Mineral-binding Affinities of Bisphosphonates Determined by Hydroxyapatite-column Chromatography. Xuchen Duan*[1], Zhidao Xia[1], Hao Zhang[1], Mike Quijano[2], Roy L M Dobson[2], James T Triffitt[1], James Dunford[1], Frank H Ebetino[3], R Graham Russell[4]. [1]Nuffield Department of Orthopaedics, Rheumatology & Musculoskeletal Sciences, The Botnar Research Centre, Oxford University Institute of Musculoskeletal Sciences, University of Oxford, United Kingdom, [2]Procter & Gamble, USA, [3]Warner Chilcott, USA, [4]University of Oxford, United Kingdom

There is abundant evidence that individual bisphosphonates (BPs) differ substantially in their binding affinities for hydroxyapatite and bone mineral and that the P-C-P moiety, the R1 OH group and the R2 side chains contribute to this binding. The differences in mineral-binding affinities among the clinically-used BPs are important since they influence their differential distributions within bone, their biological potencies, and their durations of action. In our current studies we have used column chromatography with ceramic hydroxyapatite and fluoroapatite combined with mass spectrometric identification and quantitation to assess the relative mineral-binding affinities of individual clinically-relevant BPs in mixtures of these compounds and the changes with elution pH. Although some differences are seen in the rank order of mineral binding of BPs between various adsorption assays (e.g. previous kinetic binding affinities by crystal growth assays versus column chromatography) in general, the alkyl-amino BPs, such as pamidronate, alendronate and neridronate, have the highest binding, whereas clodronate, a non-amino BP, shows the lowest binding, with risedronate displaying intermediate binding values. For example, at pHs of 5.7, 6.8 and 7.4, respectively, the peak retention times (min; mean ± SD) were as follows Pamidronate=33.3 ± 1.35, 18.55 ± 0.62, 14.55 ± 0.3; Alendronate=33.3 ± 1.14, 17.65 ± 0.62, 14.35 ± 0.17; Neridronate=22.9 ± 1.70, 13.45 ± 0.46, 11.45 ± 0.17; Zoledronate=28.2 ± 1.20, 12.85 ± 0.17, 10.45 ± 0.35; Minodronate=21.8 ± 0.30, 10.65 ± 0, 8.55 ± 0.30; Risedronate=21.2 ± 1.30, 10.65 ± 0, 7.75 ± 0.17; Etidronate=19.1 ± 0.60, 14.25 ± 0.3, 11.65 ± 0.17; Ibandronate=17.3 ± 0.60, 10.85 ± 0.17, 8.85 ± 0.52; Clodronate=10.8 ± 0.62, 8.15 ± 0.35, 7.35 ± 0.52. The results indicate that changing pH has profound effects on the binding and release from HAP, and that BPs, perhaps unexpectedly, have higher affinities at lower pH as shown by increased retention times. Changing pH will affect the ionization of the phosphonate and R2 functional groups. These observations have implications for detachment of BPs during bone resorption, and may help to explain clinical differences among BPs.

***Disclosures: Xuchen Duan**, None.*

SU0429

Bone Regeneration in Rats with Type 2 Diabetes Mellitus is Delayed due to Impaired Osteogenic Differentiation. Christine Hamann*[1], Claudia Goettsch[2], Jan Mettelsiefen[1], Veit Henkenjohann[1], Ute Hempel[1], Ricardo Bernhardt[3], Martina Rauner[4], Kathrin Wieczorek[1], Klaus-Peter Günther[1], Lorenz Hofbauer[1]. [1]Dresden Technical University Medical Center, Germany, [2]Department of Medicine III, Technical University, Dresden, Germany, [3]Technische Universität Dresden, Germany, [4]Medical Faculty of the TU Dresden, Germany

Bone regeneration in diabetes mellitus is severely impaired. The mechanisms underlying these alterations are poorly understood. Here, we analyzed the molecular and cellular differences between diabetic and non-diabetic bone regeneration using the Zucker Diabetic Fatty (ZDF) rat, an established rat model of type 2 diabetes mellitus. ZDF rats show a spontaneous diabetic phenotype and develop various macro- and microvascular diabetic complications. Diabetic rats had a reduced bone mineral density compared to non-diabetic rats as assessed by peripheral quantitative computed tomography. To assess osteoblast and osteoclast biology, bone marrow stromal cells were differentiated towards osteoblasts using osteogenic medium, and towards mature osteoclasts in the presence of RANKL and M-CSF, respectively. Osteoblast differentiation was severely impaired by diabetes as measured by lower alkaline phosphatase activity (-20%) and mineralized matrix formation (-55%). In addition, osteoblast-specific markers such as BMP-2, Runx2, osteocalcin, and osteopontin were reduced by 40-80% after osteogenic differentiation. By contrast, osteoclast functions were not affected as measured by TRAP staining, pit formation assay, and gene profiling, thus indicating a specific osteoblastic defect. To validate these findings in vivo in a clinically relevant model, a sub-critical, circumferential bone defect of 3 mm was created by microsurgical techniques at the left femur after stabilizing the femur by a 4-hole plate. Bone healing was monitored by X-ray and μCT analysis. While non-diabetic rats regenerated bone to partially fill the defects by up to 60%, diabetic rats showed delayed defect healing after 12 weeks with markedly impaired bone regeneration, resulting in only 32% filling of the defect. In conclusion, *in vitro* and *in vivo* evidence clearly identified a specific osteoblastic defect as a cause and mechanism that accounts for impaired bone regeneration in type 2 diabetes mellitus. Strategies that target this mechanism are currently being explored.

***Disclosures: Christine Hamann**, None.*

SU0430

Catechins with Gallate Moiety Suppress Bone Resorption by Inhibiting Prostaglandin Biosynthesis and RANKL Expression in Osteoblasts. Chiho Matsumoto[1], Michiko Hirata[1], Megumi Kobayashi[1], Tsukasa Tominari[1], Hideharu Takata[1], Morichika Takita[1], Masaki Inada[2], Chisato Miyaura*[1]. [1]Tokyo University of Agriculture & Technology, Japan, [2]Toyko University of Agriculture & Technology, Japan

Catechin species, a major group of polyphenol in green tea, have been shown to exhibit various biological activities including anti-oxidant, anti-cancer and anti-inflammation. However, roles of catechins in molecular mechanism of inflammatory bone diseases are unknown in bone tissues. In this study, we examined the function of various catechins in osteoclastic bone resorption. Epigallocatechin-gallate (EGCG: 1-30 μM) dose-dependently suppressed osteoclast formation induced by interleukin-1 (IL-1) in co-cultures of mouse bone marrow cells and osteoblasts. In mouse osteoblasts collected form calvariae, EGCG markedly suppressed the mRNA expression of cyclooxygenase-2 (COX-2) and membrane-bound prostaglandin E synthase-1 (mPGES-1) induced by IL-1. The level of PGE induced by IL-1 was significantly suppressed by adding EGCG in osteoblasts. In addition, EGCG also suppressed the expression of RANKL mRNA in osteoblasts. Therefore, EGCG suppresses IL-1-induced osteoclast formation by inhibiting PGE biosynthesis and following RANKL expression in osteoblasts. We compared the potency of various catechins in the suppression of osteoclast formation in co-cultures of bone marrow cells and osteoblasts, and of RANKL expression in osteoblasts induced by IL-1. EGCG, epicatechin-gallate (ECG) and gallocatechin-gallate (GCG) also suppress RANKL-dependent osteoclast formation, but epigallocatechin (EGC), epicatechin (EC), gallocatechin (GC) and catechin (C) showed much less activity. Therefore, gallate moiety is essential for the suppressive effects of catechin family on osteoclast formation. In organ culture of mouse calvaria, IL-1-induced bone resorption was completely suppressed by EGCG, indicating that EGCG is a potent anti-resorbing agent in bone tissues. To determine whether EGCG influence bone mass in vivo, mice were ovariectomized and treated with LPS, and some of the mice were treated with EGCG. We have shown that PGE biosynthesis in osteoblasts is critical for LPS-induced bone loss, and the inflammatory bone resorption is attenuated in mPGES-1-

null mice. The intake of EGCG reduced the loss of femoral bone mineral density induced by LPS in mouse by maintaining trabecular bone. These results suggest that EGCG suppresses bone resorption associated with estrogen loss and/or inflammation such as osteoporosis and periodontal diseases, and exhibits beneficial effects on bone mass by regulating osteoclastic bone resorption.

***Disclosures: Chisato Miyaura**, None.*

SU0431

Dose-dependent Effects of Blackberries in the Prevention of Boneless in Ovariectomized Rats. Lydia Kaume*[1], Vidya Gadang[2], William Gilbert[2], Yan Wang[3], Brenda Smith[3], Latha Devareddy[2]. [1]University of Arkansa, USA, [2]University of Arkansas, USA, [3]Oklahoma State University, USA

Recent studies have shown fruits rich in antioxidants such as grapes, dried plums and blueberries have bone protective properties. The objective of this study was to determine the dose-dependent effects of antioxidant-rich blackberries in preventing ovariectomy-induced bone loss. Thirty-eight, six-month-old female Sprague-Dawley rats were acclimated for 1 week before being sham-operated (Sham) or ovariectomized (Ovx). Animals were then divided into the following treatment groups: Sham, Ovx control, Ovx+ 5% blackberry (5% BB) and Ovx+ 10% blackberry (10% BB). The rats in the Sham and Ovx control groups received AIN-93M purified rodent diet, and the rats in blackberry groups received similar diet modified to contain freeze dried blackberries at levels of 5% and 10% (w/w). After 100 days of treatment, animals were euthanized and tissues were collected for further analyses. Bone mineral area (BMA), content (BMC) and density (BMD) of whole body and excised bones were measured using dual energy x-ray absorptiometry. Bone biomarkers were assessed to understand the mechanism of action of blackberries. The results of the study are presented in the table below:

Based on the findings of the study we can conclude that blackberries at the level of 5% had modest bone protective effects. The higher doses of blackberries i.e., at the level of 10% did not have any effects on bone. Blackberries may exert bone-protective effects by combating oxidative stress.

Parameter	Sham	Ovx Control	Ovx + 5% BB	Ovx + 10% BB
Tibia BMD (g/cm^2)	0.2106 ± 0.0019^{a}	0.2004 ± 0.0019^{bc}	0.2052 ± 0.0027^{ab}	0.1960 ± 0.0029^{c}
4th Lumbar Vertebra BMD (g/cm^2)	0.2295 ± 0.0036^{a}	0.2183 ± 0.0036^{b}	0.2235 ± 0.0050^{ab}	0.2135 ± 0.0049^{b}
Femur BMD (g/cm^2)	0.2386 ± 0.0029^{a}	0.2237 ± 0.0030^{bc}	0.2340 ± 0.0041^{ab}	0.2150 ± 0.0041^{c}
DPD (nmol /mmol creatinine)	16.29 ± 3.4^{c}	37.29 ± 4.95^{a}	37.6 ± 1.87^{a}	31.2 ± 1.41^{b}
Osteocalcin (ng/ml)	85.74 ± 19.46^{b}	136.89 ± 15.27^{a}	143.93 ± 25.16^{ab}	144.2 ± 16.75^{ab}

table

***Disclosures: Lydia Kaume**, None.*

SU0432

Body composition in Male (ORX) And Female (OVX) Cynomolgus Monkey Models Of Osteoporosis. Aurore Varela*[1], Nancy Doyle[2], Karen Veverka[3], Susan Y. Smith[1]. [1]Charles River Laboratories, Canada, [2]Charles River, Canada, [3]GTx, Incorporated, USA

Ovariectomized (OVX) and orchidectomized (ORX) aged non-human primates are suggested models for the evaluation of drugs for the treatment or prevention of osteoporosis. Both OVX and ORX are associated with bone loss and decreased bone strength. Changes in body composition are not clearly established for the female OVX model. The long term effect of OVX vs. ORX on body fat and muscle mass in female and male monkeys were investigated. Female (n=20/group) and male (n=20/group) Cynomolgus monkeys aged ⩾ 9 years old were assigned to two groups by gender by whole body bone mineral content. Ten females and ten males underwent OVX or ORX surgery, respectively, and 20 females or males were Sham operated. For males, body fat, muscle mass and bone density were assessed by DXA and pQCT at 4, 8, 12 and 16 months post-orchidectomy. For females, body fat, muscle mass and bone density were assessed by DXA and pQCT at 6, 12 and 15 months post-ovariectomy. Data from Sham and gonadectomized animals were derived using the same instruments and compared. Both OVX and ORX surgeries resulted in bone loss associated with increased bone turnover. Body weights for females were unaffected by OVX; however, male body weights were decreased by 20% during the first 4 months after orchidectomy and then stabilized. In males, the body weight loss was associated with an 18% decrease (compared to baseline) in muscle area measured by pQCT. Lean mass (DXA) and muscle area (pQCT) were significantly decreased for ORX animals, consistent with ORX-induced decreases in body weight. There was no effect on % body fat. In females, increased percent body fat was observed for both Sham and OVX over the course of the study up to Month 15 compared to baseline. There were no changes in lean mass (DXA) and muscle area (pQCT) following OVX when compared to sham animals. In conclusion, both ovariectomy and orchidectomy surgery in aged monkeys resulted in bone loss associated with increased bone turnover, consistent with their intended use as models of osteoporosis. However, changes in body composition differed markedly between these two models. These data suggest that the male ORX model may be useful to evaluate androgenic compounds and agents that may modify sarcopenia.

***Disclosures: Aurore Varela**, contract, 5*
This study received funding from: GTx, Inc.

SU0433

Selective Estrogen Receptor Modulators Increase the Bone Formation Activity of Mouse Osteoblasts *in Vitro*. Tiina A. Suutari*[1], Katja Fagerlund[1], Jukka Rissanen[2], Alan Chan[3], Jussi Halleen[1]. [1]Pharmatest Services Ltd, Finland, [2]Pharmatest Services,Limited, Finland, [3]Percuros B.V., Netherlands

Estrogen responsive mouse clonal osteoblast progenitor cell line KS483 can be conveniently used for studying differentiation and bone formation activity of osteoblasts *in vitro*. We have previously optimized the culture model for testing the effects of estrogen-like compounds and anabolic compounds on osteoblasts using 17β-estradiol and bone morphogenetic protein 2 (BMP-2) as reference compounds. We have now tested the culture model further by studying the effects of continuous exposure of the selective estrogen receptor modulators (SERMs) raloxifene, lasofoxifene and bazedoxifene, on osteoblast differentiation and activity. KS483 cells were cultured in phenol red-free αMEM supplemented with charcoal-stripped fetal bovine serum, ascorbic acid and β-glycerophosphate. Culture medium was changed in 3-4 –day intervals. Separate cultures were performed for studying osteoblast differentiation and osteoblast activity. Cultures for determining effects on osteoblast differentiation were stopped at day 8, and intracellular alkaline phosphatase (ALP) activity was measured in the cell lysates. Cultures for determining effects on osteoblast activity were stopped at day 13, and calcium incorporated into the formed bone matrix was measured as a marker of inorganic bone matrix synthesis by the osteoblasts. Osteoblastic bone formation was confirmed microscopically by von Kossa staining that revealed clear bone nodule formation at day 13. 17β-estradiol and BMP-2 were used as reference compounds in the study. The compounds were added into the culture medium at the beginning of the culture and when the culture medium was changed. The reference compounds 17β-estradiol and BMP-2 increased both osteoblast differentiation based on ALP activity values at day 8 and bone forming activity based on calcium values at day 13. On the contrary, raloxifene, lasofoxifene and bazedoxifene had no effect on ALP activity values, but they stimulated dose-dependently bone forming activity of osteoblasts based on calcium values. The SERMs were less efficient than 17β-estradiol or BMP-2 in increasing osteoblast activity. These results suggest that the SERMs raloxifene, lasofoxifene and bazedoxifene stimulate bone formation activity of osteoblasts without affecting osteoblast differentiation in this mouse osteoblast culture model. We conclude that the culture system can be used as a screening tool for finding SERMs with stimulatory effects on osteoblasts.

***Disclosures: Tiina A. Suutari**, None.*

SU0434

Assessment of Alterations in Internal Bone Vascularity – A Three Dimensional Approach. Jan Berry*[1], Benjamin Sinder[1], Kenneth Kozloff[2], Robert Guldberg[3], Serk In Park[1], Xin Li[1], Fabiana Soki[1], Laurie McCauley[4]. [1]University of Michigan, USA, [2]University of Michigan Department of Orthopaedic Surgery, USA, [3]Parker H. Petit Institute for Bioengineering & Bioscience, USA, [4]University of Michigan, School of Dentistry, USA

The vascular supply to tissues and organs is central to function and homeostasis, and also to the support of pathophysiologic conditions. A variety of techniques exist for the analysis of angiogenesis and vascular changes in extraskeletal sites, most of which are not feasible or are difficult to perform in skeletal tissues. Alterations in vascularity within the marrow cavity are strong modifiers of bone remodeling and regeneration. Three dimensional imaging through microCT analysis has provided valuable insights into osseous structure and function. Such analyses can be extended to dimensional studies of the vasculature within the bone. The purpose of this study was to analyze the impact of various bone active agents on changes in the internal bone vasculature. A perfusion technique using the radiopaque silicone rubber injection agent Microfil ™ followed by microCT analysis was utilized. Mice treated with vehicle or various agents that cause changes in the bone microenvironment (PTH, zoledronic acid, cyclophosphamide) were administered either acutely (cyclophosphamide) or over a 1-4 week period (PTH, zoledronic acid). At sacrifice, mice were perfused with lactated Ringer's solution containing 150 U/ml heparin, followed by 10% neutral buffered formalin, and then with Microfil ™ compound (1.04 specific gravity mixed 4:1 with the 0.92 specific gravity diluent). Femurs, tibiae and spleens were dissected and fixed, and bones were decalcified. Samples were analyzed by microradiography for gross differences in vascular morphology. Following radiography, bone samples were scanned in water using cone beam microCT, and reconstructed at 18-micron voxel size. Regions of interest were defined for both central bone vascularity and vascular regions near the growth plate, and quantitative differences in vessel numbers and sizes were determined using the stereology package of commercially available software. No significant quantitative changes were found in the volume of vasculature for PTH treated mice. Qualitative changes of altered vascular spaces were noted in femurs of mice treated with

cyclophosphamide or zoledronic acid, however changes in spleens of these mice were not observed. This technique is valuable in providing another criteria for measuring changes in the bone microenvironment.

***Disclosures: Jan Berry**, None.*

SU0435

Early Effects of Strontium Treatment Prevent Trabecular Bone Loss in Overiectomized Rats by Increasing Trabecular Thickness and Plate-like Microstructure: An *In Vivo* çCT Study. Xiaowei Liu*[1], Songlin James Peng[2], Zhaoyang Li[2], William Lu[3], X Guo[1]. [1]Columbia University, USA, [2]The University of Hong Kong, Peoples republic of china, [3]The University of Hong Kong, Hong kong

Strontium (Sr) ranelate, a therapy for postmenopausal osteoporosis, has been shown to effectively reduce the risk of fragility fractures in postmenopausal women. The early effects of Sr to help account for its efficacy remain poorly understood. To explore this point, we evaluated trabecular (Tb) bone microarchitecture of ovariectomized (OVX) rats in response to early and late Sr administrations by in vivo micro computed tomography (μCT).

Three-month-old female SD rats were divided into 3 groups: OVX treated with vehicle (OVX, n=9), or with Sr (4 mmol/kg/day) immediately after surgery (Sr @ T=0, n=10), or 4 weeks after OVX (Sr @ T=4 wk, n=10). The proximal tibia of all rats (under anesthestia) were scanned by an *in vivo* μCT system (VivaCT 40, Scanco Medical; 15 μm resolution) at 0, 4, 8, 12 weeks; Sr @ T=4 wk and OVX rats were also scanned at 16 weeks. Tb bone images of each scan were compared to baseline data using the longitudinally registered volumes of interest.

Bone volume fraction (BV/TV) and Tb thickness (Tb.Th) of Sr @ T=0 were significantly different from the OVX group over time ($p<0.05$). At week 12, BV/TV and Tb.Th of Sr @ T=0, were 32% and 7% greater than the OVX group. In addition, structure model index (SMI) decreased over time in Sr @ T=0, indicating a more plate-like structure, and was significantly different from OVX rats at week 4. Early loss of connectivity density (Conn.D) due to OVX was prevented by immediate exposure to Sr after OVX. However, early Sr @ T=0 treatment had no significant effect on Tb number (Tb.N) or Tb spacing (Tb.Sp). There was a significant decrease of Tb.N and increase of Tb.Sp in both OVX and Sr @ T=0 groups.

The Sr @ T=4 wk group began to reverse loss of BV/TV (89% at wk 16 vs. wk 0, $p>0.05$). Sr @ T=4 wk also maintained Tb.N and Tb.Sp from week 4 through 16, in contrast to an 18% decrease of Tb.N and 24% increase of Tb.Sp at week 16 compared to week 4 in the OVX group ($p<0.05$). However, Sr @ T=4 wk did not reverse Tb.N or Tb.Sp to baseline values. Although changes in SMI and Tb.Th were not significant between OVX and Sr @ T=4 wk groups, SMI significantly decreased and Tb.Th increased in the Sr @ T=4 wk.

The results show that Sr use immediately following OVX prevents bone volume loss by increasing Tb.Th and plate-like Tb structure. In addition to these mechanisms, by preventing further loss of Tb.N and increasing Tb.Sp, late Sr treatment can restore most of bone volume lost that occurs after OVX in rats.

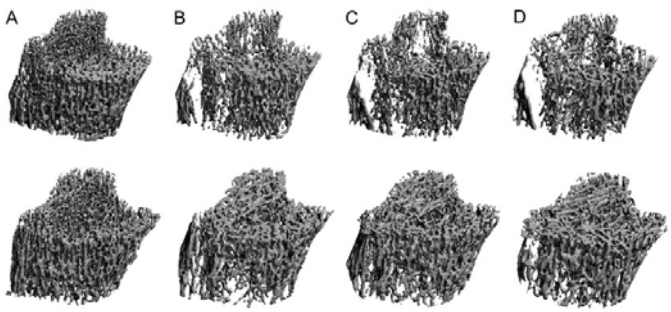

Figure 1. 3D reconstructed trabecular bone images of rat proximal tibia scanned at (A) 0, (B) 4, (C) 8, and (D) 12 weeks after OVX surgery treated with (Top) Vehicle and (Bottom) Strontium.

Figure 1

***Disclosures: Xiaowei Liu**, None.*

SU0436

Efficacy of ONO-5334, a Cathepsin K Inhibitor, on Bone Geometry and Histomorphometry in Cortical Bone in Ovariectomized Cynomolgus Monkeys. Makoto Tanaka*, Hiroyuki Yamada, Hiroshi Mori, Akiko Kunishige, Satoshi Nishikawa, Yasuaki Hashimoto, Tsutomu Shiroya. ONO Pharmaceutical Co., Ltd., Japan

We have previously reported that ONO-5334 preferentially suppressed bone resorption markers over bone formation markers and increased BMD by affecting cortical bone as well as trabecular bone in ovariectomized (OVX) cynomolgus monkeys 1). In this study, we evaluated the efficacy of ONO-5334 on cortical bone using bone geometry and histomorphometry.

Female cynomolgus monkeys were assigned to one of the following 6 groups (20 per group): sham operated, OVX control treated with vehicle, ONO-5334 1.2, 6 or 30 mg/kg, or alendronate (ALN) 0.05 mg/kg. ONO-5334 was orally administered once daily from the day following OVX surgery for 16 months. ALN was administered intravenously once every 2 weeks. Cortical geometry at the proximal tibia was evaluated by in vivo pQCT. Bone fluorochrome labeling was conducted using calcein at 15 days interval prior to necropsy and histomorphometry data was measured at the midshaft femur.

From pQCT results, OVX caused a significant decrease in cortical volumetric BMC, vBMD, bone area, cortical thickness (Ct.Th.) at 16 months (M) and periosteal circumference (PC) at 8 M (all parameters $p<0.05$ vs Sham) and a tendency to increase in endosteal circumference (EC) at 16 M. ONO-5334 at 6 and 30 mg/kg significantly increased cortical vBMC, vBMD, bone area, Ct.Th. at 16 M and PC at 8 M and significantly decreased EC at 16 M (all parameters $p<0.05$ vs OVX). ALN significantly increased cortical vBMC, vBMD and tended to increase Ct.Th at 16 M. From histomorphometry results, periosteal (Ps), endosteal (Es) and osteonal (On) bone formation rate (BFR) were significantly elevated by OVX (all sites $p<0.05$ vs Sham). ONO-5334 at all doses did not affect on PsBFR and EsBFR. ONO-5334 significantly decreased OnBFR with 6 and 30 mg/kg ($p<0.01$ vs OVX). ALN significantly decreased EsBFR ($p<0.01$ vs OVX) but not PsBFR and OnBFR.

In summary, an increase in Ct.Th. with ONO-5334 treatment results from an increase in PC and a decrease in EC of cortical bone at the proximal tibia. In addition to suppression of bone resorption, ONO-5334 does not change BFR at cortical surfaces of the midshaft femur compared with OVX.

1) Yamada H, et al. ASBMR, 2009, FR0420.

***Disclosures: Makoto Tanaka**, None.*

SU0437

Green Tea Polyphenols Supplementation Improves Bone Microstructure in Orchidectomized Middle-aged Rats. Chwan-Li Shen*[1], James K Yeh[2], Jay J Cao[3], Tom Tenner[4], Jia-Sheng Wang[5]. [1]Texas Technology University Health Sciences Center, USA, [2]Winthrop-University Hospital, USA, [3]USDA ARS Grand Forks Human Nutrition Research Center, USA, [4]Texas Tech University Health Sciences Center, USA, [5]University of Georgia, USA

We have demonstrated that green tea polyphenols (GTP) attenuate trabecular bone loss in ovariectomized middle-aged female rats. This study was designed to examine the efficacy of GTP in prevention of bone loss in middle-aged male rats with and without orchiectomy (ORX). A 2 (sham vs. ORX) × 2 (no GTP and 0.5% GTP in drinking water) factorial design using 40 middle-aged male rats was assigned to 4 groups for 16 wks. Efficacy was evaluated in femur and tibia microarchitecture by micro-CT and histomorphometric analysis, respectively. ORX decreased trabecular bone volume, number and thickness in distal femur and proximal tibia, but increased bone formation rates in cancellous of the proximal tibia as well as the endocortical tibial shaft. The results of two-way ANOVA show that GTP supplementation significantly increased trabecular bone volume (F value=5.4, P=0.025), thickness (F value = 6.5, P=0.015), and bone formation rates in both proximal tibia (F value=14.0, $P<0.001$) and periosteal tibial shaft (F value=4.1, P=0.049), but decreased eroded surface in both proximal tibia (F value=17.3, $P<0.001$) and endocortical tibial shaft (F value=4.2, P=0.047). This study demonstrates that GTP supplementation in drinking water for 16 weeks prevents trabecular bone loss through increasing bone formation while suppressing bone resorption. The results form this animal model merit investigation of a potentially significant prophylactic role of green tea in bone health of elderly men.

***Disclosures: Chwan-Li Shen**, None.*

SU0438

Lack of Intermittent PTH Response to Daily Administration of Odanacatib in Adult Ovariectomized Rhesus Monkeys. Gregg Wesolowski*[1], Patricia Rebbeck[1], Cynthia Spencer-Bauer[1], Susanne Jendrowski[1], Le Thi Duong[2]. [1]Merck & Co., Inc., USA, [2]Merck Research Laboratories, USA

Cathepsin K (CatK), the principle collagenase in osteoclasts, degrades the organic matrix during bone resorption. Odanacatib (ODN) is a selective inhibitor of Cat K, currently under development for the treatment of osteoporosis. Genetic and pharmacological evidence has demonstrated that the inhibition of Cat K leads to suppression of bone resorption without affecting bone formation. Daily administration of relacatib and balicatib, other potent cathepsin K inhibitors, was reported to produce transient PTH elevations within 2 hours post-dosing in non-human primates and in humans, respectively, suggesting a link between CatK inhibition and PTH-dependent bone anabolism. The aim of this study was to examine circulating levels of intact PTH(1-84) (iPTH) and calcium in response to ODN versus alendronate (ALN) treatment in a preclinical model of osteoporosis. Rhesus monkeys (10-22 yr-old), N=16/group) were treated with vehicle (Veh), ODN at 2mg/kg/d (L-ODN), ODN at 4 mg/kg/d (H-ODN) or ALN (15 ug/kg twice weekly, s.c.) for 20-months. A group of age matched intact animals (Int., N=12) were included as control. Following 16-mo. of treatment, the animals were fasted overnight and then bled before dosing (~ 8 AM), and again at 0.5, 1, 2, 4, 7, 12 and 24-hr after dosing. All animals were fed following the 7-hr time point. Plasma was prepared for evaluation of iPTH, and ionized calcium. Administration of ODN at both doses and ALN resulted in significant and sustained inhibition of bone resorption markers (uNTx and sCTx). Overall, iPTH profiles in all

groups followed a diurnal cycle with steady state levels in the L-ODN and ALN groups (342 and 401 pg/ml-24hr, respectively) higher than in Int, Veh, or H-ODN groups (198, 155 and 151 pg/ml-24hr, respectively). Blood ionized calcium levels increased 12-hr post-dosing, coinciding with the decline in iPTH. Ionized calcium levels did not differ among all treatment groups and there was no evidence of iPTH spikes in any group at any time point in response to daily administration of ODN post treatment for 16-months. Moreover, the steady-state circulating levels of iPTH in the ALN-treated monkeys were generally higher than those in either ODN dosed group, vehicle or intact control groups. Thus, in contrast to previous findings with other Cat K inhibitors, these data strongly indicate that the effects of ODN on bone formation, are unlikely to be due to a transient PTH response in OVX-monkeys.

***Disclosures: Gregg Wesolowski**, Merck & Co, 3*
This study received funding from: Merck & Co

SU0439

Use of Microarray Technology to Support Development of Nutraceutical Supplements to Reduce Bone Resorption and Enhance Bone Formation. Yumei Lin*[1], Shyam Ramkrishnan[2], Valentina Kazlova[2], Mary Murray[3], David Fast[4], Kevin Gellenbeck[2], Amit Chandra[4]. [1]Nutrilite, USA, [2]Nutrilite Health Institute, USA, [3]Nutrilite Health Institute.com, USA, [4]Access Business Group, USA

The purpose of the study reported here was to confirm the biochemical mechanisms used to screen natural ingredients for nutraceutical based bone health products using microarray technology in humans. Our original systematic approach included mechanism of action specific bioassays and neonatal murine calvarial organ culture systems to identify one botanical formula profile to reduce bone resorption (AR, anti-resorptive formula) and a second profile to stimulate bone growth (BF, bone formation formula). A 28-day randomized open-label study was conducted. Forty-six (n = 46) healthy non-smoking postmenopausal women (postmenopausal age from 6 months to 5 years) were recruited. Efficacy was determined by comparing changes in gene expression profiling data between Day 1 and Day 28. Safety, including anabolic effect, general safety and tolerance were also demonstrated. Cumulative results confirmed that the AR formula containing pomegranate and grape seed extracts demonstrated gene expression responses aligned with a reduction in bone resorption, and were linked to a down-regulation of RANKL, whereas the BF formula containing quercetin and ethanolic licorice extract demonstrated gene expression responses aligned with bone formation processes and up-regulation of BMP2 protein. The AR+BF combination formula showed positive effects on bone health but nullified the BMP2 effect found in the BF formula.

***Disclosures: Yumei Lin**, None.*
This study received funding from: Amway Corporation

SU0440

Eldecalcitol Improves Mechanical Strength of Cortical Bones by Both Stimulating Periosteal Bone Formation and Inhibiting Endocortical Bone Resorption. - A Comparative Study with Alfacalcidol using the Senescence-Accelerated SAM/P6 Mice -. Ayako Shiraishi*[1], Hitoshi Saito[2], Sadaoki Sakai[3], Fumiaki Takahashi[2], Masahiko Mihara[3]. [1]Chugai Pharmaceutical Co.,Ltd., Japan, [2]Chugai Pharmaceutical Company, Limited, Japan, [3]chugai pharmaceutical co., ltd., Japan

Eldecalcitol (ED-71), a 2β-hydroxypropyloxy derivative of $1\alpha,25(OH)_2D_3$, is a more potent inhibitor of bone resorption than alfacalcidol (ALF) in ovariectomized osteoporosis rat (Bone 2002). It has been reported that the senescence-accelerated mouse strain P6 (SAM/P6) showed bone loss caused by the osteoblast dysfunction (JBMR 2005). In this study, we aimed to assess the effect of ED-71 on bone in the SAM/P6 mice in comparison to ALF. Four month-old SAMP6 mice were given either ED-71 (0.025 or 0.05 μg/kg) or ALF (0.2 or 0.4 μg/kg) by oral gavages, five-times-a-week for six weeks. After the treatment, all mice were sacrificed to harvest femurs, tibiae, serum and urine samples. Both ED-71 and ALF treatment increased serum calcium (Ca) and urinary Ca excretion in a dose dependent manner. Serum Ca and urinary Ca excretion of the ED-71 0.05 μg/kg-group were comparable to those of the ALF 0.2 μg/kg-group. The mechanical strength of femoral cortex of the ED-71 0.05 μg/kg-group was significantly higher than those of the vehicle control group ($p<0.001$) and the ALF 0.02 μg/kg-group ($p<0.05$). The BMD at distal tibia of the ED-71 0.05 μg/kg-group was significantly higher than that of the ALF 0.2 μg/kg-group ($p<0.01$). Moreover, the 0.05 μg/kg of ED-71 significantly increased the cortical area of the mid-femur compared to the vehicle control ($p<0.001$), whereas the 0.2 μg/kg of ALF did not. Bone histomorphometry revealed that in the femoral endocortical surface, ED-71 suppressed bone resorption parameters such as ES/BS and N.Oc/BS greater than ALF in consistent with the effect on bone in ovariectomized high-turnover osteoporosis rat model. Particularly, the 0.05 μg/kg of ED-71 significantly increased bone formation parameters (BFR/BS, MS/BS) in the periosteal surface of femoral cortex compared to the vehicle control ($p<0.001$), however, the ALF 0.2 μg/kg-treatment did not increase these parameters. We conclude that ED-71 improves the mechanical properties not only by inhibiting the endocortical bone resorption but also by stimulating the periosteal bone formation in SAM/P6 mice, suggesting that ED-71 may be a highly potent anti-osteoporotic agent for the prevention of the long bone fracture in the osteoporosis patients.

***Disclosures: Ayako Shiraishi**, Chugai Pharmaceutical Co., Ltd., 3*
This study received funding from: Chugai Pharmaceutical Co., Ltd.

SU0441

Eldecalcitol Suppresses Trabecular and Endocortical Bone Resorption Even at Hypercalcemic Doses by Diminishing Osteoclast on Bone Surface. Hitoshi Saito*[1], Satoshi Takeda[2], Fumiaki Takahashi[1], Minqi Li[3], Paulo Luiz De Freitas[4], Norio Amizuka[5]. [1]Chugai Pharmaceutical Company, Limited, Japan, [2]Chugai Pharmaceutical Co., Ltd, Japan, [3]Hokkaido University, Japan, [4]Niigata University, Japan, [5]Hokkaido University School of Dentistry, Japan

Active vitamin D_3 is thought to be a strong osteoclast inducing agent. It stimulates osteoclastogenesis in *in vitro* co-culture or in vitro organ culture by increasing RANKL and M-CSF expression in osteoblast. Administration of excess dose of vitamin D_3 causes hypercalcemia in rats. Also, vitamin D_3 rescues hypocalcemia of the D-deficient rat fed with calcium-free diet. These observations suggested that vitamin D_3 induced both bone resorption and intestinal calcium absorption. On the contrary, we have shown that active vitamin D_3 suppressed osteoclastogenesis *in vitro* and reduced bone resorption in ovariectomized rats as well as in osteoporotic subjects. Here, we examined the effect of eldecalcitol on bone resorption at hypercalcemic doses in ovariectomized rats.

10 month-old ovariectomized rats were divided into eight groups (n=7~8 each), each group of animals were given either vehicle, eldecalcitol (10, 30 or 90 ng/kg) or calcitriol (33.3, 100, 300, 900 ng/kg), 5-times per week for 4 or 12 weeks. The rats given with 90ng of eldecalcitol or 900ng/kg of calcitriol became mild hypercalcemia, which serum calcium reached above 11mg/dL. However, both eldecalcitol and calcitriol dose dependently increased lumbar spine BMD, also, suppressed bone resorption marker, urine DPD, even at hypercalcemic doses. Bone histomorphometry revealed that eldecalcitol treatment strongly reduced osteoclast number (N.Oc/BS), osteoclast surface (Oc.S/BS) and eroded surface (ES/BS) at the trabecular region of femoral epiphysis as well as the endocortical region of femoral diaphysis. TRAP positive or catepsin K positive osteoclast diminished from the bone surface by the eldecalcitol treatment, simultaneously, ED-1 positive macrophage increased in bone marrow. The activated mature osteoblasts were unchanged, however, the ALP positive preosteoblasts diminished by the eldecalcitol treatment. The TRAP positive osteoclast-like cells became evident at the small hole-like structures in the intracortical region of femoral diaphysis.

These observations may suggest that eldecalcitol inhibited osteoclastogenesis by stimulating the osteoblast maturation *in vivo*, which consequently reduced the osteoclast supporting activity of the osteoblast. Eldecalcitol suppresses bone resorption of the trabecular bone and the endocortial surface of the cortical bone even at hypercalcemic doses, but induces the intracortical bone resorption in the femoral diaphysis.

***Disclosures: Hitoshi Saito**, Chugai Pharmaceutical Co. Ltd., 3*
This study received funding from: Chugai Pharmaceutical Co., Ltd.

SU0442

High Prevalence of Vitamin D Insufficiency in Patients with Osteogenesis Imperfecta. Barbara Santarosa Emo Peteres*[1], Marise Lazaretti Castro[1], Carlos Eduardo Andrade Chagas[2], Ailym Kurata[2], Janaina P Roque[3], Ligia Martini[4]. [1]Federal University of Sao Paulo, Brazil, [2]University of Sao Paulo, Brazil, [3]SESI-SP, Brazil, [4]University of São Paulo, Brazil

Introduction: Osteogenesis imperfecta (OI) is a systemic heritable disorder of connective tissue whose cardinal manifestation is bone fragility. Considerable attention has recently been focused on the pathogenesis, diagnosis and treatment of OI. Unfortunately, until now little is known about vitamin D metabolism as well the nutritional status of patients with OI. Purpose: The purpose of this study was to evaluate the vitamin D metabolism in a group of patients with OI. Methods: Twenty-six (26) patients, 11 male and 15 female, 13 with OI type I and 13 with OI type III, mean age 24.6 (10.2) years old, were selected at the Bone Fragility outpatient clinic of the Federal University of São Paulo in 2008. Serum levels of 25(OH)D3, PTH and CTX were measured by chemiluminescence assay (Elecsys 2010, Roche Diagnostics, EUA), and serum total calcium by colorimetrically assay. Information on dietary intake was obtained by a tree day dietary records. Results: Underweight was observed in 3.8% of subjects, normal weight in 42.3%, overweight in 30.8% and 23.1% presented obesity, according to National Center for Health Statistics growth charts (CDC, 2000) for adolescents and World Health Organization (WHO, 1997) for adults. Mean dietary vitamin D intake was 172.0 (124.0) IU/day, only 29.2% of the subjects met the adequate intake (AI) recommendation of vitamin D/day (200 IU/day). Mean supplementation vitamin D intake was 977.7 (329.1) IU/day. The mean serum levels of 25(OH)D3 was 65.5 (18.8) nmol/l, PTH was 36.8 (16.6) pg/ml, CTX was 0.368 (0.26) ng/ml and serum total calcium was 9.35 (0.43) mg/dL. Considering the 75 nmol/l cut-off for 25(OH)D3 as optimal levels, 76.9% of subjects presented vitamin D insufficiency. Only 7.7% of subjects presented elevated PTH serum level. No statistical significant difference in vitamin D intake and biochemical parameters between subjects of OI type I and III were observed. No significant correlations between 25(OH)D3, PTH and CTX were observed. Conclusion: The present study demonstrated that insufficiency of vitamin D is prevalent

in patients with osteogenesis imperfecta. The dietary intake plus vitamin D supplementation is insufficient to maintain serum levels of vitamin D adequate. Our findings suggest that nutritional strategies and higher levels of supplementation are necessary to guarantee vitamin D sufficiency.

***Disclosures: Barbara Santarosa Emo Peteres**, None.*

SU0443

Verterbral End-Plate Lesions (Schmorl's Nodes) in Lumbar Vertebrae of Cynomolgus Monkeys. Luc Chouinard*. Charles River Laboratories, PCS Montreal, Canada

The purpose of this study was to review and characterize Vertebral End-Plate lesions (Schmorl's nodes) observed microscopically in the lumbar vertebral body of skeletally mature, adult, cynomolgus monkeys. Cynomolgus monkeys (Macaca fascicularis) have been extensively used and characterized more than any other large animal model for osteoporosis research. Schmorl's nodes are considered the most common human non-intervertebral disc abnormalities in magnetic resonance imaging (MRI) and are commonly observed in routine radiographs and autopsy. They represent displacement of the intervertebral disc tissue into the adjacent end plate and/or vertebral body. There is however a high variability in the reported prevalence of Schmorl's nodes in human (38% to 78%). Schmorl's nodes are highly hereditable, occur spontaneously or are related to spine trauma. They are frequently encountered in young adolescent and in patients more than 50 years old.

A total of 77 lumbar vertebrae specimens from adult skeletally mature, intact (sham) or gonadectomized (ORX or OVX) male (37) or female (40) cynomolgus monkeys were included in this review. The vertebral body (L2) samples were embedded in methylmethacrylate, cut at 5 microns in the sagittal plane, stained with Goldner's Trichrome or Toluidine blue stain and evaluated using a conventional light microscope. Vertebral end plate lesions (VEPL) were identified in 31 of 77 monkeys; 9/37 males and 22/40 females. The change was characterized by focal to multifocal disruption of vertebral end plates and was generally limited to the ventral aspect of the vertebral body. Both cephalad and caudal ends were affected in approximately 50% of the affected animals. Herniation of fibrocartilaginous material of the nucleus pulposus was only noted in a few animals (3/31). Minimal or locally extensive osteosclerosis was noted in association with VEPL. The osteosclerosis ranged from minimal to moderate and was accompanied by marrow fibrosis. Concurrent osteophyte formation was noted in the ventral aspect of the vertebral body in 9/31 affected vertebrae. Gonadectomy had no obvious effects in the nature, incidence and/or severity of VEPL in monkeys. No fracture was noted in the any of the reviewed vertebrae. To our knowledge, this change has not been reported previously in cynomolgus monkeys.

VEPL was detected microscopically in 40% of the examined L2 vertebrae of skeletally mature adult male and female cynomolgus monkeys reviewed in this study. The presence of this change should be considered when using the lumbar vertebrae of cynomlgus monkeys in osteoporosis research most notably when considering biomechanics and histomorphometry evaluations. The pathologic features of VEPL observed in cynomolgus monkeys are comparable to the human condition and may help to understand the pathogenesis of this common entity in humans.

***Disclosures: Luc Chouinard**, None.*

SU0444

Bisphosphonate-Associated Osteomyelitis of the Jaw (BAOMJ/ONJ): Pathophysiology and Potential Mechanisms:. Sunil Wimalawansa*. Robert Wood Johnson Medical School, USA

Bisphosphonates are widely used for osteoporosis, Paget's disease, and skeletal complications associated with malignancy (1). While osteonecrosis of the jaw (ONJ) has been described for more than a century, bisphosphonate-associated ONJ (BAON) has been reported only since 2003. BAONJ has a fundamental element of inflammation (secondary to bone-infection), bisphosphonate-associated osteomyelitis of the jaw (BAOMJ) describes this entity accurately than BAON or ONJ (2).

Incidence of BAOMJ increases following oral trauma that exposes maxillary or mandibular bones such as extraction of teeth, dento-alveolar surgery or oral trauma. Contributory factors include poor oral hygiene, oral infections, periodontal disease, corticosteroid administration, chemotherapy, immune suppression, compromised immune status, diabetes, vascular insufficiency, old age, chronic diseases, and malignancies – many consists alterations of immune status. On average, one or two out of every 100,000 patients treated with bisphosphonates for osteoporosis may develop BAOMJ lesions that last over 6 weeks. In cancer patients however, the incidence of BAOMJ is over 1,000 times higher than osteoporosis patients. The greater frequency, higher dosages [e.g., intravenous administration of zoledronic acid (zometa™) or pamidronate (Aredia™), once in every 3 to 4 weeks], and the prolonged use (i.e., for more than two years) are likely to be the key factors triggering BAOMJ in such compromised patients (2).

Current evidence supports local infections and, immune impairment (aggravated by bisphosphonates) as key causes of precipitating BAOMJ (Table 1). Nevertheless, following appropriate guidelines can decrease the risks of BAOMJ in vulnerable patients. Hence, it is appropriate to use the terminology, ''bisphosphonate-associated osteomyelitis of the jaw'' (BAOMJ or OMJ), instead of BAON or ONJ (1,2), and the early use of appropriate antibiotics. The estimated incidence among non-cancer patients receiving bisphosphonate is about 0.001%, while cancer patients receiving intravenous bisphosphonate the incidence is between 0.5% to 4% depending on the dose, frequency and the duration of therapy (average ~2%). Nevertheless, the benefits of bisphosphonates especially in osteoporotic patients and in Paget's diseases of bone are far outweighing the minute risks of BAOMJ.

1. Wimalawansa S.J. Expert Opinion on Drug Safety, 7(4):491-512, 2008.
2. Wimalawansa S.J. Endocrine Practice, 14:1150-1168, 2008.

Hypotheses Illustrating Pathophysiology of BAOMJ:
1. Impaired healing hypothesis
2. Angiogenesis hypothesis
3. Oral mucosal or local bone toxicity hypothesis
4. Bone infection hypothesis
5. Impaired immune hypothesis

Table 1

***Disclosures: Sunil Wimalawansa**, None.*

SU0445

Chlorthalidone Improves Bone Quality in GeneticHypercalciuric Stone Forming Rats. David Bushinsky*[1], Thomas Willett[2], John Asplin[3], Marc Grynpas[4]. [1]University of Rochester, USA, [2]Mount Sinai Hospital, Canada, [3]University of Chicago, USA, [4]Samuel Lunenfeld Research Institute, Canada

We have bred a strain of rats to maximize urine (U) Ca excretion as a model of hypercalciuric nephrolithiasis. These GHS rats now excrete far more urine Ca than control Sprague-Dawley rats, uniformly form kidney stones and, similar to patients, demonstrate lower bone mineral density (BMD). Clinically thiazide diuretics are used to reduce UCa and prevent stone formation; however, whether they have a beneficial effect on bone is not clear. We used GHS rats to test the hypothesis that the thiazide diuretic chlorthalidone (CTD) would have a favorable effect on bone density and quality. Twenty GHS rats received a fixed amount of a standard 1.2% calcium diet and half were also fed chlorthalidone (CTD 4-5 mg/kg/day). Urine was collected weekly and at the conclusion of the 18 wk study the femurs and vertebrae were analyzed. As expected, rats fed CTD had a marked reduction in UCa. Bone quality assessment techniques were used to study the effect of CTD treatment on the axial and appendicular skeleton. CTD treatment caused a significant increase in the bone mineral content and bone mineral density of the lumbar vertebrae, measured by DEXA. Furthermore, an increase in the trabecular mineralization was observed for the CTD group. The increase in BMD in the CTD group agrees with the results from clinical studies, in which BMD measured by DEXA was increased for patients taking CTD. Treatment with CTD also improved the architecture of trabecular bones compared to the vehicle group. As indicated by the structural parameters obtained from μCT, trabecular bone volume (BV/TV), trabecular thickness and trabecular number increased significantly. Additionally, from static histomorphometry, a significant increase in trabecular thickness for the CTD group was detected. Unsurprisingly therefore, CTD also improved the connectivity of trabecular bone. However, CTD did not alter formation parameters. CTD led to a significant improvement in vertebral strength and stiffness measured by vertebral compression. CTD treatment had a greater effect on trabecular bone than on cortical bone. Thus results obtained in genetic hypercalciuric stone-forming rats suggest that CTD can favorably influence vertebral fracture risk. CTD did not alter formation parameters suggesting that the improved bone strength was due to decreased bone resorption and retention of bone structure.

***Disclosures: David Bushinsky**, None.*

SU0446

A Single High Dose of Oral Vitamin D3 Is Insufficient to Correct a Deficiency in a Rheumatologic Population. Delphine Stoll, Olivier Lamy, Marc-Antoine Krieg, Didier Hans, Jean Dudler, Alex So, Berengere Aubry-Rozier*. CHUV, Switzerland

Introduction

Vitamin D plays a major role in bone metabolism and neuromuscular function. Supplementation with vitamin D is effective to reduce the risk of fall and of fracture. However adherence to oral daily vitamin D supplementation is low. Screening and correcting vitamin D insufficiency in a general rheumatologic population could improve both morbidity and quality of life in these patients with chronic painful disorders and at high risk of osteoporosis. After determining the prevalence of vitamin D deficiency in this population, we evaluated if supplementation with a single high dose of oral 25-OH vitamin D3 was sufficient to correct this abnormality.

Methods

During one month (November 2009), levels of 25-OH vitamin D were systematically determined in our rheumatology outpatient clinic and classified into three groups: vitamin D deficiency (<10 μg/l), vitamin D insufficiency (10 to 30μg/l) or normal vitamin D (>30 μg/l). Patients with insufficiency or deficiency received

respectively a single high dose of 300'000 IU or 600'000 IU oral vitamin D3. In addition, all patients with osteoporosis were prescribed daily supplement of calcium (1g) and vitamin D (800 IU). 25-OH vitamin D levels were reevaluated after 3 months.

Results

Vitamin D levels were initially determined in 292 patients (mean age 53, 211 women, 87% Caucasian). 77% had inflammatory rheumatologic disease (IRD), 20% osteoporosis (OP) and 12% degenerative disease (DD). Vitamin D deficiency was present in 20 (6.8%), while 225 (77.1%) had insufficiency. Of the 245 patients with levels <30µg/l, a new determination of vitamin D level was available in 173 (71%) at 3 months (table 1).

Conclusion

Vitamin D insufficiency is highly prevalent in our rheumatologic population (84%), and is not adequately corrected by a single high dose of oral vitamin D3 in more than half of the patients with IRD and DD. In patients with OP, despite association of a single high dose with daily oral vitamin D supplementation, 40% of patients are still deficient when reevaluated at 3 months.

	Time 0 month			Time 3 months			
	Mean Vit D (µg/l)	Deficiency	Insufficiency	Mean Vit D (µg/l)	Deficiency	Insufficiency	Normal
All (N=173)	18.8 (1.5-29.6)	8%	92%	29.8 (7.1-85.2)	1.7%	50.3%	48%
+CaD3 (N=62, 36%)	21.6 (8.3-29.6)	5%	95%	32.4 (13.2-85.2)	0%	42%	58%
No CaD3 (N=111, 64%)	17.3 (1.5-29.1)	10%	90%	28.4 (7.1-55.5)	3%	55%	42%
IRD (N=139)	18.6 (4.3-29.2)	9%	91%	29.4 (7.1-49.8)	2%	50%	48%
+ CaD3 (N=48, 35%)	20.9 (8.3-29.2)	6%	94%	31.5 (13.2-47.9)	0%	44%	56%
No CaD3 (N=91, 65%)	17.3 (4.3-29.1)	11%	89%	28.2 (7.1-49.8)	3%	53%	44%
OP (N=25)	19.8 (1.5-29.6)	8%	92%	34.2 (12.8-85.2)	0%	40%	60%
+ CaD3 (N=19, 76%)	22.0 (9.3-29.6)	5%	95%	35.2 (19.8-85.2)	0%	37%	63%
No CaD3 (N=6, 24%)	13.0 (1.5-26.7)	17%	83%	30.7 (12.8-49.8)	0%	50%	50%
DD (N=20)	19.4 (12.1-29.1)	0%	100%	28.9 (21.2-55.5)	0%	65%	35%
+ CaD3 (N=2, 10%)	26.1 (24.4-27.8)	0%	100%	31.5 (31.5)	0%	0%	100%
No CaD3 (N=18, 90%)	18.6 (12.1-29.1)	0%	100%	28.6 (21.2-55.5)	0%	72%	28%

table 1

***Disclosures: Berengere Aubry-Rozier**, None.*

SU0447

Evaluation of a Novel Vitamin D Bioavailability Test in Normal Subjects and Subjects with Quiescent Inflammatory Bowel Disease. Hataikarn Nimitphong*[1], Francis A. Farraye[2], Arthur F Stucchi[3], Alyson B. Smith[1], Alice Vijjeswarapu[1], Andrew Tanennbaum[1], Rachael Biancuzzo[1], Tai Chen[4], Michael Holick[4]. [1]Vitamin D, Skin & Bone Research Laboratory, Department of Medicine, Endocrinology, Boston University School of Medicine, USA, [2]Center for Digestive Disorders, Section of Gastroenterology, Department of Medicine, Boston University School of Medicine, USA, [3]Department of Surgery, Boston Medical Center, USA, [4]Boston University School of Medicine, USA

Background: Vitamin D deficiency is a common problem in patients with inflammatory bowel disease (IBD). The purpose of this study was to determine the ability of normal subjects and subjects with quiescent IBD to absorb vitamin D_2 using a novel vitamin D bioavailability test. In addition we determined if the location of disease or previous surgery had any influence on the bioavailability of vitamin D_2 in IBD patients.

Methods: Ten normal subjects (50% female) and 41 IBD subjects (4 ulcerative colitis (UC) subjects and 37 Crohn's disease (CD) subjects, 46% female) were included in this study. After a baseline blood draw, all subjects were then given a single 50,000 IU oral dose of vitamin D_2 in a capsule and had their blood drawn 12 hours later to determine the vitamin D_2 level as a measure of their vitamin D_2 absorption capacity.

Results: Forty one percent and 31.3% of IBD subjects were found to be vitamin D deficient or insufficient, respectively. Twelve hours after ingesting 50,000 IU vitamin D_2, vitamin D_2 levels rose from a baseline of 0.7 ± 0.7 ng/mL (mean $\pm$ SEM) to 49.8 ± 3.0 ng/mL in normal subjects. In IBD subjects, baseline vitamin D_2 levels rose from 0 ng/mL to 35.0 ± 2.7 ng/mL. IBD subjects had on average a 30% decrease in their ability to absorb vitamin D_2 ($p<0.01$). Moreover, we found a wide variability of vitamin D_2 bioavailability in IBD subjects. One CD subject who had no gastrointestinal symptoms was found to be unable to absorb vitamin D_2. Thirty two percent and 26.8% of the IBD patients absorbed <50% and 50-80% respectively, when compared with normal subjects. Although we only evaluated 4 subjects with UC, 3 of 4 subjects had suboptimal vitamin D_2 absorption with one had 32% of normal. Anova analysis revealed no statistically difference of vitamin D_2 bioavailability between subjects in CD subgroup stratified by the location of disease, the type of surgery and receiving or not receiving surgery.

Conclusions: More than 72% of subjects with IBD were vitamin D deficient or insufficient. The ability to absorb vitamin D_2 in IBD subjects was unpredictable and the only way to determine this was to perform a vitamin D bioavailability test. There was wide variability in the bioavailability of vitamin D_2 in UC subjects which was unexpected since vitamin D is absorbed in the small intestine and not in the colon. Use of this test may guide the dosage of vitamin D for treating vitamin D deficiency in subjects with IBD.

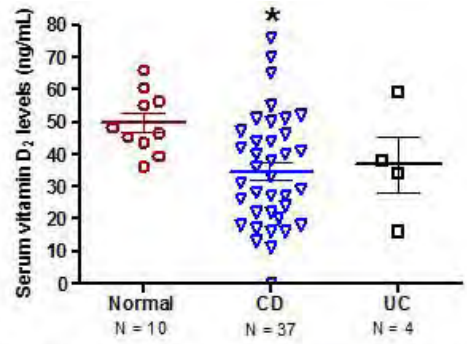

*P = 0.01 when compared the vitamin D_2 levels in subjects with Crohn's disease with vitamin D_2 levels in normal subjects. CD = Crohn's disease UC = Ulcerative colitis

Serum vitamin D2 levels 12 hours after ingesting 50,000 IU vitamin D2 in normal and IBD subjects

***Disclosures: Hataikarn Nimitphong**, None.*

SU0448

Lack of p62 Mutant (P392L) Interaction with CYLD Increases TRAF6 Ubiquitination and NF-κB Signaling in Paget's Disease of Bone. Kumaran Sundaram*[1], Srinivasan Shanmugarajan[1], Sudhaker Rao[2], Sakamuri Reddy[1]. [1]Charles P. Darby Children's Research Institute, USA, [2]Henry Ford Hospital, USA

Paget's disease of bone (PDB) is a chronic focal skeletal disorder that affects 2-3% of the population over the age of 60. PDB is inherited as an autosomal dominant trait with genetic heterogeneity. Sequestome 1 (SQSTM1/p62) UBA domain mutant (P392L) is widely associated with PDB and has been shown to increase osteoclastogenesis, however the molecular mechanisms are unclear. Recently, we showed that p62 (P392L) abolished the interaction with deubiquitinating enzyme CYLD results in up-regulation of c-Fos and NFATc1 transcription factors in preosteoclast cells. In this study, we further demonstrated by co-immune precipitation assay that p62 (P392L) significantly increased TRAF6 ubiquitination in preosteoclast cells. In contrast, no significant change in TRAF6 ubiquitination was observed in the p62 wild-type (wt) and non-UBA domain mutant (A381V) transduced cells. Furthermore, shRNA suppression of CYLD expression significantly increased TRAF6 ubiquitination in p62 wt and non-UBA mutant transduced cells. Interestingly, Western blot analysis identified that p62 (P392L) increased (3.4-fold) the levels of p-IκB in preosteoclast cells. In addition, p62 (P392L) increased (2.8-fold) NF-κB (p65) expression. In contrast, no significant change in the levels of NF-κB was observed in wt and non-UBA domain mutant transduced cells. We next determined if p62 interaction with CYLD modulate NF-κB-Luc reporter gene activity. siRNA suppression of CYLD expression increased (2.4-fold) NF-κB-Luc activity in wt and non-UBA domain mutant (A381V) transfected RAW 264.7 cells. Real-time PCR analysis further demonstrated that shRNA suppression of CYLD expression significantly increased the level of IL-6 and TRAP mRNA expression in preosteoclast cells. These results suggest that the lack of p62 UBA mutant (P392L) interaction with CYLD up-regulate NF-κB signaling and enhanced osteoclast development in PDB.

***Disclosures: Kumaran Sundaram**, None.*

SU0449

Changes in the Clinical Manifestations of Primary Hyperparathyroidism during the Past Two Decades in the Canary Islands, Spain. M del Val Groba-Marco[1], Ana Mirallave-Pescador[2], Elisa González-Rodríguez[1], Sabrina García-Santana[3], Esther González-Padilla[4], Pedro Saavedra-Santana[3], Manuel Sosa-Henriquez*[1]. [1]University of Las Palmas de Gran Canaria, Spain, [2]University Las Palmas de GC, Spain, [3]University of Las Palmas de GC, Spain, [4]University of Las Palmas GC, Spain

Introduction

Primary hyperparathyroidism (PHPT) has a variable clinical expression. Symptomatic PHPT is still the predominant form of the disease in many parts of the world, especially developing countries. Because the clinical profile of the disease has changed from that described in the past, we sought to improve our understanding of the disease

in patients in The Canary Islands and the possible changes in the clinical manifestations of the disease after two decades: 1989-1999 vs 2000-2009.

Methods

We summarized the clinical presentation, biochemical and radiological features, from the case records in the last 20 years of 221 patients at a tertiary care centre in Gran Canaria, Canary Islands, Spain, who had documented PHPT

Results

Are shown in tables.

Conclusions

The clinical pattern of PHPT has changed little. Patients are now diagnosed at an earlier age, and have greater height and weight than patients diagnosed a decade ago, but the clinical manifestations are similar in this decade compared to the previous one.

Table 1. Basal characteristics of the population studied.

	1989-1999	2000-2009	p value
Number. (Male/Female)	105 (6/99)	116 (8/108)	
Age (years)	61,2 ± 10,4	58,7 ± 9,6	0,012
Height (cm)	156 ± 6,7	158,3 ± 6,2	0,008
Weight (Kg)	70,5 ± 12,7	74 ± 12,8	0,042
BMI (Kg/m²)	28,9 ± 5,4	29,2 ± 4,8	0,662

Basal characteristics of the population

Table 2. Clinical manifestations of PHPT listed by decade

Clinical manifestations	1989-1999	2000-2009	P value
Number	105	116	
Hypercalcemia	87,1%	91%	0,649
Increase of serum PTH	100%	100%	NA
Chronic renal failure	4,1%	3,5%	0,916
Weakness/Fatigue	29,8%	42,5%	0,107
Osteitis Fibrosa	6,1%	3,7%	0,495
Urolithiasis	34%	28%	0,448
Arterial Hypertension	46,1%	51%	0,574
Depresive Symptoms	65,6%	59,3	0,470
Gatrointestinal disturbances	26,9%	30,2%	0,759
Fragility fractures	12,4%	14,3%	0,841

Clinical manifestations of PHPT listed by decade

***Disclosures: Manuel Sosa-Henriquez**, None.*

SU0450

Determinants of Plasma Parathyroid Hormone Levels in the National Health and Nutrition Examination Survey. Julie Paik*[1], Eric Taylor[2], Wildon Farwell[3]. [1]Brigham & Women's Hospital, USA, [2]Division of Nephrology & Transplantation, Maine Medical Center, USA, [3]Massachusetts Veterans Epidemiology Research & Information Center, VA Boston Healthcare System, & Division of Aging, Department of Medicine, Brigham & Women's Hospital, Harvard Medical School, USA

Background: Previous studies delineating associations between non-classic factors and parathyroid hormone levels have either been small studies or did not include non-whites or older women.

Purpose/Methods: We studied cross-sectional associations between demographic, dietary, and serum factors and intact PTH in 4,026 white, 1,792 black, and 1,834 Mexican-American adult participants without chronic kidney disease from the 2003-2004 and 2005-2006 National Health and Nutrition Examination Surveys.

Results: Median serum PTH was 39.0 pg/ml. After adjusting for 25-hydroxyvitamin D and other factors, smoking compared to non-smoking was associated with lower PTH level across races, ranging from -4.1 pg/ml (95% CI -7.2 to -0.9) in Mexican-Americans to -6.0 pg/ml (95% CI -8.7 to -3.4) in blacks. The highest compared to lowest quartile of uric acid level was associated with higher PTH across races, ranging from 4.5 pg/ml (95% CI 2.4 to 6.7) in whites to 5.7 pg/ml (95% CI 3.0 to 8.3) in blacks. PTH was higher in females compared to males, ranging from 1.8 pg/ml (95% CI -0.8 to 4.3) in Mexican-Americans to 4.4 pg/ml (95% CI 1.8 to 7.1) in blacks, and was higher in older (> 60 years) compared to younger participants (< 30 years), ranging from 3.6 pg/ml (95% CI 1.3 to 5.9) in Mexican-Americans to 7.9 pg/ml (95% CI 5.2 to 10.5) in blacks. In whites but not blacks, higher phosphorus intake, lower serum phosphorus level, and lower retinol level were associated with higher PTH. No association was found between PTH and BMI, or between menopause and PTH in women.

Conclusion: Numerous factors not classically associated with calcium-phosphorus metabolism impact PTH in adults without chronic kidney disease. In addition, these findings emphasize the need for further research in race-related differences in phosphorus handling.

***Disclosures: Julie Paik**, None.*

SU0451

Germline and Somatic Mutations of *CDKN1B*, encoding $p27^{Kip1}$, in Sporadic Parathyroid Adenomas. Jessica Costa-Guda*[1], Ilaria Marinoni[2], Sara Molatore[2], Natalia Pellegata[2], Andrew Arnold[3]. [1]University of Connecticut Health Center, USA, [2]Institute of Pathology, Helmholtz Zentrum München, Germany, [3]University of Connecticut School of Medicine, USA

Typical nonfamilial (sporadic) parathyroid adenomas are common tumors for which only a few clonally altered driver genes and no predisposing DNA mutations or variants have been identified. We considered *CDKN1B*, which encodes the cyclin-dependent kinase inhibitor $p27^{kip1}$, as a candidate gene for involvement in sporadic parathyroid adenomas because germline alterations of this gene (a) cause a complex multiple endocrine tumor phenotype in rats and (b) have been implicated a rare human familial multiple endocrine neoplasia disorder (MEN1-like), both of which can involve the parathyroid glands. We therefore sought to determine whether mutation in *CDKN1B* might be a novel contributor to the development of typical parathyroid adenomas. *CDKN1B* was sequenced in 86 adenomas from patients with typical, sporadic presentations of primary hyperparathyroidism. *CDKN1B* mutations were identified in 4 adenomas. Biallelic alteration of *CDKN1B*, resulting from somatic mutation plus acquired loss of heterozygosity, was detected in one tumor. In two cases, germline mutations were documented despite nonfamilial presentations. Another adenoma, from an unrelated patient, contained a mutation identical to one of the latter two, therefore considered likely to also be heritable despite the unavailability of matched germline DNA for this patient. None of the mutations were found in 240 *CDKN1B* alleles from normal individuals, nor among over 2000 previously reported alleles. Identified mutations reduced levels of $p27^{kip1}$ protein or altered its stability *in vitro*. In addition to the adenomas with somatic or germline intragenic *CDKN1B* mutations, 4 had acquired haploinsufficiency, i.e. clonal loss of a single allele, for a total of 9.3% of adenomas with *CDKN1B* gene abnormalities.

In typical, sporadic parathyroid adenomas, *CDKN1B* mutation can be somatic and clonal, indicative of a directly conferred selective advantage in parathyroid tumorigenesis and providing important support for *CDKN1B* as an authentic human tumor suppressor. Additionally, the presence of unexpected germline *CDKN1B* mutation in patients with sporadic disease identifies *CDKN1B* as a new susceptibility gene in the development of typical parathyroid adenomas.

***Disclosures: Jessica Costa-Guda**, None.*

SU0452

Postoperative Hypoparathyroidism Leading to Impressive Increases in Bone Mineral Density Over 6 years in a 36-year Old Woman. Karin Amrein*[1], Hans Dimai[2], Harald Dobnig[1], Astrid Fahrleitner-Pammer[2]. [1]Medical University of Graz, Austria, [2]Medical University Graz, Austria

INTRODUCTION

Permanent hypoparathyroidism is a rare complication of thyroid surgery. Treatment is symptomatic with calcium and/or calcitriol, firstly aiming at an attenuation of clinical symptoms and secondly at stabilization of serum calcium levels.

It is well known that absence of parathyroid hormone (PTH) may lead to decreased bone turnover, resulting in impressive bone mineral density (BMD) gains over time, as has been shown in several cross-sectional studies before. However, until now, no longitudinal studies or case reports documenting individual BMD increases have been published.

CASE REPORT

A 36-year-old woman with intermittent paresthesia and muscle weakness presented to the endocrinology outpatient department in 2004. She had undergone total thyroidectomy with cervical lymphadenectomy due to micropapillary thyroid carcinoma three years earlier. At the time of presentation, lab analysis revealed hypocalcaemia and hyperphosphataemia concordant with severe hypoparathyroidism. Laboratory data are shown in Table 1. Bone turnover markers were low throughout the entire observation period. Over the years, the patient was treated with 1500 – 2500mg calcium and 0.50 µg calcitriol daily, with dose adjustments depending on clinical symptoms. Additionally, the patient received 100 to 160 µg of levothyroxine as TSH-suppressive therapy. Besides laboratory assessment, DXA scans were part of routine aftercare. DXA scans revealed an impressive BMD increase (Figure 1).

DISCUSSION

Postoperative hypoparathyroidism is a complication affecting 0.2-2.5% of patients undergoing thyroidectomy. Total thyroidectomy, female sex, underlying Graves' disease and one or no identified parathyroid glands intraoperatively are associated with a higher risk. In persistent hypoparathyroidism, absent or reduced PTH leads to low bone turnover and increases in bone mineral density, mainly attributable to

increases in trabecular bone. Hypoparathyroid patients have greater cancellous bone volume, trabecular width and cortical width when compared to matched controls, while mineralising surface and bone formation rate are suppressed. Prolonged decreased bone turnover may lead to poor bone quality and elevated fracture risk. Longitudinal prospective data on BMD, bone histomorphometry and clinical endpoints like fracture risk in hypoparathyroid subjects are urgently needed.

	Normal range	Mar 04	Apr 05	Jun 06	Aug 07	Aug 08	Dec 09
TSH, µIU/ml	0.1-4.0	0.01	0.00	-	0.00	-	1.04
PTH, pg/ml	15-65	1.4	4.2	8.8	6.8	5.5	7.9
Serum calcium, mmol/l	2.2-2.65	1.80	2.24	2.11	2.23	2.18	2.06
Ionized calcium, mmol/l	1.15-1.35	0.84	0.89	0.98	1.03	0.99	0.93
Serum phosphate, mmol/l	0.84-1.54	1.71	1.65	1.66	1.58	1.47	1.40
Osteocalcin, ng/ml	1.0-35.0	7.0	6.5	14.8	11.2	6.8	9.8
ß-Crosslaps, ng/ml	0.03-0.44	0.03	0.05	0.17	0.09	0.02	0.06

Table 1

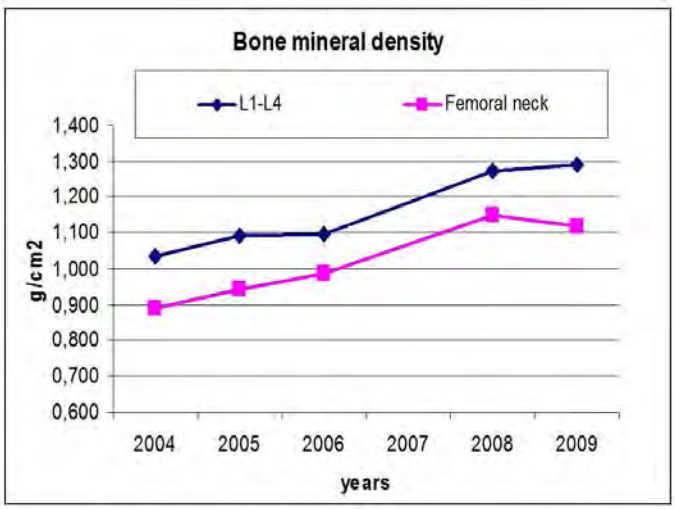

Figure 1

***Disclosures: Karin Amrein**, None.*

SU0453

Use of Cinacalcet to Normalize Serum Calcium and Clarify the Mechanism of Hypercalcemia in a Patient with Pseudohypoparathyroidism Type 1b. Rachel Hopkins*, Arnold Moses. State University of New York Upstate Medical University, USA

Cinacalcet is FDA approved for use in end-stage renal disease and parathyroid carcinoma. It also may be effective in primary hyperparathyroidism and X-linked hypophosphatemic rickets. We present the case of a 60-year-old woman with pseudohypoparathyroidism type 1b (PsHP 1b) who developed tertiary hyperparathyroidism in whom cinacalcet has been used both to treat hypercalcemia and help clarify the pathophysiology of her disease.

The patient has been followed in our clinic for 40 years for PsHP 1b. For decades her calcium levels were maintained in the normal range (mean serum Ca++ 8.9 mg/dL) with 1gram calcium and 50,000 IU ergocalciferol daily. Over the past several years her serum Ca++ gradually increased to a maximum of 11.1 mg/dL. Despite reduction of the vitamin D dose to nutritional levels, the serum Ca++ remained elevated with phosphorus levels in the low-normal range. In addition, bone specific alkaline phosphatase (BSAP) and 1,25(OH)2 vitamin D were elevated with PTH 4-5 times upper limit of normal.

In autumn of 2009, she was started on cinacalcet 60mg daily. A month later serum Ca++ had dropped to 8.0 mg/dL and PTH had decreased by half to 248 pg/ml. She developed nausea and symptoms of hypocalcemia and the dose of cinacalcet was decreased to 30mg daily. Calcium increased to 8.9 mg/dL and symptoms resolved. Serum Ca++ levels have since been between 8.7 – 9.1 mg/dL. At the same time, BSAP and 1,25 (OH)2 Vitamin D have decreased by about half and serum phosphorus and urine calcium excretion have increased.

PsHP type 1b is a condition of PTH resistance primarily in the renal tubules. In our patient, changes in BSAP before and after cinacalcet treatment provide evidence of bone response to PTH, a situation that has been described radiologically in PsHP 1b. Perhaps more intriguing is the apparent renal sensitivity to PTH as evidenced by changes in 1,25(OH)2 vitamin D and urine calcium excretion. Changes in serum phosphorus also likely represent effects of lowered PTH level on renal tubular phosphorus resorption.

To our knowledge, no other case of tertiary hyperparathyroidism has been described in PsHP 1b. Cinacalcet has been effective in lowering PTH and serum Ca++ in this patient, while concurrent biochemical responses have been useful in understanding the pathophysiology of her hypercalcemia. We continue to follow our patient closely.

***Disclosures: Rachel Hopkins**, None.*

SU0454

Vitamin D status, Physical Performance and Body Mass in Patients Surgically Cured for Primary Hyperparathyroidism Compared with Healthy Controls - A Cross-sectional Study. Anne Kristine Amstrup*, Lars Rejnmark, Tanja Sikjaer, Lars Rolighed, Peter Vestergaard, Lene Heickendorff, Leif Mosekilde. Aarhus University Hospital, Denmark

Background: Low plasma 25-hydroxyvitamin D (25OHD) levels, reduced muscle strength, and increased body mass index (BMI) are well-known characteristics of patients with primary hyperparathyroidism (PHPT). The underlying mechanism for low vitamin D levels and increased BMI and whether it changes after parathyroidectomy is however unknown. Muscle strength has been reported to increase following surgical cure, but whether the improved performance corresponds to healthy controls is largely unknown.

Methods: Between February and Marts 2009 we studied, 51 former PHPT patients (mean age 61(36-77) years) successfully treated by surgery (mean time since operation 7.4 years (range 5-15)), and 51 sex- and age matched healthy controls. We studied functional performance including "repeated chair stand" (RCS), "timed up and go" (TUG), muscle strength (hand grip, elbow flexion/extension and knee flexion/extension (60˚/90˚) on dominant hand side), and postural stability using a force platform as well as biochemistry and anthropometric indices.

Results: Among cases, 41 had pathological verified adenoma, 3 had hyperplasia, in 3 cases diagnosis was uncertain, and in 4 patients data was missing.

Dietary calcium intake and vitamin D supplementation, and biochemistry including PTH and 25OHD levels, did not differ between groups. Former patients had a significantly ($p<0.01$) higher body mass index ($28.8\pm6.0 kg/m^2$) than controls ($26.0\pm4.7 kg/m^2$ groups. Muscle pains was more frequently reported by cases than controls and cases performed RCS slower than controls ($p=0.02$). Compared with controls, female cases had lower muscle strength in knee flexion at 60˚ ($p=0.03$) and 90˚ ($p=0.06$). However, former PHPT patients did no longer differ from the controls following adjustment for BMI.

Conclusion: Following surgical cure for PHPT, 25OHD levels are normalized suggesting that vitamin D insufficiency is not a constitutional finding in these patients. However, an increased BMI seems to be sustained. Whether this is caused by decreased muscle strength or the reduced muscular performance is due to adiposity needs further investigations.

***Disclosures: Anne Kristine Amstrup**, None.*

SU0455

Differences in Structural and Material Properties of Low and High Turnover Bone. Daniel Porter[1], Raymond Wright[2], David Pienkowski[3], Marie-Claude Faugere[4], Hartmut Malluche*[4]. [1]Center for Biomedical Engineering, University of Kentucky, USA, [2]Department of Orthopedics, University of Kentucky, USA, [3]University of Kentucky, USA, [4]University of Kentucky Medical Center, USA

This IRB approved study was conducted to evaluate the relationships between bone turnover and bone quality as quantified by mineral, matrix, nanomechanical, and histomorphometric parameters of bone. Anterior iliac crest bone samples from 35 female Caucasian patients with stage-5 chronic kidney disease were studied. Eighteen patients had low bone turnover and 17 had high bone turnover as determined by qualitative and quantitative histology. For comparison, 16 additional bone samples were obtained from normal female Caucasian volunteers. Bone specimens were analyzed without mineral removal by histomorphometry, Fourier Transform Infrared (FTIR) Spectroscopy, and nanoindentation for material (mineral and matrix) and mechanical (stiffness and hardness) properties. Cancellous bone volume and trabecular thickness in high bone turnover were 27.2% and 21.8% greater ($p=0.02$ and $p=0.03$,) than in normal bone turnover. High bone turnover had 10.0% or 11.3% less ($p<0.01$) relative mineral content (mineral-to-matrix ratio) than low or normal bone turnover (Table 1). High bone turnover compared to normal bone turnover had: a) 8.7% less ($p<0.03$) mineral purity (carbonate-to-phosphate ratio), b) 4.5% smaller mineral crystals ($p<0.07$, c-axis length), c) 11.9% less stiffness ($p<0.04$), and d) 10.2% less hardness ($p=0.17$) (Table 2). Low bone turnover compared to normal bone turnover had 13.1% less mineral purity ($p<0.05$). Moreover, we found that cortical thickness, trabecular bone volume, and trabecular thickness were decreased in low bone turnover compared to normal bone

turnover. The degree of matrix crosslinking was not different among the various rates of bone turnover These data show abnormal bone quality in high and low turnover. The abnormalities in high bone turnover are primarily manifested by material properties while in low bone turnover the differences are primarily structural.

***Disclosures: Hartmut Malluche**, None.*

SU0456

Reduction of Whole PTH/Intact PTH Ratio is a Predictor of Bone Metabolism by Cinacalcet Treatment in Hemodialysis Patients with Secondary Hyperparathyroidism. Masafumi Kurajoh*[1], Masaaki Inaba[2], Senji Okuno[3], Harumi nagayama[4], Shinsuke Yamada[5], Yasuo Imanishi[1], Eiji Ishimura[2], Shigeichi Shoji[6], Tomoyuki Yamakawa[7], Yoshiki Nishizawa[8]. [1]Osaka City University Graduate School of Medicine, Japan, [2]Department of Metabolism, Endocrinology & Molecular Medicine, Internal Medicine, Osaka City University Graduate School of Medicine, Japan, [3]Shirasagi Hospital, Japan, [4]Nagayama Hospital, Japan, [5]Department of Metabolism, Endocrinology & Molecular Medicine, Osaka City University Graduate School of Medicine, Japan, [6]Minami-Osaka Hospital, Japan, [7]Shirasagi-Hospital, Japan, [8]Osaka City University Medical School, Japan

Background: Cinacalcet suppresses secretion of parathyroid hormone (PTH) partly by enhancing PTH(1-84) degradation into N-truncated PTH fragments. Objectives: To investigate the significance of N-truncated PTH/PTH(1-84) ratio to predict the effect of cinacalcet in hemodialysis (HD) patients. Subjects and Methods: Various parameters were measured in serum during 12 weeks of oral cinacalcet administration at 25 mg daily in 39 HD patients with secondary hyperparathyroidism. Results: Serum cCa, Pi, whole-PTH (W-PTH), intact-PTH (I-PTH) and W-PTH/I-PTH ratio, decreased significantly in a time-dependent manner after initiation of cinacalcet administration, which serum tartrate-resistant acid phosphatase (TRAP) 5b reflected more precisely than serum N-telopeptide of type-I collagen (NTX). At 1 week, the reduction rate of I-PTH and W-PTH correlated significantly with that of serum Pi, but not cCa. The reduction rate of serum Pi, but not cCa correlated significantly with that of serum TRAP5b at both 4 and 12 weeks. The reduction rate of serum W-PTH correlated significantly with that of serum TRAP5b at both 4 and 12 weeks, while that of serum I-PTH correlated significantly only at 12 weeks. The reduction rate of serum W-PTH/I-PTH ratio correlated significantly with that of serum TRAP5b at both 4 and 12 weeks, and that of serum W-PTH/I-PTH ratio at 4 weeks showed a tendency toward a correlation with that of serum TRAP5b at 12 weeks. HD patients with the reduction in W-PTH/ I-PTH ratio during the first 4 week showed a significantly greater rate of TRAP5b reduction during 12 week than those without. Conclusion: W-PTH and W-PTH/I-PTH ratio, which allows for estimation of the potency of cinacalcet to enhance PTH degradation, are more reliable marker than I-PTH to reflect cinacalcet-induced bone resorption.

***Disclosures: Masafumi Kurajoh**, None.*

SU0457

Serum ICTP can be a Surrogate Marker of Coronary Unstable Plaques. Itsuro Endo*[1], Mitsunori Fujimura[2], Rika Kido[1], Ken-ichi Aihara[1], Yuichi Fujinaka[1], Takashi Iwase[1], Masashi Akaike[1], Masahiro Abe[3], Toshio Matsumoto[1]. [1]University of Tokushima Graduate School of Medical Sciences, Japan, [2]Takamatsu City Hospital, Japan, [3]University of Tokushima, Japan

Coronary unstable plaques cause acute coronary syndrome including unstable angina and acute myocardial infarction. However, characterization and evaluation of coronary plaques depends on invasive examination such as intravascular ultrasonography (IVUS) and fiberscope. ICTP is a type I collagen marker produced by matrix metalloproteinase (MMP)-dependent digestion. The fact that atherosclerotic lesions, particularly coronary unstable plaques, are rich in both type I collagen and macrophages producing MMPs led us to hypothesize that serum ICTP concentrations may be a non-invasive marker of such plaques. Thus, in the present study, we examined association between serum concentrations of ICTP and coronary unstable plaques in patients with possible coronary heart disease (CHD). We recruited 46 men and 17 wemen (mean age 67.6) who underwent coronary angiography with IVUS from September 2005 to September 2007 at Takamatsu City Hospital. Written informed consent was obtained from all patients for participation in the study. Patients with renal dysfunction, metabolic bone diseases or thyroid diseases that are known to affect serum ICTP levels, were excluded. All patients evaluated for coronary risk factors including dyslipidemia, sex, current smoking, diabetes mellitus or hypertension. At the mutivariate analysis, only ICTP was independently and positively associated with necrotis core (NC) area, an index of coronary unstable plaque ($p<0.05$). Futhermore, patients with coronary plaque containing more than 10% NC area had significantly higher ICTP concentrations compared to those with plaques having less than 10% NC area (8.96 vs 4.29, $p<0.04$). We therefore conclude that serum levels of ICTP may be useful as a non-invasive marker of coronary unstable plaque in high risk patients.

***Disclosures: Itsuro Endo**, None.*

SU0458

Circulating Osteogenic Cells Increased in HIV+ Postmenopausal Women on Antiretroviral Therapy. Michael Yin*[1], J. Sanil Manavalan[1], Chiyuan Zhang[1], Stavroula Kousteni[2], Donald McMahon[3], Ivelisse Colon[2], Mishaela Rubin[1], David Ferris[4], Elizabeth Shane[3]. [1]Columbia University, USA, [2]Columbia University Medical Center, USA, [3]Columbia University College of Physicians & Surgeons, USA, [4]Bronx Lebanon Hospital Center, USA

HIV infection and antiretroviral agents (ARVs) are increasingly recognized to be associated with excess bone loss and fractures, particularly in older HIV+ adults. In this regard, we have previously reported lower BMD, higher bone turnover markers and higher rates of bone loss in HIV+ postmenopausal (PM) minority women than HIV- controls. In addition, we found increased differentiation of osteoclast-like cells from adherent peripheral blood mononuclear cells (PBMCs) exposed to autologous serum in HIV+ women on ritonavir-boosted protease-inhibitor (PI/r) based regimens compared to other regimens and to HIV- women. However, it is unclear whether cellular mechanisms underlying excess bone loss also include effects on osteoblasts and whether they are synchronous with effects on osteoclasts. We therefore characterized osteogenic cells circulating in the peripheral blood using flow cytometry and antibodies against osteocalcin (OCN), an osteoblast-specific protein product, CD34 (an early hematopoietic stem cell marker) and CD146 (an early mesenchymal stem cell marker). We evaluated the effect of HIV infection and ARVs on circulating osteogenic cells in a subset of HIV+ (N=21) and HIV- (N=25) Hispanic and African American PM women participating in a cohort study. Mean age of subjects was 59+11 and 63% were Hispanic. The percent of OCN+ osteogenic cells was slightly but not significantly higher in HIV+ than HIV- women (1.8+/-0.9% vs 1.3+/-0.5%, p=0.17). However, the proportion of OCN+ cells lacking the CD34 marker (OCN+CD34-) was significantly higher in HIV+ than HIV- women (87.8+/-8.8% vs 70.5+/-11.9% $p<0.001$). Similarly, the proportion of OCN+ cells lacking both CD34 and early mesenchymal CD146 markers (OCN+CD34-CD146-) was also higher in HIV+ women (83.8+/-14.6% vs 61.0+/-11.3%, p=0.003). Among HIV+ women, the proportion of total OCN+ cells, OCN+CD34- or OCN+CD34-CD146- cells did not differ in HIV+ women on non-nucleoside reverse transcriptase inhibitor (N=10) and PI/r-(N=10) based regimens. In summary, in HIV+ PM women on ARVs, a greater proportion of circulating OCN+ osteogenic cells lack early cell markers compared to HIV- PM women, without any discernible difference by ARV class. The increased proportion of more mature osteogenic cells among HIV+ women on ARVs is likely to be a compensatory mechanism for HIV and/or ARV induced bone resorption. However, a primary increase in osteoblast activity or maturation cannot be excluded.

***Disclosures: Michael Yin**, None.*

SU0459

Effect of Tapering Glucocorticoids for Bone and Mineral Metabolism in Patients with Rheumatoid Arthritis Taking Etanercept. Daihei Kida*. National Hospital Organization Nagoya Medical Center, Japan

Purpose: To evaluate change in bone quality in patients with rheumatoid arthritis (RA) by quantification of several bone biochemical markers, after etanercept (ETN) treatment with reductions in glucocorticoid (GC) dosages, while maintaining a clinical response. Method: Thirty patients with RA (mean age 55.3, 6 males and 24 females) were assessed and divided into two groups: treated with GC (G group; n=16) and treated without GC (C group; n=14). Demographic, clinical and laboratory features of patients are presented in Table 1. Levels of serum osteocalcin (OC), serum undercarboxylated osteocalcin (ucOC), serum bone specific alkaline phosphatase (BAP), serum tartrate resistant acid phosphatase isoform 5b (TRAP-5b), serum calcium (Ca), serum phosphorus (P) and clinical variables were measured at baseline and 24 weeks after ETN administration (25mg twice a week). Result: Clinical variables and levels of biochemical markers before and after ETN administration are presented in Table 2a and 2b. Although significant differences between G group and C group were found on mean OC levels and mean ucOC levels before treatment, no significant differences were found on mean OC levels and mean ucOC levels after treatment. Of interest, though significant strong differences between G group and C group were found on mean Ca levels ($P<0.001$) before treatment, significant weak differences were also found on mean Ca levels ($P<0.05$) after treatment. Conclusion: ETN administration significantly inhibited inflammation, disease activity and physical disability in both group. Even if GC administration inhibited bone and mineral metabolism, ETN drastically enabled tapering off of GC and prevent from GC induced bone difficulty.

Table 1

Demographic, clinical and laboratory features of patients

	Glucocorticoid Group (n=16)	Control Group (n=14)	*P-value* (G vs C)
Age (yrs.)	57.5+/4.7	52.4+/-10.8	NS
Disease duration (yrs.)	7.4+/-6.4	10.6+/-9.4	NS
Stage	2.8+/-0.9	2.8+/-1.1	NS
Class	2.6+/-0.4	2.4+/-0.5	NS

(Data are presented as the mean+/-SD.)
(Two-sided *P* value for the comparison between G Group and C Group are determined by Mann-Whitney test.)

TABLE 1

Table 2a.
Clinical variables and levels of biochemical markers before ETN administration

	Glucocorticoid Group (n=16)	Control Group (n=14)	*P-value* (G vs C)
Glucocorticoids (mg/D)	5.0+/-3.3	0.0+/-0.0	<0.001
DAS28ESR-4	6.3+/-1.2	5.6+/-1.5	NS
mHAQ	0.9+/-0.6	0.6+/-0.5	NS
BAP (U/L)	24.3+/-9.2	27.7+/-10.2	NS
ucOC (ng/mL)	2.7+/-1.5	6.1+/-3.2	<0.01
OC (ng/mL)	3.6+/-1.9	6.6+/-1.3	<0.001
NTx (nmolBCE/mmolCr)	66.7+/-34.8	61.9+/-24.4	NS
TRAP-5b (mU/dL)	251.4+/-126.4	275.5+/-100.4	NS
Ca (mg/dL)	9.7+/-0.3	9.2+/-0.2	<0.001
P (mg/dL)	3.5+/-0.6	3.3+/-0.5	NS
ucOC/OC	0.8+/-0.4	0.9+/-0.5	NS

TABLE 2A

Table 2b.
Clinical variables and levels of biochemical markers after ETN administration
(⇓:*P*<0.05, ⇓⇓:*P*<0.01, ⇓⇓⇓:*P*<0.001, vs before)

	Glucocorticoid Group (n=16)	Control Group (n=14)	*P-value* (G vs C)
Glucocorticoids (mg/D)	2.6+/-1.4 ⇓⇓⇓	0.0+/-0.0	<0.001
DAS28ESR-4	4.0+/-1.3 ⇓⇓⇓	3.6+/-1.0 ⇓⇓	NS
mHAQ	0.5+/-0.4 ⇓	0.3+/-0.3 ⇓	NS
BAP (U/L)	34.8+/-17.5 ⇑⇑⇑	32.5+/-10.7 ⇑	NS
ucOC (ng/mL)	6.9+/-4.6 ⇑⇑⇑	7.7+/-3.7	NS
OC (ng/mL)	5.7+/-2.8 ⇑⇑	7.5+/-3.1	NS
NTx (nmolBCE/mmolCr)	67.6+/-37.2	68.4+/-23.4	NS
TRAP-5b (mU/dL)	314.1+/-181.7 ⇑	323.2+/-127.1	NS
Ca (mg/dL)	9.3+/-0.3 ⇓⇓	9.1+/-0.1 ⇓	<0.05
P (mg/dL)	3.5+/-0.5	3.6+/-0.4 ⇓	NS
ucOC/OC	1.3+/-0.6 ⇑⇑⇑	1.1+/-0.5	NS

Two-sided *P* value for the comparison between G Group and C Group are determined by Mann-Whitney test.
Two-sided *P* value for the comparison between baseline and 6 months in each group are determined by Wilcoxon signed rank test.

TABLE 2B

***Disclosures: Daihei Kida**, None.*

SU0460

Hypovitaminosis D in patients with Type 2 Diabetes Mellitus: Relationship with Microvascular Complications. Hala Ahmadieh[1], Sami Azar[1], NAJLA LAKKIS[2], Maya Barake[1], Asma Arabi*[1]. [1]Internal Medicine, American University of Beirut, Lebanon, [2]Family Medicine, American University of Beirut, Lebanon

Background: Hypovitaminosis D has been reported in patients with type 2 diabetes mellitus (DM2) but studies assessing the relationship between vitamin D (Vit-D) and diabetic complications are scarce. Objectives: to assess the relationship between serum 25 (OH) VitaminD [25-OHD] and diabetes control and microvascular complications in patients with DM2. Methods: Patients attending a specialty clinic at our tertiary care center, in whom data on HbA1c, Urine microalbumin/creatinine (malb/cr) and diabetic retinopathy (DR) were checked as part of routine follow up for diabetics were invited to participate in the study. Data from 112 patients (49 men & 63 women), aged 59±11 years with a mean duration of DM2 of 8.9±7 years were collected so far. Serum calcium, phosphorous & creatinine were measured. Serum 25-OHD was measured by RIA[a] using the Immunodiagnostic System Limited, UK. The presence of diabetic neuropathy (DN) was assessed using the United Kingdom Screening Score[b]. Results: 30% of subjects were on Vit-D supplements. Mean 25-OHD level was 19.6±16 ng/ml. Women had lower levels than men (17.1±9 vs 22.8±15, p=0.03). 20% of subjects had 25-OHD levels below 10 ng/ml and 60% had levels below 20 ng/ml. The mean HbA1c was 7.9±1.6%. Serum creatinine ranged between 0.3-1.6 mg/dl and mean serum calcium & phosphorus were within normal. Serum 25-OHD correlated negatively with HbA1c (r=-0.20 p= 0.049) but not with malb/cr. Mean 25-OHD levels were lower in subjects with DR compared to those without DR (12.3±5.5 vs 21.8±13.7, p< 0.001) and in subjects with DN compared to those without DN (16.4±10.4 vs 23.5±14.5, p=0.004). Furthermore, using a cut-off value of 20 ng/ml, DR and DN were more prevalent in subjects with hypovitaminosis D than those with adequate 25-OHD levels (28% vs 7%, p=0.006 for DR and 63% vs 42%, p=0.03 for DN). This relationship persisted after adjustment for age, duration of DM2, HbA1c, gender and Vit-D intake in multivariate logistic regression analyses (p=0.001 for DR & p=0.04 for DN). No similar relationship was observed with diabetic nephropathy. Conclusion: Serum 25-OHD level correlated with diabetes control and was an independent predictor of DR and DN in patients with DM2. Correction of coexistent hypovitaminosis D may be an important step in the management of DM2 and in the prevention of its complications

[a]Our center participates in the international quality assurance program for Vit-D assays DEQAS, London, UK

[b]young et al, diabetologia 1993

***Disclosures: Asma Arabi**, None.*

SU0461

Multifocal Nodular Periostitis Associated with Voriconazole. Charles Kenney[1], Fergus McKiernan*[2]. [1]Department of Radiology, USA, [2]Marshfield Clinic, USA

A recent single case series [1] has associated voriconazole with an unusual painful condition of multifocal, nodular periostitis. We present radiographic, CT and scintigraphic findings and clinical follow-up of a similar case.

Case report: A 69 yr old steroid-dependent female with no significant past musculoskeletal history developed progressive axial and long bone pain in 8/2009 followed by acute painful swelling of the hands that led to rheumatologic consultation 2/2010. Her PMH was dominated by progressive COPD for which she underwent right lung transplant 2/2006 which was followed by multiple episodes of allograft rejection and infection. Voriconazole had been restarted 6/2009 for recurrent aspergillus pulmonary infection. Other than incapacitating musculoskeletal pain her rheumatologic ROS was otherwise unremarkable. The physical examination showed minimal nodal osteoarthritis and no active synovitis or effusion. There was a moderate distal sensory polyneuropathy. Muscle power and tone were normal. Subtle erythematous fullness of the digits and focal palpable hard tissue in the interphalangeal area of the right index finger in particular gave the appearance of "arthritis". There was no clubbing. Hand radiographs showed multiple focal areas of periostitis, nuclear scintigraphy showed extensive axial and appendicular periosteal radionuclide uptake. Chest CT showed striking nodular periosteal ossification in several ribs but no intrathoracic malignancy. (Figures) Laboratory work showed stable CKD III-IV with secondary hyperparathyroidism. The only new laboratory finding was a progressive rise in total and bone-specific Alk Phos that paralleled her symptoms. (Figures) Symptoms were treated with narcotic analgesics and a brief burst and taper of oral prednisone. Consistent with the initial case series of voriconazole associated painful periostitis, her musculoskeletal pain and elevated Alk Phos resolved quickly after drug discontinuation.

This case report strengthens the potential association of voriconazole with an unusual, painful, multifocal, nodular periostitis that resolves quickly upon drug discontinuation. Vigilance for this potential association is warranted. Potential pathophysiology is obscure.

1 Wang TF Am J Transplant 2009;9:2845-50.

***Disclosures: Fergus McKiernan**, None.*

SU0462

Older Men with Hyperkyphosis Display Worse Physical Function: the MrOS Study. Deborah Kado*[1], Stephanie Litwack[2], Howard Fink[3], Lynn Marshall[4], Eric Orwoll[4], Elizabeth Barrett-Connor[5], Peggy Cawthon[2]. [1]University of California, Los Angeles, USA, [2]California Pacific Medical Center Research Institute, USA, [3]VA Medical Center, Minneapolis, USA, [4]Oregon Health & Science University, USA, [5]University of California, San Diego, USA

Hyperkyphosis, or increased thoracic curvature, commonly affects older people, and was twice as prevalent in older men compared with older women in the Rancho Bernardo Study. In addition, men with block-measured hyperkyphosis demonstrated worse physical function and earlier mortality. To investigate whether the poor physical function associated with block-measured kyphosis might apply to other study populations, we studied men from the MrOS Study aged 71-98 (mean age 79). During their third clinic visit, 2,547 participants had the block measurement of kyphosis (number of 1.7cm blocks required to achieve a neutral head position while lying flat on the DXA table) and objective measures of physical function including grip strength, the time to stand up and sit down five times from a chair, 6-meter walking speed, ability to perform a 6-meter narrow walk (within lines 20 cm apart), and leg extension power measured using the Nottingham power rig. Only 3% (n = 73) of the participants had no kyphosis (were able to lie flat with no blocks) and 21.1% (n = 538) had severe hyperkyphosis (required >4 blocks to achieve a neutral head position). Kyphosis severity was greater with increasing age (p = 0.0001), and there were age-adjusted decreasing measures of physical performance with greater kyphosis (range in p for trends = 0.0001 – 0.02). In multivariable linear regression models adjusted for age, clinic, race, body mass index, and hip bone mineral density, compared to men without kyphosis, men with severe hyperkyphosis were more likely to display worse grip strength (p = 0.006), worse timed chair stand (p = 0.0001); slower walking speed (p = 0.0001); impaired narrow walk (p = 0.01); and weaker leg strength (p = 0.0001). The table below reports the multivariable adjusted means (95% CI) for each of the physical performance tests and demonstrates a clear trend of increasing difficulty with increasing kyphosis. These findings confirm that increasing block-measured kyphosis is strongly associated with poor physical function in older men. Clinical monitoring of physical functioning among patients with hyperkyphosis may be warranted.

Number of blocks	Grip Strength (kg)	Five repeat chair stands (seconds)	Walking speed (m/s)	Dynamic balance walk (m/s)	Leg power (watts)
0	37.2 (35.6, 38.9)	11.2 (10.4, 12.0)	1.14 (1.10, 1.19)	1.13 (1.07, 1.19)	184.5 (172.5, 196.5)
1	35.8 (35.1, 36.5)	11.0 (10.7, 11.3)	1.16 (1.14, 1.18)	1.14 (1.12, 1.17)	187.2 (182.6, 191.9)
2	36.5 (36.0, 37.0)	11.5 (11.2, 11.7)	1.15 (1.14, 1.17)	1.14 (1.12, 1.15)	183.7 (180.3, 187.2)
3	35.8 (35.3, 36.4)	12.0 (11.8, 12.3)	1.13 (1.12, 1.15)	1.11 (1.09, 1.13)	178.5 (175.8, 183.3)
4*	35.2 (34.6, 35.9)	12.6 (12.2, 12.9)	1.09 (1.07, 1.10)	1.10 (1.07, 1.12)	169.0 (164.5, 173.4)
p for trend	0.02	<0.001	<0.001	005	<0.001

*All models adjusted for age, clinic, race, education, body mass index, hip BMD, self-reported physical activity, and co-morbidities including diabetes, stroke, and Parkinson's disease

Table. Adjusted means (95% CI) for various physical performance tests*

***Disclosures: Deborah Kado**, Kyphon, 5*

SU0463

Predicting the Spinal Radiographic Severity in Ankylosing Spondylitis; Patient with Enthesitis or Arthritis of Peripheral Joints has Less Severe Radiographic Change. Sang-Hyun Kim[1], Seungwoo Han*[2], Youn-Kwan Jung[3], Seong-Ho Kim[4], Seong-Kyu Kim[5]. [1]Dongsan medical center, Keimyung university, South korea, [2]Daegu Fatima Hospital, South korea, [3]Laboratory for arthritis & bone biology, Daegu Fitima Hospital, South korea, [4]Paik-hospital, Inje University, South korea, [5]Catholic University of Daegu School of Medicine, South korea

Background; Ankylosing spondylitis (AS) is a chronic inflammatory disease, characterized by anabolic structural changes of axial skeleton such as new bone formation and ankylosis. Ankylosis of axial skeleton is a major cause of disability and there has been many clinical investigation for the prediction of radiographic damage in AS. However, most of these studies used either Bath AS Radiology Index (BASRI) or the presence of syndesmophytes or ankylosis as variable of radiologic severity, which have substantial problems of low sensitivity and ceiling effect. Objective: To develop a system that would provide prognostic information in AS, we tested the association between clinical characteristics and radiographic severity measured by the modified Stoke Ankylosing Spondylitis Spine Score (mSASSS) method. Methods: Patients with AS were enrolled in a multi-center cross-sectional study (n=248). All 248 patients had complete sets of spinal lateral radiographs of the cervical and lumbar spine and the radiographic severity were scored with mSASSS method. We assessed the association of clinical variables and mSASSS score using Student's t-test and Spearman's correlation coefficient. Based on the univariate analysis, we investigated the effect of independent variables by multiple linear regressions in which the individual clinical characteristics showing an abnormal distribution were nomally transformed. Results: In multiple linear regression models for mSASSS, the radiographic severity of AS was mainly determined by disease duration (standardized β (sβ) 0.532), older age at onset (sβ 0.352), and male sex (sβ 0.176), which account for 35% of variation in mSASSS score. Interestingly, the presence of peripheral arthritis (sβ -0.119) and enthesitis (sβ -0.114) were inversely associated with the mSASSS score. However, the cigarette smoking and the history of hip arthritis which had statistical significance in univariate analysis, were not associated with the spinal radiographic damage. Conclusion: Along with the classic risk factor such as longer disease duration, older age at onset and male sex, the presence of enthesitis or peripheral arthritis were associated with spinal changes assessed by mSASSS.

***Disclosures: Seungwoo Han**, None.*

SU0464

Reduced Cortical Density May Influence Bone Fragility in Morbidly Obese Women. Emily Stein*[1], Polly Chen[2], Halley Rogers[3], Adi Cohen[3], Marc Bessler[2], Beth Schrope[2], Akuezunkpa Ude[2], Donald McMahon[1], Elizabeth Shane[1], Shonni Silverberg[2]. [1]Columbia University College of Physicians & Surgeons, USA, [2]Columbia University, USA, [3]Columbia University Medical Center, USA

Obesity is typically thought to protect against fracture. Recent data, however, suggest that fracture rates are elevated among obese individuals with normal bone mineral density (BMD), raising the question as to whether these individuals may have an underlying deficit in bone quality.

We evaluated 16 morbidly obese (OB) and 16 normal weight women (C) matched for race and menopausal status. aBMD was measured by DXA at the lumbar spine (LS), total hip (TH), femoral neck (FN) and 1/3 radius (1/3R). Trabecular (Tb) and cortical (Ct) vBMD and Tb microarchitecture were measured by HRpQCT (Xtreme CT, voxel size ~82 μm) of the radius and tibia.

Subjects (75% Latina, 17% Caucasian and 8% African American) were of similar age (OB:41 $\pm$ 10 vs. C:44 $\pm$ 11 yrs;p=0.5) and 69% were premenopausal. Mean BMI among OB was 44 $\pm$ 6 kg/m^2 and among C 23 $\pm$ 2 kg/m^2. aBMD was 16% greater at the TH and FN in OB (both $p<0.01$) but did not differ at the LS or 1/3R. Although Z-scores were normal in OB (LS: -0.0 $\pm$ 0.2, TH: 1.0 $\pm$ 0.2, FN: 0.6 $\pm$ 0.2, 1/3R: 0.6 $\pm$ 0.2) and C (LS: -0.5 $\pm$ 0.3, TH: -0.0 $\pm$ 0.2, FN: -0.4 $\pm$ 0.2, 1/3R: 0.7 $\pm$ 0.2), they were higher in OB at the TH and FN ($p<0.004$). No differences in HRpQCT were observed at the radius, while at the tibia OB had greater total area (735 $\pm$ 37 vs. 588 $\pm$ 23 mm^2, $p<0.003$), largely due to greater Tb area (615 $\pm$ 40 vs. 479 $\pm$ 24 mm^2, $p<0.007$); Ct area did not significantly differ. While total density did not differ between groups, Ct density was lower in OB (873 $\pm$ 13 vs. 917 $\pm$ 12 mgHA/cm^3,$p<0.02$), and Tb density was greater (168 $\pm$ 8 vs. 139 $\pm$ 12 mgHA/cm^3,$p<0.05$). Central (inner) Tb density was greater in OB (128 $\pm$ 9 vs. 95 $\pm$ 12 mgHA/cm^3,$p<0.03$), while the sub-cortical (outer) Tb density did not differ from C. OB had greater Tb number (2.0 $\pm$ 0.1 vs. 1.8 $\pm$ 0.1 mm-1,$p<0.05$) and lower Tb separation (0.443 $\pm$ 0.021 vs. 0.524 $\pm$ 0.03 mm,$p<0.03$). Network heterogeneity and Ct thickness did not differ between groups. After adjustment for aBMD at the TH and bone area, the difference in Ct density between groups became less significant (p=0.057). Differences in Tb parameters were no longer observed.

In OB women, bone density is higher, but only at weight bearing sites (hip on aBMD; tibia on HRpQCT). HRpQCT demonstrates higher Tb density, particularly of the central Tb bone. However, Ct density at the tibia is reduced. This reduction in Ct density may result in abnormal bone quality in the morbidly obese, and could account for greater skeletal fragility despite greater bone size and density.

***Disclosures: Emily Stein**, None.*

SU0465

Role of 25(OH)D_3 and PTH in type 2 Diabetes Mellitus. Seong-Bin Hong*[1], Jeeyoung Han[2], JungJin Lee[2], SoHun Kim[1], Moonsuk Nam[1], Yong Seong Kim[1], Joon Ho Song[1]. [1]INHA University, South korea, [2]Inha University Hospital, South korea

Objectives: Primary or secondary hyperparathyroidism is associated with increased risk of cardiovascular disease. The risk of cardiovascular disease is increased in type 2 diabetes. Also, vitamin D has been known to predictor of mortality. To find out whether parathyroid or vitamin D might be related to the development of subclinical atherosclerosis in type 2 diabetic patients, we measured serum level of 25-hydroxyvitamin D[25(OH) D3], PTH and the carotid intima-media thickness (IMT).

Method: This cross-sectional study includes one hundreds type 2 diabetic patients aged 40-80 years without history of coronary heart disease, revascularization or stroke. The serum level of PTH was measure by immunoradiometric assay, and carotid IMT was measured with high resolution B-mode ultrasonography.

Results: The mean 25(OH) D3 was 54.9 $\pm$ 34.5 ng/ml, 26% of patients have Vitamin D deficiency. PTH was 39.7 (12.4-172.9) pg/ml. Age (r=0.453), systolic Bp (r=0.230) were related to mean carotid IMT. On the basis of linear regression analysis, the age, HbA1c and microalbuminuria predict mean carotid IMT. Serum calcium and albumin were different among 3 groups classified by the tertile of 25(OH)D3. PTH was correlated with serum creatinine, microalbuminuria and systolic blood pressure. In the lowest tertile patients have higher microabluminuria, CRP and PTH concentrations independently serum creatinine level.

Conclusions: Our results have demonstrated that both serum PTH and 25(OH)D3 are not the determinant of carotid IMT in type 2 diabetic patients. This result suggests that PTH and vitamin D might be affect the complication of diabetes differently.

***Disclosures: Seong-Bin Hong**, None.*

SU0466

Serum 25 Vitamin D Levels and Lower Extremity Strength and Coordination: a Cross-Sectional and Longitudinal Study. Nancy Lane*[1], Douglas Bauer[2], Michael Nevitt[3], Neeta Parimi[4], Kristine Ensrud[5], Jane Cauley[6], Erin LeBlanc[7], Marc Hochberg[8]. [1]University of California, Davis Medical Center, USA, [2]University of California, San Francisco, USA, [3]U.C.S.F., USA, [4]CPMC, USA, [5]Univ. of Minnesota, USA, [6]University of Pittsburgh Graduate School of Public Health, USA, [7]Oregon Health Sciences Center, Univ. of Oregon, USA, [8]Univ. of Maryland, USA

The association between vitamin D and falls and fractures may be related to a reduction in low extremity muscle strength and coordination as Vitamin D receptors are present on muscle fibers. We examined the relation of serum 25 hydroxyvitamin D [25(OH)D] levels with lower extremity strength and coordination in elderly caucasian women in both a cross-sectional and longitudinal study.

We measured 25(OH)D levels with LC-MS at the Mayo Clinic in serum archived from 6005 women who attended the 4th clinic visit (1992-1994) from the Study of Osteoporotic Fractures (SOF), a community-based cohort of women age 65 or older recruited from 4 U.S. cities. Lower extremity muscle strength was assessed using 6 meter timed walk, time to complete 5 chairs stands at visits 4 to 8 and quadriceps strength was measured using isometric leg extension chair with a load cell and was measured at visits 4 and 6. Coordination was assessed by ability to hold a tandem stand for 10 seconds or longer and measured in a subset of women at the 4th clinic visit (n=2081) and at visit 5. We used linear regression models to test the associations between quartiles of 25(OH) D levels and the lower extremity muscle strength and coordination measures. Adjusted means and 95% confidence intervals along with the p value for linear trend are reported.

Subjects with low levels of 25 (OH) D were significantly older, self-reported worse health, walked less, had less calcium and vitamin D intake, and more physical limitations compared to subjects with higher 25(OH) D levels. The cross-sectional results are listed in Table 1. Compared to subjects with higher levels of 25 (OH) D, lower levels of 25 (OH) D were significantly associated with slower walking speed, more time to complete chair stands, and reduced quadriceps strength. No association was observed for 25 (OH) D and tandem stand. Also, there was no association with 25 (OH) D and changes over the following 8 years in walking speed or chair stands and 2 year changes in quadriceps strength and tandem stand in these subjects.

In summary, low 25 (OH) D levels have only a modest association with lower extremity muscle strength in elderly women in the community and may not be clinically significant.

Table 1. Adjusted mean (95% CI) of lower extremity function by quartiles of Vitamin D status

	Multivariate Models		
Quartile 25(OH)D ng/ml	Walking Speed (m/sec)	Time to complete chair stands (sec)	Quadriceps strength (lbs)
	N=5689	N=5475	N= 5041
1 (0-14)	0.94 (0.93, 0.95)	12.44 (12.2, 12.68)	56.38 (55.09, 57.66)
2 (15-22)	0.95 (0.94, 0.96)	12.02 (11.81, 12.23)	58.18 (57.02, 59.34)
3 (23-29)	0.96 (0.95, 0.97)	11.86 (11.66, 12.07)	59.6 (58.53, 60.68)
4 (≥30)	0.96 (0.95, 0.97)	11.83 (11.59, 12.05)	58.14 (56.95, 59.28)
p trend	0.0116	0.0003	0.0357

Models adjusted for: age, clinic, season, BMI, self reported health status, education, number of medical co-morbidities, physical activity, thiazide use, vitamin D use, calcium use and estrogen use

Table 1-Lane

***Disclosures: Nancy Lane**, None.*

SU0467

Systemic Mastocytosis As A Cause Of Severe Osteoporosis In A Young Woman (Case Report). Chrysoula Liakou*[1], George Trovas[2], Evangelos Terpos[3], Nikolaos Papaioannou[4]. [1]Athens School Of Medicine, K.A.T. Hospital, Greece, [2]Laboratory for the research of Musculoskeletal System "Th. Garofalidis", KAT Hospital, Greece, [3]University of Athens School of Medicine Department of clinical Therapeutics, Greece, [4]Associate Professor of Orthopaedics at University of Athens School of Medicine, Director of Laboratory for the research of Musculoskeletal System "Th. Garofalidis" ,KAT Hospital, Greece

Purpose: We report a case of a 46-year old female suffering from a five year premenopausal osteoporosis due to systemic mastocytosis(SM).

Methods: The only clinical symptom was severe back pain and restricted spinal movements resulting from the existing vertebral compression fractures. There were not any skin lesions. Because of the severity of the case, non response to the so far administered treatment and the premenopausal initiation of her osteoporosis a further investigation for an underlying cause was accomplished.

Results: Laboratory evaluations excluded metabolic or endocrinological abnormalities. Urinary excretion of N-methylhistamine was elevated (356 ug/g creatinine, normal range 30-200), and serum tryptase (a marker for mast cell activation) level was slightly elevated (12.8 μg/l, normal<11.4 μg/l). The c-kit Asp816Val somatic activating mutation associated with SM was not detected in the patient. A diagnostic bone marrow biopsy specimen was done, after which tryptase immunohistochemistry (anti-CD117, anti-CD25, anti-CD2) confirmed the presence of mast cell infiltrates forming small aggregates. Within these infiltrates of >15 mast cells (major SM criterion), a significant percentage of the mast cells showed prominent spindling (minor criterion). Thus, the diagnostic criteria for SM were fulfilled and the diagnosis was confirmed. There was no evidence for an associated non-mast cell lineage hematological malignancy.

Conclusions: In conclusion, we report a case of severe osteoporosis as a manifestation of systemic mastocytosis which should be suspected even when there are not skin abnormalities and when there is suspicion of secondary osteoporosis. Serum tryptase and urine histamine metabolites should be measured in order to facilitate the diagnosis, and then a bone marrow biopsy should be considered. Systemic mastocytosis should be included in the differential diagnosis due to its significant morbidity and the helpful treatment options.

***Disclosures: Chrysoula Liakou**, None.*

SU0468

The Effect of Narrowband Ultraviolet B Treatment for Psoriasis on Vitamin D Status During Wintertime in Ireland. Caitriona Ryan[1], Benvon Moran[1], Malachi McKenna*[2], Barbara Murray[1], Jennifer Brady[1], Paul Collins[1], Sarah Rogers[1], Brian Kirby[1]. [1]St. Vincent's University Hospital, Ireland, [2]St. Michael's Hospital, Ireland

Objectives: To determine whether narrowband ultraviolet B radiation (NB-UVB) mediates its beneficial effect on psoriasis by increasing serum 25-hydroxyvitamin D [25(OH)D] levels, and to assess the effect of NB-UVB on vitamin D status in psoriasis patients in wintertime.

Design: A prospective controlled study from October 2008 to February 2009.

Setting: A dermatology outpatient department at a university teaching hospital.

Patients: Thirty consecutive patients with psoriasis treated with NB-UVB and 30 control patients with psoriasis were recruited. Control patients were recruited within one week of treated patients to control for seasonal variation of serum 25(OH)D levels. One patient with photoaggravated psoriasis was withdrawn from the study.

Intervention: NB-UVB was administered three times per week.

Main Outcome Measure: Serum 25(OH)D was measured at baseline, after 4 weeks and at completion of treatment.

Results: The median(range) for first dose was 299 (144-516) mJ/cm^2, for final dose was 2322 (505-3833) mJ/cm^2, and for the cumulative dose was 22508 (5773-69459) mJ/cm^2. The median (range) for number of exposures was 18 (11-47). Levels of serum 25(OH)D increased significantly ($p<0.0001$) from a median (range) of 58 (22-115) nmol/L at baseline to 126 (79-279) nmol/L at the end of NB-UVB treatment compared with no change in the control group. Ionised calcium levels did not change following NB-UVB. The change in serum 25(OH)D correlated with the number of exposures of NB-UVB ($r=0.61$; $p=0.0005$) and cumulative NB-UVB dose ($r=0.47$; $p=0.011$) but not with treatment response. In a multiple regression model, prior phototherapy was the sole predictor of baseline serum 25(OH)D ($r^2=0.13$; $p=0.006$), while the number of exposures of NB-UVB predicted change in serum 25(OH)D ($r^2=0.38$; $p=0.001$). At the end of the study, all patients in the treatment group were vitamin D sufficient but 75% of the control group were vitamin D insufficient [serum 25(OH)D<50 nmol/L].

Conclusion: NB-UVB increases serum 25(OH)D markedly while clearing psoriasis, but there was no correlation between change in serum 25(OH)D and treatment response. Up to 75% of Irish patients with psoriasis were shown to be vitamin D insufficient during wintertime,highlighting the need for seasonal supplementation in order to prevent the deleterious effects of hypovitaminosis D in this population unless phototherapy is being administered.

***Disclosures: Malachi McKenna**, Abbott pharmaceuticals, 2; Galderma, 5*

SU0469

A Novel Approach for the Repair of Segmental Long Bone Defects in Humans. Eric Hesse*[1], Gerald Kluge[2], Carl Haasper[2], Georg Berding[2], Hoen-oh Shin[2], Joerg Viering[2], Florian Laenger[2], Peter Vogt[2], Christian Krettek[2], Michael Jagodzinski[2]. [1]Harvard Schools of Medicine & Dental Medicine, USA, [2]Hannover Medical School, Germany

A large segmental defect of a weight bearing long bone can be the consequence of an infection, a congenital deformity, a tumor, but most frequently it is the result of an open fracture. The surgical repair of such a defect can be very challenging and the ideal concept has not yet been identified. Free fibula- or iliac crest grafts are mainly used for filling large bone defects. However, due to the limited availability of transplantable bone and frequently occurring donor site morbidity, current research

activities are aimed at using autologous bone marrow stromal cells in combination with a carrier to regenerate segmental bone defects. We developed a novel approach to treat a 58-year-old woman who had a 72 mm segmental defect of the distal tibia due to an open fracture (AO-classification: 43C2.3) by implanting a customized multiple disc graft. Decellularized bovine trabecular bone discs were seeded with autologous bone marrow stromal cells and cultured in a perfusion chamber for three weeks. To close the defect, the discs were implanted and fixed by an intramedullary nail. Bone formation was assessed non-invasively by plain radiographs and 18F-labeled sodium fluoride-based co-registration of positron emission- and computed tomography (PET/CT). Within regions of interest (ROI) we quantified the Hounsfield units (HUs), a measure of radiodensity, and the standard values of [18F] sodium fluoride uptake (SUVs) as a surrogate of osteoblast activity. Analysis of HUs and SUVs revealed that bone was actively formed around the grafted defect as early as six weeks after surgery. Because the tibia was sufficiently stabilized at that time, the patient was able to freely walk with full weight bearing. Three months after surgery, the callus formation reached its maximum. The two-year follow-up was uneventful, reporting no infection, failure of the graft, or loosening of the implants. Our patient was satisfied with the result, which altogether demonstrates the success of this new procedure. We conclude that the use of a multiple cell-seeded disc graft can be considered as an alternative treatment for patients with segmental long bone defects. This is the first study reporting the repair of a large segmental defect of a weight bearing long bone in humans using a cell-loaded multiple disc graft. In addition, we describe a novel application for a PET/CT-based technique to non-invasively monitor the osseointegration of a graft.

***Disclosures: Eric Hesse**, None.*

SU0470

Fluoride Related Periostitis Associated With Chronic Voriconazole Use in Solid Organ Transplants. Robert Wermers*[1], Kay Cooper[1], Gary Whitford[2], Raymund Razonable[1], Paul Deziel[1], Thomas Moyer[1]. [1]Mayo Clinic, USA, [2]Medical College of Georgia, USA

Introduction: Acquired periostitis is a rare disorder in which palpable osseous masses can develop. We describe four solid organ transplant patients evaluated at our institution who developed periostitis. After evaluation of potential causes, fluoride excess was determined to be the etiology. All of the subjects were on long term voriconazole therapy which contains 3 fluoride atoms, and in the three subjects with confirmed fluoride elevations, voriconazole was the only potential source of fluoride identified. In 2 subjects who discontinued voriconazole prompt improvement in symptoms and reduction of plasma fluoride and alkaline phosphatase levels were observed.

Methods: Fluoride in plasma was quantified using a La Motte pH PLUS Direct pH/mV/ISE/Temp meter equipped with a fluoride-specific electrode from Orion Research, Cambridge, MA. The fluoride concentration in the bone ash was determined in triplicate using the ion-specific electrode (Orion Research, Model 9409) and a minature calomel reference electrode both coupled to a potentiometer (Orion Research, Model 720A) after overnight hexamethyldisiloxane (HMDS)-facilitated diffusion.

Cases:

[See Table]

Conclusion: The temporal relationship of the initiation of voriconazole to the development of periostitis and elevated fluoride levels without another identifiable cause, as well as resolution of periostitis after voriconazole discontinuation, supports causality and that voriconazole can lead to systemic fluoride excess. We hypothesize a relationship between voriconazole metabolism and renal insufficiency in transplant patients that predisposes them to the accumulation of circulating fluoride ions.

	Case #1 (Index case)	Case #2	Case #3	Case #4	Normal Range
Age (years)	64	47	51	62	
Sex	Female	Female	Female	Female	
Voriconazole length of use before periostitis	6 months	7 months	1 year	6 months	
Transplant	Heart	Kidney	Lung	Lung	
Periostitis location	Multiple Axial and Appendicular	Multiple Appendicular	Multiple Appendicular	Multiple Axial and Appendicular	
Total Alkaline phosphatase	521 U/L (nl, 50-130)	243 U/L (nl, 50-130)	346 U/L (nl, 39-100)	378 U/L (nl, 50-130)	
Bone Alkaline phosphatase	134	72	Not done	90	Premenopausal < 14 µg/L Postmenopausal < 22 µg/L
Bone Alkaline phosphatase isoenzyme	Not done	Not done	369 U/L (nl, 11-67)	268.6 IU/L (nl, 12.1-42.7)	
Beta-CrossLaps	1765	1863	Not done	135	Premenopausal 25-573 pg/mL Postmenopausal 104-1008 pg/mL
24 hour urine: Total Pyridinoline Total Deoxypyridinoline	Not done Not done	Not done Not done	114 38.2	Not done Not done	20-62 nmol/mmol 5-22 nmol/mmol
Creatinine	1.8	1.5	1.4	1.6	0.7-1.2 mg/dL
Plasma Fluoride	20.7	7.5	Not done	27	1-4 µMol/L
Bone Fluoride (mean)	10,157 ± 890	Not done	Not done	Not done	500-1000 mg/kg

Clinical and laboratory findings in transplant patients with fluoride associated periostitis

***Disclosures: Robert Wermers**, None.*

SU0471

Gonadal Status Evolution After Liver Transplantation. Relationship with BMD Changes. Guillermo Martínez Diaz-Guerra*[1], Sonsoles Guadalix[2], Raquel Sánchez-Windt[2], Miriam Partida[3], Enrique Moreno[2], Federico Hawkins[4]. [1]Universtiy Hospital 12 de Octubre, Spain, [2]University Hospital 12 de Octubre, Spain, [3]University Hospiatl 12 de Octubre, Spain, [4]Hospital Universitario, Spain

Background: There are few data about gonadal status evolution after liver transplantation (LT) and its relationship with bone mineral density. The effect of immunosuppressive agents on gonadal function and BMD are controversial.

Patient and Methods: Prospective study in 62 Spanish males (age 56.1 ± 8.0 years) who underwent liver transplantation in our centre. Complete baseline and 12 months after LT data were available in 44 patients (Serum Total Testosterone-TT-, LH, FSH). Hypogonadism was defined as serum TT levels below 280 ng/dl. Spine BMD (L1-L4), and femoral (total, neck and intertrochanteric) BMD were measured (DEXA, Hologic QDR 4500) at 0, 6 and 12 months after LT. Accumulated dose of immunosuppressive agents were registered.

Results: Serum TT levels significantly increased 12 months after LT (343.2±137.4 vs 522.8±169.3 ng/dl, $p<0.001$), whereas serum gonadotropin levels significantly decreased (FSH: 16.8±8.6 vs 13.7±10.8 mUI/ml; p=0.035; LH: 16.3±11.6 vs 12.6±11.4 mUI/ml; p=0.007). At baseline, 29.3% of patients had primary hypogonadism decreasing to 4.3% 12 months after LT ($p<0.01$). Eugonadal patients increased from 10.3% to 46.8% ($p<0.01$). One year after LT, 94% of patients showed normal serum TT.

Accumulated dose of prednisone was 4584.0 ± 2638.6 mg; tacrolimus 1715.1 ± 883.2 mg and mophetil mycophenolate 358.5 ± 179.0 mg. No correlation was found between serum TT level at any time of the study and mean accumulated dose of immunosuppressive drugs. Baseline serum TT correlated with spine BMD change (%) at 12 months(r=0.319, p=0.018). Baseline serum FSH correlated with intertrochanteric BMD change (%) at 12 months (r= -0.306; $p<0.05$). Serum FSH level at 12 months correlated with total femoral BMD change (%) at 12 months (r= -0.300; $p<0.05$).

Conclusions: Primary hypogonadism is frequently observed in liver recipient patients, with improvement in the first year after LT. Patients with better gonadal function at baseline achieved higher BMD 12 months after LT. Long-term protocols with reduction of immunosuppresive therapy had no significant effect upon gonadal status in these patients.

***Disclosures: Guillermo Martínez Diaz-Guerra**, None.*
This study received funding from: Mutua Madrileña Foundation

SU0472

Bone Marrow Adipocytes Increase without changing 11β-Hydroxysteroid Dehydrogenase Type 1 Expression during Glucocorticoid Excess. Valentina Camozzi*[1], Chiara Franzin[1], Paola Ballanti[2], Alessandra Calcagno[1], Claudio Pagano[1], Martina Zaninotto[1], Franco Mantero[1], Roberto Vettor[1], Giovanni Luisetto[3]. [1]University of Padua, Italy, [2]University of Rome, Italy, [3]Universiy of Padua, Italy

In liver and adipose tissue, 11β-Hydroxysteroid Dehydrogenase type 1 (11β-HSD-1) is involved in activation of glucocorticoids from inactive 11-keto forms and may be up or down regulated during hypercortisolism. Since glucocorticoids (GCs) cause an increase of adipocytes and a parallel decrease of osteoblasts in bone, we aimed to study the possible role of this enzyme during the skeletal glucocorticoid-induced impairment. Eight male wild type Zucker rats were treated with methyprednisolone, 7 mg/kg, by weekly subcutaneous injection (MG) and eight rats were the controls (CG). Treatment lasted for 6 weeks. Body weight (BW), bone mineral content (BMC), bone area (BA), bone mineral density (BMD), bone GLA protein (BGP) and C-terminal peptide of type 1 collagen (CTx) were evaluated at the start and after treatment. Quantitative histomorphometric analysis was performed at the distal epiphysis of the left femur of each animal in order to evaluate bone remodelling. The expression of 11β-HSD-1, ALP, Leptin and PPARγ was evaluated by quantitative PCR in samples of the proximal epiphysis of the same femur. Tunnel reaction was performed to detect cellular apoptosis and immunohistochemistry was carried out to detect the 11β-HSD-1 localization on samples of the contralateral femur.

BW and BA increased by 40% only in controls. BMC increased in both groups, but such an increase was significantly lower in treated animals. Consequently, BMD was significantly higher and similar in the two groups. BGP and CTx decreased by 50% in CG, and by 85% in MG group ($p<0.001$). Histomorphometric parameters showed a reduction of all remodelling variables in MG. 11β-HSD1 expression in bone samples was similar in both groups, as well as PPARγ one. ALP expression was significantly decreased while leptine expression increased in the treated group. Tunnel reaction showed apoptotic osteocytes in MG. Immunohistochemistry analysis showed the presence of the enzyme in the osteoblasts and osteocytes of controls, and in the bone marrow adipocytes of the treated rats. These findings suggest that bone glucocorticoid-induced modifications are independent from 11β-HSD1 expression. Due to the

presence of the 11β-HSD-1 in the adipocytes, without changing mRNA expression, we can argue a shift of the enzyme expression and activity from bone to adipose compartment in the marrow.

***Disclosures: Valentina Camozzi**, None.*

SU0473

Developmentally-regulated Glucocorticoid-mediated Inhibition of Osteoblast Cell Cycle Progression through Repression of ATF4-Dependent Cyclin A Transcription. Yankel Gabet*, Tommy J. Noh, Sanjeev Baniwal, Christopher Lee, Baruch Frenkel. University of Southern California, USA

Synthetic glucocorticoids (GCs) such as dexamethasone (DEX) are effective immunosuppressive drugs for the management of autoimmune and inflammatory diseases. However, this treatment modality often results in GC-induced osteoporosis (GIO) and fractures. We investigated the anti-mitogenic effect of GCs in osteoblasts, which is considered a major mechanism contributing to GIO. First, we defined a commitment stage during the differentiation of newborn mouse calvarial osteoblast cultures, which occurs 3-5 days after confluence in this model system. Chronic DEX treatment commencing before commitment abrogated differentiation and mineralization, whereas treatment after the commitment stage did not inhibit the osteoblast phenotype. Interestingly, DEX administration during or after, but not before the commitment stage significantly inhibited cell cycle progression (Figure 1). To investigate the cellular mechanism by which GCs inhibit cell cycle progression in committing and committed osteoblasts, we first analyzed the effect of DEX on the proliferation-related Wnt pathway. Indeed, DEX treatment repressed the expression of the TOPGAL Wnt reporter during and after commitment. However, neither cyclin D1 nor c-Myc mRNA, well-established Wnt targets regulating cell cycle progression, were repressed by DEX. On the other hand, both acute (24-hour) and chronic (7 days) DEX treatment significantly reduced both the mRNA and the protein levels of cyclin A, another cell cycle regulator. Moreover, the effect of DEX on Cyclin A was not observed before, but only at and after the commitment stage. Using reporter constructs controlled by wild type or mutant cyclin A promoter fragments, as well as gel shift assays, we identified an ATF4 binding site critical for the DEX-mediated repression of promoter activity. Furthermore, and similar to the results with Cyclin A, ATF4 expression was repressed by DEX only during and after commitment. Our data suggest that GCs attenuate cell cycle progression in osteoblasts in a developmental stage-specific manner by repressing ATF4-dependent *Cyclin A* gene expression.

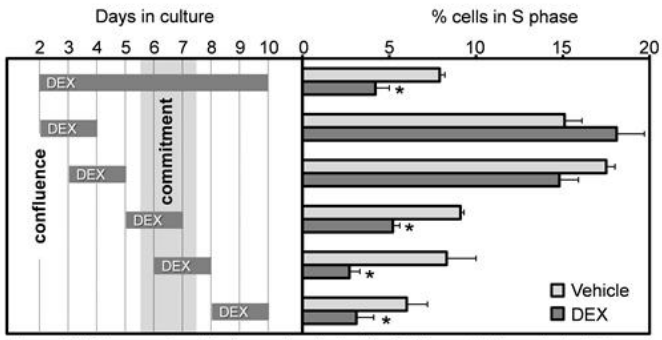

Figure 1. Primary osteoblast were treated with DEX or vehicle as indicated and %cells in S-phase was determined at the end of the treatment period. Bars represent Mean±SEM. *, *vs.* vehicle, p<0.05.

Figure 1

***Disclosures: Yankel Gabet**, None.*

SU0474

Histochemical Assessment of Altered Bone Tissue in Transgenic Mice Overexpressing Parathyroid Hormone-related Peptide (PTHrP) Driven by Type I Collagen Promoter. Minqi Li*[1], Tomoka Hasegawa[1], Sayaka Nakamura[1], Nuneteru Sasaki[1], Zhusheng Liu[2], Ying Guo[1], Reiko Suzuki[1], Tsuneyuki Yamamoto[1], Norio Amizuka[3]. [1]Hokkaido University, Japan, [2]Hokkaido Universiy, Japan, [3]Hokkaido University School of Dentistry, Japan

Purpose: This study aims to elucidate the biological function of parathyroid hormone-related peptide (PTHrP) on cell differentiation and proliferation of osteoblastic cells, by examining histologically-altered bone in PTHrP overexpressing transgenic mice.

Materials & Methods: Transgenic mice overexpressing PTHrP were generated by inserting the PTHrPcDNA downstream Collα1 promoter specific to osteoblasts. Eighteen day-old fetuses were harvested and immersed in 4% paraformaldehyde solution (pH 7.4) for 12h. After genotyping, the femora and tibiae of the transgenic mice and wild-type littermates were embedded into paraffin. Alkaline phosphatase (ALP), Runx2, type II collagen, type X collagen and proliferating cell nuclear antigen (PCNA) were examined histochemically.

Results: The epiphyseal cartilage of the PTHrP transgenic mice positive to type II collagen was markedly expanded, and there was no type X collagen positive hypertrophic zone. Further, PTHrP transgenic mice had no primary trabeculae with cartilage cores and surrounded bone matrices, indicating that intramembranous ossification but not endochondral ossification was dominant in the metaphyseal bone. Despite the overexpression of PTHrP, only few TRAP-positive osteoclasts were observed in the transgenic mice. The ALP-positive cells were mainly found in the transgenic cortical region, while the inner portion of the transgenic bone was weakly positive to ALP. The wild-type bone had ALP-positive osteoblasts covering the metaphyseal trabeculae. Cells positive to PCNA and Runx2 also tended to be present mainly in the cortical areas of the transgenic bone, while in the wild-type bone the PCNA and Runx2-reactive cells were evenly distributed. Taken together, over-expressed PTHrP appears to facilitate cells that become committed to the osteoblastic lineage and proliferate in the cortical region. However, PTHrP seems to affect other cells types negative to ALP and Runx2 in fetal bone tissue.

Conclusion: PTHrP appears to stimulate the proliferation and differentiation of the osteoblastic lineage, but may affect proliferation of other cell-types in fetal bone tissue.

***Disclosures: Minqi Li**, None.*
This study received funding from: JSPS

SU0475

In vivo Deletion of CAR Leads to Increased Bone Mass. Hwa Young Cho[1], Ju Yeon Jung[2], Solip Jung[2], Jae Yeon Yang[2], Yenna Lee[2], Ji Hyun An[2], Hyung Jin Choi[2], Sun Wook Cho[3], Sang Wan Kim[4], Young Joo Park[2], Jung-Eun Kim[5], Chan Soo Shin*[2]. [1]Department of Internal Medicine, Seoul National University College of Medicine, *Department of Internal Medicine, Hanyang University Guri Hospital, South korea, [2]Department of Internal Medicine, Seoul National University College of Medicine, South korea, [3]University of Michigan School of Dentistry, USA, [4]Seoul National University Boramae Hospital, South korea, [5]Kyungpook National University School of Medicine, South korea

Constitutive androstane receptor (CAR) belongs to a member of the nuclear receptor superfamily which induces xenobiotic, bilirubin, and thyroid hormone metabolism as a heterodimer with the retinoid X receptor (RXR). In vivo deletion of CAR has been shown to alter sensitivity to toxins and modulation of CAR activity in humans may significantly affect metabolism of drugs and other xenobiotics. To investigate the role of CAR in bone metabolism, we have analyzed the phenotypes of CAR null mice. Endogenous CAR mRNA expressions were observed during osteoblast and osteoclast differentiation. Deletion of CAR (CAR (-/-) mice) has resulted in significant increase in whole body bone mineral density (BMD) by 9.5% ($p<0.001$) in male at 10 weeks of age compared with wild-type (WT) littermates, which was maintained up to 15 weeks of age. Furthermore, micro-CT analysis of proximal tibia at 10 weeks of age demonstrated significant increase in trabecular bone volume (62.7%), trabecular number (54.1%) in CAR (-/-) mice compared with WT littermate. The mRNA expressions of Cyp2b9 and 2b10 in the liver, which regulate testosterone metabolism, were significantly downregulated while serum testosterone levels showed 4-fold increase in CAR (-/-) mice compared with WT littermate. The difference in BMD between CAR (-/-) and WT mice disappeared 8 weeks after performing orchiectomy. Primary culture of calvarial cells exhibited no significant changes in ALP activities as well as bone nodule formation assessed by Alizarin Red staining between CAR(-/-) and WT littermates. Bone marrow macrophage (BMM) culture in the presence of RANKL showed that TRAP (+) multinuclear cell formation was significantly increased in BMMs from CAR (-/-) mice compared to those from WT littermates. Taken together, these results suggest that in vivo deletion of CAR resulted in greater bone mass, which appears to be a result from reduced metabolism of testosterone due to suppressed Cy2b expression.

***Disclosures: Chan Soo Shin**, None.*

SU0477

Binding of the Homeobox Transcription Factor CDX2 at the Human Vitamin D Receptor (VDR) Gene Locus in Intestinal/Colonic Cells. Chang-Hun Lee*[1], Mark Meyer[2], Seong Min Lee[2], J. Pike[2]. [1]University of Wisconsin at Madison, USA, [2]University of Wisconsin-Madison, USA

1,25-Dihydroxyvitamin D3 (1,25(OH)2D3) regulates the intestinal uptake of calcium and phosphorus from the diet and in so doing provides minerals essential for the development and maintenance of the skeleton and other organs. These actions are mediated by the VDR, whose basal expression in intestinal epithelial cells is striking in vivo and well above that of most other target tissues. Surprisingly, while regulation of VDR expression by various hormones and other regulators has been explored, little is known of the mechanisms, signaling processes or the transcription factors that are responsible for the gene's basal and tissue-specific expression. CDX2 is one of several homeobox transcription factors that play a significant role in formation of the gastrointestinal tract in the developing embryo. It also contributes to processes inherent to intestinal function in the adult. Our early studies suggested that CDX2 might control basal expression of the VDR gene in the intestine by virtue of a CDX2 regulatory element present -3.7 kb upstream of the human gene's transcriptional start

site (TSS). Indeed, a SNP has been identified within this regulatory element that appears to correlate with intestinal VDR activity and is suggested to increase the risk of human disease. We therefore explored the role of CDX2 in VDR expression by assessing the presence of this factor and associated coregulators at the VDR locus in human intestinal/colon cells and the association of these factors with epigenetic histone modifications. ChIP-chip and ChIP-seq analyses revealed that CDX2 was residually bound to the VDR gene locus at not only the -3.7 kb site upstream of the primary VDR promoter, but also at three additional sites surrounding the promoter and at multiple sites surrounding the upstream hVDR promoter as well. A number of these CDX2 sites contained modest levels of the histone acetyltransferase CBP and the coregulator NCoR. Finally, each of these potential homeobox regulatory regions was also associated with an increase in the level of tetra-acetylated histone H4K5,8,12,16 (4AcH4), a hallmark of a transcriptionally active region. These observations suggest a role for CDX2 in the formation and/or maintenance of an active regulatory enhancer potentially capable of mediating the activity of VDR. Future studies are focused upon delineating the precise role of CDX2 and its binding sites in regulating the expression of the VDR and other vitamin D sensitive genes in the intestine.

***Disclosures: Chang-Hun Lee**, None.*

SU0478

Essential Role of Vitamin D Receptor for High Dose Vitamin D Induced Vascular Calcification in Mice. Min-Su Han*[1], Kyun Eun Lim[2], Na-Rae Park[2], Jae-Hwan Jeong[2], Shin-Yoon Kim[3], Shigeaki Kato[4], Je-Yong Choi[2]. [1]KNU, School of Medicine, South korea, [2]Kyungpook National University, School of Medicine, South korea, [3]Kyungpook National University Hospital, South korea, [4]University of Tokyo, Japan

Vascular calcification (VC) represents an important risk factor for the high mortality rates of cardiovascular diseases. High doses of vitamin D have been used to induce VC in both mice and rats. However, its molecular mechanisms have not been determined with respect to the involvement of vitamin D receptor (VDR). Here, normal and vitamin D receptor knock-out (VDR-/-) mice were subcutaneously injected with high doses of vitamin D (80 x 104 IU/kg) using previously established protocol of VC model in mice. In skeletal tissues, high doses of vitamin D injections increased TRAP activity and decreased Runx2 and Osterix expressions in normal mice. In nonskeletal tissues, Alizarin Red S and von Kossa staining showed that VC was observed in the aorta as well as the kidney and lung in normal mice. Interestingly, calcification in the medial layer of the aorta was more severe than the intimal layer. Moreover, various bone markers (Osteocalcin, Osteopontin, Osteonectin, Collagen type 1, Collagen type X, Matrix gla protein, Rankl, and Fgf-23) were increased in blood vessels. Blood calcium and alkaline phosphatase activities were increased congruently with the doses of vitamin D injections in normal mice. However, the high vitamin D injection mediated skeletal and nonskeletal tissue phenotypes were not observed in VDR-/- mice. Collectively, these results indicate that VDR is essential for high dose vitamin D induced VC model in mice.

***Disclosures: Min-Su Han**, None.*

SU0479

Evaluatern Between Serum Vitamin D Concentration and Body Mass Index in Post Menopausal Women. Hoon Choi*[1], Tak Kim[2], Heung Yeol Kim[3], Min Hyung Jung[4], Byung Ick Lee[5], Huck Jung[6]. [1]Inje University Sanggyepaik Hospital, South korea, [2]Korea University Anam Hospital, South korea, [3]Kosin University, South korea, [4]School of Medicine, Kyung Hee University, Kyung Hee Medical Center, South korea, [5]Inha University Hospital, Inha University, South korea, [6]Chosun University, South korea

Objective: To evaluate the relationship between serum vitamin D concentration and body mass in Korean postmenopausal women.

Methods: Three hundred ten healthy postmenopausal women were recruited in Korea from January, 2006 to March, 2010. The relationship between vitamin D concentration and the variables including BMI was analyzed.

Results: In Korean post menopausal women, 98.9% showed vitamin D level less than 30ng/ml and 87.8% showed vitamin D level less than 20ng/ml. The relationships between vitamin D and other factors such as age, height, weight, BMD and bone markers were not significant. The relationships between BMI and vitamin D & PTH were not significant.

Conclusion: About 90% of Korean post menopausal women showed vitamin D insufficiency and there was no relationship between vitamin D concentration and BMI.

***Disclosures: Hoon Choi**, None.*

SU0480

Inhibition of CYP24: A Novel Approach to Treat Secondary Hyperparathyroidism. Christian Helvig*[1], Dominic Cuerrier[1], Christopher Hosfield[1], Aza Kharebov[1], Rina Glozman[1], Uttam Saha[1], Gary Posner[2], Tina Epps[1], Martin Petkovich[3]. [1]Cytochroma Inc, Canada, [2]Johns Hopkins University, USA, [3]Cytochroma Incorporated, Canada

The cytochrome P450 enzyme 24-hydroxylase (CYP24) is specifically responsible for the catabolism of both 1α,25-dihydroxyvitamin D_3 (1α,25$(OH)_2D_3$), as well as the prohormonal form, 25-hydroxyvitamin D_3 (25$(OH)D_3$). The cyp24 gene responsible for encoding this enzyme is regulated by 1α,25$(OH)_2D_3$, forming a negative autoregulatory feedback loop to limit 1α,25$(OH)_2D_3$ exposure and prevent toxicity. This feedback loop can also limit the effectiveness of therapeutic doses of vitamin D analogues. In patients with chronic kidney disease (CKD), secondary hyperparathyroidism is the result of lower serum 1α,25$(OH)_2D_3$ levels caused by reduced function of the kidney to generate this active vitamin D hormone. Recently, we have demonstrated that CYP24 is profoundly elevated in kidney derived from vitamin D deficient rats with renal disease induced by adenine treatment, as well as in kidney biopsies from CKD patients. Analysis of 1α-hydroxylase expression in the kidney further revealed that loss of this enzyme is not necessarily the cause of declining 1α,25$(OH)_2D_3$ in these animals, suggesting that accelerated catabolism of 1α,25$(OH)_2D_3$ by CYP24 may play a role. To assess the role of CYP24 in a rat model of CKD induced by adenine treatment, we used the specific CYP24 inhibitor CTA091 which can effectively block CYP24 activity with an IC_{50} of approximately 7-10 nM and increase the potency of 1α,25$(OH)_2D_3$ about 700-fold. When administered to adenine-treated animals, CTA091 effectively suppresses production of intact parathyroid hormone, presumably due to elevated circulating levels of 1α,25$(OH)_2D_3$, and exhibits a wider therapeutic window superior to that for 1α,25$(OH)_2D_3$. Aberrant expression of CYP24 in the uremic kidney may potentially deprive the kidney of localized 25$(OH)D_3$ and 1α,25$(OH)_2D_3$, and thus may well contribute to disease progression. CTA091 treatment also can cause the reduction in markers of kidney fibrosis and inflammation. This suggests that inhibiting CYP24 activity may have the potential to delay progression of CKD.

***Disclosures: Christian Helvig**, None.*

SU0481

Modulation of Innate Immunity by 1,25$(OH)_2D_3$: Regulation of TREM1, a novel target of 1,25$(OH)_2D_3$. Puneet Dhawan*[1], Isaura Rigo[2], Leila Mady[3], Sylvia Christakos[1], Gill Diamond[2]. [1]University of Medicine & dentistry of New Jersey-New Jersey Medical School, USA, [2]University of Medicine & Dentistry of New Jersey-New Jersey Dental School, USA, [3]University of Medicine & Dentistry of New Jersey-New Jersey Medical School & Graduate School of Biomedical Sciences, USA

1,25$(OH)_2D_3$ has been reported to have an important role in the regulation of innate immunity. We earlier reported that cathelicidin is induced by 1,25$(OH)_2D_3$ in bronchial epithelial cells with a resultant increase in antimicrobial activity against airway pathogens. In order to examine an effect of 1,25$(OH)_2D_3$ on other factors involved in innate and adaptive immune responses an RT PCR array system (RT Profiler PCR array) which profiles the expression of genes involved in host response to bacterial infection and RNA from bronchial epithelial cells treated with vehicle or 1,25$(OH)_2D_3$ (10^{-8}M for 24h) were used. The results of the PCR array indicated that the genes that showed the greatest fold increase were two that had been previously identified as 1,25$(OH)_2D_3$-regulated, cathelicidin antimicrobial peptide and the TLR co-receptor CD14 (38 and 46-fold induction respectively). An additional gene that was induced by 1,25$(OH)_2D_3$ was TREM1 (triggering receptor expressed on myeloid cells) (21 fold induction). TREM1 is a receptor of the immunoglobulin superfamily that activates neutrophils and monocytes by signaling through the adapter protein DAP12 . The natural ligand for TREM1 is unknown. Using airway epithelial cell lines Q RT PCR showed a time dependent increase in TREM1 mRNA after treatment with 1,25(OH)2D3 (10^{-8}M) (peak induction 9.6 $\pm$ 1 fold at 12h). TREM2 mRNA was also observed in the airway epithelial cells but did not change with 1,25$(OH)_2D_3$ treatment. Combined treatment of airway epithelial cells with agonistic TREM1 antibody and 1,25$(OH)_2D_3$ (10^{-8}M) resulted in a 2-fold enhancement in the induction of human beta defensin 2 observed in the presence of 1,25$(OH)_2D_3$ alone ($p < 0.05$ compared to 1,25$(OH)_2D_3$ treatment). Putative VDREs were noted by sequence homology in both the mouse and human TREM1 promoter. 1,25$(OH)_2D_3$ (10^{-8}M 24h) stimulated TREM1 promoter (-1329/+1) activity (5. 6 $\pm$ 0.6 fold) and PU.1 transcription factor inhibited the 1,25$(OH)_2D_3$ induction. ChIP analysis indicated recruitment of VDR to the putative VDRE at -489/-477 in the hTREM1 promoter. These findings indicate for the first time that TREM1 is a novel target of 1,25$(OH)_2D_3$. Since TREM1 has been reported to accelerate the induction of the early pulmonary host response to S. pneumoniae, resulting in accelerated resolution of inflammation, 1,25$(OH)_2D_3$ induction of TREM1 may be a mechanism involved in improvement of pulmonary host defense.

***Disclosures: Puneet Dhawan**, None.*

SU0482

Suppression of PTH by the Vitamin D Analog, Eldecalcitol [1α,25-dihydroxy-2β-(3-hydroxypropyloxy)vitamin D_3], Is Modulated by Its High Affinity to the Serum Vitamin D Binding Protein and Resistance to Metabolism.

Cynthia Ritter[1], Alex Brown*[2]. [1]Washington University School of Medicine, USA, [2]Washington University in St. Louis School of Medicine, USA

The vitamin D analog, eldecalcitol [1α,25-dihydroxy-2β-(3-hydroxypropyloxy)-vitamin D3], has been shown to have greater efficacy than alfacalcidol (1α-hydroxyvitamin D3) for the treatment of osteoporosis. The explanation for the greater stimulatory effects on bone formation and inhibitory actions on bone resorption is not clear. Eldecalcitol has been found to be less potent than 1,25-dihydroxyvitamin D3 (calcitriol) in suppressing PTH in vivo. To define the mechanism for the latter observation, we compared the effects of eldecalcitol and calcitriol on PTH secretion by bovine parathyroid cells. Bovine parathyroid glands were sliced and digested with collagenase, and seeded in culture dishes in the presence of 15% newborn calf serum. After 72 hours of culture, the cells were treated with eldecalcitol or calcitriol (0, 0.1, 1, 10 or 100 nM) for 3 days with daily changes of medium. Fresh medium was added for 2 hours and the levels of PTH in the medium were measured by ELISA. Eldecalcitol was equipotent with calcitriol in regulating PTH under these conditions. Since eldecalcitol has a higher affinity for the serum vitamin D binding protein (DBP), we repeated the treatment in the absence of serum. In the absence of serum eldecalcitol was approximately 100 times more potent than calcitriol in suppressing PTH release. Therefore, DBP appears to limit the uptake and activity of eldecalcitol in parathyroid cells, providing an explanation for the lower PTH suppressing activity in vivo (100% serum). However, the 100-fold higher activity of eldecalcitol in the absence of serum was unexpected since the VDR affinity of eldecalcitol is half that of calcitriol. Preferential uptake was ruled out since tritiated eldecalcitol was taken up more slowly than tritiated calcitriol. The explanation for the greater potency of eldecalcitol in suppressing PTH in the absence of serum was revealed by metabolism studies. We measured the disappearance of radiolabeled eldecalcitol and calcitriol (1 nM) in the cultures over 24 hours. While calcitriol was completely degraded within this time, eldecalcitol was not metabolized, despite the induction of the vitamin D catabolic enzyme, 24-hydroxylase (CYP24A). The resistance to metabolism is the likely explanation for the higher potency of eldecalcitol in suppressing PTH in cell culture lacking serum. Thus, the unique properties of eldecalcitol in vivo can be attributed, at least in part, to its high DBP affinity which increases the half-life, but limits the uptake, of eldecalcitol, and to its reduced metabolism, which prolongs the activity of this analog in target tissues.

Disclosures: ***Alex Brown****, None.*
This study received funding from: Chugai Pharmaceutical Co., Ltd.

MO0001

Characterizing Cortical Bone Growth Rate Variability of Continuously Accreting Human Primary Lamellar Bone. BIN HU*[1], Santiago Gomez[2], Yusuf Juwayeyi[3], Igor Smolyar[4], Timothy Bromage[1]. [1]New York University College of Dentistry, USA, [2]Cadiz University, Spain, [3]Department of Anthropology, Long Island University, USA, [4]Ocean Climate Laboratory, National Oceanic & Atmospheric Administration, USA

Aim: The purpose of our research is to apply novel image analytical methods for characterizing cyclic - or periodic - textures manifest in bone that belong to the class we refer to as incremental patterns. Moreover, we investigate the midshaft femur histology of sub-Saharan Africans of Bantu origin and known life history with the purpose of characterizing growth rate variability for as many as five years of continuously accreting primary lamellar bone.

Methods: Bone is an incremental tissue, each increment being a distinct lamella (Bromage et al., 2009; human avg. 8-9 days), thus lamellae may be calibrated in time. Midshaft femur (N=10) montages of ground ca. 50 μm thick histological sections were imaged by circularly polarized light using Montage Explorer (Syncroscopy, Frederick, MD). First we acquire a digital monochrome image in raster format from which a binary image is rendered. Transects are semi automatically plotted perpendicular to the direction of growth, the image converted into vector format, and intersections of transects with lamellae given coordinates. Second, the impact of anisotropy on the accuracy of growth rate variability measurements is assessed by a calculation of entropy and an index of structural anisotropy. This is done by assigning a label to each intersection and evaluating all alternate possible relationships between lamellae crossed by adjacent transects.

Results: We visualize striking periodicities in lamellar growth rate, revealing cycles never before observed; e.g., we have observed cycles closely approximating a 28-day rhythm and ca. annual and even longer term (e.g. 1 and 2-year) cycles. We have also observed that secondary haversian remodeling of primary lamellar bone appears to occur preferentially within domains occupied by highly anisotropic lamellae, even though these domains are younger by as many as two years than earlier formed unremodeled primary bone.

Conclusions: To formalize the incremental pattern, we apply a discrete model based upon the parameterization of incremental structure. Information about biological periodicities, environmental and/or physiological cycles, and perturbations are all potentially contained within growth rate variability studies of lamellar incremental patterns. Because lamellae are formed within defined periods of time, quantitative measures of widths of individual lamellae provides time-resolved growth rate variability and reveal rhythms in human bone growth heretofore unknown.

***Disclosures: BIN HU**, None.*
This study received funding from: National Science Foundation (BCS-0741827)

MO0002

Do FGF23 Levels Change in Puberty in Concert with Markers of Bone Turnover? Craig Langman, Heather Price*. Children's Memorial Hospital, USA

A supply of phosphorus (Pi) is needed for bone and muscle growth in the pediatric years. Since the kidney is responsible for Pi, regulation changes with body and bone need, such as during puberty. FGF23 is a hormone that regulates kidney Pi handling. Growth and bone development markers, such as tartrate-resistant acid phosphatase5b (TRAP5b), derived from osteoclast activity, may also vary in puberty and with ethnicity. The purpose of this study was to measure serum FGF23 and TRAP5b levels in healthy children, and to determine how these values are influenced by age, gender, and ethnicity. C-Term FGF23 and TRAP5b was measured in 87 healthy children (45 females), ranging from 1-17y; Tanner stages, using a validated, self-reported method, ranged from 1-5. Self-identified ethnicity included 17 African-American (AA), 18 Asian or Hispanic (A/H), with 28 non-Hispanic white (nhW). C-Term FGF23 (RU/mL) and TRAP5b (U/L) were determined, in duplicate, using ELISAs (ALPCO Diagnostics, Windham, NH; Quidel, Santa Clara, CA), and results are reported as the median [interquartile ranges]. Boys had similar levels of FGF23 as girls across all age groups (22.5 [11.1-38] vs 28 [11.9-40.2]; p = NS). FGF23 levels were higher in early vs late puberty ($p<0.05$): pre-pubertal, 25 [9.7-37.2]; stage 1-3 puberty, 29.8 [20.3-42]; stage 4-5 puberty, 15.7 [8-27.2]. TRAP5b levels varied similarly with respect to puberty: pre-pubertal, 8.2 [4.1-10.4]; stage 1-3 puberty, 8.6 [5.7-10.5] > stage 4-5 puberty, 2.5 [1.7-3.8] ($p<0.001$). AA children had FGF23 comparable to nhW (35.1 [22.4-43.2] v 26.1 [12.5-40.3], p=0.28), while A/H children have lower levels of FGF23 (17.3 [8.1-25]) compared to AA ($p<0.01$) and nhW ($p<0.05$). However, nhW have lower TRAP5b (p = 0.05) compared to AA and A/H which were similar (6.4 [3.2-9.9; 8.3 [3.4-12]; 8.9 [5.9-10.3], respectively). In conclusion, FGF23 and TRAP5b move synchronously in puberty, but differ by ethnicity. Overall, since bone density differs between AA and nhW, simple supply of Pi cannot account for it, given the similarity of FGF23. Such control factors are demonstrated by differences at the level of bone directly, as shown by TRAP5b. FGF23 levels can be interpreted independently of ethnicity but not of pubertal stage.

***Disclosures: Heather Price**, None.*

MO0003

Evaluation of Bone Mass Adjustment By Body Size Techniques In Paediatric Population With Pathological Conditions. Elena Bonel[1], Silvana Di Gregorio*[1], Miguel Garcia[1], Luis Del Rio[2]. [1]Cetir Centre Medic, Spain, [2]Cetir Centre Medical, Spain

In paediatric population, bone mineral density (BMD) may differ from age-expected normal values, not only because of a disease, but also for height deviation. For children, BMD value is expressed as a Z score. BMD interpretation is complicated when weight or height differ from age matched children due to different pathologies that impact over growth. Aims and Population: the relation between body size deviation and bone mineral content (BMC) in total skeleton and lumbar spine was studied in 2605 subjects (1678 girls, 927 boys, age range 3 months to 18 years) by height for age percentile's group. G1:15th to 25th percentile; G2: 3rd to 15th percentile and G3 subjects below 3 rd percentile, and in turn each group was subdivided into different pathologic subgroups that are known to be associated with smaller skeleton size than age matched children . In this way, we may study the same pathology with different growth impact. Methods: total body (TB), excluding head from analysis, and lumbar spine (LS) by DXA (GE Lunar models DPX-L and Prodigy) were measured for every patient. For adjustments of bone mass the following relations were analyzed: LS-BMD/Age; Volumetric LS-BMDv/Age; TBBMC/Age; TBBMC/Height; TBBMC /Lean Mass; TBBMC/(Lean Mass /Height). Results: For low-bone-mass-for-age identification purposes, most of LS-BMD and LS-BMDv values did not show any discrepancy at any group. TBBMC identified significantly deviations in 75% of pathologic groups identify them. The results according to percentile group were as follows: G1, nobody showed any discrepancy at any TB skeletal side. G2 only found discrepancies in patient with Anorexia Nervosa (AN) and Nephritic Syndrome (NS). The best adjustment was TBBMC by age for AN, while for NS was TBBMC by height. G3: needed adjustment. Best adjustment model for most of them, was TBBMC adjusted by height, due to higher diagnostic sensibility, because this formula offered the lower Z score. The adjustment of TBBMC by lean mass was only necessary in children with Rheumatoid arthritis. Conclusion: There is no ideal adjustment method to be used in all the paediatric pathological conditions. LS-BMD seems to be the most recommended for raw application without adjustments. TBBMC without head should be adjusted in adolescent children with significantly different height for their age and sex (below 3rdP). In cases of growth deficit, the method that adapts to a greater number of pathological conditions is TBBMC adjusted by height.

***Disclosures: Silvana Di Gregorio**, None.*

MO0004

Maturation of Parathyroid Hormone Regulation by Serum Ionized Calcium in the First Year of Life. Atul Sharma*, Sherry Agellon, Sina Gallo, Catherine Vanstone, Hope Weiler, Celia Rodd. McGill University, Canada

Plasma ionized calcium (iCa) is the principle determinant of parathyroid hormone concentration (PTH), with Pearson correlations (r) from -0.38 in children to -0.66 in adults. Although the expected inverse correlation between PTH and iCa is said to be established by 6 months (mo) of age, these studies included few infants. The McGill infant vitamin D dose-response study has now recruited 122 term newborns, providing data on parathyroid gland regulation in healthy breastfed Canadian infants at 1, 2, 3, 6, 9 and 12 mo of age.

Intact PTH (ELISA, Immunotopics) increases from 19.6 $\pm$11.3 pg/ml at 1 mo to a plateau of 35-40 pg/ml between 9-12 mo. In the same period, iCa (Radiometer ICA) falls from 1.40$\pm$0.03 to 1.33-1.34 mM. The correlation between them is not statistically different from zero at any time (table 1), which is not simply a function of study size: At 1 mo, $r = \pm 0.35$ between iCa and PTH could be detected with a power of 95% (n=101, $p<0.05$).

A generalized least squares (GLS) multivariate regression was used to improve power and sensitivity by adjusting for other covariates and exploiting the repeated measures study design to increase the effective sample size and control for within-subject correlations. Main effects included iCa (mM), PO_4 (mM), 25(OH) vitamin D (nM, DiaSoran RIA), birth weight (g), age (days), and gender; and within-subject correlations were modeled as an exponential decay over time (AR1). Three significant predictors of PTH were identified, namely iCa (regression coefficient β = -50.8 $\pm$ 19.9, p=0.01), serum PO_4 (β = 11.8$\pm$3.9, p=0.003) and age (β = 0.085$\pm$0.010, $p <$ 0.001). There were no effects for 25(OH) D (p=0.6), gender (p=0.8), or birth weight (p=0.2). The regression coefficients for both iCa and PO_4 are in the expected directions, with the partial correlation between PTH and iCa =-0.2 after adjustment for other covariates. One significant two-term interaction was identified between iCa and age (β =-0.66$\pm$0.20, $p<0.001$) i.e. the relationship between PTH and iCa grows stronger with time.

Despite the absence of the expected PTH-iCa relationship before one year of age, a sensitive repeated-measure analysis in a cohort of healthy breastfed infants shows a weak relationship between concentrations of PTH and both iCa and PO_4 after adjustment for the time trend, suggesting that parathyroid gland regulation continues to mature throughout the first year of life.

Age (mo)	1	2	3	6	9	12
PTH (mean±SD)	19.6±11.3	18.2±10.0	17.1±10.5	29.9±14.5	39.9±16.7	34.6±14.3
PTH range (pg/ml)	1.3-64.6	2.2-52.0	0.4-85.9	10.0-77.8	9.2-87.9	16.2-91.1
iCa (mean±SD)	1.40±0.03	1.39±0.04	1.38±0.04	1.35±0.03	1.34±0.03	1.33±0.03
iCa range (mM)	1.29-1.52	1.38-1.48	1.30-1.46	1.28-1.42	1.28-1.43	1.26-1.39
Pearson r	0.10	-0.11	-0.14	-0.10	-0.20	-0.02
95% CI	(-0.09, 0.29)	-0.31-0.11	(-0.34,0.08)	(-0.31,0.13)	(-0.42,0.05)	(-0.29,0.26)
n	101	84	84	79	66	52

Table 1

***Disclosures: Atul Sharma**, None.*

MO0005

Normative Bone Mass for Healthy, Breast fed Infants Followed Longitudinally During the First Year of Life. Sina Gallo*, Celia Rodd, Hope Weiler, Catherine A Vanstone, Sherry Agellon. McGill University, Canada

Bone diseases are increasingly recognized as a problem in early life. For over 2 decades dual-energy x-ray absorptiometry (DXA) has been the gold standard for estimating bone mineral content (BMC) and fracture risk in adults. More recently DXA has been used to evaluate BMC in health and diseases in paediatrics. Optimal tools for the accurate assessment of bone are of importance in paediatrics, however reference data currently do not exist in infancy. We measured bone mass as part of a larger ongoing clinical trial to assess vitamin D_3 dose response in predominately breastfed infants. Healthy, term infants (weight for age between 5th and 95th percentiles, CDC growth curves) were recruited from clinics and a large primary care center located in the Montreal area and followed longitudinally from 1 to 12 months of age. Sixty percent were born during the vitamin D synthesizing period (April-October). At baseline, 3, 6, 9 and 12 months whole body (WB), femur and lumbar spine (L1-4) BMC were measured using DXA (QDR 4500A, Hologic Inc.) in array mode. A capillary blood sample was collected at each visit and analyzed for 25(OH)D using a commercially available radioimmunoassay (Diasorin). All infants included in this analysis had plasma 25(OH)D > 25 nmol/L. Using repeated measures ANOVA, a significant time effect was noted ($p<0.01$) as bone mass increases with age (Table 1). During the year, WB BMC increased by 140%, spine BMC by 120% and femur BMC by 210%. This data provides important data not currently available and as is based on a healthy sample of breast fed infants representing an appropriate standard. This, in addition to clinical data will ultimately aid in the diagnosis, interpretation and response to treatment for paediatric bone diseases.

Time Point	Whole Body BMC (g)	Lumbar Vertebrae 1-4 BMC (g)	Femur BMC (g)
1 mo	99.46 ± 17.25 (102)	2.81 ± 1.15 (103)	3.47 ± 0.72 (103)
3 mo	132.31 ± 20.35 (86)	3.35 ± 0.77 (89)	4.88 ± 0.94 (89)
6 mo	171.74 ± 27.27 (64)	4.10 ± 0.70 (71)	6.33 ± 1.28 (72)
9 mo	201.00 ± 28.83 (57)	5.06 ± 0.82 (68)	8.24 ± 1.91 (68)
12 mo	235.73 ± 31.28 (47)	6.24 ± 0.92 (60)	10.66 ± 2.50 (59)

Table 1: Mean ˘ SD (n) bone mineral content of whole body, spine and femur from 1 to 12 months

***Disclosures: Sina Gallo**, None.*

MO0006

Adolescent Dietary Intake is Associated with Adult Bone Measurements. Julie Eichenberger Gilmore*[1], Elena Letuchy[2], Trudy Burns[2], Kathleen Janz[2], James Torner[2], Linda Snetselaar[2], Steven Levy[2]. [1]Univ of Iowa, Institute for Clinical & Translational Science, USA, [2]University of Iowa, USA

Context: Calcium (Ca) and vitamin D (vit D) intake are essential for bone development. Early and continuing adequate intake has a prolonged effect on bone health in adulthood. Objective: To assess associations of dietary intake of Ca and vit D in adolescence (high school) and in adulthood with bone mineral content and density (BMC and BMD) taking into account other important factors (body size, health history, medication use, and physical activity). Participants: Subjects (542F/403M) were young to middle-age parents of child participants of the Iowa Bone Development Study. Setting: General community. Instruments and Analysis: Parents provided information regarding current and high school food intake, physical activity, health history and current medication use. Whole body (WB), hip and spine bone scans were obtained using the Hologic 4500A densitometer. Adjusted for body size and age, bi-variable associations between bone outcomes and dietary and other predictors were investigated followed by two-stage multiple regression modeling to obtain the most important predictors. Main Outcome Measures: WB without head BMC, hip BMC and BMD, and spine BMC and BMD. Results: Both men and women reported adequate intakes of Ca and vitamin D during high school years (total mean intake - 1161 mg/day Ca and 253 UI /day vitamin D for women; and 1695 mg/day Ca and 384 UI/day vitamin D for men). Adjusting for body size and age, Ca intake in high school was significantly associated with WB BMC ($p<0.01$), hip BMC ($p<0.05$) and BMD ($p<0.01$), and spine BMC ($p<0.05$) and BMD ($p<0.01$) for women; associations were similar for vit D intake. Ca intake was not as important for adult women but significant relationships remained for vit D. For men, both current and high school Ca and vit D intakes appear to be important for WB BMC ($p<0.01$). Current Ca intake was significantly associated with hip BMD ($p<0.0.5$); however, there were no significant associations with either high school or current Ca/vit D intakes and hip and spine measures. Associations with Ca intake persisted when other predictors were included in multiple regression models (health history, physical activity, medication use): high school Ca intake was statistically significantly associated with WB BMC, hip BMC and BMD, and spine BMC for women ($p<0.05$); for men current Ca intake was significantly associated with bone outcomes. Conclusions: Results suggest that early adequate Ca and vit D intake improves adult bone outcomes, especially for women.

Supported by NIH R01-DE09551, R01-DE12101, M01-RR00059.

***Disclosures: Julie Eichenberger Gilmore**, None.*

MO0007

Breastfeeding Duration is a Positive Independent Predictor of Trabecular and Cortical Bone Parameters at Age 21 Years. Emma Laing*[1], Norman Pollock[2], Ashley Ferira[3], Ruth Taylor[1], Paul Bernard[2], Richard Lewis[1]. [1]The University of Georgia, USA, [2]Medical College of Georgia, USA, [3]University of Georgia, USA

No data exist regarding the long-term effects of breastfeeding on trabecular and cortical bone geometry. In this study, relationships between duration of infant breastfeeding and subsequent young adult bone mass, density, and geometry were assessed at age 21 years. Tibial bone parameters were measured in 71 white females (aged 21 ± 0.4 years) by using peripheral quantitative computed tomography at the 4% and 20% sites from the distal metaphyses, which reflect trabecular bone and cortical bone, respectively. At the trabecular site, the following bone outcomes were assessed: total and trabecular volumetric BMD (vBMD), total bone cross-sectional area (CSA), and bone strength index (BSI; calculated as total CSA x total $vBMD^2$). At the cortical site, cortical vBMD, cortical CSA, total CSA, cortical BMC, cortical thickness, endosteal circumference, and polar strength-strain index were assessed. Breastfeeding duration was self-reported by each participant's biological mother. Fat-free soft tissue (FFST) and fat mass were measured using dual-energy X-ray absorptiometry. The independent role of breastfeeding duration on bone parameters was determined using hierarchical multiple linear regression models, including height, FFST, and fat mass as covariates. Twenty percent of the participants reported not having been breastfeed; 32% were breastfed 1-6 months; 24% were breastfed 6-12 months; and 24% were breastfed 12 months or longer. At the trabecular site of the tibia, breastfeeding duration was a positive independent predictor of total vBMD ($\beta = 0.279$, $p = 0.045$). Although breastfeeding duration was positively correlated to BSI ($r = 0.278$, $p = 0.033$), it was not an independent predictor of BSI in the regression model that included height, FFST, and fat mass as covariates. At the cortical site, breastfeeding duration was a positive independent predictor of cortical BMC ($\beta = 0.240$, $p = 0.022$), cortical CSA ($\beta = 0.232$, $p = 0.020$), and cortical thickness ($\beta = 0.357$, $p = 0.008$). There were no associations between breastfeeding duration and the other bone parameters. These results suggest that a greater duration of breastfeeding may have long-term benefits on cortical and trabecular bone. Given that our findings should be considered hypothesis generating, further studies are needed to elucidate the role of breastfeeding on bone development.

***Disclosures: Emma Laing**, None.*

MO0008

Changes in Leptin, Adiponectin, and 25-Hydroxyvitamin D as Determinants of Bone Geometry, Mass, and Density in Late-Adolescent Females: A 3-Year Study. Ashley Ferira*[1], Norman Pollock[2], Emma Laing[3], Ruth Taylor[3], Daniel Hall[3], Paul Bernard[2], Dorothy Hausman[3], Clifton Baile[1], Mark Hamrick[2], Barbara Gower[4], Richard Lewis[3]. [1]University of Georgia, USA, [2]Medical College of Georgia, USA, [3]The University of Georgia, USA, [4]University of Alabama, USA

The role of adipokines and 25-hydroxyvitamin D [25(OH)D] on trabecular and cortical bone is not well understood. Changes in leptin, adiponectin and 25(OH)D were examined with respect to changes in trabecular and cortical bone over a 3-y period in late-adolescent white females. Fasting sera were collected from participants at baseline (n=67, aged 18.2±0.4 y) and follow-up (n=67, aged 21.3±0.5 y) for assessment of 25(OH)D, leptin and adiponectin. Peripheral QCT scans of the tibia and radius were obtained at the 4% (trabecular bone), 20% (cortical bone), and 66% [muscle cross-sectional area (MCSA)] sites from the distal metaphyses. The independent role of leptin, adiponectin and 25(OH)D on tibial and radial bone outcomes was determined using hierarchical multiple linear regression models, including baseline tibial or forearm length, baseline MCSA, and change in MCSA as covariates. At baseline, mean±SD for leptin, adiponectin and 25(OH)D were 14.3±5.3ng/mL, 14.9±4.9µg/mL, and 88.6±23.7nmol/L, respectively. At follow-up, values for leptin, adiponectin and 25(OH)D were 10.9±6.3ng/mL, 13.9±5.0µg/mL and 97.2±32.2nmol/L, respectively. At the tibia, change in leptin was a negative independent predictor of changes in trabecular volumetric BMD (vBMD; β=-0.290, p=0.045), bone strength index (BSI; β=-0.314, p=0.019), cortical vBMD (β=-0.291, p=0.025), and strength-strain index (SSI; β=-0.331, p=0.011). Also at the tibia, change in 25(OH)D was a positive independent predictor of changes in total cross-sectional area [CSA; trabecular site; (β=0.371, p=0.045) and cortical site; (β=0.514, p<0.001)]

and endosteal circumference (β=0.555, p<0.001); however, it was a negative independent predictor of cortical BMC (β=-0.412, p<0.001), cortical CSA (β=-0.384, p<0.001), cortical thickness (β=-0.493, p<0.001), and endosteal circumference (β=-0.555, p<0.001). At the radius, change in leptin was a negative independent predictor of change in total CSA (cortical site; β=-0.255, p=0.044); however, change in adiponectin was a positive independent predictor of change in cortical CSA (β=0.255, p=0.044). There were no associations between changes in leptin, adiponectin and 25(OH)D and the other bone parameters. Adiponectin seems to have a minimal effect on trabecular and cortical bone; however, high levels of leptin and 25(OH)D seem to have unfavorable and favorable effects, respectively, on trabecular and cortical bone, and these effects are more pronounced at the tibia.

***Disclosures: Ashley Ferira**, None.*

MO0009

Effects of Maturational Timing on the Accrual of Adult Bone Mineral Content. Stefan Jackowski*, Marta Erlandson, Robert L. Mirwald, Robert Faulkner, Donald A Bailey, Adam Baxter-Jones. University of Saskatchewan, Canada

Purpose: A higher bone mass accrual in young adulthood may reduce the risk of osteoporosis and subsequent fracture later in life. The role of maturational timing on optimizing bone accrual is controversial. An earlier onset of maturation may expose males and females to estrogen earlier, providing bones with a greater sensitivity to mechanical loading. This enhanced sensitivity may improve bone mineralization and thus increase bone strength. However, the time prior to puberty is associated with a heightened response to osteogenic stimulation. Thus, the question that is often asked is does the duration of osteogenic stimulation prior to the onset of maturation override the effects of the hormonal influx during puberty. The purpose of this study was to examine the long term relationship between the onset of maturation and adult bone mineral content (BMC) accrual.

Methods: 230 individuals (110 males, 120 females) from the Saskatchewan Pediatric Bone Mineral Accrual Study (PBMAS) were classified based on age of peak height velocity into early, average, and late maturational groups. BMC was assessed during adolescence and in adulthood using dual energy x-ray absorptiometry (DXA). Hierarchical multilevel models were constructed to show the independent accrual of BMC by maturity group whilst controlling for sex, body size, physical activity and body composition.

Results: There were no significant difference between male maturation groups ($p>0.05$). In contrast, early maturing females developed greater total body (TB) BMC than their average and late maturing peers ($p<0.05$), with late maturing females having developed the least amount of adjusted TBBMC by adulthood.

Conclusions: In this group of healthy participants, there appears to be a gender-dependent effect on the relationship between maturational timing and TBBMC accrual, with males showing no significant difference, while late maturing females display compromised TBBMC accrual.

***Disclosures: Stefan Jackowski**, None.*

MO0010

Is Preterm Birth Detrimental to Adolescent Bone Mineral Accrual. Marta Erlandson*[1], Lauren Sherar[1], Adam Baxter-Jones[1], Stefan Jackowski[1], Heidi Ludwig-Auser[2], Chris Arnold[2], Koravangattu Sankaran[1]. [1]University of Saskatchewan, Canada, [2]Saskatoon Health Region, Canada

Purpose: Adult bone mineral content (BMC), density (BMD) and estimated strength are positively correlated with birth weight suggesting that skeletal health has its origins early in life. It has been suggested that low birth weight individuals (<2500g) have lower bone mass at birth and in adulthood compared to their normal birth weight peers. Confounding this association is the tendency for low birth weight individuals to be preterm (gestation < 37 weeks). Prematurity may be important as approximately 80% of fetal bone is produced in the last trimester, with peak accretion rates occurring at around 35 weeks of gestation. An additional critical period for bone accrual is adolescence; however, there is a paucity of information on adolescent bone status of preterm infants. The purpose of this study was to examine the associations between being born preterm and low birth weight and bone parameters in adolescence.

Methods: All preterm (<35 weeks gestation) infants who were born at the Royal University Hospital between October 1st 1989 and December 31st 1995 with a birth weight of less than 1850 grams (n= 359) were invited to take part in this study. Complete measures in adolescence were obtained for 28 males and 22 females. The preterm individuals were age and sex matched to control individuals (n=127) who were born at full term (>37 weeks gestation) and with a weight appropriate for gestational age (10th-90th percentile). Total body (TB), hip and spine bone mineral content was assessed using dual energy x-ray absorptiometry (DXA). ANOVA's were used to assess differences between the groups in height, weight, BMC, maturity, physical activity and diet. ANCOVA's were used to assess differences in TB, hip and spine BMC between groups while controlling for height, lean mass, sex, maturity, physical activity and diet.

Results: The normal birth weight controls were significantly taller and heavier than the preterm low birth weight individuals in adolescence (p<0.05). Controls also had a greater absolute BMC in adolescence than preterm low birth weight individuals (p<0.05). However, when height, lean mass, sex, diet,physical activity and maturity were controlled for there were no differences in bone parameters among the groups (p>0.05).

Conclusions: Although preterm low birth weight infants were shorter and lighter in adolescence, they had appropriate bone mineral content for their body size in this sample.

***Disclosures: Marta Erlandson**, None.*

MO0011

Lower Bone Mass in Prepubertal Overweight Children with Pre-Diabetes. Norman Pollock*[1], Paul Bernard[1], Barbara Gower[2], Karl Wenger[3], Sudipta Misra[4], Jerry Allison[5], Haidong Zhu[4], Catherine Davis[4]. [1]Medical College of Georgia, USA, [2]Department of Nutrition Sciences, University of Alabama-Birmingham, USA, [3]Department of Orthopedic Surgery, Medical College of Georgia, USA, [4]Department of Pediatrics, Medical College of Georgia, USA, [5]Department of Radiology, Medical College of Georgia, USA

Childhood studies of the fat-bone relationship are conflicting, possibly reflecting the influence of metabolic abnormalities in some but not all obese kids. In this study, we compared bone mass between prepubertal overweight children (7-11 yr) with (n=41) and without (n=99) pre-diabetes. Associations of bone mass with total and central adiposity, glucose intolerance, insulin sensitivity, lipid profile, and systemic inflammation were also determined. An oral glucose tolerance test was used to identify those with pre-diabetes and for determination of fasting glucose, 2-h glucose, glucose area under the curve (AUC), 2-hr insulin, and insulin AUC. Blood samples were also assessed for lipids and C-reactive protein (CRP). Total body bone mineral content (BMC), lean mass (LM), and fat mass (FM) were measured by DXA. Visceral adipose tissue (VAT) and subcutaneous abdominal adipose tissue (SAAT) were assessed by MRI. Total BMC was 5% lower in the pre-diabetes vs. normal-glucose group after control for sex, race, height, and weight (p<0.03). In the normal-glucose group, fasting glucose, 2-hr glucose, glucose AUC, 2-h insulin, insulin AUC, triglycerides, total cholesterol, HDL-C, LDL-C and CRP were not associated with total BMC after control for covariates. Similar findings were observed in the pre-diabetes group; however, 2-h insulin (r=-0.37), insulin AUC (r=-0.36), and CRP (r=-0.43) were inversely associated with total BMC (all p<0.03). In the total sample, FM was positively related to total BMC (r=0.23, p=0.01), after control for sex, race, height, and LM. However, VAT (r=-0.20) and SAAT (r=-0.21) were negatively correlated with total BMC (both p<0.03), after control for sex, race, height, LM, FM, and SAAT or VAT. Stepwise regression was conducted to examine the independent association of sex, race, height, weight, FM, VAT, SAAT, triglycerides, LDL-C, CRP, vigorous physical activity (VPA), and energy intake (EI) with BMC. Triglycerides, LDL-C, CRP, VPA, and EI were included in the regression model since they were related with BMC in the univariate regression models (all p<0.05). Height (11%), weight (65%), VAT (4%), and SAAT (2%) explained 82% of the variance in total body BMC, with no contribution by the other variables. Our data suggest that prepubertal overweight children with pre-diabetes may be at risk for poor skeletal development. It also appears that high levels of central, rather than total, adiposity may be deleterious for developing bone.

***Disclosures: Norman Pollock**, None.*

MO0012

Muscle Parameters are Related to Bone Strength and Microstructure in Children: A High-resolution pQCT Study. Sarah Moore*[1], Danmei Liu[1], Melonie Burrows[1], Douglas Race[2], Deetria Egeli[1], Heather McKay[1]. [1]University of British Columbia, Canada, [2]University of Victoria, Canada

Even in childhood, muscle and bone are inextricably linked. However, many questions remain as to the relation between bone microstructure and muscle during these early years. With advanced imaging systems it is now possible to assess bone microstructure *in vivo*. Thus, our objective was to examine the relationship between muscle mass, power and force, and bone microstructure in children using high-resolution (HR) pQCT (Scanco^{TM}). We assessed 120 children ages 9.2-11.6yrs (40 boys; age 10.5±0.6yrs; height 143.4±7.4cm; weight 39.3±9.0kg and 80 girls; age 10.5±0.6yrs; height 143.7±8.0cm; weight 37.1±8.5kg). We estimated muscle mass as mineral free lean body mass (LBM; kg) with dual energy X-ray absorptiometry (DXA) and muscle power (W/kg) and force (N/kg) measured during a two-footed jump via mechanography ground reaction force platform (GRFP; Novotec^{TM}). We measured the 8% site in the distal tibia using HR-pQCT which permits *in vivo* (110 slices; 9.02mm) assessment of bone microstructure. Our primary bone outcome was bone strength index [BSI, mg2/mm4 = total area (ToA; mm2) x total density (ToD2; mg/cm^3) /10,000]. We also assessed cortical [cortical density (CoD, mg/cm^3), cortical thickness (CtTh, mm)] and trabecular [trabecular density (TrD, mg/cm^3), trabecular number (TbN, mm)] bone compartments (all Table 1). We developed independent multiple regression models to evaluate the variance in bone microstructure (HR-pQCT) explained by LBM (kg; DXA), muscle power (W/kg; GRFP) or force (N/kg; GRFP), after adjusting for age (yrs), ethnicity, weight (kg) and tibial length (mm). In boys, LBM, and not power or force, predicted 22.3% of the variance in ToA ($p<0.001$). In girls, LBM, and not power or force, predicted 17.4% of the variance in BSI; 14.1% of the variance in ToD, and not ToA ($p<0.001$). Moreover, in girls, LBM predicted 14.0% and 14.7% of CrTh and TrD, respectively ($p<0.001$). The established muscle-bone link is evident in some microstructure compartments as early as childhood. Prospective studies that examine the bone microstructure-muscle relation are needed.

Table 1. Descriptives for lean body mass by DXA, muscle power and force via GRFP, and bone strength and microstructure variables measured by HR-pQCT at the distal 8% site of the tibia

Variable	Children (n=120)	
	Boys (n=40)	Girls (n=80)
Lean body mass (LBM; kg)	24.6±4.2	24.1±4.7
Muscle power (W/kg)	35.8±4.9	36.8±5.0
Muscle force (N/kg)	23.5±4.4	25.0±4.1
Bone strength index (BSI; mg²/mm⁴)	3622.5±1368.2	3094.4±1009.9
Total area (ToA; mm²)	634.0±112.8	608.7±77.8
Total density (ToD; mg/cm³)	241.4±41.6	226.9±28.1
Cortical density (CoD; mg/cm³)	638.8±33.0	629.0±37.5
Cortical thickness (CtTh; mm)	0.59±0.23	0.50±0.16
Trabecular density (TrD; mg/cm³)	184.2±28.7	174.8±22.8
Trabecular number (TrN; mm)	2.03±0.20	1.91±0.22

Data are mean±SD

Moore S, Table 1

***Disclosures: Sarah Moore**, None.*

MO0013

Reduced Mechanical Loading Results In Deficits In Cortical But Not Trabecular Bone Structure: A Study of Children With Legg-Calve Perthes Disease. Sandra Iuliano-Burns*[1], Skye Macleod[2], Ian Torode[3], Ali Ghasem-Zadeh[1], Roger Zebaze[4], Ego Seeman[1]. [1]Austin Health, University of Melbourne, Australia, [2]University of Melbourne, Australia, [3]Royal Children's Hopsital, Australia, [4]Austin Health, Australia

Physical activity during growth is associated with greater bone size, thickness and strength with these structural traits enhanced in the playing arm of racquet sport players compared to the non-playing arm in those who commenced playing before puberty. However little data are available describing the effects of mechanical loading on bone structure at weight bearing bones in children using the same unilateral model that controls for genetics, nutrition and other variables that influence bone traits. We compared the side-to-side differences in bone structure at the tibiae in children with unilateral Legg-Calve Perthes disease (limited weight bearing ability on the affected limb) to test the hypothesis that increased loading on the unaffected side would result in a wider bone with a thicker cortex while a smaller perimeter and thinner cortex would be observed at the non-weight bearing tibia.

We examined trabecular and cortical architecture at the distal tibiae using high-resolution pQCT (XtremeCT, Scanco) in 27 cases (78% male, mean age 11.1±0.5 yrs, 68% pre-pubertal, mean duration of disease 1.4±0.3 yrs) and compared the side-to-side differences to 27 healthy age- and sex-matched controls (78% males, mean age 11.6± 0.6 yrs). Differences between the affected and non-affected limbs were compared using paired t-test and comparisons of these side-to-side differences with controls determined using unpaired t-tests.

In cases, cortical area (8±4%, $p < 0.05$) and CSMI (4±3%, $p < 0.05$) were lower in the affected leg compared to the unaffected leg, with a trend towards reduced cortical thickness (7±5%, $p = 0.1$). The side-to-side difference for cortical thickness (7±5% v -3±2%, $p < 0.05$) and area (8±4% v -2±2%, $p < 0.05$) in cases was greater than for controls. In pre-pubertal cases, there was a trend for reduced cortical area of the tibia of the affected limb compared to controls after adjusting for multiple comparisons (53.9±5.1 v 64.6±1.8 mm^2, $p < 0.05$). No differences were observed for trabecular area, number, thickness, or for total cross sectional area.

Extended periods of unilateral loading was not sufficient stimulus to enhance cortical thickness and area but unloading of a limb was associated with reduced cortical thickness, area and strength but not total cross sectional area. The timing and duration of the disease would likely influence if these deficits are corrected once normal physical activity levels are re-established.

***Disclosures: Sandra Iuliano-Burns**, None.*

MO0014

Underdeveloped Trabecular Bone Microarchitecture is Related to Suppressed Bone Formation in Nonambulatory Children with Cerebral Palsy. Christopher Modlesky*[1], Mary Barbe[2], Deepti Bajaj[1], Freeman Miller[3]. [1]University of Delaware, USA, [2]Temple University School of Medicine, USA, [3]AI duPont Hospital for Children, USA

Trabecular bone microarchitecture is underdeveloped in nonambulatory children with cerebral palsy (CP). However, whether the poor bone development is due to decreased bone formation, increased bone resorption or both has not been investigated. The aim of this study was to determine if the underdeveloped trabecular bone microarchitecture in children with CP is related to markers of bone formation and bone resorption. Eleven nonambulatory children with CP and 11 typically developing children matched for age (5 to 14 y), maturity (Tanner stage) and gender participated in the study. Magnetic resonance images were collected from the lateral side of the nondominant distal femur and measures of trabecular bone micro-architecture [i.e., apparent trabecular bone volume to total volume (appBV/TV), trabecular number (appTb.N), trabecular thickness (appTb.Th) and trabecular separation (appTb.Sp)] were determined using software created with Interactive Data Language (Research Systems, Inc, Boulder CO). Serum osteocalcin (OC), a measure of bone formation, was determined using RIA. Serum cross-linked telopeptide of type I collagen (ICTP), a measure of bone resorption, was determined using ELISA. There were no group differences in age or Tanner stage ($p > 0.05$). Children with CP were shorter and had lower body mass than controls ($p < 0.05$). Children with CP also had lower appBV/TV (0.234 ± 0.049 vs. 0.314 ± 0.022), appTb.N (1.360 ± 0.213 vs. 1.690 ± 0.078 1/mm) and appTb.Th (0.170 ± 0.014 vs 0.185 ± 0.008 mm) and higher appTb.Sp (0.590 ± 0.158 vs. 0.408 ± 0.031 mm) than controls (all $p < 0.01$). Furthermore, serum OC was lower in children with CP than controls (19 ± 8 vs. 25 ± 5 ng/mL, $p = 0.027$). There was also a trend for lower ICTP in children with CP than controls (16 ± 7 vs. 21 ± 4 ng/mL, $p = 0.068$). Serum OC was positively correlated with appBV/TV ($r = 0.74$), appTb.N ($r = 0.64$) and appTb.Th ($r = 0.76$) and negatively correlated with appTb.Sp ($r = -0.71$) in children with CP (all $p < 0.05$), but no significant relationships were observed in controls ($r = -0.12$ to 0.11, $p > 0.69$). Serum ICTP was not significantly related to any measure of trabecular bone microarchitecture in children with CP ($r = -0.39$ to 0.41, $p > 0.21$) or controls ($r = -0.44$ to 0.37, $p > 0.13$). The findings suggest that the underdeveloped trabecular bone microarchitecture in children with CP is primarily related to poor bone formation. Supported by NIH HD050530

***Disclosures: Christopher Modlesky**, None.*

MO0015

Osteoclast Increases in the Brtl Mouse Model for Osteogenesis Imperfecta Occur through Marrow Mesenchymal Stromal Cell Dependent and Independent Mechanisms. Patricia Collin-Osdoby*[1], Linda Rothe[1], Matthew Kwong[1], Brianna Frigerio[1], Leanna Morinishi[1], Wayne A Cabral[2], Philip Osdoby[3], Joan C Marini[2]. [1]Washington University, USA, [2]NIH, USA, [3]Washington University in St. Louis, USA

The Brtl mouse, a knock-in model for moderately severe osteogenesis imperfecta, has a glycine substitution (G349C) in half of its type I collagen α1(I) chains, resulting in mice with reduced cortical and trabecular bone volumes, matrix insufficiency, abundant osteoclasts (OCs), and brittle bones. Bone sections from Brtl vs. WT mice exhibit more OCs that are also larger, more intensely TRAP+, and associated with greater in vivo bone resorption. We investigated mechanisms for the increase in OC bone-resorbing cells in Brtl OI mice. Although both RANKL and OPG mRNA and protein expression were increased in Brtl compared to WT bones (and in mesenchymal stromal cells (MSCs) cultured from such bones), RANKL/OPG ratios were equivalent in both genotypes. Thus, changes in RANKL relative to OPG expression do not provide a simple explanation for increased OC formation and activity in Brtl mice. Using isolated pre-OC marrow cultures, we obtained higher RANKL-induced OC formation from Brtl compared to WT mice. This suggests that an expanded OC precursor pool exists in Brtl marrow, consistent with our finding of higher RANK mRNA levels in Brtl bones. In addition, when marrow pre-OC populations (Brtl or WT) were directly co-cultured with MSCs from Brtl or WT bone and VD3 to promote osteoclastogenesis, 2-fold greater OC formation occurred in those cultures containing Brtl MSCs compared to WT MSCs. This was true regardless of the pre-OC origin (Brtl or WT). Thus, Brtl MSCs are responsible for driving enhanced osteoclastogenesis in co-cultures with pre-OCs. Because VD3 increases RANKL and decreases OPG mRNA expression similarly in both Brtl and WT MSCs, additional MSC-related mechanisms must be involved in their co-culture stimulation of OC formation. Furthermore, the enhanced OC generating capacity of Brtl pre-OCs was suppressed by their co-culture with WT MSCs, suggesting that MSCs may normally restrain OC formation under physiological conditions and that such mechanisms may be altered in Brtl MSCs. Similarly, MSCs have been shown to exert immunomodulatory and anti-inflammatory actions in other studies. Overall, we conclude that increased formation of bone-resorbing OCs in Brtl mice involves an expanded OC precursor pool and is crucially dependent on MSC-associated regulatory signals that may drive elevated osteoclastogenesis in Brtl mice but help restrain OC formation in WT mice. Further elucidation of these pathways may lead to novel therapeutic approaches for OI.

***Disclosures: Patricia Collin-Osdoby**, None.*

MO0016

Anatomical Distribution of Vertebral Fractures in the Pediatric Population. Kerry Siminoski*[1], Nathalie Alos[2], Stephanie A. Atkinson[3], David A. Cabral[4], Jacqueline Halton[5], Adam Huber[6], Brian Lentle[4], Paivi M. Miettunen[7], Helen R. Nadel[4], Frank Rauch[8], Celia Rodd[8], Johannes Roth[5], Elizabeth A. Cummings[6], Robert Couch[1], Janusz Feber[5], MaryAnn Matzinger[5], Andy Ni[5], Nazih Shenouda[5], David Stephure[7], Canadian STOPP Consortium[9], Robert Stein[10], Shayne Taback[11], Leanne M. Ward[5], and the Canadian STOPP Consortium[5]. [1]University of Alberta, Canada, [2]Université de Montréal, Canada, [3]McMaster University, Canada, [4]University of British Columbia, Canada, [5]University of Ottawa, Canada, [6]Dalhousie University, Canada, [7]University of Calgary, Canada, [8]McGill University, Canada, [9]University of Otttawa, Canada, [10]University of Western Ontario, Canada, [11]University of Manitoba, Canada

Vertebral fractures (VF) in adults occur throughout the thoracic and lumbar spine, but have the highest prevalences at T7/8 and T12/L1. As spinal shape and biomechanical forces are different in the pediatric population, fracture distribution may differ from that of adults. We explored this possibility by examining the anatomical distribution of fractures in a cohort of children with VF. Subjects (n = 44) were participants in the STOPP study of glucocorticoid-induced osteoporosis in children who had prevalent VF according to the Genant semi-quantitative method. Median age was 7.7 years (range, 2.1-16.6 years), 52% were male, and disease categories were leukemia (66%), rheumatolog conditions (21%), and nephrotic syndrome (14%). The mean lumbar spine Z-score was -1.7 (SD, 1.5) with 41% having Z-scores <-2.0. Back pain was present in 52%.

Subjects had an average of 2.1 (SD, 2.1) fractures per person. Seventy-two % of fractures were thoracic and 28% were in the lumbar spine. Fracture grade was mild (grade 1) n 62%, moderate (grade 2) in 29% and severe (grade 3) in 9%. Eighty-seven % of fractured vertebrae met the definition of wedge fracture, 5% had biconcave deformity, and 9% had crush morphology. Girls and boys did not differ in fracture number per person. Girls had a mean fracture number of 2.2 (2.3) and boys averaged 2.1 (2.0) fractures per person. Two major peaks were present when anatomic distribution was examined (see figure): T6/7 (peak 1) and L1/2 (peak 2). For all fracture grades, 31% (95% CI, 22-41%) of VF were in peak 1 and 21% (95% CI, 14-31%) were in peak 2. For moderate and severe fractures, the peaks were located in the same locations, with peak 1 containing 29% of VF (95% CI, 16-45%) and peak 2 having 23% (95% CI, 12-39%).

In this pediatric cohort, the finding of fracture foci at T6/7 and L1/2 suggests that fracture distribution in children from that of adults, perhaps resulting from the different shape of the immature spine. The thoracic focus was shifted upward and the lumbar focus downward compared to the reported distribution in adults. In addition, our findings that mild morphometric deformities (grade 1) were present in similar locations as moderate and severe fractures suggests that mild deformities are true fractures rather than congenital abnormalities.

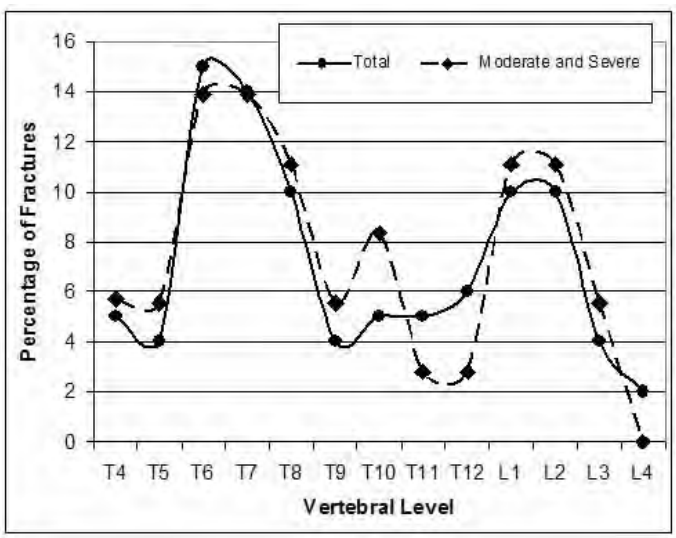

VF Distribution

***Disclosures: Kerry Siminoski**, Amgen, 5*

MO0017

Early Effects of Femoral Head Ischemia on Bone Structure-Function Relationships and Failure Patterns. Amira Hussein*[1], Harry Kim[2], Elise Morgan[1]. [1]Boston University, USA, [2]Scottish Rite Hospital for Children, USA

Purpose: Legg-Calvé-Perthes Disease is a common pediatric hip disorder and is one form of juvenile ischemic osteonecrosis (IO) that can produce permanent femoral head (FH) deformity. Early effects of IO on the biomechanics of the articular cartilage and underlying epiphyseal bone have not been fully characterized. The overall goal of this study was to assess the effect of IO on bone structure-function relationships and failure mechanisms in the FH.

Methods: IO was surgically induced in the right femur of six male piglets. Left and right hip joints were harvested two weeks post surgery. Three matching acetabular and femoral cores were machined from a central coronal area. Cores from the FH were scanned via μCT (12μm/voxel) and two regions, the cartilage bone junction and central epiphysis, were analyzed for tissue mineral density (TMD) and trabecular architecture. Each matched pair of cores was then loaded in compression to failure at a rate of 0.5% sec^{-1}. Digital images (10μm/pixel) were captured throughout the test and were used to quantify deformation patterns throughout the cores. All statistical analyses accounted for inclusion of multiple cores from each animal.

Results: Failure patterns indicated that with IO, large deformations occurred throughout the cartilage layer and underlying femoral bone, whereas in the contralateral control cores, large deformations were localized in the superficial zone of the cartilage and within the calcified cartilage. For the central epiphyseal trabecular bone, IO resulted in lower volume fraction (Vf), TMD, Tb.Th*, Tb.Sp*, and degree of anisotropy, and higher Tb.N* and connectivity density, as compared to contralateral cores ($p<0.05$). However, TMD of the calcified cartilage was significantly higher with IO. IO also resulted in decreased Young's modulus ($p=0.004$); however, no effect of IO on the relationship between modulus and microstructural properties such as Vf was found ($p>0.33$).

Conclusions: IO substantially altered the microstructure, mineralization, and failure patterns in the epiphyseal trabecular bone and calcified cartilage of the FH. Moreover, these alterations in microstructure appeared to be directly linked to changes in elastic modulus of the trabecular bone. These findings indicate that at an early disease stage, IO induces structural and compositional changes in the FH, which result in distinct differences in the way that loads applied at the hip joint are distributed throughout the femoral head.

***Disclosures: Amira Hussein**, None.*

MO0018

Osteopathia Striata with Cranial Sclerosis: Lessons from the Mutation Spectrum. Wim Van Hul, Bram Perdu*. University of Antwerp, Belgium

Osteopathia striata with cranial sclerosis (OSCS) is an X-linked dominant condition marked by linear striations mainly affecting the metaphyseal region of the long bones and pelvis in combination with cranial sclerosis. The condition is lethal in most affected males. Recently, the disease causing gene was identified as the WTX gene (FAM123B), an inhibitor of WNT signalling (Jenkins et al. Nat Genet 41(1):95-100 2009; Perdu et al. JBMR 25(1):82-90 2010). At present, we and others were able to identify 16 different mutations all expected to result in a loss of function of the WTX protein. Analysis of the mutation spectrum in OSCS patients revealed some novel insights into the pathogenesis of this rare bone dysplasia.

First, OSCS has long been considered as a radiographic finding, marked by sclerosis of the bones and linear striations in the metaphyseal region of the long bones and pelvis. However, OSCS caused by WTX mutations should also be considered in cases of cranial sclerosis in a male patient, because longitudinal striations are hardly ever seen in affected males. Recently, a male patient with longitudinal striations presented mosaicism upon DNA sequencing. These findings suggest that a mixture of affected and non-affected osteoblasts in the growth plate, due to random X-inactivation in females or mosaicism in males and females, is needed to generate longitudinal striations of the long bones.

Second, Jenkins and colleagues suggested a possible genotype-phenotype correlation that relates the position of the mutations in WTX with survival in males: only mutations that produce a WTXS1 with intact PtdIns (4,5)P2 and APCBD1 domain result in survival of males. However, close analysis of the mutation spectrum underlines the unpredictability of male survival. We identified WTX mutations in a few surviving male patients resulting in a highly truncated proteins with no intact PtdIns (4,5)P2 domain and without the APCBD1 domain. It seems likely that other modifying factors influence male survival. Therefore, although in general the condition OSCS is lethal in males, prenatal counselling must be given with caution.

In addition, the overview of all currently known mutations and their associated phenotypical features in this study provides a valuable resource for the molecular analysis of OSCS.

***Disclosures: Bram Perdu**, None.*

MO0019

Prevalent Vertebral Fractures in an Inception Cohort of Children with Glucocorticoid-Treated Illnesses: Relationship with Spine BMD and Comparison of Two Methods for Vertebral Fracture Assessment. Leanne M. Ward*[1], Nathalie Alos[2], Stephanie A Atkinson[3], David A. Cabral[4], Jacqueline Halton[1], Adam Huber[5], Brian Lentle[4], Paivi Miettunen[6], Helen R. Nadel[4], Frank Rauch[7], Celia Rodd[7], Johannes Roth[1], Elizabeth A. Cummings[5], Robert Couch[8], Janusz Feber[1], MaryAnn Matzinger[1], Andy Ni[1], Nazih Shenouda[1], David Stephure[6], Robert Stein[9], Shayne Taback[10], Kerry Siminoski[8], and the Canadian STOPP Consortium[1]. [1]University of Ottawa, Canada, [2]Université de Montréal, Canada, [3]McMaster University, Canada, [4]University of British Columbia, Canada, [5]Dalhousie University, Canada, [6]University of Calgary, Canada, [7]McGill University, Canada, [8]University of Alberta, Canada, [9]University of Western Ontario, Canada, [10]University of Manitoba, Canada

Vertebral fractures (VF) are under-recognized in childhood systemic illnesses. We studied the prevalence of VF in an inception cohort of children with glucocorticoid (GC)-treated conditions, to ascertain the clinical indices associated with VF and compare two methods for VF assessment (Genant Semi-Quantitative (GSQ) and Algorithm-Based Qualitative (ABQ) methods). Children with leukemia, rheumatic conditions and nephrotic syndrome were studied within the first month of GC initiation as follows: 1. Lumbar spine areal BMD (LSaBMD), 2. Back pain (yes or no), and 3. Lateral spine radiograph for VF assessment.

Out of 400 children enrolled (mean age 6.2 years, range 1.3-17.0; 51% male), 44 (11%, 95% CI 8-14%) manifested 94 vertebral fracture events according to the GSQ method (29/186 (16%) children with leukemia, 9/134 (7%) with rheumatic conditions and 6/80 (8%) with nephrotic syndrome). Sixty-two percent of VF were mild, 29% moderate and 9% severe. Forty-one percent of children with VF had a LSaBMD Z-score below -2 SD, 30% were between -2 and -1 SD and 29% were above -1 SD. Children with VF were similar in age and gender compared to those without. Mean LSaBMD Z-score was lower among those with VF (-1.7 ± 1.5 versus -0.8 ± 1.2, $p<0.001$). Multiple logistic regression showed that for every 1 SD reduction in LSaBMD Z-score, there was an 80% increased odds for fracture (OR 1.8, 95% CI 1.3-2.3, $p<0.001$). The odds for VF was also increased with back pain (OR 3.9, 95% CI 2.0-7.7, $p<0.001$). The underlying disease was not associated with VF after controlling for BMD and back pain. A total of 34 children had ABQ VF (9%, 95% CI 6-11%); 24 of these children also showed a GSQ VF while 10 did not (Table). Although the agreement between the GSQ and ABQ methods was only moderate (kappa = 0.53), the relationships between fractures and BMD/back pain were similar regardless of the VF assessment method used: OR for LSaBMD Z-score and VF according to ABQ = 1.7, 95% CI 1.3-2.3, $p<0.001$; OR for back pain and VF according to ABQ = 4.2, 95% CI 2.0-9.0, $p<0.001$.

In conclusion, VF occurred in 9-11% of children recently initiating GCs for the treatment of chronic illnesses. Back pain and LSaBMD Z-score were associated with an increased odds for fracture, and their relationship with VF was similar regardless of the method for VF assessment.

		# of Children with ABQ VF	
		No	Yes
# of Children with Genant VF	No	340	10
	Yes	20	24

Table: Genant versus ABQ Vertebral Fractures

***Disclosures: Leanne M. Ward**, None.*

MO0020

Proinflammatory Cytokine Expression in Bone Marrow of Colitic Mice and Children with Crohn Disease. Andrew Draghi[1], Robert Clark[2], Anthony Vella[2], Mack David[3], Leanne Ward[3], Catherine Adams[2], Francisco Sylvester*[4]. [1]Connecticut Children's Medical Center, USA, [2]University of Connecticut Health Center, USA, [3]Children's Hospital of Eastern Ontario, Canada, [4]Connecticut Children's Medical Center, USA

Inflammatory bowel disease (IBD) is associated with decreased bone mass, but the responsible mechanisms are not well known. We hypothesize that TNF (tumor necrosis factor)-α, IFN (interferon)-γ and IL (interleukin)-17, which are known inhibitors of osteoblast differentiation and function are expressed in the bone environment during intestinal inflammation. To test this hypothesis, we used two experimental models, an adoptive transfer mouse model of colitis and transiliac bone biopsies from children with newly diagnosed, untreated Crohn disease. CD4+, CD25-, $CD45^{high}$ cells sorted from spleen of C57/BL6 mice were injected intraperitoneally into Rag-1 knockout (KO) mice, which produce colitis in 6-8 weeks (n=7). Control mice received CD4+ cells (n=2). After 8 weeks, mice were sacrificed and bone marrow (BM) from femur and tibia, mesenteric lymph nodes and spleen were collected. Cells from each of these sites were immunophenotyped by flow cytometry to determine the presence of effector memory T cells (T_{EM}), central memory T cells (T_{CM}), and dendritic cells (DC). Expression of TNF-α, IFN -γ and IL -17 was measured by ELISA of conditioned medium and by flow cytometry of stained BM cells stimulated with CD3ε/CD28 or PMA/Ionomycin. Sections of bone biopsies from children with Crohn disease were examined for the presence of TNF-α by immunohistochemistry (IHC). We observed increased expression of TNF-α and IFN-γ in BM of colitic mice. Mean ± SD cytokine concentration (pg/mL, colitic/control) in cell supernatants were TNF-α 12.4 ±18.5/0 ± 0, IFN-γ 140.6 ± 265.0/4.7 ± 0.7 and IL-17 9.7 ± 15.3/9.5 ± 13.4. By flow cytometry, BM of colitic mice had a higher percentage of IFN-γ (26.7 ± 8.5/17.0 ± 8.7) and TNF-α (32.8 ± 13.3/15.4 ± 4.0) producing cells than controls. The percentage of cells expressing DC and T_{EM} surface markers was increased in BM cells of colitic mice: 3.5 ± 1.5/0.63 ± 0.5 and 3.5 ± 1.5/0.75 ± 0.6, respectively, suggesting immune activation in the bone environment. There were no differences in $\%T_{CM}$ between colitis and control. Consistent with these findings, we detected TNF-α expression in bone biopsies from children with Crohn disease by IHC (n = 2). Taken together, these data suggest that intestinal inflammation is associated with immune activation in the BM, with production of IFN-γ and TNF-α, cytokines known to inhibit bone formation. Our preliminary data raises the possibility that TNF-α and IFN-γ production in the BM is a mechanism by which IBD affects bone mass.

***Disclosures: Francisco Sylvester**, None.*

MO0021

Affects Of Allogenic Hematopoietic Stem Cell Transplantation On Bone Density Of Pediatric Patients With Beta Thalassemia Major. Zohreh Hamidi*[1], Amir Ali Hamidieh[2], Mohammad Reza Mohajeri[3], Leila Nedaeifard[2], Ramin Heshmat[3], Kamran Alimoghaddam[2], Ardeshir Ghavamzadeh[2], Bagher Larijani[3]. [1]Endocrinology & Metabolism Reserach Center of Tehran University of Medical Sci, Iran, [2]Hematology-Oncology & Stem Cell Transplantation Research Center, Tehran University of Medical Sciences, Iran, [3]Endocrinology & Metabolism Research Center of Tehran University of Medical Sciences, Iran

Introduction: Beta Thalassemia Major (a hemoglobin disorder) and it's cure by hematopoietic stem cell transplantation (HSCT) can deteriorate bone status. We assessed the effect of HSCT on growing bone of thalassemic pediatric patients.

Methods: Bone mineral density (BMD) of 20 patient, from 3 classes of thalassemia (mean age : 7.4 ± 3.8 y/o), tested before, 6 and 12 months after HSCT with a Norland XR-46 devices. Female to male ratio was one. No one had Z-score less that -2.

Results: After HSCT, at 6 and 12 months, changes of mean of BMD was not significant and BMD of no patient decreased to Z-score < -2. Class 3 thalassemia had no negative effect on BMD. Relation between corticosteroid use and BMD changes was not significant. Acute graft versus host disease (GVHD), had significant effects of BMD of femur and spine of patients after HSCT (Pvalue = 0.020 and 0.027, respectively).

Conclusion: HSCT of pediatric thalassemic patients has not positive or negative significant affects on BMD of patients.

***Disclosures: Zohreh Hamidi**, None.*

MO0022

Do Patients with Osteogenesis Imperfecta Need an Individualized Nutritional Support for Prevention of Bone Fractures. Carlos Eduardo Andrade Chagas*[1], Barbara Santarosa Emo Peteres[2], Marise Lazaretti Castro[2], Ligia Martini[3]. [1]Nutrition Depatment, School of Public Health, University of Sao Paulo, Brazil, [2]Federal University of Sao Paulo, Brazil, [3]University of São Paulo, Brazil

Osteogenesis Imperfecta (OI) is a genetic disease that involves a dysfunction in the synthesis of collagen. Bone fragility associated with reduced bone mass is the major clinical feature of OI. Thus, because of the persistent bone pain and increased risk of fractures, people diagnosed with OI have a poor quality of life. Despite the relevant role of dietary factors on bone health and metabolism, information regarding nutritional status and dietary intake of OI patients is scarce. Therefore, in the present case-control study we evaluated the nutritional status (BMI), body composition and bone mineral density (dual energy X-ray) as well as dietary intake (3-day food record) and biochemical parameters (plasma glucose, triglycerides, HDL cholesterol and insulin) of both type I OI (T1 group, n = 13) and type III OI (T3 group, n = 13) and compared with the results presented by 8 gender and age matched healthy controls. Data were analyzed by One Way ANOVA and Pearson's Correlation and the level of significance adopted was 95% ($p < 0.05$). As expected, both T1 and T3 groups presented lower bone mineral density ($p < 0.05$ vs controls). Regarding body composition, when compared to controls, T1 group presented lower ($p < 0.05$) BMI and fat free mass. Furthermore, T3 group presented the highest BMI ($p < 0.05$ vs T1 group and controls), higher percentage of body fat ($p < 0.05$ vs controls) and the lowest fat free mass ($p < 0.05$ vs T1 group and controls). Despite these results, 92%, 83%, 92% and 100% of OI patients presented normal plasma concentrations of glucose, HDL cholesterol, triglycerides and insulin, respectively. In T1 and T3 groups it was observed a positive correlation between the number of fractures and BMI ($r=0.581$; $p=0.002$) and the percentage of body fat ($r=0.451$; $p= 0.027$) while the

number of fractures was negative correlated to the fat free mass (r=-0.523; p=0.009). No differences were observed between controls, T1 and T3 groups regarding dietary intake. However, when considered total nutrient intake (dietary intake and supplements) 58% and 12% of the cases did not reach calcium and vitamin D current recommendations, respectively. In conclusion, the results of the present study suggest that body composition is a relevant factor related with the incidence of bone fractures and an individualized nutritional support may be essential to improve it and, consequently, providing a better quality of life to OI patients.

***Disclosures: Carlos Eduardo Andrade Chagas**, None.*

MO0023

Long Term Outcome in Pediatric Patients with Severe Chronic Non-Bacterial Osteitis Following Intravenous Pamidronate Therapy: Case Series with 9 Patients. Paivi Miettunen*[1], Xing-Chang Wei[2], Walid Abou Reslan[2], Deepak Kaura[2]. [1]University of Calgary, Faculty of Medicine, Canada, [2]Department of Diagnostic Imaging, Alberta Children's Hospital & University of Calgary, Canada

Objective: To describe long-term clinical outcome and bone resorption response in pediatric patients who were previously treated with intravenous pamidronate (IVP) for chronic non-bacterial osteitis (CNO).

Methods: All patients who were treated with IVP for CNO between 2003-2006 at a single center were prospectively followed until January 2010. Patients who developed recurrent pain for > 2 weeks were investigated with whole-body magnetic resonance imaging (WBMRI) to identify active CNO sites. Following confirmation of CNO, patients were offered either non-steroidal anti-inflammatory medications or re-treatment with IVP(1 mg/kg/day, maximum 60 mg/day; given as 1-day cycles/month). Patients with a single CNO lesion received 1 IVP, and patients with 2 or more lesions received monthly IVP. WBMRI was repeated every 3 months. IVP was discontinued once WBMRI revealed resolution of CNO. Visual analog scale for pain (VAS) and bone resorption marker urine N-telopeptide/urine creatinine (uNTX/uCr) were measured at baseline, at CNO relapse, and at final follow-up.

Results: Nine patients (5F, 4M) had received IVP for severe CNO at median age of 12.9(range 4.5-16.3) years and had achieved complete clinical and MRI documented remission. Median follow-up was 52 (range 40-76) months. Five patients remained asymptomatic at median 47.5(range 42-76) months. Four patients had WBMRI confirmed CNO flare at median 17 (range 7-25) months following completion of initial IVP treatment, with median 2 (range 1-13) active CNO sites. Three patients required IVP re-treatment, and one patient responded to naproxen. Mean VAS at CNO recurrence was 7/10, decreasing uniformly to 0/10 following 1st IVP re-infusion, although WBMRI resolution was slower. Median number of IVP monthly doses was 1(range 1-5). Same 4 patients had 2nd WBMRI confirmed flare at median 22 (range 5-29) months following completion of 2nd IVP treatment, but only 2 patients required IVP. For patients with no flares, median uNTX/uCr prior to 1st ever IVP was 702(range 430-945); and 104 (range 49-248) nmol/mmol/creatinine at final follow-up. For patients who flared, median uNTX/uCr prior to 1st ever IVP was 873(range 165-1361); 344 (range 98-502) at first flare; and 145(range 52-241) nmol/mmol/creatinine at final follow-up.

Conclusions: 1. IVP resulted in prolonged symptom free intervals in patients with severe CNO. 2. No patient lost the efficacy to IVP with re-treatment(s). 3. UNTX/uCr gradually decreased in all patients.

***Disclosures: Paivi Miettunen**, None.*

MO0024

Short and Long-Term Outcome of Patients With Pseudo-Vitamin D Deficiency Rickets Treated With Calcitriol. Thomas Edouard*[1], Nathalie Alos[2], Gilles Chabot[3], Francis Glorieux[4], Frank Rauch[5]. [1]CHU Sainte-Justine - Université Montréal, Canada, [2]CHU Sainte Justine, Canada, [3]Hopital Saint Justine, Canada, [4]Shriners Hospital for Children & McGill University, Canada, [5]Shriners Hospital for Children, Canada

Purpose: Pseudo-vitamin D Deficiency Rickets (PDDR, OMIM 264700) is a rare autosomal recessive disease caused by mutations in the gene encoding 25-hydroxyvitamin D-1α hydroxylase (CYP27B1), leading to an inability to synthesize 1α,25-dihydroxyvitamin D3 ($1,25(OH)_2D3$), the active form of vitamin D. Patients with the disease develop growth retardation, rickets, hypotonia, hypocalcemia and secondary hyperparathyroidism. The treatment of choice for PDDR patients has been replacement therapy with $1,25(OH)_2D3$ (calcitriol). Available reports on the effect of calcitriol treatment of PDDR included less than 10 patients and had follow up periods of less than one year. In the present study were therefore present the results of 39 patients with a diagnosis of PDDR who received calcitriol for a period of 2.0 to 26.2 years.

Methods: The patient population comprises all 39 patients (20 females; 19 males) with a diagnosis of PDDR who were followed at the Shriners Hospital for Children and at Sainte Justine Hospital in Montreal. For the purpose of the present analysis two overlapping patient groups were distinguished: a 'pediatric group' of 21 children, in whom data were available during the first 2 years of treatment, and an 'adult group' of 25 patients, who had reached their final height.

Results: In the 'pediatric group', except one asymptomatic child assessed at the age of one month because of a family history, all the patients were symptomatic. The majority of patients presented with neurological signs (17 of 20) and short stature (12 of 17), and all had signs of active rickets. Treatment with calcitriol resulted in the normalization of all biochemical parameters within 3 months. In the five patients with available bone densitometry data, lumbar spine areal BMD z-scores increased markedly in the first three months after treatment was started and then remained stable. Height z-scores increased more gradually.

In the 'adult group', patient who received calcitriol before the pubertal growth spurt had normal height, contrary to patients treated with calcitriol treatment after puberty. Lumbar spine areal BMD z-scores were normal in all adult patients. Nineteen pregnancies documented in 9 women with PDDR were normal without intra-uterine growth retardation and all newborn were eucalcemic at birth.

Conclusion: Treatment with calcitriol started in infancy results in short and long term correction of all clinical, biochemical, and radiological abnormalities related to PDDR.

***Disclosures: Thomas Edouard**, None.*

MO0025

Vitamin D Treatment in Calcium-deficiency Rickets. Tom Thacher*[1], Philip Fischer[1], John Pettifor[2]. [1]Mayo Clinic, USA, [2]Baragwanath Hospital, Republic of south africa

Introduction: Children with calcium deficiency rickets have elevated serum 1,25-dihydroxyvitamin D values. Treatment with vitamin D produces a marked short-term increase in 1,25-dihydroxyvitamin D values. We have previously shown that treatment with vitamin D alone is less effective than with vitamin D and calcium or calcium alone. We now compare the response of rickets to calcium treatment with and without vitamin D.

Methods: Nigerian children with active rickets treated with calcium carbonate as limestone (approximately 1000 mg elemental calcium daily) were, in addition, randomized to receive either oral vitamin D2 50,000 IU (Ca+D, n=44) or placebo (Ca, n=28) monthly for 6 months. The primary outcome was achievement of a 10-point radiographic score ≤1.5 and serum alkaline phosphatase ≤350 U/L.

Results: The median (range) age of enrolled children was 46 (15-102) months, and baseline characteristics were similar in the two groups. At baseline mean (±SD) 25OHD was 12.1±5.3 ng/mL, and 29 (43%) had values below 12 ng/mL. Baseline alkaline phosphatase and radiographic scores were unrelated to 25OHD levels. Of the 68 children (94% of original cohort) who completed 6 months of treatment, 29 (67%) in the Ca+D group and 11 (44%) in the Ca group achieved the primary outcome (P=0.05). Baseline 25OHD did not alter treatment group effects (P=0.99 for interaction). At the end of 6 months, 25OHD values were 22.2±6.8 ng/mL and 15.2±8.0 ng/mL in the Ca+D and Ca groups, respectively (P<0.001). In both the Ca+D and Ca groups, the final 25OHD concentration was greater in those who achieved the primary outcome (22.6±6.9 ng/mL) than in those who did not (15.1±7.4 ng/mL, P<0.001).

Conclusion: In children with calcium deficiency rickets, vitamin D improves the response to treatment with calcium carbonate as limestone, independent of baseline 25OHD concentrations.

***Disclosures: Tom Thacher**, None.*

MO0026

Adaptation to Mechanical Loading during Growth: Lumbar Spine Geometry, Density and Theoretical Strength Assessed by Antero-posterior, Supine Lateral and Paired DXA. Jodi Dowthwaite*[1], Portia Flowers[2], Karin DeJong[2], Paula Rosenbaum[2], Tamara Scerpella[3]. [1]State University of New York, Upstate Medical University, USA, [2]SUNY Upstate Medical University, USA, [3]State University of New York Upstate Medical University, USA

Purpose: Most studies use standard antero-posterior (AP) DXA and/or bone mineral apparent density (BMAD) to assess lumbar spine adaptation to mechanical loading. This study assesses AP, supine lateral (LAT) and paired (APLAT) DXA indices of bone geometry, density and compressive strength, evaluating physical maturity and gymnastic exposure during growth.

Methods: Two-factor analysis of covariance compared AP, LAT and APLAT DXA output for the third lumbar vertebra in 102 females (premenarche (pre) n= 57; postmenarche (post) n=45), adjusting for age and height. Nongymnasts (non) n=46, were compared to ex/gymnasts (ex/gym) who had engaged in gymnastic activity >4hrs/wk for at least 2 yrs during growth [pre gym n=31; pre ex n=1 (quit 0.4 yrs prior); post gym n=4; post ex n=20 (quit 0.5-10.4 yrs prior)].

Results: From AP scans, ex/gym had greater aBMD, BMC, vertebral width, cross-sectional area (CSA), axial compressive strength index (IBS)($p<0.05$), but not projected area, BMAD or volume. From LAT scans, only aBMD, BMAD and IBS were greater in ex/gym than non; non had greater area, height and volume than ex/gym ($p<0.05$). From APLAT scans, only CSA was significantly greater in ex/gym than non. Post were greater than pre for APaBMD, APBMC, APArea, LATdepth, AP/LAT/APLATCSA, AP/APLATvolume and APIBS ($p<0.05$). There were no significant maturity x gymnastics interactions.

Conclusions: Gymnastics during growth is associated with larger medial-lateral vertebral width, shorter vertebral height, greater aBMD (LAT, AP) and greater posterior element BMC, suggesting lower fracture risk. Benefits are seen in immature

girls of low gymnastic exposure and mature young women who quit gymnastics five years prior (mean). Findings were plane-specific; lateral results are not superior or equivalent to AP output. Paired DXA output does not capture differences measured in either plane alone. Thus, lumbar spine adaptation studies should evaluate AP, LAT and APLAT results.

Adjusted means and 95% confidence intervals for bone parameters by gymnastic exposure and maturity

DXA Plane	Variable	Mean (95% CI)		Mean (95% CI)	
		Ex/Gym n=56	Non n=46	Premenarche n=57	Postmenarche n=45
Postero-Anterior (AP)	APaBMD (g/cm²)	0.877 (0.850-0.907)**	0.815 (0.787-0.844)	0.790 (0.747-0.834)	0.906 (0.847-0.969)*
	APBMC (g)	10.80 (10.36-11.20)**	9.94 (9.50-10.41)	9.03 (8.40-9.73)	11.89 (10.88-13.00)***
	APArea (cm²)	12.31 (12.04-12.60) NS	12.19 (12.19-12.50)	11.45 (11.00-11.91)	13.13 (12.50-13.79)***
	APWidth (cm)	6.73 (6.50-6.96)**	6.24 (6.01-6.47)	6.10 (5.76-6.47)	6.88 (6.40-7.38) [p=0.052]
	APBMAD (g/cm²)	0.166 (0.158-0.174) NS	0.166 (0.158-0.175)	0.164 (0.152-0.179)	0.168 (0.152-0.185) NS
	APIBS (g²/cm⁴)	0.980 (0.919-1.046)**	0.846 (0.789-0.907)	0.794 (0.710-0.887)	1.045 (0.913-1.196) *
	APCSA (cm²)	35.59 (33.25-38.09)**	30.57 (28.42-32.88)	29.25 (26.02-32.85)	37.19 (32.27-42.86)*
Lateral	APVolume (cm³)	43.25 (41.76-44.79) NS	42.61 (41.06-44.26)	38.71 (36.45-41.10)	47.61 (44.26-51.16)**
	LATaBMD (g/cm²)	0.746 (0.723-0.770)**	0.696 (0.673-0.719)	0.696 (0.660-0.733)	0.746 (0.700-0.795) NS
	LATBMC (g)	5.55 (5.30-5.81) NS	5.46 (5.20-5.74)	5.10 (4.72-5.52)	5.94 (5.40-6.54) [p=0.067]
	LATArea (cm²)	7.44 (7.26-7.61)	7.35 (7.66-8.05)**	7.34 (7.04-7.64)	7.96 (7.58-8.36) [p=0.051]
	LATDepth (cm)	4.06 (3.99-4.13) NS	4.01 (3.94-4.09)	3.91 (3.80-4.03)	4.17 (4.03-4.32)*
	LATHeight (cm)	1.83 (1.79-1.87)	1.96 (1.91-2.01)***	1.88 (1.80-1.95)	1.91 (1.82-2.00) NS
	LATBMAD (g/cm²)	0.234 (0.227-0.241)**	0.220 (0.213-0.228)	0.227 (0.215-0.239)	0.227 (0.214-0.242)
	LATIBS (g²/cm⁴)	0.709 (0.667-0.754)**	0.616 (0.576-0.658)	0.616 (0.555-0.685)	0.708 (0.623-0.805) NS
	LATCSA (cm²)	12.97 (12.54-13.42) NS	12.67 (12.22-13.14)	12.01 (11.34-12.73)	13.69 (12.76-14.69)*
	LATVolume (cm³)	20.29 (19.59-21.01)	22.02 (21.20-22.87)**	19.87 (18.69-21.09)	22.49 (20.88-24.22) [p=0.051]
Paired AP/LAT	APLATBMAD (g/cm²)	0.141 (0.135-0.147)	0.142 (0.135-0.149) NS	0.145 (0.135-0.156) NS	0.138 (0.126-0.151)
	APLATIBS (g²/cm⁴)	0.428 (0.401-0.457) NS	0.397 (0.369-0.426)	0.395 (0.353-0.443)	0.429 (0.374-0.493) NS
	APLATCSA (cm²)	21.48 (20.45-22.56)*	19.69 (18.67-20.76)	18.75 (17.24-20.39)	22.56 (20.35-24.99)*
	APLATVolume (cm³)	39.33 (37.83-40.83) NS	38.47 (36.93-40.13) **	35.16 (32.92-37.60) **	43.03 (39.69-46.67)**
	Fracture Risk Index				

Means are adjusted for age and height. All variables were analyzed as natural logarithms; results are presented in antiln form.
There were no significant interactions between maturity and activity for any dependent variable.
Two-factor ANCOVA * p<0.05, ** p≤0.01, *** p≤0.001, denoting group advantage.

Table 1

***Disclosures: Jodi Dowthwaite**, None.*

MO0027

Are Children with Hutchinson-Gilford Progeria Syndrome (HGPS) Truly Osteopenic? Ara Nazarian*[1], Brian Snyder[2], Catherine Gordon[3], Leslie Gordon[4], Anita Giobie-Hurder[5], Donna Neuberg[5], Monica Kleinman[6], David Miller[6], Mark Kieran[5]. [1]Beth Israel Deaconess Medical Center, USA, [2]Children's Hospital BostonHarvard Medical School, USA, [3]Children's Hospital Boston & Harvard Medical School, USA, [4]Brown University, USA, [5]DFCI, USA, [6]Children's Hospital Boston, USA

HGPS is a rare, sporadic, autosomal dominant disorder affecting multiple organ systems that exhibit aspects of premature aging. The skeletal abnormalities observed in HGPS appear to be different from the characteristic patterns of bone turnover and demineralization seen in adults with senile osteoporosis. In children with HGPS, the accumulation of progerin within bone, cartilage and muscle cells may account for the observed phenotypical skeletal changes. The aim of this study was to evaluate the effect of HGPS on bone mineral density and the structural properties of the axial and appendicular skeleton.

Dual energy X-ray absorptiometry (DXA) of the whole body and spine were obtained on 26 children with HGPS. Peripheral quantitative computed tomography (pQCT) at serial cross-sections throughout the radius (metaphysis, meta-diaphysis and diaphysis) were also obtained and compared to 59 age-matched, normal controls. CT based structural rigidity analysis was performed on each transaxial pQCT image to calculate the resistance of the bone to axial, bending and torsional forces applied at that cross-section.

While the chronologic age of the HGPS children was 7.4 ? 3.4 yrs, their bone age trended towards advanced at 8.1 $\pm$ 4.2 yrs; however adjusting for their diminutive size, height age was 3.4 $\pm$ 1.5 yrs. Fat mass and leptin levels were low. Bone biomarker data suggest that bone turnover is normal to elevated. Thyroid function and IGF-I were normal. 14% HGPS children had low 25OH-vitamin D. Using height-age adjusted, area bone mineral density (aBMD) measured by DXA, the Z-scores were -1.7$\pm$1.4 at the spine and -2.4$\pm$0.98 for the whole body. However volumetric bone mineral density (vBMD) measured by pQCT was normal throughout the radius. Normalizing by the body mass index to eliminate differences based on size, the axial rigidity of HGPS children was 27% less at the metaphysis and diaphysis of the radius, and the bending and torsional rigidities were 55% less compared to normal controls.

HGPS appears to affect the structural geometry of the appendicular skeleton rather than the bone mineral density, which was essentially normal, suggestive of skeletal dysplasia. Since aBMD measured by DXA fails to account for differences in bone size and geometry, it is not clear that the axial bone density is actually compromised in HGPS patients. QCT of the spine will be required to evaluate this definitively.

***Disclosures: Ara Nazarian**, None.*

MO0028

Bone Phenotype in Heterozigous for a Mutation in the *GHRH* Receptor Gene. Miburge Gois-Jr*[1], Manoel Aguiar-Oliveira[2], Roberto Salvatori[3], Francisco Pereira[4], Carla Oliveira[2], Luiz Oliveira-Neto[2], Rossana Pareira[2], Francisco Paula[1]. [1]School of Medicine of Ribeirão Preto, Brazil, [2]School of Medicine, Federal University, Brazil, [3]The Johns Hopkins University School of Medicine, USA, [4]University of Sao Paulo, School of Medicine of Ribeirao Preto, Brazil

Growth hormone (GH) influences bone mass maintenance and metabolism. Homozygous mutations in the GH releasing hormone receptor (GHRHR) gene are a frequent cause of genetic isolated GH deficiency (IGHD).We had previously showed that IGHD individuals with a homozygous mutation in the GHRHR gene had a lower T-score of the stiffness, measured by calcaneal quantitative ultrasound (QUS), then matched normal homozygous individuals. Heterozygosity for this GHRHR mutation is not associated with reduction in adult stature or in serum levels of IGF-I, but is associated with reduction in body weight, body mass index (BMI), lean mass and with increased sensibility insulin, all potential interfering factors on bone strength. We hypothesized that heterozygosity for this mutation might be associated with low bone quality. We assessed the bone status by the stiffness measured by QUS and two biochemical bone markers: one of bone formation, plasma osteocalcin ng/ml and another of bone reabsorption, total urinary Crosslaps corrected by urinary creatinine µg/mmol (crosslaps) in 76 normal homozygous individuals, 68.4% of females (N/N) and 64 heterozygous individuals, 64.1% of females, for a mutation in the GHRHR gene (MUT/N), all of them from the community of Itabainainha in Brazil northeastern. Calcaneal QUS was performed with rigorous standardization of subject positioning using the Achilles Insight device (Lunar/GE). We measured: IGF-I and Osteocalcin by IRMA and Crosslaps ELISA. Data are expressed in mean (SD) and we used for all variables regressions linear models to compare N/N and MUT/N groups. There were no differences in age 44.7 (11.5) and 44.6 (14.1) years, height 157.8 (9.8) and 157.6 (10.2) cm, but Weight 65.7 (14.1) and 59.7 (11.6) Kg, p=0.007 and BMI 26.3 (4.9) and 24.0 (4.4) p=0.001 were lower in MUT/N. There were no differences in serum levels of IGF-I 139.5 (66.4) and 166.9 (101.8) ng/ml, glucose 93.7 (9.76) and 93.6 (11.6) mg/dl, T-score 0.09 (1.5) and 0.07 (1.3), Z-score 0.61 (1.4) and 0.61 (1.3), Stiffness 96.6 (23.8) and 96.3 (19.3) and osteocalcin 23.6 (11.5) and 25.5 (11.3) ng/ml but insulin 4.01 (2.7) and 2.72 (2.3) µU/ml p<0.01, HOMAir 1.00 (0.6) and 0.69 (0.5) p<0.01 and Crosslaps 350.5 (280.1) and 220.1 (150.2) µg/mmol, p<0.01 was lower in MUT/N. The present study, based on surrogate parameters, suggests that bone quality in heterozygous individuals is not impaired, and stimulates further investigation of fracture risk in this population.

***Disclosures: Miburge Gois-Jr**, None.*

MO0029

Building a Weak Skeleton Relative to Body Size During Growth Increases Fracture Risk in Adults. Karl Jepsen*[1], G. Felipe Duarte[1], Amanda Antczak[2], Yael Arbel[3], Amir Hadid[3], Ran Yanovich[3], Rachel Evans[4], Charles Negus[5], Daniel Moran[3]. [1]Mount Sinai School of Medicine, USA, [2]US Army Research Institute of Environmental Medicine, USA, [3]Heller Institute of Medical Research, Israel, [4]U.S. Army Research Institute of Environmental Medicine, USA, [5]L-3 Applied Technologies, USA

To identify bone traits that diagnose fracture risk on an individualized basis and early in life, before age-related bone loss begins and when treatments may be more effective, we assessed fracture risk in the context of functional adaptation. We tested the hypothesis that a bone which is less functionally adapted to body size during growth will show reduced adult strength and an increased risk of sustaining a bone overuse injury.

We examined two diverse cohorts of Israeli military recruits who were 17-21 years old. One cohort included 96 men (22 tibial stress-reaction diagnoses) from an elite-force undergoing intense training. The second included 151 women (12 tibial stress-reaction diagnoses) from an infantry unit undergoing less intense training. Physical traits of left tibiae were measured using pQCT (Stratec 2000L) at a site 66% from the distal end.

Bone stiffness (tissue mineral density (TMD) x moment of inertia) increased linearly with the applied force (body weight (BW) x tibial length) for both cohorts, as expected (R2=0.4-0.5, p<0.0001). Residuals from the Stiff-Force regressions quantified how well a tibia was functionally adapted to body size (i.e., negative residuals indicated tibiae with reduced stiffness). Individuals with positive and negative residuals showed no weight or height differences. However, compared to positive residuals, tibiae with negative residuals were significantly more slender relative to body weight (e.g. for women. - residual: Robust = 0.009BW + 0.58; + residual: Robust = 0.009BW + 0.77; p<0.001 for intercept, ANCOVA) and also showed reduced cortical area relative to body weight and reduced TMD relative to robustness (p<0.01, ANCOVA). Thus, having reduced stiffness relative to body size resulted from a combination of multiple trait deficits. The odds ratio calculated for bone-stress cases showed a 3.6- (women) and 3.0-fold (men) increased likelihood of developing a stress-reaction for individuals with negative residuals.

Because young adults are at the end of the growth phase, the data indicated that building a weak bone relative to body size during growth significantly increased the risk of incurring bone stress injuries as a young adult. This systems approach is novel because it does not seek a single trait to characterize injury risk in a population, but

evaluates risk based on how the set of morphological and tissue quality traits acquired by an individual during growth deviates from a functionally adapted structure.

***Disclosures: Karl Jepsen**, None.*

MO0030

Contribution of Bone Microstructural Characteristics to Mechanical Properties Evaluated at Bone Structural Unit Level. Yohann Bala*[1], Baptiste Depalle[1], Thierry Douillard[2], Sylvain Meille[2], Hélène Follet[1], Jérôme Chevalier[2], Georges Boivin[1]. [1]INSERM U831, Université de Lyon, France, [2]UMR CNRS 5510, Matériaux Ingénierie et Science, Université de Lyon, France

Bone is a multi-scale composite material made of both a type I collagen matrix and a mineral phase made of crystalline apatite. The amounts, properties and organization of its constituents at tissue level influence the mechanical properties of bone. Our purpose was to study the contributions of the quantity and quality of bone mineral and collagen matrix to the mechanical properties of bone tissue at bone structural unit (BSU) level in cortical bone.Five iliac bone biopsies were taken from untreated post-menopausal osteoporotic women and embedded in PMMA. Degree of mineralization of bone (DMB) was measured by microradiography[1] in 20 to 40 cortical BSU on 100±1µm-thick sections taken from each biopsy. On the same BSU, indentation tests were performed using a Berkovich indenter tip (NANOIndenter II, Nano Instruments Inc., US) to measure elastic modulus (E) (assuming a Poisson coefficient ν=0.3) and contact hardness (Hc)[2]. To avoid the heterogeneity of bone tissue at lamellar level, these tests were performed using sufficient load (~500mN). To exclude the variation of the measurements along the depth of the BSU, these were conducted in continuous stiffness measurement mode. Previous sections were then re-sliced to 2µm-thick for Fourier Transform Infrared Microspectroscopy analysis (FTIRM) to assess both mineral and collagen properties [Mineralization Index (MI), Mineral Maturity (MM), Crystallinity Index (CI)[3] and Collagen Maturity (CM)]. FTIRM variables were measured at the same location as DMB. DMB measurements and indentation tests were performed on 149 BSU.

Results (Mean±SD [range]) revealed that DMB=1.13±0.09 g.cm-3 [0.88-1.37], E=17.3±2.3 GPa [12.7-24.9] and Hc=0.59±0.11 GPa [0.38-0.95] and are consistent with literature[4]. At BSU level, E and Hc are positively correlated with DMB. Preliminary results show that E and Hc are correlated with MI but not with MM and CI. Only E is correlated with CM (Table).

In material field, Hc and E are related to plastic and elastic deformations respectively. Our results show that mineral quantity (DMB, MI) plays a major role in both plastic and elastic deformation. However, collagen maturity may also play an important role in the elastic behavior of bone.

1. Boivin et al. 2008, Bone 43:532
2. Oliver & Pharr 1992, J Mater Res 7:1564
3. Farlay et al. 2009, J Bone Miner Metab [epub]
4. Zysset 2009, Osteoporos Int 20:1049

	Contact Hardness (H_c, GPa)	Elastic Modulus (E, GPa)
Degree of Mineralization (DMB, g/cm^3)	0.58***	0.78***
Mineralization Index (MI)	0.63**	0.79***
Mineral Maturity (MM)	0.1	0.16
Crystallinity Index (CI)	-0.11	-0.08
Collagen Maturity (CM)	0.27	0.45*

**p<0.05, **p<0.001, ***p<0.0001*

Table: Spearmann correlation coefficients

***Disclosures: Yohann Bala**, None.*

MO0031

Cross-Sectional Circularity: A New Tomographic Variable Validates A Biomechanical Analysis of Human Distal Tibia For Diagnosing Bone Fragility and Selective Trabecular Osteopenia. Gustavo Roberto Cointry[1], Sara Feldman[1], Pablo Mortarino[1], Ivan Yelin[1], Paola Soledad Reina[1], Joern Rittweger[2], Jose Ferretti*[3], Ricardo Francisco Capozza[1]. [1]Centro de Estudios de Metabolismo Fosfocálcico, UNR, Argentina, [2]Division Space Physiology, Institute of Aerospace Medicine, German Aerospace Center, Germany, [3]National University of Rosario, Argentina

This study evaluates the structural efficiency of the distal tibia to resist compression stress employing pQCT (XCT-2000, Stratec), assuming that the adapted optimal cross-sectional design would show both a minimal cortical mass and a maximal circularity (Circ).

To show that association in the lower leg, we measured Circ = 2 √(area/perimeter), and correlated it with the total BMC (ToC) of scans taken at every 5% of the tibia length from the heel throughout the bone (C5-C95) in 21 healthy volunteers (10 men) of 20-40 yr.

The ToC was higher in men ($p<0.001$), fell by 1/3 from C5 to C15 (the lowest observed value) and then grew up to C95. Circ was inversely related to ToC throughout the bone, showing a maximal value at C15. The dispersion observed for both variables was also the lowest (CVs 8.2 & 8.5%) at C15 in both genders. Data confirmed the existence of an almost pure compression stress pattern between C15, where bone structure is almost purely cortical, and C5, where structure is combined trabecular/cortical. A separate study made at the standard 4 and 14% sites (close to C5 & C15, respectively) in 200 healthy men and pre- and post-MP women showed a linear ToC 4 (y)/14 (x) relationship ($r=.865$, $p<.001$) with a slope close to 1.5 as expected for the whole group.

Results support using the 4/14 ToC ratio from a standard pQCT study of the leg as a specific indicator of trabecular bone mass with reference to cortical mass, following a simple biomechanical criterion. 1. If only a compression stress occurs at those sites (for which only the mass of bone material in the cross-section accounts), then the 3:2 ratio between C4/C14 ToC would express the natural relationship between both the masses and structural abilities of both bone structures. 2. As long as trabecular bone tends to be lost faster than cortical bone, the C4/C14 ToC ratio would evaluate the loss in mechanical efficiency of the trabecular structure with reference to the cortical mass of the same individual, avoiding comparison with younger subjects as required by DXA. Thus, a Z-scored version of the C4/C14 graph obtained can be used as a standard reference for comparative diagnoses as well as for comparison with the muscular status of the individual.

This simple study offers a non-invasive, biomechanical diagnosis of osteoporosis as an "osteopenic fragility" in agreement with the NIH criteria, based in relevant features of the same individual, and independent of age, gender, or anthropometric traits.

***Disclosures: Jose Ferretti**, None.*

MO0032

Decay of Bone Microarchitecture in Men with Prostate Cancer During the First 12 Months of Androgen Deprivation Therapy. Emma Hamiton[1], Emily Gianatti[1], Ali Ghasem Zadeh[1], Daryl Lim Joon[2], Damien Bolton[1], Roger Zebase[1], Jeffrey Zajac*[3], Ego Seeman[4], Mathis Grossmann[1]. [1]University of Melbourne, Australia, [2]Austin Health, Australia, [3]Austin & Repatriation Medical Centre, Australia, [4]Austin Health, University of Melbourne, Australia

Context: Androgen deprivation therapy (ADT) used in the treatment of prostate cancer reduces bone mineral density (BMD) and predisposes to fractures. The structural basis of the BMD deficit and bone fragility is uncertain.

Objective and Patients: We investigated changes in bone microarchitecture in 26 men (70.6 ± 6.8 years) with non-metastatic prostate cancer during the first year of ADT using the new technique high resolution peripheral quantitative CT (HR-pQCT).

Design and Setting: We conducted a 12 month prospective observational study in the setting of a tertiary referral centre.

Results: Compared to baseline, total volumetric density decreased by 5.2 % at the distal radius and 4.2% at the distal tibia after 12 months of ADT, due to a decrease in cortical density (by 11.3% radius and 6.0% tibia, all $p<0.001$) and trabecular density (by 3.5% radius and 6.0% tibia, both $p<0.01$), the latter due to a decrease in trabecular number not thickness ($p<0.05$). Bone turnover markers (P1NP and Osteocalcin) were negatively associated with total and cortical volumetric bone density at both sites.

Conclusions: Sex steroid deficiency induced by ADT for prostate cancer, results in decay of both cortical and trabecular bone.

***Disclosures: Jeffrey Zajac**, None.*

MO0033

Determinants of the Mechanical Behavior of Human Lumbar Vertebrae after Simulated Mild Fracture. Jean-Paul Roux*[1], Julien Wegrzyn[2], Monique Arlot[1], Stephanie Boutroy[1], Nicolas Vilayphiou[1], Olivier Guyen[3], Pierre D. Delmas[1], Roland Chapurlat[1], Mary Bouxsein[4]. [1]INSERM U831, Université de Lyon, France, [2]INSERM U831, Université de Lyon, Dep. Orthopedic Surgery pavillon T Hopital E. Herriot Lyon, France, [3]Dep. Orthopedic Surgery pavillon T Hopital E. Herriot Lyon, France, [4]Beth Israel Deaconess Medical Center, USA

After sustaining an initial vertebral fracture, up to 20% of women will experience another fracture within a year. The ability of a vertebra to carry load after initial deformation and the determinants of this post-fracture (post-frx) load-bearing capacity are critical, but poorly understood. Our study aimed to determine the mechanical behavior of vertebra after simulated SQ1 fracture (grade 1 of Genant's SQ scale) and to identify the determinants of this post-fracture behavior.

We obtained 21 fresh frozen L3 vertebral bodies (10 women and 11 men, 75 ± 10 years) and assessed bone mass by DXA, and trabecular (Tb) and cortical microarchitecture by µCT (Skyscan® 1076 and Scanco® Xtreme CT). Mechanical testing was performed in 2 phases: initial compression of the vertebra to 25% deformity (SQ1), followed by 30 min of unloading, and then compression to failure, to assess the post-frx behavior. We measured: 1) initial and post-frx failure load and stiffness, 2) changes in mechanical behavior, and 3) post-frx elastic behavior, assessed by recovery of vertebral height during the unloaded phase.

Post-frx stiffness and failure load were 53 ± 18% and 11 ± 19% lower, respectively than initial values ($p < 0.0001$), with 49 to 77% of the variation in the post-frx mechanical behavior explained by the initial values. Both initial and post-frx mechanical behaviors were significantly correlated with bone mass (r = 0.49 to 0.77) and microarchitecture (r = 0.47 to 0.83; p = 0.03 to < 0.0001). Post-frx changes in mechanical parameters were independent of bone mass, but were related to trabecular and cortical microarchitecture (r = -0.46 to -0.52, p = 0.04 to 0.02). Vertebral height recovery averaged 31 ± 7% (range: 20 to 46%) and was associated with trabecular thickness (r = 0.54), cortical thickness (r = 0.64), and trabecular heterogeneity (r = 0.44) ($p < 0.05$ for all).

In summary, we found marked variation in the post-fracture load-bearing capacity following simulated mild vertebral fractures. Bone microarchitecture, but not bone mass, was associated with the post-frx change in mechanical properties and recovery of vertebral height. These results provide guidance for identifying those at highest risk for progression of vertebral fragility, and suggest that therapies that prevent bone loss and enhance bone microarchitecture may prevent worsening of prevalent fractures, and possibly delay the vertebral fracture cascade.

***Disclosures: Jean-Paul Roux**, None.*
This study was supported in part by a research grant from Eli-Lilly® to INSERM

MO0034

In-vivo and Post-mortem Investigation of Reference Point Indentation (RPI) in the Horse. Davis Brimer[1], Douglas Herthel[2], Michelle Dickinson[3], Dr Alexander Daniel*[2]. [1]Active Life Technologies, USA, [2]Alamo Pintado Equine Medical Center, USA, [3]University of Auckland, New zealand

Methods:Measuring bone quality through strength and toughness testing is crucial for disease diagnostics and monitoring treatment. This is often carried out through bone biopsies which are highly invasive. Using a novel indentation technique (RPI) which can test bone properties in-vivo, indentation distance increase (IDI-micrometers) was evaluated using a cyclic loading regime. Analysis was performed as a line profile along the dorsal aspect of the third metacarpal bone (a frequently fractured bone in the horse). Analysis in vivo:no lameness;acute or chronic lameness;casted limbs with repeated measurements on the same horse after cast removal. Analysis post-mortem:fresh bone with dermis, no dermis+/-periosteum;-frozen thawed bone (c.f.fresh tissue) no dermis+/-periosteum;a limb with osteomyelitis after one freeze thaw cycle (no dermis or periosteum). Results:In-vivo analysis;5 cases with acute onset of lameness and no pathology had similar IDI values for both the left and right limbs. Standard deviation in IDI was greater for chronic lameness (6.1,6 cases) compared to acute lameness (2.5,3 cases). Chronic severe lameness resulted in a 60% increase in IDI of the lame limb with higher standard deviation (23.2+/-8.9 versus 14.1+/-2.0). Casting;IDI increased by 43% in one case and 48% in another. Repeated testing at a 21 day interval showed similar values of IDI for both limbs (Left:14.1+/-5.7 then 13.7+/-6.0;Right:15.2+/-4.3 then 14.3+/-5.4). Post-mortem analysis:IDI on normal control limbs (no dermis or periosteum) was similar for fresh and after two separate freeze thaw cycles (Left:9.4+/-3.8,8.9+/-2.7,10.4+/-4.6;Right:8.9+/-3.2,9.4+/-2.1,11.9+/-3.7). IDI was not statistically different on fresh tissue with periosteum (6.2+/-1.2) or without (10.3+/-2.5) nor after 2 freeze thaw cycles with periosteum (12.9+/-6.0) or without periosteum (8.8+/-5.7). There was a difference between IDI for one limb before and after the dermis was removed (t-test p=0.0016) but not the other (p=0.087). Before and after the dermis removed the difference in mean IDI was 3.8 for one limb and 6.4 for the other-IDI was lower in 85% of readings. Osteomyelitis limb;mean=IDI 11.3+/-6.8 compared to the normal=7.5+/-1.7 (t-test,p=0.005). In the region with radiographic evidence of osteomyelitis IDI was 17.9+/-8.3 compared to the normal 8.0+/-2.3(p=0.005). Conclusions:RPI has been validated for use in the horse as an effective indicator of bone properties without the need for biopsy.

***Disclosures: Dr Alexander Daniel**, None.*

MO0035

Is Increased Marrow Adiposity the Cause or the Result of Bone Microstructural Abnormalities in Premenopausal Women with Idiopathic Osteoporosis? Adi Cohen*[1], David Dempster[2], Emily Stein[3], Thomas Nickolas[1], Hua Zhou[4], Donald McMahon[3], Ralph Müller[5], Thomas Kohler[5], Joan Lappe[6], Halley Rogers[1], Robert Recker[6], Elizabeth Shane[3]. [1]Columbia University Medical Center, USA, [2]Columbia University, USA, [3]Columbia University College of Physicians & Surgeons, USA, [4]Helen Hayes Hospital, USA, [5]ETH Zurich, Switzerland, [6]Creighton University Osteoporosis Research Center, USA

Our studies of premenopausal (PreM) women with idiopathic osteoporosis (IOP) have revealed disrupted trabecular (Tb) microarchitecture and thin cortices, evidence of osteoblast dysfunction (decreased osteoid width and wall thickness), and a decrease in the number of circulating putative osteoblast precursors. Given the common mesenchymal cell origin of adipocytes (Ad) and osteoblasts (Ob), we hypothesized that these changes could be due to a shift from the Ob to the Ad lineage in IOP. To test this hypothesis, we quantified marrow Ad parameters in transiliac biopsies from 63 PreM women with IOP and 39 normal PreM controls. IOPs and Controls had normal menses and no history of eating disorder. IOPs were diagnosed based on history of low trauma fracture or BMD Z score ≤ -2.0.

IOPs were similar in age and height to Controls but had lower BMI (22.9 ± 4.6 vs 25.8 ± 4.7 kg/m^2; p=0.002). BMD by DXA was significantly lower at all sites in IOP and biopsies showed lower Tb bone volume fraction (BV/TV) and markedly abnormal Tb microstructure. Adipocyte parameters differed substantially between IOPs and Controls, even after adjustment for age, BMI and Tb BV/TV (Table). Controls exhibited the expected positive correlations of Ad perimeter (Pm), Ad#, and Ad volume/marrow volume (AdV/MV) with age (R=0.4-0.5; p<0.005) and Tb separation and negative correlations with microCT-based BV/TV (R=-0.6-0.7; p<0.001), Tb#, Tb thickness, bone formation rate (BFR; R=-0.3-0.4; p<0.05) and activation frequency (ActF; R=-0.3-0.4, p<0.06). However, no such relationships were detected in IOPs (age: R=0.01-0.02; BV/TV: R=-0.1-0.2; BFR: R=0.03-0.06; ActF: R=0.02-0.06). In IOPs, but not Controls, Ad# was inversely associated with BMI (R -0.3; p=0.01) and body fat by DXA (R=-0.2; p=0.05). In contrast, AdV/MV was positively correlated with body fat by DXA in Controls (R=0.3; p=0.04).

In summary, although PreM women with IOP have lower BMI, they have significantly higher marrow adiposity than age-matched Controls. In contrast to Controls, marrow adiposity did not show expected relationships with age, bone structure or bone turnover parameters in IOPs, but did correlate inversely with BMI and body fat by DXA. These results suggest that there is an abnormal relationship between bone and energy metabolism in premenopausal women with IOP. Interactions between Ads and Obs in the bone marrow microenvironment may play a role in the pathogenesis of IOP.

	Control n = 39	IOP n = 63	p (Un-adjusted)	p (Adjusted for age and BMI)	p (Adjusted for age, BMI, BV/TV)
AdArea (mm^2)	0.236 ± 0.074	0.317 ± 0.079	<0.0001	<0.0001	0.001
Ad-Pm (mm)	24.6 ± 6.8	31.4 ± 7.1	<0.0001	0.0003	0.007
Ad# (/mm2)	170.4 ± 43.3	207.7 ± 44.9	<0.0001	0.003	0.04
AdV/MV (%)	26.6 ± 8.2	34.0 ± 8.2	<0.0001	0.0003	0.006
AdDensity	193.0 ± 48.3	223.0 ± 46.6	0.002	0.03	0.2

TABLE

***Disclosures: Adi Cohen**, None.*

MO0036

Large Inter-Scanner Differences in Measured Proximal Femur Density and Strength Remain After Correction Using QCT Standardization Phantoms. Dana Carpenter*[1], Isra Saeed[2], Carole Schreck[2], Joyce Keyak[3], Tim Streeper[2], Tamara Harris[4], Thomas Lang[1]. [1]University of California, San Francisco, USA, [2]Department of Radiology & Biomedical Imaging, University of California, USA, [3]University of California, USA, [4]Intramural Research Program, National Institute on Aging, USA

In many studies that use at least two different quantitative computed tomography (QCT) imaging systems, anthropomorphic phantoms are scanned atop the bone mineral reference phantom to standardize between systems. The purpose of this study was to determine the effects of six different standardization phantoms on inter-scanner differences in measured volumetric bone mineral density (BMD) and strength of the proximal femur. Twenty females (60-69 years old) were imaged on two CT systems (64 Slice GE Discovery VCT and 16 Slice Siemens Hi-Res Biograph) while lying on a bone mineral reference phantom (Image Analysis Inc., Columbia, KY). Identical settings (50-cm field of view, 120 kVp, 150 mAs) were used on both systems. A 2.5-mm slice thickness was used on the GE system, and a 3-mm slice thickness was used on the Siemens system. The same settings were used to scan six standardization phantoms atop the reference phantom: the European Hip Phantom (ESP), European Spine Phantom (ESP), Image Analysis Torso Phantom (IATP), QRM Hip Phantom (QRM), QRM with a 2-cm fat/tissue outer ring (QRMR1), and QRM with a 4-cm fat/tissue outer ring (QRMR2). Images of each of these phantoms were used to apply voxel-by-voxel corrections of volumetric BMD. Hip images were then processed to measure integral BMD (iBMD), trabecular BMD (tBMD), cortical BMD (cBMD), cross-sectional compressive strength (F_y), average cross-sectional bending strength (M_y), and 3D finite element-based strength in stance (FE_{stance}) and fall (FE_{fall}) loading configurations [1-3]. Inter-scanner differences in measured parameters were expressed as the coefficient of variation (CV) of repeat measures [4]. Regardless of the voxel-by-voxel correction applied, substantial inter-scanner differences in the BMD and strength of the proximal femur remained (Table 1). The inter-scanner CV was larger than the measurement precision for all parameters. Mean differences were reduced in some cases, but absolute differences (expressed as CV) remained larger than the measurement precision, suggesting a need for corrections of a higher order than those available from simple anthropomorphic phantoms. References: 1. Lang TF et al., 1997. Bone 21(1): 101-8. 2. Carpenter RD et al., 2005. J Bone Miner Res 20(9): 1533-42. 3. Keyak JH et al., 2005. Clin Orthop Relat Res 437: 219-228. 4. Glüer CC et al., 1995. Osteoporosis Int 5(4): 262-70.

Table 1. Inter-scanner differences between the two CT systems for uncorrected image pairs and for images corrected using the 6 standardization phantoms. The previously determined measurement precision (calculated as the CV of repeat measures) is provided for comparison.

	Measurement Precision (%)	Inter-Scanner CV (%)						
		Uncorrected	EHP	ESP	IATP	QRM	QRMR1	QRMR2
iBMD	1.1	4.7	4.9	4.1	4.4	3.9	3.9	3.4
tBMD	0.7	11.3	6.3	6.9	7.9	10.4	17.1	6.6
cBMD	1.4	3.8	2.0	3.2	2.5	2.9	3.9	3.4
F_y	6.6	15.5	13.4	14.0	12.6	13.1	13.5	13.4
M_y	3.9	15.7	17.1	15.7	15.6	16.2	17.1	15.9
FE_{stance}	1.6	9.2	7.4	6.5	5.9	6.9	7.4	5.9
FE_{fall}	6.4	7.3	14.1	7.7	7.6	16.0	19.6	12.5

Table 1

***Disclosures: Dana Carpenter**, None.*

MO0037

Microcrack Detection and Histomorphometric Analysis of Tibial Subchondral Bone Obtained From Patients With Severe Knee Osteoarthritis. Audray Fortin[1], Natalie Dion*[1], Andy Kin On Wong[2], Justin de Beer[2], Alexandra Papaioannou[3], Georges Boivin[4], Jonathan Adachi[5], Louis-Georges Ste-Marie[6]. [1]CHUM Research Centre, Saint-Luc Hospital, Canada, [2]McMaster University, Canada, [3]Hamilton Health Sciences, Canada, [4]INSERM, France, [5]St. Joseph's Hospital, Canada, [6]Hospital Saint-LucCHUM, Canada

Osteoarthritis (OA) is an articular cartilage degenerating disorder widespread in the aging population. It has been shown that this disease leads to the alteration of subchondral bone (SC) which is conducive to microarchitectural fragilities such as microcracks (Cr). To further characterize microdamage accumulation in relation to bone architecture alteration, 13 specimens obtained from the mid-SC tibia, were studied following a total knee arthroplasty in severe OA patients (mean age: 63,8 $\pm$ 9,7yrs). These bone cores were bulk stained with calcein, a calcium chelator, and embedded in methylmethacrylate without decalcification. Microcracks were revealed and selected on 50µm-thick sections (parallel to the long axis) under fluorescent light, based on their trabecular positioning, linear sharp edges and relative size. Their morphology was further defined with a laser confocal microscope confirming their 3D structure. Classical bone histomorphometry was performed to measure bone volume (BV/TV), Cr density (number of Cr per bone area; Cr.Dn), mean Cr length (Cr.Le) and structural parameters such as trabecular thickness (Tb.Th), separation (Tb.Sp) and number (Tb.N). Micro-computed tomography was used to assess the structure model index (SMI; plate(0) vs rod(3) - like structure). Our results show that there were no associations between Cr.Dn and age or Cr.Le. However, Cr.Dn negatively correlated with BV/TV (R^2 =0,84; p<0,0001) and a trend was noted for Tb.Th (R^2=0,42; p=0,02) and Tb.N (R^2=0,41; p=0,03). There was a significant correlation between Cr.Dn and each of Tb.Sp (R^2=0,67;p=0.0007) and SMI (R^2=0,71;p=0,0003). This last observation indicates that with a high Cr.Dn value an elevated SMI is noted. Knowing that a high SMI value corresponds to a rod-like structure, which is more prone to fatigue induced damage, our results support that Cr are associated with microarchitectural weakening. This corroborates Arlot's findings [JBMR 2008;23:1613-28] in regards to microdamage detection in vertebral trabecular bone. Moreover, the stronger correlation coefficient that was found in SC bone, compared to vertebral bone (R^2=0,35), suggests that weight-bearing bones such as tibia are more likely to accumulate Cr. Considering this, further research would be necessary to better investigate the association of Cr.Dn/SMI with bone remodelling, bone fracture and eventually, the impact on the quality of life in patients affected by OA or other bone and joint diseases.

***Disclosures: Natalie Dion**, None.*

MO0038

Motion Artifacts in High-Resolution Peripheral Quantitative Computed-Tomography of Wrist and Ankle: Usefulness of Visual Grading to assess Image Quality. Jean-Baptiste Pialat*[1], Andrew Burghardt[2], Miki Sode[3], Thomas Link[2], Sharmila Majumdar[2]. [1]INSERM U831,Université de Lyon & Hospices Civils de Lyon, France, [2]University of California, San Francisco, USA, [3]University of California San Francisco & Berkeley, USA

Purpose: Motion artifacts are common during HR-pQCT image acquisition, resulting in repeating the acquisition thereby exposing a subject to more radiation. To date no standard criterion exists to determine when to repeat a patient scan, nor when to exclude a motion degraded dataset post hoc. In this study the reproducibility of a qualitative grading score for image quality was measured and the error for repeat measurements with motion degradation was characterized.

Methods: HR-pQCTimages (XtremeCT; Scanco Medical) of the wrist and ankle of subjects enrolled in studies conducted in our laboratory over a period of 3 years were reviewed retrospectively. Exams with repeat acquisitions due to motion were graded using a qualitative scale from grade 1 (no visible motion artifact) to grade 5 (severe artifact) by two readers independently; consensus was reached in case of disagreement. Inter and intra reader reproducibility was determined using kappa statistics and Intraclass Correlation Coefficient (ICC) respectively. Standard image analysis was performed to obtain cortical and trabecular densitometric and structure measurements in paired scans with at least one grade 1 scan. The percent difference for each parameter was calculated between scan and rescan. The mean % difference for each parameter was tested against the mean % difference for pairs with two grade 1 scans using Dunnett's test.

Results: A total 912 scans were performed (53.4% Radius, 46.6% Tibia) on 250 patients. Repeated acquisitions occured for 28.5% of the exams (33.1% Radius, 23.1% Tibia). Readers evaluated 602 exams with fair agreement (inter-reader, Kappa : 0.59 and intra-reader, ICC: 0.911 and 0.917). Only 54 acquisitions with repeated scans were graded 1 (best quality) at least once. Over this subset, percent differences tended to increase as the quality grading became poorer (Figure 1). Except Tb.Ar and vBMD, grade 4 and 5 have significantly greater errors than grade 1 for most densitometric and geometric parameters, grade 5 for cortical parameters and grade 3 for microarchitectural parameters.

Conclusions: Poor image quality grades were associated with greater error in HR-pQCT measure. As expected, densitometric parameters were least affected by motion, while trabecular parameters were the most affected. These results provide a framework for standardized quality control of clinical HR-pQCT studies.

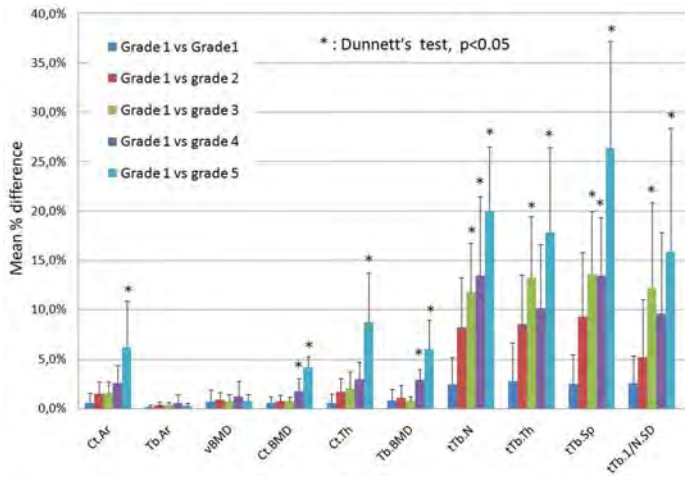

Figure 1: Mean %difference between scan and rescan for patients with best acquisition image quality

***Disclosures: Jean-Baptiste Pialat**, None.*

MO0039

Ovariectomized and Osteomalacic Rats have Altered Tissue Level Mechanical Properties as Assessed by Microindentation. Benjamin Roberts*[1], Fransisco Araiza[2], Ara Nazarian[1], Mary Bouxsein[1]. [1]Beth Israel Deaconess Medical Center, USA, [2]BIDMC, USA

Biomechanical principles dictate that whole bone strength is determined by contributions from geometry, morphology, and bone tissue material properties. However, there are few techniques for direct assessment of bone material properties, and consequently little is known about the contribution of tissue-level mechanical properties to skeletal fragility. Microindentation is an emerging method for testing the material properties of bone tissue that benefits from only being destructive to a small area of the bone, allowing for multiple tests per sample; characterization of multiple regions within each sample; and compatibility with *in vivo* testing. Our goal was to determine whether tissue-level mechanical properties and tissue mineral density differ in bones from ovariectomized (OVX) and osteomalacic (OM) rats. Methods: Adult female Sprague Dawley rats (12 wks of age, n=30) were equally assigned to control (CON, standard chow diet), ovariectomy (OVX, standard chow diet) or osteomalacia (OM, vit D deficient diet, 0.4% Ca, 0% vit D3) groups and were sacrificed 12 weeks later. Cortical bone material properties at the mid-tibial diaphysis were assessed with a microindentation system equipped with a tip sharpened to a 90˚conical, 2.5µm radius (BioDent 1000, Active Life Technologies, Santa Barbara, CA). Three to five indentation tests per specimen were performed; outcomes included total indentation distance (µm), indentation distance increase (IDI, µm), elastic modulus (E, GPa) and hardness (H, GPa). We also measured cortical tissue mineral density (TMD, $mg.cm^{-3}$) by micro-computed tomography. Results: OVX rats had higher (ie worse) IDI, a measure of post-yield mechanical competence, and lower E and H than CON ($p<0.01$, table). OM rats had lower E (-26%) and H (-28%), but IDI did not differ from CON. Cortical TMD was lower in OVX ($p<0.05$) and OM groups ($p=0.07$). Conclusion: These data illustrate the potential for microindentation to reflect differences in tissue-level mechanical properties in varied scenarios of skeletal fragility, namely OVX and OM. As tissue level mechanical properties are largely independent of BMD, these measurements have the potential to improve understanding and enhance assessment of mechanisms underlying skeletal fragility.

	CON (n=19)	OM (n=36)	OVX (n=47)
IDI (μm)	16.67 (2.96)	17.53 (4.26)	19.72 (4.84)*
Average Elastic Modulus (GPa)	1.30 (0.16)	0.96 (0.15)*	0.96 (0.25)*
Total Indentation Distance (μm)	295.1 (30.4)	348.6 (35.2)*	350.2 (49.5)*
Hardness (MPa)	63.9 (14.4)	45.1 (11.5)*	45.8 (20.0)*

*p<0.01 vs CON

table

***Disclosures:** Benjamin Roberts, None.*

MO0040

Precision of Skeletal Parameters at the Distal Radius - the Influence of Resolution Using Peripheral Quantitative Computed Tomography. Chantal Kawalilak*[1], James D. Johnston[2], Saija A. Kontulainen[3]. [1]College of Kinesiology, Canada, [2]College of Engineering; University of Saskatchewan, Canada, [3]College of Kinesiology; University of Saskatchewan, Canada

Our ability to measure cortical and trabecular bone with peripheral quantitative computed tomography (pQCT) has improved characterization of bone structure and estimated strength. However, the commonly used resolutions (400-600μm) challenge measurements of skeletal parameters at the distal radius; a common site of pediatric and osteoporotic fractures. The primary purpose of this study was to assess the precision of repeated scans and number of scans excluded when measured with a resolution of 400 and 200μm. Second, we determined whether the total, trabecular and cortical bone properties at the distal radius is similar when measured with a resolution of 400 and 200μm.

Sixty-five healthy adults (mean age ± SD, 31 ± 12 years) volunteered for the study. Repeated scans (on average 24 hours apart) of non-dominant forearm were performed using pQCT at the distal radius (4% of the radius length). We determined the precision (root means squared coefficient of variation; CV%rms) regarding the means of total (To), cortical (Co), and trabecular (Tr) bone properties at both resolutions (400μm, 200μm). Specifically, we investigated the precision between the means of: cross sectional area (ToA, CoA, TrA; mm2), volumetric bone mineral density (ToD, CoD, and TrD; g/cm^2), bone mineral content (ToC, CoC, and TrC; g), and the cortical wall thickness (CWT; mm) between the two resolutions (Table 1). We compared means and CV%rms measured with the 400 and 200μm resolutions using dependent samples t-tests, with Bonferroni adjustments for multiple comparisons. Statistical significance was set at $p<0.05$.

Precision ranged from CV%rms 1.5 to 13.6 and there was no statistically significant difference between CV%rms with 400 or 200μm resolutions for any outcome variables. The number of excluded scans was similar between the two resolutions (400μm: n=4, 3% of scans; 200μm: n=6, 5%). Significant differences were found between the resolutions in the means of: CoA, TrA, CoD, TrD, CoC, TrC, and CWT (Table 1). No significant differences were found between the two resolutions for the total bone measures (ToA, ToD, and ToC).

As the improved resolution seemed not to influence on precision and number of scans excluded skeletal researchers could consider using 200μm resolution when scanning the distal radius. Accuracy of distal radius cortical and trabecular measures, with different resolutions, is warranted as the outcomes diverged between the used resolutions.

Table 1. Mean±SD for each outcome measured with both resolutions

	400 μm	200 μm
ToA (mm²)	379.4 ± 84.3	377.8 ± 86.1
CoA (mm²)*	65.6 ± 13.5	58.4 ± 12.5
TrA (mm²)*	310.2 ± 78.5	306.7 ± 80.4
ToD (g/cm²)	337.1 ± 57.6	341.5 ± 60.1
CoD (g/cm²)*	647.4 ± 91.1	741.1 ± 88.8
TrD (g/cm²)*	245.6 ± 38.7	235.1 ± 36.4
ToC (g)	126.5 ± 31.4	127.5 ± 31.5
CoC (g)*	43.0 ± 12.8	44.0 ± 13.2
TrC (g)*	76.2 ± 23.1	72.1 ± 22.2
CWT (mm)*	1.01 ± 0.24	0.90 ± 0.22

*Significant difference ($p<0.05$)

Table 1. Mean (SD) for each outcome measured with both resolutions

***Disclosures:** Chantal Kawalilak, None.*

MO0041

Shape Based Analysis of Vertebra Fracture Risk in Post-menopausal Women. Alessandro Crimi*[1], Martin Lillholm[2], Paola Pettersen[3], Mads Nielsen[4]. [1]Nordic Bioscience & University of Copenhagen, Denmark, [2]Nordic Bioscience, Denmark, [3]Center for Clinical & Basic Research, Denmark, [4]Diku, University of Copenhagen, Denmark

Vertebral fragility fracture risk is important both in terms of early diagnosis of patients and in terms of population selection for clinical trials. The purpose of this study was to validate if the pre-fracture shape of the lumbar spine and vertebrae were predictive of future osteoporotic fractures.

This was a case-control study of 126 postmenopausal women, 25 of whom sustained at least one incident lumbar fracture and 101 controls that maintained skeletal integrity over 6.3 years from baseline to follow-up. All subjects were fracture-free at baseline and selected as a subset of the epidemiological PERF population. Case and controls were matched at baseline with respect to age, height, weight, and spine BMD. Lateral lumbar radiographs were acquired and read by an experienced radiologist to establish prevalent and incident fractures status using Genant's semiquantitative method. Furthermore, vertebrae T12-L5 had corner and midpoints of both endplates annotated using a computer tool. These 36 points describe the lumbar spine in terms of overall shape and individual vertebrae shape variations. This information was used as input to train a statistical active shape model which was regularized using Tikhonov's method. A linear classifier was trained to separate cases and controls at baseline. The fracture risk was defined as the normalized likelihood of belonging to the case group at baseline; a number between 0 and 1. The fracture risk was calculated for each subject in a leave-one-out fashion.

Results concerning the case-control group matching are given as mean ± SD for each group and tested using a Wilcoxon test. The ability to separate cases and controls at baseline are described through mean ± SEM and the p-value of a Wilcoxon test. This was further qualified through the area (AUC) under the ROC-curve.

The matching of the case and control groups yielded no significant differences at baseline: age (66.6 ± 5.9 vs. 66.9 ± 5.4, p=0.98), height (161 ± 6.0 vs. 163 ± 4.6, p=0.21), weight (65.4 ± 8.4 vs. 68.3 ± 11.7, p=0.53), BMD (0.86 ± 0.14 vs. 0.81 ± 0.14, p=0.2). There was a significant difference in fracture risk between cases and controls at baseline (0.56 ± 0.05 vs.0.27 ± 0.02, $p=3.4\times10^{-6}$). The AUC was 0.81 with a Delong p-value of 8.1×10^{-7}.

The results indicate that statistical shape analysis of overall spine and vertebrae shape are indicative of future fracture risk, and may be a useful tool for population selection in future clinical trials.

***Disclosures:** Alessandro Crimi, Nordic Bioscience, 2*
This study received funding from: Nordic Bioscience and CCBR-Synarc

MO0042

Texture Analysis of Bone Architecture in a Low Estrogen Post Pubertal Model. Theodore Raphan[1], Yongqing Xiang[1], Vanessa Yingling*[2]. [1]Brooklyn College (CUNY), USA, [2]Temple University, USA

Density measures alone, although widely used clinically, cannot identify osteoporotic subjects who will sustain fractures, due to the large overlap in bone mass measures in individuals with fractures and those without fractures. Other factors including bone size, architecture and material properties must be considered. Multiple approaches such as Mean Intercept Lengths (MIL) and the Fourier power spectrum have been used to characterize the structure of trabecular bone, particularly in describing orientation disparity or anisotropy. We have recently developed a texture analysis approach using Gabor filters, which is capable of providing insight into bone structure from localized texture information on a pixel level. Texture analysis can analyze both the global image at a low resolution and a detailed view at high resolutions. The texture approach is therefore a potentially powerful tool in analyzing trabecular bone texture where orientation, shape and architecture as well as density are the fundamental components. The following texture features were derived from the Gabor wavelets to measure properties of micro CT images of trabecular bone including: 1) Textural energy measured at 13 unique orientations analogous to density. 2) Anisotropy measures the difference between the texture energy values of the maximum and minimum orientations, normalized by the averaged texture energy. We compared texture analysis and micro CT results to a subset of data that consisted of 3 different ages of control animals (25 days, 65 days, 90 days) and 90 day old animals that received gonadotrophin releasing hormone antagonist injections to suppress estradiol for 25 days. The texture energy and anisotrophy measures from the texture analysis correlate well with the micro CT percent BV/TV and anisotrophy measurements with R2 values of 0.814 and 0.740 respectively (Figure 1A & B). However, the texture analysis is able to quantify energy values for multiple orientations and at 3 resolutions. The percent decrease in bone is dependent on orientation, a measure that is not available with micro CT analysis. The graph below illustrates the difference in the percentage of bone loss by orientation (Figure 1C). The loss of bone varies by orientation and suggests that bone loss is not similar throughout the proximal tibia.

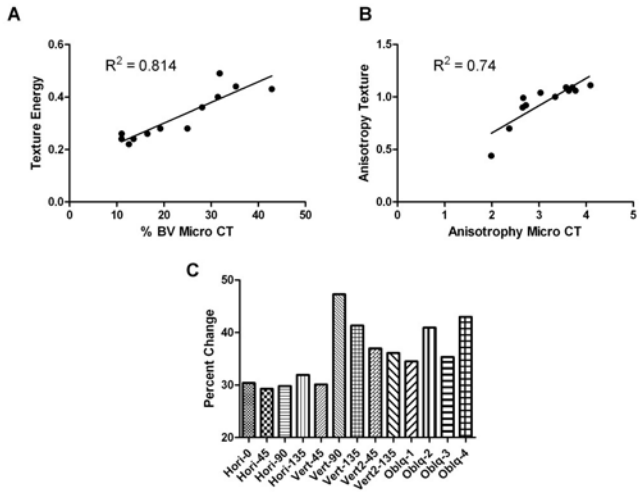

Figure 1

***Disclosures: Vanessa Yingling**, None.*

MO0043

The Accumulation of Advanced Glycation End Products and Pentosidine in Human Cancellous and Cortical Bone. Lamya Karim*[1], Grazyna Sroga[1], Simon Tang[2], Deepak Vashishth[1]. [1]Rensselaer Polytechnic Institute, USA, [2]University of California, San Francisco, USA

Non-enzymatic glycation is a spontaneous biochemical reaction occurring in bone that leads to the formation of crosslinks within and between collagen fibers known as advanced glycation end products (AGEs) [1]. AGEs accumulate with aging and cause age-related degradation of bone's mechanical properties [2]. To assess bone's mechanical integrity, pentosidine (PEN) has been used as a surrogate marker to represent AGEs [3]. However, it has not been determined whether PEN quantitatively reflects total AGEs. Thus, the goal of this study was to establish the relationship between PEN concentration and total AGE content. 56 human bone samples (37 cancellous, 18 cortical) were lyophilized and then hydrolyzed. Hydrosylates from each specimen were used to quantify PEN via ultra-high performance liquid chromatography and total AGEs with a fluorometric assay. The amount of collagen in each sample was calculated based on the determined hydroxyproline content. All crosslink quantities were normalized to the amount of collagen per sample [4]. Spearman correlations were run between PEN and AGE quantities separately in cancellous and cortical groups. PEN significantly correlated with total AGEs in cancellous bone ($r=0.752$, $p<0.0001$), but not in cortical bone ($r=0.134$, $p=0.598$). There was no correlation between age and PEN ($r=0.008$, $p=0.962$) or total AGEs ($r=0.245$, $p=0.154$) in cancellous bone. In cortical bone PEN showed no relationship with age ($r=0.154$, $p=0.546$), but there was a significant positive correlation between age and total AGEs ($r=0.842$, $p<0.0001$). Because PEN explained 75% of total fluorescent crosslink content in cancellous but not in cortical bone, we conclude that it can be used as a descriptive marker for AGEs in cancellous bone only. Our results for cortical bone emphasize the importance of quantifying total AGE content in addition to PEN rather than measurement of PEN alone. This will allow for a more comprehensive measurement of the effects of non-enzymatic glycation in bone.

1. Knott and Bailey, Bone, 1998
2. Tang et al., Bone, 2007
3. Grandhee and Monnier, J Biol Chem, 1991
4. Gross, J Exp Med, 1958

Funding source: NIH-NIA AG20618 and NIH-NIGMS T32GM067545

***Disclosures: Lamya Karim**, NIH-NIGMS T32GM067545, 2*

MO0044

A Longitudinal HR-pQCT Study of Alendronate Treatment in Post-Menopausal Women with Low Bone Density: Relations Between Bone Micro-Architecture and çFE Estimates of Bone Strength. Andrew Burghardt*[1], Galateia Kazakia[1], Miki Sode[2], Anne De Papp[3], Thomas Link[1], Sharmila Majumdar[1]. [1]University of California, San Francisco, USA, [2]University of California San Francisco & Berkeley, USA, [3]Merck & Co., Inc., USA

The purpose of this *in vivo* imaging study was to investigate the relationship between micro-architectural changes and biomechanical and bone turnover changes affected by 24-months of Alendronate treatment.In this double blind, placebo-controlled pilot study, 53 early post-menopausal women with low bone density (age=56±4yrs, femoral neck T-score=-1.5±0.6) were monitored by HR-pQCT for 24-months following randomization to Alendronate (ALN) or placebo (PBO) treatment groups. Subjects underwent annual HR-pQCT imaging of the distal radius and tibia, DXA at the spine, hip, and radius, and determination of biochemical markers of bone turnover (BSAP and uNTx). In addition to standard HR-pQCT density and structure analyses, direct measures of cortical micro-architecture (cortical thickness, porosity) were calculated. Estimates of compressive bone strength and load distribution between cortical and trabecular compartments were determined using μFE analysis. The %? at 24-months was calculated for all measures. Spearman correlation analysis was applied to determine: 1) which treatment-induced architectural changes were related to treatment-induced biomechanical and bone turnover response at 24-months, and 2) which baseline architectural properties predicted treatment-induced biomechanical and bone turnover response at 24-months.The biomechanical response to ALN was marked by a mean increase (tibia) or smaller loss of stiffness (radius) compared to placebo (Fig 1), though these effects did not reach statistical significance in this limited number of subjects. Correlation analysis revealed that the biomechanical response to ALN in the radius and tibia was specifically associated with changes in trabecular architecture ($|\rho|=0.51$-0.80, $p<0.05$), while PBO progression of bone loss was associated with a broad range of changes in density, geometry, and architecture ($|\rho|=0.56$-0.89, $p<0.05$). Unexpectedly, the %? in Tb.N was strongly negatively correlated ($\rho=-0.80$) to %? in stiffness for the radius (Fig 2). Baseline cortical load fraction and porosity measures best predicted ALN-induced change in biomechanics in the radius ($\rho>0.48$, $p<0.05$), while cortical density, geometry, and porosity predicted biomechanical and bone turnover response in the tibia ($|\rho|=0.48$-0.63, $p<0.05$). These findings suggest a positive ALN-response was manifested by prevention of trabecular plate-to-rod conversion and that HR-pQCT measures of cortical structure better predict the biomechanical and turnover response to ALN.

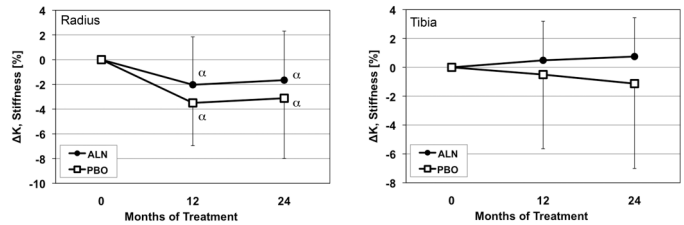

Figure 1

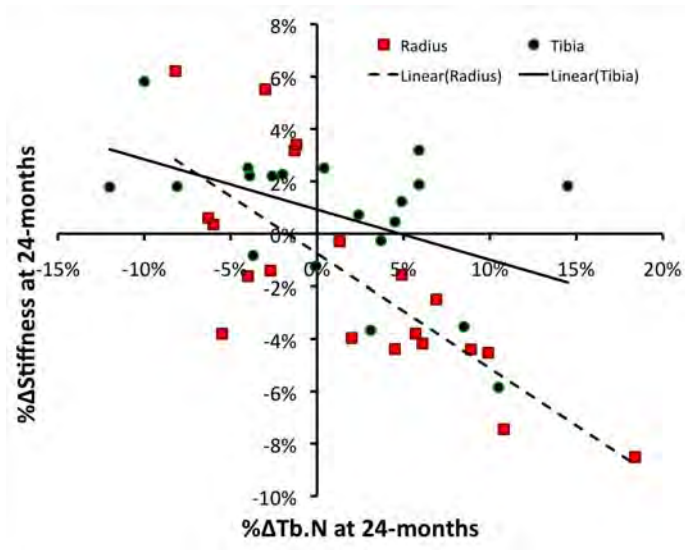

Figure 2

***Disclosures: Andrew Burghardt**, None.*
This study received funding from: Merck & Co., Inc.

MO0045

Evidence For Reduced Mineralization of Bone Matrix in Premenopausal Women With Idiopathic Osteoporosis. Barbara Misof[1], Adi Cohen[2], Paul Roschger*[3], David Dempster[4], Halley Rogers[2], Emily Stein[5], Hua Zhou[6], Thomas Nickolas[2], Donald McMahon[5], Joan Lappe[7], Robert Recker[7], Klaus Klaushofer[8], Elizabeth Shane[5]. [1]Ludwig Boltzmann Institute of Osteology, Austria, [2]Columbia University Medical Center, USA, [3]L. Boltzmann Institute of Osteology, Austria, [4]Columbia University, USA, [5]Columbia University College of Physicians & Surgeons, USA, [6]Helen Hayes Hospital, USA, [7]Creighton University Osteoporosis Research Center, USA, [8]Hanusch Hospital, Austria

Idiopathic osteoporosis (IOP) in premenopausal women (PreM) is an uncommon disorder in which fragility fractures and/or low bone mineral density (BMD) occur in otherwise healthy women with normal gonadal function. We have reported that PreM with IOP have thin cortices and cancellous (Cn) microarchitectural deterioration. However, information on bone material quality in IOP is rare. We used quantitative backscattered electron imaging (qBEI) to characterize the bone mineralization density distribution (BMDD) of Cn bone in transiliac bone biopsies from PreM with IOP. Included were 52 PreM (38+7 yrs) with IOP, 36 with Fractures, 16 with LowBMD (Z-score <-2.0 at spine and/or hip) and 37 healthy Controls (with normal BMD, Z-score >-1.0 at all sites). BMDD outcomes, the weighted mean (CaMean) and typical calcium concentration (CaPeak), the heterogeneity of mineralization (CaWidth), and the portion of low (CaLow) and high mineralized areas (CaHigh), were compared among these groups and correlation analysis was performed with mineralizing perimeter (MdPm, %), a primary determinant of bone formation rate. Comparison between IOP groups and Controls revealed that CaMean, CaPeak and CaHigh were significantly lower in both IOP fracture and LowBMD groups (CaMean -2.4% and -2.7%, CaPeak -2.3% and -2.6%, CaHigh -49% and -45%, respectively; ANOVA on ranks, all $p<0.01$) compared to Controls, with no difference between the IOP groups. MdPm by quantitative histomorphometry (median; 25th and 75th percentiles) did not differ significantly (ANOVA on ranks $p=0.064$) among IOP Fracture (3.67%; 2.37, 5.24) and LowBMD (3.93%; 2.40, 5.00) subjects and Controls (2.59%; 1.30, 3.74). In both IOPs and Controls, MdPm correlated negatively with CaMean, CaPeak, and CaHigh (r ranging from -0.33 to -0.66, p from <0.05 to <0.001), and correlated positively with CaWidth and CaLow (r ranging from 0.43 to 0.74, p from <0.01 to <0.001). The observed correlations between BMDD variables and MdPm reflect the general dependency of BMDD on the average tissue age. These findings further show that the BMDD in both IOP patients and in Controls is sensitive to variations even within the relatively narrow range of bone formation rates. We conclude that PreM with IOP have reduced mineralization of bone matrix that is not likely accounted for by differences in bone turnover. Changes in the mineralization process of the bone matrix may contribute to increased bone fragility in PreM with IOP.

***Disclosures: Paul Roschger**, None.*

MO0046

Femoroplasty Using an Injectable and Resorbable Calcium Phosphate Bisphosphonate Loaded Bone Substitute by Mini-invasive Technique to Prevent Contra-lateral Hip Fracture in the Elderly: A Cadaveric Biomechanical Study. Sébastien PARRATTE[1], Tünde AMPHOUX*[2], Sami KOLTA[3], Olivier GAGEY[4], Wafa SKALLI[5], Jean-Michel BOULER[6], Jean-Nöel ARGENSON[1]. [1]Orthopedical Surgery Department, Sainte-Marguerite Hospital, France, [2]GRAFTYS, France, [3]Paris-Descartes University, Rheumatology Department, Cochin Hospital, France, [4]Bicêtre University Hospital AP-HP & Paris-Descartes University, Service du don des corps, France, [5]Arts & Metiers ParisTech, CNRS, Laboratory of Biomechanics (LBM), France, [6]Nantes University, Laboratory of dental & osteoarticular engineering, INSERM UMR 791, France

Purpose : Prevention of hip fracture in the elderly imposes great benefit for care patient as well as for society. The incidence of contra-lateral, second hip fractures after a hip fracture surgery is as high as 20%. Femoroplasty using an injectable and resorbable calcium phosphate bisphosphonate loaded bone substitute to prevent contra-lateral hip fracture may represent a promising preventive therapy. We aimed to evaluate the biomechanical consequences of the femoroplasty using this new bone substitute.

Methods: Twelve paired human cadaveric femora from donors with a mean age of 86.3 years (7 women and 5 men) were included in this study. One femur from each donor was randomly assigned for femoroplasty and they were biomechanically tested for fracture load against their contra-lateral control. A–P and lateral radiographs and DXA scans were acquired before injection. Femoroplasty was performed under fluoroscopic guidance with an injectable and resorbable bisphosphonate loaded bone substitute. All femurs were fractured by simulating a lateral fall on the greater trochanter by an independent observer. The Wilcoxon's signed rank test was used to test for differences in fracture load between the reinforced femurs and the controls.

Results: Mean T-score of the tested femurs was -3,4 (SD $\pm$ 1,53). All the observed fractures were Kyle II trochanteric fractures. Mean fracture load was 2786 Newton in the femoroplasty group (group F) versus 2116 Newton in the control group (group C) ($p<0.001$). Fracture loads were always higher in the group F : mean 41.6% (mini: 1.2%/maxi:102.1%) and very significant ($p=0.00024$). Effect of femoroplasty was significantly superior for women (+57%) and also correlated to initial BMD ($p<0.0001$). A positive correlation between BMD and fracture load was observed both in control femurs (R2= 0.74) and reinforced femurs (R2= 0.81).

Conclusion: According to our results, femoroplasty with an injectable and resorbable calcium phosphate bisphosphonate loaded bone substitute can provide significant short term biomechanical reinforcement of the proximal femur to prevent osteoporotic contra-lateral fracture.

***Disclosures: Tünde AMPHOUX**, GRAFTYS, 5*
This study received funding from: GRAFTYS

MO0047

Effect of Dynamic Hydraulic Pressure Stimulation on Mitigation of Bone Loss in a Rat Disuse Model. Minyi Hu*[1], Jiqi Cheng[1], Suzanne Ferreri[1], Frederick Serra-Hsu[1], Wei Lin[1], Yi-Xian Qin[2]. [1]Stony Brook University, USA, [2]State University of New York at Stony Brook, USA

Bone fluid flow has been shown as a critical regulator for adaptation. Intramedullary pressure (ImP) is suggested to initiate fluid flow and then trigger bone remodeling. Such adaptive effects can be achieved via a dynamic oscillatory electrical stimulation in a rat disuse model. Other studies have shown that temporary venous ligation can also induce bone adaptation. A non-invasive manner as a direct fluid flow coupling in bone is necessary to develop new treatments for osteoporosis. Thus, it was hypothesized that direct oscillatory external hydraulic pressure stimulation can induce ImP and initiate adaptive response in a disuse osteopenia model. The aim of this study was to evaluate the effect of a novel, non-invasive, high frequency external pressure stimulus on bone structural properties. Five-month old female Sprague-Dawley virgin rats were randomly assigned to 6 groups: 1) baseline/n=10; 2) age-matched/n=9; 3) hindlimb suspended (HLS)/n=6; 4) HLS+2Hz stimulation/n=9; 5) HLS+20Hz stimulation/n=8; 6) HLS+Rest-insert Tourniquet/n=5. Pressure stimulations were given to the right mid-tibias for 10min (5min on - 10 min off - 5min on), 5 day/week, 4 weeks total. The stimulation was achieved by an inflatable cuff placed around the stimulation site with 30mmHg static+17mmHg dynamic pressures (Fig.1). At the end of the experiment, right tibial proximal metaphysis were scanned for trabecular bone morphology using μCT (μCT-40, SCANCO). The μCT analysis showed a clear trend of bone volume fraction and microarchitectural improvements in response to dynamic hydraulic pressure stimulation. While HLS reduced 32% BV/TV compared to age-matched control, 2Hz dynamic loading had a 41% increase in BV/TV, and 20Hz loading had a 33% increase in BV/TV compared to HLS. BV/TV induction was also shown in the rest-insert tourniquet group. Similar trends of improvements on bone microarchitecture were also observed in response to the stimulations (Fig.2). These encouraging results imply the mitigation affect of dynamic hydraulic stimulation in disuse bone loss. One possible underlying mechanism may be that induced ImP generated pressure gradient in bone, which initiates local fluid flow and adaptation. In contrast to previous studies, we found that the bone adaptation in response to this hydraulic stimulation was highly effective at lower frequency range. This implied that the viscoelastic property of muscle and hydraulic loader may have filtered out high frequency components.

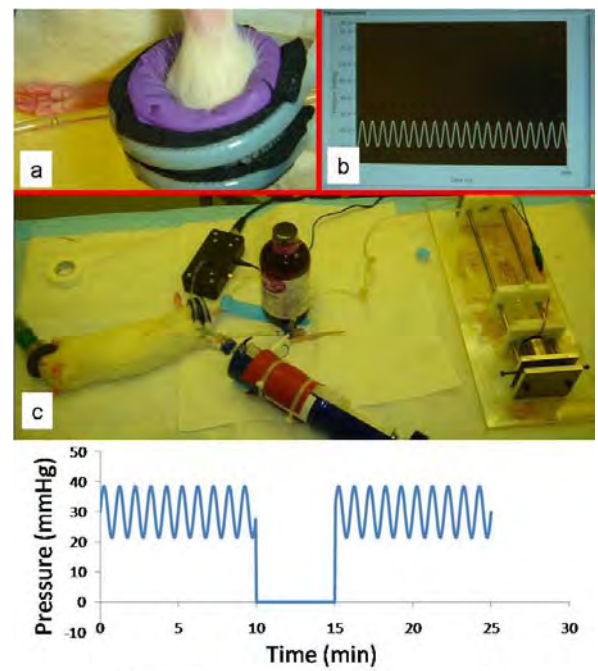

Fig. 1. *Experimental setup overview.*

Fig.1. Experimental setup overview.

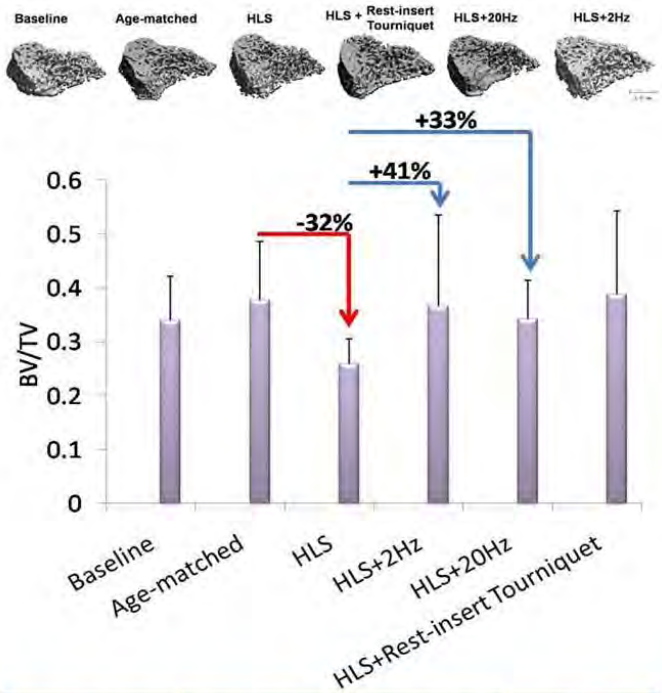

Group	ConnD	TbTh	TbSp
Baseline	90.3164±28.468	0.0988±0.007	0.1918±0.059
Age-Matched	95.749±21.177	0.105±0.0163	0.174±0.029
HLS	65.719±12.123	0.0916±0.012	0.2017±0.012
HLS + 2Hz	78.0216±27.486	0.104±0.024	0.1779±0.046
HLS + 20Hz	83.3635±28.056	0.1043±0.018	0.186±0.026
HLS+Rest-insert Tourniquet	74.4105±14.256	0.1177±0.033	0.185±0.033

Fig. 2. Right tibial trabecular bone structural quality.

Fig.2. Right tibial trabecular bone structural quality.

***Disclosures: Minyi Hu**, None.*

MO0048

Modeling Microgravity-Induced Alterations and Recovery in Metaphyseal and Diaphyseal Bone in Adult Hindlimb Unloaded Rats. Joshua Davis*, Yasaman Shirazi-Fard, Joshua Kupke, Derrick Morgan, Alyssa McCue, Joseph Thompson, Susan Bloomfield, Harry Hogan. Texas A&M University, USA

The adult hindlimb unloaded (HU) rat is a widely employed model for simulating the effects of microgravity on the musculoskeletal system. The goal of this study was to compare the changes in densitometric and geometric variables of metaphyseal bone, which contains a mix of cortical and cancellous bone, to diaphyseal bone in two different long bones (tibia and femur) after a bout of HU and over a prolonged recovery (return to weight bearing cage activity).

Adult male Sprague-Dawley rats (6-mo) were assigned to baseline (BL), cage control (CC), and hindlimb unloaded (HU) groups according to total (integral) volumetric bone mineral density (vBMD) and body weight. HU animals were further divided into sub-groups (n=15 each): HU euthanized after 28d of suspension, and HU euthanized after 28, 56, and 84 days of recovery. CC groups were euthanized at the same time 4 points. The right tibia and femur were harvested, and peripheral quantitative computed tomography (pQCT) scans were taken at the proximal tibia metaphysis (PTM), distal femur metaphysis (DFM), tibia diaphysis (TD), and femur diaphysis (FD). Results are summarized in Table 1 in terms of % changes of bone mineral content (BMC), vBMD, cross-sectional area (CSA), and compressive strength index (CSI) relative to BL (day 0) values. CSI ($vBMD^2$ *CSA) is a measure of estimated strength.

Overall, the temporal response to 28d of HU and subsequent recovery is similar at the PTM and DFM in most respects for BMC, vBMD, and CSI. The magnitude of the HU effects vary somewhat, with CSI experiencing the largest and most persistent negative effect. The main difference between the PTM and DFM is in CSA; the DFM values reflect an increase in CSA but the PTM results indicate the opposite. Thus, the DFM *ex vivo* results agree best with previously reported *in vivo* PTM results (*ASBMR* MO0041, 2009), which also show strong similarities to data from ISS astronauts (Lang et al. *JBMR* 21:1224, 2006). In the diaphysis regions, BMC, CSA, and CSI generally trend higher over time and become significantly higher than BL at the longer recovery periods (56d & 84d). However, the results at 56d and 84d of recovery are not different from corresponding aging control CC groups. The vBMD values stay essentially the same over time and are also not statistically different from CC groups. As expected, metaphyseal bone was more affected than diaphyseal bone, but the two metaphyseal sites showed some unexpected differences.

Percent Changes Relative to Baseline Values					
	Site	HU	HU+28d	HU+56d	HU+84d
BMC	PTM	-14.8%*	-10.0%*	-3.6%	-3.9%
	TD	2.0%	2.9%	8.1%*	14.7%*
	DFM	-7.2%*	-7.3%*	-3.9%	1.5%
	FD	4.1%	7.1%	11.7%*	19.9%*
vBMD	PTM	-8.7%*	-8.7%*	-4.1%	-2.0%
	TD	-1.2%	0.4%	1.3%	0.4%
	DFM	-13.5%*	-13.4%*	-9.0%*	-7.3%*
	FD	-0.1%	1.2%	3.2%	5.1%*
CSA	PTM	-5.1%	-0.9%	0.6%	-1.4%
	TD	3.4%	2.6%	6.9%	14.3%*
	DFM	7.4%	6.8%	5.6%	9.4%*
	FD	4.2%	5.9%	8.3%*	14.1%*
CSI	PTM	-24.1%*	-18.7%*	-6.4%	-4.6%
	TD	0.6%	3.7%	9.7%*	15.4%*
	DFM	-19.2%*	-18.8%*	-11.5%*	-4.4%
	FD	4.2%	8.3%	15.2%*	26.2%*

* significantly different from BL (P<0.05)

Table 1

***Disclosures: Joshua Davis**, None.*

MO0049

Cell Proliferation is Modulated by Oscillatory Accelerations but not by Differences in Fluid Shear. Gunes Uzer*[1], Ete Chan[1], Elizabeth Fievisohn[1], Suzanne Ferreri[1], Yi-Xian Qin[2], Clinton Rubin[2], Stefan Judex[1]. [1]Stony Brook University, USA, [2]State University of New York at Stony Brook, USA

Bone cells can perceive low-level accelerations, when applied at high frequencies, as an anabolic stimulus but the mechanism by which cells sense and respond to this small-magnitude signal is largely unknown. Dynamic accelerations may not only stimulate cells directly but also indirectly through the generation of fluid forces. In an effort to separate the contribution of each of the two distinct mechanical signals, here, we hypothesized that increasing vibration-induced fluid shear, while keeping the magnitude of the acceleratory oscillations constant, will not affect cell proliferation. Experiments were performed in-silico as well as in-vitro. Finite element modeling predicted the velocity profile of a viscous fluid in a rigid container oscillating horizontally at 60Hz and 1g peak acceleration. In this model, fluid-solid interactions during acceleratory oscillations were modeled by a coupled Eulerian-Lagrangian analysis. Effects of vibration-induced fluid shear stresses on MC3T3-E1 cell proliferation were then determined in-vitro at day 6. Fluid shear forces were modulated by increasing the viscosity of the fluid via the addition of dextran. In a 3% w/v dextran solution, the peak fluid shear stress between the bottom cell layer and the adjacent fluid layer (350 μm distance) was increased by 78% from the 0% dextran peak value of 0.032Pa. Increasing the dextran concentration to 6% and 9% doubled and quadrupled peak stresses compared to the 3% group. Osteoblast like cells were vibrated for 10min/day in mediums with dextran concentrations of 0%, 3%, 6% or 9% (n=3). Exposure of the cells to increased medium viscosity for 10 min/day, without the application of oscillatory accelerations, attenuated cell proliferation in a dose dependent manner at day 6. In contrast, exposure of cells to the brief mechanical stimulus increased cell proliferation in all dextran groups. However, there was no evidence of a greater vibration effect in those cells that were in a more viscous medium. These preliminary data demonstrate that brief periods of vibrations can increase cell proliferation in osteoblast like cells. Because enhanced proliferation was independent of the specific viscosity of the medium, and therefore independent of the induced fluid stress, they also suggest that the cells responded directly to the applied small-magnitude oscillatory motions. Optimal vibration parameters remain to be identified.

***Disclosures: Gunes Uzer**, None.*

MO0050

ERK/MAP Kinase-mediated Phosphorylation of Runx2 is Required for Fluid Flow Shear Stress Induction of Osteoblast Gene Expression. Yan Li*[1], Chunxi Ge[2], Rijad Tayim[3], Jose Rodriguez[4], Steven Goldstein[5], Renny Franceschi[1]. [1]University of Michigan, USA, [2]University of Michigan School of Dentistry, USA, [3]University of Michigan School of Medicine, USA, [4]University of Michigan School of Dentistry, USA, [5]University of Michigan Orthopedic Research Labs, USA

Mechanical loading is a major anabolic signal in bone that increases osteoblast differentiation, survival, motility and proliferation. Loading stimulates MAPK, PI3K/AKT and Wnt signaling, but it is not understood how these pathways regulate transcription. At last year's meeting, we reported that fluid flow shear stress (FFSS) loading of preosteoblast cells induced translocation of P-ERK and P-AKT to the nucleus where they associated with Runx2 on the chromatin of target genes. In the present report, we focus on the ERK/MAPK component of the FFSS response and involvement of the Runx2 transcription factor. Exposure of MC3T3-E1cl42 cells to cyclic FFSS (0.033Hz, 2 Pa) induced osteopontin (SPP1), bone sialoprotein (Ibsp) and osteocalcin (Bglap2) mRNAs and Bglap2 promoter activity. Induction of all 3 genes was detected within 1 h, although peak SPP1 mRNA induction occurred earlier than Ibsp and Bglap2. These events were preceded by binding of P-ERK to Runx2 on Bglap2 and Ibsp chromatin, increased histone H3 S10 phosphorylation and histone H3 and H4 acetylation. All responses to FFSS were blocked by the ERK/MAPK inhibitor, U0126. Significantly, FFSS also rapidly increased Runx2 S319 phosphorylation as measured using a specific antibody. Phosphorylation at this and a related site (S301) is necessary for maximal Runx2 transcriptional activity (Ge et al, JBC 284:32533, 2009). The importance of Runx2 phosphorylation to the FFSS response was established by transfecting Runx2-deficient C3H10T1/2 cells with wild type or S301A/S319A mutant Runx2. In the absence of Runx2, FFSS was unable to induce Ibsp and Bgalp2 mRNAs, but mRNA induction could be restored with a WT Runx2 expression vector. In contrast, the FFSS response was greatly reduced in cells transfected with mutant Runx2. Based on these observations, we propose the following novel mechanism to explain how FFSS stimulates gene expression in osteoblasts: i) FFSS directly or indirectly stimulates ERK phosphorylation and translocation to the nucleus, ii) Nuclear P-ERK specifically binds Runx2 that is already associated with the chromatin of target genes, iii) P-ERK phosphorylates Runx2 and, possibly, other substrates to form an activated complex that recruits accessory factors to the gene leading to increased histone phosphorylation and acetylation, iv) histone modifications stimulate chromatin decondensation, increased accessibility of the gene to RNA polymerase II and transcription.

***Disclosures: Yan Li**, None.*

MO0051

Load/Strain Distribution between Ulna and Radius in the Mouse Forearm Compression Loading Model. Ganesh Thiagarajan*[1], Yunkai Lu[1], Todd Bredbenner[2], Dan Nicolella[3], Mark Johnson[4]. [1]University of Missouri - Kansas City, USA, [2]Southwest Research Institute, USA, [3]South West Research Institute, USA, [4]University of Missouri, Kansas City Dental School, USA

The mouse forearm compression loading model is widely used to study bone formation in response to mechanical loading. We have shown that after a single session of forearm loading, β-catenin signaling is activated in a subpopulation of osteocytes within 1 hour in the maximal compression or tension regions predicted from finite element analysis (FEA) models, but displayed a random and heterogeneous pattern within these global strain fields. To better understand ulna strain distributions during forearm loading we have begun to develop higher resolution FEA models and apply biological metrics to validate these models. Two models were created; the Ulna Model (UM) and the Ulna-Radius Model (URM), designed to test the contribution of the radius, which is not routinely included in these FEA models. A CD-1 wildtype mice forearm was placed in a static loading device and microCT images taken at 0, 1.25 and 2.5 N of compression. The image data was imported into Slicer3D and endosteal and periosteal surfaces were manually segmented. The segmented images were imported into GeoMagic Studio 9 where the 3D object underwent smoothing, patching, curve-fitting, and surface mapping before the final CAD model was created. FEA meshes were created using automated tetrahedron mesh creation software (ABAQUA CAE). Mesh convergence was investigated using increasing numbers of both both 4- and 10-node tetrahedrons. Boundary conditions at the wrist and olecranon were included in the model to simulate the experimental loading. Displacement and strain contours resulting from a simulated load of 2 N were calculated using both the ABAQUS and LS-DYNA solvers. The results showed significant differences in the strain distributions within axial cross sections in the ulna/radius model versus ulna alone model. The maximal strain locations were located about 3-5 mm to the distal end from the mid-shaft. It is observed that the URM predicts a peak strain in the bones which is twenty percent higher than the UM prediction. The maximal compressive strain value (absolute) is 1.5 times that of the tensile strain for both ulna/radius and ulna alone models. Also, the FE analysis maximal strain values exceeded those from the strain gage readings. These data argue that the ulna/radius FEA model is a superior approach and this has important ramifications for future studies to understand strain thresholds needed to activate β-catenin signaling in osteocytes in response to mechanical loading.

***Disclosures: Ganesh Thiagarajan**, None.*

MO0052

Bone and Muscle Adaptation to High Impact Loading in Martial Artist Brick Breakers. Blair Healey, Joel Lanovaz, Ashley Gerstmar, Saija Kontulainen*. University of Saskatchewan, Canada

Unilateral models are ideal when assessing musculoskeletal adaptation to mechanical loading as between-limb comparison eliminates the confounding effects of genetics, hormones and nutrition. The unilateral activity of brick breaking within martial arts enables assessment bone and muscle adaptation to the high impact forces. Our first objective was to compare musculoskeletal properties between the dominant and nondominant forearm and upper arm in brick breakers and assess if these side-to-side differences differed from those in controls. Our second objective was to assess association between brick breaking peak impact force and bone and muscle side-to-side differences in brick breakers.

Thirteen male brick breakers' (mean age 31.1, SD 10.5 yrs) and their 13 age- and size-matched controls' wrist (4% of length), forearm (65%) and mid-upper arm were measured with pQCT(Stratec XCT2000). We calculated percent side-to-side differences for radius total area (ToA,) and estimated strength (BSIc) at wrist; cortical area (CoA), estimated strength (SSIp) and surrounding muscle cross-sectional areas (MCSA) for ulna and humeral shafts. Brick breaking impact forces were measured from the striking arm of 9 participants when they hit a vertical stack of 8 concrete patio bricks. We compared bone and muscle side-to-side differences within each group by paired t-tests and side-to-side differences between the groups by independent samples t-test. Association between brick breaking impact forces and side-to-side differences was assessed by Spearman rank correlation.

Brick breakers' both radii had similar areas and BSIc at wrist and similar ulna CoA and SSIp forearm whereas cortical area and SSIp were 5% and 7% greater ($p<0.05$) in the dominant humeral shaft. MCSA was 5% and 6% greater ($p<0.05$) in brick breakers' dominant forearm and upper arm, respectively. None of the bone side-to-side differences in brick breakers differed from those in controls. However, brick breakers' upper arm MCSA side-to-side difference was 6% greater ($p<0.05$) than that in controls. Peak impact forces ranged from 2109 N to 4511 N and were correlated ($rho=0.78$, $p<0.05$) with brick breakers' side-to-side SSIp difference in ulna only.

Brick breakers' bone in the loaded arm was not adapted for high impact forces whereas the upper arm muscle adaptation was indicated by a greater unilateral MCSA in brick breakers than in controls. Larger muscle may support humerus in withstanding high impact loading.

***Disclosures: Saija Kontulainen**, None.*

MO0053

Combined Effects of Alendronate and Low-intensity Pulsed Ultrasound in Rat Cancellous Bone Repair. Hiroshi Aonuma*, Naohisa Miyakoshi, Yuji Kasukawa, Hiroyuki Tsuchie, Yoichi Shimada. Akita University Graduate School of Medicine, Japan

Alendronate (ALN) is a bone resorption inhibitor that enhances mechanical strength at fracture sites by increasing callus volume during fracture healing in cortical bone. However, because bone remodeling is inhibited, woven bone is primarily formed. On the other hand, low-intensity pulsed ultrasound (LIPUS) is known to promote fracture healing in cortical bone in rats and humans. However, the effects of ALN and LIPUS on cancellous bone repair and their combined effects have not been elucidated. The purpose of present study was to investigate these effects in a rat cancellous osteotomy model.

Osteotomy of cancellous bone in the proximal tibia was performed in 7-month-old Sprague-Dawley rats (n=19), and the osteotomy site was closed using a nonabsorbable suture. Rats were divided into the following four groups: 1) Control group (n=4), vehicle administration + sham LIPUS; 2) ALN group (n=5), ALN administration + sham LIPUS; 3) LIPUS group (n=5), vehicle administration + LIPUS; and 4) Combination group (n=5), ALN administration + LIPUS. Subcutaneous ALN injection (10 μg/kg) and LIPUS (20 min/day) were performed daily from the third day after osteotomy for 2 weeks, after which tibial bone was harvested. After measuring bone mineral density (BMD) in the proximal tibia using the dual-energy X-ray absorptiometry method, hematoxylin and eosin-stained decalcified samples were prepared for measurement of bone union rate at the osteotomy site as well as cancellous bone volume (BV/TV), osteoid surface (OS/BS), and eroded surface (ES/BS) using bone histomorphometry.

ALN administration significantly decreased OS/BS ($p=0.0040$), but no significant differences were observed for BMD, bone union rate, BV/TV or ES/BS. LIPUS significantly increased bone union rate ($p=0.0006$), but no significant differences were observed for BMD, BV/TV, OS/BS or ES/BS. No interaction between ALN and LIPUS was observed for any of the parameters.

Although ALN did not affect cancellous bone repair, LIPUS promoted bone repair at the cancellous bone osteotomy site. No combined effects of ALN and LIPUS were observed for bone repair, BMD, or bone mass at the cancellous bone osteotomy site.

***Disclosures: Hiroshi Aonuma**, None.*

MO0054

Eccentric and Concentric Grip Strength Training on pQCT Derived Bone and Muscle Parameters in the Adult Forearm: A 26 Week Pilot Study. Andrew Frank*[1], Phil Chilibeck[2], Jonathan Farthing[3], Saija Kontulainen[4]. [1]The University of Saskatchewan, Canada, [2]University of Saskatchewan College of Kinesiology, Canada, [3]University of Saskatchewan, College of Kinesiology, Canada, [4]University of Saskatchewan, Canada

Muscles exert the greatest natural forces upon the skeleton and "muscle lengthening" eccentric (ECC) contractions produce greater tension than "muscle shortening" concentric (CON) contractions (Wright et al. *Arch Phys Med Rehabil:* 1983). Our objective was to determine whether contraction type specific training (ECC vs CON) influences forearm muscle and distal radius bone parameters in older adults.

Participants included 11 healthy men (mean age 64.5 ± SD 7.0 yr) and 18 healthy women (56.3 ± 4.8 yr). To control for limb dominance a within-subjects design was used with one arm randomized for ECC and the opposite arm for CON training. Training was progressive up to 6 sets of 8 maximal grip contractions on a Humac NORM isokinetic dynamometer, 3 times a week for 26 weeks. Peripheral quantitative computed tomography (pQCT) assessed distal radius (at 4% of radius length) total bone content, bone density, and bone area (ToA), trabecular bone content (TrC), trabecular bone density (TrD), and trabecular area (TrA) as well as forearm (at 65%) muscle cross sectional area (MCSA) and muscle density (MD). We used a time x contraction type x gender ANOVA to assess muscle and bone outcomes and paired t-test for a post-hoc analysis. Statistical significance was set at $p<0.05$.

There was a contraction type x time interaction for MSCA, where ECC increased more than CON (2.5% vs 1.2%; $p<0.05$). There was a time main effect for MD ($p<0.001$). There were no main effects for any bone parameters. However, our results did hint at a contraction type by time interaction for TrC ($p=0.13$), TrA ($p=0.11$) and ToA ($p=0.10$) with greater improvements in the ECC trained arms; and a contraction type x time x gender interaction for TrD ($p=0.06$) with a trend for greater increases in ECC trained arms of males, and in the CON trained arms of females. Our results suggested that the forearm MCSA response differs with respect to CON and ECC specific hand grip contraction training. While 26 weeks of training was adequate for muscle adaptation in the forearm, significant changes in distal radius bone may require a longer intervention. ECC grip training may provide a greater skeletal benefit in the distal radius, but a larger and longer study of these training adaptations is necessary. These results are important for optimizing the design of exercise interventions aimed at increasing bone strength at the clinically relevant distal radius.

***Disclosures: Andrew Frank**, None.*

MO0055

Effects of Prolonged Unloading on the 3D Microarchitecture of Rat Cortical Bone. Hayley Britz*[1], Jarkko Jokihaara[2], Olli Leppanen[3], Teppo Jarvinen[4], David Cooper[1]. [1]University of Saskatchewan, Canada, [2]University of Tampere, Canada, [3]University of Tampere, Finland, [4]University of Tampere/IMT, Finland

Bone is capable of adapting to changes in loading; however little is known regarding how loading affects the internal 3D microarchitecture of cortical bone. This is due to the heavy focus which is put on studying the effects of loading on trabecular bone and the gross surface changes (modeling) of cortical bone. The aim of this study was to experimentally test the hypothesis that loading is a determinant of the 3D orientation of vascular canals. This objective was addressed by observing how the primary cortical microarchitecture (canal network) of rat tibiae was affected by unloading during growth. The left tibial diaphysis from ten rats (30 weeks old) that had been immobilized by sciatic neurectomy for 27 weeks and the left tibial diaphyses from ten control rats (30 weeks old) were scanned in a micro-CT. Our lab has previously found that desktop micro-CT, operating at 3 micron nominal resolution, is an effective means of visualizing and quantifying rat cortical bone porosity. Canal volume fraction, mean canal diameter, mean canal spacing and mean canal orientation were quantitatively assessed. Qualitative observations of the canal networks in 3D revealed a marked regional variation within the tibial cross section. Both groups exhibited large numbers of radial canals with these were more predominate in the unloaded specimens. Quantitatively no differences were found between immobilized and control rats for canal volume fraction and canal separation (p=0.177 and p=0.146, respectively). Canal diameter was significantly greater in immobilized rats as compared to control rats ($p<0.001$). Canal orientation was found to be significantly different between the two groups ($p<0.001$). The mean shift in canal orientation in immobilized rats was 11° towards the transverse (radial) plane. These results suggest that cortical bone even in the rat has a highly variable microarchitecture which is directly affected by mechanical stimuli. This finding has implications for studies focusing on fluid flow and the affects of canal orientation on the mechanical properties of bone which will ultimately lead to advancements in the areas of bone adaptation, aging and disease.

***Disclosures: Hayley Britz**, None.*

MO0056

Exercise Loading Does not Account for Polar or Radial Distribution of Cortical Density at Weight-bearing Tibial Mid-diaphysis. Timo Rantalainen*[1], Riku Nikander[2], Robin Daly[3], Ari Heinonen[4], Harri Sievanen[5]. [1]University of Jyväskylä, Finland, [2]UKK Institute for Health Promotion Research, Finland, [3]The University of Melbourne, Western Hospital, Australia, [4]University of Jyvaskyla, Finland, [5]UKK Institute, Finland

Cortical bone is not a uniform tissue, and it apparent density [cortical volumetric density (vBMD)] varies around the bone cross-section as well as along the axial length of the bone. This varying vBMD distribution may be due to changes related to growth and/or aging, but it may also be modulated by regular exercise loading. Therefore, the aim of this study was to compare the cortical bone mass distribution around the centre of mass (polar distribution) and through the bone cortex (radial distribution) among 221 premenopausal women aged 17 - 40 years representing athletes involved in high impact, odd impact, high magnitude, repetitive low impact, repetitive non-impact sports and physically active referents. Bone cross-sections at the tibial mid-diaphysis were assessed with pQCT. Cortical bone was separated from the other tissues using a threshold of 690 mg/cm^3. Polar and radial vBMD distributions were analyzed in 18 sectors from the centre of mass and 8 concentric divisions from the centre of bone mass to the outer bone edge, respectively. The most inner and outer layers of pixels were excluded from the analysis to avoid partial volume effect. According to MANOVA with group as a between subjects factor and polar or radial distribution as a within subject factor, the groups differed in both polar and radial distribution (both $P<0.001$), whereas no significant group - division/sector interaction existed in either radial ($F = 0.992$, $P = 0.445$) or polar ($F = 1.377$, $P = 0.060$) distribution (Fig. 1). In radial and polar distribution post hoc testing high impact (-23 (95 % CI -16 to -32) mg/cm^3, $P < 0.001$), odd impact (-16 (-7 to -25) mg/cm^3, $P < 0.001$) and repetitive non-impact (-11 (-2 to -20) mg/cm^3, $P = 0.017$) groups differed from the referents. In conclusion, the results generate a hypothesis that, polar and radial cortical density distributions are not affected by exercise loading, while the mean vBMD is. The finding supports the notion that bone strength is mainly adapted by changing bone mineral mass and geometry rather than its material properties.

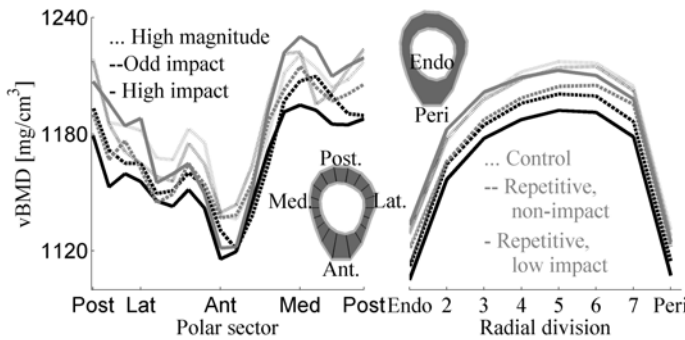

FIGURE 1. The averaged polar and radial density distributions of the exercise loading groups.

***Disclosures: Timo Rantalainen**, None.*

MO0057

Implant Microstimulation Improves Bone Implant Osseointegration. Patrick Ammann*[1], Anselm Wiskott[2], Joël Cugnoni[3]. [1]Division of Bone Diseases, Department of Rehabilitation & Geriatrics, University Hospital & Faculty of Medicine, Geneva, Switzerland, [2]Division Prothèse Conj. & Occluso, University of Geneva, Switzerland, [3]Laboratory of Applied Mechanics & Reliability Analysis (LMAF), Switzerland

The process of implant osseointegration implicates local stimulation of bone formation. This process can be stimulated by systemic treatment with antiosteoporotic treatments. External mechanical stimulation favors bone formation at the level of cortical and trabecular bone. Whether microstimulation of the implant stimulates the formation of bone in the vicinity of the implant and improves the process of osseointegration is not known. To answer this question, we devised an experimental rat model of adaptive bone modeling inducing in vivo implant activation by external microstimulation. To this end we have developed a procedure by which highly controlled stress states are induced within the bone tissue using two transcutaneous cylindrical implants. Two weeks after implantation into the proximal tibia, the rats were sedated and the two titanium cylinders were mechanically stimulated on a daily basis for four weeks. The stimulation levels selected were 1 and 2 N (corresponding to ca. 1500 and ca. 3000 microstrain respectively) or no stimulation (basal). The effects on bone micro architecture were investigated using micro computerized tomography and the following characteristics were determined: trabecular bone volume (TV/BV), bone implant contact (BIC) and trabecular thickness (TbTh). Values are means±SEM and significant differences were identified using ANOVA (*: $p<0.05$ vs basal). External micro stimulation of the implant induced a dose dependent increase

of bone mass and an enhancement of the microarchitecture in the vicinity of the implant. This increase of bone mass surrounding the implant reflects a positive bone balance and was probably obtained by stimulation of bone formation. Since the major determinants of implant osseointegration are bone implant contact and microarchitecture, an improvement of pullout force is to be expected. These data suggest that implant microstimulation could improve bone implant osseointegration

Stimulation	Basal	1N (ca. 1500με)	2N (ca. 3000με)
BV/TV	48.9±1.4	45.9±9.6	60.4±3.6*
BIC	75.2±1.7	70.3±8.3	82.2±4.11
Tb Th	0.163±0.002	0.163±0.015	0.176±0.007*

table

***Disclosures: Patrick Ammann**, None.*

MO0058

Knee Loading Promotes Bone Healing in Femoral Head Osteonecrosis. Ping Zhang*[1], Hiroki Yokota[2]. [1]Indiana University, USA, [2]Indiana University, Purdue University Indianapolis, USA

Osteonecrosis of the femoral head is one of the most serious orthopedic diseases affecting the hip joint. Using recently developed joint loading, which is capable of inducing anabolic responses in murine femora, the object of this study was to examine whether knee loading would be useful in stimulating bone healing in the necrotic femoral head. The study using 27 C57/BL/6 female mice (~ 14 wks of age) was approved by the IACUC. This induction of osteonecrosis was conducted in left and right femoral heads. In brief, the ligamentum teres were transected, two ligatures were passed around the femoral neck and tied tightly to disrupt the blood vessels that lead to the femoral head. From the fourth postoperative day, knee loading was conducted, in which 0.5 N loads were laterally applied to the left knee at 15 Hz for 5 min/day for 5 consecutive days. The contralateral femur was used as a sham loaded control. Animals were sacrificed 3 weeks after the surgery. Bone dimension was measured, and bony wet weight was determined. Using pQCT, three consecutive scans perpendicular to the femoral head axis were made at the apex, middle and base of the femoral head. Total volumetric bone mineral density and cortical bone mineral density were computed together with total bone area and cortical area. From those data, we derived total bone content, and cortical bone content. Evaluation of the femoral head supported the loading-driven bone healing. Compared to the samples with no treatment (osteonecrosis), knee loading enhanced height of the femoral head from 1.39 ˇ 0.04 mm (control) to 1.54 ˇ 0.04 mm (loaded; $p < 0.001$). The width of the femoral head were also increased from 1.49 ˇ 0.03 mm (control) to 1.56 ˇ 0.04 mm (loaded; $p < 0.001$). The femoral weight was increased from 66.2 ˇ 3.26 mg (control) to 69.3 ˇ 4.25 mg (loading) ($p < 0.01$). Although the observed pQCT increases did not show statistical significance, total vBMD was elevated from 687.1 ˇ 54.4 mg/cm^3 (control) to 698.3 ˇ 71.8 mg/cm^3 (loaded, $p = 0.20$), while cortical vBMD was increased from 815.3 ˇ 45.4 mg/cm^3 (control) to 828.9 ˇ 65.6 mg/cm^3 (loaded, $p = 0.13$). Furthermore, the total BMC was increased from 0.213 ˇ 0.055 mg (control) to 0.228 ˇ 0.058 mg (loaded, $p = 0.11$) with cortical BMC from 0.127 ˇ 0.051 mg (control) to 0.136 ˇ 0.059 mg/mm (loaded, $p = 0.23$), The murine ligation-induced osteonecrosis of the femoral head mimics children's Perthes disease, and thus this animal model seems useful for the understanding of treatment modalities for avascular osteonecrosis. The current study demonstrates for the first time that knee loading can non-invasively enhance healing of the necrotic femoral head.

***Disclosures: Ping Zhang**, None.*

MO0059

Experiment of Finding a Etchant Carrier During Acid Etching for Rap(regional acceleratory phenomenon). Seungwoo Shin*. Ujeongbu St.mary Hospital Gum O Dong, South korea

As a result of corticotomy affectiong the bone surgace, using RAP(regional accelatory phenomenon) can reduce the orthodontic treatment procedure time. But this procudure needs a surgery, and would result a damage. The goal of this research is to find the method that can reduce physilologic damage as well as nerghboring tissue damdge. Twelve 3-4kg rabbits experimental animas have been disected. 37% phosporic acid and collatape have been applied to the first group (right, experimental group) and the only phosphoricn acid was applied th the second group. (left, control group) After surgery, in each 3 days, 1 weeks, 2weeks the species gave been aquired. Each species have been stained by hematoxylin & Eosin and tartrate-resistant acid phosphatase(TRAP) and the species have been observed by light microscope. The result shows the reduction of the soft tissue damage and demineralization. It also shows the increase of the demineralization progressively.(3 days, 1 week, 2weeks) This research shows the shape of demineralization as a result of the use of phosphoric acid, and the increase of the amoynt of demineralization progressively. Even if the soft tissye damage was reduced by using carrier, demineralization was also observed. control showed more demineralization than experimental group.

***Disclosures: Seungwoo Shin**, None.*

MO0060

Micro-CT Imaging of Osteocyte Lacunae and Vascular Networks in Cortical Bone. Henry Ong[1], Alexander Wright[1], Shing Chun Benny Lam[2], Arun Tatiparthi[3], Timothy Sledz[3], Felix Werner Wehrli*[4]. [1]University of Pennsylvania, USA, [2]Laboratory for Structural NMR ImagingUniversity of Pennsylvania, USA, [3]Micro Photonics, Inc., USA, [4]University of Pennsylvania Medical Center, USA

Cortical bone is a living tissue with an elaborate inter-connected network of lacunae containing osteocytes and vascular canals containing blood vessels. Cortical bone porosity (i.e. lacunar and vascular canal volume fractions) increases with age and diseases such as osteoporosis and is a valuable metric for overall bone quality. While not directly resolvable in vivo, recent MRI and x-ray methods show potential for indirect assessment of bone porosity. Directly imaging lacunae and vascular canals could aid the development of these indirect methods and provide insight into their spatial organization. Here, we used a SkyScan 1172 μ-CT specimen scanner to obtain hi-res 3D images (reconstructed voxel size: 1 μm^3) of lacunae and vascular canal networks in cortical bone specimens from lamb (6-9 months) and human (65 year, F) mid-shaft tibiae.

The figures below show 3D volume rendering after segmentation of lacunae (blue) and vascular canals (red) in tibial cortical bone specimens from lamb and human, where z indicates the loading axis. Vascular canals tend to align along the loading axis, although the lamb specimen shows a greater number of lateral canals. The vascular canal diameters are also smaller in lamb than in human. Lacunae show the expected ellipsoidal geometry with the long axis parallel to the loading axis and encircle individual vascular canals as expected from the lamellar organization of bone. As shown in the lacunae histogram below, lacunar density and mean volume are higher in lamb (57,000/mm^3 and 360 μm^3) than human (25,000/mm^3 and 203 μm^3), which indicates a higher rate of bone remodeling as expected from the younger age of the lamb compared with human. Furthermore, human lacunar density matches literature values. Bone porosity was quantified as volume fractions of the lacunar and vascular spaces. The lamb specimen had lacunar and vascular canal volume fractions of 2.05 and 1.93%, with porosity of 3.98%, while the human specimen had lacunar and vascular volume fractions of 0.51 and 4.84%, with porosity of 5.35%. Human bone porosity was lower than expected as the image volume was too small to adequately sample large vascular canals. Bone porosity (10.4%) calculated from a low-res (16 μm^3) image sampling a larger bone volume matched literature values. These results demonstrate the utility of μ-CT for the study of 3D morphology and organization of lacunae and vascular networks in cortical bone.

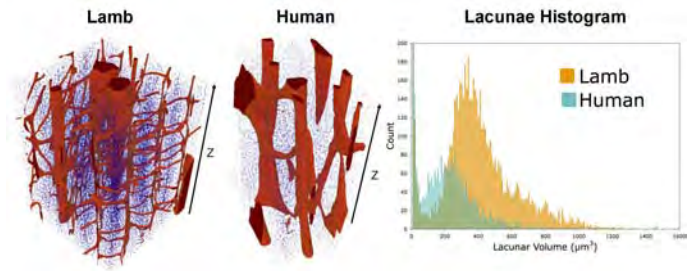

Figure1

***Disclosures: Felix Werner Wehrli**, None.*

MO0061

Non-invasive Raman Spectroscopy technique For In-vivo monitoring of Bone Graft osseointegration in Animal Models. Paul Okagbare*[1], Francis W. L. Esmonde-White[1], Steven A. Goldstein[2], Martin E. Isabelle[3], Michael D. Morris[1]. [1]Department of Chemistry, University of Michigan, USA, [2]Department of Orthopaedic Surgery, University of Michigan Medical School, USA, [3]Thayer School of Engineering, Dartmouth College, USA

The use of bone structural allografts for reconstruction following tumor resection is widespread, although successful incorporation and regeneration remains uncertain. As a result, there is still significant need for methods to follow the fate of these constructs. There are few noninvasive methods to fully assess the progress of graft incorporation. Computed tomography and MRI provide information on the morphology of the graft/host interface. Limited information is also available from DXA and ultrasound. There are few techniques to provide information on the metabolic status of the graft, such as the mineral and matrix composition of the regenerated tissue that may provide early indications of graft success or failure.

We have previously shown that non-invasive Raman spectroscopy can provide low resolution tomographic images of bone mineral composition. The techniques are similar to those used for fluorescence tomographic imaging of breast tumors. Here we discuss implementation for in-vivo assessment of allograft implantation in a rat model.

In an animal use committee approved osseointegration experiment, a 3-5 mm defect is created in the mid-diaphysis of the tibia of a Sprague-Dawley rat. The defect is reconstructed using a structural auto or allograft and stabilized using a custom

fabricated titanium internal fixation plate. Raman tomographic images are generated at several time points during healing. For tomography, the rat is anaesthetized and Raman spectra are collected using an array of optical fibers in contact with the skin of the rat over the tibia. The array allows excitation and collection of Raman spectra through the skin at various positions around the tibia. Spectra are processed using algorithms similar to those used in fluorescence tomography. These algorithms compare measured spectra to simulations from a model of the optics of the rat leg. The model is adjusted to match the experimental data and generate the Raman image. The system is calibrated against locally-constructed phantoms that mimic the morphology, optics and spectroscopy of the rat. This new technology provides a non-invasive method for in-vivo monitoring of graft osseointegration and other experiments on animals used to study skeletal biology, metabolic and other disorders and therapeutic interventions. Preliminary experiments on cadavers also suggest that the monitoring technology may be scalable for use on human subjects.

***Disclosures: Paul Okagbare**, None.*

MO0062

Notch Signaling Maintains Multipotency and Expands Human Mesenchymal Stem Cell Populations *Ex Vivo*. Regis O'Keefe[1], Matthew Hilton[2], Yufeng Dong*[1]. [1]University of Rochester, USA, [2]University of Rochester School of Medicine, USA

Human mesenchymal stem cells (hMSCs) have been studied with great interest due to their therapeutic potential for treating skeletal disease and facilitating skeletal repair, although maintaining their multipotency and expanding these cells *ex vivo* has proven to be very difficult limiting their use in clinical settings. Recently, we identified the Notch signaling pathway as an important regulator of MSC proliferation and differentiation during mouse skeletogenesis. To determine whether the Notch pathway could be utilized to promote the maintenance and expansion of hMSCs derived from bone marrow, we first analyzed the expression of all Notch receptors and each of the Hes/Hey target genes using hMSCs cultured over multiple passages. We identified *Notch2* and *Hes1* as being the most highly expressed components of the Notch pathway, data consistent with work from our previous developmental mouse studies. Interestingly, *Notch2* and *Hes1* expression levels were significantly reduced as hMSCs were cultured for multiple passages (p1 - p10), concurrent with the dramatic reduction in stem cell regulatory gene expression (*Sox2*, *Oct4*, and *Nanog*). Flow cytometric analyses of these cells at p2 and p10 demonstrates that p10 hMSCs only retain about 40% of the hMSC cell surface marker CD105, suggesting that hMSCs lose their stem cell phenotype during normal culturing and passaging of cells. To identify whether Notch activation can both enhance hMSC proliferation and maintain multipotency, we cultured hMSCs for up to 10 passages on plates coated with recombinant protein for the extracellular domain of the Notch ligand, Jagged-1 (Jag1), or control proteins. Cell proliferation assays using BrdU labeling demonstrated that Jag1 mediated Notch activation increases proliferation by more than 20% as compared to controls. Gene expression analyses also showed that Notch activation induces the stem cell transcriptional regulators, *Sox2*, *Oct4* and *Nanog*. Colony forming unit (Cfu-f) assays indicate that Notch activation enhances the number of hMSC colonies following p1, p5, and p10, suggesting an enhanced maintenance of multipotency over controls. Finally, chondrogenic and osteogenic differentiation assays demonstrate that when hMSCs are removed from Jag1/Notch activation they retain normal and possibly enhanced skeletal differentiation potential. Taken together, our study demonstrates that Jag1 mediated Notch activation facilitates the maintenance and expansion of hMSCs in culture.

***Disclosures: Yufeng Dong**, None.*

MO0063

Induction of Vasculature and Osteogenesis Using Honeycomb-shaped Ceramics with Tunnels made of β-TCP. Tohru Kaku*[1], Atsushi Niida[2], Mariko Takayama[3], Masahiko Suzuki[3], Yoshinori Kuboki[4]. [1]Division of Clinical Oral Pathology, Department of Human Biology & Pathophysiology, School of Dentistry, Health Sciences University of Hokkaido, Japan, [2]Division of Fixed Prosthodontics & Oral Implantology, Department of Oral Rehabilitation, School of Dentistry, Health Sciences University of Hokkaido, Japan, [3]Pilot Corporation, Japan, [4]Professor Emeritus, Hokkaido University, Sapporo, Japan

[Background]Geometric property of the artificial ECM is crucially important for the scaffold in bone tissue engineeringn1),2). The geometry is defined as the 3D structure of artificial ECM at the order of micrometer, which can direct growth of tissues and organs in vivo and in vitro1),2). The geometric structures were classified into 10 categories. One of them, multitunnel(honeycomb) -shape is feasible for bone formation. In the previous report that honeycomb-shaped hydroxyapatite(HC-HAP) / BMP with ca. 100-μm-pores induced endochondral ossification, while one with ca. 350-μm-pores induced direct bone formation with a single large blood vessel in the center of the 350-μm-pores of HC-HAP, resembling haversian bone formation1),2). And also we found that the concentric layered osteogenesis occurred within the tunnels of honeycomb-collagen (HC-COL)/BMP resembling the haversian-tye bone formation using a biodegradable scaffold of honeycomb structure (HC-COL and its HAP –coated product)3).

[Purpose] In this study, we studied on the haversian bone formation and an effect of the pore size using honeycomb-shaped ceramics with tunnels made ofβ-tricalcium phosphate(β-TCP) and an effect of the pore size of tunnels.

[Materials and methods] Honeycomb-shaped ceramics(HC-TCP)(Pilot Co., Japan)/BMP with tunnels were used for this study. In this bio-resorbable β-TCP, numberes and size of tunnels are strictly controllable in the production process. We used honeycomb-shaped ceramics(diameter 3mm, length 1-4mm) with 37(pore size:300μm)-,567(pore size 75μm)-, or 903(pore size:50μm) -straight- tunnels made ofβ-TCP. Those ceramics were implanted subcutaneously into 4-week-old rats. Effect of pore sizes and numbers of tunnel in HC-TCP on alkaline phosphatase (ALP) activity is examined at 2 weeks.

[Results] ALP activities and bone formation of ceramics with 75-μm(pore size)-tunnels were higher and more effective than those of ceramics with 300μm- and 50μm-pore-tunnels, respectively.

[Conclusion] HC-TCP with BMP induces haversian-type bone formation when used as a scaffold of osteogenesis. HC-TCP is useful for oriented bone formation, and also for periodontal regeneration.

References

1) Tsuruga E et al. J Biochem 121:317-24, 1997.
2) Kuboki Y et al. JBJS 83A (S-1):105-15, 2001.
3) Kuboki Y et al. Nano Biomed 1:85-94, 2009.

***Disclosures: Tohru Kaku**, None.*

MO0064

Sporadic Tumoral Calcinosis in Three Patients with Rheumatologic Diseases. Alan Burshell*. Ochsner Clinic Foundation, USA

The purpose of this study is to evaluate phosphate metabolism in three patients with sporadic tumoral calcinosis (TC) and rheumatologic disease. Tumoral calcinosis is a rare entity associated with ectopic calcifications. ESRD and familial syndromes including GALNT3, FGF23 and Klotho mutations cause TC probably through abnormal phosphate metabolism. There are sporadic cases of TC, which are not thought to be associated with abnormalities of phosphorus. We evaluated three patients with TC and rheumatologic disease.

Case 1: 25 y/o woman with juvenile dermatomyositis, osteoporosis, exogenous Cushing's syndrome and skin infections secondary to TC.

Case 2: 67 y/o woman with mixed connective tissue disease, pulmonary hypertension, CHF, S/P nephrectomy, hepatitis C and died from CHF.

Case 3: 41 y/o with polymyositis, dermatomyositis and pulmonary fibrosis

Methods: Patients had measurements of calcium, phos, FGF23, c-terminal assay Mayo Medical Laboratories and TmP/GFR before and after Sevelamer Hcl and only before in patient 3.

Results:

Conclusions: The serum phosphorus levels were in the normal range for all three patients with TC and rheumatologic disease. The TmP/GFR was elevated in cases 1 and 3. The FGF23 levels were mildly elevated in cases 1 and 2 and declined with Sevelamer Hcl therapy. There may be subtle abnormalities of phosphate metabolism in sporadic cases of TC with rheumatologic disease.

Cases	Phos (mg/dl)	Ca (mg/dl)	FGF23 (RU/ml)	1-25 Vit D (pg/ml)	TmP/GFR (mg/dl)
1	3.7 - 4.3	9.8 - 10.5	197,228	16	4.8
Sevelamer Hcl	3.0 - 3.5	9.4 - 9.7	115	47	
2	4.0 - 4.2	8.8 - 9.6	527	45	4.0
Sevelamer Hcl	3.4 - 3.8	9.2 - 9.6	337,321	30	
3	3.6	9.1 - 9.3	67	33	5

Results

***Disclosures: Alan Burshell**, None.*

MO0065

A Feedback Loop Between Sufu, Kif7, and PTHLH Coordinates Cells in the Growth Plate Chondrocyte Differentiation. Claire Hsu*[1], Chi-Chung Hui[1], Benjamin Alman[2]. [1]Sickkids Hospital, Canada, [2]The Hospital for Sick Children, Canada

--The Hedgehog (Hh) signaling pathway plays a crucial role in regulating chondrocyte development through Gli transcriptional activator and repressor function. Indian Hh (Ihh) and Parathyroid hormone-like hormone (PTHLH) control the pace of chondrocyte hypertrophy by forming a negative feedback loop. In the current study, we examined the role of the Hh signaling mediators, Suppressor of Fused (Sufu) and Kif7 in this process using genetically modified mice. We found that Sufu plays a negative role in regulating Hh transcriptional activity, and Kif7 positively regulates Hh signaling in the growth plate. However, in the absence of Sufu, maximal Hh activity also requires the absence of Kif7, showing a dual function of Kif7 as a Hh signaling mediator. PTHLH expression positively correlated with Hh signaling

activity in the growth plate, and PTHLH treatment increased the rate of chondrocyte proliferation in a Sufu and Kif7-independent manner. Sufu plays a crucial role in regulating the effect of PTHLH on chondrocyte hypertrophic differentiation. Intriguingly, PTHLH positively regulated Sufu and Kif7, and Kif7 negatively regulated Sufu, suggesting that a feedback loop between these proteins coordinates cells in the growth plate differentiating to hypertrophic chondrocytes.

***Disclosures: Claire Hsu**, None.*

MO0066

A Novel *Ex Vivo* Model for Investigating Chondrocytes Hypertrophic in OA. Pingping Chen*, Kim Andreassen, Kim Henriksen, Morten Karsdal, Anne-Christine Bay-Jensen. Nordic Bioscience A/S, Denmark

Purpose: Hypertrophic of chondrocytes lead to calcification of cartilage matrix which is a pathological event in the early phase of osteoarthritis (OA). The hypertrophic chondrocytes are locate in the deep zone of the articular cartilage and are believed to play an important part in the interaction between subchondral bone and cartilage. The aim of our work was to develop and validate an ex vivo model for OA research, in which hypertrophy chondrocytes could be induced by adding appropriate factors. This model was supposed to be used for examination of cartilage changes related to induction of hypertrophy; aiding the understanding of the role of hypertrophy chondrocytes in OA pathogenesis.

Methods: Full depth cartilage explants (from superficial to calcified cartilage) were isolated from bovine femoral condyle and cultured for 21 days with different stimulators: 1) TNF-α [20ng/ml] + Oncostatin M [10ng/ml], 2) IGF-1 [100ng/ml], 3) bFGF [50ng/ml], and 4) BMP-2[100ng/ml]. Supernatants were collected every two or three days. Safranin O/Fast Green (SaFO) and Tuludine Blue (TuB) staining were used to distinguish the morphology of the explants. Collagen type II turnover was measure by PIINP (formation) and CIIMB (degradation) assay. As a marker of hypertrophy chondrocytes, type X collagen expression was evaluated using reverse transcription followed by real-time polymerase chain reaction (PCR) at day 14 and day 21.

Results: Alarmarblue data showed that all explants were alive throughout the 21 day. Both IGF-1 and bFGF groups had enlarged cells at day 7 and 14 (TuB and SaFO stainings). CIIMB and PIINP assay results suggested that both IGF-1 and bFGF had significant ($p<0.05$) collagen type II degradation and formation at day 7, but not day 14 and 21. Gene expression of type X collagen stimulated by bFGF increased significantly at day 14 and went down at day 21 compared with control (W/O). The increased type X collagen expression confirmed that bFGF could induce chondrocytes hypertrophic in FDC model.

Conclusions: We have developed an explants culture models that include all the different layers of the articular cartilage and were able to induce hypertrophy by stimulating with bFGF. We could detect the gene expression of markers at different culture stage in the ex vivo culture model. We speculate that this model could be used as an important ex vivo model for cartilage degenerative diseases and thereby for investigating the effect of different drug candidates.

***Disclosures: Pingping Chen**, None.*

MO0067

Bmp2 Is Required for Chondrocyte Maturation and Endochondral Bone Development. Ming Zhang*[1], Bing Shu[2], Rong Xie[2], Meina Wang[2], Wei Hou[3], Dezhi Tang[2], Stephen Harris[4], Matthew Hilton[5], Yongjun Wang[3], Di Chen[1]. [1]University of Rochester Medical Center, USA, [2]University of Rochester, USA, [3]Shanghai University of Traditional Chinese Medicine, China, [4]University of Texas Health Science Center at San Antonio, USA, [5]University of Rochester School of Medicine, USA

The precise role for BMPs in chondrocyte differentiation remains to be defined. In situ hybridization assays demonstrate that both Bmp2 and Bmp4 genes are highly expressed in growth plate chondrocytes. In order to determine if Bmp2 and Bmp4 are required for chondrocyte development, we generated chondrocyte-specific Bmp2 and Bmp4 conditional knockout (cKO) mice and Bmp2/Bmp4 double KO (dKO) mice. Severe chondrodysplasia phenotypes were observed in both Bmp2/Bmp4 dKO mice and Bmp2 cKO mice. In contrast, only minor skeletal alterations were observed in Bmp4 cKO mice. The majority of skeletal elements that form through endochondral ossification were severely impaired in these mutant mice. In E18.5 Bmp2/Bmp4 dKO and Bmp2 cKO embryos, the limbs were about 30% shorter. The length of the proliferating and hypertrophic zones was significantly reduced and growth plate columnar structure was severely disorganized. Chondrocyte proliferation was significantly reduced and chondrocyte apoptosis was significantly increased in these mutant embryos. Results from in situ hybridization assays showed that the expression of chondrocyte marker genes such as Col2a1, Col10a1, and Mmp13 were significantly reduced. Immunohistochemistry (IHC) data showed that Runx2 protein levels were reduced in pre-hypertrophic and hypertrophic chondrocytes in mutant embryos. These findings demonstrate that Bmp2 is required for chondrocyte development. In contrast to the inhibition of growth plate chondrocyte development, matrix deposition at the perichondrium area was significantly increased and expanded in Bmp2 cKO embryos, suggesting a cell non-autonomous negative regulatory effect of Bmp2 on perichondrial derived bone formation. We have demonstrated that cell cycle proteins, cyclin D1 and CDK4, play an important role in Runx2 phosphorylation and ubiquitination in chondrocytes. To determine if CDK4 is involved in BMP-2-mediated chondrocyte differentiation, we examined the effects of BMP-2 on CDK4 and Runx2 expression by western blotting. Treatment of chondrocytes with BMP-2 significantly inhibited CDK4 expression and up-regulated Runx2 protein levels in RCS chondrogenic cells. Over-expression of CDK4 significantly reversed BMP-2-induced Runx2 expression in these cells, suggesting that the effect of BMP-2 on Runx2 expression is regulated in part through a CDK4-dependent mechanism. Our studies provide novel insights into the role of Bmp2 in chondrocyte development.

***Disclosures: Ming Zhang**, None.*

MO0068

Circumferential Periosteal Stripping of Femoral Diaphysis of Developing at Produces Longitudinal Overgrowth and Cortical Hypertrophy. Toshihiko Nishisho[1], Mitsuhiko Takahashi[2], Tetsuya Enishi[2], Shinjiro Takata*[3], Natsuo Yasui[4]. [1]BIGLOBE NEC, Japan, [2]Department of Orthopedics, Institute of Health Biosciences, The University of Tokushima Graduate School, Japan, [3]Institute of Health Biosciences, University of Tokushima Graduate School, Japan, [4]University, Japan

(INTRODUCTION) Unilateral circumferential periosteal division of rat tibia produces an increase in its growth rate and in the activity of both the proliferative and hypertrophic zones (Taylor FJ et al. J Anat 151:221-231,1987). This study showed that circumference periosteal stripping (CPS) of femoral diaphysis of developing rat produces longitudinal overgrowth and cortical hypertrophy.

(METHODS) Thirty-five Sprague-Dawley rats aged 8 weeks were used for this study. CPS was performed at the diaphysis of rat femur. Rats were sacrificed 4 weeks and 6 weeks after CPS. The longitudinal length of femur (n=11), rate of longitudinal growth and bone turnover by bone histmorphometry 4 weeks (n=6) and 6 weeks (n=6) after CPS, the microarchitecture of trabecular bone by trabecular analysis of secondary spongiosa by micro CT (n=6), and bone mineral density and cortical width of femoral diaphysis were compared with between ipsilateral and contralateral sides by peripheral quantitative computed tomography (pQCT) (n=6).

(RESULTS) Longitudinal length of rat femur of ipsilateral and contralateral sides were 41.793+/-0.753 mm and 40.272+/-0.690 mm, respectively ($p<0.0001$). Bone histomorphometry shows that the rate of longitudinal growth of femora of ipsilateral and contralateral sides 4 weeks after CPS was 92.3 ± 5.3 and 54.4 ± 4.6 μm/day, respectively ($p<0.0001$), and that the rate of ipsilateral and contralateral sides 6 weeks after CPS was 44.1 ± 3.4 and 27.6 ± 5.1 and μm/day, respectively ($p=0.0002$). Bone volume on ipsilateral and contralateral sides was 5.6 ± 0.9 m3 and 4.7 ± 0.8 m3, respectively (p=00416). Trabecular number on ipsilateral and contralateral sides was $3.8\pm0/4$ 1/mm and $3.4\pm0/4$ 1/mm, respectively (p=0.0116). pQCT revealed morphological changes of diaphysis of ipsilateral femur 6 weeks after unilateral CPS. Unilateral CPS caused increases of bone mineral density, bone mineral content, and cortical thickness of ipsilateral femoral diaphysis.

(DISCUSSION) These results showed that unilateral CPS produces longitudinal overgrowth and cortical hypertrophy of ipsilateral femur compared with contralateral one of developing rats. The facts suggests that unilateral CPS stimulates both endochondral and intramembranous ossification of ipsilateral femur, and that unilateral CPS might be an promising procedure to correct leg length discrepancy and bone atrophy.

***Disclosures: Shinjiro Takata**, None.*

MO0069

Differential Phenotypic Responses of Articular and Growth Plate Chondrocytes to 5-Azacytidine. Matthew Stewart*, Evelyn Caporali. University of Illinois, USA

Purpose: In osteoarthritis, articular chondrocytes (ART) undergo phenotypic changes resembling those that occur during hypertrophic differentiation, expressing collagen type X (Coll X) and alkaline phosphatase (ALP). The DNA methyl transferase inhibitor, 5-azacytidine (5-AZA) is able to induce hypertrophic differentiation in articular chondrocytes (1,2). These findings suggest that genomic methylation regulates chondrocyte differentiation and phenotype. This study assessed the phenotypic effects of 5-AZA in ART and growth plate (GP) chondrocytes, to determine whether 5-AZA directly stimulates or augments hypertrophy in these chondrocyte populations.

Methods: ART and GP chondrocytes were collected from immature horses by collagenase digestion and cultured as non-adherent aggregates in the absence (control) or presence of 5-AZA for 4 days. On day 4, the 5-AZA cultures were divided into two groups. The first group was treated continuously with 5-AZA for an additional 8 days (AZA CONT). The second group was transferred to control media for the remaining 8 days (AZA REC). Control, CONT and REC cultures were additionally maintained in the presence or absence of BMP-2 for the final 8 days. Samples were collected at days 4, 8 and 12. qPCR was used to assess changes in Coll X and ALP expression.

Results: In control cultures, there was no spontaneous expression of hypertrophic genes in ART cells while expression dropped over time in GP cells. 5-AZA, by itself, did not increase Coll X expression in ART or GP aggregates. However, continuous 5-AZA treatment of GP cells did increase ALP expression. 5-AZA did not affect the response of ART chondrocytes to BMP-2; there was no hypertrophic marker induction. In contrast, both Coll X and ALP expression by GP cells transiently

exposed to 5-AZA (AZA REC) was increased by BMP-2. The CONT GP group was not different from controls.

Discussion: This study does not support the contention that interference with DNA methylation ''trans-differentiates'' articular chondrocyte populations into the endochondral lineage. However, transient 5-AZA administration did augment the hypertrophic effects of BMP-2 on GP chondrocytes, suggesting that changes in genomic methylation profiles influence the progression of endochondral chondrocytes through hypertrophic differentiation.

References: 1. Zuscik MJ et al 2004. J Cell Biochem 92:316; 2. Ho M et al 2006. Cell Biol Int 30:288

***Disclosures: Matthew Stewart**, None.*

MO0070

Gender-Specific Rapid Membrane Responses of Rat Costochondrocytes to 17β-Estradiol are Estrogen Receptor α Dependent. Khairat ELBaradie*, Yun Wang, Barbara Boyan, Zvi Schwartz. Georgia Institute of Technology, USA

Both male and female rat growth plate chondrocytes express estrogen receptors (ERs); however, 17β-estradiol (E2) can activate protein kinase C (PKC) only in cells from female rats. The aims of the present study were: (1) to determine the pathway that mediates the membrane effect of E2 on PKC; and (2) to investigate if the gender-specific rapid membrane responses of rat costochondral chondrocytes to E2 are due to the difference in the amount or subcellular location of ERα or to differences in the potential downstream signaling pathway. Confluent, fourth passage resting zone (RC) chondrocytes from female rat costochondral cartilage were treated with E2 in the presence or absence of GDPβS (G-protein inhibitor), U73122 (inhibitor of phospholipase C [PLC]), and AACOCF3 (inhibitor of cytosolic phospholipase A2 [cPLA2]). Western blot and flow cytometry were used to analyze the expression level and the subcellular location of ERα in both male and female RC cells. To examine the similarity in the downstream signaling pathway involved in PKC activation between male and female RC cells, confluent costochondral chondrocytes isolated from both male and female rats were treated with 17β-estradiol, PLAA peptide (phospholipase A2 activator) or m-3M3FBS (phospholipase C activator) respectively and PKC activity was measured. GDPβS, U73122 and AACOCF3 inhibited E2-stimulated PKC activaty in female RC cells. Western blot and flow cytometry data showed that female chondrocytes had 2 to 3 fold greater ERα on the plasma membrane compared to male chondrocytes. Although activation of PKC by 17β-estradiol was observed only in female cells, downstream activators m-3M3FBS and PLAA induced a dose-dependent increase in PKC activity in both male and female cells with the highest increase at 10-6 M ($p<0.05$). Antibody to ERα blocked the stimulatory effect of E2 on PKC. In conclusion, our study showed that female chondrocytes expressed more ERα on the membrane than male chondrocytes while they shared similar signaling pathways. The different expression level of ERα between male and female chondrocytes might contribute to their gender-specific rapid membrane responses to 17β-estradiol.

***Disclosures: Khairat ELBaradie**, None.*

MO0071

Osterix is Required for Chondrogenesis and Skeletal Growth During Endochondral Ossification. Jung-Hoon Oh*[1], Wook-Young Baek[1], Benoit De Crombrugghe[2], Jung-Eun Kim[3]. [1]Department of Molecular Medicine, CMRI, Kyungpook National University School of Medicine, South korea, [2]University of Texas M.D. Anderson Cancer Center, USA, [3]Kyungpook National University School of Medicine, South korea

Osterix (Osx) is an essential transcription factor for osteoblast differentiation during both intramembranous and endochondral ossification. Endochondral ossification, a process in which bone formation begins from a cartilage intermediate, is crucial for skeletal development and growth. Osx was weakly expressed in differentiating chondrocytes during mouse development, but its role in chondrocytes has not been studied. Here, in vivo function of Osx in chondrocytes was examined on conditional Osx knockout model using the Cre/loxP system. Osx was inactivated in all chondrocytes by Col2a1-Cre with the Cre activity under the control of type II collagen (Col2a1) promoter. To investigate the altered skeletal development and growth, skeletal preparation and histological analysis with staining methods were performed in Osx-inactivated null mutants with Col2a1-Cre. Osx-inactivated null mutants with Col2a1-Cre died immediately in perinatal period due to a lack of endochondral bone formation. In skeletal preparation, mineralized bones were not observed at embryonic day 15.5 and severe defects in bones including ribs and limbs were examined at newborn. To further understand skeletal phenotypes, histological analysis was performed on developing long bones during embryogenesis. Both chondrocytes differentiation and bone mineralization were remarkably delayed and the formation of multinucleated osteoclasts and their invasion were also reduced. Eventually, skeletal growth was significantly reduced. Taken together, Osx that was expressed in growth plate chondrocytes regulated chondrocyte differentiation and bone growth, suggesting an autonomous function in chondrocytes during endochondral ossification.

***Disclosures: Jung-Hoon Oh**, None.*

MO0072

Overexpressing P63 in Hypertrophic Chondrocytes Impacts Endochondral Bone Formation during Skeletal Development. Sam Abbassi[1], Feifei Li[1], Ming Ding[2], Yaojuan Lu[1], Guojun Wu[3], Siying Wang[4], Qiping Zheng*[1]. [1]Rush University Medical Center, USA, [2]Rush University, USA, [3]Wayne State University, USA, [4]Anhui Medical University, China

P63 belongs to the P53 tumor suppressor gene family. Due to its different promoter usage and alternative splicing, P63 is divided into two major subtypes (TAP63 and ?NP63) and each consists of three different isoforms (-α, -β or -γ). These isoforms are known to play distinct functions in cancer and development. While it remains complex whether P63 functions as a tumor suppressor or oncogene, mouse genetic studies have clearly demonstrated that P63 play critical roles during skin and limb development. The severe limb abnormalities seen in p63 null mice suggest that p63 is essential for long bone development. However, the molecular mechanism of p63 regulation of bone formation remains largely unknown.

The type X collagen gene (Col10a1) is specifically expressed in hypertrophic chondrocytes, a critical cell stage during endochondral bone formation. We have previously shown that a 90-bp Col10a1 cis-enhancer is sufficient to mediate its hypertrophic chondrocyte-specific expression in vivo. Interestingly, by yeast one-hybrid approach using this cis-enhancer as bait, we identified p53 related proteins as candidate factors that may contribute to regulation of Col10a1 expression. In addition, both p53 and p63 are upregulated in hypertrophic MCT cells, a cell model that expresses type X collagen abundantly upon growth arrest. We therefore hypothesize that P63 may regulate cell-specific Col10a1 expression and impact chondrocyte maturation during skeletal development. To further explore the role of P63 upon skeletogenesis, we recently established two transgenic mouse lines in which HA- and Flag-tagged ΔNP63α or TAP63α is driven by the cell-specific Col10a1 regulatory element. Skeletal staining of mice at P1 stage suggests that the Col10a1-ΔNP63α mice show slightly delayed chondrocyte maturation or ossification compared to their wild-type littermates. Surprisingly, the Col10a1-TAP63α mice show accelerated ossification in long bone, digit and tail bones. We have performed real-time RT-PCR analysis and our preliminary results suggest that Col10a1 and Bcl-2 are upregulated in Col10a1-ΔNP63α mice, but downregulated in Col10a1-TAP63α mice. These results may indicate that P63 isoforms differentially regulate Col10a1 expression, lead to matrix environment change in hypertrophic zone, and therefore affect the followed chondrocyte apoptosis and bone replacement. Further phenotypic and molecular analysis is needed to define the potential mechanism of P63 upon skeletogenesis.

***Disclosures: Qiping Zheng**, None.*

MO0073

Suppressing TGF-β Signaling by SB431542 in Mesenchymal Progenitor ATDC5 Cells Promotes BMP-induced Chondrocyte Differentiation. Ichiro Kawamura*[1], Yasuhiro Ishidou[2], Takuya Yamamoto[1], Takao Setoguchi[1], Michihisa Zenmyo[1], Setsuro Komiya[1], Shingo Maeda[2]. [1]Department of Orthopaedic Surgery, Graduate School of Medical & Dental Sciences, Kagoshima University, Japan, [2]Department of Medical Joint Materials, Graduate School of Medical & Dental Sciences, Kagoshima University, Japan

Bone morphogenetic proteins (BMPs), member of transforming growth factor-β(TGF-β) superfamily, promote chondrocyte differentiation from mesenchymal progenitor cells, and are necessary for maintaining articular cartilage. Considering the case of regenerating cartilage from clinical materials by applying BMPs, its efficiency should be investigated and improved, because the materials obtained from patients are limited and generating cartilage tissue from cells is a time-consuming process. Although BMPs and TGF-βs both promote early stage of chondrocyte differentiation of mesenchymal cells in vitro, possible functional interactions of the two signaling pathways are not known. We hypothesized that endogenous TGF-β signaling could inhibit BMP signaling in chondrocytes similarly as we had reported in osteoblastic differentiation of C2C12 cells. Here, we show that deleting serum from culture medium promoted chondrocyte differentiation of ATDC5 cells induced by ITS supplement plus BMP-2. Inhibiting endogenous TGF-β signaling by a compound SB431542 further accelerated the BMP-induced chondrogenesis. Chondrocyte differentiation of ATDC5 cells was evaluated by alcian blue staining, von Kossa staining, and real time RT-PCR for chondrocyte markers. These results suggest that, in presence of exogenous BMP signaling, endogenous TGF-βs and exogenous TGF-βs in serum inhibit chondrocyte differentiation. We propose that TGF-β-induced inhibitory Smad6/7 blocked BMP signaling in ATDC5 cells. TGF-β-inhibitors may be used as an accelerator in case of BMP application in cartilage regenerative medicine.

***Disclosures: Ichiro Kawamura**, None.*

MO0074

The Expression of the *GRP* Gene, Encoding Four New Gla-rich Protein Isoforms, is Finely Regulated in Cartilage. Sébastien Flajollet[1], Tian V. Tian[1], Laurence Legeai-Mallet[2], Nathalie Tomavo[1], Anne Flourens[1], Barbara Camuzeaux[3], Muriel Holder-Espinasse[4], Philippe Galéra[5], Frédéric Mallein-Gerin[6], Marion Le Jeune[1], Martine Duterque-Coquillaud*[1]. [1]CNRS UMR8161, Institut de Biologie de Lille, Université de Lille Nord de France; Institut Pasteur de Lille, France, [2]INSERM U781, Hopital Necker-Enfants Malades, France, [3]FRE 3211, IREBS, CNRS/ Université de Strasbourg, France, [4]Service de génétique, Hopital jeanne de Flandre, CHRU, France, [5]EA 3214 Université de Caen/Basse Normandie, IFR 146 ICORE, Faculté de Médecine, France, [6]Institut de Biologie et Chimie des Protéines UMR 5086 CNRS/UCBLyon 1- IFR 128 BioSciences Gerland-Lyon Sud, CNRS UMR 5086, France

The *GRP* (Gla-rich protein) gene, firstly named as *Ucma* (Upper zone of growth plate and cartilage associated gene), has been recently identified to be expressed mainly in mouse, rat and sturgeon cartilage, as well as in rat skeletal bone tissues. The GRP protein is a novel vitamin-K dependent protein containing the highest Gla residue content of any protein known to date. We have shown that the *GRP* gene gives rise to four transcripts, which differ by exon 2, exon 4 or both. Two of the corresponding proteins are secreted while the two others accumulate in the cells. Using RT-PCR and *in situ* hybridization experiments with embryonic mouse tissues and primary chondrocytes, we studied the *GRP* gene expression from mesenchymal cells to differentiated chondrocytes in various culture cell conditions. Our results showed that, *in vivo* and *in vitro*, the *GRP* gene is not expressed in early stages of chondrogenesis in precartilaginous cells. In addition the *GRP* gene expression disappeared when chondrocyte de-differentiation occurs in culture. Moreover the four alternative transcript ratio and their expression kinetic differ during the course of cartilage differentiation and de-differentiation. This result suggests that the *GRP* gene could be a useful marker of chondrocyte-differentiated stage in culture cells and that the alternative transcript ratio is important for their function. Since the *GRP* gene expression was not defined in human cartilage, we have completed our study with the identification of the alternative transcripts in human cartilage. We showed that this gene is highly expressed in foetal cartilage but poorly in adult normal or osteo-arthritis chondrocytes. Furthermore, the *GRP* gene expression was dramatically decreased when chondrocytes are cultured *in vitro*. In conclusion, the *GRP* gene expression is finely regulated and corresponds to specific stages of cartilage differentiation. Rescuing its expression could be a positive element to maintain or control the chondrocytes differentiation in culture. In addition, although GRP gene expression regulators are not known, the Ets family transcriptional factors are good candidates since we have identified the *GRP* gene though a transgenic mouse model expressing an Ets family member dominant negative protein. Finally, we have defined in the *GRP* gene promoter a conserved and functional region, which presents Ets binding sites.

***Disclosures: Martine Duterque-Coquillaud**, None.*

MO0075

Treatment of TMJ Disease in Human with Combination of rhOP-1 and rhIGF-I Loaded on Type I Collagen Membrane; A Tissue Engineering Approach for Regenerating Articular Surface. Khalid Barakat[1], Heba Selim[2], Marina D'Angelo[3], Abdulhafez Selim*[4]. [1]Oral & Maxillofacial Surgery, Faculty of Dentistry, El-Menia University, Egypt, [2]Dental School, Ain Shams Univesity, Egypt, [3]Philadelphia College of Osteopathic Medicine, USA, [4]Center for Chronic Disorders of Aging, PCOM, USA

The temporomandibular joint (TMJ) can experience degenerative episodes initiated by disease or trauma. Tissue engineering offers potential to regenerate tissues otherwise unable to heal. TMJ engineering focuses on regenerating bony structures, articular cartilage and fibrocartilage. Animal studies have demonstrated that OP-1 as well as IGF-I have the ability to repair cartilage in vivo in various models of articular cartilage degradation. In this study we examined the use of combination of rhOP-1 and rhIGF-I loaded on collagen membrane carrier to regenerate the articular surfaces of the TMJ.

Five patients suffering TMJ arthritis were diagnosed using RDC/TMD system and MRI. Patients were treated with open arthrotomy and joint debridement. The degenerated surfaces were covered with collagen membrane pre-loaded with OP-1 (0.5 mg) and IGF-I (0.5 mg). RDC/TMD & MRI were used for evaluation of the treated joints six months post-operatively.

There were no apparent complications associated with the use of growth factors. Both axes I and II of RDC showed functional and behavioral excellent outcomes. Moreover, MRI findings detected early chondral surface regeneration. Together, these findings indicate a significant promise for the tissue engineering approach in treating TMJ disease.

***Disclosures: Abdulhafez Selim**, None.*

MO0076

Zfp521 Expression in Chondrocytes is Regulated by Ihh via BMP and PTHrP Differently During Chondrocyte Differentiation. Dutmanee Seriwatanachai*[1], Yukiko Maeda[1], Diego Correa[2], Roland Baron[3], Beate Lanske[1]. [1]Harvard School of Dental Medicine, USA, [2]Case Western Reserve University, USA, [3]Harvard School of Medicine & of Dental Medicine, USA

The balanced control of chondrocyte proliferation, differentiation and apoptosis in the developing growth plate by Ihh and PTHrP is well established. Recently zinc finger protein (Zfp) 521, a transcription factor previously studied in hematopoiesis and cancers, was found to play an important role in postnatal bone development. Since we found Zfp521 expression in early limbbuds and growth plate chondrocytes, we hypothesized its involvement in the Ihh/PTHrP feedback loop. To investigate whether Zfp521 is regulated by Ihh and PTHrP, we isolated rib chondrocytes from wild-type pups and cultured them for 5 (proliferative) and 15 days (hypertrophic). Zfp521 expression in proliferative chondrocytes was significantly upregulated by Ihh after 30 min and was accompanied by increased BMP2 and cyclinD1 expression with no changes in PTHrP expression. Addition of noggin, a BMP signaling inhibitor, completely abolished Ihh-induced expression of Zfp521 and cyclinD1, suggesting that BMP induces Zfp521 expression. Treating proliferative chondrocytes with BMP2 confirmed this. Interestingly, Ihh treatment of hypertrophic chondrocytes down-regulated Zfp521 and PTHrP expression without altering BMP2 expression, suggesting that Ihh decreases Zfp521 expression in these cells by inhibiting PTHrP expression. Consistent with this hypothesis, Zfp521 expression was significantly up-regulated in the growth plate of Jansen Tg mice, in which chondrocytes express a constitutively active PTH/PTHrP receptor, demonstrating that Zfp521 expression is affected by PTHrP signaling. Conditional deletion of Zfp521 from chondrocytes led to decreased expression of cyclinD1, ColII, and ColX, all suggesting that Zfp521 is a downstream mediator of Ihh, PTHrP, and BMP2. We are currently analyzing the effect of deleting Zfp521 from chondrocytes of Jansen Tg mice on differentiation of growth plate chondrocytes to better characterize the role of Zfp521 in mediating PTHrP control of chondrogenesis. In summary, we demonstrated that Zfp521 is expressed in chondrocytes and showed that it mediates Ihh and BMP signaling to control cyclinD1 expression in proliferative chondrocytes. Moreover, we found that Ihh decreases Zfp521 expression in hypertrophic chondrocytes, probably due to downregulation of PTHrP. Further studies will determine which effects of Ihh, PTHrP and BMP are dependent on the presence of Zfp521 during chondrogenesis.

***Disclosures: Dutmanee Seriwatanachai**, None.*

MO0077

Comparation Transcriptome in Stem Cells from Cleft Lip and Palate Patients and Controls Reveals Enrichment of Transcripts Involved in Epithelial-mesenchyme Transition During the Palatal Bone Closure. Daniela Bueno*[1], Daniele Sunaga[2], Maria Rita Passos-bueno[2], Gerson Kobayashi[2], Roberto Fanganiello[3], Meire Aguena[2]. [1]São Paulo University, Brazil, Brazil, [2]USP, Brazil, [3]Institute of Biosciences, University of Sao Paulo, Brazil, Brazil

Non-syndromic cleft lip and palate (NSCL/P) is a multifactorial disorder resulting from failure of fusion of facial primordia, a complex developmental process that involves among others the epithelial-mesenchyme transition (EMT) during the palatal bone closure. Detection of differential gene transcription between patient and normal tissues or cells is a promising approach for identifying causative pathways involved in disease manifestation. Here, we compared the transcriptome of 6 dental pulp stem cell (DPSC) cultures from NSCL/P patients and 6 normal control cultures. A total of 87 differentially expressed genes (DEGs) were identified. Four of them (MMP1, MMP3, PDGFa, EGR1) had previously been associated with NSCL/P and palatal bone closure. Functional annotation of the DEGs showed that Focal adhesion, Cell adhesion and ECM-receptor interaction were the most relevant pathways. An enrichment of genes involved with cellular movement (16 genes, $p<4.82E-02$), cellular growth and proliferation (24 genes, $p<4.98E-02$) and cellular development (24 genes, $p<4.98E-02$) was also observed. Moreover, the putative network with the largest number of DEGs (14) derived by Ingenuity analysis suggested a functional relationship among several extracellular proteins that are differentially expressed in affected DPSC, including interactions between ACAN and MMPs. We also observed a great overlap between these predicted cell functions and networks with those proposed for the EMT, which is a central component in lip and palate bone development. In conclusion, DPSCs from NSCL/P patients exhibit a gene expression signature involving enrichment of genes belonging to ECM modeling and palate EMT processes relative to normal controls. This strategy may contribute to identification of gene networks predisposing to this complex malformation. To achieve this goal we are increasing the number of sample (affected and controls) to perform microarray (Affymetrix, HumanGene 1.0 ST) assay comparisons. FAPESP.CNPq.

***Disclosures: Daniela Bueno**, None.*

MO0078

Genomic Organization of the Estrogen Receptor-related Receptor Gamma Gene: Multiple mRNA Isoforms Generated by Alternative Splicing and Differential Promoter Usage. Jane Aubin[1], Ruolin Guo[2], Ralph Zirngibl*[3]. [1]University of Toronto Faculty of Medicine, Canada, [2]University of Rochester, USA, [3]University of Toronto, Canada

Estrogen plays an important role in regulating skeletal homeostasis via direct signaling through two estrogen receptors (ERα and β) or, as recently described, by cross-talk with the estrogen receptor-related receptors (ERRα and γ). ERα has multiple promoters and protein isoforms, but a subset of these is expressed in bone. A single promoter and protein have been described for ERRα. However, multiple transcripts and protein isoforms have been described for ERRγ, but a comprehensive gene organization is still lacking. We used in silico analysis of expressed sequence tags for mouse ERRγ to determine the gene structure, then assessed whether isoform expression is different in multiple mouse tissues, including bone and cartilage. Using these analyses, we experimentally confirmed that the ERRγ gene utilizes at least 7 promoters with multiple altenative splicing of 5' untranslated regions (UTRs), which potentially leads to at least three different protein isoforms. Six of the promoters splice into a common exon 7a 5'UTR before splicing to the ERRγ coding region, but read-through into exon 7b can also occur, resulting in a nonsense transcript that codes potentially for small peptides, the largest of which would be 71 amino acids long. Intriguingly, we found evidence for a similar nonsense transcript by the in silico analysis for human ERRγ and human ERα. Different transcripts were made in different bones and bone compartments. While calvarial and trabecular bone (epiphysis/ metaphysis) use promoters 3, 4, 6, and 8, trabecular bone differs from calvaria by also transcribing the read-through transcript via promoter 6. Cortical bone (femur shaft) uses promoters 4, 6 and 8 and does not make the read-through transcript. Xiphoid cartilage uses promoters 2, 3, 4, 5, 6, and 8 to generate the protein coding transcript and promoters 1, 2, 3, 5 and 6 to make the read-through transcript. The amount of transcript generated, i.e. promoter strength, also varied in a given tissue. Promoters 3 and 8 make similar levels of transcript, but promoter 3 produces only one tenth the amount, in calvarial tissue. The amount of read-through transcript also varies in a tissue and promoter dependent manner. The ratio of coding:read-through transcript in calvaria for promoter 3 is 1:1, in cartilage it is 2:1. The conservation of the nonsense transcript between humans and mice, and its tissue specific expression suggest that it does have a functional role, which will require further study.

***Disclosures: Ralph Zirngibl**, None.*

MO0079

Identification of Coordinated Differences in the Development of Vascular Neurogenic and Skeletal Tissues During Endochondral Bone Formation of C57/B6 and C3H Strains by Comparison of the Transcriptomes of Fracture Healing. Rachel Grimes[1], Karl Jepsen[2], Jody McLean[1], Richard Marsell[3], Jennifer Fitch[1], Temple Smith[1], Thomas Einhorn[4], Elise Morgan[3], Paola Sebastiani[5], Louis Gerstenfeld*[1]. [1]Boston University School of Medicine, USA, [2]Mount Sinai School of Medicine, USA, [3]Boston University, USA, [4]Boston Medical Center, USA, [5]Boston University School of Public Health, USA

Faster fracture healing in C57/B6 (B6) mice is defined by an earlier initiation and a longer period of chondrogenesis accompanying the development of more cartilage and less bone than the C3HeJ (C3H) mice. Conversely, C3H mice initiate osteogenesis earlier and have a longer period of bone development. Comparison of the transcriptomes of endochondral bone formation across fracture healing defined the differences in timing and quantitative expression of the major transcription factors and regulatory pathways associated with the variations in skeletal development in the two strains of mice. B6 mice showed elevated expression and earlier expression of multiple components of the TGF-beta and Wnt families compared to C3H mice. C3H mice showed selective and earlier activation of specific components of the MAPK signal transduction pathway. Changes in skeletal development in the B6 strain were also coordinated with earlier expression of genes associated with neurogenic and vascular tissue development. Higher, earlier, or extended expression of genes associated with ion transport, circadian function, and innate immune function were also seen in the B6 mice. Because of the association between vasculogenesis and rates of fracture healing, a specific assessment of changes in vascular tissue gene expression were assessed in the two strains of mice. B6 mice showed a temporal foreshortening and diminished expression of genes that controlled vascular tissue development including VEGFR2, VEGFA, and PlGF in the C3H mice while mTOR signal transduction which has been associated with cardiovascular development was elevated in the B6 strain. Analysis of several transcription factors known to control cardiac tissue morphogenesis (Hand2, Twist1, and Foxc2) all showed decreased expression in C3H mice relative to B6 mice. Interestingly emerging data for all three of these transcription factors have shown that they are also crucially involved in controlling chondrocyte differentiation and endochondral bone formation. Examination of cardiovascular tissues in C3H mice showed that they quantitatively had smaller and fewer blood vessels and had ~40% smaller hearts than B6 mice. In summary, these studies show that the development of multiple tissues are linked and in particular suggest that vascular and skeletal tissue development are coordinated. These data demonstrate that genetic background is a major determinate of postnatal tissue regeneration and tissue repair.

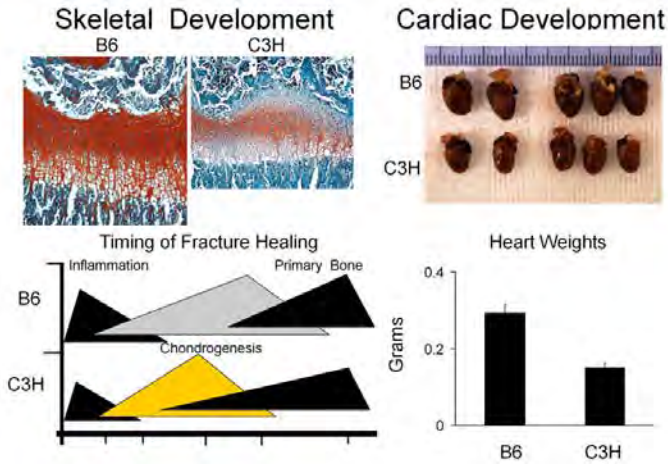

Skeletal and Cardiac Development

***Disclosures: Louis Gerstenfeld**, None.*

MO0080

Metabolic Profile of Fat in Bone. Beata Lecka-Czernik[1], Shilong Huang[2], Amrei Krings*[3]. [1]University of Toledo College of Medicine, USA, [2]University of Toledo Health Sciences Campus, USA, [3]University of Toledo Medical Center, USA

Fat in bone occupies a significant portion of bone marrow cavity. By the third decade of life almost whole cavity of human long bone is filled with fat. The metabolic activity of bone fat, or yellow adipose tissue (YAT), is unknown, but its unique location may determine its more specialized function, and distinguishes it from white (WAT) and brown (BAT) fat. YAT depot increases in its volume in response to sex hormone deficiency and in metabolic diseases, such as obesity, diabetes, and anorexia nervosa. To elucidate YAT metabolic potential we analyzed changes in gene expression profile in following murine models: 1) estrogen deficiency; 2) diabetes; and 3) improved insulin signaling due to administration of rosiglitazone (Rosi). The profile of YAT was compared to that of WAT and BAT derived from the same animal. We compared levels of expression of genes regulating energy dissipation (UCP1/2), insulin sensitivity (leptin and adiponectin), and brown adipocyte differentiation (PRDM16). Estrogen deficiency increased weight of all analyzed fat depots, however the expression of UCP1/2 was increased only in YAT and BAT, and decreased in WAT. Interestingly, lack of estrogen increased expression of adiponectin and PRDM16 only in YAT, but not in WAT and BAT. In contrast, insulin resistance did not have an effect on UCP1/2 expression, but led to increased adiponectin expression in all fat depots, despite the fact that circulating levels of this adipokine were decreased in this animal model. Administration of Rosi for 4 weeks increased expression of UCP1 in YAT and WAT by more than 10-fold in both models estrogen deficiency and diabetes. Consistent with insulin sensitizing activity of Rosi, the expression of adiponectin was increased in all fat depots, however only YAT responded to Rosi with increased expression of leptin and PRDM16. An analysis of tested genes for their relative expression per cell in YAT as compared to WAT and BAT showed that UCP1 represents less than 2%, UCP2 up to 90%, leptin and adiponectin from 5 to 40%, and PRDM16 more than 50% of combined expression. Our data indicate that YAT is metabolically active tissue and responds to changes in the energy metabolism with either WAT- or BAT-like phenotype. In conclusion, YAT may display great plasticity in acquiring different metabolic functions, which may be of local importance to bone, as well as to the systemic control of energy metabolism in conditions of functional impairment of other fat depots.

***Disclosures: Amrei Krings**, None.*

MO0081

Monocarboxylate Transporter 10 Mediates Thyroid Hormone Transport in Chondrocytes. Sanae Abe*[1], Noriyuki Namba[2], Mikihiko Kogo[3], Keiichi Ozono[2]. [1]Department of Dentistry & Oral Surgery, Sakai Municipal Hospital, Japan, [2]Department of Pediatrics, Osaka University Graduate School of Medicine, Japan, [3]First Department of Oral & Maxillofacial Surgery, Osaka University Graduate School of Dentistry, Japan

Transporters are necessary for uptake of thyroid hormone into the cell. The monocarboxylate transporter 8 (MCT8) was reported to be a highly specific transporter for thyroid hormone in 2003. Untreated congenital hypothyroidism leads to severe short stature indicating that thyroid hormone is essential for normal proliferation and differentiation of chondrocytes. The Allan-Herndon-Dudley syndrome (AHDS), caused by MCT8 mutations, is characterized by severe psychomotor retardation and elevated triiodothyronine (T_3) levels. However, growth is not as retarded as in patients with endemic hypothyroidism unless severely

malnourished. We therefore hypothesized that chondrocytes utilize transporters other than MCT8 for thyroid hormone uptake.

We first analyzed thyroid hormone transporter mRNA expression in chondrogenic ATDC5 embryonal carcinoma cells. Currently, the only transporters known to be highly specific for thyroid hormone are MCT8, MCT10, and Organic Anion Transporter 1C1 (OATP1C1). These were quantified by real-time PCR using the TaqMan® system. MCT10 was the most abundant of the three with 118,000 copies/ng RNA. Expression levels of MCT10 did not change throughout chondrocyte differentiation. siRNA mediated knockdown of MCT10 mRNA in these cells decreased [^{125}I]T_3 uptake 30~40% compared with negative control ($p<0.05$ at 30, 60, 90 min). Addition of $1x10^{-9}$ or $1x10^{-8}$ M T_3 suppresses proliferation 27.3% and 49.0%, respectively, after 5 days of culture ($p<0.05$). In contrast, when MCT10 mRNA expression was knocked down, neither the presence nor the absence of T_3 significantly altered ATDC5 cell proliferation. Culturing ATDC5 cells in alginate beads promotes differentiation and induces expression of type X collagen, a differentiation marker of hypertrophic chondrocytes. Addition of $1x10^{-9}$ T_3 to these cells further enhances differentiation ($p<0.05$ at day 3). However, when MCT10 mRNA expression was reduced, T_3 did not significantly stimulate differentiation. Thus, MCT10 knockdown diminished the effects of thyroid hormone on ATDC5 cells.

These results suggest that MCT10 might be the major thyroid hormone transporter in chondrocytes. Moreover, if MCT10 can supply chondrocytes with sufficient amounts of thyroid hormone, this could explain why AHDS patients do not exhibit significant growth impairment.

***Disclosures: Sanae Abe**, None.*

MO0082

Nkx3.2 Inhibits Chondrocyte Differentiation Through Runx2 Independent Manner. Jae-Hwan Jeong*[1], Na-Rae Park[2], Hyun-Nam Kim[2], Kyung-Eun Lim[2], Xiangguo Che[2], Sang-Min Kang[2], Dae-Won Kim[3], Je-Yong Choi[1]. [1]Kyungpook National University, School of Medicine, South korea, [2]Kyungpook National University, South korea, [3]Yonsei University, South korea

Chondrogenesis is tightly controlled by key transcription factors such as Sox trios (Sox9, Sox5, and Sox6), Nkx3.2 and Runx2. Nkx3.2 and Runx2 reciprocally express in proliferating and hypertrophic zones, respectively. Therefore, Nkx3.2 has been known as a suppressor for Runx2 expression in proliferating chondrocytes. Here, we tested whether Nkx3.2 functions as a negative regulator for Runx2 expression in cartilages. Transgenic (Tg) mice expressing Nkx3.2 or constitutively active Nkx3.2 (caNkx3.2) under the control of type II collagen promoter were obtained and their morphological characteristics were analyzed histologically. In 15.5 days embryo, the Nkx3.2 Tg mice showed short skeletal elements compared to the wild type. Interestingly, caNkx3.2 Tg mice revealed severe runted phenotypes and died just after birth. Sox trios were expressed in the skeletal elements of the caNkx3.2 mice. Surprisingly, Runx2 and Osterix were also expressed in the caNkx3.2 Tg mice with comparable levels in the wild type. These results indicate that Nkx3.2 is not a negative regulator for Runx2 expression in vivo and that Nkx3.2 inhibits chondrogenesis through Runx2 independent manner in proliferating chondrocytes.

***Disclosures: Jae-Hwan Jeong**, None.*

MO0083

Quantitative Proteome Profiling of Human Mesenchymal Stem Cell Membrane Proteins during Osteoblast Differentiation. Kenneth Hauberg Larsen**[1], Helle Christiansen*[2], Jorge S Burns[1], Irina Kratchmarova[2], Basem Abdallah[1], Jens S Andersen[2], Moustapha Kassem[3]. [1]Odense University Hospital, University of South Denmark, Denmark, [2]University of Southern Denmark, Denmark, [3]Odense University Hospital, Denmark

Understanding the biology of osteoblast differentiation has been hampered by the absence of prospective stage-specific differentiation markers for mesenchymal stem cells undergoing osteoblastic differentiation. Mass spectrometry-based proteome analyses is a powerful tool for the analysis of protein expression profiles. We employed Stable Isotope LAbeling in Cell culture (SILAC) to obtain comprehensive quantitative profiles of membrane proteins during ex vivo osteoblast differentiation in a cell model of human mesenchymal stem cells with overexpression of human telomerase reverse transcriptase gene (hMSC-tert). We quantified a total of 972 proteins in two separate SILAC experiments during several timepoints in a course of 14 days of osteogenic differentiation. Eighty percent of these proteins (778 proteins) were either integral membrane proteins, membrane associated proteins, interactors with membrane proteins or GPI-proteins. Forty-one percent (398 proteins) of the total number of proteins had a trans-membrane domain Quantitative data revealed that nearly 74 % of all proteins increased more than 2 fold as a function of control level at one or more timepoints during osteogenic induction, including several proteins well known in osteogenesis, e.g. alkaline phosphatase, CD295, CD91, Raftlin, CD107b, CD36L, integrin B5. The whole dataset was manually clustered into 10 categories of subcellular localisation. We confirmed the stage specific expression of a number of marker candidate proteins such as: CD295, alkaline phosphatase, CD10, CD44, CD49a, CD49e, CD51/61, CD29, CD63, CD73 (GPI-protein), CD146, CD166, CD107a, CD13, AnnexinA5 (secreted), LAMP2 (aka: CD36L2) and hRECK by flouresence-activated cell sorting and the presence of mRNA by polymerase chain reaction.

In conclusion, SILAC-based quantitative proteomics have provided a number of putative novel biomarkers on human mesenchymal stem cells during osteogenic induction. Several of these markers include a number of CD antigens and GPI proteins, as well as proteins not previously connected to osteogenesis. These proteins may play important roles in initiating and maintaining an osteogenic differentiation phenotype.

*Both authors contributed equally

Disclosures: Kenneth Hauberg Larsen, None.*

MO0084

The Canonical BMP Signaling Pathway Plays a Crucial Part in Stimulation of Dentin Sialophosphoprotein Expression by BMP-2. Young-Dan Cho*[1], Won-Joon Yoon[2], Kyung-Mi Woo[2], Jeong-Hwa Baek[2], Joo-Cheol Park[2], Hyun-Mo Ryoo[3]. [1]Seoul National University, South korea, [2]School of Dentistry,Seoul National University, South korea, [3]Seoul National University, School of Dentistry, South korea

Dentin sialophosphoprotein (DSPP), a typical dentin-specific protein, is mainly expressed in the dentin extracellular matrix and plays a role in dentin mineralization. BMP-2 provides a strong signal for differentiation and mineralization of odontoblasts and osteoblasts. BMP-2 treatment is reported to stimulate Dspp expression in the MD10-F2 pre-odontoblast cells through the activation of the heterotrimeric transcription factor Y (NF-Y). The canonical BMP signaling pathway is known to contribute greatly to biomineralization, however, it is not known whether it is involved in *Dspp* expression. Here, we investigated this question. Activation of the canonical BMP-2 signaling pathway by overexpression of constitutively active Smad1/5 or the downstream transcription factors Dlx5 and Runx2 stimulated Dspp expression. Conversely, knockdown of each element with siRNA significantly blocked the BMP-2-induced *Dspp* expression. To test whether these transcription factors downstream of BMP-2 are directly involved in regulating *Dspp*, we analyzed the mouse *Dspp* promoter. There are 5 well-conserved homeodomain binding elements, H1 to H5, in Dspp proximal promoter regions (-791 to +54). A serial deletion of H1 and H2 greatly changed basal promoter activity and Dlx5 responsiveness. Dlx5 has higher binding specificity to H1 than H2, whereas Msx2 has relatively higher affinity to H2. These differences in binding specificity corresponded well with Dlx5- or Msx2-mediated modulation of promoter activity. Despite their different binding specificities, the antagonism between Dlx5 and Msx2 occurs at both response elements. Thus, the canonical BMP-2 signaling pathway plays a crucial part in the regulation of *Dspp* expression through the action of Smads, Dlx5, Runx2, and Msx2.

***Disclosures: Young-Dan Cho**, None.*

MO0085

Altered Bone Repair Pattern in Ovariectomy-induced Osteoporotic Mice: A Bone Drill-Hole Healing Model. Yixin HE*[1], Ge Zhang[2], Zhong Liu[3], Xiaohua Pan[4], Xinhui Xie[5], Chun-Wai Chan[6], Kwong-Man Lee[7], Gang Li[8], Ling Qin[9]. [1]The Cuinese University of Hong Kong, Hong kong, [2]Price of Wales Hospital, Peoples republic of china, [3]The Chinese University of Hong Kong, China, [4]Department of Orthopedics, Second Hospital of Medical College of Ji Nan University, Shenzhen People's Hospital, Shenzhen 518020, China, China, [5]The Chinese University of Hongkong, Hong kong, [6]Musculoskeletal Research Laboratory, Department of Orthopaedics & Traumatology, The Chinese University of Hong Kong, Hong Kong SAR, China, China, [7]Lee Hysan Clinical Research Laboratory, The Chinese University of Hong Kong, China, China, [8]The Chinese University of Hong Kong, Peoples republic of china, [9]Chinese University of Hong Kong, Peoples republic of china

Transgenic mice provides a powerful tool to investigate the functional role of the specific genes involved in bone repair. Previously published models of osteoporotic bone repair in mice have their limitations. The internal fixation model is challenged by its angular motion and the external fixation model is challenged by its decreasing holding power of the screws in osteoporotic condition, Mouse drill-hole healing model in normal bone was established by Dr.Campbell, which showed technically simple and highly reproducible, but it has not been applied in osteoporotic mice yet. The objective of this study was to develop a bone drill-hole healing model in osteoporotic mice.

Methods: Total 112 3-month-old female C57BL/6 mice were randomizely divided into ovariectomy group (OVX) and sham-operated group (Sham). A cortical bone defect on right femur was created six weeks after OVX operation in all the mice. High resolution micro-CT (VivaCT 40, Scanco) was employed to in-vivo monitoring the repair process at day 0,3,7,10,14 and 21. Mice were sacrificed at each time point (n=8 at day 0,3,7,10,14 and n=16 at day 21). Mice callus and sera samples were collected for histology, mRNA expression, and mechanical testing.

Results: H&E staining showed that there were less granulation tissues at early stage, less woven bone and mineralized trabecular at middle stage and less organized cortical at late stage in OVX mice compared to Sham mice (Figure 1). In vivo microCT measurement showed OVX and Sham groups differed significantly in the pattern of the change in the bone volume over time in both defect region and intra-medulla space ($P<0.05$ for the interaction between time and group by the repeat measure ANOVA)

(Figure 2). Bone formation marker P1NP was increased from baseline followed by a peak at day 10 and return back to baseline at day 21 in Sham mice. The profile was shifted right in OVX mice. Bone resorption marker CTX share the similar pattern to PINP. Estrogen receptor alpha (ER alpha) expression was higher in Sham mice compared to OVX mice while estrogen receptor beta (ER beta) expression was lower in Sham mice compare to OVX mice. Sham mice showed significant higher ultimate load and energy to failure compared to the OVX mice at day 21 (Figure 3).

Conclusion: Bone drill-hole healing model is a simple way for investigating mice bone repair. Bone repair pattern in OVX-induced osteoporotic mice was altered, the altered ER alpha and ER beta expression may contribute to its underlying mechanism.

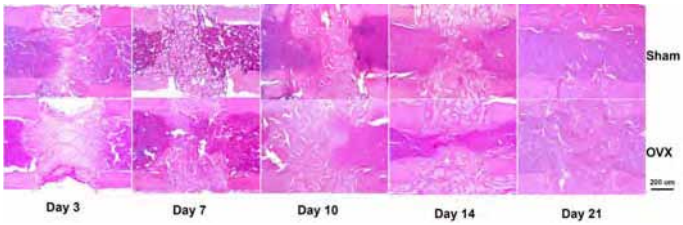

Figure 1. Histology of bone repair in H&E sections

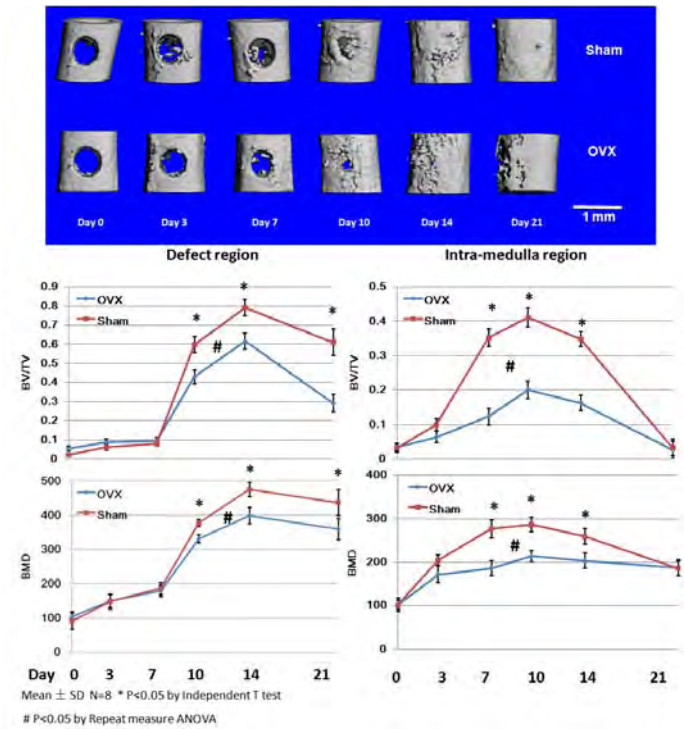

Figure 2. MicroCT monitoring of bone repiar

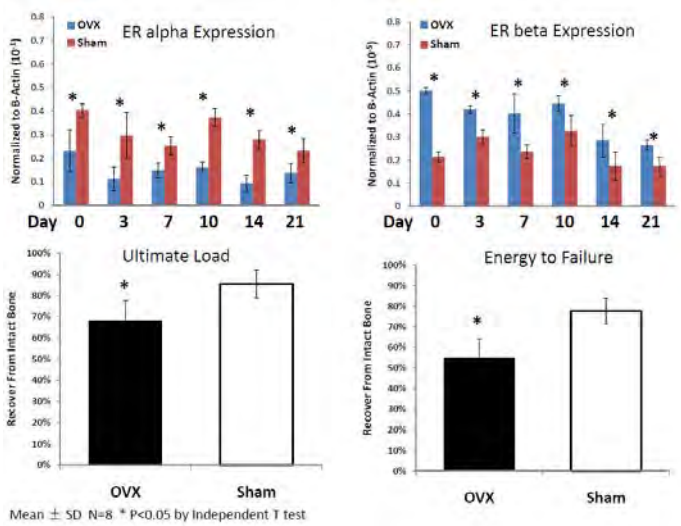

Figure 3. Estrogen receptor expression and mechanical testing of

***Disclosures: Yixin HE**, None.*

MO0086

Deciphering the Role of Parafibromin in Bone Development. Cassandra R. Zylstra*[1], Pengfei Wang[1], Bin T. Teh[1], Bart Williams[1], Heather Ramsay[2], Mohammed Farhoud[2]. [1]Van Andel Research Institute, USA, [2]MPI Research, USA

The hyper-parathyroidism-jaw tumor (HPT-JT) syndrome is an autosomal dominant disorder in which patients present with parathyroid tumors and fibro-osseous tumors of the maxilla or mandible. Studies have shown that the HPT-JT locus maps to the putative gene hyperparathyroidism type 2, HRPT2, which encodes the protein parafibromin. Parafibromin is a transcription factor associated with the PAF complex which acts as a tumor suppressor by regulating post-transcriptional events and histone modification. Others have shown parafibromin acts as a mediator of Wnt signaling by directly interacting with B-catenin and affecting Wnt target gene expression. Our lab's main interest is to understand the importance of Wnt/B-catenin signaling in bone development and disease. The importance of Wnt/B-catenin signaling in bone development has been clearly shown by many researchers. Considering that parafibromin is suggested to be a regulator of Wnt/B-catenin pathway, we are interested in learning how this gene affects osteoblast differentiation and fate. To better understand the ability of parafibromin to regulate Wnt/B-catenin signaling, we have generated a conditional mouse model of Hrpt2 where this gene is effectively eliminated specifically in osteoblasts by using the OC (Osteocalcin)-Cre mouse. Our in vivo data strongly suggests that loss of Hrpt2 in mature osteoblasts leads to increased bone mineral density compared to wildtype littermates as determined by dual energy x-ray absorptiometry (DEXA). Our in vitro data indicates loss of Hrpt2 in calvarial osteoblast cultures by Adeno-Cre infection leads to increased apoptosis and decreased cell proliferation compared to Adeno-GFP infected cells. Based on our findings we hypothesize that the timing of Hrpt2 loss during osteoblast differentiation leads to different phenotypes.

***Disclosures: Cassandra R. Zylstra**, None.*

MO0087

Effect of Platelet-Rich Plasma on Human Tenocyte Proliferation and Differentiation *In Vitro* and *In Vivo*. Xiao Wang*[1], Zhidao Xia[1], Yiwei Qiu[2], Andrew J Carr[1], James Triffitt[3], Afsie Sabokbar[4]. [1]University of Oxford, United Kingdom, [2]Botnar Reasearch Centre, United Kingdom, [3]Botnar Research Centre, United Kingdom, [4]University of Oxford, Botnar Research Centre, United Kingdom

Tendon tissue engineering provides a new approach for tendon repair. It evolves the expansion and differentiation of progenitor cells in culture. In in vitro cell culture the use of 10% Fetal Bovine Serum (FBS) to maintain cell survival and growth is commonly applied. This could potentially result in altered biological responses when using non-autologous cell populations. Platelet rich plasma (PRP) is currently used in various fields of surgery and regenerative medicine and offers an easy, cost-effective way to obtain high concentrations of autologous growth factors. This study aims to investigate (1) the effects of PRP on human tenocyte proliferation and differention *in vitro* and (2) the response of PRP-treated tenocytes when implanted in normal mice.

PRP was prepared by a two-step centrifugation procedure using blood from 3 healthy donors and activated PRP was used as a substitute for FBS. To evaluate the cellular responses of human tenocytes to activated PRP, the proliferation and differentiation of human tenocytes were examined. Proliferation was determined by the Alamar Blue® assay at days 1 and 7 and collagen production was examined by Sirius Red measurement. Differentiation of human tenocytes was determined using real time RT-PCR for the expression of scleraxis (SCX), collagen type I (COL1), collagen type III (COL3) and decorin (DCN) at Day 7. The tenocytes were implanted in Balb/c mice within diffusion chambers for 14 days, and the above differentiation makers were examined in the diffusion chambers.

The results showed that levels of collagen synthesized by tenocytes in 10% activated PRP were significantly higher than in 10% FBS. Following 7 days culture of human tenocytes, the cell numbers in 10% activated PRP were significantly higher than in 10% FBS. The mRNA levels of SCX, COL1, COL3 and DCN were decreased when tenocytes were cultured in activated PRP as compared to culture in 10% FBS after 7 days. *In vivo* implants showed tendon-like structures and normal expression of mRNA levels of tendon markers.

This study shows that tenocytes cultured in 10% activated PRP exhibit a better tenocyte growth and collagen production than in 10% FBS. The COL1 and COL3 mRNA levels decreased, suggesting a reduction in collagen production per cell. All the tendon marker expressions were restored after implantion *in vivo* for 14 days, suggesting that tenocytes cultured in activated PRP have the potential for further maturation after implantation.

***Disclosures: Xiao Wang**, None.*

MO0088

Micro-Computed Tomography Analysis of Adult Bone in Mice Expressing Reduced Levels of Perlecan/HSPG2. Peter Fomin[1], William Thompson[1], Laura Sloofman[1], Dylan Lowe[1], Christopher Price[1], Mary Farach-Carson[2], Catherine Kirn-Safran*[1]. [1]University of Delaware, USA, [2]Rice University, USA

The objective of our study is to use a mouse model of Schwartz-Jampel syndrome (SJS), a skeletal disease resulting from the reduced secretion of Perlecan/HSPG2 (PLN) to better understand the role of this large heparan sulfate proteoglycan in the establishment of bone structural properties. PLN is abundant in the pericellular matrix of non-calcified cartilage and is believed to play important regulatory functions in endochondral ossification and joint cartilage formation and maintenance. Because of profound effects on embryonic viability in the absence of PLN, only non-null allele mutations of *PLN* gene such as hypomorphic variants were characterized in adult mammals.

In this study, we observed that hypomorphic mice expressing about 10% of normal PLN levels in cartilage display a short stature phenotype accompanied by chondrodysplasias, short snout, and severe ocular abnormalities that are exacerbated during adulthood. Whereas no obvious changes are observed at ages when bone is still immature, the weight of adult PLN hypomorphs is significantly decreased by approximately 25% when compared to age-matched control animals. In adult PLN hypomorph mice, both tibial and femoral lengths were decreased when compared to controls but a concomitant decrease in PLN hypomorph wet bone weight was not observed. This observation suggests that bone mineral content is increased when PLN levels are insufficient.

For this reason, structural properties of cortical and trabecular bone are currently being examined using micro-computed tomography in both young and aged PLN hypomorphs. Our results are consistent with previous data reporting that heparan sulfate proteoglycans are strong inhibitors of hydroxyapatite crystal deposition and current work performed by our group studying PLN function in osteocytes. In conclusion, our data imply that PLN plays a regulatory function in the establishment of normal bone mass and health. Ongoing work will use the PLN hypomorph model to understand the molecular mechanisms underlying bone and cartilage pathologies in patients affected by SJS. (Supported by NIH COBRE P20 RR016458 to CKS).

***Disclosures: Catherine Kirn-Safran**, None.*

MO0089

Modulation of Bone Remodeling Activity Regulates Cartilage Response to IL-1β via Soluble Factors. Remy Nizard[1], Marie-Dominique Ah-Kioon[2], Thomas Funck-Brentano*[2], Hilene Lin[2], Marie-Christine De Vernejoul[2], Martine Cohen-Solal[2]. [1]Department of Orthopeadics, Lariboisiere Hospital, France, [2]INSERM U606, Paris VII University, France

Introduction: osteoarthritis (OA) induces both cartilage and subchondral bone changes. Bone resorption might modulate cartilage damage in mechanical conditions. The aim of our study is to investigate the ex vivo effect of bone remodeling on cartilage response to IL-1β stimulation.

Methods: explants of bone and cartilage were harvested from healthy zones in patients undergoing total replacement therapy for unicompartimental knee OA. Bone and articular cartilage were separated manually and cultured in parallel in red-phenol-free medium. Bone explants were cultured BGJb, and cartilage in DMEM. After 24h of stimulation with IL-1β (10ng/ml), bone explants were cultured in presence of estradiol at 10 or 1000 nM or pamidronate at 1μM for 72h. After changing the medium for 24h, bone culture supernatant was transferred on cartilage explants previously stimulated by IL-1β for 24h (ratio 1:3). Control cartilage explants were cultured with the same ratio of BGJb. Proteoglycan release and aggrecan neoepitops were measured as cartilage catabolism markers.

Results: IL-1β on cartilage explants induced a 24 $\pm$ 2% increase in proteoglycan release (p=0.037) compared to control explants. Supernatant of bone explants cultured with estradiol prevented this increase with a dose effect (+2.5 $\pm$ 8.2% at 10nM; -2.3 $\pm$ 7.7% at 1000nM; p=0.049) as well as with pamidronate (-2.0 $\pm$ 21.8%; p=0.049). Supernatant of bone explants stimulated by IL-1β alone did not change the response of cartilage to IL-1β.

Conclusion: These ex vivo studies suggest that bone soluble factors are capable of modulating the catabolic mechanisms of articular cartilage. This data provide further evidence of a cross-talk between bone and cartilage. They show that bone might be a target for osteoarhritis.

***Disclosures: Thomas Funck-Brentano**, None.*

MO0090

Multiple Quantum NMR Differentiates Bound and Mobile Water in Human Cortical Bone. Henry H. Ong*, Alexander C. Wright, Felix Werner Wehrli. University of Pennsylvania Medical Center, USA

NMR is a powerful tool for non-destructive study of bone water (BW), which plays a pivotal role in providing bone with its high impact strength. BW can be found in the pore space of the Haversian system and bound to the collagen matrix. Bound BW, unlike mobile BW in the pore space, has anisotropic rotational motion that gives rise to splittings in NMR spectra. Here, we use ^{1}H and ^{2}H in-phase double-quantum filtered (IP-DQF) and inversion recovery (IR) NMR to study bound and mobile BW from human tibia cortical bone specimens. Specimens were cored from posterior, medial, anterior and lateral sides of the mid-tibia of two donors (M, 37; F, 65 y). All NMR experiments were performed on a vertical-bore 9.4T spectrometer (DMX-400, Bruker). IP-DQF experiments, which allow for clear observation of the bound BW splitting, did not show any significant differences in age and tibial location. ^{1}H IP-DQF experiments revealed a large splitting of ~40 kHz (Fig. 1) that was independent of temperature and specimen orientation, suggesting it to arise from backbone collagen protons. After soaking the specimens in D_2O, ^{2}H IP-DQF experiments revealed a splitting that was dependent on specimen orientation, being halved when the specimen was perpendicular to the magnetic field (4 vs. 8 kHz, Fig. 2). As most collagen protons are non-exchangeable, we conclude that the ^{2}H splitting arises from bound BW due to the collagen fibers' alignment along the osteonal axis. ^{2}H IR NMR was used to quantify bound and mobile BW fractions based on differences in T_1 relaxation times, which allows nulling of the bound BW while preserving the mobile BW signal. Bound and mobile BW spectra could then be generated and relative fractions calculated, with the mobile BW fraction ranging from 25-40% depending on location and donor. Bone from the 65 y donor generally yielded higher mobile BW fractions. Based on the D_2O exchange, overall absolute BW concentration (BWC) was also calculated. BWCs are in good agreement with those observed *in vivo*. From total BWC and mobile BW fraction bone porosity was computed. There was excellent correlation between the NMR and μ-CT bone porosities (R=0.93, p<0.001, Fig. 3). As expected, bone from the older female donor was more porous. In conclusion, IP-DQF and IR NMR methods can used to study BW and provide insight into bone matrix nano- and micro-structure.

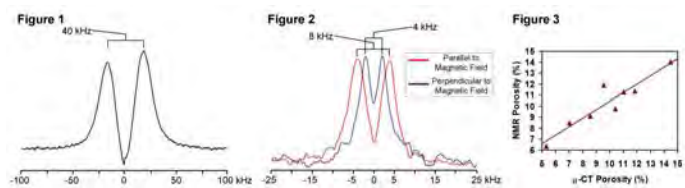

Figures

***Disclosures: Henry H. Ong**, None.*

MO0091

Site-Specific Changes in Bone Microarchitecture and Micromechanics During Lactation and After Weaning in Mice. Xiaowei Liu*[1], Laleh Ardeshirpour[2], Joshua VanHouten[3], Victor Chiang[1], X Guo[1], Elizabeth Shane[4], John Wysolmerski[3]. [1]Columbia University, USA, [2]Yale University, USA, [3]Yale University School of Medicine, USA, [4]Columbia University College of Physicians & Surgeons, USA

Despite the dramatic bone loss that occurs during lactation, BMD is rapidly restored after weaning. We used micro computed tomography (μCT), the novel technique of individual trabeculae segmentation (ITS), and micro finite element analysis (μFEA) to quantify the effects of lactation and weaning on bone microarchitecture and mechanical competence at multiple skeletal sites in mice.

Specimens from proximal tibia (PT), 3rd lumbar vertebra (L3), and distal femur (DF) were harvested from Virgin (n=5), Lactating (day 12, n=5) and Weaned (28 days post-weaning, n=4) mice and scanned using a μCT system (VivaCT 40; SCANCO Medical; 10.5 μm). Cortical thickness (Ct.Th) and porosity (Ct.Po) were evaluated for the mid femur shaft. ITS analyses were applied to trabecular (Tb) bone at PT, L3, and DF to evaluate Tb plate- and rod-microarchitecture. Whole bone stiffness of each site was estimated by μFEA of μCT scans.

Lactating mice had markedly lower Tb plate bone volume fraction (pBV/TV; 87-89%), plate tissue fraction (pBV/BV; 58-73%), plate number density (pTb.N; 19-21%), plate & rod thickness (pTb.Th; 27-31% & rTb.Th; 15-21%), and plate-rod & plate-plate junction densities (P-R & P-P Junc.D; 44-74% and 64-80%) than virgins at all 3 sites (p<0.05). Weaned mice were comparable to virgins in all ITS measures at L3 and in most ITS measures at the PT, except pBV/TV & pBV/BV, which were -16% & -38% lower in weaned vs. virgin mice (p<0.05). In contrast, at the DF, there were highly significant differences (-60 to -4%) between weaned and virgin mice (p<0.05), although pBV/BV, pTb.Th, and rTb.Th were higher in weaned vs. lactating animals (p<0.05). Ct.Th & Ct.Po of the mid femur shaft was 28% & 6% lower in lactating mice and significant differences remained in weaned mice (p<0.05 weaned vs. virgin). At L3 and PT, whole bone stiffness was 71% lower in lactating mice (p<0.05) but weaned mice did not differ from virgins (p>0.05). At DF, stiffness was 54% lower in lactating mice than virgins but only 34% lower in weaned mice (p<0.05).

In conclusion, compared to virgins, lactating mice had fewer plates, more rods, reduced plate & rod thickness, connectivity, and stiffness at PT, L3, and DF. In weaned mice, most of these differences were not apparent at PT and L3, while microarchitectural deterioration of Tb and cortical bone at the femur was still present. Our results suggest site-specific incomplete recovery of microarchitecture and stiffness after weaning.

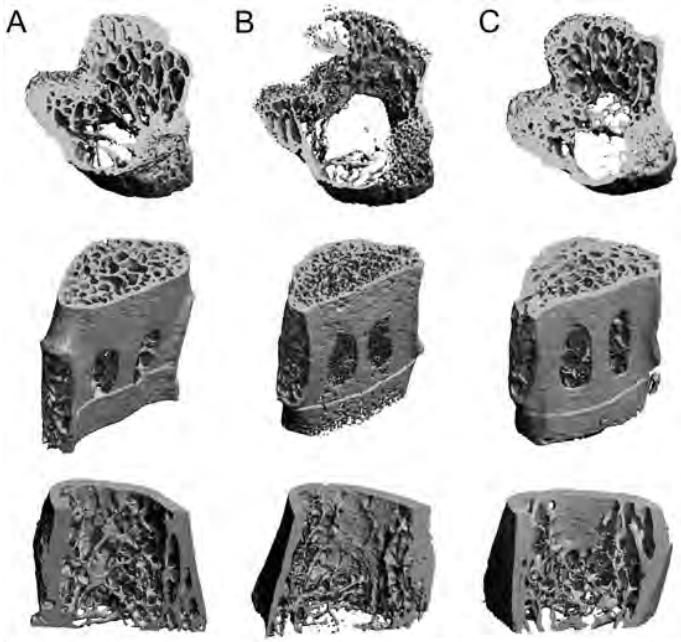

Figure 1. Three dimensional reconstruction of representative (Top) proximal tibia, (Middle) L3, and (Bottom) distal femur from (A) Virgin, (B) Lactating, and (C) Weaned mice.

Figure 1

***Disclosures: Xiaowei Liu**, None.*

MO0092

Skeletal Irradiation in Young Rodents Leads to Deficient Early Appositional Bone Growth and Remodeling. Joseph Spadaro*[1], Luis Romo[2], Timothy Damron[1], Lihini Keenawinna[3]. [1]State University of New York Upstate Medical University, USA, [2]Syracuse University, USA, [3]SUNY Upstate Medical University, USA

Radiotherapy in the treatment of childhood tumors can inadvertently involve the growth plate and cause deformity or reduction in bone length. However, the effects of radiation on other aspects of bone growth and integrity have hardly been studied. In this study, the right hind limbs of 5 groups of 32 day-old SD rats were exposed to single fraction 17.5 Gy x-irradiation collimated to include the mid-femur distally to the mid-tibia (300 KVP, 250 rads/min.). The groups were euthanized at 3 days, 1, 2, 3 and 4 weeks after exposure and Faxitron sagittal radiographs of both hind limbs where taken. Using ImageJ, measurements were made from scanned images of the femur, tibia, and fibula lengths and widths at proportional locations of the linear length over time (figure 1).

The measurements revealed that there were early, substantial differences in bone development of the irradiated limbs. Compared to the non-irradiated side, the irradiated limb was not only substantially shorter in length but smaller in diameter, even outside the targeted region. Figure 1 shows the differences in diameter of the proximal tibia with a contraction evident by 1 week and some recovery at 4 weeks. Width reductions from control were 25% for the tibia and fibula and 20% for the femur, equal to or exceeding the losses in longitudinal growth in this model. These findings suggest that, radiation causes important early changes in appositional growth and remodeling that likely weaken the structure as well as shorten it. The changes would appear to involve changes in endochondral remodeling as well as membranous (periosteal) bone formation.

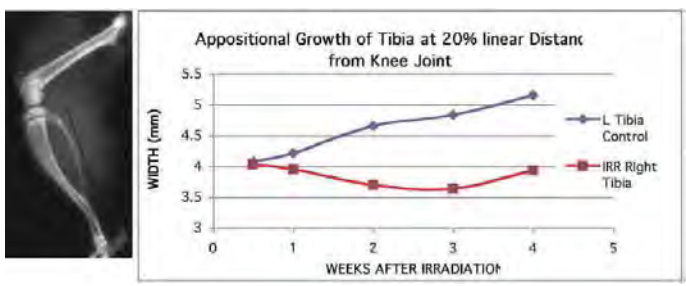

Figure 1: Appositional growth of the proximal tibia following 17.5 Gy irradiation

***Disclosures: Joseph Spadaro**, None.*

MO0093

The Bone Loss in Iron Overload is Mediated by Oxidative Stress in Mice. Maria Vogiatzi*[1], Zheiwei Yang[2], Jaime Tsay[2], Robert Grady[2], Patricia Giardina[2], Adele Boskey[3], F. Patrick Ross[3]. [1]New York Presbyterian Hospital, Weill Cornell Medical College, USA, [2]Weill Cornell Medical College, USA, [3]Hospital for Special Surgery, USA

Osteoporosis is a frequent problem in disorders associated with iron overload, such as hereditary hemochromatosis and any acquired or congenital disease, such as thalassemias, that requires chronic transfusions. The role of iron in the development of osteoporosis in these disorders is unclear. To better understand the role of iron on bone, we developed a murine model of iron overload and observed severe bone loss and increased resorption. Since oxidative stress (ROS) has been described in patients with iron overload, we sought to determine the role of ROS in iron-induced bone loss in mice. BL6C/57 mice (n=8/ group; all males; age 2 mo) were treated with placebo (PBS IP x weekly) vs. iron dextran (1g/kg /week IP) for two months. As we previously described, iron dextran (ID) resulted in significant trabecular changes, characterized by decreased bone volume fraction, trabecular number and thickness, and increased trabecular separation. Cortical changes consisted of decreased cortical thickness and area. Protein carbonyl content extracted from the bone marrow of ID treated mice (OxiBlot Detection Kit, Chemicon Int'l, CA) was increased compared to placebo indicating increased ROS with iron overload. A third group of BL6C/57 mice (n=8; all males; age 2 mo) was treated with ID (1g/kg/week) + the anti-oxidant N-acetyl-cystein (NAC; 100mg/kg/day x5days/week, sc) for 2 mo. This therapy prevented the trabecular bone changes that were induced by ID treatment alone. Cortical changes were partially reversed with ID+ NAC. As expected, both ID and ID + NAC mice had significantly elevated liver and spleen iron concentrations (> 30 fold increase compared to placebo). Serum TNFa and IL6 concentrations were elevated in ID treated mice (approximately a 2.5 fold increase compared to placebo), and returned to baseline in ID + NAC animals. Our results indicate that ROS is a mediator of bone loss in iron overload in mice. Iron overload is associated with increased bone-targeting inflammatory cytokines, such as TNFa and IL6, which normalize after anti-oxidant therapy. These data imply that the bone loss in iron excess is also mediated through an inflammatory process probably induced by ROS.

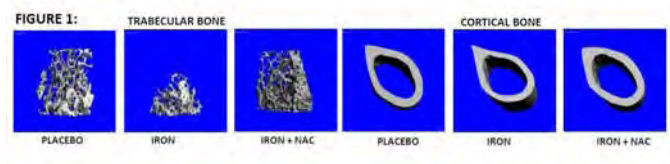

Figure

***Disclosures: Maria Vogiatzi**, None.*

MO0094

Weight Bearing in Simulated 1/6th and 1/3rd Gravity Does Not Prevent Bone Loss. Florence Lima*[1], Joshua Swift[2], Brandon Macias[1], Elizabeth Greene[1], Josh Kupke[3], Yasaman Shirazi-Fard[1], Matthew Allen[4], Harry Hogan[1], Susan Bloomfield[1]. [1]Texas A&M University, USA, [2]United States Navy, USA, [3]Texas A&M Univeristy, USA, [4]Indiana University School of Medicine, USA

The magnitude of bone loss experienced by astronauts over one month in microgravity is similar to that of postmenopausal women over one year. However, no data exist at intermediate gravity levels, such as those on the moon and Mars. We hypothesized that mice exposed to G/6 (Lunar gravity) and G/3 (Mars gravity) will experience significant reductions in bone mass and bone formation as compared to 1 G (gravity) controls, but the magnitude would be less than those of the non-weight bearing 0G mice. Methods: Female BALB/cByJ mice (4-mo, n=9/group) were randomly assigned to cage control (1G), traditional tail suspension (0G), 1/6th gravity (G/6), or 1/3rd gravity (G/3) groups for a 21-day suspension protocol. The partial G mouse model provides for titrated reductions in weight bearing to all four limbs. Bone volume (BV/TV), trabecular thickness (Tb.Th), and trabecular number (Tb.N) were measured with micro-CT scans (Skyscan 1172) of excised distal femurs. Total volumetric bone mineral density (vBMD; proximal tibia) was measured with *in vivo* pQCT scans on day 0 and 21. Bone formation rate (BFR/BS), mineral apposition rate (MAR) and mineralized surface (MS/BS) were quantified by dynamic histomorphometry. Load to failure of the right femoral neck (FN) was measured in all groups using an Instron 3345 at 1.27mm/min with a 100 N load cell. Results: After 21 d, body mass decreased significantly (-7.6%) in 0G mice but not in the G/3 or G/6 groups. Decreases in proximal tibia total vBMD were greatest in 0G (-20%) mice, with intermediate reductions in G/6 (-14%) and G/3 (-14%). Relative to the 1G group, distal femur BV/TV, Tb.Th, and Tb.N in the 0G, G/6 and G/3 groups were lower (-24%, -12%, -14%, respectively) at day 21. BFR/BS (-57%) and MS/BS (-49%) in the distal femur were significantly lower in the 0G group; similar reductions were observed in G/6 (BFR/BS: -49%, MS/BS: -43%), and G/3 groups (BFR/BS: -46%, MS/BS: -39%). Cortical bone formation in all reduced gravity groups was significantly suppressed on both the endocortical and periosteal surfaces, (BFR/BS: -79% and -86%, respectively). Load to failure of FN in the 0G group was significantly lower

(-28%) with intermediate decrements in G/6 and G/3 groups (-23% -18%, respectively) vs 1 G controls. Conclusion: These data suggest that partial weight bearing (as high as G/3) does not provide sufficient mechanical load to mitigate most of the deleterious changes in bone as observed with the non-weight bearing condition.

***Disclosures: Florence Lima**, None.*
This study received funding from: Funded by NSBRI through NASA Cooperative Agreement NCC 9-58.

MO0095

Colocalization of *In Vitro* Resorption Pits With Osteopontin, Osteocalcin, and Phosphoproteins. Colleen Janeiro*, Deepak Vashishth. Rensselaer Polytechnic Institute, USA

Osteocalcin (OCN) and osteopontin (OPN) are two non-collagenous proteins (NCPs) located in the bone matrix, and are frequently found together as a complex.[1] Each has a role in the bone resorption process. OCN attracts osteoclasts[2] (OCLs), while OPN provides an OCL attachment site. Specifically, OCLs preferentially attach to phosphorylated OPN (pOPN), while non-phosphorylated OPN (npOPN) causes OCL detachment.[3] The aim of this study is to examine the colocalization of in vitro resorption pits with OPN, OCN, and phosphoproteins. Based on current evidence that OCLs secrete TRAP, which dephosphorylates OPN and in turn causes OCL migration, it is hypothesized that the resorption pits will most frequently colocalize with npOPN and possibly nonphosphorylated OCN (npOCN).

17 transverse slices were obtained from the posterior proximal section of human tibiae. The slices were polished to 0.05 micron, and OCL precursor cells (Lonza 2T-110) were seeded at a density of 10,000 precursors/bone slice, and maintained under standard cell culture conditions for 14 days. Each bone slice was stained for OCN, OPN, and phosphoproteins. Samples were dried and mounted onto glass slides with glass coverslips. A Zeiss LSM 510 META system was utilized to visualize and image the resorption pits and colocalized proteins.

The number of resorption pits that colocalized with OPN or phosphoproteins were significantly ($p < 0.001$) higher than those colocalizing with OCN (Fig 1). However, there was no significant difference between the number of resorption pits colocalizing with OPN and those colocalizing with phosphoproteins. Fig 2 contains a sample image.

This is the first study to examine the colocalization of in vitro resorption pits with NCPs. The more frequent co-localization of pOPN than OCN with in vitro resorption pits supports the theory that OCN in bone matrix does not interact with the OCL during the attachment process, but may merely act as a chemoattractant. The pOPN, however, provides an acceptable attachment site for the OCLs and the secretion of TRAP by the attached OCL may lead to dephosphorylation of OPN, and subsequent migration.[4] Our results demonstrate that matrix bound OPN is more important than OCN for OCL bone resorption in vitro, and that the phosphorylation state of OPN may play an additional role.

1 Ritter et al, JBMRs, 1992.
2 Chenu et al, J Cell Biol, 1994.
3 Ek-Rylander et al, J Biol Chem, 1994.
4 Heinegard et al, Ann NY Acad Sci, 1995.

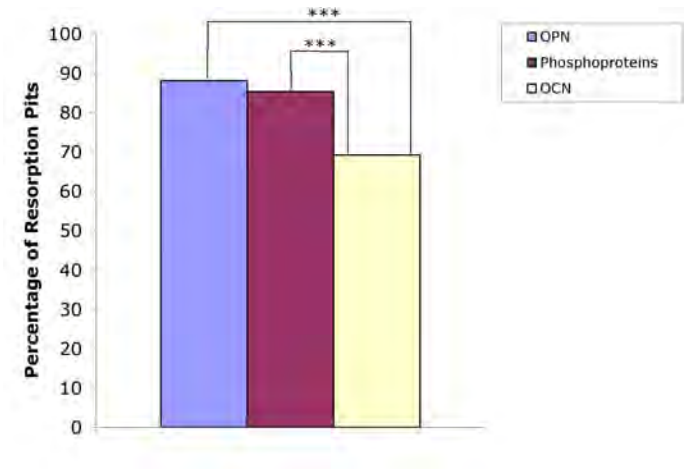

Figure 1

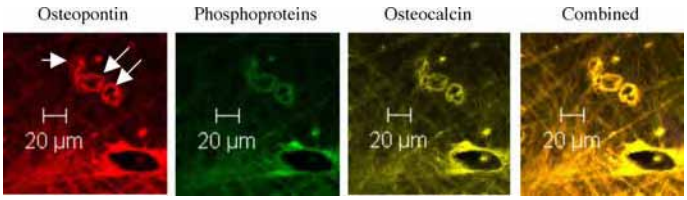

Figure 2

***Disclosures: Colleen Janeiro**, None.*
This study received funding from: AR 49635

MO0096

Microfibril-associated Glycoprotein-1 (MAGP1), an Extracellular Matrix Regulator of Bone Remodeling. Marcus Watkins[1], Roberto Civitelli[1], Matthew Silva[1], Clarissa Craft*[2], Thomas Broekelmann[2], Robert Mecham[3], Wei Zou[1], Steven Teitelbaum[1], Susan Grimston[3], Michael Brodt[2]. [1]Washington University in St. Louis School of Medicine, USA, [2]Washington University in St. Louis, School of Medicine, USA, [3]Washington University School of Medicine, USA

MAGP1 is an extracellular matrix protein that, in vertebrates, is a ubiquitous component of fibrillin-rich microfibrils. We previously reported that aged MAGP1-deficient mice (MAGP1Δ) develop lesions that appear to be the consequence of spontaneous bone fracture. We now present a more defined bone phenotype found in MAGP1Δ mice. A longitudinal DEXA study demonstrated age-associated osteopenia in MAGP1Δ animals and micro-CT confirmed reduced bone mineral density in the trabecular and cortical bone. Further, MAGP1Δ mice have significantly less trabecular bone, the trabecular microarchitecture is more fragmented, and the diaphyseal cross-sectional area is significantly reduced. The remodeling defect seen in MAGP1Δ mice is likely not due to an osteoblast deficiency since MAGP1Δ bone marrow stromal cells retain the ability to differentiate into osteoblasts and the osteoblast number to bone surface ratio is unchanged. Further, calcein-alizarin labeling demonstrated normal mineralized surface and bone formation rates in MAGP1Δ animals. Instead, our findings suggest increased bone resorption is responsible for the osteopenia. The number of osteoclasts derived from MAGP1Δ bone marrow macrophages is increased relative to WT. Additionally, osteoclast differentiation markers are expressed at earlier time points in MAGP1Δ cells. Using quantitative histomorphometry we found that the osteoclasts/bone surface ratio is significantly increased in the MAGP1Δ mice. These findings suggest that MAGP1 is a regulator of bone remodeling and its absence results in osteopenia associated with an increase in osteoclast number

***Disclosures: Clarissa Craft**, None.*

MO0097

Periostin, a Matricellular Glutamic-acid (Gla) Protein Influences Cross-linking of Bone Collagen. Evelyne Gineyts*[1], Serge Livio Ferrari[2], Nicolas Bonnet[2], Patrick Garnero[3]. [1]INSERM unit 831, Université de Lyon, France, [2]University Geneva Hospital, Switzerland, [3]INSERM unit 664, Université de Lyon & Cisbio Bioassays, France

Background: Periostin (Postn) is a non-collagenous protein preferentially localized in the periosteum which binds to collagen molecules. Studies have shown that Postn deficient mice (Postn -/-) presented with altered cortical bone bending strength compared to wild-type animals (Postn +/+). The mechanical behaviour of bone depends on its mass and architecture, but also on the properties of the organic matrix including collagen crosslinking.

Aim: The objectives of this study were to investigate whether the pattern of bone collagen crosslinking is 1) altered in Postn-/- mice compared to wild type animals and 2) associated with mechanical properties.

Methods: The cortical tibial diaphyses from 4 (n=33) and 16 (n=29)-month old Postn +/+ or Postn -/- mice were harvested. They were demineralised, reduced with NaBH4 and hydrolyzed in 6M hydrochloric acid at 110°C for 24 h. The concentration of immature (dihydroxylysinonorleucine, DHLNL and hydroxylysinonorleucine, HLNL) and mature (pyridinoline, PYD and deoxypyridinoline, DPD) crosslinks in bone extracts was measured by LC-ESI-MS. The bone femurs from the same mice were also submitted to a binding test to analyse their mechanical properties.

Results: As expected the concentration of immature crosslinks was lower in 16 compared to 4 month-old mice, whereas that of mature forms increased (Table). The bone content of both immature and mature crosslinks was lower in Postn -/- compared to Postn +/+ in the two age-groups, the difference reaching statistical significance for all molecules except for HLNL in older animals (table). In 4 month mice, the content of immature –but not mature- crosslinks was positively associated with ultimate stress (r spearman= 0.36, p=0.07 and r=0.36, p=0.08 for DHLNL and HLNL, respectively), although it failed to reach statistical significance. Conversely in 16 month mice mature –but not immature- crosslinks were positively associated with ultimate stress (r=0.45, p=0.021 and r=0.38, p=0.049 for PYD and DPD, respectively) and plastic energy (r=0.33 p=0.08 and r=0.39, p=0.044).

Conclusion: Deficiency in Postn is associated with decreased bone collagen crosslinks. These data suggest that in addition to its effects on bone formation/microstructure, Postn could modulate the properties of the organic bone matrix and thus its mechanical strength. The mechanisms, by which Postn is altering collagen crosslinking, e.g. processing and/or maturation, remain to be investigated.

Mice			Immature Crosslinks (mol/mol Collagen)		Mature Crosslinks (mol/mol Collagen)	
Age	Genotype	n	DHLNL	HLNL	PYD	DPD
4 months	Postn +/+	18	1.94 ± 0.37	0.61 ± 0. 10	0.190 ± 0.01	0.028 ± 0.005
	Postn -/-	15	1.50 ± 0.33*	0.46 ± 0. 07*	0.145 ± 0.03*	0.022 ± 0.004*
			-23%	-25%	-23%	-21%
16 months	Postn +/+	18	1.16 ± 0.21*	0.47 ± 0.09	0.31 ± 0.04*	0.040 ± 0.008*
	Postn -/-	11	0.94 ± 0.17*	0.41 ± 0.07	0.24 ± 0.02*	0.032 ± 0.006*
			-22%	-15%	-23%	-20%

* p < 0.001 vs Postn +/+ mice (Mann-Whitney test)

Table

***Disclosures: Evelyne Gineyts**, None.*

MO0098

Dynamic Loading Increases Apparent Elastic Modulus of Ex Vivo Trabecular Bovine Bone. Juan Vivanco[1], Everett Smith*[2], Sylvana Garcia-Rodriguez[3], Heidi Ploeg[3]. [1]University of Wisconsin, Material Science Program & Department of Mechanical Engineering, USA, [2]University of Wisconsin, USA, [3]University of Wisconsin, Department of Mechanical Engineering, USA

Although it is widely known that bone tissue responds to mechanical stimuli, the underlying biological response is still not completely understood. The ZETOS bone loading bioreactor system was used to test ex vivo bovine trabecular sternum in compression. The purpose of this study was to stimulate and monitor changes of apparent elastic modulus (Eapp) of viable trabecular specimens for 21 days. It was hypothesized that bone specimens (Loaded N=12) that were stimulated with a physiological load would demonstrate a greater increase of Eapp than bone specimens that were similarly prepared but not stimulated (control N=9). The response to load was examined by measuring Eapp. Trabecular bovine sternum bone was obtained from an 18 to 20 month animal free of disease and processed within 4 hr from the time of sacrifice. Twenty two trabecular bone cores of 5 mm height and 10 mm diameter were prepared under sterile conditions. Each trabecular bone core was placed inside a bone loading chamber with a DMEM culture medium maintained at 37℃ with a pH of 7.2-7.3 and perfused at 6.6 mL/hr. The medium was changed at 24 hr intervals; pH and pCO2 and pO2 were measured. During the 21 day study no contamination was observed in any bone core specimen. Two loading procedures were performed: 1) both treatment and control groups received a quasi-static load to determine Eapp on days 3, 10 and 21 (three repeats per specimen); and, 2) the treatment group were stimulated daily with a physiological load (waveform with maximum bulk strain of 4,000 με) applied twice per second for 100 cycles each day). All samples were allowed to equilibrate for 48 hr. Although there was an increase in Eapp in both groups, the treatment group presented a higher percent increase than the control. Table 1 exhibits the Eapp for both groups with their respective standard errors; and the change of Eapp from day 3 to 10, from day 11 to 21 days, and p-values between the treatment and control groups at each individual time point (fig. 1). Analysis of variance (ANOVA) demonstrated a significant overall difference (p-value < 0.05) between control and treatment groups. However, most of this change was in the first 7 days as there was no significant difference in rate of increase between groups during days 10 and 21.

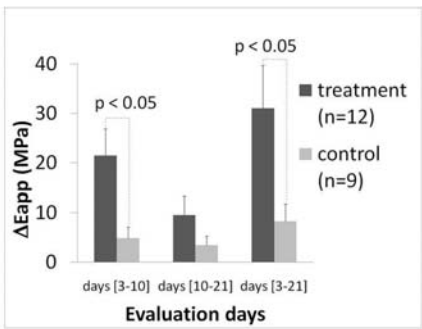

Figure 1: Change of the apparent elastic modulus Eapp (MPa)

Change of the apparent elastic modulus Eapp (MPa)

Table 1: Apparent Elastic Modulus, E_{app} (MPa) Its Change from Baseline

Group	Day	Mean (stand error)		ΔE_{app} (MPa)	p-value
Control	3	30.09 (7.70)	Days [3-10]:	4.87	
	10	34.96 (7.71)	Days [10-21]:	3.45	
	21	38.41 (8.76)	Days [3-21]:	8.32	
Treatment	3	50.77 (11.85)	Days [3-10]:	21.50	0.02
	10	72.27 (13.79)	Days [10-21]:	9.58	0.21
	21	81.85 (15.60)	Days [3-21]:	31.09	0.043

Note: P-values represent the difference between the control and treatment at each individual time point.

Apparent Elastic Modulus in MPa (Eapp) and its change from baseline

***Disclosures: Everett Smith**, None.*

MO0099

Femoral Three-Point Bending and Neck Shear in Male CD1 Mice Using the Bose ElectroForce 3300 System. Nancy Doyle*, Melanie Felx, Carle Geoffroy, Julie Plouffe. Charles River, Canada

Biomechanical strength testing of bones, considered the ultimate bone quality assessment, is a critical end-point in the evaluation of the safety and efficacy of test compounds. The purpose of this study was to assess precision and validate procedures for the biomechanical testing of mice femurs in 3-point bending and femoral neck failure using the Bose ElectroForce 3300 System, under GLP conditions.

Both femurs were collected from 6 CD1 male mice, 61 days old (approx 35 g) on the day of necropsy, and retained wrapped in saline soaked gauze and plastic wrap, and stored frozen at -20℃ until scanning and testing. Densitometry by peripheral quantitative computed tomography (pQCT) was measured at the expected 3-point bending fracture site (distal diaphysis). Both femurs underwent 3-point bending and femoral neck shear. After the 3-point bending testing was completed, the proximal end of the femur was embedded in a plastic cylinder filled with SAMPL-KWICK in an up-right ''single-legged'' position and load applied to the femoral head. Load and displacement data were collected using WinTest (version 4.1) software and biomechanics parameters derived.

Preliminary results for the 3-point bending test provided the following range of results: peak load 14 to 26 N, stiffness 44 to 111 N/mm and area under the curve (AUC) 6 to 14 N-mm as well as respective corrected parameters for specimen size, ultimate stress 702 to 1063 MPa, modulus 510 to 890 MPa and toughness 1278 to 2992 MPa. In addition, using linear regression analyses, a positive relationship between femur vBMC and peak load was obtained (r=72). Results obtained from the femoral neck testing provided the following range of results: for peak load 14 to 25 N, stiffness 53 to 144 N/mm and AUC 2 to 5 N mm. Results obtained from the left side were consistent with data obtained from the right side, supporting the reproducibility of the procedures. It was noted that peak load and parameters corrected for size: ultimate stress and modulus, were the least variable with approximately a %CV of 20% or less.

With respect to precision, these results were similar to tests performed in larger species, confirming that the current procedures used for the testing of mice femurs in 3-point bending and neck shear with the Bose ElectroForce 3300 System were adequate.

***Disclosures: Nancy Doyle**, None.*
This study received funding from: contract lab

MO0100

Indentation and Lift Generation Responses of Meniscus to Contact Loading of Various Speeds. David Burris[1], Vincent Baro[1], Liyun Wang*[2]. [1]Univ Delaware, USA, [2]University of Delaware, USA

Vincent Baro, David Burris, and Liyun WangCenter for Biomedical Engineering, Department of Mechanical Engineering, University of Delaware, Newark, DEBack-ground and Objective:Meniscus, a complex fibrocartilagenous tissue, plays important roles in load-bearing of the knee. Meniscus tear is implicated in the early development of osteoarthritis. Although meniscus contains a biphasic porous structure similar to that of cartilage, its in vivo behaviors under various loading conditions is not well characterized. The goal of this study was to characterize the mechanical behaviors of meniscus under various contact loading conditions. In particularly, we like to elucidate its indentation and lift generation response to various loading speed.-Methods:Using a custom micro-indenter, the mechanical behaviors of bovine menisci were determined.The hydrated meniscus explants (25 X 25 mm2) were indented up to 50 micrometers at various speeds to determine the effective elastic modulus and the equilibrium aggregate modulus. The spherical indenter (diameter 6.35 mm) was then moved reciprocally over 1.5 mm across the tissue at varying speeds to characterize lift generation. Articular cartilage explants from the same joints were similarly tested.Results:The biomechanical responses of meniscus to contact loadings differed from those of articular cartilage. The meniscus appeared to be less stiff than articular cartilage. In both indentation and lift generation experiments, we found that meniscus was less sensitive to loading/movement speed than articular cartilage.Discussion and

Conclusions:Our tests indicate that meniscus exhibits unique mechanical behaviors during joint loading and may account for its susceptibility to mechanical failures. We are exploring the mechanisms for meniscus' insensitivity to loading speed. Funding Acknowledgment:NIH grants (P20RR016458; RO1AR054385)

***Disclosures: Liyun Wang**, None.*

MO0101

Mapping Tibial Surface Strains Using 3D Stereo Optical System. Jonathan Hein*[1], Brian McMichen[1], Adam Stibbbe[2], Mehrdad Negahban[1], Diane Cullen[2], Joseph Turner[1], Mohammed Akhter[3]. [1]University of Nebraska, USA, [2]Creighton University, USA, [3]Creighton University Osteoporosis Research Center, USA

In vivo studies have shown that the bone adaptation response to mechanical stimulus or exercise is proportional to strains during loading. The purpose of this study is to present ex vivo tibial surface strains in three adult mouse genotypes representing HBM [high bone mass with LRP5 G171V mutation], n=5, WT [wild type, nontransgenic littermate n=4], and LRP5-KO [with Lrp5 gene knocked out KO-/-, n=4]. These genotypes represent a full range of bone mass and structural stiffness. We used a full field stereo optical measurement system (ARAMIS, GOM mbH, Germany) that provides tibial surface strain *ex vivo* (data from region of 1.5 to 4.5 mm proximal to the tibio fibular junction-TFJ). Along with quasi-static compression tests (Bose, MN), ARAMIS system provided optical 3D deformation analysis of tibial surfaces. Strain analysis with the ARAMIS system yields the equivalent of hundreds of strain gages on the surface. A set of compressive tibial loads in the longitudinal direction consist of 1, 2, 4 and 6N. Four tests were performed on each bone in order to create a 360 degree view in ARAMIS (example Figure). The average tibial surface strain was lowest in the HBM mice and highest in the KO mice (Table) for the same axial loads. These data are comparable to direct strain measurements and predicted values presented previously at ASBMR (2009 meeting). Data at 1 N may be prone to error due to the low magnitude of force and bone deformation. These data suggest that the tibial surface strains are sensitive to the structural stiffness. Smaller surface strains are measured in tibiae representing largest cross sectional moment of inertia [MOI] (tibiae from HBM mice have at least 30% greater MOI and KO 30% less than WT). These data suggest that the regional tibial strains mapped with the ARAMIS system (Figure) are comparable to the direct strain gage data at the region 1.5 to 4.5 mm proximal to TFJ. Both ARAMIS and the direct strain measuring technique can complement each other in providing reliable tibial surface strain analyses for compressive loading in small animal model of studying bone adaptation.

Table. Tibial strain (με) at lateral surface (1.5 to 4.5 mm proximal to TFJ segment) (Mean ± SD)

Load	HBM	WT	KO (-/-)
1 N	-32 ± 70	-314 ± 506	-280.03 ± 208
2 N	-119 ± 90	-395 ± 356	-483 ± 222
4 N	-268 ± 191	-545 ± 196	-763 ± 193
6 N	-479 ± 370	-639 ± 358	-837 ± 181

N-Newton load; microstrain (με)

TABLE

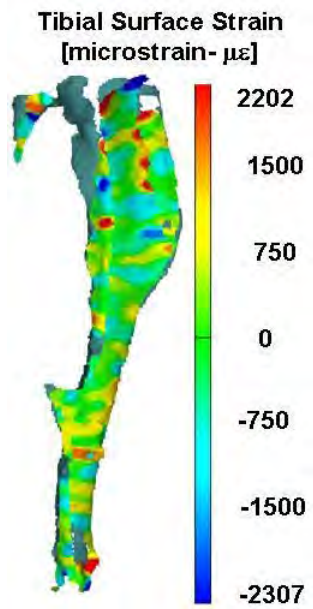

FIGURE

***Disclosures: Jonathan Hein**, None.*

MO0102

Physical Exercise Improves Bone Structural Parameters and Properties in Young Rats. Wagner Vicente*[1], Luciene dos Reis[1], Ana Paula Velosa[2], Rafael Graciolli[1], Charles Wang[3], Fabiana Graciolli[4], Keico Nonaka[3], Patricia Brum[5], Marilia Teixeira[6], Tatiana Fonseca[7], Wagner Dominguez[1], Walcy Teodoro[2], Vanda Jorgetti[8]. [1]Nephrology, School of Medicine, University of Sao Paulo, Brazil, [2]Rheumatology, School of Medicine, University of Sao Paulo, Brazil, [3]Physiological Sciences, Federal University of Sao Carlos, Brazil, [4]Nephrology, Medical School, University of Sao Paulo, Brazil, [5]School of Physical Education & Sport, University of Sao Paulo, Brazil, [6]University of Sao Paulo, Brazil, [7]Department of Anatomy, Institute of Biomedical Science, University of Sao Paulo, Brazil, [8]University of São Paulo, Brazil

This study investigated the effects of aerobic physical exercise, running on a treadmill, on the bone tissue of forty Wistar rats (21 females and 19 males), weighing between 200-300 g. The animals were divided into four groups: sedentary (10 females and 10 males) and trained (11 females and 9 males), during 12 weeks. Structural data, bone formation and resorption parameters were obtained from the histomorphometric analysis of the left femur. A mechanical test was performed on the right femur, in which maximal force, resilience and fracture load were analyzed. Quantitative real-time PCR (qPCR) was evaluated for type I collagen (COL I), osteoprotegerin (OPG), osteocalcin (OCN), alkaline phosphatase (ALP) and tartrate-resistant acid phosphatase (TRAP). Protein expression of COL I was also evaluated by means of the immunofluorescence technique. Results revealed that aerobic physical exercise significantly increased trabecular volume (BV/TV; $p<0.001$) between trained female and trained male. This increase was more accentuated in the females group than in that of the males ($p<0.001$). Trabecular thickness (Tb.Th; $p<0.001$), mineral apposition rate (MAR; $p<0.05$) and bone formation rate (BFR; $p<0.05$) increased in trained male. Eroded surface (ES/BR; $p<0.05$) and Osteoclast surface (Oc.S/BS; $p<0.004$) were increased in trained male than trained female. Physical exercise increased maximal force ($p<0.001$), resilience ($p<0.05$) and rigidity ($p<0.001$) mainly in trained male compared with trained female. We did not observe any change in the gene expression of bone formation proteins. However, TRAP by qPCR was decreased in trained animals ($p<0.001$). COL I expression in bone tissue increased ($p<0.01$) in trained male. Despite the fact that ES/BS and Oc.S/BS were increased in trained animals, their function reflected by TRAP was decreased. In conclusion, young rats of both genders submitted to aerobic physical exercise presented increased structural parameters. Maybe the increase of COL I expression, especially in males, contributed to modify bone mechanical proprieties.

***Disclosures: Wagner Vicente**, None.*

MO0103

Unloading-induced Suppression of B-lymphogenesis and Expansion of Peripheral Monocyte/macrophage Lineage Cells is Preserved in the Mice Deficient for Osteopontin. Yoichi Ezura*[1], Junji Nagata[2], Hiroaki Hemmi[2], Masashi Nagao[2], Takuya Notomi[3], Tadayoshi Hayata[4], Tetsuya Nakamoto[2], Masaki Noda[2]. [1]Tokyo Medical & Dental University, Medical Research Insititute, Japan, [2]Tokyo Medical & Dental University, Japan, [3]GCOE, Tokyo Medical & Dental University, Japan, [4]Medical Reserach Institute, Tokyo Medical & Dental University, Japan

Rodent tail-suspension experiment is a model to investigate unloading-induced bone loss in vivo. Previously, we have shown that osteopontin (Opn also known as Spp1) is required for unloading-induced bone loss. However, in this model, the cells expressing Opn could function not only in bone, but also in sympathetic nervous system or in the cells in blood circulation. Indeed, we have previously shown that the expression of Opn in the peripheral blood was significantly increased in the mice subjected to tail-suspension. The microarray analysis also indicated that tail-suspension suppressed expression of B-cell specific genes such as Ebf1, Cd19, and Cd72, in contrast to the up-regulation of genes related to monocytes/macrophage lineage cells such as Msr2, Mrc1, and Itgam were increased (29th annual meeting of the ASBMR, 2008). To examine if the causative changes in the bone marrow cells could be defined by analysis of gene expression in the bone marrow cells in this study, we examined bone marrow cells subjected to the tail-suspensioin for 2-weeks. Microarray analysis indicated the consistent suppression of the B-cell specific genes such as Ebf1, Cd19, and Cd72, in contrast to the increased expression of the T-cell receptor genes as well as the flt3l gene that is implicated to the phenomenon called ''peripheral T-cell expansion''. The expression levels of the monocytes/macrophage lineage cells were basically stable in the bone marrow cells, and the Opn showed only a weak trend to decrease, indicating that the relative increase of the Opn expression in the peripheral blood may be derived from the peripherally expanded monocyte/macrophage lineage cells. To test if the observed changes in the bone marrow and peripheral blood leukocyte fractions are dependent on the existence of the Opn, we analyzed peripheral blood and bone marrow cells of the Opn deficient mice subjected to tail-suspension by fluorescence activated cell sorting (FACS) analysis. Opn deficient mice subjected to tail-suspension showed comparable changes in the leukocyte fraction in both the peripheral blood and bone marrow to the wild type mice, while bone loss was reduced in OPN-deficient mice. Our observation suggests

that effects of tail-suspension on circulating osteopontin correlated with the change in bone mass, but not with the changes in leukocyte fraction.

***Disclosures: Yoichi Ezura**, None.*

MO0104

The Identification of the PTH Receptor in Human Osteoarthritic Chondrocytes. Hella Roachan[1], Antonio Segovia[1], Bodil Sondergaard[2], Michel Arnold[3], Markus John[4], Morten Karsdal*[1], Anne-Christine Bay-Jensen[2]. [1]Nordic Bioscience A/S, Denmark, [2]Nordic Bioscience, Denmark, [3]Novartis, Denmark, [4]Novartis Pharma AG, Switzerland

Osteoarthritis (OA) is the most common form of joint disease and a major cause of disability. PTH is known for its anabolic and catabolic effects on bone metabolism and is currently used to treat osteoporosis. Intermittent PTH administration stimulates bone formation by activation of the G-coupled parathyroid hormone receptor (PTHR1) on osteoblasts stimulating cAMP. Since both osteoblasts and chondrocytes originate from mesenchymal cells the hypothesis that chondrocytes respond anabolic to PTH treatment as well is investigated. Recent observations show that PTH may have direct effects on articular chondrocytes. During this study the presence of PTH receptor 1 (PTHR1) was investigated in human OA chondrocytes. A small fragment of PTHR1 was detected using qPCR and this verified by sequencing. Next, a nested PCR band at 2 Kb was detected by gel electrophoresis, potentially the target PTHR1 coding sequence. In order to produce enough amount of DNA material for sequencing, cloning of the PCR product was performed and sent for sequencing. These data show that PTHR1 is more than likely expressed in articular cartilage, but more evidence is required in order to verify the entire coding region of PTHR1 in human articular chondrocytes. These data support the notion that PTH has anabolic effect on cartilage.

***Disclosures: Morten Karsdal**, None.*

MO0105

A Novel Mutation of *PHEX* Gene in a Family with Hypophosphatemic Rickets. Laura Masi*, Francesco Franceschelli, Simone Ciuffi, Celestina Mazzotta, Gemma Marcucci, Loredana Cavalli, Antonietta Amedei, Alberto Falchetti, Caterina Fossi, Cristiana Casentini, Maria Luisa Brandi. Metabolic Bone Diseases Unit, Italy

X-linked hypophosphatemic rickets/osteomalacia (XLH) is a inherited disorder of phosphate (Pi) homeostasis characterized by renal phosphate wasting and hypophosphatemia, with inappropriately normal to low 1,25-dihydroxy vitamin D3 serum levels, normal serum concentration of calcium and bone deformity and rickets/osteomalacia. Mutations in PHEX gene (Xp22.2-p22.1). are responsible of this disease. PHEX encodes for an endopeptidase membre M13Zn-metalloproteinase family, involved in the regulation of phosphate homeostatis. PHEX inactivating mutations causes XLH. These mutation enable the accumulation of phosphaturic factors and/or mineralizzation inhibitors. In the present study we descrive a 2 years old boy referred to our Center, exhibiting clinical features of a clear hypophosphatemia [2.3 mg/dl (n.v.: 2.7-4.5)], normocalcemia [9.3 mg/dl (n.v.:8.6-10.3)], normal PTH circulating levels [44.8 pg/ml (n.v.:12-72)] normal values fo vitamin D [32 mg/ml (n.v.: 30-60)] and high levels of alkaline phosphatase [1055 mU/ml (n.v: 247-645)]. He showed astenia, muscle pain, bowed legs and cranial deformities. Due to the family history, the diagnosis of XLH was suspected. His mother had beend diagnosed with hypophosophatemic rickets and was of short stature and developed genu varum. A cousin and the grandfhater of the mother were affected by hypophosphatemic rickets with skeletal deformities mainly at the legs. The parents of our patients were not consanguineous. The patient and her parents underwent PHEX mutational analysis upon administration of an informed consent from (in case of minor patient signed by legal tutor). Genomic DNA has been extracted by peripheral blood leukocytes. The 22 exons and the intron-exon boundaries of PHEX have been investigated by PCR and direct –sequencing (ABI-Prism 3100) protocol. It has been identified a novel mutation of PHEX in the exon 1 at codon 2, GAA>TAA, causing a nucleotide change Glu/STOP. This nucleotide substitution has been never described on PHEX database (http://www.phexdb.mcgill.ca/). Finally, we are planning to use cellular models, either obtained from patients and engineered by transfection methods to evaluate the functionality of the mutated gene. These approaches will be helpful to better understand the molecular mechanism of PHEX action and could provide highlight for future targeted therapies.

***Disclosures: Laura Masi**, None.*

MO0106

High Phosphate Diet Accelerates Renal Glomerulus Damage in Type III Na-dependent Phosphate Transporter Overexpressing Rats. Sahoko Sekiguchi*[1], Shogo Asano[2], Megumi Shibata[1], Nobuki Hayakawa[2], Atsushi Suzuki[3], Mitsuyasu Itoh[2]. [1]Fujita Health University, Division of Endocrinology, Japan, [2]Fujita Health University, Devision of Endocrinology, Japan, [3]Fujita Health University Division of Endocrinology, Japan

Background : Phosphate (Pi) uptake at the cellular membrane is essential to maintain the cell activity because Pi has to be supplied for ATP synthesis. On the contrary, accumulating evidence suggests that Pi overload from the extracellular milieu would be stressful for the cells. We have constructed type III Pi transporter (Pit-1)-overexpressing rats (TG) and found the Pi-induced damage of filtration barrier at glomerulus in their kidney, resulting in the nephrotic syndrome. Method : In the present study, we fed normal (WT) and TG rats with 0.1% (low), 0.6% (normal) and 1.2% (high) Pi diet for three months since their 8th week of age. Results : After 1 month, the urinary protein level of TG rats taking high Pi diet (TG-HP) increased more than those taking other Pi diet in TG rats, and the massive proteinuria in TG-HP rats was more apparent until the end of the study. TG-rats taking low Pi diet (TG-LP) and those taking normal Pi diet (TG-NP) also showed proteinuria with less extent compared with TG-HP rats. Serum total cholesterol concentration in TG-HP rats increased more than TG-LP and TG-NP rats, although serum creatinine and Pi levels in TG-HP rats were same as those in the others. In addition, there was no deterioration of renal function or proteinuria in WT rats fed with low, normal and high Pi diet. Transmission electron microscopy (TEM) analysis showed that the glomerulus in the kidney of TG exhibits fusion and spread out of visceral epithelial cells (podocytes) and thickened basement membrane, and these change were the most prominent in TG-HP rats. However, low Pi-diet did not prevent glomerulus damage in TG rats. In conclusion, our findings further suggest that extracellular Pi damages filtration barrier in glomerulus in kidney.

***Disclosures: Sahoko Sekiguchi**, None.*
This study received funding from: Kyowa Hakko Kirin, Novo Nordisk, sanofi-aventis, Banyu Pharm and Ono Pharm

MO0107

Phosphate Independent Effects of Nuclear HMWFGF2 Isoforms on Bone Formation Invitro. Marja Marie Hurley*. University of Connecticut Health Center School of Medicine, USA

In humans, there are Fibroblast growth factor 2 (FGF2) high molecular weight (HMW) nuclear isoforms of 22, 23 and 24 kDa and a low molecular weight (LMW/18 kDa) FGF2 protein isoform. Mice over-expressing only HMW isoforms (HMWTg) in osteoblasts developed rickets/osteomalacia, hypophosphatemia and hyperphosphaturia, associated with increased fibroblast growth factor 23 (FGF23) in serum and increased FGF23 mRNA and protein in bone. Although several phosphatonins have been identified, FGF23 is the phosphatonin that regulates phosphate homeostasis and is responsible for phosphate wasting and the phenotypic changes observed in patients with X-Linked Hypophosphatemic rickets (XLH). Interestingly the bone phenotype of HMWTg mice is similar to human XLH and the Hyp mouse, a homologue of XLH.

The goal of the present study is to assess whether HMWFGF2 mediate phosphate independent effects on bone formation and the expression of other phosphatonins in vitro as well signaling pathway of HMWFGF2. Bone marrow stromal cells (BMSC) harvested from vector control and HMWTg were cultured for 7-21 days in osteogenic media. Cells were harvested at different time points to assess alkaline phosphatase positive (ALP) mineralized nodule formation by von-Kossa staining. Gene expression was determined by Q-RT-PCR and protein by Western blot. Total colony formation and ALP staining was increased in HMW cultures at 7 day. In contrast mineralized nodules and osteocalcin mRNA was markedly reduced in HMW cultures at 21 days. There was a significant increase in FGF2 and FGF23 mRNA at 7, 14 and 21 days in HMW cultures. The mRNA for the phosphatonins Mepe, Fgf7 and Sfrp-4 were also significantly increased between 14 and 21 days in HMW cultures. Assessment of the FGF/ FGFR/MAPK signaling pathway revealed increased FGFR1c mRNA and nuclear accumulation of FGFR1 protein in HMW cultures at 7 days. Phosphorylated ERK protein was increased in nuclear fractions from HMW at 7, 14 and 21 days. FGF23 protein accumulated in nuclear fractions of HMW cultures at 21 days.

We conclude that HMWFGF2 have phosphate independent effects on bone formation. These effects may be direct or be mediated via FGF23 or other phosphatonins. HMWFGF2 may signal via FGFR1C/FGF23/MAPK to inhibit bone formation in vitro.

***Disclosures: Marja Marie Hurley**, None.*

MO0108

Role of Processed FGF23 Fragments. Yuichiro Shimizu*, Tasuku Saito, Hisanori Suzuki, Seiji Fukumoto, Toshiro Fujita. University of Tokyo Hospital, Japan

FGF23 is a hormone that regulates phosphate and vitamin D metabolism by binding to Klotho-FGF receptor complex. Previous in vitro studies indicated that a

part of FGF23 protein is proteolytically cleaved between ^{179}Arg and ^{180}Ser by subtilisin-like proteases, and only full-length FGF23 has a biological activity to reduce serum phosphate and 1,25-dihydroxyvitamin D levels. Mutations in *GALNT3* gene which encodes an enzyme responsible for the initiation of mucin-type O-glycation cause familial hyperphosphatemic tumoral calcinosis (FTC). It has been shown that *GALNT3* gene product mediates the glycosylation at ^{178}Thr and prevents the processing of FGF23. Therefore, FGF23 protein is susceptible for the processing and there are increased FGF23 fragments in patients with FTC caused by mutations in *GALNT3* gene. However, previous reports showed that more than half of these patients had normal FGF23 values in the presence of frank hyperphosphatemia. These data suggested that the excessive amount of FGF23 fragments inhibited the action of intact FGF23. We have previously shown that about 30% of circulatory FGF23 is present in the processed form *in vivo* in the conditions other than FTC. Therefore, we have examined whether FGF23 fragments affect the activity of full-length FGF23 in the present study. R176Q mutant FGF23 protein is resistant to the processing and present almost entirely in full-length form. In contrast, T178A mutant FGF23 protein is susceptible for the processing and nearly completely cleaved between ^{179}Arg and ^{180}Ser. FGF23 activity was assessed by Klotho-dependent increase of promoter activity of *early growth response-1* (*Egr-1*) gene. Western blotting of conditioned media of cells expressing T178A and R176Q mutant FGF23 confirmed the susceptibility for, and resistance to the processing, respectively. R176Q mutant FGF23 increased *Egr-1* luciferase activity in a dose-dependent manner. T178A mutant FGF23 alone did not enhance *Egr-1* luciferase activity. However, T178A inhibited the activity of intact FGF23 when present in excess of intact FGF23. These result indicated that FGF23 fragments cannot signal through Klotho-FGF receptor complex by themselves. In contrast, excessive amount of FGF23 fragments inhibits the action of full-length FGF23. Therefore, it is possible that increased fragments of FGF23 contribute to the development of hyperphosphatemia and high 1,25-dihydroxyvitamin D in patients with mutations in *GALNT3* gene.

***Disclosures: Yuichiro Shimizu**, None.*

MO0109

Up-regulation of Stanniocalcin 2 Expression by the Abnormality of Klotho-Fgf23 Signaling and Inhibition of Phosphate-induced Calcification in Aortic Vascular Smooth Muscle Cells. Yuichiro Takei*[1], Hironori Yamamoto[2], Tadatoshi Sato[3], Masashi Masuda[4], Ayako Otani[4], Yutaka Taketani[4], Beate Lanske[5], Eiji Takeda[6]. [1]The University of Tokushima School of Medicine, Japan, [2]University Tokushima, Japan, [3]University of Harverd, USA, [4]University of Tokushima, Japan, [5]Harvard School of Dental Medicine, USA, [6]University of Tokushima School of Medicine, Japan

Ectopic calcification of soft tissues have severe clinical consequences especially when localized to vital organs such as heart, arteries and kidney. Mammalian stanniocalcin genes (STC1 and STC2) are glycoprotein hormones identified as the calcium and phosphate metabolism-related gene. It has been demonstrated previously that the mRNA expression of STCs are up-regulated in kidney of α−klotho mutant (kl/kl) mice indicating hypercalcemia, hyperphosphatemia, hypervitminosis D and ectopic calcification. In this study, to clarify the role of high-expressed STCs in kl/kl mice, we analyzed the expression and localization of STCs genes in kl/kl mice. Quantitative RT-PCR analysis firstly determined the renal mRNA expression of STC2 genes were significantly increased in both kl/kl mice and Fgf23-deficient mice having strikingly similar phenotypes. Interestingly, immunohistochemical analysis and von Kossa staining revealed the powerful expression of STC2 but not STC1 protein in the calcifying arterioles and tubular cells of kl/kl mouse kidney. Moreover, STC2 was also localized in cardiac and aortic calcifying cells. In vitro analysis using A-10 rat aortic vascular smooth muscle cells (VSMCs), the mRNA levels of STC2 were time-dependently increased by phosphate as well as that of osteocalcin, osteopontin and Pit-1, a member of the type III sodium-dependent phosphate transporter. Surprisingly, STC2 knockdown with a small interfering RNA and over-expression indicated acceleration and inhibition of the phosphate-induced calcification in A-10 cells, respectively. These results suggest that the up-regulation STC2 gene by the abnormality of klotho-FGF23 signaling may contribute to inhibit the ectopic calcification.

***Disclosures: Yuichiro Takei**, None.*

MO0110

Adrenergic Receptor Regulates Anabolic Action of Constitutively Active Form of PTH/PTHrP Receptor Signaling. Ryo Hanyu*[1], Gerard Karsenty[2], Tadayoshi Hayata[3], Tetsuya Nakamoto[1], Takuya Notomi[4], Henry Kronenberg[5], Yoshitomo Saita[6], Hiroaki Hemmi[1], Masashi Nagao[1], Masaki Noda[1], Yoichi Ezura[7], Shu Takeda[8]. [1]Tokyo Medical & Dental University, Japan, [2]Columbia University, USA, [3]Medical Reserach Institute, Tokyo Medical & Dental University, Japan, [4]GCOE, Tokyo Medical & Dental University, Japan, [5]Massachusetts General Hospital, USA, [6]Juntendo University, Department of Ortopedics, Japan, [7]Tokyo Medical & Dental University, Medical Research Insititute, Japan, [8]Keio University, Dept. of Nephrology, Endocrinology & Metabolism, Japan

Osteoporosis is one of the major issues in health care and further development of effective treatment is needed. Parathyroid hormone is anabolic to bone while the mechanism of its action is still not fully understood. Here, we examined the role of adrenergic receptor, a key molecule involved in sympathetic tone regulation. Although sympathetic tone suppresses bone mass, beta 2 adrenergic receptor (beta 2 AR) deficiency unexpectedly suppressed intermittent PTH injection (int-PTH)-induced increase in BMD and bone volume. Beta 2 AR deficiency suppressed both int-PTH-induced increase in bone resorption and decrease in bone formation. Anabolic action of osteoblast-specific PTH/PTHrP receptor (PPR) signaling on bone mass in transgenic mice was suppressed by beta 2 AR deficiency. This effect was based on beta 2 AR deficiency suppression of caPPR-induced increase in both bone formation and bone resorption in vivo. Beta 2 AR knock down in osteoblasts suppressed ca PTH receptor-induced activation of transcription through cyclic AMP response element (CRE). Constitutively active PTH-receptor signaling in osteoblasts enhanced the expression of steady-state levels of a clock gene, Per-1 in vivo. Beta 2 AR deficiency specifically suppressed caPTH receptor-induced Per-1 gene expression in double mutant mice. Knockdown of Per-1 suppressed caPTH-receptor-induced activation of CRE-dependent transcription in osteoblasts. These data indicated that PTH signaling in osteoblasts requires the presence of beta 2 AR for its anabolic action in bone at least in part through the regulation of Per-1 dependent transcriptional events.

***Disclosures: Ryo Hanyu**, None.*
This study received funding from: PTH and adrenergic signaling

MO0111

BindingCapacity to the G Protein-uncoupled PTH/PTHrP Receptor Conformation (R^0) Determines Efficacy of Calcemic Actions of PTH/PTHrP Analogs *In Vivo*. Masaru Shimizu*[1], Makoto Okazaki[1], Tatsuya Tamura[1], Thomas Gardella[2], John Potts[2], Yoshiki Kawabe[1]. [1]Chugai Pharmaceutical Co., Ltd., Japan, [2]Massachusetts General Hospital, USA

PTH and PTHrP bind to a common G-protein coupled receptor, the PTH/PTHrP receptor. (PTH1R). We have previously shown that whereas PTH and PTHrP bind similarly to the G protein-coupled PTH1R conformation (RG), PTH has a greater capacity to bind the G protein-uncoupled receptor conformation (R^0). We have also demonstrated that a PTH/PTHrP hybrid analog, M-PTH(1-14)/PTHrP(15-36) (M=Ala^{1,3,12},Gln^{10},Arg^{11,19},Trp^{14}), binds to R^0 with higher affinity than does PTH(1-34), and produces more prolonged calcemic response in rats. These observations have led us to speculate that the affinity with which a PTH or PTHrP analog binds to R^0 determines the duration and extent of that ligand's actions in vivo. To test this hypothesis, and to further delineate the ligand determinants of R^0 binding affinity, we first examined the calcemic action of [Ile^5]-PTHrP(1-36), shown previously to have higher R^0 binding affinity than PTHrP(1-36) in vitro. When injected intravenously in rats, [Ile^5]-PTHrP(1-36) showed more prolonged calcemic action than did PTHrP(1-36). The two analogs showed similar rates of disappearance from the circulation (t1/2 < 3-4 minutes), indicating that the prolonged action of [Ile^5]-PTHrP(1-36) was independent of pharmacokinetics. We next examined the effects in vivo of twelve other PTH/PTHrP hybrid analogs in which the N-terminal portions were derived from either native or M-PTH, and the C-terminal portions from PTHrP(1-36). Several of the hybrid analogs exhibited higher R^0 binding affinities than did PTH(1-34), and each of these showed prolonged calcemic actions, with M-PTH(1-14)/PTHrP(15-36) showing the highest R^0 affinity, and most prolonged calcemic action. Overall, the area-under-the-curve values for the in vivo calcemic responses correlated well with R^0 binding affinities ($R = 0.86$), but not with RG binding affinities ($R = 0.33$). These results indicate that R^0 affinity is determined by critical regions at the carboxyl terminal region of the ligand, optimally by PTHrP(15-36), together with potency-enhancing N-terminal substitutions. Controlling binding affinity to R^0 appears to be a promising strategy for identifying and optimizing long-acting PTH analogs especially for the treatment of patients with hypoparathyroidism.

***Disclosures: Masaru Shimizu**, Chugai Pharmaceutical Co., Ltd., 3*
This study received funding from: Chugai Pharmaceutical Co., Ltd.

MO0112

Distinct ß-arrestin- and G protein-dependent Signaling Pathways in Bone Revealed by Biased Agonism and Genomic Pathway Analysis. Stuart Maudsley[1], Shaoxi Liao[2], Ling Yuan[2], Robert Lefkowitz[2], Louis Luttrell[3], Diane Gesty-Palmer*[2]. [1]NIH-NIA, USA, [2]Duke University, USA, [3]Medical University of South Carolina, USA

Biased GPCR agonists are orthosteric ligands that possess pathway-selective efficacy, activating or inhibiting only a subset of the signaling repertoire of their cognate receptors. In vitro, D-Trp12,Tyr34-bPTH(7-34) (PTH-ßarr), a biased agonist for the type 1 parathyroid hormone receptor (PTH1R), antagonizes receptor-G protein coupling but activates arrestin-dependent signaling. In vivo, both PTH-ßarr and the conventional agonist PTH(1-34) stimulate anabolic bone formation. In this study we sought to understand how two PTH1R ligands with markedly different in vitro efficacy could elicit similar in vivo responses. Employing Affymetrix gene arrays and metabolic pathway analysis we compared the transcriptional profiles generated by G protein- and ß-arrestin-dependent PTH1R agonists in calvarial bone from mice treated for 8 weeks with vehicle, PTH-ßarr or PTH(1-34). Treatment of wild type mice with PTH-ßarr affected metabolic pathways that promote expansion of the osteoblast pool, notably cell cycle regulation, Akt/PI3K, p53 and ATM signaling. These responses were absent in ß-arrestin2 null mice, identifying them as downstream targets of ß-arrestin2-mediated signaling. In contrast, PTH(1-34) primarily affected pathways classically associated with enhanced bone formation, including collagen synthesis and matrix mineralization. PTH(1-34) actions were less dependent on ß-arrestin2, as might be expected of a ligand capable of G protein activation. These results illustrate the uniqueness of biased agonism and demonstrate that functional selectivity can be exploited to change the quality of PTH1R efficacy.

***Disclosures: Diane Gesty-Palmer**, None.*

MO0113

Effects of Fasting on Endogenous Parathyroid Hormone (PTH) Levels in Cynomolgus Monkeys. Caroline Ruh*[1], Nancy Doyle[2], Philip Oldfield[3], Patrick Bednarek[4], Susan Y. Smith[1]. [1]Charles River Laboratories, Canada, [2]Charles River, Canada, [3]Charles River Laboratories Montreal, Canada, [4]Cytochroma Inc, Canada

PTH is an important endocrine regulator of calcium and phosphorus concentrations and is routinely assessed in studies affecting bone metabolism. The objective of this study was to determine the effects of fasting on endogenous PTH levels in Cynomolgus monkeys.

Blood samples were taken from 6 male and 6 female Cynomolgus monkeys ranging in age from 1.5 to 3.5 years, on four occasions under fasted or non-fasted conditions and serum PTH levels were compared. Samples were analyzed using an ELISA kit (catalogue No. 60-3100) by Immutopics, Inc. All animals had access to a standard certified pelleted commercial primate food (2050C Certified Global 20% Protein Primate Diet: Harlan) twice daily and food supplements (certified treats and/or fresh fruit) daily. Blood samples were taken in the late afternoon, at approximately the same time of day on each sampling occasion, with or without a 7-hour pre sampling food deprivation period. The first set of samples was collected under fasted conditions (Day 1), the second was collected one week later under non-fasted conditions (Day 8), the third was collected approximately 4 weeks later under non-fasted conditions (Week 6) and the last sample was collected ten days later under fasted conditions (Week 7).

Day 1 samples resulted in quantifiable results for all animals with mean values of 56.78 pg/mL (SD 14.05) and 34.20 pg/mL (SD 12.83) for males and females, respectively. Day 8 samples resulted in values below the lower level of quantitation (LLOQ = 13.2 pg/mL) for 4/6 males, with a mean value of 23.15 pg/mL (SD 8.98) for the remaining 2 individuals while 4/6 females had results below LLOQ, with a mean value of 23.55 pg/mL (SD 1.90) for the remaining 2 individuals. The Week 6 samples resulted in quantifiable results for 5/6 males, with a mean value of 46.28 pg/mL (SD 28.82) while 4/6 females had quantifiable results, with a mean value of 43.75 pg/mL (SD 11.98). The last samples taken at Week 7 resulted in quantifiable results for all animals with mean values of 82.93 pg/mL (SD 14.12) and 57.38 pg/mL (SD 27.97) for males and females, respectively. Results below LLOQ were only obtained on both occasions where animals had access to food prior to blood sampling (Day 8 and Week 6), with lower mean values for PTH levels when compared to Day 1 and Week 7. Increased PTH levels following a 7-hour fasting period relative to the unfasted state provided more consistent and quantifiable values for data interpretation.

***Disclosures: Caroline Ruh**, None.*
This study received funding from: Cytochroma Inc

MO0114

Gender Specific Differences in the Skeletal Response and Endogenous PTH Levels to Continuous PTH in Mice Lacking the IGF-I Receptor. Muriel Babey*[1], Yongmei Wang[2], Hashem Elalieh[2], Daniel Bikle[2]. [1]Endocrine Research Unit, USA, [2]Endocrine Research Unit, Division of Endocrinology UCSF, USA

Intermittent administration of parathyroid hormone (PTH) stimulates bone formation, whereas continuous exposure of PTH induces bone loss. After demonstrating that IGF-I signaling is a crucial mediator of the anabolic actions of intermittent PTH, we have investigated the role of IGF-I signaling in mediating the catabolic actions of continuous PTH. We examined the degree to which continuous PTH (1-34) affects murine bone structure and endogenous PTH levels in FVB/N mice lacking the IGF-I receptor in mature osteoblasts (IGF-IR OBKO) in comparison to wildtype (WT) mice. μCT analysis of distal femurs showed that 24% of trabecular bone was lost in female PTH infused WT mice compared to vehicle infused WT mice. In female IGF-IR OBKO mice compared to female WT mice, bone volume/tissue volume (BV/TV), trabecular number (Tb.N) and trabecular thickness (Tb.Th) were increased by 43%, 21% and 8%, respectively, but PTH infusion had little or no effect on trabecular bone parameters. In male PTH infused WT mice, trabecular bone loss was minimal compared to vehicle infused WT mice. Male IGF-IR OBKO mice showed a 65% decrease in trabecular bone mass compared to WT, but PTH in these mice had little further catabolic effects in trabecular bone. The endogenous PTH levels in female mice were substantially higher by 3.4 fold than in male mice and were not suppressed by PTH infusion. In contrast, male mice showed a marked suppression of endogenous PTH levels by 95% by PTH infusion compared to vehicle. We conclude that in this strain of mice there is a remarkable gender difference in endogenous PTH levels and skeletal responsiveness to PTH as well as in the impact of IGF-IR on bone per se and its response to PTH.

***Disclosures: Muriel Babey**, None.*

MO0115

Regulation of Osteocyte Proliferation and Sclerostin Expression by PTHrP. Leonard Deftos*[1], Lynda Bonewald[2], Su Tu[1], Douglas Burton[1]. [1]Veterans Administration San Diego Healthcare System & University of California, USA, [2]University of Missouri - Kansas City, USA

Background: The signaling pathways between each bone cells are complex and involve many factors, including parathyroid hormone-related protein (PTHrP) and sclerostin (Sost). PTHrP has pleiotropic effects on the growth and differentiation in virtually every cell in the body. Many of these actions have been attributed to the amino terminal portion of PTHrP (1-34) that interacts with PTH / PTHrP receptor (PTH1R), but there are other forms of PTHrP that derive from isoform expression, proteolytic processing events and posttranslational modifications to generate peptides of distinct biological function. In bone, PTHrP is produced by preosteoblasts and bone marrow cells where it acts on preosteoblasts and mature osteoblasts through the PTH1R to stimulate osteoblast differentiation, inhibit osteoblast apoptosis, and inhibit osteocyte Sost expression. Sost, a secreted protein produced by osteocytes has been shown to inhibit osteoblast proliferation, impair mineralization by osteoblasts and to stimulate osteoblast apoptosis by interfering with Wnt and BMP signaling. In this study, we evaluated the direct effects of PTHrP, including non-amino terminal PTHrP fragments, on osteocyte proliferation and osteocyte Sost expression.

Methods: The MLO-A5 and MLO-Y4 osteocyte cell lines were treated for 8 and 2 days with PTHrP peptides (1 - 100 nM) for the cell proliferation and Sost expression studies, respectively, and compared to vehicle control treatment using MTT assays, qPCR, and westerns.

Results: Based on our preliminary results, PTHrP 1-34 and 1-86 significantly increased ($P < 0.05$) the proliferation of the MLO-A5 and MLO-Y4 cells. Conversely, PTHrP 107-138 significantly decreased ($P < 0.05$) MLO-Y4 cell growth but had no significant effect on the growth of the MLO-A5 cells. Treatment with PTHrP 107-138 significantly increased (2-fold) SOST mRNA expression in both osteocyte cell lines. The effects of PTHrP 1-34 and 1-86 on SOST mRNA demonstrated significant increases ($P < 0.5$) in the MLO-A5 cells but no significant changes were observed in the MLO-Y4 cells. The western results recapitulated the qPCR results.

Conclusions: PTHrP's actions on bone cells in orchestrating skeletal metabolism are best appreciated for osteoblasts and osteoclasts. We have demonstrated that PTHrP and its derived peptides can also regulate osteocyte proliferation and function. The modulation of osteocyte growth and Sost expression by PTHrP peptides identifies an additional pathway for bone homeostasis. Exploring this pathway in detail can identify both basic and clinical relevance for the effects of PTHrP on osteocytes.

***Disclosures: Leonard Deftos**, None.*

MO0116

Role of Osteoclasts in the COX-2-Mediated Inhibition of PTH-Stimulated Osteoblastic Differentiation *In Vitro*. Shilpa Choudhary*, Olga Voznesensky, Manshan Xu, Cynthia Alander, Lawrence Raisz, Carol Pilbeam. University of Connecticut Health Center, USA

Parathyroid hormone (PTH) is a potent stimulator of prostaglandin (PG) production via induction of cyclooxygenase-2 (COX-2) expression and PGs may modulate bone responses to PTH. Anabolic effects of intermittent PTH are increased in COX-2 knockout (KO) mice compared to wild type (WT) mice. This study examined the inhibitory effects of COX-2 on PTH-stimulated osteoblast (OB) differentiation *in vitro*. Bone marrow stromal cells (BMSCs) were cultured from COX-2 WT and KO mice and from EP2 or EP4 receptor WT and KO mice, all in a CD-1 background. PTH (10^{-8} M) was added at each media change. OB differentiation was measured by alkaline phosphatase and osteocalcin gene expression, analyzed by real time PCR, and by alizarin red staining for mineralization at d 14 or 21 of culture. PTH treatment during the first week of culture increased OB differentiation in cultures from COX-2 KO mice, but not in cultures from WT mice unless they were treated with nonsteroidal anti-inflammatory drugs to inhibit PG production. Exogenous PGE_2 (10^{-10} to 10^{-7} M) stimulated OB differentiation in COX-2 KO cultures when given alone but inhibited the stimulatory effects of PTH. Osteoclasts (OCs) were formed during the first week in both COX-2 WT and KO BMSC cultures in response to PTH. Blocking OC formation with osteoprotegerin (OPG), which interferes with RANKL/RANK interactions, had no effect on PTH-stimulated OB differentiation in COX-2 KO cultures. However, OPG reversed the inhibition of PTH-stimulated OB differentiation by exogenous PGE_2 and endogenous PGs in COX-2 WT BMSCs. Addition of COX-2 WT bone marrow macrophages (BMMs) to KO BMSCs was sufficient to inhibit the PTH stimulatory effects. PTH stimulated OB differentiation in EP4 receptor KO cultures but not in EP2 receptor KO cultures. Our results indicate that stimulatory effects of PTH on OB differentiation *in vitro* are inhibited by endogenous PGs produced by COX-2 and exogenous PGE_2 and that this inhibition is mediated by cells of the OC lineage and may involve activation of the EP4 receptor. These results suggest a novel role for PGs and non-resorbing OCs in the effects of PTH and might lead to new protocols for enhancing the therapeutic effects of intermittent PTH.

***Disclosures: Shilpa Choudhary**, None.*

MO0117

Role of PTH in Klotho Knockout Mice. Quan Yuan*[1], Michael Densmore[1], Tadatoshi Sato[1], Hiroaki Saito[1], Reinhold Erben[2], Beate Lanske[1]. [1]Harvard School of Dental Medicine, USA, [2]University of Veterinary Medicine, Austria

Klotho has been identified as the cofactor of FGF23/FGFR signaling. Klotho knockout mice exhibit a similar phenotype as *Fgf23*$^{-/-}$ mice, including growth retardation, severe hyperphosphatemia, hypercalcemia, and high serum $1,25(OH)_2D_3$ levels, abnormal bone mineralization, and decreased serum PTH levels. Our most recent study demonstrated that deletion of *PTH* may partially rescue the phenotype of *Fgf23*$^{-/-}$ mice. Here, in order to examine the role of PTH in *Klotho*$^{-/-}$ mice, we generated *Klotho*$^{-/-}$/*PTH*$^{-/-}$ double mutants and compared their phenotype to the one of wild-type, *Klotho*$^{-/-}$ and *PTH*$^{-/-}$ single knockout mice. Despite already low serum PTH levels in *Klotho*$^{-/-}$ mice, complete ablation of *PTH* in these mice resulted in larger, heavier, and more active double mutants when compared to *Klotho*$^{-/-}$ littermates. Biochemical analyses showed that serum phosphate levels in double mutants were even higher than the already high serum phosphate levels in *Klotho*$^{-/-}$ mutants. In contrast, the hypercalcemia in *Klotho*$^{-/-}$ mice was normalized in double mutants, suggesting that extremely high serum phosphate levels alone, in absence of both PTH and high serum Ca are not as detrimental to the health of the animals. We also found that renal NaPi2a expression in double mutants was further elevated, suggesting enhanced phosphate reabsorption in these mice. Moreover, both serum $1,25(OH)_2D_3$ and FGF23 levels were lower in compound mutants relative to *Klotho*$^{-/-}$ mice, but were still significantly elevated compared to WT or *PTH*$^{-/-}$ mice. Histological examination of soft tissues including lung, kidney, and aorta showed that ectopic calcification seen in *Klotho*$^{-/-}$ mice persisted in double mutants, which may be explained by the increased serum calcium/phosphate product. Finally, deletion of *PTH* rescued skeletal abnormalities of *Klotho*$^{-/-}$ mice seen by improved bone mineral density, increased length of tibiae and elevated volume of mineralized trabecular bone. In summary, our results suggest that the very low serum PTH levels found in *Klotho*$^{-/-}$ mice may contribute to the abnormalities in these mice. Further studies are required to unveil the effects of PTH in *Klotho*$^{-/-}$ mice.

***Disclosures: Quan Yuan**, None.*

MO0118

Bone Quality Characterization of a Novel Preclinical Model of Mixed Osteolytic/Osteoblastic Vertebral Metastasis. Lisa Wise-Milestone*[1], Margarete Akens[2], Marc Grynpas[3], Albert Yee[1], Brian Wilson[4], Cari Whyne[1]. [1]Sunnybrook Health Sciences Centre, Canada, [2]Sunnybrook Research Institute, Canada, [3]Samuel Lunenfeld Research Institute, Canada, [4]Ontario Cancer Institute, Canada

Breast, prostate, lung, and renal cancers are the most common primary tumours to metastasize to bone, with the vertebral column being the most frequently affected site. Spinal metastases often show patterns of mixed disease with irregular areas of enhanced bone growth (osteoblastic) in addition to areas of thinning bone (osteolytic). The underlying bone quality (structural, mechanical and material properties) of these mixed skeletal metastases has not yet been fully characterized, which is necessary in order to assess the efficacy of potential treatments. Purpose: The objective of this study is to characterize the bone quality and tumour burden of a new rat model of mixed osteolytic/osteoblastic spinal metastases. Methods: An immune compromised rat model of mixed vertebral metastases was generated via intracardiac injection of luciferase transfected Ace-1 canine prostate cancer cells. Age-matched control and tumour-bearing rats were sacrificed 21 days after tumour injection, and excised lumbar spines imaged with micro computed tomography to assess bone micro-architecture. Half of the spines were processed for histology to quantify tumour burden (parathyroid hormone-related protein) osteoclast activity (tartrate resistant acid phosphatase), osteoid formation (Goldner's Trichrome), collagen organization (picrosirius red) and turnover rate (in vivo calcein and xylenol orange fluorochrome labels). Remaining samples were stored for subsequent biomechanical testing. Results: Ace-1 metastatically-involved vertebrae exhibit significant areas of extreme osteolytic bone destruction (Figure 1; arrowhead), evident through significantly reduced trabecular bone volume (28 $\pm$ 7% bone volume vs. 51 $\pm$ 2% bone volume in controls). This decreased bone volume is due to increased osteoclast activity (2.8 $\pm$ 1.5% osteoclast activity per bone area) in tumour-bearing vertebrae compared to controls (0.4 $\pm$ 0.1% osteoclast activity per bone area). In addition to increased osteoclast activity, tumour-bearing vertebrae exhibit increased osteoid volume per bone volume (7.9 $\pm$ 3.0% vs. 3.1 $\pm$ 0.8% in controls), most strikingly on the periosteal surface of the cortical shell (Figure 1; arrow). Conclusions: Mixed osteolytic/osteoblastic spinal metastases exhibit enhanced yet decoupled bone remodelling properties, leading to decreased vertebral bone quality. This model will be used in subsequent studies focusing on therapies targeted at ablating tumour issue and improving bone quality.

Figure 1: Ace-1 metastatically involved vertebra (Goldner's Trichrome stained)

***Disclosures: Lisa Wise-Milestone**, None.*

MO0119

Breast Cancer Cell Conditioned Media Decreases Release of CXCL5 by Osteoblastic Cells. Karis Chin-quee*, Vikram Sathyendra, Alayna Loiselle, Henry Donahue. The Pennsylvania State University College of Medicine, USA

We previously demonstrated that exposure of osteoblastic hFOB1.19 cells (hFOB) to conditioned media (CM) from MDA-MET (bone metastatic-specific derivative of MDA-MB-231 breast cancer cells) resulted in the secretion of factor(s) from hFOB that functioned as a chemoattractant(s) for MDA-MET cells. In the current study, we quantified heterotypic (MDA-MET to hFOB) and homotypic (hFOB to hFOB) cell-cell adhesion in response to exposure to MDA-METCM vs hFOBCM. hFOB cells treated with MDA-METCM had decreased cell-cell adhesion for homo and heterotypic interactions compared with hFOB treated with hFOBCM. We hypothesized that a soluble factor(s) is associated with these changes in adhesion. A cytokine array was done on CM from hFOB cells exposed to hFOBCM, MDA-METCM and CM from HTERT-HME1, a normal mammary epithelial cell line. The cytokine which, demonstrated the greatest change in levels, (a decrease), in CM from hFOB exposed to MDA-METCM was CXCL5 (Epithelial Neutrophil Attracting Factor, ENA-78). The relative levels of CXCL5 were: HTERTCM treated>hFOBCM treated (2.4 fold)>MDA-METCM treated (3 fold). This finding was confirmed by assessing steady state CXCL5 mRNA levels by quantitative RT-PCR. Thus, the relative levels of CXCL5 mRNA were:HTERTCM treated>hFOBCM treated (29 fold) >MDA-METCM treated (41 fold). We also examined mRNA levels for another epithelial factor negatively associated with tumor aggressiveness, Pigment Epithelial Derived Factor (PEDF) and found it followed a similar differential expression pattern in the hFOB cells. CXCL5 is associated with an intact, continuous cell layer and is a marker of innate immunity against invading pathogens. PEDF, an anti-inflammatory factor, may be involved in pathways that preserve cell-cell adhesion and by extension, an intact cell barrier. Our data suggest that the decrease in CXCL5 and PEDF expression, as a result of exposure to MDA-METCM, is associated with decreased cell-cell adhesion and a less intact or leaky cell layer. The decreased adhesion would facilitate increased migration of breast cancer cells over osteoblastic cells and a discontinuous osteoblastic cell layer would facilitate extravasation, rendering osteoblastic bone lining cells, which cover >90% of bone extracellular matrix, more susceptible to invasion by metastatic breast cancer cells. These results suggest that increasing CXCL5 levels in the metastatic microenvironment may be a novel therapeutic approach to breast cancer bone metastasis.

***Disclosures: Karis Chin-quee**, None.*

MO0120

Effects of Different Bisphosphonates on the Apoptosis and Proliferation Rate of Breast Cancer Cell Lines. Regina Ebert*[1], Jutta Meissner-Weigl[2], Sabine Zeck[2], Ludger Klein-Hitpass[3], Nadja Raaijmakers[2], Tilman D Rachner[4], Peggy Benad[4], Lorenz Hofbauer[5], Franz Jakob[2]. [1]University of Wuerzburg, Orthopedic Center for Muskuloskeletal Research, Germany, [2]University of Wuerzburg, Germany, [3]University Hospital Essen, Germany, [4]Technical University of Dresden, Germany, [5]Dresden Technical University Medical Center, Germany

Bisphosphonates (BP) are used for the treatment of benign and malignant bone diseases such as osteoporosis, bone metastases and hypercalcemia. They inhibit bone resorption and maintain bone mass. Amino-BP show differences in their inhibitory potency of the target enzyme farnesyl pyrophosphate synthase, their binding affinity to hydroxyl apatite, and their degree of suppressing hypercalcemia. The main target of BP are osteoclasts but mesenchymal and tumor cells may also be affected, depending on the concentration and exposure time. Recent clinical studies indicate a benefit in survival and tumor relapse with the supportive treatment of ER-positive breast cancer using zoledronate (ZA), but their putative anti-tumor activity is under debate. We already reported osteogenic effects of ZA in mesenchymal stem cells (1) and analyzed the mechanism of apoptosis induction in MCF-7 and MDA-231 breast cancer cells (2). MDA-231 and MCF-7 breast cancer cells were treated for 3 h (pulse treatment) and 72 h (permanent treatment) with 5 – 100 µM ibandronate (Ibn), alendronate (Aln), risedronate (Ris) and ZA. Apoptosis and proliferation rates were determined after 72 h. To block BP effects, cells were cotreated with geranylgeranyl-pyrophosphate (GGPP). Microarray hybridizations (Affymetrix HG U133Plus2.0) were performed to identify putative target genes in MCF7 cells and the expression of candidate genes were validated by PCR. Both, permanent exposure and pulse treatment with ZA induced apoptosis and inhibited proliferation in MDA-231 cells. Permanent treatment of MDA with ZA, Ibn, Aln and Ris showed differences on proliferation inhibition and apoptosis induction. ZA was most potent, followed by Aln and Ibn, while Ris showed only minimal or no effects. In MCF-7 cells, BP were not able to induce apoptosis, while permanent treatment with either BP suppressed proliferation, which could also be observed in ZA pulse treated cells. Co-treatment using GGPP blocked the antiproliferative and antiapoptotic effects of ZA in MDA-231 cells but showed no effect in MCF-7 cells. Microarray analyses revealed 75 upregulated probesets and 111 downregulated probesets. We show here that different BP have variable efficacy of apoptosis induction and proliferation inhibition in breast cancer cells. Pulse treatment with ZA, which may mimic the clinical situation of intravenous ZA application, was also effective. In our experiments ZA was most potent to induce apoptosis in estrogen receptor (ER) negative MDA-231 cells. As GGPP treatment could not block ZA induced effects in MCF-7 cells, molecular mechanisms either upstream of farnesyl pyrophosphate synthase or independent of the mevalonate pathway might be involved. The demonstrated effects of BP on growth and apoptosis of tumor cells may be the basis for their clinical potency in the adjuvant treatment of breast cancer.

1. Ebert R et al., 2009 Bone 44:858-864
2. Rachner TD et al., 2010 Cancer Lett 287:109-116.

***Disclosures: Regina Ebert**, None.*

MO0121

Genome-Wide Reciprocal Modulation of Estrogen and Runx2 Signaling in Breast Cancer . Nyam-Osor Chimge*[1], Sanjeev Baniwal[1], Omar Khalid[2], Alice E. Kohn-Gabet[1], Gerhard A. Coetzee[1], Baruch Frenkel[1]. [1]University of Southern California, USA, [2]Univeristy of Southern California, USA

Runx2, a lineage-specific master transcription factor, and estrogen receptor α (ERα) are known to play crucial roles in both bone metabolism and carcinogenesis. We recently demonstrated that ERα physically interacts with Runx2 and that estradiol (E2) affected the expression of a few preselected Runx2 target genes. The purpose of the present study was to characterize the influence of E2 on the Runx2 transcriptome genome wide, and at the same time pursue the possible reciprocal influence of Runx2 on E2/ERα-regulated genes. To model the aberrant expression of Runx2 during tumor bone metastasis, we engineered MCF7 breast cancer (BCa) cells so that they conditionally express Runx2 in response to doxycycline (dox) at levels normally seen in osteoblasts. The cells were treated with dox, E2, or both agents, and then subjected to microarray analysis using HumanRef-8 Expression BeadChip representing well-defined 24,500 transcripts. The results revealed a total of 458 Runx2-responsive genes and 1,126 E2-responsive genes (⩾1.5-fold change, $p<0.001$). About half the Runx2-responsive genes were also E2-responsive, suggesting a tight interconnection between Runx2 and ERα signaling. In most cases, the Runx2 effects were counter-regulated by E2 treatment, thus reducing the total number of Runx2-responsive genes by 39% (from 458 to 281). Runx2 overexpression reduced the number of E2-responsive genes by 18% (from 1,126 to 919 genes). Consistent with these observations, expression data analysis of primary breast tissues from 200 patients with invasive breast carcinoma showed negative correlation (r=-0.2, p=0.003) between the Runx2 and E2 regulated genes as defined by our results. Remarkably, our microarray analyses revealed a set of 48 genes, where E2 flipped the Runx2 responsiveness either from stimulation to repression (26 genes) or from repression to stimulation (22 genes), although the individual responses to Runx2 and E2 were similar. These phenomena were confirmed by RT-qPCR analysis of selected genes. Finally, ChIP assays of four of these genes, NPNT, HS3ST3A1, MAOA and HEY2 showed occupancy by Runx2 and ERα only when cells were co-treated with both dox and E2, but not by each separately. Understanding the complex cross talk between estrogen and Runx2 signaling, a potentially crucial aspect of hormone carcinogenesis and possibly other endocrine disorders, may ultimately impact the development of improved SERMs and other novel therapeutic strategies.

***Disclosures: Nyam-Osor Chimge**, None.*

MO0122

Heel Ultrasound can Assess Maintenance of Bone Mass in Women with Breast Cancer. Gabrielle Langmann*, Karen Vujevich, Donna Medich, Megan Miller, Subashan Perera, Susan Greenspan. University of Pittsburgh, USA

Postmenopausal women with breast cancer on aromatase inhibitors (AIs) are at increased risk for bone loss and fractures. Bisphosphonates are known to prevent bone loss in women on or off AIs. While bone mineral density (BMD) can be assessed by conventional dual energy absorptiometry (DXA), little information is available on changes in bone mass assessed by portable heel ultrasound, which can be performed at a routine oncology office visit as opposed to DXA. To examine if heel ultrasound could assess changes following bisphosphonate therapy in women with breast cancer, we performed a secondary analysis of a two-year, double-blind, placebo-controlled, randomized clinical trial in 87 newly postmenopausal women, status post chemotherapy for nonmetastatic breast cancer. This included 43 patients randomized to once weekly risedronate (RIS) and 44 patients randomized to placebo (PBO). All received calcium and vitamin D if dietary intake was insufficient. Outcomes included the percent change in heel ultrasound (QUS-2 ultrasonometer, Quidel Corp, Mountainview, CA) by broadband ultrasound attenuation (BUA, dB/MHz) and conventional BMD (g/cm^2) assessed by DXA of the spine, total hip and femoral neck (Hologic Discovery, Hologic Inc, Bedford, MA).

Results: At baseline the mean age was 50 years and 49% were classified as normal, 48% had low bone mass and 2% had osteoporosis. 13% of women were on AIs at randomization and 44% at 24 months. Over 24 months, heel ultrasound bone mass remained stable in women on RIS (Table). In comparison, women on PBO had a decrease of $5.2 \pm 1.3\%$ ($p<0.05$). Total hip and femoral neck BMD assessed by DXA decreased in the PBO group ($p<0.05$) and remained stable with RIS. BMD at the spine remained stable in both groups. Heel ultrasound was moderately associated with BMD at the total hip (r=0.50), femoral neck (r=0.40) and spine (r=0.46), all $p<0.001$.

Conclusion: In women with breast cancer on or off aromatase inhibitors, RIS helps maintain skeletal integrity as assessed by heel ultrasound. Heel ultrasound is associated with bone mineral density at other major axial sites and may be used to follow skeletal health in these women.

Table: Percent Change from Baseline (mean ± SE)

	Heel U/Si	Total Hip BMD‡	Femoral Neck BMD‡	Spine BMD
PBO	-5.2 ± 1.7*	-1.6 ± 0.4*	-1.6 ± 0.7*	-1.2 ± 0.7
RIS	-0.6 ± 1.3	0.9 ± 0.6	-0.0 ± 0.6	0.4 ± 0.6

*p<0.05 change from baseline, ‡ p<0.05 PBO vs RIS

Table

***Disclosures: Gabrielle Langmann**, None.*
This study received funding from: Procter and Gamble

MO0123

Membrane Estrogen Signaling via ERα36 Leads to Crosstalk among Pathways Associated with Cell Survival and Osseous Metastases of Breast Cancer. Reyhaan Chaudhri*, Natalia Cuenca, Rene Olivares-Navarrete, Zvi Schwartz, Barbara Boyan. Georgia Institute of Technology, USA

Estrogen receptor status, particularly ERα, can determine breast cancer diagnosis and treatment. Three alternatively spliced variants of ERα have been identified: ERα66, ERα46, and ERα36. We previously reported that HCC38 breast cancer cells, commonly cited as ERα-null, are negative for ERα66 or ERα46, but positive for ERα36. We also found that activation of PKC by 17β-estradiol (E2) occurs through ERα36, which localizes in the plasma membrane. However, the physiological effects of this rapid response are not well understood. The purpose of this study was to determine the downstream effects of membrane-associated signaling of E2 via ERα36 in HCC38 cells. We hypothesized that membrane-initiated rapid signaling of E2 can enhance cell proliferation and expression of factors that promote cancer cell metastasis, particularly to bone. To evaluate our hypothesis, E2BSA treatment of HCC38 cells was performed in the presence or absence of ERα36 antibody for 24 hours, and DNA synthesis was measured by [^{3}H]-thymidine incorporation. Cells were treated with chelerythrine to inhibit PKC, and MTT and DNA fragmentation were measured after 24 hours. Cells were then treated with E2-BSA in the presence or absence of ERα36 antibody, and expression of Snail1 and RANKL was quantified by qRTPCR after 12 hours. Chelerythrine caused a dose-dependent decrease in cell viability by MTT. Cells also exhibited a dose-dependent increase in DNA fragmentation in response to chelerythrine, suggesting that inhibition of PKC by chelerythrine leads to an increase in apoptosis. E2BSA caused an increase in cell proliferation and treatment with ERα36 antibody blocked this effect, indicating that rapid signaling of E2 through ERα36 enhances proliferation of HCC38 cells. Cells treated with E2BSA showed increased expression of Snail1 and RANKL, and this was blocked by ERα36 antibody. Snail1 is a crucial factor for migration of cancer cells from their primary tumors. RANKL increases osteoclastogenesis and, consequently, bone resorption, thereby creating a fertile environment for recruitment of migrating cells. Our results show that expression of factors that may specifically be associated with breast cancer metastasis to bone can be enhanced by estrogen. ERα36 may thus be a key mediator in crosstalk of rapidly-induced E2 signaling pathways that may lead to enhanced aggressiveness of breast tumors

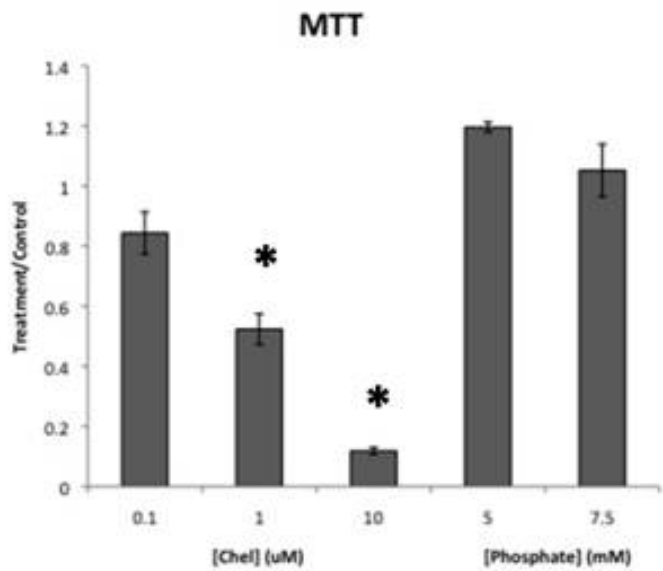

Figure 1

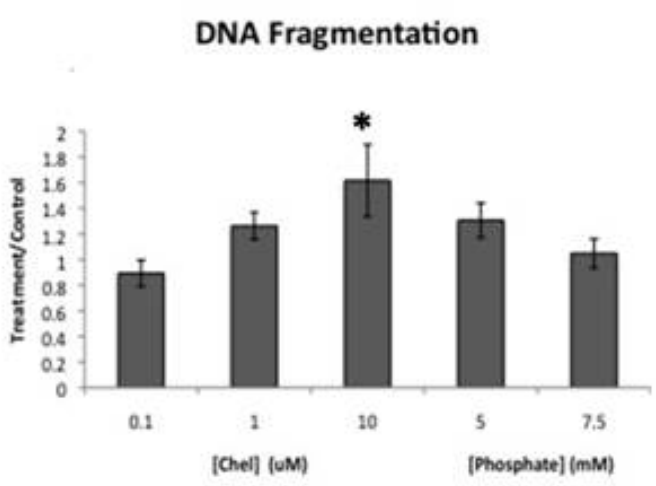

Figure 2

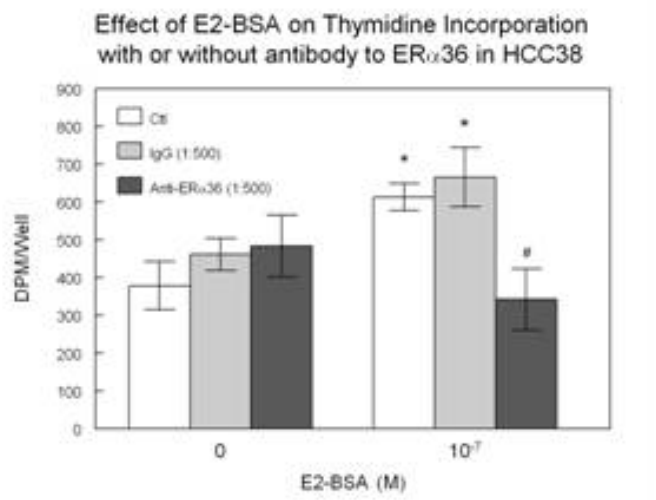

Figure 3

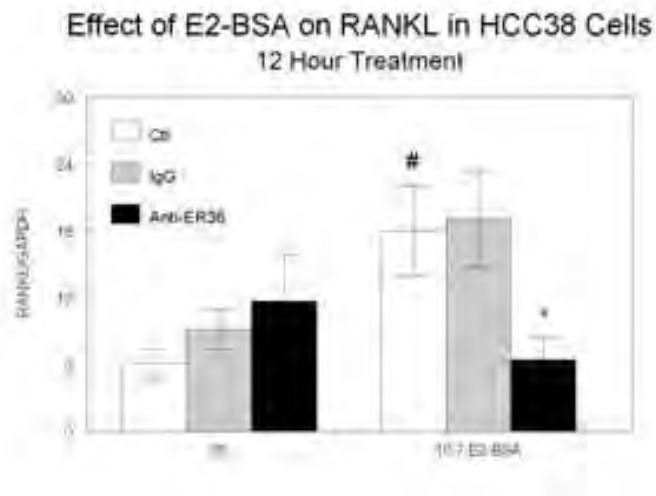

Figure 4

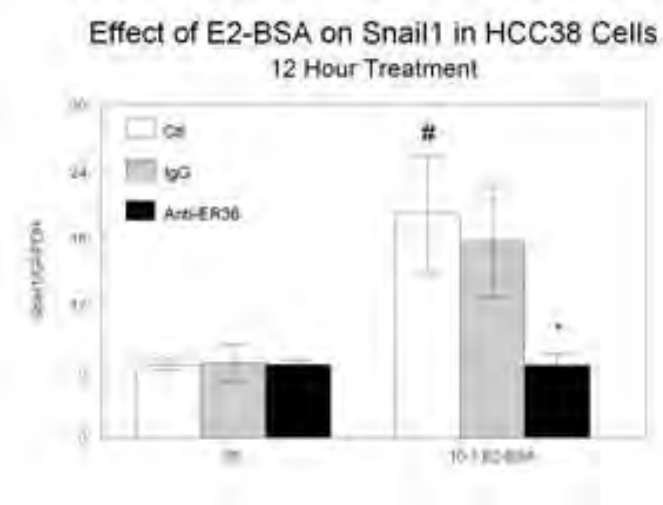

Figure 5

***Disclosures: Reyhaan Chaudhri**, None.*

MO0124

Osteocyte-derived FGF23 Acts on Bone-Metastatic Breast Cancer Cells to Increase Resistance to 1,25-dihydroxy-Vitamin D. Pierrick Fournier[1], Erik Imel[2], John Chirgwin*[1]. [1]Indiana University, USA, [2]Indiana University School of Medicine, USA

FGF23 is an endocrine hormone, uniquely secreted by osteocytes, regulating phosphate homeostasis and vitamin D metabolism by stimulating kidney cells, which express FGF receptor plus the specific co-receptor, klotho, and respond by rapid induction of the transcription factor EGR-1. Breast cancer cells also express functional klotho (Wolf et al, Oncogene 27: 7094, 2008), but responsiveness to FGF23 was not reported, while several case reports describe increased serum FGF23 concentrations in patients with tumor in bone. We report molecular responses of breast cancer cells to recombinant FGF23, which parallel those seen in the kidney.

MCF7 human breast cancer cells cause osteoblastic metastases in nude mice and express klotho and the FGF receptor 1iiic isoform. The cells were treated in triplicate with 100ng/ml recombinant human (rh)FGF23 (R&D Systems) and analyzed by real-time PCR. EGR-1 mRNA increased 18X at 1hr ($p< 0.0001$) and returned to baseline by 2 hrs. Expression of mRNA encoding the vitamin D-inactivating 24α-hydroxylase, CYP24A1, increased 10X at 2 hrs ($p<0.005$) and 6X at 4hrs ($p<0.05$), returning to baseline at 8hrs. There was little change in tumor cell expression of 1α-hydroxylase, CYP27B1, which converts 25-hydroxy-vitamin D to the active 1,25-dihydroxy metabolite. Treatment of MCF7 cells with 100nM 1,25-dihydroxy-vitamin D3 for 6 days caused 90% inhibition of growth by MTT assay. Addition of 100ng/ml rhFGF23 caused a 215% increase in cell number ($p<0.05$), despite co-treatment with 1,25-dihydroxy-vitamin D3. This response was not seen with MDA-MB-231 breast cancer cells, which express very low klotho. We found that several tumor lines which cause osteoblastic metastases had very high klotho expression, suggesting that FGF23/klotho signaling may contribute to osteoblastic metastases through unknown downstream mediators.

PTH receptor ligands, such as PTHrP, increase production of FGF23 by osteocytes, while other factors important in the bone-metastatic microenvironment, including hypoxia and TGFβ, can activate EGR-1, which is increased in metastatic breast and prostate cancer cells. The data suggest that a local FGF23/klotho/EGR-1 signaling axis may sustain a novel vicious cycle of bone metastases, and may be a novel target for bone-specific therapeutic intervention against metastatic breast cancers, such as with FGF23-neutralizing antibodies.

***Disclosures: John Chirgwin**, None.*

MO0125

Osteoimmunology of Breast Cancer Bone Metastasis: Possible Mechanisms and Therapeutic Approaches. Anandi Sawant, Diptiman Chanda, Jonathan Hensel, Selvarangan Ponnazhagan*. The University of Alabama at Birmingham, USA

Osteolytic bone metastasis is common among carcinomas of the breast, lung, thyroid and kidney. Dissemination of the primary tumor to the bone triggers the production of osteolytic cytokines and growth factors that not only result in osteoclast activation but also promotes the growth of tumor cells and immune suppression in the bone microenvironment. Thus, understanding the influence and interaction of metastasizing cancer cells with cells of the skeletal system and the immune system will provide clues towards designing preventive and therapeutic strategies for osteolytic bone metastasis.

Towards this goal, mice were injected with 10^5 osteolytic mouse breast cancer cell line 4T1, expressing firefly luciferase via intra-cardiac route. Mice were sacrificed when bone metastasis was observed. Immunophenotyping and intracellular staining was performed on cells obtained from the bone marrow to enumerate the various immune cells by flow cytometry. Micro-CT and histological analysis were performed on femur and tibia. Results of this study indicated that with increased bone metastasis, there was a significant increase in plasmacytoid dendritic cell (pDC) population in the bone, which resulted in increased Th2 response through CD40/CD40L interaction and IL-3 production. The number of pDC and CD4T cells producing osteolytic cytokines IL-3, IL-15 and IL-17 increased with increased tumor burden in the bone. Micro-CT and histological analysis of bone showed significant destruction of femur and tibia.

The significance of this finding was further confirmed by depleting pDC population in vivo which led to a significant decrease in the tumor burden and absence of bone metastasis. Depletion of pDC population also increased Th1 response and decreased levels of osteolytic cytokines. Collectively, the data suggest that pDC play a pivotal role in bone metastasis of the breast cancer cells by skewing Th1 response to Th2 during progressive stages of cancer dissemination to the bone. Thus, depletion of pDC during cancer progression may provide a therapeutic opportunity and further may be combined as an adjuvant to conventional therapies.

***Disclosures: Selvarangan Ponnazhagan**, None.*

MO0126

Prevention of Androgen Deprivation Therapy-Induced Bone Loss and Fractures in Men with Non-Metastatic Prostate Cancer: a Systematic Review and Meta-analysis. Adrian Lau*[1], Ophir Vinik[1], Shabbir Alibhai[2], George Tomlinson[2], Angela Cheung[2]. [1]University of Toronto, Canada, [2]University Health Network, Canada

Background: Androgen deprivation therapy (ADT) for non-metastatic prostate cancer has been shown to induce bone loss and increase fracture risk. We conducted a systematic review and meta-analysis to evaluate the efficacy of different pharmacologic agents used in the prevention of ADT-induced bone loss.

Methods: We searched MEDLINE (1950 to September 2009) for original English-language articles of randomized controlled trials of therapy that reported outcomes of bone mineral density (BMD), bone turnover markers or fractures in men with prostate cancer on medical ADT or who had orchiectomy. BMD sites analyzed included lumbar spine (LS), total hip (TH), and femoral neck (FN). Bone turnover markers analyzed included serum bone-specific alkaline phosphatase (bone ALP), urinary collagen type I cross-linked N-telopeptide (NTX), and urinary deoxypyridinoline (D-PYR). Dersimonian and Laird random-effects models were used to compute summary estimates of the effect of different pharmacologic agents on BMD and bone turnover markers at 6 and 12 months as compared to controls.

Results: Of 2,171 potentially relevant citations, we identified and included 12 trials involving 2,556 men. Mean age was 74 years, and 84% were Caucasian. Eleven trials included men on luteinizing hormone releasing hormone agonists, 2 included men on non-steroidal anti-androgens, 4 on complete androgen blockade, and 6 with men who had orchiectomy. Nine trials examined bisphosphonates, 2 examined selective estrogen receptor modulators (SERMs), and 1 examined denosumab as therapy. Compared to controls, men on ADT treated with bisphosphonates and denosumab showed increases in BMD at 6 and 12 months, while men treated with SERMs showed increases in BMD at 12 months (Table). Bisphosphonate therapy decreased bone turnover markers at 6 and 12 months. There was insufficient fracture data in studies with bisphosphonates and SERMs; however, the study on denosumab showed a decreased cumulative incidence of new vertebral fractures with denosumab at 36 months [1.5% vs. 3.9% (p=0.006)].

Conclusion: Pharmacologic therapy with bisphosphonates, SERMs or denosumab is effective in preventing ADT-induced bone loss in men with non-metastatic prostate cancer. Denosumab decreased vertebral fractures in this population. More studies are required to examine the effect of bisphosphonates and SERMs on fractures.

Table: Changes in BMD and Bone Turnover Markers as compared to controls (95% confidence interval)

			Bisphosphonates	SERMs	Denosumab
BMD	LS	6 months	+4.2% (+3.2%, +5.2%)		+3.3% (+3.0%, +3.7%)
		12 months	+6.2% (+5.3%, +7.1%)	+2.3% (+1.4%, +3.1%)	+4.9% (+4.5%, +5.3%)
	TH	6 months	+1.1% (+0.5%, +1.8%)		+1.9% (+1.7%, +2.1%)
		12 months	+2.8% (+2.1%, +3.6%)	+2.8% (+1.1%, +4.5%)	+3.0% (+2.7%, +3.3%)
	FN	6 months	+0.9% (-0.02%, +1.8%)		+1.6% (+1.2%, +2.0%)
		12 months	+2.9% (+2.1%, +3.8%)	+1.6% (+0.7%, +2.6%)	+2.6% (+2.2%, +3.0%)
Bone Turnover Markers	Bone ALP	6 months	-31% (-41%, -21%)		
		12 months	-44% (-55%, -33%)		
	NTX	6 months	-52% (-71%, -34%)		
		12 months	-60% (-77%, -43%)		
	D-PYR	6 months	-38% (-70%, -7%)		
		12 months	-50% (-85%, -16%)		

Table: Changes in BMD and Bone Turnover Markers as compared to controls (95% confidence interval)

***Disclosures: Adrian Lau**, None.*

MO0127

Role of Tumor-derived OPG in Supporting Cancer Growth within Bone Tissue. Marc Ryser*[1], Nilima Nigam[2], Svetlana Komarova[3]. [1]Department of Mathematics & Statistics, McGill University, Canada, [2]Department of Mathematics, Simon Fraser University, Canada, [3]McGill University, Canada

The roles of RANKL as a key osteoclast stimulator and OPG as osteoclast inhibitor are firmly established. During metastases to bone, breast cancer cells are known to produce PTHrP, which stimulates RANKL production by osteoblasts, which in turn simulates osteoclastogenesis. Moreover, systemic application of OPG has been shown to prevent bone destruction during cancer metastasis to bone. However, several facts have been established, which apparently disagree with this model: a) expression of OPG by cancer cells has been shown to significantly increase local osteolysis, and b) high circulating OPG levels in prostate cancer patients predict increased bone metastases. To assess potential differences between tumor-derived and bone-derived OPG, we have used previously developed mathematical model that describes changes in time and space in RANKL and OPG concentrations and in bone cell numbers. We have introduced in the model tumor cells, which were able to produce RANKL or OPG at variable levels. In addition, we varied the bone tissue levels of RANKL and OPG. Osteoclast activation and movement were affected by the level and gradient of RANKL respectively. Osteoclast function resulted in changes in bone mass, and the growth of tumor cells was assumed to occupy all the space free of bone tissue. We have found that increase in the level of RANKL in the bone tissue significantly increased osteoclast activation, bone loss and tumor growth, which was prevented by systemic application of OPG. Next, we assumed that OPG is produced by tumor cells and diffuses through the bone tissue. We have found that depending on its level, tumor-derived OPG may act as a stimulator or inhibitor of osteoclastic bone resorption. At moderate expression values, OPG acts to reinforce the RANKL gradient by removing the RANKL in the back of the cutting cone. As a result, the cutting cone moves faster and resorbs more bone, thus supporting tumor growth. At high levels of OPG production by tumor cells, diffusing OPG overtakes osteoclastic resorption front, removing RANKL required for osteoclast stimulation, and thus inhibiting bone destruction and tumor growth. Thus, our data demonstrate how the establishment of the RANKL gradient critical for osteoclast movement can be supported by localized production of OPG by tumor cells, resulting in apparent paradox of known osteoclast inhibitor OPG acting as a stimulator of tumor-induced bone osteolysis.

***Disclosures: Marc Ryser**, None.*

MO0128

Targeted Inhibition of GLI2 Blocks Cancer Bone Disease I*n Vivo*. Rachelle Johnson*[1], Mai Nguyen[2], Susan Padalecki[3], Barry Grubbs[3], Alyssa R. Merkel[1], Babatunde Oyajobi[3], Gregory Mundy[1], Julie Sterling[1]. [1]Vanderbilt University Medical Center, USA, [2]Vanderbilt University, USA, [3]University of Texas Health Science Center at San Antonio, USA

Breast cancer remains the second leading cause of cancer deaths in women, mainly due to its propensity to metastasize to distant organs such as lung and bone. Once tumor cells have metastasized to bone, they secrete osteolytic factors including Parathyroid Hormone-related Protein (PTHrP), which is mediated upstream by the Hedgehog signaling molecule GLI2. PTHrP inhibition by neutralizing antibody prevents tumor-induced bone destruction, while over-expression of GLI2 in tumor cells *in vivo* increases osteolysis. Given that PTHrP inhibition prevents tumor-induced osteolysis *in vivo* and that downstream GLI2 over-expression enhances cancer bone disease, we hypothesized that GLI2 inhibition *in vivo* may elicit anti-osteolytic effects in a breast cancer model. MDA-MB-231 cells stably transfected with a GLI2-Repressor (GLI2-Rep) construct significantly reduced endogenous PTHrP mRNA expression by real-time RT-PCR (73.63%), but did not alter tumor cell proliferation. Furthermore, mice inoculated with MDA-GLI2-Rep by intracardiac injection exhibited a significant inhibition in the number and size of osteolytic lesions by 41.19% by ex-vivo μCT. Due to the success of the GLI2-Rep construct *in vivo*, we desired to move toward a more translational approach to GLI2 inhibition, and therefore chose to target GLI2 through the use of small molecule inhibitors. Since GLI2 expression is up-regulated in osteolytic tumor cells, we used the MDA-MB-231 intracardiac model of bone metastasis, and first treated these mice with the Hedgehog signaling antagonist cyclopamine. However, cyclopamine had no effect on tumor burden or osteolysis *in vivo*, due to the lack of expression of the Hedgehog signaling receptor Smoothened. Since GLI2 inhibition was proven ineffective at the extracellular level, we therefore moved to specific GLI inhibition utilizing the small molecule inhibitor GANT58, a known inhibitor of GLI-mediated transcription. GANT58 induces a GLI conformational change, which compromises DNA binding. We found that GANT58 significantly inhibited PTHrP mRNA expression (62.57%) by real-time RT-PCR and promoter activity (84.66%) *in vitro*. Efforts are currently underway to target Gli2 by GANT58 in bone *in vivo*. Taken together, these data suggest that inhibition of GLI2 by small molecule inhibitors is a potential therapeutic avenue to treat breast cancer bone metastasis.

***Disclosures: Rachelle Johnson**, None.*

MO0129

The Early Effect of Aromatase Inhibitors on Bone Metabolism and Bone Density in Postmenopausal Women with Breast Cancer: An Interim Analysis. Pamela Taxel*, Faryal Mirza, Pamela Fall, Richard Feinn, Susan Tannenbaum. University of Connecticut Health Center, USA

Aromatase Inhibitors (AIs) are effective for secondary prevention of postmenopausal breast cancer and are first-line treatment of hormone-sensitive breast cancer. Reduction in estradiol (E2) levels by these medications leads to substantial bone loss, as reported in clinical trials. Antiresorptive medications prevent this bone loss, but they have frequent side effects and expense. Thus, treating all women receiving AIs with bisphosphonates might not be the most prudent approach. We hypothesized that women who demonstrate high bone turnover in the first 3 to 6-months on treatment, will have greater bone loss. The current study evaluated women with normal or moderately low bone mass during their first year of treatment with anastrozole or letrozole to determine if early changes in bone turnover markers correlate with bone loss at one year. We present an interim analysis of the first 12 women who have completed the study.

Hormones including E2 and sex hormone binding-globulin (SHBG) and bone turnover markers including type-1 procollagen peptide (P1NP), urine N-terminal collagen crosslinks (UNTX) and serum C-telopeptide collagen crosslinks (sCTX) were measured at baseline, 1, 3, 6 and 12 months. Bone Mineral Density (BMD) was measured at baseline, 6 and 12 months at the Lumbar spine (LS), Femoral Neck (FN) and Total Hip (TH) using a Lunar DXA (Prodigy). L-spine and Total hip BMD decreased significantly by 2% and 1.4% ($p<0.05$ respectively) at 6- months and by 3.4% and 2.0% ($p<.01$ and $p<.05$, respectively, at 12 months). E2 levels decreased from BL values (P=.03), as did SHBG although not significant. sCTX and PINP increased significantly from BL to 12 months, $p < .001$, p=.003, respectively), along with a trend for increase of UNTx (p=.096). Vitamin D increased from a BL of 33 to 42 ng/ml at 12 months due to supplementation. The higher the % increase in vitamin D at 6-months, the lower the % increase in UNTX at 3-months (p=.009), and the less the decline of BMD at the total hip (p for trend = .09).

We conclude that women receiving AIs for breast cancer show bone loss at the spine and hip during the first year of therapy. The data suggests an interaction between bone turnover markers, vitamin D and BMD; however, further analysis of these parameters in the complete study group is necessary to determine if these relationships remain and thus can identify those women at highest risk of bone loss.

***Disclosures: Pamela Taxel**, Amgen, 8; Novartis, 8*

MO0130

Anticancer Efficacy of Apo2L/TRAIL is Retained in the Presence of High and Biologically Active Concentrations of Osteoprotegerin I*n Vivo*. Irene Zinonos[1], Agatha Labrinidis[1], Michelle Lee[1], Vasilios Liapis[1], Shelley hay[2], Vladimir Ponomarev[3], Peter Diamond[4], David Findlay[1], Andrew Zannettino[4], Andreas Evdokiou*[1]. [1]University of Adelaide, Australia, [2]Royal Adelaide Hospital, Australia, [3]Sloan-Kettering Cancer Center, USA, [4]IMVS, Australia

Osteoprotegerin (OPG) is a secreted member of the TNF receptor superfamily, which binds to the ligand for receptor activator of nuclear factor kB (RANKL) and inhibits bone resorption. OPG can also bind and inhibit the activity of the TNF-related apoptosis inducing ligand (Apo2L/TRAIL), raising the possibility that the anticancer efficacy of soluble Apo2L/TRAIL may be abrogated in the bone microenvironment where OPG expression is high. In this study we used a murine model of breast cancer growth in bone to evaluate the efficacy of recombinant soluble Apo2L/TRAIL against intratibial tumours, which were engineered to overexpress native full-length human OPG.

In vitro, OPG-overexpressing breast cancer cells were protected from Apo2L/TRAIL-induced apoptosis, an effect that was reversed with the addition of soluble RANKL or neutralizing antibodies to OPG. In vivo, mice injected intratibially with cells containing the empty vector developed large osteolytic lesions. In contrast, OPG overexpression preserved the integrity of bone and prevented breast cancer–induced bone destruction. This effect was primarily due to the complete absence of osteoclasts in tibiae of mice inoculated with OPG transfected cells, confirming the biological activity of the transfected OPG in vivo. Despite the secretion of supra-physiological levels of OPG, treatment with Apo2L/TRAIL resulted in complete responses with strong growth inhibition of both empty vector and OPG overexpressing intratibial tumours. While Apo2L/TRAIL-induced apoptosis may be abrogated in vitro by OPG overexpression, the in vivo anticancer efficacy of recombinant soluble Apo2L/TRAIL is retained in the bone microenvironment where biologically active OPG is present at high concentrations.

***Disclosures: Andreas Evdokiou**, None.*

MO0131

Bone Mineral Content Deficits Are Present in Childhood Cancer Survivors. Lynda Polgreen*[1], Anna Petryk[1], Andrew Dietz[1], Leisenring Wendy[2], Pam Goodman[2], Lyn Steffen[1], Donald Dengel[1], K. Scott Baker[2], Alan Sinaiko[1], Julia Steinberger[1]. [1]University of Minnesota, USA, [2]Fred Hutchinson Cancer Research Center, USA

Purpose: Childhood cancer survivors (CCS) frequently have poor growth, hormonal deficiencies, and altered body composition; however the impact on bone acquisition in CCS remains unclear. The objectives of this study were to assess whole body bone mineral content (WBBMC) and lumbar spine bone mineral content (LBMC) and to identify factors that may effect bone mineral content (BMC) in CCS, using their healthy siblings as a control group.

Methods: WBBMC, LBMC, lean body mass (LBM), and percent body fat were measured by dual-energy x-ray absorptiometry (DXA) in CCS $\geq$ 5 years after diagnosis and healthy sibling controls; both groups aged 9 to 18 years. Anthropometrics, sexual development, and bone age were assessed on all subjects; steroid exposure was assessed on all CCS. Multivariable linear regression with generalized estimating equations and robust variances to account for intra-sibling correlations was utilized to evaluate the relation of anthropometrics, body composition, endocrine function, and steroid exposure to BMC, adjusted for chronologic age, gender, and race.

Results: 309 CCS (46% female) and 200 healthy siblings (46% female) were evaluated. Compared to healthy siblings, CCS had impaired growth (height SDS 0.1 ± 1.1 vs. 0.4 ± 1.0, $p<.001$), and older age (14.6 ± 2.5 years vs. 13.7 ± 2.4 years, $p<.001$). There was no difference in relative bone age or Tanner stage. In multivariable analyses (adjusted means $\pm$SE), CCS had lower WBBMC (2180 ± 39 gm vs. 2284 ± 48 gm, p=.01), lower LBMC (39 ± 0.8 gm vs. 41 ± 0.9 gm, p=.004), higher percent body fat (28 ± 0.8% vs. 26 ± 1.0%, p=0.03), and lower LBM (39 ± 0.6 kg vs. 41 ± 0.7 kg, $p<.001$) compared to healthy siblings. WBBMC and LBMC increased with an increase in percent body fat and LBM, and a decrease in body mass index (BMI). Although growth hormone (GH) status did not have a direct effect on WBBMC, the positive effect of increasing LBM on WBBMC was attenuated in GHD subjects. There was a decrease in WBBMC and LBMC in all CCS with a cumulative steroid exposure of $\geq$6.6g prednisone equivalents.

Conclusions: Childhood cancer survivors, $\geq$ 5 years after diagnosis, have significant bone deficits in bone mineral content. Alterations in body composition are major predictors of bone health in childhood cancer survivors, and differ for subjects with and without GHD. These bone deficits may predict an increased risk of fracture and early osteoporosis.

***Disclosures: Lynda Polgreen**, None.*

MO0132

LAO, A Novel Lung Cancer Cell Line Inducing Bone Metastatic Osteosclerotic Lesions through a Wnt-dependent Mechanism. Iker Anton*[1], Diego Luis-Ravelo[2], Jose L Lafarga[2], Carolina Zandueta[2], Karmele Valencia[2], Susana Martinez[2], M Dolores Lozano[3], Alfonso Gurpide[3], Fernando Lecanda[2]. [1]Foundation for Applied Medical Research, Spain, [2]Center for Applied Medical Research, Spain, [3]CUN, Spain

Bone microenvironment homeostasis is frequently subverted by metastatic cells leading to osteosclerotic and /or osteolytic lesions. The mechanisms involved in *de novo* bone formation are poorly understood. To this aim, we isolated a novel lung adenocarcinoma cell line from a patient with metastatic osteosclerotic lesions. Tumor cells displayed positive immunoreactivity for epithelial pan-cytokeratin, vimentin and TTF-1 markers. Consistently, LAO cells express low levels of prosteoclastogenic PTHrP, IL-6 and IL-11 and high levels of OPG. In basal conditions, osteogenic factors EDN1, BMP-2 and 4 were expressed at high levels. In conditions of LAO coculture with MC3T3-E1 or C3H10T1/2 cells a marked increase in osteocalcin (OC) was detected by RT-PCR as compared to these cells cultured alone. Moreover, using a Runx2-response element, transcriptional promoter activity of OC was associated with a 2- to 3-fold increase in LAO coculture with NIH3T3 cells as compared to cells alone, or in coculture with an osteolytic cell line. Systematic analysis by RT-PCR revealed the relevance of the Wnt pathway. Wnt activity assessed by transcriptional promoter using Top-flash reporter was upregulated 2-3-fold whereas no effects were detected in mutant Fop-flash promoter activity under these conditions indicating critical induction by tumor-stromal interactions. Consistently, intratibial inoculation of LAO cells in athymic nude mice induced overt osteosclerotic lesions, whereas subcutaneous injection led to the development of tumors with no heterotopic ossification. Interestingly, intracardiac inoculation of LAO cells after luciferase transduction showed a selective bone tropism by bioluminescence imaging with a time of latency of 28-35 days and high frequency. X-ray image analysis and μCT scans revealed patches of osteoclerotic lesions in the endocortical surface of long bones. Histological examination showed abundant osteoblasts at tumor-bone interphase and concomitant induction of TRAP+ multinucleated cells resulting in altered bone homeostasis. Thus, these data indicate that tumor-stromal interactions are critical for the development of osteosclerotic lesions, by a mechanism involving Wnt activation and Runx2-mediated induction of OC. We suggest that LAO represents a unique cell line to study tumor-induced osteogenesis. This model will help to test novel therapeutic targets to prevent bone metastasis.

***Disclosures: Iker Anton**, None.*

MO0133

p62-ZZ and p38 Domains as a Therapeutic Target for Myeloma Cell Growth and Osteoclast Formation. Fumito Ishizuka[1], Shunqian Jin[2], Jolene Windle[3], G. David Roodman[4], Noriyoshi Kurihara*[2]. [1]Center for Bone Biology,University of Pittsburgh, USA, [2]Center for Bone Biology, University of Pittsburgh, USA, [3]Virginia Commonwealth University, USA, [4]VA Pittsburgh Healthcare System (646), USA

We reported that sequestosome 1 (p62) plays a critical role in the formation of signaling complexes that result in NF-κB, p38 MAPK, and PI3K activation in the marrow microenvironment of patients with multiple myeloma (MM), suggesting that p62 is a potential therapeutic target for MM. In contrast to treating patients with inhibitors for each of the multiple signaling pathways activated in marrow stromal cells by MM cells, blocking the function of p62 should inhibit the activation of multiple signaling pathways and have a broader effect on the bone marrow microenvironment in MM. The goal of this study was to identify the domains of p62 responsible for increased MM cell growth and osteoclast (OCL) formation mediated by NF-κB and p38 MAPK signaling in marrow stromal cells when they interact with MM cells, and to develop inhibitory peptides as potential therapeutic agents that interfere with p62's role in these signaling complexes. To pursue this objective, we generated the deletion constructs of p62 that lacked specific p62 domains: ΔSH2, ΔPB1, ΔZZ, Δp38, ΔTBS and ΔUBA domains. GFP-labeled MM1.S myeloma cells or normal CFU-GM, a source of OCL precursors, were co-cultured with $p62^{-/-}$ and WT marrow stromal cells transduced with the different p62 deletion constructs. Transduction of $p62^{-/-}$ stromal cells with the ΔSH2, ΔPB1, Δp38 and ΔUBA construct restored stromal cell support of MM growth. However, transduction of $p62^{-/-}$ stromal cells with the ΔZZ construct resulted in an inability of the stromal cells to increase support for MM cell growth. Transduction of the ΔZZ and Δp38 constructs did not restore the capacity of the $p62^{-/-}$ stromal cells to support OCL formation. Further, we determined the effects of transfecting the full-length, ΔZZ and Δp38 deletion constructs in $p62^{-/-}$ stromal cells on VCAM-1 expression and p38 signaling induced by TNF-α. Transduction of $p62^{-/-}$ stromal cells with the full-length and Δp38 deletion construct restored VCAM-1 and phospho-IκBα levels. Transduction of $p62^{-/-}$ stromal cells with the ΔZZ construct resulted in an inability of VCAM-1 and phospho IκBα activation. These results demonstrate that the ZZ and p38 MAPK domains of p62 together are required for stromal cell support of MM cell growth and OCL formation and suggest that generating dominant negative constructs for p62 may be a feasible blocking p62 function in the MM marrow microenvironment.

***Disclosures: Noriyoshi Kurihara**, None.*

MO0134

Percutaneous Kyphoplasty for Palliation of Thoracolumbar Spine Fractures Due to Malignancy - Procedure Indications, Limitations and Results out of 5 years. Dr. Max Markmiller*. Klinikum Kempten, Germany

Purpose of the study: Affection of the spine by metastases threatens the patients with pain, loss of mobility and neurologic defects. Treatment options have to meet concerns of the short term prognosis, the limited operability and should allow quick mobilisation and short hospital stay. An answer is the minimally–invasive percutaneous augmentation of the vertebra by CT – guided dilatation and injection of bone cement (methylmethacrylate). The patients are able to stand up immediately after the procedure, surgical trauma and complication rates are minimized. There is no need of an additional spine orthesis.

Methods: The patients were documented prospectively by ASA – Score and Karnovsky – Index. Percutaneous kyphoplasty was guided with CT and combined with fluoroscopy. All patients were aftertreated functionally with early mobilisation. Epidural tumor involvement was no contraindication.

Results: From 05/2004 to 09/2009 out of 1117 kyphoplasties 115 patients with metastatic lesions were treated. The localisation favorites the thoracolumbar junction. The subjective evaluation using the Visual Analog Scale showed a decrease of the pain level of 60 % in 80% of the patients. All patients were mobile without orthesis after the procedure. The clinical and radiological 6 – months followup confirmed the good results however 24 patients had died in between. Radiologically, all survivers showed an unaltered mechanical sufficient bone cement material. The complication rate is on the lower limit of the literature (7 %). Complications refer to paravasations of the cement: two patients showed temporary radiculopathy, three patients with intervertebral disc paravasation stayed asymptomatic. Three patients showed epidural paravasation without neurological impairment, but no oncologic patient required surgical revision.

Conclusion: Percutaneous kyphoplasty is an excellent method of palliation for pain relief and mobility in oncologic patients with cancer metastases of the spine.

***Disclosures: Dr. Max Markmiller**, None.*

MO0135

Pharmacokinetic and Pharmacodynamic Effects of Antiresorptive Agents on Bone in Patients With Metastatic Bone Disease. Peyman Hadji*. Philipps-University of Marburg, Germany

Purpose: Patients with bone metastases from advanced cancer require antiresorptive therapy to reduce the risk of skeletal-related events (SREs). Although continuous therapy is most effective, patients may miss appointments or experience delays in treatment, and protection during these prescription refill gaps is an important consideration. The pharmacokinetics and pharmacodynamics of antiresorptive agents might also influence clinical outcomes.

Methods: A systematic literature review was performed to identify studies documenting the pharmacokinetic and pharmacodynamic effects of antiresorptive agents in patients with metastatic bone disease from advanced cancer. Data from bone loss studies were used when data from cancer studies were unavailable.

Results: Bisphosphonates (BIS) have a high affinity for calcified tissue and prolonged accumulation in bone with local release at sites of active bone remodeling. The anti-RANKL antibody, denosumab, can be detected in serum several weeks after administration, but is not targeted to or stored in bone. After stopping bisphosphonates, bone resorption markers gradually increase. Stopping denosumab results in rapid increases in bone resorption marker levels that exceed baseline levels and leads to a significant decrease in bone mineral density. In patients with bone metastases, compliance with monthly intravenous BIS (eg, zoledronic acid) provided the greatest protection against SREs (0.16 vs 0.43 SREs/month), but less frequent dosing was still superior to no treatment (0.31 vs 0.43 SREs/month).

Conclusions: The pharmacokinetics and pharmacodynamics of antiresorptive therapies could greatly affect efficacy, duration of clinical effect, and safety in metastatic bone disease. Further pharmacodynamic studies are needed to elucidate the effects of discontinuations on SRE-prevention activity of BIS and denosumab. The pharmacodynamics of BIS therapy is well established in this setting, and BIS have been shown to effectively normalize bone resorption marker levels with continuous monthly treatment. Although regular and persistent treatment is associated with the greatest SRE-preventing efficacy, planned or unplanned discontinuations do not appear to correlate with dramatic SRE-risk increase versus no treatment, suggesting that BIS-treated patients continue to derive residual benefit in case of unavoidable delays in therapy.

***Disclosures: Peyman Hadji**, GlaxoSmithKline, 2; AstraZeneca, 2; Eli Lily,1; Amgen, 2; GlaxoSmithKline, 2*
This study received funding from: Amgen, AstraZeneca, Eli Lilly, GlaxoSmithKline, Novartis, Novo Nordisk, Organon, Pfizer, Procter & Gamble, Roche, sanofi-aventis, Solvay, and Wyeth.

MO0136

Ribonomics Approach to Study a Complex Inherited Tumor Predisposing Disorder: the Multiple Endocrine Neoplasia Type 1 as a Model. Ettore Luzi*, Francesca Marini, Isabella Tognarini, Sergio Fabbri, Francesca Giusti, Alberto Falchetti, Annalisa Tanini, Maria Luisa Brandi. Department of Internal Medicine, University of Florence, Italy

Purpose: Multiple Endocrine Neoplasia Type 1 (MEN1) is an inherited cancer syndrome characterized by tumors of parathyroids, neuroendocrine gastro enteropancreatic tract and anterior pituitary. MEN1 oncosuppressor gene is the responsible gene. We previously analyzed the MEN1 mRNA and menin expression in fibroblasts from normal skin biopsies and from MEN1 patients [two with a frame-shift 738del4 (exon 3) mutation, introducing a premature stop codon, and an individual with a R460X (exon 10) nonsense mutation], finding that the expression of full length menin protein did not differ between MEN1 and normal fibroblasts with both wild type and mutated alleles mRNAs being expressed in MEN1 patients, and, thus, suggesting a mechanism of compensation for mRNA loss by up regulating the expression of menin oncosuppressor at a post transcriptional level. We propose to study molecular mechanisms responsible for this compensation. A ribonucleoprotein structure in which multiple mRNAs were coordinately regulated by RNA binding proteins and small non-coding RNA could be hypothesized involving a menin-mRNA-microRNA(s) complex.

Methods: Menin-RNA complex formation has been investigated by gel retardation assay (REMSA) and RNA-immunoprecipitation chip (RIP-chip). In silico analysis with Target Scan, Miranda and Pictar-Vert softwares for the prediction of miRNA targets indicated miR-24 as capable to bind to the 3'UTR of MEN1 mRNA. MiR-24 expression profiles will be performed in cells and tissues through Real-Time RT-PCR and Northern blot.

Results: Result from REMSA and RIP-chip evidenced that menin recognized its mRNA in vitro and that a specific RNA proteins complex bound to MEN1 mRNA, thus indicating that induction of menin oncosuppressor compensation could have been regulated through RNA protein driven post transcriptional mechanisms. Analysis of miR-24 expression profiles performed in parathyroid and pancreatic endocrine tissues from MEN1 mutation carriers, in their sporadic non-MEN1 counterparts and in normal tissues, showed that the expression profiles of miR-24 mRNA and menin protein were inversely correlated, suggesting a negative post-transcriptional control of miR-24 on MEN1 expression.

Conclusions: The interplay between menin and miR-24 suggested an autoregolatory feedback loop with functional significance in MEN1 tumorigenesis thus also opening new avenues for future developments of RNA-based strategies in the in vivo control of tumorigenesis in MEN1 carriers.

***Disclosures: Ettore Luzi**, None.*

MO0137

Skeletal 45Ca Pharmacokinetics Following Irradiation and Administration of Zoledronic Acid. Susanta Hui*[1], Manju Sharma[1], Gregory Fairchild[1], Louis Kidder[1], Maryka Bhattacharyya[2], kathleen Coghill[1], Seymor Levitt[1], Douglas Yes[1]. [1]University of Minnesota, USA, [2]Medical College of Georgia, USA

Purpose: In order to model the skeletal effects of therapeutic radiation on the post-menopausal cancer patient, this investigation sought to describe the skeletal pharmacokinetics of 45Ca in mice following ovariectomy, and exposed to a clinically relevant radiation dose. In addition, the temporal effect of a bisphosphonate commonly used as a treatment adjunct for this cohort, zoledronic acid (ZA), was also examined. Methods: Five groups of skeletally mature BALB/c mice (n=5-7 per group) were used for this study. Mice were either intact, intact + 18 Gy (single fraction), ovariectomized (OVX), OVX + 18 Gy radiation, or OVX + 18 Gy + ZA. Delivered dose was verified by microTLD. This exposure was the radiobiological equivalent of a radiation treatment of endometrial cancer. Radiation was targeted to both the cranial and caudal limbs while shielding the radiosensitive organs (lung, heart, kidney, intestines, brain, etc) with lead. 14 days after radiation exposure, all mice were injected i.v. with 45Ca. Thirty days after radioisotope administration, the OVX + 18 Gy + ZA group was injected with 500 µg/kg ZA to in order to examine the effect of an antiresorptive on irradiated skeletal kinetics. Feces and urine were collected for 24 hours periods in metabolic cages at various time points. Excreted radioisotope was measured by liquid scintillation (Beckmann Coulter LS 6500). The observed data point was fit to our compartmental model. Following sacrifice at 80 days post-45Ca, all major tissue systems were segregated to measure radioisotope uptake, and bone architectural parameters were quantified at the distal femur (0.6mm away from the growth plate) using Scanco microCT scan. Results: Steady state was attained between 25-28 days post 45Ca administration in all groups. 45Ca was rapidly removed from kidney, gut, liver, and muscle. The majority of the isotope was incorporated into the skeleton within 5 days. Rapid urinary excretion of 45Ca is observed early (0-6 days; slope = -55830), followed by decreasing excretion in the feces (6-15 days; slope -1054), followed by minimal change in excretion rate (15-28 days; slope = -139). Modeled excretion rate (Figure 1A) fit the observed data well. Ovariectomized and irradiated mice treated with ZA exhibited a rapid increase in bone formation / decrease in resorption after ZA administration (reflected by decreased 45Ca in excreta, Figure 1) over the course of the study. Trabecular histomorphometry validated the expected patterns of bone loss & gain as determined by microCT. Conclusions: The time course required to attain equilibrium following overiectomy and/or radiation is independent of skeletal status. 45Ca can be used as an effective biomarker to monitor temporal bone remodeling response after systemic antiresorptive therapy.

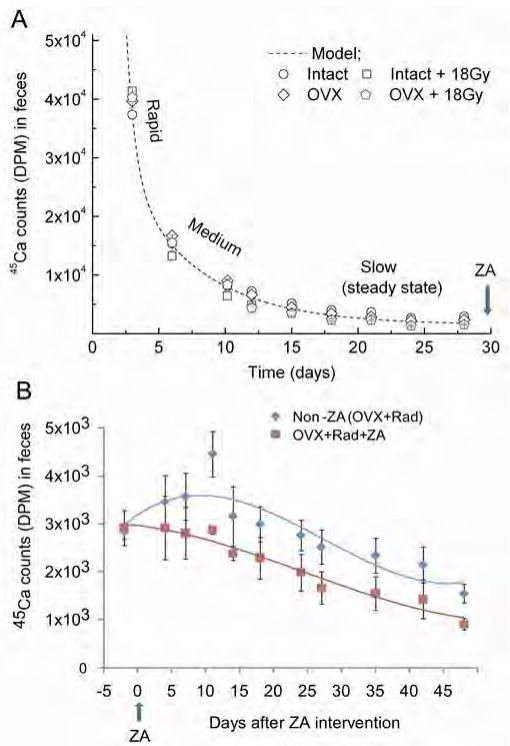

Figure 1. A. skeletal PK of 45Ca in mice B. reduced excretion of 45Ca in feces in BP-treated mice

***Disclosures: Susanta Hui**, None.*

MO0138

The Effect of Risedronate on Serum Dickkopf-1, Osteoprotegerin, and RANKL in Patients with Hematologic malignancies following HSCT. Eunhee Jang*[1], Kihyun Baek[2], Sunhee Ko[3], Moo-Il Kang[3]. [1]St.Mary's Hospital, South korea, [2]St. Mary's Hospital, South korea, [3]Seoul St. Mary's Hospital, South korea

Dickkopf-1(dkk1) is an soluble inhibitor of Wnt/ß-catenin signaling, which is implicated in the regulation of osteoblas differentiation. Dkk1 overexpression causes osteopenia and inhibits fracture repair in vivo, while Dkk1 activation seems to involve in the pathogenesis of glucocorticoid-induced and cancer-related bone disease. However, there is no informations for the serum Dkk1 in bone metabolism after HSCT except multiple mylema.

In this prospective, double- blind clinical trial, 121 patients undergoing HSCT for hematologic diseases were randomly assigned to receive calcium (1tablet bid, Adcal?R) plus either risedronate (35mg/week, Actonel?R,Procter & Gamble Pharmaceuticals Inc.) or placebo. During the study, 48 patients dropped out for several reasons, 73 patients(37 placebo/36 risedronate) were performed for 12months. Serum concentrations of alkaline phophatase, Dkk1, Osteoprotegerin (OP-G),RANKL were measured before HSCT and 1, 4, and 12 weeks, 6 months, and 1 year after HSCT in 73 patients. BMD was measured with dual-energy X-ray absorptiometry before HSCT and 6months, 1 year after HSCT.

At baseline, there was no significant difference between placebo and risedronate in dkk-1,OPG, RANKL, RANKL:OPG ratio and BMD. Serum dkk1 decreased progressively until 1 weeks after HSCT and thereafter, it continued to increase at post-HSCT 1year. Other bone turnover markers, like osteocalcin and 1CTP,had recovered baseline levels after 1years, while Dkk1 maintained increasing tendency above baseline. Patients with risedronate had lower dkk1 after 4weeks compared with placebo group, which was associated with BMD decrease after HSCT. RANKL:OPG ratio increased until 4weeks, thereafter it showed decreased pattern like 1CTP. RANKL:OPG ratio in risedronate group showed lower trends than placebo group continuously. No distinct differences were observed in the serum dkk1, RANKL:OPG ratio between gender, total body irradiation status, myeloablative regimen or not, cyclosporine use or not, acute leukemia or MDS and GvHD status.There was a negative correlation between serum dkk1(3months and 6 months after HSCT) and BMD values at the lumbar spine, total femur and femur neck (p=0.001, regardeless of risedronate or placebo).

We conclude that increased serum Dkk1 and decreased RANKL:OPG ratio explain the pathogenesis of bone loss after HSCT. Our results suggest that Dkk1 as a possible target for the development of novel agents for the management of HSCT-related osteoporosis.

***Disclosures: Eunhee Jang**, None.*
This study received funding from: Sanofi-Aventis Korea

MO0139

The Effect of sFRP3 Expression in Myeloma on MSC Differentiation and Their Biological Function. Ya-Wei Qiang*, Bo Hu, Yu Chen, Bart Barlogie, John Shaughnessy. University of Arkansas for Medical Sciences, USA

Bone disease is one of several complications patients with multiple myeloma (MM). The molecular mechanisms by which MM-triggered bone disease develops have not been fully understood. We have previously demonstrated that Dkk1, an antagonist of canonical Wnt signaling, is associated with bone disease in MM patients. Dkk1 expression, however, is found less frequently in MM cell lines, which represent the late stages of MM during the disease's progression. These results indicate that other molecules may be involved in bone disease at this stage of the disease. The sFRPs family of secreted proteins (including sFRP1, 2, 3 and 4) acts as decoy receptors and directly binds to Wnts, thereby altering the ability of Wnts to bind to the cellular Wnt receptor complex. Like sFRP2 mRNA, sFRP3 mRNA is highly expressed in myeloma plasma cells. However, it remains to be seen if sFPF3 is involved in myeloma-triggered bone disease. In present studies, we have sought to investigate the role of sFRP3 in MM-triggered bone lesions using OB cell lines, MSC from MM patients, and serum from a MM cells that express high level of sFRP3. RT-PCR analysis showed sFRP-1, -2 and -3 were expressed in the mouse MSC cells. q-PCR analysis demonstrated that sFRP3 was weakly expressed in human OB-like cells lines, while sFRP1 expressed highly in MG63, as did sFRP2 in Saos-2. High levels of sFRP3 and sFRP2 mRNA were detected in RNA from MSC in one of 6 MM patients. sFRP3 was also detected in 50% of MM cell lines. Unexpectedly, recombinant sFRP3 protein did not inhibit, but synergized with Wnt3a-induced increased beta-catenin in mouse MSCs. Similarly, sFRP3 treatment of the MSC cells increased Wnt-3a induced TCF transcript activity when transfected with TOPflash luciferase report constructs. sFRP3 also increases MSC differentiation, evidenced by an increase in ALP activity, and Alizarin red staining analysis in MSC cells. sFRP3 treatment also increases OPG mRNA and protein production. This data suggests that sFRP3 synergized Wnt signaling induces MSC differentiation, and indirectly inhibits osteoclastogenesis via regulating OPG in MSC cells. Further experiments are being performed to determine if serum from sFRP3 high expression MM cells has effect on MSC differentiation and the molecular mechanisms of sFRP3 activity in bone disease of MM patients.

***Disclosures: Ya-Wei Qiang**, None.*

MO0140

Two Novel *HRPT2* Mutations In The Nucleolar Localization Signal Of Parafibromin. Vito Guarnieri*[1], Valerio Pazienza[2], Filomena Baorda[3], Dieter Kotzot[4], Klaus Kapelari[5], David E. C. Cole[6], Geoffrey Hendy[7], Leonardo D'Agruma[3], Massimo Carella[3], Alfredo Scillitani[8]. [1]Medical Genetics Service, IRCCS Casa Sollievo della Sofferenza Hospital, Italy, [2]Unit of Gastroenterology, IRCCS "Casa Sollievo della Sofferenza" Hospital, Italy, [3]Medical Genetics Service, IRCCS "Casa Sollievo della Sofferenza" Hospital, Italy, [4]Division of Clinical Genetics, Department of Medical Genetics, Molecular & Clinical Pharmacology, Innsbruck Medical University, Austria, [5]Clinical Department of Pediatrics, Innsbruck Medical University, Austria, [6]Banting Institute, University of Toronto, Canada, [7]McGill University, Royal Victoria Hospital, Canada, [8]Casa Sollievo Della Sofferenza Scientific Institute, Italy

Parafibromin is a 531 amino acid tumor suppressor encoded by the HRPT2 gene that when inactivated causes the HPT-JT syndrome characterized by parathyroid tumors – with carcinoma being frequent – and jaw tumors. Inactivating mutations in HRPT2 are also frequent in sporadic parathyroid carcinoma and atypical adenoma. Parafibromin interacts with the RNA polymerase II-associated PAFI complex important for chromatin remodelling. Here, we report two novel mutations lying in the nucleolar localization signal (NoLS; amino acids 76-92) of parafibromin. One, a somatic mutation (R77P) in a subject with recurrent parathyroid carcinoma, is located at the beginning of the NoLS. The second, p.82_83delVV, a germline mutation in a patient with an atypical parathyroid adenoma, is an in-frame deletion of two valines in the middle of the NoLS. While these mutations may not alter the expression of parafibromin, they may impair the nucleolar localization of the protein.

***Disclosures: Vito Guarnieri**, None.*

MO0141

A *Gja1* Mutant with Dominant-Negative Action in the Osteogenic Lineage is Sufficient to Cause a Skeletal Phenotype Resembling Oculodentodigital Dysplasia. Roberto Civitelli[1], Bertrand Guillotin[2], Jin-Yi Norris[2], Susan Grimston[3], Marcus Watkins*[1]. [1]Washington University in St. Louis School of Medicine, USA, [2]Washington University in St. Louis, USA, [3]Washington University School of Medicine, USA

Oculodentodigital dysplasia (ODDD) is an autosomal dominant disorder linked to mutations of the connexin43 gene (*Gja1*), and characterized by craniofacial and dental defects, type III syndactyly, and eye abnormalities. We have reported craniofacial abnormalities and osteopenia in a mouse model of ODDD, in which one copy of *Gja1* is globally replaced by the $Gja1^{G138R}$ mutant. To determine whether this skeletal phenotype is due to inherent defects in bone cells caused by the mutant Gja1, we have induced a $Gja1^{G138R}$ mutation in osteo-chondroprogenitors, using the *Dermo1* (*DM1*) promoter. Replacement of a single wild type (WT) allele with $Gja1^{G138R}$(*DM1;G-ja1*$^{G138R/+}$:cODDD), reproducing the genetic defect of the human disease, results in a phenotype very similar to conditional Gja1 ablation (*DM1;*$Gja1^{flox/-}$:cKO), though less severe. The skull of cODDD mice is normally mineralized, but whole body bone mineral density (BMD) is significantly reduced (–17±5% at 2 months), differences persisting up to 12 months of age. As in cKO, cODDD mice have shortened long bones (–10±4% femur length), with tubulation and larger cross-section of the femoral diaphysis, larger total tissue (54±6%) and marrow area (30±6%). Cortical thickness and cortical BMD are significantly decreased in cODDD mice (20±7% and 4±2%, respectively); whereas no differences in trabecular bone parameters are observed relative to WT littermates. Also similar to cKO, endocortical osteoclast number is increased in cODDD mice. Hence, cODDD bone marrow stromal cells induce higher number of osteoclasts when co-cultured with WT or cODDD osteoclast precursors, and express higher RANKL mRNA relative to WT cells. However, osteoblastic gene products in cortical bone are not significantly altered in cODDD. Intriguingly, $Gja1^{G138R}$ allele replacement in a *Gja1* null background (*DM1;*$Gja1^{G138R/-}$) has far worse consequences than conditional *Gja1* ablation (cKO), as no viable mice are retrieved, whereas cKO mice are obtained at the expected Mendelian frequency with modest dysmorphic features at birth. Thus, conditional induction of an ODDD *Gja1* mutation in osteo-chondroprogenitor cells is sufficient to produce an ODDD skeletal phenotype, which is primarily due to indirect endocortical osteoclast activation. The more severe phenotype of *DM1;*$Gja1^{G138R/-}$ mice relative to cKO demonstrates that the $Gja1^{G138R}$ mutant is not only dominant negative for Cx43, but may interfere with other connexins or non-gap junction related cell functions.

***Disclosures: Marcus Watkins**, None.*

MO0142

An Antagonist of Interleukin-15 Inhibits Weight and Bone Loss in a Mouse Model of Inflammatory Bowel Disease. Dominique Pierroz*[1], Sylvie Ferrari-Lacraz[2], Xin X Zheng[3], Serge Ferrari[4]. [1]University Hospital of Geneva, Switzerland, [2]Transplantation Immunology Unit, Geneva University Hospital & Faculty of Medicine, Switzerland, [3]Transplantation Unit, University of Pittsburgh, USA, [4]Geneva University Hospital & Faculty of Medicine, Switzerland

IL-15 is a T cell growth factor produced by monocytes/macrophages. In turn, activated T lymphocytes secrete cytokines, which are key regulators of osteoclast and osteoblast activity. In patients with inflammatory bowel disease (IBD), high levels of IL-15 in blood parallel high levels of IL-15 in the inflamed rectal mucosa, and colitis is associated with low BMD and increased fracture risk. We reported that IL-15a$^{-/-}$ mice have increased bone mass compared to WT, before and after ovariectomy. We hypothesized that inhibition of IL-15 signaling might prevent bone loss in a mouse model of IBD. Colitis was induced in 10-week-old mice by adding 2% of dextran sulphate sodium (DSS) to drinking water for 1 week, followed by 1% DSS for 2 weeks. During the last 14 days, mice received an IL-15 antagonist (CRB-15, 5mg/day) or IgG2a. IgG2a was also administered to control mice (Ctrl) without colitis. According to the severity of colitis, mice were divided in two groups. In mice with severe colitis, mortality was high during the 2nd week (6/8 in IgG2a) and partially prevented by CRB-15 (3/8). In these mice, BW loss was stopped after 2 days of CRB-15 administration and reached -7.3% at day 11, compared to -22.4% in those receiving IgG2a ($p=0.001$). By week 3, BW returned to Ctrl levels in both groups. Circulating IGF-I levels, a marker of nutritional status, paralleled changes in BW, reaching -52% after 1 week in DSS-treated mice ($p=0.002$ vs Ctrl) and returning to Ctrl values at week 3. These changes were independent of CRB-15. In 3-week-survivors, a loss of femur BMD occurred in the IgG2a ($p<0.03$ vs Ctrl), which was prevented by CRB-15. Moreover, trabecular BV/TV, number and connectivity at the distal femur were decreased in IgG2a (-14% to -42%, $p<0.05$ vs Ctrl), whereas CRB-15 preserved trabecular microstructure. Serum osteocalcin declined after 2 weeks (-59.7% in IgG2a vs Ctrl, $p<0.001$), but remained higher with CRB-15 ($p<0.04$ vs IgG2a). In mice with light colitis, death rate was minimal, BW, femoral BMD, microarchitecture, osteocalcin and IGF-I levels were modestly and only transiently decreased, and not influenced by CRB-15.

In summary, antagonizing IL-15 may exert favorable effects on weight and bone loss caused by severe colitis, whereas its effects are undetectable in milder colitis. These results suggest that the protective effects of CRB-15 on the skeleton in IBD might be mediated by a control of the inflammatory processes, independently of IGF-I.

***Disclosures: Dominique Pierroz**, None.*

MO0143

Bone Loss in Aging Mice Correlates with Increased, not Decreased Vascular Density. Bernard Roche*[1], Arnaud Van den Bossche[1], Françoise Peyrin[2], Cecile Olivier[2], Laurence Vico[1], Marie-Helene Lafage-Proust[1]. [1]Université de Lyon, INSERM U890, France, [2]CREATIS-LRMN-CNRS UMR 5220, France

The functional relationships between bone and vessels are not well understood. Studies in humans and rats showed a decreasing bone blood flow with aging. However, structural changes in the vascular network are poorly described. Thus, we designed a quantitative assessment and imaging of this network during aging in mice, the most used animal model in our research field. After sacrifice, 3 groups of 11 CD-1/129 male mice, respectively 3, 7 and 17- month-old (M), were infused with barium sulphate through the aorta. Femora and tibiae were then embedded in methylmetacrylate. Bone Volume, (BV/TV, %), Vessel density (V.Nb/mm^2), Vascular Volume/Marrow Volume (VV/Mar.V) and mean Vessel Area (V.Ar, μm^2) were quantitated on 7 sections/bone sample in both metaphysis and diaphysis (Fig1 Top: longitudinal sections). Additionally, 15 samples, chosen from histological assessment as representative for the mean vascular density of each age group were imaged using synchrotron radiation microtomography (SR-μCT, voxel size 1.5 μm^3). Data are expressed as mean ± SEM.

As expected, BV/TV decreased with aging (femur: 14.9±1.7, 5.4± 0.5 and 1.5±0.2%, tibiae: 11.4±0.6, 2.7±0.5 and 0.7±0.3%, at 3M, 7M, and 17M, respectively, $p<0.001$). Between 3 and 7M, V.Nb/mm2 decreased significantly by 67 and 34% in both femoral and tibial metaphyses (97±6 vs 32±4 and 102±5 vs 67±3, respectively, $p<0.0001$) with no significant change in the diaphysis. Surprisingly, between 7 and 17M, V.Nb/mm^2 increased by 84% in femur metaphysis (17M: 59 ± 4.6, $p<0.001$ 17 vs 7M) and not significantly (+15%) in the tibia (17M: 77± 5.2). V.Ar increased significantly only between 7M and 17M (1144 ± 58 μ^2 vs 1429 ± 118 μ^2, $p=0.02$). Femoral and tibial vascular densities were significantly correlated ($r=0.75$, $p<0.001$). VV/TV correlated with vascular density ($r=0.83$, $p<0.0001$) and showed a similar evolution with aging (femur: 8.5±2.8, 3.7±1.5 and 13.2±2.9% at 3, 7 and 17M, respectively, $p<0.0001$). Finally, BV/TV correlated negatively with VV/Mar.V in femora of aging (7 and 17M) mice ($r=0.75$, $p<0.0001$). SR-μCT illustrated and confirmed our histomorphometry data (Fig 1 Bottom: 2D projections of 10 cross-sections).

In conclusion, such a biphasic evolution of microvessels in mouse long bone metaphysis needs to be further explored in other mouse strains and other animal

models. A confirmation would lead to reconsider the paradigm of a coupled involution of bone and vessels during physiological aging.

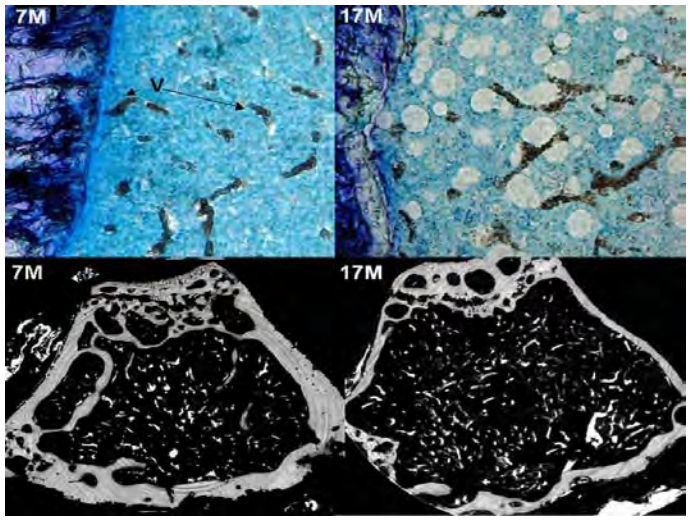

Figure 1

***Disclosures: Bernard Roche**, None.*

MO0144

Effects of Fish Oil and Exercise on Postmenopausal Bone Loss. Erika Varela[1], Ali Bahadur[1], Nishu Kazi[1], Jameela Banu*[2], Gabriel Fernandes[3]. [1]UTHSCSA, USA, [2]University of Texas Health Science Center at San Antonio, USA, [3]University of Texas Health Science Centre, USA

There is increasing evidence that fish oil decreases bone resorption by decreasing osteoclastogenesis and that increase in physical activity increases bone mass. The combined effects of fish oil intake and physical activity may have additive effects by both increasing bone formation as well as decreasing bone resorption. We used middle aged mice to study the effects of fish oil and exercise on bone after ovariectomy induced bone loss.

12 months old C57BL/6 mice were either sham operated or ovariectomized and divided into the following groups: Group 1 LC S Sed; Group 2 LC S EX; Group 3 LC O Sed; Group 4 LC O EX; Group 5 18/12 S Sed; Group 6 18/12 S EX; Group 7 18/12 O Sed; Group 8 18/12 O EX; Group 9 30/20 S Sed; Group 10 30/20 S EX; Group 11 30/20 O Sed; Group 12 30/20 O EX. Mice were fed respective diets and on a treadmill exercise regimen soon after surgery. Mice were maintained in the respective treatments for 3 months and then sacrificed. The femur was removed and stored for pQCT and mCT densitometry.

pQCT densitometry: In the distal femur, the total BMC was significantly higher in the 18/12 and 30/20 S Sed groups when compared to that of the LC S Sed groups. 30/20 O Sed mice had higher total BMC when compared to that of LC O Sed mice. Exercise significantly increased BMC in the LC O and 18/12 O mice when compared to their respective sedentary mice. The total BMD was higher in the 18/12 and 30/20 fed sham Sed mice. 30/20 O Sed mice had higher BMD when compared to that of LC O mice. Exercise significantly increased BMD in the LC O and 18/12 O mice. Cortical BMC, in the distal femoral metaphysis, increased after EX and with both fish oil diets.

?CT densitometry: In the distal femur there were no significant changes in the trabecular thickness. However the trabecular number increased in mice on 18/12 fish oil diet and exercise. 30/20 O Sed mice showed more trabecular number than LS O Sed and this did not change after exercise. Trabecular separation was increased in the 18/12 fish oil fed mice and was lower in the LC and 30/20 fish oil fed animals.

In conclusion, fish oil fed mice showed increased BMD in the distal femur, however, only 30/20 fish oil showed higher trabecular number and decreased trabecular separation.

Supported by NIH ROIAG023648-01A1, ROIAT004259-03

***Disclosures: Jameela Banu**, None.*

MO0145

InppA as a Modulator of Bone Formation. Maya Boudiffa*[1], Mohammad Rashed[1], Monica Pata[1], Jean Vacher[2]. [1]IRCM, Canada, [2]Institut De Recherches Cliniques De Montréal, Canada

Bone remodeling relies on a strict balance between bone formation by the osteoblast and bone resorption by the osteoclast. Differentiation and activation of these cells are regulated by multiple signaling pathways, including the PI3kinase. Upon external stimulation phosphatidylinositol kinases and phosphatases are activated and produce short-lived phosphatidyl inositol second messengers essential in intracellular signaling cascades for cell growth, survival and activation. Two inositol polyphosphate 4-phosphatase isoenzymes (Inpp4b and Inpp4a) have been identified. We have characterized Inpp4b that is expressed throughout the osteoclast lineage. Inpp4b enhanced ex vivo expression in osteoclast precursors caused significant decrease in differentiation whereas in vivo ablation leads to an osteoporotic phenotype with increased osteoclast resident population. The second isoenzyme Inpp4a (type I) has been associated with a preponderant role in neuronal cell survival since spontaneous loss of function in weeble mice leads to severe neurodegeneration with premature death at ~3 weeks of age. Because Inpp4b is a negative regulator of osteoclastogenesis, we investigated whether Inpp4a has a potential role in bone cells. We first established that in contrast to Inpp4b, Inpp4a is highly expressed in osteoblasts but not in osteoclasts. Second, phenotypic analysis of 3 weeks old weeble mice exhibited delayed growth and skeletal development with smaller bones. Bone tissue analysis revealed 4-fold reduction in the number of resident osteoblast, correlating with decreased bone density and mineralization compared to wild-type controls. In addition, weeble osteoblasts were deficient in supporting osteoclast differentiation in coculture experiments. Importantly, osteoclastogenesis occurs normally in weeble mice. These findings indicate a preponderant role of Inpp4a in osteoblast lineage independent of the coupling osteoblast-osteoclast mechanism. Our results unraveled major and distinct roles for Inpp4a in osteoblasts and Inpp4b in osteoblastogenesis and are thus key regulators of bone cell physiology.

***Disclosures: Maya Boudiffa**, None.*

MO0146

A Case of Camurati-Engelmann Disease with a *TGFβ1* R218C Mutation. Line Vautour*[1], Geoffrey Hendy[2]. [1]McGill University Health Centre Royal Victoria Hospital, Canada, [2]McGill University, Royal Victoria Hospital, Canada

Hyperostosis of the skull can be associated with the rare Camurati-Engelmann disease (CED) (OMIM #131300) and several other bone disorders making the differential diagnosis problematic. We report a case of a 26-year-old woman who presented with headaches, vomiting, and visual loss. Non-contrast CT revealed hyperostosis of the skull with loss of diploic spaces; sclerosis was particularly marked at the base of the skull. Magnetic resonance imaging showed medial displacement of both unci and an acquired Chiari malformation – a downward displacement of the cerebellar vermis and medulla potentially causing obstruction of cerebral spinal outflow. Intracranial pressure was markedly increased. A reduction craniotomy with subtemporal decompression was performed with good clinical improvement. Later radiological evidence was obtained of diaphyseal dysplasia of the femora and tibiae. The autosomal-dominant CED is due to mutations in the transforming growth factor (TGF)-β1 gene (Gene map locus 19q13.1). *TGFβ1* mutation analysis was performed on leukocyte DNA from the proband and her parents who are clinically unaffected. All seven *TGFβ1* exons were PCR amplified from genomic DNA, the amplicons gel-purified and sequenced directly. The proband is heterozygous for an R218C (CGC>TGC) mutation in exon 4 whereas both her parents are of wild-type sequence. Ten different *TGFβ1* mutations have been identified in 46 CED families worldwide. The majority (7/10) are missense mutations located in exon 4 coding for the latency-associated peptide (LAP) of the TGF-β1 precursor. The mutations destabilize the intermolecular disulphide bridging of the LAP and cause premature activation of the mature TGF-β1 leading to disordered bone remodeling. Arginine 218 is the most commonly mutated residue. Therefore, genetic analysis clarified the underlying molecular defect in the present case that typifies the extreme variability in phenotypic expression of CED.

***Disclosures: Line Vautour**, None.*

MO0147

Impaired Generation of Reactive Oxygen Species in Nox4-deficient Mice Results in a High Bone Mass Phenotype Due to an Osteoclast Defect. Claudia Goettsch*[1], Reinhold Erben[2], Stefan Rammelt[3], Martina Rauner[4], Christiane Schüler[2], Lorenz Hofbauer[5], Ralf P. Brandes[6], Katrin Schroeder[6]. [1]Department of Medicine III, Technical University, Dresden, Germany, [2]University of Veterinary Medicine, Austria, [3]Department of Trauma & Reconstructive Surgery, Technical University, Dresden, Germany, [4]Medical Faculty of the TU Dresden, Germany, [5]Dresden Technical University Medical Center, Germany, [6]Institut für kardiovaskuläre Physiologie, Goethe-Universität Frankfurt am Main, Germany, Germany

Reactive oxygen species (ROS) have been implicated in osteoclastogenesis. NADPH oxidases of the Nox family are important sources of ROS. The contribution of individual Nox proteins, however, is unknown. We generated a Nox4-deficient mouse and determined the impact of Nox4 on osteoclastogenesis and subsequently bone mass in mice. Eight-week-old wild type and Nox4-/- mice were studied. Bone mineral density (BMD) was measured at the distal femur by peripheral quantitative computed tomography ex vivo. Bone histomorphometry was performed on undecalcified bone sections of the distal femoral metaphysis. In addition, osteoclast numbers were assessed in decalcified sections stained for tartrate-resistant acid phosphatase (TRACP). Protein expression in bone extracts was analyzed by Western blot. Osteoclasts were cultured ex vivo by differentiating bone marrow cells using

RANKL and M-CSF for 7 days. Deficiency of Nox4 in mice led to an increase in trabecular BMD of the distal femur by 30% compared to wild-type litter mates, whereas cortical/subcortical BMD did not differ between the two groups. Bone formation rate and mineral apposition rate were not affected by Nox4-deficiency. Interestingly an increase in trabecular thickness and width was observed in Nox4-/- mice, whereas trabecular number and separation were not altered when compared to their wild type litter mates. In addition, the number of osteoclasts per perimeter was significantly lower in Nox4-/- mice (-54%) which was also confirmed by TRACP staining. These data point towards an osteoclast phenotype in Nox4-/- mice. Indeed bones form Nox4-/- mice showed lower expression of OSCAR and higher level of osteopontin, when compared to wild type mice. Moreover, during osteoclast differentiation by RANKL and M-CSF an upregulation of Nox4 was observed, indicating a potential role of Nox4 in this process. Importantly, in Nox4-/- mice, the RANKL and M-CSF-induced differentiation of bone marrow stromal cells into osteoclasts was reduced by 44% as compared to wild type cells. In conclusion, deficiency of Nox4 causes a high bone mass phenotype due to impaired osteoclastogenesis.

***Disclosures: Claudia Goettsch**, None.*

MO0148

Increased Bone Resorption in a Mouse Model of Mucolipidosis II. Jan M. Pestka*[1], Katrin Kollmann[2], Robert P. Marshall[1], Michaela Schweizer[3], Michael Amling[1], Thomas Braulke[2], Thorsten Schinke[1]. [1]Dept. of Osteology & Biomechanics, University Medical Center Hamburg-Eppendorf, Germany, [2]Dept. of Biochemistry, University Medical Center Hamburg-Eppendorf, Germany, [3]ZMNH, University Medical Center Hamburg-Eppendorf, Germany

Mucolipidosis II (ML-II) is a lysosomal storage disorder caused by mutations in the *GNPTAB* gene, which is required for the generation of the mannose 6-phosphate recognition marker. The disease is characterized by an impaired targeting of lysosomal enzymes, thereby causing an intracellular accumulation of various undegraded macromolecules in different cell types. The clinical features of ML-II include facial dysmorphism, short stature, organomegaly, retarded psychomotor development and premature death. To study, how missorting of lysosomal enzymes would affect skeletal remodeling, we generated a mouse model of ML-II by introducing an inactivating mutation into the murine *Gnptab* gene. As expected, these mice displayed several features of ML-II, such as increased lethality, reduced body weight and skeletal growth, as well as defective mannose 6-phosphorylation and targeting of lysosomal enzymes. Histomorphometric analysis revealed that the trabecular bone volume was decreased compared to wildtype littermates at 4 and 12 weeks of age, while cortical bone was characterized by osteolytic lesions. Our cellular analysis of bone remodeling demonstrated that the bone formation rate was significantly reduced in ML-II mice, which could be explained by the existence of lysosomal inclusion bodies in osteoblasts, as observed by electron microscopy. In contrast, similar morphological abnormalities were not found in osteoclasts from ML-II mice, which is in line with the finding that the amount of bone-specific collagen degradation products was significantly increased compared to wildtype littermates. Unexpectedly, the number of osteoclasts was more than 3-fold higher in ML-II mice, albeit these cells did not stain in TRAP-activity assays, thereby confirming the defective targeting of this lysosomal enzyme. Taken together, our results demonstrate that osteoclast function is not impaired by the absence of mannose 6-phosphorylation on lysosomal enzymes and that the skeletal abnormalities caused by *Gnptab* inactivation are primarily the consequence of increased bone resorption. Given the fact, that osteolytic lesions have been observed in ML-II patients, our results are also of immediate clinical relevance, since they suggest that the skeletal manifestations of ML-II can be prevented by anti-resorptive therapies, such as bisphosphonate administration.

***Disclosures: Jan M. Pestka**, None.*

MO0149

Mouse Models of Hermansky-Pudlak Syndrome, a Lysosome-related Organelle Biogenesis Disorder, Exhibit Osteopenia. Cheryl Ackert-Bicknell*, Jordanne Dunn, Babette Gwynn, Beverly Paigen, Luanne Peters. The Jackson Laboratory, USA

Hermansky-Pudlak syndrome (HPS) is a rare recessive disorder caused by defects in the biogenesis of lysosome-related organelles (LROs). The classical triad of HPS defects include oculocutaneous albinism due to melanosome defects, prolonged bleeding due to absent or defective platelet dense bodies, and ceroid pigment accumulation in lysosomes. As defects in lysosomal biogenesis/trafficking in osteoclasts are predicted to result in osteopetrosis due to defective bone resorption, we examined the bone phenotype of mouse models of HPS. All known mutations for HPS fall in genes that are members of the biogenesis of lysosome related organelle complex (BLOC) -1, -2, -3, or the AP-3 sorting complex. We examined the bone phenotype of 3 HPS mouse models: cappuccino (*cno*), a member of BLOC-1; ruby-eye/HSP-6 (*ru*), a member of BLOC-2; and pale ear/HPS-1 (*ep*), a member of BLOC-3. Whole body aBMD was measured in 16 week old female mice by dual X-ray absorptiometry (DXA, PIXImus) and periosteal circumference and cortical thickness at the femoral mid-shaft were examined by peripheral quantitative computed tomography (pQCT). We observed a decrease in aBMD in cno null mice (*cno*/*cno* = 0.0499 +/- 0.0003 g/cm^2) as compared to littermate controls (*cno*/+ = 0.0516 +/- 0.0003 g/cm^2, P=0.0051). The *cno*/*cno* mice also had a decrease in periosteal circumference (*cno*/*cno* = 4.82 +/- 0.02 mm vs. *cno*/+ = 4.91 +/- 0.02 mm, P=0.0041), but no change in cortical thickness. We then examined aBMD in 16 wk old female *ru*/*ru* mice as compared to C57BL/6J (B6) controls. Like the *cno*/*cno* mice, a reduction in aBMD was observed in the null mice (*ru*/*ru* = 0.0505 +/- 0.0008 g/cm^2, B6 = 0.0529 +/- 0.0004 g/cm^2, P=0.0193). The *ru* null mice had a reduced cortical thickness at the mid-shaft (*ru*/*ru* = 0.174 +/- 0.002 mm vs. B6=0.183 +/- 0.003 mm, P=0.0186), but no change in periosteal circumference. A reduction in total femoral vBMD was noted in *ep*/*ep* null mice, as measured by pQCT (*ep*/*ep* = 0.548 +/- 0.007 mg/mm^3, B6 = 0.569 +/- 0.006 mg/mm^3, P=0.0382). This was coincident with a decrease in cortical thickness (*ep*/*ep* = 0.171 +/- 0.003 mm vs. B6=0.183+/- 0.003, P=0.020). In summary, we have examined 3 mouse models for HPS, 1 model for each of BLOC-1, -2 and -3. All 3 models exhibited an osteopenic phenotype, not the predicted osteopetrotic phenotype. Thus, mouse models for HPS represent novel models for study of bone mass homeostasis and may be useful for understanding lysosomal trafficking in the osteoclast.

***Disclosures: Cheryl Ackert-Bicknell**, None.*

MO0150

New siRNA-based Therapy For Autosomal Dominant Osteopetrosis. Andrea Del Fattore*, Marta Capannolo, Nadia Rucci, Anna Teti. University of L'Aquila, Italy

Autosomal Dominant Osteopetrosis (ADO) is a rare genetic disease characterized by sclerosis of the skeleton due to impaired osteoclast bone resorption. Clinically, ADO is extremely heterogeneous, ranging from asymptomatic to severe. Patients with the severe forms are subjected to multiple fractures and high morbidity. Unfortunately, no therapeutic approach is available so far for this disease. Since 70% of ADO patients harbors single allele dominant negative mutations of the CLC7 gene, we hypothesized that silencing the mutant allele by small interfering (si)RNA could lead to a condition of haplosufficiency, thus rescuing a nearly normal phenotype. To this aim we generated plasmids containing the entire human ClC7 cDNA and inserted four ADO mutations, R767W, G215R, A788D and R286W. We then designed mutation-specific siRNAs and tested them in HEK293 cells transfected with the wild type or the mutant vectors. Using siRNAs perfectly complementary to the mutant transcripts, we obtained effective but poorly specific silencing of the mutant alleles. To improve allele specificity, we inserted a mismatch within the siRNAs and obtained up to 90% reduced expression of the mutant ClC7, with no effect on the normal allele. Human osteoclasts transfected with the mutant ClC7 constructs showed a reduced bone resorbing ability similar to that observed in osteoclasts from ADO patients (about 30% compared to control), thus representing an effective cellular model for this form of osteopetrosis. Treatment of these transfected cells with mutation specific-siRNAs rescued their resorbing ability, which was increased by two-fold compared to irrelevant siRNA-treated cells. Moreover, Cy3-tagged siRNA was taken up by human osteoclasts without transfection agents, paving the way for their use in vitro and in vivo. Notably, treatment of control osteoclasts with mutation-specific siRNAs did not affect normal allele expression, nor their resorbing ability, confirming the allele specificity of these siRNAs. To set a siRNA-based therapy in vivo, due to the unavailability of mouse models of ADO, we treated CD1 mice for 24-48h with wild type-specific siRNA. We retrieved several organs, including tibia, brain, liver, kidney, spleen, heart and lung, and observed organ targeting of fluorescent siRNA along with a time-dependent clc7 mRNA reduction in all of them but the brain, suggesting the in vivo feasibility of a siRNA−based therapy to cure ClC7−dependent ADO.

***Disclosures: Andrea Del Fattore**, None.*

MO0151

OPG Rather Than RANKL Regulates Alveolar Bone Loss. Masanori Koide*[1], Tadashi Ninomiya[2], Midori Nakamura[2], Yasuhiro Kobayashi[2], Hisataka Yasuda[3], Naoyuki Takahashi[2], Nobuyuki Udagawa[2]. [1]Matumoto Dental University, Japan, [2]Matsumoto Dental University, Japan, [3]Oriental Yeast Company, Limited, Japan

Alveolar bone resorption in periodontitis is induced via enhancement of RANKL expression and suppression of OPG expression. Therefore, we have believed that the RANKL/OPG ratio determines the intensity of alveolar bone resorption. However, it is not known which of the induction of RANKL or the suppression of OPG is a more important determination factor in periodontitis-induced alveolar bone loss (ABL). To address this question, we compared alveolar bone resorption in RANKL-transgenic mice (RANKL-Tg), OPG-deficient mice (OPG-KO) and wild type littermates (WT) using histological and micro-CT analyses. Bone resorption-related serum parameters such as soluble RANKL and TRAP5b were also measured in those mice.

Serum concentrations of RANKL and TRAP5b were markedly increased in RANKL-Tg and OPG-KO in the comparison with WT. Serum levels of RANKL in RANKL-Tg and OPG-KO were approximately 200-fold and 20-fold higher than those in WT, respectively. However, the serum concentration of TRAP5b in OPG-KO was much higher than that in RANKL-Tg. The distance from the cement-enamel junction to the alveolar bone crest was measured on micro-CT images as ABL, a clinical parameter in periodontology. OPG-KO showed approximately 2-fold increase in ABL when compared to WT. Bone volume (BV) of alveolar bone was markedly reduced in OPG-KO. In contrast, ABL in RANKL-Tg was comparable to that in

WT, though BV of alveolar bone was significantly decreased in RANKL-Tg. In histological analysis, both OPG-KO and RANKL-Tg mice showed increased number of osteoclasts in comparison with WT. Again, the osteoclast number was significantly higher in OPG-KO than RANKL-Tg. Prominent bone resorption in the cortical bone area was remarkably observed in OPG-KO. Thus, bone resorption was much more remarkably induced in OPG-KO than RANKL-Tg. Finally, we examined whether administration of a bisphosphonate (BP, risedronate) can prevent the ABL in OPG-KO. Administration of BP to OPG-KO recovered the state of bone to the level of WT. Serum levels of TRAP5b in OPG-KO were significantly decreased by the treatment with BP as well. These results suggest that the suppression of OPG is much more important to induce osteoclastic bone resorption than the enhancement of RANKL expression, and that OPG-KO is a useful model for in vivo screening of therapeutic agents for the treatment of diseases with enhanced osteoclastic bone resorption.

***Disclosures: Masanori Koide**, None.*

MO0152

Physiological Control of Bone Resorption by Semaphorin4D is Dependent on Ovarian Function. Romain DACQUIN*[1], Chantal Domenget[1], Pierre Jurdic[2], Irma Machuca-Gayet[1]. [1]IGFL, Ecole Normale Superieure de Lyon, France, [2]Ecole Normale Superieure de Lyon, France

Semaphorin4D is a homodimeric transmembrane semaphorin sharing structural similarities with αVβ3 integrin, which is the most abundant integrin expressed in bone resorbing ostoclasts, playing a major role in osteoclast function both *in vitro* and *in vivo*. We found that SEMA4D is not detected in osteoblasts but is present at the osteoclast cell surface, suggesting that it might play a role in bone resorption. Indeed, we show that, *in vitro*, *Sema4D-/-* osteoclast differentiation is delayed when compared to WT. Similarly to *β3 integrin*-deficient osteoclasts, *Sema4D-/-* osteoclasts displayed defective spreading, migration and reduced resorption due to altered β3 integrin downstream signalling, namely hyper phosphorylation of c-Src and Pyk2. In accordance with these *in vitro* data, histomorphometrical analysis of 3 and 6-month-old *Sema4D*-deficient females revealed a 30% increased bone mass phenotype compared to WT animals. The analysis of dynamic and biochemical marker of bone resorption and formation, indicated that this high bone mass phenotype was due to a decreased bone resorption as only urinary deoxypyridinoline were decreased in *Sema4D-/-* mice compared to WT. Neither the number nor the size of osteoclast of the mutant mice was affected, indicating a functional defect of osteoclasts in those mice. Surprisingly, mutant males display normal bone mass, suggesting that female *Sema4D-/-* bone resorption phenotype is not osteoclast autonomous. To prove it, we performed *Sema4D-/-* and WT cross bone marrow transplantation in irradiated *Sema4D-/-* and WT mice. The bone phenotype of the engrafted animals was not dependent of the donor mice genotype but of the recipient one, confirming that indeed *Sema4D* controls resorption through an indirect mechanism. We had noticed that *Sema4D-/-*mice were less fertile than WT mice; both the number of pups per brood and the number of litters per breeding period were decreased in *Sema4D*-deficient mice. In addition, the female osteopetrotic phenotype was detected at the onset of sexual maturity suggesting a link between the observed phenotype and ovarian functions. Indeed, after ovariectomy *Sema4D-/-* and WT mice exhibited similar bone volume demonstrating that the bone resorption phenotype of *Sema4D-/-* mice is dependent on female reproductive function. Altogether, this study suggests that *Sema4D* is a regulator of the interactions between bone resorption and reproduction.

***Disclosures: Romain DACQUIN**, None.*

MO0153

Reduced Bone Turnover in Mice Lacking the P2Y13 Receptor. Ning Wang*[1], Bernard Robaye[2], Ankita Agrawal[3], Gwendolen Reilly[4], Jean-Marie Boeynaems[2], Alison Gartland[5]. [1]The University of Sheffield, United Kingdom, [2]Institute of Interdisciplinary Research, IRIBHM, Université Libre de Bruxelles, Belgium, [3]The Mellanby Centre for Bone Research, Department of Human Metabolism, The University of Sheffield, United Kingdom, [4]University of Sheffield, United Kingdom, [5]The Mellanby Centre for Bone Research, The University of Sheffield, United Kingdom

The P2Y13 receptor is one of the new members in the P2Y receptor family and is abundantly expressed in the nervous, haematopoiesis, and immune systems. Expression of P2Y13 receptor by osteoblasts has been confirmed, indicating a potential role in bone formation and homeostasis. The aim of this study was to examine the bone phenotype of P2Y13 receptor knockout (KO) mice and to investigate the role of the P2Y13 receptor in the skeletal system. Bone morphometric analysis was performed on tibae of 16 week-old female mice using a Skyscan 1172 MicroCT machine at the scan resolution of 4.3μm. Results showed the KO mice had 37.5% lower trabecular bone volume/tissue volume, 37.8% less trabecular number and 10.5% increased cortical bone thickness. Histomorphometric analysis showed a significant decrease in both osteoblast and osteoclast number on the tibial endocortical surface (42.6% and 48.0% respectively) of the KO mice. For dynamic histomorphometry analysis, mice were given intraperitoneal injections of calcein (30 mg/kg) 14 days and 2 days prior to the sacrifice. KO mice had 49.7% reduced endocortical mineral apposition rate and 48.9% lower bone formation rate. Mechanical properties tested by femur midshaft three-point bending on Bose EnduraTEC ELF3200 materials testing machine revealed that the KO mice had increased bone strength. In vitro, primary osteoblasts derived from the calvaria of neonatal KO mice showed reduced alkaline phosphatase (ALP) activity. In addition, multinucleated osteoclasts were derived from the mononuclear hematopoietic cell population of 10 weeks old female mice long bone marrow in the presence of murine macrophage colony stimulating factor (M-CSF) and receptor activator of NF-κB ligand (RANKL). There was a 49.45% reduction in the number of Tartrate Resistant Acid Phosphatase (TRAP) positive osteoclasts derived from KO mice and 66.14% reduced total resorption when compared to wild type osteoclasts. In summary, deletion of the P2Y13 receptor in mice leads to an abnormal bone phenotype, including less trabecular bone but thicker cortical bone. This is a consequence of reduced rates of bone turnover caused by decreased number and function of both osteoblasts and osteoclasts. The reduced bone turnover activities of the P2Y13 receptor KO mice may present a novel potential target to create new effective pharmaceuticals for fighting bone diseases such as osteoporosis.

***Disclosures: Ning Wang**, None.*

MO0154

Sphenoid Wing Dysplasia in Neurofibromatosis Type 1 (NF1) is Recapitulated in the Nf1 Osteoblast Conditional Knockout Mouse. Regina O'Sullivan*[1], Roberto Fajardo[2], Zhenxin Shen[3], Merrilee Flannery[3], Kevin McHugh[3]. [1]Center for Advanced Orthopaedic Studies, Harvard Medical School, USA, [2]UT Health Science Center, San Antonio, USA, [3]Beth Israel Deaconess Medical Center, USA

A range of cranial bone abnormalities are seen in NF1 patients with Sphenoid Wing Dysplasia (SWD) as the most severe. SWD is seen in 7-11% of NF1 patients. SWD is progressive and results in unilateral proptosis of an eye and the distinct facial appearance of NF1. In Nf1ob-/- mice, the neurofibromin gene (Nf1) is conditionally deleted in osteoblasts under the control of col-1Cre. Nf1ob-/- mice display a cranial dysplasia remarkably similar to SWD. We undertook characterization of this phenotype to establish the Nf1ob-/- mouse as a model of SWD in NF1.

Founding Nf1ob-/- mice were the generous gift of Dr. Florent Elefteriou, Vanderbilt University. Whole mouse skulls were scanned using a high-resolution desktop μCT system (micro-computed tomography) (μCT-40; Scanco Medical) at a voxel size of 36μm^3, 70kV, 114 μAmps and 200 mS. Analyze 7 was used for image analysis.

Proptosis of an eye and malocclusion, characteristics of SWD, were observed (Figure 1) in 50% of Nf1ob-/- mice at 10 weeks, 75% at 16 weeks, and 100% of mice 18 weeks and greater. Malocclusion normally has an incidence rate of 8.9 per 10,000 in the background C57BL6 strain (Jackson Labs, 2002). μCT analysis of Nf1ob-/- mice at 16 and 25 weeks shows a marked cranial asymmetry including the squamosal/temporal bone, sphenoid bone, and the frontal bone (Figure 2). Morphometric analysis indicates that the nasal and premaxilla bones are curved in the horizontal plane and twisted in the sagittal plane. Nf1ob-/- skulls are significantly shorter at 25 weeks than controls (floxed). Maxilla and lacrimal bones are thinned. Cranial sutures are also thickened relative to controls. μCT imaging of animals at 16, 19, 20, and 25 weeks of age indicate a progressive phenotype.

μCT of these animals show a progressive loss of craniofacial symmetry at the sphenoid bone and other cranial bones, in a manner similar to SWD in NF1. In these animals, we see deviation of the nasal bones associated with malocclusion.

The similarities between human SWD and the Nf1ob-/- mouse cranial dysplasia are remarkable. There are currently no treatments to block or slow the progression of SWD in NF1. We have characterized a novel and relevant mouse model which recapitulates the phenotype of SWD. Using this mouse model we are positioned to test the effects of currently approved drugs on the progression of SWD. The long-term goal of these studies is to identify treatments to treat NF1 patients with sphenoid wing dysplasia.

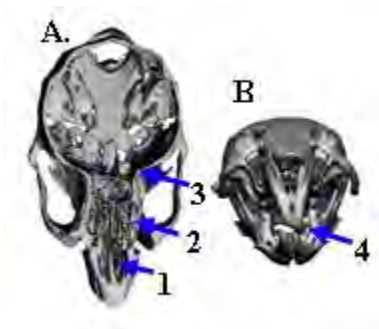

Figure 2. Horizontal cutaway image at the level of the eye (A) and frontal view (B).

Figure 1. Proptosis of an eye is apparent in a 36 week old Nf1ob-/- male mouse

***Disclosures: Regina O'Sullivan**, None.*

MO0155

The Adipogenic Potential of Mesenchymal Stem Cells (MSCs) Isolated from the Bone Marrow of Osteoporotic Postmenopausal Women Is Higher than in Control Cells. Juan Rodriguez*[1], Ana María Pino[2], Mireya Fernández[2], Oscar Donoso[2], Celeste Avalos[2], María Elena Ponce[2], César Navea[2], Julio Tapia[3], Nelson Osses[4]. [1]INTA Universidad De Chile, Chile, [2]Laboratorio de Biología Celular y Molecular, INTA, Universidad de Chile, Chile, [3]Laboratorio de Transformación Celular, ICBM, Facultad de Medicina, Universidad de Chile, Chile, [4]Facultad de Ciencias, Universidad Católica de Valparaíso, Chile

Postmenopausal osteoporosis is characterized by decreased bone quality and mineral density. The origin of this pathology is not well understood, but the activities of osteoclasts, osteoblasts, and mesenchymal stem cells (MSCs) have been proposed. MSCs found in bone marrow, are multipotent cells able to differentiate into several phenotypes, among others into osteoblasts and adipocytes. In the human bone marrow, the osteogenic differentiation pathway appears favored in normal conditions. In contrast, in osteoporosis the balance between osteoblast/ adipocyte commitment and differentiation is broken favoring adipocyte formation. In this work, the adipogenic potential of MSCs obtained from control and osteoporotic donors was studied by measuring the expression of genes involved in cells commitment into adipogenesis. For this purpose, MSCs were isolated from bone marrow samples obtained by iliac crest aspiration from volunteer postmenopausal women donors, after signing an informed consent. MSCs were expanded in culture and mRNA was extracted, samples were classified as control (c-) or osteoporotic (o-) according to donors bone density determined by DEXA. The relative abundance of genes for peroxisome proliferator-activated receptor gamma (PPARγ), beta-catenin, glycogen synthase kinase-β (GSK-3β), Dickkopf-1 (Dkk-1), bone morphogenic protein receptors IA and IB (BMPRIA and BMPRIB) were determined by RT-PCR. After adipogenic differentiation of cells, the adipocytes number and its morphological characteristics were analyzed by flow cytometry. Results show that under basal conditions the level of mRNAs for PPARγ, β-catenin, Dkk-1 and BMPRIB are similar in both control and osteoporotic cells, while GSK-3β and BMPRIA genes expression are significantly higher in o-MSCs than in c-MSCs. After adipogenic treatment, o-MSCs originated higher adipocyte number than c-MSCs, while the adipocytes size was higher in those derived from c-MSCs. The increased BMPRIA gene expression found in o-MSCs under basal conditions suggests improved adipogenic cell commitment; further the increased GSK-3βgene expression in this cell type implies diminished potential for Wnt activity favoring early adipogenic differentiation.

***Disclosures: Juan Rodriguez**, None.*

MO0156

The Dominant V-ATPase a3 Mutation, R740S, Results in Perinatal Lethality in Homozygous Mice. Noelle Ochotny*[1], Ann Flenniken[2], Celeste Owen[2], Irina Voronov[1], Morris Manolson[1], Jane Aubin[3]. [1]University of Toronto, Canada, [2]Centre for Modeling Human Disease, Canada, [3]University of Toronto Faculty of Medicine, Canada

Mutations in vacuolar-type H+-ATPases (V-ATPases) disrupt bone resorption, leading to osteopetrosis in mice and humans. V-ATPases are proton pumps composed of 14 subunits, including the 'a' subunit. Of the 4 'a' isoforms in mammals a3 is enriched in osteoclasts where it is essential for bone resorption. Humans with inactivating mutations to both a3 alleles are severely osteopetrotic and do not live past 6 years without treatment, while their heterozygous parents have no detectable phenotype. Homozygous a3-/- mice have severe osteopetrosis and die by 6 weeks, while a3 +/- mice have no phenotype. During a mouse genome-wide ethylnitrosourea (ENU) mutagenesis screen for dominant mutations affecting bone mineral density (BMD), we identified a mouse with a high BMD/osteopetrotic phenotype carrying a dominant V-ATPase a3 missense mutation replacing arginine 740 with serine (R740S). The mouse a3 R740 residue is perfectly conserved in human and mouse 'a' isoforms. The heterozygous +/R740S mice have normal appearance, size and weight but, despite a greater number of osteoclasts, exhibit increased bone density due to defective osteoclast resorption. To determine the phenotype of mice homozygous for R740S, we conducted intercross breedings of +/R740S mice. There were no differences in appearance, size or weight of R740S/R740S, +/R740S or WT pups at P0. Although R740S/R740S mice were born alive, none lived past 3 weeks of age. Whole mount staining of mice collected within 12 hours of birth to visualize mineralization of the skeleton revealed that the R740S/R740S pups had mineralization deficits, i.e., the ribs and the supraoccipital bone were poorly mineralized. No detectable abnormalities in morphology or cellularity of major organ systems were detected by a trained mouse pathologist. Osteoclasts were clearly present in R740S/R740S bones, however, isolation of osteoclasts by flushing bone marrow failed to yield any osteoclasts from R740S/R740S pups. Osteoblast number, differentiation time course and activity were similar in cultures isolated from the calvaria of newborn R740S/R740S, +/R740S and WT pups. Conclusion: Mice homozygous for R740S are born at the expected Mendelian ratio but die soon after birth. Studies are in progress to determine what causes R740S/R740S pups to die soon after birth.

***Disclosures: Noelle Ochotny**, None.*

MO0157

The High Bone Mass Phenotype is Characterised by Reduced Endosteal Expansion, Increased Thickness and Density of Trabeculae, but not Number. Celia Gregson*[1], Margaret Paggiosi[2], Eugene McCloskey[3], Jon Tobias[4]. [1]University of Bristol, United Kingdom, [2]Northern General Hospital, United Kingdom, [3]University of Sheffield, United Kingdom, [4]Clinical Sciences at North Bristol, University of Bristol, United Kingdom

High Bone Mass (HBM) is an uncommon sporadic finding of raised bone density on DXA scanning in otherwise asymptomatic individuals. Some cases have been reported in association with activating *LRP5* gene mutations suggested to enhance osteoblast activity; X-rays have shown widened long bones and cortices in-keeping with increased bone formation. However our HBM cases have previously shown reduced bone turnover markers suggesting a low bone turnover state. As part of the first systematic evaluation of the HBM skeletal phenotype we performed High Resolution peripheral Quantitative Computed Tomography (HRpQCT) measurements in a unique collection of HBM cases.

69 HBM index cases were identified by screening a hospital DXA database (n=60319). HBM was defined as a)L1 Z score of ⩾ +3.5 plus total hip Z score of ⩾ +1.2 or b)total hip Z score ⩾ +3.5. Cases with significant osteoarthritis and/or other causes of raised BMD were excluded. First-degree relatives and spouses were recruited, in whom HBM affectation status was defined as L1 Z plus total hip Z scores of ⩾ +3.5. Controls comprised unaffected relatives & spouses. HRpQCT was performed at the 4% radius & tibia using a Scanco XtremeCT. Cases were compared with controls using linear regression adjusting for age, sex, weight & height.

26 HBM cases (21 index & 5 affected relatives) (54% female) & 15 controls (27% female) underwent HRpQCT; mean age 58.4 & 57.9years, height 170 & 167cm, weight 89 & 81kg respectively. As shown in the table, compared with controls HBM cases had considerably higher trabecular BMD at both the radius and tibia, reflecting greater trabecular thickness rather than number. HBM cases had increased cortical thickness, particularly in the radius. Whilst total bone area in HBM cases was similar to controls, cortical bone area was higher (22.1 vs 13.6%, p=0.01, and 19.7 vs 14.3%, p=0.08, percentage cortical bone area of the radius and tibia respectively).

We conclude that, the greater bone mass seen in HBM is due to a combination of thicker trabeculae and cortices. Interestingly, total bone area, an indicator of periosteal apposition, is unaffected. Taken together, the bone phenotype of HBM cases is more in-keeping with a primary role of reduced bone resorption than increased formation. Though consistent with our previous finding of reduced bone turnover markers in this group, these results would seem at odds with reports that these cases arise from mutations causing excessive osteoblast activation.

	HBM Cases (n=26) [95% CI]†	Family Controls (n=15) [95% CI]†	P value†
RADIUS			
Trabecular BMD (mg/cm^3)	224.2 [201.9, 246.5]	161.7 [129.0, 194.3]	<0.01
Trabecular No. (1/mm)	2.32 [2.17, 2.47]	2.21 [1.99, 2.43]	0.38
Trabecular Thickness (μm)	81 [73, 88]	60 [49, 72]	0.01
Cortical Thickness (mm)	0.93 [0.77, 1.08]	0.58 [0.35, 0.81]	0.01
Total Bone Area (mm^2)	352.5 [332.3, 372.7]	360.6 [331.1, 390.1]	0.64
TIBIA			
Trabecular BMD (mg/cm^3)	234.5 [215.0, 254.0]	193.4 [164.9, 222.0]	0.02
Trabecular No. (1/mm)	2.35 [2.20, 2.51]	2.33 [2.11, 2.56]	0.89
Trabecular Thickness (μm)	84 [78, 89]	70 [62, 77]	<0.01
Cortical Thickness (mm)	1.41 [1.17, 1.65]	1.03 [0.67, 1.39]	0.07
Total Bone Area (mm^2)	833.1 [786.4, 879.9]	825.2 [756.57, 893.9]	0.84

†adjusted for age, sex, weight & height
HBM:High Bone Mass, CI:Confidence Interval, BMD:Bone Mineral Density

Table: HRpQCT measures from the radius & tibia in High Bone Mass cases and their family controls

***Disclosures: Celia Gregson**, None.*

MO0158

Pleiotropic Genetic Effects Contribute to the Correlation Between Bone Mineral Density and Quantitative Ultrasound Measurements. Sing Nguyen*, Nguyen Nguyen, Jacqueline Center, John Eisman, Tuan Nguyen. Garvan Institute of Medical Research, Australia

The heritability of bone mineral density (BMD) has long been established using both twin and familial models. Similarly, various quantitative ultrasound (QUS) parameters of bone have been shown to be under genetic influence. BMD is correlated with QUS, but it is not known whether this is due to genetic or environmental influences. The present study was designed to examine whether BMD and QUS are affected by the same genetic factors.

The study involved 622 individuals from 33 multigenerational families who were part of the Dubbo Osteoporosis Genetics Study, all aged 18+ at the time of participation. BMD at the femoral neck (FNBMD), lumbar spine (LSBMD) and total body (TBBMD) was measured by DXA (GE-Lunar Corp, Madison, WI, USA). Speed of sound (SOS) at the distal radius (DRSOS), midshaft of tibia (MTSOS) and proximal phalanges (PPSOS) were measured by Sunlight Omnisense (Sunlight Medical). The indices of heritability (h^2) of BMD and QUS measurements were estimated using the variance components model as implemented in the SOLAR program, taking into account the effects of age, sex, and anthropometric variables. Moreover, the genetic and environmental correlations were estimated by bivariate genetic analysis. The genetic correlation represents a measure of pleiotropic effects of genes influencing both traits concomitantly.

Between 42% and 59% of the variation in BMD at different skeletal sites was attributable to genetic factors (h^2 for FNBMD 0.42 (standard error: 0.09), LSBMD: 0.59 (0.07), and TBBMD: 0.54 (0.14)). The effect of genetic factors on QUS was slightly lower than for BMD (DRSOS: 0.21 (0.09), MTSOS: 0.39 (0.12), and PPSOS: 0.23 (0.12)). More importantly, there was a strong genetic correlation between the three BMD measurements (FNBMD vs. LSBMD: 0.55 (0.10), FNBMD vs. TBBMD: 0.77 (0.06), and LSBMD vs. TBBMD: 0.81 (0.09)). Moreover, there was a genetic correlation between DRSOS and FNBMD (0.52 (0.22)) and LSBMD (0.40 (0.17)), but the correlation was not statistically significant for other QUS measurements (0.08 to 0.40; $P > 0.05$). Furthermore, a modest genetic correlation was observed between total fat mass and LSBMD: 0.38 (0.17).

These results suggest that pleiotropy contributes to the additive genetic variation in BMD measurements, and to a lesser extent, between BMD and QUS measurements. The presence of genetic correlation provides the rationale for multivariate analyses to identify novel genetic loci with pleiotropic effects on these bone traits.

***Disclosures: Sing Nguyen**, None.*

MO0159

Significant Quantitative Trait Loci on Chromosomes 3 and 16 Linked to Proximal Hip Geometry in the Fels Longitudinal Study. Miryoung Lee*[1], Audrey Choh[1], Bradford Towne[1], Thomas Dyer[2], Dana Duren[3], Ramzi Nahhas[1], Richard Sherwood[4], Wm. Chumlea[1], Roger Siervogel[1], Shelley Cole[2], Stefan Czerwinski[1]. [1]Wright State University Boonshoft School of Medicine, USA, [2]Southwest Foundation for Biomedical Research, USA, [3]Wright State University, USA, [4]Lifespan Health Research Center,Wright State University, USA

Purpose of the study: Osteoporosis leads to loss of bone strength and increases risk of fracture. Different measures of bone strength (e.g., hip geometry) may well be influenced to varying degrees by different genes or sets of genes. We performed genome-wide quantitative trait linkage analysis on hip structure phenotypes collected in a sample of 724 family members (340 males, 384 females) aged 18 – 91 years participating in the Fels Longitudinal Study. Methods: Hip structure parameters were obtained from existing dual energy X-ray absorptiometry scans collected using the Hologic Discovery A bone densitometer and Hip Structure Analysis (HSA) software (Hologic, Inc., Waltham, MA). All participants were genotyped for 400 autosomal short tandem repeat (STR) markers spaced approximately every 10 cM. Our analyses focused on four HSA phenotypes (i.e., cortical buckling ratio, cross-sectional area, endocortical diameter and section modulus) collected at three regions of the femoral neck (i.e., shaft, intertrochanteric and narrow neck). Using a variance-components based maximum likelihood method for pedigree data (SOLAR), we calculated initial heritability estimates (h^2) and identified quantitative trait loci influencing variation in each of the four HSA phenotypes. Results: Each HSA trait measured was highly heritable (h^2 range = 0.44 - 0.66, all $p < 0.000001$) after adjusting for the effects of age, sex, age^2, age-by-sex, age^2-by-sex, height, and body mass index. Significant evidence for linkage was found on chromosome 3p (50cM) near marker D3S1266 for cross-sectional area at all three anatomic regions (maximum LOD = 4.1 at the intertrochanteric region). Significant evidence for linkage was also found on chromosome 16q (73cM) near marker D16S3140 for endocortical diameter in the intertrochanteric region (maximum LOD = 3.2). Conclusion: These results provide evidence of replication of linkage signals between our study and other previous studies of bone strength phenotypes.

***Disclosures: Miryoung Lee**, None.*

MO0160

Association between Polymorphisms in Wnt Signaling Pathway Genes and Bone Mineral Density in Postmenopausal Korean Women. Dong-Yun Lee[1], Hoon Kim[2], Seung-Yup Ku[3], Young- Min Choi[3], Jung-Gu Kim*[3]. [1]Samsung Medical Center, South korea, [2]Seoul National Univeristy Hospital, South korea, [3]Seoul National University Hospital, South korea

Objective: The purpose of this study was to investigate the association between single nucleotide polymorphism (SNP) in Wnt signal pathway genes and circulating osteoprotegerin (OPG), soluble receptor activator of NF-κB ligand (sRANKL) levels, bone turnover markers, and bone mineral density (BMD) in postmenopausal Korean women.

Methods: Wnt9a c256G>A, low density lipoprotein receptor-related protein (LRP) 5 c266A>G, c2245C>G, c3893C>T, c4099G>A, secreted frizzled-related protein (sFRP) 4 c1019G>A, axin II c148C>T, c1615G>A, glycogen synthase kinase binding protein (GBP) c455C>A, β-catenin c94G>T, c101G>T, T cell factor (Tcf) 1 c663G>T, c734C>T and c766G>A, and adenomatous polyposis coli c5465T>A polymorphisms were analyzed in 392 postmenopausal Korean women. Serum levels of OPG, sRANKL, and bone turnover markers were measured, and BMDs at the lumbar spine and femoral neck were examined.

Results: Wnt9a c256G>A, LRP 5 c2245C>G and c4099G>A, axin II c1615G>A, GBP c455C>A, β-catenin c94G>T and c101G>T, Tcf 1 c663G>T and c734C>T SNPs were not observed. Among genes showing polymorphisms, only the sFRP4 c1019G>A polymorphism was associated with BMD. The AA genotype in the sFRP4 c1019G>A polymorphism showed significantly lower lumbar spine BMD and a higher serum bone alkaline phosphatase level than the GG genotype, and showed a 6.39 times higher risk for osteoporosis at the lumbar spine compared with the GG genotype. No significant differences in bone turnover markers, OPG, and sRANKL were detected among other single genotypes or the LRP haplotype genotype.

Conclusions: Our results indicate that the sFRP4 c1019G>A polymorphism is one of the genetic factors affecting lumbar spine BMD in postmenopausal Korean women.

Funding Support: This study was supported by a grant (A080012) from the Korea Health technology R&D project, Ministry of Health, Welfare & Family Affairs, Republic of Korea

***Disclosures: Jung-Gu Kim**, None.*

MO0161

Functional Relevance of the BMD-associated Polymorphism rs312009. Novel Implication of Runx2 in *LRP5* Transcriptional Regulation. Daniel Grinberg*[1], Lidia Agueda[2], Rafael Velazquez[2], Roser Urreizti[2], Patricia Sarrion[2], Susana Jurado[3], Guy Yoskovitz[4], Roberto Güerri[4], Natalia Garcia-Giralt[4], Xavier Nogues[5], Leonardo Mellibovsky[4], Adolfo Diez-Perez[6], Susana Balcells[2]. [1]The University of Barcelona, Spain, [2]Universidad de Barcelona. Dep of Genetics, Spain, [3]Hoospital del Mar-IMIM, Spain, [4]Hospital del Mar-IMIM, Spain, [5]Institut Municipal D'Investigació Mèdica, Spain, [6]Hospital del Mar-IMIM-Autonomous University of Barcelona, Spain

LRP5 is a known osteoporosis susceptibility gene. Association analyses allow for the discovery of individual SNPs that determine variation in bone mineral density (BMD) among individuals as well as fracture risk. In a previous work, we identified a lumbar spine BMD-associated SNP, rs312009, located in the *LRP5* 5' region. By gel shift experiments a Runx2 binding site was identified at that site. The purpose of this work was to test the functionality of this SNP and to analyze whether Runx2 is indeed a regulator of *LRP5* expression.

The 3kb region upstream of *LRP5* was screened for Runx2 binding elements using bioinformatic predictive tools. Gel shift and gene reporter assays were used to test the functionality of the sites and of the two alleles of site 1. Site-directed mutagenesis as well as Runx2 cotransfection were undertaken to assess Runx2 involvement. Constructs were transfected in the osteoblastic cell lines U2OS and Saos2 as well as in HeLa cells.

Allelic differences in transcriptional activity of rs312009 were observed in the two osteoblastic cell lines, the T allele being a better transcriber than the C. Runx2 cotransfection in HeLa cells revealed that *LRP5* 5' region was able to respond to Runx2 in a dose-dependent manner and that the previously identified Runx2 binding site participated in this response. Four other Runx2 binding sites were identified in the 5' region of *LRP5*. Luciferase experiments, where each Runx2 binding site was individually mutated, revealed the implication of all of them in the Runx2-response.

The allelic differences observed point to rs312009 as a functional SNP implicated in the observed association. To our knowledge, this is the first time that a direct action of Runx2 on *LRP5,* an important element of the Wnt β-catenin pathway, is described. This adds evidence to previously described links between two important bone regulating systems: the Runx2 transcription factor cascade and the Wnt signaling pathway.

***Disclosures: Daniel Grinberg**, None.*
This study received funding from: Instituto Carlos III. RETICEF. Spanish Ministry of Science and Technology

MO0162

Genome-wide Association Study for Femoral Neck Bone Geometry. Fei-Yan Deng*[1], Xiang-Hong Xu[2], Yong-Jun Liu[1], Hui Shen[1], Shu-Feng Lei[1], Jian Li[1], Yan Guo[2], Tie-Lin Yang[2], Hong-Wen Deng[3]. [1]University of Missouri - Kansas City, USA, [2]Xi'an Jiaotong University, China, [3]University of Missouri, Kansas City Medical School, USA

Hip fractures are the most severe clinical outcome of osteoporosis due to its serious impact on quality of life and excessive therapeutic costs. Femoral neck (FN) bone geometry is an important predictor of bone strength and risk of hip fractures. FN bone geometry is under strong genetic control, but the specific genes influencing FN bone geometry remain largely unknown. To identify such genes, we conducted a genome-wide association study (GWAS) for FN bone geometry using the Affymetrix Genome-Wide Human SNP Array 6.0 in a large cohort of 2,500 unrelated Caucasian subjects.

After applying rigorous quality-control criteria, 2286 individuals (558 males and 1,728 females) and 730,349 single nucleotide polymorphisms (SNPs) were retained for association analyses. SNPs were tested for association with FN bone geometry by the quantitative association tests implemented in PLINK, while controlling for potential confounding factors, such as age, gender, height and weight.

A common genetic variant rs6578987 located approximately 8kb downstream of the insulin-like growth factor 2 (IGF2) gene was identified in association with two indices of FN bone geometry, cortical thickness (CT, p=1 x 10-7) and bucking ratio (BR, p=1 x 10-6). Our findings, together with the well-known function of IGF2 in bone metabolism, provided compelling evidence that IGF2 may affect FN bone geometry variation and thus risk to hip fractures.

***Disclosures: Fei-Yan Deng**, None.*

MO0163

Large Scale Human SNP Analysis Revealed an Association of GPR98 Gene Polymorphisms with Bone Mineral Density in Postmenopausal Women and Gpr98 Deficient Mice Display Osteopenia. Tomohiko Urano*[1], Masataka Shiraki[2], Hideshi Yagi[3], Makoto Sato[3], Yasuyoshi Ouchi[1], Satoshi Inoue[1]. [1]Department of Geriatric Medicine, Graduate School of Medicine, The University of Tokyo, Japan, [2]Research Institute & Practice for Involutional Diseases, Japan, [3]Division of Cell Biology & Neuroscience, Department of Morphological & Physiological Sciences, Faculty of Medical Sciences, University of Fukui, Japan

Genetic factors are important for the development of osteoporosis. Our objective is to search for novel genes that regulate BMD. We performed a large scale search for 50K single-nucleotide polymorphisms (SNPs) associated with BMD by using SNP arrays in Japanese postmenopausal women. We focused on a SNP of G protein-coupled receptor gene 98 (GPR98) that showed a significant P value after the multiple comparison tests. We then discovered that GPR98 gene polymorphisms were significantly associated with total body BMD in 750 postmenopausal Japanese women. These data suggest that the genetic variations in the GPR98 gene would influence the risk of osteoporosis. The associations of the GPR98 gene polymorphisms with femoral neck and lumbar spine BMD were also observed *in silico* database of Framingham Heart Study in Caucasian women. These replicable associations of GPR98 SNPs with BMD in different races further encourage us to consider that this gene may contribute to the development of osteoporosis. Therefore, we have analyzed whether the deficiency of Gpr98 gene is involved in the control of BMD in the mouse model. Compared with 12 weeks-old wild-type mice (n=6), femur BMD in 12 weeks-old Gpr98 knockout mice (n=5) was significantly lower ($P<0.001$). These data indicated that Gpr98 KO mice display osteopenic phenotype. Thus, genetic analyses in both human and mouse models uncovered the importance of GPR98 gene in the regulation of the BMD.

***Disclosures: Tomohiko Urano**, None.*

MO0164

Mouse QTL-directed Analysis of Homologous Human Chromosomal Regions in a Large Scale Meta-analysis of Genome-wide Association Studies of the GEFOS Consortium Reveals Novel Genetic Associations with Bone Mineral Density. Carrie Nielson*[1], Karol Estrada[2], Robert Klein[1], Fernando Rivadeneira[2], Andre Uitterlinden[3], Eric Orwoll[1], GEFOS Consortium[4]. [1]Oregon Health & Science University, USA, [2]Erasmus University Medical Center, The netherlands, [3]Rm Ee 575, Genetic Laboratory, The netherlands, [4]Erasmus Medical Center, Netherlands

Background: In mouse models, quantitative trait locus (QTL) linkage analyses identify regions highly associated with bone mineral density (BMD) that contain too many genes to be easily assessed in functional or human studies. Analyses of homologous human chromosomal regions in large genome-wide association studies (GWAS) of BMD may help focus follow-up studies on the genes most likely to be relevant to human BMD.

Methods: From analyses of a C57BL/6 (B6) x DBA/2 (D2) mouse model of peak BMD, we selected 3 QTLs strongly linked to BMD: mouse proximal chromosome (Chr) 12 (homologous to human Chr2p23-25), mid Chr8 (human Chr16q12-23), and proximal Chr7 (human Chr19q12-13.3). We interrogated these regions in humans using the results of the published GEFOS GWAS meta-analysis on femoral neck (FN) and lumbar spine (LS) BMD in 19,195 individuals. All available association results from the imputed SNPs in the 3 specific homologous human regions (27,679 SNPs on Chr2; 22,059 on Chr16; and 11,024 on Chr19) were adjusted for multiple testing by the false-discovery-rate (FDR) method where a FDR<0.05 was considered significant.

Results: Of the three loci, two were associated. On human Chr19, 3 novel genes (*GPATC1* encoding G-patch domain containing 1 a member of a family of proteins known to play important roles in RNA processing; *RHPN2* encoding rhophilin, a member of the Rho GTPase binding protein family that controls osteoclast podosome arrangement; and *PEPD* encoding prolidase, a cytosolic imidodipeptidase that regulates collagen biosynthesis) were identified with multiple SNPs significantly associated with LS BMD after adjustment for multiple testing (FDR<0.05; Table). Two genes on Chr2 (*ASXL2* encoding additional sex combs-like 2, a protein that participates in murine axial skeleton patterning and *TPO* encoding thyroid peroxidase, a member of the NADPH oxidase family involved in thyroid hormone synthesis) had multiple SNPs with p=0.0001 but FDR~0.1. No significant associations were observed for Chr16 or for FNBMD in any of the 3 regions after adjustment for multiple testing.

Conclusions: BMD is a complex trait determined by numerous genetic variants. By interrogating selected human SNPs in regions homologous to previously identified mouse BMD QTLs, we have identified two novel loci. Some of the genes in these loci have known skeletal function in model organisms and may contribute to genetic control of human BMD.

Gene symbol	Locus	SNPs significant*/ genotyped	SNP most strongly associated with LSBMD					
			SNP	A1/A2	Freq. A1	Effect	P value	FDR
ASXL2	2p24.1	60/86 (70%)	rs10469884	T/G	0.30	0.05	0.0001	0.11
TPO	2p25	24/184 (13%)	rs10204647	T/C	0.52	0.05	7.8×10^{-5}	0.11
GPATC1	19q13.11	36/42 (86%)	rs2287679	T/C	0.75	-0.07	8.1×10^{-8}	0.0002
RHPN2	19q13.11	14/60 (23%)	rs8106453	T/C	0.25	0.07	4.3×10^{-7}	0.0003
PEPD	19q13.11	13/143 (9%)	rs3786913	A/G	0.86	0.08	7.7×10^{-6}	0.004

* Unadjusted p < 0.0001
A1: allele1, A2: allele2, Freq.: frequency, FDR: false-discovery rate

Table

***Disclosures: Carrie Nielson**, None.*

MO0165

Novel Loci on the X Chromosome for Musculoskeletal Traits: the Framingham Osteoporosis Study. Yue Fang*[1], Yi-Hsiang Hsu[2], Yanhua Zhou[3], Serkalem Demissie[3], Josee Dupuis[3], Adrienne Cupples[3], Douglas Kiel[4], David Karasik[4]. [1]Hebrew Seniorlife Center at Harvard Medical School, USA, [2]Hebrew SeniorLife & Harvard Medical School, USA, [3]Department of Biostatistics, Boston University School of Public Health, USA, [4]Hebrew SeniorLife, USA

Genome Wide Association (GWA) studies have provided significant evidence of sequence variations that influence genetic susceptibility to many common complex diseases. Using a candidate gene approach, genes on the X-Chromosome have been found to be related to several clinical disorders, including bone and muscular disorders. However, most GWA studies have focused only on the autosomes. In this study, we performed an X-chromosome focused association study between single nucleotide polymorphisms (SNPs) and multiple musculoskeletal parameters in the Framingham Original and Offspring cohorts. Multiple musculoskeletal parameters [including heel ultrasound as well as bone mineral density (BMD) at femoral neck (FN) and lumbar spine (LS) sites, whole body and appendicular lean body mass (wbLM and aLM), and 5 hip geometry indices] were measured by DXA. We genotyped 3,391 Caucasians (mean age of 65 years; 1,462 Men and 1,929 women) with the Affymetrix 500+50K Genechips, and imputed X-chromosome wide SNPs with the HapMap CEU phase II panel using "IMPUTE". A total of 57,197 SNPs with minor allele frequency $> 1\%$ and imputed ratio of observed/expected variance of allele frequency >0.3 were included in our association analyses. To correct for multiple testing, for each trait X-chromosome-wide cut-off p-values were estimated by the False Discovery Rate at 0.05 level, and the lowest trait-specific cut-off p-value ($=3.8 \times 10^{-6}$) was set as the common significant p-value for all association analyses. After adjusting for age, sex (for sex-combined data), BMI, height and population structure in linear mixed effect models (including sex-specific), we observed significantly associated loci: the *DMD* gene (involved in Duchenne Muscular Dystrophy) with aLM ($p=3.3 \times 10^{-6}$) and *PIGA* gene (involved in acquired hematologic disorder) with femoral neck cross-sectional area (NeckCSA, $p=9.0 \times 10^{-7}$) for both men and women. The *FIGF* gene (involved in endothelial cell growth) was found to be specifically associated with female NeckCSA ($p=1.9 \times 10^{-6}$). We also examined the association between 314 SNPs in previously reported candidate genes (e.g., *AREG*, *PHEX*, *ARSE* and *PIR*) and musculoskeletal phenotypes in our study. No SNPs in these genes were significantly associated at the trait-specific and entire X-chromosome significant level. In conclusion, three novel loci on the X-chromosomewere associated with appendicular lean mass and femoral neck cross-sectional area in the Framingham Osteoporosis Study, including a gene with potential important for muscle. Future GWAS analyses should include the X-chromosome because of potentially important loci for musculoskeletal traits.

***Disclosures: Yue Fang**, None.*

MO0166

Osteoprotegerin Gene Haplotype CT Is Associated With Lumbar Spine BMD in Osteoporotic Postmenopausal Women. Simona Mencej Bedrac[1], Janez Prezelj*[2], Tomaz Kocjan[3], Misa Pfeifer[4], Janja Marc[1]. [1]University of Ljubljana, Faculty of Pharmacy, Department of Clinical Biochemistry, Slovenia, [2]Medical faculty, University of Ljubljana, Slovenia, [3]University Medical Centre Ljubljana, Slovenia, [4]University Medical Centre Ljubljana, Department of Endocrinology & Metabolic Diseases, Slovenia

Osteoprotegerin (OPG) acts as a decoy receptor for receptor activator of nuclear factor κB ligand (RANKL) and inhibits osteoclast differentiation, survival and function. Due to its important role in bone biology, *OPG* gene has been considered as a candidate gene for osteoporosis. Additionally, recently published genome-wide association studies all identified the *OPG* gene as having a key role in the genetic background of osteoporosis. The aim of the present study was to investigate the influence of haplotypes of K3N (rs2073618) and 245T>G (rs3134069) *OPG* gene polymorphisms on bone mineral density (BMD) and serum OPG concentrations in postmenopausal women.

478 postmenopausal women, 243 osteoporotic and 235 non-osteoporotic, were enrolled in the study. BMD at lumbar spine, total hip and femoral neck were measured by dual energy X-ray absorptiometry (DXA). Serum OPG levels were measured by an enzyme immunoassay. Genotyping was performed by Taqman allelic discrimination method for K3N and by PCR-RFLP for 245T>G. Haplotypes were inferred using PHASE software. To evaluate the association of haplotypes with BMD and OPG levels, one-way ANOVA or Kruskal-Wallis test were used.

In our study, two common *OPG* gene haplotypes CT (52.4%) and GT (41.2%) were inferred. In osteoporotic postmenopausal women, lumbar spine BMD (BMD-ls) showed significant association with CT haplotype (p=0.006), whereas no association was observed for femoral neck or total hip BMD (p=0.161 for BMD-fn and p= 0.289 for BMD-th). In BMD-ls, the presence of CT haplotype was associated with higher BMD-ls. No association with BMD was found in GT haplotype (p=0.728, p=0.950 and p=0.134 for BMD-fn, BMD-th and BMD-ls, respectively). In non-osteoporotic postmenopausal women, no association with BMD was found in CT and GT haplotypes. The influence of studied haplotypes on OPG levels was not statistically significant.

Our results indicate the association of *OPG* gene haplotype CT with BMD-ls in osteoporotic postmenopausal women. The presence of CT haplotype seems to have a protective effect on BMD-ls, but the results need to be further confirmed in larger cohorts.

***Disclosures: Janez Prezelj**, None.*

MO0167

***In vivo* Bone Formation is Induced by Blocking Bone Morphogenetic Protein Receptor Type Ia Interaction with Casein Kinase II.** Beth Bragdon*[1], Shayamala Thinakaran[2], Lauren Gurski[2], Oleksandra Moseychuk[2], Wesley Beamer[3], Anja Nohe[2]. [1]University of Maine University of Delaware, USA, [2]University of Delaware, USA, [3]The Jackson Laboratory, USA

Bone Morphogenetic Proteins (BMPs) are potent growth factors, with robust osteoinductive properties a prominent characteristic of BMP2. Currently, rhBMP2 is used in treatment for vertebral fusion and long bone fractures. Disadvantages of rhBMP2 are high cost, need for high doses to induce adequate bone formation, and large variations in response among patients. An alternative to the rhBMP2 is desirable to exploit downstream molecules of the mechanism at which BMP2 is osteogenic.

BMPs signal through a hetero-oligomeric complex of BMP type I and type II receptors that activate multiple pathways including Smad and p38. Previous work identified Casein Kinase II (CK2), a ubiquitous protein kinase, as an interacting protein with the BMP type Ia receptor at the membrane of mesenchymal stem cells (C2C12 cells). A peptide was designed to block this interaction, which included an antennapedia homeodomain signal sequence for cellular uptake. In C2C12 cells, this peptide initiated a BMP-induced Smad signal and increased mineralization in the absence of BMP2. The purpose of this study was to test the osteoblastic differentiation properties of the osteogenic peptide for induction of bone in vivo. The peptide was injected sc once per day for 5 days, over the right side calvaria of 4 week old C57BL/6J mice (n= 21 per group). Mice were necropsied at 8 weeks of age and calvaria were measured by PIXImus dual energy X-ray densitometry for area BMD (aBMD). Results showed a significant increase in aBMD (0.00105 $1/cm^2$, +/- 0.00003 SEM) compared to groups without injection (0.00089 $1/cm^2$, +/- 0.00002), PBS injection (0.000855 $1/cm^2$, +/- 0.00004), and control peptide injection (0.00091 $1/cm^2$, +/- 0.00003) containing only the antennapedia homeodomain signal sequence. Histologically examined calvaria showed an increase in bone width. Further, calcein injections confirmed the new bone area increased with peptide injections. Taken together these data suggest the osteogenic peptide does induce in vivo bone growth and could provide a cost effective alternative to rhBMP2 for orthopedic surgeries that is small in size and more specific downstream of BMP2.

***Disclosures: Beth Bragdon**, None.*

MO0168

All IFITMs, except IFITM5, Inhibit Osteoblast Differentiation and Bone Formation. Hui Liu[1], Yunshan Liu*[2], Scott Boden[3], Louisa Titus[3]. [1]Emory University & Sun Yat-sen University, USA, [2]Emory University, USA, [3]VAMC & Emory University, USA

It has long been observed that first passage rat calvarial osteoblast cells (ROBs) lose their ability to spontaneously form bone nodules compared to primary cultures. Instead, a stimulus such as glucocorticoid or BMP-2 is needed for these secondary ROB cells to differentiate. It is reasonable for one to speculate that the expression level of critically important factor(s) is changed during the culture procedure. We analyzed the expression profiles of primary and secondary ROB cells for known bone differentiation factors as well as several other related factors, including Interferon induced transmembrane proteins (IFITMs), BMP-2 and osterix.

It appeared that primary and secondary ROB cultures have different gene expression patterns. The expression of IFITM5 and BMP2 is higher in primary ROB cells while other IFITMs show the reverse trends. IFITM2 and IFITM3 are the most abundant forms in both primary and secondary ROB cultures. In the mouse pre-osteoblast cell line MC3T3 sub-clone 24, which can be induced towards osteogenic differentiation and bone nodule formation by BMP-2, siRNAs against IFITM1, 2, 3, 6 and 7 all enhanced BMP-2-induced bone nodule formation. IFITM siRNAs alone, however, had little effect on bone nodule formation in these cells.

IFITM5 forced expression, has been reported to enhance bone formation in primary ROB cultures and in UMR106 cultures while knockdown of IFITM5 resulted in reduced mineralization of MC3T3 spontaneously differentiating cultures. Our data suggest that, in contrast, other IFITMs exhibit inhibitory effects on osteoblast differentiation and bone nodule formation. The mechanism by which IFITMs regulate osteoblast differentiation needs to be further investigated.

***Disclosures: Yunshan Liu**, None.*

MO0169

Osteoblast-Specific Enhancers of *Bmp2* Gene Expression: Anatomical Specificity and *Bmp2* Stimulation by FGF2 *In Vitro* and *In Vivo*. Eva Broeckelmann*, Steven Pregizer, Douglas Mortlock. Vanderbilt University Medical Center, USA

Bmp2 is a member of the TGF-β superfamily of secreted signaling molecules that plays a critical role not only in bone formation during early embryonic development but also in bone maintenance and fracture repair in adult life. Previous studies have shown that *Bmp2* gene expression is stimulated by FGF2 signaling in both endochondral and intramembranous bones *in vivo* as well as in cultured osteoblasts. Similarly, the activity of an evolutionarily conserved region (ECR1) 156kb downstream of *Bmp2*, which is known to function as an osteoblast-specific enhancer of *Bmp2* expression, can also be upregulated by FGF2. Here we show that ECR1 function *in vivo* is restricted to osteoblasts in specific anatomical regions, as it exhibits robust activity in endochondral bones, but expression is highly mosaic in intramembranous bones of the face and undetectable in cranial intramembranous bones. Therefore we hypothesize that the expression of *Bmp2* in osteoblasts is regulated by multiple enhancers that act in a highly modular fashion specific to different anatomical domains within the skeleton, but share upstream activation signals through FGF2-mediated pathways. In order to further explore these mechanisms *in vitro,* we have analyzed several osteoblast cell lines in comparison to primary calvarial osteoblasts. *Bmp2* expression was found to be inducible by 20ng/ml FGF2 in both MN7 and U-33 cells, whereas an MC3T3-E1 subclone lacked any *Bmp2* expression measurable by real-time RT-PCR even after FGF2 treatment. In MN7 cells, the immediate 3.5-fold induction after 24 hours of FGF2 treatment closely mirrored the effect observed in primary osteoblasts, whereas U-33 cells exhibited a delayed response with an average 48-fold increase in *Bmp2* expression seen only after 24 hours post FGF2 treatment (serum-starved). However, despite the significant induction by FGF2, the overall level of *Bmp2* expression in U-33 cells was several orders of magnitude lower than in MN7 cells or primary osteoblasts. Therefore, MN7 cells stand out as a very suitable osteoblast cell line for further in vitro studies of *Bmp2* regulation. Future studies will employ ChIP and Chromosome Conformation Capture (3C) assays in MN7 cells to investigate the molecular mechanism by which ECR1 induces *Bmp2* expression, and to identify additional *Bmp2* enhancers.

***Disclosures: Eva Broeckelmann**, None.*

MO0170

Regulation of BMP3 Expression in Postnatal Bone. Laura Gamer*[1], Dorothy Pazin[2], Karen Cox[1], Regina Raz[3], Aris Economides[3], Vicki Rosen[1]. [1]Harvard School of Dental Medicine, USA, [2]Harvard School of Medicine, USA, [3]Regeneron Pharmaceuticals, Inc., USA

BMP3 is a negative regulator of bone formation. Mice with excessive BMP3 production display decreased osteogenesis and incur spontaneous fractures. In contrast, mice lacking BMP3 do not lose bone mass with age. By 7 months, and continuing out to one year of age, BMP3 null mice have significantly more bone (BV/TV), greater numbers of bone trabeculae, higher connectivity density, decreased trabecular separation and reduced marrow adiposity. These data suggest that controlling the amount of BMP3 present in bone may be a novel means to regulate bone mass. To examine where and when BMP3 is expressed and identify factors that regulate its expression, we created a BMP3LacZ knock-in mouse where the first exon of BMP3 was replaced in frame with a LacZ reporter and used these mice to monitor BMP3. During endochondral ossification, BMP3 is first expressed exclusively in the perichondrium (E14.5). Once osteogenesis begins (E16.5), BMP3 can be found in the osteoprogenitor layer of the periosteum and is also produced by osteoblasts. In postnatal bone, BMP3 is detected in the periosteum, osteoblasts and osteocytes. These data identify BMP3 as an osteoblast lineage specific gene product. To determine potential regulators of BMP3, we analyzed the BMP3 genomic locus for regions of sequence conservation across multiple species (ECRs) and found several ECRs 50 kb upstream of the BMP3 start site. We then analyzed these sequences for potential transcription factor binding sites and found predicted sites for signals that have been reported to modulate BMP3 expression including BMP2, Wnts, FGFs, Ihh, PTH and TNF alpha. Several of these factors were then tested in cultures of embryonic mouse metatarsals, mouse calvaria and bone marrow stromal cells harvested from BMP3LacZ mice, and activity was monitored by changes in X-gal staining and BMP3 mRNA levels. From these studies, we know that BMP2 and bFGF down regulate BMP3 expression in osteoblast-lineage cells, providing us with candidate molecules for further testing. We believe our studies on the function and regulation of BMP3 during adult bone formation will provide us with new approaches for controlling postnatal bone mass.

***Disclosures: Laura Gamer**, None.*

MO0171

Fibroblast Growth Factor 23 (FGF23) Concentrations in Low Birth Weight Infants during the Early Postpartum Period and FGF23 Expression in Placenta. Masanori Takaiwa*[1], Koji Kadoya[2], Kunihiko Aya[3], Kosei Hasegawa[3], Motofumi Yokoyama[4], Youichi Kondo[1], Tsuneo Morishima[3], Hiroyuki Tanaka[5], Nobuyuki Kodani[1]. [1]Dept. of Pediatrics, Matsuyama Red Cross Hosp., Japan, [2]Dept. of Pathology, Matsuyama Red Cross Hosp., Japan, [3]Dept. of Pediatrics, Okayama University Graduate School of Medicine, Dentistry & Pharmaceutical Sciences, Japan, [4]Dept. of Obstetrics & Gynecology, Matsuyama Red Cross Hospital, Japan, [5]Okayama Saiseikai General Hospital, Japan

Early postpartum infants show intriguing changes in Ca, Pi, PTH and 1,25-(OH)2D levels. However, the role of FGF23 in neonatal mineral metabolism remains unclear. Previously, we reported that serum intact FGF23 levels in healthy term infants are significantly low at birth (30th Annual Meeting, Sa165). In this study, we firstly examined the circulating FGF23 levels in low birth weight infants using an intact FGF23 and a C-terminal FGF23 ELISAs during the early postpartum period (day 0-LBW and day 5-LBW groups). We also compared these ranges with those of healthy term infants (day 0-term infant and day-5 term infant groups) and adults (healthy adult group). Data was expressed as mean ± SEM and analyzed by the Steel-Dwass test. C-terminal FGF23 in the day 0-LBW, the day 5-LBW, the day 0-term infant, the day-5 term infant and the healthy adult groups were 163.4 ± 26.0, 155.6 ± 31.9, 73.2 ± 4.9, 81.0 ± 6.3 and 39.0 ± 2.4 RU/ml, respectively. Intact FGF23 in the day 0-LBW, the day 5-LBW, the day 0-term infant, the day-5 term infant and the healthy adult groups were 8.6 ± 2.7, 14.7 ± 4.4, 3.9 ± 0.4, 21.8 ± 3.7 and 27.6 ± 2.2 pg/ml, respectively. The ratio between the intact and the C-terminal FGF23 levels (intact/C-FGF23 ratio) in the day 0-LBW, the day 5-LBW, the day 0-term infant, the day-5 term infant and the healthy adult groups were 0.047 ± 0.060, 0.138 ± 0.017, 0.055 ± 0.005, 0.287 ± 0.060 and 0.726 ± 0.058, respectively. We also performed immunoprecipitation assays using anti FGF23 antibodies. This assay demonstrated that FGF23 is mainly detected as fragmented 18 kDa FGF23 in plasma obtained from a neonate at birth. We also recovered the 18 kDa FGF23 from homogenates of a human placenta. An immunohistochemical test using an anti C terminal FGF23 antibody detected focal positive staining in the trophoblast layer of the placenta. Additionally, we confirmed FGF23 mRNA expression in the placenta by RT-PCR. Our observation indicated that the intact FGF23 level and the intact/C-FGF23 ratio were very low due to the fragmentation of FGF23 during the early postpartum period, particularly in the low birth weight infants. These results also suggested that placenta is one of the potent sources of the fragmented FGF23 during the late third trimester. Hence, further investigation is necessary to clarify the role of placenta in FGF23 production and inactivation from late gestational to intrapartum periods.

***Disclosures: Masanori Takaiwa**, None.*

MO0172

Nuclear HMWFGF2 Isoforms are Novel Regulators of Fgf23 Promoter Activity in ROS17/2.8 Osteoblasts. Liping Xiao*[1], Alycia Esliger[1], Marja Marie Hurley[2]. [1]University of Connecticut Health Center, USA, [2]University of Connecticut Health Center School of Medicine, USA

X-Linked Hypophosphatemic rickets (XLH) is a X-linked dominant form of rickets which is characterized by growth retardation, rachitic/ osteomalacic, hypophosphatemia and renal defects in phosphate reabsorption and vitamin D metabolism. Recent studies have shown that fibroblast growth factor 23 (FGF23) is a phosphatonin made by osteoblasts (OBs)/osteocytes that regulates phosphate homeostasis and is responsible for the phenotypic changes in patients with XLH. However the mechanism involved in the regulation of FGF23 is not defined.

In humans, there are high molecular weight (HMW) nuclear isoforms of 22, 23 and 24 kDa and a LMW/18 kDa Fibroblast Growth Factor (FGF2) protein isoform. Our published data showed that mice over-expressing only HMW FGF2 in OBs developed bone phenotype and hypophospatemia which is similar to human XLH and the Hyp mouse, a homologue of XLH. We hypothesized that HMWFGF2 could be important in regulating FGF23 expression in OBs/osteocytes in XLH.

To determine whether increased Fgf23 mRNA is due to HMWFGF2 activation of the Fgf23 promoter, ROS17/2.8 OBs were co-transfected with the Col3.6/HMWFGF2/GFP or Col3.6/GFP as control and p3550Fgf23-luc reporter construct or pGL3-Basic-luc. Luciferase activity was increased by 48% in p3550-luc/Col3.6/HMWFGF2/GFP group compared with p3550-luc/Col3.6/GFP.

To assess which TFs were involved in HMW FGF2 up-regulating Fgf23, ROS17/2.8 OBs were stably transfected with Col3.6/GFP or Col3.6/HMWFGF2/GFP. Nuclear proteins were extracted for Protein/DNA Array analysis. Fifty-three out of 345 TFs were altered by over-expressing HMWFGF2. Among these 53 TFs, were binding sites for CREB-2, VDR/DR-3 and E4F/ATF that were previously found in the mouse Fgf23 promoter. Nuclear FGFR1 and FGF2 were reported to activate tyrosine hydroxylase promoter through the camp-responsive element in adrenal cells. Therefore we determined the involvement of FGFR1c in the up-regulation of Fgf23. FGFR1c mRNA expression was increased by 66% in ROS17/2.8 OBs over-expressing HMWFGF2.

These data indicate that HMWFGF2 increases Fgf23 mRNA through activation of the Fgf23 promoter via modulation of FGFR1c and CREB in ROS17/2.8 OBs. HMWFGF2 might be a therapeutic target for XLH.

***Disclosures: Liping Xiao**, None.*

MO0173

Adiponectin Induces Interferon-Response Genes in Mouse Bone Marrow Cultures. Dorit Naot*, Garry Williams, Jian-ming Lin, Greg Gamble, Andrew Grey, Ian Reid, Jillian Cornish. University of Auckland, New zealand

Adiponectin is a cytokine produced by adipocytes, with circulating levels that are inversely related to both fat mass and bone mass. In postmenopausal women, circulating adiponectin levels are more strongly related to bone density than leptin or fat mass itself, indicating that adiponectin might play a role in mediating the relationship between fat mass and bone mass. Adiponectin is a pleiotropic factor, affecting energy homeostasis, glucose and lipid metabolism and inflammatory pathways. A number of studies have shown that adiponectin directly affects osteoblasts and osteoclasts, although the results of some of the published studies are inconsistent. Investigations in our laboratory have shown that adiponectin has a proliferative effect on osteoblasts and an inhibitory effect on osteoclast formation in vitro.

The aim of the current study was to investigate the mechanisms involved in the inhibition of osteoclastogenesis in bone marrow cells treated with adiponectin, by determining changes in gene expression in adiponectin-treated cells. RNA was extracted at different time points from mouse bone marrow cells cultured in the presence of $1,25(OH)_2D_3$ to promote osteoclastogenesis, and differential gene expression was determined by Affymetrix GeneChip® Mouse Gene 1.0 ST arrays. Unexpectedly, we found that a large number of type I interferon-response genes were induced by adiponectin, including IRF7, Ifit1, Ifit2, Ifit3, Ifi44, Oas3, Stat1, Stat2, Mx1, Mx2, Ccl5 and Cxcl10. The response appears to be elicited by adiponectin and not by contaminants as the adiponectin preparation used was purified from mammalian cells stably transfected with adiponectin and is not of viral origin, and analysis of the adiponectin by QSTAR®System mass spectrometer showed no contaminating peptides that might have induced an interferon response. The microarray analysis has not identified significant changes in the levels of any of the interferon genes themselves. In subsequent experiments we measured similar increases in interferon-response genes in the murine macrophage cell line RAW264.7 but not in ST2 cells, which are of mesenchymal origin.

The induction of interferon-response genes could be contributing to adiponectin's inhibitory effect on osteoclasts, as interferons are known to inhibit osteoclastogenesis. Furthermore, crosstalk between adiponectin and interferon pathways has much broader implications for the understanding of the physiological activities of adiponectin.

***Disclosures: Dorit Naot**, None.*

MO0174

Attenuation of Receptor Tyrosine Kinase Degradation by Targeting Cbl Promotes Osteogenic Differentiation in Human Mesenchymal Stromal Cells. Pierre Marie[1], Hichem Miraoui[2], Nicolas Sévère*[2]. [1]INSERM Unit 606 & University Paris Diderot, France, [2]Inserm U606 & University Paris Diderot, France

Elucidating the mechanisms underlying mesenchymal stromal cell (MSC) osteogenic differentiation is critical to develop strategies to promote osteogenic differentiation and bone formation. The E3 ubiquitin ligase Cbl is an important protein controlling the ubiquitination and degradation of several signalling proteins. In osteoblasts, we previously demonstrated that Cbl controls the degradation of Src (Lyn and Fyn) molecules, PI3K, integrin alpha5 and fibroblast growth factor receptor 2 (FGFR2), resulting in modulation of cell proliferation, differentiation and survival. We now hypothesized that attenuation of Cbl-mediated degradation of signalling molecules may promote osteogenic differentiation in MSCs. In this study, we tested the effect of a Cbl mutant (G306E) that abolishes the binding ability of Cbl phosphotyrosine-binding domain (PTB) to receptor tyrosine kinase (RTK) on osteoblast differentiation in MSCs. We showed that expression of mutant G306E Cbl by lentiviral infection increased Runx2, alkaline phosphatase (ALP) and type 1 collagen (COL1A1) expression in human clonal Stro-1+ (F/Stro-1+) MSCs. Additionally, the Cbl mutant G306E expression increased matrix mineralization in F/Stro-1+ cells, whereas cell proliferation and cell survival were not adversely affected. Similar results were obtained in human primary bone marrow stroma derived MSCs. Immunoprecipitation analyses showed that the mutant Cbl decreased FGFR2 and PDGFRalpha protein levels associated with Cbl and ubiquitin, indicating that the mutant Cbl increased MSC osteoblast differentiation via attenuation of FGFR2 and PDGFRalpha ubiquitination and degradation. Western blot analysis showed that the increased FGFR2 and PDGFRalpha protein levels induced by the mutant Cbl resulted in increased ERK1/2 and PI3K phosphorylation. The results indicate that: 1) the osteogenic differentiation program in human MSCs can be promoted by Cbl-mediated attenuation of RTK degradation, and 2) PDGFRalpha/ERK1/2 and PI3K signalling may mediate the osteogenic differentiation program induced by the mutant Cbl in MSCs. This study shows that Cbl is an important factor regulating osteoblast differentiation in human mesenchymal stromal cells. This also provides ''proof-of-concept'' that attenuation of RTK degradation by targeting Cbl promotes MSC osteogenic differentiation, thus identifying a target that could potentially be used in the treatment of skeletal disorders where MSC osteogenic differentiation is compromised.

***Disclosures: Nicolas Sévère**, None.*

MO0175

Calcitriol Decreases the Expression of Importin Alpha3 in Human Bronchial Smooth Muscle Cells. Tanupriya Agrawal*, Devendra Agrawal. Creighton University School of Medicine, USA

Purpose: Vitamin D plays an important role in the immunomodulation by affecting both innate and adaptive immune systems. NF-?B is a transcriptional factor that activates many genes involved in inflammatory response. The nuclear import of p65 and p50 subunits of activated NF-?B is dependent on Importinα3 (KPNA4). In this study, we examined the effect of calcitriol on the protein and mRNA expression of Importinα3 in human bronchial smooth muscle cells (HBSMCs). We also analyzed the effect of calcitriol on the nuclear expression of NF-?B. Methods: HBSMCs were cultured in smooth muscle cell media containing 10% FBS. Cells in the passages 3-7 were used to stimulate with calcitriol in different doses (0.1 – 100 nM) for 24hrs. Protein and mRNA Expressions of Importin α3 were analyzed using Western Blot and qPCR, respectively. To analyze the effect of calcitriol on activated NF-?B, nuclear protein was extracted after stimulating the cells with 10ng/ml of TNF-α with and without various doses of calcitriol for 24 hr. Protein Expression of nuclear NF-?B was analyzed by Western Blot. Results: There was significant expression of mRNA and protein of Importinα3, VDR, CYP24A1 and CYP27B1 in HBSMCs. Treatment with increasing doses of calcitriol significantly increased VDR protein expression and significantly decreased the protein and mRNA expression of Importinα3 as compared to control. There was a significant decrease in the nuclear protein expression of NF?B after stimulation with TNFα (10ng/ml) and calcitriol (0.1nM-100nM) as compared to the cells treated with TNFα alone. Conclusions: These data suggest that calcitriol decreases the expression of Importinα3 thereby decreasing the import of NF?B to the nucleus. This could be one of the potential mechanisms underlying anti-inflammatory effect of vitamin D in allergic airway inflammation and airway hyperresponsiveness in asthma.

***Disclosures: Tanupriya Agrawal**, None.*

MO0176

Fam3c - a Novel Factor in Bone Biology. Jorma Määttä*[1], Kalman Büki[2], Pia Rantakari[3], Johanna Saarimäki[2], Matti Poutanen[4], Pirkko Härkönen[2], Kalervo Väänänen[2]. [1]Institute of Biomedicine, Department of Cell Biology & Anatomy, Turku Center for Disease Modeling, University of Turku, Finland, [2]Institute of Biomedicine, Department of Cell Biology & Anatomy, University of Turku, Finland, [3]Institute of Biomedicine, Department of Physiology, Turku Center for Disease Modeling, University of Turku, Finland, [4] Institute of Biomedicine, Department of Physiology, Turku Center for Disease Modeling, University of Turku, Finland

Fam3c (also known as ILEI) is a cytokine-like growth factor, the function of which has been attributed to epithelial-mesenchymal transition (EMT) and tumor growth and metastasis. Recently, a large genome-wide single nucleotide polymorphism (SNP) analysis on Asian populations revealed that a SNP affecting bone mineral density is located at the first intron of the Fam3c gene. Independently of that, we have found Fam3c to be expressed in osteoclasts, and thus, we have generated a $Fam3c^{-/-}$ mouse strain to examine the role of the gene in bone biology *in vivo*.

Rat osteoclasts were differentiated from spleen cells on plastic and bone slices, cDNA libraries were generated from both cultures. With substraction method one of the isolated cDNA:s specific for osteoclasts cultured on bone was found to encode Fam3c.

$Fam3c^{-/-}$ mice were generated by utilizing a commercial gene-trap ES (129SvEv) cell clone (LST057) from Bay Genomics, USA. The gene-trap construct carries beta-geo- and placental alkaline phosphatase reporter genes, and it has been localised to the intron region between exons 3 and 4 of the Fam3c gene. The ES cells were injected to C57BL/6N blastocysts to generate chimeric littermate, and finally homozygous $Fam3c^{-/-}$ mice were generated by breeding heterozygous littermates. The analysis of $Fam3c^{-/-}$ mice and their wild-type littermates were carried out at the F3 generation. The $Fam3c^{-/-}$ mice were found to have normal appearance, behaviour and fertility. However, micro-CT analysis of tibia revealed reduced trabecular bone content in the $Fam3c^{-/-}$ mice as compared to the wild-type mice at the age of 3 months, due to smaller number of bone trabeculi.

Although Fam3c has been attributed to be developmentally important for the EMT, our results indicate that the gene is not essential for normal mouse development. However, the reduced number of bone trabeculi in $Fam3c^{-/-}$ mice indicates a role of Fam3c in bone remodelling.

***Disclosures: Jorma Määttä**, None.*

MO0177

High Circulating Levels of Osteopontin Are Associated with Idiopathic Scoliosis Onset and Spinal Deformity Progression. Alain Moreau*[1], Anita Franco[2], Pierre H. Rompré[3]. [1]Sainte-Justine Hospital, Canada, [2]Viscogliosi Laboratory in Molecular Genetics of Musculoskeletal Diseases, Sainte-Justine University Hospital Research Centre, Canada, [3]Faculty of Dentistry, Université de Montréal, Canada

The etiology of idiopathic scoliosis (IS), the most common form of scoliosis, remains poorly understood resulting in the traditional paradigm that IS is a multifactorial disease with a genetic predisposition. We hypothesized that scoliosis development in patients with idiopathic scoliosis (IS) and different melatonin-deficient animal models could be induced by a similar mechanism involving a common downstream effector regulated by melatonin. Indeed, the study of the molecular changes occurring in pinealectomized chickens revealed an increased production of Osteopontin (OPN), at the mRNA and protein levels, in paraspinal muscles of scoliotic chickens. Therefore, we investigated the involvement of OPN, a multifunctional cytokine, in IS pathomechanism. A group of 683 consecutive patients with IS were compared with 262 healthy control subjects and 178 asymptomatic offspring, born from at least one scoliotic parent, who are considered at-risk of developing this disorder. Plasma OPN and soluble CD44 receptor (sCD44) levels were measured by enzyme-linked immunosorbent assays. Contributions of OPN to IS were validated using wild-type and genetically modified C57Bl/6j mice, a well known scoliosis animal model. Mean plasma OPN levels were significantly increased in IS patients and correlated with disease severity, with average values of 655 ± 279 ng/ml and 812 ± 363 ng/ml for moderate (10-44♂) and severe (⩾ 45♂) spinal deformities, respectively, when compared to the healthy control group (537 ± 233 ng/ml). Elevated plasma OPN levels were also found in the asymptomatic at-risk group (733 ± 3336 ng/ml), suggesting that these changes precede scoliosis onset. Mean plasma sCD44 levels were significantly lower in IS patients with Cobb angle ⩾ 45♂ (359 ± 190 ng/ml) compared to healthy control subjects (505 ± 108 ng/ml). Generation of bipedal C57Bl/6 mice (after forelimbs amputation under anesthesia), a known scoliosis animal model, induced scoliosis in 46% of bipedal females and 24% of males, although females were more severely affected with scoliotic ones having higher plasma OPN levels than non-scoliotic bipedal mice. Using the same strategy, we found that none of the bipedal C57Bl/6 OPN-null mice developed scoliosis. Our clinical data and experiments on animals demonstrate that high circulating OPN and low sCD44 levels herald scoliosis formation in IS; thus offering a first molecular concept to explain the pathomechanism leading to IS. OPN and sCD44 could be useful markers for IS.

***Disclosures: Alain Moreau**, Paradigm Spine LLC, 5; Paradigm Spine LLC, 2*
This study received funding from: Paradigm Spine LLC (NYC, USA)

MO0178

Probable Roles of Adiponectin Functional Domains in Osteoblastic Differentiation. Aiko Kamada*, Takashi Ikeo, Yoshihiro Yoshikawa, Eisuke Domae, Seiji Goda, Isao Tamura. Osaka Dental University, Japan

Adiponectin is abundantly present as a plasma protein, and exhibits various biological functions, such as regulating energy homeostasis and increasing insulin sensitivity in the liver and skeletal muscle. It is ~30-kDa polypeptide containing N-terminal signal sequence, variable domain, collagen-like domain, and C-terminal globular domain. Recent studies have demonstrated both a positive and negative action of adiponectin on bone formation, and it was thought that these different actions might be attributed to its multifunctional domains. In this study we investigated effect of adiponectin functional domains on gene expression during osteoblast differentiation.

Recombinant murine adiponectin domains were designed and produced. Osteoblastic differentiation of a murine pro-osteoblastic cell line, MC3T3-E1 cells, was induced by differential medium including ascorbic acid and beta-glycerophosphate with or whithout functional domain peptides. Three days after stimulation, RNA was extracted and reverse-transcribed. Gene expression was determined by RT-PCR analysis,

The collagen-like domain peptide induced expression of genes related to various signaling pathways (MAPK, Ca^{2+}, Wnt, Jun) and BMP family involved to osteoblastic differentiation. In contrast, the globular domain suppressed the above genes, and induced expression of genes related to cell morphogenesis and neurological system processes. Interestingly, the three-dimensional structure of the globular domain of adiponectin is shown to have homology to that of TNF-alpha. Therefore these characteristic effects of the globular domain may be attributed to its structural resemblance to TNF-alpha.

Our study suggests that functional domains of adiponectin act on osteoblasts through different manners, and the collagen-like domain may be involved to osteoblast differentiation.

***Disclosures: Aiko Kamada**, None.*

MO0179

Regulation of Colon Hyperplasia by the Calcium Channel TRPV6. Shahid Umar[1], Sara Peleg*[2]. [1]University of Oklahoma Health Science Center, USA, [2]University of Texas M.D. Anderson Cancer Center, USA

The transient receptor potential of the vanilloid subfamily, member 6 (TRPV6) is best known for its role in regulating intestinal calcium (Ca) absorption, but in vitro studies imply that it also regulates cellular growth signaling. To determine the contribution of TRPV6 to cell growth in vivo we have used mice infected by the enteropathogenic bacterium *citrobacter rodentium* (CR). In these mice the injured colonic epithelium responds by a profound activation of several growth-promoting signals, leading to crypt hyperplasia. This hyperplasia is also characterized by a 20-fold increase in TRPV6 mRNA and protein, and a switch in its localization from the apical membrane of the absorptive epithelium into the membrane of proliferating cells in the hyperplastic crypts. A high Ca diet, which suppresses the hyperplasia, also restored TRPV6 expression and localization to their normal status. These findings led to the hypothesis that TRPV6 is an important component in the wound healing response of the injured mucosa to CR infection. We tested this by infecting WT and TRPV6-knockout (KO) mice with CR and assessing their response to the infection. We found that the time course for colonization and clearance of CR from the colon and the spleen was similar for the two groups of mice, indicating that the adaptive immune response to CR is effective in the TRPV6-KO mice. However, bacterial dissemination to the spleen was significantly greater in the TRPV6-KO mice than in WT mice, indicating a more severe barrier breach in the mutant mice. Furthermore, while in WT mice colonic crypt length increased up to 90% over that of uninfected mice, this cellular response was delayed and modest in the TRPV6-KO mice (20-40% increase in crypt length). These results implied that TRPV6 contributes to intestinal barrier integrity and to epithelial cell proliferation. However, global ablation of TRPV6 causes systemic changes in vitamin D and Ca metabolism, which could alter colon response to CR indirectly. Therefore, we used the colon carcinoma cells, Caco-2, to determine directly the role of TRPV6. Transfecting these cells with TRPV6 siRNA diminished TRPV6 expression, decreased proliferation by 40% and increased apoptosis by 150%. In conclusion, we have shown that TRPV6 is an important contributor to intestinal mucosal health in vivo and this is due at least in part to the growth-promoting and anti-apoptotic activity of this channel in injured or malignant intestinal epithelial cells.

***Disclosures: Sara Peleg**, None.*

MO0180

Regulation of Gene Expression and Subcellular Protein Distribution in Murine Osteocyte-Like Cells by the Lipid Growth Factor Lysophosphatidic Acid. Katrina M. Waters, Jon M. Jacobs, Marina A. Gritsenko, Norman Karin*. Pacific Northwest National Laboratory, USA

Osteoblasts and osteocytes are highly responsive to the lipid growth factor lysophosphatidic acid (LPA) but the mechanisms by which LPA alters bone cell functions are largely unknown. We found that a major effect of LPA on osteocytic cells was the stimulation of dendrite membrane outgrowth, and predicted that this process required changes in osteocyte gene expression and protein distribution. DNA microarrays were employed for global transcriptional profiling of MLO-Y4 osteocytic cells grown for 6 hr and 24 hr in the presence or absence of LPA. We identified 932 transcripts that displayed statistically significant changes in abundance in response to LPA treatment. Gene ontology (GO) analysis revealed that the regulated gene products were associated with a diverse set of cellular processes, which is consistent with the pleiotropic nature of this growth factor. The most robust changes in gene expression were linked to the regulation of actin microfilament dynamics. We determined that LPA-induced dendritogenesis *in vitro* was blocked by the stress fiber inhibitor cytochalasin D. Mass spectrometry (MS)-based proteomic profiling of osteocytes revealed significant LPA-induced changes in the abundance of 284 proteins at 6 hr and 844 proteins at 24 hr. GO analysis of the proteomic data linked the effects of LPA to cell processes that control protein distribution and membrane outgrowth, including *protein localization*, *protein complex assembly*, *Golgi vesicle transport*, *cytoskeleton-dependent transport*, and *membrane invagination/endocytosis*. Dendrites were isolated from LPA-treated MLO-Y4 cells and subjected to MS-based proteomic analysis to quantitatively assess the subcellular distribution of proteins in the membrane extensions relative to whole osteocytes. Sets of 129 and 36 proteins were enriched in the dendrite fraction after 6 hr and 24 hr of LPA exposure, respectively. Marker protein profiles indicated that organelles were largely excluded from the dendrites. Highly represented among the proteins with elevated abundances in dendrites were molecules that regulate cytoskeletal function, cell motility and membrane adhesion. Our combined transcriptomic-proteomic analysis of the response of MLO-Y4 osteocytic cells to LPA indicates that dendritogenesis is a cytoskeleton- and membrane-driven process with actin dynamics playing a particularly critical role.

***Disclosures: Norman Karin**, None.*

MO0181

The Effect of Electrical Stimulation on Osteogenesis-related Cytokine Production in Three Dimensionally Cultured Human Mesenchymal Stromal Cells. In Sook Kim, Ri Youn Kim*. Seoul National University, South korea

Purpose: Electrical stimulation exerts bio-stimulatory effects on bone metabolism such as proliferation, osteoblast differentiation and the production of cytokines. This study investigated the effect of electrical stimulation on osteogenesis-related cytokine production in human mesenchymal stromal cells (hMSCs) via three-dimensional (3D) culture on the scaffold.

Methods: hMSCs were cultured in vitro culture system by 3D plating on collagen sponge. Electrical stimulation was delivered in a form of biphasic current with a magnitude of 1.5 $\mu A/cm^2$, 250 μs in monolayer culture, and at 40 $\mu A/cm^2$, 125μs in 3D culture at common frequency of 100 Hz. Cell proliferation was measured using evaluated using tetrazolium salt, WST-8. Cytokine production from 3D culture was assessed by real time RT-PCR and ELISA, compared with that from monolayer culture.

Results: Electrical stimulation significantly increased the expression of VEGF, IGF-1 and BMP-2 in the 3D culture of hMSCs, consistently with monolayer culture. Resorption inhibitory factor, osteprotegerin and a chemokine, interleukin-8, expressed in an increased level under electrical stimulation. ELISA for VEGF, IGF-1, BMP-2 and bFGF showed a significant increase in electrically stimulated hMSCs, compared to unstimulated group.

Conclusions: These results showed that electrical stimulation enhanced cell proliferation and the production of diverse cytokines in 3D-cultured hMSCs. Thus, we suggest that electrical stimulation might be a critical signal in the regulation of local bone cell function.

***Disclosures: Ri Youn Kim**, None.*

MO0182

Understanding the Differences Between LRP5 and LRP6. Bryan MacDonald*[1], Mikhail Semenov[2], He Huang[2], Xi He[2]. [1]Children's Hospital Harvard Medical School, USA, [2]Children's Hospital, Harvard Medical School, USA

The low-density lipoprotein related receptors LRP5 and LRP6 are the vertebrate homologs of *Drosophila* Arrow and serve as Wnt co-receptors for the canonical Wnt/β-catenin pathway. These receptors all contain five highly conserved PPPSP motifs in the intracellular region which collectively serve as phosphorylation dependent binding sites for Axin, however most *in vitro* data comparing the activity of LRP5 and LRP6 suggests that LRP6 is much more effective at transducing Wnt signaling. Additionally both LRP5 and LRP6 are reported to be ubiquitously expressed, yet there are striking differences in the severity of the *Lrp5-/-* and *Lrp6-/-* mouse phenotypes indicating that LRP6 is responsible for a majority of *in vivo* Wnt/β-catenin signaling during development. To identify the regions that correlate with the highest Wnt signaling activity, we generated several chimeric receptors and examined their signaling strength using the TOPFLASH reporter assay. By swapping the intracellular region of LRP5 and LRP6, we found that the LRP5N/6C receptor was highly active while the LRP6N/5C receptor exhibited little activity. Our results indicate that most of the differences in signaling strength for LRP5 and LRP6 are contained in the intracellular region. These results are surprising considering the PPPSP Axin binding sites in LRP5 and LRP6 are nearly identical, suggesting other portions of the intracellular region are critical for conferring signaling strength. We have performed *in vitro* Axin binding experiments to compare the ability of GST purified LRP5C and LRP6C to bind Axin. We find that when phosphorylated to similar extent by GSK3 and CKI, phosphorylated LRP5C binds to Axin at equivalent levels compared to phosphorylated LRP6C. In addition we find that phosphorylated LRP5C and LRP6C appear to directly bind Axin and they do not require indirect GSK3 protein-protein interactions to bridge this complex. Our results suggest that phosphorylated LRP5C is capable of strong, direct Axin binding which should correlate with active Wnt signaling, however we hypothesize that the full-length LRP5 receptor is less active due to reduced phosphorylation. The intracellular region of LRP6 is slightly larger than LRP5 with LRP6 containing extra amino acids between each of the PPPSP motifs. We have generated new LRP5/6 chimeric receptors altering the spacing between the PPPSP motifs and we will investigate their effect on Wnt activity and PPPSP phosphorylation levels.

***Disclosures: Bryan MacDonald**, None.*

MO0183

Wnt10b Expression Stimulates NF-kappaB Activity in Osteoblasts. David Monroe[1], Ulrike Moedder*[2]. [1]Mayo Foundation, USA, [2]Mayo Clinic College of Medicine, USA

The Wnt family of secreted cytokines regulates numerous aspects of development including the formation and maintenance of bone. Activation of Wnt signaling by Wnt10b has been shown to enhance osteogenesis by increasing expression of key osteogenic transcription factors in cell culture models. Furthermore, genetic deletion of Wnt10b in mice is associated with a decrease in bone mineral density whereas transgenic overexpression is associated with a significantly higher bone mineral density, suggesting that Wnt10b is a positive endogenous regulator of bone formation. To identify the transcriptional targets of Wnt10b signaling in osteoblasts, we stably introduced Wnt10b in the U2OS osteosarcoma cell model and performed microarray analysis. A total of 370 genes were significantly regulated, including classical Wnt targets (i.e. Axin2, Lef1) and the bone morphogenetic protein family, confirming the role of Wnt10b as an activator of bone formation. Metacore pathway analysis revealed that the Wnt developmental pathway ($p=0.0016$) and the NF-kappaB pathway ($p=0.003$) were significantly upregulated by Wnt10b. Furthermore, increased expression of known NF-kappaB pathway activators, such as TNFα (7.57-fold, $p<0.001$) and IL1α (8.72-fold, $p<0.001$), was also observed. To confirm specificity of this response, a Wnt10b-specific siRNA significantly inhibited activation of TNFα and IL1α. To investigate these findings in a physiologically more relevant cell system, conditioned media (CM) generated from U2OS or U2OS-Wnt10b cells was used to treat primary mouse calvarial osteoblasts and mouse bone marrow stromal cells (BMSCs) transduced with a NF-kappaB reporter vector. Wnt10b CM stimulated reporter activity 10.5-fold ($p=0.0027$) and 2.5-fold ($p=0.015$) in these models respectively, demonstrating NF-kappaB pathway activation by Wnt10b in multiple systems. Furthermore, BMSCs maintained in osteoblastic differentiation media exhibited a steady decrease in Wnt10b expression throughout differentiation, suggesting that Wnt10b-mediated stimulation of the NF-kappaB pathway may be necessary at early stages of osteoblastic differentiation, however is downregulated for terminal differentiation to occur. This is in agreement with a report demonstrating that inhibition of NF-kappaB signaling in mature osteoblasts enhances bone formation in young mice. In summary, this study identifies the NF-kappaB pathway as a novel Wnt10b target in osteoblasts.

***Disclosures: Ulrike Moedder**, None.*

MO0184

Bioavailable IGF-I is Reduced in Female Recruits Sustaining Stress Fractures during Military Basic Training. Cassi Strohbach*[1], Dennis E. Scofield[1], Amanda Antczak[1], Bradley C. Nindl[1], Rachel Evans[2], Ran Yanovich[3], Yael Arbel[3], Daniel C. Moran[4]. [1]US Army Research Institute of Environmental Medicine, USA, [2]U.S. Army Research Institute of Environmental Medicine, USA, [3]Heller Institute, Sheba Medical Center, Israel, [4]Heller Institute, Sheba Medical Center & Ariel University Center of Samaria, Israel

During military training, musculoskeletal overuse injuries, such as stress fractures, result in increased lost duty time, medical costs, and attrition of new recruits. Despite the research on stress fracture occurrence and changes to military training programs, stress fractures still occur at a higher rate in female recruits than male recruits. Insulin-like growth factor-I (IGF-I) is an important mediator of bone remodeling and has been reported to be correlated with bone mineral density, especially in women, and is influenced by physical training. This study examined the response of total and free (i.e. bioavailable) IGF-I concentrations between female soldiers that sustained a stress fracture (SF, n=13) during basic training (BT) and female soldiers who did not (NSF, n=49). Female soldiers (n=72, 18.8 ± 0.6 yr) from 2 companies of a gender-integrated combat battalion in the Israeli Defense Forces participated in this study. Height, weight and blood draws were taken upon entry to BT (preBT) and at the end of a four month BT program (postBT). Stress fractures were diagnosed by bone scan. Serum was analyzed for total IGF-I, free IGF-I, BAP, calcium, CTx, IL1β, IL6, PINP, PTH, TNFα, TRAP, and VitD. Statistical differences between SF and NSF groups were detected by two-way ANOVA with Fisher post-hoc ($p<0.05$). The SF group was taller (165.8 ± 4.5 vs 161.4 ± 6.7cm) and had lower BMI (21.4 ± 2.2 vs $23.7 \pm 3.5 kg/m^2$) than the NSF group (both $p<0.05$). Serum concentrations of total IGF-I, bioavailable IGF-I, other bone biomarkers, and cytokines were not significantly different between SF and NSF groups preBT. However, a significant difference was observed in the bioavailable IGF-I response pre to postBT. The SF group demonstrated a significant decrease in bioavailable IGF-I pre to postBT (preBT: 0.580 ± 0.580ng/mL; postBT 0.393 ± 0.478) whereas the NSF group demonstrated a significant increase in bioavailable IGF-I pre to postBT (preBT: 0.527 ± 0.370ng/mL; postBT: 0.629 ± 0.448). No difference in the change of total IGF-I pre to postBT was observed between SF (preBT: 432.0 ± 120.1ng/mL; postBT: 442.6 ± 137.8) and NSF groups (preBT: 501.2 ± 164.6ng/mL; postBT: 535.7 ± 156.9). Our results indicate that women sustaining stress fracture during BT demonstrate a significant decrease in bioavailable IGF-I, unlike their uninjured counter parts, which increase bioavailable IGF-I. This suggests that bioavailable IGF-I may have utility as a biomarker for musculoskeletal injury risk potential.

***Disclosures: Cassi Strohbach**, None.*

MO0185

PAPP-A Regulates PTH-IGF Interactions in Bone. Kari Clifton*, Cheryl Conover. Mayo Clinic College of Medicine, USA

The ability of intermittent parathyroid hormone (PTH) to increase bone formation in several animal models and in humans has led to the approval of PTH as the first truly anabolic treatment for osteoporosis. However, the underlying mechanisms for its potent anabolic effect in bone are not fully understood. Early in vitro studies indicated that PTH treatment increased production of insulin-like growth factor (IGF)-I in

bone cells. Several recent in vivo studies highlighted the importance of IGF-I signaling for mediating the anabolic actions of PTH in bone. Regulation of local IGF-I signaling is complex and can be modulated not only by changes in ligand or receptor levels, but also by expression and post-translational modification of IGF binding proteins (IGFBPs). IGFBP-4 is the most abundant IGFBP in bone and has been shown in vitro and in vivo to bind and prevent IGF-I from interacting with its receptor. Furthermore, cleavage of IGFBP-4 by the metalloproteinase PAPP-A markedly decreases IGFBP-4 affinity for IGF-I, thereby increasing local IGF-I bioavailability. PTH is known to stimulate IGF-I and IGFBP-4 production in vitro, and PTH mimetics have been shown to stimulate PAPP-A expression by bone cells in vitro. We hypothesized that PTH increases not only the expression of IGF-I and IGFBP-4, but also PAPP-A in vivo, thereby establishing a pericellular reservoir of IGF-I through proteolysis of IGFBP-4 in the bone microenvironment, leading to increased bone formation. Secondarily, we predicted that loss of PAPP-A would attenuate the anabolic effects of PTH in bone. Female wildtype (WT) and PAPP-A knockout (KO) mice received 80μg/kg PTH or vehicle 5 days/wk for 6 weeks. Expression of PAPP-A, IGF-I, IGFBP-4, and IGFBP-5 (an IGF-responsive gene) in the tibia was measured by qPCR. PAPP-A expression was upregulated 3-fold in WT, and other genes were upregulated 1.5 to 2–fold. In the PAPP-A KO mice, PTH increased expression of IGFBP-4, but there was no change in IGF-I or IGFBP-5. BMD of the femur was measured before and after treatment by DEXA. PTH increased BMD in both WT and KO, but the increase in BMD was significantly higher ($p>0.001$) in WT animals treated with PTH than in PAPP-A knockouts. These results provide evidence that PAPP-A regulates IGF-dependent effects of PTH in bone.

***Disclosures: Kari Clifton**, None.*

MO0186

Prostaglandin E_2 Increases Cancellous Bone Mass and Formation in Dwarf Rats Despite a Depressed GH/IGF-I Axis. Ana Cristina Bassit*[1], Jose Aguirre[2], Tamashbeen Rahman[2], Thomas Wronski[2]. [1]University of Florida - Veterinary College, USA, [2]University of Florida, USA

Insulin-like growth factor I (IGF-I) is thought to be a potential mediator for the skeletal effects of bone anabolic agents such as prostaglandin E_2 (PGE_2). In support of this hypothesis, PGE_2 stimulates IGF-I synthesis in cultured osteoblast-like cells, and gene expression for IGF-I is upregulated in bone cell cultures treated with PGE_2. The objective of this study is to determine whether the bone anabolic effects of PGE_2 are blunted in dwarf rats with a depressed growth hormone (GH)/IGF-I axis. In these animals, GH synthesis is selectively reduced to about 6% of normal in females, and serum IGF-I levels are less than a third of normal. Bone mass, bone growth, and osteoblast activity are decreased in dwarf rats, but these animals are healthy and without skeletal malformations. At 9 weeks of age, female Lewis (background strain) and dwarf rats were injected SC daily for 2 weeks with vehicle or PGE_2 at a dose of 3 mg/kg body weight (N=7-10/group). Serum IGF-I was measured by ELISA, and cancellous bone histomorphometry was performed in the lumbar vertebral body. Serum levels of IGF-I were significantly decreased in dwarf rats compared with Lewis rats ($P<0.0001$). PGE_2 treatment did not increase serum IGF-I in either Lewis or dwarf rats. However, PGE_2 significantly increased cancellous bone volume in both dwarf ($20.1 \pm 4.2\%$ vs. $16.0 \pm 4.4\%$, $P=0.09$) and Lewis rats ($31.2 \pm 4.3\%$ vs. $26.4 \pm 6.4\%$, $P=0.03$) when compared to vehicle-treated rats, which was associated with increased trabecular number and decreased trabecular separation. PGE_2-treated dwarf rats also exhibited 3-4 fold increases in cancellous mineralizing surface and bone formation rate compared to vehicle-treated dwarf rats. PGE_2 treatment of Lewis rats induced 2-fold increases in mineralizing surface and bone formation rate compared to vehicle-treated Lewis rats. Mineral apposition rate, an index of osteoblast activity, was not increased by PGE_2 treatment in either dwarf or Lewis rats, which indicates that PGE_2 stimulates bone formation primarily by increasing osteoblast numbers rather than their activity. In conclusion, PGE_2 induced significant anabolic effects in vertebral cancellous bone despite low circulating levels of IGF-I in dwarf rats.

***Disclosures: Ana Cristina Bassit**, None.*

MO0187

Runx2 Deficiency Promotes Adipogenesis by Regulating Insulin Signaling. Mitra Adhami*[1], Farah Ghori[1], Haiyan Chen[1], Soraya Gutierrez[2], Amjad Javed[1]. [1]University of Alabama at Birmingham, USA, [2]Universidad de Concepción, Chile

Insulin signaling is critical for the regulation of glucose homeostasis and energy metabolism. Insulin pathway is altered in aging, obesity, and diabetes, all of which are associated with a concomitant increase in fat formation and a decrease in bone synthesis. Fat producing adipocytes and bone forming osteoblasts are derived from a common mesenchymal progenitor. Runx2 is essential for skeletal cell differentiation but its role in commitment of mesenchymal cells (MC) to other lineages and insulin signaling is not known. To investigate this, we isolated MC from Runx2 null mice and established monoclonal lines. These cells exhibits increased proliferative capacity but fails to undergo osteoblast differentiation when cultured in osteogenic media. Surprisingly, Runx2 deficiency resulted in a preferential commitment of mesenchymal cells to the adipocyte lineage. It is well established that anabolic actions of insulin are essential for the conversion of MC into adipocytes. However, addition of insulin to the Runx2 null MC strongly inhibited adipocyte formation. Moreover, treatment with rosiglitazone alone induced robust adipogenesis. Reconstitution of these cells with Runx2 restores insulin response. These results suggest that Runx2 deficient MC bypass the critical requirement of insulin for adipogenesis. To understand the molecular regulatory network responsible for this paradox, we performed gene microarray analysis of control and insulin treated Runx2 null and 3T3L-1 pre-adipocyte. Surprisingly, more than 95% of the genes (122/128) associated with insulin signaling were expressed at higher levels in control Runx2 null MC compared to pre-adipocytes. Thus the observed increase in proliferative capacity of Runx2 null MC reflects an elevated state of basal metabolism. Insulin evoked a differential response, with 85% genes induced in 3T3L-1 but only 3% in Runx2 null MC. Shockingly, a strong suppression of all components of the insulin signaling pathway was evident in insulin treated Runx2 null MC. For a mechanistic understanding, we performed in situ and biochemical analyses. Insulin receptor was expressed in both cell types but Runx2 null MC utilized a differential isoform during adipocyte formation. We further demonstrate that impaired internalization of the activated insulin receptor contributes to the paradoxical insulin response in Runx2 null MC. In conclusion, Runx2 regulates adipocytic lineage commitment as well as energy metabolism.

***Disclosures: Mitra Adhami**, None.*

MO0188

CTGF/CCN2 is a Downstream Target Gene of Ets-1 in Osteoblasts. Randy Astaiza[1], Max Geisinger[1], Tiffany Butler[1], Steven Popoff[2], John Arnott*[1]. [1]The Commonwealth Medical College, USA, [2]Temple University School of Medicine, USA

Erythroblastosis virus E26 oncogene homologue 1 (Ets-1) is the founding member of the Ets family of transcription factors that control a wide variety of important biological processes, including cell proliferation, differentiation and ECM regulation. Recent studies have demonstrated that Ets-1 plays a role in osteoblast differentiation and bone development; however, its mechanism of action and essential downstream target genes in osteoblasts remains largely undetermined. Connective tissue growth factor (CTGF/CCN2) is a cysteine rich, extracellular matrix protein that acts as an anabolic growth factor to regulate osteoblast differentiation and function. In osteoblasts, CTGF is induced by transforming growth factor beta 1(TGF-β1) where it acts as a downstream mediator of TGF-β1 induced matrix production. The molecular mechanisms that control CTGF induction by TGF-β1 in osteoblasts are not understood. In this study, we investigate the role of Ets-1 in CTGF induction by TGF-β1 in primary osteoblasts. We demonstrate that Ets-1 is expressed in primary osteoblasts, and that its expression is induced by TGF-β1 treatment. When we overexpressed Ets-1 in osteoblasts using a CMV-Ets-1 expression construct, it induced CTGF promoter activity at a level similar to TGF-β1 treatment alone. CTGF promoter activation was enhanced further with both TGF-β1 treatment and Ets-1 expression beyond the level achieved using either TGF-β1 or Ets-1 individually, suggesting that both synergize to induce CTGF promoter activation in osteoblasts. When we used Ets-1 siRNA to impair Ets-1 expression, it also impaired CTGF expression at a similar level, further demonstrating the importance of Ets-1 for CTGF induction by TGF-β1. Transcriptional activation by Ets-1 proteins function in a combinatorial manner through association with other transcriptional co-factors (including Smads) that facilitate binding of Ets-1 to the Ets-1 binding motifs (EBE) in the promoters of target genes. Bioinformatic analysis identified putative Ets-1 binding motifs in the CTGF promoter. Using site-directed mutagenesis, multiple constructs were generated that contain point mutations in the EBE sites in the CTGF promoter upstream of a luciferase reporter. Using this approach, we found that mutation of EBE sites in close proximity to the SBE had a more severe impact on CTGF expression suggesting that the Ets-1 sites may cooperate with Smads to achieve CTGF expression following TGF-β1 treatment in osteoblasts.

***Disclosures: John Arnott**, None.*

MO0189

Loss of Matrix Metalloproteinase-13 Increases Bone Matrix Heterogeneity and Decreases Fracture Resistance. Simon Tang*, Tamara Alliston. University of California, San Francisco, USA

Matrix metalloproteinase-13 (MMP-13) is a proteolytic enzyme that degrades collagen fibrils and has significant roles in bone development and in the matrix remodeling of connective tissues. MMP-13 is regulated by TGF-β, and TGF-β has been demonstrated to regulate bone matrix material properties (BMMP) to affect fracture resistance. Preliminary data suggest that MMP-13 may be downstream of the TGF-β regulation of BMMP. However, the role of MMP-13 in maintenance of BMMP and subsequent fracture resistance remains relatively unknown. We hypothesized the deficiency of MMP-13 may affect bone fragility through alterations in the bone matrix that may alter BMMP and bone fracture resistance.

Tibiae and femora were collected from 2 month old MMP-13 deficient (-/-) mice and their WT littermates (n=6-9). Using microCT (5-10μm voxels), structural, histomorphometric, and mineralization indices were determined from the tibiae. Microindentation was performed on the transverse sections of the tibiae using a 2μm spherical tip. Whole bone mechanical behavior was determined by loading the femora to fracture in 3-point bending. Fracture toughness was determined by propagating a razor-notched flaw in 3-point bending. Femoral cortical bone was demineralized, and

analyzed for advanced glycation end-products (AGEs). AGEs are biomarkers for post-translational collagen crosslinking that have been associated with bone fragility.

MMP-13-/- mice showed increased fragility through reduced post-yield deflection ($p<0.001$) and post-yield work-to-fracture ($p<0.001$). This loss of fracture resistance is associated with inferior BMMP shown through reduced fracture toughness ($p<0.001$) and increased accumulation of AGEs ($p<0.05$). These changes occurred with no significant changes in structural parameters of the cortical bone. MMP-13-/- mice also showed increased heterogeneity in the mineral distribution within the bone matrix ($p<0.01$; Fig. 1). Specifically, the MMP-13 -/- bone matrix has hypo- and hyper- mineralized regions distributed throughout the diaphyseal cortical bone. These changes were coupled with increased variability in local tissue elastic modulus. Taken together, MMP-13-/- mice showed a significant loss of bone fracture resistance that is due to structure-independent changes in the bone matrix including increased mineral heterogeneity and reduced BMMPs. Ongoing studies are investigating the extent to which these effects are directed by the actions of TGF-β.

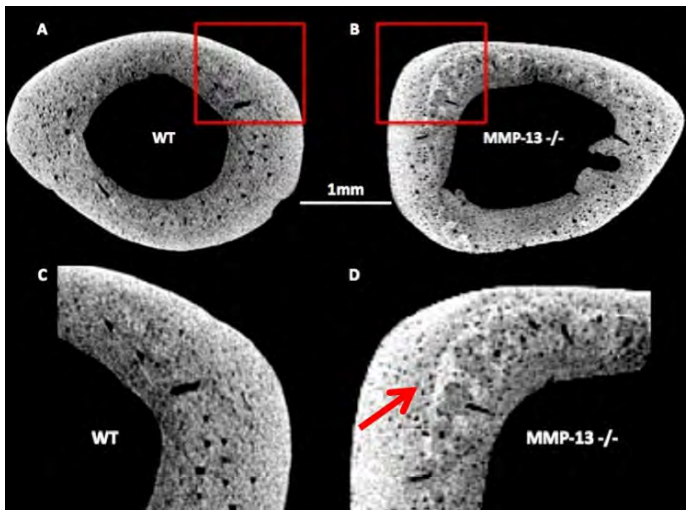

Figure 1: The MMP-13 deficient animals exhibit increased heterogeneity of the matrix.

***Disclosures: Simon Tang**, None.*

MO0190

Oscillatory Fluid Shear Stress Inhibits TNF-α-induced Apoptosis in MC3T3 cells via Blocking of TNFR1 Signaling. Haifang Wang[1], Fredrick Pavalko*[2]. [1]Indiana University School of Medicine, & Key Laboratory for Space Bioscience & Biotechnology, Northwestern Polytechnical University, USA, [2]Indiana University School of Medicine, USA

Previous work indicates that application of steady fluid shear stress (SFSS) inhibits TNF-α-induced activation of caspase-3 in osteoblasts and protects these cells from apoptosis. However, we and others have suggested that oscillatory fluid shear stress (OFSS) may be a more physiological biophysical signal than SFSS for bone cells.

Purpose: We sought to determine the effect of pre-exposing osteoblasts to OFSS on TNF-α-induced apoptosis in vitro and to identify the relevant molecular mechanisms that mediate the protective effects of OFSS against TNF-α-induced apoptosis.

Methods: MC3T3 cells were subjected to 2 hr of OFSS (10 dynes/cm^2), followed by induction of apoptosis by TNF-α for 4 hr.

Results: TNF-α-induced activation of caspase-3 and cleavage of PARP were nearly completely inhibited and phosphorylation of histone was significantly suppressed by pre-exposure of cells to 2 hr of OFSS. In contrast, phosphorylation of histone induced by 250 mM H2O2 in MC3T3 cells was not inhibited by 2 hr of OFSS. Unexpectedly, the ability of OFSS to inhibit TNF-α-induced apoptosis was not affected by treatment with inhibitors of several pro-survival signaling pathways including pI3-Kinase (LY294002), MAPK/ERK kinase (PD98059 or U0126), NO production (L-NAME) or protein synthesis (cycloheximide) during the period of exposure to OFSS. In addition, TNF-α-induced phosphorylation and degradation of IκBα were also blocked by pre-exposure of cells to OFSS. These results suggest that the anti-apoptotic effect of OFSS is conferred on cells by preventing the upstream initiation of TNFR1 signaling. To test this possibility we used a cell surface protein labeling and isolation technique combined with immunobloting to investigate the effect of OFSS on cell surface TNFR1 protein expression and TNF-α-stimulated internalization of TNFR1. Cell surface expression of TNFR1 was significantly down-regulated by 2hr of OFSS (about 35%), without changing the total cellular level of TNFR1. Surprisingly, TNF-α-induced internalization of TNFR1 was not inhibited by OFSS, on the contrary, a trend toward enhanced TNFR1 internalization was consistently observed.

Conclusions: In conclusion, the current study strongly suggests that the anti-apoptotic effect of OFSS results from the inhibition of TNF-α-induced pro-apoptotic signaling which can be explained, at least partially, by the down-regulation of TNFR1 on the cell surface by OFSS, rather than activation of pro-survival signaling pathway by OFSS.

***Disclosures: Fredrick Pavalko**, None.*
This study received funding from: NIH AR052682

MO0191

A Possible Role of Adipocytes in Bone in Osteoblastogenesis. Hengwei Zhang[1], Weida Lu[2], Yingchun Zhao[3], Robert Recker[4], Gary Guishan Xiao*[2]. [1]Creighton University Medical Center, USA, [2]Creighton University, USA, [3]Genomics & Functional Proteomics Laboratory, Osteoporosis Research Center, Creighton University Medical Center, USA, [4]Creighton University Osteoporosis Research Center, USA

Accumulative adipocytes in the aged bone were well documented and have been reported to associate with a reduced osteoblastic bone formation and bone mass loss. However, the role of bone marrow adipocytes remains unknown. Although several recent studies show that adipocytes may regulate the proliferation and differentiation of osteoblasts, the exact mechanism of how adipocytes regulate osteogenesis is not clear. In the present study, we used two different modes of co-cultures of adipocytes and osteoblasts which were derived from human mesenchymal stem cells (hMSC), to study the effects of hMSC-derived adipocytes on osteoblastogenesis. We found that alkaline phosphatase (ALP) positive areas, ALP activity, and calcification positive area decrease significantly as adipocyte density increases from low to high after 14-day or 28-day co-culture of adipocytes and osteoblasts using both co-culture modes. However, this effect was caused more by indirect co-culture mode than direct co-culture mode, suggesting that adipocytes significantly affected osteoblastogenesis mainly through indirect inhibitory pathway (indirect co-culture mode). To further understand the mechanism of the inhibitory adipocytes' effects on bone formation, the levels of both mRNA and protein expression in osteoblasts in the lower layer of the indirect co-culture mode were analyzed, leading to identification of two genes/proteins, S100A6 and calreticulin, both of which are related to bone formation. The differential expression of these two proteins can synergistically regulate the activity of canonical Wnt signaling pathways. Two proteins differentially expressed were confirmed in the bone tissue slides from young (4-week-old) and old (6-month-old) mice. Further, decreased nuclear expression level of β-catenin in osteoblasts was observed in 6-month-old mice. The analyses of antibody-based protein microarrays showed that the expression level of TGF-beta1 increased with the increase in adipocytes in the medium. In conclusion, above data suggest adipocytes in bone inhibit bone formation through their secreted factors.

***Disclosures: Gary Guishan Xiao**, None.*

MO0192

Acoustic Radiation Force on MC3T3-E1 Cells Modulates Calcium Transient in a Strain and Frequency-Dependent Manner. Yi-Xian Qin[1], Jiqi Cheng[2], Shu Zhang*[2]. [1]State University of New York at Stony Brook, USA, [2]Stony Brook University, USA

Purpose: Mechanotransduction has demonstrated potentials for tissue adaptation. It is well documented that ultrasound, as a mechanical signal, can produce a wide variety of biological effects in vitro and in vivo. Although a wide range of studies have been done, mechanism for therapeutic effect of ultrasound on bone healing still remains unclear. The present study investigated the influence of acoustic radiation force generated by ultrasound on intracellular Ca^{2+} signaling in MC3T3-E1 osteoblast-like cells. Methods: A therapy focused transducer with frequency of 3.3MHz, pulse duration of 300 ms and duty factor of 0.15 was used. Two power levels of 1W and 6W were chosen. Cells labeled with Calcium Green-1 were visualised using confocal microscopy following acoustic force stimulation. The effects of two intensities of acoustic forces with a cycle of stimulation of 60 seconds (strain modulation) and a period of 3 cycles of acoustic force between 10 and 30 seconds with 60 seconds rest time in each cycle (frequency modulation) were evaluated in our study. Results: In MC3T3-E1 cells, not subjected to acoustic force, no more than 1% of the relative intensity of the spontaneous global Ca^{2+} transient was exhibited. Acoustic force modulated global Ca^{2+} signaling by increasing the relative intensity of Ca^{2+} transients by 10%. The higher acoustic force generated by 6W ultrasound induced a significantly higher Ca^{2+} transient than that of lower acoustic force (10% *vs.* 3%, $P<0.05$) (Fig.1). The lower frequency of acoustic force induced higher Ca^{2+} transient in the last two cycles and lower residual Ca^{2+} concentration at the end of each cycle (Fig.2). Conclusions: The strain and frequency of acoustic force differentially modulated these Ca^{2+} signaling characteristics providing a potential mechanism through which osteoblasts may distinguish between different stimulation conditions. In our previous study, we have confirmed this newly developed methodology allowed manipulating of osteoblastic cells without the effects of acoustic streaming and ultrasound-induced temperature rise. We also found that acoustic force could deform the well-adhered cells and cause bending movement of primary cilium which acts mechanosensor on the surface of cell. Further studies to explore the relationship of these morphological changes with Ca^{2+} transient induced by ultrasound may lead to improve our knowledge of fundamental mechanotransduction pathway.

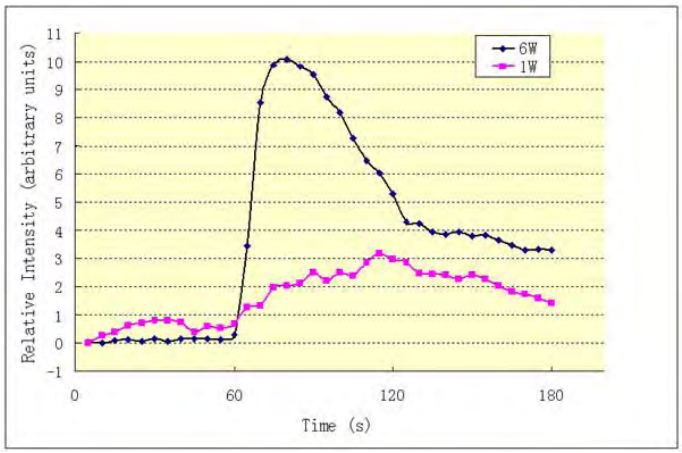

Fig.1 The influence of strain on the Ca2+ signaling in cells subjected to acoustic radiation force

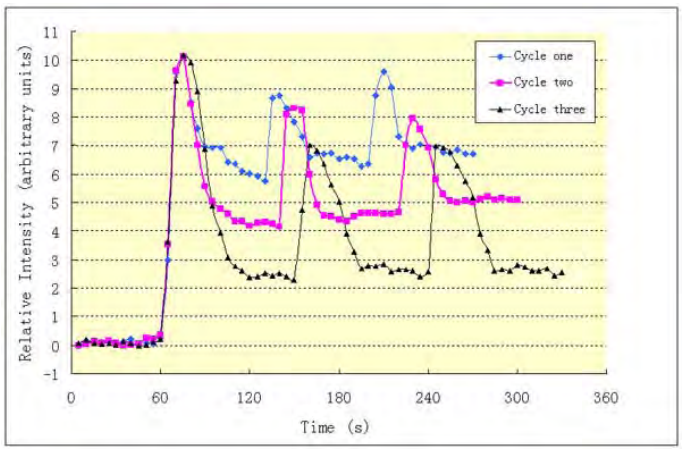

Fig.2. The influence of stimulation frequency on the Calcium signaling in cells.

***Disclosures: Shu Zhang**, None.*

This study received funding from: NIH (AR49286 and AR52379), National Space Biomedical Research Institute through NASA Cooperative Agreement NCC 9-58, and US Army Medical Researc.

MO0193

Acute-phase Serum Amyloid A Enhances Mineralization Processes and Cellular Senescence in Mesenchymal Stem Cells *In Vitro*. Peggy Benisch*[1], Sabine Zeck[2], Melanie Kober[2], Martina Regensburger[2], Jutta Meißner-Weigl[2], Moustapha Kassem[3], Regina Ebert[4], Franz Jakob[2]. [1]University of Wuerzburg, Germany, [2]Orthopedic Center for Musculoskeletal Research University of Wuerzburg, Germany, [3]Odense University Hospital, Denmark, [4]University of Wuerzburg, Orthopedic Center for Muskuloskeletal Research, Germany

Differentiation of human mesenchymal stem cells (hMSC) into osteoblasts is a major step for maintaining bone homeostasis and fracture repair. Human MSC stop proliferation and enter replicative senescence in vitro after several months in culture. Thereby they lose their potential for multilineage differentiation and self-renewal. Acute-phase Serum Amyloid A proteins (AP-SAA) have been demonstrated to be important players and mediators of the acute phase response in infection and chronic inflammation. They have also been linked to the pathogenesis of aging and age-associated diseases like atherosclerosis and tumor development. In the present study we analyzed the influence of AP-SAA – as pro-inflammatory proteins – on in vitro aging and differentiation into osteoblast-like-lineage of hMSC. Primary hMSC obtained from the bone marrow were cultured without any morphogen till growth arrest due to replicative senescence confirmed by senescence-associated beta-galactosidase staining. We detected a continuous increase of AP-SAA gene expression during the course of in vitro aging. By treating hMSC with high concentrations of rhAP-SAA we observed an increase in mineralization during osteogenic differentiation. High mineralization levels were also inducible in telomerase immortalized hMSC lines (hMSC-TERT) stable transfected with AP-SAA. AP-SAA overexpressing hMSC-TERT also exhibited a higher number of cells positive for senescence-associated beta-galactosidase compared to control cells. We conclude that increased expression of SAA1 and SAA2 is a hallmark of cellular senescence in in vitro aged hMSC and that endogenous AP-SAA overexpression propagates signs of senescence even in telomerase immortalized hMSC lines. Furthermore recombinant AP-SAA as well as overexpression of AP-SAA enhances mineralization during osteogenic differentiation in vitro. Taken together, AP-SAA may contribute to both physiological and pathological calcification in bone and in aseptic inflammation induced calcification, as well as atherosclerotic lesions.

***Disclosures: Peggy Benisch**, None.*

MO0194

Adherent Lipopolysaccharide Inhibits Osteoblast Differentiation on Titanium Alloy Substrates without Affecting Attachment, Spreading or Growth. Lindsay Bonsignore*, Victor Goldberg, Edward Greenfield. Case Western Reserve University, USA

Soluble lipopolysaccharide (LPS) from Gram-negative bacteria inhibits osteoblast differentiation and residual bacterial debris containing LPS adheres to implant surfaces sterilized and packaged by an orthopaedic implant manufacturer. Therefore, the purpose of this study was to determine whether bacterial-derived molecules adherent to implant surfaces inhibit osteogenesis through direct effects on osteoblasts.

To test this hypothesis, titanium alloy discs (13mm in diameter, Ti Industries) were made "LPS-free" by ten alternating treatments with 0.1N NaOH-95% ethanol and 25% nitric acid. Adherent LPS on the discs was measured using the Limulus Amoebocyte Lysate assay. LPS was adhered to the "LPS-free" discs (3.3 ± 0.9 Endotoxin Units (EU)/m^2) by incubation with various concentrations of LPS (ultra pure *E. coli*) in PBS followed by extensive washing. MC3T3-E1 pre-osteoblast cells were plated on discs at $2.5x10^3$ cells/cm^2 and the parameters of osteogenesis were examined. Statistical analysis was done by Two Way ANOVA with Bonferroni post-hoc tests.

Incubation with various concentrations of LPS provided discs with a range of adherent levels of LPS (between 5-20,000 EU/m^2). Adherent LPS had no affect on osteoblast attachment, spreading or growth as assessed by DNA quantification and staining with Texas Red X Phalloidin and DAPI. However, adherent LPS significantly impaired osteoblast differentiation in a dose dependent manner as measured by alkaline phosphatase activity and staining for mineralization with xylenol orange. Thus, at 8 days after plating, 5 EU/m^2 inhibited alkaline phosphatase activity by 21%, 100 EU/m^2 inhibited by 28%, 860 EU/m^2 inhibited by 52% ($p<0.05$) and 21,000 EU/m^2 inhibited by 68% ($p<0.02$). Also, 100 EU/m^2 partially inhibited mineralization 30 days after plating and 21,000 EU/m^2 almost completely inhibited mineralization.

Our results demonstrate that adherent LPS significantly impairs osteogenesis through direct effects on osteoblasts and that these effects are primarily due to inhibition of osteoblast differentiation without substantial effects on osteoblast spreading, attachment or growth. Previously reported levels of adherent LPS of 10-15 EU/m^2 on implant surfaces may have negative effects on osteoblasts as these levels are in the range shown here to impair osteoblast differentiation. These results provide further rationale for development of better detection and removal methods for residual bacterial debris on implant surfaces.

***Disclosures: Lindsay Bonsignore**, None.*

MO0195

Cnot3, a Novel Critical Regulator of a mRNA Stability, is Involved in the Maintenance of the Bone Mass and the Bone Structure in Senile Osteoporosis Model. Chiho Watanabe*[1], Masahiro Morita[2], Yoichi Ezura[3], Tetsuya Nakamoto[1], Tadayoshi Hayata[4], Hiroaki Hemmi[1], Takuya Notomi[5], Keiji Moriyama[1], Tadashi Yamamoto[2], Masaki Noda[1]. [1]Tokyo Medical & Dental University, Japan, [2]Division of Oncology, Institute of Medical Science, University of Tokyo, Japan, [3]Tokyo Medical & Dental University, Medical Research Insititute, Japan, [4]Medical Reserach Institute, Tokyo Medical & Dental University, Japan, [5]GCOE, Tokyo Medical & Dental University, Japan

Bone mass levels are determined by the balance of continuous remodeling that is based on bone formation and bone resorption. Although modulators for transcription and epigenetic control have been known to regulate the bone mass under the influences of cytokines and hormones, there is no knowledge to date, on the roles of regulation of mRNA stability in the regulation of bone remodeling. Cnot3 is one of the CCR4-NOT complex components that are critical for the mRNA stability in eukaryotic cells including yeast to mammalian cells and therefore we examined the possible role of this molecule in bone. We found that Cnot3 is expressed in bone in vivo and in osteoblasts in vitro. To address the in vivo role of Cnot3 in regulation of bone metabolism, bone structure of the Cnot3+/- mice in comparison to wild-type mice were examined (-/- is lethal). The longitudinal dimension of the femur of the Cnot3+/- mice was almost identical to that in wild-type mice. However, bone mineral density of the femur of Cnot3+/- mice was significantly suppressed compared to that in wild-type mice. With regard to the structures of the bone micro architectures, micro CT pictures of the Cnot3+/- mice exhibited sparsity of the trabecular bone pattern compared to wild-type. Quantification indicated that Cnot3+/- mice exhibited low bone mass phenotype in the secondary trabeculae of the femur. Bone volume per tissue volume (BV/TV) was reduced compared to wild-type mice. The bone mass in mice was dependent on the age. When we compared young adult mice about 10 weeks to 2 years old mice, base line levels of BV/TV for wild-type decreased with age

significantly. Cnot3+/- decreased BV/TV in young adult mice. In aged Cnot3+/- mice the levels of a reduction due to the deficiency was more than that due to age-dependent decrease indicating the importance of Cnot3. With respect to the three dimensional structural element analysis, trabecular number and trabecular thickness were suppressed in Cnot3+/- mice. Cnot3 +/- mice exhibited enhancement in trabecular separation and trabecular spacing. Preliminary bone marrow cells cultures in osteogenic (beta-glycerophosphate and ascorbic acid) or osteoclatogenic conditions showed similar levels of mineralized nodule formation and osteoclast development regardless of the presence or absence of Cnot3, suggesting the role of Cnot3 to be specific to in vivo environment. In conclusion, our data indicates that Cnot3 is required for the maintenance of bone mass.

***Disclosures: Chiho Watanabe**, None.*

MO0196

CREB Mediates Brain-derived Serotonin Regulation of Bone Mass Accrual. Gerard Karsenty, Franck OURY*, Vijay Yadav. Columbia University, USA

Serotonin is a bioamine synthesized in neurons of the brainstem and in enterochromaffin cells of the duodenum that does not cross the blood brain barrier. In the brain, serotonin is a well characterized neurotransmitter affecting cognitive functions whereas in the periphery, it is thought to act locally in the gut and at a distance as a hormone whose spectrum of functions only begins to be delineated. Besides its well known role in influencing cognitive functions brain-derived serotonin emerged recently as a molecule regulating, centrally, three homeostatic functions, bone remodeling, appetite and energy expenditure. Briefly, following its binding to the Htr2c receptor in neurons of the ventromedial hypothalamus (VMH) nuclei serotonin favors bone mass accrual, while following its binding to the Htr1a and Htr2b receptors in neurons of the arcuate hypothalamus nuclei, serotonin favors appetite and decreases energy expenditure. Recently, gut-derived serotonin was described as an inhibitor of bone formation by acting directly on osteoblasts. Gut-derived serotonin binds to the Htr1b receptor present on osteoblasts and through a PKA-dependent pathway uses cAMP response element binding protein (CREB) as a transcriptional mediator to inhibit osteoblast proliferation.

CREB is a broadly expressed leucine zipper-containing transcription factor implicated in the control of differentiation and proliferation of multiple cell types. Although it acts in many different cellular contexts CREB is a major regulator of multiple aspects of neurobiology such as neuron survival, axon growth and synaptic transmission. In this context it is important to note that CREB activation is a cAMP/PKA-dependent or a Calcium/Calmodulin-dependent kinase (CaMK) process. These roles of CREB in neurobiology together with the fact that it mediates the function of gut-derived serotonin raised the testable hypothesis that CREB could also mediate some of the homeostatic functions of brain derived-serotonin.

We show here, through cell-based assays and cell-specific gene inactivation studies, that brain derived-serotonin uses calmodulin-dependent kinases that are expressed in VMH neurons and calmodulin as second messenger downstream of the Htr2c receptor. We further show that CREB mediates brain-derived serotonin regulation of bone mass accrual. These data along with the one already gathered identify CREB as the main effector of the regulation of bone mass by serotonin, regardless its site of synthesis and of action. As such they further underscore the role of this transcription factor in regulating bone mass.

***Disclosures: Franck OURY**, None.*

MO0197

Does PTHrP Plays a Role in the Stimulatory Effect of Strontium on Osteoblast like Cells UMR 106.1 Mineralization? Pierre Bergmann[1], Rafik Karmali[2], Nicole Nijs-De Wolf*[3]. [1]Centre Hospitalier Universitaire Brugmann, Belgium, [2]Dept of Medicine, CHU Brugmann, ULB, Belgium, [3]Lab Exp Medicine, CHU Brugmann, ULB, Belgium

AIM: Sr2+ increases bone mass both by increasing bone formation and decreasing resorption (Bone 2007; 40S1:S5).PTHrP production by osteoblast like cells could regulate bone formation (J Clin Invest 2005; 115:2402). Sr2+ increases PTHrP mRNA expression by osteoblast like cells UMR 106.1 (JBMR 2008:23; SU016). In this study, we investigated the effect of Sr2+ on UMR 106.1 mineralization in the absence or presence of a PTH antagonist (PTH 7-34) to elucidate a possible role of local PTHrP in transducing the stimulation of osteoblast function by Sr2+.

METHOD: Confluent UMR 106.1 cells were trypsinized and plated onto 24-wells plates at 104 cells/well in MEM medium with 10 % fetal calf serum (FCS), 50 ng/mL ascorbic acid, 10 mM glycerophosphate and 10-8M dexamethasone (DEXA) $\pm$ 1 mM Sr2+ during 1 to 14 days. The effect of 1 µmol PTH 7-34.added with Sr2+ or 24H later was tested after 6 days. At the end of the incubation, the mineralized matrix was stained for calcium by Alizarin-red 2% (Endocrinology 1995; 270:9420-9428). The optical density (OD) of the supernatant was read at 562 nm after destaining (Bone 2001; 29:323-330). The results were expressed as mean of OD ($\pm$ SD).

RESULTS: OD was significantly higher in the presence of Sr2+ after 6 to 10 days of incubation (OD day 6 w/o Sr2+ =0.60 ($\pm$0.13) and + Sr2+ = 1.47 ($\pm$0.21), $p<0.00001$, n=12; day 7 w/o Sr2+ =1.28 ($\pm$0.17) and + Sr2+ = 1.84 ($\pm$0.19), $p<0.00001$, n=18; day 10 w/o Sr2+ =1.78 ($\pm$0.10) and + Sr2+ = 2.03 ($\pm$0.3), $p<0.0002$, n=6). There was no significant effect of PTH 7-34 on mineralization in the presence or absence of Sr2+, whether when added simultaneously (Table), or when added 24h after the incubation of Sr2+ to allow an effect of Sr2+ on UMR 106.1 proliferation.

CONCLUSION: Incubation with 1 mM Sr2+ during 6 to10 days increases significantly the OB-like cells mineralization. There was no significant inhibitory effect in the presence of PTH 7-34. These results demonstrated that PTHrP does not take part in the effect of Sr2+ on bone formation in this system.

Experience	DEXA	DEXA + Sr^{2+}	DEXA + PTH 7-34	DEXA + Sr^{2+} + PTH 7-34
1	0.57 (0.14) (n=12)	1.54 (0.26) (n=12)	0.48 (0.15) (n=12)	1.30 (0.38) (n=12)
2	0.36 (0.08) (n=12)	1.56 (0.15) (n=12)	0.35 (0.08) (n=12)	1.74 (0.09) (n=12)

Table

***Disclosures: Nicole Nijs-De Wolf**, None.*

MO0198

EGLN Inhibitor Promotes Bone Fracture Healing by Induction of VEGF. Yan Wang*[1], Bruce Hopkins[1], Masahiko Sato[2], Mary Adrian[1], Leah Helvering[1]. [1]Eli Lilly & Company, USA, [2]Lilly Research Labs, USA

Hypoxia-inducible factor (HIF) signaling is important to the initiation of angiogenesis following a bone fracture (Riddle et al. 2009. J. Mol. Med. 87:583). HiF1a transcriptionally upregulates VEGF in multiple cell types, including osteoblasts, which in turn promotes the coupling of angiogenesis to osteogenesis at the fracture site. Thus, strategies that promote HIF1/2α signaling in osteoblasts may accelerate bone healing and bone formation activity by increasing VEGF levels at the fracture site. EGLNs (EGLN1, EGLN2, and EGLN3) are members of egg-laying-defective nine prolyl-hydroxylases which during normoxia catalyze hydroxylation of HIFs which leads to its subsequent ubiquitination and proteosomal degradation. We hypothesized that inhibition of EGLNs would enhance the stability of active HIFs which in turn would potentiate VEGF secretion and speed bone healing. EGLN inhibitors were evalutated for their ability to enhance HIF signaling and downstream target genes in multiple osteoblast cell lines (primary rat marrow stromal cells, primary human osteoblasts, and U2OS). All of inhibitors induced HIF1a protein expression in 293 cells after 6 hours of treatment and increased VEGF secretion from 2-5 fold in human osteoblasts after 2 days of treatment. One of the EGLN inhibitors was further evaluated in a cortical defect model with osteopenic ovariectomized SD rats (Harlan) that were 8 months old (2 months post-ovariectomy) (Komatsu et al. 2009. Endocrinology 150:1570). However, region specific QCT analyses showed that 0.2 to 30 mg/kg/d of the EGLN inhibitor was ineffective at enhancing bone healing after 5 weeks of oral dosing. Taken together, these studies establish that EGLN inhibitors can stimulate VEGF secretion in osteoblasts but were ineffective in stimulating bone formation in a cortical defect model.

***Disclosures: Yan Wang**, None.*
This study received funding from: Eli lilly and campany

MO0199

EP1$^{-/-}$ Mice Are Resistant to Both Age-induced and Ovariectomy-induced Bone Loss. Minjie Zhang*[1], Hsin Chiu Ho[2], Tzong-Jen Sheu[2], Edward Schwarz[2], Regis O'Keefe[2]. [1]University of Rochester Medical Center, USA, [2]University of Rochester, USA

PURPOSE:

In our previous study, we provided novel findings showing that the absence of EP1 signaling results in accelerated endochondral ossification, earlier bone formation and remodeling, enhanced osteoblast differentiation, and accelerated fracture healing. Since fracture healing recapitulates the post-natal developmental process, we hypothesize that the EP1-/- mice may exhibit distinct bone properties, so that the regulation of EP1 receptor function could have a potential role in osteoporosis and its treatment.

METHODS:

Micro-computed tomography and 3-point bending test was used to determine the bone properties. Ovariectomy was used as an osteoporosis model. Calcein double labeling and TRAcP staining were performed to study the bone formation and resorption.

RESULTS:

Analysis of the µCT data on the cortical region showed significant increased of bone mineral density and minimum bending moment of inertia in EP1-/- mice compared to WT, indicating EP1 had a significant impact on the cortical bone geometry. Consistently, 3-point bending mechanical test results showed that EP1-/- mice had significantly increased maximum load, yield load and stiffness. µCT data collected from the trabecular region showed that EP1-/- mice have higher bone volume (BV/TV) (Table).

The changed bone properties of EP1-/- mice may result from either increased bone formation or decreased bone resorption. Calcein labeling showed that the mineralization apposition rate and bone formation rate were significantly higher in EP1-/- than in WT (Fig.1) while TRAcP staining showed similar resorption surface between EP1-/- and WT.

Ovariectomy (OVX) was performed in EP1-/- and WT mice at the age of four months and bone properties were evaluated 2 months later. Both EP1-/- and WT OVX mice have significantly lower BV/TV compared to sham mice, suggesting OVX accelerate trabecular bone loss (Fig.2). However, EP1-/- OVX mice have twice as much BV/TV as WT OVX mice suggesting that EP1-/- mice are resistant to the bone loss caused by OVX.

CONCLUSION:

Our findings demonstrated the EP1-/- mice have stronger cortical bone and more bone mineral density, more trabecular bone volume and delayed trabecular bone loss with aging, further supporting that EP1 negatively regulates bone formation. Using the ovariectomy model, we found that the EP1-/- mice are resistant to the ovariectomy-induced trabecular bone loss. These findings suggest EP1 as a potential target for the treatment of metabolic bone disease.

	2Mo WT Ave	EP1-/- Ave	T-test	6Mo WT Ave	EP1-/- Ave	T-test	1Yo WT Ave	EP1-/- Ave	T-test
MicroCT Data - evaluation of cortical diaphyseal bone									
Minimum Bending Moment of Inertia (mm^4	0.135	0.163	0.148	0.164	0.198	**0.030**	0.181	0.234	**0.001**
BMD (mgHA/cc)	1141.104	1148.439	0.273	1207.212	1238.534	0.096	1270.271	1308.906	**0.008**
Mechanical Testing - 3 point bending of femurs									
Max Load (N)	16.801	20.850	**0.026**	17.543	21.515	**0.033**	14.903	20.370	**0.002**
Max Bending Moment (N*mm)	67.204	83.401	**0.026**	70.173	86.062	**0.033**	59.611	81.480	**0.002**
Max Stiffness (N/mm)	100.910	125.998	0.175	114.064	135.643	0.394	134.930	145.241	**0.046**
Yield Load (N)	11.112	12.823	0.152	13.110	17.484	0.103	10.312	15.188	**0.005**
Energy to Max (N*mm)	3.153	4.212	0.053	2.603	3.491	**0.026**	1.817	3.599	**0.004**
MicroCT Data - evaluation of trabecular metaphyseal bone									
Bone Volume/Total Volume	0.340	0.327	0.796	0.234	0.316	**0.028**	0.124	0.198	**0.021**
Trabecular Number	6.746	6.342	0.567	5.520	5.208	0.118	3.032	3.894	**0.030**
BMD(mgHA/cc)	706.381	713.269	0.801	690.607	730.851	**0.001**	794.536	798.879	0.423
Trabecular Thickness	0.079	0.069	0.105	0.062	0.073	**0.040**	0.064	0.068	0.171

Table

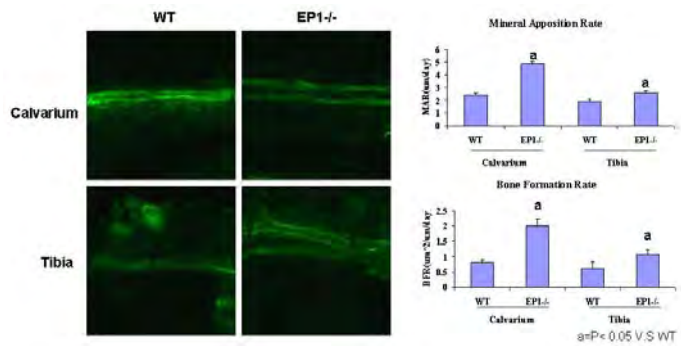

Fig.1

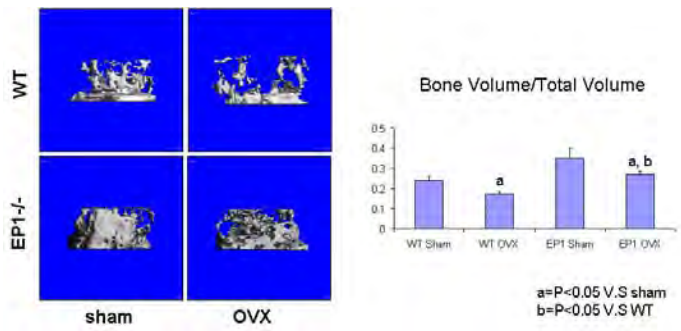

Fig.2

***Disclosures: Minjie Zhang**, None.*

MO0200

Extracts of the Nutritional Supplement, Bone builder™, and the Herbal Supplement, Greens+™, Synergistically Stimulate Bone Formation by Human Osteoblast Cells in Vitro. Dawn Snyder*[1], A. Venketeshwer Rao[1], Balachandran Bashyam[1], Jaclyn Beca[2], Honglei Shen[1], Salva Sadeghi[2], Ayesha Quireshi[2], Erin MacKinnon[3], Leticia Rao[3]. [1]University of Toronto, Canada, [2]St. Michael's Hospital, Canada, [3]University of Toronto, St. Michael's Hospital, Canada

The standard dietary recommendation for osteoporosis prevention and treatment includes supplementation with calcium and vitamin D. However, other nutrients have been found to be beneficial to bone health, including those in the nutritional supplement, bone builder™. The objective of our study was to investigate the effects on bone formation in vitro, of a water-soluble extract of bone builder™ (bb) alone and in combination with the antioxidant-rich, polyphenolic extract of the herbal supplement, greens+™ (g+). Our experimental design used human osteosarcoma SaOS-2 or cloned CD34+ cells cultured in HAM's F-12-supplemented media. Varying combinations of bb and g+ were added on day 8 and every 2-3 days thereafter. Cells were stained by vonKossa method, and subjected to image analysis to quantified bone formation. Alkaline phosphatase activity (ALP) was measured from sonicates. Results showed that bb had a significant time-dependent (two-way ANOVA, $p< 0.001$), and dose-dependent effect (one-way ANOVA, $P<0.0001$), in both cell lines. When compared to 1 mg/ml calcium, the effect of 1.0 mg/ml bb was found to be 2.35 $\pm$ 0.28x more effective than calcium alone. This could indicate that the other components of bone builder™ are necessary for the stimulation of bone formation. When varying doses of bb were combined with 1.2 mg/ml g+, results similarly showed a significant dose-dependent effect (one-way ANOVA, $P<0.001$). At 0.8 mg/ml bb plus g+ was 6x more effective than bb alone (t-test, $P<0.05$). Varying doses of g+ alone or combined with 0.5 mg/ml bb showed that at all concentrations tested, 0.8-2.0 mg/ml g+, the effect was significantly higher in the presence of bb. The highest concentration of g+ treated in combination with bb was 6x more effective than 2.0 mg/ml g+ alone (t-test, $P<0.005$). ALP activity showed that treatments of both bb and g+ alone, and in combination resulted in the maturation of the cells. In conclusion, bone formation in vitro was significantly enhanced over and above the effect of calcium when treated with a combination of nutrients, as found in the water-soluble extract of the bone builder™ supplement. This effect was further enhanced by the addition of a polyphenol extract with antioxidant properties. The results could suggest that use of greens+bone builder™ may be a good alternative or complementary supplement for the prevention and treatment of osteoporosis.

***Disclosures: Dawn Snyder**, None.*

MO0201

Function of OPG as a Traffic Regulator for RANKL is Crucial for Controlled Osteoclastogenesis. Shigeki Aoki*[1], Masashi Honma[1], Yoshiaki Kariya[1], Yuko Nakamichi[2], Tadashi Ninomiya[2], Naoyuki Takahashi[2], Nobuyuki Udagawa[2], Hiroshi Suzuki[1]. [1]The University of Tokyo Hospital, Japan, [2]Matsumoto Dental University, Japan

The amount of RANKL on the osteoblastic cell surface is considered to determine the magnitude of the signal input to osteoclast precursors and the degree of osteoclastogenesis. Previously, we have shown that most of the newly synthesized RANKL is transferred from the Golgi apparatus to the lysosomal storage compartment via the route involving Vps33a in osteoblastic cells. There also exists the minor pathway transporting RANKL from the Golgi apparatus to the plasma membrane. However, there still remains a problem that RANKL molecules are mostly transferred to the cell surface when expressed in non-osteoblastic cells, while Vps33a is ubiquitously expressed in these cell lines. In order to explain this discrepancy, it should be assumed that there are additional machineries which are required for RANKL transport from the Golgi apparatus to the secretory lysosomes in osteoblastic cells. Here, we have examined the involvement of OPG, which is currently recognized as a decoy receptor for RANKL, in the regulation of RANKL subcellular behavior using confocal laser scanning microscopic analyses. From a series of experiments using various OPG mutants, it has been suggested that OPG already makes a complex with RANKL in the Golgi apparatus and the complex formation is necessary for RANKL sorting to the secretory lysosomes. Co-precipitation assay showed that the interaction between RANKL and Vps33a is greatly enhanced by co-expression of OPG, also supporting the OPG function as a traffic regulator for RANKL. It was also shown that each structural domain of OPG is indispensable for exerting OPG function as a traffic regulator. In particular, heparin binding domain of OPG, whose physiological function has been almost unclear, was indicated to be important in sorting RANKL molecules to the lysosomes from the Golgi apparatus. In addition, the over-expression of RANK-OPG chimeric protein, which retained OPG function as a decoy receptor but lost the function as a traffic regulator, inhibited endogenous OPG function as a traffic regulator selectively in osteoblastic cells and resulted in the up-regulation of osteoclastogenic ability despite the increased number of decoy receptor molecules. Conclusively, OPG function as a traffic regulator for RANKL is crucial for regulating osteoclastogenesis at least as well as that as a decoy receptor.

***Disclosures: Shigeki Aoki**, None.*

MO0202

Functional Adaptation of the Skeleton may be Regulated by CGRPα Through a Neuronal Mechanism. Susannah Sample*[1], Jason Bleedorn[2], Zhengling Hao[3], Peter Muir[4]. [1]UW-Madison School of Veterinary Medicine, USA, [2]University of Wisconsin-Madison, USA, [3]University of Wisconsin - Madison, USA, [4]University of Wisconsin, Madison, USA

Purpose: The mechanisms that regulate load-induced bone formation are currently not understood. Bone innervation has been shown to regulate load-induced bone formation. The present study was designed to determine whether the sensory innervation of bone, specifically calcitonin gene related peptide-α (CGRPα) peptidergic innervation, is involved in the neuronal regulation of load-induced bone formation.

Methods: 48 male C57B6 mice aged 19-21 weeks were used for the study; 24 were CGRPα knockouts and 24 were wildtypes. 8 mice in each group were used as sham controls and the remaining 16 had their right ulna loaded at 2Hz for 800 cycles at -3,500με. Half of the loaded mice were given perineural anesthesia of the right brachial plexus with bupivacaine before loading to induce temporary neuronal blocking. Mice were injected with calcein immediately after loading and alizarin 7

days later, and were euthanatized at 10 days. Normalized periosteal labeled ulna bone areas were determined using confocal microscopy.

Results: Brachial plexus anesthesia resulted in decreased bone formation in both the loaded and contralateral ulna in the wildtype group, but did not affect load-induced bone formation in the knockout group. Loading, with or without brachial plexus anesthesia, resulted in greater bone formation in the knockout mice compared to the wildtype mice.

Conclusion: These data suggest that CGRPα is involved in the neuronal regulation of functional adaptation. Bone does not have motor innervation, and it has been shown that the sympathetic innervation is not involved in mechanotransduction. Collectively, these findings suggest that peptidergic sensory innervation is involved in mechanotransduction, and that CGRPα signaling has a role in the neuronal blocking effect seen in this model with brachial plexus anesthesia. It should be noted that CGRPα knockout mice have a low bone mass phenotype. Further work is needed to understand the relationship between skeletal mechanosensitivity and systemic changes in bone remodeling in this knockout mouse.

Figure 1: Unlike the wildtype mice, abrogation of load-indiced bone formation did not occur in the CGRPα knockout mice with of brachial plexus anesthesia, suggesting that CGRPα may have a role in the neuronal regulation of functional adaptation. Bars represent the mean ? standard deviation, n=7-9 mice/group. # - P = 0.10; * - P < 0.05; ** - P < 0.01 as indicated or versus the same bone in the wildtype group.

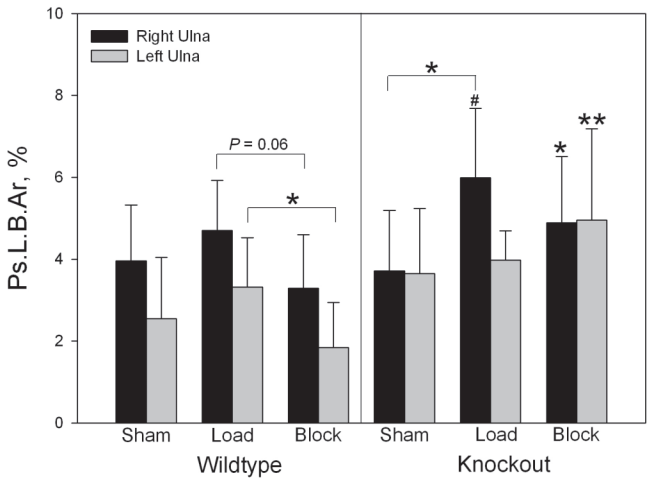

Figure 1

***Disclosures: Susannah Sample**, None.*

MO0203

Important Role of Non Canonical Pathways in Controlling the Proliferation and Differentiation of Osteoblastic Cells Induced by Wnt Proteins. Cyril Thouverey, Joseph Caverzasio*. Service of Bone Diseases, Dept of Rehabilitation & Geriatrics, University Hospital of Geneva, Switzerland

In vitro and in vivo data indicate that Wnt proteins (Wnts) stimulate the proliferation of osteoblastic cells but their effect on the differentiation of these cells remains unclear. Enhanced proliferation of osteoblastic cells by Wnts involves the canonical ß-catenin and the non canonical Src, ERK, PI3K pathways. Signaling implicated in the regulation of osteoblastic cell differentiation induced by Wnts are not known and have been investigated in MC3T3-E1 cells in response to Wnt3a. Recombinant Wnt3a (100 ng/ml) enhanced MC3T3-E1 cell proliferation by 1.9 fold ($p<0.01$). Excess of DKK1 (1 µg/ml), a natural antagonist of the ß-catenin pathway, completely blunted activation of the ß-catenin promoter TOPflash induced by Wnt3a but only reduced the enhanced cell proliferation by 25% ($p<0.01$) suggesting a predominant role of non canonical pathways in this response. Selective inhibitors of Src kinases (SU6656, CGP77675, 5 µM) and of PKC (Go6983, 5 µM) strongly inhibited the Wnt3a-induced cell proliferation (> 80%, $p<0.01$). Associated with these effects, Wnt3a induced an increase in protein tyrosine phosphorylation detected after 12-24h incubation with a concomitant increased activation of Src and PKC kinases, as well as of PDGF and EGF receptors. Enhanced proliferation induced by Wnt3a was associated with a strong inhibition of MC3T3-E1 cell differentiation (complete inhibition of osterix, type 1 collagen, BSP and alkaline phosphatase expression after 5-7 days). This effect was partially prevented by the Src inhibitor SU6656 and was reversible upon further incubation of cells in absence of Wnt3a.

In conclusion, data presented in this study indicate that non canonical pathways play a predominant role in controlling the proliferation and differentiation of osteoblatic cells induced by Wnt proteins. The Src and PKC pathways as well as PDGF and EGF receptors are involved in the stimulation of cell proliferation induced by Wnts whereas a Src kinase(s) is probably responsible for inhibition of their differentiation. These data also indicate that Wnt proteins increase the number of osteoblatic cells. During this process, osteoblastic markers are repressed but cells recover their phenotype in absence of agonists.

***Disclosures: Joseph Caverzasio**, None.*

MO0204

Lrp5 Receptor and PGE2 in Bone Response to Mechanical Loading. Bryan Hackfort*[1], Gwendolin Alvarez[1], Mohammed Akhter[2], Diane Cullen[1]. [1]Creighton University, USA, [2]Creighton University Osteoporosis Research Center, USA

Increased mechanical loading is known to stimulate new bone formation in vivo; however the pathways are poorly understood. Two pathways that have been identified include the Lrp5 receptor and PGE2 signaling. PGE2 is released by osteoblasts and osteocytes in response to loading with Cox-2 as the rate limiting enzyme in its production. In this study we examine Lrp5 effects by using mice with three different levels of expression and to examine PGE2's role by using NS-398 as a selective Cox-2 inhibitor. We hypothesize that there will be an interaction between Lrp5 (Wnt signaling) and PGE2 inhibition with mechanical loading. Adult (4 month old, 23 ± 2g), virgin female mice included HBM high bone mass phenotype (G171V mutation), WT C57/B6, and Lrp5-/- KO mice were divided into groups of 15 control and 15 treated. They were injected with either 10 mg/kg NS-398(Cayman Chemical) in DMSO, or vehicle (DMSO) 3 hours prior to loading. Right tibiae were loaded via tibial compression on Mon, Wed, and Fri for 100 cycles at 2 Hz for a total of 10 days. Left and right tibiae were sectioned at 1-3 mm proximal to the tibia fibula junction. Histomorphometry was collected for periosteal and endocortical MS/BS, MAR, and BFR. NS 398 did not have an effect on the nonloaded leg formation parameters. There was an increase in formation with loading for all groups. The loads were selected based upon previous testing to create strains of 650 µε HBM, 1060 µε Wt and 1500 µε KO. For BFR vehicle groups showed a significant increase (10 to 40 um/yr) after 28 days. Surprisingly, the NS398 groups showed an even greater response (40 to 65 um/yr). NS 398 was expected to decrease PGE2 and therefore the response to mechanical loading. Previous studies in rats with four-point bending have shown a 50% reduction over a 21 day period with indomethacin and others complete suppression with NS398 after a single extremely high load above injury level with a possible inflammatory response dependent upon PGE2 levels. It seems in this study that the long term load adaptation process was able to overcome the suppression of PGE2, perhaps by utilizing other redundant stimulatory processes.

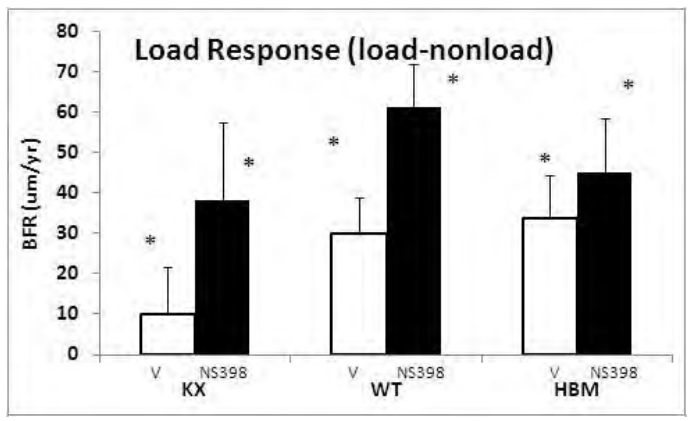

fig 1

***Disclosures: Bryan Hackfort**, None.*

MO0205

Osteoblast Growth and Differentiation in Three-Dimensional Collagen Gels. Brya Matthews*[1], Karen Callon[1], Rachel Locklin[2], Philippa Hulley[2], Dorit Naot[1], Jillian Cornish[1]. [1]University of Auckland, New zealand, [2]University of Oxford, United Kingdom

Osteoblastic cells cultured in two dimensions (2D) on plastic surfaces have long been used as a tool for studying bone cell growth, differentiation and response to growth factors or therapeutic agents, with the results extrapolated to the *in vivo* situation. In bone *in vivo*, however, osteoblasts are operating within a complex interconnected three-dimensional (3D) microenvironment which bears little relation to the situation in a culture flask. Type I collagen, which sets as a gel at appropriate temperature and pH, can be used as a scaffold for 3D culture of cells. The aim of this study was to compare growth and differentiation of osteoblasts cultured in collagen gels with cells cultured using standard 2D methodologies.

Primary rat osteoblasts were cultured in parallel in standard plastic dishes and in 3D cultures, incorporated into 3mg/ml type I collagen minigels. Cell proliferation was measured by thymidine incorporation and differentiation was assessed using von Kossa and alizarin red staining. Gene expression during differentiation was examined by qRT-PCR.

Cells cultured in 3D responded to anabolic factors such as TGFβ, PDGF and lactoferrin over a similar concentration range as in 2D, but the magnitude of the response in the gels was much larger. For example, 10pM TGFβ increased thymidine incorporation 1.6x in 2D and 3.3x in 3D. The targeted tyrosine kinase inhibitor imatinib, whose targets include the PDGF receptor, inhibited cell proliferation in both systems, with inhibition occurring at concentrations at least 10x lower in 3D. 3D

culture also appeared to promote cell differentiation. Osteoblast differentiation markers were up-regulated earlier in 3D, with approximately 20x higher alkaline phosphatase, 40x higher bone sialoprotein and 250x higher osteocalcin mRNA levels in 3D cultures in the first week of the mineralisation assay. In addition, staining indicated mineralisation occurred earlier in 3D than in 2D.

Cultures in 3D collagen minigels are simple to set up and produce reproducible results. 3D culture of rat osteoblasts appears to amplify the effect of selected anabolic agents. It also promotes osteoblast differentiation and mineralisation. This type of methodology may provide a better indication of *in vivo* effects of potential anabolic therapeutics.

***Disclosures: Brya Matthews**, None.*

MO0206

Osteoblast IL-33 mRNA Expression is Regulated by PTH, and IL-33 Treatment Causes both Increased Osteoblastic Matrix Mineralisation and Reduced Osteoclast Formation In Vitro. Julian Quinn*[1], Hasnawati Saleh[2], Matthew Gillespie[1]. [1]Prince Henry's Institute of Medical Research, Australia, [2]Prince Henry's Institute, Australia

IL-33 is a Th2 stimulating pro-inflammatory cytokine related to IL-1 and IL-18, with actions mediated by receptor ST2L. Like IL-18, IL-33 does not directly affect osteoclast formation from RANKL- and M-CSF-stimulated immature bone marrow macrophages (BMM) but strongly inhibits such osteoclast formation when T cells are present.

In mouse bone sections, anti-IL-33 immunostaining was observed in osteoblasts and chondrocytes but few osteocytes or bone marrow cells. DNA microarray array and qRT-PCR studies found that PTH treatment increases IL-33 and ST2L mRNA expression in matured osteoblastic Kusa O cells and cultured calvarial osteoblasts. Oncostatin M, which (like PTH) has both anabolic and catabolic influences on bone, similarly regulated IL-33 and ST2L mRNA.

Since osteoblasts express ST2L we investigated IL-33 action on osteoblasts to identify possible autocrine actions. IL-33 promoted matrix mineralisation by primary osteoblasts. Furthermore, in long term ascorbate stimulated primary osteoblasts in which expression of osteocytic features are apparent (i.e., sclerostin and DMP-1 expression), IL-33 reduced sclerostin mRNA levels after 6 and 24 hours of treatment, although other PTH regulated genes in these cells such as ephrin B2 were not affected.

We also investigated IL-33 effects on osteoblastic support of osteoclastogenesis. Like PTH and oncostatin M, IL-33 increased RANKL mRNA levels. However, in co-cultures of BMM with osteoblasts (or Kusa O pre-osteoblastic cells) osteoclasts did not form. Indeed, when osteolytic factors such as 1,25 dihydroxyvitamin D3 were present, IL-33 treatment (20ng/ml) inhibited osteoclast formation, indicating induction of an inhibitor. This inhibitory influence was confirmed to be a diffusible factor and was ablated by anti-GM-CSF antibody. GM-CSF mRNA was also strongly upregulated by IL-33 treatment. However, Kusa O/BMM co-cultures treated with IL-33 and anti-GM-CSF antibody (without other stimulus) induced osteoclast formation only weakly.

In summary, IL-33 stimulates osteoblastic function in vitro but also indirectly inhibits osteoclast formation through at least two separate mechanisms. Autocrine actions of IL-33 thus may play a role in maintaining bone mass, perhaps participating in the anabolic actions of PTH.

***Disclosures: Julian Quinn**, None.*

MO0207

Regulation of Osteoblast Function and Bone Remodeling by Phosphatidylinositol Transfer Protein-alpha (PITP-alpha). Zheng Zhou*, Lin Mei, Wencheng Xiong. Medical College of Georgia, USA

Phosphatidylinositol transfer proteins a (PITPa) is an ubiquitous expressed protein that transfers phosphatidylinositol (PI) or phosphatidylcholine (PC) between cell membranes. It is essential for membrane trafficking and signal transduction through PLC-mediated phosphatidylinositol bisphosphate (PIP2) hydrolysis. Reduced expression of PITPa in mice leads to defective neurite outgrowth, aponecrotic spinocyerebella disease, hypoglycemia, and intestinal and hepatic steatosis. However, its role in bone remodeling is unclear. Here we present evidence for PITPa in this event. PITPa deficient mice showed reduced bone mineral density and bone mass. These defects were caused by aberrant osteoblast proliferation and differentiation. The osteoclast differentiation and function are relatively normal in vitro and in vivo. We are further investigating molecular mechanisms underlying PITPa regulation of osteoblast differentiation and function.

***Disclosures: Zheng Zhou**, None.*

MO0208

The Effect of Oral Glucose Tolerance Test on Serum Osteocalcin and Other Bone Turnover Markers in Young Adults. Paivi Paldanius*[1], Kaisa Ivaska[2], Petteri Hovi[3], Sture Andersson[4], Eero Kajantie[3], Kalervo Vaananen[5], Outi Makitie[6]. [1]University of Helsinki, Finland, [2]University of Turku, Department of Cell Biology & Anatomy, Finland, [3]National Institute for Health & Welfare, Finland, [4]Hospital for Children & Adolescents, Institute of Clinical Medicine, University of Helsinki, Finland, [5]Department of Cell Biology & Anatomy, Institute of Biomedicine, University of Turku, Finland, [6]Hospital for Children & Adolescents, University of Helsinki, Finland

Serum osteocalcin (OC) is an osteoblast-derived protein which has recently been implicated in the regulation of glucose tolerance and energy metabolism. This endocrine function of OC is most likely exerted via its uncarboxylated form which has been shown to induce expression of adiponectin, insulin, and markers of pancreatic islet cell proliferation. The aim of the present study was to evaluate the effect of a standard 75-g oral glucose tolerance test (OGTT) on serum osteocalcin, carboxylated osteocalcin (cOC) and bone turnover markers C- terminal telopeptide of type I collagen (bCTX) and amino-terminal propeptide of type I collagen (PINP). Serum samples at baseline and at 120 min were analyzed in a cohort of normoglycemic young adults (n=23; 12 females, 11 males; mean age 23.6 years, range, 18.5 to 26.4). During OGTT a statistically significant decrease was observed for all bone turnover markers from baseline to 120 min (paired t-test, $p< 0.001$ for all variables). The median ($\pm$SE) decreases for OC, cOC, bCTX, and PINP were -32.1 ($\pm$2.9)%, -34.4 ($\pm$2.9)%, -61.4 ($\pm$2.4)% and -26.8 ($\pm$2.5)%, respectively. The observed changes were independent of the time of collection (baseline samples between 6:00 and 11:00 am). A strong association between the changes in serum OC and cOC was observed (Pearson's correlation, r=0.86, $p< 0.001$). Also the decrease in PINP values was associated with changes in OC (r=0.76, $p<0.001$) and cOC (r=0.78, $p<0.001$) whereas the change in resorption marker bCTX was not associated with OC or cOC (r=0.34 and 0.36, respectively, p=ns). The observed OGTT-induced changes in these different bone-derived proteins are independent of each other and maybe mediated by separate different mechanisms which require further studies. The magnitude of change in bCTX after the OGTT was similar to the effect of food intake as reported previously by others and was moderately associated with the reduction in PINP (r=0.46, p=0.034). Further studies to characterize the effect of glucose on serum osteocalcin and its degree of carboxylation in a larger population are warranted.

***Disclosures: Paivi Paldanius**, None.*

MO0209

C/EBPβ Binds Multiple Distal Regulatory Sites in the *Rankl* Gene Locus and Modulates the Gene's Expression in Osteoblasts. J. Pike, Melissa Martowicz*. University of Wisconsin-Madison, USA

RANKL is a TNF-like factor that is synthesized in osteoblasts and controls the differentiation, activation and life-span of the osteoclast. Its expression is therefore a primary determinant of both normal as well as pathological bone turnover. Given this linkage to the osteoporotic state, an understanding of the mechanisms that govern *Rankl* expression from osteoblasts is of emerging interest. Our previous studies in mouse ST2 cells defined a series of six distal enhancers located up to 88 kb from the mouse *Rankl* transcriptional start site (TSS) that mediate regulation of *Rankl* expression by $1,25(OH)_2D_3$, PTH and the gp130-activating cytokines IL-6 and OSM. Recent ChIP-chip analyses in these cells revealed that both $1,25(OH)_2D_3$ and PKA activators such as forskolin also strongly induced the binding of C/EBPβ to these enhancers as well, suggesting a potential role for this transcription factor in *Rankl* expression in the osteoblast. Surprisingly, however, siRNA knockdown of C/EBPβ mRNA levels resulted in upregulation of *Rankl* mRNA expression in response to $1,25(OH)_2D_3$. Overexpression of C/EBPβ, on the other hand, increased basal *Rankl* expression and blunted the capacity of $1,25(OH)_2D_3$ to induce the mRNA. Interestingly, C/EBPβ binding was most strongly observed at the -75 kb mRLD5 enhancer, a region that mediates highly robust *Rankl* regulation by both $1,25(OH)_2D_3$ and PTH. We thus assessed the ability of C/EBPβ to modulate both basal and inducible levels of this fragment following cotransfection with an expression vector for C/EBPβ. C/EBPβ strikingly increased basal activity of the *Rankl* enhancer while simultaneously suppressing the ability of $1,25(OH)_2D_3$ and Fsk to induced this reporter. This inhibitory activity of C/EBPβ was also observed in sub-fragments of the mRLD5 enhancer that mediated either $1,25(OH)_2D_3$ or Fsk response. These findings suggest a more complex role for C/EBPβ in the regulation of *Rankl* expression in osteoblasts than anticipated. Interestingly, $1,25(OH)_2D_3$ also induced *C/EBPβ* mRNA expression in osteoblastic cells and strongly upregulated the level of C/EBPβ protein. Since C/EBPβ binding to the *Rankl* gene precedes this upregulation, however, we suggest that the actions of $1,25(OH)_2D_3$ on C/EBPβ DNA binding are likely mediated through a posttranslational mechanism. We conclude that C/EBPβ does not play a direct role in upregulating *Rankl* expression, but may influence the basal state of *Rankl* expression in osteoblastic cells.

***Disclosures: Melissa Martowicz**, None.*

MO0210

DExH-box Helicase DHX36 Mediates Histone Deacetylase Inhibitor MS-275-induced Bone Formation. Ha-Neui Kim*[1], Kyoungsuk Jung[1], Hyunil Ha[1], Jea Seung Ko[2], Zang Hee Lee[1]. [1]Seoul National University School of Dentistry, South korea, [2]Seoul National University, School of Dentistry, South korea

Histone deacetylase (HDAC) enzymes are known to modify core histones and to be involved in oncogenic transformation by regulating the transcriptional activity. Thus, HDAC inhibitors represent a new strategy in mechanism-based cancer therapeutics regulating chromatin remodeling and gene expression. In this study, we investigated the effects of MS-275, a HDAC inhibitor, on bone regeneration. The effects of MS-275 on in vivo bone formation were evaluated both in a critical size calvarial bone defect rat model and in a recovery model after soluble receptor activator of nuclear factor ?B ligand-induced mouse trabecular bone loss. Radiographic and histomorphometric analyses indicated that MS-275 administration substantially increases the osteogenic capacity to repair bone lesion in the two animal models. In addition, treatment of osteoblastic cells with MS-275 strongly increased early osteogenic marker alkaline phosphatase (ALP) mRNA levels, enzymatic activity, and its promoter activity. By analyzing a series of murine ALP promoter deletion constructs and purifying DNA binding proteins, we identified DExH-box helicase DHX36 which binds to the MS-275 responsive region between nucleotides -117 and -97 of the ALP promoter. Down-regulation of endogenous DHX36 using shRNA potently inhibited MS-275-induced osteoblast differentiation by abrogating ALP activity. In contrast, overexpression of DHX36 promoted MS-275-induced osteoblast differentiation, as reflected by stimulation of ALP activity and bone nodule formation. Taken together, these results demonstrate that MS-275 has a bone anabolic effect via DHX36-dependent ALP up-regulation.

***Disclosures: Ha-Neui Kim**, None.*

MO0211

Epigenetic Bookmarking of Osteoblast Growth and Differentiation Related Genes by Runx2 During Mitosis. Syed Ali*, Jason Dobson, Sayyed K. Zaidi, Andre Van Wijnen, Jane Lian, Janet L. Stein, Gary Stein. University of Massachusetts Medical School, USA

The osteogenic Runx2 transcription factor regulates key genes required for osteoblast growth, proliferation and differentiation. However, mechanisms controlling inheritance of osteoblast growth and differentiation potential are not known. We have found that Runx2, unlike many other transcription factors, associates with its target genes during mitosis. These include RNA Pol I-transcribed ribosomal RNA (rRNA) genes that are linked with bone cell growth, as well as RNA Pol II-transcribed genes that are involved in osteoblast proliferation (e.g., p21) and differentiation (e.g., Smads). Runx2 marks these genes for transcriptional regulation in post-mitotic progeny cells, thus maintaining cellular memory for key biological parameters of lineage commitment and maintenance. Ribosomal RNA genes are suppressed by Runx2, indicating that Runx2 plays a key role in balancing osteoblast growth with differentiation. At a mechanistic level, the transcriptional co-repressor Transducin Like Enhancer-1 (TLE1), a known Runx2 co-regulator, associates with rRNA genes through its interaction with Runx2 during mitosis and interphase. We further show that Runx2 and TLE1 cooperate to suppress rRNA transcription. Functionally, TLE1 depletion relieves Runx2-mediated rRNA gene suppression and selectively increases histone modifications (H4Ac, H3Ac and H3K9Ac) that represent a code for open chromatin structure. Importantly, relieved suppression coincides with increased global protein synthesis and cell proliferation. Our findings reinforce the concept of architectural epigenetics through recruitment of cell type specific regulators, which convey cellular memory to progeny cells by bookmarking of fate determining genes.

***Disclosures: Syed Ali**, None.*

MO0212

Fluid Flow Activation of Osteoblasts and the Interaction of PKA and AKT. Jacob Miller*[1], Gwendolin Alvarez[1], John Yee[2], Diane Cullen[1]. [1]Creighton University, USA, [2]Creighton University School of Medicine, USA

Mechanical loading stimulates an anabolic bone response that results in osteoprogenitor proliferation and de novo bone formation in vivo through the Wnt signaling pathway. G-coupled protein receptors activated by mechanical loading can activate both PKA and Akt pathways which in turn can increase β-catenin transfer to the nucleus independent of Wnt signaling. The relative role of PKA and Akt pathways in osteoblast response to mechanical stimulation is not known. In this study we use pulsatile fluid flow (PFF) to create shear stress on bone cells and simulate in vivo loading to examine G-coupled pathways known to be associated with the loading response. Neonatal mouse calvarial osteoblasts were collected at 3-5 days, grown in flasks, and cultured on collagen coated slides. Slides were expose to pulsatile fluid flow (PFF) (16 ± 2 dyn/cm^2) for 1 hr at 1 Hz. Samples were collected from static control and PFF exposed cells immediately after exposure or 1 hr later (n=6/grp). All inhibitors were applied from 30 min prior to PFF through 1 hr of recovery. Inhibitors included NS398 (Cox2, 0.0031g/l, Caymen), PTH7-34 (PTH receptor, 0.0034g/l, Bachem), H89 (PKA, 0.0156 g/l, Biomol), and Akti (Akt kinase, 0.0058g/l, Calbiochem). mRNA expression was quantified (ABI 7500) for PTGS2 and PTHrP, both mechanosensitive genes with PTGS2 a Wnt target gene. NS398 suppressed PGE2 levels, but did not suppress PTGS2 or PTHrP gene expression with PFF. PTH7-34 decreased PTGS2 response to PFF by 50%, but not PTHrP expression. The PKA and Akt inhibitors alone did not block gene expression, but when combined suppressed expression of both PTGS2 and PTHrP at 1 hr after fluid flow. These data show that increased production of PGE2 is not essential to the PTGS2 and PTHrP mRNA responses to PFF and that other signals such as PTHrP may contribute to the response. It also suggests that PKA and Akt may have overlapping roles and that both must be blocked to suppress the load response. Mechanical loading creates a complex set of signals in osteoblasts with overlapping or redundant pathways to allow for appropriate bone adaptation and strength.

***Disclosures: Jacob Miller**, None.*

MO0213

Gene Expression Patterns in Bone Following Mechanical Loading. Sara Mantila Roosa*[1], Yunlong Liu[2], Charles Turner[3]. [1]Purdue University, USA, [2]Indiana University School of Medicine, USA, [3]Indiana University, Purdue University Indianapolis, USA

The advent of high-throughput measurements of gene expression and bioinformatics analysis methods offers new ways to study gene expression patterns. The goal of this study was to determine the time sequence for gene expression in a bone subjected to mechanical loading, during key periods of the bone formation process including expression of matrix genes and the appearance of active osteoblasts. We used the rat forelimb loading model, in which the right forelimb was loaded axially for 3 minutes, while the left forearm served as a non-loaded control. Animals were subjected to loading sessions every day, with 24 hours between sessions. Ulnae were sampled at 11 time points, from 4 hours to 32 days after beginning loading. The time points are referenced to the number of hours or days after the first bout of bone loading was applied. RNA was isolated and mRNA abundance was measured at each time point using Affymetrix exon arrays (GeneChip® Rat Exon 1.0 ST Arrays). Differentially expressed genes were identified across the time course, and genes were grouped into unique cluster patterns using a k-means algorithm. Groups of genes within the clusters were then defined based on gene and associated protein function.

We identified 1051 differentially expressed genes across the time course. These genes were grouped into 6 distinct, time-dependent patterns of gene expression and categorized into three primary clusters: genes upregulated early in the time course, genes upregulated during matrix formation, and genes downregulated during matrix formation. Many gene groups known to be important in loading-induced bone formation were identified within the clusters, including AP-1-related genes in the early response cluster (Fosl1 and Junb), matrix-related genes in the upregulated gene clusters (Alpl, Bglap, and Col1a2), and Wnt/β-catenin pathway inhibitors in the downregulated gene clusters (Sost and Sfrp4). In addition, we observed numerous genes encoding chemokines that were upregulated early. These may be involved in osteoblast recruitment. During matrix formation, a large number of solute carrier genes were regulated, including amino acid transporters that were upregulated. Finally, we observed many muscle-related genes that were primarily downregulated. In conclusion, we determined the time sequence of gene expression in a bone subjected to mechanical loading, and identified known and novel gene groups that shared loading-induced, time-dependent gene expression patterns.

***Disclosures: Sara Mantila Roosa**, None.*

MO0214

Histone Demethylase NO66 is a Negative Regulator of Osterix and Osteoblast Diffrentiation. Krishna Sinha*[1], Qin Chen[2], Hideyo Yasuda[2], Benoit De Crombrugghe[3]. [1]UT MD Anderson Cancer Center, USA, [2]M. D. Anderson cancer Center, USA, [3]University of Texas M.D. Anderson Cancer Center, USA

Osterix (Osx) is an osteoblast-specific transcription factor required for osteoblast differentiation, and bone formation and homeostasis. Osx null mice do not form bone but have a normal cartilage skeleton. To better understand the control of transcriptional activation by Osx, we recently showed that a Jumonji C (JmjC)-domain containing protein NO66 directly interacts with Osx and inhibits Osx target gene activation. We hypothesized that NO66 is a negative regulator of osteoblast differentiation and bone formation. Knockdown of NO66 in preosteoblast cells triggers accelerated osteoblast differentiation and mineralization and markedly stimulates expression of Osx target genes. NO66 exhibits a JmjC-dependent histone demethylase activity specific for both H3K4me and H3K36me in vitro and in vivo, and this activity is needed for the regulation of osteoblast-specific promoters. NO66 is a chromatin protein and its interaction with chromatin of Osx target genes influences both the levels of methylation states of histone H3 and expression of these genes. In undifferentiated MC3T3 preosteoblasts or in differentiation-arrested Osx null primary calvarial osteoblasts, NO66 remains bound to the promoter of the Bsp gene where Bsp expression remains in a repressed state. In contrast, in differentiating MC3T3 cells induced by BMP-2 and in differentiating primary mouse calvarial cells, there was a decrease in occupancy of NO66 at the Bsp gene but an increase in the occupancy of both Osx and trimethylated lysine 4 and 36 of histone H3, which are associated with

marked stimulation in Bsp expression. A decreased NO66 occupancy thus correlates with increased Osx occupancy at Osx-target promoters during osteoblast differentiation. The mechansim by which NO66 is depleted from chromatin is not clearly understood, however we postulate that an Osx-containing activator complex may be invloved in displacing an NO66-repressor complex during sequential activation of osteoblast-specific genes. Our results suggest the hypothesis that interactions between NO66 and Osx regulate expression of a repertoire of Osx target genes in osteoblasts by modulating histone methylation states.

***Disclosures: Krishna Sinha**, None.*

MO0215

Identification of Osteoblast-Specific *cis*-acting Regulatory Elements in the *Bmp2* and *Bmp4* Gene Deserts: *Effect of Chromatin Context on Transcription Regulation*. Steven Pregizer*, Douglas Mortlock. Vanderbilt University Medical Center, USA

Bone Morphogenetic Proteins 2 (*Bmp2*) and *4* (*Bmp4*) are closely-related members of the Transforming Growth Factor-β super-family that are redundantly required for endochondral bone development. They are both situated in the middle of large, conserved gene deserts and are transcriptionally regulated during development by tissue-specific *cis*-regulatory sequences scattered throughout these deserts. In an attempt to locate the sequences that drive *Bmp2* and *Bmp4* expression in osteoblasts, we mapped ''active'' chromatin marks throughout the gene deserts in MC3T3 and MN7 cells, a pair of osteoblast-derived cell lines that express robust levels of *Bmp4* and *Bmp2* mRNA, respectively. These marks (acH3K9, mono-meH3K4, H2A.Z) were ubiquitous throughout the *Bmp2* gene desert in MN7 cells; however, there was an obvious paucity of marking in the *Bmp4* gene desert. In MC3T3 cells, we found the opposite situation: strong marking across the *Bmp4* gene desert but a paucity of marking in the *Bmp2* gene desert. This strong correlation between "active" chromatin marks and expression suggests that the marked regions play a role in transcriptional regulation. To address this possibility, we cloned several regions from the *Bmp2* gene desert that were specifically marked in MN7 cells and tested them in the context of a minimal promoter-reporter vector. Surprisingly, upon transfection into MN7 cells, they repressed transcriptional activity. Likewise, regions from the *Bmp4* gene desert that were uniquely marked in MC3T3 cells exhibited repressor activity in this cell line. None of the regions had repressor activity in NIH3T3 fibroblasts, which express neither *Bmp2* nor *Bmp4*. These results demonstrate that the cloned regions can act as repressors of transcription in an osteoblast-specific manner; however, their effect on transcription may also depend upon chromatin context. This idea is consistent with our observation that ''active'' chromatin marking in the *Bmp2* and *Bmp4* gene deserts correlates strongly with expression status of these genes. Future studies with stably-integrated constructs should help us to address the role these *cis*-acting regulatory regions play in the transcription of *Bmp2* and *Bmp4* in osteoblasts.

***Disclosures: Steven Pregizer**, None.*

MO0216

Iron Inhibits Osteoblast Differentiation and Maturation of Mesenchymal Stem Cells Origin. Qing Yang[1], Florence Huang[2], Jinlong Jian[3], Xi Huang*[4]. [1]NYU School of Medicine, USA, [2]Bergen County Academy, USA, [3]New York University Medical Center, USA, [4]New York University School of Medicine, USA

Women after menopause are at high risk of developing osteoporosis. We have previously shown that postmenopausal women experience not only estrogen deficiency due to ceases of ovarian functions but also iron accumulation as a result of cessation of menstruation. In the present study, we have tested a hypothesis that increased iron contributes to postmenopausal osteoporosis by affecting mesenchymal stem cells (MSCs) differentiation and maturation in adult life. The abilities of mouse MSCs to differentiate into osteoblasts were tested in the osteoblast induction media in the presence of iron. We have shown that the expression and activity of alkaline phosphates, which is a pivotal early marker of osteoblast differentiation, were significantly suppressed by iron. Iron so far has been known to directly regulate only eight genes through iron regulatory proteins (IRPs), which bind to the iron responsive element (IRE) of the genes at either 3' or 5'-untranslated regions (UTR). Six of the eight genes are related to iron metabolisms. Interestingly, HIF-2alpha which contains a IRE at 5' UTR and is activated by high iron, was shown to completely suppress ALP activities. The terminal differentiation represented by matrix mineralization, was also significantly inhibited by iron. Expression of Runx2, an essential transcription factor for osteoblast differentiation, along with other osteoblast differentiation and maturation markers including osterix, osteocalcin, collagen I, and osteopontin, were significantly decreased by iron treatment. Currently, we are investigating whether CDC14A, a dual specificity phosphatase, which contains a IRE at 3' UTR and is downregulated by high iron, lead to the observed downregulation of osteoblast differentiation and maturation markers. Our in vitro findings provide further novel mechanistic explanations on clinical observations that, in addition to estrogen deficiency, menopausal women lose bone mineral density due to iron increase.

***Disclosures: Xi Huang**, None.*

MO0217

Metformin, an Oral Anti-diabetic Drug, Stimulates Osteoblast Diferentiation via AMPK-activated SHP Expression in Mouse Calvarial Cells. Won Gu Jang*[1], Eun Jung Kim[1], Kkot-nim Lee[2], Sin-Hye Oh[2], In-Ho Bae[1], Hye-Ju Son[2], Shee-Eun Lee[1], Sun-Hun Kim[1], Jeong-Tae Koh[1]. [1]Chonnam National University, South korea, [2]Chonnam National University School, South korea

The association between glycemic control of type 2 diabetes mellitus (type 2 DM) and severity of osteoporosis has been investigated. Metformin, an oral anti-diabetic drug of biguanide class, is commonly used for the treatment of obese type 2 diabetes. The drug has been introduced to improve glucose metabolism via activation of AMP-activated protein kinase (AMPK) and small heterodimeric partner (SHP; NR0B2). Recently SHP is also known to be a positive regulator of osteoblastic differentiation. This study was to explore the effect of metformin on osteoblast differentiation and its molecular mechanism.

Metformin (100-500 μM) significantly increased expression of key osteogenic genes, alkaline phosphatase (ALP), osteocalcin (OC), bone sialoprotein (BSP) as well as SHP in MC3T3E1 cells. Metformin-induced SHP mRNA and protein levels were demonstrated to be mediated via activation of the AMPK signaling pathway. To confirmed metformin-induced AMPK effect, we performed transient transfcetion with SHP promoter (SHP-luc) and osteocalcin promoter (OG2-luc) in MC3T3E1 cells. Promoter study showed that metformin (100 μM) stimulated the transcriptional activity of SHP or OG2 gene, and the metformin effect was inhibited by DN-AMPK or Compound C. Adenoviral overexpression of SHP significantly increased ALP staining and OC production. We confirmed that upstream stimulatory factor-1 (USF-1) specifically mediated metformin effect on SHP gene expression, and inhibition of USF-1 by dominant negative USF-1 (DN-USF-1) significantly abrogated metformin-mediated activation of the SHP promoter. Furthermore, we determined that induced-SHP physically interacts and forms a complex with Runx2 on the osteocalcin gene promoter in MC3T3E1 cells. On the other hands, metformin-induced AMPK increased Runx2 mRNA and protein levels. However, USF-1- SHP signaling pathway was not involved in Runx2 expression. Finally, we evaluated the effect of SHP gene using primary calvarial cells from wild type mice and SHP-/- mice. In primary calvarial cells of SHP-/- mice, ALP, OC and BSP mRNA expression and ALP activity were suppressed compare with wild type primary calvarial cells in the presence of metformin. Taken together, these results indicate that metformin could stimulate the osteoblast differentiation through AMPK-activated SHP expression.

***Disclosures: Won Gu Jang**, None.*

MO0218

NFATc1 Interacts With CSL and Suppresses Canonical Notch Signaling. Stefano Zanotti*[1], Anna Smerdel-Ramoya[2], Ernesto Canalis[2]. [1]Saint Francis Hospital & Medical Center, USA, [2]St. Francis Hospital & Medical Center, USA

Nuclear Factor of Activated T-Cells (NFAT)c1 is a transcription factor that regulates cell differentiation and function. The effect of NFATc1 in osteoblasts is controversial and both suppressive and stimulatory effects on osteoblastic differentiation have been reported. Notch are evolutionary conserved transmembrane receptors that determine cell fate. In the Notch canonical pathway, activation of signaling results in the cleavage and nuclear translocation of the Notch intracellular domain (NICD). In the nucleus, NICD associates with the DNA-binding protein Epstein-Barr virus latency C Promoter Binding Factor 1, Suppressor of Hairless and Lag-1 (CSL) to activate the transcription of target genes, such as *Hairy enhancer of split 1 related with a YRPF motif* (*Hey)1* and *Hey2*. NICD inhibits NFAT transactivation in osteoblasts, and Notch suppresses osteoblastogenesis. To test whether NFATc1 regulates Notch canonical signaling, osteoblasts from $Rosa^{Notch}$ mice, where NICD is induced following the deletion of a STOP cassette by CRE recombination, were used. $Rosa^{Notch}$ osteoblasts were transduced with an adenoviral vector expressing constitutive active (ca)NFATc1 in the context, or not, of NICD expression. NICD induced the transactivation of a reporter construct containing 12 copies of a CSL consensus sequence directing luciferase expression (12xCSL-Luc), and induced HEY1 and HEY2 transcripts. caNFATc1 inhibited the transactivation of the 12xCSL-Luc reporter and of fragments of the *Hey1* and *Hey2* promoters directing luciferase expression. Accordingly, caNFATc1 suppressed HEY1 and HEY2 transcript levels. The mechanism of action of NFAT on Notch transactivation was analyzed by electrophoretic mobility shift assay, using a radiolabeled DNA probe containing a CSL consensus sequence. In control cells a DNA-protein complex was observed, and this complex was shifted in cells expressing NICD. In cells transduced with caNFATc1 an additional DNA-protein complex, which was shifted by an antibody recognizing NFATc1, was observed. Formation of a protein complex between NFATc1 and CSL was demonstrated by immunoprecipitation. Accordingly, co-localization of dual immunofluorescence labeling for CSL and NFATc1 was reported by confocal microscopy, demonstrating direct NFATc1-CSL interactions in osteoblasts. In conclusion, NFATc1 inhibits Notch canonical signaling by interacting with CSL, and as a consequence modulates Notch actions in osteoblasts.

***Disclosures: Stefano Zanotti**, None.*

MO0219

Nuclear Factor of Activated T cells Mediates Osteoblastic Regulation of Hematopoiesis in the Bone Marrow Microenvironment. Laurel Druschitz*[1], Jennifer Paige-Robinson[2], Christopher Klug[2], Majd Zayzafoon[2]. [1]University of Alabama, USA, [2]University of Alabama at Birmingham, USA

The Nuclear Factor of Activated T Cells (NFAT) family of transcription factors are best known for their role in T lymphocyte activation. However, recent studies are increasingly revealing new roles for NFAT proteins in diverse organs, including the heart, blood vessels, central nervous system and during skeletal development. We previously reported that NFAT signaling negatively regulates osteoblast differentiation and bone formation both *in vitro* and *in vivo*. In addition to bone formation, osteoblasts are also known to support hematopoietic cell development and have been implicated in the regulation of B lymphopoiesis. To determine whether NFAT signaling in osteoblasts exerts direct action over bone formation and hematopoietic development *in vivo*, we generated mice expressing a dominant-negative form of NFAT (dnNFAT) driven by the 2.3kb fragment of the Collagen I promoter to disrupt NFAT activity specifically in osteoblasts ($dnNFAT^{OB}$). Male mice were examined at 12 weeks of age and μCT analysis of tibiae showed that $dnNFAT^{OB}$ mice have significant increases in bone volume and mineral apposition rate as compared to controls. In addition, $dnNFAT^{OB}$ mice displayed significant increases (72%) in the $Lineage^{-}cKit^{+}Sca\text{-}1^{+}$ (LSK) cells in the bone marrow. $dnNFAT^{OB}$ mice also showed significant decreases in $B220^{+}$ B lymphocytes (42%), but no significant differences in $B220^{+}CD19^{+}IgM^{-}$ or $B220^{+}CD19^{+}IgM^{+}$ cells as compared to controls. Concurrent with these findings, the *in vitro* expression of dnNFAT in primary calvarial cells significantly diminished (43%) the ability of LSK cells to differentiate into $B220^{+}$ cells. The gene expression and protein levels of Jagged-1, which has been shown to be important during early hematopoietic development, was significantly decreased in $dnNFAT^{OB}$ mice as well as dnNFAT calvarial cells. In addition, the gene expression and protein levels of the vascular cellular adhesion molecule (VCAM-1), which is required for B cell development, were also significantly decreased. Taken together, these data suggest an important role for osteoblast-specific NFAT activity during early hematopoietic differentiation as well as during early B lymphopoiesis.

***Disclosures: Laurel Druschitz**, None.*

MO0220

pRB/p107 and BRG1 Coordinate Transcriptional Activation of Alkaline Phosphatase in Osteoblasts. Stephen Flowers*[1], George Beck[2], Elizabeth Moran[3]. [1]NJMS-UH Cancer Center, University of Medicine of Dentistry of New Jersey, USA, [2]Emory University School of Medicine, USA, [3]University of Medicine & Dentistry of New Jersey, Cancer Center, USA

The retinoblastoma susceptibility gene, Rb1, is closely linked with osteosarcoma as well as retinoblastoma. The basis of such ties between individual susceptibility genes and tumors of specific tissue origin is a central question in cancer biology. Functional analysis of pRB and the closely related family members, p107 and p130, has tended to focus on repression of proliferation, but genetic evidence from our lab and others indicates an active requirement for pRB in osteoblast differentiation that might relate more directly with osteosarcoma susceptibility. Our previous studies linked pRB with activation of the early osteoblast marker, alkaline phosphatase (the product of the Akp2 gene). Here we have investigated the functional relationships between pRB and the SWI/SNF complex in Akp2 activation. Chromatin immunoprecipitation (ChIP) assays reveal the Akp2 promoter is targeted directly by all three pRB family members. Only p130 occupies the promoter prior to induction, while pRB and p107 target Akp2 directly during activation, and concurrent with association of the global co-activator p300. Akp2 is also a direct target of SWI/SNF chromatin remodeling complexes. These ATPase-powered complexes help orchestrate the programmatic shifts in gene expression necessary for progression from a self-renewing precursor state to a state of terminal differentiation. In osteoblasts, SWI/SNF complexes that repress osteogenic gene expression in order to maintain the precursor state are characterized by inclusion of the BRM ATPase. The alternative ATPase, BRG1, characterizes complexes that activate osteogenic genes during terminal differentiation. Thus, the onset of osteoblast differentiation is marked by a switch from BRM to BRG1 complexes on the Akp2 promoter. Our analysis shows that the BRM to BRG1 switch is accomplished in a precise two-step mechanism, with dissociation of BRM-containing SWI/SNF dependent on p300, and association of BRG1-containing SWI/SNF dependent on pRB/p107. Binding of RNA polymerase-II is dependent in turn on BRG1. Thus, in contrast to their widely studied role in cell cycle repression, pRB/p107 play a directly activating role in osteogenic gene expression, specifically in recruitment of the activating SWI/SNF complex.

***Disclosures: Stephen Flowers**, None.*

MO0221

Transcriptional Control of FIAT Expression in Osteoblasts. Bahareh Hekmatnejad*[1], Claude Gauthier[2], Rene St-Arnaud[3]. [1]McGill University, Canada, [2]Shriners Hospital for Children, Canada, [3]Shriners Hospital for Children & McGill University, Canada

FIAT (Factor Inhibiting ATF4-mediated Transcription) represses osteocalcin gene transcription and inhibits osteoblast activity by heterodimerizing with ATF4 and preventing it from binding to DNA. It thus becomes important to identify and characterize the mechanisms that control FIAT gene expression. We investigated the regulation of FIAT transcription following treatment of osteoblastic cells with the osteogenic cytokine BMP2. Using Reverse Transcription quantitative PCR, we measured a transient inhibition of FIAT expression upon BMP2 treatment. A 1.4 kb fragment of the proximal FIAT promoter was subcloned upstream from the luciferase reporter gene and transfected into osteoblastic MC3T3-E1 cells. BMP2 treatment of the transfected cells transiently inhibited the expression of the reporter gene, demonstrating that the response element is contained within the proximal promoter fragment. Using in silico analysis of the promoter sequence combined with Electrophoretic Mobility Shift Assays, we identified a canonical GC box that binds the Sp1 and Sp3 transcription factors from osteoblastic nuclear extracts. Chromatin immunoprecipitation (ChIP) confirmed binding of both factors to the FIAT promoter GC box in living osteoblasts. Overexpression of Sp1 in MC3T3-E1 cells resulted in a dose-dependent activation of the expression of the FIAT-luciferase reporter construct. Interestingly, transfection of osteoblastic cells with expression vectors for both isoforms of Sp3 led to dose-dependent inhibition of FIAT-luciferase transcription. To further confirm the involvement of Sp1 in FIAT gene transcription, we have applied RNA knockdown technology using siRNAs to inhibit expression of Sp1, which led to a reduction in steady-state FIAT expression. In parallel, we treated MC3T3-E1 cells with anthracycline WP631, which binds G/C-rich domains in DNA and thus inhibits Sp1-DNA interaction. A four-hour treatment with WP631 inhibited the expression of FIAT by 80% and decreased the binding of Sp1 to its cognate site within the FIAT promoter, as detected by ChIP. Our results show that the Sp1 and Sp3 transcription factors modulate the expression of the FIAT gene in opposing fashion and suggest that they are implicated in the BMP2-dependent regulation of FIAT transcription.

***Disclosures: Bahareh Hekmatnejad**, None.*

MO0222

Differential Regulation of Cortical and Trabecular Bone by Secreted Frizzled-Related Protein 4 (Sfrp4). Richard Kao*[1], Alyssa Louie[2], Wei-Dar Lu[2], Robert Nissenson[3]. [1]UCSF/VAMC, USA, [2]VAMC, USA, [3]University of California, San Francisco, USA

Previously we found that Sfrp4 is markedly up-regulated during the differentiation of primary osteoblasts in vitro. Deletion of canonical Wnt signaling inhibitors such as Dkk1 and SOST in vivo led to an increase in both trabecular and cortical bone mass. Secreted frizzled-related proteins (Sfrp), belonging to a class of Wnt signaling inhibitors that bind Wnts directly, could antagonize both canonical and non-canonical Wnt pathways. Interestingly, Sfrp1 null mice exhibited increased bone formation in metaphysis but no change in cortical BMD. To further address the function of Sfrp class of Wnt antagonists in the skeleton, a global Sfrp4 knock-out (KO) mouse model was generated by a polyA trapping method. Embryonic stem cells harboring a trapped Sfrp4 gene were obtained from Toronto Centre for Phenogenomics and used to generate chimeric mice. Both heterozygous (het) and homozygous (hom) mice for the trapped Sfrp4 gene were generated for phenotypic analysis. Cortical and trabecular bone parameters from 12-week old male and female mice were determined by μCT. Hom KO of Sfrp4 produced a reduction in BV/TV (-10.4%, $p<0.001$; $n\geq19$) and cortical thickness (-16.3%, $p<0.001$) and a concomitant increase in the medullary volume (+27.4%, $p<0.05$) of the tibia-fibular junction as compared to wild-type (WT) littermates. In trabecular bone of the distal femur, TV (+21.7%, $p<0.001$), BV (+41.8%, $p<0.05$), connectivity density (+42.6%, $p<0.01$), and trabecular number (+19.2%, $p<0.01$) of hom KO were increased while there was a decrease in trabecular spacing (-21.6%, $p<0.01$%) as compared to WT littermates. Significant reduction in these parameters was also detected between het and hom KO mice. No changes in serum markers of bone formation and resorption were detected in Sfrp4 KO mice. Sfrp4 has been postulated to play a role in systemic mineral balance. However, no abnormalities in serum calcium or phosphate levels were detected in Sfrp4 KO mice. In summary, mice lacking Sfrp4 have reduced cortical thickness and display an increased amount of trabecular bone. These results are consistent with the preliminary findings of Saito et al. (JMBR 23:S3;2008) and Brommage et al. (JBMR 24:S1;2009). While the positive effects of Sfrp4 deficiency on trabecular bone may well result from enhanced canonical Wnt signaling, the negative effects of Sfrp4 deficiency on cortical bone are likely to be mediated by other actions such as an increase in non-canonical Wnt signaling.

***Disclosures: Richard Kao**, None.*

MO0223

Gα12-RhoA Signaling in Osteoblasts Antagonizes PTH/Calcitriol-Stimulated Osteoclastogenesis and Effects on RANKL and OPG: A Potential Homeostatic Mechanism in Bone. Jun Wang*, Paula H. Stern. Northwestern University, USA

Osteoblast-stimulated osteoclastogenesis is an important component of bone remodeling as well as a potential limitation in the therapeutic use of parathyroid hormone (PTH) to build bone. Factors that modulate this osteoclastogenic effect are important for understanding bone physiology and could lead to new therapeutic agents. Gα12 – RhoA signaling has recently been recognized as a PTH-stimulated pathway that mediates effects in bone and that may have a role in the genetic susceptibility to osteoporosis. To further elucidate the effects of the pathway in osteoblasts, we have stably transfected UMR-106 osteoblastic cells with constitutively active (ca) RhoA (RhoA63N), caGα12 (Gα12Q231L), dominant negative (dn) RhoA (RhoA19L), or empty vector (pcDNA) and determined the effects of the constructs on osteoclastogenesis, assessed by tartrate resistant acid phosphatase activity, in co-cultures with RAW 264.7 osteoclast precursor cells. None of the constructs elicited osteoclastogenesis in untreated co-cultures. Also, none of the constructs affected the osteoclastogenic response to receptor activator of NFκB ligand (RANKL) in the co-cultures. However, whereas UMR-106 cells transfected with pcDNA or dnRhoA stimulated osteoclastogenesis when the co-cultures were treated for 5 days with 30nM PTH plus 100nM calcitriol (PTH/D), the osteoclastogenic effect of PTH/D was markedly attenuated or absent in the UMR-106 cells stably expressing either caRhoA or caGα12. The effect of the constructs was not due to differences in osteoblast viability or proliferation, as assessed by MTT assay. The inhibitory effect of the caRhoA or caGα12 could be partially antagonized with the Rho kinase inhibitor Y27632. To investigate the mechanism of the inhibitory effects, the expression of RANKL and osteoprotegerin (OPG) in the UMR-106 cells was examined by RT-PCR. Cells transfected with pcDNA, dnRhoA, caRhoA or caGα12 were treated with PTH/D for 16hr. PTH/D treatment increased RANKL mRNA and decreased OPG mRNA in the cells transfected with pcDNA or dnRhoA, whereas PTH/D failed to elicit these effects in cells expressing caGα12 or caRhoA. Basal expression of RANKL and OPG was unaffected by the constructs. The results suggest that Gα12 – RhoA signaling could inhibit hormone-stimulated osteoclastogenesis by effects on expression of RANKL and OPG. Since PTH can stimulate the Gα12 – RhoA pathway, the current findings could represent a homeostatic mechanism for regulating PTH action in bone.

***Disclosures: Jun Wang**, None.*

MO0224

Heat Shock Protein 25 Induced by Dexamethasone is Associated with Osteoblast Differentiation via GSK3ß. Sun-Il Yun, Hyung-Young Yoon, Yoon-Sok Chung*. Ajou University School of Medicine, South korea

Purpose: Dexamethasone (Dex) was shown to increase the expression of heat shock protein 25 (HSP25) in osteoblasts. However, the functional role of HSP25 induced by Dex in osteoblasts remains unknown. In this study, the role of HSP25 in osteoblast was investigated.

Method: The effect of Dex on osteoblast mineralization was examined by alizarin red S staining. The mRNA changes of osteogenic differentiation markers were analyzed by RT-PCR; osteocalcin, osteopontin, Runx2, and type I collagen. To determine whether HSP25 is associated with osteoblast MC3T3-E1 cells differentiation, HSP25 was knock-downed by siRNA.

Results: Dex decreased mineralization and accumulated HSP25 during differentiation. Dex significantly decreased osteocalcin, but had no effects on osteopontin, Runx2, and type I collagen. The knock-down of HSP25 did not recover the decreased osteocalcin mRNA by Dex. To determine whether the HSP25 expression was related to Wnt signaling, LiCl, a GSK3β inhibitor, was treated, and then analyzed the level of HSP25 expression. Interestingly, LiCl significantly overcame the effect of Dex on both mRNA and protein of HSP25 and osteocalcin mRNA.

Conclusion: This study suggests that HSP25 is associated with osteoblast differentiation through the control of osteocalcin, which is modulated by GSK3β.

This research was supported by the "GRRC" Project of Gyeonggi Provincial Government, Republic of Korea.

***Disclosures: Yoon-Sok Chung**, None.*

MO0225

MMP14 Mediates PTH-induced Soluble RANK Ligand Release from Osteoblasts. Mei-ling Zhu*[1], Christine Simpson[2], Karl Insogna[3]. [1]Yale School of Medicine, USA, [2]Yale University, USA, [3]Yale University School of Medicine, USA

RANKL is produced by osteoblasts and bone marrow stromal cells primarily as the transmembrane isoform. Transmembrane RANKL can be cleaved from the cell surface to release a 21 kD soluble isoform. The biological significance of this process in bone is unclear. It has been suggested that release of sRANKL serves to restrain bone resorption by removing RANKL from the bone microenvironment. However, it has also been reported that sRANKL production is increased in states of accelerated bone loss such as hyperparathyroidism and sex-steroid deficiency. Matrix metalloproteinase-14 (MMP14) and ADAM 10 (A Disintegrin And Metalloproteinase domain) have both been suggested as sheddases for RANKL in osteoblasts. Although PTH can induce RANKL production, its effects on sRANKL release have not been extensively studied. We found that PTH increased sRANKL release in primary murine osteoblasts and in the PTHR1-over expressing osteoblast/stromal cell line, UAMS P32. In the UAMS P32 cells, PTH induced sRANKL expression by 26-fold (as assessed by RIA of conditioned media) and confirmed by Western blotting using an OPG pull down assay. GW4133X, a TACE and MMP inhibitor suppressed PTH induced sRANKL release by 70%. PTH rapidly induced RANKL transcript expression in osteoblasts but had no effect on ADAM 17 (also known as TACE, TNF-alpha converting enzyme), ADAM 10 or MMP14 transcript levels. PTH did induce a slight increase in MMP14 protein levels (1.8 fold). In UAMS P32 cells, an RNAi to MMP14 reduced release of sRANKL by 59% percent (838 to 349 pg/ml, p=0.04). In contrast, an RNAi to ADAM10 did not affect sRANKL release (3% change, p= NS). We conclude that PTH induces sRANKL release primarily by stimulating the activity of MMP14 by post-transcriptional mechanisms.

***Disclosures: Mei-ling Zhu**, None.*

MO0226

Oxytocin Receptor Nuclear Translocation Could Be A Novel Mechanism Mediating Osteoblast Differentiation Induced By Oxytocin. Adriana Di Benedetto*[1], Graziana Colaianni[1], Stefania Dell'Endice[1], Roberto Tamma[1], Cosima Damiana Calvano[2], Carlo Giorgio Zambonin[2], Bice Chini[3], Li Sun[4], Mone Zaidi[4], Alberta Zallone[5]. [1]University of Bari, Medical School, Italy, [2]University of Bari, Chemistry, Italy, [3]Neuroscience, CNR, Italy, [4]Mount Sinai School of Medicine, USA, [5]University of Bari Medical School, Italy

We recently demonstrated a direct anabolic effect of oxytocin (OT) on bone (Tamma et al., 2009). OT upregulates expression of osteoblast markers and transcription factors as Osterix, Schnurri, Atf-4, Osteocalcin and Osteopontin. This effect is mediated by the seven-transmembrane G-protein coupled receptor (GPCR) OTR expressed by osteoblasts. We investigated how OT-OTR promote osteoblast differentiation and activity. Recently several reports suggest a novel pathway for GPCRs: the receptors upon ligand triggering are found in the nucleus and a nuclear localization of OTR in neoplastic cells and fibroblasts has been reported (Kinsey,2007); however how this is accomplished is still not clear. Accordingly we found by western blot OTR in osteoblast nuclear extracts after OT stimuli (15-30 min); this result was confirmed by confocal microscopy of OTR-GFP in fixed or living cells and by immunogold identification of the receptor by TEM. MALDI-TOF analysis was performed on nuclear proteins immunoprecipitated with anti-OTR and analysis of the spectra with FindPept database revealed the presence of four peptides corresponding to OTR intracellular loops. We further analyzed OTR trafficking and nuclear transport following OT stimulation. Exogenous OTR-GFP fusion protein transfected in primary osteoblasts, colocalizes with β-arrestin1/2 within 2-3 min after OT treatment, thereafter the receptor dissociates from β-arrestins and localizes in endosomal compartment. By the time OTR-GFP is sorted to the nucleus. Transportin-1 silencing in osteoblasts affects OTR nuclear localization, suggesting this protein mediates OTR nuclear translocation. We hypothesized a possible role for OTR in regulating transcription. By immunoprecipitation, we found physical interaction of native OTR with the osteoblast transcription factor Runx-2 and with the transcription co-activator Schnurri-2, in response to OT stimulus. Furthermore simultaneous stimulation of osteoblast with OT and BMP2 induced OTR/Smad4 interaction in the nucleus. Blocking OTR endocytosis by silencing β-arrestins, prevented OT induced up-regulation of genes as ATF-4, Osteocalcin and FAS-L. In conclusion some OT anabolic effects on bone are mediated by a novel mechanism initiated by OTR internalization and nuclear translocation.

***Disclosures: Adriana Di Benedetto**, None.*

MO0227

Age and *in vivo* Clinical Characteristics of Subjects Influence *in vitro* Vitamin D Action in Human Bone Marrow Stromal Cells. Shuanhu Zhou*, Julie Glowacki, Meryl Leboff. Brigham & Women's Hospital, USA

Vitamin D deficiency and osteoporotic fractures are prevalent disorders in older adults. We recently reported that human marrow stromal cells (hMSCs, a.k.a. mesenchymal stem cells) express vitamin D hydroxylases and produce 1,25-dihydroxyvitamin D_3 ($1,25(OH)_2D_3$) *in vitro*, and that 1α-hydroxylase gene expression is influenced by the *in vivo* vitamin D status of the subjects whose MSCs were studied [*Endocrinology* 2010; 151:14-22]. In this study we test the hypothesis that age and other *in vivo* clinical characteristics influence the *in vitro* effect of $1,25(OH)_2D_3$ on hMSCs differentiation to osteoblasts. First, in a series of MSCs obtained from 13 de-identified, unconsented men (age 27-79 years), we found that there was an age-related decline in the magnitude of stimulation of ALP activity by $1,25(OH)_2D_3$ ($r=-0.803$, $p=0.0009$). Subjects scheduled for total hip replacement (as a source of discarded marrow) were recruited to an IRB-study for research serum and other tests. In a series of 49 consented subjects (age 41-83 years, 43% men), there were wide ranges of values for clinical characteristics of subjects with significant age-related declines in bone

mineral density (BMD), BMI, and renal function (eGFR) (Table 1). *In vitro* stimulation of osteoblast differentiation by $1,25(OH)_2D_3$ was significantly greater for hMSCs obtained from subjects who had lower serum 25(OH)D, higher serum PTH, better renal function, more STRO-1^+ cells in their marrow, or higher whole body BMD (Table 2). Stimulation of osteoblastogenesis by $1,25(OH)_2D_3$ in hMSCs obtained from subjects who were vitamin D deficient (<20 ng/mL serum 25OHD) was 50% greater than vitamin D "insufficient" (20-32 ng/mL) group and 55% greater than the vitamin D sufficient (>32 ng/mL) group ($p<0.05$). In summary, these data indicate greater stimulation of osteoblast differentiation by $1,25(OH)_2D_3$ in hMSCs from younger subjects and from vitamin D-deficient subjects; this suggests that repletion of vitamin D-deficient subjects may lead to more vigorous bone formation. These data also show that age-related declines in BMD may be related to reductions in renal function. Thus, responsiveness of hMSCs to vitamin D is influenced by age and *in vivo* clinical characteristics of subjects. Further studies of *in vivo* and *in vitro* models of human cells may greatly enhance our understanding of skeletal aging and the role of vitamin D in skeletal health.

Table 1. Age *vs.* clinical parameters

	BMD (FN)	BMD (FN) T-score	BMD (WB) T-score	BMI	eGFR
r	-0.32	-0.33	-0.47	-0.34	-0.36
n	42	42	28	46	36
p	0.037	0.030	0.013	0.020	0.032

Table 2. ALP of hMSCs *vs.* clinical parameters

	BMD (WB)	s25OHD	sPTH	eGFR	% of STRO-1^+ cells
r	0.35	-0.34	0.49	0.37	0.43
n	36	37	38	31	32
p	0.038	0.030	0.0016	0.039	0.014

r: Pearson correlation coefficient,
n: number of subjects,
p: two-tailed *p* value,
BMD: bone mineral density,
FN: femoral neck,
WB: whole body,
BMI: body mass index,
eGFR: estimated glomerular filtration rate.

table

***Disclosures: Shuanhu Zhou**, None.*

MO0228

Binge Alcohol Exposure Disrupts Wnt Signaling in the Fracture Callus. Kristen Lauing*[1], Ryan Himes[2], John Callaci[3]. [1]Loyola University Medical Center, USA, [2]Loyola University Medical Center, Dept of Orthopaedics, USA, [3]Loyola University of Chicago, USA

Binge alcohol consumption is a contributing factor in up to 40% of all orthopaedic trauma cases and is associated with delayed or incomplete fracture healing. We have shown that binge alcohol treatment significantly modulates gene expression of several canonical Wnt signaling proteins, particularly β-catenin and Lrp5. Canonical Wnt signaling is known to promote osteoblast and chondrocyte formation from mesenchymal stem cells through tight regulation of β-catenin signaling. To elucidate the effects of binge alcohol on canonical Wnt signaling during fracture healing, we utilized a murine tibial fracture model. TCF reporter mice were used to visualize areas of activated canonical Wnt signaling in the fracture callus; all other studies were performed in C57BL/6 mice. The mice were administered alcohol (2 g/kg) or saline intraperitoneally once per day for 3 consecutive days. Mice were then subjected to a stabilized, mid-shaft tibial fracture and sacrificed 3, 6, 9, or 14 days post-fracture.

Histological analysis showed that binge alcohol treatment prior to fracture significantly decreased the volume and altered the matrix composition of the callus tissue. Biomechanic studies performed on mouse tibias using a 4-point bending apparatus show that alcohol-treated calluses are significantly weaker than controls at day 14 post-fracture. Western blot analysis of isolated fracture calluses revealed a time-dependent increase in β-catenin protein levels following injury, peaking at day 9. Binge alcohol exposure disrupted the expression pattern of β-catenin and decreased protein levels at days 9 and 14 post-fracture. Analysis of Wnt-mediated transcriptional activation in fracture calluses from TCF-reporter mice showed that alcohol exposure deregulates canonical Wnt signaling both spatially and quantitatively in the callus at all time points during healing. We performed immunofluorescence studies of early osteoblast and chondrocyte markers, Runx2 and Sox9, which are also gene targets of canonical Wnt signaling. These studies revealed that binge alcohol treatment decreases the amount of bone and cartilage present in the callus, in part by modulation of the expression of these downstream Wnt target genes. We conclude that alcohol-induced deficient fracture repair is caused, in part, by deregulation of the canonical Wnt signaling pathway, contributing to delayed fracture healing and impaired osteoblast and chondrocyte differentiation from mesenchymal precursors.

***Disclosures: Kristen Lauing**, None.*

MO0229

Carboxyl-Modified Single-Wall Carbon Nanotube Substrates Induce Expression of Osteoblast Differentiation Markers Associated With Matrix Attachment and Formation. Navasard Ovasapians, Dulce Padilla, Antonio Barrientos-Duran, Laura Zanello*. University of California, USA

One main goal in bone tissue regeneration is to identify new highly osteoinductive materials for use in orthopedic surgery. Due to their superior physical properties, we have investigated the use of carbon nanotubes (CNT) for bone cell growth. We showed previously that chemically modified CNT substrates sustain osteoblast proliferation and mineralization in vitro. However, comprehension of the molecular mechanisms of osteoinduction by CNT is only partial. Here, we studied gene induction of osteoblast precursors grown on carboxyl (COOH)-modified single-wall (SW) CNT. SWCNT-COOH were chosen for their high water solubility and biocompatibility. With the purpose to identify mechanisms of early osteoinduction, we grew human pre-osteoblasts (hFOBs) and mouse embryonic stem cells (mESCs) on SWCNT-COOH sprayed on glass, and collagen or gelatin-covered glass (for hFOBs and mESCs, respectively) and glass alone as controls. We induced osteoblast differentiation with 10 nM $1\alpha,25(OH)_2$vitamin D_3 added to the medium. We used RT-PCR to measure the expression of a number of osteoblast markers at 1-week intervals for a period of 5 weeks. We found that SWCNT-COOH significantly increased expression of the transcription factors osterix and Cbfa-1 in hFOBs and mESCs respectively, as compared to collagen or gelatin and glass as early as day 7, and remained high for the entire length of the experiment. Collagen substrates induced transient Osx expression at day 7, while glass did not significantly induce Osx. Highly significant induction of bone sialoprotein, which induces nodule formation, was also measured for the entire 5 weeks in hFOB cultures, and this was similar to collagen. In addition, SWCNT-COOH induced expression of osteopontin, which anchors cells to the mineral matrix and binds to integrin receptors, at days 7 and 14 in hFOBs and mESCs. Osteocalcin was highly induced in mESC grown on SWCNT-COOH as compared to control on gelatin. Collagen type I and alkaline phosphatase were expressed at similar levels on all substrates studied. We found that CNT induction of osteoblast differentiation correlated with higher expression of integrins α_v and β_3 in hFOBs as compared to glass and collagen, suggesting an integrin-initiated signaling leading to osteogenesis. We conclude that SWCNT-COOH substrates might be seen as effective inducers of new bone formation, and could be used as an interfase material in orthopedic devices to improve osteointegration with the host's native bone.

***Disclosures: Laura Zanello**, None.*

MO0230

Comparison of Human and Minipig Bone Marrow Derived Mesenchymal Stem Cells. Terhi Heino*[1], Jessica Alm[2], Niko Moritz[3], Hannu Aro[4]. [1]Department of Cell Biology & Anatomy, University of Turku, Finland, [2]Orthopaedic Research Unit, Finland, [3]Orthopaedic Research Unit, University of Turku, Finland, [4]University of Turku, Turku, Finland, Finland

Minipigs are claimed to have bone physiology closest to human. Therefore, minipigs are a recommended large-animal model for preclinical testing of human bone implants. However, the basic characteristics of their mesenchymal stem cells (MSCs) are poorly defined. The aim of this study was to isolate and characterize minipig MSCs in comparison to human MSCs.

Bone marrow (BM) samples (1-4 ml) were aspirated from the posterior iliac crests of five male minipigs with closed epiphyses of the distal femur (weight 36.2 ± 2.2 kg, age 15 ± 1 mo). Mononuclear cells (MNCs) were isolated and MSCs were selected by plastic adherence. Cell morphology, proliferation capacity and osteoblastic differentiation of minipig BM-MSCs were examined using standard protocols developed for human BM-MSCs.

MNCs were successfully isolated from all minipig BM samples. After two weeks of culture, plastic-adherent cells with a fibroblast-like morphology were observed. The proliferative capacity varied highly between cells from individual minipigs with an average maximum population doubling of 3.4 ± 0.7. Upon low density plating, MSCs from all minipigs formed fibroblastic colonies (CFUs), on average 16 ± 6 CFUs per well. Minipig MSCs differentiated into alkaline phosphatase (ALP) positive osteoblasts. An occasional presence of von Kossa-stained mineralized bone nodules was also observed. Data on minipig MSCs was further evaluated against data on identically isolated and cultured human BM-MSCs from adult fracture patients (n=13, age 19-60 yr). The fraction of plastic adherent MSCs in the MNC population was similar in minipigs and humans and no differences were observed in proliferation or colony formation capacities of minipig and human MSCs. However, the quantification of ALP and von Kossa positive areas as well as the measurement of

cellular ALP activity demonstrated that the osteoblast formation capacity of minipig BM-MSCs was significantly ($p<0.01$) poorer than that of human BM-MSCs.

The current study demonstrates that the proliferation and colony formation capacity of minipig BM-MSCs corresponds to human BM-MSCs but unexpectedly minipig MSCs have a significantly lower ability than human MSCs to form differentiated and functional osteoblasts. The observation urges a systematic characterization of MSCs in miniaturized large animal models in relation to skeletal growth and bone repair.

***Disclosures: Terhi Heino**, None.*

MO0231

Hedgehog Signaling Mediates BMP2-induced Osteogenic Differentiation of Bone Marrow Stromal Cells In Vitro and Spinal Fusion in Rats In Vivo. Jared Johnson*[1], Jeong-Hyun Yoo[1], Vicente Meliton[2], Woo Kyun Kim[2], Jeff C. Wang[1], Renata Pereira[3], Theodore Hahn[4], Farhad Parhami[5]. [1]Department of Orthopedics, UCLA, USA, [2]Department of Medicine, UCLA, USA, [3]UCLA, USA, [4]VA Greater Los Angeles/ UCLA, USA, [5]University of California, Los Angeles, USA

Hedgehog (Hh) and BMP signaling are important for osteoblast generation and bone formation, and have been shown to act synergistically in stimulating osteogenic differentiation of bone marrow stromal cells (MSC). However, the role of basal Hh signaling in BMP-induced osteogenic differentiation of MSC and bone repair has not been defined. Here we examined the effect of cyclopamine (Cyc), a specific Hh signaling inhibitor, on BMP2-induced osteogenic differentiation of MSC in vitro, and BMP2-mediated bone formation and spinal fusion in rats in vivo. M2-10B4 MSC (M2) cells were treated with control vehicle or 50ng/mL BMP2 with or without 2 μM cyclopamine. Cyc significantly inhibited BMP2-induced mRNA expression of osteogenic differentiation markers osterix, alkaline phosphatase (ALP) and bone sialoprotein, as well as ALP activity, in M2 cells and in primary mouse MSC, suggesting a role for basal Hh signaling in BMP2-induced osteogenic differentiation of MSC. BMP2 itself did not induce the expression of Shh, Ihh, or Hh target genes in M2 cells. Furthermore, Cyc did not inhibit BMP2-induced SMAD1/5/8 phosphorylation or the expression of Runx2, Id1, or Msx2, suggesting that Hh signaling mediates some but not all responses to BMP2. Moreover, Cyc did not inhibit BMP2-induced adipocyte formation by MSC despite partial but significant inhibition of some but not all adipogenic genes. To examine the role of Hh signaling in BMP2-induced bone formation in vivo, 26 Lewis rats divided into 4 groups underwent posterolateral intertransverse process spinal fusion at L4-L5 with implantation of a collagen sponge carrier containing control vehicle, 5μg BMP2, 5μg BMP2 + 2 mg Cyc, or Cyc alone. At 4, 6 and 8 weeks, bone formation was assessed by plain radiographs, and manual palpation of excised spines was performed after sacrifice at 8 weeks to assess the final degree of spinal fusion. MicroCT scanning and histological analyses were performed on select specimens from each group. No fusions or new bone formation were found in control or Cyc treated rats. All specimens from BMP2 treated rats demonstrated complete fusion with robust bone formation. Bone formation in rats that received BMP2+Cyc, although greater than that seen in control or Cyc treated animals, was significantly inhibited when compared to BMP2 treated rats, with none of the specimens showing complete fusion. These findings suggest an important role of Hh signaling in BMP2-induced osteogenesis in vitro and in vivo.

***Disclosures: Jared Johnson**, None.*

MO0232

Highly Osteogenic Multipotent Mesenhymal Stromal Cells from Human Breast Adipose Tissue Express High Levels of Stage specific Antigen-4 (SSEA-4). Christopher Niyibizi*[1], Feng Li[2], Jacquelyn Maddox[2]. [1]The Pennsylvania State University College of Medicine, USA, [2]Penn State College of Medicine, USA

Stage specific embryonic antigen 4 (SSEA-4) was previously shown to identify multipotent mesenchymal stromal cells (MSCs) isolated from bone marrow; however there are no other studies that have examined its expression by MSCs harvested from other sources. We assessed expression of this antigen by MSCs isolated from different sources of human adipose tissues and determined its effectiveness in identifying MSCs with potential to differentiate into various cell lineages including osteogenic lineage. Human adipose was obtained from abdominal and breast tissues of patients undergoing gastric bypass and breast reduction respectively with approved institutional protocol. Following collagenase digestion, tissues were centrifuged; the pellets were resuspended in sterile PBS and filtered. The filtrates were centrifuged and resulting pellets were suspended in DMEM supplemented with 10% FBS, 1% penicillin/ streptomycin v/v (P/S) and incubated at 37 oC in 5% CO2. Immediately after cell isolation and at different passages cells were assessed for expression of selected surface antigens including SSEA-4 by FACS. At passage 3, cells were sorted for SSEA-4 and the sorted and unsorted cells were assessed for differentiation toward osteogenic, adipogenic and neuralgenic cell lineages. SSEA-4 enriched and unenriched cell fractions were also assessed for healing critical sized defects in mice. The results showed that at passage 0, about 10 % of the cells from abdominal fat expressed SSEA-4 while about 50% from breast fat tissue were positive for this antigen. This high level of SSEA-4 expression by cells from breast fat tissue was maintained with cell expansion in vitro. Nearly 100% of cells expressed SSEA-4 following cell sorting. Adipose derived stromal cells (ADSCs) enriched in SSEA-4 were more efficient in differentiating toward osteogenic, adipogenic and neuralgenic cell lineages in vitro than nonenriched population. In addition, SSEA-4 positive cells exhibited a higher tendency to deposit more bone in calvarial defects especially when stimulated by BMP-2 than low SSEA-4 expressing cells. Taken together, the data indicate that SSEA-4 enriches for MSCs that exhibit higher osteogenic potential and that breast adipose tissue is enriched with cells expressing SSEA-4 antigen. The presence of a higher level of ells in breast tissue expressing SSEA-4 and its implication remains to be further explored.

***Disclosures: Christopher Niyibizi**, None.*

MO0233

Localization of Tie-2 Expression in Mice Skeletal Unloading Model. Kuniaki Moridera*, Kunitaka Menuki, Toshitaka Nakamura, Akinori Sakai, Soshi Uchida. University of Occupational & Environmental Health, Japan

Introduction: Vascular factors play an important role in the bone formation and remodeling. Mechanical unloading causes bone loss in loaded bones. Not much has been done to clarify the relationship between osteogenesis and vasculogenesis in skeletal unloading as well as reloading. It has been recognized that Angiopoiein-1/Tie-2 system plays a pivotal role during skeletal system. The purpose of this study was to clarify whether angiogenic factor is associated with osteogenesis in mice hindlimb skeletal unloading model.

Materials and Methods: C57BL/6J male 8-week-old mice were assigned to three groups: ground control(GC), tail suspension(TS), and reloading after one week TS (RL). In TS group, mice's hindlimb were elevated by tail suspending for one week. Bilateral femur were used for analyses. Immnocytochemistries and Real-Time PCR for expressions of osteogenic and angiogenic molecules such as Osteocalcin, Angiopoietin-1, Tie-2, were assessed.

Results: The expression levels of Tie-2 and Osteocalcin mRNA in femoral bone in TS significantly decreased compared to those in GC . ALP as well as osteocalcin positive cells around secondary spongiosa were dramatically decreased in the TS compared to GC. Immunoreactivity for Tie-2 was mainly located on vascular endothelium surrounding secondary spongiosa at metaphysis of femur in the GC group. In contrast, it was located on vascular endothelium along with primary spongiosa and endosteal osteoblast at metaphysic of femur in the TS group.

Conclusion: We demonstrated that reduced osteogenic activity is closely correlated with the suppression of Tie-2 expression in metaphysis of femur after skeletal unloading in mice. This finding suggests that Angiopoietin-1/Tie-2 system plays a crucial role in bone adjustment for skeletal unloading.

***Disclosures: Kuniaki Moridera**, None.*

MO0234

NF-kB RelB/p52 Non-canonical Signaling Regulates Hematopoietic Stem Cell Maintenance. Chen Zhao*[1], Yan Xiu[1], John Ashton[2], Lianping Xing[2], Craig Jordan[2], Brendan Boyce[1]. [1]University of Rochester Medical Center, USA, [2]University of Rochester, USA

RelB and p52 mediate non-canonical NF-κB signaling and have critical roles in many pathologic processes, including pathologically stimulated osteoclast (OC) formation. RelB-/- mice have myeloid proliferation, multi-organ inflammation, and impaired dendritic and B cell development. However, it is not known if RelB and p52 are important for maintenance of hematopoietic stem cells (HSCs) from which OCs and other cells arise. To investigate this, we generated RelB/p52 double knockout (dKO) mice: they have increased short-term HSC numbers (dKO 11+/-5.7 vs control 4.6+/-4 %) and proliferation (21+/-4 vs 7+/-4%) but decreased long-term HSCs (4 +/- 1.5 vs 10+/-3%). dKO bone marrow cells did not efficiently reconstitute lethally-irradiated WT recipient mice, suggesting dKO mice have an intrinsic defect in HSCs. With the increased cell proliferation we hypothesized that the dKO mice may succumb to 5-FU treatment, which kills cycling cells. Surprisingly, dKO mice are resistant to 5-FU (32+/-1.5% KLS in dKO vs 1.6+/-0.7% of HSCs in control post-treatment). Since hematopoiesis is regulated not only by intrinsic signals in HSCs but also the microenvironment (mainly bone marrow stromal and bone-lining cells), we next investigated if RelB/p52 affect HSCs also through regulation of these osteoblastic niche cells. We used CD45-Ter199-OPN+ bone-lining cells purified from collagenase digestion and cultured marrow stromal cells as sources of niche cells. We co-cultured these cells from control or dKO mice with WT bone marrow cells for 24hr or 2wk and assessed HSC frequency and colony formation. Both dKO primary bone-lining cells and cultured marrow stromal cells support more progenitor cells (KLS percentage: 6.4+/-1.8 vs 1.1+/-0.6% in controls; colony number: 151+/-21 vs 32+/-13 in controls). Finally, we transplanted WT bone marrow cells into irradiated dKO mice and found that after engraftment, the wT cells in dKO mice developed increased myeloid proliferation and decreased B cell development, recapitulating the characteristics of RelB/p52 null hematopoietic cells. In summary, we have identified a new role for RelB/p52 coordinating hematopoietic and stromal cell functions. They point to a potential role for non-canonical NF-κB pathway inhibitors to promote bone marrow recovery after chemotherapy.

***Disclosures: Chen Zhao**, None.*

MO0235

Novel Osteogenic Oxysterols Induce Osteogenic and Inhibit Adipogenic Differentiation of Marrow Stromal Cells In Vitro and Stimulate Bone Formation and Spinal Fusion In Vivo. Jared S. Johnson*[1], Vicente Meliton[1], Woo Kyun Kim[1], Kwang-Bok Lee[1], Jeffrey C. Wang[1], Khanhlinh Nguyen[1], Dongwon Yoo[1], Michael E. Jung[1], Elisa Atti[1], Sotirios Tetradis[1], Renata Pereira[1], Theodore Hahn[2], Francine Farouz[3], Scott Thies[3], Farhad Parhami[4]. [1]UCLA, USA, [2]VA Greater Los Angeles/UCLA Medical Center, USA, [3]Fate Therapeutics, Inc., USA, [4]University of California, Los Angeles, USA

We previously reported that specific naturally occurring oxysterols including 20(S)-hydroxycholesterol (20S) induce the osteogenic differentiation of pluripotent mesenchymal cells, while inhibiting their adipogenic differentiation. Here we report on the synthesis and characterization of two potent structural analogs of 20S, Oxy34 and Oxy49, which induce the osteogenic differentiation of bone marrow stromal cells (MSC) and inhibit their adipogenic differentiation through activation of Hedgehog (Hh) signaling. Treatment of M2-10B4 (M2) MSC with 0.1-5 uM of Oxy34 or Oxy49 induced the mRNA expression of early osteogenic differentiation markers Runx2, Osterix (Osx) and alkaline phosphatase (ALP), and ALP activity. Late osteogenic differentiation markers bone sialoprotein (BSP) and osteocalcin (OCN) as well as robust mineralization were also induced by Oxy34 or Oxy49. Furthermore, treatment with Oxy34 or Oxy49 together with PPARgamma activator, troglitazone (Tro), caused a complete inhibition of Tro-induced expression of adipogenic genes PPARgamma, LPL, and aP2 mRNA, and inhibited the formation of adipocytes as assessed by oil red O staining.

In previous studies we have found only modest stimulation of bone formation in vivo by naturally occurring osteogenic oxysterols. In the present study, the efficacy of Oxy34 and Oxy49 in stimulating bone formation in vivo was assessed using the posterolateral intertransverse process rat spinal fusion model. This procedure is similar to posterior spinal fusion performed in humans and is used frequently to test the efficacy of osteoinductive materials in vivo. 60 Lewis rats were divided into 6 groups and underwent fusion procedure at L4-L5 with bilateral implantation of a collagen sponge carrier containing: 1) control vehicle, 2) 5ug rhBMP2, 3) 0.2mg Oxy34, 4) 2mg Oxy34, 5) 20mg 0xy34, or 6) 20mg Oxy49. At 4, 6 and 8 weeks, bone formation was assessed by plain radiographs. Definitive fusion in all specimens was then determined at 9 weeks by manual palpation and MicroCT of the excised spines. Manual assessment revealed fusion in 0/10 Group1, 10/10 Group 2, 0/10 Group 3, 5/10 Group 4, 10/10 Group 5 and 10/10 Group 6. Micro CT showed fusion in 0/10 Group 1, 10/10 Group 2 (8 bilateral/2 unilateral), 0/10 Group 3, 5/10 Group 4 (3 bilateral/2 unilateral), 10/10 Group 5 (8 bilateral/2 unilateral) and 10/10 Group 6 (8 bilateral/2unilateral). Altogether, these data suggest that Oxy34 and Oxy49 are potent novel osteoinductive molecules with the ability to induce significant dose-dependent osteogenesis in vitro as well as in vivo, and may be suitable candidates for development into osteogenic therapeutic agents.

***Disclosures: Jared S. Johnson**, None.*
This study received funding from: Fate Therapeutics, Inc.

MO0236

Osteoblast Lineage Cells Expressing High Levels of Runx2 Enhance Hematopoietic Stem Cell Maintenance and Function. Brahmananda R. Chitteti[1], Ying-Hua Cheng[2], Sonia Rodriguez-Rodriguez[3], Nadia Carlesso[3], Edward F. Srour[4], Melissa Kacena*[5]. [1]Department of Medicine, Indiana University School of Medicine, USA, [2]Department of Orthopaedic Surgery, Indiana University School of Medicine, USA, [3]Department of Pediatrics, Indiana University School of Medicine, USA, [4]Departments of Medicine, Pediatrics, & Microbiology & Immunology, Indiana University School of Medicine, USA, [5]Indiana University School of Medicine, USA

We previously demonstrated that osteoblasts (OB) significantly enhance in vitro proliferation and functional capacity of primitive hematopoietic progenitor cells and maintain the marrow repopulating potential of hematopoietic stem cells (HSC). While these activities were clearly attributable to OB, the exact definition, both phenotypically and hierarchically, of OB responsible for these functions is yet to be determined. Although our data suggested that early stage OB maintained HSC function better than late stage OB, a more precise definition and identification of cells mediating these functions is required. Unlike HSC, the phenotypic definition of different stages of OB development is not well characterized. Using flow cytometric cell sorting, we recently began to fractionate OB to stratify OB lineage cells based on their maturational status and to segregate the hematopoiesis enhancing activity into a phenotypically defined group of cells. Isolated cells were examined by classical OB functional assays (calcium deposition and alkaline phosphatase activity) and by QRT-PCR quantification of OB-specific lineage markers (Runx-2, osteocalcin, and type I collagen) and were assessed for their hematopoiesis enhancing activity in co-cultures with marrow-derived Lin-Sca1+CD117+ (LSK) cells. LSK cells co-cultured with populations of OB cells were examined for cell proliferation, maintenance of primitive phenotype and expansion of clonogenic cells. Limited consensus is that OB lineage cells are Lin-Sca1- cells. We further separated these cells based on ALCAM and OPN expression. While we were able to identify Lin-Sca1-OPN+ALCAM+ as less mature OB in contrast to the more mature Lin-Sca1-OPN+ALCAM- cells, these fractionations did not compartmentalize the hematopoiesis enhancing activity. These populations were then further separated based on CD44 and CD90 expression. Using this strategy we found that the Lin-Sca1-OPN+ALCAM+CD44+CD90+ cells exhibit a >5-fold increase in Runx2 expression compared to fractionated counterparts, with a concomitant >4.6-fold increase in the sustained proliferation and production of primitive hematopoietic cells. Other hematopoietic studies including in vivo repopulating potential of LSK progeny from various OB fractions are underway. These studies begin to define the hierarchical organization of osteoblastic cells and provide a more refined definition of OB that can mediate hematopoiesis enhancing activities.

***Disclosures: Melissa Kacena**, None.*

MO0237

Platform for Comparing In Vivo Bone Formation by Different Osteoprogenitor Cell Populations. Liping Wang*, Xi Jiang, Jianping Huang, David Rowe. University of Connecticut Health Center, USA

Progenitor cells capable of osteogenic differentiation can be derived from a wide variety of adult and ES cell sources using multiple production protocols. Discerning their relative osteogenic potential and utility as a cell source for tissue engineering has been difficult due to the lack of uniformity of a testing platform and comparison to a reference source. Here we propose a model that could be a useful platform for assessing osteogenesis of a test cell population relative to a reference. The critical size calvarial defect has been modified to have two 3.5 mm in diameter circular defects introduced into the parietal bone and is fitted with a collagen-hydroxyapetite scaffold (Healos). The host mice carry a Col3.6GFPtpz reporter to follow host ingress into the scaffold, and the donor cells to be tested, which are derived from mice carrying a Col3.6GFPcyan reporter, are added directly to the scaffold. The extent of bone formation is assessed by photography, digital X-ray and cryohistology in which osteogenic differentiation is based on Col3.6GFP expression overlying an fluorescent mineralization line. To assess the in growth of host cells into the scaffold, mice receive the scaffold without addition of donor cells. After 8 weeks, approximately 1/3 of the defect is filled centripetally. To test the inherent osteoprogenitor potential of a donor source, the host mice received total body irradiation and bone marrow transplantation, which suppresses host in growth into the scaffold. In all experiments a contrast between two difference cell sources is made in which neonatal calvarial osteoblast (mCOb) or bone marrow stromal (BSMC) cultured cells are used as a reference. When directly compared, mCOb make an irregular membraneous bone structure with limited bone marrow while BMSC produce a cortical like structure with an ample marrow space. mCOb derived bone forms rapidly but rarely joins the host bone and by 8-12 weeks begins to resorb. However BSMC derived bone extends over the surface of the host bone and persists for at least 20 weeks. Progenitors derived from long bone outgrowth cells for a structure that is intermediate between mCOb and BMSC while adipocyte stromal cells do not form bone. The combined host and donor interaction can be assessed with inbred C57Bl/6 reporter mice. The model is well tolerated by *NOD/Scid/IL2rg null* mice making the analytical platform available for assessing osteogenic potential of human progenitor cells.

***Disclosures: Liping Wang**, None.*

MO0238

Role of Alpha-Linolenic Acid (ALA) in the Regulation of Differentiating Preadipocyte-Like MC3T3-L1 and Preosteoblast-Like MC3T3-E1 Cell Metabolism. Youjin Kim*[1], Owen Kelly[2], Jasminka Ilich-Ernst[3]. [1]The Florida State Univesity, USA, [2]Texas Woman's University, USA, [3]Florida State University, USA

A high n-6 to n-3 polyunsaturated fatty acids (PUFA) ratio (~20:1) in the typical Western diet may be associated with some inflammatory diseases, including osteoporosis and obesity. Hence, there is great interest in increasing dietary n-3 PUFA including ALA, rich in flaxseed and canola oils. ALA is also a major n-3 PUFA in dairy products existing with linoleic acid (LA) (n-6 LA:n-3 ALA ratio=~2-5:1). The aim of this study was to investigate how ALA at a relatively low n-6:n-3 ratio (1-5:1) modulates adipogenesis and osteoblastogenesis and the involvement of prostaglandin E2 (PGE2) in the regulatory process using preadipocyte-like MC3T3-L1 and preosteoblast-like MC3T3-E1 cells. Cells were grown in typical cell culture conditions (5% CO2 at 37oC). Following the exposure to PUFA (n-6:n-3 ratio=20:1), cells were differentiated by culturing in adipogenic media (0.5mM IBMX+1mM dexamethasone+1μg/ml insulin) for MC3T3-L1 or in osteogenic media (5mM β-glycerophosphate+100μg/ml ascorbic acid) for MC3T3-E1 cells (6-well plates; 1x105 cells/well). A range of different concentrations of ALA (35-7μM for MC3T3-L1; 200-40μM for MC3T3-E1) was adapted to constitute the n-6:n-3 ratio as 1-5:1 (6 days). Oil red O and Alizarin red S staining were performed to determine the adipogenicity and mineralization of MC3T3-L1 and MC3T3-E1 cells respectively, followed by a quantification of each. The level of the inflammatory mediator, PGE2, was measured using a commercial ELISA kit. ANOVA with a Tukey's post-hoc test was performed using SPSS with the level of significance at $p<0.05$. At all ratios of ALA, the production of lipid droplets in differentiating MC3T3-L1 cells was significantly reduced compared to the control (DMSO). The lowest adipogenicity was observed at 4:1 ratio of ALA. The mineralization of differentiating MC3T3-E1 cells were significantly increased at ALA ratios of 3-5:1, showing highest increase at 4:1 ratio of ALA. Although there was tendency to increase the PGE2 production in both

differentiating cell lines, it was not significant except at 5:1 ALA ratio in MC3T3-E1 cells. Overall, during MC3T3-L1 and MC3T3-E1 cell differentiation, the favorable effect of ALA in reducing lipid formation and enhancing calcification would be maximized when the ratio of n-6:n-3 is 4:1 which may not be modulated by PGE2. This study, although in-vitro, confirms the benefits of reducing n-6:n-3 ratios for higher osteogenic and lower adipogenic outcomes. Funded: DMI#1673&FSU-CRC#119532

***Disclosures: Youjin Kim**, None.*

MO0239

Serum from Patient with High Bone Mass Phenotype Due to lrp5 T253I Mutation, Contain Factors Independent of Serotonin that Stimulate Osteoblast and Inhibit Adipocyte Differentiation of Mesenchymal (skeletal) Stem Cells. Tom Andersen*[1], Morten Nielsen[1], Basem Abdallah[2], Moustapha Kassem[1]. [1]Odense University Hospital, Denmark, [2]Odense University Hospital, University of South Denmark, Denmark

The mechanism mediating high bone mass phenotype due to Lrp5 gene mutation is not known in details. Recently, Lrp5 activating mutation was demonstrated to enhance mature osteoblast function indirectly by reducing blood levels of gut-derived serotonin. We have previously demonstrated that MSC carrying lrp5 T253I mutation exhibit enhanced osteoblast and impaired adipocyte differentiation. Thus, we examined the cellular phenotype and effects of serum and serotonin on MSC proliferation and differentiation. Adipose tissue-derived MSC and sera were obtained from 5 patients with HBM due to Lrp5 T253I mutation and 10 sex and age-matched controls. MSC differentiation in vitro to osteoblast (OB) was quantified by ALP activity and adipocyte (AD) differentiation by Nile red staining. No significant differences in HBM and control MSC proliferation or OB differentiation.

Pooled sera from HBM individuals had lower level of serotonin than control (72 ng/ml $\pm$ 5,5 ng/ml SD versus 86 ng/ml $\pm$5,1 ng/ml SD). HBM serum increased MSC proliferation (38,5% $\pm$6,9) and OB differentiation (5,1 $\pm$1.0 fold induction versus 3,3 $\pm$0,3 in ctrl serum) while AD differentiation was reduced (24.8% $\pm$ 1.0 adipocytes in HBM serum versus 35.0% $\pm$ 3,9 in control serum). Interestingly, addition of increasing amounts of serotonin to serum, had no effect on cell proliferation but increased OB differentiation. In conclusion, patients with HBM exhibit no intrinisic defects in their MSC but their serum contain factors, other than serotonin that influence MSC biology and possibly increase bone mass.

***Disclosures: Tom Andersen**, None.*

MO0240

Short-Term Hypoxia Enhances the Mobilization of Hematopoietic Progenitors and Decreases the Number of SDF-1 Positive Osteoblasts in Endosteum. Marjorie Durand*[1], Pascal Pradeau[1], Marina Trouillas[2], Denis Clay[3], Jean Jacques Lataillade[2], Marie Caroline Le Bousse Kerdiles[3], Xavier Holy[4]. [1]Institut de Recherche Biomédicale des Armées, BP73, France, [2]Centre de Transfusion des Armées, France, [3]INSERM U972, France, [4]IMASSA, France

Purpose: Bone formation and repair are controlled by dynamic processes involving osteoblasts and osteoclasts. Osteoblasts are derived from Mesenchymal Stem Cells (MSC) while osteoclasts derived from Hematopoeitic Stem Cells (HSC). Hypoxia is thought to be a key regulator of osteogenesis by interacting with mobilization and/or differentiation of both HSC and MSC. However, a few data suggest that the number of mesenchymal and hematopoietic progenitor cells in bone marrow remains unchanged under long-term hypoxic conditions. Here, we investigate the effects of short-term hypoxia on hematopoietic progenitor cells and on osteoblast expressing SDF-1 (Stromal Derived Factor-1) in endosteum.

Methods: Male BalbC mice (n=8) were housed into a hypobaric chamber at 50kPa corresponding to a Fraction of inspired Oxygen (FiO_2) of 10% for four days and sacrificed afterwards. Reticulocytes were scored in blood stained with cresyl blue. Effects of hypoxia on bone marrow and spleen hematopoietic progenitors were assessed by clonogenic tests. SDF-1 immuno-staining was performed on tibia sections. Normoxic control mice (n=8, FiO_2 = 21%) were similarly treated.

Results: Hypoxia increases the number of reticulocytes in blood and tends to increase the number of hematopoietic progenitors (especially erythroid progenitors) in spleen. By contrast, a significant decrease in the number of hematopoietic progenitors was evidenced in bone marrow of hypoxic mice. This decrease affects both multipotential (CFU-GEMM progenitors) and lineage-restricted progenitors (erythroid/BFU-E and granulo-macrophagic/ CFU-GM progenitors). In addition, we demonstrate that hypoxia reduces by more than 50% the number of SDF-1 positive osteoblasts in endosteum.

Conclusions: These results suggest that respiratory hypoxia in the mouse enhances the mobilization of hematopoietic progenitors from bone marrow to spleen and reduces the number of SDF-1 labeled osteoblasts in endosteum. These data need to be interpreted taking into account the dialogue between osteo-competent cells (osteoblasts, osteoclasts) in response to hypoxia.

***Disclosures: Marjorie Durand**, None.*

MO0241

Strontium Role on Adipose Tissue Mesenchymal Stem Cells Osteogenic Induction. Isabella Tognarini*[1], Roberto Zonefrati[1], Gianna Galli[1], Carmelo Mavilia[1], Giorgia Donata Zappoli Thyrion[1], Anna Maria Carossino[1], Valentina Vitale[1], Simone Ciuffi[1], Annalisa Tanini[2], Maria Luisa Brandi[2]. [1]Department of Internal Medicine, University of Florence, Italy, [2]University of Florence, Italy

Strontium Ranelate is a drug used in osteoporosis in order to reduce bone fractures incidence. It is composed by Ranelic acid as a carrier and 2 atoms of stable Strontium (Sr^{2+}), an alkaline trace earth metal with high affinity to hydroxyapatite, able to produce skeletal effects. The aim of the present study was to evaluate the effect of Sr^{2+} on osteogenic differentiation of adipose tissue mesenchymal stem cells (AMSCs). We have previously demonstrated that AMSCs have the same ability to produce bone matrix as bone marrow derived stem cells, while being a better source of stem cells according to their abundance and accessibility. In this study in vitro tests were used to evaluate the ability of Sr^{2+} to promote the osteogenic differentiation on AMSCs primary cultures and to evaluate their response in terms of cell proliferation and differentiation.

Cell growth and viability were assessed in all cell lines, in presence of Sr^{2+} 1, 10 and 25 μg/ml, by manually cell counting directly on growth support, by phase contrast microscopy. The expression of the osteoblastic phenotype was evaluated in cells treated with different concentrations (from 0.5 to 100 μg/ml) of Sr^{2+} after 7, 14, 21, 28 days from osteogenic induction, monitoring quantitative alkaline phosphatase (ALP) activity, and calcium mineralization by fluorometric assay and Alizarin Red S assay respectively.

Statistically significant difference was observed in cell proliferation for all primary cell lines cultured in presence of 1% FCS and Sr^{2+} 25 μg/ml, with a population doubling time of 5 days vs 15 days in not treated cells. No effect of $Sr^{2+}$was observed for the ALP activity during osteoblast differentiation. Sr^{2+} 0.5, 1, 5 μg/ml treatment strongly increased hydroxyapatite deposition levels in all cell lines, after 7 days from osteogenic induction. No statistically significant difference at the mineral level was observed in cells treated with same concentration of Sr^{2+} at 14, 21, 28 days from induction.

In conclusion our preliminary results confirm that the Sr^{2+}, at appropriate concentration, can promote both AMSCs growth and osteoblast differentiation throughout the induction of calcium mineral deposition. These findings open the possibility of the use of Strontium ranelate for the in vivo treatment of cell transplantation in bone regenerations programs.

***Disclosures: Isabella Tognarini**, None.*

MO0242

The Effect of Mild Heat Shock on Osteoblast Proliferation and Differentiation. Adel Al-Enazy, Nasser Alqhtani, Ada Armstrong, Vasilis Bousdras, Sajeda Meghji*. UCL Eastman Dental Institute, United Kingdom

We have previously shown that physiological stresses such as changes in pH or oxygen tension can affect bone remodeling (1,2). Preliminary work in our laboratory has shown that mild thermal stress of osteoblasts increases the ratio of OPG to RANKL (3).

In this study we have investigated the effect of mild heat stress on osteoblasts and the effect of conditioned media from the heat stress together with heat shock proteins (hsp) on osteoblast proliferation and differentiation. Osteoblastic cell line; MG63 cells were exposed to 32°C, 37°C, 42°C and 47°C for 30 seconds, 2 and 5 minutes, then incubated for 24 hours at 37°C. We assayed for heat shock proteins 27, 60 and 70 synthesis using an ELISA kit (R&D Systems). The hsp 27,60 and 70 and the conditioned medium for the treated cells was tested for ability to stimulate osteoblast proliferation and differentiation (alkaline phosphastase activity) over 1, 3 and 6 days.

Preliminary results show that osteoblast treated at 47°C for 5 minutes synthesized hsp60 and hsp70. The conditioned medium from the cells treated at 42°C for 5 minutes stimulated osteoblast proliferation, there was no effect on alkaline phosphatase. The heat shock proteins stimulated osteoblast proliferation, again there was no effect on alkaline phosphatase activity.

These results show that conditioned media from osteoblasts cell line exposed to 42°C stimulates osteoblasts proliferation. Likewise the heat shock protein tested stimulated cell proliferation. There was no effect on osteoblast differentiation.

These experiments show that mild heat shock may modulate bone turnover by stimulating cell proliferation.

***Disclosures: Sajeda Meghji**, None.*

MO0243

Wnt7b Plays a Unique and Essential role in Osteoblast Differentiation. Xinyu Shao[1], Colette Fong-Yee[2], Karin Lyon[2], Weiping Jia[3], Colin Dunstan[4], Di Chen[5], Markus Seibel[1], Hong Zhou*[1]. [1]Bone Research Program, ANZAC Research Institute, The University of Sydney, Australia, [2]Bone Research Program, ANZAC Research Institute, University of Sydney, Australia, [3]Department of Endocrinology & Metabolism, Shanghai Jiao Tong University Affiliated Sixth People's Hospital, China, [4]University of Sydney, Australia, [5]University of Rochester Medical Center, USA

Activation of the Wnt signaling pathway is vital for osteoblast differentiation. We previously found that the mRNA expression of Wnt7b and Wnt10b increases linearly with osteoblast differentiation (1). To define the individual roles of Wnt7b and Wnt10b in the control of osteoblast differentiation, we knocked down Wnt7b or Wnt10b expression by shRNA stable expression in MC3T3-E1 cells.

Knockdown of Wnt7b in MC3T3-E1 cells resulted in a complete failure of mineralized nodule formation, while non-target (NT) control cells formed significant amounts of nodules under the same osteogenic conditions by day 7. When Wnt10b mRNA was knocked down, the mineralized nodule formation was delayed and reduced by 75% compared to NT control cells. Real time PCR revealed that when Wnt10b mRNA expression was knocked down, Wnt7b mRNA expression increased, reaching 50% of the levels seen in NT cells at day 4, 100% at day 6 and 400% of NT control levels by day 8 suggesting Wnt7b may compensate for reduced Wnt10b expression during osteoblast differentiation. In contrast, Wnt10b is unable to compensate for a reduced expression of Wnt7b in Wnt7b shRNA cells. Consequently, while mRNA for ALP and osteocalcin was suppressed in Wnt7b shRNA cells, expression was delayed in Wnt10b shRNA cells. Interestingly, Runx2 and Osx mRNA expression was reduced and delayed in Wnt10b shRNA cells but expression was remained at similar levels to NT cells in Wnt7b shRNA cells. In addition, the osteopontin mRNA levels were 2 and 2.5 fold higher in Wnt7b shRNA cells than seen in NT cells at day 2 and day 4 respectively, indicating that differentiation in these cells was arrested at an early stage. Importantly, treatment of Wnt7b shRNA cells with recombinant BMP2 rescued the phenotype as the cells formed same amount of mineralized nodules as seen in BMP2 treated NT cells, suggesting that BMP may be an important downstream mediator of Wnt7b signaling. Our results indicate that knock-down of either Wnt7b or Wnt10b severely impairs osteoblast differentiation. Wnt7b appears to play an essential role in osteoblast differentiation and is able to partially compensate for a reduced expression of Wnt10b. We conclude that both members of the Wnt family are relevant to normal osteoblast differentiation and nodule formation but that Wnt7b has a unique function in the control of bone formation, as a ''feed-forward'' loop that promotes osteoblast differentiation and mineralization.

(1) J Biol Chem. 283: 1936-1945, 2008.

***Disclosures: Hong Zhou**, None.*

MO0244

Comparison of the Biological Activities of Vitamins D_2 and D_3 on Osteoblast Differentiation and Activity. Allahdad Zarei*[1], Francis Lam[2], David Mahoney[1], Guillaume Mabilleau[1], Afsie Sabokbar[3], Morovat Alireza[2]. [1]University of Oxford, United Kingdom, [2]John Radcliffe Hospital, United Kingdom, [3]University of Oxford, Botnar Research Centre, United Kingdom

In the UK, deficiency of vitamin D is usually treated by oral supplementation with vitamin D_2 (ergocalciferol) rather than D_3 (cholecalciferol). This is based on the assumption that both forms are equipotent in raising circulating concentrations of the active metabolites of vitamin D, though there is hardly any scientific evidence for this. Since an increase in osteoblastic activity is one aim in the treatment of osteoporotics, who are the largest group of patients receiving vitamin D, we compared the effects of 25(OH)- and 1,25$(OH)_2$-vitamins D_2 and D_3 on osteoblast proliferation, activation and biological responses.

Murine osteoblast cells derived from the marrow stroma (MBA-15.4) and calvaria (MC3T3-E1) were seeded on 24-well plates (1.25 x 10^4 cells/ml), and grown for 3-7 days at 37♂C in media supplemented with 10% (v/v) stripped foetal bovine serum, 10 mM glutamine, and antibiotics (100 IU/mL penicillin and 10 μg/mL streptomycin). Metabolites of vitamin D were added at physiological concentrations – i.e. 0-1000 nM 25(OH)-vitamins D_2 or D_3, and 0-1000 pM 1,25$(OH)_2$-vitamins D_2 and D_3. After lysing washed cells, total protein concentration and alkaline phosphatase activity were determined chemically in both cells lines, and Western blots of MBA-15.4 cell lysates were used to compare osteopontin expression.

Cellular proliferation, as assessed by protein content, was inhibited in a dose-dependent manner for all metabolites of vitamin D tested. In this respect, 25(OH) D_3 was more potent than 25(OH) D_2 (1000 nM; $p<0.05$ on days 3 and 5, and $p<0.001$ on day 7). Similarly, 1,25$(OH)_2$ D_3 had a greater proliferating effect than 1,25$(OH)_2$ D_2 (1000 pM; $p<0.05$ on days 3 and 5, and $p<0.0001$ on day 7). All forms of vitamin D also reduced alkaline phosphatase activity per gram protein, with 25(OH) D_3 being more active than 25(OH) D_2 (1000 nM; after 7 days of culture), and 1,25 $(OH)_2$ D_3 eliciting a greater response than 1,25 $(OH)_2$ D_2 (1000 pM; $p<0.05$ after 5 days, and $p<0.001$ after 7 days of incubation). Vitamin D metabolites up-regulated osteopontin expression, with 10 nM 25(OH) D_3 eliciting a significantly greater response than the same concentration of 25(OH) D_2 after 5 days of incubation ($p<0.001$).

These preliminary results indicate that (cholecalciferol) vitamin D_3 is more potent than vitamin D_2 in stimulating the proliferation and the maturation of pre-osteoblasts, possibly through increasing osteopontin expression.

***Disclosures: Allahdad Zarei**, None.*

MO0245

Identification and Functional Analysis of a Novel Regulator of Actin-ring Formation in Osteoclasts. Norihiro Ishida-kitagawa*, Bao Xilinqiqige, Kunitaro Tanaka, Takanori Kimura, Tadashi Miura, Takuya Ogawa, Tatsuo Takeya. Nara Institute of Science & Technology, Japan

Osteoclasts are multinucleated giant cells and present only in osseous tissue with capacity to resorb bone. Osteoclastogenesis is preceded by a commitment, differentiation to polykarion formation by cell fusion and cytoskeletal rearrangement. Our group previously reported that transcription factor NFAT2/NFATc1 acts as a key regulator for osteoclastogenesis (Ishida et al. *J. Biol. Chem.* 277. p41147-56). Since NFAT2 is essential for inducing the entire processes of multinucleated cell formation, it seems to be reasonable to speculate that NFAT2 may regulate the expression of membrane proteins which control cell fusion and bone resorption.Here, to understand the mechanism of cell fusion and/or bone resorption, we tried to screen membrane proteins whose expressions are controlled by NFAT2. We conducted SST-REX (signal sequence trap by retrovirus-mediated expression screening) to screen genes encoding secreted/membrane proteins from RAW264-derived osteoclasts cDNA library, and identified 56 genes including #16. #16 mRNA appeared to be induced 48 hours after RANKL treatment in osteoclast precursor bone marrow macrophages and RAW264 cells and sustained until 96 hours when multinucleated osteoclasts were formed. When cells were treated with Cyclosporin A or applied by an RNA interference method for NFAT2, the expression of #16 was significantly suppressed at both mRNA and protein levels. Although multinucleated osteoclasts were formed in #16 knock-down bone marrow macrophages, cells showed contracted form with disordered actin-ring structure, accompanying significant reduction of bone resorption activity. These results suggest that #16 is a NFAT2-inducible gene and essential for the formation of functional osteoclasts through the regulation of actin reorganization.

***Disclosures: Norihiro Ishida-kitagawa**, None.*

MO0246

Fluid Pressure and Titanium Particles Induces Osteoclast Activation Via Alternative Pathways. Göran Andersson[1], Anna Nilsson[2], Maria Norgård[1], Anna Fahlgren*[2]. [1]Karolinska Institute Huddinge, Division of pathology, Sweden, [2]Linköping University, Division of Orthopaedics, Sweden

Despite rigorous research the mechanism behind the osteolytic process is not fully understood. Most focus has been on wear-related inflammatory effects in the periprosthetic area. One less explored risk factor for osteolysis is the force-induced mechanical stimulus within the bone-implant interface. The hypothesis was that these 2 stimuli act through different cytokine networks for differentiation, activation and localization of osteoclasts. We also hypothesized that pressure- induced osteolysis acts through a molecular signaling pathway less dependent on pro- and anti-inflammatory cytokines. To test this hypothesis, we used an animal model in which osteoclasts and bone resorption can be induced either by fluid pressure or particles. Osteoclast activation and localization was evaluated by morphometrical assessment of Cathepsin K positive large cells, and cytokine signaling pathways were evaluated by RT-qPCR of selected genes for pro-inflammatory cytokines, chemokines, target genes (IL-6, IL-1β, TNF-α, iNOS, PGES, TGF-β, CCL2 and CX3CL1) and for osteoclasts (RANKL, OPG and Cathepsin K). We report a distinct difference in osteoclast activation and molecular signaling pathway between titanium particles- and fluid pressure- induced osteolysis. Titanium particles recruit and activate osteoclasts within the soft tissue with direct contact to particles, meanwhile fluid pressure recruits and activates osteoclasts with bone marrow contact at a certain distance from the fluid pressure exposure zone. At day 1, 6 of 8 pro-inflammatory genes and anti-inflammatory genes were strongly up regulated by titanium particles, meanwhile 3 of 8 genes were more weakly up regulated after fluid pressure, both compared to internal control. Furthermore, at 3 days, 4 of 8 genes were up regulated after titanium particle and none was up regulated after fluid pressure. All genes except for IL-1β and IL-6 were moderately correlated with RANKL and Cathepsin K ($R2=0.48$-0.76, $p<0.05$) after titanium particles, meanwhile only CCL2 ($R2=0.94$, $R2=0.39$, $p<0.05$) and iNOS were correlated both to RANKL and Cathepsin K after fluid pressure exposure. Also, IL-6 was correlated to RANKL ($R2=0.34$, $p=0.01$) after fluid pressure, which was not observed with titanium particles. These results demonstrate that fluid pressure induces osteoclast activation at a different localization than titanium particles by a signaling pathway distinct from or acting in parallel to a classical innate immune response.

***Disclosures: Anna Fahlgren**, None.*

MO0247

Hypoxia-Inducible Factor (HIF) Regulates Osteoclast-Mediated Bone Resorption: Role of Angiopoietin-like 4 (ANGPTL4). Helen Knowles[1], Anne-Marie Cleton-Jansen[2], Eberhard Korsching[3], Nicholas Athanasou*[1]. [1]University of Oxford, United Kingdom, [2]Leiden University Medical Centre, Netherlands, [3]University of Munster, Germany

The transcription factor HIF regulates osteoblastic promotion of angiogenic-osteogenic coupling. Osteoclast-mediated bone resorption is also enhanced by hypoxia in a HIF-dependent manner. We have investigated mechanisms linking HIF expression and osteoclast activation to determine how HIF might co-ordinate osteoclast and osteoblast function.

Osteoclasts were differentiated from CD14+ monocytes with M-CSF (25 ng/ml) and RANKL (50 ng/ml) for 16 days. An Illumina HumanWG-6 v3.0 48k array compared 6 paired samples of normoxic versus hypoxic (2% O_2, 24 h) osteoclasts. Expression of genes of interest was confirmed by real-time PCR, Western blotting and ELISA. Effects on the viability (number of vitronectin receptor-positive multi-nucleated cells) and resorption activity (lacunar resorption of dentine slices) of mature osteoclasts were assessed on differentiation day 12-14. Effects of isoform-specific HIF siRNA were assessed 48 h post-transfection with 50nM siRNA and RNAiMAX.

A panel of normoxic inducers of HIF revealed that HIF expression itself is sufficient to enhance osteoclast resorption in the absence of a hypoxic stimulus. Analysis of microarray data therefore focussed on HIF target genes. A role for the adipokine ANGPTL4 in osteoclast resorption was postulated based on associations with MMP expression, cartilage degradation and rheumatoid arthritis. We have confirmed O_2 concentration-dependent induction of ANGPTL4 in both osteoclasts and osteoblasts. ANGPTL4 expression was increased by normoxic inducers of HIF and selectively inhibited by siRNA targeting HIF-1α. Exogenous ANGPTL4 (100 ng/ml) caused a 2.5-fold increase in osteoclastic bone resorption that was independent of, but augmented by, RANKL. It could also rescue the hypoxic induction of osteoclast activity inhibited by HIF-1α siRNA. However, ANGPTL4 did not affect either osteoclast differentiation or monocyte survival / proliferation. In osteoblastic cells ANGPTL4 caused a dose-dependent increase in both proliferation and mineralisation.

This data demonstrates that HIF is sufficient to enhance osteoclast-mediated bone resorption in the absence of a hypoxic stimulus. ANGPTL4 can compensate for HIF-1α deficiency with respect to stimulation of osteoclast activity and augments osteoblast proliferation and differentiation. This is the first description of a role for ANGPTL4 in bone biology and represents a mechanism whereby HIF could couple osteoclastic and osteoblastic components of the osseous niche.

***Disclosures: Nicholas Athanasou**, None.*

MO0248

The Role of CX3CL1/CX3CR1 on the Osteoclastogeneis in a Mice Model of Radiation Induced Bone Loss. Chang Sun whang*[1], So Young Park[2], Seoung Mi Choi[1], Yun Kyung Yu[1], Chang Hoon Yim[1], Sung Hoon Kim[1], Hyun-Koo Yoon[3], Ki Ok Han[1]. [1]cheil hospital, South korea, [2]Kwandong University College, South korea, [3]Cheil Hospital & Women's Healthcare Center, South korea

Chemokines regulate cell migration and adhesion. Fractalkine (Fkn/CX3CL1), the sole member of the CX3C chemokine, has dual functions for cells expressing its receptor CX3CR1: it acts as a chemotactic factor in its soluble form and an adhesion molecule in its membrane-bound form. In our study, the expression of Fkn in bone was observed to increase dramatically after exposure to 5, 10, 20 Gy radiation in a dose dependent manner; osteoclast precursors expressed CX3CR1 and its expression was rapidly decreased according to differentiation. In vitro transmigration assay showed that Fkn significantly induced the migration of preosteoclasts, RAW 264.7. In immunohistochemistry on sections from decalcified tibia, we found that Fkn expression was localized mainly in the vascular endothelium and increased dose-dependently after exposure to radiation. To test whether circulating preosteoclastic cells increased to recruit into irradiated bone and this process was mediated by Fkn, we isolated GFP^+ CD^{11b+} cells from a C57BL/6 transgenic mice strain expressing GFP ubiquitously and injected them into the wild type (WT) mice via tail vein after 3 days of 5 Gy dose of irradiation. Compared to the non-irradiated control, the GFP expressions significantly increased at 2 hours, 24 hours, and 1 week after injection in the irradiated bone. When we injected GFP^+ CD^{11b+} cells from a $CX3CR1^{-/-}$, a C57BL/6 mouse in which the CX3CR1 gene was replaced by a GFP reporter gene, no significant increment of GFP expression could be found in bone after 2 hours of injection. At 6 weeks after bone marrow transplantation, BMD in WT mice received transplantation of BMCs from CX3CR1 deficient mice ($WT/CX3CR1^{-/-}{}_{BM}$) was significantly preserved compared to WT/WT_{BM} (0.4087 ± 0.011 vs 0.3808 ± 0.0201 g/cm^2 in $WT/CX3CR1^{-/-}{}_{BM}$ and WT/WT_{BM}, respectively. n=18 each, $p<0.001$). BMD of $CX3CR1^{-/-}/CX3CR1^{-/-}{}_{BM}$ was 6.1% higher than that of WT/WT_{BM}. Our results suggest that Fkn(CX3CL1)-CX3CR1 system is important for osteoclastogenesis by regulating the recruitment of preosteoclasts to bone through activated endothelium.

***Disclosures: Chang Sun whang**, None.*

MO0249

Twisted-gastrulation, a Negative Regulator of BMP-signaling in Osteoclasts. Lan Pham*[1], Eric Jensen[2], Kayla Beyer[3], Charlie Billington[3], Julia Davydova[3], Julio Rodriguez[3], Masato Yamamoto[3], Anna Petryk[3], Kim Mansky[1], Raj Gopalakrishnan[1]. [1]University of Minnesota, USA, [2]University of Minnesota School of Dentistry, USA, [3]University of MN, USA

We have previously shown that mice deficient for the BMP antagonist Twisted-gastrulation (*Twsg1*) display severe osteopenia resulting from increased osteoclastogenesis. We also showed that exogenous BMP2 synergized with RANKL to enhance osteoclastogenesis. We detected pSMAD-1,5,8 in the nuclei of osteoclasts, and showed increased expression of pSMAD, BMP2, and BMPRs during osteoclast differentiation. This suggested that BMP-signaling directly regulates osteoclastogenesis. To further test the hypothesis that *Twsg1* is a negative regulator of osteoclast differentiation, murine bone marrow cells were allowed to differentiate into mature osteoclasts following overexpression of *Twsg1* using adenoviral vectors. Over-expression of *Twsg1* showed decreased number and size of TRAP positive multinucleated osteoclasts, decreased expression of osteoclast-specific genes and reduced resorptive ability. Further, we show that exogenous BMP2 treatment reversed *Twsg1*-mediated attenuation of osteoclastogenesis confirming that *Twsg1* acts by modulating BMP-signaling pathway. The significance of BMP pathway in osteoclast differentiation was further confirmed when similar attenuation of differentiation and gene expression was noted when osteoclast differentiation was allowed to proceed in cells where BMPRII was knocked down using lentiviral shRNA vectors. Taken together, our results reveal that BMP-signaling directly promotes the differentiation of multinuclear osteoclasts and further clarifies a novel anti-resorptive role for *Twsg1* by modulating BMP-signaling.

(NIH/NIDCR: T32DE007288(L.D.P.);R01DE016601(A.P.); AHC(R.G.))

***Disclosures: Lan Pham**, None.*

MO0250

Cortical Bone Stimulates Osteoclast Formation and Calvarial Bone Does Not. Teun De Vries*[1], Ton Schoenmaker[2], Vincent Everts[1]. [1]ACTA, Vrije Universiteit, The netherlands, [2]ACTA, Netherlands

Osteoclasts form in the vicinity of bone. Yet, remarkably little is known about the possible influence of the diverse bones of the skeleton on the formation of osteoclasts. Here, we investigated the influence of bovine femoral cortical bone and calvarial bone on osteoclast formation. Mouse bone marrow cells were seeded on plastic, cortical bone and calvarial bone in the presence of M-CSF and RANKL and the formation of TRACP+ multinucleated cells (TRACP+MNC) was assessed. In addition, the formation of TRACP+MNC was assessed with conditioned medium (CM) obtained from cultures on plastic, cortical or calvarial bone, which was collected early (days 0-3) and late (days 3-6) in osteoclastogenesis experiments (CM w cells). To assess whether bones release osteoclastogenesis stimulating factors, CM was collected from plastic, cortical or calvarial bone which were not exposed to any cells (CM w/o cells). The number of TRACP+MNC was 3-5 fold higher on cortical bone compared to plastic or calvarial bone ($p<0.05$). More compelling was the difference in large TRACP+MNC containing more than 10 nuclei, which was 13-fold higher on cortical bone compared to plastic or calvarial bone ($p<0.01$). To assess whether TRACP+MNC grown on plastic or on bones release factors that influence osteoclastogenesis, we next cultured freshly isolated bone marrow cells in the presence of CM 1:1 diluted with medium containing M-CSF and RANKL. Strikingly, CM w cells collected after the first three days of osteoclastogenesis did not affect osteoclast formation, whereas CM w cells of the last three days completely prevented osteoclast formation. This accounted for CM collected from all three substrates. Most intriguing results, however, were obtained with CM w/o cells at time point 3-6 days from plastic, cortical bone and calvarial bone that was kept without cells. CM from cortical bone induced significantly higher numbers of TRACP+MNC ($p<0.001$) compared to CM from plastic or calvarial bone. Again, large TRACP+MNC were found nearly exclusively in cultures with cortical bone CM.

Our results indicate that osteoclasts may release soluble inhibitors that act as a feed-back on osteoclast formation. Furthermore, certain bones may release factors that stimulate osteoclast formation. These results may help explain why the skull is relatively protected against osteoclastic degradation in diseases such as osteoporosis or when the calcium reservoir of bone is challenged in case of a calcium deficit.

***Disclosures: Teun De Vries**, None.*

MO0251

Cross-talk between Phagocytic and Osteoclastogenic Pathways Determine Myeloid Cell Fate in Granulomatous Inflammation. Ed Purdue*, Douglas James, Bryan Nestor, Thomas Sculco, F. Patrick Ross, Steven Goldring. Hospital for Special Surgery, USA

Phagocytosis of non-degradable materials is a common feature of a number of granulomatous human diseases, including periprosthetic osteolysis after joint replacement, which specifically targets skeletal tissues, The cellular and molecular processes by which phagocytosed materials influence the potential for myeloid cells to differentiate into bone resorbing osteoclasts, activated macrophages or macrophage

polykaryons have not been fully defined. To address this issue, human peripheral blood monocytes were challenged with non-degradable particulates during M-CSF/RANKL-mediated osteoclast differentiation. We found that phagocytosis of particulate polymethylmethacrylate dose-dependently inhibited M-CSF and RANKL-mediated osteoclastogenesis. Expression patterns in cells treated with or without particles were analyzed by quantitative RT-PCR. Analyses revealed that phagocytosis was associated with strong repression of c-fms and RANK mRNA consistent with effects on gene transcription, and that this was dependent, at least in part, upon MAP kinase activation. In addition, c-Fms expression was regulated by post-translational mechanisms involving shedding of the ectodomain from the cell surface. The metalloprotease inhibitor TAPI partially prevented this effect, implicating involvement of metalloprotease-mediated receptor shedding. Of interest, RANKL pretreatment of monocytes averted particle-induced down-regulation of c-fms and RANK expression, and cells progressed in a predicted fashion to osteoclast formation, even though they retained phagocytic activity. Surprisingly, phagocytosis strongly induced expression of several NFATc1-dependent genes associated with cell fusion, including DC-STAMP and ATP6v0d2, although cells pretreated with particles prior to RANKL, did not become terminally differentiated osteoclasts. The activation of these fusogenic gene products may be responsible for maintaining the ability of the cells to form nonresorptive polykaryons. These studies provide further insights into the cellular and molecular mechanisms involved in the determination of myeloid cell fate and provide potential therapeutic targets and strategies for modulating the skeletal complications associated with granulomatous inflammation.

***Disclosures: Ed Purdue**, None.*

MO0252

HDAC3 and HDAC7 Have Opposite Effects on Osteoclast Differentiation. Eric Jensen[1], Lan Pham[2], Bria Kaiser[2], Amanda Romsa[2], Toni Schwarz[2], Raj Gopalakrishnan[2], Kim Mansky*[2]. [1]University of Minnesota School of Dentistry, USA, [2]University of Minnesota, USA

Histone deacetylases (HDACs) are negative regulators of transcription. Endochondral bone formation including chrondocyte and osteoblast maturation is regulated by HDACs. Very little is known about the role HDACs play in osteoclast differentiation. Suppression of HDAC3 expression mimics the previously described repression of osteoclastogenesis from HDAC inhibitors TSA and NaB, while osteoclasts suppressed for HDAC7 expression had accelerated differentiation compared to control cells. Mitf is a transcription factor necessary for osteoclast differentiation. We demonstrate that Mitf and HDAC7 interact in osteoclasts in a RANKL antagonized manner. Mitf's transcriptional activity is repressed by HDAC7. Lastly, we show that either the amino or carboxy terminus of HDAC7 is sufficient for transcriptional repression and that HDAC7's repression is insensitive to TSA, indicating that HDAC7 represses Mitf at least in part by deacetylation-independent mechanism. Understanding the mechanisms by which HDAC7 represses Mitf function, the significance in the context of the larger transcription complex (c-fos/Mitf/PU.1/Nfatc1) at osteoclast promoters and the regulatory inputs that coordinate their activity will be significant areas for future studies.

***Disclosures: Kim Mansky**, None.*

MO0253

Isoquinoline Alkaloids Attenuate Osteoclast Differentiation and Function Through Regulation of RANKL and OPG Gene Expression in Osteoblastic Cells. Ji-Won Lee*[1], Nam-Kyung Im[2], Takayuki Yonezawa[3], Hwa-Jeong Seo[4], Won Bae Jeon[4], Byung-Yoon Cha[1], Kazuo Nagai[5], Je-Tae Woo[1]. [1]Research Institute for Biological Functions, Chubu University, Japan, [2]Dept. of Food Science & Technology, Keimyung University, South korea, [3]The University of Tokyo, Japan, [4]Daegu Gyoengbuk Institute of Science & Technology, South korea, [5]Department of biological chemistry, Chubu university, Japan

The isoquinoline alkaloids including berberine, coptisine and palmatine, from several medicinal plants, have been studied extensively with antipyretic, antiphotooxidative, dispelling dampness, antidote, antinociceptive and anti-inflammatory activities *in vitro* and *in vivo*. Recently, berberine has been reported to inhibit RANKL-induced osteoclast differentiation from osteoclast precursors, survival of mature osteoclasts and ovariectomy-stimulated bone resorption in rats. Although berberine directly acts on osteoclast precursors and inhibits osteoclast differentiation through blocking RANKL signaling pathways, the detailed effect of berberine on osteoblastic cells to support osteoclast differentiation remains unknown. This study focused on the effects of these three isoquinoline alkaloids on osteoblastic cells as well as osteoclast precursors for osteoclastogenesis in vitro. Addition of three alkaloids with same concentration (10 μM) to co-cultures of MCSF-dependent cells derived from mouse bone marrow cells and primary osteoblastic cells with 10-8 M $1\alpha,25(OH)_2D_3$ caused significant inhibition of osteoclast formation. Berberine and coptisine inhibited RANKL-induced osteoclast formation from MCSF-dependent cells but not palmatine. And RT-PCR analysis showed that berberine and coptisine inhibited the expression of RANKL gene and stimulated the expression of OPG gene induced by $1\alpha,25(OH)_2D_3$ in osteoblastic cells, but palmatine only inhibited the expression of RANKL gene. In addition, three alkaloids at 10 μM concentration inhibited resorption pit formation by mature osteoclasts with osteoblastic cells on dentin slices, although the inhibitory effect of berberine is stronger than that of the other two alkaloids. Taken together, these results suggest that isoquinoline alkaloids attenuate osteoclast differentiation and function through not only blocking RANKL signaling pathways in osteoclast precursors and ostelclasts but also regulating the expression of RANKL and OPG gene in osteoblastic cells.

***Disclosures: Ji-Won Lee**, None.*
This study was supported by a grant for Biodefense Programs of the Ministry of Education, Science and Technology of the Republic of Korea

MO0254

Osteocytic MLO-Y4 Cells Inhibit Osteoclastogenesis by a Soluble Factor(s), Independent of Modulation of RANKL/OPG Productions by Stromal Cells. Takuya Sato*[1], Chiyomi Hayashida[2], Mari Okayasu[2], Yoshiyuki Hakeda[3]. [1]Meikai University School of Dentistry, Jpn, [2]Meikai University Graduate School of Dentistry, Japan, [3]Meikai University School of Dentistry, Japan

Osteocytes regulate bone resorption dependent on mechanical loading. Selective ablation of osteocytes *in vivo* stimulated bone resorption under normal loading, indicating that physiological role of osteocytes on osteoclastogenesis is inhibitory. However, the mechanisms of this inhibitory effect remain unclear, in part, due to a lack of suitable culture systems to analyze the relationship between osteocytes, bone lining/stromal cells and osteoclast precursors. Osteocytic MLO-Y4 cells have been shown to express RANKL mRNA and support osteoclastogenesis from bone marrow (BM) cells in the presence of $1,25(OH)_2D_3$ (VD_3), suggesting that *in vitro* cocultures of MLO-Y4 cells and osteoclast precursors are incompatible with functions of osteocytes as observed *in vivo* osteocyte ablation model. Therefore, we developed a culture system reflecting *in vivo* function of osteocytes.

MLO-Y4 cells were first cultured in collagen gel to form a 3-D cellular network, followed by seeding of stromal ST2 cells on the gel. After formation of ST2 cell layer on the gel, BM cells were seeded and osteoclastogenesis was induced by addition of osteoclastogenic factors. In this culture system, the presence of MLO-Y4 cells in the gel negatively regulated osteoclastogenesis induced by VD_3, depending on densities of MLO-Y4 cells. When MLO-Y4 cell apoptosis in the gel was induced by exposure of UV-light prior to seeding, the inhibitory effect of MLO-Y4 cells on osteoclastogenesis was diminished. Next we analyzed whether the presence of MLO-Y4 cells in the gel affects RANKL and/or OPG productions. ST2 cells were cultured on the gel with or without MLO-Y4 cells in the presence of VD_3 and RANKL mRNA expression was examined. The results showed that RANKL mRNA expressions were not significantly different, irrelevant to the presence or absence of MLO-Y4 cells in the gel. In addition, OPG mRNA expression as well as OPG concentration in culture medium were not significantly changed by the presence of MLO-Y4 cells in the gel. When osteoclastogenesis from BM cells was induced by exogenous addition of soluble RANKL, the presence of MLO-Y4 cells in the gel similarly decreased the osteoclastogenesis as induced by VD_3. Furthermore, the conditioned medium of MLO-Y4 cells inhibited the osteoclastogenesis induced by M-CSF and soluble RANKL.

These data suggested that osteocytes produce a soluble factor(s) to decrease osteoclastogenesis independent of modulation of RANKL/OPG productions by stromal cells.

***Disclosures: Takuya Sato**, None.*

MO0255

PGC1β Mediates PPARγ Activation of Osteoclastogenesis and Rosiglitazone-Induced Bone Loss. Wei Wei[1], Xueqian Wang[1], Marie Yang[1], Leslie Smith[2], Paul Dechow[2], Yihong Wan*[3]. [1]UT Southwestern Medical Center, USA, [2]Baylor College of Dentistry, Texas A&M University Health Sciences Center, USA, [3]University of Texas Southwestern Medical Center, USA

Long-term usage of rosiglitazone, a synthetic PPARγ agonist, increases fracture rates among diabetic patients. PPARγ suppresses osteoblastogenesis while activating osteoclastogenesis, suggesting that rosiglitazone induces skeletal fragility by decreasing bone formation while sustaining or increasing bone resorption, leading to the uncoupling of bone remodeling. Using several mouse models with genetically altered PPARγ, PGC1β or ERRα, here we show that PGC1β is required for the pro-osteoclastogenic and resorption-enhancing effects of rosiglitazone. PPARγ activation indirectly induces PGC1β expression by down-regulating β-catenin and derepressing c-jun. PGC1β in turn functions as a PPARγ coactivator to stimulate osteoclast differentiation. Complementarily, PPARγ also induces ERRα expression, which coordinates with PGC1β to enhance mitochondrial biogenesis and osteoclast function. ERRα knockout mice exhibit osteoclast defects, revealing ERRα as a novel regulator of osteoclastogenesis. Strikingly, PGC1β deletion in osteoclasts confers complete resistance to rosiglitazone-induced bone loss. These findings identify PGC1β as an essential mediator for the PPARγ stimulation of osteoclastogenesis by targeting both PPARγ itself and ERRα, thus activating two distinct transcriptional programs.

***Disclosures: Yihong Wan**, None.*

MO0256

Regulation of Osteoclast Differentiation by Adenylate Cyclase 3 Through PKA-Mediated NFATc1 Inactivation. Woo-shin Kim*, SOO-HYUN YOON, Hong-Hee Kim. Seoul National University, South korea

Woo-shin Kim, Soo-Hyun Yoon, Ji yoon Ryu, Youngkyun Lee, Zang Hee Lee, Hong-Hee Kim

Department of Cell and Developmental Biology, Seoul National University, Seoul, Korea

Summary

By a DNA microarray analysis, we found that adenylate cyclase 3 (AC3) was up-regulated by > 3-fold after treatment of bone marrow macrophages (BMMs) with receptor activator of NF-κB ligand (RANKL), the osteoclast differentiation factor. Unexpectedly, however, cAMP increasing agents, forskolin and PGE2 inhibited RANKL-induced osteoclast formation in cultures of BMMs. Furthermore, rolipram, a phosphodiesterase 4 (PDE4) inhibitor, also suppressed RANKL-induced osteoclastogenesis. By introducing siRNA against AC3 and PDE4 to BMMs, we confirmed the inhibitory action of cAMP on osteoclast differentiation. In vivo administration of forskolin reduced osteoclastogenesis and bone resorption in RANKL treated mice calvariae. Furthermore, we revealed that the inhibitory action of cAMP was mediated by protein kinase A (PKA). The nuclear accumulation and subsequent induction of nuclear factor of activated T cells c1 (NFATc1) was strongly blocked by cAMP-PKA. Additionally, intracellular cAMP levels were down-regulated by calmodulin kinase II (CaMKII) that mediates NFATc1 induction during osteoclastogenesis. Treatment of KN63, the CaMKII inhibitor elevated intracellular cAMP levels. Moreover, CaMKII silencing resulted in elevation of intracellular cAMP levels and inhibition of osteoclastogenesis. Taken together, these results suggested that the AC3-cAMP-PKA signaling pathway negatively regulated osteoclast differentiation through NFATc1 inactivation and that CaMKII counter-balanced the inhibitory cAMP pathway during osteoclastogenesis.

***Disclosures: Woo-shin Kim**, None.*
This study received funding from: 21c Frontier functional proteomics project(FPR08B1-170)

MO0257

RelB, and not p65, Regulates Osteoclast Differentiation via Direct Binding to κB sites in c-fos and NFATc1 Genes. Jennifer Davis*[1], Chang Yang[2], Kathleen McCoy[1], Roberta Faccio[2], Deborah Novack[3]. [1]Washington University School of Medicine, USA, [2]Washington University in St Louis School of Medicine, USA, [3]Washington University in St. Louis School of Medicine, USA

RANKL stimulation activates the classical and alternative pathways of NF-κB leading to nuclear translocation of p65 and RelB, respectively. In the classical pathway, p65 is critical for osteoclast (OC) precursor survival, and when apoptosis is prevented, p65-/- bone marrow macrophages (BMMs) can make functional OCs in vitro. In contrast, RelB in the alternative pathway is required for OC differentiation, and RelB-/- BMMs fail to produce mature OCs in culture. The goal of this study was to delineate the mechanism by which the different members of the NF-κB family orchestrate OCgenesis. Analysis of subunit binding to a κB consensus oligo revealed distinct kinetics for p65 and RelB. We found that activation of p65 is rapid and transient (on/off within 15-60 min), whereas RelB exhibited much slower and sustained activation from 4 to 72 hours. To explore whether persistent NF-κB activation, by either subunit, is sufficient to mediate OCgenesis, we retrovirally expressed a constitutively nuclear form of p65 in RelB-/- cells, and found that it was not able to rescue the OCs. This data suggests that differences in activation kinetics are not sufficient to explain the unique functions of p65 and RelB in OC differentiation. While induction of the key osteoclastogenic genes, c-fos and NFATc1, is known to be NF-κB dependent, it is not known which subunit(s) regulate their transcription. Quantitative RT-PCR and immunoblot of BMMs stimulated with RANKL from 0 to 4 days showed intact expression of c-fos and NFATc1a in p65-/- samples, consistent with the ability of these cells to differentiate in these culture conditions. However, both c-fos and NFATc1a mRNA induction were blunted in RelB-/- cells, and c-fos and NFATc1 protein was not detectable in RelB-/- cells. The sustained activation kinetics of RelB match the expression profiles of c-fos and NFATc1, suggesting direct modulation by this NF-κB subunit. Chromatin immunoprecipation of RANKL-stimulated WT BMMs showed binding of RelB to κB sites within the first intron of c-fos at 24 hours and in the NFATc1 promoter at 48 and 72 hours. Collectively, our data demonstrate that it is RelB, not p65, which controls induction of these osteoclastogenic transcription factors via direct binding to κB sites. Understanding the transcriptional targets of RelB may aid in the design of alternative NF-κB pathway inhibitors for the prevention of pathological bone loss.

***Disclosures: Jennifer Davis**, None.*

MO0258

Sirtuin Activating Compounds Inhibit Rac1 Activation, Actin Ring Formation, and Osteoclastogenesis. Manhui Pang*[1], Mireya Hernandez[1], Isabel Fernandez[1], María Rodríguez-Gonzalez[1], Bruce Troen[2]. [1]Miami VA GRECC, Geriatrics Institute, University of Miami Miller School of Medicine, USA, [2]Miami VA GRECC, University of Miami Miller School of Medicine, USA

Osteoporosis is a widely prevalent contributor to frailty and results from an imbalance between bone resorption and bone formation leading to progressive bone loss, fractures, and increased morbidity and mortality. Sirtuin activating compounds (STACs) such as resveratrol (RSV) are pro-longevity agents that can extend healthspan in vertebrates. RSV enhances bone mineral density in mice, and sirtuin knockout mice exhibit increased osteoclastogenesis. We are therefore investigating the impact of novel sirtuin1 (Sirt1) specific activating compounds (SRT2183 and SRT1720) on bone during aging.

Both RAW264.7 cells and bone marrow cells can be induced to form functioning multinucleated osteoclasts. We now show that SRT2183 and SRT1720 inhibit osteoclast formation in a dose-dependent manner in both RAW264.7 cells and bone marrow cells, whereas RSV does not. SRT2183 also inhibits resorption of dentine by osteoclasts. Since rac1 activation and subsequent actin ring formation play a critical role in the formation and function of osteoclasts and therefore bone resorption, we investigated the impacts upon both of these events. SRT2183 and SRT1720 markedly suppress the stimulation of rac1 and cdc42 activation by RANKL. Furthermore SRT2183 and SRT1720 dose-dependently inhibit actin ring formation, whereas RSV does not. In contrast, RSV increases mineralization by osteoblasts in vitro, and microCT analysis reveals that RSV treatment of older mice for six weeks markedly increased bone volume.

These results suggest that STACs may disrupt osteoclastogenesis and osteoclast function by suppressing rac1 and cdc42 activation and subsequent actin ring formation. STACs also enhance osteoblastogenesis. Interestingly, RSV is not effective in vitro, but appears to exert potent effects in vivo. Consequently, STACs appear to exert novel anti-resorptive and anabolic effects upon the skeleton. They offer significant potential as therapeutic agents to regulate the balance between osteoclastic bone resorption and osteoblastic bone formation to enhance bone mineral density and bone quality.

***Disclosures: Manhui Pang**, None.*
This study received funding from: Sirtris - GSK

MO0259

The p66, p52, and p46 Isoforms of the Adaptor Protein Shc Play Critical but Distinct Roles in Osteoclast Differentiation. Haibo Zhao*[1], Maria Jose Almeida[1], Xiaohua Qiu[2], Shiqiao Ye[1], Aaron Warren[2], Charles O'Brien[1], Stavros Manolagas[1]. [1]University of Arkansas for Medical Sciences, USA, [2]Center for Osteoporosis & Metabolic Bone Diseases, University of Arkansas for Medical Sciences & Central Arkansas Veterans System, USA

P66, p52 and p46 are three isoforms of Shc proteins encoded by the ShcA locus in vertebrates and mammals. $p52^{Shc}$ and $p46^{Shc}$ act as adaptor proteins that specifically bind to phosphorylated tyrosines on the cytoplasmic motif of growth factor receptors upon stimulation. $p52^{Shc}/p46^{Shc}$ then recruit the Grb2-Sos complex on the plasma membrane and subsequently activates RAS and the mitogen-activated protein kinase (MAPK) cascade. Although $p66^{Shc}$ shares the same amino acid sequence at the C-terminus, $p66^{Shc}$ has different functions to those of $p52^{Shc}/p46^{Shc}$ as it does not activate the RAS/MAPK signaling pathway. Instead, $p66^{Shc}$ regulates intracellular redox balance and oxidative stress levels. Given that both MAPK and reactive oxygen species (ROS) are critical for osteoclast differentiation and function, Shc proteins might play an important role in osteoclast regulation. However, this hypothesis has not been tested. To do so, we examined protein expression of the three Shc isoforms during osteoclast differentiation. While all three isoforms were present at the same level in macrophages, pre- and mature-osteoclasts, the $p52^{Shc}/p46^{Shc}$ isoforms were approximately 20-fold more abundant than $p66^{Shc}$ in both osteoclast precursors and mature cells. To elucidate the role of Shc proteins in osteoclast differentiation we used two genetic modification approaches. First, we knocked down the expression of all three isoforms by lenti-viral vectors mediated shRNA expression. All three Shc isoform levels decreased by 70% in Shc shRNA transduced osteoclasts as compared with control cells. The reduction of expression of all three Shc proteins resulted in a dramatic reduction of TRAP+, multinucleated OC formation and elimination of bone resorption, as measured by resorption pit staining and the level of the resorption marker CTx in the culture medium. Second, we isolated bone marrow macrophages from mice in which only the p66 isoform was deleted (provided by T. Prolla, Univ of Wisconsin) and cultured them with M-CSF and RANKL. $P66^{Shc}$, but not $p52^{Shc}/p46^{Shc}$, protein level was eliminated in knockout cells. Unexpectedly, the number of TRAP+ multi-nucleated OC in the p66 null cells was increased by 30% compared with WT cultures. Consistent with this, M-CSF induced ERK activation was enhanced. We conclude that $p66^{Shc}$ exerts a cell autonomous suppressive effect on OC generation, perhaps by antagonizing $p52^{Shc}/p46^{Shc}$ binding to Drb2/Sos complex and therefore terminating Ras/MAPK signaling.

***Disclosures: Haibo Zhao**, None.*

MO0260

Zoledoronic Acid Inhibits TNF-α Induced RANK Expression and Migration in Osteoclast Precursors. Keiichiro Kimachi[1], Tetsuro Ikebe[2], Fujio Okamoto[1], Hiroshi Kajiya*[1], Koji Okabe[1], Shuji Nakayama[1]. [1]Fukuoka Dental College, Japan, [2]Fukuoka Dental College., Japan

Bisphosphonates have been known to directly inhibit bone resorption and promote apoptosis in mature osteoclasts. However, little is known about the effect of bisphosphonates and their exact molecular mechanism on osteoclast differentiation, but not on resorption activity. Although they have been recognized as the most effective drugs to treat osteoporosis and cancer bone metastasis, an adverse effect that has recently emerged is bisphosphonate-related osteonecrosis of the jaw (BRONJ). To understand the first step in its pathobiology in abnormal osteoclast differentiation mechanism, it is crucial to investigate the effect of bisphosphonate on inflammation-induced osteoclast differentiation and recruitment since BRONJ often occurs with osteomyelitis in the jaw following tooth extraction. To exactly clarify whether nitrogen-containing bisphosphonates affect recruitment and differentiation in osteoclast precursors, in particularly inflammatory bone osteolysis, we examined the effect of zoledronic acid on TNFα-induced RANK expression and cell migration in two types of osteoclast precursors, RAW264.7 cells and mouse bone marrow cells. TNF-α up-regulated RANK expression in RAW264.7 as well as bone marrow cells in the presence of macrophage colony stimulating factor in a time-dependent manner using RT-PCR, Western blot, and FACS analysis. Zoledronic acid had no effect on cell viability in these osteoclast precursors after 2 days of cultivation. Zoledronic acid strongly inhibited TNF-α-induced up-regulation of RANK in a dose-dependent manner. The inhibitory effects on RANK expression was likely to be involved with the suppression of IκBα phosphorylation and then κB transcriptional activity in the NFκB pathway, but not the other downstream signaling pathways. Interestingly, zoledronic acid also suppressed the TNF-α-induced migration of precursors through inhibiting the mevalonic acid pathway. In summary, zoledronic acid suppressed TNFα-induced recruitment and RANK expression in osteoclast precursors. Our results suggest that nitrogen-containing bisphosphonates not only inhibit mature osteoclasts, but also prevent osteoclast precursors from differentiating and migrating to inflammatory lesions.

***Disclosures: Hiroshi Kajiya**, None.*

MO0261

Development of Cell-based Assays for Identifying Inhibitors of RANK Intracellular Signaling. Jason Ashley*[1], Erin McCoy[1], Zhenqi Shi[1], Daniel Clements[1], Taosheng Chen[2], Xu Feng[1]. [1]University of Alabama at Birmingham, USA, [2]St. Jude Children's Research Hospital, USA

Bone loss due to metabolic or hormonal disorders and osteolytic tumor metastasis continues to be a costly health problem that will likely become even more prevalent as life expectancy increases. As such, the discovery of more and better antiresorptives remains an attractive goal. Unraveling of the critical role for the receptor activator of NF-κB ligand (RANKL) and its receptor, RANK, in osteoclast biology provides an unprecedented opportunity to develop more effective antiresorptive drugs, and the effectiveness RANKL inhibitors such as Denosumab clearly demonstrate the potency of the RANKL/RANK system as a drug target. Here, we report the development of cell-based assays for high throughput screening (HTS) to identify compounds that inhibit signaling from two RANK cytoplasmic motifs ($PVQEET^{559-564}$ and $PVQEQG^{604-609}$), which play potent roles in osteoclast formation and function. We hypothesize that inhibitors of these motifs' signaling can be developed into new anti-resorptive drugs that can compliment current and future therapies. The cell-based assays consist of cell lines generated from the RAW 264.7 macrophage line stably expressing an NF-κB-responsive *Luciferase* reporter and a chimeric receptor containing the human Fas external domain linked to a murine RANK intracellular domain in which only one of either PVQEET or PVQEQG is fully functional. When the cells are treated with an anti-human Fas activating antibody, signaling through the chimeric receptor's functional motif is initiated leading to an increase in NF-κB translocation to the nucleus which can be measured as an increase in *Luciferase* activity. Inhibition of intracellular signaling will result in a reduced Luciferase response following treatment. In 96-well plates, both assays demonstrated a greater than 300% increase in *Luciferase* activity following RANK motif activation and Z' scores over 0.8, indicating low well-to-well variability. Furthermore, assay cell lines are capable of RANKL-induced osteoclastogenesis, indicating that RANK intracellular signaling is intact within these cells. After adapting our assays into HTS systems, we will screen compound libraries for molecules that exhibit inhibitory activity against these critical intracellular motifs. Follow up assays using a chimeric receptor in which all motifs except target motifs are functional and cell viability assays will allow us to refine initial hits to a smaller group of more specific inhibitors of intracellular RANK signaling.

***Disclosures: Jason Ashley**, None.*

MO0262

Elucidating the Mechanism by which the Human R444L and G405R Point Mutations in the V-ATPase 'a3' Subunit Leads to Osteopetrosis. Ajay Bhargava*[1], Michael Glogauer[2], Morris Manolson[2]. [1]Dental Research Institute, Canada, [2]University of Toronto, Canada

The vacuolar H+ ATPase (V-ATPase) is a conserved proton pump located on the ruffled border of osteoclasts and is responsible for the acidification of bone resorption lacunae. It consists of fourteen subunits, with the 'a3' isoform preferentially enriched in osteoclasts. Autosomal recessive osteopetrosis (ARO) is a disease characterized by decreased bone resorption. Without treatment, the outcome is fatal. Mutations in the human V-ATPase a3 subunit account for over 50% of ARO. Two of the point mutations in human a3 resulting in ARO (G405R and R444L), when recreated in the yeast ortholog Vph1p, did not affect V-ATPase assembly or activity, suggesting that these mutations have an osteoclast-specific effect (Ochotny et al., J. Biol. Chem. 2006). Here we ask whether these a3 point mutations affect V-ATPase trafficking in mammalian cells. To first ask whether these mutations affect membrane insertion, a3-GFP fusion proteins harboring both mutations were constructed and transfected into HeLa cells, and microsomal fractions were obtained. Immunoblots of resulting whole cells extracts, soluble proteins and microsomals pellets revealed that a3-GFP containing either the R444L and G405R mutations were properly inserted into the membrane. Epifluorescence analysis of transfected HeLa cells immunostained with Rab7 and LAMP1 suggest that these mutant V-ATPases may not appropriately localize to the lysosomal vesicles. Future analysis includes investigating V-ATPase assembly and trafficking through confocal analysis of osteoclasts transduced with WT and mutant a3-GFP constructs, and in-vitro immunoprecipitation studies to ascertain if mutant V-ATPases interact with cellular trafficking factors. Our results to date suggest that the human ARO mutations R444L and G405R do not affect a3 assembly and membrane insertion. Considering that these mutations did not affect V-ATPase activity in yeast, our data suggest that these human mutations may affect appropriate targeting of the V-ATPase complex to the ruffled border.

***Disclosures: Ajay Bhargava**, None.*

MO0263

In Vivo Imaging of Osteoclast Precursor Recruitment to the Inflammatory Site where Extensive Bone Destruction Occurs. Keiko Suzuki*[1], Fumitaka Takeshita[2], Kenji Yamamoto[3], Shoji Yamada[1], Hisashi Shinoda[4], Takahiro Ochiya[2]. [1]Department of Pharmacology, School of Dentistry, Showa University, Japan, [2]Section for Studies on Metastasis, National Cancer Center Research Institute, Japan, [3]Research Institute, National Center for Global Health & Medicine, Japan, [4]Tohoku University Graduate School of Dentistry, Japan

Bacteria are a common cause of inflammatory bone diseases including periodontitis and osteomyelitis. Since mediators associated with the innate immune response, such as TNFalpha, IL-1 and IL-6, significantly contribute to the disease process, in addition to local and systemic factors that regulate bone remodeling, the mechanism underlying bacteria-induced bone destruction is thought to be complicated. In the present study, we investigated the mobilization of osteoclast precursor cells (OCPs) in living mice, in which the interrelationship among different cell types are maintained, by using in vivo imaging techniques. OCPs derived from luciferase (Luc)- or EGFP-transgenic (Tg) rats were systemically injected into SCID mice, after inducing inflammatory osteolysis by injecting lipopolysaccharide (LPS) or Pam_3CSK_4 (Pam3) onto the skull of mice. Luc- or EGFP-expressing cells in living mice were monitored by noninvasive bioluminescence or fluorescence imaging up to 2 weeks. Bone morphometry, gene expression and histological changes were analysed at the end of the experiment. The results showed that; 1) In LPS- or Pam3-administered mice, inflammatory symptoms were observed within a day and subsequent osteolysis was detected on day 5, furthermore, expression of TNFalpha, IL-1beta, IL-6, MCP-1 and MIP-1alpha mRNAs were significantly increased in calvaria; 2) Within 3 days of Luc-Tg OCPs injection, Luc-positive cells were detected in the inflammation site, secondary lymph nodes and spleen; 3) EGFP-positive multinuclear cells were observed in the calvaria of EGFP-Tg OCP-injected living mice, and immunohistochemical analyses revealed that EGFP-positive cells differentiated into TRAP-positive OCs to make resorption lacunae in calvaria; 4) In calvaria from Luc-Tg OCPs-injected mice, expression of Luc and rat TRAP mRNAs was detected, which was significantly diminished by treatment with zoledronate or [4-(Methylthio)phenylthio] methanebisphosphonate (MPMBP). Together, these findings indicate that OCPs circulating in the bloodstream migrate into the local inflammation site through MCP-1/MIP-1alpha activation and can take part in the rapid and extensive bone destruction. Furthermore, the BPs tested in this study, including zoledronate and MPMBP, are able to inhibit the process of OCP mobilization and/or differentiation into the TRAP-positive OC, suggesting that BPs are promising drugs in inflammatory osteolysis as well as age-related osteoporosis.

***Disclosures: Keiko Suzuki**, None.*

MO0264

Isoprostane Levels are Altered in Rheumatoid Arthritis and Suppress NFκB Activity to Inhibit Osteoclast Formation. Seint Lwin*[1], Josh Brooks[1], Rick Jacobson[1], Lynett Danks[2], Karin Lundberg[2], Erin Terry[1], Stephanie Sanchez[1], Gregory Mundy[1], Jason Morrow[1], Ginger Milne[1], James Edwards[1]. [1]Vanderbilt University Medical Center, USA, [2]Imperial College London, United Kingdom

Excessive osteoclastic resorption is a defining feature of rheumatoid arthritis (RA), resulting in devastating bone loss and pain. Omega-3 fatty acids (Ω3-FA) are suggested to protect against RA, however the mechanism through which this occurs remains unknown. Isoprostanes (IsoPs) are formed in situ as oxidation products of Ω3-FA. We hypothesize that a beneficial effect of Ω3-FA in RA occurs following the formation of IsoPs, to suppress osteoclast formation and activation. To test this notion, we used GC-mass spectrometry to analyze the IsoP profile in human serum from age-, sex-matched RA patients or controls (n=9). RA patient samples were confirmed as CEP1 and CCP positive. In addition we employed osteoclast formation assays using RAW 264.7 cells treated with A3-IsoP in addition to RANKL and M-CSF. The molecular mechanism through which IsoP affects osteoclast formation was assessed using an NFκB-reporter macrophage cell line, to recapitulate and quantify NFκB signaling in osteoclast precursors. These studies were supported by immuno-fluorescent staining for nuclear/cytoplasmic p65 and western blot analysis for phosphorylated IκBα. To confirm the role of NFκB in IsoP mediated osteoclast inhibition, site-directed mutagenesis was employed to alter a putative IsoP binding region of IKK (C179). The osteoclast formation rate and NFκB activation status was assesed in mutated and unmodified cells. Our studies show that the IsoP levels within RA serum are significantly altered, compared to normal control patients. In addition, osteoclast precursor cells treated with A3-IsoP (15uM) formed significantly fewer TRAP+ multinucleated cells (26.3 ± 5.3) compared to vehicle treated controls (46.3 ± 4.3, $p<0.05$). Moreover, osteoclast precursor cells treated with 15-A3-IsoP demonstrated up to 60% decrease in NFkB reporter activity (25uM, $p<0.01$), phosphorylated IκBα protein levels and nuclear localization of the p65 protein. Mutation of C179 on IKK resulted in a loss of inhibition of NFκB activity and osteoclast formation, following A3-IsoP treatment compared to WT cells ($p<0.01$). These findings show that the A3-IsoP molecule inhibits osteoclast formation through interactions with C179 on the IKK molecule, to reduce IκBα phosphorylation and suppress NFκB activation. Moreover, we identified a significant change in IsoP levels in RA patients compared to controls, suggesting that Ω3-FA metabolites may contribute in part, to the increased osteoclastic resorption of RA.

***Disclosures: Seint Lwin**, None.*

MO0265

Osteoclast Retraction Induced by Isoform-Specific PI3-kinase Inhibitors. S. Jeffrey Dixon[1], Stephen Sims[2], Frank Jirik[3], Ryan Shugg*[1]. [1]The University of Western Ontario, Canada, [2]Supervisor, Canada, [3]Co-supervisor, Canada

Common human cancers, including lung, prostate and breast often metastasize to bone. Tumors in bone frequently promote the formation and activation of osteoclasts, leading to bone resorption and subsequent tumor growth. Phosphatidylinositol-3 kinases (PI3-kinases) regulate fundamental cellular processes such as cytoskeletal remodeling, growth and survival. Different PI3-kinase isoforms have distinct biological roles downstream of specific receptors in various cell types. Studies using pan-PI3-kinase inhibitors have suggested roles for PI3-kinases in osteoclasts, such as controlling cytoskeleton function during spreading and chemotaxis, but little is known about the function of specific PI3-kinase isoforms in these cells. We are studying the PI3-kinase Class I p110 isoforms α, β, γ and δ, with the goal of identifying inhibitors which may be useful for treating metastatic bone disease. The following inhibitors are being investigated (targets in parentheses): wortmannin (pan-p110), BEZ-235 (pan-p110), PIK-75 (α), GDC-0941 (α and δ), TGX-221 (β) and AS-252424 (γ). To assess possible toxicity, we incubated RAW-264.7 cells with inhibitors (100 pM to 10 μM) for 24 h, after which viability was assessed using an MTT assay. Toxic effects were observed only for PIK-75, at concentrations of 1 and 10 μM. Next, we assessed the effects of selected inhibitors on osteoclast morphology and motility. Osteoclasts were isolated from long bones of neonatal rats and plated on glass cover slips. Following 1 h incubation, preparations were washed to remove non-adherent cells and incubated for a further 0.5-2 h to permit osteoclast spreading. Osteoclasts were monitored using time-lapse phase-contrast microscopy and planar area was quantified by image analysis. Within 25 min, GDC-0941 (1 μM) induced retraction of osteoclasts to approximately 50% of their initial area. Retraction was sustained for at least 55 min and, despite marked retraction, osteoclasts remained motile. In contrast, there was no significant effect of AS-252424 (1 μM) or vehicle, consistent with the involvement of specific PI3-kinase isoforms in regulating cytoskeletal remodeling in osteoclasts. Future studies will examine the effects of isoform-specific PI3-kinase inhibitors on osteoclast survival and resorptive activity. Thus, the potential exists for identifying isoform-specific PI3-kinase inhibitors that target both osteoclasts and tumor cells for the treatment of metastatic tumors in bone.

***Disclosures: Ryan Shugg**, None.*

MO0266

The Benzohydrazide Derivative KM91104 Inhibits Osteoclast Mineral Resorption at çM Concentrations that do not Affect Osteoclast Differentiation or Fusion. Gazelle Crasto*[1], Norbert Kartner[1], Keying Li[2], Yeqi Yao[2], Alessandro Datti[3], Morris Manolson[1]. [1]University of Toronto, Canada, [2]Dental Research Institute, Faculty of Dentistry, University of Toronto, Canada, [3]Samuel Lunenfeld Research Institute, Mt. Sinai Hospital, Canada

V-ATPases are proton pumping enzymes highly expressed in ruffled borders of bone-resorbing osteoclasts, where they play a crucial role in skeletal remodeling by acidifying the resorption lacunae. V-ATPases are multimeric enzymes composed of at least 14 subunits with the a3, B2 and d2 isoforms highly enriched in the osteoclast ruffled border. Using yeast two hybrid and ELISA binding assays, we show that the 50 kDa N-terminus of the a3 subunit interacts with the B2 and d2 subunits. Solid-phase binding assays were subsequently used to screen a chemical library for inhibitors of a3-B2 interaction. One inhibitor of the a3-B2 interaction, the small molecule benzohydrazide derivative, 3,4-dihydroxy-N'-(2-hydroxy-benzylidene)benzohydrazide (KM91104), did not affect RAW264.7 cell viability at concentrations up to 2.5 μM on the basis of total protein concentration and the MTS assay. When RAW264.7 cells where differentiated into osteoclasts using 100ng of RANKL for 5 days, TRAP activity and osteoclast numbers (TRAP positive cells with >3 nuclei) were unaffected by concentrations up to 20 μM and 1.2 μM KM91104 respectively. Nevertheless, 1.2 μM KM91104 reduced osteoclastic resorption on the Corning Osteo Assay surface by ~50%. To summarize, here we show that KM91104 effectively inhibits osteoclast mineral resorption at μM concentrations without significantly affecting RAW 264.7 cell viability or RANKL-mediated osteoclast differentiation or fusion. A therapeutic that reduces osteoclastic resorption without affecting osteoclastogenesis could preserve osteoclast-osteoblast signaling and would be ideal for combination therapy with an anabolic agent such as parathyroid hormone

***Disclosures: Gazelle Crasto**, None.*

MO0267

Krox20/EGR2 Deficiency Accelerates Osteoclast Growth and Differentiation and Decreases Bone Mass. Yankel Gabet*[1], Nathalie Leclerc[2], Sanjeev Baniwal[1], Yunfan Shi[2], Alice E. Kohn-Gabet[2], Jon Cogan[2], Alexis Dixon[2], Marilyn Bachar[3], Lixin Guo[1], Jack E. Turman[1], Baruch Frenkel[1]. [1]University of Southern California, USA, [2]Institute for Genetic Medicine, University of Southern California, USA, [3]Faculty of Dental Medicine, Hebrew University of Jerusalem, Israel

Krox20/EGR2, one of the four early growth response (EGR) genes, is a highly conserved transcription factor implicated in hindbrain development, peripheral nerve myelination, tumor suppression and monocyte/macrophage cell fate determination. Here, we determined a novel role for Krox20 in the monocytic lineage, which affects postnatal skeletal metabolism. Due to the perinatal lethality of *Krox20* null mice, we employed the viable heterozygous animals. Micro-CT analysis of 4- and 8-week old mice revealed a low bone mass (LBM) phenotype in both the distal femur and the vertebra of *Krox20*$^{+/-}$ mice. This was attributable to increased bone resorption as demonstrated *in vivo* by the higher number of TRAP+ lining osteoclasts and higher serum levels of CTX, a marker for bone resorption. We also found a significant increase in bone marrow CD115+/CD62L- cells, resident monocytes that give rise to osteoclasts. *Krox20* haploinsufficiency did not reduce bone formation *in vivo*, nor did it compromise osteoblast differentiation *in vitro*. In contrast, growth and differentiation were significantly stimulated in preosteoclast cultures derived from *Krox20*$^{+/-}$ splenocytes, suggesting that the LBM phenotype is attributable to *Krox20* haploinsufficiency in the monocytic lineage. Furthermore, silencing of Krox20 expression in preosteoclasts enhanced proliferation due to the cell-autonomous stimulation of cell cycle progression. Our data establish an anti-mitogenic role for Krox20 in preosteoclasts, which is the predominant mechanism underlying the LBM phenotype of *Krox20*-deficient mice. Maintenance or stimulation of Krox20 expression in preosteoclasts may present a viable therapeutic strategy for high-turnover osteoporosis.

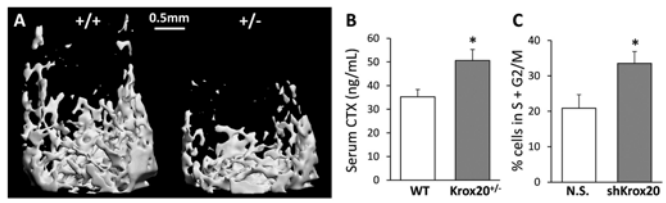

Figure 1. A, μCT images of representative distal femoral trabecular bone of *Krox20*$^{+/+}$ (*left*) and *Krox20*$^{+/-}$ (*right*) mice. B, Serum CTX levels in 8 WT and 4 *Krox20*$^{+/-}$ 6-week old mice indicate increased bone resorption. C, Accelerated cell cycle progression in preosteoclasts after Krox20 shRNA silencing (shKrox20). *, vs. control, $p<0.05$.

Figure 1

***Disclosures: Yankel Gabet**, None.*

MO0268

Egr2, a Zinc-finger Transcription Factor, Negatively Modulates Osteoclastogenesis by Up-regulation of Id2 helix-loop-helix Protein and Suppression of c-fos Expression. Jung Min Hong*[1], Tae-Ho Kim[1], Shin-Yoon Kim[2], Hyun-Ju Kim[1]. [1]Kyungpook National University School of Medicine, South korea, [2]Kyungpook National University Hospital, South korea

The Egr2/Krox-20 transcription factor regulates macrophage cell fate by up-regulating the expression of macrophage-specific genes. Osteoclasts are bone-resorbing polykaryons that are derived from monocyte/macrophage lineage cells. In this study, we show that Egr2 negatively regulates osteoclast differentiation. Overexpression of Egr2 in bone marrow-derived macrophages (BMMs) inhibits the formation of multinuclear osteoclasts and the expression of osteoclastogenic markers including nuclear factor of activated T cells c1 (NFATc1) during osteoclastogenesis, but it does not affect the gene expression of macrophage markers. Overexpression of Egr2 up-regulates the expression of the inhibitor of helix-loop-helix protein Id2, which acts as an important repressor in osteoclast differentiation, and induces Id2 promoter activity. Furthermore, Egr2-dependent induction of Id2 promoter activity is abrogated by overexpression of the Egr2 repressor, NGFI-A binding protein 2 (NAB2). In addition, overexpression of Egr2 inhibits RANKL-induced IkB? phosphorylation and the expression of a key osteoclastogenic transcription factor, c-fos. Taken together, our results reveal that Egr2 plays as a negative modulator of RANKL-mediated osteoclastogenesis.

***Disclosures: Jung Min Hong**, None.*

This study was supported by a grant of the Korea Healthcare technology R&D Project, Ministry for Health, Welfare & Family Affairs, Republic of Korea (Project No.: A010252)

MO0269

ITAM Adapter Signals and Generation of Reactive Oxygen Species During Osteoclastogenesis. Yalei Wu*[1], Julia Charles[1], Erene Niemi[1], Mary Nakamura[2]. [1]UCSF, USA, [2]University of California, San Francisco, USA

Bone is a dynamic organ, undergoing constant remodeling by osteoblasts that make new bone, and osteoclasts that degrade bone. The resorption of bone is the unique function of the osteoclast, a cell type derived from hematopoietic cells in the myeloid lineage. Osteoclast development requires receptor stimulation through RANK (receptor for activation of NFkappaB), and c-fms (receptor for macrophage colony stimulating factor, M-CSF). We and others demonstrated an additional requirement for costimulatory signals through ITAM (immunoreceptor tyrosine based activation motif) signaling receptors during normal osteoclast differentiation and function. Interestingly we also found that ITAM-adapter deficient mice lose bone under conditions of rapid bone remodeling induced by estrogen deficiency, a low calcium diet or LPS (lipopolysaccharide). Thus, other costimulatory signals and/or receptors can substitute for ITAM-adapter mediated signals in osteoclastogenesis under these pathologic conditions of bone remodeling. In osteoclastogenesis, ITAM-signaling receptors primarily provide a Ca2+ signal to activate the critical transcription factor for osteoclastogenesis, NFATc1 during RANKL stimulation. We are interested in determining what other signals are provided by ITAM-signaling receptors that are also critical for osteoclastogenesis to help us understand the requirements for costimulatory signals. In other cell types, ITAM signals also lead to production of reactive oxygen species (ROS). ROS have been previously demonstrated to be important regulators of osteoclast differentiation and function in vitro and in vivo. RANKL has been shown to stimulate ROS production during osteoclastogenesis. We observed that RANKL stimulated ROS production in preosteoclasts does not occur in the absence of ITAM adapters thus ITAM-adapters provide both a Ca2+ signal and a ROS signal to osteoclast precursors that together are required for osteoclastogenesis. We propose that without ITAM signaling in osteoclast precursors, osteoclasts can only be generated under stressful or inflammatory conditions where reactive oxygen species are prevalent. Our data suggests that osteoclasts differentiate under distinct stimuli under basal and inflammatory conditions, and may reveal subtypes of osteoclasts that can be differentially regulated.

***Disclosures: Yalei Wu**, None.*

MO0270

Osteopontin Increases Osteoclast Survival through an NFAT-Dependent Pathway. Natsuko Tanabe*, Hong H. Chen, Ryan P. Shugg, Stephen M. Sims, Harvey A. Goldberg, S. Jeffrey Dixon. The University of Western Ontario, Canada

Osteopontin (OPN) is a phosphorylated extracellular matrix glycoprotein that binds integrins. OPN enhances osteoclast activity; however, its mechanism of action has remained elusive. The transcription factor NFATc1 plays a critical role in osteoclast differentiation. Activation of NFATc1 involves its dephosphorylation by the calcium-dependent phosphatase calcineurin and subsequent translocation from the cytoplasm to the nuclei. The purpose of this study was to determine the effects of OPN on NFATc1 activation and survival of osteoclasts. Native OPN (nOPN, post-translationally modified) from rat long bones and rat recombinant OPN (rOPN, prokaryotically expressed without post-translational modifications) were purified to homogeneity using FPLC. Osteoclasts were isolated from the long bones of neonatal rabbits and rats, and plated on coverslips – uncoated or coated with nOPN, rOPN or bovine albumin. NFATc1 activation was assessed by immunofluorescence as the percentage of osteoclasts demonstrating nuclear localization of NFATc1. Osteoclast survival was quantified as the percentage of osteoclasts surviving following 18 h incubation. Nuclear localization of NFATc1 was significantly enhanced in osteoclasts plated on coverslips coated with nOPN or rOPN. Maximal activation of NFATc1 was observed 3 h after plating osteoclasts on rOPN. An RGD-containing, integrin-blocking peptide inhibited the translocation of NFATc1 induced by rOPN. Moreover, mutant rOPN lacking RGD failed to induce translocation of NFATc1. Thus, activation of NFATc1 is dependent on integrin binding. rOPN also enhanced osteoclast survival. The intracellular calcium chelator BAPTA inhibited both the translocation of NFATc1 and the increase in osteoclast survival induced by rOPN, implicating elevation of cytosolic calcium in the signaling pathway. A cell-permeable peptide inhibitor of NFAT activation (11R-VIVIT) suppressed the effects of rOPN on nuclear localization of NFATc1 and osteoclast survival. The effectiveness of both rOPN and nOPN indicates that post-translational modifications are not essential for activation of NFATc1; however, activation is dependent on integrin binding. This is the first demonstration that OPN activates NFATc1 and enhances osteoclast survival through a calcium- and NFAT-dependent pathway. Increased NFATc1 activity and enhanced osteoclast survival may account for the stimulatory effects of OPN on osteoclast function *in vivo*.

***Disclosures: Natsuko Tanabe**, None.*

MO0271

PLCγ2 SH2 Domain Targeting Leads to Blockade of Osteoclastogenesis in vitro and in vivo. Corinne Decker*[1], Kaihua Zhang[2], Roberta Faccio[3]. [1]Washington University in St. Louis, Department of Orthopaedic Surgery, USA, [2]Washington University, USA, [3]Washington University in St Louis School of Medicine, USA

We have previously reported that phospholipase C gamma-2 (PLCγ2) deficient mice are osteopetrotic due to defective osteoclast (OC) formation and are protected from inflammatory bone loss. These findings position PLCγ2 as a promising candidate for anti-resorptive therapies. In order to design an efficient strategy to block PLCγ2, we first performed a structure-function study to determine the critical domains of PLCγ2 involved in osteoclastogenesis. We found that PLCγ2 catalytic activity modulates OC differentiation by affecting NFATc1 induction. Surprisingly, PLCγ2 adapter function, conferred by the tandem N and C-terminal SH2 motifs, is also required to generate OCs. Specifically, we found that PLCγ2 adapter motifs recruit the docking protein GAB2 to the RANK/TRAF6 complex, leading to NF-KB, AP-1, and JNK activation. In order to direct the design of small molecules blocking endogenous PLCγ2 activity in WT OCs, we focused on the unique SH2 domains of PLCγ2, since the catalytic domain shares high homology to the more ubiquitously expressed PLCγ1. Therefore, we generated retroviral constructs harboring the N-SH2 or C-SH2 PLCγ2, alone or in combination (N+C-SH2). WT pre-OCs expressing either N-SH2 or C-SH2 PLCγ2 developed similar numbers of TRAP positive OCs as empty-vector pMX control (N-SH2:143 ± 10; C-SH2:140 ± 12; pMX:150 ± 10). In contrast, N+C-SH2-expressing pre-OCs failed to form mature OCs (3 ± 1) due to a block in RANK signaling, as evidenced by a loss of cFos, p65 and NFATc1 nuclear translocation and JNK phosphorylation. Mechanistically, N+C-SH2 disrupts PLCγ2-GAB2 association in pre-OCs stimulated with RANKL. Importantly, our in vitro findings are mirrored in vivo using an established model of osteoclastogenesis initiated by a single LPS injection on the calvaria of WT mice. Following LPS stimulation, 10^7 PFU of N+C-SH2-adenovirus or control LacZ-adenovirus were injected over the calvaria for five days. WT mice receiving N+C-SH2 developed half the number of TRAP-positive OC/μm bone surface compared to LacZ-injected controls (SH2: 3.4 ± .77, LacZ: 6.5 ± .13, p=.018). Collectively, these data indicate that inflammatory-mediated osteoclastogenesis can be abrogated by treatment with a small molecule composed of the tandem SH2 domains of PLCγ2. This novel method of specific PLCγ2 inhibition by small molecule blockade may hold clinical relevance for pathological bone loss therapies.

***Disclosures: Corinne Decker**, None.*

MO0272

RANKL Regulates the Non-canonical NF-kB Pathway in Osteoclasts by Promoting TRAF3 Degradation Through Lysosome. Yan Xiu*[1], Zhenqiang Yao[2], Lianping Xing[2], Brendan Boyce[1]. [1]University of Rochester Medical Center, USA, [2]University of Rochester, USA

RANKL activates the RelB/NF-κB2 non-canonical pathway by promoting NIK-mediated processing of the NF-κB2 precursor protein, p100, to p52. However, how RANKL controls NIK activity in osteoclasts (OCs) has not been investigated. TNF receptor-associated factor 3 (TRAF3) negatively controls NIK levels in B cells by facilitating NIK proteasomal degradation, but its role in OCs is not known. In this study, we asked two questions. 1) Does TRAF3 affect RANKL-induced OC formation? 2) Does RANKL control TRAF3 levels in OCs and through what mechanism? To address the 1st question, we generated a retroviral expression vector for TRAF3, infected WT OCPs with TRAF3 retrovirus, and cultured them with

RANKL to form OCs. TRAF3 over-expression significantly reduced the number and size of RANKL-induced OCs (OC#/well: 159±14 vs 342±7; Area (mm2)/OC: 0.030±0.002 vs 0.080±0.003 with GFP retrovirus). To study the 2nd question, we treated WT OCPs with RANKL for various times and examined TRAF3 protein levels by Western blot. RANKL markedly reduced TRAF3 protein levels (>50% vs PBS-treated controls) as early as 1 hr after treatment but had no effect on TRAF3 mRNA expression, suggesting that RANKL promotes TRAF3 degradation. We found that, as reported in B cells, TRAF3 binds to NIK in OCPs using immunoprecipitation assays. So to test if RANKL-induced TRAF3 degradation is proteasome-mediated, we treated cells with the proteasome inhibitor MG132 in the presence of RANKL. MG132 did not prevent TRAF3 degradation. To determine if the lysosome, another cell organelle that destroys proteins and large molecules mediates degradation of TRAF3 by RANKL, we treated OCPs with the lysosome inhibitor NH4Cl and found that it prevented RANKL-induced TRAF3 protein degradation, an effect that was confirmed using another lysosome inhibitor, Chloroquine. Our findings show that TRAF3 negatively regulates RANKL-induced OC formation and fusion, and that RANKL promotes lysosome-mediated TRAF3 degradation. They link TRAF3-NIK together as signaling proteins downstream from RANKL/RANK interaction, providing a molecular explanation for RANKL-induced activation of the non-canonical pathway in OCPs: RANKL increases NIK levels in OCPs to mediate their differentiation by reducing NIK degradation through stimulation of lysosomal breakdown of TRAF3. Stabilization of TRAF3 levels in OCPs should present a new strategy to inhibit osteoclast formation.

***Disclosures: Yan Xiu**, None.*

MO0273

Effect of Variable Oscillatory Fluid Flow Conditions on Osteocyte Activity. Emily Rose[1], Lidan You[2], Jason Li*[1]. [1]University of Toronto, Canada, [2]Mechanical & Industrial Engineering, University of Toronto, Canada

Proper bone health and metabolism relies on the delicate balance between osteoclastic bone resorption and osteoblastic bone formation. Bone atrophies during disuse and adapts to physiological loading. This indicates that tissue deformation and subsequent dynamic flow of interstitial fluid in the lacuno-canalicular network is required for maintaining bone homeostasis and remodelling. Osteocytes are believed to sense and respond to dynamic fluid flow-induced shear stress by releasing cytokines that regulate osteoblast and osteoclast activity.

This study aims to elucidate how osteocytes respond to different modes of shear stress in vitro by subjecting MLO-Y4 osteocyte-like cells (gift from Dr. Lynda Bonewald, University of Missouri-Kansas City) to oscillatory fluid flow stimulus of different shear magnitudes (0.5-5 Pa), frequencies (0.5-2 Hz), and durations (1-4 hrs). These parameters are selected to mirror the in vivo flow regime during normal loading conditions and thus encompass the predicted physiological range of each respective variable.

Specifically, we examine the mRNA expression levels of receptor activator of nuclear factor kappa B ligand (RANKL), osteoprotegerin (OPG), and cyclooxygenase-2 (COX-2). RANKL binds to the RANK receptor on osteoclast precursor membranes leading to osteoclast differentiation while OPG inhibits osteoclastogenesis by blocking the receptor site. The ratio RANKL/OPG is therefore an important indicator of bone resorption. COX-2 has been identified as a necessary enzyme for promoting bone formation by indirectly stimulating osteoblast proliferation through prostaglandin-E2 production.

Findings from this study suggest that increasing the applied shear stress magnitude results in significantly elevated COX-2 expression (Fig. 1A) as well as decreasing RANKL/OPG expression (Fig. 1B), suggesting that larger loading favors bone formation. Additionally, COX-2 expression levels were found to peak at a frequency of 1Hz (Fig. 1C) while RANKL/OPG expression also decreased at this frequency (Fig. 1D). This indicates that this loading frequency around 1Hz may be optimal for bone formation. Finally, COX-2 levels increased with exposure time (Fig. 1E) while the RANKL/OPG ratio remained unaffected (Fig. 1F), suggesting that longer flow times favor osteogenesis. These findings will aid in our understanding of bone metabolism and may yield an optimized exercise protocol for better bone health, disease treatment and prevention.

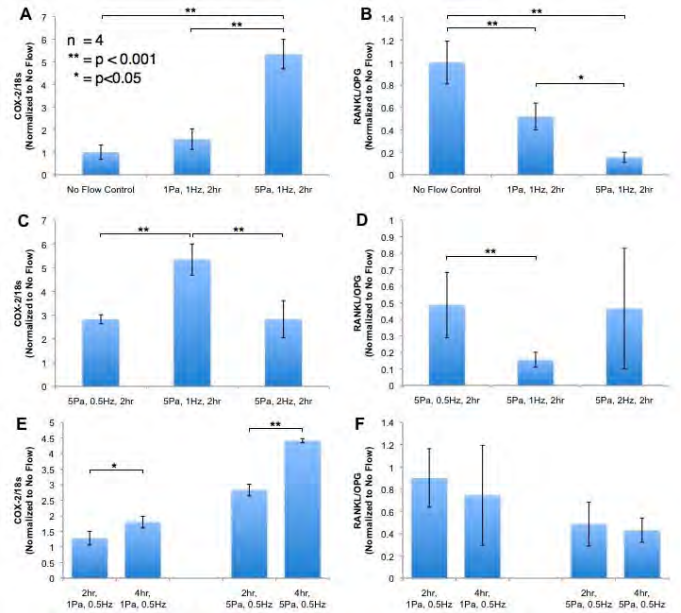

Figure 1: RANKL/OPG & COX-2 mRNA expression of MLO-Y4 cells subjected to different flow conditions.

***Disclosures: Jason Li**, None.*

MO0274

Effects of Cyclic Hydraulic Pressure on Osteocytes. Yan Zhao[1], Chao Liu*[1], Wing-Yee Cheung[1], Ronak Gandhi[1], Liyun Wang[2], Lidan You[3]. [1]University of Toronto, Canada, [2]University of Delaware, USA, [3]Mechanical & Industrial Engineering, University of Toronto, Canada

Background: Bone is able to adapt its composition in order to suit its mechanical environment. Osteocytes, the bone cells embedded in the calcified matrix, are believed to be the mechanosensors and responsible for orchestrating the bone remodeling process. Recent in vitro studies have shown that osteocytes are able to sense and respond to substrate strain and fluid shear [1, 2]. However the capacity of osteocytes to sense cyclic hydraulic pressure (CHP) induced by physiological mechanical loading is not well understood. The objective of this study is to investigate the effect of CHP on osteocytes. We hypothesize that osteocytes are able to sense CHP, and respond by changes in the level of intracellular calcium concentration ([Ca2+]i)., gene expression of regulators of bone remodeling, and apoptosis.

Methods: We subjected osteocyte-like MLO-Y4 cells to CHP of 68 kPa at 0.5 Hz, and measured intracellular calcium concentration ([Ca2+]i) using Fura-2 AM dye, mRNA expression of genes related to bone remodeling (COX2, RANKL, OPG) using reverse transcription and RT-PCR, and osteocyte apoptosis was induced by serum starvation, then measured using Apopercentage. Student t-tests were used to determine significance ($p < 0.05$).

Results: As tested in the present study with a cyclic pressure at 68 kPa level, 21% of the MLO-Y4 cells responded to the simulation by increasing the [Ca2+]i 40 s after the onset of loading, compared with only 4.2% in the non-loaded group (Fig. 1). In terms of apoptosis, 1 additional hour of incubation after CHP was needed to observe sufficient apoptosis attenuation in the loaded samples (Fig. 2). The COX-2 mRNA level increased after 1 hour of loading and the RANKL/OPG ratio increased significantly after 2 hours (but not 1 hour) of loading (Fig 3).

Conclusions: This study is the first to show that osteocytes were able to sense CHP and respond by increased intracellular calcium concentration, altered microtubule organization, a time-dependent increase in COX-2 mRNA level and RANKL/OPG mRNA ratio, and decreased apoptosis. Load-induced cyclic hydraulic pressure in bone may serves as a mechanical stimulus to osteocytes and may play a role in regulating bone remodeling in vivo. These results could lead to improved pharmaceutical agents and exercise regimens for bone diseases such as osteoporosis, and enhancement of bone health.

References: [1] Rubin, J., J. Cell. Physiol. 170 (1), 81 (1997) [2] Qin, Y.X. et al., J Biomech 36 (10), 1427-1437 (2003)

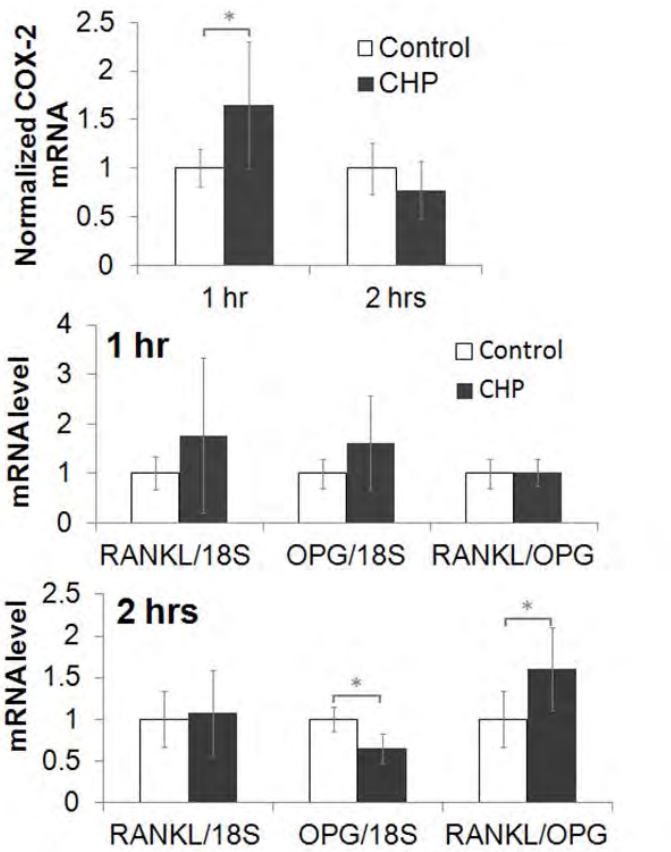

Fig. 3. Relative mRNA levels of COX-2, OPG, RANKL and RANKL/OPG ratio (n = 12).

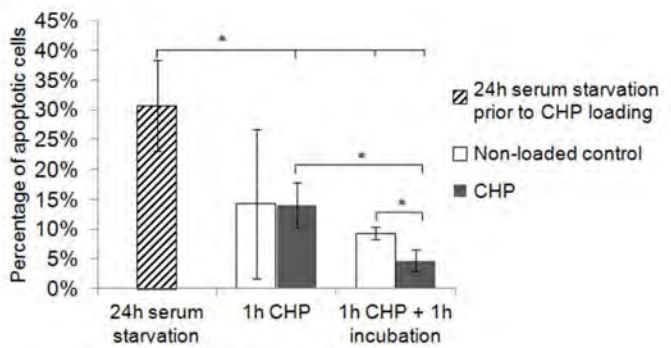

Fig. 2. Apoptotic cells after 24 hrs of serum starvation, 1 hr of CHP (n = 8) plus 1 hr incubation.

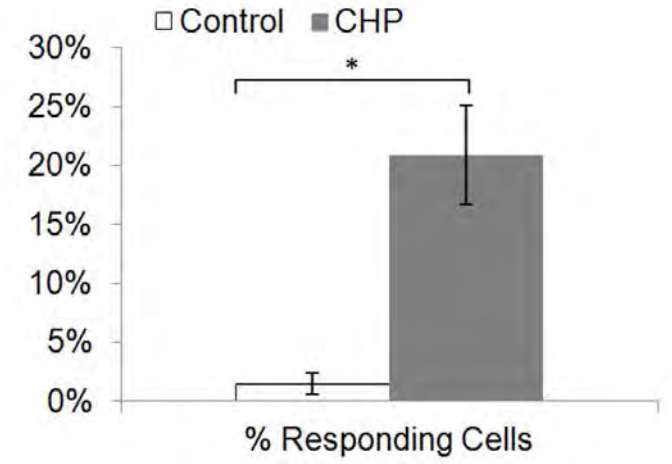

Fig 1. Effect of CHP on intracellular [Ca2+] in MLO-Y4 cells (n = 5).

***Disclosures: Chao Liu**, None.*

MO0275

Mechanical Loading Affects IL-6 Expression in Osteocytes: Is IL-6 a Novel Factor Regulating Bone Homeostasis? Astrid Bakker*[1], Jolanda M.A. de Blieck-Hogervorst[2], Rishikesh N. Kulkarni[3], Willem Lems[4], Jenneke Klein-Nulend[5]. [1]Academic Centre for Dentistry Amsterdam, UvA & VU, Research Institure MOVE, The netherlands, [2]ACTA-University of Amsterdam & VU University Amsterdam, Dept Oral Cell Biology, Research Institute MOVE, Netherlands, [3]ACTA-University of Amsterdam & VU University Amsterdam, Dept Oral Cell Biology, Research Intitute MOVE, Netherlands, [4]Vrije Universiteit Medical Centre, The netherlands, [5]ACTA-VU University Amsterdam, The netherlands

Mechanical adaptation of bone is brought about by the actions of osteoclasts and osteoblasts, their activity being coordinated by signaling molecules that are produced by mechanically stimulated osteocytes. Interleukin 6 (IL-6) may act as such a signalling molecule since high amounts of IL-6 are produced by mechanically active muscle cells, and IL-6 enhances osteoclastogenesis during inflammation. We investigated whether mechanical loading stimulates IL-6 expression in osteocytes, and whether IL-6 modulates osteocyte-induced osteoclastogenesis.

MLO-Y4 osteocytes were incubated for 24 h in αMEM containing IL-6 (0, 1 or 10 pg/ml), and subjected to 60 min of static culture or mechanical loading by pulsating fluid flow (PFF; 0.7 ± 0.3 Pa at 5 Hz) in the presence of IL-6 (0, 1 or 10 pg/ml). Expression of mRNA for IL-6, RANKL, OPG and M-CSF were analyzed by taqman PCR. Nitric oxide (NO) production was quantified using Griess reagent. The effect of IL-6 on actin was quantified by extraction of phalloidin-stained F-actin and apoptosis was quantified as caspase 3/7 activity. In some experiments $1x10^6$ mouse bone marrow cells were cultured for 7 days on top of IL-6 treated osteocytes. Tartrate-resistant acid phosphatase positive multinucleated cells were counted to determine osteoclast formation.

PFF increased IL-6 mRNA expression by 11.7-fold. IL-6 at 1 and 10 pg/ml inhibited PFF-stimulated NO production at 5 min, but not at 60 min. This effect of IL-6 on the NO-response to PFF was probably not caused by alterations in the actin cytoskeleton, as IL-6 did not affect F-actin content in osteocytes. Cultured osteocytes supported osteoclastogenesis, which was unaltered by the addition of IL-6 at 1 and 10 pg/ml. This is not surprising, as treatment with IL-6 did not significantly affect caspase 3/7 activity in osteocytes, nor did IL-6 affect OPG, RANKL or M-CSF expression by osteocytes.

In summary, osteocytes express high levels of IL-6, and loading boosted this expression even further. IL-6 alone did not affect osteocyte-stimulated osteoclastogenesis at a concentration present in serum of healthy humans during rest (1 pg/ml) or after exercise (10 pg/ml), or in humans with rheumatoid arthritis (10 pg/ml). However IL-6 may reduce the effect of PFF on osteocyte-stimulated osteoclastogenesis, since IL-6 reduced the NO response to PFF. In conclusion, IL-6 is a novel factor that may play a role in the regulation of bone homeostasis by mechanically stimulated osteocytes.

***Disclosures: Astrid Bakker**, None.*

MO0276

Mechanism of Action of Sclerostin: Sclerostin Interacts with the Carboxyl Terminal Region of ErbB3. Rajiv Kumar[1], THEODORE CRAIG*[2]. [1]Mayo Clinic College of Medicine, USA, [2]Mayo Clinic, USA

Sclerostin, an osteocyte-derived, cystine-knot protein, interacts with bone morphogenic proteins (BMPs), LRP 5/6 and cysteine-rich protein 61 (Cyr61) to influence osteoblast, fibroblast, and vascular endothelial cell function. Structural studies of sclerostin reveal a well-structured cystine-knot region and relatively unstructured amino-terminal and carboxyl-terminal domains within sclerostin that might potentially interact with proteins. To identify other novel binding partners of sclerostin, we performed yeast two-hybrid experiments using a Normalized Universal Human Mate & Plate Library and the Matchmaker Gold System (Clontech, Mountainview, CA). Human SOST cDNA was amplified by PCR methods with appropriate primers. The PCR construct was cloned in-frame with the GAL4 DNA-BD of the pGBKT7 DNA-BD vector using EcoRI and BamHI restriction sites within the multiple cloning site. The SOST pGBKT7 plasmid was used to transform Y2H Gold yeast cells. Appropriate positive and negative control mating, auto-activation and toxicity experiments were performed. 1 mL of the Mate and Plate Library was combined with 5 mL of the bait strain and 45 mL of 2X YPDA medium (50 ?g/mL kanamycin). Cells were incubated for 24 h at 30℃ with shaking. Following the manufacturer's instructions, positive colonies were identified and re-analyzed by streaking onto quadruple dropout (SD/-Leu/-Trp/-His/-Ade) plates containing X-?Gal/Aureobasidin A. Aliquots of blue colonies that had been serially selected were used for PCR with flanking primers specific for the pGAD-T7-RecAB plasmid, to generate insert DNA for sequencing. Plasmids were rescued from yeast and were used to transform E. coli grown on ampicillin-containing plates to isolate the "prey" plasmid. Protein interactions were confirmed in transformed yeast cells using HA, c-myc or sclerostin antibodies for immuno-precipitation (IP) and/or detection.

Results: Several positive clones were identified that expressed proteins interacting with sclerostin. DNA sequencing revealed that one of the positive clones expressed the intracellular domain of the erbB3 receptor. IP experiments confirmed the interaction of sclerostin with erbB3 receptor.

Conclusions: Our experiments suggest that sclerostin might influence EGF function by interacting with the intracellular domain of the erbB3 receptor. The mechanism of action of sclerostin involves interactions with the BMPs, LRP 5/6, cyr61 and the erbB3 receptor.

***Disclosures: THEODORE CRAIG**, None.*

MO0277

Osteoprotegerin Prevents Glucocorticoid-induced Osteocyte Apoptosis, Decreased Bone Interstitial Fluid, and Reduced Strength in Mice. Robert Weinstein*, Charles O'Brien, Haibo Zhao, Paula K Roberson, Stavros Manolagas. University of Arkansas for Medical Sciences, USA

Glucocorticoid excess decreases bone strength by direct effects on osteoblasts or osteocytes, but it remains unknown which of the two is the primary target of this deleterious action, and whether osteoclasts participate. To dissect the contribution of osteocytes, we administered recombinant osteoprotegerin (OPG-Fc), 10 ug/g subcutaneously three times a week, as a means of decreasing the number of both osteoblasts and osteoclasts, alone or in combination with prednisolone pellets, 2.1 mg/kg/d, to 6-month-old C57BL/6 mice for 28 days. As expected, both prednisolone and OPG-Fc administration decreased osteocalcin mRNA levels in whole vertebrae. However, expression of the osteoclast-specific transcripts cathepsin-K and calcitonin receptor was unaffected by prednisolone alone but dramatically decreased with the administration of OPG-Fc. The suppressive effect of prednisolone on spinal bone mineral density (BMD), vertebral cortical thickness (micro-CT), and vertebral compression strength was prevented by OPG-Fc. Prednisolone decreased osteoid area and perimeter, osteoblast number, and bone formation rate by 33 to 50%, but osteoclast number was not significantly different from placebo as predicted by the maintenance of cathepsin-K and calcitonin receptor expression in the mice receiving prednisolone alone. OPG-Fc, with or without prednisolone, profoundly reduced the number of osteoclasts and osteoblasts, and the rate of bone formation. More strikingly, OPG-Fc prevented the prednisolone-induced increase in the prevalence of osteocyte apoptosis and reduction in solute transport from the systemic circulation to the osteocyte-lacunar-canalicular network, as determined by procion red fluorescence in the bone interstitial fluid. The procion fluorescence in the osteocyte-lacunar-canalicular system was inversely related to the prevalence of osteocyte apoptosis and directly related to BMD. Consistent with the *in vivo* findings, OPG-Fc abrogated dexamethasone-induced apoptosis of MLO-Y4 osteocytic cells. In addition to antagonizing RANKL, OPG binds to the TNF-related, apoptosis-inducing ligand (TRAIL). Based on this evidence and the results of the present report, we suggest that OPG-Fc prevented the glucocorticoid-induced decrease in bone strength not only by its anti-resorptive actions but also by directly antagonizing TRAIL-mediated osteocyte apoptosis.

***Disclosures: Robert Weinstein**, None.*
This study received funding from: Amgen

MO0278

Decrease in the Osteocyte Lacunae Density Accompanied by Hypermineralized Lacunar Occlusion Reveal Failure and Delay of Remodeling in Aged Human Bone. Bjoern Busse*[1], Danijela Djonic[2], Petar Milovanovic[2], Michael Hahn[1], Klaus Püschel[1], Robert Ritchie[3], Marija Djuric[2], Michael Amling[1]. [1]University Medical Center Hamburg-Eppendorf, Germany, [2]University of Belgrade, Serbia, [3]University of California, USA

Aging decreases the human femora's ability to withstand maximum weight, pressure, and strength. Changes in the osteocyte distribution as well as their elemental composition might be involved in the age-related impairment of bone tissue. To address this question, we carried out a histomorphometric assessment of the osteocyte distribution in the periosteal and endosteal human femoral cortexes of 16 female and 16 male donors with a focus on age- and gender-related bone remodeling. Measurements of the bone mineral density distribution (BMDD) by quantitative electron backscattered imaging (qBEI) and energy dispersive x-ray analysis (EDX) were carried out to evaluate the osteocyte's capability to engage the mechanisms of mineralization. Age-dependent decreases in the total osteocyte lacunae per bone area (Tt.L.N/B.Ar) were measured in all of the investigated cases that favored dysfunction of the bone's safety. Subdivision of the bone into periosteal and endosteal regions of interest emphasized that, in the female and male cases, primarily the endosteal cortex ($y_{(endo,female)}$ = Intercept: 355.0, Slope: -1.74, r = -0.835, $p < 0.001$ and $y_{(endo,male)}$ = Intercept: 346.3, Slope: -1.93, r= -0.837, $p < 0.001$) is affected by age-dependent losses in osteocyte lacunae, whereas the periosteal compartment showed a less pronounced osteocyte lacunae deficiency ($y_{(peri,female)}$ = Intercept: 380.1, Slope: -1.74, r = -0.785, $p < 0.001$ and $y_{(peri,male)}$ = Intercept: 462.8, Slope: -2.64, r = -0.944, $p < 0.001$). Predominantly in aged bone tissue (> 80 years), osteocyte lacunae showed an increased amount of hypermineralized calcium phosphate occlusions (Mn.L.N./B.Ar.) in comparison to younger cases (< 39 years) ($Mn.L.N./B.Ar._{endo}$: 33.04 ± 16.73 vs. 3.6 ± 1.62, $p < 0.001$ and $Mn.L.N./B.Ar._{peri}$: 19.25 ± 2.28 vs. 3.58 ± 1.89, $p < 0.001$). With respect to Frost's early delineation of micropetrosis, the recent microanalyses, however, reveal that altered osteocytes are subject to hypermineralization. Intra-lacunar hypermineralization accompanied by a decrease in the total osteocyte lacunar density can account for a failure or long delay in the bone repair process in aging femoral bone. Decreased osteocyte density may cause deteriorations in canalicular fluid flow and reduce detection of microdamage, which counteracts the bone's structural integrity, where hypermineralized osteocyte lacunae may increase bone brittleness that renders bones fragile.

***Disclosures: Bjoern Busse**, None.*

MO0279

Increased Density of Hypermineralized Osteocyte Lacunae and Microdamage Accumulation in Fragility Hip Fracture Patients. Julia Kuliwaba*, Vincent Carpentier, Helen Tsangari, Shruti Shah, Peter Sutton-Smith, Ian Parkinson, Arash Badiei, Nick Fazzalari. SA Pathology, Australia

The phenomenon of hypermineralization of osteocyte lacunae (micropetrosis; Frost 1960 JBJSA 42-A:144-50), has received little attention in the literature. While hypermineralized lacunae are a known feature of the aging human skeleton, no data are available for fragility fracture. Therefore, the purpose of this study was to determine the extent of hypermineralized osteocyte lacunae in relation to bone architecture, mineralization and accumulated microdamage for fragility hip fracture patients compared to non-fracture controls. Intertrochanteric bone cores were obtained from patients at surgery for non-traumatic femoral neck fracture (FNF: 10F, 4M, 65-94y) and from cadaveric controls (C: 5F, 13M, 60-84y). All bone samples were resin-embedded for quantitative backscattered electron imaging (qBEI) of the degree of mineralization. Using a custom image-processing algorithm for qBEI images, hypermineralized and total lacunar densities were quantified. A subset of 8 FNF (4F, 4M, 65-94y) and 12 C (4F, 8M, 64-84y) cases were initially micro-CT imaged for 3D measures of trabecular architecture, and en bloc-stained in basic fuchsin before resin-embedding for histomorphometric assessment of microdamage and eroded surface (resorption). Bone tissue mineralization (wt%Ca) was not different between FNF and C (24.46 vs 24.77%). Mean values for lacunar and total lacunar density were similar between FNF and C. Strikingly, hypermineralized lacunar density (HL.Dn[#/mm^2]: 28.9[23.7-42.0] vs 10.2[4.8-32.5], $p<0.02$; median[quartiles]) and percent hypermineralized lacunae (HL/TL[%]: 9.5[8.0-15.6] vs 5.2[1.7-13.7], $p<0.04$) were significantly higher in FNF compared to C. For the subset of cases examined, FNF was associated with trabecular architectural insufficiency. Specifically, BV/TV ($p<0.02$), Tb.N ($p<0.01$), DA ($p<0.04$) were reduced and Tb.Sp ($p<0.02$) was increased in FNF. Microcrack density (Cr.Dn, $p<0.002$) and diffuse microdamage (DxV/BV, $p<0.02$) were increased in FNF, coupled to elevated bone resorption (ES/BS, $p<0.01$; Rs.Dn, $p<0.0001$). In conclusion, these study data suggest that in addition to architectural decay, fragility hip fracture is associated with an increased density of hypermineralized lacunae and an accumulated microdamage burden. Unlike empty osteocyte lacunae, hypermineralized lacunae do not permit extracellular fluid circulation, and therefore their presence may contribute to microdamage accumulation by inhibiting damage detection and signalling for repair.

***Disclosures: Julia Kuliwaba**, None.*

MO0280

Transcription of Collagens I and XI, Phex, Dmp1, and Fibronectin by Osteoblastic/Osteocytic Cells is Co-ordinately Regulated. Jeffrey Gorski*[1], Nichole Huffman[2], Sridar Chittur[3], Ronald Midura[4], Dina Black[2], Julia Oxford[5], Nabil G. Seidah[6]. [1]University of Missouri, Kansas City, School of Dentistry, USA, [2]Sch. Dentistry, Univ. of Missouri-Kansas City, USA, [3]Center for Functional Genomics, Univ. of Albany, USA, [4]Lerner Research Institute of Cleveland Clinic, USA, [5]Boise State University, USA, [6]Laboratory of Biochemical Neuroendocrinology, IRCM, Canada

Mineralization, a characteristic property of differentiated osteoblastic/osteocytic cells, can be blocked completely by either the covalent serine protease inhibitor AEBSF or by the peptide decanoyl-RRLL-chloromethyl ketone. Since both inhibitors inactivate the proprotein convertase SKI-1, a Golgi protease required for the activation of SREBP and CREB/ATF family transcription factors, in a whole genome array study we examined the effect of these inhibitors on gene expression in the cell line UMR106-01. Short term (12h) treatment of serum-fed cultures with a minimum concentration of AEBSF sufficient to block mineralization, decreased expression of 85 genes by 1.5-3.0-fold including *Phex, Dmp1, COL1A1, COL1A2, tenascin-N, tenascin-C, COL11A1,* and *fibronectin*. Additional comparisons of the effect of AEBSF or dec-RRLL-cmk on the expression of a subset of these genes in serum depleted UMR106-01 cells revealed two outcomes. First, *Phex, Dmp1, COL11A1,* and *fibronectin* were significantly reduced by both inhibitors while *COL1A2* and *HMGCS1* were each only inhibited by AEBSF. Second, AEBSF and dec-RRLL-cmk also reduced the nuclear content of SKI-1 activated forms of the transcription factors SREBP-2 and OASIS, while at the same time increasing the nuclear content of caspase-3 activated SREBP-1 and OASIS forms. Importantly, activation and turnover of the cytosolic caspase-3 was differentially modified depending upon the covalent inhibitor used, e.g., AEBSF, dec-RRLL-cmk, or Z-DVED-fluoromethyl ketone. In addition, the caspase-3 inhibitor Z-DVED-fmk increased the nuclear contents of SREBP-1 and CREB-H, which are subject to ubiquitination. Our findings suggest that caspase-3 inhibition can independently block proteasomal degradation of SREBP-1 and CREB-H, and, cause a transient increase in their nuclear content. Finally, over-expression of the SKI-1-activated forms of SREBP-1a and of CREB-H in UMR106-01 cells increased the number of mineralized foci or altered their local distribution, respectively. Taken together, these results suggest that SKI-1 and caspase-3 together regulate the activation of a small group of transmembrane transcription factor precursors required for expression of key genes (*Phex, Dmp1, COL11A1,* and *fibronectin*) needed for mineralization of UMR106-01 cultures in vitro and bone formation in vivo. Our results indicate that the differentiated phenotype of osteoblastic/osteocytic cells is regulated by SKI-1 and the non-apoptotic activity of caspase-3.

***Disclosures: Jeffrey Gorski**, None.*

MO0281

Characterization of Osteocyte Lacunae in Adult Human Bone by 3D X-ray Microscopy. Mohammed Akhter*[1], Susan Candell[2], Robert Recker[1], Tiffany Fong[3], Jack Coats[4], Donald Kimmel[5]. [1]Creighton University Osteoporosis Research Center, USA, [2]Xradia, Inc, USA, [3]Xradia, Inc., USA, [4]Xradia, USA, [5]Kimmel Consulting Services, USA

Osteocytes (Ocy) may alter their lacunar density and volume in response to pharmacologic and mechanical stimuli. Ocy lacunar (Ocy.La) properties are poorly understood. A method that reproducibly identifies large numbers of whole Ocy.La from different regions of bone tissue is ideal. Current imaging technology has difficulty resolving structures the size of Ocy.La in intact bone specimens. The purpose of this project is to quantify Ocy.La properties in various bone microarchitectural regions in adult human bone.

A transilial biopsy from a healthy post-menopausal woman was embedded undecalcified in methyl methacrylate. Sections were prepared for standard histomorphometric evaluation. The portion of the plastic-embedded specimen left after sectioning was trimmed to 2mm X 2mm X 8mm and scanned at 125μm^3 voxel resolution (VR) (5µm pixel resolution [PR]) with a 3D Xray microscope (MicroXCT-200). Images were reconstructed in which nodes, struts, and the cortex could be clearly identified in both 2D slices and 3D images. Subregions (1mm diameter X 0.5mm long) containing trabecular nodes and struts and the cortex were re-scanned at 0.125μm^3 VR (0.5µm PR). Subregions were analyzed by segmentation software (Ratoc System Engineering Co., Ltd.; Tokyo, JP) for individual Ocy.La volume (iOcy.LaV), Ocy.La density (Ocy.LaD), and total Ocy.La volume/bone volume (ΣOcy.LaV/BV). Ocy.La were defined as voids in mineralized bone tissue with volume >25 and <500μm^3.

3D bone tissue volumes of nodes, struts, and the cortex were identified separately and analyzed three times on three separate days. Ocy.La were distributed non-uniformly (Figure) and contained 1850$\pm$981voxels. Means are presented (Table). The coefficients of variation for the three iOcy.LaV, Ocy.LaD, and Ocy.LaV/BV analyses were 3%, 5%, and 6%, respectively. While iOcy.LaV varied little (~9%) among the regions, Ocy.LaD was 45% higher in nodes, and 17% higher in struts, than in the cortex. Void volume due to Ocy.La is 63% higher in trabecular nodes than in cortical bone.

These data, that appear very reproducible, compare favorably to previous measurements of Ocy.La attributes taken by 2D methods. The data suggest that though Ocy.LaV is constant among bone regions that seem likely to experience different mechanical stresses, there are more Ocy.La in nodes, making node void volume higher than in cortical bone. Additional regions are under study in this and other specimens from both pre- and post-menopausal women.

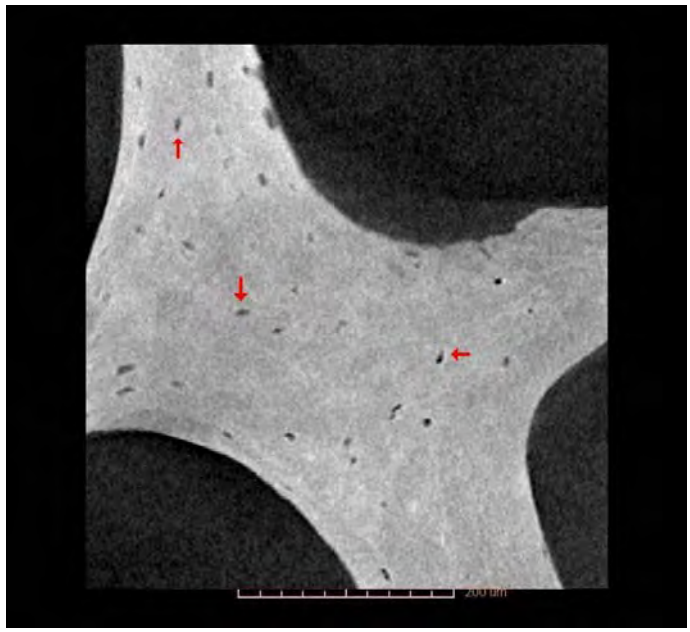

0.5çm pixel resolution slice from trabecular node. Note uneven distribution of Ocy.La (arrows).

Variable	Units	Trab Node	Trab Strut	Cortex
Volume (BV)	mm^3	0.0160	0.0067	0.0026
Ocy.La#	#	514	174	59
Ocy.LaD	mm^3	32272	26062	22232
iOcy.LaV	μm^3 (mean±SD)	237±125	216±111	227±124
ΣOcy.LaV/BV	%	0.75	0.56	0.46
Ocy.La#-# of Ocy analyzed; Trab-trabecular				

Osteocyte lacunar properties in trabecular node and strut, and cortical regions of adult human bone

***Disclosures: Mohammed Akhter**, Xradia, 5*
This study received funding from: Xradia, Inc.

MO0282

Structural Basis of Osteocytic Osteolysis during Lactation in Mouse Fibula. Koichi Matsuo*[1], Yoshihiro Takeda[1], Yasunari Takada[1], Takashi Nakamura[1], Makoto Suematsu[1], Wataru Yashiro[2], Nobuhito Nango[3], Atsushi Momose[2]. [1]School of Medicine, Keio University, Japan, [2]The University of Tokyo, Japan, [3]Ratoc System Engineering Co., Ltd., Japan

During lactation, the maternal bone surface is massively resorbed by osteoclasts in order to transfer significant amounts of calcium to infants. Although osteoclasts are the only professional bone resorbing cells, the possibility of osteocytic osteolysis has been suggested for decades, and recent evidence suggests that osteocytes indeed participate in bone resorption. The purpose of this study is to investigate whether osteocytes resorb bone matrix surrounding the lacuna in which they reside, and if so, to to determine their identity. We analyzed the organization and volume of osteocyte lacunae in mouse fibulae by three-dimensional imaging with an X-ray phase-contrast microscope using synchrotron radiation.

We found that mouse fibula harbors cylindrical bone layers surrounding the central bone marrow cavity and resembles a single osteon or Haversian system in larger mammals. Each osteocyte lacuna was boat-shaped and was aligned largely parallel to the long axis of the fibula. The "keels" of osteocyte lacunae faced either toward the bone marrow in the central osteon-like structure or away from it in the peripheral bone matrix. These two distinguishable organizations of osteocyte lacunae may reflect inward endochondral and outward intramembranous ossification during development, giving rise to the central osteon-like structure and the peripheral bone matrix, respectively. Importantly, in lactating mice, the volume of osteocyte lacunae was increased around blood vessels and near the boundary between the central osteon-like structure and the peripheral bone matrix, indicating active resorption. This study provides the first evidence for osteocytic osteolysis using three-dimensional measurement. These and other biochemical data reveal a structural basis for position-dependent responses of fibular osteocytes to metabolic changes during lactation.

***Disclosures: Koichi Matsuo**, None.*

MO0283

Antibody Array Technology Identifies Differentially Expressed Proteins in Postmenopausal Women with Osteopenia and Osteoporosis. Laura Corrigan*[1], Kellie Adamson[1], Joseph Browne[2], Kara Fitzgerald[3], Guan Choon Chan[4], Siobhain Kennelly[5], Joseph Marry[5], Mary Nash[5], Daniel Ryan[5], Davinia Ryan[5], Neasa Fallon[5], Georgina Steen[5], Miriam Casey[5], James Walsh[6], Thomas Clive Lee[1], Jacqueline Daly[1]. [1]Royal College of Surgeons in Ireland, Ireland, [2]St James's Hospital, Ireland, [3]St. James' Hospital, Ireland, [4]Bone Health & Osteoporosis Unit, St James's Hospital, Ireland, [5]St James' Hospital, Ireland, [6]Trinity College Dublin, The University of Dublin, Ireland

Antibody arrays provide a platform to simultaneously study the expression of a large number of proteins in individuals with a given condition compared to healthy controls. The RayBio Biotin Label-based Antibody Array was used to identify differentially expressed protein in serum taken from postmenopausal women with osteopenia and osteoporosis. The array assays 507 proteins qualitatively including cytokines, chemokines and growth factors. Serum was taken from otherwise healthy postmenopausal women with osteopenia n=33, osteoporosis n=32 and a control group n=36. An equal volume of each sample was pooled into three groups and applied to the array. All participants were Caucasian Irish nationals, subject to DXA, LVA, biochemical tests for markers of bone turnover, had no history of other bone metabolic disorders and were not prescribed any medication altering bone metabolism. A ratio threshold of 1.5 and 0.5 was applied for a protein to be considered up and down-regulated respectively. A p value threshold of <0.05 was also applied. DAVID analysis of Gene Ontology (GO) was carried out on the top 5% up-regulated and down-regulated proteins across the 3 groups. Proteins were classified into functional groups based on their involvement in biological processes as provided by the GO framework. Large numbers of proteins were up and down regulated among the 507 proteins assayed. In the Osteopenia group compared with Normal 12 proteins were down-regulated and 167 proteins up-regulated. In the Osteoporosis group compared with Normal 154 proteins were down-regulated and 6 up-regulated. In the Osteopenia group compared with Osteoporosis 164 proteins were down-regulated and no proteins were up-regulated. GO analysis revealed that the largest proportion of differentially expressed proteins identified are involved in signal transduction (n=15). Other differentially expressed proteins are involved in ligand-mediated signaling (9), cell surface receptor-mediated signal transduction (13), cytokine and chemokine mediated signaling pathway (7), cell communication (10). The RayBio Biotin Label-based Antibody Array identified a large number of differentially expressed proteins in the serum of postmenopausal women with osteopenia and osteoporosis. This study provides an insight into the molecular changes in the serum of postmenopausal women with osteopenia and osteoporosis thus providing new opportunities to assess the disease at the biochemical level.

***Disclosures: Laura Corrigan**, None.*

MO0284

Association Between Serum Osteocalcin and Markers of Metabolic Syndrome in Overweight/Obese Postmenopausal Women. Hyehyung Shin*[1], Pei-Yang Liu[1], Owen Kelly[2], Jasminka Ilich-Ernst[1]. [1]Florida State University, USA, [2]Texas Woman's University, USA

Some recent research shows that osteocalcin may be associated with glucose and insulin metabolism and possibly with markers of metabolic syndrome (MetS). MetS is diagnosed when 3 or more of the following conditions are present: fasting glucose (FG) $\geqslant$100mg/dL; high-density lipoproteins (HDL) $<$50mg/dL; triglycerides (TG) $\geqslant$150mg/dL; blood pressure (BP) $\geqslant$130/85mm Hg; and waist circumference $\geqslant$88cm (for women)(National Cholesterol Education Program Adult Treatment Panel III). Our objective was to evaluate serum osteocalcin level in overweight/obese postmenopausal women with or without MetS. Participants included 176 Caucasian women age 55.8 ± 4.3y; BMI 31.6 ± 5.6kg/m2 (mean $\pm$ SD), without diabetes, osteoporosis, or other diseases/medications known to affect bone metabolism. Weight and height were measured in indoor clothing without shoes and used to calculate BMI for classification into overweight/obese groups. Waist circumference was measured by tape placed around the smallest circumference of the torso and parallel to the floor. BP was measured in a non-dominant arm, 3 times with 1-2 minute intervals and average taken. Overnight fasting blood samples were obtained by venous puncture and serum separated from red blood cells. HDL, TG and FG were analyzed by the contracting laboratory. Serum osteocalcin was measured by ELISA. The mean waist circumference and BP were 97.3 ± 12.0cm and $122.0 \pm 15.0/80.7 \pm 9.6$mmHg respectively. The mean serum HDL, TG, FG and osteocalcin concentrations were 56.8 ± 16.3mg/dL, 136.7 ± 75.7mg/dL, 99.9 ± 15.5mg/dL and 19.8 ± 7.6ng/mL, respectively. 34% of our cohort had MetS with mean serum osteocalcin concentration of 17.6 ± 6.6ng/mL compared to 20.9 ± 7.9ng/mL ($p<0.01$) in those without MetS. Among MetS criteria items, osteocalcin was positively associated with HDL and negatively with waist circumference ($p<0.05$). 54% of the cohort was categorized as obese, with osteocalcin concentration of 18.2 ± 7.6ng/mL; significantly lower than that in the overweight group (21.7 ± 7.2ng/mL). When participants were divided into four groups (overweight/obese; with/without MetS), ANCOVA controlled for age demonstrated significant differences in osteocalcin among the groups; with obesity having the significant effect on osteocalcin, but not the presence of metabolic syndrome ($p<0.01$). Our results support the hypothesis that osteocalcin may play a role in metabolic regulation, however, the relations are complex and more research is warranted. USDA/CSREES/NRI#2004-05287.

***Disclosures: Hyehyung Shin**, None.*

MO0285

Identification of Protein Biomarkers for Postmenopausal Bone Mineral Density in the Aberdeen Prospective Osteoporosis Screening Study. David A Stead, Evelyn A Argo, David Reid, Blair H Smith, Phillip Cash, Alistair JP Brown, Lynne Hocking*. University of Aberdeen, United Kingdom

Osteoporosis (OP) is a skeletal disorder characterized by low bone mineral density (BMD), increased bone fragility and increased risk of fracture. Individuals with OP often go undetected until after they sustain a fracture as mass screening by Dual-energy X-ray Absorptiometry (DXA) is not recommended. New methods are required to rapidly, reliably and cheaply identify individuals with low BMD to effectively target interventions for fracture prevention. The aim of this study was to identify protein biomarkers in urine and serum samples that discriminated between individuals with high or low BMD. Such biomarkers offer the attractive prospects of earlier screening for disease and initiation of treatment before a fracture occurs.

The longitudinal Aberdeen Prospective Osteoporosis Screening Study (APOSS) comprises women from north east Scotland who have been extensively characterised for OP risk; women are being reassessed using imaging DXA (iDXA) bone scans (GE Lunar), and providing biological samples for biomarker detection. Urine and serum samples provided by 6 APOSS participants were selected for analysis, 3 from each extreme of both hip (femoral neck, FN) and lumbar spine (LS, L2-L4) BMD as determined by iDXA. Urinary proteomic profiles were generated by GeLC-MS/MS and proteins identified by Mascot database searching. Corresponding spectral counts were used as measures of protein abundance, and differences between high-low BMD groups examined using GeneSpring GX. Serum samples were depleted of high abundance proteins and paired high-low BMD samples analysed by 2D-DIGE; groups were compared using Progenesis SameSpots software. Associations with BMD were assessed by linear regression in SPSS.

Among the 6 samples, 384 urinary proteins and 335 serum protein spots were identified. Preliminary analyses identified a urinary protein signature comprising 5 proteins that differentiated between the high and low BMD groups ($p<0.05$), 3 of which reside within chromosomal regions previously linked to BMD, and one of which was associated with FN and LS BMD ($p_{FN}=0.002$, $p_{LS}=0.006$). Two serum protein spots had significantly altered abundance between the high and low BMD groups ($p=0.01$, power$>$86%, 1.5- & 1.8-fold differences), with 1 associated with FN and LS BMD ($p_{FN}=0.03$, $p_{LS}=0.004$).

These results suggest that proteomic biomarkers will be useful for identifying individuals with low BMD for further examination, and may provide insight into the underlying pathophysiology.

***Disclosures: Lynne Hocking**, None.*

MO0286

Are Fragility Fractures Osteoporotic Fractures. Arne Hoiseth*. Curato Rtg., Norway

Fractures caused by low energy trauma are often considered fragility fractures and denoted osteoporotic. The purpose of this paper is to question the rationale for considering such fractures as osteoporotic without a fracture independent measure of bone strength. BMC/BMD, as measured by DXA, is the best available bone strength surrogate. By using this surrogate detailed analyses of the associations between fractures and bone strength was performed. Fracture history was obtained from and BMC/BMD measured in total of 13 741 females. Fractures were classified as number of fractures and into 4 fracture groups: 1) Having had at least a femoral fracture, 2) at least a clinical vertebral fracture but not a femoral fracture, 3) a fore-arm fracture only and 4) "other fractures". BMD and BMC were ranked and divided into 20 equally large groups. The age of the patients ranged from 40->90 years. Analyses was done with all patients pooled and in age specific groups. The results showed only a weak or no association between BMC/BMD and the number of fractures per patient. Nor were there associations between fore-arm fractures and ''other fractures'' and BMC/BMD. For femoral fractures there was a slight increase in frequency of the fractures by lower BMC/BMD. An exponential increase in fractured cases was seen only in 5% of cases with lowest BMC/BMD; in the oldest age group ($>$75 years) in 10% of cases. The general finding was thus that fractures occurred in all BMC/BMD groups and the occurrence of fractures was basically independent of bone strength. BMC/BMD seemed to have an effect on femoral fractures, and to a lesser extent on vertebral fractures, only in 5 to 10% of cases with low BMC/BMD. It seems that most fractures, even femoral fractures, occur independent of variation in bone strength. It is hypothesized that bone strength, probably being strongly dependent on bone mass and thus on the weight of the bones, is being balanced to allow a variety of physical activities (some dependent on low body weight) at the cost of a ''baseline fracture risk'' in humans. Such a fracture risk, being almost independent on bone mass, may explain why fracture risk intervention has insignificant effect on some fracture types. It is suggested that fractures caused by low energy trauma should not be considered as osteoporotic without a fracture independent measure to confirm high bone fragility.

***Disclosures: Arne Hoiseth**, None.*

MO0287

Body Composition Analyzes in Healthy Brazilian Women: Normative Data. Maria das Graças Barbosa Sousa*[1], Marcelo Pinheiro[2], Vera Szejnfeld[3], Charlles Castro[1]. [1]Universidade Federal de São Paulo, Brazil, [2]Sao Paulo Federal University/ Unifesp/ Escola Paulista De Medicina, Bra, [3]UNIFESF/EPM, Brazil

The lack of representative body composition reference values has limited their potential application in clinical and research settings. No reference values for the Brazilian population are available. In the present study we aim to determine the reference values for body composition parameters in the Brazilian women and compare to published databases. A total of 500 healthy Brazilian women will be recruited for body composition measurements. Healthy women aged 20 years and older with BMI lower than 30 kg/m^2 will be consecutively selected to participate. Women with history of fragility fracture, liver, renal, endocrine, gastrointestinal, neurological, rheumatological, pulmonary or coronary disease, as well as AIDS and use of silicone prosthesis and drugs that affect the muscle, bone and mineral metabolism will be excluded. Body composition will be performed using DXA (GE DPX densitometer). Total and regional body composition analyzes will include arms, legs and trunk. For statistical purposes, women will be divided into groups according to age: 20-29, 30-39, 40-49, 50-59, 60-69, 70-79 and over 80 years. For each age group, data sets will comprise whole body DXA measurements of bone mineral content (BMC, g), areal bone mineral density (BMD, g/cm^2), fat mass (g) and lean mass including BMC (g) and percent fat, calculated as (fat mass divided by total mass)x 100. Whole body fat and lean mass measurements and appendicular lean mass were normalized to height^2. From the whole body measures the following derivative values were calculated: FMI (arms and legs fat mass/height^2), lean mass/height^2, appendicular lean mass/height^2. The comparison between groups was performed using Student t test or ANOVA. At the present, a total of 200 healthy Brazilian women were included (age 43.8$\pm$17.3 years old; BMI 23.8$\pm$2.9 kg/m2). Mean appendicular lean mass/height^2 was 6$\pm$0.64 kg/m^2 and about 20 women (10%) were considered sarcopenic (<5.45 kg/m^2). There was a significant decline in lean mass parameters with age ($p<0.001$). On the other hand, fat mass increased with age ($p<0.001$). Mean FMI was 4$\pm$1.13 kg/m^2. The highest value for FMI was 7.69, so none of the women had excess fat or obesity. Brazilian women had significantly lower lean and fat mass parameters for almost all age-groups when compared to NHANES population ($p<0.01$). Our data suggest that regional data sets for body composition are needed to provide a better understanding of bone and metabolic syndromes.

***Disclosures: Maria das Graças Barbosa Sousa**, None.*

MO0288

Comparability and Precision of Appendicular Lean Mass and Android/ Gynoid Fat Mass Measurement: Comparison of Prodigy With iDXA. Bjoern Buehring*[1], Nellie Vallarta-Ast[2], Jessie Libber[3], Diane Krueger[4], Neil Binkley[5]. [1]Cleveland Clinic, USA, [2]UW Osteoporosis Research, USA, [3]University of Wisconsin Osteoporosis Clinical Research Program, USA, [4]University of Wisconsin, Madison, USA, [5]University of Wisconsin, USA

Sarcopenia is increasingly being recognized as contributing to falls and fracture risk. While consensus does not yet exist regarding a clinical definition of sarcopenia, it seems probable that appendicular lean mass as measured by DXA will be part of such a definition. Additionally, DXA measurement of regional body fat is becoming more widely utilized. However, the comparability of these measurements between instruments and their short-term reproducibility (precision) has received little study. As such, the purposes of this study were to compare appendicular lean mass, and android/gynoid fat mass measurements obtained by total body DXA with a GE Healthcare Lunar Prodigy and iDXA densitometer. Additionally, the reproducibility of these measurements was evaluated. Eighty individuals (38 women/42 men) age 20 to 85.4 years had total body measurements performed on both instruments in routine clinical manner by ISCD certified technologists. Precision assessment was conducted in a randomly-selected subset (n = 30). Software versions 9.2 (Prodigy) and 9.3 (iDXA) were used for acquisition; versions 11 (iDXA) and 11.4 (Prodigy) for analyses. The ISCD precision calculating tool was used to determine precision of regional (android, gynoid and appendicular) soft tissue measurement. Tissue composition results were compared by linear regression and Bland-Altman analyses using Analyze-it software. Instrument precision was compared by f-test. Appendicular lean mass was highly correlated between instruments (r2 = 0.97). Bland-Altman analysis revealed little bias in appendicular lean mass measurement (bias -451.6, CI -682.1 to -221.1). Android and gynoid fat mass measurements were similarly highly correlated, r2 = 0.99 for both. Bland-Altman analysis demonstrated only slight bias with iDXA measuring slightly higher fat mass than Prodigy (android: bias 101.7, CI 62.6 to 141.0, gynoid: bias 272.5, CI 223.6 to 321.6) . Precision (%CV) for appendicular lean, android fat and gynoid fat mass were similar with iDXA and Prodigy (Table).

In conclusion, appendicular lean mass and android/gynoid fat mass measurements with Prodigy and iDXA densitometers is highly correlated to each other. Changes of <400 grams in fat mass and ~600 grams in appendicular lean mass are detectable with these instruments.

	Prodigy		iDXA		Difference
	LSC (grams)	CV (%)	LSC (grams)	CV (%)	p-value
Android fat (grams)	152	3.41	114	2.37	<0.0001
Gynoid fat (grams)	378	2.95	418	3.02	<0.0001
Appendicular lean (grams)	635	0.95	572	0.77	0.33

Table 1

***Disclosures: Bjoern Buehring**, None.*

MO0289

FRAX is Able to Discriminate Fracture Status in Patients with Chronic Kidney Disease. Sophie Jamal*[1], Lisa Langsetmo[2], Ryan Chauncey[3], Sandhya Thomas[3], Sarah West[4], Thomas L. Nickolas[3]. [1]The University of Toronto, Canada, [2]Canandian Multicenter Osteoporosis Study, Canada, [3]Columbia University Medical Center, USA, [4]University of Toronto, Canada

Purpose: Since half of osteoporotic fractures occur in patients with bone mineral density (BMD) above the diagnostic threshold for osteoporosis, further risk assessment is necessary. The limited ability of BMD measurement to identify patients at high fracture risk is even more marked among patients with chronic kidney disease (CKD). The FRAX tool uses BMD and additional risk factors for fracture to determine absolute fracture risk. We hypothesized that among patients with CKD FRAX would result in better fracture discrimination than BMD alone. Methods: We combined data from two ongoing observational studies of men and women 18 years and older with CKD stages 3 to 5 not on dialysis. We evaluated the discriminative ability of FRAX, without/with femoral neck (FN) BMD and assuming no prior fracture to determine prevalent osteoporotic fracture status. We also considered the ability of FRAX without/with BMD including prior clinical fracture to determine prevalent morphometric vertebral fractures. We compared results using FRAX to the ability of age alone to determine fracture status. Results are expressed as areas under the receiver operating characteristic curves (AUC) with 95% confidence intervals (CI). Results: We enrolled 109 men and 81 women of whom 187 had BMD measurements. Mean age was 66.5 yrs, BMI was 28.5 kg/m2, and FN BMD was 0.722 g/cm^2; 49 had osteoporotic fractures, 44 had vertebral fractures, 20 had a family history of fractures, 19 were taking steroids, 3 had RA, 15 were smokers and one person consumed $\geqslant$ 3 units of alcohol/day. Excluding prior clinical fractures, fracture status discrimination for osteoporotic fracture using age alone gave an AUC=0.60 (95% CI:0.52-0.69) for FRAX without BMD: AUC=0.63 (95% CI:0.54-0.71) and for FRAX with BMD: AUC= 0.67 (95% CI:0.58-0.75). Including prior clinical fractures, discrimination for vertebral fracture status using age alone gave an AUC= 0.68 (95% CI:0.59-0.77), for FRAX without BMD: AUC=0.70 (95% CI:0.62-0.78) and for FRAX with BMD the AUC= 0.66 (95% CI:0.57-0.75). There were no statistically significant differences between the AUCs for either outcome when using age, FRAX without BMD, or FRAX with BMD. Conclusions: FRAX, with or without BMD, discriminates between CKD patients with and without clinical fractures and may be clinically superior to age alone. For vertebral fractures the discriminative ability of FRAX is not improved by including BMD and FRAX is no better than age alone.

***Disclosures: Sophie Jamal**, None.*

MO0290

Hypoparathyroidism (HP) Protects Bone Mass but is Highly Associated with Lumbar Morphometric Fracture. Francisco Pereira*[1], Maira Mendonça[2], Marcello Nogueira-Barbosa[3], Plauto Watanabe[4], Sara Teixeira[5], Lucas Monsingnore[6], Léa Maciel[3], Francisco Paula[3]. [1]University of Sao Paulo, School of Medicine of Ribeirao Preto, Brazil, [2]Internal Medicine, School of Medicine of Ribeirao Preto, Brazil, [3]Internal Medicine, School of Medicine of Ribeirao Preto, University of Sao Paulo, Brazil, [4]School of Dentistry of Ribeirao Preto, University of Sao Paulo, Brazil, [5]Internal Medicine, School of Medicine of Ribeirão Preto, University of Sao Paulo, Brazil, [6]Internal Medicine, School of Medicine of Ribeirao Preto, University of Ribeirao Preto, Brazil

Objectives: To use different imaging techniques to assess bone mass, bone quality and morphometric vertebral fractures in patients with hypoparathyroidism (HP). Methods: Sixteen women with HP (HPG) and seventeen control women (CG) were evaluated. The following biochemical parameters were determined: calcium, albumin, inorganic phosphorus, alkaline phosphatase, creatinine, parathyroid hormone, 25–OH vitamin D, osteocalcin and IGF–1 in serum, and deoxypyridinoline/creatinine in urine. DXA of L1-L4, femoral neck, total hip, distal 1/3 of the forearm, whole body, and body composition were determined. Vertebral morphometry was performed by measuring the anterior, middle and posterior heights of each vertebra and a reduction of more than 20% in each segment was considered to be a fracture. Mandibular analysis was performed by measuring the inferior mandibular cortical thickness bilaterally in the region of the mental foramen and of the mandibular angle. Results: Age = 62.3$\pm$8.9 y, weight = 72.6$\pm$10.9 kg, height = 1.54$\pm$7.87 m, and BMI = 30.3$\pm$4.2 kg/m2 of CG did not differ from those of HPG (age = 58$\pm$6.0 y, weight =

71.7 ± 13.7 kg, height = 1.58 ± 6.4 m and BMI = 28.5 ± 55 kg/m2). Also, there was no significant difference between groups in alkaline phosphatase, 25–OH vitamin D or deoxypyridinoline/creatinine levels. Calcium and osteocalcin levels were significantly lower in HPG. HPG presented bone mineral density similar to that of CG at all sites analyzed (e.g. L1-L4: GH = 1.090 ± 0.3 vs CG = 0.970 ± 0.2 g/cm^2; p = 0.2). HPG had a significantly smaller mandibular cortical thickness at the level of the mental foramen than CG. Regarding vertebral morphometry, the presence of fractures was observed in 11 of HPG subjects (62.5%) and only in 2 of CG subjects (11.7%). Conclusion: The present results indicate that, despite the preservation of bone mass, primary HP seems to be associated with a greater risk of fracture, at least at the vertebral level. Mandibular cortical bone seems to be an important site for the assessment of bone involvement in primary HP.

***Disclosures: Francisco Pereira**, None.*

MO0291

IVA, in Addition to BMD can Change the Osteoporosis Management in 25% of Clinical Routine Patients. Berengere Aubry-rozier*[1], Delphine Stoll[2], Marc-Antoine Krieg[1], Olivier Lamy[1], Didier Hans[3]. [1]University Hospital, Switzerland, [2]Center of Bone Unit - DAL - Lausanne University Hospital, Switzerland, [3]Lausanne University Hospital, Switzerland

Vertebral fracture is one of the major osteoporotic fractures which are unfortunately very often undetected. In addition, it is well known that prevalent vertebral fracture increases dramatically the risk of future additional fracture. Instant Vertebral Assessment (IVA) has been introduced in DXA device couple years ago to ease the detection of such fracture when routine DXA are performed. To correctly use such tool, ISCD provided clinical recommendation on when and how to use it. The aim of our study was to evaluate the ISCD guidelines in clinical routine patients and see how often it may change of patient management.

During two months (March and April 2010), a medical questionnaire was systematically given to our clinical routine patient to check the validity of ISCD IVA recommendations in our population. In addition, all women had BMD measurement at AP spine, Femur and 1/3 radius using a Discovery A System (Hologic, Waltham, USA). When appropriate, IVA measurement had been performed on the same DXA system and had been centrally evaluated by two trained Doctors for fracture status according to the semi-quantitative method of Genant. The reading had been performed when possible between L5 and T4.

Out of 210 women seen in the consultation, 109 (52%) of them (mean age 68.2 ± 11.5 years) fulfilled the necessary criteria to have an IVA measurement. Out of these 109 women, 43 (incidence 39.4%) had osteoporosis at one of the three skeletal sites and 31 (incidence 28.4%) had at least one vertebral fracture. 14.7% of women had both osteoporosis and at least one vertebral fracture classifying them as ''severe osteoporosis'' while 46.8% did not have osteoporosis not vertebral fracture. 24.8% of the women had osteoporosis but no vertebral fracture while 13.8% of women did have osteoporosis but vertebral fracture (Clinical osteoporosis).

In conclusion, in 52% of our patients, IVA was needed according to ISCD criteria. In half of them the IVA test influenced of patient management either my changing the type of treatment of simply by classifying patient as ''clinical osteoporosis''. IVA appears to be an important tool in clinical routine but unfortunately is not yet very often use in most of the centers.

***Disclosures: Berengere Aubry-rozier**, None.*

MO0292

Peak Bone Mineral Density in Healthy Chinese Young Men of Han Ethnicity. Jing Yang[1], Jin Sun[1], Fengtao Luo[1], Yue Shen[2], Lin Chen*[1]. [1]State Key Laboratory of Trauma, Burns & Combined Injury, Center of Bone Metabolism & Repair, Trauma Center, Institute of Surgery Research, Daping Hospital, Third Military Medical University, China, [2]State Key Laboratory of Trauma, Burns & Combined Injury, Trauma Center, Institute of Surgery Research, Daping Hospital, Third Military Medical University, China

Peak bone mass is an important factor for the occurrence of osteoporotic fracture in adulthood. Obtaining high peak bone mineral density (BMD) at adolescence could reduce the fracture risk. Genetic factors explain more than 60% variance of the peak BMD. Male Caucasian obtains peak BMD of lumbar and hip around age 19 years. We try to measure the BMD in healthy Chinese young men of Han ethnic group and subsequently find the ages reaching peak BMD and bone mineral content (BMC) at lumbar and hip. This study involved 823 Chinese men of Han ethnicity aged ranging from 16 to 23 years. The BMD, BMC and the area of lumbar (L1-4), left femoral neck and total hip were measured by using the dual-energy X-ray absorptiometry The height, weight, waist circumference and hip circumference were also measured simultaneously. The average age was 19.17 ± 1.54 years. BMD at lumbar, femoral neck and total hip reached a plateau at the age of 21 years. The peak value of BMD at these three sites was 1.161 ± 0.17, 1.075 ± 0.17 and 1.085 ± 0.15, respectively. The peak value of BMC at femoral neck, lumbar and total hip was observed in group aged 20 years (5.707 ± 1.129), 21 years(69.89 ± 12.62) and 23 years (16.353 ± 16.69), respectively. The area of femoral neck, lumbar and total hip in group aged 23 years increased by 7.12%, 9.32% and 1.05% compared with that in group aged 16 years. Pearson's correlation analysis showed a significant correlation between the body weight (or hip circumference) and BMD (or BMC) at all sites, respectively ($P<0.001$). In conclusion, we established the value of BMD and BMC at lumbar, femoral neck and total hip in Chinese young men belong to Han ethnicity. The average age reaching peak BMD and BMC in Chinese men of Han ethnicity is delayed than that in the male Caucasian.

***Disclosures: Lin Chen**, None.*

MO0293

Profile of Elderly Met with Diagnosis of Osteoporosis and Falls History in Outpatient Physician in the City of Guarulhos in the State of São Paulo, Brazil. Ana Segantin, Fabiana Fonseca*, Ana Elisa Klein, Paulo Montenegro, Mariana Yoshida. PUC sp, Brazil

INTRODUCTION: people of all ages have with drops, however for elderly they have something very important, because they can lead you to incapacity and death. Its social cost is immense and becomes greater when the elderly has reduced autonomy and independence or shall require institutionalization (FABRÍCIO, ET AL, 2004). GOAL: • Characterize the profile of elderly people with osteoporosis who suffer drops, making possible measures for the prevention of falls; Assess major susceptibility to falls; Information that could be used for improvement and the establishment of new programmes of prevention and rehabilitation of patients experiencing drops or reduce the recurrence of the same. METHODOLOGY: Questionnaire semi structured, containing 15 questions;Describe the studied population, second socio-economic variables and health;Information that could be used for improvement and the establishment of new programmes of prevention and rehabilitation of patients experiencing drops or reduce the recurrence of the same. RESULTS: Fractures osteoporosis produce several psychological and physical consequences, affecting the quality of life of patients and their people, and has high socioeconomic impact to society. Noted that the main factors for drops are:, postural Instability; The shoes are inadequate; furniture poorly adapted; The presence of obstacles which enable falls. Noted that after deployment methods and measures for the prevention of falls patients present improves the quality of life and greater independence for activities of daily life. CONCLUSION: In the cases studied it was noted that the osteoporóticas fractures occur in higher prevalence in reason poor adherence to treatment, factors for falls and even external factors. Causing expenses with hospital admissions and even deaths by immobility syndrome which could be avoided with effective approaches.

***Disclosures: Fabiana Fonseca**, None.*

MO0294

Scanning the Head in all DXA Whole Body is not Medically Justifiable. John Shepherd, Bo Fan*. University of California, San Francisco, USA

Background: ISCD position states that the headless whole body DXA analysis should be used for children and adolescents. Head DXA values have long been known to be less accurate and reliable than other DXA measures because of the inability to directly sample the soft tissue independently of bone. In addition, the head is rarely if ever reported as a valid clinical trial finding. However, the head is always included in a whole body scan and thus receives a radiation dose. Recently, there has been much attention to the need to reduce unnecessary radiation dosage to patients. The purpose of this study is to further investigate whether the head provides accurate information for adults and children and discuss the implications of not scanning the head.

Methods: We used published whole body DXA results from the 1999 to 2004 NHANES Study. Head BMD, BMC and %FAT were compared to other whole body subregions including the Total, Arms, Legs, Trunk Mean values, which were calculated as a function of age for each ethnicity. Univariate analyses were used to investigate the distribution of the variables.

Results: A total of 10,696 with mixed ethnicity and sex scans were included in this data analysis. The age of subjects ranged from 8 to 85 years old and their weight ranged from 18 to 138 kg. The head BMD and BMC were normally distributed and with a broad range of values. However, the changes of head FAT and %FAT did not track other regions and show little or no change over time. The correlation of head BMD, BMC, FAT and %FAT to whole body and other subregions in general were better in young subjects (age<=20) than adults subjects. The adult head BMD, BMC weakly correlated with other regions, the r value for subtotal BMD and BMC were 0.4, while adult head FAT and %FAT had poor with other regions, r value for subtotal FAT and %FAT were 0.2.

Discussion and conclusion: The head %FAT does not track other %fat values and most likely is not an accurate reference for head BMD and BMC. In addition, head %fat has the potential of being a large error source of body composition results. Even though the DXA dose to the head is very low, the potential for more harm than good exists because of the inaccuracies it adds to the whole body composition results. From our study results, there is no medical justification for scanning the head and the option for scanning the whole body without dosing the head should be considered and provided on DXA systems.

***Disclosures: Bo Fan**, None.*

MO0295

Spinal Trabecular Volumetric Bone Mineral Density (vBMD) in Japanese Subjects: The Relationships of Thoracic, Lumbar, and Lumbosacral vBMD on Multi-detector Row Computed Tomography Images. Tatsuro Hayashi*[1], Huayue Chen[1], Kei Miyamoto[1], Xiangrong Zhou[1], Takeshi Hara[1], Ryujiro Yokoyama[2], Masayuki Kanematsu[1], Hiroaki Hoshi[1], Hiroshi Fujita[1]. [1]Gifu University Graduate School of Medicine, Japan, [2]Gifu University Hospital, Japan

Purpose: Multi-detector row computed tomography (MDCT) can be used to estimate spinal trabecular volumetric bone mineral density (vBMD). Despite a moderate amount of literature on correlates of areal BMD few comprehensive studies have examined correlates of spinal trabecular vBMD on nearly isotropic MDCT images. The objective of this research was to examine spinal trabecular vBMD on isotropic MDCT images, and to compare vBMD in each vertebral level.

Materials and Methods: The study sample enrolled Japanese sebjects with MDCT images, which is included thoracic, lumbar, and lumbosacral vertebrae, and were scanned for each subject using standard settings (120 kV, Auto mAs, 1.25-mm section thickness, and 0.6-mm reconstruction overlap). Some subjects were excluded because of normal variants, bone pathology, vertebral fractures, or reasons other than mild degenerative changes at vertebrae. As a result, the study subjects consisted of 1031 individuals: 490 men and 541 women. The study subjects were then subdivided into five age categories in order to observe age differences; < 41 (154 subjects), 41 - 50 (127 subjects), 51 - 60 (271 subjects), 61 - 70 (255 subjects), and 70 < years (224 subjects). In the current research, central locations of the vertebral trabecular bones were measured and their relations in each vertebral level based on Th7 and Th12 were computed by Tukey multiple comparison test.

Results: Age- and gender- dependent vBMDs of spinal trabecular bones at thoracic, lumbar, and lumbosacral vertebrae were shown in the Table. This table showed L3 had the lowest vBMD among vertebrae and vBMD tended to increase gradually from L3 to Th1. Tukey test indicated that there were no significant differences among Th6 - Th10 as compared with Th7 as well as Th11 - L2 as compared with Th12, in all age categories in both genders. Therefore, among these vertebrae, if the BMD of one vertebra is known, the BMD of the other vertebrae can be used as the initial estimation in place of the undetermined value of a target vertebra.

Conclusions: This research examined spinal trabecular vBMD in Japanese subjects, and showed the relations between vertebral levels and their vBMD. The experimental results suggested that vBMD among spinal level had similar distributions regardless of age and gender. These knowledge may help the decision of the vertebral level which should be scanned by QCT.

Table Trabecular vBMDs (mg/cm³) in each age and gender category.

(BMDs describe mean ± standard deviation)

Level	Age (yrs)									
	<41		41 - 50		51 - 60		61 - 70		70<	
	Male (n = 78)	Female (n = 76)	Male (n = 52)	Female (n = 75)	Male (n = 112)	Female (n = 159)	Male (n = 126)	Female (n = 129)	Male (n = 122)	Female (n = 102)
Th1	214.2±45.1	235.7±44.3	193.0±38.5	220.0±47.3	197.8±43.3	188.3±43.5	183.9±43.3	162.7±46.2	168.3±42.8	142.4±39.4
Th2	211.2±43.7	221.6±41.9	192.0±48.0	212.7±49.1	200.0±45.2	183.3±44.0	185.2±49.2	159.2±44.2	165.0±45.3	137.9±43.5
Th3	212.7±44.5	218.5±39.8	192.2±50.9	211.9±49.6	200.3±52.1	182.4±42.5	190.5±56.4	157.9±47.3	162.5±48.9	133.8±43.0
Th4	206.4±45.4	212.5±39.1	182.3±44.3	206.9±46.4	189.8±49.3	181.5±42.8	178.2±48.9	155.1±47.1	153.4±48.1	122.7±38.6
Th5	200.9±41.5	209.2±37.4	173.6±36.6	203.5±46.2	184.0±47.6	172.0±39.3	166.6±46.6	144.5±45.8	144.6±40.3	114.6±37.5
Th6	195.1±41.5	202.6±39.0	168.1±34.5	191.2±45.1	169.0±43.4	163.5±39.4	156.0±43.7	136.4±42.5	134.1±39.0	105.9±38.5
Th7	188.2±40.0	196.6±37.6	159.5±34.9	185.7±42.3	159.9±39.7	155.1±38.6	145.7±41.4	129.7±39.6	122.4±36.7	98.0±37.4
Th8	187.6±41.3	194.6±37.8	157.1±34.1	184.5±43.2	157.3±42.4	153.5±39.1	142.6±42.1	124.4±38.7	119.8±36.2	97.1±36.3
Th9	194.0±41.3	197.9±37.8	160.3±32.3	188.9±42.8	158.5±40.3	156.3±40.0	146.6±43.4	126.9±42.9	125.6±37.2	96.9±37.7
Th10	192.8±41.6	200.2±41.3	159.4±36.0	185.5±43.9	155.5±36.7	154.2±39.5	144.2±41.9	125.9±40.4	123.1±36.1	98.5±37.6
Th11	183.2±41.0	190.2±39.3	150.2±35.3	176.0±40.5	141.9±36.7	142.1±34.5	124.8±37.7	113.7±35.5	109.0±33.9	89.2±37.1
Th12	176.0±40.0	182.1±38.8	142.5±33.0	167.4±37.3	133.2±33.5	133.9±32.8	114.0±31.8	105.8±33.5	95.7±30.6	82.6±34.2
L1	175.6±40.0	180.7±38.3	138.5±34.9	163.4±36.3	130.3±33.3	129.4±32.6	109.7±32.7	99.6±33.6	91.1±32.4	78.6±31.4
L2	172.2±40.6	176.0±36.8	132.9±37.2	159.6±36.6	125.9±36.5	123.3±34.1	106.2±33.2	95.9±35.6	91.6±33.7	76.4±32.8
L3	166.7±40.1	171.0±37.9	130.0±39.2	153.1±39.8	120.3±35.9	116.8±32.3	99.8±34.5	87.2±36.0	85.9±35.8	69.9±32.3
L4	170.1±40.1	176.0±40.0	133.6±39.8	154.8±41.4	123.1±36.9	119.8±36.7	103.3±34.1	90.4±35.1	88.8±32.9	74.5±34.9
L5	177.8±46.1	181.6±44.2	135.4±43.3	164.6±42.0	134.8±37.1	129.1±37.3	113.4±34.4	96.1±35.8	99.9±33.8	81.6±38.5
S1	217.2±56.1	240.3±52.1	181.6±52.0	215.4±56.9	178.8±45.0	175.9±48.5	148.8±46.5	144.3±43.1	134.8±45.1	115.2±50.4

Table

***Disclosures: Tatsuro Hayashi**, None.*

MO0296

The Working Definition of Sarco-Osteopenia in Estonia. Mart Kull*, Riina Kallikorm, Margus Lember. University of Tartu, Department of Internal Medicine, Estonia

Purpose: To define sarco-osteopenia in a population based cohort of young healthy Estonians using both quantitative and functional muscle indicators.

Methods: 304 subjects (age 25-70 years) were randomly selected from the registers of general practitioners in Estonia. To define sarco-ostepenia 77 young and healthy subjects (44 women, 33 men, age 25-39) were selected. Exclusion criteria and the femur neck bone mineral density (BMD) normative data for these individuals have been described elsewhere(1). Appendicular lean mass (ALM) was measured with the Lunar DPX-IQ densitometer and hand grip strength (GS) with a dynamometer. Sarcopenia was defined if either the height adjusted ALM (kg/m2) or GS (kg/cm^2) was 2 SD below the mean for healthy young individuals and sarco-osteopenia if this was accompanied by low bone mass (T-score <-1SD). These criteria were applied in the remainder of the population sample (N=227, age 40-70). Descriptive statistics were used in analysis. The study has Tartu University Ethics Committee approval and all subjects signed an informed consent form.

Results: For women the mean (±SD) height-adjusted ALM was 6708 (± 920) g/m^2 and for men 8791 (± 1095) g/m^2. The mean GS in women was 24.7 (± 9.1) kg/cm^2 and for men 51.8 (±13.7) kg/cm^2. Based on the predefined criteria women were sarco-osteopenic if their ALM was <4868 g/m^2 or GS <6.5 kg/cm^2 and femur neck sBMD <813 mg/cm^2 and men if ALM <6601 g/m^2 or GS <24.4 kg/cm^2 and femur neck BMD <882 mg/cm^2. The application of these criteria into diagnosis identifies 3-9% of middle aged individuals as sarco-osteopenic (Table).

Conclusion: The literature is supportive of the benefits of utilising additional "markers" of frailty when predicting osteoporotic fractures (2). In the current sarcopenia definitions muscle functional parameters have not been incorporated (3). The cross-sectional nature and modest sample size of our study limit us from assessing the impact of this sarco-osteopenia definition in osteoporosis management, therefore future studies in Estonia are needed. As fractures occur in individuals with BMD above the thresholds for osteoporosis, our proposed definition of sarco-osteopenia might be an option when trying to identify subjects with higher fracture risk in the non-osteoporotic low bone mass population.

References: 1. Kull M et al. J Clin Densitom 12:468-474,2009.
2. Lang T et al. Bone 42:798–805, 2008.
3. Delmonico MJ et al. J Am Ger Soc. 55:769–774, 2007.

Table. Classification into osteopenia, sarcopenia and sarco-osteopenia

		Osteopenia	Sarcopenia	Sarco-osteopenia
	N	N (%)	N(%)	N(%)
Women	130	46 (35%)	26(20%)	12(9%)
Men	97	42(43%)	7(7%)	3(3%)
Combined	227	88 (39%)	33(15%)	15 (6%)

Table

***Disclosures: Mart Kull**, None.*

MO0297

What if we had used FRAX®? - a retrospective analysis using the FRAX® tool in patients treated for osteoporosis. Carmen Barbu[1], Alina Roman[2], Dariana Ionita[2], Magda Giscan[2], Cristina Stefan[2], Alice Curaj[1], Mara Carsote[3], Catalina Poiana*[3], Simona Fica[2]. [1]Carol Davila University, Romania, [2]Elias Hospital, Romania, [3]C I Parhon Institute, Romania

Aim of our study is the retrospective analysis of medical records of 1050 patients who received treatment in National Program for Osteoporosis in Elias Hospital and C.I. Parhon Institute (Dr. Poiana database) in order to appreciate the impact of FRAX® use in such patients.

Material and methods. We analyse medical records of 1050 patients (987 women and 63 men with mean age of 67.7 years) who received treatment between 2006-2009 in two endocrine departments in Bucharest. They received antiosteoporotic treatment based mainly on the diagnosis of osteoporosis, but they have very good evaluation at baseline to record all clinical risk factors and to rule out secondary causes of osteoporosis . We use The FRAX® tool to assess the fracture risk at the moment of starting treatment in the National Program of Osteoporosis based on their medical records.

Results. From the 1080 cases, only 652 were suitable for FRAX® analyze, the other ones being treated before. Among the 652, only 41.4% had hip BMD available. After risk assessment, only 11% were found to have significant risk for major fracture and 25% significant risk for hip fracture according to NOF criteria . In the subgroup of the patients with not significant risk fracture (according to FRAX® evaluation and NOF criteria), 18% had prevalent spine fractures and 10% nonvertebral prevalent fractures. As long as romanian reference population is not available in the FRAX® tool, we use german population, but changing the reference population from german to austrian, in almost 12% from cases the predictive value was significantly changed in terms of inclusion/ exclusion from treatment recomandation group.

Conclusion. Treatment initiation based solely on osteoporosis diagnosis allowed inclusion of some low risk population in the treatment group but on the other hand, lack of romanian reference population makes the use of FRAX® model not appropriate. !8% patients with prevalent spine fracture were excluded from the high risk group. Using the "closest reference population" might be tricky since this concept could significantly alter the outcome in individuals.

***Disclosures: Catalina Poiana**, None.*

MO0298

Which FRAX Database to Use in Measuring Absolute Risk of Major Osteoporotic Fracture in Guatemala? Stuart Silverman[1], Alejandro Quiñónez Obiols[2], Keaton Nasser*[3]. [1]Cedars-Sinai/UCLA, USA, [2]Universidad Mariano Gálvez de Guatemala, Guatemala, [3]Osteoporosis Medical Center, USA

Introduction: The FRAX calculator combines a set of clinical risk factors with country-specific incidence rates to determine the ten year absolute risk of major osteoporotic fracture and hip fracture. However, data on country specific fracture rates for Central American countries does not exist. Our objective was to see which database (US Hispanic or Spain) was better in separating fracture from nonfracture patients in Guatemala.

Methods: We enrolled postmenopausal women greater than age 40 in Guatemala with no history of bone medication use with a history of clinical fracture and a history of no clinical fracture. A random sample of 194 women in 34 different regions in Guatemala City was visited in their homes to complete the surveys. Due to literacy, a member of the study staff completed the survey with the participants in an oral interview. We collected FRAX clinical risk factor data on the participants, without BMD results, and calculated the FRAX absolute risk of major osteoporotic fracture and hip fracture using both the US Hispanic and Spain database.

Results: Of the 194 participants, 55 participants had a history of non-traumatic clinical fracture. Mean participant age was 60 years, mean height was 152cm, and mean weight was 62.3kg. Using the Spain FRAX database, subjects with a prior clinical fracture had a mean 10-year absolute risk of major osteoporotic fracture of 9.97% (median 6.9%) versus 4.03% (median= 2.30%) for subjects with no fracture history. Using the US Hispanic database, subjects with a prior clinical fracture had a greater absolute difference between mean 10-year absolute risk of major osteoporotic fracture 11.43% (median 9.30%) versus 4.60% (median= 3.80%) for subjects with no fracture history. The mean values are confirmed to be significantly different between the fracture and nonfracture groups by a Wilcoxon signed rank test.

Conclusion: Until regional or country-specific FRAX data is available, using the US Hispanic database, as opposed to the Spain database, provides a greater absolute difference in absolute fracture risk between Hispanic White women in Guatemala with prior clinical fracture and those without.

***Disclosures: Keaton Nasser**, None.*

MO0299

Assessment of Bone Microarchitecture in Cronic Kidney Disease Patients Using High Resolution Peripheral Computerized Tomography. Maria Belen Zanchetta*[1], Armando Negri[2], Elisa del Valle[2], Fernando Silveira[3], Mariela Sesta[3], Cesar Bogado[1], Jose Ruben Zanchetta[1]. [1]Instituto de Investigaciones Metabolicas (IDIM), Argentina, [2]El Casasco, Argentina, [3]Idim Technologies, Argentina

Bone fragility is a common complication of chronic kidney disease (CKD).

The aim of this study was to assess whether bone microarchitecture and volumetric BMD (vBMD) is impaired in CKD patients undergoing chronic dialysis.

We consigned clinical history (mean time in dialysis, BMI, CKD etiology, co-morbidities, fracture history, medications, history of surgery) and performed calcium homeostasis lab evaluations (serum calcium, phosphate, iPTH, ALP) in 20 CKD stage V men (mean age 59.1 ± 11.0 years, mean time on dialysis 2.8 ± 1.4 years and mean BMI 27.2 ±3.7). Bone microarchitecture and vBMD were assessed at the distal radius and tibia using a three-dimensional HR-pQCT system (XtremeCT; Scanco Medical AG). For comparison, HR-pQCT scans were also obtained in a cohort of 11 healthy young men (mean age 48 ± 9.1 years). None of the subjects had a history of fragility fracture. Comparisons between groups were assessed by the two-sample T test. When the distribution of the variables was not normal, the Wilcoxon Rank Sum Test was used. A p value <0.05 was considered statistically significant.

Compared to the young healthy men cohort, CKD patients showed a significant impairment of the trabecular bone compartment (trabecular bone volume, density and thickness) at both the radius and tibia (Table 1). As expected, cortical density and thickness was severely compromised at both radius and tibia compared to healthy controls. Additional data, including results in women will be presented.

Our results, using a non-invasive bone imaging technique, suggest that in addition to the previously described cortical bone impairment, trabecular bone density and microarchitecture are severely affected in CKD patients on chronic dialysis treatment. Further longitudinal studies should be performed to validate HR-pQCT as a tool for predicting fracture risk in these patients.

	CKD (n=20)	Control Group (n=11)	p	CKD	Control group	p
Age (years)	59.1 ± 11.0	48.1 ± 9.6	0.0092			
DISTAL RADIUS				**DISTAL TIBIA**		
Total density	259.8 ± 68.4	346.0 ± 46.3	0.0008	235.5 ± 67.7	321.8 ± 69.1	0.0021
Cortical density	752.9 ± 91.6	884.4 ± 47.8	<0.0001*	780.4 ± 85.9	863.4 ± 54.6	0.0027*
Cortical thickness	0.550 ± 0.222	0.834 ± 0.176	0.0010	0.899 ± 0.399	1.321 ± 0.399	0.0087
Trabecular Density	158.8 ± 40.6	195.1 ± 26.6	0.0057*	140.6 ± 38.2	191.4 ± 28.3	0.0006
BV/TV (%)	0.132 ± 0.034	0.162 ± 0.022	0.0058*	0.117 ± 0.032	0.160 ± 0.024	0.0006
Trabecular number	1.93 ± 0.33	2.05 ± 0.31	0.3972ns	1.82 ± 0.37	2.07 ± 0.29	0.0698
Trabecular thickness	0.068 ± 0.014	0.080 ± 0.010	0.0185**	0.064 ± 0.011	0.078 ± 0.012	0.0043

Table 1

***Disclosures: Maria Belen Zanchetta**, None.*

MO0300

Comparison of Aqueous Storage Solutions of Bone. Ericka Calton*[1], Lyudmila Lukashova[1], Kostas Verdelis[1], Marjolein Van Der Meulen[2], Adele Boskey[1]. [1]Hospital for Special Surgery, USA, [2]Cornell University, USA

Cancellous bone architectural changes seen with microCT [Judex et al. 2008] can be affected by storage-related degradation, which may prevent observation of early indications of osteoporosis [Parfitt et al. 1987]. The purpose of this study was to determine if saline solutions saturated with hydroxyapatite (HA) reduce cancellous bone mineral dissolution assessed by microCT. There is no consensus as to how to optimally store bone for long periods prior to evaluation; storage may also affect bone mechanical properties [Linde et al. 1993]. Freezing of samples is desirable, and non-aqueous media are preferable but prevent future analysis of cells and risk the possibility of lysing cell membranes. Calcium-buffered saline solutions that provide an adequate initial calcium ion concentration reduce mineral dissolution and bone stiffness changes [Gustafson 1996]. Chemical preservation (i.e. protease inhibitors, PI) can help maintain mechanical integrity [Martin et al. 2001]. HA is an analogue of bone mineral, and HA-supersaturated saline solutions may reduce the driving force for mineral dissolution of stored bone.

Methods

Storage in 70% ethanol was compared to four (4) solutions prepared with phosphate buffered saline: 1xPBS, HA-supersaturated PBS, PBS supplemented with PI, and HA-supersaturated PBS with PI. Cancellous cores (8-mm diameter, n=6/group) removed from fresh lumbar vertebrae of Columbia-Rambouillet cross ewes were stored at -20℃ in solution-soaked gauze. MicroCT data at t=0 (GE) and after 6 mo. (Scanco) were processed using central 4-mm diameter regions of interest. MicroCT parameters (bone volume fraction, BV/TV; trabecular thickness, TbTh; trabecular number, TbN; trabecular separation, TbSp), important determinants of mechanical strength [Odgaard et al. 1997] were determined using Scanco software and compared.

Results

All parameters showed the fewest change at 6 mo. for bone stored in EtOH. For bones in aqueous solutions, BV/TV and TbTh had fewer storage-related changes than TbN and TbSp. Bones stored in HA-supersaturated PBS with PI had the smallest changes for TbN (28.4%) and TbSp (15.2%) compared to other aqueous solutions.

Conclusions

This study indicates that relative to ethanol, HA-supersaturated saline solutions better preserve bone than saline solutions alone; however, no storage prevented dissolution, which is preferable when assessing cancellous bone architecture using microCT and subsequent histology and mechanical testing.

***Disclosures: Ericka Calton**, None.*

MO0301

Creating a BMD Image Using MDCT to Evaluate the Lumbar Bone Fragility Arising from Osteoporosis. Masafumi Machida[1], Nobuhito Nango*[2]. [1]Murayama Medical Center, Japan, [2]Ratoc System Engineering Co., Ltd., Japan

Previously, we proposed the Connective Path method to evaluate the fragility of lumbar bone using Multi-detector CT images. This was able to analyze the connective paths which support the dynamic load of trabecular bone in a loading direction. Applying this method, an evaluation of the effect of osteoporosis medication treatment was reported at last ASBMR. This method quantified the thickness, length, BMD value of each trabecular bone and the network connections within trabecular bone. Using the hydroxiapatite phantom, CT scanning was acquired the BMD value in the method. In this study, we clarified whether it is possible to create an image equivalent to the BMD value and determine a measurement process using the MDCT image only. Two tasks exist, however. One is to eliminate the partial volume effect that occurs when the MDCT image resolution is larger than the thickness of lumbar trabecular bone. The other is the method to create the BMD image.

A specimen from a cadaver sample with osteoporosis from an anatomy lab using the vertebrae T12, L1, L2, L3 was scanned. The Voxel size is 50μm at the μCT. The

Voxel size of MDCT is 200μm. The μCT and MDCT images were aligned at each vertebra three dimensionally. Using a calibration curve for BMD from a phantom image scanned by μCT, we created a BMD image whose image intensity is used as the BMD value. Using the BMD image acquired through μCT scanning, it was compared to an MDCT image, and created a calibration curve for the MDCT image and acquired a BMD image from the MDCT images.

Result: the figure represents the T12 BMD images processed from the μCT and MDCT scan images.The following are the measurement results calculated from the μCT images, MDCT images respectively.

The trabecular bone thickness: 213, 502(μm).The cortical bone thickness: 305, 820(μm)The trabecular bone BMD value: 229, 167(mg/cm^3)The cortical bone BMD value: 401, 308(mg/cm^3)

The figure revealed that MDCT image was similar to μCT image, however, the bone thickness became greater in the MDCT image compared to the μCT image. Contrarily, the BMD value became lower. MDCT provided the good image quality, and the obtained data were correlated with μCT data, except thickness error.

Using the CT value of bone in the MDCT images, a calibration curve equivalent to BMD value may be calculated and it may be possible to create a BMD image from the MDCT for calculating Conn. Path Method.

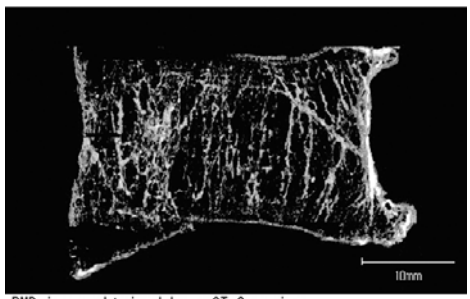

BMD image obtained by μCT Scanning

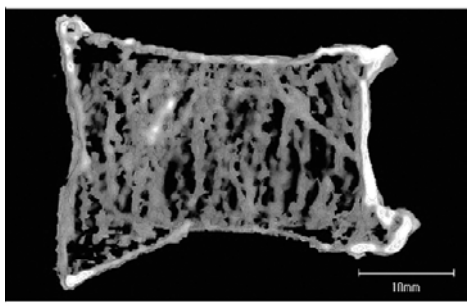

BMD image obtained by MD CT Scanning

BMD image

***Disclosures: Nobuhito Nango**, None.*

MO0302

Defining the Surface/Volume Ratio of Bone Identifies the Susceptibility of Bone to Being Remodelled and Lost and Individuals at Risk for Fracture Better than Bone Density Measurements. Ali Ghasem-Zadeh, Roger Zebaze, Sandra Iuliano-Burns, Kylie King, Ego Seeman*. Austin Health, University of Melbourne, Australia

Background Bone densitometry is used to estimate fracture risk. However, the measurement is neither sensitive or specific. Fracture is structural failure so that specific structural changes need to be quantified. More specifically, bones surface/volume ratio determines susceptibility of matrix to being remodeled so that an in vivo estimate of this geometric property may better predict fracture risk than bone 'density' studies. We tested this hypothesis by quantifying bone structure using Strax 1.0, image analysis method allow estimation of structural decay in vivo.

Material & Methods We studied women with forearm fracture and their age, height and weight matched controls using HR-pQCT images of the distal radius (in 23 cases and 50 controls), tibia (in 32 cases and 53 controls) and fibula (32 cases and 52 controls) measuring total volumetric bone mineral density (TvBMD), cortical vBMD (CtvBMD), and trabecular vBMD (TrvBMD) using the Scanco software and processed using a new software (Strax1.0) to estimate the fraction of the bone within the subperiosteal envelope accessible to remodeling (FBAR %); this is an estimate of surface/volume as bone requires a surface to be remodeled.

Results At the distal radius, FBAR (%), correlated weakly with CtvBMD (r = 0.18, NS) but strongly with TvBMD (r= 0.67 p <0.0001) and TrvBMD (r = 0.87 p<0.0001). Similar correlations were obtained at the tibia (CtvBMD r = 0.27, p = 0.01) TvBMD r = 0.77, p<0.0001 and TrvBMD r = 0.92, p<0.0001). At the distal radius, FBAR was 18.5% lower in cases than controls (22.48 ± 1.17 vs 27.61 ± 0.96; p = 0.0029)(mean ± SEE). Whilst densities were lower in cases than controls, differences were relatively modest, 4.5% for CtvBMD (847.9 ± 13.12 vs 858.3 ± 11.4; NS), 10% for TvBMD (261.69 ± 12.9 vs 291.0 ± 9.68; p = 0.08), and 16.6% for TrvBMD (-16.6%)(109.8 ± 8.14 vs 131.84 ± 5.51; p = 0.028). The odds ratios for fracture were 5.68 (95% CI: 1.49 - 21.57; p <0.05) for FBAR, 1.54 (95% CI: 0.39-6.1; NS) for Ct vBMD, 2.9 (95% CI: 0.92-9.14; NS) for TvBMD, and 2.03 (95% CI: 0.73-5.64; NS). Similar results were obtained at the tibia and at the fibula.

Conclusion Bone fragility is not captured by 'density'; in vivo identification the structural configuration of cortical and trabecular bone accessible to being remodeled, and so decayed, is likely to improve identification of individuals at risk for fracture.

***Disclosures: Ego Seeman**, None.*

MO0303

Geometrical and Trabecular Parameters Derived from Radiographs Can Discriminate Cervical Hip Fracture Patients from Controls in Non-Osteoporotic Individuals. Pasi Pulkkinen*[1], Juha Partanen[2], Pekka K.A. Jalovaara[3], Miika T Nieminen[1], Timo Jamsa[1]. [1]University of Oulu, Finland, [2]Oulu Deaconess Institute, Finland, [3]Oulu University, Finland

Purpose

Majority of hip fractures occur in individuals with BMD in the non-osteoporotic range (BMD T-Score>-2.5). This suggests that factors other than BMD are associated with increased fracture risk in these individuals. These additional factors, however, are not well understood.

The aim of this study was to test the hypothesis that the combination of radiograph-based trabecular and geometrical parameters is able to discriminate cervical hip fractures from controls in the individuals with non-osteoporotic BMD.

Methods

The study subjects consisted of 39 postmenopausal females with non-pathologic cervical hip fracture. Nineteen of the fracture patients (48.7%) had non-osteoporotic BMD and they constituted a fracture group. The control group consisted of 35 age-matched non-osteoporotic females.

Femoral neck BMD was measured with a Lunar DPX scanner and calibrated pelvic radiographs of the fracture patients and controls were taken. Geometrical parameters were measured from radiographs, including femoral neck and head diameters, femoral neck axis length, femoral neck cortical thickness (FNC) and neck-shaft angle (NSA). Trabecular bone was segmented from a square region of interest (20mm x 20mm) at the femoral head, and trabecular parameters, including trabecular bone area (TBA), Euler's number (EN) and homogeneity index (HI), were calculated from the segmented images.

A combined multiple regression model was constructed to identify the best explanatory variables for the discrimination of fractured subjects and controls. Measured geometrical and trabecular parameters were included as the covariates into the regression analysis. Receiver operating characteristics (ROC) analysis was used to study the ability of the combined model to discriminate fracture subjects from controls.

Results

Among the geometrical parameters, FNC was significantly lower (p=0.002) and NSA higher (p<0.001) in the fracture patients than in the controls. In the trabecular parameters, TBA was significantly lower and HI higher in the fractured subjects than in the controls (p=0.001). There was no statistically significant difference in BMD between the groups (p=0.92). Area under the ROC curve was 0.993 (95% CI 0.977–1.008) for the combined model, in which FNC, NSA and HI were as explanatory variables. The sensitivity of 100% was achieved with the specificity of 94%.

Conclusions

The combination of radiograph-based trabecular and geometrical parameters was able to discriminate the cervical fracture cases from controls, although the BMD values were similar in both groups.

***Disclosures: Pasi Pulkkinen**, None.*

MO0304

Intra- and Inter-Reader Reproducibility of a New Clinical Tool for Quantitative Vertebral Morphometry. Daniele Diacinti[1], Romano Del Fiacco*[2], Nathaniel Steiger[3], Davide Diacinti[1], Joes Staal[4], Peter Steiger[5], Emilio D'Erasmo[6], Salvatore Minisola[7], Roberto Passariello[6]. [1]Dept. of Radiology, University "SAPIENZA" Rome, Italy, [2]University "Sapienza" - Rome, Italy, [3]Boston University Medical School, USA, [4]Optasia Medical, United Kingdom, [5]Optasia Medical, USA, [6]Dept. of Clinical Sciences, University "SAPIENZA" Rome, Italy, [7]University of Rome, Italy

Purpose: Quantitative Vertebral Morphometry (QM) provides important information in support of vertebral fracture diagnosis. However, QM is time-consuming with existing clinical tools. The purpose of this study is to evaluate intra- and inter-reader reproducibility of a new clinical tool for QM.

Methods: Twenty subjects (18 women, 2 men, aged 34-82 yrs, mean 66 yrs) who visited the clinic for evaluation of osteoporosis were included in the study. QM was performed twice using a novel semi-automated clinical workflow tool (SpineAnalyzer, Optasia Medical) by three different readers: two experienced radiologists and one first year medical student with no prior experience in QM. All readers were trained on the

use of the software using a different set of subjects. The readers analyzed the images independently without knowledge of their own previous or other readers' results in two sessions, separated by 5 days or more. Intra- and inter-reader reproducibility was evaluated by using the root mean squared error of coefficients of variation (RMS CV) of all heights (anterior: ha, mid: hm, and posterior: hp) and RMS standard deviations (RMS SD) of height ratios (ha/hp, hm/hp). Vertebrae that were inconsistently labeled on one of the 6 reads were excluded from analysis, resulting in the inclusion of 239 of the possible 260 vertebrae analyzed. 34 vertebrae (14%) of the vertebrae were deformed as defined by one of the height ratios being lower than 0.8 (or 20% deformed).

Results: Intra- and inter-reader reproducibility of vertebral heights and ratios are summarized in the table. Shown are the ranges of RMS estimates across the three readers.

Conclusions: Intra- and inter-reader reproducibility of both vertebral heights and height ratios are consistent with those observed in previously published studies. Reproducibility was twofold better in normal versus deformed vertebrae. Our results showed that after brief training an inexperienced operator can obtain QM results that are consistent with those of more experienced readers.

	Intra-Reader Heights RMS CV	Inter-Reader Heights RMS CV	Intra-Reader Ratios RMS SD	Inter-Reader Ratios RMS SD
All vertebrae (n=239)	2.1% - 3.7%	2.8% - 4.0%	0.021 - 0.039	0.025 - 0.048
Fractured (n=34)	4.1% - 5.7%	4.9% - 6.8%	0.031 - 0.056	0.029 - 0.079
Normal (n=205)	1.7% - 3.5%	2.5% - 3.6%	0.019 - 0.035	0.021- 0.042

Table of Inter- and Intra-Reader Reproducibility Results

***Disclosures: Romano Del Fiacco**, None.*

MO0305

Quantitative Morphometry on Spinal X-Rays: Initial Evaluation of a New Workflow Tool for Measuring Vertebral Body Height in Fractured Vertebrae. Klaus Engelke*[1], Thomas Fuerst[2], Bernd Stampa[3], Harry Genant[4]. [1]University of Erlangen, Germany, [2]Synarc, Inc., USA, [3]Synarc Inc, Germany, [4]UCSF/Synarc, USA

Vertebral body height assessed by 6-point quantitative morphometry (QM) provides useful information for the diagnosis of prevalent and incident vertebral fractures. The aim of this study was to evaluate a new QM tool SpineAnalyzer, Optasia Medical Ltd, Cheadle, UK) in a research setting for the measurement of vertebral body height in fractured and non-fractured vertebrae.

In this study the default placement provided by SpineAnalyzer was compared with a standard manual 6-point placement, which was used as a reference standard. In contrast to clinical routine, default placements were not corrected by the reader even if they were obviously incorrect. Lateral lumbar and thoracic x-rays from 100 osteoporotic postmenopausal women (73.8 $\pm$ 5.2 y) with prevalent vertebral fracture (femoral neck T-score = -2.7 $\pm$ 0.6) were used. As arbitrarily classified in this study, 50 subjects had milder fractures (deformed >20% but <30%) and 50 subjects had more severe fractures (>30%). For each patient T4 to L4 levels were analyzed except for 30 vertebrae judged unreadable due to low image quality. Anterior (HA), mid (HM) and posterior (HP) heights and height ratios were calculated from the 6 points using standard algorithms. The root mean square coefficient of variation (rmsCV) of the 3 heights of the default placements relative to the reference standard were computed for each vertebral level.

The table shows the percent rmsCV of automatic compared to manual analysis. In non-fractured vertebra the agreement was good (4.0-4.8%) and comparable to inter-reader agreement of manual analysis (3-4%). However, default point placements for fractured vertebrae were not as effective. In the mild-moderate fractures the percent rmsCV was ~2 times larger (7.2-8.5). Similar results were found for the rmsCVs of the height ratios. Default point placement failed for more severe fractures.

The performance of the default point placement algorithm compared well with manual QM analysis in non-fractured vertebrae, even in this difficult osteoporotic population. However, consistent with the intended use of the tool, fractured vertebrae require manual adjustment. This study did not evaluate the expected performance of the tool in a clinical setting, where such adjustment is expected to improve agreement. We expect that the performance of default point placement can be improved by developing a more sophisticated placement model for fractured vertebrae.

	No fractures (n=1066)			Milder fractures, (n=61) deformation >20% but <30%			More severe fractures (n=143) deformation >30%		
	HA	HM	HP	HA	HM	HP	HA	HM	HP
Mean	4.8	4.6	4.0	7.8	7.2	8.5	14.2	8.0	13.5
SD	0.8	0.5	0.9	4.8	2.0	3.6	7.4	2.1	5.5
Min	3.8	3.9	3.1	1.9	4.0	2.9	5.3	4.1	5.3
Max	7.0	5.8	6.2	18.3	10.6	14.3	27.7	11.2	23.0

Table

***Disclosures: Klaus Engelke**, Synarc, 3*

MO0306

Meta-Analysis of Genome-Wide Association Studies for Quantitative Ultrasound of the Heel: The GEFOS Consortium. Alireza Moayyeri*[1], Yi-Hsiang Hsu[2], Karol Estrada[3], Suzanne Brown[4], Sumei Xiao[5], Wilmar Igl[6], Ozren Polasek[7], Scott Wilson[8], Kay-Tee Khaw[9], Nicholas J Wareham[10], Pak Sham[11], Caroline Hayward[12], Ulf Gyllensten[6], Harry Campbell[13], Andre Uitterlinden[14], Tim Spector[15], Annie Kung[16], Douglas Kiel[17], Fernando Rivadeneira[3], David Karasik[17]. [1]University of Cambridge, United Kingdom, [2]Hebrew SeniorLife & Harvard Medical School, USA, [3]Erasmus University Medical Center, The netherlands, [4]Department of Twins Research & Genetic Epidemiology, Kings College London, United Kingdom, [5]HONG KONG UNIVERSITY, Peoples republic of china, [6]Department of Genetics & Pathology, Sweden, [7]Andrija Stampar School of Public Health, University of Zagreb, Croatia, [8]Sir Charles Gardner Hospital, Australia, [9]Department of Public Health & Primary Care, University of Cambridge, United Kingdom, [10]MRC Epidemiology Unit, United Kingdom, [11]Department of Psychiatry, University of Hong Kong Queen Mary Hospital, China, [12]MRC Human Genetics Unit, United Kingdom, [13]Public Health Sciences, Teviot Place, United Kingdom, [14]Rm Ee 575, Genetic Laboratory, The netherlands, [15]King's College London, United Kingdom, [16]Department of Medicine, University of Hong Kong, Hong kong, [17]Hebrew SeniorLife, USA

Quantitative ultrasound (QUS) of the heel is a convenient and affordable method that predicts osteoporotic fractures comparably to DXA.

In this GEFOS project, we performed meta-analysis of seven genome-wide association (GWA) studies with heel QUS (12,286 participants) and two studies with heel pDXA (1,377 participants). Sex-specific analyses were performed by each cohort using broadband ultrasound attenuation (BUA) or heel pDXA-derived BMD applied to one or both calcanei in additive regression models adjusted for age, weight, height and machine type (total of 13,663 participants: 9,693 women, age range 18-91 years). All cohorts had imputed GWA data (~2.5 million SNPs). Evidence of genome-wide significance (GWS) was set at p-value<5x10-8 in inverse-variance fixed-effects meta-analysis.

There was a strong association signal for heel BUA on chromosome 7q31 (29 significant SNPs; top SNP, rs718766: p=1.8x10-20) in three genes (FAM3C, WNT16 and C7orf58) (Figure). Three significant SNPs in C6orf97 (close to ESR1) on chromosome 6q25 (top SNP, rs4869742: p=1.5x10-9) were also associated with BUA. Both signals became more significant after inclusion of studies with heel pDXA (38 significant SNPs on 7q31 and 6 significant SNPs on 6q25). Effect sizes for the significant hits ranged between 0.05 and 0.16 SD difference per copy of effect allele. There was suggestive evidence of association (p-value<5x10-6) on chromosomes 6q22 (RSPO3), 16p13 (near FLYWCH1), 2p21 (near SPTBN1) and 20q13 (near RPS4X). FAM3C was reportedly associated with heel DXA by a Korean GWA study (Nat Genet 2009(41)527) and ESR1 and SPTBN1 by the GEFOS BMD meta-analysis.

In conclusion, this study identifies two previously-suggested GWS loci associated with heel QUS and proposes four new loci with suggestive significance. Interest centres on the very strong signal on chromosome 7q31 and the partial overlap of signals with GEFOS BMD study. We plan to double our study population by including additional cohorts. Follow-up replication genotyping of the top hits and evaluation of their effect on other bone phenotypes and fracture risk will be done in GEFOS consortium. This should provide novel insights into genetic mechanisms that determine variations in bone phenotypes and fracture risk among individuals and populations.

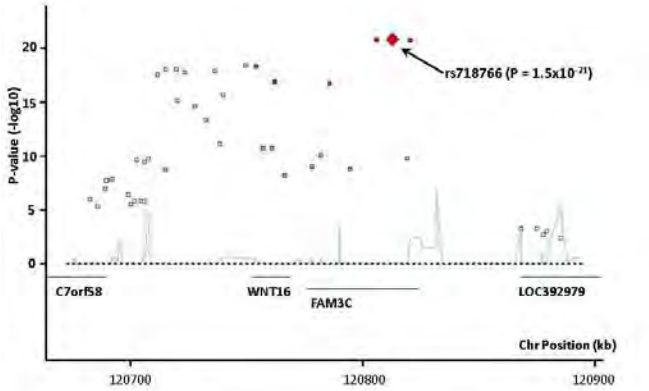

Regional association plot for heel BUA in chromosome 7q31

***Disclosures: Alireza Moayyeri**, None.*

MO0307

Prediction of Non-vertebral Fractures by Calcaneal Quantitative Ultrasound in Older Chinese Men. Timothy Kwok*. The Chinese University of Hong Kong, Hong kong

Kwok T, Khoo CC, Leung PC for MrOs (Hong Kong)

Jockey Club Centre for Osteoporosis Care and Control, the Chinese University of Hong Kong

Background

There is lack of data to evaluate the use of QUS to predict fracture risk in older Chinese men. We therefore compared the predictive power of QUS and that of DXA for incidence of non-vertebral fractures in older Chinese men.

Method and Material

2000 Chinese community dwelling, independently mobile men aged 65 and above, were recruited in 2001-2003. They were followed up once every two years for an average of 6.5 $\pm$ sd 1.68 years. The incidence of fractures was primarily based on reviewing electronic medical records of all outpatient and inpatient episodes in public hospitals in Hong Kong. It was supplemented by self reports during follow-up visits. All fractures were confirmed by X ray.

At baseline, Sahara clinical bone sonometer (Hologic, Bedford, MA, USA) was used to scan the heel of the subjects to obtain broadband ultrasound attenuation (BUA) and speed of sound (SOS) and quantitative ultrasound index (QUI).Hip and spine BMD were measured using Hologic QDR 4500 W bone densitometers (Hologic, Waltham, MA, USA).

Results

The average age of the cohort was 72.5 years. BUA and QUI, but not SOS were moderately correlated with hip bone mineral density (BMD) (correlation

coefficient 0.43, 0.42 respectively, $P<0.01$). There were 131 new non-vertebral fractures, 107 of which (81.7 %) were considered to be fragility fractures. Subjects with non-vertebral fractures were significantly older and had lower scores in BUA, QUI and hip and lumbar spine BMD than those who did not have fracture. On logistic regression, adjusting for age, QUI was significantly associated with non-vertebral fractures as well as fragility non-vertebral fractures (OR 1.33 and 1.30 respectively). BUA was associated with non-vertebral fractures only. SOS was not associated with fractures. None of the three QUS parameters was associated fractures when hip BMD was included in regression model. After adjustment for age, the areas under the ROC curve of QUI were comparable to those of hip BMD by DXA (0.628 and 0.626 versus 0.650 and 0.650 for non-vertebral and fragility non-vertebral fractures respectively).

Conclusion

Quantitative ultrasound index of heel had comparable predictive power for non-vertebral fractures to that of DXA in older Chinese men.

***Disclosures: Timothy Kwok**, None.*

MO0308

Screening of Low Bone Mass in Japanese Elderly Men using Quantitative Ultrasound. Akira Minematsu*[1], Kan Hazaki[2], Akihiro Harano[3], Masayuki Iki[4], Nozomi Okamoto[5], Norio Kurumatani[5]. [1]Kio University, Japan, [2]Osaka Electro-Communication University, Japan, [3]Higashiosaka City General Hospital, Japan, [4]Kinki university, Japan, [5]Nara Medical University, Japan

Bone mass decreases with aging. It is important that we pick out low bone mass person to start a treatment of osteoporosis early. However, it is difficult to measure bone mineral density (BMD) by dual-energy X-ray absorptiometry (DXA) of many people at a time in a group examination because it takes much time and cost. The purpose of this study was to investigate whether sound of speed (SOS) by quantitative ultrasound (QUS) measurement is useful to pick out low BMD in Japanese elderly men.

Of 785 Japanese elderly men (65-84 years old), BMD of lumber spine (LS), total hip (TH) and femoral neck (FN) were measured by DXA, and SOS of cancellous bone was measured by QUS. We presented 5-year age-specific mean value. Difference among age-specific groups was determined by one-way analysis of variance (ANOVA) and post hoc test. Relationship among BMD, SOS, age and body characters (height and weight) were fined. Logistic regression analysis was conducted to evaluate low BMD as -1 SD or more below the young adult means.

Low BMD as -1 SD or more below the young adult means was found in 29.7%(LS), 34.2% (TH) and 48.0% (FN) of subjects. Compared with 65-69 group, BMD at all skeletal sites of 75-79 group and SOS of 80-84 group were low significantly. Relationship between age and BMD at all skeletal sites ($r = -0.072$/LS, -0.113/TH, -0.128/FN) and SOS ($r = -0.113$) were low ($p<0.05$). Significant positive correlation coefficients between BMD at all skeletal sites and SOS were observed even after adjusting for the effect of age and body characters (height and weight), ($r = 0.385$/L5, 0.498/TH, 0.418/FN, $p<0.0001$). Logistic regression analysis showed that BMD (T-score) decreased by about 0.3 to 0.4 per 10 m/s reduction of SOS.

Though rapid bone loss was not occurred in men like women, bone mass was decreased with aging. Compared with 60's men, BMD in over 70's men and SOS in over 80's men were lower in this study. Relationship between SOS and BMD, especially hip, was found and reduction of SOS showed decrease of BMD (T-score). It was concluded that SOS was useful to pick out low BMD men because SOS was measure for a short time at low cost with high probability. But this study had limitations. The study area was not randomly selected from all the municipalities in Japan. The subjects might not be representative samples of the Japanese elderly male population.

***Disclosures: Akira Minematsu**, None.*

MO0309

Association Between Serum Bone-specific Alkaline Phosphatase Activity and Biochemical Markers, Dietary Nutrients, and Functional Polymorphism of the Tissue-nonspecific Alkaline Phosphatase Gene in Healthy Young Adults. Natsuko Sogabe*[1], Rieko Maruyama[2], Mayu Haraikawa[2], Yutaka Maruoka[3], Takayuki Hosoi[4], Masae Goseki-Sone[5]. [1]Japan Women's University, Komazawa Women's University, Japan, [2]Japan Women's University, Japan, [3]National Center for Global Health & Medicine, Japan, [4]National Center for Geriatrics & Gerontology, Japan, [5]Japan Women's University, Japan

Alkaline phosphatase (ALP) is present mainly on the cell membrane in various tissues and hydrolyzes a variety of monophoshate esters into inorganic phosphoric acid and alcohol. Human ALPs are classified into four types: tissue-nonspecific, intestinal, placental, and germ cell types. Based on studies of hypophosphatasia, which is a systemic skeletal disorder resulting from TNSALP deficiency, TNSALP was suggested to be indispensable for bone mineralization. Recently, we demonstrated that there was a significant difference in the BMD among genotypes, being lowest among TNSALP 787T homozygotes (TT-type), highest among TNSALP 787T>C homozygotes (CC-type), and intermediate among heterozygotes (TC-type) in postmenopausal women. We investigated the effects of the TNSALP genotype on associations among serum bone-specific ALP (BAP), osteocalcin (OC), calcium, phosphorus, 1α, 25(OH)2D3, and FGF23 in healthy young males (n=97, age: 22.6$\pm$1.7 y; mean$\pm$standard deviation) and females (n=96, age: 21.8$\pm$1.8 y). Dietary nutrient intakes were measured based on 3-day food records before the day of blood examinations. All subjects were genotyped for the polymorphism (TNSALP 787T>C). As the results, there was a significant negative correlation between the levels of BAP and phosphorus in all male subjects ($r=-0.201$, $p<0.05$). Moreover, grouped by the TNSALP genotype, a significant negative correlation between serum BAP and phosphorus was observed in 787T>C homozygotes (CC-type) ($r=-0.402$, $p<0.05$), but not in heterozygotes (TC-type), nor in 787T homozygotes (TT-type). No significant correlation was noted between the levels of BAP and phosphorus in all female subjects, nor on grouping by the TNSALP genotype. In the present study, we revealed that the single nucleotide polymorphism of 787T>C in the TNSALP gene affected the correlation between serum BAP and phosphorus in young males. These results suggest that TNSALP variation may be an important determinant of phosphate metabolism. Our data may be useful for planning strategies to prevent osteoporosis.

***Disclosures: Natsuko Sogabe**, None.*

MO0310

BMD in American Indian Men and Women. Maureen Murtaugh*, Tracy Frech, Khe-ni Ma, Molly McFadden, Lillian Tom-Orme, Laurie Moyer-Mileur, Tom Greene, Martha Slattery. University of Utah, USA

Little is known about bone mineral density (BMD) in US American Indian populations. The purpose of this work is to describe current bone BMD in Ameican Indian men and women in the southwest US. Participants for the Navajo Bone Health Study were randomly selected to age and gender group (n=454 men and n=646 women) from a larger population-based study of lifestyle and health (EARTH). BMD measurements of the total hip, total femoral neck, lumbar spine (L1-L4), and whole

body BMD were measured in Shiprock, NM on one Hologic Discovery W DEXA using standard protocols. We present cross-section means for BMD at these sites and T-scores for hip by age and gender groups. Femoral neck BMD decreased across age and gender groups as expected. Other BMD measures were stable or slightly increased among the 30-40 year group as compared to the <30 group and decreased over time except for lumbar spine BMD that increased across age groups in men. We believe this is the first description of BMD in American Indian men. The cross-sectional design prevents us from discriminating between age and temporally related differences in BMD, but these data will help to formulate direction for future studies.

Navajo Men	Age ≤ 30	Age 30-40	Age 40-50	Age 50-60	Age > 60
	N=123 Mean (SD)	N=89 Mean (SD)	N=108 Mean (SD)	N=90 Mean (SD)	N=44 Mean (SD)
Total Hip BMD (g/cm^2)	1.04 (0.12)	1.05 (0.12)	1.02 (0.13)	1.02 (0.14)	0.96 (0.14)
Femoral Neck BMD (g/cm^2)	0.95 (0.13)	0.89 (0.12)	0.86 (0.12)	0.84 (0.12)	0.78 (0.12)
Lumbar Spine BMD (g/cm^2)	1.06 (0.13)	1.07 (0.12)	1.06 (0.14)	1.09 (0.15)	1.11 (0.15)
Whole body BMD (g/cm^2)	1.17 (0.1)	1.19 (0.10)	1.18 (0.10)	1.18 (0.11)	1.15 (0.11)
DEXA Hip T-score	0.07 (0.81)	0.12 (0.77)	-0.10 (0.87)	-0.11 (0.93)	-0.46 (0.90)
Navajo Specific Hip T-score	0.01 (1.00)	0.06 (0.95)	-0.21 (1.07)	-0.22 (1.15)	-0.65 (1.12)
Navajo Women	Age ≤ 30	Age 30-40	Age 40-50	Age 50-60	Age > 60
	N=152 Mean (SD)	N=120 Mean (SD)	N=159 Mean (SD)	N=119 Mean (SD)	N=96 Mean (SD)
Total Hip BMD (g/cm^2)	0.97 (0.13)	1.00 (0.12)	0.98 (0.12)	0.90 (0.12)	0.81 (0.14)
Femoral Neck BMD (g/cm^2)	0.88 (0.13)	0.87 (0.12)	0.84 (0.10)	0.76 (0.10)	0.70 (0.11)
Lumbar Spine BMD (g/cm^2)	1.06 (0.11)	1.09 (0.10)	1.07 (0.12)	0.96 (0.13)	0.70 (0.11)
Whole body BMD (g/cm^2)	1.12 (0.10)	1.15 (0.08)	1.14 (0.08)	1.05 (0.11)	0.98 (0.11)
DEXA Hip T-score	0.25 (1.10)	0.48 (1.02)	0.34 (1.00)	-0.36 (0.96)	-1.06 (1.13)
Navajo Specific Hip T-score	0.05 (1.0)	0.26 (0.920)	0.13 (0.90)	-0.50 (0.86)	-1.13 (1.02)

table

***Disclosures: Maureen Murtaugh**, None.*

MO0311

Bone Mineral Density in Men with and Without Hip Fracture. Laura Yerges-Armstrong*[1], Marc Hochberg[2], William Hawkes[3], Lisa Reider[4], Thomas Beck[5], Richard Hebel[3], Denise Orwig[6], Jay Magaziner[6]. [1]University of Maryland, USA, [2]University of Maryland School of Medicine, USA, [3]Epidemiology & Preventive Medicine, University of Maryland, USA, [4]School of Public Health At Johns Hopkins, USA, [5]Johns Hopkins Outpatient Center, USA, [6]University of Maryland, Baltimore, USA

While hip fracture is more common in older women, hip fracture is also a substantial public health burden in older men. The goal of this analysis was to compare bone mineral density (BMD) in the contralateral proximal femur of male fracture cases to non-fracture male controls. This was accomplished by comparing data on 58 white men from the Baltimore Hip Study (BHS)-7, a prospective cohort study of hip fracture outcomes in older community-dwelling men and women conducted in the greater Baltimore area, to 498 white men who had participated in the Baltimore Male Osteoporosis Study (MOST), a prospective cohort study of men age 65 and older from the Baltimore area recruited without regard to their skeletal health (George A et al; JBMR 2003). Height, weight and age-adjusted T-scores from the total hip and femoral neck were calculated for men from both studies. Height and weight adjusted mean BMD was also calculated by 10 year age group. Overall, men who had a hip fracture had a 44% lower T-score at the total hip and a 31% lower T-score at the femoral neck compared to men without hip fractures. This pattern was consistent across ten year age groups (see table). At the femoral neck, 32.7%(SE=4.0) of men with a hip fracture had a T-score less than -2.5 compared to only 8.6%(SE=1.3) of men from the control group. Similarly, 27.7%(SE=3.2) of men who had a hip fracture had a total hip T-score less than -2.5 compared to only 4.2%(SE=1.0) in the control group. These data are consistent with the following conclusions: 1) men who fracture have lower BMD at the contralateral hip compared to men in the general population, and 2) fewer than half of older men who sustain a hip fracture have a T-score of -2.5 or below at the time of fracture as has previously been reported for older women (Wainwright SA, et al: JCEM 2005).

		BHS-7	MOST
Total Hip BMD T-scores	Overall	-1.64 (0.12)	-0.92 (0.04)
	65-74 years	-1.53 (0.23)	-0.72 (0.05)
	75-84 years	-1.62 (0.17)	-1.04 (0.06)
	85+ years	-2.19 (0.19)	-1.32 (0.13)
Femoral Neck BMD T-scores	Overall	-1.98 (0.11)	-1.36 (0.04)
	65-74 years	-1.74 (0.22)	-1.19 (0.05)
	75-84 years	-2.08 (0.17)	-1.48 (0.06)
	85+ years	-2.40 (0.18)	-1.69 (0.13)

Table1

***Disclosures: Laura Yerges-Armstrong**, None.*

MO0312

Does Prevalent Vertebral Fracture Status (PVFx) Modify the Association Between Bone Mineral Density and Incident Hip and Incident Radiographic Vertebral Fractures in Older Women? Findings from SOF. John Schousboe*[1], Lisa Palermo[2], Kathy Wilt[3], Dennis Black[2], Kristine Ensrud[4]. [1]Park Nicollet ClinicUniversity of Minnesota, USA, [2]University of California, San Francisco, USA, [3]California Pacific Medical Center, USA, [4]Minneapolis VA Medical Center / University of Minnesota, USA

Purpose: Prevalent radiographic vertebral fractures (PVFx) and bone mineral density (BMD) are well established independent predictors of incident vertebral and hip fractures. Recent published data from the MORE and FPT trials suggest that the association between bone mineral density and incident radiographic vertebral fracture may be modified by PVFx status, being stronger in those with PVFx and weaker in those without PVFx. If this were so, then BMD may be less predictive of fracture in that subset of women without prevalent vertebral fracture. We used data from the Study of Osteoporotic Fractures (SOF) to test whether or not the associations between BMD (lumbar spine and femoral neck) and risk of incident radiographic vertebral and hip fractures are modified by PVFx.

Methods: 6,351 women were evaluable for PVFx on baseline lateral spine radiographs and for incident radiographic vertebral fracture on lateral spine radiographs taken at the 3rd SOF visit (mean 3.7 years later), and had complete covariate data, including BMD at the 2nd SOF visit. Incident hip fractures (over the first five years after measurement of BMD at the 2nd SOF visit) were detected by self-report every 4 months and confirmed by review of the radiographic reports. Two sets of multivariable-adjusted logistic regression and proportional hazards models were used to estimate the associations of, respectively, incident radiographic vertebral fracture and incident hip fracture with BMD; a) separately in the subsets having 0 or ⩾1 PVFx, and b) in the entire cohort including an interaction term between PVFx (absent or present) and BMD.

Results: The odds ratios of incident radiographic vertebral and the hazard ratios of incident hip fractures associated per one standard deviation decrease of BMD in the subset with ⩾ 1 prevalent vertebral fracture were not different than those in the subset with zero prevalent vertebral fractures (table). The p-values for the interaction terms PVFx*BMD parameter estimates were all > 0.10.

Conclusion: The associations of bone mineral density at either the lumbar spine or femoral neck with incident radiographic vertebral or incident hip fracture are not modified by PVFx status in community dwelling women elderly women. Irrespective of prevalent vertebral fracture status, BMD is a robust predictor of incident radiographic vertebral and hip fractures.

Table – Associations of BMD with incident fractures in subsets defined by PVFx

***Disclosures: John Schousboe**, None.*

MO0313

DXA Screening and Use of Osteoporosis Medications in Two Large Healthcare Systems. Amy Warriner*[1], Ryan Outman[2], Jeffrey Curtis[2], Adrianne Feldstein[3], Harry Glauber[4], Junling Ren[5], Douglas Roblin[5], Ana Rosales[3], Robert Unitan[4], Kenneth Saag[2]. [1]UAB, USA, [2]University of Alabama at Birmingham, USA, [3]Kaiser Permanente Center for Health Research, USA, [4]Kaiser Permanente Northwest, USA, [5]Kaiser Permanente Georgia, USA

Purpose: To compare the effect of a patient panel-support tool (PST) vs. standard of care on dual energy x-ray absorptiometry (DXA) screening in two large healthcare systems. Despite U.S. guideline recommendations for all women 65 years and older to

have a screening bone density scan with central DXA, less than one-third of eligible U.S. women have undergone DXA testing.

Methods: We evaluated DXA receipt and use of prescription osteoporosis medications among women aged 65 - 90 in two large healthcare systems. Women were eligible for inclusion in the analysis if they had at least 24 months of enrollment at Kaiser Permanente Georgia (KPGA) or Northwest (KPNW). Primary outcomes included a DXA scan in the past 5 years and use of osteoporosis medications in the past year. The analysis included data obtained in 6 month intervals from January 2005 through July 2009. From this data, we examined the effect of a PST (KPNW) vs. standard of care (KPGA). The PST uses EMR data to graphically display "care gaps" for each patient, based on current evidence. Through this mechanism, primary care physicians within the KPNW system are alerted to order a DXA in patients without a DXA in the previous 5 years (start date February 26, 2007).

Results: The number of women undergoing screening DXA increased significantly in the KPNW group with the proportion increasing from 25.3% in January 2005 to 58.7% in July 2009 (Risk Difference {RD} 33.3%, 95% CI 32.5 – 34.1%). This differs from KPGA, in which minimal change in DXA scan use occurred between January 2005 and July 2009, 43.1% and 45.3%, respectively (RD 2.2%, 95% CI 0.6 – 3.9%). The majority of the increased DXA use was seen following the implementation of the PST, Figure 1. However, the number of women taking an osteoporosis medication did not increase significantly over the 5 year period in either region, +3.4% in KPNW and +1.3% in KPGA.

Conclusions: Among older women, DXA testing increased incrementally over the past 3 years in the KPNW healthcare system, following the implementation of a PST. However, despite the increased screening, the use of osteoporosis-specific medications for fracture risk reduction did not increase significantly. In a similar healthplan that did not implement such a program, the rates of DXA testing remained relatively flat. Further randomized studies are needed to confirm effectiveness of methods to improve appropriate DXA utilization.

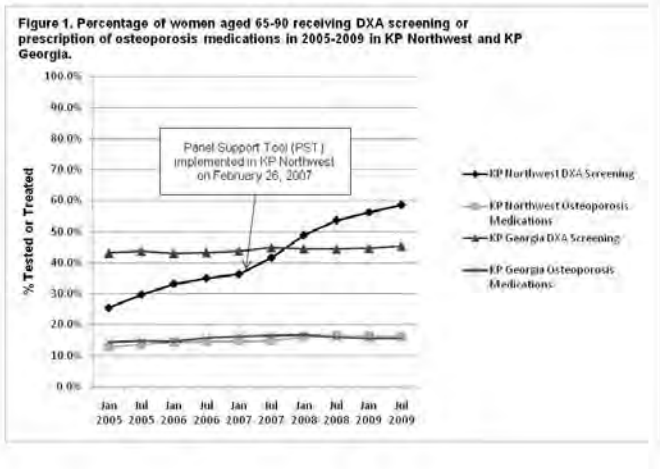

Percentage of women receiving DXA or osteoporosis medications

***Disclosures: Amy Warriner**, None.*

MO0314

Genetic and Phenotypic Correlation between Bone Mineral Density and Subclinical Cardiovascular Disease in Multi-generational Families of African Ancestry. Allison Kuipers*[1], Genevieve A. Woodard[2], Kim Sutton-Tyrrell[2], Iva Miljkovic[2], Hu Li[2], Clareann H. Bunker[2], Alan L. Patrick[3], Victor W. Wheeler[3], Candace Kammerer[1], Joseph Zmuda[1]. [1]University of Pittsburgh Graduate School of Public Health, USA, [2]University of Pittsburgh, USA, [3]Tobago Health Studies Office, Trinidad & tobago

Osteoporosis and cardiovascular disease are chronic diseases associated with the aging process. However, it is unclear whether these diseases progress together due to shared environmental and genetic determinants, or if they are coincident conditions of aging. We quantified the genetic and phenotypic correlations between these two disease processes in 377 individuals aged 18 years and older (mean age, 42.7 years) belonging to seven large, multi-generational families of African ancestry on the island of Tobago (19-125 individuals per family; 4,676 relative pairs). Bone mineral density (BMD) was measured with dual x-ray absorptiometry (DXA) and peripheral quantitative computed tomography (pQCT). Subclinical indices of atherosclerotic cardiovascular disease were assessed using carotid artery ultrasound images for calculation of common carotid artery intima-media thickness and adventitial diameter. After the traits were adjusted for age, sex, height and weight, genetic and environmental correlations were estimated using maximum likelihood variance component methods. Heritability of the BMD and CVD traits ranged from 0.51 ± 0.10 to 0.68 ± 0.10. We observed a significant phenotypic (P=-0.23, P=0.001) and genetic (rhoG=-0.47, P=0.002) correlation between mean arterial diameter and DXA total hip BMD. Adventitial diameter also had significant phenotypic and genetic correlation with pQCT measures of trabecular volumetric BMD at the radius (P= -0.247, P<0.001; rho G: -0.48, P=0.001). Similar findings were observed at the tibia. We did not detect significant correlations between intima-media thickness and BMD. Our results suggest that there may be significant shared (pleiotropic) genetic factors underlying variation in subclinical atherosclerosis and BMD.

***Disclosures: Allison Kuipers**, None.*

MO0315

High Bone Mineral Density is Associated with Metabolic Syndrome. Adarsh Sai*[1], Xiang Fang[2], J. Christopher Gallagher[1]. [1]Creighton University Medical Center, USA, [2]Creighton University, USA

Introduction: We examined the association of bone mineral density (BMD) with various parameters of metabolic syndrome.

Methods: 489 postmenopausal women with osteopenia and osteoporosis, mean (Standard Deviation) age 71.5(3.6) yrs were enrolled in an interventional treatment study (STOP IT). These results are from the baseline data. Serum bioavailable estradiol, testosterone and sex hormone binding globulin (SHBG) were measured by radioimmunoassay. Serum total cholesterol and triglycerides (TGs) were analyzed by enzymatic methods. High Density lipoprotein (HDL) cholesterol was estimated after pretreatment of the sample to precipitate Low Density Lipoprotein (LDL) cholesterol and Very Low density Lipoprotein (VLDL) cholesterol. VLDL cholesterol level was calculated as triglyceride/5. LDL cholesterol was calculated as [total cholesterol-(HDL+VLDL)]. Bone Mineral Density (BMD) measurements at the femoral neck were done on DPXL scanner. We divided study population into tertiles of femoral neck BMD and compared the groups with one-way ANOVA.

Results: Amongst femoral neck BMD tertiles the differences in various parameters were compatible with Metabolic Syndrome. In the highest tertile of femoral neck BMD, body mass index was higher ($p<0.01$), serum TGs were higher ($p<0.05$) and HDL was lower (<0.01)(Table 1). There was no difference in serum LDL cholesterol. Fasting serum glucose was significantly higher only in tertile 2 as compared to tertile 1 (Table1). Systolic blood pressure was significantly higher in tertile 3 vs 1 of BMD (142.59 ± 1.6 mm of Hg vs 134.8 ± 1.4 mm of Hg, $p<0.01$) and diastolic blood pressure was significantly higher in tertiles 2 and 3 vs 1 (75.3 ± 0.6 mm of Hg in tertile 1 vs 78.6 ± 0.8 in 2 and 78.6 ± 0.7 mm of Hg in tertile 3; $p<0.01$). Bioavailable estradiol and testosterone were significantly increased (Table1) and SHBG was significantly lower among higher BMD tertiles (168.82 ± 6.16 nmol/L in tertile 1 vs 144.02 ± 5.3 in tertile 2 and 125.85 ± 5.45 in tertile 3; $p<0.01$).

Conclusions: Women with higher BMD have several features of Metabolic Syndrome. This association between femoral neck BMD and the parameters of metabolic syndrome might imply a higher risk of cardiovascular and metabolic diseases in women with higher BMD at femoral neck.

Tertiles of		1	2	3
Femoral neck BMD	(g/cm^2)	(0.55-0.72)	(0.73-0.82)	(0.83-0.94)
BMI (Body Mass Index)		25.22±0.3	27.72±0.4**	28.37±0.4**
Serum Triglycerides	(mg/dl)	131.15±5.6	155.52±6.8	161.91±7*
Serum HDL	(mg/dl)	54.09±1	50.85±0.91*	49.97±0.9**
Serum LDL	(mg/dl)	139.75±2.5	145.41±3	142.23±2.4
Fasting serum glucose	(mg/dl)	89.34±1.27	96.21±2*	94.79±1.6
Bio-Estradiol	(pg/ml)	2.73±0.12	3.74±0.17**	4.25±0.21**
Bio-testosterone	(ng/ml)	21.08±1.23	26.16±1.31*	33.48±1.73**

*P<0.05 and **p<0.01 as compared to tertile 1 after Tukey's post-hoc correction
Data expressed as Mean ± 1 SE

Table 1

***Disclosures: Adarsh Sai**, NIH (Grants AG28168, UO1-AG10373 and RO1-AG10358), 2*

MO0316

Vertebral Body Dimensions Increase in Young Women Independently From BMD: a Longitudinal *in vivo* Study. Sami Kolta*[1], Samar Kerkeni[2], Christophe Travert[3], Wafa Skalli[4], Christian Roux[1]. [1]Paris Descartes University, Rheumatology Department, Cochin Hospital, France, [2]Paris Descartes University, Cochin Hospital, France, [3]Arts et Metiers ParisTech, CNRS, LBM, France, [4]Arts et Metiers ParisTech, CNRS, France

Introduction: Bone geometry is known to be an important determinant of bone strength. We have previously shown, in a cross sectional study, that vertebral body parameters adjusted to body height, are larger in postmenopausal women than in young premenopausal women (1).

Aim of study: Our study aimed to assess changes in vertebral geometric parameters in young women using 3D-XA method in vivo.

Patients and Methods: Subjects were women participating in the European population-based Osteoporosis and Ultrasound Study (OPUS) (2). This longitudinal study was conducted in young women (20–40 years, N=53), without prevalent or incident vertebral fracture. All participants had an anterior-posterior and a lateral measurement of thoracic and lumbar spine using Instant Vertebral Assessment software on a standard Hologic QDR4500A device at baseline and 6 years later. Legible vertebrae from T4 to L4 were studied. Three-dimensional reconstruction of vertebrae using 3D-XA method was performed according to our previously published methodology (3). Several geometric parameters of vertebral bodies were measured from the 3D-XA including anterior, middle and posterior heights (aH, mH and pH),

vertebral body depth, vertebral body width, vertebral volume, and minimal cross sectional area (CSA).

Results: There was no significant difference between BMD results at the spine between baseline and 6 year follow-up results (p=0.09). Height has not changed during follow-up period (166.5±6.2 cm vs 166.4±6.3 cm). Six years follow-up using 3D-XA method revealed no significant change in vertebral body heights (aH, mH or pH). However, there was a significant increase in vertebral body width (+0.3 mm, p<0.0001), vertebral body depth (+0.2 mm, p<0.001), vertebral volume (+175.2 mm3, p=0.003) and CSA (+8.1 mm^2, p<0.0001).

Conclusion: This study shows that vertebral dimensions vary with age in young adults. It suggests that vertebral body growth in women still continues after 20 years of age, independently from BMD and that these changes in dimension can be detected by the 3D-XA method.

(1) Kerkeni et al ASBMR 2008.
(2) Gluer et al J Bone Miner Res 2004; 19: 782-793.
(3) Kolta et al Osteoporos Int 2008; 19: 185-192.

***Disclosures: Sami Kolta**, None.*

MO0317

Food Supplementation with 2,200 IU Vitamin D_3 Daily Is Safe, but Does Not Assure Adequacy. Irina Haller*[1], Diane Krueger[2], Mary Checovich[2], Jean A Engelke[3], Neil Binkley[4]. [1]Essentia Institute of Rural Health, USA, [2]University of Wisconsin, Madison, USA, [3]University of Wisconsin-Madison, USA, [4]University of Wisconsin, USA

Food fortification with vitamin D (D) amounts greater than currently used is a reasonable approach to improve D status on a population level. However, provision of larger amounts of D in food has received little study. This randomized, double-blind, placebo-controlled trial evaluated serum 25-hydroxyvitamin D [25(OH)D] response to daily ingestion of D_3 fortified food for 4 months in 99 women from 3 age groups (20-30, 55-65 and 75+ years). Women were randomly assigned in 1:1 ratio to receive either a low calorie chocolate disk fortified with ~2,300 IU of D_3 or an identical placebo disc. Body composition was determined at baseline by total body DXA. Serum calcium, 25(OH)D concentration and 24-hour urinary calcium excretion were measured at baseline and months 1, 2 and 4. Serum chemistries, parathyroid hormone (PTH) and markers of bone turnover were measured at baseline and 4 months. Data were analyzed using t-test, chi-square test and general linear model.

Baseline differences ($p < 0.05$) in BMI, creatinine, albumin, PTH and bone-specific alkaline phosphatase (BSAP) were observed between age groups: young women had lower weight, creatinine, PTH, BSAP and higher albumin. There were no baseline differences in 25(OH)D or other clinical characteristics between placebo and D groups. While the mean [SEM] baseline 25(OH)D concentration was 31.4 [1.0] ng/ml, 44% of women had low D status (25(OH)D < 30 ng/ml). Compliance exceeded 90% in all groups resulting in an average daily D intake of ~2,200 IU. At 4 months, 25(OH)D concentration increased ($p < 0.01$) by 14.2 [1.3] ng/ml on average in those receiving D, however 11% of them remained below 30 ng/ml. Serum and 24-hour urinary calcium were unaffected by D intake. There was no age-group effect on the 25(OH)D increase. Total body mass, fat mass and lean mass were negatively correlated ($p < 0.05$) with baseline 25(OH)D. However, the change in 25(OH)D following 4 months of D intake was unrelated to total body mass, fat mass or lean mass.

In conclusion, food fortification is a safe and effective approach to improve D status. The increment in 25(OH)D (~6 ng/1,000 IU D_3 daily) observed with ingestion of fortified food was similar to that reported with supplements and does not differ by age or amount of body fat. Daily D_3 intake will likely need to exceed 2,200 IU to assure adequacy for all women. The mechanisms underlying the differences in 25(OH)D response to oral D intake require further evaluation.

***Disclosures: Irina Haller**, None.*

MO0318

Adherence to the Current Physical Activity Guidelines Is Not Associated with a Reduced Fracture Incidence in Older Adults? A National, Population-based Prospective Study (AusDiab). Robin Daly*[1], Riku Nikander[2], Claudia Gagnon[3], David Dunstan[4], Peter Ebeling[5], Dianne Magliano[4], Paul Zimmet[4], Jonathan Shaw[4]. [1]The University of Melbourne, Western Hospital, Australia, [2]Department of Medicine, The University of Melbourne, Australia, [3]Department of Medicine, University of Melbourne, Western Hospital, Australia, [4]Baker IDI Heart & Diabetes Institute, Australia, [5]University of Melbourne, Australia

Current physical activity (PA) guidelines recommend that older adults accumulate at least 2.5 hrs/wk of moderate (mod) intensity aerobic PA, or at least 20 min/d of vigorous (vig) PA 3 d/wk and resistance training 2-3/wk. There is also increased emphasis on reducing sedentary behaviour (prolonged sitting), which has been associated with adverse cardiometabolic outcomes. However, whether adherence to these guidelines will reduce the risk of fractures in the elderly is unknown. This study aimed to examine whether: 1) older adults who meet the current PA guidelines are at a reduced risk of fracture; 2) fracture risk varies by PA frequency and intensity; and 3) prolonged TV viewing time is associated with a greater fracture risk. This national, population-based prospective study, undertaken in 1999/2000 with a 5-yr follow-up, included 2780 postmenopausal women (mean±SD; 60±10 yrs) and 2129 men aged ≥50 yrs (62±9 yrs). Incident non-traumatic clinical fractures (eg. fall from a standing height or less) were self-reported. Self-reported (previous week) PA [total = walking + mod-vig] and TV viewing time were assessed using interview-administered questionnaires. Overall, 307 (6.3%) participants sustained at least one fracture (women 9.3%; men 2.3%). After adjusting for age, BMI and physical functioning (SF36), women who accumulated at least 2.5 hrs/wk of PA were not protected from fractures [OR (95% CI), 1.06 (0.81, 1.39)]. When walking and mod+vig PA time (hr/wk) or frequency (≥10 min continuous walking or mod-vig PA) were entered separately into the model, each 1-hr increment in weekly walking time [OR 1.05 (1.00, 1.10)] and walking frequency [OR 1.06 (1.02, 1.09)] were associated with a significant 5-6% increased risk of fracture. Mod-vig PA time or frequency was not protective of fractures [OR time 0.98 (0.94, 1.02); frequency 0.98 (0.93, 1.04)]. When walking time and frequency were entered together in the model, only walking frequency remained significant [OR 1.06 (1.01, 1.10)]. Similar results were observed in men, and after adjusting for other potential confounders, including previous fracture history, serum 25OHD levels, smoking and alcohol intake. TV viewing time was not associated with fracture risk in men or women. In conclusion, middle aged and older adults who met the current PA guidelines do not appear to be protected against fragility fractures, and more frequent walking appears to be associated with an increased fracture risk.

***Disclosures: Robin Daly**, None.*

MO0319

Association of Diet Quality Measured by Healthy Eating Index and Bone Turnover Biomarkers among Postmenopausal Women in the National Health and Nutrition Examination Survey 1999-2002. Maryam Hamidi*[1], Valerie Tarasuk[2], Paul Corey[3], Angela Cheung[4]. [1]University of Toronto/University Health Network-TGH, Canada, [2]Professor- Department of Nutritional Sciences- University of Toronto, Canada, [3]Professor- Dalla Lana School of Public Health-University of Toronto, Canada, [4]University Health Network, Canada

Background: Diet is one of the major modifiable risk factors in the prevention and treatment of postmenopausal osteoporosis. There is evidence that overall diet quality, not just single nutrients like calcium or vitamin D, is important for bone health.

The objective of this study was to examine the association between overall diet quality and bone turnover biomarkers (BTB) among postmenopausal women, using the original Healthy Eating Index (HEI) and HEI 2005 developed by the United States Department of Agriculture. Unlike HEI, HEI 2005 scores are expressed per 1000 calories.

Methods: We used cross-sectional data from two cycles (1999 and 2002) of National Health and Nutrition Examination Survey (NHANES). Ambulatory postmenopausal American women ≥ 45 years, free from diseases and medications that affect bone metabolism were included. HEI and HEI 2005 scores were calculated based on a validated 24-hour dietary recall and used as continuous variables as well as tertiles in regression models. Survey procedures with appropriate weights were used for all analyses.

Bone Alkaline Phosphatase (BAP), a biomarker of bone formation, and Urinary N-Telopeptides (U-NTx), a biomarker of bone resorption were the outcome variables and were logarithmically transformed to reduce the within person variability and to avoid inappropriate exclusion of outliers. Weighted multiple regressions with adjustments for relevant confounders were used to assess the relationship between HEIs and BTB.

Results: The relationship between HEI and BTB was not linear. Those in the highest tertile of HEI (healthiest) had lowest BAP and U-NTx levels, but this was only statistically significant when second and third tertiles were compared (p=0.030 and 0.049 respectively). HEI 2005 was not associated with BTB. Models for BAP were adjusted for nicotine exposure, alcohol intake, income, calcium or vitamin D supplements and sedentary lifestyle. Models for U-NTx were adjusted for central obesity, education and nicotine exposure. The correlation between dairy intake and total HEI score was low (r=0.15, p<0.0001) and not statistically significant between dairy intake and total HEI2005 score (r=0.01, p=0.790).

Conclusion: Our results suggest that HEI and HEI 2005 are not good measures of healthy eating for optimal bone health. Further research is needed to develop an overall dietary assessment tool in relation to bone health for postmenopausal women.

***Disclosures: Maryam Hamidi**, None.*

MO0320

Effect of Milk Product with Soy Isoflavones on Bone Metabolism in Spanish Postmenopausal Women: A Randomized Controlled Trial. Antonia García-Martín*[1], María Dolores Avilés-Pérez[1], Miguel Quesada-Charneco[1], Juristo Fonollá-Joya[2], José J Jiménez-Moleón[3], Manuel Muñoz-Torres[1]. [1]Bone Metabolic Unit. Endocrinology Division. San Cecilio University Hospital, Granada, Spain, [2]Investigation Department Puleva Biotech, Granada, Spain, [3]Epidemiology & Preventive Medicine Department, University of Granada, Spain

Recent studies have been conducted to determine the role of isoflavones in the prevention of postmenopausal osteoporosis with conflicting results. The aim of this study is to evaluate the effects of nutritional intervention with a milk product enriched with soy isoflavones on bone metabolism in postmenopausal Spanish women. We performed a double-blind controlled randomized trial in ninety-nine postmenopausal women: 48 subjects (group S) were randomized to consume milk product enriched with soy isoflavone (50 mg/day) while 51 subjects (group C) consumed product control for 12 months. Hormonal parameters and biochemical markers of bone were analyzed. We used calcaneus ultrasound (QUS, Hologic Sahara®, NC, USA) as method to examine bone mass at baseline and after 1-year. Overall, serum levels tartrate resistant acid phosphatase and osteoprotegerin decreased (2.18 $\pm$0.8 vs 1.76 $\pm$0.54 IU/l, $p<0.001$ and 5.21 $\pm$3.36 vs 3.89 $\pm$1.47, $p=0.007$) and serum concentrations 25-OH-vitamin D increased (24.48 $\pm$9.85 vs 28.18 $\pm$10.45, $p<0.001$) without differences between groups. There were no significant variations in hormonal parameters and other bone markers. About QUS, in total sample there were increases of speed of sound (1517.86 $\pm$38.13 vs. 1525.11 $\pm$35.6 m/s, $p=0.036$), stiffness (76.37 $\pm$19.87 vs 80.82 $\pm$18.26, $p=0.012$), estimated bone mineral density (0.408 $\pm$0.13 vs 0.435 $\pm$0.12 g/cm^2, $p=0.013$) and T-score (-1.55 $\pm$1.12 vs -1.31 $\pm$1.03, $p=0.019$). In the group S, there were positive changes in stiffness (74.37 $\pm$18.87 vs 78.83 $\pm$13,68, $p=0.032$) and estimated bone mineral density (0.397 $\pm$0.12 vs 0.423 $\pm$0.09 g/cm ^{2}, $p=0.04$) while the group C showed no significant differences. We conclude that daily consumption of milk products increases levels of 25-OH-vitamin D and decreases bone remodelling markers. Additional supplementation with soy isoflavones improves QUS parameters in Spanish postmenopausal women.

***Disclosures: Antonia García-Martín**, None.*

MO0321

Factors Influencing Vitamin D Deficiency in Saudi Arabian Children and Adolescents: Impact of Age, Gender, Lifestyle and Nutrition. Susan Lanham-New[1], Jalal Jalal[2], Maryam AL-Ghamdi*[3]. [1]University of Surrey, United Kingdom, [2]King Abdula-Aziz University, Saudi arabia, [3]King Abdulaziz University, Saudi arabia

Few data exist on the effects of age, gender and life-style factors (including nutrition) on vitamin D status among Saudi Arabian children and adolescents, for both male and female. The aim of this study was to determine the extent of poor vitamin D status in school children (boys and girls, pre- and post-pubertal) and examine if there were any differences in vitamin D status with chronological age, physical activity and extent of veiling and the concomitant effects on bone health. This research forms part of on-going work on vitamin D and bone health at the King Abdul Aziz University (KAAU) in Jeddah. Weight and height was recorded and subjects were asked to complete a lifestyle questionnaire which asked about their physical activity levels and dietary habits. A total of 150 boys (7–16 years) and 150 girls (6–18 years) from schools in Jeddah were recruited. A fasted blood sample was collected for assessment of vitamin D (25OHD) status; parathyroid hormone (PTH), sCa, saAlbumin. sALK.phosphates, sOsteocalcin and sCTx. . BMD was assessed using DXA (Lunar Corp., DPX version 4.7). Calcaneal bone mass was measured by BUA (CUBA plus+ softwareV4). The mean age was 10.3$\pm$ [3.49] yrs for Pre-Pubertal boys vs. 8.53$\pm$ [1.29] yrs for Pre-Pubertal girls; Post-Pubertal boys 14.6$\pm$ [0.6] yrs vs 12.69$\pm$ [1.28] yrs for the Post-Pubertal girls. 25OHD status was significantly lower in the girls than the boys generally ($P<0.001$). There was difference in 25OHD status between the pre-pubertal boys and post-pubertal boys and between the pre-pubertal girls vs. the post-pubertal girls, which remained significant after adjustment for weight and height (Pre Boys: 56.1 [13.9] vs. Post Boys 50.5b [11.9] nmol/l; Pre Girls 40.4. [8.9] vs. Post Girls 28.8 [9.4] nmol/l. In parallel, PTH was significantly higher in the post-pubertal boys and girls compared to their younger age counterparts. However, the difference in PTH was markedly higher in the post-pubertal v pre-pubertal comparisons in the girls compared with the differences in the boys. There were no differences in serum Ca levels between any of the groups. Alkaline phosphatase was significantly higher in the older boys but significantly lower in the older girls. .These data suggest significant hypovitaminosis D in older adolescent females than males, which may be particularly influenced by the extent of veiling. These data are a cause for concern given that there is currently no public health policy for vitamin D in the Kingdom of Saudi Arabia. Further work is underway to examine the impact of low 25OHD on PBM attainment.

***Disclosures: Maryam AL-Ghamdi**, D3Tex Ltd, 1*

MO0322

High Vitamin A serum Levels Are Associated with Low Bone Mineral Density (BMD) in postmenopausal osteoporotic women. Jose Maria Mata-Granados*[1], Jose Manuel Quesada Gomez[1], Manuel Diaz Curiel[2], Manuel Sosa-Henriquez[3], Xavier Nogues[4], Victor Vila Fagos[5], Jose Luis Pérez-Castrillón[6], Javier Calvo Catalá[7], Carlos Gomez[8], Jorge Malouf[9], Pau Lluch Mezquida[10], Javier Pino Montes[11], Xavier Cortés[10], Joaquín Delgadillo[10]. [1]Gabinete Quesper, Spain, [2]Jimenez Diaz Fundacion, Spain, [3]University of Las Palmas de Gran Canaria, Spain, [4]Institut Municipal D'Investigació Mèdica, Spain, [5]Hospital, Spain, [6]University Hospital Rio HortegaValladolid Spain, Spain, [7]Hospital de Valencia, Spain, [8]Hospital Central de Asturias, Spain, [9]Hospital de la Santa Creu i Sant Pau, Spain, [10]Barcelona, Spain, [11]University of Salamanca, Spain

A cohort of treated and non-treated osteoporotic postmenopausal women [Previcad study] was identified. The prevalence of high serum levels of vitamin A, vitamin D deficiency & insufficiency and its association with bone mineral density (BMD) in relation with osteoporosis treatment was assessed.

A total of 358 osteoporotic postmenopausal women [WHO criteria] 65 years and older were identified: group 1: treated for osteoporosis (n=204) and group 2: non-treated for osteoporosis (n=154). BMD was measured by DEXA. Vitamins A and D (25OHD3) were measured by an automated HPLC method previously reported by our group.

The prevalence of vitamin D deficiency (25(OH)D3< 20 ng/ml) was higher in the non-treated group (42.8%) than in the treated group (29.4%). Vitamin D insufficiency (25(OH)D3< 30 ng/ml) was also higher in the non-treated group (75.7%) than in the treated group (62.8%). High serum levels of vitamin A (>80 µg/dl) were slightly more prevalent in the non-treated group (25.8%) as compared to the treated group (22.5 %). Among subjects with vitamin D deficiency (n = 152), 60.4% (n=92) had high serum levels of vitamin A. MANOVA in a multivariate linear model for BMD as continuous variable showed a statistically significant effect of serum vitamin A levels in quintiles ($p<0.01$) in both LS and FN [age and weight were included in the model as inputs ($R=0.342$, $p<0.0001$)]. Statistically significant differences ($p<0.05$) were found for BMD-LS running the Bonferroni test between first quintile (-2.48 $\pm$ 0.16) and second (-2.89 $\pm$ 0.11), third (-2.84 $\pm$ 0.09), fourth (-3.06 $\pm$ 0.10) and fifth (-3.64 $\pm$ 0.19). In FN ($R=0.260$, $p< 0.001$), BMD was significantly lower for 5th (-2.43 $\pm$ 0.17), 4th (-2.44 $\pm$ 0.12), 3rd (-2.21 $\pm$ 0.11) and 2nd (-2.25 $\pm$ 0.10) quintiles of vitamin A compared to the 1st (-1.79 $\pm$ 0.20) quintile as reference, running Bonferroni test.

The treated group showed the same trend that it in whole population: BMD in LS spine was significantly lower in 5th (-3.75 $\pm$ 0.22), 4th (-3.20 $\pm$ 0.12), 3rd (-3.12$\pm$ 0.16) and 2nd (-2.93 $\pm$ 0.18) than in 1st (-2.56 $\pm$ 0.14) quintiles of vitamin A. In the non-treated group the effect was less intense than in the treated group, although significant differences were found between 1st (-2.45$\pm$ 0.34) and 4th (-3.21 $\pm$ 0.12), 5th (-3.45 $\pm$ 0.38) quintiles.

High serum levels of vitamin A, especially in vitamin D deficient patients are associated with low BMD, in treated and not treated osteoporotic women.

***Disclosures: Jose Maria Mata-Granados**, None.*

MO0323

Is there a Relation Between Dietary Protein and Bone Loss in Men, Premenopausal Women or Postmenopausal Women in the Framingham Osteoporosis Study? Marian Hannan*[1], Shivani Sahni[2], Robert McLean[3], Kerry Broe[4], L. Adrienne Cupples[5], Katherine Tucker[6], Douglas Kiel[7]. [1]HSL Institute for Aging Researchand Harvard Medical School, USA, [2]Hebrew SeniorLife, Institute for Aging Research, Harvard Medical School, USA, [3]Hebrew SeniorLife, Harvard Medical School, USA, [4]Hebrew Senior Life, USA, [5]BUSPH, USA, [6]Northeastern University, USA, [7]Hebrew SeniorLife, USA

Our prior work showed a link between low protein intake and greater bone loss in elderly Framingham Study men and women. It is unclear if this relation exists in middle-aged adults and if it depends upon calcium intake, as higher protein intake may enhance calcium absorption. Thus, we examined the relation between baseline dietary protein and subsequent annualized change in bone mineral density (BMD) over follow-up by calcium intake levels for 495 men, 105 premenopausal women and 550 postmenopausal women from the Framingham Offspring Study. We hypothesized lower dietary protein to be associated with BMD loss, and in those with calcium intakes <800 mg/d, a greater bone loss. BMD (g/cm^2) was assessed using Lunar DPX-L in 1996-01 and repeated using Lunar Prodigy in 2002-5 at total hip (TH), femoral neck (FN), and trochanter (TR), adjusting for change in technology. %Protein (percent of energy from protein intakes), calcium and other dietary intakes were estimated via a 126-item food frequency questionnaire.

Multivariable linear regression was used to calculate the association (β) between %Protein and annualized BMD % change for men and pre/post menopausal women separately and also by calcium intake groups (<800 mg/d: y/n). Analyses were adjusted for age (y), height (in), weight (kg), current smoker (y/n), physical activity, intakes of total energy (Kcal/d), dietary and supplemental calcium (mg/d), dietary and supplemental vitamin D (IU/d), alcohol (g/d), caffeine (g/d) and in postmenopausal women, current estrogen use (y/n). We then stratified by calcium < 800 mg/d

adjusting for calcium intake within strata. %Protein was evaluated as a continuous variable and as quartiles. 60 osteoporosis medication users were excluded.

Mean age at baseline was 61y (range 29-86) with mean follow-up of 4.6y; see table for participant characteristics. Contrary to our hypothesis, women showed no associations between %Protein and bone loss, either as a whole or by calcium groups (all sites p>0.21). Only those men with calcium intakes ⩾ 800 mg/d showed a link between higher protein and BMD loss, but only at TR & TH, not FN. Results from quartile analyses were similar. Our results suggest protein intake is not linked to bone loss in pre- or postmenopausal women, regardless of calcium intake. Yet, in middle-aged men, higher protein is linked to bone loss but only in men with calcium ⩾ 800 mg/d, perhaps due to poor dietary habits of high fat, high protein diets. Future studies should examine patterns of dietary intakes rather than individual nutrients for their effect on bone in middle-aged, healthy adults.

Table. Characteristics of the Framingham Offspring cohortwith BMD change and annualized %BMD change model beta coefficients and standard errors.

Descriptive Variables	Mean ± SD		
	Men	Pre-menopausal women	Post-menopausal women
Age (years)	61 ± 9	48 ± 4	62 ± 8
BMI (kg/m^2)	28.8 ± 4.4	27.2 ± 6.6	27.6 ± 5.4
Total protein intake (g/d)	81 ± 28	82 ± 25	76 ± 26
Total protein %	16.9 ± 3.4	18.2 ± 3.2	17.8 ± 3.4
Baseline Total Hip BMD (g/cm^2)	1.041 ± 0.14	1.009 ± 0.13	0.900 ± 0.14
Baseline Femoral Neck BMD (g/cm^2)	0.970 ± 0.13	0.972 ± 0.13	0.856 ± 0.13
Baseline Trochanter BMD (g/cm^2)	0.883 ± 0.14	0.787 ± 0.12	0.705 ± 0.13
Total Hip BMD ?% (g/cm^2)	-0.012 ± 0.04	-0.022 ± 0.04	-0.015 ± 0.04
Femoral Neck BMD ?% (g/cm^2)	-0.012 ± 0.04	-0.024 ± 0.06	-0.001 ± 0.05
Trochanter BMD ?% (g/cm^2)	-0.018 ± 0.04	-0.026 ± 0.05	-0.022 ± 0.06
% Calcium supplement users	24%	39%	58%
% Current smokers	11%	12%	13%
% Dietary calcium intake <800 mg/d	42%	66%	65%
% Current estrogen users	-	-	37%
	Beta ± SE, p-value	Beta ± SE, p-value	Beta ± SE, p-value
Annualized TH-BMD ?% (adjusted for covariables)	-0.0339 ± 0.014, 0.01	-0.0072 ± 0.034, 0.83	-0.0171 ± 0.0157, 0.27
Annualized FN-BMD ?% (adjusted for covariables)	-0.0102 ± 0.019, 0.60	-0.0552 ± 0.054, 0.31	-0.0231 ± 0.0187, 0.21
Annualized TR-BMD ?% (adjusted for covariables)	-0.0580 ± 0.020, 0.005	-0.0428 ± 0.049, 0.39	-0.0250 ± 0.027, 0.34
-Men, calcium intakes = 800 mg/d	-0.096± 0.035, 0.0007	-	-
-Men, calcium intakes < 800 mg/d	-0.037± 0.025, 0.13		

Table

***Disclosures: Marian Hannan**, None.*

MO0324

Long-Term Effect Of Phytoestrogens On The Ovariectomy Response In The Cynomolgus Monkey Model Of Osteoporosis. Aurore Varela*, Susan Y. Smith. Charles River Laboratories, Canada

Phytoestrogens (PEs) are naturally occurring plant derived polyphenols with estrogenic activity. They are ubiquitous in diet and generally consumed. The 2056 Soy Protein-Free Primate Diet excludes alfalfa and soybean meals, minimizing the presence of phytoestrogens. The purpose of this study was to evaluate the long term effects of this diet on bone turnover and on bone mass over a 15 month period in aged ovariectomized monkeys. Animals older than 9 years were obtained from established colonies in Mauritius. Animals were fed with 2056 Soy Protein-Free Diet. The effects of OVX were monitored in vivo using DXA (whole body, lumbar spine and proximal femur), pQCT (proximal tibia metaphysis and diaphysis) and biochemical markers of bone turnover. Twenty females underwent OVX, 20 females were Sham operated. Data were compared to our laboratory historical dataa obtained from animals fed with a standard diet (2050C Teklad Global 20% Protein Primate Diet).

Relative to Sham controls, decreases were obtained in whole body DXA BMD of 4.2% and 5.5% at Months 12 and 15, respectively. Relative to Sham controls, decreases were obtained in lumbar spine DXA BMD of 6.4% and 8.8%, at the proximal femur 7.9% and 13.4% at Months 12 and 15, respectively. Decreases in DXA BMD were more marked relative to historical data obtained at Month 16 which showed decreases at the lumbar spine of 4.8% and at the proximal femur 5.1%. Decreases in trabecular pQCT BMD at the proximal tibia were 12.6% and 21.2% at Months 12 and 15 in low PEs OVX animals. Compared to sham, OVX decreased cortical BMD at the tibial diaphysis by 6.1% and 4.7%. These decreases were more marked compared to historical data at Month 16 which showed trabecular BMD decreases of 9.3% with similar cortical data. Biochemical markers were markedly elevated in the soy-free diet OVX compared to Sham controls at Months 12 and 15: OC 2-fold and 5-fold, serum CTx 82% and 50%, PINP 2-fold at each occasion, Bone-ALP 69% and 78%. Compared to historical data at Month 16: OC increased of 93% and 54%, serum CTx 77% and 45%, Bone-ALP 31% and 62%, increases in bone turnover was larger.

These data suggested that controlling PEs in the diet may be important in the OVX response in aged monkeys as evidenced by a more important increase in bone turnover and loss of bone mass measured by densitometry techniques especially after 15 months. The influence of diet should be considered in this model to better discriminate potential bone anabolic or anti-catabolic agents in the preclinical evaluation of potential anti-osteoporosis agents.

[a]Smith SY, Jolette J, Turner CH, Skeletal health: primate model of postmenopausal osteoporosis. *Am J Primatol*. 2009;71(9):752-65.

***Disclosures: Aurore Varela**, None.*

MO0325

Plant Protein Intake is Associated with Bone Mineral Density (BMD) in Older Puerto Rican Women: The Boston Puerto Rican Health Study. Shilpa Bhupathiraju*[1], Marian Hannan[2], Katherine Tucker[3]. [1]Tufts University, USA, [2]HSL Institute for Aging Researchand Harvard Medical School, USA, [3]Northeastern University, USA

Protein intake is known to influence BMD in older Caucasians. Yet, little is known about this association in Puerto Ricans, a group with documented health disparities. Therefore, we evaluated cross-sectional associations of protein intakes (total, animal, and plant) with BMD of the total hip (TH), femoral neck (FN), trochanter, and lumbar spine (L2-L4) among 402 women in the Boston Puerto Rican Health Study. BMD was measured in 2007-09 using dual energy X-ray absorptiometry (Lunar Corp, WI). Dietary protein intake was estimated using a food frequency questionnaire, developed and validated for this population. Tertiles of protein intake (for each definition of total, animal, plant) were created, adjusting for total energy intake (residual method). General linear models were constructed to assess associations between protein intake and bone measures. Models were sequentially adjusted for age (y), weight (lb), height (cm), current smoking (Y/N), alcohol (g/d), season of BMD measurement (spring/summer/fall/winter), total energy (kcal), total calcium (mg/d), vitamin D (IU), osteoporosis medication use (Y/N), physical activity score, and income ($/year). Animal and plant protein intakes were adjusted for each other. Because protein, in our population, is typically consumed with rice, we also adjusted for total carbohydrate (CHO) intake (g/d). Mean age was 60.1 ± 7.1 (46-79 y). Mean total, animal, and plant protein intakes (SD) were 77.2 g (36.5), 52.2 g (27.4), and 24.5 g (11.4). Plant protein intake was positively associated with TH BMD ($\beta \pm SE = 0.003 \pm 0.001$, P=0.008) and trochanter BMD ($\beta \pm SE = 0.003 \pm 0.001$, P=0.02) but not LS BMD ($\beta \pm SE = 0.001 \pm 0.002$, P=0.39). No associations were found between intakes of total and animal protein and various bone sites. There was a positive linear trend of adjusted mean TH and trochanter BMDs across tertiles of plant protein intake (P-trend≤0.05). LS BMD tended to decrease (non-significantly) across tertiles of animal and total protein (Table 1). Our results suggest that for older Puerto Rican women, plant protein may be beneficial to both TH and trochanter. Our findings of lower, albeit non-significant, LS BMD across total and animal protein tertiles should be interpreted with caution. While we adjusted for CHO intake, residual confounding remains a possibility. Further studies are needed to explore this relation longitudinally in both men and women. Future work should focus on the differential effects of plant protein on LS and TH.

Table 1: Adjusted least square mean (SE) bone mineral density (g/cm^2) across energy-adjusted tertiles of plant, animal, and total protein intakes (g) in the Boston Puerto Rican Health Study

	Plant Protein				Animal Protein				Total Protein			
	1	2	3	P-trend	1	2	3	P-trend	1	2	3	P-trend
Median (range)	19.9 (5.7 – 22.5)	24.4 (22.5 – 26.1)	28.6 (26.1 – 49.6)		39.6 (7.8 – 46.7)	51.4 (46.7 – 55.5)	65.0 (55.6 – 115.7)		65.7 (35.9 – 71.6)	75.9 (71.6 – 80.1)	88.9 (80.3 – 267.7)	
Femoral Neck	0.882 (0.013)	0.898 (0.012)	0.901 (0.012)	0.23	0.894 (0.013)	0.878 (0.013)	0.909 (0.013)	0.34	0.896 (0.013)	0.889 (0.012)	0.899 (0.013)	0.80
Total Hip	0.966 (0.014)	1.003* (0.013)	1.002 (0.013)	0.04	0.991 (0.013)	0.977 (0.014)	1.005 (0.015)	0.42	0.991 (0.014)	0.977 (0.014)	1.005 (0.015)	0.51
Trochanter	0.762 (0.012)	0.801* (0.012)	0.793 (0.012)	0.05	0.784 (0.013)	0.777 (0.012)	0.797 (0.013)	0.42	0.783 (0.013)	0.785 (0.012)	0.791 (0.013)	0.60
Lumbar Spine (L2-L4)	1.075 (0.017)	1.113 (0.016)	1.109 (0.016)	0.11	1.109 (0.017)	1.098 (0.017)	1.090 (0.018)	0.11	1.110 (0.017)	1.105 (0.016)	1.083 (0.017)	0.13

Adjusted for age (y), weight (lb), height (cm), current smoking (Y/N), alcohol (g/d), season of BMD measurement (spring, summer, fall, winter), total energy (kcal), intakes of total calcium (mg/d), vitamin D (IU), carbohydrate intake (g/d), osteoporosis medication use (Y/N), physical activity score, and income ($/year)
*P≤0.05 relative to the lowest tertile (Dunnett adjustment)

Adjusted mean BMD across tertiles of protein intake

***Disclosures: Shilpa Bhupathiraju**, None.*

MO0326

10-Year Fracture History in Seniors with Acute Hip Fracture: Are we Missing an Opportunity? Andreas Egli*[1], Robert Theiler[2], Bess Dawson-Hughes[3], Jana Henschkowski[4], Hannes B Staehelin[5], Heike Bischoff-Ferrari[6]. [1]Centre on Ageing & Mobility, Switzerland, [2]Triemli City Hospital, Switzerland, [3]Tufts University, USA, [4]University Hospital Zurich, Switzerland, [5]University of Basel, Switzerland, [6]University of Zurich, Switzerland

Background: Severe vitamin D deficiency and lack of treatment after hip fracture has been demonstrated in many studies.

Methods: We reviewed hospital charts (internal medicine, orthopaedic surgery/traumatology and radiology in- and outpatient reports) and contacted general practitioners of 173 acute hip fracture patients age 65 and older admitted to one large centre hospital, 79% were women, and 77% were living at home prior to their hip fracture. A previous fracture was classified as confirmed, if either an x-ray showed the fracture, or an x-ray report clearly described the fracture, or a surgical or medical report described the fracture repair.

Results: Upon admission to acute care, 51% of hip fracture patients had severe vitamin D deficiency with 25(OH)D levels below 30 nmol/l and 98% had levels below 75 nmol/l; less than 10% had any dose of vitamin D. Further, 82 of 173 patients (47.4%) had one or more confirmed fractures in the 10 years preceding their hip fracture: 12 of 173 (6.9%) had a confirmed prior hip fracture, and 59 of 173 (34.1%) had a confirmed non-vertebral fracture other than the hip. For non-vertebral fractures other than the hip, 22 of 173 patients (12.7%) had a forearm fracture, 18 of 173

(10.4%) had a humerus fracture, 15 of 173 (8.7%) had a rib fracture, 11 of 173 had a pelvis fracture (6.4%), and 13 had other non-vertebral fractures.

Conclusion: Based on these data, seniors with non-vertebral fractures are undertreated, despite their high risk of hip fracture as documented in this study.

***Disclosures: Andreas Egli**, None.*
This study received funding from: Amgen (Investigator initiated study), Swiss National Foundations

MO0327

An epidemiological study of fragility fracture incidence and associated mortality. Sonia Jean*[1], Etienne L. Belzile[2], Louis Bessette[3], K. Shawn Davison[2], Bernard Candas[4], Sylvie Dodin[5], Suzanne Morin[6], Jacques Brown[2]. [1]Institut National De Sante Publique, Canada, [2]Laval University, Canada, [3]Centre Hospitalier De L'Universite Laval, Canada, [4]Institut national de santé publique du Québec, Canada, [5]Université Laval, Canada, [6]McGill University Health Centre, Canada

Purpose: Although osteoporosis-related fractures are an important and growing public health problem, research has primarily focused on hip fractures. The purposes of this study were to describe the incidence of fragility fractures (FF), and evaluate the impact of FF on relative four-year survival.

Methods: Using a validated algorithm, women ⩾50 years old with incident fractures of an osteoporotic site were identified in the physicians' claims databases in three health regions of the Province of Québec. For each fracture site, fracture incidence was tabulated by calendar year and five-year age groupings. To calculate age-specific incidence rates, the population of women ⩾50y of age (from the same health regions) was used as the denominator. Finally, for each fracture type, annual age-standardized fracture rates per 100,000 person-years was calculated and rates were directly-adjusted to the 2001 age-structure of the Québec population. To assess the impact of FF on mortality, vital statistics were obtained for women who sustained a fracture (until December, 31, 2007) and relative survival analyses were performed. In these analyses, we assumed that fracture-related deaths were attributable to the fracture, or its complications, and to other causes unrelated to the fracture. By assessing the mortality rate in the general population, which reflects deaths associated with other causes, we hypothesized the increases in mortality were directly attributable to the fractures.

Results: During the study period, 16,361 fractures were identified. The most frequent fractures were at the hip, wrist, humerus and ankle, with age-standardized incidence rates of 365.1, 289.3, 244.6 and 194.8 (per 100,000 person/y), respectively (Table 1). Except for tibia/fibula and ankle fracture, incidence increased with age, exponentially for hip fracture and linearly for other fracture sites. A significant decrease in relative survival was observed in women who sustained hip, pelvis, humerus, forearm or tibia/fibula fractures (Table 2). Following a hip fracture, there was a fracture-attributable excess mortality at 12 and 48 months of 16% and 27%, respectively.

Conclusions: Hip and non-hip fractures are common and are associated with significantly decreases in survival. These fractures have a significant impact on individuals and the healthcare system. Therefore, in the assessment of burden related to fragility fractures, non-hip fractures, such as humerus and pelvis, must be included.

Fracture Type	2004 age-standardized rate (95% CI)	2005 age-standardized rate (95% CI)
Hip	365.1 (351.0-379.5)	344.5 (330.9-358.5)
Wrist	289.3 (275.5-303.5)	299.7 (285.7-314.0)
Humerus	244.6 (232.0-257.5)	247.6 (235.0-260.5)
Ankle	194.8 (183.2-206.7)	180.0 (168.9-191.4)
Forearm	145.5 (135.7-155.6)	144.8 (135.0-154.8)
Tibia, fibula	76.1 (69.0-83.6)	76.7 (69.6-84.1)
Pelvis	24.8 (21.1-28.8)	24.7 (21.0-28.7)

Incidence rate (per 100,000 person-years) of osteoporotic fractures in women > 50 yrs, 2004-2005

Fracture Type	12-mo RS (95% CI)	24-mo RS (95% CI)	36-mo RS (95% CI)	48-mo RS (95% CI)
Hip	84.1 (82.9-85.3)	80.5 (79.0-81.9)	76.7 (74.9-78.4)	73.3 (70.8-75.7)
Wrist	99.5 (98.8-100.1)	100.0 (99.1-100.0)	99.9 (98.7-100.0)	99.4 (97.6-100.0)
Humerus	96.6 (95.6-97.5)	95.3 (94.1-96.5)	94.3 (92.8-95.8)	93.5 (91.2-95.5)
Ankle	99.5 (98.7-100.0)	99.5 (98.5-100.0)	99.2 (98.0-100.0)	99.1 (97.2-100.0)
Forearm	98.5 (97.4-99.4)	97.1 (95.6-98.5)	96.6 (94.8-98.3)	94.6 (91.7-97.2)
Tibia, fibula	97.7 (96.0-98.9)	96.3 (94.1-98.0)	95.9 (93.3-98.0)	93.3 (89.1-96.7)
Pelvis	89.7 (85.2-93.3)	90.6 (85.5-94.8)	87.8 (81.6-93.1)	87.7 (79.0-95.1)

Relative survival (RS) at 12, 24, 36, and 48 months following osteoporotic fracture

***Disclosures: Sonia Jean**, None.*
This study received funding from: Warner Chilcott, sanofi-aventis, Merck, Amgen, Novartis, Eli Lilly, Servier

MO0328

Burden of Non-Hip-Non-Vertebral Fractures in Postmenopausal Women: Prospective Data From the Global Longitudinal Study of Osteoporosis in Women. Christian Roux*[1], Frederick Hooven[2], Steven Boonen[3], Roland Chapurlat[4], Cyrus Cooper[5], Adolfo Diez-Perez[6], Andrea Lacroix[7], Stuart Silverman[8], Grigor Nika[9], Ethel Siris[10]. [1]Hospital Cochin, France, [2]University of Massachusetts Medical School, USA, [3]Center for Metabolic Bone Disease, Belgium, [4]E. Herriot Hospital, France, [5]University of Southampton, United Kingdom, [6]Hospital del Mar-IMIM-Autonomous University of Barcelona, Spain, [7]Fred Hutchinson Cancer Research Center, USA, [8]Cedars-Sinai/UCLA, USA, [9]COR, UMass Medical School, USA, [10]Columbia University College of Physicians & Surgeons, USA

Purpose: The consequences of fractures on quality of life as people age are increasingly recognized, but most emphasis has been placed on hip and vertebral fractures. However, the impact of non-hip, non-vertebral (NHNV) fractures is under-recognized. We sought to assess the incidence of NHNV fractures, and disability related to these fractures. Methods: The observational Global Longitudinal Study of Osteoporosis in Women (GLOW) study was established to provide a comprehensive community-based evaluation of osteoporosis and related risk factors in women ⩾55 years recruited through primary physician practices. EQ-5D scores and SF-36 physical function (PF) and vitality scores (VT) were computed. NHNV fractures were grouped into the categories of major (pelvis, upper leg, lower leg, arm, shoulder fractures) and minor (clavicle, arm, wrist, rib) fractures. In order to estimate the independent effect of each fracture, declines in EQ-5D and in other scores vs baseline were analyzed in both unadjusted analysis and in multiple regression analysis adjusting for all other fracture types. Results: 952 new NHNV fractures were reported in the first year of follow-up. The overall incidence of NHNV fractures was 2.0% compared to hip (0.2%) and clinical spine (0.2%). Mean ages were 76, 73, 72 and 69 years for those experiencing hip, clinical spine, major NHNV and minor NHNV fractures, respectively. The table shows the independent effect of fracture types on change in EQ-5D, PF and VT. A decline in PF of 5.2 for those with major fractures was smaller than for those with spine fractures (6.9) but greater than those with hip fractures (3.7). Vitality scores declined more for spine fractures than for any other category (5.6). EQ-5D index was reduced by 0.04 for major fractures, 0.04 for hip and 0.05 for spine, but only 0.02 for minor fractures. A significant interaction between hip and major fracture was found for the EQ-5D difference score. Conclusions: Patients experiencing major NHNV fractures show important declines in quality of life and physical function that are comparable to those associated with hip and spine fractures.

	EQ-5D (N=44,996)		PF (N=46,822)		VT (N=46,464)	
Variable	Estimate	p	Estimate	p	Estimate	p
Hip	−0.04	<0.02	−3.7	<0.05	−1.3	<0.5
Spine	−0.05	<0.002	−6.9	<0.0001	−5.6	<0.001
Major	−0.04	<0.002	−5.2	<0.0001	−2.1	<0.02
Minor	−0.02	<0.005	−0.4	<0.6	−1.3	<0.05
Hip (major)	−0.18	<0.0001	–	–	–	–

Mean adjusted change in difference in EQ-5D, PF and VT scores (1 year minus baseline)

***Disclosures: Christian Roux**, Alliance, Amgen, Lilly, Merck Sharp and Dohme, Novartis, Nycomed, Roche, GlaxoSmithKline, Servier, Wyeth, 5; Alliance, Amgen, Lilly, Merck Sharp and Dohme, Novartis, Nycomed, Roche, GlaxoSmithKline, Servier, Wyeth, 9*
This study received funding from: The Alliance for Better Bone Health (sanofi-aventis and Warner Chilcott)

MO0329

Corticosteroid Use Predicts Fractures Differentially according to Site of Fracture. Risto J Honkanen*[1], Heli Koivumaa-Honkanen[2], Kari Salovaara[3], Marjo Tuppurainen[3], Joonas Sirola[3], Heikki Kröger[1]. [1]University of Kuopio, Finland, [2]University of Oulu, Finland, [3]Kuopio University Hospital, Finland

Use of corticosteroids has deleterious effects on bone. The purpose of this study was to examine 1) if the fracture risk related to corticosteroids (CORT) varies by site of fracture and 2) if nutritional calcium or estrogen prevent this CORT effect. The study population consisted of 9759 women of the Kuopio Osteoporosis Risk Factor and Prevention (OSTPRE) Study. The OSTPRE cohort was established in 1989 by selecting all women borne in 1932-41 and living in the Kuopio Province, Finland (n=14220). The subject was eligible if she had responded at baseline in 1989 and at every follow-up enquiry in 1994, 1999 and in 2004(n=9759). Duration of CORT use in tablet form up to the time of the year 1999 enquiry was the independent variable and follow-up fractures during 1999-2004 was the dependent variable. Duration of CORT use was self-reported and was categorized as follows: 1=no use (90.7%), 2=use of 1-59 months (8.2%) and 3=use of more than 59 months (1.2%). Self-reported fractures in 1999-2004 were validated by perusal of radiological reports from patient records. Fracture risks were estimated with the Cox proportional hazards model. Several variables such as age, height, weight, year of menopause, fall and fracture history, nutritional calcium, estrogen use, number of chronic health disorders, smoking, use of alcohol and life satisfaction were tried as covariates. A total of 905 validated follow-up fractures were in use for the study. Wrist fracture was most common (351 women), followed by ankle fracture (158 women). 461 women had sustained an osteoporotic fracture (wrist (351), hip (30), spine (56), humerus (67)); 21 women had a pelvic fracture. CORT use predicted any fracture with a hazard ratio (HR) of 1.3 (95%CI 1.03-1.6) for <5 years of use and with a HR of 2.8 (95%CI 1.9-4.1) for 5 years or more of use ($p<0.001$). The 5 years or more of CORT use predicted strongly fractures at the spine (HR 7.1 (95%CI 2.6-19.8) and pelvis (OR 15.1 (95%CI 4.3-52)), but not at the wrist (HR 1.3(95%CI 0.85-1.73) or ankle (HR 1.6 (95%CI 0.52-5.1). Multivariate adjustments did not affect CORT effects and risk estimates were similar for women with vs. without sufficient calcium or estrogen intake. Causes of differential corticosteroid effects on fractures according to site of fracture need further clarification.

***Disclosures: Risto J Honkanen**, None.*

MO0330

Factors Associated with Fracture Free Survival. Jane Cauley*[1], Susan Ewing[2], Li-Yung Lui[3], Teresa Hillier[4], Steven Cummings[5], Kristine Ensrud[6]. [1]University of Pittsburgh Graduate School of Public Health, USA, [2]University of San Francisco, USA, [3]California Pacific Medical Center Research Institute, USA, [4]Kaiser Center for Health Research, USA, [5]San Francisco Coordinating Center, USA, [6]Minneapolis VA Medical Center / University of Minnesota, USA

Successful aging is multidimensional; many phenotypes including bone mineral density (BMD) have been proposed. Women who remain "fracture free" may share unique characteristics. To test this hypothesis, we examined women enrolled in the Study of Osteoporotic Fractures. We limited our analysis to women who had at least 10 years of follow-up and compared women who remained fracture free (n=2047) with women who experienced at least one incident clinical or vertebral fracture (n=3830). Fracture free women did not have a baseline prevalent morphometric vertebral fracture, did not self-report a fracture since age 50 and did not experience an incident morphometric vertebral or clinical fracture. Logistic regression was used to identify factors associated with fracture free survival; odds ratios and 95% confidence intervals were calculated. Of the women with at least one incident fracture, 2020 (52.7%) experienced 1 fracture; 1021 (26.7%), 2 fractures; 454 (11.8%), 3 fractures and 335 (8.7%), 4+ fractures. Women who remained fracture free compared to women with a fracture, respectively were younger at baseline (69.9 vs 71.2 yrs). Despite the strong link between age and fracture, age was weakly associated with fracture free survival (Table). Women with a one SD lower BMI at baseline were 20% more likely to remain fracture free. Lower BMD and faster BMD loss were both independently associated with a lower likelihood of remaining fracture free. A higher supplemental calcium intake was associated with lower odds of remaining fracture free perhaps reflecting an indication bias. Higher alcohol intake, history of falling, poor depth perception, greater height loss and more IADL impairments were associated with lower odds of remaining fracture free. Finally, history of MI and higher systolic blood pressure were unexpectedly associated with remaining fracture free. Use of estrogen at baseline, resting pulse, contrast sensitivity, poor health status, grip strength, history of stroke or COPD, current smoking and nulliparity have been previously identified as risk factors for fracture but were unrelated to fracture free survival.

In conclusion, characteristics of remaining fracture free are not consistently the mirror image of risk factors for fracture.

Multivariable (MV) determinants of fracture free survival: Odds ratio (95% CI) of remaining fracture free (referent group: women with incident fracture)

	Unit	OR	95% CI	p
Age	5 yr	0.93	(0.85, 1.01)	0.08
BMI (kg/m^2)*	4.6 kg/m^2	1.20	(1.11, 1.31)	≤ 0.0001
Total hip BMD*	-0.13 g/cm^2	0.50	(0.46, 0.55)	< 0.0001
Change in hip BMD*	-0.004 g/cm^2/yr	0.85	(0.79, 0.92)	≤ 0.0001
Supplemental calcium intake*	594 mg/d	0.87	(0.80, 0.94)	0.0003
Drinks/wk*	3.95	0.89	(0.83, 0.96)	0.002
Fall last 12 months	Yes	0.80	(0.68, 0.93)	0.004
Depth perception (Q4 vs Q1,2,3)	1.0	0.86	(0.73, 1.02)	0.08
Systolic BP*	18mmHg	1.09	(101, 1.16)	0.02
MI history	Yes	1.34	(1.00, 1.79)	0.05
Height change (since age 25)*	-2.8	0.89	(0.82, 0.96)	0.004
V1 # IADL impairments (range 0-6)	1	0.94	(0.88, 1.00)	0.07

* unit is expressed as one standard deviation (SD)

Table

***Disclosures: Jane Cauley**, None.*

MO0331

Outcomes from the First 10years of the Fracture Liaison Service, a Systems-based approach to Fracture Secondary Prevention. Mayrine Fraser[1], Frances Lovell[2], Alastair McLellan*[1]. [1]Western Infirmary, United Kingdom, [2]Royal Infirmary, United Kingdom

The Fracture Liaison Service (FLS) provides a systems-based approach to post-fracture assessment for fracture secondary prevention. Established in 1999, the FLS now operates from 5 centres covering an entire NHS healthcare region's population of 1.4million. All women and men age 50 & over who present with a new fracture (occurring outside RTA or fall from above head-height) to A&E / trauma / orthopaedics or radiology departments are identified and offered a one-stop post-fracture assessment of future fracture risk, incorporating DXA, where appropriate. Fracture case-identification and the subsequent post-fracture assessment with recommendation of treatment (where necessary) are undertaken by nurse specialists. Additional management options include falls-risk assessment, tiered exercise classes and a patient education programme. Since 1999, the North Glasgow FLS, the largest component of this regional service, and the longest established, comprising 2 FLS centres, with coverage of a patient population of 600,000 has processed 30622 fractures (of which 28% were of radius /ulna, 20% of hip, 14% of humerus, 10% of ankle, 13% of hand /foot, 4% of vertebrae and the remainder of other sites) in 26363 patients (74.1% women) age (mean(SD))70.6(12.1)yr. 52% underwent DXA as part of their post-fracture assessment. 31% were treated with bisphosphonate, usually with calcium & vitaminD, 20% received calcium & vitaminD alone and 1% received other bone-active treatments. During follow-up of up to 10years (median 39months), 19% died, and 13.2% had at least one further fracture presentation and 0.3% had at least 2 further presentations. A previous study has established that the FLS is the most effective current service model for effecting fracture secondary prevention (http://www.nhshealthquality.org/nhsqis/files/99_03FullReportFINAL_040705.pdf), and a recent health economic analysis has shown the FLS to be cost effective.

The current data provide evidence of the sustainability of the FLS over 10years; generation of long term outcome data including mortality and incidence of secondary fractures should be required of all services that aspire to effect fracture secondary prevention, as quality indices.

***Disclosures: Alastair McLellan**, None.*

MO0332

Population-based Canadian Estimates of 10-year Fracture Risk by Age, Sex, Fracture Site and Trauma Status. Lisa Langsetmo*[1], Claudie Berger[2], David Goltzman[3], Jerilynn Prior[4], Christopher Kovacs[5], Stephanie Kaiser[6], Alexandra Papaioannou[7], Jonathan Adachi[8], Robert Josse[9], Tassos Anastassiades[10], Tanveer Towheed[10], W.P. Olszynski[11], Nancy Kreiger[12]. [1]Canandian Multicenter Osteoporosis Study, Canada, [2]McGill University, Canada, [3]McGill University Health Centre, Canada, [4]University of British Columbia, Canada, [5]Memorial University of Newfoundland, Canada, [6]Dalhousie University, Canada, [7]Hamilton Health Sciences, Canada, [8]St. Joseph's Hospital, Canada, [9]St. Michael's Hospital, University of Toronto, Canada, [10]Queen's University, Canada, [11]Midtown Medical Center (#103), Canada, [12]University of Toronto, Canada

Background: International comparisons have shown age-dependent differences in hip fracture incidence. There are also possible age-dependent differences in the burden of hip fracture relative to overall fracture burden. Our objective was to determine skeletal site-, sex- and trauma-specific 10-year absolute risk of clinical fracture by age group in the Canadian Multicentre Osteoporosis Study (CaMos).

Methods: We studied 2814 men and 6405 women, aged 25 to 95 years. Fracture cases were identified at annual follow-ups with structured interview to determine site and circumstance. Fractures of the skull, hands, ankles or feet were excluded. Low-trauma fractures occurred without trauma or from a fall of standing height or less. The "main" fracture sites were hip, clinical spine, wrist and humerus. The 10-year absolute risk of fracture was calculated by the Kaplan-Meier method.

Results: Figure 1 shows the 10-year fracture risk (overall, main, low-trauma, hip) by sex and age group. Clear sex differences are apparent. Men have higher overall fracture risk than women from ages 25-45 years, similar risk from ages 45-55 years, and lower risk from ages 55-85 years. The risk of the four main fractures was roughly similar to the risk of all low trauma fractures. In the youngest age group (25-35 years) only 27% of the overall fracture risk in both men and women was due to low-trauma fractures, whereas in the oldest group (75-85 years) this increased to 79% in men and 89% in women. The percentage of overall fracture risk due to high trauma was at least 10% higher in men than in women in all age groups other than the youngest age group (25-35 years). The risk of hip fracture by age was similar in men and women. In the youngest age group (25-35 years) essentially none of the overall fracture risk in men and women was due to hip fractures, whereas in the oldest group (75-85 years) this increased to 44% in men, but only to 26% in women.

Conclusions: Age is more strongly related to fracture risk in women than in men. In men much of the age-related increase in fracture risk is accounted for by hip fracture, whereas in women there is also a substantial age-related increase at non-hip sites.The contribution of hip fracture to all fractures varies by sex and age indicating that hip fracture risk and overall fracture risk are different measures of skeletal fragility.

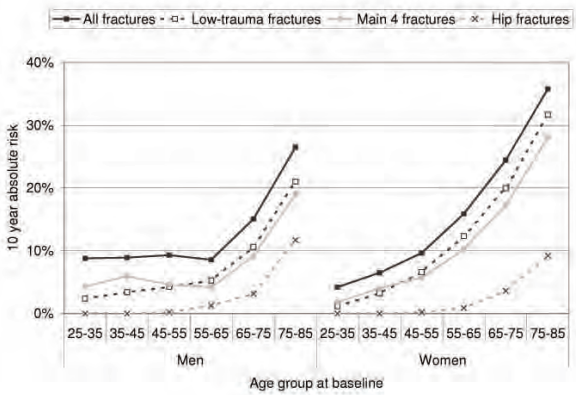

Figure

***Disclosures: Lisa Langsetmo**, None.*

MO0333

Prediction of Short-Term Fracture Risk in Patients Presenting with a Non-Vertebral Fracture. Kirsten Huntjens*[1], Tineke Geel van[2], Joop Bergh van den[3], Svenhjalmar Helden van[4], Piet Geusens[5]. [1]Maastricht University, The netherlands, [2]Maastricht University, Netherlands, [3]VieCuri, Netherlands, [4]MUMC, Netherlands, [5]University Hasselt, Belgium

Background:

Patients with a recent fracture are at risk for subsequent fracture, especially at short term.

Objective:

To investigate in patients presenting at the time of a non-vertebral fracture (NVF) to what degree clinical risk factors (CRF), osteoporosis and fall-related risk factors separately or in combination are related to subsequent fractures.

Methods:

In total, 957 patients who agreed and were able to participate were evaluated by the specialist fracture nurse at the Fracture and Osteoporosis Outpatient Clinic and followed during 2 years for subsequent fractures and mortality. Three groups of risk factors (GRF) were assessed, namely CRF (e.g. previous fracture ⩾50 years), osteoporosis and fall risks (e.g. previous falls in preceding 12 months). Patients were treated according to the Dutch Guidelines. We prospectively studied the distribution of GRFs in patients with and without a subsequent fracture using multivariable Cox regression (adjustment for age, sex and baseline fracture location).

Results:

Of the 957 patients, 32% had osteoporosis, 51% had at least one CRF and 60% had at least one fall risk factor. Combining GRFs, 15% of these patients had all 3 GRFs, 31% at least 2 GRFs and 36% at least 1 GRF.

In total, 71 (7.4%) sustained a subsequent fracture within 2 years of follow-up. On its own, osteoporosis, bone-related risk factors and fall-related risk factors were no significant predictors for a subsequent fracture in multivariable Cox regression analysis. However, the combination of the 3 GRFs, was significantly more predictive than any of these GRFs separately or a combination of two GRFs (3 GRF vs. 2 GRF p=0.03; 3 GRF vs. 1 GRF p=0.01, respectively).

The prevalence of 3 GRFs was 8% in patients with one fracture, 18% in patients who also had a prior fracture (n=228), and 32% in patients who had also a subsequent fracture.

Conclusion:

The combination of all three GRFs was significantly predictive for subsequent fracture risk, but not the individual GRFs. The clinical consequence is that all three GRFs should be evaluated in patients at the time they present with a fracture.

***Disclosures: Kirsten Huntjens**, None.*

MO0334

Prevalence and Treatment Rate of Vertebral Fractures Detected by Densitometric Vertebral Fracture Assessment (VFA) in Swiss Mountain and Plain Areas: a Pilot Study. Jotinder Schuematschek-Kainth*[1], Sebastian Bellwald[1], Albrecht Popp[1], Günter Menz[2], Oswald Lang[3], Matthias Stahl[4], Christoph Senn[1], Antonella Berlingieri[1], Romain Perrelet[1], Kurt Lippuner[1]. [1]Osteoporosis Policlinic, University of Bern, Switzerland, [2]Hochgebirgsklinik Davos, Switzerland, [3]HFR Tafers, Switzerland, [4]Kantonsspital Olten, Switzerland

Purpose: Little is known about the prevalence and treatment rate of osteoporotic vertebral fractures in Switzerland. Differences with respect to life-style and environmental factors between urban and rural areas on the one hand, and mountain areas and plain country on the other could significantly influence both, the risk of suffering a fracture, and the individual likelihood of being diagnosed and treated.

Methods: In a pilot of a future larger cohort study, a mountain area (Davos, 1600 m.a.s.l.), a plain rural area (Tafers, 651 m.a.s.l.) and a plain urban area (Olten, 396 m.a.s.l.) were chosen. Two hundred thirty-eight community dwelling women aged 65 to 80 years were randomly selected from the inhabitants' address lists. In a mobile investigational unit (Osteomobil^{TM}) equipped with a DXA scanner (Hologic Discovery C^{TM}), our experienced study team consisting of a study physician and a study nurse examined the selected persons near their place of residence. Vertebral fractures were assessed by VFA and defined using the Genant visual semi-quantitative approach. Among additional procedures, subjects were specifically asked about previous diagnostic and therapeutic measures.

Results: Fifty-four vertebral deformities were detected in 40 out of the 238 women (16.8%). In 10 subjects (4.2%) multiple (up to 5) fractures were present. A total of 11 severe and 16 moderate fractures were diagnosed in 4 and in 11 subjects, respectively. Vertebral deformities were more prevalent in the plain urban area (20%) than in the mountain area of Davos (15%), although not reaching statistical significance. The prevalence in the plain rural area at intermediate altitude was 17%. Only 8 of the 40 women (20%) with ⩾1 vertebral deformities had ever received a bone active medication (a bisphosphonate in all cases, one followed by teriparatide). Of these, only 5 patients (12.5%) received current treatment other than Ca/D supplements. No regional differences could be detected in the treatment rate. Compared to untreated women, treated women were more likely to have a history of inadequate clinical fracture (50 vs. 3%, $p<0.001$) and to have undergone earlier DXA examination (87.5 vs. 22%, $p<0.001$).

Conclusions: Most patients with vertebral deformities detected by VFA were unaware, undiagnosed, and untreated. Further study of regional differences in the prevalence of vertebral fractures and their determinants requires a large countrywide study.

***Disclosures: Jotinder Schuematschek-Kainth**, None.*

MO0335

Prevalence of Symptomatic Vertebral Fractures in Premenopausal Women Newly Treated with High-Dose Glucocoriticoid. Tomohiko Yoshida*. Chiba University Hospital, Japan

Objective: The treatment and prevention of glucocorticoid-induced osteoporosis, especially bisphosphonate therapy during childbearing age has been controversial. This study aimed to investigate the incidence and risk factors for symptomatic vertebral fracture in childbearing age of women newly treated with high-dose glucocorticoid.

Methods: Chiba-Shimoshizu Rheumatic Cohort (CSRC) is an observational cohort study from 1986 to 2006 at the rheumatic center of Shimoshizu National Hospital in Japan. Data were extracted from the CSRC study, and 292 patients newly treated with high-dose glucocorticoid (⩾20 mg/day prednisolone equivalent) and 81 patients with non-glucocorticoid control group in premenopausal women aged less than 50 years were analyzed. If the back pain corresponded to the radiographic findings, it was defined as symptomatic vertebral fracture.

Results: The high-dose glucocorticoid group had a significantly higher incidence of symptomatic vertebral fracture (11.3%) than the non-glucocorticoid group (1.2%). Kaplan-Meier analyses demonstrated that the incidence rate of fractures in 40s ($40\leq age<50$) was significantly higher than those in 20s ($age<30$) or 30s ($30\leq age<40$). Cox proportional hazard model demonstrated that every 10 years of initial age increases the risk with the hazard ratio (HR) 2.267, every number of times glucocorticoid dose has increased rises the risk with HR 2.282, and every additional 1 gram of cumulative glucocorticoid dose decreases the risk with HR 0.953.

Conclusions: High-dose glucocorticoid therapy was shown to be associated with significantly higher prevalence of symptomatic vertebral fracture in premenopausal women. However, it was found the fracture risk in the women of 20s and 30s was considerably low, suggesting that for women in childbearing age prophylactic therapy for prevention of glucocorticoid-induced osteoporosis should be carried out with caution.

***Disclosures: Tomohiko Yoshida**, None.*

MO0336

Rate of Proximal Humerus Fractures in a Defined Urban Population. Thomas Westphal[1], Kathrin Baessgen[2], Veronika Rattay[2], Julia Wiedbusch[2], Thomas Mittelmeier[2], Hans-Christof Schober*[3], Patrick Haar[2]. [1]Klinikum Südstadt Rostock, Germany, [2]University of Rostock, Germany, [3]Klinikum Südstadt RostockKlinik Für Innere Medizin I, Germany

Introduction

There is a substantial variation in fracture incidence among different populations. Epidemiological studies of osteoporosis related fractures applied different methods and sources: analysis of health registries, hospital or GP databases. Among these data missclassification or doubling of cases might occur. We therefore conducted a study to detect all osteoporosis related fractures in the city of Rostock at the Baltic Sea, relying on primary data only.

Methods

Data collection was made in a prospective fashion. Included were all citizens of the city of Rostock (200413) who attended one of the two hospitals or one of the 16 surgical outpatient departments from 10/2008 to 10/2009. For every patient the type of fracture (distal forearm, proximal humerus, proximal femur, vertebrae) was ensured by X-Ray. The patients were subdivided in 10 years groups. Statistic was performed using SPSS.

Results

Among 200413 citizens 1204 fractures occured in one year. Humerus fractures were as frequent as femur fractures (282 vs. 279, incidence rate per 100000: 141 vs. 139,5)

The incidence rate in percent in different age groups are the following :

Female

Age group (years):	50-60	60-70	70-80	80-90	90 -
humerus	0,17	0,20	0,56	0,76	0,56
femur	0,03	0,09	0,35	1,50	1,67

Male

Age group (years)	50-60	60-70	70-80	80-90	90 -	.
humerus	0, 16	0,07	0,19	0,66	0,0	
femur	0,09	0,11	0,19	1,12	1,47	

A significant increase ($p< 0,001$) in the number of humerus fractures occured in females after the age of 70 y, in males after the age of 80 y.

Conclusion

Humerus fractures are increasing significantly with age but not with the same incidence as in femur fractures. These data underscore the importance of humerus fractures as osteoporosis related. With regard to osteoporosis diagnosis and treatment fractures of the proximal humerus seem to be an early sign.

***Disclosures: Hans-Christof Schober**, None.*

MO0337

Searching for Atypical Subtrochanteric Femoral Shaft Fractures. Fergus McKiernan*[1], Quang Ton[2], Andrew Neviaser[2], Joseph Lane[2]. [1]Marshfield Clinic, USA, [2]Hospital for Special Surgery, USA

Case reports, small case series and lay media have implicated prolonged bisphosphonate (BP) exposure in the etiology of atypical subtrochanteric femoral shaft fractures (ASFSF). On the contrary, reviews of large pharmaceutical databases1 and national health registries 2 have failed to detect any signal to indicate an excess rate of ASFSF in BP users. Black 1 searched for ASFSF among >14,000 enrollees of three major pharmaceutical BP trials but examined only 1 radiograph out of 12 radiographic reports of subtrochanteric fracture. Abrahamson 2 and Curtis 3 searched for ASFSF amongst >71,000 persons with hip fractures in national health registries using ICD-10/-9 diagnosis codes for sub-trochanteric femur fracture (S72.2 and 820.22 respectively). The aim of this study is to determine whether our confirmed cases of ASFSF would have been detected using these ICD diagnosis codes or without review of the primary radiographic data.

Local IRB approved the retrospective review of billing records and radiographs of 40 confirmed cases of ASFSF. Only 11 of 38 confirmed ASFSF cases (29%) were initially assigned the ICD-9 diagnosis code for subtrochanteric fracture (820.22). No case would have been confirmed without examination of the primary radiographic data. Conclusions made from X-ray reports are dependent on reviewer inference, reporting diligence and radiologist familiarity with ASFSF. Furthermore, incompleted ASFSF, asymptomatic ASFSF and pre-symptomatic contralateral ASFSF may not have been detected by either search strategy.

We conclude that the majority of our confirmed cases of ASFSF would have been missed by the published search strategies employed in reviews of large pharmaceutical databases and national health registries. While ASFSF appears to be rare the potential association of ASFSF with BPs could be profound given that 1.7x108 BP prescriptions had been dispensed by 2006. Furthermore, a potential risk horizon could linger long after drug discontinuation since the residence time of BP in bone is prolonged. Until the prevalence and incidence of ASFSF are accurately established, an association with any exposure variable will remain speculative. Reports on prevalence, incidence or those suggesting that BPs are not associated with ASFSF will not be reassuring if the search strategy from which they are derived is flawed.

1. Black DM NEJM 2010 ePub ahead of print, 2. Abrahamsen B JBMR 2009;24:1095, 3. Curtis J ASBMR 2009 AnnualMeeting/Abstr

***Disclosures: Fergus McKiernan**, None.*

MO0338

More Women than Men Require Hospital Admission after an Osteoporotic Fracture. Christian Marcelli[1], Anne Billon[2], Johann Césini*[2]. [1]University Hospital, France, [2]Division of Rheumatology, University Hospital, France

Purpose: although the incidence of osteoporotic fractures is higher in women than in men, it is not well known if the consequences of theses fractures are the same in both genders. As less elderly men than women live alone at home, we speculated that less men than women would require hospital admission after a low-trauma fracture. Therefore, we conducted this retrospective study to compare hospital admission rate (HAR) after an osteoporotic fracture between men and women.

Methods: all the patients aged 55 to 99 referred to our hospital with low-trauma fractures (femur, spine, radius and humerus) during the Nov 2007-Oct 2008 period were retrospectively included in the study. Clinical parameters, lifestyle characteristics and outcome after fracture were recorded from patients' charts. To compare the outcome between both genders, each man was compared with a randomly selected woman matched for age, fracture site and the period of year. Correlations between HAR and other parameters were explored by simple and multiple linear regression analysis. Differences between both genders were analyzed by Fisher or Student's t-test.

Results: 341 patients, 75 males (22%) and 266 females (78%), aged 55-99 were included. Fracture sites: femur, n=161, 47.2%; humerus, n=93, 27.2%; radius, n=71, 20.8%; spine, n=16, 4.6%. 66% of men (n=50) and 83% of women (n=221) required hospital admission while 33% of men (n=25) and 17% of women (n=45) were able to go back to home straight after orthopedic treatment. In the whole group of patients, HAR was significantly lower in men than in women ($p=0.002$) and in subjects aged 50-70 than in those aged 71-99 ($p=0.003$). It was significantly lower for fractures located at humerus, radius, and spine than for femoral fractures ($p<0.0001$). HAR did not significantly differ among different periods of year. In a multivariate analysis, HAR was significantly associated with gender ($p=0.001$) and fracture site ($p<0.0001$). Among patients who required hospital admission after the fracture, when men were compared to matched women, 27.7% of men and 42.6% of women were previously living alone while 23.4% of men and 14.9% of women were living in aged care facilities.

Conclusions: although low-trauma fractures are 3.5 times more frequent in women than in men, HAR is 70% lower in men than in women. It appears from this study that, together with gender and fracture site, lifestyle characteristics could interfere with the outcome after the fracture.

***Disclosures: Johann Césini**, None.*

MO0339

Body weight but not Serum C-Telopeptide Predicts Rate of Bone Loss During Menopausal Transition. Elaine Cheung[1], Cora Bow*[2], Shirley Tsang[3], Cissy Soong[3], Shirley Yeung[3], Connie Loong[3], Anita Kan[4], Sue Lo[5], Grace Tang[4], Annie Kung[1]. [1]Department of Medicine, University of Hong Kong, Hong kong, [2]Department of Medicine, The University of Hong Kong, Hong kong, [3]Department of Medicine, University of Hong Kong, China, [4]Department of Gynaecology, University of Hong Kong, China, [5]Family Planning Association of Hong Kong, Hong kong

Objective: To investigate the predictors for rapid bone loss in Asian women during menopausal transition.

Material and Methods: A total of 161 treatment-naïve Chinese women aged 45-55 years were followed annually for 5 years. BMD at the spine and hip, demographic characteristics, lifestyle habits and clinical risk factors for osteoporosis, serum estradiol (E2), testosterone (TA), Sex hormone binding globulin (SHBG), parathyroid hormone (PTH), follicular stimulating hormone (FSH) and C-terminal collagen crosslinks (CTx) were obtained at baseline and yearly for 5 years. Menstrual status at each visit was recorded and determined according to Stages of Reproductive Aging Workshop (STRAW) of the Practice Committee of American Society for Reproductive Medicine.

Results: The mean age at baseline was 47.7 $\pm$ 2.2 yr. At the baseline visit, 80.1%(n= 129) of the subjects were classified as premenopausal, 19.3%(n=31) perimenopausal and 0.6%(n=1) postmenopausal. At the end of 5 years, 12.4%(n=20) of the subjects remained in premenopausal stage (group 1), 31.1%(n=50) changed from pre- to perimenopausal (group 2), 34.2%(n=55) from pre- through peri- to post-menopausal (group 3) and 21.7%(n=35) from peri- to postmenopausal (group 4). The annualized bone loss at the spine in groups 3(-1.6$\pm$1.1%) and 4(-1.7$\pm$1.5%) were significantly greater than groups 1(0$\pm$0.8%) and 2(-1$\pm$1.1%). CTx did not correlate with annualized bone loss at any site. There was no difference in CTx between the subjects with rapid bone loss (>3%/year) and normal bone loss (<3% /year). Among all risk factors, only body weight (50 vs 56kg,

p=.016, 95% CI =1.19 to 11.06) and body mass index (BMI) (21.0 vs 23.4 kg2/m2, p = 0.026, 95% CI = 1.30 to 4.30) were significantly different between those with rapid and normal bone loss. Subjects with weight <50kg have an odds ratio of 5.5 having rapid bone loss. Similarly, subjects with BMI<20kg/m2 have a 3.5-fold increased risk of rapid bone loss.

Conclusion: The rate of bone loss occurs most significantly at the perimenopausal stage of menopausal transition. Body weight and BMI but not serum CTx predicts the likelihood of having rapid bone loss. Strategies to prevent bone loss should best be reinforced to perimenopausal women with low body weight and BMI.

***Disclosures: Cora Bow**, None.*

MO0340

Total, Android and Gynoid Fat Mass in Normal Weight and Overweight Women. The Influence of Menopause. Silvina Mastaglia*[1], Fabiana Solís[2], Alicia Bagur[3], Carlos Mautalen[4], Beatriz Oliveri[5]. [1]Seccción Osteopatía Médicas, Hospital de Clínicas, Universidad de Buenos Aires, Argentina, [2]Centro de Osteopatìas Médicas Dr. Carlos Mautalen, Buenos Aires, Argentina, [3]Sección Osteopatías Médicas, Hospital de Clínicas, Universidad de Buenos Aires. Centro de Osteopatìas Médicas Dr. Carlos Mautalen, Buenos Aires, Argentina, [4]Sección Osteopatías Médicas, Hospital de Clínicas, Universidad de Buenos Aires. Centro de Osteopatías Mèdicas Dr. Mautalen, Buenos Aires, Argentina, [5]Sección Osteopatías Médicas, Hospital de Clínicas, Universidad de Buenos Aires. Centro de Osteopatías Médicas Dr. Carlos Mautalen, Buenos Aires, Argentina

Obesity is a world public health problem. It is an independent risk factor for cardiovascular disease and increases morbimortality. Dual X-ray absorptiometry is a valid method to estimate body composition. Objectives: 1-to study a population of women aged 20 to 69 years to obtain normal values for total (TF), android (AF), and gynoid (GF) fat, and android/gynoid coefficient (A/G); 2- to evaluate whether menopause (MP) affects TF, AF, and GF distribution similarly in normal weight and overweight women. Material and Methods: Seventy seven women, average age (X ±DS) 49±14 years (range 20-69 years) and body mass index (BMI) between 18.5-24.9 Kg/m2 and thirty two women, average age 48±12 years with overweight (BMI 25.0-29.9 Kg/m2), were studied. Those receiving hormonal contraceptives, hormone replacement therapy, or medication affecting adipose tissue, or participating in weight loss programs were excluded. TF, GF, AF were determined using a GE Lunar Prodigy densitometer (Encore V 8.1). Statistical analysis (SPSS software) was used to compare pre vs. postmenopause, dividing the population according to BMI. Results: 33 pre-MP (BMI 21±2 Kg/m2) and 44 post-MP (BMI 22±2 Kg/m2) women were normal weight (control group); 13 pre-MP (BMI 26±1 Kg/m2) and 19 post-MP (BMI 27±1Kg/m2) women were overweight. Results are shown in Table (X±DS). During menopause, normal weight women showed changes in TF distribution (18.3±5 vs. 19.6±3 kg, ns) at the expense of AF (1.3±0.5 vs. 1.5±0.5kg, p<0,04) and increase in A/G index (0.7 vs. 0.8, p<0.01). Results showed no significant changes in GF. During menopause, overweight women no exhibited significant changes (GT: 27.6±3 vs. 27.0±4 kg; ns; GA: 2.2±0.5 vs. 2.3±0.5kg; ns, GG: 5.5±0.8kg vs. 5.0±0.8; ns; and A/G:0.9vs.0.9;ns).

Conclusion: 1- Fat redistribution during menopause in normal weight women involves greater android fat deposit. 2- Android and gynoid fat deposits increase equally in overweight women. 3- Peripheral conversion to estrogens may contribute to lessening changes in fat compartments in overweight women.

Table: Results of total, android and gynoid fat in the control group (X±DS)

				Normal Women						
	Characteristics			TF		AF		GF		A/G
	n	Age	BMI	Kg	%	Kg	%	Kg	%	
Pre-MP	33	34±9	21±2	18.3±5	31.9±7	1.3±0.5	33.3±9	4.2±0.9	43.4±5	0.7
Post-MP	44	59±9	22±2	19.6±3	34.1±4	1.5±0.5	37.2±8	4.0±0.7	44.1±4	0.8
p	___	0.00	ns	ns	ns	0.04	ns	ns	ns	0.01

Table

***Disclosures: Silvina Mastaglia**, None.*

MO0341

Elevated incidence of Fractures in Solid Organ Transplant Recipients on glucocorticoid-sparing immuno-suppressive regimens. Beatrice Edwards*[1], Amishi Desai[2], Joy Tsai[3], Hongyan Du[4], Andrew Bunta[5], Gabrielle Edwards[6], Allison Hahr[6], Michael Abecassis[6], Stuart Sprague[7]. [1]Northwestern University Medical School, USA, [2]University of Chicago, USA, [3]Medicine, Northwestern University, USA, [4]Northshore Healthcare System, USA, [5]Northwestern University Feinberg School of Medicine, USA, [6]Northwestern University, USA, [7]Northwestern University Evanston Northwestern Healthcare Center, USA

Objective: To assess the occurrence of fractures in solid organ transplant recipients

Methods: In a cohort study conducted from Jan 2001 to December 2007, participants were recruited from the Transplant Service clinical registry at Kovler Transplant Center at Northwestern Memorial Hospital. Medical record review, telephone and mailed surveys were conducted. Patients received less than 6 months of glucocorticoids as part of the immune-suppressive regimen.

Results: Of 351 transplant patients (Jan 2001-Dec 2007), 175 patients provided fracture information, with 48 (27.4%) having fractured since transplant (2-6 years). Organ transplants included 19 kidney/liver, 47 kidney/pancreas, 92 liver and 17 pancreas transplants. Age at transplant was similar (p=0.146) in fracture (47.3± 12.1 years) and non-fracture groups (50.8 ±10.3 yrs). Fractures were equally seen (p=0.214) in both genders [68 female (33.8 %) and 100 male (25.0 %)]. Fractures were equally distributed (p=0.683) across all transplant types; (15.8%, 29.8%, 23.5%, and 21.4% respectively). Fracture location included 8 (16.7%) foot (metatarsal), 12 (25.0%) vertebral, 3 (6.3 %) hand, 2 (4.2%) humerus, 5 (10.4%) wrist fractures, 10 (20.8%) occurred at other sites, and 7 (14.6%) occurred at multiple sites.

Discussion: Our findings confirm a high frequency of fractures in transplant recipients. Previously, fractures had been attributed to glucocorticoid use. We identify that fractures in solid organ transplant recipients occur despite avoidance of glucocorticoids.

Conclusion: Fractures remain a common occurrence in organ transplant recipients in spite of glucocorticoid-sparing immuno-suppressive regimens. Further research in this area is needed.

Figure 1 Site of fractures in solid organ transplant recipients

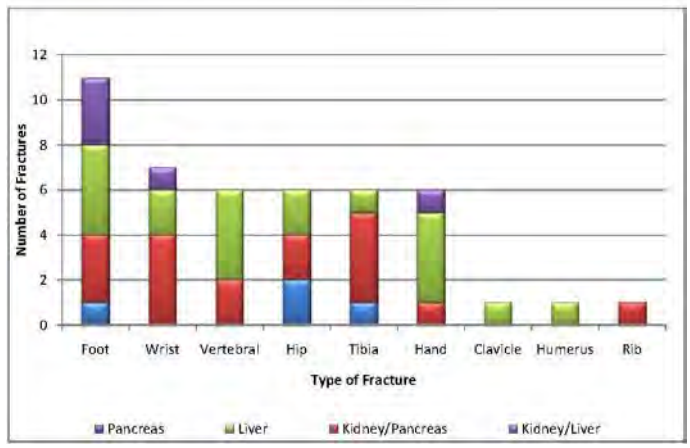

Figure 1 Site of Fracture

***Disclosures: Beatrice Edwards**, Novartis, 5; Amgen, 5; Procter and Gamble, 2; Roche, 5; Amgen, 5; Eli Lilly, 5*
This study received funding from: Procter and Gamble

MO0342

Evaluation of Contributors to Secondary Osteoporosis and Bone Loss in Patients Presenting with a Clinical Fracture. Sandrine Bours*[1], Tineke Van Geel[2], Piet Geusens[3], H. Janzing[4], Marcel Janssen[4], G. Hoffland[4], P. Willems[5], Joop van den Bergh[4]. [1]Maastricht University Medical Centre, The netherlands, [2]Maastricht University, The netherlands, [3]University Hasselt, Belgium, [4]Viecuri MC Venlo, Netherlands, [5]Maastricht University Medical Centre, Netherlands

Background: Previously undetected contributors to secondary osteoporosis and bone loss (SECOB) are frequently found in patients with osteoporosis, but the prevalence in patients at the time they present with a clinical fracture is unknown.

Methods: Of 893 consecutive fracture patients, 626 (482 women, 144 men, age range: 45-97 years) had bone mineral density (BMD) testing and laboratory investigations [serum calcium, phosphate, 25(OH)D, protein electrophoresis, creati-

nine, PTH, TSH, free T4, and in men serum testosterone in all and 24 hrs urinary calcium excretion on clinical indication].

Results: Known SECOB were present in 23.0% of patients and previously undetected SECOB in 28.3%, including paraproteinemia (n=14), renal insufficiency grade ⩾III (n=54), primary (n=17), secondary (n=62) and idiopathic hyperparathyroidism (n=8), hyperthyroidism (n=39), hypercalciuria (n=4 out of 16 measured) and hypogonadism in men (n=12). In patients with a normal BMD we found a newly diagnosed factor in 25% of the male and in only 7,1% of the female patients. With osteopenia we found a new factor in 30,0% and 28,2% in men and women, respectively. In the patients with osteoporosis a new factor was diagnosed in 45,0% in men and 32,0% in women. 52.5% of the SECOBs were found in fracture patients without BMD-osteoporosis (6.2% with normal BMD and 46.3% with osteopenia).In addition, only 8.6% of patients had a daily dietary calcium intake of ⩾1200 mg combined with a serum 25(OH)D level ⩾50 nmol/l (only 1.8% combined with ⩾ 75 nmol/l). Risk factors for undetected SECOB were increasing age (OR: 1.04, CI: 1.02-1.05), being male (OR: 1.77, CI: 1.16-2.73), osteopenia (OR 2.67, CI: 1.34-5.32) and osteoporosis (OR: 2.98, CI: 1.47-6.05; normal BMD as reference).

Conclusion: Since more than 50% of newly detected SECOBs are present in patients without BMD osteoporosis, systematic screening for SECOBs, dietary calcium intake and vitamin D status needs to be performed in all patients who present with a fracture. This allows for identification of potentially reversible SECOBs and correction of calcium and vitamin D deficiency, in addition to the possibility of treatment with anti-osteoporosis medication in these high risk patients.

***Disclosures: Sandrine Bours**, None.*

MO0343

Fractures in Obese Postmenopausal Women: Prevalence, Skeletal Location and Risk Factors. The Global Longitudinal Study of Osteoporosis in Women. Juliet Compston*[1], Robert Lindsay[2], Cyrus Cooper[3], Adolfo Diez-Perez[4], Susan Greenspan[5], Frederick Hooven[6], Andrea Lacroix[7], Maurizio Rossini[8], Julie Flahive[9], Coen Netelenbos[10]. [1]University of Cambridge School of Clinical Medicine, United Kingdom, [2]Helen Hayes Hospital, USA, [3]University of Southampton, United Kingdom, [4]Hospital del Mar-IMIM-Autonomous University of Barcelona, Spain, [5]University of Pittsburgh, USA, [6]University of Massachusetts Medical School, USA, [7]Fred Hutchinson Cancer Research Center, USA, [8]Department of Rheumatology, University of Verona, Italy, [9]COR, UMass Medical School, USA, [10]VU Medical Center, The netherlands

Obesity is believed to be protective against fracture, although in a recent study a high prevalence of obesity was reported in postmenopausal women with fragility fracture. We compared the prevalence and location of fractures in obese and non-obese postmenopausal women in a large multinational study and examined risk factors for fracture in these women. GLOW is an observational longitudinal study of non-institutionalized women aged ⩾55 years recruited from 723 primary physician practices in 10 countries. Practices typical of each region were identified. All women visiting practices within the prior 2 years were eligible. Self-administered questionnaires were mailed and data collected included demographics, medical history, fracture occurrence, medications and risk factors for fracture. We performed a cross-sectional analysis of data on history of fracture in obese and non-obese women. Baseline data on body mass index (BMI) were available in 57,555 women, mean (±SD) age 68.5(8.83) years. The prevalence of obesity (BMI ⩾30 kg/m2) was 23.8%. A history of fracture after age 45 was observed in 23% of obese and 24% of non-obese women. The upper arm, ankle, upper leg and lower leg were significantly more likely to be affected in obese than non-obese women with a prevalent fracture (14% vs 12%; p=0.010, 34% vs 25%; p<0.0001, 5.1% vs 4.1%; p =0.015 and 13% vs 10%; p<0.0001, respectively), whilst fractures of the wrist (31% vs 39%), hip (5.8% vs 8.3%) and pelvis (2.9% vs 4.9%) were significantly less common than in non-obese women (p<0.0001 for all sites). Compared to non-obese women, obese women with a prevalent fracture were more likely to be current cortisone users (5.6% vs 4.3%), to report early menopause (20% vs 13%), to report fair or poor general health (39% vs 29%), to use arms to assist standing from a sitting position (63% vs 40%), and to report ⩾2 falls in the past year (26% vs 21%) (all p<0.0001). We conclude that fractures in obese postmenopausal women contribute significantly to the overall fracture burden in this population, fractures of the upper arm, ankle and leg being more common and hip, pelvis and wrist less common than in non-obese women. Poor mobility and increased falls risk may play an important role in the pathogenesis of fractures in obese women. Our findings have significant public health implications in view of the rapidly increasing prevalence of obesity and emphasize the need for appropriate preventive strategies in this population.

***Disclosures: Juliet Compston**, Servier, Procter & Gamble, Eli Lilly, 8; Servier, Shire, Nycomed, Novartis, Amgen, Procter & Gamble, Wyeth, Pfizer, Alliance for Better Bone Health, Roche, GlaxoSmithKline, 5; Servier R&D and Procter & Gamble, 2*
This study received funding from: The Alliance for Better Bone Health (sanofi-aventis and Warner Chilcott)

MO0344

High Prevalence of Hypovitaminosis D in Japanese Pregnant Women with Threatened Premature Delivery. Megumi Shibata*[1], Atsushi Suzuki[2], Takao Sekiya[3], Sahoko Sekiguchi[1], Shogo Asano[1], Yasuhiro Udagawa[3], Mitsuyasu Itoh[1]. [1]Fujita Health University, Division of Endocrinology, Japan, [2]Fujita Health University Division of Endocrinology, Japan, [3]Fujita Health University, Department of Obstetrics & Gynacology, Japan

Background: Hypovitaminosis D in mother has been reported to affect bone mass and the incidence of neuromuscular diseases of their children. In addition, low maternal 25-hydroxyvitamin D (25-OHD) level could increase the risk of preeclampsia, cesarean section, and craniotabes. We have previously found that rather low 25-OHD levels in Japanese mother compared with age-matched non-pregnant females. In the present study, we investigated the relationship of maternal hypovitaminosis D in Japanese pregnant women and their clinical complications around their delivery.

Methods: Serum concentration of 25-OHD in 93 pregnant women after 30th weeks of their gestation was determined by direct radioimmunoassay. Results: Over all, hypovitaminosis D, which was defined as serum 25-OHD concentration was equal to or less than 20 ng/ml, was revealed in 85 mothers (89.5%), including vitamin D deficiency (25-OHD < 10 ng/ml) in 10 subjects. Maternal hypovitaminosis D did not affect corrected calcium concentrations but associated with serum Pi level and several bone markers. In addition, serum albumin concentration was associated with serum 25-OHD levels suggesting the modification of 25-OHD levels in pregnant women. Serum concentration of 25-OHD in mothers of 10 babies with clinical complications (6 cases of intrauterine growth retardation, 2 cases of 18-trisomy, 2 cases of external malformation) were not lower than others. However, serum 25-OHD levels (11.2 ±3.2 ng/ml) in preterm threatened delivery mother were significantly lower than others (15.2 ±5.1 ng/ml). Conclusion: The present data suggest the high prevalence of hypovitaminosis D in Japanese perinatal pregnant women, which seems to affect bone metabolism and to be associated with threatened premature delivery in these subjects.

***Disclosures: Megumi Shibata**, None.*
This study received funding from: Novo Nordisk, sanofi-aventis, Banyu Pharm,and Ono Pharm

MO0345

Long-term Survivors of Advanced Head and Neck Cancer are not at Increased Risk for Osteoporosis or Fragility Fractures. Siu-Ling Ma, Victoria Villaflor, Ezra Cohen, Everett Vokes, Tamara Vokes*. University of Chicago, USA

PURPOSE: Advanced head and neck cancer (HNC) patients suffer severe malnutrition and weight loss, which may increase their risk for osteoporosis. In this cross-sectional study, we evaluated bone mineral density (BMD) and presence of vertebral fractures in long-term survivors of HNC.

METHODS: HNC survivors who finished chemoradiotherapy at least 12 months prior, had no bone metastases, and were disease free were contacted by telephone. Participating subjects had BMD measured at the L1-L4 spine (LS), femoral neck (FN) and total hip (TH), and a lateral thoracolumbar spine image taken for Vertebral Fracture Assessment (Lunar Prodigy, GE Medical Systems). A vertebral fracture was defined as a grade 2 or higher fracture.

RESULTS: Of 134 contacted patients, 74 (55%) participated, of whom 68 had complete data that was used in analysis: 56 males (82%), 12 females; 56 Caucasians, 10 African-Americans, 1 Asian, 1 Hispanic; age 59±9 (SD) years, range 37-77 years. Time since treatment was 59±28 months. Weight loss during treatment was 12±7 kg, and weight regained was 9±11 kg. Compared to those who did not participate, study subjects were heavier (p<0.01) and finished treatment more recently (p<0.05), but did not differ by age, race, sex, HNC stage, amount or percentage of weight loss.

The lowest Z-score between the hip and spine (LowZ) was -0.64±1 (range -2.7 to 1.3), and was ≤-2 in 7 subjects (10%; 6 males, 1 female). LowZ did not correlate with amount (r=0.14, p=0.25) or percentage of weight lost (r=0.11, p=0.39), or amount regained (r=-0.16, p=0.20). Five subjects (all males, aged 61±5 years) had a vertebral fracture but did not differ from those without any vertebral fracture in LowZ (-0.7±0.4, range -0.3 to -1.3), weight lost (16±6 kg), and weight regained (11±12 kg). Only one subject (52 year-old male with LowZ=-2.6, weight loss=12.6 kg, weight regained=11.6kg) sustained a peripheral fracture after treatment. Six subjects (3 males, 3 females) with osteoporosis by T-score criteria had lower baseline (66 vs 101 kg, p<0.01) and current weight (68 vs 94 kg, p<0.01), but less weight loss during treatment (7 vs 15 kg, p<0.01) than those with a normal T-score.

CONCLUSION: Long-term survivors of advanced head and neck cancer who regain most of their weight are not at increased risk for osteoporosis.

***Disclosures: Tamara Vokes**, None.*

MO0346

Measures of Body Fat are Associated with Prevalent Vertebral Deformities in Older Women. Laura Laslett*[1], Stella Last[1], Stephen Quinn[1], Tania Winzenberg[1], Graeme Jones[2]. [1]Menzies Research Institute, Australia, [2]Menzies Centre for Population Health Research, Australia

Low body weight has long been recognised as a risk factor for osteoporosis, but it is unclear whether high body weight is protective or deleterious. The aim of this population-based cross-sectional study was to describe the relationship between weight-related factors and anterior wedge deformities.

Anterior wedging of T4-L4 were determined by morphometric dual-emission X-ray absorptiometry (MXA), and the ratio was appropriately used as a continuous variable; the mean number of assessable vertebrae in each patient was 12.6 (range 3-13). Body fat was assessed as weight, body mass index (BMI), waist-hip ratio (WHR), waist circumference, trunk fat (%) and total fat mass using a combination of measurement and dual-emission X-ray absorptiometry (DXA). Mixed models were used to take into account the correlated readings of vertebral deformities within patients, and were adjusted for age, hip BMD and spine BMD. The mean age of participants (N=1007) was 62.6 years (range 50-80 years); mean BMI was 27.7 (range 17.6 - 52.9) and 51.4% were female. The prevalence of anterior wedge deformities using a definition of 20% reduction in anterior height was 36.6% in women and 47.4% in men in the thoracic spine; and 1.4% in women and 5.3% in men in the lumbar spine.

As body fat increased, the ratio of anterior to posterior vertebral heights decreased, indicating worsening vertebral deformity. In women in the thoracic region, this association was present for weight (Sβ 0.006, p=0.001), BMI (Sβ 0.007, $p<0.001$), trunk fat (%) (Sβ 0.004, p=0.006), waist circumference (Sβ 0.005, p=0.003), and total body fat mass (adjusted for lean mass) (Sβ 0.005, p=0.012); but not waist-hip ratio or total lean mass (adjusted for fat mass). No significant association was present between measures of body fat and deformities in the thoracic region in men or the lumbar region in either men or women.

In conclusion, there is a deleterious association between thoracic anterior wedge deformities and body fat in women but not in men. The associations with waist circumference and trunk fat in women suggest a direct effect from increased skeletal loading on the thoracic spine, and indicate that the obesification of western society may not be protective against fractures as previously thought.

***Disclosures: Laura Laslett**, None.*

MO0347

Relationship Between Osteopenia and Sexual Hormones in Human Immunodeficiency Virus-infected Patients. Sharona Azriel*[1], Rafael Rubio[2], Federico Hawkins[2]. [1]Hospital Infanta Sofia, Spain, [2]University Hospital 12 de Octubre, Spain

Reduced bone mineral density (BMD) is considered a metabolic complication among HIV-infected patients on highly active antiretroviral therapy (HAART). Multiple factors associated with abnormalities in the bone mineral metabolism have been postulated, including the direct effect of virus, the antiretroviral drugs or risk factors of osteopenia, like hypogonadism. Objectives: 1) Evaluate the prevalence of reduced BMD HIV-infected patients and the prevalence of sexual hormonal alterations and its association with the osteopenia. 2) Estimate longitudinal changes of BMD at 12 and 24 months. Patients and methods: This is a prospective cohort study. 100 HIV-infected caucasian outpatients were recruited during 24 months and studied over 2 years of follow-up. Exclusion criteria were any condition that could cause loss of BMD and use of medications that interfere with mineral metabolism in the past 6 months. 68% were males; all the females were premenopausic; mean age of the cohort was 40 years (SD: 9);mean BMI was 24 kg/m2 (SD: 3.6). 95% had undetectable virus load. 77% was taking a HAART regimen (65% included a protease inhibitor), 18% bitherapy (2 nucleoside reverse-transcriptase inhibitors) and 5% was ART-naïve. BMD (L1-L4, femoral neck, total hip and radium) and body composition (total body fat mass, % total fat, trunk fat mass, % trunk fat and lean mass) were assessed by DXA Hologic QDR 4500. Osteopenia (op) and osteoporosis (OP) was defined according to WHO criteria. Results: Prevalence of total op was 63.6% and 13.1% of OP. The incidence of male hypogonadism was 2%. Serum total testosterone (TT) levels were increased > 800 ng/dl in 25.4% of males, mean TT was 646 ng/dl (SD: 248). No differences in immunological and virological parameters were found between patients with increased TT and normal values. In the univariate statistical analysis, male patients with femoral neck T-score <-1 SD vs normal T-score >-1 showed significantly greater TT concentrations [517.22 (353.08) vs 340.95 (340.19), p=0.021]. Multivariate regression logistic model showed that for each additional 100 ng/ml of serum TT, there was for femoral neck BMD a RR: 35% (11.96-64.21%), p=0.003). Total body fat mass (kg) and trunk fat mass (kg) were significantly lower in males with op and elevated TT vs. those with normal T-scores. No significant changes in BMD and TT levels were found after 2 years of follow-up. Summary: Prevalence of op in HIV-infected patients is high, but does not progress after 24 months of follow-up. Lower total and visceral fat mass could be implicated in this femoral neck bone loss and aromatization failure of androgens should be further studied in this condition.

***Disclosures: Sharona Azriel**, None.*

MO0348

Renal Function and Fracture Risk in a Cohort of Community Dwelling Elderly Adults. Lekshmi Nair, Thomas Weber*, Carl Pieper, Cathleen Colon-Emeric. Duke University Medical Center, USA

Patients with chronic kidney disease (CKD) appear to be at a higher risk for fractures, though the mechanism(s) underlying this observation remain poorly understood. This analysis sought to determine if progressive decline of renal function is independently associated with a higher risk of any new fracture as the primary outcome, and new hip fracture as the secondary outcome in community-dwelling older adults.

The Established Population for Epidemiologic Studies of the Elderly (EPESE), designed to estimate the incidence and prevalence of chronic conditions and impairments in the elderly, was utilized to assess the relationship of glomerular filtration rate (GFR) with subsequent self-reported hip fracture or fracture. Over a four-year follow-up period (1992-96), 147 subjects reported a new hip or any new fracture and 1120 subjects reported no fractures. Logistic regression was employed to assess the association of GFR (calculated by a single serum creatinine at study entry) with any new fracture or new hip fracture.

GFR was significantly lower in fracture relative to non-fracture subjects (50.9 vs. 56.3 ml/min, $p<0.0001$. respectively). Univariate analysis demonstrated a significant association between GFR and any new fracture, with an odds ratio (OR) of 2.7 for every 30 cc/min decrease in GFR (95% CI 1.8-4.0). In addition, there was also a significant association between decline in GFR and new hip fracture (OR =3.4, 95% CI 1.7-7.1). After adjustment for covariates (age, sex, race, BMI, history of stroke, history of prior fracture at any site or hip alone, current smoking status, current alcohol intake, Rosow-Breslau score, SPMSQ score and corrected calcium), a decrease in GFR of 30 cc/min was still significantly associated with an increased risk for any new fracture (OR = 1.6 ,95% CI 1.0-2.7), but not with new hip fracture (OR =2.1,95% CI 0.9-4.8).

These data suggest that decline in renal function may independently increase the risk for any new fracture in community dwelling elders. If confirmed by further studies, assessment of renal function may provide insight into additional mechanisms that increase an older individual's risk for fracture.

***Disclosures: Thomas Weber**, None.*

MO0349

Risk Factors For Fractures Over Aged 50 In A Population-Based Cohort Of Older Women From The UK. Emma Clark*, Miranda Cuming, Virginia Gould, Leigh Morrison, Jon Tobias. University of Bristol, United Kingdom

Purpose: Assessing an individual's fracture risk using clinical risk factors is increasingly important, as shown by the development of tools such as the fracture-risk predictor FRAX. Many previous studies have looked at various groups of risk factors for fracture such as osteoporosis risk factors, or risk factors for falls. There are very few studies in the literature that have looked at the effects of osteoporosis risk factors and falls risk factors combined with co-morbidities. We have the ability to do this, with our unique population-based cohort of elderly women that contains detailed data on individual risk factors.

Methods: The Cohort for Skeletal Health in Bristol and Avon (COSHIBA) is a population-based cohort of 3200 women aged 65-84 from south-west England. Cross-sectional self-reported data were collected on history of fracture after aged 50 years. Data was also collected on age, socioeconomic status e.g. housing tenure, co-morbidities e.g. stroke, mobility including use of walking aids, current and previous alcohol and smoking intake, habitual exercise such as brisk walking, dietary calcium intake, family history, age at menopause, anthropometrics including reported height loss, past history of steroid use for >3 months and current and previous use of HRT, calcium and vitamin D supplements and bisphosphonates or other bone protective therapies. Logistic regression was used to calculate odds ratio (OR) for fracture risk and to adjust for potential confounders.

Results: Unadjusted models showed associations between age, history of falls, co-morbidities, use of walking aids, early menopause, dietary calcium intake, current bisphosphonate treatment and calcium and vitamin D supplements, and previous steroids and HRT use– see Table. Adjustment for all variables in the table showed that independent risk factors for fracture were age, history of falls, bisphosphonate use and calcium and vitamin D supplementation, and previous HRT use.

Conclusion: There appear to be relatively few risk factors for fractures in the elderly independent of age and falls, that are detectable in a population based setting. Other than age and falls, the strongest independent risk factors for fracture were current bisphosphonate use and calcium and vitamin D supplementation, confirming that fracture liaison services operating in our region have successfully targeted bone protective therapy to individuals with a history of fracture.

Risk factor:	Unadjusted OR for fracture risk OR (95%CI)	OR for fracture risk adjusted for all other variables in the table OR (95%CI)
Age (per year)	1.06 (1.04 to 1.08)	1.04 (1.03 to 1.07)
Falls	1.68 (1.49 to 1.89)	1.68 (1.46 to 1.92)
Co-morbidities	1.23 (1.05 to 1.44)	NS
Early menopause	1.26 (1.06 to 1.50)	NS
Use of walking aids	1.31 (1.09 to 1.59)	NS
Dietary calcium intake	1.19 (1.02 to 1.40)	NS
Current bisphosphonates	3.33 (2.54 to 4.36)	2.30 (1.64 to 3.25)
Current calcium and vit D supps	2.48 (2.01 to 3.06)	1.67 (1.26 to 2.21)
Steroids	1.24 (1.05 to 1.46)	NS
Previous HRT use	0.72 (0.60 to 0.85)	0.79 (0.65 to 0.97)

Table

***Disclosures: Emma Clark**, None.*

MO0350

Risk Factors for Subtrochanteric and Diaphyseal Femur Fractures: An Analysis from the Study of Osteoporotic Fractures. Michael Kelly*[1], Rosanna Wustrack[1], Douglas Bauer[1], Lisa Palermo[1], Shane Burch[1], Katherine Wilt[2], Jane Cauley[3], Nicola Napoli[4], Marc Hochberg[5], Dennis Black[1]. [1]University of California, San Francisco, USA, [2]California Pacific Medical Center, USA, [3]University of Pittsburgh Graduate School of Public Health, USA, [4]University Campus Biomedico, Italy, [5]University of Maryland School of Medicine, USA

Purpose: Recent reports have linked the long-term use of bisphosphonates with low energy subtrochanteric and diaphyseal femur fractures, but little is known about the risk factors for these fractures. The purpose of this study was to examine risk factors for subtrochanteric and diaphyseal fractures from the Study of Osteoporotic Fractures (SOF) a prospective study of 9704 women at least 65 years of age, begun in 1986. Methods: Radiographic reports of femur fractures from the SOF were reviewed and classified as: femoral neck (FN), all hip (HP), and subtrochanteric/diaphyseal (SH). Demographic variables, including age, total hip bone mineral density (BMD), body mass index (BMI), history of prior fractures, and history of prior falls were collected. In addition, current use of bisphosphonates (yes/no), hormone replacement therapy (HRT), and corticosteroid use was recorded at each visit at two to five year intervals. We compared predictors of SH fractures to predictors of other types of hip fractures using multivariable, time-dependent cox proportional hazards models to calculate relative hazard (RH) of fracture. Results: Forty five women sustained 48 subtrochanteric/diaphyseal femur fractures and 746 sustained femoral neck fractures over a total follow up of 142,000 person years. Significant univariate predictors for SH fractures included age (HR/5 years, 2.04, 95% CI%: (1.59, 2.63), $p<0.0001$), total hip BMD (RH/SD decrease: 1.52, (1.11, 2.08), $p = 0.0098$) and history of falls (2.04, (1.13, 3.66), $p = 0.0174$). Only increasing age remained significant in multivariate models. Nine women with SH fractures reported any previous bisphosphonate use and no significant association between bisphosphonate use and SH fractures was observed. Predictors of FN fractures were similar including age, total hip BMD, and a history of falls. Conclusions: In SOF, women of older age, with lower BMD, and histories of prior falls were at an increased risk for SH fracture. These risk factors were common to both FN and HP fractures as well. There were too few events to draw conclusions regarding medication use and SH fractures.

***Disclosures: Michael Kelly**, None.*

MO0351

Selective Serotonin Reuptake Inhibitor Use and Change in Bone Mineral Density Among Older Men. Elizabeth Haney*[1], Smriti Shrestha[1], Susan Diem[2], Kristine Ensrud[3], Jane Cauley[4], Katie Stone[5], Eric Orwoll[1], Michael Bliziotes[6]. [1]Oregon Health & Science University, USA, [2]University of Minnesota, USA, [3]Minneapolis VA Medical Center / University of Minnesota, USA, [4]University of Pittsburgh Graduate School of Public Health, USA, [5]California Pacific Medical Center-Research Institute, USA, [6]OHSU/Portland VA Medical Research Center, USA

Background: Antidepressants have been linked to osteoporosis through various direct and indirect mechanisms. Recent interest in the serotonin system focuses attention on selective serotonin reuptake inhibitors (SSRI's) and their potential effect on bone. We evaluated the association between use of SSRI's and change in bone mineral density (BMD) at the total hip, subregions and lumbar spine. Methods: We evaluated change in BMD using data from the Osteoporotic Fractures in Men (MrOS) Study. 39 men were excluded because they had no medication information, leaving 5,956 eligible for analysis. We assessed medications at baseline and 3 additional visits over the course of approximately 10 years to compare rates of bone loss among men who used SSRI medications at any of the four time points compared to non-users (defined as those using no antidepressant medication at any time point). We used multivariable linear regression to create models adjusting for covariates. We evaluated potential covariates from a list of variables used in prior analyses of SSRI use and BMD, and included those that were associated with both SSRI use and change in BMD, and those provided the best model fit.Results: Compared to non-users, SSRI users were heavier, with greater fat mass and greater changes in weight since age 25; had lower physical activity scores, lower grip strength, and more impairments in IADLs; reported lower self-rated health and more comorbidities, higher SF-12 mental component scores; and greater history of falls. In adjusted models, SSRI users had higher rates of bone loss at the total hip compared to non-users (Table). Results were similar at the trochanter and femoral neck. There was no significant difference between users and non-users at the spine. Conclusion: In multivariable analyses, SSRI use was associated with increased loss of BMD at the total hip and subregions. These results are consistent with prior literature, but limited by incomplete ability to control for confounding by indication (depression). The potential for antidepressant medications to contribute to bone loss is clinically important, and warrants further research to understand how they contribute to mechanisms for bone loss.

Table: Annualized %change in BMD, mean (95% confidence interval)

	SSRI Users (n=347)	Non-Users (n=5,168)
Total hip*	-0.72 (-0.83, -0.61)	-0.57 (-0.66, -0.48)
Femoral neck*	-0.73 (-0.87, -0.59)	-0.61 (-0.72, -0.50)
Trochanter*	-0.65 (-0.78, -0.52)	-0.48 (-0.59, -0.38)
Total spine	0.50 (0.35, 0.65)	0.60 (0.49, 0.72)

*p<0.05; models adjusted for age, race, site, weight change, BMI, vitamin D from diet and supplements, average grip strength, walking speed, alcohol use, self-reported health, co-morbidity, other antidepressant use and baseline BMD.

Table

***Disclosures: Elizabeth Haney**, None.*

MO0352

Statin Use is Associated with Increased Bone Mineral Density in Women, but not in Men. Wei Zhou*[1], Wilma Hopman[2], Claudie Berger[3], Suzanne Morin[1], Lisa Langsetmo[4], Tanveer Towheed[2], Tassos Anastassiades[2], Rick Adachi[5], David Goltzman[1]. [1]McGill University Health Centre, Canada, [2]Queen's University, Canada, [3]McGill University, Canada, [4]Canandian Multicenter Osteoporosis Study, Canada, [5]McMaster University, Canada

Purpose: Observational studies, clinical trials and meta-analyses have found mixed results regarding the association between statin use and bone mineral density (BMD), partly due to differences in study design and length of exposure. This study adds to the literature due to the large sample, the ability to assess men and women separately, the lengthy follow-up of up to 10 years and the ability to adjust for a large number of potential confounders.

Methods: Participants in the Canadian Multicentre Osteoporosis Study (CaMos) were randomly selected from a 50 km radius of 9 cities across Canada. Participation involved a detailed, in-person interview to collect sociodemographic information, medical and family history, food intake, lifestyle (alcohol, smoking, activity level), quality of life assessment and current use of medications and supplements. Bone mineral densitometry (BMD) was scheduled as part of the study protocol, and height and weight were measured. Participation is on-going; results are based on a cross-sectional analysis of year 10 data. Multivariable models of BMD of the lumbar spine (L1-L4), total hip and femoral neck were constructed using linear regression, adjusting for known confounders (see Table 1).

Results: 4899 participants had BMD and questionnaire data at year 10. Mean age for the 3477 women was 68.8 years (SD 11.3); statin use increased from 141 (4.1%) at baseline to 704 (20.3%) by year 10. Mean age for the 1422 men was 66.1 years (SD 12.5); statin use increased from 76 (5.3%) at baseline to 388 (27.3%) at year 10. Median (interquartile range) duration of use in months was 60 (30, 72) for women and 60 (36, 74) for men. Mean BMD for women was 0.958 (SD 0.163) for lumbar spine, 0.845 (0.137) for total hip and 0.699 (0.113) for femoral neck. For men, values were 1.084 (0.178) for lumbar spine, 0.993 (0.144) for total hip and 0.787 (0.121) for femoral neck. Table 1 presents the results of the multivariable regressions. Women taking statins had significantly higher BMD at all three sites than those not using a statin, although the estimates are modest, ranging from 0.015 (femoral neck) to 0.025 (lumbar spine). For men, estimates were negative in direction, but 95% confidence intervals included zero.

Discussion: These data provide support for a positive but small association between statin use and BMD in women, but results are inconclusive for men.

Sex	Site	Adjusted Estimate (95% CI)
Women (n=3477)	Lumbar Spine	0.025 (0.010, 0.039)
	Total Hip	0.021 (0.010, 0.032)
	Femoral Neck	0.015 (0.006, 0.024)
Men (n=1422)	Lumbar Spine	-0.013 (-0.036, 0.011)
	Total Hip	-0.006 (-0.024, 0.011)
	Femoral Neck	-0.014 (-0.029, 0.001)

- Reference category = No statin use
- Adjusted for age, height, BMI, education, centre (9), smoking status, alcohol use, calcium intake, regular activity, sedentary time, use of antiresorptives, use of corticosteroids (women), menopausal status (women), the Physical Component Summary of the SF-36, family history of fracture, history of fracture, IBD and rheumatologic disease.

Table 1: Adjusted Estimates for Bone Mineral Density at Three Sites, by Sex

***Disclosures: Wei Zhou**, None.*

MO0353

TSH Directly Modulates Human Bone Metabolism Irrespective of Thyroid Hormone: Clinical Evaluation of 21 Patients with TSH Producing Pituitary Adenoma. Nobuaki Ito*[1], Akira Takeshita[2], Megumi Miyakawa[2], Noriaki Fukuhara[3], Kenich Oyama[3], Shozo Yamada[3], Yasuhiro Takeuchi[4]. [1]University of Tokyo Hospital, Japan, [2]Toranomon Hospital Endocrine Center, Japan, [3]Department of Hypothalamus-Pituitary Surgery, Toranomon Hospital, Japan, [4]Toranomon Hospital, Japan

Thyrotoxicosis along with suppressed serum TSH level stimulates bone turnover that results in bone loss. Among subjects with serum thyroid hormone level within reference range, less serum TSH level might be associated with less bone mineral density (BMD). TSH receptor-null mice present less BMD than controls with supplementation of thyroid hormone or not, and accumulating evidence suggests that TSH directly inhibits osteoclastogenesis to suppress bone turnover and increases bone mass in rodents. However, it is yet uncertain if this is the case in human. The aim of this study is to clarify whether or not circulating TSH is correlated with BMD in human even in the presence of inappropriately high level of serum thyroid hormone. To this end, we examined BMD with DXA and biochemical bone markers in 21 patients with TSH producing pituitary adenoma (TSHoma) but without any other hormonal disorders, because circulating TSH is active even in the presence of thyrotoxicosis in TSHome patients. Serum free thyroxine (FT4), free triiodethyronine (FT3), TSH, bone markers, bone alkaline phosphatase (BAP), osteocalcin (OC), urinary NTX (uNTX) and deoxypyridinoline (DPD), and lumbar BMD (Z-score) before surgery were measured. Nor FT3 or FT4 but TSH was correlated with lumbar BMD ($r=0.614$, $p=0.003$). Bone markers were all positively correlated with either serum FT3 or FT4 ($p< 0.01$) but not with TSH or BMD. These observations indicate that, independent of thyroid hormone, TSH is involved in bone metabolism to increase BMD in TSHoma patients. This is the first report suggesting direct anabolic effects on bone of TSH in human. Although the mechanism is unknown yet, TSH itself may have anabolic effects on bone in human.

***Disclosures: Nobuaki Ito**, None.*
This study received funding from: Okinaka Memorial Institute for Medical Research

MO0354

Vitamin D Levels and Incident Frailty Status in Older Women. Kristine Ensrud*[1], Susan Ewing[2], Lisa Fredman[3], Marc Hochberg[4], Jane Cauley[5], Teresa Hillier[6], Steven Cummings[7], Kristine Yaffe[2], Peggy Cawthon[8]. [1]Minneapolis VA Medical Center / University of Minnesota, USA, [2]University of California - San Francisco, USA, [3]Boston University, USA, [4]University of Maryland School of Medicine, USA, [5]University of Pittsburgh Graduate School of Public Health, USA, [6]Kaiser Center for Health Research, USA, [7]San Francisco Coordinating Center, USA, [8]California Pacific Medical Center Research Institute, USA

Vitamin D deficiency and frailty are increasingly common with aging, but the association between these conditions is uncertain. To determine whether non-frail older women with lower serum 25-hydroxyvitamin D (25(OH)D) levels are at increased risk of greater frailty status at follow-up, we measured 25(OH)D levels (liquid chromatography-tandem mass spectroscopy) in 4242 non-frail women (mean age 75.9 years) at baseline and re-examined frailty status 4.5 years later. Using criteria similar to those used in the Cardiovascular Health Study index, frailty status was classified as robust (n=1843) or intermediate stage (n=2399) at baseline; and robust (n=985), intermediate stage (n=2165), frail (n=693) or dead (n=399) at follow-up. Logistic regression models were used to examine the association between baseline 25(OH)D levels and incident frailty status. Median 25(OH)D level at baseline was 23.0 ng/mL (interquartile range 17.0-29.0 ng/mL). After adjustment for age, site, season, smoking, health status, education, estrogen use, medical conditions, cognition, and body mass index, there was no association between 25(OH)D levels and risk of being classified as intermediate/frail/dead (vs. robust) at follow-up (Table). Compared with women with 25(OH)D levels 20.0-29.9 ng/mL (referent group), women with levels 15.0-19.9 ng/mL (but not those with levels <15 ng/mL or those with levels ⩾30 ng/mL) were at higher risk of being classified as frail/dead (vs. robust/intermediate) at follow-up. The risk of being classified as dead (vs. robust/intermediate/frail) at follow-up was higher among women with levels <15 ng/mL (but not among those with levels 15.0-19.9 ng/mL or those with levels ⩾30 ng/mL). Further adjustment for baseline frailty status (intermediate vs. robust) or expressing 25(OH)D as quartiles did not substantially alter these results. In this cohort of community-dwelling older women not frail at baseline, lower serum 25(OH)D levels (<20 ng/mL) were modestly associated with an increased risk of being classified as frail at follow-up or dying in the interim period.

	Odds Ratio (95% CI) by Category of 25(OH)D Level (ng/mL)			
	<15.0 (n=725)	15.0-19.9 (n=792)	20.0-29.9 (n=1675)	≥30.0 (n=921)
Mutivariate Model[†]				
Intermediate/frail/dead vs. robust	1.19 (0.95-1.50)	0.97 (0.79-1.20)	1.00 (referent)[‡]	1.04 (0.86-1.27)
Frail/dead vs. robust/intermediate	1.08 (0.87-1.34)	1.23 (1.00-1.51)	1.00 (referent)[‡]	0.92 (0.75-1.13)
Dead vs. robust/intermediate/frail	1.36 (1.00-1.85)	1.27 (0.94-1.72)	1.00 (referent)[‡]	1.05 (0.77-1.43)

[†]4113 women with complete data on all covariates included in multivariable model

[‡]25(OH)D level expressed as a categorical variable due to evidence of a U-shaped association between 25(OH)D level and odds of greater frailty status among the entire cohort (n=5873) at baseline with nadir of risk among those with levels 20.0-29.9 ng/mL (referent group)

Table. Association between 25(OH) D Level and Odds of Greater Frailty Status

***Disclosures: Kristine Ensrud**, None.*

MO0355

Warfarin Use and Osteoporosis: Results of a Selected Screening Program. Christine Simonelli*[1], Mary Schoeller[2], Julie Morancey[2]. [1]HealthEast Osteoporosis Services, USA, [2]HealthEast Osteoporosis Care, USA

Osteoporosis and fracture rates have been reported to be increased in some studies of patients using chronic warfarin. Warfarin competitively inhibits vitamin K an important co-factor for an enzyme that catalyzes the carboxylation of glutamic acid to gamma-carboxyglutamic acid (bone-Gla-protein or osteocalcin).

The purpose of this pilot project was to see the impact of a program to assess prevalence of osteoporosis and fracture risk using DXA in patients being followed in a warfarin management clinic.

A protocol was initiated that allowed the Registered Nurse managing the anticoagulation clinic to recommend bone density testing with DXA to the provider caring for a patient who had not previously undergone BMD testing with DXA within five years. Adults at least age 50 using warfarin for at least 6 months were included.

During August, 2009, 240 patients were seen and 81 patients (50 female, 31 male) underwent BMD testing with DXA. Mean age for women was 67.2 (49, 85) and men 69.4 (52, 84). Of these, 18 (26%) were found to have osteoporosis (BMD T-score ≤-2.5 at femoral neck, total femur or lumbar spine), 23 (33%) with low bone mass (BMD T-score ≤-1, >-2.5) and 28 (40%) with normal bone mass (BMD T-score >-1). At 6 months following their DXA 12 of the 18 patients with osteoporosis were treated with a bisphosphonate, calcium and vitamin D (none on teriparatide or raloxifene); 1 with calcium alone; 2 on calcium and vitamin D and one on vitamin D alone. Three patients were newly diagnosed with vitamin D deficiency and placed on vitamin D replacement. Two patients were on no treatment. The mean Z-score of the osteoporotic patients was -1.5 (-0.2, -2.7). We were able to perform FRAX calculation on 22 of 23 patients with low bone mass and 1 patient had a ⩾20% 10-year fracture risk and ⩾3% 10-year hip fracture risk and 4 others had ⩾3% hip fracture risk. Of these 5 patients with low bone mass considered at highest risk, 1 was treated with a bisphosphonate, calcium and vitamin D, 3 with calcium and vitamin D alone and one on no treatment.

Adults being managed in a warfarin clinic who have not undergone recent BMD testing have a significant risk for undiagnosed osteoporosis and low bone mass. The Z-scores suggest that in a population of patients on chronic warfarin therapy bone density values are lower than would be predicted in the general population of age, sex and ethnicity-matched adults. This presents an opportunity for selective osteoporosis screening in a captive and high risk population.

Not all patients who were recommended for DXA scans by the anti-coagulation nurse were referred for bone density testing. Individuals on warfarin have at least one underlying medical problem and this may explain their lower bone density relative to their peers not on warfarin.

***Disclosures: Christine Simonelli**, None.*

MO0356

Lumbar Densitometry Analysis of Sequential Bone Mineral Density Gradient in the Evaluation of Vertebral Fractures. Sumiaki Okamoto*[1], Sumitada Okamoto[1], Akira Itabashi[2], HItoshi Noguchi[3], Hiroyuki Suzuki[4]. [1]Okamoto Clinic SORF, Japan, [2]Saitama Center for Bone Research, Japan, [3]Noguchi Thyroid Clinic & Hospital Foundation, Japan, [4]Suzuki Orthodontic office, Japan

DXA morphometry (DVA) in the evaluation of vertebral fractures has low diagnostic value due to its coarse imagery compared to plain x-ray. Only the bare outlines of wedge shaped vertebrae can be traced but not the minute fracture lines of fish like vertebrae. A new modality of vertebral fracture analysis is presented. Schmorl's nodes are present in the early stages of most vertebral fractures but it is reported that only 0.3% of them are diagnosed by conventional methods. We present examples of callus formation and sclerotic changes surrounding multiple Schmorl's nodes detected through changes in bone mineral density (BMD). We found that BMD, through L1 to L4, sequentially increase in young healthy controls and surmised that the disruption of this sequence implied vertebral fracture. Since 1994, we have analyzed proximately 3500 cases in the out patient setting, positioning patients to align the distal and proximal ends of the vertebrae for both horizontal rotation and vertical tilt and manually mapping each picture so that the ROI outline matches the perimeter of the vertebrae in every case. We first took lumbar DXA measurements of 20 young volunteers, aged 22-28, and found that L1 had lower BMD than L2 in all subjects, L2 had lower BMD than L3 in 16 of 20 subjects (80%), L3 had lower BMD than L4 in 12 subjects (60%), L1 always had the lowest BMD of the four and the BMD of L3 was never higher than L4 by more than 5%. Thus even when L3 had BMD higher than L4, the sequence was considered askew if the BMD of L3 surpassed that of L4 by more than 5%. 1540 patients of osteoporosis were examined by DXA and three dimensionally analyzed by CT under fully informed consent. We present a series of cases in which the disruption in the sequence of BMD in the lumbar vertebrae was verified for vertebral fracture by CT. The increase in the BMD was caused by (1) compaction of the vertebrae, (2) callus formation and sclerotic changes surrounding Schmorl's nodes and (3) calcification at the facet joint and the point of contact between spinous processes. The analysis of BMD sequence disruption will be useful not only in the detection of vertebral fractures but also in the detection of false negatives in the diagnosis of osteoporosis due to erroneously elevated BMD measurements.

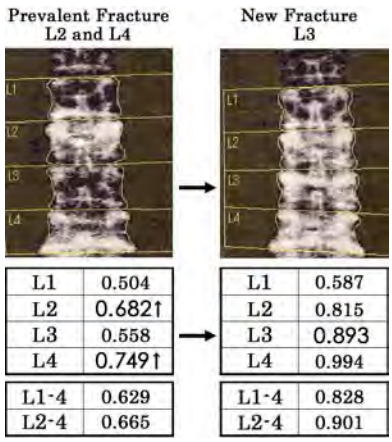

fracture detection

***Disclosures: Sumiaki Okamoto**, None.*

MO0357

Low Areal Bone Mineral Density and Trabecular Microarchitectural Changes in Premenopausal Women with Epilepsy Treated with Antiepileptic Drugs. Alison Pack*[1], Adi Cohen[2], Robert Pelgrift[1], Chiyuan Zhang[1], Donald McMahon[3], Elizabeth Shane[3]. [1]Columbia University, USA, [2]Columbia University Medical Center, USA, [3]Columbia University College of Physicians & Surgeons, USA

Purpose

Many studies report lower areal bone mineral density (aBMD) in persons with epilepsy. Whether low aBMD is due to deficits in cortical or trabecular bone is unknown. We evaluated aBMD using dual energy X-ray absorptiometry (DXA) and volumetric BMD (vBMD) and bone microarchitecture using high resolution peripheral quantitative tomography (HR-pQCT) in premenopausal women with epilepsy (WWE) treated with AEDs.

Methods

Premenopausal Caucasian WWE treated with AEDs for at least 6 months (n=24) and controls with normal aBMD at all sites (n=39; Z score + -1.0) were compared. Women with known bone disease, medical conditions or taking medications known to affect bone were excluded. Areal BMD was measured by DXA (Hologic QDR 4500) and expressed as absolute BMD (g/cm^2) and Z scores at the lumbar spine (LS), total hip (TH), femoral neck (FN), and 1/3 radius (1/3 R). Volumetric BMD (vBMD) and trabecular and cortical microarchitecture were measured at the nondominant distal radius and tibia by HR-pQCT using the SCANCO Xtreme CT (voxel size, ~82 um).

Results

WWE and controls did not differ in age (38 $\pm$ 1.5 vs 37 $\pm$ 1.4 years). As BMI was higher in controls ($p = 0.03$), all analyses were adjusted for BMI. aBMD was lower at the LS ($p=0.003$), TH ($p=0.005$), and FN ($p=0.001$) in WWE. Similarly, BMI adjusted Z scores were lower at the LS ($p<0.001$), TH ($p<0.001$), and FN ($p<0.001$). BY HR-pQCT, WWE had 10.3% lower total area and 14% lower trabecular area at the radius. Cortical vBMD was higher at the radius ($p=0.04$) and lower at the tibia ($p=0.06$). WWE tended to have lower radius trabecular vBMD ($p=0.06$). At both radius and tibia, trabecular number was lower and trabecular separation higher in WWE (all $p<0.02$). There were no differences in cortical microarchitectural parameters.

Conclusion

In summary, aBMD by DXA was lower at the spine and hip in WWE treated with AEDs. HR-pQCT revealed that WWE had smaller bones than Controls. The between-groups differences in aBMD by DXA were more highly significant than differences in vBMD by HR-pQCT, suggesting that the DXA results were influenced by the smaller bone size of WWE. However, WWE also had significantly fewer and more widely spaced trabeculae at both the radius and tibia. These findings, already detectable in premenopausal women, are consistent with trabecular drop out, may result in significant decreases in strength and could contribute to increased fracture risk later in life in persons with epilepsy.

Supported by NIAMS

HR-PQCT Results	Radius			Tibia		
	WWE	Control	p-value	WWE	Control	p-value
Total Area	226.1 ± 6.9	252.3 ± 5.8	0.007	658.6 ± 18.9	664.3 ± 16.0	0.82
Cortical Area	55.4 ± 2.4	54.1 ± 2.0	0.35	110.2 ± 4.2	120.1 ± 3.5	0.08
Trabecular Area	170.7 ± 7.1	198.2 ± 6.0	0.006	548.6 ± 19.9	544.2 ± 16.8	0.87
Total vBMD	343.3 ± 12.7	328.3 ± 10.7	0.38	281.5 ± 10.3	298.4 ± 8.7	0.22
Cortical vBMD	940.8 ± 12.3	905.3 ± 10.4	0.04	898.6 ± 8.0	918.8 ± 6.8	0.06
Trabecular vBMD	137.3 ± 7.3	156.5 ± 6.2	0.06	151.6 ± 7.3	156.2 ± 6.2	0.64
Cortical Thickness	0.87 ± 0.04	0.81 ± 0.03	0.17	1.09 ± 0.05	1.19 ± 0.04	0.11
Trabecular Thickness	0.065 ± 0.002	0.066 ± 0.002	0.79	0.071 ± 0.002	0.068 ± 0.002	0.32
Trabecular Number	1.77 ± 0.07	1.98 ± 0.06	0.02	1.77 ± 0.05	1.94 ± 0.05	0.03
Trabecular Spacing	0.52 ± 0.02	0.45 ± 0.02	0.014	0.51 ± 0.02	0.46 ± 0.01	0.02

Pack Table

***Disclosures: Alison Pack**, None.*

MO0358

Postmenopausal BMD Loss is Partially Compensated by Increased Bone Size during the First 15 Years but not Beyond. Henrik Ahlborg[1], Magnus Karlsson[2], Ola Svejme*[3]. [1]Malmo University Hospital, Sweden, [2]Skåne University Hospital Malmö, Lund University, Sweden, [3]Lunds Universitet, Sweden

Aim: This prospective population-based study aimed to investigate whether increased bone size through periosteal apposition could compensate for bone loss (at least partly preserving bone strength) in women not only in the decade following menopause, but also in the remote post-menopausal period when the incidence of fragility fractures rises exponentially.

Methods: Included were 81 population-based selected women who were pre-menopausal and 48 years at study start. All were of Caucasian origin and none were during the study period exposed to diseases or medication known to interfere with bone metabolism. Bone mineral density (BMD), bone size and a bone strength index, calculated by taking both BMD and bone size into account, were regularly evaluated in the distal forearm by single-photon absorptiometry at 12 different occasions during a 29-year follow-up period. Age at menopause was determined prospectively by repeated hormone assessments and fragility fractures were recorded continuously through questionnaires and the hospital's radiographic archives. The last measurements were carried out at age 77 years, in average 24 years (range 18-29) after the menopause which had occurred at a mean age of 52 years (range 48-59). Data is presented as mean with 95% confidence interval (95% CI).

Results: At age 67 (in mean 15 years after menopause), bone width had increased by 8.5% (95% CI 7.0, 9.9),compared to study start, from mean 13.0 mm to mean 14.1 mm. This partly compensated for the 23.2 % (95% CI 20.3, 26.1) loss in BMD, from mean 0.56 g/cm^2 to 0.42 g/cm^2, that had occurred during the same period, resulting in decrease in the bone strength index, of no less than 8.9 % (95% CI 5.9, 11.9). Ten years later (in mean 24 years after menopause), there had been a further 13.6% (95% CI 10.7, 16.4) loss in BMD (compared to the age 67 value) whereas bone width was unchanged, resulting in a marked reduction in the bone strength index from age 67 and onwards.

Conclusions: This prospective study suggests that increase in bone width through periosteal apposition could be a compensatory mechanism that counteracts the fast postmenopausal BMD loss in cortical bones during the first decades following menopause but also that the periosteal apposition is reduced in older ages. This could, at least partly, explain the exponential rise in the incidence of distal radius fractures and other cortical fractures in the seventh decade in life.

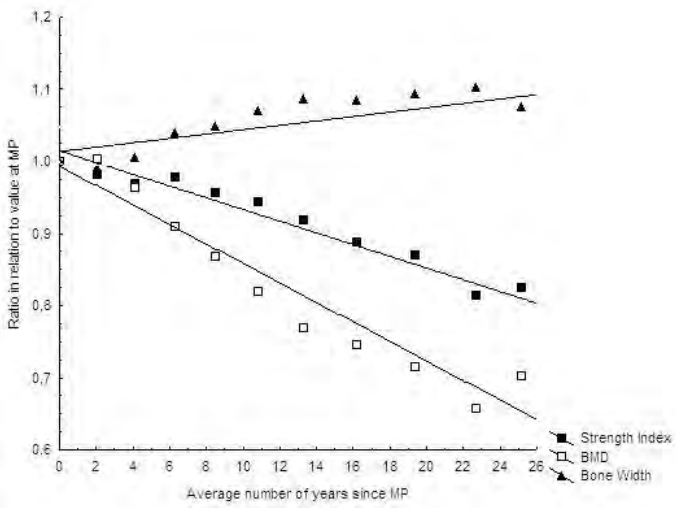

Development of BMD, bone size and bone strength after menopause

***Disclosures: Ola Svejme**, None.*

MO0359

Iron Deficiency Negatively Affects Spine Bone Mineral Density and Bone Microarchitecture in Weanling Sprague Dawley Rats. Krista Shawron*, McKale Davis, Elizabeth Rendina, Yan Wang, Edralin Lucas, Brenda Smith, Stephen Clarke. Oklahoma State University, USA

Iron deficiency anemia and osteoporosis are two common nutrition-related diseases primarily affecting women. The accretion of peak bone mass is a key determining factor in an individual's risk for developing osteoporosis, with ~25% of the accumulation occurring between the ages of 12-14 years. This is also a time period during which females are at heightened risk of iron deficiency. Emerging research has identified the possibility of iron's role in bone physiology. In particular, in animal models of severe iron deficiency, BMD was decreased with alterations in the rate of bone turnover.

Thus, the objective of this study was to examine the effects of severe and moderate iron restriction on bone microarchitecture and osteoblast and osteoclast lineage allocation. Weanling Sprague Dawley rats were assigned to one of five dietary treatments for 35 days (n=6/group): severe iron restriction (2-5 mg Fe/kg diet), moderate iron restriction (10-12 mg Fe/kg diet), control (50 mg Fe/kg diet), or pair-fed control diet to the level of intake of both the 2-5 and 10-12 mg Fe/kg diets. Analysis of bone mineral density (BMD) and microarchitecture were obtained by DXA and microcomputed tomography (μCT) in both the tibia and spine. RNA was extracted from bone marrow cells and used to synthesize cDNA for quantitative real-time polymerase chain reactions (qPCR).

Iron deficiency was confirmed by the expression of transferrin receptor mRNA in bone marrow cells (3.6-fold higher in iron-restricted animals, $p<0.05$). Both BMD (-12%) and bone microarchitecture of spines from animals receiving both levels of iron restriction were decreased ($p<0.05$), whereas no changes were observed in the tibia. A lower BMD and alterations in spine microarchitecture suggest that iron plays a critical role in bone modeling, although the exact mechanism remains unclear. Ongoing ex vivo studies are currently being conducted to further examine cellular mechanisms through which iron functions in osteogenesis, with a focus on the activity of genes involved in osteoblastogenesis. Although site-specific changes in BMD and micro-architecture are not uncommon, it is unclear why iron deficiency appears to be affecting the spine over the tibia. Currently, our work is focused on examining molecular mechanisms contributing to the negative effects of iron deficiency on osteoblastogenesis and osteoclastogenesis that may be the result of alterations in lineage allocation.

***Disclosures: Krista Shawron**, None.*

MO0360

Body Composition and Bone Mineral Density in Patients with Multiple Sclerosis Treated with Low Dose Glucocorticoids. Vit Zikan*[1], Michaela Tyblova[2], Ivan Raska[1], Eva Havrdova[2], Dana Michalska[1], Maria Luchavova[1]. [1]Department of Internal Medicine 3, Charles University Faculty of Medicine, Czech republic, [2]Department of Neurology, Charles University Faculty of Medicine, Czech republic

The purpose of the present study was to examine the relationship between body composition and bone mineral density (BMD) in ambulatory patients with multiple sclerosis (MS). We studied 225 premenopausal women, 125 postmenopausal women and 95 men with MS long term treated with low dose glucocorticoids. Methods: Dual-energy X-ray absorptiometry was used to analyze body composition and BMD. Motor function of the patients was evaluated using the Kurtzke Expanded Disability Status Scale (KEDSS). Results: Total femur and femoral neck BMD (T-score) was positively correlated with % trunk fat both in postmenopausal and premenopausal MS women (p ? 0.05), but not in men with MS. Fat body mass (FBM, % total body mass) and lean body mass (LBM %) did not significantly correlate with BMD in each group of patients. LBM % and bone mineral content (BMC % total body mass), but not FBM % and % trunk fat mass, significantly correlated with KEDSS. No significant correlation was observed between glucocorticoid treatment and either body composition parameters or BMD. Conclusion: The present study suggest that % trunk fat is related to total femur and femoral neck BMD both in premenopausal and postmenopausal women, but not in men with MS long term treated with low dose glucocorticoids. To verify whether the parameters of body composition will also affect the risk of fractures are needed to further study.

***Disclosures: Vit Zikan**, None.*

MO0361

Subclinical Ovulatory Disturbances within Regular Menstrual Cycles are associated with Spinal Bone Loss−a meta-analysis of prospective data. Jerilynn Prior*, Christine Hitchcock. University of British Columbia, Canada

Introduction: Amenorrhea and oligomenorrhea are recognized risks for post-menopausal osteoporosis; decreased estrogen levels are important. Regularly cycling women with subclinical ovulatory disturbances (OD, anovulation or short luteal phases) have adequate estrogen, but lower progesterone levels. Subclinical ovulatory disturbances were associated with cancellous spine (LS) bone loss in healthy, weight-stable regularly cycling premenopausal women (Prior NEJM 1990). Our purpose was to determine whether combined data support this early observation.

Methods: Systematic review and meta-analysis. All prospective LS-BMD, and menstrual cycle-ovulation data in regularly menstruating premenopausal women were included. Study characteristics, group mean/SD and sample size from published data or authors were used. Meta-analysis was performed using the metan (Ross 2006) module within Stata (version 9.2).

Results: A systemic review of prospective studies in predominantly white premenopausal women documenting LS-BMD, menstruation and OD yielded 5 studies (Prior NEJM 1990; Prior Bone 1996; Waller JCEM 1996; Waugh Am J Clin Nut 2007; Bedford JCEM 2010 in press). Studies were of varying aged women (mean 31 y), methods used to document ovulation?Quantitative Basal Temperature (Prior 1990 & 96; Bedford) uLH peak (Waugh), and uPdG (Waller)?monitored cycles (1.5-10 #/y, mean 6.6), criteria for diagnosing OD and BMD method (DXA or QCT). Cycle lengths averaged 28.9 d. Ovulatory disturbances were documented in 4-58% of cycles/y. In studies with OD monitoring for ?5 cycles/y, yearly rates of LS-BMD change were: OD –1.0%; normally ovulatory +1.2%. At abstract deadline, data from 4 of 5 studies were available; 75% showed an association between OD and more negative LS-BMD change. The pooled effect size was 0.35 (95% CI: 0.10 to 0.60) (Figure). There was significant heterogeneity, however, among studies ($^2(3)=13.26$; $p = 0.004$). Factors explaining this include cycle# monitored/y, cohort age (mean mid-30s except mean 22 y (Bedford)), BMI range, whether or not PCOS was excluded and when cycle/OD data were collected relative to BMD change.

Conclusion: Clinically important, silent bone loss occurs in regularly menstruating women with lower progesterone levels but normal estrogen levels. Cyclic progestin treatment of abnormal cycles/OD increases LS-BMD (Prior Am J Med 1994). The contribution of subclinical ovulatory disturbances to risk for postmenopausal osteoporosis needs to be examined.

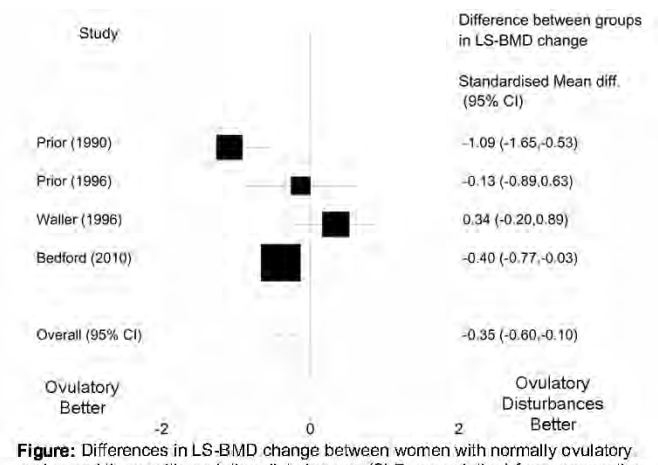

Figure: Differences in LS-BMD change between women with normally ovulatory cycles and those with ovulation disturbances (SLP, anovulation) from prospective observational studies. Data are shown as standardized mean differences (no units).

***Disclosures: Jerilynn Prior**, None.*

MO0362

Older Men with High Osteoprotegerin Concentration Have Lower Cortical Density and Thickness - the STRAMBO Study. Pawel Szulc*[1], Gerhard Hawa[2], Stephanie Boutroy[1], Nicolas Vilayphiou[1], Ali Chaitou[1], Pierre Delmas[1], Roland Chapurlat[1], Lorenz Hofbauer[3]. [1]INSERM 831 Unit, Université de Lyon, France, [2]BIOMEDICA, Austria, [3]Dresden Technical University Medical Center, Germany

Osteoprotegerin (OPG) and RANK ligand (RANKL) are major regulators of bone remodeling. The relationship between the OPG/RANKL system and bone microarchitecture in men is poorly defined. We studied this association in 1,160 men aged 20 to 87. We assessed bone microarchitecture and volumetric bone mineral density (vBMD) at the distal radius and distal tibia by high resolution peripheral QCT (HR-pQCT, XtremeCT, Scanco, Switzerland). We measured serum OPG and RANKL levels and bone turnover markers (BTM): serum bone alkaline phosphatase, osteocalcin, P1NP, and CTX-I, and urinary deoxypyridinoline. Serum OPG levels increased with age, whereas RANKL level and the RANKL/OPG ratio decreased (log-transformed: r=0.52, r= -0.15 and r= -0.22, all $p<0.001$). Further analyses were adjusted for age, weight, height, physical activity, diabetes, serum free testosterone (fT), bioavailable 17β-estradiol (bioE), 25-hydroxyvitamin D (25OHD) and parathyroid hormone (PTH). Men in the highest quartile of the OPG level (>4.55 pmol/L) had lower cortical thickness (-9.4%, -0.34SD, $p<0.001$) and vBMD (-2.9%, -0.39SD, $p<0.001$) at the distal radius compared with the three lower quartiles, which contributed to a 6.2% lower total vBMD (-0.31SD, $p<0.001$) at this site. At the distal tibia, men in the highest OPG quartile had a 4.8% lower cortical thickness (-0.21SD, $p<0.05$) and a 1.8% lower cortical vBMD (-0.27SD, $p<0.005$) compared with men in the three lower quartiles. By contrast, association between the OPG level and trabecular microarchitecture (trabecular vBMD, number, thickness and distribution) was not significant, even for the analyses performed separately in the inner (central 60%) and in the subendocortical regions of the trabecular area. After adjustment for age, weight, height, physical activity, diabetes, fT and bioE, men in the highest OPG quartile had higher BTM levels (7 to 23%, 0.21 to 0.37SD, $p<0.01$-0.001) than men in the three lower quartiles. This association slightly weakened after adjustment for PTH and 25OHD. RANKL serum level and the RANKL/OPG ratio were neither associated with the BTM levels nor with bone microarchitecture regardless of the age, skeletal site, bone compartment or statistical model.

Thus, men with high serum OPG level have lower cortical thickness and vBMD, which may partly depend on the faster bone turnover in this subgroup. High OPG serum levels may reflect the impairment of the cortical bone mass and microarchitecture in men.

***Disclosures: Pawel Szulc**, None.*

MO0363

Osteoporosis in Asian men: Effect of Vitamin D. Lan T Ho-Pham*[1], Thai Lai[2], Tong Nguyen[3], Tuan Nguyen[4]. [1]Pham Ngoc Thach University of Medicine, Vietnam, [2]People's Hospital 115, Vietnam, [3]MEDIC Pathology Center, Vietnam, [4]Garvan Institute of Medical Research, Australia

Risk factors for osteoporosis in men, particularly in Asian men, has not been well documented. In recent years, the role of vitamin D in bone health has been intensively studied in Caucasians, but little is known about vitamin D status and bone health in Asian populations. This study sought to examine the association between vitamin D status, parathyroid hormone (PTH) and bone mineral density (BMD) in a Vietnamese population.

The study was designed as a cross-sectional study, which involved 357 men aged between 18 and 85 years. The men were randomly recruited from various districts within Ho Chi Minh City, Vietnam. BMD at the femoral neck, lumbar spine, and whole body was measured by DXA (Hologic QDR4500, WI, USA). Among the men, fasting blood samples were available in 205 men. Serum concentration of 25(OH)D and PTH were measured by the Electrochemiluminescence immunoassay on the Roche Elecsys 10100/201 system (Roche Diagnosis Elecsys). In addition, a structured questionnaire was used to collect data concerning anthropometric, demographic, clinical history, and lifestyle factors from all individuals. Vitamin D insufficiency was quantified as 25(OH)D levels below 30 ng/ml (or 75 nmol/L).

The average age among the men was 46.3 ± 17.6 years (mean $\pm$ SD). The prevalence of osteoporosis (T-scores $\leq$ -2.5) among men aged 50+ years was 10.4%. The mean 25(OH)D and PTH concentration was 36.8 ± 10.2 ng/mL and 30.6 ± 11.2 ng/L, respectively. There was a linear inverse relationship between serum 25(OH)D and PTH concentrations with r = -0.12, but there was no threshold of 25(OH)D at which PTH levels plateaued. After adjusting for age, body weight and lifestyle factors in a multiple linear regression analysis, 25(OH)D levels were positively associated with BMD at the lumbar spine (P=0.003), but not with BMD at the femoral neck (P=0.18) and whole body (P=0.09). The amount of variance in BMD that could be "explained" by 25(OH)D levels was around 7%. The prevalence of vitamin D insufficiency in men was 20% (41/205). Men with vitamin D insufficiency were more likely to have osteoporosis (odds ratio: 2.54; 95% CI: 1.22 – 5.28) than those who had adequate vitamin D. There was no significant association between PTH levels and BMD at any skeletal site.

These results indicate that the prevalence of osteoporosis in Vietnamese men is as high as in Caucasian men of the same age group, and vitamin D insufficiency was a significant risk factor for osteoporosis or low BMD in men.

***Disclosures: Lan T Ho-Pham**, None.*

MO0364

Evaluation of Bone Mineral Density and Body Composition in Women with Dunnigan-Type Partial Familial Lipodystrophy. Francisco Pereira[1], Luciana Monteiro*[2], Milton Foss[2], Maria Cristina Freitas[2], Renan Montenegro Júnior[3]. [1]University of Sao Paulo, School of Medicine of Ribeirao Preto, Brazil, [2]University of São Paulo, Brazil, [3]Faculty of Medicine of the Federal University of Ceará, Brazil

Objective: The objective of the present study was to determine the anthropometric indices, bone mineral density (BMD) and body composition of patients with Partial Familial Lipodystrophy (PFLD). Methods: A quantitative, descriptive cross-sectional study was conducted on 18 women diagnosed with PFLD and 18 control women (CG), with the determination of anthropometric variables (weight, height, BMI, abdominal and hip circumference, and waist-hip ratio, WHR). We determined BMD of the total spine (L1-L4), total femoral head, total hip, forearm and body composition, lean mass (LM), fat mass (FM), and % fat by DXA (Hologic 4500 W). Results: The data for women with PFLD were: age = 35.6 ± 13 years, weight = 64.7 ± 14.1 kg, height = 1.61 ± 0.07 m, BMI = 24.8 ± 4.2 kg/m2, abdominal circumference = 81.8 ± 11.1 cm, hip circumference = 93.61 ± 12.01 cm, and WHR = 0.87 ± 0.04 cm, and GC data were: age = 35.6 ± 13 years, weight = 63.9 ± 12.4 kg, height = 1.62 ± 0.07 m, BMI = 24.4 ± 4.8 kg/m2, abdominal circumference = 78.5 ± 12.5 cm, hip circumference = 97.94 ± 10.81 cm, and WHR = 0.80 ± 0.05 cm. There was no significant difference between groups regarding BMD of total hip (PFLD = 0.875 ± 0.10g/cm^2 vs CG = 0.894 ± 0.09 g/cm^2), forearm (PFLD = 0.616 ± 0.06 g/cm^2 vs CG = 0.650 ± 0.04 g/cm^2), total spine (PFLD = 0.994 ± 0.14 g/cm^2 vs CG = $1,011 \pm 0.12$ g/cm^2), femoral head (PFLD = 0.795 ± 0.18 g/cm^2 vs CG = 0.810 ± 0.83 g/cm^2) or subtotal BMD (PFLD = 0.872 ± 0.08 g/cm^2 vs CG = 0.889 ± 0.78 g/cm^2), even though the values of the lipodystrophic group were slightly lower than those of the control group. As expected, % fat (PFLD = 23.51 ± 9.5% vs CG = 36.02 ± 6.1% $p<0.05$) and LM (PFLD = 42,88 kg vs CG = 35.95 kg $p<0.05$) differed significantly between groups. Conclusion: The present data demonstrate that individuals with the PFLD syndrome present significant differences regarding LM, FM and % fat, but no alterations of BMD.

***Disclosures: Luciana Monteiro**, None.*

MO0365

Helicobacter Pylori CagA Positive Strains Negatively Affect Bone Health: a Population Based Study. Luigi Gennari*[1], Natale Figura[2], Daniela Merlotti[1], Maria Stella Campagna[2], Maria Beatrice Franci[2], Annalisa Avanzati[2], Barbara Lucani[2], Anna Calabrò[2], Stefania Lardiello[2], Giuseppe Martini[1], Ranuccio Nuti[1]. [1]University of Siena, Italy, [2]Department of Internal Medicine, Endocrine-Metabolic Sciences & Biochemistry, University of Siena, Italy

Helicobacter pylori (HP) infection is a leading world-wide infectious disease as it affects more than 30-40% of the world population. The infection elicits a chronic cellular inflammatory response in the gastric mucosa that may persist for long period, possibly for life. Moreover, the effects of this local inflammation may not be confined solely to the digestive tract but may spread to involve extra-intestinal tissues and/or organs. In particular, HP strains that possess a chromosomal insertion called Cag (secreting a highly immunogenic protein called CagA) are endowed with an increased inflammatory potential, which is generally associated with increased oxidative stress and higher local and systemic levels of cytokines such as TNF-α, IL-1, and IL-6 with potential negative effects on several tissues including bone. In this study we investigated serum antibodies to HP and the CagA protein in relation to bone mineral density (BMD) and bone markers in a large epidemiological cohort of 1118 male and female subjects from the "Siena Osteoporosis Study".

Overall, 53% of males and 43% of females were positive for HP infection, while CagA positive strains were observed in 28% and 26% of males and females, respectively. The prevalence of HP infection did not differ among patients with normal BMD, osteoporosis, or osteopenia. However, the prevalence of patients with CagA positive strain was significantly higher ($p=0.01$) in osteoporotic (30%) and osteopenic (26%) patients than in subjects with normal BMD (21%). Moreover, anti CagA autoantibody titer was significantly and negatively associated with BMD at different sites (spine, hip, hand and total body) in males as well as in females. Above the median CagA autoantibody level, only 14% and 30% of males and females, respectively had normal BMD.

Finally, prevalent symptomatic fractures of the hip and the vertebral bodies were reported in 4%, 2% and 0.8% of patients with CagA positive HP strain, CagA negative HP strain and non affected subjects, respectively ($p<0.05$ CagA positive patients vs. not affected HP subjects). In conclusion, HP infection by strains expressing CagA may therefore be considered a risk factor for osteoporosis and fractures in males as well as in females. Further studies are required to clarify the underlying pathogenetic mechanism of this association.

***Disclosures: Luigi Gennari**, None.*

MO0366

The Association Between Serum Osteocalcin Levels and Metabolic Syndrome. Sung Jin Bae*[1], Jae Won Choe[2], Yun-Ey Chung[3], Beom-Jun Kim[4], Seung Hun Lee[5], Ha Young Kim[6], Jung-Min Koh[1], Hong Kyu Kim[2], Ghi Su Kim[7]. [1]Asan Medical Center, South korea, [2]Health Promotion Center, Asan Medical Center, University of Ulsan College of Medicine, South korea, [3]Department of Internal Medicine, Seoul Veterans Hospital, Seoul, Korea, South korea, [4]Division of Endocrinology & Metabolism, Asan Medical Center, University of Ulsan College of Medicine, South korea, [5]Asan Medical Center, University of Ulsan College of Medicine, South korea, [6]Wonkwang University Sanbon Medical Center, Korea, [7]University of Ulsan, South korea

Objective: Osteocalcin has recently been shown to affect glucose and lipid metabolism. However, the association between serum osteocalcin and metabolic syndrome (MS) has not yet been investigated. In the present study, we investigated the possible association between osteocalcin and metabolic syndrome in Korean individuals.

Design: A cross sectional community (health promotion center)-based survey.

Subjects and measurements: For 567 subjects (including 198 men and 369 postmenopausal women) who participated in routine health screening examination, we measured serum osteocalcin, C-telopeptide, high-density lipoprotein cholesterol (HDL-C), triglycerides (TG), fasting glucose, HbA1c, fasting insulin, blood pressure (BP), height, weight, and waist circumference. Degree of insulin resistance was assessed by homeostasis model assessment-insulin resistance (HOMA-IR).

Results: Serum osteocalcin concentrations were significantly correlated with age, height, weight, systolic BP, diastolic BP, BMI, waist circumference, and/or levels of fasting glucose, HbA1c, fasting insulin, HOMA-IR, TG and HDL-C in men and women ($p < 0.001$ to 0.043). After adjustments for sex, age, height, and weight, serum osteocalcin levels were significantly lower in subjects with MS than those without ($P < 0.001$). Subgroup analysis revealed that the difference in serum osteocalcin levels by MS status was noted in both normal glucose tolerance (NGT) and abnormal glucose tolerance (impaired fasting glucose (IFG) or diabetes) group ($P = 0.034$ and $P < 0.0001$, respectively). According to the increased number of MS components, serum osteocalcin levels decreased in order (P for trend < 0.0001). Compared with those of the highest quartile of osteocalcin (Q4), those with Q1 and Q2 had remarkable increased risks of MS (OR = 4.98, CI = 2.52 – 9.87; OR = 3.31, CI = 1.65 – 6.63, respectively).

Conclusion: These findings suggest that osteocalcin may be associated with MS, and suggesting a need of a prospective study.

***Disclosures: Sung Jin Bae**, None.*

MO0367

Vertebral Compression Fractures Resulting from Strenuous Recreational Exercise: When Good Intentions Crumble. Mehrsheed Sinaki*[1], Daniel Hurley[2], Robert Wermers[1], Peter Tebben[1], Kurt Kennel[3], Matthew Drake[3]. [1]Mayo Clinic, USA, [2]College of Medicine, Mayo Clinic, USA, [3]Mayo Clinic College of Medicine, USA

Back strengthening exercises are important to reduce osteoporosis (OP) related vertebral compression fractures (VCF's) and improve bone mineral density (BMD) in the clinical management of OP. We previously reported on subjects with known OP who developed VCF's after spine flexion exercises (SFE's), and recommended that SFE's not to be prescribed in patients with OP of the spine.

Here, we report four previously healthy individuals with low bone mass and exercise-induced fractures.

Patient #1

An 87 yo F had severe back pain while performing SFE's during strenuous yoga with instructor supervision:

• Spine x-rays: L2 VCF and mild anterior wedging of several thoracic vertebrae
• Lumbar spine (LS) OP with T Score - 4.3
• Physical examination: tandem test -3, LS pain with extension, and ¾ inch leg length discrepancy with lumbar curve.

Patient #2

A 61 yo F with osteopenia had severe back pain with strenuous SFE's during yoga:

• Spine x-rays: T4 VCF
• LS BMD T Score -1.8.

Patient #3

A 76 yo M with osteopenia had severe back pain while lifting 35-40 lbs using an exercise machine anterior to his chest with spine flexion at his local physical therapy facility:

• Spine x-rays: L1, L2, and L5 VCF's
• Hip T-score -1.2.

Patient #4

A 73 yo M had acute back pain while jogging in preparation for a triathlon:

• Spine x-rays: T7 VCF
• LS BMD T Score -1.9.

SUMMARY:

OP is characterized by low bone mass, loss of bone microstructure and ↑ fracture risk. OP musculoskeletal rehabilitation is a non-pharmacologic approach to limit bone loss. Although exercise has been shown to be an effective method for improving BMD and ↓ fracture risk, our subjects developed VCF's while engaged in exercise. Of note, three of four patients reported here did not have OP by BMD criteria. This suggests that factors other than bone mass should be considered for exercise counseling in patients with bone loss. The ↑ torque pressure applied to vertebral bodies during SFE's may be one such risk and requires further study in patients with any degree of bone loss.

CONCLUSIONS:

Although exercise is effective and important in the treatment of OP, individuals with bone loss should be educated in proper exercise technique, and exercise in at risk individuals should be performed in a safe and appropriate manner. Fracture risk assessment in older individuals performing SFE's and other high impact exercises may be an important clinical consideration.

***Disclosures: Mehrsheed Sinaki**, None.*

MO0368

A Developmental Perspective on Metacarpal Radiogrammetry and Trabecular Architecture from an Imperial Roman Skeletal Population. Luca Bondioli[1], Patrick Beauchesne[2], Sabrina Agarwal*[2]. [1]Luigi Pigorini Museum, Rome, Italy, [2]University of California, USA

This paper explores patterns of age and sex-related cortical and trabecular bone loss from a skeletal population excavated from the Imperial Roman port city of Velia (1st and 2nd century AD). The ancient city of Velia functioned as an important trading centre and port for Imperial Rome and is situated on the west coast of Italy, south of Salerno, in the Campania region. The null hypothesis of this research was that patterns of bone loss (assessed by metacarpal radiogrammetry (n=79) and analysis of vertebral trabecular architecture (n=46) in this well represented Roman sample would mirror modern patterns of age and sex-related change. Changes in the cortical bone across three age cohorts (18-29yrs, 30-45yrs, 45+yrs) are significant in both males and females, however the pattern of bone loss differs between the sexes. Females lose bone in young reproductive age and then maintain bone into old age, while male cortical levels remain high until old age where cortical bone values drop rapidly. The radiogrammetry results show no sex differences at any age group. There is also no significant sex difference in trabecular architecture in any age cohort. The only exception is the Conn.D measure in young adults, where males are significantly higher than females. These data suggest the null hypothesis should be refuted, as significant sex differences, particularly in mid to old age, are expected based on modern patterns of bone loss in Western cultures. A life course approach is used to explain these observations. Specifically, developmental pathways are offered as one explanatory factor in these deviations from modern populations, including considerations of culturally specific activity and reproductive history. Future avenues of research are also outlined.

***Disclosures: Sabrina Agarwal**, None.*

MO0369

The Effect of Endogenous Parathyroid Hormone on Iliac Bone Structure and Turnover in Healthy Postmenopausal Women. D. Sudhaker Rao*[1], Shijing Qiu[1], Saroj Palnitkar[1], A. Michael Parfitt[2]. [1]Henry Ford Hospital, USA, [2]University of Arkansas for Medical Sciences, USA

It is known that the moderate increase in PTH resulting from mild primary hyperparathyroidism can preserve the skeleton enriched with cancellous bone, such as the lumber spine and the femoral neck, in postmenopausal women. To our knowledge, little is known about the effect of the variation in endogenous PTH on the skeleton in postmenopausal women without hyperparathyroidism. In the present study, the effects of serum PTH on bone were investigated in iliac crest biopsies obtained from 37 healthy white postmenopausal women aged 50-73 years. There was no woman associated with vitamin D deficiency (serum 25 (OH)D <10 ng/mL) and hyperparathyroidism (abnormal high serum calcium and PTH). Neither cancellous nor cortical bone structure was changed with PTH levels. In cancellous bone, the bone formation (wall thickness, osteoid surface, osteoblast surface, mineralizing surface and mineral formation rate) and turnover (bone formation rate at the surface and the volume levels and activation frequency) variables increased with increasing PTH levels (all $p < 0.05$) in univariate analysis. Multiple linear regressions, adjusted for 25(OH)D, Ca, ALP, age and BMI, showed that PTH was independently associated with wall thickness, osteoid surface, osteoblast surface, mineralizing surface, and bone formation rate at the surface and the volume levels (all $p < 0.05$). No histomorphometric variable in cortical bone was significantly correlated with PTH levels. On the endosteal surface, some of the bone formation (osteoid surface, osteoblast surface, mineralizing surface) and turnover (bone formation rate at the bone surface levels and activation frequency) variables were positively correlated with PTH levels (all $p < 0.05$). None of these variables could be independently predicated by PTH variation. We conclude that cancellous bone is the only place that can respond anabolically to the increased endogenous PTH in healthy postmenopausal women. The effects of PTH on the endosteal surface may probably be confounded by other factors.

***Disclosures: D. Sudhaker Rao**, None.*

MO0370

Characteristics of a Puerto Rican Population Initiating Teriparatide Therapy in the DANCE Study. Valerie Ruff*[1], Agaph Acosta[2], Oscar Soto[3], Xiaohai Wan[1], Yuqin Li[4], Kathleen Taylor[1]. [1]Eli Lilly & Company, USA, [2]Lilly Puerto Rico, Puerto rico, [3]SARC San Juan Arthritis & Research, Puerto rico, [4]Inventiv Clinical, USA

It has been observed that there are population differences in the risk of osteoporosis and fractures; however, there is a great need to obtain more data on osteoporosis diagnosis and treatment in various ethnic and/or geographical populations. The prospective, observational Direct Assessment of Non-vertebral Fracture in Community Experience (DANCE) study was designed to examine the long-term efficacy and safety of teriparatide therapy in 4220 patients with osteoporosis in the United States including Puerto Rico. Study investigators prescribed teriparatide (TPTD) 20 µg/d for up to 24 months for patients, and followed them for up to 24 months after treatment cessation. This analysis compared baseline characteristics, persistence to therapy, and reasons for discontinuation between the Puerto Rican population (n=212, 98% Hispanic) and the mainland US population (n=3452, 94% Caucasian). Although similar proportions in each population had prior osteoporosis therapy (86%), 39% of the Puerto Rican population had a prior fragility fracture compared to 58% in the US mainland population ($P<0.0001$). Significantly fewer patients in the Puerto Rican population reported risk factors such as family history of hip fracture (9% vs.21%), tobacco (3% vs.14%), or alcohol use (10% vs.27%). Additionally, even though there was no significant difference in average age (68 vs.69 yrs), the Puerto Rican population had significantly more comorbid conditions (2.1 vs.1.8, p=0.003). Overall, 62% of enrolled patients persisted with therapy through 18-24 months, but fewer patients in the Puerto Rican population were persistent at each time point examined. The highest proportion of enrolled patients in the Puerto Rican population (n=55, 26%) discontinued TPTD within the first 6 months and financial reasons were cited as the major reason for discontinuation. This data suggests that there may be differences in physician reasons for initiating TPTD therapy as well as persistence to therapy between Puerto Rican and US mainland populations in the community setting.

***Disclosures: Valerie Ruff**, Eli Lilly and Company, 1; Lilly USA, LLC, 3*
This study received funding from: Eli Lilly and Company

MO0371

Clinical Evaluation of a Nasal Spray Formulation of Teriparatide Demonstrates Rapid Absorption and Similar Systemic Exposure to Marketed Subcutaneous Teriparatide. Stephan Bart[1], Kristen Armstrong[2], Brian MacDonald*[3], Ruth Ann Subach[4], Gene Merutka[5]. [1]SNBL Clinical Pharmacology Center Inc, USA, [2]Zelos Therapeutics, Canada, [3]Zelos Therapeutics Inc, USA, [4]Travena Inc, USA, [5]Zelos Therapeutics, USA

PTH (1-34) (teriparatide rDNA origin, Forteo®) is an effective drug in the treatment of osteoporosis but the need for daily injection is suboptimal. Nasal spray administration is simple and convenient, does not require sterile technique and could improve the willingness of patients to consider and/or continue PTH therapy. Previously (Krause et al., ASBMR 2009) we have shown that N-dodecyl-β-maltoside (DDM; Intravail® A3) is an effective permeation enhancer that improves the absorption of nasally administered ZT-034 (synthetic teriparatide) in rats and monkeys. Long term non-clinical safety studies have found no evidence of nasal epithelial or bone toxicity (P Eddy this meeting). We evaluated the pharmacokinetic (PK) and pharmacodynamic profile of nasal ZT-034 formulated with DDM in an inpatient clinical study. Healthy postmenopausal women were enrolled in a double blind, dose escalating study. ZT-034 doses of 20, 40, 80, 120 and 160 µg/day or placebo were administered daily for 7 days by nasal spray with another group receiving subcutaneous Forteo (20 µg/day). 4-6 women were treated at each dose level. PK and serum calcium profiles were obtained on Days 1 and 7 of the study. Serum calcium was also measured daily, 4 hours after dosing. Nasal spray ZT-034 was well tolerated at all tested doses. Adverse events related to nasal administration were minor and not dose related. PTH related adverse events (headache, nausea) were reported in the 120 and 160 µg and Forteo dose groups. Measurable blood levels were observed at all doses with rapid absorption (Tmax ≤15 minutes). The duration of measurable PTH (1-34) levels was generally less in nasal spray treated than in Forteo treated patients with higher Cmax at comparable exposure. Dose normalized bioavailability, relative to subcutaneous Forteo was approximately 22% and similar systemic exposure was achieved in the range of 80-120 µg/day. Post dose serum calcium increases were higher in Forteo than in nasal spray subjects. Post dose hypercalcemia (>10.6 mg/dL, 2.64 mmol/L) was observed in 2 of the 5 subjects receiving Forteo and in 1 of the 20 subjects receiving nasal spray ZT-034 (at the 80 µg dose). The results of this study warrant further exploration of nasal spray teriparatide as a convenient alternative to Forteo for patients with high fracture risk.

***Disclosures: Brian MacDonald**, Zelos Therapeutics, 5*

MO0372

Effect of Treatment with Strontium Ranelate on Bone Turnover Markers and Bone Mineral Density in Women with Postmenopausical Osteoporosis without Prior Treatment. María J. Moro-Álvarez*[1], Susana Sanz-Baena[1], Francisco Cogolludo-perez[2], Marjorie Andrade[2], Manuel Díaz-Curiel[2], Concepción de la Piedra[3]. [1]Department of Internal Medicine, Metabolic Bone Disease Unit, H. Central Cruz Roja, Spain, [2]Department of Internal Medicine, Metabolic Bone Disease Unit, Fundación Jiménez Díaz, Spain, [3]Department of Clinical Biochemistry. Fundación Jiménez Díaz, Spain

Objectives: To evaluate the effect of SR on bone turnover markers and bone mineral density in postmenopausical osteoporosis without previous treatments.

Material and Methods: We enrolled 41 postmenopausal women, mean age 68 years (r= 54-87), treated with RE 2 grs/day during 12-24 months. Calcium, phosphorus, and bone turnover markers of formation (P1NP) and resorption (CTX) basal, at 12 and 24 months were measured in serum by the following techniques: CTX by electro-chemisluminescence (0,064-0,548 ng/ml) and PINP by RIA (10,4-62 ng/ml). Bone mineral density (BMD) was measured by dual energy X-ray (c.v. in vivo 1,2%), at lumbar spine (L2-L4) (LS), femoral neck (FN) and total hip (TH) over 2 years.

Statistical analysis was carried out by using descriptive summaries of each variable and Wilcoxon test for comparisons. The Spearman correlation was utilized to relate the bone turnover markers and the values of BMD.

Results: The BMI did not vary throughout the study. The treatment with RE did not produce significant variations in serum calcium and phosphorus levels. CTX decreased 4.3% at 12 months and 9,01% at 24 months. P1NP increased 5.5% at 12 months and 24.01% at 24 months. RE increased the BMD in LS 2.3% at 12 months and 6.7% at 24 months, in CF 3.5% at 12 months and 1.6% at 24 months, and in FT 3.1% at 12 months and 0.7% at 24 months. The gain of BMD at LS, FN y TH were statistically significant at 12 months ($p<0,05$) but the gain at 24 months was only statistically significant at CL. We did not find significant differences in the response of BMD related with clinical variables as: age, existence of previous fracture or basal BMD. We found a powerful correlation ($p<0.05$) between the decrease of the CTX and the BMD in LS (r=0.89) and FN (r=0.75). We did not found any correlation between increase of the P1NP and the BMD.

Conclusion: We found that the treatment during 12 or 24 months with RE causes a decrease in the bone resorption marker and an increase in the bone formation marker. The magnitude of antiresorptive effect is correlated significantly with the increase in the BMD in LS and FN. We observed that these effects do not depend on the basal clinical variables as age, previous fracture or BMD.

***Disclosures: María J. Moro-Álvarez**, None.*

MO0373

Micro-MRI Based Virtual Bone Biopsy Detects Structural Remodeling Effects upon Anabolic Drug Treatment. Yusuf Bhagat*[1], Jeremy Magland[1], Chamith Rajapakse[2], Michael Wald[3], Theresa Scattergood[1], Felix Werner Wehrli[3], Peter Snyder[1]. [1]University of Pennsylvania, USA, [2]University of Pennsylvania School of Medicine, USA, [3]University of Pennsylvania Medical Center, USA

So far, remodeling induced changes upon anabolic treatment could only be observed by bone biopsy and there only in paired biopsies representing different anatomic locations. In this pilot study we provide direct evidence of trabecular bone (TB) topological changes accompanying teriparatide (Forteo, Eli Lilly) treatment (20 µg daily; s.c.) in a small group of women (N=6, ages 65-81 years) with osteoporosis studied at three time points, in serially acquired and mutually registered virtual cores. Images were acquired at baseline, 9 months and 18 months by high resolution 3D micro-MRI from the left distal tibia at 1.5T as previously described [1], and resulted after processing, in a 3D grayscale image of 137x137x410 μm^3 voxel size with each voxel representing bone volume fraction (BVF). The follow-up images were co-registered to the baseline reconstruction grid using rigid body registration. Data were then subjected to virtual bone biopsy (VBB) processing yielding 3D skeleton maps with TB plates represented by surfaces and rods by curves. Parameters quantifying scale and topology included BVF, surface/curve (S/C) ratio and erosion index (EI) [2]. The co-registered images and the 3D rendered VBB cores (23x23x68 μm^3 voxels) from a 73-year old subject (Figure 1) highlight the level of reproducibility achievable across the time series (color coding: surface interior – gray, surface edges – red, curves – blue). While most structural features are replicated in repeat VBBs, some remodeling changes are clearly detectable manifesting as small plate perforations (green arrows) observed at baseline, diminishing and filling in over the course of the treatment (Figure 1). In this subject, even though full tibial cross-section analysis showed moderate improvements in BVF, S/C and EI at 9 and 18 months post treatment, topological changes in a posterior sub-region exhibited increases up to 30% and reductions up to 14% over time for S/C and EI, respectively (Figure 2). Four out of six patients demonstrated a strong anabolic response as evidenced by changes in their individual parameters. Sample size was too small to reach overall statistical significance. However, visually observed changes such as closure of perforations agreed with the changes in topological parameters.

References: [1] Magland and Wehrli. Acad Radiol 15:1482 (2008); [2] Gomberg et al. IEEE Trans Med Imaging 19:166 (2000)

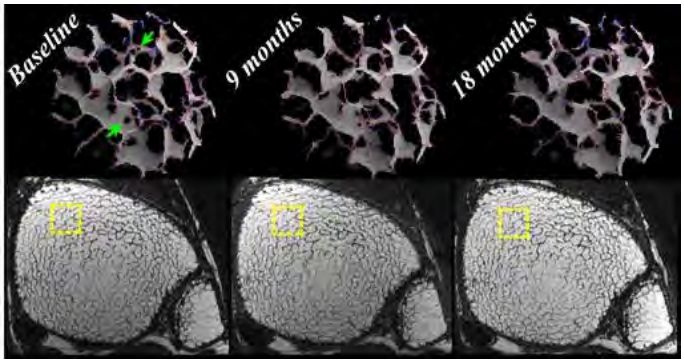

Figure 1: Co-registered tibia TB images of a 73 year-old woman with virtual biopsy cores (top)

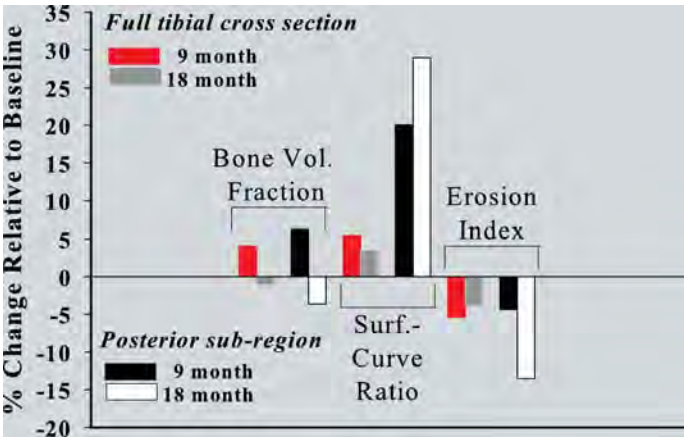

Figure 2: Changes from baseline in DTA parameters in a patient (Fig 1) upon teriparatide treatment

***Disclosures: Yusuf Bhagat**, Micro MRI Inc., 5*
This study received funding from: Eli Lilly

MO0374

PTH (1-84)-induced Bone Accrual is Accompanied by Enhanced Endothelium-dependent Vasodilation of the Bone Vasculature in Rats. Rhonda Prisby*. University of Texas at Arlington, USA

Intermittent administration of parathyroid hormone (PTH) redistributed bone blood vessels closer to sites of new bone formation. Furthermore, PTH-induced bone anabolism was not related to angiogenesis; i.e., tibial and femoral blood vessel number was reduced vs. CON rats. Adequate circulation to bone is requisite for normal growth, remodeling and repair. Since PTH has been shown to enhance skeletal blood flow, perhaps a contributing mechanism(s) for bone accrual is related enhanced bone vasodilator capacity. The principal nutrient artery (PNA) is the primary conduit for blood flow to long bones; therefore, the purpose of the study was to assess whether PTH augments bone vasodilator function of the femoral PNA. Endothelium-dependent and –independent vasodilations were determined following 2 weeks of intermittent PTH (1-84) administration. Male Wistar rats (300g) were administered PTH 1-84 (100 µg/ kg/d) or a saline solution (CON) s.c. for 5 d/wk for 2 weeks. The right PNA was dissected and cannulated to assess endothelium-dependent (acetylcholine [ACh]: $10^{-9} - 10^{-4}$ M) and -independent (sodium nitroprusside [SNP]: $10^{-10} - 10^{-4}$ M) vasodilation. Right femora (n=5 per group) were analyzed by bone histomorphometry. Expectedly, PTH augmented BV/TV by 23% vs. CON via thicker and more numerous trabeculae (Tb.Th: PTH = 62 $\pm$ 4 µm vs. CON = 41 $\pm$ 4 µm: $p < 0.05$; Tb.N: PTH = 3.7 $\pm$ 0.2 /mm vs. CON = 2.9 $\pm$ 0.2 /mm; $p < 0.05$). Preliminary analyses indicate a tendency ($p = 0.1$) for enhanced OS/BS (59%) with PTH treatment. Analyses of additional bone static and dynamic parameters are currently being conducted. Augmented bone mass corresponded with enhanced vasodilator capacity of the femoral PNA (PTH: n =8; 85 $\pm$ 5% maximal dilation; CON: n=8; 68 $\pm$ 5% maximal dilation). Endothelium-independent vasodilation did not differ between groups, indicating no change in smooth muscle cell responsiveness following PTH treatment. As hypothesized, 2 weeks of PTH administration augmented vasodilator capacity of bone vasculature via endothelium-dependent mechanisms. More importantly, these modifications were associated with augmented bone parameters (i.e., BV/TV, Tb.Th, Tb.N). Future analyses of bone static and dynamic properties will elucidate the relationship between bone cellular activity and bone blood vessel function. In conclusion, these results suggest that PTH-induced bone anabolism is presumably related to enhanced skeletal perfusion. Further work needs to be conducted.

***Disclosures: Rhonda Prisby**, None.*

MO0375

Teriparatide [rhPTH (1-34)] can Improve the Osteosynthesis results in Unstable Hip Fractures. A series of 6 Clinical Cases. Angel Oteo-Alvaro*[1], Lorenzo Castrejon[2], Ricardo Larrainzar[2], Pablo Maseres[2], Tomas Pampliega[2], Pablo Sarcangelo[2]. [1]Hospital General Universitario Gregorio Marañón, Madrid, Spain, [2]MD, Spain

Purpose of the study. To describe the osteosynthesis results in 6 unstable hip fractures treated with teriparatide.

Methods. A retrospective case analysis based on monthly radiological studies and pain VAS scores.

Results. In each of the 6 fractures (4 subtrochanteric and 2 intertrochanteric fractures), all of a multiple-fragment and/or unstable nature due to poor bone quality, a lack of bone stock, lesser trochanter rupture and/or the absence of posteromedial bony contact, an accelerating effect was observed in fracture healing after teriparatide treatment, with filling of the bone defect and early callus development that stabilized the fracture, accompanied by a considerable reduction of pain VAS score cerrelated to clinical improvement of the patient (Graphic 1).

Conclusion. Unstable intertrochanteric and subtrochanteric fractures present a high rate of complications. Implant fixation failure, particulary in osteoporotic bone, and delayed fracture healing are more frequent in intertrochanteric fractures. Non-union is more common in subtrochanteric fractures, since they affect a region with cortical bone, this favoring comminution and involving great biomechanical stress. The recommendations for the management of these patients focus on the importance of controlling co-morbidities, with a view to securing early mobilization and functional recovery. In this context, early and stable fixation must be attempted, with adequate treatment of osteoporosis,and the control of postoperative pain.

In our 6 clinical cases teriparatide was seen to accelerate the fracture healing process, showing exuberant callus growth within 2-6 months, the restoration of posteromedial bony contact and filling of the bone defects, with the stabilization of osteosynthesis. This in turn was accompanied by important clinical and functional improvement as a result of reduction in pain (level IV evidence).

References

Cipriano CA, Issack PS, Shindle L, Werner CM, Helfet DL, Lane JM. Recent advances toward the clinical applicaton of PTH (1-34) in fracture healing. HSSJ 2009;5(2):149-153

Morrison RS, Magaziner J, McLaughlin MA, Orosz G, Silberzweig SB, Koval KJ, Albert L. The impact of postoperative pain on outcomes following hip fracture. Pain 2003;103(3):303-311

Chong CP, Savige JA, Lim WK. Medical problems in hip fracture patients. Arch Orthop Trauma Surg. 2010;[Epub ahead of print]

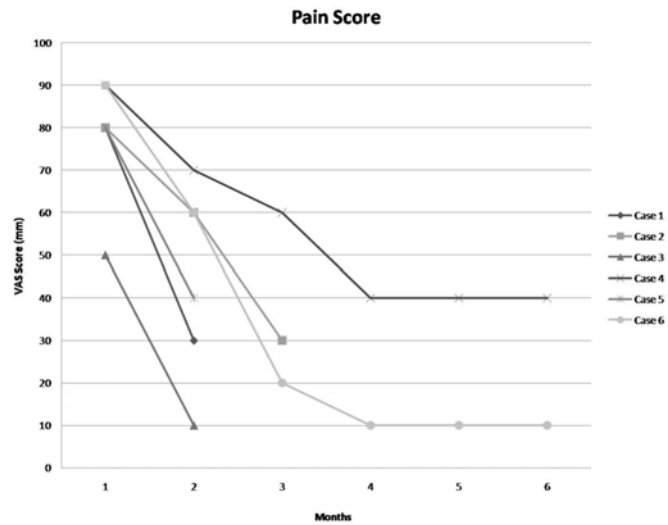

Graphic 1

***Disclosures: Angel Oteo-Alvaro**, Lilly Es, 8*

MO0376

Addressing Unmet Need - Setting up an IV Bisphosphonate Infusion Service for High Risk Patients Post Fractured Neck of Femur. Eamonn Brankin*[1], Robin Munro[2], Wendy Feeney[2], Margaret Yates[2], Paul Mitchell[3], Andrew Gallagher[4], John Hinnie[5], Stephen Gallacher[6]. [1]NHS Lanarkshire Osteoporsosis Service, United Kingdom, [2]NHS Lanarkshire Osteoporosis Service, United Kingdom, [3]University of Derby, United Kingdom, [4]Victoria Infirmary, United Kingdom, [5]South Glasgow Osteoporosis Service, United Kingdom, [6]Southern General Hospital, United Kingdom

A large percentage of patients who suffer fractured neck of femur currently require long term residential / nursing care. Historically few of these patients, who are at very high risk of subsequent fracture due to their frailty, are considered suitable for current 'gold standard' therapy with oral bisphosphonates, thereby leaving them relatively unprotected from further fractures. In addition, for those who are on oral secondary prevention therapies, concordance in this group is notoriously poor, resulting in large drug wastage which is relatively cost inefficient to the NHS. To address this suboptimal situation and unmet need we have recently set up an IV infusion service, sitting truly between primary and secondary care. This innovative service is aimed at two patient groups : the initiation of treatment for post operative patients with incident fracture prior to discharge, and secondly, working in primary care within community hospitals, nursing and residential homes to treat those with prevalent fractured neck of femur, which had occurred within the last year.

A new fracture liaison service nurse was appointed, and in addition to running 'standard fracture liaison' services, 50% of her time was allocated to setting up and running an IV bisphosphonate infusion service, using once yearly zoledronic acid both in the 3 local NHS hospitals, and in community care. Within NHS Lanarkshire, approximately 800 patients suffered a fractured neck of femur in the last year, from a population approximately 633,000. At full capacity, 5 patients can be treated by one nurse in one morning / afternoon session. Co-morbidities commonly associated with this patient group [physical and mental health related] dictate the numbers who can be safely treated by one nurse per session. Assuming 5 sessions per week running 46 weeks of the year, a total of 1150 patients per year may be treated, allowing us to treat both incident and prevalent fracture patients in an evidence based, cost effective manner by a simple once yearly infusion, delivered wherever the patient currently resides.

We feel that this new service, which we believe to be the first of its kind in the UK, represents high quality cost effective patient care for a very high risk patient population. It greatly improves concordance with therapy, reduces oral therapy wastage, ensures optimal secondary prevention is instituted and addresses a significant area of current unmet need in fracture liaison services.

***Disclosures: Eamonn Brankin**, MSD, 2; The Alliance for Better Bone Health, 5; MSD, 5; Novartis, 2; Roche, 5*
This study received funding from: Novartis Pharma

MO0377

Bone Histomorphometry Analyses in a Sub-Group of Patients with Glucocorticoid-Induced Osteoporosis Treated with Once-Yearly Zoledronic Acid 5 Mg or Daily Oral Risedronate 5 Mg Over 1 Year. Robert Recker*[1], David Reid[2], Philemon Papanastasiou[3], Daniel Chappard[4]. [1]Creighton University Osteoporosis Research Center, USA, [2]University of Aberdeen, United Kingdom, [3]Novartis Pharma AG, Switzerland, [4]INSERM, U922- LHEA, France

Glucocorticoids (GCs) have various effects on bone metabolism, including inhibition of osteoblast function, leading to reduced bone formation.[1,2] Histomorphometric analyses of bone biopsies from GC-treated patients vs postmenopausal women have shown lower bone volume, trabecular thickness, wall thickness, osteoid thickness and mineral apposition rate, and higher resorption parameters.[1,2] Bisphosphonates (BPs) are proven to decrease bone loss in GC-treated patients.[3,4] This substudy of patients from the HORIZON-Glucocorticoid-Induced Osteoporosis (GIO) trial[5] evaluated the effects of BPs on bone quality, remodelling, morphology, and possible mineralization defects.

This was a double-blind, active-controlled study in 833 men and women taking GCs. Patients were randomized 1:1 to receive a single iv infusion of zoledronic acid 5 mg plus daily oral placebo, or daily oral risedronate 5 mg plus a single iv placebo for 12 months. Patients were stratified into two sub-groups according to duration of prior GC treatment (≤3/>3 months).[5] Trans-iliac crest bone biopsies were performed at Month 12 on patients who agreed to participate in this sub-study, regardless of treatment group. Only samples containing the inner and outer cortex, and intact trabecular bone were considered suitable for histomorphometric analysis.

Twenty one biopsies were analyzed. Patients from the two sub-groups and two treatment groups were analyzed as a single cohort and these data are presented together. Baseline characteristics were comparable within the bone biopsy population. Qualitative analysis showed that newly formed bone was of normal quality in terms of lamellar structure. There was no evidence of pathological findings, osteomalacia, marrow dyscrasia, marrow fibrosis, or woven bone. Results of the quantitative histomorphometric and microCT analyses are presented in the table.

In conclusion, in patients with GIO, 1 year of treatment with zoledronic acid or risedronate did not have detrimental effects on bone quality. In the absence of pretreatment biopsies and a placebo group, it is difficult to establish the effect of bisphosphonates on preservation of bone remodelling capacity in this study.

1. Carbonare LD, et al. J Bone Miner Res 2001;16:97–103.
2. Dempster DW. J Bone Miner Res 1989;4:137–41.
3. Reid DM, et al. J Bone Miner Res 2000;15:1006–13.
4. Saag KG, et al. N Engl J Med 1998;339:292–9.
5. Reid DM, et al. Lancet 2009;373:1253–63.
6. Recker RR, et al. J Bone Miner Res 1988;3:133–44.

Table. Quantitative histomorphometric bone biopsy indices and micro CT results at 12 months* (reference data from 34 normal women[6] are shown in italics, where available)

VARIABLE	MEAN	STANDARD DEVIATION	RANGE
QUANTITATIVE HISTOMORPHOMETRY			
STRUCTURAL AND SURFACE RELATED			
Cortical thickness (Ct.Th), µm	628	318	217–1408
Wall thickness (W.Th), µm	31.3	3.2	26.3–37.6
	30.9	*4.0*	*25.0–39.0*
Osteoid thickness (O.Th), µm	4.7	0.9	3.7–7.2
	9.27	*2.10*	*5.50–12.00*
Osteoid volume (OV/BV), %	0.26	0.30	0.05–1.30
	1.65	*1.07*	*0.30–5.10*
Osteoid surface (OS/BS), %	2.90	2.75	0.65–12.31
	14.3	*6.3*	*7.0–25.0*
Kinetic indices			
Mineral apposition rate (MAR), µm/day	0.49	0.11	0.28–0.66
	0.53	*0.09*	*0.36–0.63*
Bone formation rate/volume referent (BFR/BV), %/yr	2.3986	4.7706	0.0000–20.4947
	13.0	*9.0*	*0.7–28.0*
Mineralization lag time (Mlt), days	86.7	88.6	8.1–279.6
	108.1	*149.0*	*25.0–480.0*
Activation frequency (AcF), year^{-1}	0.00	0.00	0.00–0.01
MicroCT			
Trabecular bone volume (BV/TV), %	17.65	5.04	2.64–28.14
	21.17	*4.90*	*14.00–30.00*
Trabecular thickness (Tb.Th), µm	124	30	70–195
	132.4	*27.9*	*93.0–185.0*
Trabecular separation (Tb.Sp), µm	785	451	384–2659
	629	*134*	*480–850*

*Sample size: n=21, except for mineralization lag time (n=19) and activation frequency (n=14)

Table

***Disclosures: Robert Recker**, None.*
This study received funding from: Novartis Pharma

MO0378

Comparison of Oral and Intravenous Ibandronate on Acute Phase Response in Osteoporotic Patients. Won Park[1], Seong Ryul Kwon[1], Min Jung Son[1], Mie Jin Lim*[2], Ji Yeol Youn[1], Chang Gi Moon[1]. [1]Inha University Hospital, South korea, [2]Inha University Hospital, Korea

Introduction

Ibandronate may be administered in two ways, via either oral or intravenous (IV) routes. Although acute phase response (APR) is expected to be prominent in intravenous regimen than oral route, it was not yet studied in osteoporotic patients.

Objective

We analyzed the difference of APR after administration of oral and IV ibandronate.

Methods

Total of twenty one osteoporotic patients was enrolled. Sixteen patients took 150mg of oral ibandronate (oral group) whereas eight patients were given IV ibandronate 3mg (IV group). Acute phase reactants including ESR and CRP were measured at baseline, 1, 2, 3 and 7 days after administration. Serum tumor necrosis (TNF)-α level was assessed using an immunoenzymetric assay (TNF-α: R&D Systems, Minneapolis, Minn., USA). Serum calcium level and hematologic parameter such as differential WBC count were also done. Results

Intravenous group showed significant rise in serum CRP level during initial 2 days ($p = 0.021$, 0.036 at 24 and 48 hours, respectively) as oral group showed modest increase. There was no marked change in ESR between two groups. Serum TNF elevation was not significant in both groups. Serum calcium level decreased significantly for 2 days after oral ibandronate administration ($p = 0.003$, 0.003 at day 1 and day 2) while it was slight in IV group. Neither groups showed any significant change on hematologic parameters.

Conclusion

This study proved that acute phase response is prominent after intravenous administration. Therefore more attention is required for early APR when IV BP is administered and attention for serum calcium level after both IV and oral intermittent large dose bisphosphonate regimen should be taken.

Acute phase reactants, serum calcium and WBC count after oral and IV ibandronate administration

***Disclosures:** Mie Jin Lim, None.*

MO0379

Effect of Alendronate on Radiographic Fracture Healing after Surgery for Low-energy Distal Radius Fractures. Shigeharu Uchiyama*[1], Toshirou Itsubo[2], Koichi Nakamura[3], Yasunari Fujinaga[4], Toshihiko Imaeda[5], Shota Ikegami[6], Mikio Kamimura[7], Masumi Kadoya[4], Hiroyuki Kato[2], Shinshu Society for Surgery of the Upper Extremities Investigators[8]. [1]Shinshu University, School of Medicine, Japan, [2]Department of Orthopaedic Surgery, Shinshu University School of Medicine. Shinshu Society for Surgery of the Upper Extremities, Japan, [3]Department of Orthopaedic Surgery, Shinshu Univesrity School of Medicine. Shinshu Society for Surgery of the Upper Extremities, Japan, [4]Department of Radiology, Shinshu University School of Medicine, Japan, [5]Department of Food & Nutritional EnvironmentKinjo Gakuin University, Japan, [6]Department of Orthopaedic Surgery, Shinshu University School of Medicine, Japan, [7]Center for Osteoporosis & Spinal Disorders, Kamimura Orthopaedic Clinic, Japan, [8]Shinshu University, Japan

We conducted a multicenter prospective randomized clinical trial to determine whether early alendronate (ALN) administration delayed radiographic fracture healing after surgical treatment of distal radius fractures. The study population comprised 39 patients with fresh low-energy distal radius fractures that required surgery. The patients were randomized to 2 groups: the ALN group and the no-ALN group. In the ALN group (n = 21), oral administration of ALN (35 mg, once weekly) was initiated within a few days after the surgery and continued for 6 months. In contrast, in the no-ALN group (n = 18), oral ALN administration was not initiated until at least 4 months after the surgery. Open reduction and internal fixation with a volar locking plate and screws were performed for all the patients. Posteroanterior (PA) and lateral X-rays of the affected wrist were taken every month till 6 months after the surgery. Central radiographic assessment was performed by 3 independent raters: 2 orthopedic surgeons and 1 radiologist. All the raters were blinded to the information regarding ALN therapy. Four parameters related to the fracture healing process were radiographically evaluated using the X-rays obtained in the PA and lateral views: time to early trabecular healing (initial and maximum) and time to cortical bridging (initial and complete). The Mann-Whitney test was used to compare these parameters between the 2 groups. The reliability of the raters' assessments was also determined. The ethical committee of each hospital approved the study protocol, and written informed consent was obtained from all the patients. No differences were observed between the 2 groups with regard to sex, age, AO fracture classification, and bone mineral densities at the hip or spine. No significant differences were noted between the 2 groups with respect to the parameters related to fracture healing (Table) in both PA and latetral X-rays. In both groups, the initial anatomical reduction was well maintained, with minimum displacement until the final follow-up. The reliability of the raters' assessments ranged from moderate to good. The surgeons confirmed that their patients took ALN tablets at predetermined intervals, without any side effects. On the basis of our results, we conclude that early ALN administration after surgery for fresh low-energy distal radius fractures does not affect the radiographic fracture healing process in humans.

Mean and median time to radiographic changes indicating fracture healing, according to one rater

		Early trabecular healing				Cortical bridging			
		Initial		Max		Initial		Complete	
		PA	Lateral	PA	Lateral	PA	Lateral	PA	Lateral
no-ALN	n	18	18	18	17	17	18	18	16
	mean (month)	1.17	1.06	1.56	1.47	1.82	1.72	3.67	3.63
	median (month)	1.00	1.00	1.00	1.00	2.00	2.00	4.00	3.50
	Standard deviation	.383	.236	.784	.624	.636	.575	1.138	.957
	percentile 25	1.00	1.00	1.00	1.00	1.00	1.00	3.00	3.00
	75	1.00	1.00	2.00	2.00	2.00	2.00	4.25	4.00
ALN	n	21	21	21	21	21	21	21	20
	mean (month)	1.29	1.19	1.81	1.81	1.86	1.76	3.62	3.35
	median (month)	1.00	1.00	1.00	1.00	2.00	2.00	3.00	3.00
	Standard deviation	.784	.512	1.436	1.401	.854	.700	1.284	1.089
	percentile 25	1.00	1.00	1.00	1.00	1.00	1.00	3.00	3.00
	75	1.00	1.00	2.00	2.00	2.00	2.00	5.00	4.00

No signifcant differences were observed between the 2 groups, with regard to the 4 parameters of radiographic healing (p>0.05). PA:posteroanterior view, ALN:alendronate.

Table

***Disclosures:** Shigeharu Uchiyama, None.*
This study received funding from: Univers foundation, Local medical reserach foundation, Banyu Co., Teijin Co.

MO0380

Effect of Once-yearly Zoledronic acid in Men after Recent Hip Fracture: Results from HORIZON Recurrent Fracture Trial. Steven Boonen*[1], Eric Orwoll[2], Jay Magaziner[3], Cathleen Colon-Emeric[4], Jonathan Adachi[5], Christina Bucci-Rechtweg[6], Patrick Haentjens[7], Jean-Marc Kaufman[8], Dirk Vanderschueren[9], Kenneth Lyles[4]. [1]Center for Metabolic Bone Disease, Belgium, [2]Oregon Health & Science University, USA, [3]University of Maryland, Baltimore, USA, [4]Duke University Medical Center, USA, [5]St. Joseph's Hospital, Canada, [6]Novartis Pharmaceuticals, USA, [7]CEBAM, Belgian Centre for Evidence Based Medicine, Belgium, [8]University Hospital of Ghent, Belgium, [9]Catholic University of Leuven, Belgium

Purpose: Osteoporosis is an under-recognized problem in men, which often goes untreated in majority of men sustaining fragility fractures. Mortality is also higher in osteoporotic men sustaining fracture compared to women. HORIZON-Recurrent Fracture Trial (RFT) explored efficacy and safety of once-yearly i.v. zoledronic acid (ZOL) 5mg compared to placebo (PBO) in reducing the risk of subsequent clinical fractures in patients following recent hip fracture[1]. This report summarizes the findings of the male sub-set of patients enrolled in HORIZON-RFT.

Methods: In HORIZON-RFT, a multicenter, double-blind, placebo-controlled trial involving 2127 patients with a recent low-trauma hip fracture. 508 male patients (age ⩾50 years) were randomized to receive either once-yearly i.v. ZOL 5 mg (n=248) or PBO (n=260), within 90 days after the surgical hip repair. All patients received daily supplementation with oral calcium (1000 to 1500 mg) and vitamin D (800 to 1200 IU) and were followed to assess the incidence of new clinical fractures.

Results: The percentage change from baseline in total hip (TH) bone mineral density (BMD) at Month 24 was significantly greater with ZOL (3.81%; p=0.0021) *vs.* PBO. In fact, THBMD, at Month 24 increased with ZOL but decreased with PBO treatment (3.59% *vs.* -0.22%, respectively). At Months 12 and 36, greater increases in THBMD were observed with ZOL (2.01% and 7.06%, Months 12 and 36, respectively; both $p<0.005$) *vs.* PBO. New clinical fractures occurred in 36 (7.1%) of the study male subset (16 ZOL; 20 PBO). The two-year cumulative clinical fracture event rates were 7.45% and 8.70% for ZOL and PBO, respectively (Kaplan-Meier estimates). No treatment-by-gender interaction (p=0.34) was observed indicating a lack of association between treatment and gender with respect to fracture risk reduction. Adverse events (AEs) and seriousAEs were comparable between treatment groups. There were no significant differences in cardiovascular or long-term parameters of renal function. No spontaneous or adjudicated cases of osteonecrosis of the jaw were reported.

Conclusion: Once-yearly i.v. ZOL 5 mg infusion within 90 days after repair of a low-trauma hip fracture significantly increased THBMD in men. The increases in BMD in this study were in line with those seen in women, both in women with recent hip fracture in the RFT as well as in women with postmenopausal osteoporosis participating in the PFT.

Reference: Lyles KW *et al. NEJM* 2007; 357:1799–1809.

***Disclosures: Steven Boonen**, Eli Lilly, Novartis, Pfizer, Procter & Gamble, Sanofi-Aventis, and Roche, GlaxoSmithKline, 2; Amgen, Eli Lilly, Merck, Novartis, Procter & Gamble, Sanofi-Aventis, and Servier,, 8*
This study received funding from: Novartis

MO0381

Effect on Bone Mineral Density of Oral Bisphosphonates In Women with Osteoporosis and Breast Cancer Treated with Aromatase Inhibitors. Are Bone Turnover Markers Useful In These Patients? Enrique Casado*[1], Ivonne Vázquez[1], Marta Larrosa[1], Elsa Dalmau[2], Miquel Angel Seguí[2], Jordi Gratacós[1]. [1]Rheumatology. University Institute Parc Taulí (UAB), Spain, [2]Oncology. University Institute Parc Taulí, Spain

Purpose: To evaluate the effect on bone mineral density (BMD) of 2-years treatment of oral BP in women with osteoporosis and breast cancer treated with aromatase inhibitors. To evaluate the effect on bone resorption of this treatment measuring the urinary cross-linked N-telopeptides of type I collagen (u-NTX).

Methods: Longitudinal study. Period of inclusion September 2005-July 2008. All women with osteoporosis by bone densitometry (Hologic), who had started in the previous 12 months treatment with aromatase inhibitors (anastrozole, letrozole exemestane) received treatment with oral BP (weekly alendronate or weekly risedronate) and were followed for 2 years. Thoracic and lumbar spine X-ray was performed in all patients at inclusion and after 2 years of bisphosphonate therapy to assess the presence of vertebral fractures (VF). The presence of non-vertebral fractures during the follow-up was assessed by reviewing medical history. All patients underwent determination of u-NTX (ELISA, normal <65 nmol/mmol) before and after 6 months of BP.

Results: 55 women were included. Mean age 63.1 $\pm$ 8 years (49-80). Baseline BMD was 0.744 $\pm$ 0.099 g/cm^2 (T-score -2.7 $\pm$ 0.7) at lumbar spine, and 0.671 $\pm$ 0.090 g/cm^2 (T-score 2,1 $\pm$ 0.9) at femoral neck. 16.6% of patients had suffered one or more non-vertebral fractures and 19% had at least one morphometric VF before the inclusion. After 2 years of treatment, BMD increased by 5.5% in lumbar spine and decreased by 3.9% in femoral neck. Only one patient with 2 previous VF suffered 2 new VF during the 2-years of follow-up. We didn't observe any new non-vertebral fracture in any patient.

The mean baseline u-NTX was 80.0 ± 38.8 nmol/mmol. 62.2% of patients had a high bone resorption (increased levels of u-NTX). After 6 months of treatment the mean u-NTX decreased by 36.4% and only 21% of patients maintained levels of u-NTX above the normal range. Patients who maintained a high resorption after 6 months of treatment with BP BMD increased by only 2.8% in lumbar spine and decreased by 6.3% in femoral neck.

Conclusions: Treatment with oral BP in women with osteoporosis and breast cancer treated with aromatase inhibitors seems able to increase BMD in cancellous bone, but not in cortical bone. BP are also able to maintain at 6 months, a low bone turnover in almost 80% of patients. Patients who do not achieve a normal u-NTX after 6 months of treatment fail to increase BMD at lumbar spine and femoral neck.

***Disclosures: Enrique Casado**, None.*

MO0382

Effects of Intravenous Ibandronate Injection on Renal Function in Postmenopausal Women With Osteoporosis at High Risk for Renal Disease Compared With Ibandronate Infusion or Oral Alendronate-the DIVINE study. Paul Miller*[1], Sergio Ragi Eis[2], Carlos Mautalen[3], Francisco Ramirez[4], Iris Jonkanski[5]. [1]Colorado Center for Bone Research, USA, [2]Cedoes - Centro de Diagnósticos e Pesquisa, Brazil, [3]Centro de Osteopatías Médicas, Argentina, [4]Roche Products Limited, United Kingdom, [5]F. Hoffmann-La Roche Ltd, Switzerland

PURPOSE: The Designed for IV Ibandronate ReNal Safety Evaluation (DIVINE) study evaluated the renal safety of quarterly (q3mo) ibandronate IV injection (over 15-30s; INJ) compared with q3mo ibandronate IV infusion (over 15 min; INFU) and weekly oral alendronate (ALN) for 1 year in women with postmenopausal osteoporosis (PMO) at increased risk for renal disease.

METHODS: This was a randomized, open-label, multicenter study of women aged ⩾60 years with PMO at high risk for renal disease. At least half of patients had ⩾1 of the following: hypertension, diabetes, or actual glomerular filtration rate (aGFR) <60 mL/min, where aGFR was determined using an abbreviated MDRD.[1] Women received ibandronate q3mo as 3 mg INJ or 3 mg INFU, or 70 mg weekly oral ALN, for 12 months. The primary endpoint was the absolute change from baseline in mean post-dose aGFR at 9 months (10-21 and 3-12 days post ibandronate and ALN dose, respectively) in the per-protocol population. Treatment was interrupted/stopped if the patients met prespecified criteria for serum creatinine (sCr), aGFR or urine albumin-to-Cr ratio. Secondary endpoints included absolute and relative changes in aGFR at month 12 and estimated GFR using Cockcroft-Gault (CG). An ANOVA noninferiority test was used to compare the INJ, INFU, and ALN groups. The INJ regimen was considered noninferior to INFU and ALN with regards to aGFR if the lower bound of the 2-sided 95% CI of the mean of the difference was ⩾-3 mL/min for both comparisons.

RESULTS: A total of 801 women were randomized: 268 to ibandronate INJ, 264 to ibandronate INFU, and 269 to oral ALN. Over 75% of patients had at least 1 risk factor for renal disease. Mean absolute aGFR change from baseline in the INJ group was noninferior to the INFU and ALN groups at 9 months (Table). Similar results were observed at 12 months and using CG at both time points. Adverse events generally were comparable between groups and consistent with what has been reported for ibandronate. Interruption/stopping criteria were met by 3.4%, 2.7%, and 6.7% of patients in the ibandronate INJ, ibandronate INFU, and oral ALN groups, respectively.

CONCLUSIONS: Ibandronate INJ was shown to be noninferior to INFU and weekly oral ALN with regards to renal function as assessed by change in aGFR. The licensed dosing of ibandronate INJ q3mo is safe and well tolerated in women with PMO and at high risk for renal disease.[1]Levey AS, et al. 2003, Ann Intern Med 139, 137-147.

	Ibandronate 3 mg q3mo injection (N=246)	Ibandronate 3 mg q3mo infusion (N=243)	Alendronate 70 mg oral weekly (N=241)
Actual GFR (mL/min, SD)			
Baseline	72.5 (18.3)	71.5 (18.1)	70.5 (16.7)
9 months	71.4 (17.7)	71.4 (18.0)	68.0 (16.2)
Change from baseline, mean (SD)	-1.3 (7.14)	0.5 (7.86)	-1.6 (5.89)
Difference of means to INJ (95% CI)*	NA	-0.74 (-1.98, 0.50)	0.66 (-0.60, 1.91)

*ANOVA adjusted for baseline GFR and randomization factors; non-inferiority margin: -3 mL/min

Table. Change from baseline in actual GFR at 9 months' post-dose (per-protocol population)

***Disclosures: Paul Miller**, Procter & Gamble, Sanofi-Aventis, Merck, Eli Lilly, Amgen, NPS, Novartis, Roche, and GlaxoSmithKline, 5; Procter & Gamble, Sanofi-Aventis, Roche, Eli Lilly, Merck, Novartis, and Amgen, 2*
This study received funding from: F. Hoffmann-La Roche Ltd

MO0383

Efficacy Of Zoledronic Acid In Bone Mineral Density Increases In Postmenopausal Osteoporosis. Corina Galesanu*[1], Mihail Romeo Galesanu[2]. [1]University of Medicine & Pharmacy, Romania, [2]Centre of Imaging & Radiologic Diagnostic, Romania

Osteoporosis in a chronic disorder that has significant consequences including increased morbidity and mortality, that is manifest clinically after a fracture has occurred. Bisphosphonate therapy is the standard of care in osteoporosis.

Zoledronic acid (ZOL) 5 mg, once-yearly infusion is the most recent drug approved for the treatment of postmenopausal osteoporosis. Strong evidence supports reported a risk-reduction in all clinical fractures along with significant increases in bone mineral density (BMD).

We proposed to evaluate the effect of ZOL treatment on BMD change in a group of postmenopausal osteoporotic women (PMO) assessed by DXA-BMD using a Hologic bone densitometer.

Osteoporosis was defined as a BMD T-score in lumbar spine and/or total hip of -2.5 or less. Among 520 PMO registered in the years 2008-2009, 17 women were treated with ZOL iv 5 mg/yearly. DXA measurement for BMD change was used at baseline and after 12 months. The mean age of the patients was 58.43 ± 3.43 years. Time since menopause was 10.2 ± 17 years. Lumbar spine mean BMD was: 0.665 ± 0.028 g/cm^2 and increased at 0.700 ± 0.006 g/cm^2 (+5.2%). Total hip mean BMD was: 0.714 ± 0.042 g/cm^2, increased at 0.749 ± 0.023 g/cm^2 (+4.9%). Femoral neck mean BMD was: 0.549 ± 0.015 g/cm^2 and increased at 0.572 ± 0.010 g/cm^2 (+4%).

Significantly reduced the hyperalgesia after a mean of 6.7 weeks (4-12 weeks). Adverse events after infusions were flu-like syndrome transient: 4 cases (23.5%), arthromyalgias 2 cases (11.7%), arterial hypertension 1 case (5.8%). No cardiac arrhythmias or bone necrosis.

In our experience iv Zoledronic 5 mg/once yearly has demonstrated to be an effective antiosteoporotic treatment increasing BMD in patients suffering from osteoporosis. It is now well accepted that increases in bone mass. The women who take bisphosphonate will have a decrease in fracture risk.

***Disclosures: Corina Galesanu**, None.*

MO0384

Experience with Intravenous Zoledronic Acid Treatment for Osteoporosis in the Real Clinical Practice. Diana Gonzalez De Bertini*[1], Beatriz Oliveri[2], Alicia Bagur[3], Carlos Mautalen[2]. [1]Centro de Osteopatías Medicas, Argentina, [2]Centro De Osteopatías Médicas, Argentina, [3]Hospital De Clinicas, Argentina

Randomized controlled trials have demonstrated that IV Zoledronic acid (ZOL) ensures an effective anti-osteoporotic treatment. In the pivotal trials previous use of IV bisphosphonate was an exclusion criteria and previous oral bisphosphonate was allowed after a long wash out period. However, we cannot apply these measures in the real clinical practice. Aim: to share our experience in the utilization of Zol in osteoporosis during 2007-2010. Methods: patients that had been treated at least with one dose of ZOL were included. We analyzed: a) Changes in serum calcium (sCa), 25OHD, PTH, CrossLaps (CTX), Bone alkaline phosphatase (BAP) 1 to 3 months and 1 year post ZOL. b)Changes in BMD of the lumbar spine (LS), femoral neck (FN) and total femur (TF) one year after ZOL. Results: 71 women of 66.8 + 8.1 years old were included. Only 6 women were naive of bisphosphonate treatment. Four patients presented celiac disease, all of them in effective compliance with their gluten free diet. Fifty eight patients had history of fragility fractures (n=23) and/or BMD T-score < -2.5. Thirteen patients had BMD T-score>-2.5. Biochemical and BMD values at baseline, 1-3 months and 1 year post ZOL are shown in the Table. BMD increased 3.6 % in LS, 2.7% in FN and 2.1% in TF. The increments in LS and FN were significant in both osteopenic and osteoporotic patients. No patient presented hypocalcemia in the post dose control, however sCa levels were significantly lower compared to baseline values. A very significant 73% decrease was observed in the 1-3 months CTX values. CTX levels were at or below the lowest normal limit for premenopausal women in 6 patients. After one year post dose levels were 37% decreased compared to baseline and were still 50% decreased from baseline in 23 out of 50 patients. We found a positive correlation between the % change of CTX 1-3 months post dose and % change BMD TF(r=0.3; p=0.05) and the % change CTX one year post ZOL and BMD FN (r= -0.4; p=0.05). Three patients with previous fractures suffered from a new fracture after ZOL, one of them occurred 1 month after dose. Up-to-day 15 patients received a second ZOL dose. Conclusion: In our experience, IV ZOL has been an effective anti-osteoporotic treatment even in those patients previously treated with oral or IV bisphosphonates. CTX appears to be an interesting option in monitoring the duration of the IV ZOL effect and could be useful to decide in certain cases a longer time for re dosing patients.

Table: Biochemical and BMD (GE LUNAR) values at baseline, 1-3 months and 1 year post IV ZOL

	Baseline	1-3 months	1 year
sCa (mg/dl)	9.5±0.4	9.4±0.4 *	9.4±0.4 #
25 OHD (ng/ml)	34.5 ±8.2	33.8±10.9	36.6±11.5
PTH (pg/ml)	46.8 ± 14.7	57.2±22.5	49.7±15.2
BAP (UI/L)	54.4 ± 15.2	48.9±15.8 **	57.1±28.9
CTX (ng/L)	346 ± 167.5	84.7±55.2 ***	187.4 ± 90.6***
BMD-LS	0.894±0.131		0.929±0.151##
BMD-FN	0.699±0.08		0.711 ±0.08 ##
BMD-FT	0.716±0.08		0.717±0.08***

*p= 0.028 compared to basal

** p<0.05 compared to basal

*** p= 0.0001 compared to basal

p= 0.007compared to basal

p= 0.002 compared to basal

Table

***Disclosures: Diana Gonzalez De Bertini**, None.*

MO0385

Potential Under-treatment of Male Veterans with or at risk for Osteoporotic Fractures. Robert Adler*[1], Todd Semla[2], Fran Cunningham[3], Leonard Pogach[4]. [1]McGuire VA Medical Center, USA, [2]Dept of Veterans Affairs National Pharmacy Benefits Management Services, USA, [3]Dept of Veterans Affairs Pharmacy Benefits Management Services, USA, [4]Dept of Veterans Affairs National Program Director for Endocrinology, USA

Despite increased knowledge of osteoporosis and the availability of generally safe and effective therapy, many patients, especially men, with osteoporosis and/or fractures do not have adequate evaluation and therapy. To determine the extent of under-treatment in a large medical system, we compared medication use in patients with the following categories of future fracture risk: Previous osteoporotic fracture (hip,spine, forearm, humerus), oral glucocorticoid use (> 90 days), diagnosis of osteoporosis or osteopenia in the medical record, androgen deprivation therapy for prostate cancer (ADT), or anti-seizure medication (AED). We used administrative databases for the entire Department of Veterans Affairs (approximately 5.1 million patients, 91% male) for 2.25 years (2007-2009). The percentages of patients on different therapies are shown in the table. As can be seen, adequate therapy was prescribed for only a minority of patients with osteoporotic fractures, on oral glucocorticoids, on androgen deprivation therapy, or on anti-epileptic drugs. Only about half of patients with a diagnosis of osteoporosis or osteopenia receive pharmacologic treatment or calcium/vitamin D supplements. In a medical system with an excellent electronic medical record, few barriers to DXA, and relatively inexpensive medication costs, most patients at risk for fracture are not treated adequately. Since the time the data were derived, an algorithm for evaluation and treatment of male osteoporosis has been sent to all V.A. Medical Centers. We will determine if the algorithm changes the proportion of veterans treated.

Condition	Patients (1000's)	Calcium (%)	Vitamin D (%)	Bisphosph. (%)	Teriparatide (%)
Fracture	178.9	13.8	15.4	9.1	0.2
GIOP Risk	72.7	32.2	33.4	26.0	0.2
OP/Penia	115.8	50.4	46.2	26.0	0.6
ADT	29.6	27.6	28.9	12.3	<0.1
AED	50.5	11.2	12.8	4.8	<0.1

Treatment of Veterans with Fracture Risk

***Disclosures: Robert Adler**, GTX, Inc., 5; Eli Lilly, 5; Genentech, 2; Novartis, 2; Eli Lilly, 2; Merck, 5; Amgen, 2*

MO0386

Serum 25 Hydroxyvitamin D Concentrations and the Risk of Atypical Femoral Fractures Associated with Bisphosphonate Use : A Case Control Study. Alvin Choong-Meng Ng*, Joyce Suang-Bee Koh, Seo-Kiat Goh, Tet-Sen Howe. Singapore General Hospital, Singapore

There have been several recent reports of atypical femoral fractures occurring in patients treated with bisphosphonates; these occur mostly in the subtrochanteric region, have transverse or short oblique configurations and thickened cortices. While the primary hypothesis has centered on over-suppression of bone turnover, there have been suggestions that vitamin D deficiency might be an important risk factor. Vitamin D deficiency is associated with impaired calcium absorption, compensatory hyperparathyroidism, increased bone resorption and an increase in fracture risk.

We hypothesize that vitamin D deficiency is a risk factor for atypical femoral fractures associated with bisphosphonate use. In our case series of such fractures which presented between May 2004 to March 2010, 16 female subjects, age 52 to 91 years, had a serum 25-hydroxyvitamin D (25OHD) level ascertained at the time of presentation. Each case was age and sex matched to two controls; the controls being patients admitted for low-energy femoral neck or intertrochanteric femoral fractures. Vitamin D deficiency was defined as serum 25OHD < 20 ng/mL. We used Fisher's exact test and Wilcoxon rank-sum test to compare the vitamin D status and serum 25OHD levels respectively.

Baseline characteristics including age, sex and ethnicity were similar between cases and controls. Duration of bisphosphonate use ranged from 2 to 10 years, with 15 cases treated with alendronate and one with risedronate. The median serum 25OHD was 26.2 ng/mL in cases vs 19.0 ng/mL in controls (p=0.013). 3 of 16 cases (18.75%) were vitamin D deficient vs 17 of 32 controls (53.13%) (p=0.031). The odds-ratio for vitamin D deficiency in cases vs controls was 0.20 (95% CI : 0.03 - 0.97). Corrected serum calcium was 2.36 mmol/L in cases vs 2.31 mmol/L in controls (p=0.094); serum intact PTH was 5.2 pmol/L in cases vs 4.9 pmol/L in controls (p=0.961).

While our study has shown that vitamin D status was better in cases vs controls, it does not preclude the possibility that low serum 25OHD might still have a role in pathogenesis. Notably, 14 of 16 cases (87.5%) had serum 25OHD lower than 30 ng/mL (range: 12.6 - 31.4 ng/mL). We acknowledge that a better comparison group would have been controls that were also matched for bisphosphonate exposure. Another important limitation is the possibilty of reverse causation as the serum 25OHD was measured at the time of presentation rather than at the initiation of bisphosphonate therapy.

***Disclosures: Alvin Choong-Meng Ng**, None.*

MO0387

Subtrochanteric Femoral Stress Fractures in Patients on Chronic Bisphosphonate Therapy: A Case Series. Jason Nitche[1], Carlos Sagebien[2], Robert Masella[2], Daniel Redziniak[2], Sunil Wimalawansa*[3]. [1]Dept. Orthopedic, UMDNJ-RWJMS, USA, [2]Orthopedic, UMDNJ-RWJMS, USA, [3]Robert Wood Johnson Medical School, USA

Bisphosphonates modulate bone resorption at the level of the osteoclast. Recent articles have suggested an association of stress fractures with prolonged bisphosphonate use. In addition to the classic thickened cortices, bone biopsies from some of these patients showed markedly suppressed bone turnover at the sites of such fractures. In general, bisphosphonate therapies significantly reduce fractures including hip fractures. However, with prolonged use of bisphosphonate, there is some evidence to suggest that it may increase the atypical subtrochanteric fractures. Here we report six patients with antecedent thigh pain who suffered subtrochanteric femoral stress fractures. All patients had been treated for osteoporosis with bisphosphonate alendronate, for at least six years. All these patients sustained a low energy subtrochanteric femur fracture through a clear region of chronic stress reaction in the bones and had choke-stick-like horizontal fractures (Figure 1 to 3). Moreover, there was no radiographic evidence of thin, osteoporotic cortices at any of the fracture sites; instead, all had thickened cortices around the fracture sites, bilaterally.

The numbers of such fractures reported to-date are insufficient to make firm conclusions of its etiology. Although there could be a number of reasons for such fractures including genetic susceptibilities, preexisting conditions, inappropriate treatment with bisphosphonates (i.e., treatment of patients with normal BMD) etc, there may also be an association between long-term bisphosphonate use and atypical subtrochanteric femoral stress fractures. We also speculate that such fractures and the correlation of the use of long term bisphosphonates may have been overlooked. This is particularly important that bisphosphonates such as alendronate now has been in the market for over 13 years, and such long term complications may only beginning to surface with increasing numbers of patients who use bisphosphonates for prolong periods. We suggest that treating physicians should have an index of suspicion for any patient on bisphosphonates longer than 5 years, who present with thigh pain or dysfunction. Imaging with a 99Tc-bone scan or MRI may be helpful in identifying patients vulnerable for such fractures (Figure 1), whereas in most circumstances, plain radiograph will be negative, till a fracture is established.

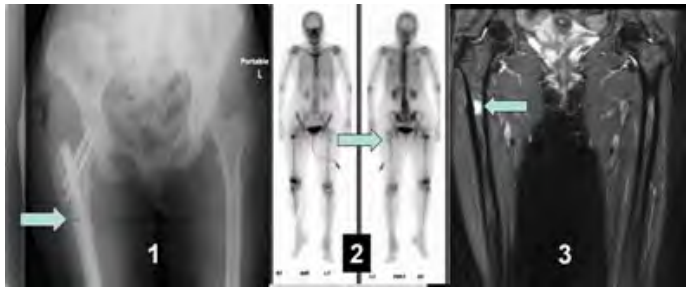

Figure 1

***Disclosures: Sunil Wimalawansa**, None.*

MO0388

Switching Patterns Over 12 Months in Postmenopausal Women Initiating or Receiving Bone Loss Medications in the POSSIBLE EU® Study. Luc Martinez*[1], Christian Roux[2], Rob Horne[3], Adolfo Diez-Perez[4], Francis Guillemin[5], Sergio Ortolani[6], Anne Marciniak[7], Matt Gitlin[8], Susan Shepherd[7], Gerd Moeller[8], Nick Freemantle[9]. [1]Société Française de Médecine Générale, Issy les Moulineaux, France, France, [2]Hospital Cochin, France, [3]School of Pharmacy, University of London, United Kingdom, [4]Hospital del Mar-IMIM-Autonomous University of Barcelona, Spain, [5]Nancy-University, EA 4360 Apemac, France, [6]Istituto Auxologico Italiano, Italy, [7]Amgen Ltd, United Kingdom, [8]Amgen (Europe) GmbH, Switzerland, [9]Birmingham University, United Kingdom

Aims: As treatment effectiveness with bisphosphonates may depend on whether patients regularly take their prescribed medication, it is important to understand treatment patterns, such as switching among these patients. POSSIBLE EU® is an observational study, describing the baseline characteristics of postmenopausal women receiving bone loss medication (N = 3402) in 5 European countries (France, Germany, Italy, Spain, UK)[1]. In this analysis, switching patterns were explored at baseline and over a 12-month-follow-up period.

Methods: Patients were recruited by their general practitioner into one of three cohorts: inception (newly starting treatment, no previous therapy within 12 months of entry [1787/3402, 53%]), established (receiving therapy for at least 12 months [1041/3402, 31%] or switch (had been receiving a therapy during previous 12 months and changed at enrollment [574/3402, 17%]). We analyzed individual medications at baseline across the 3 cohorts and then the first-switch post-baseline, ie, over the 12-month follow-up period. A switch was defined as a change in medication, or frequency, but not a change in dose. Significance between cohorts was performed using the chi-squared test.

Results: Mean age (SD) for all patients was 68.2 (9.8) years. Bone loss medications were identified for 3121 patients at baseline. Most patients were receiving bisphosphonates 2633/3121 (84%) at baseline. The most common medications were: alendronate (49%), risedronate (18%) and ibandronate (13%). A total of 9% (308/3402) of patients switched medication during the 12-month follow-up period. The percentage of patients switching was significantly higher in the switch cohort vs the established cohort (switch cohort vs established cohort, 13% [77/574] vs 7% [74/1041], $p<0.0001$) whereas for the inception cohort vs the established cohort the difference was not significant (9% [157/1787] vs 7% [74/1041]). Most patients (69%, 154/224) who switched during follow-up switched from a bisphosphonate to a bisphosphonate. Among patients who switched medication 14% (42/308) switched again at least twice.

Conclusions: Switching bone loss medication is more common in postmenopausal women who have a history of switching than in patients who are naïve to therapy or already established on treatment.

1. Freemantle N, et al. Arch Osteoporos 2010. In print.

***Disclosures: Luc Martinez**, Amgen, Sanofi, Pfizer, Roche, Novonordisk, Mayoli-Spindler, 5*
This study received funding from: Amgen (Europe) GmbH

MO0389

The Effect of a Single Infusion of Zolendronic Acid 5mgs Intravenously (iv) on Bone Density and Strength in Patients with Postmenopausal Osteoporosis. A Peripheral Quantitative Computed Tomography (pQCT) Study. Konstantinos Stathopoulos*[1], Pelagia Katsimbri[2], Eratw Atsali[3], Euaggelia Kataxaki[4], Loukas Papas[5], Aristidis B. Zoubos[5], Grigoris Skarantavos[5]. [1]"Attikon" Athens University Hospital, Greece, [2]Bone Metabolic Unit, 1st Orthopedic UniversityClinic, "Attikon" Athens University Hospital, Greece, [3]3rd Pediatric University Clinic, "Attikon" Athens University Hospital, Greece, [4]Department of Rheumatology, Eleusina General Hospital "Thriassion", Greece, [5]Bone Metabolic Unit, 1st Orthopedic University Clinic, "Attikon" Athens University Hospital, Greece

Purpose: We assessed the effect of Zolendronic Acid (ZOL) 5 mgs iv on volumetric densities and strength in postmenopausal osteoporotic women using tibia pQCT.

Methods: We reviewed medical records of 30 postmenopausal women who received 1 infusion of ZOL in our department. Inclusion criteria: 1) age>50y 2) menopause>2y, 3) DXA measurement (Spine/Hip) with Tscore<-2,5 SD 4) Tibia pQCT before and 1 y after treatment. Exclusion criteria: 1) Secondary osteoporosis' conditions 2) Other bone metabolic diseases 3) Previous use of bone anabolic agents 4) Previous use of bisphosphonates > 2 y 5) malignancies. Biochemical markers of bone formation (Osteocalcin, bone ALP) and resorption (serum CTX, NTX) were tested before and 1y after treatment. All patients had tibia pQCT (Stratec Medizintechnik, Pforzheim, Germany), 3 slices were obtained at the 4% (trabecular), 14% (subcortical and cortical) and 38% (cortical bone) of tibia length sites. We studied 15 variables for each slice, mainly total bone content (TOT_CNT), total density (TOT_DEN), cortical content (CRT_CNT), cortical density (CRT_DEN), subcortical content (CRTSUB_CNT), subcortical density (CRTSUB_DEN), total area (TOT_A),cortical area (CRT_A), subcortical area (CRTSUB_A), mean cortical thickness (CRT_THK), Stress Strength Indexes (SSIs). We performed statistical analysis (t-test, ANCOVA), data expressed as mean ± standard deviation (S.D.)

Results: Patients' mean age was 65,3 ± 8,6y and mean object length 359,83 ± 22,1mm. After treatment, we report increases at the 14% site in TOT_CNT (324.08 ± 54.53 vs 329.89 ± 55.85, p = 0.012), CRT_DEN (994.91 ± 51.89 vs 1005.45 ± 56.62, p=0.006) and SSI2 (1000.7 ± .208.05 vs. 1026.6 ± 215.21, p<0.0005). At the 38% site we report increases in TOT_CNT (272.66 ± 41.08 vs 279.94 ± 41.13, p<0.0005), in SUBCRT_CNT (205.98 ± 22.32 vs 210.99 ± 24.50, p<0.0005), CRTCNT (152.04 ± 52.03 vs 165.87 ± 54.78, p<0.0005), TOTDEN (700.53 ± 102.64 vs 711.03 ± 104.83, p=0.008), CRT_DEN (1198.77 ± 24.58 vs 1213.10 ± 25.76, p<0.0005), CRT_A (126.42 ± 42.10 vs 136.29 ± 43.74, p< 0.0005), CRT_THK (2.02 ± 0.76 vs 2.19 ± 0.79, p<0.0005) and SSI3 (1259.0 ± 205.01 vs. 1297.0 ± 237.39, p=0.001). All biochemical markers were decreased 12 months after the infusion, but remained within normal premenopausal range.

Conclusions: Our results indicate that i.v. ZOL 5 mgs once yearly increases significantly bone content, volumetric cortical densities, cortical thickness and bone strength in postmenopausal osteoporotic women.

***Disclosures: Konstantinos Stathopoulos**, None.*

MO0390

Time to Onset of Efficacy of Antiresorptive Treatments for Osteoporosis is Important. Charles Inderjeeth*[1], Kien Chan[2], Kevin Kwan[2], Michelle Lai[2]. [1]Sir Charles Gardner Hospital, Australia, [2]Sir Charles Gairdner Hospital, Australia

Objective

Osteoporosis and fracture are important causes of morbidity and mortality and at significant cost. Treatment and prevention of future fracture is an important goal in those at risk. Most agents report similar 3 year efficacy. Early onset of efficacy is important. Efficacy in non vertebral and hip fracture reduction in addition is desirable.

Methods

We reviewed the peer reviewed literature to ascertain the rapidity of onset of efficacy of commonly prescribed antiresorptive treatments. Only published data were used. Studies included original studies, post hoc and subgroup analysis and observational cohort studies. All papers were reviewed independently and summarised by at least 2 reviewers for onset of efficacy for vertebral (VF), non vertebral (NVF), hip (HF) and any clinical fracture (CF).

Results

Risedronate studies report efficacy by 6 months for all types of fracture (VF, NVF, HF, CF) and was superior to Alendronate (NVF, HF) and Calcitonin (NVF) in cohort studies . Alendronate is reported to be effective by 6 months (VF), 1 year (CF, NVF) and 2 years (HF). Zoledronic Acid studies report efficacy of 1 year (VF, CF) and 3 years (NVF, HF). Ibandronate is reported effective for VF only (1 year). Strontium Ranelate is effective at 1 year (VF) and 3 years (NVF, HF, CF). Raloxifene is effective at 1 year (CF) and 2 years (VF). Denosumab is effective at 3 years (VF, NVF, HF, CF).

Conclusions

Literature reports of early fracture reduction with current agents are very limited. It would be useful to have data on early efficacy with currently available agents in the published domain. Current evidence for the early onset of efficacy is strongest for

Risedronate. Onset of efficacy may be an important consideration in the selection of treatment for many patients.

***Disclosures: Charles Inderjeeth**, Sanofi Aventis Australia, 2*
This study received funding from: Sanofi Aventis Australia

MO0391

Vitamin D Cut-off Level for Maximum Increase in Bone Mineral Density with Bisphosphonate Treatment in Osteoporotic Women. Ippei Futami[1], Yuko Sakamoto[1], Tokuhide Doi[2], Kazuo Kaneko[1], Akifumi Tokita[1], Haruka Kaneko[1], Makoto Yamanaka[1], Muneaki Ishijima*[1], Lizu Liu[1]. [1]Juntendo University, School of Medicine, Japan, [2]Fukuoka Clinic, Japan

It is important to identify clinical conditions that might induce maximum increase the bone mass by the treatment of osteoporosis. We have shown that vitamin D status may affect the increase in lumbar spine (LS)-BMD with bisphosphonates (BPs) treatment in individuals being treated for osteoporosis and calculated the minimum vitamin D (serum 25-hydroxyvitamin D (s25(OH)D)) level that required for an optimal LS-BMD response (Calcif Tissue Int, 09). In this study, we have calculated the cut-off levels of s25(OH)D that induce the maximum increase in the LS-BMD by BPs using the Akaike information criterion (AIC) statistical criteria. A total of 75 postmenopausal Japanese osteoporotic women (avr. 70y of age) enrolled in this study. They were treated with BPs (either 35 mg/w alendronate or 17.5 mg/w risedronate). A total of 68 patients completed this study. The s25(OH)D were measured by a radioimmunoassay. The AIC statistics were defined by AIC = (-2)*log(maximum likelihood)+ 2*(number of parameter in the model), and have been widely used to compare different models with same data. A smaller AIC value indicated a more reliable model for predicting the outcome.

The s25(OH)D of the subjects at baseline was 21.7 ng/ml, and no significant difference in the s25(OH)D of the patients after 1y of BP treatment was observed in comparison to that seen at baseline. The LS-BMD after the BP treatment significantly increased by 6.3% (min; -6.9%, max; 26.2%). In the ranges of both 5 to 40 ng/ml of s25(OH)D and -6 to 26% of changes in LS-BMD in response to BPs, the smallest AIC value for the most appropriate cut-off levels of both the s25(OH)D and changes in LS-BMD in response to BPs were 28 ng/ml and 12%, respectively. More than the patients with s25(OH)D above 28 ng/ml increased in 12% or more changes of LS-BMD in response to BPs than did those lower than 28 ng/ml ($\chi 2=8.2$, $p<0.01$). The changes of urinary levels of NTx in response to BPs in the patients with s25(OH)D above 28 ng/ml (-59.9%) were significantly reduced in comparison to those lower than 28 ng/ml (-45.2%) ($p<0.01$).

In this study, the vitamin D cut-off levels for maximum increase in LS-BMD ($\geqslant$12%) with BP were calculated using AIC statistical criteria, suggesting that vitamin D may have some roles for the inhibition of bone resorption by BPs. In conclusion, the vitamin D is involved in the induction of a maximum increase in bone mass by BPs in osteoporotic women.

***Disclosures: Muneaki Ishijima**, None.*

MO0392

Zoledronic Acid Reduces Femoral Bone Loss Following Total Hip Arthroplasty. Dr. David Scott*[1], Jennifer Woltz[2], Christine Loiseau[2]. [1]Orthopaedic Specialty Clinic/ Spokane Joint Replacement Center, USA, [2]Spokane Joint Replacement Center, USA

Introduction: Significant proximal femoral remodeling occurs after total hip arthroplasty (THA), with regions of bone loss and hypertrophy. We evaluated the effect of zoledronic acid (ZOL) on femoral bone mineral density (BMD) for 2 yrs following primary uncemented THA. Methods: Fifty-one patients (mean age, 61.2 yrs; range, 33-84 yrs) participated in a prospective, blinded, randomized, placebo-controlled study. Exclusion criteria included osteoporosis, inflammatory arthritis, severe renal impairment, and medications that affect BMD. ZOL 5 mg intravenous infusion (n=27) or saline placebo (n=24) was administered at 2 weeks and 1 yr after surgery. Dual energy X-ray absorptiometry (DXA) scans of the 7 femoral region Gruen zones were performed preoperatively and 3-7 days, 6 weeks, 6 months, and 1 & 2 yrs postoperatively. Urine and serum markers of bone turnover were measured preoperatively and 6 weeks, 6 months, 1 yr, and 2 yrs postoperatively. 2-yr data were available for a subset of pts (ZOL, n=18; placebo, n=16). A single type of implant/articulation was used for all cases. Harris hip scores were recorded to assess post-arthroplasty pain and functionality. Results: There were no statistical differences in age, gender, or BMI between groups. BMD in Gruen zone 1 decreased 2.8% at 2 yrs in the placebo group, but increased 16.8% in the ZOL group ($P<.0001$, Wilcoxon/Kruskal-Wallis test). BMD in Gruen zone 7 decreased 25.5% at 2 yrs in the placebo group, but decreased 7% in the ZOL group ($P<.0001$). Urine N-telopeptide of type I collagen (NTX) was significantly reduced in the ZOL group vs. the placebo group at 6 weeks, 6 months, 1 yr, and 2 yrs ($P<.01$, ANOVA); serum bone-specific alkaline phosphatase was significantly reduced in the ZOL group vs. the placebo group at 6 and 12 months ($P<.05$). Harris hip scores were not statistically different between groups at 6 wks, 6 mos, 1 yr, or 2 yrs ($P<0.5$, $P<0.35$, $P<0.83$, $P<0.14$, respectively [chi-square test]). Conclusion: Percentage BMD loss at the proximal femur after cementless THA was significantly reduced with ZOL vs. placebo at 2 yrs. By preserving bone, ZOL has the potential to improve long-term outcomes in THA.

***Disclosures: Dr. David Scott**, None.*
This study received funding from: Novartis

MO0393

3-year Adherence to the Treatment of Osteoporosis in National Center of Osteoporosis in Poland. POMOST Study. Jerzy Przedlacki*, Krystyna Księżopolska-Orłowska, Artur Grodzki, Dorota Bartuszek, Tomasz Bartuszek, Andrzej Świrski, Jan Musiał, Ewa Loth, Paweł Teter, Andrzej Łasiewicki. National Center of Osteoporosis, Poland

Purpose: The purpose of the study was to assess the adherence to the pharmacological treatment of osteoporosis and to assess the possibility of its prediction at the beginning of treatment.

Methods: All 1189 patients (152 men and 1037 women) admitted the first time to National Center of Osteoporosis (KCO) during 1 year (2006/2007) were taken into consideration. Two hundred ten patients (21 M and 189 W) aged 69.0 ± 7.0 years were qualified for pharmacological treatment with antifracture medicines, mostly with oral bisphosphonates in weekly regime on the basis on our local qualitative method (excluding 229 patients already previously treated). Next, all of them were asked for the visits in KCO at least once a year. Other visits have taken place in Family Doctors Centers. Observation was done for 3 years. The persistence of treatment was assessed on the basis of real visits in KCO during 3 years and compliance on patients's oral information.

Results: After 1 year 178 patients (83.8%; 18 men and 160 women) have been continuing treatment, after 2 years 100 (47.6%; 10 M and 90 W), and after 3 years 78 (37.1%; 8 M and 70 W). Compliance was positive (>80% of taken medicines) in all patients visited our Center on the basis on patients information. The persistence of treatment was the same in men and women. There was not statistically important difference in persistence of treatment after 3 years when the following data were taken into consideration: age, presence of previous osteoporotic bone fracture, hip fracture in parents, smoking, alcohol abuse, chronic steroids treatment, the presence and number of concomitant chronic diseases. We asked all patients at the first visit, who was the initiator of referring them to our center to begin diagnostic procedures, their doctors (mostly primary) or patients themselves, but there was no difference also. The same results were obtained when all these data were evaluated after 2 years of treatment.

Conclusions: We were not able to predict the further adherence to pharmacological therapy of osteoporosis on the basis of any available clinical data at the begining of observation. The negative surprise was the lack of positive influence of patients willingness to begin the diagnostic procedures and the previous osteoporotic fractures on the adherence to therapy.

***Disclosures: Jerzy Przedlacki**, None.*

MO0394

Attitudes Toward Compliance of Patients Participating in a Randomized Controlled Trial. Deborah Gold*[1], Stuart Silverman[2], April Naegeli[3], Steven Watts[3], Russel Burge[3]. [1]Duke University Medical Center, USA, [2]Cedars-Sinai/UCLA, USA, [3]Eli Lilly & Company, USA

Community-dwelling individuals have low compliance and persistence with oral osteoporosis (OP) medications (Gold, et al. CMRO, 25:1831-9, 2009; Silverman, et al. So Med J, 100;1214-8, 2007). Due to frequent healthcare provider interactions, compliance and persistence to trial medications is usually better in randomized controlled trials (RCT) (Schmuely, et al. Maturitas, 46:33-44, 2003). Little is known about the underlying factors for compliance and persistence in osteoporosis RCT patients; therefore, we asked postmenopausal women participating in an RCT [teriparatide Fracture Prevention Trial (FPT)] about their attitudes toward compliance.

US FPT participants (n=478) were asked upon enrollment and at study end to complete an eight-question survey, the Attitudes Index (Callahan LF, J Rheum, 15:418-26, 1988). Five of the eight questions form a Learned Helplessness Scale; the remaining three are questions related to medication use. Study participants' demographics were: (mean) age, 71 years; 24 years postmenopausal; body mass index, 26.54 kg/m^2; 97% Caucasian. At baseline, 33.2% of individuals did not disagree or strongly disagree with the statement that concerned medicines cannot help. 38.5% did not disagree or strongly disagree with the statement that the side effects of medicines were worse than the disease. However, only 9.2% of the individuals reported that they often do not take medicines as directed. There were no significant changes between baseline and endpoint or between treatment groups. The Learned Helplessness Scale showed that 38% did not disagree or strongly disagree with the statement that their OP was controlling their life, 28% felt helpless, 17% were not coping effectively with their OP, and 37% felt factors beyond their control were affecting their condition. There was a trend ($p=0.09$) towards worsening of self-report of coping effectively with their condition between baseline and endpoint.

Although individuals in an RCT of an OP medication report having excellent compliance with medication, we find a large proportion have concerns about whether their medications can help them and whether medications side effects may be worse than their disease. Learned helplessness toward their diagnosis of OP is common in this population. Further research on patient attitudes and behaviors toward OP medications within RCTs may be useful in developing new methods to improve therapy compliance and persistence in RCTs and actual clinical practice.

***Disclosures: Deborah Gold**, Novartis, 2; Amgen, 8; Sanofi-Aventis, 5; Amgen, 5; Novartis, 5; Eli Lilly and Company, 8; Sanofi-Aventis, 8; Eli Lilly and Company, 5; Novartis, 8*
This study received funding from: Eli Lilly and Company

MO0395

Bone Density and Vitamin D Status in Liver Transplant Patients 10 Years After the First Assessment. Elena Segal*[1], Yaakov Baruch[2], Marina Nodelman[3], Sophia Ish-Shalom[4]. [1]Rambam Health Care Campus, Israel, [2]Liver Diseases Unit, Rambam Health Care Campus, Israel, [3]Bone Metabolic Diseases Unit, Rambam Health Care Campus, Israel, [4]Rambam Health Care Campus, Technion Faculty of Medicine, Israel

Osteoporosis represents a serious problem in liver transplant patients. Ten years ago we evaluated 29 liver transplant patients. Nineteen (65.5%) had decreased bone mass, 11 (37/8%) were osteoporotic, 28 (96.5%) had serum level of 25(OH)D<20 ng/ml, mean 12.52?3.19, mean PTH 59.67 ng/l?29.78. The patients received letters containing the diagnosis and treatment recommendations. Now we re-evaluated charts of 20 patients', 10 men, 10 women (postmenopausal), age 58.8?15.8. Fifteen fractures were reported following transplantation, 10 (75%) within the first year, none in the last ten years. Four (20%) patients were followed-up in the Bone Diseases Clinic, all received 600 mg of elemental calcium, 1200-1600 IU of vitamin D daily, and bisphosphonates. PTH levels ranged 29-71 ng/l, 25OHD levels- 24-42 ng/ml. Eleven patients (55%) received 600-1200 mg of elemental calcium, 400 IU of vitamin D daily. After sending letters to the family physicians with request to perform 25OHD and PTH levels and BMD tests, we received six PTH and seven 25OHD results, range 32-71 and 14-22 ng/ml, respectively. Mean PTH 56.11?48, p=0.68; mean 25OHD 28.97±8.62, p=0.003 compared with the first evaluation. Cocnclusion: osteoporosis in liver transplant patients in Israel is underdiagnosed and undertreated. Vitamin D supplementation might have some positive effect on patients' metabolic status.

***Disclosures: Elena Segal**, None.*

MO0396

Predicting Patient's Readiness to Accept Osteoporosis Treatment: Application of the Stages of Change Model to Post Fracture Context. Rebeka Sujic*[1], Dorcas Beaton[2], Morgan Slater[3], Earl Bogoch[1]. [1]St. Michael's Hospital, Canada, [2]Keenan Research Centre, St Michael's Hospital, Canada, [3]Mobility Program Clinical Research Unit, St. Michael's Hospital, Canada

Introduction: The Stages of Change model suggests that people move through five distinct stages of change (pre-contemplation, contemplation, preparation, action and maintenance) when adopting a new health behaviour such as treatment initiation. The purpose of this study is to examine whether this model is applicable to osteoporosis (OP) treatment initiation in a cohort of fragility fracture patients.

Methods: This prospective cohort study uses self-reported data collected as part of a provincial OP screening initiative targeting low trauma fracture patients over the age of 50. We examined the distribution of stages of change at baseline and follow up. Logistic regression was used to identify baseline factors associated with patients moving from the first stage at baseline to more advanced stages at follow up.

Results: At baseline, 93% (883/952) of patients were in the pre-contemplation stage. This first stage is characterized by a lack of awareness of OP and its treatment or a decision against the treatment. Of baseline pre-contemplators, 76% remained at the same stage at follow up, 2% moved to contemplation and preparation while 22% jumped to either action (stage in which a significant effort to change behaviour has been made within the previous six months) or maintenance (the most advanced stage in which patients sustained a behaviour change for a period of at least six months). Those who jumped from pre-contemplation to action or maintenance shared the following baseline characteristics: previous fracture OR 1.8 (1.2-2.7), history of oral steroid use OR 2.1(1.0- 4.1), higher perceived benefits to OP drug treatment OR 2.8 (1.2- 6.7), they were less likely to believe they were taking too many medications OR 0.6 (0.4- 0.9) and they were unsure whether OP caused their current fracture OR 2.0 (1.2-3.1).

Conclusion: The distribution of stages found in our sample suggests that the Stages of Change model may not be applicable to the initiation of OP treatment in post-fracture population: contrary to what the model would predict, most patients occupied the first stage while those who changed stages jumped from the first to the last two stages without occupying the middle stages. The fact that most patients stayed in the first stage points to the need for more patient education on OP and treatment risks and benefits. Modifiable factors that we identified as predictors of change could be used in post-fracture interventions to facilitate this change.

***Disclosures: Rebeka Sujic**, None.*

MO0397

Systematic Review on Interventions to Improve Osteoporosis Investigation and Treatment in Fragility Fracture Patients. Joanna Sale*, Dorcas Beaton, Joshua (Harry) Posen, Victoria Elliot-Gibson, Earl Bogoch. St. Michael's Hospital, Canada

Purpose: Initiatives to improve osteoporosis (OP) investigation and treatment in fracture patients have been identified worldwide. The purpose of this systematic review was to determine the outcomes of post-fracture initiatives regarding OP investigation and treatment with medication.

Methods: A systematic review was conducted in multiple databases up to September 2009 to identify relevant publications. Abstracts were read by two independent reviewers who selected articles for full-article review if they met inclusion criteria. Selected articles were reviewed by four teams of two researchers based on the following eligibility criteria: hip fracture plus all other fracture patients presenting with a fragility fracture; orthopaedic environment or setting where orthopaedic physicians/staff were involved; intervention aimed at improving access or care to initiate or maintain OP management; primary data on ⩾20 patients from randomized controlled trials (RCTs) and other observational studies. Data abstraction was conducted independently by two reviewers on all eligible articles. Outcome data within six months of screening were calculated from an intention-to-treat perspective to derive an equated proportion (EP) across interventions. Primary outcomes were: 1) proportion of patients investigated with bone densitometry; 2) proportion of patients initiating OP medication; 3) proportion of patients taking OP medication.

Results: We identified 2,259 citations; 422 of these were eligible for full-article review, of which 57 articles (54 studies that included 64 intervention groups) were eligible for data abstraction. Of the 54 studies, 10 were RCTs. The total number of patients enrolled per study ranged from 23-7713 in 11 countries. The EP for patients investigated ranged from 3-100%; the median was 43% and the 75th percentile was 71%. The EP for medication initiation ranged from 0-65%; the median was 22% and the 75th percentile was 34%. The EP for medication taking ranged from 0-83%; the median was 27.5% and the 75th percentile was 43%.

Conclusions: In the majority of interventions with an EP, up to 71% of patients were investigated, but <35% initiated medication, and <45% were taking medication within 6 months of screening. While we could not calculate an EP for all interventions, calculating an EP allowed us to compare outcomes across the studies, therefore capturing both RCTs and observational studies typical of real-world settings.

***Disclosures: Joanna Sale**, None.*

MO0398

Use of Bisphosphonates and Calcium/Vitamin D Supplementation Following Low Trauma Hip Fracture - How well are we doing? Yew-Xin Teh*[1], Gregor Freystaetter[2], Nitin Trivedi[1]. [1]Saint Vincent Hospital, USA, [2]St Vincent Hospital, USA

Purpose: Osteoporosis-related fractures carry a heavy economic burden. Hip fractures account for approximately 14% of osteoporotic fractures and 72% of fracture-related costs. Personal history of fragility fracture is a major risk factor for future fragility fractures. Treatment with bisphosphonates effectively reduces the risk of fragility fractures, particularly in high risk patients. Nonetheless, recognition and treatment of osteoporosis is often overlooked. We performed a retrospective chart review to assess the trends in pharmacological intervention with bone specific medication(s) in patients admitted with low-trauma hip fracture for surgical repair at a community-based hospital.

Methods: Charts of 86 patients with a diagnosis of low-trauma hip fracture, admitted between June 2009 and November 2009 were reviewed. Exclusion criteria included non-fragility fractures and fractures involving sites other than the hip.

Results: Females comprised 73% of the sample size. Ages ranged from 44 to 99 years, with 56% falling in the 80-89 years range. All patients were of Caucasian ethnicity except for one female who was of Asian Filipino origin. Forty one percent had a past history of fragility fracture. A total of 36 patients (42%) and 32 patients (37%) had a bone densitometry and vitamin D level respectively prior to this current hospitalization for hip fracture. Post-hip fracture, only 5 patients (6%) underwent a bone densitometry and 20 patients (23%) had a vitamin D level measured. Upon discharge from hospital, close to one third (29%) of our patients were not placed on any form of pharmacotherapy such as calcium, vitamin D, multivitamin or bisphosphonates. Only 8% of patients were discharged on a bisphosphonate, 30% on calcium, 31% on vitamin D and 61% on a multivitamin. Two patients were discharged on calcitonin nasal spray and 1 patient on raloxifene. Within 5 months of this study, 4 patients (5%) sustained a subsequent low-trauma fracture, and 17 patients (20%) died, out of which 12 were females.

Conclusions: Our study demonstrates low rates of evaluation and pharmacological intervention following low trauma hip fracture. This study suggests that there is still lack of awareness of osteoporosis among many health care providers. There exists an opportunity to educate health care providers on the importance of osteoporosis treatment, as well as implementation of a protocol to ensure adequate osteoporosis management following a fragility fracture.

***Disclosures: Yew-Xin Teh**, None.*

MO0399

Changes of Volumetric Bone Densities and 3D-Bone-Structures under Therapy with Raloxifene measured with HRpQCT. Maximilian Dambacher*[1], Maurus Neff[2], Radspieler Helmut[3]. [1]Metabolic Bone Diseases, Switzerland, [2]Osteoporosezentrum Zuerich, Switzerland, [3]Osteoporosezentrum Muenchen, Germany

Introduction: Data of the MORE-Study demonstrated that areal bone densities measured with DXA showed only a small increase which could not explain the reduction of vertebral fracture risk of at about 50%. Therefore, "bone quality" should be improved by raloxifene, which, however, cannot be evaluated by DXA-

measurements but with HRpQCT (XtremeCT, SCANCO Medical AG, Zurich). In 2008 we started a prospective study to demonstrate the effects on volumetric trabecular and cortical bone densities and on microarchitectural parameters (bone quality) in postmenopausal osteoporotic and osteopenic women, taking raloxifene.

Methods: Altogether we included more than 40 postmenopausal osteoporotic and osteopenic women taking raloxifen in this trial until now. After a baseline measurement with HRpQCT two control measurements after one and after two years are planned or already done. Furthermore, in about one half of the patients measurements of bone markers (beta-crosslaps, bone specific alkaline phosphatase, calcium, vitamin D and parathyroid hormone) in the blood before starting therapy and after 3 to 6 month are planned or have taken place already. Until now, data of 15 paients for HRpQCT measurements and laboratory results of more than 15 patients are available. Additionally to raloxifene all patients receive individual dosage of calcium and vitamin D, depending of the individual vitamin-D blood levels.

Results: After the first control measurement we find a significant increase in volumetric trabecular bone densities up to 6% resp. 2,9% in cortical bone. Furthermore, we found significantly improvements in microarchitectural parameters like BV/TV, trabecular number, trabecular thickness and cortical thickness. Bone markers showed significant decreases in all patients as expected, vitamin D leves grew up in all patients.

Summary: As shown already in a retrospective trial, under raloxifene we found not only a significant increase in volumetric trabecular and cortical bone densities but also an improvement of microarchitectural parameters (bone quality) in this prospective trial, which is still ongoing. Furthermore, we could demonstrate even clearly visible improvements in 3D-bone-imaging after therapy with raloxifene.

***Disclosures: Maximilian Dambacher**, None.*

MO0400

Determinants of Health-Related Quality of Life (HRQoL) in Postmenopausal Women Receiving or Initiating Bone Loss Medications: POSSIBLE EU® and POSSIBLE US™. Nick Freemantle*[1], Francis Guillemin[2], Luc Martinez[3], Melanie Calvert[1], Cyrus Cooper[4], Ted Ganiats[5], Matthew Gitlin[6], Rob Horne[7], Anne Marciniak[8], Johannes Pfeilschifter[9], Susan Shepherd[8], Sally Wade[10], Anna Tosteson[11]. [1]University of Birmingham, United Kingdom, [2]Nancy University, EA 4360 Apemac, France, [3]Société Française de Médecine Générale, France, [4]University of Southampton, United Kingdom, [5]University of California San Diego School of Medicine, USA, [6]Amgen (Europe) GmbH, Zug, Switzerland, [7]School of Pharmacy, University of London, United Kingdom, [8]Amgen Ltd, United Kingdom, [9]Alfried Krupp Krankenhaus, Germany, [10]Wade Outcomes Research & Consulting, USA, [11]Dartmouth Medical School, USA

Purpose

The POSSIBLE EU® and POSSIBLE US™ studies are prospective, observational studies describing the characteristics and management of postmenopausal women receiving bone loss medication in the European Union (France, Germany, Italy, Spain and the UK; N=3402) and in the United States (N=4994), respectively. This analysis of baseline data evaluates the association between patient characteristics and HRQoL.

Methods

Clinical and health utility data (including health utility measured by EQ-5D[1] and fear of falling from the OPAQ[2] scale) were available from 7897 patients (94%) continuing (treated ⩾1 year), initiating (not treated for ⩾1 year) or switching (treated ⩾1 year and changed at enrollment) bone loss medication at baseline. We developed parsimonious multivariable mixed models, using a prespecified list of patient characteristics at baseline (N=34; including age, BMI, prior fractures, bone loss and concomitant medications, comorbidities and fear of falling), to identify important determinants of health utility score.

Results

At baseline, median age (Q1, Q3) was 65 (57, 73) years. A total of 538 patients (6.8%) had a prevalent vertebral fracture and many patients (6477 [82%]) had ongoing comorbid conditions. Median EQ-5D health utility score was 0.796, but varied substantially (-0.594 [a score of worse than death] to 1.0 [the score denoting optimal health]). In our model, any prior vertebral fracture, number of ongoing comorbid conditions, fear of falling, higher BMI, ongoing depression and patients who initiated or switched treatments at baseline were found to have significantly lower health utility scores.

Conclusions

Combined data from these two large observational studies showed that a prior vertebral fracture, number of comorbid conditions, and fear of falling were key factors associated with significantly lower HRQoL among women receiving or initiating bone loss medications.

1. Brooks R. Health Policy. 1996;37:53-72.
2. Silverman SL. Qual Life Res. 2000;9:767-774.

***Disclosures: Nick Freemantle**, Amgen, 2; Amgen, Eli Lilly, Pfizer, Sanofi-Aventis, 5 This study received funding from: Amgen*

MO0401

Direct Medical Costs Attributable to Peripheral Fractures in Postmenopausal Women. Louis Bessette*[1], Sonia Jean[2], Marie-Pierre Lapointe-Garant[3], Etienne Belzile[1], K. Shawn Davison[3], Louis-Georges Ste-Marie[4], Jacques Brown[1]. [1]Laval University, Canada, [2]Institut National De Sante Publique, Canada, [3]Centre de recherche du CHUQ, Canada, [4]Hospital Saint-LucCHUM, Canada

Purpose: To obtain Canadian-specific data regarding the direct medical cost of peripheral osteoporotic fracture treatment.

Methods: Based on a validated algorithm, 15,827 women ⩾50 years old with incident fractures of an osteoporotic site were identified from health administrative databases (2004 through 2005) of the province of Quebec, Canada. Fractures were grouped as occurring at the hip, wrist or another osteoporotic site. To establish fracture-related costs for each fracture case, health resource use in the year following the fracture was identified in physicians' fee-for-service claims (RAMQ)) and hospital discharge (Med-Echo) databases. Data were linked by a unique personal identifier creating a longitudinal cohort of health resource utilization for all fracture cases. The one-year post-fracture direct cost was calculated for each fracture case selected, which included: total cost of physician claims (visit and procedure claims), total cost of hospital use associated with physicians' visits to emergency rooms and outpatient clinics (staff and hospital support at the emergency room (ER) and outpatient clinics (OC)), and total cost of hospital stay. Costs of hospitalization for complications post-fracture were not included. Preliminary analyses are presented below.

Results: The table provides the fracture incidence per site, the mean patient age, and the mean direct medical cost of treatment for each fracture site grouping (in 2009 $CAN). At least one hospitalization directly related to the fracture was reported for 89.5% of the hip fractures; for 31.3% of the wrist fractures, and for 27.8% of fractures of other sites in the year following the fracture.

Conclusions: The direct medical costs associated with peripheral fracture are considerable. Although hip fractures are associated with the highest economic burden, other peripheral fractures account for a significant portion of the total direct medical costs for the treatment of osteoporotic fracture.

	Hip fracture (n = 4,536)	Wrist fracture (n = 3,157)	Other fracture (n = 8,134)
Mean patient age in y (± SD)	80.7 (10.1)	69.1 (11.6)	68.4 (11.8)
Mean cost related to physician claims (± SD)	$1,091 (497)	$306 (200)	$326 (374)
Mean cost related to ER and OC (± SD)[a]	$426 (291)	$657 (357)	$573 (347)
Mean cost related to hospitalization[b] with a principal or secondary diagnosis of fracture at the same site in the year[a] following fracture (± SD)	$41,441 (39,847)	$4,011 (18,227)	$8,530 (24,521)

[a] Unit of price related to hospital use and hospital stay are based on the *Ontario hospital corporate costing model* but will be changed when the unit price for Québec is available.
[b]These preliminary results include costs for direct hospitalization but do not include costs for re-hospitalization associated to post-fracture complications.

Treatment cost of fractures by site

***Disclosures: Louis Bessette**, Amgen, 8; Abbott, 2; Abbott, 5; Amgen, 5; Warner Chilcott, 8; Eli Lilly, 2; Merck, 2; Amgen, 2; Novartis, 8; Pfizer, 5; Novartis, 5; Roche, 5; Roche, 2; Merck, 8; Roche, 8; Bristol-Myers-Squibb, 2; Merck, 5; Pfizer, 8; Pfizer, 2 This study received funding from: Warner Chilcott, sanofi-aventis, Merck, Amgen, Novartis, Eli Lilly*

MO0402

Fractures in Commercial and Medicare Patients Treated with Raloxifene or Alendronate: A Retrospective Database Analysis. Shonda Foster*[1], Suellen Curkendall[2], Nianwen Shi[2], John Stock[1], Bong-Chul Chu[2], Russel Burge[1], David Diakun[2], John Krege[1]. [1]Eli Lilly & Company, USA, [2]Thomson Reuters, USA

The purpose of this study was to evaluate fracture rates in a commercial/Medicare population treated with raloxifene (RLX) or alendronate (ALN). Female beneficiaries (45 years and older) with claims for RLX or ALN between January 1998 to December 2006 were identified in the Thomson Reuters MarketScan® Commercial and Medicare Claims Databases. Members with continuous enrollment 12 months prior to and at least 12 months after the treatment initiation date who were adherent (medication possession ratio 80% or greater) to therapy were included. Six cohorts were identified based on the number of years of adherent therapy: 1 year (RLX [N= 23,243], ALN [N=72,055]); 3 years (RLX [N= 9,758], ALN [N=24,221]); 5 years (RLX [N=3,141], ALN [N=6,652]); 6 years (RLX [N=1,246], ALN [N=2,465]); 7 years (RLX [N=650], ALN [N=1,053]); and 8 years (RLX [N=217], ALN [N=331]). Propensity weights were calculated based on demographic and clinical variables such as age, health status, confounding medical conditions and medications, and pre-index fractures to adjust for imbalances between treatments. Marginal proportional hazards models were used

to assess the relative risk of nonvertebral fractures, and standard Cox models were used to obtain the relative risk of vertebral fractures in 3 years of adherent treatment with RLX compared with ALN. There were no statistically significant differences in the percentage of patients with vertebral fractures after propensity weighting between RLX and ALN in any of the cohorts. There was a significant difference in the percentage of patients with nonvertebral fractures in the 3-year cohort after propensity weighting (7.3% RLX vs. 6.7% ALN, p=0.034), with no significant differences in the other cohorts. Multivariate models showed no difference in the relative risk of vertebral or nonvertebral fractures in the 3-year cohort. In summary, the occurrence of propensity-weighted vertebral fractures was not significantly different between RLX and ALN in any of the cohorts. Also, propensity-weighted nonvertebral fractures were not significantly different in any of the cohorts with the exception of a lower rate of nonvertebral fractures with ALN versus RLX in the 3-year cohort; this difference was not observed in the 3-year multivariate analysis. In conclusion, patients treated with ALN and RLX had similar propensity-weighted fracture rates in up to 8 years of retrospective database claims.

***Disclosures: Shonda Foster**, Eli Lilly and Company, 3*
This study received funding from: Eli Lilly and Company

MO0403

Health Services Utilization after Fractures: Recent Evidence from Medicare.
David Becker*[1], Huifeng Yun[2], Meredith Kilgore[3], Jeffrey Curtis[1], Elizabeth Delzell[1], Lisa Gary[1], Kenneth Saag[1], Michael Morrisey[1]. [1]University of Alabama at Birmingham, USA, [2]Univiersity of Alabama at Birmingham, USA, [3]University of Alabama At Birmingham School of Public Health, USA

Purpose: Osteoporosis related fractures impose a large and growing societal burden, including adverse health effects and direct medical costs. This study estimates the incremental health services utilization associated with these fractures.

Methods: We use a 5% random sample of Medicare claims data to construct annual cohorts (2000-2004) of beneficiaries diagnosed with incident fractures at one of seven sites – clinical vertebral, hip pelvis, femur, tibia/fibula, humerus and distal radius/ulna. We use person-specific changes in health services utilization (e.g. inpatient acute/post-acute days, home health visits, physical and occupational therapy) before/after fractures and probabilities of entry into (long-term) nursing home residency to estimate the utilization burden associated with fractures.

Results: (Please see attached table)

Relative to the prior six-month period, rates of acute hospitalization are between 19.5 (distal radius/ulna) and 72.4 (hip) percentage points higher in the six months after fractures. Average acute inpatient days are 1.9 (distal radius/ulna) to 8.7 (hip) higher in the post-fracture period. Fractures are associated with large increases in all forms of post-acute care, including rates of post-acute hospitalizations (13.1-71.5 percentage points), post-acute inpatient days (6.1-31.4), home health care hours (3.4-8.4), and hours of physical (5.2-23.6) and occupational (4.3-14.0) therapy. Among patients who were community dwelling at the time of the initial fracture, 0.9-1.1% (2.4-4.0%) were living in a nursing home six months (1-year) after the fracture.

Conclusions: Fractures are associated with significant increases in health services utilization relative to pre-fracture levels. Additional research is needed to assess the determinants and effectiveness of alternative forms of fracture care.

Key Words: Medicare, fractures, osteoporosis, utilization

Results:

Change in Utilization in the 6 Months After (vs Before) Incident Fracture by Site (2000-2004)

	Clinical Vertebral	Hip	Pelvis	Femur	Tibia/ Fibula	Humerus	Distal Radius/ Ulna
Acute inpatient stay, %	29.0	72.4	62.6	55.2	47.4	42.5	19.5
Post-acute inpatient stay, %	24.3	71.5	58.5	57.1	39.6	30.2	13.1
Home health care, %	14.5	30.8	28.2	26.1	24.8	21.7	12.1
Acute inpatient days	3.7 (11.5)	8.7 (11.3)	7.1 (11.7)	7.6 (13.3)	5.3 (11.4)	4.6 (10.6)	1.9 (7.6)
Post-acute inpatient days (total)	9.5(29.5)	31.4(42.5)	23.5(37.4)	30.4(40.2)	19.9(39.9)	14.4(33.3)	6.1(27.0)
Home health care hours (total)	3.5(27.1)	8.3(61.4)	6.4(29.2)	7.8(32.2)	6.6(25.9)	6.1(23.4)	3.7(61.0)
Physician visits (total)	1.0 (5.8)	1.2 (6.3)	1.1 (6.0)	1.3 (6.8)	1.8 (5.7)	1.5 (5.6)	1.3 (4.6)
Outpatient visits	0.6 (4.5)	0.8 (4.9)	0.3 (4.6)	0.9 (5.3)	1.0 (4.7)	1.2 (4.7)	1.2 (4.0)
Physical therapy, hours	6.8 (31.5)	23.6(49.0)	17.1(36.9)	23.1(102)	14.9(39.1)	12.5(31.4)	5.2 (28.2)
Occupational therapy, hours	4.3 (25.1)	14.0(38.6)	10.9(32.0)	12.6(37.2)	8.5 (33.3)	9.2 (29.7)	5.0 (23.5)
N	36,458	50,778	10,379	6,154	5,306	16,160	20,373

Notes: We report unconditional means of each category of utilization (i.e. based upon full sample with and without utilization of given type of service). Standard deviations are reported in parentheses.

Results Table

***Disclosures: David Becker**, Amgen, Inc., 2*
This study received funding from: Amgen, Inc.

MO0404

Incremental Cost of Osteoporosis-related Fractures in a Large U.S. Managed Care Population.
H Viswanathan[1], J White[2], SW Wade*[3], J Yu[4], JR Curtis[5], B Stolshek[1], C Merinar[1], J Kallich[1], A Balasubramanian[1], J Adams[6]. [1]Amgen Inc, USA, [2]Wellpoint Inc., USA, [3]Wade Outcomes Research & Consulting, USA, [4]HealthCore, USA, [5]University of Alabama at Birmingham, USA, [6]RAND Corp, USA

Purpose: While incremental or attributable costs of osteoporosis (OP)-related fracture have been reported, data on the economic impact of OP-related fractures in commercial health plan populations are limited. The objective of this study was to quantify the incremental cost of OP-related fractures in a large U.S. managed care population between 2004 and 2008.

Methods: Patients were identified from a large, commercially-insured population with integrated pharmacy and medical claims. Patients were included if they were age 45-64 years, new to OP therapy (no OP medication claims in prior year) with the first (index) OP medication claim between 1/1/2005 and 4/30/2008, and had continuous coverage for 12 months pre-index. Patients were excluded if they had: pre-index Paget's disease or malignant neoplasm, were in a skilled nursing facility or on combination therapy at index, or had a fracture ≤ 6 months post-index. Clinically-diagnosed and coded fractures were identified using published claims criteria; total direct costs were assessed in the 6 months pre- and post-fracture event date. Event dates were assigned to patients with no fracture; propensity score weighting was used to increase comparability of fracture and non-fracture patients. A generalized linear model was used to compare differences in 6 month pre-/post-event cost for patients with fracture and those without fracture. Covariates included demographics, prior fracture, comorbidities, and other potential confounders. Generalized estimating equations methods were used to account for repeated measures.

Results: The sample included 49,680 patients (2,613 with fracture) with a mean (± SD) age of 56.4 ± 4.7 years; 95.9% were female. Mean unadjusted total costs showed minor variation in the 6 months pre-event vs post-event for non-fracture patients. Mean pre-/post-event cost differences were substantially larger for patients with vertebral, hip, or non-hip, non-vertebral fractures (Table). After adjusting for covariates, OP-related fractures increased the direct health care costs by an estimated $9,996 (95% CI: $8,838, $11,154, $p<0.0001$) per patient across all fracture types during the 6 months immediately after the fracture.

Conclusion: On average, patients with an OP-related fracture incurred nearly $10k in additional health care costs in the 6 months post-fracture, compared to patients with no fracture. Efforts to reduce fracture risk may ultimately lower associated direct health care costs.

Table: Unadjusted Mean Total Direct Costs Per Patient*

	Patients With:			
	Vertebral Fracture	Hip Fracture	Other Fracture	No Fracture
6 Months Pre-Event	$12,955 $8,617, $17,293	$8,195 $5,912, $10,478	$5,599 $5,085, $6,112	$3,354 $3,272, $3,436
6 Months Post-Event	$27,004 $21,339, $32,668	$24,857 $19,893, $29,823	$13,181 $12,043, $14,319	$3,372 $3,285, $3,460
Post-Event Minus Pre-Event (Difference)	$14,049 $7,670, $20,428	$16,663 $11,690, $21,636	$7,582 $6,532, $8,632	$18 $-60, $96

*Values are means and 95% confidence intervals

Table

***Disclosures: SW Wade**, Amgen Inc., 1; Amgen Inc., 3*
This study received funding from: Amgen Inc.

MO0405

Denosumab Administration is Not Associated With Fracture Healing Complications in Postmenopausal Women With Osteoporosis: Results From the FREEDOM Trial.
Silvano Adami*[1], Cesar Libanati[2], Jonathan Adachi[3], Steven Boonen[4], Steven Cummings[5], Luiz de Gregorio[6], Nigel Gilchrist[7], George Lyritis[8], Gerd Moeller[9], Santiago Palacios[10], Karel Pavelka[11], Heinrich Resch[12], Christian Roux[13], Daniel Uebelhart[14], Andrea Wang[2], Ethel Siris[15]. [1]University of Verona, Italy, [2]Amgen Inc, USA, [3]St. Joseph's Hospital, Canada, [4]Center for Metabolic Bone Disease, Belgium, [5]San Francisco Coordinating Center, USA, [6]Center for Clinical & Basic Research, Brazil, [7]CGM Research Trust, New zealand, [8]University of Athens, Greece, [9]Amgen (Europe) GmbH, Switzerland, [10]Instituto Palacios, Salud y Medicina de la Mujer, Spain, [11]Institute of Rheumatology, Charles University Prague, Czech republic, [12]Medical University Vienna, Austria, [13]Hospital Cochin, France, [14]University Hospital of Zurich, Switzerland, [15]Columbia University College of Physicians & Surgeons, USA

Aims:

A fracture occurrence provides a window of opportunity to intervene in patients with osteoporosis. However, concerns about potential complications of fracture

healing may be a barrier to the timely initiation of therapy at the time of fracture. In the FREEDOM trial, denosumab (DMAb), a fully human MAb against RANKL, significantly reduced the risk of new vertebral, hip and nonvertebral fractures compared with placebo over 3 years in women with osteoporosis (Cummings NEJM 2009;361:756). In this prespecified analysis, we report all complications associated with the management or healing of nonvertebral fractures.

Methods:

FREEDOM was a 3-year, randomized, double-blinded trial in postmenopausal women aged 60–90 years with low BMD. Women were assigned to receive SC DMAb 60mg SC every 6 months or placebo, and daily elemental calcium and vitamin D. Nonvertebral fractures were radiologically confirmed. Complications associated with the management or healing of each nonvertebral fracture were reported by the investigator on specific case report forms. Delayed healing was defined as fracture healing not completed within 6 months post fracture. We also evaluated fracture healing complications as a function of time from DMAb administration.

Results:

A total of 851 nonvertebral fractures (465 placebo, 386 DMAb) in 667 subjects were documented in FREEDOM. 120 fractures (26%) in the placebo group and 79 (21%) in the DMAb group underwent surgical intervention. Among patients with a nonvertebral fracture, complications associated with the fracture or surgical management of the fracture occurred in 5.5% of placebo subjects and 1.7% of DMAb subjects ($p<0.01$) (table). Fracture occurrences were evenly distributed throughout the 6-monthly dosing intervals. Overall, there were 6 reports of delayed union (4 placebo, 2 DMAb) and one non-union case (placebo) (table). No complications associated with delayed healing/non-union were reported for any of the non-vertebral fracture cases (n=115) where DMAb was administered within 4 weeks before or after fracture occurrence.

Conclusions:

Over 3 years, compared with placebo, DMAb significantly reduced the risk of nonvertebral and hip fractures without an increased rate of fracture healing complications, regardless of time of administration. DMAb provides an opportunity to safely and conveniently address osteoporosis treatment needs before and after fracture occurrence.

Subject incidence of complications associated with delayed healing, fracture or surgical management of fracture

	Placebo (N = 364)	DMAb 60 mg Q6M (N = 303)
Number of subjects with delayed healing	5* (1.4%)	2 (0.7%)
Number of subjects with complications associated with fracture or surgical management	20 (5.5%)	5 (1.7%)
Other†	14 (3.8%)	4 (1.3%)
Infection	3 (0.8%)	1 (0.3%)
Thromboembolic events	0 (0%)	1 (0.3%)
Avascular necrosis	2 (0.5%)	0 (0%)
Neurologic and vascular injury	1 (0.3%)	0 (0%)
Posttraumatic arthritis	1 (0.3%)	0 (0%)

N = number of subjects who received ≥1 dose of placebo or DMAb and experienced a nonvertebral fracture regardless of trauma severity and location

*One case was nonunion.

†Other includes reduced mobility, pain, ulcer, pneumonia, carpal tunnel syndrome, tachycardia, bedsore, dislocation of bone and anemia.

Table

***Disclosures: Silvano Adami**, Merck, Amgen, Roche GSK, 5; Amgen, Roche, Merck, Eli Lilly, 8*

This study received funding from: Amgen Inc.

MO0406

Effect of 24-week Green Tea Polyphenols Supplementation and Tai Chi Exercise on Bone Biomarkers in Postmenopausal Osteopenic Women.

Chwan-Li Shen*[1], Ming-Chien Chyu[2], James K Yeh[3], Yan Zhang[4], Barbara C Pence[4], Carol K Felton[4], Raul Y Dagda[4], Susan Doctolero[4], Jia-Sheng Wang[5]. [1]Texas Technology University Health Sciences Center, USA, [2]Texas Tech University, USA, [3]Winthrop-University Hospital, USA, [4]Texas Tech University Health Sciences Center, USA, [5]University of Georgia, USA

Osteoporosis is a major health problem in postmenopausal women. We have demonstrated supplementation of green tea polyphenols (GTP) in drinking water increase bone formation biomarker in ovariectomized middle-aged female rats. The objective of this study was to examine if 24 weeks consumption of GTP along with Tai Chi exercise (TC) exerts beneficial effects on bone turnover biomarkers in postmenopausal women with low bone mass. 171 postmenopausal women with osteopenia (57.4 yr, BMI 28.4 kg/m2) were recruited and randomly assigned to 4 treatments groups: placebo (500 mg starch/day), GTP (500 mg GTP/day), placebo+TC (60 min TC/session, 3 times per week), and GTP+TC for 24 weeks. Fasting serum samples were analyzed for bone-specific alkaline phosphatase (BAP, bone formation biomarker) and tartrate resistant acid phosphatase (TRAP, bone resorption biomarker) at baseline, 4, 12, and 24 weeks. After 24 weeks intervention, 21 participants dropped out (12% attrition rate) due to loss of interest or any other condition unrelated to the study protocols. The compliance rates for GTP pills and TC exercise were 89% and 83%, respectively. ANOVAs were applied to examine the difference of the outcomes among the groups and that of over time. At the baseline, there were no differences in any demographic parameters and bone biomarkers among 4 treatment groups. GTP supplementation significantly increased BAP after 4 weeks ($F=4.396$, $P < 0.05$), while TC exercise significantly enhanced BAP after 12 weeks ($F=4.150$, $P < 0.05$). After 24 weeks, the order of BAP was GTP+TC > GTP = placebo+TC > placebo. However, neither GTP supplementation nor TC exercise affected TRAP throughout the study period. This clinical trial demonstrated that 24 weeks GTP supplementation and TC exercise positively modulated bone formation biomarker in postmenopausal women with low bone mass. Study was supported by NCCAM/NIH 1R21AT003735-01A1 (CLS).

***Disclosures: Chwan-Li Shen**, None.*

MO0407

Effects of Low Dose Calcium and Vitamin D Supplementation on Bone Density and Structure Measured In Vivo by CT at the Distal Tibia in Postmenopausal Women with Osteopenia or Mild Osteoporosis.

Hendrikje Börst[1], Oliver Bock*[2], Gisela Beller[1], Martina Kratzsch[1], Heike Profittlich[1], Marlies Kalbow[1], Ralf Legler[1], Gabriele Armbrecht[3], Peter Martus[4], Dieter Felsenberg[2]. [1]Charité - Universitätsmedizin Berlin, Campus Benjamin Franklin, Germany, [2]Charité - Campus Benjamin Franklin, Germany, [3]Centre of Muscle & Bone Research, Charite-CBF, Germany, [4]Charite University Medicine, Germany

Objectives: To examine in vivo the effect of low dose supplementation of calcium 500 mg and vitamin D 400 IU daily on bone density and structure at distal tibia in postmenopausal women with osteopenia or mild osteoporosis.

Patients and Methods: 68 postmenopausal women with low bone mass and without prevalent vertebral fractures were equally randomized into a mono-centric, placebo-controlled, double-blind study of one year (SPIMOS-3D). All patients received calcium 500 mg and vitamin D3 400 IU daily (CaD). Bone density and structure were measured in vivo by µCT (XtremeCT, Scanco Medicals) at the distal tibia (DT). These are the results of a post-hoc analysis of the placebo group only (n = 33; mean age 68.6 ± 3.2 years; mean T-score of DXA-BMD at lumbar spine and total hip -2.47 ± 0.47 and -0.86 ± 0.75 SD, respectively) showing the effects of calcium and vitamin D alone on the above mentioned parameters. µCT values at baseline and after one year of treatment were available for 29 patients in this group.

Results: Over the one year treatment period, there was a significant increase of tBV/TV by 1.21% ($p=0.002$) and a reduction of tTbSp by -6.94% ($p<0.001$) in the placebo (calcium and vitamin D only) group as compared to baseline. In addition, there was also a significant change in other parameters possibly relevant for bone strength at the distal tibia (table).

Serum bone turnover markers as CTx and P1NP showed significant changes in accordance to those of the µCT parameters. CTx decreased by 16.78% ($p=0.006$), P1NP increased by 8.68% ($p=0.048$) as compared to baseline. On the other hand no significant changes could be detected in DXA BMD measurements at lumbar spine and total hip (+0.16% and +0.24%; $p=0.755$ and 0.569, respectively).

Conclusions: After one year of low dose calcium and vitamin D supplementation, bone density and structure as measured by µCT at the distal tibia, but not DXA BMD at lumbar spine and total hip, show significant changes in postmenopausal women with low bone mass. Further analysis is needed in order to explain the study outcome. For the purpose of a deeper understandig of treatment effects on bone, DXA can not be considered to be a viable measurement.

parameters of bone density and structure	baseline (mean values)	12 months (mean values)	changes (%)	*p* values
Trab. Bone Volume to Tissue Volume (**tBV/TV [1]**)	0.1153	0.1167	1.214	**0.002**
Trabecular Separation (**tTbSp [mm]**)	0.5981	0.5568	-6.939	**< 0.001**
Cortical Area (**CortArea [mm²]**)	80.3276	82.8207	3.104	**< 0.001**
Trabecular Area (**TrabArea [mm²]**)	594.9882	593.2310	-0.295	**< 0.001**
Cortical Bone Density (**Dcomp [mg HA/ccm]**)	773.2000	770.2241	-0.385	0.220
Trabecular Bone Density (**Dtrab [mg HA/ccm]**)	138.2552	140.0552	1.302	**0.001**
Cortical Thickness (**CtTh [mm]**)	0.7824	0.8069	3.131	**< 0.001**
Cortical, Periosteal Perimeter (**CtPm [mm]**)	103.7828	103.6414	-0.136	0.104
Number of Trabeculae (**tTbN [1/mm]**)	1.5179	1.6352	7.728	**< 0.001**
Trabecular Thickness (**tTbTh [mm]**)	0.0758	0.0714	-5.805	**< 0.001**

table

***Disclosures: Oliver Bock**, None.*

This study received funding from: Roche Pharma

MO0408

Efficacy and Safety of Oral Salmon Calcitonin in Postmenopausal Osteoporosis: Randomized, Double-Blind, Placebo-Controlled Trial. Luis Augusto Russo[1], Edith Lau[2], Hai Tang[3], Milos Rajman[4], Christence Teglbjarg[5], Hans Christian Hoeck[5], Peter Alexandersen[6], Ivo Valter[7], Roland Chapurlat[8], Maria Luisa Brandi[9], Zydrune Visockiene[10], Henry G Bone[11], Michael McClung[12], Markus John[13], Juergen Loeffler[13], Michel Arnold[13], Bente Juel Riis[14], Moise Azria[13], Claus Christiansen*[14]. [1]Center for Clinical & Basic Research, Brazil, [2]Hong Kong Orthopaedic & Osteoporosis Center for Treatment & Research, Hong kong, [3]Beijing Friendship hospital, China, [4]Center for Clinical & Basic Research, Czech republic, [5]Center for Clinical & Basic Research, Denmark, [6]Center for Clinical & Basic Research A/S, Denmark, [7]Center for Clinical & Basic Research, Estonia, [8]E. Herriot Hospital, France, [9]University of Florence, Italy, [10]Center for Clinical & Basic Research, Lithuania, [11]Michigan Bone & Mineral Clinic, USA, [12]Oregon Osteoporosis Center, USA, [13]Novartis Pharma AG, Switzerland, [14]Nordic Bioscience A/S, Denmark

Purpose: Postmenopausal osteoporosis is a systemic skeletal disease characterized by low bone mass and micro-architectural deterioration with a subsequent increase in bone fragility and susceptibility to fractures. Calcitonin (CT), a natural hormone secreted by the parafollicular cells of the thyroid gland, is a potential therapeutic agent for osteoporosis due to its anti-resorptive effects on bone and analgesic properties. As long-term administration of subcutaneous and intranasal salmon CT (sCT) is hampered by local irritation and administration difficulties, a convenient oral formulation of sCT using a 5-CNAC carrier (based on Eligen® technology from Emisphere) was developed. The objective of this study is to evaluate the efficacy and safety of oral sCT in the treatment of osteoporosis in postmenopausal women also taking calcium and vitamin D.

Methods: A total of 4500 postmenopausal women with osteoporosis (aged 55–85 years) were planned to be enrolled in this multi-center, double-blind, placebo-controlled study. The subjects received (1:1) oral sCT 0.8 mg daily or placebo, both along with vitamin D (400 to 800 IU) and calcium (800 to 1000 mg) for 36 months. Inclusion criteria were BMD T-score ≤–2.5 at lumbar spine (LS), femoral neck (FN) or total hip (TH) or a T-score ≤ –1.5 at LS, FN or TH along with osteoporotic fracture(s) located at the spine. Primary endpoint is the number of patients with new vertebral fractures. Secondary endpoint is the number of patients with non-vertebral fractures (including hip). Safety is assessed by adverse event incidence and changes in laboratory profiles including antibodies, which is monitored by an independent Data Monitoring Committee (DMC). After interim analysis of 12 month efficacy and safety data for futility, the DMC concluded not to recommend discontinuation of the study. Final analysis of all efficacy endpoints will be done after 36 months.

Results: This ongoing trial has completed recruitment of 4665 postmenopausal women with osteoporosis (age 66.7 ± 6.14 years, BMI: 26.1 ± 4.16; Baseline T-score: <-2.5) randomized at 16 study sites in 12 countries till 16 June 2008. Study results will be available in late 2011.

Conclusions: This is a Phase III, randomized, placebo-controlled trial to demonstrate the efficacy and safety of oral sCT plus calcium and vitamin D compared with calcium and vitamin D alone to reduce the incidence of new vertebral and non-vertebral fractures in postmenopausal women with osteoporosis.

***Disclosures: Claus Christiansen**, None.*
This study received funding from: Novartis Pharma AG, Basel, Switzerland

MO0409

Safety and Effectiveness Profile of Raloxifene in Long-term, Prospective, Observational Study (Final Report). Etsuro Hamaya*[1], Noriko Iikuni[2], Shigeru Nihojima[3], Shunji Yokoyama[3], Wakana Goto[2], Masanori Taketsuna[2], Akimitsu Miyauchi[4], Hideaki Sowa[5]. [1]Eli Lillly Japan KK, Japan, [2]Eli Lilly Japan KK, Japan, [3]Chugai Pharmaceutical Co., Ltd., Japan, [4]Omura municipal Hospital, Japan, [5]Eli Lilly Japan K.K., Japan

This large-scale postmarketing surveillance of raloxifene (60 mg/day) was conducted to assess the safety of raloxifene in Japanese postmenopausal osteoporosis patients in long-term practical use (three years). The baseline examination included 6967 patients (mean age 70.4 years). The subject completed observation after 6, 12, 24, and 36 month of therapy. The persistence rate after three-year treatment of raloxifene was 42.3%. Adverse drug reactions were reported in 776 patients (11.14%). A total of 87 serious adverse drug reaction cases occurred in 76 patients (1.09%). Most frequent adverse drug reactions were peripheral oedema (45/6967, 0.65%), followed by abdominal discomfort (39/6967, 0.56%). Eleven patients (0.16%) of venous thromboembolism (VTE) were reported. There were no specific adverse drug reactions seen in this study compared with the clinical trial in Japan. We also assessed effectiveness of raloxifene in this study. Of 6967 patients, 2784 patients were included for effectiveness analysis. Lumbar spine bone mineral density (BMD) increased significantly ($p<0.001$, paired t-test) compared with baseline at 6-, 12-, 24-, and 36 months (2.51, 2.85, 4.76, and 3.51%, respectively). Significant decreases in serum and urinary cross-linked amino-terminal telopeptide of type I collagen (NTX) and urinary Deoxypyridinoline levels from baseline were observed as early as 3 months, followed by a significant decrease of serum bone alkaline phosphatase at 6 months ($p<0.001$ for all comparisons except serum NTX [$p=0.011$], Wilcoxon signed-rank test). This decrease in bone turnover markers persisted up to 36 months overall. Early reduction in the bone turnover marker (urinary NTX) at 3 months with raloxifene treatment correlates negatively with subsequent increase in lumbar spine BMD at 1 year ($r=-0.347$, $p=0.008$). The incidence of any new clinical fractures within 3 years was 1.18% (82/6967 patients). In summary, no new signals in safety were observed in the daily use of raloxifene, and the incidence of VTE was lower in Japanese than in Caucasian women. Moreover, profiles of post-treatment increase in BMD, and change in bone turnover markers were similar to those of the Japan clinical trials, confirming the effectiveness profile of a selective estrogen receptor modulator in practical use by this large-scale, long-term post-marketing observational study.

***Disclosures: Etsuro Hamaya**, Eli Lilly Japan, 3*

MO0410

Semi-mechanistic PK/PD Model of the Effect of Odanacatib, a Cathepsin K Inhibitor, on Bone Turnover to Characterize Lumbar Spine Bone Mineral Density in Two Phase II Studies of Postmenopausal Women. Julie Stone[1], Le Thi Duong[2], Albert Leung[2], Jill Fiedler-Kelly[3], David Jaworowicz[3], Dosinda Cohn[1], Nadia Verbruggen[4], Julie Passarell[3], Aubrey Stoch[1], Stefan Zajic*[5]. [1]Merck & Co., Inc., USA, [2]Merck Research Laboratories, USA, [3]Cognigen, USA, [4]Merck & Co., Inc., Belgium, [5]Merck, USA

Odanacatib (MK-0822), a potent oral inhibitor of cathepsin K, is under development for treatment of postmenopausal osteoporosis. A semi-mechanistic model of bone turnover was developed to describe creatinine adjusted urinary aminoterminal crosslinked telopeptides of Type I collagen (uNTx), a bone resorption biomarker, and lumbar spine bone mineral density (lsBMD) data from two Phase IIb studies. Data from 391 postmenopausal women receiving placebo, 3, 10, 25 or 50 mg weekly odanacatib for up to 2 years and 266 Japanese postmenopausal women receiving placebo, 10, 25 or 50 mg weekly odanacatib for up to 1 year were utilized. In the first study, patients who completed 2 years of treatment were re-randomized to placebo or 50 mg weekly odanacatib and followed for an additional year. Odanacatib concentration, biomarker, and BMD data were collected.

A population PK model was used to estimate individual exposures. An indirect response model characterizes the timecourse of lsBMD as a function of bone formation and resorption rate. The PK/PD model characterizes the action of odanacatib through an inhibitory sigmoid Emax function applied to the bone resorption rate and the release rate of uNTx which is a function of resorption. Transiently elevated bone resorption biomarkers after cessation of treatment is described by incorporating active and inactive osteoclast numbers as system variables and including an osteoclast turnover component with an inhibitory sigmoid Emax function describing odanacatib inhibition of osteoclast apoptosis rate to reflect an increase in osteoclast numbers during therapy. A modest decrease in bone formation on treatment with odanacatib was included using an empirical, time-dependent term to better account for the shape of the BMD response in the first year of treatment.

Population PK/PD modeling was performed with the model simultaneously fit to uNTx and lsBMD data from all treatments. Goodness of fit diagnostics and visual predictive checks indicate that the model well characterizes the uNTx and lsBMD data. The model supports that a combination of drug effects on bone resorption (Emax 67.9%, EC50 38.1 nM) and osteoclast cycling (Emax 72.0%, EC50 17.9 nM) can generate the range of behaviors observed in the Phase II data, including a non-monotonic dose-response relationship and enhanced bone resorption post cessation of therapy. The model also suggests that odanacatib only modestly (15.9%) reduces bone formation rate with long term therapy.

***Disclosures: Stefan Zajic**, Merck & Co., Inc., 3; Merck & Co., Inc., 1*
This study received funding from: Merck & Co., Inc.

MO0411

In Balloon Kyphoplasty for Osteoporotic Vertebral Body Fractures, the Potential of Reduction is Depending on the Time to Surgery. Thomas Blattert*. Leipzig University Hospital, Germany

PURPOSE: For the treatment of osteoporotic vertebral body fractures, balloon kyphoplasty has been shown to be highly efficient in pain reduction. This technique can restore patient mobility and enhance quality of life. Fracture reduction is resulting in part from positioning of the patient and from balloon expansion. This prospective study tries to investigate whether the potential of reduction is depending on the time to surgery in these patients.

METHODS: Inclusion criteria: t-score < 1.0, thoracolumbar fractures types. Exclusion criteria: more than two fractures, previous fractures, additional posterior instrumentation, age > 90 years, cardiac arrhythmia. 71 patients (47 female, 24 male; average age 74 years) with 101 fractures were included. 62 patients concluded follow-up (FU) at 2 years post op. The following clinical and radiological data were collected pre and post op, after 6 weeks, and after 3, 6, 12 and 24 months: Bisegmental endplate angle, anterior vertebral body height, Visual-Analog-Score (VAS; 0 no pain; 100 worst possible pain), Oswestry-Disability-Questionnaire (ODQ).

Surgical technique follows the standard protocol for balloon-kyphoplasty (Medtronic). Fractures were defined acute, if fracture age was less than two weeks. Fractures were defined chronic, if fracture age was two weeks or more. Conventional X-rays were provided in an upright position during all post op FU visits.

RESULTS: 61 patients suffered from osteoporosis, 10 from osteopenia. For the acute fracture group (n=54), bisegmental endplate angle was improved by 8,6° on average. For the chronic fracture group (n=47), however, bisegmental endplate angle was improved by 3,7° only. This difference between groups is statistically significant ($p<0.05$). For the acute fracture group, anterior vertebral body height was restored from 48% to 81% ($p<0.05$). For the chronic fracture group, anterior vertebral body height was restored from 41% to 60% (not significant).

CONCLUSIONS: If osteoporotic vertebral body fractures are being surgically treated within the first two weeks of injury, restoration of the sagittal spinal profile is significantly improved as compared to older fracture age. The pain reducing effect of the procedure, however, occurs independent of fracture age. As the leading clinical sign for osteoporotic fracture augmentation is persistent pain, cement injection remains an option even in older fractures with reduced potential for sagittal correction.

***Disclosures: Thomas Blattert**, Medtronic, 5*

MO0412

Kyphoplasty In Fresh Osteoporotic Vertebral Body Fractures - For How Long Should the Preceding Intensive Conservative Pain therapy Be Conducted? Janos Borgulya[1], Christian Günther*[2]. [1]Abt.Wirbelsäulenchirurgie, Germany, [2]Johannesbad Reha-Clinics, Germany

Introduction: We aimed at reassessing the reasonability of the DVO Guideline 2009, setting a time frame for conservative treatment of 3 weeks prior to performing balloon kyphoplasty. Methodology: Following this aim we re-evaluated balloon kyphoplasties, conducted between May 2001 and October 2003 in 85 vertebral bodies of 54 patients (48 females, 6 males, with a mean age of 72.7 years). 49 of the 85 treated vertebral fractures were acute fractures (intervention within the first 4 weeks), 20 were subacute fractures (intervention within 4 to 8 weeks after fracture occurrence). All patients were submitted to a first out-patient follow-up examination at 3-4 weeks postoperatively. Follow-up was conducted on average for 13 months (3-28 months). We assessed pain intensity using the VAS score and determined the kyphotic angle using lateral radiographs of the spine. Results: The 49 patients with acute fractures showed an immediate postoperative correction in the kyphotic angle of 11.5° and of 10.7° at 3-4 weeks. The 20 patients with subacute fractures showed a correction in the kyphotic angle of 1.8° only after surgery and of 1.7° during follow-up. The VAS score of the patients with acute fractures was 8.8 preoperatively, 4.1 immediately postoperatively and 3.2 during follow-up, whereas the patients with subacute fractures showed scores of 8.3 preoperatively, 4.7 postoperatively and 4.2 during follow-up. Summary: 1. Acute fresh fractures allow for good restoration in vertebral height within 4 weeks, with a negligible re-collapse in the range of measurement errors. 2. The restoration in height of subacute fractures is harder to achieve, however consistent pain relief is nonetheless achieved. 3. Based on our experience, balloon kyphoplasty is a safe procedure for treatment of fresh osteoporotic vertebral body fractures and thus an important adjuvant procedure within the overall concept of osteoporotic therapies. 4. On the day of surgery at the latest an effective basic and medicinal therapy should be started in accordance with the DVO Guidelines 2009 for osteoporotic treatment. Conclusions: 1. The 3-week period of conservative therapy, as recommended in the DVO Guidelines 2009, and interdisciplinary consultations in individual cases are acceptable or even required. These 3 weeks should also particularly be used for accurate determination of the surgical indication so as to counteract uncontrolled minimally-invasive surgical excesses! 2. The scientific proof of the - from our point of view - very good clinical results of the balloon-kyphoplasty still require extensive research, however.

***Disclosures: Christian Günther**, None.*
This study received funding from: Medtronic

MO0413

25-Hydroxyvitamin D Levels Increase Progressively With Higher Vitamin D Doses in Elderly Long-Term Care Residents. Alexandra Papaioannou*[1], Jenna Johnson[2], Courtney Kennedy[2], George Ioannidis[3], Laura Pickard[2], Janet Pritchard[2], Joanne Dykeman[4], Sandra Dudziak[4], Jonathan Adachi[5]. [1]Hamilton Health Sciences, Canada, [2]McMaster University, Canada, [3]Sympatico, Canada, [4]Revera Inc., Canada, [5]St. Joseph's Hospital, Canada

Background: Residents living in long-term care (LTC) are at a greater risk of experiencing falls and fractures. Meta-analyses suggest 25 hydroxyvitamin D (25-OHD) levels of ⩾ 75 nmol/L to achieve fracture prevention. Few studies have assessed the vitamin D status of LTC residents.

Purpose: 1) To determine the level of vitamin D insufficiency in the elderly living in LTC; 2) To examine the relationship between vitamin D supplementation and 25-OHD levels.

Methods: LTC residents ⩾ 65 years of age and not in palliative care in 3 LTC homes were eligible. Informed consent was provided by either the resident and/or their legal representative. Health and demographic data were collected from medical charts by staff at each LTC home. Laboratory measures in Dec 2009 and Jan 2010 included: 25-OHD, calcium, and albumin serum levels. The prevalence of vitamin D insufficiency was determined based on the laboratory reference ranges: Insufficiency < 75 nmol/L; Sufficiency 75 – 250 nmol/L.

Results: Data collected for 69 consenting LTC residents. The mean age of the sample was 83.5 years (SD 8.98), and 67% were female. Twenty-five percent of participants had a documented diagnosis of osteoporosis. The method of transfer in our sample, an indicator of mobility, was 55% ambulatory and 45% required transfer assistance. Overall, 42% of participants were taking ⩾ 800IU of vitamin D daily; the other 58% were taking ≤ 400IU daily. Mean 25-OHD, calcium, and albumin levels were 78.0 (SD 31.5) nmol/L, 2.24 (SD 0.18) nmol/L and 37.8 (SD 3.8) g/L, respectively. Overall, 49% of participants had insufficient levels of 25-OHD; age and gender were not related to 25-OHD status. Of the residents who were taking <800IU of vitamin D daily, 70% had insufficient blood levels of 25-OH D, versus only 21% of those taking recommended amount of vitamin D (⩾800IU daily; $p<0.001$). The figure below shows the trend of increasing 25-OHD sufficiency across vitamin D dosage groups ($p<0.001$).

Conclusion: Nearly 80% of LTC residents taking the recommended dose of vitamin D had 25-OHD levels in the range associated with fracture prevention. There was a progressive increase in 25-OHD with increasing dose. Given that 60% of LTC residents were taking an inadequate dose of vitamin D (≤ 400IU daily), strategies are needed to reduce the "knowledge into practice" gap. We are currently conducting a knowledge translation initiative to increase the rate of appropriate vitamin D use in LTC (ViDOS Study).

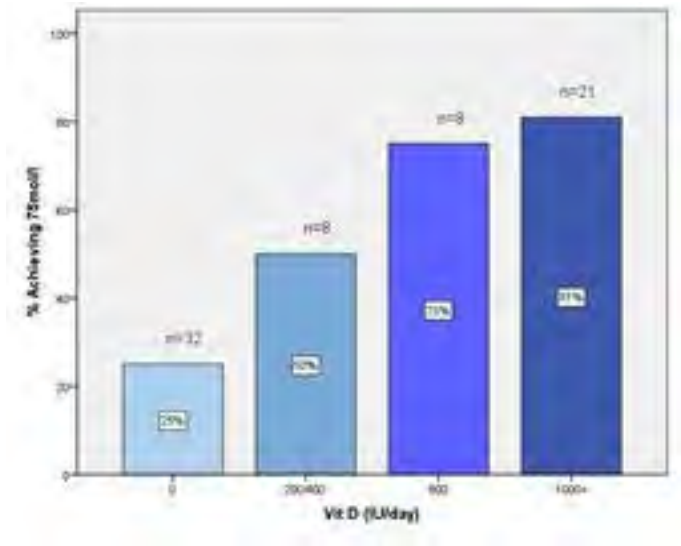

Percent Achieving 75 nmol/l by Dosage Group

***Disclosures: Alexandra Papaioannou**, Amgen, 2; Eli Lilly, 8; Procter and Gamble, 2; Novartis, 2; Merck Frosst, 8; Merck Frosst, 2; Eli Lilly, 2; sanofi-aventis, 8; Amgen, 8; Servier, 8*

MO0414

A New Active Vitamin D Analog, Eldecalcitol, Positive Effect on Hip Structural and Biomechanical Properties. Masako Ito*[1], Toshitaka Nakamura[2], Masao Fukunaga[3], Masataka Shiraki[4], Toshio Matsumoto[5]. [1]Nagasaki University Hospital, Japan, [2]University of Occupational & Environmental Health, Japan, [3]Kawasaki Medical School, Japan, [4]Research Institute & Practice for Involutional Diseases, Japan, [5]University of Tokushima Graduate School of Medical Sciences, Japan

[PURPOSE] The effects of an active vitamin D analog, eldecalcitol (ELD), on bone mineral density (BMD), geometry and biomechanical properties of the proximal femur were investigated using clinical CT in a subgroup of a randomized, active comparator, double blind study to compare its anti-fracture efficacy with alfacalcidol (ALF). [METHOD] The subjects were 189 postmenopausal women and 4 men ambulatory patients with osteoporosis (age range: 52-85 years old, 71.2 ± 7.1 in ELD and 70.6 ± 6.8 in ALF groups) enrolled at 11 centers in Japan. CT data acquisition was performed at baseline and at the end of drug administration including the complete treatment for 144 weeks or after continuous treatment for more than 48 weeks. Projectional and cross-sectional (CS) densitometric and geometric parameters were calculated based on three-dimentional CT data. Biomechanical properties including cross-sectional moment of inertia (CSMI), section modulus (SM) and buckling ratio (BR) of the femoral neck (FN), and CSMI of the femoral shaft (FS) were also calculated. [RESULTS] 1) Projectional data of the FN; areal BMD and bone mass significantly decreased from baseline at the FN, trochanter and FS in the ALF group, while they were maintained in the ELD group. 2) Total FN CS; in the ALF group, BMD decreased but bone mass was maintained and cross-sectional area (CSA) increased. In contrast, ELD maintained BMD with a significant increase in bone mass and increased trend for CSA. 3) Cortical FN CS; in the ALF group, bone mass/BMD increased while CSA was maintained and cortical thickness (CoTh) decreased. In the ELD group, bone mass/BMD/CSA all increased with maintained CoTh. 4) Biomechanical properties of the FN; ELD improved CSMI and SM to a greater extent than ALF. Neither ALF nor ELD improved BR. 5) FS parameters; the

overall results of total and cortical CSAs and CSMI of the FS were similar to those of the FN, but the trends of changes in cortical BMD were completely different between the FN and FS; cortical BMD decreased significantly in both ELD and ALF. [CONCLUSION] Our longitudinal analysis of hip geometry by clinical CT has disclosed an unexpected potential of ELD to increase the cortical CSA, BMD and bone mass and to maintain cortical thickness, probably through a more potent effect of ELD in mitigating endocortical bone resorption compared to ALF. By improving biomechanical properties of the proximal femur, ELD may have the potential to reduce the risk of hip fracture.

***Disclosures: Masako Ito**, Chugai, Takeda, Eli Lilly Japan, 2; Chugai, Astellas, Daiichi-Sankyo, JT,Asahi Kasei Pharma, Ono Pharm, 5*

MO0415

Chart Review Initiative to Characterize the Assessment and Management of Vitamin D Levels in Osteoporosis Patients in Clinical Practice. Jonathan D. Adachi[1], Jacques Brown*[2]. [1]McMaster University, Canada, [2]Laval University, Canada

Purpose: This chart review initiative aimed to better understand how vitamin D levels are assessed and managed in Canadian osteoporosis patients.

Methods: Using an online tool or paper forms, specialists and primary care practitioners from Ontario and Quebec completed a practice profile questionnaire, as well as profiles for each of ~20 patients in their practice being treated to prevent fractures and last seen between November 2008 and April 2009. Information collected included demographics, BMD and fracture risk factor information, availability and level of serum vitamin D measurements, and information on osteoporosis medications and calcium and vitamin D supplementation. Participants also evaluated patients' current regimens and detailed any proposed changes, if applicable.

Results: Information was collected from 52 physicians in Ontario and Quebec on 983 patients. Over 85% of patients were female and 64% was 60 to 79 years of age. Mean BMD ± SD based on most recent lowest T-score was -2.15 ± 1.55. A total of 28% of patients had had a previous fragility fracture and 8.5% had received systemic glucocorticoid therapy for >3 months. Nearly 80% of patients were treated with a bisphosphonate and 85% were prescribed calcium and vitamin D supplements, with 50% being prescribed ⩾5800 IU/week of vitamin D. Of the 73% of patients for whom serum 25(OH)D levels were available, ~50% had levels <80 nmol/L. This contrasts with the 37% thought to have "unsatisfactory" vitamin D levels based on physician perceptions. Similarly, 37% of patients were considered to have "unsatisfactory" change in BMD and 16% to have both "unsatisfactory" BMD and vitamin D. Of these patients, ~70% were thought to require changes to their osteoporosis regimen. The most common changes suggested for these patients (n=286) was to add or increase the dose of vitamin D supplementation (78%), though no change was suggested for 48% with "unsatisfactory" vitamin D levels. Participants felt almost two-thirds of the 385 patients for whom a question about combination therapy was answered might benefit from combination therapy with vitamin D.

Conclusions: This initiative provided insight into vitamin D assessment and management in Canadian clinical practice. Although most physicians recommend calcium and vitamin D supplementation, vitamin D levels appear to be insufficient in half of patients. The results underscore the importance of considering vitamin D status when looking to optimize bone health.

***Disclosures: Jacques Brown**, Wyeth, 9; AstraZeneca, 5; Servier, 5; Nycomed, 5; Wyeth, 5; Bristol-Myers Squibb, 5; Eli Lilly, 9; Novartis, 9; sanofi aventis, 5; Roche, 9; Novartis, 5; sanofi aventis, 9; Eli Lilly, 5; Pfizer, 9; Pfizer, 1; Merck, 9; Roche, 5; Procter & Gamble, 9; Bristol-Myers Squibb, 1; GlaxoSmithKline, 5; Amgen, 9; GlaxoSmithKline, 9; Amgen, 5; Merck, 5; Procter & Gamble, 5*
This study received funding from: Merck Frosst Canada

MO0416

Clinical History is Unreliable in Assessment of Vitamin D Status: To Know Your Patient's Vitamin D Status, 25(OH)D Measurement is Needed. Neil Binkley*[1], Ellen Fidler[2], Diane Krueger[3]. [1]University of Wisconsin, USA, [2]University of Wisconsin Osteoporosis Clinical Research Program, USA, [3]University of Wisconsin, Madison, USA

Vitamin D inadequacy is common. Assessing an individual's vitamin D status by simple clinical history would be desirable. However, the capability of clinically applicable questionnaires to predict 25(OH)D concentration has received only limited evaluation. The purpose of this study was to evaluate the utility of a simple one-page questionnaire assessing self-reported vitamin D intake from diet and supplements to predict circulating 25(OH)D status in older adults. In this study, 125 postmenopausal women mean age 65.1 (range 55-90) years who were being enrolled into studies of vitamin D supplementation completed a questionnaire evaluating vitamin D intake from supplements plus diet including milk, eggs, yogurt, fortified orange juice and cereals, sun-dried mushrooms and fish. Serum 25(OH)D was measured by HPLC. Estimated mean daily vitamin D intake was 659 IU; (SD 583; range 52-2901). Serum 25(OH)D ranged from 9.1 to 56.8 ng/ml (mean 32.1) and was lower ($p < 0.0001$) in those with higher body weight and BMI. Mean serum 25(OH)D did not differ ($p = 0.43$) by season. Estimated total daily vitamin D intake and weight-corrected intake (IU/kg/day) were positively correlated with 25(OH)D ($p < 0.0001$). Body weight was unrelated to estimated daily vitamin D intake. A substantial range in 25(OH)D concentration was observed at "usual" levels of vitamin D intake. For example, among the 46 women with an intake of <400 IU daily, 25(OH)D ranged from 9 to 57 ng/ml. Similarly, for the 17 with intakes of 800 to 1,200 IU, 25(OH)D ranged from 17 to 54 ng/ml; in this subcohort, 25(OH)D was below 30 ng/ml in 6/17. While the small numbers limit generalizability, only the 7 women whose estimated intake exceeded 2,000 IU daily reliably had a 25(OH)D concentration > 30 ng/ml. When these evaluations are limited to those enrolled during the winter and spring (n = 93), similar patterns were observed. In conclusion, in this cohort of older women, estimated vitamin D intake does correlate with serum 25(OH)D. However, at estimated intakes up to 2,000 IU daily, some individuals have sub-optimal vitamin D status. As such, on an individual patient level, estimating vitamin D intake does not allow reliable prediction of 25(OH)D status. The factors leading to variation in 25(OH)D level between individuals with similar vitamin D intakes needs further clarification. Measurement of 25(OH)D is needed to determine an individual's vitamin D status.

***Disclosures: Neil Binkley**, None.*

MO0417

The Effect of cis-9, trans-11 Conjugated Linoleic Acid on Parathyroid Hormone in Middle-Aged Men. Jason DeGuire*[1], Nour Makarem[1], Catherine Vanstone[2], Suzanne Morin[3], Hope Weiler[1]. [1]McGill University, Canada, [2]Research coordinator, Canada, [3]McGill University Health Centre, Canada

There is evidence suggesting that cis-9, trans-11 conjugated linoleic acid (CLA) decreases PTH in male rats as soon as 4 weeks after supplementation. The purpose of this study is to determine if cis-9, trans-11 CLA can reduce PTH in healthy men. The first 12 participants in a RCT involving healthy (BMI 25.9±2.4) middle-aged men (age 47.1±4.2 y) were divided into 3 blinded treatment groups (0, 1.5, or 3 g/d of CLA, 75.2% cis-9, trans-11 isomer). Plasma PTH, 25(OH) vitamin D (vitD), and serum total ionized calcium (ical), were collected between 7:00-10:00am and were measured at 3 different time points (baseline, month 1, and month 2). Dietary calcium intake was estimated using the Harvard/Willett food frequency questionnaire (FFQ). Differences between groups were calculated using a mixed model approach where the level of significance was set at $p<0.05$. The study remains blinded and thus the 3 groups presented are A, B, and C. There were no differences between treatments for dietary calcium intake (A: 1461.2±470.1 vs. B: 870.0±213.5 vs. C: 1171.7±574.4 mg, p=0.227) and no differences between treatment and time points for age (A: 49.4±5.7 vs. B: 45.5±2.1 vs. C: 45.8±2.5 y p=0.303), BMI (A: 27.4±1.9 vs. B: 25.1±1.4 vs. C: 24.8±2.7, (p=0.556), ical (A: 1.25±0.04 vs. B: 1.25±0.04 vs. C: 1.24±0.04 mmol/L, p=0.175). There was a time point main effect for vitD (p=0.005). VitD levels at baseline (74.8±31.0 nmol/L) were higher than at 2 months (56.9±21.7 nmol/L, p=0.002). There was also a treatment and time point interaction (p=0.008). In treatment B, vitD levels were higher at baseline (100.2±44.5 nmol/L) when compared to 1 and 2 months (60.7±29.2 and 52.8±32.3 nmol/L respectively, $p<0.001$ for both). The differences in PTH between groups and assessment time point are shown in the table below. These data suggest that in treatment A there is a statistically significant increase in PTH after two months of supplementation. Regarding treatment C, there is a main effect for PTH when compared to treatment A and B. Most participants started the study in the Fall. This could partly explain the decline in vitD status from baseline to month 2, which in turn could lead to an increase in PTH. Further investigation, will use a larger sample size and a final time point of 4 months and will include body composition data using DXA, bimonthly 24h food recalls to further assess diet, and plasma total lipid CLA composition determined by gas chromatography.

PTH (pg/mL) [1,2]	A* (n=5)	B* (n=3)	C§ (n=4)
Baseline	39.5±3.8 a	40.3±13.7	61.4±10.7
Month 1	41.5±3.2 a	43.5±5.7	55.5±10.7
Month 2	55.5±11.0 b	47.1±26.9	60.1±17.6

[1]Within columns, values with different letters are significantly different (P<0.05).
[2]Within rows, main effects with different symbols are significantly different (P<0.05).

Table 1

***Disclosures: Jason DeGuire**, None.*
This study received funding from: Dairy Farmers of Canada

MO0418

A Nasal Spray Formulation of Teriparatide Produces Supratherapeutic Systemic Exposure But Does Not Cause Turbinate Bone Damage in a 3-Month Monkey Study. Christopher Jerome[1], Gene Merutka[2], E. Priya Eddy*[2], Brian MacDonald[3]. [1]Think Bone Consulting, USA, [2]Zelos Therapeutics, USA, [3]Zelos Therapeutics Inc, USA

PTH (1-34) (teriparatide rDNA origin, Forteo®) is an effective drug in the treatment of osteoporosis but the need for daily injection is suboptimal. Nasal spray administration is simple and convenient, does not require sterile technique and could improve the willingness of patients to consider and/or continue PTH therapy. We (Krause et al., ASBMR 2009) have shown that N-dodecyl-β-maltoside (DDM; Intravail® A3) enhances the absorption of nasally administered ZT-034 (synthetic teriparatide) in rats and monkeys. Nasal spray formulations for efficient peptide absorption may have toxic effects on the nasal epithelium leading to erosions and

inflammation. A particular concern with nasal administration of PTH is that prolonged high local concentrations or direct exposure through epithelial erosions may cause turbinate bone perforation through excessive osteoclast activation. We therefore examined the safety of prolonged daily nasal administration of ZT-034 formulated with DDM. Seven groups of 8 adult female Cynomolgus monkeys received daily doses of 5, 10, 25 or 50 μg/kg of ZT-034 with 0.18% DDM via a hand-held spray device (50μL) for 3 months in alternating nostrils. Vehicle only, DDM only and 10 μg/kg subcutaneous ZT-034 control groups were included. Plasma samples were obtained on Day 1 and 91 for toxicokinetic evaluation. Macroscopic and microscopic pathology particularly of the nasal epithelium and the bony structures within and around the nasal cavity were evaluated. Nasal spray ZT-034 had a half-life of 25-35 minutes with no accumulation after repeat dosing and achieved exposures that were 2.6 to 22 fold higher, depending on dose, than human exposure obtained with 20 μg/day subcutaneous Forteo using the same assay. No ZT-034 related adverse effects were observed on the nasal epithelium. Normal levels of bone remodeling activity were observed in the nasal turbinates of all groups, including non-PTH controls. No evidence of increased osteoclast activation, substantial loss of bony elements orbony plate perforation was found. This study indicates that teriparatide can be administered nasally for prolonged periods in combination with DDM, to produce high systemic exposure without causing nasal epithelial toxicity or damage to underlying bony elements. Nasal administration of teriparatide in humans is feasible and likely to be safe.

***Disclosures: E. Priya Eddy**, Zelos Therapeutics, 5*

MO0419

A Novel Parathyroid Hormone Fusion Protein Causes Sustained Increases in Bone Mineral Density in Ovarectomized Rat After Monthly or Single Dosing. Ranjitha Katikaneni[1], Tulasi Ponnapakkam[1], Elease Bradford[1], Satish Pasala[1], Osamu Matsushita[2], Joshua Sakon[3], Robert Gensure*[1]. [1]Ochsner Clinic Foundation, USA, [2]Kitasato University Medical School, Japan, [3]University of Arkansas, USA

Daily subcutaneous injections of parathyroid hormone (PTH) stimulates bone growth and has been used as a treatment for osteoporosis. We have shown previously in normal mice that a hybrid protein of human PTH(1-33) and the collagen binding domain of *Clostridium histolyticum* collagenase (PTH-CBD) has a prolonged anabolic effect in bone with no apparent side-effects. We now show effects of PTH-CBD in the ovarectomized (OVX) female rat, an animal model of postmenopausal osteoporosis. OVX and sham 3 month old female Sprague Dawley rats were purchased from Charles River (Cambridge, MA). Bone mineral density (BMD) was measured monthly. After 6 months, there was a 17.0% reduction in bone mass in OVX rats, confirming significant osteoporosis. OVX rats were divided into 5 groups (12 animals/group) and treated with one of the following regimens: vehicle s.q.x1, human PTH(1-34) 20/ug/kg/day s.q.x14, PTH-CBD 320 ug/kg s.q.x1, PTH-CBD 320 ug/kg/month s.q., and CBD 320 ug/kg s.q.x1. Sham animals received vehicle s.q.x1. BMD was measured monthly. Blood samples were obtained at baseline, 20 minutes, 1 month, 3 months, and at 6 months. Samples will be analyzed for calcium, PTH (rat and human). and markers of bone turnover (total and bone-specific alkaline phosphatase, osteocalcin, CTX, and P1NP). Urine samples were collected at baseline, 4 hours and 24 hours, 3 months, and 6 months. Samples were analyzed for creatinine and cAMP. Animals will be sacrificed at the end of 6 months; femur, tibia, and spine will be harvested for histological and micro-CT analysis. Complete analysis of these results will be available for presentation. Preliminary analysis at the 4th month of the study showed the following: BMD increased significantly (4.0%) in the PTH-treated group after 1 month, declining to control levels thereafter. Monthly treatment with PTH-CBD showed significantly increased BMD (9.1%) after 2 months, sustained thereafter. BMD increased slowly after a single dose of PTH-CBD, to 3.5% after 4 months. CBD alone had no effect on BMD. Serum calcium increased significantly 20 minutes after PTH injection, but not after PTH-CBD injection. Likewise, urinary cAMP increased significantly both 4 and 24 hours after PTH injection, but not after PTH-CBD injection. Overall, compared to PTH(1-34), PTH-CBD showed greater and more sustained increase in BMD in the OVX rat without causing hypercalcemia, and required far fewer injections to achieve these results.

***Disclosures: Robert Gensure**, None.*

MO0420

Alendronate and Parathyroid Hormone Treatment Improve Bone and Metabolic Health in the OVX Rat. Andrea Trinward*[1], Steven Tommasini[2], Lisa Miller[3], Stefan Judex[4]. [1]State University of New York at Stony Brook, USA, [2]SUNY Stony Brook, USA, [3]Brookhaven National Laboratory, USA, [4]Stony Brook University, USA

Post-menopausal osteoporosis is associated with bone loss but may also increase body mass and abdominal adiposity, factors that can pose a secondary risk to skeletal health. Drugs such as alendronate (ALN) or parathyroid hormone (PTH) target bone loss but their effects on adiposity, metabolism, and the interrelationship between bone and fat are largely unknown. To this end, we subjected OVX rats to short-term (2mo) and long-term (6mo) treatments of different doses of ALN and PTH and analyzed vertebral bone, abdominal fat volume, liver fatty acids, and serum leptin and IGF-I. Six-month old Sprague-Dawley rats were assigned to age-matched controls, untreated OVX, OVX treated with high (H), medium (M), or low (L) doses of hPTH (60, 15, or 0.3μg/kg/d), or OVX treated with H, M, or L-ALN (100, 10, or 1μg/kg/2xwk). Rats were sacrificed at 6, 8, and 12mo of age (n=10/group/age). At 8mo, H- and M-ALN as well as H- and M-PTH showed had higher bone volume and vertebral apparent density (μCT) than OVX controls ($p<0.05$). At 12mo and compared to OVX controls, apparent vertebral density remained significantly higher in H-, M-, and L-ALN as well as H-, and M-PTH groups. Liver triglyceride (TG) and esterfied free fatty acid concentrations were smaller in 8mo H-PTH rats compared to OVX controls. At 12mo, all groups except M-ALN had lower liver TG and NEFA concentrations than OVX controls. Further, IGF-I serum concentrations were lower in H-ALN and H-PTH than in OVX controls at 12mo. Body mass was positively correlated to bone volume and density for the combined dataset of age-matched controls and high dose treatment groups ($r2= 0.36$, $p<0.01$), but was not correlated in the combined dataset of OVX controls and low dose treatments. Liver TG content was not correlated to apparent mineral density in OVX controls ($r2=0.001$, $p<0.93$), but ALN and PTH treatment normalized this relationship to that of age-matched control rats. These data demonstrate that treatment with moderate to high doses of ALN and PTH can normalize bone morphology and indices of fat metabolism to those of normal age-matched controls but also indicate that high drug doses can suppress IGF-I levels. Through their effects on adiposity, both drug therapies may also reduce the incidence of liver steatosis and type 2 diabetes.

***Disclosures: Andrea Trinward**, None.*

MO0421

Bone Mineral Quality Assessed at Bone Structural Unit Level in Macaca fascicularis Monkeys is not modified by a 52-week treatment with Strontium Ranelate. Audrey DOUBLIER*[1], Delphine Farlay[2], Yohann Bala[3], Xavier JAURAND[4], Dominique BERTRAND[5], Georges Boivin[1]. [1]INSERM, France, [2]University of Lyon, France, [3]Université De Lyon, France, [4]Centre Technologique des Microstructures, Université de Lyon, France, [5]INRA, France

Interactions between strontium (Sr) and bone mineralization have been investigated in animals (1,2) and women treated with strontium ranelate (SrRan) for 3 (3,4) to 5 years (5). Our purpose was to evaluate the impact of Sr on bone mineral quality at Bone Structural Unit (BSU) level, which has never been investigated in details. Sixteen iliac crest samples were taken from monkeys receiving 0, 200, 500 or 1250 mg/kg/day of SrRan for 52 weeks. Degree of mineralization (DMB) and the heterogeneity index (Hi) were measured by quantitative microradiography, Vickers microhardness (Hv) was assessed (6), and focal bone Sr content and distribution were quantified by X-ray microanalysis (1,3), on the same 607 BSUs. Fourier Transform Infrared Microspectroscopy allowed the quantification of mineral maturity and crystallinity index of mineral (7,8) in 737 BSUs. Chemometric analyses (MATLAB) were done on each wavenumber of infrared spectra. ANOVA and Fisher test were performed on 4 clusters (cortical old and new, cancellous old and new). At BSU level, focal DMB and Hv were greater in old than in recent bone in untreated monkeys (+12.5% and +19.1%, respectively), but also in the 3 groups of treated animals (+9.5% to +13.2% and +17.3% to +18.9%, respectively). DMB and Hv were not significantly different between treated and untreated monkeys. Thus, these variables depended mainly on the age of the BSU (physiological evolution of the secondary mineralization), and were not influenced by the focal bone Sr content. Mineral maturity and crystallinity index were not significantly modified in treated versus untreated monkeys. Chemometric analyses of whole infrared spectra showed no statistical difference between treated and untreated groups, confirming the absence of a Sr effect on bone mineralization. To conclude, after a 52-week treatment with strontium ranelate, mineralization and hardness assessed at BSU level in monkeys were unchanged, leading to the same bone mineral quality than untreated animals.

1. Farlay et al. J Bone Miner Res 2005, 20:1569.
2. Bain et al. Osteoporos Int 2009, 20:1417.
3. Boivin et al. Osteoporos Int 2010, 21:667.
4. Li et al. J Bone Miner Res 2009 (online).
5. Doublier et al. J Bone Miner Res 2009, 24(Suppl 1):S41.
6. Boivin et al. Bone 2008, 43:532.
7. Bala et al. Bone 2010, 46:1204.
8. Farlay et al. J Bone Miner Metab 2009 (online).

***Disclosures: Audrey DOUBLIER**, SERVIER, 2*
This study received funding from: SERVIER Laboratories

MO0422

Dietary Dried Plum Increases Bone Mass. Bernard Halloran*. VA Medical Center (111N), USA

Bone is progressively lost with advancing age. Therapies to treat age-related bone loss are limited and the only effective pro-anabolic regimen available to restore bone is intermittent treatment with teriparatide (parathyroid hormone, PTH 1-34). Recent evidence suggests that dietary supplementation with dried plum can prevent and reverse bone loss due to estrogen deficiency. To determine whether dietary dried plum supplementation can prevent the loss of bone with aging and whether bone that has already been lost can be replaced, we used a mouse model of age-related bone loss. Adult (6 m) and old (18 m) male mice were fed a normal diet or diets supplemented

with dried plum (15% and 25% by weight) for 6 months. MicroCT analysis and bone histomorphometry were used to assess bone volume, structure and metabolic activity before, during and after dietary supplementation. Animals consuming the control diet lost bone while both adult and old animals consuming the dried plum diets gained bone. Cancellous bone volume in animals receiving the highest dietary level of dried plum exceeded baseline levels by 40-50%. After 6 months on their respective diets bone volumes in adult and old mice were 80% and 33% greater, respectively, in those animals receiving the 25% plum diet than in the control group. Trabecular thickness (+12%) and connectivity density (88%-268%) increased with dietary plum while the structure model index decreased (19%-22%), demonstrating a change in trabecular structure from rod-like to more plate-like. Responses in old animals were generally blunted. Trabecular, but not cortical, mineral density increased with age but was unaffected by diet. Cancellous bone formation rate was lower in old than adult mice but did not differ among the diet groups. Cortical bone thickness increased (20%) and medullary area decreased (-19%) on the plum diet but only in the old mice. Measures of bone anabolic activity were lower in old animals. Our results suggest that dried plum contains factors that can dramatically increase bone volume and restore bone that has already been lost due to aging. As such dried plum may prove to be an effective therapeutic agent for the treatment of patients with osteoporosis.

***Disclosures: Bernard Halloran**, None.*
This study received funding from: California Dried Plum Board

MO0423

Effects of an Anti-resorptive and Anabolic Agent Alone or in Combination on the Micro-architecture and Mineralization of an Ovariectomized Rat. Graeme Campbell*[1], Ricardo Bernhardt[2], Dieter Scharnweber[3], Steven Boyd[1]. [1]University of Calgary, Canada, [2]Technische Universität Dresden, Germany, [3]Technische Universitaet Dresden, Germany

The mechanical integrity of bone tissue is determined by both architecture and tissue properties, which are affected differently by anabolic and anti-resorptive treatment. We examined the recovery of bone architecture and tissue mineralization in rats treated with anabolic agent parathyroid hormone (PTH) or anti-resorptive agent alendronate (ALN) alone and in combination (PTH+ALN) after overiectomy (OVX).

Female Wistar rats aged 7-9 months were assigned to one of five groups: (1) sham + vehicle, (2) OVX + vehicle, (3) OVX + 40 µg/kg hPTH(1-34), (4) OVX + 0.015mg/kg ALN, (5) OVX + 40 µg/kg hPTH(1-34) and 0.015mg/kg ALN. Surgery was performed at wk 0, and treatment was from wk 6 to wk 14. This study was divided into an *in vivo* component, which consisted of micro-CT scans (vivaCT 40, Scanco Medical, Switzerland) of the right proximal tibial metaphysis at wks 0, 6, 8, 10, 12 and 14, and an *ex vivo* component of synchrotron radiation micro-CT (SRµCT) scans of the same site at the endpoint. Standard bone architectural parameters were measured from the *in vivo* data, and the mean bone tissue mineral density (TMD) of *surface* (0.013mm thick) and *inner* bone tissue (>0.034mm from surface) of trabecular subvolumes was determined from the *ex vivo* scans.

Significant changes ($p<0.05$) in all measured architectural parameters except for Tb.Th were observed between wk 0 and wk 6 in all groups subject to OVX (BV/TV shown in Fig 1). Alendronate treatment prevented further OVX-induced declines in the trabecular architecture throughout the treatment period. With PTH treatment, BV/TV returned to baseline values and Tb.Th increased to 150% of baseline by week 14, while Tb.N and Conn.D remained unchanged during the treatment phase. Combined PTH+ALN treatment resulted in similar changes to Tb.Th and Conn.D as the PTH group, and improved BV/TV. The Tb.N increased to baseline values at wk 14. From SRµCT, there was no difference detected in TMD of the inner bone tissue for all groups. But, the ratio of surface-to-inner TMD was higher in the ALN group than all others (FIg 2).

Combined, these data indicate that the trabecular architecture can be altered to restore bone that has been lost through ovariectomy, and that the recovery is maximized when using a combined treatment of an anabolic and anti-resorptive agent. Furthermore, ALN leads to increased surface TMD compared to both normal and osteoporotic bone, whereas TMD is at normal levels with PTH and combined ALN+PTH treatment.

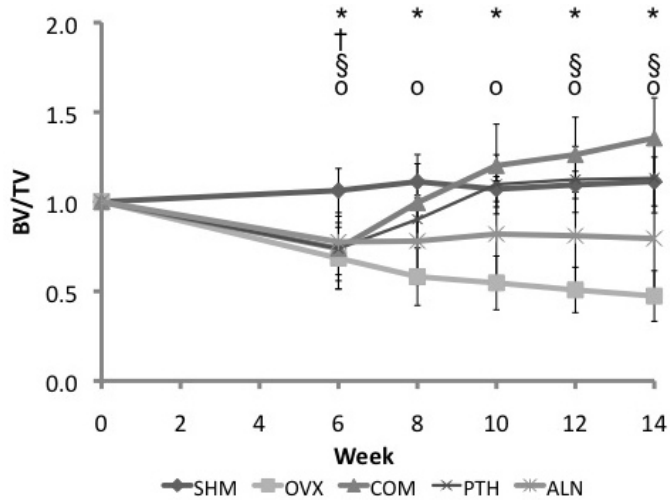

Fig 1: BV/TV normalized to wk0. *,†,Ï,o,-sig change from wk0 in ALN, PTH, combined, OVX respectively

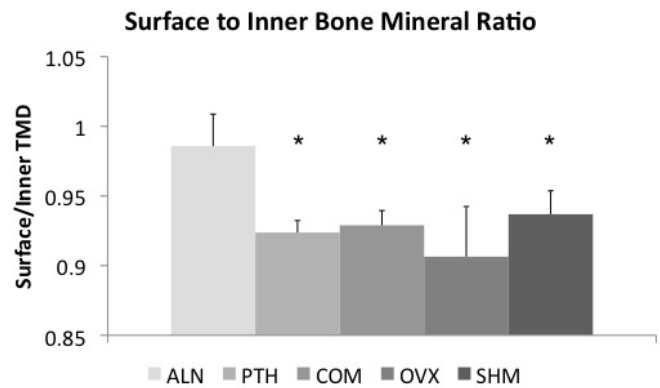

Fig 2: Ratio of surface to inner region TMD of the bone tissue. * - Significant difference from ALN

***Disclosures: Graeme Campbell**, None.*

MO0424

Optimization of the Pharmacodynamic Response to the Calcium-Sensing Receptor (CaSR) Antagonist MK-5442 (JTT-305) in the Sprague-Dawley Rat and Beagle Dog. Helmut Glantschnig*[1], Tara Cusick[2], John Fisher[2], Bindhu Karanam[2], Pascale Nantermet[2], Kevin Scott[2], Monica Tijerina[2], Nan Wei[2], Le Thi Duong[1]. [1]Merck Research Laboratories, USA, [2]Merck & Co., Inc., USA

The current anabolic standard of care in patients with severe osteoporosis is daily injection of recombinant parathyroid hormone (PTH). The CaSR allosteric antagonist MK-5442/JTT-305 provides as a PTH secretagogue a promising alternative oral osteoanabolic candidate. Here we describe the use of different formulations of MK-5442 to optimize preclinical pharmacokinetic and pharmacodynamic parameters in rat and dog. Single-doses of MK-5442 were administered in selected formulations as suspensions (0.5% methylcellulose, MC; nanosuspension, NS) or solutions (10% Tween-80, Tw; 30% b-cyclodextrin, BC; 100% PEG400, P4) to fasted Sprague-Dawley rats (0.1 to 3.0 mg/kg, p.o.; n=4/group) or Beagles (0.4 to 2.0 mg/kg, p.o.; n=3/group). Plasma PK, drug metabolism, iPTH(1-84) and serum calcium/phosphate responses to treatment were monitored over 24hr. MK-5442 was rapidly absorbed (Tmax ~15-30 min) and eliminated in a dose-related manner, with substantially greater exposures achieved using soluble preparations (Tw, BC) in rats. Dose-related increases in plasma iPTH levels were dynamic (Tmax ~15-30 min, up to 4-5 fold) and observed to larger degree and more consistently in Tw and BC vs. MC groups, with iPTH rapidly returning towards baseline one to two hours or thereafter. Dietary Ca-content was varied from 0.4-0.8% to study effects of MK-5442 (Tw) in a 1-wk multi-dose study. sCa-peaks and 24hr-trough levels, but not iPTH responses, were attenuated by the 0.5% Ca-diet vs. 0.8% Ca-diet. Serum-P1NP levels were numerically increased (10%, 0.7 mg/kg, Tw, ns) while urinary-NTX was found elevated only when dosed at 3 mg/kg in MC ($p<0.05$). Similarly, in Beagles bioavailability of MK-5442 was greater using P4 and NS formulations (34%) vs. MC (25%), resulting in pulsatile PK (Tmax 0.8 hrs) and dose-related exposures over 24hrs. The canine iPTH profile indicated a dynamic, dose-related increase (Tmax 1 hr, up to 7-fold), returning to baseline at 3-4 hrs post-dose. Minimal effects on sCa level were observed in dog up to the highest

dose level tested (2 mg/kg, P4 and NS). In summary, these data indicate that pharmacodynamic parameters, i.e. pulsatile PTH profiles, mediated by MK-5442 could be optimized by altered formulations. This is thought to be crucial for the bone-anabolic actions of a CaSR antagonist in preclinical models.

***Disclosures: Helmut Glantschnig**, Merck & Co, 3*
This study received funding from: Merck & Co

MO0425

Rapid-Onset Anabolic Actions on Bone of 2-Methoxyestradiol. Khalid Mohammad*[1], Lauren Dunn[2], Holly Davis[2], Xianghong Peng[1], Maria Niewolna[1], Theresa Guise[1], John Chirgwin[1]. [1]Indiana University, USA, [2]University of Virginia, USA

2-Methoxyestradiol (2ME2) is an anti-hypoxic agent in clinical trials in cancer. We previously found that 150mg/kg/day 2ME2 for six months increased bone mass and strength in nude mice, with significant changes by one month. The responses differ from published results in rats given 100mg/kg/day oral liposomal 2ME2, which inhibited longitudinal bone growth, by suppression of proliferation and increased apoptosis of growth plate chondrocytes in vivo and inhibition of osteoclast formation in vitro.

Female nude mice (8 animals per group) were treated once daily for 10 days by intraperitoneal injection with vehicle or 2ME2 at doses of 150, 30 or 5 mg/kg/day as a water-soluble, nanocrystalline formulation (EntreMed). Bone mineral density (BMD) was determined by DEXA. 2ME2 increased BMD at the tibia at 7 and 10 days of treatment at all doses ($p<0.01$ & $p<0.001$ respectively). Significant changes were seen as early as 4 days in mice treated with the lowest dose. 2ME2 also increased femoral BMD ($p<0.001$) at 10 days with all doses. 2ME2 at 30mg & 150mg doses increased femoral BMD at 7 days ($P<0.001$ & $P<0.05$) respectively). Mice treated for 10 days with 30 or 150 mg/kg/day showed higher BMD at the tibia ($p<0.01$ or $p<0.001$, respectively) than mice receiving the 5mg dose, with similar responses at the femur.

Histomorphometry showed an increase in tibial TBV in mice treated with all doses of 2ME2 ($p<0.01$), accompanied by increased trabecular number and reduced trabecular separation, with no changes in growth plate cartilage or morphology. Mouse bone marrow cells were cultured for 10 days from animals pre-treated with 2ME2 or vehicle. CFU-fibroblast numbers were unchanged. CFU-osteoblast numbers were decreased from mice treated with any dose of 2ME2 compared to vehicle. Formation of TRAP+ multinucleated osteoclasts was reduced from mice treated with 2ME2. However, 100nM 2ME2 increased osteoclast number 10X in 7-day neonatal mouse calvarial organ cultures.

Overall, we observed rapidly increased BMD and trabecular bone in mice receiving the lowest dose of 2ME2. These changes are largely opposite those seen in rats Differences may be due to species-specific responses to 2ME2 or to different formulation and pharmacokinetics of drug delivery. Our results suggest that nanocrystalline 2ME2 may be a useful, rapidly-acting bone anabolic treatment and a bone-sparing anti-tumor agent.

***Disclosures: Khalid Mohammad**, None.*

MO0426

A Pilot Study on the Synergistic Effect of Anti-resorptive and Anabolic Treatment on Ovariectomized Rat. Xiao Yang*[1], Yong Hoow Chan[1], Padmalosini Muthukumaran[1], Xiuli Chen[1], Taeyong Lee[2]. [1]nus, Singapore, [2]National University of Singapore, Singapore

Osteoporosis is a progressive debilitating disorder associated with reduction in bone mass often leading to fractures. Commonly used anabolic drug is the recombinant parathyroid hormone (PTH) [1]. The third generation nitrogen-containing bisphosphonates (Ibandronate) is being used as an anti-resorptive agent [2]. Whether the use of both bisphosphonate and PTH would have a synergistic effect on osteoporosis is still controversial [3]. We aim to investigate the effect of individual and combined administration of ibandronate and PTH on the ovariectomized (OVX) rat models in terms of structural and mechanical analyses.

60 female Sprague-Dawley rats of age 8 to 10 weeks were divided into 5 groups (SHAM, OVX+VEH, OVX+PTH, OVX+IBAN, OVX+PTH+IBAN). The rats were subjected to ovariectomy or sham surgery. PTH and/or ibandronate or its vehicle was administered subcutaneously to the respective groups from 4th week post-surgery. 3 rats from each group were euthanized every 2 weeks. The tibiae were subjected to metaphyseal 3-point bending (Fig. 1), pQCT and micro-CT analysis. Serum biomarkers for both bone formation (P1NP) and resorption (LAPs) were studied.

The results showed a significant difference between SHAM and OVX+VEH suggesting the establishment of osteoporosis (Fig. 2). pQCT analysis showed that the treatment groups had significantly higher bone mineral density (BMD) than OVX+VEH, with OVX+IBAN and OVX+PTH+IBAN groups showing significantly higher BMD than OVX+PTH (Table 1). BMD, cortical density and mechanical properties of OVX+PTH+IBAN group is higher than the mono-treatment groups (Table 2) and OVX+VEH. Micro-CT analysis showed OVX+PTH+IBAN has significant beneficial effects on trabecular bone at 6 weeks after OVX surgery compared to OVX+PTH.

Synergistic effects were observed in the 10th week mean BMD and P1NP result (Table 3). Mean value of cortical density, micro-architecture morphology of trabecular bone, stiffness and maximum load of OVX+PTH+IBAN group have conferred beneficial effects than those of other mono-treatment groups, whilst previous studies claim a negative effect of bisphosphonate on PTH. Synergistic effect may exist in low dosage on a weekly regimen with proper ratio of anabolic and antiresorptive drugs. Large-scale studies are in progress to prove the effect of concurrent and sequential treatments.

References

1.Gabet Y,et al., OI 2005,16(11):1436-1443.
2.Fleisch H,et al., OI 1996,6(2):166-170.
3.Garcés C,et al., Maturitas 2006,54(1):47-54.6.

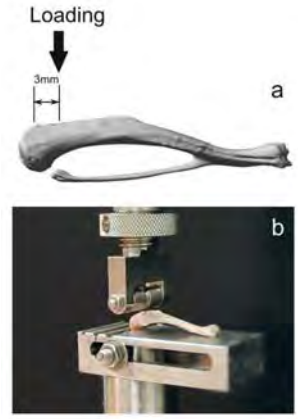

Figure 1 (a) MicroCT rendered image of rat tibia; (b) metaphyseal three-point bending test.

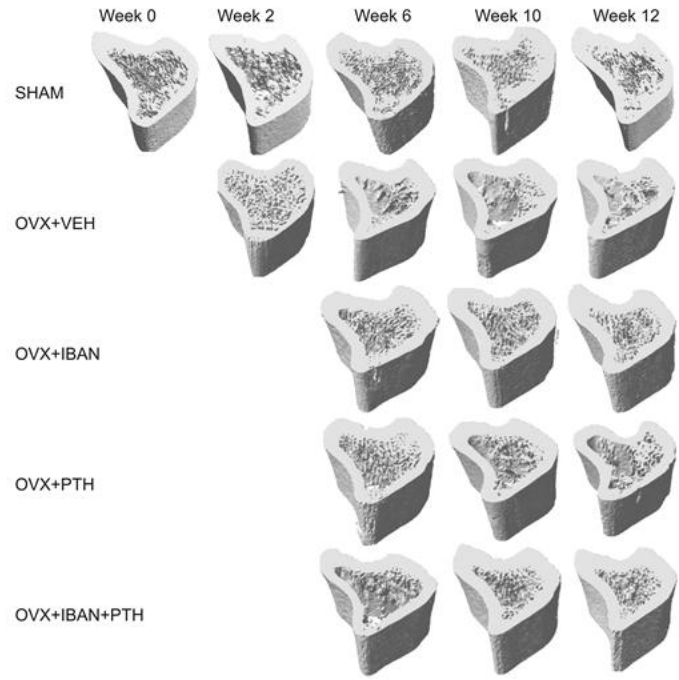

Figure 2 Visualization of bone loss in a transaction of the tibial metaphysis of rat

		Transaction Surgery (Wks)						
		0	2	4	6	8	10	12
Mean BMD (mg/cm³)	SHAM	631 ± 16	742 ± 14	743 ± 20	749 ± 8	786 ± 70	759 ± 22	780 ± 11
	OVX+VEH		643 ± 24	686 ± 29*	684 ± 33*	692 ± 14*	673 ± 4*	642 ± 28*
	OVX+PTH				817 ± 33	847 ± 30*	869 ± 29*^	864 ± 24*^
	OVX+IBAN				802 ± 9	798 ± 49*	875 ± 19*^	784 ± 29*
	OVX+PTH+IBAN				857 ± 63	781 ± 39*	721 ± 23*	782 ± 13
Tb. D (mg/cm³)	SHAM	358 ± 19	448 ± 13	439 ± 9	392 ± 16	406 ± 18	392 ± 16	407 ± 8
	OVX+VEH		322 ± 29*	273 ± 27*	192 ± 19*	200 ± 17*	190 ± 15*	170 ± 15*
	OVX+PTH				212 ± 12*	231 ± 20*^	218 ± 22*^	217 ± 20*^
	OVX+IBAN				256 ± 41*	285 ± 27*^	281 ± 34*^	316 ± 17*^
	OVX+PTH+IBAN				256 ± 36*	280 ± 50*^	244 ± 30*	270 ± 20*^
C.t.D (mg/cm³)	SHAM	1043 ± 1	1038 ± 8	1061 ± 28	1095 ± 26	1080 ± 13	1113 ± 65	1128 ± 22
	OVX+VEH		1026 ± 26	1004 ± 24	1095 ± 20	1110 ± 22	1102 ± 23	1136 ± 16
	OVX+PTH				1124 ± 28	1156 ± 21*^	1147 ± 13*^	1171 ± 16*^
	OVX+IBAN				1127 ± 22	1161 ± 16*^	1153 ± 15*^	1168 ± 21*
	OVX+PTH+IBAN				1122 ± 19	1150 ± 15*^	1132 ± 9*	1170 ± 14*^

*Significant difference from SHAM (p<0.05)
^Significant difference from OVX+VEH (p<0.05)
Sol=Sline (p<0.05)

Table 1 Volumetric density changes by treatment groups measured using pQCT.

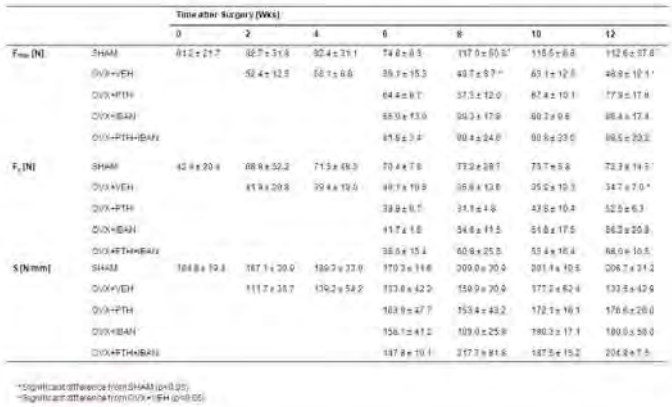

Table 2 Mechanical property changes by treatment groups measured using 3-point bending test

a) Concentrations of Bone formation marker. Values are represented as (mean ± SD).

		Time after Surgery [Wks]		
		0	6	12
P1NP	SHAM	19.9±11.6	14.4±7.2	7.8±0.1
	OVX+VEH	17.3±7.9	7.8±1.1	7.6±0.2
	OVX+PTH	19.61±11.9	10.3±0.7	28.6±3.6*+
	OVX+IBAN	13.3±2.1	9.3±2.3	6.1±0.3
	OVX+PTH+IBAN	21.6±3.1	12.9±1.8	48.9±4.0*+

b) Concentrations of Bone resorption marker. Values are represented as (mean ± SD).

		Time after Surgery [Wks]		
		0	6	12
CTX	SHAM	21.4±0.1	28.3±5.0	15.2±2.8+
	OVX+VEH	21.6±3.0	32.6±21.2	32.4±4.1*
	OVX+PTH	23.3±9.0	36.6±7.4	41.4±1.8*+
	OVX+IBAN	20.5±3.8	29.8±11.0	14.3±4.56+
	OVX+PTH+IBAN	26.2±0.2	14.1±1.6	17.5±3.6+

*Significant difference from SHAM ($p<0.05$)
+Significant difference from OVX+VEH ($p<0.05$)
Solid line $p<0.01$

Table 3 a) Concentrations of formation marker; b) Concentrations of resorption marker

***Disclosures: Xiao Yang**, None.*

MO0427

Effect of Bisphosphonates on Menaquinone-4 Biosynthesis in Human Osteoblasts. Toshio Okano*[1], Kimie Nakagawa[1], Naoko Okuda[1], Yoshitomo Suhara[2], Yoshihisa Hirota[1]. [1]Kobe Pharmaceutical University, Japan, [2]Yokohama College of Pharmacy, Japan

Vitamin K is a cofactor for γ-glutamyl carboxylase (GGCX), an enzyme that converts specific glutamic acid residues in several substrate proteins to γ-carboxyglutamic acid residues. It has three major forms, the plant-derived vitamin K1 (phylloquinone: PK), the bacterium-derived vitamin K_2 (menaquinone-4: MK-4), and the synthetic homologue vitamin K_3 (menadione: K_3). Vitamin Ks have been shown to play a role in bone formation besides classical blood coagulation. MK-4, but not PK, functions as a transcriptional regulator of extracellular matrix-related genes that are involved in the collagen assembly in bone by activating the steroid and xenobiotic receptor (SXR). Independent of SXR pathway, MK-4 modulates its target gene expressions in osteoblastic cells by enhancing the phosphorylation of protein kinase A. Moreover, clinical and nutritional studies have indicated that vitamin K is effective for prevention of osteoporotic fractures in postmenopausal women. Thus, vitamin K is believed to play a significant role in bone homeostasis. We recently reported that dietary PK is converted to MK-4 in the body and accumulates in bone (Okano *et al*., *J Biol Chem*.,2008, 283;17:11270-9). A proposed mechanism for this conversion is that the side chain moiety is released from PK after reduction of naphthoquinone ring, and then resulting intermediate, K_3 hydroquinone, is subsequently converted to MK-4 hydroquinone by a bond-forming reaction with a geranylgeranylpyrophosphate (GGPP) derived from the mevalonate synthetic pathway. Finally, the produced MK-4 hydroquinone is oxidized to MK-4 under atmospheric conditions. In this study, we examined in human osteoblastic MG-63 cells whether GGPP exogenously added to the medium is utilized to convert K_3 to MK-4, and whether bisphosphonates, well known inhibitors of the mevalonate pathway that produces GGPP, inhibit MK-4 biosynthesis by MG-63 cells. In these experiments, we used deuterium labeled compounds and LC-APCI-MS/MS methods for the structural assignments. As the results, the conversion of K_3 to MK-4 was significantly decreased, leading to decrease of vitamin K-dependent carboxylation of osteocalcin by treatment with nitrogenous bisphosphonates, but not by treatment with a non-nitrogenous bisphosphonate. Our results suggest that vitamin K supplementation would be required to maintain bone homeostasis for osteoporotic patients with nitrogenous bisphosphonate treatment.

***Disclosures: Toshio Okano**, None.*

MO0428

Segregation of Pro-apoptotic and Anti-resorptive Functions of Risedronate In Vivo. Takumi Matsumoto*[1], Yuichi Nagase[1], Tetsuro Yasui[2], Hironari Masuda[1], Kozo Nakamura[1], Sakae Tanaka[1]. [1]The University of Tokyo, Japan, [2]University of Tokyo, Japan

Nitrogen-containing bisphosphonates (N-BPs) are potent anti-resorptive agents, and one of the most successful therapeutics for the treatment of osteoporotic patients. However, the molecular mechanism of action of N-BPs in vivo has not been fully clarified yet. In particular, it remains elusive whether the anti-resorptive effect of N-BPs is mediated by its apoptosis-inducing activity in osteoclasts (OCs) or through the suppression of bone-resorbing function of OCs. In the last ASBMR meeting, we reported that the apoptosis-inducing activity of risedronate (RIS) in osteoclasts is much reduced in *bim*$^{-/-}$ OCs in vitro. In this study, we analyzed the effect of RIS in *bim*$^{-/-}$ mice and normal mice in vivo, and tried to elucidate whether or not the anti-resorptive effect of RIS in vivo is through the induction of OC apoptosis.

RIS (0.01 mg/kg body weight) or normal saline was subcutaneously injected into14-week-old *bim*$^{-/-}$ and wild type (WT) mice once a day for 14 days. Next day after the final injection, the mice were sacrificed and were analyzed radiologically, biochemically and histologically.

Histological analysis of proximal tibial metaphysis showed that OC apoptosis induced by RIS was prominently suppressed in *bim*$^{-/-}$ mice compared to WT mice as determined by TUNEL staining. However, RIS treatment induced increase in bone mass and decrease in serum type I collagen crosslinks at the comparable levels in both *bim*$^{-/-}$ and WT mice. RIS treatment induced about 50% increase in OC number per bone perimeter in WT mice as compared to untreated mice, while RIS-induced increase in OC number was not observed in *bim*$^{-/-}$ mice. Giant OCs detached from bone surfaces were similarly observed in both *bim*$^{-/-}$ and WT mice in response to RIS treatment.

These results suggested that anti- resorptive effect of RIS in vivo is due to other mechanism than induction of OC apoptosis.

***Disclosures: Takumi Matsumoto**, None.*

MO0429

Lovaza® Prevents Aging Associated Bone Loss in C57BL/6 Mice by Inhibiting Inflammation and Bone Resorption. Md Rahman*[1], Ganesh Halade[2], Jyothi Veigas[2], Kazi Nishu[2], Paul Williams[2], Gabriel Fernandes[2]. [1]University of Texas Health Science Center, USA, [2]UTHSCSA, USA

Aging associated bone mineral density (BMD) loss is becoming a significant, worldwide social and financial health care problem. In this study, we demonstrated the beneficial role of FDA approved prescription omega-3 fatty acids, Lovaza® against BMD loss during aging. To determine the effect of Lovaza® on BMD during aging, 12 month old C57BL/6 mice were fed for 12 months. DXA scan was performed once before starting the diet at 12 month of age and again after 12 months of feeding with experimental diets at 24 month of age. Mice were fed with 1% and 4% of Lovaza® and 1% and 4% placebo diets including a group with 4% regular fish oil (18/12 (EPA/DHA)) diet. After analyzing the BMD of different bone regions, we found that 4% Lovaza® prevents age-associated BMD loss while 1% Lovaza® offers mild protection against age-associated bone loss. However, 1% Lovaza® showed better protection against age-associated bone loss than that of commercially available 4% regular fish oil. We also measured the effect of LPS-stimulated cytokines production in bone marrow cells collected from mice fed different experimental diets. Interestingly, 4% Lovaza® showed decreased production of pro-inflammatory cytokines, TNF-α, and IL-6 and increased production of anti-inflammatory cytokines IL-10 and IFN-γ as compared to that of other groups. We also analyzed RANKL-stimulated activation of inflammatory and pro-osteoclastogenic signaling molecules p38 MAPK and JNK in bone marrow cells from mice fed different experimental diets using Fast Activated Cell-based ELISA (FACE) assay system. Interestingly, both 1% and 4% Lovaza® showed reduced activation of both p38 MAPK and JNK. Further, we analyzed the components of bone remodeling (bone turn over markers) in serum samples for TRAP5b, PINP, RANKL and OPG. Bone resorption marker, TRAP5b level was dramatically reduced in 4% Lovaza treated mice, whereas, bone formation marker, PINP level was unaffected. Moreover, the osteoclast stimulating factor, RANKL was significantly reduced in 4% Lovaza treated mice whereas, the decoy receptor for RANKL, OPG level was unaffected. These data indicate that Lovaza® protects age-associated bone loss in C57BL/6 mice by modulating inflammatory signaling molecules and related bone resorption.

***Disclosures: Md Rahman**, None.*

MO0430

Recommended Intake of Vitamin D2 is not as Effective as Vitamin D3 in Recovering Serum 25OHD in Vitamin D Insufficient Sham and OVX Rats. Silvia Friedman[1], Clarisa Marotte[2], Macarena Gonzales Chaves*[3], Gabriel Bryk[4], Gretel Pellegrini[5], Susana Zeni[6]. [1]PhD, Argentina, [2]Biologist, Argentina, [3]Odontologist, Argentina, [4]Biochemist, Argentina, [5]seccion osteopatias medicas, Hospital de Clínicas José de San Martín, Argentina, [6]University of Buenos Aires, Argentina

D3 according to previous works is almost twice more potent than D2 in raising 25OHD levels (J Clin Met endoc 93:3015, 2008). We performed a study using our model of vit D insufficiency in adult SHAM and OVX rats refeeding with 2 isocaloric diets that supplied the recommended dietary vitamin D intake which only differed in the source of vit D (Bone 39: 837-844, 2006). During 15 days post-surgery all rats fed a diet containing 15% protein, 200IU% vit D and 0.6% calcium followed by an additional period of 45 days with diet lacking of vit D (0 IU%) to obtain vit D insufficiency. After the105-days, rats were divided into 4 groups that fed a diet containing 100UI% of D2 (OVX+D2 and SHAM+D2) or D3: (OVX+D3 and SHAM+D3).

Baseline, 60, 85 and 105 days serum 25HOD (ng/ml) levels were measured in each group by a methodology recognized both 25OHD3 and 25OHD2 (125I RIA Kit, DiaSorin, Stillwater, MN, USA). Results of SHAM and OVX rats are show in figures 1 and 2, respectively.

(*) p? 0.01 compared to baseline and (**) $p<0.05$ compared to D2

Conclusions: Under our experimental conditions, recommended dietary intake of vitamin D supplied by adding D3 in the diet is more effective than supplying D2 in raising 25OHD levels during a 45 day period in both estrogen conditions. PIP 6483

Figure 1

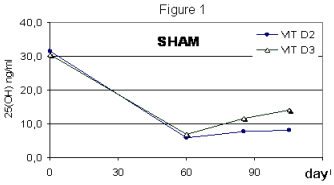

Figure 2

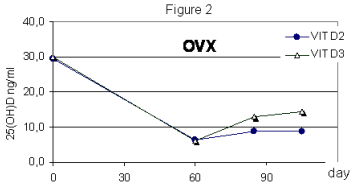

figures 1 and 2

***Disclosures: Macarena Gonzales Chaves**, None.*

MO0431

The Effects of Colored Rice in the Prevention of Bone Loss in Ovarectomized Rats. Jordan Teeple*[1], William Gilbert[1], Priyanka Sharma[1], Vidya Gadang[1], Yan Wang[1], Brenda Smith[2], Latha Devareddy[1]. [1]University of Arkansas, USA, [2]Oklahoma State University, USA

In recent years, there has been an increased interest in the use of functional foods in the prevention of chronic diseases. Colored rice, particularly black and red rice are rich in antioxidants that have been shown to prevent bone loss. Therefore, the objective of this study was to assess the effects of red and black rice in preventing bone loss in an ovariectomized rat model. Forty-eight Sprague-Dawley rats were either sham operated (Sham) or ovariectomized (Ovx) and randomly divided into four groups (n=12): Sham control, Ovx control, Ovx + red rice, or Ovx + black rice. The Sham and Ovx controls received AIN-93M diet. The rats in the red and black rice groups received similar diets in which the cornstarch was replaced with red or black rice flour (approximately 20% w/w). After 100 days of treatment, rats were euthanized and tissues were collected for analysis. Bone mineral density (BMD) of whole body, fourth lumbar vertebra, femur, and tibia were measured by dual-energy X-ray absorptiometry. Biomarkers of bone metabolism were assessed using enzyme-linked immunoassays. The findings of the study are presented below:

Values are presented as mean ± SEM. Values within rows that do not share a common letter are significantly different ($P<0.05$). Abbreviations: Deoxypyridinoline (DPD); Bone Mineral Density (BMD).

Preliminary data analyses indicate that red and black rice are effective in prevention of bone loss as indicated by increased femur BMD values compared to Ovx control. The bone protective mechanism of colored rice needs to be elucidated.

	Sham	Ovx Control	Red Rice	Black Rice
Femur BMD (g/cm^2)	0.2386 ± 0.0028^a	0.2237 ± 0.0029^b	0.2325 ± 0.0029^a	0.2312 ± 0.0029^a
4th Lumbar BMD (g/cm^2)	0.2295 ± 0.0038^{ab}	0.2183 ± 0.0038^b	0.2221 ± 0.0040^{ab}	0.2195 ± 0.0040^b
Osteocalcin (ng/mL)	85.74 ± 19.46^b	136.89 ± 15.27^a	161.88 ± 15.70^a	154.33 ± 13.87^a
DPD (nmol/mmol creatinine)	16.29 ± 4.06^b	37.29 ± 4.06^a	41.09 ± 4.76^a	38.34 ± 4.26^a

Table

***Disclosures: Jordan Teeple**, None.*

MO0432

Short Term Effects of a Transdermal Contraceptive Patch on Bone Turnover in Premenopausal Women. Jason Vescovi*[1], Robert Foulds[1], Bruce Bain[2], Ira Jacobs[1]. [1]York University, Canada, [2]Defence Research & Development Canada Toronto, Canada

Sex steroid hormones are potent regulators of bone metabolism thus there is concern about the effects of exogenous hormonal contraceptives on bone health in premenopausal women (Martins et al. 2006; Herrmann and Seibel, 2009). The combination estrogen-progestin pill is the most widely used reversible contraceptive method, however newer technologies that do not call for daily compliance have been developed. Use of the transdermal contraceptive patch results in a 60% greater estrogen exposure compared to oral contraceptives (Devineni et al., 2007), therefore it is plausible that alterations to bone turnover would exceed those previously observed while using oral contraceptives. We used a prospective open labelled study design to examine the short term effects of the transdermal contraceptive patch (EVRA®) on markers of bone formation and resorption in young women. Nine healthy premenopausal women volunteered for this study and were prescribed one cycle of EVRA® containing 6.0 mg norelgestromin/0.6 mg ethinyl estradiol, with the first patch being placed on day 2-5 of menses. Fasting venous blood samples were taken for 5 consecutive weeks between 0800-1000 hr to assess bone turnover markers BSAP and SCTX-I. A repeated measures ANOVA was used to assess changes in bone turnover concentrations. Compared to Baseline (25.8 ± 6.8 U•L-1) mean serum BSAP levels were 12% (22.8 ± 6.6 U•L-1, p=0.486) and 18% (21.2 ± 5.9 U•L-1, p=0.249) lower after two and three weeks, respectively, but returned to 94% (24.4 ± 6.2 U•L-1) of Baseline values following the withdrawal week. Compared to Baseline (0.61 ± 0.16 ng•mL-1) mean SCTX-I was reduced by 40% (0.36 ± 0.10 ng•mL-1; p=0.002) after only one week of the patch and tended to remain suppressed by 26-30% ($p\leq0.10$) through the third week, returning to 90% of Baseline (0.54 ± 0.15 ng•mL-1) after the withdrawal week. No adverse events were reported and side effects included minor headaches, breast tenderness, itchiness at the application site and weight gain (~1.5 kg; $p\leq0.02$). These data indicate that the transdermal contraceptive patch rapidly reduced bone resorption, but has a delayed and less suppressive effect on bone formation. Despite these short term effects of the patch on BSAP and SCTX-I, the concentrations remained within normal reference ranges for premenopausal women (Glover et al., 2008, 2009; De Papp et al., 2007) and do not appear to have deleterious consequences on BMD with use during 12 months (Massaro et al., 2010).

***Disclosures: Jason Vescovi**, None.*
This study received funding from: Janssen-Ortho Inc.

MO0433

The Novel Selective Androgen Receptor Modulator (SARM) ORM-11984 Prevents the Development of Osteopenia in Aged Orchidectomized Rats. Jukka Morko*[1], Jukka Rissanen[2], ZhiQi Peng[3], Mari Suominen[3], Katja Fagerlund[3], Laura Ravanti[4], Riikka Oksala[4], Pekka J. Kallio[4], Jussi Halleen[3]. [1]Pharmatest Services Ltd, Fin, [2]Pharmatest Services,Limited, Finland, [3]Pharmatest Services Ltd, Finland, [4]Orion Corporation, Finland

Selective androgen receptor modulators (SARMs) are androgen receptor ligands with oral bioavailability and tissue-selective effects on sex organs, skeletal muscle and bone. We have recently demonstrated that a novel SARM, ORM-11984, exhibits efficacy sufficient to prevent the development of osteopenia induced by ovariectomy and disuse, and to treat established osteopenia induced by orchidectomy (ORX) in young adult rats. The purpose of this study was to characterize effects of ORM-11984 on the prevention of osteopenia in aged ORX rats. Male Sprague-Dawley rats were operated at the age of 12 months and treated once a day for 4 months. The following study groups were included, with 12 animals in each group: 1) Sham-operated group receiving vehicle; 2) ORX group receiving vehicle; 3) ORX group receiving a subcutaneous dose of 0.6 mg/kg/d testosterone propionate (TP) used as a reference compound; 4) ORX group receiving an oral dose of 0.5 mg/kg/d ORM-11984; 5) ORX group receiving an oral dose of 3.0 mg/kg/d ORM-11984. Treatment effects were analyzed by peripheral quantitative computed tomography and bone histomorphometry. Biochemical markers of bone turnover, including osteocalcin, C-terminal cross-linked telopeptides of type I collagen (CTX-I) and tartrate-resistant acid phosphatase isoform 5b (TRACP 5b) were determined in fasting serum samples before the start of treatment and at 1, 2 and 4 months. Development of metaphyseal and diaphyseal osteopenia was observed in ORX rats treated with vehicle. Treatment with ORM-11984 at the doses of 0.5 and 3.0 mg/kg/d prevented ORX-induced reduction in trabecular bone mineral density in tibial metaphysis and ORX-induced reduction in cortical thickness in tibial diaphysis. Treatment with ORM-11984 also decreased serum levels of biochemical markers of bone turnover and parameters of dynamic histomorphometry on the trabecular bone surface, indicating anti-catabolic activity. The bone effects observed in ORX rats treated with ORM-11984 were similar to corresponding effects observed in ORX rats treated with TP. In addition, treatment with ORM-11984 and TP decreased body weight and prevented ORX-induced reduction in prostate weight. Treatment with ORM-11984 maintained the prostate weight at the sham-level, whereas treatment with TP increased it above the sham-level. We conclude that ORM-11984 is a novel SARM with efficacy sufficient to prevent the development of osteopenia in metaphysis and diaphysis of aged ORX rats.

***Disclosures: Jukka Morko**, None.*
This study received funding from: Orion Corporation

MO0434

A Hypertensive Drug Telmisartan Selectively Activates PPARg Pro-Adipocytic but not Anti-Osteoblastic Activities in Marrow Mesenchymal Stem Cells (MSCs). Beata Lecka-Czernik[1], Vipula Petluru*[2]. [1]University of Toledo College of Medicine, USA, [2]University of Toledo Medical Center, USA

Anti-diabetic drugs TZDs improve insulin sensitivity by activating PPARγ nuclear receptor, however their prolonged use causes bone loss and increases fracture risk. In marrow MSCs, activation of PPARγ2 with TZD rosiglitazone (R) induces adipocyte and suppresses osteoblast differentiation. The beneficial anti-diabetic and pro-adipocytic (pro-AD) activities of PPARγ2 can be separated from the unwanted anti-osteoblastic (anti-OB) activity by using selective PPARγ agonists. The anti-hypertensive drug Telmisartan (TEL), which binds to and inhibits the activity of Angiotensin II receptor, also acts as a selective PPARγ agonist. Activation of PPARγ with TEL improves insulin resistance and lipid profile by upregulating GLUT4 expression, increasing glucose uptake, and by increasing serum adiponectin levels. To date, there are no reports on the effects of TEL on human skeleton. We tested the effect of TEL on MSCs lineage commitment using U33/γ2 cell model of MSCs differentiation under the control of PPARγ2. TEL (50 μM) did not affect osteoblast phenotype as assessed by an alkaline phosphatase (ALP) enzyme activity and expression of Runx2 and Dlx5, however it induced adipocyte phenotype typified by accumulation of fat droplets and significant increase in the gene expression for aP2 (56-fold) and adiponectin (5.6-fold). Next, we tested whether TEL may protect against the anti-OB effect of R. U33/γ2 cells were treated with R alone (1 μM) or in combination with TEL (50 μM). As expected, R alone suppressed osteoblast phenotype, however combined treatment with TEL and R did not affect ALP activity nor expression of Runx2 and Dlx5, indicating that TEL selectively inhibits R-induced PPARγ2 anti-OB activity. Previous studies have showed that R-activated PPARγ2 suppresses an activity of TGFß/BMP signaling by decreasing expression of TGFß3, BMP4, TGFßR2 and Smad6. TEL not only did not affect the TGFß/BMP pathway activity, but it protected TGFß/BMP pathway from negative effects of R. In summary, our data reveal that TEL selectively induces pro-AD but not anti-OB PPARγ activity and, in the presence of R, it protects integrity of TGFβ/BMP signaling. Currently, TEL effect on the skeleton, alone and in combination with R, is tested in the murine model of type 2 diabetes, A^{vy}/a mice. In conclusion, TEL may represent a drug, to be used alone or in combination with R, for simultaneous treatment of hypertension and diabetes without adverse effects on bone.

***Disclosures: Vipula Petluru**, None.*

MO0435

CEA Enantiomers Exerts Different Effects on Estrogen-Sensitive Bone and Cancer Cells. Man-Sau Wong[1], Man-Chun Law[2], Tak-Hang Chan[3], Ka-chun Wong*[4]. [1]Hong Kong Polytechnic University, Hong kong, [2]Co-lab, Hong kong, [3]Co-supervisior, Hong kong, [4]The Hong Kong Polytechnic University, Hong kong

4b-carboxymethyl-(-)-epiafzelechin acid (CEA) is a flavan-3-ol previously identified as active ingredient in Chinese herbal medicine *Drynaria fortunei (Kunze) J. Sm. that exert osteoprotective effects.* CEA, previously synthesized in our laboratory as racemic mixture, was shown to be able to stimulate osteoblastic functions through the activation of estrogen receptor (ER). We hypothesized that the two CEA enantiomers might interact differently with ER and exert different effects on osteoblastic-like cells.

The present study aims to compare the estrogenic properties of the CEA enantiomers (stereospecific CEA(-) and CEA(+)) in rat osteoblastic UMR 106 cells and human breast cancer MCF-7 cells. UMR 106 cells or MCF-7 cells were treated with 10^{-14} to 10^{-6}M, of CEA (racemic mixture), CEA(-) or CEA(+), estradiol (E2, 10^{-8}M) or its vehicle. The effects of CEAs on cell proliferation were assessed by MTS assay and the effects on osteoblast differentiation were studied by measurement of alkaline phosphatase (ALP) activities. The ability of CEAs to transactivate estrogen response element (ERE)-dependent transcription was determined in UMR 106 cells co-transfected with either ER-α or ER-β construct and ERE-luciferase construct.

Both CEA(-) and CEA(+) are able to promote the growth of UMR-106. Only CEA(-) is able to increase the ALP activity but not CEA(+). However, the proliferation of CEA(-) and CEA(+) are not as potent as the racemic mixture of CEA (CEA: ↑ 52% vs Ctrl, 10^{-8}M;CEA (-) ↑ 22% vs Ctrl, 10^{-8}M; and CEA (+) ↑ 28% vs Ctrl, 10^{-14}M) while the ALP activity in both CEA(-) and CEA(+) are weaken when compared to the racemic mixture. Transfection assay indicated that CEA(+), but not CEA(-), could activate ERE-dependent luciferase activities via ER-α and ER-β in UMR 106 cells in a dose-dependent manner. CEA(+) could activate ERE-dependent luciferase activities via ER-α with a comparable effect to E2(10^{-8}M). This imply that the ERE-dependent luciferase activities of CEA racemic mixture is mainly due to CEA(+). For MCF-7 breast cancer cells, both CEA(-) and CEA(+) would slightly increase the proliferation of cells at relative high concentrations. These demonstrate that CEA exert different effect on different estrogen-sensitive cell types. Further characterization of CEA enantiomers on estrogen-sensitive cells may be able to select a CEA enantiomer to use as a bone protective agent.

***Disclosures: Ka-chun Wong**, None.*
This study received funding from: RGC General Research Fund

MO0436

Inhibition of the Angiotensin Pathway Increases Bone Mass by Reducing Osteoclastogenesis. Shan Chen*[1], Tarek Sibai[1], Tao Yang[1], Jianning Tao[1], Dobrawa Napierala[1], Brian Dawson[1], Jennifer Black[2], Yuqing Chen[1], Ming-Ming Jiang[1], Brendan Lee[1]. [1]Baylor College of Medicine, USA, [2]Vanderbilt University School of Medicine, USA

Hypertension and osteoporosis are common diseases affecting an increasingly aging population. The angiotensin pathway plays a central role in controlling blood pressure and is an important target for anti-hypertension drugs. Interestingly, through epidemiological studies in human as well as animal experiments, it has been found that the blockage of this pathway is associated with reduced risk of fractures, while activation of this signaling leads to bone loss. However, the mechanistic basis is largely unknown. Our aim in this study is to understand the effects of inhibiting the angiotensin pathway on bone homeostasis using the mouse model. We administered Losartan, an angiotensin II type I receptor antagonist in both wild-type (WT) and the ovariectomized (OVX) mice. After 6 weeks, Losartan-treated WT mice showed a significant increase in femoral cortical thickness, increased in trabecular bone volume/total bone volume (BV/TV), trabecular thickness, and trabecular number, and corresponding decrease of trabecular separation. Interestingly, we observed that osteoclast numbers were significantly decreased whereas osteoblast numbers did not change. Similarly, OVX mice treated with Losartan showed a significant improvement in trabecular BV/TV, trabecular thickness and bone mineral density. In conclusion, the inhibition of angiotensin signaling by Losartan shows beneficial effects on bone mass via reduction of bone resportion secondary to a decrease in osteoclast numbers. These data suggest that use of angiotensin receptor antagonists may have added beneficial effects beyond treatment of hypertension.

***Disclosures: Shan Chen**, None.*

MO0437

Melatonin Functionalized on Novel Bone Regenerating Scaffolds Enhances Bone Remodeling Activity in a Model of Calvaria Defects. William Clafshenkel*[1], James L. Rutkowski[2], Rachelle Palchesko[3], Jared Romeo[3], Kenneth McGowan[4], Ellen S. Gawalt[3], Paula A. Witt-Enderby[1]. [1]Graduate School of Pharmaceutical Sciences, Duquesne University, USA, [2]Department of Restorative Dentistry, State University of New York at Buffalo, USA, [3]Department of Chemistry & Biochemistry, Duquesne University, USA, [4]Westmoreland Advanced Materials, USA

The prevalence of osteonecrosis of the jaw (ONJ) is increasing in menopausal patients taking bisphosphonates for the prevention and treatment of osteoporosis. Incorporating bone autografts into reconstructive procedures for patients with ONJ is complicated by poor bone integrity and limited bone quantity. Patients with ONJ may benefit from novel approaches in optimizing synthetic bone grafting materials. The use of platelet-rich plasma (PRP) in oral surgery reduces healing time and increases the quality and quantity of reformed bone. Melatonin aids bone formation by enhancing osteoblast differentiation and inhibiting osteoclast-mediated bone resorption. Thus, the use of synthetic materials combined with melatonin and PRP may provide adequate scaffolding and local stimuli necessary for new bone generation in oral graft procedures. It is hypothesized that the cooperative effects between the novel bone regenerating scaffold (BRS), melatonin, and PRP will enhance bone regeneration in a model of calvarial bone defects. Initial *in vitro* assessments demonstrate that melatonin functionalized on the BRS (BRS-Mel) had a significant preference for the adherence of normal human osteoblasts versus NIH3T3 fibroblasts. Chick chorioallantoic membrane assays indicate that the novel BRS is nontoxic. Ovariectomized rats underwent osteotomy and implant procedures in four groups: BRS, BRS-Mel, BRS plus PRP, and BRS-Mel plus PRP. Bone regeneration was assessed by histology and double-fluorochrome labeling at three and six months. Histological examination indicates scaffold integration, tissue infiltration into scaffold pores, and osteoid synthesis along the scaffold surface for all groups. Groups implanted with BRS-Mel showed a significantly greater degree of bone remodeling activity across the scaffold surface at three and six months, and significantly more regions of bone remodeling activity at six months when compared to other treatment groups and control. This suggests that BRS-Mel may significantly impact the degree and rate of osteoid tissue mineralization and bone formation in this model and that the implanted BRS is biocompatible. Cooperative interactions between the novel BRS and melatonin may create a synthetic bone graft therapy that surpasses traditional grafting methods for post-menopausal women exhibiting ONJ.

***Disclosures: William Clafshenkel**, None.*

MO0438

Nanobodies Targeting RANK-Ligand are Strong Inhibitors of Human Osteoclast Differentiation *in Vitro*. Jussi Halleen*[1], Katja Fagerlund[1], Hans Ulrichts[2], Els Beirnaert[3], Sigrid Cornelis[2], Jukka Rissanen[4]. [1]Pharmatest Services Ltd, Finland, [2]Ablynx NV, Belgium, [3]Ablynx, Belgium, [4]Pharmatest Services,Limited, Finland

Nanobodies® are a novel class of antibody-derived therapeutic proteins that combine the advantages of conventional antibodies with important features of small molecule drugs. We studied the effects of three Nanobodies, #60, #130 and #180 that target the ligand for receptor activator of nuclear factor kappa B (RANKL) on differentiation of human osteoclasts *in vitro*. Human bone marrow-derived CD34-positive osteoclast precursor cells were cultured on bovine bone slices in the presence of M-CSF and RANKL. The cells were cultured on 96-well plates, each plate containing 8 replicates of a baseline group including vehicle, a control group including 5.0 nM osteoprotegerin (OPG) as a reference inhibitor, and 7 different concentrations (0.05, 0.3, 1.0, 3.0, 10, 50 and 250 nM) of one of the Nanobodies. The cultures were stopped at day 7, and the cells were fixed with paraformaldehyde and stained for tartrate-resistant acid phosphatase (TRACP). Secreted TRACP 5b was measured from the culture medium collected at day 7 as an index of the number of osteoclasts formed during the differentiation period. The reference inhibitor OPG inhibited significantly human osteoclast differentiation. All three Nanobodies inhibited dose-dependently osteoclast differentiation with similar inhibition profiles. Their half maximal inhibitory concentrations (IC50) were 1.56 nM for compound #60, 1.18 nM for compound #130 and 1.14 nM for compound #180. Maximal inhibition was observed with 3.0 nM concentrations of all three Nanobodies. Morphological studies demonstrated that cultures treated with 3.0 nM concentrations of the Nanobodies contained a large number of TRACP-positive mononuclear osteoclast precursor cells, but no multinuclear TRACP-positive osteoclasts. TRACP 5b secretion was, however, strongly decreased, confirming the earlier findings observed in mouse osteoclast cultures that TRACP-positive mononuclear osteoclast precursor cells do not secrete enzymatically active TRACP 5b. These results demonstrate that the tested Nanobodies targeting RANKL inhibited strongly osteoclast differentiation, with their IC50 values between 1.1 – 1.6 nM concentrations.

***Disclosures: Jussi Halleen**, IDS Ltd, 7; IDS Ltd, 5*
This study received funding from: Ablynx NV

MO0439

Preclinical Assessment of Cell Based Therapies to Treat Type II Osteoporosis. Jeffrey Kiernan*, William Stanford. University of Toronto, Canada

Osteoporosis affects more than 1.4 million Canadians, costing >$1.3 billion a year in Canada. Osteoporosis can be divided into two categories, postmenopausal osteoporosis (type I) and age-related osteoporosis (type II). Therapeutics targeting type II osteoporosis remain underdeveloped. Our lab has generated the Sca-1 null mouse that closely approximates human type II osteoporosis. Sca-1 null mice display decreased mesenchymal progenitor cell (MPC) self-renewal and expansion capabilities. This model strongly suggests that age-related osteoporosis can be attributed to MPC defects; thus, MPCs and their progeny could be therapeutic targets. While drugs would be the optimal therapy, the appropriate first step is to validate that increasing the MPC pool via MPC transplantation is therapeutic. We have isolated a Sca-1+CD44+CD45-CD11b- plastic adherent cell population that retains osteogenic capacity. To enrich for these MPCs, we utilized compact bone along with bone marrow as a cell source. In addition, we have optimized dissociation conditions where released cells are enriched for the desired population, leaving unwanted hematopoietic cells attached to the tissue culture vessel. To allow subsequent in vivo tracking of donor cells, we transduced passage 0 cells with eGFP via retrovirus, resulting in approximately 60% eGFP+ cells, with 95% of eGFP+ cells being mesenchymal. Isolated eGFP+Sca-1+CD44+CD45-CD11b- are to be used in a series of transplants into Sca-1 null neonates and adults, with the aim of rescuing the osteoporotic phenotype, thus showing proof of principle that increasing the local MPC population may relieve the human form of the disease. Preliminary transplant data display the presence of transplanted MSCs within the bones of recipient mice after 1 week. Long-term transplant studies are currently underway to determine donor contribution to bone quality and strength.

***Disclosures: Jeffrey Kiernan**, None.*

MO0440

Vitamin K2 Prevents Hyperglycemia and Cancellous Osteopenia in Rats with Streptozotocin-induced Type 1 Diabetes. Jun Iwamoto*[1], Azusa Seki[2], Tsuyoshi Takeda[1], Hideo Matsumoto[1], James Yeh[3]. [1]Keio University School of Medicine, Japan, [2]Hamri. Co., Ltd., Japan, [3]Winthrop University Hospital, USA

The purpose of the present study was to examine the effect of vitamin K2 on cancellous and cortical bone mass in rats with streptozotocin (STZ)-induced type 1 diabetes. Twenty-seven 12-week-old male Sprague-Dawley rats were randomized according to the stratified weight method into three groups: age-matched controls, STZ + vehicle, and STZ + vitamin K2. STZ (40–50 mg/kg) was administered intravenously twice during the initial one-week period. Vitamin K2 (menatetrenone, 30 mg/kg) was administered orally five times a week. After 12 weeks of treatment, serum glucose levels and femoral length and weight were measured and bone histomorphometric analysis was performed on cancellous and cortical bone of the distal metaphysis and diaphysis of the femur, respectively. STZ administration induced hyperglycemia, decreased femoral weight, but not femoral length, induced cancellous osteopenia as a result of decreased number of osteoblasts/bone surface (N.Ob/BS) and osteoblast surface (ObS)/BS without significantly affecting bone resorption parameters, but did not significantly decrease cortical bone mass. Vitamin K2 administration to STZ-administered rats prevented development of hyperglycemia, did not induce a decrease in femoral weight, without significantly affecting femoral length, prevented cancellous osteopenia by inhibiting decreases in N.Ob/BS and ObS/BS without significantly affecting bone resorption parameters, but did not significantly increase cortical bone mass. These results suggest the beneficial effects of vitamin K2 on glucose metabolism and cancellous bone mass in rats with STZ-induced type 1 diabetes.

***Disclosures: Jun Iwamoto**, None.*

MO0441

The Combined Therapy of Alendronate and Eldecalcitol has Therapeutic Advantages over Monotherapy by Improving Bone Strength. Sadaoki Sakai*[1], Masahiko Mihara[2], Hitoshi Saito[3], Fumiaki Takahashi[3], Ayako Shiraishi[4]. [1]Chugai Pharmaceutical Co., LTD., Japan, [2]Chugai Pharmaceutical Co., LTD, Japan, [3]Chugai Pharmaceutical Company, Limited, Japan, [4]Chugai Pharmaceutical Co.,Ltd., Japan

Eldecalcitol (ED-71), a 2β-hydroxypropyloxy derivative of 1α,25$(OH)_2D_3$, is a more potent inhibitor of bone resorption than alfacalcidol while maintaining osteoblastic function in estrogen-deficient high-turnover osteoporosis rat model. Alendronate (ALN) has been reported to increase bone mass by suppressing bone resorption mainly by inducing apoptosis of osteoclasts. The aim of this study was to clarify the synergistic effect of ED-71 and ALN on bone loss in ovariectomized (OVX) rats. Ninety-six, 32 week-old Wistar rats were OVX and randomly assigned 10 groups (n=9~11), and 11 rats were sham-operated (SHAM). Rats were received either vehicle, ALN (0.05, 0.2 mg/kg), ED-71 (0.015, 0.03 mg/kg) alone or a combination with ALN and ED-71. The treatment started 2 weeks after surgery and continued for 12 weeks by oral gavages. The ALN monotherapy or the ED-71 monotherapy significantly inhibited bone loss in lumbar spine, and improved bone mechanical strength. The combination of ALN and ED-71 significantly increased bone mineral density (BMD) greater than the ALN monotherapy. Interestingly, the combination therapy improved the bone mechanical strength of lumbar spine significantly greater than the monotherapy, suggesting that the combination therapy may be beneficial not only for the BMD, but also for the bone quality. Furthermore, the urinary deoxypyridinoline, a bone resorption marker, was rapidly declined by the 4-week the combination therapy. The ED-71 dose-dependently increased serum calcium (Ca). The ALN counteracted the elevation of serum Ca by the ED-71 treatment. The serum Ca of the combination therapy (ALN 0.2 mg/kg + ED-71 0.03 mg/kg) was significantly lower than serum Ca of the ED-71 monotherapy (0.03mg/kg). In conclusion, the combination therapy of ALN and ED-71 has therapeutic advantages over the monotherapy not only by reducing the occurrence of hypercalcemia, but also by improving bone mechanical strength.

***Disclosures: Sadaoki Sakai**, Chugai Pharmaceutical Co., LTD, 3*
This study received funding from: Chugai Pharmaceutical Co., LTD.

MO0442

Vitamin D_3 Enhances Collagen Maturation in Ovariectomized Rat Bones. Hideaki Nagaoka*, Marnisa Sricholpech, Masahiko Terajima, Mitsuo Yamauchi. University of North Carolina, Chapel Hill, USA

Fibrillar type I collagen is the structural basis of bone formation. Recently we have reported that 1,25$(OH)_2$ vitamin D_3 (VD_3) regulates the post-translational modifications of collagen, a critical determinant of bone quality, in an osteoblastic cell culture system. In the present study, we investigated the effects of VD_3 on the quality and quantity of bone collagen using an ovariectomized rat model. Female Sprague Dawley rats (12 wk-old) were ovariectomized (OVX) - or sham-operated. At 4 weeks post-surgery, rats were divided into six groups (7/group, a total of 42 rats): sham + vehicle (S), OVX + vehicle (OVX), and OVX treated with 4 different doses of 1α$(OH)D_3$, a vitamin D_3 analog, (ALF) (0.007, 0.022, 0.067 and 0.2 μg/kg/day). Each drug was administered orally five times a week for 12 weeks and the animals were sacrificed. The tibiae were dissected, and the proximal metaphyses were subjected to biochemical (5/group) and histological (2/group) analyses. For the former, the specimens were pulverized, demineralized, reduced with standardized NaB^3H_4, and subjected to quantitative amino acid and cross-link analyses. For the latter, the bone collagen matrix was evaluated by picrosirius red staining (PSR) under polarized light microscope. The results of biochemical analyses demonstrated that the collagen content was significantly decreased in (OVX) compared to (S) ($p<0.05$) but, with the (ALF) treatment, it increased to the level comparable to (S). Two major reducible/immature cross-links, dihydroxylysinonorleucine and hydroxylysinonorleucine, and

two nonreducible/mature cross-links, pyridinoline and deoxypyridinoline, were identified in all samples. In (OVX), the mature cross-links were significantly diminished compared to (S) ($p<0.05$). However, even with the lowest dose of (ALF), the levels returned to those comparable to (S), and further increased in a dose-dependent manner. The total number of aldehyde (both free and cross-linked) in the group treated with highest dose of (ALF) was significantly higher than the rest of the groups ($P<0.05$). By PSR staining, collagen in (OVX) appeared as immature and poorly organized matrix, however with the (ALF) treatment, both maturation and organization were significantly improved with dose. These data strongly indicate that VD_3 enhances not only collagen deposition but also the maturation and stability of collagen in osteoporotic bones, which likely contributes to the improvement of bone quality.

***Disclosures: Hideaki Nagaoka**, None.*

MO0443

Bone Histomorphometry in Hypophosphatasia Diagnosed in Adults. Robert Wermers*[1], Theresa Hefferan[1], Kathryn Berkseth[1], Donna Jewison[1], Matthew Drake[2], Michael Yaszemski[1], Peter Tebben[1]. [1]Mayo Clinic, USA, [2]Mayo Clinic College of Medicine, USA

Introduction: Hypophosphatasia (HPP) is a rare disorder marked by low serum alkaline phosphatase (AP) levels due to ↓ tissue-nonspecific AP (TNSALP) in bone and liver. Limited data exists relating bone histomorphometric findings and clinical presentation in adults with HPP.

Aim: To characterize bone histomorphometric findings in adults with HPP and assess the relationship to clinical and biochemical findings.

Methods: All Mayo Clinic patients diagnosed with HPP as adults from 1976 through 2009 were identified. Patients were included if they met the following criteria: age >18 years at diagnosis, low serum AP in the absence of bisphosphonate therapy, and one additional supporting element including ↑ pyridoxal 5'-phosphate or phosphoethanolamine (PEA), evidence of osteomalacia (OM) such as pseudofracture or stress fracture, family history, or positive genetic testing for HPP.

Results: Of 22 HPP patients identified, 4 had iliac crest bone biopsies. Despite biochemical findings consistent with HPP in all 4 subjects, only 2 (50 yo M and 57 yo F) had histomorphometric evidence of OM with ↑ osteoid volume (OV) (Z-scores 6.3 and 3.9), osteoid width (OW) (Z-score 1.3 and 2.0), and osteoid covered surface (OS) (Z-scores 4.6 and 2.8) [Table]. One of these 2 patients received a single tetracycline label, but had little uptake. The other subjects (34 yo F and 42 yo F) had unremarkable OV (Z-score -0.1 and -0.9), OW (1.7 and -0.8), and OS (Z-score -0.9 and -0.7), and double tetracycline label and bone histomorphometric measures consistent with normal mineralization. Cortical and trabecular volumes were well preserved in all 4 subjects. Both patients with OM on biopsy had a history of "rickets" as children, dentures, and lower extremity pain with fracture on presentation. Patients without OM had diffuse musculoskeletal pain as a primary feature, normal dentition, and history of childhood fracture in one and adult fractures in the other. AP levels were 48% and 35% of the lower normal limit (NL) in patients with OM, and 46% and 64% in patients without OM. Urine PEA was 131% and 240% of the upper NL in patients without OM and 921% and 480% in the patients with OM.

Conclusion: Adults with HPP may not demonstrate mineralization defects by bone histology. Adult HPP patients with OM on bone biopsy have clinical features often seen in childhood onset HPP such as tooth loss. While urine PEA levels were higher in adult HPP patients with OM, AP levels showed overlap.

Patient	Bone Biopsy	Alkaline Phosphatase (% Low Limit of Normal)	Urine Phosphoethanolamine (% Upper Limit of Normal)
Subject 1	Osteomalacia	48%	921%
Subject 2	Osteomalacia	35%	480%
Subject 3	Normal Osteoid	46%	131%
Subject 4	Normal Osteoid	64%	240%

Relationship of Biochemical Markers to Bone Histomorphometry in Adults Diagnosed with Hypophosphatas

***Disclosures: Robert Wermers**, None.*

MO0444

ERCC-XPF Nuclease Is Required for Bone Homeostasis. Qian Chen*[1], Andria Robinson[1], Paul Robbins[1], Laura Niedernhofer[2], Hong-Jiao Ouyang[3]. [1]UPMC, USA, [2]Hillman Cancer Center, UPMC, USA, [3]University of Pittsburgh, USA

ERCC1-XPF is a heterodimeric nuclease that plays important roles in DNA damage repair. Mutations in *XPF* or *ERCC1*, affecting expression of the nuclease leads to spontaneous and rapid premature aging in both humans and mice. To determine if DNA damage affects bone homeostasis and aging, we examined bones from ERCC1-XPF hypomorphic mice (*Ercc1*$^{-/\Delta}$ mice). *Ercc1*$^{-/\Delta}$ mice exhibit severe progressive osteoporosis as early as 8 weeks. At 22 weeks, radiograph, microCT analysis, and HE staining revealed a decrease in bone density at all skeletal sites in *Ercc1*$^{-/\Delta}$ mice compared with the age- and gender-matched wild-type (WT) littermates (fig A). MicroCT analysis indicated 70% reduction of bone volume/tissue volume with reduced trabecular thickness, reduced trabecular number and increased trabecular space in *Ercc1*$^{-/\Delta}$ mice (fig A). Calcein labeling over a 7-day period on 3 pairs of 8 week old *Ercc1*$^{-/\Delta}$ mice revealed reduced bone formation rate compared to WT mice (fig B). At 22 weeks of age, *Ercc1*$^{-/\Delta}$ mice displayed reduced expression of Runx2, Osterix, Osteocalcin, and Bone Sialoprotein in bone tissues compared to WT littermates, as measured by qPCR (fig C). To discover the mechanism behind reduced bone formation, primary calvarial osteoblasts (p-OB) and bone marrow stromal cells (BMSCs) were isolated from ERCC1-deficient mice and WT littermates. . The p-OBs of *Ercc1*$^{-/-}$ mice exhibited reduced mineralization, compared with WT, as shown by von kossa staining. Induction of osteoblastic markers were detected in the p-OBs of *Ercc1*$^{-/-}$ mice but severe suppression of ALP, Runx2 and Osterix occurred in BMSCs of *Ercc1*$^{-/-}$ mice. These data suggest that ERCC1 deficiency blunted differentiation of bone marrow progenitor cells to osteoblasts; however, it paradoxically accelerated differentiation from pre-OB to OB. Severely reduced cell proliferation was detected in p-OB, BMSC of *Ercc1*$^{-/-}$ mice compared to WT, as evidenced by measuring cell number, Ki67 and cyclin D1 in tibia sections and p-OBs and BMSCs cultures. Accumulation of DNA damage in the p-OBs and BMSCs of *Ercc1*$^{-/-}$ mice was detected by increased γH2AX staining. This was associated with increased cellular senescence as measured by staining for senescence-associated β-galactosidase and p16 staining in tibia sections, p-OB and BMSCs. Together these data indicate that unrepaired DNA damage due to deficiency of ERCC1, dramatically affects bone homeostasis and promotes osteoporosis. Loss of bone mineralization arises in response to damage as a consequence of impaired proliferation and increased senescence of osteoblasts and altered differentiation of osteoblastic cells. This work has important implications for cancer survivors treated with genotoxic agents and the cause of osteoporosis with aging.

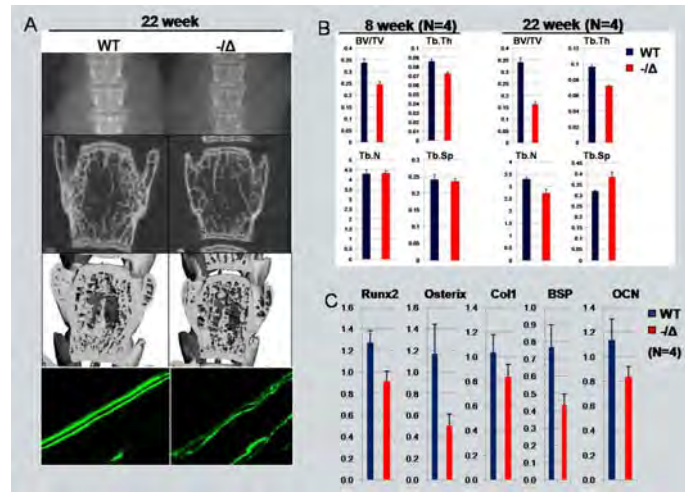

Osteoporosis in Ercc1 Deficient Mice

***Disclosures: Qian Chen**, None.*

MO0445

Increased Vitamin D Receptors in Genetic Hypercalciuric Stone Forming Rats are Biologically Active. Kevin Frick*[1], John Asplin[2], Murray Favus[2], Christopher Culbertson[1], Stephanie Yee[1], Nancy Krieger[1], David Bushinsky[1]. [1]University of Rochester, USA, [2]University of Chicago, USA

We have selectively bred a strain of rats to maximize urine (U) Ca excretion as a model of hypercalciuric nephrolithiasis. These genetic hypercalciuric stone-forming GHS rats now excrete far more UCa than do Sprague-Dawley (SD) controls, uniformly form kidney stones and express an increased number of vitamin D receptors (VDR) in the kidney, intestine and bone. To assess the biological activity of the GHS VDR, we injected vitamin D replete GHS and control Sprague-Dawley (SD) rats with either vehicle (Veh) or 25 ng/d $1,25(OH)_2D_3$ (Vit D) for 7 d while rats ate a constant amount of a Ca replete (1.2% Ca) diet. We then determined serum (S) and U chemistries and gene expression of Ca transport proteins. Administration of Vit D to both SD and GHS rats increased SCa equally (increase of ~1.5 mg/dl) and suppressed PTH to undetectable levels in both. UCa in GHS+Veh (10.5 mg/d) was elevated compared to SD+Veh (1.7 mg/d) and UCa was increased in SD+Vit D to 24.4 mg/d, which was further increased in GHS+Vit D to 41.9 mg/d (all groups n=8, all comparisons $p<0.01$). To examine expression of genes important for renal tubular Ca reabsorption, total RNA was isolated from kidneys and analyzed by QRT-PCR. As expected VDR was increased in SD+Vit D and GHS+Vit D. Expression of the distal luminal renal Ca transporter TRPV5, calcium binding protein calbindin D_{28K} and the basolateral Na/Ca exchanger NCX were all similarly increased in SD+Vit D and GHS+Vit D. Expression of klotho, which activates TRPV5, was decreased in GHS+Vit D. The Ca transporter TRPV6 was increased in SD+Vit D and was increased further in GHS+Vit D. Levels of the basolateral Ca ATPase PMCA were inhibited in GHS+Vit D but not in SD+Vit D. There were no differences in thick ascending limb gene expression of paracellular protein claudin 16, the sodium potassium 2 chloride transporter NKCC2 and the potassium channel ROMK between the SD+Vit D and GHS+Vit D groups. Thus the marked increase in UCa with Vit D in GHS, which exceeded the increase induced by Vit D in SD, indicates that the

enhanced number of VDR in GHS rats results in greater biological response to administered Vit D. The mechanism of the increased UCa in GHS+Vit D may be secondary to a reduction in klotho, which activates TRPV5, and/or a reduction in the basolateral Ca ATPase PMCA, either of which may result in less tubular Ca reabsorption and greater hypercalciuria in the GHS+Vit D compared to SD+Vit D.

***Disclosures: Kevin Frick**, None.*

MO0446

Higher Vitamin D Requirements in Older Persons. Silvina Levis*. University of Miami School of Medicine, USA

Hypovitaminosis D has become a major concern in the elderly population. In the United States, reported prevalence rates are >50%. The optimal serum 25-hydroxyitamin D (25-OH-vitD) concentration is still being debated, but most investigators agree that levels >30 ng/ml can be considered normal. However, the question of optimal dosing still remains to be resolved, particularly in at-risk populations such as the elderly and the obese. The vitamin D content of standard multivitamins appears not to be sufficient to prevent hypovitaminosis D in most adults. In order to help determine the effectiveness of two vitamin D doses in maintaining normal 25-OH-vitD concentrations and/or preventing hypovitaminosis D (25-OH-vitD <30 ng;/ml), we randomized 66 persons (82.6% women) mean age 72.7 ± 6.4 (range 64 - 92), to vitamin D3 daily 400 IU or 2000 IU for 6 months. Results are presented in the Table.

None of the participants developed hypercalcemia or hypercalciuria.

Conclusion: In persons age 64 and older, vitamin D3 400 IU daily over 6 months does not significantly increase 25-OH-vitD concentrations, while 2000 IU daily raises 25-OH-vitD to levels >30 ng/ml in most but not all individuals. Larger vitamin D doses might be needed to reach and maintain 25-OH-vitD concentrations ⩾30 ng/ml in all persons in this age group.

Treatment arm	25-OH-D at baseline (ng/ml)[a]	25-OH-D at 6-months (ng/ml)[b]	% LoD at baseline[c]	% LoD at 6-months[d]
vitD3 400 IU/d	25.6 ± 7.7	28.7 ± 5.3	65.2%	55.2%
vitD3 2000 IU/d	27.0 ± 8.7	36.8 ± 9.9	60.5%	17.2%

Comparisons between treatment arms: (a) p=0.5; (b) p<0.0001; (c) p=0.7; (d) p<0.001

***Disclosures: Silvina Levis**, None.*

MO0447

Vitamin D Deficiency vs Vitamin D Insufficiency: An Example of How This Distinction Cannot Be Made. Barbara Silva*[1], Carolina Kulak[2], Eduardo Dias[3], Bruno Camargos[4], John Bilezikian[5], Marta Sarquis[6]. [1]Columbia University Medical Center, USA, [2]Federal University of Parana, Brazil, [3]Endocrinology Unit, Felicio Rocho Hospital, Brazil, [4]Rua Padre Francisco Arantes, USA, [5]Columbia University College of Physicians & Surgeons, USA, [6]Department of Internal Medicine, Federal University of Minas Gerais, Brazil

Low levels of 25-hydroxyvitamin D (25OHD), the best indicator of vitamin D (Vit D) sufficiency, are associated with increased risk of osteoporosis, muscle weakness, falls and fractures. Low Vit D status has also been linked to nonskeletal conditions, such as cancers, cardiovascular diseases, diabetes, autoimmune diseases, and all-cause mortality. Despite these real or perceived benefits of Vit D, inadequate levels are still common. We aimed to evaluate the prevalence of Vit D deficiency and insufficiency in community-dwelling patients, followed in an endocrinology clinic in Belo Horizonte (19♂ S), a sunny urban center in Southeast Brazil. In addition, we sought to determine what serum concentration of 25OHD in this population defines Vit D insufficiency vs Vit D deficiency. To this point, we sought a relationship between PTH and 25OHD. This study was conducted by reviewing medical records of 310 patients who had serum 25OHD measured in the same laboratory and did not have conditions or were taking drugs that could interfere with calcium homeostasis. The majority of subjects (n=275) were women (mean age, 57.2 ± 17 years (range 18-92). There was no age, sex or BMI influence on 25OHD values. The mean ± SD serum 25OHD was 36.7 ± 18.0 ng/mL. A significant inverse correlation was noted between serum PTH and 25OHD, r= -0.404; P< 0.0001; and between CTX and 25OHD, r= -0.271; P= 0.03. PTH levels started to rise significantly when serum 25OHD fell to < 30 ng/mL. We then compared means of serum PTH, CTX, BSAP, and BMD in patients whose serum 25OHD was less than 20 ng/mL to those whose 25OHD was between 20 and 30 ng/mL. The comparison of means was not different between these two groups of individuals currently classified as Vit D deficient or insufficient, respectively among all comparative indices. Subjects whose 25OH D levels were <20 ng/mL constituted 18.7% of the population while those whose 25-OH D levels were <30 ng/mL constituted 45.5% of the population. The results show a high prevalence of reduced Vit D levels in a community-dwelling population from Southeast Brazil. While we are able to define a threshold of 30 ng/mL for serum 25OHD that defines Vit D insufficiency, there was no distinction between Vit D insufficiency and deficiency based upon other calciotropic indices. For this, and perhaps for other populations, we propose a unitary concept of Vit D insufficiency rather than the distinction between Vit D insufficiency and deficiency.

***Disclosures: Barbara Silva**, None.*

MO0448

Detection of Low Copy Numbers of Mutant *SQSTM1* Alleles in DNA from Peripheral Blood Cells in Paget's Disease of Bone. Laetitia Michou*[1], Edith Gagnon[2], Jean Morissette[2], Jacques Brown[2]. [1]Centre De Recherche Du Chuq-Chul, Canada, [2]Laval University, Canada

Purpose: Paget's disease of bone (PDB) has a strong genetic component, and has been linked to the *PDB3* and *PDB4* loci in the French-Canadian population. In the *PDB3* locus, mutations have been reported in the *SQSTM1* gene. The *P392L* mutation, which is the only *SQSTM1* mutation in French-Canadian PDB patients, was identified in 46% of familial forms and in 16% of sporadic cases. A recent study reported the presence of the *P392L* mutation in affected bone tissue, but not in peripheral blood in sporadic PDB patients, suggesting the presence of somatic *SQSTM1* mutation in PDB. However, contrary results were reported in an independent study. The purpose of this study was to develop a method to detect low copy numbers of mutant *SQSTM1* alleles in DNA extracted from peripheral blood cells from PDB patients non-mutated in *SQSTM1* gene.

Methods: We studied genomic DNA extracted from peripheral blood cells from 13 PDB patients from familial forms who were considered "phenocopies" and from three unrelated affected patients without the *P392L* mutation. We used a highly-sensitive locked nucleic acid (LNA) clamping polymerase chain reaction (PCR) method in order to detect low copy numbers of mutant *SQSTM1* alleles. LNA are a new generation of peptide nucleic acids (PNA) which specifically block synthesis from the wild-type allele. This approach has been successfully used for the detection of *GNAS* somatic mutation in genomic DNA extracted from peripheral blood cells in fibrous dysplasia. We amplified exon 8 of the *SQSTM1* gene with the following primers: TGGCTAACTGCCTGTTCTT as forward primer and AATGGCTTCTTGCACCC-TAA as reverse primer, in the presence and absence of a LNA oligonucleotide with the following sequence: 5'TCAGCCGCGGGTCAGCC3'. Amplification products were further purified and sequenced on a 3700 ABI sequencer. Both strands were analyzed with comparison to a reference sequence. These results are preliminary.

Results: In the presence of the LNA, the PCR product-intensity was reduced by > 50%. Our preliminary analysis of chromatogram sequence suggested the presence of low numbers of mutant *SQSTM1* alleles with the *P392*L mutation in two familial form PDB patients and in one sporadic PDB patient.

Conclusions: The inclusion of a specific LNA primer may allow the selective amplification of low numbers of mutant *SQSTM1* alleles in genomic DNA from peripheral blood cells in PDB patients, suggesting that somatic *SQSTM1* mutations may occur in PDB.

***Disclosures: Laetitia Michou**, None.*

MO0449

Effect of Parathyroidectomy on Structural Cardiac Indices and Diastolic Dysfunction in Mild Primary Hyperparathyroidism. Marcella Walker*, Marco Di Tullio, James Lee, Shunichi Homma, Chiyuan Zhang, Donald McMahon, Jessica Fleischer, Tamara Taggart, Julia Udesky, Rui Liu, Shonni Silverberg. Columbia University, USA

Severe primary hyperparathyroidism (PHPT) is associated with cardiovascular (CV) calcification and increased CV mortality. To determine the presence and reversibility of subclinical CV abnormalities in mild PHPT, we used echocardiography to evaluate structural and functional cardiac indices pre-parathyroidectomy (PTX) and 1 yr post- PTX.

Results: Patients (N=42) were typical of those with PHPT: 79% female, age ± SD 62 ± 7 yrs, serum calcium (Ca) 10.6 ± 0.5 mg/dl, PTH 97 ± 47 pg/ml. Baseline values for blood pressure, left ventricular mass index (LVMI) and diastolic function [mitral inflow E/A ratio (E/A), tissue Doppler e' wave (e'), mitral deceleration time (DT) and isovolumic relaxation time (IVRT)] were all normal. At baseline, LVMI was associated with 25OHD (r=-0.38, p=0.01) and isovolumic relaxation with Ca (r=0.30, p=0.05), while none of the measures correlated with PTH levels.

One yr after PTX, there was no change in BP or LV calcifications. LVMI, IVRT and tissue Doppler e' (e') worsened after PTX, although mean values for all measures remained within the normal range (Table). The association between LVMI and 25OHD levels weakened (r=0.20, p=0.21) after PTX, while the association between IVRT and serum calcium levels persisted (r=0.32, p=0.04). DT and E/A were unchanged.

Subgroups with abnormal LVMI or diastolic function indices prior to PTX were examined for post-PTX improvement. LVMI did not decline in those with high LV mass (n=5), but the strong baseline association between LVMI and PTH in this group (r=0.90; p=0.04) weakened (r=0.65; p=0.23). In those with prolonged IVRT, suggestive of decreased compliance, IVRT normalized (n=7; 114 ± 11 to 98 ± 9 msec; p=0.01). This decline was associated with change in 25OHD (r=0.76; p=0.05) but not in Ca or PTH. Although E/A normalized in 4/10 with low baseline values (also suggesting decreased compliance), group levels did not quite normalize (0.68 ± 0.14 to

0.74±0.14, p=0.23; nl >0.75). There were too few people with abnormal DT (n=1) and e' (n=2) at baseline to assess their change after PTX.

Conclusions: In the 1st yr after PTX, structural cardiac indices and diastolic function did not improve in this cohort with mild PHPT. Improvements were seen only in the subset of patients who had prolonged isovolumic relaxation time prior to surgery. We conclude that there is no evidence that PTX improves cardiac structure or function, except in selected patients with diastolic dysfunction at the time of diagnosis.

	Normal Range	Baseline Mean ± SD n = 42	12 month Mean ± SD n = 42	p-value Baseline vs. 12 months
Blood Pressure (mmHg)	<140/90	121±15/74±10	122 ± 14/76 ± 9	0.74/0.12
LVMI (g/m^2)	♀≤ 108 ♂≤ 131	96 ± 21	99 ± 23	0.03
E/A	0.75-1.5	1.1 ± 0.4	1.1 ± 0.4	0.12
DT (msec)	≤ 220	161 ± 31	169 ± 34	0.35
IVRT (msec)	50-102	85 ± 18	93 ± 14	0.01
Tissue Doppler e' (cm/sec)	≤ 7	11.4 ± 2.9	10.2 ± 2.4	0.04

Echocardiographic Studies

***Disclosures: Marcella Walker**, None.*

MO0450

Ethnic Differences in the Presentation of Primary Hyperparathyroidism. Naim Maalouf*[1], Jacob Grange[2]. [1]University of Texas Southwestern Medical Center, Dallas, USA, [2]University of Texas Southwestern Medical Center, USA

Background: Ethnic differences exist in the physiological responses to parathyroid hormone (PTH), but little is known about the ethnic differences in the clinical presentation of primary hyperparathyroidism (PHPT).

Objective: To compare the clinical findings of PHPT patients of different ethnicities.

Methods: Records of patients with PHPT who underwent parathyroidectomy between 2003-2009 at a County Hospital in a large metropolitan U.S. city were reviewed. Data on demographic, historical, laboratory, imaging and surgical findings were collected and compared across ethnic groups. Indications for parathyroidectomy according to the 2009 updated guidelines by the 3rd International Workshop on Primary Hyperparathyroidism were compared across ethnic groups.

Results: Records of 82 consecutive patients were included in this analysis. Ethnic distribution was African-American 38%, Caucasian 19%, and Hispanic 42%. 87% of patients were women, the mean age was 59 years, and the mean BMI was 30.8 kg/m^2, with similar demographic characteristics across ethnic groups. Median serum calcium and PTH were not significantly different between the ethnic groups. The prevalence of kidney stones was highest in Caucasians (56%), intermediate in Hispanics (37%), and lowest in African-Americans (23%). The prevalence of osteoporosis (by DXA scan) was highest among Hispanics (57%), intermediate in Caucasians (40%), and lowest in African-Americans (21%). There was no significant difference in the proportion of patients with age < 50 years, serum calcium > 1 mg/dl above upper limit of the reference range, estimated glomerular filtration rate (eGFR) < 60 ml/min, or hypercalciuria (defined as 24hr urine calcium > 400 mg/day) (Table).

Conclusions: Ethnic differences exist in the clinical presentation of primary hyperparathyroidism. In our cohort, despite similarities in serum calcium and PTH, Hispanics were more likely to present with osteoporosis while Caucasians were more likely to have a history of nephrolithiasis.

	African-Americans		Caucasians		Hispanics		p-value*
	N	%	N	%	N	%	
Age <50 years	6/31	19.4%	5/16	31.3%	6/35	17.1%	0.521
History of Kidney Stones	7/31	22.6%	9/16	56.3%	13/35	37.1%	0.073
History of Osteoporotic Fractures	0/31	0.0%	1/16	6.3%	1/35	2.9%	NED
Serum Ca^{2+} > 11.2 mg/dL	19/31	61.3%	11/16	68.8%	24/35	68.6%	0.466
Urine Ca^{2+} > 400 mg / day	1/29	3.2%	1/12	8.3%	9/29	31.0%	0.028
Estimated GFR <60 mL/min	5/31	16.1%	2/15	13.3%	6/34	17.6%	1.0
Osteoporosis (any T-Score ≤ -2.5)	5/24	20.8%	4/10	40.0%	13/23	56.5%	0.039

* p-value determined by Fisher's exact test. NED: Not enough data

Criteria for Parathyroidectomy According to the 2009 Int'l Workshop on 1ry Hyperparathyroidism

***Disclosures: Naim Maalouf**, None.*

MO0451

Genetic Analysis of HRPT2 Gene in a Large Series of Parathyroid Tumors. Filomena Cetani*, Chiara Banti, Elena Pardi, Simona Borsari, Feredica Saponaro, Claudio Marcocci. University of Pisa, Italy

Parathyroid carcinoma is a rare endocrine malignancy. It accounts for <1% of cases of sporadic primary hyperparathyroidism (PHPT) and is usually associated with more severe clinical manifestations than its much more common benign counterpart, parathyroid adenoma. The etiology of parathyroid carcinoma is largely unknown, but recently, it has been shown that mutations in the HRPT2 gene are associated with the development of parathyroid carcinoma. The aim of this study was to further evaluate the role of HRPT2 mutations in a series of sporadic parathyroid tumors. We studied a large series of parathyroid carcinomas (45 primary tumors and 1 lung metastasis) and 7 atypical adenomas. DNA was extracted from paraffin-embedded material. All coding regions and splice site junctions of the HRPT2 gene were PCR-amplified. PCR products were purified and nucleotide sequences were determined on double strands by direct sequencing.

In 28 out of 46 parathyroid carcinomas, the sequences of 20% of the HRPT2 genes could be analysed in the fragmented DNA. Herein we report the results of tumors in which the entire coding sequence was performed. Three HRPT2 mutations were identified in parathyroid carcinomas. Case 1 (lung metastasis) harboured a double somatic mutation in exon 1 (c.60delG) and in exon 3 (c.248delT), resulting both in a premature stop codon. Case 2, had a germline mutation in exon 4 (c.343G>T), resulting in a premature stop codon. Case 3 harboured a germline mutation in exon 4 (c.343G>T) and a somatic mutation in exon 1 (c.64G>T), resulting in a premature stop codon. No HRPT2 mutations were identified in atypical adenomas.

In summary, we detect only 3 inactivating HRPT2 gene mutations in our series of parathyroid carcinomas. The overall frequency of HRPT2 mutations detected in this study is substantially lower than recently described. The selection of parathyroid carcinomas is different compared to previous study, in which only cases with metastasis or recurrence were included (unequivocal carcinoma). It might be speculated that parathyroid tumours fulfilling only the classic histological features, but without signs of recurrence or metastasis, should be considered as less aggressive carcinomas, in contrast to unequivocal carcinoma with HRPT2 mutations.

***Disclosures: Filomena Cetani**, None.*

MO0452

Identification and Characterization of a Novel C106R Mutation in the DNA Binding Domain of the GCMB Gene in a Family with Autosomal Dominant Hypoparathyroidism. Sihoon Lee*[1], Hyon-Seung Yi[1], Young Sil Eom[1], Sangho Lee[2], Suntaek Hong[1], Harald Jueppner[3], Michael Mannstadt[4]. [1]Gachon University of Medicine & Science, South korea, [2]Sungkyunkwan University, South korea, [3]Massachusetts General Hospital, USA, [4]Massachusetts General Hospital Harvard Medical School, USA

Background: Most hypoparathyroidism(HP) patients appear to be sporadic. However, familial forms of the disease have been described, which show either an autosomal recessive(AR) or autosomal dominant(AD) mode of inheritance. Causes of AD-HP can be activating mutations in the gene encoding the calcium sensing receptor(CaSR) or mutations in pre-pro-PTH that impair processing and thus secretion of the wild-type hormone. GCMB is a transcription factor that is expressed in the PTH-secreting cells of the parathyroid glands. everal mutations in GCMB have been reported to cause AD-HP or AR-HP.

Method: We identified two individuals in two generations, who are affected by AD-HP. The proband, aged 41 years, and her son, aged 16 years had been diagnosed as having idiopathic HP. We performed mutational analysis of the genes encoding GCMB, pre-pro-PTH, and CaSR using PCR-amplified genomic DNA. A novel heterozygous C106R mutation was identified in the DNA-binding domain of GCMB in both affected individuals; no mutation was found in pre-pro-PTH and CaSR. Functional studies including electrophoretic mobility shift assay(EMSA) and luciferase-reporter assay were performed to assess DNA-binding ability and transactivation of the GCMB mutation. C106R as well as two previously reported mutations, R47L and c.1389delT, were introduced into both pcDNA3 and pET-28a; plasmids were transfected into DF-1 cells and BL21 cells, respectively. We performed homology modeling to generate a three-dimensional structural model for the DNA binding domain of GCMB.

Results: Four healthy family members including proband's parents did not carry the mutation and 100 normal chromosomes did not reveal the mutation either. As determine by EMSA, the C106R mutant of GCMB failed to interact with the DNA consensus recognition motif of the CaSR promoter P1. Our studies with the C106R mutant furthermore revealed, in comparion to wild-type GCMB, reduced transactivation of the luciferase-reporter using DF-1 cells; however, the mutant GCMB failed to reduce the activity of the wild-type protein. Consistent with these findings, homology modeling analysis suggested that C106R mutant protein is unable to bind to DNA.

Conclusion: We have identified a novel GCMB mutation that may explain HP in our family. However, functional studies have thus far failed to show a dominant-negative effect of the mutant, and it therefore remains possible that a different mechanism or a mutation in another gene is responsible for the disease.

***Disclosures: Sihoon Lee**, None.*

MO0453

Implications of Vitamin D Status in Patients with Primary Hyperparathyroidism. Liana Tripto Shkolnik*[1], Rafit Drori[1], Tali Schiller[1], Orit Twito[1], Pinchas Klein[1], Yair Liel[2], Anat Jaffe[1]. [1]Hillel Yaffe Medical Center, Israel, [2]Soroka University Medical Center, Israel

Background: Primary hyperparathyroidism (PHP) and vitamin D deficiency are connected on several levels. Epidemiological data suggests that vitamin D deficiency is more prevalent in PHP patients than in control subjects.

Moreover, there is data indicating, that PHP manifestations are more severe in patients with vitamin D deficiency. This is true in respect to the severity of the bone involvement and parathyroid adenoma weight.

Scant data exists regarding vitamin D status normalization in this patient population, which shows that PTH might even be lowered by vitamin D supplementation. Little is known about the safety aspects of vitamin D replenishment in PHP patients, and there has been some concern about worsening hypercalcemia and hypercalciuria.

Methods: We retrospectively examined the electronic database of patients treated in our department since 2005. Medical records of patients with a diagnosis of ''hyperparathyroidism'' were reviewed. Normocalcemic patients, those with impaired kidney function and patients with only one measurement of 25-OH- D or without increment of vitamin D during the years of follow up were excluded from the analysis. The remaining cohort was analyzed for calcium metabolism parameters at two different time points: lowest and highest vitamin D measurement. The parameters selected were blood calcium, phosphorus, albumin, PTH concentration, and 24-hour urinary calcium and creatinine.

Results: Forty patients met the sample criteria. The mean age was 63 and ninety percent were women. Vitamin D status changed significantly during the follow up years, due to supplementation. Mean vitamin D level at the lowest point was 15.4 + 6 ng/ml. The mean 25-OH-D concentration was 33.2+8 ng/ml at the highest measurement. Neither of the parameters examined was influenced by vitamin D status. Serum calcium, phosphorus, and PTH were not significantly changed by vitamin D replenishment: 10.7+ 0.4 mg/dl, 3+0.4 mg/dl and 130+39.5 pg/ml at lowest vitamin D value as compared with 10.7+0.36, 2.9 +0.4 and 133+55, at the highest, respectively.

Twenty-four hour urinary calcium excretion had not significantly changed between the two time points (220+110 vs. 260+140 mg Ca/ gr Cr, respectively).

Conclusions: Vitamin D replenishment in patients with primary hyperparathyroidism does not cause worsening of hypercalcemia and hypercalciuria, and thus, is safe. As opposed to previous reports, we did not find significant improvement in the degree of PTH elevation.

***Disclosures: Liana Tripto Shkolnik**, None.*

MO0454

PTH Regulates the Distribution of Trabecular and Cortical Compartments of Bone. Mishaela Rubin*[1], Hua Zhou[2], Shonni Silverberg[1], James Sliney[1], David Dempster[1], John Bilezikian[3]. [1]Columbia University, USA, [2]Helen Hayes Hospital, USA, [3]Columbia University College of Physicians & Surgeons, USA

The skeleton is divided into trabecular and cortical compartments, yet how this distribution is regulated is unknown. We compared trabecular and cortical compartments of bone in disorders characterized by either excessive PTH [primary hyperparathyroidism (PHPT)], and deficient PTH [hypoparathyroidism (HypoPT)]. In HypoPT, we also compared the 2 skeletal compartments before and after administration of PTH(1-84) for 12 (n=14) and 24 (n= 16) months. Seventy-five subjects (n= 27 PHPT; n= 48 HypoPT) underwent tetracycline-labeled percutaneous iliac crest bone biopsies. As compared to controls (C), PHPT showed higher trabecular bone volume (24.25$\pm$1.25 vs 19.70$\pm$1.35 %; $p < 0.02$) and trabecular number (2.0 $\pm$ 0.06 vs1.5$\pm$0.04 #/mm; $p < 0.001$) but reduced cortical width (630 $\pm$ 40 vs 1030$\pm$ 80 μm; $p < 0.001$). HypoPT also had higher trabecular bone volume (HypoPT: 23.35 $\pm$ 7.33 vs C:19.84 $\pm$ 4.45%; p= 0.007) and trabecular width (HypoPT:129.17 $\pm$ 36.31 vs. C:114.81$\pm$ 20.18 μm; p= 0.02), but in contrast to PHPT, showed greater cortical width (HypoPT: 872. 18 $\pm$ 392.67 vs C: 748.36 $\pm$ 247.27 μm; p=0.08). In HypoPT, PTH(1-84) treatment decreased trabecular width from baseline to 12 months (pre: 143.83 $\pm$ 34.40 vs post: 127.51 $\pm$ 33.8 μm; p =0.03) and trabecular number increased from baseline at both 12 months (pre:1.71$\pm$ 0.35 vs post:2.12 $\pm$ 0.60 #/mm; p =0.02) and 24 months (pre:1.74 $\pm$ 0.34 vs post:2.07 $\pm$ 0.50 #/mm; p= 0.02) due to intra-trabecular tunneling. Cortical width did not change, but cortical porosity increased at both 12 months (pre:7.01 $\pm$ 4.13 vs post:10.22 $\pm$ 4.08%; p=0.01) and 24 months (pre:7.40 $\pm$ 3.22 vs post:9.22 $\pm$ 2.41%; p= 0.03). This was accompanied by a significant increase in remodeling rate on the endocortical surface. These results suggest that PTH excess leads to a thinning, or ''trabecularization,'' of cortical bone while PTH deficiency leads to a thickening, or ''corticalization,'' of trabecular bone. Raising PTH levels in HypoPT restores trabecular bone properties. Whether lowering PTH levels in PHPT by parathyroidectomy also restores cortical bone properties remains to be seen. We hypothesize that parathyroid hormone (PTH) plays an important role in controlling the balance between the trabecular and cortical compartments of the skeleton.

***Disclosures: Mishaela Rubin**, None.*

MO0455

Reduced Physical and Mental Health in Patients with Long Standing Hypoparathyroidism Compared to Healthy Controls. Tanja Sikjaer*, Anne Kristine Amstrup, Lars Rejnmark, Leif Mosekilde. Aarhus University Hospital, Denmark

BACKGROUND: Hypoparathyroidism is known to be associated with mental- and neuropsychiatric-disturbances as well as impairment in well-being and mood.

Furthermore in chronic hypoparathyroidism, fatigue and a reduced endurance is a common complaint despite standard treatment with calcium and vitamin D.

However, only few data are available on mental and physical health in patients with hypoparathyroidism.

AIM: In a cross-sectional design, we compared quality of life (QoL) in patients with longstanding hypoparathyroidism with QoL in healthy controls.

SUBJECTS AND METHODS: 39 patients with hypoparathyroidism recruited from our hospital outpatient clinic, who have been treated with oral calcium and a 1α-hydroxylated vitamin D preparation for a minimum of 6 months. The patients were compared with 39 age- and gender-matched healthy controls randomly selected from the local background population. We assessed QoL using the SF36v2 questionnaires and WHO-Five Well-Being Index (WHO-5)-survey.

The SF36v2 is 36 questions differentiated in to 8 subcategories (physical functioning, role physical, role-emotional, bodily pain, vitality, mental health, social functioning and general health) and 2 main categories consisting of Mental component score (MCS) and Physical component score (PCS). The WHO-5-survey consists of five 6 point-rated questions on well being.

RESULTS: Patients and healthy controls were well matched by age (median 59, range 32-79 years) and gender (85 % females). The patients had a median duration of disease of 8.5 yrs. (1-37yrs. -) years. Most of the patients had post-surgical hypoparathyroidism (92%). All patients had plasma calcium levels within or slightly below the lower limit of the reference range and all were normothyroid as assessed by plasma TSH levels. Compared with healthy controls, patients had a significantly lower score in all of the 8 subcategories, and significantly lower physical ($p<0.01$) and mental- ($p<0.01$) component scores.

CONCLUSION: In patients with hypoparathyroidism, quality of life is significantly reduced due to an impaired mental as well as physical functioning. Further studies should address how to improve quality of life among these patients.

Disclosure: No conflicts of interest.

***Disclosures: Tanja Sikjaer**, None.*

MO0456

Bone Mineral Density and Bone Structure Discriminate Among Those With and Without Fractures in Early Stage Chronic Kidney Disease. Sarah West*[1], Charmaine E. Lok[2], Angela Cheung[2], Sophie Jamal[3]. [1]University of Toronto, Canada, [2]University Health Network, Canada, [3]The University of Toronto, Canada

Purpose: The ability of bone mineral density (BMD) by dual x-ray absorptiometry (DXA) and bone structure by high resolution peripheral quantitated computed tomography (HR-pQCT) to discriminate among fractured and non-fractured patients with stages 3 to 5 chronic kidney disease (CKD) has not been well studied.

Methods: We utilized baseline data from an ongoing observational study of individuals 18 yrs and older with stages 3-5 CKD to determine if BMD by DXA (Hologic) at the lumbar spine (LS), total hip (TH), ultradistal radius (UDR); and/or cortical area, density & thickness, trabecular density, thickness, separation & number by HR-pQCT (XtremeCT) at the radius could discriminate between those with and without self-reported low trauma fractures occurring after age 40. Results are expressed as areas under the receiver operating characteristic curves (AUC) with 95% confidence intervals (CI).

Results: Data was available for 71 men and 45 women. The mean age was 61.8$\pm$15.7 yrs, weight was 78.7$\pm$17.6 kg, the most common cause of CKD was diabetes (43.4%) and most subjects (62.9%) were Caucasian. Just under half (46.4%) had a history of fractures and 1/3 (34.6%) reported a fall in the past year. BMD by DXA was able to discriminate among those with and without fractures at all sites (AUC for LS: 0.72 [95% CI: 0.61-0.84]; AUC for TH: 0.74 [95% CI: 0.61-0.88]; AUC for UDR: 0.69 [95% CI: 0.57-0.81]). HR-pQCT also performed well for cortical measures (AUC for area: 0.63 [95% CI: 0.49-0.78]; density: 0.65 [95% CI: 0.53-0.78] and thickness: 0.65 [95% CI: 0.53-0.78]) as well as trabecular measures (AUC for density: 0.69 [95% CI: 0.55-0.82]; number: 0.73 [95% CI: 0.61-0.86]; thickness: 0.65 [95% CI: 0.53-0.78], and separation: 0.69 [0.56-0.83]). There were no statistical differences in the performance characteristics of any of these tests.

Conclusions: Among patients with stages 3 to 5 CKD not on dialysis, BMD by DXA and HR-pQCT parameters are able to successfully discriminate among those patients with and without self-reported low trauma fractures.

***Disclosures: Sarah West**, None.*

MO0457

Changes in Poorly Mineralized Bone area after Parathyroidectomy for Renal Hyperparathyroidism. Shigeru Otsubo[1], Aiji Yajima*[2], Kosaku Nitta[3]. [1]Department of Nephrology, Sangenjaya Hospital, Japan, [2]Towa Hospital, Japan, [3]Department of Medicine, Kidney Center, Tokyo Women's Medical University, Japan

Purpose; Patients with renal failure characteristically show a great deal of poorly mineralized bone area, which may be the cause of the high fracture rate in these patients. Therefore, the changes in the poorly mineralized bone area were investigated after parathyroidectomy for renal hyperparathyroidism as an acute mineralization at the lacunar wall through the canaliculi both before and after osteocyte death was found early after parathyroidectomy (JBMR in press).

Methods; The first bone biopsy specimen was obtained from the left iliac crest just prior to parathyroidectomy, while the second specimen was obtained from the right iliac crest after the surgery. Prior to the biopsy performed post-parathyroidectomy, the patients underwent double tetracycline labeling of bone prior to biopsy using oral administration of tetracycline hydrochloride. Oral administration of alfacalcidol (1α-hydroxyvitamin D3; Chugai Pharmaceutical Co. Ltd, Tokyo, Japan) at doses of 0.5–2.0 μg/day with intravenous calcium (Ca) gluconate or oral Ca carbonate was administered during the observation period after parathyroidectomy. Changes in poorly mineralized bone volume (PM.BV) in basic multicellular units (PM.BV/BV(BMU)) and bone structural units (PM.BV/BV(BSU)) were investigated at 2 to 4 weeks after parathyroidectomy in 17 patients with renal hyperparathyroidism.

Results; The PM.BV/BV(BSU) decreased significantly from 16.4 ± 15.5 to 2.9 ± 3.1 % ($P < 0.01$), and the PM.BV/BV(BMU) decreased significantly from 19.8 ± 16.9 to 3.7 ± 4.7 % ($P < 0.05$) after parathyroidectomy. And the tetracycline-labeled bone volume was greater in the BSU than at the mineralization front early after parathyroidectomy (JBMR in press).

Conclusion; The poorly mineralized bone area was well mineralized early after parathyroidectomy, due probably to the movement of mineral and fluid from the bone marrow to the osteocyte-canalicular system. Maintenance of osteocyte function plus supplementation of adequate Ca, phosphorus and vitamin D will be needed to prevent increase of poorly mineralized bone area in patients undergoing parathyroidectomy for secondary hyperparathyroidism.

***Disclosures: Aiji Yajima**, None.*

MO0458

Changes in Trabecular and Cortical Volumetric Bone Mineral Density and Cortical Geometry after Renal Transplantation in Adults. Mary Leonard*[1], Babette Zemel[1], Simin Goral[2], Debbie Foerster[3], Yusuf Bhagat[2], Felix Werner Wehrli[4]. [1]Children's Hospital of Philadelphia, USA, [2]University of Pennsylvania, USA, [3]The Children's Hospital of Philadelphia, USA, [4]University of Pennsylvania Medical Center, USA

End-stage renal disease is associated with increased risk of fracture, and fracture rates increase further following renal transplantation (RTxp). The discrete effects of RTxp on trabecular and cortical volumetric bone mineral density (vBMD) and cortical geometry have not been established. Tibia quantitative CT scans were obtained in 30 RTxp recipients (ages 41 + 11 yr; 16 male) at RTxp and 6 months later. Patients with systemic inflammatory diseases (e.g. systemic lupus erythematosis, Wegener's, viral hepatitis) and those treated with glucocorticoids within the prior 6 months were excluded. Race, sex, and age-specific Z-scores were generated for trabecular vBMD (TrabBMD), cortical vBMD (CortBMD), and cortical thickness using reference data in 540 healthy controls. At the time of RTxp, TrabBMD ($p < 0.001$) and cortical thickness ($p < 0.01$) Z-scores were significantly lower, compared with controls (Table). At baseline, cortical BMD Z-scores were significantly lower in subjects requiring dialysis, compared with pre-emptive Rtxp recipients ($p < 0.05$). Following transplantation, TrabBMD and CortBMD decreased significantly (Table); cortical thickness did not change. All patients were treated with glucocorticoids following RTxp and the cumulative exposure (mg/kg) was not associated with changes in bone outcomes. PTH levels decreased significantly following transplantation; however, PTH levels were not associated with bone Z-scores. Future studies are needed to determine the fracture implications of these changes and to identify therapies to restore bone density and structure.

	Baseline	6 Months	Change p-value
Body Mass Index (kg/m^2)	25.4 ± 4.8	27.4 ± 5.8	< 0.0001
TrabBMD (mg/cm^2)	223 ± 36	219 ± 35	< 0.001
TrabBMD Z-Score	-0.68 ± 0.98*	-0.81 ± 0.97*	< 0.001
CortBMD (mg/cm^2)	1181 ± 38	1177 ± 36	< 0.01
CortBMD Z-score	0.05 ± 1.61	-0.10 ± 1.47	< 0.01
Cortical Thickness (mm)	5.27 ± 0.97	5.26 ± 1.01	0.25
Cortical Thickness Z-score	-0.77 ± 1.32**	-0.80 ± 1.39**	0.35

* $p < 0.001$ compared with controls. ** $p < 0.01$ compared with controls

Table

***Disclosures: Mary Leonard**, None.*

MO0459

Leads and Target Validation for the Treatment of Medial Vascular Calcification. Tina Kiffer-Moreira*[1], Yalda Mostofi[2], Russell Dahl[2], Marc F. Hoylaerts[3], Sonoko Narisawa[1], Ying Su[2], W. Charles O'Neil[4], Nicholas D. P. Cosford[2], Jose Luis Millan[1]. [1]Sanford Children's Health Research Center, Sanford-Burnham Medical Research Institute, USA, [2]Program on Apoptosis & Cell Death & Conrad Prebys Center for Chemical Genomics, Sanford-Burnham Medical Research Institute, USA, [3]Center for Molecular & Vascular Biology, University of Leuven, Belgium, [4]Emory University, Renal Division, USA

Calcification of the medial layer of arteries is common in patients with chronic kidney disease (CKD) and correlates with cardiovascular events and death. Research in our laboratories has demonstrated that vascular calcification is normally inhibited by extracellular pyrophosphate (PPi) produced by vascular smooth muscle (Narisawa et al., 2007; Lomashvili et al., 2008). Plasma PPi concentrations are reduced in hemodialysis patients and are inversely correlated with vascular calcification. We have shown that medial calcification in uremic rats is prevented by PPi. The key regulator of extracellular PPi is the tissue-nonspecific isozyme of alkaline phosphatase, (TNAP), an ectoenzyme present in vascular smooth muscle, that hydrolyzes PPi thus destroying its ability to suppress calcification. Addition of TNAP to culture medium or transgenic expression of TNAP in tissues expressing type I collagen is sufficient to cause calcification. We have also shown that TNAP is upregulated in uremic aortas and mouse models of idiopathic infantile arterial calcification, suggesting the putative mechanism linking PPi deficiency to medial calcification in patients with CKD (Narisawa et al., 2007; Lomashvili et al., 2008). Using high throughput screening, we have identified potent inhibitors of TNAP that prevent calcification of aortas in culture (Sergienko et al., 2009). Third generation TNAP inhibitors MLS-0010847 and MLS-0038949 (Dahl et al., 2009) proved to be superior inhibitors of TNAP function than levamisole or the previously described MLS-5804079 (Narisawa et al., 2007). Docking studies and kinetic analysis of TNAP mutants have helped us model the likely binding of MLS-0010847 and MLS-0038949 in the TNAP active site. Here we report ongoing structure-activity-relationship studies that are leading to derivatives of the MLS-0038949 scaffold that have improved solubility while retaining high affinity and good pharmacokinetic properties suitable for testing in vivo in models of medial vascular calcification.

***Disclosures: Tina Kiffer-Moreira**, None.*

MO0460

Adiposity, Fat Distribution, Adipokines and Ghrelin Serum Levels in Knee Osteoarthritis. Eric Toussirot*[1], Nhu Uyen Nguyen[2], Daniel Wendling[1], Gilles Dumoulin[3]. [1]Department of Rheumatology University Hospital, France, [2]Department of Physiology University Hospital, France, [3]Department of Physiology, University Hospital, France

Introduction: overweight subjects are prone to develop knee osteoarthritis (OA). It has been suggested that adipokines may contribute to OA pathophysiology and may explain the link between obesity and the development of OA. There are limited data on body composition in OA. In this study, we explored the amount of adipose tissue in the whole body and its distribution in patients with knee OA compared to healthy subjects. In parallel, the serum levels of the adipokines leptin and adiponectin, and also ghrelin, a gastric-derived peptide involved in appetite control, were evaluated.

Patients and methods: 30 patients with knee OA (ACR criteria and Kellgren-Lawrence grade ⩾ II), 14 M, mean age ± SD 64.7 ± 9.1 years, mean body mass index-BMI: 30.23 ± 6.5 kg/m2) and 30 healthy controls (17 M, mean age: 45.5 ± 11.7, BMI: 25.3 ± 5.7) were evaluated.13 subjects in the OA group and 4 in the control group were in the obese category (BMI > 30 kg/m2).Total and regional body fat and lean masses were measured by total body DEXA (Lunar iDXA). Adiposity was determined as the ratio between total fat tissue and total lean mass + total fat tissue. Fat distribution was evaluated as the relative proportion of fat tissue in the

android (central) and the gynoid (hip and thigh) regions. Adipokines and ghrelin were evaluated by immunoradiometric assays (IRMA).

Results: Patients with OA were older and had higher BMI than control subjects ($p< 0.001$). OA patients had significantly high measures of adiposity (total fat or regional fat mass, adiposity, android and gynoid fat regions) compared to controls (all $p < 0.05$) while lean mass did not differ between the 2 groups. Serum leptin was increased in OA patients (OA vs Controls: 21.3 $\pm$ 4.2 vs 14.4 $\pm$ 3.3 ng/ml; $p< 0.05$) and there was a tendency for higher adiponectin in the OA group (OA vs Controls: 12.4 $\pm$ 0.9 vs 9.7 $\pm$ 0.6 pg/ml; $p = 0.054$). Ghrelin levels did not differ between the 2 groups. Serum leptin levels were strongly correlated with all measures of fat tissue (total fat, adiposity, android and gynoid fat; all $p < 0.005$), with laboratory parameters of inflammation (ESR and CRP: $r= 0.38$ and $p<0.05$) and with Lequesne score ($r= 0.43$, $p< 0.05$), but not with the severity of OA as evaluated by Kellgren-Lawrence grade. Pain score (VAS) weakly correlated with serum leptin ($r= 0.38$, $p= 0.07$).

Conclusion: in this study, patients with OA were characterized by increased overall adiposity compared to healthy subjects but without preferential fat distribution or parallel increase in lean mass, giving additional data for the link between fat tissue and OA. Serum leptin was markedly elevated and strongly correlated with all measures of adiposity, systemic inflammation and to the functional impairment but not to the severity of OA. Thus, serum leptin could be a relevant marker in knee OA.

***Disclosures: Eric Toussirot**, None.*

MO0461

Association Between Hypovitaminosis D and Mortality in type 2 diabetes Patients during 7-years Follow-up. Shogo Asano*[1], Atsushi Suzuki[2], Sahoko Sekiguchi[3], Megumi Shibata[3], Kumiko Jo[3], Maiko Kimura[3], Nobuki Hayakawa[3], Shigeo Imamura[1], Mitsuyasu Itoh[3]. [1]Toyokawa City Hospital, Japan, [2]Fujita Health University Division of Endocrinology, Japan, [3]Fujita Health University, Division of Endocrinology, Japan

Background: Accumulating evidences suggests that vitamin D could play important roles in modifying risk for not only osteoporosis but also cardiovascular events in type 2 diabetes mellitus. However, systemic review of longitudinal ovservational studies suggested that the association of cardiometabolic disorders and vitamin D status is still uncertain (Pittas et al., Ann Int Med 2010). In addition, chronic kidney disease complicated with diabetes mellitus could affect both vitamin D status and cardiovascular events in these patients. In 2002, we performed the observationa study of vitamin D status in type diabetes patients with their serum creatinine levels below 2.0 mg/dl, and found high prevalence of hypovitaminosis D in these patients (Suzuki et al., 2006). The aim of this study is to assess the association of low vitamin D status with survival rate and their cause of death during 7-years follow up in type 2 diabetes population. Methods: Subjects were 577 type 2 diabetes patients (M/F=313/264, age 61.6$\pm$11.5) in our out-patient clinic, who were evaluated their 25-hydroxyvitamin D (25-OHD) levels (17.0$\pm$7.0 ng/dl) in 2002. Results: During 7 years, 44 patients died (Died), 353 patients completed the study (Survival), 100 moved to another hospital or clinic, and 80 peoples were lost. Average of their follow-up periods was 2199$\pm$839 days (2130-2267 days, 95% C.I.). Serum concentration of 25-OHD (14.9$\pm$6.3 ng/dl) in Died group was significantly lower than that (17.0$\pm$7.0 ng/dl) in Survival group ($p=0.04$). When we divided the patients into three groups according to 25-OHD levels (Deficiency <10 ng/ml, Insufficiency 10-19 ng/ml, Sufficiency ?20 ng/ml), survival rate of Deficiency group was significantly lower than Insufficiency and Sufficiency groups ($p = 0.0298$). The cause of their death were cancer (N=15), acute myocardial infarction (N=6), chronic heart failure (N=9), apoplexy (N=4), liver cirrhosis (N=2), pneumonia (N=3) and others (N=5). Conclusion: hypovitaminosis D could be associated with lower survival rate in type 2 diabetes patients.

***Disclosures: Shogo Asano**, None.*

MO0462

Effect of Bisphosphonate Therapy on Changes in Volumetric BMD at the Metacarpal Bone in Patients with Rheumatoid Arthritis on Therapy with Biologics: A Pilot Study. Daniel Aeberli*[1], Prisca Eser[2], Jolanda Widmer[2], Peter M Villiger[2]. [1]Inselspital Bern, University Hospital, Switzerland, [2]Department of Rheumatology, Clinical Immunology & Allergology, Inselspital Bern, Switzerland

Objective: To assess the effect of bisphosphonate (BP) therapy on changes in volumetric BMD measured by peripheral quantitative computed tomography (pQCT) at juxta-articular metacarpal bone in RA patients on therapy with biologics.

Methods: Consecutive RA patients fulfilling the ACR criteria starting or switching to a new biological were included. Retrospective analysis of their bisphosphonate use were assessed. PQCT scans were performed at the distal epiphysis of the third metacarpal bone at baseline and at 12 months follow-up. Therapy with BP, glucocorticoids (GC) and biologics was monitored on the basis of patient records from baseline to follow-up measurement as well as during the 12 months preceding baseline. Disease activity score (DAS28) was also monitored at baseline and follow-up. Mann-Whitney test were performed to compare baseline values and 12-months changes in DAS28, GC cumulative doses and metacarpal vBMD. Fisher's exact test was performed to compare the number of individuals with measurable increases in vBMD to those with stable vBMD or vBMD losses. VBMD gains or losses were defined as changes greater than the least significant change, which was determined to be 7.2 mg/cm^3. Spearman correlation coefficients were calculated between changes in cumulative GC doses of the previous and the concerned year and changes in vBMD.

Results: Thirty-two subjects were included (14 subjects in BP and 18 in no-BP group). There were no significant differences between the BP and no-BP group in DAS baseline values and DAS 12-months changes. There were also no between group differences in cumulative GC doses from baseline to follow-up and in changes in cumulative GC dose between the preceding and concerned year. Metacarpal vBMD was comparable between groups at baseline. Gain of vBMD in the no-BP group was significantly increased (median 4.7 mg/cm^3) compared the BP group (median 1.1 mg/cm^3), one-sided Mann-Whitney test p-value of 0.03. There were significantly more subjects in the no-BP group with a measurable gain in vBMD at the distal metacarpal bone (7 versus 10 with stable vBMD or vBMD losses) than in the BP group (1 versus 13 with stable vBMD or vBMD losses, $p=0.046$, Figure 1). There were significant negative correlations between changes in cumulative GC doses between the preceding and measured year and changes in vBMD in both groups ($r=-0.56$ in both groups, Figure 1).

Conclusions: The results of this pilot study indicate that BP may limit bone recovery but cannot pre-vent bone loss at the inflammation prone site of the juxta-articular metacarpal bone in RA patients.

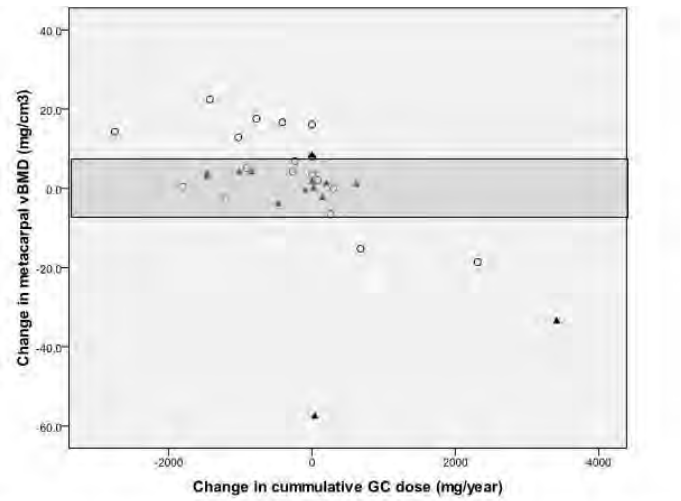

Figure 1: Change in metacarpal vBMD versus change in cumulative GC dose between the year pre-ceding the measurements and from baseline to 12-months follow-up of RA patients with BP therapy (filled triangles) and those without BP therapy (empty circles). Symbols within the shaded area depict changes smaller than the least significant change.

Figure 1

***Disclosures: Daniel Aeberli**, None.*

MO0463

Effect of Tocilizumab on Bone Metabolism in Patients with Rheumatoid Arthritis. Daihei Kida*. National Hospital Organization Nagoya Medical Center, Japan

Purpose: Tocilizumab (TCZ) is a monoclonal antibody directed against the IL-6 receptor, blockade of which represents a molecular target for rheumatoid arthritis (RA). The aim of this study is to evaluate change in bone quality in patients with RA by quantification of several bone biochemical markers, after TCZ treatment. Method: Eighteen patients with RA treated with TCZ (8mg/kg once a month), were enrolled. Levels of serum osteocalcin (OC), serum undercarboxylated osteocalcin (ucOC), serum bone specific alkaline phosphatase (BAP), serum tartrate resistant acid phosphatase isoform 5b (TRAP-5b), urinary N-teropeptide of type I collagen/creatinine (NTx), serum calcium (Ca) and serum phosphorus (P), 1,25-dihydroxy-vitamin D3 (1,25D3), intact parathyroid hormone (iPTH) and calcitonin (CT) were measured at baseline and 52 weeks after TCZ administration. To evaluate inflammation, disease activity and physical disability, ESR, CRP, Disease activity score (DAS28ESR-4) and modified Stanford Health Assessment Questionnaire score (mHAQ) were also measured. Result: Changes of clinical variables and levels of biochemical markers during therapy with TCZ were samarized in Table 2. While levels of DAS28ESR-4, mHAQ, BAP, OC, ucOC and Ca were changed significantly, but levels of NTx, TRAP-5b, P, iPTH, 1,25(OH)D and CT were not significantly changed after TCZ administration. Conclusion: TCZ administration significantly inhibited inflammation, disease activity and physical disability. Furthermore, TCZ administration may not inhibit bone resorption, but may stimulate bone formation and may play a beneficial roll to prevent the elution of Ca from bone. Consequently, this effect may be due to a roll of IL-6 blockade on bone turnover in RA patients.

Demographic, clinical and laboratory features of RA patients

Features	
Female/Male	15/3
Age (yrs.)	43.3+/-14.8
Disease duration (yrs.)	9.7+/-10.8
mHAQ	0.83+/-0.55
Stage	2.6+/-1.1
Class	2.1+/-0.5

(Data are presented as the mean +/-SD)

TABLE 1

Changes of clinical variables and levels of biochemical markers during therapy with TCZ

	Before treatment	After treatment	P-value
DAS28ESR(4)	6.1+/-1.0	2.7+/-1.4	***
mHAQ	0.83+/-0.55	0.56+/-0.60	*
BAP (U/l)	21.8+/-6.7	25.6+/-7.8	**
OC	5.0+/-1.9	6.6+/-4.2	*
ucOC	2.7+/-1.4	6.6+/-11.0	**
NTx (nmolBCE/mmol.Cr)	47.4+/-21.0	41.7+/-21.1	NS
TRAP-5b	272+/-149	305+/-173	NS
Ca	9.4+/-0.1	8.9+/-0.3	***
P	3.4+/-0.3	3.4+/-0.4	NS
iPTH	37.3+/-14.8	44.1+/-17.1	NS
1.25(OH)D	44.1+/-14.4	43.7+/-16.1	NS
CT	36.3+/-13.0	38.6+/-7.0	NS

(Mean +/-SD. NS: Not significant, *: p<0.05, **: p<0.01, ***: p<0.001)

TABLE 2

***Disclosures: Daihei Kida**, None.*

MO0464

Exercise Improves Glucose Control in Patients with Type 2 diabetes through Undercarboxylated Osteocalcin. Itamar Levinger*[1], Roger Zebaze[2], George Jerums[3], David Hare[4], Steve Selig[5], Ego Seeman[6]. [1]Victoria University, Australia, [2]Austin Health, Australia, [3]University of Melbourne & the Department of Endocrinology, Austin Health, Australia, [4]University of Melbourne & the Department of Cardiology, Austin Health, Australia, [5]Institute for Sport, Exercise & Active Living, School of Sport & Exercise Science, Victoria University, Australia, [6]Austin Health, University of Melbourne, Australia

Background: Bone via osteocalcin (OC) in its undercarboxylated (unOC) form may contribute to glucose homeostasis. Exercise improves insulin sensitivity. We examined whether acute aerobic and power exercise mediate the beneficial effects on glycaemic control through unOC in individuals with type 2 diabetes (T2DM).

Methods: Men and women aged 52.5±1.0 (mean±SEM) with (n=23) and without T2DM (n=26) were randomised to 45min of aerobic (cycling at 75% of VO_{2peak}) or power (leg press at 75% of 1RM plus jumping sequence) exercises. Blood samples were taken at baseline and up to 2h post-exercise.

Results: Diabetics had lower OC (3.2±0.3 versus 5.7±0.4ng•mL-1,p<0.001), unOC (4.0±0.4 versus 5.2±0.4ng•mL-1, p=0.004) and high-molecular-weight adiponectin (HMW-AN, 1.7±0.3 versus 2.6±0.44ng•mL-1, p=0.061) compared to non-diabetics. In diabetics, aerobic and power exercise reduced serum glucose (p<0.05). Aerobic exercise increased unOC (7.1±2.6%, p=0.029) and unOC/OC ratio (28.2±9.9%, p=0.022) whilst power exercise improved the unOC/OC ratio (16±4.4%, p=0.003). Changes in glucose levels correlated inversely with changes in unOC (r=-0.45, p=0.021). Neither form of exercise altered HMW-AN.

Similar results were observed in non-diabetics, but HMW-AN increased with both forms of exercise and changes in HMW-AN correlated inversely with glucose (r=-0.52, p=0.005).

For the whole cohort, those with higher baseline glucose levels had a greater reductions in glucose after exercise (r=-0.30, p=0.02). LBM and muscle strength correlated inversely with the change of unOC (r=-0.34, p=0.049, r=-0.27, p=0.032 respectively).

Conclusions: Acute aerobic and power exercise increased serum unOC, associated with lower serum glucose after exercise in diabetics. Those with low muscle mass and muscle strength and those with higher glucose exhibited larger increase in unOC and reduction in glucose levels. Benefits of exercise on glucose metabolism may be explained partly by effects on a bone derived protein.

***Disclosures: Itamar Levinger**, None.*

MO0465

Hip Bone Geometry in HIV/HCV Co-infected Men and Age-, Race-matched Controls. David Thomas[1], Thomas Travison[2], Shruti Mehta[1], Gretchen R Chiu[2], Mark S Sulkowski[1], Andre Araujo[2], Yvonne Higgins[1], Catherine G Sutcliffe[1], Thomas Beck[3], Todd Brown*[1]. [1]Johns Hopkins University, USA, [2]New England Research Institutes, USA, [3]Johns Hopkins Outpatient Center, USA

Objective: Hepatitis C co-infection is an independent risk factor for fragility fracture among HIV-infected populations. Whether bone strength is compromised in HIV/HCV co-infected patients is unknown.

Methods: We compared DXA-derived hip geometry in 88 HIV/HCV co-infected men from the Johns Hopkins HIV Clinic to 289 race-matched men without HIV or HCV from the BACH/Bone Survey, a community based cohort in Boston, MA. Hip geometry was assessed at the narrow neck (NN), intertrochanteric (IT), and shaft (S) regions using Hip Structural Analysis. Lean body mass (LBM), total fat mass (FM), and fat distribution (Trunk Fat: Lower Extremity Fat Mass Ratio [FMR]) were measured by whole body DXA. Linear regression was used to assess for differences in bone geometry between the two cohorts with and without adjustment for body composition parameters.

Results: Age (mean±SE) was similar between the two cohorts (51.6±6.3 vs. 50.7±8.5 years, p=0.31). HIV/HCV co-infected men had lower BMI, lower LBM, lower FM, and higher FMR compared to the control men (all p<0.05). In the NN region, significant differences were observed between HIV/HCV co-infected men and controls in BMD (-0.063±0.023 g/cm^2), cross-sectional area (-0.17±0.079 cm^3), section modulus (-0.13±0.061 cm^3), buckling ratio (BR; 0.96±0.29), and centroid position (CP; -0.0096±0.0023). After adjustment for race, age, smoking status, height, and weight, only BR (0.54±0.28, p=0.05) and CP (-0.0087±0.0024, p=0.0003) at the NN remained significantly different between the two cohorts. Similar differences in BR and CP between the cohorts were obtained when LBM, FM, and FMR were substituted for weight in the multivariate models, with LBM, but not FM, significantly associated with all NN geometry parameters. Geometry parameters did not differ between the two cohorts at the IT or S regions. NN geometry parameters were not associated with CD4 cell count, specific antiretroviral therapies, the degree of HIV suppression, or liver disease severity.

Conclusion: Differences in lean body mass, but not fat mass or fat distribution, account for most, but not all, of the differences in narrow neck hip strength in HIV/HCV co-infected men and uninfected controls. The etiology and clinical consequences of the residual differences in buckling ratio and centroid position in HIV/HCV co-infected men require further clarification.

***Disclosures: Todd Brown**, None.*

MO0466

Prevalence and Risk Factors Associated with Sarcopenia in Brazilian Community-dwelling Elderly Women: Comparison Between 2 Different Methodologies for Definition. Diogo S Domiciano*[1], Jaqueline B Lopes[1], Camille Danilevicius[2], Marcelo Pinheiro[3], Liliam Takayama[1], Valeria F Caparbo[1], Rosa Pereira[1]. [1]Faculdade de Medicina da Universidade de São Paulo, Brazil, [2]Universidade De São Paulo, Brazil, [3]Sao Paulo Federal University/ Unifesp/ Escola Paulista De Medicina, Bra

Purpose: Sarcopenia is defined when relative skeletal muscle index [RSMI = appendicular muscle mass (kg)/ height2 (m2)], based on DXA, is below 2 SD compared to young population, matched to gender (Baumgartner, 1998). However, some studies have suggested RSMI could underestimate the prevalence of sarcopenia in overweight/obese people (Newman, 2003). Thus, this author has proposed new definition criteria considering appendicular muscle mass adjusted to total fat mass, based on residuals from linear regression models. The aim of this study was to evaluate the prevalence and risk factors associated with sarcopenia, accordingly Baumgartner and Newman's criteria in elderly Brazilian women.

Methods: A total of 611 community-dwelling women, aged over 65 years, from Butantã area, São Paulo/Brazil were enrolled in this cohort. Anthropometric data, lifestyle habits and medical history were assessed by a specific questionnaire. Laboratory tests were also performed (lipid profile, 25 hydroxyvitamin D and intact parathormone, calcium, phosphorus, creatinine, glucose, and thyroid function). Bone mineral density (BMD) at lumbar spine, femoral neck and total femur, and body composition were evaluated by DXA measurements. Thoracic and lumbar spine X-ray was performed for identifying vertebral fracture, accordingly Genant's semiquantitative method. Logistic regression models were used to identify risk factors related to sarcopenia in each one method. Results: The prevalence of sarcopenia was

3.7% and 19.9%, accordingly Baumgartner and Newman's criteria, respectively. After adjustments for age, risk factors associated with sarcopenia were different for each method. In agreement with Baumgartner, the risk factors observed in logistic regression models were fat mass index (OR= 2.95; 95%CI 1.64-5.31, p=0.002) and body mass index (OR = 0.29; 95%CI 0.18-0.46; p<0.0001). On the other hand, creatinine (OR = 0.16; 95%CI 0.05-0.51; p=0.002) and body mass index (OR = 0.93; 95%CI 0.89-0.97; p=0.003) showed significant association with sarcopenia, accordingly Newman criteria.

Conclusion: Our results demonstrated the prevalence of sarcopenia was extremely different using the Baumgartner (3.7%) or Newman's definition (19.9%). Besides, risk factors were also distinct. These aspects may have relevant implications and should be considered for diagnosing sarcopenia in elderly women.

***Disclosures: Diogo S Domiciano**, None.*
This study received funding from: FAPESP, CAPES, CNPQ

MO0467

Subclinical Carotid Atherosclerosis in Subjects with Low 25-Hydroxyvitamin D Levels. Angela Carrelli*[1], Hyesoo Lowe[2], Marcella Walker[3], Donald McMahon[2], Tanja Rundek[4], Ralph Sacco[4], Shonni Silverberg[3]. [1]New York Presbyterian- Columbia University, USA, [2]Columbia University College of Physicians & Surgeons, USA, [3]Columbia University, USA, [4]University of Miami Miller School of Medicine, USA

Indices of mineral metabolism have been linked to cardiovascular disease. We assessed the association of serum calcium (Ca), phosphorus (PO4), vitamin D, and parathyroid hormone (PTH) with subclinical carotid markers and early predictors of coronary and cerebrovascular events. 203 consecutive community-dwelling adults from the Northern Manhattan Study (age: 68±11 (SD), range: 50-93) had measurements of serum Ca, PO4, vitamin D and PTH and carotid ultrasound (plaque presence, maximal carotid plaque thickness [MCPT] and intima-media thickness [IMT]).

Results: Ca (9.1±0.4 mg/dl), PO4 (3.7±0.7 mg/dl), PTH (40±22 pg/ml) and $1,25(OH)_2D$ (35±16 pg/ml) were normal, while 25OHD levels were suboptimal (22±10 ng/ml; 48%<20 ng/ml; 17%>30 ng/ml). Carotid measures were highly correlated with traditional vascular risk factors. Age was the strongest predictor (IMT: r=0.41, p<0.0001; plaque number: r=0.44, p<0.0001; MCPT: r=0.48, p<0.0001). Over half had plaque (N=116; 57%). When we controlled for age, race, sex, renal function, BMI, and vascular risk factors, inverse associations were found between 25OHD and MCPT (r=-0.20, p<0.05) and IMT (r=-0.18, p=0.056). Ca-PO4 product also emerged as an independent predictor of carotid plaque number (r=0.23, p<0.05) and IMT (r=0.19, p<0.05). Although no independent association was found with serum Ca, PO4 levels were positively correlated with carotid plaque number (r=0.24, p<0.05), MCPT (r=0.19, p<0.05), and a trend with IMT (r=0.18, p=0.07). There were no independent associations between PTH or $1,25(OH)_2D$ and any carotid measures. To test the interdependence of the associations discovered, indices of mineral metabolism were simultaneously entered into a final model with carotid measures adjusted for the presence of cardiovascular risk factors. The inverse associations of 25OHD with MCPT (r=-0.19, p<0.05) and IMT (r=-0.19, p<0.05) persisted. The positive relationship of PO4 with MCPT (r=0.18, p<0.05) also persisted, while there was no evidence for an independent relationship of carotid measures with Ca-PO4 product.

Conclusion: We report an independent association between low 25OHD levels and subclinical carotid atherosclerosis. We conclude that in this cohort of older adults, vitamin D deficiency is common and is associated with subclinical markers of cardiovascular disease. The precise nature of this association and the optimum levels of vitamin D for vascular health remain to be elucidated.

***Disclosures: Angela Carrelli**, None.*

MO0468

TNF-alpha Blocking Therapy Induces an Early Shift in the Bone Turnover Balance in Ankylosing Spondylitis Patients with Active Disease. Suzanne Arends[1], Elisabeth Brouwer[2], Anneke Spoorenberg[3], Martha Leijsma[2], Pieternella Houtman[3], Cees Kallenberg[2], E. Van Der Veer*[4]. [1]University Medical Center Groningen, The netherlands, [2]University Medical Center Groningen, Netherlands, [3]Medical Center Leeuwarden, Netherlands, [4]Groningen University Hospital, Laboratory Medicine, The netherlands

Purpose: Ankylosing spondylitis (AS) is characterized by both bone formation and bone loss in the spine. The aim of the present study was to investigate the early effects of tumor necrosis factor-alpha (TNF-α) blocking therapy on bone turnover markers (BTM) in AS patients with active disease.

Methods: Forty-eight consecutive AS outpatients, fulfilling the modified New York criteria, who started TNF-α blocking therapy because of active disease were included. Excluded were patients with recent fractures or drug intake affecting bone metabolism (bisphosphonates or corticosteroids). Infliximab (5mg/kg) was administered intravenously at 0, 2, and 6 weeks and then every 8 weeks; etanercept (50mg once a week or 25 mg twice a week) and adalimumab (40mg on alternate weeks) were given subcutaneously. Bath AS Disease Activity Index (BASDAI), erythrocyte sedimentation rate (ESR), C-reactive protein (CRP), bone formation markers bone-specific alkaline phosphatase (BALP) and procollagen type 1 N-terminal peptide (PINP), and bone resorption marker serum C-telopeptides (sCTX) were assessed at baseline and after 6 weeks and 3 months of TNF-α blocking therapy. Z-scores of BTM were used to correct for the normal influence that age and gender have on bone turnover. Z-scores were calculated using matched 10-years-cohorts of a Dutch reference group (150 men or 350 women), checked for normal serum 25-hydroxyvitamin D levels as well as for normal bone mineral density after 50 years of age.

Results: Mean age of the 48 AS patients was 37.9 years (SD ± 10.4), mean disease duration was 13.7 years (SD ± 7.8), and 56% were male. TNF-α blocking therapy resulted in a significant improvement in BASDAI, ESR, CRP, and ASDAS scores. Furthermore, there was a significant increase in BALP and PINP Z-scores and a significant decrease in sCTX Z-score after 6 weeks of therapy. However, only the increase in BALP Z-score remained statistically significant after 3 months of therapy (Table 1).

Conclusion: This study indicates that the bone turnover balance favors bone formation in AS patients during the first 3 months of TNF-α blocking therapy.

Table 1. Clinical and laboratory measures at baseline and after 6 weeks and 3 months of etanercept (n=34), infliximab (n=1), or adalimumab (n=13) treatment.

	Baseline	6 weeks	P-value†	3 months	P-value†
BASDAI	6.2 ± 1.7	3.4 ± 2.2	0.000	3.1 ± 2.1	0.000
ESR	24 (2-101)	6 (2-41)	0.000	6 (1-47)	0.000
CRP	14 (2-82)	3 (1-41)	0.000	3 (1-42)	0.000
ASDAS	3.7 (2.5-5.8)	2.2 (0.8-3.6)	0.000	2.1 (0.8-3.9)	0.000
BALP Z-score	0.68 ± 1.35	1.31 ± 1.38	0.000	1.28 ± 1.41	0.000
PINP Z-score	0.56 ± 1.16	0.80 ± 1.09	0.032	0.70 ± 1.15	0.422
sCTX Z-score	-0.12 ± 0.93	-0.41 ± 0.85	0.045	-0.31 ± 0.74	0.500

Values are mean ± SD or median (range). † P-value calculated with respect to baseline values.

Table 1

***Disclosures: E. Van Der Veer**, None.*

MO0469

Decreased Bone Mineral Density in Patients Submitted to Kidney Transplantation Is Related to Age, Hyperparathyroidism, Time on Dialysis and Low Body Mass Index. Mario Sergio Zen[1], Paulo Gustavo Lacativa[1], Carolina Hammes Torres[1], Renato T. Gonçalves[2], Laura Maria Mendonça[3], Maria Lucia Farias*[4]. [1]Division of Endocrinology, UFRJ, Brazil, [2]Division of Nephrology, UFRJ, Brazil, [3]Division of Densitometry, UFRJ, Brazil, [4]Federal University of Rio de Janeiro, Brazil

Post-transplantation (post-TX) osteoporosis has been the focus of many studies and several factors seem to be involved. In patients with renal failure, hyperparathyroidism (HPT) is an important factor for bone loss that may persist after kidney transplantation (TX) and superimpose to the deleterious skeletal effects of immunosuppressive drugs necessary to prevent graft rejection. We evaluated 88 patients submitted to kidney TX, 43 from live donor (16 females:27 males) and 45 from dead donor (20 F:25 M) who maintained glomerular filtration rate at or above 60 ml/min. Bone mineral density (BMD) was measured at lumbar spine and proximal femur by DXA (Prodigy Advance, GE). Simultaneously blood was taken to measure calcium, phosphate, albumin, creatinin and parathormone (PTH). Mann Whitney test compared females vs. males, live vs. dead donor and patients with lower than expected BMD (Z-score at or below -2 SD) at any site of the skeleton vs. all others. Pearson test, Kendall.s Tau_b test and multivariate regression analysis (stepwise) were used to evaluate correlations between BMD Z-scores and time on dialysis, time from TX–BMD and biochemistry. A p value lower than 0.05 was considered significant. Results in median and quartiles: time on hemodialysis= 5 (1–7.6) years; age= 44.3 (37.2-52.5) years; time TX-BMD= 2.17 (1.3-5.2) years. BMD Z-scores did not differ between men and women nor between live and dead donor patients, although the former had been less time on dialysis (p<0.005). No clinical fracture was reported, but 3 in 12 postmenopausal women and 5 in 17 men over 50 years had a T-score equal or below -2.5 SD (27.6%). Also, a Z-score equal or lower than -2 SD was found in 24 (28.4%) of all patients. Serum PTH was elevated in 42% of the patients associated with low-normal serum calcium in most, as only five were hypercalcemic. The only difference between patients with low Z-score and the remaining subjects was serum PTH: median and quartiles= 83.3 (49.1–137.8) pg/ml and 48.2 (33.1–79.3) pg/ml (p=0.016). Multivariate analysis identified age, PTH, time on dialysis and body mass index as the main factors associated with low bone density. In conclusion, there was a high prevalence of hyperparathyroidism and decreased BMD after kidney TX. Post-TX hyperparathyroidism might be related to pre-TX PTH levels, which were not available, but could also be secondary to vitamin D deficiency, as no supplementation is prescribed after kidney transplantation.

***Disclosures: Maria Lucia Farias**, None.*

MO0470

Demineralized Allogenic Dentin Matrix Increases the Bone Formation Rate. Neema Bakhshalian*, Shirin Hooshmand, Sara Campbell, Bahram Arjmandi. Florida State University, USA

The objective of this study was to evaluate the osteopromotive property of allogenic Demineralized Dentin Matrix (DDM) using a rabbit model of surgical bone defect. Bone deficiency is a major problem in the elderly, individuals with traumatic injuries, undergoing cosmetic/constructive surgeries, and those with periodontal diseases. There are different kinds of grafts and biomaterials being used for bone regeneration which are neither cost effective nor free of complications. Therefore, introducing an improved and feasible bone regenerative material is of great importance. Autogenous Demineralized Dentin Matrix has been shown to accelerate bone regeneration. The major concern with using autogenous DDM is its impracticality. In order to obtain the autogenous DDM, one needs to sacrifice his/her own healthy tooth to rebuild bone and obviously this is not possible in edentulous patients. To overcome this concern, it is best to utilize teeth that are extracted from other individuals (due to orthodontic treatments or wisdom teeth extractions which are routinely discarded) to make an appropriate bone regenerative material, allogenic DDM. Based on our preliminary observations regarding the bone regenerative properties of allogenic DDM, we have hypothesized that allogenic DDM has bone regenerative properties. To test our hypothesis we used rabbit model to evaluate the extent to which allogenic DDM increases bone formation and to determine the quality of the newly-formed bone. The allogenic DDM specimens were obtained from the mandibular incisors of rabbits. Surgical bone defects were created on the skull of 30 New Zealand White rabbits (two defects in each rabbit). The experimental defect was filled with allogenic DDM applying the guided bone regeneration technique while the control defect surfaces, both inner and outer surface, were covered by a membrane with no material in between. Rabbits were divided into four groups and sacrificed after 15, 30, 60, and 90 days. Specimens from each group were utilized for Micro-Computed Tomography (μCT). The μCT results showed that Trabecular Number, Trabecular Thickness, Bone Surface, Bone Surface/Bone Volume, and Connectivity Density were significantly higher and Bone Separation and structure model index were significantly lower in experimental group after 60 days. These results indicate that in the experimental group, both bone quantity and bone quality were significantly improved compared to control group in 60 days.

***Disclosures: Neema Bakhshalian**, None.*

MO0471

Effect of Vitamin D on Clinical Outcomes of Lung Transplant Recipients. Thomas Cascino*[1], Ramon Durazo[2], Charles Alex[2], Pauline Camacho[3]. [1]Loyola University Chicago Stritch School of Medicine, USA, [2]Loyola University Medical Center, USA, [3]Loyola University of Chicago, USA

Purpose: Vitamin D deficiency is highly prevalent among lung transplant recipients. The role of vitamin D in T cell-mediated immunity has been an area of great interest recently. The possible immune-regulatory effect of vitamin D in human lung transplants is not known. We hypothesized that Vitamin D exerts immuno-modulatory effects in patients who have undergone a lung transplant resulting in immunosuppression and improved outcomes.

Methods: A retrospective cohort study was performed on 122 patients who underwent lung transplantation at Loyola University Medical Center between January 2005 and June 2008. Vitamin D status was assessed post transplantation. Vitamin D sufficiency was defined as a 25 hydroxyvitamin D >30 ng/ml. The primary outcomes were one year survival, acute rejection, and airway inflammation as determined by accepted histological grading of the Lung Rejection Study Group.

Results: The cohort consisted of 122 patients with a mean age of 49.2 +- 14.8 years. There were 64 males (52.5%) and 58 females (47.5%). Of the 122 patients, 50% (61) were vitamin D deficient, 18% (22) were Vitamin D sufficient, and 32% (39) were unidentified as to their Vitamin D status post transplant. The most common causes of lung transplant were idiopathic pulmonary fibrosis (36.9%), cystic fibrosis (18.0%), emphysema (15.6%), and chronic obstructive pulmonary disease (11.5%). Vitamin D deficiency was associated with a significant increase in acute rejection of any grade (51.7% vs. 19 %, P=0.012) and minimal acute rejection (A1) (38.3% vs. 14.3%, P=0.049) during the first year following transplant. Vitamin D deficiency showed a trend towards increased occurrence of minimal airway inflammation (B1) (16.7% vs. 0 %, P=.081). Vitamin D status did not influence 1 year survival (83.61% in the deficient group vs. 95.45% in the sufficient group, P=.32).

Conclusion: The study shows that vitamin D, perhaps through its immunologic effects, alters lung transplant outcomes. To our knowledge, this is the first study that has shown an association between vitamin D deficiency and rejection among lung transplant recipients. A follow up study will be looking at the effect of vitamin D therapy on acute and chronic rejection rates, pulmonary function, and long term survival.

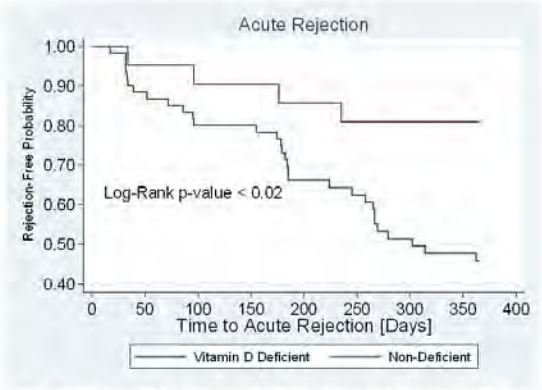

Fig. 1: Incidence of acute rejection (A1, A2, A3, A4) during the first year following transplant (51.7% vs. 19%, P=0.012).

Incidence of Acute Rejection During the First Year

***Disclosures: Thomas Cascino**, None.*

MO0472

Time-dependent Effects of Glucocorticoids on Osteocyte Autophagy In Vivo. Wei Yao*[1], Junjing Li[2], Mohammad Shahnazari[2], L. Darryl Quarles[3], Weiwei Dai[2], Min Guan[4], Lynda Bonewald[5], Nancy Lane[1]. [1]University of California, Davis Medical Center, USA, [2]UC Davis Medical Center, USA, [3]University of Tennessee Health Sciences Center, USA, [4]UC DavisMedical Center, USA, [5]University of Missouri - Kansas City, USA

Glucocorticoid (GC) use results in rapid bone loss and an elevated fracture risk due to changes in bone cell lifespan and metabolism. In this experiment we evaluated time-dependent changes in osteocyte autophagy and apoptosis and serum mineral metabolism in male mice exposed to GCs for 28 and 56 days. Three month old male Swiss-Webster mice were implanted with GC or placebo pellets (5 mg/60 day slow release pellets). At sacrifice, minerals and calcitrophic hormones were assayed. The percentages of osteocytes undergoing apoptosis or autophagy were measured by RT-PCR and immunohistochemistry. Results. Twenty-eight days of GC exposure decreased serum phosphorus, 1,25 Vitamin D and increased FGF23 levels; all returned to control levels by day 56. Real-time RT-PCR revealed a significant increase in the activation of DNA damage repair gene pathway together with the presence of autophagy at day 28 of GC treatment. In addition, messenger RNA levels and protein levels of several autophagy markers including LC3, Beclin 1, and autophagy-related 7 were elevated in bone samples of the mice treated for 28 days with GCs. When GC treatment was prolonged for another 28 days to day 56, all of the genes expressed for DNA damage repair either did not change or decreased (except for. P53). In the contrast, genes associated with apoptosis (Foxo1, Fas, Bcl2, Casp8, Casp3) increased by day 56. GCs increased the percentage of LC3-II positive osteocytes in the trabecular bone by 38% at day 28 but with continued GC treatment to day 56, LC-II positive osteocytes were not significantly different from PL group. In contrast, GC treatment increased apoptotic osteocytes/total osteocytes to 19% as compared to 13% in the PL group) at the cortical bone region of the LVB at day 28 and the apoptotic osteocytes increased to 25% at day 56(P Value). GC exposure did not significantly change osteocyte apoptosis n the trabecular bone region of the LVB either at day 28 or at day 56. Conclusions. Mice exposure to GCs for 28 days resulted in osteocyte autophagy and an elevation in FGF23 production. Additional exposure of osteocytes to GCs resulted in osteocyte apoptosis only in the cortical bone. These data suggest that the acute GC exposure may have created a ''stress'' that induced osteocyte autophagy and the production of FGF23 which together may contribute to the localized changes around the osteocyte in the mineral and material properties that may contribute in bone fragility observed GC use.

***Disclosures: Wei Yao**, None.*

MO0473

Characterizing the Tissue-Specific Properties of Selective Estrogen Receptor Modulators in Breast, Uterine and Bone Cells. Robert Nerenz*, Mark Meyer, J. Pike. University of Wisconsin-Madison, USA

17-β Estradiol (E2) regulates proliferation, differentiation and cellular function in breast, uterine and skeletal tissues. Selective estrogen receptor (ER) modulators (SERMs) function as mixed agonist/antagonists with consequential differential actions in these tissues. Our work is therefore aimed at identifying and characterizing E2 target genomes in breast MCF-7, endometrial ECC-1 and osteoblastic HOB cells using gene expression analysis and exploring the underlying mechanisms that facilitate the differential activities of the SERMs on these target genes using ChIP-chip analysis.

Earlier work defined both a target genome in MCF-7 cells and the ability of E2 as well as the SERMs to promote ER DNA binding, cofactor recruitment and changes in H4ac at these and additional locations. SERMs, however, functioned largely as antagonists. Current studies examine the actions of E2 in uterine ECC-1 cells. The ECC-1 target genome is almost entirely unique, and comprised of genes involved in angiogenesis, cell growth and survival, and tissue development and morphogenesis. Interestingly, while the SERM tamoxifen (T) was found to function as an antagonist in MCF-7 cells, it manifested significant partial agonist activity in uterine cells. Importantly, the expression of CTAG1B, a cancer-specific antigen known to elicit immune responses, was increased in response to T but not E2. At other target genes, the induction of ER DNA binding and gene expression by T was delayed relative to E2. Indeed, this subset of E2 target genes manifested a reduced sensitivity to inhibition by actinomycin D, suggesting a fundamentally different mechanism of gene regulation which may help explain the tissue-specific nature of estrogenic ligands. In the osteoblastic cell HOB, E2 activity is limited by the reduced level of endogenous ER. To circumvent this limitation, we developed a transfection method whereby levels of ER can be supplemented in a controlled fashion to enhance response to E2. Our studies are now focused upon defining the effects of increased ER expression on the target genome in these osteoblasts, assessing the ER cistrome, and defining the partial agonist actions of T and other SERMs. We conclude that these multiple cell line models will permit delineation of the mechanisms that enable ER interacting ligands to function as antagonists in one cell type and differential partial agonists in another.

Disclosures: Robert Nerenz, *None.*

MO0474

Early Programming of Reproductive Health by Soy Isoflavones. Wendy Ward, Elsa Dinsdale*. University of Toronto, Canada

Background: Soy based infant formula can be a significant source of soy isoflavones during early life. Because soy isoflavones have the capacity to mimic endogenous estrogen and thereby exert hormone-like effects, there is concern regarding adverse effect on reproductive health. Previous studies have shown that early exposure to environmental estrogens such as diethylstilbestrol (DES) has adverse effects on reproductive health that are transferred to subsequent generations. It is uncertain whether soy isoflavones, at physiologically relevant doses, modulate reproductive health and whether such effects are multigenerational. Objectives: To assess the safety of neonatal exposure to soy isoflavones on female reproductive health and to determine if potential effects on reproductive health are transferred to subsequent generations. Study Design: soy isoflavones, 7 mg/kg body weight, were administered to the F1 generation of CD-1 mice (n=8-13/group) from postnatal day (PND) 1-10 or from PND 1-21. These mice were subsequently bred to control CD-1 mice on PND 56 to obtain the F2 generation. Outcomes included anogenital distance (AGD), age at vaginal opening and fertility. Results: In the F1 generation, accelerated vaginal opening was observed in the group exposed to isoflavones for 21 days. Lengthened anogenital distance at PND 65, but not at PND 21, was observed in both treatment groups. Fertility, which was measured as successful delivery of live pups, was markedly reduced in both treatment groups. Pups exposed to isoflavones for 10 and 21 days of neonatal life had a 55% and a 60% success rate of delivering live pups, respectively. There were no significant differences in length of gestation, sex ratio of offspring and litter size. In the F2 generation (n=24-50/group), accelerated vaginal opening, and lengthened AGD was observed in the mice exposed to isoflavones for the first 10 days of life. Summary: Findings suggest that early exposure to soy isoflavones at levels comparable to those which human infants are exposed to alter fertility in the F1 generation and sexual maturation in the F1 and F2 generation. Fertility assessment in F2 generation is currently underway.

Disclosures: Elsa Dinsdale, *None.*

MO0475

GPR30 Deficiency Causes Increased Bone Mass, Growth Plate Proliferation, and in vitro Mineralized Nodule Formation in Male Mice. Jeffery Ford[1], Asghar Hajibeigi[2], Deborah Clegg[3], Joseph Zerwekh[4], Orhan Oz*[4]. [1]Department of Radiology, UT Southwestern Medical Center, USA, [2]Department of Radiology, UT Southwestern Medical Center at Dallas, USA, [3]Department of Internal Medicine, UT Southwestern Medical Center at Dallas, USA, [4]University of Texas Southwestern Medical Center, Dallas, USA

Estrogen regulation of the male skeleton was first clearly demonstrated about a decade ago with the discovery of patients' deficient in aromatase or with a mutation in the ERα gene. Estrogen action on the skeleton is thought mainly to occur through the action of the nuclear receptors ERα and ERβ, with ERα apparently being more important in males. Recently, in vitro studies have suggested that the G-protein coupled receptor GPR30 is a functional ER. The purpose of this study was to evaluate its role in the male skeleton using a global GPR30 knockout (GPR30KO) mouse model. All mice were of a mixed C57Bl6/129 background. Bone mass and body composition was assessed in 4 month old male GPR30KO mice and their WT littermates (n=18-22 per genotype) by DEXA. Nasal anal length and femur length were measured with digital calipers. Trabecular bone volume and microarchitecture were assessed by microCT. In vivo BrdU labeling was performed to assess the proliferation of chondrocytes in the tibial growth plate. Static and dynamic histomorphometry was performed on excised non-decalcified tibia following in vivo labeling with tetracycline. GPR30KO mice weighed significantly more ($p<0.01$) and had longer nasal anal length ($p<0.01$). Nasal anal and femur lengths were significantly greater in GPR30KO mice ($p<0.05$ for both). By DEXA analysis, GPR30 KO mice had significantly greater %body fat, areal whole body, spine, and femoral bone mineral density ($p<0.01$). MicroCT evaluation of the femur revealed a significant increase in trabecular bone volume and thickness along with significantly decreased trabecular spacing in the knockout mice. GPR30KO mice had significantly increased BrdU incorporation when compared to WT littermates. Femoral bone marrow cells, cultured in osteogenic medium, had fewer alkaline phosphatase positive colonies in early differentiating osteoblast cultures but showed significantly increased mineralized nodule deposition in mature osteoblast cultures. Mineralized surface (MS/BS) was elevated in GPR30KO mouse bone. These data suggest, that in male mice, GPR30 action regulates body size, bone growth and mass, and body composition. Its role in proliferation may be cell lineage and its action may inhibit bone mineralization.

Disclosures: Orhan Oz, *None.*

MO0476

A Gene Expression Profile of Keratinocyte Stem Cells from the VDR Null Mouse. Marie Demay[1], Hilary Luderer*[2]. [1]Massachusetts General Hospital & Harvard Medical School, USA, [2]Massachusetts General Hospital, USA

The vitamin D receptor (VDR) is an important regulator of mineral ion homeostasis. Mutations of the VDR in humans causes Hereditary Vitamin D Resistant Rickets, which is often accompanied by alopecia totalis. Mice lacking a functional VDR phenocopy the human disease. While the rickets observed in these mice can be rescued by restoration of mineral homeostasis, the alopecia persists, suggesting a unique role of the VDR in the skin. Hair follicle morphogenesis is normal in the VDR-/- animals, however; they are unable to initiate postnatal hair cycling due to functional deficits in the Keratinocyte Stem Cells (KSCs). KSCs are not only essential for hair follicle regeneration but also contribute to wound repair, therefore, elucidating the functional role of the VDR in the KSC has implications for understanding multiple biological processes.

To identify the molecular mechanism of VDR action in KSCs, microarray analysis was performed. Flow cytometry was used to select α-CD34, α-CD49 double positive KSCs isolated from Wt and VDR-/- mice at 28 days of age, the beginning of the first postnatal hair cycle in normal mice. RNA was extracted and hybridized to Affymetrix Mouse Gene 1.0 ST arrays. Arrays were performed in triplicate for each genotype. To identify differentially regulated genes, arrays were compared using dChip analysis. We detected 99 genes with a fold change of at least ± 1.3. Functional annotation clustering performed using DAVID analysis identified 27 gene clusters downregulated and 10 gene clusters upregulated in the VDR-/- KSCs compared to Wt controls. Genes downregulated in the VDR-/- KSCs included those important for cholesterol, lipid and vitamin metabolic processes, as well as metal ion binding. Genes upregulated in the VDR-/- KSCs included those important in enzyme regulation, signal transduction, and developmental processes. In sum, these data identify multiple molecular pathways in the KSC that are altered in the absence of the VDR. A better understanding of the VDR's role in KSC may provide potential therapeutic targets for regeneration of the epidermis and its appendages.

Disclosures: Hilary Luderer, *None.*

MO0477

Direct Effects of 25-Hydroxyvitamin D_3 on Proliferation, Apoptosis, Cell Cycle, and Osteoblast Differentiation in Human MSCs Depend on CYP27B1/1a-Hydroxylase. Shuo Geng*, Shuanhu Zhou, Julie Glowacki. Brigham & Women's hospital, USA

Vitamin D secosteroids are important regulators of mineral and bone metabolism and have many non-calcemic actions that rest on inhibition of proliferation. Anti-proliferative effects of 1,25-dihydroxyvitamin D_3 ($1,25(OH)_2D_3$) have been demonstrated in many malignant and normal cell types, but less is known about effects of 25-hydroxyvitamin D ($25OHD_3$). The CYP27B1/1α-hydroxylase (1α) that converts $25OHD_3$ into $1,25(OH)_2D_3$ is expressed in some but not all preparations of hMSCs (human mesenchymal stem cells). Our hypothesis is that direct effects of $25OHD_3$ on cell proliferation, apoptosis, cell cycle progression, and differentiation depend on CYP27B1. To test this hypothesis, we used hMSCs that expressed high ($hMSC^{hi\text{-}1\alpha}$) or low ($hMSC^{lo\text{-}1\alpha}$) levels of CYP27B1. Cells were cultured in growth medium (10% FBS) with concentrations of $1,25(OH)_2D_3$ (1,10,100nM) or $25OHD_3$ (1,10,100nM) added daily. After 3 days, cells were counted, PCNA and cell cycle regulators (P53, P21 and cyclin D1) were measured by Western immunoblot, apoptosis-related Bax and Bcl-2 were measured by RT-PCR and Western immunoblot, and osteoblast marker genes were assessed by RT-PCR. A cytochrome P450 inhibitor ketoconazole (10 μM) was added to some cultures. Both $25OHD_3$ and $1,25(OH)_2D_3$ inhibited proliferation of $hMSC^{hi\text{-}1\alpha}$; at 100 nM, cell numbers were reduced by $25OHD_3$ (56%, $p<0.001$) and by $1,25(OH)_2D_3$ (50%, $p<0.001$). In contrast, $hMSC^{lo\text{-}1\alpha}$ were resistant to $25OHD_3$ (96%), yet were inhibited by $1,25(OH)_2D_3$ (17%, $p<0.001$). Consistent with effects on cell numbers, PCNA was decreased by both $25OHD_3$ and $1,25(OH)_2D_3$ in $hMSC^{hi\text{-}1\alpha}$, but for $hMSC^{lo\text{-}1\alpha}$ there was less effect by $25OHD_3$ than by $1,25(OH)_2D_3$. Both $25OHD_3$ and $1,25(OH)_2D_3$ reduced Bax/Bcl-2 ratio in $hMSC^{hi\text{-}1\alpha}$; but for $hMSC^{lo\text{-}1\alpha}$, there was no effect by $25OHD_3$. The downregulation of Bax/Bcl-2 ratio by $25OHD_3$ in $hMSC^{hi\text{-}1\alpha}$ was reduced by ketoconazole. Such anti-apoptotic effects in $hMSC^{hi\text{-}1\alpha}$ of

vitamin D differ from pro-apoptotic effects in many cancer cells. Both $25OHD_3$ and $1,25(OH)_2D_3$ downregulated P53 and cyclin D1 and upregulated P21 in $hMSC^{hi\text{-}1\alpha}$, but only $1,25(OH)_2D_3$ had those effects in $hMSC^{lo\text{-}1\alpha}$. Further, both $25OHD_3$ and $1,25(OH)_2D_3$ upregulated RUNX2, Osterix, Alkp and BSP in $hMSC^{hi\text{-}1\alpha}$ and the effect of $25OHD_3$ was reduced by ketoconazole. These data show that $25OHD_3$ had no effects in hMSCs that lack CYP27B1. In sum, the anti-proliferative, anti-apoptotic, and pro-differentiation effects of $25OHD_3$ depend on CYP27B1.

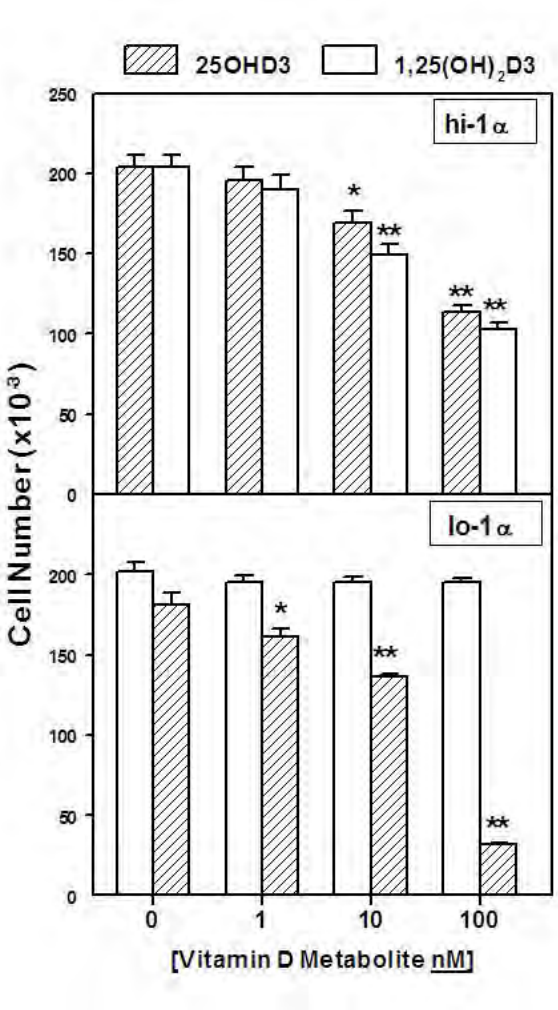

Figure

***Disclosures: Shuo Geng**, None.*

MO0478

Effect of Calcitriol on Vitamin D Receptor, its Metabolizing Enzymes and Cell Proliferation in Porcine Coronary Artery Smooth Muscle Cells. Gaurav Gupta*[1], Devendra Agrawal[2]. [1]Creighton University, USA, [2]Creighton University School of Medicine, USA

Purpose: A growing body of research on non-skeletal actions of vitamin D indicates that most cells in the body have vitamin D receptors. Calcitriol has a great spectrum of biological activities as it directly or indirectly controls more than 200 heterogeneous genes including the genes for the regulation of cellular differentiation and proliferation. Intimal hyperplasia, containing mainly smooth muscle cells, occurs following coronary intervention due to injury to the luminal surface of arteries. We examined the effect of calcitriol on vitamin D receptors, enzymes involved in vitamin D metabolism and proliferation of porcine coronary artery smooth muscle cells (PCASMCs).

Methods: Porcine model has been established as a valuable model for cardiovascular research and lesions following coronary interventions in pig heart are very close, if not identical, to human. PCASMCs were isolated from the coronary arteries of domestic swine and cultured in smooth muscle cell media with 10% FBS. Cells were characterized by positive immunostaining with α-smooth muscle actin and smooth muscle-myosin heavy chain. Cells were stimulated with different concentrations (0.1 nM, 1 nM, and 10 nM) of calcitriol for 24 hours. The mRNA and protein expression of cathelicidin, vitamin D receptor (VDR) and vitamin D metabolism enzymes, including CYP24A1 and CYP27B1, were analyzed by real-time PCR and Western blot, respectively. Cell proliferation and apoptosis assays were performed by radiolabeled-thymidine incorporation and PI-annexin V labeling, respectively.

Results: Treatment of PCASMCs with calcitriol significantly increased the mRNA and protein expression of cathelicidin, VDR and CYP24A1 in a dose-dependent manner while expression of CYP27B1 was significantly decreased as compared to control. Calcitriol treatment significantly decreased the proliferation at supraphysiological (10 nM) concentration of calcitriol. However, there was no significant effect on the apoptosis of the cells.

Conclusion: These data suggest that PCASMCs express VDR and vitamin D metabolizing enzyme machinery. High concentration of calcitriol inhibits the proliferation without inducing a significant apoptosis in PCASMCs. Thus, it is possible that the patients prone to develop intimal hyperplasia following coronary intervention are vitamin D-deficient and vitamin D supplementation prior to interventional procedures might be helpful in the prevention of intimal hyperplasia in coronary artery disease patients.

***Disclosures: Gaurav Gupta**, None.*

MO0479

Fifty Mutations of 25-OH-D3-24-Hydroxylase (hCYP24A1) Provide Insights into its Regioselectivity & Substrate Specificity. Martin Kaufmann*, David E Prosser, Tessa Mathew, Glenville Jones. Queen's University, Canada

CYP24A1 catabolizes $1\alpha,25\text{-}(OH)_2D_3$ to calcitroic acid or a 26,23-lactone via C24- or C23-hydroxylation respectively. Our work has identified key residues involved in substrate-binding and regioselectivity, namely A326 [PNAS 104:12673-8] which is a major determinant of the regioselectivity differences between human (24-hydroxylating) and opossum (23-hydroxylating) CYP24A1. We have recently focused on identifying residues that could potentially alter the substrate specificity of CYP24A1, using a homology modeling, mutagenesis, and activity assay-based approach. We selected over 50 mutations in the substrate binding domain and stably expressed these in a novel Flp-In host cell (Chinese hamster lung fibroblast cell line, V79-4) lacking background CYP24A1 activity. The Flp-In system allowed for stable and consistently-high expression levels of wild-type and mutant CYP24A1. With the wild-type enzyme, we observed a typical pattern of catabolism of $1\alpha,25\text{-}(OH)_2D_3$ via the C24 hydroxylation pathway whereas with some the mutants, most notably A326G, favored catabolism via 23-hydroxylation. Other mutations including Q82V, L148A, I131A also increased the degree of 23-hydroxylation. Several mutations (V391L, M252L) increased total enzyme activity as compared to wild-type. The mutation V391L dramatically altered the substrate specificity

of the enzyme towards $1\alpha\text{-OH-}D_3$ forming $1\alpha,25\text{-}(OH)_2D_3$, an activity absent from the wild-type enzyme. The unexpected production of $1\alpha,25\text{-}(OH)_2D_3$ by V391L was accompanied by its catabolic products in the 24-hydroxylation pathway. Using the recently published crystal structure of rat CYP24A1, we rationalized the enzymatic results that we obtained from the 50 mutants from a structural perspective. The A326G mutation enables the substrate to enter deeper into the binding pocket to position a different carbon (C-23 rather than C-24) over the heme group. The other mutations alter potential contacts with A-ring, CD-ring or side chain moieties of the substrate; or because of their proximity close to substrate access channels are able to influence substrate access or product egress. Taken together, we have successfully developed an approach that has identified key structural and functional insights into the mechanism of action of CYP24A1 that can be potentially applied to study other CYPs.

***Disclosures: Martin Kaufmann**, None.*

MO0480

Human Colon and Serum Concentrations of 1,25-dihydroxyvitamin D are Positively Correlated. Dennis Wagner*[1], Andre Dias[1], Theodorus van der Kwast[2], Reinhold Vieth[3]. [1]University of Toronto, Canada, [2]University Health Network, Canada, [3]Mount Sinai Hospital, Canada

Purpose: Several tissues, including colon, express the vitamin D receptor (VDR) and the vitamin D-activating enzyme CYP27B1, which mediate the anti-proliferative effects of 1,25-dihydroxyvitamin D [1,25(OH)2D], the active vitamin D metabolite. However, in vivo evidence for this has been lacking because of the technical difficulty in measuring 1,25(OH)2D in human tissue. We have developed a robust method to measure 1,25(OH)2D concentration in human tissue. The objectives of this study were: 1) to determine whether 1,25(OH)2D is present in human colon tissue, and 2) to characterize the relationship between human colon and serum 1,25(OH)2D concentrations. Methods: Serum and normal colon specimens were obtained from 28 patients who had undergone colectomy surgery. Total colon (i.e. mucosa + muscularis) 1,25(OH)2D concentrations were determined by lipid extraction followed by immunoextraction and quantitation by IDS enzyme immunoassay (EIA). Serum 1,25(OH)2D and 25(OH)D were measured by IDS EIA and DiaSorin LIAISON EIA, respectively. Results: The mean ($\pm$ SD) concentrations of colon 1,25(OH)2D, serum 1,25(OH)2D, and serum 25(OH)D were 28 $\pm$ 8 pmol/kg, 61 $\pm$ 41 pmol/L, and 62 $\pm$ 26 nmol/L, respectively. Serum and colon tissue 1,25(OH)2D concentrations correlated significantly as expected for a hormone and its target tissue ($r = 0.56$, $p = 0.002$). Regression analysis indicated a significantly positive slope of colon tissue 1,25(OH)2D (pmol/kg) versus serum 1,25(OH)2D (pmol/L) that was 0.12 (95% CI = 0.05-0.19). The corresponding intercept at zero serum 1,25(OH)2D was significantly

positive, 21.4 pmol/kg (95% CI = 16.66-26.18), consistent with local, paracrine production of 1,25(OH)2D. Colon 1,25(OH)2D did not correlate significantly with serum 25(OH)D (r = 0.09, p = 0.66). Conclusions: The hormone 1,25(OH)2D was detected in human colon tissue at physiologically relevant concentrations largely determined by serum 1,25(OH)2D. These results also demonstrate local synthesis of 1,25(OH)2D within colon tissue in vivo.

***Disclosures: Dennis Wagner**, None.*

MO0481

The Vitamin D Analog, Eldecalcitol [1α,25-dihydroxy-2β-(3-hydroxypropyloxy)vitamin D_3], Is a Potent Regulator of Calcium and Phosphate Metabolism. Alex Brown*[1], Jane Finch[2], Eduardo Slatopolsky[3], Cynthia Ritter[1]. [1]Washington University School of Medicine, USA, [2]Washington Univeristy School of Medicine, USA, [3]Washington University in St. Louis School of Medicine, USA

The vitamin D analog, 1α,25-dihydroxy-2β-(3-hydroxypropyloxy)vitamin D3 (eldecalcitol), stimulates bone formation and reduces bone resorption, and has been shown to increase bone mineral density in ovariectomized rats and in post-menopausal women. The present study compared the effects of eldecalcitol and 1,25-dihydroxyvitamin D3 [calcitriol] on calcium and phosphate (Pi) metabolism in normal rats. In the first protocol, eldecalcitol and calcitriol (0. 7.5, 20 or 50 pmol) were administered orally every other day for two weeks. The highest dose of eldecalcitol elevated ionized Ca, enhanced intestinal Ca absorption and increased urinary Ca excretion, while calcitriol had no significant effects at these doses. The high dose eldecalcitol did not alter serum Pi, but stimulated both intestinal Pi absorption and urinary Pi excretion. The increased Pi excretion was attributable, in part, to an increase in serum FGF-23. In a second protocol, the effects of the high-dose eldecalcitol on Ca and Pi absorption and urinary excretion, as well as the increased FGF-23, were found to persist for several days following cessation of treatment, likely due to its higher DBP affinity and slower clearance than calcitriol. Because vitamin D compounds can modulate mineral metabolism indirectly via altering PTH levels, a third protocol examined the effects of eldecalcitol and calcitriol in parathyroidectomized rats that were infused with PTH to normalize Ca levels. Eldecalcitol (50 pmol) had greater effects than calcitriol on serum Ca and urinary Ca excretion. In this model, eldecalcitol and, to a lesser extent, calcitriol (50 pmol) increased intestinal Pi absorption, but decreased serum Pi. This was due to a greater increase in urinary P excretion, secondary to elevations in FGF-23. These studies indicated that with chronic administration, eldecalcitol is more potent than calcitriol in stimulating intestinal Ca and Pi absorption and renal excretion of Ca and P. The higher urinary Pi with eldecalcitol is due to a greater stimulation of FGF-23. The greater effects of eldecalcitol on mineral metabolism are not due to VDR affinity, which is lower, but likely to its higher DBP affinity. The role of DBP binding in the beneficial effects of eldecalcitol on bone is under investigation.

***Disclosures: Alex Brown**, Chugai Pharmaceutical, 2*
This study received funding from: Chugai Pharmaceutical Co., Ltd.

MO0482

Vitamin D_2 from Light-exposed Mushrooms: Bioavailability and Capacity to Suppress the Pro-inflammatory Response to LPS Challenge in Rats. Mona Calvo*[1], Uma S. Babu[1], Larry H. Garthoff[2]. [1]Food & Drug Administration, USA, [2]Food & Drug Adminsitration, USA

High prevalence of poor vitamin D (vit D) status is significantly linked to risk of chronic and infectious diseases due in part to limited intake of naturally rich or vit D-fortified foods. Our objectives are to develop and test UVB-exposed edible mushrooms as a source of vit D that would effectively support vit D status and innate and acquired immunity. We exposed white button mushrooms to UVB light which markedly increased vit D2 content, creating a naturally rich food source. The vit D2 was analyzed in dried mushroom powder from both UVB-exposed (post-harvest) and unexposed mushrooms from the same crop. These mushroom flours were then incorporated into defined rodent diets at the expense of non-nutritive fiber to determine vit D2 bioavailability and function in modulating innate immune response in rats challenged with lipopolysaccharide (LPS). For 10 wk, 300 weanling female rats were fed 1 of 5 diets, all formulated based on AIN93G to contain: 1) Control diet vit D, 1 IU/g; 2) No Vit D; 3) No vit D + 5% unexposed mushroom, 0.12 IU/g; 4) No vit D + 2.5% exposed mushroom, 15 IU/g and 5) No vit D + 5% exposed mushroom, 30 IU/g (Research Diets, New Brunswick, NJ). The rats were estimated to consume 20, 0, 2.4, 300 and 600 IU of vit D2 /d, respectively. At wk 10, rats were challenged with either saline (immune control) or LPS. Blood and tissue were collected at 3, 24 and 72 h post-challenge. Bioavailability was assessed by RIA for plasma total 25-hydroxyvitamin D (25OHD) (DiaSorin, Stillwater, MN) and pro-inflammatory cytokine suppression was assessed by ELISA measuring plasma TNF-α and IL1-β levels at 3 h post LPS. In the table below, we report significant (*p<0.006, **0.01) bio-availability of vit D2 from the UVB-mushroom diets and compared to LPS control-fed rats, we show significant (§p< 0.006) suppression of TNF-α and a trend (p<0.056) toward inhibition of IL1-β levels. In our rat model, chronic intake of vit D2 from UVB exposed mushrooms effectively raises circulating 25OHD and is capable of suppressing induced inflammation.

Diet Group	25OHD x±sem, ng/ml, (n)	TNF-α x±sem, pg/ml, (n)	IL 1-β x±sem, pg/ml, (n)
1) Control vit D,	31.8 ± 1.7 (46)	190 ± 35 (9)	956 ± 140 (9)
2)Control, No Vit D	3.5 ± 0.3 (47)	156 ± 23 (9)	957 ± 142 (9)
3) 5% unexp.mushroom	4.1 ± 0.4 (48)	127 ± 26 (9)	1415 ± 160 (9)
4) 2.5% UVB mushroom	114.1 ± 4.2** (45)	50 ± 7§ (8)	1110 ± 205 (8)
5) 5% UVB mushroom	157.7 ± 4.3* (38)	43 ± 7§ (10)	789 ± 173 (10)

Table 1

***Disclosures: Mona Calvo**, None.*
This study received funding from: The Mushroom Council

MO0483

Vitamin D3 and D2-Rich Yeast are Equally Effective in Improving Trabecular Bone Quality in Vitamin D Deficient Rats. Emily Hohman*[1], Berdine Martin[1], Pamela Lachcik[1], Dennis Gordon[2], James Fleet[1], Connie Weaver[1]. [1]Purdue University, USA, [2]North Dakota State University, USA

Vitamin D (VD) is a major regulator of calcium absorption, and therefore, bone acquisition. It is metabolized to a hormone and works through either endocrine or autocrine mechanisms. Few foods are naturally rich in VD, so new food sources of VD are in high demand. Foods may contain either vitamin D3 (VD3) or vitamin D2 (VD2). We previously reported bioequivalency of VD3 and bread made with VD2-rich yeast on VD status (Hohman et al. 2009 JBMR 24(Supp 1)) and here we report the effects of VD3 and VD2-rich yeast on bone quality in growing VD deficient rats.

4-wk-old male Sprague Dawley rats were fed a VD3 deficient diet (25 IU/kg feed) for 7 weeks. After VD deficiency was established (plasma 25 hydroxyvitamin D (25OHD) = 6.3 nmol/L), the rats were randomized to diets containing either 25 or 1000 IU/kg of either crystalline VD3 or bread made with VD2-rich yeast for 8 weeks. At sacrifice, blood and bones were harvested. Plasma 25OHD was determined by radioimmunoassay. Bone microarchitecture is a determinant of bone strength, so left femurs were scanned by pQCT and microCT at 18 and 50% from the distal end. The effects of VD dose and source on bone parameters were assessed by 2-way ANOVA.

As previously reported, plasma 25OHD level was significantly increased by dietary VD supplementation (15.2 vs. 138.8 nmol/L for VD3, 16.5 vs. 188.2 nmol/L for VD2-rich yeast). pQCT results showed that, compared to rats on the 25 IU VD diet, rats fed 1000 IU VD had 15% greater trabecular BMC and 6% greater trabecular BMD in the distal femur. MicroCT results indicated that rats fed 1000 IU VD had 14% greater trabecular bone and 13% greater connectivity density in the distal femur. There were no statistically significant effects of VD source; nor was there an interaction between VD source and dose, indicating that the bone effects did not differ between VD3 and VD2. No differences were seen at the femoral midshaft, suggesting that the effect of VD was limited to trabecular bone. Our results suggest that VD2-rich yeast baked into bread is equally effective as VD3 at improving trabecular bone quality in VD deficient rats.

***Disclosures: Emily Hohman**, None.*
This study received funding from: Lallemand/American Yeast

MO0484

ACTH Ameliorates Glucocorticoid-Induced Osteonecrosis of Bone. Mone Zaidi[1], Li Sun[2], Lisa Robinson[3], Irina Tourkova[4], Li Liu[3], Yujuan Wang[4], Ling-Ling Zhu[5], Xuan Liu[5], Jianhua Li[6], Yuanzhen Peng[7], Jammel Iqbal*[5], Beatrice Yaroslavskiy[4], Xingming Shi[8], Alice Levine[5], Alex Kirschenbaum[5], Carlos Isales[9], Harry Blair[3]. [1]Mount Sinai Medical Center, USA, [2]Mount Sinai School of Medicine, USA, [3]University of Pittsburgh, USA, [4]Departments of Pathology & of Physiology & Cell Biology, University of Pittsburgh School of Medicine, & the Pittsburgh Veterans Affairs Medical Center, USA, [5]The Mount Sinai Bone Program, Mount Sinai School of Medicine, USA, [6]Tount Sinai School of Medicine, USA, [7]The Mount Sinai School of Medicine, USA, [8]Department of Orthopedic Surgery, Medical College of Georgia, USA, [9]Medical College of Georgia, USA

The long-term use of corticosteroids has given rise not only to a variety of metabolic complications, mainly diabetes and osteoporosis, but also to a painful debilitating condition, osteonecrosis, most commonly involving the femoral head. Osteonecrosis almost invariably requires surgical debridement of dead bone, and contributes to ~10% of the 120,000 hip replacements annually in the US. We report that the anterior pituitary hormone ACTH protects against osteonecrosis of the femoral head induced by depot methylprednisolone acetate (depomedrol), in essence, testifying to its direct effect on the skeleton. Depomedrol (4 mg/kg, daily, s.c.) induced dramatic regional necrosis of the femoral head and suppressed pituitary-derived ACTH in rabbits. This osteonecrosis, visualized as deep tetracycline labeling, was reduced by ~65% when synthetic ACTH was co-administered daily (0.05 μg/kg). This dramatic therapeutic response was associated with an equally profound local up-regulation of VEGF mRNA. In keeping, ACTH also induced VEGF production from mineralizing human osteoblasts in culture. The VEGF up-regulation was associated with a significant increase in osteoblast maturation, seen as an elevation in the marker genes Runx2, osterix, alkaline phosphatase and bone sialoprotein. That the osteoblast maturation induced by ACTH was VEGF-dependent was tested in VEGF shRNA-transfected cells, in which the effect of ACTH was abolished. Furthermore, ACTH withdrawal from osteoblast cultures containing dexamethasone and

ACTH, leaving cells in dexamethasone alone for 36 hours, caused a marked increase in annexin V-positivity, proving that ACTH was critical for cell survival. VEGF production was also induced by co-culturing human osteoblasts with CD14+ osteoclast precursors. Glucocorticoids abolished this effect, showing that endogenous VEGF in bone was sensitive to glucocorticoid inhibition, and was perhaps causal to the osteonecrosis. Finally, a modest stimulation of early osteoclastogenesis was noted in RAW264.7 cells and murine osteoclast precursors, with little or no effects on bone resorption by mature osteoclasts. The results not only substantiate our view regarding a novel pituitary-bone axis, in which stimulating hormones, such as ACTH, FSH and TSH, bypass traditional endocrine targets to effect the skeleton directly, but also, on a broader clinical front, call for studies to examine the efficacy of ACTH in preventing human osteonecrosis

***Disclosures: Jammel Iqbal**, None.*

ADULT BONE AND MINERAL WORKING GROUP

WG1

Bilateral Atypical Subtrochanteric Femoral Fractures in Patients on Chronic Bisphosphonate Therapy. Esther Lee, Chaaya Makjija, and Sunil Wimalawansa, Division of Endocrinology, Department of Medicine, UMDNJ, Robert Wood Johnson Medical School, USA.

Bisphosphonate have been available for over two decades. Long-term bisphosphonate therapy will maintain BMD, but with reduced bone remodeling as demonstrated by biochemical markers of bone turnover. Furthermore, there is no credible evidence indicating that continuation of bisphosphonate therapy beyond 5 to 6 years has added beneficial effects on fracture reduction.

Recent reports suggest an association of atypical subtrochanteric femoral fractures with prolonged use of bisphosphonate. These factures have some commonalities including prodromal symptoms such as thigh pain prior to sustaining a fracture, thickened cortices, and having transverse fractures. Although bisphosphonates significantly reduce fractures including hip fractures, the prolonged use may increase the atypical subtrochanteric fractures; a relatively uncommon event. Recently, we had six patients who sustained atypical subtrochanteric femoral fractures. Here we report two postmenopausal women who had antecedent thigh pain, and subsequently suffered bilateral subtrochanteric femoral fractures. Both subjects had been treated with oral bisphosphonate, alendronate for over six years, and sustained, non-traumatic bilateral subtrochanteric femoral fractures. Instead of osteoporotic thin cortices, both had thickened cortices around the fracture sites, bilaterally. Such hyper-mineralization does not seem to add strength to the bones.

The numbers of such fractures reported to date are insufficient to make firm conclusions of its etiology. Although there could be a number of reasons for such fractures including genetic susceptibilities, preexisting conditions, inappropriate treatment with bisphosphonates (e.g., treatment of patients with normal BMD) etc., there may also be an association between long-term bisphosphonate use and atypical subtrochanteric femoral stress fractures. The correlation of long term use of bisphosphonates and such fractures may have been overlooked. This is important since bisphosphonates such as alendronate have been in the market for over 13 years and if such an association exist, then this complication may augment with time. Physicians should have a high index of suspicion for patients present with thigh pain or dysfunction, and who are treated with a bisphosphonates longer than 5 years. Imaging with a ^{99}Tc-bone scan or MRI are helpful in identifying patients vulnerable for such fractures, when in most circumstances, plain radiographs are likely negative.

***Disclosures:** Sunil Wimalawansa has nothing to disclose.*

WG2

Cortical Thickening and Fissure Fracture of Outer Cortex of Femoral Mid-Shaft: An Early manifestation of SSBT Following Long-term Biphosphonate Therapy? S. Qiu, L.F. Rojas, R. Greenberg, M. Samuel, T. Guthrie, D. Sudhaker Rao. Henry Ford Hospital, U.S.A.

Femoral mid-shaft fractures following long-term bisphosphonate (BP) therapy have received much attention recently. However, very little is known about pathogenesis of these fractures. We encountered 3 women on long-term BP therapy who presented with what appears to be the earliest manifestation of severely suppressed bone turnover (SSBT) fractures.

Materials & Methods: Three post-menopausal white women (78y, 87y, and 61y) each developed localized mid thigh pain 3-6 months before an x-ray diagnosis of fissure fractures of the outer cortex of femoral mid-shaft associated with cortical thickening and irregularities. Each patient had low initial BMD (lowest T-scores: -3.9 at spine; -1.5 at hip; & -3.0 at spine respectively) before BP therapy, which they took for 5-13 years before the onset of mid thigh pain. In 2 patients prophylactic intra-medullary rod was placed and the other is being considered for the same. A tetracycline labeled bone biopsy was performed from the iliac crest and from the distal femur in the first 2 patients.

Results: The x-rays showed incomplete outer cortical irregularities with confirmed fissure fracture by MRI. Bone specific alkaline phosphatase was normal in the first 2 patients (26 & 24) and not measured in the third. Urine NTX was normal in the first 2 patients (41 & 29) and low in the third (12). Bone histomorphometry was consistent with SSBT. BP therapy was discontinued with only calcium and vitamin D supplements.

Conclusions: We suggest that prodromal bone deterioration (PBD) associated with localized mid thigh pain appears to be the earliest manifestations of SSBT resulting in femoral shaft fractures in some patients with long-term BP therapy. Further studies are needed to fully characterize the pathogenesis of such fractures.

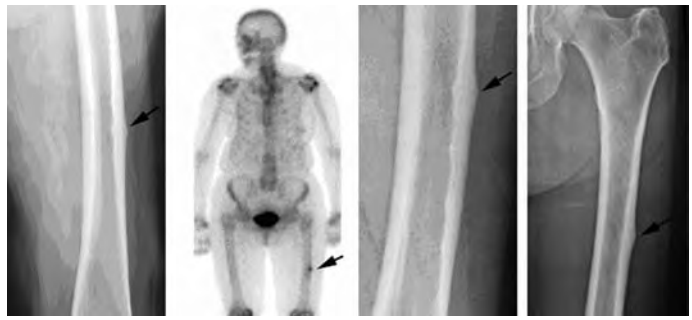

***Disclosures:** Sudhaker Rao has nothing to disclose.*

WG3

Atypical Subtrochanteric Femoral Shaft Fractures Detected by Dual X-ray Absorptiometry. McKiernan FE, Cournoyer S, Hocking J. Marshfield Clinic, USA.

Case reports and small case series have implicated prolonged bisphosphonate (BP) exposure in the etiology of atypical subtrochanteric femoral shaft fractures (ASFSF). On the contrary, reviews of large pharmaceutical databases and national health registries have failed to detect any signal to indicate an excess rate of ASFSF in BP users. Recent high profile reports in the lay media have fueled patient and physician anxiety about monitoring for this potential association. While ASFSF appears to be rare the potential association of ASFSF with BPs could be profound given that $1.7x10^8$ BP prescriptions had been dispensed by 2006. Furthermore, a potential risk horizon could linger long after drug discontinuation since the residence time of BP in bone is prolonged. Periodic bilateral femur X-ray screening of all patients on bisphosphonates would result in excessive radiation exposure and unnecessary cost. Nearly all persons taking BPs and a substantial number of demographically similar persons have periodic DXA examinations. DXA captures the proximal femur and ASFSF has been shown to be apparent by DXA at the point of routine scheduled monitoring, at no extra cost and without the additional radiation exposure of plain radiography. [1] The DXA images of 6 established cases of ASFSF were reviewed retrospectively; 1 case of ASFSF was plainly evident on serial DXA images over 4 years, 3 cases could be appreciated only after very close scrutiny of the DXA image and 2 cases occurred outside the predetermined femoral ROI and therefore could not be seen. None of the 6 cases of ASFSF had been appreciated by the densitometrist on the original clinical DXA interpretation. As a quality improvement initiative 4000 DXA scans of the proximal femur performed consecutively between 2008 and 2009 (including the 6 previously identified cases) were blindly re-reviewed for evidence of ASFSF and no additional case was found. Since there is precedent for the detection of ASFSF by DXA densitometrists should be vigilant for these fractures in patients presenting for routine DXA. A prospective observational study is underway.

1. J Clin Densitom 2010;13:102-3.

***Disclosures:** McKiernan FE has received consulting fees from Amgen.*

WG4

Postmenopausal Female with Pycnodysostosis and Bilateral Mid-femoral Fractures. Clarke BL. Mayo Clinic Division of Endocrinology, Diabetes, Metabolism, and Nutrition, and Mayo Clinic College of Medicine, USA.

Purpose To describe a single postmenopausal female with pycnodysostosis and bilateral mid-femoral fractures.

Methods The case history and laboratory data of a 57 year-old postmenopausal female with pycnodysostosis referred for evaluation and management of left mid-femoral fracture non-union were reviewed.

Results A 57 year-old female was referred for evaluation and management of left femur mid-shaft fracture nonunion. She had been treated with focal ultrasound for one month after orthopedic surgery to stimulate fracture healing, with slow improvement in her x-rays. She had a right femur mid-shaft stress fracture precipitated by a fall on her driveway 18 months earlier. She developed her left femur mid-shaft stress fracture about six months after her right femur stress fracture, which was followed by a completed fracture after another fall. She had no previous fractures, and had never taken oral or IV bisphosphonates, or other antiresorptive therapy.

She had been diagnosed with pycnodysostosis 44 years earlier, based on her x-rays, physical appearance, and laboratory evaluation. She had previously declined genetic

testing for cathepsin K deficiency. She had an affected sister, but no other affected family members, and no consanguinity in her family. Her physical examination at age 13 years showed frontal bossing, thickening of her calvarium, malar hypoplasia, proptosis, slight esophoria with down-slanting palpebral fissures, small mandible with persistent primary teeth, loss of her mandibular angle, dental malalignment, severe caries, hypoplasia of her distal phalanges, and increased skeletal x-ray density throughout.

Her past medical history was unremarkable, and was taking no medications. Her supplements included black cohosh for hot flashes, calcium citrate + D 600 mg/200 IU twice daily, and one multivitamin each day.

Her laboratory studies were normal, with her serum BSAP 12 mcg/L (normal postmenopausal female, <22), and serum CTx-telopeptide 422 pg/mL (normal postmenopausal female, 104-1,008).

Her BMD in 2003 showed her lumbar spine T-score +3.6, right femoral neck T-score +5.0, and right total hip BMD T-score +5.8. Her BMD on the same densitometer in 2008 showed her lumbar spine T-score +2.6 (6.7% decrease), right femoral neck T-score +4.1 (7.1% decrease), and right total hip T-score +4.1 (11.5% decrease). Her skeletal survey showed diffuse patchy sclerosis throughout, shortening of her forearms, and acro-osteolysis of her left fifth distal phalanx.

Conclusions This case report illustrates that decreased bone turnover resulting from cathepsin K deficiency may be associated with bilateral mid-femoral fractures, similar to that associated with long-term bisphosphonate therapy.

Disclosures: *Bart L Clarke does not have any relationships to disclose.*

WG5

Total parathyroidectomy for Tumor Induced Hypophosphatemic Osteomalacia: A Novel Curative Surgical Therapy? Sanjay Bhadada, Gary B. Talpos and D. Sudhaker Rao. Postgraduate Institute of Medical Education & Research, Chandigarh, India, and, Henry Ford Hospital, USA.

Introduction : Tumor induced osteomalacia (TIO) is an acquired disorder of phosphate metabolism in which phosphate wasting is mediated by phosphatonins secreted by the tumor. Excision of the tumor is desirable and is almost always curative, but the detection of tumor is often elusive. Life long treatment with large and frequent daily doses of oral phosphate with varying doses of calcitriol is necessary. Focused radiation of the lesion or calcimimetics are other alternative therapies. We report an unusual case of TIO with 19 year follow-up during which he required subtotal parathyroidectomy (PTX) for hypercalcemic hyperparathyroidism, but normalization of serum P was ultimately achieved with deliberate total PTX based on a report published in 1969.

Case report: A 56y old white man was first seen in 1990 in the Bone & Mineral Clinic at the age of 36y and was diagnosed to have acquired hypophosphatemic OM by bone biopsy. His case was reported as an atypical form of hypophosphatemic OM sharing several features of the genetic form of the disease (Bone 1985). From 1990 to 1998 he was treated with oral phosphate and calcitriol with clinical, biochemical, and bone histologic improvement, but required chronic therapy to maintain serum phosphate around 2.3 mg/dl (<2.5 mg/ml most of the time). All available imaging techniques (whole body CT, MRI, PET and octreo scans) failed to localize the tumor except for a 3 x 5 cm lytic lesion in the distal left femur. After extensive discussion with the patient and his family medical therapy was opted because the lesion did not resemble mesenchymal tumor and potential for complete resection was considered high risk due to its proximity to the knee joint.

At age 44y, he developed hyperpcalcemic autonomous hyperparathyroidism as result of long term phosphate therapy, a well known complication of chronic phosphate therapy. Despite lowering and discontinuing calcitriol therapy hypercalcemia persisted requiring sub-total PTX with removal of 3½ glands. He did well from July 1998 to December 2003 on oral phosphate and calcitriol therapy, but serum phosphate was still <2.5 mg/dl. Serum PTH increased from 10 pg/ml to 75 pg/ml over the next 4 years. Serum FGF-23 was 1495 RU/ml (reference range: ≤180 RU/ml). Because of poor response to medical treatment, deliberate total PTX was considered based on a report published in 1969. After discussion with the patient and an experienced parathyroid surgeon (GBT), the decision was made to remove the remaining half parathyroid gland. After total PTX on November 3, 2008, serum PTH became undetectable (<10 pg/ml) and serum phosphate normalized almost immediately and remained within the reference range (always >2.5 mg/ml) over the next 18 months (April 2010) without oral phosphate therapy and despite elevated serum FGF-23 levels. The calcitriol dose was reduced to maintain serum calcium ~8.5 mg/dl.

Conclusion: To the best of our knowledge, this is first case of TIO in which normalization of serum P was achieved after deliberate PTX despite elevated FGF-23 levels. This implies that PTH plays a permissive role in mediating (or requires?) phosphaturic effect of FGF-23. Further research on the relative contributions of PTH and FGF-23 to hypophosphatemia are warranted.

Disclosures: *Sudhaker Rao has nothing to disclose.*

WG6

Treatment With Teriparitide Of A Persisting Metatarsal Stress Fracture In A Woman With Hypophosphatasia. Irinel Stanciu; Idaho Endocrinology; Boise, ID; Steven Mumm; Washington University School of Medicine, USA; Michael P. Whyte; Washington University School of Medicine, USA; Joseph L. Shaker, Medical College of Wisconsin, USA.

Hypophosphatasia (HPP) is caused by deficiency of the tissue-nonspecific isoenzyme of alkaline phosphatase (TNSALP). Affected adults often develop insufficiency fractures which heal poorly, but may mend with teriparitide (PTH 1-34) treatment whereby osteoblasts can be stimulated to increase alkaline phosphatase (ALP) activity. A 43 year-old woman born with a bowed right leg was diagnosed with HPP at age 8 years. At that time, she reportedly had normal serum calcium, elevated serum phosphorus, markedly reduced ALP, and elevated urinary phosphoethanolamine consistent with HPP. She had suffered premature loss of her baby teeth, as well as multiple cavities and dental procedures. About 14 months before referral, pain developed across the instep of her right foot. A stress fracture involved the right fifth metatarsal in a "splay" foot. Her height was 145 cm, weight 60.9 kg, and BMI 29. The right foot was wider than the left, and tender across the dorsal surface; other bones were not tender. The right lower extremity was about 5 cm short. Surgical intervention for the stress fracture was considered. She had normal serum calcium, albumin, inorganic phosphate, 25-hydroxyvitamin D, and intact PTH levels, but ALP was markedly low at 3 IU/L (25-150), and bone-specific ALP (BAP) was 0.9 µg/L (less than 21.3). Radiographs revealed a nondisplaced transverse fracture of the proximal right fifth metatarsal where technetium bone scan showed increased activity. TNSALP gene analysis showed two missense mutations: exon 5, c.422C>A, p.Thr141Asn and exon 6, c.535G>A, p.Ala179Thr. After about 18 months without radiographic healing, teriparitide was administered 20 µg subcutaneously daily. Soon after, serum BAP was increased. After five months of therapy, there was significant clinical improvement with some evidence of radiographic healing. Teriparitide was stopped after 10 months because clinical symptoms resolved together with radiographic healing. There is no established medical treatment for HPP. Recently, enzyme replacement therapy with TNSALP bioengineered for targeting to bone has been effective in short-term studies of pediatric patients. In our patient, and two previously reported cases, teriparitide seemed effective for unhealed stress fractures in adults with HPP.

Disclosures: *Joseph L. Shaker has nothing to disclose; Irinel Stanciu had nothing to disclose.*

WG7

A Case Report of PTHrP Mediated Hypercalcemia during Pregnancy. AL Carrelli, G Page-Wilson, TJ Reid, SJ Silverberg. Columbia University College of Physicians & Surgeons, USA.

We were called to see a 36-year-old female G1P0 at 22 wks gestation for hypercalcemia. At 14 wks she developed persistent nausea and vomiting, associated with intermittent abdominal pain and constipation. When a 9-pound wt loss was noted at 18 wks, she was admitted. Corrected calcium was 14.8 mg/dL. She was treated with IV fluids and anti-emetics. She was readmitted at 22 wks with an additional 11-pound weight loss. Past history: Notable for a large uterine fibroid, 15.9 x 9.1 x 12 cm prior to pregnancy. No family history of cancer. Home medications: prenatal vitamin and metoclopramide.

Physical exam: Cachectic. No lymphadenopathy. A 1 cm mobile nodule in the right breast. Abdominal exam: 15-cm tender mass in the right lower quadrant. Gravid uterus.

Labs: calcium 13.3 mg/dL, phosphorus 2.3 mg/dL, BUN 11 mg/dL, creatinine 0.6 mg/dL. albumin 2.9 g/dL, alkaline phosphatase 165 U/L, amylase 149 IU/L, lipase 182 U/L, SPEP normal. CBC: hemoglobin 7.8 g/dL, hematocrit 24.3%, white cell count 21,900/mm^3, platelets 570,000/mm^3. Hormonal evaluation: PTH <3 pg/mL, 25-hydroxyvitamin D 19 ng/mL, 1,25-dihydroxyvitamin D 73 pg/mL, AM cortisol 32.8 µg/dL, TSH 1.44 mU/L. PTHrP 51 pg/mL (nl range: 14-27 pg/mL). Repeat PTHrP one week later remained elevated (40 pg/mL).

Work up: Normal breast ultrasound. MRI chest/abdomen: marked enlargement of the known fibroid, now 23 x 15 x 14.7 cm; no significant lymphadenopathy. Peripheral flow cytometry and a bone marrow biopsy: no lymphoma or acute leukemia.

The patient required continuous IV fluids, steroids, and intermittent IV furosemide to keep her corrected calcium around 11 mg/dL. Urgent cesarean section was done at 33 wks for pre-eclampsia and vaginal bleeding. She delivered a male infant, Apgar 8/9, wt 1955 gm, with normal calcium levels. The patient's hypercalcemia resolved within 48 hrs of delivery. She remains normocalcemic 2 months post-partum. Repeat PTHrP is pending.

This case highlights the rare occurrence of PTHrP-mediated hypercalcemia during pregnancy. Malignancy work-up was negative. There are case reports of PTHrP mediated hypercalcemia in non-pregnant women due to uterine fibroids. However, the patient's hypercalcemia resolved promptly following delivery without removal of the fibroid. In this patient, the PTHrP is more likely to have been placental in origin. This rare cause of hypercalcemia and other sources of PTHrP-mediated hypercalcemia during pregnancy will be reviewed.

Disclosures: *Angela L Carrelli has nothing to disclose.*

WG8

Primary Hyperparathyroidism and Severe Hypocalciuria in a Patient with Three Homozygous Mutations of the CASR Gene. Pauline Camacho, MD, Monica Komorowski, MD and Steven Dejong, MD Loyola University Medical Center, USA.

Objective: To describe the first case of primary hyperparathyroidism, corrected surgically, in a patient with persistent and severe hypocalciuria and three homozygous mutations of the CASR gene (3031 G>C, 492+19G>A, 2244 G>C).

Case presentation: Pt is a 51 yr old female with a history of sickle cell disease and gout was referred to the endocrine service in 2007 for hypercalcemia. There was no family history of hypercalcemia or personal history of nephrolithiasis or intake of medications affecting calcium metabolism. Physical examination was unremarkable. Her serum calcium was 10.9 mg/dL (normal range: 8.9-10.3 mg/dL), ionized calcium 1.46 (normal range: 1.15-1.30 mm/L), phosphorus 3.8 mg/dL (normal range: 2.5-4.7 mg/dL), intact PTH 235 pg/mL (normal range: 10-65 pg/mL). Vitamin D-1,25 OH was 15.9 pg/mL (normal range: 15-75 pg/mL). Vitamin D-25 OH was 7 ng/mL and a 24 hour urine calcium level was 62 mg/24 hours (normal range: 150-250 mg/24 hours). TSH was 0.36 UU/mL (normal range: 0.4-4.4 UU/mL) and free T4 was 0.8 ng/dL (normal range: 0.8-1.7 ng/dL). (attributed to sick euthyroid syndrome). DXA scan revealed lumbar spine BMD of 1.007 gm/cm2 with a T score of -1.6 and femoral neck BMD of 0.810 gm/cm2 with a T score of -1.6.

She was initially started on cholecalciferol 1000 international units daily and was referred to the endocrine surgeon. Subsequent labs showed an ionized calcium 1.48 mmol/L, calcium 10.9 mg/dL and PTH 311 pg/mL. 24 hour urine calcium was undetectable despite weeks of weekly ergocalciferol 50,000 IU. Sestamibi scan showed uptake near the inferior pole of the left lobe of the thyroid.

The patient underwent a subtotal parathyroidectomy with excision of an 870 mg left inferior parathyroid adenoma. Post op serum calcium was 9.3 mg/dL. Repeat labs revealed ionized calcium 1.25 mmol/L, phosphorus 4.1 mg/dL PTH 108 pg/mL, vitamin D-25 OH 16 ng/mL and 24 hour urine calcium < 2mg/24 hours. At this time, the patient was taking ergocalciferol weekly for 3 months but was not as compliant with her calcium intake. She was then prescribed calcitriol 0.25 mcg daily in addition to ergocalciferol 50,000 international units weekly and was advised to take 1200 mg of calcium carbonate daily.

In 6/2008, labs were obtained showed near normalization of 25- OH D and PTH levels but persistent hypocalciuria: The patient was found to have three homozygous mutations, 3031 G>C, 492+19G>A, 2244G>C that have not previously been associated with familial hypocalciuric hypercalcemia (FHH).

Conclusion: To our knowledge, this is the first report of simultaneous primary hyperparathyroidism and hypocalciuria, associated with three homozygous mutations of the CASR gene not previously linked to FHH.

Disclosures: *Pauline Camacho, MD has received research grants from Eli- Lilly and Procter & Gamble Pharmaceuticals, Inc.. Monica Komorowski has nothing to disclose.*

WG9

Fluorosis Associated With Chronic Voriconazole Therapy. Robert A. Wermers, M.D.[1], Kay Cooper, M.D.[2], Gary M. Whitford Ph.D., D.M.D.[3] Raymund R. Razonable, M.D.[4,5], Paul J. Deziel, P.A.-C.[5], and Thomas Moyer, Ph.D.[6] [1]Department of Internal Medicine and the Division of Endocrinology, Diabetes, Nutrition, and Metabolism, Mayo College of Medicine, Mayo Clinic, Rochester, Minnesota, USA., [2]Department of Radiology, Mayo College of Medicine, Mayo Clinic, Rochester, Minnesota, USA., [3]School of Dentistry Medical College of Georgia, Augusta, Georgia, USA, [4]Department of Internal Medicine and the Division of Infectious Diseases, Mayo College of Medicine, Mayo Clinic, Rochester, Minnesota, USA., [5]William J von Liebig Transplant Center, Mayo Clinic, Rochester, Minnesota, USA, and [6]Department of Laboratory Medicine, Mayo College of Medicine, Mayo Clinic, Rochester, Minnesota, USA.

Introduction: Voriconazole, a triazole antifungal agent, contains 3 fluoride atoms. Although voriconazole has not been previously associated with fluoride toxicity, it was the only identified source of fluoride in this patient with fluorosis.

Methods: Fluoride in plasma was quantified using a La Motte pH PLUS Direct pH/mV/ISE/Temp meter equipped with a fluoride-specific electrode from Orion Research, Cambridge, MA. The fluoride concentration in bone ash was determined using the ion-specific electrode (Orion Research, Model 9409) and a minature calomel reference electrode coupled to a potentiometer (Orion Research, Model 720A) after overnight HMDS-facilitated diffusion.

Case: A 64 year-old female presented with diffuse bone pain 4 years after a heart transplant for idiopathic dilated cardiomyopathy. Her immediate postoperative course was complicated by aspergillus pneumonia treated with voriconazole, which she remained on since. Six months after the transplant, she experienced painful bony growths, starting with her fingers, which progressed to her wrists, elbows, legs, and feet requiring the use of hydrocodone and fentanyl. Skeletal x-rays revealed innumerable heterotopic and periosteal ossifications arising from the cortical surfaces of multiple bones in the axial and appendicular skeletal. A bone scan limited to the shoulders, head, and thorax showed multiple foci of increased tracer uptake in both of the scapulae, ribs, and thoracic spine. Laboratory findings revealed high bone turnover and an elevated plasma fluoride level (20.7 μMol/L). She denied typical sources of fluoride. Fluoride water testing from her primary residence and lake-home were 0.70 mg/L and 0.17 mg/L respectively. A transiliac crest bone biopsy showed thickened and increased osteoid covered surfaces with poorly resolved tetracycline labels consistent with a mineralization defect. Bone fluoride levels were 10,964 mg/kg ash (ppm), 9202 mg/kg ash, and 10,305 mg/kg ash consistent with fluorosis. Shortly after the patient discontinued voriconazole her pain symptoms improved, the alkaline phosphatase level dropped by 50% and her plasma fluoride level decreased to13.2 μMol/L.

Conclusion: Chronic voriconazole therapy appears to be an important cause of systemic fluoride excess.

Disclosures: *Robert A. Wermer has nothing to disclose.*

Numeric

B

C

D

E

F

G

H

I

J

K

L

M

N

O

P

Q

R

S

T

U

V

W

X

Y

Z

(Key: 1001-1300 = Oral, FR = Friday Plenary poster, SA = Saturday poster, SU = Sunday poster, MO = Monday poster)

(Key: 1001-1300 = Oral, FR = Friday Plenary poster, SA = Saturday poster, SU = Sunday poster, MO = Monday poster)

C

(Key: 1001-1300 = Oral, FR = Friday Plenary poster, SA = Saturday poster, SU = Sunday poster, MO = Monday poster)

(Key: 1001-1300 = Oral, FR = Friday Plenary poster, SA = Saturday poster, SU = Sunday poster, MO = Monday poster)

D

(Key: 1001-1300 = Oral, FR = Friday Plenary poster, SA = Saturday poster, SU = Sunday poster, MO = Monday poster)

E

F

(Key: 1001-1300 = Oral, FR = Friday Plenary poster, SA = Saturday poster, SU = Sunday poster, MO = Monday poster)

G

(Key: 1001-1300 = Oral, FR = Friday Plenary poster, SA = Saturday poster, SU = Sunday poster, MO = Monday poster)

H

(Key: 1001-1300 = Oral, FR = Friday Plenary poster, SA = Saturday poster, SU = Sunday poster, MO = Monday poster)

(Key: 1001-1300 = Oral, FR = Friday Plenary poster, SA = Saturday poster, SU = Sunday poster, MO = Monday poster)

I

J

K

(Key: 1001-1300 = Oral, FR = Friday Plenary poster, SA = Saturday poster, SU = Sunday poster, MO = Monday poster)

L

(Key: 1001-1300 = Oral, FR = Friday Plenary poster, SA = Saturday poster, SU = Sunday poster, MO = Monday poster)

M

(Key: 1001-1300 = Oral, FR = Friday Plenary poster, SA = Saturday poster, SU = Sunday poster, MO = Monday poster)

(Key: 1001-1300 = Oral, FR = Friday Plenary poster, SA = Saturday poster, SU = Sunday poster, MO = Monday poster)

N

(Key: 1001-1300 = Oral, FR = Friday Plenary poster, SA = Saturday poster, SU = Sunday poster, MO = Monday poster)

O

(Key: 1001-1300 = Oral, FR = Friday Plenary poster, SA = Saturday poster, SU = Sunday poster, MO = Monday poster)

P

(Key: 1001-1300 = Oral, FR = Friday Plenary poster, SA = Saturday poster, SU = Sunday poster, MO = Monday poster)

Q

R

(Key: 1001-1300 = Oral, FR = Friday Plenary poster, SA = Saturday poster, SU = Sunday poster, MO = Monday poster)

S

(Key: 1001-1300 = Oral, FR = Friday Plenary poster, SA = Saturday poster, SU = Sunday poster, MO = Monday poster)

(Key: 1001-1300 = Oral, FR = Friday Plenary poster, SA = Saturday poster, SU = Sunday poster, MO = Monday poster)

T

(Key: 1001-1300 = Oral, FR = Friday Plenary poster, SA = Saturday poster, SU = Sunday poster, MO = Monday poster)

U

V

(Key: 1001-1300 = Oral, FR = Friday Plenary poster, SA = Saturday poster, SU = Sunday poster, MO = Monday poster)

W

(Key: 1001-1300 = Oral, FR = Friday Plenary poster, SA = Saturday poster, SU = Sunday poster, MO = Monday poster)

X

Y

Z

(Key: 1001-1300 = Oral, FR = Friday Plenary poster, SA = Saturday poster, SU = Sunday poster, MO = Monday poster)